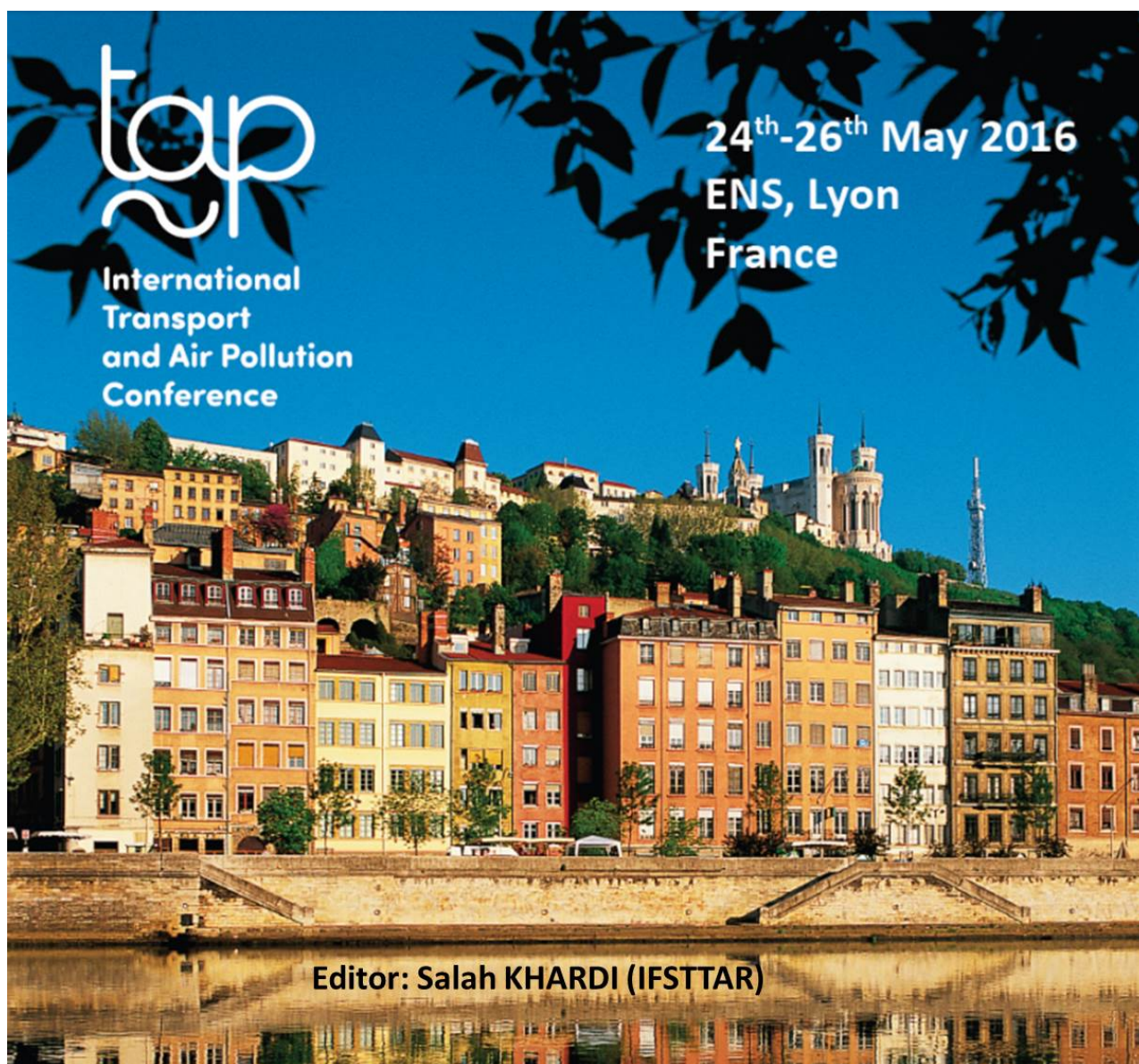


*The provisional proceedings of the
21st International Transport and Air Pollution Conference
"TAP 2016"*



Towards energy transition and cleaner transport



ISBN N°: 978-2-85782-716-0

GENERAL REMARKS

Provisional proceedings

- Abstracts and papers appear by author, in alphabetic order
- This provisional version contains papers submitted up to May 13th 2016 whereas the deadline was April 29th 2016
- In the following final program:
 - two sub-topics have been removed because no abstract has been submitted in those,
 - a few sub-topics have been combined under the main heading of the session each time the number of the accepted abstracts was not sufficient to constitute a thematic session
- The table of contents indicates only the names of the first author of each abstract
- Some abstracts and papers were partially submitted or not submitted on-line but were sent directly to the TAP 2016 chairman (S. Khardi):
 - these papers have been added at the end of the table of contents and at the end of the proceedings
 - the authors of these papers do not appear in the “Author Index” but only in the participant list
- **A final version will be available after the conference**
- **The best 40 papers will be selected to be published in the Journal of Earth Sciences & Geotechnical Engineering**

Welcome message

Dear Colleagues and Friends,

On behalf of the Organizing Committee, it is my great pleasure to cordially welcome all the participants to the 21st International Transport and Air Pollution Conference "TAP 2016", held in Lyon, France from May 24th to 26th, 2016.

The scientific program provides an opportunity for participants to exchange new ideas and information on many important issues in the fields of transport, air pollution and control systems. High keynotes and tutorial lectures have been prepared by outstanding scholars invited both from academia and industry. TAP 2016 will be the place to be for the participants to make new acquaintance and strengthen cooperative relationships.

France is one of the most dynamic countries in the world acting for environmental improvement. Good facilities and its sharp beauty combined with its historical heritage makes France an attractive country to visit, where science, art, and society coexist in harmony.

I wish to express my warm welcome to you all and to encourage for active participation at the TAP 2016 Conference. I hope you will enjoy both the conference and your stay in Lyon.

Thank you very much.



*Salah KHARDI, PhD HDR, Senior Researcher
French Institute of Science and Technology for Transport, Development and
Networks (IFSTTAR)
Transport and Environment Laboratory*

A handwritten signature in blue ink, consisting of a stylized 'S' followed by a horizontal line and a small vertical tick at the end.

21st International Transport and Air Pollution Conference

**Salah KHARDI PhD HDR, Research Director (IFSTTAR, France)
President of TAP 2016**

International Transport and Air Pollution Conferences have been held since 1986 in Graz (Austria), Zurich (Switzerland), Avignon, Reims and Toulouse (France), Boulder (Colorado, USA), Thessaloniki (Greece), the last one being again in Graz. The 21st TAP conference will take place in Lyon (France) with the aim of bringing together scientists, international experts, users and decision makers to share their contributions on the current scientific knowledge of air pollution due to emissions from transport systems. Public authorities and state or local government agencies with jurisdiction over transport or air quality, community groups, operators, commercial carriers, nonprofit and other business entities are invited to participate and are welcome.

Transport sectors play a strategic and major role in the global market and fast changing economic and societal frame. Technologies, policies and citizen behaviors must be continually adapted towards the reduction of fossil energy and the increasing demand for mobility etc.

The 21st International Transport and Air Pollution Conference, organized by the French Institute of Science and Technology for Transport, Development and Networks ([IFSTTAR](#)) - Mobility, Planning and Environment Department (AME) will take place from May 24th (8:30 am) to 26th, 2016 (6:00 pm) in Lyon (France) at the Ecole Normale Supérieure (ENS of Lyon). Its aim is to create a stage for exchanging the latest research results and sharing the advanced research methods and technologies.

The aim of TAP 2016 will be “Towards energy transition and cleaner transport” and their implication to air quality, with an emphasis on the programme topics.

Key issues

1. Emission sources and future trends for emission control
2. Impacts, green mobility, transport policies, control strategy, societal challenges and counter-measures
3. Vehicle technological improvement, traffic management, infrastructures, green integrated transport, smart cities and mobility
4. Turning scientific breakthroughs into innovative products and services that provide environmental security and improve people's health

Main Topics

The aim of TAP 2016 will be “Towards energy transition and cleaner transport” and their implication to air quality, with an emphasis on the following topics:

- **Exhaust and non-exhaust emissions from transport modes: measurements and modelling**
- Characteristics of primary and secondary air pollutants (gases and aerosols, particles, VOCs, GhG, ...)

- Physical, chemical processes and mechanisms of air pollution
- Real driving emissions (RDE)
- **Emission control and technologies**
 - Emission Control Technologies of primary air pollutants of road and non-road transport
 - Electric and Hybrid Vehicles induced emission control
 - Building and maintenance of road infrastructures (roads, tunnels, new materials and technologies)
 - Cleaner trucks, buses and non-road machines
- **Transport, energy consumption and greenhouse gas emissions**
 - Energy efficient technologies and alternative fuels
 - Energy optimization of transportation systems
- **Urban and suburban air quality**
 - Air quality measurement, monitoring and modelling
 - Transport and non-transport emission interactions
 - Human exposure and health impacts
 - Impacts on ecosystems: ground and water contamination, assessment methodologies, impact models
- **Transport policies and mobility challenges towards cleaner cities**
 - Intelligent Transport Systems and traffic management
 - Environmental legislation, green mobility and teleworking
 - Economic impacts and instruments
 - Societal challenges (perception of air quality and acceptability)
- **Tutorial on modelling and energy management of hybrid electric vehicles coping with environmental issues**

Part 1 – Modelling and Part 2 - Energy Management

Modes addressed

Road: highways, urban, suburban and rural roads, passenger and freight transport, motor vehicles (cars, trucks, buses, powered 2-wheelers)

Rail and Air: passenger and freight

Waterborne: maritime, in-land waterborne, short sea shipping, passenger transport and cruises, containers, dredging

Cross-modality: co-modality, inter-modality, combined transport, public transport

TAP 2016 is an opportunity and a multi-disciplinary event, to bring together all the actors in order to exchange ideas about transport and environment questions, with a particular emphasis on truck emission control (technical, management, economic and policy matters). It will contribute to the European transport competitiveness. The conference topics address the main challenges in transport, with respect to energy, environment and economy issues. TAP 2016 aims to explore the most advanced research works and innovations, the latest technological and industrial developments and implementations, and innovative policies, in Europe and worldwide.

TAP 2016 comprises:

- plenary sessions with invited speakers,
- scientific and technical sessions on the conference topics, where the accepted papers will be presented, either as oral or poster presentations,
- invited sessions, to be suggested and organized by project leaders, submitted to the organizers committee for acceptance, without published papers.

Exhibition will be held during the conference, aimed at governmental and professional organisations, public and private research organizations, and industrial companies.

Networking event (Side event)

**M.F. Sherratt-Roux (IFSTTAR - DAEI)
National Contact Point (NCP) - Transport**

Within the framework of the international conference TAP 2016, the French National Contact Point (N.C.P.), in the field of Transport, organizes a networking event on 25 May 2016 from 10.30 a.m. to 12.30 p.m.

This networking event will provide an opportunity for the participants of the conference looking for partners, in the context of the 2017 calls, to meet and present their work and their organization, in relation to the Work Programme for Research and Innovation Horizon 2020.

The calls 2017 being dealt with will refer to the topics and modes being covered during TAP 2016, based on the Transport Work Programme 2016-2017 as well as other challenges (Energy, Environment, Climate...).

To be noted:

- The calls planned for 2017 are announced in the preliminary Work Programmes 2016-2017 which are in the process of being revised
- The changes will be very limited and will be based on either a clarification of the existing texts or a very slight revision of the budgets
- The Work Programmes should be adopted by the European Commission in July 2016 and the opening date of the calls is planned on 20 September 2016

Organising Committee

TAP 2016 chairman

Salah KHARDI, PhD HDR, Senior Researcher

French Institute of Science and Technology for Transport, Development and Networks (IFSTTAR).

Transport and Environment Laboratory

Cité des Mobilités.25, avenue F. Mitterrand. 69675 Bron -France

Email: Salah.khardi@ifsttar.fr

Tel.: + 33 4 72 14 24 79

Fax: +33 4 72 37 68 37

Main organiser

French Institute of Science and Technology for Transport, Development and Networks (IFSTTAR)

Mobility, Planning and Environment Department (AME Department)

Transport and Environment Laboratory (LTE)

<http://www.ifsttar.fr>

IFSTTAR Organising Committee

S. Khardi (LTE), S. Pelissier (LTE), G. Da Silva (LTE), N. Teillac (DG - COM), M.F. Sherratt-Roux (DAEI), D. Pillot (LTE), R. Trigui (LTE).

Registration

Alexandra Richard (IFSTTAR AME)

Co-organisers

- *LUTB Transport & Mobility Systems*
Rhône-Alpes Automotive Cluster
www.lutb.fr - www.automotive-cluster.fr
- *European Commission*
Joint Research Centre. Institute for Energy and Transport
Sustainable Transport Unit. Ispra, Italy
<https://ec.europa.eu/jrc/>

International Scientific Committee

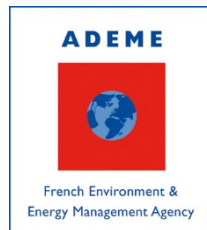
Jürgen Blassnegger (TUG, Austria)
Pierre Bonnel (JRC, European Commission)
Alain Bouscayrol (Lille University, France)
Thomas Bütler (EMPA, Switzerland)
Aurélie Charron (IFSTTAR, France)
Panagiota Dilara (DG-GROW, European Commission)
Asif Faiz (FA, USA)
Laurent Gagnepain (ADEME, France)
Maria-Cristina Galassi (JRC, European Commission)
Christian George (IRCELYON, France)
Stefan Hausberger (TUG, Austria)
Mario Keller (MKC, Switzerland)
Salah Khardi (IFSTTAR, France)
Norbert Ligterink (TNO, NL)
Raphael Luz (TUG, Austria)
Joeri Van Mierlo (Vrije Universiteit Brussel, Belgium)
Nikolas Moussiopoulos (LHTEE/AUTH, Greece)
Leonidas Ntziachristos (LAT/AUTH, Greece)
Martin Rexeis (TUG, Austria)
Zisis Samaras (LAT/AUTH, Greece)
Ernesto Sanchez-Triana (World Bank, USA)
Ake Sjödin (IVL, Sweden)
Robin Smit (DSITI and University of Queensland, Australia)
Peter Sturm (TUG, Austria)
Martin Weilenmann (MODESTIA, Switzerland)

Chairmen of sessions

Tim Wallington (Ford Motor Company, USA)
Norbert Ligterink (TNO, NL)
Thomas Bütler (Automotive Powertrain Technologies Laboratory, EMPA, Switzerland)
Ms Joanna Szychowska (European Commission, Belgium)
Christian George (IRCELYON, France)
Nour-Eddin El-Faouzi (IFSTTAR, France)
Dilara Panagiota (JRC, European Commission)
Mario Keller (INFRAS, Switzerland)
Stefan Hausberger (TUG, Austria)
Laurent Gagnepain (ADEME, France)
Salah Khaldi (IFSTTAR LTE, France)
Åke Sjödin (IVL, Sweden)
Ernesto Sanchez-Triana (World Bank, USA)
Klaus Schäfer (IMK-IFU, Germany)
Serge Pelissier (IFSTTAR LTE, France)
Zisis Samaras (LAT/AUTH, Greece)
Leonidas Ntziachristos (LAT/AUTH, Greece)
Jürgen Blassnegger (TUG, Austria)
Maria-Cristina Galassi (JRC, European Commission)
Nikolas Moussiopoulos (LHTEE/AUTH, Greece)
Asif Faiz (FA, USA)
Tim Wallington (Ford Motor Company, USA)
Michel DEPROST (Editor-in-Chief Enviscope, France)
Peter Sturm (TUG, Austria)
Marc Lejeune (LUTB / Renault Trucks, France)
Yinon Rudich (Weizmann Institute, Israel)
Pierre Bonnel (JRC, European Commission)
Barbara D'Anna (Ircelyon, France)
Aurélie Charron (IFSTTAR, France)
Rochdi Trigui (IFSTTAR, France)
Harikishan Perugu (Univ. of Cincinnati, USA)
Robin Smit (DSITIA and University of Queensland, Australia)

Acknowledgments for supporting partners

- François Boguet (Accountancy, IFSTTAR)
- Yannick Barborini (CNRS/CSSD/IN2P3) is acknowledged for the great support he provided to the TAP 2016 organisation in its intensive and successful use of Scienceconf (<http://www.sciencesconf.org>).



ARISTOTLE
UNIVERSITY OF
THESSALONIKI



TAP 2016 Final Program

Please note that only the name of the first author is indicated. However, TAP proceedings will include the names of all the contributors.

Day 1: Tuesday 24th May 2016

8:00	Registration - coffee
PLENARY SESSION (Amphitheater)	
8:45	<p>Opening – Welcome</p> <p><i>Chairmen: Salah Khardi (Senior Researcher, IFSTTAR, France) and Thomas Bütler (Head of Vehicle Systems Group. Automotive Powertrain Technologies Laboratory, EMPA - Switzerland)</i></p> <p><i>Hélène Jacquot-Guimbal (General Directorate, IFSTTAR)</i></p> <p><i>Philippe Grand (President of LUTB Transport & Mobility Systems and IVECO France)</i></p>
9:00	Ms. Ségolène Royal (Minister of the Environment, Energy and Marine Affairs, responsible for International Climate Relations - France) or her representative: to be confirmed
9:30	<p>Ms Joanna Szychowska (European Commission. DG Internal Market, Industry, Entrepreneurship and SMEs. Unit - Automotive and Mobility Industries, Belgium)</p> <p><i>The EU regulatory system for Type Approvals of Motor Vehicles and how to avoid another Dieseldate</i></p>
10:00	<p>Pr Tim Wallington (Ford Motor Company, USA)</p> <p><i>Light-Duty Vehicles Emissions and Urban Air Quality: Past, Present, and Future Perspectives</i></p>
10:45 Amphitheater	
Exhaust and non-exhaust emissions from transport modes : measurements and modelling	
Chairmen: Christian George (IRCELYON, France) and Norbert Ligterink (TNO, NL)	
	<p>In service CO2 and NOX emissions of Euro 6/VI cars, light- and heavy-duty goods vehicles in real London driving: Taking the road into the Laboratory</p> <p><i>James Tate (Institute for Transport Studies - University of Leeds, United Kingdom)</i></p> <p>PM10 emission effects of new studded tyre regulations</p> <p><i>Mats Gustafsson (Swedish National Road and Transport Research Institute, Sweden)</i></p> <p>Portable Emissions Measurement System (PEMS) data for Euro 6 diesel cars and comparison with emissions modelling</p> <p><i>O'Driscoll Rosalind (Imperial College London, United Kingdom)</i></p> <p>Emissions of NO, NO2, and PM from inland water transportation</p> <p><i>Ralf Kurtenbach (Bergische Universität Wuppertal, Germany)</i></p>

10:45 Room B

Transport policies and mobility challenges towards cleaner cities

Chairmen: Tim Wallington (Ford Motor Company, USA) and Asif Faiz (FA, USA)

Evaluation of E-mobility co-benefits in Klagenfurt

Ulrich Uhrner (Traffic & Environment, IVT, Graz University of Technology, Austria)

ESPRIT: a new carsharing concept - A socio-economic assessment from Lyon region, France

Sadeghian Shadi (VEDECOM Institute, France)

Analyzing effectiveness of air quality management policies in Peru: improvements and challenges

Gomes Lima Ana Luisa (World Bank, USA)

Vehicle fleet composition in urban environment

Eijk Arjan (TNO, Netherlands)

Decomposition of Low emission zone strategies into mechanisms and methodology for assessing their impacts on air pollution

Pasquier Anaïs (IFSTTAR, France)

Combined air quality and noise evaluation of transport policies: methodology and feedbacks

Philippe Dunez (CEREMA, France)

Reducing Freight Transport Pollution by using Electric good vehicles in Paris region

Montenon Antoine (LUTB-RAAC, France)

10:45 Room C

Intelligent Transports Systems and traffic management

Chairman: Nour-Eddin El-Faouzi (IFSTTAR, France)

Air pollution and energy consumption mitigation by Parking Guiding System

Benhassine Sana (Ecole Supérieure Commerce Tunis, Tunisia)

Sustainability Enhancement of Urban Traffic Routing via Multi Criteria Optimisation

Nai Oleari Alberto (Automotive, Infrastructure & Transportation Division, Altran Technologies, France)

Combining microscopic traffic modelling and 3 pollutant emission modellings to assess modifications of traffic supply and demand

Badin Anne-Laure (Cerema, France)

truckRCS - Truck Rail Cargo System - Road & Rail Network Innovation

Korn Patrick (Voith Engineering Services GmbH, Germany)

An Efficient Lane-based Strategy to provide an Eco-Signal Pre-emption Control System Using Connected Vehicles Technology

Noaen Mohammad (Department of Electrical and Computer Engineering, University of Calgary, Canada)

12:30 Lunch Break

13:30 Poster session

Chairmen: Serge Pelissier and Didier Pillot (IFSTTAR, France)

14:30 Amphitheater**Exhaust and non-exhaust emissions from transport modes : measurements and modelling**

Chairwoman: Dilara Panagiota (JRC, European Commission)

Particle mass size distribution relation to train traffic and type in a railway tunnel

Mats Gustafsson (Swedish National Road and Transport Research Institute, Sweden)

Modelling non-exhaust emissions of road salt using the NORTRIP model

Rolstad Denby Bruce (Norwegian Meteorological Institute, Norway)

DPF regeneration of Euro5 Diesel vehicles as source of fine and ultrafine particles in the atmosphere

Barbara D'Anna and R'mili Badr (IRCELYON, France)

Intercomparison of three modeling approaches for road dust resuspension using two experimental data sets

Thouron Laëtitia (CEREA, France)

How selection techniques on traffic data sets can help in estimating network vehicle emissions

*Schiper Nicole (IFSTTAR ENTPE, France)***14:30 Room B****Building and maintenance of road infrastructures (roads, tunnels, new materials and technologies)**

Chairman: Mario Keller (INFRAS, Switzerland)

Influence of pavement management on road traffic emissions and associated costs

Pellecier Luc (Département de génie de la construction, École de technologie supérieure, Canada)

Potential and methods to reduce GHG emissions from road infrastructure

Johansson Håkan (Swedish Transport Administration, Sweden)

BIOTAIR : Biofiltration treatment, promising results for reducing road traffic pollutants

Petit Jean-François (CEREMA, France)

Use of cement-based materials containing activated carbon to improve air quality in road-transport infrastructures: pilot field tests done in France & Spain

*Isabelle Dubois-Brugger (LafargeHolcim R&D, France)***14:30 Room C****Transport, energy consumption and Greenhouse Gas emissions**

Chairmen: Stefan Hausberger (TUG, Austria) and Laurent Gagnepain (ADEME, France)

ITS environmental monitoring: Development of an innovative method based on unique data for traffic management and traffic user information

Heidegger Fabian (ITS Vienna Region, Public Transport Authority Eastern Region, Austria)

The most promising environmental innovations in inland waterway transport

Consuegra Sara (Verbeek, Netherlands)

<p>Monitoring Specific Energy Consumption and CO2 Emissions from Rail Traction Activity <i>A. Braschi (Sustainable Development Unit, International Railways Union, France)</i></p> <p>Using a simplified Willans line approach as a means to evaluate the savings potential of CO2 reduction measures in Heavy-Duty Transport <i>Zyl Stephan (TNO, Netherlands)</i></p> <p>Impact assessment of vehicle technology, fuel, and ICT measures on CO2 emissions from road traffic to 2030 <i>Papadimitriou Giannis (Emisia S.A., Greece)</i></p> <p>Modal Shifting Effects and Climate Impacts through Electric Bicycle Use in Germany <i>Kaemper Claudia (Institut für Energie- und Umweltforschung, Germany)</i></p>
--

16:00 Coffee Break

16:30 Amphitheater

Exhaust and non-exhaust emissions from transport modes : measurements and modelling

Chairmen: Salah Khaldi (IFSTTAR, France) and Peter Sturm (TUG, Austria)

<p>An emissions inventory for non-road mobile machinery (NRMM) in Switzerland <i>Notter Benedikt (INFRAS Research and Consulting, Switzerland)</i></p> <p>Evaluation of emissions and fuel consumption of Heavy-Duty Vehicles in urban areas <i>Zamboni Giorgio (Dept. MEMTE - University of Genoa, Italy)</i></p> <p>Development of Road Transport Emissions: Case Study of Singapore for 2004-2014 <i>Arimbi Jinca (TUM CREATE, Singapore)</i></p> <p>RemIAG model: Bottom-up emissions inventories for cities with lack of data <i>Ibarra Sergio (Instituto de Astronomia, Geofisica e Ciencias Atmosfericas, Sao Paulo - Brazil)</i></p> <p>A comprehensive evaluation method for instantaneous emission measurements <i>Weller Konstantin (Graz University of Technology, Austria)</i></p>
--

16:30 Room B

Transport and non-transport emission interactions

Human exposure and health impacts

Chairman: Åke Sjödin (IVL, Sweden)

<p>Investigation on lowering commuters' in-vehicle exposure to ultrafine particles <i>Xu Bin (Tongji University, Shanghai - China)</i></p> <p>Air quality in urban Mass Transit Systems: indoor/outdoor interrelations <i>Muresan Bogdan (IFSTTAR, France)</i></p> <p>Risk Exposure of BTEX Emissions from a Diesel Refuelling Station in Johannesburg, South Africa <i>Moolla Raesa (University of the Witwatersrand, South Africa)</i></p> <p>Reconstructing past and present dioxins atmospheric pollution scenarios in the city of Lyon <i>Coudon Thomas (Santé Individu Société – SIS, France)</i></p>

	Effects of bike lane features on cyclists' exposure to black carbon and ultrafine particles <i>Lonati Giovanni (Politecnico di Milano, Italy)</i>
16:30 Room C	
Transport, energy consumption and Greenhouse Gas emissions	
Chairman: Ernesto Sanchez-Triana (World Bank, USA)	
	<p>Analysis of Diurnal Trends in Vehicle Fleet Composition and their Emission Contribution on an Urban Arterial Road in Leeds, UK <i>Wyatt David (University of Leeds, United Kingdom)</i></p> <p>Vehicle emissions in Turkey: Current status and policy options for the future <i>Mock Peter (International Council on Clean Transportation, Germany)</i></p> <p>Market fuel properties and CO₂ emissions for mobility <i>Ligterink Norbert (TNO, Netherlands)</i></p> <p>Scenario analysis of CO₂ emissions in the period 2015-2035 from passenger vehicles in Ireland <i>Alam Md Saniul (Environmental Protection Agency, Ireland)</i></p> <p>Prospective of the city and the daily mobility: which tools for the environmental assessment? <i>Francois Cyrille (LET ENTPE, France)</i></p> <p>An Alternative Energy Efficiency Index Offer to Reduce CO₂ Emissions from Ships: Fleet Energy Efficiency Management Index <i>Gorkem Kokkulunk (Yildiz Technical University, Turkey)</i></p> <p>A real-world test and demonstration project for assessing consumption and emission of Natural Gas Heavy Good Vehicles: Equilibre Project <i>F. Baouche (IFSTTAR, France)</i></p>
16:30 Room D	
PRESS CONFERENCE	
18:00 End of day 1 sessions	
19:15 - Welcome Cocktail	

Day 2: Wednesday 25th May 2016

8:00	Registration - coffee
PLENARY SESSION (Amphitheater)	
Chairmen: Klaus Schäfer (IMK-IFU, Germany) and Zissis Samaras (LAT/AUTH, Greece)	
8:30	Marie-Françoise Sherratt-Roux (French National Contact Point - Transport, France) <i>Presentation of Horizon 2020 calls for 2017 in the area of Transport and air pollution</i>
9:00	Dr Rodolfo Lacy Tamayo Ph.D. (Subsecretario de Planeación y Política Ambiental, México) <i>Air Pollution Control and Fuel Subsidies in Mexico</i>
9:30	Pr Sergio Sanchez (CEO and Executive Director - Clean Air Institute) <i>Analyzing effectiveness of air quality management policies in Peru: improvements and challenges</i>
10:00 Coffee Break	
10:30 Amphitheater	
Exhaust and non-exhaust emissions from transport modes : measurements and modelling	
Chairmen: Leonidas Ntziachristos (LAT/AUTH, Greece) and Jürgen Blassnegger (TUG, Austria)	
	<p>Vehicle emission model for traffic simulations <i>Ligterink Norbert (TNO, Netherlands)</i></p> <p>Numerical investigation of diesel particulate matters in the exhaust tailpipe <i>Talebizadeh Pouyan (Amirkabir University of Technology, Iran)</i></p> <p>The relative importance of tailpipe and non-tailpipe emissions on the oxidative potential of ambient particles in Los Angeles, CA <i>Shirmohammadi Farimah (University of Southern California, USA)</i></p> <p>Elucidating the origin of the enrichment in aromatic compounds in Paris megacity atmosphere <i>Salameh Thérèse (LISA, France)</i></p> <p>Effect of Lane Closure on Vehicle Trajectories and Emissions: Simulation and Real-World Evaluation <i>Hartmann Martin (Institute for Transportation Research and Education, North Carolina State University, USA)</i></p> <p>Laboratory and Field Measurements of Solid Particle Number Concentration <i>Tritscher Torsten (TSI GmbH, Germany)</i></p>
10:30 Room B	
Real driving emissions (RDE)	
Chairwoman: Dilara Panagiota (JRC, European Commission)	
	<p>Quality Assurance of PEMS Emissions Data aimed for the Development of Real-world Vehicle Emission Factors <i>Katsis Petros (EMISIA S.A., Greece and School of Civil Engineering, University of Queensland, Australia)</i></p>

	<p>Variations of real world NOx emissions of diesel Euro 5 and 6 light-duty vehicles <i>Kadijk Gerrit (TNO, Netherlands)</i></p> <p>How vehicle emissions vary through the day, week and year: Evidence from telematics data <i>Luc Pellecuer (Département de génie de la construction, École de technologie supérieure, Canada)</i></p> <p>Exhaust emissions from in-service inland waterways vessels <i>Pillot Didier (IFSTTAR, France)</i></p> <p>Real driving emissions as a determinant for the sustainable transport system development <i>Merkisz Jerzy (Poznan University of Technology, Poland)</i></p>
10:30 Room C	
Environmental legislation, green mobility and teleworking	
Chairman: Maria-Cristina Galassi (JRC, European Commission)	
	<p>Amending EU Regulations 443/2009 and 510/2011 on CO2 emissions from Light Duty Vehicles following the introduction of the WLTP <i>Pavlovic Jelica (European Commission, Joint Research Centre, Italy)</i></p> <p>On the potential for lightweight electric vehicles to facilitate one-way trips in and around city centres <i>R. Mounce (Centre for Transport Research, University of Aberdeen, UK)</i></p> <p>Developments on Eco-innovations: procedure and calculation examples <i>Malfettani Stefano (European Commission, Joint Research Centre, Italy)</i></p>
10:30 Room D	
Networking event	
<p>Networking event with the opportunity to present your organization, project ideas and your skills <i>The French National Contact Point – Transport (France)</i></p>	
12:30 Lunch Break	
13:30 Poster session - Rochdi Trigui (IFSTTAR, France) and Didier Pillot (IFSTTAR, France)	
14:30 Amphitheater	
Exhaust and non-exhaust emissions from transport modes : measurements and modelling	
Chairmen: Norbert Ligterink (TNO, NL) and Nikolas Moussiopoulos (LHTEE/AUTH, Greece)	
	<p>PM10 non-exhaust emission factors from tunnel measurements using a novel approach accounting for wall deposition and resuspension <i>Ulrich Uhrner (Traffic & Environment, IVT, Graz University of Technology, Austria)</i></p> <p>Effect of measurement protocol on organic aerosol measurements of exhaust emissions from gasoline and diesel vehicles <i>Kim Youngseob (CEREA, France)</i></p> <p>Urban Taxis and their contribution to the air pollution and CO2 emission: Case study of Singapore <i>Arimbi Jinca (TUM CREATE, Singapore)</i></p>

	<p>Dilution and temperature effects on ultrafine particle emissions at the exhaust outlet of Diesel and gasoline passenger cars <i>Louis Cédric (IFSTTAR, France)</i></p> <p>VOC emissions from the vehicle evaporation process: species and underestimation <i>Man Hanyang, School of Environment, Tsinghua University (China)</i></p> <p>Uncertainty estimation of road transportation emissions at metropolitan scale <i>Chen Ruiwei (CEREA, France)</i></p>
14:30 Room B	
Emission Control Technologies of primary air pollutants	
Chairmen: Asif Faiz (FA, USA) and Tim Wallington (Ford Motor Company, USA)	
	<p>Low-temperature catalytic oxidation of vinyl chloride emission over Ru modified Co₃O₄ catalysts <i>Chao Wang (East China University of Science and Technology, China)</i></p> <p>Development of a resistive soot sensor <i>Grondin Didier (IRCELYON, France)</i></p> <p>Performance of in-use buses retrofitted with diesel particle filters <i>Rafael Fleischman (Technion - Israel Institute of Technology, Israel)</i></p> <p>Active Diesel Particulate Filters and Nitrogen Dioxide Emission Limits</p> <p>Potential of In-Motion-Charging buses for the Electrification of Urban Bus Lines <i>Fabian Bergk (ifeu – Institut für Energie, Germany)</i></p>
14:30 Room C	
Tutorial on modelling and energy management of hybrid electric vehicles coping with environmental issues	
Part 1 – Modelling	
Alain Bouscayrol (Lille University - MEGEVH Network, France)	
<ul style="list-style-type: none"> - <i>Structural and functional descriptions / Backwards and forwards approaches</i> - <i>Different modeling objectives / Graphical descriptions</i> - <i>Requirements for energy management of HEVs</i> 	
14:30 – 17:00 Room D	
ROUND TABLE	
Air pollution in the cities	
Air quality improvement for the well-being of citizens	
Moderator: Michel DEPROST (Editor-in-Chief Enviscope, France)	
	<p>Debate involving journalists, scientific and political personalities (in French):</p> <ul style="list-style-type: none"> • Actions for the present and the future based on the following topics: air quality monitoring, health and environmental impacts, new fuels, abatement devices and technologies of emissions, urban traffic management, ... • How to act on the citizen behaviors to reduce health, environmental and climatic impacts of pollutant emissions?

	<p>Participants:</p> <ul style="list-style-type: none"> - Marie-Blanche Personnaz (General Directorate, Air Rhône Alpes) - Bernard Garnier (President ATMO France) - Laurent Gagnepain (ADEME, France) / Salah KHARDI (IFSTTAR, France) - Gilles Vesco (Responsible for Soft mobility in Grand-Lyon ; Inventor of Velo'Ov) - Lionel Brard (Deputy Mayor of Valence - France, Vice-President of the Urbail Community of Valence Romans Sud-Isère, Former President of "France Nature Environnement") - Eric Wiart (Municipal Councillor – Urban logistics and mobility, Grenoble)
<p>16:00 Coffee Break</p>	
<p>16:30 Amphitheater</p>	
<p>Air quality measurement, monitoring and modelling</p>	
<p>Chairmen: Zissis Samaras (LAT/AUTH, Greece) and Peter Sturm (TUG, Austria)</p>	
	<p>Wireless sensor networks deployment for air pollution monitoring <i>Boubrima Ahmed (URBANET, France)</i></p> <p>Coupling traffic and emission models: dynamic driving speed for emissions assessment <i>Lejri Delphine (IFSTTAR-ENTPE, France)</i></p> <p>Traffic-related and meteorological influences on air pollutant concentrations at an urban background station in Berlin during BÄRLIN2014 <i>Schäfer Klaus (Karlsruhe Institute of Technology, Institute of Meteorology and Climate Research, Department of Atmospheric Environmental Research, Germany)</i></p> <p>Evaluation of Black Carbon sources and geographical origins in Lorraine: multi-site approach and near real time data <i>Petit Jean-Eudes (Air Lorraine, France)</i></p>
<p>16:30 Room B</p>	
<p>Emission Control Technologies of primary air pollutants</p>	
<p>Chairmen: Marc Lejeune (LUTB / Renault Trucks, France) and Asif Faiz (FA, USA)</p>	
	<p>Impact of engine warm-up and DPF active regeneration on regulated & unregulated emissions of a Euro 6 Diesel vehicle equipped with urea SCR catalyst <i>Leblanc Mickaël (IFP Energies Nouvelles, France)</i></p> <p>Active Diesel Particulate Filters and Nitrogen Dioxide Emission Limits <i>Ibrahim Osama (Department of Mechanical Engineering, College of Engineering & Petroleum, Kuwait University, Kuwait)</i></p> <p>Real time measurements of VOCs by transportable mass spectrometry using chemical ionization methods: a breakthrough innovative product for air quality analysis <i>Leprovost Julien (AlyXan, France)</i></p> <p>A simplified temperature model for the three way catalytic converter <i>Varun Pandey (IFSTTAR, France)</i></p>

16:30 Room B

**Transport and non-transport emission interactions
Human exposure and health impacts**

Chairmen: Yinon Rudich (Weizmann Institute, Israel) and Maria-Cristina Galassi (JRC, EC)

Effective air quality management: lessons from Latin America

Enriquez Santiago (The World Bank, USA)

Possible health effects of repeated exposures to re-suspended urban dust: the effect of non-tailpipe emissions

Rudich Yinon (Weizmann Institute of Science, Israel)

Evaluation of exposure to particulate air pollution and its lung deposition among cyclists in the Perth Metropolitan Area

Shrestha Anu (Curtin University, Australia)

New compact technology for cabin air purification

Lamaa Lina (Brochier Technologies, France)

Does air pollution modify the impact of aircraft noise on mortality from cardiovascular disease? Results of an ecological study in France

Evrard Anne-Sophie (IFSTTAR, France)

16:30 Room C

**Tutorial on modelling and energy management of hybrid electric vehicles
coping with environmental issues**

Part 2 - Energy Management

Rochdi Trigui (IFSTTAR - MEGEVH Network, France)

- *Energy management definition*
- *Rule based approaches*
- *Optimization based approaches*
- *From offline assessment to online implementation*
- *Pollutant emissions as constraints*
- *Pollutant emissions as part of the optimization*

16:30 Room D

PRESS CONFERENCE

18:00 End of day 2 sessions

 **Departure from conference venue to conference dinner (coach organized)**

19:00 - GALA DINNER

Day 3: Thursday 26th May 2016

8:00	Registration - coffee
PLENARY SESSION (Amphitheater)	
Chairman: Christian George (IRCELYON, France) and Ernesto Sanchez-Triana (World Bank, USA)	
8:30	Dr Yewande Awe (World Bank, Washington DC, USA) <i>The World Bank's work on "Clean air and healthy lungs"</i>
9:00	Pr Sergio Sanchez (CEO and Executive Director - Clean Air Institute) <i>Effective air quality management: lessons from Latin America</i>
9:30	Pr Yinon Rudich (Department of Earth and Planetary Sciences, Weizmann Institute, Israel) <i>Health effects of repeated exposures to re-suspended urban dust</i>
10:00 Coffee Break	
10:30 Amphitheater	
Real driving emissions (RDE)	
Chairmen: Laurent Gagnepain (ADEME, France) and Pierre Bonnel (JRC, European Commission)	
	<p>A new approach for systematic use of PEMS data in emission simulation <i>Claus Matzer (Technical University of Graz, Austria)</i></p> <p>Real life emissions of Euro 6 diesel cars and operation of emission control systems <i>Cuenot Francois (Transport and Environment, Belgium)</i></p> <p>Real-world driving cycles for light-duty vehicles in the Netherlands <i>Geilenkirchen Gerben (Netherlands Environmental Assessment Agency – PBL, Netherlands)</i></p> <p>Modelling the effect on air quality of Euro 6 emission factor scenarios <i>Toenges-Schuller Nicola (AVISO GmbH, Germany)</i></p> <p>Recent remote sensing measurements of emissions from heavy-duty buses and passenger cars in Sweden <i>Jerksjö Martin (IVL Swedish Environmental Research Institute, Sweden)</i></p>
10:30 Room B	
Air quality measurement, monitoring and modelling	
Chairman: Tim Wallington (Ford Motor Company, USA)	
	<p>Investigating the influence of the calibration and validation of cell-transmission traffic flow model on average-speed based emissions prediction <i>Sayegh Arwa (University of Leeds, United Kingdom)</i></p> <p>Urban air: An operational air quality management tool at high resolution for cities <i>Galineau Julien (NUMTECH, France)</i></p> <p>Air-noise observatory regional and local scale exposure to air and noise pollution <i>Didier Chapuis (Air Rhône-Alpes, France)</i></p>

	<p>Investigation of Volatile Organic Compounds Exposure inside Vehicle Cabins in China <i>Xu Bin (Tongji University, Shanghai - China)</i></p> <p>Exposure Analysis in Pearl River Delta (PRD) Based on Land Use Regression (LUR) <i>Xiaofan Yang (School of Environment, Tsinghua University, Beijing, China)</i></p>
<p>10:30 Room C</p>	
<p style="background-color: #00b050; color: white; text-align: center;">Transport, energy consumption and Greenhouse Gas emissions</p>	
<p style="text-align: center;">Chairman: Nikolas Moussiopoulos (LHTEE/AUTH, Greece)</p>	
	<p>Quantification of the effect of WLTP introduction on CO2 emissions from passenger cars <i>Tsokolis Dimitris (Laboratory of Applied Thermodynamics, Greece)</i></p> <p>Transport energy consumption in Tunisia: growth which needs to be stopped <i>Harizi Besma (High School of Business Tunis, University of Manouba, Tunisia)</i></p> <p>The validation of CO2MPAS tool for supporting the introduction of WLTP in the European CO2 certification scheme <i>Fontaras Georgios (European Commission, Joint Research Centre, Italy)</i></p> <p>Real-world driving, energy demand and emissions of electrified vehicles <i>Kugler Ulrike (German Aerospace Center, Germany)</i></p> <p>Greenhouse gas emissions from heavy duty vehicles using upgraded biogas as a fuel <i>Winther Morten (Department of Environmental Science, Aarhus University, Denmark)</i></p>
<p>10:30 Room D</p>	
<p style="background-color: #00b050; color: white; text-align: center;">Exhaust and non-exhaust emissions from transport modes : measurements and modelling</p>	
<p style="text-align: center;">Chairwoman: Barbara D'Anna (Ircelyon, France)</p>	
	<p>MOVES-Matrix Energy Consumption and Emission Modeling Applied to Individual Vehicles <i>Liu Haobing (Georgia Institute of Technology, USA)</i></p> <p>Calculating emissions from road transport on a street level with COPERT4 and COPERT street level, a case study <i>Kouridis Chariton (EMISIA SA, Greece)</i></p> <p>An investigation of evaporative VOC emissions from petrol light duty vehicles in Europe using different oxygenated fuels <i>Mellios Giorgos (EMISIA SA, Greece)</i></p> <p>Physical characterization of fine and ultrafine particle emissions from non-exhaust road transport in urban and suburban areas. New project development <i>Khardi Salah (IFSTTAR, France)</i></p> <p>Experiences and Results with different PEMS <i>J. Czerwinski (University of Applied Sciences, Switzerland)</i></p> <p>Quantifying the air pollutants from construction and service life of roads <i>Younes Mohamed (Menoufia University, Egypt)</i></p>
<p>12:30 Lunch Break</p>	

14:00 Amphitheater**Real driving emissions (RDE)****Chairmen: Pr Sergio Sanchez (Clean Air Institute) and Harikishan Perugu (Univ. of Cincinnati, California Air Resources Board, USA)**

Measurement of late-model diesel automobile real driving emissions of reactive nitrogen compounds with on-board FTIR analyzer

Vojtisek Michal (Czech Technical University in Prague, Czech Republic)

Modelling exhaust emissions of normal driving and crossings, respectively, using the PHEM model

Janhäll Sara (Swedish National Road and Transport Research Institute, Sweden)

High-resolution mapping of vehicular emissions for the entire municipality of Beijing based on real-world dynamic traffic data

Yang Daoyuan (State Key Joint Laboratory of Environment Simulation and Pollution Control, Tsinghua University, China)

Experiences and Results with different PEMS

J. Czerwinski (University of Applied Sciences, Switzerland)

Why do diesel cars emit more NOX on the road than during certification?

Bart Degraeuwe (European Commission, JRC - Institute for Environment and Sustainability, Air and Climate Unit, Italy)

Study of Traffic Real Driving Emissions in Madrid in 2015 and conclusions

De La Fuente Josefina (Remote Sensing Laboratory, Spain)

14:00 Room B**Air quality measurement, monitoring and modelling****Chairman: Aurélie Charron (IFSTTAR, France)**

Ultrafine particle measurement and characterization for air quality monitoring

E. Zimmermann (CEA, France)

Assessment of the area affected by particulate matter generated by freight transportation over unpaved roads using computational fluid dynamics

Prato Daniel (Instituto Tecnológico de Estudios Superiores de Monterrey, Mexico)

Dust absorption performance of urban trees in roadsides of Ho Chi Minh city

Huynh Trong Nguyen (Ho Chi Minh City University of Technology, Vietnam)

Influence of Gaps Between Buildings on Air Quality in Cities, Two Case Studies

Gruber Karin (consulting gruber, Austria)

Analysing impacts of intense ethanol fuel use on urban VOCs burden and composition

Dominutti Pamela (Department of Atmospheric Sciences - University of São Paulo, Brazil)

Determination of the influence of meteorological parameters on the ambient VOC concentrations in an industrial town located Aegean coast of Turkey

Doğan Güray (Akdeniz University, Turkey)

14:00 Room C

Economic impacts and technological instruments

Chairman: Rochdi Trigui (IFSTTAR, France)

Why Own a Hybrid? A Global Total Cost of Ownership Analysis for the Private and Company Car Driver

Palmer Kate (University of Leeds, United Kingdom)

Personal mobility choices and climate change: which incentives are effective?

Raux Charles (Laboratoire d'économie des transports, France)

Economies of scale and density in the public road transport sector in Tunisia

Ezghani Amine (Department of Management, University of Sfax, Tunisia)

Can electric delivery vans compete with internal combustion engine ones? A constraint analysis

Camilleri Pierre (IFSTTAR University of Paris-Est, France)

Parametric study on trajectory optimization

Setareh Javanmardi (IFSTTAR, France)

An Investigation for the Fuel Price Escalations on Optimum Speed in Maritime Transportation

Eda Turan (Yildiz Technical University, Turkey)

15:45 Coffee Break

15:45 - 16:30 Amphitheater

TAP 2016 CLOSING PLENARY SESSION

Chairman: Thomas Bütler (Automotive Powertrain Technologies Laboratory, EMPA, Switzerland)

+ others to be confirmed

POSTER SESSION 1

Day 1: Tuesday 24th May 2016 from 13:30 (for 24 hours)

Title	Author
ERMES - Providing Consolidate Emissions Factors for European Road Transport	<i>M. C. Galassi (Institute for Energy and Transport of the Joint Research Centre (EC, DG JRC), Italy)</i>
CadnaA Model and GIS (Case Study: IKIA Airport)	<i>Kiani Sadr Maryam (Islamic Azad University of Hamedan, Iran)</i>
Light Duty Vehicle Emission Modelling for Indian Cities: Application of US-EPA'S MOVES Model in Hyderabad, India	<i>Perugu Harikishan (Univ. of Cincinnati, USA)</i>
Study of NH ₃ - Standard SCR reactions over a commercial catalyst on powder and mini-SCRF forms	<i>Molina Gonzalez Sonia (IRCELYON, France)</i>
NOX Emission Performance of Vans in Real Urban Driving Using A Remote Sensing Device	<i>Rushton Christopher (Institute for Transport Studies, University of Leeds, United Kingdom)</i>
Fe zeolite supported catalysts for the SCR-NH ₃ reaction	<i>Anguita Paola (IRCELYON, France)</i>
Methods to comply with sulphur regulation for shipping and resulting particle emissions	<i>Fridell Erik (IVL Swedish Environmental Research Institute, Sweden)</i>
Impact of aftertreatment device and driving conditions on PAHs, BTEX, Carbonyl compounds, black carbon, ultrafine particle and NO ₂ emissions for Euro 5 Diesel and gasoline vehicles	<i>Liu Yao (IFSTTAR, France)</i>
Manganese-based catalysts for toluene combustion	<i>Sihaib Zakaria (IRCELYON, France)</i>
VOC emissions from the vehicle evaporation process: species and underestimation	<i>Man Hanyang (School of Environment, Tsinghua University, China)</i>
A semi-empirical comparison of CO ₂ emissions and energy demands of vehicles under the NEDC and WLTP type approval test procedures	<i>Pavlovic Jelica (European Commission, Joint Research Centre, Italy)</i>
Identification of anthropogenic and natural sources of atmospheric particulate matter and trace metals in Constantine, Algeria	<i>Ali-Khodja Hocine (Université des Frères Mentouri, Algeria)</i>
Mixing state and size distribution of aerosols during the tropospheric evolution of urban and industrial plumes	<i>Deboudt Karine (ULCO-LPCA, France)</i>
The interactions of the Exhaust Ultrafine Particle with the vehicle near-wake flow	<i>Mehel Amine (Laboratoire de l'Ecole Supérieure des Techniques Aéronautiques et de Construction Automobile, France)</i>

Assessment of traffic congestion in arterial roads of Tunisian Metropolitan City	<i>Benhassine Sana (Ecole Supérieure Commerce Tunis, Tunisia)</i>
Effect of Road Grade, Vehicle Speed and Vehicle Types on NO2 Emission in Urban Roads in Jordan	<i>Al-Rifai Jawad (Philadelphia University, Jordan)</i>
Traffic emissions study and development of a legal framework in Spain	<i>De La Fuente Josefina (Technet, sostenibilidad en transporte, Spain)</i>
Improved catalyst for decreasing methane emissions from natural gas vehicles	<i>Caravaggio Gianni (Natural Resources Canada, Canada)</i>
Metrological characterization of a remote sensing equipment for on-road emission measurements: Considerations for detecting high-emitter vehicles	<i>Pujadas Manuel (Centro de Investigaciones Energéticas, Medioambientales y Tecnológicas, Spain)</i>
A Combined Method of PAMS and Modelling to Quantify the Emission Benefits of Switching to Hybrid Vehicles in Taxi Fleets	<i>Riley Richard (University of Leeds, United Kingdom)</i>
Space, transport and fuel: District of Tunis	<i>Azaiez Mohamed (Faculty of Economics and management, Tunisia)</i>
Empirical study for absolute relation between GDP per capita and CO2 emissions from transportation, industrialization and an energy mix	<i>Akter Shamema (Bangladesh Economic Association, Bangladesh)</i>
Pre-normative Research on E-mobility: the new European Interoperability Centre	<i>M. C. Galassi (Institute for Energy and Transport of the Joint Research Centre (EC, DG JRC, Italy)</i>

POSTER SESSION 2

Day 2: Wednesday 25th May 2016 from 13:30 (for 24 hours)

Title	Author
ERMES - Providing Consolidate Emissions Factors for European Road Transport	<i>M. C. Galassi (Institute for Energy and Transport of the Joint Research Centre (EC, DG JRC), Italy)</i>
GRETA: Gridding Emission Tool for ArcGIS	<i>Schneider Christiane (AVISO GmbH, Germany)</i>
Output growth, energy consumption and reduction potential of CO2 emission in Pakistan transport sector	<i>Ahmad Izhar (China Center for Energy Economics Research, Xiamen University, China)</i>
Effects of Alternative Drivetrain Technologies and -Fuels on CO2-Emissions from Road Traffic in Germany	<i>Piasecki Conrad (Bundesanstalt für Straßenwesen, Germany)</i>
Evolution of traffic related air pollutants in Veszprém County over the past 15 years	<i>Georgina Nagy (University of Pannonia, Hungary)</i>
Non-Intrusive Reduced Basis Methods Applied to Outdoor Pollutant Transport Models	<i>Hammond Janelle Katharine (Laboratoire Instrumentation, Simulation et Informatique Scientifique, France)</i>
PMx traffic resuspension estimation over a Milan area domain	<i>Pepe Nicola (Politecnico di Milano, Italy)</i>
Impact of train braking systems on particle levels in the Paris subway	<i>Molle Romain (RATP, France)</i>
Polybrominated Diphenyl Ethers (PBDEs) Levels in Indoor Dust	<i>Basaran Bilgehan (Dept. of Environmental Engineering, Kocaeli University, Turkey)</i>
Risk estimation of halogenated POPs in indoor dust in an industrialized city	<i>Civan Mihriban (Kocaeli University, Turkey)</i>
Analysis of spatiotemporal ozone concentrations considering traffic flows and solar radiations in Seoul, Korea	<i>Kim Youngkook (Youngkook Kim, South Korea)</i>
Photocatalytic Oxidation of VOCs for Cleaning Vehicle Cabin Air	<i>M. Bouhatmi (IRCELYON, France)</i>
Contribution of traffic to local PM10 concentrations in urban space? example of Wrocław, SW Poland	<i>Muskala Piotr (Department of Climatology, University of Wrocław, Poland)</i>
Real world performance of ventilation systems for reducing nitrogen oxides or particulate matter levels in road tunnels	<i>Vidal Bruno (CETU, France)</i>
Innovative and efficient novel smart sensors for air pollution monitoring in urban area	<i>Fertier Laurent (ECOLOGICSENSE, France)</i>

Comparative study of three digestion methods for airborne PM10-bound metallic elements in an urban site	<i>Ali-Khodja Hocine (Université des Frères Mentouri-Constantine, Algeria)</i>
Monitoring, assessing, and following up on people's health of air pollution emissions from transport in urban area in Moldova	<i>Stratulat Tatiana (Grigori Friptuleac, Moldova)</i>
Estimation of atmospheric pollutant emissions by transport at Mytilene, Greece, during the tourist season	<i>Kotrika Anna (Inst. for Environmental Research and Sustainable Development, Greece)</i>
Sustainability evaluation of electric taxi fleet in the city of Poznan	<i>Merkisz-Guranowska Agnieszka (Poznan University of Technology, Poland)</i>
Development of Eco-Friendly Vehicle Choice Model	<i>Hahn Jin-Seok (Hye Ran Kim, South Korea)</i>
Pre-normative Research on E-mobility: the new European Interoperability Centre	<i>M. C. Galassi (Institute for Energy and Transport of the Joint Research Centre (EC, DG JRC, Italy)</i>

Timetable summary

	8:00	8:45-10:30	10:30-10:45	10:45-12:30	12:30-14:30	13:30-14:30	14:30-16:00	16:00-16:30	16:30-18:00	19:30
Day 1 Tuesday 24 th May 2016	Registration Coffee	Opening session Plenary session (A)	Coffee Break	Scientific sessions (A, B, C)	Lunch	Poster session 1 (hall)	Scientific sessions (A, B, C)	Coffee Break	Scientific sessions (A, B, C) Press conference (D)	Welcome Cocktail
	Press conference									

	8:00	8:30-10:00	10:00-10:30	10:30-12:30	12:30-14:30	13:30-14:30	14:30-16:00	16:00-16:30	16:30-18:00	19:30
Day 2 Wednesday 25 th May 2016	Registration Coffee	Plenary session (A)	Coffee Break	Scientific sessions (A, B, C)	Lunch	Poster session 2 (hall)	Scientific sessions (A, B, C) Special session HEV (Room C)	Coffee Break	Scientific sessions (A, B, C) Special session HEV (Room C)	Gala Dinner
	Networking event - Room D						Round table (private session - Room D) Press conference			

	8:00	9:00-10:00	10:00-10:30	10:30-12:30	12:30-14:00	14:00-15:30	15:30-15:45	15:45-16:30
Day 3 Thursday 26 th May 2016	Registration Coffee	Plenary Session (A)	Coffee Break	Scientific sessions (A, B, C)	Lunch	Scientific sessions (A, B, C)	Coffee Break	Closing plenary session (A)

A: Amphitheater - B, C and D: Meeting rooms

ISBN N°: 978-2-85782-716-0

Table of contents

Page_Garde1.pdf	1
PROGRAMME_TAP2016_May_13_2016.pdf	12
Empirical study for absolute relation between GDP per capita and CO2 emissions from transportation, industrialization and an energy mix, Akter Shamema	1
Contribution of local Traffic to PM10 Levels and trace metals in Constantine, Algeria, Ali-Khodja Hocine [et al.]	21
Combining microscopic traffic modelling and 3 pollutant emission modellings to assess modifications of traffic supply and demand, Badin Anne-Laure [et al.]	27
Air pollution and energy consumption mitigation by Parking Guiding System, Benhassine Sana [et al.]	38
Wireless sensor networks deployment for air pollution monitoring, Boubrima Ahmed [et al.]	50
Real life emissions of Euro 6 diesel cars and operation of emission control systems, Cuenot Francois [et al.]	66
An assessment of present and future competitiveness of electric commercial vans, Camilleri Pierre [et al.]	80
The most promising environmental innovations in inland waterway trans-	

port, Consuegra Sara	98
Experiences and Results with different PEMS, Czerwinski Jan	104
Combined air quality and noise evaluation of transport policies: methodology and feedbacks, Dunez Philippe [et al.]	112
Analysing impacts of intense ethanol fuel use on urban VOCs burden and composition, Dominutti Pamela [et al.]	125
Determination of the influence of meteorological parameters on the ambient VOC concentrations in an industrial town located Aegean coast of Turkey, Doğan Güray [et al.]	136
Does air pollution modify the impact of aircraft noise on mortality from cardiovascular disease? Results of an ecological study in France, Evrard Anne-Sophie [et al.]	146
Estimation of atmospheric pollutant emissions by transport at Mytilene, Greece, during the tourist season, Fameli Kyriaki-Maria [et al.]	152
The validation of CO2MPAS tool for supporting the introduction of WLTP in the European CO2 certification, Fontaras Georgios [et al.]	160
Prospective of the city and the daily mobility: which tools for the environmental assessment?, Francois Cyrille [et al.]	172
Development of a resistive soot sensor, Grondin Didier [et al.]	188
URBAN AIR: AN OPERATIONAL AIR QUALITY MANAGEMENT TOOL AT HIGH RESOLUTION FOR CITIES, Galineau Julien	200
Real-world driving for light-duty vehicles in the Netherlands, Geilenkirchen Gerben [et al.]	208
A new approach for systematic use of PEMS data in emission simulation, Hausberger Stefan [et al.]	225

RemIAG model: Bottom-up emissions inventories for cities with lack of data, Ibarra Sergio [et al.]	239
On-road emission measurements in Sweden 2007-2015, Jerksjö Martin	240
Potential and methods to reduce GHG emissions from road infrastructure, Johansson Håkan [et al.]	255
Modal Shifting Effects and Climate Impacts through Electric Bicycle Use in Germany, Kaemper Claudia [et al.]	263
Quality Assurance of PEMS Emissions Data aimed for the Development of Real-world Vehicle Emission Factors, Katsis Petros [et al.]	273
Comparative study of three digestion methods for airborne PM10-bound metallic elements in an urban site, Kemmouche Amina [et al.]	291
Calculating emissions from road transport on a street level with COPERT4 and COPERT street level, a case study, Kouridis Chariton [et al.]	300
New compact technology for cabin air purification based on photocatalytic optical fiber textile, Lamaa Lina [et al.]	314
Impact of engine warm-up and DPF active regeneration on regulated & unregulated emissions of a Euro 6 Diesel vehicle equipped with urea SCR catalyst, Leblanc Mickael [et al.]	319
Coupling traffic and emission models: dynamic driving speed for emissions assessment., Lejri Delphine	338
Market fuel properties and CO2 emissions for mobility, Ligterink Norbert [et al.]	346
Developments on Eco-innovations: procedure and calculation examples, Malfetani Stefano [et al.]	354
The interactions of the Exhaust Ultrafine Particle with the vehicle near-wake flow, Mehel Amine [et al.]	363

An investigation of evaporative VOC emissions from petrol light duty vehicles in Europe using different oxygenated fuels, Mellios Giorgos	373
Vehicle emissions in Turkey: Current status and policy options for the future, Mock Peter	382
Sustainability Enhancement of Urban Traffic Routing via Multi Criteria Optimisation, Nai Oleari Alberto [et al.]	401
An emissions inventory for non-road mobile machinery (NRMM) in Switzerland, Notter Benedikt [et al.]	409
Exhaust emissions from in-service inland waterways vessels, Pillot Didier [et al.]	423
Why Own a Hybrid? A Global Total Cost of Ownership Analysis for the Private and Company Car Driver., Palmer Kate [et al.]	438
Impact assessment of vehicle technology, fuel, and ICT measures on CO ₂ emissions from road traffic to 2030, Papadimitriou Giannis [et al.]	453
Influence of pavement management on road traffic emissions and associated costs, Pellecuer Luc	473
PM _x traffic resuspension estimation over a Milan area domain, Pepe Nicola [et al.]	480
Evaluation of Black Carbon sources and geographical origins in Lorraine: multi-site approach and near real time data, Petit Jean-Eudes [et al.]	486
Effects of Alternative Drivetrain Technologies and -Fuels on CO ₂ -Emissions from Road Traffic in Germany, Piasecki Conrad	495
Metrological characterization of a remote sensing equipment for on-road emission measurements: Considerations for detecting high-emitter vehicles, Pujadas Manuel [et al.]	500
Personal mobility choices and climate change: which incentives are effec-	

tive?, Raux Charles	508
Real-world CO2 emission, and cost benefit, of a switch to hybrid electric vehicles in taxi fleets, Riley Richard [et al.]	519
NOX Emission Performance of Vans in Real Urban Driving Using A Remote Sensing Device, Rushton Christopher [et al.]	530
ESPRIT: a new carsharing concept - A socio-economic assessment from Lyon region, France, Sadeghian Shadi [et al.]	537
Elucidating the origin of the enrichment in aromatic compounds in Paris megacity atmosphere, Salameh Thérèse [et al.]	550
Investigating the influence of the calibration and validation of cell transmission traffic flow model on average speed-based emission predictions, Sayegh Arwa [et al.]	559
GRETA: Gridding Emission Tool for ArcGIS, Schneider Christiane [et al.]	573
Intercomparison of three modeling approaches for road dust resuspension using two experimental data sets, Thouron Laëtitia	585
Modelling the effect on air quality of Euro 6 emission factor scenarios, Toenges-Schuller Nicola [et al.]	605
Quantification of the effect of WLTP introduction on passenger cars CO2 emissions, Tsokolis Dimitris [et al.]	621
Real world performance of ventilation systems for reducing nitrogen oxides or particulate matter levels in road tunnels, Vidal Bruno [et al.]	636
A comprehensive evaluation method for instantaneous emission measurements, Weller Konstantin [et al.]	656
Greenhouse gas emissions from heavy duty vehicles using upgraded biogas as a fuel, Winther Morten [et al.]	670

Analysis of Diurnal Trends in Vehicle Fleet Composition and their Emission Contribution on an Urban Arterial Road in Leeds, UK., Wyatt David [et al.]	679
Study on reducing commuters' in-vehicle exposure to ultrafine particles, Xu Bin [et al.]	698
Exposure of Volatile Organic Compounds inside Vehicle Cabins in China, Xu Bin [et al.]	710
TOWARDS AN INTEGRATED TOOL OF A LIFE CYCLE ASSESSMENT FOR CONSTRUCTION OF ASPHALT PAVEMENTS IN EGYPT, Younes Mohamed [et al.]	719
Evaluation of emissions and fuel consumption of Heavy-Duty Vehicles in urban areas, Zamboni Giorgio [et al.]	726
Study of Traffic Real Driving Emissions in Madrid in 2015 and conclusions, De La Fuente Josefina [et al.]	742
Prediction of Airport Noise with CadnaA Model and GIS (Case Study: IKIA Airport), Kiani Sadr Maryam [et al.]	752
Economies of scale and density in the public road transport sector in Tunisia, Mezghani Amine	763
Air quality in an urban public transportation network: local-scale determinants, Muresan Bogdan [et al.]	772
Using a simplified Willans line approach as a means to evaluate the savings potential of CO2 reduction measures in Heavy-Duty Transport, Van Zyl Stephan [et al.]	784
Alikhodja.pdf	798
ali_khodja_Kadja.pdf	807
Baouche.pdf	813

Bergk.pdf	814
Bouhatmi.pdf	828
Chen.pdf	834
ERNESTO.pdf	849
Fleischman.pdf	850
Gustafsson1.pdf	865
Gustafsson2.pdf	873
Ibarra.pdf	880
Ibrahim.pdf	888
Jinca.pdf	895
Kadijk.pdf	911
Kugler_etal.pdf	929
Kurtenbach.pdf	941
Lonati2.pdf	955
Mehel2.pdf	964
molle.pdf	974
MoodyTate.pdf	976

Mounce.pdf	985
ODriscoll.pdf	993
Olivier.pdf	1006
PellecuerTate_Chapman.pdf	1014
Rizet.pdf	1022
Rmili_2015_Rege_DPF_Euro5_29042016.pdf	1037
Schiper.pdf	1053
Setare_Trigui.pdf	1071
Sibarra.pdf	1073
uhrner_cemobil.pdf	1081
uhrner_tunnel_emissions.pdf	1090
Wallington.pdf	1099
Author Index	1100
List of participants	1103

Empirical study for absolute relation between GDP per capita and CO₂ emissions from transportation, industrialization and energy mix

Shamema Akter¹

¹Transport Economist, ACE Consultants Ltd. Bangladesh (a subsidiary of SMEC International), Dhaka, 1206, Bangladesh

shamema.akter@smec.com

Abstract *The range of carbon dioxide (CO₂) emission is snowballing which is one of the most important causes for air pollution. It emphasizes that all kinds of pollutions are liable for global heating and climate change negative outcome on human being, animals as well as on earth. The objective of the research is to explore the absolute relationship between the CO₂ emission and GDP² per capita. So, for this reason, I have used cross countries data from the World Development Indicators (WB³) for scrutinizing bi-variant linear regression model (such as scatter plot, histogram, correlation coefficient etc.) by using SPSS software. It is found, here is a positive linear correlation of CO₂ emissions with the escalation of GDP per capita. The present topic can be further studied including other determining parameters as independent variable, eg; transportations (such as highways motorize vehicles, water, air and rail), energy mix, industrialization, etc for multivariate analysis. I have accomplished this analysis using an OLS⁴ method. This research paper demonstrates that there is a strong positive correlation between GDP per capita and CO₂ emissions. In addition, the global economy is extremely dependent on fossil fuels burning. So, this is much more challenging for the global economy to minimize carbon dioxide emissions. Therefore, we should be very cautious in order to maintain a sustainable development as well as a healthful environment for the present and forthcoming generation.*

Keywords: GDP per capita, CO₂ emission, Cross Countries data, Bi-variate regression, Kuznets Curve (EKC).

¹Carbon Dioxide emission (metric tons per capita)

²Gross Domestic Product (current US\$)

³www.worldbank.org, last updated date, 9/18/2015

⁴OLS is one of the simplest methods of the econometrics model. The objective of OLS is to methodically accept a function with the data set. It does so by minimizing the sum of squared errors from the data.

1 Introduction

Now a day, Carbon dioxide emissions are one of the focal global anxieties. Usually, there are two main sources, e.g.; burning of fossil fuels (such as coal, gasoline, natural gas, and diesel) and industrial sources of chemical reactions emit carbon dioxide. Countries using more petrochemical fuels for transportations and having more manufacturing factories are considered as the main CO₂ emitters. It could be assumed, countries use more energy sources give escalation GDP per capita resulting emissions of pollutant gases.

There are many number of authors has revealed and described 'causal relationship between economic development and different indicatorsof environmental quality'country wise and internationally newly by the support of EKC⁵models. EKC hypothesis was first used by Grossman and Krueger for several environmental indicators and CO₂ emissions at all in 1991. So, CO₂emissions was typically described by linear, quadratic cubic polynomial functions of per capita income(S.Boopen and S.Vinesh,the Mauritian Experience). The EKC hypothesis stated an upturned U-shape relation among various indicators of environment and per capita income. Usually, it is emphasizes that, carbondioxide emissions, which is extremely connectedwith the environmental degradation is roaming equivalent with economic development.Thus,theappropriate choice of goal oftheenvironmental emittershas become a crucial decision in economics. According to global economy isextremely dependentonfossilfuels burning as well as industrial manufacturing developments. So, thereductionofcarbondioxide emissions is asolemn environmental challenge forthe globaleconomy.Carbon dioxide emissions are those stemming from the burning of fossil fuels (oil, gasoline, natural gas, and diesel) and the manufacture of cement. They include carbon dioxide produced during consumption of solid, liquid, and gas fuels and gas flaring. This paper has the latest values, historical data, graphs, statistics, and an economic research. CO₂ created by human activities. It is most harmful for urban environment as well as human being. It has been producing by Transportations such as highways motorize vehicles (cars, bus, trucks, pick up etc), Electricity, Manufacturing Industries and Construction and Residential Buildings and Commercial and Public Services. In this paper, review of literature on similar studies is mentioned in section 2, presents the methodology and data are Section 3, Descriptive findings are discussed in section 4, and Section 5 Conclusions of the research, there are Acknowledgement in section 6 and Appendix in section 7.

1.1 Global Carbon dioxide emissions trends

The explanation of cross countries composition is given in Appendix A and descriptive statistics for principal data set are given in Table 4. The 200 countries of data set cover 78% of worldwide CO₂ emissions. As per WB 2011, the twelve countries with the highest level of per capita emissions are Qatar (44.02), Trinidad and Tobago(37.14), Kuwait (28.10) ,Brunei Darussalam (24.39),Aruba (23.92),Luxembourg (20.90),United Arab Emirates (20.43) Oman (20.20), Saudi Arabia (18.07),Bahrain (17.95), United States (17.02) and Australia(16.52). In 2011, a per capita CO₂ emission was the highest in the Qatar (44.02) and the lowest in the Burundi (0.2). On the other hand, the highest level of GDP per capita is Monaco \$163351.64, Luxembourg \$113731.65, Norway \$100575.11, Qatar \$89115.9, Switzerland \$88002.6, Bermuda\$ 85973.1, China (Macao SAR) \$67012.89, Australia \$62133.6, Denmark \$61304.06. In 2011, GDP per capita was the highest in the Monaco \$163351.6 and the lowest in the Burundi \$240.

1.1.1 Sector wise Carbon dioxide emissions trends and Forecasting of CO₂ emissions (metric tons per capita) and GDP per capita (current US\$) up to 2050

Global CO₂ emissions from electricity, industry, transport and residential in 2012, CO₂ emissions from electricity and heat production, by far the largest, accounted for 41%, while transport accounted for 31%. CO₂ emissions from manufacturing industries and construction are 19% and residential

⁵ Kuznets curve demonstration an inverted "U" curve. This curve first advanced by economist Simon Kuznets in 1950.

buildings and commercial and public services are 9% (Fig.1 (a)). There is forecasting of CO₂ emissions (metric tons per capita) and GDP per capita (current US\$) up to 2050 (see fig.1 (b) and Appendix A). Compound growth rate of GDP per capita (2005-2014) (for 9 years) and CO₂ emissions (2005-2011) for 6 years (see fig. 2 and Appendix A, table 4).

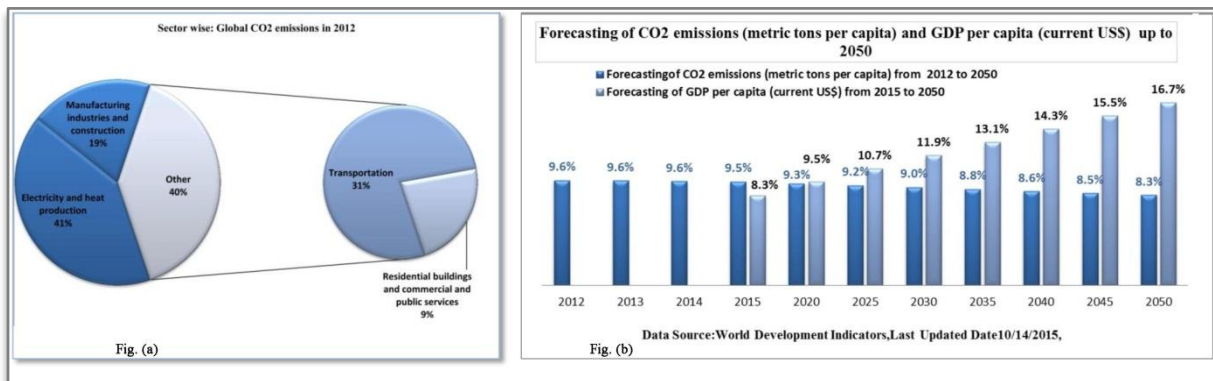


Fig. 1: (a) Sector wise: Global CO₂ emissions in 2012 and (b) Forecasting of CO₂ emissions (metric tons per capita) GDP per capita (current US\$) and up to 2050

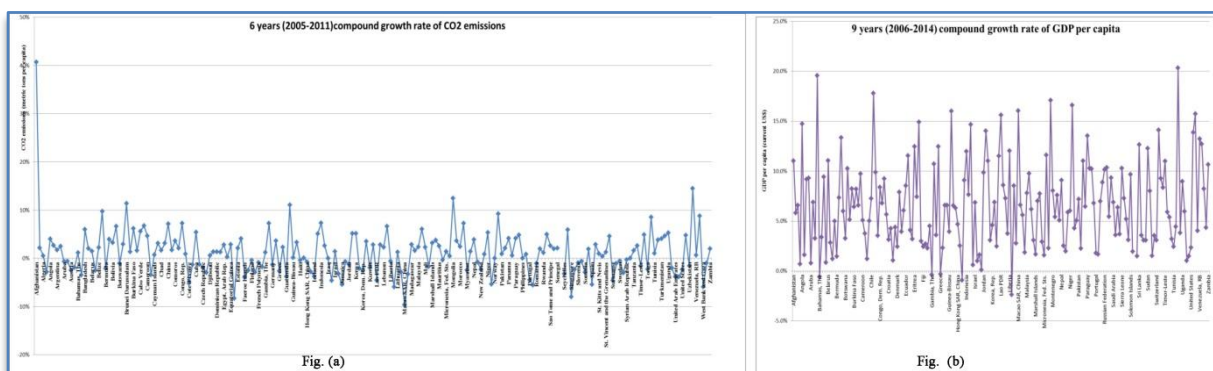


Fig. 2: Compound growth rate of GDP per capita (2005-2014) and CO₂ emissions (2005-2011)

1.1.2 GDP per capita and Carbon dioxide emissions trends by region

Regional differences in contributions to global emissions cover even larger differences among individual countries. In 2012, Europe & Central Asia 27.5%, East Asia & Pacific 22.1%, Latin America & Caribbean 16.1%, Middle East & North Africa 15.7%, Sub-Saharan Africa 8.6%, North America 2.6%, Arabian Peninsula, Middle East 1.9%, Southern Europe 1.1%, Northern Europe 1.1%, Central Africa 1%, South Asia 0.7%. There are highest CO₂ emissions in Europe & Central Asia 27.5% and lowest Eastern Africa 0.012% (see fig.3)

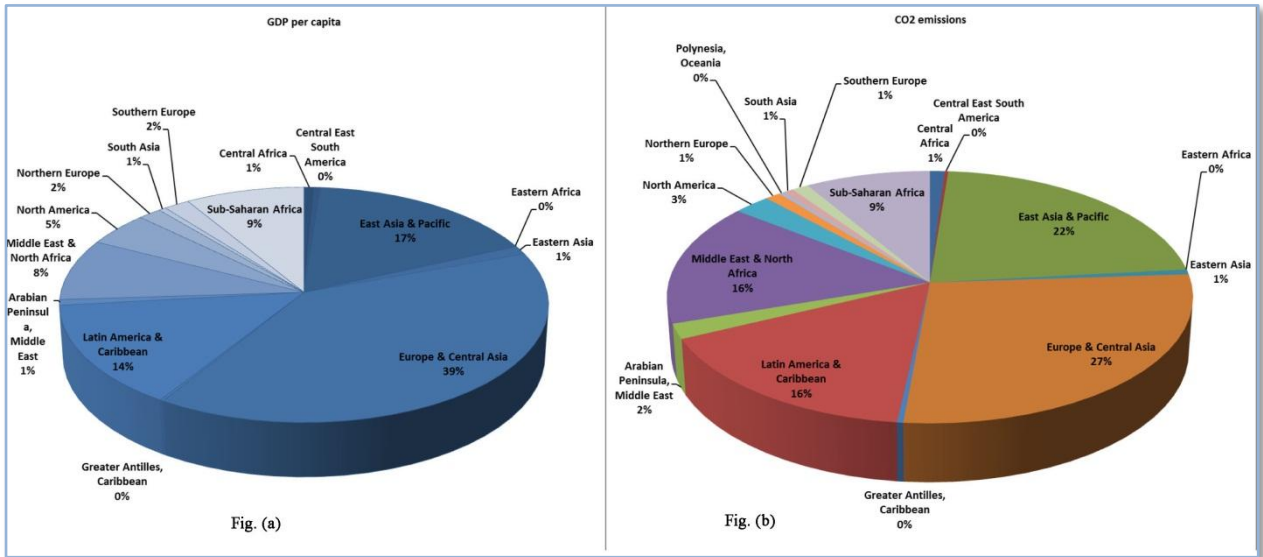


Fig. 3: Regionwise: GDP per capita and Carbon dioxide emissions in 2012 (Data source: WB)

1.1.3 CO2 emissions trends on the top 14 emitting countries and SAARC region in 2012

From Fig. 3 (a) show the top 14 emitting countries of global CO2 emissions trends from Manufacturing industries and construction, Transportation, Residential buildings and commercial and public services, and Electricity and heat production (see Table 1).CO2 emissions trends on SAARC⁶ countries. Carbon dioxide emissions (metric tons per capita) in India 1.66, Pakistan 0.94, Maldives 3.26, Sri Lanka 0.73,Nepal 0.16,Afghanistan 0.43, Bhutan 0.77 and Bangladesh were reported 0.37 in 2011, according to the World Bank (see Appendix A, table 4). The population of Bangladesh is 159.1 million GDP \$ 173.8 billion, GDP growth 6.1% and inflation 7.0% (WB, 2014). Fig.3 (b) demonstration that CO2 emissions trends of SAARC countries from Manufacturing industries and construction, Transportation, Residential buildings and commercial and public services, and Electricity and heat production.

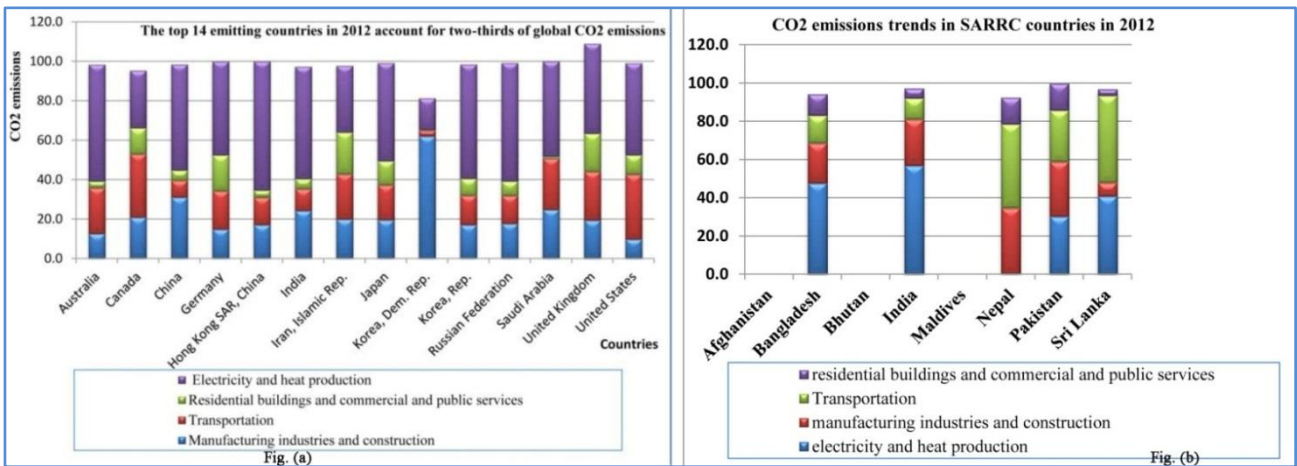


Fig. 4: (a). The top 14 emitting countries and (b).SAARC region in 2012 account for CO2 emissions trends (Data source WB)

⁶The South Asian Association for Regional Corporation is an economic and geopolitical organization of eight countries which is located in South Asiawhich are categorized by relatively high densities of population, low per capita income and literacy rate, and unplanned use of technology in several sectors that causes environmental dilapidation.

Table 1: CO₂ emissions trends on the top 14 emitting countries (in 2012)

Country Name	Manufacturing industries and construction	Transportation	Residential buildings and commercial and public services	Electricity and heat production
Australia	12.6	23.2	3.3	59.2
Canada	20.9	32.1	13.2	29.2
China	31.0	8.6	5.1	53.7
Germany	14.8	19.5	18.1	47.5
Hong Kong SAR, China	17.1	13.9	3.6	65.4
India	24.2	11.1	5.1	56.9
Iran, Islamic Rep.	20.0	22.8	21.2	33.8
Japan	19.6	17.6	12.2	49.8
Korea, Dem. Rep.	62.1	2.9	0.3	16.1
Korea, Rep.	17.1	14.9	8.6	57.9
Russian Federation	17.7	14.2	7.3	60.0
Saudi Arabia	24.8	26.0	0.9	48.3
United Kingdom	19.4	24.7	19.4	45.6
United States	9.8	32.9	9.8	46.7

Data source: World Development Indicators, Last Updated Date 9/18/2015

Objective of the Research

The purpose of the research is to discover the absolute relationship between carbon dioxide emissions and GDP per capita. The findings of the report will give us way and means to take resistance mechanism against the CO₂ emission to support the growth of the economic development which will eventually support in the growth of GDP per capita. In this research, cross country data of 200 countries from the World Bank is taken and OLS linear regression is done.

2 Literature Review

Now a day, there is a global apprehension about the CO₂ emissions which is one of the main indications liable for worldwide warming. This literature review analyzed the association between CO₂ emissions and GDP.

There is CO₂ emissions which create by human activities (WB). It is burning of, coal, natural gas and oil for energy. The core reasons for transportation, industry and electricity (www3.epa.gov)⁷. Firstly, CO₂ emission and 31% of total U.S. greenhouse gas emission due to electricity generated in 2012. Secondly, CO₂ emission and 27% of total U.S. greenhouse gas emission due to transportation (for burning of fossil fuels such as diesel, gasoline, petrol). Moreover, CO₂ emission and 12% of total U.S. greenhouse gas emission due to industrial. Electricity is an important source of energy and it is used to power, business as well as industry besides the kind of fossil fuel used to generate electricity which produces CO₂ emissions. Therefore, the burning coal produces more CO₂ emission than oil and natural gas. Transportation is similarly a main source of worldwide pollutants, which is responsible for the greenhouse effect. The fossil fuel burning related with transportation outcomes in emissions of pollutants which root harm to human health, agriculture, and contribute to global climate change. Transportation can too support to the erosion of urban environments, with damage of value of life and economic efficiency from the obstacle and defeat caused by traffic jam and oppression from traffic noise which pollutants are produced in that proportions depend on a number of factors, including the vehicles and fuel (diesel, gas, petrol) used and the driving situations of a specific trips. The IEA⁸ predictions, CO₂ emissions will escalation 92% (percent) by 1990 to 2020 due to transportation

⁷ <http://www3.epa.gov/climatechange/ghgemissions/sources.html>

⁸ The International Energy Agency

(Roger Gorham, 2002). Every day, people and goods are moved by various types of transports (highway vehicles, air transportation, marine transportation and rail) which use fossil fuel. Accordingly, the burning of petrol, diesel and gas produces more CO₂ emissions. Several industrial processes produce CO₂ emissions because they use chemical, natural gas and oil, Electricity which create CO₂ emissions.

Bo Xu, R. W (2013) in this paper they have analyzed the EKC relationship between China's CO₂ (capita) and GDP (capita) in the period 1980-2008. The analysis of the EKC hypothesis only worries the statistical association between empirical CO₂ emissions and their impact factors in principle, rather than a fundamental theorem expecting a fact that will occur regardless. From their study emphasizes that CO₂ emissions will not impulsively decline if China country to develop its economy without adopting instruments for extenuating climate change; on the other hand, CO₂ emissions could start to reduction if substantial efforts are made. In addition, China's wealth gap and its role in international trade are reflected as two possible elements to affect EKC hypothesis. So, internal income discrimination reduction and international discussions to allocate clear responsibilities between China and developed countries for CO₂ emissions relationship with China's product exports are suggested to the more efforts.

Roger Gorham (2002) analyzed of the transportation sector's involvement to local and global air pollution, and the strategic and planned choices existing the problem in an environment of development and economic growth. The report examines the roots of, and the damages caused by, air pollution from transport; it assesses the causal causes, surveys the main planned methods applied to solving the problem. The study demonstrated that negative impact on environment by transport-related air pollution.

SS Sharma (2011) studied a dynamic panel data consisting of 69 countries which were used that explored the causes of carbon dioxide emissions (CO₂) and the time component of data set is 1985–2005. There was found that for all countries, except for those with high income, only per capita GDP and urbanization are determinant for CO₂ emissions. It was also highlighted that for the global panel, only GDP per capita and per capita total primary energy consumption were found to be statistically significant determinants of CO₂ emission.

Dinda (2004) analyzed a dynamic panel data consisting of 88 countries which was collected on the source geographic area to observe the correlation between per capita CO₂ emissions and per capita GDP. In that study, IPS panel root test and Engel-Granger methodology of co-integration were used. The objective of the study was to expose how the emission of carbon dioxide changes as the economic development of country changes, which was essentially a test of the EKC hypothesis. The result shows that there is an inverted-U-shaped relationship between different pollutants and per capita income, such as environmental burden rises up to a certain level as income goes up and vice versa. In other hand, CO₂ emissions increases faster than income at initial periods of development and slows down relative to GDP growth at higher income levels.

Wadud (2014) analyzed that the long-run causal relationships between CO₂ emissions and economic growth in SAARC countries during the period of 1972-2012. They put on cointegration and Vector Error Correction Modeling (VECM) to calculate the association. Empirical results advise that a long run relationship exist between CO₂ emissions and economic growth in SAARC countries. The performance of the cointegration based "Granger Causality test" found that there is a long run and short run too relationship between economic growth and CO₂ emissions that is energy consumption granger causes CO₂ emissions and economic growth.

3 Methodology and Data analysis

I have used annual unstable cross countries data covering in 2011 for 200 countries. I also used a supplementary data set which acceptable to perform ranked huddling. I am going to use descriptive statistics main to describe the nature of the variables. I have used bi-variate models such as scatter plot, histogram, correlation coefficient etc. to see if there is association between economic variables. I

want to estimate the value of the dependent variable (y) based on fixed value of the independent variable (x). I have used the regression model. Give reference from previous studies that they also used or proposed to use regression model. The regression equation is a mathematical equation which defines the relationship between Carbons Dioxide emissions and Gross Domestic product per capita. I have accomplished this analysis using an OLS method.

I stipulate the following bi-variant regression equation for seeing the absolute relationship between economic variables:

$$y_i(\text{CO}_2\text{emission}) = \alpha + \beta x_i(\text{GDP per capita}) + \mu_i \text{----- (i)}$$

$$\frac{dy}{dx} = \beta \text{ and } 0 < \beta < 1$$

Where,

y_i (emission of CO₂) =dependent variable and estimate value of y for a fixed value of x;

x_i (GDP per capita) = independent variable;

α = y- intercept which represents the estimate value of y (part of y axis from origin) when x = 0;

β = the slope of co-efficient of independent variable;

μ_i = error term

The coefficient of regression of y on x and α regression constant. The coefficient β is computed first using the formula-

$$\beta = \frac{n \sum xy - (\sum x)(\sum y)}{n \sum x^2 - (\sum x)^2} \text{----- (ii)}$$

Having estimated β and constant α is computed from the observed data using the formula

$$\alpha = \frac{\sum y}{n} - \beta \frac{\sum x}{n} = \bar{y} - \beta \bar{x} \text{----- (iii)}$$

My suggested null hypothesis H₀: $\beta = 0$; there is no relation between CO₂ emission and GDP per capita. And alternative hypothesis H₁: $\beta \neq 0$; there exists association between carbon dioxide (CO₂) emission and GDP per capita.

Data: I have used secondary cross country data of 200 countries for my study which is show Table-4 (AppendixA)⁹. The data of GDP per capita and CO₂ emission from World Bank Indicators (WDI) of World Bank (2015).I have used a simple liner regression model. It has independent variable i.e. GDP per capita and dependent variable is CO₂ emission. Now, I have tried to draw a connection between the two variables. Here α is a constant term and β is the coefficient of x variable that denotes GDP per capita. GDP per capita is gross domestic product divided by midyear population. GDP is the sum of gross value added by all resident producers in the economy plus any product taxes and minus any subsidies not included in the value of the products. There is calculated without creation deductions for depreciation of fabricated assets or for exhaustion and lack of natural resources. Data are in current U.S. dollars.CO₂ are those stemming from the burning of fossil fuels and the manufacture of cement. They comprise carbon dioxide output during consumption of solid (Mt), liquid (Mt), and gas (Mteo) fuels and gas flaring. Here, μ is the error term. It is a variable in a statistical or mathematical model, which is made when the model does not fully signify the actual association between the independent variable (GDP per capita) and the dependent variable CO₂ emission.

⁹ Large Tables are set aside at the end of this chapter (Appendix) to boost readability.

4 Descriptive Findings

I have a large number of data set comprehending data from 200 countries. Range of our data set is very high for GDP per capita range is 163111 and for CO₂ emission it is about 44.2. The explanation of cross countries composition is given Annex A and descriptive statistics for main data set are given in Table 1. There are 200 countries of data set cover 78% of global CO₂ emissions as well as 14 countries with the highest mean per capita emissions.

Table 2: Descriptive statistics

GDP per capita (current US\$)		CO ₂ emissions (metric tons per capita)	
Mean	15440.18	Mean	4.81
Standard Error	1619.09	Standard Error	0.4413
Median	5813.11	Median	2.80
Standard Deviation	22897.5	Standard Deviation	6.24
Sample Variance	5.24	Sample Variance	38.95
Kurtosis	11.12	Kurtosis	11.93
Skewness	2.87	Skewness	2.93
Range	163111.03	Range	44.0
Minimum	240.61	Minimum	0.02
Maximum	163351.64	Maximum	44.0
Count(N)	200	Count(N)	200

I can observe from the above mention table measures of central tendency of the variables used in study. For GDP mean, median is 15440.18 & 5813.11 respectively, values are quite low. For CO₂ emission mean, median is 4.81 & 2.80 respectively. GDP skewness, Kurtosis is 3 & 11 respectively. For CO₂ emission skewness, Kurtosis is 2.93 & 11.93 respectively. GDP Standard Deviation, Variance is 22897.5 & 5.24 respectively. For CO₂ emission Standard Deviation, Variance is 6.24 & 38.95 respectively. Here, observation (N) is 200.

I can see from the skewness and kurtosis values that data set is not normally distributed. Thus I have used log values to solve this matter. I can see from the histogram that after the log transformation the data set is normally distributed.

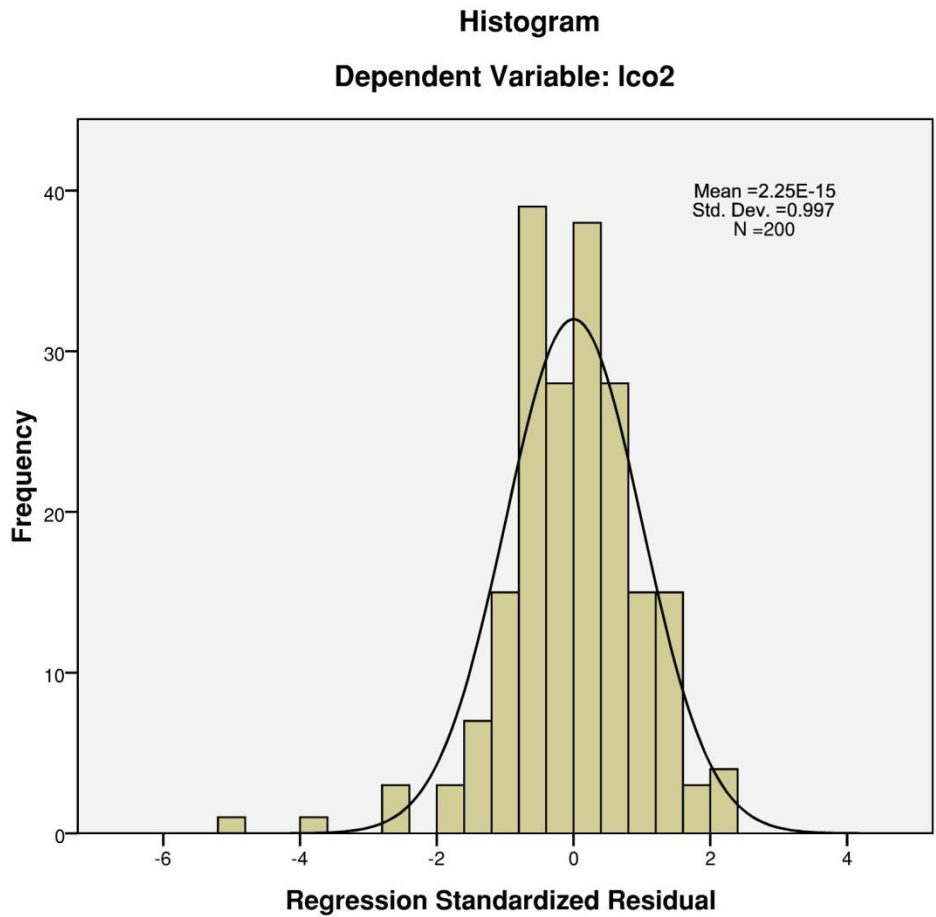


Fig.5: Histogram

By using the log values I have the following scatter plot:

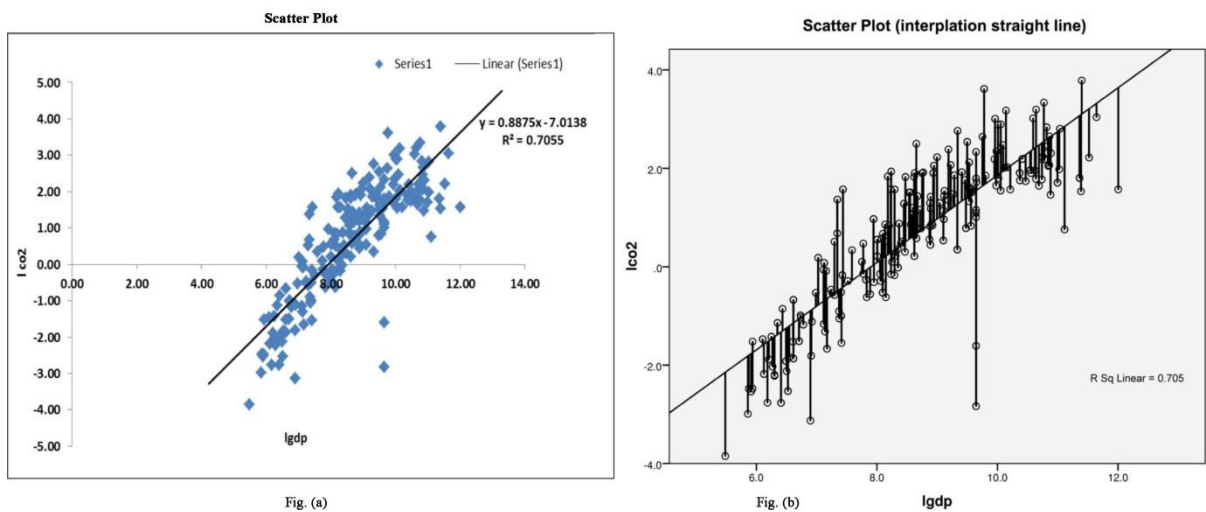


Fig. 6: Scatter Plot (World Bank data)

As a result, from the scatter plot I can observe a likely positive relation between C02 and GDP variables. The value of β is positive 0.8875. This is also the slope term. The intercept term α has a value of -7.0138.

The coefficient of determination $r^2 = 0.705$. This is also high. Which states almost 70 % (percent) of the total variation in Carbon-dioxide (Co2) explained by the regression model.

The coefficient of correlation $r = \pm 0.84$. We can clearly see that there is strong positive correlation between GDP per capita and carbon-dioxide (CO2) emission.

By using SPSS data analysis software I have derived linear regression analysis and the result is as followed:

Table 3: regression results

Variable/parameter	Coefficients	Standard Error	t Stat	P-value	Lower 95%	Upper 95%
Intercept	2.18	0.463	4.711	0.000	1.25	3.06
x Variable 1	0.000	0.000	10.014	0.000	0.000166	0.000247

Estimation of the Econometric Model

Regression analysis is the main tool used to obtain the estimates. Using this technique and the data given in Table 4, I obtain the following estimates of α and β , namely, 2.18 and 0.000. Thus, the estimated equation is:

$$y_i(\text{CO}_2\text{emission}) = 2.18 + 0.00 x_i(\text{GDP per capita}) + \mu_i \text{----- (iv)}$$

Where,

α = the intercept term is 2.18 this is a constant term and

β = the GDP coefficient is 0.00. It is a log-liner model.

The estimated regression line is shown in Fig. 5. The regression line fits the data quite well. The slope coefficient was about 0.000,

From these results I see that coefficient of GDP per capita is positive + 0.000206. It is emphasizes that, 1 percent increase in the GDP per capita, the emission of carbon dioxide CO2 on the average increases by about 0.000206 percent. I can say that there is positive relation between GDP per capita and CO₂ emission.

To find out if the parameters are statistically significant I have used t-test, p value & confidence interval approach.

So, the calculated t-values for both the variables are much higher that the crucial t-values, therefore the parameters are statistically significant at 1% level.

P-values are also very low consequently variables are statistically significant.

The values of Standard error (SE) are also very low compared to the constant term & coefficient which states these values are statistically significant.

Observing the upper and lower values of confidence interval, so I can say zero is not included in this range. Thus β cannot be zero ($\beta \neq 0$), this supports alternative hypothesis (H_1).

Using the above test, it is emphasizes that $\beta \neq 0$ therefore, I canvisibly reject the null hypothesis (H_0). There is no relation between GDP per capita and CO₂ emission.

As a consequence, I cannot find that findings are equivalent alternative hypothesis (H_1). Moreover, there are a positive association between GDP per capita and CO₂ emission. If GDP per capita increases by 1 percent then the CO₂ on the average increases by about 0.000206 percent.

5 Conclusions

To long years, the level of carbon dioxide emissions is escalation which is main liable for air pollution. It is thought that all kinds of pollutants are liable for global warming and climate change resulting harmful effect on human being, animals and plant kingdom. Carbon dioxide emissions created by human activities. CO₂ emissions are those stemming from the burning of fossil fuels and the manufacture of cement (WB). According to global economy is enormously dependent on fossil fuels burning as well as industrial manufacturing developments. So, this is the challenging for global economy of minimize of carbon dioxide emissions. The objective of the research is to pursue the association between the emission of carbon dioxide (CO₂) and Gross Domestic Product per capita (GDP). So, for this reason, I have used cross countries data from the World Development Indicators (WB, last updated date, 9/18/2015) for scrutinizing bi-variant linear regression model by using SPSS software. It is found, there is a positive linear association between CO₂ emissions and GDP per capita. Here, CO₂ (Metric tons per capita) and GDP per capita (current US\$). We should have to very cautious in order to maintain a sustainable development as well as a healthful environment for the present and future generation. Although, there are somewhat limitations such as I have used only cross country data (WB) and one independent variable GDP per capita, this study has opportunity for more improvement. It can be more studied along with additional determining parameters as independent variable, eg; energy, transportation, industrialization, urbanization etc for multivariate analysis. It can also include several methods, different data set, particular country's outlook using panel data, comparing between several countries etc. This will not only enhance my knowledge but also will be obliging for taking suitable measures to confirm getting up economy.

6 Acknowledgement

I am Shamema Akter, Transport Economist, ACE Consultants Ltd. Bangladesh a subsidiary of SMEC International. I have some experience on PPP Elevated Expressway and Rail Project. My projects Team Leader Mr. Martin Kerridge encourage me to research about air pollution. Therefore, I have enthusiastic to research on GDP per capita and CO₂ emissions. I'm thankful to him.

7 Appendix A

Table 4(a): GDP per capita (current US\$) and CO2 emissions (metric tons per capita)

Country Name	GDP per capita (current US\$) (2005-2014)											9 years compound growth rate	Forecasting of GDP per capita from 2015 to 2050						
	2005	2006	2007	2008	2009	2010	2011	2012	2013	2014	2015		2020	2025	2030	2035	2040	2045	2050
Afghanistan	257.2	280.2	380.4	384.1	459.0	569.9	622.4	690.8	662.0	659.0	11.0%	785.4	1048.0	1310.6	1573.2	1835.8	2098.4	2361.1	2623.7
Albania	2781.6	3051.8	3603.0	4370.5	4114.1	4094.4	4437.8	4256.0	4458.1	4619.2	5.8%	4973.0	5876.9	6780.9	7684.8	8588.7	9492.7	10396.6	11300.5
Algeria	3102.0	3467.5	3939.6	4912.3	3875.8	4473.5	5421.7	5457.6	5504.2	5498.1	6.6%	6083.1	7463.1	8840.9	10222.9	11602.8	12982.7	14362.6	15742.5
Andorra	39903.0	42417.2	47523.5	46736.0	42701.4	39639.4	41630.1	39666.4	42806.5	42537.9	0.7%	41515.8	40586.6	39657.4	38728.3	37799.1	36869.9	35940.7	35011.6
Angola	1576.2	2253.8	3151.0	4242.4	3678.9	3886.5	4745.0	5084.3	5295.2	5423.6	14.7%	6177.0	8216.3	10255.7	12295.0	14334.4	16373.7	18413.1	20452.5
Antigua and Barbuda	12079.9	13599.9	15276.1	15786.2	13979.3	13017.3	12817.8	13525.6	13342.1	13961.7	1.6%	13622.3	13516.6	13411.0	13305.3	13199.6	13093.9	12988.2	12882.5
Argentina	5694.4	6649.4	8250.2	10054.1	9277.4	11227.8	13439.9	14436.6	14623.5	12568.6	9.2%	15979.7	20850.2	25720.7	30911.1	35461.6	40332.1	45202.5	50073.0
Armenia	1625.4	2126.6	3081.0	3920.0	2915.6	3124.8	3417.2	3343.4	3486.1	3619.8	9.8%	3982.0	4814.7	5647.4	6480.1	7312.8	8145.5	8978.2	9810.9
Aruba	23302.8	24015.4	25921.5	27549.9	24640.4	24289.1	25353.8	25010.4	25010.4	25010.4	0.0%	25371.7	25700.1	26028.6	26357.0	26685.5	27013.9	27342.3	27670.8
Australia	33995.9	36100.6	40976.5	49650.4	42702.2	51801.0	62133.6	67511.8	67473.0	61887.0	6.9%	73084.9	92777.5	112470.0	131262.5	151855.0	171547.5	191240.0	210932.5
Austria	38242.1	40431.0	46586.6	51386.4	47654.2	46593.4	51131.0	48348.2	50513.4	51127.1	3.3%	53652.1	59516.4	65380.7	71245.1	77109.4	82973.7	88838.1	94702.4
Azerbaijan	1578.4	2473.1	3851.4	5574.6	4950.3	5842.8	7189.7	7938.8	7811.6	7884.2	19.6%	9374.0	12936.8	16499.6	20062.4	23625.1	27187.9	30750.7	34313.5
Bahamas, The	23405.9	23721.2	24306.1	23657.4	22043.0	21920.5	21514.9	22112.6	22315.6	22217.5	-0.6%	21453.1	21030.0	19146.9	17993.8	16840.7	15687.6	14534.5	13381.5
Bahrain	18418.1	19669.3	21167.6	23043.0	19166.7	20386.0	22238.7	23063.1	24378.9	24868.4	3.4%	24950.1	27959.3	30968.6	33977.8	36987.0	39962.2	43005.4	46014.6
Bangladesh	485.9	495.9	543.1	618.1	683.6	760.3	838.5	858.9	954.4	1092.7	9.4%	1099.4	1432.4	1765.4	2098.4	2431.4	2764.3	3097.3	3430.3
Barbados	14201.9	15646.8	16641.8	16569.6	16526.3	15901.4	15530.9	15317.1	15153.8	15343.4	0.9%	15577.2	15497.2	15417.1	15337.0	15257.0	15176.9	15066.9	15016.8
Belarus	3126.4	3848.6	4736.0	6376.2	5176.0	5818.9	6305.8	6721.8	7722.1	8040.0	11.1%	8510.5	10986.2	13461.9	15937.6	18413.4	20891.1	23364.8	25840.5
Belgium	36928.0	38936.3	44449.7	48561.4	44999.2	44360.9	47801.6	44818.0	46927.2	47516.5	1.8%	49535.1	54085.4	58635.6	63185.8	67736.0	72286.2	76835.6	81386.7
Belize	3933.2	4187.2	4324.8	4470.2	4258.8	4344.1	4517.1	4674.3	4719.1	4381.0	2.8%	4705.2	5000.0	5294.7	5589.5	5884.6	6179.0	6473.7	6768.4
Benin	532.6	557.2	633.0	739.2	712.5	690.0	745.4	750.6	804.8	825.3	5.0%	864.1	1014.1	1164.2	1314.2	1464.3	1614.3	1764.3	1914.4
Bermuda	75882.0	83912.7	90849.6	93605.7	88463.3	88207.3	85973.2	85458.5	85748.1	86455.6	1.5%	88358.6	90140.2	91894.7	93649.3	95403.8	97153.4	98912.9	100667.5
Bhutan	1257.5	1346.1	1755.2	1810.6	1786.8	2201.3	2485.8	2452.2	2360.4	2380.9	13.4%	2754.9	3455.9	4157.0	4858.1	5559.2	6260.3	6961.3	7662.4
Bolivia	1046.4	1233.6	1389.6	1736.9	1766.9	1981.2	2376.3	2640.5	2942.4	3235.8	7.3%	3370.7	4584.1	5797.5	7010.9	8224.3	9437.7	10651.1	11864.6
Bosnia and Herzegovina	2844.4	3269.5	4020.7	4873.2	4498.7	4392.8	4780.0	4415.9	4668.8	4805.2	6.0%	5224.7	6104.6	6984.3	7864.1	8743.9	9623.7	10503.5	11383.3
Botswana	5327.9	5322.2	5666.6	5561.9	5115.1	6244.0	7504.9	6935.6	6882.3	7123.3	3.3%	7514.4	8738.1	9961.8	11185.5	12409.2	13629.3	14856.6	16080.3
Brazil	4733.2	5809.1	7241.1	8700.6	8462.4	11124.1	13042.2	11922.7	11711.1	11384.6	10.2%	14088.8	18339.4	22590.1	26840.7	31091.4	35342.0	39922.6	43843.3
Brunei Darussalam	26338.0	31157.0	32707.7	37799.3	27727.1	31453.0	41786.6	41808.8	39152.3	41344.0	5.1%	43534.5	51177.4	58820.3	66463.2	74106.0	81748.9	89391.8	97034.7
Bulgaria	3075.6	4320.6	5783.4	7115.9	6738.1	6580.8	7588.8	7198.5	7498.8	7712.8	8.2%	8623.3	10610.5	12597.8	14580.0	16572.3	18559.5	20546.8	22340.0
Burkina Faso	407.0	422.5	474.7	569.0	551.8	574.5	665.8	673.0	709.8	713.1	6.4%	778.5	962.4	1146.4	1340.4	1514.3	1689.3	1882.2	2066.2
Burundi	140.8	154.9	159.3	182.7	190.4	214.2	240.6	244.2	259.4	286.0	8.2%	295.9	376.5	457.1	537.7	618.3	699.0	779.6	860.2
Cabo Verde	2049.6	2316.5	3145.7	3698.3	3517.4	3393.9	3766.1	3497.7	3623.2	3641.1	6.6%	4108.6	4875.6	5642.6	6409.6	7176.6	7943.6	8710.6	9477.6
Cameroon	472.4	537.8	629.3	742.9	735.4	782.7	879.2	947.6	1009.9	1090.1	9.7%	1146.4	1477.1	1807.7	2138.3	2468.9	2799.6	3130.2	3460.8
Canada	915.1	965.4	1071.0	1191.7	1164.7	1164.7	1258.9	1222.3	1312.1	1429.3	5.1%	1440.6	1686.9	1933.3	2179.6	2425.9	2672.2	2918.6	3164.9
Central African Republic	36202.2	40243.6	44328.5	46400.4	40764.1	47463.6	52086.5	52733.5	52053.5	50271.1	3.8%	55542.5	63978.9	72415.2	80851.6	89280.0	97724.4	106160.7	114957.1
Chad	332.9	357.1	404.1	463.8	454.4	446.8	484.6	469.7	327.9	371.1	1.2%	428.6	444.4	460.3	476.1	491.9	507.7	523.5	539.3
Chile	660.2	712.0	801.4	929.3	803.9	895.9	988.4	972.7	985.1	1024.7	7.0%	1087.9	1279.4	1470.8	1662.3	1853.7	2045.2	2236.6	2428.0
China	727.6	9500.8	10513.5	10791.0	10217.3	12785.1	14582.2	15253.3	15741.7	14528.3	3.3%	16915.0	21233.9	25522.8	29871.7	34190.6	38809.5	42824.4	47147.3
China	1740.1	2082.2	2673.3	3441.2	3800.5	4514.9	5574.2	6264.6	6991.9	7593.9	9.7%	8205.1	11602.7	15003.3	18398.0	21795.6	25193.2	28890.9	31988.5
Colombia	3386.0	3709.1	4674.2	5433.7	5148.4	6250.7	7227.8	7885.1	8028.0	7903.9	19.8%	9079.1	11910.4	14741.6	17527.9	20404.2	23235.5	26066.7	28989.0
Comoros	614.9	640.7	712.1	786.2	768.7	759.3	818.9	778.1	823.0	841.2	3.5%	878.9	991.8	1104.9	1217.9	1331.0	1444.1	1557.2	1670.2
Congo, Dem. Rep.	213.3	246.8	273.5	310.7	286.0	311.2	350.3	390.7	413.7	440.2	8.4%	455.0	574.4	693.8	813.2	932.6	1052.0	1171.4	1290.8
Congo, Rep.	1737.6	2144.8	2259.3	3094.1	2428.3	2953.2	3453.2	3191.2	3205.5	3137.8	6.8%	3636.7	4433.3	5229.9	6026.5	6832.1	7619.7	8416.3	9212.8
Costa Rica	4700.0	5228.0	6024.1	6736.2	6546.6	7986.0	8963.7	9733.4	10461.6	10415.4	6.9%	11504.2	14981.3	18458.3	21933.5	25412.4	28890.4	32366.5	35843.5
Cote d'Ivoire	942.2	962.9	1078.5	1257.7	1233.3	1236.1	1231.9	1281.4	1447.2	1545.9	5.7%	1547.2	1843.0	2138.9	2434.7	2730.6	3026.4	3322.3	3618.1
Croatia	10224.2	11359.5	13544.2	15887.4	14142.2	13805.8	14539.2	13236.0	13979.9	13807.4	3.1%	14654.2	18353.9	21701.5	25199.2	28860.5	32652.5	37441.1	42295.8
Cuba	3786.9	4677.7	5193.5	5385.7	5494.9	5688.7	6092.6	6448.2	6789.8	5506.4	4.2%	6801.4	7978.6	9155.9	10333.1	11510.4	12687.6	13864.8	15042.1
Cyprus	24738.0	26455.1	30915.5	34950.4	31673.5	30438.9	31836.6	28868.3	27910.6	27194.4	1.1%	29880.9	30228.9	30769.6	30924.9	31272.9	31620.9	31968.9	32316.9
Czech Republic	13317.1	15159.1	18333.9	22649.4	19698.5	19764.0	21656.4	19670.4	19858.3	19533.9	4.8%	22059.1	24870.9	27682.7	30494.5	33306.3	36118.1	38929.9	41741.7
Denmark	48016.8	52044.0	58501.1	64182.0	57895.5	57647.7	61704.1	57631.6	59818.6	60834.4	2.4%	62767.6	67240.1	71712.7	76185.3	80575.8	85130.4	89603.0	94075.5
Djibouti	910.4	974.6	1060.8	1234.0	1462.0	1358.5	1472.0	1586.8	1684.5	1805.0	7.9%	1896.9	2389.7	2882.5	3375.3	3868.0	4360.8	4853.6	5346.4
Dominica	5250.4	5621.1	6058.2	6615.2	7027.1	6926.8	7121.9	7181.6	7175.4	7433.9	3.9%	7892.7	9028.9	10167.1	11304.3	12441.5	13578.7	14715.9	15853.2
Dominican Republic	3619.0	3818.0	4596.4	4931.6	4902.8	5359.0	5786.9	5951.9	5952.3	6147.3	6.1%	6689.7	8128.9	9568.1	11007.4	12446.6	13888.8	15325.1	16764.3
Ecuador	3021.9	3350.8	3590.7	4274.9	4255.6	4657.3	5223.4	5682.6	6032.2	6322.3	8.5%	6713.9	8598.1	10482.3	12366.6	14250.8	16135.1	18019.3	19903.6
Egypt, Arab Rep.	1196.7	1409.2	1681.3	2061.6	2349.3	2668.0	2816.7	3068.2	3104.2	3198.7									

Country Name	GDP per capita (current US\$) (2005-2014)											9 years compound growth rate	Forecasting of GDP per capita from 2015 to 2050						
	2005	2006	2007	2008	2009	2010	2011	2012	2013	2014	2015		2020	2025	2030	2035	2040	2045	2050
Liberia	165.8	178.5	209.8	231.4	302.3	326.6	378.8	414.2	453.3	461.0	12.0%	514.5	698.4	882.4	1066.3	1250.3	1434.2	1618.2	1802.1
Libya	8159.0	9304.3	11219.4	14231.6	10151.6	11933.8	5517.8	13035.2	10454.8	6569.6	-2.4%	9340.0	8627.5	8035.1	7382.6	6730.1	6077.2	5425.2	4772.7
Lithuania	7863.5	9240.3	12298.2	14961.7	11837.1	11976.9	14360.4	14333.2	15689.0	16444.8	8.5%	17263.3	21229.5	25195.7	29161.9	33128.0	37074.2	41060.4	45026.6
Luxembourg	79595.5	88400.2	102523.4	112477.1	100735.4	102863.1	113731.7	106022.8	110664.8	101890.4	2.8%	114553.6	126065.6	137577.6	149089.5	160601.5	172113.5	183625.4	195137.4
Macao SAR, China	25189.8	30368.7	36620.4	40867.5	40876.6	53045.9	67012.9	77079.2	90332.3	96037.7	16.0%	100752.3	141669.7	182587.2	223504.6	264422.1	305339.5	346257.0	387174.4
Macedonia, FYR	3063.6	3351.3	4063.7	4821.5	4566.3	4561.2	5080.0	4709.5	5195.3	5455.6	6.6%	5768.0	6932.7	8097.3	9262.0	10426.7	11591.4	12756.1	13920.8
Madagascar	275.5	293.0	379.1	472.4	417.2	414.1	456.3	445.0	463.0	449.4	5.6%	507.6	599.5	691.4	783.3	875.2	967.2	1059.1	1151.0
Malawi	216.1	237.7	270.2	307.6	351.1	365.5	369.6	270.1	239.9	255.0	1.9%	307.1	324.3	341.4	358.5	375.7	392.8	409.9	427.0
Malaysia	5564.2	6194.7	7240.7	8486.5	7312.0	8802.9	10125.9	10507.8	10628.0	10933.5	7.8%	11983.0	15077.0	18170.9	21264.9	24358.9	27452.9	30546.8	33640.8
Maldives	3671.9	4754.5	5533.8	6596.9	6630.7	7013.4	7266.9	7350.4	7704.5	8483.8	9.8%	9015.1	11301.0	13586.8	15872.7	18158.5	20444.4	22730.2	25016.1
Mali	411.9	460.0	519.3	614.3	610.1	621.2	680.8	641.8	669.7	706.7	6.2%	758.4	908.2	1058.0	1207.9	1357.7	1507.5	1657.4	1807.2
Malta	14834.4	15705.3	18357.0	20895.8	19636.0	19694.1	22347.7	21176.3	22776.2	19491.4	3.1%	23155.4	26486.3	29817.2	33148.1	36479.0	39809.9	43140.8	46471.7
Marshall Islands	2646.0	2757.6	2877.9	2925.7	2907.4	3126.5	3291.8	3500.7	3616.8	3072.3	1.7%	3548.4	3981.2	4414.0	4846.8	5279.6	5712.4	6145.2	6578.0
Mauritania	692.6	938.0	1008.6	1180.5	1045.8	1207.8	1390.9	1282.8	1306.0	1275.0	7.0%	1465.5	1768.0	2070.5	2370.3	2675.5	2978.0	3280.5	3583.0
Mauritius	5116.0	5455.1	6285.8	7749.3	7082.3	7772.1	8984.6	9110.8	9476.8	10005.6	7.7%	10726.5	13474.4	16222.2	18970.1	21717.9	24465.8	27213.7	29961.5
Mexico	7894.0	8680.6	9222.9	9578.6	7661.2	8861.5	9730.3	9721.1	10200.8	10230.2	2.9%	10371.9	11457.2	12542.4	13627.7	14712.9	15798.2	16883.5	17968.7
Micronesia, Fed. Sts.	2352.6	2393.9	2435.2	2501.5	2669.4	2838.4	2998.6	3150.8	3049.1	2730.0	1.6%	3144.7	3539.8	3935.0	4330.2	4725.3	5120.5	5515.7	5910.8
Moldova	831.2	950.6	1230.4	1690.6	1525.5	1631.5	1970.6	2046.5	2244.0	2233.8	11.6%	2525.6	3334.3	4143.0	4951.6	5760.3	6569.0	7377.7	8186.4
Monaco	126599.4	135629.6	170472.3	193648.1	152877.4	145221.2	163351.6	155399.9	155399.9	155399.9	2.3%	162856.3	169634.8	176413.2	183191.7	189907.2	196748.7	203527.2	210305.7
Mongolia	998.8	1344.6	1633.4	2138.4	1717.1	2052.1	2472.2	4377.2	4387.7	4129.4	2.7%	50176.4	7111.5	9205.6	11299.6	13397.3	15487.8	17581.9	19675.9
Montenegro	3674.5	4383.6	5957.1	7325.7	6698.1	6636.9	7249.9	6519.2	7110.8	7370.9	8.0%	8121.9	9784.9	11447.9	13110.9	14773.9	16436.9	18099.9	19762.9
Morocco	1931.8	2107.9	2389.7	2792.0	2822.1	2782.7	3001.2	2860.9	3056.1	3103.2	2.4%	3355.6	3965.4	4575.3	5185.1	5794.4	6408.7	7014.6	7624.5
Mozambique	311.4	326.4	407.7	480.6	453.3	416.1	527.5	580.4	584.0	602.1	7.6%	648.5	811.7	974.9	1138.1	1301.3	1464.6	1627.8	1791.0
Namibia	3582.2	3884.6	4195.9	3999.6	4123.5	5139.1	5540.3	5681.6	5511.1	5589.0	5.1%	6141.7	7430.0	8718.2	10066.4	11294.7	12582.9	13871.1	15159.4
Nepal	318.7	350.6	396.2	476.6	483.4	595.4	695.9	685.5	691.4	696.9	9.1%	805.9	1048.5	1291.1	1553.7	1776.3	2018.9	2261.5	2504.1
Netherlands	41199.7	44011.3	50861.1	56628.8	51909.6	50341.3	53537.3	49128.1	50792.5	51900.0	2.5%	54049.1	57730.1	61411.1	65092.2	68773.2	72454.2	76135.2	79816.3
New Zealand	27833.6	26630.4	32382.3	30972.1	27998.6	33394.1	37896.9	39573.8	42409.0	33232.3	2.0%	40044.5	47306.5	54088.5	60710.5	67412.5	74144.5	80816.5	87518.5
Nicaragua	1175.1	1245.1	1350.6	1517.8	1479.0	1523.5	1679.7	1779.9	1825.0	1963.1	5.9%	2014.8	2433.8	2852.8	3271.8	3690.8	4109.8	4528.8	4947.8
Niger	252.5	260.6	295.4	358.2	344.4	351.0	378.2	393.6	418.5	427.4	6.0%	455.9	554.0	652.1	750.2	848.3	946.4	1044.5	1142.6
Nigeria	804.0	1014.7	1131.1	1376.9	1092.0	2315.0	2514.1	2739.9	2979.8	3203.3	16.6%	3518.0	4973.4	6428.8	7884.2	9339.5	10794.9	12250.3	13705.7
Norway	66775.4	74114.7	85128.7	96880.5	80017.8	87466.3	100575.1	101563.7	102832.3	97363.1	4.3%	108529.7	126206.0	143511.5	161002.4	178493.3	195984.2	213475.2	230966.1
Oman	12398.6	14575.2	16225.7	22963.4	17518.8	19920.6	21164.3	21533.8	20011.3	19309.6	5.0%	22688.7	26440.2	30191.6	33943.1	37694.5	41446.0	45197.4	49848.9
Pakistan	714.0	877.0	953.8	1042.8	1009.8	1230.8	1266.4	1282.0	1334.1	1334.1	7.2%	1428.0	1748.5	2069.0	2389.5	2710.0	3030.5	3351.0	3671.5
Palau	9721.5	9719.1	9726.1	9837.4	9183.1	9004.6	9765.3	10397.8	10926.3	11879.7	2.3%	11044.0	11978.5	12912.9	13847.4	14781.9	15716.3	16650.8	17585.3
Panama	4659.0	5072.2	6129.1	7124.4	7283.6	7958.6	9036.0	10138.5	11206.4	11948.9	11.0%	12954.9	16645.0	20535.0	24825.1	29915.1	35005.2	37995.2	41185.3
Papua New Guinea	799.4	886.4	992.7	1232.2	1210.9	1418.9	1838.7	2151.2	2108.8	1403.4	6.5%	2131.3	2793.1	3454.9	4116.7	4778.6	5440.4	6102.2	6764.0
Paraguay	1507.1	1809.7	2312.2	3059.9	2600.2	3228.3	3988.0	3855.6	4469.2	4728.7	13.5%	5113.9	6893.9	8673.9	10453.9	12233.9	14013.9	15793.9	17573.9
Peru	2714.5	3143.6	3611.3	4244.5	4178.8	5056.3	5713.3	6388.8	6620.6	6550.9	10.3%	7472.2	9793.6	12160.1	14526.5	16893.0	19259.4	21625.9	23992.3
Philippines	1196.5	1395.2	1678.9	1929.1	1836.9	2145.2	2371.9	2606.2	2788.4	2870.5	10.2%	3118.3	4060.4	5002.6	5944.8	6886.9	7829.1	8771.3	9713.4
Portugal	17875.0	18921.4	22780.1	24815.6	23064.0	22540.0	23194.7	20577.4	21507.7	22080.9	1.8%	22752.3	23511.9	24271.5	25031.1	25790.7	26550.4	27310.0	28069.6
Puerto Rico	21959.3	22935.9	23664.9	24898.3	25768.7	26435.7	27752.0	28681.7	25479.6	1.7%	28811.8	31841.2	34870.5	37899.9	40929.2	43958.6	46987.9	50017.3	
Qatar	53207.3	61593.7	67612.5	82990.1	61463.9	70870.2	89115.9	94236.1	96719.3	97518.6	7.0%	104385.5	128797.1	153208.8	177201.0	200322.0	224443.6	250855.2	275266.8
Romania	4651.7	5789.2	8170.0	9949.2	8069.0	8139.1	9063.7	8445.3	9489.7	9996.7	10.0%	10603.0	12809.0	15015.0	17210.0	19427.0	21633.0	23839.0	26045.1
Russian Federation	5323.5	6920.2	9102.3	11635.3	8562.8	10675.0	13323.9	14078.8	14487.3	12735.9	10.2%	15742.6	20341.1	24939.5	29537.6	34136.3	38734.7	43331.4	47931.5
Rwanda	286.6	336.9	398.2	491.9	529.6	553.6	606.9	667.4	679.0	695.7	10.4%	784.3	1020.4	1256.5	1492.6	1728.7	1964.8	2200.9	2437.0
Samoa	2587.5	2793.5	3130.4	3375.8	3173.5	3530.6	4066.0	4258.0	4180.6	4173.1	5.5%	4595.1	5566.2	6537.2	7508.3	8479.4	9450.5	10421.5	11392.6
Sao Tome and Principe	804.8	863.3	901.3	1121.5	1175.1	1176.5	1421.7	1475.4	1703.4	1797.2	9.3%	1863.5	2426.7	2989.9	3553.1	4116.2	4679.4	5242.6	5805.8
Saudi Arabia	13273.7	14826.9	15947.4	19436.9	15655.1	18754.0	23256.1	24883.2	24646.0	24161.0	6.9%	27015.8	33862.9	40710.0	47557.2	54404.3	61251.4	68098.5	74945.6
Senegal	772.7	808.3	948.5	1094.6	1018.4	998.1	1081.1	1019.3	1040.1	1061.8	3.6%	1134.9	1271.8	1408.7	1545.6	1682.5	1819.5	1956.4	2093.3
Serbia	3528.1	4129.8	5458.1	6701.8	5821.3	5411.9	6423.3	5659.4	6353.3	6101.9	6.4%	6862.5	8042.8	9223.2	10403.6	11584.0	12764.3	13944.7	15125.1
Seychelles	11086.9	12014.4	12155.7	11123.0	9707.3	10861.1	12189.0	12844.8	15695.6	15359.2	3.7%	14968.8	16877.4	19058.0	21238.6	23419.2	25599.8	27780.4	29611.1
Sierra Leone	321.0	359.5	400.4	453.7	434.5	446.3	496.2	627.0	797.6	774.6	10.0%	791.8	1047.0	1302.2	1552.7	1812.6	2067.8	2323.0	2578.2
Singapore	29869.6	33579.8	39223.5	39722.1	38577.0	46569.7	53122.2	54578.2	55979.8	56286.8	7.3%	62068.3	77811.6	93554.8	109298.1	125041.3	140784.5	156527.8	172271.0
Slovak Republic	11620.5	13111.8	16006.9	18558.9	16455.2	16509.9	18065.7	17151.4	18050.2	18416.5	5.2%	19200.0	22739.0	25758.0					

Table 4(b): CO2 emissions (metric tons per capita)

6 years Compound growth rate and forecasting (2012 to 2050) of CO2 emissions (metric tons per capita)																			
Country Name	2005	2006	2007	2008	2009	2010	2011	6 years compound growth rate	2012	2013	2014	2015	2020	2025	2030	2035	2040	2045	2050
Afghanistan	0.1	0.1	0.1	0.2	0.2	0.3	0.4	40.7%	0.4	0.5	0.6	0.6	0.9	1.3	1.6	1.9	2.2	2.5	2.8
Albania	1.4	1.3	1.5	1.6	1.5	1.5	1.6	2.2%	1.6	1.7	1.7	1.8	1.9	2.1	2.3	2.5	2.7	2.9	3.1
Algeria	3.2	3.0	3.2	3.2	3.4	3.3	3.3	0.5%	3.4	3.4	3.5	3.5	3.7	3.9	4.2	4.4	4.6	4.8	5.0
Andorra	7.1	6.6	6.4	6.3	6.0	6.1	6.0	-2.8%	5.7	5.5	5.4	5.2	4.4	3.6	2.8	2.0	1.2	0.4	-0.4
Angola	1.1	1.2	1.3	1.4	1.4	1.4	1.4	4.0%	1.5	1.6	1.6	1.6	1.9	2.1	2.4	2.6	2.9	3.1	3.4
Antigua and Barbuda	5.0	5.1	5.6	5.6	5.9	6.0	5.8	2.7%	6.2	6.4	6.6	6.8	7.6	8.4	9.3	10.1	11.0	11.8	12.7
Argentina	4.1	4.4	4.5	4.7	4.4	4.3	4.6	1.7%	4.6	4.6	4.7	4.7	4.9	5.1	5.4	5.6	5.8	6.0	6.2
Armenia	1.4	1.5	1.7	1.9	1.5	1.4	1.7	2.5%	1.6	1.6	1.7	1.7	1.7	1.8	1.9	1.9	2.0	2.1	2.2
Aruba	25.0	24.8	25.6	24.8	24.9	24.2	23.9	-0.7%	24.0	23.8	23.6	23.5	22.6	21.7	20.8	19.9	19.0	18.1	17.2
Australia	17.2	17.3	17.5	17.7	17.6	16.7	16.5	-0.6%	16.8	16.7	16.6	16.5	15.9	15.4	14.9	14.4	13.8	13.3	12.8
Austria	9.0	8.7	8.4	8.3	7.6	8.1	7.8	-2.5%	7.5	7.2	7.0	6.8	5.8	4.8	3.7	2.7	1.7	0.6	-0.4
Azerbaijan	4.1	4.6	3.6	4.1	3.6	3.4	3.6	-1.9%	3.3	3.2	3.0	2.9	2.2	1.6	0.9	0.2	-0.5	-1.1	-1.8
Bahamas, The	4.9	4.5	4.5	3.0	4.6	6.8	5.2	11.1%	5.6	5.8	6.0	6.2	7.3	8.3	9.3	10.3	11.4	12.4	13.4
Bahrain	22.2	20.0	21.4	21.5	18.1	18.4	17.9	-3.4%	17.2	16.5	15.9	15.2	11.8	8.4	5.0	1.5	-1.9	-5.3	-8.7
Bangladesh	0.3	0.3	0.3	0.3	0.4	0.4	0.4	6.0%	0.4	0.4	0.4	0.4	0.5	0.6	0.7	0.8	0.8	0.9	1.0
Barbados	4.9	5.0	5.2	5.9	5.8	5.4	5.6	2.1%	5.9	6.0	6.1	6.3	6.9	7.5	8.1	8.7	9.4	10.0	10.6
Belarus	6.1	6.4	6.3	6.6	6.3	6.6	6.7	1.5%	6.7	6.8	6.9	6.9	7.3	7.6	8.0	8.3	8.7	9.1	9.4
Belgium	10.3	10.1	9.7	9.7	9.6	10.0	8.8	-2.6%	9.1	8.9	8.7	8.6	7.7	6.8	6.0	5.1	4.3	3.4	2.6
Belize	1.5	1.5	1.5	1.5	1.5	1.7	1.7	2.2%	1.7	1.7	1.8	1.8	2.0	2.2	2.4	2.6	2.8	2.9	3.1
Benin	0.3	0.5	0.5	0.5	0.5	0.5	0.5	9.7%	0.6	0.6	0.7	0.7	0.8	1.0	1.1	1.3	1.4	1.6	1.7
Bermuda	6.9	8.1	8.0	6.0	7.1	7.3	6.1	-2.1%	6.4	6.2	6.0	5.8	5.0	4.1	3.2	2.3	1.5	0.6	-0.3
Bhutan	0.6	0.6	0.6	0.6	0.5	0.7	0.8	3.9%	0.7	0.7	0.8	0.8	0.9	1.0	1.1	1.2	1.3	1.5	1.6
Bolivia	1.3	1.6	1.3	1.4	1.5	1.5	1.6	3.2%	1.6	1.6	1.7	1.7	1.8	2.0	2.2	2.3	2.5	2.6	2.8
Bosnia and Herzegovina	4.2	4.6	4.6	5.2	5.4	5.5	6.2	6.6%	6.3	6.6	6.9	7.2	8.8	10.3	11.8	13.4	14.9	16.4	18.0
Botswana	2.5	2.5	2.4	2.5	2.2	2.6	2.3	-1.1%	2.4	2.3	2.3	2.3	2.2	2.1	2.0	1.9	1.9	1.8	1.7
Brazil	1.8	1.8	1.9	2.0	1.9	2.1	2.2	2.9%	2.2	2.2	2.3	2.4	2.6	2.9	3.2	3.5	3.8	4.1	4.4
Brunei Darussalam	12.8	11.6	24.2	26.3	22.1	21.9	24.4	21.4%	28.1	30.0	31.9	33.8	43.3	52.9	62.4	71.9	81.5	91.0	100.5
Bulgaria	6.2	6.4	6.9	6.8	5.7	6.0	6.7	1.4%	6.3	6.3	6.3	6.3	6.2	6.1	6.1	6.0	5.9	5.9	5.8
Burkina Faso	0.1	0.1	0.1	0.1	0.1	0.1	0.1	6.1%	0.1	0.1	0.1	0.1	0.2	0.2	0.2	0.2	0.2	0.3	0.3
Burundi	0.0	0.0	0.0	0.0	0.0	0.0	0.0	1.6%	0.0	0.0	0.0	0.0	0.0	0.0	0.0	0.0	0.0	0.0	0.0
Cabo Verde	0.6	0.6	0.8	0.6	0.6	0.6	0.9	5.6%	0.7	0.8	0.8	0.8	0.9	1.0	1.1	1.1	1.2	1.3	1.4
Cambodia	0.2	0.2	0.3	0.3	0.3	0.3	0.3	6.7%	0.3	0.4	0.4	0.4	0.5	0.6	0.6	0.7	0.8	0.9	1.0
Cameroon	0.2	0.2	0.3	0.3	0.3	0.3	0.3	4.7%	0.3	0.4	0.4	0.4	0.5	0.6	0.6	0.7	0.8	0.9	1.0
Canada	17.4	16.9	17.1	16.4	15.1	14.6	14.1	-3.4%	13.6	13.0	12.4	11.8	8.9	6.0	3.0	0.1	-2.9	-5.8	-8.7
Cayman Islands	9.9	9.7	11.3	11.2	10.3	10.2	10.3	0.7%	10.6	10.6	10.7	10.7	11.0	11.2	11.4	11.7	11.9	12.1	12.3
Central African Republic	0.1	0.1	0.1	0.1	0.1	0.1	0.1	3.1%	0.1	0.1	0.1	0.1	0.1	0.1	0.1	0.1	0.1	0.1	0.1
Chad	0.0	0.0	0.0	0.0	0.0	0.0	0.0	1.7%	0.0	0.0	0.0	0.0	0.1	0.1	0.1	0.1	0.1	0.1	0.1
Chile	3.8	4.0	4.4	4.3	4.0	4.2	4.6	3.1%	4.5	4.6	4.7	4.8	5.3	5.7	6.1	6.6	7.0	7.5	7.9
China	4.4	4.9	5.2	5.3	5.8	6.2	6.7	7.1%	6.9	7.3	7.6	8.0	9.8	11.6	13.3	15.1	16.9	18.7	20.5
Colombia	1.4	1.4	1.4	1.5	1.5	1.7	1.6	1.7%	1.6	1.7	1.7	1.8	2.0	2.2	2.3	2.5	2.7	2.9	3.1
Comoros	0.2	0.2	0.2	0.2	0.2	0.2	0.2	3.6%	0.2	0.2	0.2	0.2	0.2	0.3	0.3	0.3	0.3	0.3	0.4
Congo, Dem. Rep.	0.0	0.0	0.0	0.0	0.0	0.0	0.1	2.1%	0.1	0.1	0.1	0.1	0.1	0.1	0.1	0.1	0.1	0.1	0.1
Congo, Rep.	0.4	0.3	0.3	0.3	0.4	0.5	0.5	7.2%	0.5	0.6	0.6	0.6	0.8	1.0	1.2	1.3	1.5	1.7	1.9
Costa Rica	1.6	1.6	1.9	1.9	1.7	1.7	1.7	0.9%	1.7	1.7	1.8	1.8	1.8	1.8	1.8	1.9	1.9	1.9	1.9
Cote d'Ivoire	0.4	0.4	0.4	0.4	0.3	0.3	0.3	-5.2%	0.3	0.2	0.2	0.2	0.1	0.0	-0.1	-0.2	-0.3	-0.4	-0.5
Croatia	5.2	5.2	5.5	5.3	4.9	4.7	4.8	-1.3%	4.7	4.6	4.5	4.4	3.9	3.4	2.9	2.4	1.9	1.4	0.9
Cuba	2.3	2.4	2.4	2.7	2.6	3.4	3.2	5.4%	3.4	3.6	3.7	3.9	4.8	5.6	6.5	7.3	8.2	9.0	9.9
Cyprus	7.3	7.4	7.7	7.9	7.4	7.0	6.7	-1.3%	7.0	6.9	6.8	6.7	6.2	5.7	5.2	4.7	4.2	3.7	3.2
Czech Republic	11.8	11.9	12.0	11.2	10.3	10.6	10.4	-2.0%	10.0	9.7	9.4	9.1	7.6	6.1	4.7	3.2	1.7	0.2	-1.3
Denmark	8.7	10.1	9.2	8.5	8.1	8.4	7.2	-3.0%	7.3	7.0	6.7	6.4	4.8	3.2	1.6	0.0	-1.6	-3.2	-4.7
Djibouti	0.5	0.5	0.6	0.6	0.6	0.6	0.6	0.6%	0.6	0.6	0.6	0.6	0.7	0.7	0.8	0.8	0.8	0.9	0.9
Dominica	1.6	1.6	2.1	1.8	1.8	1.9	1.7	1.3%	1.9	1.9	2.0	2.0	2.1	2.3	2.4	2.6	2.7	2.8	3.0
Dominican Republic	2.0	2.1	2.2	2.2	2.1	2.2	2.2	1.3%	2.2	2.2	2.2	2.3	2.3	2.4	2.5	2.6	2.7	2.8	2.8
Ecuador	2.2	2.1	2.2	2.1	2.4	2.3	2.4	1.3%	2.4	2.4	2.5	2.5	2.7	2.9	3.1	3.3	3.5	3.7	3.9
Egypt, Arab Rep.	2.2	2.3	2.5	2.5	2.5	2.5	2.6	2.8%	2.7	2.7	2.8	2.8	3.1	3.4	3.6	3.9	4.2	4.4	4.7
El Salvador	1.1	1.1	1.2	1.1	1.1	1.0	1.1	0.3%	1.1	1.1	1.0	1.0	1.0	1.0	0.9	0.9	0.8	0.8	0.7
Equatorial Guinea	7.5	7.4	7.2	6.6	6.5	6.4	8.9	2.8%	7.4	7.5	7.6	7.6	7.9	8.2	8.5	8.7	9.0	9.3	9.6
Eritrea	0.2	0.1	0.1	0.1	0.1	0.1	0.1	-8.3%	0.1	0.1	0.1	0.1	0.0	0.0	-0.1	-0.1	-0.2	-0.3	-0.3
Estonia	12.4	12.0	14.1	13.1	11.0	13.8	14.0	2.1%	13.7	13.9	14.1	14.3	15.3	16.2	17.2	18.2	19.2	20.2	21.2
Ethiopia	0.1	0.1	0.1	0.1	0.1	0.1	0.1	4.1%	0.1	0.1	0.1	0.1	0.1	0.1	0.1	0.1	0.2	0.2	0.2
Faeroe Islands	14.9	14.0	14.2	13.0	11.8	13.0	11.7	-4.0%	11.2	10.7	10.2	9.7	7.2	4.7	2.2	-0.3	-2.8	-5.3	-7.8
Fiji	1.7	1.6	1.4	1.3	1.0	1.5	1.4	-2.5%	1.2	1.2	1.1	1.1	0.8	0.6	0.3	0.0	-0.2	-0.5	-0.7
Finland	10.4	12.6	12.1	10.7	10.0	11.5	10.2	-0.4%	10.3	10.2	10.0	9.8	8.9	8.0	7.1	6.3	5.4	4.5	3.6
France	6.2	6.0	5.9	5.8	5.5	5.5	5.2	-2.9%	5.1	4.9	4.8	4.6	3.9	3.1	2.3	1.5	0.8	0.0	-0.8
French Polynesia	3.3	3.3	3.2	3.3	3.3	3.3	3.2	-0.9%	3.2	3.2	3.2	3.2	3.1	3.0	2.9	2.8	2.7	2.7	2.6
Gabon	1.6	1.5	1.4	1.4	1.4	1.5	1.4	-1.8%	1.4	1.4	1.3	1.3	1.2	1.2	1.1	1.0	0.9	0.8	0.7
Gambia, The	0.2	0.2	0.3	0.3	0.3	0.3	0.2	1.2%	0.3	0.3	0.3	0.3	0.3	0.4	0.4	0.4	0.4	0.5	0.5
Georgia	1.2	1.4	1.5	1.5	1.4	1.5	1.8	7.3%	1.7	1.8	1.9	1.9	2.3	2.6	3.0	3.3	3.6	4.0	4.3
Germany	9.7	9.8	9.5	9.5	8.8	9.2	8.9	-1.3%	8.7	8.6	8.5	8.3	7.6	6.8	6.1	5.3	4.6	3.9	3.1
Ghana	0.3	0.4	0.4	0.4	0.3	0.4	0.4	3.6%	0.4	0.4	0.4	0.4	0.4	0.5	0.5	0.5	0.5	0.5	0.5
Greece	8.9	8.7	8.8	8.7	8.5	7.8	7.6	-2.7%	7.5	7.3	7.1	6.9	5.7	4.6	3.5	2.4	1.3	0.1	-1.0
Grenada	2.1	2.2	2.3	2.5	2.4	2.5	2.4	2.3%	2.6	2.6	2.7	2.7	3.0	3.3	3.6	3.8	4.1	4.4	4.7
Guatemala	0.9	0.9	0.9																

6 years Compound growth rate and forecasting (2012 to 2050) of CO2 emissions (metric tons per capita)

Country Name	2005	2006	2007	2008	2009	2010	2011	6 years compound growth rate	2012	2013	2014	2015	2020	2025	2030	2035	2040	2045	2050	
Lao PDR	0.2	0.3	0.2	0.2	0.2	0.2	0.2	-4.5%	0.2	0.1	0.1	0.1	0.1	0.0	0.0	-0.1	-0.2	-0.2	-0.3	
Latvia	3.2	3.4	3.8	3.6	3.4	4.0	3.8	2.8%	4.0	4.0	4.1	4.1	4.2	4.7	5.1	5.6	6.0	6.5	6.9	7.3
Lebanon	4.1	3.6	3.3	4.2	5.0	4.6	4.7	2.3%	5.0	5.2	5.4	5.6	6.6	7.6	8.6	9.6	10.6	11.6	12.6	
Lesotho	0.7	0.7	0.8	1.1	1.1	1.1	1.1	6.6%	1.2	1.3	1.4	1.5	1.8	2.2	2.6	3.0	3.3	3.7	4.1	
Liberia	0.2	0.2	0.2	0.2	0.1	0.2	0.2	-0.6%	0.2	0.2	0.2	0.2	0.1	0.1	0.1	0.1	0.1	0.0	0.0	
Libya	9.0	9.2	8.8	9.1	10.0	10.5	6.2	-6.0%	8.4	8.2	8.0	7.9	7.1	6.3	5.5	4.6	3.8	3.0	2.2	
Lithuania	4.2	4.4	4.6	4.6	3.9	4.3	4.5	1.3%	4.4	4.4	4.4	4.4	4.5	4.5	4.5	4.6	4.6	4.7	4.7	
Luxembourg	24.8	24.0	23.0	22.4	20.9	21.6	20.9	-2.8%	19.9	19.2	18.5	17.9	14.5	11.2	7.9	4.6	1.2	-2.1	-5.4	
Macao SAR, China	3.9	3.4	3.1	2.6	2.8	2.2	2.1	-9.7%	1.7	1.5	1.2	0.9	-0.5	-2.0	-3.4	-4.8	-6.3	-7.7	-9.2	
Macedonia, FYR	5.5	5.3	4.6	4.6	4.2	4.2	4.5	-3.3%	3.9	3.7	3.5	3.3	2.2	1.2	0.2	-0.8	-1.9	-2.9	-3.9	
Madagascar	0.1	0.1	0.1	0.1	0.1	0.1	0.1	2.9%	0.1	0.1	0.1	0.1	0.1	0.1	0.2	0.2	0.2	0.2	0.2	
Malawi	0.1	0.1	0.1	0.1	0.1	0.1	0.1	1.6%	0.1	0.1	0.1	0.1	0.1	0.1	0.1	0.1	0.1	0.1	0.1	
Malaysia	6.9	6.5	7.0	7.7	7.4	8.0	7.9	2.3%	8.2	8.5	8.7	8.9	10.1	11.2	12.3	13.5	14.6	15.8	16.9	
Maldives	2.3	2.9	2.9	3.1	3.3	3.2	3.3	6.0%	3.6	3.7	3.8	4.0	4.7	5.4	6.1	6.8	7.6	8.3	9.0	
Mali	0.1	0.1	0.1	0.1	0.1	0.1	0.1	2.3%	0.1	0.1	0.1	0.1	0.1	0.1	0.1	0.1	0.1	0.2	0.2	
Malta	6.7	6.4	6.7	6.3	5.8	6.3	6.0	-1.7%	5.9	5.8	5.7	5.6	5.1	4.5	4.0	3.5	3.0	2.4	1.9	
Marshall Islands	1.6	1.8	1.9	1.9	2.0	2.0	2.0	3.2%	2.1	2.1	2.2	2.2	2.5	2.8	3.0	3.3	3.5	3.8	4.1	
Mauritania	0.5	0.5	0.6	0.6	0.6	0.6	0.6	3.7%	0.7	0.7	0.7	0.7	0.8	0.9	1.1	1.2	1.3	1.4	1.5	
Mauritius	2.7	2.9	3.0	3.0	3.0	3.1	3.1	2.6%	3.2	3.3	3.3	3.4	3.7	4.0	4.3	4.6	4.9	5.2	5.5	
Mexico	4.0	4.0	4.1	4.1	3.9	3.8	3.9	-0.4%	3.8	3.8	3.7	3.7	3.5	3.4	3.2	3.0	2.8	2.7	2.5	
Micronesia, Fed. Sts.	1.1	1.2	1.4	1.2	1.6	1.2	1.2	1.4%	1.3	1.4	1.4	1.4	1.5	1.6	1.7	1.8	1.9	2.0	2.1	
Moldova	1.4	1.4	1.3	1.3	1.3	1.4	1.4	0.4%	1.4	1.4	1.4	1.4	1.4	1.4	1.4	1.4	1.4	1.4	1.4	
Mongolia	3.4	3.7	3.9	3.8	4.1	4.2	6.9	12.4%	6.0	6.4	6.8	7.3	9.4	11.5	13.6	15.7	17.8	19.9	22.0	
Montenegro	3.3	3.9	3.7	4.5	3.0	4.2	4.1	3.6%	4.1	4.2	4.3	4.4	4.8	5.2	5.6	6.0	6.4	6.8	7.2	
Morocco	1.5	1.5	1.6	1.7	1.7	1.7	1.7	2.4%	1.8	1.8	1.9	1.9	1.9	2.1	2.3	2.5	2.7	2.9	3.1	3.3
Mozambique	0.1	0.1	0.1	0.1	0.1	0.1	0.1	7.2%	0.1	0.1	0.1	0.2	0.2	0.2	0.3	0.3	0.3	0.4	0.4	
Myanmar	0.2	0.3	0.2	0.2	0.2	0.2	0.2	-2.4%	0.2	0.2	0.1	0.1	0.1	0.0	0.0	-0.1	-0.1	-0.2	-0.2	
Namibia	1.1	1.1	1.2	1.7	1.5	1.4	1.2	1.4%	1.5	1.6	1.6	1.6	1.9	2.1	2.3	2.5	2.8	3.0	3.2	
Nepal	0.1	0.1	0.1	0.1	0.1	0.2	0.2	3.9%	0.2	0.2	0.2	0.2	0.2	0.3	0.3	0.4	0.4	0.5	0.5	
Netherlands	10.5	10.2	10.5	10.5	10.2	10.9	10.1	-0.8%	10.4	10.4	10.4	10.4	10.3	10.3	10.3	10.2	10.2	10.2	10.1	
New Zealand	8.2	8.0	8.0	8.0	7.5	7.3	7.1	-2.3%	7.0	6.8	6.6	6.5	5.5	4.6	3.7	2.8	1.9	0.9	0.0	
Nicaragua	0.8	0.8	0.8	0.8	0.8	0.8	0.8	0.8%	0.8	0.8	0.8	0.8	0.8	0.9	0.9	0.9	0.9	0.9	0.9	
Niger	0.1	0.1	0.1	0.1	0.1	0.1	0.1	5.3%	0.1	0.1	0.1	0.1	0.1	0.2	0.2	0.2	0.2	0.2	0.3	
Nigeria	0.7	0.7	0.6	0.6	0.5	0.5	0.5	-5.4%	0.4	0.4	0.4	0.3	0.1	-0.1	-0.3	-0.5	-0.7	-0.9	-1.1	
Norway	9.2	9.5	9.6	10.6	10.8	11.6	9.2	0.0%	10.9	11.0	11.2	11.4	12.4	13.4	14.4	15.4	16.4	17.4	18.3	
Oman	11.9	15.5	17.2	14.5	13.9	19.1	20.2	9.2%	20.2	21.2	22.2	23.3	28.4	33.5	38.7	43.8	49.0	54.1	59.2	
Pakistan	0.9	0.9	1.0	1.0	1.0	1.0	0.9	0.9%	1.0	1.0	1.0	1.0	1.0	1.1	1.1	1.1	1.1	1.2	1.2	
Palau	9.6	10.1	10.4	10.3	10.3	10.6	10.9	2.1%	11.0	11.1	11.3	11.5	12.3	13.1	14.0	14.8	15.7	16.5	17.3	
Panama	2.1	2.2	2.1	2.1	2.4	2.4	2.6	4.1%	2.6	2.7	2.8	2.9	3.4	3.8	4.3	4.7	5.2	5.6	6.1	
Papua New Guinea	0.7	0.7	1.0	0.7	0.8	0.7	0.7	0.6%	0.7	0.7	0.7	0.7	0.7	0.7	0.6	0.6	0.6	0.6	0.5	
Paraguay	0.7	0.7	0.7	0.7	0.7	0.8	0.8	4.1%	0.9	0.9	0.9	1.0	1.1	1.3	1.4	1.6	1.7	1.9	2.0	
Peru	1.3	1.3	1.5	1.4	1.8	2.0	1.8	4.8%	2.0	2.1	2.2	2.3	2.9	3.4	3.9	4.5	5.0	5.5	6.1	
Philippines	0.9	0.8	0.8	0.8	0.8	0.9	0.9	0.0%	0.9	0.9	0.9	0.9	0.9	1.0	1.0	1.1	1.1	1.2	1.2	
Poland	7.9	8.4	8.3	8.3	7.8	8.3	8.3	0.8%	8.3	8.3	8.3	8.4	8.5	8.6	8.8	8.9	9.0	9.1	9.3	
Portugal	6.2	5.6	5.8	5.2	5.2	4.7	4.7	-4.5%	4.3	4.1	3.8	3.6	2.3	1.1	-0.2	-1.4	-2.6	-3.9	-5.1	
Qatar	62.0	57.4	55.3	48.6	44.8	42.6	44.0	-5.5%	37.3	33.9	30.6	27.2	10.4	-6.3	-23.1	-39.9	-56.7	-73.4	-90.2	
Romania	4.5	4.8	4.9	4.7	4.0	3.9	4.2	-1.1%	3.9	3.8	3.7	3.5	2.9	2.3	1.6	1.0	0.4	-0.3	-0.9	
Russian Federation	11.3	11.7	11.7	12.0	11.0	12.2	12.6	2.0%	12.4	12.6	12.8	12.9	13.7	14.6	15.4	16.2	17.0	17.8	18.6	
Rwanda	0.1	0.1	0.1	0.1	0.1	0.1	0.1	1.2%	0.1	0.1	0.1	0.1	0.1	0.1	0.1	0.1	0.1	0.1	0.1	
Samoa	0.9	1.0	1.0	1.0	1.1	1.1	1.3	4.9%	1.2	1.3	1.3	1.4	1.6	1.8	2.0	2.3	2.5	2.7	2.9	
Sao Tome and Principe	0.5	0.5	0.5	0.5	0.5	0.6	0.6	2.6%	0.6	0.6	0.6	0.6	0.7	0.8	0.8	0.9	1.0	1.0	1.1	
Saudi Arabia	16.1	17.0	15.1	15.6	17.7	19.0	18.1	2.0%	18.7	19.2	19.6	20.1	22.3	24.5	26.8	29.0	31.2	33.5	35.7	
Senegal	0.5	0.4	0.4	0.4	0.5	0.6	0.6	2.1%	0.6	0.6	0.6	0.7	0.8	0.9	1.0	1.1	1.3	1.4	1.5	
Serbia	7.3	7.1	7.1	7.1	6.3	6.3	6.8	6.8%	6.3	6.1	5.9	5.8	5.0	4.3	3.5	2.7	1.9	1.2	0.4	
Seychelles	8.3	8.7	7.5	8.0	8.5	7.7	6.8	-3.2%	7.1	7.0	6.8	6.6	5.6	4.6	3.6	2.6	1.7	0.7	-0.3	
Sierra Leone	0.1	0.1	0.1	0.1	0.1	0.1	0.2	5.9%	0.1	0.1	0.1	0.2	0.2	0.2	0.2	0.2	0.2	0.3	0.3	
Singapore	7.1	7.0	4.0	4.9	4.8	2.7	4.3	-8.0%	2.6	2.1	1.5	0.9	-2.0	-4.9	-7.8	-10.7	-13.6	-16.5	-19.4	
Slovak Republic	7.3	7.3	6.8	7.0	6.3	6.7	6.4	-2.3%	6.2	6.0	5.9	5.7	4.9	4.1	3.3	2.5	1.7	0.9	0.1	
Slovenia	7.9	8.1	8.0	8.5	7.5	7.5	7.5	-0.9%	7.5	7.4	7.3	7.2	6.6	6.1	5.6	5.1	4.6	4.0	3.5	
Solomon Islands	0.4	0.4	0.4	0.4	0.4	0.4	0.4	-0.6%	0.4	0.4	0.4	0.4	0.4	0.3	0.3	0.3	0.3	0.3	0.3	
Somalia	0.1	0.1	0.1	0.1	0.1	0.1	0.1	-2.9%	0.1	0.1	0.1	0.1	0.0	0.0	0.0	0.0	0.0	0.0	0.0	
South Africa	8.3	8.8	9.1	9.5	9.5	9.0	9.3	1.9%	9.6	9.7	9.9	10.0	10.7	11.3	12.0	12.7	13.3	14.0	14.7	
Spain	8.1	7.9	7.9	7.2	6.2	5.8	5.8	-5.4%	5.2	4.7	4.3	3.8	1.5	-0.8	-3.0	-5.3	-7.6	-9.9	-12.2	
Sri Lanka	0.6	0.6	0.6	0.6	0.6	0.6	0.7	2.9%	0.7	0.7	0.7	0.8	0.8	0.9	1.0	1.1	1.2	1.2	1.3	
St. Kitts and Nevis	4.8	4.7	4.9	4.9	5.0	5.0	5.1	0.9%	5.1	5.2	5.2	5.3	5.5	5.8	6.0	6.3	6.6	6.8	7.1	
St. Lucia	2.2	2.2	2.3	2.3	2.2	2.3	2.3	0.4%	2.3	2.3	2.3	2.3	2.4	2.4	2.5	2.5	2.5	2.6	2.6	
St. Vincent and the Grenadines	2.0	2.0	2.1	2.1	2.1	2.1	2.2	1.3%	2.2	2.2	2.3	2.3	2.4	2.6	2.7	2.8	3.0	3.1	3.2	
Sudan	0.3	0.3	0.3	0.3	0.3	0.3	0.3	4.6%	0.4	0.4	0.4	0.4	0.5	0.6	0.6	0.7	0.8	0.9	0.9	
Suriname	4.9	4.9	4.9	4.8	4.8	4.6	3.6	-4.6%	4.0	3.9	3.7	3.6	2.8	2.0	1.3	0.5	-0.3	-1.0	-1.8	
Swaziland	0.9	0.9	0.9	1.0	0.9	0.9	0.9	-1.1%	0.9	0.9	0.8	0.8	0.8	0.7	0.7	0.6	0.6	0.5	0.5	
Sweden	5.7	5.5	5.3	5.3	4.7	5.6	5.5	-0.6%	5.2	5.2	5.2	5.2	5.0	4.9	4.7	4.6	4.4	4.3	4.1	
Switzerland	5.6	5.6	5.0	5.3	5.4	5.0	4.6	-3.0%	4.7	4.5	4.4	4.3	3.6	2.9	2.2	1.6	0.9	0.2	-0.4	
Syrian Arab Republic	2.8	2.9	3.4	3.4	3.0															

Table 5: CO₂ emissions from electricity, industries, Transportation and Residential buildings and commercial trends on the 172 emitting countries

SL No.	Country Name	Electricity ^a	Manufacturing industries and construction ^b	Transportation ^c	Residential buildings and commercial and public services ^d	SL No.	Country Name	Electricity	Manufacturing industries and construction	Transportation	Residential buildings and commercial and public services
1	Albania	2.6	26.4	58.2	6.5	85	Latin America & Caribbean (all income levels)	33.2	21.9	35.8	6.1
2	Algeria	38.5	11.9	32.0	14.6	86	Latin America & Caribbean (developing only)	31.3	20.3	39.9	5.3
3	Angola	14.5	16.8	44.0	24.5	87	Latvia	28.0	15.8	38.9	12.1
4	Arab World	46.8	22.7	24.5	4.5	88	Least developed countries: UN classification	28.3	20.4	34.3	10.6
5	Argentina	37.7	18.0	25.6	14.0	89	Lebanon	56.8	5.9	25.2	12.1
6	Armenia	26.2	12.5	23.8	23.2	90	Libya	47.5	10.2	37.5	4.7
7	Australia	59.2	12.6	23.2	3.3	91	Lithuania	34.5	23.8	32.0	8.0
8	Austria	34.1	19.1	32.9	12.7	92	Low & middle income	49.7	26.3	14.9	6.8
9	Azerbaijan	47.9	8.7	21.9	17.7	93	Low income	16.3	39.8	26.1	5.5
10	Bahrain	78.2	10.1	10.9	0.8	94	Lower middle income	48.9	22.9	17.7	7.5
11	Bangladesh	47.7	20.9	14.5	11.1	95	Luxembourg	11.0	9.1	64.3	15.2
12	Belarus	46.7	26.1	16.3	7.8	96	Macedonia, FYR	64.0	16.2	15.9	3.5
13	Belgium	24.2	28.4	23.3	20.2	97	Malaysia	54.9	19.4	21.9	2.2
14	Benin	2.4	3.0	69.9	24.4	99	Mauritius	60.2	8.9	26.3	4.6
15	Bolivia	28.6	11.3	38.4	8.4	100	Mexico	43.9	13.4	35.1	5.4
16	Bosnia and Herzegovina	69.9	8.3	14.9	2.4	101	Middle East & North Africa (all income levels)	44.6	21.4	23.6	8.5
17	Botswana	8.3	30.2	48.8	3.1	102	Middle East & North Africa (developing only)	39.6	16.5	26.2	14.8
18	Brazil	18.6	27.6	45.2	4.5	103	Middle income	49.9	26.2	14.8	6.8
19	Brunei Darussalam	59.0	23.8	15.8	1.2	104	Moldova	46.6	13.4	13.9	24.1
20	Bulgaria	68.6	8.6	18.4	3.2	105	Mongolia	60.4	13.6	15.2	6.4
21	Cambodia	18.2	16.1	51.8	14.1	106	Montenegro	67.4	3.9	27.4	0.9
22	Cameroon	32.3	7.2	53.3	7.0	107	Morocco	39.2	14.7	27.9	8.0
23	Canada	29.2	20.9	32.1	13.2	108	Mozambique	2.3	19.2	72.3	5.0
24	Caribbean small states	38.5	48.9	10.8	1.4	110	Namibia	1.3	9.4	54.7	0.3
25	Central Europe and the Baltics	52.8	13.9	18.3	12.5	111	Nepal	0.2	34.6	43.8	13.9
26	Chile	46.9	16.6	28.5	6.8	112	Netherlands	37.4	23.3	18.7	16.8
27	China	53.7	31.0	8.6	5.1	113	New Zealand	29.0	19.5	41.7	4.4
28	Colombia	22.6	23.2	40.9	7.9	114	Nicaragua	39.5	12.3	40.9	6.7
29	Congo, Dem. Rep.	1.2	6.2	91.7	1.2	115	Nigeria	36.5	12.1	39.0	2.4
30	Congo, Rep.	14.2	5.0	74.8	6.0	116	North America	45.0	10.8	32.8	10.1
31	Costa Rica	8.6	15.1	69.8	4.0	117	Norway	34.8	19.5	36.6	2.8
32	Cote d'Ivoire	46.4	12.8	30.0	7.4	118	OECD members	45.5	13.5	27.5	11.8
33	Croatia	33.2	17.2	32.6	13.1	119	Oman	34.2	46.7	16.3	0.5
34	Cuba	59.4	27.8	6.8	2.2	120	Other small states	32.2	17.5	37.2	3.4
35	Cyprus	52.9	7.0	30.8	7.7	121	Pakistan	30.3	28.6	26.9	14.0
36	Czech Republic	57.5	16.7	15.0	9.5	122	Panama	28.3	27.8	36.9	6.3
37	Denmark	46.0	9.9	30.5	8.6	123	Peru	33.1	21.2	38.7	5.8
38	Dominican Republic	47.7	11.5	33.4	7.0	124	Philippines	48.0	14.2	30.5	6.6
39	East Asia & Pacific (all income levels)	52.7	27.7	12.2	5.8	125	Poland	55.1	11.5	15.5	14.4
40	East Asia & Pacific (developing only)	52.2	30.3	10.7	5.1	126	Portugal	42.7	14.4	34.2	6.4
41	Ecuador	26.6	14.3	48.4	8.4	127	Qatar	62.2	23.5	13.9	0.4
42	Egypt, Arab Rep.	44.5	18.5	25.6	7.8	128	Romania	50.0	18.2	18.8	10.9
43	El Salvador	23.4	16.7	50.4	9.6	129	Russian Federation	60.0	17.7	14.2	7.3
44	Equatorial Guinea	55.6	3.7	29.6	11.1	130	Saudi Arabia	48.3	24.8	26.0	0.9
45	Estonia	76.2	5.8	13.7	2.5	131	Senegal	37.4	19.7	36.9	5.1
46	Ethiopia	0.5	40.6	40.7	11.1	132	Serbia	69.9	11.4	11.5	6.2
47	Euro area	39.0	16.5	25.9	16.6	133	Singapore	56.7	28.3	13.9	1.1
48	Europe & Central Asia (all income levels)	47.4	16.8	19.8	13.8	134	Slovak Republic	39.7	24.5	20.1	14.6
49	Europe & Central Asia (developing only)	47.8	20.1	13.2	15.0	135	Slovenia	40.3	11.5	37.5	8.8
50	European Union	42.3	15.0	24.6	16.1	136	Small states	36.8	40.5	17.8	1.9
51	Finland	49.0	17.4	23.6	5.1	137	South Africa	62.9	15.6	12.9	5.9
52	Fragile and conflict affected situations	46.9	11.5	30.3	7.9	138	South Asia	54.7	24.3	12.5	5.9
53	France	18.1	18.2	36.8	22.5	139	Spain	41.1	16.1	30.8	9.2
54	Gabon	40.5	30.4	19.4	8.5	140	Sri Lanka	40.9	7.1	45.5	3.4
55	Georgia	19.4	19.5	35.7	19.8	141	Sub-Saharan Africa (all income levels)	50.4	15.8	23.6	6.4
56	Germany	47.5	14.8	19.5	18.1	142	Sub-Saharan Africa (developing only)	50.4	15.8	23.6	6.4
57	Ghana	24.8	14.1	52.6	5.8	143	Sudan	14.4	15.8	59.8	7.3
58	Greece	58.6	9.0	21.0	9.5	144	Sweden	25.0	20.3	49.6	3.9
59	Guatemala	23.7	16.6	52.3	7.1	145	Switzerland	9.0	13.0	41.2	35.0
60	Haiti	32.9	17.4	45.9	3.9	146	Syrian Arab Republic	47.6	14.9	23.9	10.1
61	Heavily indebted poor countries (HIPC)	23.8	15.6	49.1	7.3	148	Tanzania	31.7	10.1	54.0	3.4
62	High income	47.6	15.5	25.2	10.3	149	Thailand	41.0	27.1	23.7	3.7
63	High income: nonOECD	54.0	22.4	17.5	5.2	150	Togo	1.2	9.3	77.2	12.3
64	High income: OECD	45.7	13.4	27.5	11.9	151	Trinidad and Tobago	38.5	52.4	8.3	0.9
65	Honduras	33.8	15.7	39.8	3.9	152	Tunisia	36.4	21.7	27.4	10.2
66	Hong Kong SAR, China	65.4	17.1	13.9	3.6	153	Turkey	41.1	18.1	17.2	19.8
67	Hungary	36.9	12.3	24.6	24.2	154	Turkmenistan	36.5	8.6	10.9	25.4
68	India	56.9	24.2	11.1	5.1	155	Ukraine	49.1	25.3	10.7	13.2
69	Indonesia	42.1	21.6	29.5	4.7	156	United Arab Emirates	36.5	46.6	16.6	0.3
70	Iran, Islamic Rep.	33.8	20.0	22.8	21.2	157	United Kingdom	45.6	9.6	24.7	19.4
71	Iraq	30.8	8.7	30.9	9.7	158	United States	46.7	9.8	32.9	9.8
72	Ireland	36.1	10.7	28.9	22.7	159	Upper middle income	50.1	27.3	13.9	6.6
73	Israel	68.5	2.6	17.6	2.3	160	Uruguay	38.6	9.7	39.0	7.0
74	Italy	38.1	14.2	27.2	18.5	161	Uzbekistan	36.2	17.5	7.0	35.9
75	Jamaica	38.8	30.7	23.6	4.2	162	Venezuela, RB	33.9	32.8	29.4	3.9
76	Japan	49.8	19.6	17.6	12.2	163	Vietnam	31.3	35.4	23.7	8.4
77	Jordan	51.9	5.9	31.3	8.6	164	World	48.7	21.1	19.9	8.5
78	Kazakhstan	55.3	27.6	6.4	7.2	165	Yemen, Rep.	26.9	15.4	38.9	9.0
79	Kenya	18.7	25.6	44.9	9.1	166	Zambia	3.3	55.8	32.6	2.9
80	Korea, Dem. Rep.	16.1	62.1	2.9	0.3	167	Zimbabwe	33.9	19.5	13.6	9.8
81	Korea, Rep.	57.9	17.1	14.9	8.6	168	Tajikistan	1.8		10.9	
82	Kosovo	76.5	7.3	12.5	3.4	169	Paraguay		5.1	89.5	4.2
83	Kuwait	67.4	18.4	13.6	0.6	170	Myanmar	25.7	33.1	26.3	
84	Kyrgyz Republic	19.5	16.1	41.0	2.7	171	Malta	79.4		18.3	2.4
						172	Iceland		26.1	42.9	1.1

Data Source: World Development Indicators, Last Updated Date:10/9/2015

(a). CO₂ emissions from electricity and heat production, total (% of total fuel combustion)

(b). CO₂ emissions from manufacturing industries and construction (% of total fuel combustion)

(c). CO₂ emissions from transport (% of total fuel combustion)

(d). CO₂ emissions from residential buildings and commercial and public services (% of total fuel combustion)

Table 6: CO₂ emissions from Transportation

CO ₂ emissions from transport (% of total fuel combustion)																										
Year	Arab World	East Asia & Pacific (all income levels)	East Asia & Pacific (developing only)	Europe & Central Asia (all income levels)	Germany	Highly indebted poor countries (HIPC)	High income	High income: OECD	India	Indonesia	Latin America & Caribbean (all income levels)	Least developed countries: UN classification	Low & middle income	Lower middle income	Malaysia	Mexico	Middle East & North Africa (all income levels)	Middle income	North America	OECD members	South Asia	United Arab Emirates	United Kingdom	United States	Upper middle income	World
1971	230	116	8.1	12.3	10.1	192	191	38.1	31.9	32.1	32.7	16.1	26.8	31.8	30.8	30.8	16.5	25.1	19.3	23.8	16.3	11.8	25.2	14.1	18.7	
1972	228	116	8.2	12.6	10.3	191	194	38.4	32.2	32.6	32.9	16.2	26.9	32.2	31.2	31.2	16.5	25.3	19.4	23.9	11.9	12.6	25.2	14.2	18.8	
1973	230	117	8.5	12.7	10.1	193	195	38.5	32.3	32.6	32.9	16.2	26.8	32.3	31.2	31.2	16.5	25.6	19.6	24.1	12.7	12.8	25.6	14.3	18.9	
1974	242	119	8.9	12.6	9.9	196	195	38.6	32.0	32.0	33.4	16.4	25.6	32.2	29.9	31.9	17.0	25.8	19.7	21.8	20.9	13.2	25.8	15.1	19.1	
1975	241	120	8.5	13.4	10.8	195	207	38.6	31.3	30.4	34.4	15.6	26.7	31.6	30.4	32.3	16.6	27.2	20.8	21.3	18.1	13.4	27.2	14.8	19.8	
1976	246	119	8.3	13.2	10.4	197	205	38.4	31.3	31.2	34.2	15.7	26.0	31.0	30.6	32.3	16.4	26.9	20.6	19.8	21.2	13.8	26.5	14.8	19.5	
1977	253	118	8.1	13.7	11.1	191	207	38.6	31.7	31.7	33.7	15.7	26.2	29.5	30.7	33.9	15.9	26.6	20.8	19.9	21.6	13.9	26.5	14.2	19.6	
1978	267	119	7.8	13.8	11.5	193	215	38.7	31.1	31.6	34.4	15.4	26.3	28.4	30.0	34.8	16.6	27.6	21.1	21.1	20.8	14.6	27.4	13.8	20.0	
1979	246	122	7.9	13.7	11.4	210	209	38.0	31.0	31.0	33.4	15.4	26.4	28.6	31.4	33.6	15.5	26.9	21.1	20.7	22.7	14.1	26.6	13.8	19.7	
1980	236	123	7.9	14.1	12.1	43.3	211	21.0	20.0	25.7	33.1	34.0	15.4	24.9	26.0	31.5	23.1	18.6	26.8	21.2	20.7	36.1	15.6	26.5	13.7	19.7
1981	246	124	8.0	14.4	12.1	43.4	214	21.4	19.2	26.1	32.8	34.8	15.6	23.8	26.2	31.7	23.8	18.8	27.1	21.6	19.0	34.8	15.4	26.7	14.4	20.0
1982	252	123	8.1	14.0	12.6	43.4	221	21.9	18.6	26.8	33.8	35.6	15.2	23.6	26.5	31.2	24.2	18.5	28.0	22.2	16.0	35.3	16.2	26.0	14.0	20.3
1983	267	124	8.1	15.2	12.8	41.8	226	22.4	18.2	25.9	32.7	35.4	14.8	23.0	27.7	28.6	25.8	18.1	28.5	22.5	15.5	37.2	16.9	28.4	13.6	20.5
1984	279	124	7.8	15.8	12.8	41.6	226	22.4	18.0	26.6	32.8	34.6	14.4	23.0	26.0	28.8	26.4	18.7	28.1	22.8	14.4	38.8	18.3	28.3	13.4	20.4
1985	281	121	7.9	15.4	12.8	41.7	226	22.4	18.1	25.7	32.1	34.0	14.4	22.9	26.6	27.9	26.4	14.7	28.3	23.5	14.5	36.2	17.6	28.3	13.4	20.3
1986	258	123	7.9	16.0	13.4	43.8	231	23.0	18.1	22.6	32.3	34.7	14.3	19.1	28.4	27.9	25.0	14.6	28.9	23.1	13.6	23.2	18.3	28.9	13.4	20.6
1987	258	123	7.8	16.4	14.0	43.2	234	23.4	18.0	24.0	31.2	32.4	14.0	18.6	28.0	27.5	24.8	14.3	29.0	24.5	13.4	22.7	18.8	29.0	13.2	20.6
1988	256	122	7.9	17.2	14.6	44.7	238	23.8	17.6	23.1	31.5	33.0	14.0	18.6	30.0	27.9	24.5	14.2	29.0	23.9	13.2	22.8	20.1	29.0	13.1	20.9
1989	254	125	8.0	18.2	15.3	44.1	240	24.1	17.7	24.0	31.6	33.8	14.2	18.8	28.4	29.1	24.1	14.5	28.8	24.2	13.2	20.6	21.4	28.9	13.3	21.0
1990	267	126	7.6	18.5	16.6	40.0	236	24.5	17.1	24.8	31.4	34.1	13.9	18.7	27.0	31.4	24.8	13.0	29.1	24.6	12.8	21.8	20.8	29.2	12.7	19.8
1991	274	127	7.7	18.8	17.3	40.0	236	24.4	16.8	24.4	31.3	37.5	13.2	14.7	24.6	30.7	25.3	13.4	28.8	24.5	12.3	19.4	20.3	28.8	12.8	19.5
1992	269	129	8.0	18.4	18.4	48.9	233	25.0	16.5	22.5	33.4	37.3	13.2	14.3	25.0	30.7	24.7	13.3	29.1	25.1	12.2	20.6	21.0	29.1	12.9	19.9
1993	258	131	8.2	18.7	19.0	48.6	238	25.2	16.1	22.1	34.2	34.1	13.4	14.5	25.6	31.5	24.6	13.5	28.9	28.4	12.0	20.9	21.8	28.9	13.4	20.0
1994	254	129	7.9	17.0	19.0	48.8	239	25.6	16.8	23.4	33.7	38.1	13.3	15.1	24.4	30.6	24.3	13.3	29.5	28.7	11.8	18.9	22.2	28.4	12.7	20.3
1995	242	129	8.0	17.2	19.2	48.0	240	25.8	16.0	22.7	34.1	33.8	13.4	15.6	22.9	30.0	23.2	13.4	29.7	28.8	11.9	18.6	22.4	29.8	12.6	20.2
1996	241	134	8.5	17.4	18.7	49.0	238	26.2	16.2	23.3	33.8	34.0	13.5	16.7	24.0	29.6	23.4	14.5	28.5	28.7	12.1	16.9	22.1	29.6	13.2	20.6
1997	234	136	9.2	18.0	19.5	47.4	240	26.7	16.9	23.9	33.5	32.6	14.5	17.2	22.7	29.8	23.8	14.5	29.1	28.7	12.1	17.0	23.6	29.1	13.4	20.7
1998	240	133	8.8	18.0	19.9	46.3	247	26.3	16.1	23.1	33.3	33.2	14.4	17.1	23.9	29.0	23.2	14.4	29.7	26.2	12.4	16.4	23.2	29.8	13.4	21.0
1999	241	138	9.5	18.2	21.2	44.4	251	26.8	16.9	24.3	33.3	31.3	14.8	16.5	22.0	30.2	23.6	14.8	30.4	28.8	12.1	16.5	24.0	28.3	14.2	21.5
2000	244	143	11.1	19.0	20.8	45.4	247	26.5	16.6	23.8	32.7	31.3	15.4	16.6	26.3	30.2	23.9	15.5	29.8	30.4	11.6	17.2	23.3	30.0	15.1	21.3
2001	242	145	11.2	19.1	19.9	45.6	247	26.5	16.4	23.8	32.9	31.2	15.6	16.7	27.2	30.6	23.6	15.6	30.0	30.5	11.5	18.8	22.6	30.1	15.2	21.4
2002	239	143	11.1	19.4	19.8	45.8	250	26.8	16.4	23.7	32.8	31.0	15.5	16.7	26.6	30.6	23.6	15.5	30.6	30.8	11.4	19.3	22.4	30.3	15.1	21.4
2003	238	136	10.5	19.2	19.5	45.8	249	26.7	16.4	23.1	33.2	32.3	14.9	16.4	27.1	32.0	23.7	14.9	30.5	30.7	11.4	20.4	23.2	30.4	14.4	21.0
2004	242	132	10.4	19.6	19.9	45.8	251	26.8	16.4	23.3	33.9	33.4	14.8	16.7	26.5	31.2	23.8	14.8	30.6	30.8	11.4	19.6	23.4	30.7	14.2	21.0
2005	241	125	9.8	19.8	19.3	44.8	252	27.0	16.5	22.0	33.7	33.5	14.4	16.3	24.8	31.6	23.7	14.4	30.9	27.0	11.3	20.6	23.7	31.0	13.8	20.6
2006	240	121	9.5	20.0	18.7	44.8	253	27.2	16.2	19.9	33.9	33.0	14.0	15.5	22.7	31.7	23.6	14.0	31.3	27.3	10.9	20.4	23.9	31.4	13.4	20.3
2007	248	116	9.6	20.3	18.9	45.6	253	27.1	16.0	20.1	34.5	33.6	14.1	16.0	23.3	31.3	23.6	14.1	30.9	27.2	11.7	19.9	24.6	31.0	13.4	20.2
2008	243	119	9.7	20.4	18.8	46.9	249	26.7	15.8	22.5	34.4	33.8	14.4	16.8	22.1	31.5	23.5	14.3	30.3	26.9	12.3	17.9	23.8	30.3	13.5	20.0
2009	242	120	9.9	21.1	20.0	48.9	254	27.4	16.5	24.5	34.6	34.1	14.4	16.9	24.0	30.8	23.7	14.4	31.0	27.5	11.9	17.7	25.2	31.0	13.4	20.1
2010	242	123	10.4	20.4	19.1	48.5	249	26.8	16.8	26.9	34.5	34.4	14.8	17.4	22.7	30.2	23.2	14.7	30.7	26.9	12.3	17.6	24.2	30.6	13.6	20.0
2011	241	121	10.5	20.3	20.0	49.2	249	27.0	17.2	28.7	35.2	35.1	14.6	17.6	22.4	30.2	23.2	14.6	31.0	27.0	12.7	17.1	26.0	31.0	13.7	19.7
2012	245	122	10.7	19.8	19.5	49.1	252	27.5	17.1	29.5	35.8	34.3	14.9	17.7	21.9	31.1	23.6	14.8	32.8	27.5	12.8	16.6	24.7	32.9	13.9	19.9
2020	243	134	10.8	22.0	24.3	51.2	273	30.3	4.0	20.8	34.4	33.3	13.7	11.8	20.7	34.8	24.2	13.5	32.9	30.3	6.7	13.9	29.5	33.0	13.2	21.1
2025	242	135	11.2	24.0	25.8	52.3	284	31.4	2.4	20.1	34.6	33.2	13.5	10.5	19.7	35.5	24.2	13.3	33.6	31.3	5.3	12.5	31.2	33.8	13.5	21.2
2030	241	137	11.5	25.1	27.3	53.5	288	32.5	0.7	19.4	34.8	33.1	13.4	9.2	18.6	36.1	24.3	13.1	34.3	32.4	3.8	11.0	32.9	34.5	13.4	21.3
2035	240	138	11.9	26.1	28.7	54.7	292	33.6	-1.0	18.7	34.9	33.0	13.2	7.9	17.6	36.7	24.4	12.8	35.0	33.5	2.4	9.2	34.6	35.2	13.4	21.2
2040	239	139	12.2	27.2	30.2	55.8	30.3	34.6	-2.6	18.0	35.1	32.9	13.0	6.7	16.5	37.4	24.5	12.6	35.7	34.5	1.0	8.0	36.3	36.0	13.3	21.6
2045	238	141	12.6	28.3	31.7	57.0	31.0	35.7	-4.3	17.2	35.3	32.8	12.8	5.4	15.5	38.0	24.5	12.4	36.4	35.6	-0.4	6.5	37.9	36.7	13.3	21.8
2050	237	142	12.9	29.3	33.1	58.1	31.8	36.8	-5.9	16.5	35.5	32.7	12.6	4.1	14.5	38.6	24.6	12.1	37.1	36.7	-1.9	5.0	39.6	37.4	13.2	21.9
10 Years (2002-2012) Compound Growth rate	0.2%	-1.6%	-0.4%	0.2%	-0.2%	0.7%	0.1%	0.2%	1.6%	2.2%	0.9%															

8 References

- Climate Change Indicators in the United States. (2015). Retrieved 2015, from <http://www3.epa.gov/climatechange/science/indicators/ghg/>
- Sources of Greenhouse Gas Emissions. (2015). Retrieved October 2015, from EPA Transportation: <http://www3.epa.gov/climatechange/ghgemissions/sources/transportation.html>
- Bo Xu, R. W. (2013). China's CO₂ emissions an analysis of Environmental Kuznets Curve for China. Teknikringen 34, SE 114 28 Stockholm, Sweden: Department of Industrial Ecology, Royal Institute of Technology (KTH).
- Doda, B. (2013, June). Emissions-GDP Relationship in Times of Growth and Decline. UK: Grantham Research Institute on Climate Change and the Environment London School of Economics and Political Science.
- EPA. (2015, September). Climate Change Indicators in the United States . Retrieved September 2015, from Climate Change Indicators in the United States : <http://www3.epa.gov/>
- Gorham, R. (2002). The Global Initiative on Transport Emissions. United Nations and the World Bank.
- Jos G.J. Olivier, G. J.-M. (2013). Trends in global CO₂ emissions: 2013 Report. PBL Netherlands Environmental Assessment Agency,978-94-91506-51-2.
- Lee, J. W. (2014). The Impact of Product Distribution and Information Technology on Carbon Emissions and Economic Growth: Empirical Evidence in Korea. The Journal of Asian Finance,, Economics and Business Vol.1 No.3, pp.17-28.
- Michael Grubb, 1. M. (2004). The relationship between carbon dioxide emissions and economic growth. (p. 19). University of Cambridge.
- OECD/IEA. (2014). CO₂ EMISSIONS FROM FUEL COMBUSTION Highlights. France: International Energy Agency, www.iea.org.
- Robert W. Bacon, S. B. (October 2007). Growth and CO₂ Emissions:How do Different Countries Fare? Environment Department,The World Bank.
- S.S.Sharma. (2011). "Determinants of carbon dioxide emissions: empirical evidence from 69 countries,". Applied Energy,vol.88,pp.376-382.
- Stolyarova, E. (2013). Carbon Dioxide Emissions, economic growth and energy mix: empirical evidence from 93 countries. Climate Economics Chair. Paris Dauphine University.
- T.Selden, D.-E. a. (1995). Stoking the fires? CO₂ emissions and economic growth,. Journal of Public Economics,vol.57,, pp.85-101.
- Théophile Azomahou, F. L. (2005, July). Economic Development and CO₂ Emissions:A Nonparametric Panel Approach. France;; ZEW, Center for European Economic Research, Mannheim.
- Tiwari, A. K. (2011, JANUARY). A Structural VAR Analysis of Renewable Energy consumption, real GDP andCO₂ emissions: Evidence from India . Economics Bulletin, Vol. 31 no.2 pp. 1793-1806.
- U.S. Environmental Protection Agency. (2006). Greenhouse Gas Emissions from the U.S. Transportation Sector, 1990-2003. Virginia: The United States Environmental Protection Agency (EPA).
- Vinesh, S. B. (n.d.). On the Relationship between Co₂ Emissions and Economic Growth. University of Mauritius.

Wadud, M. M. (June 2014). CARBON EMISSION AND ECONOMIC GROWTH OF SAARC COUNTRIES:A VECTOR AUTOREGRESSIVE (VAR) ANALYSIS. International Journal of Business and Management Review, Vol.2, No.2, pp.7-19,.

WB. (2015). World Bank Bangladesh. Retrieved 9 18, 2015, from <http://www.worldbank.org/en/country/bangladesh>

WB. (n.d.). <http://data.worldbank.org/indicator/EN.ATM.CO2E.PC>. Retrieved 9, 18, 2015, from CO2 emissions (metric tons per capita) : <http://data.worldbank.org/indicator/EN.ATM.CO2E.PC>

Contribution of local Traffic to PM10 Levels and trace metals in Constantine, Algeria

Hocine ALI-KHODJA**, Mahfoud KADJA**, Ahmed TERROUCHE* & Kanza LOKORAI*

* *Laboratoire Pollution et Traitement des Eaux, Université des Frères Mentouri, Constantine, Algérie*

** *Laboratoire d'Energétique Appliquée et de Pollution, Université des Frères Mentouri, Constantine, Algérie*

Abstract

The purpose of this study was to study the time evolution of PM10 in a traffic and urban background sites. This work aims also to study the influence of weather conditions on levels of particulate matter emitted by vehicles and to assess the evolution of the difference in concentration of PM10 between traffic and urban background sites and the contribution of road traffic to PM10 and some metal elements.

Keywords: *Traffic site, PM10, urban background site, trace metals.*

Introduction

Motor vehicles strongly affect air quality within urban areas (Pastuszka et al. 2010). Several studies have provided evidence that the exposure to high concentrations of aerosols is associated with adverse health effects (Pateraki et al. 2012). Multi-city extensive studies conducted in the United States and in Europe reported positive associations between PM10 and death. In a multicentre study involving four European cities, consistent positive associations were found between coarse particles central sites concentrations and prevalence of respiratory symptoms. Another particulate matter health study in China revealed a 10- $\mu\text{g}/\text{m}^3$ increase in 2-day moving-average PM10 was associated with a 0.35% increase of total mortality, 0.44% increase of cardiovascular mortality and 0.56% increase of respiratory mortality (Chen et al, 2012). In a study that examines the relation of lung cancer incidence with long-term residential exposures to ambient particulate matter, it was established that a 10- $\mu\text{g}/\text{m}^3$ increase in 72-month average PM10 was positively associated with lung cancer. Moreover, adverse health effects may be caused by mineral dusts originating from the Sahara.

Lim et al. (2012), in the framework of the WHO driven evaluation of the Global Burden of Disease (GBD), evidenced that particulate atmospheric pollution is the 4th cause of worldwide mortality in developing countries and the 11th one in central Europe. REVHHAAP (Review of evidence on health aspects of air pollution) (WHO, 2013) evidenced that mean life expectancy of European citizens is reduced by 9 months due to increase on premature mortality due to cardiovascular, respiratory and cerebro-vascular causes. These reports also indicate that atmospheric particulate matter (PM) is the main pollutant causing these health outcomes.

Studies on traffic-related airborne particulate matter, are scarce or even not available in many cities in the developing world and particularly in Africa. This is in spite of the high levels of atmospheric particulate pollution observed in African cities.

In the developing countries, the particulate matter forms the major contributor to air pollution and hence the pressure to understand its sources better. Emissions from combustion of fossil fuels are expected to increase significantly in African cities in the near future. Atmospheric particulate pollution is more severe in developing countries than in developed countries because of rapid urbanization and a sudden expansion in the number of vehicles. It was reported that annual PM levels in Northern Africa exceeded annual and 24-h WHO guidelines, with annual PM10 levels exceeding 150 $\mu\text{g}/\text{m}^3$ in different sites of Cairo while mean PM10 levels across a network of four monitoring stations that was established in Algiers ranged from approximately 38 to 129 $\mu\text{g}/\text{m}^3$ between 2002 and 2003.

The Mediterranean area is also affected by natural mineral dust transport from the Sahara (Rodriguez et al. 2007).

The main objectives of this work were to study the influence of weather conditions on levels of particulate matter emitted by vehicles and to assess the evolution of the difference in concentration of

PM10 between traffic and urban background sites and the contribution of road traffic to PM10 and some metal elements

1. Methods

Site description

The sampling site was located at the entrance to the campus of the Faculty of Earth Sciences located at Zouaghi, Constantine, nearby National Road 79, which is one of the busiest traffic highways in the city of Constantine, (36°22'N, 6°40'E, 640 m.a.s.l), Algeria. The sampling devices were placed about 3 m above the ground, and about 6 m from the road for the traffic site and about 200 m away from the road for the urban background site. The traffic site was directly influenced by vehicular emissions while the urban site was sufficiently distant from the road as to be considered as a background site. Sampling was scheduled at midnight.

Measurement of fine particulate matter

A portable low volume air sampler Model Minivol TAS with a rate of 5 liters/minute was used. Ambient air particulates were trapped by a quartz filter (47 mm in diameter with a porosity of 0.2 microns). After each sampling interval, the collection media were returned to the weighing laboratory and allowed to equilibrate for 24 h in a dessicator before weighing to a precision less than ± 0.01 mg using a Shimadzu balance (model AUW120D). The initial weights were determined after a similar period of desiccation.

Analysis of trace elements

Each filter was digested according to the method of Kuvarega and Taru (2008). A Shimadzu-7000 AAS supporting an acetylene flame was used to analyse metallic elements Fe, Na, Mg, Ca, Zn and K, while Pb and Cu were analysed using polarography (VA Computrace797). To minimize the effects of matrices, the standard addition technique was used for the determination of all metals. The results of the analysis of ten blank samples were used to estimate the element concentration produced by the filter and sample preparation.

2. Results

2.1. Contribution of local Traffic to PM10 Levels

Figure 1 shows the evolution of the difference in concentration of PM10 between the traffic and background sites. Daily concentrations of roadside PM10 are almost always higher than those of background site (positive days), but for 9 days (of 116 days), background pollution exceeds the pollution along road (negative days) and for 22 days, the levels of PM10 in the background and roadside sites are identical.

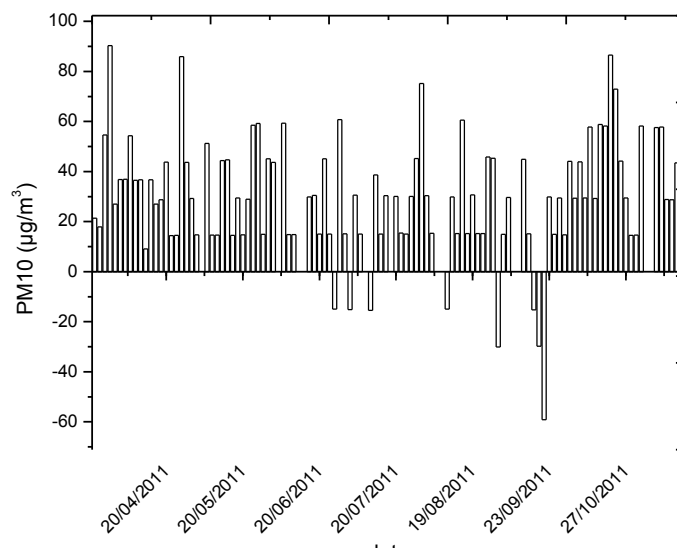


Figure 1. Time variation of the difference in PM10 concentrations between traffic and background sites

Several studies (Charron & Harrison, 2003) reported the influence of weather conditions on levels of particulate emitted by vehicles. To understand well this phenomenon, we analyzed the meteorological data during the positive and negative days (Table 1, Figure 2).

In the positive days, the temperature and humidity are different from those observed during the negative days (Table 1). These two parameters have a significant influence on the number and size of particles. A rise in temperature favors the formation of finer and thus more mobile particles. In addition, a high temperature and a high air humidity effectively reduce the density of air causing a reduction in the oxygen content in the air and thus influence the air-fuel ratio of the burnt mixture resulting in elevated levels of particle emissions (Jamriska et al., 2008).

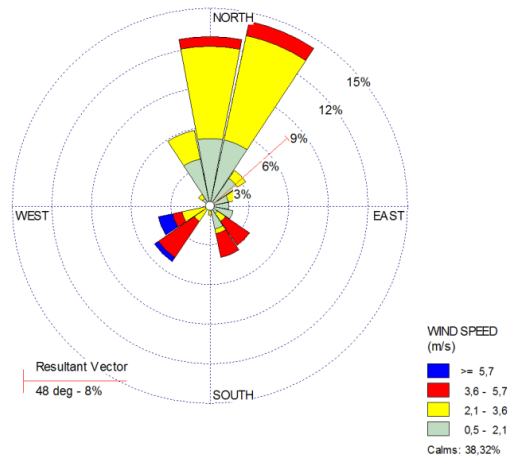
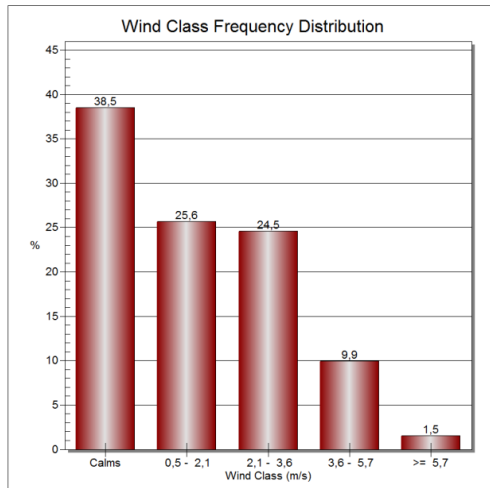
Table 1. Average values of some meteorological parameters

	Negative days	Positive days
Wind speed	1.4	1.2
Rainfall	0.7	2.2
Temperature	22.6	19.4
Humidity	31.8	41.4
Pressure	948	968.2

We also observe that the average wind speed is higher during the negative days than during the positive days (1.4 and 1.2 m/s respectively). The wind speed is greater than 3.6 m/s in 12% of the time during the negative days (Fig. 2) and only in 5% of the time during the positive days (Fig. 2B). High wind speeds promote the dispersion of the particles and eliminate the difference between traffic and background sites. The predominance of light winds at measurement sites promotes the accumulation of dust from transportation on the roadside leading to higher pollution than in the background site.

We also note that for the positive days, prevailing winds are westerly and tend to bring dust from arid lands situated to the west of National Road 79.

A



B

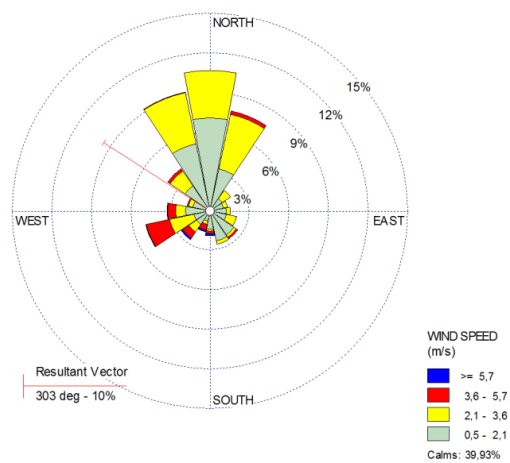
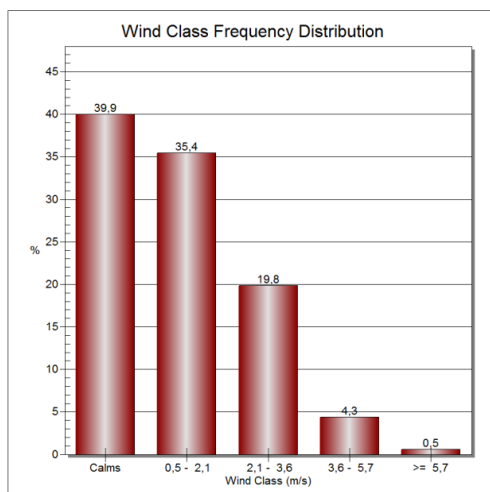


Figure 2. Wind roses in Zouaghi, Constantine (A) Negative days (B) Positive days

Table 2 shows the contribution of road traffic to PM₁₀ and some metal elements. Traffic contributes 39.8% to PM₁₀, either by direct emissions such as Pb (62.4%), Zn (50.3%), Cu (55.6%), and/or the resuspension of soil dust originating from earth such as Fe (57.9%), Ca (65.1%), K (56.8%) and from marine elements like Na (29.5%) and Mg (49.6%). It is assumed that traffic emits Pb, Zn and Cu by a single channel (direct emission) and the other elements are resuspended by vehicle movement. The direct emission and resuspension contribute up to 55.49% and 49.55% respectively to PM₁₀ levels.

Table 2. Difference in pollution between traffic and the background sites

	<i>Traffic site</i>	<i>Background site</i>	<i>Increment*</i>	<i>Contribution due to traffic**</i>
	$\mu\text{g}/\text{m}^3$		$\mu\text{g}/\text{m}^3$	%
PM ₁₀	81,71	49,23	32,48	39.75
Pb	1,09	0,41	0,68	62.39
Cu	0,63	0,28	0,35	55.56
Zn	1,47	0,73	0,74	50.34
Direct emission	3.19	1.42	1.77	55.49
Fe	4,11	1,73	2,38	57.90
Ca	3,93	1,37	2,56	65.14
K	5,93	2,56	3,37	56.83
Mg	2,34	1,18	1,16	49.57
Na	6,92	4,88	2,04	29.48
Resuspension	23.23	11.72	11.51	49.55

*Increment = concentration in traffic site - concentration in background site

**Contribution = [(concentration in traffic site – concentration in background site) / concentration in traffic site]* 100

Conclusion

PM10 concentrations were measured at a traffic sampling site situated at Zouaghi, Constantine between 23 March 2011 and 22 November 2011. The results presented in this work allow us to conclude that PM10 concentrations are excessive in light of the WHO and the EU standards. The latter seem hardly feasible in view of the contribution of natural aerosols to ambient PM levels. The average daily concentration of PM10 was 80,42 $\mu\text{g}/\text{m}^3$ was observed for the period of study. During the study period implying the sampling of PM10, the average concentration of PM10 was 105.2 $\mu\text{g}/\text{m}^3$. Sources of PM10 particles are related to the significant contribution of resuspended coarse particles and Saharan dust intrusions.

Traffic contributes 39.8% to PM10, either by direct emissions, the resuspension of soil dust originating from earth and from marine elements.

References

- Charron A., Roy M. Harrison (2003): Primary particle formation from vehicle emissions during exhaust dilution in the roadside atmosphere. *Atm. Environ.*, vol. 37, p 4109–4119.
- Chen R., H. Kan, B. Chen, W. Huang, Z. Bai, G. Song & G. Pan (2012): Association of particulate air pollution with daily mortality: the China Air Pollution and Health Effects Study. *Am J Epidemiol* 175(11), p 1173-1181.
- Lim S.S., T.D. Vos, A.D. Flaxman, G. Danaei & K. Shibuya (2012): A comparative risk assessment of burden of disease and injury attributable to 67 risk factors and risk factor clusters in 21 regions, 1990-2010: a systematic analysis for the Global Burden of Disease Study 2010. *Lancet* 380, p 2224-2260.
- Pastuszka J.S., W. Rogula-Kozłowska, E. Zajusz-Zubek (2010): Characterization of PM10 and PM2.5 and associated heavy metals at the crossroads and urban background site in Zabrze, Upper Silesia, Poland, during the smog episodes. *Environ Monit Assessment* 168: 613-627.
- Pateraki St., D.N. Asimakopoulos, H.A. Flocas, Th Maggos & Ch Vasilakos (2012): The role of meteorology on different sized aerosol fractions (PM10, PM2.5, PM2.5–10). *Sci Total Envir* 419, p

124-135.

Rodriguez S., X. Querol, A. Alastueya & J. de la Rosa (2007): Atmospheric particulate matter and air quality in the Mediterranean: a review. *Environ. Chem. Lett.*, 5, p 1–7.

Jamriska, M., L. Morawska & K. Mergersen (2008): The effect of temperature and humidity on size segregated traffic exhaust particle emissions. *Atmos. Environ.*, 42, p 2369-2382.

WHO (2013): Review of evidence on health aspects of air pollution- REVHIHAAP. WHO Regional Office for Europe.

Combining microscopic traffic modelling and 3 pollutant emission modellings to assess modifications of traffic supply and demand

Anne-Laure Badin*, Aurore Clavel*, Thérèse Vittoz*, Caroline Sorand*, Delphine Lejri**, Ludovic Leclerc** and Xavier Olny*

* Cerema CE, Bron, 69500, Bron

** COSYS-LICIT, IFSTTAR, ENTPE, Université de Lyon, 69000, France

Keywords: dynamic traffic modelling, traffic management, emissions, scenario, sensitivity

Author email: anne-laure.badin@cerema.fr

Abstract

Traffic management definition and assessment strategies rely on results from successive stages of modelling: from traffic to air pollution concentrations. The objective of this study was to improve this modelling process. Combining microscopic traffic modelling and 3 pollutant emission modellings was performed: two using aggregated traffic estimates (HBEFA, Copert) and the other using vehicle trajectory (Phem).

The studied area is part of the Lyon urban area (6,2 km², 2091 road sections). Traffic and emissions were simulated for 16 scenario resulting from modifications of supply or demand (traffic calibration on the afternoon rush hour).

Copert and HBEFA estimations show many similarities and differences with Phem. Ranking of scenarios on the basis of their variation to the reference was performed and analysed. Copert and HBEFA provide the same ranking. To focus on the analysis of two scenarios, difference of NO_x emissions per link were mapped (only the higher variations). The relevance of dealing with both the network and the links spatial scales to assess the impact of the scenario was clearly shown.

Number of outlooks ensue from this work.

Résumé

La définition des mesures de gestion de trafic repose sur des étapes successives de modélisation: des trafics aux concentrations de polluants dans l'air. Il est nécessaire d'améliorer ces méthodes. Le travail présenté s'inscrit dans cet objectif.

Des couplages de modélisation de trafic dynamique à une échelle microscopique et de modélisation des polluants ont été réalisés. Trois méthodologies d'estimation des polluants ont été mises en oeuvre: deux utilisant des paramètres de trafic agrégés en entrée (Copert et HBEFA) et une utilisant les trajectoires des véhicules (Phem).

Le réseau étudié est un quartier urbain de la périphérie lyonnaise qui comprend un peu plus de 2000 noeuds et tronçons routiers. Des simulations de trafic et des calculs d'émissions ont été réalisés sur un ensemble de 16 scénarios de modification de l'offre et de la demande de trafic afin d'évaluer la sensibilité des modélisations couplées (sur l'heure de pointe du soir).

Au delà des éléments comparatifs entre les modèles d'émissions (Copert/HBEFA vs Phem), les résultats montrent des évaluations des scénarios différentes suivant l'échelle spatiale d'analyse considérée (réseau/tronçons les plus variables). De nombreuses perspectives sont ouvertes par ce travail.

Mots clés : modélisation dynamique du trafic, gestion du trafic, émissions, scénario, sensibilité

1. Introduction

Health impact of air pollution is largely referenced; road traffic is one of the main source of some pollutants (NO_x, particulate matter) (Pascal et Medina 2012). Local air quality results from the combination of regional air quality and local emissions of pollutants. As road traffic is a major source of pollution,

policies aiming at improving air quality target it. Pollutants emissions from road traffic depend in particular on volumes of traffic, vehicle fleet and vehicle dynamic. Thus policies aim at having an impact on these parameters, by improving car fleet renewal, promoting public transport and car sharing, and implementing traffic management. Implementation of traffic management and promotion of public transport and car sharing could be efficient more rapidly than car renewal. In order to define operational policies and measures impacting traffic, their efficiency needs to be assessed. Stakeholders require this assessment to base their decision on it. Analysis and ranking of scenarios regarding their impact on air pollution and health therefore has to be performed.

In France, these assessments are commonly conducted on the basis of results of traffic static modelling; these studies are performed to assess the impact of a new road on air quality. Temporal and spatial precisions of those modellings are quite insufficient to assess the impact of traffic management measures. Thus it is needed to develop some methods using dynamic traffic modelling as input of emissions modellings. The mid term aim of our work is to define a methodology to assess traffic management strategies regarding their environmental impacts.

We have performed couplings of results from a microscopic dynamic modelling with pollutant emissions modellings. Different modifications of traffic supply and demand were modeled and analyzed in terms of traffic and environmental impacts. Some analyses of these results are presented in this paper.

2. Methods

The studied area

The studied area is part of the Lyon urban area (6,2 km², 2091 road sections). It is considered as an urban area. Speed limits are, respectively, 50, 30 and 70 km/h, for 89, 10 and 1% of the links.

The microscopic traffic simulations

The microscopic traffic simulations were modeled with Aimsun (Transport Simulation System, s. d.) for 1 hour (the traffic was loaded 15 min before the beginning of the simulation, on an empty network). Real data of the 5-6 PM period were used for the calibration. The reference simulation was sufficiently stabilized to allow the assessment of the sensitivity to supply and demand variations. Its own variability was assessed (10 runs performed).

The studied scenarios

To assess sensitivity of the joint modellings, 16 scenarios of modified traffic supply and demand were simulated (table 1).

The following mean traffic parameters were recorded: flow (veh/h), density (veh/km), total run distance (km). Microscopic traffic simulation is stochastic, so in order to qualify the variability of the estimated traffic parameters, the simulation of the reference was repeated 10 times with a random seed pace (sec/km), total run time (h), mean speed (km/h). Results are presented in the table 2.

The modelling of pollutant emissions

The configuration of the emission modellings benefited from previous works: i, the development of an information system called TRAPS (Trafic Related Air Pollution Simulator), that establishes the link between modellings of traffic and emissions, ii, TRAPS calibration with appropriated fleet composition and traffic situation iii, sensibility analyses that settled an optimal time aggregation of 15 min, and the use of mean spatial speed.

Pollutant emissions were calculated using: Copert IV, HBEFA and PHEM (Hausberger, Stefan). Only exhaust emissions were calculated, and cold start excess emissions were not taken into account. Fuel consumption (FC) and the following pollutants: CO, NO_x, hydrocarbons (HC) were considered.

As any aggregated emission model, Copert IV uses mean driving speed and total travelled distance for a given time period to predict the related exhaust emissions. The total emissions are calculated as the product of the travelled production (vehicle.distance) and the unitary emission factors (expressed in g.km⁻¹). Unitary emission factors consist of speed-continuous functions that have been constructed over driving cycles of about 6mn-length, which are representative of encountered traffic conditions. These unitary emission functions are defined for each vehicle technology. The unitary emission functions of a specific vehicle category (passenger cars, light commercial vehicles, heavy duty vehicles or buses) are obtained by operating a weighted average of the vehicle technologies that compose the category.

Table 1: description of the simulated scenarios

Simulation	Description	Named as
Reference		Ref
Supply modification	Capacity of the street called <i>bvd du 11 novembre</i> was reduced to 400 vehicles/hour (instead of 1300)	O11nov
	The street called <i>rue Francis de Pressensé</i> was settled as a one way street; journeys from west to east were made impossible	OPr
Modification of the overall matrix of demand: for all the O-D the number of journeys increase / decrease in the given proportion	- 30%	Dm30MG
	- 20%	Dm20MG
	- 10%	Dm10MG
	+ 10%	Dp10MG
	+ 20%	Dp20MG
	+ 30%	Dp30MG
Modification of part of the matrix of demand	Demand modification of the O-D submatrix constituted from the O-D that use the streets called <i>bvd Stalingrad</i> and <i>bvd du 11 novembre</i>	Dm20S11
	- 20%	Dm10S11
	- 10%	Dp10S11
	+ 10%	Dp20S11
	+ 20%	
Modification of part of the matrix of demand	Demand modification of the O-D submatrix constituted from the O-D that use the streets called <i>bvd Emile Zola</i> and <i>rue Francis de Pressensé</i>	
	- 20%	Dm20ZP
	- 10%	Dm10ZP
	+ 10%	Dp10ZP
	+ 20%	Dp20ZP

Table 2: traffic parameters mean and SD for 10 replicates of the reference scenario

	Unit	Mean value	Standard deviation
Traffic flow	veh/h	13747	156
Density	veh/km	8,0	0,4
Traveled total distance	km	29588	522
Mean speed	km/h	25,1	0,6

Copert IV (Ntziachristos et al., 2009) has been widely used in most European Countries to elaborate the national emission inventories, but it is also extensively used for network emission modelling (Borge et al., 2012; Samaras, Christos et al., 2014). However, its use at spatial scales lower than the driving cycles is subject to questions, since the speed distribution might differ and lose representativeness over too small samples or specific traffic conditions (e.g. in the vicinity of intersections).

HBEFA is another aggregated emission model. It provides emission factors, i.e. the specific emission in g/km for all current vehicle categories (PC, LDV, HDV, buses and motor cycles), each divided into different technologies segments, for a wide variety of traffic situations. Traffic situations were not provided by the microscopic traffic modelling. Thus, a conversion method was defined to estimate the traffic situation from the mean speed occurring on the links and some characteristics of the link. Then, emissions are calculated with the HBEFA methodology.

PHEM (Passenger Car and Heavy Duty Emission Model) calculates the fuel consumption and emissions of vehicles based on the vehicle longitudinal dynamics and on-engine emissions maps, with a 1s time resolution. The model provides an estimate of the engine power of a vehicle at each time step (1s), based on its speed time series and road gradient. The engine speed is estimated based on the transmission ratios and a gear shift model. The model also includes transient correction functions, and a cold start tool, to finally provide the evolution with time of fuel consumption and emissions of CO, CO₂, HC, NO_x, NO, particle mass (PM). Cold start emissions will be however disregarded in this paper.

PHEM has been coupled with dynamic traffic platforms at several occasions, in order to test the impact on emissions of road traffic strategies that modifies the vehicle kinematics behavior. However, the inadequacy between its required high traffic data resolution and the available dynamic traffic model outputs, which are much less refined, is subject to debate.

Data analysis has been performed using Rdata project (R Core Team, 2015) and Qgis (QGIS Development Team).

3. Results

Comparison of emission modellings

Ranges of pollutant emissions and fuel consumption differ between emission modellings as illustrated on figure 1. Range of Phem estimated emissions is much larger than ranges of emissions calculated with mean speed models. Moreover Phem estimates are always higher than Copert and HBEFA estimates: from 1.4 to 2 times the Copert estimates, and from 1.5 to 2.8 the HBEFA estimates.

A better consideration of the diversity of speeds by Phem could explain part of the variability of estimated environmental parameters.

The higher estimations of environmental parameters with Phem could result from the vehicle acceleration calibration of of the traffic modelling. Indeed, the modelling may not necessarily be well calibrated for environmental impact assessment. This was identified in the CoERT-P project.

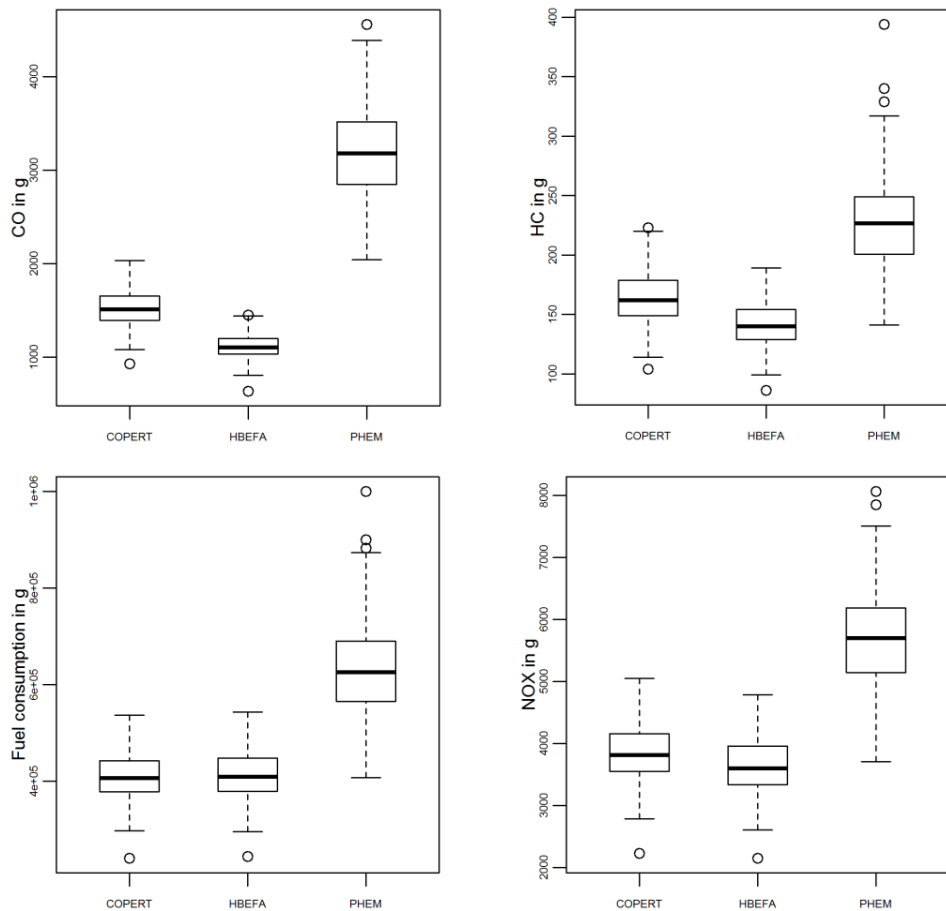


Figure 1: boxplot of the environmental parameters calculated with the different emission modellings for all the scenarios for the 4 periods of 15 min aggregated at the network scale

Table 3: global traffic estimates for the reference and all the scenarios

Scenario	Production in 1h (veh.km)	Production relative to ref	Spatial mean speed in m/s (over the 4 periods) (range)
ref	29 240	-	5.2-5.9
O11nov	28 230	-3%	3.9-5.2
OPr	29 010	-1%	5.1-5.6
Dm30MG	22 130	-24%	6.5-7.6
Dm20MG	24 987	-15%	6.2-6.8
Dm10MG	26 789	-8%	5.7-6.1
Dp10MG	31 100	6%	4.2-5.1
Dp20MG	33 370	14%	3.9-4.3
Dp30MG	25 570	-13%	1.3-3.6
Dm20S11	28 550	-2%	5.3-5.7
Dm10S11	28 370	-3%	5.2-6.8
Dp10S11	30 520	4%	4.7-5.4
Dp20S11	30 780	5%	4.6-5.0
Dm20ZP	28 150	-4%	5.3-5.7
Dm10ZP	27 290	-7%	5.3-6.6
Dp10ZP	30 160	3%	4.6-5.3
Dp20ZP	30 910	6%	4.6-5.3

Comparisons of all the scenarios at the network scale

The table 3 presents the traffic global estimates. Traffic production varies from 22 130 to 33 370 veh.km for two scenarios that impact the global OD matrix, respectively the Dm30MG and the Dp20MG scenario. Surprisingly, the scenario that impacts the most the demand (Dp30MG) do not show the greater production; mean speeds are much lower than for other scenarios: 1.3 to 3.6 m/s. In this scenario, grid lock occurred, no more vehicle could enter the network. Thus this scenario was considered to be out of the traffic legitimate domain we do not further consider it in this study. Regarding all the other scenarios, mean speed ranges from 3.9 m/s for both O11nov / Dp20MG to 7.6 m/s for the Dm30MG scenario.

Comparison of scenarios is first performed using the aggregation of environmental parameters on the overall network; the relative difference to the reference scenario is considered.

Relative difference of scenario to the reference ranges from -35% to 49%, respectively for HC Dm30MG and HC Dp10MG scenarios, both being Phem estimates. The ranking of scenarios from the less emissive to the more emissive is similar whatever environmental parameters is considered when considering HBEFA and Copert estimates, and it is the same regarding the Phem NOx estimates: Dm10ZP, O11nov, Dm10S11, OPr, Dp10ZP, Dp10S11, Dp20ZP, Dp20S11, Dp10MG, Dp20MG.

Whereas Phem NOx estimates rank scenarios as all Copert and HBEFA environmental estimates, Phem estimates of HC, fuel consumption or CO rank differently the scenarios (figure 2). The HC and FC appear to evolve in the same way whereas CO evolves differently. As an example, Dp10MG is the most emissive scenario regarding HC (+48%) and is expected to lead to the higher fuel consumption (+42%), whereas it leads to only +5% of CO emissions.

Whatever method is used for emissions estimations, pollutant emissions and fuel consumption are significantly (more than 5% of difference relative to the reference values) higher in the followings scenarios, from the higher to the lesser increase: Dp20MG, Dp10MG, Dp20S11, Dp20ZP, Dp10S11, and significantly lower in the following scenarios, from the higher to the lesser decrease: Dm30MG, Dm20MG, Dm10MG, Dm20ZP, Dm20S11.

Minor relative differences are noticed for the following scenarios: Dm10ZP (-4% whatever the parameters and emissions modelling used), O11nov (from -3 to 4%), Dm10S11 (from -6 to -2%), OPr (from -1 to 0%), Dp10ZP (from 3 to 9%).

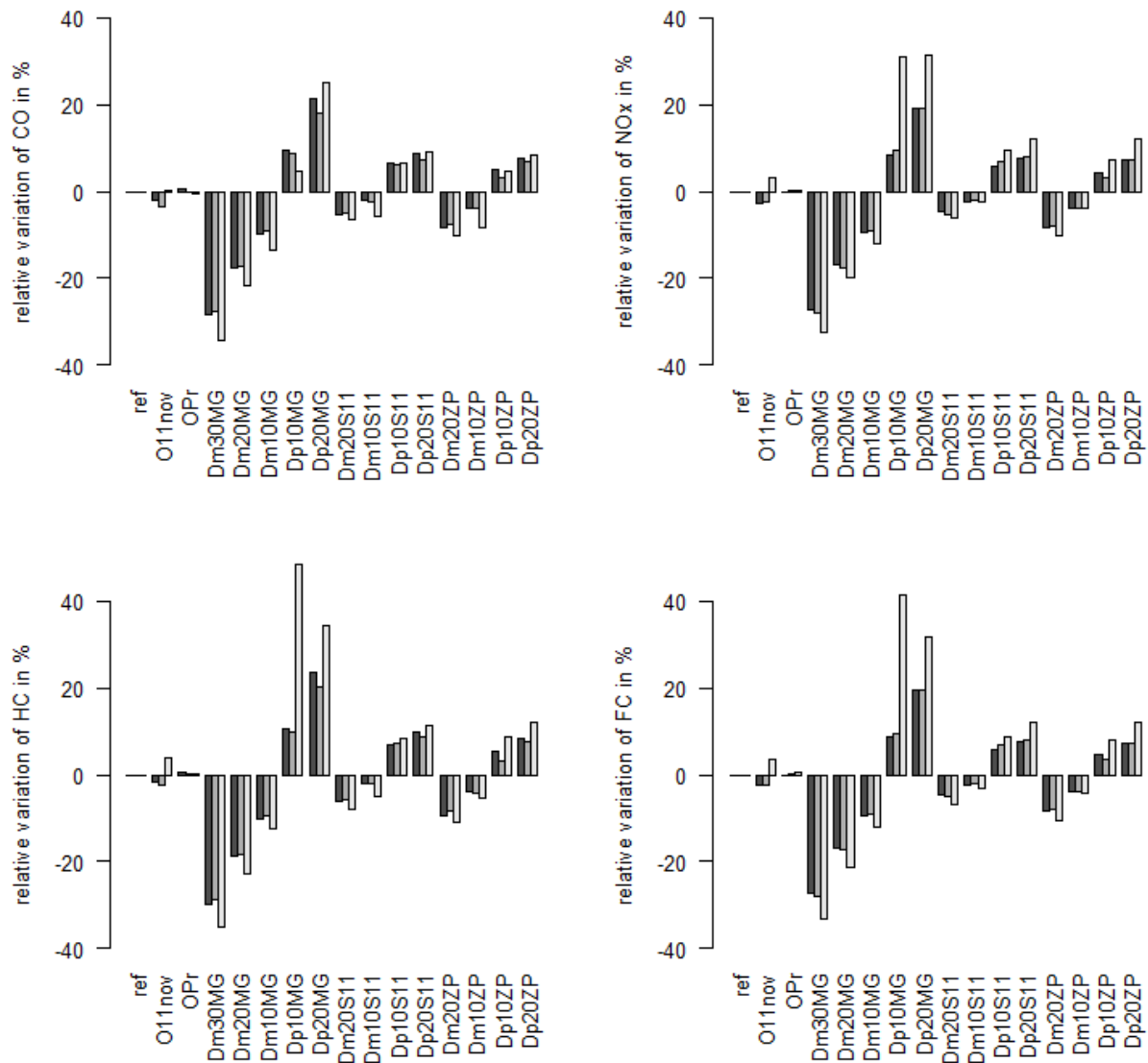


Figure 2: relative variation of the environmental parameters calculated for each scenario to the reference scenario. The darker grey: Copert, medium grey: HBEFA, light grey: Phem estimations.

Analysis of two scenarios on the basis of the difference of NOx emission between scenario and reference over the 2091 links

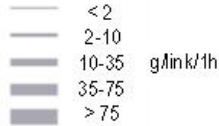
Focus was directed on the analysis of NOx emissions in the following analysis. We have chosen to further analyze two scenarios that have presented moderate variations of emissions at the network scale: Dm20ZP and the O11nov scenarios. Their variations of environmental parameters rank from -8 to -11% and -3 to +4% to the reference scenario, respectively. Both are quite realistic scenarios that could be analyzed as part of a transport local policy.

Maps are presented in the figures 3 and 4. As to highlight the major trends, a selection of the links that show the higher difference in NOx emissions between scenario and reference was performed. D is defined as $D = \text{NOx emissions of the scenario} - \text{NOx emissions of the reference}$. Figured links have absolute value of $D > 10 \text{ g of NOx / h / link}$. This means that Positive D means more emissions (figured in solid line); negative D means less emissions (dashed line). All links and nodes are included in the analysis, whereas only links are figured. Details of the distribution of D regarding the threshold of 10 g and the quantiles 0.05 and 0.95 are provided in table 4.

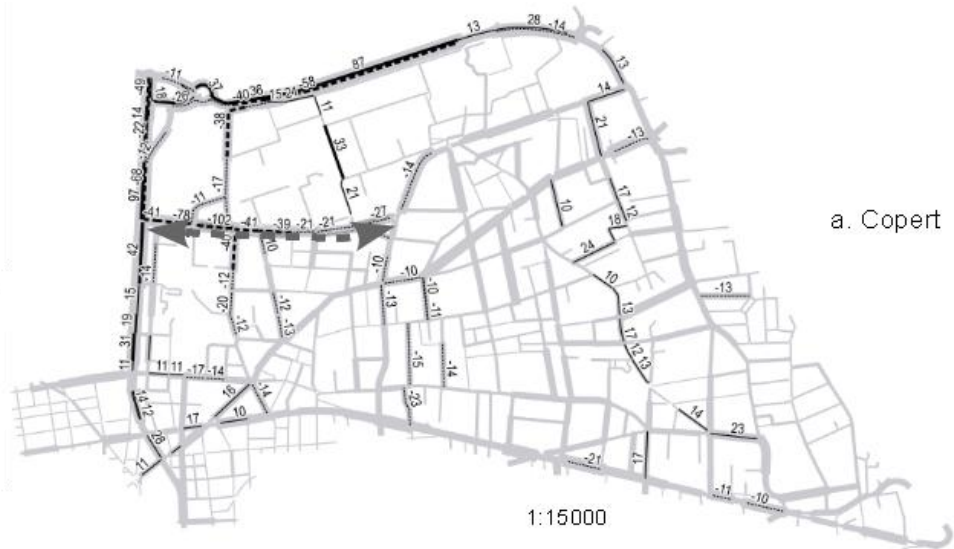
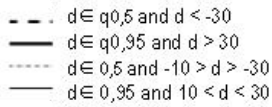
Legend

Supply modification:
Capacity of the street
called bvd du 11 novembre
was reduced to be 400
vehicles/hour (instead of
1300) 

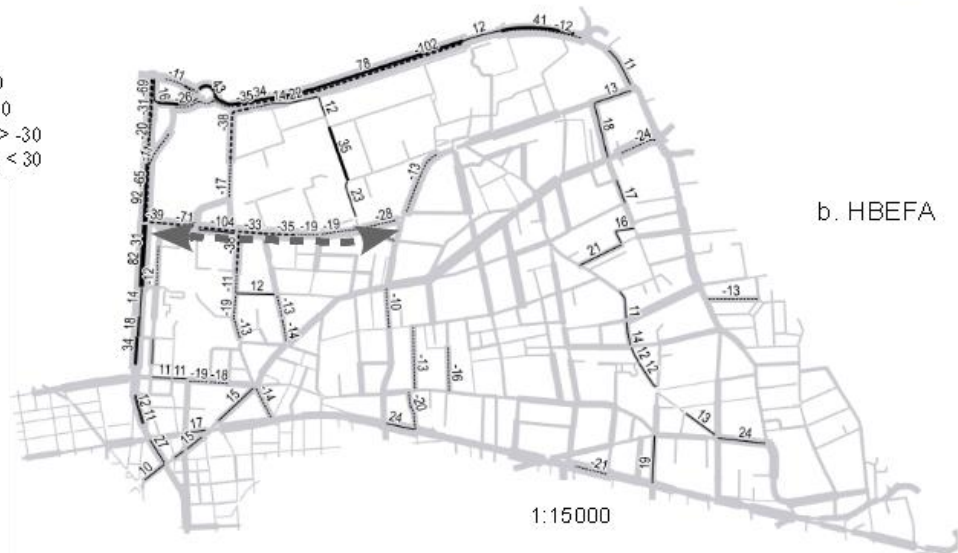
NOx emissions of the
reference scenario



Major differences of
NOx emissions in g
per link /1h:
 $D = \text{NOx(O11nov)} -$
 NOx(ref) (labels)



a. Copert



b. HBEFA



c. Phem

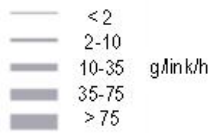
Figure 3: impact of the O11nov scenario on the estimated NOx emissions. NOx emissions of the reference scenario is figured in lighth grey, major differences of O11nov to the reference in dark. More explanations of method in the text.

Legend

Demand modification of the O-D submatrix constituted from the O-D that use the streets called Blvd Emile Zola and rue Francis de Pressensé : -20 %

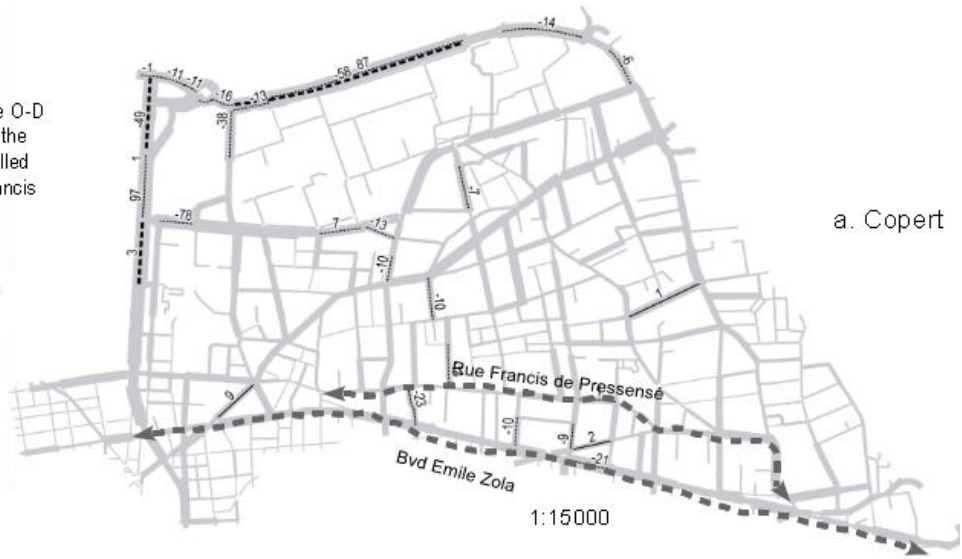
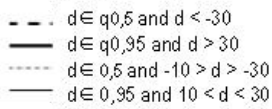


NOx emissions of the reference scenario



Major differences of NOx emissions in g per link / 1h:

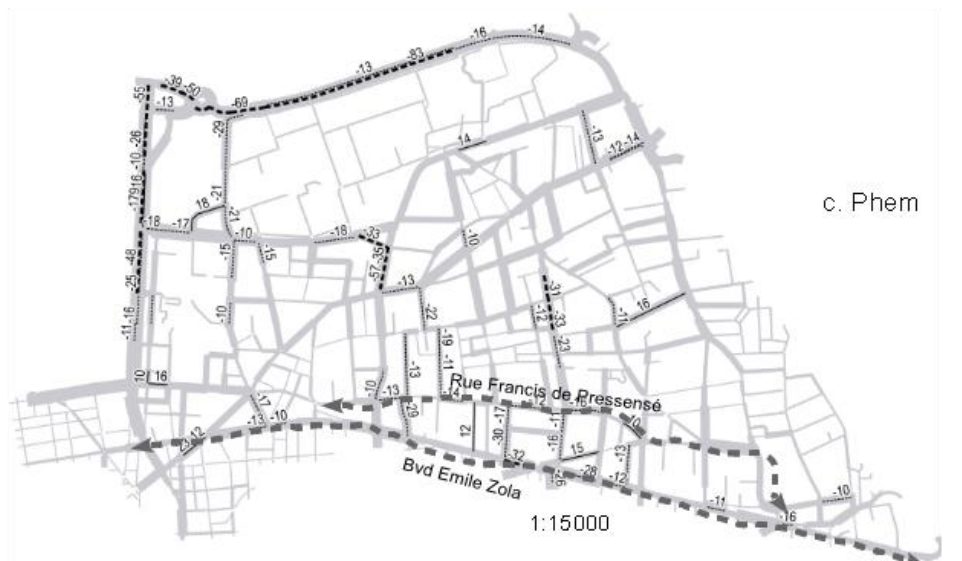
$D = \text{NOx}(\text{Dm 20ZP}) - \text{NOx}(\text{ref})$ (labels)



a. Copert



b. HBEFA



c. Phem

Figure 4: impact of the Dm20ZP scenario on the estimated NOx emissions. NOx emissions of the reference scenario is figured in ligh grey, major differences of O11nov to the reference in dark. More explanations of method in the text.

Table 4: absolute differences of NOx emissions between scenarios and reference taken into account in different subsets of data, q0.05 and q0.95 are quantiles of the differences (D) of emissions of the 2091 links and nodes. a, NOx emissions are summed over the different subsets of links (in g / h); b, percents are given relatively to the sum of negative and positive differences of emissions; c, number of links per subsets

		Sum of NOx emissions differences in the following subsets						Values of difference of NOx emissions per link (in g/h)		
		D < -10	D < q0.05	D < 0	D > 0	D > q0.95	D > 10	Quantile 0.05	Quantile 0.95	
Dm20ZP – ref	Copert	a	-625	-1072	-1698	428	318	47	-3.67	1.14
		b	37%	63%	100%	100%	74%	11%		
		c	29	106	921	515	105	4		
Dm20ZP – ref	HBEFA	a	-666	-1090	-1661	474	368	98	-3.54	1.17
		b	40%	66%	100%	100%	78%	21%		
		c	29	106	919	514	106	7		
Dm20ZP – ref	Phem	a	-1732	-2007	-3078	742	542	171	-7.30	1.90
		b	56%	65%	100%	100%	73%	23%		
		c	73	106	932	516	106	13		
O11Nov – ref	Copert	a	-1271	-1622	-2301	1899	1457	1101	-5.10	4.07
		b	55%	70%	100%	100%	77%	58%		
		c	56	106	766	681	106	51		
O11Nov – ref	HBEFA	a	-1215	-1637	-2289	1915	1508	1150	-5.22	4.18
		b	53%	72%	100%	100%	79%	60%		
		c	48	106	771	672	106	51		
O11Nov – ref	Phem	a	-2197	-2357	-3423	4135	3189	3094	-8.81	9.17
		b	64%	69%	100%	100%	77%	75%		
		c	89	106	769	698	106	96		

The table 4 shows the quantities of NOx emissions that are generated or avoided thanks to the scenarios over different subsets of links. Regarding the two studied scenarios, quantiles 0.05 and 0.95 of NOx differences are very similar for Copert and HBEFA resulting estimates (maximal difference of 0.13), whereas absolute values of these quantiles are higher for Phem. The distribution of differences of NOx emissions is thus more dispersed. Phem calculations result in more frequent large differences between scenarios and reference.

The proportions of links with less emissions (ie negative D) over the links with supplementary emissions (ie positive D) are different for the two studied scenarios: 1.8 for the Dm20ZP and 1.1 for the O11nov (ratio similar whatever emissions modelling used).

At least 63% of the emissions variation are taken into account when considering 5% of the links included in one of the tails of the distribution of D (with values of difference inferior to quantile 0.05, or superior to quantile 0.95). It reaches 79% for the O11Nov scenario estimated with HBEFA. More than 200 links are considered ($2 \times 0.05 \times 2091$ links and nodes).

More than 200 links represented on the map may result in a confusing map, thus we have applied a threshold at 10 g/link on D. When applying this threshold value, the number of links is reduced to 33 to 185 and the representativeness of these links as supporting a large amount of NOx variation is also reduced up to 11%. The two scenarios present noticeable differences: i, in terms of number of links having a $D > 10$ (33 to 86 for Dm20ZP, 99 to 185 for O11Nov), ii, the representativeness of the subset is more reduced in the case of Dm20ZP (11% to 23% of the positive emissions, and 37% to 56% of the negative emissions) than in the case of O11Nov, in which the reduction due to the threshold still represents more than the half of the emission variations. These differences must result from the scenario design. One is a very local operation, O11Nov, resulting in high local variation of emissions. The Dm20ZP scenario induced a much more global variation; indeed it affects two very long and travelled roads of Villeurbanne. It must trigger an impact on the overall urban area but with less intense variation per link than the O11Nov scenario (ie less links showing differences > 10).

The analysis of maps (figures 3 and 4) show some similarities and some dissimilarities. As previously presented, more links are figured for the O11Nov than the for the Dm20ZP. More links are figured when Phem was the modelling used. Each modelling highlights some links that do not appear in the other. For each scenario, some links are figured whatever the emissions modelling is used. The larger solid and dashed dark lines highlight the difference of emissions that are higher than 30 g. For instance, this helps to

identify the links that would support major variation of pollution, especially noticeable on the Op11nov map (figure 3).

4. Discussion

Several environmental parameters were calculated with 3 different emissions modellings on the basis of a microscopic dynamic modelling of a French urban network. As far as we know, very few studies reported that kind of data (Borge et al., 2012).

Investigating various spatial scales

Air quality results from phenomena that occur at different spatial scales. Emissions from traffic are local, but emitted pollutants can be transported far away from their sources. This supports the idea of analysing scenarios with different levels of spatial aggregation.

Interestingly, the analysis of the two selected scenario is very different at the two considered scales. At the network scale, no clear conclusion could be drawn for the O11nov scenario. But when highlighting the links that represent the higher variations, impact of the O11nov scenario could be clearly noticed on some roads whose emissions were largely modified. . No aggregation was performed at the road scale, the two directions of traffic were considered. So, for some roads emissions increase on the links of one direction, and decrease on the links of the opposite direction. Aggregation has to be performed to provide better clarity concerning the variation of the emissions in a given road. Dispersion phenomena, largely influenced by the weather, and population allocation must also be taken into account in the future methodology.

Does the choice of the modelling of pollutants influence the scenario ranking?

Whereas estimations of emissions largely differ between the two aggregated modellings (Copert and HBEFA) and the instantaneous modelling (Phem), the differences of scenario emissions relative to the reference emissions are much less significant.

As a stakeholder could proceed, we have conducted an analysis by ranking the scenarios from the less emissive to the more emissive one. Rankings based on fuel consumption and pollutant estimates were performed. Whatever environmental parameter considered, the two aggregated modellings provided the same ranking of scenarios. Part of the rankings based on Phem estimates could be similar or different depending on the environment parameters considered (HC and FC vs CO vs NOx).

As Phem considers vehicle trajectories and speed, it might be more sensitive to variations of traffic condition and speed variation. Further investigations of the traffic dynamic in those scenarios would provide explanations, but has not been performed yet.

Combining a dynamic traffic modelling and emissions modellings

This study is one stage of development of a much longer line of modelling that goes from the traffic characterization to the health impact assessment.

The analysis of the microscopic simulation results would allow to further characterize the traffic conditions.

Comparisons between emissions modellings were made possible because ensuring consistency of emissions factors, vehicle fleets and other hypothesis were performed previously in the CoERT-P project. To improve the combining of dynamic traffic modelling and emissions modelling, other developments are needed: integration of the fleet of heavy duty vehicles, and calculation of cold start excess emissions. These developments would integrate the TRAPS interface.

A weak representativeness of accelerations for the traffic simulation is suspected to explain the high values of Phem estimates. The mean speed used for Copert and HBEFA calculations might be more realistic. Previous work have already discussed the relevance of combining microscopic traffic simulation with estimations of environmental parameters (Vieira da Rocha et al, 2015).

Ranking of scenarios on the basis of relative difference to the reference is often used. However, accurate estimations of real pollutant emissions are needed because they enter the calculations of pollutant concentrations. Monitoring air pollution can only be performed on pollutants concentrations.

In order to value the emissions estimations and their trends, comparisons with measures would be necessary. Following this idea, experimentations could be designed on the basis of the results of modelling. Locations for the measuring apparatus and period of observation could be defined thanks to modelling results. This is one perspective of this work.

Dynamic traffic modellings are usually made for dealing with rush hours and their constraints. However, pollutant emissions in each hour of the day contribute to the air quality. Thus, methodologies of traffic modellings have to evolve to also take into account environmental requirements and not only traffic management ones.

Acknowledgments

This work was supported by the PREDIT IV fund of the French ministry of environment and transport (Medde). The authors are grateful to F. Golay for preliminary work, to M. André, and O. Charnay for useful help for data analysis, and L. Chauvin for proofreading.

References

- Borge R., I. de Miguel, D. de la Paz, J. Lumbreras, J. Pérez & E. Rodríguez (2012): Comparison of road traffic emission models in Madrid (Spain). Atmospheric Environment, 62, p 461–471.
- Ntziachristos L., D. Gkatzoflias, K. Chariton & Z. Samaras (2009): COPERT: A European Road Transport Emission Inventory Model - In "Information Technologies in Environmental Engineering", Ioannis N Athanasiadis, Andrea E Rizzoli, Pericles A Mitkas et Jorge Marx Gómez, Berlin, 491-504.
- Samaras C., L. Ntziachristos & Z. Samaras (2014): COPERT Micro: a tool to calculate the vehicle emissions in urban areas, Paris, France, 14-17 April, 2014, Transport Research Arena, 10.
- COPERT 4 (version 4.10) (2012): Emisia. <http://emisia.com/copert>.
- Hausberger S (s. d.): PHEM (version 11.2.17): Graz University of Technology.
- HBEFA (version expert version 3.1v5) (2014): Infras: <http://www.hbefa.net/e/index.html>.
- QGIS Development Team (2016): QGIS Geographic Information System, Open Source Geospatial Foundation.
- R Core Team (2015): R: A language and environment for statistical computing, Vienna, Austria: R Foundation for Statistical Computing.
- Transport Simulation System (s. d.): Aimsun, Transport Simulation System: <https://www.aimsun.com/>
- Vieira da Rocha T., L. Leclercq, M. Montanino, C. Parzani, V. Punzo, B. Ciuffo & D. Villegas (2015): Does traffic-related calibration of car-following models provide accurate estimations of vehicle emissions?, Transportation Research Part D, 34(c), 267–280.

Air pollution and energy consumption mitigation by Parking Guiding System

Sana BENHASSINE*, Elyes KOOLI** & Rafea MRAÏHI*

sana.benhassine@ymail.com ; elyes_kooli@yahoo.fr ; rafea_mraihi@yahoo.fr

*The Higher School of Business of Tunis, University of Monouba, Tunisia.

**The Higher Institute of Technological Studies of Ksar-Hellal, Tunisia

Abstract

Find a vacant parking space in the center of large cities, especially at peak times, is always a source of additional air pollution and loss of productivity, time and fuel, harmful to the drivers. This damage affects not only drivers looking for a parking, but all drivers who follow vehicles searching for a parking space. Referring to the objective which aims to examine the impacts of minimizing search time of a parking space on CO₂ emissions and energy consumption, an intelligent parking system is proposed. Our system offer three services: searching for a vacant parking place, directions to that parking place and booking the place for parking. This study takes on optimal route guidance algorithms, which are simulated and analyzed on Tunis urban network. The results of this study generated by the platform MATSim transport simulation; show that our system can reduce the CO₂ emissions and the energy consumption.

Keys-words: *Intelligent parking, Guigance cars, CO₂ emissions, road traffic, energy consumption.*

Introduction

The parking holds an important role in access, mobility and economic development of cities [1]. It is an essential daily need for residential neighborhoods, as for the proper functioning of businesses, economic and social activities. A good parking management can better understand the movements and thus improve the vehicle turnover, facilitate access to downtown, revitalize business districts and stimulate purchases, leisure, etc. Parking can be the most powerful tool that governments have to manage mobility in dense urban areas.

The parking plays an integral part in the circulation system. A car parked on average over 95% of its lifetime, which is not without impact on urban traffic conditions [2]. Initially, a parking was not problem, simply locate a lawful place to store a car. However, in the thirties and with the growth of motorization, the issue of parking begins to be felt [3]. Major cities attend a growing demand for parking and an increase in traffic and CO₂ emissions related to the search of parking spaces.

The parking offer is no longer sufficient to meet the rhythm of household car ownership. Meanwhile, scarcity of urban spaces and the ineffective regulation of parking are major causes that triggered the problem of finding a parking space. This problem arises in a particularly increased manner. It remains quite serious, because vehicles in search of a parking space represent a part that cannot be ignored in urban traffic. According [4]: if we spend a third of our lives asleep, we spend a whole year of our life to look for a parking space.

Finding a parking space remains a problem increasingly severe in the most densely populated cities in the world [5]. It has become the daily concern for most drivers [6], except for those with a reserved parking destination. However, each driver is competing with other drivers in order to claim the vacant parking spaces.

According to a recent survey, researchers showed that during peak hours for most of the big cities, generated traffic by vehicles looking for a parking space up to 40% of total traffic [7]. Another survey revealed that the share of urban traffic generated by the flow of vehicles in search for a vacant parking space is between 5% and 10% of world traffic [8]. According [4], the average time to find an on-street parking space can vary from 3,5min to 14 min. He also estimated that on-street parking space, with a turnover of 10 cars per day, generates total search time of 30 minutes if the search time is only 3 min.

However, [9] stated that during peak hours nearly half of the cars in the centers of large cities are searching for a free parking space. [10] reported that nearly 30% of cars on the road in the city center of major cities seem to be looking for parking spaces, for an average of 7.8 min.

Several studies were conducted to discover the magnitude of nuisance of looking for a parking space (such as congestion, pollution, insecurity, etc.) on the environment, society and the economy. For example, [11] argue that parking is a source of congestion. They show that the car consumes a lot of space, considerably inflates the demand for urban land, and causes excessive congestion in cities. As they confirmed that the massive use of cars has not only an impact on traffic congestion, but also leads to decrease the effectiveness of public transit, creating difficulties movements in cities. [4] proves that finding a place to park creates a queue of cars. He asserts that the problem is not measurable, because the cars in search for a parking space are blended with other vehicles in transit. Moreover, [12] conducted a study on the parking situation in Schwabing (a Germany district). They showed that an annual economic damage was estimated at 20 million Euros, due solely to the research of free parking spaces.

In addition, looking for a parking space is wasteful of time and fuel. [4] Consider a crowded area where it takes three minutes to find on-street parking space and where turnover is ten cars per space per day. For each site, the search time is equivalent to thirty minutes of movement per day. If the average search speed is ten miles an hour, he obtained a distance of five miles traveled by vehicles per place per day. For one year, this conduct amounts to 1825 miles and to 10950 minutes for each on-street parking space.

The search for a parking space contributes also to increase atmospheric pollution. Observations made by [2], for more than a year in a business district of Los Angeles, have shown that cars in search for a parking space have created the equivalent of 38 turned around the world, burning 47,000 gallons of gasoline and producing 730 tons of carbon dioxide. These emissions can be generated by slowdowns induced by drivers who want to park. For example, [13] considers that the offer of a new parking place in the workplace causes the emission of 750 kg of CO₂ per year. 40-50 kg of CO₂ are emitted directly following construction and operation of the garages. The rest is induced indirectly through the motion generated by this instead. The study made by [14] showed that the implementation of an intelligent parking system in Paris, could save the community two million tons of CO₂ per year.

The objective of our work is to attenuate the CO₂ emission and the energy consumption. This study integrates a multi-agent network. In fact, with rapid technological advancement in computing and telecommunications, Multi-Agent approach may be appropriate to minimize the time spend for looking to a vacant parking space and to reduce the negative effects on society and the environment. To emphasize our goal, a comparison among two methods is imposed. For the first method, the cars travel in the hope of finding a vacant place. Here, the strategy adopted by the driver during his research depends on both the urban context in which they are searched and the individual characters. For the second method, the cars will be guided to a parking space around their destinations through our system.

Following the enumeration of the most interesting studies that revolves around the problem of searching for a parking space, the rest of the paper is organized as follows. Section 2 described operation of our proposed solution. Section 3 deals with the implementation of the proposed system, in the simulation model MATSim, results, their analysis, and interpretation. Conclusions are drawn in the last section.

1 Methodology

When a group of vehicles are simultaneously searching for parking places in a city area, it is required to allocate each car to the most suitable parking facility in an efficient way, which is the intention of the parking guidance system. The parking decision process is complex since they are influenced by many factors. On the one hand, the route choice for parking will be influenced by the distance between the parking and the final destination affects the parking movement [23,24,25]. the travel time of the route and the walking time from the parking to final destination also have effects on this resolution [23,25].

On the other hand the parking indicators, price and parking occupancy and average parking occupancy can be utilized to measure the effectiveness of the parking usage [26]. The parking occupancy indicator is a proportion of spaces taken in a defined time interval. Besides, the vehicle travel time, including travel time from the driver's vehicle current location at the car park and the

searching time for the parking space at the parking will attract drivers choose parking space [27]. Hence, this travel time can be used to measure the effectiveness of the parking lot. The values of the utility function is used to select the most appropriate parking facility. The detailed procedure will be explained in the following subsections.

The conceptual model of our system is based on Multi-Agent network. This model is a way of representing our real world. This allows us to represent the dynamics of resource parking use, namely the interactions regarding the use of parking resources among vehicles which are the main actors of our system. Here, we assume that all cars and parking places are fully connected to the information network. The basic organizational structure of our system is a hierarchical structure. The hierarchical organization of agents allows a default message routing which facilitates the development of agents. There are five types of agents having each one characteristic that distinguish it from others: vehicle agent, traffic agent, global traffic agent, parking agent and station agent.

The smart parking system that we propose is illustrated by a parking procedure in a cooperative environment of agents. The idea is to develop a practice which coordinates road between driver and car parks in order to provide more convenience and comfort in terms of conduct. New information technologies such as GPS and GIS are used to facilitate the process of parking.

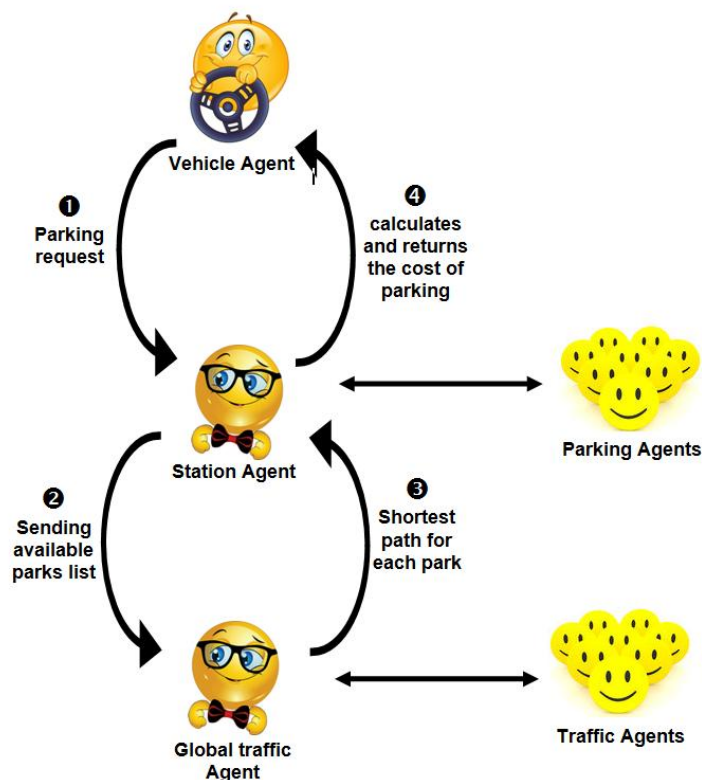


Figure 1. Parking guidance system

1.1 The search for a place to park

Once the driver reaches the air in "D" where he wants to park, it must register with the station agent by entering its destination: the GPS accurately measures the coordinates of the current location of driver [15]. Through the GIS, the positioning of this point will be located on a map displayed in the GUI man-machine. The user can then view its destination and highlight it. Besides the destination, the driver must specify certain personal data such as length and type of parking. At this point, the vehicle is the agent responsible for transmitting all information to the station agent. The latter that has, in real time, the list of car parks with open space, interacts with the global traffic agent and asked him to find the shortest path associated with each parking space [16]. The global traffic agent refers to the current location of the driver and contact information for each parking space contained in the list.

The idea of looking for the shortest path can lead to beneficial results not only in terms to reduce the spent time on the road but also in terms to improve traffic efficiency and to reduce the consumption of fuel (energy saving). In our study, we propose the optimal route guidance algorithms: A* algorithm.

Based on the information transmitted by the global traffic agent and on the price and duration of parking, the agent assigns a cost to each parking space. Indeed, the cost (C) is the combination of three elements. The first element is the multiplication between the travel

time of the shortest path (K) leading to the parking and fuel consumption (F). The second element is the multiplication between the parking price (P) and the parking duration (D) of the driver. Finally, a multiplication of the length of the distance in feet to walk (M : distance between parking and destination) and the time's value of the driver and his companions (R). Afterwards, all costs will be sorted in ascending order from minimum to maximum, which is likely to allow the solicitor the opportunity to choose the most convenient parking.

$$C = (K \times F) + (P \times D) + (M \times R) \quad (1)$$

Where C is the evaluated cost, K is the travel time by car (h : hours), F is the fuel consumption, P is the price of parking, D is the parking time (h : hours), M is the travel time to work in feet (h : hours), R is the time value of the driver and the number of people in the car.

1.2 The guidance to a Parking Place

As soon as the calculations are completed, the list of free parking places (unoccupied) appears instantly on the screen of the dashboard: the GIS produced a map that illustrates consulting geographical positioning of each parking place compared to the driver's location and destination. Several information associated with each parking are also displayed: name parking, type of parking (on-street or off-street ...), cost (C), parking price (P)...

The driver can select the parking that suits him on the basis of the cost function calculated by the station agent, or according to its time value, calculated on the basis of the distance of walking. This latter is between the parking and the chosen destination target.

A simple touch of the screen and the selected car park is designated by the user. Following this choice will start two steps: (1) The GIS produces a path map that guides the driver's current location to the desired parking location (display the shortest path already computed by the global traffic agent). (2) The station agent must sign a seat booking contract with the vehicle agent.

1.3 The Reservation of a Parking Place

The system ensures, through the principle of reservation, a parking place available for the driver. Indeed, the station agent must provide to the vehicle agent a reservation guarantee, if we fall back into the same conflict of lost time due to the search for a place. While the concept of reservation is not guaranteed by our system, there are certainly other cars currently looking for a place to park. When the driver reaches the target location, it will most likely find its space already occupied by another vehicle. Subsequently, our driver must try to do another search [17] [18].

Once the order booking is confirmed by the station agent, the vehicle agent and the parking agent must inform each other to follow the progress of the vehicle. When the space detects the presence of a car, the parking agent must check the identity of the agent vehicle. If the identity is not confused, the agent must warn the car driver through the vehicle agent, that this place is reserved.

2 Travel demand simulator MATSim

MATSim is a transport simulation framework designed to simulate large-scale scenarios in reasonable computation time [21]. It is therefore chosen for all simulation runs. Minimal inputs to the model are network data and daily plans of all individual travelers represented as agents, forming the initial demand (see Fig. 2), as well as various configuration parameters.

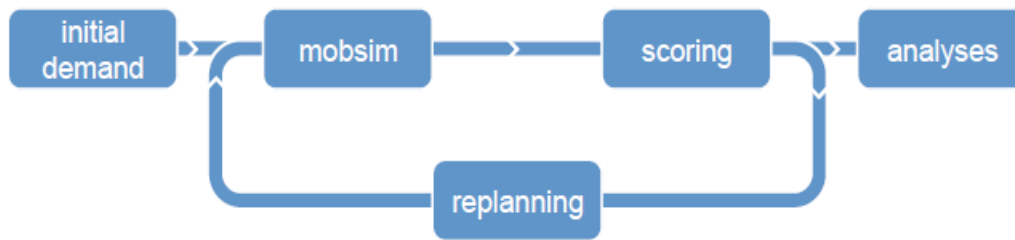


Figure 2. MATSim cycle

Every agent in the simulation, learns and adapts to the system within an iterative process. This process is composed of the following three steps:

- a. Simultaneous execution of plans (mobsim): In the first step, daily plans of all individuals are executed simultaneously on the network. In this study, a state-of-the-art queuing model [22] is used which follows the traditional “first-in-first-out” queuing logic.
- b. Evaluation of plans (scoring): In order to model the choice between multiple potential daily plans, executed plans of all agents are evaluated using a utility function, indicating the performance (or score) of the plan.
- c. Change of plans (replanning): After executing and scoring plans, a new plan is generated for a predefined share of agents. The new plan is generated by modifying an existing plan according with respect to predefined choice dimension.

3 Simulation and results

The economic growth achieved in the 1990s in Tunisia contributed to the development of the supply of transport [19]. Furthermore, the blast of the vehicle fleet, the rapid growth of urban population, the extension of the national road network, motorization, fuel prices, government subsidies etc, accordingly led to serious environmental and economic problems. For example, energy consumption and CO₂ emissions have significantly increased.

The transport sector in Tunisia comes second in terms of energy consumption. It represents 34% of total energy consumption in 2010 [20]. In particular, road transport appropriates 82% of consumption in the sector, followed by air transport then by the maritime and rail transport. On the other hand, the emission of carbon dioxide CO₂ is one of the major impacts of transport on the environment. Official reports show that the emission of this gas continue to grow in Tunisia (National Institute of Statistics, 2013).

The network created in our project is an excerpt from Open Street Map (Fig. 2) containing only roads in the study area, Tunis city center. This sample contains about 100000 vehicles / day (randomly generated). This network includes only roads with cars of 2500 links and 1000 nodes.

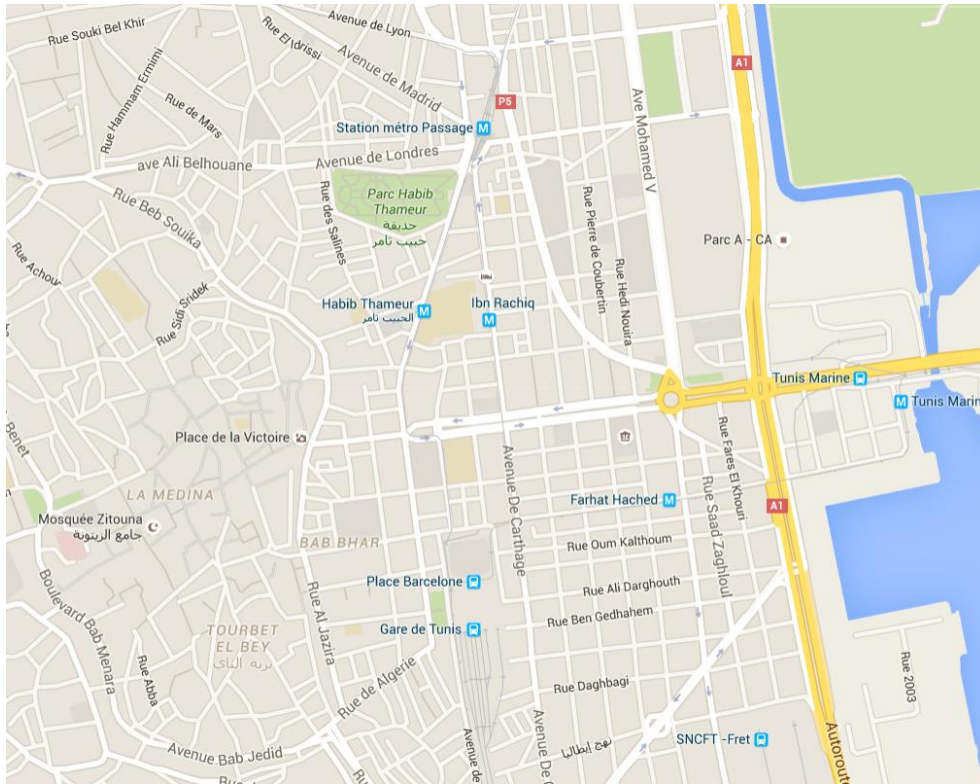


Figure 3. Study Area

According to the municipality of Tunis, the selected area has a capacity of 11.201 parking spaces divided into two categories: off-street parking and on-street parking (fig4).

The municipality of Tunis attempted to increase the capacity of the off-street parking by the construction of car parks intended primarily to capture migrants (merchants and employees), residents and partly those who have a need for long-term parking. Off-street parking of Tunis offers 6001 seats.

To reduce the on-street parking, the center of Tunis has several parks with capacity reached 5200 seats. The on-street parking offer the paid parking or Parking in the blue zone. Following the creation of a blue area, the municipality of Tunis has made the generalization of short-term parking in the street, this type of paid parking and limited in duration. Parking in the blue zone of Tunis offers 5200 seats including parking time shall not exceed two hours and this is what allowed from 8:00 until 20:00. The unit price of a place to park is 0.500 TND per hour.

The generalization of paid parking policy with short-term parking in the city center is implemented to improve the management of the supply of available parking on public highway this is by setting the rotary parking with the installation of parking meters. The objective of this new technique of payment in the blue areas is to facilitate the process of paid parking allowing drivers to have a simple method, faster and more secure.

We have developed a simulation's environment in the software simulation MATSim (Multi-Agent Transport Simulation). As a matter of fact this software provides a toolbox to implement large-scale transport simulations based agents.

Moreover, for the project described, two methods were highlighted. For the first method, people can move randomly in the hope of finding places to park their vehicles in the area of their destinations. However, in the second method, drivers are guided to parking places. Thus, a comparison between the two methods was established. Figure 3 provides an overview of the data structure.

Network:

- 1) Node: each node is identified by a unique id and has x , y attributes which are converted from geographical location.
- 2) Link: each link has a unique id and is defined by a start and end node. Further important link attributes are length, capacity (vehicles per hour), free-flow speed and number of lanes

Plan:

- 3) Agent person: each agent person refers to a citizen.
- 4) Itinerary: each itinerary contains the trips and activities done by the agent throughout a given time period. Within that period, each agent only has one itinerary. Each agent should and only have one itinerary for one day.
- 5) Trip: each trip contains multiple nodes and has distance, start and end time attributes. Hence the exact location of an agent at certain time can be retrieved.
- 6) Activity: each activity is what the agent is doing at a given time. It contains the activity type, such as shopping and education, location, start and end time attributes. Activity can also be considered as a trip with an event type and no change in the location.

3.1 Traffic jams

In order to examine the results of both methods, we proceed by comparing stuck in traffic jam .

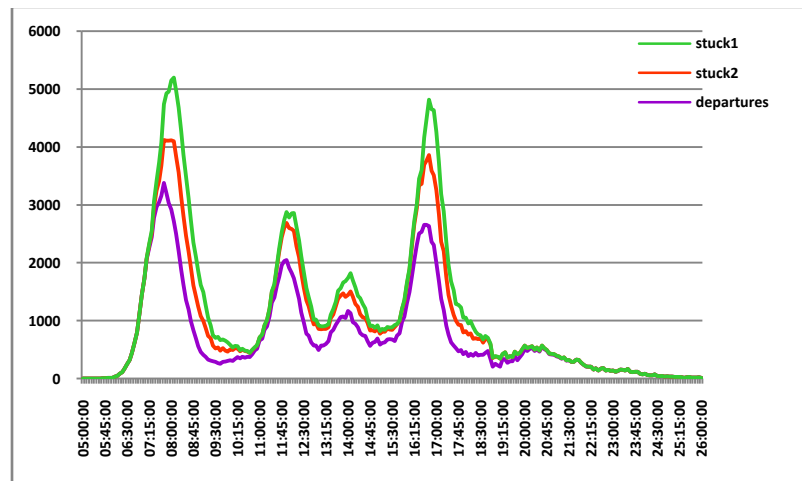


Figure 4. Stuck in traffic jams

We notice that the departure of vehicles is consistent with the traffic congestion rates. Then we can notice that the curves have three peaks:

- Bottling in the morning, the maximum number of car (pic) is 5200 veh for method 1 against 4100 veh for method 2. It can be concluded that the traffic for method 2 is proportionally more fluid than the traffic of method 1.
- Bottling in the middle, the peaks are not too high. Indeed already parked vehicles, more precisely of those commuters, do not leave their parking spaces. This peak represents the flow of vehicles of those visitors, or those who have a specific reason such as lunch... It can be concluded also that the traffic for method 2 is proportionally more fluid than the traffic of method 1
- Bottling in the evening was recorded by 4800 veh for method 1 against 3900 veh for method 2, which reinforces the idea of fluidity of traffic.

3.2 Changes in the number of vehicles in circulation over time

Figures 5 and 6 show the traffic for one day, during the week, by the two different methods. These are curves that reflect the number of staff vehicles arriving and moving every hour of the day. The green and blue curves represent the number of cars circulating in the street. The yellow and pink curves show the number of vehicles that have reached their destinations.

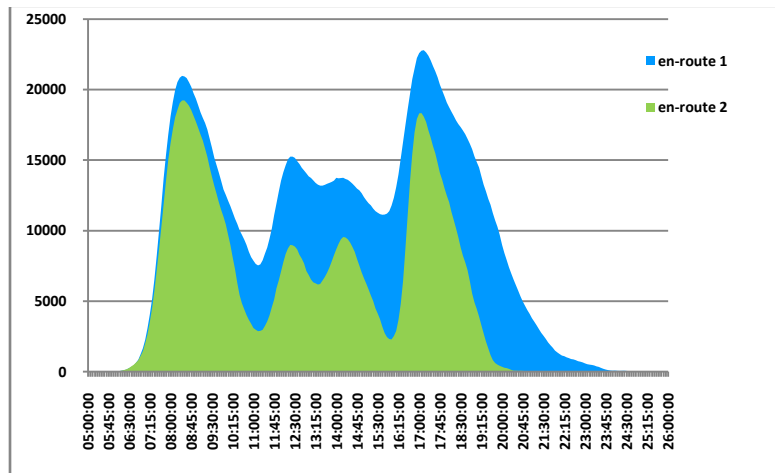


Figure 5. Vehicles in circulation

In the morning; a comparison between the method 2 and method 1 has contributed to a reduction of 2% of vehicles in circulation. The percentage of vehicles reduced for method 2 represent the proportion of motorists who were currently looking for places to park. Therefore this result represents a reduction of travel time and an increase in the number of drivers who reaches their destination which has positive repercussions on the psychology of drivers, especially in the morning. Indeed, if the motorist reaches the workstation with good humor (no stress of driving), it will perform better;

In the evening, the percentage of reduced vehicle traffic is currently equal to 5.5% (comparing the method 2 to method 1). It reflects the number of cars that have been in search for a vacant parking place. It's lower than that found in the morning because the conductive agents who broke away from their Workstations will move toward the periphery of the city center (away) or they will move downtown to a pattern of leisure or purchase; they are more likely to find vacancies. Similarly, for people arriving from the outskirts of the city center will be guided to parking spaces unoccupied;

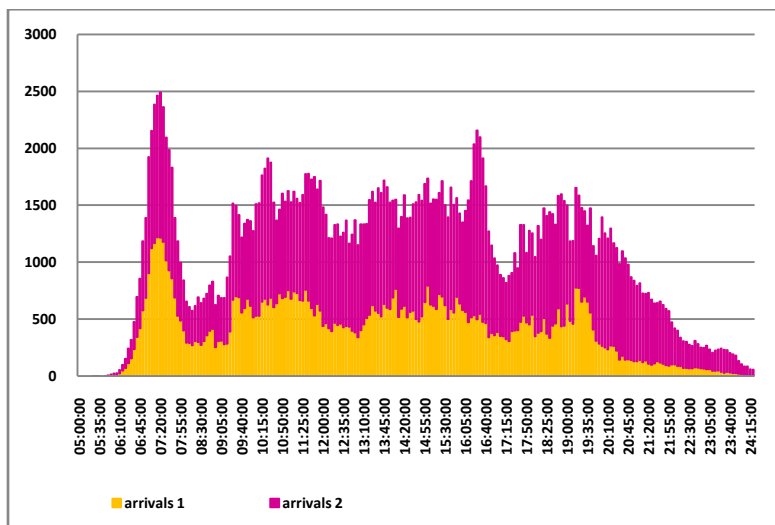


Figure 6. Arrivals vehicles

The pink curves show that the number of vehicles that have led to their destinations on the 24 hours studied is higher in the case of method 2. This implies that if drivers are guided to parking spaces, first the number of cars circulating in the street is fewer, and second the number of vehicles which have reached their destinations is higher despite that the number of vehicles which have left their places of origin is more important than if drivers are moved randomly in the hope of finding places to park their vehicles. This is can be explained by traffic that has become more fluid

3.3 Changes in the energy consumption over time

Figure 7 show the evolution of the traveled distance by the 100000 vehicles for each hour. We notice that the average distance traveled by cars to Method 2 is less than the distance traveled to Method 1.

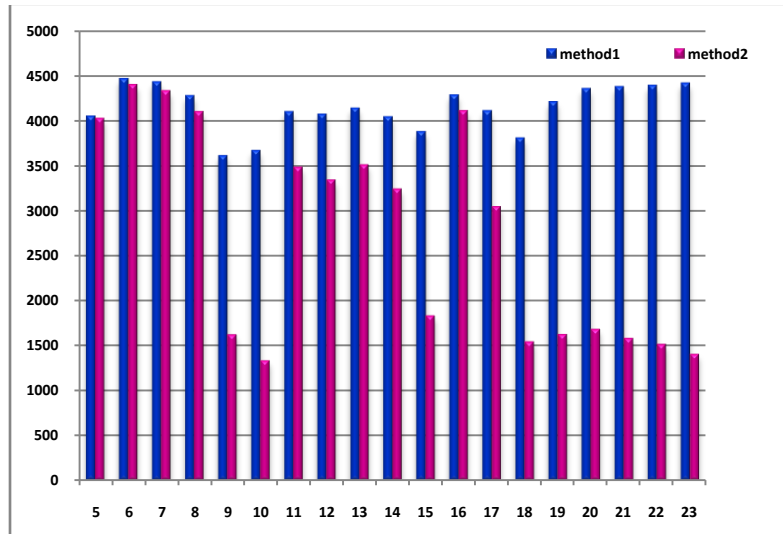


Figure 7. Statistics on Travel Distance (over time)

An impressive difference between the two proposed methods appears in the average distance traveled. Indeed, the average traveled distance by vehicles is 78443.7 km by method 1 against 51854 km by method 2, so there's been down for 26589.7 km through the park during the 24 hours studied. This decrease is synonymous with significant decrease energy consumption.

Table 1 presents the main differences between the two methods in term of the average distance traveled, and the associated average saving of energy consumption. Results (Table 1) show also that method 2 is more efficient and more effective than Method 1.

Depending on the distance traveled, the average saving of energy consumption can be measured as:

$$ASEC = NV \times AFC \times DT \times APD \quad (1)$$

Where, *ASEC* is the Average Saving of Energy Consumption, *NV* is the number of vehicles (100000), *AFC* is the average fuel consumption per 100 km (7 liters/100 km = 7%), *DT* is the distance traveled, and *APD* is the average price of fuel (1.250 TND). According the method 1, the average saving of energy consumption is:

$$6.8638 \times 10^{11} = (100000 \times 7\% \times 78443.7 \times 1.250).$$

However, according method 2, it's:

$$4.5372 \times 10^{11} = (100000 \times 7\% \times 51854 \times 1.250).$$

A decrease in daily distance traveled by the resulting method 2 causes a reduction in average savings of energy consumption of 2.3266×10^{11}

TABLE I. COMPARATIVE STATISTICS

	Method 1	Method 2
Average distance traveled	78443,7 km	51854 km
<i>ASEC</i>	6.8638×10^{11}	4.5372×10^{11}

The results show that finding a parking place is now guided. It can also provide a time saving, less congestion, less mileage, less movement and energy consumption (Fig8) and therefore less pollution.

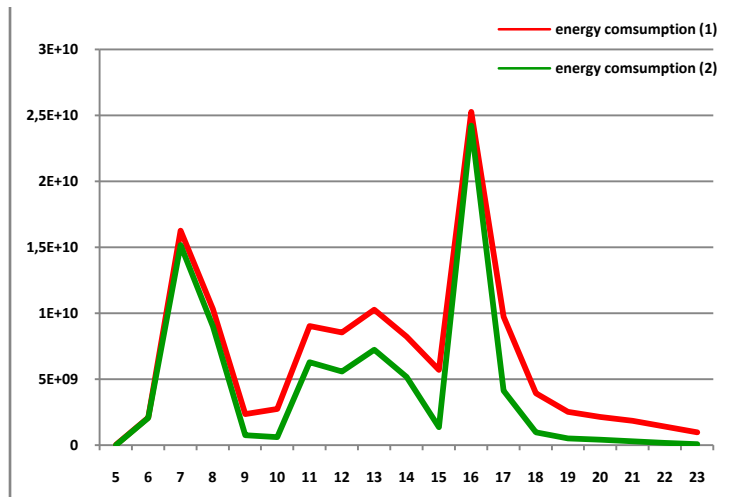


Figure 8. Changes in the energy consumption over time

3.4 Changes in the CO₂ emission over time

Urban pollution is a local issue; the consequences appear in the short term. This pollution is mainly related to increased traffic. A decrease in the number of vehicles on the road, allowed a reduction of the amount of CO₂ emitted for each hour of travel. Method 2 admitted a decrease of 31% of the total amount of carbon dioxide (CO₂) emitted by cars. This result reinforces the idea that method 2 is more efficient than method 1.

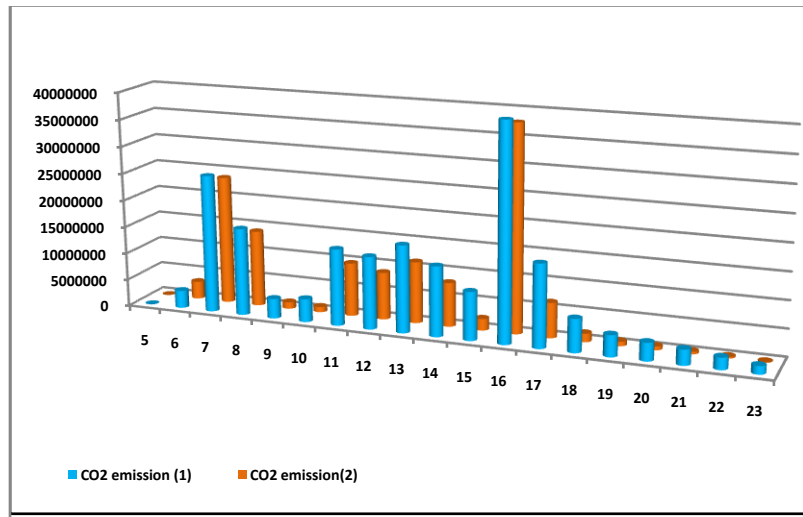


Figure9. Changes in the CO₂ emission over time

Conclusion

In order to research an intelligent car parking management system, this paper proposed a multi-agent system for mitigation Air pollution and energy consumption. It starts with the description of the considered system organization in order to arrange the interactions, communications and coordination between agents. The coordination between them implies to find a vacant parking place, guide the driver to this area, and guarantee the reservation of the targeted area. Faced with all the possibilities that are available, the agents try to optimize the choice of driver for convenience and comfort.

Simulations established in this work show the differences between two methods. The first involve that people can move randomly in the hope of finding places to park vehicles and the second supposes however that our people are guided to park places. The results of the simulations from downtown Tunis are considered quite satisfactory. It shows the importance of our model of multi-agent in the reduction of time looking for a vacant parking place. The consequences of this minimization of search time

generates a positive impact : a reduction of the distance traveled, traffic jams, energy consumption, air pollution, noise and other benefits such as improving the psychology of drivers...

3.5 References

- [1] Guido Ferilli « An analysis of the city centre car parking market: The supply side point of view » A thesis for the award of Doctor of Philosophy, Edinburgh Napier University, December 2008
- [2] Manville, M. et Shoup, D. « Parking, People, and Cities». *Urban Planning and Development*, vol. 131, no 4, 2005, p. 233-245
- [3] A. Diallo, J.-S. Bourdeau, C. Morency, N. Saunier. 'Methodology of Parking Analysis'. *Canadian Journal of Civil Engineering*, 42(4), 2015, pp 281-285.
- [4] D.C., Shoup, "Cruising for parking". *Transport Policy*, 2006, 13, 479-486.
- [5] LI Zhichun, Huang Haijun, William H. K. Lam and S. C. Wong, « Optimization of Time-Varying Parking Charges and Parking Supply in Networks with Multiple User Classes and Multiple Parking Facilities ». *Tsinghua Science And Technology*, 2007, pp167-177
- [6] Jong-Ho Shin, Hong-Bae Jun, « A study on smart parking guidance algorithm ». *Transportation Research Part C: Emerging Technologies*, July 2014, pp299-317
- [7] Paul Steely White. « No vacancy: Park slope's parking problem». *Transportation alternatives*, 2007. <http://www.transalt.org/newsroom/releases/126>
- [8] Sareco « time looking for a parking space» Tome 1: Repport, SA117Q, Prédit – Ademe, Février 2005
- [9] Arnott, R., Inci, E. « An integrated model of downtown parking and traffic congestion». *J. Urban Economic* vol60, 2006, pp418–442
- [10] Arnott, R., Rave, T., Schob, R. «Alleviating Urban Traffic Congestion». MIT Press. 2005
- [11] Takyi Harriet, Kofi Poku, Anin Kwabena Emmanuel « An Assessment of Traffic Congestion and Its Effect on Productivity in Urban Ghana » *International Journal of Business and Social Science*, Vol 4, March 2013, pp1-10
- [12] Caliskan, M., Barthels, A., Scheuermann, B., Mauve, M., 2007. « Predicting Parking Lot Occupancy in Vehicular Ad Hoc Networks». *IEEE 65th Conference on Vehicular Technology*, 2007
- [13] Christophe Begon, "Parking and reducing CO₂ emissions." *Proceedings of the international conference, Hammamet (Tunisia), French Development Agency Research Department, Sareco 2007*
- [14] VOUILLON, C. "With SmartGrains find a parking space is no longer an ordeal." *TechCrunch France*, November 23, 2010 <url: <http://fr.techcrunch.com/2010/11/23/SmartGrains-find-with-a-place-of-parking-not-be-more-a-Calvary/>
- [15] Y.C. Shiue, J. Lin, S.C. Chen, "A Study of Geographic Information System Combining with GPS and 3G for Parking Guidance and Information System". *World Academy of Science, Engineering and Technology*, 2010, pp. 418-423
- [16] F. Baumarius, "A multi-agent approach towards modeling urbain trafic scenarios". *The Research report RR- 92-47, Deutsches Forschungszentrum fOR KOnstliche Intelligenz GmbH*, 1992, pp. 2-16.
- [17] H. Wang, W. He, "A reservation-based smart parking system". In *Proc. 5th International Workshop on Cyber-Physical Networking Systems (colocated with IEEE INFOCOM)*, April 2011.
- [18] M.T. Tsai, C.P. Chu, "Evaluating parking reservation policy in urban areas: An environmental perspective". *Transportation Research, Part D*, 17, 2012, pp. 145-148.
- [19] Rafea Mraih, Talel Mraih, Riadh Harizi, Mohamed Taoufik Bouzidi "Carbon emissions growth and road freight: Analysis of the influencing factors in Tunisia". *Transport Policy*, Vol 42, 2015, pp. 121–129
- [20] Rafea Mraih, Khaled ben Abdallah, Mehdi Abid « Road transport-related energy consumption: Analysis of driving factors in Tunisia ». *Energy Policy*, Vol 62, 2013, pp. 247–253
- [21] M. Balmer, M. Rieser, K. Meister, D. Charypar, N. Lefebvre, K. Nagel, and K. Axhausen. *MATSim-T: Architecture and simulation times*. In A. Bazzan and F. Klugl, editors, *Multi-Agent Systems for Traffic and Transportation*, pages 57{78. IGI Global, 2009.

- [22] N. Cetin, A. Burri, and K. Nagel. A large-scale agent-based tra_c microsimulation based on queue model. In Proceedings of the Swiss Transport Research Conference (STRC), Monte Verita, Switzerland, 2003.
- [23] P. Bonsall, I. Palmer, Modelling drivers' car parking behaviour using data from a travel choice simulator, *Transp. Res. Part C Emerg. Technol.* 12 (2004) 321–347.
- [24] R.G. Thompson, A.J. Richardson, A Parking Search Model, *Transp. Res. Part A Policy Pract.* 32 (1998) 159–170.
- [25] W. Young, parking design Young1986.pdf, *Traffic Eng. Control.* 12 (1986) 606–613.
- [26] Mathew V.T., Chapter 41 Parking Studies, 2014. Engineering, Transportation Systems, IIT Bombay;
- [27] P. van der Waerden, A. Borgers, H. Timmermans, Travelers Micro-Behavior at Parking Lots : A Model of Parking Choice Behavior 1, (2003) 1–20. Urban Planning Group, Eindhoven University of Technology.

Wireless Sensor Networks Deployment for Air Pollution Monitoring

Ahmed Boubrima¹, Walid Bechkit¹, Hervé Rivano¹, and Anne Ruas²

¹ Univ Lyon, Inria, INSA Lyon, CITI, F-69621 Villeurbanne, France

² IFSTTAR, Paris, France

Abstract. Recently, air pollution monitoring emerges as a major issue of the development of smart cities and the well-being of citizens. Air pollution is traditionally monitored using some measuring stations that are accurate but expensive, big and inflexible. This leads to bad global estimations of pollution concentrations. The emergence of air quality sensors, which are less expensive, allows to consider a new pollution monitoring paradigm based on the wireless interconnection between these sensors. This allows to ensure a district-wide air pollution monitoring. In this paper, we tackle the minimum-cost node positioning issue for the detection of air pollution thresholds. We propose two models for wireless sensors deployment while taking into account the air pollution modelling and the probabilistic sensing of nodes. We evaluate our deployment models on a real data set of Greater London and conduct extensive simulations to study the impact of some parameters, among which sensors' height. Results show that the deployment cost depends on the dispersion of pollutants in the area of interest and can be minimized by placing sensors at a height close to the one of pollution sources.

Keywords— Air pollution monitoring, Detection of threshold crossings of pollutants, Atmospheric dispersion modeling, Wireless sensor networks (WSN), Deployment, Coverage, Connectivity.

1 Introduction

Air pollution affects human health dramatically. According to World Health Organization (WHO), exposure to air pollution is accountable to seven million casualties in 2012 [17]. In 2013, the International Agency for Research on Cancer (IARC) classified particulate matter, the main component of outdoor pollution, as carcinogenic for humans [14]. Air pollution has become a major issue of modern megalopolis, where the majority of world population lives, adding industrial emissions to the consequences of an ever denser urbanization with traffic jams and heating/cooling of buildings. As a consequence, the reduction of pollutant emissions is at the heart of many sustainable development efforts, in particular those of smart cities. Monitoring urban air pollution and detecting pollution peaks is therefore required by both municipalities and the civil society, wanting to design and assess, or ask for, pollution mitigation public policies.

Most of actual air quality monitoring is operated by independent authorities. Conventional measuring stations are equipped with multiple lab quality sensors

[1]. These systems are however massive, inflexible and expensive. An alternative – or complementary – solution would be to use wireless sensor networks (WSN) which consist of a set of lower cost nodes that can measure information from the environment, process and relay them to some base stations, denoted sinks [18]. The main advantages of a WSN infrastructure, namely self-organization and healing as well as energetic autonomy of the nodes, for air pollution monitoring is to obtain a finer spatiotemporal granularity of measurements, thanks to the resulting lighter installation and operational costs [2]. Pollution monitoring may target two objectives: i) the periodic air quality sampling and mapping; and ii) the detection of threshold crossings in order to trigger adequate alerts [5]. In this work, we focus on the second application where sensors are deployed to control concentrations of pollutants released by pollution sources like factories, sewage treatment plants and urban traffic [7]. We investigate on the computation of minimum-cost optimal deployments that ensure both pollution coverage and network connectivity while considering the phenomenon dispersion.

Minimizing the deployment cost is a major challenge in WSN design. The problem consists in determining the optimal positions of sensors and sinks so as to cover the environment and ensure the network connectivity while minimizing the deployment cost [20]. The deployment is constrained by the cost of the nodes and sinks, but also by operational costs such as the energy spent by the nodes [8][11][10]. The network is said connected if each sensor can communicate information to at least one sink [19]. Many papers on the deployment issue have assumed that two nodes are able to communicate with each other if the distance between them is less than a radius called the communication range [3]. The coverage issue has often been modeled as a k -coverage problem in which at least k sensors should monitor each point of interest [6]. Most research work on coverage uses a simple detection model which assumes that a sensor is able to cover a point in the environment if the distance between them is less than a radius called the detection range [6]. This can be true for some applications like presence sensors but is not suitable for pollution monitoring. Indeed, a pollution sensor detects pollutants that are brought in contact by the wind. The notion of detection range is therefore irrelevant in this context. In order to define a realistic formulation of pollution coverage, we consider pollution propagation models that take into account the inherently stochastic weather conditions.

In this paper, we propose two optimization models for the deployment of WSN for air pollution monitoring. The expected deployment should ensure pollution coverage and network connectivity while minimizing the deployment cost. Based on the pollution dispersion modeling and the related work on ILP formulations of WSN coverage and connectivity, we first propose an optimization model where pollution coverage and network connectivity are modeled independently. Then, we propose a more effective model in which we give a joint formulation of coverage and connectivity using only the flow concept. The second model is compact and tighter than the first one. In both of the two models, we take into account the probabilistic sensing of pollution sensors.

The remainder of this paper is organized as follows. We first present and analyze the atmospheric dispersion modeling of pollutants in section 2. Then, section 3 details our two proposed optimization models while section 4 presents the simulation dataset and the obtained results. Finally, we conclude and propose some perspectives in section 5.

2 Atmospheric dispersion modeling

As claimed in the previous section, generic detection models using the notion of detection range are not suitable to the sensing of air pollutants. In particular, a realistic formulation of pollution coverage has to capture the dispersion in the atmosphere. The atmospheric dispersion of pollutants was extensively studied in the literature and several models have been proposed and validated. These models are of major interest for many applications such as weather forecasting, assessment of contamination, poisoning, etc. The theoretical study of pollutant atmospheric dispersion is mainly based on fluid mechanics theory [4]. For the sake of clarity, we focus in this work on steady state dispersion models, in particular on Gaussian dispersion. Our approach is however more generic and can be adapted to more sophisticated dispersion models.

The basic Gaussian model estimates the concentrations of a pollutant gas released by a pointwise pollution source in a free space environment [12]. The estimated value C (g/m^3) at a measurement location (x, y, z) is given by Formula (1). Table 1 details the parameters of the model. The pollution source is located at the point $(0, 0, h_s)$ and the measurement point location is given according to a 3D coordinate system where the x-axis is oriented in the wind direction D_w . Parameters σ_y and σ_z describe the stability of the atmosphere and can be approximated using Briggs formulas: $\sigma_y = a_y \cdot |x|^{b_y}$ and $\sigma_z = a_z \cdot |x|^{b_z}$. The parameter H , which represents the pollutant effective release height, is equal to the sum of the pollutant source height h_s , and the plume rise Δh . Briggs formulas are commonly used for the calculation of the Δh parameter. To simplify the analysis, we only consider the case where the temperature of the pollutant T_s is greater than the ambient air temperature T , which is usually the case. In this case, the value of Δh is given by Formula (2) where F , which denotes the pollutant gas buoyancy, is computed using Formula (3).

$$C(x, y, z) = \frac{Q}{2\pi V_w \sigma_y \sigma_z} e^{-\frac{y^2}{2\sigma_y^2}} \left(e^{-\frac{(z-H)^2}{2\sigma_z^2}} + e^{-\frac{(z+H)^2}{2\sigma_z^2}} \right) \quad (1)$$

$$\Delta h = \frac{1,6 \cdot F^{1/3} \cdot x^{2/3}}{V_w} \quad (2)$$

$$F = \frac{g}{\pi} \cdot V \cdot \left(\frac{T_s - T}{T_s} \right) \quad (3)$$

Formula (1) takes into account only pointwise pollution sources, and thus cannot be applied to area sources like crossroads and line sources like highways. Multiple extensions were proposed in the literature to deal with these kinds of

Pollution source	
h_s	Pollutant source height (m)
Δh	Plume rise (m)
H	Pollutant effective release height (m)
Measurement location	
x	Downwind distance from the pollution source (m)
y	Crosswind distance from the pollution source (m)
z	Hight (m)
Pollutant gas	
Q	Mass flow rate at the emission point (g/s)
V	Volumetric flow rate at the emission point (m^3/s)
T_s	Pollutant temperature at the emission point (K)
Weather	
T	Ambient air temperature (K)
V_w	Wind velocity (m/s)
D_w	Wind direction (degree)
Constants	
a_y, b_y	Horizontal dispersion coefficients
a_z, b_z	Vertical dispersion coefficients
g	Gravity constant ($9.8m/s^2$)

Table 1: Parameters of the Gaussian dispersion model

pollution sources. In addition, many enhanced systems were developed based on the Gaussian model to take into account complex meteorological data, effect of obstacles on pollution dispersion, etc.

3 Deployment models

In this paper, we propose two integer programming formulations for optimal deployment of wireless sensor networks to efficiently monitor air pollution. Our formulations rely on a pollution dispersion model. For the sake of clarity, we use the aforesaid Gaussian dispersion model in this work. Our approach is however more generic and can be adapted to more sophisticated dispersion models and environments. We consider pollutants that can be released by industrial sources like factories, sewage treatment plants, etc, as well as traffic sources such as highways and crossroads. In the first model, we formulate pollution coverage and network connectivity independently. In the second one, we propose a more sophisticated formulation in which coverage and connectivity are joint in a common network flow problem. Table 2 depicts the notations used in the integer programming formulations.

Sets	
\mathcal{P}	Set of potential positions of sensors and sinks
\mathcal{N}	Number of sensors and sinks potential positions
\mathcal{I}	Set of pollution sources
\mathcal{M}	Number of pollution sources
Parameters	
\mathcal{Z}_i	The pollution zone formed by source i
\mathcal{B}_{ip}	Define whether the position p belongs to the zone \mathcal{Z}_i or not
$\Gamma(p)$	The neighborhood of the potential position p
c_p^{sensor}	The cost of deploying a sensor at position p
c_p^{sink}	The cost of deploying a sink at position p
β	Coverage requirements of each zone
\mathcal{W}_i	The probability of detecting the zone \mathcal{Z}_i
C_0	Pollutant concentration threshold
Variables	
x_p	Define whether a sensor is deployed at position p or not $x_p \in \{0, 1\}, p \in \mathcal{P}$
y_p	Define whether a sink is deployed at position p or not $y_p \in \{0, 1\}, p \in \mathcal{P}$
g_{pq}	Flow quantity transmitted from node p to node q $g_{pq} \in \{0, 1, \dots\}, p \in \mathcal{P}, q \in \Gamma(p)$
f_{ip}	Flow quantity transmitted from zone \mathcal{Z}_i to node p $f_{ip} \in \{0, 1\}, i \in \mathcal{I}, p \in \mathcal{Z}_i$

Table 2: Notations used in deployment models.

3.1 Model 1

In smart cities applications, some restrictions on node positions may apply because of authorization or practical issues. For instance, in order to alleviate the energy constraints, we may place sensors on lampposts and traffic lights as experimented in CitySense [9]. In the following, we consider a set of a pre-defined potential positions, denoted \mathcal{P} , which is obtained using a discretization of the deployment field restricted to allowed positions. In free space environments without deployment restrictions, that would be a regular grid. We denote $\mathcal{N} = |\mathcal{P}|$ the number of potential positions. The locations of pollution sources, e.g. factories, sewage treatment plants, crossroads, highways..., is denoted \mathcal{I} . \mathcal{M} denotes the number of pollution sources. The binary decision variables x_p , resp. y_p , define if a sensor, resp. a sink, is placed at position p .

We consider that sinks are equipped with pollution sensors. They are also connected to a backbone network. Deploying a sink is therefore more expensive than a regular sensor node. The cost of deploying a sensor, resp. a sink, at position p is denoted c_p^{sensor} , resp. c_p^{sink} . Our optimization models minimize the sensors and sinks overall deployment cost. Thus, the objective function is the following.

$$\mathcal{F} = \sum_{p \in \mathcal{P}} c_p^{sensor} * x_p + \sum_{p \in \mathcal{P}} c_p^{sink} * y_p \quad (4)$$

Since a sink embeds sensing capabilities, a sink and a sensor cannot be deployed at the same potential position p as formulated in constraint 5.

$$x_p + y_p \leq 1, \quad p \in \mathcal{P} \quad (5)$$

Pollution coverage The coverage constraints rely on the modeling of the atmospheric dispersion. We assume that pollution sources release pollutants independently and may have simultaneous release. Our formulation ensures the coverage of threshold crossings in all cases.

Using an atmospheric dispersion model, we determine the set of generated pollution zones. Each zone \mathcal{Z}_i corresponds to the geographical area, i.e. set of positions, where the pollution threshold is crossed when the pollution source i is releasing pollutants. Let the binary parameter \mathcal{B}_{ip} denote whether a position p belongs to \mathcal{Z}_i or not. A pollution zone \mathcal{Z}_i is therefore the set $\{p \in \mathcal{P} \text{ where } \mathcal{B}_{ip} = 1\}$. When using the pointwise Gaussian dispersion model, the value of \mathcal{B}_{ip} is calculated using Formula (6) where σ_y, σ_z, Q and H are the parameters presented in Section 2, $p = (x, y, z)$ and C_0 is the threshold of pollutant concentration above which a point is considered as polluted.

$$\mathcal{B}_{ip} = \begin{cases} 1 & \text{if } \frac{Q}{2\pi V_w \sigma_y \sigma_z} e^{-\frac{y^2}{2\sigma_y^2}} (e^{-\frac{(z-H)^2}{2\sigma_y^2}} + e^{-\frac{(z+H)^2}{2\sigma_y^2}}) \geq C_0 \\ 0 & \text{otherwise} \end{cases} \quad (6)$$

We assume that a sensor exposed to a given pollutant will detect its concentration with a probability that is different from a pollution zone to another. We denote $\mathcal{W}_i \in]0, 1[$ the probability of detecting the pollution source i by a sensor located within its zone.

Once the pollution zones \mathcal{Z}_i are identified and the sensing parameters \mathcal{W}_i are computed, we formulate the coverage of each pollution source i with a probability β in constraint 7.

$$\prod_{p \in \mathcal{Z}_i} (1 - \mathcal{W}_i * (x_p + y_p)) \leq (1 - \beta), \quad i \in \mathcal{I} \quad (7)$$

When a sensor or a sink is placed at position p , i.e. $x_p + y_p = 1$, $1 - \mathcal{W}_i * (x_p + y_p)$ is then equal to $1 - \mathcal{W}_i$, the probability that the node deployed at p does not cover the pollution zone \mathcal{Z}_i at position p . Assuming that the detection events are independent among all potential positions, constraint 7 ensures therefore that each zone \mathcal{Z}_i is covered with a probability $\beta \in]0, 1[$.

Constraint 7 should be linearized in order to get an ILP formulation. The process of linearization is done through formulas 8, 9 and 10. Hence, we get the linear form in constraint 11.

$$\prod_{p \in \mathcal{Z}_i \text{ where } (x_p + y_p = 1)} (1 - \mathcal{W}_i) \leq (1 - \beta), \quad i \in \mathcal{I} \quad (8)$$

$$(1 - \mathcal{W}_i)^{\sum_{p \in \mathcal{Z}_i} (x_p + y_p)} \leq (1 - \beta), \quad i \in \mathcal{I} \quad (9)$$

$$\left(\sum_{p \in \mathcal{Z}_i} (x_p + y_p) \right) * \log(1 - \mathcal{W}_i) \leq \log(1 - \beta), \quad i \in \mathcal{I} \quad (10)$$

$$\sum_{p \in \mathcal{Z}_i} (x_p + y_p) \geq \frac{\log(1 - \beta)}{\log(1 - \mathcal{W}_i)}, \quad i \in \mathcal{I} \quad (11)$$

Connectivity We formulate in this first model the connectivity constraint as a network flow problem. We consider the same potential positions set \mathcal{P} for sensors and sinks and we do not assume that potential positions of sinks are known or different from those of sensors. We first denote by $\Gamma(p)$, $p \in \mathcal{P}$ the set of neighbors of a node deployed at the potential position p . This set can be computed using any adequate propagation models. Then, we define the decision variables g_{pq} as the flow quantity transmitted from a node located at potential position p to another node located at potential position q . We suppose that each sensor of the resulting WSN generates a flow unit in the network, and verify if these units can be recovered by sinks. The following constraints ensure that deployed sensors and sinks form a connected wireless sensor network; i.e. each sensor can communicate with at least one sink.

$$\sum_{q \in \Gamma(p)} g_{pq} - \sum_{q \in \Gamma(p)} g_{qp} \geq x_p - \mathcal{N} * y_p, \quad p \in \mathcal{P} \quad (12)$$

$$\sum_{q \in \Gamma(p)} g_{pq} - \sum_{q \in \Gamma(p)} g_{qp} \leq x_p, \quad p \in \mathcal{P} \quad (13)$$

$$\sum_{q \in \Gamma(p)} g_{pq} \leq \mathcal{N} * x_p, \quad p \in \mathcal{P} \quad (14)$$

$$\sum_{p \in \mathcal{P}} \sum_{q \in \Gamma(p)} g_{pq} = \sum_{p \in \mathcal{P}} \sum_{q \in \Gamma(p)} g_{qp} \quad (15)$$

Constraints 12 and 13 are designed to ensure that each deployed sensor, i.e. such that $x_p = 1$, generates a flow unit in the network. These constraints are equivalent to the following.

$$\sum_{q \in \Gamma(p)} g_{pq} - \sum_{q \in \Gamma(p)} g_{qp} \begin{cases} = 1 & \text{if } x_p = 1, y_p = 0 \\ = 0 & \text{if } x_p = y_p = 0 \\ \leq 0, \geq -\mathcal{N} & \text{if } x_p = 0, y_p = 1 \end{cases}$$

The first case corresponds to deployed sensors that should generate, each one of them, a flow unit. The second case, combined with constraint 14, ensures that absent nodes, i.e. $x_p = y_p = 0$, do not participate in the communication. The third case concerns deployed sinks, and ensures that each sink cannot receive more than \mathcal{N} units. The case $x_p = y_p = 1$ is not possible because of constraint 5. Constraint 14 ensures also that deployed sinks cannot transmit flow units, and only act as receivers. Constraint 15 means that the overall flow is conservative. The flow sent by deployed sensors has to be received by deployed sinks.

ILP Model At the end, our first optimization model can be written as follows.

[*Model1*]

Minimize (4)

Subject to. (5), (11), (12), (13), (14) and (15)

3.2 Model 2

Despite the huge progress made in solving ILPs, the first formulation cannot deal with large-scale instances. One of the main reasons is that the two sub-problems, namely connectivity and coverage, are formulated as set of constraints of different natures. The underlying writing of coverage is an instance of set cover, a very complex combinatorial problem that does not combine efficiently with the network flow problem of connectivity. In particular, solvers might not be able to use their computation optimization tailored for network flow. To cope with this, we propose in this section a more efficient modeling. By considering pollution sources as a part of the network, we obtain a homogeneous coverage/connectivity formulation as a network flow problem.

In this second model, each pollution source i should transmit some flow units to potential nodes p which are located within its pollution zone. In addition, sensors are flow conservative and the sinks receive the flow units generated by pollution sources. Therefore, the definition of the joint coverage/connectivity is to ensure that sinks will be informed each time that a threshold crossing occurs. In this regard, a sensor has to receive at most one unit from a given pollution zone. We hence define the binary decision variable f_{ip} as the flow quantity from the pollution source i to the potential node p . The following constraints ensure coverage and connectivity for pollution monitoring.

$$\sum_{p \in \mathcal{P}} f_{ip} \geq \frac{\log(1 - \beta)}{\log(1 - \mathcal{W}_i)}, \quad i \in \mathcal{I} \quad (16)$$

$$\sum_{i \in \mathcal{I}: p \in \mathcal{Z}_i} f_{ip} + \sum_{q \in \Gamma(p)} g_{qp} - g_{pq} \leq \mathcal{N}\mathcal{M}y_p, \quad p \in \mathcal{P} \quad (17)$$

$$\sum_{i \in \mathcal{I}: p \in \mathcal{Z}_i} f_{ip} + \sum_{q \in \Gamma(p)} g_{qp} - g_{pq} \geq 0, \quad p \in \mathcal{P} \quad (18)$$

$$\sum_{q \in \Gamma(p)} g_{pq} \leq \mathcal{N}\mathcal{M}x_p, \quad p \in \mathcal{P} \quad (19)$$

$$f_{ip} \leq x_p + y_p, \quad p \in \mathcal{P}, i \in \mathcal{I} \quad (20)$$

Coverage is formulated in constraint 16, which ensures that each pollution source i generates a sufficient number of flow units in the network. Constraint 20 enforces that all the flow units are received by deployed nodes. The flow is conservative on deployed sensors thanks to constraints 17 and 18. These two constraints combined with constraints 19 and 20 also ensure that absent nodes do not participate in the communication. Flow conservation on sensors ensures that the deployed sinks will receive all the flow units generated by the pollution sources. The second optimization model can then be written as follows.

[Model2]

Minimize (4)

Subject to. (5), (16), (17), (18), (19) and (20)

4 Simulation results

In this section, we present the simulations that we have performed to evaluate our deployment models. We first present the data set of Greater London that we used in simulation. Next, as a proof of concept we apply our models to the London Borough of Camden. Then, we investigate the performance of the two optimization models in terms of computational burden. Finally, we investigate some engineering insights while we study the impact of the height, the number and the coverage requirements of pollution sources on the deployment cost.

4.1 Greater London dataset

We evaluate our deployment models on a data set provided by the Greater London community [15]. London is one of the most polluted cities in Europe [16]. The data set corresponds to the locations of urban pollution sources. In

this data set, mostly urban facilities have the potential to affect the air quality such as petrol stations, waste oil burners, cement works, etc. The set of pollution sources is spread over the 32 boroughs of Greater London. Overall, 1090 pollution sources are considered. Pollution sources distribution per borough depends on the surface of the borough and ranges from 6 sources to 161 sources.

ILP formulations are implemented using the IBM ILOG CPLEX Optimization Studio and executed on a PC with Intel Xeon E5649 processor under Linux. The ILP solver is executed with a time limit of 30 minutes. The default values of simulation parameters are summarized in Table 3. We simulate the Gaussian dispersion model with the parameters depicted in table 4. Moreover, we define the nodes neighboring I based on a given transmission range. We assume that the cost of nodes is independent from the position of the node, i.e. $c_p^{sensor} = c^{sensor}$ and $c_p^{sink} = c^{sink}$.

Parameter	Value
Nodes transmission range	100m
Nodes height	10m
Sensors cost (c_p^{sensor})	1 monetary unit
Sinks cost (c_p^{sink})	10 monetary units
Coverage requirements of pollution zones (β)	0.90
Detection sensitivity of sensors (\mathcal{W}_i)	0.80
Pollution threshold (C_0)	$20\mu g/m^3$

Table 3: Summary of default simulation parameters of the ILP models.

Parameter	value
h_s	25m
Q	5g/s
V	$1.9mm^3/s$
T_s	30°C
D_w	225°
V_w	5m/s
T	7°C
a_y	1.36
b_y	0.82
a_z	0.275
b_z	0.69

Table 4: Default simulation parameters of the Gaussian model

4.2 Application to the London Borough of Camden

As a proof of concept, we first execute our models on the London Borough of Camden. We use streetlights as potential positions of sensors in order to alleviate the energy constraints. The streetlights data set was provided by the Camden DataStore [13]. Camden is spread over an area of around $8km \times 6km$ and contains 19 pollution sources. Fig. 1 depicts the pollution zones obtained by running of the Gaussian dispersion model. Fig. 1 also shows the obtained positions of wireless sensor network nodes computed by the deployment models. We notice that sensors are placed at the intersections of the different pollution zones in order to minimize the coverage deployment cost. Moreover, the resulting network consists of 7 sub-networks, a sink is deployed in each one and some sensors are added to ensure connectivity.

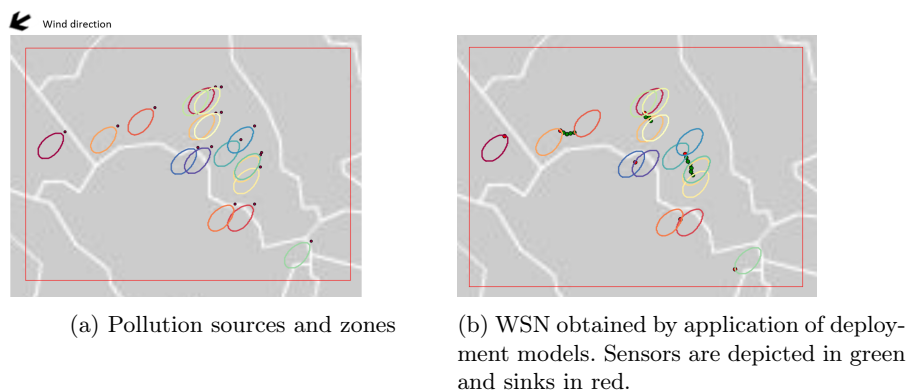


Fig. 1: Application of our deployment models to the London Borough of Camden

The following results have been obtained by running our deployment models on a hundred of $1200m \times 1200m$ blocks extracted from the Greater London map. The density of pollution sources varies between 3 and 18 sources per block. We discretize each block with a resolution of $100m$ to get a $2D$ grid of points that we consider as potential positions of WSN nodes.

4.3 Computational comparison between the proposed models

In order to show the impact of the complexity of the block instances on the tractability of our models, we consider the area of interest as a complexity metric. For a given block b , let C_b be the set of potential positions of sensors that are at least within a pollution zone generated by the block pollution sources under the weather scenarios that are considered. The metric value is defined as the area of the convex envelope of the set C_b . This means that the area of interest includes all the potential positions needed for pollution coverage, i.e. C_b , and

also the area where relay nodes may be placed. Indeed, neither coverage sensors nor relay nodes will be placed in the block area that is not included in the area of interest.

After executing the two models, we got the same objective values; this was expected since the second model is derived from the first one. We depict in table 5 the execution time of the models depending on the area of interest of block instances. Results have been averaged with respect to the complexity metric class of each instance. We notice that the instances that are more complex take more time to be resolved when using both of the two models. Moreover, the joint formulation allows to enhance the total mean execution time with a factor of around 8. This is due to the fact that in the second model, coverage and connectivity are modeled in joint way.

Area of interest (km^2)	CPU time (seconds)	
	Model 1	Model 2
[0.00 – 0.20[7.460	0.890
[0.20 – 0.45[20.400	2.810
[0.45 – 0.70[29.830	3.360
[0.70 – 0.95[68.200	8.820
Mean	31.470	3.970

Table 5: Model 1 VS Model 2.

4.4 Engineering insights

Impact of the height of pollution sources We now study the impact of the height of pollution sources on the deployment cost. We assume that nodes are placed on a height equal to $10m$, and all the pollution sources have the same height, which is considered in the range from 0 meters to 25 meters. We plot in Fig. 2 the sensors and sinks overall deployment cost depending on the height of pollution sources while considering two different values of the wind direction. The results are averaged over all the London blocks. On the one hand, we notice that the deployment cost is minimal when the nodes height is close to the effective release height of pollution sources H , which is nearly equal to the height of the sources in our case. This is explained by the fact that pollution concentration gets the highest values when being near to the pollutant effective release height H . On the other hand, pollutants are more likely to drop than to increase, which is due to gravitation. Indeed, the deployment cost when pollution sources are $5m$ above sensors is less than the deployment cost when pollution sources are $5m$ below sensors. Fig. 2 also shows the impact of wind on the deployment cost which is different in the two considered cases. Indeed, weather conditions impact the disposition of pollution zones allowing for more or less intersections. As a

result, the obtained WSN topology depends on the weather conditions taken into account.

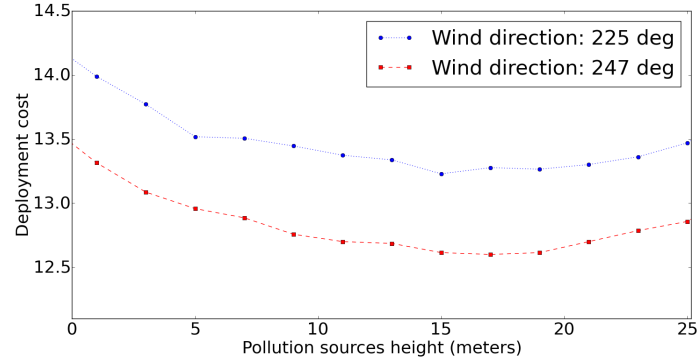


Fig. 2: Deployment cost average depending on pollution sources height while considering different wind directions.

Impact of the number of pollution sources In this scenario, we study the impact of pollution sources density on the deployment cost. For this purpose, we take the results of the previous scenario where the wind direction is equal to 225° . The results are averaged with respect to the number of pollution sources of each instance, i.e. the number of pollution sources within each block instance. We plot in Fig. 3 the deployment cost variations depending on the pollution sources height while considering three different densities: 4, 5 and 6 pollution sources per instance. Fig. 3 shows that the more there are pollution sources in the environment, the more there are sensors required and thus higher is the deployment cost. This can be explained by the number of pollution zones that increases with the number of pollution sources, and thus requires much sensors to ensure the coverage requirements. In addition, the increasing in the deployment cost from 5 sources density to 6 sources density is less than the increasing from 4 sources density to 5 sources density. This is because when the number of pollution sources increases, more intersections between pollution zones appear and affect the increasing of the deployment cost.

Impact of the coverage requirements of pollution sources The coverage requirements of pollution sensors is one of the most important factors that affect the topology of sensor networks used for pollution monitoring. Fig. 4 depicts the average cost of the resulting deployments of the block instances while considering two values of the minimum requirement of coverage probability: $\beta = 0.90$ and $\beta = 0.98$. As expected, the deployment cost increases with the coverage requirements. We notice that the ratio between the two curves is around 1.1. This

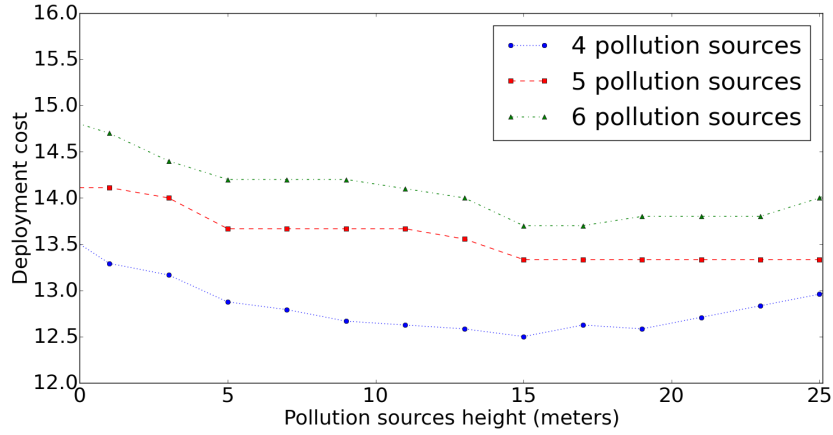


Fig.3: Deployment cost average depending on the height and the density of pollution sources.

is explained by the intersection existence between the different polluted zones, which means that in some cases a sensor can monitor more than one pollution source.

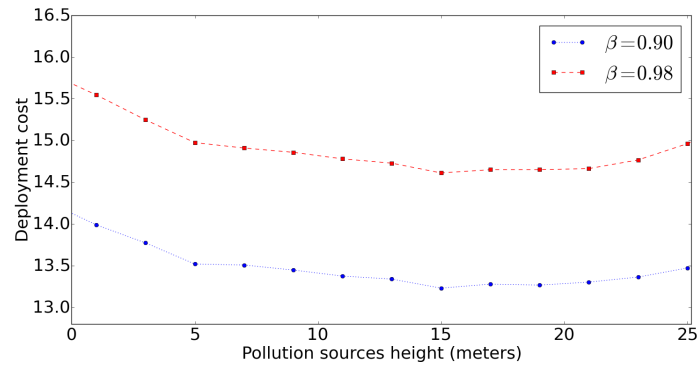


Fig.4: Deployment cost average depending on the height and the coverage requirements of pollution sources.

5 Conclusion and future work

Air pollution is becoming a major problem of smart cities due to the increasing industrialization and the massive urbanization. In this paper, we focused on a

new paradigm of pollution monitoring based on a set of interconnected and tiny sensor nodes. We addressed the deployment issue and proposed two optimization models ensuring pollution coverage and network connectivity with the minimum cost. Unlike the inadequate related works, which do not take into account the pollution propagation, we based on atmospheric dispersion modeling to take into account the nature of the addressed phenomenon.

We investigated some engineering insights on the deployment of sensor nodes while we evaluated the impact of the model parameters on the deployment results. We concluded that sensors should be placed at a height close to the one of pollution sources. We also studied the impact of the coverage requirements of pollution sources and have shown that the higher is this parameter, the higher is the deployment cost.

As a future work, we plan to consider the energy consumption in our models while maintaining their tractability. Another perspective would be to consider the impact of the nature of pollutants and the urban topography on the coverage results.

Acknowledgment

This work has been supported by the "LABEX IMU" (ANR-10-LABX-0088) and the "Programme Avenir Lyon Saint-Etienne" of Université de Lyon, within the program "Investissements d'Avenir" (ANR-11-IDEX-0007) operated by the French National Research Agency (ANR).

References

1. AirParif: The air quality monitoring organization of the paris agglomeration, <http://www.airparif.fr/en/index/index>
2. Akyildiz, I.F., Su, W., Sankarasubramaniam, Y., Cayirci, E.: Wireless sensor networks: a survey. *Computer networks* 38(4), 393–422 (2002)
3. Cardei, M., Pervaiz, M.O., Cardei, I.: Energy-efficient range assignment in heterogeneous wireless sensor networks. In: ICWMC'06. International Conference on. pp. 11–11. IEEE (2006)
4. Daly, A., Zannetti, P.: Air pollution modeling—an overview. *Ambient air pollution* (2007)
5. ETSI: Electromagnetic compatibility and radio spectrum matters (erm); system reference document (srdoc): Spectrum requirements for short range device, metropolitan mesh machine networks (m3n) and smart metering (sm) applications, available on http://www.etsi.org/deliver/etsi_tr/103000_103099/103055/01.01.01_60/tr_103055v010101p.pdf, last access: 2016-01-20
6. Ghosh, A., Das, S.K.: Coverage and connectivity issues in wireless sensor networks. *Mobile, wireless, and sensor networks: Technology, applications, and future directions* pp. 221–256 (2006)
7. Kadri, A., Yaacoub, E., Mushtaha, M., Abu-Dayya, A.: Wireless sensor network for real-time air pollution monitoring. In: ICCSPA, 2013 1st International Conference on. pp. 1–5. IEEE (2013)

8. Keskin, M.E., Altinel, İ.K., Aras, N., Ersoy, C.: Wireless sensor network lifetime maximization by optimal sensor deployment, activity scheduling, data routing and sink mobility. *Ad Hoc Networks* 17, 18–36 (2014)
9. Murty, R.N., Mainland, G., Rose, I., Chowdhury, A.R., Gosain, A., Bers, J., Welsh, M.: Citysense: An urban-scale wireless sensor network and testbed. In: *Technologies for Homeland Security, 2008 IEEE Conference on*. pp. 583–588. IEEE (2008)
10. Rebai, M., Snoussi, H., Hnaien, F., Khoukhi, L., et al.: Sensor deployment optimization methods to achieve both coverage and connectivity in wireless sensor networks. *Computers & Operations Research* 59, 11–21 (2015)
11. Sengupta, S., Das, S., Nasir, M., Panigrahi, B.K.: Multi-objective node deployment in wsns: In search of an optimal trade-off among coverage, lifetime, energy consumption, and connectivity. *Engineering Applications of Artificial Intelligence* 26(1), 405–416 (2013)
12. Stockie, J.M.: The mathematics of atmospheric dispersion modeling. *Siam Review* 53(2), 349–372 (2011)
13. Camden Data: Camden lighting point, on <http://www.camdendata.info/Pages/Home.aspx> [2015-07-15]
14. International Agency for Research on Cancer: Iarc: Outdoor air pollution a leading environmental cause of cancer deaths, on http://www.iarc.fr/en/media-centre/iarcnews/pdf/pr221_E.pdf [2016-02-20]
15. London DataStore: London atmospheric emissions inventory 2010, on <http://data.london.gov.uk/dataset/london-atmospheric-emissions-inventory-2010> [2016-01-15]
16. The guardian: London ranks among worst european cities for air pollution, on <http://www.theguardian.com/environment/2011/sep/07/london-worst-european-cities-air-pollution> [2016-02-15]
17. World Health Organization: Burden of disease from household air pollution for 2012, on http://www.who.int/phe/health_topics/outdoorair/databases/FINAL_HAP_AAP_BoD_24March2014.pdf [2016-02-27]
18. Yick, J., Mukherjee, B., Ghosal, D.: Wireless sensor network survey. *Computer networks* 52(12), 2292–2330 (2008)
19. Younis, M., Akkaya, K.: Strategies and techniques for node placement in wireless sensor networks: A survey. *Ad Hoc Networks* 6(4), 621–655 (2008)
20. Zhu, C., Zheng, C., Shu, L., Han, G.: A survey on coverage and connectivity issues in wireless sensor networks. *Journal of Network and Computer Applications* 35(2), 619–632 (2012)

Real life emissions of Euro 6 diesel cars and operation of emission control systems

Francois CUENOT*, Julia POLISCANOVA* & Greg ARCHER*

*Transport & Environment, 18 Square de Meeûs, Brussels, 1050, Belgium
email: francois@transportenvironment.org

Abstract

NO_x and CO₂ emissions are much higher in real life than during laboratory type approval tests. Are those exceedances due to the driving cycle, driving dynamics and ambient conditions differences or is that a deliberate engineering choice to alter the environmental performance of the vehicles? This paper shows results of two Euro 6 diesel cars fitted with a PEMS and independent instrumentation to measure exhaust emissions and emission control systems operation to identify the use of defeat devices. Results show that engine calibration is vastly responsible for emissions exceedances, with most emission control system under-used in conditions not covered by the laboratory test.

The first vehicle tested (a Peugeot 2008) shows consistent behavior on NEDC drives, but clearly indicated that the emissions control system is sized and fully operating mainly on NEDC conditions. Beyond those, the SCR reaches its limit rapidly and the EGR remained closed. The second vehicle (an Opel Insignia) showed a much more erratic behavior with questionable results when performing an NEDC on a test track, on both CO₂ and NO_x emissions. GM staff to which the results have been presented could not explain it either. Degraded operation of the EGR remains the most plausible explanation.

Keys-words: NO_x emissions, RDE test, emission control system operation, defeat devices.

Introduction

Evidence of wide exceedances in some exhaust gases (especially NO_x and CO₂) emissions have emerged over the years (EU JRC, 2010, Carslaw, 2011 and ICCT, 2014), especially more recently on Euro 5 and Euro 6 light duty diesel cars. The increasing gap between type approval values and real life values has widened significantly and has caused concerns that vehicles manufacturers can be tampering with emission control systems.

Many tests performed by independent parties either on more demanding test cycles on the chassis dynamometer, or more recently using Portable Equipment Measurement Systems (PEMS) highlighted the fact that the vast majority of recent diesel cars are widely exceeding the type approval values.

There is limited evidence on the reasons for such wide exceedances publically available in the literature. Recently some OEMs have add to justify their emissions in front of investigations committee set-up by some European Member States following the VW revelations in the US. Independent bodies usually do not provide detailed technical explanations on how such difference in emissions were being obtained by potentially altering the operation of the emission control systems. Some tests performed on an unidentified vehicle showed that NO_x emissions could be drastically cut in real life conditions (AECC, FEV, 2015) by recalibrating the engine. Open access to a development Engine Control Unit (ECU) was necessary to change the vehicle's cartographies, which is difficult to get and would require the consent of the OEM or of the vehicle development team sub-contracted by OEMs.

1. Objectives and test procedure

In order to find defeat devices, performing emission measurements are not enough. The tests performed for this paper were aiming at detecting potential defeat devices, according to the definition from EC regulations 715/2007, article 3 (10). In article 5 (2) of the same regulation, not all defeat devices are prohibited, listing three exemptions that make some "defeat devices" legal. This paper summarizes tests contracted by Transport & Environment to measure CO₂ and pollutant emissions under different driving conditions and also looking at the operation of key emission control systems during the tests. The hypothesis was that higher pollutant (in particular NO_x) emissions would be potentially associated with modulation or deactivation of one of the emission control systems of the

vehicle. That would indicate the use of defeat devices, whether legal or illegal ones.

In order to truly reveal the emission behavior of the tested vehicles, several tests have been performed to highlight the different calibration strategies used by the Original Equipment Manufacturer (OEM). The tests consisted of four tests:

- a coast-down test in order to measure the road load curves of the vehicles tested. Those are needed in order to perform the laboratory test on a chassis dynamometer as the official values from OEMs are not public. The vehicle was specifically instrumented to comply with UNECE regulation 83 specifications. No emission are measured during this test.

- a Type I test, as per UNECE regulation 83. This is the official test that is performed by official authorities to type approve the vehicle under a laboratory NEDC test. Pre conditioning tests (three EUDC) were performed, as allowed by the legislation, to prepare the vehicle for the test. This test is later referenced as the “lab test”. In order to be operative, the vehicle had to be switched to a “dyno mode”, so that the vehicle would not send error message with the powered wheels rolling while the rest of the vehicle remains stationary. This test has been performed with the measured road loads, which differ substantially from the official road loads used for type approval, as CO2 emissions shows.

- a NEDC test cycle on the test track, in order to validate emissions of the vehicle when the drive cycle is left unchanged, with only ambient conditions (atmospheric temperature and pressure) are changing. The road load tests were performed on the same test track, so rolling resistance of the vehicle can be considered to be similar to the one of the “lab test”. This test is later referred to as the “track test”.

- a RDE-compliant test; even though, at the time the tests were performed, the Real Driving Emissions (RDE) legal text was not finalized, its main content had been voted in May 2015, with limited changes expected to the test procedure. The test provider (Idiada) had some RDE routes ready to be used. In order to test the vehicle under stringent conditions, the hilliest route was chosen, within the authorized limits by the legislation (Figure 1). Minimum altitude was 40m above sea level and maximum altitude was 356m according to on-line mapping software. Cumulative altitude gain reached 1125m per 100km. This test is later referred to as the “RDE test”.



Figure1. RDE route profile.

2. Vehicle selection and instrumentation

Within the budget allowed for the test campaign, two vehicles have been tested. To make sure the vehicles were representative of the vehicle sold by the OEM, vehicles were rented from dealers or specialized agencies without them knowing what the vehicles were intended to. The vehicles tested were:

- A Peugeot 2008 All Blue Hdi 100
- An Opel Insignia Sports Tourer SW

Both vehicles are Euro 6 diesel vehicles. Their emission control systems include a high pressure Exhaust Gas Recirculation (EGR) system and a Selective Catalytic Reduction (SCR) as the main exhaust after treatment system for NOx. There are two main after-treatment systems OEMs have adopted to treat NOx emissions in the exhaust line: the SCR, and the Lean NOx Trap (LNT), also sometimes called NOx Storage Catalyst (NSC). For the test campaign presented here, SCR vehicles have been chosen mainly because it was easier and less resource-intensive to measure the operation of such system.

Indeed, to know if a SCR is in operation, urea injection can be monitored as a reliable proxy for SCR efficiency. To be able to monitor LNT operation, more instrumentation is needed to be able to know when LNT regenerations occur: instantaneous fuel consumption and above all lambda signal must be monitored, which required heavy vehicle modifications.

The test campaign aimed at being as independent from on-board signals as possible, with separate instrument measuring the operation of emission control systems. SCR vehicles were assumed to be easier to measure by fitting a urea flowmeter into the urea injection line and a clamp into the urea injector electrical signal to monitor whether the injector is in operation or not. Fitting an independent lambda to measure LNT regeneration was much more costly and time intensive according to the test provider.

Some of the vehicle sensors' signals were nevertheless logged in order to corroborate the operation of the vehicle and of the emission control systems (Table 1). CAN signals were taken from the OBD and decrypted by Berton, a company contracted by the test provider. CAN signals have been minimized in order to rely as much as possible on information that is not under the control of the OEM. Finally, a Portable Equipment Measurement System (PEMS) was fitted to the vehicle in order to measure exhaust emissions and other parameters independently.

Signals logged		
PEMS	Instrumented	CAN
CO	Accelerator pedal position	Engine speed
CO ₂	Urea injector signal	Vehicle speed
HC	Urea flow	Engine load
NOx NO	Engine coolant temperature	Urea injector signal
Exhaust gas flow	Engine oil temperature	EGR monitoring
Exhaust gas temperature	Gearbox oil temperature	
Exhaust gas pressure	Air intake temperature	
Ambient temperature		
Ambient pressure		
Ambient humidity		
Latitude		
Longitude		
Altitude		
Speed		
Fuel consumption		

Table1. Signals acquisition during the tests at 1hz.

3. Tests results

1. Peugeot 2008 : Higher NOx in real life is partly due to emission control systems deactivation / modulation.

Over the 3 exhaust measurement tests performed for the Peugeot, average urea dosing per unit of distance varies substantially (Table 2). If CO₂ is considered as a proxy for test severity, then the RDE trip is not much more demanding than the laboratory, with about 1% CO₂ difference over the lab and RDE test.

Urea dosage is cut by a third under RDE conditions of use; lowering the performance of the NOx emission control system under normal condition of use. This leads to a wide exceedance of the NOx emissions during the RDE drive, by a factor of 4.4 compared to the legal limit.

	CO ₂ (g/km)	urea injection (g/km)	NOx emissions (mg/km)	averageEGR rate (%)
Official Type approval value	95	NA	33	NA
Laboratory test	119	0.91	46	NA
NEDC on test track	116	0.93	71	16.3%
RDE trip	118	0.60	344	14.9%

Table 2: urea dosage versus NOx emissions for the Peugeot 2008 tested

During the RDE test, the SCR system operated about 30% less than when performing a NEDC test, whether on the lab or on track. This constitutes a strong indication that urea injection seems to be reduced in order not to treat all engine operations to the full potential of the SCR, where NOx emissions occur. Further data analysis have been in order to try and identify that.

Differences during NEDC tests in the lab and on the track

The testing procedure included performing a NEDC test in the lab (as per the legal requirement of the Type 1 test), and repeat a similar driving profile on a test track, with similar road loads. NOx emissions have increased by more than 50% on the test track, but remain below the 80mg/km legal barrier. Overall urea injection is quite similar, but when looking more closely at the different NEDC phases (Part I is the urban phase, part II is the extra urban drive cycle), the vehicle's main emission control system (the SCR and the related urea injection) behaves differently during each phase (Figure 2 and Figure 3). In the phase I, average urea injection times are half those on the laboratory when tested on the test track, and average NOx emissions increase by 50%.

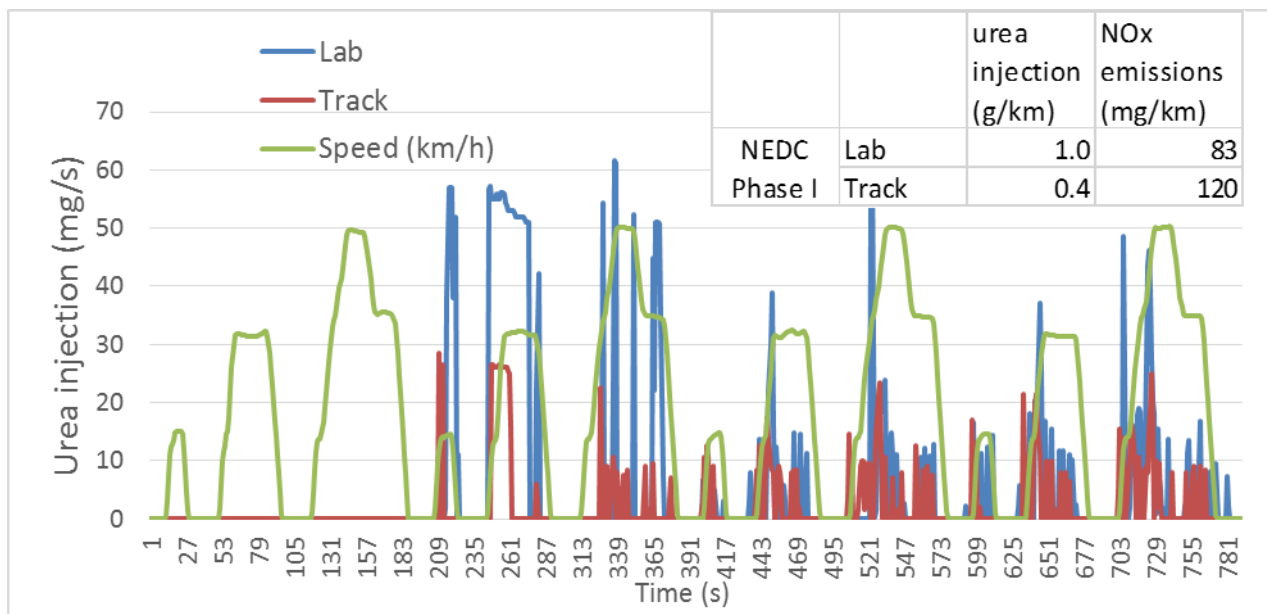


Figure 2: Urea injection times on NEDC phase I, in the laboratory and on the test track

During phase II, when the vehicle is driven at higher speeds, the SCR have an opposite behavior, with more urea injected on the track than in the lab. Surprisingly, NOx emissions are higher on the track, despite the higher urea dosage. This could be explained by the Ammonia load of the SCR prior to the test, as no preconditioning was done for the track test. Some of the differences found might also be due to OBD requirements, occasionally testing the effectiveness of the SCR system.

Overall, this does not seem to indicate that the vehicle detects laboratory conditions, and NOx emissions when performing NEDCs are pretty consistent and well within legal limits.

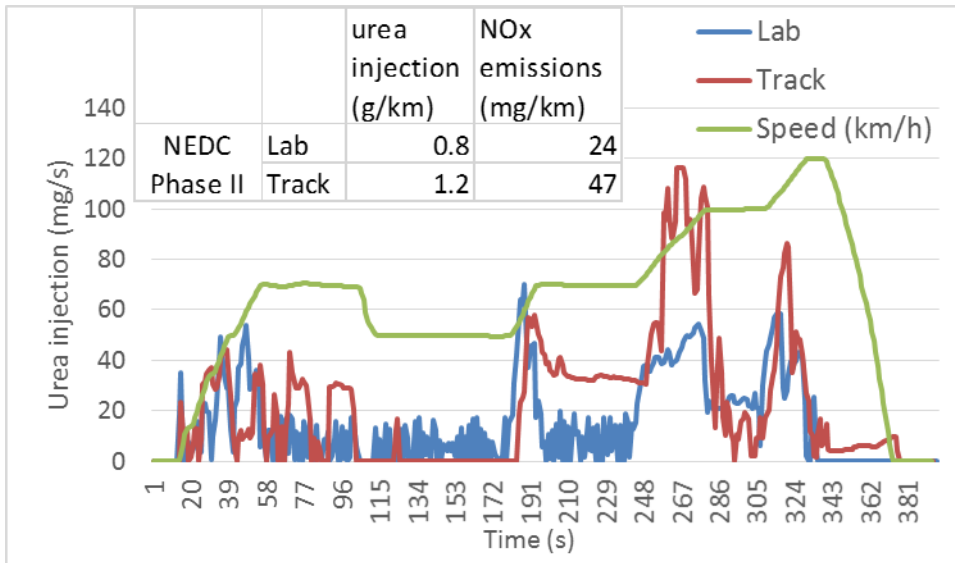


Figure 3: Urea injection times on NEDC Phase II, in the laboratory and on the test track

Detailed behavior of the tested vehicle in real life conditions.

Looking closely at the reasons why the NOx emissions in real life conditions are so high, it is surprising to notice that there is no urea injection for the first half of the RDE trip. This might be due to a low exhaust temperature as the first part of the trip is in urban condition, and there is altitude loss of about 100 meters early on, preventing a quick warming-up of the engine (Figure 4). This urban drive part is likely not to have reached the sufficient exhaust temperature conditions for the SCR to work effectively and for the urea to be injected.

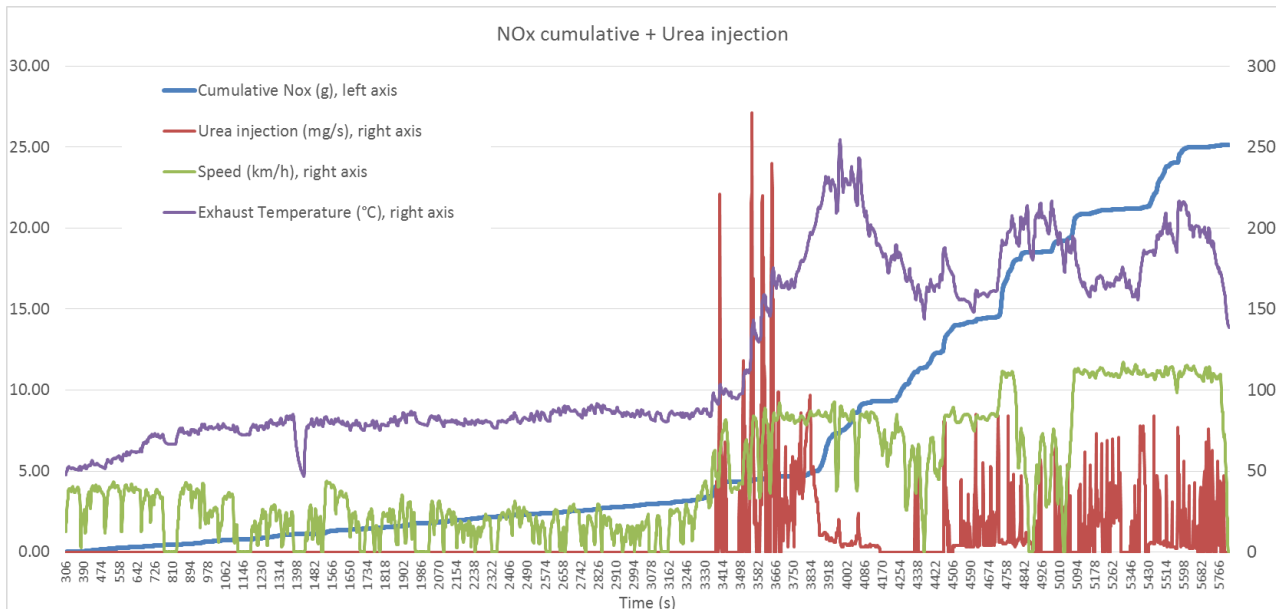


Figure 4: NOx emissions versus urea injection time, vehicle speed and exhaust temperature over typical RDE drive.

Note: time starts at around 300 sec as the cold start (as defined by the RDE legal text) has been removed from the analyzed data.

The whole of the urban part nevertheless represents a small share (about 12% of total emissions). Most of the emissions occur during high engine load events (rather strong acceleration of vehicle going uphill) in rural / motorway sections.

When looking closely at a steady speed section in rural driving condition (between seconds 3700 and 4000 of the drive, Figure 5), the impact of modulating/reducing urea injection can clearly be seen on NOx emissions. It is not clear why urea injection declines, but the effect on NOx emissions is immediate and significant.

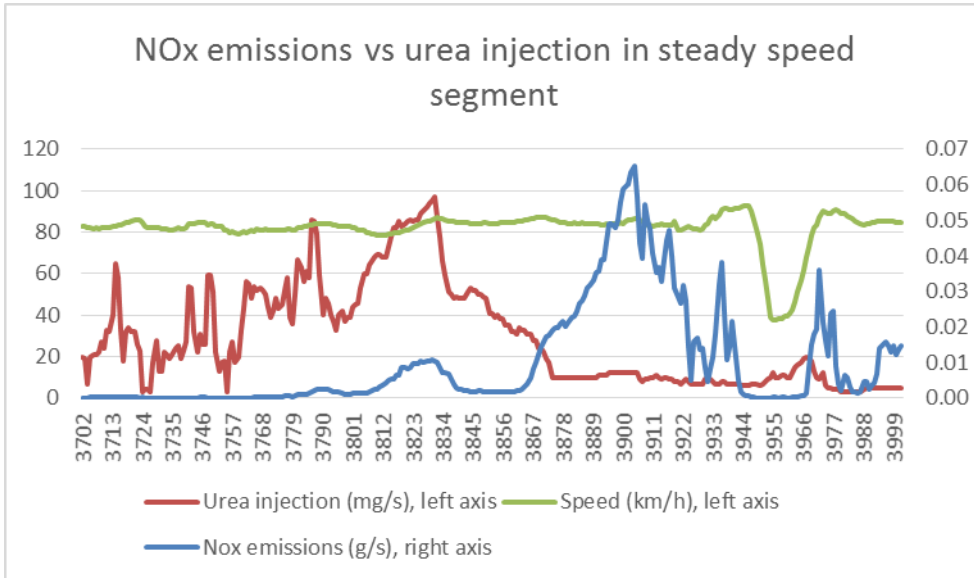


Figure 5: Close up on a steady state segment, showing urea and NOx emissions interactions

When driven on the NEDC, in the laboratory or on the track, the tested vehicle never exceeded 2250 rpm, and the throttle position never got beyond 57% (Figure 6). The RDE trip has therefore been split into 2 parts: one part that include all the operating points within the NEDC (All operating points with throttle position <57%, and engine speed <2250 rpm, labelled as “RDE trip inside NEDC”), and another part with all the remaining operating points “RDE trip outside NEDC” (Table 3).

	CO ₂ (g/km)	urea injection (g/km)	NOx emissions (mg/km)	EGR average rate (%)
RDE trip outside NEDC	310	2.49	1113	0.7%
RDE trip inside NEDC	108	0.48	301	16.0%

Table 3: urea dosage versus NOx emissions for the Peugeot 2008 tested

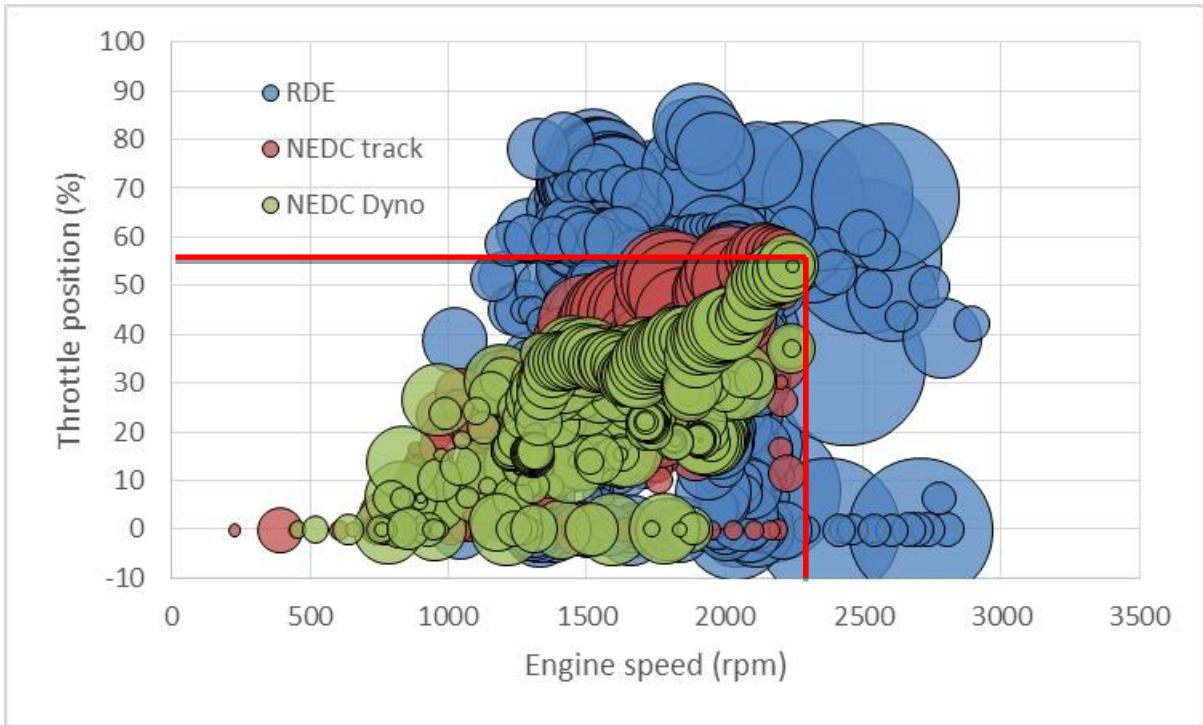


Figure 6: Urea injection time (proportional to bubble size) versus throttle position and engine speed

Closing fully the EGR when not under NEDC operating point can probably not be only explained by the gas dynamics within the engine, and likely is a deliberate choice not to alter the engine performance when outside of NEDC driving conditions.

When comparing the RDE operating points within the NEDC operating points with the actual NEDC results in the lab and on the track, the difference in urea injection is substantial, so are the NOx emissions in RDE drive (Figure 7). Most of the high NOx emission events are only partially treated on the RDE drive, showing a lack of urea injection or a sizing issue of the SCR that is not able to post treat the vast amount of NOx emitted under more demanding circumstances under normal driving.

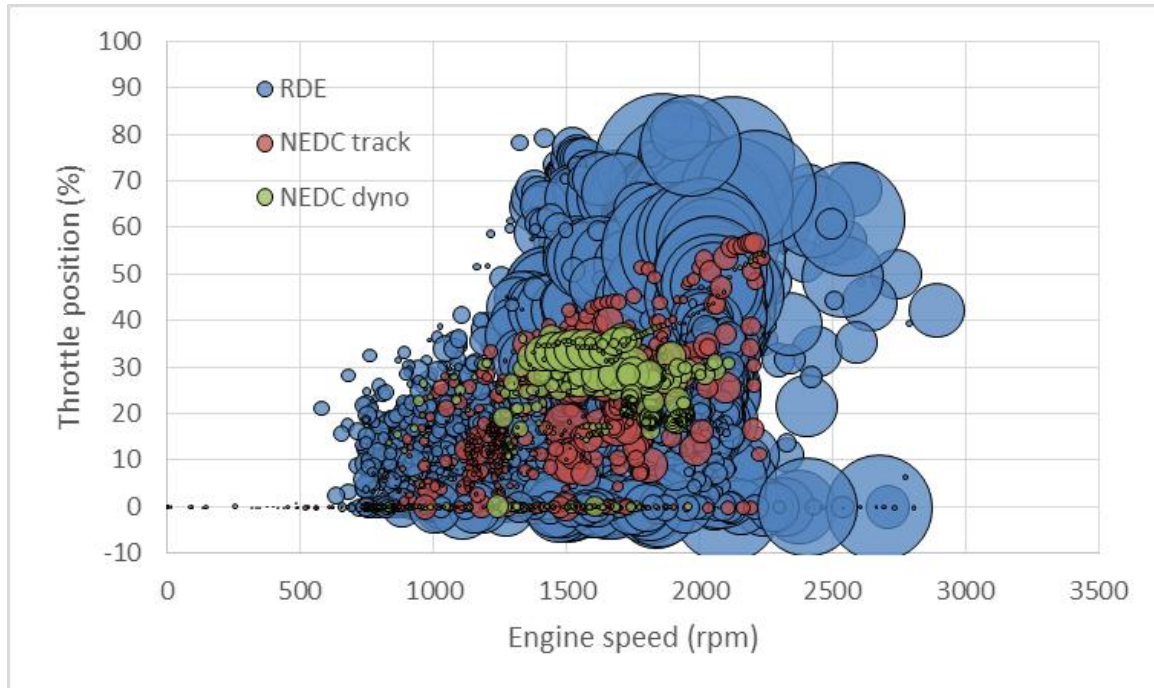


Figure 7: NOx emissions (proportional bubble size) displayed on an engine speed versus throttle position map

Such behavior of the SCR system highlights the fact that this vehicle has sized the post treatment capabilities of the vehicle on the NEDC needs, largely ignoring NOx emissions occurring under more demanding driving conditions. Such performance has nevertheless been classified as not suspicious by the Commission set-up in France to check 100 vehicles following the VW scandal.

2. Vehicle 2, Opel Insignia: Strategy to mitigate NOx emissions during the NEDC raises questions

The car tested (an Opel Insignia 2.0 CdtiEcoFlex) is fitted with SCR and EGR technologies that are used quite differently from Vehicle 1. The car's NOx emissions skyrocketed during the NEDC on the track, from 40mg/km in the laboratory to almost 200mg/km during a similar drive on the track (Table 4).

	CO ₂ (g/km)	urea injection (g/km)	NOx emissions (mg/km)	EGR average rate (%)
Official Type approval value	124	NA	27	NA
Laboratory test	157	1.06	40	40.9%
NEDC on test track	189	0.98	198	34.1%
RDE trip	151	0.92	121	32.4%

Table 4: Summary values for the Opel Insignia; NOx and CO₂ emissions on the test track raises questions about the car's calibration.

When looking at the NOx emissions second by second, it appears that on-track NEDC NOx emissions exceed Laboratory NOx emissions just after 210 seconds of the 1200 seconds of the NEDC test (Figure 8), with a uniform exceedance distributed across the whole cycle. Explaining why NOx emissions over the NEDC track test are so high is challenging, and requires looking at several sensor signals.

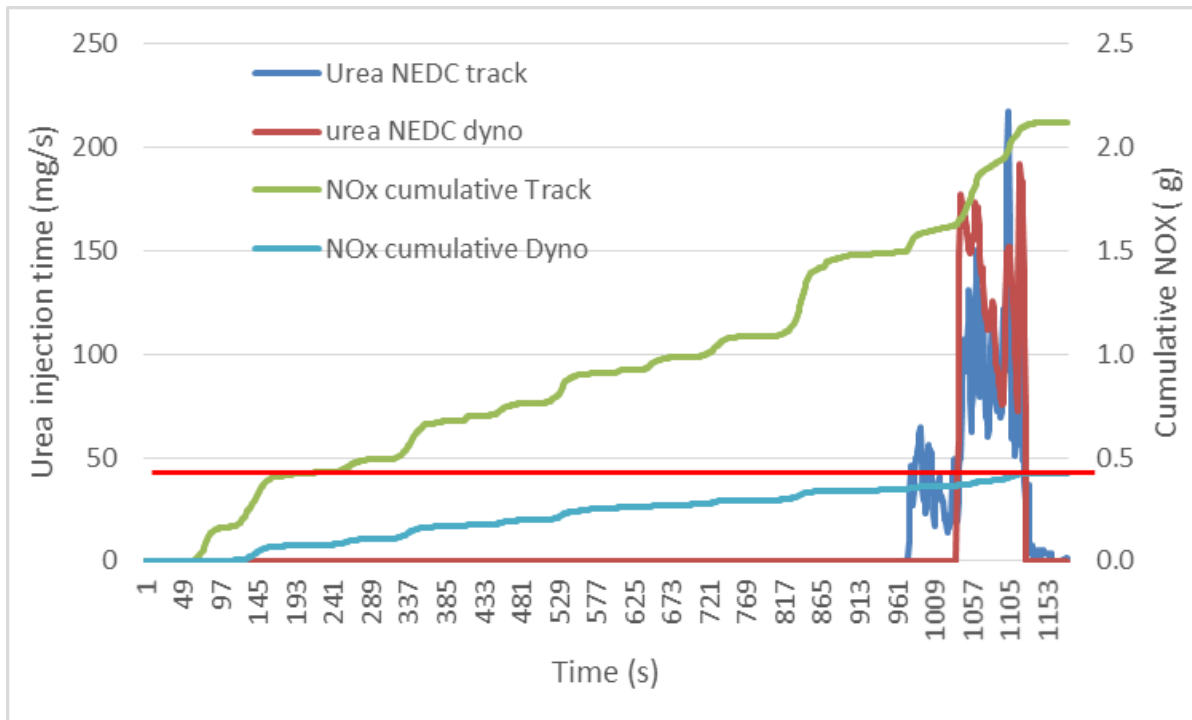


Figure 8: Cumulative NOx emissions on the NEDC, on the laboratory and the track, together with Urea injection time

Why are NOx emissions so much different in the lab and on the track pose questions about the vehicle emission control system calibration. Looking at the specific instrumentation fitted to the vehicle, there are no clear explanation of what happened to the vehicle to lead to such high level of NOx emissions.

SCR behavior during NEDC tests

Urea injection is barely used on the NEDCs driven, only used very late on the extra urban cycle (Figure 8). Over this short time interval, almost the same quantity of urea is injected compared with vehicle#1 over a much longer time period. Such late urea injection might be due to exhaust gas temperature not reaching the required value in the early part of the cold NEDC. Light off temperatures for the SCR seem to be reached earlier on the track, allowing for an earlier urea injection to help reduce NOx. This nonetheless does not seem to have a substantial impact on tailpipe NOx emissions that exceeds 2 g over the 11km drive.

EGR behavior during NEDC tests

EGR opening rate have an inconsistent behavior on the track; the 2 NEDCs performed on the track (and averaged) are not really consistent and quite far apart from the NEDC laboratory test (Figure 9). Overall, the average EGR opening rate is quite high, especially for a high pressure system. This seems to indicate that the Opel relies mostly on EGR to control NOx emissions, using high rates of gas recirculation into the inlet.

EGR opening rates has been particularly looked upon when the vehicle is moving, with speed above 2km/h. Vehicle stationary points were disregarded as the engine is usually switched off, but EGR position can be different according to our test results. Some substantial differences can be noticed, especially in the first urban cycle that can be mainly attributed to the engine speed and Stop & Start system behaving differently in the lab and on the track.

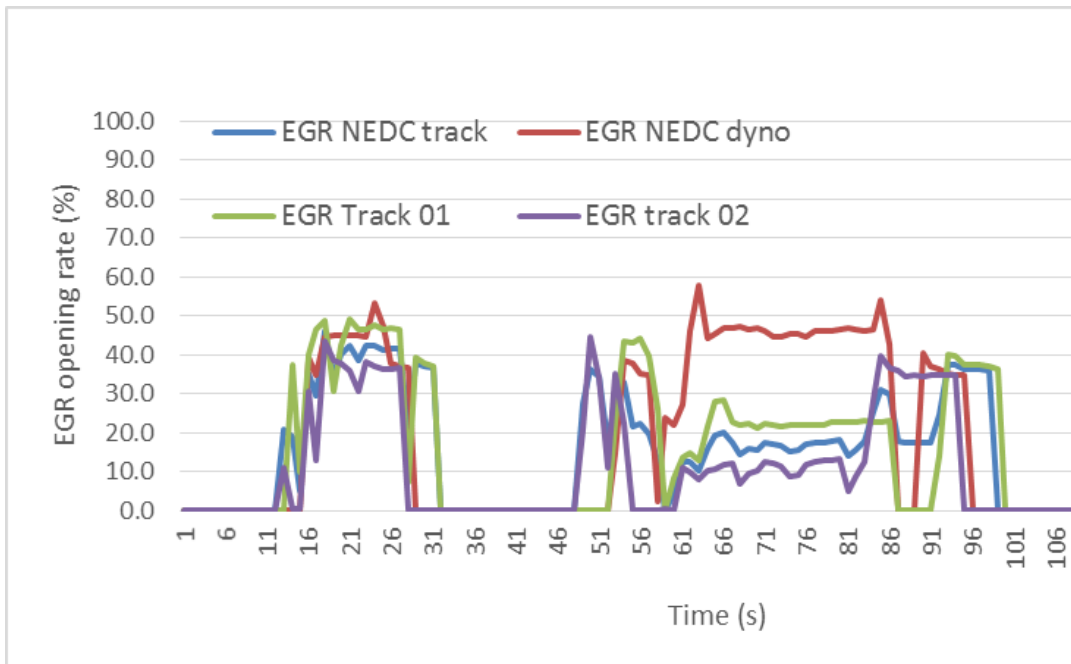


Figure 9: EGR opening rates on the 100 first seconds of the NEDCs performed on the dynamometer and on the track

Engine speed

When looking into some of the engine operation to try and explain this huge gap between laboratory and track NOx emissions, it can be noted that the stop and start system behaves differently on the track and in the lab. The engine stops during the first few stationary operation points during the NEDC performed in the laboratory, whereas it is idling on the track (Figure 10). When stopped, the engine does not create any exhaust gases, and the after treatment systems temperature is not altered by the exhaust flow which, at idling, can cool down the filters.

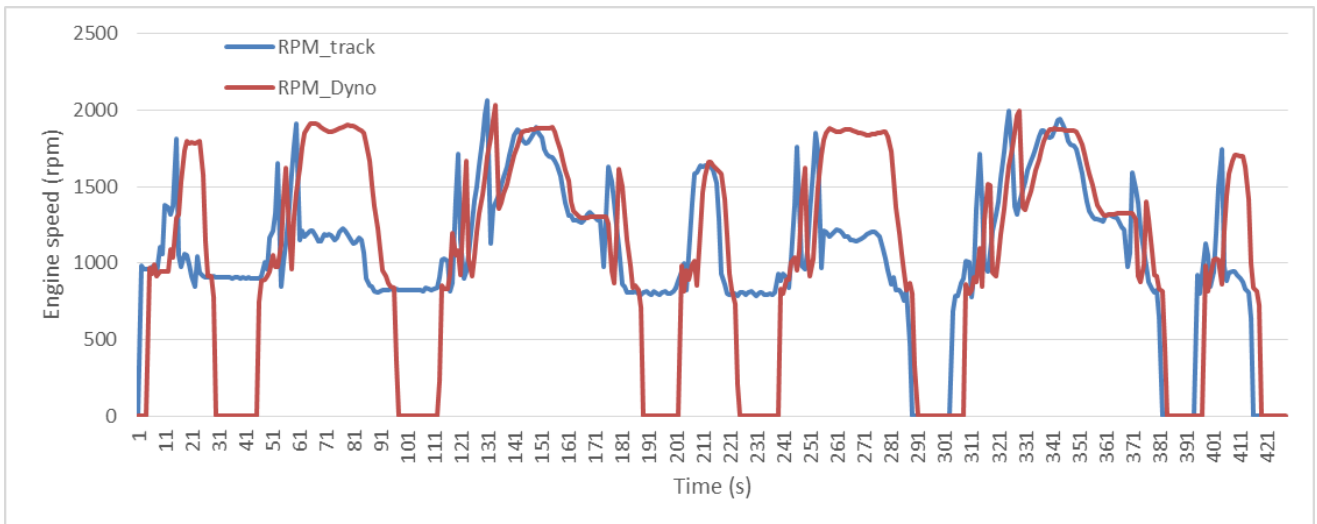


Figure 10: Engine speed on the first 400 seconds of the NEDC, on the track and on the chassis dynamometer.

Overall, the parameters looked after can explain some NOx differences in part of the NEDC, but no explanation can be found for the continuous and systematic gap that opens over the course of the NEDCs run in the lab and on the track.

Contacted over the matter, GM could not find any explanation either for the reasons behind this difference. Some of their views included an abnormality of the engine load parameter (taken from the

CAN bus and which indeed showed a strange behavior for some operating points, indicating this signal cannot easily be interpreted).

The differences in CO₂ emissions could also not be explained by T&E nor by GM. Even though the NEDC on the track has more transient, throttle position never exceeds 45% showing the limited power demand of the NEDC (Figure 11), even with the car that has an extra load on-board, with the PEMS and co-driver needed to perform the NEDCs on the test track.

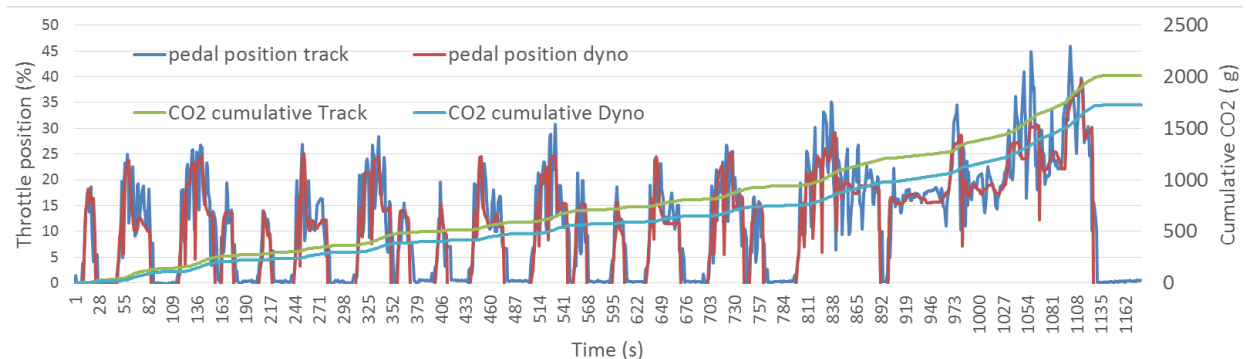


Figure 11: Cumulative CO₂ and pedal for the dyno and track NEDCs.

RDE test

When looking at the RDE drive, the results are much better than the NEDC on the test track, which is surprising, with NO_x emissions just reaching 120mg/km. That would make the vehicle pass the RDE test as proposed by the Commission, under the drive performed here. The driving style seems to be not demanding for a 170hp engine, and the driver never had to accelerate more than 62% of the throttle pedal, which still leave the top third of engine performance not monitored. The average $v^*a(pos)$ does not exceed 5 m²/s³ on the motorway section, far below the dynamic boundary conditions defined in the RDE legal text.

When compared with vehicle #1, vehicle #2 has been driven in a less demanding way, because of the vehicle specifications, and maybe also because of driver's behavior (Figure 12). Both vehicle were driven on the same route, with similar ambient conditions, with vehicle #1 average speed slightly higher than vehicle#2 (45.2km/h average versus 43.5km/h)

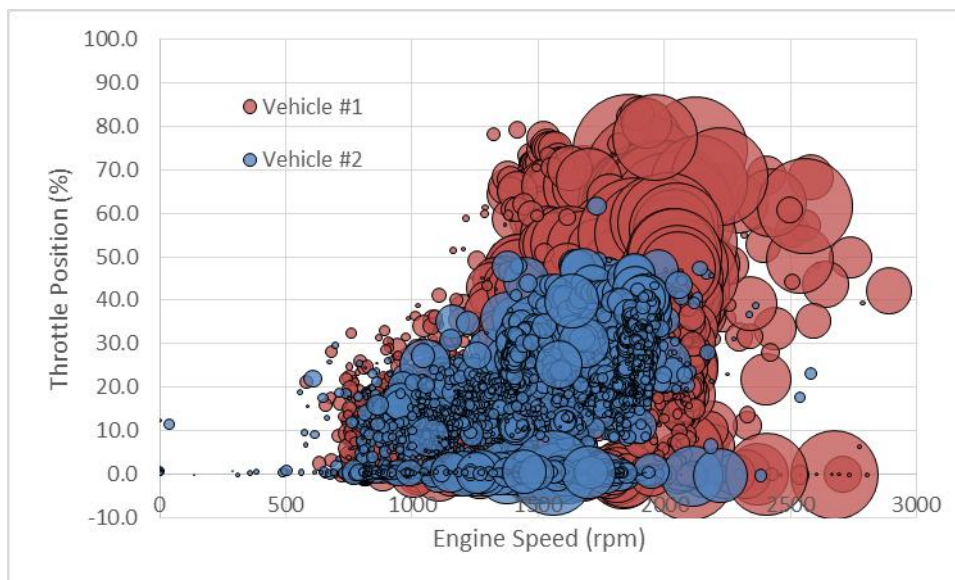


Figure12: RDE trip operating points for both vehicle tested (bubble size being instantaneous NO_x emissions)

Tests comparison

When shown on the same figure, all tests performed on the Opel seem to have been driven in rather similar driving conditions. The RDE test was pretty conservative and most of the time has been spent in non-demanding operation point (Figure 13).

When looking at the instantaneous NO_x emissions, only the lab NEDC was able to deliver low NO_x emissions over all driving conditions encountered during the test. All other tests showing much higher NO_x emissions under most operating conditions.

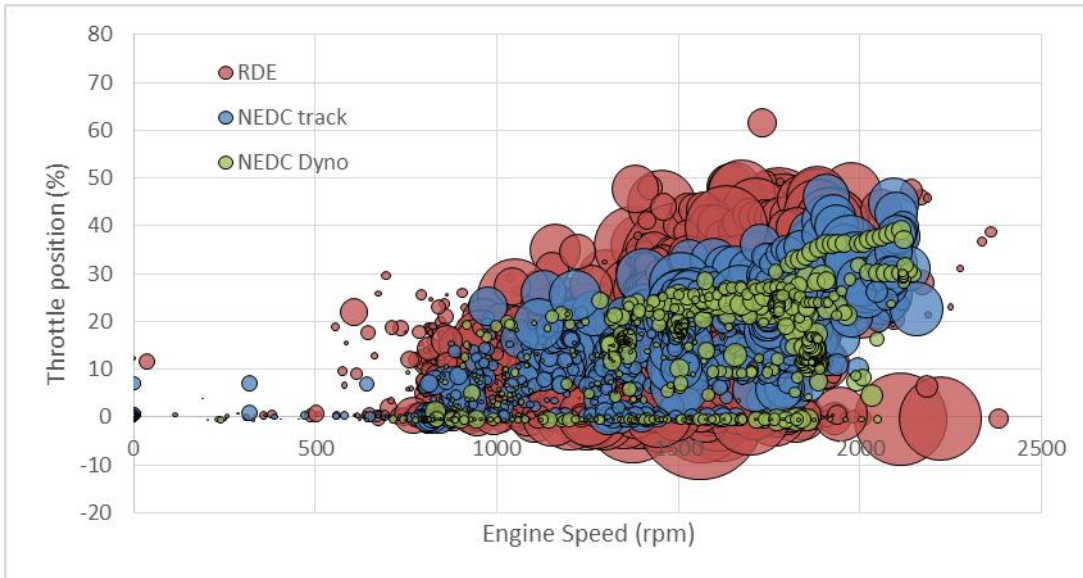


Figure 13: Instantaneous NO_x emissions (bubble size) for NEDC on lab, NEDC on track and RDE tests

Such a disparity in NO_x emissions is, at this stage, unexplainable, and further investigation from third parties, preferably official bodies, should be pursued in order to shed some light on such different behavior between the lab and other operating conditions.

Even though less visible than for NO_x, CO₂ emissions seem to be equally optimized for the laboratory conditions, especially for the low rpms, low throttle positions area of the engine map (Figure 14).

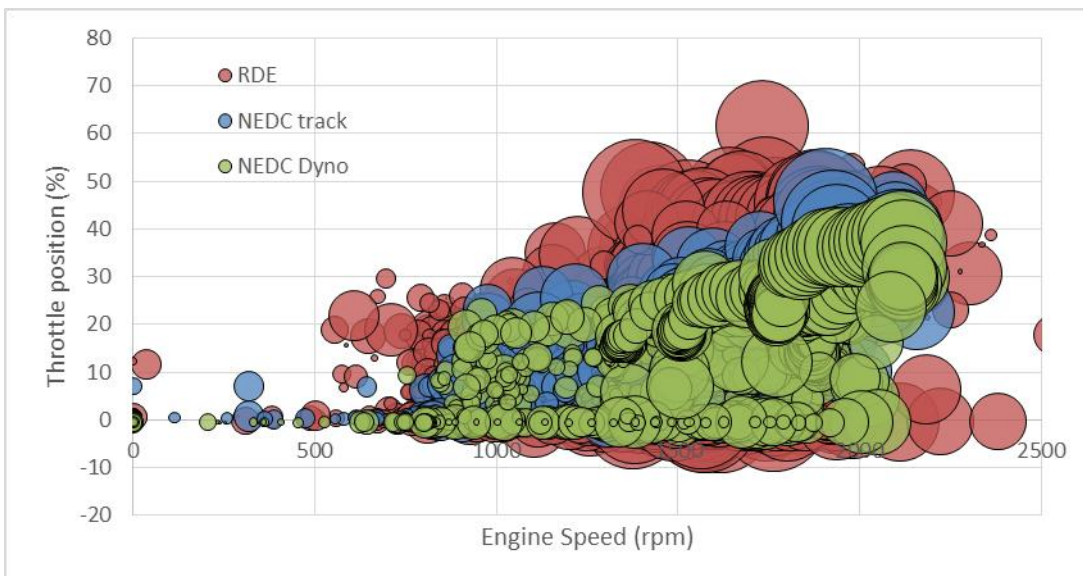


Figure 14: Instantaneous CO₂ (bubble size) on the throttle position versus engine speed engine map

Conclusion

Measuring not only emissions from the exhaust, but also the operation of emission control system is a complex and expensive process for which NGOs have limited resources. Nevertheless, two Euro 6 diesel cars have been tested and instrumented in order to show emissions and operation of the emission control devices under different testing conditions. Results show that emission control systems are operative when tested under type approval conditions, and also show questionable behaviors when tested on a test track or on the road.

The Peugeot 2008 showed lower urea injection time when tested on open roads, and no operation of the EGR when outside of the NEDC operating conditions, together with much higher NO_x emissions under those more demanding engine operation points. The SCR is used intensively, though urea is under dosed in order to make sure that the urea tank is only filled during vehicle maintenance operation (Assemblée Nationale, 2016).

The Opel is performing well on the road, but the RDE journey performed in this test campaign was not very demanding for such a high powered vehicle, and the vehicle has not been driven in an aggressive way. NO_x and CO₂ emissions on the NEDC on the test track triggers questions on the vehicle operation. The average EGR rate is lower and the stop and start was not operational on the test track, but it remains unclear whether this could explain the wide differences in exhaust emissions.

In European legislation, software does not need to be declared or specified during the type approval process. The vast majority of vehicle's hardware equipment need to be type approved. With the key role played by computer controlled devices in modern vehicles, there is today a need to also declare software algorithms to authorities in order to make sure vehicles are performing as expected according to the legal obligations. If software codes would need be released during type approval, then authorities need to strengthen their capability to closely monitor the operation of emission control systems.

Instrumenting vehicles in order to find out the use of defeat devices is tedious, expensive and resource intensive. To the author's knowledge, no type approval authorities have ever carried such investigation by instrumenting emission control systems to understand its operation that would nevertheless be necessary in order to ensure that the legislation is respected around Europe.

When applied with not to exceed limits in 2017, the new RDE requirements will hopefully solve most of the NO_x emissions exceedances highlighted in this paper; but in the meantime, vehicle are emitting vast amounts of NO_x emissions whilst not using the emission control systems to their full potential. Once RDE is in place, a close look at ammonia slip would also be required on vehicle that are fitted with an SCR. OEMs are likely to inject bigger quantities of urea to lower the NO_x emissions, running the risk of Ammonia passing by the SCR and released in the atmosphere. A problem should not be solved by creating another one.

Acknowledgments

The authors would like to thank the Life+ Clean Air project and the European Climate Foundation for funding the tests and are grateful to Idiada for carrying the tests and answering all questions related to the vehicles tested and the instrumentation fitted.

References

- AECC, FEV(2015), Potential for Euro 6 Passenger Cars with SCR to meet RDE Requirements, 36th International Vienna Motor Symposium. <http://www.aecc.eu/content/pdf/150507%20FEV-AECC%20paper%20Potential%20for%20Euro%206%20Passenger%20Cars%20with%20SCR%20to%20meet%20RDE.pdf>
- Assemblée Nationale (2016), Mission d'information sur l'offre automobile française dans une approche industrielle, énergétique et fiscale, Audition de M. Gilles Le Borgne, directeur de la la recherche et du développement, membre du comité exécutif de PSA Peugeot Citroën, http://videos.assemblee-nationale.fr/video.3795832_56fa8bb322856.offre-automobile-francaise--m-gilles-le-borgne-psa-peugeot-citroen-29-mars-2016

- Carslaw et al. (2011). Recent evidence concerning higher NOX emissions from passenger cars and light duty vehicles. *Journal of Atmospheric Environment* 45 (2011) 7053-7063.
- EU JRC. (2010) Analyzing on-road emissions of light-duty vehicles with Portable Emission Measurement Systems (PEMS), JRC Scientific and Technical Reports.
- ICCT (2014) Real World Exhaust Emissions from Modern Diesel Cars, <http://www.theicct.org/real-world-emissions-diesel-cars>

An assessment of present and future competitiveness of electric commercial vans

Pierre CAMILLERI* & Laetitia DABLANC*

*IFSTTAR, University of Paris-Est, 77447 Marne la Vallée, France

Email: pierre.camilleri@ifsttar.fr

Abstract

As electric vehicles appear as a potential solution for cleaner deliveries, several constraints affect the attractiveness of electric light commercial vehicles (eLCVs). Our research aims at identifying these constraints as well as quantifying their respective weight.

We investigate two types of constraints: operational and economic. Operational constraints determine if an electric vehicle is suitable for a given use; for example, the limited range of operation due to the necessity to recharge the battery. Economic performance, which we examine through Total Cost of Ownership (TCO) computations for electric and conventional vehicles, sheds light upon the trade-offs faced by business users when they have to choose between several technologies. We then present the results of a disaggregated constraints analysis made on a French database about light commercial vehicles, which assesses the proportion of vehicles that could be replaced by electric ones, and at what costs.

This study shows that, today, eLCVs are competitive for some specific uses, but do not cover the needs of every freight transport operator. Our analysis also shows that even if fuel prices remain low and financial incentives decline, the competitiveness of electric vehicles could grow in the future.

Key-words: *electric vehicles, light commercial vehicles, constraints analysis, total cost of ownership*

Introduction

The environmental impact of light commercial vehicles is high and freight transport, which represents a non-negligible proportion of road traffic, contributes significantly to the urban pollution – even more so than its mere physical presence in the streets, as shown by Dablanç (2008).

The use of alternative fuels brings good prospects for a more sustainable transport. In particular, battery electric vehicles raise a growing interest (Hanke et al. 2014), even if other alternative fuels are contenders. The environmental performance of electric vehicles is promising. Moreover, it raises interesting opportunities in interaction with the energy system and renewable energies (Held and Baumann 2011; Van Vliet et al. 2011; Helmers and Marx 2012).

Although electric vehicles have existed for more than a century, the last decade has witnessed a new enthusiasm, driven by the lithium-ion battery technology. Numerous carmakers have brought out several models, and new competitors have entered the market.

Light commercial vehicles (LCVs) seem to be good candidates to be replaced by electric vehicles, as most of them are used in built-up areas (IFEU 2012; Taefi et al. 2015). An urban use of LCVs, by freight companies for instance, seems particularly relevant (Lee et al. 2013; Macharis et al. 2013; CGDD 2014), since:

- They are driven at a low average speed.
- Driving conditions impose numerous slowdowns and stops. In these conditions, electric vehicles may take better advantage of regenerative braking.
- Some delivery companies drive the same route every day.
- The driven distances may be relatively short.
- The frequent use of the vehicle allows a better profitability.
- Vehicles may return to company's garage at the end of operation.

- Companies may benefit from a positive image.

It is interesting to notice that already in 1992, Brunel and Perillo(1992) identified business users as relevant early adopters for electric vehicles. However, the sales of Electric Light Commercial Vehicles (eLCVs) remain marginal in Europe, including in countries offering substantial financial incentives. In France for instance, despite a grant of 6300€ for the purchase of an electric vehicle, the market share of eLCVs in 2014 reached only 1.21%. There has been zero growth between the first semesters of 2014 and 2015 unlike the market for private cars. In Norway, a leading country in electromobility, eLCV market share is 1.87%, far behind that of passenger cars.

How can we explain this apparent lack of attractiveness? Is the LCV market an actual fertile ground for the development of electromobility?

The article is built as follows: in part 1, we discuss the methodology we use and present the database we worked with. In part 2, we examine and discuss the state of the art of operational and economic performance of electric light commercial vehicles. Part 3 looks at TCO computations for light commercial vehicles, and presents the numeric assumptions used for our computations. Our constraints analysis' results are exposed in part 4. Finally, we discuss the study's limitations in part 5, and conclude.

1. Objectives and methodology

The aim of this study is to quantify the impacts of operational and economic constraints of electric light commercial vehicles on business-type mobility. We put a special attention on freight transport operators. We assess the performance of vehicles currently on the market as well as the projected performance of vehicles in the future, taking into account expected rapid technological improvements. In this way, while not providing detailed market forecasts, we question the market development potential for electric commercial vehicles.

Approach

Our research relies on an agent-based disaggregated study. We do not target a comprehensive socio-economic evaluation. We investigate Light Commercial Vehicles (LCVs), i.e. commercial vehicles up to 3.5 ton gross weight. This corresponds to the N1 category of the European general classification of vehicle categories. The quantitative study will be limited to small vans, which we define as LCVs of less than 2.5 ton gross weight. This category is a rather common one within the car manufacturing industry, corresponding for instance to the market segment of the Renault Kangoo model.

We chose to compare conventional commercial vehicles (the most widely used internal combustion engine, or ICE vehicle), to the lithium-ion electric vehicles, mentioned as eLCV (for electric Light Commercial Vehicles) in the rest of the article. Switching from ICE to eLCV demands some operational adaptations that we will explore.

The spatial scale of our research is the use of commercial vehicles within France.

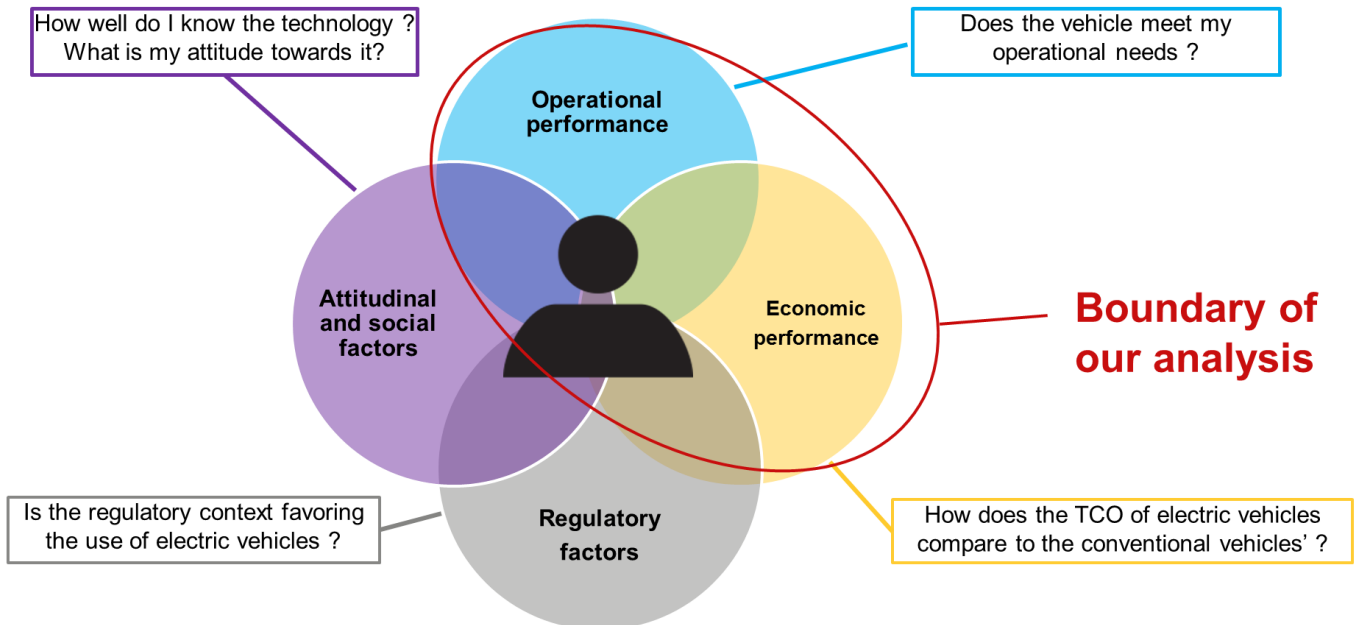


Figure 1. Schematic representation of the topics investigated (based on FREVUE project success factors (Nesterova et al. 2013))

Figure 1 presents four key factors (and briefly, some interrogations they raise) that impact the choice of a vehicle user to purchase an electric car. The choice of factors was based on Nesterova et al. (2013). We merged technical and operational factors. As shown on Figure 1, we only look at the economic and operational performances. Regulations vary a lot from one city to another, and they are difficult to take into account for a quantitative analysis at the scale of France. Cognitive perceptions cannot be quantified within a database either, and attitudinal and social factors will be researched further through interviews, and presented in a follow-up paper.

The uses of commercial vehicles are numerous and diverse. To comprehend this diversity, we started our research with a global understanding of the economic and operational performances of the lithium-ion technology. We explored constraints and opportunities of eLCV through a literature review and state of the art, as well as preliminary interviews with several companies already operating them.

Economic performance is investigated through computations of Total Cost of Ownership (TCO). We use the Present Net Value method of computation for life costs analyses, presented for example in Tim Mearig et al. (1999):

$$PV = A_t \cdot \frac{1}{(1 + d)^t}$$

With:

PV : Present Value

A_t : Amount of costs at year t

d : Real discount rate

t : Time, in number of years

TCO can be computed over two different study periods: over the lifetime of the vehicle (with no residual value for the vehicle), or over a given length of time (the vehicle still has a residual value at the end of this period). The electric mobility system can be broken down to three independent systems, namely the vehicle without battery, the battery, and the charging infrastructure. As each has its own life cycle, we chose to make the analysis on a given period, which lasts four years. We took a real discount rate of 7%.

Nesbitt and Sperling (1998) had shown that the selection of a type of vehicle was largely driven by purchase costs, which is also the cost difference amongst vehicles which is the easiest to estimate. According to (OVE) cited in Boutueil (2015), more comprehensive assessments of the real costs, which take into account maintenance costs, fuel costs, tax expenses and vehicle resale value, are becoming more common. Though companies do not always have a precise knowledge of their costs, we also

want to investigate how they are impacted if they switch to electric vehicles. Therefore, TCO comparisons seem to be a good method for the economic performance valuation.

Then, we tried to quantify how LCVs are impacted by the identified constraints with a *constraints analysis*. It is a disaggregated approach, applied on a database about uses of conventional LCVs. For each entry, we apply specific criteria to determine if the current vehicle could be replaced by an electric one, or in the words of Windisch(2014), if the use is *EV-qualifying*. If it is the case, we examine what would be the TCO comparison for this given use between conventional and electric vehicles. We obtain the proportion of vehicles that are impacted by one constraint or another. We can cross operational and economic performances. The same approach can be found for private car users, with a comprehensive literature review, in Windisch(2014).

Our analysis is not a market forecast: first, we do not look at all the constraints (for example, as mentioned earlier, cognitive and regulatory factors are left apart); non-monetary features are mentioned, but not integrated into the TCO computations. Taking only our indicators as market predictors would be strongly biased. TCO has its limitations, as it implies that agents have a perfect rational behavior. However, as stated for example in Nesbitt and Sperling(1998), companies do not always know precisely the cost structure of their vehicle fleet. In this article, or else in other words in Crane (1996), suitability and experience with the vehicle and technology are presented as two other important factors for pre-selection. Boutueil(2015) also underlines the complexity of decision-making processes for car fleet acquisition. Despite its drawbacks however, the constraints analysis gives a glimpse on the choices that are to be made by economic agents when faced with several technologies – ICE vehicles and EVs in the present case.

The disaggregated approach allows us to limit one drawback of TCO calculations when comparing two technologies, namely the difficulty of interpretation and generalization. Even when sensitivity analyses are conducted, it is not always easy to make a link between the results and the reality of LCV uses. This difficulty, and the fact that TCO varies from one country to another, justifies a multitude of computations, to confront several results with different assumptions. So we made our own assumptions for the TCO computations. The constraints analysis enables us to cross the operational and economic constraints and to have easier to interpret results: a result does not summarize a price difference between two technologies, but a price difference gradient for a big quantity of users.

We applied this methodology for two electric vehicles: a small van that is today on the market (based on the electric Renault Kangoo Z.E., on the market since 2011), and an imaginary comparable small van, projected in 2021 (in five years' time); and we compared both vehicles to a conventional small van (based on the non-electric Renault Kangoo), with only slight differences for 2021. All computations have been done under R.

Nature of the database

The database we worked with is a French "Survey on the uses of light commercial vehicles" ("Enquête sur l'utilisation de véhicules utilitaires légers"), conducted in 2010-2011 by the SOeS ("Service de l'Observatoire et des Statistiques"), the French environment ministry's statistics service. Light Commercial Vehicles are defined as vehicles of the N1 category according to the European general classification of vehicle categories. As such, private cars transformed into LCVs, usually by condemning the backseats and often for fiscal reasons, are integrated into the scope of the database.

The survey is vehicle-based and the answers are brought by the users (which are not always the owners) of the vehicles. Freight transport activities have been oversampled on purpose, to have a more accurate representation of this specific use. The same has been applied for recent vehicles, as they drive a great deal.

French LCVs represented approximately 5,800,000 vehicles in 2011. The database represents a subset of around 15,000 exploitable answers. We extracted from the database the vehicles of under 2.5 ton gross weight (small vans). As we are interested exclusively in business uses (as opposed to the use of commercial vehicles by households), we filtered vehicles that are only driven for private purposes, as well as the vehicles that were not driven at all in the year surveyed (2010). Thus, we used a database of around 7700 vehicles.

A statistical adjustment was conducted on the database by the SOeS, by a marginal calibration, relying on several variables (energy used, vehicle gross weight, vehicle main use and vehicle age) to

define 32 strata. 20 variables have been adjusted to make up for partial non-responses. The maximum partial non-response rates account for approximately 20% of the respondents, and affect the driven distance in 2010 and daily driven distance declarations, which are unfortunately important variables for our study. As a result, these two values are sometimes non consistent with each other, forcing to make choices on which one to choose.

The available data describes: the vehicles (gross weight and payload, year of purchase, age, etc.), the users (legal situation, main activity of the company they are working for, etc.), the driven distance (driven distance in 2010, typical daily driven distance, mileage at purchase, distribution of driven distances in city, on roads or highways, etc.) and the specific uses (frequency of uses, per distance brackets or weight of cargo brackets, category of use, etc.).

The size of the fleet of one company is unfortunately not available, although that would have been interesting to have. Geographic data is also missing, so there is no way to differentiate between a vehicle operated in the Paris region or in medium size cities, in the north or the south of France, etc.

To determine the annual driven distance for TCO calculations, we chose the declared driven distance in 2010 if the vehicle had been first sold in 2009 or before (as it is more accurate than what follows), else we multiplied the declared daily driven distance by 254, the number of working days in the year surveyed. In order not to have to cross the two most adjusted variables, which could give misleading results as mentioned before, we chose to stick to the previous choice when dealing with range constraints.

2. Barriers and opportunities for electric light commercial vehicles

Electric vans are not suited to every use that can be covered by ICE vehicles. Low driving range and long charging duration are considered in the literature the most restricting factors for the use of eLCVs (Frenzel 2016). However, eLCVs present other advantages compared with conventional LCVs. We discuss these barriers and opportunities in this section.

Range

Range is one of the most common constraints associated with battery electric vehicles. We make a distinction between the range that allows *most* everyday trips, which we define as covering the average daily driven distance; and the range that covers *all* the trips and that allows unchanged mobility patterns. It is clear that the latter is more demanding than the first one.

The range limitations are similar for the private use of a car by households. Based on GPS data, Pearre et al. (2011) show that even if most of the mobility needs are covered by electric vehicles, the possibility of adaptation (like charging during the trip / traveling by train / renting a car / sharing a car etc.) for a little amount of long trips in the year can multiply the potential for EVs (on the contrary, the absence of alternatives penalizes EVs heavily). To our knowledge, no such study has been conducted for business van users.

It is important to note that the range is not constant, because it varies with the consumption, dependent on many parameters, among which: (1) the driving profile, which depends both on the context (consumption in cities will be less than on highways), and the driving behavior (an aggressive driving style will consume more than a relaxed one); and (2) the temperature. The colder the weather is the higher the fuel consumption, compounded by the use of auxiliary equipment. The heater is by far the most consuming auxiliary component and is usually supplied by the power of the traction battery. Heater consumption depends on working time, not on distance (Helms et al. 2010). Solutions exist to minimize overconsumption and the lack of predictability of the range, for example an additional fuel heater or pre-heating scheduling as the vehicle is still charging (Taefi et al. 2015).

For regular delivery rounds, these seasonal range variations limit the maximal possible route to the minimal range (reached during winter, with the heater on, and with the worst driver). Frenzel (2016) shows that 18% of eLCV users who plan their trips try to exploit the range to its full extent.

Charging

Charging is another well-known constraint of using an electric vehicle. We will focus on charging facilities owned by companies, as it seems the most likely way companies deal with charging.

Indeed, in our opinion, it is unlikely that the use of electric vehicles develop if dependent on public

charging infrastructure. In case of a problem (such as a charging station is down or occupied by somebody else), there are few alternatives. Frenzel(2016)calculated that, for commercial uses,only 5% of planned trips actually recharge during the trip, which is a small but not insignificant share. This raises the interesting question of the role of public charging stations for professional users.

In all cases, today, charging takes place essentially overnight and on company grounds (Nesterova et al. 2013), and we make the assumption that it will stay so.

In this configuration, charging might raise several problems:

- Vehicles are generally immobilized for a long duration. The time it takes to charge a vehicle depends on the power of the stations. If a charging problem occurs during night for instance, the vehicle is not usable for an appreciable length of time.
- Availability of overnightparking facilities is not systematic.Browne et al. (2007)indicate that almost two thirds of LCVs are taken home by drivers overnight, and one third are parked off-street at premises, as a result of a study conducted in 2005 in the London boroughs of Southwark and Lewisham. We expect that ad-hoc acquisition of facilities is unlikely.Observations in Frenzel(2016) tend to confirm this, as early adopters have mostly “trip-profiles which allow usage without any adjustments or adaptations regarding technical conditions.”

Counter-examples exist: for example “La Petite Reine,” a French urban freight deliverycompany, which operates about 50 electric LCVs and 100 electric cargo bikes;also“Citylogin” (a collaboration of FM logistics and Mag.Di),which operates several electric LCVs and trucksin Rome (among other places). Both companies useproximity hubs where electric vehicles are parked overnight. However, it is not obvious that this solution can be applied to the majority of LCV users, and both examples are from companies trying out innovative logistics schemes.

- Implementationof charging stations is more expensive than the mere costs of the stations: extra costs can occur due to works, for example to bring electrical system up to standard.Companies willing to convert to electric vehicles often find themselves surprisedin this regard(Van Amburg and Pitkanen 2012). Fire safetyregulations can represent a significant financial burden too, especially when facilities are shared and considered as “establishment open to the public” (*Établissement recevant du public*, or ERP in French, such as underground car parks).

We will not discuss in details the possibility of charging the electric vehicles at the home of employees, but it seems to present several drawbacks:no guaranty that the installation of infrastructure is possible, the difficulty to assess the security of charge and to intervene in case of a flaw, the legal complexity to pay for electricity and infrastructure at the driver’s home; or the turnaround of employees.

Constraints linked to the novelty of the electric vehicle market

Today’s electric vehicle market is rather small and comparatively new (compared to the conventional vehicle market).Several drawbacks ensue:

- Existing eLCVmarket is relatively limited, especially for vans with higher payload (Frenzel 2016).
- Customer service and maintenancemay be rather poor(Nesterova et al. 2013). Companies are used to put local garagesin competition butcannot do so with electric vehicles, which can translate in an immediate monetary loss.
- Downtimes for repairs can be long, sometimes because of a lack of experience aboutelectric vehicles by car mechanics, which goesalong with the previous point.

More generally speaking, the novelty of the market generatesbig uncertainties, on the reliability of the technology in the long term, on the residual value of used vehicles... Prospects on improvements in the technology can also cause wait-and-see behaviors, and residual value deterioration due to obsolescence.

Other constraints

To what is described above, we can add some other potential problems: as the weight of battery and electric engine widely exceeds the weight of the internal combustion engine and fuel tank, payload can be affected; especially for the heaviest of LCVs (near 3.5t gross weight), whose overall weight cannotexceed 3.5t without changing their regulatory category. It looks like in Europe a regulatory

solution already exists for heavier trucks, which can benefit from a weight overrun of up to one ton compared with conventional ones, if they are equipped with a heavier technology using alternative energies (EU, 2015).

If reliability has been a recurring problem in the past, with the newest vehicles, it seems to be less so, because the vehicles are no longer trial products but mass-produced (Nesterova et al. 2013).

Opportunities

Electric LCVs are not only about new constraints. Opportunities can be numerous too.

- Electric vehicles are subsidized in many countries. In France today, each vehicle benefits from 6300€ from the state.
- They can be a mean of communication: the image associated with an electric vehicle is very positive. Brand image is one of the main drivers of the adoption of electric vehicles today (Boutueil 2015).
- They free the user from refueling the vehicle, which simplifies the shared use of the vehicle.
- Comfort of electric vehicles, due to less noise and vibrations (at low speeds), is very appreciable for drivers who use their vehicle intensively. EVs are more responsive when the vehicle starts, and they have no gearbox, which is valuable when activities include numerous stops and urban trips.
- Less maintenance overall is necessary compared with a conventional LCV.
- Paradoxically, conventional vehicles have their own uncertainties too: the fuel, which can be a big expenditure item, has a very unforeseeable price. EV users have more visibility on this expenditure item and are able to have a more resilient planning (McMorrin et al. 2012).

The constraints taken in our constraints analysis

We considered the following constraints in our quantitative analysis:

- A first range constraint for the vehicles which daily driven distance is higher than the calculated range (given the driving profile and the mean consumptions in city environments, on roads and on highways). We will call this constraint "insufficient range for daily use".

- A second constraint will be on the declared frequency of long trips. The constraint will be called "insufficient range for peak use". For the current eLCVs, we will consider that any trip exceeding 80 kilometers is a limiting factor. For the future eLCVs, the data is insufficient to do the same, as in the upper bracket for the frequency of trips is 150 kilometers and more. So when the range is more than 150 kilometers, we can't determine if the trip is feasible or not. Therefore, we chose to add a constraint called "Uncertainties on peak use".

- A third and last constraint affects the vehicles used for daily commute. For reasons exposed before, we consider that this is an important obstacle for the use of electric vehicles.

We warn that even if we try at the most to personalize the treatment of each vehicle, we are necessarily restricted by the availability of data in the database. Some assumptions necessarily average the real use.

One example is the number of working days: some professions use the vehicle more than the 254 working days used in the computations, and this affects greatly the economic results. For example, post activities can use the vehicle more than 300 days a year (Infini-drive, 2015), but this will not be taken into account in our analysis, the number of working days being fixed at 254 for every vehicle.

To conclude this section, we see that the use of electric vehicle requires careful planning and anticipation. However, electric vehicles have also non-monetary benefits that can possibly outweigh disadvantages. The question of the TCO is an important arbitrator: if it costs more, how much (if any) are users ready to pay extra for the benefits of EVs? If on the contrary, eLCVs cost less, are the companies ready to shift their habits despite the complexity of the change? We do not answer these questions, raised only to underline the importance of the TCO difference between the two technologies, but we calculate these TCO for each vehicle of the database, in order to shed light upon the trade-offs

faced by users.

3. TCO computations and numerical assumptions

Several TCO analyses have been conducted to compare the costs of ICE and EVs, which range from small LCVs to medium sized trucks.

Lee et al. (2013), Van Amburg and Pitkanen(2012) and Davis and Figliozzi(2013) have investigated the US case for medium-sized trucks (around 7t gross weight). Lee et al. (2013) use a statistical distribution of numerical hypotheses to take into account uncertainty, and find (in the baseline) a TCO distribution around zero, which shows that electric vehicles might be competitive in some scenarios. Van Amburg and Pitkanen(2012) insist on the potentially surprising high costs that can occur for installation of infrastructure and the need to carefully plan in advance the deployment of further vehicles. Hidden costs linked to the infrastructure seem to affect large fleets in particular. Davis and Figliozzi(2013) use modeling and optimization to evaluate input assumptions for the TCO. The final conclusion is that even if at the time of the study, electric vehicles are not competitive in most scenarios, "it is highly plausible that a confluence of rising energy costs and falling battery costs will create an environment where EVs will prevail in most scenarios."

There are European studies as well. Lebeau et al. (2015) consider a wide range of different light commercial vehicles. TCO calculations are made for the Belgian market. In general, the results put electric vehicles between their diesel counterpart (cheaper) and their petrol counterpart (more expensive). In France, Crist (2012) studies the TCO and socio-economic impact of three vehicles, including one LCV (the Renault Kangoo). The research shows that TCO is more suited for a business rather than a private use, with almost comparable TCO between conventional and electric LCVs after only three years. However, assumptions are rather optimistic for the professional user given the range of the vehicle (90km/day for 260 days a year). It also finds unfavorable societal costs, with an additional cost over the vehicle life of almost 7000€.

Infini-drive (2015) makes a review of a French experimentation of small electric vans by La Poste (the French postal operator) and ERDF (network manager of electricity distribution in France). Almost 100 vehicles were tested for 20 months, in about 15 locations. The study focuses mainly on charging and infrastructure optimization, but real life TCO are computed as well. Three results caught our attention: a possible gain of 3 to 7% for mixed fleet optimization (i.e. use of both ICE and electric vehicles); an estimation of 3% savings made possible by charging optimization in the most favorable case; and as in Van Amburg and Pitkanen(2012), a high variability of infrastructure costs, that range from 5% to 15% of the vehicle TCO.

Some studies focused on companies. The Observatory of Company Vehicles (*Observatoire du Véhicule d'Entreprise*, (OVE2015)) presents a TCO study for France, mainly about conventional LCVs, but with a section about electric vehicles. At last, we can mention tools available online for businesses willing to calculate TCO within their own operational conditions: the tool from Van Amburg and Pitkanen(2012) where a user can enter their own data, or the I-Cvue decision support model (I-Cvue n.d.), which has preloaded data for several European countries and several car models, including LCVs, and which gives also other information, such as reduced CO₂ emissions for instance.

We can conclude from these studies that electric vehicles can be, according to the cases, in the same price range as ICE vehicles, or a bit more expensive. This applies to different countries and different sizes of LCVs or trucks. There is a general agreement over the following: the more intensive the use, the more competitive the electric vehicle. All in all, this seems to us a rather positive signal, as the lithium-ion electric vehicle market development seems to be in its early stages, even if we have to keep in mind that the current financial incentives will perhaps not last forever.

For each period of time (2016 and 2021), we investigate two equivalent LCVs, one with an ICE and one full electric with a lithium-ion battery. In **Erreur ! Source du renvoi introuvable.** and Table 2, we present the numerical assumptions taken for the computations. Sources and short discussions are presented after.

Vehicle Data	 Small ICE Van 2016	Small ICE Van 2020	 Small Van EV 2016	Small Van EV 2020
Purchase price (excluding VAT)¹	17450 €	17950 €	21850 €	20350 €
Incentives²	0	0	6300 €	3300 €
Battery Size³	-		22 kWh	40 kWh
Battery Rental (excluding VAT)⁴	-		From 79€/month (less than 10000km/year) to 106€/month (more than 20000km/year)	The same, with a quadratic interpolation for higher mileages
Infrastructure⁵	-		2500 € amortized on 8 years + 200€/year maintenance and supervision	
Mean consumption city⁶	7,4 L / 100 km		17,5 kWh/100km	
Mean consumption road⁶	6,4 L / 100 km		19,5kWh/100 km	
Mean consumpt. Highway⁶	7,4 L / 100 km		24 kWh/100km	
Worst heating power⁶	-		2.5 kW (energy consumption depends on time driven)	
Residual Value⁷	Identical in €			
Maintenance⁸	3,77c€/km		1,885c€/km	

Table 1. Numerical assumptions for the vehicle data

Contextual Data	Diesel	Electricity
Fuel prices in 2016 (excluding VAT) ⁹	84,88 c€/L	8,936 c€/kWh
Fuel prices in 2021 (excluding VAT) ⁹	84,88 c€/L	8,936 c€/kWh
Study period	4 years	
Discount rate	7%	
Number of working days ¹⁰	254	

Table 2. Numerical assumptions for the contextual data

Assumptions:

1. Purchase price: the small ICE van is inspired from Renault Kangoo Express ConfortdCi 90model, and the EV is based on the Renault Kangoo Z.E. Confort model. Assumptions for future projections are, that ICE will cost 500€ more due to more demanding air-pollution treatment devices, and that electric vehicles (without battery) will benefit from a decrease of 1500€ in purchase prices, thanks to economies of scale and technologic advances.
2. Incentives: 6300€ is the current bonus from the French administration for the purchase of an electric vehicle. Other subsidies exist from local governments, but they are different from one place to another, so we did not include them. Incentives cannot remain as high as they are today if the market takes off and the vehicle technology improves (Fearley et al. 2015), so our baseline's assumption is a 3000€ cut into the incentives by 2021.
3. EV battery sizes: for the current eLCVs, we take the battery size of the Kangoo Z.E. model. For the projected battery size, our baseline takes the more conservative battery's cost decrease of 6% from Nykvist and Nilsson (2015). From this, we assume that for the same price, we will have a progress of 80% in 10 years over the battery of the 2011-brought-out Kangoo Z.E., which results in a 40 kWh battery. This is in line with announcements that have been made by carmakers, even if there is no mention of the price (LesEchos.fr 2015).
4. EV battery rental: we base our analyses on a Renault-like battery rental business model. This has benefits and drawbacks. The main benefit is that we don't have to care about battery ageing, second life and residual value, which are all very uncertain. The major drawback is that we have to rely on the carmakers' outlooks. We have no visibility on their evolution nor on the factors which impact rental rates. Today's rental prices are based on Kangoo Z.E. prices, projected prices are the same for low driven distances, and we make a quadratic interpolation of today's prices to determine the rental for higher annual driven distances.
5. Infrastructure costs: Values have been taken in line with the order of magnitude given by our preliminary interviews.
6. Mean consumptions: for the conventional LCV, we corrected NEDC consumption in cities and on roads to account for real driving conditions. Based on findings of ICCT (2015), we increased them by 37%. Consumption on highway is assumed equal to consumption in cities. For eLCVs, we take the mean consumptions of Helms et al. (2010). When computing worst range, we assume a 10% increase of consumptions due to cold temperature, and take into account the heating consumption separately, based on data from Kavalchuk et al. (2015). We assume an 85% charging efficiency rate.
7. Residual values: they are a great unknown today. As the purchase price of electric vehicles is higher, and under the assumption of the same life span of electric and conventional vehicles, we could make the hypothesis that residual values will be greater for eLCVs than for conventional vehicles. However, residual values might be affected by obsolescence of the technology, and uncertainties on the ageing of the vehicle. By lack of evidence and of quantitative data, we choose to put residual values equal, in euros, for conventional and electric vehicles. So we do not have to take them into account in the comparison. For illustrative purposes, residual values in Figure 2 and Figure 3 are respectively 33.8% and

19.7% of the ICE purchase price to calculate vehicle depreciations.

8. Maintenance: The ICE maintenance costs are proportional to the driven distance. We make the assumption that it is constant over our study period. The value is an average of 28 declared real-use costs on (entretien-auto.com). Moreover, we assume savings of 50% of maintenance costs for electric vehicles, in accordance with Lee et al. (2013) and with our preliminary interviews.
9. Energy prices: in our baseline, we consider energy constant over the 10 next years. As many expect the fuel prices to raise in the future, this may be a conservative assumption. Changes in electricity prices are less crucial as the part of costs for electricity represents a more marginal proportion of the TCO. We take the fuel and electricity prices of January 2016 as baseline (MEEM 2016; SOeSn.d.).

Electricity costs are taken for off-peak hours, for the “blue rate” (*Tarif bleu*), which power is limited at 36 kW. This assumption suits better to small businesses than to big fleets. If it is necessary to switch from the “blue rate” to the “yellow rate” because of an increased need in power due to charging stations, extra-costs can be penalizing (920€/year according to Infiniti-drive (2015). This might encourage ‘smart’ recharge management.

10. The number of working days chosen is the number of working days of the year surveyed (2010). Even if we are well aware that the vehicles are not necessarily used every working day or on the contrary can be driven on non-working days, daily driven distances are computed as if it were the case.

No taxes and insurance differences have been taken into account, so we can leave them out for our comparison. Business users get important commercial discounts when they buy new vehicles. We do not take any commercial discount rate. This is the same as considering they are identical in euros for both vehicle technologies.

Several scenarios are investigated from this baseline.

4. Main results of the constraints analysis

As previously stated, this section will only cover the market of small vans (<2500kg gross weight). On Figures 2 and 3 the TCO for two specific vehicle uses are represented, for illustrative purposes. The first one illustrates a daily driven distance of around 50kilometers; the second one of 160kilometers a day.

Based on Figure 2, we can make the following statements:

- For small driven distances, the main expenditure item of the TCO is the vehicle’s depreciation. Therefore, the current 6300€ state incentives enable to have less depreciation on the electric vehicle than on the conventional one. This is still the case in 2021, despite the lower incentives, thanks to the purchase price decline.
- Electricity expenses are much lower than ICE fuel expenses. But as diesel prices are currently very low, electricity and rental expenses together exceed by far these fuel expenses.
- Maintenance cost savings are rather significant, as are infrastructure costs, and should not be neglected.
- All in all, TCO of conventional and electric vehicles are comparable in 2016, and eLCVs slightly more expensive in 2021 for moderate driven distances (which are the only ones which we consider as being covered by eLCVs today). If there is a 3000€ cut in incentives as in our baseline, tomorrow’s projected eLCVs may be more expensive than the current eLCVs for this user’s profile.

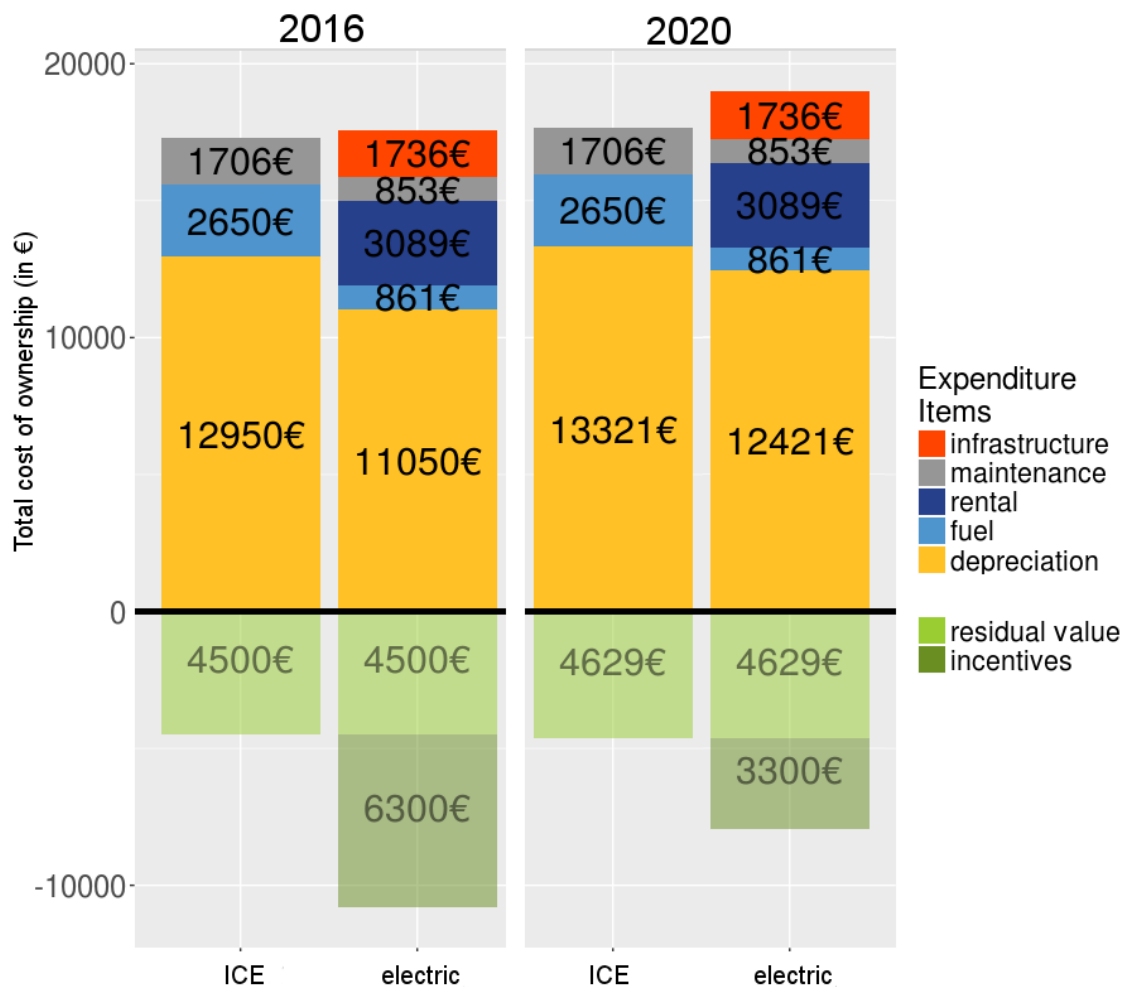


Figure 2. Current and projected TCO comparisons between electric and conventional LCVs in 2021, for a specific use, driving in average 50 kilometers a day.

Figure 3 represents the projected TCO for a user who drives 160 kilometers every day. The following can be said:

- Today's eLCVs have a range that doesn't fit this user's needs. However, the projected eLCVs will be adequate.
- Fuel costs represent a much more important proportion of the TCO than in the first case.
- With our assumptions, the electric vehicle is competitive with the conventional one in this case. However, we also see that without projected battery prices and if diesel prices remain as low as today, it may lead to smaller fixed costs and higher operational costs for eLCVs, even for higher mileages. Indeed, we can see that battery rental and electricity account for one third more than fuel expenses.

This being said, how many business users resemble the first user presented, and how many the second user?

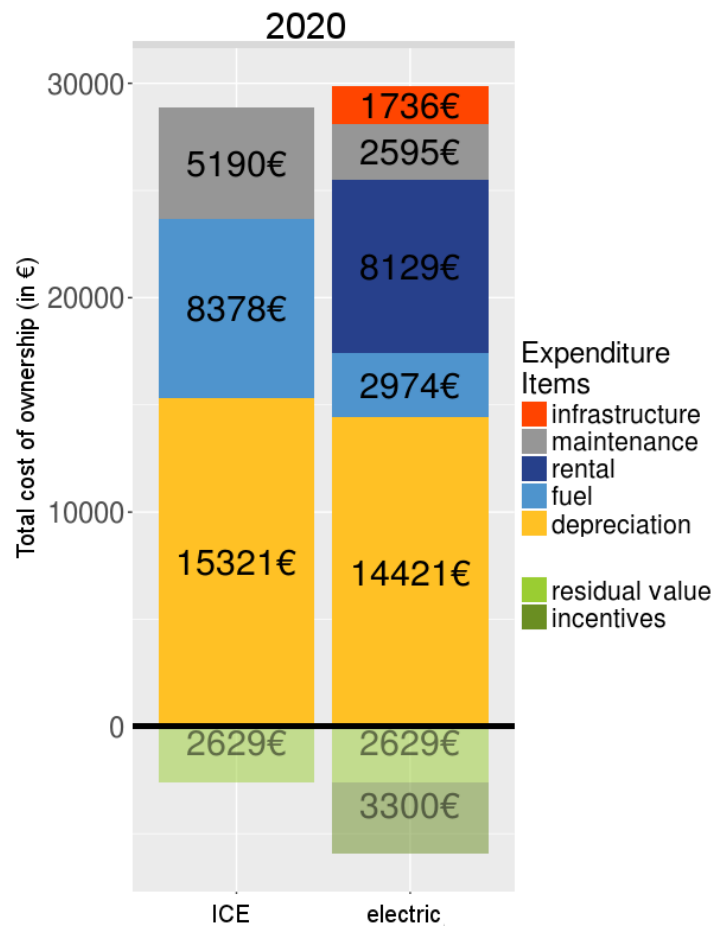


Figure 3. Projected TCO comparison between electric and conventional LCV in 2021, for a specific use, driving in average 160 kilometers a day.

The constraints analysis

Figures Figure 5 show the constraints analysis as we described it in the previous section, for today and for a 2021 projection. The sum of percentages does not always reach 100% due to rounding-off errors. For each, the first line represents the operational constraints and the second the distribution of TCO comparisons between EV and ICE. A positive TCO difference favors eLCVs. TCO differences are given by ranges of 50€. Results can be interpreted as follows: percentages in yellow have comparable TCO for conventional and electric LCVs, orange shades represent extra-costs for the use of an electric vehicle (the darker the greater the extra-costs).

In Figure 4, we identified 26% of the vehicles that are used for the drivers' commute. We consider this as a negative constraint, due to the difficulties to install charging infrastructure at the driver's home. When we look at the range issues, we see that more than 35% of them would be constrained by the use of electric vehicles, a majority of them on a regular basis, and a bit more than a third at least on a monthly basis. All in all, 38% of the vehicles seem to be EV-qualifying.

Among these EV-qualifying vehicles, a bit more than half (19% of the total) could be replaced by an electric vehicle at no additional costs, according to our computations. The other half would be penalized by around 50€ monthly extra-costs per vehicle.

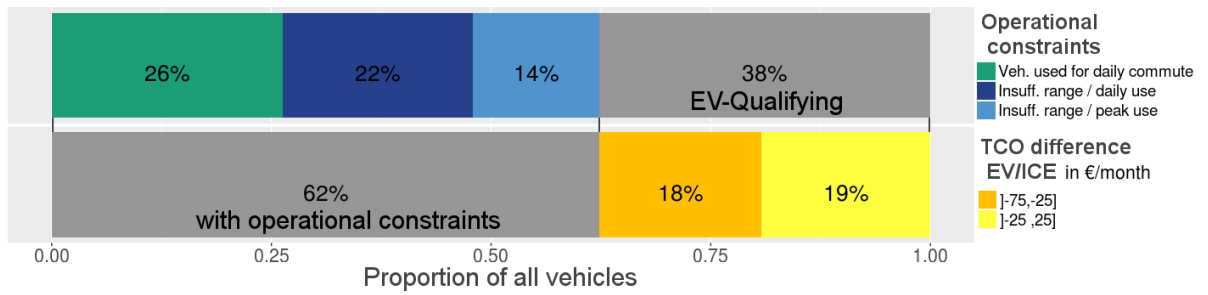


Figure 4. Constraints analysis for eLCVs compared to conventional LCVs, in 2016

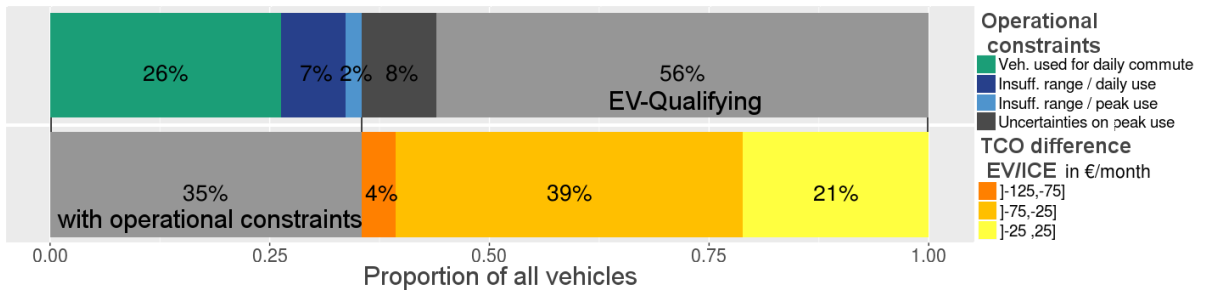


Figure 5. Projected constraints analysis for eLCVs compared to conventional LCVs, in 2021

In Figure 5, which represents the same analysis with our projected vehicles in 2021, we can see that the operational constraints are less stringent. The charging constraint remains identical, but the range constraint impacts only 7% of the vehicles in their daily use. From 2% to 10% of vehicles may have a range problem during peak uses, but the data we have don't allow us to decide. Indeed, 8% have a range of more than 150 kilometers, and all we know is that they make regularly trips of over 150 kilometers, but we do not have further details about the exact distance of these trips.

All in all, between 56% and 64% of vehicles could be electric without changing operators' organization.

Among these EV-qualifying vehicles, our pessimistic baseline assumptions give an extra-cost of more than 25€/month per vehicle for 43% of the total, and a comparable TCO for 21%.

5. Discussion

The important amount of operational constraints shows that today, electric vehicles are not appropriate for all commercial fleet operators, if we make the assumption that use patterns stay identical. Peak uses seem almost as constraining as average uses: this shows that it is important not to take into account only the average daily driven distance to assess the relevancy of electric vehicles. Peak uses, that we considered disqualifying, are peak trips made with at least one occurrence per month. We have no data on rarer events, so the constraint could be greater than identified here. On the contrary, it would be interesting to investigate mixed fleet uses – i.e. with vehicles of both technologies. Then, rare longer trips could be covered by conventional vehicles and would not stop the operational use of electric vehicles for a portion of the fleet. This would minimize the range constraint for peak uses.

Electric vans are still a bit more expensive in average than conventional ones. 19% of vehicles present comparable costs, which represents an important proportion, far more than the actual market shares. This is not surprising, as switching from one technology to another requires careful preparation, and a change in operational habits, which can discourage some operators. Moreover, these operators do not have a detailed knowledge of the technology and of its costs. Operators who value their image, have a specific environmental commitment or want to be at the leading edge of innovation, and/or have specific uses, are more inclined to be favorable to EVs. Moreover, with relatively moderate ranges (less than 80km in worst conditions for current LCVs), even if the vehicle's range apparently covers all the

needs of the user, the mere hypothetical possibility that they could need more range one day can prevent them from buying an electric vehicle (even if costs are comparable).

If we project ourselves into 2021, this cognitive barrier will be partly reduced as the average range potential grows. And even if diesel prices remain low and with a decrease in incentives, there is some potential for competitive electric vehicles. To specify this interpretation, a comprehensive sensitivity analysis is necessary, but is still in progress. Instead, Table 3 shows the variation in the potential market for EVs, depending on two varying parameters: fuel prices and fixed costs. The number presented is the proportion of vehicles for which operating an EV would cost as much or less than a conventional vehicle, the number in the parentheses represents the proportion that would potentially save money by operating an eLCV.

		Fuel prices scenarios (without VAT)		
		0.85€/L (base.)	1€/L	1.15€/L
Fixed costs scenarios	+1500 €	1% (0%)	8% (0%)	21% (1%)
	baseline	21% (0%)	34% (1%)	40% (9%)
	-1500 €	53% (2%)	55% (18%)	57% (29%)

Table 3. Potential for the economic competitiveness of eLCVs, according to two varying parameters: fuel prices and fixed costs. Numbers in the parentheses represent the proportion of electric vehicles saving more than 25€ per month and vehicle.

Fixed costs variations can be interpreted as one, or any combination, of the following factors:

- Different financial incentives (3300€ for the baseline, 1800€ or 4800€ incentives from the state, or other incentives such as local ones).
- Different purchase prices (if economies of scale are lower or higher than expected from the baseline for example).
- Different residual values than for conventional LCVs (to be weighted by the discount rate as the revenue is four years after the purchase).

In this table, we see that more optimistic assumptions (for the electric vehicle) give much more potential for the electric vehicle in 2021 than our baseline. Some scenarios give even a significant amount of vehicles which could lead to savings, which would certainly give a real boost to the EV market.

We can see that high fuel prices could make it possible to reduce the incentives without penalizing the eLCVs market's growth. If fuel prices remain low, the decrease in incentives would be possible without penalizing eLCVs, but with a constant potential (which is not inconsistent with a growing market). Lowering the amount of financial incentive too fast (from 6300€ in 2016 to 1800€ in 2021 for example) would impact the EV potential market very much. On the contrary, if we have a combination of increasing fuel prices and decreasing vehicle prices, we could see an actual breakthrough for the electric commercial vehicle market, even with cuts in subsidies.

All this brings a rather positive signal for electromobility in the freight transport business: if the financial incentives are carefully adapted to the economic context, there is a huge development potential. Still, there will be a certain amount of costs to absorb to be competitive without incentives. This will probably slow down the expansion of electric vehicles, but history gave us many examples of rapidly falling costs for new technologies, more rapidly than we assumed in this paper.

There are some limitations to our approach. First, we considered only one type of vehicle, whether for conventional or electric vehicles. This is a great restriction, as results might be different depending on the specific needs of each operator (one operator can favor volume while another can favor weight). This is even more penalizing for tomorrow's projections, as we could imagine a more diverse supply of electric vehicles: several battery sizes, but also several business models, with the battery either leased or sold.

Another limitation is that the vehicles we considered represent only a portion of all light commercial vehicles, as we didn't account for medium-sized and larger vans.

The constraints analysis is inevitably limited by the availability of data. That is why we tried to give a broader qualitative picture of constraints and opportunities associated to electric vehicles, which are important to keep in mind. Charging might be the real constraint of tomorrow, as batteries grow and as this constraint may remain the same in the future, unlike range. Charging difficulties are rather hard to account for given the available data of the database we are working on.

The quality of the results is also strongly linked to the quality of data, and partial adjustments made on the database might introduce some discrepancies.

Cognitive and regulatory factors have not been examined in this study, but can have great effects on the rise of freight transport electromobility.

Conclusion

Examining the potential market for electric vehicles in the freight sector is relevant when looking at the future sustainability of our communities. Light commercial vehicles are among the most rapidly expanding types of vehicles on roads, especially in urban areas. A significant proportion of them are used for freight and delivery activities, and this trend is growing as consumer demand for e-commerce and home deliveries is increasing at a fast rate in metropolitan areas around the world. Another interesting characteristic of the urban freight market is that, currently, the vehicles used are rather old, more so than in the longer haul freight sector. Freight commercial vehicles' environmental impact in terms of global (CO₂) and local (NO_x, particulate matters) emissions is therefore poor, and their share in total emissions is growing.

This study focused on the market development potential for small electric commercial vans. We were able to use a comprehensive database of light commercial vehicles in France with very detailed characteristics of their uses and users for year 2010. Current users and their operating attributes constituted the baseline of our analysis, which makes our research rather close to the reality of the current market. From that basis, and taking into account that our analysis misses important issues, as discussed in the methodology section, our results are - from a mostly economic point of view - somewhat positive towards the market potential of electric vans. Even if fuel prices in 2021 remain as low as they are today, which is a realistic assumption given that oil production continues to increase faster than oil demand, a rather small decrease in EV fixed costs (including purchase prices), which could be brought by several factors many of them being realistic today, could translate into a significant market potential for freight electric vans.

Acknowledgements

This research work was supported by the French Institute of Science and Technology for Transport, Development and Networks (IFSTTAR) and the MetroFreight VREF Centre of Excellence in the framework of a PhD research (supervised by Dr. Dablanç).

References

- Boutueil V (2015): Towards a sustainable mobility system : Leveraging corporate car fleets to foster innovations. Doctoral dissertation. University of Paris-Est.
- Browne M, Allen J, Woodburn A, Piotrowska M (2007): Literature review WM9: part II-light goods vehicles in urban areas.
- Brunel P, Perillo T (1992): La voiture propre. Econ Stat 258:89–94.
- CGDD (2014) : Les véhicules utilitaires légers : une bonne complémentarité avec les poids lourds. Le point sur. N°190. Retrieved from : http://www.statistiques.developpement-durable.gouv.fr/fileadmin/documents/Produits_editoriaux/Publications/Le_Point_Sur/2014/lps_190-vul.pdf. Accessed 20 Aug 2015
- Crane SS (1996): An empirical study of alternative fuel vehicle choice by commercial fleets: lessons in transportation choices, cost efficiency, and public agencies' organization. Doctoral dissertation. University of California Irvine

- Crist P (2012): Electric Vehicles Revisited. International Transport Forum Discussion Paper
- Dablanc L (2008): Urban goods movement and air quality policy and regulation issues in European cities. J Environ Law 20:245–266.
- Davis BA, Figliozzi MA (2013): A methodology to evaluate the competitiveness of electric delivery trucks. Transp Res Part E LogistTransp Rev 49:8–23.
- Entretien-auto.com : Statistiques du modèle RENAULT Kangoo. Retrieved from www.entretien-auto.com/statistiques_membres_modele.php?constructeur=2&nom=Kangoo. Accessed 27 Apr 2016
- EU (2015):EU directive 2015/719 of the European parliament and the council. Official journal of the European Union, n°58
- Fearnley N, Pfaffenbichler P, Figenbaum E, Jellinek R (2015): E-vehicle policies and incentives: assessment and recommendations. Compett deliverable D
- Frenzel I (2016): Who Are the Early Adopters of Electric Vehicles in Commercial Transport—A Description of Their Trip Patterns. In: Clausen U, Friedrich H, Thaller C, Geiger C (eds) Commercial Transport. Springer International Publishing, pp 115–128
- Hanke C, Hüelsmann M, Fornahl D (2014): Socio-Economic Aspects of Electric Vehicles: A Literature Review. In: Evolutionary Paths Towards the Mobility Patterns of the Future. Springer, pp 13–36
- Held M, Baumann M (2011): Assessment of the environmental impacts of electric vehicle concepts. In: Towards Life Cycle Sustainability Management. Springer, pp 535–546
- Helmers E, Marx P (2012) Electric cars: technical characteristics and environmental impacts. Environ SciEur 24:1–15.
- Helms H, Pehnt M, Lambrecht U, Liebich A (2010) Electric vehicle and plug-in hybrid energy efficiency and life cycle emissions. In: 18th International Symposium Transport and Air Pollution, Session. p 113
- ICCT (2015) From laboratory to road. A 2015 update of official and “real-world” fuel consumption and CO2 values for passenger cars in Europe. Retrieved from http://www.theicct.org/sites/default/files/publications/ICCT_LaboratoryToRoad_2015_Report_English.pdf. Accessed 23 Apr 2016
- I-Cvue Incentives for Cleaner Vehicles in Urban Europe - Decision support model. Retrieved from <http://icvue-dsm.maxapex.net/apex/f?p=ICVUE:WELCOME:11695356204827:::::> Accessed 18 Apr 2016
- IFEU (2012) Aktualisierung” Daten-und Rechenmodell: Energieverbrauch und Schadstoffemissionen des motorisiertenVerkehrs in Deutschland 1960-2030 “(TREMODO, Version 5.3) für die Emissionsberichtserstattung 2013 (Berichtsperiode 1990-2011). Final report
- Infini-drive (2015) Pour un futur [simple] du véhicule électrique. Final report
- Kavalchuk I, Arisoy H, Stojcevski A, Oo AMT (2015) Advanced Simulation of Power Consumption of Electric Vehicles.International Journal of Electrical, Computer, Energetic, Electronic and Communication Engineering 9.1 (2015): 53-59.
- Lebeau P, Macharis C, Van Mierlo J, Lebeau K (2015): Electrifying light commercial vehicles for city logistics? A total cost of ownership analysis. EJTIR 15:551–569.
- Lee D-Y, Thomas VM, Brown MA (2013): Electric urban delivery trucks: Energy use, greenhouse gas

- emissions, and cost-effectiveness. Environ SciTechnol 47:8022–8030.
- LesEchos.fr (2015): Renault-Nissan/Electrique-Autonomie doublée en 2020. Retrieved from <http://investir.lesechos.fr/actions/actualites/renault-nissan-electrique-autonomie-doublee-en-2020-nikkei-1048785.php>. Accessed 25 Apr 2016
- Macharis C, Lebeau P, Van Mierlo J, Lebeau K (2013): Electric versus conventional vehicles for logistics: A total cost of ownership. Electric Vehicle Symposium and Exhibition (EVS27), 2013 World.IEEE, 2013. p. 1-10
- McMorrin F, Anderson R, Featherstone I, Watson C (2012): Plugged-in fleets: A guide to deploying electric vehicles in fleets. Retrieved from http://www.theclimategroup.org/_assets/files/EV_report_final_hi-res.pdf Last Accessed 27 Apr 2014.
- MEEM (2016) : Prix de vente moyens des carburants, du fioul domestique et des fiouls lourds en France, en € - Ministère de l'Environnement, de l'Energie et de la Mer. Retrieved from <http://www.developpement-durable.gouv.fr/Prix-de-vente-moyens-des,10724.html>. Accessed 23 Apr 2016
- Nesbitt K, Sperling D (1998): Myths regarding alternative fuel vehicle demand by light-duty vehicle fleets. Transp Res Part Transp Environ 3:259–269.
- Nesterova N, Quak H, Balm S, et al (2013): Project FREVUE deliverable D1. 3: State of the art of the electric freight vehicles implementation in city logistics. TNO SINTEF EurComm Seventh FramewProgramme accessed from <http://frevue.eu/wp-content/uploads/2014/05/FREVUE-D1-3-State-of-the-art-city-logistics-and-EV-final-.pdf>. Accessed 29 Apr 2015.
- Nykvist B, Nilsson M (2015): Rapidly falling costs of battery packs for electric vehicles. Nat Clim Change 5:329–332. doi: 10.1038/nclimate2564
- OVE (2015) TCO Scope 2015 | OVE Retrieved from: <http://www.observatoire-vehicule-entreprise.com/tco-scope-2015>. Accessed 15 Jul 2015
- Pearre NS, Kempton W, Guensler RL, Elango VV (2011): Electric vehicles: How much range is required for a day's driving? TranspRes Part C EmergTechnol 19:1171–1184. doi: 10.1016/j.trc.2010.12.010
- SOeS Pégase [Données en ligne, Énergies et climat] : Observation et statistiques. Retrieved from <http://www.statistiques.developpement-durable.gouv.fr/donnees-ligne/r/pegase.html>. Accessed 23 Apr 2016
- Taefi TT, Kreutzfeldt J, Held T, et al (2015): Comparative analysis of European examples of Freight electric vehicles schemes. In: Proceedings of Dynamics in Logistics: Fourth International Conference.
- Tim Mearig, Nathan Coffee, Michael Morgan (1999): Life Cycle Cost Analysis Handbook. First Edition.
- Van Amburg B, Pitkanen W (2012): Best fleet uses, key challenges and the early business case for e-trucks: findings and recommendations of the e-truck task force. Calstart
- Van Vliet O, Brouwer AS, Kuramochi T, et al (2011): Energy use, cost and CO 2 emissions of electric cars. J Power Sources 196:2298–2310.
- Windisch E (2014): Driving electric? A financial assessment of electric vehicle policies in France.Doctoral dissertation.Ecole des Ponts ParisTech

The most promising environmental innovations in inland waterway transport (IWT)

Sara CONSUEGRA*, Ruud VERBEEK, Jorrit HARMSSEN, Gerrit KADIJK & Pim VAN MENSCH
Research group Sustainable Transport and Logistics, TNO, Delft, The Netherlands
*sara.consuegra@tno.nl

Abstract

Traditional engine requirements are insufficient to improve the current environmental performance of the inland shipping industry. Therefore, alternative policy that focuses on real-life emissions is needed. On-Board Monitoring (OBM) of emissions could be the instrument in this evolution. On-Board Monitoring allows to measure the emission reduction effect of various environmental innovations, including technical, operational and logistical innovations. By creating policy on the real-life emission reduction rather than by setting norms to the engine performance, shipping companies would enjoy a larger freedom in choosing to adopt the environmental innovations they prefer. This is particularly important because of the diversity in the inland shipping industry. IWT has many market segments which can be identified by their large differences in ship design, operations, financial structures and stakeholder considerations. For the segment of bulk materials, operational innovations are the most promising for a fast, cost- and effort effective adoption. For the container segment is are operational innovations and logistical innovations which are most promising. Most technical innovations still require more financial support or R&D development than operational and logistical innovations. The industry is therefore advised to focus on the latter ones to effectively reduce real-life emissions in a fast way.

Key-words: Inland waterway transport, On-Board Monitoring, real-life emissions, stakeholders

Introduction ^{1, 2}

The environmental performance of inland waterway transport (IWT) has historically been better than that of its main competitor: road transport. While the emissions of greenhouse gases per tonkm are lower for IWT than for other modalities, modern trucks are currently outperforming inland ships when it comes to the emission harmful air pollutants like NO_x and PM.

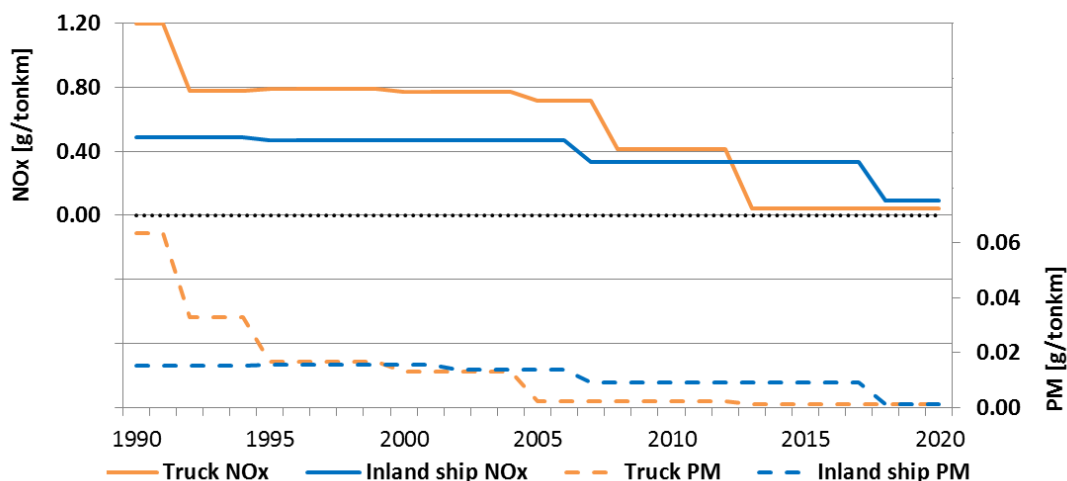


Figure 1. NO_x and PM emissions of road and inland waterway transport.

Because IWT has a strong position in the modal split (Eurostat data of 2015 show that IWT has a share in the modal split of 38% in the Netherlands, 19% in Belgium and 12% in Germany) the industry's relatively high emissions of air pollutants are concerning and are gaining attention from regulating authorities. These regulating authorities traditionally focus on setting stricter emission

requirements for new engines. The Stage V requirements that are expected to go into effect in 2019/2020 are an example of stricter emission requirements in IWT, as these norms are more ambitious than the current CCNR2 requirements.

However, engines of inland ships commonly have a lifespan of around 30 to 35 years. Research by Verbeek, Harmsen and Van Mesch (2015) shows that there is only a minority of ships which have modern engines.

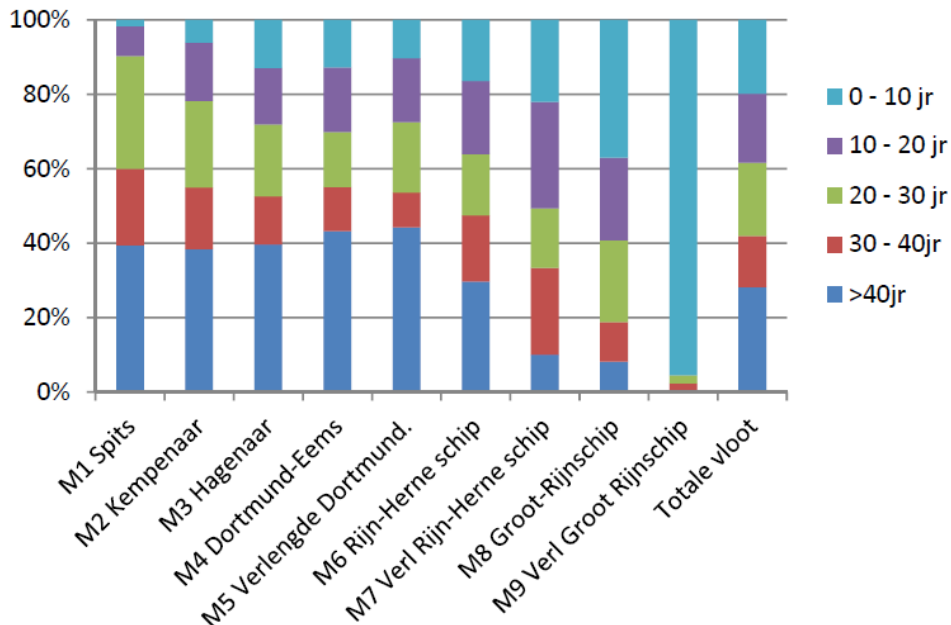


Figure 2. The age distribution of main engines of the European IWT fleet

This long lifetime of IWT engines means there is a delayed effect on the reduction of the emissions when stricter norms are set for new engines. That is why alternative policy instruments are needed to reduce the current emission levels. For an effective policy it is also necessary to know which innovations can be successfully adopted by the inland shipping industry in a short time span.

1. On-Board Monitoring ^{1, 3}

On-Board Monitoring has recently been identified as a method to reduce the emission of greenhouse gases and air pollutants in IWT. Verbeek, Harmsen and van Mensch (2015) show that when On-Board Monitoring is combined with feedback to the captain, it enables them to adjust their sailing techniques and save up to 7% fuel.

On-Board Monitoring also allows regulating authorities to set requirements for the real-life emissions, rather than lab-emission. This already happens for heavy duty road transport (trucks) and it has also gained attention in light duty vehicles (cars) after the recent events concerning defeat devices. Kadijk et al (2015) show that On-Board Monitoring as a certification, monitoring and enforcement option is particularly interesting in IWT due to the high number of retrofit emission reduction technologies. These technologies (including diesel particulate filters and selective catalytic reduction) can be installed on board without replacing the main engine and can effectively reduce emissions. However, an adequate legislative framework is missing for these after treatment solutions.

The European research project PROMINENT (under the Horizon 2020 research grant number 633929) is investigating how On-Board Monitoring could be set up, both from a policy point of view as a technical point of view. From a policy-perspective large efforts are required, since there are no procedures yet that allow certification to be granted on basis of real world emission measurement. The increasing technical possibilities on real-life emission measurements, like PEMS (portable Emission Measurements System) are motivating authorities to find appropriate legislative frameworks for On-Board Monitoring. That On-Board Monitoring is practically possible and can be

used to effectively reduce real-life emissions of the inland fleet, is being demonstrated by real-life pilots in which ships sail with On-Board Monitoring equipment. These pilots are currently being carried out in the PROMINENT research project. During several weeks these ships are monitored during their regular operations, providing valuable data on their real-life emissions and enabling the IWT industry to gain experience with On-Board Monitoring.

2. Environmental innovations ^{1, 2}

On-Board Monitoring allows emission legislation to focus on real-life emissions. This means that the industry, instead of purely focusing on the engine's emissions, could be stimulated to use a much wider array of environmental innovations to reduce the emissions of IWT. Aside from alternative fuels and efficient engines, technical innovations that reduce the energy demand of a ship could also be used to realize a reduction of real-life emissions. The same goes for operational and logistical innovations. More than 30 environmental innovations in the inland shipping industry can be identified.

Table 1. Some environmental innovations that can reduce emissions of IWT

Improved fuel quality	Improved maintenance	SCR
Fuel additives	New components	Particle filters
Lubrication oil additives	Diesel-electric hybrids	Water injection
Biofuels	Exhaust gas recirculation	Advanced route planning
LNG	Waste heat recovery	Fuel-efficient sailing techniques
CNG	Hull shape optimization	Cold ironing
GTL	LED lighting	Hubs & spokes
Electric powering	Friction reducing coatings	Hops
Wind energy	Propeller optimization	Fairway infrastructure information sharing
Solar energy	Whale tale propulsion	Chain partner planning integration
Fuel cells	Flexible tunnels	Network cooperation

For certification purposes, the emission levels would need to be expressed gr/tonkm rather than in gr/kWh for (some of) these innovations. This would require a mind shift from regulating authorities, but would stimulate the IWT industry to work on multi-level energy optimization and the reduction of current real-life emissions.

3. Stakeholder considerations ¹

The reduction of emissions is not the shoulders of regulating authorities alone. It is a shared responsibility of all the actors in the inland shipping network, as they each have an influence on the market adoption of innovations.

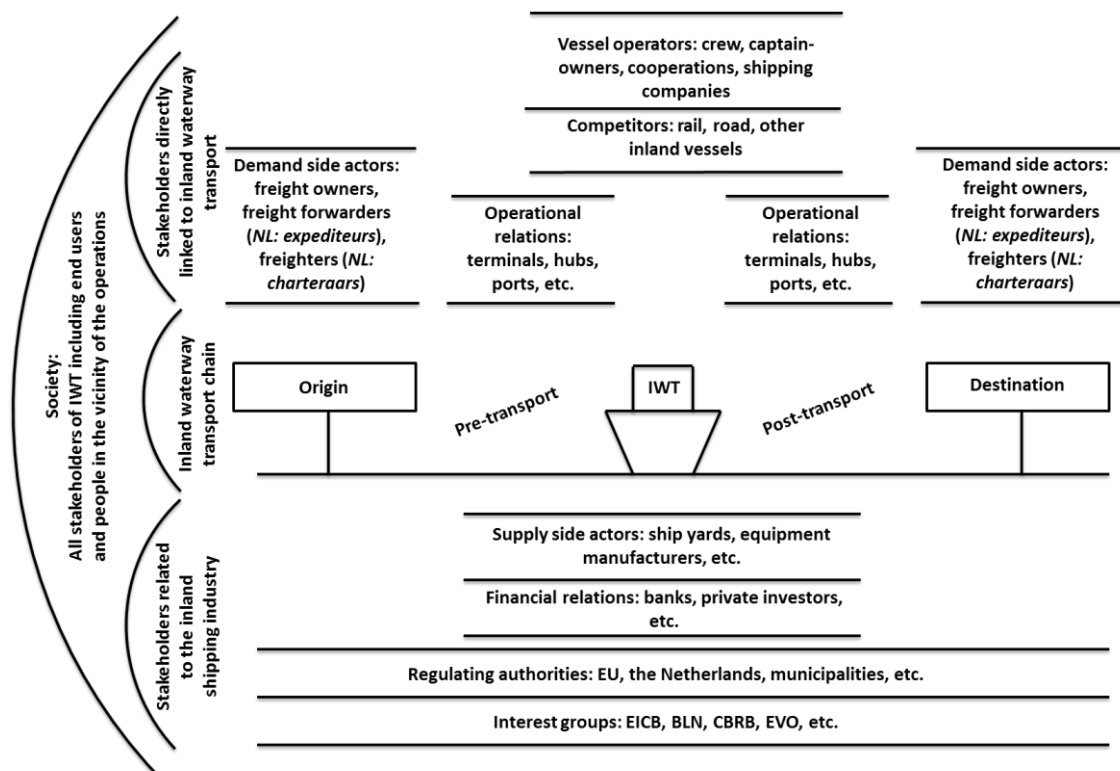


Figure 3. The stakeholders in the IWT network

While regulating authorities have an influence via policy, financial organizations for example can provide the funds required for investments in environmental innovations, and demand-side actors can choose to impose their standards. Because owner-operators of inland ships have the final decision to adopt innovations, they are at the center of the network.

Through stakeholder interviews, the attitudes of these various actors were analyzed in the thesis research of Consuegra, S.C (2016). The stakeholders' opinions about emission reduction are found to be diverse. Owner-operators and demand-side actors for example want to reduce fuels costs, so they are focused on innovations which reduce the fuel consumption. In other words: they are focused on the reduction of CO₂. Regulating authorities and operational relations (e.g. ports) on the other hand want to improve the air quality in their area so they want to reduce harmful emissions like NO_x and PM. Apart from this difference, there are also conflicting interests. Some are evident: owner-operators want to minimize their investment costs when adopting an innovation, while the supply-side actors who offer these products want to maximize their profits. Some are less evident: owner-operators want to have an edge over their competition but most of them also prefer to not be the first to try out something new.

4. Diversity in market segments ^{1,2,3}

Different stakeholder considerations are most apparent in different segments of IWT. Some factors which characterize market segments in the inland shipping industry are:

- The type of cargo: ore, petroleum, containers, coal, chemicals, ro-ro, etc
- The geographical area of operations: Rhine corridor, North-South corridor, etc.
- The size of the vessels: from CEMT 0 to CEMT VIIIb
- The age of the vessels: from newbuilds to 70+
- The ownership of the vessels: from single-ship captain-owners to shipping companies with 20+ vessels
- The freight contracts: spot market, bareboat charter, voyage charter, time charter, own account

In addition to stakeholder considerations varying in each market segment, the diversity in ship design, operations and financial structures also influence the cost-effectiveness of each innovation. These factors all contribute to the inexistence of 'one size fits all solutions' for the inland shipping industry. This means that some innovations may be effective in one segment but not in another. An example of this is waste heat recovery. Waste heat recovery can reduce emissions for the larger chemical tankers which must keep their cargo warm, but is not interesting for other ships. Another example is LNG. The fuel can currently only be bunkered in Amsterdam, Rotterdam and Antwerp, meaning it is still only an option for ships that operate in this particular area.

Determining which innovations are most promising for a fast, cost and effort effective adoption in IWT, cannot be done for the IWT industry as a whole. It must be done for specific cases. Two of the largest market segments in the Dutch inland shipping industry are the segment of containers, and the segment of sand, stone and gravel. Together, these case studies represent about 40% of the Dutch inland shipping industry, and have been studied in the thesis research of Consuegra (2016).

5. Case study: sand stone and gravel market ¹

Most vessels in the sand, stone and gravel market are small or medium-sized. Most of these ships are owned by single-ship captain-owners which operate on the spot market. The project cargoes they carry often originate from quarries near smaller waterways, and are destined to building sites.

Consuegra (2016) uses the theory of Suurs (2009) to show the characteristics which are essential for innovations to be adopted in a fast, cost- and effort effective way in this market segment. These characteristics include:

- Innovations must not still require any R&D
- Innovations must be well-known (established knowledge diffusion)
- Innovations must not require exemptions from regulations
- Innovations must have low investment costs
- Innovations must have low pay back periods (i.e. save fuel)

There are only a couple of innovations which currently meet these criteria. These are LED lighting and operational innovations: advanced route planning, cold ironing, and On-Board Monitoring combined with fuel-efficient sailing techniques. These innovations may have a limited emission reduction potential, but they are inexpensive ways to effectively reduce the real-life emissions of the sand, stone and gravel market. Most technical innovations are too costly or still require R&D.

Table 2. The most promising innovations in the sand stone and gravel market

Innovation	Savings potential	Costs
LED lighting	Less than 1%	Less than €5 per light
Advanced route planning	Less than 10%	Less than €2000
OBM and fuel-efficient sailing	Less than 10%	Between €10.000 and €15.000
Cold ironing	100% during cold ironing	Comparable to on-board generated power

6. Case study: container market ¹

The container market is dominated by shipping companies that own several vessels. They own mostly large Rhine ships and have long term freight contracts with their clients. Freight is carried between large sea ports and inland container terminals.

Consuegra (2016) shows the characteristics which are essential for innovations to be adopted in a fast, cost- and effort effective way in this market segment. These characteristics include:

- Innovations must improve the throughput, punctuality, customer services or freight tariffs
- Innovations must not require exemptions from regulations
- Innovations must have low pay-back periods (i.e. reduce fuel costs)

Apart from advanced route planning and On-Board Monitoring combined with fuel-efficient sailing techniques, several logistical innovations meet these criteria: hubs & spokes, hops, fairway infrastructure information sharing, chain partner planning integration and network cooperation. These logistical innovations have a remarkably high emission savings potential but their costs are hard to quantify. This is because there is no traditional investment like for a piece of equipment, but there are man-hours invested and for example administrative costs for the setting up of agreements.

Table 3. The most promising innovations in the container market

Innovation	Savings potential	Costs
Advanced route planning	Less than 10%	Less than €2000
OBM and fuel-efficient sailing	Less than 10%	Between €10.000 and €15.000
Hubs & spokes and hops	Less than 40% per tonkm	Various value cases
Fairway infrastructure information sharing	Less than 10% per tonkm	Various value cases
Chain partner planning integration	Less than 10% per tonkm	Various value cases
Network cooperation	Less than 20% per tonkm	Various value cases

Conclusion

There are numerous environmental innovations and their cost-effectiveness differs for each market segment of IWT. This is also the case for the stakeholders' considerations. To determine which innovations are most promising for an fast, cost- and effort effective reduction of real-life emissions, these aspects must be evaluated for a particular cases rather than for the IWT industry in its entirety. After performing two important case studies, it appears technical innovations are not the most promising innovations. They are often too costly or still require R&D. Operational and logistical innovations do not have these issues and could be adopted by the industry faster than technical innovations. To measure the emission reduction effect of these innovations, On-Board Monitoring of real-life emissions is needed.

Acknowledgments

This work was supported by H2020 project PROMINENT under grant number 633929

References

- 1: Consuegra, S.C. (2016), The analysis and adoption of environmental innovations in inland waterway transport, Delft, TU Delft & TNO
 - 2: Verbeek, R., Harmsen, J. and van Mensch P. (2015), Visie On-Board Monitoring in de binnenvaart + Bijlagen visie On-Board Monitoring in de binnenvaart, Delft, TNO
 - 3: Kadijk, G. et. Al. (2015), PROMINENT WP3.1: State of the art report, TNO & TUV & IMST & SGS
- Suurs, R. (2009), Motors of sustainable innovation, Universiteit Utrecht

Experiences and Results with different PEMS

J. Czerwinski¹, Y. Zimmerli¹, P. Comte¹, Th. Bütler²

¹University of Applied Sciences, 2500 Biel-Bienne, AFHB^{*}, Switzerland

²Federal Laboratories, 8600 Dübendorf, EMPA^{*}, Switzerland

Keywords: PEMS, RDE, HD-vehicles and LD-vehicles

Author email: jan.czerwinski@bfh.ch

Abstract

PEMS – portable emissions measuring systems were introduced in the last stage of exhaust gas legislation for HD-vehicles in order to measure and to limit the real driving emissions (RDE). PEMS were also confirmed by EU to be applied for the LD-vehicles in the next legal steps.

In the present paper, the results and experiences of testing different PEMS on the chassis dynamometer and on-road are presented.

The investigated PEMS were: Horiba OBS ONE, AVL M.O.V.E and OBM Mark IV (TU Wien).

The measuring systems were installed on the same vehicle (Seat Leon 1.4 TSI ST) and the results were compared on the chassis dynamometer in the standard test cycles: NEDC, WLTC and CADC.

As reference, the results of the stationary laboratory equipment (CVS and Horiba MEXA 7200) were considered.

For the real-world testing a road circuit was fixed: approximately 1h driving time with urban/rural and highway sections.

Comparisons of results between the PEMS and with stationary reference system show different tendencies, depending on the considered parameter (NO_x, CO, CO₂) and on the test cycles. In this respect all investigated PEMS show similar behavior and regarding over average of all parameters and tests no special preferences or disadvantages can be declared.

Repeated test on the same road circuit produce dispersing emission results depending on the traffic situation, dynamics of driving and ambient conditions. Also the calculated portions of urban, rural and highway modes are varying according to the traffic conditions.

Test vehicle

The rented test vehicle was a Seat Leon 1.4 TSI (GDI, TWC) in used state (1½ year, 20'800 km). During the tests approximately 2000 km were driven.

The above mentioned vehicle is presented in [Fig. 1](#) and [Tab. 1](#).

The gasoline used was from the Swiss market, RON 95, summer quality, according to SN EN228.

In the present tests the lube oil was not changed, or analyzed – the same oil was used for all tests.



Figure 1a. Vehicle used for research on PEMS

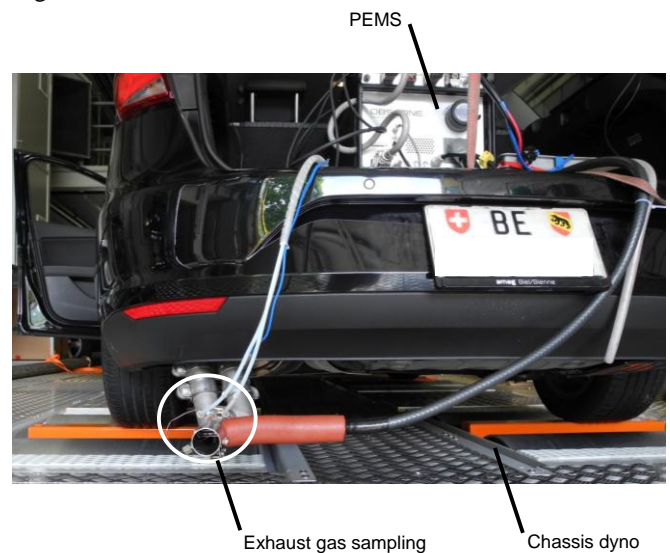


Figure 1b. Test vehicle with installed PEMS on chassis dynamometer

Vehicle	SEAT Leon 1.4 TSI ST
Number and arrangement of cylinder	4 / In line
Displacement cm ³	1395
Power kW	103 @ 4500 - 6000 rpm
Torque Nm	250 @ 1500 - 3500 rpm
Injection type	Direct Injection (DI)
Curb weight kg	1275
Gross vehicle weight kg	1840
Drive wheel	Front-wheel drive
Gearbox	M 6
First registration	21.01.2014
Exhaust	EURO 5b

Table 1. Data of tested vehicle

^{*}) Abbreviations, see at the end of this paper

Test equipment

Part of the tests were performed on the 4WD-chassis dynamometer of AFHB (Laboratory for Exhaust Emission Control of the Bern University of Applied Sciences, Biel, CH).

The stationary system for regulated exhaust gas emissions is considered as reference

This equipment fulfils the requirements of the Swiss and European exhaust gas legislation.

- regulated gaseous components:
 - exhaust gas measuring system Horiba MEXA-7200
 - CO, CO₂... infrared analysers (IR)
 - HCFID... flame ionisation detector for total hydrocarbons
 - CH₄FID... flame ionisation detector with catalyst for only CH₄
 - NO/NO_x... chemoluminescence analyser (CLA)

The dilution ratio DF in the CVS-dilution tunnel is variable and can be controlled by means of the CO₂-analysis.

The overview of used PEMS is given in the Table 2. Let us remark that the OBM Mark IV system does not use any flowmeter for exhaust flow measurement. It calculates the necessary parameters from the on-board data. Thanks to that this apparatus can be much simpler and quicker adapted on the vehicle.

	HORIBA MEXA 7100	HORIBA OBS ONE	AVL M.O.V.E	TU Wien OBM Mark IV
	4x4 chassis dyno CVS	PEMS ① wet	PEMS ② dry	PEMS ③ dry
CO	NDIR	heated NDIR	NDIR	NDIR
CO ₂	NDIR	heated NDIR	NDIR	NDIR
NO _x	CLD	CLD	NDUV	Zirkonium- dioxid
NO	CLD	CLD	-	Electro- chemical + NDIR
NO ₂	calculated	calculated	NDUV	-
O ₂	-	-	electro- chemical	electro- chemical
HC	FID	-	IR	IR
PN	not measured	-	-	-
OBD logger	-	yes	yes	yes (Bluetooth dongle)
GPS logger	-	yes	yes (Garmin GPS16)	yes (GPS - Bluetooth receiver)
ambient (p, T, H)	yes	yes	yes	no
EFM	-	pitot tube	pitot tube (SEMTECH- EFM HS)	no
PN		Particles Number		
OBD		On Board Diagnostics		
EFM		Exhaust Flow Meter		
OBS - one		H ₂ O monitored to compensate the H ₂ O interference on CO and CO ₂ sample cell heated to 60°C dry to wet correction applied		
AVL - Move				

Table 2. Overview of used measuring systems.

Test procedures

Driving cycles on chassis dynamometer

The vehicle was tested on a chassis dynamometer in the dynamic driving cycles: NEDC, Fig. 2, WLTC, Fig. 3 and CADC, Fig. 4.

The first NEDC of each test series was performed with cold start (20-25°C) and further cycles followed with warm engine. Between the cycle always 3 minutes of constant speed 80 km/h in 4th gear were performed as conditioning.

The braking resistances were set according to legal prescriptions they were not increased i.e. responded to the horizontal road.

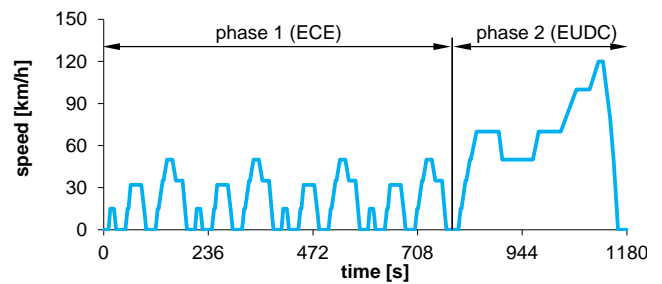


Figure 2. NEDC European driving cycle

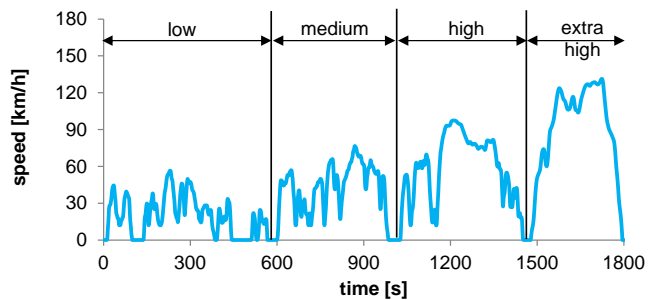


Figure 3. WLTC driving cycle

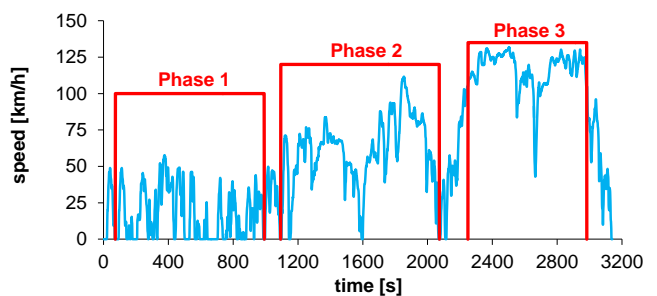


Figure 4. CADC driving cycle

On-road testing

With each PEMS several road tests were performed. The used road circuit was always the same with approximately 1h duration and parts of urban, rural and highway roads (see Fig. 9).

Results

Comparisons of PEMS on chassis dynamometer

All three PEMS were tested on chassis dynamometer in the driving cycles NEDC_{cold}, NEDC_{warm}, WLTC_w and CADC_w and the results were compared with the stationary CVS-installation (with Horiba MEXA 7100), which is shortly called here “CVS”.

Fig. 5 gives an example of correlations of NO_x, CO and CO₂ measured with PEMS and with “CVS” in NEDC_{cold} (which is still the legal test procedure of today). The emission components are given in [mg/km] or [g/km].

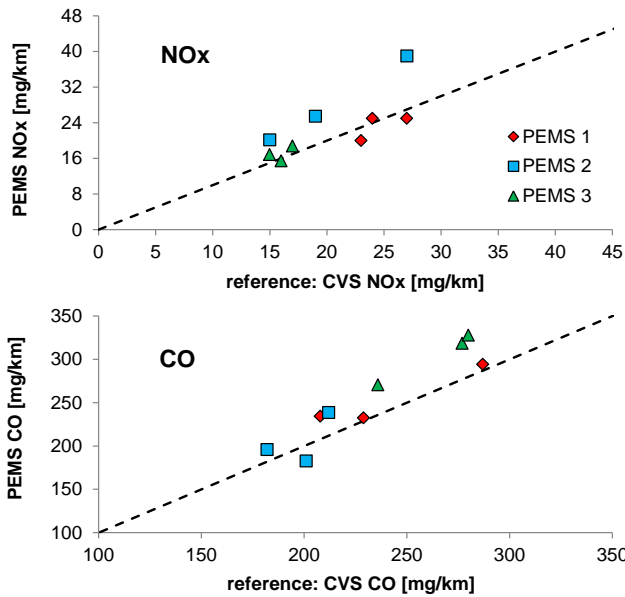


Figure 5a. Correlations of emissions measured with PEMS and with stationary CVS-installation in NEDC cold.

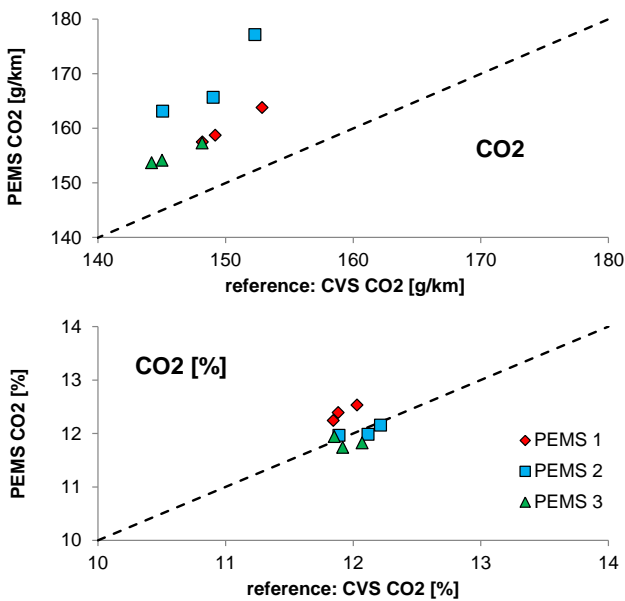


Figure 5b. Correlations of emissions measured with PEMS and with stationary CVS-installation in NEDC cold.

The correlations for NO_x and CO are in an overall view quite good, but there is tendency of too high NO_x-values with PEMS2 and too high CO-values with PEMS1 and PEMS3. For CO₂, which is naturally presented in much higher concentrations, than NO_x & CO, the deviations – too high values obtained with all PEMS – are clearly pronounced.

What can be the reasons of these deviations?

The mass flow (\dot{m}_x) of an emissions component “x” is calculated as:

$$\dot{m}_x = \dot{V}_{exh} \cdot k_x \cdot \rho_x$$

$$\left[\frac{kg_x}{s} = \frac{m^3_{exh}}{s} \cdot \frac{m^3_x}{m^3_{exh}} \cdot \frac{kg_x}{m^3_x} \right]$$

where:

\dot{V}_{exh} ... volumetric flow of exhaust gas

k_x ... volumetric concentration of component “x” in the exhaust gas

ρ_x ... density of the component “x”

For dynamic measurements with PEMS in the real-world transient operation there is a challenge to well synchronize the signals of all three parameters, which are continuously changing with the operating conditions. (The instantaneous density varies with the pressure and temperature of exhaust gas).

All PEMS try to perform this synchronization as to the best, but the authors presume that this is the major reason for the indicated differences. Of course the measuring accuracy of the parameters also contributes to the results. In measurements of concentrations there are for the different PEMS’s different: measuring principles, wet-dry-corrections and linearisations.

In order to exclude the influence of volumetric flow (V_{exh}) and density (ρ_x) the concentrations of CO₂ were correlated: integral averages measured with PEMS against the bag-concentrations (diluted) recalculated to the non-diluted concentrations at tailpipe. This is represented at the bottom of Fig. 5b as CO₂ in [%].

The comparison of concentrations indicates much better correlations.

About the magnitude of values obtained in NEDC_{cold} it can be remarked:

- NO_x results are lower than the Euro 6 limit (60 mg/km)
- CO results are lower than the Euro 6 limit (1000 mg/km)
- CO₂ results are greater than 119 g/km (manufacturer specifications)

⇒ average of all CVS results: 148 g/km [average of all road measurements (different PEMS): 134g/km]

The correlations of emissions measured with all three PEMS and with “CVS” in all driving cycles are represented in Fig. 6. The tendencies of the too high indications with PEMS’s are confirmed: too high NO_x-values with PEMS2, high CO₂-values with all PEMS’s.

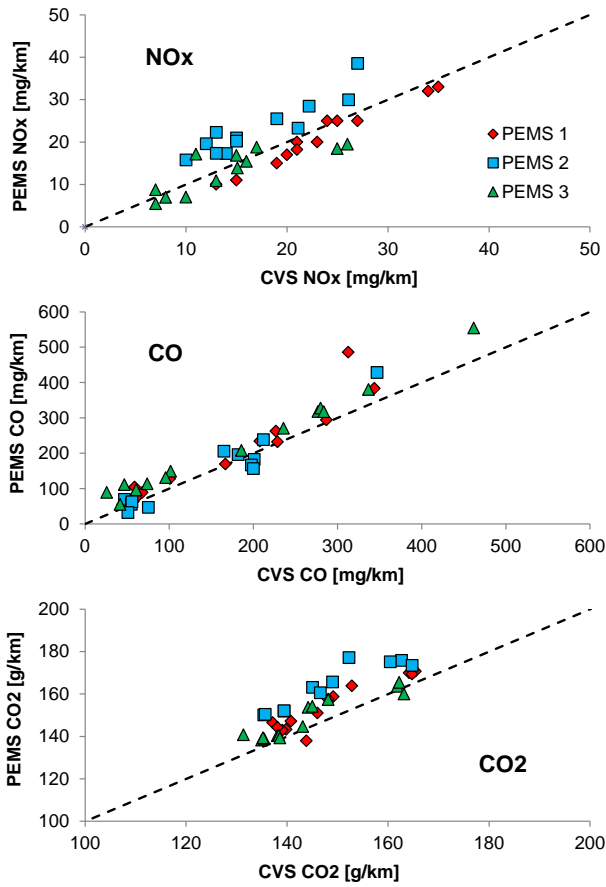


Figure 6. Correlations of emissions measured with PEMS and with stationary CVS-installation in all investigated driving cycles: NEDC cold, NEDC, WLTC, CADC.

As already demonstrated in Fig. 5, the major reason for the higher CO₂ mass-emissions with PEMS’s is the insufficient synchronization and accuracy of transient parameters. The average CO₂ concentrations are in a much better accordance.

A general comparison of average results: CVS versus all PEMS’s is represented in Fig. 7 for NEDC_{cold} only and for all performed driving cycles. The higher readings with PEMS’s are confirmed. CO and NO_x have very low concentrations, so they have generally higher standard deviations, than CO₂. For “all cycles” the standard deviations of CO are higher, because of considering the cold start cycle.

Fig. 8 summarizes the average deviations between the PEMS- and CVS – values considering all cycles, including NEDC_{cold}. Considering the maximum deviations: for NO_x at 37% and for CO at 67%, it seems too much, but on the other hand taking in view the very low absolute values of NO_x and CO these deviations become more comprehensible.

Each of the tested systems has some little and some big deviations. This conducts us to the statement that in the average view there is no best or worst system. All of them represent a similar balance of advantages and disadvantages and their measuring quality can be regarded as similar. There are of course still big potentials for improvements.

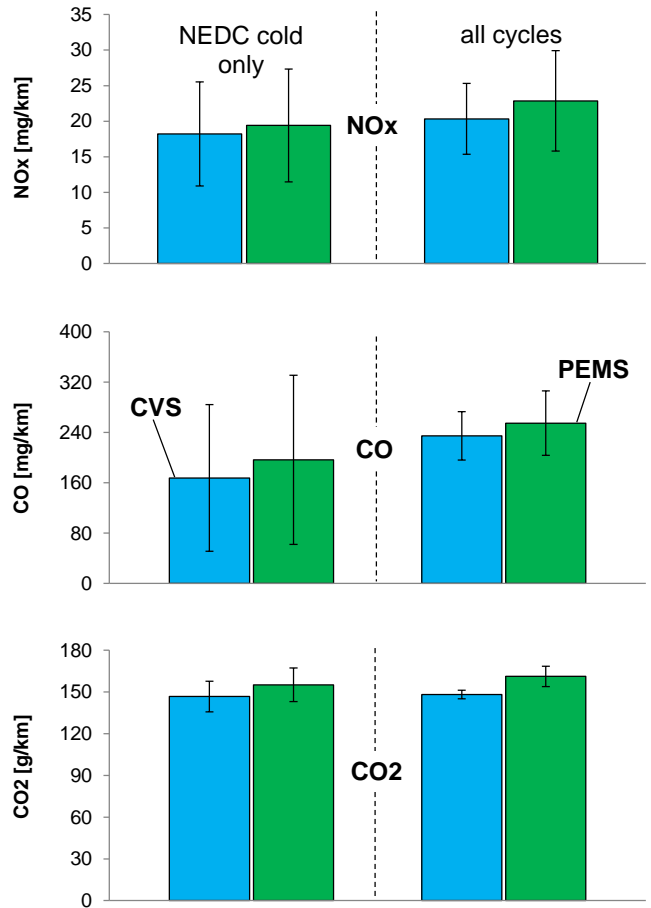


Figure 7. Comparisons of average results: CVS versus all PEMS’s.

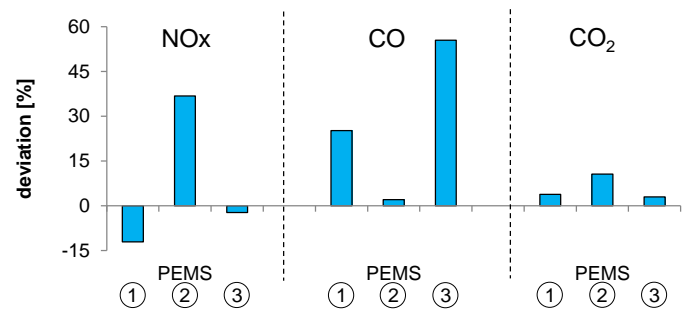


Figure 8. Average deviations between PEMS and CVS values; all cycles.

Road tests and comparisons with chassis dynamometer

The road test route used for the tests is described in Fig. 9.

The time and the average speed in each type of (urban, rural, highway) may vary according to the traffic situation. Testing in peak traffic hours was avoided. The distinction between the driving modes: urban, rural, highway is performed by the evaluating program according to the RDE requirements (see next section). All cycle parts below 60 km/h are considered as “urban” all intervals with [60 km/h < 90 km/h] are rural and all driving with vehicle speeds $v > 90$ km/h is highway.

This means, that the distinction is only performed according to the driving speed and not (as usually supposed) according to the type of road.

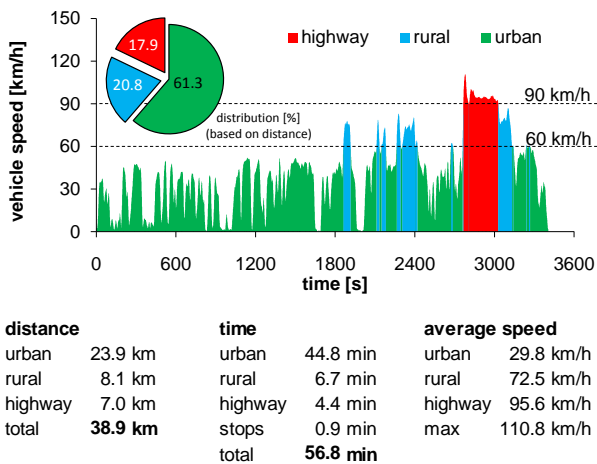


Figure 9. AFHB Road-Test Route. PEMS 2, Seat Leon 1.4 TSI Euro 5b

Fig. 10 shows a comparison of accumulated results from five road trips with PEMS1.

From all performed trips can be followed that:

- CO₂ emissions are well repetitive,
- there is a lot of dispersion in the measured NO_x; differences happen mainly during the first 10km in the urban part of the circuit; the dynamics of driving (traffic) influences strongly the accumulated NO_x,
- a CO peak occurs at the beginning of the highway part; this suddenly increasing CO-amount during entering highway attains different levels depending on acceleration and on the initial state of engine exhaust system; this peak influences massively the accumulated end result.

Fig. 11 summarizes the results from several road tests with all three PEMS. Following can be remarked:

- The trip composition (operation mode urban, rural, highway) is relatively constant. If there is some congestion or dense traffic on the highway parts, this can influence significantly the share between rural and highway operation.
- CO₂ measurements are repetitive.
- CO results show more dispersion – the level of CO emissions for the whole road trip is below 300mg/km, a sudden acceleration during the measurement can influence greatly the final results.

- The vehicle has not constant NO_x emissions. This tendency is confirmed by the comparison of the results in different cycles with different instruments.
- CO and NO_x measured levels are relatively low (concentrations not represented here: NO_x average <50ppm; CO average <300ppm).
- The results from the PEMS3, which has no EFM (Exhaust mass Flow Meter), are similar to the results of other measuring systems.

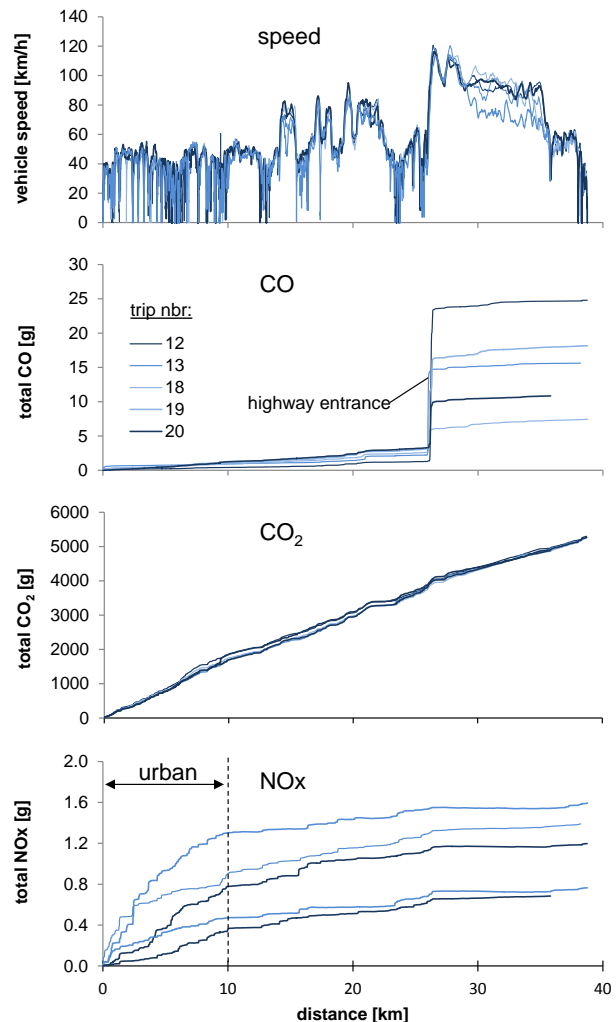


Figure 10. Comparison of accumulated results from five road trips.

Fig. 12 compares the average values from measurements performed on chassis dynamometer and in the road trips. There is a strong dispersion of CO & NO_x in the road trips. This is especially caused by the quite dynamic driving style in the first part of road tests.

It can be said for CO and NO_x that the WLTC depicts the best the average road driving in this circuit. CO₂-emissions measured on road are lower, than on chassis dynamometer.

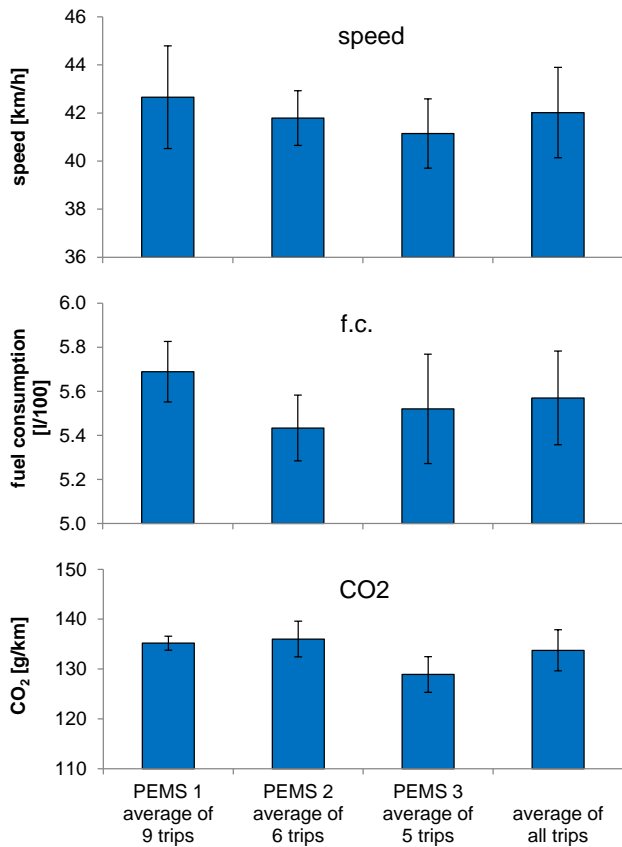


Figure 11a. Results from road trips (38 km) with different PEMS. PEMS 1, 2, 3; Seat Leon 1.4 TSI Euro 5b.

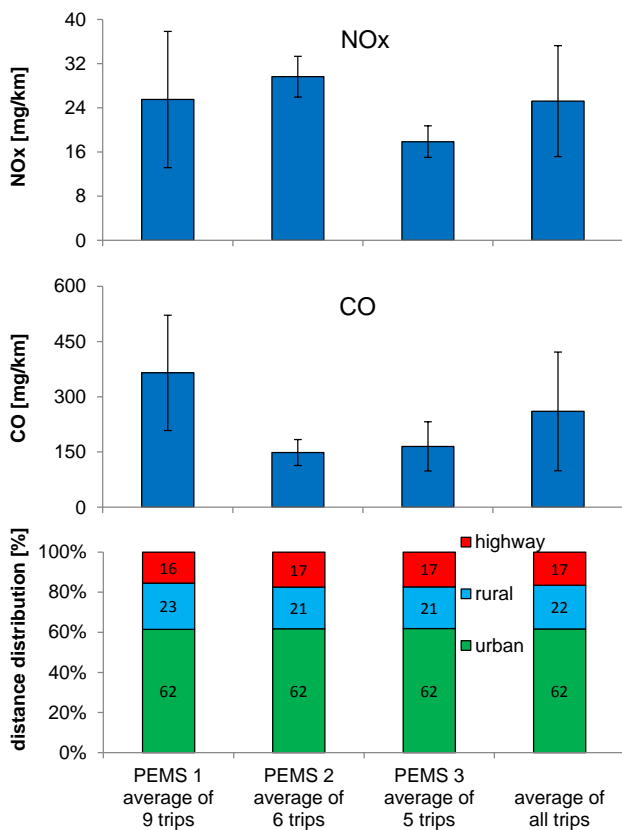


Figure 11b. Results from road trips (38 km) with different PEMS. PEMS 1, 2, 3; Seat Leon 1.4 TSI Euro 5b.

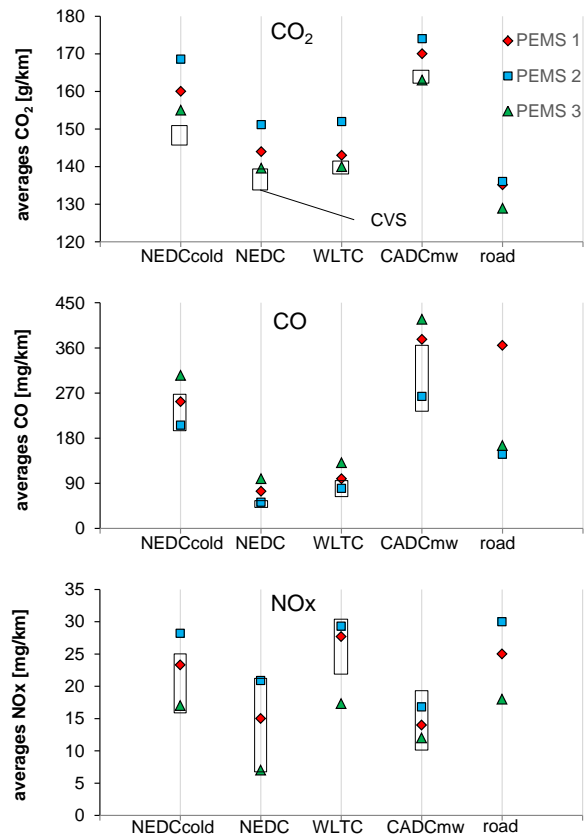


Figure 12. Comparisons of average values between road trips and cycles on chassis dynamometer. PEMS 1, 2, 3; Seat Leon 1.4 TSI Euro 5b.

RDE requirements for road testing

The requirements concerning: vehicle, test circuit, test equipment, boundary conditions, emission trip validation and evaluation are given in the preliminary version of the Euro 6c Norm, [1, 3]. Useful information and explanations can be found in literature, [2, 4, 5, 6].

The objective of this section is to give a possible short summary of the requirements of this testing method.

An extract of the requirements regarding trip validation is:

- DAQ at least at 1Hz
- percentage of total trip distance (34% - 33% - 33%)
- urban → rural → highway (continuously run)
- urban: < 60 km/h; rural: 60-90 Km/h; highway: > 90 km/h (≠ 50 - 80 - 120 km/h)
- max velocity 145 km/h
- average speed in urban including stops = 15-30 km/h
- stops = vehicle speed < 1km/h
- urban stops = at least 10% of the time duration of urban operation
- urban shall contain several stop periods of 10s or longer
- highway speed at least 110km/h
- highway at least 5 minutes above 100 km/h
- trip duration: 90-120 minutes
- start and end point elevation difference < 100m

- minimum distance of each mode (urban, rural highway) > 16 km
- measured vehicle speed (GPS or ECU) have to be checked
- shall be conducted on working day
- off road operation is not permitted
- it shall not be permitted to combine data of different trips or to modify or remove data from a trip
- cold start shall be recorded but excluded from the emissions evaluation → but included in trip validation

Conclusions

Following conclusions can be mentioned:

- Comparisons of PEMS's with a stationary measuring system (CVS) on a chassis dynamometer show similar behaviour for all investigated instruments – different dispersion of results, depending on the considered parameter and driving cycle.
- All PEMS's indicated more CO₂ than the "CVS". The reason is most probably the insufficient synchronization of the transient parameters: exhaust gas mass flow, concentration and density of the measured parameter. Further clarifications will be undertaken.
- From the road testing of the present vehicle it can be stated:
 - CO₂ emissions are repetitive,
 - there is a lot of dispersion in the measured NO_x; differences happen mainly during the first 10 km in the urban part,
 - a CO peak occurs at the beginning of the highway part; this peak influences massively the accumulated end result,
 - the results from the OBM system (TU-Wien), which has no EFM (Exhaust mass Flow Meter), are well correlating with the results of other measuring systems.
- There are quite numerous requirements for a trip validation of the RDE-procedures. The road traffic influences some of the validation parameters. It is recommended to select a "flexible" road circuit, which can be adapted to the actual traffic situation.

Summarizing: the PEMS and RDE testing is a new challenging task for the test laboratories.

Acknowledgement

The authors express their thanks to the Swiss Federal Office of Environment BAFU, Dr. M. Schiess and Mr. G. D'Urbano for the financial support and inspiration of the project.

Literature

- [1] COMMISSION REGULATION (EC) no 692/2008 of 18 July 2008 implementing and amending Regulation (EC) No 715/2007 of the European Parliament and of the Council on type-approval of motor vehicles with respect to emissions from light passenger and commercial vehicles (Euro 5 and

Euro 6) and on access to vehicle repair and maintenance information

Available at: <http://eur-lex.europa.eu/legal-content/en/ALL/?uri=CELEX:32008R0692>

- [2] Brüne, H.-J.; Bittermann, A.; Fortner, T.: *RDE – The challenge for future Diesel Powertrains*. 8. Internationales Forum, Abgas- und Partikel-Emissionen, 1-2. April 2014 / Ludwigsburg
- [3] Darft of the Annex IIIa: *Verifying Real Driving Emissions amending Regulation (EC) No 692/2008 as regards emissions from light passenger and commercial vehicles (Euro 6)*.
Available at: <http://ec.europa.eu/transparency/regcomitology/index.cfm>
keyword: D040155/01
- [4] Anderson, J.; May, J.; Favre, C.; Bosteels, D. et al.: *On-Road and Chassis Dynamometer Evaluations of Emissions from Two Euro 6 Diesel Vehicles*. SAE Paper 2014-01-2826. SAE Detroit, April 2014.
- [5] Vlachos, T. G.; Bonnel, P.; Weiss, M.: *Die Bewertung des Abgasverhaltens von Fahrzeugen im realen Fahrbetrieb – Eine Herausforderung für die europäische Emissionsgesetzgebung*. 36. Internationales Wiener Motorensymposium, 2015.
- [6] Hofacker, A.: *Abgasnorm und Wirklichkeit Eine Annäherung*. Springer: MTZ-Motortechnische Zeitschrift, January 2015, Vol. 76, Issue 2, pp 8-13.

Abbreviations

AFHB	Abgasprüfstelle FH Biel, CH
ASTRA	Amt für Strassen (CH)
BAFU	Bundesamt für Umwelt, (Swiss EPA)
BC	board computer
CADC	Common Artemis Driving Cycle
CLA	chemiluminescent analyzer
CLD	chemiluminescent detector
CVS	constant volume sampling
DAQ	data acquisition
DF	dilution factor
DI	Direct Injection
EC	European Commission
ECE	Economic Commission Europe
ECU	electronic control unit
EFM	exhaust flow meter
EMPA	Eidgenössische Material Prüf- und Forschungsanstalt
EUDC	Extra Urban Driving Cycle
Q_x	density of the component "x"
HC	unburned hydrocarbons
k_x	volumetric concentration of component "x" in the exhaust gas
\dot{m}_x	mass flow of emission component "x"
MFS	mass flow sensor
NEDC	New European Driving Cycle (ECE+EUDC)
NO	nitrogen monoxide
NO ₂	nitrogen dioxide
N ₂ O	nitrous oxide
NO _x	nitric oxides
OBD	on-board diagnostics
PEMS	portable emission measuring systems

PN	particle number
RDE	real driving emissions
TWC	three way catalyst
V_{exh}	Volumetric flow of exhaust gas
WLTC	worldwide harmonized light duty test cycle
WLTP	worldwide harmonized light duty test procedure
3WC	three way catalyst

Combined air quality and noise evaluation of transport policies: methodology and feedbacks

Philippe DUNEZ*, Virginie DUNEZ* & Christine BUGAJNY*

**Departement Bâtiment Energie Environnement, Groupe Air et Bruit, Direction Territoriale Nord-Picardie CEREMA, 42 bis rue marais –Sequedin- 59482 Haubourdin, France*

Author email: philippe.dunez@cerema.fr; virginie.dunez@cerema.fr; christine.bugajny@cerema.fr

Abstract

This article is about the evaluation of transport policies, for example, relating to PPA 'Atmosfer Protection Plan'.

In France, the environmental assessment includes the four key principles of the code of the environment (Article L. 110-1): the principles of integration, participation, precaution and prevention. The negative effects of a project must be avoided, reduced or compensated.

The evaluation of transport policies is really important, first to know the expected impacts on population exposition and then to quantify the real efficacy of these policies. Few publications and feedbacks are published about methodology for environmental evaluation of transport policies. One other challenge of these evaluations is to reach a coherence between air quality and noise evaluation, by using similar methodologies.

The article describes necessary input data, models used and common methodology for the two thematics. Difficulties and ways to improve methodology will be traited from feedback on two operational projects. The first project studied was evaluated from modeling and the second one from measurements.

The first project concerns the PPA (Atmosfer Protection Plan) of the Île-de-France region which mentions that road transport is responsible for 54% of NOx emissions, 25% of PM10 and PM2.5. Trucks are contributing to 30 and 10% of these emissions respectively. Restrictions on heavy trucks transit in the dense heart of the Paris agglomeration exist as a regulatory measure in case of pollution peak. This policy has to be used continuously. Cerema has established a methodology to measure the effects of these project on noise and pollutants, in correlation with traffic data and based on air and noise modellisation results.

The second project is about VDTB (Dedicated ways for Taxis and Bus) on roadways. The VDTB have vocation to be developed as part of Master Plans of Transportation. The DRIEA has planned to set up an experimental VDTB on the highway A1, to facilitate the connection between Roissy airport and Paris. The project consists in dedicating the left lane for taxis and buses, between Bourget and Landy tunnel, direction province-Paris, from 06:30 to 10 am every day.

In this second project, the use of emission models is really impossible to evaluate air and noise impacts because of the difficulties for having a prospective scenario on traffic data; the evaluation is based on measurements.

This work should answer to these important questions about transport policies evaluation:

-What are the important data to use for a good evaluation on air quality and noise?

-How can we improve the common methodology about air quality and noise impacts?

Keywords : evaluation, impact, transport policies, environment, traffic, air quality, noise

Résumé

Le sujet de cet article est l'évaluation des politiques de transports à travers d'exemples comme un Plan de Protection de l'Atmosphère.

En France, l'évaluation environnementale comprend les quatre principes clés du code de l'environnement (article L. 110-1) : les principes d'intégration, de participation, de précaution et de prévention. Les effets négatifs d'un projet doivent être évités, réduits ou compensés.

L'évaluation des politiques de transport est importante pour connaître les impacts attendus sur l'exposition de la population puis quantifier l'efficacité réelle de ces politiques. Peu de publications et de retours d'expérience ont été publiés sur une méthodologie à mettre en place pour l'évaluation environnementale des politiques de transport. Un autre défi de ces évaluations, est de parvenir à une cohérence entre les études sur la qualité de l'air d'une part et les études acoustiques d'autre part, en utilisant des méthodologies identiques.

L'article décrit les données d'entrée nécessaires, les modèles utilisés et les méthodologies communes pour les deux thématiques. Les difficultés et les pistes d'amélioration sont évoquées suite à un retour d'expérience sur deux projets opérationnels. La première étude a été évaluée à partir d'une modélisation et la seconde à partir de mesures.

La première étude concerne le PPA (Plan de Protection de l'Atmosphère) de la région Île-de-France, qui relate que le transport routier est responsable de 54% des émissions de NOx, 25% des PM10 et PM2,5. Les poids-lourds contribuent respectivement à 30 et 10% de ces émissions.

Les restrictions sur les poids-lourds en transit dans le cœur dense de l'agglomération parisienne existent en tant que mesure réglementaire en cas de pic de pollution. Cette mesure doit être mise en place de manière permanente. Le Cerema a mis en place une méthodologie basée sur la modélisation pour mesurer les effets du projet sur le bruit et les polluants atmosphériques, en corrélant avec les données de trafic.

La deuxième étude porte sur une VDTB (voies dédiées pour les taxis et bus) sur une voie autoroutière.

Les VDTB ont vocation à être développées dans le cadre des Schémas Directeurs des Transports. La DRIEA a prévu de mettre en place une VDTB expérimentale sur l'autoroute A1, afin de faciliter la connexion entre l'aéroport de Roissy et Paris. Le projet consiste à dédier la voie de gauche pour les taxis et les bus. La zone concernée se situe entre Le Bourget et le tunnel du Landy, dans le sens province-Paris et de 06h30 à 10h00 tous les jours.

Pour ce projet, l'utilisation de modèles d'émission est quasiment impossible de par les difficultés d'avoir un scénario prospectif sur les données de trafic.

Ce travail devrait répondre à ces questions importantes sur l'évaluation des politiques de transport :

-Quels sont les données importantes à utiliser pour une bonne évaluation de la qualité de l'air et du bruit ?

-Comment pouvons-nous améliorer la méthodologie commune sur les impacts de la qualité de l'air et du bruit ?

Mots-clés : *évaluation, impact, politiques de transport, environnement, trafic, qualité de l'air, bruit*

Background

Transportation of people and goods interact in three areas of sustainable development: economic, social and environmental, including greenhouse gases emissions (GHG) and noise pollution.

Public transport policies should support sustainable development. They play a role in the organization and management of transport. They must attempt to reduce transport demand by including town and country planning, behaviour and lifestyles.

In France, these are organised on a regional scale, mainly at departmental level, with national and European coordination.

They are the subject of public debate through regional integrated development plans (Schémas de Cohérence Territoriale - SCOT) and transport framework plans.

Limiting environmental impact is one of the key objectives. To do this, it is appropriate to assess these inconveniences.

In France, environmental assessment includes integration, participation, precaution and prevention (article L. 110-1 of the Environment Code). Environmental and health aspects should be examined as early as possible. The negative effects of a project should be avoided, reduced or compensated for.

The evaluation of public transport policies is important in order to learn the effects of exposure of the population and to quantify the real impact of these policies.

CEREMA Nord-Picardie performs these environmental studies, especially on the topics of air quality and noise. Joint air and noise studies began in 2001. These studies, as part of project evaluation, are not yet often carried out using homogenized approaches.

Air-noise evaluations can be made by on-site measurement and/or modelling, the ideal solution being to use both. The article describes the methodologies used in the context of two studies in the Ile-de-France (Paris) region: the HGV diversion in the Ile de France region as part of the Ile de France Atmospheric Protection Plan (PPA) (evaluation by modelling) and creating a taxi and bus dedicated lane on the A1 (evaluation by measurements).

Feedback is presented on the difficulties of combining air and noise initiatives and the expected areas for improvement.

1. Theoretical notions

A sound is quantified by the amplitude of pressure fluctuations and is expressed in decibels (dB). The decibel is a ratio between a measured quantity and a reference level.

Its scale is logarithmic. A weighting called A is applied in order to approximate to human auditory perception.

Frequencies audible by humans range from 20 to 20,000 Hz. These figures may vary according to age and the people concerned. Below 20 Hz are infrasounds and above 20 kHz, ultrasounds. These do not give any sensation of sound. The human ear is more sensitive to midrange and high frequencies corresponding to the frequencies of the voice (from 500 to 10,000 Hz). To account for this sensitivity that varies with frequency, a type A weighting is applied.

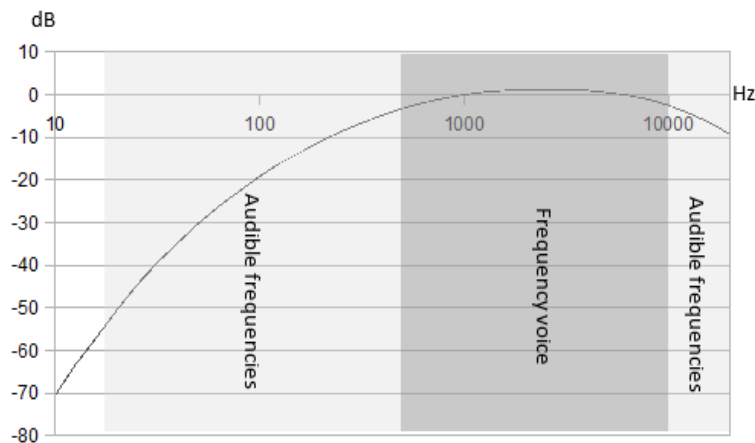


Figure 1. Type A acoustic weighting (dB according to frequency in Hz)

The propagation of sound in air is uniform in all directions. It is related to a number of factors, some of which are in common with air quality:

- geometric divergence
- atmospheric absorption
- topography
- ground effect
- weather conditions

In theory, doubling the distance in an open field and in normal sound propagation conditions, reduces the noise level by 3dB(A), loss by geometric divergence. Under these conditions, the decrease in sound level between a distance d1 from the road and a point distant from d2 is expressed in the form:

In fact, the perceived loudness away from a noise source (> 200m) is very much influenced by the ground effect and atmospheric absorption (weather).

If there is an obstacle, part of the sound is reflected, part absorbed, and the rest will be transmitted through the obstacle or diffracted.

The influence of weather conditions on propagation may be great: they influence the shape of the acoustic radiation (depending on the temperature gradient, speed and wind direction).

The acoustic impact of road infrastructure is dependent on traffic, traffic speed, emitter-receiver distance and angle of view. For example, in open fabric (building) and regardless of the nature of soils and topography, the following formula can be used to estimate the noise level on house front:

$$L A e q = 20 + 10 * \log \square(Q e) + 20 * \log \square(V) - 12 * \log \square\left(d + \frac{L c}{3}\right) + 10 \log \square\left(\frac{T \acute{e} t a}{180}\right)$$

LAeq: the equivalent A-weighted noise level in dB (A)

Qe: the equivalent representative hourly flow of traffic LV-HGV in veh/h

V: speed, in km/h

d: the distance between the receiver and the side of the roadway in m

Lc: the width of the roadway in m

Theta: angle at which the source is seen in degrees

It should be remembered that of air pollutant emissions can be quantified by the following equation for a traffic source:

$$E = FE * Qe$$

with: E: Pollutant emission per time step, in g/h

FE: Unit emission factor of pollutant per kilometre, at a given speed (g/km)

Qe: the hourly rate of equivalent traffic, in veh/h (LVs, as HGVs are often expressed as a percentage of traffic)

The relation between pollutant emission and traffic is linear.

Evolution equation of chemical species "i" in 3D model:

$$\underbrace{\frac{\partial C_i}{\partial t} + u_x \frac{\partial C_i}{\partial x} + u_y \frac{\partial C_i}{\partial y} + u_z \frac{\partial C_i}{\partial z}}_{\text{advection}} = \underbrace{\frac{\partial}{\partial x} \left(K_{xx} \frac{\partial C_i}{\partial x} \right) + \frac{\partial}{\partial y} \left(K_{yy} \frac{\partial C_i}{\partial y} \right) + \frac{\partial}{\partial z} \left(K_{zz} \frac{\partial C_i}{\partial z} \right)}_{\text{diffusion}} + \underbrace{R_i(c_1, c_2, \dots, c_n)}_{\text{chimie}} + \underbrace{E_i(x, y, z, t)}_{\substack{\text{sources} \\ \text{(émis.)}}} - \underbrace{S_i(x, y, z, t)}_{\substack{\text{puits} \\ \text{(dépôt)}}$$

2. Importance of taking co-exposure into account

First, multi-exposure and co-exposure must be distinguished. Multi-exposure is the exposure of a receiver, in our case the population, to the same type of inconvenience (air quality, noise or vibration) from several sources: for example, a resident subject to noise from a road, a railway line and a factory. Co-exposure is exposure of a receiver to multiple inconveniences from the same source.

Air quality and noise affect the health of people living near road, rail and airport infrastructure (HEI 2010).

People living close to road, rail and aircraft noise are likely to experience negative health effects.

For air pollution, in addition to the risk of cancer, acute effects must be distinguished from chronic effects. Road traffic is a major source of pollution. Epidemiological models indicate that cardiovascular and respiratory systems are most affected by oxidative stress and inflammation. Other organs may also be affected.

Health effects of air pollution can be distinguished to acute, chronic not including cancer and cancerous. Epidemiological and animal model data indicate that primarily affected systems are the cardiovascular and the respiratory system. However, the function of several other organs can be also influenced (Kunzli and al, 2000; Cohen and al., 2005; Huang and Ghio, 2006).

Long-term noise exposure may lead to problems with their heart and circulatory (cardiovascular) system and night-time noise is particularly disruptive of sleep patterns, which in turn may lead to cardiovascular health problems (Münzel and al, 2014). Traffic noise can cause numerous health problems such as sleep disturbance, high bloodpressure and psycho-physiological symptoms (King and al, 2003; WHO, 2011)

Noise is defined as a sound without regular harmony, which affects the health of man and his physical, mental and social well-being. Different people perceive it differently according to its components. Excess noise has an impact on hearing, with effects ranging from simple ear fatigue to hearing loss. Over the long term, the cardiovascular system is also affected. Night-time discomfort disrupts sleep and increases cardiovascular risks (ANSES 2013).

Studies on health and noise are more numerous and have allowed the World Health Organization (WHO) to determine guideline values for the specific effects of noise on health. A day sound level (L_{day}) of 57.5 dB(A) can lead to cardiovascular events. By night (L_{night}) sound levels from 40 to 55 dB (A) can generate a risk of hypertension and myocardial infarction or cardiovascular effects above 55 dB (A).

Although the mechanisms leading to an impairment of the cardiovascular system do not always follow the same pattern, it has been shown that there may be an interaction between the two sources of inconvenience - air quality and noise - and cardiovascular risk.

Some studies exist about potential cofounders between air pollution and noise in studies about association between air pollution due to traffic and CVD or noise due to traffic and CVD (Selander and al, 2009; Beelen and al, 2008)

Moreover, it may be appropriate to take into account co-exposure to other elements such as drugs (e.g. ototoxic for noise, antihistamine for air), population age and health, vibration, etc.

3. Feedback from the Ile de France PPA

Presentation of the study on the Ile de France PPA

The Atmospheric Protection Plan for the Île-de-France region for the period 2005-2010 was approved in 2006 and its revision approved on March 25, 2013. It notes that road transport is responsible for 54% of NO_x emissions, 25% of PM₁₀ and PM_{2.5} emissions. HGVs account for 30 and 10% respectively.

As part of the 2013 revision of the Île-de-France PPA, a study entrusted to Cerema focused on assessing the real impact of a bypass for HGVs in transit in the heart of the Ile-de-France region as it could actually be implemented, subject to a study on the legal basis and means of controlling it.

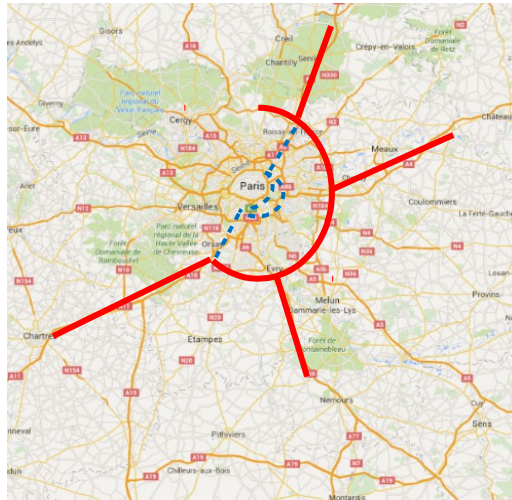


Figure 2. Bypass project for HGVs in transit

The studies by Cerema Nord-Picardie focus on human exposure to the effects of air quality and noise.

Study methodology

The field of study of the project is large and complex. This conditioned the choice of a methodology based primarily on air and noise modelling, using available traffic data, with and without the project.

Ideally, measurements to reinforce the initial draft-project diagnosis would have been required, but the time available for the study and the complexity of the terrain did not allow this measurement process to be completed.

The study is one relative to a baseline scenario and not an accurate model of pollutant and noise emission levels.

For noise, the routes affected by the HGV bypass were acoustically characterized (Paris ring road, A86 and Francilienne).

An enumeration of the population exposed to changes in sound levels, and especially to "significant" changes in sound levels, was made.

An assessment of the degree of sensitivity of routes was performed using predefined exposure limits and the risk of exposure to multi-sources noise, mainly airport and railway noise.

The study is one relative to a baseline scenario and not an accurate model of noise levels.

The proposed methodology is based on an estimate of noise levels from traffic according to the noise guide. It has limits which are listed below:

- the choice of the reference road section with the maximum sound level for the exposure study
- increased noise level is calculated at the infrastructure level, at the place where it is theoretically maximum. This causes noise levels to be overestimated
- propagation: a section A, noisier (95 dB (A) for example) than a section B (94.9 dB (A) for example) is taken into account, whereas a building may be located at 290m from section A and 10m from section B.
- existing noise protection (screens or mounds) and indirect protection related to the presence of buildings of different heights are not taken into account
- the difference in maximum acoustic levels selected for buildings is the effect of the buffer with the highest sound level of the baseline scenario encompassing the building. The sound level of the section is considered as having greater impact in terms of discomfort than the effect related to changes in traffic.

Sound emissions of the routes concerned are calculated as relative values from the land-based transport noise guide - forecasting sound levels (CETUR November 1980) and 2020 traffic, according to the steps listed below,

Step	Action
Calculation of traffic	$Q=Q_{LV} + 10Q_{HGV}$
Choice of speed	$V=Max (V_{LV};V_{HGV})$
Finding one-way streets	If $Q=0$ and $V=0$ then $LA_{eqAB}=0$
Noise levels in U streets	If $V<50\text{km/h}$ then $LA_{eqAB}=55+10\log(Q)$
Noise levels in open fabric	If $V>50\text{km/h}$ then $LA_{eqAB}=20+10\log(Q)+20\log(V)$
Addition of both directions of travel	$LA_{eq}=LA_{eqAB}+LA_{eqBA}$
Acoustic impact	$I=LA_{eqf} - LA_{eqi}$, if LA_{eqf} ou $LA_{eqi} = 0$ then I not considered

For each road segment, the emissions are calculated for periods of Day and Night.

The differences in noise levels compared to the baseline are sorted by class, as is the case for air quality.

The class boundaries chosen correspond to:

- a significant noise reduction impact [-5 dB, -2dB] (positive impact)
- a perceptible noise reduction impact [-2 dB, -0.5dB] (positive impact)
- a negligible variation [-0.5dB, +0.5dB].
- a perceptible noise increase impact [+0.5, +2dB] (negative impact)
- a significant noise increase impact [+2dB, +5dB] (negative impact)

The limit of 2 dB (A) was chosen in reference to the noise law which defines this threshold as a significant change and forces the manager to protect residents from reaching or exceeding this threshold (protection at source or at the façade).

The results of the acoustic study are cross-referenced with land use in terms of buildings and population in a buffer area of 300m around the roads examined in the main network.

The population data are identical to those used for the air quality study.

The choice of acoustic impact per building is made as follows:

- find the buffer corresponding to the road with the highest noise level (baseline scenario) containing the building
- take the difference in sound levels associated with the maximum sound level chosen

The Bruitparif association makes noise maps for the Ile de France region available to the public. They give an idea of the original acoustic status in the area examined.

The Bruitparif maps show areas already highly affected by noise pollution, and areas identified as potentially affected by the proposed HGV diversion as part of the PPA. Adding traffic would be likely to cause buildings to be defined as noise black spots with compulsory protection for local residents. Crossing railways and the Le Bourget airport area need to be analysed in more detail also with regard to multi-source sound exposure of these sectors.

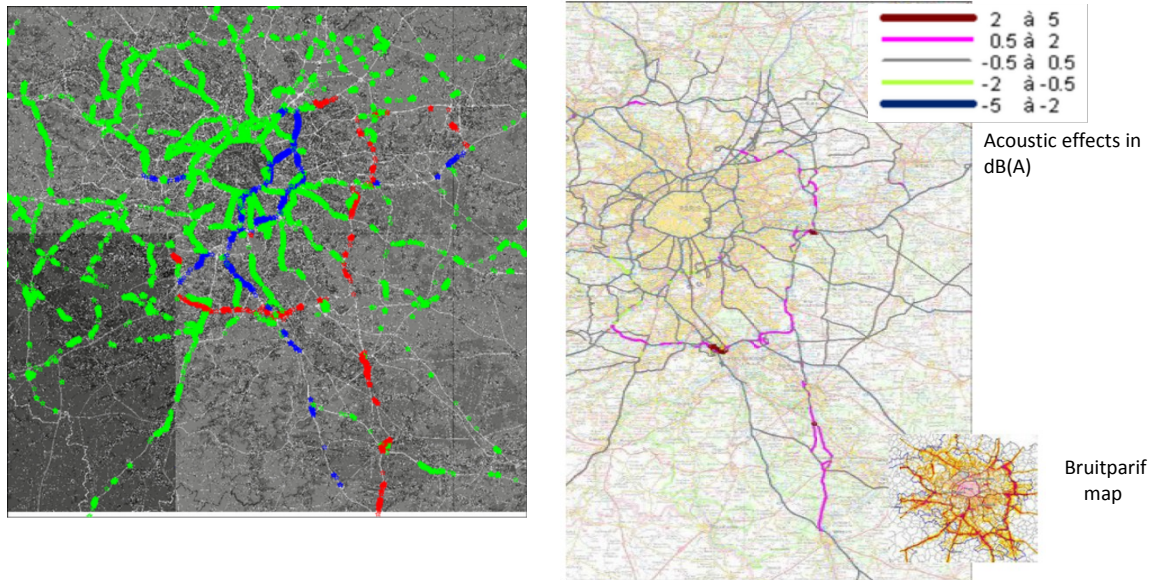


Figure 3. Acoustic and air impacts of the diversion project (in dB(A))

For air quality, the work focused on nitrogen oxides NOx and particulate matter (PM10) and especially:

- modelling NOx and PM emissions along major routes,
- an assessment of populations exposed to these pollutants (number of people affected by a rise or fall of emissions, and a "significant" increase or reduction in emissions),
- an assessment of the impact on CO2 emissions will also be conducted across the region (irrespective of areas that have no meaning for this component, the effect of which is not local).

The calculation of emissions from road traffic is performed using COPCETE software developed by Cerema as part of the Scientific and Technical Network of the French Ministry of Ecology, Energy, Sustainable Development and the Sea.

This software is based on the COPERT 4 methodology. Traffic data used are AADT (Annual Average Daily Traffic). Only the main road network was taken into account, because of the density of road infrastructure in this area.

The unit emissions factors correspond to the mass of pollutant emitted by a vehicle for a given trip length. They are expressed in kg/km/vehicle.

The composition of the motor vehicle fleet taken into account in this study is that established by IFSTTAR (French Institute of Science and Technology for Transport, Development and Networks), which provides a distribution based on age and fuel for each vehicle class, and also the gross vehicle weight rating for HGVs.

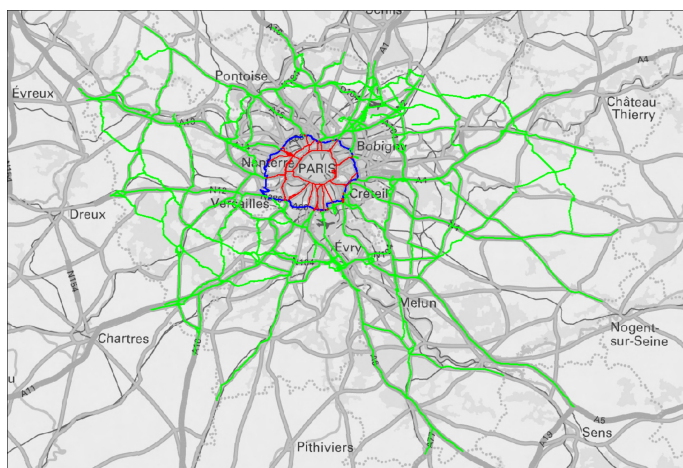


Figure 4. Main network taken into consideration in calculating population exposure

The population was enumerated by plot in a study strip of 300m around each road of the main network.

For NO_x, the affected population taken into account is that present in this 300m buffer area. For PM, only the population within a 150m buffer area around the roads was considered (this is the particle impact distance).

First, the slight changes in emission percentages (increasing or decreasing) may largely result from uncertainties in modelling. It is necessary to be careful when interpreting these lower data, which are at the limit of the models. Out of 27,393 sections examined, only 2,981 did not vary between the different scenarios. The project does not however concern all the sections which show a variation: these are modelling uncertainties.

The affected population is distributed according to the roads into 3 classes. Insignificant changes in emissions were defined on the basis of calculations of the excess concentrations produced. Below an emission of 100 g/km (positive or negative) for a road section, we were able to consider the over-concentration as negligible.

- population affected by falling significant emissions (positive impact) greater than -100g/km for a road section and by pollutant,
- population not affected or affected by insignificant changes in emissions for a road section and by pollutant; the insignificant emissions are in the range [-100, 100] in g/km,
- population affected by rising significant emissions (negative impact) greater than 100g/km for a road section and by pollutant.

Excess concentrations of pollutants were modelled from emissions, knowing that a change in emissions may seem significant without resulting in a significant excess concentration. In addition, the excess concentrations do not accumulate in one zone, unlike emissions.

4. Feedback on the VDTB- A1

Presentation of the VDTB-A1 study

On the A1 motorway, an experimental lane dedicated to taxis and buses (VDTB) was set up to facilitate the connection with Roissy airport in Paris.

The development involves dedicating the left-hand lane for taxis and buses, between Le Bourget and the Le Landy tunnel, in the province-Paris direction, from 06:30 to 10:00 am. The dedicated lane runs from La Courneuve to the Le Landy tunnel.

The move from three to two lanes creates additional congestion on the A1 motorway. To make it easier for vehicles from the A1 to get onto the Paris ring road and limit congestion, the right-hand lane of the ring road will be closed at the level of Porte de la Chapelle, increasing the insertion distance. This arrangement should make traffic on the A1 more fluid.

The VDTB will be activated by a dynamic system of road signs.

An initial experimental phase was carried out in 2008-2009 with the study of traffic, greenhouse gas emissions and noise impact.

Cerema was asked to conduct a more complex assessment of the impact of the arrangement in order to better understand the effects on exposure. The traffic studies are also entrusted to Cerema.

The study extends to the length of the A1 concerned and to the ring road from Porte de la Chapelle to Porte de Bagnolet.

Study methodology

The assessment for this project was made by means of measurement campaigns. The use of models is almost impossible because of the difficulties in obtaining a prospective scenario on traffic data.

An initial status report, before implementing the measurement has been made, followed by a conclusion after commissioning (not yet done).

The aim is to establish a methodology for measuring the impact of setting up the VDTB at the level of the A1 on significant noise and pollutants in the Île-de-France region, from measurements made in situ. The challenge is a substantial one because VDTBs are likely to develop as part of the urban framework transport plan.

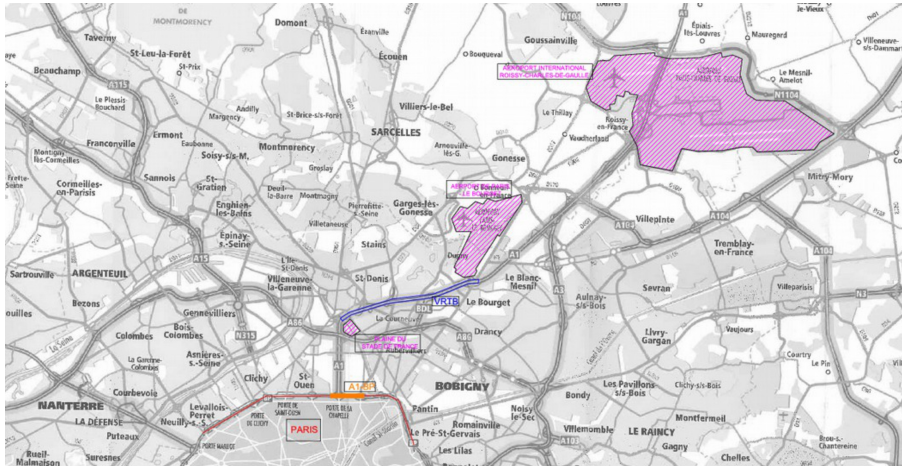


Figure 5. The VDTB on the A1, between Roissy and Paris

For noise, measurement points are set up throughout the length of the proposed VDTB, mainly on the province-Paris side (the direction of the VDTB) and in keeping with the site and safety imperatives.

The measurement campaigns were broken up by route: A1 and ring road.

The site is highly urbanized with much road infrastructure. A quiet area extends along the project: the Georges Valbon park in La Courneuve.

On the A1 motorway, three sound-level meters have been installed for 24h measurements. Acoustic mapping is complemented by short-term measurements (30 minutes) readjusted to the 24h points. On the ring road, 3 sound-level meters are also in use for 24h measurements.

The study focuses mainly on the period 6:00 am to 10:00 am, corresponding to the period when the signage for the VDTB is in use.

The measurements are validated on the basis of meteorological data - wind and rainfall - from the nearest Météo-France weather station.

Sound levels measured hourly and modelled for different cross sections before and after commissioning the VDTB, are adjusted according to hourly traffic road by road, then compared.

The study of the initial status by measurements is based on the same measurement sites as for the air and noise studies, while respecting the specific imperatives of each of the two subjects. These respective imperatives reduce the choice of potential sites to be instrumented, which may ultimately, but only in certain cases, lead to a decrease in measurement quality for one of the subjects. Care therefore needs to be taken with the choice of air-noise sites.

The approach to representativeness of the measurements compared to the annual situation for example is not based on the same methodology as for the noise field: measurements are recalculated taking into account the hourly traffic measured in terms of AADT.

Despite the efforts made in this study to achieve as uniform an air-noise assessment as possible, the duration of the air and noise measurements, taking into account the equipment and the respective methodologies in use, are different.

The initial assessment presented will be reproduced as soon as measurement has been implemented in a stabilized manner to make it possible to determine the impact of the proposed VDTB.

The impact on air quality of the project is characterized by means of measurements points by passive tubes. They are installed along the A1 motorway and the ring road. These passive tubes are placed there for two weeks. The pollutant measured will be NO₂, the tracer for car pollution.

AirPointer, a multi-pollutant measurement unit, is installed alongside the A1 and is used to display

concentrations during the measurement period and also outside this period, with a fine time step. The unit measures O₃, NO₂ and PM₁₀.

Six passive tubes will be placed along the A1, including one on the Airparif measuring station and one on the Airpointer. Three passive tubes have been installed on the ring road.

Measurements by passive tubes take place over a period of one week, with fitting on Monday and removal the following Monday.

Airpointer measurements take place over a two-week period.

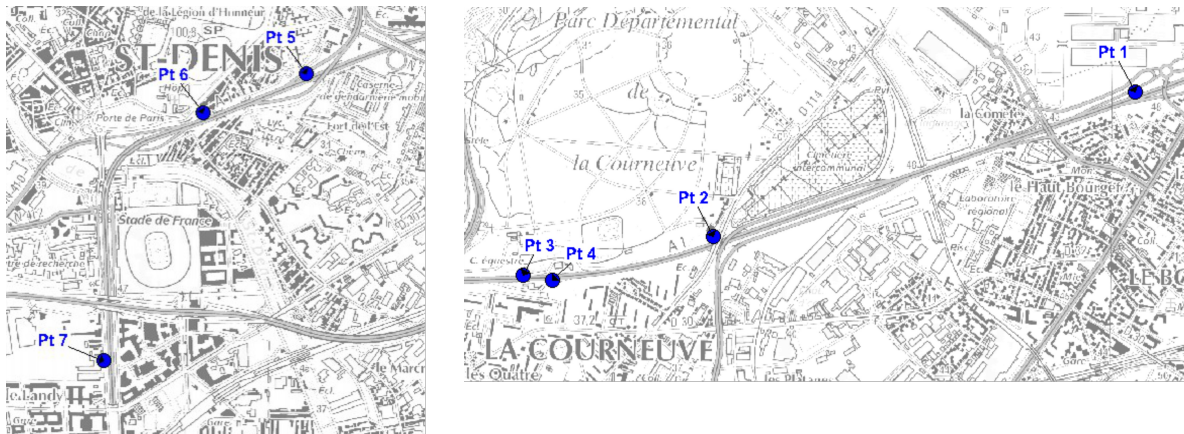


Figure 7. Acoustic and air measurement points on the A1

5. Experience feedback and suggestions for improvement of air-noise co-exposure studies

This feedback is done from the studies presented in this article and, in addition, many other studies conducted by Cerema Nord-Picardie as part of road projects, improvements to waterways and urban development.

It should answer these important questions about the assessment of transport policies:

- What are the important data to be used for proper assessment of air quality and noise?
- How can the common methodology for air quality and noise impacts be improved?

The various input data common to both themes are given below:

- The project and any variants,
- Traffic (annual average daily traffic, speed, percentage of HGVs),
- The population,
- Sensitive institutions such as schools and hospitals,
- The various sources of pollution present (other infrastructure, industries),
- The topography,
- Buildings,
- Meteorology observed over the long term on the field examined and that observed during any measurement campaigns.

All of these are necessary for environmental impact surveys and air and noise modelling. It is imperative that these data come from the same data sources for air and noise, which is not always the case.

In general, complying with regulatory requirements or recommendations in the strict sense on air and noise may lead to a heterogeneous approach that may be detrimental. It is often necessary to go beyond regulatory requirements in order to achieve a consistency of approach. The main points requiring care relate to the points listed below:

- the study field or area

Implementing an assessment in a common air and noise study field or area. The 2005 air health circular concerning road infrastructure impact studies recommends taking into account a field of study consisting of the project examined and all roads whose traffic varies by plus or minus 10% as a result of implementation of the project. Noise regulations require an assessment around the project only

- time frame of the study

In a study on the impact of a development project, noise regulations require an assessment of this impact at a time equal to "commissioning date + 20 years". The annex to the circular of 12/12/1997 relating to the consideration of noise in the construction of new roads or the development of existing roads in the national system actually indicates that compliance with maximum permitted noise levels is compulsory throughout the service life of the infrastructure.

In practice, noise levels will be evaluated, in general, 20 years after commissioning, taking into account the high-case estimates of traffic growth. As regards air quality, no study time frame is imposed.

It would therefore seem appropriate to keep the study time frame imposed by the acoustic requirements. This time frame, however, is not what has the greatest impact on air quality, because of favourable technological developments for reducing unit emissions factors and also because of uncertainties about the way the motor vehicle fleet is changing. Commissioning the project may in fact be the scenario that has the most impact for air quality due to favourable technological developments.

For noise, the increased traffic expected for a "commissioning date + 20 years" scenario will have more impact than during commissioning.

- measurement periods

During in situ measurements, the measurement periods for air quality and noise are often different, particularly because of imperatives relating to the equipment. Moreover, regarding air quality, good measurement representativeness makes it necessary to measure concentration levels for at least 8 weeks distributed over the year, in different seasons.

As far as noise is concerned, NFS31-085 standard describes the in situ measurement method for noise resulting from road traffic on existing infrastructure. Three methods are described: observation measurement, measurement and estimation of a traffic long-term sound level, measurement and interpretation of a long-term sound level with respect to long-term weather conditions.

For the last two methods which make it possible to obtain an annual type representation of the measurement, it is possible to readjust measurements in relation to traffic data representative of a long-term situation, or even with representative meteorological data.

This approach is different from that for air quality: the representativeness of air measurements is based on a measurement time, without analysis of the observed traffic.

- protection devices

For noise, acoustic protections of the sound barrier type are taken into account as part of the modelling done. These protections have an impact on air quality which is most often not taken into account in the appropriate models. But they do have a potential impact on the dispersion of gaseous and particulate pollutants, for residents of the infrastructure concerned.

Moreover, in the study phase, it is increasingly necessary to analyse a common approach to air and noise, leading to an optimized assessment of the impacts of a project on population exposure. Attempting to achieve good air quality in an urban type sector for example can actually cause a significant increase in noise levels following the shift in traffic, leading to a risk of complaints and additional costs related to the protections that need to be fitted. For example, for the Ile de France PPA, the diversion of HGVs in transit, would generate discomfort greater than 2 dB(A), in the night-time, on an estimated population of 30,000 people.

These air and noise studies have shown the recurring need for a good relationship with departments that have competency in the field of traffic. Communication between air quality, acoustic and traffic departments would require a common glossary (technical terms and units of measurement) to be drawn up. Common databases, using topography, buildings, traffic, population, etc., must be

standardized. Projects are under way such as the Shared Assistance Environmental Diagnosis platform by Cerema (PLAteforme Mutualisé d'Aide au Diagnostic Environnemental - PLAMADE). These databases must ultimately be used on both a regional and a local scale (district, development, diversion).

Acknowledgements

We would like to thank DIRIF (Direction des Routes Île de France), DRIEA (Direction Régionale et Interdépartementale de l'Équipement et de l'Aménagement d'Île de France) and our partners for their participation to this studies and specially Philippe QUOY and the service Transport-Mobility of CEREMA Nord-Picardie

References

- ANSES – Evaluation des impacts sanitaires extra-auditifs du bruit environnemental – Rapport d'expertise collective, février 2013.
- Beelen R., Hoek G., Van Den Brandt P.A., Goldbohm A., Fischer P., Schouten L.J., Jerret M., Hugues E., Armstrong B., Brunekreef B.-Long-Term Effects of Traffic-Related Air Pollution on Mortality in a Dutch Cohort (NLCS-AIR Study)-*Environ Health Perspect.* 2008 Feb; 116(2): 196–202.
- Circulaire du 12/12/1997 - Prise en compte du bruit dans la construction de routes nouvelles ou l'aménagement de routes existantes du réseau national (annexe).
- Code de l'environnement (France) : article L. 110-1.
- Cohen A. J., Anderson H. R.; Ostr, B., Pandey K. D., Krzyzanowski M., Kunzli N., Gutschmidt K., Pope C. A., Romieu I., Samet J. M., Smith K. R.-The global burden of disease due to outdoor air pollution-*J. Toxicol. Environ. Health, Part A* , 2005, 68, 1301–1307.
- Health Effects Institute-Traffic-Related Air Pollution : a critical review of the literature on emissions, exposure, and health effects-January 2010.
- Huang Y.-C. T., Ghio A.- Vascular effects of ambient pollutant particles and metals. *Curr. Vasc. Pharmacol.*, 2006 4:199–203.
- International Journal of Hygiene and Environmental Health*, 2003, 206(2), 123-131.
- King R. P., Davis J. R. - Community noise : health effects and management-*International Journal of Hygiene and Environmental Health*, 04/2003, 206 (2), 123-31.
- Kunzli N., Tager I. B. - Long-term health effects of particulate and other ambient air pollution: research can progress faster if we want it to *Environmental Health Perspectives*, 2000, 108, 915-918.
- Münzel T, Gori T, Babisch W, Basner M.-Cardiovascular effects of environmental noise exposure-*Eur Heart J.* 2014 Apr;35(13):829-36.
- Norme AFNOR NFS 31-085 - Caractérisation et mesurage du bruit dû au trafic routier.
- Selander J., Nilsson M.E., Bluhm G. Rosenlund M., Lindqvist M., Nise G., Pershagen G.-Long terme exposure to road traffic noise and myocardial infarction- *Epidemiology (Cambridge, Mass.)*,. 03/200,; 20(2):272-9.
- WHO-Europe - Night noise guidelines for Europe 2009).
- WHO-Burden of disease from environmental noise: Quantification of healthy life years lost in Europe- WHO Regional Office for Europe, 2011.

Analyzing impacts of intense ethanol fuel use on urban VOCs burden and composition

Pamela A. DOMINUTTI^{1,2}, Agnes BORBON², Thiago NOGUEIRA¹ and Adalgiza FORNARO¹

¹Department of Atmospheric Sciences, University of São Paulo, São Paulo, Brazil
Rua do Matão, 1226, CEP 05508-900, São Paulo, SP Brazil.
E-mail address: pamela.alejandra@iag.usp.br; Fax: +55-11-3091-4713.

²Laboratoire de Météorologie Physique LaMP/CNRS, Université Blaise Pascal
4 av. Blaise Pascal, 63178 Aubière Cedex - France

Abstract

São Paulo Megacity (MASP), with more than 20 million inhabitants, is among the world's most populous cities. Brazil is the only area in the world where fuel with a high ethanol content has been used since 1975 and its usage has increased in the last decade with the development of flex-fuel vehicles. Here, we discuss the biofuel effects on VOCs burden and composition by a crossed analysis of long-term ambient data and emission data over the last decades in MASP. In particular a very detailed and comprehensive database of gaseous Non-Methane hydrocarbons (NMHC) were hourly collected in 2013, completed by near source campaigns. The ambient concentrations were submitted to an exhaustive verification before analyzing the diurnal, seasonal and spatial variability. The most abundant NMHCs were propane (5.02 ± 5.94), ethylene (3.97 ± 4.55), ethane (2.28 ± 1.89), acetylene (1.98 ± 2.11), 2,2,4-trimethylpentane (2.05 ± 1.48), *i*-propylbenzene (1.96 ± 1.85), *n*-butane (1.97 ± 2.24), toluene (1.62 ± 2.02), *i*-pentane (1.30 ± 1.61) and propylene (1.26 ± 1.54). The comparison with studies performed in MASP over the last 15 years show a decrease in the NMHC levels, in spite of the growth of the vehicular fleet and fuel consumption. However, VOC mean concentrations are higher in MASP compared to other megacities worldwide (Paris, Los Angeles and London) by a factor of 1.5 to 20 but shows similar composition. This suggests that VOC distribution is dominated by traffic emission regardless of regional characteristics like fuel characteristics. Diurnal profiles of NMHC in MASP confirm these findings by all showing the same patterns as CO and acetylene, both recognized as vehicular emission tracers. Finally ethanol would not affect the distribution of NMHCs in MASP area.

Keys-words: VOCs, vehicular emissions, megacity, ethanol

Résumé

La mégapole de São Paulo (MASP), avec plus de 20 millions d'habitants, compte parmi les villes les plus peuplées au monde. Au Brésil, le carburant avec une teneur élevée d'éthanol a été introduit depuis 1975 et son utilisation a largement augmenté au cours de la dernière décennie avec le développement et la mise sur le marché des véhicules hybrides Flex-Fuel. Ici, nous discutons les effets de l'utilisation de l'éthanol comme biocarburant sur la composition et les niveaux des COVs par une analyse croisée des données ambiantes et des données d'émission d'hydrocarbures non-méthaniques (HCNM) au cours des dernières décennies à MASP. Un jeu de données des HCNM gazeux très détaillé a été recueilli avec résolution horaire en 2013, complété par campagnes proches des sources d'émission. Les concentrations ambiantes ont été soumises à un contrôle qualité exhaustif avant d'analyser leur variabilité diurne, saisonnière et spatiale. Les HCNM les plus abondantes sont le propane (5.02 ± 5.94), éthylène (3.97 ± 4.55), éthane (2.28 ± 1.89), acétylène (1.98 ± 2.11), 2,2,4-triméthylpentane (2.05 ± 1.48), *i*-propylbenzène (1.96 ± 1.85), *n*-butane (1.97 ± 2.24), toluène (1.62 ± 2.02), *i*-pentane (1.30 ± 1.61) and propylène (1.26 ± 1.54). La comparaison avec des études effectuées dans MASP au cours des quinze dernières années montre une réduction des niveaux COVs, malgré l'augmentation du nombre de véhicules et de la consommation de carburants. Cependant, les concentrations moyennes restent plus élevées dans MASP par rapport aux autres mégapoles (Paris, Londres et Los Angeles) même si les profils montrent une composition similaire. Ceci suggère que la distribution des HCNM est dominée par les émissions du trafic quel que soit la zone urbaine et les pratiques réglementaires. L'analyse des profils diurnes des HCNM confirme ce

résultat en montrant des profils similaires à ceux du CO et de l'acétylène, tous deux reconnus comme traceurs d'émission véhiculaire. Finalement, l'utilisation de bioéthanol n'affecte pas la distribution en NMHC à São Paulo.

Mots clés : COVs, émission véhiculaire, mégapole, éthanol

1. Introduction

Non-methane hydrocarbons (NMHCs) are important pollutants present in urban atmospheres and these are mainly emitted by primary anthropogenic sources. Once emitted into the atmosphere, NMHCs can react with atmospheric oxidants to produce other pollutants like ozone and Secondary Organic Aerosol (SOA). Field observations of NMHCs can provide relevant information for a better prediction of ozone, SOA and other oxidant estimations, as well as for building up emission inventories, which strongly depend on an accurate knowledge of the primary NMHC emissions.

The population density in large urban areas has grown alarmingly in recent decades. Currently, there are close to 30 megacities (over 10 million inhabitants) worldwide, while in the early 70s there were only three (UN, 2014). These areas have serious problems that affect the quality of life of its inhabitants, including water supply, sewage treatment, housing, air pollution and mobility. São Paulo megacity (MASP), the most important economic region in Brazil, is one of the largest urban agglomerations in the world. The region covers an area of 8051 km², being the urban area 2000 km² with 21 million inhabitants and more than 11 million of licensed vehicles (IBGE, 2014).

The vehicular fleet has been considered the main source of air pollutants in the MASP and responsible for more than 90% of CO, NO_x and hydrocarbons emissions in 2013 (CETESB, 2014). This vehicular fleet burn gasohol (25% anhydrous ethanol and 75% gasoline), hydrated ethanol (5% of water content) and diesel (5% biodiesel). It is important to highlight that the consumption of the total ethanol (anhydrous + hydrated) was higher than that of gasoline for the first time during 2008-2010. Since 2003, the number of flex-fuel vehicles (burn ethanol or gasohol) increased, reaching almost 6 million and 83% of MASP vehicular running fleet.

The use of ethanol or gasohol by flex-fuel vehicles depends on the relationship between price and fuel consumption, making ever more complex the evaluation of emissions of air pollutants by the vehicle fleet. The Brazilian fuel characteristics make of MASP an especial scenario for air pollutants studies. Since 1986, the Brazilian air pollution control program for vehicles (PROCONVE) has been established new fuel quality and technological innovations, such as electronic injection and catalytic converters, apart from increasing bio-fuels production, reducing emissions limits and changing vehicular fleet. Despite the increasing number of vehicles during this period, the reduction of air pollutants concentrations has been significant (CETESB, 2013; Nogueira et al., 2014). MASP has an important air quality monitoring network, managed by the São Paulo State Environmental Agency (CETESB). More than 20 years of CETESB data show a strong decrease in the concentration of SO₂, CO, NO and PM (by a factor of 8, 5.15, 3.1 and 2.3 respectively, while the maximum O₃ concentrations has remained unchanged (Carvalho et al., 2015; Pérez-Martínez et al., 2015).

Tropospheric ozone (O₃) is one of the main atmospheric pollutants in MASP, being the exceeding of the Brazilian standard air quality (1 hour, 160 µg m⁻³) most frequent from September to March (Spring and Summer), during hot days and higher incidence of solar radiation (Carvalho et al., 2015). This O₃ situation is worrying and raises the question of the role of non-methane hydrocarbons (NMHC) as one of their major precursors, especially in urban areas with VOC-limited photochemical regimes (Fujita et al., 2003; Qin et al., 2004; Silva Júnior et al., 2009).

In order to characterize the NMHCs composition in MASP atmosphere, few ambient campaigns have been conducted over the last twenty years. In addition, campaigns for determining NMHCs were carried out in inside urban tunnels (Alvim, 2013; Martins et al., 2006; Vasconcellos et al., 2005). Nevertheless, few studies were performed since the flex-fuel fleet increase and after the switch to ethanol usage. Even though ethanol has been considered a less polluting bio-fuel (Goldemberg, 2007), little is known on its impact on VOC emission levels and composition due to limited temporal and spatial measurements in the MASP or even in Brazil (Brito et al., 2015).

This work aims to analyze the composition of NMHC profile in the metropolitan area of São Paulo by performing online sampling during the whole year of 2013. We also analyzed the multiyear trends in NMHCs levels in MASP and the spatial variations of these compounds among other megacities worldwide. An evaluation of the vehicular and urban background profiles is also provided by

comparing to profiles available in studies before. Finally, the impact of the use of intense ethanol in the vehicular fleet and its consequences in the NMHCs profile is approached regarding the implication in fuel-vehicular improvements and air quality.

2. Materials and methods

Sampling point

The MASP is located in southeast of Brazil at approximately 800 meters above sea level (m.a.s.l.), 60 km far from Atlantic Ocean (Fig. 1). The climate in MASP is characterized by a dry season in winter (June, July and August) with minimum mean temperatures values (monthly mean 12°C), precipitation (< 60 mm/month) and cloudiness, and a wet season in summer (December, January and February) with maximum mean temperatures values (monthly mean 27°C) and precipitation > 170 mm/month (IAG, 2014). The other seasons present the intermediary conditions between dry and wet characteristics.

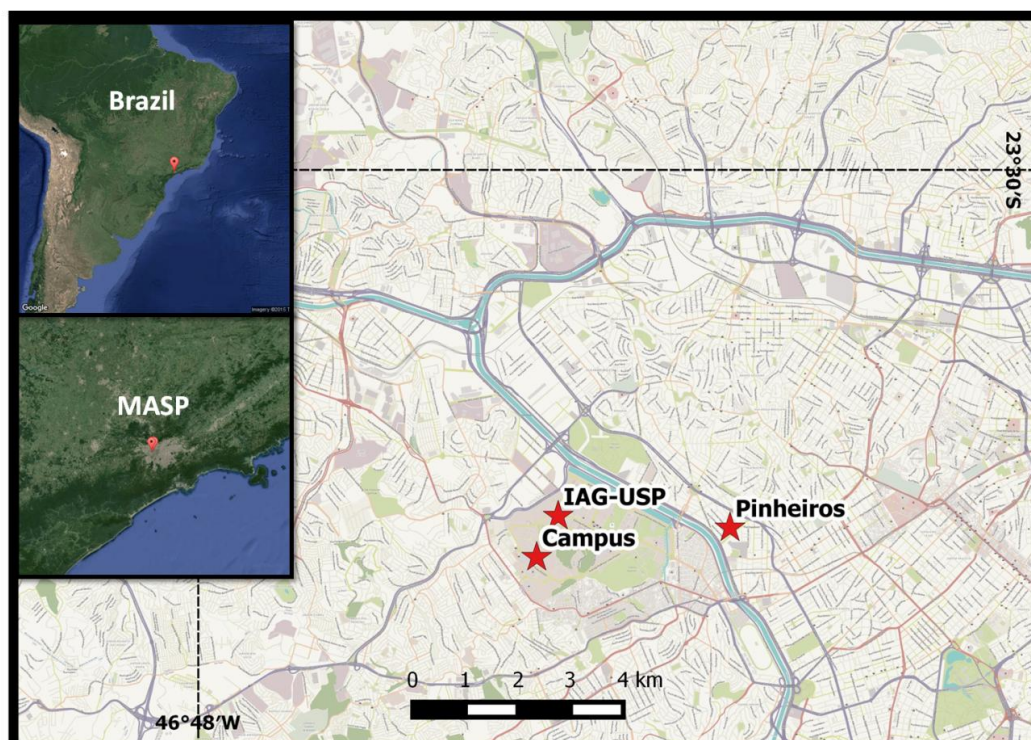


Figure 1. Location of measurement points: IAG for the NMHCs monitoring point; Pinheiros and Campus are the official Air Quality Monitoring Stations (CETESB).

The sampling site (figure 1, IAG) is located inside the University of São Paulo campus (USP), in the western region of MASP (23°33'33.6" S, 46°44'0.3" W), 750 m above sea level. USP campus is a little green-park (~7.5 km²), with traffic along the day, and surrounded by important roads with intense traffic of light and heavy-duty vehicles. We sampled the NMHCs on the rooftop of a building at the Institute of Astronomy, Geophysics, and Atmospheric Sciences (IAG/USP) for 2998 hours during the whole year of 2013. We considered this point as urban background due to the distance of the major suspected vehicular sources.

NMHCs measurement system

NMHCs mixing ratios were measured using the Ozone Precursors Analyzer System (Perkin-Elmer, Waltham, MA, USA), an equipment composed of an air sampler accessory, a thermal desorption unit (Turbo Matrix 650 ATD) and a double gas chromatography. The last one has two flame ionization detectors (GC-FID Clarus 500), including a dual capillary system supplied with a switching mechanism: PLOT column (Al₂O₃ / Na₂SO₄, 50 m × 0.32 mm × 5 μm) for C₂-C₅ compounds and BP1 dimethyl siloxane column (50 m × 0.22 mm × 1 μm) for the C₆-C₁₂ range. The

dried air sample is concentrated (15 mL min⁻¹) on an electrically Peltier cooled sorbent trap (- 30 °C) in the ATD during 40 min. This trap contained two carbon-based adsorbents: a graphitized carbon black to collect the less volatile compounds and a carbon molecular sieve to collect the most volatile analytes (C2–C4). The trap undergoes a rapid thermo-desorption at a 40 °C s⁻¹ up to 325 °C rate, transferring the air sample into the CG-FID. Ultra-pure helium (6.0) was used as carrier gas, and the temperature program for the GC oven was held at 46 °C (15 min), up to 170 °C (5 °C min⁻¹), up to 200 °C (15 °C min⁻¹), and finally maintained at 200 °C (6 min). Under these analytical conditions more than 55 NMHCs C2–C12 were sorted out in 47.8 min. The Ozone Precursors Analyzer System was optimized by systematic online hourly operation and controlled by Perkin-Program. This measurement system is part of the Compendium of Methods for Toxic Organic Air Pollutants TO-17 (US EPA, 1997), which describes the atmospheric air VOCs monitoring by sorbent tube or thermal desorption and analysis by gas chromatographic-based system. The air samples were drawn through a Nafion permeation dryer (Nafion®, Permapure Inc, Toms Rivers, NJ, USA) which, even though causing loss of some polar VOCs, is suitable for the sampling of other hydrocarbons.

Data analysis and quality control procedures

Two raw chromatograms, which were integrated by the software, were produced for each sampled hour, producing two reports with each distinct hydrocarbons identified and quantified. The quantification limit (QL) for most of compounds was less than 100 pptv, being the maximum value for the detection limit (DL) 30 pptv, and lower than 15 pptv for 45 NMHCs. We validated continuously the compounds identification. The automatic peaks recognition was constantly verified and eventually the retention times were manually adjusted. Concentration reproducibility as well as peak area and retention times were tested frequently. Missing data was observed in case of trap substitution, blank analysis and corrective/preventive maintenance. Mixing ratios below DL were replaced by DL/2. In this work we evaluated those NMHCs compounds which presented precision and analytical quality which parameters.

Supplementary measurements

To support NMHC data analysis and interpretation, we completed the NMHC database by air pollutants data for CO, PM_{2.5} and O₃ provided by the São Paulo State Environmental Agency (CETESB, 2015) from two air quality monitoring stations. The first is an urban background station, located at the Institute for Energy Research and Nuclear Science in the University of São Paulo campus (Campus, figure 1), 800 m far away from the IAG NMHCs sampling point (23°33'58.96"S 46°44'15.57"W). The second station (Pinheiros, figure 1) is an urban site, located in São Paulo State Environmental Agency (23°33'39.77"S 46°42'6.62"W), 4000 m from the IAG sampling point and near one of the most important roadways in MASP. Pollutants measurements were performed every hour in both stations. CO data were obtained by an analyzer based on IR absorption (48i, Thermo Scientific™ Electron Corporation, USA). For ozone was used an analyzer based on UV absorption (49i, Thermo Scientific™ Electron Corporation, USA) and for the particulate matter (PM_{2.5}) concentrations by Beta continuous ambient particulate monitor (5014i, Thermo Scientific™ Electron Corporation, USA).

Basic meteorological data (temperature, precipitation, relative humidity, cloudiness and solar radiance) were provided by the Meteorological Station of IAG/USP (IAG, 2014). Synoptic analysis were obtained from the Center of Weather forecast and Climate studies (CPTEC-INPE) reports (INPE/CPTEC, 2013). In this work, seasons are defined as follows: summer from December to February, autumn from March to May, winter from June to August and spring from September to November

3. Results and discussion

Overview of meteorology conditions in 2013

Although the total precipitation in 2013 (1501 mm) was higher than climatologic average values (1419 mm/year, from 1933 to 2013), the amount of rain was not well distributed along the year. The precipitation of 2013 showed that the winter months of June (130 mm) and July (82 mm) were surprisingly rainy, while in December (72 mm) rained one third of the average amount (200 mm/month, from 1933 to 2013). The excess of rain registered in June and July was due to a high number of frontal systems over the region. February (281 mm) was the month with more precipitation and August (10 mm) was the driest month. July and August reached the lowest temperatures.

Figure 2. Average mixing ratios comparison for different NMHCs measurements in MASP. Urban data refer to measurements performed downtown or in intense vehicular sites during the day. Urban background measurements were performed inside urban green areas (Ibirapuera Park and Campus). References: 1996 (Gee e Sollars, 1998), 1998 (Colón et al., 2001), 2003 (Martins et al., 2008), 2006 (Alvim et al., 2011), 2008 and 2011 (Alvim, 2013), 2013 (Brito et al., 2015) and 2013* this study.

In terms of spatial variability, the São Paulo NMHCs annual average presented the similar profile compared with those in megacities such as Los Angeles, Paris and London (Fig. 3). The most abundant compounds measured in MASP were propane, ethylene, ethane, n-butane, acetylene, toluene, i-butane, i-pentane and propylene, which were similar to those measured in other cities worldwide (Fig. 3). In spite of these good profile agreement, the average mixing ratios of NMHCs were higher in MASP when compared to those in the other cited megacities (by a factor of 1.5 to 20), except for ethane and i-pentane that showed higher levels in Los Angeles. Concerning propane and ethane, the higher level of the former in São Paulo reveals the influence of liquefied petroleum gas (LPG) emissions, as observed in the enrichment of urban background profiles (discuss in next section). The considerable propane and butane concentrations from LPG use were reported in other studies worldwide (Barletta et al., 2008, 2002; von Schneidemesser et al., 2010). Regarding aromatics compounds, these were higher in São Paulo by an average factor of 4 respect to Paris, by a factor of 5 to Los Angeles and by a factor of 12 to London. The differences observed in NMHCs levels could be correlated to the distinctive fleet and fuel usage in these megacities, highlighting the intensive use of ethanol in Brazil (Anderson, 2009; Goldemberg, 2007; Niven, 2005). In addition we observed that fleet size per 1000 inhabitants are quite similar between São Paulo, Los Angeles and Paris (586, 590 and 509 respectively) while in London the number of vehicles are lower (370). Even though these contrasts the same fingerprint is observed in São Paulo with background cities worldwide. This suggest that vehicle emission dominate NMHC distribution but regional practices and regulation (vehicle fleet composition and type of fuel usage) does not seem to affect NMHC composition.

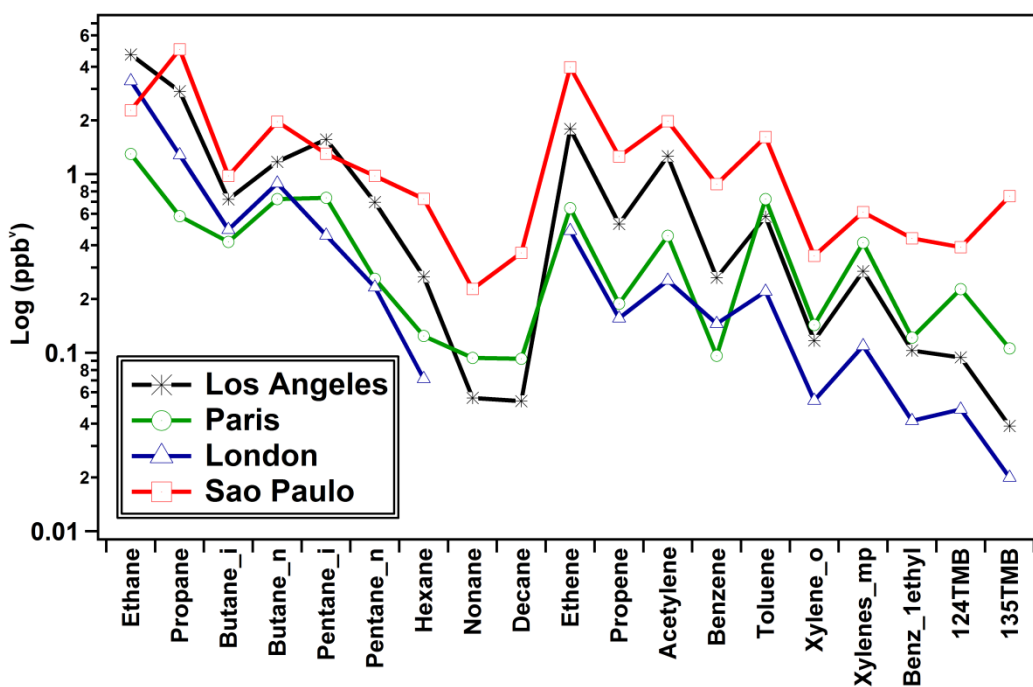


Figure 3. NMHCs average mixing ratios in São Paulo compared with those in other megacities. Paris and London data were obtained in urban background air quality stations (Evry (AIRPARIF, 2013) and London Eltham site (DEFRA, 2013), respectively). Los Angeles data were attained from CalNEx study in 2010 (ref) (CalNex, 2010).

NMHCs urban composition: from road emission profiles to urban background

Figure 4 reports the NMHCs fractional contribution in mass from urban road tunnel (Alvim, 2013), urban road traffic (Alvim, 2013) and urban background (this study) measurements. Alkanes (>C4) presented a slightly higher contribution inside the tunnel, nonetheless the same levels were noted in

urban and background profiles. Regarding light alkanes (C2-C3) it was observed a progressive enrichment from traffic emissions (tunnel) to urban background. This could be associated to the presence of LPG emissions, adopted extensively for domestic use in MASP. For alkenes it was observed higher levels from vehicle emissions than from urban and background profiles. This decay may be due to the consumption or reactions losses of these compounds by photochemistry or/and the dilution atmospheric processes. Comparing alkenes levels from urban road traffic to background, they show the same mass contribution. A little enrichment was observed for aromatics (C7-C9) in urban profile, although this contribution was lower in background profile, denoting the presence of other sources. For tunnel profile an appreciable contribution from benzene was reported, while in urban profile this contribution is lower (Alvim, 2013). We found that the urban background fingerprint is consistent with the one of tunnel and urban emissions except for the enhancement of light alkanes due to presence of LPG sources.

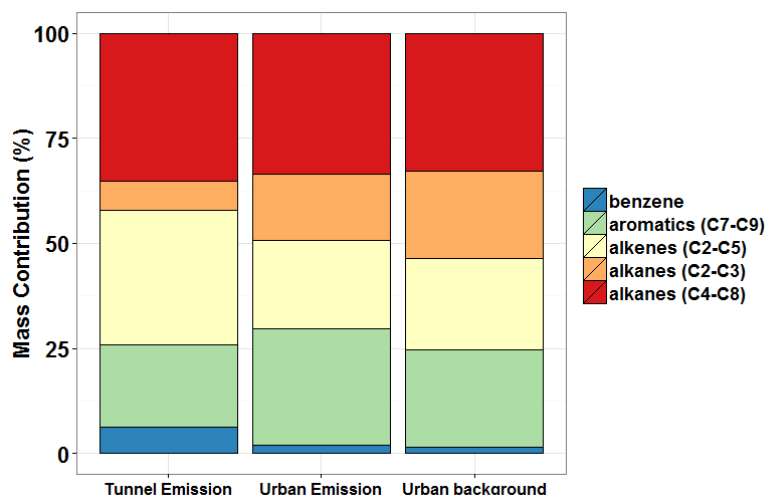


Figure 4. NMHCs composition in mass (%) in MASP during daytime (6a.m.-6p.m.); from urban road tunnel in 2011 (Alvim, 2013), urban road traffic in winter 2008 (Alvim, 2013) and urban background in winter 2013 (this study) experiments. Aromatics integrate toluene, ethylbenzene, *m,p*-xylenes, *o*-xylene, 135-TMB and 124-TMB data, alkenes (C2-C5) ethylene, propene, 1-butene, *trans*-2-butene, *cis*-2butene, *trans*-2-pentene and 1-pentene contributions, alkanes (C2-C3) refer to ethane and propane, and alkanes (C4-C8) to *i*-butane, *n*-butane, *i*-pentane, *n*-pentane, *n*-hexane, *n*-heptane and *n*-octane.

Concurrently, we calculated the fractional mass contribution by season for every group of compounds, such as aromatics, light alkanes (C2-C6), heavy alkanes (C7-C11), alkenes and acetylene on a ppbC basis. For this calculation, we analyzed mixing ratios measured between 6 and 9 a.m., conditions out of photochemistry reactions. Aromatic compounds presented higher contributions during winter (28.4 %) and autumn (26.2 %), while the alkenes were predominant during spring (29 %), being the maximum contribution (47 %) of the light alkanes (C2-C6) during summer. Heavy alkanes presented a strong increase during winter (17%) and acetylene contribution remained almost constant during all seasons of 2013 with a higher contribution during spring (4.7 %). These changes in contribution are related to meteorology conditions which drive the pollutants levels in MASP.

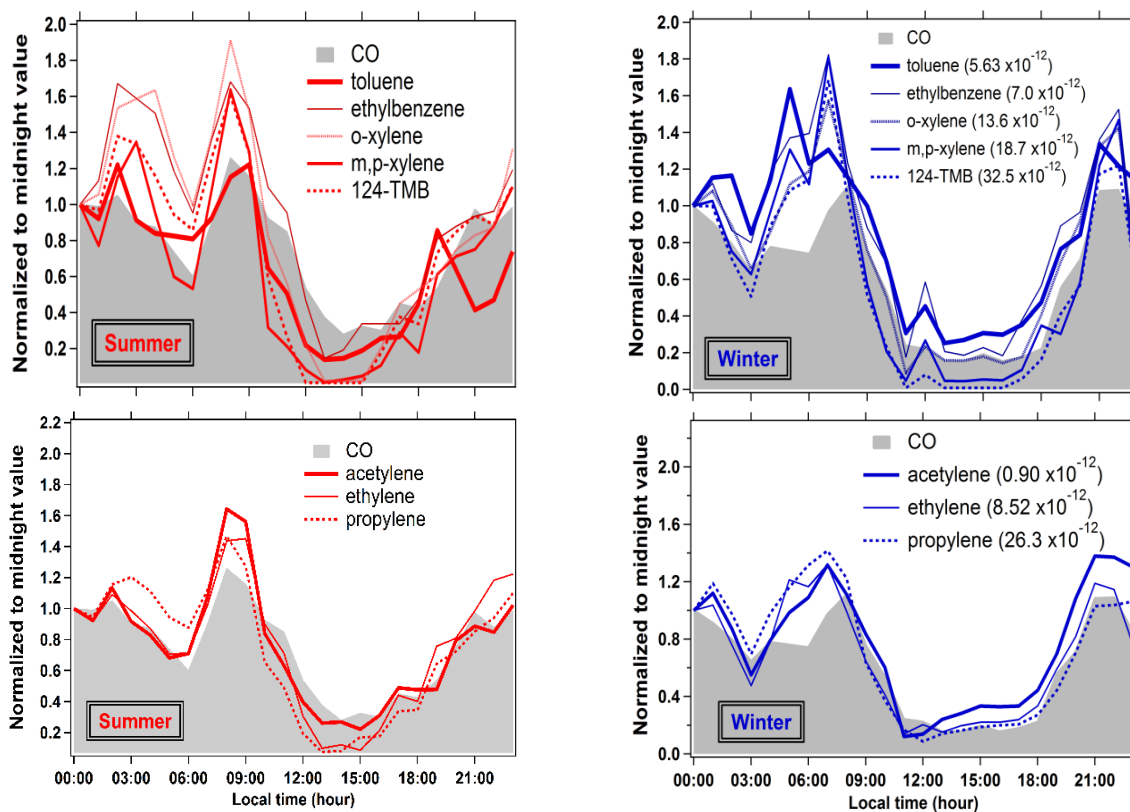
Previous results obtained in MASP showed that alkanes compounds represented 55 %, alkenes 29.2 % and aromatics 13.6 % of the total VOCs sampled during 2006 (Alvim, 2013). In our study the mean annual contribution regardless the season suggests a higher contribution of total alkanes (49.6 %) followed by aromatics (24 %) and alkenes (24 %). These differences could be related, not only to distinct places sampling, but to changes in the gasoline composition and ethanol use in the last years. Nonetheless, this pattern was in agreement with other urban areas, such as French cities (Boynard et al., 2014), wherein total alkanes contribution was larger in summer and winter, followed by aromatics, alkenes and acetylene. In MASP, this seasonal contribution for summer and winter was higher for total alkanes (51 and 50 %), aromatics (22 and 28 %), alkenes (23 and 20 %) and

acetylene (3 and 1.5 %) respectively.

Although the light alkanes were the most abundant compounds regarding the total NMHCs mass; the alkenes contributed to over 50% for ozone forming potential, in all seasons. The ozone forming potential (OFP) corresponds to the ozone mass produced per each gram of NMHC emitted, being calculated from the maximum incremental reactivity (MIR) scale (Carter, 2010). We calculated the OFP for each NMHC only for samples from 6 a.m. to 9 a.m. The OFP in mass average was higher in winter, reaching 88.6 g O₃/g NMHC, and lower in spring (32.8g O₃/g NMHC). We considered that, once the anthropogenic emissions were similar during all year long, these differences among the seasons could be due to the meteorological conditions. The temperature and solar radiation affect the photochemical process, besides being the boundary layer lower than 200m during the winter, hindering the pollutants dispersion (CETESB, 2014).

Variability on diurnal basis

For a better understanding of the meteorology effects, emissions and chemistry processes on diurnal profiles of NMHC concentrations, two specific periods were selected (Figure5). One in the summer (12-19 February) rainy (100 mm, all events after 6 p.m.) and hot ($23.8 \pm 4.0\text{C}$, reaching up to 33.1C), and the latter in the winter (30 July - 07 August) dry and cool ($17.2 \pm 5.3\text{C}$, reaching down to 7.2C). The average diurnal profiles of the absolute mixing ratios normalized to the midnight



value of each compound represent tracers of different emission sources (Fig. 5).

Figure 5. Normalized hourly profiles to midnight values of the mixing ratios of selected NMHCs and carbon monoxide (CO) during summer (red lines) and winter (blue lines) 2013. Numbers in parentheses are the rate coefficient with OH (kOH) in $\text{cm}^3 \text{ molecule}^{-1} \text{ s}^{-1}$ (Atkinson e Arey, 2003).

CO and acetylene, well known as traffic inert tracers, presented similar diurnal profile for both periods. The NMHCs maximum levels at morning during the traffic rush hours was also reported in other megacities worldwide (Borbon et al., 2013). These same average profiles during the morning in both seasons can suggest that NMHCs emissions are always constant in MASP. In addition, a suchlike profile was observed for CO, toluene and acetylene suggesting a common traffic-related

emission, considered the principal source in MASP (CETESB, 2014; Nogueira et al., 2015). On the other hand, high concentrations were measured at night (after 7 p.m.) as a result of absence of photochemistry reactions and the accumulation of local emissions into the nocturnal boundary layer (Fig. 5). Simultaneously, the number of heavy-duty vehicles increase after 10 p.m., when the circulation restriction implemented for truck traffic finishes, in the workdays from 4 a.m. to 10 p.m. (Nogueira et al., 2014). In contrast, maximum concentrations at night during winter were higher than in summer which could be related to removal processes by precipitation or absence of thermal inversion.

The kOH reactivity coefficient is an index of the photochemistry removal intensity which increases with kOH values. All compounds exhibited an analogous well-defined pattern, with afternoon minimum concentrations. Nevertheless, there is not a clear evidence concerning decrease in concentrations during afternoons by either chemical removal or dilution into the diurnal boundary layer. Despite their different levels between summer and winter, the hourly profiles were similar, showing that the traffic emissions along with meteorological conditions were the major control processes of the NMHCs variability in MASP

4. Conclusions

More than 50 NMHCs (C2–C11) were identified and quantified hourly during one year in Sao Paulo megacity. A very detailed database enabled a first insight into NMHCs sources as well as the analysis of temporal and spatial variability of these compounds. We found that meteorological conditions were responsible for one of the principal drivers of NMHCs concentrations in MASP, inducing or impeding photochemistry as well as favoring dilution or stagnation processes. The evaluation based on long-lived species variability like CO, showed that the sampling site could be a good reference in terms of regional fingerprint of air pollutants and NMHCs compounds. A good correlation in diurnal profiles of many NMHCs with those of typical traffic markers (CO, acetylene) reinforced the importance of sources linked to traffic activities in MASP. High levels of C2-C4 alkanes were observed, suggesting the presence of other sources as domestic usage of LPG. Comparisons with others megacities NMHCs concentrations showed higher levels of most of compounds in MASP. Nevertheless, the NMHC composition profile obtained was relatively consistent with those in other megacities, suggesting that fleet and fuel usage are not a dominating factor in the composition and spatial variability of NMHC. In addition NMHC average concentrations were compared with previous studies performed in São Paulo reporting a decrease of NMHC levels in the last fifteen years. It will be important to analyze deeply the relation of these concentrations, fuel usage and improvements in vehicular emissions as well as in fuel contents. A further analysis about the emissions will allow a better assessment of the sources contribution into ambient levels of NMHCs in MASP.

Acknowledgments

The authors gratefully acknowledge the financial support from the Fundação de Amparo à Pesquisa do Estado de São Paulo (São Paulo Research Foundation - FAPESP) and Instituto Nacional de Análise Integrada do Risco Ambiental (INAIRA). We also thank CAPES (PROEX, Meteorology Post-Graduation Program at USP), CNPq and FAPESP for the grants provided. The authors also thankfully acknowledge the PVE-CAPES program (Project N: 88881.068087/2014-01).

The authors would like to gratefully thank the French network AIRPARIF (www.airparif.asso.fr) as well as the United Kingdom air quality network - DEFRA (www.uk-air.defra.gov.uk) for providing NMHCs data from monitoring stations. J. Gilman, J. A. de Gouw and B. Kuster are kindly acknowledged for providing the NMHC data for Los Angeles. We also thank the air quality data supported by São Paulo State Environmental Agency (CETESB - www.cetesb.sp.gov.br) and fuel sales data provided by the Agência Nacional do Petróleo (National Petroleum Agency- ANP- www.anp.gov.br), as well to IAG Weather Station (www.estacao.iag.usp.br) for the meteorological data provided.

References

- Alvim, D.S., (2013). Estudo dos Principais Precusores de Ozônio na Região Metropolitana de São Paulo. University of Sao Paulo. PhD thesis in portuguese.
- Alvim, D.S., Gatti, L. V., dos Santos, M.H., Yamazaki, A., (2011). Estudos dos compostos orgânicos voláteis precusores de ozônio na cidade de São Paulo. Eng Sanit Ambient 16, 189–196.
- Anderson, L.G., (2009). Ethanol fuel use in Brazil: air quality impacts. Energy Environ. Sci. 2, 1015. doi:10.1039/b906057j

- ANP, 2014. Agência Nacional de Petróleo, Gás Natural e Biocombustíveis (National Agency for Oil, Natural Gas, and Biofuels). URL <<http://www.anp.gov.br/>> (access 8.20.15).
- Atkinson, R., Arey, J., (2003). Gas-phase tropospheric chemistry of biogenic volatile organic compounds: a review. *Atmos. Environ.* 37, 197–219. doi:10.1016/S1352-2310(03)00391-1
- Barletta, B., Meinardi, S., Simpson, I.J., Khwaja, H. a, Blake, D.R., Rowland, F.S., (2002). Mixing ratios of volatile organic compounds (VOCs) in the atmosphere of Karachi, Pakistan. *Atmos. Environ.* 36, 3429–3443. doi:10.1016/S1352-2310(02)00302-3
- Barletta, B., Meinardi, S., Simpson, I.J., Zou, S., Sherwood Rowland, F., Blake, D.R., (2008). Ambient mixing ratios of nonmethane hydrocarbons (NMHCs) in two major urban centers of the Pearl River Delta (PRD) region: Guangzhou and Dongguan. *Atmos. Environ.* 42, 4393–4408. doi:10.1016/j.atmosenv.2008.01.028
- Borbon, A., Fontaine, H., Veillerot, M., Locoge, N., Galloo, J.C., Guillermo, R., (2001). An investigation into the traffic-related fraction of isoprene at an urban location. *Atmos. Environ.* 35, 3749–3760.
- Borbon, A., Gilman, J.B., Kuster, W.C., Grand, N., Chevallier, S., Colomb, A., Dolgorouky, C., Gros, V., Lopez, M., Sarda-Esteve, R., Holloway, J., Stutz, J., Petetin, H., McKeen, S., Beekmann, M., Warneke, C., Parrish, D.D., de Gouw, J.A., (2013). Emission ratios of anthropogenic volatile organic compounds in northern mid-latitude megacities: Observations versus emission inventories in Los Angeles and Paris. *J. Geophys. Res. Atmos.* 118, 2041–2057. doi:10.1002/jgrd.50059
- Boynard, A., Borbon, A., Leonardis, T., Barletta, B., Meinardi, S., Blake, D.R., Locoge, N., (2014). Spatial and seasonal variability of measured anthropogenic non-methane hydrocarbons in urban atmospheres: Implication on emission ratios. *Atmos. Environ.* 82, 258–267. doi:10.1016/j.atmosenv.2013.09.039
- Brito, J., Wurm, F., Yáñez-Serrano, A.M., de Assunção, J.V., Godoy, J.M., Artaxo, P., (2015). Vehicular Emission Ratios of VOCs in a Megacity Impacted by Extensive Ethanol Use: Results of Ambient Measurements in São Paulo, Brazil. *Environ. Sci. Technol.* 150923141509009. doi:10.1021/acs.est.5b03281
- Carter, W.P.L., (2010). Updated maximum incremental reactivity scale and hydrocarbons bin reactivities for regulatory applications.
- Carvalho, V.S.B., Freitas, E.D., Martins, L.D., Martins, J.A., Mazzoli, C.R., Andrade, M.F., (2015). Air quality status and trends over the Metropolitan Area of São Paulo, Brazil as a result of emission control policies. *Environ. Sci. Policy* 47, 68–79. doi:10.1016/j.envsci.2014.11.001
- CETESB, (2015). Companhia ambiental do estado de Sao Paulo [WWW Document]. URL <http://www.cetesb.sp.gov.br/> (access 8.25.15).
- CETESB, (2014). Qualidade do Ar no Estado de São Paulo -2013.
- CETESB, (2013). PCPV - Plano de Controle de Poluição Veicular do Estado de São Paulo 2011-2013.
- Colón, M., Pleil, J.D., Hartlage, T.A., Guardani, M.L., Martins, M.H., (2001). Survey of volatile organic compounds associated with automotive emissions in the urban airshed of São Paulo, Brazil. *Atmos. Environ.* 35, 4017–4031.
- DEFRA, (2013). UK Hydrocarbon Monitoring Network. Department for environment food and rural affairs.
- Fujita, E.M., Campbell, D.E., Zielinska, B., Sagebiel, J.C., John, L., Goliff, W.S., Stockwell, W.R., Lawson, D.R., Bowen, J.L., (2003). Diurnal and Weekday Variations in the Source Contributions of Ozone Precursors in California ' s South Coast Air Basin Diurnal and Weekday Variations in the Source Contributions of Ozone Precursors in California's South Coast Air Basin. *J. Air Waste Manage. Assoc.* 53, 844–863.
- Gee, I.L., Sollars, C.J., (1998). Ambient air levels of volatile organic compounds in Latin American and Asian cities. *Chemosphere* 36, 2497–2506. doi:10.1016/S0045-6535(97)10217-X
- Goldemberg, J., (2007). Ethanol for a Sustainable Energy Future. *Science* 315, 808–810. doi:10.1126/science.1137013
- IAG, (2014). Weather station bulletin <http://www.estacao.iag.usp.br/> [WWW Document]. URL <http://www.estacao.iag.usp.br/>
- IBGE, (2014). Estimativa da população residente no Brasil. Diretoria de Pesquisas - Coordenação de População e Indicadores Sociais [WWW Document]. URL <http://www.ibge.gov.br/> (access 9.1.15).
- INPE/CPTEC, 2013. CLIMANÁLISE. Boletim de Monitoramento e Análise Climática.
- Martins, L.D., Andrade, M.D.F., Ynoue, R.Y., Albuquerque, Ê.L. de, Tomaz, E., Vasconcellos, P.C., 2008. Ambiental volatile organic compounds in the megacity of São Paulo. *Quim. Nov.* 31, 2009–2013.
- Martins, L.D., Andrade, M.F., Freitas, E.D., Pretto, A., Gatti, L. V., Albuquerque, E.L., Tomaz, E., Guardani, M.L., Martins, M.H.R.B., Junior, O.M.A., 2006. Emission Factors for Gas-Powered Vehicles Traveling Through Road Tunnels in Sao Paulo, Brazil. *Environ. Sci. Technol.* 40, 6722–6729.
- Niven, R.K., (2005). Ethanol in gasoline: environmental impacts and sustainability review article.

- Renew. Sustain. Energy Rev. 9, 535–555. doi:10.1016/j.rser.2004.06.003
- Nogueira, T., de Souza, K.F., Fornaro, A., Andrade, M.D.F., de Carvalho, L.R.F., (2015). On-road emissions of carbonyls from vehicles powered by biofuel blends in traffic tunnels in the Metropolitan Area of Sao Paulo, Brazil. *Atmos. Environ.* 108, 88–97. doi:10.1016/j.atmosenv.2015.02.064
- Nogueira, T., Dominutti, P.A., Carvalho, L.R.F., Fornaro, A., Andrade, M.D.F., (2014). Formaldehyde and acetaldehyde measurements in urban atmosphere impacted by the use of ethanol biofuel: Metropolitan Area of Sao Paulo (MASP), 2012 – 2013. *Fuel* 134, 505–513. doi:10.1016/j.fuel.2014.05.091
- Pérez-Martínez, P.J., Andrade, M.F., Miranda, R.M., (2015). Traffic-related air quality trends in São Paulo, Brazil. *J. Geophys. Res. Atmos.* 1–15. doi:10.1002/2014JD022812.
- Poulopoulos, S.G., Samaras, D.P., Philippopoulos, C.J., (2001). Regulated and unregulated emissions from an internal combustion engine operating on ethanol-containing fuels. *Atmos. Environ.* 35, 4399–4406. doi:10.1016/s1352-2310(01)00248-5
- Qin, Y., Tonnesen, G.S., Wang, Z., 2004. Weekend/weekday differences of ozone, NO_x, Co, VOCs, PM 10 and the light scatter during ozone season in southern California. *Atmos. Environ.* 38, 3069–3087. doi:10.1016/j.atmosenv.2004.01.035
- Silva Júnior, R.S. Da, Oliveira, M.G.L. De, Andrade, M.D.F.(2009). Weekend/weekday differences in concentrations of ozone, nox, and non-methane hydrocarbon in the metropolitan area of São Paulo. *Rev. Bras. Meteorol.* 24, 100–110. doi:10.1590/S0102-77862009000100010
- UN, (2014). World Urbanization Prospects-The 2014 Revision. <http://esa.un.org/unpd/wup/Publications/Files/WUP2014-Highlights.pdf>
- Vasconcellos, P.C., Carvalho, L.R.F., Pool, C.S.(2005). Volatile Organic Compounds Inside Urban Tunnels of São Paulo City , Brazil. *J. Braz. Chem. Soc.* 16, 1210–1216.
- von Schneidemesser, E., Monks, P.S., Gros, V., Gauduin, J., Sanchez, O., (2011). How important is biogenic isoprene in an urban environment? A study in London and Paris. *Geophys. Res. Lett.* 38, 1–7. doi:10.1029/2011GL048647
- von Schneidemesser, E., Monks, P.S., Plass-Duelmer, C., (2010). Global comparison of VOC and CO observations in urban areas. *Atmos. Environ.* 44, 5053–5064. doi:10.1016/j.atmosenv.2010.09.010

Determination of the influence of meteorological parameters on the ambient VOC concentrations in an industrial town located Aegean coast of Turkey

Güray DOĞAN^{1,*}, Mihriban YILMAZ CİVAN², Öznur OĞUZ KUNTASAL³, Aysen MÜEZZİNOĞLU⁴, Abdurrahman BAYRAM⁴, Mustafa ODABAŞI⁴, Tolga ELBİR⁴, Sait SOFUĞLU⁵, Remzi SEYFİOĞLU⁴, Yetkin DUMANOĞLU⁴, Beyhan PEKEY², Hakan PEKEY² & Gürdal TUNCEL⁶

^{1,*}Akdeniz University, Dumlupınar Boulevard, 07058 Antalya, Turkey
Fax +90 242 310 63 - email: gdogan@akdeniz.edu.tr

²Kocaeli University, 41380 Kocaeli, Turkey

³United Nations Development Program, 06610 Ankara, Turkey

⁴Dokuz Eylül University, 35370 İzmir, Turkey

⁵İzmir Institute of Technology, 35430 İzmir, Turkey

⁶Middle East Technical University, 06530 Ankara, Turkey

Abstract

In this study, the relationship between ambient volatile organic compound (VOC) concentrations in an industrial town with the wind speed, mixing height, ventilation coefficient, temperature and relative humidity data obtained from meteorological station at the region are investigated.

VOC sampling was carried out in an industrial town located on the Aegean Sea coast of Turkey, namely Aliğa. Petrochemical complexes, petroleum refinery, ship breaking facilities, iron steel plants are the major industrial facilities in the Aliğa region. Air quality in the area was monitored via two monitoring stations during summer and winter seasons of the years 2005 and 2006. One of the monitoring station was located at downtown Aliğa and the other monitoring station was located at downwind direction of the industrial facilities (Horozgediği). In each station more than 50 compounds were measured. However, for this study, relation of benzene, toluene, m,p-xylene, o-xylene and ethylbenzene (BTX) with the meteorological parameters were investigated.

The VOC monitoring was held with on-line GCs. In Aliğa station Syntech Spectras GC955 series 600 and 800 model GC was used. Approximately 50 VOCs were quantified with 30 minute resolution. In downwind station, Agilent 6890 N Network GC-FID was used. The temporal resolution of this GC was approximately 45 minutes and the integration of a sample took about an hour. With this GC, around 150 VOCs could be quantified.

Generally, the relation of meteorological parameters with the BTX concentrations at downtown Aliğa are more representative and are highly correlated than those observed for downwind station. High regression coefficients are observed at downtown Aliğa because station is located within Aliğa town whose emissions are always correlated with the meteorological parameters. However, at downwind station, VOC concentrations increases when northern winds are effective in the region. Thus, other meteorological parameters are not as decisive at downwind station as they are at Aliğa on VOC concentrations.

Keys-words: *Aliğa, Volatile organic compounds, On-line GC, Meteorological parameters.*

Introduction

The reactions of organic gases with NO_x play important role in tropospheric chemistry. Organic gases are compounds of primarily carbon and hydrogen. These compounds include reactive organic gases, also known as Volatile Organic Compounds (VOCs), in addition to low reactivity compounds and organics that have aerosolized. There are many definitions of VOCs. The most common definition of VOC is that carbon containing gases and vapors whose vapor pressure at 20°C is less than 760 torr (101.3 kPa) and greater than 1 torr (0.13 kPa) excluding carbon dioxide, carbon monoxide, methane and chlorofluorocarbons. They are typically classed as containing up to 12 carbon atoms per molecule (Derwent, 1995; Blake and Blake, 2002).

Although there are thousands of organic compounds in the natural and polluted troposphere that meet the definition of a VOC, most measurement programs have concentrated on the 50 to 150 most abundant hydrocarbons depending upon the characteristics of the specific environment and the effects of the VOCs to both the environment and the human. Volatile organic compounds (VOCs) have large impact on atmospheric chemistry contributing to ground level ozone formation, stratospheric ozone depletion, and secondary particle formation. Organic compounds in the atmosphere also have health effect, because many of them are carcinogens or suspected carcinogens. Volatile organic compounds also enhance global warming. Some of these compounds, not volatile ones, are persistent in the atmosphere and thus accumulate in various compartments.

The most important sources of VOC emissions are motor vehicles, organic solvents, the oil and chemical industries, combustion sources and natural sources. Other minor VOC sources include food and drink manufacturing, the metals industries, waste disposal, and straw and stubble burning. Natural and biogenic processes produce significant amounts of VOCs (Derwent, 1995; Passant, 1995). A recent estimate of anthropogenic non-methane VOC emissions indicates a global release of about 140 Tg y⁻¹. However, natural sources make a significantly larger contribution to total emissions, with about 1150 Tg y⁻¹ (Blake and Blake, 2002).

Natural and biogenic sources, trees, plants, wild animals, natural forest fires, and anaerobic processes in bogs and marshes, also contribute significantly to VOC emissions (Derwent, 1995). Estimates of biogenic emissions vary considerably; still, biogenic emissions represent a high fraction of total emissions in some regions (Passant, 1995).

Emissions from motor vehicles can be divided into two categories. These are emissions as a result of incomplete fuel combustion (exhaust emissions) and emissions due to losses of fuel prior to combustion (evaporative emissions).

A major use of solvents is in the formulation of industrial coating materials such as paints, inks and adhesives. Solvent evaporation after application is the most important emission source. Through coating processes, some part of the emission is controlled and this is referred as a fugitive emission; handling and storage of coating materials, washing of equipment, and spillages. Solvents are also used in other industrial processes, for instance the extraction of vegetable oil from oil seeds, the cleaning of metal and plastic components, and dry cleaning of textiles. Another important use of solvents is in the formulation of products for use by consumers, for example aerosols, cosmetics and household paints.

Major emissions from crude oil production are flaring and venting of gases from production facilities, together with displacement of vapor during loading of crude oil tankers. Oil refineries and chemical plants also emit enormous quantities of VOCs. Emissions occur from storage of volatile materials, venting and flaring of gases and fugitive emissions from valves and pumps. The distribution of fuel is another important source of VOCs; emissions occurring during loading of road tankers, filling station storage facilities and during vehicle refueling. Emissions from stationary combustion sources are much less significant. Aliağa is an important industrial region with a large number of industries, including a petrochemical complex (PETKİM) and a refinery (TÜPRAŞ).

Local meteorology is one of the most important factors affecting measured concentrations of not only VOCs but also most of the other air pollutants, particularly at urban and industrial atmospheres. Another important factor is the emissions. Upper atmospheric transport of pollutants from other emission areas can also affect concentrations of pollutants (Kindap, 2006), but this factor, which is important at rural atmosphere, is small and can be neglected in urban and industrial regions, because local emissions are high and can completely mask influence of distant sources.

Meteorological influence on concentrations of species can occur in two forms, horizontal ventilation process, which is caused by winds and vertical ventilation, which refers to convective stability of the atmosphere (Şen, 1998; Yang et al., 2011). Absence of horizontal ventilation is called "calm" and absence of vertical ventilation is called "inversion". Combination of calm and inversion is referred to as "stagnant". Stagnant conditions correspond to highest pollution episodes in an urban and industrial airshed, as emitted pollutants are not removed horizontally and vertically from the emission area (Bustamante et al., 2011; Wallace et al., 2010).

In this study, the influence of meteorological parameters like wind speed, mixing height, ventilation coefficient, temperature and relative humidity on VOC levels at two locations in Aliağa industrial town were inspected.

1. Method

Aliağa is located 50 km north of İzmir on the coast of Aegean Sea. The town is surrounded by the Dumanlı Mountains and Yunt Mountains. The town located along D550 Çanakkale - İzmir highway. Typical Mediterranean climate is observed in the town. Almost all of the precipitation events occur during winter. Northerly winds dominate during winter whereas local sea breezes (etesian winds) are particularly effective on summer afternoons. Average daily temperatures are 25°C and 7°C in summer and winter, respectively (Municipality of Aliağa, 2009).

The economy of Aliağa, which was based on agriculture until early 1960's, has gained an industrial character after the 1970's as the town was declared as a "heavy industrial zone" in the first five year development plan. Aliağa Organized Industrial Zone was established in 1977 and Aliağa became an industrial center. Today, Aliağa produces 1-1.3% of Turkey's gross national product per capita (Aliağa Chamber of Commerce, 2011). The population of Aliağa municipality according to 2007 statistics is approximately 60 000 and is expected to rise to 300 000 by 2015 (Turkish Statistical Institute, 2012).

Various industrial facilities in different production sectors were established, once the Organized Industrial Zone was established. These include refinery (TÜPRAŞ), petrochemical complex (PETKİM), petroleum products storage and filling facilities, iron steel industries, power plants, shipbreaking facilities, pulp and paper factory, and fertilizer factory. Locations of major facilities are given in Figure 1.

The crude oil demand of Turkey is about 694 000 tons and one third of this demand is processed by TÜPRAŞ. A natural gas fired thermal power plant, with a capacity of 1520 MWh was built by ENKA in 2002. Another major industry in Aliağa is the petrochemical complex, PETKİM, which became operational in 1985. PETKİM has production capacity of 3.2 million tons. Aside from these three major complexes, a number of harbors, including PETKİM terminal, Nemrut Port, Refinery Port, Port of Aliağa, and ship breaking facilities played significant roles in the development of the area. These harbors are especially important for the transportation of crude oil, distilled products, petrochemical products and various chemicals to and from the region. The scrap for iron steel industry, ammonia and phosphoric acid for fertilizer factories, pulp for paper industry and raw materials for petrocokes industry are also supplied from these harbors. There are 25 ship breaking units are located in the shoreline of the Nemrut area. Approximately 10 iron and steel factory are located in the Horozgediği area. These factories use the steel and iron recovered from ships and metals recovered from metal recovery factories.

In order to quantify the contribution of industrial facilities to Aliağa region and downtown Aliağa VOC concentrations, sampling was conducted at two monitoring stations through winter and summer campaigns. One of the sampling stations was located in downtown Aliağa and the other one was established approximately 500 m to the south east of Horozgediği village. Stations consisted of containers with dimensions 4m x 6m x 2m and equipped with a bench, an air conditioner and uninterruptible power supply.

According to 2007 census, downtown Aliağa had a population of 52 000 (Turkish Statistical Institute, 2012). Aliağa station was located at the Demokrasi Square in downtown Aliağa (38°48'N, 26°58'E). This station will be referred as Aliağa Station throughout the manuscript.

Various commercial and non-commercial facilities, including a municipality building, restaurants, banks, grocery stores and offices of non-governmental organizations and lawyers were located around the square. Bankalar Street and İstiklal Street were two frequently used road in the town. These two streets were also used for parking. The station was located 50 m and 30 m from İstiklal Street and Bankalar Street, respectively. It was also approximately 500 m from the Aegean Sea. The distance between D550 Çanakkale-İzmir highway and station was 300 m. The closest industries to the sampling site were TÜPRAŞ and PETKİM, which were located 2 km to the west and 3.3 km to south west of the station, respectively. A paper and pulp factory was located approximately 4 km to northwest of the station. The station was also approximately 5.5 km from the Nemrut Bay.

VOCs were not the only species measured in this station. In addition to organic compounds, daily trace element samples were also collected using a dichotomous sampler and trace elements in collected samples were analyzed using x-ray fluorescence (XRF) technique. Inorganic pollutants, namely SO₂, NO, NO₂, O₃ and PM₁₀ mass were also measured on an hourly basis along with the VOCs. Results of these non-VOC measurements were not evaluated in this thesis. However, the results of those data are not discussed in this manuscript.

Horozgediği Station was located 350 m north east of Horozgediği Village (38°43'N, 26°55'E). The

station was installed near an air quality monitoring station operated by ENKA gas-fired power plant. This was necessary, because data on air quality parameters, SO₂, NO, NO₂ and PM₁₀ mass were obtained from their measurements. The station was 500 m south of Yeni Foça-İzmir road and 4.5 km west of D550 Çanakkale-İzmir highway. Industries were located to the north and northeast of the station. Horozgediği station was particularly close to iron and steel industries. There were 7 of these plants located between 640 m – 3900 m from the station. TÜPRAŞ and PETKİM are relatively further away. These two important VOC emitters are located approximately 7.5 km to the NW of the Horozgediği station. Sampling site is 2.7 km and 8.2 km away from Nemrut Bay and from Aliğa downtown, respectively. Çakmaklı, Cumhuriyet, Bozköy and Kozbeyli were other villages around the sampling site.

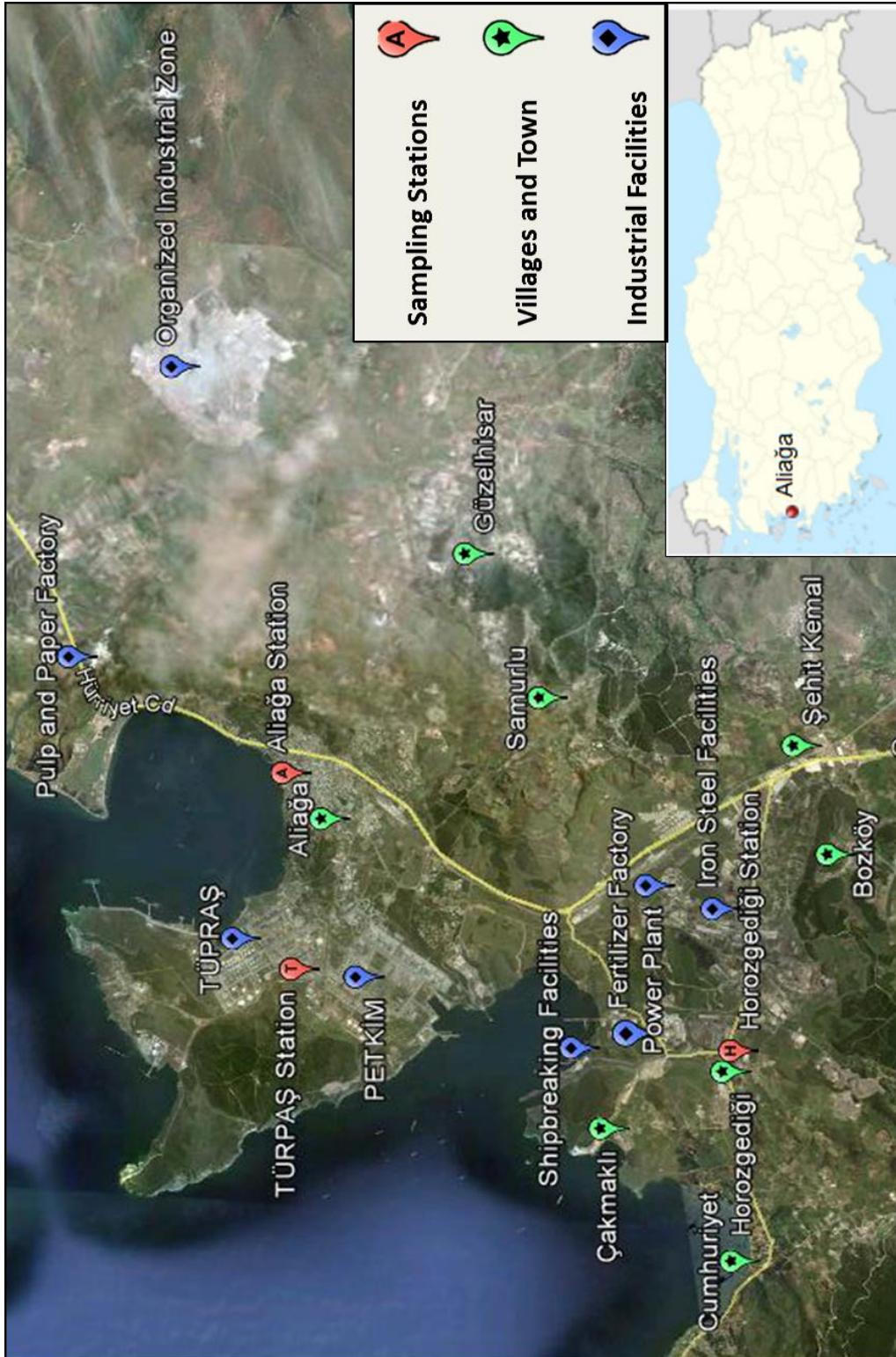


Figure 1 Sampling Site

The VOC measurement method used in this study was online gas chromatograph with FID and PID detectors. Online GC systems, which includes deploying a specially designed gas chromatograph equipped with a sampling system to field has few advantages compared to other sampling techniques, briefly described above. Main advantage is their capability of generating high resolution data. Hourly data or data with 30 min resolution can be generated. They also have lower detection limits and they can measure larger spectrum of VOCs than those measured in adsorbent or canister samples.

The working principle of online GC is composed of four steps. These are sampling, preconcentration, separation and quantitative analyses. During separation of VOCs, instruments are capable of sampling and preconcentrating the next sample.

Two different on-line GC systems, one located at the Aliğa station and the other one at Horozgediği station, were used in this study. Two field campaigns were conducted in 2006. Winter campaign was started in November 2005 and continued until March 2006. Summer campaign started in August 2006 and continued until October 2006. The samplings were carried out simultaneously in Aliğa and Horozgediği stations.

At Aliğa Station, The Syntech Spectras GC955 series 600 and 800 online GCs were used. An Agilent 6890N Network GC-FID system was used for Horozgediği measurements.

In this study more than 50 species were measured in approximately 7500 measurement cycles (chromatograms). Some errors during generation of such vast data matrix is inevitable. That is why protocols which includes procedures to detect potential errors and thus to assist generating reliable data set, which is known as quality assurance-quality control is becoming more and more important.

In this study QA/QC protocol included:

- Estimation of detection limits and quantification limits
- Determination of the precision of the measurement system
- Parallel measurements using the two GC systems
- Proper calibration of the instruments
- Investigation of the role of below LOQ values on average and median concentrations
- Data quality control

All these activities, except for data quality control, are related to ensure accuracy of measurements but cannot identify potential errors that can occur during processing of chromatograms. The objective of the last step in the QA/QC protocol, namely "Data Quality Control" is to identify possible errors that can occur during manual determination of peak areas (peak fitting). Considering that approximately 375 000 peaks were fitted in this study (7500 chromatograph x 50 VOC in each chromatograph), data quality control was a very important component of the QA/QC program performed in this study.

Meteorological data is used to understand the variations in concentrations of pollutants. In this study, the data from two meteorological stations were used. One of the stations was operated by Turkish State Meteorological Service at downtown Aliğa. The other meteorological station was located just nearby Horozgediği station and was operated by ENKA (power plant). The meteorological data was used to determine effect of temperature, relative humidity, wind speed, mixing height, ventilation coefficient and wind direction on concentrations of pollutants.

Mixing height is the height to which the lower troposphere will undergo mechanical or turbulent mixing, producing a nearly homogenous air mass (NOAA, 2011). In this study, mixing height is calculated on an hourly basis using PCRAMMET software program. For PCRAMMET to run, wind direction, wind speed, dry bulb temperature, opaque cloud cover, cloud ceiling height, morning and afternoon mixing height data are supplied from meteorological station operated by General Directorate of Meteorology at Aliğa. Another meteorological parameters used in this study was "ventilation coefficient". Concentrations of VOCs and other pollutants in an airshed are primarily determined by vertical and horizontal ventilation mechanisms. Horizontal ventilation occurs winds and vertical ventilation is caused by convective stability of the atmosphere. Wind speed and mixing height are two indicators for horizontal and vertical ventilation process. Because of this in many studies pollutant concentrations in airshed is found to be more strongly correlated with ventilation coefficient than wind speed and mixing height alone (Manju et al., 2002; Goyal and Rao, 2007; Genç et al., 2010). Ventilation coefficient is also considered as an indicator for assimilation capacity of the atmosphere (Goyal and

Rao, 2007).

The effect of wind speed, relative humidity and temperature on VOC concentrations will also be discussed. The effect of these parameters on VOC concentrations are fitted to a model using a statistical program, Statgraphics v16.1 Centurion. The statistical program can fit data set to twenty-seven linear and nonlinear models. At first linear ($y=ax+b$) and logarithmic ($y=\ln x+b$) models are tested. If there is a statistically significant relationship between the selected parameters, then these models are used. If there is no linear or logarithmic relation between the parameters, then rest of the nonlinear models are run and best R-squared valued model is selected.

2. Results and Discussion

Although there is a close relationship between pollutant concentrations and local meteorology, quantifying that relation is not always straightforward, because atmospheric concentrations of pollutants depend on a number of factors, such as chemical processes they may undergo, different scavenging processes, such as wet removal with rain and dry deposition, in addition to meteorology and emissions. The relation between VOC concentrations measured at Aliğa and Horozgediği stations and prevailing surface meteorology are discussed in this section. Meteorological parameters investigated include wind speed, which is indicator for the effectiveness of horizontal ventilation mechanism in the study area, mixing height, which is an indicator for the vertical ventilation. In addition to these two major parameters the relation between VOC concentrations and ventilation coefficient is also investigated. Ventilation coefficient (VC) is the product of wind speed and the mixing height, thus it combines the influence of horizontal and vertical ventilation mechanisms on measured concentrations of pollutants (Goyal and Chalapati, 2007; Rao et al., 2003). Ventilation coefficient is considered as the assimilative capacity of the atmosphere and it is shown to be better related with measured concentrations of air pollutants than mixing height and wind speed alone (Genç et al., 2010). The relation between measured VOC concentrations and temperature and relative humidity is also discussed. However, it should be noted that relation between VOC levels and temperature can be indirect, because emissions can change with seasons, which can appear as the influence of temperature on measured concentrations.

Visualization of the relation between VOC concentrations and meteorological parameters is difficult. This is shown in Figure 2 where the scatterplot between BTX concentrations measured at Aliğa station and wind speed is depicted. Although there is a general decreasing trend in concentrations of BTX compounds with increasing wind speed it is difficult to see if the decrease follow a linear or other pattern and it is impossible to see if there are different type of variation for different BTX compounds. To avoid this difficulty, median concentrations of the compounds are calculated for different intervals of meteorological parameters and concentration vs. meteorology plots are prepared for these median values.

Meteorological data used in calculations are the data obtained from General Directorate of Meteorology (GDM). For the further regression analyses, Statgraphics Centurion 16.1 software is used.

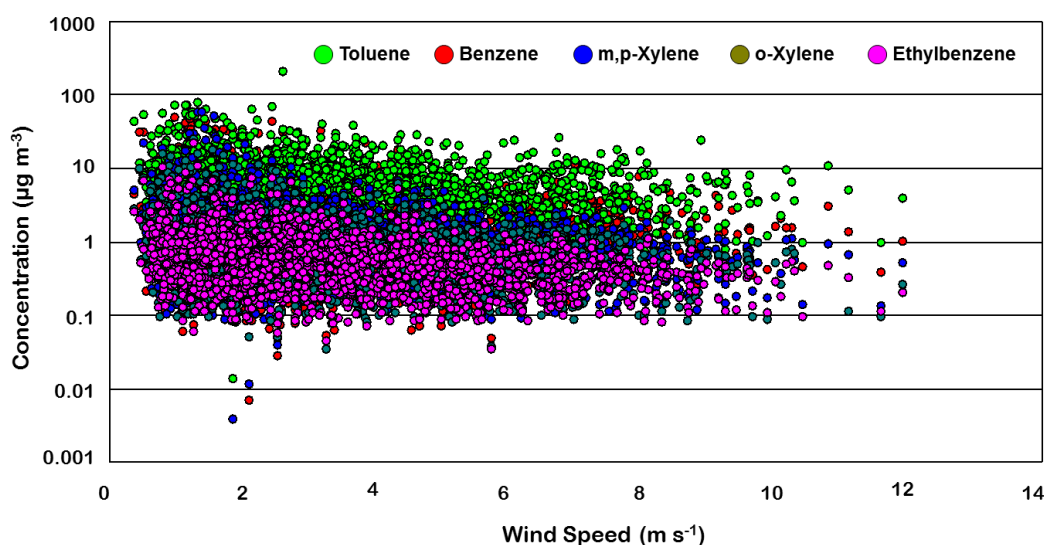


Figure 2. The relation between wind speed and BTX concentrations at Aliğa station, using all available data

Models fitted to BTX data for different meteorological parameters are given in Table 1. Wind is the main horizontal ventilation mechanism for VOCs (and for most of the other pollutants as well). Since pollutants emitted to Aliaga atmosphere will be diluted with increasing wind speed, a decrease in VOC concentrations is expected with increasing wind speed. At Aliaga station concentrations of all five BTX compounds decrease, as expected. The decrease is logarithmic for all five compounds. The “p” values (probability of chance correlation) of the fitted models are 1% or less for all of them, indicating a very good agreement between the model and data. Fitted models explained 84% of the variance in benzene, 85% of the variance in toluene data, 93% of the variance in m,p-xylene data, 91% of the variance in o-xylene data and 93% of the variance in ethylbenzene data. These values clearly demonstrate that VOC concentrations at the town of Aliaga, are strongly dependent on the wind speed as expected. This is an indication that VOC emissions that influence the data at Aliaga station are in the immediate vicinity of the station and horizontal transport of emissions is an important ventilation mechanism in the city.

On the contrary, the relation between wind speed and BTX concentrations at Horozgedigi station is not as strong as the relation observed at Aliaga station. Toluene data fitted to log model with 95% confidence. Benzene fitted to a double reciprocal y model.

Concentrations of the other three compounds, namely m,p-xylene, o-xylene and ethylbenzene did not fit to any of the 27 models with statistical significance > 95%. This clear difference in response of VOC concentrations to WS in the two stations can be explained with more rural nature of the Horozgedigi station. The station is not in the immediate vicinity of the VOC emission sources. VOCs are transported to the station from refinery, petrochemical complex and roads. Winds do not transfer the VOCs from the station, but brings them to the station. In such a case, we do not expect to see a categorical decrease in VOC concentrations with increasing wind speed, because high concentrations of VOCs will be measured when winds blow from the direction of the refinery and petrochemical complex, even if the winds are strong. On the other hand, low VOC concentrations can be measured during low wind speeds if that wind is blowing from a clean sector. However, at Aliaga station VOC sources are around the measurement point and winds transport emissions from the station, as well as diluting them. This results in a well-defined decrease in concentrations with increasing wind speed.

Mixing height is a measure of vertical ventilation of the region. As long as emissions are constant, concentrations of VOCs (and other pollutant as well) are expected to decrease with increasing mixing height. The mixing height calculations were done by using PCRAMMET software. Patterns observed in the figure are not substantially different from the patterns observed in relation between concentrations and WS.

Table 1. Relations of compounds with meteorological parameters and their regression coefficients

Compounds	Wind Speed		Mixing Height		Ventilation Coefficient		Temperature		Relative Humidity	
	Model	R ²	Model	R ²	Model	R ²	Model	R ²	Model	R ²
Aliaga										
Benzene	Log	0.84	-	-	Log	0.86	-	-	Log	0.35
Toluene	Log	0.85	Linear	0.40	Log	0.63	Linear	0.64	Linear	0.77
m,p-Xylene	Log	0.93	Linear	0.41	Log	0.75	Linear	0.60	Log	0.88
o-Xylene	Log	0.91	Linear	0.45	Log	0.66	Linear	0.61	Log	0.88
Ethylbenzene	Log	0.93	Linear	0.36	Log	0.78	Linear	0.64	Log	0.89
Horozgedigi										
Benzene	DR [*]	0.15	RySx ^{**}	0.23	Linear	0.30	Linear	0.51	Linear	0.34
Toluen	Log	0.13	Log	0.40	Linear	0.17	Linear	0.38	-	-
m,p-Xylene	-	-	-	-	DS [“]	0.16	Linear	0.11	-	-
o-Xylene	-	-	SR ^{***}	0,15	-	-	Linear	0.13	DS [“]	0.20
Ethylbenzene	-	-	-	-	Linear	0.19	-	-	-	-

^{*}DR: $y=1(a+b/x)$, ^{**}RySx: $y=1/(a+bx^2)$, ^{***}SR: $y=(a+b/x)^{1/2}$, [“]DS: $y^2=a+bx^2$

Concentrations of all BTX compounds, except for benzene, show poor correlation with mixing height at Aliağa station. Toluene, m,p-xylene, o-xylene and ethylbenzene showed linear correlation. However, the correlation coefficients are lower than wind speed. This indicates that mixing height is not as strong parameter as wind speed at Aliağa.

At Horozgediği data set, concentrations of benzene, toluene and o-xylene decrease with increasing mixing height. The decrease in m,p-xylene and ethylbenzene concentrations observed at the Horozgediği station did not fit to any model with statistical significance better than 95%. Benzene fitted to a reciprocal y squared x, toluene fitted to logarithmic model and o-xylene fitted to a “square-y reciprocal-x” model. Variance explained (R^2) varies between 0.15 for o-xylene and 0.40 for toluene. All these relatively marginal significance of fitted models in both stations indicate that variations of concentrations of VOCs can be partly due to variations in mixing height, but obviously there are other factors which also contribute to temporal variations in their concentrations.

Ventilation coefficient is the product of mixing height and wind speed. Since it encompasses most important indicators of horizontal and vertical ventilation processes, it is generally believed that it is a better parameter to investigate dependence of pollutant concentrations to local meteorology than wind speed and mixing height alone (Chan et al., 2012; Genç et al., 2010; Ashrafi et al., 2009). There is fairly strong decreasing trend in concentrations of not only all BTX compounds, but also most of the VOCs measured in this study at Aliağa station. All BTX compounds fit to “log” model indicating that fits are robust. Variances of BTX compounds explained by ventilation coefficient vary between 0.63 for toluene and 0.86 for benzene. Such a strong relation between BTX concentrations and VC is not surprising, because concentrations of VOCs at Aliağa station correlated strongly with both mixing height and wind speed and they are expected to be correlated with the product of these two parameters.

VOCs measured at Horozgediği, on the other hand is not strongly correlated with ventilation coefficient. Benzene, toluene and ethylbenzene fitted to linear model and m,p-xylene fitted to double squared model. O-Xylene did not fit to any of 27 models. Variances of BTX compounds explained by ventilation coefficient vary between 0.16 for m,p-xylene and 0.30 for benzene.

VOC's depicted interesting dependence to temperature in both Aliağa and Horozgediği stations. Concentrations of toluene, m,p-xylene, o-xylene, ethylbenzene at Aliağa station and m,p-xylene at Horozgediği station showed increasing trend with > 0.95 statistical confidence. Concentrations of benzene, toluene and o-xylene at Horozgediği station presented decreasing trend. Benzene at Aliağa station and ethylbenzene at Horozgediği station did not fit to any model.

The increasing trend in VOC concentrations with temperature can be expected in Aliağa station, because of several reasons, including increased traffic activity during summer months, increased evaporation from painted surfaces and from solvents in summer.

Benzene at Aliağa station and benzene and o-xylene at Horozgediği station showed increasing trend with relative humidity. Toluene, m,p-xylene, o-xylene and ethylbenzene at Aliağa station showed decreasing trend. Toluene, m,p-xylene and ethylbenzene at Horozgediği station did not fit to any model.

Relatively low R^2 values observed in the relations between VOC concentrations, temperature and relative humidity indicates that these two parameters can explain only a small part of the variations in VOC concentrations at the Aliağa region.

Conclusion

This lack of strong relation between VOC concentrations and WS, MH and VC clearly demonstrate that it may not be a very good idea to attempt to explain measured concentrations of pollutants with meteorology in rural airshed. In an urban airshed, pollutants are emitted within the city and dispersed by meteorology. Measurement of VOCs and other pollutants in the city is a measure of this dispersion process. Because of this mechanism, pollutant concentrations including VOCs show fairly well-defined and foreseeable variations with meteorological parameters, such as wind speed, mixing height and ventilation coefficient. However, at a rural airshed, relation between pollutant levels and meteorology is much more complicated. First of all rural station was not located in the immediate vicinity of the emission sources, which means that there is no dispersion or dilution of pollutants from the measurement point, which can be related to meteorology. Furthermore, VOCs and other pollutants can be transported from source regions which are not related to meteorological parameters. The only exception to this is the dependence VOC concentrations on wind direction. In addition to these, which are common to all pollutants, VOCs have also chemistry in the atmosphere, which further complicates the relation between

concentrations and meteorology. To summarize this discussion it can be said that, at a rural station high VOC concentrations are measured when wind blows from the direction of sources (PEKTİM and TÜPRAŞ in our case), not when mixing height is low or when wind is strong, because that strong wind may be blowing from the direction of PETKİM and TÜPRAŞ, in that case high VOC levels are measured even when the wind is strong.

Acknowledgments

This work was supported by The Scientific and Research Council of Turkey (104Y276) and State Planning Organization (BAP-08-11-DPT.2011K121010), Aliğa Municipality and PETKİM. The authors would like to thank Mürsel Cila for his contributions during sampling campaigns.

References

- Aliğa Chamber of Commerce (2011): Economy of Aliğa. <http://www.alto.org.tr/en/aliaga/aliaga-economy.html>, access date December 10, 2012.
- Ashrafi, Kh., Sharife-Pour, M. & Kamalan, H. (2009): Estimating temporal and seasonal variation of ventilation coefficients. International Journal of Environmental Research, vol. 3, p 637-644.
- Blake, N.J. & Blake, D.R. (2003): Tropospheric chemistry and composition: VOCs overview. In H. Holton, J. Pyle and J. Curry (Eds.). Encyclopedia of Atmospheric Sciences, Amsterdam: Elsevier, p 2438-2446.
- Bustamante, E.N., Monge-Najera, J. & Lutz, M.I.G. (2011): Air pollution in a tropical city: The relationship between wind direction and lichen bio-indicators in San Jose, Costa Rica. Revista de Biología Tropical, vol 59, p 899-905.
- Chan, L., Deng, Q.-H., Liu, W.-W., Huang, B.-L. & Shi, L.-Z. (2012) : Characteristics of ventilation coefficient and its impact on urban air pollution. Journal of Central South University of Technology (English Edition), vol. 19, p 615-622.
- Derwent, R.G. (1995): Sources, distributions, and fates of VOCs in the atmosphere. Volatile Organic Compounds in the Atmosphere. In R.M. Harrison and R.E. Hester (Eds), Volatile Organic Compounds in the Atmosphere, Cambridge: The Royal Society of Chemistry, pp 1-15.
- Genç, D.D., Yeşilyurt, C. & Tuncel G. (2010): Air pollution forecasting in Ankara, Turkey using air pollution index and its relation to assimilative capacity of the atmosphere. Environmental Monitoring and Assessment, vol. 166, p 11-27.
- Goyal, S.K. & Rao, C.V.C. (2007): Assessment of atmospheric assimilation potential for industrial development in an urban environment: Kochi (India). Science of the Total Environment, vol. 376, p 27-39.
- Kindap, T., Ünal, A., Chen, S.-H., Hu, Y., Odman, M.T. & Karaca, M. (2006): Long range aerosol transport from Europe to Istanbul, Turkey. Atmospheric Environment, vol. 40, p 3536-3547.
- Manju, N., Balakrishnan, R. & Mani, N. (2002): Assimilative capacity and pollutant dispersion studies for the industrial zone of Manali. Atmospheric Environment, vol. 36, p 3461-3471.
- Municipality of Aliğa (2009): Coğrafyası. <http://www.aliaga.bel.tr/cografyasi-32.html>, access date December 11, 2012.
- NOAA (2011): Mixing Height (ft). <http://graphical.weather.gov/definitions/defineMixHgt.html>, access date December 16, 2012.
- Passant, N.R. (1995): Source inventories and control strategies for VOCs. In R.M. Harrison and R.E. Hester (Eds), Volatile Organic Compounds in the Atmosphere, Cambridge: The Royal Society of Chemistry, pp 51-64.
- Rao, S.T., Ku, J.-Y. Bermen, S. Zhang, K. & Mao, H. (2003): Summertime characteristics of the atmospheric boundary layer and relationships to ozone levels over the Eastern United States. Pure and Applied Geophysics, vol. 160, p. 615-622.
- Şen, O. (1998): Air pollution and inversion features in İstanbul. International Journal of Environment and Pollution, vol. 9, p 371-383.
- Turkish Statistical Institute (2012): Adrese Dayalı Nüfus Kayıt Sistemi (ADNKS) Sonuçları, http://rapor.tuik.gov.tr/reports/rwservlet?adnksdb2&ENVID=adnksdb2Env&report=turkiye_ilce_koy_sehir.RDF&p_il1=35&p_ilce1=442&p_kod=2&p_yil=2007&p_dil=1

&desformat=pdf, access date December 11, 2012.

Wallace, J., Corr, D. & Kanaroglou, P. (2010) : Topographic and spatial impacts of temperature inversions on air quality using mobile air pollution surveys. Science of the Total Environment, vol . 408, p 5086-5096.

Yang, X., Dong, W. & Liu, F. (2011): Impact of air pollution on summer surface winds in Xi'an. Acta Meteorological vol. 25, p 527-533.

Does air pollution modify the impact of aircraft noise on mortality from cardiovascular disease? Results of an ecological study in France

Anne-Sophie Evrard¹, Liacine Bouaoun^{1,2}, Marie Lefèvre¹, Patricia Champelovier³, Jacques Lambert^{3,4} & Bernard Laumon⁵

¹Univ Lyon, IFSTTAR, Univ Lyon 1, UMRESTTE, UMR_T9405, F-69675, Bron, France
email: anne-sophie.evrard@ifsttar.fr

²Current address: International Agency for Research on Cancer, F- 69372 Lyon, France

³IFSTTAR, Planning, Mobilities and Environment Department, Transport and Environment Laboratory (LTE), F-69675 Bron, France

⁴Currently retired

⁵IFSTTAR, Transport, Health and Safety Department, F-69675 Bron, France

Abstract

The reduction of aircraft noise nuisance has been considered to be the main issue for a long time but in recent years, the question of air pollution around airports and concerns for disentangling the effects of air pollution and of noise on cardiovascular outcomes has been raised. We performed an ecological study addressing the issue of an association between exposure to aircraft noise and mortality from cardiovascular disease, and the impact of air pollution on this association. The study was based on 161 communes (the smallest administrative unit in France) close to three major French airports: Paris-Charles de Gaulle, Lyon Saint-Exupéry and Toulouse-Blagnac. The mortality data were provided by the French Center on Medical Causes of Death. Based on noise maps produced by the French Civil Aviation Authority, a population-weighted average exposure to aircraft noise was computed at the commune level. The average air pollution exposure for both NO₂ and PM₁₀ indicators was estimated with dispersion modelling. The present study seems to confirm the findings of recent studies suggesting that air pollution does not appear to modify the impact of aircraft noise on mortality from cardiovascular disease. However, further individual studies are necessary in order to better understand this association.

Keys-words: *air pollution; aircraft noise; mortality; health.*

Résumé

La réduction des nuisances sonores des avions a été considérée comme une préoccupation majeure pendant longtemps mais depuis quelques années, la problématique liée à la pollution de l'air à proximité des aéroports a été soulevée. Cela pose également la question de dissocier les effets du bruit de ceux de la pollution de l'air, en particulier sur les maladies cardiovasculaires. Nous avons réalisé une étude écologique originale s'intéressant non seulement à l'existence d'une association entre l'exposition au bruit des avions et la mortalité cardiovasculaire, mais aussi à l'impact de la pollution de l'air sur cette association. Cette étude est basée sur 161 communes situées à proximité de trois aéroports français majeurs : Paris-Charles de Gaulle, Lyon Saint-Exupéry et Toulouse-Blagnac. Les données de mortalité ont été transmises par le Centre d'épidémiologie sur les causes médicales de décès de l'Institut national de la santé et de la recherche médicale. L'exposition moyenne au bruit des avions pondérée par la population a été calculée au niveau de chaque commune à partir des cartes de bruit produites par la Direction Générale de l'Aviation Civile. L'exposition moyenne à la pollution de l'air en termes de NO₂ et de PM₁₀ a été estimée avec des modèles de dispersion. Notre recherche confirme les résultats des études récentes qui suggèrent que la pollution de l'air ne modifie pas l'impact de l'exposition au bruit des avions sur la mortalité cardiovasculaire. Cependant d'autres études individuelles sont nécessaires pour mieux comprendre les associations mises en évidence ici.

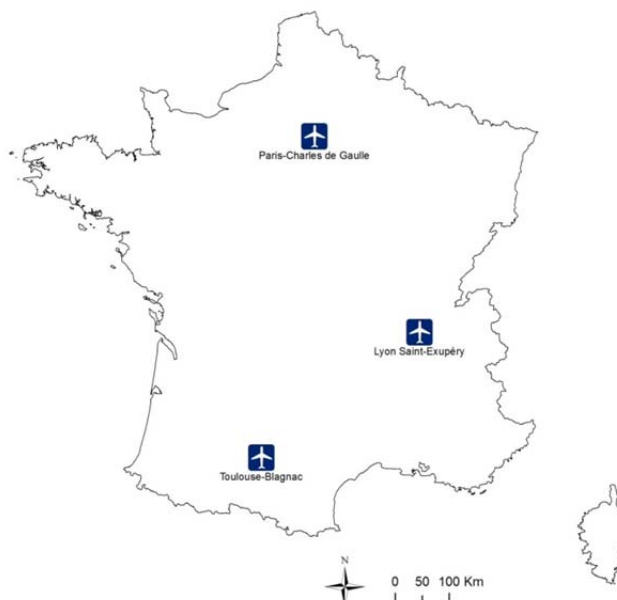
Mots-clés: *pollution de l'air ; bruit des avions ; mortalité ; santé.*

Introduction

Health issues related to airport noise pollutions became over the last years one of the key-questions which public policies want more to take into account. In 2004, the French High Council for Public Hygiene delivered its recommendation related to the health protection of people exposed to airport noise: noise around airports is considered as a public health problem. It recommended that the knowledge of the French health situation resulting from aircraft noise exposure is improved by performing epidemiological studies. Further to this recommendation, the French Ministry of Health (DGS), in co-operation with the Airport Pollution Control Authority (Acnusa) asked the French Institute of Science and Technology for Transport, Development and Networks (Ifsttar) to implement an epidemiological research program named “Discussion sur les Effets du Bruit des Aéronefs Touchant la Santé” (DEBATS).

DEBATS is an on-going research program (2011-2018) involving adult residents around three French airports (Evrard et al. (2011)): Paris-Charles de Gaulle, Toulouse-Blagnac, and Lyon Saint-Exupéry (Cf. Figure 1). It aims to characterize the relations between the aircraft noise exposure and the health status of the French population living in the vicinity of airports, both physically and mentally but also in terms of annoyance. In particular, it includes an ecological study aiming to investigate the relationship between weighted average exposure to aircraft noise and drug prescriptions, non-prescription drug sales, hospital admissions and mortality at the commune level (the smallest administrative unit in France).

Figure 1. The three airports included in DEBATS



If the reduction of aircraft noise nuisance has been considered to be the main issue for a long time, in recent years, the question of air pollution around airports has been raised. Indeed, air pollution exposure has been found to be associated with cardiovascular morbidity and mortality (Brook et al. (2010)). As several studies have shown an association between aircraft noise exposure and hypertension (Babisch and van Kamp (2009)) or mortality from cardiovascular disease (Huss et al. (2010), Hansell et al. (2013)), concerns for disentangling the effects of air pollution and of noise on cardiovascular outcomes have increased (Lekaviciute et al. (2013)). Therefore, DEBATS has attempted to take into account the issue of confounding air pollution and its impact on the association between aircraft noise exposure and cardiovascular disease.

1. Objectives

The present paper refers to the ecological study included in the DEBATS research program. It addresses the issue of an association between exposure to aircraft noise or to air pollution and mortality for cardiovascular disease, coronary heart disease, myocardial infarction and stroke. It focuses on the impact of air pollution on the association between aircraft noise exposure and mortality.

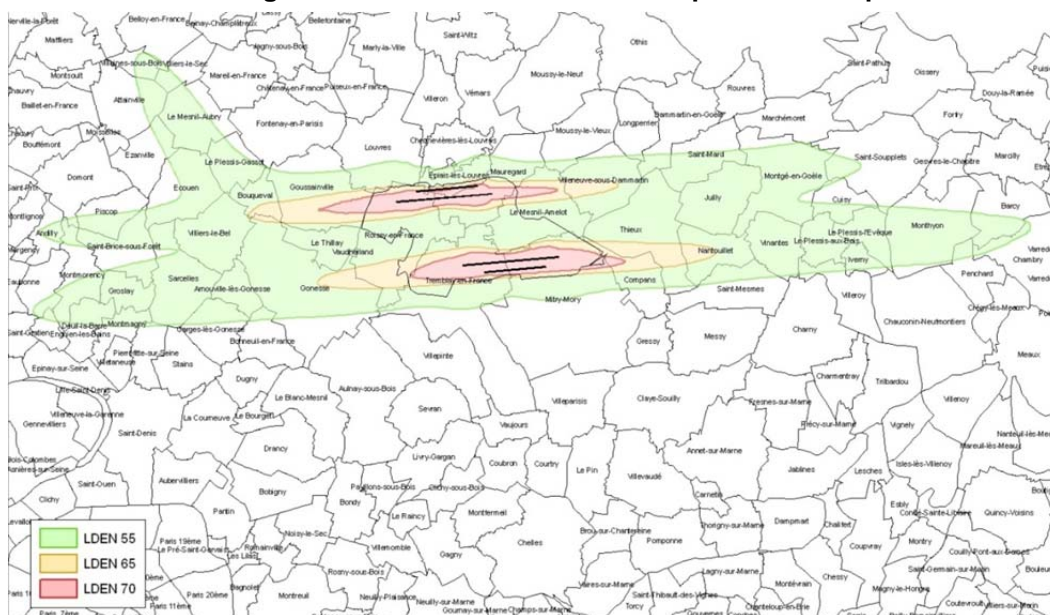
2. Methods

The study was based on 161 communes (the smallest administrative unit in France) close to the three above-mentioned French airports: Paris-Charles de Gaulle (108 communes), Lyon Saint-Exupéry (31 communes) and Toulouse-Blagnac (22 communes); these areas are hereafter referred to as the areas of Paris, Lyon, and Toulouse, respectively.

The mortality data were provided by the French Center on Medical Causes of Death for the period 2007-2010. The tenth revision of the International Classification of Diseases (ICD-10) was used to code and classify the mortality data based on the death records. The commune of residence, which is systematically included in the death record, was used as the spatial location. The following four underlying causes of death were investigated in the present study: 1) cardiovascular disease (including diseases coded from I00 to I52), 2) the sub-group called "coronary heart disease" (I20-I25), 3) in this sub-group, myocardial infarction (I21-I22), and finally, 4) stroke (including diseases coded from I60-I64, excluding I63.6).

Aircraft noise exposure at the commune level has been estimated using noise maps. Residents living near France's largest airports can get noise insulation grants for their homes. To select which residents are eligible for this funding, noise exposure maps are drawn up for each of these airports by the French Civil Aviation Authority with the 'Integrated Noise Model'. The INM is an internationally well-established computer model that evaluates aircraft noise impact in the vicinity of airports. The INM outputs noise contours for an area. They consist of three areas (Cf. Figure 2): the first one indicates a very high level of noise pollution limited by the L_{den} 70 index curve; the second one indicates a high level of noise pollution between the L_{den} 70 and L_{den} 65 index curves; and the last one indicates a moderate level of noise pollution between the L_{den} 65 and L_{den} 55 index curves. Aircraft noise contours were available for the year 2008 for Paris-Charles de Gaulle airport, 2003 for Lyon-Saint-Exupéry airport, and 2004 for Toulouse-Blagnac airport. These contours were considered to be representative of the years preceding the mortality assessment.

Figure 2. Paris-Charles de Gaulle airport noise map



For each commune in the study area, the number of inhabitants of the commune living within these noise levels with a 1-dB(A) resolution was assessed by the French Civil Aviation Authority. Noise levels were aggregated to obtain an estimate of commune-level exposure to aircraft noise. A population weighted average called average energetic index was estimated by weighting for a given commune, the noise level by the number of inhabitants living within this noise level.

The average air pollution exposure for each commune of the Paris and Lyon areas was estimated for both NO_2 and PM_{10} indicators with dispersion modelling. Data for the Toulouse area were missing. Briefly, modelled concentrations were provided at a $50\text{ m} \times 50\text{ m}$ resolution by Airparif institute for the Paris area, and at a resolution of $1,000\text{ m} \times 1,000\text{ m}$ by Air Rhône-Alpes institute for the Lyon area. For both areas, modelled concentrations were validated by comparison with

concentrations measured by a monitoring station network. The average air pollution exposure (for both NO₂ and PM₁₀ indicators and expressed in µg/m³) for the years 2008-2010 was used in the statistical analyses.

Correlations between aircraft noise and air pollution exposure were assessed using Spearman's rank correlation coefficients. The effects of aircraft noise or of air pollution on mortality rates were examined with Poisson GLMMs.

The models were adjusted for the following covariates, at the commune level, considered to be a priori confounding factors: gender, age, log-population density, lung cancer mortality (used as a proxy measure for commune-level smoking), and a deprivation index based on the median household income, the percentage of high school graduates in the population aged 15 years and above, the percentage of blue-collar workers in the active population, and the unemployment rate (Rey et al. (2009)).

The impact of air pollution on the relationship between aircraft noise exposure and mortality was examined by introducing simultaneously aircraft noise exposure and air pollution (NO₂ or PM₁₀ concentrations) in the models.

3. Results

The average concentration in NO₂ was estimated to 22.3 µg/m³, the average concentration in PM₁₀ to 23.9 µg/m³ and the average exposure to aircraft noise to 49.6 dBA, as shown in Table 1. NO₂ concentrations varied more widely than PM₁₀ concentrations (Table 1).

Table 1. Air pollution concentrations (NO₂ and PM₁₀) and aircraft noise levels^a.

NO ₂ (µg/m ³)	PM ₁₀ (µg/m ³)	Aircraft noise (dBA)
22.3 (12.0-36.3)	23.9 (22.3-27.1)	49.6 (42.0-64.1)

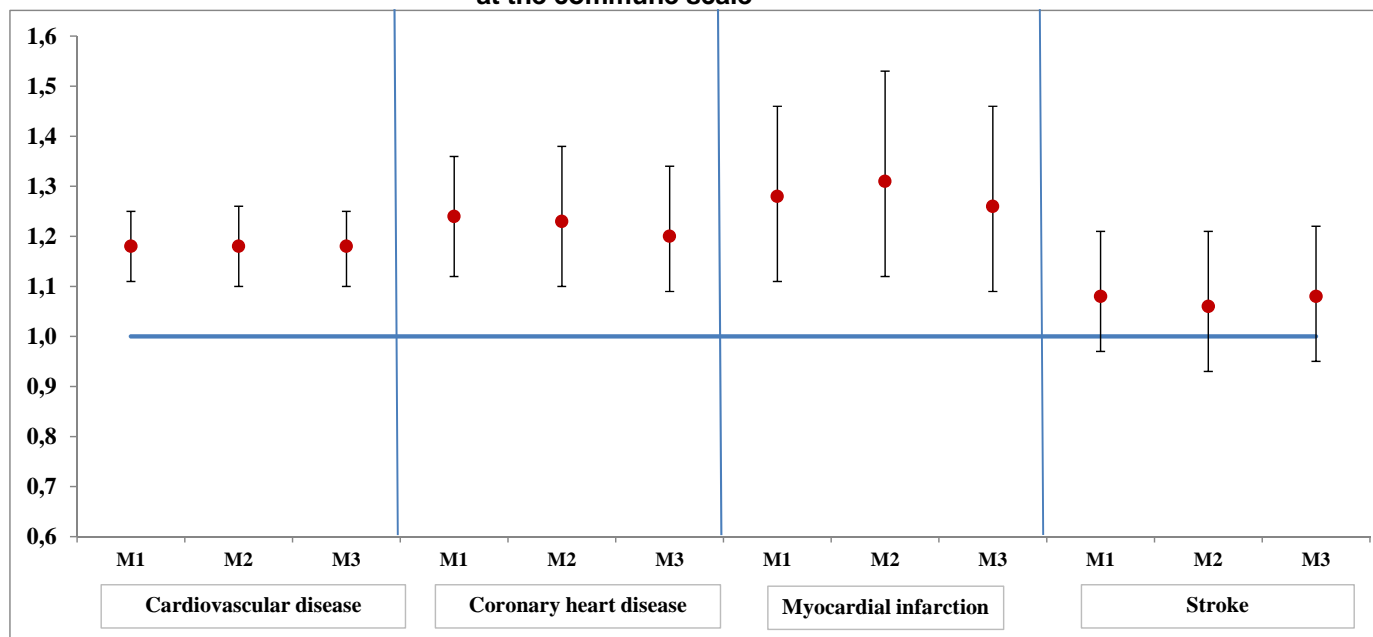
^aMean (range).

The highest average of aircraft noise exposure was observed in the Paris area. Moreover, aircraft noise exposure varied more widely in the Paris area. The NO₂ concentration was higher in the Paris area (mean: 24.0 µg.m⁻³) than in the Lyon area (mean: 16.5 µg.m⁻³) and varied more widely in the Paris area. The PM₁₀ concentrations were very similar in both the areas (mean: 24.2 µg/m³ in the Paris area and 23.9 µg/m³ in the Lyon area).

NO₂ and PM₁₀ concentrations were positively correlated (Spearman's rank correlation coefficient = 0.64). NO₂ concentrations were moderately correlated to aircraft noise levels (Spearman's rank correlation coefficient = 0.45) while PM₁₀ concentrations were not (Spearman's rank correlation coefficient = 0.06).

Regardless of aircraft noise, neither NO₂ nor PM₁₀ concentrations were significantly associated with mortality. However, the p-values were at the borderline of statistical significance. Positive associations were observed between exposure to aircraft noise and mortality for all causes of interest except stroke. As shown in Figure 3, these associations were not attenuated when NO₂ or PM₁₀ concentrations were included in the models.

Figure 3. Mortality rates ratios related to an 10 dBA-increase in aircraft noise exposure at the commune scale



M1: Noise level, gender, age, log-population density, lung cancer mortality, and deprivation index were included in the model.
M2: M1 + NO₂ concentrations.
M3: M1 + PM₁₀ concentrations.

4. Discussion

The present study is the first ecological study investigating the relationship between exposure to aircraft noise or to air pollution and the mortality of the population living in the vicinity of the airports in France. Regardless of aircraft noise, neither NO₂ nor PM₁₀ concentrations were significantly associated with mortality. In contrast, the present study seems to confirm the findings of recent studies, suggesting that high levels of aircraft noise are associated with mortality from cardiovascular disease and coronary heart disease and with mortality from myocardial infarction. Accounting for NO₂ or PM₁₀ concentration did not change the results — air pollution does not seem to be a confounding factor in the relationship between aircraft noise and mortality from all causes of interest. These results are consistent with previous studies.

The major strength of the present study is both the accuracy and the exhaustiveness of the mortality data provided by the French Center on Medical Causes of Death (CépiDc-Inserm) and the large number of deaths from cardiovascular disease (7,450) for a 4-year period (2007-2010). The second point of interest in the present study is that the ecological approach allowed us to take advantage of larger contrasts in aircraft noise and air pollution exposures between geographical units than between individuals.

One limitation of the present study relates to the fact that data about air pollution were missing for the Toulouse area. Therefore, analyses carried out to examine the impact of air pollution on the relationship between aircraft noise exposure and mortality were restricted to 139 communes instead of 161, thus limiting the statistical power to detect an association between air pollution and mortality from cardiovascular disease if it exists. Air pollution modelling is still ongoing in the Toulouse area within the framework of the Atmosphere Protection Plan. Data will be available in the next future.

Currently, ultrafine particle (UFP) emissions from aircrafts and its health effects around airports are an important issue. UFP is one of the new issues in air pollution epidemiology and toxicology and UFP exposures are present at all airports. Unfortunately, exposure data based on this indicator are not yet available around airports in France.

Conclusion

The present research seems to confirm the findings of recent studies suggesting that air pollution does not modify the impact of aircraft noise exposure and mortality from cardiovascular disease,

coronary heart disease and myocardial infarction. However, the potential for ecological bias and the possibility that this association could be due to unmeasured factors cannot be excluded. Further individual studies are necessary in order to better understand this association.

Acknowledgments

This work was supported by funds from the French Ministry of Health, the French Ministry of Environment, and the French Civil Aviation Authority.

The Airport Pollution Control Authority (Acnusa) requested the French Institute of Science and Technology for Transport, Spatial Planning, Development and Networks (Ifsttar) for carrying out the present study. We would like to thank them for their confidence in us.

The authors are grateful to the CépiDc-Inserm for providing mortality data from the database of the French Center on Medical Causes of Death and to Aéroports de Paris and the French Civil Aviation Authority for providing noise exposure maps produced with the Integrated Noise Model. We are also grateful to Airparif and Air Rhône-Alpes for providing background air pollution concentrations.

References

- Brook, R.D., Rajagopalan, S., Pope III, C.A., et al. (2010): Particulate matter air pollution and cardiovascular disease: an update to the scientific statement from the American Heart Association. Circulation 121(21):2331-7238.
- Babisch W. and van Kamp I. (2009): Exposure-response relationship of the association between aircraft noise and the risk of hypertension. Noise&Health 11(44):161-168.
- Evrard A.S., Barthélémy L., Champelovier P., Chiron M., Jähi H., Lambert J., and Laumon B. (2011): The DEBATS Study: Health effects of aircraft noise near three French airports. 10th International Congress on Noise as a Public Health Problem organized by the International Commission on the Biological Effects of Noise (ICBEN). London (United Kingdom), July 2011.
- Huss, A., Spoerri, A., Egger, M., Röösli, M. (2010): Aircraft noise, air pollution, and mortality from myocardial infarction. Epidemiology 21(6):829-836.
- Hansell, A.L., Blangiardo, M., Fortunato, L., et al. (2013): Aircraft noise and cardiovascular disease near Heathrow airport in London: small area study. BMJ 347:f5432.
- Lekaviciute J. Kephelopoulos S., Stansfeld S., Clark C. (2013): Final Report of the ENNAH (European Network on Noise and Health) project. Publications Office of the European Union.
- Rey G., Jouglé E, Fouillet A, Hémon D. (2009): Ecological association between a deprivation index and mortality in France over the period 1997-2001: Variations with spatial scale, degree of urbanicity, age, gender and cause of death. BMC Public Health 9:33.

Estimation of atmospheric pollutant emissions by transport at Mytilene, Greece, during the tourist season

Kyriaki-Maria FAMELI* & Anna-Maria KOTRIKLA**

**Institute for Environmental Research and Sustainable Development, National Observatory of Athens, 152 36 Athens, Greece - email:kmfameli@noa.gr*

***Department of Shipping, Transport and Trade, University of the Aegean, Chios, 82100 Greece, e-mail : akotr@aegean.gr*

Abstract

In the Greek islands tourism is one of the main economic activities. However due to its seasonality, tourism results in adverse environmental and health effects including traffic congestion, noise and atmospheric pollution. The aim of this study is to estimate emissions from road transport and navigation for the pollutants PM₁₀, NO_x, CO and SO₂, at the city of Mytilene (the capital of the north eastern Aegean island of Lesbos) for a typical weekday during the summer period. Road transport emissions were calculated following the top-down approach, with the use of the programme COPERT 4 for five distinct vehicle types. The annual emissions were disaggregated on a temporal scale of 1 hour. The emissions from maritime transport were estimated using a bottom-up approach based on the ships activity at the port of Mytilene. Comparing emissions from both sources, road transport is the greatest contributor to the local pollution levels regarding CO. Both road transport and navigation affect NO_x and PM₁₀ emissions. The emissions of SO₂ are solely due to shipping because marine fuel contains 0.1-1.5% S compared to 10 ppm of the diesel oil for road transport.

Keys-words: *Road transport, navigation, emissions, Mytilene, Greece.*

Introduction

The passenger and freight transport with cars, trucks, boats, buses, motorcycles and other motorized vehicles is responsible for the majority of the polluting emissions found in both developed and developing cities (Ald, 2012). Vehicles are a major source of nitrogen oxide (NO_x), leading to acidification and ozone formation. In 2011, the contribution of road transport emissions to the NO_x and carbon monoxide (CO) in Europe amounted to 40% and 26%, respectively (EEA, 2013). Road transport is also the dominant source of inhalable particles (those particles that are able to penetrate deep into the lung, affecting health) typically described as PM_{2.5} (Pant and Harrison, 2013) while passenger cars alone are among the top five key categories for CO emissions (EEA, 2013). More specifically, diesel engines emit significantly more organic compounds and elemental carbon compared to new gasoline engines. Gasoline vehicles emit relatively low amount of particulate matter but the potential for inhalation of gaseous and semi-volatile compounds is greater (Ald, 2012). Additionally, in cities connected with their ports, a considerable amount of atmospheric pollution results by the maneuvering and berthing of ships at the port. The main pollutants emitted by ships are SO₂, because of the high sulphur content of marine bunkers, PM and CO which are emitted as a result of incomplete combustion of the low quality marine fuels and finally NO_x that are emitted due to the high temperatures and pressures inside internal combustion engines. Gaseous oxides of sulphur produced during combustion of fossil fuels can be oxidized to particulate sulphates. In addition particulate emissions from shipping include OM (organic matter) and BC (black carbon) (Lack et al, 2009).

The emission of atmospheric pollutants has adverse effect on human health and ecosystems, damages materials and affects atmospheric visibility. In a study considering the effects of the emissions of PM by ships to public health, Corbett et al (2007) estimated that shipping-related PM emissions are responsible for approximately 60,000 cardiopulmonary and lung cancer deaths annually, with most deaths occurring near coastlines in Europe, East Asia, and South Asia. Additionally to the toxic atmospheric pollutants, as in every hydrocarbon's combustion process, carbon dioxide (CO₂) is emitted by transport modes that use combustion of fossil fuels. CO₂ is not toxic at current levels; however it is the main greenhouse gas and contributes to global warming. The transport sector accounts for 26% of global CO₂ emissions (Chapman, 2007) and road transport is the biggest producer of greenhouse gases in the transport sector. Therefore, studying accurately

emissions can enrich our knowledge towards the formulation of efficient air quality management schemes (Tsilingiridis et al. 2002, Giannouli et al. 2011), since the emission inventory is a key component of any air pollution control program (Souza et al. 2013).

In this framework, the purpose of the present study is to construct an emission inventory from road transport and navigation for the city and port of Mytilene which is the capital and the most populated city of the north eastern Aegean Island Lesvos (Figure 1). Since summer tourism is one of the main economic activities in the Greek islands, a typical weekday during the summer period was selected for the estimation of PM₁₀, NO_x, CO and SO₂ emissions, at the city of Mytilene.



Figure 1. Lesvos Island (left) and the city of Mytilene (right).

1. Methodology

Road transport emissions for Lesvos Island were calculated following the top-down approach based on the EMEP/ CORINAIR methodology (EMEP/EEA, 2013). For the estimation of annual emissions from five distinct vehicle types (passenger cars, light commercial vehicles, heavy duty vehicles, urban buses and coaches and two wheelers) the programme COPERT 4 was used (EMISIA, 2014) firstly at national level (Greece) and secondly at regional level (Lesvos Island) for the year 2014. The emissions were distinguished according to the fuel type used (gasoline, diesel, liquid petroleum gas, compressed natural gas), the EU Directives to which they conform in terms of emissions (PRE ECE, ECE 15/00-01, Euro 1, Euro 2, etc.) and the engine capacity (e.g. <1.4lt, 1.4-2.0lt, >2.0lt for passenger cars, <3.5t or >3.5t for commercial vehicles) of each vehicle. Detailed fleet composition data (vehicles number for each of the five categories, per fuel type, engine technology and capacity) were provided by the Greek Ministry of Transport for the year 2006 for Greece. In order to construct the annual fleet for the year 2014 for Greece new vehicle registrations were obtained from ACEA, the Association of Motor Vehicle Importers Representatives (AMVIR), the Hellenic Statistical Authority (ELSTAT) and the International Council on Clean Transportation. For the development of the vehicle fleet for Lesvos Island for the year 2014 statistical data from the Hellenic Statistical Authority (ELSTAT, 2014) were used (passenger cars: 26,190 vehicles - 40%, trucks: 16,226 vehicles - 25%, buses: 106 vehicles - 0% and two wheelers: 22,547 vehicles - 35%, percentages refer to the part of the total fleet for each vehicle category) and the engine technology speciation used for Greece was applied (Table 1). The National Observatory of Athens provided the mean minimum and maximum monthly temperature values and the mean monthly relative humidity required by COPERT (Table 2).

The necessary activity data (share of driving condition and mean travelling speeds in different driving conditions) were collected by Ntziachristos et al. 2008 and are provided by Emisia SA for Greece (www.emisia.com). For the purposes of this study, only 40.45% of total emissions on Lesvos were attributed to the road network of the Mytilene according to population data from Hellenic Statistical Authority.

Table 1. Vehicle fleet for the year 2014 for Greece and Lesvos Island (Number of vehicles, source: Hellenic Statistical Authority).

Vehicle category	Greece	Lesvos
Passenger Cars	5,110,873 (64%)	26,190 (40%)
Trucks	1,317,945 (16%)	16,226 (25%)
Buses	26,691 (0%)	106 (0%)
Two-wheelers	1,582,818 (20%)	22,547 (35%)
Total	8,038,327	65,069

Table 2. Mean monthly temperature and relative humidity values for Mytilene (Source: National Observatory of Athens, www.meteo.gr).

Month	Mean minimum monthly temperature (°C)	Mean maximum monthly temperature (°C)	Mean monthly relative humidity RH(%)
January	8.5	12.9	71
February	8.5	13.2	70
March	9.6	14.8	68
April	12.4	18.4	64
May	15.9	22.8	63
June	19.8	27.1	57
July	21.8	28.1	56
August	21.6	27.6	57
September	19.6	25.2	60
October	16.1	21.3	66
November	13.1	18.0	71
December	10.3	14.6	72

The temporal disaggregation of the annual emissions to monthly, weekly and diurnal values was based on the equation:

$$E_{h,i} = E_i \times M_i \times D_i \times H_i,$$

where $E_{h,i}$ is the hourly emissions of pollutant i , E_i is the annual emissions of pollutant i and M , D and H are the monthly, daily and hourly coefficients, respectively. Due to the increased influx of vehicles during the tourist season higher values were attributed to summer months, especially to August, May and September as well (Table 3). Regarding the weekly coefficients, they were derived from traffic counts recorded by the University of the Aegean. According to Table 4, the highest traffic in Mytilene is observed in Friday and Saturday. This is probably due to the fact that residents use their vehicle more these days, firstly during the working hours and secondly in the evening. Finally, the necessary allocation of emissions on an hourly scale was based on hourly coefficients derived from hourly traffic data for each day of the week for Athens (Fameli and Assimakopoulos 2015), considering that they reflect adequately the movement of vehicles in Mytilene. This was necessary because of the lack of detailed hourly traffic data for Mytilene.

Table 3. Monthly temporal coefficients for Mytilene.

Month	Monthly coefficient	Month	Monthly coefficient
1	0.081	7	0.086
2	0.081	8	0.088
3	0.082	9	0.085
4	0.083	10	0.082
5	0.085	11	0.081
6	0.085	12	0.081

Table 4. Daily temporal coefficients for Mytilene.

Day	Monday	Tuesday	Wednesday	Thursday	Friday	Saturday	Sunday
Daily coefficient	0.133694	0.128095	0.14661	0.13839	0.164873	0.155156	0.133182

Regarding emissions from maritime transport, the emissions of NO_x, PM, SO₂ and CO of the ships approaching the port of Mytilene were estimated for two days: Friday 3/7/2015 and Friday 10/7/2015. On 3/7/2015 there were 6 calls of passenger or ro-ro passenger ships that connect the island with the Greek mainland and with Turkey. On 10/7/2015 marine traffic doubled (12 calls of ships including two cruise ships).

Estimations of the shipping emissions were performed using a bottom-up methodology (EMEP/EEA, 2013; ENTEC, 2007). According to that, the emissions for a single trip of a vessel are determined using the following equation:

$$E_{trip,i,m} = \sum_p [t_p (P_e \times LF_e \times EF_{e,i,m,p})]$$

Here EF is the emission factor for the particular pollutant in g per kWh (g/kWh), LF the engine load factor (%), P the engine nominal power (kW), and t time (hours). Subscript e refer to the different engine category (main, auxiliary), i to the engine type (slow-, medium-, and high-speed diesel), m to the fuel type (Heavy Fuel Oil - HFO, Marine Diesel Oil – MDO or Marine Gas Oil - MGO), and p to the different phases of the trip (berthing, maneuvering). Regarding the different phases of the trip, maneuvering refers to the slow movement of the ship between the port's breakwater (entry/exit) and point of berth, whereas berthing refers to the dockside mooring of the ship. The total inventory is the sum over all trips of all vessels during the period we investigated. Information relevant to ship calls at the ports of Chios and Mytilene, involving the date of call, the vessel's name, as well as the call duration (i.e. arrival and departure time) were gained by the Port Authorities of Chios and Mytilene. Details of the ships (IMO number, type of ship, gross tonnage, engine model, main engine power) were obtained from internet data bases (Equasis 2015; Marine Traffic, 2015). The type of main engines, the fuels as well as the power of the auxiliary engines of the ships were inferred by the literature (ENTEC 2007; Tzanatos 2010). The average load factors and emission factors of the main and auxiliary engines suggested by the study of EMEP/EEA (2013) were used in this study.

2. Results and Discussion

The results from the estimation of the emissions from navigation and road transport for a typical working day (Friday) are presented in Table 5. Concerning road transport emissions, it is obvious that CO emissions (2294.7 kg/day) outweigh the other emissions while those of NO_x (1181.5 kg/day) follow. Generally emissions are highly correlated with the type of fuel used by vehicles as it determines the type of pollutant emitted. Gasoline is linked to CO, VOC and NMVOC emissions (Ban-Weiss et al., 2008), while diesel vehicles mainly contribute to NO_x and PM emissions. In Greece most passenger vehicles, two wheelers and part of light commercial vehicles using gasoline, while trucks, buses, the rest of light commercial vehicles and taxis use diesel fuel. As shown in figure 2, two wheelers and

trucks (more specifically light commercial vehicles) contribute mostly to CO emissions (54.73%, and 29.87% respectively). This is because the usage of two wheelers, instead of passenger cars, is very popular in Greek islands. According to a study for the Greater Athens Area by Fameli and Assimakopoulos 2015, two-wheelers contribute by 25.31% to the total CO emissions for Athens while passenger cars are the main contributor (56.53%) revealing the difference in residents' habits as far as the vehicle category preferred for transportation is concerned. Moreover higher annual mileage is attributed to light commercial vehicles compared to passenger cars. Regarding PM₁₀ emissions trucks (heavy duty trucks and light commercial vehicles) affect the total value by 80.29% due to the use of diesel fuel. Trucks hold a significant part of the total fleet (25%) and in combination with the fact that the daily mileage attributed to them is high, they have much higher fuel consumption compared with passenger cars, resulting in high emissions of PM₁₀. The second largest contribution (9.11%) comes from passenger cars. The diesel penetration on the total passenger cars fleet is only 2%. The involvement of motorcycles is 8.93%.

As for emissions from navigation, the emissions on 10/7/2015 are 1.7 – 2 times the emissions on 3/7/2015 because the ship arrivals/departures have doubled. The passenger ship itineraries from Mytilene to Piraeus and Ayvalik, Turkey become more frequent during the summer months reflecting the increased tourist activity. The pollutants that are emitted in greater quantities (in terms of mass) from the ships at the port of Mytilene are the NO_x, followed by SO₂ and CO and finally by PM₁₀ (Table 5). NO_x are emitted in every internal combustion engine process due to the high temperatures in the combustion chamber. SO₂ is due the high sulphur content of the marine fuels. Passenger ships in European ports use marine fuel that contains 0.1-1.5% S (EC, 2005) compared to 10 ppm of the diesel oil for road transport. CO from the ships is due to the incomplete combustion of the fuels. PM from the ships contains soot, unburned fuel and sulphate particles.

Table 5. Emissions from road transport and navigation at Mytilene.

Pollutant	Emissions (kg/day)		
	Navigation, Friday 3/7/2015	Navigation, Friday 10/7/2015	Road transport, Friday
PM ₁₀	24.6	41.8	57.6
NO _x	373.0	678.0	1181.5
CO	50.7	89.8	2294.7
SO ₂	59.2	122.0	-

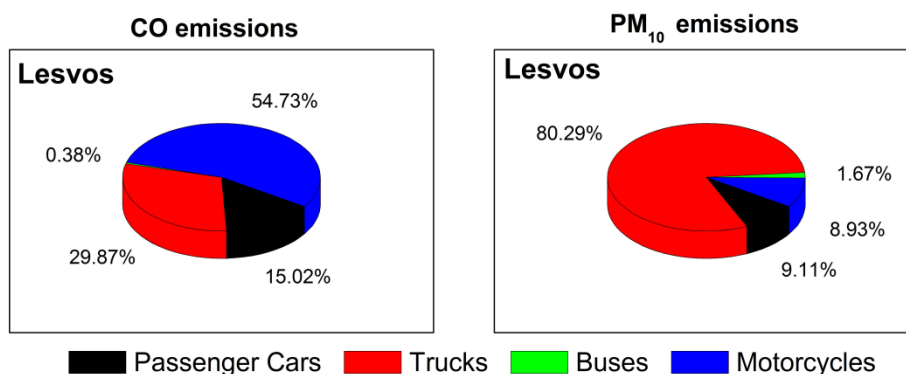


Figure 2. Percentage contribution of each vehicle category to the daily CO (left) and PM₁₀ (right) emissions.

Comparing emissions from both sources (Table 5), it is obvious that road transport is the greatest contributor to the local pollution levels, especially regarding CO emissions. Much higher NO_x levels are also estimated to arise from road transport compared to ships. Both road transport and navigation affect PM₁₀ emissions. On the other hand, the emissions of SO₂ are solely due to the ships, due to the high sulphur content of the marine bunkers compared to road diesel and gasoline.

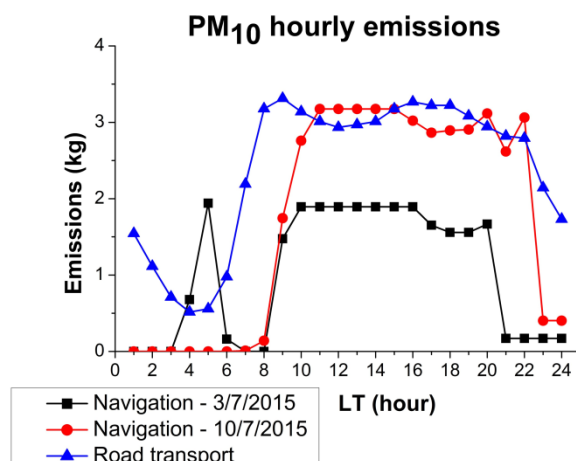


Figure 3. The diurnal variation of PM₁₀ emissions from road transport and navigation for a typical weekday.

The diurnal variation of PM₁₀ emissions is shown in figure 3 for both road transport and navigation emissions. It is obvious that road transport emissions profiles are highly correlated with the working hours having a morning peak at 9.00 LT and a second one from 15.00 to 19.00 LT since the working hours vary. Concerning the diurnal variation of ship emissions, it is generally higher during the day corresponding to the arrival/departure and berthing of most of the ships.

Conclusion

In the Greek islands tourism often has negative environmental and health effects including congestion, noise and atmospheric pollution. In this work the emissions of atmospheric pollutants from road and maritime transport were estimated at Mytilene for a typical summer weekday. The results indicated that road transport is the greatest contributor to the local pollution levels. It mostly affects CO emissions (two wheelers and trucks are the main contributors). However, both road transport and navigation affect NO_x and PM₁₀ emissions. More specifically trucks (heavy duty trucks and light commercial vehicles) affect the total value of PM₁₀ emissions by 80.29% due to the use of diesel fuel. The emissions of SO₂ are solely due to ships due to the high content of the marine fuel. The development of the emission inventory for the city of Mytilene will lead to the modelling of the pollutants' dispersion and chemical transformations and consequently to the assessment of different mitigation strategies on the local air quality.

Acknowledgments

This research has been co-financed by the European Union (European Social Fund – ESF) and Greek national funds through the “Operational Program “Education and Lifelong Learning” of the National Strategic Reference Framework (NSRF) – Research Funding Program: THALES – “Green Transport in Island Areas (GreTIA)”.

References

- Ald K. (2012): Air pollution in the urban atmosphere: sources and consequences. *Metropolitan Sustainability: Understanding and Improving the Urban Environment*, 231.
- Ban-Weiss G.A., McLaughlin J.P., Harley R.A., Lunden M.M., Kirchstetter T.W., Kean R.A., Strawa A.W., Stevenson E.D., Kendall G.R. (2008): Long-term changes in emissions of nitrogen oxides and particulate matter from on-road gasoline and diesel vehicles. *Atm. Env.*, vol. 42, p220-32. <http://dx.doi.org/10.1016/j.atmosenv.2007.09.049>

- Chapman L. (2007): Transport and climate change: a review. Journal of transport geography, vol. 15, n°5, p354-367.
- Corbett J.J., Winebrake J.J., Green E.H., Kasibhatla P., Eyring V., & Lauer A. (2007): Mortality from ship emissions: a global assessment. Environmental Science & Technology, vol. 41, n°24, p8512-8518.
- EC (2005): Directive 2005/33/EC of the European Parliament and of the Council of 6 July 2005 amending Directive 1999/32/EC, as regards the sulphur content of marine fuels, Official Journal of the European Union, L 191/59.
- EEA (European Environmental Agency), (2013): European Union emission inventory report 1990–2011 under the UNECE Convention on Long-range Transboundary Air Pollution (LRTAP). EEA Technical report No 10/2013.
- ELSTAT (2014): Vehicle fleet / January 2014 <http://www.statistics.gr/statistics/-/publication/SME18/>
- EMEP/EEA (2013): EMEP/EEA air pollutant emission inventory guidebook, Technical guidance to prepare national emission inventories. Retrieved April 24, 2015 from <http://www.eea.europa.eu/themes/air/emep-eea-air-pollutant-emission-inventory-guidebook/emep>.
- EMISIA (2014): COPERT 4. Available at <http://emis.com/copert>
- Entec UK Limited (2007): Ship Emissions Inventory – Mediterranean Sea, Final Report for Concaawe, April 2007.
- Equasis (2014): Ship search, viewed 27 March 2015, <http://www.equasis.org/EquasisWeb/public/HomePage?fs=HomePage>
- Fameli K.M. and Assimakopoulos V.D. (2015): Development of a road transport emission inventory for Greece and the Greater Athens Area: Effects of important parameters. Sci Total Environ, vol.505, p770-786.
- Giannouli M., Kalognomou E.A., Mellios G., Moussiopoulos N., Samaras Z., Fiala J.(2011): Impact of European emission control strategies on urban and local air quality. Atm. Env., vol45, n°27, p4753-62. <http://dx.doi.org/10.1016/j.atmosenv.2010.03.016>
- Lack D.A., Corbett J.J., Onasch T., Lerner B., Massoli P., Quinn P.K., Bates T.S., Covert D.S., Sierau B., Herndon S., Allan J., Baynard T., Lovejoy E., Ravishankara A., & Williams E. (2009): Particulate emissions from commercial shipping: Chemical, physical, and optical properties. Journal of Geophysical Research: Atmospheres (1984–2012), vol.114(D7), DOI: 10.1029/2008JD011300.
- Marine Traffic (2014) Ships. Viewed 27 March 2015, <http://www.marinetraffic.com/gr/ais/index/ships/range>
- Ntziachristos L., G. Mellios, Ch. Kouridis, Th. Papageorgiou et al. (2008): European Database of Vehicle Stock for the Calculation and Forecast of Pollutant and Greenhouse Gases Emissions with TREMOVE and COPERT – Final Report. LAT/AUTh Report No. 08.RE.0009.V2, Thessaloniki, Greece, p.250.
- Pant P. and Harrison R.M. (2013): Estimation of the contribution of road traffic emissions to particulate matter concentrations from field measurements: A review. Atm. Env., vol.77, p78-97. <http://dx.doi.org/10.1016/j.atmosenv.2013.04.028>
- Souza CDR, Silva SD, Silva MAV, D'Agosto MA, Barboza AP.(2013): Inventory of conventional air pollutants emissions from road transportation for the state of Rio de Janeiro. Energ Policy, vol.53, p125-35. <http://dx.doi.org/10.1016/j.enpol.2012.10.021>
- Tsiliniridis G, Zachariadis T, Samaras Z. (2002): Spatial and temporal characteristics of air pollutant emissions in Thessaloniki, Greece: investigation of emission abatement measures. Sci Total

Environ, vol.300, p99-113. [http://dx.doi.org/10.1016/S0048-9697\(02\)00170-5](http://dx.doi.org/10.1016/S0048-9697(02)00170-5)

Tzannatos, E. (2010): Cost assessment of ship emission reduction methods at berth: the case of the Port of Piraeus, Greece. Marit. Pol. Mgmt., vol.37, n°4, p427-445.

The validation of CO₂MPAS tool for supporting the introduction of WLTP in the European CO₂ certification

Georgios FONTARAS*, Víctor VALVERDE*, Stefanos TSIKMAKIS*, Vincenzo ARCIDIACONO*, Konstantinos ANAGNOSTOPOULOS* and Biagio CIUFFO*

Anastasios KONTSES**, Dimitrios TSOKOLIS**, Athanasios DIMARATOS** and Zissis SAMARAS**

*Joint Research Centre, Ispra, Via Enrico Fermi 2749, I – 21027, Ispra (VA), Italy, Contact E-Mail: georgios.fontaras@jrc.ec.europa.eu, Tel. +39 0332 786425, Fax +39 0332 786671

**Laboratory of Applied Thermodynamics, Aristotle University of Thessaloniki, P.O. Box 458, GR 54124

Abstract

To support the transition from NEDC-based CO₂ monitoring to the WLTP-based one, the Joint Research Centre (JRC) of the European Commission develops the CO₂ Model for Passenger and commercial vehicles (CO₂MPAS), to be used for correlating the measured WLTP CO₂ emissions to their NEDC equivalent ones. Scope of CO₂MPAS is to calculate NEDC CO₂ emissions based on limited information collected during the WLTP test at vehicle type-approval. The model also attempts to provide a flexible yet robust basis for testing the CO₂ reduction potential of different technology packages and for analyzing different policy options for curbing CO₂ emissions in the future. This paper demonstrates a first validation of the model. Synthetic and real data were obtained from simulations and tests, respectively, that were performed at the Laboratory of Applied Thermodynamics of the Aristotle University and the JRC's VELA laboratories over both cycles. A pool of 22 sets of real tests and more than 2000 simulation cases were developed for running the validation exercise. Results suggest a good operation of CO₂MPAS with an error of the CO₂ emission prediction on NEDC below ±4% in 90% of the cases.

Key-words: CO₂MPAS, WLTP, NEDC, CO₂, Fuel consumption

1. Introduction

Curbing CO₂ from road transport has been a key policy target in the European Union (EU) for the past 20 years. So far, a number of measures and policy initiatives have been established in order to reduce light duty vehicle CO₂ emissions and fuel consumption (FC). In particular, EU Regulations 443/2009 and 510/2011 set European targets for average CO₂ emissions from light duty vehicles for 2015 and 2020 (for passenger cars: 130 gCO₂/km from 2015 and 95 gCO₂/km from 2020). The targets are not uniform for all vehicle manufacturers (OEMs) but are correlated to the average mass of the vehicles sold, allowing higher emissions for heavier vehicles. However the system is set up in such a way that the global CO₂ average of the new sales should not exceed the abovementioned target values. Each year, the average CO₂ emissions of each manufacturer's newly registered vehicle fleet during the year before are compared to the corresponding targets. In case an OEM does not comply with the target, costly penalties are applied which can range up to 100 €/gCO₂ in excess per each vehicle registered (for a thorough and detailed description please refer to (European Commission 2009; European Commission 2011)).

A continuous decrease in the officially reported fleet-wide average CO₂ emissions has been achieved as a result of the above mentioned policy. Recent data (EEA, 2014) suggest that OEMs have achieved their 130 g CO₂/km targets ahead of time, as the average test-cycle based EU emissions of all manufacturers in 2014 was 123.4 g CO₂/km. Nonetheless, there are increasing indications that these reductions do not entirely appear under real world driving conditions and that the shortfall between the existing certification test in Europe and real-world fuel consumption is increasing with time (ECMT 2005; Mellios 2011; Ligterink *et al.*, 2013; Mock *et al.*, 2013; Mock *et al.*, 2014). In their study, Mock *et al.* (2014) have found that the gap has been constantly increasing from 7% in 2001 to 23% in 2011 and 30% in 2013. Other studies report deficiencies of the existing test procedure in accurately capturing CO₂ emissions of modern vehicles too (Fontaras and Samaras 2007; Fontaras and Dilara 2012; Dings 2013). For strengthening the current certification framework for both, CO₂ and pollutant emissions control, the European Union has decided the introduction of the recently developed Worldwide harmonized Light duty vehicle Test Protocol (WLTP) in the

European light duty certification procedures.

The introduction of the WLTP requires the adaptation of the entire certification scheme for light duty vehicle CO₂ emissions. As expected the CO₂ emissions of the vehicles under the new protocol will be different from those of the current New European Driving Cycle (NEDC), with first information showing higher values when the entire certification process is taken into account (Ciuffo *et al.*, 2015; Marotta *et al.*, 2015). As a result an adaptation of the CO₂ targets set by the relevant European Regulations would be necessary. The NEDC/WLTP correlation project has started with this aim and its final objective is to identify the most appropriate strategy to introduce the new procedures without having to radically amend the targets set for the 2015-2021 period. Such an amendment could potentially create significant disturbance in the European automotive market. The chosen solution is the development of a correlation model able to estimate the difference in terms of CO₂ emissions between the two test-procedures rather than revisiting the established targets (Ciuffo *et al.*, 2015). The approach selected by the European Commission to deal with this issue, required the development of a technology oriented vehicle simulation model, CO₂ Model for Passenger and commercial vehicles (CO₂MPAS). In order to assist the development of such a combined testing-modelling approach a pool of 15 passenger cars, representative of the 2014 European fleet were selected and their corresponding simulation models were developed by the Laboratory of Applied Thermodynamics (LAT) of the Aristotle University and the European Commission's Joint Research Centre (JRC) in a commercial vehicle simulation software (AVL's Cruise). Data for building these simulation models were provided by the corresponding OEMs, with the objective to enable modelling with the highest possible accuracy, while real chassis dyno measurements were also performed independently as part of the study in order to thoroughly validate the results of the models (Tsokolis *et al.*, 2015). All models were validated against these measurements for both NEDC and WLTP test procedures.

CO₂MPAS has been extensively validated against simulated and real data in order to demonstrate its capacity to capture the differences between the two certification procedures. In this paper a first validation of the model is being presented. Synthetic and real data were obtained from simulations and tests respectively which were performed at the Laboratory of Applied Thermodynamics of the Aristotle University and the JRC's VELA laboratories over both cycles. A pool of 22 sets of real tests and more than 2000 simulation cases were developed for running the validation exercise.

2. Methodology

CO₂MPAS model description

CO₂MPAS follows a hybrid approach between a more general purpose emission model and a fully developed vehicle simulation model. The key design objectives of the model, which were set from the beginning, are:

- Capacity to capture the effect of specific fuel/energy consumption reduction technologies, when individually applied or in combination, at vehicle level with good accuracy (e.g. < 2.0% as compared to the measurement);
- Ability to perform accurate simulation of vehicle fuel consumption/CO₂ emissions under different operating conditions/mission profiles using mainly physical models and by limiting statistical factors as much as possible;
- Formulation of testing cases based on real fleet data and possibility to screen out unrealistic and implausible cases;
- Fast simulation times in order to allow simulation of large number of cases (>10⁴ representative samples of an actual vehicle fleet) in reasonable time;
- Possibility to link with other models/components such as traffic simulation models, GPS provided info, cost calculation modules, etc. for future usage;

A dedicated energy consumption-CO₂ emissions calculation component, for passenger cars and light commercial vehicles, has been developed to support the simulation activity. The core of the simulation module is a physical-based model based on standard vehicle longitudinal dynamics and energy consumption simulation. Initial investigations indicated that the 4 most important factors affecting CO₂ emissions over given driving conditions are:

- Accurate calculation of power;
- Driving (gear-shifting, acceleration patterns);

- Powertrain operation and efficiency;
- Cold start – temperature conditions;
- Controls of secondary systems – power sources;

In the power – driving submodule, vehicle energy demand is calculated via simple vehicle longitudinal dynamics. A gear-shifting model based on the WLTP gear-shifting rules is included in order to back calculate engine rpm and torque based on the velocity and acceleration of the vehicle. In addition to the WLTP- based driving and gear shifting, dedicating machine learning methods are incorporated in order to identify the gear shifting logic of automatic transmission vehicles, calibrate the respective model, and apply it to NEDC or other driving profiles.

The engine – cold start submodule consists of two main modules. The engine fuel consumption module and the temperature prediction, additional fuel consumption module. The engine fuel consumption module is based on an extended 2nd degree Willans model operating with normalized quantities (effective pressures). The engine fuel consumption map is reduced to an equation consisting of 6 factors, which are calibrated based on the provided WLTP CO₂ measurements (bag values). Cold start and its impact on fuel consumption are captured by CO₂MPAS through an engine temperature prediction sub-module and a cold start extra-fuel consumption function that is directly coupled with the engine fuel consumption function. The temperature prediction model is calibrated based on the evolution of the engine temperature as a function of the engine power, the rpm and the vehicle velocity recorded over the WLTP test. The function defining the extra fuel consumption due to cold start is a two parameter exponential function and the unknown factors are calibrated based on the measured emissions of the WLTP cold phase (Low phase).

A generic gearbox temperature model is also included to account for the changes in gearbox torque losses due to cold start. Some common energy saving technologies such as engine start stop and brake energy recuperation are simulated based on a generic operating strategy which takes into account vehicle motion status and other vehicle characteristics (battery state of charge, engine coolant temperature, etc.). Functions to cover additional technologies such as Constant Variable Transmission gearboxes and hybrid vehicles are currently under development.

CO₂MPAS is an open-source project developed with Python-3.4, using Anaconda & WinPython under Windows 7, Anaconda under MacOS, and Linux's standard python environment. It runs as a console command. The tool is licensed under the EUPL II open-source license. Further information regarding the model, its submodules and physical functions can be found in <http://co2mpas.io/reference.html>.

Description of the dataset used for validation

The validation is based on two datasets, i) a large collection of synthetic data (2520 cases), and ii) a set of real vehicles (22 cases). CO₂MPAS version 1.2.2 was used in this exercise.

The synthetic data are generated by the LAT using pre-defined vehicle models in AVL CRUISE™ simulator (Tsokolis *et al.*, 2015). The CRUISE-based synthetic collection, referred to as batch data in the upcoming pages, is based on 13 vehicle models developed by LAT and JRC. The initial 13 vehicle simulation models were developed based on measurements conducted at the two labs also with the support of the respective OEMs. The results of the Cruise simulator runs are used as if they were real type approval test data over WLTP (cycle used for CO₂MPAS calibration) and NEDC (prediction cycle) measurements. Hence the necessary input data (vehicle characteristics, time series over the WLTP cycle, etc.) to run CO₂MPAS and the necessary reference data (fuel consumption time series, NEDC vehicle operation timeseries) to validate it, are produced.

The initial pool of the 13 simulation models correspond to the baseline cases (cases 0). In order to create a comprehensive testing dataset for CO₂MPAS, the various vehicle characteristics of the original 13 vehicle models are varied and new test cases are created. The following parameters are varied:

- vehicle mass;
- vehicle road loads;
- gear box configuration;
- Application of brake energy recuperation;
- Application of Start Stop system;
- Different engine technologies such as variable valve actuation (VVL), direct/port injection (DI/MPI), different temperature management strategies (ThM);

- Combinations of the above technologies/characteristics;

The mass and road load variations are applied over the NEDC, WLTP-H, and WLTP-L. Each vehicle was run with 2 different gear configurations (GCA: one extra gear as compared to the base case; GCB: another extra gear or one gear less depending on the car), and 5 vehicle technologies which were recognized as important contributors to the reduction of CO₂ emissions over the certification test. The Start/Stop and the Brake Energy Recuperation technologies are considered to be present by default, and they are removed in some simulations to test their influence on the vehicle's emissions (NoSS and NoBERS, respectively). The remaining three technologies (VVL, DI/MPI, and improved ThM) are activated for selected cases on top of the base case. It is worth mentioning that VVL and DI/MPI technologies are tested only in 8 of the 13 batch models representing gasoline vehicles in the batch pool (Table 1). More information about the investigated vehicle technology variations can be found in Table in Annex I.

Table 1. Tested vehicle technologies and acronyms

Technology	Variation	Technology Acronym
Base variation Weight	± 100kg	
Base variation Road load	± 10% in F0, F1	
	± 10% in F2	
Gearbox: Number of gears	+1 gear ratio, +2 gear ratios	+ 1 gear (GCA) + 2 gears (GCB)
Start-stop	Active – Inactive	Base case with tech. Alternative case (NoSS)
Brake Energy Recuperation (BERS)	Active – Inactive	Base case with BERS Alternative case (NoBERS)
Variable Valve Actuation	Present/not present	Base case without tech Alternate case with (VVL)
Direct Injection/Multiple Injection	Present / not present	Base case without tech. Alternate case with (DI/MPI)
Thermal Management	Faster warm-up	Base case without tech. Alternate case with (ThM)

In addition to the synthetic test cases, data from laboratory tests were collected in order to produce a pool of validation cases based on real measurement data. It is important to note that the availability of these real measurements is limited for various reasons most important of which being the fact that the WLTP measurement process was finalized only late during the correlation process. The initial measurements performed and the respective data collected were not entirely compliant to the final WLTP test protocol and thus were not considered sufficiently representative of the two test procedures. In addition the measurement procedures themselves contain a level of uncertainty which is reflected in the variability of the results and which eventually may propagate in the model's calculations. However, considering that the input data to be eventually used for running CO₂MPAS may contain some degree of inaccuracy, it is important to validate CO₂MPAS also under these working conditions and demonstrate its capacity to operate accurately with real measurement data. More information about the real vehicles used in the study can be found in Table in Annex I.

3. Results

In this section the results of the predictions of the CO₂ emissions are presented for the whole set of simulated results (differentiating manual and automatic cases), and then an analysis based on the specific technology tested is shown. The validation of the results is done for the whole NEDC cycle, and for its Urban (UDC) and Extra Urban sub-cycles (EUDC). For real cars, the validation is also done for the CO₂ emission prediction over NEDC, UDC, and EUDC cycles. In addition, for specific vehicle signals, we present a temporal comparison of the target (measured signal on NEDC) and the NEDC prediction of CO₂MPAS to provide insight of the model performance beyond the CO₂ emission parameter.

In order to compare the evolution of the performance of the CO₂MPAS model along its versions (v.1.1.0, v.1.1.1, and v.1.2.2), a brief analysis is presented comparing the CO₂ emission (on NEDC, UDC, and EUDC)

for the whole batch of manual vehicles and for the real cars.

Simulation-based validations

The average error on the NEDC CO₂ emission prediction for the manual transmission vehicles (2169 cases on 11 vehicle models) is 0.03 gCO₂/km with a standard deviation of 2.17 gCO₂/km (Table 2). All the cases have an error within ± 5% of their target CO₂ emission on NEDC, 98% have an error lower to ±4%, and 83% have an error lower to ±2.5%. The median of the distribution of the error is centered in 0.10 gCO₂/km with 51% of the cases showing an overestimation of the error and 49% an underestimation (Figure 1). The maximum underestimation and overestimation in the NEDC CO₂ emission prediction are -5.56 and 6.05 gCO₂/km, respectively. Considering all the manual cases, the model performance is satisfactory on NEDC although there is a slight underestimation of the emissions in the UDC (median UDC error: -0.75 gCO₂/km) due to the cold start effect and a compensatory slight overestimation of the error in the Extra Urban part of the cycle (median EUDC error: 0.17 gCO₂/km). The performance for the batch vehicles with automatic transmission is not as good as for the manual cases, with an overall underestimation of the error on NEDC, which is larger for UDC than for EUDC (Table 2). However, 98% and 78% of the cases lie within the ±4% and ±2.5% error on NEDC, respectively. Despite the -1.39 gCO₂/km of underestimation in EUDC, the standard deviation on automatics is lower than on vehicles with manual transmissions pointing at UDC as the largest contributor to the error on the whole NEDC cycle.

Table 2. Basic statistics for CO₂ emission prediction error for batch and real cars on NEDC

		NEDC	UDC	EUDC
Batch (manuals) 2169 cases	Average error [gCO ₂ /km]	0.03	-0.41	0.26
	Std. dev error [gCO ₂ /km]	2.17	3.86	1.89
Batch (automatics) 351 Cases	Average error [gCO ₂ /km]	-2.09	-3.29	-1.39
	Std. dev error [gCO ₂ /km]	2.88	5.38	1.64
Real cars 22 cases	Average error [gCO ₂ /km]	0.25	-0.80	0.89
	Std. dev error [gCO ₂ /km]	3.43	7.69	3.35

NEDC results per technology

For manual vehicles, 307 cases form the base subset of cases (BC). The average and the standard deviation values of the CO₂ emission error on NEDC, UDC, and EUDC are slightly lower for this subset as compared to the whole batch (Average: 0.00/-0.27/0.13 gCO₂/km; Std. dev: 1.75/2.90/1.58 gCO₂/km, respectively). Furthermore, the BC performs better, in terms of average and standard deviation of the CO₂ emission error, than any other technological subset of the batch on NEDC, UDC, and EUDC with the exception of the NoBERS subset. However, the distribution of the error on all three cycles and for all the technologies is alike with no particular outliers Figure 1. The VVL subset shows the largest underestimation on NEDC (median error: -1.24 gCO₂/km) as well as the largest standard deviation. Equivalent results are found on the UDC for VVL cases proving that further improvements are needed to correctly simulate the effect of this technology on CO₂ emission on cold start.

Regarding the automatic vehicles batch, 56 cases form the BC subset that averages larger errors on all cycles than the full batch (Average: -3.15/-4.87/-2.16 gCO₂/km; Std. dev: 0.60/0.89/0.81 gCO₂/km, respectively). For NEDC, UDC, and EUDC, the technological subset with a largest average overestimation is GCB (4.24/9.01/1.48 gCO₂/km, respectively), whereas the largest average underestimation corresponds to the VVL cases (-4.20/-6.07/-2.76 gCO₂/km, respectively). At this point it should be noted that contrary to the case of manual vehicles the batch simulations for A/Ts were based on only two vehicles available at the time this paper was drafted. Additional batch cases for A/Ts are scheduled and will be added in the analysis in the months to come. It is worth mentioning that there are not particular reasons why CO₂MPAS should operate differently in the case of AT vehicles as regards engine or electrical system related technologies as compared to manual transmission vehicles. In this sense the main differences observed in the accuracy and the stability of CO₂MPAS should originate from errors in the prediction of the gearshifting over the NEDC. Given the complexity however of gearshifting algorithms it is concluded that the performance of the module is good while additional improvements will be investigated once more data becomes available.

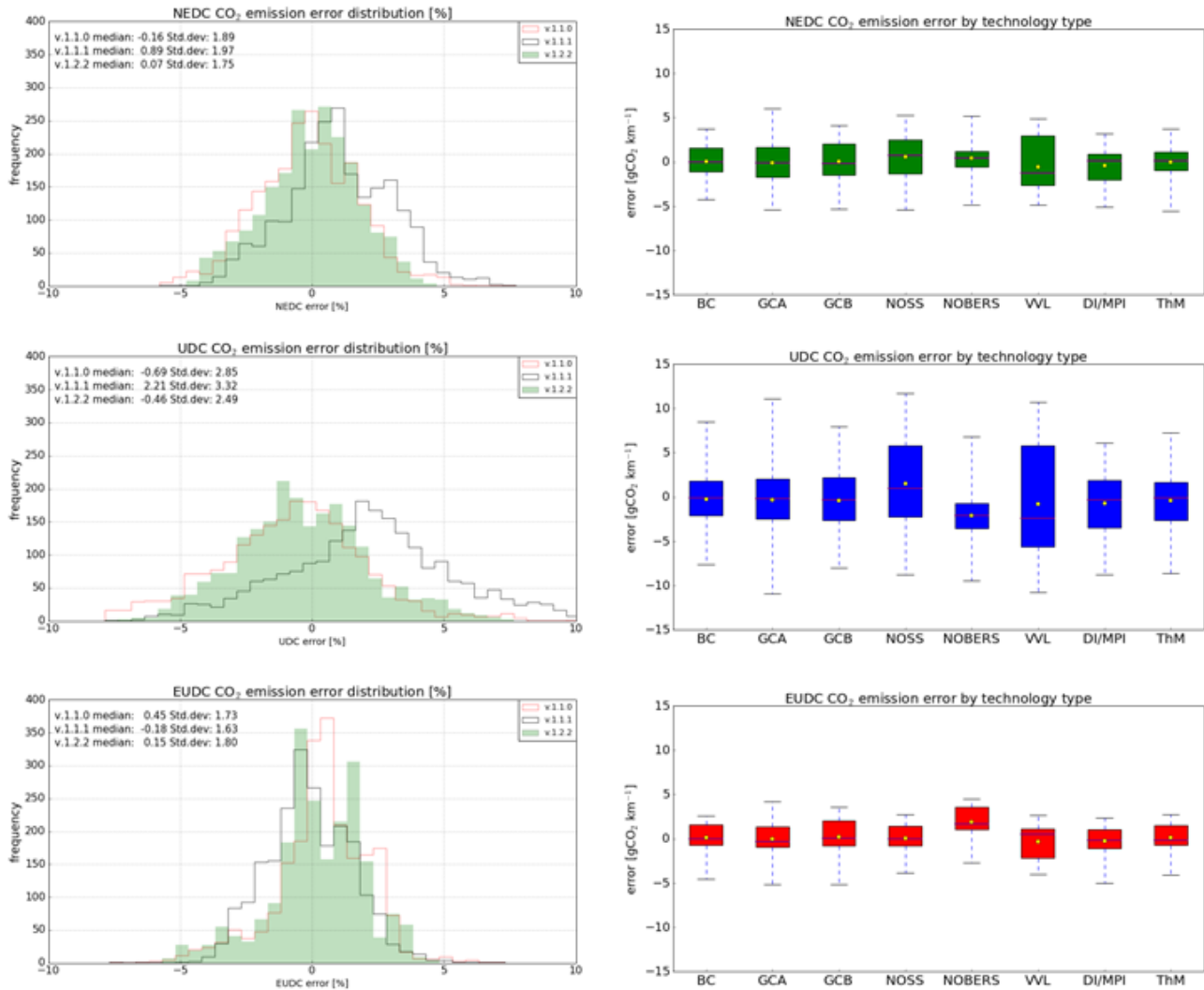


Figure 1. Results of the simulation-based validation. Charts on the left report the NEDC, UDC, and EUDC error distributions [%] for the whole batch of manual vehicles on the v.1.1.0, v.1.1.1, and v.1.2.2 versions of the CO₂MPAS model. Charts on the right report the error distributions per technology for the batch of manual vehicles on the v.1.2.2 version of CO₂MPAS. The boxplots represent the 1st and 3rd quartile, with the dark purple line indicating the median and the yellow dot, the mean. The whiskers show the minimum and maximum values of the error

NEDC results per individual vehicle model

Per individual vehicle model, the standard deviation of the NEDC error is alike for all the manual vehicles with the minimum value for B7 (0.59 gCO₂/km) and the maximum for B4 and B6 (~1.30 gCO₂/km). The cases with an error of CO₂ emission prediction over NEDC larger than 4% occur in 4 out of the 11 manual vehicles (essentially in B6). Regarding the automatics, the B13 has three times more variability in its predicted CO₂ emission error as compared to the B12 case, which has a standard deviation in the range of the manuals (1 gCO₂/km). All the automatic cases with a CO₂ emission error on NEDC larger than 4% correspond to B13.

Beyond the capacity of CO₂MPAS to accurately predict the CO₂ emissions, the performance of the model can also be assessed analyzing the time series that are simulated as compared to the measured time series (target series). The time series of the main quantities affecting the fuel consumption on a test case with good model performance (NEDC prediction error less than 1%) are provided in Figure 2. The NEDC time series as predicted by CO₂MPAS and as measured for the same vehicle show a good correlation and a reduced bias along the cycle proving the good performance of the different CO₂MPAS submodules.

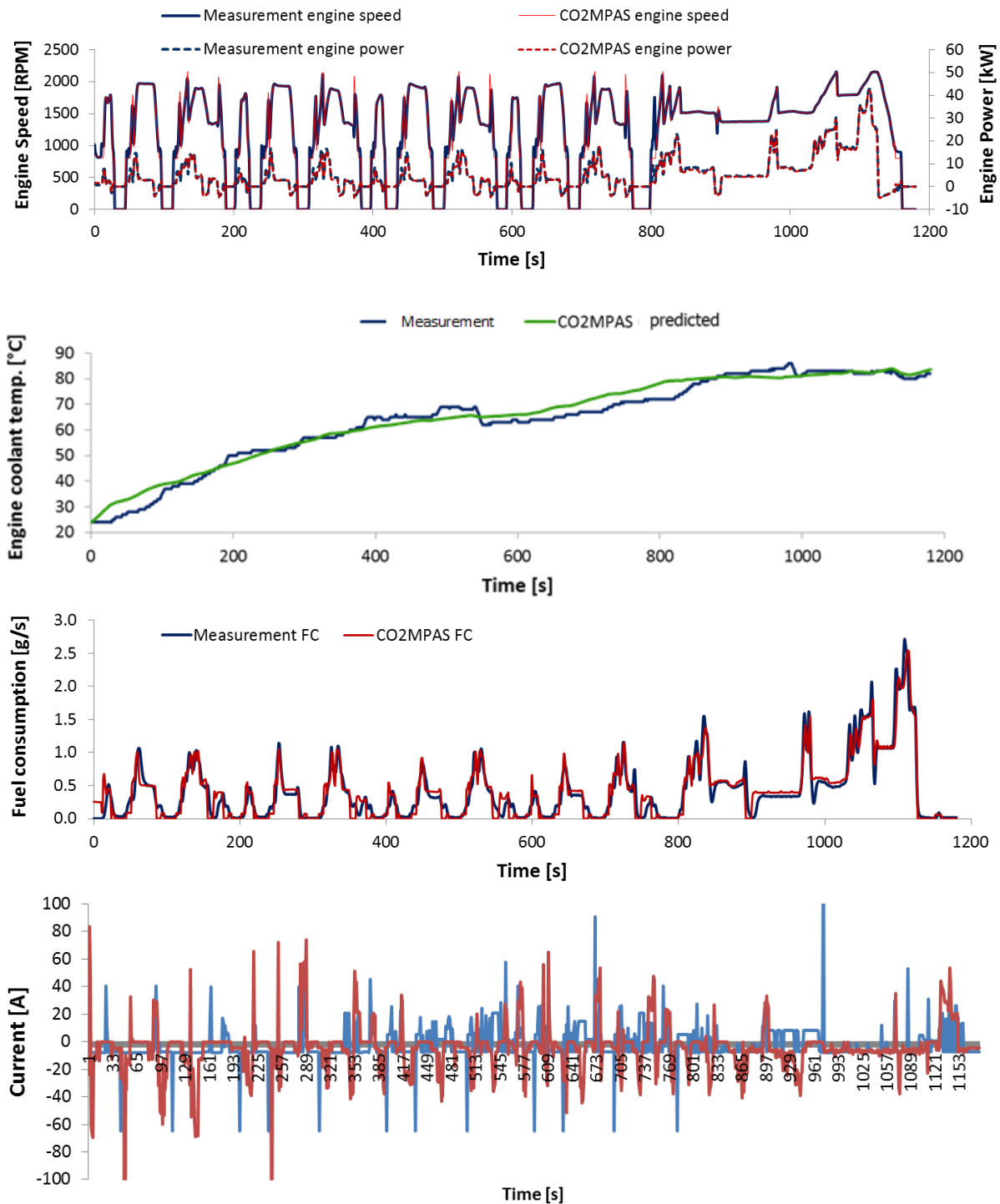


Figure 2. Measured vs NEDC predicted time series for the main quantities affecting CO₂ emissions for a typical case (prediction error less than 1%)

Real cars validation

On average, for the real cases, the NEDC CO₂ emission prediction appears to be slightly overestimated (average and median error = 0.25 and 1.38 gCO₂/km, respectively) and the standard deviation of the error is 1.58 times higher than the one for the batch cases (Table 2). On the measured vehicles, 90% and 68% of the cases have an error lower than ± 4% and ± 2.5% of their target CO₂ emission on NEDC and there are no vehicles with an error higher than ±5%. For an individual vehicle, the maximum underestimation (AT04) and overestimation (MAN11) in the NEDC CO₂ emission prediction are -6.76 and 5.91 gCO₂/km, respectively. The error in NEDC is mainly driven by the CO₂ emission prediction on UDC (Figure 3) for which 50% of the cases show an underestimation with 2 cases particularly underpredicted (AT03, and AT04) that cause an overall reduction of the performance of the model for real cars. Both of them are automatic vehicles (Table 2 in

Annex). On the EUDC, CO₂MPAS performs better than on UDC, however, the standard deviation is almost two times larger as compared to batch cases (Std. dev EUDC error: 3.35 gCO₂/km).

On NEDC, the error of the CO₂ emission prediction for all the real vehicles is in the range of the error of the CO₂MPAS model for the synthetic cases (Figure 3). The same occurs on UDC and EUDC (except for the MAN03 vehicle) proving that the model is able to perform well on all three cycles when using as inputs time series that may contain inaccuracies from the measurements. The comparison between synthetic and real cases shows however that the batch cases do not cover the whole range of CO₂ emission variability existing among the real vehicles: 6 of the 22 real vehicles have largest emission on NEDC than the batch case with highest emission (> 160 gCO₂/km) (Figure 3). It is worth noting that for these 6 cases, the error on CO₂ emission prediction still lies in the ± 4% range.

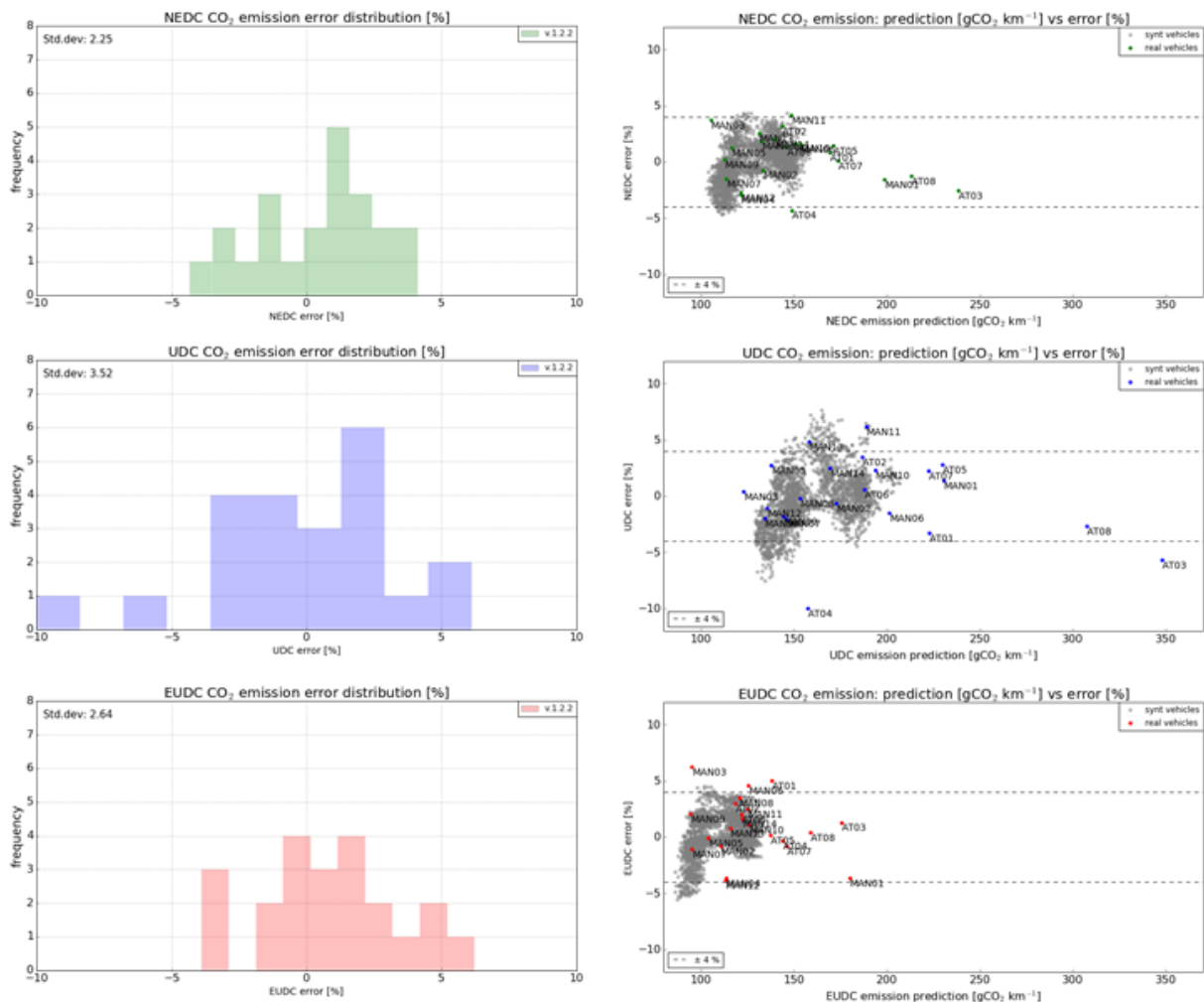


Figure 3. Results of the real cars validation. Charts on the left report the distribution of the NEDC, UDC, and EUDC CO₂ emission error [%] on 22 real vehicles. Charts on the right report CO₂ emission error [%] as a function of the predicted CO₂ emission [gCO₂/km] on NEDC, UDC, and EUDC for real vehicles (colored dots) and synthetic vehicles (grey dots). Dashed lines indicate ± 4% error (v.1.2.2 version of CO₂MPAS)

It is noteworthy that the model performance on NEDC is rather independent on the provision as input of one or two WLTP cycles (WLTP-High and/or WLTP-Low) (Figure 3). Furthermore, no particular under performance of CO₂MPAS is found for either gasoline/diesel real vehicles. However, the three cases with largest overestimations and underestimations on NEDC correspond to gasoline (MAN11, MAN03, AT02) and diesel (MAN12, MAN04, AT04) vehicles, respectively.

Considering all the real cases, the performance of the model throughout its development has improved in terms of the reduction of the standard deviation of the error on all three cycles. The NEDC/UDC/EUDC error has passed from 4.77%/8.86%/4.38% on v.1.1.0 to 3.43%/7.69%/3.35% in v.1.2.2. When checking individual vehicles, 6 of the 8 automatics have lower NEDC error on v.1.2.2 version than on previous versions (Figure 4). However, for manual vehicles, only 6 out of 14 vehicles have lower NEDC error on v.1.2.2 than on previous versions. Further developments are needed to improve the performance of the model on these

particular real vehicles.

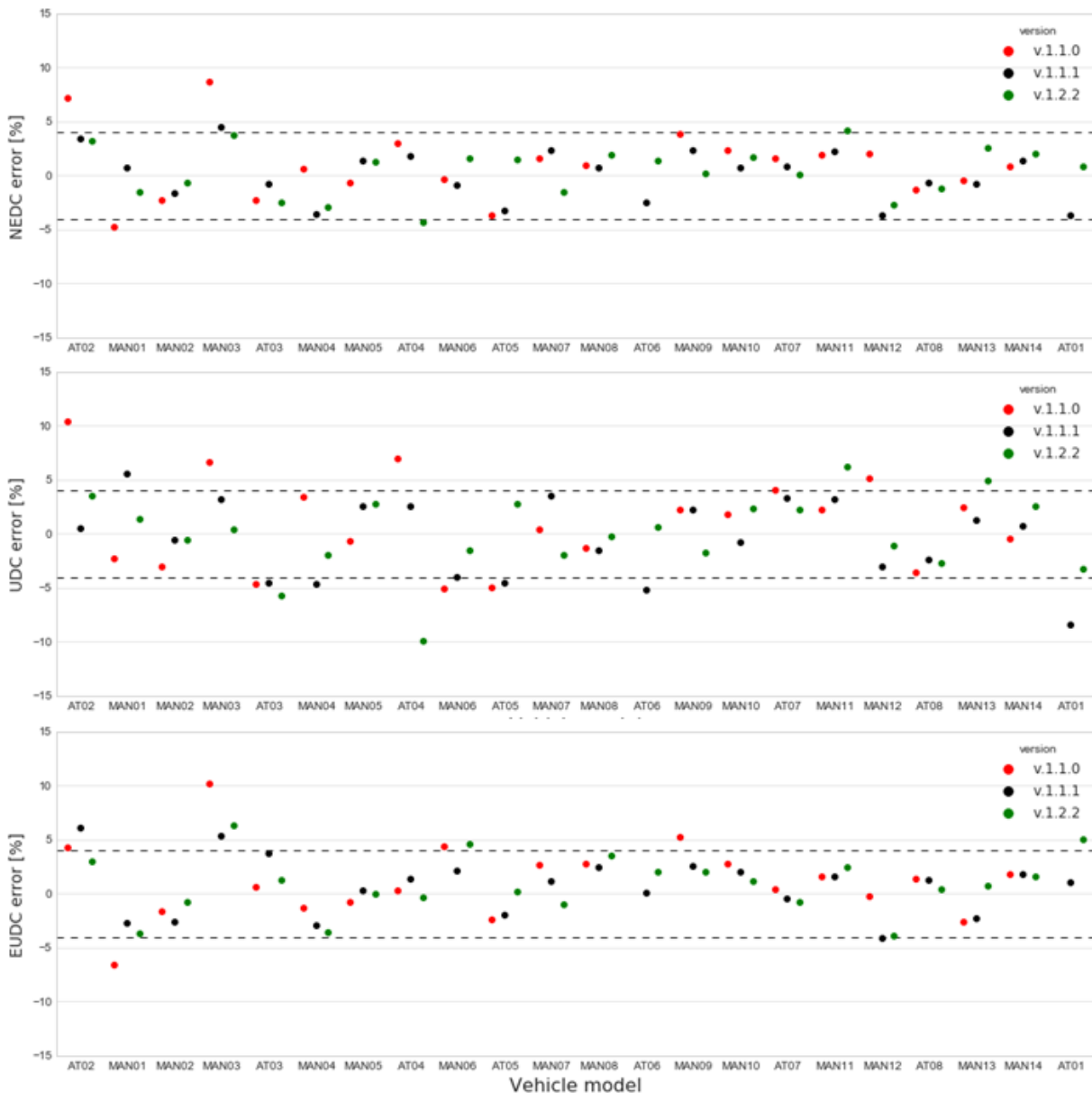


Figure 4 NEDC, UDC, and EUDC CO₂ emission prediction error [%] for real vehicles on the v.1.1.0, v.1.1.1, and v.1.2.2 versions of the CO₂MPAS model. The dash lines indicate $\pm 4\%$ error

4. Conclusion

Based on the findings of the validation campaign presented above, it can be concluded that CO₂MPAS has the capacity to predict NEDC CO₂ emissions when calibrated over the WLTP test with good accuracy. For the current version of the model (v.1.2.2), in all of the cases, simulated and measured, the error falls within $\pm 5\%$ of the reference NEDC CO₂ value. The percentage of cases falling within the acceptance limits ($\pm 4\%$) exceeds 98% on batch cases and 90% on measured vehicles. The Urban part of the NEDC cycle has 2 times higher standard deviation of the error than the Extra Urban part due to the cold start effect, both in manual simulated and real measured cases. On simulated automatics, the CO₂ emission prediction error has larger spread than manuals on UDC but not on EUDC.

The effect of different technologies on CO₂ emissions is well captured by the model with no particular outliers appearing for specific technologies. Overall, the model is stable with very few cases of errors or inability to calculate the NEDC result appearing during the validation. Additional effort is scheduled by the developers for enhancing error reporting and user interface. The possibility to use the model without the need of WLTP measured data is being considered for research purposes.

If such performance is achieved in reality during the certification procedure it means that potentially no double testing will be required for 90% of the vehicles undergoing the WLTP certification procedure. Of

course real measurements are influenced by a series of factors hence the variability of the input data may influence CO₂MPAS and increase the uncertainty of the results. Given the present performance it is estimated that CO₂MPAS could capture at least two thirds of the new registrations in the worst case while respecting the ±4% limit. This fact may help vehicle OEMs to significantly reduce the costs for vehicle certification by avoiding excessive measurements and can also assist in better validation and understanding of the WLTP measurement results from the side of the technical services and type approval authorities. Additional effort will be put in improving the accuracy and stability of the model in order to further facilitate the correlation process and support WLTP introduction in European vehicle certification scheme.

Acknowledgments

Authors would like to acknowledge the contribution of the following people in the development of the test cases and the validation of CO₂MPAS: JelicaPavlovic, Simone Serra, BarouchGiechaskiel, Alessandro Marotta, Renata Praxova, Udo Gerke, Thomas Vogel, Stephane Rimaux, Stylianos Doulgeris, Georgios Triantafyllopoulos.

References

- Ciuffo, B., A. Marotta, M. Tutuianu, G. Fontaras, K. Anagnostopoulos, J. Pavlovic, S. Serra, S. Tsiakmakis and N. Zacharof (2015). The development of the World-Wide Harmonized Test Procedure for Light Duty Vehicles (WLTP) and the Pathway for its Implementation into the EU Legislation. Transportation Research Records, Journal of the Transportation Research Board, vol. 2503, pp. 110-118
- Dings, J. (2013). "Mind the Gap! Why official car fuel economy figures don't match up to reality." Brussels: Transport and Environment.
- ECMT (2005). "European Conference of Ministers of Transport (ECMT). (2005). Making cars more fuel efficient. Technology for Real Improvements on the Road. International Energy Agency. Paris."
- EEA (2014) "Monitoring CO₂ emissions from passenger cars and vans in 2013." EEA Technical Report DOI: 10.2800/23352.
- European Commission (2009). Regulation (EC) No 443/2009 of the European Parliament and of the Council setting emission performance standards for new passenger cars as part of the Community's integrated approach to reduce CO₂ emissions from light-duty vehicles . European Union. Brussels, Official Journal of the European Union.
- European Commission (2011). "REGULATION (EU) No 510/2011 OF THE EUROPEAN PARLIAMENT AND OF THE COUNCIL setting emission performance standards for new light commercial vehicles as part of the Union's integrated approach to reduce CO₂ emissions from light-duty vehicles." Official Journal of the European Union 145/1.
- Fontaras, G. and P. Dilara (2012). "The evolution of European passenger car characteristics 2000–2010 and its effects on real-world CO₂ emissions and CO₂ reduction policy." Energy Policy 49(0): 719-730.
- Fontaras, G. and Z. Samaras (2007). "A quantitative analysis of the European Automakers' voluntary commitment to reduce CO₂ emissions from new passenger cars based on independent experimental data." Energy Policy 35(4): 2239-2248.
- Ligterink, N., Kadijk, G., Hausberger, S., Rexeis, M. (2013). "Investigations and real world emission performance of Euro 6 light-duty vehicles. ." TNO. Dutch Ministry of Infrastructure and the Environment.
- Marotta, A., J. Pavlovic, B. Ciuffo, S. Serra and G. Fontaras (2015). "Gaseous Emissions from Light-Duty Vehicles: Moving from NEDC to the new WLTP test procedure." Environmental Science and Technology 49(14): 8315-8322.
- Mellios, G., Hausberger, S., Keller, M., Samaras, C., Ntziachristos, L. (2011). "Parameterisation of fuel consumption and CO₂ emissions of passenger cars and light commercial vehicles for modelling purposes".
- Mock, P., J. German, A. Bandivadekar, I. Riemersma, N. Ligterink and U. Lambrecht (2013). From laboratory to road: A comparison of official and 'real-world' fuel consumption and CO₂ values for cars in Europe and the United States, International Council on Clean Transportation.

Mock, P., U. Tietge, V. Franco, J. German, A. Bandivadekar, N. Ligterink, U. Lambrecht, J. Kühlwein and I. Riemersma (2014). From Laboratory to Road: A 2014 update of official and "real - world" fuel consumption and CO₂ values for passenger cars in Europe, International Council on Clean Transportation, TNO, IFEU.

Tsokolis, D., S. Tsiakmakis, G. Triantafyllopoulos, Z. Toumasatos, G. Fontaras, A. Dimaratos, B. Ciuffo, J. Pavlovic, A. Marotta and Z. Samaras (2015). Development of a Template Model and Simulation Approach for Quantifying the Effect of WLTP Introduction on Light-Duty Vehicle CO₂ Emissions and Fuel Consumption. SAE-12th International Conference on Engines & Vehicles. Capri, Italy, SAE.

Annex I

Table 1. General characteristics of the batch vehicles

Vehicle ID	Fuel type	Engine capacity [cc]	Transmission	Vehicle mass on NEDC* [kg]	Target NEDC CO ₂ * [gCO ₂ /km]	Tested technologies	No of cases simulated
B1	diesel	1560	manual	1360	115.1	BC, GCA, GCB, NoSS, NoBERS, ThM	163
B2	gasoline	1798	manual	1470	145.0	BC, GCA, GCB, NoSS, NoBERS, VVL, DI/MPI, ThM	217
B3	diesel	1248	manual	1360	117.1	BC, GCA, GCB, NoSS, NoBERS, ThM	163
B4	gasoline	875	manual	920	109.9	BC, GCA, GCB, NoSS, NoBERS, VVL, DI/MPI, ThM	215
B5	gasoline	999	manual	1250	111.0	BC, GCA, GCB, NoSS, NoBERS, VVL, DI/MPI, ThM	217
B6	gasoline	1195	manual	1130	117.0	BC, GCA, GCB, NoSS, NoBERS, VVL, DI/MPI, ThM	217
B7	diesel	1995	manual	1590	129.0	BC, GCA, GCB, NoSS, NoBERS, ThM	163
B8	diesel	1598	manual	1700	129.7	BC, GCA, GCB, NoSS, NoBERS, ThM	163
B9	gasoline	1598	manual	1360	135.2	BC, GCA, GCB, NoSS, NoBERS, VVL, DI/MPI, ThM	217
B10	gasoline	1368	manual	1360	146.1	BC, GCA, GCB, NoSS, NoBERS, VVL, DI/MPI, ThM	217
B11	gasoline	1368	manual	1130	139.7	BC, GCA, GCB, NoSS, NoBERS, VVL, DI/MPI, ThM	217
B12	diesel	1686	automatic	1470	143.7	BC, GCA, NoSS, NoBERS, ThM	135
B13	gasoline	1995	automatic	1700	164.4	BC, GCA, GCB, NoSS, NoBERS, VVL, DI/MPI, ThM	216

* referred to the base case

Table 2. General characteristics of the real vehicles

Vehicle ID	Fuel type	Engine capacity [cc]	Transmission	Vehicle mass on NEDC [kg]	Target NEDC CO ₂ emission [gCO ₂ /km]	Provided series
AT01	gasoline	1995	automatic	1700	168.1	NEDC, WLTP-H,
AT02	gasoline	1991	automatic	1470	139.4	NEDC, WLTP-H, WLTP-L
AT03	gasoline	2995	automatic	1700	245.0	NEDC, WLTP-H
AT04	diesel	1969	automatic	2040	155.9	NEDC, WLTP-H, WLTP-L
AT05	diesel	2967	automatic	1930	169.1	NEDC, WLTP-H
AT06	gasoline	3099	automatic	1470	144.5	NEDC, WLTP-H, WLTP-L
AT07	diesel	1995	automatic	1700	173.9	NEDC, WLTP-H, WLTP-L
AT08	gasoline	2497	automatic	1590	216.1	NEDC, WLTP-H
MAN01	diesel	3157	manual	2040	202.2	NEDC, WLTP-H, WLTP-L
MAN02	gasoline	1595	manual	1360	134.7	NEDC, WLTP-H, WLTP-L
MAN03	gasoline	999	manual	1250	101.9	NEDC, WLTP-H, WLTP-L
MAN04	diesel	1598	manual	1360	125.2	WLTP-H
MAN05	diesel	1598	manual	1470	115.4	WLTP-L
MAN06	diesel	1798	manual	1470	151.5	NEDC, WLTP-H
MAN07	diesel	1248	manual	1360	115.8	NEDC, WLTP-H
MAN08	diesel	1995	manual	1590	130.6	WLTP-H, WLTP-L
MAN09	gasoline	875	manual	1020	112.8	NEDC, WLTP-H,
MAN10	gasoline	1368	manual	1360	148.8	NEDC, WLTP-H
MAN11	gasoline	1368	manual	1130	143.0	NEDC, WLTP-H
MAN12	diesel	1598	manual	1360	125.2	WLTP-H
MAN13	diesel	1995	manual	1590	128.4	NEDC, WLTP-H
MAN14	diesel	1598	manual	1700	137.2	NEDC, WLTP-H

Prospective of the city and the daily mobility: which tools for an environmental assessment?

Cyrille FRANCOIS*, Jean-Pierre NICOLAS* & Natacha GONDRAN**

*Laboratoire Aménagement Economie Transports (UMR CNRS 5593), Ecole Nationale des Travaux Publics de l'État, Lyon, Rhône-Alpes, France
Email: cyrille.francois@entpe.fr

** UMR CNRS 5600 Environnement Ville Société, Ecole des Mines de Saint-Etienne, Rhône-Alpes, France

Abstract

Today cities and urban mobility are two main challenges for global and local impacts on environment. Both are changing quickly through social, technological and urban developments and the evaluations of these evolutions need to be done. Then this study aims at defining the parameters that will have to be tracked by a methodology aiming to assess the environmental impacts of the future daily mobility of a given city. Thus urban mobility was evaluated through assessments of the transport system and travel habits, by applying life cycle assessment methods to the results of mobility simulations that were produced by a Land Use and Transport Interactions (LUTI) model. The environmental impacts of four life cycle phases of urban mobility in the Lyon area (exhausts, fuel processing, infrastructure and vehicle life cycle) were estimated through nine indicators (global warming potential, particulate matter emissions, photochemical oxidant emissions, terrestrial acidification, fossil resource depletion, metal depletion, non-renewable energy use, renewable energy use and land occupancy). GHG emissions were estimated for 2006 to be 2.83 kg CO₂-eq inhabitant⁻¹ day⁻¹, strongly linked to car use, and indirect impacts represented 33% of GHG emissions, which is consistent with previous studies. Combining life cycle assessment (LCA) with a LUTI model allows implementations of mobility scenarios, either social or technological, in view of proposing prospective analysis. Moreover by linking emissions with emitters, environmental perspectives analyses are more detailed and helpful for transport policy makers and urban planners.

Résumé

Aujourd'hui les villes et leurs mobilités sont deux importants défis à considérer pour améliorer l'environnement aux échelles mondiale et locale. Il est donc nécessaire d'évaluer leurs différentes évolutions, qu'elles soient sociale, technologique ou liée à l'aménagement urbain. L'objectif de cette étude est donc d'évaluer la mobilité urbaine en incluant le système de transport et les habitudes de mobilité. L'évaluation repose sur la méthode d'Analyse de Cycle de Vie (ACV) appliquée aux résultats d'un modèle transport-urbanisme. Les impacts environnementaux des quatre phases du cycle de vie de la mobilité de l'aire urbaine de Lyon (échappements, carburants, infrastructures et vie des véhicules) ont été estimés pour neuf indicateurs (réchauffement climatique, particules, oxydants photochimiques, acidification terrestre, ressources métallique et fossile, énergies renouvelable et non-renouvelable et l'occupation au sol). Les émissions de GES ont été estimées pour 2006 à 2,83 kg CO₂-eq par habitant par jour, liées principalement à l'utilisation de la voiture, et les émissions indirectes représentent 33% de ces émissions. Coupler ACV et modèle transport-urbanisme permet d'évaluer différents scénarios de mobilité, qu'ils soient sociaux ou technologiques. De plus en reliant les émissions aux émetteurs les différentes politiques urbaines (transport ou aménagement) peuvent être évaluées plus précisément.

Keys-words: urban mobility, Land Use and Transport Interactions model, environmental assessment, life cycle analysis, urban prospective.

Mots-clés : Mobilité urbaine, Modèle Transport-Urbanisme, Évaluation environnementale, Analyse de Cycle de Vie, prospective urbaine ;

Introduction

The transport sector has become the main source of GHG emissions in France, producing 136.4 Mt CO₂-eq (carbon-dioxide equivalent), 27.8% of the total GHG, in 2012. Personal vehicles represent 57% of these emissions, and individual mobility accounts for approximately two-thirds of total transport emissions – the other third being generated by freight transport (MEDDE, 2014a). Individual mobility comprises local and long-distance mobility (above 80 km from home). In 2008, local mobility represented 99% of individual journeys, 59% of total distance and 69% of greenhouse gas emissions. The total GHG emissions from internal travel by French residents increased by 14% between 1994 and 2008, due to a significant increase in local travel emissions (+17%) compared to long-distance travel emissions (+8%), mainly linked with population growth (+6%) (Nicolas et al., 2013).

At local scale the population growth is unequal, the urban part of the population is still growing. The UN predict that 70% of the 2050 population is going to be urban at a world scale (80% in Europe). Today most carbon emissions and most energy consumptions take place in cities areas with 70% of the global CO₂ emission and two thirds of global energy consumption (United Nations, 2014). These impacts, which would increase with urban growth, highlight the major role of cities at global scale. However cities are exposed directly or indirectly to their own emissions and their high densities of population and activities increase their vulnerability. Cities are both sources and targets of ecological risks. Nevertheless urban high densities improve efficiency of local actions due to economy of scale. Cities are both problems and solutions. The challenge for local authorities is to take decisions to improve local and global environmental impacts without increasing social disparities.

This paper focuses on the concept and the development of new environmental assessment tools to help urban planning decision making. It is based on four assumptions: (1) the environmental assessment should be large enough to avoid excessive blind spots for public decisions; (2) it is important to link emission and emitters, which is not easy in the case of transport; (3) urban modelling now furnishes operational tools which are efficient enough to guide an assessment at a conurbation scale; (4) mobility need forward-looking vision in order to prevent technologic or social evolutions, or ruptures.

Firstly, in the field of environmental assessment for public policies, although some scientific reviews now provide a good survey of the environmental impacts of transport (Joumard and Gudmunsson, 2010), most applied studies still focus on direct emissions from vehicle operation and their spatial distribution inside the defined perimeter. However, research on life cycle analysis shows the importance of including indirect impacts resulting from other stages, such as infrastructure, fuel production, car manufacturing, maintenance and disposal (Le Féon, 2014). It is also important to enlarge the scope by considering different kinds of emissions and impacts, which can be cumulative or can compensate each other. Indeed, public policies may have both environmental advantages and disadvantages if various environmental impacts and the whole lifecycle of transport are taken into account. For example, promoting electric vehicles may reduce urban atmospheric pollution, but it also generates additional environmental impacts during the fabrication of batteries and electricity production. This study contributes to identifying some of these combined factors in order to simulate cascading effects of transport policy in a more realistic manner.

Secondly, it is necessary to link emissions with emitters to be able both to evaluate policies more accurately and to take social inequality into account. Many studies give good estimates of transport emissions and their impacts at various territorial scales (for example, EEA, 2012 at the European level, or, for France, Citepa, 2014 at a national level and Aurenche, 2010 at a local scale), allowing estimation of the importance of the issue and the economic activity at stake. However, in the case of transport, as these emissions are due to a multitude of individuals who move for many reasons and have different constraints, that link is more difficult to establish. Assessments often simply link emissions to traffic levels, with no precise knowledge of who emits, which is not helpful in defining fairer and more efficient public policies. To overcome this limitation,

some research has employed household travel surveys enhanced with emission estimates, allowing a better understanding of who emits what, how much and why (Brand and Preston, 2010; Dupont-Kieffer et al., 2010; Nicolas and David, 2009). This may help local authorities to better target their actions towards the social groups that are the greater emitters.

Thirdly, evaluating environmental impacts of urban mobility is not an easy task because urban mobility is part of the urban system and interacts with the rest of this complex urban system. Three main subsystems can be defined: location, transport and relationship systems. These three subsystems interact with others with different temporality (Bonnafous and Puel, 1983). To develop prospective views of this urban mobility land use and transport interaction models (LUTI models) allow long-term scenarios to be tested and give outputs for large scale urban transport systems. On the one hand, such a choice encounters some limitations: the simplifications and hypotheses intrinsic to modelling allow a limited range of prospective scenarios, as well as introducing some biases and uncertainties. But on the other hand, once the initial investment to develop such a tool is made, its use simplifies data acquisition from a complex system, and it facilitates simulations to test the effect of developments in the overall context (public policies, economic trends, demographic evolutions, behaviour changes, etc.) on emission levels. Several models exist at a sufficiently disaggregated level to give a good picture of the emitters (see Antoni, 2010 for France and Hund et al, 2005 or Wegener et al., 2004 at an international level). The model selected for this study is SIMBAD (Simuler les MoBilités pour une Agglomération Durable, ie Simulate Mobility for a Sustainable City), which has been developed for the Lyon urban area (Nicolas et al., 2009).

Lastly, transport technological changes affect urban mobility and its environmental assessment. For example, by reducing fuel consumption of vehicles, EURO norms implementation probably impacted, not only atmospheric emissions but also transport systems, trip generations and social habits. Technological changes have to be foresighted to evaluate urban policies. Some evolution can be estimated by trends, but recent scandals on car exhausts highlight the difficulties for car manufacturers to further reduce emissions rates and comply with new norms. However new transport technologies are in progress and mobility may face technological breakthroughs in the next few years. For some breakthroughs, such as electric cars, the democratisation already begins, for others such as autonomous vehicles, the knowledge is still restricted.

Our final aim is to demonstrate the relevance and the feasibility of combining these four assumptions by providing a clear and structured environmental assessment of urban mobility in Lyon. In order to achieve this goal, several objectives were set:

- To undertake a life cycle assessment of the environmental impacts of Lyon's urban transport system using a multi-indicator evaluation
- To integrate the LCA with dynamic data from a LUTI model
- To link emissions with emitters.
- To foresight different urban developments and potential technologic and behaviour changes.

This paper presents the method of calculation and its application on the Lyon urban area for the year 2006. Then the potential of this method for a prospective application will be discussed.

Methods

To create a strong method of assessment of urban mobility that can oversee urban, technologic and social evolution, the method should be built from currents or old data in order to compare environmental results from model with environmental impacts from household travel survey and with others mobility assessment studies.

To assess the environmental impacts of urban mobility, estimates were made using a method based on standard LCA methods (ISO, 2006). Urban mobility was considered as a system whose function is to enable people living within an urban area to travel during a working day. Using this

functional definition, urban mobility is defined not only by the transport system, but also includes journey habits and locations of both activities and households (Geurs and Van Wee, 2004). Locations and journey habits are important because they characterise the demand of mobility. This boundary includes all personal journeys made by every inhabitant of the urban area, it includes all purposes and all modes of transportation. Goods transport is not included in this study. In order to assess the whole system, the functional unit was expressed as per inhabitant day to take into account the transport system, the distance and the number of trips. To provide comparison points with other studies and to discuss functional unit choices, some results were expressed in different units, such as per person kilometre (pkm) and per trip.

SIMBAD is a Land Use and Transport Interactions model developed by the Laboratoire Aménagement Économie Transports (LAET) (Nicolas et al., 2009). It is designed on a city commuting scale, in order to estimate economic, environmental and social impacts of alternative public policies in urban and transport planning. It simulates the location changes for households and companies over a 25 year timeframe, in interaction with a complete urban transport system (public transport, car and non-motorized modes for individuals, and goods movements due to economic activities).

It has been applied to the case of Lyon, the second most populous area in France, covering 3,300 km² distributed in 296 municipalities and 777 IRIS, which are used as the spatial unit basis and are represented in Figure 1 (INSEE, 2016b). The location modelling has been calibrated and estimated using 1999 census data for households and 1999 SIRENE data for companies (INSEE, 2016a). Public transport and road networks have been built and validated in the model for the same year and are regularly updated to take changes into account. Goods movements are generated with the FRETURB model, which is a model developed by the Laboratoire Aménagement Économie Transports (LAET) to simulate the transport of goods in urban areas (Routhier and Toilier, 2007), and the individual trip model has been calibrated using the 2006 Lyon household travel survey (SYTRAL, 2006).

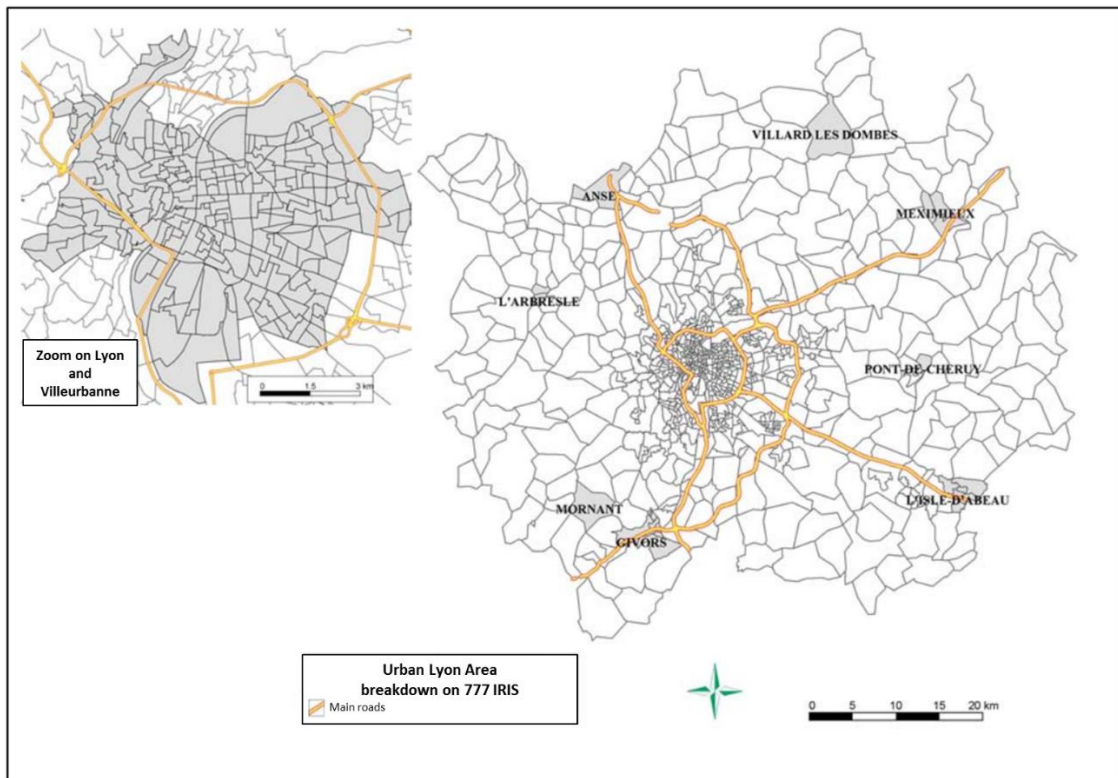


Figure 1. SIMBAD perimeter and the 777 IRIS of Lyon urban area (Nicolas et al., 2009)

For the case study presented here, which tests the feasibility and relevance of combining LUTI output with a life cycle assessment to assess an urban transport system, a 2006 simulation was conducted and used. This study focused on individual daily mobility; goods movements were not considered. In 2006 the area had a population of 1,900,000 people, and the model calculates 5,700,000 journeys per day distributed among individual car, public transport and non-motorized modes. All motorized trips were allocated to the road network and public transport network in one representative peak hour or one representative off-peak hour of an average working day. The flows of vehicles simulated on each network section for 2006 were used as input data for environmental impact assessment, based on the LCA methodology (ISO, 2006).

In order to estimate the environmental impacts of the transport system, nine indicators were selected. Global warming potential and energy use measure the achievement of global environmental targets to reduce GHG emissions and improve energy efficiency (MEDDE, 2011). However, the transport sector is a large user of fossil resources, so their utilization should be monitored (Wall, 2002). Metal depletion and land occupancy were also included. Some environment impacts are local, especially in cities with high density and population. Particulates and tropospheric ozone are local pollutants, which particularly impact human health through respiratory diseases. Acidification damages terrestrial ecosystems and may migrate to oceanic ecosystems. The ReCiPe method (Goedkoop et al., 2008) was used to normalize these impacts because it evaluates the chosen indicators at a midpoint level using a standard method, rather than endpoint indicators, which aggregate impacts. The environmental calculation was based on the traffic on each section of the network. In particular, the input data, for each road section, included the speed and the vehicle load estimated by the SIMBAD model for an average off-peak and an average peak hour. The vehicle fleet details were obtained from the household travel survey. The public transport calculation was based on the same equations as for cars, but with a specific network. The same method was used for every indicator.

Table 1. Assessed impacts categories

Impact categories	Units	Substances
Global warming potential (100 years)	kg CO ₂ -eq	All Greenhouse gases
Particulate matter emissions	kg PM ₁₀ -eq	PM, SO ₂ , NO _x , NH ₃
Photochemical oxidant emissions	kg NMVOC-eq	NMVOC ¹ and other photochemical oxidants
Terrestrial acidification (100 years)	kg SO ₂ -eq	NH ₃ , SO ₂ , NO _x
Fossil depletion	kg oil-eq	Coal, gas, oil
Metal depletion	kg Fe-eq	All metals
Non-renewable energy	MJ-eq	Coal, gas, oil, peat, uranium, primary forest
Renewable energy	MJ-eq	Hydro, wind, geo, solar, biomass energies
Land occupation	m ² a ⁽²⁾	Agricultural and urban lands

¹ Non-Methane Volatile Organic Compounds ² square meters annum

Four independent calculations were made for each section:

- indirect impacts that are related to the production, maintenance and disposal of vehicles;
- indirect impacts that are generated by fuel extraction and refining;
- indirect impacts that are generated by the construction of infrastructure (road, tracks, etc.);
- direct emissions that are generated by the use of vehicles.

The environmental impacts of the production, maintenance and disposal of vehicles on the network model were estimated by

$$I_{veh} = i \sum_{s \in sections} L_s C_s \quad (1)$$

where

- I_{veh} is the total impact due to car production, maintenance and disposal [impact/day]
- L_s is the length of the section s [km]
- C_s is the daily load of vehicles on the section s [vehicles/day]
- i is the impact due to an average vehicle (v) on one kilometre [impact/vkm]

The impacts i per vehicle km were obtained from the Ecoinvent database which is one of the most commonly used databases for LCA in the European context. This Swiss national database accommodates more than 2500 background processes often required in LCA case studies (Frischknecht and Rebitzer, 2005). As data is often based on the Swiss demand patterns some data were adapted to better represent the description of the French context. In particular, some modifications were based on vehicle weight and car occupancy rate.

The second calculation evaluated the impacts that are generated by the extraction and refining of the fuels that are consumed during the journeys. Three fuels were considered, diesel, petrol and LPG. The consumption estimates were based on the average speed of each section and consumption curves (Grassot, 2011) derived from COPERT IV (Computer Program to calculate Emissions from Road Transport) (Gkatzoflias et al., 2012) for the defined vehicle fleet. The SIMBAD model describes two types of traffic, off-peak and peak traffic (7 to 9 a.m. and 4 to 6 p.m.).

$$I_{fuel} = \sum_{s \in sections} L_s \sum_{f \in fuels} i_f (20 F_{sf}^{off} C_s^{off} + 4 F_{sf}^{peak} C_s^{peak}) \quad (2)$$

where

- I_{fuel} is the total impact due to fuels production and transport [impact/day]
- L_s is the length of the section s [km]
- i_f is the impact due to one kilogram of fuel f [impact/kg]
- F_{sf}^{off} and F_{sf}^{peak} are fuel consumption factors on an off-peak and a peak hour on the section s for the fuel f [kg/vkm]
- C_s^{off} and C_s^{peak} are the hourly vehicle loads in an off-peak and a peak hour on the section s [V/hour]

The environmental impacts of fuel were obtained directly from Ecoinvent database, considering fuels that were entirely made from fossil sources. The electricity consumption and impact were calculated using average emission factors with the French electricity mix.

The third calculation assessed the infrastructure impacts. Only linear infrastructure types were assessed, excluding infrastructures such as stations and car parks.

$$I_{infra} = \sum_{s \in sections} \frac{1000 L_s i_s}{365} \quad (3)$$

where

- I_{infra} is the total impact due to infrastructures [impact/day]
- L_s is the length of the section s [km]
- i_s is the annual impact due to one meter of section s [impact/(m.a)]

Infrastructures were divided into categories of section (4 roads, 1 tram track and 1 subway track) and their impacts were obtained from Ecoinvent database.

The last calculation evaluated direct pollutant emissions due to vehicle operation. As for fuel consumption, emissions were calculated from section speeds using COPERTIV for 9 pollutants (CH₄, CO, CO₂, VOC, PAH, NH₃, N₂O, NO_x, PM).

$$I_{exhaust} = \sum_{s \in sections} L_s \sum_{p \in pollutants} i_p (20 E_{sp}^{off} C_s^{off} + 4 E_{sp}^{peak} C_s^{peak}) \quad (4)$$

where

- $I_{exhaust}$ is the total impact due to exhaust pollutants [impact/day]
- L_s is the length of the section s [km]
- i_p is the impact due to one kilogram of pollutant p [impact/kg]
- E_{sp}^{off} and E_{sp}^{peak} are emissions factors on an off-peak and a peak hour on the section s for the pollutant p [kg of pollutant/(km.vehicle)]
- C_s^{off} and C_s^{peak} are hourly charge of vehicles on an off-peak and a peak hour on the section s [vehicles/hour]

Each ecological indicator was evaluated for the four steps and summed to obtain the total amount for the whole transport life cycle.

This study contains uncertainty due to the quantity of data needed to assess this urban mobility system. The Ecoinvent database describes and, sometimes, quantifies uncertainty of material flow data on the level of each individual input and output of the unit processes (Frischknecht and Rebitzer, 2005). However, uncertainty is very difficult to estimate for the simulations of flows of vehicles because the input data are subject to model errors and also temporal and spatial errors. Because of the unknown errors embedded in data, uncertainty was not estimated in this prospective study. However, a comprehensive sensitivity analysis was undertaken on several parameters. Several car fleets were created to compare the technological dependency of the results. Sensitivities to land occupancy, speed and modal share were assessed.

Results and discussion

The environmental impacts of transport in the Lyon urban area are determined by the technology mix (engine specifications, public transport, etc...), modal share and mobility habits, in terms of the number of trips and their distances. The method used in this study assesses the mobility effectiveness, and reports the environmental impact in four categories (car exhaust, fuel production, car life cycle and infrastructure) and the distribution of impact between personal vehicles and public transport. Data from the LUTI model allow assessment of the impact distribution by types of households in order to link emissions with emitters.

In the model, urban mobility was divided into three mode of transport categories – personal vehicles (as driver and passenger), public transport and non-motorised modes – according to

modal shares. The average trip length was 13.64 km in personal vehicles, 1.57 km on public transport and 0.96 km for non-motorized modes (Figure 2, estimates made with the LUTI model, SIMBAD). The environmental impacts of non-motorised modes were assumed to be negligible. The vehicle occupancy rate in the Lyon urban area is 1.33 persons per car, which is lower than the national rate of 1.4 for local mobility (MEDD, 2010).

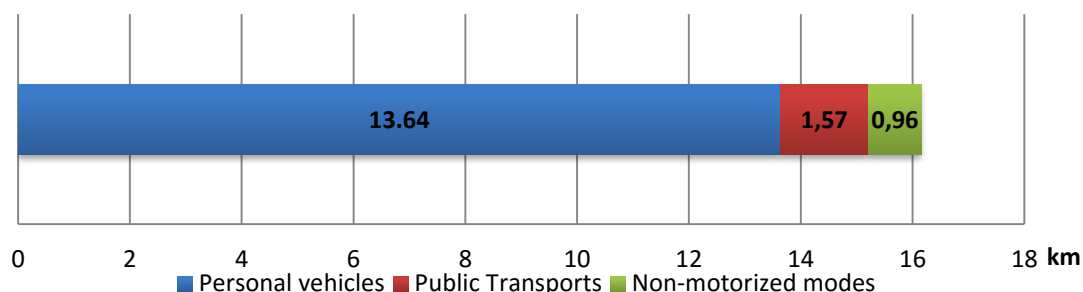


Figure 2: Modal share of the distance travelled for an average trip in 2006

Average impacts

For each environmental indicator, the results for each life cycle phase (car exhaust, fuel production, car life cycle and infrastructure) and the total are presented in Table 2. The estimated global warming potential from urban mobility in Lyon was 2.83 kg CO₂-eq person⁻¹day⁻¹. The main source of these emissions was exhaust from cars, which represented about two-thirds of the total. The average transport GHG emissions in Lyon were estimated to be 175 g CO₂-eq/pkm, which is within a range of estimates for French cities (Le Féon, 2014) and is less than an estimate for New York City of 220 g CO₂-eq/pkm (Chester et al., 2010). Including the distance dependency, the average emissions were 969 g CO₂-eq/trip. The GHG emissions were highly correlated with fossil resource use and non-renewable energy use through fuel combustion. Note that French electricity, which is the main source for public transport such as trams or underground railways, is mainly produced by nuclear plants, which have low GHG emissions, but depend on a non-renewable resource with specific risks for its production and waste management.

Table 2. Total and sub-total environmental impacts of transport in Lyon urban area

Impact per inhabitant	Exhausts	Fuel	Infrastructure	Vehicles life cycle	Total	Unit
Global warming potential	1.88	0.33	0.22	0.41	2.83	kg CO ₂ -eq/day
Photochemical oxidant emissions	10.54	2.05	2.49	1.61	16.69	g NMCOV-eq /day
Terrestrial acidification	5.43	3.23	1.37	2.19	12.22	g SO ₂ -eq /day
Particulate matter emissions	2.31	0.90	0.65	0.93	4.80	g PM-eq /day
Metal depletion	0	8.73	43.17	161.65	213.55	g Fe-eq /day
Fossil depletion	0	0.69	0.13	0.15	0.98	kg Oil-eq/day
Non-renewable energy resources	0	30.55	10.76	6.42	47.73	MJ-eq /day
Renewable energy resources	0	0.14	0.33	0.42	0.89	MJ-eq /day
Land occupancy	0	1.83	51.92	4.69	58.44	m ² /annum

For the other air pollutants, the main source of emissions was also exhaust from cars. For photochemical oxidant emission, it represented 63% of the lifecycle impact. Infrastructure impacts were the second largest, at 15% of the total. The emission of particulates by cars engines represented 48% of the total emissions. Fuel production and car life cycle each represented 19% of particulates emissions; however their emissions are unlikely to be located in cities with air quality issues. Exhaust gas represented 44% of the acidification potential and the second largest source of emissions was fuel production (26%). Unlike the two previous categories, acidification may have impacts on ecosystems at a continental scale. Energy consumption during car operation was included in the fuel category.

Fossil resource use and non-renewable energy use were both mainly correlated with the use of fuel in engines, representing 71% of fossil resource use and 64% of non-renewable energy use. For non-renewable energy use, infrastructure represented 23% of the total use. The use of around 1 kg oil-eq person⁻¹day⁻¹ highlights the dependency on a limited and imported resource. The proportion of renewable energy was low, at 1.8% of the total energy use.

The average land occupancy resulting from urban mobility for a Lyon inhabitant was at least 58 m²/year, and infrastructure accounted for 89% of the total land occupancy. The total land occupancy for Lyon urban mobility was bounded below by 113 ha of land. This result is probably underestimated because it only takes into account road width, neglecting non-linear infrastructure, such as stations or car parks. The average metal depletion was about 214 g Fe-eq person⁻¹day⁻¹, mainly due to car manufacturing.

The previous figures describes direct and indirect impacts of mobility. Direct emissions are link to car use and can be spatialize on the road network with the traffic description. This spatialization of emissions can be used in dispersion model then in an exposure analysis. Indirect emissions from background processes can't be spatialize. This spatial analysis might be interested in a prospective approach when introducing new urban form or new technology which influence traffic distribution and relocate emissions.

Influence of household characteristics

The LUTI model is based on household travel survey in which households characteristics were declared. The model reduced the numbers of household's parameters but many remain such as the income, the age of the head of the household, the head activity, the household size, the number of cars, the number of children. The location of households are known then analysis can be made on location parameters (distance from centre, density, functional mixing, accessibility, land price).

For this paper, two household characteristics strongly linked with daily mobility and its environmental impacts were considered: the income per consumption unit, in 3 classes (the 20% lowest incomes, the 60% median and the 20% wealthier), and the distance from centre, also in 3 classes (centre, inner suburbs and outer suburbs), creating 9 classes of households. The results from SIMBAD showed that the location had a big effect on the distance travelled and car use; there was also an effect of income, but it was smaller. Although the environmental impact of income was small, it was retained to highlight the social dimension of the conclusions for public policies. It would have been possible to choose other variables within SIMBAD, such as the age of the head of the household, the head activity, the household size, or the number of cars but, as stated in the introduction, the main purpose of this research was to test the methodology.

Figures 3 and 4 show that there are different GHG contributions for each type of inhabitant. Indeed one person in the outer suburbs with high income may emits almost six times the GHG emissions of a person with low income in the urban centre. The impacts increased with household income, particularly from low income households, which emitted around 2.14 kg CO₂-eq/person.day, to medium and high income households, which emitted 2.99 and 3.05 kg CO₂-eq/person.day respectively. This was primarily due to the smaller proportion of working people in the low income class, with more students, retired, etc. In that class, the car was used less, both

due to income constraints and to shorter journeys (the number of home-work trips longer than the average, was lower). For the location characteristic, emissions increased with the distance of the household from the urban centre. The average GHG emissions were 1.34 kg CO₂-eq/day for an inhabitant in the centre, 2.73 kg CO₂-eq/day in the inner suburbs and 5.19 kg CO₂-eq/day in the outer suburbs. Thus impacts were more dependent on the location than on the income of households.

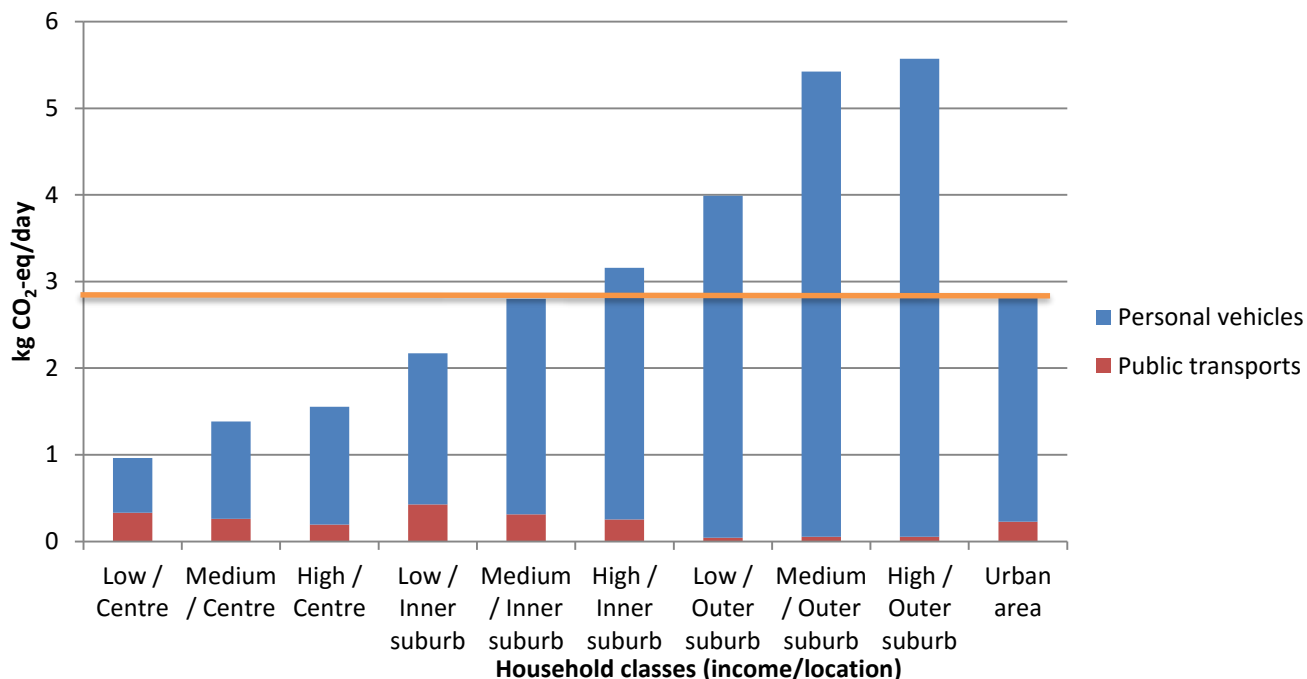


Figure 3. GHG emissions by household class in 2006

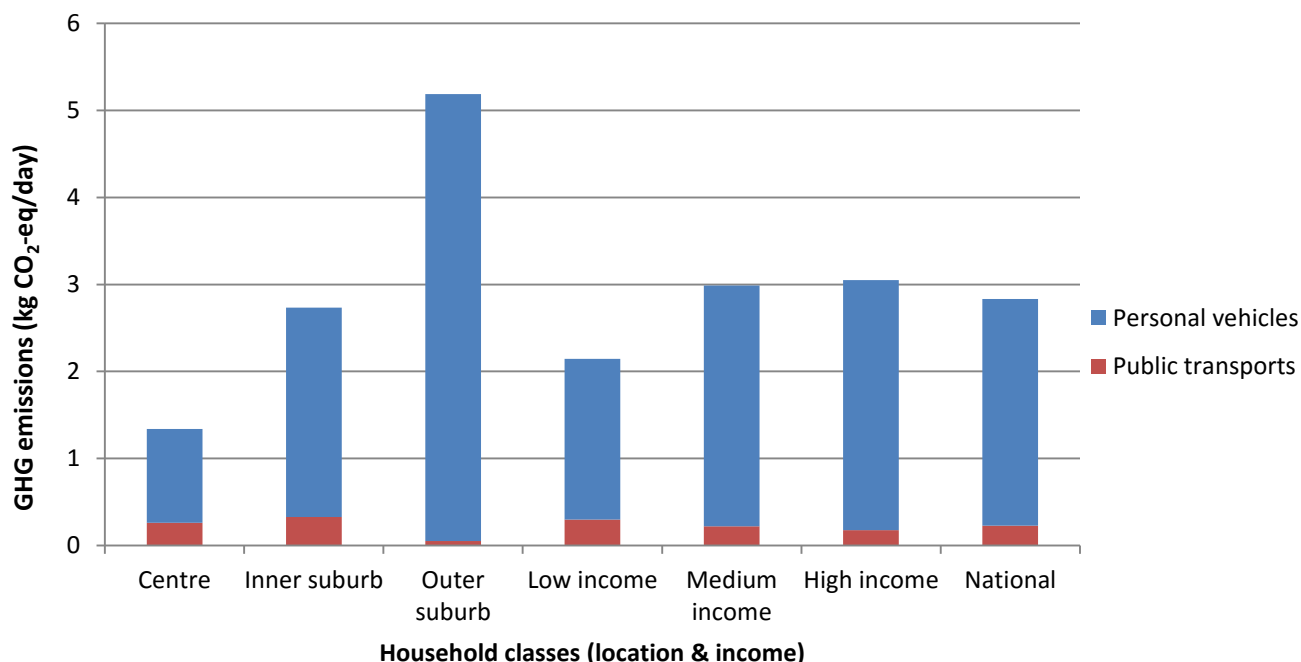


Figure 4. GHG emissions by household location and income level in 2006

For the eight other indicators, the conclusions were similar to those for global warming

potential, with an increase of impacts with the income and the distance from the centre.

The distance travelled was strongly related to the location of the household. The average distance by car was 5.5 km/day for an inhabitant in centre, 12.7 km for an inhabitant in the inner suburbs, and 27.2 km in the outer suburbs. The distance travelled also depended on the household income: wealthier households travelled further and the largest difference was between low and medium income households. Moreover households with low income used cars less and public transport more than higher income households. In the city centre, households with low income travelled 2.5 km/person.day by public transport. In the outer suburbs, public transport is less accessible and car share represented almost the entire distance travelled. The number of trips per day also affected the total distance travelled: people in the outer suburbs travelled more often than those in the centre or inner suburbs, and wealthier households travelled more than poorer households.

By disaggregating results by household types, analysis is more detailed and provides better understanding of origin of trips and impacts. This kind of disaggregation may be conducted on prospective scenarios and may reveal a homogenisation or greater inequalities between household types. Moreover, others household characteristics can be added to the analysis and provide additional conclusions. Analysis can be enriched with others location parameters such as density, accessibility. This data wealth may be used on different topics such as socio-environmental inequalities or urban planning debates.

Modal and technological sensitivity analysis

With technological development and behavioural changes, modal share, occupancy rate and vehicle efficiencies are expected to change. These variations will influence the final impacts, so sensitivity analyses were undertaken to estimate them. For all sensitivity analyses the baseline was the Lyon vehicle fleet, to which changes were applied. A change from the Lyon vehicle fleet to the national vehicle fleet increased the use of fossil resources, because the national vehicle fleet contains more powerful cars than an urban fleet as in Lyon. However, local air pollutant emissions were lower with the national fleet (Table 4).

Table 3. Modal and speed sensibility analysis

Impact per inhabitant	Lyon 2006	Car occupancy +10%	Car occupancy -10%	Average speed +10%	Average speed -10%	Modal transfer 10% from car to public transp.
Global warming potential	2.8 kg CO ₂ -eq /day	-7.8%	9.5%	0.8%	0.5%	-7.1%
Photochemical oxidant	16.7 g NMCOV-eq /day	-6.6%	8.0%	2.6%	-0.4%	-5.2%
Terrestrial acidification	12.2 g SO ₂ -eq /day	-7.1%	8.7%	2.1%	-0.7%	-6.0%
Particulate matter	4.8 g PM-eq /day	-6.9%	8.4%	2.4%	-0.9%	-5.6%
Metal depletion	213.6 g Fe-eq /day	-7.1%	8.7%	0.04%	0.02%	-6.7%
Fossil depletion	0.98 kg Oil-eq /day	-7.4%	9.0%	0.7%	0.4%	-6.7%
Non-renewable energy	47.7 MJ-eq /day	-6.5%	7.9%	0.6%	0.3%	-5.6%
Renewable energy	0.9 MJ-eq /day	-5.1%	6.1%	0.08%	0.05%	-3.9%
Land occupation	58.4 m ² a	-2.0%	2.3%	0.03%	0.02%	-2.0%

Table 4. Technological sensitivity analysis on the Lyon vehicle fleet basis

Impact per inhabitant	Lyon 2006	National 2006	Diesel +10%	Gasoline +10%	electric 10% FR	electric 10% EU	Hybrid 10%	Biofuel 10%
Global warming potential	2.8 kg CO ₂ -eq /day	3.0 kg CO ₂ -eq /day	-0.4%	0.4%	-5.7%	-2.6%	-2.9%	3.1%
Photochemical oxidant emissions	16.7 g NMCOV-eq /day	14.7 g NMCOV-eq /day	-1.6%	1.6%	-5.7%	-4.1%	-4.8%	1.3%
Terrestrial acidification	12.2 g SO ₂ -eq /day	11.6 g SO ₂ -eq /day	-1.4%	1.4%	-3.5%	-0.9%	-3.8%	4.5%
Particulate matter emissions	4.8 g PM-eq /day	4.6 g PM-eq /day	0.8%	-0.8%	-3.0%	-1.0%	-3.8%	2.6%
Metal depletion	213.6 g Fe-eq /day	221.2 g Fe-eq /day	0.6%	-0.6%	38.2%	38.1%	9.8%	2.3%
Fossil depletion	0.98 kg Oil-eq /day	1.03 kg Oil-eq /day	0.1%	-0.1%	-5.3%	-2.6%	-2.7%	-3.9%
Non-renewable energy resources	47.7 MJ-eq /day	50.2 MJ-eq /day	0.1%	-0.1%	-0.03%	-1.5%	-2.3%	-3.2%
Renewable energy resources	0.9 MJ-eq /day	0.9 MJ-eq /day	0.2%	-0.2%	13.9%	24.1%	0.6%	256%
Land occupation	58.4 m ² a	58.8 m ² a	0.05%	-0.05%	0.8%	1.9%	-0.04%	183%

For the same number of trips by car, a variation in the occupancy rate would have a complementary effect on car use. A 10% increase in the occupancy was estimated to decrease all environmental impacts by around 7%, because the infrastructure and public transport impacts remained constant. Conversely, a decrease of the car occupancy rate by 10% was estimated to increase impacts by around 8%, except for the land occupancy, which would increase by 2% (Table 3). A decrease in the occupancy rate may happen in the case of a sprawling city where people are more isolated.

The network could be modified to increase or reduce the traffic speed. A global increase or decrease of 10% in the traffic speed would not significantly change the impact on greenhouse gas emissions, but an increase of 10% in the traffic speed was predicted to cause an increase of about 2% in emissions of local air pollutants. Conversely, decreasing the traffic speed by 10% reduced local air pollutant emissions by less than 1%. For both sensitivity analyses, traffic congestion was not recalculated with the new car flows. A modal transfer from personal vehicles to public transport would decrease the environmental impact of urban mobility. A transfer of 10% of travelled distance from car to public transport would decrease almost all environmental impacts by 5-7%, depending on the public transport offered (Table 3).

These sensitivity analyses highlight the effects of behavioural changes on environmental stress. Technological developments that change the characteristics of the vehicle fleet also have effects on environmental impacts. Table 4 shows six vehicle fleet developments and the predicted effect on impacts, based on the Lyon vehicle fleet in 2006. Globally changes in fleet technology have heterogeneous impacts on the nine environmental indicators, for example electric cars contribute to reduce GHG and local air pollutants emissions but increase the use of metal (especially during vehicle fabrication) as well as energy consumption for the whole lifecycle. It is also noticeable that technological changes have less impact than behavioural changes, which impacts are homogeneous between indicators.

Sensitivity analysis on diesel and gasoline rate in the car fleet shows tiny variations. Significant variations occur for local pollutants, particles emissions decrease with more gasoline cars but photochemical oxidant emissions and terrestrial acidification increase. These results are estimated for the entire life cycle. For local pollutants, conclusions may vary on the scope of analysis. In this case looking at direct emissions from exhaust does not change conclusions.

Electric and hybrid technologies have convincing impacts on atmospheric emissions during the use phase. They reduce both local pollutants and GHG emissions. Nevertheless, these vehicles need batteries and electric motors whose fabrication gobbles rare metal, increasing significantly metal depletion (lower increase for hybrid car). In this sensitivity analysis, the difference between French electric cars and European electric cars is the origin of the electricity. Indeed, French electricity mix has low carbon footprint but has a low rate of renewable energy, while the European electricity mix is more fossil dependant but with higher renewable energy rate. This difference explains the lower interest for electric cars in Europe, but renewable energy programs will change this conclusion.

Finally the blending of biofuel deteriorates many environmental indicators, biofuel increases local pollutants and GHG emissions and needs significantly more land. Nonetheless biofuel appears efficient to introduce renewable in the transport sector which is mainly based on fossil energy. In the reference case it was assumed that fuels contains no biofuels, in 2006 French incorporation rate was equal to 1.75% of the PCI value, today it is 7%.

All these sensitivity analyses highlight potential of several transport policies, some on transport technologies others on transport habits. They are all based on marginal variation and are not time dependant but despite this simplicity they show some key parameters that need to be assessed more precisely. Car occupancy is one key parameter while speed seems less important, then car sharing scenarios may present great environmental advantage. For technological parameters biofuel blending ratio, electric cars seem relevant for some environmental indicators. The electricity mix has also an impact on results, especially with electric cars. Diesel and gasoline ratio in the car fleet is less influencing for global impacts but for local pollutants it has influence, especially on direct emissions.

The aim of the prospective approach is to estimate transport trends to predict future impacts, indeed car fleets are evolving and technologies are improving years after years. Moreover some objectives on transport and energy are set by the French and the European government for the next few years and their applications will have impacts on environmental impacts of mobility. Nevertheless some other technologies are emerging and can be the future of the urban mobility, making breaks in current trends about transport systems. For example autonomous vehicles may emerge quickly in the next years. In any case technological prospective brings high uncertainty due to the lack of data on recent technologies and the difficulties from cars manufacturers to meet governmental objectives, but it may highlight key parameters influencing various environmental indicators.

Conclusions

In the course of this study, an urban mobility assessment tool was created and applied on the Lyon urban area. This tool is based on the Life Cycle Assessment method. On the one hand, it needs a lot of data about foreground and background activities which are numerous for the transport system of Lyon. On the other hand, it provides a full analysis of environmental impacts because it takes all phases of the life-cycle of the system into account and returns several indicators concerning different environmental impacts.

The results of the nine chosen indicators represent different tendencies according to the five technologies that were observed in this study. Technological development actions, such as electric cars, hybrid cars or biofuel, mitigate some environmental issues but also exacerbate others. This diversity of chosen indicators may enrich and enhance policy debates about the development of urban transport systems and actions to take on its different subsystems. Therefore, forecast scenarios for technological development or modal share will have to be assessed using these nine indicators.

This method distinguished four phases into the life-cycle of the transport system: vehicle life cycle, fuel life cycle, infrastructure life cycle and the use of vehicles with exhausts. This distinction may highlight some potential transfers of environmental issues from one impact to another, or one life cycle phase to another. For instance, if only the use phase was considered, electric vehicles would have appeared preferable to diesel or gasoline cars. If vehicle and fuel fabrications are taken into account, electric vehicles present more impacts on some impacts such as metal depletion and energy consumption. Thus, an assessment methodology aiming to evaluate prospective changes of daily urban mobility will have to take into account these four phases. Furthermore, in the context of prospective debate, the infrastructure fabrication phase may not be neglected. Indeed, some infrastructure and planning choices, such as the decision to invest in an underground construction may have important environmental impacts. These four phases contribute differently on the total impacts and cannot be ignored.

Moreover, this LCA method is mainly proportional and additional, then, impacts can be easily disaggregated by life cycle phases or by modes of transportation (cars or public transport) or by road sections. With these detailed results, impacts can be used for spatial analysis such as dispersion and exposure analyses. Nonetheless, the LCA method is data consuming and requires updated databases to assess recent transport systems, this barrier may get bigger and more problematic in a prospective approach.

In addition to the LCA method, a Land-Use and Transport Interaction model was used for this study. Based on land-use data, transport systems and household travel survey, the LUTI model simulates the complex urban system (or a part of it). Due to the complexity, this kind of models needs time to be developed but when developed it makes the data collection for the urban system easier. Then environmental results can be analysed in relation to town-planning and social characteristics of the urban area. Furthermore, in the used model, SIMBAD, scenarios of urban-development or transport development can be implemented then evaluated through the LCA

method. Nevertheless, LUTI models are still a representation of the urban system and may introduce bias and errors through its process.

This wealth of data from both the LUTI model and the LCA method allows to get at the root causes of emissions, households and inhabitants. By estimating the environmental impacts for each household and knowing their characteristics, emitter profiles can be drawn and compared. Households are characterised by many socio-economic parameters and by many town-planning characteristics linked to their location in the urban area. The evaluation undertaken on income and distance to centre showed a great heterogeneity between households with a group emitting six time more GHG than another. Household analysis highlights the great socio-environmental inequality due to mobility present in urban area. Such analysis can be implemented on prospective scenarios to highlight inequality evolutions for different urban and transport policies.

The developed assessment tool is now effective and functional and provides detailed results for previous years with different environmental indicators, urban characteristics and emitter profiles. To go further, the method should include prospective scenarios in order to foresight potential technological and societal evolutions and urban developments. The LUTI model used in the evaluation process provides dynamic data from different scenarios of urban and transport development. Based on an incremental process, the model creates and moves households and activities every year, then assigns traffic on transport networks. Depending on the implemented scenario, households move in some specific area. For example compact scenario creates and moves households in the city centre. Others scenarios such as urban sprawl or transit oriented development can be implemented in order to enrich urban planning debates. Others social and demographic scenarios can be implemented to explore generational issues or new transport habits such as car-sharing or teleworking. For technological prospective, assessment can be based on evolution trends of technologies. Indeed, year after year, vehicle mix, fuel composition and emission factors evolve. Nonetheless, many new technologies are in development and may change significantly the transport system such as autonomous vehicles. The implementation of these different scenarios in the developed tool will return detailed analysis of different policies and approach numerous environmental and social issues.

References

- Antoni J-P. (ed.), (2010), *Modéliser la ville. Forme urbaine et politiques de transport*. Paris, Economica, coll. Méthodes et Approches.
- Bonnafeous A., Puel H., 1983, *Physionomies de la ville*. Paris, Les Editions ouvrières, 165p.
- Brand C., Preston J., 2010, '60-20 emission' - The unequal distribution of greenhousegas emissions from personal, non-business travel in the UK. *Transport Policy* 17, pp. 9–19
- Chester, M. V., Horvath, A. and Madanat, S. (2010), "Comparison of life-cycle energy and emissions footprints of passenger transportation in metropolitan regions", *Atmospheric Environment*, no. 44, pp. 1071-1079.
- CITEPA - Centre Interprofessionnel Technique d'Etudes de la Pollution Atmosphérique (2014), *Inventaire des émissions de polluants atmosphériques et de gaz à effet de serre en France – Format Secten. Rapport pour le Ministère de l'Ecologie, du Développement Durable et de l'Energie*.
- Goedkoop, M., Heijungs, R., Huijbregts, M., De Schryver, A., Struijs, J., van Zelm, R. (2008), *ReCiPe 2008 A life cycle impact assessment method which comprises harmonised category indicators at the midpoint and the endpoint level*.
- Dupont-Kieffer A., Merle N., Hivert L., Quételard B., (2010), *Environment Energy Assessment of Trips (EEAT): An updated approach to assess the environmental impacts of urban mobility. The case of Lille Region*. 12th World Conference on Transport Research, Lisbon, 11-15 July 2010.

- Geurs K.T., Van Wee B., (2004), "Accessibility evaluation of land-use and transport strategies: review and research directions", *Journal of Transport Geography* n°12, pp. 127-140.
- Grassot, L. (2011), Estimation des émissions de CO₂ & NO_x liées au trafic : impact des hypothèses de composition du parc, Laboratoire d'Economie des Transport, Vaulx-en-Velin.
- EEA - European Environment Agency, 2012, The contribution of transport to air quality - TERM 2012: Transport indicators tracking progress towards environmental targets in Europe. Copenhagen, EEA Report No 10/2012.
- INSEE. 2016a. « Connaître et comprendre le répertoire SIRENE », available at: <http://www.insee.fr/fr/service/default.asp?page=entreprises/sirene/institutionnel.htm> (assessed 27 April 2016).
- INSEE. 2016b. « Définitions, méthodes et qualité - Découpage infracommunal en IRIS », available at: <http://www.insee.fr/fr/methodes/default.asp?page=zonages/iris.htm> (assessed 27 April 2016).
- Joumard R., Gudmundsson H. (ed.), (2010), Indicators of sustainability in transport – an interdisciplinary approach to methods. INRETS research report, Bron, France.
- Le Féon, S. (2014), Evaluation environnementale des besoins de mobilité des grandes aires urbaines en France : approche par analyse de cycle de vie, Ecole Nationale Supérieure des Mines de Saint-Etienne.
- MEDDE, Ministère de l'Écologie du Développement Durable et de l'Énergie (2011), Les modalités du Paquet Énergie Climat, available at: <http://www.developpement-durable.gouv.fr/Les-modalites-du-Paquet-Energie.html> (assessed 18 June 2014).
- MEDDE, Ministère de l'Écologie, du Développement Durable et de l'Énergie (2014a), Émissions de gaz à effet de serre (Monde, Europe, France), available at: www.developpement-durable.gouv.fr/Emissions-de-la-France,33791.html (assessed 20 May 2014).
- Nicolas, J-P., Verry, D. and Longuar, Z. (2013), "Évolutions récentes des émissions de CO₂ liées à la mobilité des Français : analyser les dynamiques à l'œuvre grâce aux enquêtes nationales Transports de 1994 et 2008", *Economie et Statistique*, no. 457-458, pp. 161-183.
- Nicolas J-P. (dir), Bonnel P. (dir), Cabrera J., Godinot C., Homocianu M., Routhier J-L., Toilier F., Zuccarello P., (2009), Simuler les mobilités pour une agglomération durable. Laboratoire d'Economie des Transport, Vaulx-en-Velin. 211 p.
- Nicolas J.-P., David D., (2009), Passenger transport and CO₂ emissions: What does the French transport survey tell us? *Atmospheric Environment* n°43, pp. 1015-1020.
- SYTRAL (Syndicat mixte des Transports pour le Rhône et l'Agglomération Lyonnaise) (2006) Enquête Ménages et Déplacements 2006 de l'aire métropolitaine lyonnaise. 2006
- United Nations, Department of Economic and Social Affairs and Population Division. 2014. World Urbanization Prospects: The 2014 Revision : Highlights.
- Verdon, B., Varnaison – Revolle, P., Lebondidier, C., Verry, D., (2008). Mobilité urbaine et réduction des émissions de gaz à effet de serre, TEC n°198 – avril - juin 2008
- Wall, G. (2002), "Conditions and tools in the design of energy conversion and management systems of a sustainable society", *Energy Conversion and Management*, no. 43, pp. 1235-1248.

Development of a resistive soot sensor

Didier. GRONDIN*^{&***}, Alexandre. WESTERMANN**, P. BREUIL*, J.P. VIRICELLE* & P. VERNOUX**

*Ecole Nationale Supérieure des Mines, SPIN-EMSE, CNRS:UMR5307, LGF, 42023 Saint-Etienne, France

Fax +33 4 77 49 96 94 - email: viricelle@emse.fr

**Université de Lyon, Institut de Recherches sur la Catalyse et l'Environnement de Lyon, UMR 5256, CNRS, Université Claude Bernard Lyon 1, 2 avenue A. Einstein, 69626 Villeurbanne, France

Abstract

This paper is a comprehensive study dealing with the parameters that influence the response of a resistive soot sensor which was developed for Diesel Particulate Filter (DPF) failure detection in a past project. From the conductance measurement between two Pt electrodes, and a regeneration strategy, this kind of sensor can provide the weight concentration of particulate matter (PM). In this study, we have characterized and determined the key parameters such as the PM distribution size and the polarization voltage between the electrodes that could influence the sensor response. First results show that the sensor response strongly depends on the polarization voltage applied between the two electrodes.

Keys-words: Soot sensor; Resistive sensor, Particle Matter, On-Board diagnosis (OBD); Diesel particulate filter monitoring.

Résumé

Les paramètres clés qui gouvernent la réponse d'un capteur de suie de type résistif ont été étudiés. Le capteur testé a été développé pour le diagnostic embarqué d'un filtre à particules diesel lors d'un projet précédent. A partir de la mesure de la conductance électrique entre deux électrodes de platine, et d'une stratégie de régénération, ce type de capteur peut fournir la concentration en masse de suie. Dans cette étude, nous avons déterminé et caractérisé les principaux paramètres, tels que la distribution de taille des particules et la tension de polarisation entre les électrodes qui influencent la réponse du capteur. Les premiers résultats montrent que l'analyse de la réponse pourrait permettre de remonter à des informations concernant la taille des particules.

Mots clefs: Capteur de suie; Capteur résistif, Particules, Diagnostique embarqué, Filtre à particules, Diesel.

Introduction

Studies on vehicles exhausts have clearly demonstrated the negative effect of these emissions on the environment and the health [Barbusse and Plassat (2005)]. Emission legislations for Diesel engines become more and more stringent. The Particulate Matter (PM) emissions of automotive engines are now regulated in terms of mass and number. Since Euro 4 standards, Diesel light-duty vehicles have been equipped with Diesel particulate filters (DPF) to strongly reduce PM emissions. The PM accumulation into the inlet channels is determined by the pressure difference between the inlet and the outlet of the DPF. However, this system is not suitable to detect leaks and gives no information on the PM mass and number concentrations [Barbusse and Plassat (2005), Walker (2004)]. In order to meet the next European standards for PM emissions of Diesel light duty vehicles, an on-board diagnostic (OBD) sensor, able to detect DPF failures, is required. Therefore, the development of a cheap sensor effective for the measurement of both mass and particle number (PN) concentration is necessary. Resistive sensors are ones of the most promising solution for that purpose [Brunel *et al.* (2013), Grob *et al.* (2012), Hagen *et al.* (2010)]. They are typically composed of an alumina substrate, where the sensing face consists of two interdigitated platinum electrodes [Brunel *et al.* (2013), Hagen *et al.* (2010), Husted *et al.* (2012), Ochs *et al.* (2010)]. The sensor response is the conductance (or the resistance) between these two electrodes, measured as a function of the soot loading. The distance between these two electrodes may be around 10 μm to 100 μm [Noulette and Duault (2014)]. During soot loading, an initial threshold time is required to observe a significant increase in the conductance because the PM collection does not yet form any electrical connections between the electrodes. The second phase corresponds to an increase of the conductance with time

explained by soot bridges which are continuously formed between the electrodes [Brunel *et al.* (2013)]. When a polarization voltage is applied between the electrodes, the blind state (threshold time) is shorter because the production of dendrite-like paths is promoted [Brunel *et al.* (2013), Ochs *et al.* (2010)]. On the other side of the substrate, a platinum resistance is used to monitor and control the sensor temperature. Periodically, the soot accumulated on the sensing electrodes is removed during active regenerations by heating the sensor at around 600°C. By performing several cycles of soot loading/regeneration, the sensor can give the PM mass concentration in pseudo real time with a response time of around 3 minutes [Brunel *et al.* (2013)].

Starting from past results on a resistive soot sensor development in the frame of “Ciclamen 2” French National project [Brunel *et al.* (2013)], the objective of the present study is to determine the impact of the PM size and concentration on the sensor response. Model soot particles issued from a gas burner have been produced with various characteristics in terms of size distributions, PN and mass concentrations. For each kind of model soot, the response of the sensor has been monitored versus time as a function of the polarization voltage between the two Pt electrodes. Although model soot may have slightly different physico-chemical properties than those of real diesel one, their size distribution, mass and number concentrations are realistic for the application. Moreover, the interest of model soot is obviously to have more reproducible conditions than with working with a real engine.

1. Materials and methods

Soot sensor

The sensor was developed in a previous work (“Ciclamen 2” national project) in collaboration with Electricfil Automotive car supplier Company. The sensor is made of an alumina substrate (5*0.5 mm²). A platinum heater is deposited on opposite side to the sensing element which consists in interdigitated platinum electrodes deposited by screen-printing and laser engraving technics (Figure 1a-b) [Brunel *et al.* (2013), Noulette and Duault (2014)]. Using this latter method, the space between the two Pt electrodes is around 20 μm as shown by SEM image in Figure 1c. Which also reveals an Insulating layer (blue color in Figure 1b) as deposited on the sensing side to define the collecting area of the soot particles as well as on the whole heater side to protect it against short circuits that could be provoked by the soot.

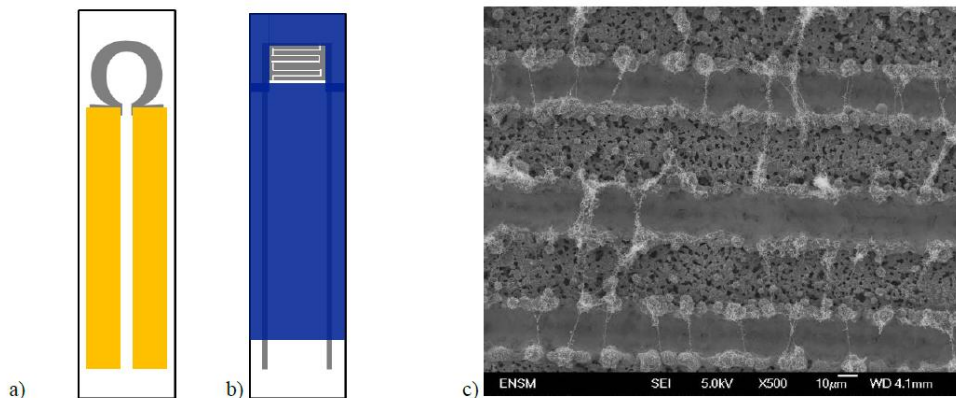


Figure 1. Schematic of the soot resistive sensor a) heater side, b) sensing side and c) SEM image of electrode area showing soot bridge.

The response of the sensor is defined as the conductance (or resistance) which is measured between the two platinum electrodes as a function of time, under controlled temperature and PM flow. Indeed, a stream of soot particles creates bridges between the two Pt electrodes (Figure 1c), by increasing the conductance. A polarization voltage is applied between the electrodes with a Keithley 6430 Sub-Femtoamp Remote Sourcemeeter which records the sensor conductance with time. The apparatus is monitored with a specific LabVIEW software.

Soot generation

The soot generation was performed on a synthetic gas bench described elsewhere [Lopez-Gonzalez *et al.* (2015)] and shown schematically in Figure 2.

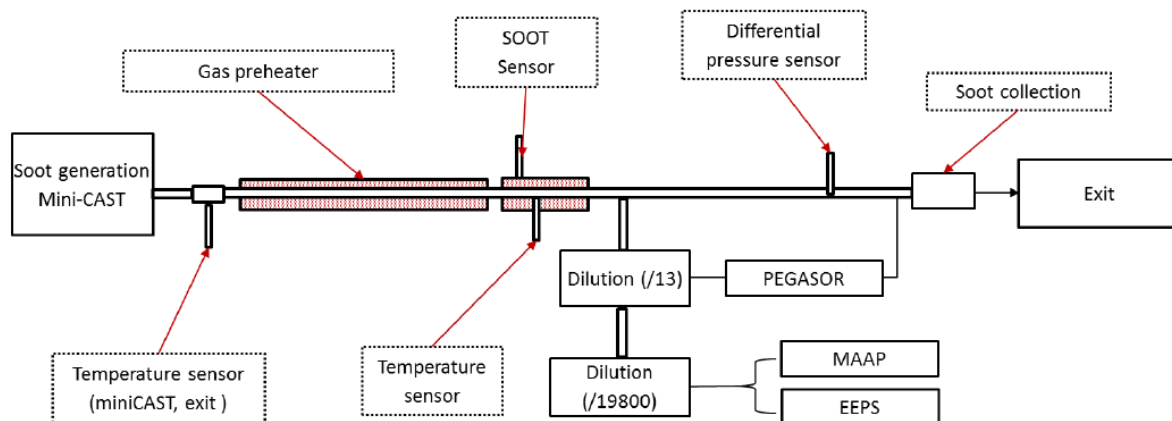


Figure 2. Schematic diagram of the synthetic test bench.

The bench is divided in 4 parts, the soot particles generator, a tubular oven to pre-heat the PM stream, the sensor and PM analytical tools.

Soot particles were produced with a mini Combustion Aerosol Standard burner (miniCAST 4202, Jing Ltd. Switzerland). Soot particles are formed within a co-flow diffusion flame due to the hydrocarbon pyrolysis (propane was used as a fuel) which takes place as a consequence of the heat provided by the oxidation at the flame front. The produced flame is quenched by a stream of nitrogen that enables at the same time the pyrolysis of the fuel, and the escape without being oxidized of the generated particles. The fuel to air ratio can be customized in order to obtain a broad range of flame conditions and consequently different types of soot particles (PN and size distribution) [Moore *et al.* (2014)]. An air flow of 1200 NL/h was added to dilute the PM stream. Four different operating points (OP) of the CAST burner, corresponding to four propane/air ratios (Table 1) have been used to produce different sizes and concentrations of soot particles. For each of these operating points, soot particles have been collected for ex-situ analysis. The soot collection was performed by thermophoretic deposition on the internal surface of an aluminum perforated block (1 inch diameter) and located just before the outlet of the bench.

The PM stream was preheated in a tubular furnace (THERMCONCEPT). The temperature control was performed by a retrofitted closed loop control system which controls the gas temperature at the exit of the oven (so close to the sensor).

The sensor is placed downstream the oven, perpendicularly to the pipeline with the sensing side back on stream to avoid direct impacts of particles on the sensing surface which could lead to a noisy signal. A K-type thermocouple was placed near the sensor (1 cm after the sensor) to record the gas temperature (180°C). In order to control and characterize the PM produced, several on-line analyzers were positioned after the sensor as detailed in paragraph 2.3).

The conductance measurements were performed at the steady state conditions after the stabilization of temperature at the output of the miniCAST (around 1 hour after the flame ignition). The regeneration of the sensors was performed at 650°C for 3 min.

On-line Soot analysis

Three complementary analyzers were used to characterize soot particles (size distribution, mass and number concentrations) generated by the miniCAST burner in our experimental tests conditions,

The PN and the size distribution were measured by an engine exhaust particle sizer spectrometer (EEPS model 3090, TSI Inc.) which can quantify PM size from 22 to 560 nm with a sizing resolution of 16 channels per decade (i.e., total 32 channels). Measurements are performed at a frequency of 10 Hz allowing a real time analysis. Overview of the principle can be found in reference [Burtscher (2005)].

In addition, the black carbon concentration in the soot was measured with a Multi-angle Absorption Photometer (MAAP). This analysis is based on the light absorption of the black carbon that is collected on a fiber glass [Burtcher (2005)] Hence, MAAP analyzer does not give any information on the organic fraction. Although the specific extinction coefficient may slightly vary with the PM size [Fuller *et al.* (1999)], it was kept constant for the various OPs used in our study. Indeed, MAAP measurements applied to urban and background aerosol have shown a strong correlation between black carbon mass concentration and aerosol light adsorption despite a wide size distribution [Petzold and Schönlinner (2004)].

Three ejector diluters (2 Palas VKL 10, 1 Palas VKL 100) [Burtcher (2005)] have been connected in series to achieve soot concentrations levels below the upper measurement ranges of the EEPS and the MAAP. The overall dilution ratio was 19800.

Finally, a PEGASOR particle sensor analyzer (PPS) was placed after the first diluter system (VKL 10 diluter, dilution ratio 13) to online follow the soot mass concentration. This latter is measured from the leak current of charged particles [Ntziachristos *et al.* (2013)]. The trap was set at 400V as recommended by the constructor. PPS response is sensitive to soot composition and size, and should be calibrated for each OP to perform an accurate quantitative analysis. However, in the present study, PPS analyzer was mainly used to check the reproducibility between various tests at a given OP, and the stability of soot generation over time.

Characterizations of collected soot.

The structure and size of the collected soot at each mini-CAST operation conditions have been observed with a Transmission Electronic Microscope (TEM, JOEL 2010 LaB6). The acceleration voltage applied was 200 kV and the resolution point was 0.19 nm. The samples were previously dispersed in ethanol using an ultrasonic bath and deposited on a measurement grid.

Temperature programmed oxidation (TPO) measurements have been performed to evaluate the reactivity of the different soot. The collected soot was mixed with an inactive SiC powder (weight ratio soot/SiC = 1/5) for 5 minutes with a ball-grinder. TPO were also conducted using Printex U, a commercial black carbon powder, for comparison. The soot weight varies in the range 2 – 5 mg (Table 2). The samples were then introduced in a tubular furnace. The reaction temperature was measured with a K-type thermocouple located close to the sample. The temperature was increased at the rate of 10°C/min up to 750°C. The composition of the gas mixture was 5 % of oxygen (Linde Gas, 99.995% purity) in helium. The flow rate was kept constant at 6 L/h. Gas emissions were recorded during the heating ramp. CO and CO₂ production were monitored using an infrared analyzer (EMERSON NGA 2000) while O₂ concentrations were measured by gas chromatography using a micro-chromatograph (SRA 3000). Soot conversion (%) was calculated as the ratio of cumulative (CO + CO₂) quantity at the considered temperature, to the total (CO + CO₂) quantity at the end of TPO experiment where we assume that soot is totally converted. In addition, a mass spectrometer (Pfeiffer vacuum PrismaPlus QME220) was used to obtain complementary qualitative information on the soot chemical composition.

Raman spectra of the collected soots were recorded with a LabRam HR Raman spectrometer (Horiba-Jobin Yvon) equipped with BXFM confocal microscope, interference and Notch filters and CCD detector. The exciting line at 514.5 nm of a 2018 RM Ar⁺ laser (Spectra Physics) was focused using a x 50 long working distance objective. The influence of the laser power was investigated from 10 to 1000 μW (not discussed in this study) and P = 100 μW was chosen as the working power. Indeed, the focusing of a laser on materials can locally heat depending on its power and lead to structural and chemical evolutions. Spectra collected with gratings of 300 grooves.mm⁻¹ were accurate within 4 cm⁻¹ (with a laser spot diameter of 1 μm). The instrument was calibrated against the Stokes Raman signal of pure Si at 521 cm⁻¹ using a silicon wafer ((111) crystal plane surface). All recorded data were treated using the Labspec software (Horiba-Jobin Yvon). Spectra were fitted after the multi-point baseline correction by combination of five Lorentzian-shaped G, D1, D2, D3 and D4 bands at about 1580, 1350, 1620, 1500 and 1200 cm⁻¹ [Sadezky *et al.* (2005), Ivleva *et al.* (2007)].

The apparent electrical conductivity of soot was estimated at room temperature in air by using a specific cell developed to fit with the low soot quantity that can be collected during the test. The cell consists in a Teflon block with an internal diameter of 1.5 mm with a brass piston at the top and a brass plate at the bottom, connected to a resistor meter. However, conductivity values were found to be strongly dependent on the soot packed-bed arrangement in the cell. Only range of order could be determined, leading to around 50 S.m⁻¹ for OP1 and to nearly 0.3 S.m⁻¹ for OP5 at 20°C. It must be taken into account that these values do not represent the intrinsic soot conductivity but an overall conductivity including carbon and organic fractions. In addition, the conductance measured on sensors may strongly depend on the structure of soot bridges between electrodes.

2. Results and discussion

On-line PM characterizations.

The soot produced by the CAST burner depends on the richness of the propane/air mixture (Table 1). Size distributions measured by the EEPS analyzer are shown in Figure 3.

Table 1. Soot characteristics produced by the soot generator (MiniCAST) depending on the operating point (OP).

Operating Point	Richness of propane/air mixture	PN (EEPS) particles/cm ³	Mass concentration (PEGASOR) mg/m ³	Carbon black (MAAP) mg/m ³
OP1	0.97	1.7 E+8	94	143
OP1B	0.97	1.2 E+8	61	81
OP4	1.00	2.5 E+8	91	70
OP5	1.02	2.1 E+8	55	22

Four operating Points (OP) of the burner have been defined to produce various PM sizes and concentrations. Two OPs (OP1 and OP1B) correspond to the same richness but with lower propane and air flows for OP1B (Table 1). The two instruments, PEGASOR and MAAP, give quite different values of mass concentrations. According to the photometer, the PM mass concentration strongly decreases with richness in the flame from OP1 to OP5 (Table 1). These measurements are based on the light absorption of black carbon. Therefore, one can assume that this apparatus is more sensitive to large soot particles, mainly composed of a carbon core. This is in good agreement with the drop of PN above 100 nm when the richness in the flame increases (Figure 3).

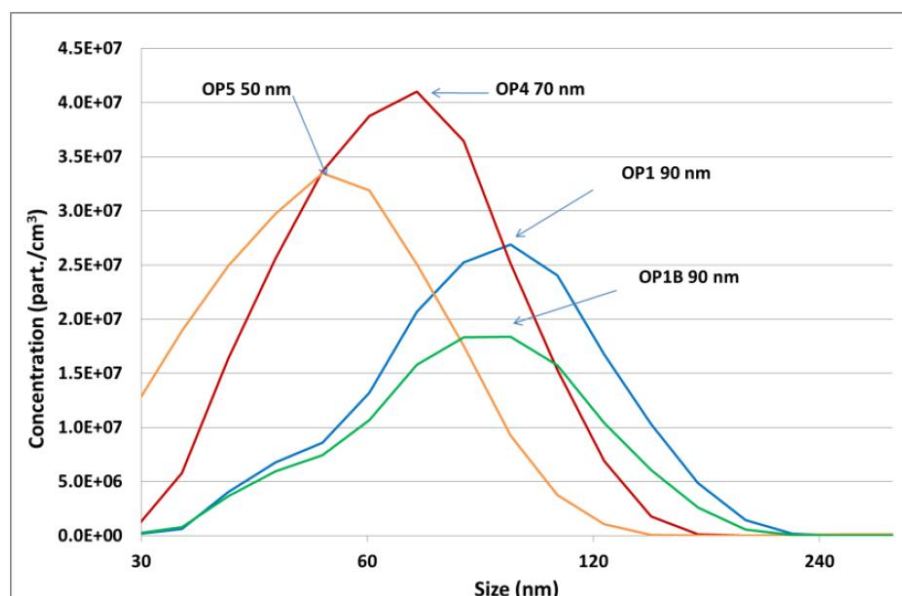


Figure 3. Size distribution of the different OPs (EEPS measurement). Concentrations correspond to values before dilution (dilution factor = 19800).

On the other hand, the PEGASOR analyzer is measuring a leak current extracted from the PM electrical charge. This latter parameter most probably varies with the CAST OP, i.e. the chemical nature of the soot, leading the comparison between the different OPs quite speculative. For OP1 and OP1B, two similar tunings, the responses of the PEGASOR show similar trends than those of the photometer but for OP4 and OP5, results are quite different. Therefore, we have considered that the PM mass concentration estimated by the MAAP is more suitable to compare the different OPs.

When the propane/air ratio in the flame increases, the PM mass concentration decreases while the size distribution is shifted to lower values (Figure 3 and Table 1). For instance, the PM diameter at the maximum of the Gaussian distribution is around 90 nm for OP1 and OP1B, 70 nm for OP4 and 50 nm for OP5. As expected, OP1 and OP1B lead to a similar size distribution (Figure 3), but with a lower mass and PN concentration for OP1B. The ratio of the propane flows between OP1 and OP1B was approximately 1.2. This value is fairly similar to the mass concentration ratios between OP1 and OP1B measured by the different instruments: 1.4 (EEPS), 1.5 (PEGASOR) and 1.8 (MAAP). Regarding the overall PN, concentrations are fairly similar at around $2 \cdot 10^8$ part/cm³ for OP1, OP4 and OP5 (Table 1). For OP1B, the lower flow of propane explains the smaller PN around 10^8 part/cm³.

Temperature Programmed Oxidation of collected soot

The reactivity of the soot was evaluated from Temperature Programmed Oxidation (TPO) experiments (Figure 4).

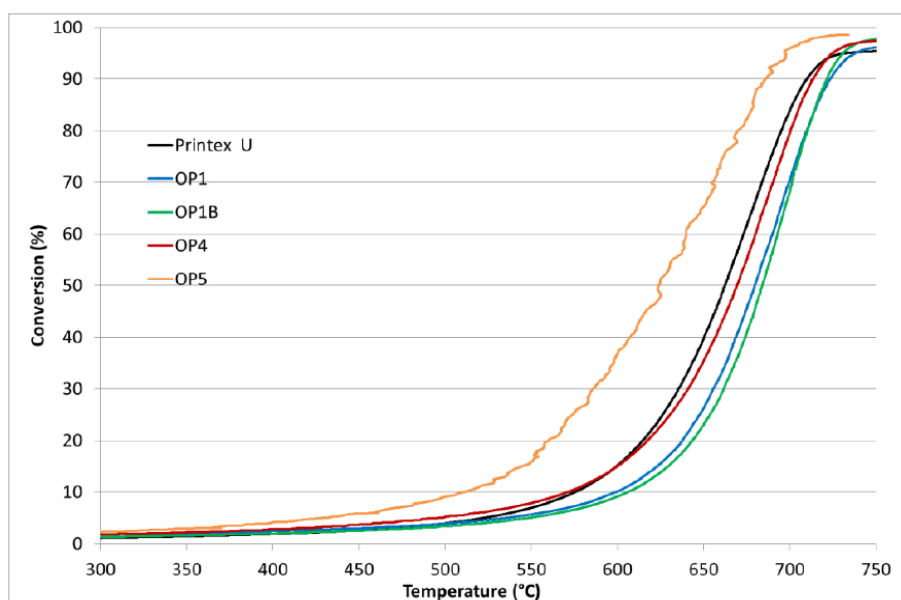


Figure 4. Soot conversion as a function of temperature for the different CAST soot measured from TPO experiments.

The soot oxidation beginning was fixed when the derivative of the conversion curve was higher than an arbitrary value (0.03). The soot oxidation starts at 326°C for OP5, 493°C for Printex U, 496°C for OP4, 525°C for OP1 and 529°C for OP1B (Table 2 and Figure 4).

Table 2. TPO results summary for the different OPs ($T_{\text{oxidation}}$ is the observed starting oxidation temperature; T_{10} is the temperature corresponding to 10% conversion of the soot).

Operating Point	Soot mass mg	$T_{\text{oxidation}}$ °C	T_{10} °C
Printex U	5.3	493	575
OP1	2.4	525	599
OP1B	3.1	529	606
OP4	2.2	496	571
OP5	3.5	326	510

The parameters T_{10} (Table 2), corresponding to the temperature at 10% conversion of soot, was used to compare the reactivity. Values of T_{10} (Table 2) follow this rank: OP5 (510°C) < OP4 ≈ Printex U (570°C) < OP1 ≈ OP1B (600°C). This indicates that soot reactivity increases with the richness in the flame. This difference in reactivity may be due to different chemical compositions or surface specific areas or also soot structure organization, as observed by Grob *et al* (2012). However, one can note that TPO experiments confirm that OP1 and OP1B produce similar PM with the same reactivity. Three kinds of PM can be determined from TPO (Figure 4) and on-line characterizations (Table 1). OP5 produces more reactive particles containing a higher organic fraction compared to those generated by OP1 and OP1B. This was also supported by Temperature-Programmed Desorption (TPD) under vacuum of the different soot up to 850°C (not shown here). In particular, the monitoring of m/z 15 and 29 signals during a heating ramp (20°C/min) has confirmed the highest concentration of organic compounds on the OP5 soot. OP4 soot particles present intermediate properties whereas the desorption of organics from OP1 and OP1B only takes place from 750°C and is rather limited. Such classification is also in agreement with MAAP measurements (Table 1) which point out that the black carbon content decreases from OP1 to OP5. It appears also coherent with apparent soot electrical conductivity measurements (section 2.4) as lower black carbon fraction leads to lower conductivity.

TEM observations

The PM structure and size have been observed by TEM. The results presented in Figure 5 show that the produced PM have the same structure as emitted by a Diesel engine [Liaty *et al.* (2013)]. The soot is composed of primary spherical particle agglomerated in a bigger particle with a fractal shape (Figure 5 a,b,c). The primary particles have a similar size for each OPs, around 20 nm organized with a turbostratic arrangement of the graphene lamellae spaced of around 0.3 nm (Figure 5 d,e,f). No significant difference was found between each OPs.

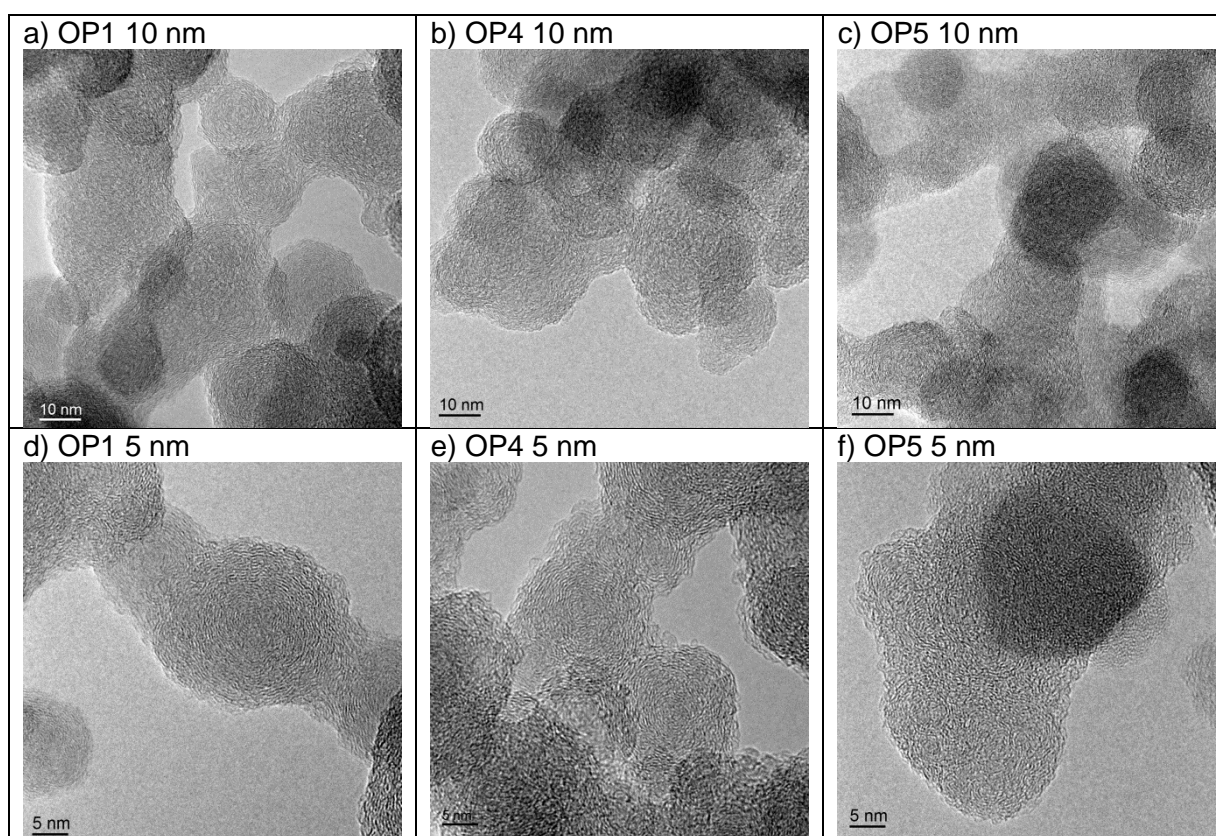


Figure 5. TEM observations for OP1 a), d), OP4 b) e), and OP5 c), f) at 10 nm a), b), c) and 5 nm d), e), f) scale.

Raman spectroscopy characterizations

Figure 6 shows characteristic visible Raman spectra of the collected PM with no correction of the baseline.

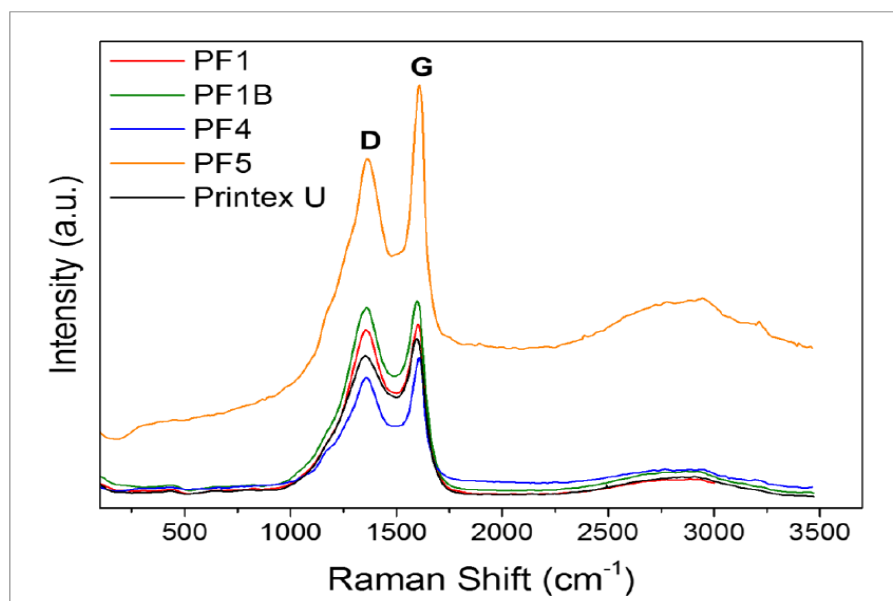


Figure 6. Characteristic Raman spectra of the collected soot using an exciting line at 514.5 nm.

We have observed quite different backgrounds due to fluorescence between OP5 soot spectra and those of the others PMs. This level of fluorescence is mainly due to presence of adsorbed organics on the surface [Uy *et al.* (2014)]. This indicates that OP5 PMs contain a much larger surface concentration of organic compounds. This confirms the result observed on OP5 soot with TPO experiments. The Raman spectra are all composed of two broad and overlapping bands centered at 1355-1360 cm^{-1} (with a shoulder at 1180 cm^{-1}) and 1575-1595 cm^{-1} corresponding respectively, according to the literature, to the D and G of amorphous and graphitic carbon [Ivleva (2007)]. According to previous studies [Sadezki *et al.* (2005)], these broad bands can be fitted in multiple D bands, i.e. D1, D2, D3, D4 located at about 1350 cm^{-1} (D1), 1620 cm^{-1} (D2), 1500 cm^{-1} (D3), 1220 cm^{-1} (D4) as well as the G band at 1580 cm^{-1} . This latter corresponds to the ideal graphitic lattice (E_{2g} -symmetry) while the D bands (or “Defect” bands) are associated with disordered graphitic lattice and amorphous carbon for D3. The lower the G/D intensity ratio, the more disordered (less graphitic) the material is. The A_{D1}/A_G band area ratios are commonly used to describe the structural order of soot. Values of this ratio are quite similar and comprised between 3.1 and 6.25 for OP5 and OP1B, respectively (Table 3).

Table 3. Main characteristics of the different soot Raman spectra.

Soot type	Band position (cm^{-1})			FWHM (cm^{-1})			A_{D1}/A_G
	D1	D3	G	D1	D3	G	
Printex U	1357	1504	1581	213 ± 13	135 ± 24	69 ± 11	4.68 ± 1.6
OP1	1357	1509	1579	194 ± 6	120 ± 16	70 ± 12	5.97 ± 2.0
OP 1B	1355	1511	1578	200 ± 6	119 ± 17	67 ± 12	6.25 ± 2.0
OP 4	1358	1512	1589	170 ± 4	128 ± 13	64 ± 6	4.25 ± 0.9
OP 5	1365	1530	1594	151 ± 4	239 ± 11	56 ± 4	3.10 ± 0.5

For comparison, the A_{D1}/A_G ratio of the pure graphite is approximately 0.2 while that of a Diesel soot is around 4.2 [Sadezki *et al.* (2005)]. This underlines that PMs produced by the CAST burner have a similar carbon organization than that of real Diesel soot. The A_{D1}/A_G ratio seems to slightly decrease with the richness in the flame, suggesting that OP5 PMs are more graphitic than OP1 soot. If soot reactivity was only linked to graphitic state, this result would be in contradiction with TPO experiments (Figure 4). It means that the main difference is the organic fraction content, higher for OP5, in agreement with TPO results and the background of Raman spectra. The difference in the graphitic level is rather small as also observed by TEM. In addition, the difficult deconvolution of the broad spectral range into multiple and strongly overlapping bands leads to inaccurate determination of the A_{D1}/A_G ratio (with a standard error up to 30% for OP1 and OP1B PMs). It was shown by Sadezki *et al.* (2005), that the full widths at half maximum (FWHM) of the different bands, and specifically that of D1, is more precise to estimate the degree of the structural order of PMs. The FWHM of the D1 peak was found to decrease with the graphitic organization. Table 3 shows that the D1 band FWHM is in the range $151\text{-}194\text{ cm}^{-1}$ while that of the graphite is approximately at 45 cm^{-1} and a Diesel soot at 174 cm^{-1} . These results confirm that the structural order of the CAST soot is similar to that of Diesel soot. Raman spectroscopy also clearly underlines that OP1 and OP1B soot present similar structural order.

Soot sensor responses

The variations of the sensor conductance with time during the soot loading for the different OPs upon different polarizations voltage are reported on Figure 7.

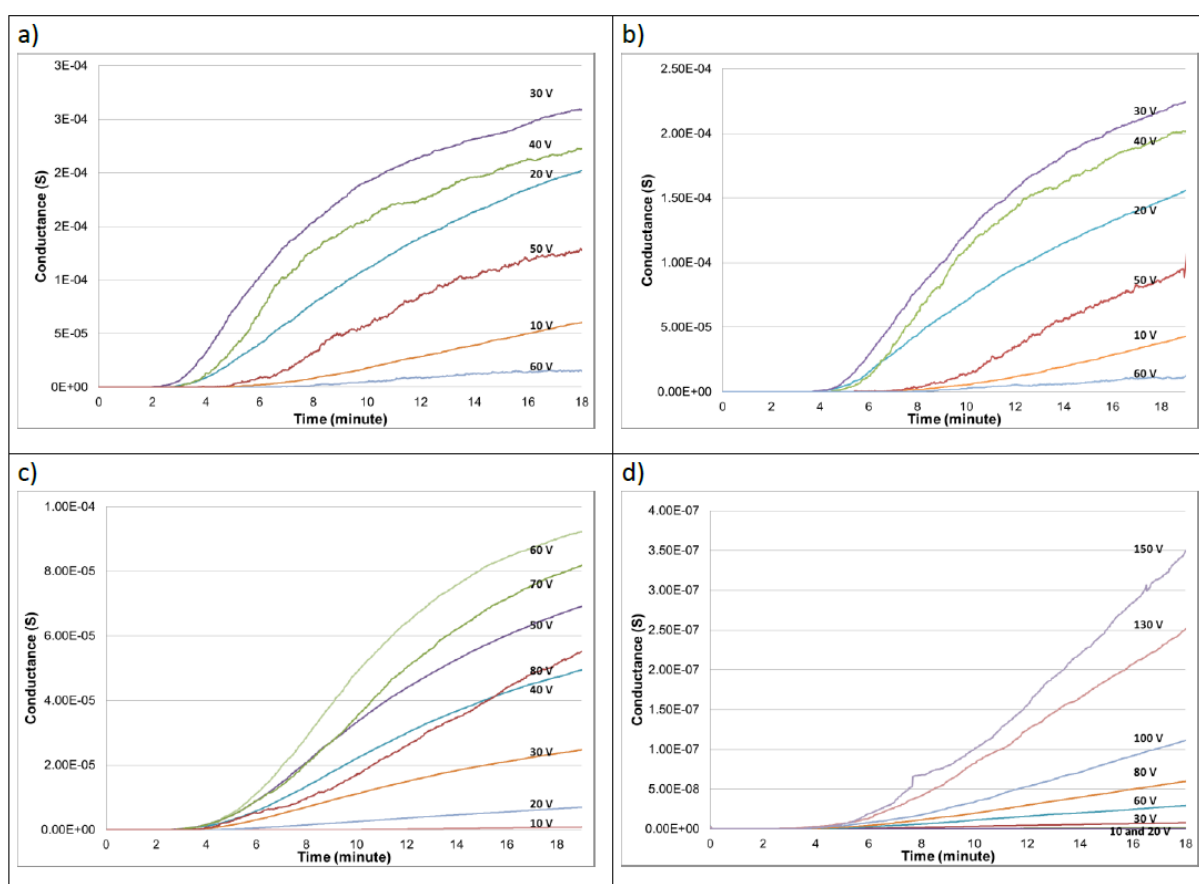


Figure 7. Variation of the conductance with time for different polarization voltages and mini-CAST OPs: OP1 a) OP1B b) OP4 c) and OP5 d).

These tests were carried out on the same sensor for each OP. The polarization voltage range was 10-60 V for OP1 and OP1B, 10-80 V for OP4 and up to 150 V for OP5. The conductance measurements were performed during several cycles (soot loading / regeneration) for a stable temperature at 180°C of the PM stream. The initial time on Figure 7 corresponds to the end of a regeneration phase, i.e. no PM collected on the sensing Pt electrodes. The conductance was measured for 18 minutes. The curves present a sigmoid profile. The first part of these curves corresponds to the formation of the first connections (percolation time), i.e. first bridges between the two Pt electrodes. Then, the second part corresponds to the continuous formation of soot bridges between the electrodes as shown in Figure 1. Once the inter-electrodes space becomes more or less saturated with soot bridges for longer exposure time (not shown in Figure 7), the conductance reaches more or less a plateau. Soot continues to deposit on the sensing element as a layer but the contribution to the global conductance becomes negligible as no additional conducting bridge is formed between electrodes. Moreover, this situation has no real interest regarding neither comprehension of size or number effect as the sensor is saturated, nor application as the sensor will have to be regenerated at quite lower accumulation time. The conductance increase rate, corresponding to the soot collection rate on sensing electrodes strongly depends on the polarization voltage (Figure 7). Except for OP5, there is an optimal voltage corresponding to the higher collection rate. This latter is 30 V for OP1 and OP1B, and 60 V for OP4. For OP5, despite the fact that the voltage applied reached 150 V, no optimal voltage has been achieved (Figures 7 and 8).

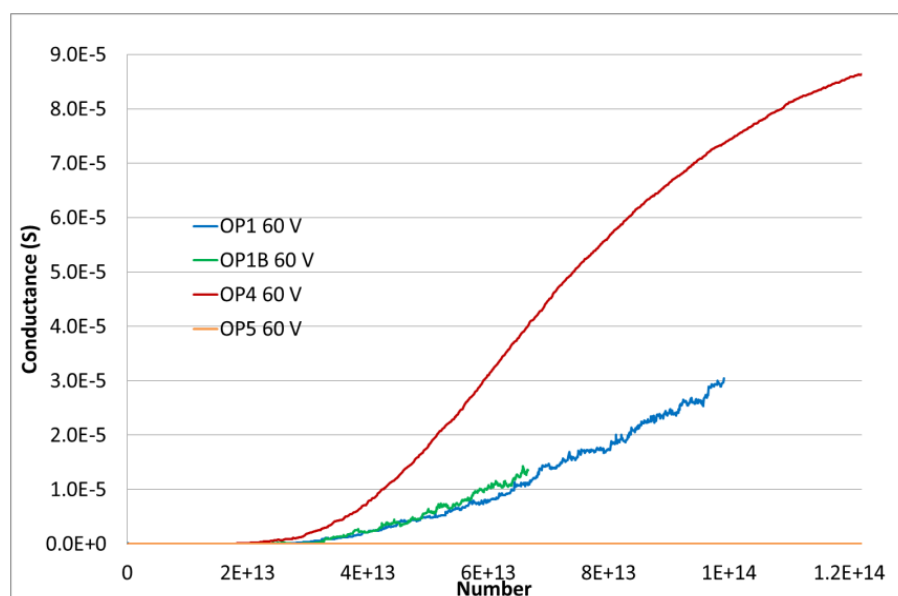


Figure 8. Variation of the conductance as a function of cumulative particle exposed number for 60 V polarization for each OP.

Upon optimal polarization, the sensor responses are different for each OPs. After 18 min on PM stream, the conductance values, for the optimum voltage, follow this rank: 300 μ S (OP1) > 225 μ S (OP1B) >> 90 μ S (OP4) >> 0.4 μ S (OP5) (Figure 7). This is in good agreement with the mass concentration measured by the MAAP (table 1) which gives the same ordering. Therefore, the value of conductance measured at a given time after percolation step, under optimal polarization, is linked to the black carbon content into the soot. This result is also coherent with both the apparent electrical conductivity measurement of OP5 soot which is two orders of magnitude lower than that of OP1 (section 2.4), as well as the TPO experiments which indicate that the reactivity increases (decreases) with the organic (black carbon) content.

Figure 7 also allows to determine the percolation times as a function of the polarization voltage for each OP. They are in the range 1.8 - 3.9 min for OP1, 3 - 5 min for OP1B, 1.6 - 6.3 min for OP4 and 2.5 - 7 min for OP5. Percolation times are not so different and cannot be linked to the PM mass concentration. For instance, a 4 times smaller mass concentration does not significantly modify the percolation time recorded for OP5 compared to OP1B (Table 1). On the other hand, the twice PN of OP1 compared to OP1B leads to a shorter percolation time: 1.8 min instead of 3 min. This indicates that the percolation time could be linked to the number of particles for similar size distribution. To check this hypothesis, conductance variations are represented as a function of the cumulative PM number calculated as the product of PN concentration measured by EEPS (particle/cm³) by the flow (cm³/h) and the time (h). Figure 8 reports such curves for each OP at a fixed polarization voltage of 60 V. It can be seen that sensor responses for OP1 and OP1B having the same size distribution (Figure 3) but different PN concentrations are similar. Hence, the correlation between percolation time and particle number seems to be valid for a given type of particles. Moreover, Figure 8 also reveals that OP1, OP4 and OP5 curves are different, highlighting that size distribution and electrical apparent conductivity are the key parameters.

In order to point out the optimal polarization voltage corresponding to each OP, Figure 9 presents the time to achieve a conductance value of 10⁻⁷ S versus the polarization voltage extracted from Figure 7 results. The optimum polarization voltages, corresponding to the minima of the inverted-vulcano curves, seem to be inversely proportional to the PM size. The smallest the PM size, the highest the optimal polarization voltage is. Indeed, despite different PM mass concentrations, the optimal polarization voltage of the sensor exposed to a PM stream produced by OP1 and OP1B is similar.

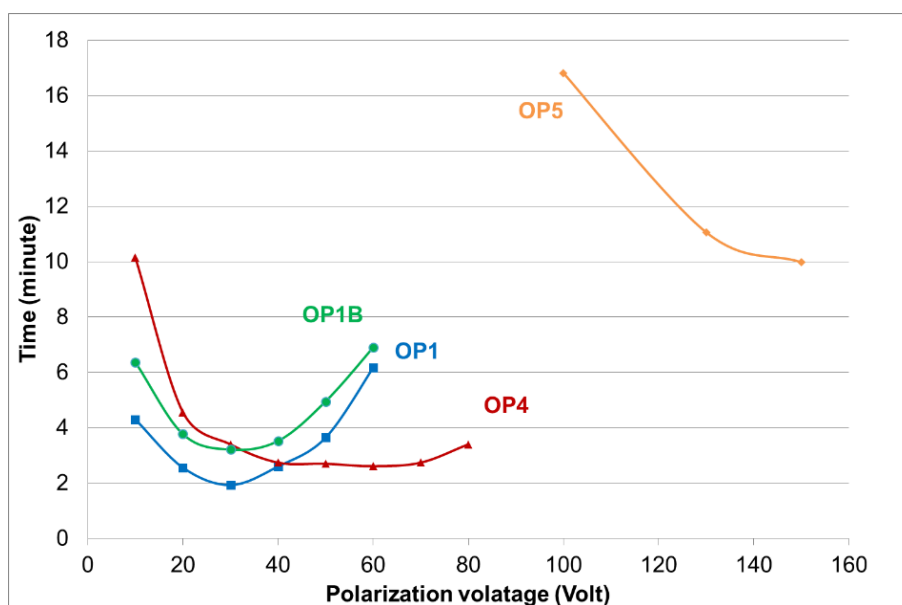


Figure 9. Loading time to reach 10⁻⁷ S versus the polarization voltage for the different OPs.

Conclusion

This study describes the impact of the PM size and concentration on the responses of a resistive sensor. Model soot particles have been produced with various characteristics in terms of size distributions, number and mass concentrations and collected onto two interdigitated Pt electrodes upon different polarization voltages. Analysis of the sensor responses curves, i.e. variation of the conductance with time, allowed to draw correlations between some characteristics like the percolation time, the optimal polarization voltage and the conductance value with the soot properties. This conductance value is clearly linked to the PM mass concentration and PM composition (organic fraction), while the percolation time seems to be more related with the PN concentration.

Finally, the optimal polarization voltage appears to be dependent on the PM size. These demonstrative results will be useful in the development of a soot sensor for PN measurement. In order to go further, a physical model based on soot collection between polarized electrodes is under development.

Acknowledgments

The authors wish to acknowledge “Arc Environnement” from Region Rhone-Alpes for the funding and EFI automotive car supplier for sensors manufacture.

References

- Barbusse S. & Plassat G. (2005): Particules de combustion automobile et leurs dispositifs d'élimination (Les). ADEME report, n°5728, France, 128 p.
- Brunel O., Duault F., Lavy J., Creff Y. & Youssef B. (2013): Smart Soot Sensor for Particulate Filter OBD. SAE International Journal of Passenger Cars - Electronic and Electrical Systems, Vol 6, p 307–327.
- Burtscher, H. (2005): Physical characterization of particulate emissions from diesel engines: a review. Journal of Aerosol Science, Vol36, n°7, p 896-932.
- Fuller, K. A., Malm, W. C., & Kreidenweis, S. M. (1999): Effects of mixing on extinction by carbonaceous particles. Journal of Geophysical Research, Vol 104, n°15, p 941-954.
- Grob B., Schmid J., Ivleva N.P. & Niessner R. (2012): Conductivity for Soot Sensing: Possibilities and Limitations, Anal. Chem., Vol 84, p 3586–3592.
- Hagen G., Feistkorn C., Wiegärtner S., Heinrich A., Brüggemann D. & Moos R. (2010): Conductometric Soot Sensor for Automotive Exhausts: Initial Studies. Sensors, Vol. 10, p 1589–1598.
- Husted H., Roth G., Nelson S., Hocken L., Fulks G. & Racine D. (2012): Sensing of Particulate Matter for On-Board Diagnosis of Particulate Filters. SAE Int. J. Engines, Vol 5, p 235–247.
- Ivleva, N. P., Messerer, A., Yang, X., Niessner, R., & Pöschl, U. (2007): Raman microspectroscopic analysis of changes in the chemical structure and reactivity of soot in a diesel exhaust aftertreatment model system. Environmental science & technology, Vol 41, n°10, p 3702-3707.
- Liati, A., Eggenschwiler, P. D., Schreiber, D., Zelenay, V., & Ammann, M. (2013): Variations in diesel soot reactivity along the exhaust after-treatment system, based on the morphology and nanostructure of primary soot particles. Combustion and Flame, Vol 160, n°3, p 671-681.
- Lopez-Gonzalez D., Tsampas M.N., Boréave A., Retailleau-Mevel L., Klotz M., Tardivat C., Cartoixa B., Pajot K. & Vernoux P. (2015): Mixed Ionic–Electronic Conducting Catalysts for Catalysed Gasoline Particulate Filters. Top. Catal., Vol 58, n°18, p 1242–1255.
- Moore, R. H., Ziemba, L. D., Dutcher, D., Beyersdorf, A. J., Chan, K., Crumeyrolle, S., ... & Anderson, B. E. (2014): Mapping the operation of the miniature combustion aerosol standard (Mini-CAST) soot generator. Aerosol Science and Technology, Vol48, n°5, p 467-479.
- Noulette J. & Duault F. (2014): Sonde de mesure de depot de suie dans l'échappement et son procede de fabrication. WO2014044965 A1, 2014.
<http://www.google.com/patents/WO2014044965A1> (accessed June 29, 2015).
- Ntziachristos, L., Amanatidis, S., Samaras, Z., Janka, K., & Tikkanen, J. (2013): Application of the Pegasor Particle Sensor for the measurement of mass and particle number emissions. SAE International Journal of Fuels and Lubricants, Vol 6, n°2, p 521-531.
- Ochs T., Schittenhelm H., Genssle A. & Kamp B. (2010): Particulate Matter Sensor for On Board Diagnostics (OBD) of Diesel Particulate Filters (DPF). SAE Int. J. Fuels Lubr., Vol 3, p 61–69.
- Petzold, A., & Schönlinner, M. (2004): Multi-angle absorption photometry—a new method for the measurement of aerosol light absorption and atmospheric black carbon. Journal of Aerosol Science, Vol 35, n°4, p 421-441.
- Sadezky, A., Muckenhuber, H., Grothe, H., Niessner, R., & Pöschl, U. (2005): Raman microspectroscopy of soot and related carbonaceous materials: spectral analysis and structural information. Carbon, Vol 43, n°8, p 1731-1742.
- Uy, D., Ford, M. A., Jayne, D. T., Haack, L. P., Hangas, J., Jagner, M. J., ... & Gangopadhyay, A. K. (2014): Characterization of gasoline soot and comparison to diesel soot: Morphology, chemistry, and wear. Tribology International, Vol 80, p 198-209.
- Walker A.P. (2004): Controlling Particulate Emissions from Diesel Vehicles, Topics in Catalysis, Vol. 28, n°1, p 165–170.

URBAN AIR: AN OPERATIONAL AIR QUALITY MANAGEMENT TOOL AT HIGH RESOLUTION FOR CITIES

Fabien BROCHETON*, Benjamin CHABANON*, Julien GALINEAU*, Verónica MIRA JUST*, Céline PESIN* & David POULET*

*NUMTECH, 6 allée Alan Turing, Aubière, France

Tel+33 4 73 28 75 95-email:julien.galineau@numtech.fr

Abstract

Air quality and its health effects is an important preoccupation for local authorities and air quality management has been taken into account in public policies.

Urban Air is an operational system designed for local authorities and air quality monitoring organisms to map and to forecast air quality at the scale of an urban area, a town or a district. Air Quality calculation is performed every day in analysis and forecast mode, and can integrate measurements from pollution sensors from AQMS to improve the quality of the analysis results. Alert module, and scenarios mode can help public authorities to manage high levels of pollution episodes.

First version of the system had been installed in 2005 on Strasbourg. Nowadays it provides daily real-time results and forecasts in more than 20 cities all over the world.

Keys-words: *Air Quality Modelling, Operational system, air quality policies management, health exposure.*

Résumé

La qualité de l'air et ses effets sont une préoccupation importante pour les collectivités territoriales et la gestion de la qualité de l'air est à présent prise en compte dans la mise en place des politiques publiques.

Urban Air est un système opérationnel développé pour les collectivités territoriales et les organismes en charge de la surveillance de la pollution de l'air dans le but de cartographier et de prévoir la qualité de l'air à l'échelle d'une zone urbaine, d'une ville ou d'un quartier. Les calculs sont réalisés chaque jour en analyse et en prévision et peuvent intégrer des mesures issues de capteurs permanents pour améliorer la qualité des résultats en analyse. Des modes alertes et scénarios sont présents pour aider les autorités locales dans la gestion des épisodes de pollution aigue.

La première version du système a été installée en 2005 sur la ville de Strasbourg. Aujourd'hui, il fournit des prévisions en quasi temps réel dans plus de 20 villes de par le monde.

Mots-clés : *Modélisation de la qualité de l'air, Système opérationnel, politiques de management de la qualité de l'air, exposition sanitaire*

Introduction

Air quality and its health effects is an important preoccupation for local authorities and air quality management has been taken into account in public policies.

Urban Air is an operational system designed for local authorities and air quality monitoring organisms to map and to forecast high-resolution air quality at the scale of an urban area, a town or a district. First version of the system had been installed in 2005 on Strasbourg.

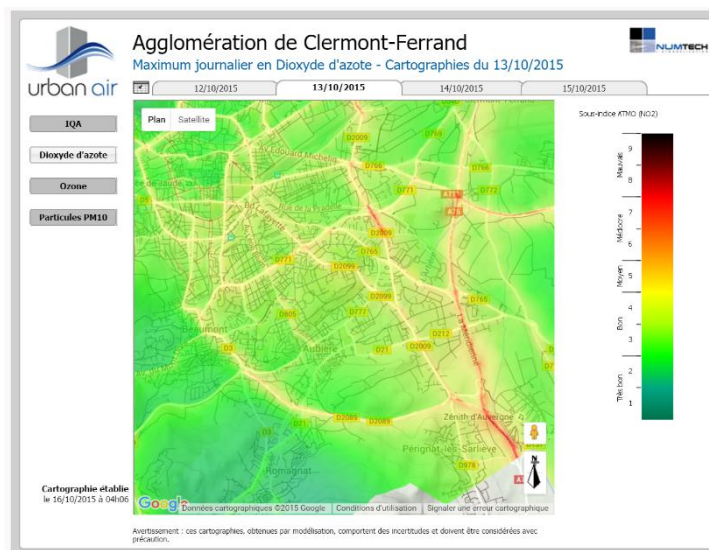


Figure1. Air Quality Forecast in Clermont-Ferrand using Urban Air (ATMO Auvergne, 2015).

1. Method

Urban Air is an automated platform using recognized and validated Hanna et al. (1999) air quality model ADMS Urban, developed by Cambridge Environmental Research Consultants (CERC).

ADMS-Urban is a comprehensive system for modelling air quality in large urban areas, cities and towns. It incorporates the latest scientific understanding, explicitly represents the full range of source types occurring in an urban area, takes account of complex urban morphology including street canyons, and provides output from street-scale to urban-scale and, with the regional model link, to even larger scales.

Air Quality calculation is performed every day in analysis and forecast mode (day, day+1 and day+2). The platform is able to automatically download air quality data from an air quality monitoring network or can be coupled with regional and national pollution models to get pollutants concentrations imported in the urban area. These background levels are then added to local emissions sources integrated in ADMS Urban model during dispersion calculation using local meteorological data.

Setting up ADMS Urban model for the area

The first step of the use of Urban Air in an area is to set up ADMS Urban for the modeled area.

Urban areas are complex domains with a lot of variables that have an impact on the dispersion of the pollutants emitted. The Figure 2 show all the input data that are used to set up ADMS Urban model for an urban area.

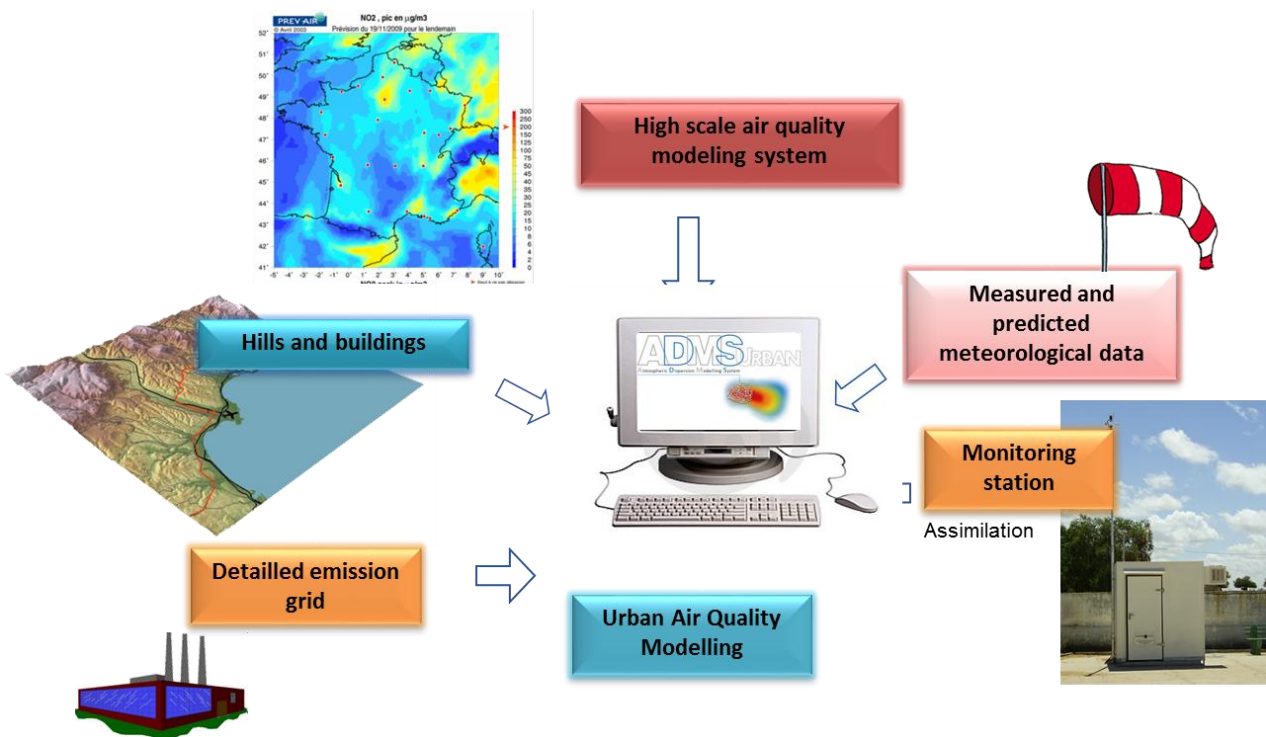


Figure 2. Input data used to set up ADMS Urban models (NUMTECH, 2016)

Input data can be classified in two different type:

- Emission sources data (description, localization, emissions...)
- Environmental data

Emission sources that have to be imported in ADMS Urban (as shown in 3) are:

- Road traffic: main road network described as line sources: this is the most important data needed to get good representation of the spatial distribution of the concentrations of urban pollutants such as NO_x and particulate matter (PM).
- Most important emissions sources of the area (or close to the area) like: principal industrial activities (stack emissions or industrial diffuse emissions), harbor activity, airport activity...
- Other emissions sources: Combustion in residential and tertiary activities, secondary road network described as volume sources, railway traffic, biogenic sources...

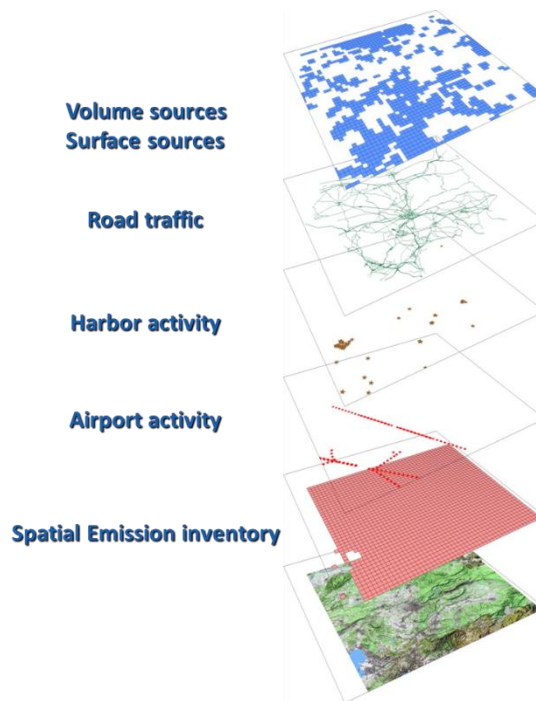


Figure 3. Sources integrated in urban air quality dispersion model (NUMTECH, 2016)

To model the contribution of the most important emissions sources, different data sources are available in ADMS Urban: point sources (for industrial stacks), line source (for road traffic), surface sources (storage areas, settling basin...) and volume sources (use to model the contribution of secondary road network or residential and tertiary emissions).

In order to model any type of source, several information have to be supplied to the dispersion model:

- Emission data (for each activity/source for a period),
- Metadata associated with emission data :
 - Spatial description : localization, physical characteristics
 - Temporal distribution of the emission

The temporal allocation (monthly and/or diary) of the emissions also have to be integrated in ADMS Urban to get the best results. Indeed, most emissions are not constant during the day (figure 4) and it is very important to be able to model this at the urban area scale, in order to get consistent hourly results throughout the day.

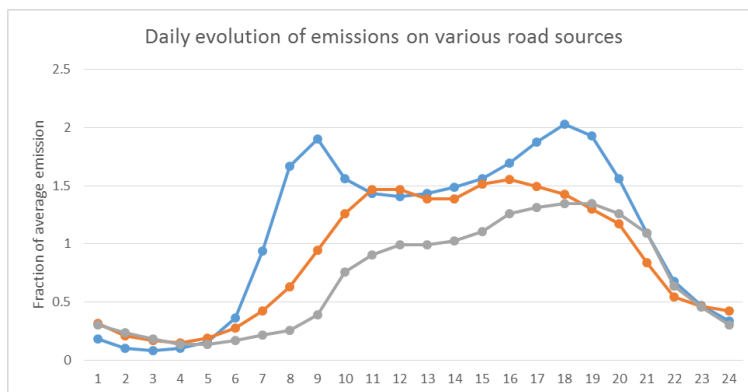


Figure 4. Example of temporal allocation for road transport emissions (NUMTECH, 2016)

Main environmental data required for air quality modelling purpose are:

- Topography : In complex domain areas, the terrain height variation has an important impact on plume dispersion so in this cases, it is important to set it up in ADMS Urban
- Meteorological data (measures and forecast): A variety of meteorological data can be used for input. Parameters are needed at an hourly scale to estimate the variability of the stability of the atmosphere. Wind speed, wind direction and temperature are required along with cloud cover, heat flux or solar radiation. The meteorological pre-processor then calculates the necessary boundary layer parameters from the inputs.

Air quality concentration data (measures and forecast): these data are used for model validation and to estimate background levels on the modelling domain. A dataset of a year is required to validate the results in a lot of different meteorological conditions.

Validation

The second step of the use of Urban Air in Urban Air is a validation phase.

The pollution levels are calculated as pollutant concentrations, and as spatialized air quality index (CITEAIR index for example). It is calculated on a specific non regular grid that allow to realize a high-resolution dynamic display of pollutants concentrations in the city (Figure 1), and that is optimized to limit computation times.

To ensure the quality of the results produced, pollution levels are also automatically calculated in the location of air quality monitoring stations (AQMS) so Urban Air can calculate performance scores based on statistical indicators such as correlation, RMSE or bias. These indicators are calculated by comparing hourly levels modelled by the system and measured by the AQMS as shown in Figure 5.

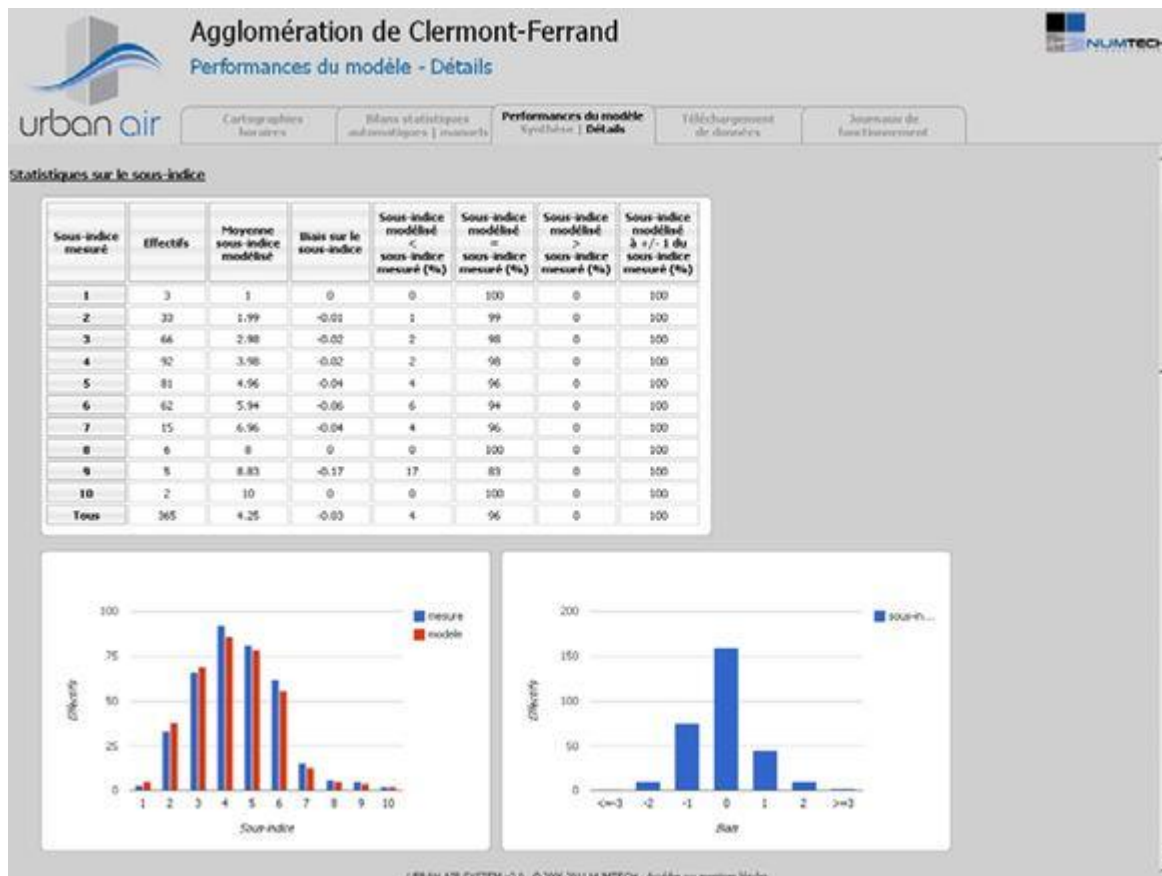


Figure 5. Automatic performance scores computed (NUMTECH, 2016).

Air quality sensor data assimilation

To improve the quality of the analysis results, Urban Air is able to integrate in the system measurements from pollution sensors from AQMS to perform data assimilation (Tilloy et al. (2013)). Data assimilation is quite unique in Urban Air because the corrections of the pollution levels modelled in ADMS Urban is spatially variable depending on the location and the road network expressed in the simulation. It allow to improve the results near the road traffic, where pollution levels are the most important.

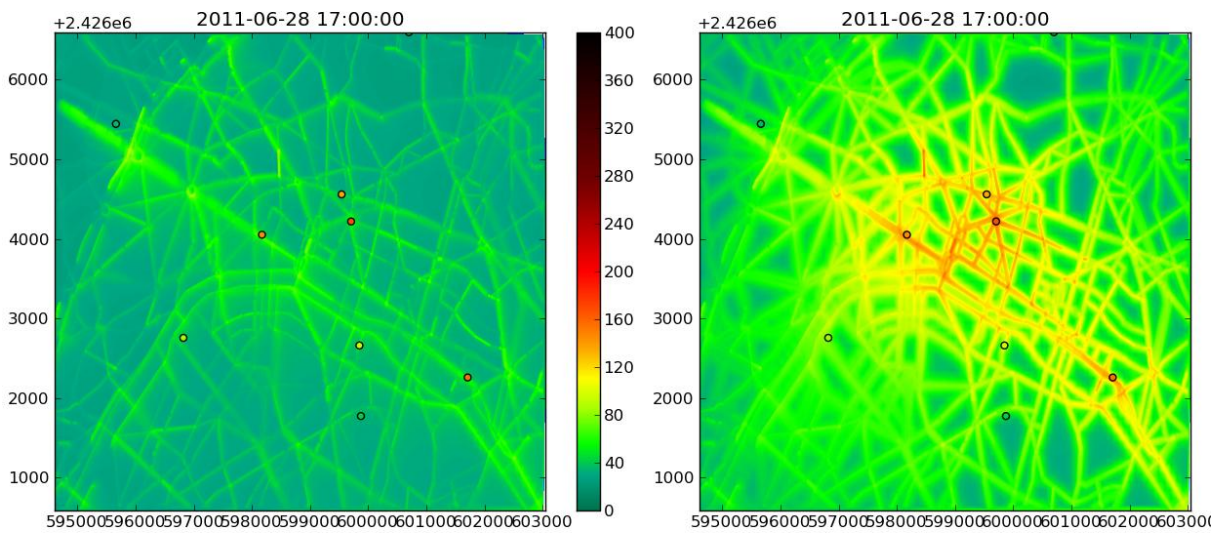


Figure 6. Maps of nitrogen dioxide concentrations over a quarter of Paris on 28 June 2011 at 17 UTC, in $\mu\text{g}/\text{m}^3$. Points represent the concentrations measured at AQMS.

Alert module

To help public authorities to manage high levels of pollution episodes, Urban Air integrate an Alert Module that can detect and inform users that a specific threshold has been exceeded. In this case, Urban Air automatically estimate the area concerned by the threshold exceedance and then calculate the population potentially exposed.

Urban Air offers then the possibility to run different scenarios including emergency measures (low emission zones, alternating traffic, speed limit reduction...). All the scenarios can be performed in Urban Air to compare pollutions levels of the current situation to the predicted situation with the emergency measures, helping the decision-makers to choose the most efficient way to reduce air pollution levels during peak of pollution.

2. Deployment

Urban Air is already fully operational in several cities and urban communities. It provides daily real-time results and forecasts in more than 20 cities all over the world such as Marseille, Lille, Strasbourg, Clermont-Ferrand, Dubaï or Casablanca... It is becoming an important communication way for decision-makers to take into account of the environmental dimension of public policies and actions in the city.

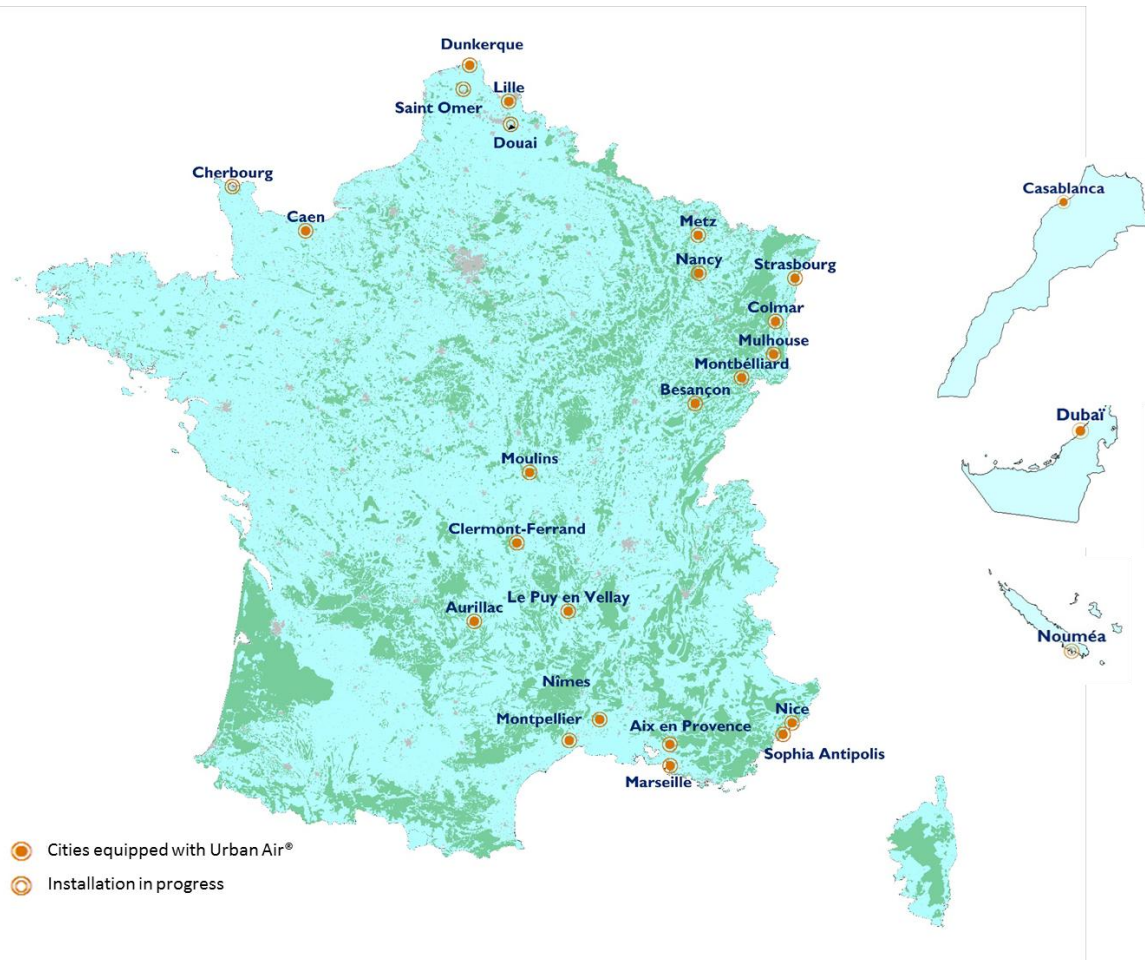


Figure 7. Cities using Urban Air (NUMTECH, 2016)

Conclusion

Urban Air is becoming an important tool to help public authorities to manage air quality at the scale of an urban area, a town or a district. Working complementary with the AQMS network, it allows to get spatial real time information and forecast of pollutants levels at high resolution. Decision-makers can have access to this information to deal with high level of pollution episodes or to measure the efficiency of the public policies on air quality.

References

Hanna S.R., Egan B.A., Purdum J. and Wagler J. (1999), *Evaluation of ISC3, AERMOD, and ADMS Dispersion Models with Observations from Five Field Sites*. HC Report, API, 1220 L St. NW, Washington, DC 20005-4070

A. Tilloy, V. Mallet, D. Poulet, C. Pesin and F. Brocheton (2013), *BLUE-based NO₂ data assimilation at urban scale*, *Journal of Geophysical Research: Atmospheres*, Vol. 118, 2031–2040

Real-world driving for light-duty vehicles in the Netherlands

Gerben GEILENKIRCHEN* & Norbert LIGTERINK**

*PBL Netherlands Environmental Assessment Agency, PO Box 30314, 2500GH The Hague, The Netherlands; Fax +31 70 328 87 00 – email : Gerben.Geilenkirchen@pbl.nl

**Sustainable Transport and Logistics, TNO, PO Box 49, 2600 AA Delft, The Netherlands

Abstract

Pollutant emissions from light duty vehicles are strongly influenced by driving circumstances. Representative real-world driving data are required to determine real-world emission factors. Driving behaviour for light duty vehicles in the Netherlands has been updated based on an extensive measurement programme. Measurements were performed on-road by a professional driver using the car-chasing technique. In total 108 hours of on-road driving were recorded, distributed over urban roads, rural roads and motorways with varying speed limits. Different time periods are covered, including evening trips.

Urban driving shows a rather large variations in driving speeds from 0 to 50 km/h. Rural driving shows a clear peak at 80 km/h, the national speed limit on rural roads, but also shows a rather large variations below 80 km/h. Motorway driving shows peaks just below 100 km/h and 120 km/h, the speed limits at most motorways in the Netherlands. A second peak at 100 km/h is related to the dynamic speed limits on Dutch motorways. It was concluded that real-world driving is more dynamic than previously assumed, especially on motorways.

Key-words: *real-world driving, driving cycles, light-duty vehicles, emission factors, car-chasing*

Introduction

The national emission totals for road transport and the modelling of (future) local air quality rely on accurate estimates of pollutant emissions by road transport at different locations and under different driving circumstances. The driving dynamics and the level of congestion play an important role in the emission levels of road transport. Deriving appropriate emission factors for emission inventories and local air quality modelling requires associating generic traffic situations: i.e. road types, speed limits, and congestion levels to specific driving behaviour. This paper establishes this relation anew for the Netherlands. The emission factors are the average emissions in grams per vehicle kilometre for a given traffic situation.

The Dutch national emission factors that are derived annually by TNO and PBL (TNO, 2016) for modelling local air quality near roads and for the national emission inventory are a combination of the vehicle emissions for different driving behaviour combined with the driving behaviour in different traffic situations for which the emission factors are provided. A main distinction is made between urban, rural, and motorway driving. For urban and motorway driving different levels of congestion are provided. Moreover, for motorways the different speed limits and speed-limit enforcement levels in the Netherlands are distinguished, as driving behaviour and resulting emission levels differ.

Previously, driving behaviour in the Netherlands was derived from a mix of studies, some of which are over ten years old. Some of these studies on driving behaviour were conducted right after the introduction of specific speed limits, such as the 80 km/h zones on the motorways surrounding the four major cities in the Netherlands and more recent the introduction of the 130 km/h speed limit. It is unclear if the driving behaviour that was derived from these studies is still representative for current driving, years after the introduction with perhaps some habituation having occurred.

Moreover, after the adaption of the VERSIT+ emission model, this model no longer requires a small set of representative driving data, i.e., velocity profiles, to predict the emission for a specific traffic situation. Rather, a limit to the amount of data which can underpin an emission factor no longer exists. Hence, the use of more data on real-world driving will lead to more statistics and a better prediction of the average driving behaviour in the Netherlands. This takes away an intermediate filtering, and

resulting bias, of driving behaviour from a large set of driving data and a true average can be determined based on hundreds of hours of data.

Lastly, nowadays on-road emission measurements are used to determine real-world emission factors. In the past, specific real-world driving cycles were executed in the emission laboratory. Today, the driving behaviour in the emission tests on the road is more arbitrary; it is merely dictated by the driver and the traffic situation on the road. And what is more, ambient conditions vary on road as well. This study gives further understanding of representative driving behaviour and it will help to ensure vehicle emissions are to be tested in a representative manner for the Dutch situations.

All in all, many good reasons exist for updating the driving behaviour underlying the emission factors for road transport used for air quality modelling and for estimating national emission totals from road transport in the Dutch Pollutant Release and Transfer Register. This study offered the opportunity to execute a measurement program enabling a general overhaul of the understanding of driving behaviour. The results of this research were submitted as Dutch input in discussions on representative driving behaviour forming a basis for Real Driving Emission (RDE) testing for future legislation.

1. Objectives

In the past, velocity profiles were central to the determination of driving behaviour for estimating real-world emission factors. Despite their shortcomings, velocity profiles are still used in many cases today. Velocity profiles originate from the need to repeat driving behaviour in the laboratory during emission tests. Using real-world on-road driving behaviour was a manner to ensure real-world emission tests in the laboratory. However, it has grown into a research effort of its own with its own jargon and methods, which, with today's possibilities of on-road emission testing and ever deviating laboratory tests, and the use of Markov chain methods to generate driving cycles (Balau et al., 2015), is largely outdated.

A velocity profile is a selection of data from a large set of driving data that is representative for on-road driving. There is a large history of "trip characteristics", or average trip properties, which are meant to determine the driving behaviour and the representativeness of the velocity profile for normal driving behaviour and normal vehicle use (Barlow et al., 2009). The selection of the velocity profile, from parts of the data, is a manual process flawed by the fact that the representative velocity profile, or the driving cycle, must be short, and it is built up of parts of driving data, typically separated by stops. Long parts in the data, between stops, are therefore inappropriate to derive a test with specific trip characteristics. Hence, the short parts, or sub-cycles, are therefore selected. Instead, a normal driver may go for half an hour or more without stops; such data is unsuited for laboratory tests.

Another major fault with the standard velocityprofile approach is the aim at average driving. Given the fact that emissions are produced intermittently, the average driving is not a good way of determining the average emissions. The total span of driving behaviour must be weighed according to their occurrences in real-world conditions to arrive at the average emissions, as a small part of driving behaviour may result in a large part of the emissions. This may even be driving behaviour which lies outside the physical realm of the average car with a limited engine power. As was shown by André et al. (2006), using the same set of driving cycles for all cars can lead to strong differences in emission estimates then using specific driving cycles depending on vehicle characteristics.

The emission model VERSIT+ was adapted to limit the effects of these drawbacks (Ligterink & De Lange, 2009). Moreover, new test cycles were developed to ensure a full span of driving behaviour as observed on the Dutch roads. In particular, the TNO Dynacycle covers the hard accelerations normally excluded in laboratory driving cycles. Since 2009, the Dynacycle has been used commonly in laboratory tests by TNO, in order to augment the emission data collection. However, this artificial cycle was only meant to compensate the lack of high-acceleration data experienced with most real-world cycles. Most standard driving cycles are designed so that low-powered vehicles can drive them, and the somewhat circular reasoning is that high-powered vehicles are driven in the same manner as low powered vehicles. The notable exception, to these low-powered cycles are the De-Lijn bus cycle of the Belgian research institute VITO (Lenaers et al. 2007), with maximal acceleration to set points, and the maximal acceleration segment in the ERMES cycle (www.ermes-group.eu).

In the past, the velocity profiles underlying the Dutch emission factors were based on one to five separate representative trips weighed together. Only recently, this restriction has been abandoned, and the intermediate step via representative trips is no longer required. Current study is to make a

complete adaptation from so-called average, or representative, driving to the full-span of driving, to be used in the determination of emission factors.

Driving data is collected on-road using the car-chasing technique that was also applied by Pathak et al. (2016). Cars are followed in the normal traffic flow in the relevant conditions. From 2009 and earlier this data is no longer available for re-analysis, hence a detailed comparison with the findings of previous studies cannot be made. There are five major studies for driving behaviour from which data is currently used in the Netherlands:

- The ARTEMIS project has led to the Common Artemis Driving Cycle (CADC) which is commonly used across Europe to test the real-world emission performance of vehicles in the laboratory (André, 2004).
- The OSCAR project performed within the European 5th Framework project, resulted in a number of driving cycles which are used for urban driving with different degrees of congestion (Boulter et al., 2005).
- The Files-and-Emissies project of TNO is the main understanding of Dutch motorway driving behaviour (Gense et al., 2001).
- The Overschie project was carried out to determine driving behaviour in newly formed 80 km/h zones on the motorway with strict speed-limit enforcement (Smit et al., 2006).
- The 130 km/h motorway project was set up to study the driving behaviour on motorway stretches where the newly introduced speed limit of 130 km/h applies (De Lange et al., 2011).

These studies were performed in the 2001-2011 period. Little information and data remains from the earlier studies. Typically, only the selected, or constructed “representative velocity profiles” have been carried over in time. Hence, there is little understanding of whether and how driving behaviour changes over time, due to changes in vehicle power, drivers getting used to new traffic situations, and the manner in which speed limits are enforced.

In the meantime, GPS has become ubiquitous. Several projects were carried out collecting GPS velocity data, e.g., UDRIVE (Eenink et al., 2014). There are major flaws in this data. For starters, the quality of the velocity data is generally poor. It may look smooth and appropriate but it can in fact deviate significantly from the actual velocity, as will be shown in the current paper. Moreover, the selection of vehicles, drivers, and routes is generally aimed to represent the ‘fallacious average’. Hence, the average in many different ways will not lead to the appropriate span of driving behaviour. What is more, it will not lead to any understanding of the missing data.

It is therefore essential to collect a large amount of random driving behaviour on the road with a good coverage of all aspects which may determine the complete span of driving behaviour for emissions and the weighing of the different data therein. Hence, a proper set-up of a test program from modern driving behaviour must be as wide as possible, without preselecting in any manner of what may be representative or average. A common fallacy is that the average driving behaviour will produce the average emissions. The aim of this project is to provide an appropriate set of Dutch driving data which spans all situations on the road.

2. Driving behaviour in the VERSIT+ model

In 2009, the VERSIT+ emission model underwent a major update (Ligterink & De Lange, 2009) to make the model ready for improved real-world emission measurement techniques: second-by-second data and results from on-road testing. The three essential features of the new model version are:

1. The use of a map with emission rates [g/s] for the velocity and acceleration of the vehicle as a basis for the emission model. Such a map is linear, which ensures exact post-diction and allows for averaging.
2. Dividing the map into segments relevant for road type and emission rates, as shown in Figure 1, such that the velocities are typical for urban (0-50 km/h), rural (50-80 km/h) and motorway (>80 km/h) driving, and a line of equal emission rates similar to a large share (~65%) of smooth driving, a smaller share (~30%) of mild accelerations and an even smaller share (~5%) of hard acceleration; all three contributing a similar amount to the total emissions.
3. A least-square regression fit of each segment of all the relevant emission data collected per

vehicle category. This method ensures appropriate total emissions, as the focus is on the average emissions. The quality of the model determines to what extent each specific case is represented. Generally, for driving for which no data is collected the predictability is lower, as expected. When the predictability is low, the results default to the average emissions by design.

Essential to this approach is the collection of representative data and the full variation therein. The main principle is that the emission tests must already include the typical velocities and accelerations which are used to determine the emission factors. In that manner, the emission model is little more than a re-weighing of the emission measurement data, for variations, or selections, of velocities and accelerations.

Representative driving behaviour, in other words, is essential to estimate accurate real-world emissions in a particular situation. A slightly smaller or larger time share of accelerations will affect the outcome significantly. In particular, the roughly 5% of the time of hard accelerations contributes typically about a third to the total emissions. A 1% change from 5% to 4% or 6% harder accelerations will lead to a significant change in emissions of about 5% down or up.

Personal driving style can deviate a lot from the average driving style. Moreover, the power-to-mass ratio may limit the driving style with certain vehicles. Eventually, everybody drives in the same traffic flow, hence globally, or on average, there may be little differences in driving behaviour, but in the details large differences can be observed. For example, accelerating from a stop to 100 km/h on the motorway may take as short as 10 seconds for a high powered car, or as much as 60 seconds behind a heavy-loaded truck. In both cases the total $v \cdot a_{\text{pos}}$ (velocity times the positive acceleration), which is a commonly-used trip characteristic, is the same (i.e. $\sim v^2$). If this total is combined with data of constant driving to make up the total distance, the average will be the same as well. On the other hand, emissions in the first case can be twentyfold higher than in the second case, which is not compensated by the shorter period of acceleration.

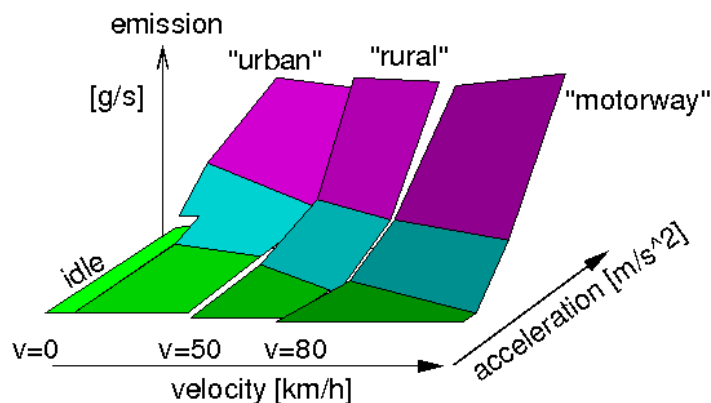


Figure1. The emission rates in VERSIT+ are fitted as ten piecewise constant and linear parts which shapes follow the general contour lines of the emission maps.

3. Data collection

The test program was set up to cover many eventualities, and to collect as much data as possible. Moreover, the data itself, i.e. without any analysis or filtering, should be representative for the span, the variation, and the average of Dutch driving behaviour. The program was carried out by randomly following vehicles across the Netherlands. The velocity was recorded in different ways, as is shown in Figure 2. The calibrated wheel rotation sensor, part of the ABS, was determined to be the most accurate. The signal was robust as well, as the signal was always available. The velocity reported by the on-board diagnostic (OBD) is somewhat stylized, as shown in the figure. The optical sensor gave a poor signal, whereas the GPS does not follow the true velocity but instead seems to be filtered and delayed with fast connections from time to time.

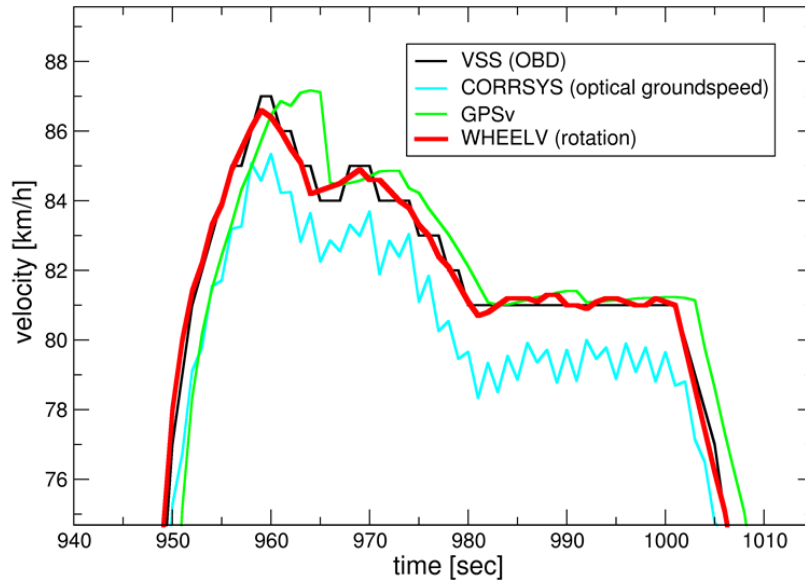


Figure2. Comparison of different velocity signals what were recorded during the test program

The vehicle used for the test program was high-powered with automatic transmission to allow for the following of all other vehicles in normal Dutch driving. The program was carried out by a professional driver. The driver used the navigation system to drive from one location to the next. These locations usually were inner-city locations that were 30-40 km apart, resulting in a proper distribution of urban, rural, and motorway driving, as is shown schematically in Figure 3. On a single day, about 10 such sub-trips were driven. A greater part of the Netherlands was covered.

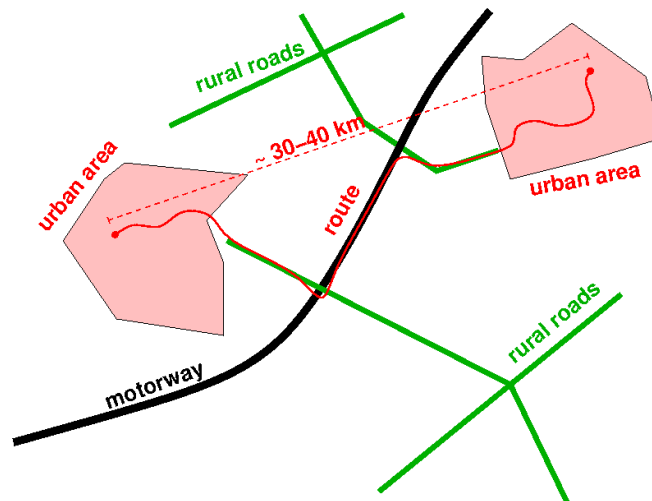


Figure3. A typical trip driven during the test program, including urban driving, rural driving and motorway driving

The driver was given the following instructions:

- The first priority is safe and legal driving. If a car is speeding and the driver considers it safe to follow, than the speeding car should be followed for 30 seconds. In the course of the project, one speeding ticket was obtained on an 80 km/h rural road with an actual speed of 90 km/h. More incidents of speeding did occur.

- After every sub-trip, a five to ten minutes pause is taken, at an appropriate parking space. The equipment is left running. During the day one or two longer breaks must be taken, to avoid drowsiness.
- The driver will follow cars in the same direction at a constant distance, so to reproduce the driving of the car in front. The driver will attempt to follow the passenger cars and vans with the license plate where the first number is the lowest. If a car passes, or is passed, in the lane directly adjacent with a lower number this car will be followed for as long it drives in the same direction.
- If a car is going in a different direction the nearest vehicle in front is to be followed.
- If no car is available to be followed, the driver will drive the speed limit (on the vehicle display) for that road section.

In total about fifteen days of driving were planned. This included the morning rush-hour, starting at 7:30, and two evenings of driving to monitor the driving behaviour on the parts of the motorway network where higher speed limits apply during evening and night (from 7 PM to 6 AM). An appropriately large headway distance was used during driving, such that the actions, i.e., braking and accelerations, of the car in front were not enhanced by the car follower, in order to maintain constant headway. Slower vehicles using the right-lane on motorways were included as well. Cars stuck behind trucks on the motorway are easily ignored due to the lack of space and time to merge behind smoothly. During the first days of testing the instructions were augmented to include the following:

- Each car is to be followed at least for a few kilometres, before a lower license plate number is selected. This was done in order to avoid constant switching of cars.
- If the driver of the car in front appears to be aware that he or she is being followed, the following is to be abandoned. This phenomenon occurred a couple of times in the 15 days of driving.

The experiences of the driver were the following. In urban driving there was very little choice but to follow the car in front. This means that in urban trips usually only a few cars were followed. On the motorway, some cars accelerated quite aggressively, in particular if a slower vehicle was blocking the left lane for some time. As the slower vehicle vacated the left lane, some tailing cars sped off. The 130 km/h sections on the motorway were often short and/or the 130 km/h stretch was poorly indicated. As a result, many cars drive at a slower velocity. Only in the northern provinces the long stretches of daytime 130 km/h speed-limit motorways seem to have led to a substantial velocity increase in (average) driving velocity compared to the 120 km/h speed limit.

In total, the project resulted in 108 hours of recorded driving time. In this time, a distance of 6640 kilometres was travelled, consisting of 180 trips. Of this time, twelve days consisted of typically 11 ordinary trips per day. To increase the share of rural driving the motorway was avoided on one testing day. The testing period started at the end of the last school summer holiday period on August 31st 2015 and ended on September 21st 2015. It included two weekday evenings, a Saturday, and a Sunday. On some days a substantial amount of motorway congestion was observed, typically associated with traffic incidents.

The collected data consists of velocity signal and latitude and longitude information. During the trip, a front-view camera was recording, making it possible to check particular incidents in the velocity data. In practice, the camera recording did not add much to the current study. The velocity data was accurate and did not contain unexpected, or improbable, results. The velocity data is very rich and diverse. For example, as Figure 4 shows, congestion on the motorway does not have a natural pattern which uniquely identifies congestion, but varies smoothly from free-flow towards stop-and-go. However, notably is the oscillatory behaviour of variations of 40 km/h while entering and leaving a region of heavy congestion on the motorway.

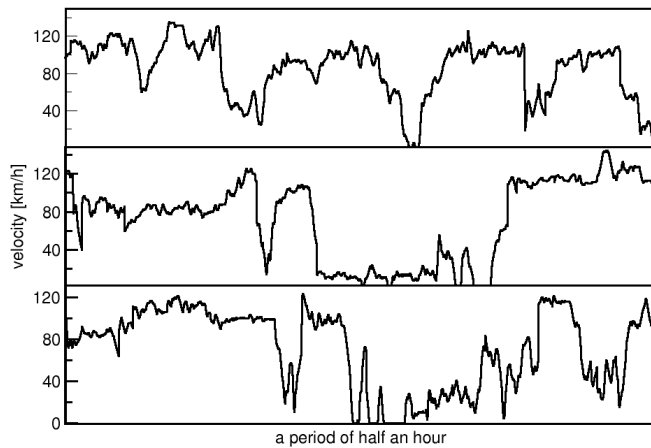


Figure 4. Three arbitrary selections of motorway driving in the case of reduced velocity. The dynamics seems especially large around 50 km/h.

4. Verification using radar data

The car-chasing technique is a method to collect a representative sample of driving behaviour on roads and routes of interest. The accuracy and representativeness of the collected data depends on the capabilities of the driver in the instrumented car. In a later stage of the project, a radar was instrumented in the chase-car to not only collect the data of the instrumented car itself, but also the velocity and acceleration data from the car in front. The radar determines the distances and relative velocities of multiple targets. The radar also detects stationary objects and objects further away. If the stationary targets are removed and the closest target from the remainder is selected, a majority of the radar data has a target identified as a car in front.

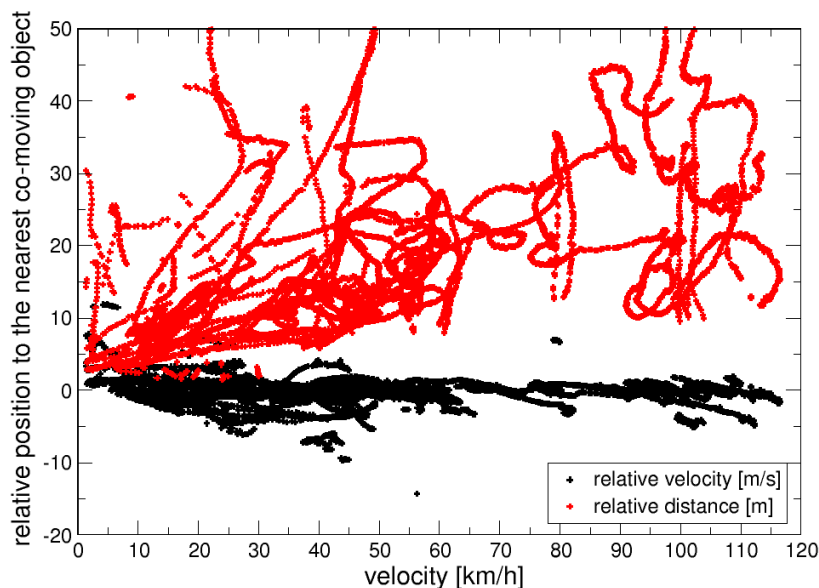


Figure 5. The radar data from a trip of 1800 seconds, with the relative velocity [m/s] in black, and the relative distance [m] in red. For 64% of the time a co-moving object is identified.

From the radar data it seems more appropriate to use the combination of vehicle velocity and radar distance to determine the driving behaviour of the cars in front, with respect to the instrumented car, than to use relative velocity or relative acceleration, as shown in Figure 5.. The reason is simple: there is no instantaneous relation between the two vehicles, but a delayed reaction dependent of the velocity and inter-vehicle distance. In the case of a perfect car-chase: a 3 seconds delay with the car in front, with a slow change to the ideal car distance of 15 metres and the additional distance associated with one second delay. The simulation shows a natural variation the in the inter-vehicle distance, even if the driving behaviour is perfectly replicated with a delay.

Even in an ideal case the variation of the inter-vehicle distance is 10-15 metres. The variation observed in the radar data therefore seems only natural. Hence it is not expected, due to the delay of the car-follower, that the velocity difference is always zero. However, the velocity difference is centred tightly around zero.

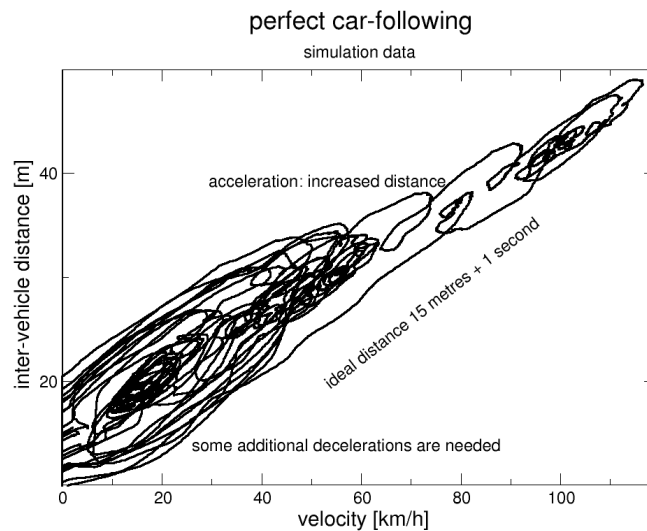


Figure 6 The perfect car following with a constant time delay is possible, except for a few cases of hard decelerations, where additional braking of the car-follower may seem required.

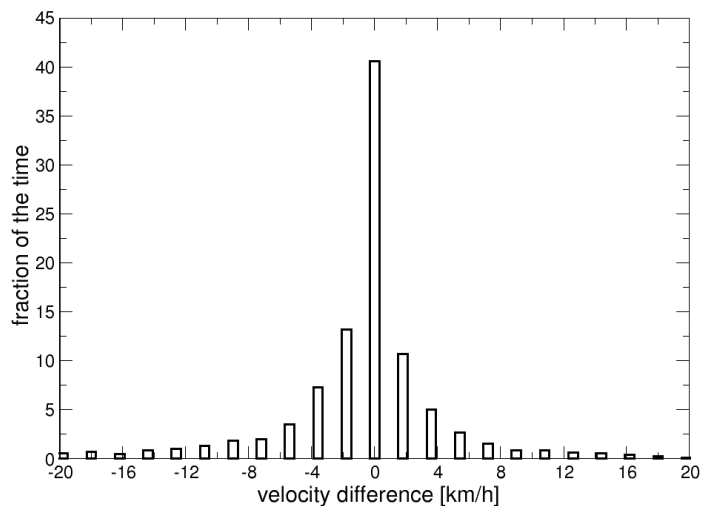


Figure 7. The time shares of velocity differences with the car in front from the radar data.

Figure 7 shows the time shares of the velocity differences with the car in front as derived from the radar data. The difference in velocity is smaller than ± 0.5 m/s for 41% of the time, despite the delayed reaction from the chase-car. If a delay, or reaction time, is assumed, the velocity differences of the car in front and the following car is even smaller than based on the radar-based velocity difference alone. In that case almost 50% of the time the velocity difference is in between the ± 0.5 m/s. The comparison of accelerations is less straightforward as the numerical differences of the radar and vehicle velocity signals are somewhat noisy, which affects the quality of the comparison of accelerations. The symmetric distribution of the velocity differences, as shown in Figure 8, indicates there is limited bias. If the car accelerates harder to catch up than decelerates to keeps its distance, the positive velocity difference would be larger than the negative velocity difference.

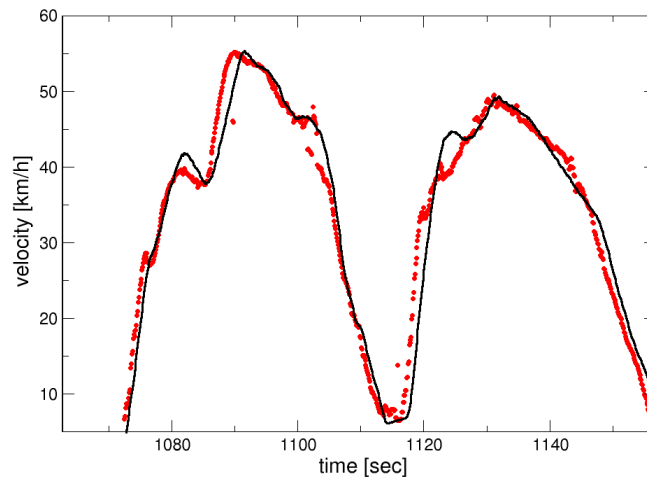


Figure 8. A sample of typical data of the chase car in black and the radar data in red. Occasional signal loss in the 10 Hz radar data can be observed, and the car in front reacting about one second ahead of the chase car.

From these preliminary analyses it is clear radar data can assist to check the accuracy of the car-chasing technique. In over 40% of the time the velocity difference is less than ± 0.5 m/s. Moreover, the correlation between the acceleration of the instrumented car and the velocity difference with the car in front is:

$$v_{\text{difference}}[\text{m/s}] \sim 0.84 * a_{\text{chase}} [\text{m/s}^2]$$

which corresponds with a delayed reaction of 0.84 seconds in both the case of acceleration and deceleration. The systematic deviation occurs in transients where the instrumented car reaches the same velocity about 0.84 seconds later. Such delay is common for human reaction times. Velocity differences occur mainly at low acceleration. Hence they are not related to increased dynamics for transient driving. The data shows little hints of deviating dynamics apart from the delayed reaction. Therefore it is concluded that some deviation exists between the driving behaviour of the car in front and the chase car. However, these differences are small. Moreover, there are no indications that a systematic bias is introduced with this method, and with this driver, of obtaining representative behaviour on the road.

5. Data processing and analysis

The velocity data was linked to the different road types using the National Road Database NWB of January 1st 2015. The NWB contains all road segments in the Netherlands per maintainer (national government, province or municipality). These maintainers have been used as a proxy for the generic definitions of motorway, rural, and urban. Since the GPS data has limited accuracy, the map of the Netherlands was divided into 0.00250×0.00250 squares. In the case a motorway was present in a square, the data was assigned to the motorway, if a provincial road was present the road type was designated rural, and otherwise a urban road was assumed. Periods of limited accuracy and signal

loss, for example caused by driving through tunnels, sometimes occurred on motorways and rural roads. In such cases, the last-registered road type was retained for a period of 50 seconds.

The resulting breakdown of the recorded data is shown in Table 1. The high fraction of motorway seems natural for Dutch driving. However, the data is slightly biased by a number of special motorway trips in the evening to cover the evening driving styles, resulting from different speed limits.

Table 1. Total distance covered in the test program by road type

Road type	Distance covered (km)	Driving time (h)	Average speed (km/h)
Urban	835	32	26
Rural	1,179	22	53
Motorway	4,625	53	87
Total	6,640	108	62

Time dependence of driving behaviour

The test program was performed throughout the day, including at least one rush hour, but in many cases both the morning and the evening rush hour was included. Nowadays the traffic intensity in the Netherlands varies only limitedly throughout the day from 7:00-18:30, and only a few percent more traffic in the rush hour periods is enough to tip the balance and generate congestion. Hence, the program is more or less representative for the total distance travelled.

In order to estimate the effect of the morning rush hour on the average velocity, the data was grouped into start times before 9:00, the period 9:00-16:00, and after 16:00. A full trip is used to avoid bias from a long congestion period spilling over after the normal rush hour. The trips that start before 9:00 have an average velocity of 70.8 km/h +/- 12.6 km/h. The 9:00-16:00 trips have an average velocity of 72.1 km/h +/- 11.5 km/h. After 16.00 the average is 65.8 km/h +/- 22.1 km/h. The evening rush-hour seems to have some heavy congestion periods, typically caused by incidents, yielding a lower average velocity and larger variation, unlike the morning rush hour which yields a similar velocity distribution as the rest of the day.

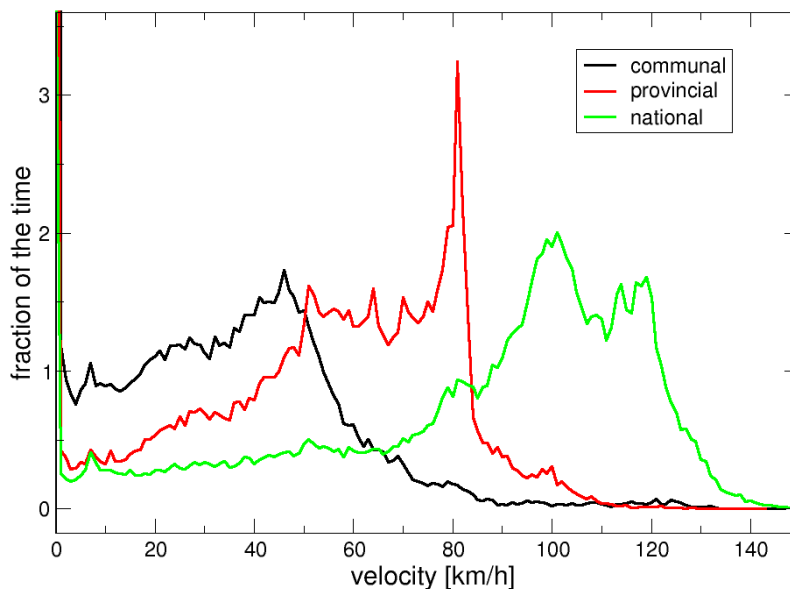


Figure 9. The distribution of velocities for the main road types. Speed limits show up as spikes. Above 120 km/h the picture is more diffuse because drivers do not always try to maintain the speed limit as their driving velocity.

Motorway driving

In the case of motorways the different speed limits were deduced from the information published by the Dutch road authority. The coloured maps in Figure 10 for daytime (left) and evening (right) speed limits were used to match the velocity data to the different speed limits on the motorway. This data does not include the dynamic speed limits, associated with an additional congestion lane ("spitsstrook"). This kind of information is not used separately in the current set of emission factors for air quality modelling in the Netherlands. The main speed limit is used for the road segment, not the dynamic speed limit. Hence the lower, yet constant, velocity observed in the case of 120 km/h and 130 km/h, as shown in Figure 11, are probably associated with a reduced speed limit applying throughout parts of the day. The data probably contains significant fractions of reduced speed limits. If the usage of the default emission factors is changed to separately incorporate lower speed limits, e.g. in the case of congestion lanes, this will require an update of the driving behaviour. The frequency of occurrences is hopefully well-represented by the collected velocity data.

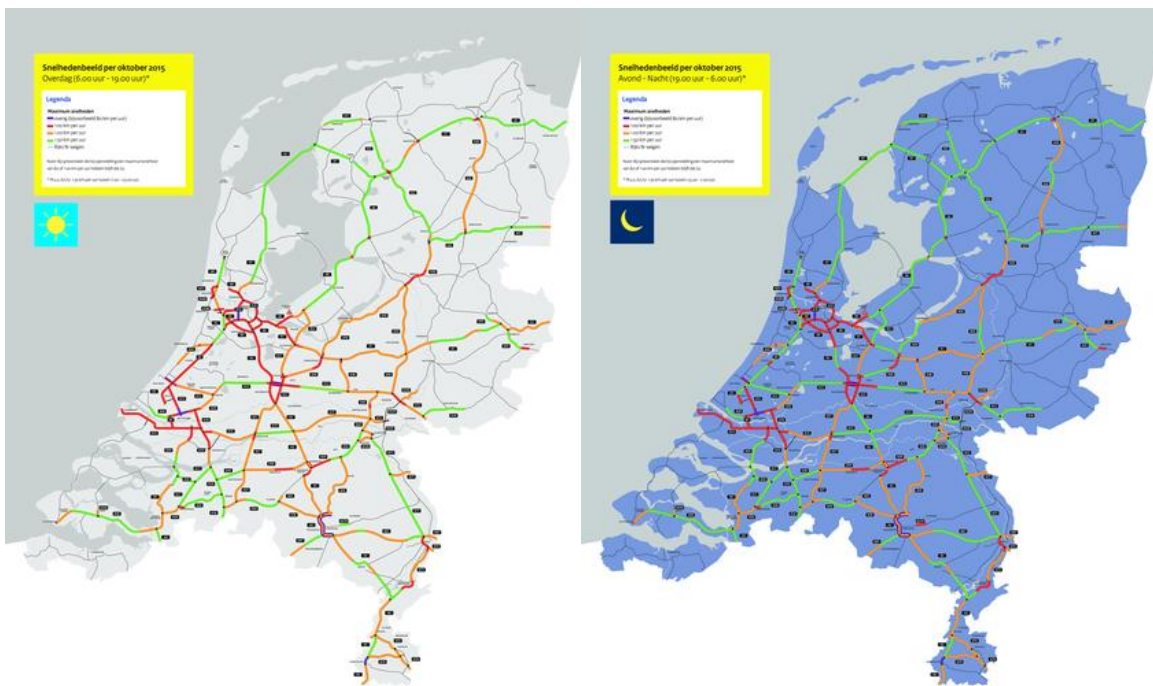


Figure 10. The daytime (6:00-19:00) and night-time (19:00-06:00) velocity limits on the motorway as published by the Dutch road authority for the period during which the current study was executed (green: 130 km/h, orange: 120 km/h, red: 100 km/h, and purple: 80 km/h).

The data assigned to motorways is divided into the different speed limits on the basis of the maps shown in Figure 10. However, the maps are not very accurate. Therefore 2 x 2 km blocks are used to assign velocity data to the appropriate speed limits. This poses a minor problem for the identification of the limited number of road sections of 80 km/h, which are typically short. An overlap of 2 kilometres already will lead to a significant misrepresentation. In this specific case the velocity data was filtered further.

The emission factors are generated for different situations on the motorway. The following velocity data is underlying the different categories:

- Motorway average: all motorway data (used for determining national emission totals);
- Motorway congestion: all motorway data below 50 km/h;
- Motorway 80 km/h with strict enforcement: motorway data at 80 km/h speed limit locations, truncated at 80 km/h and standard above 50 km/h for all free flow situations;
- Motorway 80 km/h without strict enforcement: motorway data at 80 km/h speed limit locations

truncated at 90 km/h (to exclude crossover data to higher speed limits);

- Motorway 100 km/h with strict enforcement: motorway data at 100 km/h speed limit locations truncated at 100 km/h;
- Motorway 100 km/h without strict enforcement: all motorway data at 100 km/h speed limit locations;
- Motorway 120 km/h: all motorway data at 120 km/h speed limit locations;
- Motorway 130 km/h: all motorway data at 130 km/h speed limit locations;

It should be noted that the velocity distribution obtained in this study is slightly higher: a few km/h than observed in averaged, and localized, data from different motorway induction loops. The amount of low velocity data is representative for the amount of congestion observed in 2015, prior to the last quarter.

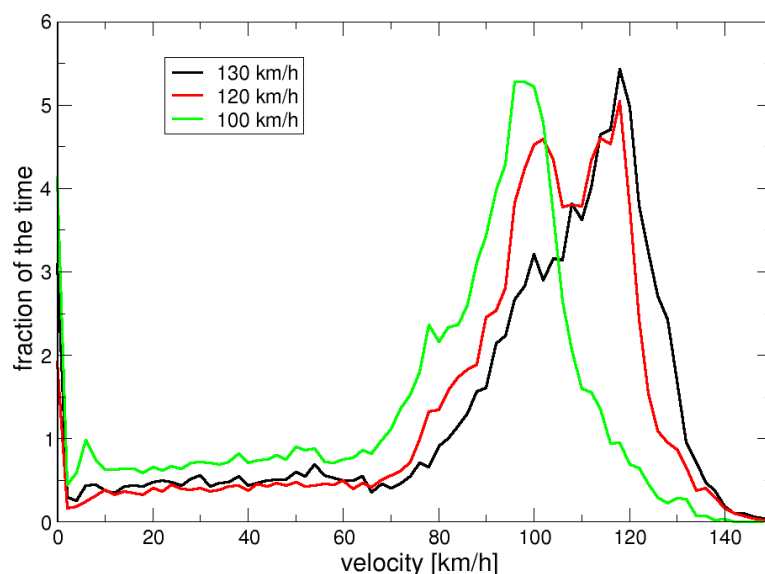


Figure 11. The distribution of velocities for the three main motorway velocity limits. The second peak at 100 km/h at the 120 km/h speed limit may be partly due to congestion lanes (additional lanes that are made available during rush hour), with a reduced dynamic speed limit.

The definition of strict enforcement and the implementation thereof in the driving behaviour has been a matter of some debate in the Netherlands. The enforcement by camera's to register the time travelled over a longer distance is usually assumed. There is no data available of the road segments where such enforcement was present during the study period. Instead, the data was separated into all velocity data for a given speed limit as the normal situation. A subset of velocity data with only data below the actual speed limit is used as the velocity data in the case of strict enforcement of the speed limits.

Congestion driving on motorways

From the velocity data there are strong indications that the driving dynamics at intermediate velocities (40 km/h – 70 km/h) are larger than at low or high velocities (Figure 12). At the onset or end of heavy congestion, with an average velocity below 20 km/h, drivers seem eager to maintain a high(er) desired velocity, which leads to velocity oscillations in the traffic flow, with high dynamics and, consequently, high pollutant emissions as a result. At the moment, in the determination of emission factors in the Netherlands, congestion is defined as all speeds under 50 km/h. This means the highly dynamic driving behaviour at velocities between 50 and 70 km/h, and the high pollutant emissions

associated with this, go unnoticed in the current approach, and is part of the dynamics underlying the emission factors in the free-flow situations.

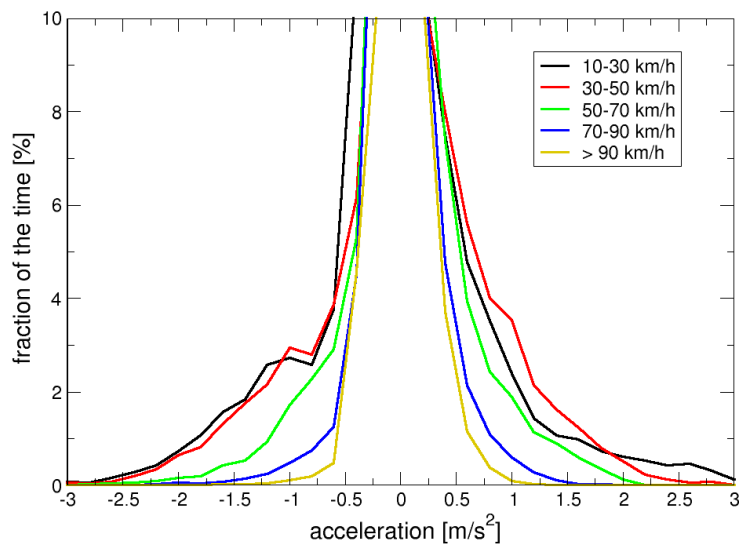


Figure 12. The distribution of accelerations in different velocity ranges on the motorway. Notably, the 30-50 km/h range has more accelerations of 1 m/s^2 .

In urban driving, the magnitude of acceleration decreases with increasing velocity, as shown in Figure 13. This is not the case however on the motorway: the high accelerations ($> 1 \text{ m/s}^2$) occur mostly at velocities in between 30-50 km/h. The actual magnitude of the fraction is determined by the amount of deliberate accelerations over the amount constant driving. Rural driving has more stops and therefore a higher fraction of deliberate accelerations, above 1 m/s^2 , but from a stop the high accelerations occurs mainly at lower velocity.

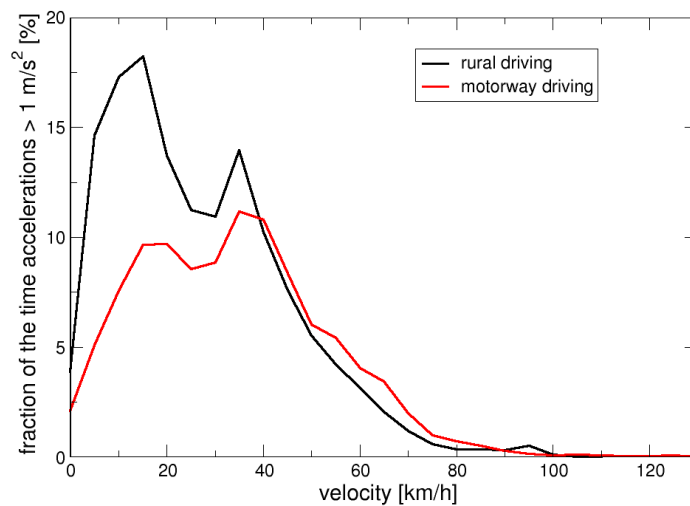


Figure 13. The fraction of accelerations above 1 m/s^2 decreases with velocity for rural driving, while a maximum occurs at 40 km/h for motorway driving.

The maximum acceleration of the vehicle strongly depends on the velocity. Given an average car of 75 kW and a weight of 1300 kg, the maximum acceleration, ignoring gear ratios and driving resistance is:

$$a_{\max} [\text{m/s}^2] < 200/v [\text{km/h}]$$

Hence, as the velocity increases the physical limitations for hard accelerations are large. Given the increase in air-drag and rolling resistance with velocity, this limitation is an over-estimation. Generally, it is therefore expected that the magnitude of acceleration decreases with velocity. The fact that most hard accelerations occur at 40 km/h on the motorway is due to the specific driving dynamics related to traffic intensities close to the critical intensity. These types of oscillations are well-known phenomena in the study of phase transitions and critical, i.e., unstable processes. Hence, the current decision to set the boundary of motorway congestion at 50 km/h in the Netherlands is, in hindsight, an unfortunate one for determining representative real-world emission factors for different driving dynamics. The data collected in the current study indicates that a boundary at 65-70 km/h is more natural. In the latter case the increased vehicle dynamics, with an associated increase in pollutant emissions, is properly assigned to the change due to the increased congestion.

Rural driving

The rural driving data is associated with provincial roads where on the through roads the typical speed limit is 80 km/h, but occasionally 60 km/h and 100 km/h speed limits occur as well. The definition of rural roads in the current study is based on the road maintainer and it usually transcends the local roads and the different city limits. The 80 km/h speed limit shows up very neatly as an isolated peak in the velocity data, as Figure 9 shows.

Contrary to general understanding, the number of stops and driving at low velocity is limited on rural roads in the Netherlands. Only in the case of agricultural mobile machinery situations of low velocity and even stop-and-go traffic occur. Clearly, in many cases these roads do not reach their maximum capacity, and free-flow conditions are common. Very likely the bottlenecks for the intensity lie at the urban or the motorway end of the rural road. It is also possible that the capacity is not tuned across the network, and a few bottlenecks ensure a limited intensity in general and free-flow conditions on the remainder of the network. On motorways, on the other hand, with the removal of successive bottlenecks the whole network is, more or less, critical for congestion and reduced velocity.

Urban driving

The pollutant emission factors for urban roads in the Netherlands are derived for three different driving situations: congestion, normal driving and free-flow driving. In order to make the distinction between these three, according to the official definitions in the air quality assessment of average velocity and number of stops, the average velocity over a kilometre was determined in the urban velocity data. The instantaneous velocity data would lead to a strange bias where stops are associated with congestion only, as is shown in Figure 14. The distance of 500 metres behind and 500 metres ahead are included in this determination of the average velocity. Driving behaviour associated with congestion may not necessarily be associated with a high urban traffic intensity (i.e., stop-and-go traffic), but a low average velocity can also be the result of traffic lights, narrow streets, sharp bends, consecutive junctions, speed bumps, or 30 km/h zones.

The three congestion classes for emissions (congestion, normal and free flow) are based on representative situations. These situations are assumed to be the middle of the band in which all the driving behaviour lies. Therefore the velocity data is binned according to the average velocity below 20 km/h and above 30 km/h. Normal urban driving is at an average velocity in between 20 km/h and 30 km/h. This definition deviates slightly from the official definition in the air quality assessment of velocities below 15 km/h. The average velocity at a location is slightly lower than the average velocity over a kilometre, as the parts with the highest velocity usually dominate the latter. Therefore, in light of the different average velocity determination, instead of a lower limit of 15 km/h for normal driving a limit of 20 km/h is used. The resulting velocity distributions are shown in Figure 15.

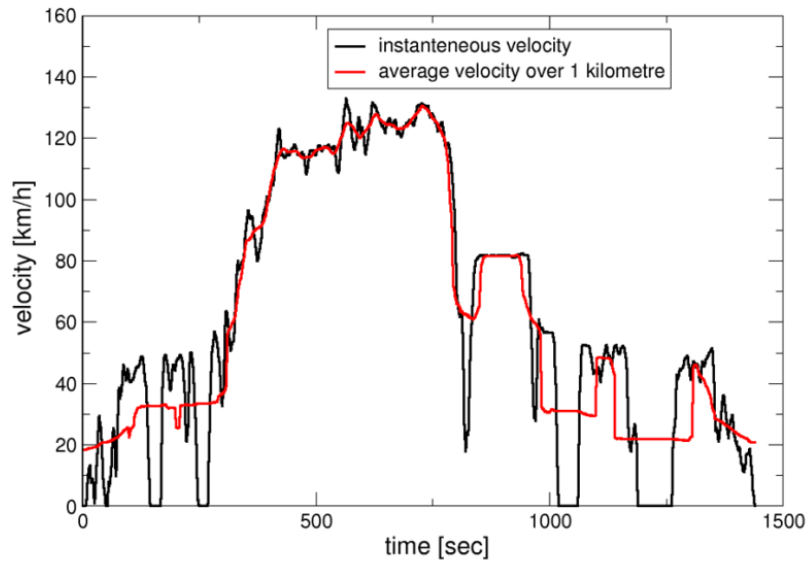


Figure 14. The instantaneous velocity and the resulting average velocity by averaging over one kilometre (500 metre before and 500 metre after). Despite the stops, the average velocity is associated mainly with normal and free flow driving.

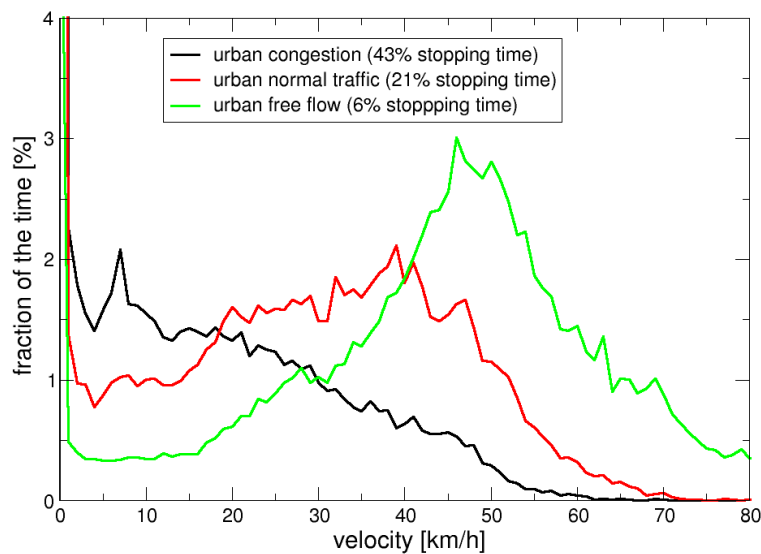


Figure 15. The velocity distribution of urban driving in the three urban classes. The fraction of stopping time ($v < 1$ km/h) is off the scale and they are indicated in the legend.

Prior to the current study, the “average urban driving”, as used in the Dutch emission inventory (PRTR) for air pollutants, was assumed to be identical to the “normal urban driving”, as used in the in the Dutch default calculating method (SRM I) for air quality modelling. Given the representative collection of velocity data, a distinction between average and normal is now possible. The sum of congested, normal, and free-flow driving can be weighed to an average based on the frequency of

occurrences in normal trips throughout the Netherlands including both large and smaller cities. In the current study, 18% congested, 25% normal, and 57% free-flow urban distance at average velocities of 12 km/h, 25 km/h, and 44 km/h respectively are found. Consequently, the average driving that is used for the PRTR leads to a slightly higher average velocity and lower dynamics than normal driving used for SRM I, due to the relatively large share of free-flow driving at relatively high velocity.

A substantial part of urban free-flow driving is above the typical Dutch urban speed limit of 50 km/h. In part this may be the result of speeding, but in part this also is the result of higher speed limits on the main access roads into different cities.

The driving behaviour as was determined in the current study serves as input for the emission model VERSIT+. VERSIT+ uses tables with the fractions of time of driving at different velocities and accelerations normalized to 1 kilometre of total distance travelled (Ligterink & De Lange, 2009). The driving behaviour vectors allow for different emissions to occur in the case of hard accelerations in urban, rural, and motorway driving. Generally, the emissions do vary in the three cases as, for example, accelerations in urban situations are usually hard but short, while on the motorway, due to the limited power available, accelerations are lower but more prolonged. The emission measurements determine the actual effect of hard accelerations in the different cases.

Conclusions

For the first time the driving behaviour recorded on the road is directly translated to the driving behaviour underlying the Dutch pollutant emission factors for air quality modelling and for the national emission inventory, without restrictions, pre-selection, or filtering of the data. Moreover, all driving behaviour is determined in the same period, and can be characterised as the state of affairs in 2015, producing a coherent picture across the different traffic situations for the current driving behaviour on the Dutch roads. The velocity data in itself is collected in a manner representative for the average driving on the Dutch roads. Velocity data is collected from the wheel rotation sensor, which is much more accurate and reliable than GPS velocity.

The changes from previous studies and results are not major, but some changes are systematic. The driving dynamics are larger across all traffic conditions than previously assumed, which makes the pollutant emission factors less dependent on the average velocity alone. In particular, the reduced velocity on the motorways, still above 50 km/h, increases the dynamics in motorway driving. This type of driving dynamics is the result of the onset of congestion, where cycles of acceleration and deceleration occur. The current study indicates that motorway congestion should be defined as driving below 65-70 km/h, instead of the current limit of 50 km/h. Because of the current limit of 50 km/h these driving dynamics between 50 and 70 km/h are included in the emission factors for non-congested driving. Since these dynamics can contribute significantly to total emissions, the effects from reduced speed limits on the motorway itself are, for example, expected to be somewhat smaller, as part of the emissions result from dynamic driving.

Major cities are incorporated several times in the typical trips, smaller cities are included fewer times, but do add up to about half of the urban driving. The trip length ensures a proper representation of urban, rural, and motorway driving in the total data. Navigation equipment is used for the actual route. The fraction of rural driving is somewhat lower than expected. This may in part be due to the definition of urban, rural, and motorway, based on the road maintainers from the national road database, instead of speed limits or road signs. However, an additional route was designed to enhance the rural velocity data.

These results apply to passenger cars and vans and reflect the situation on-road in 2015 in the Netherlands. In order to keep the driving behaviour underlying the pollutant emission factors up-to-date, new data should be collected on-road every few years. A similar study should be carried out for trucks as well, as there is very limited, and largely outdated information on the driving behaviour of trucks in the Netherlands.

Acknowledgments

This work was supported by the Dutch Pollutant Release and Transfer Register.

References

André, M. (2004) : The ARTEMIS European driving cycles for measuring car pollutant emissions. Science of the Total Environment, p. 73-84.

André, M., R. Joumard, R. Vidon, P. Tassel & P. Perret (2006) : Real-world European driving cycles, for measuring pollutant emissions from high- and low-powered cars. Atmospheric Environment 40, p. 5944-5953.

Balau, A.E., D. Kooijman, I. Vazquez Rodarte & N. Ligterink (2015) : Stochastic Real-World Drive Cycle Generation Based on a Two Stage Markov Chain Approach, SAE Int. J. Mater. Manf. 8(2):390-397..

Barlow, T.J., S. Latham, I.S. McCrae & P.G. Boulter (2009) : A reference book of driving cycles for use in the measurement of road vehicle emissions, Version 3. TRL Limited.

Boulter, P.G., T. Barlow, I.S. McCrae, S. Latham, D. Elst & E. van der Burgwal (2005) : Road traffic characteristics, driving patterns and emission factors for congested situations, TRL Limited, Wokingham & TNO, Delft.

Eenink, R., Y. Barnard, M. Baumann, X. Augros & F. Utesch (2014), UDRIVE: the European naturalistic driving study, Transport Research Arena 2014, Paris.

Gense, N.J.J., H.C. van de Burgwal & D.A.C.M. Bremmers (2001) Emissies en files. Bepalen van emissiefactoren. TNO 01.OR.VM.043.1/NG, TNO Automotive, Delft.

Lange, R. de, A. Eijk, T. Kraan, U. Stelwagen & A. Hensema (2011) Emissiefactoren voor licht wegverkeer bij maximum snelheid van 130 km/u op autosnelwegen, TNO-060-DTM-2011-03219, TNO, Delft.

Lenaers, G., K. Scheepers & G. Camps (2007), Vergelijkende metingen van emissies en verbruik aan een bus van De Lijn rijdend op PPO, biodiesel en diesel, VITO.

Ligterink, N.E. & R. de Lange (2009) : Refined vehicle and driving behaviour dependencies in the VERSIT+ emission model. ETTAP Conference Toulouse.

Pathak, S.K., V. Sood, Y. Singh & S.A. Channiwala (2016) : Real world vehicle emissions : Their correlation with driving parameters. Transportation Research Part D, p. 157-176.

Smit, R., M. Keuken, A. Hensema, R. van Mieghem & P. Zandveld (2006) Effecten van 80 km/uur in combinatie met "compact rijden" op netwerk- en wegvakemissies van PM₁₀, NO_x, CO₂ en brandstofverbruik en immissies van PM₁₀ en NO₂ in 2010 rondom snelwegen bij Amsterdam, Rotterdam, Utrecht en Den Haag (Fase 2). TNO IndustrieenTechniek, Delft.

TNO (2016) Performance and analysis of vehicle emission measurements, TNO, Delft.

A new approach for systematic use of PEMS data in emission simulation

C. Matzer¹, S. Hausberger¹, S. Lipp¹ and M. Rexeis¹

(1) Institute for Internal Combustion Engines and Thermodynamics, Graz University of Technology, Inffeldgasse 19, 8010 Graz, Austria

Fax +43 316 873 30262 - email: matzer@ivt.tugraz.at

Abstract

Using on-board emission tests from portable emission measurement systems (PEMS) is becoming more and more a common approach for real world emission testing of passenger cars (PC), light commercial vehicles (LCV) and heavy duty vehicles (HDV). The advantages against chassis dyno tests are the high robustness to obtain unbiased emission levels and to cover a lot of real world driving situations. Disadvantages for the use in emission modelling are the high influence of the route, the driver, traffic conditions and ambient temperature on the resulting emissions. Consequently test results show a high variability for single vehicles and can hardly be used directly to obtain emission factors. Figure 1 shows as example test data from one EU 6 diesel car in 25 PEMS trips and in New European Drive Cycle (NEDC), Worldwide Harmonized Light-Duty Vehicles Test Procedure (WLTP) and European Research Group on Mobile Emission Sources cycle (ERMES) as chassis dyno tests. NO_x measured in the PEMS tests had a factor of 7 between lowest and highest test value. Obviously ambient temperature, engine load and cycle dynamics have high influence on the measured emissions and should be considered in a systematic way to elaborate reliable fleet emission values.

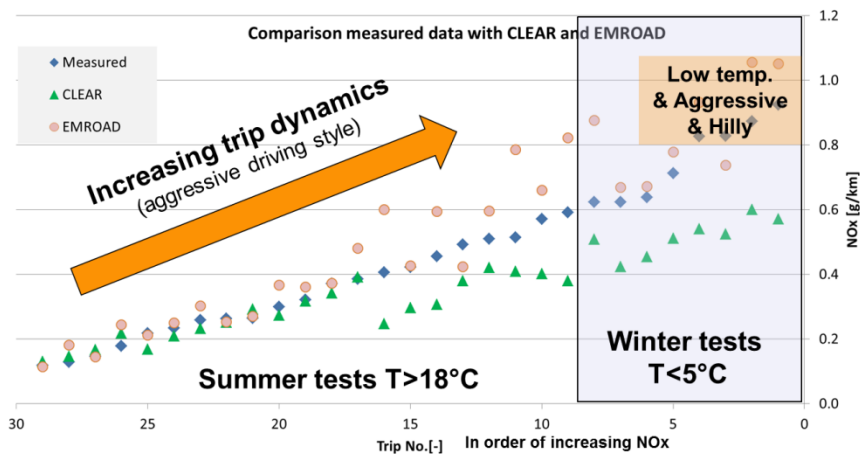


Figure 1: Example for NO_x emissions measured at a EU 6 diesel car in 28 trips (Hausberger S. et al. (2016)).

To solve the new issues in emission simulation the Institute for Internal Combustion Engines and Thermodynamics (IVT) at TU Graz has developed a novel approach to integrate PEMS tests into the Passenger car and Heavy duty Emission model (PHEM). The model PHEM is used to calculate real world emissions for PC, LCV and HDV, e.g. (Rexeis M. et al. (2013)). PHEM simulates engine power and engine speed based on longitudinal dynamics and interpolates base emission values then from engine emission maps. Depending on vehicle class and technologies also the influences of dynamic load changes and of the space velocity and temperature in the exhaust gas after treatment systems are considered for the tailpipe emissions.

To simulate representative fleet average emissions per vehicle class, from all vehicle emission measurements engine emission maps are calculated. The emission maps are produced by PHEM by sorting the instantaneously measured emissions into standardized maps according to the actual engine speed and torque. Average emission maps from all tests are obtained by averaging the single maps in normalized formats. To produce representative engine maps tests from many vehicles shall be included and realistic driving situations shall be used. Consequently the inclusion of PEMS data would be very beneficial for the PHEM simulation if done properly.

Since a reliable torque signal most often is missing in PEMS test data, PHEM offers now a new option to calculate the engine power from measured CO₂ mass flow (or fuel flow) and engine speed based on generic engine efficiency maps (Figure 2). Thus only engine speed needs to be measured beside the standard emission components to compile engine emission maps for the measured vehicle. To improve the accuracy of the allocation of emissions and engine speed the method to correct for variable transport times of the exhaust gas implemented in the ERMES Tool can be applied.

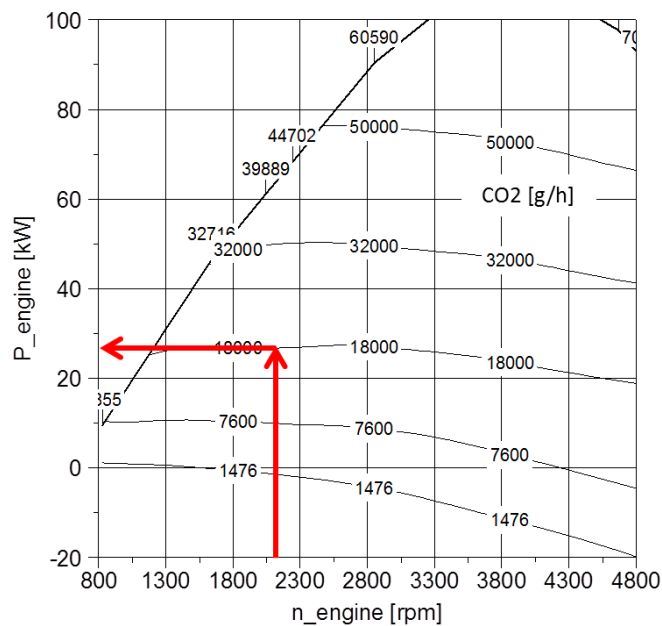


Figure 2: Example for interpolation of the engine power from a generic CO₂ map.

With this method all new data from PEMS tests can be integrated into the existing data base from the model PHEM to have a broader number of vehicle tests as basis for future updates of emission factors. The paper describes the method and validation results.

Keys-words: CO₂ interpolation method, engine map, emission, simulation, PEMS.

Introduction

The discussions on defeat device software together with the introduction of on-board emission tests in the vehicle type approval procedure for PC, LCV and HDV led to increasing number of vehicles tested in real traffic with PEMS (Table 1). For EU 5 cars 18% of the vehicles were tested with PEMS while for EU 6 cars already 60% of the vehicles are tested with on-board equipment.

Table 1: Vehicle tests available within the ERMES group.

Category	Test category	No. of vehicles
PC EU 5	Total: Chassis dyno + PEMS (1)	119
	Share PEMS, SEMS	18%
PC EU 6	Total: Chassis dyno + PEMS	93
	Share PEMS, SEMS	60%
LCV EU 5	Total: Chassis dyno + PEMS	24
	Share PEMS, SEMS	42%
HDV EU V	Total: Chassis dyno + PEMS	20
	Share PEMS, SEMS	50%
HDV EU VI	Total: Chassis dyno + PEMS	40
	Share PEMS, SEMS	65%

(1)...additional 190 EU 5 cars shall be available from the SE In-use Compliance test program

Actual emission models have to react on this trend and have to find proper ways to consider the PEMS test data for model parameterization. In the past the main problem was the rather unknown driving conditions during PEMS tests. Nearly none of the PEMS data included a reliable engine torque signal and a simulation of the engine torque with the uncertainties concerning real world air drag, rolling resistance, gradient and loading lead to quite inaccurate assessments of the engine power. Thus from the typically available PEMS data an assessment of the representativeness of the trip was hardly possible.

If the PEMS test data is used only to calculate average emission factors for urban, road and motorway driving, testing on well-defined routes and with “representative drivers” can reduce the uncertainties. However, this approach does rather not allow to elaborate more detailed emission information, e.g. for uphill, downhill driving at different gradients, driving with different loads etc. If the routes used for the measurement campaign prove not to produce representative emission levels in future, approaches based on simple averaging of emissions measured cannot adjust the results ex post. Also a fair comparison of PEMS results from different sources is hardly possible since typically different routes, drivers, loadings and weather conditions are different.

To use emission test data in a highly flexible way the model PHEM converts any emission test on a vehicle into engine emission maps with normalized engine speed and normalized power as parameters. PHEM needs for the map creation engine speed, engine power and emissions measured instantaneously as input.

With the engine emission maps emissions can be simulated for any driving condition. The engine power and speed are in this application computed instantaneously for the given velocity and road gradient cycle and for the user defined vehicle properties and loading situation. Emissions are then just interpolated from the emission map for the power and rpm values. By changing the gear shift model also adjustments in driver behavior and/or transmission systems can be made.

The main obstacle to convert data from PEMS tests into engine maps was so far the missing or unreliable engine power signal. The paper describes a novel method which can solve this problem for any measurement as long as signals for CO₂ and engine speed are available.

The approach was developed after an analysis of engine fuel maps in a PHEM application to assess future CO₂ reduction potentials of different technologies (Hill N. et al. (2015)). The maps measured steady state on engine test beds showed a much better quality than the maps produced

from transient chassis dynamometer tests. Main reasons for the poorer quality of transient maps are the uncertainties in the time alignment between engine torque and fuel flow or CO₂ mass flow.

On the other hand pollutant emission maps are not very representative if measured steady state on an engine test bed. Since vehicle emission tests hardly take place on engine test beds but use typically the entire vehicle either on a chassis dynamometer or with PEMS, in the past the pollutant maps and the fuel consumption maps were calculated from transient vehicle tests as basis for the model PHEM.

The new approach combines now the advantages of both data sources:

- The fuel consumption and CO₂ engine maps are gained from existing engine steady state tests from representative engines. Since the engine efficiencies from engines with similar technology differ only by a few percent between makes and models, the uncertainty from the small engine sample is much lower than the uncertainty coming from inaccurate time alignment when the map was produced from transient tests. The accuracy of the CO₂ simulation thus is increased in PHEM by using generic fuel maps.
- Since the fuel consumption and CO₂ engine maps are defined now by generic maps, the engine power can easily be interpolated from the instantaneous engine speed and CO₂ mass flow or fuel flow as shown in the abstract. Since engine power is calculated from CO₂ errors in the time alignments between engine power and pollutant emissions can be excluded, as long as the time alignment between the different exhaust gas components is not wrong. Thus signal misalignments are restricted to engine speed and CO₂. Since engine speed usually changes less dynamically than the torque, the influence of misalignments is reduced compared to the former method. To reduce the remaining uncertainty also a new method for variable time alignment of exhaust emissions and engine torque and rpm was elaborated (Weller K. et al. (2016)).
- Since engine speed can be measured quite easily and accurately also in PEMS tests, the new method allows also to convert on-board emission test data into PHEM engine maps as long as CO₂, rpm and some pollutant emissions are recorded instantaneously.

The following chapters describe the new method and show the results of the validation work done so far.

1. Input data for CO₂ interpolation method

To apply the new CO₂ interpolation method for power interpolation, the measured CO₂ and engine speed must be known for each trip. Also a generic CO₂ map is necessary for the interpolation method.

The CO₂ and other emissions are measured and recorded by PEMS in an adequate temporal resolution (1Hz or better). If possible the PEMS also records the engine speed. The signal could be obtained from the CAN-Bus in most of the cases. If not, an additional engine speed sensor could be installed for the tests. Due to a time shift between the measured CO₂ and load signal the CO₂ should be time aligned to the engine speed in an appropriate way. Following options for the time alignment have been investigated by TU Graz (Weller K. et al. (2016)):

- Constant time shift: With a constant offset the CO₂ signal is shifted over the time axis according to a reference signal.
- Variable time shift: The instantaneous emission signals are time shifted for the transport time computed for each time step based on the exhaust gas mass flow rates.

The constant time shift was used for all validations described in the next chapter since the variable time shift was implemented in the software too late to be presented in this paper. In the next months possible improvements in the model accuracy due to the better time alignment shall be analyzed.

The vehicle speed and the altitude for gradient calculations in this paper were recorded by a global positioning system (GPS).

The generic CO₂ map describes the correlation between CO₂, engine speed and engine power. Since engine maps usually are not provided by the OEMs and measurements on the engine test bed from a third party are expensive due to the high effort such data are rarely available. Thus generic maps were elaborated which represent average engine technology for 2013 and 2015 diesel and petrol engines. The data are gained from a CO₂ study for the European Commission (EU), executed

by Ricardo and TU Graz (Hill N. et al. (2015)). Also estimated engine maps for a 2020 engine technology are available.

The generic maps are normalized to allow their application for all power classes. The simplified approach is to scale the same CO₂ map for vehicles with similar engine technologies but different engine capacities. For a validation of the best method for normalization measured maps were normalized and then de-normalized according to the data from another measured engine. The criterion for “best normalization” was to get lowest differences in the de-normalized fuel maps from one engine compared to the original fuel map of other engines with different power. Following cases for investigation of the best normalization were done:

- Case 1: $FC = f(n, P_{engine})$
 - n normalization with $(n-n_{idle})/(n_{rated}-n_{idle})$
 - P_{engine} normalization with P_{engine}/P_{rated}
 - FC normalization with FC/P_{rated}

n ... engine speed in [rpm]
 n_{idle} ... idle speed in [rpm]
 n_{rated} ... engine speed @rated engine power in [rpm]
 P_{engine} ... engine power in [kW]
 P_{rated} ... rated engine power in [kW]
 FC ... fuel consumption in [g/h]
- Case 2: $FC = f(n, p_e)$
 - n normalization with $(n-n_{idle})/(n_{rated}-n_{idle})$
 - p_e normalization with p_e/p_{emax}
 - FC normalization with FC/P_{rated}

p_e ... mean effective pressure in [Pa]
 p_{emax} ... max. mean effective pressure in [Pa]
- Case 3: $FC = f(c_m, p_e)$
 - c_m not normalized
 - p_e normalization with p_e/p_{emax}
 - FC/ normalization with FC/P_{rated}

c_m ... mean piston speed in [m/s]
- Case 4: $FC = f(c_m, p_e)$
 - c_m not normalized
 - p_e normalization with p_e/p_{emax}
 - FC normalization with FC/V_H

V_H ... engine capacity in [l]
- Case 5: $FC = f(c_m, p_e)$
 - c_m not normalized
 - p_e normalization with p_e/p_{emax}
 - FC normalization with FC/h

h ... stroke in [mm]

To find out the best case 2 diesel and petrol engines with similar engine technology but different engine capacity were measured on the engine test bed. As an example, the diesel engine comparison is presented.

Table 2 shows the deviation between two maps, namely of the averaged measured FC from the steady state map of the original 2.0l engine and the averaged FC from the steady state map of the 3.0l engine de-normalized to a 2.0l engine according to the described cases. Similar exercise was done for upsizing the 2.0l engine to 3.0l. The corresponding deviations are also shown in Table 2.

Table 2. Average FC deviations.

	Case 1	Case 2	Case 3	Case 4	Case 5
Deviation between the averaged measured FC from the steady state map of the original 2.0l engine and the averaged FC from the steady state map of the 3.0l to 2.0l de-normalized engine	3.44%	1.87%	5.80%	-4.54%	43.19%
Deviation between the averaged measured FC from the steady state map of the original 3.0l engine and the averaged FC from the steady state map of the 2.0l to 3.0l de-normalized engine	3.22%	2.05%	5.37%	-4.88%	-30.08%

Additionally one significant load point at 1400rpm and 4.7kW was investigated. Table 3 shows the results for the de-normalized engines.

Table 3. FC deviations for one significant load point.

	Case 1	Case 2	Case 3	Case 4	Case 5
Deviation between the averaged measured FC from the steady state map of the original 2.0l engine and the averaged FC from the steady state map of the 3.0l to 2.0l de-normalized engine	0.78%	-2.86%	4.30%	-5.90%	41.16%
Deviation between the averaged measured FC from the steady state map of the original 3.0l engine and the averaged FC from the steady state map of the 2.0l to 3.0l de-normalized engine	1.47%	3.85%	3.50%	6.95%	-28.70%

Case 1 and 2 show the lowest deviations for normalization of diesel and petrol engine maps. Since case 1 was already implemented in the simulation tool PHEM before, this option was chosen to normalize and de-normalize the engine maps according to the fuel map. CO₂ is treated like the fuel flow as separate column in the engine map or simply computed from the carbon content of the fuel as basis for the CO₂ interpolation method.

Furthermore, measurements from the diesel engine show, that the engine out temperature is similar between an engine with small and large cylinder displacement in an engine map with the normalized engine speed and power axis. The same is valid for petrol engines. Therefore the temperature value in the map points is not normalized for engines with different cylinder displacement but engine power and speed are normalized as for fuel consumption and for pollutants as described in case 1.

2. Validation of CO₂ interpolation method

To validate the previously described CO₂ interpolation method, four diesel vehicles with EU 5 and EU 6 exhaust emission standard were measured on the chassis dynamometer and on the road with

PEMS. Table 4 shows main data of the investigated vehicles. The investigation of petrol and of further diesel vehicles will follow.

Table 4. Vehicles investigated in the validation.

Vehicle ID	Segment	Exhaust emission standard	After treatment	Transmission
1	D-segment, 2.0l, 120kW	EU 6	NSC and DPF	6-speed MT
2	D-segment, 1.6l, 77kW	EU 5	DOC and DPF	7-speed AT
3	SUV, 3.0l, 160kW	EU 6	DOC, DPF and SCR	8-speed AT
4	D-segment, 2.0l, 105kW	EU 5	DOC and DPF	6-speed MT

For the measurements on the chassis dynamometer the appropriate settings for Worldwide Harmonized Light-Duty Vehicles Test Cycle (WLTC), ERMES and Common Artemis Driving Cycles (CADC) were used. This means that the road load and test masses in WLTC settings are adjusted according to the WLTP draft, the ERMES and CADC settings according to real world standard. To validate the CO₂ interpolation method a benchmark was necessary. On the chassis dynamometer as reference signal the wheel power from the investigated vehicle provided by the chassis dynamometer in 1Hz was chosen. For the comparison with the power interpolated from the CO₂ map the measured power was recalculated to the clutch with an estimated constant transmission efficiency of 92%. The inertia of the rotational accelerated components was considered in the comparison since the CO₂ interpolation method delivers the “quasi-stationary engine power”. As an example, the comparison for the WLTC with vehicle no. 4 is presented in detail. Since the CO₂ method cannot describe the braking power (lowest value is the motoring power with zero CO₂ mass flow), only the positive power is compared. For the CO₂ interpolation method the measured CO₂, the measured engine speed and the generic CO₂ map from PHEM for 2013 EU 5 diesel engines was used. The measured CO₂ signal was time shifted according to the measured wheel power by a constant offset as explained before. In Figure 3 the measured positive power at the clutch is shown in grey. The dotted black line is the interpolated power at clutch. The interpolated power matches the measured power with an average deviation of -3%.

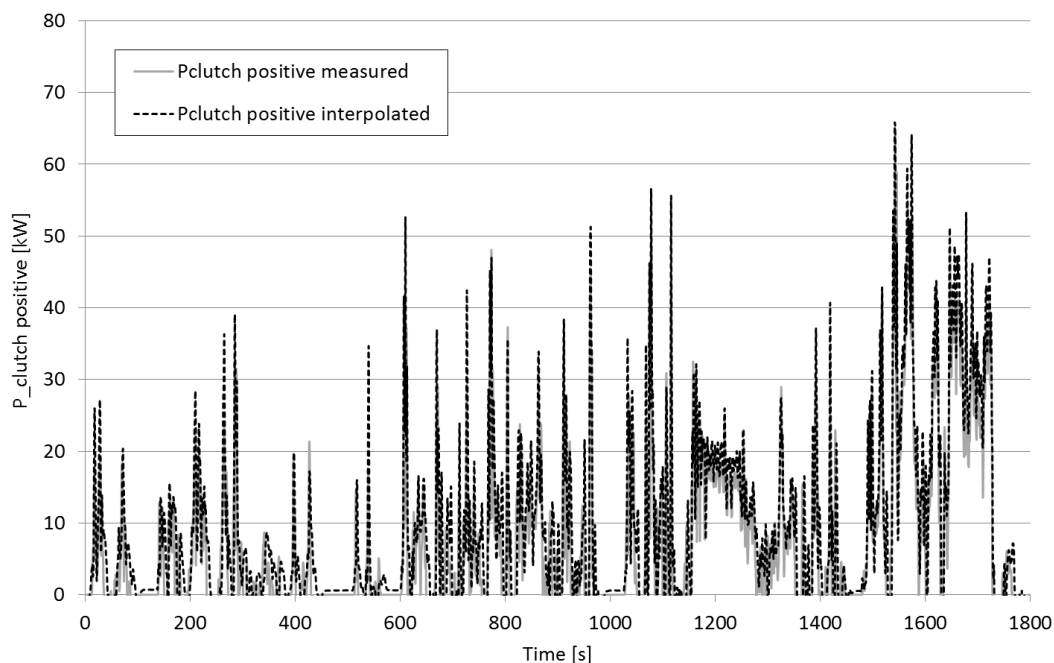


Figure 3: Positive power validation for a D-segment diesel vehicle in WLTC.

The same exercise was done for the CADC urban, CADC road, CADC motorway and ERMES. For the ERMES cycle the average deviation between measured and interpolated positive power was 6%, for CADC between -12% and 8%. In consideration of the generic CO₂ map used for the calculation and the uncertainties in measurement and transmission efficiencies the deviations are in an acceptable range.

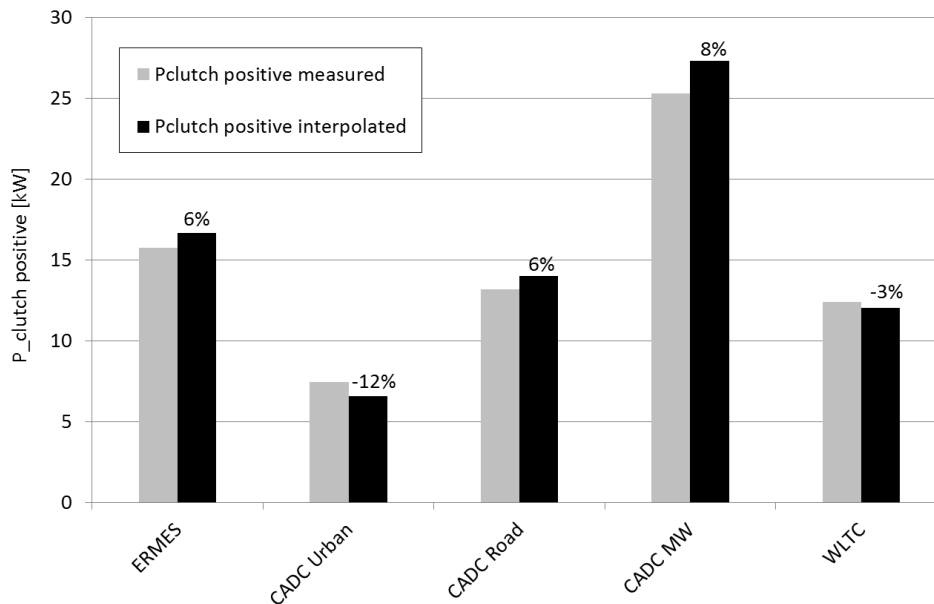


Figure 4: Power deviations between measured and simulated data from a D-segment diesel vehicle.

With improvements of the CO₂ map according to the engine technology of the vehicle investigated the deviations may be reduced (i. e. a higher efficiency in the part load area for this vehicle) but the effort seems not to be justified due many other and larger uncertainties in the emission factors (representative driving cycles and driver behavior, real world rolling and air resistance, average loading, etc.).

The measurements on the road were carried out in accordance with the actual real driving emissions (RDE) draft regulation. The analysis shown includes hot starts. The vehicles were driven by different drivers on different routes. For completeness it is mentioned that not all vehicles were measured on all routes and for testing the repeatability some routes were measured several times with the same vehicle.

The first route is called Ries-Route, which leads from Graz to Sinabelkirchen (east of Graz). The second route leads from Graz to Köflach (west of Graz) and is called Köflach-Route and the third one is from Graz to Arzberg (north of Graz), called Arzberg-Route. To investigate different driving and ambient conditions the measurements were done for one vehicle in winter and in summer. The average ambient temperature was between 1.5°C and 30°C.

A similar exercise was done for the RDE trips as described before for the chassis dynamometer tests. As an example, the following figure shows the load points interpolated with the CO₂ method for vehicle no. 4 driven on the Ries-Route. Each grey point describes one load point, calculated in 1Hz. The black points describe the stationary full load and drag curve for the generic diesel engine with 2013 technology standard. Resulting from the generic full load curve, transient measurement and measurement uncertainties some data points are above the full load curve.

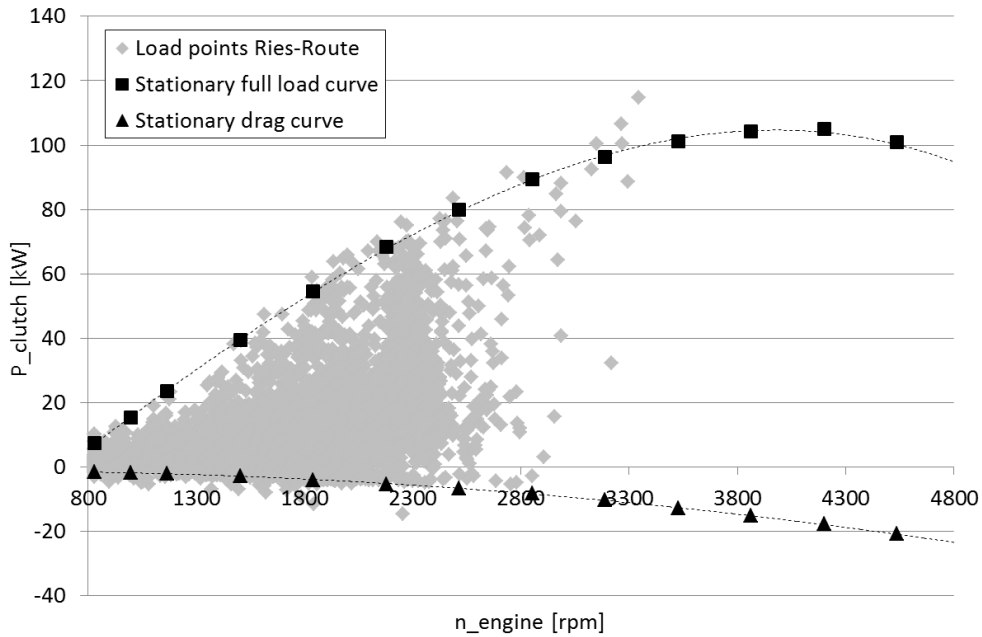


Figure 5: Interpolated load points from a RDE trip with a D-segment diesel vehicle.

Due to missing engine power data during the RDE trip from the CAN-Bus and in absence of torque measuring wheel hubs, no measured reference signal for the engine power for validation is available at the moment for PEMS tests. Thus the validation is based on the simulation of the engine power via longitudinal dynamics from the measured vehicle speed and road gradient data as shown later. All measured pollutant emissions i.e. NO_x , CO and others were matched in the engine map as described before, using the rpm signal as x-axis and the power interpolated from CO_2 as y-axis. The CO_2 and fuel map used for map production and for the vehicle simulation was always the generic map. The emission map was then used to simulate the pollutant emissions in the RDE trips. In Figure 6 the generic CO_2 basis map is shown as function of P_{engine} and rpm (both normalized according to the described case 1). Figure 7 and Figure 8 represent the NO_x and CO map gained from the measured data.

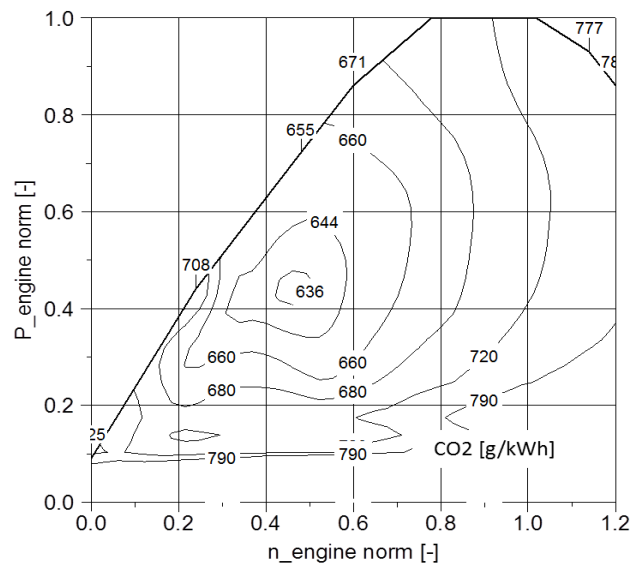


Figure 6. CO_2 in [g/kWh] as function of P_{engine} and n normalized.

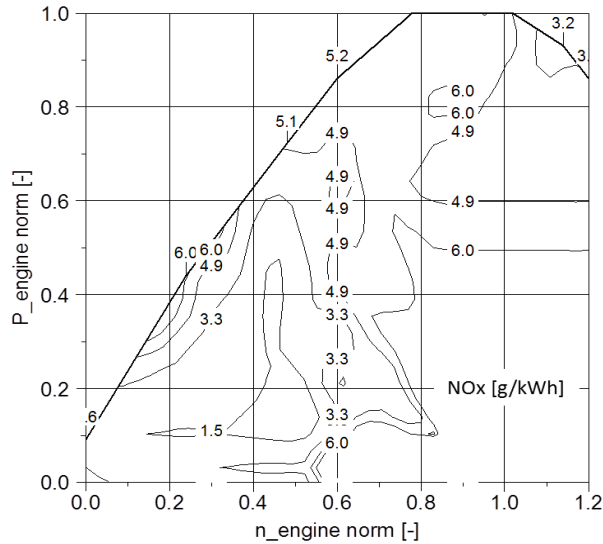


Figure 7. NO_x in [g/kWh] as function of P_{engine} and n normalized.

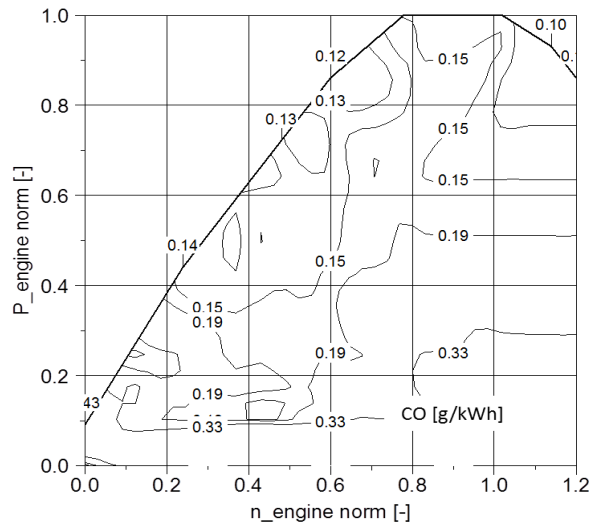


Figure 8. CO in [g/kWh] as function of P_{engine} and n normalized.

For the validation all driven routes were simulated using PHEM with the engine map elaborated from a PEMS test with following steps:

- Option 1: Simulation with measured engine speed and engine power as input (engine power interpolated from CO₂ and rpm) to check the quality of the interpolation method.
- Option 2: Simulation with measured engine speed, but vehicle velocity and road gradient input to check additional to option 1 the quality of power calculation based on the longitudinal dynamics model.
- Option 3: Simulation with velocity and gradient input to check additional to option 2 the quality of the gear shift model from the simulation tool.

With the deviation between the measured and the simulated data a qualitative assessment of the interpolation method can be done. It has to be noted that the uncertainties cover the entire chain from production of the emission map up to simulation of the trip for the vehicle. Following tables show in extracts the results of the comparison for vehicle no. 4 with validation option 1 and option 3. The Ries-Route was driven five times with the vehicle no. 4. One trip was invalid according to the RDE regulation draft, thus the trips Ries no. 2 to no. 5 were inputs for the simulation.

It shall be mentioned that the simulation is not optimized yet. The effect of the interpolation routines

used for the interpolation from the engine map is quite large and seems to need further analysis. The deviations include also several other uncertainties such as:

- Default CO₂ map for the interpolation method
- Road gradients are based on the GPS data (relevant for option 2 and 3)
- Power calculations based on default road load resistances (relevant for option 2 and 3)
- Unknown power of auxiliary demand (relevant for option 2 and 3)
- Default gear shift model (relevant for option 3)

Figure 9 contains the CO₂ comparison between the measured and simulated data. As mentioned before, option 1 gives an overview on the quality of the interpolation method. In this case the “bi-linear” interpolation method shows good results; the simulated CO₂ (grey bar) is equal to the measured one (black bar).

Simulation results with option 3 include a lot of uncertainties as mentioned before. Different gear shift behavior from driver compared to the simulated behavior can be one reason for the different deviations between -8% and 1%. One further reason could be the different auxiliary power demand and different state of charge (SOC) from the battery at the end of each measured trip. In the simulation the same average auxiliary power demand for all trips was estimated and the SOC was not corrected.

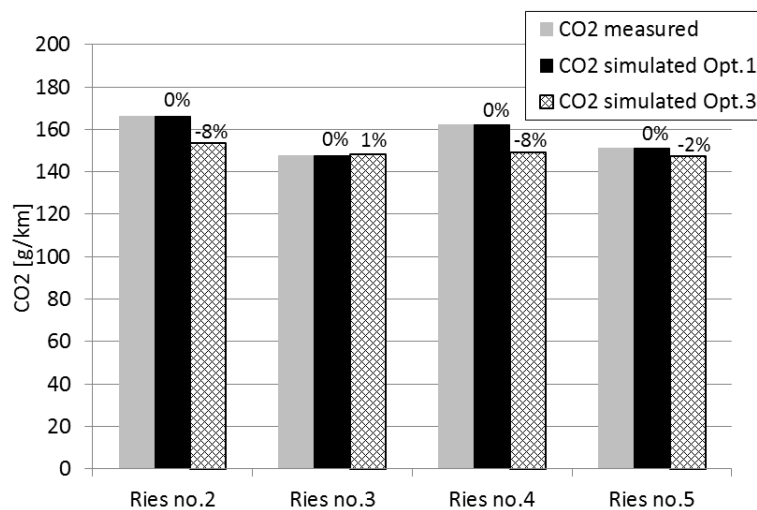


Figure 9. CO₂ deviations between measured and simulated data.

In Figure 10 the measured and simulated NO_x levels for four RDE trips are shown. The simulation overestimates the NO_x up to 25%. The bars in black represent the simulated data with option 1, the crosshatched bars show the simulation results with option 3. Possible reason for the high deviations with option 3 could be the steep gradient of NO_x in the engine map (Figure 7). Minor deviations in engine power calculations due to the uncertainties mentioned before, could be lead in a higher deviation of NO_x.

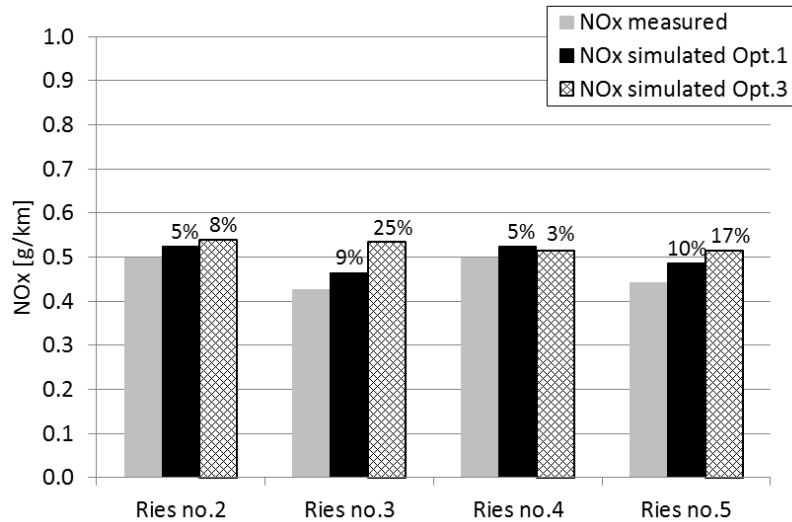


Figure 10. NO_x deviations between measured and simulated data.

Figure 11 contains the CO comparison. The grey bars show the measured CO values for the same trips mentioned before. The black bars represent the simulation results with option 1. In one case the CO value is underestimated. In all other cases the simulation overestimates the CO values. The crosshatched bars show the simulation results with option 3. The deviation trend is identical with option 1. The deviations up to 33% could also come from minor deviations in engine power calculation.

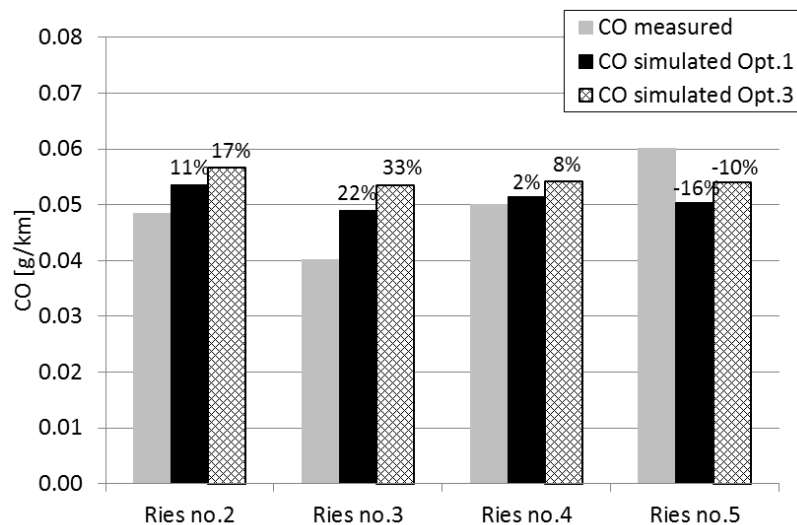


Figure 11. CO deviations between measured and simulated data.

First investigations of the simplified power determination approach show a good accordance with the measured data. With elimination of uncertainties mentioned before, the deviations could be further reduced. With this method it is possible to create engine maps from vehicles driven on RDE trips.

3. Effect of the ambient temperature

Since chassis dynamometer tests are typically measured between 20°C and 30°C while RDE tests can be done at any ambient condition, the effect of ambient temperature on emissions have to be considered when emission maps are produced in future. The influence of the temperature under hot start conditions on emissions, especially for NO_x, was investigated on a few vehicles so far. As mentioned before the RDE trips were performed in summer and winter. The average ambient temperature from the trips was between 1.5°C and 30°C. Due to the other influencing parameters

(driving style, traffic conditions) the influence of the temperature is not directly visible from the PEMS data but a trend to higher NO_x at lower ambient temperatures is visible for several cars, e.g. Figure 1.

To assess temperature effects chassis dyno tests are preferable, because only temperature can be changed while all other parameters are kept constant over the tests. Four diesel vehicles with EU 5 and EU 6 exhaust emission standard were tested. As driving cycle the ERMES cycle with hot start was chosen. Each vehicle was measured under hot engine conditions at 0°C and at 23°C ambient temperature. All other settings were identical with the settings described before. The small test campaign shows that the NO_x level is higher for lower ambient temperatures for several vehicles, but not for all (Figure 12).

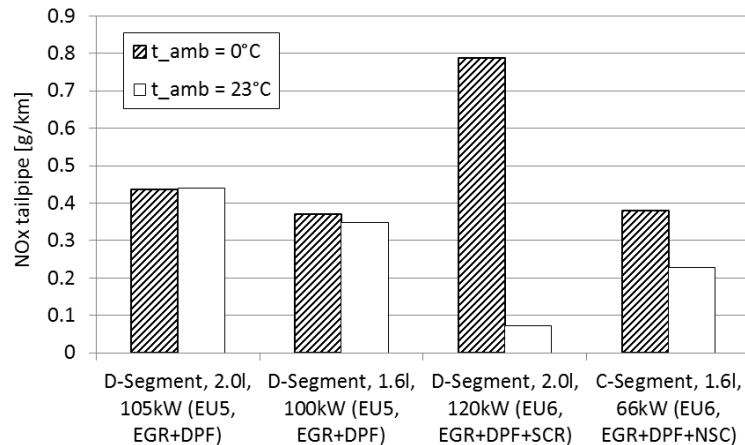


Figure 12: NO_x dependency on ambient temperature.

A recent publication (BMVI (2016)) measured a larger number of diesel cars and shows significant increases in NO_x emissions in NEDC after a hot start with 10°C compared to a hot start at 20°C to 24°C (on average 1.6 times higher for EU 5 and 2 times higher for EU 6).

Possible reasons are the reduction of exhaust gas recirculation (EGR) rates to prevent condensation effects in EGR cooler or/and intake system and lower temperature levels in the exhaust gas after treatment system which can lead to lower NO_x conversion efficiencies at low engine loads.

Especially for the D-segment vehicle with 120kW and selective catalytic reduction (SCR) the deviation is very high in Figure 12. This may be a result of the engine control unit (ECU) application as mentioned before and the operational range of the SCR, which has less than 200°C a poor efficiency (Hausberger S. et al. (2016)). The conclusion of this investigation is that different NO_x engine maps for different ambient temperatures shall be used for accurate simulation. Most likely the core engine maps for PHEM will be produced from tests at 20°C and 30°C since all chassis dynamometer tests from EU 0 to EU 5 used this temperature range for hot start emission tests.

In addition the quite high number of PEMS tests for EU 5 and EU 6 cars shall cover also lower temperature levels (e.g. in ranges such as 0°C to 10°C and 10°C to 20°C). Possibly from this data a 4 dimensional map can be produced with power, rpm and temperature as axis. Effects from exhaust gas after treatment temperatures can be simulated by the existing catalyst models in PHEM. The analysis on this issue is ongoing.

Conclusion and outlook

The application of real world tests as basis for emission simulation for vehicles will become more important in future. The novel method calculating the actual engine power instantaneously from engine speed and CO₂ mass flow signals allows the use of PEMS test data to set up engine emission maps with good accuracy. For the interpolation of the power signal generic engine fuel maps are used which shall be representative for actual engine technologies. The error from using generic fuel maps due to variations in engine efficiencies from engines with similar technology but from different OEMs is much smaller than the uncertainty in the fuel maps gained from transient chassis dynamometer tests in the former method. Thus the quality of CO₂ simulation for different traffic situations is assumed to be clearly improved. The new method is also less sensitive against inaccurate time alignment between

exhaust gas emission and engine speed and torque recording since the power is calculated from the CO₂ signal which shall have the same transport time as all other exhaust gas components.

Validations by simulation of measured RDE trips show a good accordance. In the simulation of the RDE trips the uncertainties due to the unknown auxiliary power demand, gear shifts, real world vehicle driving resistances and engine specific data are included. For overall high model accuracy beside emission maps also accurate vehicle input data are necessary (i.e. real world rolling resistance, air resistance, weight, etc.) for the simulation tool PHEM. A novel method to assess the driving resistances and auxiliary power demand from the data recorded usually in RDE tests is under development based also on the power interpolated from the CO₂ map. If this method is successful, also the data quality on real world vehicle data could be improved leading to a better overall model accuracy.

Acknowledgments

The work was supported by fund of UBA Germany and UBA Austria. We want to acknowledge the very good cooperation and the support.

References

- BMVI (2016): Bericht der Untersuchungskommission „Volkswagen“ Untersuchungen und verwaltungsrechtliche Maßnahmen zu Volkswagen, Ergebnisse der Felduntersuchung des Kraftfahrt-Bundesamtes zu unzulässigen Abschaltvorrichtungen bei Dieselfahrzeugen und Schlussfolgerungen, BM für Verkehr und digitale Infrastruktur, April 2016
- Hausberger S., Lipp S., Matzer C. (2016): Requirements on the RDE regulation. 18th VDA Technical Congress, March 2016, Ludwigsburg
- Hill N., Windisch E., Hausberger S., Matzer C., Skinner I., et.al. (2015): Improving understanding of technology and costs for CO₂ reductions from cars and LCVs in the period to 2030 and development of cost curves; Service Request 4 to LDV Emissions Framework Contract; Final Report for DG Climate Action. Ref. CLIMA.C.2/FRA/2012/0006; Ricardo AEA, UK
- Rexeis M., Hausberger S., Kühlwein J., Luz R.: Update of Emission Factors for EURO 5 and EURO 6 vehicles for the HBEFA Version 3.2. Final report No. I-31/2013/ Rex EM-I 2011/20/679 from 06.12.2013
- Weller K., Rexeis M., Hausberger S., Zach B. (2016): A comprehensive evaluation method for instantaneous emission measurements. TAP 2016, Lyon

RemIAG model: Bottom-up emissions inventories for cities with lack of data

S. Ibarra¹ Ynoue R¹.

¹Department of Atmospheric Sciences, Institute of Astronomy, Geophysics and Atmospheric Sciences, University of São Paulo, São Paulo, 05508-090, Brazil

Keywords: vehicular, emissions, R, estimation, inventory.

Author email: sergio.ibarra@iag.usp.br, zergioibarra@gmail.com

“Emission Inventories always seem to be available at a very late point in time ... and are easily seen as the scapegoat if a mismatch is found between modelled and observed concentrations of air pollutants” Tim Pulles (2010)

Emissions inventorying is a complex task with regulatory and/or scientific environmental purposes. In South American cities, if the task is performed, the common denominator is lack of data and documentation, and vehicles are usually the main source of pollutant of emerging and consolidated megacities. Therefore, emissions inventories is becoming more important, especially for mobile sources.

This work consists in present the model remIAG for developing bottom-up emissions inventory for vehicles in cities with lack of data (Ibarra, 2016). The program was written in R using libraries maptools and ggplot2. The characteristics and process of the model are described as follows:

Activity: Reads traffic simulations, traffic counts and interpolates, or road network and assigns interpolation. Splits categories by fuel, size of motor, use and gross weight annually up to 50 years. Data classification is according to EEA/EMEP guidelines and Copert (Ntziachristos, 2014).

Emission factors: Reads local emission factors of new vehicles given by emission test in g/km and uses Copert factors to obtain speed variation and especiation. Reads deterioration factor to obtain deteriorated emission factors. Reads experimental emission factors to obtain especiations.

Estimation: Emission estimation for morning peak hour. Extrapolation to 24 h, 7 days of the week by city data. Results in tables, images and shapefiles. Exportation to WRF Chem and other models. Estimates 25 pollutants of 110000 links of road network in 2 hours. It takes 30 min to estimate traffic simulation emission of 25000 links.

Some results:

Megacity of São Paulo, Brazil: Vehicular emissions for 2012 with traffic simulations and vehicular counts: CO = 158834 (t/y), NO_x = 129317 (t/y), THC = 21025 (t/y), MP2.5 = 4118 (t/y), CO₂ = 15141643 (t/y) (Ibarra, 2016), very similar to official Top-down estimations. Results with traffic simulations as inputs are twice higher, not showed here.

Santiago, Chile: Assigned interpolation. MP2.5 = 1221 (t/y), CO = 335777 (t/y), NO_x = 43979 (t/y) and THC = 36393 (t/y). WRF Chem simulations showd good agreement with CO superficial observations (Ibarra *et al*, 2015).

South America: Emissions estimation of 58 urban centers of South American cities. It was associated average age of type of vehicles with GDP. MP2.5 = 27329 (t/y), CO = 4459961 (t/y), NO_x = 773432 (t/y) and THC = 485745 (t/y) (Ibarra *et al*, 2015).

Future work

So far the model has assumes one zone with homogeneous characteristics like daily profile and age. In the future the model will identify different zones inside city with different age, profiles for different type of vehicles and other specifications. Also, include HBEFA emission factors.

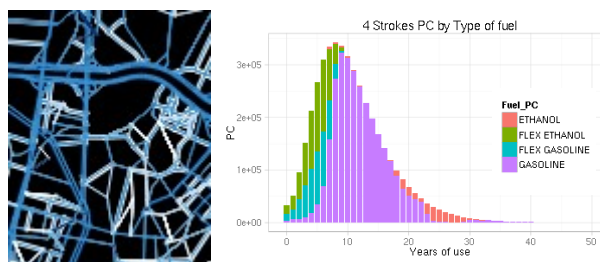


Figure 1. Some outputs of remIAG model.

This work was supported by the Capes, Brazil and Conicyt, Chile funds.

Pulles, T., and D. Heslinga. "The art of emission inventorying." *TNO, Utrecht* (2010).

Ntziachristos, L.; Zissis, S. Passenger cars, light commercial trucks, heavy-duty vehicles including buses and motor cycles. IN: EMEP, EEA. EEA air pollutant emission inventory guidebook 2013. Copenhagen: European Environment Agency, 2014

Ibarra, S., Vara A., Ynoue R. (2015) *Proc. 11th Int. Conf. on Southern Hemisphere Meteorology and Oceanography, Santiago, Chile*.

Ibarra, S., Ynoue R. (2016) *High resolution emission inventory for the megacity of São paulo*. In preparation to be sent to Atmospheric Environment.

Keller, M. Handbook of emission factors for road transport (HBEFA) 3.1. Quick reference. Tech. rep., INFRAS. <http://www.hbefa.net>, 2010.

R Core Team (2015). R: A language and environment for statistical computing. R Foundation for Statistical Computing, Vienna, Austria. URL <https://www.R-project.org/>.

On-road emission measurements in Sweden 2007-2015

Martin JERKSJÖ

*IVL Swedish Environmental Research Institute, Aschebergsgatan 44, Gothenburg, Sweden
Fax+4610 788 68 90-email:martin.jerksjo@ivl.se

Abstract

In different studies reaching from 2007 through 2015 on-road emission measurements on heavy-duty buses and passenger cars have been conducted in Gothenburg, Sweden. Measurements of bus emissions have been carried out both from the roadside during real-world driving conditions with a remote sensing instrument, and during controlled driving conditions with both a remote sensing instrument and an Engine Exhaust Particle Sizer Spectrometer (EEPS).

All measured emissions (CO, HC and NO_x) from gasoline cars have continuously decreased from Euro 1 to Euro 6. Regarding diesel vehicles, emissions of nitrogen oxides from buses and passenger cars have not decreased significantly from the Euro 3 to the Euro 5 emission standard. A few diesel passenger cars and buses of the Euro 6 emission standard are included in the data set, which show a lower average emission of nitrogen oxides compared to Euro 5 vehicles. For buses a comparison between diesel and RME (Rapeseed Methyl Ester) was conducted. It was found that particle emissions from buses driving on 100% RME were 88% lower compared to emissions from buses fueled with conventional diesel.

Key-words: (5 words) on-road emissions, heavy duty buses, passenger cars, NO_x, particles.

1. Introduction

This paper summarizes the on-road vehicle emission measurements conducted by means of remote sensing in Sweden between 2007 and 2015. The work was carried out within several different research projects, financed by the Swedish Transport Administration, Västtrafik (a public transport company serving Southwest Sweden) and the Foundation for IVL Swedish Environmental Research Institute (SIVL).

2. Background

In the summer of 2007, a series of remote sensing measurements were conducted in Gothenburg by means of the fourth generation of the Denver University FEAT instrument, the first remote sensor measuring NO₂ ("FEAT 4"). Apart from NO₂, this instrument measures CO, HC, opacity, NO, NH₃ and SO₂. This instrument has been described in detail earlier by e.g. Burgard *et al.* (2006). Measurements were carried out at four different sites, of which three had mixed traffic (with respect to vehicle categories), and the fourth site was a road operated by buses only. The main objective of the 2007 study was to measure on-road NO_x and NO₂ emissions for the first time in Sweden, and to gather on-road emission data in general for validation of the ARTEMIS/HBEFA emission models (Sjodin and Jerksjö, 2008). After the 2007 study (2010-2015), the main focus of the on-road emission/remote sensing studies in Sweden has been to measure emissions from heavy duty buses operating for public transport services. The main purpose of these measurements – carried out during controlled driving conditions – has been to screen the bus fleet for high-emitters, and to find out how reliable and useful remote sensing is for this purpose. Most of the measurements have been conducted with an RSD AccuScan RSD 3000 instrument, which measures HC, CO, NO and opacity, along with an EEPS (Engine Exhaust Particle Spectrometer) for particle measurements (number and mass divided by particle size). However, in the summer of 2014, the Denver University FEAT 4 instrument was hired by IVL again, both for the controlled measurements on buses and for a series of roadside measurements on mixed traffic. The measurements 2010-2015 have resulted in emission data for 218 unique buses, the roadside measurements in 2007 and 2014 excluded. Among the 218 buses, different Euro classes, model years, fuels, exhaust after-treatment systems, etc., are represented. The number of Euro VI buses measured was 15 (two methane fueled, nine RME fueled and four electrical hybrids fueled with RME). The measurements have been carried out at 17 different bus depots in Southwest Sweden, of which some has been visited more than once. The measurements with the FEAT 4

instrument were conducted at two of the bus operators and during a five day roadside measurement campaign. In this paper no analysis regarding high-emitters is presented, instead emissions from vehicles representing different Euro standards and operating on different fuels are compared.

3. Bus emissions during controlled driving conditions

Experimental

Emissions from the buses were measured during full throttle accelerations from stand still. Prior to the test, a warm-up route was driven, typically 5-10 minutes, to prevent cold engines. The length and driving conditions during the warm-up routes varied depending on where the buses were stationed. After being warmed up, the bus stops right before the instrument set-up. On a given signal it accelerates, passing the instruments and the emissions are measured. After the first measurement the bus turns to do a few more accelerations past the instruments until at least three valid measurements have been obtained. The aim has been to test ten buses at each bus garage; this is often accomplished during a workday including time for the set-up of instruments. The testing conditions are similar to conditions when buses accelerate in real-traffic, e.g. from a bus stop or a traffic light. This means that the measured emissions are representative for "stop and go" traffic normally occurring in city centers, but not for emissions during e.g. motorway driving.

The gaseous species have been measured using either of two different remote sensing instruments. Both instruments generate a light beam across the driving lane and measure concentration ratios of the pollutants to the concentration of CO₂ by measuring absorption at certain wavelengths used for detecting each species. Relating pollutant concentrations to CO₂ facilitates quantitative measurements of pollutant emissions despite not knowing the extent of exhaust gas dilution. Emissions measured by remote sensing are often expressed as ratios to CO₂, or mass of pollutant per mass of fuel. In this report the latter is used.

Most measurements were performed with an AccuScan RSD-3000 instrument. One main drawback of this instrument is its inability to measure NO₂ and therefore it only measures a part of the total NO_x emissions. The NO₂/NO_x-ratio varies between different manufacturers, emission standards and exhaust aftertreatment systems, and in some cases the total NO_x emissions is dominated by NO, and primary emitted NO₂ only contributes to a few percent. In other cases though, the shares of NO, and primary emitted NO₂ are equal. If there is a good knowledge of NO₂/NO_x -ratios by certain exhaust aftertreatment systems etc., total NO_x can be estimated by only measuring NO, but preferably both NO and NO₂ should be measured. For measuring NO₂ the Denver FEAT was used.

Both the AccuScan RSD-3000 and the Denver FEAT also measures opacity in the IR-range. This parameter gives an approximation of the particle emissions but it was not evaluated in this study since it is considered to be a too uncertain estimate of the particle emissions. Instead an EEPS (Engine Exhaust Particle Sizer Spectrometer, TSI Inc. Model 3090) was used. This instrument measures the number size distribution of particles in the range from 5.6 to 560 nm with a time resolution of 10 Hz. When estimating the particle mass, spherical particles with a density of 1 g cm⁻³ was assumed. The measured particle emissions were also related to CO₂ as is the case for the gaseous species measured with the RSDs. CO₂ concentrations used for relating to the particles measurements was measured using a non-dispersive infrared gas analyzer (LI-840A) with a time resolution of 1 Hz. The sampling of the particle and CO₂ emissions was conducted by using an extractive sampling of the passing bus plumes, where the sample was continuously drawn through a cord-reinforced flexible conductive tubing. To prevent the influence of the ambient temperature on the measurement a thermodenuder (TD) was used in front of the EEPS (298K). Figure 1 shows a schematic of the experimental setup.

Today many buses use SCR (Selective Catalytic Reduction) systems for reducing nitrogen oxides. The efficiency of these is strongly dependent on the exhaust (catalyst) temperature. Since the temperature was not measured during these tests, it was not possible to determine if high NO_x emissions from SCR-equipped buses was a consequence of low temperature or a malfunctioning SCR system.

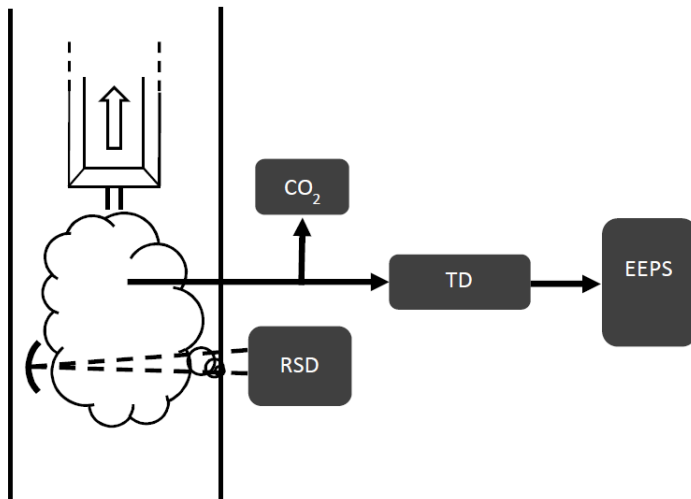


Figure 1. Schematic of the experimental set-up used (Hallquist *et al.* 2013).

Results

Most of the measurements of nitrogen oxides during full throttle acceleration in the studies conducted from 2010 to 2015 were done with the AccuScan RSD 3000, which does not measure NO_2 . The total NO_2 emission have instead been estimated by using general NO_2/NO_x ratios from the HBEFA road emission model (HBEFA, 2016) or ratios estimated by IVL from measurements with the Denver FEAT. Since the NO_2 part in most cases is approximations, some of the figures in this paper instead present measured NO (as NO_2 equivalents). In general, median emission values of e.g. different Euro standards are presented. This will give a value more representative of the Euro standard compared to the mean, since the mean maybe affected by high-emitters. However, in some cases the averages are presented with a 95% confidence interval. All measured emission factors are expressed as mass of pollutant per kg fuel burnt and are notated as EF_{NO} , EF_{PM} etc.

In total 218 unique buses were measured at the depots during the period 2010-2015. Fifteen of the buses were measured twice and one was measured three times during the six year period. The emission standard of the tested buses ranged from Euro II to Euro VI. Some of the tested Euro V diesel buses were in the Swedish vehicle register referred to as EEV. According to Västtrafik, and in some cases the bus operator, these buses were specified to comply with the Euro V standard, but not the EEV standard. Since it was not clear how to classify these vehicles all diesel buses referred to as EEV in the register is referred to as Euro V vehicles in this paper. Also different techniques for reducing NO_x and particles are represented among the buses. Information about the Euro standard and exhaust aftertreatment systems was obtained from the bus operators or Västtrafik. Some of the information from the operators did show up to be wrong during the data evaluation, especially regarding information on the presence of particle reduction systems for Euro IV and Euro V buses. However, most of this incorrect information could be corrected by contacting the vehicle manufacturers. All manufacturers also have their own implementation of the aftertreatment system that differs from the other brands, even though they are similar. This is important to bear in mind since the emissions will depend not only on the technique but also on bus/engine manufacturer. Table 1 shows a summary of all the measured buses with respect to fuel type, Euro class and technology. Also the measured mean and median emissions of NO_x (EF_{NO_x}) and PM (EF_{PM}) are presented. Information about the fuel was obtained from the bus operators. Some buses, mostly Euro V and Euro VI, were fueled with 100% RME (Rapeseed Methyl Ester). When it comes to diesel there may be a mix of different low blends of RME and HVO (Hydrotreated Vegetable Oil). Since IVL does not have this detailed information all low blends are termed as diesel.

Table 1. Number of tested buses and EF_{NOx} and EF_{PM} by fuel, Euro standard and exhaust aftertreatment system. HEV = Hybrid electric vehicle, DF = dual fuel (diesel and methane). Dual fuel buses where operated on diesel when tested.

Fuel	Euro std.	Technology	#*	#**	EF_{NOx}			EF_{PM}		
					Median	Mean	95% CI	Median	Mean	95% CI
Diesel	E II		2	2	22	22	69	819	259	2325
Diesel	E III		11	7	12	14	6	1571	1794	668
Diesel	E III	DPF	17	16	13	16	5	188	229	134
Diesel	E III	SCR+DPF	5	4	22	26	19	6	507	1360
Diesel	E III	EGR+DPF	1	1		18			61	
Diesel	E IV	SCR	4	4	10	13	21	222	746	1746
Diesel	E IV	EGR	12	12	14	15	7	650	1151	719
Diesel	E V	SCR	42	42	22	27	6	257	301	66
Diesel	E V***	SCR+DPF	4	4	20	21	9	1	1	2
Diesel	E V	EGR+DPF	5	5	11	13	8	36	54	62
Diesel (HEV)	E V	SCR	7	7	30	27	1	41	45	23
RME	E III	SCR+DPF	2	2	38	38	4		68	
RME	E IV	SCR	6	6	40	39	24	233	268	262
RME	E IV	EGR	2	2	13	13	16	72	72	197
RME	E V	SCR	23	22	38	38	7	28	59	26
RME	E V	EGR+DPF	7	7	10	10	5	61	64	35
RME (HEV)	E V	SCR	10	10	42	39	11	19	21	9
RME (DF)	E V	SCR	10	10	36	35	2	77	82	7
RME	E VI	EGR+SCR	9	9	4	4	2	1	2	2
RME (HEV)	E VI	EGR+SCR	4	4	7	13	24	1	1	1
Methane	EEV		50	46	0	30	11	8	23	13
Methane	E VI		2	2	0.45	0.45	0.32	2	2	17
Total			235	224						

* In this column every bus that were tested two or three times are counted two or three times respectively.

** In this column every bus that were tested two or three times and not have changed from diesel to RME are counted only once. Six of the buses were tested both on diesel and RME, hence these buses are included twice in this column.

*** mini buses

NO_x emissions by Euro standard

Measured EF_{NOx} from all buses are shown in Figure 2, together with the median values of each Euro class/technology. The figure shows that there is no decrease in NO_x emissions going from Euro III to Euro V for the conditions valid in the controlled measurements. As is seen in Figure 2, buses equipped with an SCR-catalyst have approximately twice the emissions of their EGR equivalents. This is most likely due the SCR not operating at optimal conditions during the tests. The tested Euro VI (diesel) buses though, use both SCR and EGR and the measured NO_x emissions from these buses were several times lower than the emissions from the Euro V buses, and did not show any sign of significant increases in NO_x even after longer periods of stand still. When it comes to methane powered buses, the very high median emissions are due to some groups of buses emitting high amounts of NO_x.

Figure 3 shows EF_{NO} for methane powered buses by manufacturer (M1-M4), model year and age of the vehicle when tested. In a complete analysis of the emission behavior from the different manufacturers there are even more parameters that should be considered, e.g. different models from the same manufacturer, kilometers driven and maintenance. The differences between models from the same manufacturer did not show any significant differences, and this information was chosen not to be included in the analysis. When it comes to driven kilometers, IVL did get information about only a few of the buses and no information at all about when the buses were serviced. Emissions of NO from two of the manufacturers (M3 and M4) were low regardless of vehicle age (median 1.5 g kg fuel⁻¹ and 4.9 g kg fuel⁻¹). M2 showed a bit higher median emission (20 g kg fuel⁻¹) compared to M3 and M4, also two really high emitters were identified from M2. The highest median emission was measured from manufacturer M1 (67 g kg fuel⁻¹), and the variation in NO-emissions between the different individual buses within this brand was relatively large. Also, all the buses from M1 were

owned by the same operator which may have an influence on the emissions, e.g. that all the buses have higher yearly driving distances than other buses and that the maintenance scheme differed from other operators. However, the reason for these differences between manufacturers was not further investigated.

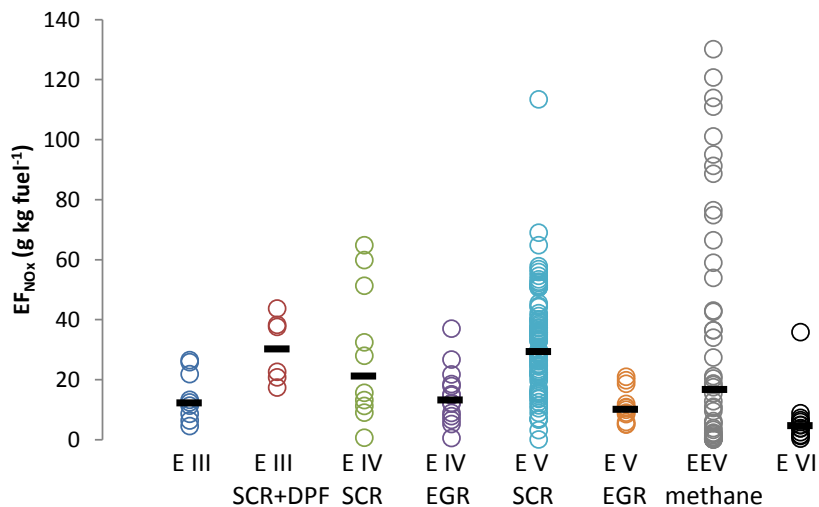


Figure 2. Measured EF_{NOx} from all buses by Euro standard and aftertreatment system (circles) and median EF_{NOx} (black lines).

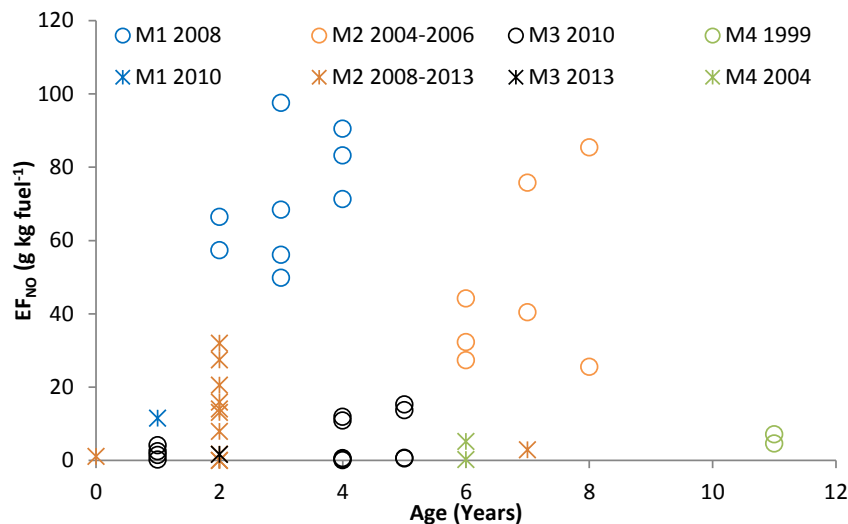


Figure 3. EF_{NO} from methane powered buses by manufacturer, model year and age.

Particle emissions by Euro standard

In Figure 4 the particle emissions (by mass) for all the tested buses are shown. There is a large variation in emissions between different classes but also within the Euro classes. Euro III (without DPF) and IV (EGR) have the highest median EF_{PM} (1571 and 649 $mg\ kg\ fuel^{-1}$ respectively) and the EEV (methane fueled) and the Euro VI buses the lowest (8 and 1 $mg\ kg\ fuel^{-1}$ respectively).

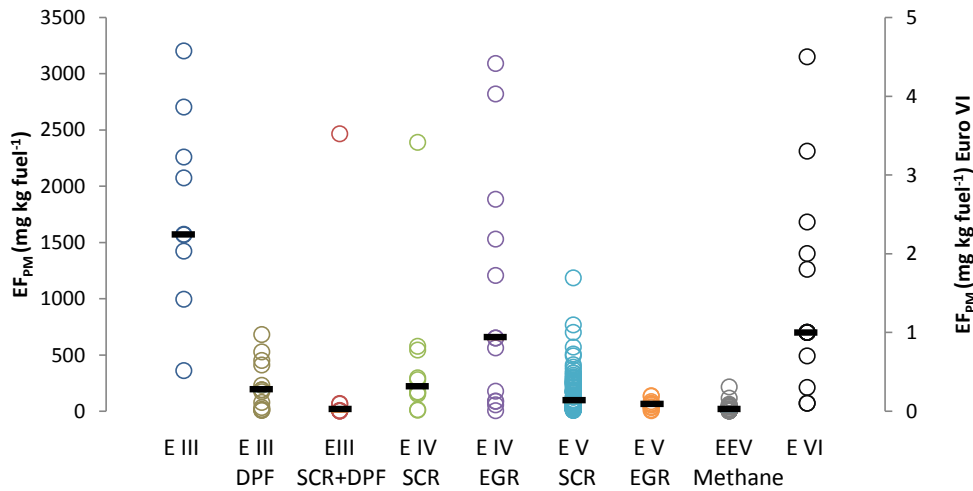


Figure 4. Measured EF_{PM} from all buses by Euro standard/aftertreatment system (circles) and median EF_{PM} (black lines). The secondary axis is for Euro VI.

Buses equipped with diesel particulate filter (DPF) are emitting significantly less particle mass compared to similar buses without DPF as is illustrated in Figure 5 for Euro III buses. The median EF_{PM} with DPF is 188 $mg\ kg\ fuel^{-1}$ and the median EF_{PM} without 1571 $mg\ kg\ fuel^{-1}$, respectively. The reason for high masses for some buses equipped with DPF may be malfunction of the DPF.

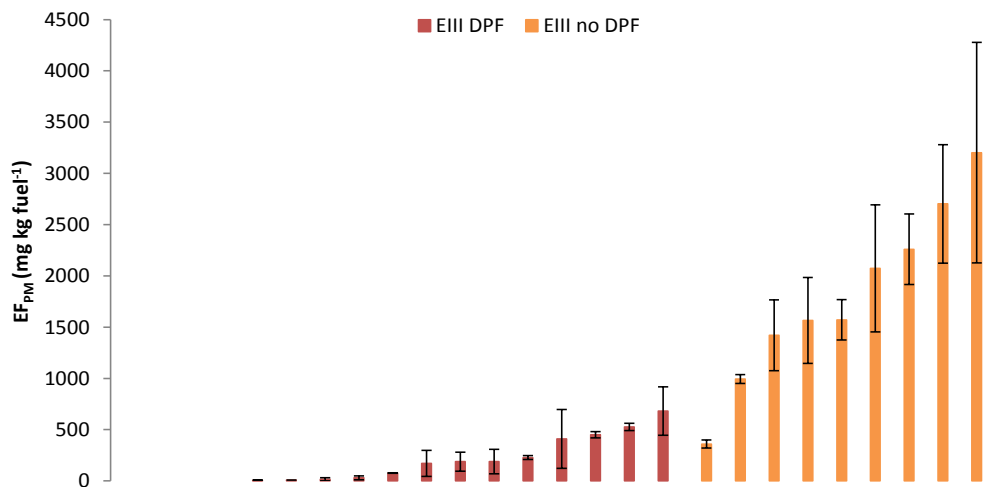


Figure 5. EF_{PM} of Euro III buses equipped with (red) and without DPF (orange). Stated errors are at the statistical 95% confidence level.

Buses corresponding to the Euro V standard were the most frequently tested. In Figure 6, all the Euro V buses are shown and subdivided depending on fuel and NO_x abatement technology. For SCR buses the median EF_{PM} was higher for diesel buses compared to RME fueled buses. For the EGR buses the median EF_{PM} was very similar between the different fuel types, 36 and 61 $mg\ kg\ fuel^{-1}$, respectively. However, these buses were equipped with DPF. Additionally, for the RME buses, the median EF_{PM} was similar for the EGR+DPF and SCR technologies (61 and 28 $mg\ kg\ fuel^{-1}$, respectively).

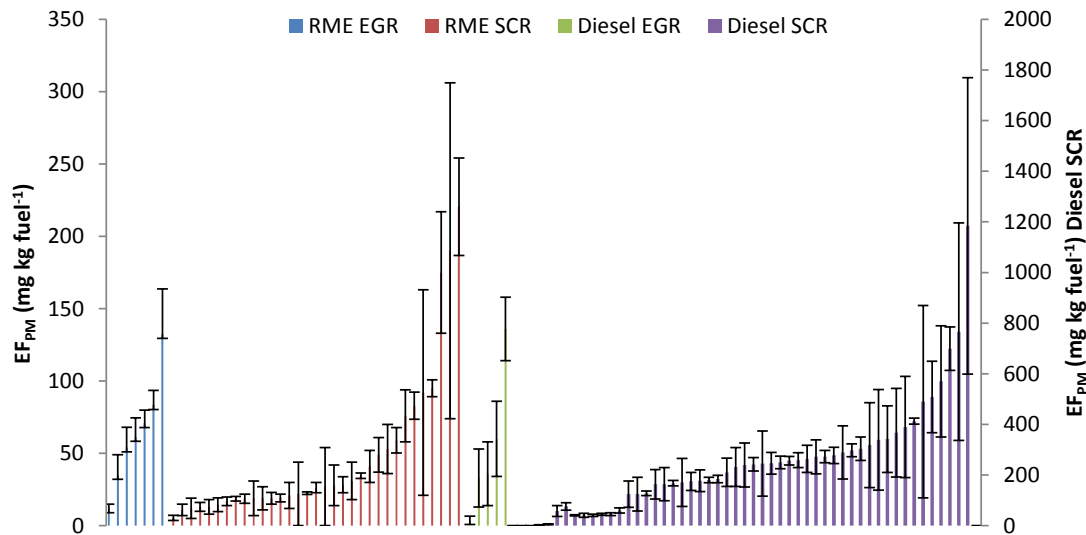


Figure 6. EF_{PM} of the tested Euro V buses with respect to fuel and NO_x abatement technology. The secondary y-axis is for Diesel SCR buses. Stated errors are at the statistical 95% confidence level.

Particle and NO_x emissions from diesel vs RME fueled buses

Among the tested diesel buses there was a mixture between buses fueled with conventional (low blended) diesel and buses fueled with 100% RME. This enabled an analysis of differences in emissions depending on the type of fuel. To minimize the number of parameters other than the fuel that may influence the emissions, only Euro V buses with SCR from one manufacturer were considered. However, different models from this manufacturer were included. When it comes to particle mass, the median emission from RME fueled buses was 88% lower than the median for buses fueled with low-blended diesel ($30 \text{ mg kg fuel}^{-1}$ and $249 \text{ mg kg fuel}^{-1}$, respectively), see Figure 7. The particle emissions from the RME fueled buses were generally low, $<100 \text{ mg kg fuel}^{-1}$, whereas the scatter for diesel fueled buses was much larger, ranging from 41 to $1200 \text{ mg kg fuel}^{-1}$.

Any differences in NO_x -emissions between the fuels are not as clear as for particle mass, Figure 8. This is in line with expectations as the NO_x reduction system (SCR) is dependent on parameters such as the exhaust temperature which was not controlled in this study. However, the median NO_x emission from buses fueled with low blended diesel was 35% higher than for RME fueled buses ($25 \text{ g kg fuel}^{-1}$ and $33 \text{ g kg fuel}^{-1}$, respectively). Still it is not possible to determine if the measured difference in this study is fuel dependent, or if it is a consequence of different exhaust gas temperatures of the tested buses. Most likely it is an effect of both fuel and temperature.

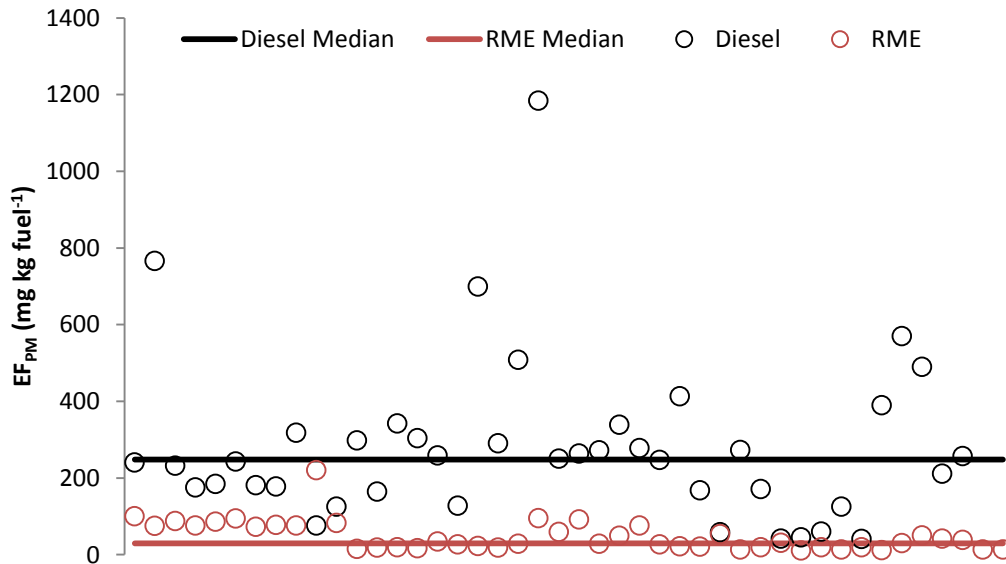


Figure 7. Median EF_{PM} for Euro V busses running on RME (red symbols) and diesel (black symbols).

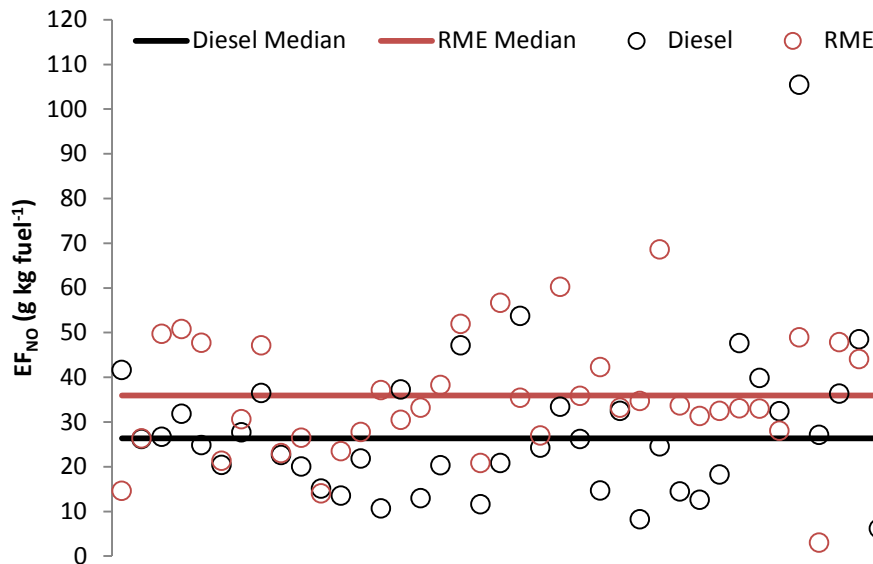


Figure 8. Median EF_{NO} for Euro V busses running on RME (red symbols) and diesel (black symbols).

Emissions from buses tested both on diesel and 100% RME

Seventeen of the buses were analyzed more than once, with one year or more between each occasion. For six of these buses (here named B1, B2, B3, B4, B5 and B6) there was a fuel switch from diesel to RME between the two occasions the bus was tested, and both a decrease (B1, B2 and B3) and an increase (B4, B5 and B6) in EF_{PM} when running on RME compared to diesel were observed. The emission standard of B1, B4 and B6 was Euro IV and Euro V for B2, B3 and B5.

B1 was converted to be operated on 100% RME in 2014. Also the particulate filter was washed in March 2015 (four months before the measurements). The lower emissions in 2015 compared to 2010 may be a consequence of both the conversion to RME and/or the newly washed particulate filter. Both B2 and B3 were converted to be operated by 100% RME and the particle emissions were

significantly lower in 2015 compared to 2012 (Figure 9). Common for these buses is that the combustion conditions were similar (i.e. small difference in EF_{CO}) at both occasions the bus was tested, indicating a general reduction in EF_{PM} when running on RME compared to diesel (Figure 9).

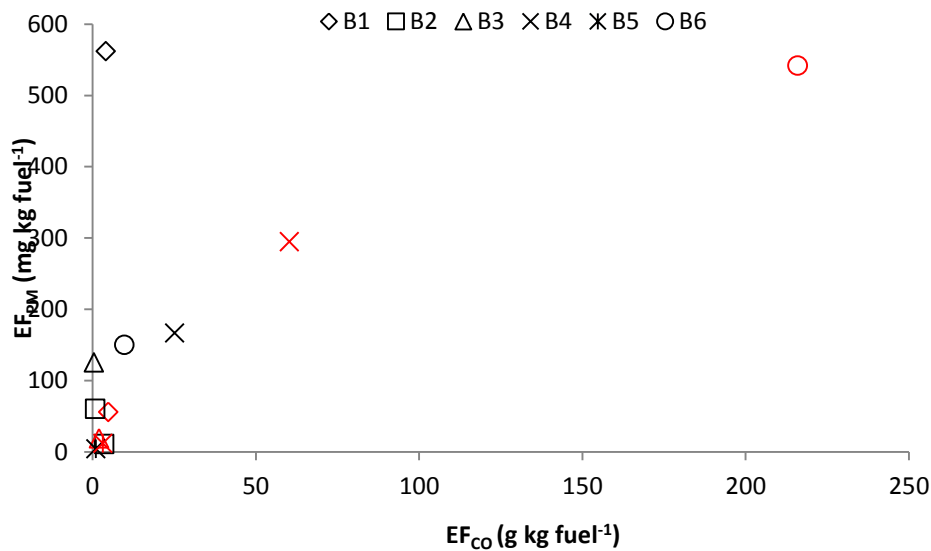


Figure 9. EF_{PM} for buses that have been tested at multiple years and where there has been a fuel switch (red symbols are EF_{PM} when fueled with RME).

For B4, B5 and B6 the particle emissions were higher when running on RME compared to diesel. B4 was converted to RME operation sometime between 2011 and 2015, and B11 was converted sometime between 2014 and 2015. However, for B4 and B6 also the EF_{CO} was much higher when running on RME (Figure 9), indicating a more incomplete combustion, hence favoring soot formation. It is therefore difficult to distinguish between impact of fuel and impact of different combustion conditions on the emissions.

B5 was converted to RME operation sometime between 2010 and 2015. There was a slight increase in particle mass emitted when running on RME, and also the CO emission increased somewhat. However, the CO emission was much lower compared to B4 and B6. Additionally, B5 was equipped with a DPF, so another possibility for the increase in particle mass emitted, besides fuel and combustion conditions, is the performance of the DPF.

For three of the buses (B2, B3 and B6) the measured difference in EF_{NO} was statistically significant (Figure 10). B2 and B3 showed an increase of NO emissions when fueled with RME compared to diesel, whereas B6 showed the opposite trend. B6 did even show a significant increase of EF_{PM} and EF_{CO} , but the reason for the lower NOx emission is hard to determine without knowing more about the bus/engine. Since it was equipped with an SCR catalyst it may just be a consequence of better operating conditions of the catalyst at the second measurement occasion.



Figure 10. EF_{NO} for buses that have been tested at multiple years and where there has been a fuel switch (red symbols are EF_{NO} when fueled with RME).

3. On-road measurements

Buses

This section presents NO_x emissions and NO₂/NO_x ratios measured from the roadside with the Denver FEAT in 2014. For comparison, measured NO₂/NO_x ratios are compared to ratios measured during the controlled acceleration measurements and also to ratios from the HBEFA model.

The by far most frequent emission standard measured among the buses from the roadside was Euro V (this was also the case with the controlled measurements at the bus depots). Among the measured Euro V buses one manufacturer was dominating. There were also three other manufacturers that were represented to an extent that an analysis of differences in NO_x between the brands was considered possible. This is interesting since different manufacturers may use different versions of exhaust aftertreatment systems that may result in e.g. different levels of emitted NO_x and NO₂/NO_x ratios. It is also interesting to compare NO_x emissions measured from the roadside with measured emissions from the controlled acceleration measurements.

Table 2 presents measured NO_x emissions together with information on emission standard, NO_x reducing technology, manufacturer and number of measurements. Comparing emissions from the SCR equipped Euro V buses (M1 and M2) show that the differences in median and average NO_x emissions are quite large. However the number of measurements of M2 is low and this is reflected in the confidence interval. If comparing to the measured NO_x during the controlled acceleration measurements from the same manufacturers, the difference is similar to what is observed from the roadside which may indicate lower on-road NO_x emissions from M2 compared to M1. The NO₂/NO_x ratio between M1 and M2 are similar though.

The EGR equipped buses (M3 and M4) shows similar levels of NO_x emissions but the average NO₂/NO_x ratio differs greatly (5 vs 41%). One possible reason may be due to different techniques used for particle reduction, but this could not be confirmed during this study.

Only two unique Euro VI buses were measured from the roadside (total 6 measurements) and the NO_x emissions were low, similar to the observations from the controlled measurements during acceleration. The NO₂/NO_x ratio was measured to 29% from roadside and 22% during the controlled measurements. It should be noted though that this is a ratio of two low averages based on a small number of measurements which makes the ratio uncertain.

Table 2. EF_{NOx} emissions (g kg fuel⁻¹) measured from the roadside and NO₂ share of NO_x measured during the controlled acceleration measurements, from the roadside and ratios taken from the HBEFA model.

Euro Standard	Technol.	Brand	# (total)	# (unique)	EF _{NOx}			NO ₂ /NO _x		
					Median	Average	95% CI	Roadside	Controlled	HBEFA
E III	-	Mix	10	7	43	42	7	5%	-	7% (30%)
E V / EEV	SCR	M1	246	116	41	43	3	2%	1%	7% (25%)
E V	SCR	M2	8	4	26	29	19	2%	-	7% (25%)
E V / EEV	EGR	M3	173	79	20	25	2	5%	-	21% (25%)
E V	EGR	M4	19	13	21	21	4	41%	-	21% (25%)
E VI	SCR+EGR	M1	6	2	1	2	3	22%	29%	-

Passenger cars

The roadside measurement campaigns in 2007 and 2014 resulted together in 20 000 valid measurements on passenger cars. This is a quite low number compared to many other similar remote sensing studies from which data have been published. Still our results are similar to those presented in e.g. Carslaw *et al.*(2013) and Borken-Kleefeld and Chen(2013), which indicates that the amount of data is still sufficient to use for some analyses, even though the uncertainties in the means in some cases are high.

All figures in this section are presented as average emissions by Euro class with error bars showing the 95% confidence interval of the mean. Pre-Euro 1 vehicles are divided into three groups, Pre-Euro cars with a three way catalyst, vehicles of model year 87-88 where there is a mix of vehicles with and without three-way catalysts, and Pre-Euro which only includes cars without three-way catalysts. Only vehicles with a measured vehicle specific power between 2.5 and 22.5 are included.

Figure 11 - 14 show emission trends of CO, HC, NO_x and NH₃ from pre-Euro to Euro 6 for gasoline passenger cars. Other remote sensing studies of European passenger car emissions, e.g. Carslaw *et al.* (2013) and Borken-Kleefeld and Chen(2013), have shown that these emissions have decreased for every new Euro standard from Euro 1 through Euro 5. Carslaw *et al.* (2013) have also shown that ammonia from gasoline cars is predominantly emitted from the first model years that were equipped with three-way catalysts. Then the emissions have decreased through the emission standards to be at approximately the same level for Euro 6 vehicles as for pre-Euro non-catalyst vehicles. Results from Carslaw *et al.* (2013) and Borken-Kleefeld and Chen (2013) also clearly show that when it comes to diesel cars newer cars emit about the same level of NO_x that new cars did 20 years ago. Data from the measurements in Gothenburg in 2007 and 2014 show the same trends. Moreover, when comparing average emissions by Euro standard between the 2007 and 2014 measurements, the NO_x emissions seem to have increased within the same emission standard. If analyzing NO and NO₂ separately it shows that NO has increased and at the same time NO₂ has decreased, also leading to a decreased NO₂/NO_x ratio. The reason for the increase in NO_x and at the same time lower NO₂/NO_x comparing the measurements in 2007 with 2014 is not clear. Some of it may be attributed to the uncertainty due to a relatively low number of measurements. But it may also be deactivation of the diesel catalyst which causes deterioration of the NO_x reduction performance and the ability to produce NO₂. This may also be the reason for the difference between the 2007 Gothenburg measurements and data presented in Carslaw (2013). Other differences between the measurements in Sweden and the UK may be a different mix of engine sizes. In Carslaw (2013b) the NO₂/NO_x ratios for diesel cars are presented separately for <2 liter engines and >2 liter engines. This shows a higher NO₂ share for the larger engines in a certain VSP range with a maximum of about 47% for Euro 4 cars with low VSP. The diesel vehicles measured had an average cylinder volume of 2.3 l and 2.2 l for Euro 3 and Euro 4 vehicles respectively in 2007. In 2014 the averages were 2.3 l and 2.1 l. Another difference may be a possibly higher share of Euro 3 vehicles with DPF in Sweden compared to the UK.

Figure 4 shows that the NO₂/NO_x ratio measured in 2007 increased from about 15% for Euro 2 cars to about 47% for Euro 3 cars and 56% for Euro 4 cars. The increase from Euro 2 to Euro 3 is due to the introduction of diesel oxidation catalysts (DOC) in Euro 3 vehicles. Some Euro 4 cars were equipped with DOC + diesel particulate filter (DPF) which may explain the higher NO₂/NO_x ratio from

Euro 4 compared to Euro 3, Carslaw *et al.* 2016. Data presented in Carslaw *et al.* (2013) also show this stepwise increase of the NO_2/NO_x ratio from Euro 2 to Euro 4.

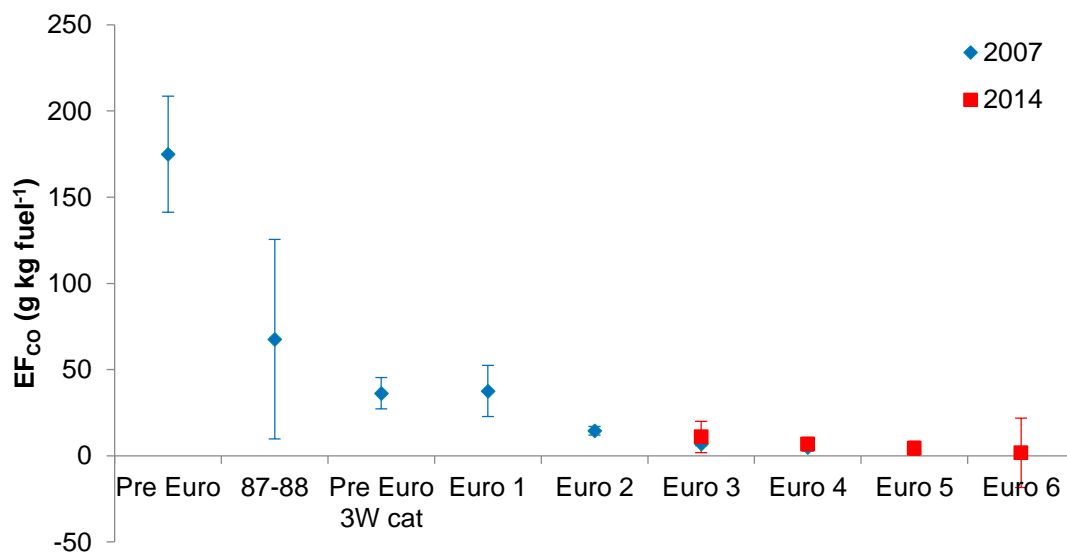


Figure 11. CO emissions from gasoline cars as measured in Gothenburg 2007 and 2014.

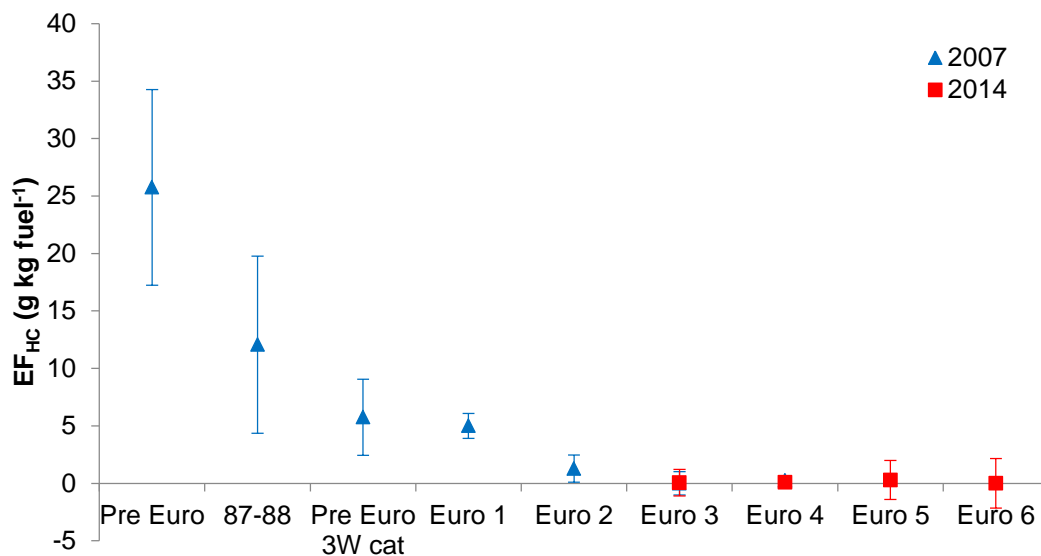


Figure 12. HC emissions from gasoline cars as measured in Gothenburg 2007 and 2014.

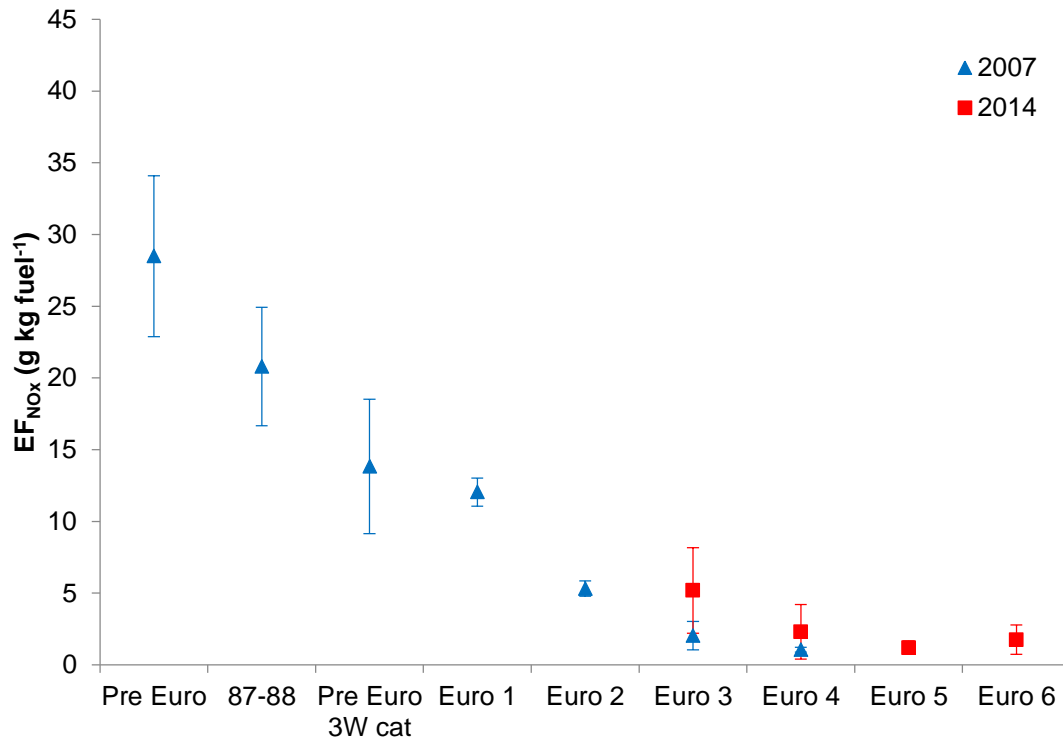


Figure 13. NO_x emissions from gasoline cars as measured in Gothenburg 2007 and 2014.

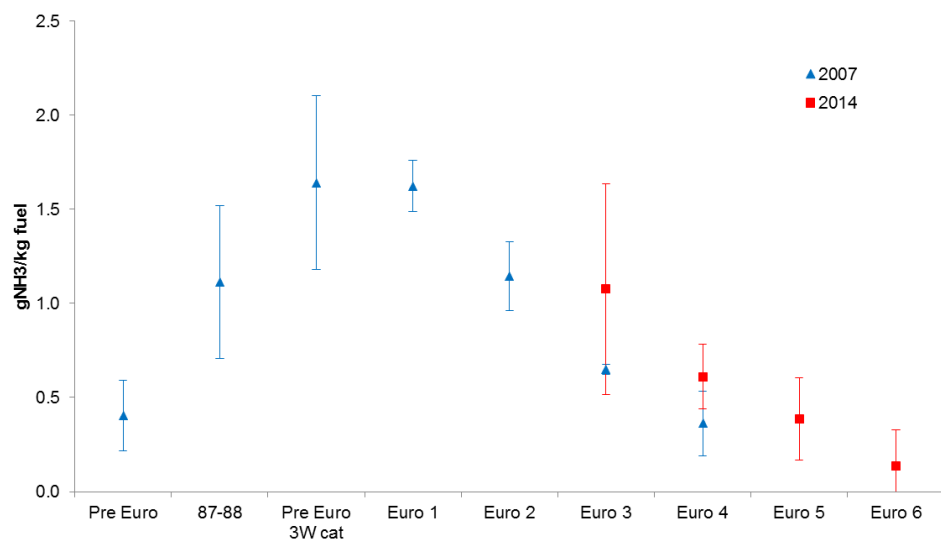


Figure 14. NH₃ emissions from diesel cars as measured in Gothenburg 2007 and 2014.

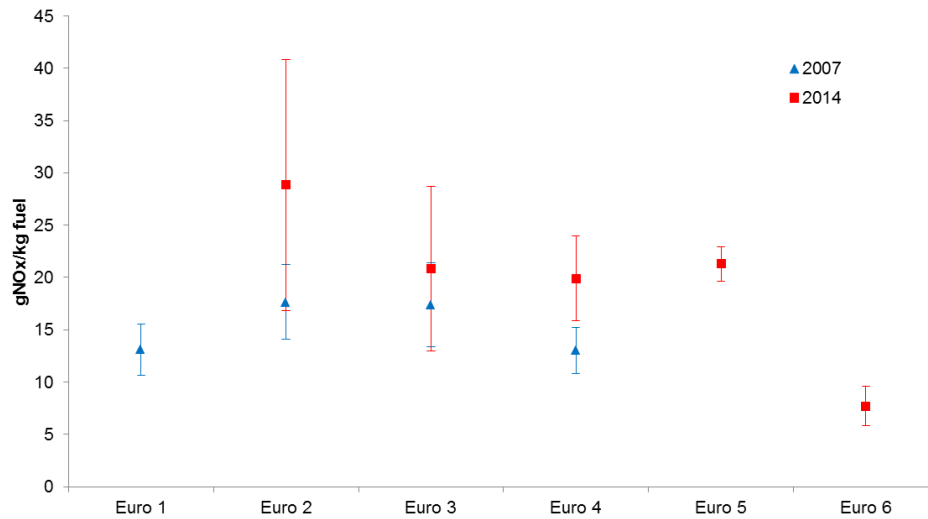


Figure 15. NO_x emissions from diesel cars as measured in Gothenburg 2007 and 2014.

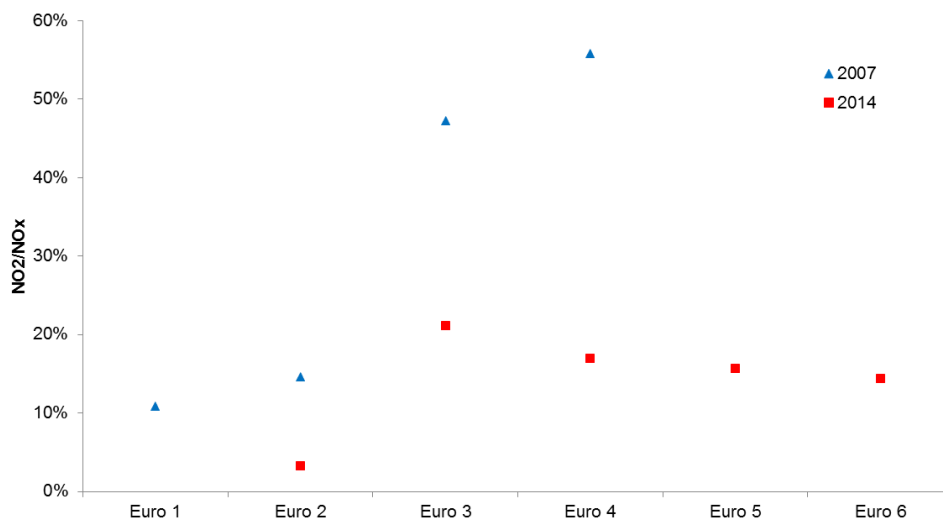


Figure 16. NO₂/NO_x ratio in exhausts from diesel cars as measured in Gothenburg 2007 and 2014.

Conclusion

During 2007-2015 on-road emission measurements by means of remote sensing were conducted in Sweden, mainly on heavy-duty buses and passenger cars. The number of measured vehicles in the studies is relatively small compared to other similar studies in Europe and the United States. However, the Swedish data shows comparable results with other studies. What differs from most other published studies on roadside emission measurements, is the use of an Engine Exhaust Particle Sizer Spectrometer for measuring particle mass and number (of which only particle mass has been presented in this paper) on heavy-duty buses. These measurements have shown differences in emission behavior between different emission standards and emission reduction technologies. More over the roadside measurements on passenger cars in 2007 were probably the first of its kind in Europe including NO₂. The following measurement in 2014 enabled an analysis of changes in NO and NO₂ emissions from diesel passenger by emission standard over a seven year period (2007 to 2014).

Acknowledgements

Gary Bishop at the University of Denver is deeply acknowledged for big support in both measurements and data analysis, and Annette Bishop for her work on license plate recognition.

The drivers and the personnel at the bus depots are acknowledged for their assistance and hospitality.

References

- Burgard D.A, Bishop G. A., Stadtmuller R. S., Dalton T. R. Stedman D. H., Spectroscopy Applied to On-Road Mobile Source Emissions, Applied Spectroscopy 2006 May; 60(5): 135A-148A
- Carslaw D. C., Murrells, T. P., Andersson J. & Keenan M., (2016) : Have vehicle emissions of primary NO₂ peaked ? Faraday Discuss, Advance Article, DOI 10.1039/C5FD00162E
- Carslaw D. C. & Rhys-Tyler, G., (2013): New insights from comprehensive on-road measurements of NO_x, NO₂ and NH₃ from vehicle emission remote sensing in London, Atmospheric Environment 81 (2013) 339-347
- Carslaw D. C. & Rhys-Tyler, G., (2013b): Remote sensing of NO₂ exhaust emissions from road vehicles – A report to the City of London Corporation and London Borough of Ealing,, DEFRA Project Reference 332c2011 (City of London Corporation), 334c2011 (London Borough of Ealing)
- Chen Y., Borcken-Kleefeld J., (2013): Real-driving emissions from cars and light commercial vehicles – Results from 13 years remote sensing at Zurich/CH, Atmospheric Environment 88 (2014) 157-164
- Hallquist Å. M., Jerksjö M., Fallgren H., Westerlund J. & Sjödin Å., (2013): Particle and gaseous emissions from individual diesel and CNG buses, Atmos. Chem. Phys., 13, 5337-5350
- HBEFA (2016), www.hbefa.net

Potential and methods to reduce GHG emissions from road infrastructure

Håkan JOHANSSON*, Kjell Ottar SANDVIK**, Jozséf ZSIDÁKOVITS*** and GrzegorzŁUTCZYK****

*Swedish Transport Administration, 781 89 Borlänge, Sweden
hakan.johansson@trafikverket.se

**Norwegian Public Roads Administration, PO Box 8142 Dep N-0033 Oslo, Norway

***Hungarian Transport Administration, Lövöház u. 39, Budapest 1024, Hungary

****General Directorate for National Roads and Motorways, Wronia 53, 00-874 Warsaw, Poland

Abstract

The transport sector is a major contributor to GHG emissions and there is an urgent need to reduce these emissions. About 5-10 percent of the emissions from road transport are not traffic related but generated during construction and maintenance. The emissions are dominated by the use of concrete, steel, asphalt and fuel consumed by vehicles and machines in these processes.

In the paper the CEDR I4 climate mitigation group give recommendations how GHG emissions from road infrastructure can be reduced. Methods have been developed to calculate the GHG emissions from construction and maintenance of infrastructure in a life cycle perspective. In countries like Sweden and Norway it is now mandatory to use these methods in all major projects.

Consultants contracted for planning should deliver calculations of emissions for different alternatives and measures that can be taken into consideration by the administration.

At procurement of construction the recommendation is to have requirements on a certain level of reduction of the GHG emissions instead of pointing on certain measures. This gives the contractor a degree of freedom to choose the most cost-effective way to reduce the emissions to the required level, which should be verified at the end of contract.

Keys-words: low carbon, infrastructure, construction, maintenance

Introduction

Present trends in global emissions of greenhouse gases will give rise to increases of the global mean temperature of 4-5 degrees Celsius. If this trend is maintained it will result in dire consequences for life on earth that will be difficult to estimate. However, it is not too late to shift the trend and there is also a possibility to limit the temperature increase to 1.5 - 2 degrees Celsius or less in line with Paris Climate Agreement (United Nations, 2015). An objective all countries have agreed to. Limiting the temperature increase to less than 1.5 degrees Celsius means that the global emissions have to be reduced to zero in period between 2045 - 2060 and the emissions after that must be negative (Rogelj et.al., 2015). For example - the latter can be achieved by burning biomass in power plants together with carbon capture and storage (BECCS). Transport sector is one of the most significant contributors to emissions of greenhouse gases, responsible for 26 percent of the global emissions and the share is increasing (IEA, 2015). Of the emissions in the transport sector road transport is dominating, therefore it must contribute to meet the goals set by global climate agreement.

Besides the traffic on the roads, the maintenance, operation and construction of new infrastructure leads to GHG emissions. It is highly important to consider not only the direct emissions from machinery and trucks, but also the indirect emissions from materials and energy including extraction of raw material, processing of materials and transport in all phases, including to the production site or maintenance area. Also dismantling of old infrastructure should be included. In Sweden it is estimated that emissions from infrastructure in a life cycle perspective stands between 5 to 10 percent of the total emissions from traffic and infrastructure. This is a rough estimate but give a picture of emissions magnitude. Even if the emissions are not as high as the emissions from traffic it is emissions that the road administrations can affect either directly or through setting the requirements in procurements for construction and maintenance of infrastructure.

This paper is a result of work done within the CEDR I4 group on mitigation and adaptation to climate change. Based on examples especially from Sweden and Norway within the group the paper will give recommendations on how to calculate emissions from road infrastructure and how requirements for consultants and contractors during procurement can be used to reduce the GHG emissions from the infrastructure in a life cycle perspective (LCA). One basis for the paper is an enquiry that was done within the CEDR I4 group that was answered by all countries that belonged to the group, which at that time included, Norway, Sweden, Denmark, Ireland, Poland, Hungary, Austria, Switzerland and Italy. All CEDR I4 countries take emissions from traffic into account during planning of infrastructure. When coming to emissions from the infrastructure in a life cycle perspective the picture is however somewhat mixed. Denmark, Ireland, Italy, Norway and Sweden also take emissions from materials used for the road construction into account. Except Denmark these countries and Hungary also considers emissions from machinery and trucks used during construction. Emissions from maintenance of constructed infrastructure are taken into account by Hungary, Ireland, Norway and Sweden. Finally emissions from changed land use are considered by Denmark, Italy and Norway. The conclusion is that only Norway take all emissions from traffic, maintenance of constructed roads, changed land use, materials, machinery and trucks into account.

Figure 1 shows an example from Norway of how the emissions of GHG emissions are distributed between different materials and energy in a motorway project. Figure 2 shows another example for all major road projects included in the Swedish National Transport Plan 2014-2025. From both pictures it can be concluded that GHG emissions are dominated by concrete, steel for reinforcement and other construction, diesel fuel for machines and trucks and asphalt. Reducing need of materials through lighter elements of construction, reducing mass of transports and using more efficient vehicles and machines together with materials and energy with less GHG emissions are ways to reduce the overall GHG emissions from the projects. Examples from Norway and Sweden shown below depict how one can work to achieve better control of the emissions and their reduction.

There are of course also other methods for calculations and establishing the requirements for reduction of GHG emissions from infrastructure than described below. This paper does not serve as an overview of different methods, but instead gives practical examples on calculation methods from Norway and Sweden and procurement requirements from Sweden.

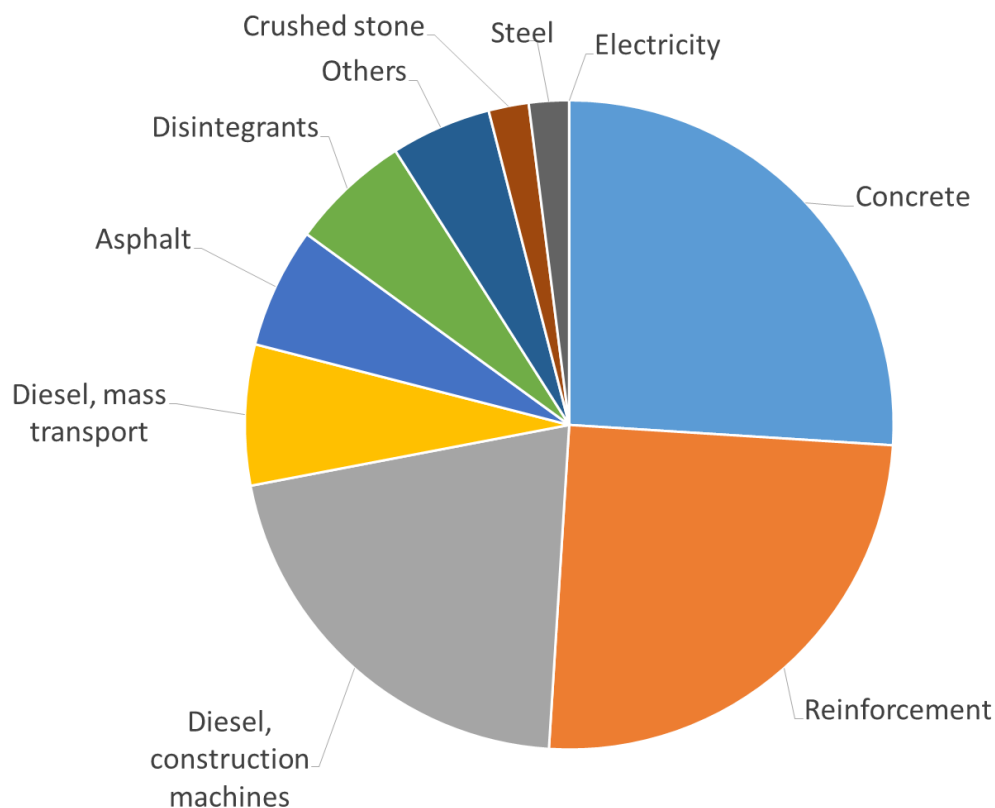


Figure 1 Distribution of GHG emissions for a motorway project in Norway (Norwegian Public Roads Administration, 2015)

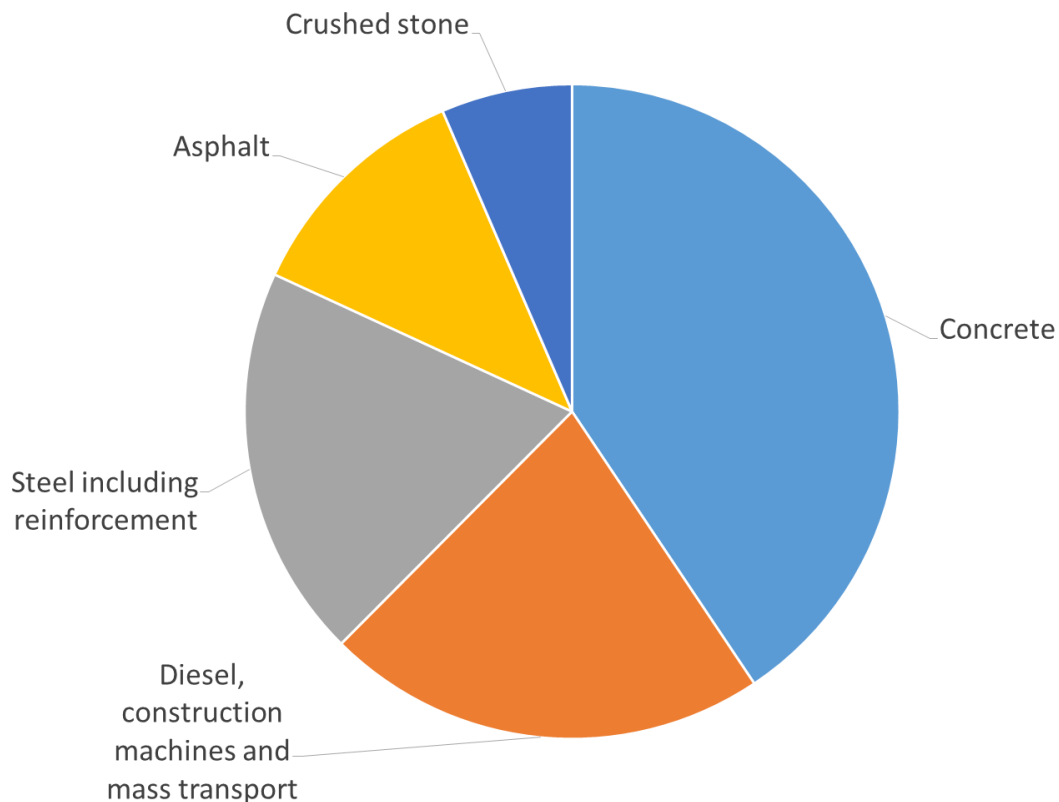


Figure 2. Distribution of GHG emissions for major road projects in Sweden (WSP, 2015)

1. Calculation of emissions from infrastructure

Proper calculation of emissions from infrastructure is a key to all further actions which include reduction and mitigation goals. It is the most complex part of entire process and only few polled CEDR I4 countries have already developed methodologies. Doing calculations is a first step to get a picture of GHG emissions and energy use from construction of infrastructure. From this large emitters and potential reductions can be identified. As described above the emissions of GHG emissions from infrastructure in a life cycle perspective is dominated by the use of concrete, steel, asphalt and fuel consumed by vehicles and machines.

The methodology that was recently developed in Norway incorporates the impact of GHG emissions during the construction phase and from relevant maintenance works performed throughout the lifetime of the project (Norwegian Public Roads Administration, 2015). These indirect emissions, together with direct emissions from traffic, are incorporated into the cost-benefit-analysis (CBA) that is performed. The methodology has been operationalized and is integrated into the standard software package EFFEKT used for performing CBA.

Regarding construction the methodology summarizes emissions from the extraction of raw materials, processing of materials and construction. The underlying principle for calculation is that GHG emissions are equal to input factors multiplied by emission factors. Input factors may include concrete, steel, explosive, transport, etc. Emission factors are derived for all input factors from the environmental database Ecoinvent and adapted to Norwegian conditions. The reason for the small number of input factors used (around 20) is that this analysis is carried out at an early planning stage when knowledge about the material used in construction is limited. For example, only one quality of steel is used; the same applies to concrete. The closer it gets to the start of construction work, the easier it should be to differentiate more and use more specified input factors.

The emissions consisting of CO₂ (carbon dioxide), N₂O (nitrous oxide), and CH₄ (methane) are calculated in tons of CO₂ equivalents. To convert this volume into monetary terms for CBA applications, a unit value of NOK (Norwegian Kroner) per ton is used.

This methodology is primarily designed for calculating GHG emissions from ordinary roads in open terrain, steel and concrete bridges, ferries and tunnels all of which are elements that may be part of an ordinary transport project. The method is now used for most of the project candidates in the new National Transport Plan.

As mentioned above what have been done so far is calculation of GHG at an early planning stage. However, experience shows, that the closer it gets to construction phase, the more precise calculation is needed. For this reason there is an ongoing development of a more detailed calculation program for GHG where the results are supposed to be part of the tender documents and constructors are prompted to reduce the GHG emission.

Calculations of GHG emissions and energy use during the life cycle have also been done in Sweden for all projects included in the National Transport Plan for the years 2014–2025. A methodology has been developed and used to make calculations for the largest projects and a number of 'standard projects'. The total GHG emissions during the life cycle (including traffic) was calculated for the largest projects, standard projects and indicative parameters. This gave an estimation of GHG emissions and energy use for the whole National Transport Plan.

The method used for the national plan has been developed into a tool, Klimatkalkyl that can be used for operational calculations of GHG emissions and energy use for new infrastructure projects. In April 2015 the Swedish Transport Administration made it mandatory to use Klimatkalkyl to calculate GHG emission and energy use during life cycle for all new infrastructure projects with total cost over 50 million SEK (5,4 million €). Successive calculations shall be done from early planning till the infrastructure project is completed and ready to open for traffic. This can be basis to utilize the potential in every step. Klimatkalkyl is updated regularly. In future updates of the method it will also be possible to make calculations not only for new infrastructure projects but also for the operation and maintenance of existing one.

Methods to calculate and work for reduced GHG emissions in a LCA perspective in planning and procurement of infrastructure have not yet been implemented in Poland or Hungary. In Poland there are however plans to introduce it. The Strategic Environmental Impact Assessment (SEIA), included in Prognosis of Environmental Impact made for the National Road Construction Program for years 2014 – 2023 clearly states, that continuing trend of emissions release to atmosphere will in future contribute to results of climate change. SEIA identifies, that emissions from transport sector stand at 23 percent of those from energy sector. It is also underlined that, mitigating measures must be assessed at every stage during planning phase, i.e. selection of route variant, feasibility studies and design, so they can be introduced during construction, operation, maintenance and dismantling of road projects.

2. Basic principles for reducing GHG emissions from infrastructure

Based on the experience developed from calculations of GHG emissions and energy use from infrastructure the Swedish Transport Administration started a work to develop requirements to reduce GHG emissions and energy use from infrastructure in 2014. The purpose of the requirements was that they would be used during procurement of consultants and contractors. Early in the process some basic principles were identified:

- The requirements should be long term so that the consultants and contractors get sufficient time to develop cost efficient strategies to develop solutions to deal with them. Rather more ambitious requirements later than less ambitious requirements with no lead time.
- The requirement on reduction of GHG emissions for a certain year about 5 years from now should be supplemented with an indicative more long term target 10 years from now. This will give the consultants and contractors long-term rules to develop solutions for the future.
- Technically neutral requirements on reductions of GHG emissions that describe what should be achieved instead of how it should be achieved. In this way the consultants and contractors can chose the most cost efficient solution.
- Monitoring should be mandatory for every contract that is subject to the requirements. Monitoring of separate contractors for all contracts that they have can also be done. By comparing results of different contractors and benchmark them a form of competition between them can be established.
- The requirements should be complemented with research and development activities together with

the consultants and contractors. Focus should be put to reducing the cost of promising solutions with large potential to reduce GHG emissions.

- Barriers for using cost efficient solutions should be identified as well as solutions to unlock these.

It was decided that the requirements should include the whole infrastructure including construction, operation and maintenance of existing infrastructure and also the procurement of railway-specific materials that the Transport Administration provides to the contractors. The requirements should include consultants for planning and design as well as contractors for construction, operation and maintenance.

3. Setting targets as basis for technically neutral requirements

In 2014 the Swedish National Transport Administration derived preliminary targets to reduce the GHG emissions and use of energy from infrastructure from national climate and energy targets. The purpose of these targets was employing them as basis for technically neutral requirements at procurement. A research project was conducted during 2014 and 2015 to describe the consequences of the preliminary targets and two alternative levels (WSP, 2015). The research project also provided basis for designing requirements in procurement. Potential reductions of GHG emissions for different measures including design and materials were identified in the project. These measures were put together in scenarios that fulfilled the different target levels. The scenarios were then presented and discussed together with possible requirements in a number of workshops with consultants and contractors. It is very difficult to establish a potential for reduction of GHG emissions in the planning phase, but it is probably large if GHG emissions are considered in the decisions.

The overall conclusion was that the target derived from the national GHG objective, standing at 15 percent reduction of GHG emissions from new infrastructure projects between 2015 and 2020, could be achieved in the design and construction phase without extra cost. Also a 30 percent reduction to 2025 could be achieved but here the costs are less certain. To achieve a 100 percent reduction and thereby contribute to the national objective of Sweden (no net emissions of GHG emissions to 2050) new processes are needed such as carbon capture and storage in plants producing cement and steel are necessary. Other methods like using hydrogen instead of coal as reduction agent in steel production can also be used. The consultants and contractors that took part in the workshops generally regarded the Transport Administration intended requirements for GHG reduction in procurement as positive.

4. Requirements in all phases

Based on the results from the research project the Swedish Transport Administration introduced requirements on all new contracts for consultants and contractors to new infrastructure projects (with total cost over 50 million SEK) starting from 2016 and concluded in 2020 or later. Pilot programs will also be made for projects with shorter lead time. Requirements on contractors for operation and maintenance as well as for smaller projects (50 million SEK or less) will be developed in a later stage.

The requirements are put on consultants and contractors during both planning and construction phase (see figure 3). During the planning phase the exact location of the road is still open and the design is also not well defined. Depending on decision for later solution, the GHG emissions can vary a lot. They are however only one of many parameters that will be considered when the Transport administration chooses the final solution. When procuring the consultant for the planning phase there are requirements that must be fulfilled:

- make climate calculations for the different alternatives
- present the most important aspects for GHG emissions for the different alternatives
- present measures that can reduce the GHG emissions.

To encourage the consultant to deliver a good product, bonuses can be used. This can also affect future possibilities to win contracts. From the proposals on measures to reduce GHG emissions and other important factors the Transport Administration makes a decision on an alternative. To encourage the region within the Transport Administration that makes the decision to choose alternatives with low GHG emissions internal performance management is used with annual emission objectives per region.

The Swedish Transport Administration uses both construction contracts and turnkey (design) contracts for contractors. The objective is to increase the latter. When decision has been taken to use

construction contracts a consultant is first procured to do the design of the project. Before doing the procurement the Transport administration calculates the potential to reduce GHG emissions in the project using a specified method. On average this meets the objectives mentioned above (15 percent reduction to 2020 compared to 2015). In the procurement it is required that during work the consultant shall propose measures that fulfills the specified reduction of GHG emissions (in percent) compared to a certain base level. The consultant shall specify the proposals divided on:

- design measures that can be decided by the Transport administration
- quantitative reduction requirements that can be used in procurement of contractor.

The consultant also makes an update of the climate calculation for the project.

In next phase, procurement of the contractor for construction of works is done. During this the Transport Administration uses the input from the design phase to undertake decision on project design and a quantitative reduction of GHG emissions compared to a certain base level, that the contractors have to fulfill. This is then specified in the procurement. In the end of the contract the contractor has to show certified climate declaration using a third party, that the requirement on reduction of GHG emissions has been fulfilled. For larger reduction than required the contractor can be awarded a bonus. How large the reduction should be is specified in the procurement. The results also affect future possibilities to acquire contracts.

For turnkey (design) contracts it works essentially in the same way as for construction contracts. The difference is mainly on requirements level which are higher, since it also includes the design phase.

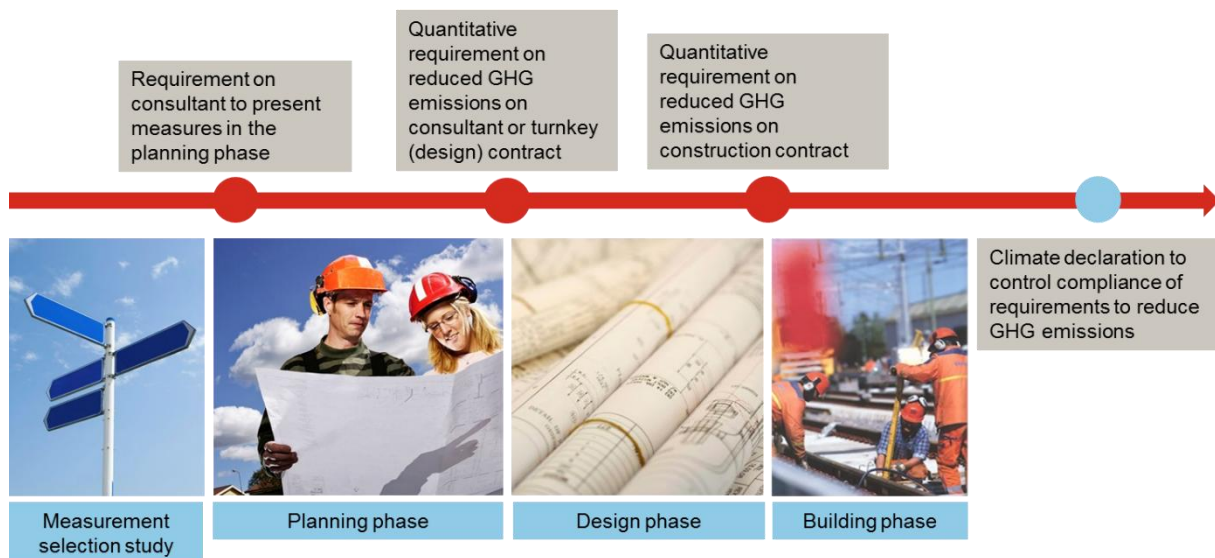


Figure 3. Requirements on consultants and contractors in different phases

Conclusion

Reduction of emissions from infrastructure in a life cycle perspective is essential to meet climate objectives. It is also something that road administrations have influence over either directly or indirectly through procurement. Performing the climate calculation for infrastructure, both planned, existing and its maintenance, will provide good basis for measures to reduce the GHG emissions.

The road administration can act in different ways to reduce the GHG emissions from infrastructure. In early planning phases the potential is high but also influenced by other criteria for selecting an alternative. Basis for reducing the GHG emissions should be included as requirements for consultants and contractors, with purpose to reduce GHG emissions from infrastructure and maintenance in a lifecycle perspective. Follow up at the end of contracts, to ensure that requirements have been fulfilled is obligatory. Bonuses can be used as incentives for further accomplishments. The requirements at procurement should be complemented with identifying possible barriers for utilization of methods that are already cost efficient today. Also financing and taking initiative in research over future promising techniques, which will help reduce GHG emissions from transport is necessary.

References

IEA, 2015, Energy Technology Perspectives 2015 - Mobilizing Innovation to Accelerate Climate Action, Paris: <http://www.iea.org/etp/>

Norwegian Public Roads Administration (2015a) Klimagassutslipp fra utbyggingen av E18 Sky – Langangen (GHG emissions from building E18 Sky – Langangen), 31.08.2015 Statens vegvesen, Vegdirektoratet, TMT (In Norwegian)

Norwegian Public Roads Administration (2015b) Dokumentasjon av beregningsmoduler i EFFEKT 6.6. (Documentation of calculation modules in EFFEKT 6.6.) (In Norwegian). http://www.vegvesen.no/fag/Publikasjoner/Publikasjoner/Statens+vegvesens+rappporter/_attachment/113240?ts=14e2ea3bec0&download=true&fast_title=Dokumentasjon+av+beregningsmoduler+i+EFFEKT+6.6

Rogelj J, Luderer G, Pietzcker R. C., Kriegler E, Schaeffer M, Krey V, Riahi K (2015) Energy system transformations for limiting end-of-century warming to below 1.5 °C, Nature Climate Change, 21 May 2015, DOI:10.1038/NCLIMATE2572

United Nations (2015) Adoption of the Paris Agreement, <https://unfccc.int/resource/docs/2015/cop21/eng/l09r01.pdf>

WSP (2015) Konsekvensanalys av klimatkrav för byggande och underhåll av infrastruktur (Impact of climate requirements for the construction and maintenance of infrastructure) (In Swedish): <http://fudinfo.trafikverket.se/fudinfoexternwebb/pages/PublikationVisa.aspx?PublikationId=2800>

Swedish Transport Administration (2015) Klimatkalkyl version 3.0– model for calculating energy use and greenhouse gas emissions of transport infrastructure from a life cycle perspective, Report 2015:063.

http://www.trafikverket.se/contentassets/eacf8784f0b341c4a4198d40eb620134/2015_063_klimatkalkyl_version_30-eng_report.pdf

Prognosis for Environmental Impact of National Road Construction Program for years 2014 – 2023 (in Polish)

https://www.gddkia.gov.pl/userfiles/articles/k/konsultacje-spoleczne-prognozy-o_18875/TOM%20A%20-%20czesc%20tekstowa.pdf

Modal Shifting Effects and Climate Impacts through Electric Bicycle Use in Germany

ClaudiaKAEMPER*, Hinrich HELMS* & Julius JOEHRENS*

*ifeu – Institut für Energie- und Umweltforschung Heidelberg GmbH, Heidelberg, Germany
Fax+494115124625-email:claudia.kaemper@ifeu.de

Abstract

Sales rates of electric bicycles (e-bikes) have grown rapidly over the last ten years, not only in Germany but all over Europe. Thus, the strongest movement towards electric mobility on German roads is yet dominantly pushed by e-bikes, whereas electric cars need to catch up. So far, there are hardly any reliable investigations about everyday use patterns, modal shift effects and potentials to reduce climate impact. An assessment of the significance of e-bikes for achieving climate and energy policy guidelines from the "German Federal Government's National Energy Concept" from 2010 has not been possible so far. The project "Pedelection" analysed these questions by conducting a field test focused on people who purchased their e-bike only recently. The main finding from the field test is that e-bikes have the potential to substitute a considerable amount of car mileage. Since the climate balance of distance travelled by e-bikes is by factor 10 better, additional induced traffic or shifting from bicycle/walking is negligible to a certain degree. Bicycles – with or without electric assistance – are serious means of transport and a genuine alternative to passenger cars on short and medium distances up to 15 km.

Key-words: electric mobility, two-wheeler, environmental impact, mobility patterns.

Introduction

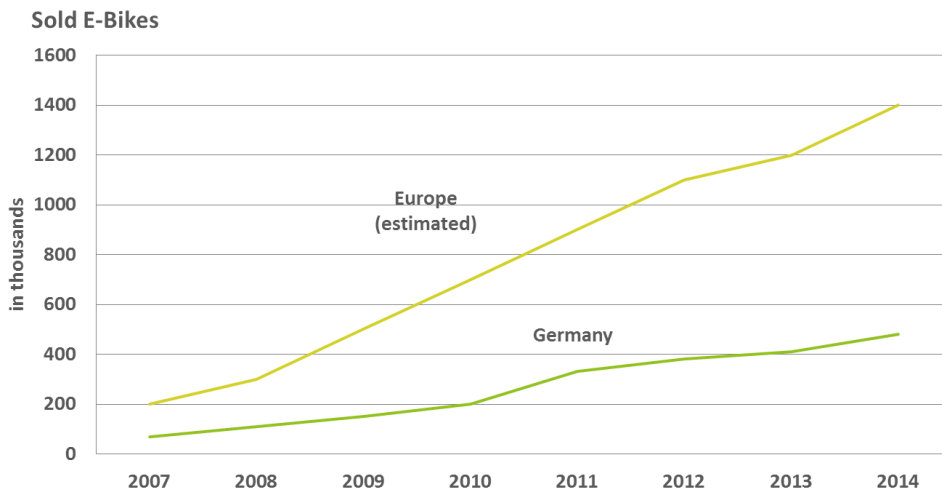
Mobility is an important basis for many economic and private activities and thus is a crucial part of our life. However, mobility is also energy consuming and leads to substantial environmental problems. In 2015, the transport sector was responsible for 28% of the final energy consumption in Germany. More than 80% of the transport energy consumption is thus consumed by road traffic, and more than 90% of this energy consumption is based on the use of fossil fuels. This leads to a share of 18% of CO₂ emissions caused solely by the transportation sector (Umweltbundesamt, 2015). Although air quality improved over the last decades in Germany, NO_x concentration and noise in urban areas still remain a problem. The current challenges for the road transport are the reduction of energy consumption, greenhouse gas (GHG) emissions and other air pollutants. This demands for new and improved technologies in the transportation system. However, the ambitious national goals to reduce CO₂-emissions and energy consumption cannot be met by only using more efficient vehicles. A broader transformation of the transport sector is needed which also focuses on mobility patterns of people in general.

Electric mobility is discussed as the main choice to reduce fossil fuel consumption and integrate renewable energies into the transportation sector. Until now, the discussion of electric mobility is mainly focused on electric cars. But other modes of transport offer electric mobility choices, too, such as the electric bicycle (e-bike). The concept is not completely new since they were introduced to our roads in the 90s. But advances in technology (e.g. lithium-ion battery) helped the e-bike to reinvent itself and gain popularity for different mobility purposes in Germany and other European countries (Budde et al., 2012). There are two general concepts of e-bikes available: (1) E-bike with pedal electric assistance and (2) E-bikes with exclusive electric propulsion. This article is focused on the first concept which requires pedalling by the cyclist because this vehicle is still treated like a conventional bicycle by German law.

As figure 1 indicates, sales rates of e-bikes have grown rapidly over the last ten years, not only in Germany but all over Europe (ZIV, 2015). The image of e-bikes has improved due to a broader range of models from an everyday-bike to an ambitious sport vehicle or lifestyle product. E-bikes can be used as conventional bikes but the electric assistance may have an impact on use patterns since distances and difference in altitude become less relevant. So far, there are hardly any reliable investigations about everyday use patterns, modal shifting effects and potentials as well as use and non-use motives of German e-bikes users. An assessment of the significance of e-bikes for achieving climate and energy

policy guidelines from the "German Federal Government's National Energy Concept" from 2010 has not been possible so far. The project "Pedelection" closed this research gap (Lienhop et al, 2015).

Figure 1. Number of electric bikes sold in Germany and Europe per year (ZIV, 2015).



1. Method

The project "Pedelection" had a comprehensive research design by using qualitative as well as quantitative methodology in order to answer the broad set of questions. Modal shifting effects and climate impacts by e-bike usage were primarily answered with quantitative methodology but also findings from the qualitative assessments had an impact on the research progress.

Outline of the field test

In order to analyse the modal shifting effects and climate impacts, a field test in Germany was conducted with two groups with a different volume of data collected. The core group was selected from four metropolitan regions: (1) Munich, (2) Frankfurt, (3) Brunswick-Hannover and (4) Bremen-Oldenburg. Participants were not required to live directly in the city itself, the intention was rather to have participants from different regions in Germany to gain a higher representativeness of the results. The core group (70 participants) was equipped with data loggers in order to record driving and charging data. Every participant was instructed to provide data for four separate weeks throughout one year to cover different seasons. Additionally, participants logged all their daily trips for the same four weeks. The core group was accompanied by a second group (312 participants) which only participated in the online survey to log their daily trips for four weeks throughout the year. The online survey did not have any regional constraint. The field test started with 382 participants in the first week and ended with 216 participants in the last week due to panel mortality. To get data covering the whole year, the weeks were scheduled in advance for the different participants.

The sample

The aim of the sample selection was to gain a high representativeness concerning German e-bike users. Nevertheless, it was challenging to spread the sample throughout different social groups, since e-bike users are currently predominantly male, older than 40 years and bike enthusiasts. Therefore, the sample comprised of only 30% female users against 70% male users. Young e-bike users were underrepresented since only 15% of the sample was under 45 years old, 23% was over 65 years. Up to 47% of the sample had a university degree which is higher than average share. Concerning the work situation, 64% were either in a full-time or part-time employment. 27% of the users were pensioners. In addition to covering different social groups, it was aimed to get participants into the sample which only recently used an e-bike. The average e-bike experience of the sample at the beginning of the field test was eight months.

E-bikes in Germany follow mainly two concepts due to legal regulation. An e-bike is treated by German law as a normal bicycle, if it has an engine performance of maximum 250 W and electric pedal assistance up to a speed limit of 25 km/h (e-bike-25). Higher engine performances or assistance up to higher speeds require registration of the vehicle and are accompanied with certain obligations

such as mandatory helmets (e-bike-S). Today the concepts of “e-bike-25” and the “e-bike-S” are established on the German market. 84% of the sample possessed an “e-bike-25” and only 10% an “e-bike-S”, the rest were retrofitted bicycles.

The sample was analysed for three different user groups who shared similar mobility profiles: (1) Commuter, (2) Everyday user and (3) Leisure user. The group “Commuter” consisted of participants who had a significant number of trips to work in their total journey protocol. The group “Everyday user” made 50% of their trips for daily purposes such as shopping, private errands or undefined purposes. “Leisure users” used their e-bikes mainly for leisure trips to relax or for physical activity. 41% of the sample belonged to the group of “Commuters”, 40% to the group of “Everyday users” and 19% to the group of “Leisure users”.

Compilation of data

In order to answer the research questions three sources of primary data were available: (1) GPS-data of journeys, (2) charging data for the battery and (3) metadata for single trips. Further information to assess climate impacts of vehicles and mobility patterns was also derived from secondary data such as results from a lifecycle assessment of different vehicle concepts (Helms et al., 2011, 2016; Weidema et al., 2013). Compiling the primary data was a complex task because there were no standard compiling systems available and the two logging systems produced different data formats. The main challenge was to match the data and find inconsistencies due to handling errors of the participants. Unfortunately, 12% of the submitted data could not be used because of handling errors.

2. Results and Discussion

The motorization of the e-bike enables the cyclist to cover larger distances and/or shorter travel durations in comparison to the conventional bike. The average travel distance on an e-bike is 11.4 km and the average duration is about 50 minutes. Compared to average results for a conventional bicycle and a car, the e-bike is closer to the bicycle in terms of travel distance (see figure 2). The relatively high average duration is due to constraints in data measurement (stops up to 30 minutes are included) and a considerable amount of leisure day trips. 90% of all e-bike trips are under 26 km and under 120 minutes. The frequency distribution of trip distances shows a peak at 4 km, after that it decreases constantly. Examining the distribution of duration, it peaks between 20 to 30 minutes.

Figure 2. Potential range of individual means of transport.

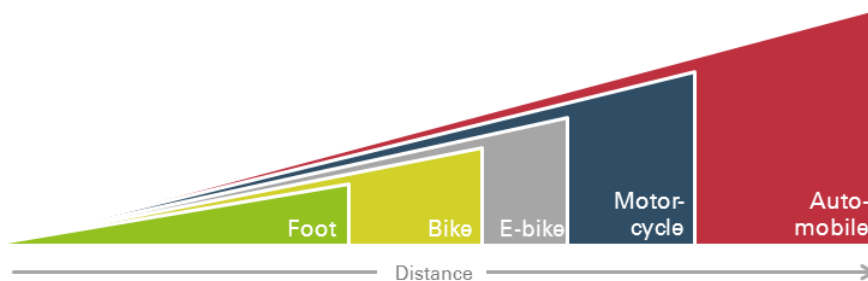
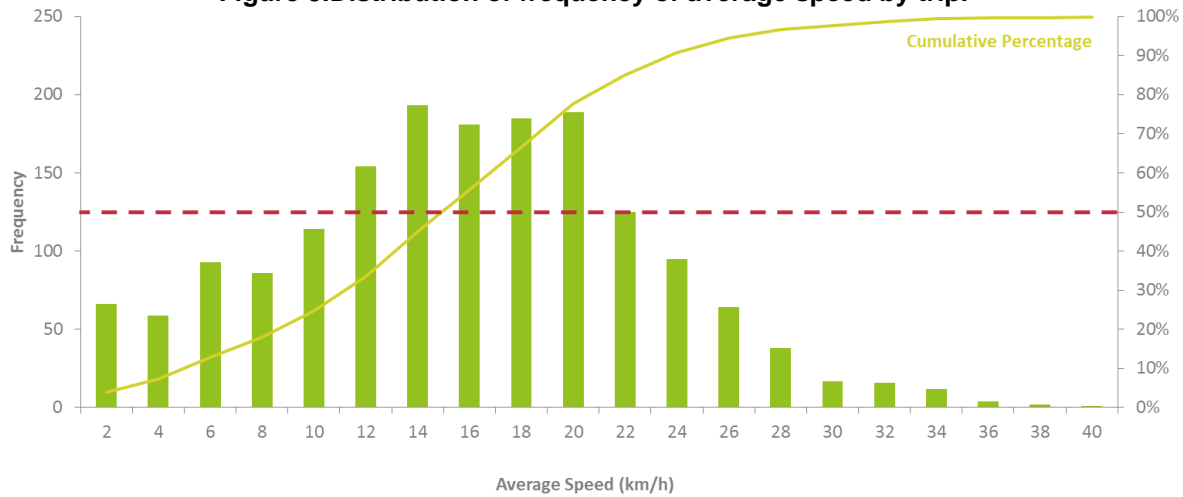


Figure 3 shows the analysis of the speed distribution. The average speed is 15 km/h for all e-bike trips, with the majority ranging between 12 and 20 km/h. After 20 km/h follows an abrupt decline due to the high number of e-bike-25 owners in the sample. The average speed of 20 km/h for e-bike-S owners is considerably higher. The same accounts for the group of commuters which travels with an average speed of 17 km/h. Selected participants were equipped with a cadence sensor. The average cadence was 59 rpm which is a rather low value for cyclists. The study of DHBW (2014) observed the same pattern with a 30% lower cadence as for conventional cyclists. They also concluded that e-bike cyclists pedal less continuously due to the combination of fast acceleration and followed freewheeling. The aspect of lower exertion to cover higher elevations was less distinctive in the field test than expected since 45% of trips only covered a positive change in elevations of 20 meters. This especially accounts for daily trips and of course for trips in Northern Germany. The average for South German trips was a cumulative change in altitude of 68 meter per trip.

Figure 3. Distribution of frequency of average speed by trip.



The analysis of the mobility patterns of e-bike users shows that in general only 21% use their e-bike exclusively for leisure and holiday trips, while around 80% use it as a full means of transport for commuting and other everyday trips. Distances and duration show a high dependency on the purpose of the trip. Table 1 summarises the distribution of distance and duration by trip purpose. It has to be noted that the duration not only includes the actual moving time but also stops up to 30 minutes. It is thus the duration of the whole journey. Long stopping periods especially account for shopping and private duty trips, because the shopping itself is often included in the data. The overall duration of the journey to and from the workplace shows no relevant stopping times except for normal traffic stops. The field test showed sensitivity due to seasons: 70% of e-bike trips were completed from April to September; winter use was considerably lower.

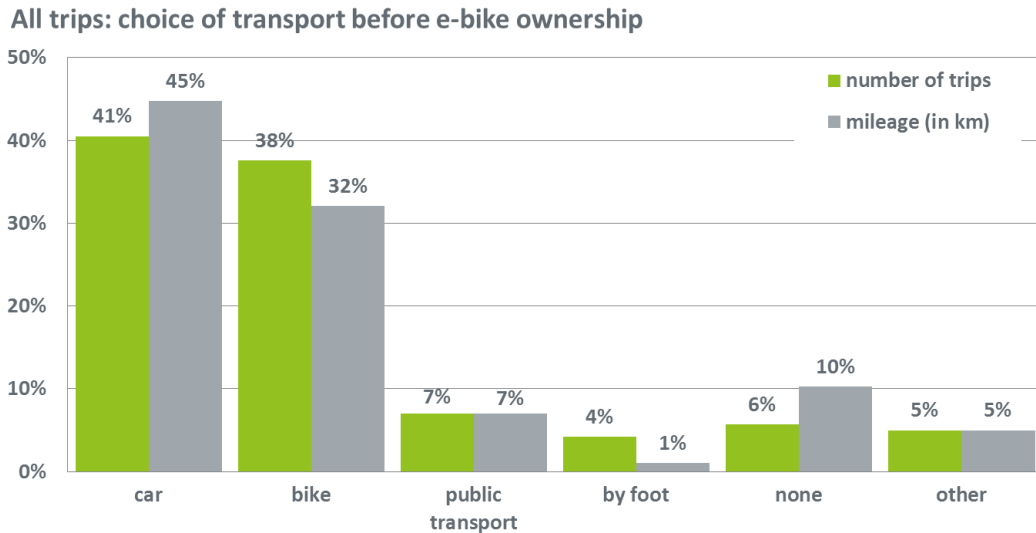
Table 1. Purpose of e-bike trips.

	Work related		Leisure / Everyday			
	Workplace	Business trip	Leisure/ Holiday	Private duty	Shopping	Other
Total Share	38%	2%	21%	18%	12%	9%
Ø distance (km)	11.7	-	17.8	7.5	6.1	10.3
Ø duration (minutes)	46.3	-	98.2	54.6	64.6	53.5

Modal Shifting Effects through E-bike Use

An important focus of the study is the modal shift induced by e-bikes: 41% of the e-bike trips and 45% of the e-bike mileage replaced car trips (respectively car mileage), while 38% of the e-bike trips and 32% of the distance were completed with a conventional bicycle before buying an e-bike (see figure 4). The participants only marginally substituted other means of transport like public transport or walking. Nevertheless, an additional traffic of 10% is induced by e-bike ownership if the mileage is considered. Especially the replacement of car mileage is noteworthy, since it has the potential for a considerable decrease of environmental impacts as well as other related effects such as urban congestion. Car mileage replacement was also much higher in the group of e-bikes-S users (70%), aged under 45 (57%), employees (57%) and frequent cyclists (47%).

Figure 4. Modal shift induced by e-bikes.



The modal shift effects clearly differ between different mobility profiles and are highest for the group of “commuters”, with over 60% of the e-bike mileage substituting passenger car mileage (see figure 5). On the other hand, “leisure users” largely substitute conventional bicycle mileage by e-bikes (60%) and thus potentially lead to an increase in energy consumption and environmental impacts. For this group, there is also a considerable share of additionally induced mileage, which is also evident for the “everyday user”. The impact on public transport is in general low but the group of “commuters” at least substituted 10% of their mileage. This could have a negative impact on passenger numbers of public transport. However, e-bikes have the potential to reduce pressure on public transport during the rush hour.

Figure 5. Modal shift induced by different e-bike user groups.

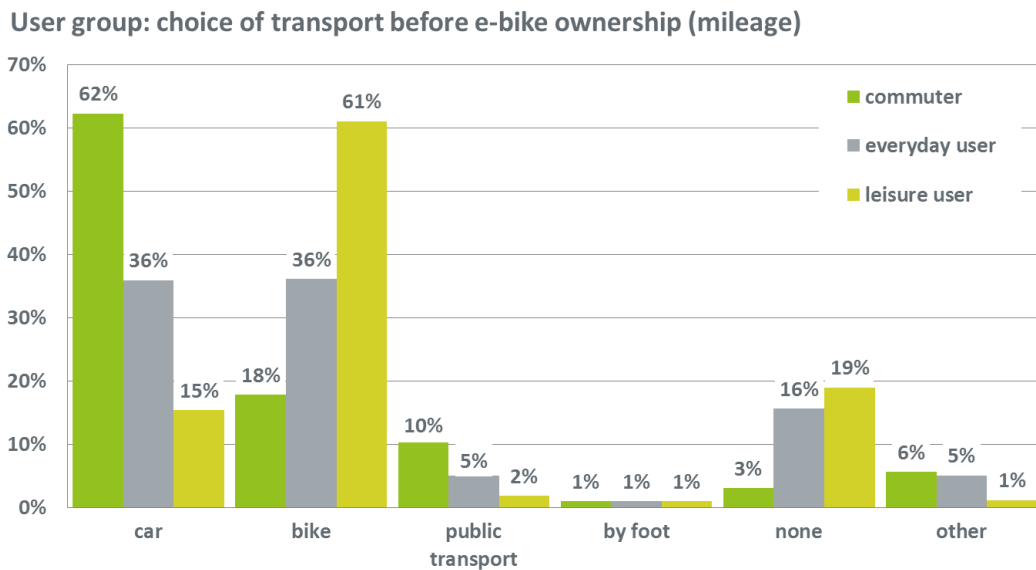
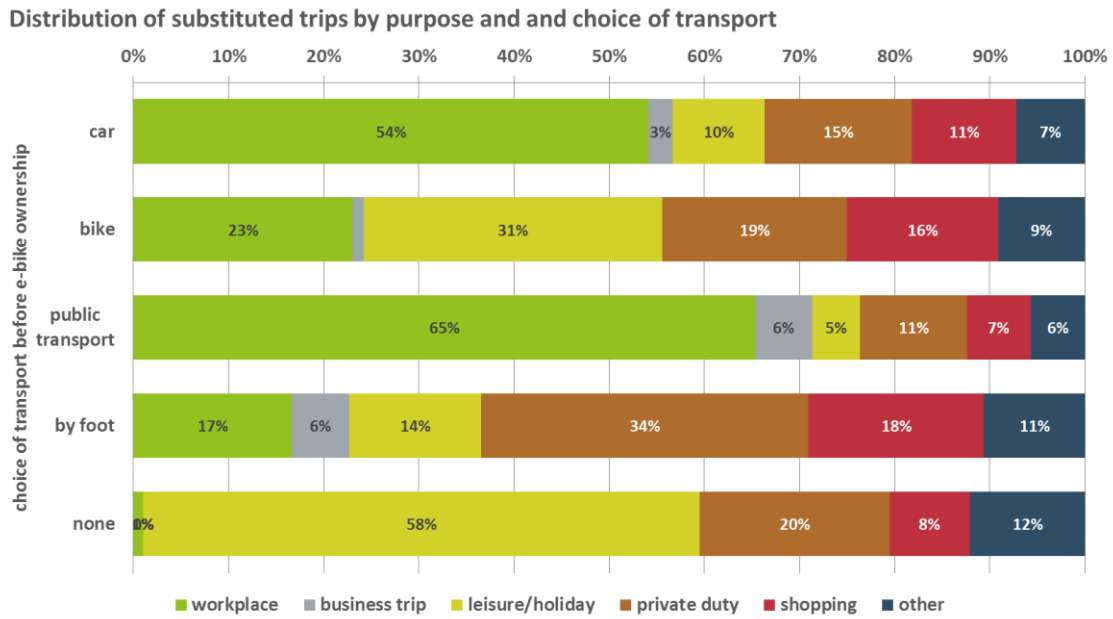


Figure 6 shows the result of combining the aspect of trip purpose and modal shifting effect. Again, it can be observed that car and public transport trips were mainly to travel to and from the workplace. A negative effect results from the shift between using the conventional bike and walking and by inducing new traffic (represented by “none” in the choice of transport). These categories show high shares of leisure trips and private duties. Shopping has the highest share for the transport categories “by foot” (18%) and “bike” (16%). The question arises how much additional traffic and negative modal shifting can be levelled out by positive modal shifting effects (from motorised vehicles). The following section therefore analyses and compares the environmental impacts of different vehicle types in more detail.

Figure 6. Combination of trip purpose and modal shifting effect.



Climate Impacts through Electric Bicycle Use

In order to assess climate impacts of these modal shifts, a life cycle assessment (LCA) approach was applied to different modes of transport. The scope of the analysis comprises the entire life-cycle from vehicle manufacturing to the use phase and to end-of-life treatment. All environmental impacts directly associated with these processes have been considered, as well as upstream emissions for provision of materials and fuels. In this study traffic infrastructure has been neglected. The analysis does not reflect a specific vehicle, but rather aims at representing defined generic reference vehicles. This is regarded as a suitable approach for comparing different modes of transport. The functional unit is the mobility service expressed as passenger kilometres (pkm) driven. Hereby, all environmental impacts of vehicles along the life cycle are allocated to average lifetime mileage and degree of capacity utilisation in Germany.

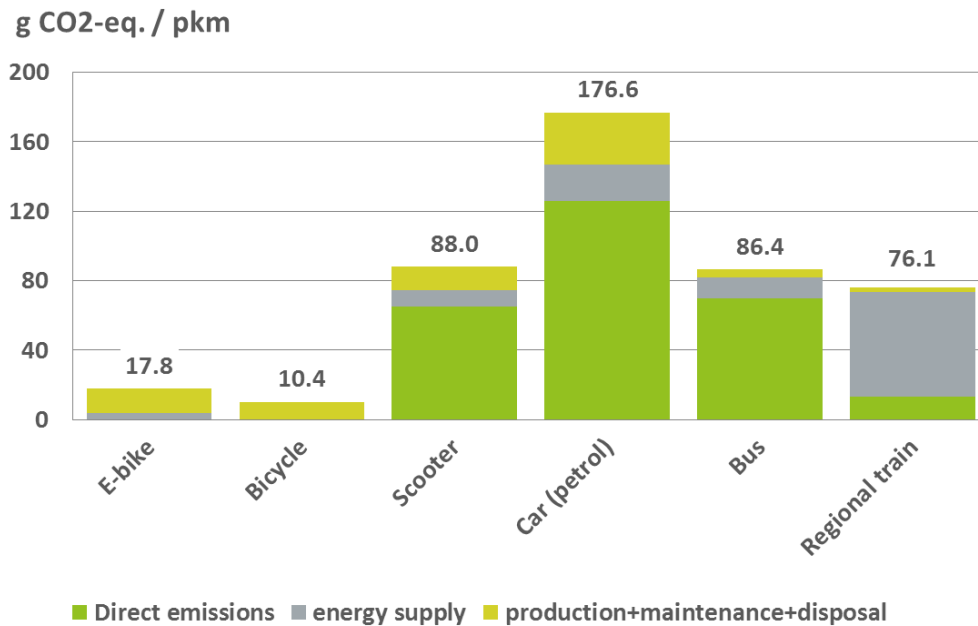
The reference vehicles are: (1) e-bike, (2) bicycle, (3) scooter, (4) petrol car, (5) bus and (6) regional train. The data basis for modelling different modes of transport was collected fromecoinvent 3.1 (Weidema et al., 2013) and results from eLCAR (Helms et al., 2016). Additionally, results from the field test have been used to adapt the LCA of the e-bike. This accounts for battery size, mileage and energy consumption. Table 2 summarizes the input data which was used for adapting the e-bike LCA.

Table 2. Input data for e-bike lifecycle assessment.

	value	unit
Battery size	300	Wh
Mileage	2,500	km per year
Energy consumption	0.73	kWh/100 km

Figure 7 shows the result of the climate impacts for different modes of transport measured in greenhouse gas emissions (GHG) per pkm. Since the electricity consumption of the e-bike is low, the manufacturing process was found to be far more relevant for its overall environmental impact. The e-bike has an advantage of at least 25% compared to all other motorized modes of transport. However, the highest advantage arises by shifting from car to e-bike because GHG emissions of e-bikes per passenger kilometre merely amount for 10% of the petrol car emissions. In absolute numbers this shift saves almost 150 g GHG emissions per pkm. The only negative shift in terms of additional climate impact is of course from the conventional bicycle. Nevertheless, the conventional bike itself is also not free from GHG emissions due to its manufacturing but additional components and electricity contribute to additional GHG emissions of 7,4 g per pkm for the e-bike.

Figure 7. Greenhouse gas emissions for different vehicles.

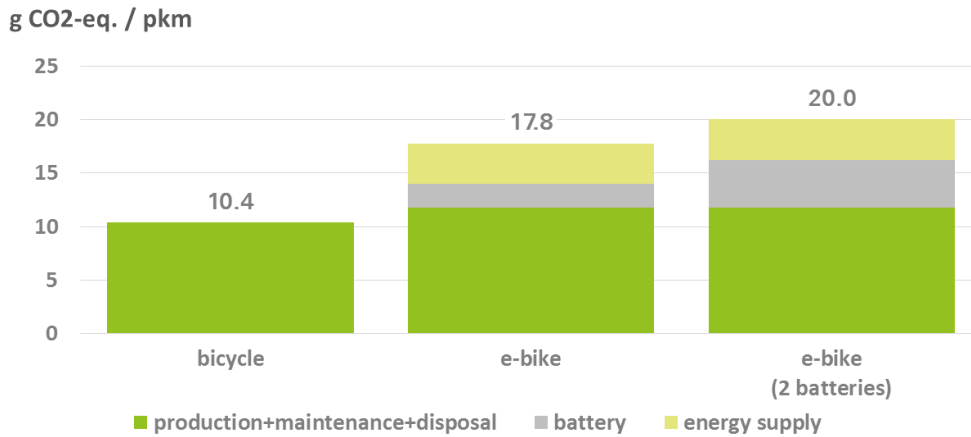


The environmental burden of the battery in electric vehicles is often controversially discussed. This is also true for the electric bike (Wachotsch et al., 2014). The battery results in higher prices and an increased material consumption of the vehicle. Currently most e-bikes use lithium-ion (Li-Ion) batteries with considerable higher energy densities compared to older technologies such as lead or nickel based batteries. The higher energy density of Li-Ion batteries helped the e-bike concept to gain new popularity because of the significant weight reduction. Nevertheless, the production of the Li-Ion battery is associated with additional material consumption and thus environmental burdens. Nearly all Li-Ion cells for e-bikes are manufactured in Southeast Asia where national environmental regulation is less strict and quality demands differ by supplier. Low quality batteries have been used in some e-bike models and led to early replacements which caused costs for the owner and additional environmental burdens. Problems with the life expectancy have been observed during the field test but were not a constant problem. Less than 20% of the participants reported technical problems with the battery. However, stockpiling has been found to contribute to a multiplication of environmental burdens caused by the battery. 13% of the participants already purchased a second (or even third) spare battery. The reported reasons were either range extensions or fear of not getting the vehicle specific battery system at a later stage.

In order to highlight the effect of an additional battery over the lifetime, a sensitivity analysis has been conducted. It also represents the recent tendency of bigger battery systems because the battery size of 300 Wh observed in the early phase of the field test does not reflect recent average sizes of new e-bike models. The base e-bike in this analysis uses a 300 Wh battery over the whole lifetime (15,000 km mileage). Figure 8 compares the conventional bicycle and the base e-bike with an e-bike with two 300 Wh batteries (or an e-bike with a single battery of 600 Wh). The results show that the battery of the base e-bike contributes 12% to the total climate impact, this share rises up to 22% for the scenario with two batteries. From an environmental perspective it is advisable to only purchase a new battery as a replacement for a deteriorated battery or if required by special use patterns. Long storage of batteries also has a negative effect on lifetime and energy capacities.

Another relevant effect on vehicle climate impacts is the lifetime mileage. Since e-bikes are associated with higher emissions as normal bicycles they should be considered as full means of transport. An integration of e-bikes into daily trips and even into commuting generally increases the mileage. If the e-bike is used just for a few leisure trips during the year it is not considered to be a full means of transport but rather a hobby equipment. This effect is illustrated by the extreme assumption of an e-bike lifetime mileage of only 1.500 km which would result in the same GHG emission per pkm as for cars which generally have a much higher mileage (176.6 g GHG emissions per pkm).

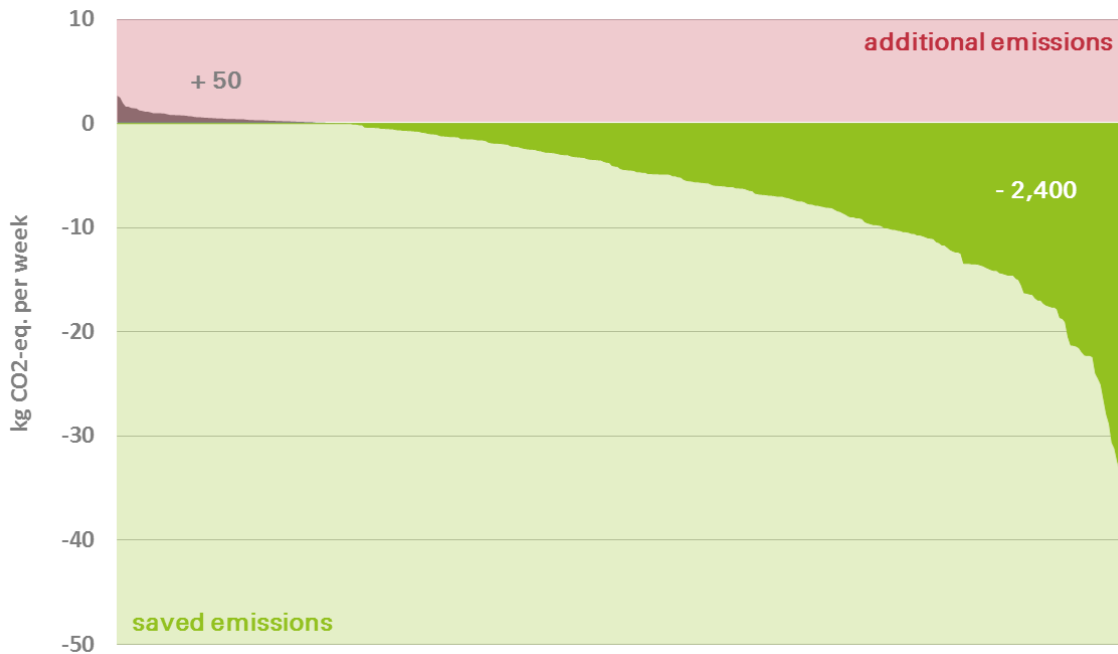
Figure 8. Sensitivity analysis of battery consumption by e-bikes.



Climate Impacts of Modal Shifting of E-bike Users

Due to modal shift induced by e-bikes, relevant car mileage can be substituted. The LCA results quantify the climate advantage of e-bikes compared to cars. But the key question to be answered at this point is how additional emissions caused by negative shifting from bicycle and walking contribute to the overall climate balance of e-bike users. Figure 9 summarises the overall average weekly GHG balance of the field test participants with e-bike compared to the previous mobility profile. The results are sorted from highest additional emissions to highest saved emissions. Significant GHG reductions owing to the observed modal shift have been achieved in the field test for most of the participants. Thus, 2,400 kg of GHG emissions have been saved by the field test participants per week. 50 kg GHG emissions have been additionally emitted due to a negative shift from bicycle and walking. In total, e-bike use saves far more emissions than it causes additionally. This even justifies the small amount of additional traffic and shifting from bicycle.

Figure 9. Average weekly GHG balance of the field test.



Conclusion

According to the presented results, minimization of climate relevant emissions through e-bike usage is especially large where frequent car trips are replaced. This is the case particularly for commuter traffic, where up to 80 million pkm of car trips could be substituted in Germany through the usage of e-bikes on distances up to 15 kilometres. Furthermore, e-bike-S users have been found to be

replacing significantly more car trips than conventional e-bike users. In addition to promoting the modal shift, environmental impacts of e-bikes could be further reduced. Especially the lifetime of e-bike components (like the battery) highly influence the environmental impact of e-bikes. Several conclusions can be drawn from the presented results which point out the direction for relevant policy makers. Though most conclusions have been drawn for Germany, they may be valid for other European countries as well disregarding legislative constraints.

- Legislative frameworks need to be adjusted: The general differentiation between bike and motor vehicle, which is currently often made based on EU directive 2002/24 can be an obstacle for the integration, especially of e-bikes-S in the overall traffic. In Germany, for instance, bicycle lanes are not officially available to e-bike-S users. This often makes orientation difficult during cycling.
- Infrastructure needs to be improved: Environmental benefits of e-bikes are high, while costs for the improvement of their infrastructure are comparably low. E-bikes do not require any different infrastructure as conventional bicycles. An improvement of infrastructure supports e-bikes and un-motorised bicycles likewise. Despite an official commitment towards increased share of cycling in the modal split, this is hardly reflected in the public funding yet.
- Use of e-bike batteries should be optimised: Battery treatment until sale should be improved and possibly separated from the bike sales. Considerable capacity losses can occur even before the first use of the e-bike by the end consumer. E-bike retailers suggested delivering new batteries directly from the factory together with the purchase of the bike. Also battery rental could be expanded.
- Technical upgrades should be enabled: Retailer and participants expressed the demand for upgrade possibilities, especially due to the fast innovation cycle in the battery sector. Upgrading and retrofitting should be possible even after several years of use and could be supported by the introduction of consistent standards. Consistent standards would also contribute to consumer trust and prevent stockpiling of spare batteries.
- Potential users and new segments need to be directly addressed: Currently e-bike use with a high environmental benefit (especially commuting) correlates with the level of education. More emphasis on e-bikes as a “hip” means of transport could motivate potential new users. Also currently underrepresented segments such as young adults and women could be directly addressed. One way to overcome prejudices towards e-bikes is campaigns which allow for testing of e-bikes.
- Promotion of e-bikes should not cannibalise conventional bicycles: The focus of promotion should centre on bike transportation in general. E-bikes are one option equal to bicycles as means of transport depending on the use patterns.

Bicycles – with or without electric assistance, with two or more wheels – are serious means of transport and a genuine alternative to passenger cars on short and medium distances up to 15 km. In combination with public transport even longer distances are possible. If the trend of increasing sales rates continues as the German Two-Wheeler Industry Association predicts (ZIV, 2016) over 3.5 Mio. e-bikes could be on the road by 2020. Mobility research neglected the topic for many years, despite the environmental and health benefits. In Germany, even though further projects such as Pedelec have been initiated in the past years, many research questions have not been addressed yet. Therefore, the establishment of a continuous research and improved communication towards policy makers is necessary.

Acknowledgments

The study “Pedelec” was funded by the German Federal Ministry for the Environment, Nature Conservation, Building and Nuclear Safety. The project has been conducted by the Institut für Transportation Design (ITD) and ifeu - Institut für Energie- und Umweltforschung in collaboration.

References

Budde, A., T. Dagers, A. Fuchs, T. Lewis, H. Neupert, N. Manthey & W. Vogt (2012): Go Pedelec! Handbuch. Utrecht: Go Pedelec Projektkonsortium.

DHBW (2014): Pedelec vs. Fahrrad: Vergleich Leistungsbezogener Daten auf einer Langstrecke. Duale Hochschule Baden-Württemberg (DHBW). Friedrichshafen.

Helms, H., J. Jöhrens, J. Hanusch, U. Höpfner, U. Lambrecht & M. Pehnt (2011): Umbrella: Umweltbilanzen Elektromobilität - Grundlagenbericht. Wissenschaftlicher Grundlagenbericht funded by Bundesministerium für Umwelt, Naturschutz und Reaktorsicherheit. ifeu - Institut für Energie- und Umweltforschung Heidelberg GmbH. Heidelberg. <http://www.emobil-umwelt.de/>

Helms, H., J. Jöhrens, C. Kämper, J. Giegrich, A. Liebich, R. Vogt & U. Lambrecht (2016): Weiterentwicklung und vertiefte Analyse der Umweltbilanz von Elektrofahrzeugen. ifeu- Institut für Energie- und Umweltforschung. Umweltbundesamt. UBA Texte: 177. Dessau-Roßlau. <http://www.umweltbundesamt.de/publikationen/weiterentwicklung-vertiefte-analyse-der>

Lienhop, M., D. Thomas, A. Brandies, C. Kämper, J. Jöhrens & H. Helms ifeu (2015): Pedelection: Verlagerungs- und Klimaeffekte durch Pedelec-Nutzung im Individualverkehr. Institut für Transportation Design. Institut für Energie- und Umweltforschung. Braunschweig, Heidelberg. http://www.transportation-design.org/cms/upload/DOWNLOADS/150916_Abschlussbericht_Pedelection_final.pdf

Umweltbundesamt (2015): Environmental Trends in Germany: Data on the environment 2015. Umweltbundesamt . Dessau-Roßlau. https://www.umweltbundesamt.de/sites/default/files/medien/378/publikationen/data_on_the_environment_2015.pdf

Wachotsch U., A. Kolodziej, B. Specht, R. Kohlmeyer & F. Petrikowski (2015): Electric bikes get things rolling: The environmental impact of pedelecs and their potential. Umweltbundesamt. Dessau-Roßlau. https://www.umweltbundesamt.de/sites/default/files/medien/378/publikationen/hgp_electric_bikes_get_things_rolling.pdf

Weidema, B. P., C. Bauer, R. Hischier, C. Mutel, T. Nemecek, J. Reinhard, C. O. Vadenbo & G. Wernet (2013): The ecoinvent database: Overview and methodology, Data quality guideline for the ecoinvent database version 3. Ecoinvent Center. Zürich. www.ecoinvent.org

ZIV (2016): Pressemitteilung: Zahlen – Daten – Fakten zum Deutschen E-Bike-Markt 2015 (03.03.2016). German Two-Wheeler Industry Association (ZIV). Bad Soden. http://www.ziv-zweirad.de/fileadmin/redakteure/Downloads/Marktdaten/PM_2016_08.03._E-Bike-Markt_2015.pdf

ZIV(2015): ZIV-Jahresbericht 2015. German Two-Wheeler Industry Association (ZIV). Bad Soden. http://www.ziv-zweirad.de/nc/presse/themen-dossiers/?download=ZIV_Jahresbericht_2015.pdf&did=10

Quality Assurance of PEMS Emissions Data aimed for the Development of Real-world Vehicle Emission Factors

Petros KATSIS*, Robin SMIT**, LeonidasNTZIACHRISTOS***, Ting-Shek LO**** & Carol WONG****

* *Emisia S.A., Antoni Tritsi 21, P.O. Box 8138, Thessaloniki, GR-57001, Greece*
- email: petros.k@emisia.com

** *School of Civil Engineering, University of Queensland, Brisbane, 4072, Australia*

*** *Laboratory of Applied Thermodynamics, Department of Mechanical Engineering, Aristotle University, Thessaloniki, GR-54124, Greece*

**** *Environmental Protection Department, the Hong Kong SAR Government*

Abstract

Portable Emission Measurement Systems (PEMS) have recently become widespread in collecting real-world emission information from vehicles. The Environmental Protection Department of Hong Kong (HKEPD) has been carrying out vehicle emission measurements by means of PEMS. The collected data are used to generate real-world emission factors for the particular environment and vehicle types. For this reason, emission information needs to be verified in a systematic manner by using extensive Quality Assurance / Quality Control (QA/QC) methods.

In this study, the authors attempt to devise proper criteria to verify PEMS data measurements and subsequently develop corresponding automated algorithms aiming to highlight a variety of potential abnormalities such as single or clustered outliers, analyser measurement saturation and zero drift.

Results show that the proposed set of detection and verification algorithms can be used for PEMS data to create a robust, efficient and cost-effective screening protocol that will guarantee a quality level, adequate enough to check the data prior to using them for emission factor development. Visual time-series analysis is still a necessary tool to rule out any prediction errors.

Key-words: (5 words) PEMS, vehicle measurements, quality assurance, quality control, real-world.

Introduction

Portable Emission Measurement Systems (PEMS) have been under the spotlight as of late, in view of the developments and resulting need for accurate emission measurements in realistic driving conditions. PEMS systems are versatile emission and exhaust flow measurement equipment with the capacity to provide accurate, second-by-second emission information for gaseous and particulate pollutants. PEMS are installed on board the vehicle and are powered by an independent source (on-board batteries). With PEMS on, each vehicle can be operated in its usual driving conditions, while its emissions are being measured. PEMS therefore provide realistic emission information of high resolution, which is difficult, if not impossible, to obtain otherwise.

As a result of the high resolution, PEMS generate large datasets with pollutant emission rates as well as other secondary information. From the perspective of accurate vehicle emission prediction, a large database of empirical data is essential to adequately reflect the large variability in real-world emission profiles from different vehicles and different engine and driving conditions. However, it is also vital to use verified emissions data in emission factor development to prevent prediction errors. Given the large amount of data, efficient and effective screening methods are needed to filter out erroneous measurements. Even data from high quality test facilities such as certification-grade laboratories require scrutiny and verification as there are several steps in data collation that can lead to errors, e.g. manual data entry typos and erroneous data can still be overlooked and included in the database.

The Environmental Protection Department of Hong Kong (EPD) has collected and continues to collect a large number of vehicle emission measurements utilizing PEMS. The large number of emission data produced even on a single vehicle are useful to check the emission performance of the particular vehicle, but also, more generally, to understand emission phenomena. Combined with

emission measurements from other vehicles and properly processed, these data may generate real-world emission factors for the particular environment and vehicle types. For this reason, the collected emission information needs to be verified and organized systematically; the sheer quantity of available PEMS data requires effective quality control and assurance (QA/QC) methods that use specific verification statistics and automated computation and visualisation techniques to ensure invalid data are flagged, corrected or removed, while ensuring that valid outliers are maintained.

The Hong Kong landscape combined with the driving regulations and typical traffic conditions constitute a measurement environment with certain characteristics; it is mainly an urban area with a hilly terrain. The speed is controlled by traffic lights and is usually maintained below 50km/h in urban areas and between 80 and 110 km/h in highways, while the speed limit for heavy duty vehicles is set to 70 km/hr.

The PEMS measurements conducted by EPD are mainly focused on NO_x and PM emissions. Moreover, On-Board Diagnostics (OBD) are not readily provided for most vehicles. Because of Hong Kong landscape particularities, i.e. high buildings in dense urban environment, GPS recordings may contain gaps due to satellite signal loss. Due to that, speed measured by a speedometer on the wheel of the tested vehicle with dead reckoning is used alongside GPS. Finally, the entire procedure for PEMS data measurement, collection and processing is consistent with the requirements of CFR1065, ISO16183 and Regulation (EU) No 582/2011 with corresponding UNECE Regulation No 49.

EPD has already in place an established method to collate and organize data from different PEMS measurement campaigns. With regard to measurements, five main components are being recorded:

- Gaseous pollutants, including CO, CO₂, NO, NO₂, and total hydrocarbons (THC), utilizing a number of different PEMS systems of different manufacturers and generations.
- Integrated particulate matter (PM) and real-time PM, again utilizing different PEMS units.
- Pollutants speciation and non-regulated pollutants, like NH₃, N₂O using Fourier-Transform Infrared Spectroscopy (FTIR).
- Global Positioning System (GPS) data, including position, altitude and speed.
- Vehicle relevant information, including speed measured on the wheel of the tested vehicle and OBD data if available.

Vehicles equipped with PEMS devices and peripherals will follow a target vehicle with the similar characteristics, which will then operate on its regular driving route (car chasing). Apart from this method, PEMS-equipped vehicles can also follow a fixed course. Both of these approaches are used for all vehicles except buses.

The current measurement sample exceeds 250 vehicles in several categories by using a variety of PEMS and other monitoring and recording devices over a range of routes and operational conditions.

Various data summary statistics can be used in a quality assurance and screening process to identify unrealistic and suspicious data. They range from basic statistics such as 'maximum value' and 'number of missing values' to the results produced by specific verification algorithms. A challenge with the use of summary statistics is the determination of accurate and robust pass/fail criteria. These criteria are developed through inter-comparison of PEMS data with vehicle-specific data, and, in some cases, for several vehicles within a particular vehicle class.

In this paper, we present different QA/QC procedures in order to verify the PEMS data being collected by EPD. The analysis focused on second-by-second data of gaseous and particulate pollutants. The proposed screening protocol applies algorithms to detect issues in the overall test statistics and includes data pre-processing, speed smoothing, driving behaviour verification and basic statistical analysis of emission rates. A second step examination focuses on specific pollutant traces and includes specific routines for clipping detection, statistical analysis indices, baseline drift

detection and outlier detection. The criteria behind these procedures aim to pinpoint a variety of abnormalities such as single or burst outliers, analyser measurement saturation and zero drift.

1. Methodology

The proposed methodology applies verification procedures in two consecutive phases, each applied at a different level of detail:

- verification of overall test validity and integrity, and
- verification of individual pollutant trace integrity.

The concept of this approach is first to subject the data to a general screening, so as to remove any obviously compromised measurements and ensure that abnormalities are detected and flagged or corrected; this would often mean that entire tests would be discarded or modified as a whole. Then, the second phase deals with more specific issues, focusing on individual pollutant traces to identify occurrence of errors either at a test level or at a time stamp level (single errors or bursts of errors).

In order to apply the verification protocol, first a number of statistics have to be calculated using the original dataset. The proposed screening protocol is designed to handle issues on gaseous and particulate real-time (second-by-second) PEMS data measurements in conjunction with real-time speed data measurements. The two distinct levels of verification steps will hereinafter be denoted as Phase 1 (overall test level) and Phase 2 (individual trace level) respectively, while the preparatory step will be referred to as Phase 0. A summary of the approach is presented in Figure 1. Details for each procedure are provided in the following paragraphs.

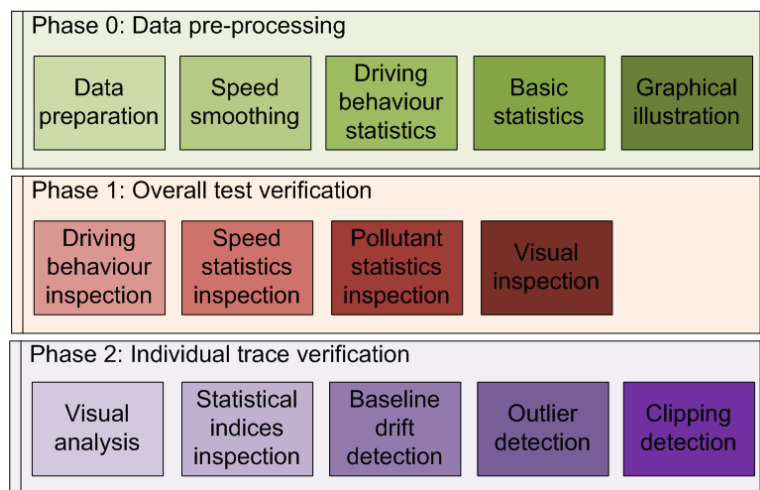


Figure 1. Screening protocol process

Phase 0: Data pre-processing

This first step addresses time gaps developed when intermediate time-stamps are missing from the PEMS data set e.g. due to transcription errors. This step enables the application of the follow-up verification phases, which require complete time series at least split on a sub-trip level. Sub-trips are defined as continuous and uninterrupted periods of travel time for a unique vehicle. Sub-trips are identified by computing the time difference (Δt) between consecutive time stamps, and flagging $\Delta t > 1$ s.

The addition of this metadata yields continuous second-by-second values within each sub-trip; this is necessary to allow speed smoothing to take place and more importantly to calculate acceleration values as part of the Phase 1 verification.

Speed smoothing may be optionally applied to the speed-time column to account for measurement noise and to prevent unrealistic computations of acceleration and engine power, in particular at higher speeds. A T4253H smoothing can be used in this approach (Velleman 1975, Velleman 1980); T4253H is a nonlinear data smoothing filter which can provide a practical method of

finding smooth traces for data confounded with possibly long-tailed or occasionally spiky noise. The smoothing algorithm is resistant to the effects of extreme observations that are not part of the local pattern and capable of responding rapidly to well-supported patterns. Speed-time smoothing is also conducted at the sub-trip level within each vehicle data test to prevent unrealistic jumps at sub-trip end points.

In the next part, statistics pertaining to second-by-second speed and individual pollutant traces will be extracted. It is useful to examine derived variables as they can readily reveal unrealistic recordings, which can then be traced back to particular issues with the PEMS measurements. The following speed trace summary statistics are computed for each unique vehicle data test:

- idle time (s),
- proportion of idle time (-),
- number of missing values in the speed trace (s),
- proportion of missing values in the speed trace (-),
- total length of all trips (s),
- average absolute deviation (AAD) in between raw and smoothed speeds (km/h),
- maximum absolute deviation (MAD) in between raw and smoothed speeds (km/h),
- minimum/maximum speed (km/h),
- minimum/maximum acceleration (m/s^2), with acceleration being computed using smoothed speed.

A number of basic statistics are computed for the pollutant emission rates (expressed in g/s) at test level:

- minimum, mean, maximum (MIN, MEAN, MAX),
- proportion of zero values (PZERO),
- proportion of missing values (PNA),
- proportion of negative values (PNEG),
- standard deviation (SDEV),
- coefficient of variation (COV),
- peak-to-mean ratio (PTM).

Figure 2 illustrates an example of the basic statistics table for PM sec-by-sec data, containing the metrics described above.

trip	min	mean	max	pzero	pna	pneg	sdev	cov	ptm
PM_1	0	0.0014	0.0418	0.0	0.0	0.0	0.004	2.96	30.5
PM_2	0	0.0023	0.1000	0.0	0.0	0.0	0.007	2.97	44.3
PM_3	0	0.0026	0.0602	0.0	0.0	0.0	0.005	2.10	23.0
PM_4	0	0.0012	0.0725	0.0	0.0	0.0	0.005	3.89	62.2
PM_5	0	0.0023	0.1024	0.0	0.0	0.0	0.009	3.81	45.4
PM_6	0	0.0018	0.0942	0.0	0.0	0.0	0.007	3.89	51.8
PM_7	0	0.0017	0.0697	0.0	0.0	0.0	0.006	3.41	41.3

Figure 2. Example of summary statistics table (PM)

Finally, before proceeding to the actual verification algorithms, visualisation of empirical data is an effective way of summarizing various key aspects of PEMS data, and facilitating further detailed analysis of potential issues. Time-series and other summary plots need to be generated for each vehicle data set for different variables, and saved for possible use in the screening process.

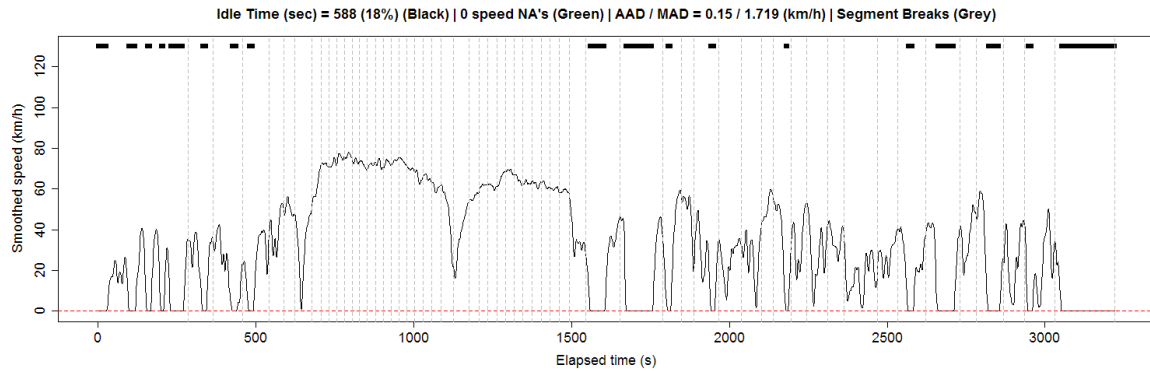


Figure 3. v-t-power plot example

Figure 3 shows an example of a ‘v-t-power’ plot which depicts the vehicle speed versus the elapsed test time derived from a PEMS data test. Coloured bars are used in these plots to provide additional time-series information, such as ‘idling’ (black bars), and ‘missing/not available values’ (green bars, not visible in this plot). The vertical grey dotted lines show 500 m drive segments. On the top of this figure, additional average statistics, as noted previously, are illustrated: Idling time and its proportion vs. the total test time, the average absolute deviation between raw and smoothed speeds and the maximum absolute deviation in between raw and smoothed speeds.

Phase 1: Overall test validity and integrity

The goal of this verification phase is to study the pre-processed data provided after the completion of Phase 0 in order to investigate whether basic trip metrics such as speed, acceleration and pollutant basic statistics at an aggregated test level fall within plausible ranges. The approach is valid only for real-time, sec-by-sec measurement data.

The overall test integrity procedures are expected to target the following issues:

- Instrument errors, including calibration and zero/span issues, data gaps in the recordings, misalignment in synchronization and time scales, measurements below detection limits, over the range (instrument saturation) values, etc.
- Errors in the transcription of the different files, such as value separation issues, digits changes (often confusion with point or comma decimal separator), unknown or variable units scales, lack or erroneous transfer of manual information stored in log files, etc.
- Vehicle operation specific abnormalities, e.g. cold start operation, regeneration modes, in particular for DPF equipped vehicles, and specific operation windows.
- Protocol gaps, including lack of correct monitoring of environmental conditions (e.g. on-road water load during rainy conditions), lack of monitoring of vehicle and instrument preconditioning patterns, etc.
- Other reasons which may be random or systematic, but may not be possible to identify (i.e. specific instrument errors in the recordings, PEMS system faults, etc.)

A number of procedures were developed to address these issues. The procedures fall in the following four categories:

1. Operation feasibility verification
2. Speed trace statistics verification
3. Pollutant trace average statistics verification
4. Visual time-series inspection

The first three procedures provide methods to verify statistics related to the speed trace or pollutant traces at an aggregated level (overall test). The fourth procedure can be used to verify the validity of

the potential issues raised by procedures 2 and 3. These procedures are analysed below.

Operation feasibility verification

Ideally, second-by-second engine power could be used to identify unrealistic vehicle operation. This could be done by using either measured or computed instantaneous engine power and normalizing these values over rated engine power. Any exceedance of a value of 1 (plus an error margin, e.g. 25%) would indicate unrealistic operation, i.e. an erroneous recording. The issue with this approach is that there is often a lack of accurate road gradient information to be used to predict second by second engine power.

For this reason, an alternative approach was implemented. The operation feasibility verification algorithm aims to flag extreme accelerations for vehicles falling into different power-to-weight ratios (PTW). In order to accomplish this, a model was devised to portray the relationship between acceleration and vehicle class. The maximum possible acceleration is expected to be a function of rated engine power, or rather PTW ratio. For example, heavy duty vehicles (HDVs) with a low PTW ratio will not be able to accelerate as quickly, as light duty vehicles (LDVs) with a high PTW ratio.

First, a range of typical drive cycles per vehicle type and driving mode were designed (Smit, 2006), on the basis of statistical analysis of smoothed speed-trace data of the vehicles in the sample. Different driving profiles were designed according to the vehicle PTW ratio, defined as rated engine power divided by Gross Vehicle Weight (GVW).

Examples of this procedure are shown in Figure 4 for passenger cars and buses, which represent two different PTW classes. This is essentially a scatter plot of all individual speed points and associated accelerations of the drive cycles. It is clear that the maximum possible acceleration is a function of both instantaneous speed and vehicle class.

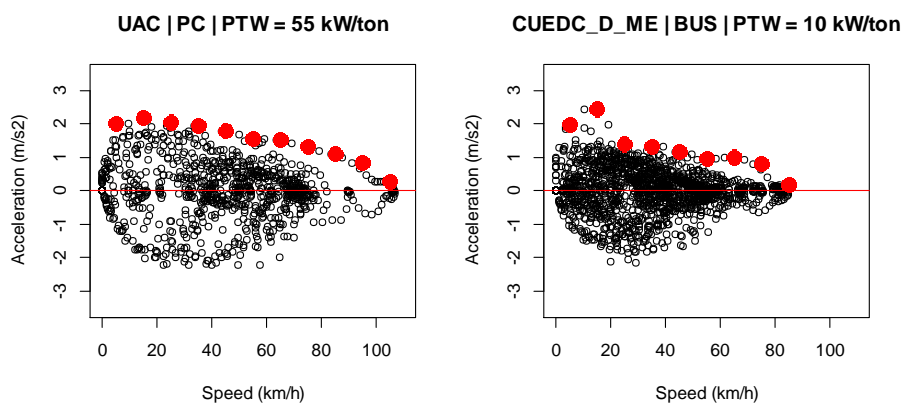


Figure 4. Scatter plots of instantaneous speed versus acceleration (Left: PC; Right: BUS).

To complete the model, first the maximum acceleration was computed for 10 km/h speed bins for each PTW class. These values are depicted as red dots in Figure 4. A non-linear regression model was fitted to these data. It was assumed that a reverse sigmoid function would best describe a maximum feasible acceleration model for each drive cycle. Figure 5 shows the results of the regression for four PTW classes and two vehicle types, i.e. HDVs (PTW of 8 or 15 kW/ton GVW) and LDVs (PTW of 25 or 55 kW/ton GVW). In general, the reverse sigmoid functions appear to fit the data well, in particular for the HDVs, but they may overestimate maximum feasible acceleration at higher speeds (>90 km/h). An error margin of 30% was added to the model and this constitutes the limit above which acceleration appears infeasible.

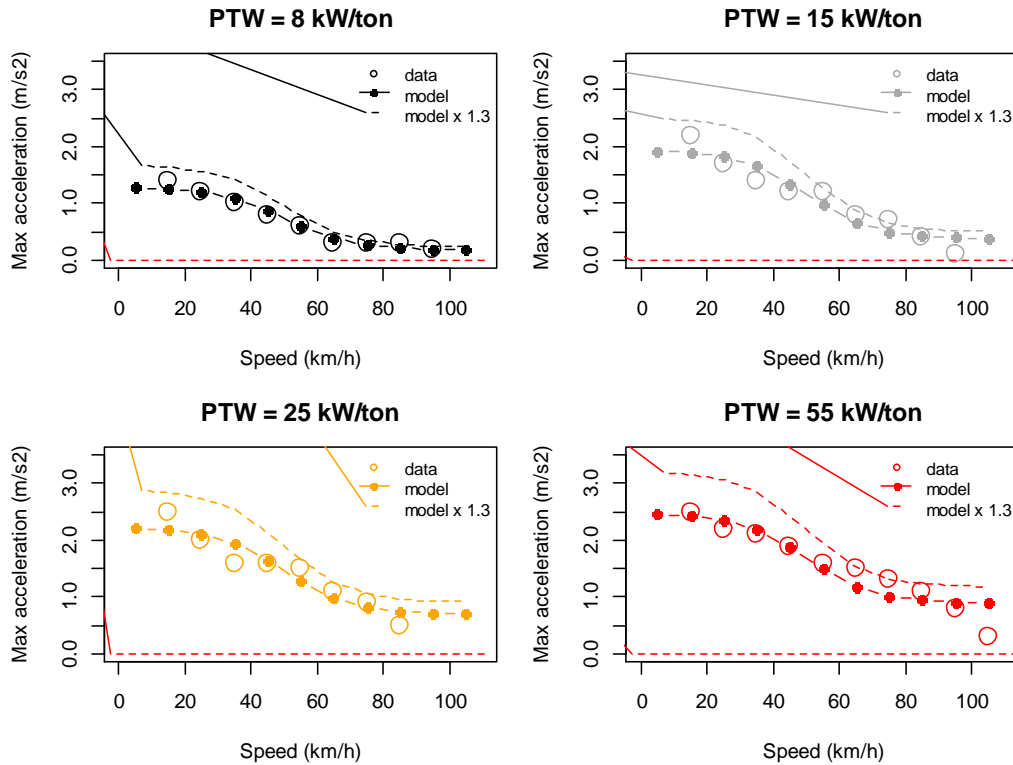


Figure 5. Maximum feasible acceleration models

The final models for LDVs and HDVs extracted via this process are shown by the following equations:

$$LDV: a_{max} = (-0.25 + 0.01 PTW) + 1.30 \left(0.70 + \frac{1.53}{1 + EXP\left(\frac{v-50}{10}\right)} \right)$$

for $PTW \geq 25 \text{ kW/ton GVW}$

$$HDV: a_{max} = (0.43 + 0.07 PTW) \times 1.30 \left(0.18 + \frac{1.11}{1 + EXP\left(\frac{v-50}{10}\right)} \right)$$

for $PTW \geq 8 \text{ kW/ton GVW}$

Here, a_{max} represents the maximum feasible acceleration (m/s^2), v is the instantaneous vehicle speed (km/h) and PTW is the ratio of rated engine power to GVW.

With the maximum acceleration – PTW – vehicle class modelling in place, the operation feasibility verification procedure only requires the vehicle information, which is casually available with the PEMS data. With this data, the verification procedure calculates the PTW of the vehicle and classifies the vehicle as either LDV or HDV. It then uses the respective equation above to verify whether the calculated acceleration values of the PEMS data are acceptable or not, flagging such test/time stamps as having a suspicious driving behaviour.

Speedtrace statistics verification

This procedure was used to investigate whether other basic speed-time statistics comply with expected values:

- The proportion of idling time may indicate a problem in the test (measurement issue).
- The proportion of missing values in the speed trace.
- Large deviations between the smoothed and original speed traces.

The exact limits for these metrics may need to be customized to the studied data set, but e.g. if the missing speed values percentage within a test is close to 100%, it should probably be discarded.

Pollutant trace average statistics verification

This procedure requires a blanket screening of basic pollutant trace statistics in the overall test level to conduct a high level scan of the integrity of pollutant measurements and identify any issues. This verification procedure uses the minimum/maximum pollutant recording in the dataset and the proportion of zero values, negative values and missing values in the entire test duration.

This inspection allows the identification of traces within each data test that should not be used. The specific limits need to be calibrated on each measured dataset, but some general guidelines are quite straightforward:

- When maximum/minimum values are way off expected limits. This is vehicle- and test-dependent (driving conditions).
- When the proportion of missing values reaches 100% (e.g. no data if all data are missing). Obviously, a lower value should also invalidate the values of this trace in the data test.
- When the proportion of negative values is too high. This also raises the issue of how to proceed, i.e. whether the test will be discarded or if remedial action is needed before further usage (e.g. correction of negative values by zeroing or marking them as missing).
- For tests with too many zero values, similar action could be taken, especially in comparison with the speed behaviour. Some situations are quite intuitive, e.g. a large percentage of zero CO₂ values while not idling is suspicious.

Visual time-series inspection

In Phase 1, the overall test examination focuses on the visual examination of second-by-second speed values. While, the previous verification procedures may suggest potential issues, a visual inspection is necessary to corroborate such erroneous behaviour and flag or correct those tests or identify situations where average statistics check may not be sufficient.

Moreover, the computed summary statistics guide the selection of datasets that require visual examination and vice versa to identify untypical errors. For instance, visual examination may point out issues that were actually missed by the operation feasibility verification procedure.

Phase2: Individual data trace validity and integrity

This phase specifically focused on second-by-second pollutant data trace validity and integrity. The individual pollutant trace verification algorithms included:

- Use of test statistics values such as coefficient of variation and peak-to-mean ratios of recorded data. A challenge with these new statistics is to create accurate and robust pass/fail criteria, as no generic limits can be applied.
- The identification of transient operation conditions, such cold start, fuel enrichment periods, regeneration patterns for DPF devices, etc.
- Methods to detect untypical analyser drift, which may lead to shift in the measured levels or even saturation.

The proposed verification procedures used for the data trace validity and integrity testing were:

1. Visual time-series analysis (pollutant trace level),
2. Clipping detection,
3. COV-PTM analysis,
4. Baseline drift detection,

5. Outlier detection.

Visual time-series analysis

Information-dense time-series plots are created for each individual pollutant trace, and they can be called upon when necessary to examine second-by-second data traces combined with the speed-time behaviour.

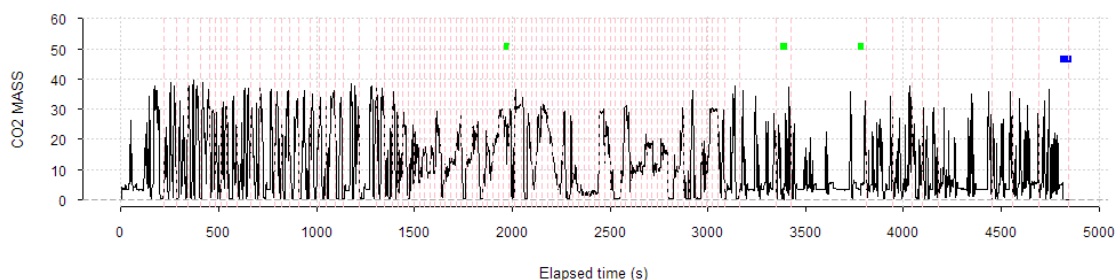


Figure 6. CO₂rate time-series plot.

In these plots, blue bars indicate zero values, green bars indicate missing values and red bars indicate periods with constant and high values. These situations may be indicative of periods with e.g. clipping and DPF regeneration. This figure also contains additional statistics to enable a combination of visual and statistical analysis.

Clipping detection

Clipping is defined as the replacement of measured concentrations with the analyser's maximum range value, when the concentration exceeds the analyser's range. Clipping results to characteristic plateaus for a few seconds in the measured signal. Clipping may occur e.g. due to improper calibration during the PEMS spanning process or if the measured quantity trace is actually outside the instrument range.

Clipping correction is required when high constant values are monitored for a given period. In this approach "clipping" is quantified with vector C , which is computed as follows:

$$C = e/m$$

where e and m represent the actual and maximum measured emission rate in g/s for a particular pollutant and particular vehicle. An indicator which illustrates how frequently clipping appears in a test is calculated by dividing the number of flagged values by the total trip duration; this indicator is noted as PCLIP.

COV-PTM analysis

Tests with relatively low PTM and COV values may reflect a significant proportion of clipped emissions data, or have small emission peaks, or experience a combination of both. Tests with relatively high PTM and COV values are indicative of data with large emission peaks ('spiky' data). This is the context around which this verification procedure is built.

COV is computed as the standard deviation divided by the mean. COV is a normalized measure of the dispersion in the data. PTM is a dimensionless indicator reflecting the relative magnitude of spikes in the data. This 'validation by comparison' approach is an effective way to visually identify outliers in large datasets that warrant further analysis. It is noted that the PTM/COV data can vary substantially with pollutant, as well as with engine and emission control technology. The data should therefore be examined for each pollutant individually, and the data need to be categorized using an appropriate vehicle classification.

Baseline drift detection

A measurement drift algorithm was developed to quantify analyser zero drift and at the same time indicate the possibility for other emission events such as distinction between cold/hot conditions. Measurement drift represents a shift in measured values under the same conditions at different points in time. Significant drift results in erroneous emission results, so this test parameter is quite important for emissions level accuracy. Despite the fact that measurement drift is usually automatically

verified before and after a test, it is still necessary to identify tests with potential issues.

The verification procedure aims to extract emission values for homogeneous engine conditions at different time intervals throughout the test. To quantify the level of measurement drift, idling segments need to be identified first. An idling segment is defined as a chronological time period of a few seconds duration with engine on and zero vehicle speed. The measured emission rates in these idling segments are then extracted. A certain amount of time before and/or after the idling period may be omitted to prevent boundary effects related to transient engine operation and extract stabilized emission rates.

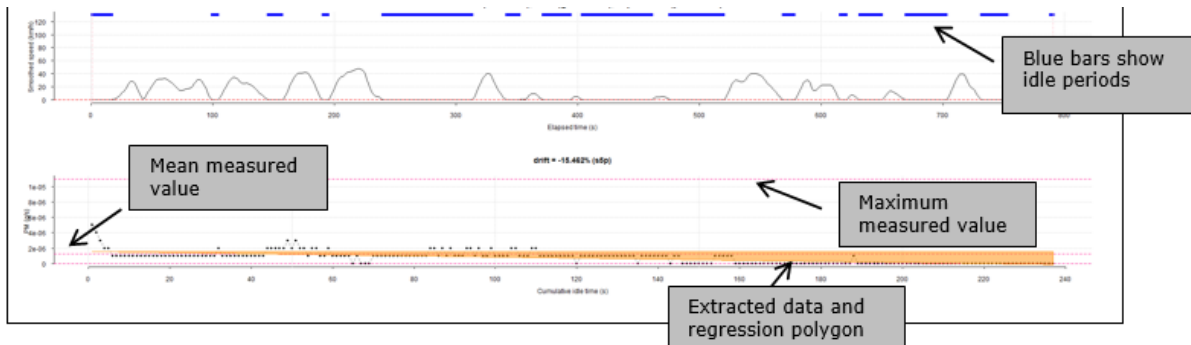


Figure 7. Example of speed and baseline drift time-series plots.

A robust least-squares linear model (RLM) is then fitted to the extracted data, and a drift variable D is computed as follows:

$$D = 100 n b / m$$

where n represents the number of extracted idling data points (s), b represents the regression coefficient in g/s and m represents the maximum measured emission rate in g/s for a particular pollutant and particular test. RLM is not sensitive to outliers, and is expected to better quantify any general trends.

Therefore, D quantifies the percentage change in idling emission rates over time relative to the peak emission value. It can produce meaningful results for time-aligned hot running tests with a significant number of idling segments. Cold start tests will create large D values due to highly elevated emission levels at the start of the test. Finally, the 95% confidence interval (CI) for D can be compared with the intercept to verify if D is statistically significant (i.e. D is outside the 95% CI). An example of this procedure is shown in Figure 7.

Outlier detection

Outliers are observations with characteristics that are distinctly different from the other observations. Before PEMS data are used in, e.g. emission factor development, it is vital to identify these outliers and determine if they are valid data points. They can also have a significant impact on emission factors. Outliers can also arise from specific situations or issues, including errors that were produced during testing (e.g. incorrect measurement settings) or during the data transfer and reporting phase (e.g. data entry error). Outliers can be determined in various ways such as via examination of univariate and multivariate distributions and at different scales. The scale of outlier assessment can be at data trace level (single test), vehicle level (all tests) or vehicle class level (all pooled test data for all vehicles with similar characteristics).

The method proposed here focuses on univariate data trace level, as any outliers detected and verified at this fundamental level, will prevent propagation of data issues to higher scales of assessment. Nevertheless, it is still recommended that emission factors based on PEMS data are compared at vehicle and vehicle class level to ensure any suspicious data are investigated further.

It is noted that observations may occur normally in the outer ranges of the distribution, so the analysis attempts to identify those distinctive observations and designate them as outliers. Outliers can be detected using 'standard z-scores'. A z-score represents the distance between the observation and the mean in terms of the number of standard deviations. The z-score is negative when the observation is below the mean value and positive when it is above.

There is, however, one issue with this approach. Vehicle emissions are typically highly skewed with long tails to the right, reflecting occasional emission spikes. On the other hand, outlier detection using z-scores assumes an approximately normal distribution. As a consequence, PEMS emissions data need to be transformed before outlier detection can be applied. The aim is to achieve a more or less symmetrical and normal distribution of observed emission rates.

Due to the large number of data sets, the Box-Cox procedure has been used to automatically select the best data transformation from a family of power transformations, and compute the transformation variable 'lambda' (λ). Transformed data equals the actual data to the power of lambda where, by definition, $\lambda=0$ suggests a log-transformation.

The z-scores are computed for pollutant traces for each test as follows:

$$d_i^* = 1 + d_i + |\min(d_i)|$$

$$d_i^{*\prime} = (d_i^*)^\lambda$$

$$z_i = (d_i^{*\prime} - d^{*\prime})/s_{d^{*\prime}}$$

where d_i is an actual pollutant data point, d_i^* represents a vector of shifted d_i values, $d_i^{*\prime}$ represents a vector of transformed d_i^* values, z_i represents the computed z-score for transformed data point i , $d^{*\prime}$ and $s_{d^{*\prime}}$ are the mean and standard deviation of the vector of $d_i^{*\prime}$ values, respectively. Using the previous conversion, the minimum of d_i^* is achieved when d_i is minimum or:

$$\min(d_i^*) = 1 + \min(d_i) + |\min(d_i)| \geq 1$$

The d_i^* term is computed in order to create data values greater than zero; this is required for the Box-Cox procedure, which includes a log transformation of d_i^* (thus the logarithm must be higher than zero). Z-scores have a mean of zero and a standard deviation of one. Z-score values are then used to determine if an observation d_i qualifies as an outlier. An example of this transformation is illustrated in Figure 8.

In addition, the impact of removing outliers is quantified to assess the relevance of the outliers with respect to computed emission factors (expressed in g/km). The relevance is computed as the ratio of the test averaged emission factor with outliers removed (expressed in g/km) to the emission factor with all data included. Significant deviation from unity indicates remarkable impacts of the outliers. An outlier relevance impact greater or equal to 0.95 is not considered significant given the uncertainties in the PEMS measurements.

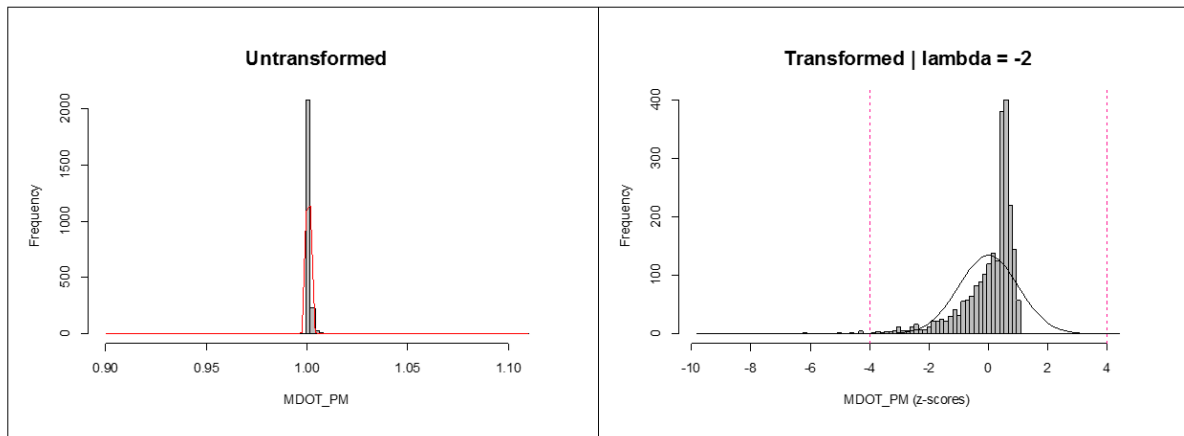


Figure 8. Example of outlier detection in pollutant traces using z-scores

The equivalent real-time plot for the bottom example is shown in Figure 9. The red bubbles indicate the time-stamps where the z-scores method has identified as suspicious if the z-score limit is set to 4.

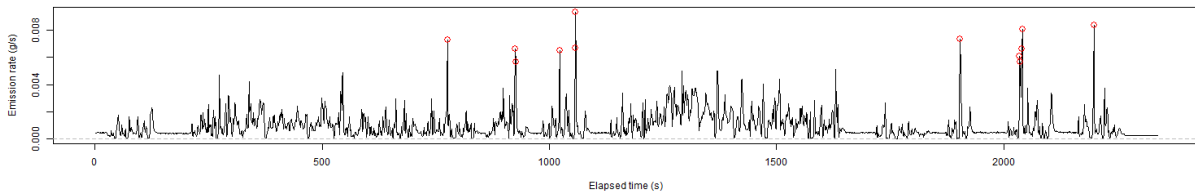


Figure 9. Real-time plot corresponding to the transformed data above (Figure 8)

After outliers have been identified, a decision must be made on the retention or deletion of each outlier. Outliers are not by definition invalid as they may be indicative of specific cases that, although relatively unique, are part of real-world vehicle emissions behaviour (e.g. emission spikes).

Given the large variability in vehicle emissions and especially if high emitters are present in a dataset, outliers should be initially retained, unless there is clear evidence that the data are invalid due to e.g. errors in recording, miscalculation, malfunctioning test equipment or other technical reasons.

2. Results and Discussion

The methodology analysed in the previous paragraphs was developed into verification routines using custom coding. The methodological approach was then tested on the EPD PEMS dataset in order to suggest calibration parameters and demonstrate examples of application for the screening. The pre-processing phase has been carried out prior to proceeding with the verification phases.

Overall test verification

For the first phase, the driving behaviour verification scheme application can outline tests with exceeding maximum acceleration values. Figure 10 shows an example of the summary statistics table extracted from a sample array of second-by-second data tests. The highlighted fields indicate maximum/minimum acceleration exceedance as defined in the developed maximum acceleration model (Operation feasibility verification procedure).

segm	idle_time	idle_prop	na_time	Pna_spd	length_cycle	AAD	MAD	min_speed	max_speed	min_acc	max_acc
PM_9	1	0.00	0	0	459	0.2	1.2	0.0	55.4	-1.2	1.0
PM_10	18	0.06	0	0	301	0.1	1.2	0.0	43.3	-1.2	0.7
PM_1	786	0.29	0	0	2,698	0.1	1.1	0.0	67.8	-1.6	1.0
PM_2	531	0.20	0	0	2,595	0.1	1.3	0.0	81.4	-1.9	17.3
PM_3	215	0.08	0	0	2,629	0.1	1.3	0.0	64.6	-2.0	1.2
PM_4	762	0.23	0	0	3,316	0.1	1.2	0.0	56.4	-1.7	1.0
PM_5	225	0.09	0	0	2,472	0.1	1.3	0.0	84.9	-2.3	1.2
PM_6	1,233	0.32	0	0	3,854	0.1	1.3	0.0	60.9	-1.7	1.1
PM_7	58	0.35	0	0	164	0.1	0.7	0.0	34.7	-1.2	0.8
PM_8	247	0.10	0	0	2,527	0.1	1.7	0.0	74.0	-8.8	1.3
PM_9	649	0.19	0	0	3,467	0.1	1.4	0.0	72.3	-4.1	1.1
PM_10	633	0.21	0	0	3,067	0.1	2.1	0.0	79.7	-2.1	1.2
PM_11	783	0.23	0	0	3,419	0.1	1.5	0.0	67.6	-2.2	1.2
PM_12	797	0.22	0	0	3,625	0.1	1.9	0.0	66.4	-1.8	1.1
PM_13	769	0.23	0	0	3,349	0.1	1.3	0.0	93.1	-2.1	1.0
PM_14	238	0.07	0	0	3,471	0.2	1.7	0.0	71.8	-1.9	1.1
PM_15	34	0.12	0	0	274	0.1	0.6	0.0	56.9	-10.6	0.8
PM_16	1,135	0.17	0	0	6,819	0.1	1.5	0.0	76.9	-2.7	1.2
PM_17	208	0.29	0	0	723	0.1	1.1	0.0	73.1	-1.8	1.1

Figure 10. Example of outlier detection in pollutant traces using z-scores

The obtained statistical properties of the speed-time trace are also presented. A similar table for individual trace (PM) statistics was presented in Figure 2. A visual analysis of the speed trace is necessary to validate possible issues.

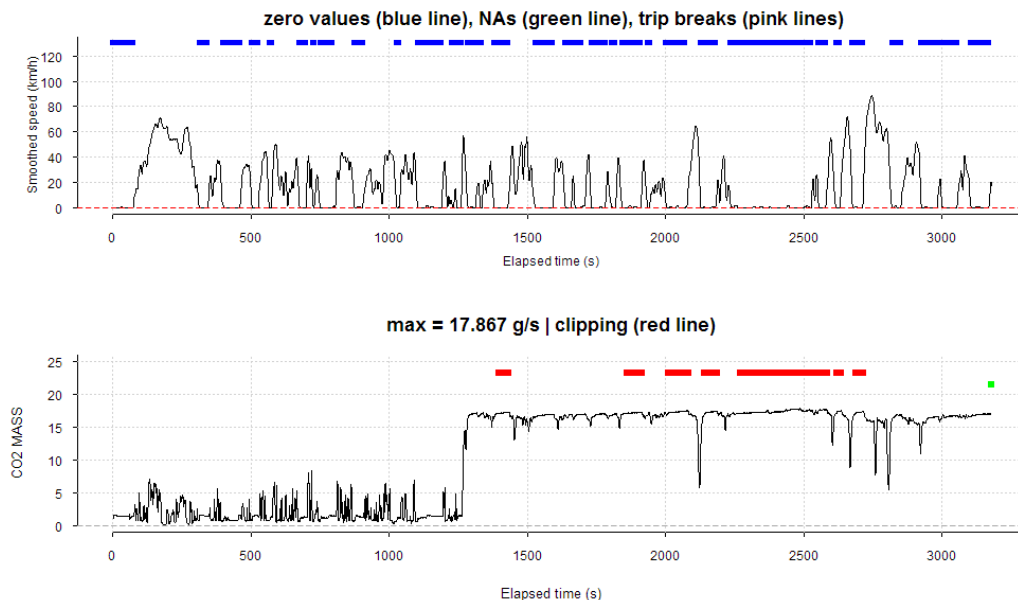


Figure 11. Example of gaseous file with a PCLIP value of 0.11 for CO₂.

Individual traces verification

For the practical application of the clipping detection algorithm, the following approach can be used: potential clipping is flagged whenever $C > 0.995$ and the number of consecutive potentially clipped values is at least 15 s long. In this example, the idling segment is defined as a duration of at least 9 s while the first 5 s and the last 3 s of each idling segment are omitted.

An example of application is shown in Figure 11; it corresponds to a trip travelled by a petrol Euro 4 passenger car with questionably steady CO₂ values for most of the trip duration, despite the fluctuations in vehicle speed. Another sample test which demonstrates potential clipping is shown in Figure 12. The same, relatively low clip value is observed for both NO_x and NO measurements. This trip was performed by a heavy Euro II bus equipped with DPF.

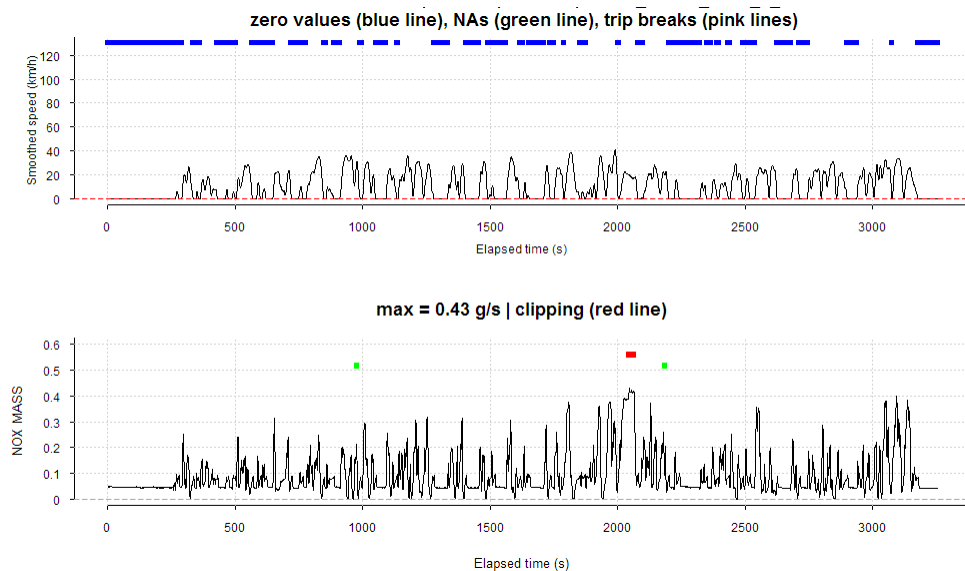


Figure 12. Example of gaseous file with a PCLIP value of 0.006 for NO_x.

In order to apply the COV/PTM analysis procedure, previous lab-based work was used to define typical COV/PTM criteria for modal emission traces (Smit, 2013), as shown in Table 1. Note that the criteria for PM in this table reflect HDV vehicle technology classes up to Euro IV.

Table 1. Emission trace verification criteria for PTM/COV

Variable	CO, HC, NO _x	CO ₂ , FC	PM
COV	> 1.0	> 1.2	> 1.0
PTM	> 2.5	> 2.5, < 12	> 2.5, < 50

To apply this verification procedure, the comparison may use these limits for modal emission traces from laboratory experiments as a starting point. Differences between PEMS and laboratory testing (sensitivity, stability, etc.) may affect the specific PTM/COV threshold values; thus, a further calibration is required to account for PEMS testing upon careful data inspection.

PEMStests of the EPDdataset indicate that there is general compliance with the lab-level criteria of Table 1, although it appears that PEMS PM data for newer technology vehicles exceed the PTM threshold of 50, indicating more spiky PM data than were observed in laboratory test conditions for Euro I-III HDVs. This does not mean that the PEMS data are invalid, as lower baseline PM emission rates with relatively high spikes are expected for vehicles with advanced emission control (in particular DPF).

For this particular data set, the following PEMS outlier identification criteria for PM can be adopted instead:

- COV < 0.7
- PTM < 2.5 or PTM > 60 (no DPF technology)
- PTM < 2.5 or PTM > 150 (with DPF technology)

Figure 13 is an example of a vehicle test with very large PTM (304) and COV (10) values. This is a light bus with a DPF and has essentially zero PM emission levels (blue bar) throughout the trip, except for two consecutive peaks in the middle of the trip.

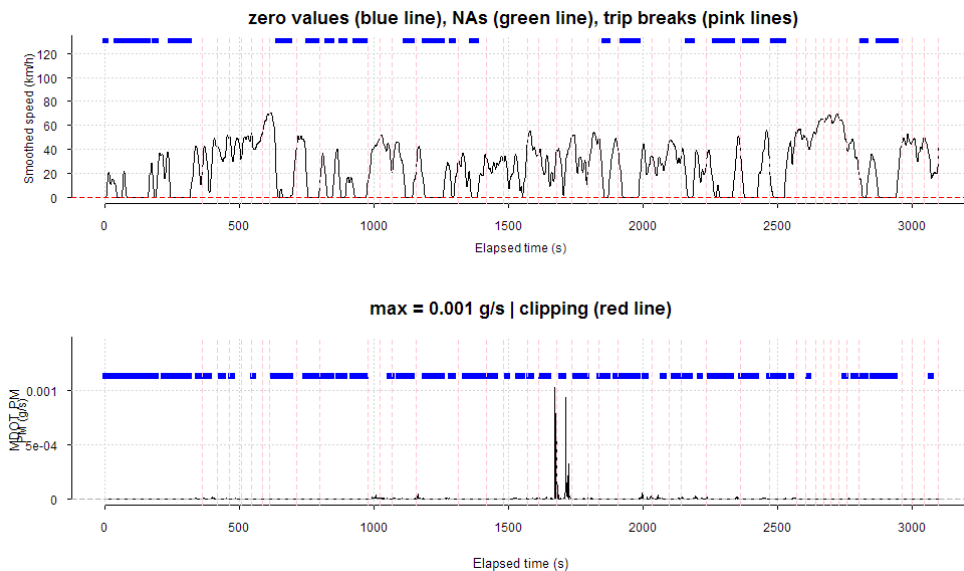


Figure 13. Example of PM traces with large PTM (304) and COV (10) values

For the gaseous emission, a minimum COV limit of 0.7 has been initially used for CO, NO_x, THC and CO₂. Upon reviewing the CO₂ data results visually, new boundaries that denote potential outliers are suggested to account for real-world measurements:

- COV < 0.25, for passenger cars
- COV < 0.65 for all other vehicles

Figure 14 shows an example of a vehicle test with very low PTM (1.1) and COV (0.11) values for CO₂ data. CO₂ are unrealistically steady and stay so even during idling periods.

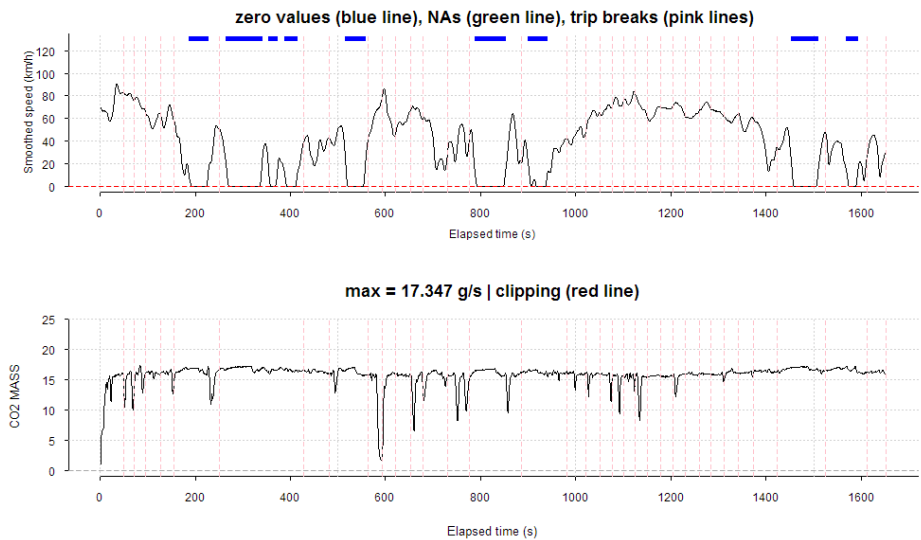


Figure 14. Example of CO₂ trace with very low PTM and COV values.

For the other gaseous pollutants, application of COV and PTM limits individually may flag several normal-looking trips as possible outliers; therefore a combination of COV/PTM boundaries was tested instead. The final thresholds were set

- COV<0.5 and PTM<3 for CO
- COV<0.5 and PTM<2.5 for NO_x
- COV<0.5 and PTM<2.5 for THC

In order to test the baseline analyser drift algorithm, the limit for computed drift variable D (as defined in the methodology) values was set to less than -5% or more than +5%. These values are flagged as showing significant drift. The example illustrated in Figure 15 yields a very high positive D value equal to 113% for CO₂ emissions. It corresponds to the same data test depicted in Figure 11 (clipping detection application). The top part of Figure 15 shows the speed-time visualisation of the observed test, while the bottom part illustrates the cumulative idling time of the same test. The orange-coloured shape is the regression polygon representing the drift. Zero values in the beginning of this test are around 2 g/s, but they exceed 15 g/s later on through the test. The combination of clipping and high drift will result in marking this trip as an outlier.

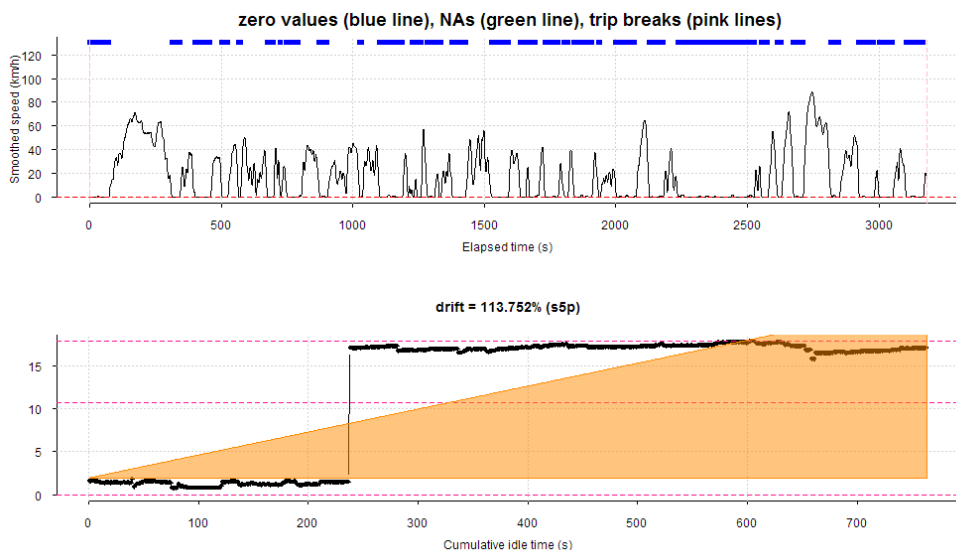


Figure 15. Example of CO₂ trace with large positive baseline drift value (+113%).

Figure 16 shows the THC drift plot of a petrol passenger car with a negative D value of -91%. The plots show a large negative drift of the THC emissions traces over time as shown in the bottom part starting from 0.012 g/s and reaching 0 g/s; this clearly illustrates a cold start and this trip is flagged as

such. The corresponding speed-time visualization of this test is shown in Figure 17.

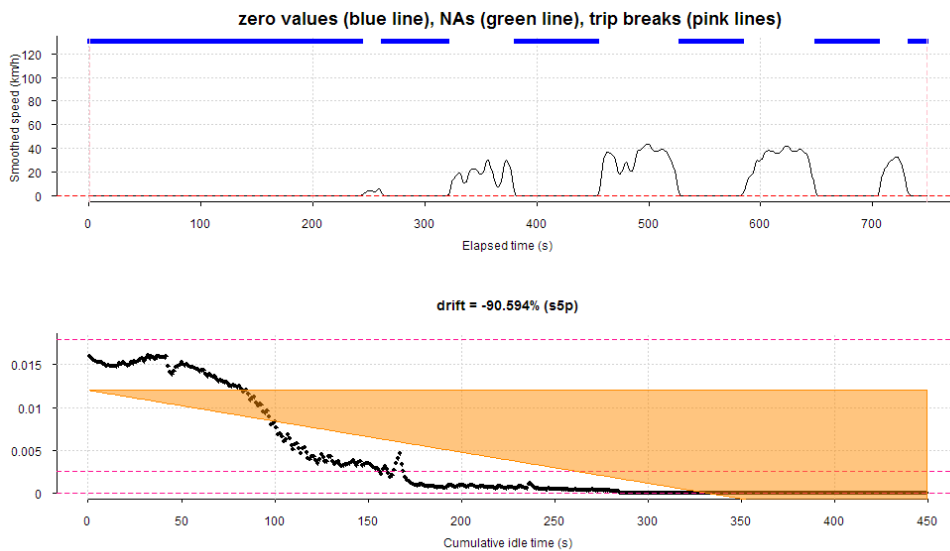


Figure 16. Example of CO trace with large negative baseline drift value (-21%). Drift time-series plot

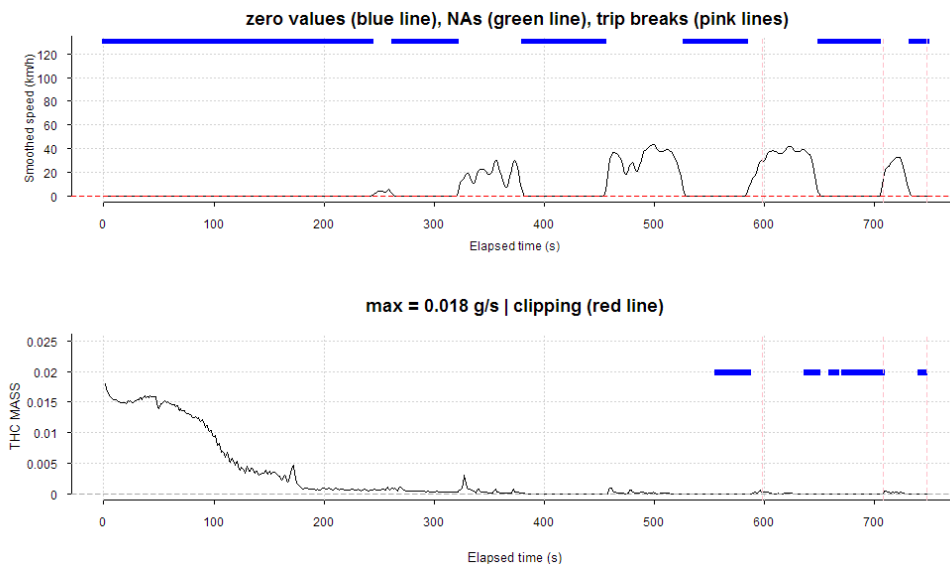


Figure 17. Example of CO trace with large negative baseline drift value (-21%). Speed time-series plot

For the application of the outlier detection scheme, the z-score limits must be defined. The sample test size in this dataset is typically large ($n \sim 3000$ s on average), so an absolute z-score threshold value larger than 3-4 could typically be used to flag potential outliers for normally distributed data. Should the transformed PEMS data exhibit notable, non-normal behaviour, a more conservative value of 5 can make the method more robust.

The outlier relevance is probably a more important metric to judge if the validity of a possible outlier. Initial visual examination of these pollutant plots may not yield unrealistic behaviour, so the outliers should probably be retained.

Examples of outlier detection results are shown in Figure 18 and in Figure 19; the former one shows THC emissions and is indicative of cold start, while the latter one shows a trip with a single spike in NO_2 values which yields a relevance of 0. It is however, recommended that further checks are performed for some of the extreme cases.

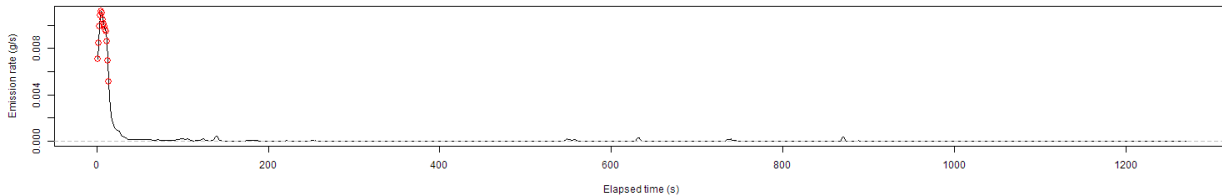


Figure 18. Examples of trip with identified outliers (THC, z-score = -11, relevance = 0.25)

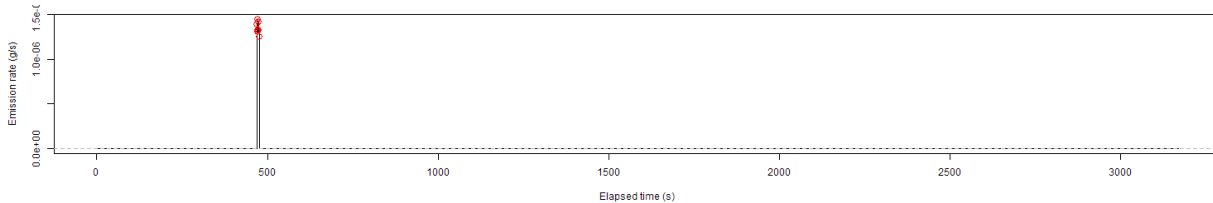


Figure 19. Examples of trip with identified outliers (NO₂, z-score = -23, relevance = 0)

The application of the visual time-series analysis is useful tool to validate issues raised by the other verification procedures and especially for outlier detection.

3. Further work

So far, a comprehensive approach for the verification of a variety of PEMS data measurements has been presented. Nevertheless, there is room for further enhancements. An option for consideration is to use verification algorithms that apply multivariate analysis across a number of pollutants. Univariate analysis does not reveal observations that fall within the ordinary range of values on each of the pollutants, but are unique in their combination of values for the different pollutants.

This option would require an analysis of multivariate distributions and could be achieved e.g. by using a statistical variable called the Mahalanobis Distance, which measures the distance in multi-dimensional space of each observation from the mean centre of the observations.

Also, it is recommended that emission factors based on PEMS data are compared at both vehicle and vehicle class level to ensure any suspicious data are further investigated. As a first step, the data need to be categorized to ensure comparison of emission tests for similar vehicles in similar test conditions. An example is illustrated in Figure 20, where several buses with similar characteristics (vehicle class, emission control technology, fuel, euro standard) are depicted together in terms of PTM vs. COV.

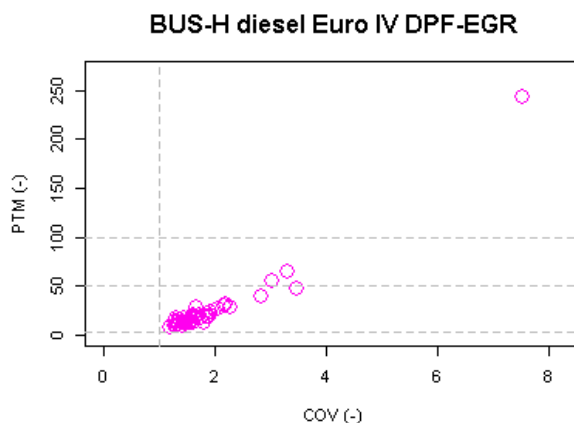


Figure 20. COV-PTM plots for PM emissions for individual vehicle classes.

Therefore, subsets of test data (denoted as groups) can be created, where each subset represented a particular combination of vehicle class, driving conditions and driving mode (hot, cold). Secondly, the data need to be shifted and transformed and z-scores computed for each data point. Thirdly, univariate or multivariate analysis can be used to detect outliers.

To the extent possible, additional protocols should also be devised to deal with missing values,

including consideration of possible imputation methods, and outliers (valid, invalid).

Summary and Conclusion

This study aimed to devise a set of automated procedures to extract verification statistics and visualization schemes in order to quality assure PEMS data. The overall goal is to ensure invalid data are flagged, corrected or removed, while at the same time valid outliers are maintained. During the first step of the procedure, a pre-processing of the PEMS data set is carried out to extract useful information for the verification process. Then, in the first verification step, an assessment of overall PEMS test validity is performed. Basic trip metrics are investigated to establish that general abnormalities are detected and flagged. The verification algorithm included a procedure to detect unrealistic accelerations as a function of instantaneous vehicle speed, generic vehicle type and power-to-weight ratio. A non-linear model was fitted to these data by adopting a reverse sigmoid function. The next verification phase focused on individual pollutant traces to identify occurrence of such errors in the dataset. For the gaseous and PM data, apart from visual analysis, the verification algorithms examined clipping, coefficient of variation / peak-to-mean ratio (COV/PTM) analysis, analyser drift and outlier detection. Initial comparisons used verification criteria for modal emission traces from laboratory experiments, but these must be modified to account for PEMS testing upon careful data inspection. The baseline analyser drift algorithm was developed to quantify analyser drift and indicate the possibility for other emission events such as cold/hot operation conditions. The outlier detection method used in this analysis focused on univariate data trace level, as any outliers detected and verified at this fundamental level, will prevent propagation of data issues to higher scales of assessment. Standard z-scores were used to implement the outlier detection protocol and the review was based on outlier relevance to measure their impact.

These QA/QC procedures were applied to the Hong Kong dataset collected by EPD to illustrate how they can be fitted to take account of any particularities of the PEMS measurements in general as well as environment-specific ones.

The overall approach provides a variety of tools to tackle different types of data measurements and examples of application indicate that it can successfully detect a variety of issues and suspicious behaviours. This verification methodology can be further expanded to include multivariate analysis across a number of pollutants. Also, emission factors based on PEMS data can be compared at both vehicle and vehicle class level to ensure any suspicious data are investigated further.

Acknowledgments

This work was carried out in the framework of the project "Provision of Services for Quality Assurance of the Portable Emission Measuring Systems (PEMS)", funded by the HKEPD.

References

- Smit, R. (2006), An Examination of Congestion in Road Traffic Emission Models and Their Application to Urban Road Networks, Ph.D. Dissertation, Griffith University, Brisbane, Australia.
- Smit, R. (2013), A procedure to verify large modal vehicle emissions databases, Proceedings of the CASANZ Conference, Sydney, 7-11 September 2013.
- Velleman, P. F. (1976), Robust Nonlinear Data Smoothers; Theory, Definitions, and Applications, PhD thesis, Princeton University.
- Velleman, P. F. (1980), Definition and Comparison of Robust Nonlinear Data Smoothing Algorithms, Journal of the American Statistical Association, vol. 75, number 371, pages 609-615.

Comparative study of three digestion methods for airborne PM10-bound metallic elements in an urban site

Amina Kemmouche*, [Hocine Ali-Khodja*](#), Xavier Querol**, Fayrouz Bencharif-Madani*

*Laboratoire Pollution et Traitement des Eaux (LPTE), Département de Chimie, Faculté des Sciences Exactes, Université des Frères Mentouri, Constantine, Algérie.

** Institut de l'Evaluation Environnementale et de la Recherche sur l'Eau (IDAEA), Conseil Supérieur de la Recherche Scientifique (CSIC), Barcelone, Espagne.

Author email: hocine_ak@yahoo.fr

Abstract

A comparative study of three different aerosol extraction processing techniques was carried out on ten quartz fiber PM10 sampling filters and a standard material (P1633b Fly Ash). Simultaneous sampling of PM10 was conducted at an urban background site in the town of Constantine. Three different mixtures of reagents were chosen in order to achieve the extraction procedure: mix 1 (HF / HClO₄ / HNO₃), mix 2 (HCl / HNO₃), mix 3 (HCl / H₂O₂ / HNO₃). A standard material (P1633b) was used to quantify and compare the extraction efficiencies of the three techniques. The solutions obtained after dust mineralization were analyzed by two analytical techniques. Pb, Cu, Co and Ni were analyzed by ICP-MS, while Zn and Mn were determined by ICP-AES. The first digestion technique proved to be the most efficient for all samples. The differences in extraction efficiencies between the three techniques varied from one sample to another according to the element analyzed.

Keywords: PM10, partial extraction, metallic elements, digestion methods

Introduction

Particulates are compounds with a health issue and their study is important because they are small enough to penetrate the respiratory system (Al Masri *et al.*, 2005). These pollutants can be primary when they are directly emitted to the atmosphere or secondary when they result from the transformation of gaseous pollutants. The emission sources of aerosols are diverse. They may be natural such as soil erosion, the bursting of waves bubbles allowing the formation of sea spray, volcanic activity, etc. (Azimi, 2004). Anthropogenic sources are also responsible for particulate pollution; farming activities using fertilizers and pesticides, industry with the various pollutants it rejects, petroleum refining, combustion and finally road transport (Lamaison 2006; Tombette, 2007; Han *et al.*, 2006). According to the IUPAC definition, MTE (metallic trace elements) is: "Anything with an average concentration below 100 ppm." The term "ultra-trace" is a name that has no strict definition, but which is frequently used in the literature (Brown & Milto, 2005). MTE are part of air pollutants and their determination in the fine particles is an important parameter in the assessment of the health risk induced by these particles (Perez *et al.*, 2004). Recent studies have developed methods for the determination of harmful MTE such as: Cd, Co, Cr, Cu, Ni and Pb present in aerosols (Castillo *et al.*, 2008; Moreno *et al.*, 2006). Analysis of MTE present in dust samples taken from the ambient air at very low concentrations is a challenge. The low weights of the samples increase the risk of loss and contamination. Research has mainly focused on the development of new methods to increase the sensitivity and selectivity of the analysis of trace elements. Direct methods include X-ray fluorescence (XRF), X-ray emission induced by proton (PIXE) analysis and instrumental neutron activation (INAA). However, matrix effects can cause major interferences while using these techniques. The most common methods used today for the determination of metallic elements in environmental samples involve highly sensitive spectroscopic techniques, such as atomic absorption spectroscopy (FAAS, ETAAS), inductively coupled plasma mass spectrometry and inductively coupled plasma atomic emission spectrometry (ICP-MS and ICP-AES). The use of these techniques requires dissolving the samples before the determination of the metal contents. In recent years, analysts have

recognized increasingly that most systematic errors could be introduced during the sampling and sample preparation steps. Currently, the influence of the sample preparation step on the quality of the analysis results is recognized worldwide (Ehi-Eromosele et al., 2012). Different digestion methods for trace metals present in aerosols can be used. The extraction efficiency depends on several factors: the sample nature and its matrix, the time available for analysis and the optimal time of acid digestion (Ehi-Eromosele et al., 2012).

In the scientific literature, several extraction protocols of trace elements in aerosols are reported without specifying whether the type of extraction is exhaustive allowing the total dissolution of metals or selective for a specific metallic fraction. Several techniques are used for the extraction of metal elements contained in solid environmental matrices (aerosols, sediments, soil, marine and dust samples). Some studies are based on the extraction in a single step and use different mixtures of reagents such as: $\text{HNO}_3 + \text{HCl}$ (aqua regia), HNO_3 alone, $\text{HNO}_3 + \text{H}_2\text{O}_2$, $\text{HNO}_3 + \text{HF} + \text{H}_2\text{O}_2 + \text{H}_3\text{PO}_4$, $\text{HNO}_3 + \text{HCl} + \text{HF}$, $\text{HNO}_3 + \text{HF}$, etc. (Pérez et al., 2004; Petterson & Olsson, 1998; Ragosta et al., 2008; Bettinelli et al., 2000). Other studies implement the sequential extraction based on the principle of the attack of the sample by gradually stronger mineralizing solutions (Grotti et al., 2002; Ryan et al., 2008; Jimoh, 2012). A total digestion method must include the use of hydrofluoric acid HF which, despite its harmful health effects, remains the only reagent capable of releasing the silicates bound metal fraction. However, in many studies, other techniques such as aqua regia proved equally effective for some metals (Sastre et al., 2002).

The purpose of this study is to conduct a comparative study between a total digestion technique ($\text{HF} / \text{HNO}_3 / \text{HClO}_4$) and two partial extraction techniques ($\text{HNO}_3 / \text{HCl}$) and ($\text{HNO}_3 / \text{HCl} / \text{H}_2\text{O}_2$) to measure the efficiency of such techniques towards the metallic elements: Cd, Co, Cr, Cu, Ni and Pb.

1. Material and methods

1.1. Samples

A standard material (UPM 1648 Fly Ash) and ten PM10 quartz fiber filters were used for sampling PM10 in the period between 15/01/2015 and 13/03/2015 at the Slimane Zouaghi campus of the university of Constantine using a high volume sampler, model Tisch-TE-6001 (Fig. 1).

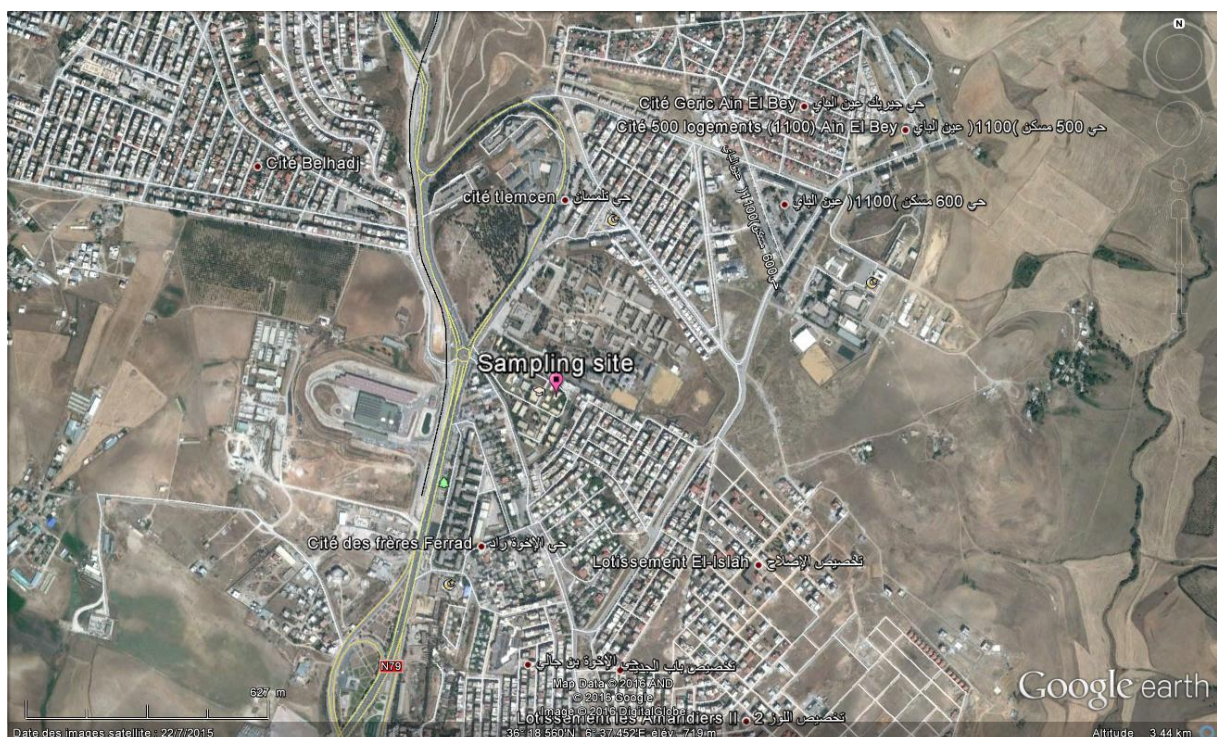


Figure 1. Map of PM10 sampling site

1.2. Dust mineralization

Experimental protocols used for PM₁₀ sample dissolution are shown below. To complete each extraction protocol, circular 30 mm diameter discs were cut from the ten PM₁₀ filters.

1.2.1. First Protocol (P1)

Samples were digested in a solution containing 1 ml HNO₃ and 2 ml HF in a closed PFA bottle at 90 °C for at least 8 hours. After cooling, the containers were opened and 1 ml of HClO₄ was added. The acids were then completely evaporated by placing the PFA containers on a hot plate at 240 °C. The remaining dry residue was dissolved with 2.5 ml of HNO₃ before being diluted with distilled water (MilliQ) to 25 ml, to obtain solutions of 10% HNO₃ that were centrifuged for 20 minutes at 3000 rpm (Querol et al., 2001).

1.2.2. Second Protocol (P2)

The samples were introduced into PFA vials. A 10 ml solution of a (3:1) mixture (12M HCl and 17M HNO₃) was left at room temperature for 24 h. Then the solution was digested on a hot plate at 130 °C for 15 min. After cooling at room temperature, the suspension was filtered and diluted to 25 ml with 0.17 M HNO₃ (Pena-Icart et al., 2011).

1.2.3. Third Protocol (P3)

The extraction of the filters was carried out using the following reagents: HCl (37%), H₂O₂ (35%) and HNO₃ (65%). Samples were put in a PFA flask and a solution containing 30 ml HCl and 5 ml H₂O₂ was added. After heating for 1 hour on a hot plate at 120 °C, the solution was filtered and 20 ml HCl (1+1) were added to the residue for 15 min to complete the extraction. The PFA flask content was filtered again and the filtrate was added to the filtrate of the previous step. The solution was concentrated on a hot plate until a small volume was left in the flask. The latter was then transferred to a volumetric flask of 25 ml. This volume was filled up with a HNO₃ solution (2+98) (Awan et al., 2011).

1.2.4. Analytical techniques

The resulting solutions were then analyzed by ICP-AES (IRIS Solutions Advantage Thermo TJA) for elements, Zn and Mn and by ICP-MS (X Series II Thermo) for elements Cu, Pb, Co and Ni.

2. Results and discussion

2.1. Evolution of PM₁₀ concentrations

Ten PM₁₀ samples were collected during from 15/01/2015 to 13/03/2015. The daily concentrations of PM₁₀ are shown in Fig. 2.

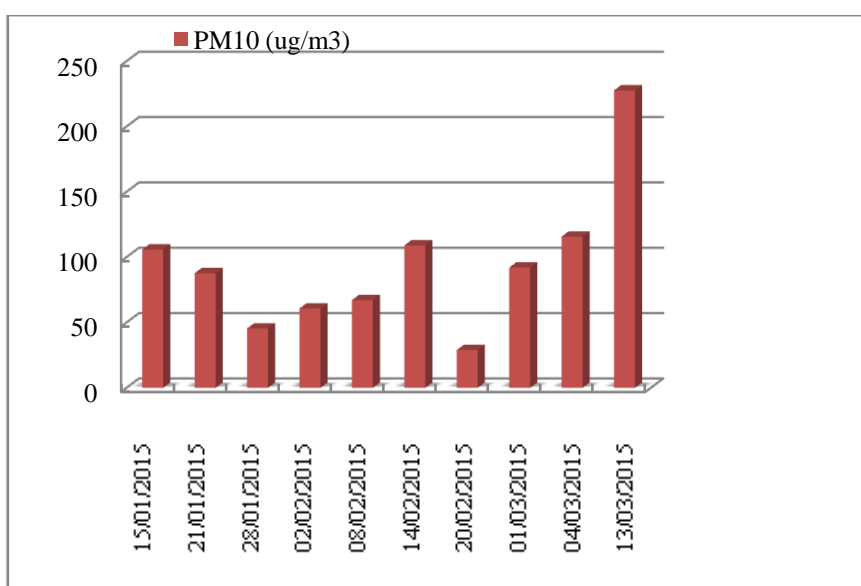


Figure 2. Daily atmospheric levels of PM₁₀

Table 1 summarizes the results for PM10.

Table 1. PM10 concentrations measured at the study area

Number of samples	10
Sampling period	15/01/2015 - 13/03/2015
Unit	$\mu\text{g}/\text{m}^3$
Average daily concentration	94
Maximum daily concentration	227
Minimum daily concentration	28

PM10 concentrations range from 28 $\mu\text{g}/\text{m}^3$ to 227 $\mu\text{g}/\text{m}^3$ with an average value of 94 $\mu\text{g}/\text{m}^3$. The results obtained show that daily levels of PM10 vary widely. This variation is linked both to fluctuations in the intensity of emission sources (road traffic, various industrial activities) and to natural influences (desertic sand, biomass fires, dust resuspension) and weather parameters (wind direction and intensity, humidity, precipitation, temperature) (Kerbach et al., 2009).

2.2. Concentrations of the standard material (P1633b) bound metal elements extracted according to the three extraction protocols

The most common approach for measuring the efficiency of digestion procedures is the estimation of the percentage recovery of metals contained in standard materials having a composition and a structure similar to those of the samples (Celo et al., 2010). Table 2 shows the certified values and reference values of the six studied metallic elements contained in the standard material (P1633b) and the measured concentrations obtained after analysis of the same material using the three extraction protocols.

Using the data from Table 2, we calculated the percentage recovery of each metal element and for each extraction protocol. The results are shown in Table 3.

Table 2. Certified values and reference values and measured concentrations for Cu, Pb, Zn, Co, Mn and Ni contained in the standard material (P1633b)

Element	Certified and reference values	Measured concentrations		
		P1	P2	P3
Cu (mg/kg)	113	102	47	68
Pb (mg/kg)	68	58	31	37
Zn (mg/kg)	210	266	123	173
Co (mg/kg)	50	40	17	24
Mn (mg/kg)	131,8	137	65	81
Ni (mg/kg)	120	130	44	59

Table 3. Percentage recovery of metal elements contained in the standard material (P1633b)

R%	P1	P2	P3
Cu	90%	42%	60%
Pb	85%	46%	54%
Zn	127%	59%	83%
Co	80%	34%	48%
Mn	104%	49%	61%
Ni	108%	37%	49%

In order to interpret the observed differences between the three extraction techniques, it is essential to define the metallic fraction targeted by each extraction method. The mixture HF / HClO_4 / HNO_3 (P1) allows the determination of the total contents of the analyzed elements (Bettineli et al., 2000). The aqua regia extraction method (P2) is a technique that is frequently used for the extraction of metals in different environmental matrices. This technique solubilizes most of the residual minerals (Bettineli et al., 2000). The addition of oxygenated water in the third solution (P3) makes it possible to solubilize the oxidizable phase metals such as sulphides and organic matter (Grotti et al., 2002).

The extraction efficiency is relatively better for method P3 compared to method P2 for all studied elements with percentage recoveries ranging from 48% to 83% for P3 and from 34% to 59% for P2. The addition of H₂O₂ in method P3 improved the percentage recoveries by 18% for Cu, 8% for Pb, 24% for Zn, 14% for Co, 12% for Mn and Ni.

The addition of HF in the first extraction protocol P1 improved significantly the extraction efficiency for all elements with percentage recoveries ranging from 85% to 127%. This method improved the percentage recoveries achieved by protocol P3 by 50% for Cu, 31% for Pb, 32% for Co, 39% for Mn and 51% for Ni, considering that percentage recoveries cannot exceed 100%. The overestimated observed Zn concentration was due to possible contamination.

2.3. Concentrations of the metal elements contained in aerosols and obtained according to the three extraction protocols

Figure 3 allows a comparison between the mean concentrations of six metallic elements present in the solutions obtained by the three extraction protocols for ten PM10 samples represented by: S1, S2, S3, S4, S5, S6, S7, S8 S9 and S10.

P1 allows the highest extraction efficiency of the three digestion methods for the elements determined, in most individual samples. Exceptions concern Pb contained in samples S3 and S8, Ni contained in samples S1, S3, S8 and S10 and Zn contained in samples S3 and S10. This may be due to possible contamination of the samples while performing protocols P2 and P3.

P2 and P3 protocols are two partial extraction techniques. The absence of HF in the P2 and P3 reagent mixtures does not allow the release of the metal bound silicate fraction (Hong et al., 2005). This fraction varies from one sample to another depending on the element considered and this explains the significant difference in extraction efficiency between the total extraction protocol P1 and the two partial extraction protocols P2 and P3. Both protocols present a more or less similar efficiency for elements Mn, Ni and Co. Protocol P2 is on average more efficient than P3 protocol for the extraction of Cu and Zn.

The behavior of Pb is exceptional with concentrations very close to each other for protocols P1, P2 and P3 for almost all samples. This element has a high affinity for organic matter (Mathews et al, 2012). The organic fraction may well be completely dissolved by the various mixtures used in the three digestion methods.

For sample S7 which shows the minimum PM10 concentration, significant differences were not found in the amounts of metal elements extracted by the three digestion methods in each studied sample.

2.4. Comparison of the results obtained for the standard material (P1633b) and PM10 samples

The efficiency of an extraction technique can only be quantified by using standard samples having certified values and reference values for the elements of interest. Because these materials are easier to analyze than real environmental samples (Gerboles et al., 2011), such standard samples can not confirm the digestion efficiency of real samples because of different inherent matrices and element concentration ranges (Celo et al., 2010). Figure 4 compares the concentrations of metal elements extracted by the three extraction methods on standard material and the average concentrations of the same elements contained in the ten studied PM10 samples.

For Pb, Zn, Co, and Mn and despite the different concentrations ranges between samples and between samples and the standard material, the same findings apply for the three extraction protocols for the standard material (P1633b) and for the studied PM10 samples. The extraction efficiency increases in the order P2, P3, P1.

The total digestion method P1 is most efficient for the six elements analyzed in both the standard material and the studied PM10 samples.

The addition of H₂O₂ in the third method has improved the percentage of recovery of all elements contained in the standard material (P1633b) in comparison to the second extraction method. However, the average concentrations of Cu, Zn and Ni contained in the PM10 samples are higher when they are extracted by method P2 in comparison to method P3. This could be explained by the difference in composition of the samples studied in both cases.

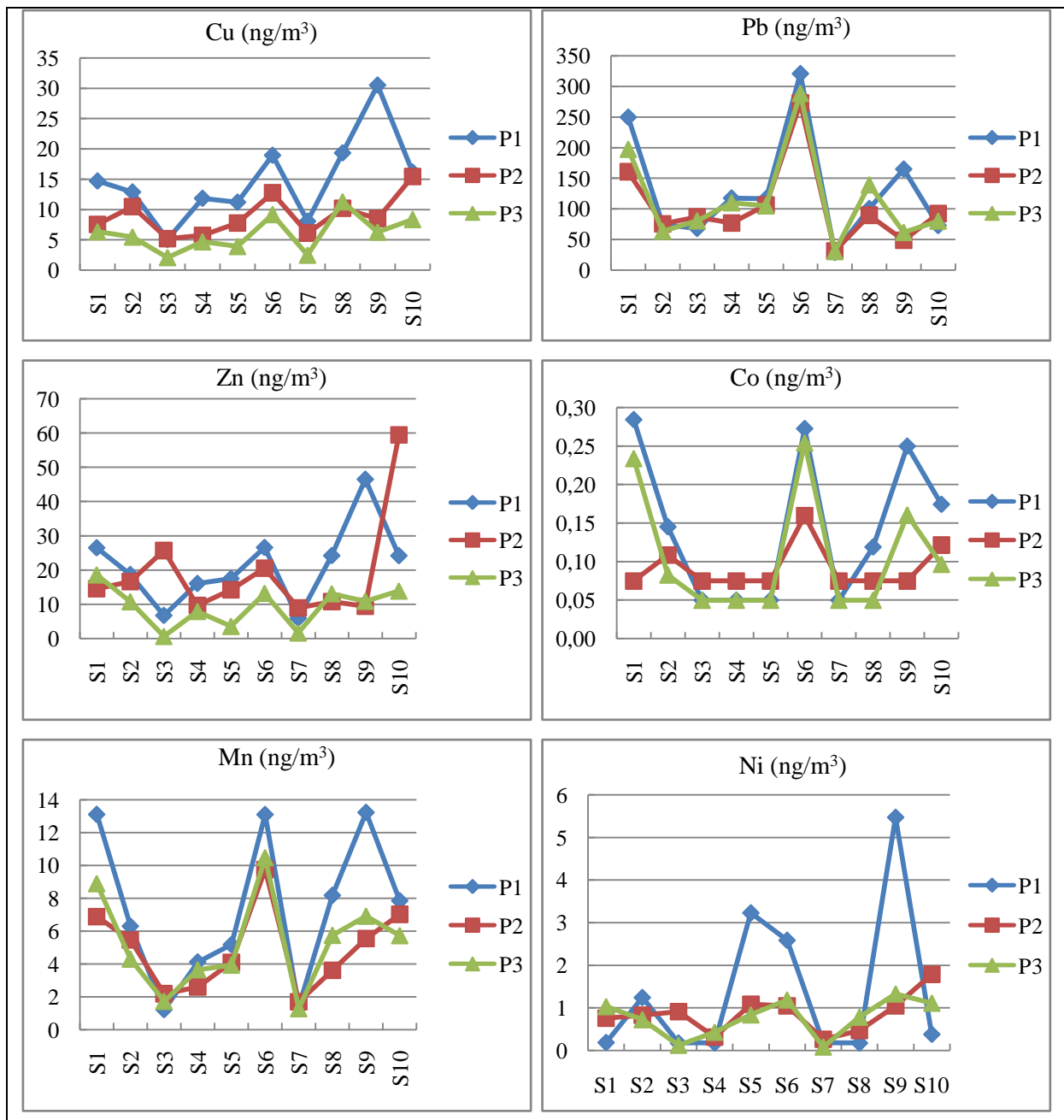
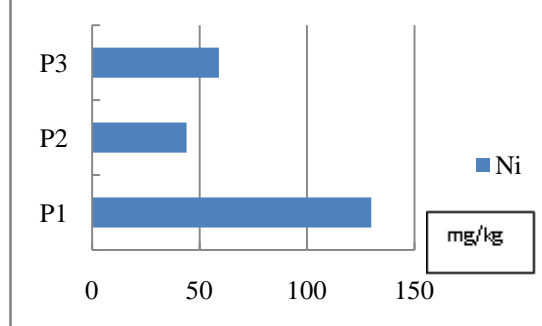
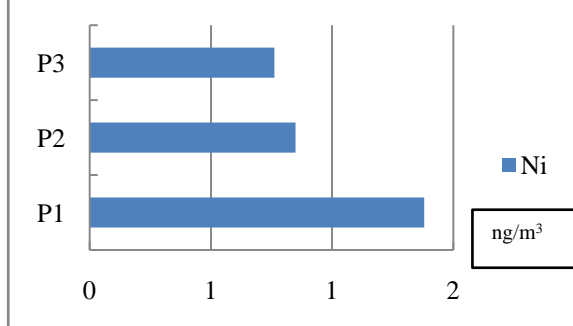
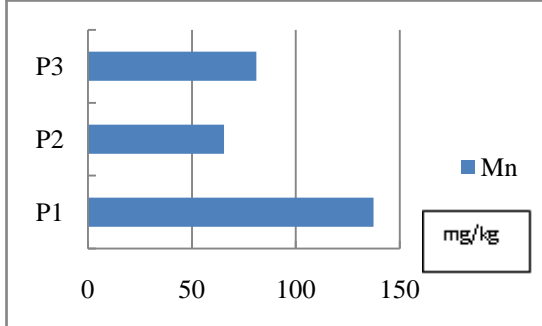
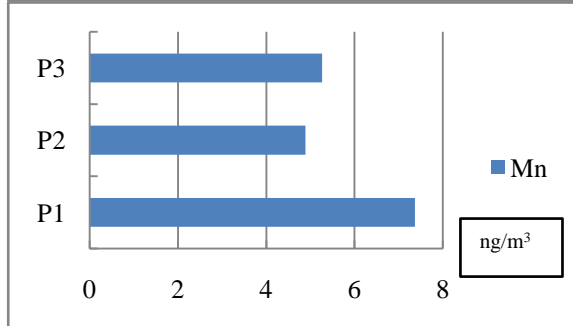
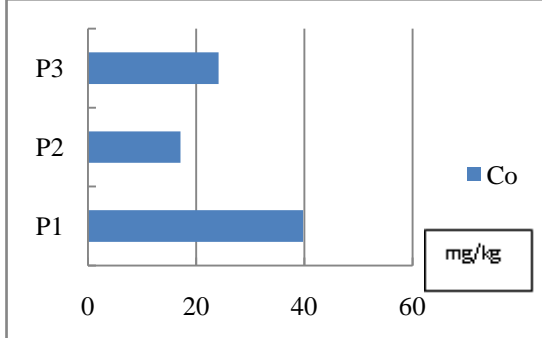
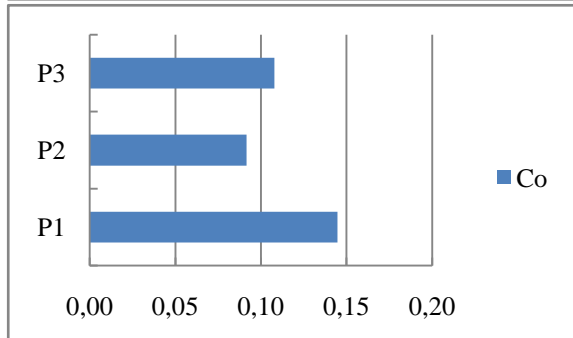
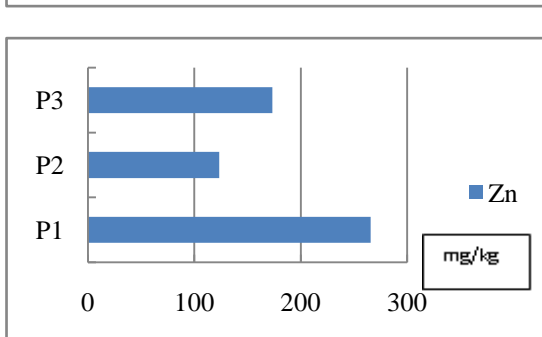
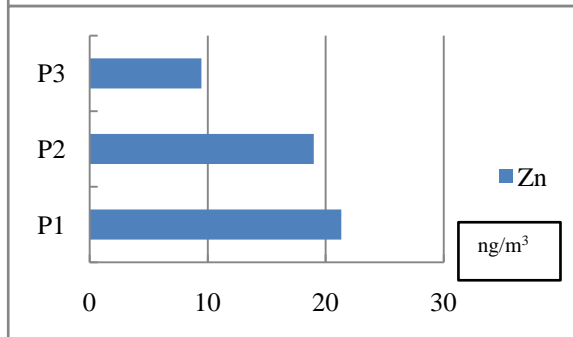
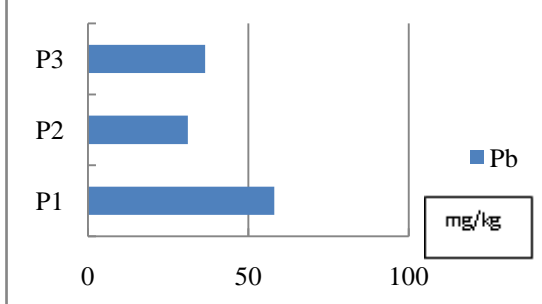
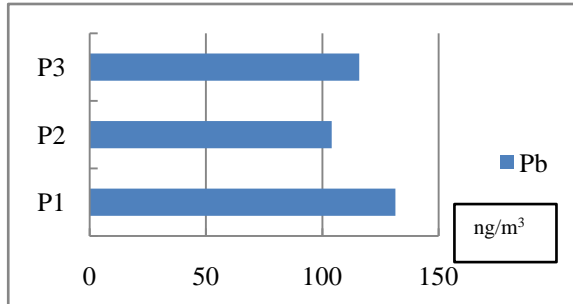
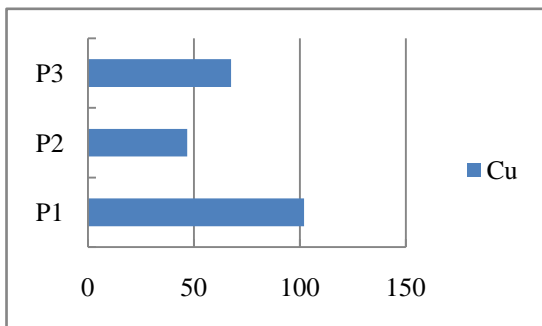
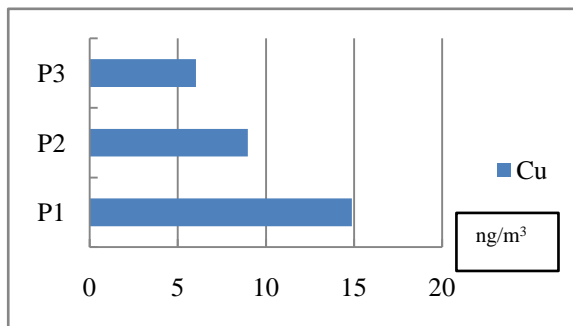


Figure 3. Comparison of the concentrations of Cu, Pb, Zn, Co, Mn, and Ni extracted from PM10 by the three digestion methods

Figure 4. Comparison of the concentrations of metal elements extracted from the PM10 samples (left) and the certified material P1633b (right) by the three digestion methods



Conclusion

This study highlights the different metal extraction capacities of three digestion methods. Extraction efficiencies were shown to vary greatly between these methods. This emphasizes the need for normalization of digestion methods in order to be able to harmonize results for comparison purposes.

The addition of H₂O₂ to aqua regia has improved the percentage of recovery of all elements contained in the standard material (P1633b). Such an improvement concerned only Co and Mn and to a lesser extent Pb. Extraction of Cu, Zn and Ni in PM10 samples was better with aqua regia. The silicate phase could be poorly attacked by the solvents used with respect to some elements. Mn oxides and hydroxides which are not completely dissolved by aqua regia could explain the small amount of extracted Mn.

The total digestion method proved to be the most efficient for extracting Cu, Pb, Zn, Co, Mn and Ni in a standard material and in ten PM10 samples. No reagent mixture can replace the presence of HF which, despite its harmful effects, is the only reagent capable of releasing the metal fraction associated with silicates. Significant differences between extraction protocols vary with samples, matrices and elements. The efficiency of an extraction technique depends on several factors: the extraction solution, the nature of the sample matrix, the analysis time available as well as the optimal time of digestion acids (Ehi-Eromosele et al., 2012).

References

- Al Masri, M.S, K. Al-Kharfan, & K. Al-Shamali (2005). Speciation of Pb, Cd and Zn determined by sequential extraction for identification of air pollution sources in Syria. *Atm. Environ.*, 40 (2006) p 753–761.
- Awan, M.A., S.H. Ahmed, M.R. Aslam & I.A. Qazi (2011). Determination of total suspended particulate matter and heavy metals in ambient air of four cities of Pakistan. *Iran. J. Energ. & Environ.* 2 (2): 128-132.
- Azimi, S. (2004). Sources, flux et bilan des retombées atmosphériques de métaux en Ile-de-France. Thèse présentée pour l'obtention du diplôme de docteur de l'Ecole nationale des ponts et chaussées, spécialité : sciences et techniques de l'environnement. 30-36.
- Bettinelli, M., G.M. Beone, S. Spezia, & C. Baffi (2000). Determination of heavy metals in soils and sediments by microwave-assisted digestion and inductively coupled plasma optical emission spectrometry analysis. *Anal. Chim. Act.* 424, p 289-296.
- Brown, R & M. Milto (2005). Analytical techniques for trace element analysis : an overview. *Trends Anal. Chem.*, vol. 24, n°3, p 266-274.
- Castillo, S., T. Moreno, X. Querol, A. Alastuey, E. Cuevas, L. Herrmann, M. Mounkaila, M & W. Gibbons (2008). Trace element variation on size-fractionated African Desert dusts. *J. of Arid Environ.* vol. 72, p 1034-104.
- Celis, E.D. Zlotorzynska, D., Mathieu, & I. Okonskaia (2010). Validation of a simple microwave-assisted acid digestion method using microvessels for analysis of trace elements in atmospheric PM2.5 in monitoring and Fingerprinting studies. *Open Chem. Biomed. Method. J.* 3, p 143-152.
- Ehi-Eromosele, C.O., A.A. Adaramodu, W.U., Anake, C.O., Ajanaku & A., Edobor-Osoh (2012). Comparison of three methods of digestion for trace metal analysis in surface dust collected from an e-waste recycling site. *Nat. Sci.* vol. 10, n° 10, p 1-6.
- Gerboles, M et al. (2011). Interlaboratory comparison exercise for the determination of As, Cd, Ni and Pb in PM10 in Europe. *Atm. Environ.* vol. 45, n° 20, p 3488-3499.
- Grotti, M. C., Ianni, & R. Frache (2002). Inductively coupled plasma optical emission spectrometric determination of trace elements in sediments after sequential selective extraction: effects of reagents and major elements on the analytical signal. *Talanta*, vol. 57, n° 6, p 1053–1066.
- Han, X. & Luke P. Naeher (2006). A review of traffic-related air pollution exposure assessment studies in the developing world. *Environ. Int.* p 106-120.
- Nguyen, H.L., M. Braun & M. Leermakers (2005). Comparison of two digestion procedures used for trace metals extraction from reference sediments. *Environ. Tech.* ES04.
- Jimoh, W. (2012). A sequential extraction method for the chemical speciation of metals in Harmattan dust collected from Kano and Zaria cities in Northern Nigeria. *Int. J. Res. Chem. Environ.*, vol. 2, n° 2, p 76-82.

- Kerbachi, R., N. Oucher, A. Bitouche, N. Berkouki, B. Demri, M. Boughedaoui, & R. Jourmard (2009). Pollution par les particules fines dans l'agglomération d'Alger. Colloque international Environnement et Transports dans des Contextes Différents, Ghardaïa, Algérie, 16-18 février 2009.
- Lamaison, L. (2006). Caractérisation des particules atmosphérique et identification de leurs sources dans une atmosphère urbaine sous l'influence industrielle. Thèse de doctorat en Structure et dynamique des systèmes réactifs, Lille, France.
- Mathews, A., C. Omono, C. & S. Kakulu (2012). Comparison of digestion methods for the determination of metal levels in soils in Itakpe, Kogi State, Nigeria. *Int. J. Pure Appl. Sci. Technol.*, 13(2) p 42-48.
- Moreno, T., X. Querol, A. Alastuey, M. Viana, P. Salvador, A. Sanchez, A. Begona, S. Dela Rosa, & W. Gibbons (2006). Variation in atmospheric PM trace metal content in Spanish towns: Illustrating the chemical complexity of the inorganic urban aerosol cocktail. *Atm. Environ.* 40, p 6791-6803.
- Pena-Icart, M. (2011). Comparative study of digestions methods EPA 3050B (HNO₃, H₂O₂, HCl) and ISO 11466.3 (aqua regia) of Cu, Ni and Pb contamination assessment in marine sediments. *Marine Environmental Research* 72, p 60-66.
- Querol, X., A. Alastuey, S. Rodriguez, F. Plana, E. Mantilla, & C.R. Ruiz (2001). Monitoring of PM10 and PM2.5 ambient air levels around primary anthropogenic emissions. *Atm. Environ.* vol. 35, n° 5, p 848–858.
- Pérez, C., J. Pinerio, P. Mahia, S. Lorenzo, E. Fernandez, & D. Rodriguez (2004). Hydride generation atomic fluorescence spectrometric determination of As, Bi, Sb, Se(IV) and Te(IV) in aqua regia extracts from atmospheric particulate matter using multivariate optimization. *Anal. Chim. Act.*, vol. 526, p 185-192.
- Petterson, R.P. & M. Olsson (1998). A nitric acid–hydrogen peroxide digestion method for trace element analysis of milligram amounts of plankton and periphyton by total-reflection X-ray fluorescence spectrometry. *J. Anal. At. Spectrom.*, vol. 13, p 609–613.
- Ragosta, M., R. Caggiano, M. Macchiato, S. Sabia, & S. Tripetta (2008). Trace elements in daily collected aerosol : Level characterization and source identification in a four-year study. *Atm. Res.*, vol. 89 p 206-217.
- Ryan, P.C., S. Hillier, & A.J. Wall (2008). Stepwise effects of the BCR sequential chemical extraction procedure on dissolution and metal release from common ferromagnesian clay minerals: A combined solution chemistry and X-ray powder diffraction study. *Sci Total Environ.*, vol. 407,
- Sastre, J., A. Sahuquillo, M. Vidal, & G. Rauret. (2002). Determination of Cd, Cu, Pb and Zn in environmental samples: microwave-assisted total digestion versus aqua regia and nitric acid extraction. *Anal. Chim. Act.*, vol. 462, n° 1, p 59-72.
- Tombette, M. (2007). Modélisation des aérosols et de leurs propriétés optiques sur l'Europe et l'Ile de France : validation, sensibilité et assimilation de données. Thèse présentée pour l'obtention du diplôme de docteur de l'Ecole nationale des ponts et chaussées, spécialité : sciences et techniques de l'environnement, p 30-36.

Calculating emissions from road transport on a street level with COPERT4 and COPERT Street Level, a case study

Chariton KOURIDIS*, Leonidas NTZIACHRISTOS**, Thomas PAPAGEORGIOU*

* EMISIA SA, Thessaloniki, 57001, Greece

Fax +30 23 10 80 41 10 - email: charis.k@emisiasa.com

** Laboratory of Applied Thermodynamics, Aristotle University of Thessaloniki (LAT/AUTH), Thessaloniki, 54124, Greece

Abstract

This paper compares two road transport emission calculation models: COPERT4 and COPERT Street Level. COPERT4 has been developed to facilitate experts to compile national emission inventories. COPERT Street Level has been developed in order to allow a more detailed emission calculation, based on a single road segment rather than the entire country. The comparison was made for 3 different cases in the city of Thessaloniki. One "business as usual" case describing a typical working day. The second case based on the latest Greek implemented policy with the legalization of diesel passenger cars use in the metropolitan area of Thessaloniki. The third case is based on the effect of the subway on urban transport emissions that will be in use in the next years. Data was collected from various sources, such as previous studies, the WISERIDE tool and traffic models. All this information was inserted to both models and emissions were calculated for 4 main pollutants, CO₂, NO_x, PM and VOC. Comparison was made with quantitative (time required for the calculations, accuracy, calculation time) but also qualitative criteria (ease of use, data visualization).

Keys-words: COPERT Street Level, CO₂ emissions, road transport, emission factor, COPERT4.

1. Introduction

Ever since the first significant air pollution event of London in 1952 raising awareness that urban pollution will be a major issue in the next years, scientists have been trying to identify and quantify the most important sources of pollution in an urban area. With the strong increase of road transport it is now evident that vehicle emissions play a significant role to the urban air quality. A number of models have been developed to calculate emissions from road transport in a micro, meso and macro scale.

This paper compares two such models: COPERT4¹ and COPERT Street Level². The development of COPERT4 has been coordinated by the European Environmental Agency (EEA) to facilitate experts compile their national emission inventories. COPERT Street Level has been developed by EMISIA SA and is based on the COPERT methodology in order to allow a more detailed emission calculation, based on a single road segment rather than the entire country. The comparison was made for 3 different cases in the city of Thessaloniki.

Both models are able to calculate emissions in the metropolitan area of Thessaloniki. However, there are major differences both in the calculation process as well as the accuracy of the results. COPERT4 requires significantly more time to calculate emissions since it is designed to compile an emission inventory, which means that the model must calculate all emissions for all vehicle categories. COPERT Street Level was designed specifically to reduce calculation time even if a large number of data was used. COPERT4 requires post processing to display the emissions on a road level, while COPERT Street Level already includes a GIS library to facilitate this task. Most importantly COPERT Street Level can more accurately calculate emissions for a road network since it uses average speed and traffic composition per road segment rather than average values over the entire network like COPERT4 does.

The paper is divided in 5 sections. The first one is the introduction to the work performed. The second section describes both models as well as their methodological elements. The third section

¹ <http://emisiasa.com/products/copert-4>

² <http://emisiasa.com/products/copert-street-level>

presents the input data used as well as the 3 scenarios and outlines the differences. The fourth section compares the results as calculated by the models for all scenarios and finally the fifth section presents the conclusions as they were drawn by the analysis of the results.

2. Model description

COPERT4

COPERT4, developed by EMISIA SA, is a model used world-wide to calculate air pollutant and greenhouse gas emissions from road transport. The development and continuous update of COPERT4 is coordinated by the European Environment Agency (EEA). The COPERT4 methodology is part of the EMEP/EEA air pollutant emission inventory guidebook and is consistent with the 2006 IPCC Guidelines for the calculation of greenhouse gas emissions.

COPERT4 has been initially developed to help national experts compile their emission inventories. However, due to the high demand for accurate emission calculation, it has also been further developed to be used for urban emission inventories, policy assessment, scenario formulation and modelling.

COPERT4 is an average speed emission model. The main equation used to calculate emissions is the following:

$$Emission[g] = VehiclePopulation[veh] \times AnnualMileage[km] \times EmissionFactor\left[\frac{g}{veh\ km}\right]$$

The emission factor is calculated based on the average speed of a vehicle. This average speed is provided for three driving modes: urban, rural and highway. The emission factor calculation function is different for each vehicle category and pollutant. There are 2 main sources for providing the data for the emission calculation functions, laboratory measurements and simulations from microscale models. An example of a typical graph describing the measured data, as well as the underlying function, is provided below.

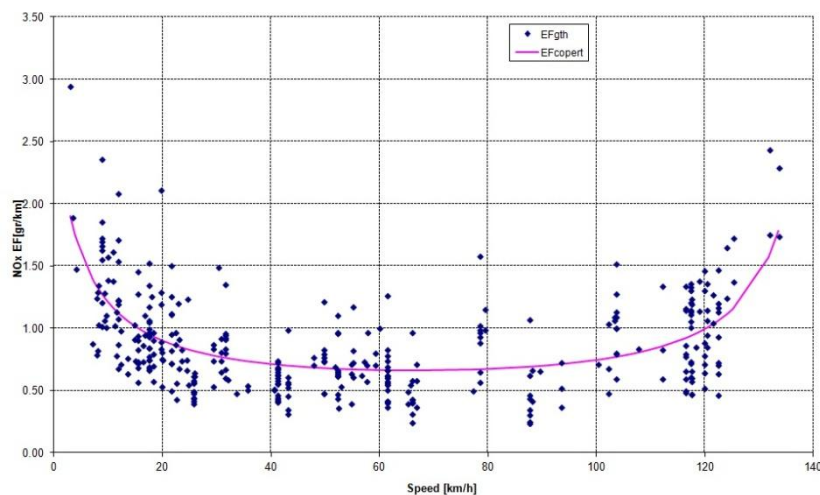


Figure 1. NO_x emission factor [g/km] for a EURO 3 medium sized diesel passenger car

The model consists of 5 modules:

- Hot emission calculation
- Cold emission calculation
- Evaporation emission calculation

- Total emission calculation
- Advanced characteristics use

COPERT4 calculates emissions of all major air pollutants (CO, NO_x, VOC, PM, NH₃, SO₂, heavy metals) produced by different road vehicle categories, as well as GHG emissions (CO₂, N₂O, CH₄) and energy/fuel consumption. It also provides speciation for NO/NO₂, elemental carbon and organic matter of PM and non-methane VOCs, including PAHs and POPs.

It is build around an extensive database containing all factors and functions to calculate the emission factors for 266 vehicle categories. However, additional user input is required to calculate the emissions.

Data required for the hot emission calculation is the average vehicle speed, the road slope and vehicle load (for HDVs only). For the cold emission calculation the input needed is the average vehicle speed, trip length and min and max ambient temperature. For the evaporation emission calculation the input is the fuel tank and canister size, the parking time distribution, the Reid vapour pressure, the average trip duration and the mean fleet mileage. Moreover, additional input needed is the transport activity split into the urban, rural and highway driving mode. However, COPERT4 already includes part of the abovementioned information, so the required input for a complete inventory is mainly the following:

- Activity data for the 3 driving modes
- Average vehicle speed
- Ambient temperature
- Reid Vapour Pressure

COPERT4 provides a detailed output of the calculated emissions at a vehicle technology level. The intermediate results of the emission factors are provided in g/km for urban, rural and highway driving modes for both hot and cold engine conditions. Evaporative emission factors are provided in g/day. The final output of the emissions is calculated in tones for urban, rural and highway driving modes for both hot and cold engine conditions as well as the fuel evaporation.

COPERT Street Level

COPERT Street Level is a new model developed by EMISIA SA. It constitutes an evolution of the standard COPERT4 model. COPERT Street Level was designed in such a way as to fill the gap between macro and micro emission calculation models.

A significant part of COPERT4 use was the calculation of emissions for traffic analysis models. However, it was clear that COPERT4 was not suitable for direct use with traffic models for 2 main reasons. The first was that it required a high enough spatial analysis for the results to be reliable and the second was that the model was in no way compatible with any form of traffic analysis model output. It was those 2 disadvantages that COPERT Street Level was designed to overcome. The model still uses an average speed approach.

The core of the model is the hot emission calculation methodology as described in the EMEP/EEA air pollutant emission inventory guidebook. At this stage only 4 pollutants were covered, CO₂, NO_x, VOC and PM. The resulting hot emissions are calculated based on the following equation:

$$HotEmissions[g] = VehiclePopulation[veh] \times AnnualMileage[km] \times HotEmissionFactor\left[\frac{g}{veh\ km}\right]$$

This method of calculation was applied to each segment describing the road network for which the traffic analysis would occur. The available output from a number of traffic models contains the average speed for each segment, the characteristics of the segment such as type and length, the traffic volume and, if required, the traffic composition in different vehicle categories. This output is essentially the input for COPERT Street Level.

Te model can directly use the average speed, the segment length and the traffic volume but requires some additional information to calculate the total emissions. This information is the fleet

composition for each area in question. In order to minimise the required information, an extensive database of different fleet compositions already exists in COPERT Street Level. This composition is based on the SIBYL model and is different for each country and year. The level of detail is up to the engine technology of each vehicle. So, even if no information on the fleet composition is available, the user can select a predefined dataset to use along with the traffic volume to calculate each vehicle type activity and, thus, increase the accuracy of the calculations by using the extensive COPERT4 database for the emission calculation. Figure 2 illustrates the methodology used to calculate the emission level for each road segment.

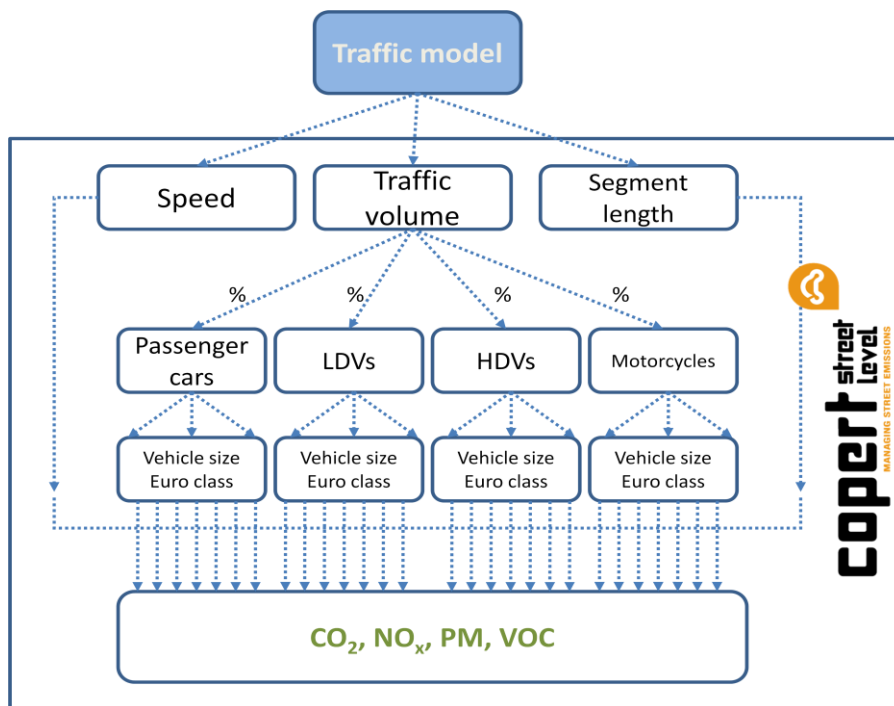


Figure 2. COPERT Street Level emission calculation flowchart for a single road segment

Great effort was also given in the calculation speed even if the size of the road network is significant. COPERT Street Level can calculate up to 1million unique segments in a relatively short amount of time which covers an extensive area, depending on the road segmentation.

It is also possible to differentiate the segments into different categories based on their characteristics (one way, single lane etc) but also perform the calculations for different time periods. The user can provide his/her own fleet composition if more reliable information is available.

In addition to the resulting dataset with the emission levels, the model can produce maps illustrating the emissions on each road to facilitate the identification of “hot spots”, areas where the emission levels are high.

3. Scenario description and input data

In order to evaluate the differences of the models and identify weaknesses and strengths, 3 scenarios were designed in such a way as to highlight specific characteristics.

All scenarios were executed by calculating emissions (CO₂, NO_x, PM and VOC) for a single day, for the city of Thessaloniki, for the year 2015, as well as 3 projected years (2020, 2025 and 2030). The city of Thessaloniki was selected for two main reasons. The first one is that EMISIA has developed a traffic monitoring tool (WISERIDE) which estimates city traffic as well as vehicle volumes for the larger area of Thessaloniki and Chalkidiki by using GPS from TAXIs. This data can be used by the COPERT Street Level tool to calculate emissions for a typical day for 24 hours. The second reason is that the city of Thessaloniki is a large enough area to allow COPERT4 to perform average calculations with

appropriate post processing and aggregation.

Both models require the same basic input information to calculate emissions which is the activity of the fleet (vehicle kilometres), the average vehicle speed and the vehicle fleet breakdown in the different vehicle sizes and engine technologies. This information was extracted from the WISERIDE database and was used either as is in the case of COPERT Street Level or aggregated in the case of COPERT4.

The database of WISERIDE collects GPS information from 1,200 taxis driving in the larger Thessaloniki and Chalkidiki area. This information is collected and through appropriate post processing translated into average vehicle speed and traffic volume for all road segments existing in the network. Furthermore, the road segments are separated into 9 major categories distinguished by their use and infrastructure characteristics (2 lanes, one way, width, etc.), which leads to different fleet categorization. This categorization includes the 5 major vehicle categories which are: passenger cars, light duty vehicles, heavy duty vehicles, buses, and two wheelers. The information extracted from the database and used in this study was the vehicle speed, the road segment length, the road segment category and the traffic volume for all segments in the city of Thessaloniki for 24 hours of a typical day. The following table includes a sample of the WISERIDE database.

Table 1. Data included in the main WISERIDE database table

hour_id	link_id	length	avg_speed	total_veh_number	link_type
6	255559	42.04	32.90	45.15	DS_XX
6	257331	80.91	29.12	1869.03	KA_1K
6	259107	32.97	29.44	1758.40	KS_1K
6	259108	22.06	28.59	2054.64	KS_1K
6	260382	46.94	29.31	1802.42	KS_1K
6	260661	87.04	31.78	66.33	KT600
6	262123	47.90	28.44	2114.05	KS_1K
6	262217	167.35	26.99	407.18	KT600
6	268997	23.54	28.78	1986.73	KS_1K
6	275075	54.98	27.66	310.72	KT600
6	278357	20.94	28.27	2182.24	KS_1K
6	290091	110.31	32.15	58.32	DS_XX
6	317437	33.92	27.14	3923.45	KA_1K
6	329140	79.60	28.95	61.77	DA_2K
6	488570	123.55	32.87	45.55	DS_XX
6	490566	90.60	32.87	45.66	DS_XX

COPERT Street Level is designed in such a way as to directly import this information in the highest possible detail. The structure of the model allows calculations to be made for a single road segment. Moreover, the road segments were split into 9 different categories and the calculations were performed for a 24 hour day. As previously mentioned, COPERT Street Level already includes a very detailed fleet categorization, different for each EU country from 2010 to 2050. However, in order to improve the calculations, the split in the 5 main vehicle categories for the 9 different road types as well as the 24 hours was updated based on the database findings.

COPERT4 on the other hand requires aggregated data, and for this reason the WISERIDE database required significant post processing to produce the necessary input for the model. This was completed in 3 steps. In the first step the total activity was calculated for all vehicles for the entire day. The activity was calculated as the product of the road segment length and the vehicle volume.

$$Activity = \sum_{r=1}^9 \sum_{h=1}^{24} RoadSegmentLenght \times RoadSegmentVehicleVolume$$

Where r corresponds to each of the 9 road segment categories and h to each of the 24 hours of the typical day.

COPERT4 however includes a more detailed vehicle categorization. To split the activity in the different vehicle types, vehicle sizes and engine technologies data from the SIBYL model was used. SIBYL is a vehicle stock projection tool with (internally implemented) energy consumption and emission calculation algorithms. It includes a complete database of the vehicle fleet and the split in the highest level of detail. By using the vehicle split provided by SIBYL along with the calculated activity it was possible to populate the required information in COPERT4. The same split has also been introduced as a default vehicle split in COPERT Street Level although modified according to the WISERIDE input data.

The same averaging approach was used to calculate the vehicle speed in COPERT4.

$$AverageSpeed_i = \frac{\sum_{r=1}^9 \sum_{h=1}^{24} RoadSegmentLenght \times RoadSegmentVehicleVolume_i \times RoadAverageSpeed}{\sum_{r=1}^9 \sum_{h=1}^{24} RoadSegmentLenght \times RoadSegmentVehicleVolume_i}$$

Where r corresponds to each of the 9 road segment categories and h to each of the 24 hours of the typical day. The resulting speed used in all scenarios and years was 19.2 km/h.

Further disaggregation of the speed to more detailed vehicle type (such as vehicle size or engine technology) was not possible due to lack of detailed statistical data, so the same value (speed) was used for all vehicles under the same category.

The following table summarises the input information used, the sources and the level of aggregation for both models.

Table 2. Input information: level of detail and sources

	COPERT Street Level		COPERT4	
	Aggregation level	Source of information	Aggregation level	Source of information
Activity	Road segment, hour, major vehicle category	WISERIDE	Vehicle type	WISERIDE, SIBYL
Speed	Road segment, hour, major vehicle category	WISERIDE	Vehicle Type	WISERIDE
Vehicle categorization	Vehicle type (included in the model)	SIBYL	Vehicle type	SIBYL

Regarding projections for the years 2020, 2025 and 2030 the total activity and average vehicle speed were considered to remain unchanged. So the WISERIDE database was used for all years. However the technological improvement of the fleet was taken into consideration. This means that the engine technology split is different for the future years based on the SIBYL fleet projection.

Scenario 1 - BAU

This is a “business as usual scenario”. The database of WISERIDE contains information for the city of Thessaloniki in real time. WISERIDE includes the information on the current state of the city’s road network which may include extraordinary events such as accidents. These events affect the average speed and the traffic flow. However the database also maintains historical information for all road segments, for two 24 hour days (business and weekend). The “business as usual scenario” uses the information collected for a business day and provides the input information to both models for the emission calculation as described above.

Scenario 2 - Dieselisation

This is the “dieselization” scenario. Greece used to ban diesel passenger cars from the two major cities, Athens and Thessaloniki up to 2011. Since 2011 however this restriction was lifted for both new, old and second hand vehicles. Lower diesel price and improved engine performance led buyers to switch to diesel engines. In this scenario additional statistical information was collected, mainly from the Association of Motor Vehicle Importers Representatives³ which identified a clear trend in the vehicle engine selection. In 2011, when the ban was lifted, only 10% of newly registered vehicles had diesel engines. In 2014 however more than 60% were equipped with a diesel engine. In order to simulate the evolution of the diesel engine percentage growth it was assumed that in 2030 newly registered vehicles would be about 77% diesel. This is the percentage of the newly registered diesel vehicles in Belgium for 2030 according to SIBYL. The following table describes the evolution of the Gasoline and Diesel percentage for the newly registered passenger cars for scenario 2.

Table 3. Scenario 2 passenger cars new registrations evolution

%	2015	2020	2025	2030
Gasoline	36	32	28	23
Diesel	64	68	72	77

This assumption was incorporated in the vehicle fleet composition, thus modifying the percentages used to calculate the individual activity data.

Table 4. Diesel passenger cars percentage evolution in the total fleet for scenario 1 and 2

%	2015	2020	2025	2030
Diesel - Scenario 1	3.8	7.2	10.9	12.4
Diesel - Scenario 2	4.5	8.0	11.9	13.6

The increase in the total fleet is not high for two main reasons, the first reason is that there was already an increase in the diesel vehicles in 2015 and the second reason is that in Greece the life expectancy of a vehicle is significantly high, therefore new registrations are consequently low. This delays the effect of the changes in the characteristics of new registrations to the total fleet.

All other input data for both models were the same with “business as usual scenario”.

Scenario 3 - Metro

This scenario evaluates the introduction of a metro in the city of Thessaloniki. Thessaloniki is constructing a new metro to reduce city traffic but also to reduce emissions from road transport. Focus is especially given in particulate emissions which proved to be a major issue in the last years. The new public transport system is not yet available, however in order to evaluate the model capabilities it was assumed that already in 2015 all metro lines would be available for use. The following picture⁴ illustrates the main but also secondary lines which are under construction for the city of Thessaloniki.

³ source: <http://www.seaa.gr/en>

⁴ source: <http://www.ametro.gr/page/default.asp?la=1&id=8>



Figure 3. Main and secondary metro lines in Thessaloniki

The total length of the metro lines will be about 31 km and the passenger kilometres have been estimated at around 2.7 million per day. For the purposes of the current study and in lack of more detailed information it was assumed that almost half of the metro passenger kilometres would replace passenger kilometres driven by cars. The other half would replace passengers kilometres travelled with buses. Although this means a reduction in the passenger car activity this is not the case for the activity of the buses. The urban planning of Thessaloniki indicates that at least for the first operating years of the metro the bus routes and timetables would remain unchanged pending evaluation once enough statistical data will be gathered to justify modifications.

To introduce this passenger car activity decrease the city was divided in two zones. One zone consists of areas around the metro lines and in proximity to the metro stations. The second zone consists of the rest of the examined area. In the first zone it was assumed that a higher decrease of passenger car activity would occur, while in the second zone a lower one. In order to achieve a total decrease of 1.35 million passenger kilometres overall it was calculated that a 5% drop in passenger car activity would occur in the first zone while a 2% drop in the rest of the city. This is a simplification made to allow a simple calculation of the overall activity. Normally a more complicated study would describe in detail the impact of the introduction of a metro in a city. However, the scope of this paper is to demonstrate the capabilities of the two environmental models which are designed to work along with traffic simulation tools.

As far as the rest of the input data is concerned, the basis of the calculations will be scenario 2. This means that the dieselisation effect in the fleet breakdown and the vehicle speed will be the same in scenario 2 and 3.

4. Results

In total, each one of the 3 different scenarios produced 4 different datasets for the current year (2015) and 3 projection years (2020, 2025 and 2030). The following table summarises the results for all datasets and pollutants calculated.

Table 5. Scenario results in tonnes

Scenario	Model	Pollutant	2015	2020	2025	2030
BAU	COPERT4	CO ₂	6,265,966	5,996,888	5,720,345	5,538,284
		NO _x	13,802	10,504	8,121	6,943
		PM	615	452	315	249
		VOC	31,431	23,157	16,943	15,457
Dieselisation		CO ₂	6,263,614	5,994,773	5,718,047	5,535,765
		NO _x	13,847	10,548	8,164	6,986
		PM	615	452	315	249
		VOC	31,430	23,156	16,942	15,456
Metro		CO ₂	6,046,740	5,787,296	5,520,204	5,344,217
		NO _x	13,361	10,180	7,881	6,744
		PM	593	436	304	240
		VOC	30,319	22,335	16,341	14,908
BAU	COPERT SL	CO ₂	7,752,144	7,679,065	7,554,748	7,338,186
		NO _x	18,327	15,212	11,634	8,230
		PM	665	533	391	216
		VOC	19,491	13,997	9,335	7,018
Dieselisation		CO ₂	7,741,458	7,674,841	7,552,600	7,335,325
		NO _x	17,247	14,780	11,772	8,300
		PM	668	536	394	216
		VOC	17,356	13,049	9,440	7,049
Metro		CO ₂	7,471,683	7,407,274	7,289,041	7,079,190
		NO _x	16,639	14,260	11,359	8,009
		PM	645	517	380	209
		VOC	16,751	12,593	9,109	6,802

It is evident that results differ according to the model used. However both show similar behaviour in each scenario and time series evolution. The following paragraphs will demonstrate the underlying reason for this.

Time series evolution

As previously mentioned the total activity was constant in all scenarios and models for all years calculated. However the fleet technological evolution was included in the input data through the different fleet distribution which demonstrated the improvement on the engine technology. The population of newer engine technologies increases with time. The following table describes the difference in the population for an older and a newer vehicle type used in COPERT4. Since both models use the SIBYL database as a starting point this evolution is apparent in both COPERT4 and COPERT Street Level.

Table 6. COPERT4 vehicle population for the Dieselisation scenario

Sector	Subsector	Technology	2015	2020	2025	2030
Passenger Cars	Gasoline 0,8 - 1,4 l	PC Euro 1 - 91/441/EEC	291,667	90,571	10,864	0
Passenger Cars	Gasoline 0,8 - 1,4 l	PC Euro 6 - EC 715/2007	95,833	634,835	990,319	1,296,855

Newer engine technologies have lower emission limits and perform better compared to older ones. For this reason one would expect emissions to drop in 2030 compared to 2015. The following figure demonstrates this for both models for the NO_x emission calculation of the Dieselisation and the Metro scenarios.

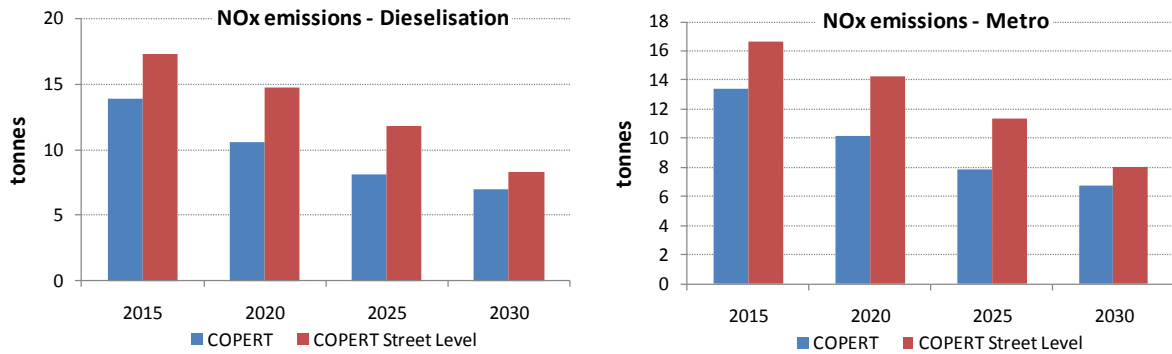


Figure 4. NO_x emissions in two scenarios for both models

Scenario comparison

All 3 scenarios were designed in such a way as to demonstrate the model capabilities. In the Dieselisation scenario a more aggressive evolution of the Diesel Passenger car fleet was introduced. Diesel vehicles are characterised by lower CO₂ but higher PM emissions than gasoline vehicles. The following figures demonstrate that both models calculate this trend in the respective results. However since the scenario only affects a small part of the passenger car fleet the difference in the two scenarios are negligible compared to the total emissions.

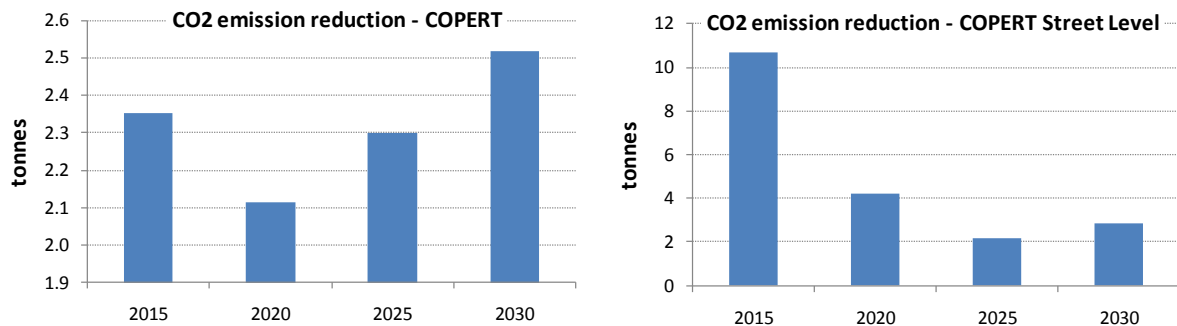


Figure 5. CO₂ emission reduction in the Dieselisation scenario compared to BAU

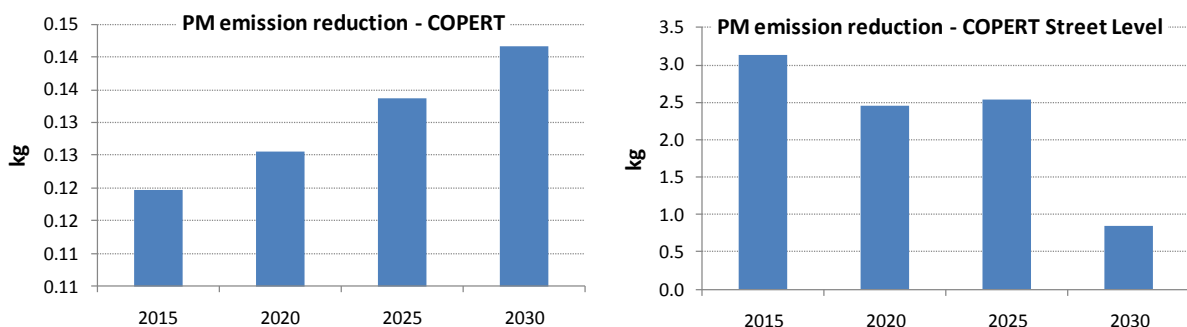


Figure 6. PM emission reduction in the Dieselisation scenario compared to BAU

On the other hand the Metro scenario was designed in such a way as to demonstrate the effect of the new public transport network in the city's emissions. A reduction in the total activity of the passenger cars was introduced proportional to the metro activity. The resulting decreased emissions could be observed in both models and all emissions. The following figures present the emission reduction for both models for CO₂ and NO_x emissions.

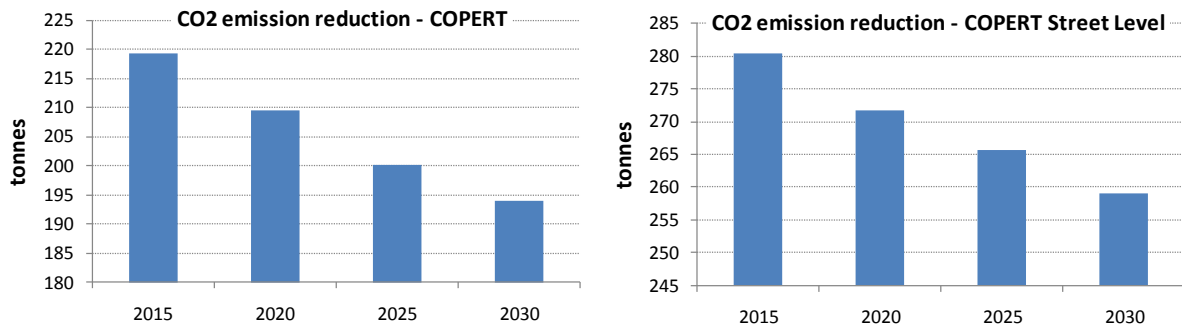


Figure 7. CO₂ emission reduction in the Metro scenario compared to BAU

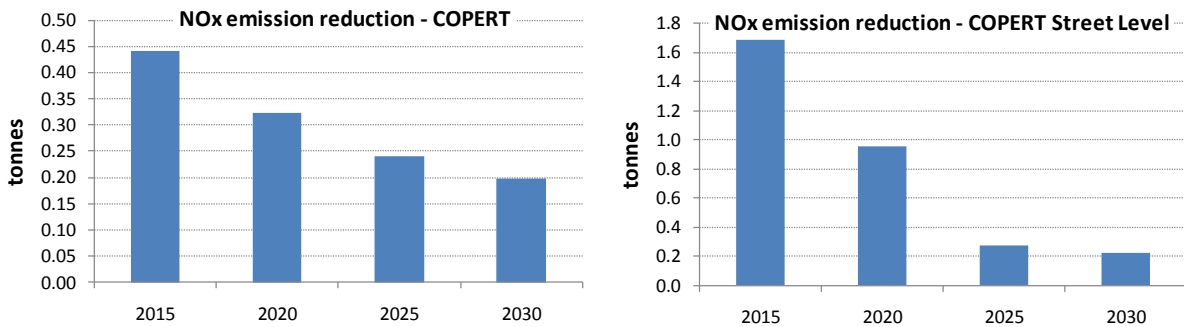


Figure 8. NO_x emission reduction in the Metro scenario compared to BAU

The results show that both models present the same trend in all scenarios. Emissions for CO₂ and NO_x are reduced in the two scenarios compared to the BAU scenario. This reduction however is becoming smaller as time progresses since it corresponds to total emissions which are also reduced due to the improvement of the engine technology.

Software comparison

Table 5 summarises the emission results in both models for all scenarios and years. However it is clear that the results can be quite different although the initial database was the same. A closer analysis of both models shows that there are two main reasons for these differences which are the result of the different level of detail available in each model.

While COPERT Street Level calculates emissions in each road segment, using different input data COPERT4 cannot facilitate this calculation and requires a single speed for the complete dataset. In chapter 2 it has been shown that this is possible using the weighted average speed for the whole Thessaloniki road network for 24 hours. However this has one major disadvantage and this is the elimination of hot spots in the city network caused by increased traffic. To demonstrate the effect of hot spots in the entire dataset and in order to eliminate all other parameters a single vehicle type has been selected (Heavy Duty Vehicle <7.5t Euro I) and only NO_x emissions have been calculated using two methods. The first one (applied in COPERT4) calculates total emissions based on the weighted average speed and the second one (applied in COPERT Street Level) based on the distribution of the speed across the entire network. The weighted average speed has been calculated at 30 km/h, while Figure 9 describes the speed distribution according to the activity.

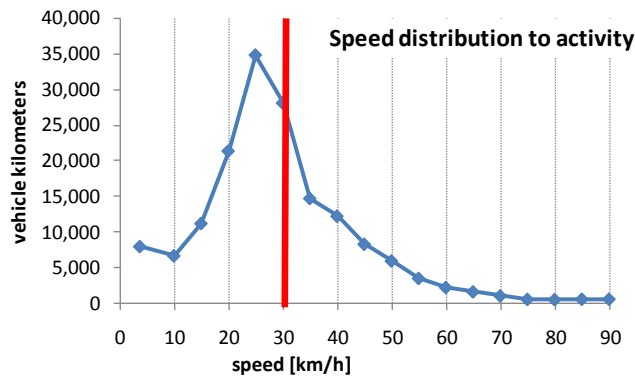


Figure 9. Speed distribution

By using both methods with the same emission calculation function for NO_x emissions two different results occur, 586 kg with the detailed while 500 kg with the average approach. This shows that by using the average speed we underestimate the emission level by ignoring hot spots in the network. This explains the increased emissions calculated by COPERT Street Level compared to COPERT4 for all emissions and scenarios with the exception of VOC. VOC emissions are significantly lower when calculated by COPERT Street Level compared to COPERT4. This difference is the result of the second reason leading to different results, namely the different vehicle distribution used in COPERT Street Level for different road types and hours of the day. WISERIDE provides not only the vehicle speed and total vehicle population but also the vehicle distribution in the 6 major categories (passenger cars, light duty vehicles, heavy duty vehicles, buses, motorcycles and mopeds) for different road types and hours of a day. COPERT4 cannot use this information since each run can only include one distribution. However COPERT Street Level is able to calculate emissions using the maximum level of detail and information provided by the initial database, in this case WISERIDE. As already mentioned the WISERIDE database provided information for all the city's road network distinguished in 9 different road types. When combined with the 24 hours a total of 216 different vehicle distributions have been used by COPERT Street Level. These 216 distributions when used to calculate emissions can each produce a completely different result when compared to the average distribution used by COPERT4. To demonstrate how large this difference can be especially for VOC the following example has been calculated by COPERT4 using both methods. In the first case the single COPERT4 distribution has been used to calculate an average emission factor for all 6 major vehicle categories as well as the total VOC results. In the second case however a different distribution has been used and more specifically a distribution for a 4 lane road with 2 directions for hour from 09:00 to 10:00 as included in the WISERIDE database. Using the average emission factor calculated in the first case a completely different result has been calculated, almost 1/4 of the COPERT4 value. Although this was selected especially to demonstrate an extreme case it can clearly show that it is possible for both models to vary significantly in the final emission results. Table 7 and Table 8 include the results for both cases.

Table 7. VOC emissions calculated with COPERT4 for year 2030

Vehicle category	Fleet distribution (COPERT4 default)	Activity [vehkm]	VOC emission factor [g/vehkm]	VOC emissions [t]
Passenger Cars	54%	12,665,371,729.7	0.013	163.9
Light Commercial Vehicles	11%	3,030,954,215.0	0.016	48.3
Heavy Duty Trucks	2%	797,844,662.1	0.161	128.6
Buses	0%	42,757,019.5	1.056	45.1
Mopeds	19%	7,203,148,971.9	1.578	11,367.8
Motorcycles	15%	5,558,812,048.4	0.666	3,703.2
Sum	100%	29,298,888,646.6		15,456.9

Table 8. VOC emissions calculated with COPERT4 for year 2030 (alternative fleet distribution)

Vehicle category	Fleet distribution (4 lane road, hour 09:00-10:00)	Activity [vehkm]	VOC emission factor [g/vehkm]	VOC emissions [t]
Passenger Cars	88%	12,665,371,729.7	0.013	332.1
Light Commercial Vehicles	1%	3,030,954,215.0	0.016	5.7
Heavy Duty Trucks	1%	797,844,662.1	0.161	28.8
Buses	0%	42,757,019.5	1.056	75.3
Mopeds	5%	7,203,148,971.9	1.578	2,136.1
Motorcycles	6%	5,558,812,048.4	0.666	1,119.1
Sum	100%	29,298,888,646.6		3,697.1

5. Conclusions

The analysis of the results shows that both models can correctly calculate the trends and verify the expected results based on the designed scenarios. However the assumptions used to in COPERT4 to facilitate the calculations can have a significant effect on the results. On one hand the use of an average speed necessary for the COPERT4 calculations normalises the results and eliminates the hotspots in the city's network. COPERT Street Level on the other hand can calculate the different levels of emissions in the different road segments. Figure 10 demonstrates how COPERT Street Level identifies the CO₂ emissions hotspots in the Business As Usual scenario (BAU) and displays them on the city's road network.

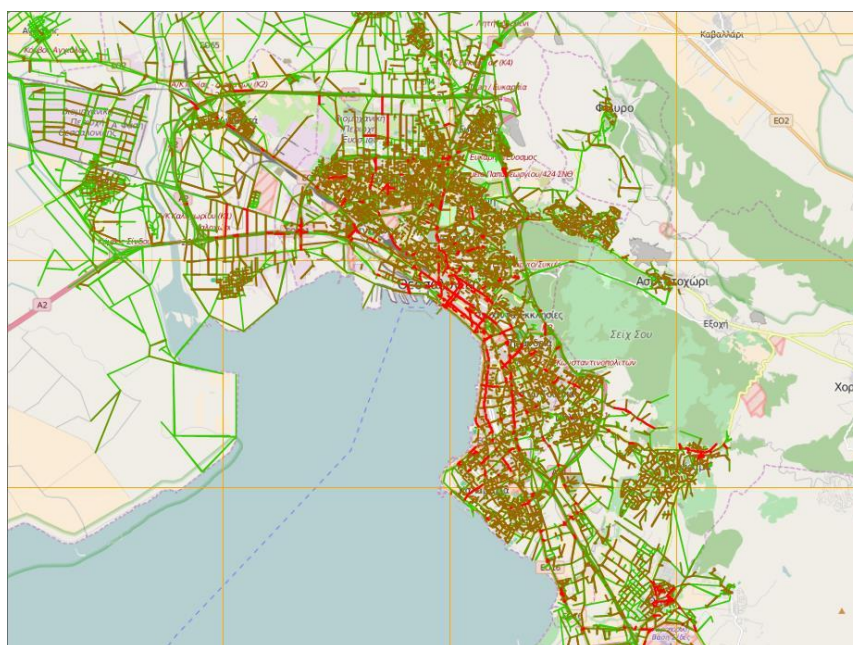


Figure 10. CO₂ emissions for BAU scenario in year 2015

On the other hand COPERT4 cannot use the different fleet distributions of the different road types and hours and requires additional averaging of the input data. As demonstrated for VOC this can greatly overestimate the results.

Both cases show that the process of transforming the input data (in this case the WISERIDE database) can have an effect on the results which is not easy to quantify due to the complexity and size of data. In order to accurately calculate emissions it is important to eliminate any uncertainty originating

from underlying assumptions and use the dataset as produced by the traffic model.

On a more quantitative comment, while COPERT Street Level directly interfaces with any traffic model database, COPERT4 requires post processing which increases the calculation working hours. Moreover the post processing requires significant calculation time mainly because when working with large amount of data (in this case over 500 MB) data processing and calculations can be extremely cumbersome.

In conclusion both models can calculate emissions from road transport. However when dealing with a city's road network COPERT Street Level can more adequately deal with the large amount of data produced from a traffic model. COPERT4 can also perform the same calculations but it requires a large number of runs to calculate emissions for all road segments and therefore aggregations of the input data is required. This aggregation leads to significant differences in the emission results compared to the detailed calculation.

References

- L. Ntziachristos, Z. Samaras et al. (2014), EMEP/EEA air pollutant emission inventory guidebook - 2013, Exhaust emissions from road transport
- H. Kouridis (2015), COPERT Street Level User's Manual, <http://emisiasa.com/products/copert-street-level>
- EMISIA SA (2015), WISERIDE, <http://www.wiseride.gr>
- P. Katsis (2015), SIBYL manual

New compact technology for cabin air purification based on photocatalytic optical fiber textile

Lina LAMAA*, Laure PERUCHON*, Cedric BROCHIER* & Chantal GUILLARD**

*Brochier Technologies, 90 Rue Frédéric Faÿs, 69100, Villeurbanne, France

**IRCELYON, Institut de Recherche et de Catalyse sur l'Environnement de Lyon, CNRS-UMR 5256, 2 avenue Albert Einstein, F-69626 Villeurbanne Cedex

Abstract

An innovative photocatalytic media was developed by Brochier Technologies. The new media is based on the combination of UVtex® technology, a luminous optical fiber fabric connected to UV LED, and the photocatalysis. Photocatalysis, as an Advanced Oxidation Process (AOP), is an effective method in the field of air and water treatment due to its complete mineralization of organic compounds.

To optimize photocatalysis, the interaction between photocatalyst and UV irradiation needs to be maximized. Due to a microtexturation of the optical fibers, the light emitted by the LED is distributed over the surface of the textile. Thus, by photocatalyst deposition on these woven optical fibers, the contact between photocatalyst and UV can be radically improved. The photocatalytic woven optical fibers is an innovative solution to treat air that allows to design compact reactor ideal for restricted environment such as vehicle cabin. Optical properties ageing and photocatalytic performances were investigated.

For the ageing, it remains essential to protect the textile by a layer of silica to avoid the photocatalytic degradation of the optical fiber. The photocatalytic performances in the measured conditions are significant with the conversion rate about 90%.

Keys-words: (5 words) photocatalysis, vehicule cabin air, optical fiber textile.

Abstract

FRANCAIS

Le textile lumineux photocatalytique innovant est développé par Brochier Technologies. Son principe repose sur le couplage de la technologie UVtex®, un textile lumineux en fibres optiques connecté à une LED UVA, et la photocatalyse, un procédé d'oxydation avancé (POA) classiquement utilisé dans le traitement de l'eau et de l'air car il permet la dégradation des composés organiques jusqu'à minéralisation complète.

Le tissu photocatalytique - LED se démarque de façon significative des systèmes classiques existants qui utilisent des médias photocatalytiques recevant l'irradiation d'une source ponctuelle extérieure projetée. Le textile UVtex® sert à la fois de source d'irradiation UV et de support du photocatalyseur, ce qui crée une surface de contact maximum entre ces deux éléments, permettant d'optimiser la réaction photocatalytique. Le dimensionnement en multicouche du textile permettra la conception d'un réacteur compact idéal pour des applications en milieu confiné tel que l'habitacle véhicule. La durabilité et les performances photocatalytiques du textile lumineux ont été étudiées.

Concernant la durabilité du textile, il a été démontré qu'il est nécessaire de protéger les fibres optiques de l'action de la photocatalyse par une couche intermédiaire de silice. Les performances photocatalytiques du tissu sont significatives avec des taux de conversion de 90% dans nos conditions expérimentales.

Introduction

Outdoor air pollution is a major environmental risk to human health. Air in the vehicle cabin is one of the first areas affected by this pollution and passengers are ones of the main pollution victims. Cabin air is impacted by particles, Volatile Organic Compounds (VOCs), NOx.... which can provoke respiratory problems, severe headache, and certain skin allergies.

In 2013, a study carried out by the laboratory of hygiene of the city of Paris (LHVP), evaluated the Indoor Air Quality (IAQ) of over a hundred vehicles. Results revealed that 23% of the samples exceed the threshold limit of formaldehyde exposure, which was fixed by the World Health Organization (WHO) to $10 \mu\text{g}/\text{m}^3$ (the guideline for formaldehyde is set for a long-term exposure to $30 \mu\text{g}/\text{m}^3$ at 1 Jan. 2015 and $10 \mu\text{g}/\text{m}^3$ at 1 Jan. 2023 (<http://www.developpement-durable.gouv.fr/Valeurs-guides-de-l-air-interieur.html>)). This pollutant is associated by WHO with carcinogenic risks, migraine, fatigue and irritation. The study also showed that 43% of vehicles exceed the limit for total VOCs ($300 \mu\text{g}/\text{m}^3$).

Some depollution systems exist on the market: filtration, adsorption and ionization, but act only on some pollutants. In the case of the adsorption, activated carbon will trap some VOCs better than others until saturation of device, then releasing. Ionization aggregate particles and can generate VOCs and NOx. Moreover, there is no degradation of pollutants with these systems. Photocatalytic oxidation is a very promising technology for VOCs degradation. The main advantage of this process is its capability to remove and mineralize VOCs at room temperature and atmospheric pressure due to generation of reactive oxygen species, $\cdot\text{OH}$, $\text{O}_2^{\cdot-}$ and HO_2^{\cdot} from air and photocatalytic phenomena is illustrated in figure 1.

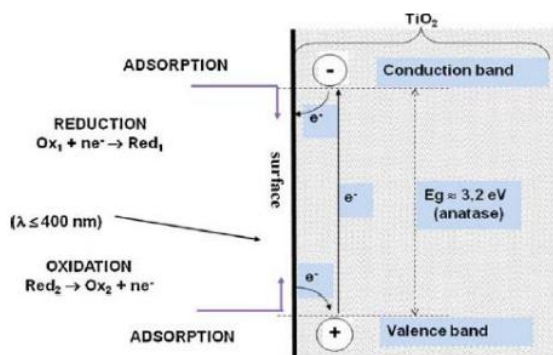


Figure 1. Photocatalytic scheme (Herrmann, 2010).

Commercial photocatalytic systems use external light and have several disadvantages:

- Important volume of set/up;
- Scattering of light;
- High energy consumption.

Unlike classical systems, the use of optical fibers fabric connected to LEDs developed by Brochier technologies allows:

-Designing of a compact reactor using textile on multistage adapted to limited spaces such as vehicles.

-Saving energy: LEDs require only a low power consumption (3W) compared to external lamps (100W).

-Optimizing the contact between UV/photocatalyst and pollutant

In this work we focused on the optimization of the durability and efficiency of the innovative photocatalytic optical fiber textile. Tests were conducted on the degradation of model pollutants, formaldehyde and toluene.

1. Methods

Optical fiber fabric is produced by Brochier Technologies Company (UVtex®). It is composed of optical fibers in polymethyl methacrylate (PMMA), made by Mitsubishi, and textile fibers in polyester (Trévira

CS™ fibers). All optical fibers are woven in the same direction, in parallel, and the extremities are gathered, altogether thanks to a cylindrical connector. In order to allow light emission over the entire surface of the fabric, a treatment of micro-texturation is performed. Micro-texturation is carried out by mechanical abrasion specific technique developed by Brochier Technologies, Brochier et al. (2007) (2009). The active surface is a square of 10 cm. In order to have some photocatalytic activity, fabrics are coated with titanium dioxide suspension.

Local emitted light intensities were measured by a CCD Spectrometer. Measurements were performed under radiometric mode, using a CCD Spectrometer Avantes AvaSpec- ULS2048. Before analysis a calibration was carried out by using a Deuterium Halogen Light Source (AvaLight- D (H)-S, Avantes, and Apeldoorn, Netherlands). A fiber-optic cable with a cosine corrector (CC-UV/VIS) enables punctual light emission measurements. The cosine corrector diameter is 3.9mm for a measurement area of 12mm². Spectra in UVA region (320-400nm) were recorded and processed with AvaSpec 7.0 software via USB. Emitted light intensity was measured through 25 points on the surface of the fabrics (10cm *10cm), as shown on the insert of Figure 2.

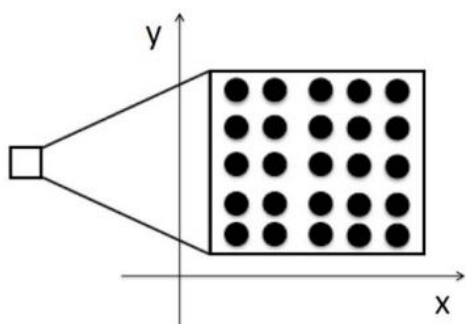


Figure 2. Measured points used to characterize light emission evolution over exposure time to UVA irradiation. 25 measurements dots.

The degradation of toluene during the reaction was monitored every 10 min using an online instrument GC–PID Chromatograph GC8900. Photoionization detectors is efficient way to detect low VOC levels.

For the experimental conditions, photocatalytic degradations were performed in gaseous flow, in one pass. Pollutant was generated using permeation system. Relative humidity was fixed at 50% and total flow at 1mL min⁻¹.

2. Results and discussion

Ageing:

The polymeric optical fiber selected to transmit UV light is a PMMA optical fiber. Due to the organic nature of optical fiber, it is important to study the durability of fibers during exposure to UVA in presence of TiO₂.

Optical fiber textiles coated by TiO₂ were exposed to UVA at 365nm emitted by LED with an irradiation of 240mW/cm² distributed throughout optical fiber textile. On a textile surface 200 cm², irradiance is measured at 50 points to have representative measurement using radiometric measurements along exposure time to UVA light.

An important ageing under UVA irradiation of the photocatalytic fabrics non protected by a SiO₂ layer, leading to an inhomogeneous light distribution at the surface of the textile was observed in figure 3a. This could be explained by the fact that the organic nature of the optical fiber is degraded by TiO₂ deposited on the textile. Indeed, the photocatalysis is known to involve the mineralization of a large variety of organic compounds, Gaya and Abdullah (2008); Mills and Hunte (1997). In fact hydroxyl radicals formed at the surface of the photocatalyst, TiO₂, are very reactive and non-selective. The photocatalytic degradation of PMMA was demonstrated by Vinu and Madra (2008). In presence of TiO₂ (Degussa P25) and UVA high pressure mercury vapor lamp (predominant radiation at 365 nm), PMMA and others MMA (methyl methacrylate) co- and homopolymers are degraded randomly along the chain. For this reason, it remains essential to find a solution that can protect the optical fiber from the photocatalysis and did not modify light absorption. So before coating TiO₂, a layer of silica which do not

absorb UV light, was deposited in the textile to protect the optical fiber textile from ageing. The ageing of photocatalytic textile protected by silica layers after 71 days of UVA irradiation is represented in figure 3b.

In presence of SiO₂ layer between woven optical fibers and TiO₂ layer, no ageing was observed. Moreover, these textiles protected by silica layer show similar photocatalytic efficiency to non-protect textiles due to the transparency of silica to UV. This results are in agreement with the work of Alobaidani et al. (2010).

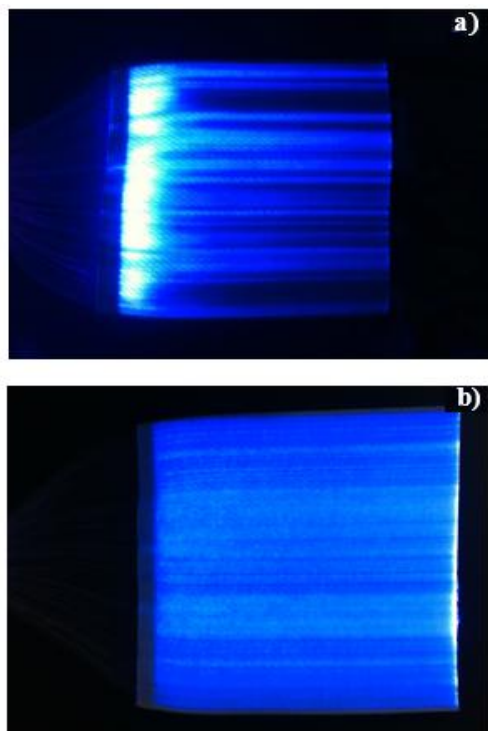


Figure. 3 Photography of light emission distribution on the overall surface of the TiO₂ coated textile unprotected by silica after ageing under UVA irradiation (a), and coated textile protected by silica after ageing under UVA irradiation (b).

Photocatalytic performances

Previous experiments performed on the photocatalytic degradation of formaldehyde have showed the efficiency of these photocatalytic textiles, Bourgeois et al. (2012).

In order to optimize photocatalytic performances of optical fiber textile, different types of TiO₂ coating were compared under the same conditions by using toluene, the concentration of toluene is fixed at 1 ppmv. Results are represented in the table 1, for reasons of confidentiality the nature of different coating are named BR1, BR2 and BR3. For both Br1 and Br2 results are similar, and comparing to a commercial material they showed slightly better performance. To choose the suitable coating, several tests in vehicle should be realized in real conditions.

Table 1. Comparison of different types of TiO₂ coating

Types of coating	toluene conversion (%)
SiO ₂ +Br1	94
Luminous textile + photocatalytic commercial material	82
SiO ₂ +BR2	87

Conclusion

For the ageing study:

The protection of the woven optical fibers by an intermediate layer of silica is essential to protect the optical fibers from degradation by photocatalysis.

For the photocatalytic performances, results show highperformances for different types of TiO₂.

The results of this innovative photocatalytic optical fiber textile are very encouraging and open new perspectives in photocatalytic reactor design, as these textiles allow a three-dimensional source of light, irradiate not only the surface, but also the heart of the photocatalytic bed. The innovative textile will be used in multistage in order to design 3D compact treatment system ideal to treat pollution in vehicle cabin air.

References

- Alobaidani A.D., D. Furniss, M.S. Johnson, A. Endruweit & A.B. Seddon (2010): Optical transmission of PMMA optical fibres exposed to high intensity UVA and visible blue light. *Optics and Lasers in Engineering*, vol 48, p 575 – 582.
- Bourgeois P.A, E. Puzenat, L. Peruchon, F. Simonet, D. Chevalier, E. Deflin, C. Brochier & C. Guillard (2012) : Characterization of a new photocatalytic textile for formaldehyde removal from indoor air. *Applied Catalysis B: Environmental*, vol 128, p 171– 178.
- Brochier C., D. Malhomme & E. Deflin - Brevet (2007) : « Nappe textile présentant des propriétés dépolluantes par photocatalyse » - n°de délivrance FR2910341, 2008-06-27 (A1) et FR2910341, 2009-02-06 (B1).
- Brochier C. & E. Deflin (2008) : - Brevet N°WO 2008/062141, Complexe éclairant verrier. FR2908864 (A1) - 2008-0523.
- Gaya U. I. & A. H. Abdullah, (2008): Heterogeneous photocatalytic degradation of organic contaminants over titanium dioxide: A review of fundamentals, progress and problems. *Journal of Photochemistry and Photobiology C: Photochemistry Reviews*, vol 9, p 1-12.
- Herrmann JM, (2010): Photocatalysis fundamentals revisited to avoid several misconceptions. *Applied Catalysis B: Environmental* vol 99(3-4), p 461-468
- Indermühle C., E. Puzenat, F. Simonet, L. Peruchon, C. Brochier & C. Guillard (2016): Modelling of UV optical ageing of optical fibre fabric coated with TiO₂. *Applied Catalysis B: Environmental*, Vol 182, p 229-235.
- Mills A. & Le Hunte S., (1997): An overview of semiconductor photocatalysis. *Journal of Photochemistry and Photobiology A: Chemistry* vol 108, p 1-35.
- Vinu R.&G. Madras, (2008):Photocatalytic degradation of methyl methacrylate copolymers *Polymer Degradation and Stability*,vol 93, p 1440-1449.

Impact of engine warm-up and DPF active regeneration on regulated & unregulated emissions of a Euro 6 Diesel vehicle equipped with urea SCR catalyst

M. Leblanc*, L. Noël*, B. R'Mili**, A. Boréave**, B. D'Anna**, S. Raux*

* IFP Energies nouvelles - Etablissement de Lyon, Rond-point de l'échangeur de Solaize - BP 3, 69360 Solaize, France

email: mickael.leblanc@ifpen.fr

** CNRS - UMR 5256 IRCELYON - Université Claude Bernard Lyon 1, 2 avenue A. Einstein, 69626 Villeurbanne, France

Abstract

The latest improvements achieved thanks to stringent regulations, Diesel engine design and control developments or after treatment evolutions, contribute to the global reduction of Diesel vehicle emissions. This study proposes an extensive assessment of the gaseous and particulate emissions of a Euro 6b Diesel vehicle equipped with a DOC+SCR+DPF exhaust line, under different transient driving conditions reproduced on a roller test bench. It highlights the negative impact of engine warm-up and DPF active regeneration on the regulated and unregulated gaseous and particulate emissions of this vehicle, in particular:

- Engine cold starts and warm up, lead to HCs, CO, CO₂, N₂O and CH₂O global increase for the gaseous phase, the two first however remaining compliant with their related emission limits, as well as higher particle number (also under Euro 6b limit),
- DPF active regenerations lead to more important HCs, CO, CO₂ and CH₂O emissions, dramatic NH₃, SO₂ and particle number (PN) increase, but is above all characterized by significant HCN and nucleation mode particles formation.

It finally tackles the need to further improve the related after-treatment's efficiencies, as well as to consider additional pollutant emissions limits for passenger cars for the future standards.

Keys-words: *Selective Catalytic Reduction, Diesel Particulate Filter regeneration, Hydrogen cyanide, sulfur dioxide, size distribution*

Mots clés: *Réduction Catalytique Sélective, régénération de Filtre à particules, cyanure d'hydrogène, dioxyde de soufre, granulométrie*

Introduction

Diesel exhaust emissions are classified by the international agency for research on cancer since 2012 as "carcinogenic to humans" (IARC group 1) and are also related to other health concerns among which lung or heart diseases [7]. The toxicity of Diesel exhaust is due to the individual substances contained in their gaseous or particulate fractions (among which for example: unburnt HCs, aldehydes, CO/CO₂, NO/NO₂, SO_x, N₂O, PAHs,... for the gaseous phase or carbon, organic/metallic compounds, ashes, sulfates, salts, PAHs... from the particulate phase), as well as to the potential combined effects of these numerous deleterious substances.

Despite of the improvements achieved with the spread of Diesel particulate filter (DPF) or more recently with NO_x abatement systems such as selective catalytic reduction (SCR) or lean NO_x trap (LNT), recent Diesel vehicles remain considered as not environmentally friendly and of a public health concern. From one hand, the particulate and NO_x emissions of their predecessors still tarnished during

the last years the improvements achieved thanks to the most recent standards. On the other hand, the recent discovery of defeat devices on brand new Volkswagen group model cars to comply the most stringent standards [15], as well as higher NO_x emissions under real driving conditions [5] [6] [8] [14], highlight the need to carry on improving these after treatment devices and their control strategies to allow a better efficiency, in terms of real driving emissions (RDE).

Moreover, the later improvements achieved in terms of toxicity thanks to stringent regulations (regarding to exhaust emissions and fuel quality as well), better Diesel engine design and control, new after treatment devices, or lubricants and related additives evolutions, all contribute to a global reduction of Diesel exhaust emissions, but their respective potential benefits remain insufficiently studied, uncertain and need to be better assessed[2] [11]. This is particularly true in terms of potential side effects or contribution to secondary organic aerosols (SOA) formation in the atmosphere of the later NO_x emissions control devices that are SCR or LNT, considering their growing market penetration [16], their specificities (Diesel exhaust fluid (DEF) use in the SCR case, or rich purges occurrence for the LNT), as well as their growing contribution to NO_x reduction with a view to the relevant RDE regulation.

The CAPPNOR2 project has been launched from 2013, in order to improve detailed knowledge related to the emissions of Euro 6b compliant vehicles equipped with Diesel engine and to precisely assess their gases and particles emissions, the impact of their after treatment devices, as well as their secondary organic aerosol's (SOA) forming potential. The first vehicle studied is equipped with a close-coupled Diesel oxidation catalyst (DOC) and underfloor SCR catalyst + fuel borne catalyst DPF (FBC-DPF). The second one is equipped with close-coupled LNT and catalyzed DPF (cDPF).

This article focusses on the SCR equipped vehicle emissions, extensively studied. It highlights the negative impact of engine warm-up and DPF's active regeneration on the regulated and unregulated gaseous and particulate emissions of the DOC+SCR+DPF equipped vehicle. It also tackles the need to further improve the related after-treatment's efficiencies, particularly during the previously introduced conditions, as well as to consider additional pollutant emissions limits for passenger cars, as already introduced for heavy-duty vehicles standard.

1. Experimental setup

The results presented in this study were obtained during transient tests conducted on a Euro6b compliant chassis dynamometer.

The tested vehicle is a 7 seats family car which complies with the latest Euro 6b standard and whose unladen mass is 1430 kg. It is equipped with a 110 kW, 2.0 liter, four-cylinder Diesel engine, with common-rail direct injection, cooled turbocharger, cooled exhaust gases recirculation (EGR) and a 6 speeds gearbox.

In order to improve the representativeness of our results compared to similar European real cars on the roads, this car was specially hired for the project nearby a specialized company. Its mileage was 19700 km when it arrives. It first goes to the mechanical workshop to be implemented with needed instrumentation (vehicle speedometer, exhaust line temperatures, pressures and flow meter, O₂ sensor, engine mass air flow, as well as dedicated analyzers branching pipes along the exhaust line) to control the vehicle's behavior during the tests and to allow to calculate and interpret the pollutants emissions.

The main vehicle's parameters and their emissions were then acquired and analyzed on the chassis dynamometer during approximately 4275 km, under various driving conditions that will be described afterwards. At the end of the tests, the dedicated instrumentation was completely removed and the original exhaust line of the vehicle replaced by a brand new one.

The fuel used during this study is a European EN 590 compliant Diesel fuel. Its measured cetane number is equal to 52.1 and its measured PCI to 42.74 MJ/kg. It contains 4.8% of fatty acid methyl ester (FAME), 3.3% of poly-aromatic compounds and 8.3mg/kg of sulfur. The engine lubricant has been replaced by a new one before the beginning of the tests. So, a low SAPS lubricant, as preconized by the vehicle manufacturer for such engine and after-treatment technologies, is used. Finally, the Diesel exhaust fluid (DEF) that is necessary for the proper SCR catalyst functioning, is an aqueous solution named Adblue containing 32.5 % of urea (CO(NH₂)₂), which comply with

international standards DIN 70070 and ISO 22241-1.

Diesel Oxidation Catalyst principle

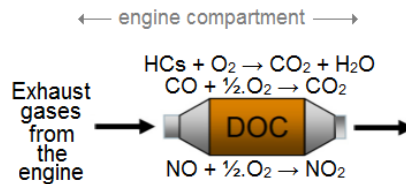


Figure1.Schematic diagram of DOC catalyst functioning

The Diesel oxidation catalyst (DOC) mainly allows to oxidize unburnt hydrocarbons and carbon monoxide coming from the engine, as soon as the catalyst temperature is high enough to oxidize it, via the following main chemical reactions:

- Hydrocarbons oxidation : $C_xH_y + (x + \frac{y}{4}).O_2 \rightarrow x.CO_2 + (\frac{y}{2}).H_2O$ (reaction 1)
- Carbon monoxide oxidation : $CO + \frac{1}{2}.O_2 \rightarrow CO_2$ (reaction 2)[1]

The DOC also contributes via the chemical reaction 3, to the oxidation of the nitric oxide (NO) emitted by the engine to nitrogen dioxide (NO₂) which then, favor the continuous regeneration of the Diesel particulate filters located downstream, throughout the covered mileage of the vehicle, reducing consequently, the DPF active regeneration frequency.

- NO conversion to NO₂ : $NO + \frac{1}{2}.O_2 \rightarrow NO_2$ (reaction 3)[1]

Selective Catalytic Reduction principle

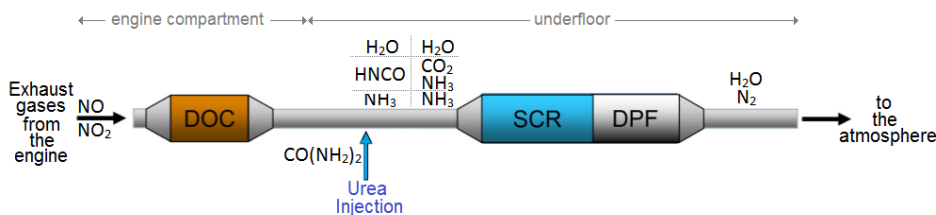


Figure2.Schematic diagram of SCR catalyst functioning

The SCR catalyst allows to reduce nitrous oxides emissions thanks to the injection in front of the catalyst of a Diesel exhaust fluid, here named Adblue, which is an aqueous solution containing 32.5% of urea and whom main characteristics are defined by the international standards DIN 70070 and ISO 22241-1. As soon as the SCR catalyst and exhaust gases temperatures near the urea injector are high enough ($\geq 160^\circ C$) to allow the smooth progress of the urea vaporization and decomposition, as well as the NO_x reduction by the catalyst, the urea injection can be activated and the following steps occur[9]:

- Adblue vaporization,
- Urea thermolysis: $CO(NH_2)_2 \rightarrow NH_3 + HNCO$ (reaction 4)
- Urea hydrolysis: $HNCO + H_2O \rightarrow NH_3 + CO_2$ (reaction 5)

Once the molecules of ammonia formed inside the exhaust line, the reactions leading to the nitrous oxides reduction by the selective catalytic reduction take place on the catalyst, via the following main chemical reactions[9]:

- Fast SCR: $4.NH_3 + 2.NO + 2.NO_2 \rightarrow 4.N_2 + 6.H_2O$ (reaction 6)
- Standard SCR: $4.NH_3 + 4.NO + O_2 \rightarrow 4.N_2 + 6.H_2O$ (reaction 7)
- NO₂ SCR: $8.NH_3 + 6.NO_2 \rightarrow 7.N_2 + 12.H_2O$ (reaction 8)

Diesel Particulate Filter principle

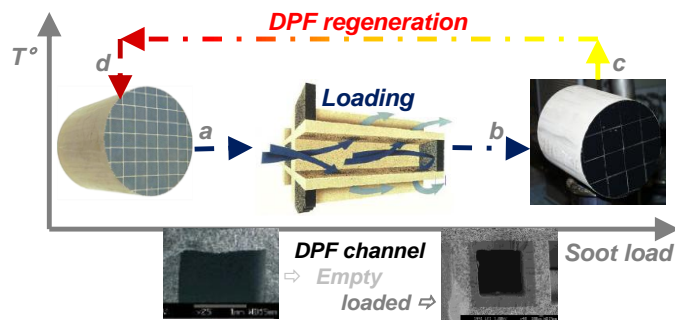


Figure3.Schematic diagram of DPF loading and cleaning

The operating principle of a Diesel Particulate Filter (DPF) is introduced in figure 3. The DPF first of all goes from clean to soot loaded state (stages a \Rightarrow b), because of the gradually loading of trapped particles (Diesel soot and other particles like for example ash, salts, metals...). The particles filtration efficiency of the DPF simultaneously increases thanks to the soot cake contribution to the filtration mechanism, as the DPF loading goes along. When soot loading of the DPF is estimated appropriate by the engine control unit (ECU) to perform a successful regeneration of the filter (that is to say, not too low to avoid a fuel consumption penalty and nor too high to avoid a possible DPF failure; stage b), a DPF active regeneration is triggered (stage c). It mainly consists to increase the DPF temperature (target usually $\geq 600^{\circ}\text{C}$; stages c \Rightarrow d) via a Diesel fuel post-injection, to allow the combustion of the previously trapped particles. As a result of the gradual soot cake removal, the particles filtration efficiency of the DPF simultaneously decreases. At the end of this process, a new DPF loading phase restarts (stages a \Rightarrow b), for a mileage that varies for this vehicle during this study between 670 and 1040 km.

In addition to the particulate emissions impact of the DPF regeneration process, the combustion of the soot particles previously trapped inside the DPF leads to the following main chemical reactions (reaction 9 and 10), while the not catalyzed DPF used here, does not allow (or very few) to convert the CO formed in case of incomplete combustion of soot (reaction 11):

- Incomplete combustion of soot: $\text{C} + \frac{1}{2}\text{O}_2 \rightarrow \text{CO}$ (reaction 9)
- Complete combustion of soot: $\text{C} + \text{O}_2 \rightarrow \text{CO}_2$ (reaction 10)
- CO oxidation by catalyzed DPF: $\text{CO} + \frac{1}{2}\text{O}_2 \rightarrow \text{CO}_2$ (reaction 11)

Emissions analysis

The IFPEN's chassis dynamometer used during the study is equipped with a full flow Constant Volume Sampling (CVS), three simultaneous raw gases analyzers and a dedicated one for diluted gases; all of them include CO and CO₂ measurement by Non-Dispersive Infrared Sensor (NDIR), total hydrocarbons and CH₄ by Flame Ionization Device (FID), NO/NO_x by Chemi-Luminescence Detector (CLD) and O₂ by Paramagnetic Detector (PMD). Particulate Matter (PM) measurement by conventional gravimetric procedure of normalized filters and Particle Number (PN) characterization via Particle Measurement Programme (PMP) protocol (dedicated to particles with $\phi > 23 \text{ m}$), are also available.

Besides these conventional equipments, a wide variety of less usual devices and analyzers are used. The diagram introduced by the Figure 4 shows the complete set of instruments and their different ways of exhaust sampling, while the analyzers whose results are presented in this paper are introduced below:

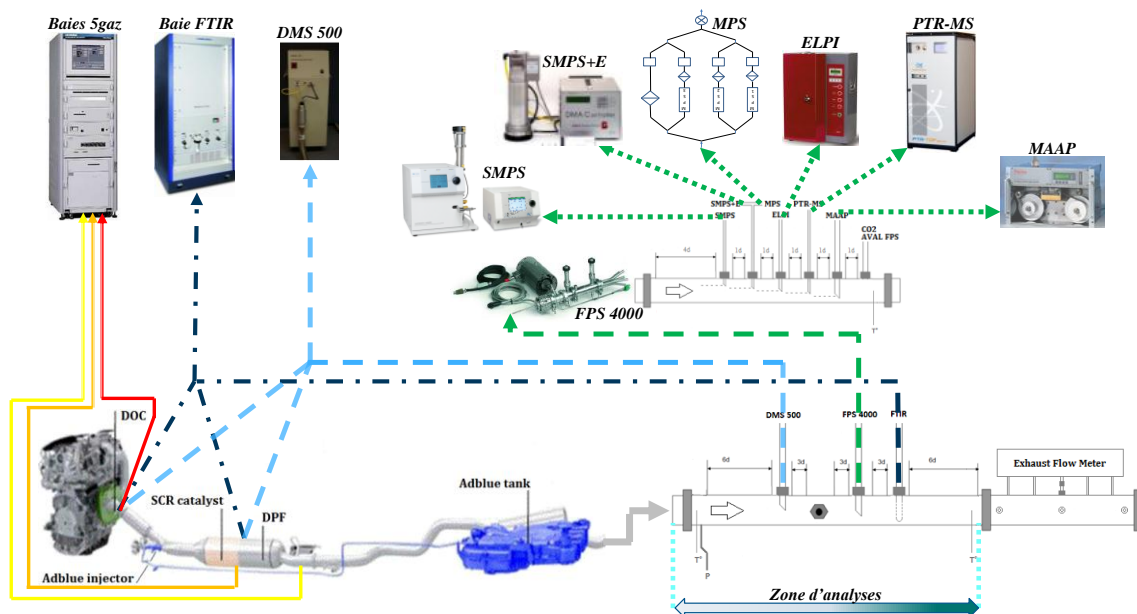


Figure4. Diagram of the exhaust line and analyzers samplings

A fine particle sampler (DekatiFPS4000) operates the sampling and a fast double dilution of a part of the exhaust gases prior to their analyze by some of the following instruments. It is only used at the DPF's outlet, with areal dilution ratio chosen during the whole tests described to be 11, the first dilution being hot and the second one cold.

A Fourier transform infrared spectroscopy (AVL FTIR), broadens the composition characterization of the raw gas phase along the exhaust line with additional compounds among which: NH_3 , N_2O , SO_2 , CH_2O , $\text{C}_2\text{H}_4\text{O}$, HCN or 9 hydrocarbons speciation, with a minimum detectable concentration (MDC) comprised between 0.25 and 5 ppm.

A differential mobility spectrometer (CambustionDMS500) analyzes in real-time the number and size of the particles of the exhaust aerosol in the range 5-1000 nm. This instrument has its own sampling and dilution device which is heated and set during the whole tests described (DPF downstream measures), between 4 and 5 with a hot first dilution only.

A scanning mobility particle sizer (TSI SMPS) analyzes the number and size of the particles in the range 14-674 nm with the chosen configuration made up of 3081 differential mobility analyzer (DMA) + 3775 condensation Particle Counter (CPC). This device analyzes previously diluted aerosols coming from the FPS4000. Due to its functioning, it is used as an SMPS during steady state tests to obtain both number and size information, but as a CPC during the transient tests to obtain continuous total particle concentration in the range 4 to 1000 nm.

During some cold tests, the polycyclic aromatic hydrocarbons (PAHs) content of the soluble organic fraction (SOF) of the emitted particles, as well as the emitted hydrocarbon's composition were also analyzed accordingly to specific or standard methods (PAHs: tailpipe ELPI sampling and gas chromatography (GC); HCs speciation: CVS sampling and HCs speciation by high performance liquid chromatography (HPLC) and gas chromatography (GC).

Tests plan

The two Euro 6b vehicles emissions were first of all assessed under steady state conditions corresponding to New European Driving Cycle (NEDC) speed steps at 15, 32, 50, 70, 100 and 120 km/h.

Then, they were assessed during many days under transient conditions consisting of successive NEDC, WLTC (Worldwide harmonized Light vehicles Test Cycle) and CADC (Common Artemis Driving Cycles). Figure 5 introduces the vehicle speed evolution during these 3 driving cycles. The NEDC is the current normalized cycle for passenger cars approval. With its 1180s long, 11.007 km covered, particularly smooth profile and a maximum vehicle speed equal to 120 km/h, it is considered as not representative of real world driving and will be replaced from 2017. The two others cycles are

considered more representative of real driving conditions. It's about the future normalized WLTC which lasts 1800s during which the car covers 23.262 km and achieve 130 km/h, or the CADC which lasts 3143s for 51.687 km covered and achieves an even higher vehicle speed of 150 km/h.

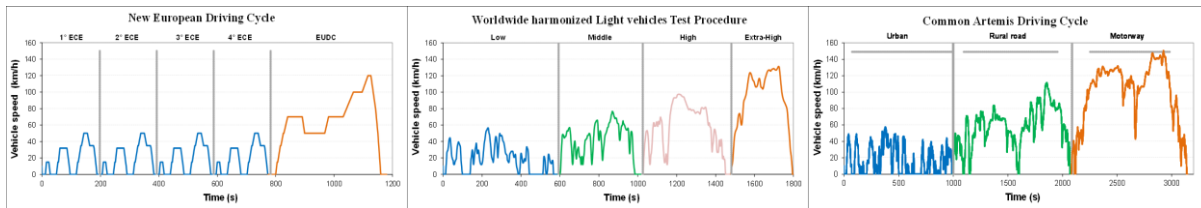


Figure 5. NEDC, WLTC and CADC cycles

In order to increase the vehicle mileage by day, necessary to broaden the driving conditions studied and try to increase the DPF active regeneration number of occurrences, a succession of these cycles were done day by day according to the following number of cycles: 10 NEDC, 6 WLTC and 4 CADC. In order to avoid a too long length of driving, harmful for reproducibility and analyzers dirtying, a maximum one hour per test was chosen, leading to 4 individual CADC by day, 3 series of 2 WLTC and 4 series of NEDC (2-3-2-3). This protocol leads to different engine starting conditions, ranging from ambient temperature of the engine fluids, DOC, SCR and DPF (called "cold start" when previous test was done the day before) to hot temperatures starting (called "hot start", for few minutes since last cycle's end) and additional conditions named "q-cold" (following a longer stop of the engine of approximately one hour) and cycles without engine start named "hot".

At the end of each 3 days series of driving, another series started with a different order of cycles, to mix the conditions and avoid a potential systematic bias between the two vehicles, due to their different emissions and control devices. Moreover, to avoid to miss an interesting period of emissions like for example potential DPF active regenerations that are automatically triggered by the engine control unit (ECU) in relation to the estimated DPF soot mass load, the whole vehicle driving conditions were acquired and analyzed for each tests and day after day.

2. Results

This article addresses the exhaust emissions of the Euro 6b vehicle equipped with close-coupled DOC and underfloor SCR + DPF. It mainly focusses on the results obtained during the transient conditions tests under NEDC, WLTC and CADC cycles, depending on the different starting conditions introduced previously and the presence or not of a DPF active regeneration.

The results introduced in the following figures, synthesize for most of them, up to 58 cycles with the following distribution:

- 30 NEDC (3 "cold start", 3 "q-cold start", 6 "hot start" and 18 "hot"),
- 18 WLTC (3 "cold start", 3 "q-cold start", 3 "hot start" and 9 "hot"),
- 10 CADC (2 "cold start", 3 "q-cold start" and 5 "hot start").

The particulate mass results (Figure 20) take into account a lower number of cycles (14, including 5 NEDC, 5 WLTC and 4 CADC, different of the previous ones), since only the cold and hot start conditions were tested. Finally, the particle size distributions include as for them, only one mean value for each introduced conditions.

It is important to bear in mind that these results are not obtained during normalized tests, under related conditions and with normalized instruments and protocols, but under various conditions and with a variety of instruments, with the aim of finely assess the regulated and unregulated emissions of the vehicle, nearer of realistic conditions. This, as well as the mileage and history of the vehicle, its estimated road law, the absence of vehicle preconditioning before each cycle can contribute to slightly different results compare to their theoretical certification values.

Moreover, due to the intermittent character of the Diesel Particulate Filter active regeneration, it is necessary to remember that their related emissions must be weighted according to their frequency. To make easier their comparison with the other studied conditions reported in this article (made up of the three cycles and the four starting conditions), the emissions reported afterwards are not strictly those of the regeneration phase, but are expressed in terms of emissions per kilometer on the whole cycle

length, including an active regeneration.

Gaseous emissions

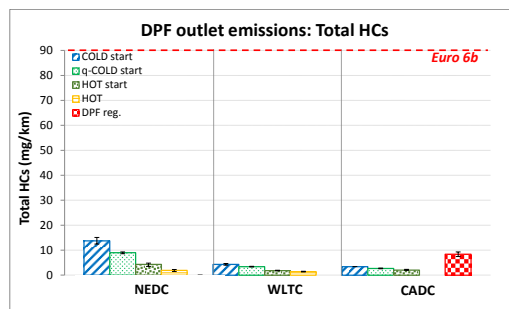


Figure6. Total HCs

The total hydrocarbons emissions of the Euro 6b SCR Equipped vehicle during the 3 cycles and different starting conditions are synthesized in figure 6 which highlights the extremely low amount of HCs emitted, whatever the conditions, those remaining well below the indirect tolerance fixed by the HC+NO_x Euro 6b limit, since they never exceed 15 mg/km.

The impact of the warm-up phase of the engine (calculated between "cold start" and "hot start" conditions) ranges from 1.7* to 3.2* for CADC and NEDC respectively and is equal to 2.4* for WLTC. These differences depends on the engine solicitation and the cycle length which causes a temperature increase of the DOC more or less fast and outlines its contribution. These emissions are mainly observed during the first minutes of the cycles, until the DOC's temperature becomes sufficient to oxidize it (reaction 1). As an example, the first ECE phase of the NEDC cycle only represents 16% of the cycle length but 58% of the whole cycle emissions, while the contribution of the first two ECE reach 75% of the emissions for a third of the length only.

The effect of the occurrence of a DPF active regeneration is more important, since the HCs emissions during the CADC are increased by a factor of 4.1 compared to the mean value of the hot CADC. This is due to the activation of the post-injection of Diesel fuel necessary to achieve the high temperatures (≥ 600°C) needed to burn the particles trapped inside the filter and this, despite the high oxidation efficiency of the DOC for such temperatures.

The hydrocarbons emitted during the cycles without DPF active regeneration are composed of a wide variety of species, since 16 to 37 different compounds are detected and 15 to 24 quantified, during the cold tests (HPLC analyses), most of them with extremely low contents. The mono and cyclo-olefins family is always the main contributor (46-76%) of the total measured hydrocarbons, before aromatics, naphthene and paraffin (n+i). Regarding to individual compounds, the main contributors are methane (CH₄), ethene (C₂H₄), propene (C₃H₆), formaldehyde (CH₂O) and acetaldehyde (C₂H₄O). During the regenerations, the total hydrocarbons emissions remain too low when analyzed downstream the DOC, to allow their partial speciation via the FTIR analyzer.

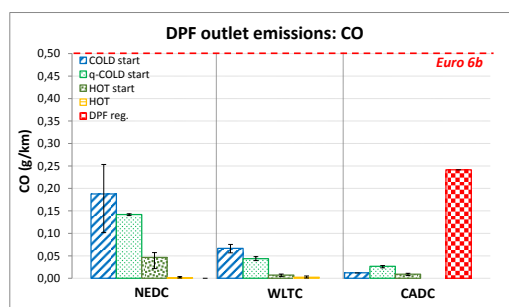


Figure7. CO

The carbon monoxide (CO) emissions synthesized in figure 7 remain in line with the Euro 6b standard whatever the conditions, since they never exceed half of the corresponding emission limit. The highest emissions are measured during the NEDC following a cold start that involves on average 0.188 g/km of CO.

The impact of the warm-up phase ranges from 1.3* to 9.4* for CADC and WLTC respectively and is equal to 4* for NEDC, depending on the speed of the temperature increase of the DOC and raw CO emissions of the engine. Like HCs, these emissions are mainly observed during the first minutes of cycles, until the DOC reach its light-off temperature and become efficient enough to oxidize it (reaction 2).

The effect of a DPF cleaning is higher than the cold start impact, since the CO emissions during the CADC including an active regeneration are increased by a factor of 27. This increase is mainly due to the combustion of the soot trapped inside the filter, which causes the release of CO₂ (reaction 10) if the combustion is complete and CO (reaction 9) otherwise. The DPF here being a Fuel Born Catalyst DPF and not a catalyzed one, the CO emitted in case of incomplete combustion of the particles, is not converted to CO₂ (reaction 11) and contributes to the increase of the CO emissions.

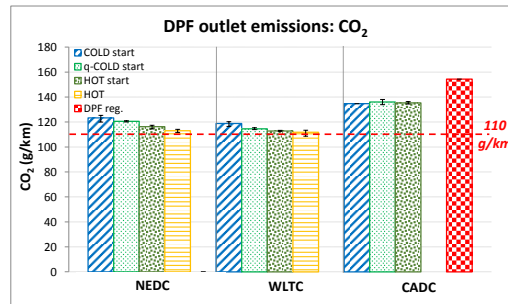


Figure8. CO₂

The carbon dioxide (CO₂) emissions of the vehicle synthesized in figure 8 are higher than the reference value of 110 g/km claimed by the manufacturer. For example, the difference varies between 1.7% and 12.2% on the NEDC and WLTC cycles for the different starting conditions. It even reaches up to 23% on the CADC, which presents the highest CO₂ emissions whatever the conditions, with an average value of 135 g/km.

The over emissions observed during this study, even on NEDC cycles that differs from the exact certification conditions, agree with the recent results of the investigation commission of the French environment ministry, that reports for equivalent vehicles tested and slightly different NEDC conditions, a 13.7% difference [5]. The gap measured on the CADC during this study compared to the reference value of 110 g/km, is also consistent with those regularly assessed under real driving conditions, as reported by the EEA [12] with a 20% gap for a similar 2 liter Diesel engine (based on new passenger cars registration in Eu-27 between 2010 and 2013) or by the ICCT [13] that even reports a growing gap from 2001 to 2014 reaching of 37% for the latest passenger cars models.

Although it is non-existent on CADC, our study underlines the impact of the warm-up phase of the engine and the potential dedicated strategy to accelerate the temperature rise of the DOC, since CO₂ cold emissions are from 5.4 to 6.1% higher after cold start than after hot start (for WLTC and NEDC respectively).

The effect of a DPF active regeneration on CO₂ emissions is higher than the one observed for engine cold start and reaches 14%, almost exclusively because of the catalytic oxidation of the Diesel fuel post-injected to increase the DPF temperature and to a lesser extent, of the complete combustion (reaction 10) of a part of the previously trapped soot.

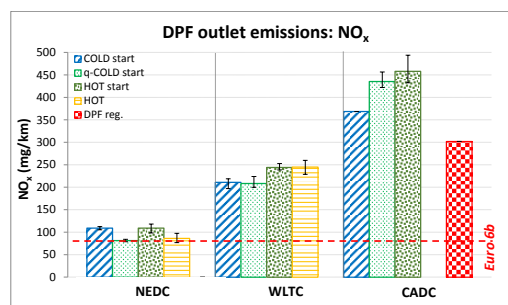


Figure9. NO_x

The nitrous oxides (NO_x) emissions of the vehicle synthesized in figure 9 vary considerably during

our tests, depending on the starting conditions, but even more on the driving cycle. Thus, the lowest emissions are encountered with NEDC for which they range from 76 to 118 mg/km (respective min/max values), the highest with CADC (average value of 421 mg/km), the average emissions for WLTC being 227 mg/km. Moreover, higher engine temperatures involve additional emissions.

Consequently, the average NO_x emissions measured during this study exceed most of time, the Euro 6b emission limit of 80 mg/km. For example, it exceeds during the NEDC cycles by 1.7 to 36.5% this limit, depending on the starting conditions. The gaps for WLTC and CADC are greatly higher with respective 2.6 to 3.1* and even 4.6 to 5.7 factors. The variations observed between the 3 cycles are mainly due to the raw NO_x emissions of the engine which does not allow to maintain a constant efficiency of the SCR, particularly during the CADC. Indeed, the SCR catalyst efficiency remains equivalent whatever the cycle in case of cold start (51 to 55% of efficiency), while it varies between 38 to 60% (CADC and NEDC respectively) after hot start and reach up to 73% during NEDC hot cycles (on average).

The NO_x results obtained during this study are in good agreement with those reported by Kadijk & Al. [8] or the recent French, English and German investigation commissions [5] [6] [14]. The 3 later confirm in particular: from one hand, the absence of defeat devices or cycle recognition strategies on vehicles commercialized in the last years in Europe and on the other hand, the large variety of NO_x emissions measured under real driving emissions tests (on tracks or on the road) or equivalent laboratory conditions. This study, as well as the three investigation commissions, particularly highlights the impact of the driving conditions (vehicle speed and acceleration) and engine temperatures on the level of emitted NO_x. The origin of the engine temperature effect seems to be the exhaust gas recirculation [6] (EGR, which contributes to the engine NO_x raw emissions reduction) and is accordingly differently settled, whether it be to protect the engine at the lowest temperatures or at higher, to achieve a better NO_x/fuel consumption compromise.

The occurrence of a DPF active regeneration during a CADC, lower by 66% the NO_x emissions compared to the average value observed during the cycles without regeneration with similar starting conditions (hot start). This decrease is due to the higher amount of ammonia (NH₃) available in the exhaust line during this phase (as shown by figure 10) and to a lesser extent, to the higher exhaust temperatures.

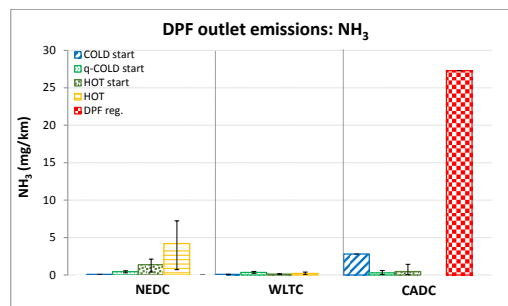


Figure 10. NH₃

This study highlights as shown by figures 10 and 11, the very negative impact of the DPF active regenerations on ammonia (NH₃) emissions, which are 60* higher than those observed otherwise. Indeed, a similar effect (not presented in this article) is also noticed via the FTIR results upstream the DPF during another active regeneration, while a third occurrence, does not show any impact on NH₃ emissions upstream of the SCR catalyst. It can be affirmed from these results, that the engine raw emissions or the DOC, have nothing to do with this NH₃ emissions increase, contrary to the SCR catalyst and its related urea injection, whose contribution via the chemical reactions 4 and 5 is essential, especially in case of high urea quantity injection.

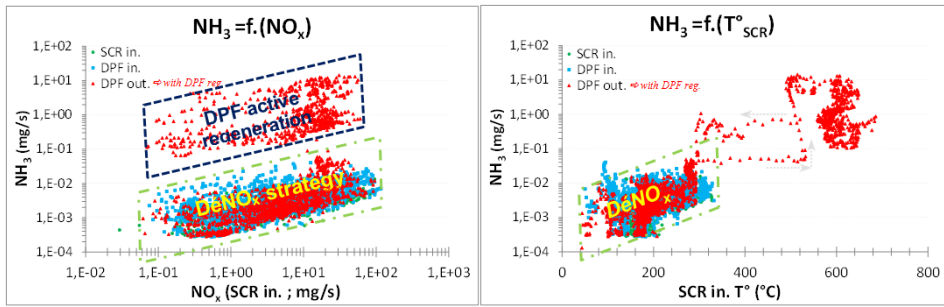


Figure 11. CADC hot w/wo DPF reg. - NH_3 slip (DPF out.) = $f.(\text{NO}_x \text{ abatement} \ \& \ T^\circ \text{SCR in.})$

Two main potential causes have to be considered in the case of the CADC with the DPF active regeneration introduced on figure 10: from one hand (the most likely), the urea injection increase needed at the highest exhaust temperatures to cool down the urea injector to avoid damage (as seemed underlined by the right graph) and on the other hand, the possible salt formation in the exhaust line, coming from the urea partial decomposition under cold conditions for instance, previously and gradually accumulated inside the exhaust line and that could be released later, undercover of favorable thermal conditions.

The NH_3 emissions during the cycles without DPF active regeneration always remain under 7.5 mg/km and most of time (as observed for WLTC), similar to minimum detectable concentration (MDC) of the compound. However, it can be noticed from figure 10 that significant differences occur during NEDC and CADC.

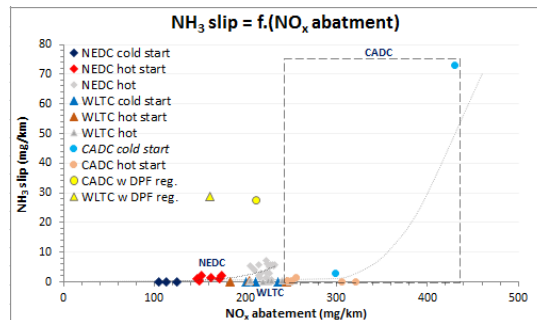


Figure 12. NH_3 slip (DPF out.) = $f.(\text{NO}_{x \text{ DPF out.}} - \text{NO}_{x \text{ SCR in.}})$

Figure 12 synthesizes and links the undesired emissions of NH_3 to the calculated NO_x abatement during the cycles. The variations of NH_3 emissions during NEDC are mainly associated to NO_x reduction efficiencies which varies from 53 to 73 % (from cold start to hot cycles) and to engine raw emissions (the higher the DeNO_x efficiency, the higher the NH_3 slip). During CADC cold, the higher quantity of NO_x to convert by the SCR catalyst compared to the 2 other cycles, also lead to an increase in urea injection, as well as to a lower SCR efficiency and higher NH_3 slip (also intensified by the lower temperatures involved by the engine cold start). The NH_3 slip during cycles including a DPF active regeneration, clearly appears to be higher than the equivalent cycles without and not related to the NO_x abatement by the SCR.

These observations emphasize the need of a fast introduction of a new emission limit for passenger cars towards NH_3 , in accordance with continuous engines and after treatments evolutions and improvements, as already implemented for heavy-duty vehicles [4]. This is particularly true in the real driving emissions prevision. Indeed, as suggested by this study, NO_x emissions under more realistic driving conditions are higher than those measured under certification conditions and involve higher quantities of NO_x to reduce. The necessary higher NO_x abatement and the related need of a high efficiency, may involve potentially higher NH_3 emissions. It is therefore essential to include all realistic and normal operating conditions in the future certification procedures, as for example the DPF active regeneration, and not to authorize some certification tests to be voided [3], to allow an extensive and reliable limitation of the exhaust emissions.

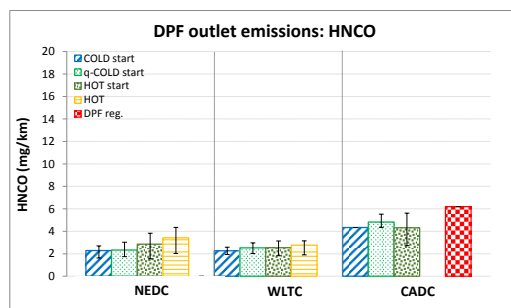


Figure13. HNCO

Figure 13 emphasize the lack of significant evolutions of isocyanic acid (HNCO) emissions depending on the starting conditions and the occurrence of a DPF active regeneration, compared to the FTIR's minimum detectable concentration of this compound, since all calculated emissions remain lower than this later. It is however necessary to specify that the FTIR signal to noise ratio (SNR) regarding to the HNCO measurement, is the poorest of all measured compounds with a ≤ 5 ppm equivalent background noise.

Nevertheless, this study confirms the efficient decomposition of the injected urea and more particularly the hydrolysis decomposition of the HNCO (chemical reaction 5), particularly during the CADC with the DPF active regeneration, since these emissions do not follow the previously introduced surge in NH_3 emissions.

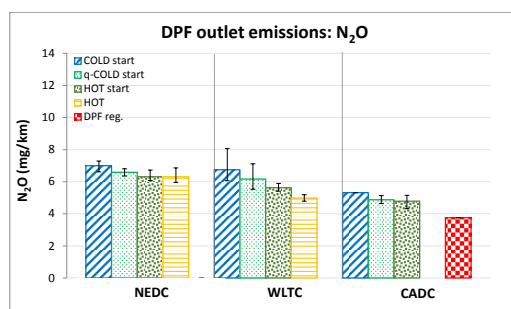


Figure14 N₂O

This study highlights the presence of significant emissions (compared to analyzer's MDC) of nitrous oxide (N_2O) whatever the cycle, the starting conditions, or the presence or not of a DPF active regeneration. The average emissions during the cycles without DPF regeneration (synthesized on figure 14), vary between 4.8 and 7 mg/km from CADC hot to NEDC cold.

The N_2O emissions are not constant whatever the driving conditions, but regularly appear during the cycles, mainly during the speed vehicle accelerations for which the air to fuel ratio (AFR) of the exhaust gases is increased, while the catalysts temperatures sharply rise. Then, the higher amount of unburnt hydrocarbons associated to the catalysts temperatures variations can in a specific range of these latter (depending on the catalyst characteristics), favor the occurrence of undesirable chemical reactions leading to the formation of N_2O .

The temperature range for which this undesired reaction occurs being rather low, cold start cycles tend to increase the spent time in the N_2O emission temperature window, leading to an increase of these emissions from 11 to 20 % depending on the cycle.

During the DPF active regenerations, the N_2O emissions are on the whole lowered (as observed for the dedicated CADC), because of the strong catalysts temperatures increase, but two different effects need to be specified. Indeed, the N_2O emissions are firstly increased during the few seconds following the post-injection activation, because of the exhaust AFR increase whereas the catalyst temperatures remain as usual. Afterwards, the higher temperatures do not favor the N_2O formation anymore and contribute to its global reduction at the time scale of the whole cycle. The emissions during the CADC including the DPF active regeneration is equal to 3.8 mg/km and represents a 21.5 % reduction compared to the equivalent CADC hot start without DPF Cleaning.

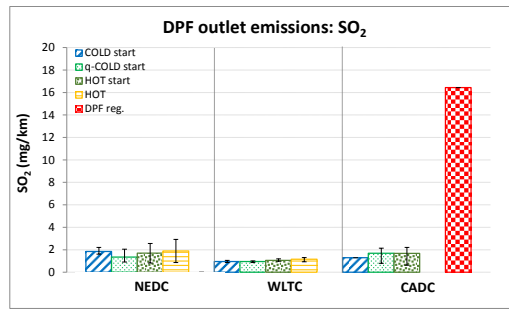


Figure15.SO₂

The sulfur dioxide (SO₂) measurements (synthesized on figure 15), reveal the lack of significant emission and evolution during the cycles without DPF active regeneration and this, whatever the starting conditions since the values always remain equivalent or lower than the MDC of this compound. These emissions, except during the DPF active regeneration, are particularly low because of the gradual poisoning of the catalyst, due to the continuous storage of the main part of the emitted sulfur species coming from fuel and lubricant, by the catalysts during normal conditions (that is to say, when exhaust temperatures remain those usually encountered on Diesel exhaust gases).

However, during the regeneration process of the DPF, the temperature rise of the catalysts (which achieve temperatures higher than 600°C because of the exothermic reaction due to the post-injected HCs oxidation by the DOC), allow to desorb the sulfur species previously trapped on the DOC or the SCR, involving in the gas phase the formation of sulfur compounds among which SO₂, as already observed during DPF active regenerations of Euro 5 Diesel vehicles [10]. Because of this considerable effect, the SO₂ emissions during the CADC cycle with an active regeneration are multiplied by almost 10 and achieve 16.4 mg/km.

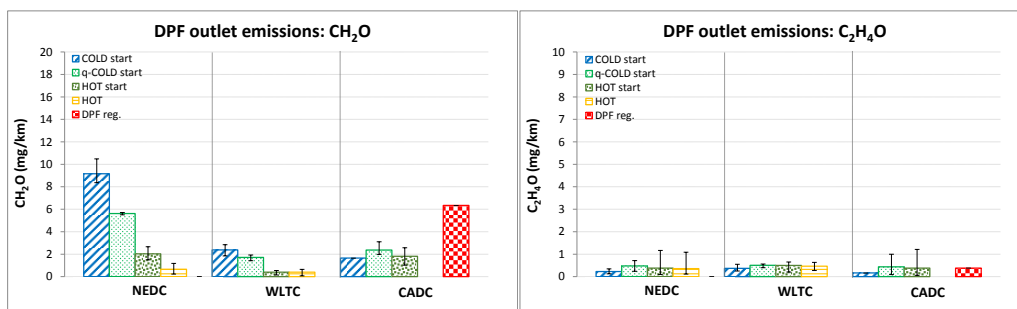


Figure16.CH₂O (left graph) & C₂H₄O (right graph)

The evolutions of formaldehyde (CH₂O) and acetaldehyde (C₂H₄O) measured during this study are synthesized on figure 16 (left and right graphs respectively).

While formaldehyde shows significant emissions and variability in accordance with the starting conditions or the presence of a DPF regeneration, acetaldehyde still remains near or lower its MDC and most of time, lower than formaldehyde. Thus, the C₂H₄O results obtained with FTIR, do not allow to give a verdict on the emitted quantity or on the possible effect of the warm up phase of the engine or of the DPF active regeneration, except that their emissions remain low, whatever the studied conditions.

At the opposite and in good agreement with the previously introduced hydrocarbon emissions, formaldehyde is largely emitted during the warm up phase of the engine following a cold start (compared to the other starting conditions) and during DPF active regeneration as well. Thus, the emissions globally vary from 0.4 to 9.2 mg/km on average during the cycles without DPF active regeneration and are mainly observed during the first minutes of the cycles, until the DOC's temperature becomes sufficient to oxidize it (reaction 1).

The CH₂O average emissions during a cycle following a cold start are, for NEDC and WLTC respectively, 4.5 to 6.1 times higher than for equivalent cycle with hot start, while the DPF active regeneration multiplies by 3.5 the emissions in the case of the studied CADC cycle (compared to the equivalent cycle and starting conditions).

Considering the quality characteristics of Adblue according to the ISO 22241-1 standard and its

potential formaldehyde small content of maximum 5 mg/kg, its maximum potential contribution to the measured CH₂O exhaust emissions is estimated, considering an Adblue content of formaldehyde equal to the previous standard limit and the calculated Diesel exhaust fluid consumption, during the whole cycles synthesized in this article.

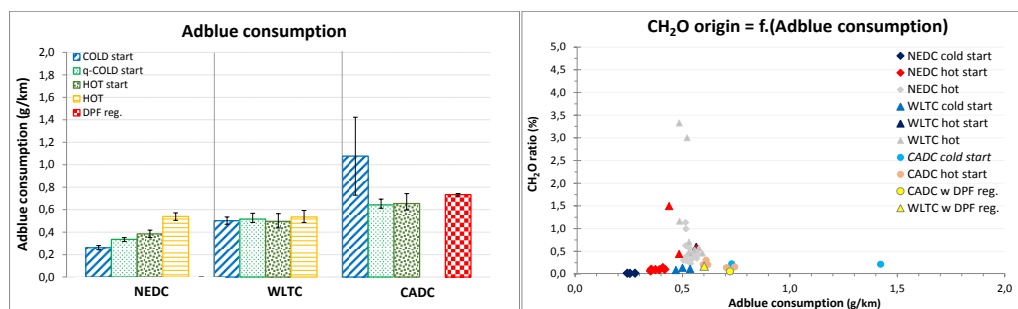


Figure 17. Estimated Adblue consumption/cycle (left graph) & Adblue's maximum potential contribution to CH₂O (right graph)

To do this, the Adblue consumption which is not measured, is estimated for each of the synthesized driving cycles covered by the vehicle, from the amount of NO_x treated by the SCR catalyst (calculated from the difference of SCR upstream and DPF downstream NO_x measurements) and also taking into account the amount of undesired NH₃ emitted.

These estimated average consumptions (summarized in the left graph of figure 17), vary from 0.26 to 0.54 g/km during NEDC cycles (following the NO_x emissions and the efficiency of the SCR catalyst) and are stable during WLTC (0.5-0.54 g/km) for which SCR efficiency is more stable. They finally achieve during CADC, 0.64 and even 1.08 g/km for the cold start cycles, because of their higher NO_x and NH₃ slip emissions.

The ratio between CH₂O potentially resulting from the consumption of the Diesel exhaust fluid and CH₂O measured at the outlet of the vehicle exhaust line via the FTIR, can then be calculated and plotted for each cycle and all starting conditions to adequately represent the diversity of testing conditions and results (right graph of figure 17). These results highlight the limited contribution of the injected Diesel exhaust fluid to the formaldehyde emissions of the evaluated Diesel SCR equipped vehicle. Indeed, its theoretical maximum potential contribution never exceeds 3.5 % (whatever the cycle and the starting conditions) of the CH₂O measured downstream the DPF and is most of time lower than 1.5 %.

Figure 18 and 19 respectively introduce the emissions of hydrogen cyanide (HCN), nitric acid (HNO₃) and formic acid (CH₂O₂), measured during the study.

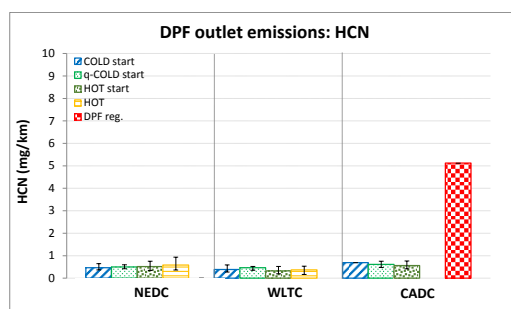


Figure 18. HCN

The hydrogen cyanide (HCN) emissions still remain quite stable and below its MDC during the cycles without DPF regeneration and this, whatever the starting conditions. Thus, the results do not allow to provide a verdict on the emitted quantity or on the possible effect of the warm up phase of the engine, except that their emissions remain low, whatever the starting conditions considered.

While hydrogen cyanide emissions during the CADC cycle including a DPF active regeneration, strongly increase and achieve 5.1 mg/km, considerably higher than its MDC in that case. Moreover, a similar effect (not presented in this article) is also noticed via the FTIR results upstream the DPF during another active regeneration on a WLTC cycle, while a third DPF regeneration during another CADC, does not show any impact on HCN emissions upstream of the SCR catalyst.

It can thus be affirmed from these results, that DPF active regeneration of the evaluated Euro 6b Diesel vehicle equipped with SCR, causes significant emissions of hydrogen cyanide, whether it be in terms of instantaneous emissions or at the scale of the whole cycle. Elsewhere, the engine or the DOC, have nothing to do with this substantial HCN emissions increase, which only comes from the SCR catalyst and its related urea injection, under the DPF regeneration conditions that involve high temperatures, high NH₃ emissions mainly related to the urea injector cooling and increased emissions of hydrocarbons due to the post-injection activation.

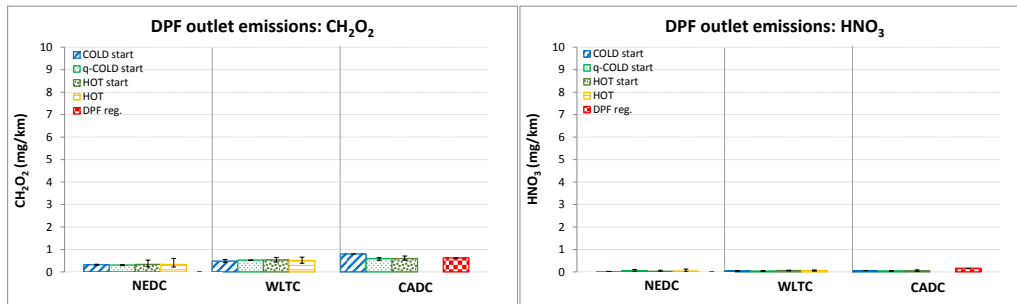


Figure 19. CH₂O₂ (left graph) & HNO₃ (right graph)

The nitric acid (HNO₃) and formic acid (CH₂O₂) emissions reported on the figure 19, whose values still remain well below their respective MDC, do not highlight significant emissions or variations of this 2 compounds, whatever the cycle, the starting conditions or the presence or not of a DPF active regeneration. Thus, this study does not allow to give a verdict on the emitted quantity, on the possible effect of the warm up phase of the engine or of the DPF active regeneration on these two last gaseous compounds, except that their emissions remain low, whatever the studied conditions.

Particulate emissions

In addition to the gaseous regulated and unregulated pollutants, the particles emitted by the vehicle also were analyzed among others, in terms of particulate matter (PM), particle number (PN) and size distribution.

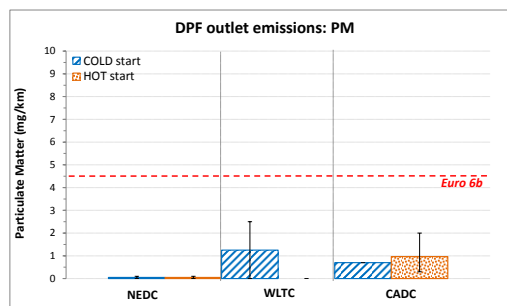


Figure 20. Particulate Matter (PM)

As shown by Figure 20, the PM of the emitted aerosol, measured with the conventional gravimetric method, remains for the three cycles and for cold as well as hot conditions, widely under the Euro 6b emission limit of 4.5 mg/km, since the mean values never exceed 2.5 mg/km.

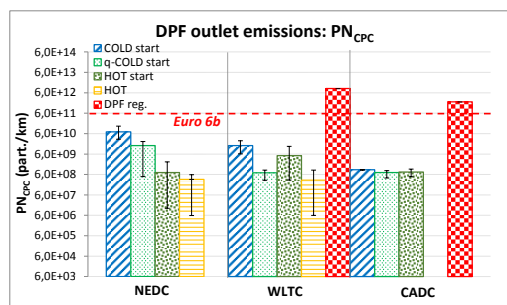


Figure 21. Particle Number (PN)

The particle number (PN) synthesized in figure 21, measured thanks to the specific protocol defined

for the project and described in figure 4, remains for the three cycles and for each starting conditions under the Euro 6b emission limit of 6.10^{11} particle/km, except for the two cycles including a DPF active regeneration, for which the number of emitted particles is widely increased. Thus, the PN emissions varies whatever the cycle and the starting conditions considered, within $3,14.10^8$ part./km and $7,23.10^{10}$ part./km if no DPF active regeneration occurs, while it achieves $2,13.10^{12}$ part./km and $9,61.10^{12}$ part./km (respectively for CADC and WLTC) for cycles including an active regeneration.

Whatever the measurement protocol (PMP protocol with volatile particle remover [VPR] and CPC_{PMP} with cut-off diameter [d50] equal to 23 nm; or specific protocol with FPS4000 dilution, TSI $CPC_{R\&D}$ with d50 = 4nm and without VPR), the impact of the warm-up phase is more easily observed with NEDC than with WLTC, while CADC cycle does not show any significant effect. Indeed, the impact varies between 98* and 162* (comparison between cold start and hot start) for NEDC, from 3.1* to 5.1* for WLTC and is not so obvious for CADC for which it never exceeds a 34% increase.

If the sizeable difference between PMP and CPC for NEDC results can seem excessive, it is necessary to keep in mind that these two analyzes, besides their significantly different protocols, are not simultaneous. Consequently, the raw emissions of the engine are first of all not exactly equal for both tests. Furthermore, the DPF downstream particulate emissions, also vary accordingly to the DPF soot cake thickness which greatly depends on the vehicle mileage since the previous regeneration (whether it be a partial in the case of a continuous regeneration, or a more complete in the case of an active regeneration), as emphasized by the right graph of the figure 22.

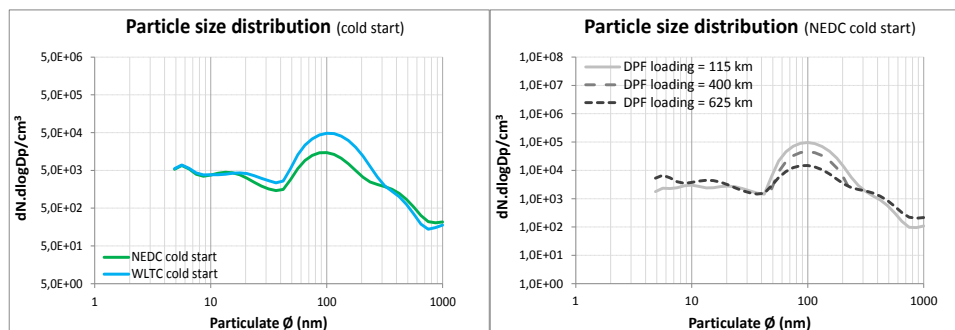


Figure 22. Mean particle size distribution during cold cycles without DPF regeneration

This graph indeed (left one), highlights the progressive reduction of the accumulation mode of the aerosol between 3 cold start NEDC cycles, for 3 different vehicle mileage (from 115 to 625 km) since the previous active regeneration. This evolution is linked to the DPF filtration efficiency increase, which results from the gradual growth of the DPF soot cake thickness. This accumulation mode is centered at 100nm (count median diameter (CMD), calculated on the range 23-1000nm) and does not vary as a function of the DPF loading. These particles, also extensively assessed (the results will be later published) includes typical Diesel soot aggregates, mainly composed of a carbonaceous fraction on which are adsorbed a variety of volatile compounds, stem from engine fuel, lubricant as well as from Diesel exhaust fluid.

It is useful to precise here, that these 3 size distribution curves, are measured downstream the Diesel particulate filter with the DMS500. Consequently, the number of particles to be measured is extremely low due to the filtration efficiency of the DPF and is near or lower than the background noise of the electrometers. Thus, if the signal on the range corresponding to the accumulation mode ($40nm < CMD < 200nm$) is significant because of the cold start impact on the number of emitted particles of this mode, the evolution of the curves outside this range is mainly due to electrometers noise and should not be taken into account.

The impact of the DPF soot load having been previously underlined, the cycles can now be compared in terms of particle size distribution. Because of the absence of impact of cold start conditions on CADC cycles as already shown in figure 21 and of the exclusively transient conditions reported in this article (DMS results, no SMPS measurements available), the particles size distribution related to CADC is not shown. Thus, left graph of figure 22 compare the average particles size distributions measured during NEDC and WLTC cycles following a cold start of the engine. It shows a slightly increased diameter (CMD, calculated on the range 23-1000nm) during the WLTC compared to the NEDC, with respective 105 and 99 nm.

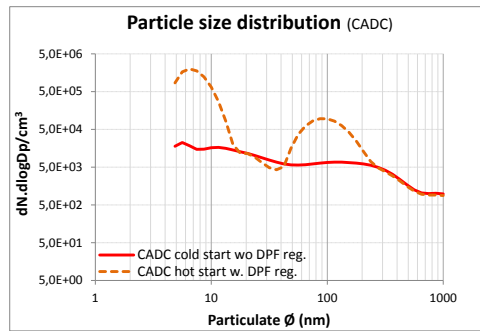


Figure 23. Particles size distribution (CADC, w/wo DPF regeneration)

The impact of a DPF active regeneration is more dramatic than that of cold starts previously studied, since the 2 events that occurred during WLTC and CADC cycles (as shown on figure 21, measured with the implemented specific protocol based on TSI 3775 CPC), cause a great exceeding of particle number (PN) emissions compared to the other studied conditions. The two DPF active regenerations also exceed the emissions limit of 6.10^{11} part/km defined by the Euro 6b standard (based on the PN_{PMP} protocol), the gap reaching respectively 3.6 and 16* this limit during CADC and WLTC respectively.

The analysis of the mean particle size distribution of the CADC including the DPF active regeneration (figure 23), highlights the bimodal distribution of the aerosol during the active regeneration of the DPF. This bimodal distribution is made up of a nucleation mode centered on 6.5 nm (nucleation mode CMD), containing extremely small particles and an accumulation mode centered on 94 nm (accumulation mode CMD), containing in particular the typical Diesel soot aggregates.

The nucleation mode encountered during the DPF active regeneration on the CADC cycle, essentially results from the high temperatures reached ($\geq 600^{\circ}\text{C}$), that cause an intense sulfur desorption from the catalysts of the previously trapped sulfur, and the appearance of sulfur compounds (among which SO_2 which is measured by the FTIR) in the gaseous phase of the exhaust aerosol, that are major precursors of nucleation processes (as already observed during Euro 5 vehicles DPF active regeneration[10]). Inversely to the gradual DPF loading previously shown, the DPF active regeneration causes the progressive but faster combustion of the previously trapped particles and as a result, the progressive soot cake removal, the gradual decrease of the particles filtration efficiency of the DPF, leading to the accumulation mode appearance downstream the DPF[10].

Conclusion

The variety of driving and starting conditions covered in this article, composed of 3 cycles and 4 engine warm up conditions, as well as the large reproducibility offered by the 58 cycles synthesized, offer an extensive assessment of the vehicle emissions, further improved by the complementarity of the implemented analysis.

It highlights the negative impact of engine warm-up and DPF active regeneration on the regulated and unregulated gaseous and particulate emissions of the Euro 6b Diesel vehicle studied, in particular during the warm up phase of the engine and even more, during DPF active regenerations.

Total hydrocarbons emissions of the vehicle are whatever the conditions, well below the indirect tolerance fixed by the $\text{HC}+\text{NO}_x$ Euro 6b limit. The warm up phase of the engine have a negative impact, particularly acute during the first minutes of the cycles and the DPF active regeneration have an even higher.

Carbon monoxide emissions remain in line with the Euro 6b standard

whatever the conditions, whether it be with or without DPF regeneration. The warm-up phase have a negative effect, particularly during the first minutes of cycles, while the DPF regeneration further increase the emissions because of the incomplete combustion of soot trapped inside the filter.

Carbon dioxide emissions are up to 23% higher than the reference value claimed by the manufacturer. The emissions are also increased during the warm up phase of the engine and even more during the DPF active regeneration.

Nitrous oxides emissions vary considerably during the tests, depending on the starting conditions, but even more on the driving cycle. They are lower during the NEDC for which they are equivalent to the Euro 6b limit, than the WLTC and furthermore the CADC, these differences being mainly due to the variations of the raw engine emissions. The DPF active regeneration lower NO_x emissions because of the higher amount of NH_3 emphasized during this phase.

Ammonia emissions are highly increased during the DPF active regeneration and are released exclusively by the SCR catalyst and its urea injection and being neither correlated to the NO_x abatement nor to the SCR Efficiency.

Significant emissions of nitrous oxides are highlighted by this study, whatever the studied conditions, these emissions regularly appearing along the cycles, mainly during the speed vehicle accelerations.

Whatever the starting conditions, there is no sulfur dioxide emissions during the cycles without DPF active regeneration because of its continuous storage on the catalysts. At the opposite, the temperature rise of the catalysts during the active regeneration of the DPF, allow to desorb the previously trapped sulfur species.

Formaldehyde shows significant emissions, in good agreement with those of hydrocarbons. The ratio between CH_2O potentially resulting from the consumption of the Diesel exhaust fluid (which can contain a small content) and CH_2O emitted by the vehicle, never exceeds 3.5%.

The studied vehicle presents globally stable and extremely low emissions of hydrogen cyanide during the cycles without DPF active regeneration, while they are significantly increased during the cycles including a DPF active regeneration.

Low emissions of Acetaldehyde, nitric acid and formic acid are observed during this study, whatever the studied conditions. Isocyanic acid also, which highlights the efficient decomposition of the injected urea, particularly during the DPF active regeneration, for which the NH_3 emissions dramatically increase.

The particulate mass (PM) of the aerosol emitted by the vehicle, always remains widely under the corresponding Euro 6b emission limit, as well as the particle number (PN) which remains under the Euro 6b emission limit of $6 \cdot 10^{11}$ particle/km in the absence of DPF

active regeneration.

This study also underlines the impact of cold starts and warm up phase of the engine on the particulate emissions, which can in the worst case, be multiplied by more than 100. It also highlights the progressive reduction of the accumulation mode of the aerosol, depending on the vehicle mileage since the previous DPF active regeneration, whereas the median diameter does not vary.

The DPF active regenerations cause a great increase of the emitted number of particles, which easily overtake the PN Euro 6b limit. The analysis of the mean particle size distribution during a cycle including a DPF active regeneration, shows a bimodal distribution of the aerosol during the regeneration, made up of a nucleation mode (essentially resulting from the desorption of the previously trapped sulfur from the catalysts) and a lower accumulation mode (which results from the progressive soot cake removal).

Taking into account the results achieved, the study finally tackles the need to further improve the related after-treatment's efficiencies, especially during the studied phases that remain major contributors to the pollutants emission of recent Diesel vehicles.

Furthermore, even if the latest European regulation improvements (in particular the WLTC cycle introduction and the incoming of the new real driving emission (RDE) test procedure) are positive ways to further reduce the automotive emissions, additional efforts are still needed. Indeed, the results also bring to light the necessity to abolish some remaining invalidations (first and foremost, regarding to the DPF active regeneration that remains insufficiently taken into account, including on the latest commission regulation 2016/427[15] dedicated to the new Euro 6 passenger cars RDE tests), whilst considering the need of additional pollutant emissions limits for passenger cars (primarily regarding to the ammonia due to the SCR technology spread, as well as the <23nm particles which are often emitted during the DPF active regeneration process).

In the same way, the hydrogen cyanide emissions revealed by this study during the DPF active regeneration of this Euro 6b DOC+SCR+DPF Diesel equipped vehicle, deserves to be additionally studied.

Acknowledgments

This study has been performed within the framework of the CAPPNOR2 project (ADEME convention1366C0033), selected in the context of the call for projects CORTEA. The authors would thank the French Environment and Energy Management Agency (ADEME) for their financial support to the project.

References

[1] Ambs J.L., McClure B.T. (1993): The influence of oxidation catalysts on NO₂ in Diesel exhaust. SAE

technical paper: 932494, doi:10.4271/932494.

- [2] Claxton L.D. (2014): The history, genotoxicity and carcinogenicity of carbon-based fuels & their emissions. Part 3: Diesel and gasoline. Elsevier Ltd.: [dx.doi.org/10.1016/j.mrrev.2014.09.002](https://doi.org/10.1016/j.mrrev.2014.09.002)
- [3] Commission regulation (EU) 2016/427 of 10 March 2016 amending Regulation (EC) n°692/2008 as regards emissions from light passenger and commercial vehicles (Euro 6). Official journal of the European Union; 31/03/2016.
- [4] Delphi (2015): worldwide emissions standards, heavy-duty and off-highway vehicles.
- [5] French ministry of the environment, energy and the sea (media kit; 2016): Contrôles des émissions de polluants atmosphériques et de CO₂ : Résultats détaillés des 52 premiers véhicules testés.
- [6] German federal ministry of transport and digital infrastructure (report; 2016): Volkswagen investigation commission report.
- [7] International agency for research on cancer (IARC monographs, volume 105; 2013): Diesel and gasoline engine exhausts and some nitroarenes.
- [8] Kadijk G., Ligterink N., van Mensch P., Smokers R. (TNO report; 2016): NO_x emissions of Euro 5 and Euro 6 Diesel passenger cars – test results in the lab and on the road.
- [9] Koebel M., Elsener M., Kleemann M. (2000): Urea-SCR: a promising technique to reduce NO_x emissions from automotive Diesel engines, Catal. Today 59 (2000) 335–345.
- [10] Leblanc M., Noël L., D'Anna B., Boreave A., R'Mili B., Raux S., Vernoux Ph. (2014): Unregulated Gaseous and Particulate Emissions During Active Regeneration of Diesel Particulate Filters. 18th ETH-Conference on Combustion Generated Nanoparticles, Zurich, Switzerland.
- [11] McClellan R.O., Hesterberg T.W., Wall J.C. (2012): Evaluation of carcinogenic hazard of Diesel engine exhaust needs to consider revolutionary changes in Diesel technology. Elsevier Ltd.: [dx.doi.org/10.1016/j.yrtph.2012.04.005](https://doi.org/10.1016/j.yrtph.2012.04.005)
- [12] Pastorello C, Mellios G. (EEA technical report; 2014): Monitoring CO₂ emissions from passenger cars and vans in 2013.
- [13] Tietge U., Zacharof N., Mock P., Franco V., German J., Bandivadekar A., Ligterink N., Lambrecht U. (ICCT white paper; 2015): From laboratory to road-a 2015 update of official and real-world fuel consumption and CO₂ values for passenger cars in Europe.
- [14] UK Department for transport (Report; 2016): Vehicle Emissions Testing Programme.
- [15] US environmental protection agency (US EPA; 2015): Notice of violation to Volkswagen AG.
- [16] Yang L., Franco V., Campestrini A., German J. and Mock P. (ICCT white paper; 2015): NO_x control technologies for Euro 6 Diesel passenger cars: Market penetration and experimental performance assessment.

Coupling traffic and emission models: dynamic driving speed for emissions assessment.

D. Lejri*, A. Can**, L. Leclercq*

*Laboratoire Ingénierie Circulation Transport (LICIT), ENTPE/IFSTTAR, Lyon, 69518, France
email:delphine.lejri@entpe.fr

**Laboratoire d'Acoustique Environnementale (LAE), IFSTTAR, Nantes, 44344, France

Abstract

Emission models can provide an estimation of the environmental impact of road traffic. However, decision makers need to be confident in these assessments in order to implement reduction strategies. The key issue at stake, especially in dense urban zone, is to describe accurately the traffic dynamic and particularly the congestion periods. The proper definition of the link mean speed is the ratio of total travelled distance and total time spent during a given period. This spatial speed description can be easily obtained from a dynamic traffic simulation. However, in operational conditions, it is often deduced from observed speeds on loop detectors or speed limit, which inevitably implies a bias on related emissions to be quantified. For this study we focused on vehicle trajectories in the morning peak for a typical weekday in a 3km² urban network. These detailed traffic data represent a considerable amount of data, but allows us to operate any spatiotemporal aggregation used for emission assessment sake. The emission calculations were made at link level each 6 minutes, combining the various traffic indicators and either the Copert emission factors database or Phem model. The related fuel consumption and NO_x emissions are compared.

Keys-words: road traffic emissions, emission models comparison, dynamic traffic variable, driving speed.

Introduction

Road traffic emissions are known to make large contribution to air pollution in urban areas. In 2013, the transport sector is the largest contributor to Nitrogen Oxides emissions (NO_x), accounting for 46% of total EU emissions (European commission, 2015). Exposure to NO_x pollutants concentrations has been demonstrated to have detrimental impacts on human health (Shaughnessy & al. 2015), while CO₂ road traffic emissions highly contribute to global warming. Therefore, in the last few years, many efforts have been made to quantify the contribution of greenhouse gas emissions and other pollutants from transportation. Various emission models can provide an estimation of the environmental impact of road traffic, which can range from very local (e.g. for some road traffic facilities assessment) to global investigations (e.g. for inventories elaborations). A detailed review of the vehicle emission models can be found in (Smit & al. 2010) (Franco & al. 2013), while (Fallah Shorshani & al. 2015) provides a review of the complete modeling chain (traffic, emission, dispersion and stormwater).

However, decision makers need to be confident in these assessments in order to implement reduction strategies. Therefore the inaccuracies and inconsistencies associated to emission estimations cannot be minimized. The urban scale concentrates the main current research efforts, because urban road traffic causes the vehicle kinematics that generate the higher emissions and are the most difficult to take into account, namely rapid speed variations and congestions (Ma & al. 2015) (Ahn & al. 2009), (De Vlieger & al. 2000) (Zhang & al. 2011) (Qu & al., 2015).

1. Objectives

Classical methods for assessing road traffic emissions are based on an aggregated kinematic characterisation of the vehicles flow. Thus, emission model, such as Copert (Gkatzoflias, 2012) needs mean speed and total distance travelled for a given time period to estimate the related emissions. On the contrary, instantaneous models, such as Phem (Zallinger, 2009) provide dynamic emission estimation directly from the vehicle trajectories, taking into account the whole traffic dynamic.

Microscopic traffic models, being good providers of traffic data adapted to emission models, are now considered as relevant for emission estimations (Vieira da Rocha & al.2013). These models are especially used to provide modal emission models for testing local development scenarios (Xu & al. 2016)(Erdman & al.2016). The sensitivity studies that explored the impact of car-following calibration on emissions(Vieira da Rocha & al.2015)(Lu & al. 2016) give some insights to use them wisely in that purpose. The main benefit of traffic dynamic modelling, especially in dense urban zone, is to describe accurately the vehicles kinematics and particularly the congestion periods. In parallel, it can help evaluating the bias introduced when using aggregated traffic representations at different temporal and spatial scales.

The main objectives of this work are (i) to compare road traffic emission models (Phem and Copert) applied to a large network and (ii) to test innovative ways to transfer information from the traffic model to a « mean-speed » emission model (Copert).

The section 2 presents the simulation framework and the tested models. The section 3 compares the emission estimations.

2. Material

Traffic simulation

The network under study is a 3-km² zone covering part of the cities of Le Perreux-sur-Marne and Neuilly-Plaisance, in the Parisian area. The traffic network, displayed in Figure 1, has been selected during the Trafipollu research project, for its high range of traffic conditions. For this study we focused on the morning peak hour for a typical weekday.

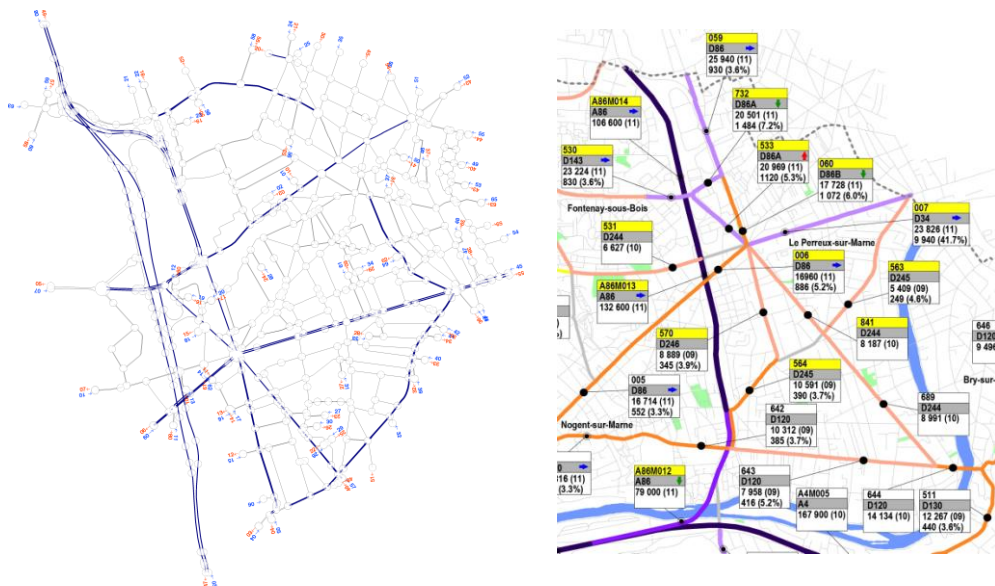


Figure 1 Network of the traffic microsimulation (left) ; traffic experimental data (right) - Trafipollu project

The traffic microsimulation has been implemented within the Symuvia platform, which gives access to the position, speed and acceleration of each vehicle on the network with a 1s-resolution. Vehicles routing choices are governed by a dynamic traffic assignment model, which guides each vehicle on the network on the route that minimizes its travel time towards its initially affected destination. Vehicles movements at the microscopic scale are governed by a set of rules, including car-following modeling (Leclercq & al., 2007), lane-changes (Laval & al., 2008) and specific movements at intersections. The platform also copes with the cohabitation on the network of vehicle with different kinematics, including passenger cars, buses and heavy-duty vehicles. This detailed traffic data represents a considerable amount of data, but allows us to operate any spatiotemporal aggregation used for emission assessment sake.

All vehicles second-by-second trajectories during the morning peak are extracted from the traffic microsimulation. These speed profiles are either: (i) directly formatted to correspond to Phem model input data, which are 1s-speed time series, or (ii) used to produce aggregated traffic variables, characterizing road segments for each 6min period, in order to correspond to Copert model input data. These aggregated data are composed of a mean speed and a distance travelled, for each road segment and time period.

Various speed definitions are compared for qualifying the vehicles kinematics on each road segments, which correspond to an increasing level of detail that aim to reduce the associated potential errors:

1. The operational (or default) definition describes the speed as the speed limit V_{limit} , which is the first available information. Associating the road segments to V_{limit} instead of the actual vehicles speeds might however result in high errors.
2. The speed experimented at one specific location on the road segment V_{loop} corresponds to the local insight that can be obtained through electromagnetic loops. Associating the road segment to V_{loop} amounts to assuming that vehicle speeds are homogeneous along the segment.
3. The speed characterizing the vehicles kinematics on the whole road segment $V_{spatial}$ can be determined thanks to the Edie's definition (Edie, 1963), in which the spatial speed is the ratio between the total travelled distance and the total spent time. This speed definition is the more accurate and compatible with the emission estimations, but it relies unfortunately on data not available on a real network.

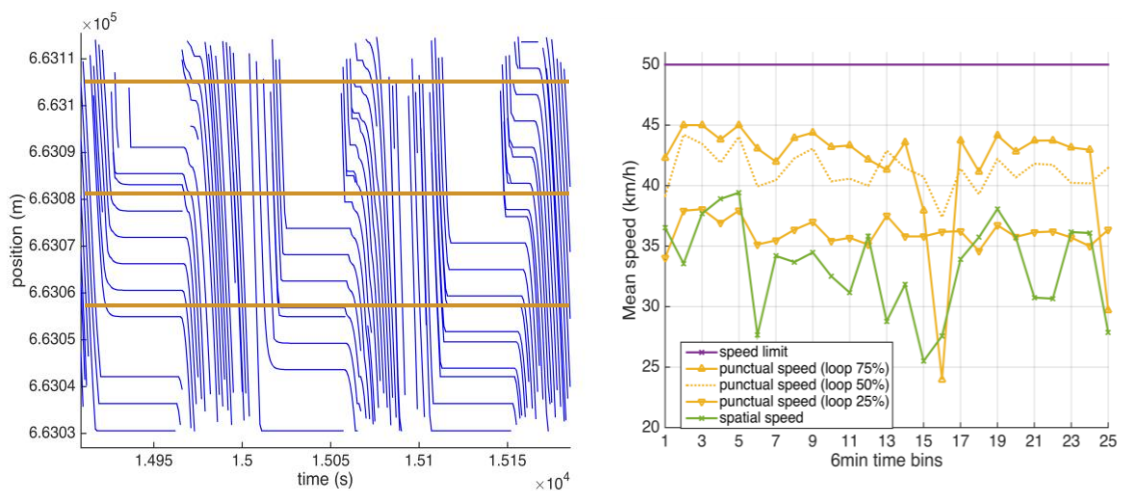


Figure 2 Traffic data: vehicle trajectories (left) – a link mean speed through 5 definitions (right)

These three speed definitions can differ significantly, in particular under congestion, as shown in Figure 2. As expected, the speed limit V_{limit} overestimates the actual speeds. Punctual loops often also result in speed overestimations, which is a long date acknowledged bias. Additionally, the dispersion between the speeds provided by each loop is significant. The resulting emission errors are estimated in the section 3.

Emission modelling

The two investigated emission model types are the modal model and the aggregated model, the implemented models being Phem and Copert IV, respectively. Only hot exhaust emissions are considered. The emission calculations were made at link level, combining the various traffic indicators to the two emission databases. The emissions have been estimated according to the Ifsttar French urban vehicle fleet for the year 2015.

COPERT

CopertIV has been widely used in most European Countries for elaborating the national emission inventories, but it is also extensively used for network emission modeling (Borge et al., 2012, Samaras et al., 2014). However, its use at spatial scales lower than the driving cycles is subject to questions, since the speed distribution might differ and lose representativeness over too small samples or specific traffic conditions (e.g. in the vicinity of intersections)(André & al. 2009). Different speed definitions are investigated in section 3.

As any aggregated emission model, Copert IV needs mean driving speed v (in km/h) and total distance d (in km) travelled for a given time period to predict the related exhaust emissions. The total emission e (in g) is derived from the unitary emission factors f (expressed in $g \cdot km^{-1}$), according to formula (1). Unitary emission factors consist of speed continuous functions constructed over driving cycles of about 6mn-length, which are representative of encountered traffic conditions. They are defined for each pollutant k and each vehicle technology l .

$$e^{k,l} = d^l \cdot f^{k,l}(v^l) \quad (1)$$

We will here consider the simplified formula including the repartition of vehicles over the various technologies for each category (passenger cars, light commercials vehicles, heavy duty vehicles and urban buses). The unitary emission function of a specific category is obtained by operating a weighted average of the vehicle technologies that compose the category. Indeed, even with the finest traffic information, the technology of the vehicle is not individually defined and the emission calculation is generally made at global fleet scale.

$$E^{k,c} = D^c \cdot F^{k,c}(V^c) \quad (2)$$

with $F^{k,c}$ the unitary emission factor (g/km) of pollutant k of one of the four categories.

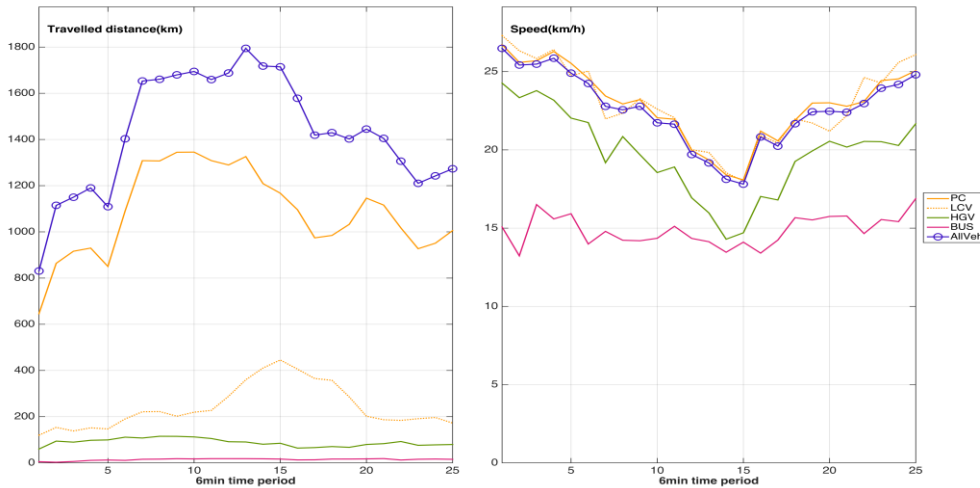


Figure 3 Macroscopic traffic variable experimented each 6min during the morning peak

The emission factors $F^{k,c}$ (in g/km) are defined for the French urban fleet in 2015, in function of the mean speed, over 10km/h, as described by Copert methodology. Though, at link scale, some of the 6mn mean speeds are assigned to a value lower than 10km/h. As emissions are definitely not insignificant at that speed range, the Copert emission curves were extended maintaining the emission factor value at that of 10km/h (straight extension).

PHEM

Phem (Passenger Car and Heavy Duty Emission Model) calculates the fuel consumption and emissions of vehicles based on the vehicle longitudinal dynamics and on engine emission maps, with a 1s time resolution. The model provides an estimate of the engine power of a vehicle at each time step (1s), based on its speed time series and road gradient. The engine speed is estimated based on the transmission ratios and a gearshift model.

Phem has been coupled with dynamic traffic platforms at several occasions, in order to test the impact on emissions of road traffic strategies that modify the vehicle kinematics behavior (Erdman & al. 2016). However, the inadequacy between its required high traffic data resolution and the available dynamic traffic model outputs, which are much less refined, is sometimes matter of questions.

3. Results

This section is devoted to the analysis of the emissions calculations. We will first observe the results with Copert and the impact of the speed definition on emissions assessment. The shape of the Copert emission curves motivates this first study. Indeed, a consequence of this particular shape is that the potential error on emissions is maximum around 35km/h for NOx emissions (respectively around 23km/h for fuel consumption), which is a common mean speed in a city center. Thus, relative error on emissions due to a bias on mean speed is expected to be significant at speed range corresponding to urban scale.

Here, the emissions were calculated at link scale every 6mn thanks to the corresponding traffic variables: distance travelled and mean speed for each vehicle category c . The emission for link-period (j,i) is defined for each pollutant k by the following formula :

$$E_{i,j}^{k,c} = D_{i,j}^c \cdot F^{k,c}(V_{i,j}^c) \quad (3)$$

where $V_{i,j}^c$ is deduced from traffic microsimulation from spatial or punctual virtual sensors. Summing on all the links, we can then observe the impact of speed definition on the emissions over the network.

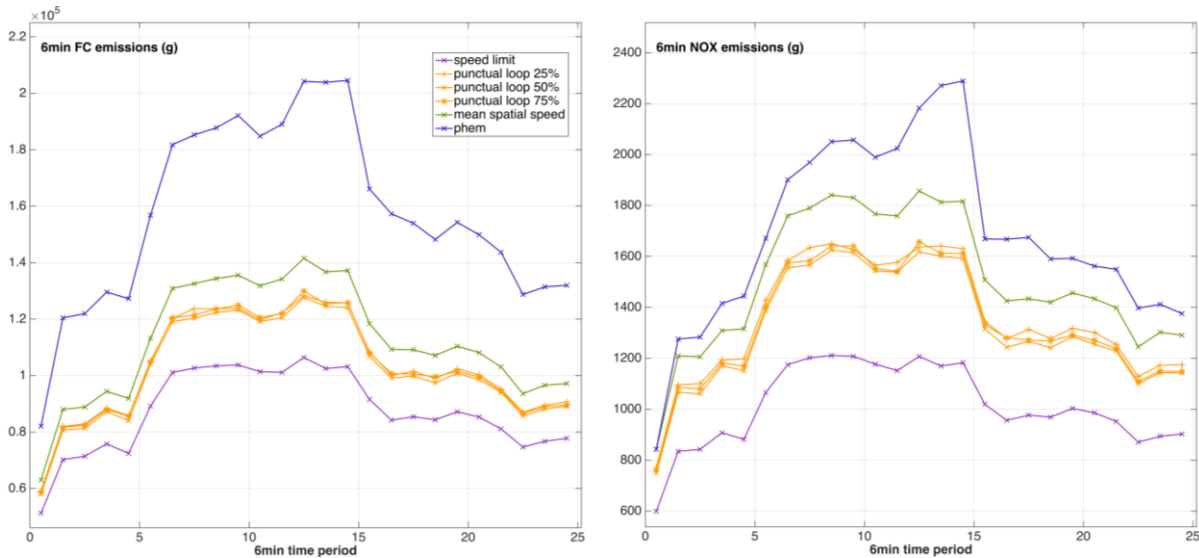


Figure 4 6min fuel consumption (left) and NOx emissions (right) over the network during the morning peak for the various speed definitions

The figure 4 represents the network emissions for each 6min period, obtained with Copert and the various speed definitions. Degraded speed definitions (speed limit and punctual loops) lead globally to underestimate the emissions. The discrepancies between the calculated emissions are also depending on time, with a maximum gap occurring at the more congested period.

The first observation is that, at network scale, the position of the virtual loop does not have a significant impact on the emission levels. We will then focus on the virtual loop positioned in the middle of the link (50% loop). The relative error compared to spatial mean speed has been quantified for each 6min period: for FC, this global error is varying between -3 and -5% with a loop detector (respectively -3 and -5% for NOx) and between -11 à -15% with speed limit (respectively -15 and -21% for NOx).

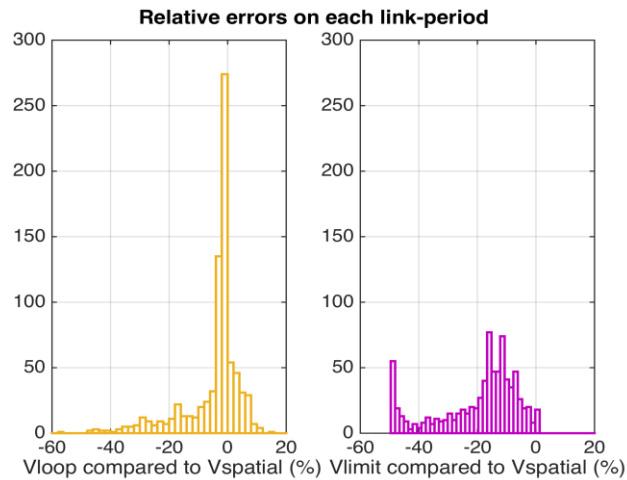


Figure 5 Distribution of relative errors on fuel consumption on links associated to a degraded definition of speed: Vloop (left); Vlimit (right).

The spatial analysis represented in figure 5 shows that the mean relative error for fuel consumption can be ranged from -60% to +20% locally, when using punctual loop definition. Yet, with speed limit definition, the fuel consumption is always underestimated, even locally and the relative error can reach -50%.

The figure 4 also represents the emissions evaluated thanks to the instantaneous model Phem. The implementation of this emission model being stochastic (see fig.6), the curve printed in figure 4 is the mean emission value over 10 replications. Indeed, the stochastic fleet definition impacts not only the local emission but also the network emissions. The mean global gap reaches 5.3% for fuel consumption, respectively 12.5% for NOx emissions.

This modal emission model admits the finest dynamic traffic representation (i.e. speed profiles) as input data. It is then not surprising to achieve higher emissions levels, especially for congestion periods. The gap between Copert emissions (with spatial mean speed) compared to Phem emissions has been quantified: the relative errors reach -33% for fuel consumption (respectively -21% for NOx emissions). We can observe a constant gap between the two models for fuel consumption, independent of the congestion. However, the relative errors are always more important in congested periods than in free-flow conditions.

In other words, the congestion peak is particularly underestimated with an aggregated emission model, which leads us to conclude that this bias is partially due to the use of mean speed, that poorly represents vehicle kinematics in bad traffic conditions.

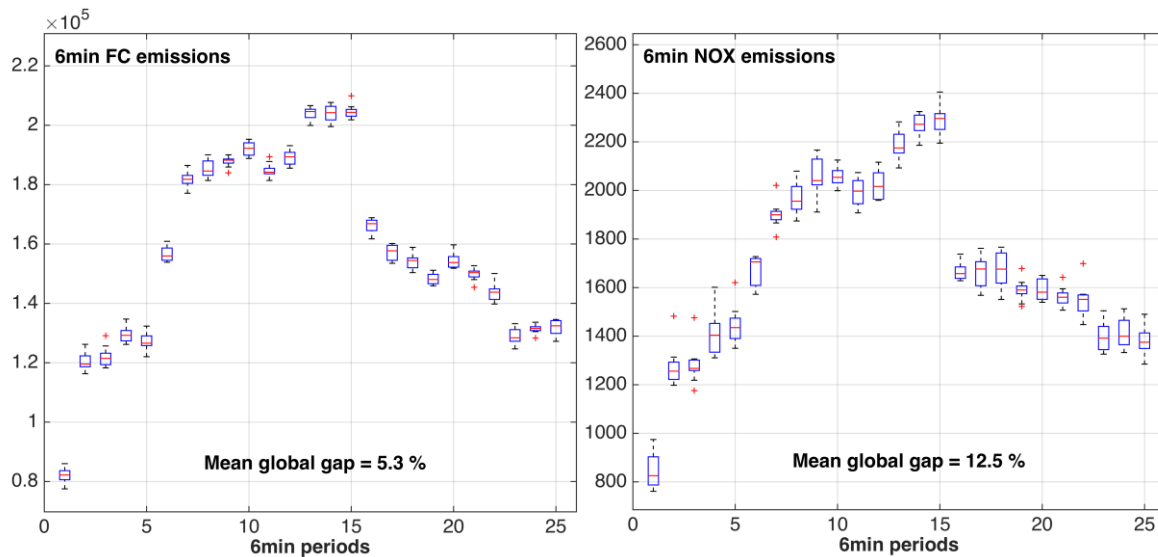


Figure 6Dynamic network Phem emissions resulting of ten replications.

Conclusion

This work proposed a comparison between emissions calculations from a traffic microsimulation, at large urban scale during the morning peak. The testing focused here on looking at the impact of dynamic traffic representations on emissions. This was made in comparing (i) the speed definition as an input data of aggregated emission model and (ii) the emissions evaluated dynamically with a macroscopic traffic variable on one-hand and speed profiles on the other hand.

We confirmed that an accurate representation of vehicles kinematics is needed in order to cope with congestion at urban scale. The use of a degraded speed definition in place of the spatial speed does impact the emissions: the global relative error on fuel consumption (respectively NOx emissions) is -3.8% (-4.3%) with loop detectors and -13.8% (-19.2%) with speed limit. This effect is reinforced in the most congested period and locally.

The use of the finest traffic representation (i.e. trajectories) can also conduct to inaccuracy: the parameter identified is the stochastic way to define the fleet that induces highly variable local emissions.

The differences between the twomodeling approaches can be partly explained by the differences between the two databases (hypothesis independent of traffic). However, we think it is possible to work at more coherent results between both models. In order to reach this goal, we will go ahead in working at (i) a better macroscopic traffic indicator compatible with Copert input data and (ii) taking into account more coherently the fleet definition in the two approaches, which is definitively a source of discrepancies.

Acknowledgments

Trafipollu project was supported by the National Research Agency fund *ANR-12-VBDU-0002-01*.

References

- Ahn, K., & Rakha, H. (2009). A field evaluation case study of the environmental and energy impacts of traffic calming. *Transportation Research Part D: Transport and Environment*, 14(6), 411–424.
- André, M., & Rapone, M. (2009). Analysis and modelling of the pollutant emissions from European cars regarding the driving characteristics and test cycles. *Atmospheric Environment*, 43(5), 986–995.
- Borge, R., de Miguel, I., de la Paz, D., Lumbreras, J., Pérez, J., & Rodríguez, E. (2012).

Comparison of road traffic emission models in Madrid (Spain). Atmospheric Environment, 62, 461–471.

De Vlieger, I., De Keukeleere, D., & Kretzschmar, J. . (2000). Environmental effects of driving behaviour and congestion related to passenger cars. Atmospheric Environment, 34(27), 4649–4655.

Edie, L.C., (1963). Proc. 2nd International Symposium on the Theory of Traffic Flow. OECD, pp. 139–154

Erdmann, J. (2016). Benefits of Using Microscopic Models for Simulating Air Quality Management Measures, 95th Annual Meeting of the Transportation Research Board.

European Commission (2015). European Union energy and transport in figures: statistical pocketbook. Luxembourg: Office for Official Publications of the European Communities.

Fallah Shorshani, M., André, M., Bonhomme, C., & Seigneur, C. (2015). Modelling chain for the effect of road traffic on air and water quality: Techniques, current status and future prospects. Environmental Modelling & Software, 64, 102–123.

Franco, Vicente, Marina Kousoulidou, Marilena Muntean, Leonidas Ntziachristos, Stefan Hausberger, and Panagiota Dilara (2013): Road Vehicle Emission Factors Development: A Review. Atmospheric Environment 70, 84–97.

Gkatzoflias, D., Chariton, K., Ntziachristos, L. and Samaras, Z. (2012) COPERT 4, European Environmental Agency.

Laval, J., Leclercq, L. (2008). Microscopic modeling of the relaxation phenomenon using a macroscopic lane-changing model. Transportation Research Part B, 42(6), 511-522.

Leclercq, L. (2007). Hybrid approaches for the solutions of the Lighthill-Whitham-Richards model. Transportation Research part B, 41 (7), 701-709.

Lu, X. C. (2016). A comparison and modification of car-following models for emission estimation. 95th Annual Meeting of the Transportation Research Board.

Ma, H., Xie, H., Huang, D., & Xiong, S. (2015). Effects of driving style on the fuel consumption of city buses under different road conditions and vehicle masses. Transportation Research Part D, 41, 205–216.

Qu, L., Li, M., Chen, D., Lu, K., Jin, T., & Xu, X. (2015). Multivariate analysis between driving condition and vehicle emission for light duty gasoline vehicles during rush hours. Atmospheric Environment, 110, 103–110. <http://doi.org/10.1016/j.atmosenv.2015.03.038>

Samaras, C., Ntziachristos, L., & Samaras, Z. (2014). COPERT Micro: a tool to calculate the vehicle emissions in urban areas. Transport Research Arena 2014, 10.

Shaughnessy, W. J., Venigalla, M. M., & Trump, D. (2015). Health effects of ambient levels of respirable particulate matter (PM) on healthy, young-adult population. Atmospheric Environment, 123, 102-111.

Smit, R., Ntziachristos, L., & Boulter, P. (2010). Validation of road vehicle and traffic emission models – A review and meta-analysis. Atmospheric Environment, 44(25), 2943–2953.

Vieira da Rocha, T., Can, A., Parzani, C., Jeanneret, B., Trigui, R., & Leclercq, L. (2013). Are vehicle trajectories simulated by dynamic traffic models relevant for estimating fuel consumption? Transportation Research Part D, 24, 17–26.

Vieira da Rocha, T., Leclercq, L., Montanino, M., Parzani, C., Punzo, V., Ciuffo, B., & Villegas, D. (2015). Does traffic-related calibration of car-following models provide accurate estimations of vehicle emissions? Transportation Research Part D, 34(c), 267–280.

Xu, X., Liu, H., Anderson, J. M., Xu, Y., Hunter, M. P., & Rodgers, M. O. (2016). Estimating Project-Level Vehicle Emissions with VISSIM and MOVES-Matrix. 95th Annual Meeting of the Transportation Research Board.

Zallinger M., Tate J., Hausberger S., Goodman P., (2009) Air Quality Conference, Istanbul.

Zhang, K., Batterman, S., & Dion, F. (2011). Vehicle emissions in congestion: Comparison of work zone, rush hour and free-flow conditions. Atmospheric Environment, 45(11), 1929–1939.

Market fuel properties and CO₂ emissions for mobility

Norbert E. Ligterink* & Gerben Geilenkirchen**

*Sustainable Transport & Logistics Group TNO Delft, Van MourikBroekmanweg 6, 2628 XE Delft The Netherlands, email: norbert.ligterink@tno.nl

**PBL Netherlands Environmental Assessment Agency, PO Box 30314, 2500GH The Hague, The Netherlands

Abstract

For international reporting of CO₂ emissions from road transport the Netherlands uses national figures on the CO₂ emissions for transport fuels, such as the CO₂ per kilogram fuel, and the CO₂ per MJ energy content. This study provides data to update the fuel-based CO₂ emission factors to the current situation. Fuels were collected at consumer fuel stations across the Netherlands in 2015. Both summer and winter fuels, of petrol and diesel, were included and analyzed for relevant physical-chemical properties. Heating value, density and carbon content were determined, among other aspects.

For diesel fuel the findings are in line with previous and international results. About 3.2% FAME is added to diesel, slightly lowering the heating value. The fossil component remains similar to the fossil diesel. For petrol fuel, the fossil component in fuel with bio-admixture is different from traditional fossil petrol without bio-admixture. In particular the heating value is lower, yielding a lower CO₂ reduction of the admixture of ethanol than based on the separate properties of traditional fossil petrol and ethanol. The variation of the fossil component also differs substantially between summer and winter petrol. Moreover, despite the constant admixture of ethanol in petrol, at 4.7%, the variations of the petrol lower heating value are substantial.

Keys-words: fuels, GHG emissions, carbon content, lower heating value.

1 Introduction

The Netherlands reports the CO₂ emission of road transport internationally as part of a number of international agreements (Coenen et al., 2016). Foremost, CO₂ is an important Greenhouse Gas (GHG) contributing to global warming. The total CO₂ emission is reported to the UNFCCC. Moreover, the monitoring of mitigation measures to reduce the GHG emissions relies on the accurate monitoring of relevant properties and quantities. The admixture of biofuels, which targets are set in the Renewable Energy Directive (RED), ensures the energy usage from renewable sources. For proper monitoring appropriate basic numbers are needed, such as the CO₂ emissions related to fuel sold [CO₂ g/g] and CO₂ emission related to the energy consumption [CO₂ g/MJ]. The Fuel Quality Directive (FQD) regulates that the appropriate values are used in the monitoring. The Netherlands uses specific national values for international reporting. In 2004 these numbers were last updated (Olivier, 2004), and with the increasing admixture of biofuels an update was appropriate. This paper presents an extended measurement campaign of fuel samples taken at the consumer fuel stations across the country.

The admixture of biofuels reduces the energy content of market fuels, because ethanol, FAME, MTBE, and ETBE do not have the same energy density as fossil fuels, petrol and diesel, from the refinery. In the national energy statistics of Statistics Netherlands (CBS), this effect is compensated for. However, the actual energy density of the fossil component of the mixture is unknown. Olivier (2004) already reported that the energy density exhibited the largest variation of all the relevant fuel properties, such as density and carbon fraction, affecting the CO₂ emissions. With the admixture of biofuels that was introduced since, it was unclear how this situation changed.

Underlying this discussion is not only the heating value but also the carbon content of the fuels. The carbon content of automotive fuels determines the greenhouse gas emissions of road transport. Hence, a good understanding of this carbon content and its variability in market fuels is also essential in determination of greenhouse gas emissions and the effectiveness of mitigation measures. In

particular, biofuel admixture is meant to reduce the total greenhouse but will affect the fuel composition, and therefore the carbon content. Moreover, it affects the fuel quality and therefore the variation in the amount of fuel needed for the same transport demand.

The different metrics of reporting carbon content are aimed at different ways of reporting greenhouse gas emissions:

- [g/g] carbon content is used to report the CO₂ emissions based on the fuel sold in weight units, typically at the source and in trade.
- [g/liter] carbon content is used to report CO₂ emissions based on refuelling information from consumer's fuel stations.
- [g/MJ] carbon content is used to compare different types of fuels and handle bio-admixture in a uniform manner.

In 2004 the last Dutch study was performed to determine the carbon content in the metrics above (Oliver, 2004), and these results have been used until now in the official reporting of greenhouse gas emissions by road transport in the Netherlands (Coenen et al., 2016). Separately, JRC/CONCAWE has provided in the past the carbon content in all of these three metrics, as shown in Table 1. The 2006 IPCC guidelines are roughly based on this information.

Table 1 JRC/Concawe typical values for market fuels

Fuel		Density	LHV	Carbon	CO ₂ emissions		
		kg/m ³	MJ/kg	%m	kg/kg	g/MJ	g/l
Gasoline	2002	750	42.9	87.0	3.19	74.35	2393
	2010	745	43.2	86.5	3.17	73.38	2362
Ethanol		794	26.8	52.2	1.91	71.38	1517
Diesel	2002	835	43.0	86.2	3.16	73.54	2639
	2010	832	43.1	86.1	3.16	73.25	2629

Already in 2004 it was observed that the largest variability in the fuel was the heating value, and not the density or weight fraction of carbon. Hence, in the current study special attention was given to ensure sufficient data was collected to investigate issues concerning the caloric value. With bio-admixture, the heating value is expected to decrease according to the weight fractions of the different components in the fuel. For example, based on standard JRC/Concawe figures as shown in Table 1, one could conclude that the lower heating value of e.g. 4.5% mass fraction of ethanol admixture will lead to a reduction of the heating value from 43.20 MJ/kg to 42.46 MJ/kg. This is a 1.7% reduction of energy in a kilogram of fuel. The fossil component has a higher energy density, and replacing it with ethanol will reduce the energy density. Consequently, a 4.5% admixture of ethanol does not yield a similar percentage reduction in CO₂ emissions for the same energy. The admixture of 4.5% ethanol, without associated CO₂ emissions, corresponds to 2.8% reduction in CO₂ emissions based on the energy from renewable sources, in this case. These effects are taken into account in the national energy statistics, as shown in Table 2, where the fossil component of the fuel and the bio-admixture are reported separately. The fossil component has a caloric value of 44 MJ/kg, combined with 5% ethanol, a net market fuel of 43.2 MJ/kg is reported as expected based on the exercise above.

Table 2 The data used to determine energy usage and CO₂ emissions for road transport fuels, as provided by Statistics Netherlands for the Dutch emission inventory

basis data IPCC as used by CBS		year	2002	2003	2004	2005	2006	2007	2008	2009	2010	2011	2012	2013	
density	benzine	kg/liter	0.747	0.750	0.750	0.749	0.750	0.750	0.748	0.748	0.748	0.748	0.748	0.747	
	biobenzine	"					0.750	0.750	0.748	0.750	0.748	0.748	0.750	0.750	
	dieselolie	"	0.836	0.837	0.837	0.836	0.836	0.837	0.837	0.836	0.837	0.838	0.838	0.837	
	biodiesel	"		0.885	0.885	0.885	0.885	0.885	0.879	0.884	0.884	0.882	0.884	0.884	
heating value															
heating value	benzine-totaal	MJ/kg	44.0	44.0	44.0	44.0	43.9	43.5	43.4	43.1	43.2	43.1	43.2	43.2	bioadmixture
	benzine-fossiel	"	44.0	44.0	44.0	44.0	44.0	44.0	44.0	44.0	44.0	44.0	44.0	44.0	
	biobenzine	"					27.9	27.9	27.8	27.1	27.0	27.0	27.0	27.0	
	dieselolie-totaal	"	42.7	42.7	42.7	42.7	42.5	42.5	42.5	42.6	42.5	42.5	42.5	42.5	bioadmixture
	dieselolie-fossiel	"	42.7	42.7	42.7	42.7	42.7	42.7	42.7	42.7	42.7	42.7	42.7	42.7	
	biodiesel	"		36.9	36.9	36.9	36.9	36.9	36.9	37.1	37.0	37.0	37.0	37.0	37.0

The reduction of the lower heating value of different bio-admixtures for the market fuels is known and understood. However, most bio-admixtures are oxygenated fuels. The burn characteristics of oxygenated fuels are typically good, and lead to a fast and stable flame. Hence it is possible to achieve the proper fuel quality, as required by the Fuel Quality Directive (FQD), with the use of oxygenated fuels, from a base fuel outside the fuel specification. Therefore, it may be possible to use a different base fossil component; not satisfying the fuel specifications from the FQD, and bring it into specification by the use of bio-admixture. The quality of the base fuel and how it will affect the market fuel is part of this study. Therefore, there is some redundancy build into the chemical analyses. In the case of similar bio-admixture, it can be tested whether the main fuel characteristics are the same. Variations in the fuel composition with the same bio-admixtures means that the here relevant fuel properties are not fully controlled by assigning only end criteria of market fuels. The original fuel specification was based on refinery products, with further adaptations to allow for bio-admixture. For example, fossil fuel can contain only a very minor amount of water, but with the admixture of ethanol, the amount of water petrol can contain increased manifold. There is, however, no specification for water content beyond the "clear and bright" requirement, i.e., no separated water or bubbles.

The water content in fuels is therefore another aspect of this new fuel landscape, which is the result of bio-admixture. Oxygenated fuel may contain a substantial amount of water without separation occurring. Pure hydrocarbons allow only very little water before the fuel turns cloudy. Well known is the water in ethanol, which is difficult to remove completely. In the EN 228 fuel specification there is no specification for water content, except for the "clear and bright", and it was impossible to have much water blended in hydrocarbons. The ethanol added to the fuel may contain 0.3% water, according to EN 15376, tested according EN 15489. This would mean that with the typical admixture of 4.5% ethanol, 0.0135% water can be in petrol as result of the ethanol admixture. In practice the water content is always higher. With the other oxygenated components: MTBE, ETBE, and methanol some additional water can be in the fuel, but the water concentration almost always exceeds the maximum allowable fraction that can arise from the oxygenated components. In hydrocarbon fuels, large amounts of water will separate from the hydrophobic fuel and a small amount of water will show as cloudiness. This effect will depend strongly on the temperature.

In 2015 fuel samples were collected from fuel stations for consumers. Due to the high cost of chemical analyses, special care is taken to have a representative sampling, rather than a random sampling of market fuels.

2 Sample collection

It is expected that different fuel companies use the same depot fuels. Hence, it is essential to ensure a proper variation in the collected fuels to collect across the Netherlands in different distribution and safety regions because fuel transport is not likely to be interregional. In this manner different depot fuels are sampled.

Moreover, the fuel is collected at different fuel companies to ensure the fullest variation. The collection was carried out in three periods of about ten days each:

- The first winter fuel samples (24 - 31 March 2015);
- The summer fuel samples (14 - 26 August 2015);
- The second winter fuel samples (23 December 2015).

The fuel was collected by TNO employees who participated according to their travelling to different regions of the Netherlands. The sample bottles were special wide-neck fuel-sample bottles of glass with a double cap (soft plastic inner cap to reduce spillage, and a hard outer cap to avoid diffusion of volatile fractions). The bottles were handed out closed, and opened solely at the moment of collecting at the refuelling stations.



Figure 1 The sample bottles of the summer fuel collection: all clear and bright, but with a large variation in colour.

The refuelling stations were of nine different fuel companies, including brand names and budget stations. No brand-less stations (“wittepompen”) were selected. Fuel companies who advertise with special fuels, outside the diesel and petrol (Euro-95 and Euro-98, suitable for Euro-4 and older vehicles) specification were excluded from the sample collection. In this paper “premium” petrol is the octane 98 petrol suitable for certain older vehicles. In the Netherlands “premium” is also understood as brand fuels with special additives (Shell Fuel Save, BP Excellium, Texaco XL, Esso Synergy, etc.). These fuels were not selected. “Premium” refers in this study to regular Euro-98 “Super”. No other premium fuels were sampled, only regular fuels with the two octane numbers. Since only a few samples were collected per brand, the brand names are not reported. The deviating findings may have been accidental for the particular brands and it is not known if findings are systematic.

The number of samples is limited, due to the high cost of chemical analyses. The variations for some fuel properties are large, but are expected to give the bandwidth of common Dutch market fuels.

3 Sample analysis

In the first chemical analyses of the first batch of winter fuels, the composition of petrol was not requested. The results, showing large variation in caloric value, raised questions about the actual composition of the fuels, so that in the subsequent analyses the composition was determined as well.

The chemical analyses were carried out by a specialized and certified chemical laboratory. It contained the following analyses:

- regular petrol (Euro-95):
determination of density, C-H-N fractions, LHV, aromatics content, H₂O
- “premium” petrol (Euro-98): (~3% market share)
determination of density, C-H-N fractions, LHV, aromatics content, H₂O
- Diesel:
determination of density, C-H-N fraction, FAME content, LHV

The analysis methods used were:

For all fuels:

- C,N,H content fractions via ASTM D5291
- Density via EN ISO 12185
- Heating value (LHV) via ASTM D240 (using ASTM D5291)

Specific analysis for diesel:

- FAME content via EN 14078

Specific analyses for petrol and premium (second and third batch):

- Chemical composition via EN ISO 22854
- Water content via EN ISO 12937

In principle all fuels satisfy the EN 590 (Diesel) or the EN 228 (Petrol) fuel specifications. In the Netherlands there is only a legal obligation to satisfy the reduced specification of the Fuel Quality Directive. The Inspection authority of Transport and Environment (ILeT) sees to that. The current analyses only have a minor overlap with these specifications (density and aromatics content) and implicitly via EN ISO 15376, for the requirements of the ethanol prior to admixture, some upper limit to the consequent water content of petrol is determined.

4 Results

The current results should be compared with the official numbers, for fossil fuels, used in the UNFCCC and EU reporting by the Netherlands:

- Petrol 72.0 g/MJ, 44.0 MJ/kg (IPCC 2006: 44.3, RED: 43.0)
- Diesel 74.3 g/MJ, 42.7 MJ/kg (IPCC 2006: 43.0, RED 43.0)

The national numbers take prevalence over the IPCC guidelines. In particular the current findings show a deviation for petrol, also after being compensated for the ethanol content.

Especially the heating value of petrol shows unexplained variations across the samples, as shown in Table 3. Given that the same test method yields very stable results for diesel, and the re-testing of samples shows minimal variations, it is expected the results can be taken at face value. The issues concerning the fuels are not limited to particular brands or brand segments.

Table 3 The results from the test program, with the variations therein defined as the standard deviation divided by the average. This includes the bio-admixtures, the fossil components are determined from subtracting the average admixtures.

	petrol				diesel			
	winter	variation	summer	variation	winter	variation	summer	variation
density [g/ml]	730.4	0.7%	745.5	0.6%	835.4	0.4%	833.6	0.5%
heating value [MJ/kg]	42.34	1.2%	40.96	5.5%	42.98	0.8%	43.05	0.4%
carbon content [%]	83.88	1.1%	84.23	0.7%	85.19	1.1%	84.98	0.6%
total CO ₂ emissions								
CO ₂ [g/g]	3.076		3.088		3.124		3.116	
CO ₂ [g/MJ]	72.64		75.39		72.68		72.38	
CO ₂ [g/l]	2246		2302		2609		2597	
fossil only	excluding 4.69% ethanol				excluding 3.18% FAME			
CO ₂ [g/g]	3.133		3.146		3.133		3.125	
CO ₂ [g/MJ]	72.69		75.52		72.59		72.27	
heating value [MJ/kg]	43.10		41.66		43.17		43.24	

The caloric value results of the summer petrol are heavily influenced by one outlier at 34.87 MJ/kg. This sample was tested again a few weeks later (some deterioration may have occurred) with a similar result at 34.76 MJ/kg. Excluding this exceptional sample the average of summer petrol was 41.71 MJ/kg (+/- 1.7%). However, without an apparent fault in either the measurement, other properties, and the collection of the sample, the sample should be included in the average. These values are much lower than the value of 43.2 MJ/kg (44 MJ/kg for the fossil component, therefore based on 5% ethanol admixture) currently used by Statistics Netherlands, as shown in Table 1.

The physical properties, such as carbon content, heating value, and density are based on the available samples. The detailed composition is only available for a limited subset. In this set there is a clear distinction between Euro-95, the largest fuel group, and Euro-98 which plays a minor role in total sales. The former has mainly ethanol admixture at 4.69% and some MTBE at 1.84%, while the latter has a substantial amount of MTBE but no ethanol. From bio-MTBE only 36% is bio-component, and the heating-value attribution should be based on methanol. However, MTBE is also added as anti-knocking agent and possibly not from renewable sources. The bio-MTBE altogether is not fully renewable, as it is derived from bio-methanol and hydrocarbons. The latter is typically fossil and has the higher heating value of the two components. Assigning the CO₂/MJ according to weight to the bio-admixture overestimates the CO₂ reduction of MTBE. Currently, only a minor fraction of the MTBE and ETBE are bio-admixture. It is therefore assumed the MTBE found in the samples is fossil only.

The winter samples were collected in two consecutive winters. The results of the first winter show a much wider variation in heating values than the results of the second winter. The second set of samples, collected in December 2015, were more homogeneous.

In the results the carbon content is somewhat lower than would be expected on the basis of the common used data from the literature. This lowers the CO₂ emissions based on fuel sold, in weight units, somewhat. On the other hand the density of petrol is lower than both the CBS and JRC use, which means that the energy content per litre of fuel sold is lower compared to the commonly used figures, based on the density and energy per kilogram.

The diesel results are very stable for heating value, density, and carbon content, although the variation of FAME content is large for both the summer and winter fuels. Higher FAME content yields on average a marginally lower heating value and density. The FAME has average admixtures fractions in the winter fuel of 3.1% and the summer fuel of 3.2%. The annual average from these samples is 3.18%, with a wide variation. The consequences thereof are limited, as FAME has a relatively high heating value at 37.2 MJ/kg. (Concawe/JRC, 2013) On average the reduction of caloric value per kilogram is therefore only 0.4%.

In the future it is expected HVO will be added to diesel, as there is no restriction on the amount of HVO that can be added. Using HVO it is therefore easier to achieve the renewable energy targets of the RED. Currently, negligible other oxygenated components, apart from FAME were established. However, for future fuel monitoring this must be taken into consideration.

For the petrol fuels different analyses were performed, based on the expected admixture of ethanol. Water was determined in most of the samples. The amount of water is well below 1% with an average of 0.032% with a variation around it, but large compared to the expected value based on the admixture of dry ethanol, which is in the order of 0.015%. None of the samples has this low amount of water. In some cases ETBE and MTBE were added, but this cannot explain the amount of water either, except in a single case where 12% MTBE with the allowable 5% water would result in 0.6 g/kg water in the fuel.

In particular the premium petrol ("super" or Euro-98) does not contain much ethanol, but mainly MTBE and some ETBE instead. Clearly, these chemical components are even better suited to improve the fuel specification of petrol. The admixture of MTBE and ETBE is allowed to a higher fraction than ethanol. This may lead to a lower heating value, as both MTBE and ETBE have lower heating values than the fossil fuel. The reduction of heating value is shown in Table 4.

Table 4 The reduction of heating value from the admixture of different components: for example, 4.5% weight admixture of ethanol will result in $4.5\% \times 0.38\% = 1.7\%$ lower heating value.

	reduction in LHV
Ethanol	38.0%
MTBE	18.8%
ETBE	16.0%
FAME	13.7%

The actual petrol composition was determined only later in the project, as the first results showed large and unexplained variation. Based on the last three sets of samples, ethanol has a very constant admixture in Euro-95 of 4.69% with a relative variation of 2.9% (absolute 0.14%). This can therefore not explain the variation in heating values at all, which would be, based on the variation in ethanol admixture, is the order of 0.05%. Likewise, the different Euro-98 samples have similar compositions with MTBE and ETBE which differ only marginally, and the variation in heating value cannot be explained from the bio-admixtures. The origin of the unexpected low heating values of petrol must therefore be in the base, or refinery, fuel. No proper explanation, for example in the detailed composition, is found as yet.

5 Discussions and conclusions

In the discussions regarding fuels and the GHG emissions they produce during combustion there are many stakeholders and different contexts. The stakeholders often have complementary views:

- Consumers would like the fuel, for which they pay per litre, to provide the energy for the propulsion of their vehicle. The relevant unit is therefore MJ/litre. Moreover, they assume the fuel to satisfy specification which will not lead to damage of the engine.
- The official CO₂ emissions in the national inventory are reported based on fuel sold. These figures are reported to Statistics Netherlands in kilogram. The total GHG emissions are therefore related to the carbon content in g/g.
- The total bio-admixture as specified in the Renewable Energy Directive and monitoring requirements in the Fuel Quality Directive is based on the replacement of fuels according to the energy they supply, as different fuels have different heating values per litre or kilogram. In

particular ethanol has a lower heating value, adding 5% ethanol will not reduce the CO₂ emission by 5%, but by a lower number. The relevant unit for such reporting is the CO₂ emissions in g/MJ.

- Engine manufacturers design and calibrate their engines and fuel systems on the basis of fuel specifications. If these fuel specifications allow for a large variation in the composition from bio-admixture, it may lead to reduced engine power, engine malfunctioning and maintenance problems.

The main problem observed in the chemical analyses of the market fuel is the low heating value of petrol and the large variation therein. In particular the summer petrol is affected. Consequently, consumers will have less energy per litre, and it requires more fuel to fulfil the same mobility demand. The results are not explained by the bio-admixture. The 4.69% ethanol admixture would lead to 1.8% lower heating value in MJ/kg, from 44 MJ/kg down to 43.2 MJ/kg. Instead the heating value (average over summer and winter petrol) is 3.5% lower. This indicates that the effect GHG emission reduction of bio-admixture in petrol is less than half of what is now assumed. With the bio-admixture there is generally a lower heating-value of the fossil component than the fossil petrol, and more fuel is needed for the same energy demand. For the determination of bio-admixture, and fossil CO₂ emission reduction, the results presented here may have most consequences.

The different conversion numbers used by the stakeholders involved in the Fuel Quality Directive, in particular the effectiveness of bio-admixture based in the metric of g/MJ CO₂ emissions, should be reviewed. This study, carried out by a single chemical laboratory, is only limited in the number of samples and the explanations of the differences that were found. The most likely cause of the differences found are the properties of the base fuel, or refinery product. It is unlikely the base fuel, prior to bio-admixture, already satisfies the fuel specification.

The large variation in petrol properties across the samples and the significant change from the currently used values should be examined further. In particular, a monitoring of average heating value over time should be set up. This can be performed by collecting several samples for a single analysis of the heating value and composition, and repeat this several times a year.

Given the variation of heating value of petrol with oxygenated components, it may also be that in the type-approval test high quality fuel is selected with lower CO₂ emissions, different from the market fuels. So far, with the current fuel specifications does not seem adapted fully to the modern fuel blends.

Acknowledgments

This study was carried as part of the Dutch Program on Pollutant Release and Transfer Register (www.emissieregistratie.nl).

References

- Coenen, P.W.H.G., Maas, C.W.M. van der, Zijlema, P.J., et al. (2016), Greenhouse gas emissions in the Netherlands 1990-2014. National Inventory Report 2016, RIVM Report 2016-0047, National Institute for Public Health and the Environment, Bilthoven.
- Olivier, J.G.J. (2004), Netherlands' CO₂ emission factors for petrol, diesel, and LPG, J.G.J., MNP memorandum, December 200.
- Kyriakides, A., et al. (2013), Evaluation of gasoline–ethanol–water ternary mixtures used as a fuel for an Otto engine, *Fuel* 108 (2013) p. 208-215.
- P.J. Zijlema (2015), Nederlandse energiedrager lijst en standaard CO₂ emissiefactoren, versie april 2015, RVO.
- CBS website: www.cbs.nl
- JRC/Concawe (2013), TTW report.

Developments on Eco-innovations: procedure and calculation examples

Stefano MALFETTANI*, Chiara LODI*& Pierre BONNEL*

**European Commission, Joint Research Centre, Institute for Energy and Transport, Sustainable Transport Unit, Via E. Fermi 2749, 21027 Ispra (VA), Italy
Tel +39 0332 789424 - email stefano.malfettani@jrc.ec.europa.eu*

Abstract

The transport sector is the second largest source of GHG emissions in the EU with road transport being responsible for more than two thirds of transport-related GHG emissions. Passenger cars alone represent around 12% of total European CO₂ emissions. The EU has adopted a range of policies aiming at lowering emissions from the transport sector.

This paper focuses on the latest developments in the European eco-innovation scheme for reducing CO₂ emissions from vehicles, with a focus on electrical components. The European eco-innovation scheme is a part of the legal framework to reduce the CO₂ emissions from vehicles. To help manufacturers to meet their CO₂ emissions targets, Regulation (EC) No 443/2009 and Regulation (EU) No 520/2011 provide the opportunity to take into account CO₂ savings from innovative technologies, 'eco-innovations', which cannot demonstrate their CO₂-reducing effects under the Type 1 test procedure used for vehicle type approval.

The process for approving applications for eco-innovations is illustrated: discussion on the candidate application, official assessment, Decision publication and type approval certification. In order to analyse the overall procedure, LED technology is taken as relevant examples. The paper presents how a simplified reproducible and wide applicable testing procedure has been defined. The differences between the comprehensive methodology and the simplified approach are identified. The impact of different eco-innovations fitted to one vehicle on the total CO₂ savings is also briefly discussed.

Keys-words: *Transport Technologies, CO₂ emissions, Energy Efficiency, Real World Driving, Eco-innovation.*

Introduction

The European Union (EU) is committed to reducing greenhouse gas emissions (GHG) under the Europe 2020 Strategy (EC 2010) and the Kyoto Protocol's second period (2013-2020). The second biggest source of GHG emissions in the EU is the transport sector; in particular road transport is responsible for more than two thirds of transport-related GHG emissions (EC 2016b). Transport is the only sector that increased emissions in the EU over the period 1990-2012: an increase of over 14 %, yet with a downward trend since 2007 (EC 2014c). Passenger cars alone represent around 12% of total European CO₂ emissions (Hill et al. 2012). A range of policies aiming to lower emissions from the transport sector has been adopted by the EU (EC 2011c). For example, the EU legislation sets binding CO₂ emissions targets for new passenger car (M1) and light commercial vehicle (N1) fleets (EC 2009; EC 2011b). In 2015, newly registered cars were required to emit no more than an average of 130 grams of CO₂ per kilometre (gCO₂/km), expressed as fleet average per car manufacturer. By 2021, phased in from 2020, the objective for all new cars is 95 grams of CO₂ per kilometre. Compared with the 2007 fleet average, the 2015 and 2021 targets represent reductions of 18% and 40% respectively. Light commercial vehicle (N1) fleets are also required to meet average fleet target of 175 gCO₂/km by 2017 and 147 gCO₂/km by 2020.

The technical procedures to assess the CO₂ performance of cars and vans in Europe are twofold. First, the traditional laboratory test based on a driving cycle (currently the New European Driving Cycle, NEDC) provides the CO₂ emissions under reference conditions, . Because of the inadequacy of the NEDC and other elements of testing procedure to catch the actual vehicle performance (Meyer & Wessely 2009; Fontaras & Samaras 2010; Weiss et al. 2011; Fontaras & Dilara 2012; Sileghem et al. 2014; Martin et al. 2015), additional procedures - the so called eco-innovation scheme (EC 2011a; EC 2014b) – have been proposed to assess the performance of technologies whose effects cannot be observed or quantified properly while driving the vehicle on the laboratory Type 1 test, e.g. electrical consumption under real-word conditions or the use of ambient energy sources.

Applications for eco-innovations may be submitted by either vehicle manufacturers or components suppliers. The application must include the necessary evidence that the eligibility criteria are fully met, including a methodology for measuring the CO₂ savings from the innovative technology (EC 2011a). One of the eligibility criteria is that the minimum reduction achieved by the innovative technology has to be 1 g CO₂/km; this minimum threshold (MT) can be reached also combining technologies with similar technical features and characteristics (technology package). The decision to approve the technology as eco-innovation shall specify the information required for the certification of the CO₂ savings and it may be used by manufacturers for the purpose of certifying the CO₂ savings as part of the type approval process. The total contribution that a manufacturer may take into account for reducing its specific emissions target in a given calendar year is 7 gCO₂/km.

For the quantification of the CO₂ savings of the innovative technologies, the approved methodologies have to be used (EC 2011a). Two types of methodologies have been defined within the legislative framework: the simplified approaches, based on predefined functions and average data, and the comprehensive methodologies, defined with the use of extensive vehicle and hardware testing. In order to facilitate a wide application of the eco-innovation scheme, methodologies for the quantification of the CO₂ savings should be based on simple, stable, reproducible and general procedures. Another important aspect is the combination of approved methodologies for the evaluation of the total CO₂ savings when a vehicle is fitted with more than one eco-innovation.

To accomplish these needs, this paper presents how the methodologies for the evaluation of the CO₂ savings have been modified to reach a more simplified testing procedure. The differences between comprehensive methodology and simplified approach are identified and a relevant example on LED lighting is presented. The impact of different eco-innovations fitted to one vehicle on the total CO₂ savings is also briefly discussed.

1. Methods

1.1 Legal background

Regulation (EU) No 725/2011 and Regulation (EU) 427/2014 establish a procedure for the approval and certification of innovative technologies for reducing CO₂ emissions from passenger cars and light commercial vehicles pursuant to Regulation (EC) No 443/2009 and Regulation (EU) No 510/2011. These Regulations specify the eligibility criteria and sets out the procedures. The Technical Guidelines for the preparation of applications for the approval of innovative technologies (EC 2015b) provide additional information on how to prepare the applications as well as practical examples of potential technologies and testing methodologies.

The European eco-innovation procedure can be summarized in the following phases (see Figure 1):

- Discussion on the draft application (optional): an informal discussion between the potential applicant and the EC may be beneficial to set up the basis of the application and define a methodology to evaluate the benefits of the technology. The results of the informal discussion do not constitute any legal commitment on the part of the Commission.
- Submission of the official application by the applicant: the application should contain the description of the technology and the corresponding methodology and the report of an independent verifier.
- Assessment of the application: once the application is found to be complete, the Commission has 9 months to finalize the assessment and take a decision to approve or reject it. In case of complex application, the assessment period may be extended by 5 months. In practice this work is divided between the EC Joint Research Centre (JRC) that carries out the technical assessment and the Directorate General for Climate Action that is responsible for preparing the final decision to be adopted by the Commission.
- Approval of the eco-innovation: following a consultation of other Commission services the decision is finally adopted by the Commission and is published in the Official Journal of the European Union.
- Recording of the eco-innovation savings: the type approval authority certifies the savings if the manufacturer can demonstrate that they are 1gCO₂/km or more for the relevant vehicle version. When a vehicle is fitted with more than one eco-innovation, the effect of interaction on

the total CO₂ savings has to be taken into account. The certified savings will be indicated in the certificate of conformity of the vehicles concerned.

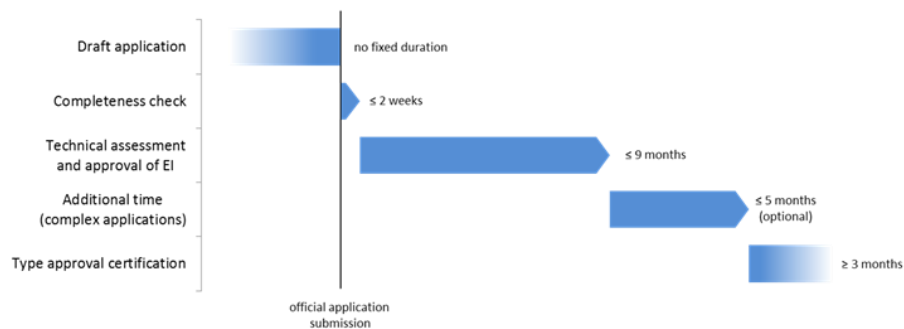


Figure 1. The eco-innovation procedure.

As of February 2016 fifteen applications for eco-innovation have been approved, seven applications are under assessment and several applications are expected to be submitted within the near future. The currently approved technologies are concerning the improvement of electrical and mechanical components, the storage and use of wasted energy and the use of potential energy.

The application for an approval of an innovative technology as eco-innovation has to include a testing methodology which is suitable to quantify the CO₂ saving effect of the technology. The methodology has to provide accurate and verifiable results. In principle, a measurement, a modelling approach or a combination of both may be applied. Two types of methodologies have been defined: simplified approaches, based on predefined functions and average data, and comprehensive methodologies, defined with the use of extensive vehicle and hardware testing. A mixture of the 'comprehensive methodology' and the 'simplified approach' is in principle possible. A list of approved eco-innovative technologies and their corresponding testing methodologies is presented in Table 1. Both simplified approaches and comprehensive methodologies are normally based on input data which represent values for mean European conditions.

Table 1. Summary of approved eco-innovative technologies and corresponding type of methodology (as of February 2016)

Eco-innovative technology	Applicant	Type of methodology
LED lighting	AUDI AG	Comprehensive
Efficient alternator	Valeo Equipments Electriques Moteur	Simplified
Engine compartment encapsulation	Daimler AG	Comprehensive
Navigation-based preconditioning of battery state of charge	Robert Bosch Car Multimedia GmbH	Comprehensive
LED lighting	Automotive Lighting Reutlingen GmbH	Simplified
Efficient alternator	Denso Corporation	Simplified
Battery charging solar roof	Webasto Roof & Components SE	Simplified
Efficient alternator	Robert Bosch GmbH	Simplified
LED lighting	Daimler AG	Simplified
Battery charging solar roof	Asola Technologies GmbH	Simplified
Efficient alternator	Mitsubishi Electric Automotive Europe BV	Simplified
Coasting	Porsche AG	Comprehensive
Efficient alternator	Denso Corporation	Simplified
LED lighting	Toyota Motor Europe	Simplified
Efficient motor generator	Mitsubishi Electric Automotive Europe BV	Simplified

1.2 Methodology

Our analysis is focused on the methodologies for the evaluation of the CO₂ savings from eco-innovation. An example is presented on the evolution of methodologies from comprehensive to simplified approaches. The example is based on LED technology. The effect of different EIs fitted to one vehicle is also evaluated and a calculation of the effect of interaction in final CO₂ savings is presented.

2. Results

2.1 LED lighting: from comprehensive methodology to simplified approach

In a vehicle, 12 exterior lights can be fitted with efficient lighting: low beam headlamp, high beam headlamp, daytime running light (DRL), front position, fog–front, turn signal–front, turn signal–side, center high-mount stop light (CHMSL), rear position, stop, fog–rear, turn signal–rear, license plate and reversing lamps. While the technological improvement for DRL, CHMSL and stop lamps is fully covered by the standard type approval measurements, for the other lighting functions a testing methodology has been developed to evaluate their off-cycle CO₂ benefits.

In March 2013 LED (Light-Emitting Diode) lighting technology has been approved as innovative technology. This innovative technology replaces conventional (halogen) lights for more efficient exterior lighting. As of February 2016, four applications have been approved for LED lighting (EC 2013; EC 2014a; EC 2015a; EC 2016a).

To evaluate the benefits of LED lighting, two different methodologies have been approved: a comprehensive methodology (EC 2013) and a simplified approach (EC 2014a; EC 2015a; EC 2016a).

The comprehensive testing methodology for LED lighting consists of the following 3 steps:

- Step 1 – Determination of the electrical power savings by measuring the average electrical power of innovative lamps and comparing the result with the average electrical power of conventional lamps (baseline)
- Step 2 – Determination of the CO₂ savings due to the saved electrical power by comparing CO₂ emission measurements of the vehicle on a chassis dynamometer with and without an electrical consumer. In order to ensure repeatability of the measurement, the power of the additional electrical load must be significantly higher than the potential electrical power saving of the efficient lighting system (i.e. 750W)
- Step 3 – Calculation of the CO₂ savings by relating the measured electrical power savings (under Step1) to the CO₂ savings determined in Step 2. The results are then weighted to consider the (time share) real-world usage factor of each lighting functions

This approach requires several vehicle tests on a chassis dynamometer. To overcome this burden, a simplified approach has been approved to evaluate the benefits of LED lighting. It requires only measurements of the average power consumption for each efficient exterior LED light, as required also in step 1 of the comprehensive methodology. The CO₂ savings are deducted using average 'consumption of effective power' values. The 'consumption of effective power' has been evaluated following the 'Willans' approach (Heywood 1988).

The simplified approach is defined by the following equation:

$$C_{CO_2} = \left(\sum_{i=1}^m \Delta P_i \cdot UF_i \right) \cdot \frac{V_{Pe} \cdot CF}{\eta_A \cdot v} \quad (1)$$

The mean driving speed of the NEDC (v) is 33.58 km/h (EC 2014a).

It has been demonstrated that CO₂ savings are higher than 1 gCO₂/km with a pack-age composed by at least LED low beam headlamps (EC 2013). Other common packages are also including high beam headlamp, front position and license plate LED lightings (EC 2013; EC 2014a; EC 2016a).

For both the comprehensive and simplified approaches, the statistical errors have to be quantified. It must be demonstrated for each type, variant and version of a vehicle fitted with the

package of the efficient exterior LED lights that the error in the CO₂ savings is not greater than the difference between the total CO₂ savings and the minimum threshold (MT) i.e. 1 gCO₂/km. In addition, the standard deviation of the determined total CO₂ saving of the proposed testing methodology cannot exceed 0.5 g CO₂/km.

Considering the current technology developments, the resulting CO₂ savings range is from 1 to 1.5 gCO₂/km, depending on the efficiency and the type of lightings. In view of future improvements in lightings technologies (Altingöz 2014), a wider CO₂ savings range can be expected.

2.2 LED lighting: from comprehensive methodology to simplified approach

Based on the experience gained from the applications on LED exterior lighting systems, the Commission finds that it has been satisfactorily and conclusively demonstrated that combinations of efficient exterior LED lights, including low beam head-lamp, high beam headlamp, front position, front fog, rear fog, front turn signal, rear turn signal, license plate and reversing lamps meet the eligibility criteria referred to in Article 12 of Regulation (EC) No 443/2009 and Implementing Regulation (EU) No 725/2011 and provides a reduction in CO₂ emissions of at least 1g CO₂/km as compared to a baseline exterior lighting package including the same combination of vehicle lights.

With a view to facilitating the further deployment of efficient exterior LED lighting systems in new vehicles, it was therefore found appropriate to consolidate the conditions for determining the CO₂ savings from this type of lighting.

A generic Decision on LED lighting is planned to be published: by reference to this Decision, a manufacturer should have the possibility to apply for the certification in accordance with Article 11 of Regulation (EU) No 725/2011 by a type approval authority of the CO₂ savings of an appropriate combination of efficient exterior LED lights. That application for certification should be supported by a verification report as specified in Article 7 of Regulation (EU) No 725/2011.

The type approval authority should verify that the package of efficient exterior LED lights provides the minimum threshold of CO₂ savings required and that the testing methodology used is in accordance with the one defined in the generic Decision. If the type approval authority finds that the application for certification of the savings does not satisfy the conditions referred to in the generic Decision or in Regulation (EU) No 725/2011, the application for certification should be rejected.

2.3 The quantification of interaction between LED lighting and efficient alternator

When several eco-innovations are fitted to one vehicle type, variant or version, their interaction on the total CO₂ has to be taken into account. The manufacturer shall quantify the impact of the interaction in the application to the approval authority and shall provide a report from the independent and certified body(IEC 2011a). In this Chapter a methodology is presented to evaluate the interaction between LED lighting and efficient alternator.

As shown in equation1, the CO₂ savings for LED lighting are influenced by the alternator efficiency: in particular, the installation of the same LED lights leads to decreasing values of CO₂ savings with increasing values of the vehicle alternator efficiency. In fact, increasing values of alternator efficiency mean lower CO₂ emissions for the same electrical energy consumption. This effect is illustrated in Figure2, which refers to a package including 9 LED lights installed in a petrol-fuelled passenger car. The following lights are included in the package: low beam headlamp, high beam headlamp, front position, fog – front, turn signal – front, fog – rear, turn signal – rear, license plate and reversing.

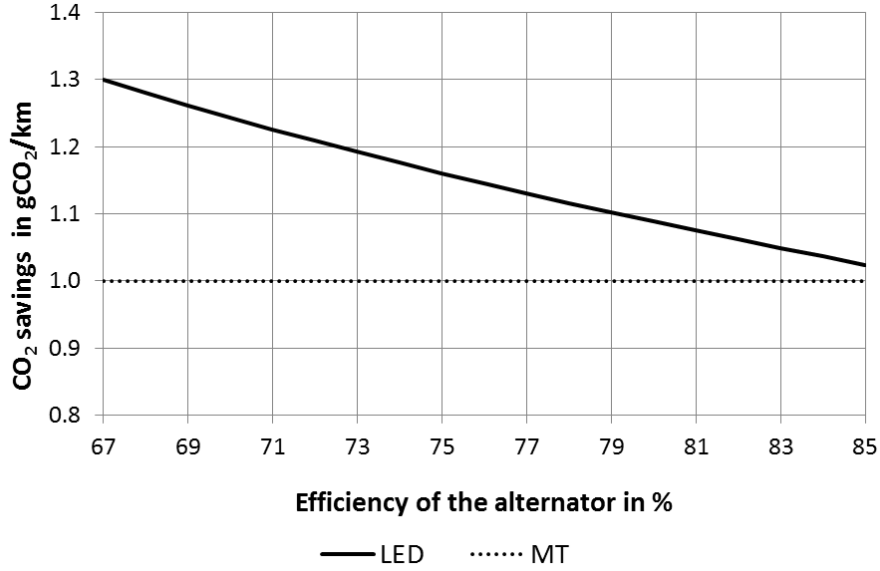


Figure 2. Influence of the alternator efficiency on CO₂ savings of a LED lighting package.

Therefore, if a vehicle is fitted with LED lighting and an efficient alternator, the combined effect on the total CO₂ savings has to be evaluated. The following equation is proposed to evaluate the total CO₂ savings ($C_{CO_2}|_{tot}$):

$$C_{CO_2}|_{tot} = C_{CO_2}|_{eff.alt.}^{LED} + C_{CO_2}|_{halogen}^{eff.alt.} \quad (2)$$

Where:

$C_{CO_2}|_{eff.alt.}^{LED}$ are the CO₂ savings due to the installation of the LED lighting in a vehicle equipped with an efficient alternator

$C_{CO_2}|_{halogen}^{eff.alt.}$ are the CO₂ savings due to the installation of the efficient alternator in a vehicle equipped with baseline (halogen) lighting

Therefore, equation (2) can be rewritten as:

$$C_{CO_2}|_{tot} = \left(\sum_{i=1}^m \Delta P_i \cdot UF_i \right) \cdot \frac{V_{Pe} \cdot CF}{\eta_A \cdot v} + (P_{RW} - P_{TA}) \cdot \frac{V_{Pe} \cdot CF}{v} \cdot \left(\frac{1}{\eta_A} - \frac{1}{\eta_{EI}} \right) \quad (3)$$

The average European value for the total electric power requirement in real world (P_{RW}) is assumed to be 750W, considering the use of conventional halogen lighting.

In Figure 3, a numerical example is presented to show the combined effect of efficient alternator and LED lighting upon CO₂ savings. The results refer to the LED package described above, installed in a petrol-fuelled passenger car.

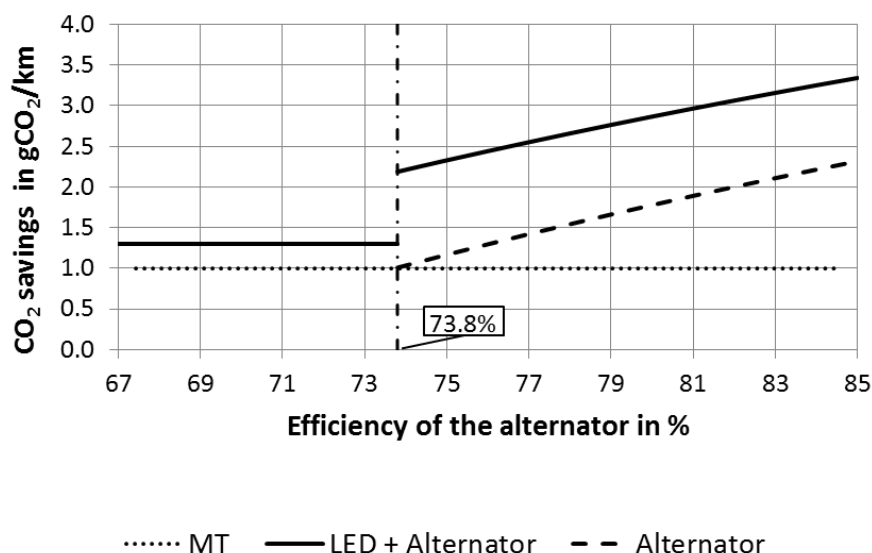


Figure 3. Combined effect of efficient alternator and LED lighting on CO₂ savings.

As it is possible to observe, if the alternator efficiency is below 73.8% (for petrol-fuelled vehicles), the CO₂ savings are only given by the presence of the LED lighting because the CO₂ savings given by the efficient alternator are lower than 1 gCO₂/km (i.e. below the minimum threshold). When the alternator efficiency is higher than 73.8%, savings for the LED lighting and the efficient alternator are combined and interaction is taken into account.

Conclusions

In this paper methodologies for the evaluation of the CO₂ savings from eco-innovation were presented. An example is given on the evolution of methodologies from comprehensive to simplified approaches, based on the LED lighting technology.

Simplified approaches are envisaged for the future as they do not require testing of the whole vehicle on a chassis dynamometer and can be applicable to a wide range of vehicles. Generic, simplified approaches make it easier for car manufacturers to have similar eco-innovations technologies assessed by using the same approach. The example of LED lights also demonstrates the possibility to bundle eco-innovations into packages, which consist of different components, but the CO₂ emission reductions of each component can be quantified by using the same methodology.

The effect of different EIs fitted to one vehicle has also been evaluated and a calculation of the effect of interaction in final CO₂ savings is presented for LED lighting and efficient alternator. The suggested methodology to quantify interactions is simple and can be applied to any combination of innovative technologies for the evaluation of their interaction on the total CO₂ savings.

Acknowledgments

We thank the colleagues of the European Commission Joint Research Centre who provided insight and expertise that greatly assisted the work.

Disclaimer

The views expressed here are purely those of the authors and may not, under any circumstances, be regarded as an official position of the European Commission.

Nomenclature

Latin symbols	Quantity	Unit
C_{CO_2}	CO ₂ savings	gCO ₂ /km
CO ₂	Carbon dioxide	
CF	Conversion factor	gCO ₂ /l

m	Number of efficient exterior LED lights	
MT	Minimum threshold	gCO ₂ /km
P	Power consumption of the vehicle light	W
UF	Usage factor	
v	Mean driving speed of the New European Driving Cycle	km/h
V _{pe}	Consumption of effective power	l/kWh

Greek symbols	Quantity	Unit
Δ	Difference	
η	Efficiency	%

Subscripts

Index (i) refers to vehicle lights

A	Alternator
EI	Eco-Innovation
TA	Type approval
RW	Real world

References

Altingöz, C., 2014. Laser technology in automotive lighting. In pp. 896518–896518–11. Available at: <http://dx.doi.org/10.1117/12.2036519> [Accessed July 30, 2015].

EC, 2013. Commission Implementing Decision 2013/128/EU. Available at: <http://europa.eu/Ch46gt> [Accessed July 22, 2015].

EC, 2014a. Commission Implementing Decision 2014/128/EU. Available at: <http://europa.eu/!CU64Wd> [Accessed July 22, 2015].

EC, 2015a. Commission Implementing Decision (EU) 2015/ 206 -. Available at: <http://europa.eu/!kx66Gw> [Accessed July 22, 2015].

EC, 2016a. Commission Implementing Decision (EU) 2016/160. Available at: http://data.europa.eu/eli/dec_impl/2016/160/oj [Accessed April 29, 2016].

EC, 2014b. Commission Implementing Regulation (EU) No 427/2014. Available at: <http://europa.eu/!nY68hV> [Accessed July 28, 2015].

EC, 2011a. Commission Implementing Regulation (EU) No 725/2011. Available at: <http://europa.eu/!Nj39TU> [Accessed July 22, 2015].

EC, 2010. Communication from the Commission to the European Parliament, the Council, the European Economic and Social Committee and the Committee of Regions. Energy 2020 A strategy for competitive, sustainable and secure energy. SEC(2010) 1346 COM(2010) 639 final, Brussels, 10.11.2010. Available at: <http://europa.eu/!wf67Jf> [Accessed July 24, 2015].

EC, 2014c. Progress towards achieving the Kyoto and EU 2020 objectives - Progress report 2014.

EC, 2016b. Reducing emissions from transport. Available at: <http://europa.eu/!ju43KU> [Accessed July 24, 2015].

EC, 2009. Regulation (EC) No 443/2009 setting emission performance standards for new passenger cars as part of the Community's integrated approach to reduce CO₂ emissions from light-duty vehicles. Available at: <http://europa.eu/!Xu63JC-> [Accessed July 23, 2015].

EC, 2011b. Regulation (EU) No 510/2011 setting emission performance standards for new light commercial vehicles as part of the Union's integrated approach to reduce CO₂ emissions from light-duty vehicles. Available at: <http://europa.eu/!Pd74mD> [Accessed July 23, 2015].

EC, 2015b. Technical Guidelines for the preparation of applications for the approval of innovative

technologies pursuant to Regulation (EC) No 443/2009 and Regulation (EU) No 510/2011 - Revision: October 2015. Available at: <http://europa.eu/!ch88vv> [Accessed September 29, 2015].

EC, 2011c. White Paper – Roadmap to a Single European Transport area – Towards a Competitive and Resource Efficient Transport System. COM(2011) 144 final, Brussels. Available at: <http://europa.eu/!Pc33hk> (2011)_144_en.pdf [Accessed July 27, 2015].

Fontaras, G. & Dilara, P., 2012. The evolution of European passenger car characteristics 2000–2010 and its effects on real-world CO₂ emissions and CO₂ reduction policy. *Energy Policy*, 49, pp.719–730.

Fontaras, G. & Samaras, Z., 2010. On the way to 130 g CO₂/km—Estimating the future characteristics of the average European passenger car. *Energy Policy*, 38(4), pp.1826–1833.

Heywood, J.R., 1988. *Internal combustion engine fundamentals* 1st ed., New York: McGraw-Hill Education.

Hill, N. et al., 2012. EU transport GHG: routes to 2050 II - Developing a better understanding of the secondary impacts and key sensitivities for the decarbonisation of the EU's transport sector by 2050 - Final report. Available at: <http://www.eurtransportghg2050.eu/cms/assets/Uploads/Reports/EU-Transport-GHG-2050-II-Final-Report-29Jul12.pdf> [Accessed July 30, 2015].

Martin, N.P.D. et al., 2015. Can UK passenger vehicles be designed to meet 2020 emissions targets? A novel methodology to forecast fuel consumption with uncertainty analysis. *Applied Energy*, In Press, Corrected Proof. Available at: doi:10.1016/j.apenergy.2015.03.044 [Accessed July 27, 2015].

Meyer, I. & Wessely, S., 2009. Fuel efficiency of the Austrian passenger vehicle fleet—Analysis of trends in the technological profile and related impacts on CO₂ emissions. *Energy Policy*, 37(10), pp.3779–3789.

Sileghem, L. et al., 2014. Analysis of vehicle emission measurements on the new WLTC, the NEDC and the CADC. *Transportation Research Part D: Transport and Environment*, 32, pp.70–85.

Weiss, M. et al., 2011. On-Road Emissions of Light-Duty Vehicles in Europe. *Environmental Science & Technology*, 45(19), pp.8575–8581.

The interactions of the Exhaust Ultrafine Particle with the vehicle near-wake flow

Amine MEHEL*, Frederic MURZYN** & Romain RODRIGUEZ**

*Department of Composite Materials Mechanics and Environment, ESTACA, 78180, Montigny-Le-Bretonneux, France Fax+33 0176 52 11 43 -email:amine.mehel@estaca.fr

**Department of Composite Materials Mechanics and Environment, ESTACA, 53061, Laval, France

Abstract

Reduction of pollution emission coming from automotive engines has become a key strategy leading to some significant improvements in the last two decades in Europe with the implementation of new and tighter regulations. To date, the most important remaining problem concerns the increased emission of ultrafine particles (nanoparticles) especially with the reduction of larger and solid carbonaceous particles. Recent studies have shown that these ultrafine particles (most important in number rather than in mass) are the worst and most harmful particles in terms of health effects. Indeed, they are able to reach the respiratory system in its deepest part, the alveolar region where they can readily penetrate the blood stream leading to major cardiovascular diseases or cancer. Furthermore, it is well-known that these ultrafine particles can infiltrate the vehicle in-cabin and accumulate inside. This enhances the risk exposure of the passengers. In this study, we are not only interested in investigating their dispersion downstream of a reduced-scale square-back car model, but also in studying their interaction with the dynamic of the model near-wake flow turbulence in a wind tunnel. The results show that a high correlation is found between the ultrafine particles dispersion/accumulation zones and the turbulent vortices that are generated in the vehicle near-wake.

Keys-words: Aerosol dispersion, Ultrafine Particles, Particle concentration, Turbulence, Wind tunnel, LDV

Introduction

For many decades the particles emissions were not regulated or only limited to the mass concentration. This explains why road traffic has become one of the major sources of fine and ultrafine particles number concentrations (PNC). Emission measurements campaigns suggest that motor vehicles are the primary direct emission sources of fine and ultrafine particles to the atmosphere in urban areas (Shi et al., 1999; Hitchins et al., 2000; Biswas et al., 2008). They roughly count for 90% or more of the total particle number in areas influenced by on-road vehicles emissions (Morawska et al., 2008). They are in the size range 20–130 nm for diesel engines (Morawska et al., 1998) and 20–60 nm for gasoline engines (Ristovski et al., 1998). The exposure to such ultrafine particles result in causing several adverse health effects. Recent toxicological studies have showed that these ultrafine particles are more toxic than larger particles with the same chemical composition and at the same mass concentration (Brown et al., 2000; Oberdorster, 2001). Indeed, they are able to reach the respiratory system in its deepest part, the alveolar region where they can readily penetrate the blood stream leading to major cardiovascular diseases or cancer (Valberg, 2004; Silverman et al., 2012; Ostro et al., 2015). Thus, the need of particle number concentration (PNC), together with the size distribution (PSD) of ultrafine particles, has led to several studies where measurements have been conducted to better assess ambient air quality and its potential health effects. Among them, Zhu et al. (2002), Janssen et al. (2001), Kozawa et al. (2012) assessed PNC and PSD near major highways and roads. These ultrafine particles are then transported from these regions with very high concentrations all over the surrounding local environments where they can infiltrate vehicles in-cabin, buildings, schools and indoor environments. Consequently they can cumulate resulting in the exposure of the passengers, pedestrians, bikers... The exposure to such pollutants has been assessed through local/individual measurements. Particularly, recent studies have evaluated the individual exposure when commuting in the transportation microenvironment (Adams et al., 2001; Zuurbier et al., 2010), buses or bicycle (Gee & Raper; 1999), vehicles in-cabin

(Joodatnia et al., 2013; Zhu et al., 2007). Other investigations have been conducted to compare exposure depending on transport mode (Panis et al., 2010; Knibbs et al., 2011) or during day-time activities including, outdoor commuting in traffic environments (Gu et al. 2015). All these studies have underlined the importance of two major parameters (among others) in assessing the exposure, i.e. the concentration and particle size. This has led some authors to characterize them during different stages of the transportation process. During the infiltration process, it has been shown that parameters such as vehicle mileage, age and ventilation fan speed have strong influence on the indoor to outdoor concentration ratio (Hudda et al., 2012). The pollutants dispersion is also influenced by the local topology as mentioned in Goel & Kumar (2015) or Takano and Moonen (2013). They showed the influence of signalized traffic intersections or of the street canyon roof shape on PNC respectively on pollutants concentration levels.

This brief overview demonstrates the importance of treating particle dynamics at different urban scales as concluded by Kumar et al. (2011). This is the reason why we focus on the dispersion of the UFP in the vehicle wake flow where the PNC levels are very high and the risk due to exposure elevated. The dispersion process of the UFP at this stage is mostly influenced by the flow and particularly by the turbulent structures. Studying their correlations with PNC would be helpful to identify some key-parameters that may affect particle dispersion. To achieve this goal, we undertake wind tunnel investigations. Across the literature, we notice that only very few experimental studies dealt with that topic (Kanda et al., 2006; Carpentieri et al., 2012). Then, we present new wind tunnel experiments to assess the dynamic of carbonaceous UFP downstream of a reduced-scale truck model. While Carpentieri et al. (2012) used a passive tracer gas, we resort to solid particles. Furthermore, in our experimental conditions, the tailpipe flow and wind tunnel flow mixing are supposed to be representative of an urban vehicle moving at 30 km/h (kinematic scale). PNC and velocity field measurements are achieved to bring new understanding regarding UFP interaction with the vehicle near wake flow and its consequence on their dispersion. Results are mostly compared and discussed with Carpentieri et al. (2012). Further perspectives and future works are presented.

1. Experimental method

The present experiments are conducted in two different wind tunnels. The Particle Number Concentrations (PNC) measurements are undertaken in the experimental facility located at ESTACA Paris. The corresponding wind tunnel has a test section of 800 mm in length, a width of 600 mm and a height of 600 mm. The velocity measurements are recorded at ESTACA Laval in the second wind tunnel which is 1 m in length, 0.3 m in width and 0.3 m in height. The same upstream air velocity is ensured and set at $U_{\text{mean}}=14.4\text{ m/s}$ so as to get the same flow conditions in both wind tunnels. This velocity is recorded either with a Pitot tube (Paris) or with a 2D LDV system (Laval). Walls are made of transparent altuglass allowing flow visualization and use of optical devices. The studied car model is shown in Fig. 1 (left). It has a common rear part of a truck with a reduced size. Here, the scale factor is 1/20 compared to a real prototype. The length of the model is $L=122\text{ mm}$, its width is $W=49\text{ mm}$ and its height is $H=65\text{ mm}$. For all conditions, the blockage ratio was less than 4%. No raised false floor is installed contrary to Carpentieri et al. (2012) where one was used for some experimental conditions. Nevertheless, a calibration of the wind tunnel is carried out prior to the present experiments to ensure a well-defined knowledge of the undisturbed flow developing in the measurement section. For both wind tunnels, the turbulence intensity of the incoming flow is less than 1%.



Figure 1. Car model used during the experiments (Left) and the Cartesian coordinate system with incoming flow from top left to bottom right (Right)

The experimental conditions are supposed to correspond to a real truck prototype speed $U_p=8.33\text{m/s}$ (30km/h) according to an imposed kinematic scale of 1.73 (U_{mean}/U_p). This scale is imposed by some experimental constraints related to the flow rate of the exhausted particles. Hence, the dynamic similarity of the tailpipe jet and wind tunnel air flows is ensured. The associated Reynolds number based on the truck height and kinematic viscosity of air is 6.10^5 ($Re=U_{\text{mean}}*H/\nu=6.10^5$). This is significantly larger than critical value of 10^4 from which the boundary layer at the rear of the car becomes turbulent. According to Hucho (1998), above this limit, little sensitivity to the Reynolds number is expected. During the experiments, the kinematic scale between prototype and model is kept constant for exhausted gas/particle velocity considering a given engine speed of 2500 rpm. It is worthwhile to note that this condition is a novelty in comparison to the previous studies on pollutant dispersion in wind tunnels. The nanoparticles are generated by a PALAS DNP 2000 spark discharge aerosol generator using graphite electrodes and Nitrogen. The aerosol is injected in the model tailpipe at a given flow rate of $Q_{cp}=0.133\text{L/s}$. The size distribution of ultrafine carbon particles ranges from 20 to 100nm. An Electrical Low Pressure Impactor (ELPI) is used for Particle Number Concentration (PNC) measurements. Altogether these experimental conditions are supposed to be typical of urban areas. Additional details dealing with experimental conditions are given by Mehel and Murzyn (2015).

The Particle Number Concentrations are measured at 66 different locations downstream of the car corresponding to distinct positions in the longitudinal (x), vertical (y) and transversal (z) directions. Altogether they cover a domain given by $0.25 < X=x/H < 5$, $0.25 < Y=y/H < 1$ and $-0.5 < Z=z/H < 0.5$ where H is the height of the truck. This finite volume is imposed by the size of the wind tunnel section. Therefore, according to the dimensions of the experimental facilities, we are mostly focused on the near-wake region ($x/H < 5$). For completeness, the origin of the axis system (Fig. 1, right) is taken on the centerline of the wind tunnel ($z=0$), on the ground ($y=0$) and on the rear face of the car model ($x=0$). In the dimensionless coordinate system, the injection point representing the tailpipe is located at $X=x/H=0$, $Y=y/H=0.25$ and $Z/H=-0.25$.

For PNC measurements, data acquisition lasts 120 seconds and the data rate is kept constant and equal to 1 Hertz. The acquisition duration is long enough compared to the time scale of the flow. So the convergence of the concentration data is ensured.

The velocity fields are measured using a 2D LDV system (DANTEC) mounted on a 2D displacement table. Both streamwise (U) and vertical (V) components of the velocity are recorded at 560 different locations downstream of the truck. The corresponding investigated area spreads such as $0.25 < X < 5$, $0.25 < Y < 1$ and $-0.55 < Z < 0$. The measurement grid consists of $20 \times 7 \times 4$ points. On the x-axis, the step between 2 points is 16.25mm while it is 8.25mm on the y-axis and 12mm on the z-axis. Data acquisition lasts 60 seconds or ends as soon as 5000 samples are acquired. To avoid any erroneous measurements, velocity data are filtered based on the rms value of U and V. That is, if $U-U_{\text{mean}}$ (or $V-V_{\text{mean}}$) is larger than $3u'$ ($3v'$ respectively) where u' and v' are the rms values of U and V, then the pair (U, V) is replaced by $(U_{\text{mean}}, V_{\text{mean}})$. This filtering technique only concerns few points (less than 1%) and does not significantly affect U_{mean} , V_{mean} , u' and v' (Murzyn and Belorgey, 2005). Furthermore, measured points where data rate is below 5Hz are systematically removed as they may not represent the real flow dynamic where rapid fluctuations occur. Nevertheless, this only represents a very low number of points (less than 2%) and may be explained by possible invisible scratches on the wind tunnel walls for instance.

For all measurements, we acknowledge a constant air speed (steady conditions) and no heat flux from engine is considered. Lastly, it should be noticed that even if the aerosol is not heated, the particles are less sensitive to the buoyancy effect than if a gaseous passive tracer was used. Indeed, their density is approximately 2000kg/m^3 (carbon particle). This point is a main difference compared to the experimental investigations of Kanda et al. (2006) and Carpentieri et al. (2012) where a gas tracer was used.

2. Results and Discussion

For the following figures, black marks indicate the measurement positions. An absence of symbol means unavailable data due to data rate below 5Hz and/or possible scratch on the side of the wind tunnel.

Mean velocity fields

Figure 2 presents a 2D vertical map (xy) of the dimensionless mean streamwise velocity (U/U_{mean}) measured at the centreline of the channel ($z/H=0$). Our results indicate that a negative streamwise velocity component is found close to the rear of the vehicle ($x/H < 1$) over a height which approximately corresponds to $0.80H$. The minimum streamwise velocity ($U \sim -0.23\text{m/s}$) is found at $x/H=0.5$ and $y/H \sim 0.38$. Overall, this finding is in accordance with results from Carpentieri et al. (2012). Out of this very near-wake region, positive streamwise velocities are measured with increasing values when the distance to the vehicle increases. This characterizes a recirculating flow that appears in the near-wake of the vehicle Ahmed et al (1984). From the present measurements, the length of this region is estimated at approximately $1H$ when Carpentieri et al. (2012) suggested $2H$. This is not in contradiction as they did not strictly use the same shape for the vehicle model. Far downstream (top right of figure 2), the flow recovers the same mean streamwise velocity as upstream ($U/U_{\text{mean}} \sim 1$) for $x/H > 4$ and $y/H > 0.90$. The transition between the recirculation and the “far wake” regions is gradual. This is also in agreement with Carpentieri et al. (2012).

Figure 3 presents the same 2D vertical map for the dimensionless mean vertical velocity (V/U_{mean}) measured at the centreline of the channel ($z/H=0$). For $0 < x/H < 0.75$ and y/H up to 0.90 , positive values are found depicting an upward mean flow motion. Similarly, at $x/H=0.50$, an upward motion occurs up to $y/H \sim 0.50$. Everywhere else, negative values are encountered. For $x/H > 0.75$, dimensionless values are between -0.20 and -0.05 (-2.90m/s and -0.7m/s). Far downstream ($x/H=5$), the dimensionless vertical component of the velocity is roughly homogeneous with an average value of -0.05 . The flow is back to a quasi 1D structure similar to the upstream conditions. Combining with the above results, this clearly denotes the apparition of recirculation vortex in the vicinity of the car model. From the mean velocity field, we put in evidence its development close to the car model. This is in accordance with past results (Carpentieri et al., 2012). The structure and the dynamic of the flow in this near-wake region are of importance and have significant impact on the PNC measurements as it will be seen in the next section.

For completeness, Figs 4 and 5 present the same characteristics relative to the mean flow but for a different 2D cross section. Here, the (yz) map is considered at $x/H=0.50$ (near-wake). It only represents half of the symmetrical near-wake flow. Taking into account the width of the car model, it is worthwhile to note that the lateral sides of the car are situated at $z/H \sim \pm 0.38$. From these figures, some relevant information can be deduced. From the lower vertical position $y/H=0.25$ to $y/H \sim 0.75$, negative horizontal streamwise velocities are encountered when $z/H < 0.20$. In the same time, vertical component of the velocity vector is mostly positive when $y/H < 0.50$ whatever z/H is. It is believed that the recirculation area may be symmetrical but does not spread over the whole width of the vehicle. Out of this very near-wake region (for $x/H > 2$), our results show that horizontal streamwise velocity is always positive. This is also true at $x/H=1$ except for the position $y/H=0.25$ and $z/H=0$ where a negative horizontal streamwise velocity is recorded. This reveals that the recirculation region is limited to the closest vicinity of the car model.

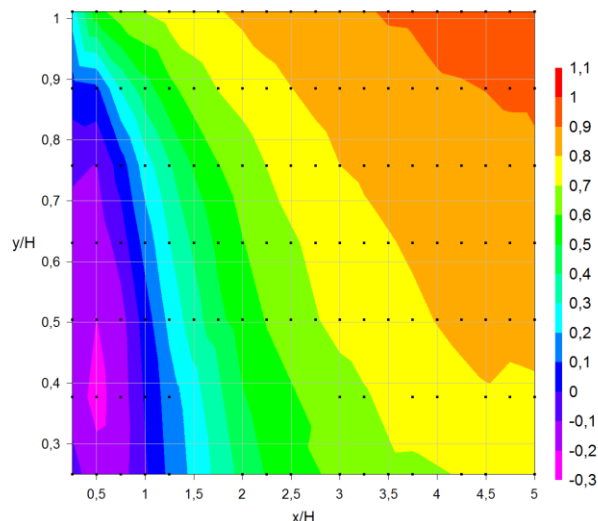


Figure 2. 2D map (xy) of dimensionless mean streamwise velocity ($z/H=0$)

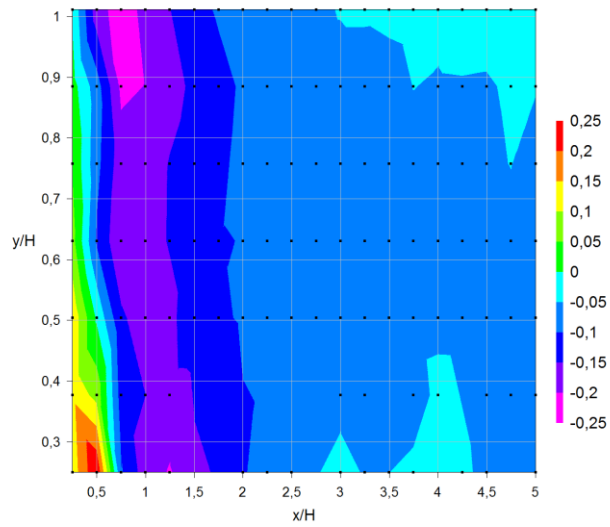


Figure 3. 2D map (xy) of dimensionless mean vertical velocity ($z/H=0$)

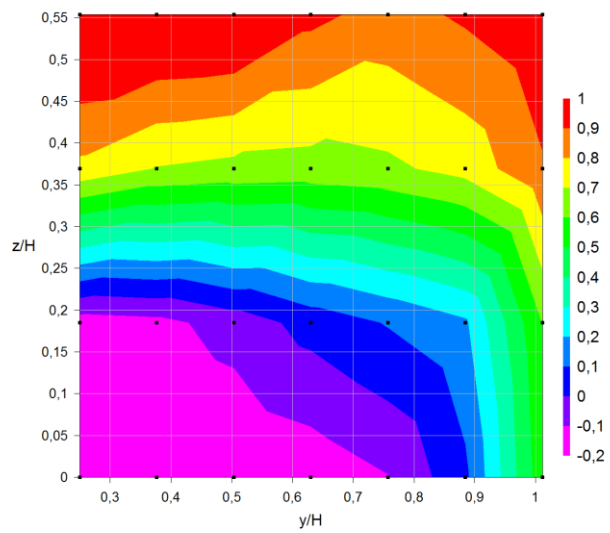


Figure 4. 2D map (yz) of dimensionless mean streamwise velocity ($x/H=0.50$)

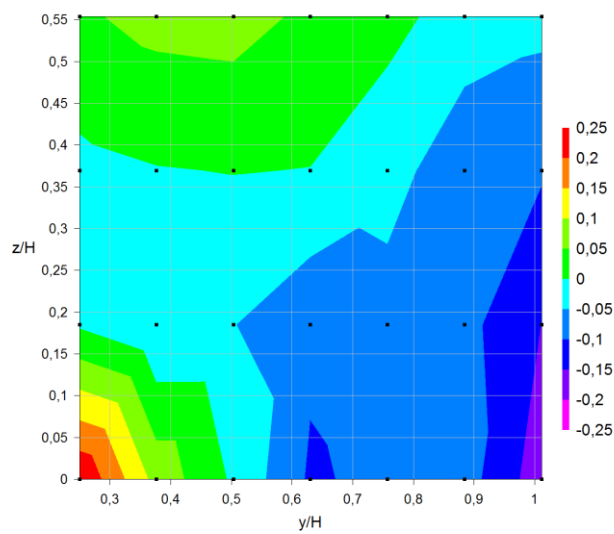


Figure 5. 2D map (yz) of dimensionless mean vertical velocity ($x/H=0.50$)

Turbulent velocity fields

Figures 6 and 7 present the turbulence intensity in both longitudinal (I_x) and vertical (I_y) directions respectively. I_x and I_y are expressed as the ratio between rms of the corresponding velocity component and U_{mean} . The displayed data correspond to the centreline of the wind tunnel ($z/H=0$). Note that the scale is kept identical to make the comparison easier.

For the given transverse position $z/H=0$, our results for the turbulence intensity levels (Figs 6 and 7) exhibit that the turbulence level is overall more intense close to the vehicle and decreases with the dimensionless distance x/H . Except for one position ($x/H=0.50$ and $y/H=0.25$ where I_x reaches 25.5%) the turbulence intensity does not exceed 17%. Peaks are mainly measured at heights corresponding to upper ($0.80 < y/H < 1$) and lower ($y/H < 0.40$) surfaces of the car model. This behaviour was previously observed by Carpentieri et al. (2012) within a comparable range. Furthermore, a similar behaviour is highlighted. Indeed, at the roof height ($y/H \sim 1$), we found the highest turbulence level at $x/H=0.75$ ($I_x=16.8\%$). Close to the ground, the maximum is measured at $x/H=0.50$ ($I_x=25.5\%$). This longitudinal gap between both peaks has been reported by Carpentieri et al. (2012) as well. Regarding I_y (Fig. 7), the highest level is estimated slightly below 20% but average results are pretty much the same as I_x (Fig. 6).

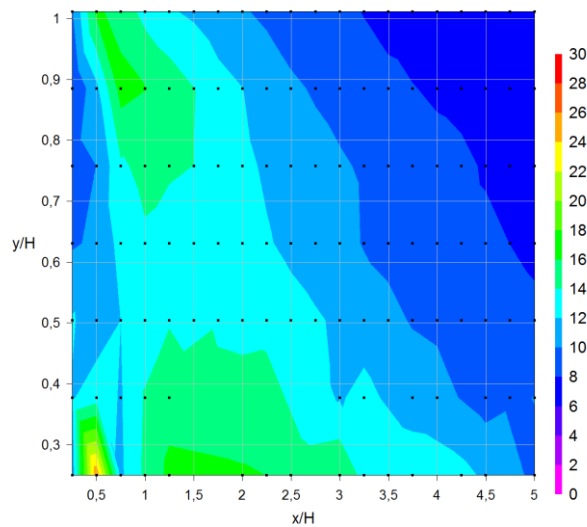


Figure 6. 2D map (xy) of turbulence intensity I_x ($z/H=0$)

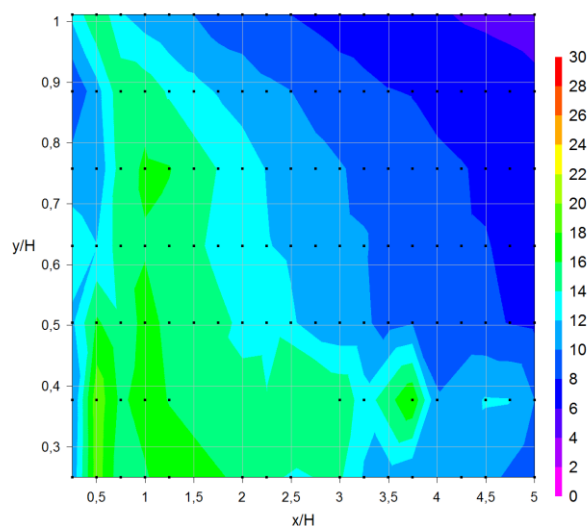


Figure 7. 2D map (xy) of turbulence intensity I_y ($z/H=0$)

Far downstream, both average levels of turbulence (I_x and I_y) fall below 10%. The wake is still disturbed compared to the upstream flow conditions and a larger distance is required to get back to the upstream flow conditions.

Particle Number Concentration (PNC)

Two different 2D maps of Particle Number Concentrations are presented on Figs 8 and 9.

Figure 8 corresponds to a vertical section at the centreline of the channel ($z/H=0$). It shows that the most important PNC ($\text{PNC} > 2 \cdot 10^6$) is observed in the vicinity of the car ($x/H < 1$). This is not surprising since it corresponds to the emission point region. The maximum PNC reaches $3.38 \cdot 10^6$ for $x/H=0.50$ and $y/H=0.25$ (height of the tailpipe). In the spanwise direction (vehicle width), the PNC evolves according to a particular behaviour: close to the vehicle ($x/H < 1$), nanoparticles are entrapped by the recirculation cell leading to highest concentrations in the centreline at $z/H=0$. By looking at these PNC contours for $z/H=-0.30$ (approximated position of the tailpipe), the maximum of PNC is found between $x/H=0.50$ and 1 for $y/H=0.25$. The corresponding levels are $1.21 \cdot 10^6$ ($x/H=0.50$ and $y/H=0.25$) and $1.29 \cdot 10^6$ ($x/H=1$ and $y/H=0.25$). For $z/H=-0.50$ and 0.50 (outer of the vehicle width), peaks are mostly found from $x/H=5$ rather than in the very near wake region ($x/H < 1$).

This is strongly related to the near wake flow structure pointed out from the velocity measurements. At $z/H=0$, nanoparticles are sucked by this large recirculating structure and accumulate in this part of the flow. It has an approximated size of 0.50 to $1H$ in length and 0.50 to $0.80H$ in height. Once the nanoparticles are trapped by the large recirculating vortex, the mechanism of turbulence diffusion takes place driving them to the area where I_x and I_y are lower which corresponds to $x/H < 0.75$ and $y/H > 0.5$ as noticed above (Figs 6 and 7). As a result, the plume is enhanced in the vertical direction. The highest PNC correspond to highest levels of I_y . Interaction between turbulence and particles is then obvious. This behaviour was previously mentioned by Mehel and Murzyn (2015) and illustrates the strong influence of the vehicle wake on the development of the plume.

In the cross-section at $x/H=1$ (Fig. 9), the cloud of dispersed nanoparticles enlarges and spreads in the spanwise direction. At $x/H=1$, the shape of the plume is roughly Gaussian but not centred around $z/H=0$. Far downstream ($x/H=2$ to 5), we show that a clear dissymmetry appears and the most important PNC are found between $z/H=-0.50$ and -0.30 (Fig. 10). This clearly denotes that the dynamic of the nanoparticles is strongly influenced by the pair of lateral longitudinal outer vortices that develop and propagate from both edges of the car. The highest number of particles is also found in the lower part of the flow ($y/H < 0.50$) which corresponds to the position of the tailpipe. For $x/H=0.50, 1, 2$ and 5 , the highest PNC values are $3.38 \cdot 10^6$ ($y/H=0.25$ and $z/H=0$), $1.29 \cdot 10^6$ ($y/H=0.25$ and $z/H=-0.30$), $0.548 \cdot 10^6$ ($y/H=0.25$ and $z/H=-0.30$), $0.293 \cdot 10^5$ ($y/H=0.25$ and $z/H=-0.30$). Therefore, the decay rate is inversely proportional to the dimensionless distance to the car model and is related to the dilution process.

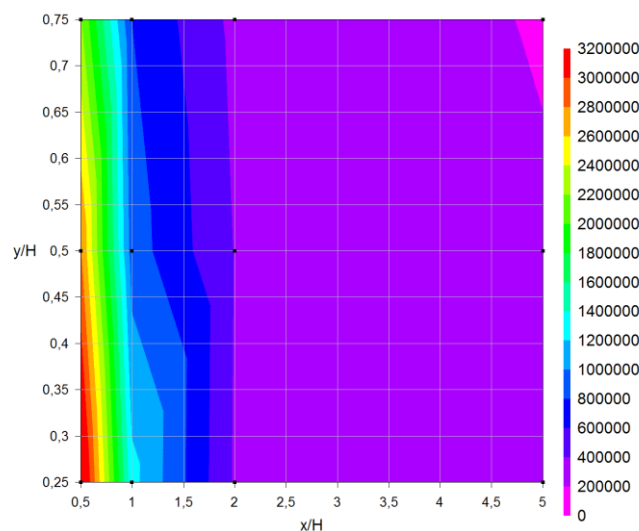


Figure 8. 2D map (xy) of PNC ($z/H=0$)

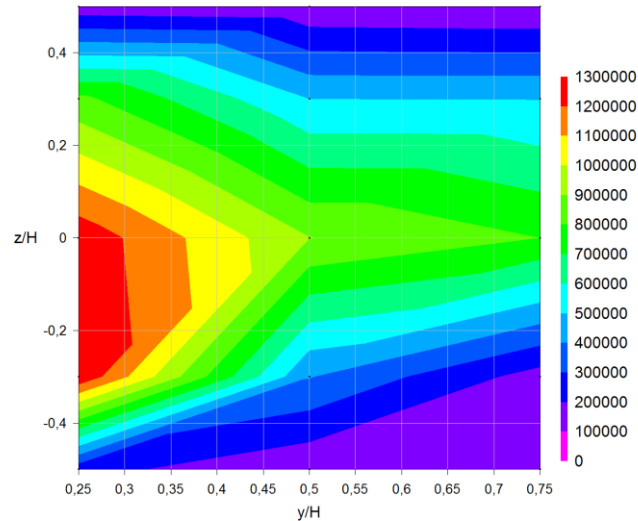


Figure 9. 2D map (yz) of PNC (x/H=1)

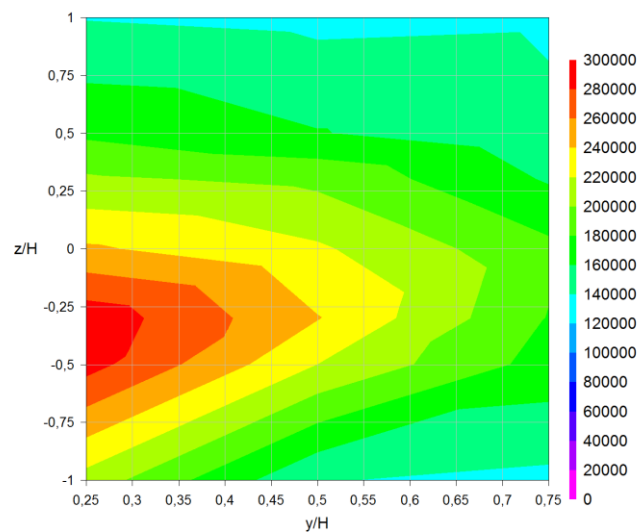


Figure 10. 2D map (yz) of PNC (x/H=5)

At the same time, at $x/H=0.50$, the maximum PNC is found at $z/H=0$ while it is shifted to $z/H=-0.30$ for $x/H=1, 2$ and 5 . It is worthwhile to note that $z/H=-0.30$ roughly corresponds to the position of the lateral side of the car model and the tailpipe position. For $x/H=1$, a second peak close to the first one ($PNC=1.27 \cdot 10^6$) is measured showing that lateral dispersion really starts downstream of $x/H=1$. According to the literature, this is also related to lateral vortices that develop in this region from the edge of the car (Hucho, 1998). Our results confirm that the vortices appearing in the near wake flow strongly influence the dispersion of the emitted particles. Accordingly, the turbulence plays an important role in the dispersion of nanoparticles emitted from the tailpipe of a car and the development of the corresponding plume.

Conclusion

In the present paper, we present experimental results of wind tunnel investigations regarding the correlation between flow dynamic and Particle Number Concentration in the wake of a vehicle model. Prior to this contribution, only few studies have been undertaken to assess this link. Here, we measure the mean and turbulent properties of the near-wake flow developing downstream of a passenger car and the Particle Number Concentration (PNC). The experimental flow conditions are defined so as to be representative of a real car at 30km/h (urban cycle) according to a kinematic scale. The flow developing downstream of the car is characterized using a 2D LDV system and a grid of 560 points is defined for velocity measurements while PNC are recorded at 66 locations. Although we acknowledge that some

improvements may be brought by reducing the step between 2 measurement points, by exploring the 3D flow or by considering more accurately the boundary layer effect, it is also expected that these preliminary results will be helpful for the community. From the measurements, our main conclusions highlight that:

- A recirculating flow develops in the close vicinity of the car model which size is estimated and compared with the previous work of Carpentieri et al. (2012) showing interesting consistency;
- The longitudinal and vertical turbulence intensities are investigated showing peaks around 25% and 20% for I_x and I_y respectively;
- Two main regions of intense turbulence activity are revealed either at the roof level or close to the ground with a longitudinal gap;
- PNC measurements in the near-wake depict a strong influence of the recirculation region which is able to suck particles leading to highest concentrations at the centreline of the channel for lowest values x/H . Then they are diffused in the vertical direction towards low level of turbulence intensities I_x and I_y ;
- When increasing the distance to the vehicle, our results indicate that lateral vortices developing from the edge of the car are capable of trapping particles. This is put in evidence by looking at the off-centre distribution of PNC. Far downstream, the peak of PNC is found to be in-line with the tailpipe. This point is important for numerical modelling as the position of the tailpipe must be taken into account with accuracy.

Altogether, these results are an added value to the existing literature and supplement interestingly some preliminary PNC measurements published earlier(2015). They particularly show the narrow relation existing between flow turbulence dynamics and particle dispersion. Nevertheless, the remaining questions are still numerous. As a consequence, some further experimental measurements and in-situ campaigns will be scheduled in the context of two new PhD research project startings focusing on correlation between wake flow and PNC.

References

- Adams, H. S., Nieuwenhuijsen, M. J., Colvile, R. N., McMullen, M. A. S., & Khandelwal, P. (2001). Fine particle (PM 2.5) personal exposure levels in transport microenvironments, London, UK. *Science of the Total Environment*, 279(1), 29-44.
- Ahmed, S. R., Ramm, G., & Faitin, G. (1984). Some salient features of the time-averaged ground vehicle wake (No. SAE-TP-840300). Society of Automotive Engineers, Inc., Warrendale, PA.
- Brown, D. M., Stone, V., Findlay, P., MacNee, W., & Donaldson, K. (2000). Increased inflammation and intracellular calcium caused by ultrafine carbon black is independent of transition metals or other soluble components. *Occupational and Environmental Medicine*, 57(10), 685-691.
- Carpentieri, M., Kumar, P., & Robins, A. (2012). Wind tunnel measurements for dispersion modelling of vehicle wakes. *Atmospheric environment*, 62, 9-25.
- Janssen, N. A., van Vliet, P. H., Aarts, F., Harssema, H., & Brunekreef, B. (2001). Assessment of exposure to traffic related air pollution of children attending schools near motorways. *Atmospheric environment*, 35(22), 3875-3884.
- Joodatnia, P., Kumar, P., & Robins, A. (2013). The behaviour of traffic produced nanoparticles in a car cabin and resulting exposure rates. *Atmospheric environment*, 65, 40-51.
- Gee, I. L., & Raper, D. W. (1999). Commuter exposure to respirable particles inside buses and by bicycle. *Science of the Total Environment*, 235(1), 403-405.
- Goel, A., & Kumar, P. (2015). Zone of influence for particle number concentrations at signalised traffic intersections. *Atmospheric Environment*, 123, 25-38.
- Gu, J., Kraus, U., Schneider, A., Hampel, R., Pitz, M., Breitner, S., ... & Cyrus, J. (2015). Personal day-time exposure to ultrafine particles in different microenvironments. *International journal of hygiene and environmental health*, 218(2), 188-195.
- Hitchins, J., Morawska, L., Wolff, R., Gilbert, D., (2000). Concentrations of submicrometer particles from vehicle emissions near a major road. *Atmospheric Environment* 34,51–59.
- Hucho W.H. (1998), *Aerodynamics of road vehicles: From fluid mechanics to vehicle engineering*, Society of Automotive Engineering.
- Kanda, I., Uehara, K., Yamao, Y., Yoshikawa, Y., & Morikawa, T. (2006). A wind-tunnel study on exhaust gas dispersion from road vehicles—Part I: Velocity and concentration fields behind single vehicles. *Journal of wind engineering and industrial aerodynamics*, 94(9), 639-658.

- Knibbs, L. D., Cole-Hunter, T., & Morawska, L. (2011). A review of commuter exposure to ultrafine particles and its health effects. *Atmospheric Environment*, 45(16), 2611-2622.
- Kozawa, K. H., Winer, A. M., & Fruin, S. A. (2012). Ultrafine particle size distributions near freeways: Effects of differing wind directions on exposure. *Atmospheric Environment (Oxford, England: 1994)*, 63, 250–260.
- Kumar, P., Ketzel, M., Vardoulakis, S., Pirjola, L., & Britter, R. (2011). Dynamics and dispersion modelling of nanoparticles from road traffic in the urban atmospheric environment—a review. *Journal of Aerosol Science*, 42(9), 580-603.
- Mehel, A., & Murzyn, F. (2015). Effect of air velocity on nanoparticles dispersion in the wake of a vehicle model: Wind tunnel experiments. *Atmospheric Pollution Research*, 6(4), 612-617.
- Morawska, L., Ristovski, Z., Jayaratne, E.R., Keogh, D.U., Ling, X. (2008). Ambient nano and ultrafine particles from motor vehicle emissions: characteristics, ambient processing and implications on human exposure. *Atmospheric Environment* 42, 8113-8138.
- Morawska, L., Bofinger, N.D., Kocis, L., Nwankwoala, A., (1998). Submicrometer and super micrometer particles from diesel vehicle emissions. *Environmental Science and Technology* 32, 2033–2042.
- Murzyn, F. and Belorgey, M. (2005). Experimental investigations of the grid-generated turbulence features in a free-surface flow, *Experimental Thermal and Fluid Science*, 29, pp925-935.
- Oberdorster, G., (2001). Pulmonary effects of inhaled ultrafine particles. *International Archives of Occupational and Environmental Health* 74 (1), 1–8.
- Ostro B, Hu J, Goldberg D, Reynolds P, Hertz A, Bernstein L, Kleeman MJ. 2015. Associations of mortality with long-term exposures to fine and ultrafine particles, species and sources: results from the California Teachers Study cohort. *Environ Health Perspect* 123:549–556
- Panis, L. I., De Geus, B., Vandenbulcke, G., Willems, H., Degraeuwe, B., Bleux, N., ... & Meeusen, R. (2010). Exposure to particulate matter in traffic: a comparison of cyclists and car passengers. *Atmospheric Environment*, 44(19), 2263-2270.
- Ristovski, Z.D., Morawska, L., Bofinger, N.D., Hitchins, J., (1998). Submicrometer and supermicrometer particles from spark ignition vehicles. *Environmental Science and Technology* 32, 3845–3852.
- Shi, J.P., Khan, A.A., Harrison, R.M., (1999). Measurements of ultrafine particle concentration and size distribution in the urban atmosphere. *Science of the Total Environment* 235, 51–64.
- Takano, Y., & Moonen, P. (2013). On the influence of roof shape on flow and dispersion in an urban street canyon. *Journal of Wind Engineering and Industrial Aerodynamics*, 123, 107-120.
- Zhu, Y.; Hinds, W.C., Kim, S., Shen, S. & Sioutas, C., (2002). Study of ultrafine particles near a major highway with heavy-duty diesel traffic, *Atmospheric Environment*, Volume 36, Issue 27, Pages 4323-4335
- Zhu, Y., Eiguren-Fernandez, A., Hinds, W. C., & Miguel, A. H. (2007). In-cabin commuter exposure to ultrafine particles on Los Angeles freeways. *Environmental science & technology*, 41(7), 2138-2145.
- Zuurbier, M., Hoek, G., Oldenwening, M., Lenters, V., Meliefste, K., van den Hazel, P., & Brunekreef, B. (2010). Commuters' exposure to particulate matter air pollution is affected by mode of transport, fuel type, and route. *Environmental health perspectives*, 118(6), 783.

An investigation of evaporative VOC emissions from petrol light duty vehicles in Europe using different oxygenated fuels

Giorgos MELLIOS* & Thomas PAPAGEORGIOU*

*EMISIA S.A., Antonitritsi 21, Thessaloniki, GR-57001, Greece
Fax+302310 804110-email:giorgos.m@emisiam.com

Abstract

This paper presents the outcome of a study aiming at investigating the impact of typical fuel ethers and ethanol blends on evaporative VOC emissions from petrol cars. The COPERT model has been used to simulate the effect on the current and future European petrol light duty vehicle fleet.

In order to investigate whether fuel ethers can offer any environmental benefits compared to ethanol containing fuels, the main parameters of typical ETBE and ethanol blends having an effect on evaporative emissions were assessed. The parameters mostly affected are permeation emissions and the activated carbon canister durability. These were modelled in COPERT to estimate the expected evaporative emissions for a number of scenarios, including (i) pure hydrocarbon petrol (basecase scenario); (ii) ethanol-containing petrol at 5% v/v (ethanol scenarios); and (iii) ETBE-containing petrol at 11% v/v ETBE (ETBE scenarios).

All scenarios result in a reduction in the total evaporative emissions. These reductions are of the same order of magnitude – in absolute terms – for the different scenarios. However, the ethanol scenarios result in considerably higher VOC emissions levels compared to the basecase and the ETBE scenarios.

Overall, there are significant emissions reductions associated with the use of ETBE instead of ethanol for blending into petrol. This is due to the increased activated carbon durability and lower permeability of ETBE blends compared to equivalent (in terms of oxygen content) ethanol blends.

Key-words: evaporative emissions, COPERT, fuel ethers, ethanol, petrol vehicles.

Introduction

The Renewable Energy Directive (2009/28/EC) and the Fuel Quality Directive (2009/30/EC) are the two major policy instruments supporting the increased use of renewable fuels in the European Union (EU). Both Directives encourage the use of bio components such as ETBE (ethyl tertiary butyl ether) and ethanol in petrol. Fuel ethers can significantly contribute to the different fuel-related environmental targets set out in EU legislation.

In earlier studies conducted for the European Commission, such as the joint JRC/CONCAWE/EUCAR study on evaporative emissions (Martini et al. 2007) and the recent review of the European evaporative emission test procedure (Haq et al. 2013), fuel ethers were excluded from the analyses conducted. Yet, fuel ethers can offer significant environmental benefits (in terms of lower evaporative emissions) compared to ethanol containing fuels. In both studies the COPERT model has been used for the calculation of emissions from the road vehicle fleet.

1. Objectives

The present paper investigates the impact of fuel ethers on evaporative emissions and demonstrates the relative advantages compared to ethanol blends.

Hence, the principal objectives of this study are:

- To investigate the main parameters of fuel ethers having an effect on evaporative emissions and how these can be modelled in COPERT.
- To apply the COPERT model to estimate the expected evaporative VOC emissions for each of the scenarios considered.

- Provide recommendations on the relative advantages of fuel ethers over ethanol blends.

2. Refining/calibration of the COPERT model

As a first step, the applicability of the latest version of the COPERT model (v11.3 – June 2015) to estimate the evaporative emissions from fuel ethers (mainly ETBE) has been assessed. The impact of ethanol and fuel ethers on the following parameters affecting evaporative emissions was investigated:

- Fuel tank permeability
- Activated carbon degradation

The effect on carbon canister emissions was also investigated and it was concluded that there is no measurable effect of ethanol and ETBE on canister emissions for new cars.

To this aim, several literature sources have been consulted. These are summarised in Table 1 below, in which the following key information is included:

- The name of the study or scientific paper;
- The test fuels and vehicles used in the study;
- The effect on evaporative (canister breakthrough, permeation, total) emissions;
- Data on VOC speciation;
- Any other useful information relevant for the present study.

In general, there are a sufficient number of sources – including experimental test data – on the effect of ethanol on different aspects of evaporative VOC emissions, such as canister breakthrough, permeation and VOC speciation. For the effect of fuel ethers there is unfortunately much less information available, mainly from older US studies.

Table 1: Summary of literature review on permeation emissions from fuel ethers compared to ethanol and oxy-free fuels

Study / Paper	Fuels compared	Test vehicles	Canister breakthrough	Permeation	Total evap	Speciation	Comments
Influence of Oxygenated Fuels on the Emissions from Three Pre-1985 LD Passenger Vehicles (Stump et al. 2012)	Base (HC only) vs 10% MTBE	3 pre-1985 US cars	--	--	Diurnal emissions decrease 5 to 60% for MTBE	--	Hot soak emissions also decreased by same order of magnitude
Review of Organic Gas Speciation Profiles of Exhaust and Evaporative Emissions from Alternate Gasoline Formulations	Oxy-free gasoline, MTBE @ 2 wt% oxygen, EtOH @ 2 and 3.5 wt% oxygen	--	--	--	--	Detailed weight percent in head space for different species	RVP of tested fuels were 7.1, 7.6, 8.3 and 8.5 psi respectively
Air Quality Impacts of the Use of Ethanol in California Reformulated Gasoline (CARB, 1999)	Oxy-free gasoline, MTBE @ 2 wt% oxygen, EtOH @ 2 and 3.5 wt% oxygen	7 US cars, MY 75-92	--	--	--	Detailed weight percent in head space for different species	Results based on both emissions testing and mathematical models
Fuel permeation from automotive systems, CRC Project E-65 (Haskew et al. 2004; 2006)	Oxy-free gasoline, MTBE @ 2 wt% oxygen, EtOH @ 2 wt% oxygen	10 California vehicles, MY 78-02	--	- EtOH vs MTBE: 1.4 g/day (or 65%) higher - EtOH vs oxy-free: 1.1 g/day (or 45%) higher	--	Example speciation results provided for one rig and one fuel	Both diurnal and steady-state tests conducted
Effects of Ethanol or ETBE Blending in Gasoline on Evaporative Emissions for Japanese In-Use Passenger Vehicles (Tanaka et al. 2007)	Base, E3 (L-H RVP), E10 (L-H RVP), E20, ETBE8, ETBE17	2 Japan cars, MY 2000	--	--	- E3 vs base: from 2 to 6-fold higher - ETBE8 vs base: almost identical	--	- Effect on refuelling losses also estimated - All fuel blends (except E3 H-RVP) had matched RVP
Effects of Ethanol and ETBE Blending in Gasoline on Evaporative Emissions (Tanaka et al. 2006)	Base, E3 (L-H RVP), E10, ETBE8	3 cars, MY 98-00	- E3 vs base: RL tend to increase - ETBE8 vs base: no increase in RL	--	--	--	- Effect on refuelling losses also estimated - All fuel blends (except E3 H-RVP) had matched RVP
Kautex measurement	10% MTBE vs 10% EtOH	One fuel tank (2006 PZEV system)	--	40% increase for 10% EtOH	--	--	Absolute emission rates very low (20 to 28 mg/day)

On the basis of the information collected from these literature sources and in order to enable the use of COPERT for evaluating the emissions performance of the different scenarios, the following

modifications have been introduced to the model:

Effect of ethanol and fuel ethers on permeation emissions

Based on relevant data found in the literature, different permeation rates are proposed for fluorinated (0.6 g/day) and for multi-layer (0.2 g/day) tanks containing pure hydrocarbon (oxy-free) fuels. For ethanol containing fuels (E5 – E10), 0.3 g/day additional emissions from the fuel and vapour control system were assumed based on relevant US studies and confirmed by tests conducted by the Association of European Plastic Fuel Tanks and Systems Manufacturers (PlasFuelSys). These include permeation, as well as other sources, such as small leakages.

Table 2 below summarizes the proposed emission factors to be used in the COPERT model. Permeation depends on fuel polarity, solvency and volatility (Haskew et al. 2004), which explains why fuel ethers perform better than ethanol in terms of permeation emissions.

Table 2: Suggested permeation rates for different fuels and fuel tank structures (values in grams of VOC emissions per day)

Fuel tank structure	Oxy-free fuels	Ethanol blends	ETBE blends
Fluorinated (mono-layer) fuel tanks	0.6	0.9	0.55
Multi-layer fuel tanks	0.2	0.5	0.175

Activated carbon canister durability

Based on information received from MeadWestvaco (the largest activated carbon provider), two classes of durability of carbons are currently used in Europe:

- Low Degradation Carbons: these carbons lose about 4% to 9% of their capacity over the lifetime of the vehicle, due to repeated cycling with petrol fuel.
- High Degradation Carbons: these carbons lose about 12% to 20% of their capacity over the lifetime of the vehicle, due to repeated cycling with petrol fuel.

In order to estimate the canister performance deterioration with mileage, data from the in-service conformity testing programs conducted in Germany and Sweden (Schmidt 2007; 2008; 2009) were analysed. The two datasets contain information on the SHED (Sealed Housing for Evaporative Emission Determination) test emissions measured over the type approval test procedure (type IV) for a large number of vehicles. Other information, such as vehicle mileage, engine capacity, Euro standard, and fuel tank structure (for the Swedish program only) was also available.

The main difference between the Swedish and the German testing programs is the ethanol content of the fuel in the two countries. The use of ethanol is widespread in Sweden, typically in the range of 5-10% blended in petrol, whereas there was no ethanol in the fuel used in Germany at the time the testing program was carried out.

Table 3 summarises the tests from the Swedish in-service program. Vehicles are grouped into three engine capacity classes (small: <1.4 litres; medium: >1.4 & <2.0 litres; large >2.0 litres), and are further differentiated by fuel tank structure (selar, monolayer, multilayer, steel, and undefined). Average values for the evaporative emissions measured over the diurnal test and vehicle mileage are included in the same table for each vehicle configuration (number of tests shown in parentheses).

Based on the results of the Swedish (100 tests) and the German (26 tests) programs, it was found that the degradation of the activated carbon is higher for small cars and lower for medium and large cars. The effect of ethanol is also important as the in-service emissions in Sweden are consistently higher than in Germany for all vehicle classes.

Table 3: Summary of tests conducted for the Swedish in-service conformity testing program.

Fuel tank structure	Small cars		Medium cars		Large cars	
	Diurnal (g/day)	Mileage (km)	Diurnal (g/day)	Mileage (km)	Diurnal (g/day)	Mileage (km)
All (100)	2.48	41,832	1.49	44,509	1.20	47,003
Selar (6)	-	-	3.58	60,180	3.51	69,868
Monolayer (21)	3.35	36,487	1.83	42,344	-	-
Multilayer (31)	1.98	42,856	1.03	41,829	0.78	43,126
Steel (4)	1.06	45,720	0.48	67,244	-	-
Not defined (38)	2.66	48,113	0.73	37,519	0.75	37,710

In order to quantify this emissions deterioration effect, the latter was simulated with the revised COPERT code assuming a variable decrease in the efficiency of the activated carbon.

Based on these simulations for ethanol blends it was found that the efficiency of the activated carbon decreases by 1% every 8 000 km for small cars (i.e. about 20% decrease over vehicle lifetime), and by 1% every 32 000 km for medium and large cars (i.e. about 5% decrease over vehicle lifetime). For non-ethanol containing fuels the respective deterioration factors over the vehicle useful life are 13% and 4% respectively. Table 4 summarizes the results for ethanol (Sweden) and non-ethanol (Germany) fuels for the different vehicle classes.

Table 4: Effect of carbon degradation on evaporative emissions for ethanol and non-ethanol containing fuels based on the Swedish and German in-service test programs.

Vehicle category (engine capacity classes)	Measured emissions (g/day)	Modelled emissions (g/day)	Degradation	Fuel tank structure
Sweden				
Small (<1.4 l)	2.48	2.56	1% ~ 8000 km 20% over lifetime	35% fluorinated 65% multi-layer
Medium (>1.4, <2.0 l)	1.49	1.48	1% ~ 32000 km 5% over lifetime	35% fluorinated 65% multi-layer
Large (>2.0 l)	1.20	1.32	1% ~ 32000 km 5% over lifetime	0% fluorinated 100% multi-layer
Germany				
Small (<1.4 l)	1.94	1.92	1% ~ 12000 km 13% over lifetime	35% fluorinated 65% multi-layer
Medium (>1.4, <2.0 l)	0.95	1.05	1% ~ 40000 km 4% over lifetime	35% fluorinated 65% multi-layer
Large (>2.0 l)	0.86	0.95	1% ~ 40000 km 4% over lifetime	0% fluorinated 100% multi-layer

This ethanol effect on durability is largely due to the polarity of the ethanol molecules. For fuel ethers – on the other hand – there was no indication of any effect in carbon efficiency found in the literature that was consulted. Hence, it is assumed that fuel ethers behave similarly to non-oxy fuels in terms of carbon capacity loss with vehicle mileage.

3. Definition of scenarios and running of the model

The following scenarios were evaluated:

- Basecase scenario, assuming pure hydrocarbon petrol, i.e. no oxygenates (oxy-free)
- Ethanol scenarios, assuming ethanol-containing petrol at 5% v/v (E5). The following two variants were considered:
 - o All EU Member States (MS) with no bioethanol waiver (Ethanol-1)
 - o All EU MS with bioethanol waiver (except those MS granted an “arctic” vapour pressure waiver) (Ethanol-2)
- ETBE scenarios, assuming ETBE-containing petrol at 11% v/v ETBE (E5 equivalent). The following two variants were considered:
 - o Smart blending to maintain the 60 kPa vapour pressure (ETBE-1)
 - o Splash blending, i.e. the blended fuel has a lower vapour pressure (ETBE-2)

An important element in simulating the above scenarios is the vapour pressure of the summer grade petrol available in the different EU MS. For the basecase scenario, these values were taken from the annual summary reports on the quality of petrol and diesel used for road transport that EU MS transmit to the European Commission in line with their obligations set in the Fuel Quality Directive (Directive 98/70/EC as amended by Directive 2009/30/EC).

The above scenarios were simulated in COPERT taking into account the adjustments in the model as described in section 2. The modified COPERT model was then used for calculating the evaporative VOC emissions from the petrol passenger car fleet for the basecase and the ethanol and ETBE scenarios. It should be noted here that any effect on exhaust emissions was not taken into account in the present study. The calculations have been performed for the EU-27 Member States (all except Croatia for which no information is available) and for selected years including 2015, 2020, 2025 and 2030.

The main scenario assumptions and specifications are summarised in Table 5 below.

Table 5: Summary of main scenario assumptions and specifications.

Basecase scenario	Ethanol Scenarios	ETBE Scenarios
<ul style="list-style-type: none">• Oxy-free fuel• Current RVP values from Fuel Quality reports	<ul style="list-style-type: none">• 5% v/v EtOH in petrol• RVP values with and without waiver• Higher permeation• Higher degradation	<ul style="list-style-type: none">• 11% v/v ETBE in petrol• RVP values with and without waiver• Lower permeation• Same durability as base fuel

4. Results and discussion

Emissions results are presented for the EU as a whole in the following tables (Table 6 through Table 8). Each table contains the calculated evaporative VOC emissions for the basecase, the ethanol and ETBE scenarios for the years 2015 to 2030 (in five year intervals) using different metrics.

Table 6 shows total calculated evaporative emissions (in tonnes of VOCs) from the entire petrol vehicle fleet and from the Euro 6 fleet only. Euro 6 (and later) vehicles are shown separately to demonstrate the effect on latest technology vehicles, whereas the entire petrol fleet includes all vehicle technologies from pre-Euro (i.e. more than 20 years old) to Euro 6. As shown in the table the share of

Euro 6 cars in the petrol fleet is relatively small in 2015, whereas it is the dominant technology in 2030.

Table 7 shows the same results expressed in kilograms of VOC emissions per vehicle and Table 8 shows the calculated average diurnal emission factors in grams of VOCs per vehicle per day for the basecase and the different scenarios.

Table 6: Total calculated evaporative VOC emissions (in tonnes of VOC) for the entire petrol passenger car fleet and for the Euro 6 car fleet in the EU-27.

	2015	2020	2025	2030
	Total evaporative emissions – All petrol cars			
Vehicle population	167,163,118	175,716,100	167,983,699	153,447,560
Base	165,255	148,860	139,215	134,766
Ethanol-1	213,040	198,948	191,090	188,757
Ethanol-2	243,975	227,224	218,030	215,617
ETBE-1	162,867	146,749	137,446	133,277
ETBE-2	158,156	142,575	133,597	129,570
	Total evaporative emissions – Euro 6 petrol cars			
Vehicle population	13,248,596	74,039,151	109,664,298	123,560,526
Base	6,376	40,370	71,682	95,154
Ethanol-1	8,099	53,524	96,952	131,001
Ethanol-2	9,144	60,521	109,267	148,338
ETBE-1	6,223	39,697	70,722	94,071
ETBE-2	6,035	38,490	68,686	91,438

Table 7: Average yearly evaporative emissions (in kilograms of VOC per vehicle per year) for the entire petrol passenger car fleet and for the Euro 6 car fleet in the EU-27.

	2015	2020	2025	2030
	Average yearly emissions – All petrol cars			
Base	0.99	0.85	0.83	0.88
Ethanol-1	1.27	1.13	1.14	1.23
Ethanol-2	1.46	1.29	1.30	1.41
ETBE-1	0.97	0.84	0.82	0.87
ETBE-2	0.95	0.81	0.80	0.84
	Average yearly emissions – Euro 6 petrol cars			
Base	0.48	0.55	0.65	0.77
Ethanol-1	0.61	0.72	0.88	1.06
Ethanol-2	0.69	0.82	1.00	1.20
ETBE-1	0.47	0.54	0.64	0.76

ETBE-2	0.46	0.52	0.63	0.74
--------	------	------	------	------

Table 8: Average daily evaporative emissions (in grams of VOC per vehicle per day) for the entire petrol passenger car fleet and for the Euro 6 car fleet in the EU-27.

	2015	2020	2025	2030
	Average daily emissions – All petrol cars			
Base	2.71	2.32	2.27	2.41
Ethanol-1	3.49	3.10	3.12	3.37
Ethanol-2	4.00	3.54	3.56	3.85
ETBE-1	2.67	2.29	2.24	2.38
ETBE-2	2.59	2.22	2.18	2.31
	Average daily emissions – Euro 6 petrol cars			
Base	1.32	1.49	1.79	2.11
Ethanol-1	1.67	1.98	2.42	2.90
Ethanol-2	1.89	2.24	2.73	3.29
ETBE-1	1.29	1.47	1.77	2.09
ETBE-2	1.25	1.42	1.72	2.03

As shown in Table 6, total evaporative VOC emissions for the basecase decrease by about 20% from 2015 to 2030 due to fleet renewal, i.e. more vehicles with latest emissions control technology (bigger carbon canisters and low permeability fuel tanks) substituting older uncontrolled vehicles. This is reflected in the average emissions factors of Table 8 showing a decrease from 2.71 g/day in 2015 to 2.27 g/day in 2025. The emission factor increases to 2.41 g/day in 2030 because of the activated carbon degradation effect for canister-equipped vehicles. This effect is lower in the previous years (i.e. 2015-2025) because the share of uncontrolled vehicles (for which there is no degradation) is larger.

When looking at petrol Euro 6 vehicles only, emissions for the basecase increase steadily from 2015 to 2030 due to the combined effect of Euro 6 population growth and degradation. The population of Euro 6 cars in the EU27 is projected to grow (9-fold) from about 13.2 million vehicles in 2015 to about 124 million vehicles in 2030. The increase in emissions, however, is projected to be even higher (15-fold) over the same period, due to the carbon efficiency loss with mileage accumulation.

Emissions of the ethanol scenarios are significantly higher compared to the basecase due to the higher permeation emissions and higher carbon degradation of ethanol compared to non-oxy fuel and ETBE as explained in section 2. For the Ethanol-2 scenario in particular the calculated emissions are 50 to 60% higher compared to the basecase. This is because the Ethanol-2 scenario assumes a bioethanol waiver for all MS – except those with an “arctic” waiver – and hence vapour pressure values up to 68 kPa are allowed for summer fuel.

The Ethanol-1 scenario assumes no bioethanol waiver, which means that all MS have to comply with the 60 kPa summer fuel vapour pressure requirements of the Fuel Quality Directive. The lower – compared to Ethanol-2 scenario – fuel volatility results in reduced fuel vapour generation in the fuel tank of the vehicles and hence lower evaporative emissions.

The ETBE scenarios on the other hand deliver slightly improved emissions results compared to the basecase, due to the somewhat lower permeation rates assumed for ETBE over non-oxy fuels.

The ETBE-2 scenario delivers slightly higher emissions reductions compared to the ETBE-1 scenario, as a result of the lower vapour pressure when ETBE is splash blended into petrol. Typically,

the resulting blend has a vapour pressure of approximately 56.5 kPa for a 60 kPa base petrol fuel. The ETBE-1 scenario assumes that fewer amounts of lighter components (e.g. butane) will have to be removed from the blendstock so that the final blend will have a vapour pressure of 60 kPa.

All three scenarios (including variants) result in a reduction in the total evaporative emissions (Table 6). These reductions are of the same order of magnitude – in absolute terms – for the different scenarios and variants. However, the ethanol scenarios result in considerably higher VOC emissions levels compared to the basecase and the ETBE scenarios.

The following Table 9 compares the ethanol and ETBE scenarios and summarises the emissions reductions potential of ETBE over ethanol for the entire petrol light duty vehicle fleet.

Table 9: Emissions reduction potential of ETBE blends over Ethanol blends and over oxy-free petrol fuel.

	2015	2020	2025	2030
	ETBE vs Ethanol scenarios			
ETBE-1 vs Ethanol-1	-24%	-26%	-28%	-29%
ETBE-1 vs Ethanol-2	-33%	-35%	-37%	-38%
ETBE-2 vs Ethanol-1	-26%	-28%	-30%	-31%
ETBE-2 vs Ethanol-2	-35%	-37%	-39%	-40%
	ETBE vs Basecase			
ETBE-1 vs Basecase	-1.4%	-1.4%	-1.3%	-1.1%
ETBE-1 vs Basecase	-4.3%	-4.2%	-4.0%	-3.9%

Overall, there are significant emissions reductions associated with the use of ETBE instead of ethanol for blending into petrol. This is due to the increased activated carbon durability and lower permeability of ETBE blends compared to equivalent (in terms of oxygen content) ethanol blends.

References

- Haq G., G. Martini & G. Mellios (2013): Estimating the Costs and Benefits of Introducing a New European Evaporative Emissions Test Procedure. Institute for Energy and Transport, [EUR 26057 EN](#).
- Haskew H., T. Liberty & D. McClement (2004): Fuel permeation from automotive systems. [Final Report, CRC Project No. E-65](#).
- Haskew H., T. Liberty & D. McClement (2006): Fuel permeation from automotive systems: E0, E6, E10, E20 and E85. [Final Report, CRC Project No. E-65-3](#).
- Martini G., U. Manfredi, G. Mellios, V. Mahieu, B. Larsen, A. Farfaletti, A. Krasenbrink, et al. (2007): Joint EUCAR/JRC/CONCAWE Study on: Effects of Gasoline Vapour Pressure and Ethanol Content on Evaporative Emissions from Modern Cars, Institute for Environment and Sustainability, [EUR 22713](#).
- Mellios G. & Z. Samaras (2007): An empirical model for estimating evaporative hydrocarbon emissions from canister-equipped vehicles, [Fuel](#), 86, 2254–2261.
- Schmidt H. (2007): Swedish In-Service Testing Program 2006 on Emissions from Passenger Cars and Light-Duty Trucks. [Vägverket, Publication 2007:43](#).
- Schmidt H. (2008): Swedish In-Service Testing Program 2007 on Emissions from Passenger Cars and Light-Duty Trucks. [Vägverket, Publication 2008:121](#).

- Schmidt H. (2009): Swedish In-Service Testing Program 2008 on Emissions from Passenger Cars and Light-Duty Trucks. Vägverket, Publication 2009:145.
- Stump F., K. Knapp, W. Ray, P. Siudak&R. Snow (2012): Influence of Oxygenated Fuels on the Emissions from Three Pre-1985 Light-Duty Passenger Vehicles. Air & Waste Management Association 44: 781-186.
- Tanaka H., T. Kaneko, T. Matsumoto, T. Kato& H. Takeda (2006): Effects of Ethanol and ETBE Blending in Gasoline on Evaporative Emissions. SAE Technical Paper Series 2006-01-3382.
- Tanaka H., T. Matsumoto, R. Funaki, T. Kato, K. Mitsutake, M. Sekimoto & H. Watanabe (2007): Effects of Ethanol or ETBE Blending in Gasoline on Evaporative Emissions for Japanese In-Use Passenger Vehicles. SAE Technical Paper Series 2007-01-4005.

Vehicle emissions in Turkey: Current status and policy options for the future

Peter MOCK*, **

* Istanbul Policy Center, Sabancı University, Istanbul, 34420, Turkey

**International Council on Clean Transportation (ICCT), Berlin, 10178, Germany

email: peter @theicct.org

Abstract

Passenger cars and light commercial vehicles account for three-quarters of the vehicle fleet in Turkey. When taking into account differences in fleet characteristics, such as vehicle weight, size, and engine power, fuel consumption and CO₂ emission levels for new vehicles in Turkey tend to be similar to those on the EU market. While taxes on sales and ownership of passenger cars in particular are relatively high in Turkey, these taxes currently are not directly linked to the CO₂ emissions and fuel consumption of a vehicle. Furthermore, Turkey is one of the few key automotive markets worldwide not yet having introduced mandatory CO₂ standards for cars and light commercial vehicles. The same is true for heavy-duty vehicles, which are responsible for more than half of total fuel consumption and CO₂ emissions. In addition to these policy measures at the national level, urban areas can take complementary action, for example, to incentivize the deployment of low-emission vehicles. This is of particular relevance for Turkey, where about half of new cars are first registered in the Istanbul area.

Keywords: road transport, greenhouse gas emissions, exhaust emissions, modeling, policy instruments

Introduction

Turkey is among the most important vehicle manufacturing countries in the world. Of the more than 1.1 million vehicles produced in Turkey every year, about three quarters are currently being exported abroad (OSD, 2014). At the same time, the number of vehicle sales in Turkey itself is growing quickly – recently at a rate of about 8% per year (TUIK, 2015). As a result, the automotive sector in Turkey is a vital part of the national economy, with numerous production plants and employees in the vehicle and vehicle parts manufacturing industry.

Given the strong dependence of the Turkish economy on the automotive industry, it is of particular importance to ensure that this industry sector is ready to meet current and future challenges, such as local air pollution, climate change, and energy security, by offering innovative vehicles that can compete on the global and national market. An extensive set of policy measures can help drive forward the necessary innovations.

It is the objective of this paper to describe the current structure of the vehicle fleet in Turkey, in particular with respect to its fuel consumption and emissions level, as well as to assess a set of potential policy measures that could help driving down fuel consumption and emissions from the road transport sector in Turkey in future years¹.

1. Vehicle fleet structure

In Turkey, there are about 17 million vehicles currently on the road (TUIK, 2015). This is significantly less than, for example, in Germany (52 million) (KBA, 2015), despite both countries having about the same population. As a result, the number of passenger cars per 1,000 inhabitants in Turkey is only around 120, compared to 550 on average in Germany. The annual growth rate in vehicle stock is comparably high in Turkey though, at around 8% in the 2000-2014 timeframe (Figure 1 and Figure 2).

¹ A more detailed assessment can be found in (Mock, 2016a) and (Mock, 2016b).

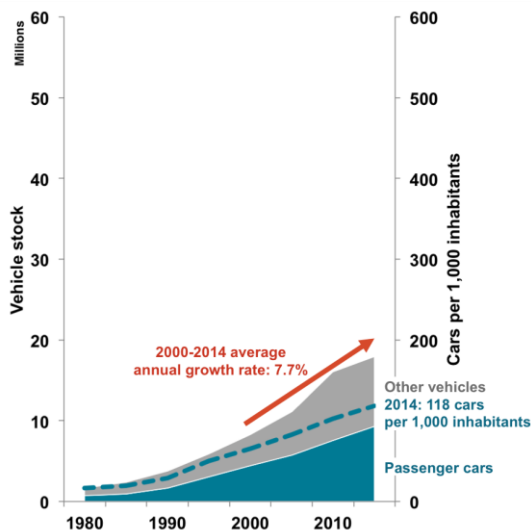


Figure 1. Historic development of vehicle stock in Turkey. Data source: (TUIK, 2015).

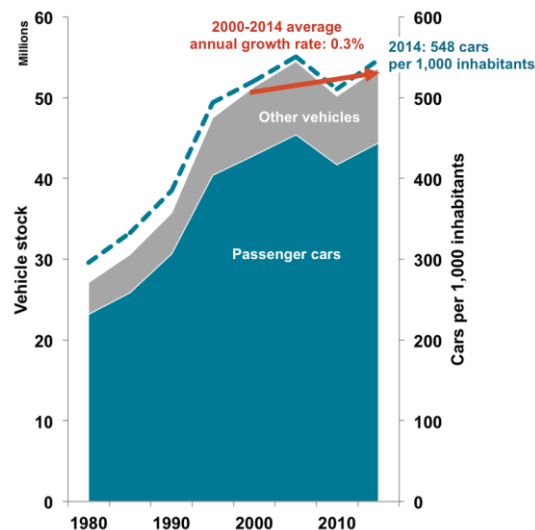


Figure 2. Historic development of vehicle stock in Germany. Data source: (KBA, 2015).

Passenger cars account for the majority of vehicle sales in Turkey, with about 60% of the 1 million new vehicles sold every year being cars (Figure 3 and Figure 4). Light commercial vehicles (also called “light trucks”) are significantly more popular in Turkey than in Germany (15% vs. 7% market share). A key underlying reason is the fact that light commercial vehicles in Turkey are subject to a drastically lower vehicle sales tax than passenger cars (4-15% “Special Consumption Tax” instead of 45-145%) (ACEA, 2015). Motorcycles are also more popular in Turkey, accounting for 16% of vehicles in Turkey but only 8% in Germany.

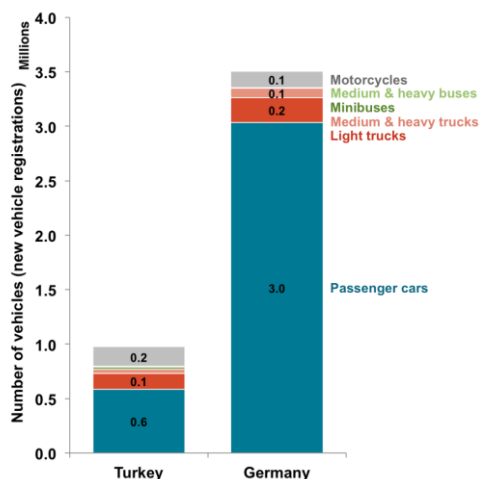


Figure 3. New vehicle registrations (2014), differentiated by vehicle type, in absolute numbers. Data sources: (ACEA, 2015a), (KBA, 2015), (TUIK, 2015).

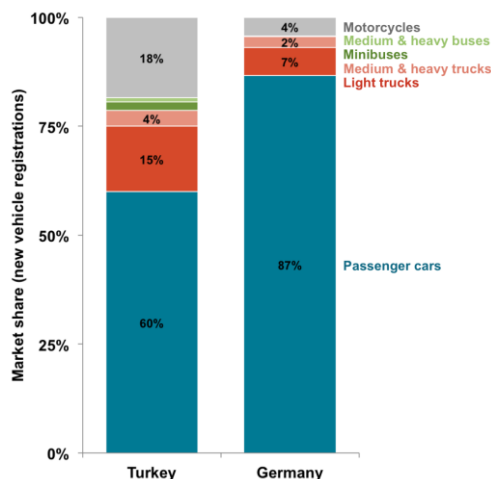


Figure 4. New vehicle registrations (2014), differentiated by vehicle type, in percentage. Data sources: (ACEA, 2015a), (KBA, 2015), (TUIK, 2015).

The automotive sectors in Turkey and Germany are very similar in the sense that both countries have a large number of vehicle manufacturing plants and are exporting a majority of their local vehicle production abroad. In fact, the automotive sector is the number one export sector in both nations. In 2014, 0.7 million passenger cars were produced locally in Turkey, with about 79% of these being exported abroad (OSD, 2014). In addition, another 0.4 million commercial vehicles were produced locally, with 0.3 million being exported abroad. The importance of vehicle exports in Turkey is particularly strong for buses and trucks. In comparison, 77% of the 5.6 million passenger cars produced in Germany were exported abroad (VDA, 2015). In Turkey, exports from the automotive sector overall account for about 12% of the country’s total export volume (TUIK, 2015). In Germany, automotive exports comprise about 18% of total exports (DESTATIS, 2015).

Around half of new passenger car registrations in Turkey take place in the region of Istanbul (Figure 5). However, throughout the lifetime of a vehicle, it is likely to shift eastward. The statistics show that of

the total number of passenger cars on the road, only around 23% are still registered in the Istanbul area (Figure 6). This pattern suggests that many new vehicles are first registered in Istanbul but are then sold as secondhand cars to other regions in Turkey. Overall, the average age of passenger cars in Turkey is 12 years, with the vehicle fleet in Istanbul being significantly younger than that.



Figure 5. New passenger car registrations (2014) in Turkey by region². *Data source: (TUIK, 2015).*

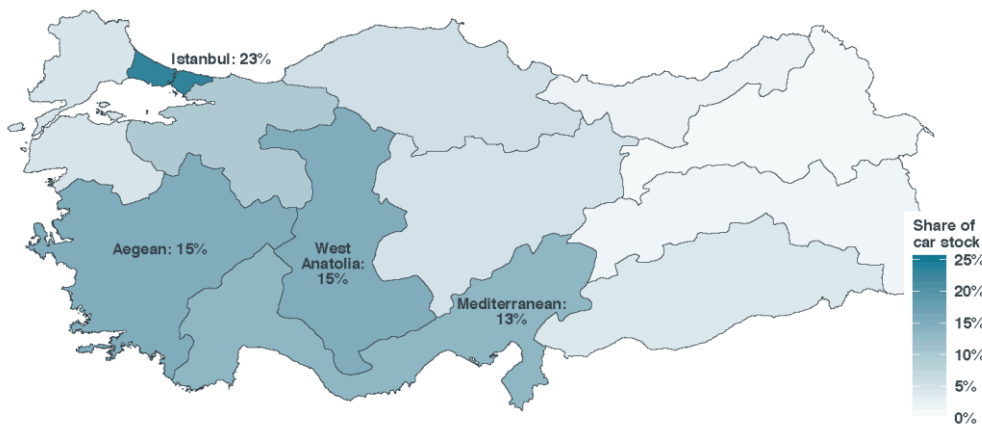


Figure 6. Passenger car stock (2014) in Turkey by region. *Data source: (TUIK, 2015).*

In Turkey, more than half of all new passenger cars are from the lower medium segment (Figure 7). Within this segment, it is in particular the Renault Fluence and Fiat Linea models that are most popular. In Germany, the lower medium segment only accounts for 32% of new car registrations, with the VW Golf being the most popular model. Vehicles from the mini segment, such as the VW up! or smart fortwo, are largely absent from the Turkish market. At the other end of the spectrum, the market share of larger vehicles, including sport utility vehicles (SUV), is significantly lower in Turkey than in Germany.

² Regions with a market share at 10% or above are annotated in the maps.

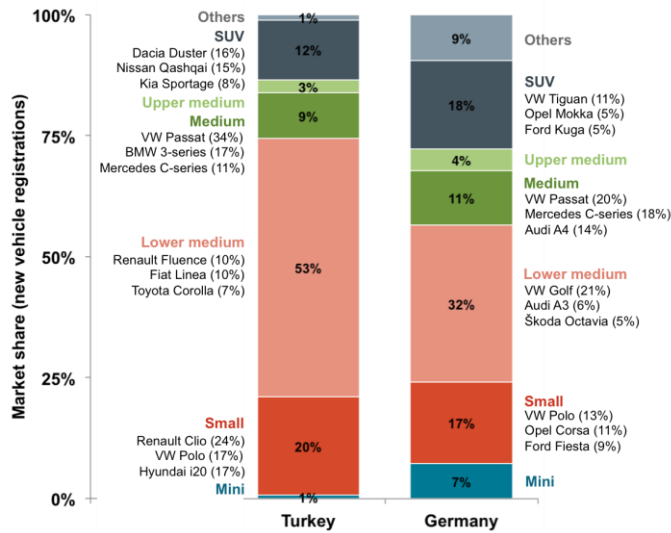


Figure 7. New passenger car registrations (2014) by segment, including top three vehicle models for selected segments. *Data source: (ICCT, 2015a).*

Looking at the distribution of sales by vehicle manufacturers, it can be seen that Renault and Volkswagen both account for about 22% of all new passenger cars in Turkey. The majority of car sales are divided among a number of other manufacturers, unlike in Germany where the Volkswagen group alone sells about 40% of all new cars, and BMW and Daimler account for another 19% of the market (Figure 8).

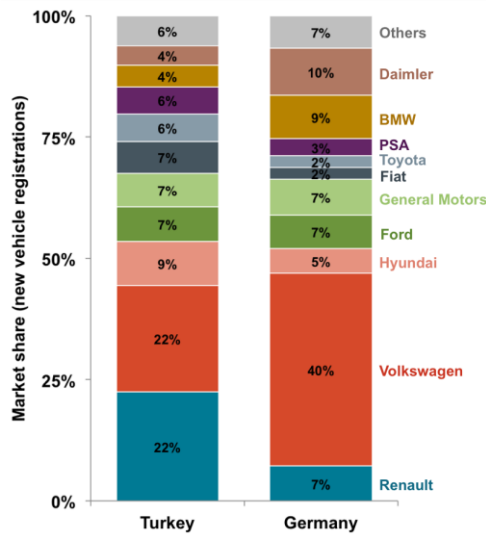


Figure 8. New passenger car registrations (2014) by manufacturer. *Data sources: (ICCT, 2015a), (TUIK, 2015).*

In terms of technical characteristics, it is particularly remarkable that 95% of all new cars in Turkey have an engine displacement of 1.6 liters (l) or less, while in the EU about 30% of new cars have an engine displacement above 1.6l (Figure 9). Underlying reason for this phenomenon is the vehicle taxation scheme in Turkey that is based on engine displacement and includes an important tax threshold at 1.6l engine displacement.

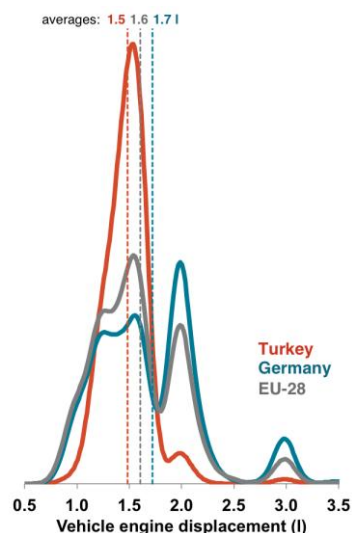


Figure 9. New passenger car registrations (2014) by engine displacement, estimated probability density function. *Data source: (ICCT, 2015a).*

In comparison to other key automotive markets worldwide, it can be seen that in terms of average engine displacement (1.5l) and engine power (80 kW), the market in Turkey is most similar to those in the EU-28, China, Japan, and Brazil (Table 1). In terms of average vehicle weight (1.3 metric tons) and size (4.0 m²), new cars in Turkey are most similar to those sold on average in the EU-28 and in China. The power-to-weight ratio is a measure for expressing how powerful the engine of a vehicle is in comparison to its weight. Here the average for Turkey (0.059 kW/kg) is most similar to the average value for the EU-28.

Table 1. International market comparison of new passenger car fleet characteristics.³ *Data sources: (ICCT, 2015a), (Posada and Façanha, 2015).*

	Turkey (2014)	Germany (2014)	EU-28 (2014)	U.S. (2014)	China (2012)	Japan (2011)	Brazil (2013)	India (2012)	S. Korea (2013)
Sales (million)	0.6	3.0	12.5	7.9	15.5	3.5	3.0	2.6	1.3
Number of cylinders	4.0	4.0	3.9	4.6	--	3.8	4.0	3.6	4.3
Engine displacement (l)	1.5	1.7	1.6	2.5	1.6	1.4	1.4	1.3	1.9
Engine power (kW)	80	103	90	150	86	78	76	55	120
Curb weight (metric tons)	1.3	1.5	1.4	1.6	1.3	1.2	1.1	1.1	1.5
Footprint (m ²)	4.0	4.1	4.0	4.3	3.8	3.7	3.7	3.4	4.2
Power-to-weight-ratio (kW/kg)	0.059	0.070	0.065	0.093	0.066	0.065	0.067	0.052	0.084
Energy consumption - U.S. CAFE (MJ/km)	1.6	1.7	1.6	2.0	2.2	1.8	2.0	1.8	1.9
Current emission standard	Euro 5	Euro 6	Euro 6	Tier 2	Euro 4 _{eq}	Euro 6 _{eq}	Euro 5 _{eq}	Euro 4 _{eq}	Euro 6 _{eq}
Petrol	38%	50%	43%	93%	99%	86%	6%	56%	46%
Diesel	62%	48%	53%	2%	1%	0%	0%	40%	42%
Hybrid-electric	0%	1%	2%	6%	0%	13%	0%	0%	0%
Others	0%	1%	2%	0%	0%	1%	94%	4%	12%
Manual transmission	54%	70%	77%	5%	60%	1%	83%	98%	9%
Automatic transmission	46%	30%	23%	95%	40%	99%	17%	2%	91%

The market share of diesel cars in Turkey (62%) is among the highest in the world. Only some EU member states (such as Luxembourg, Ireland, and Portugal) have a higher diesel share than Turkey. Outside of Europe, only India and South Korea have a significant diesel market share among passenger cars. Of the 40% of new cars that are petrol-fuelled, a large portion is being converted to run on gas, taking advantage of tax incentives (WLPGA, 2015). With respect to hybrid-electric vehicles, Japan and the United States are the leading markets. Meanwhile, in the EU the current market share is only 2% and for Turkey the number of hybrid-electric vehicles is currently insignificant.

³Sales / registration weighted averages; energy consumption data was converted using the methodology described in (Yang, 2015).

For light commercial vehicles, more than half of the market in Turkey is dominated by Fiat and Ford (Figure 10). While Volkswagen and Renault are the largest passenger car manufacturers, for light commercial vehicles they are only third and fourth, with about 20% market share altogether. In Germany, it is particularly the Mercedes-Benz Sprinter that is a popular light commercial vehicle. In Turkey on the other hand, it is smaller vehicles, such as the Fiat Fiorino and Fiat Doblo, that are most popular in the light commercial vehicle segment. New light commercial vehicles in Turkey are running entirely on diesel fuel.

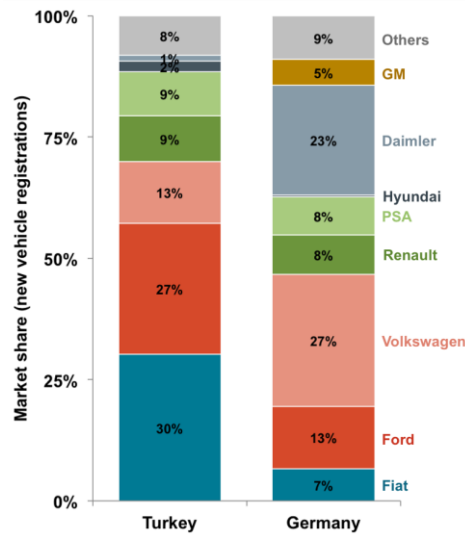


Figure 10. New light commercial vehicle registrations (2014) by manufacturer. *Data source: (ICCT, 2015a).*

The market for heavy-duty trucks in Turkey is dominated by Daimler, accounting for about half of new truck sales (Figure 11). The remaining 50% of the market is split between several companies, with Ford Otosan (owned by Ford Motor Company and Koç Holding) being the second largest truck manufacturer (16%) and Volkswagen being third (10%).

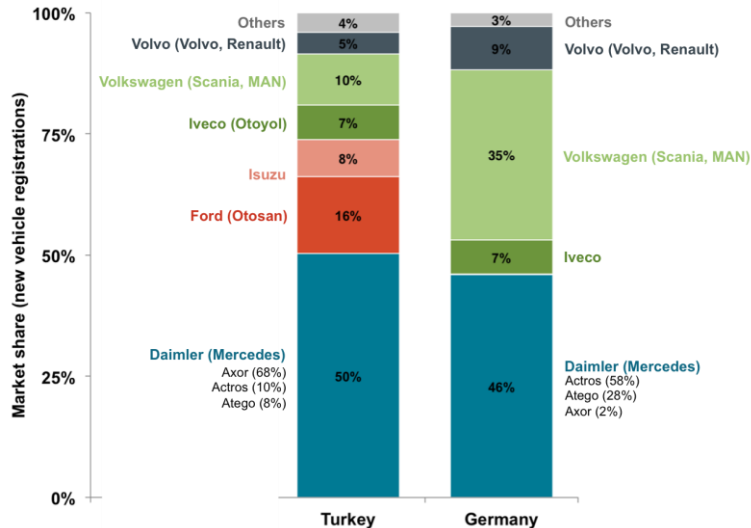


Figure 11. New heavy-duty truck registrations (2014) by manufacturer, including top-3 vehicle models for Daimler. *Data sources: (ICCT, 2015a), (TUIK, 2015).*

2. Fuel consumption and emissions

New passenger cars in Turkey in 2014 had an average CO₂ emission level of 121g/km (ICCT, 2015a). As CO₂ emissions and fuel consumption of a vehicle are directly proportional, the value of 121g/km is equal to a fuel consumption of approximately 4.8l/100km. For light commercial vehicles, the average level in 2014 was 157g/km, or about 6.2l/100km. These values are according to the official type-approval test procedure in Europe, the New European Drive Cycle (NEDC).

In the EU, a mandatory CO₂ emission target for new passenger cars is in place, fixed at 130g/km for 2015 for the average new vehicle fleet. Targets for individual manufacturers depend on the weight of the vehicle fleet though: the heavier a vehicle, the more CO₂ emissions it is allowed to emit. Applying this weight-based target function at country level, the new passenger car fleets in EU-28 and Germany are below their respective 2015 target threshold (Figure 12). It can be seen that the new car fleet in Germany is heavier than for the EU average, thereby resulting in a higher target value for the German car market. New passenger cars in Turkey are lighter than in Germany and also slightly lighter than the EU average. If the EU CO₂ target line would also apply to Turkey, it would have already been met in 2014 as well.

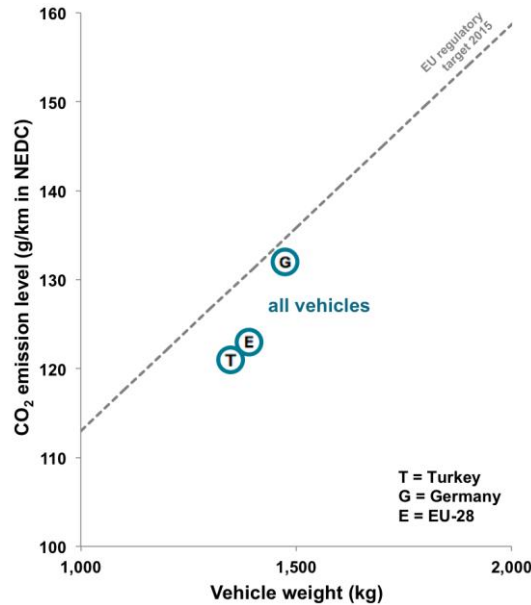


Figure 12. Average CO₂ emission level of new registration passenger car registrations (2014), all vehicles by vehicle weight. *Data source: (ICCT, 2015a).*

A differentiation between vehicles with different fuel types allows for a better interpretation of the data. Figure 13 shows again new passenger car weight vs. CO₂ emissions, with petrol and diesel cars shown separately. It can be seen that petrol cars in Turkey and Germany tend to have nearly the exact same average weight and CO₂ emission levels, while petrol cars at the EU average are about 70 kg lighter and emit about 5g/km less of CO₂. For diesel cars, the differences are much bigger, with these vehicles weighing about 250kg less on average in Turkey than in Germany. Similarly, the difference in CO₂ emissions between average diesel cars in Turkey and Germany is around 15g/km. It is remarkable to see that, despite their absolute differences, the efficiency (in terms of fuel consumption/CO₂ emission level per kg of vehicle weight) of the average vehicle fleets is about the same in all three markets.

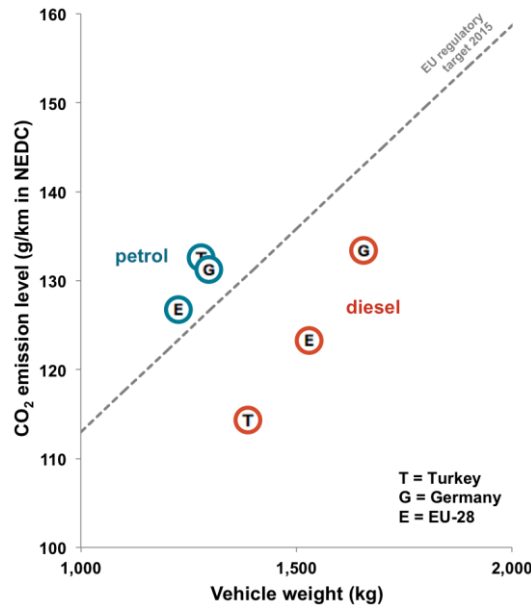


Figure 13. Average CO₂ emission level of new registration passenger car registrations (2014), all vehicles by fuel type and vehicle weight. *Data source: (ICCT, 2015a).*

Figure 14 provides a further break down into individual vehicle segments. For most of the vehicle segments, the average weight, size, and also CO₂ emission levels are very similar for all three markets levels. The only exception is the SUV segment, where vehicles in Germany tend to be significantly heavier and larger and emitting higher CO₂ emission levels than in Turkey and the EU average. Again, this is an indication that the efficiency of new cars in all markets is similar and that the resulting lower overall CO₂ emission level in Turkey is mostly due to differences in the fleet mix, i.e. more vehicles from the smaller segments being sold in Turkey.

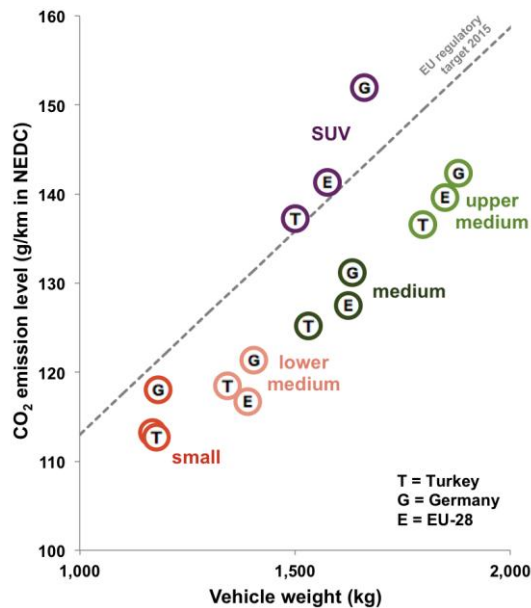


Figure 14. Average CO₂ emission level of new registration passenger car registrations (2014), all vehicles by vehicle segment and weight. *Data source: (ICCT, 2015a).*

Total oil demand in Turkey is estimated at 670,000 barrels per day (IEA, 2013). Nearly all of this oil is imported from abroad, with Iran, Saudi Arabia, and Russia being the main sources. Transport accounts for about half of the total oil consumption. In terms of greenhouse gas (GHG) emissions, the transport sector accounts for about 15% of total GHG emissions, with CO₂ being the highest contributing emissions category (UNFCCC, 2013).

As part of the analysis, a business-as-usual scenario for future vehicle emissions and fuel consumption in Turkey was developed. It is important to emphasize that the objective of this modeling exercise is not to produce a highly accurate reflection of the current emission situation in both countries and future developments. Instead, the modeling results are intended to allow for approximate estimates and for highlighting similarities and differences to other markets. For the modeling, the ICCT Global Transportation Roadmap Model was applied (ICCT, 2015b).

In a business-as-usual scenario, fuel consumption of road transport in Turkey is estimated to almost double by 2030. As Turkey is importing most of its oil from abroad, this would be linked to a doubling also of its oil imports, thereby implicitly weakening national energy security. With fuel consumption and CO₂ emissions being directly linked to each other, CO₂ emissions would approximately double by 2030, from about 40 million metric tons (Mt) in 2010 to 79Mt in 2030 (Figure 15). The expected increase would be due mostly to trucks and buses, while the CO₂ emissions from passenger vehicles would increase to a lesser extent.

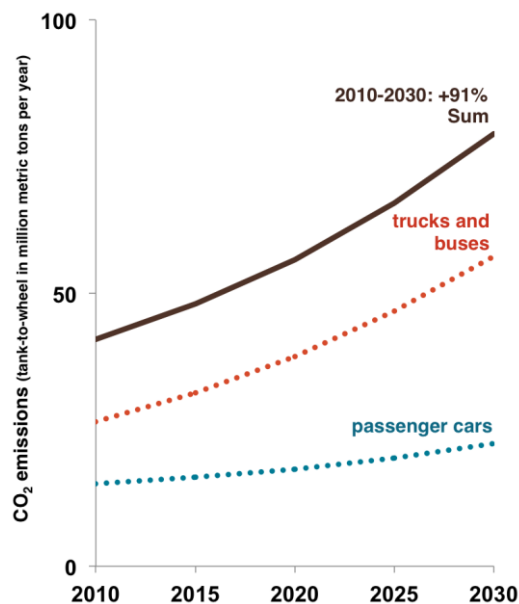


Figure 15. Estimated CO₂ emissions from road transport in Turkey (2010-2030) in a business-as-usual scenario.

About 45% of overall nitrogen oxides (NO_x) emissions in Turkey come from the road transport sector (EEA, 2013). For heavy-duty vehicles, nitrogen oxides emissions are expected to significantly decrease in future years as new trucks and buses that fulfill the latest Euro VI emissions standard will penetrate the vehicle fleet. For passenger cars, Turkey is introducing the Euro 6 standard from 2016/17 onwards. However, even with Euro 6, real-world nitrogenoxides emissions from diesel cars are expected to remain at high levels. As a number of recent studies demonstrate, the emission levels, and particularly the NO_x emissions of diesel cars, are much higher under real-world driving conditions on the road than during laboratory testing (Franco et al., 2014). This problem is expected to be even more relevant in Turkey than in the EU, given the particularly high share of diesel cars in Turkey (Mock, 2015a).

3. Potential policy instruments

Vehicle CO₂ standards

A CO₂ standard requires vehicle manufacturers to ensure that the emissions of their new vehicles sold are below a certain target value by a certain target year. Usually CO₂ standards are applied at the fleet level, i.e. a manufacturer can continue selling some vehicles with emissions above the target value, as long as the sales-weighted average for the new vehicle fleet remains below the respective target level.

With a total of about 1.1 million new vehicle sales (including passenger cars, light commercial vehicles and heavy duty vehicles) per year. Turkey ranks among the G20 countries. Altogether, the G20 countries account for more than 80 million vehicle sales per year and thereby more than 90% of global annual vehicle sales. By now, half of the G20 countries have implemented mandatory CO₂reduction standards for new passenger cars and light commercial vehicles (Table 2).

Table 2. Overview of mandatory CO₂ emission standards for new passenger cars and light commercial vehicles in the G20 countries⁴. Data sources: (ICCT, 2016), (Kodjak, 2015), (OICA, 2016).

Region	Total vehicle sales in 2015		Passenger cars - Standards CO ₂ reduction					Light-commercial veh. - Standards CO ₂ reduction						
			2015	2020	2025	Total	Annual	2015	2020	2025	Total	Annual		
China	24,597,583	28%	■	■	■	■	■	■	■	■	■	■	■	■
EU	15,786,092	18%	■	■	■	■	■	■	■	■	■	■	■	■
U.S.	17,470,659	20%	■	■	■	■	■	■	■	■	■	■	■	■
Japan	5,046,511	6%	■	■	■	■	■	■	■	■	■	■	■	■
India	3,425,336	4%	■	■	■	■	■	■	■	■	■	■	■	■
Brazil	2,568,976	3%	■	■	■	■	■	■	■	■	■	■	■	■
Canada	1,939,949	2%	■	■	■	■	■	■	■	■	■	■	■	■
South Korea	1,833,786	2%	■	■	■	■	■	■	■	■	■	■	■	■
Russia	1,437,930	2%	■	■	■	■	■	■	■	■	■	■	■	■
Mexico	1,351,648	2%	■	■	■	■	■	■	■	■	■	■	■	■
Australia	1,155,408	1%	■	■	■	■	■	■	■	■	■	■	■	■
Indonesia	1,031,422	1%	■	■	■	■	■	■	■	■	■	■	■	■
Turkey	1,011,194	1%	■	■	■	■	■	■	■	■	■	■	■	■
Saudi Arabia	830,100	1%	■	■	■	■	■	■	■	■	■	■	■	■
South Africa	617,749	1%	■	■	■	■	■	■	■	■	■	■	■	■
Argentina	605,933	1%	■	■	■	■	■	■	■	■	■	■	■	■
All G20 countries	80,710,276	91%												
All countries	88,677,983	100%												

The United States (U.S.) and Canada currently have the furthest reaching standard, in terms of target year. Both markets have set a mandatory CO₂ target for 2025, for passenger cars requiring a 35-39% reduction compared to 2015 levels, which equals an annual reduction rate of 3.5-3.9%. South Korea is the market that currently has the most stringent standard in terms of required total and annual CO₂ reduction, having set a mandatory standard for 2020 that will bring down new car CO₂ emissions by 34% compared to 2015 at a rate of 6.8% per year. The EU requires new cars to emit – on average – not more than 95 g/km⁵ of CO₂ by 2021, which is equivalent to a reduction of 21% compared to 2015 at an annual rate of 3.6%. China requires a 27% reduction (5.4% per year) to meet its 2020 target. Japan also has set a mandatory CO₂ target for 2020 (122 g/km), but it has already been met well in advance so that the current regulation does not require any further improvements of vehicles. India, Brazil, Mexico and Saudi Arabia are other G20 countries with mandatory CO₂ emission standards for new passenger cars in place. Most markets with CO₂ emission standards for passenger cars also have similar standards for light commercial vehicles in place.

Turkey is one of the G20 countries not having implemented mandatory CO₂ standards for new cars or light commercial vehicles at this point. For passenger cars, the average CO₂ emission level in Turkey (121 g/km in 2014) is slightly below the EU-28 average (123 g/km) (Figure 16). For the years 2012-2014, for which data on the new car CO₂ emissions is available, the annual rate of reduction is similar to that in the EU. Other markets, like the U.S., China and South Korea, come from a higher baseline CO₂ emission level but require a steeper reduction rate than Turkey and the EU in order to meet their respective 2020-2025 emission targets for new cars.

⁴While Germany, France, UK and Italy are members of G20, for this overview table the EU-28 was included instead.

⁵All CO₂ emission targets and reduction rates given are expressed as being measured in the New European Driving Cycle (NEDC) vehicles test procedure. The conversion factors for non-NEDC test procedures can be found in (ICCT, 2016).

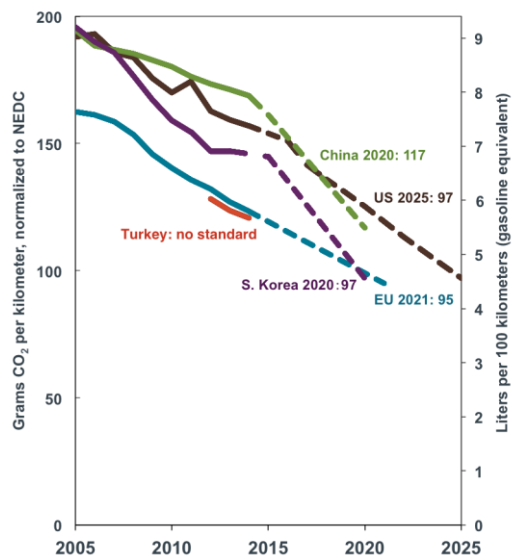


Figure 16. Average new passenger car CO₂ emission levels for selected countries/regions, normalized to NEDC. Data source: (ICCT, 2016).

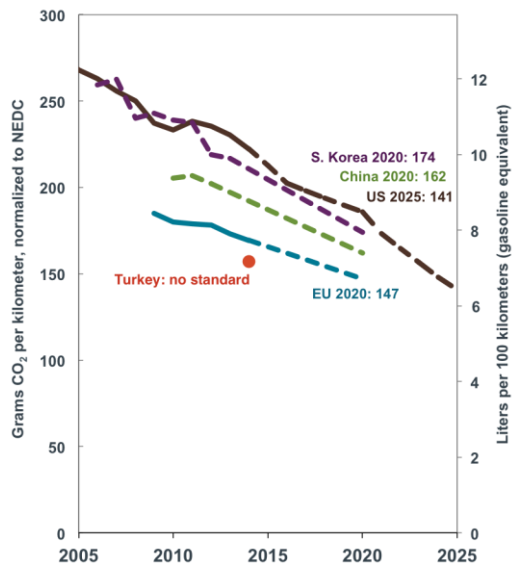


Figure 17. Average new light commercial vehicle CO₂ emission levels for selected countries/regions, normalized to NEDC. Data source: (ICCT, 2016).

For light commercial vehicles, the average new vehicle CO₂ emission level for Turkey in 2014 (157 g/km) was below the EU average (171 g/km) (Figure 17). Historical data was not available for the analysis within this paper. The annual CO₂ reduction rate in the EU, China and South Korea is at a similar level, with a somewhat steeper reduction pathway for the U.S. market.

For Turkey, despite not having introduced any mandatory CO₂ regulation for new cars at this point, the annual reduction rate for new vehicle CO₂ emission levels is similar to that in the EU. This is most likely due to the fact that the market in Turkey is indirectly affected by the CO₂ regulation in the EU and other markets, given that about 79% of Turkey's car production is exported abroad and about 73% of new cars sold in Turkey are imported from abroad (OSD, 2014). As a result, there are spill-over effects from vehicle regulations abroad that have an influence on the vehicle market, and also CO₂ emission levels, in Turkey. In addition, fuel and vehicle taxation levels tend to be among the highest in the world, thereby driving the new car market towards models with smaller engine size, lower engine power and – indirectly – also lower CO₂ emission levels (Mock, 2016a).

For the future, it is expected that if Turkey would introduce mandatory CO₂ emission standards, the annual CO₂ emission reduction rate could be increased significantly. Simply applying the existing EU CO₂ regulation to the Turkish market would not result in any significant additional CO₂ reductions though, as the EU's 95 g/km CO₂ target for passenger cars for 2021 would translate into an approximately 3.4% annual CO₂ reduction for Turkey – not much higher than the current business-as-usual rate without any CO₂ regulation. The same is true for the light commercial vehicles market.

Figure 18 illustrates the current situation of the new passenger car market in Turkey by including all vehicle model variants of which more than 100 vehicles were registered in 2014. Nine selected vehicle model variants were specifically highlighted. These selected vehicle models include some of the top-selling vehicle models within their segment, all of them being diesel (D) powered, except the Toyota Yaris which was chosen as an example for a hybrid (H) vehicle that is available on the Turkish market.

The 2015 and 2021 CO₂ emission targets that apply to new passenger cars in the EU are also shown. It can be seen that the majority of vehicle models registered in Turkey already outperform the EU 2015 target line⁶. Furthermore, some vehicle models already today comply with the CO₂ emission target that will apply in the EU in 2021. Specific examples include the Toyota Yaris hybrid, as well as variants of the Peugeot 208 and Renault Mégane.

⁶ The current vehicle CO₂ emission standards in the EU for 2015 and 2021 use vehicle weight as the underlying target parameter. This means that the heavier a vehicle, the higher its allowed CO₂ emission level.

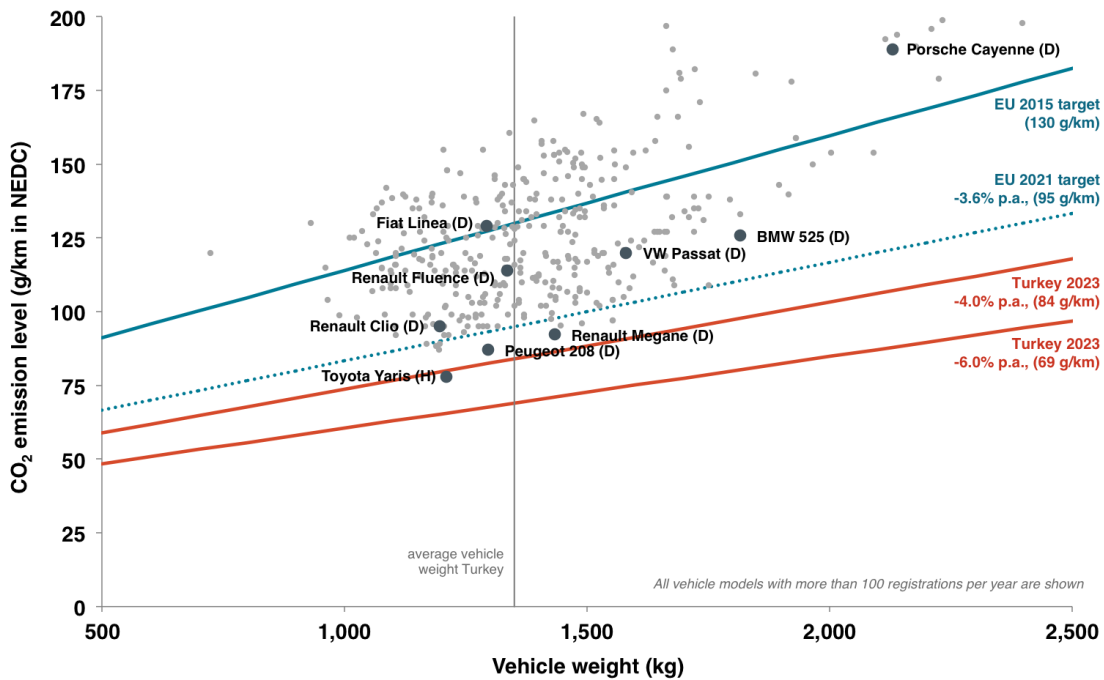


Figure 18. New passenger car registrations in Turkey in 2014, differentiated by vehicle weight and CO₂ emission levels. Some selected vehicle models are highlighted. *Data source: (ICCT, 2015a).*

Looking at the target lines for a hypothetical 2023 (the 100th year anniversary of the Turkish Republic) new car CO₂ standard in Turkey, it can be seen how these would go one step beyond the current EU 2021 regulation, if an underlying annual reduction rate of 4.0% or 6.0% (compared to a 3.6% reduction rate in the EU) is assumed. At the same time it is noteworthy that already in 2014 – nearly ten years before the standard would apply – some vehicle models, such as the Toyota Yaris hybrid, would already comply or nearly comply with the respective CO₂ emission targets. This observation is in line with the expectation that a 4.0% per year (p.a.) and even a 6.0% p.a. 2023 CO₂ standard could largely be met by further improving conventional combustion engine vehicles and also making use of the mild and full hybrid electric vehicle technology.

Using the ICCT Global Transportation Roadmap Model, the estimated fuel consumption and CO₂ emissions impact of introducing a mandatory standard for new cars in Turkey is assessed (ICCT, 2015b). In a business-as-usual scenario, without a CO₂ standard, the daily fuel consumption is expected to rise from about 83,000 barrels of oil equivalent per day in 2010 to 116,000 barrels per day by 2030 (Mock, 2016a) (Figure 19). Introducing a CO₂ standard equivalent to 84 g/km for the average new vehicle by 2023 would reduce the 2030 level to 98,000 barrels per day, a 15% decrease compared to the business-as-usual scenario. With a 69 g/km standard in place the daily fuel consumption level would drop to about 87,000 barrels of oil equivalent by 2030 – 25% lower than in the business-as-usual scenario.

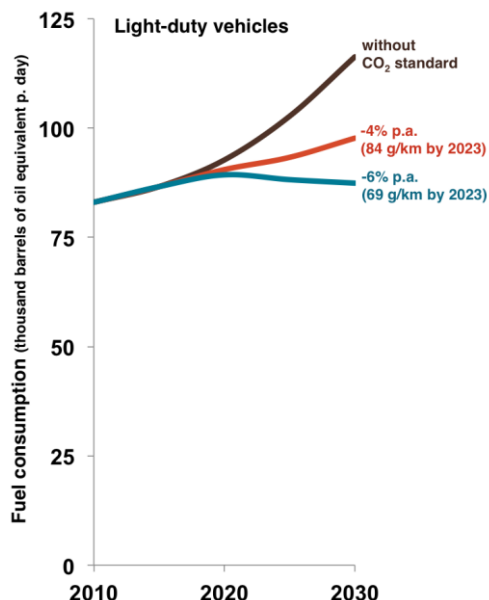


Figure 19. Estimated fuel demand from light-duty vehicles in Turkey (2010-2030).

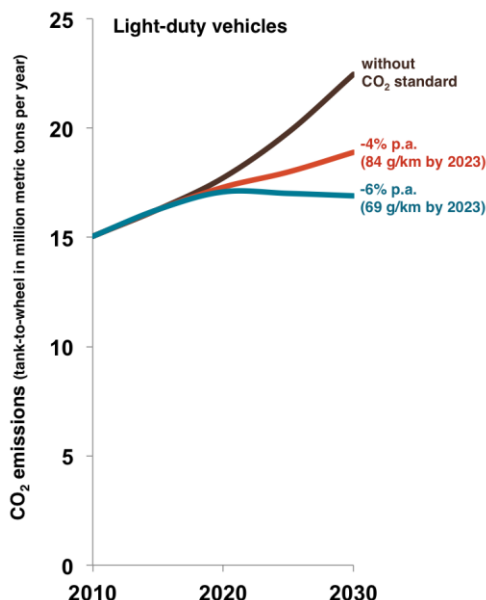


Figure 20. Estimated CO₂ emissions from light-duty vehicles in Turkey (2010-2030).

For CO₂ emissions, the expected impacts are similar, with an increase from 15 million metric tons (Mt) per year in 2010 to 22 Mt/year by 2030 in a business-as-usual scenario (Figure 20). Introducing a 84 g/km CO₂ standard by 2023 would reduce the annual emission level to 19 Mt (-15%) while a 69 g/km standard would bring emissions down to 17 Mt per year (-25%).

Vehicle CO₂based taxation

A CO₂ based vehicle taxation scheme can help to further leverage any reductions in CO₂ achieved by vehicle standards. In Turkey, currently new passenger cars are subject to the general value added tax (VAT, or Katma Değer Vergisi – KDV – in Turkish), which is 18% and applies to all goods. In addition, a special sales tax is levied, the Motorlu Taşıtlar Araçlarının ÖZel Tüketim Vergisi (ÖTV), also called Special Consumption Tax (SCT). Besides for cars, ÖTV is also levied upon some other goods categories, such as petroleum products, tobacco, alcohol as well as luxury products.

The amount of ÖTV to be collected depends on the engine displacement of a vehicle and ranges from 45% to 145% (Table 3). Calculation basis is the net price of the vehicle, i.e. without any taxes. VAT is then added to the sum of net price and ÖTV to result in the gross sales price of the vehicle. In addition to these taxes that apply once at vehicle purchase, any passenger car in Turkey is subject to an annual ownership tax, the Motorlu Taşıtlar Vergisi (MTV). This annual tax is again linked to the engine displacement of the vehicle and it decreases with the age of the vehicle.

Table 3. Overview of passenger car vehicle taxes in Turkey in 2015. *Data source: (ACEA, 2015).*

Engine displacement (l)	Special sales tax ("ÖTV"), one-time	Value added tax ("KDV"), one-time	Ownership tax ("MTV"), annual (in TL), based on age of vehicle				
			year 1-3	year 4-6	year 7-11	year 12-15	older than 16
≤ 1.3	45% of net sales price	18% of net sales price + special sales tax	591	412	231	175	63
> 1.3 and ≤1.6			945	709	412	291	112
> 1.6 and ≤1.8	90% of net sales price		1,667	1,304	786	469	182
> 1.8 and ≤2.0			2,626	2,024	1,189	709	280
> 2.0 and ≤2.5	145% of net sales price		3,939	2,860	1,787	1,068	423
> 2.5 and ≤3.0			5,491	4,777	2,985	1,607	591
> 3.0 and ≤3.5			8,362	7,524	4,553	2,263	831
> 3.5 and ≤4.0			13,147	11,352	6,686	2,985	1,189
> 4.0		21,516	16,135	9,556	4,296	1,667	

In particular the ÖTV strongly influences customer purchase behavior. An indication is the fact that 95% of all new cars in Turkey have an engine displacement of 1.6l or less. In comparison, in the EU it is only about 70% of all new cars that are equipped with an engine of 1.6l or smaller. In fact, 40% of cars in Turkey are right at the tax threshold of 1.6l, indicating the importance of this step in the tax rate. Figure 21 illustrates the current situation, using the example of a new car with a net

sales prices of 66,000 Turkish Lira (TL) ($\approx 20,000$ EUR). The tax difference between a vehicle with 1.6l engine and one with 1.7l engine then is 29,700 TL ($\approx 9,000$ EUR) if only considering ÖTV and 31,866 TL ($\approx 9,700$ EUR) if also taking into account MTV for the first three years of ownership. This significant difference in taxation levels provides a strong incentive for consumers for picking a vehicle with an engine displacement of 1.6l or less. A similar tax threshold can be found at 2.0l engine size. Again using the example of a 66,000 TL vehicle, the tax difference between 2.0l and 2.1l engine size amounts to 40,239 TL ($\approx 12,200$ EUR). As a result, another clustering of new car sales around the 2.0l tax threshold is observed, accounting for nearly 5% of vehicle sales. Vehicles above 2.0l engine size are very rarely found in the Turkish new car fleet.

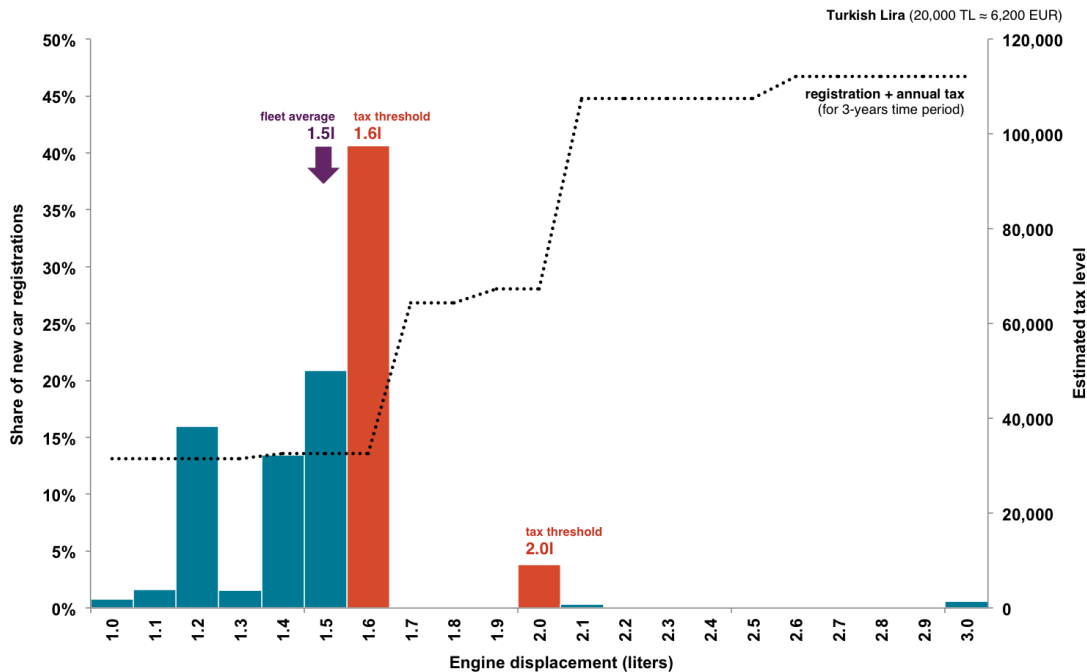


Figure 21. Taxation levels for a 66,000 TL ($\approx 20,000$ EUR) new car in Turkey and distribution of new car sales by engine displacement. *Data source: (ACEA, 2015), (ICCT, 2015a).*

In order to assess the effect of the current vehicle taxation scheme in Turkey on consumer prices, five vehicle models were selected and put in comparison to the same vehicle models in Germany, France and the Netherlands (Figure 22). Each of the selected vehicle models belongs to the most popular ones within its respective vehicle size segment.

The first three models, a VW Polo, Golf and Passat fall below the 2.0l threshold and therefore in Turkey are subject to 45% ÖTV. It can be seen how the impact of ÖTV increases with increasing vehicle value, being highest for the Passat. In Germany there is no vehicle sales tax equivalent to the ÖTV in Turkey. In France, a vehicle sales tax is in place but only applies to vehicles above 130 g/km of CO₂. As all of the vehicle models examined are below this CO₂ threshold, they are not subject to a sales tax in France. In the Netherlands vehicle sales tax is linked to the CO₂ emissions of a vehicle. It is lowest for the VW Polo but increases significantly, as the other vehicle models examines have higher CO₂ emission levels. An annual vehicle ownership tax does not exist in France and ownership tax rates are very low both in Turkey, Germany and the Netherlands when compared to the sales price of the vehicle. VAT rates are similar in all four markets.

The fourth vehicle, again a VW Passat, falls above the 2.0l engine displacement tax threshold in Turkey and therefore is subject to 90% ÖTV. The impact of the ÖTV is even stronger in the case of the fifth vehicle, a 3.0l engine Mercedes-Benz E350. In comparison, these two vehicles in France are neither subject to a sales tax nor an annual tax and in only to a minimal annual ownership tax. In the Netherlands, the sales tax increases notably for the 2.0l VW Passat and the E350. It is, however, still only about half of the tax level in Turkey for the Passat and about one-fifth for the E350.

Overall, it can be seen that gross vehicle prices (i.e. including taxes) for the vehicles below 1.6l engine size are relatively similar for Turkey, Germany and France, with the prices in the Netherlands being notably higher than in the other three markets. For the 2.0l Passat and the 3.0l E350 though consumer prices in Turkey are significantly higher than in Germany and France. Even though tax levels for these two vehicles are comparably high in the Netherlands, vehicle prices are still lower than in Turkey. It is remarkable that for all five vehicles examined net vehicle prices are lower in

Turkey than in Germany, France and also the Netherlands. This is potentially an effort of vehicle manufacturers to compensate for the relatively high vehicle taxation rates in Turkey by offering the vehicles with a lower profit margin in Turkey than it is the case in other markets.

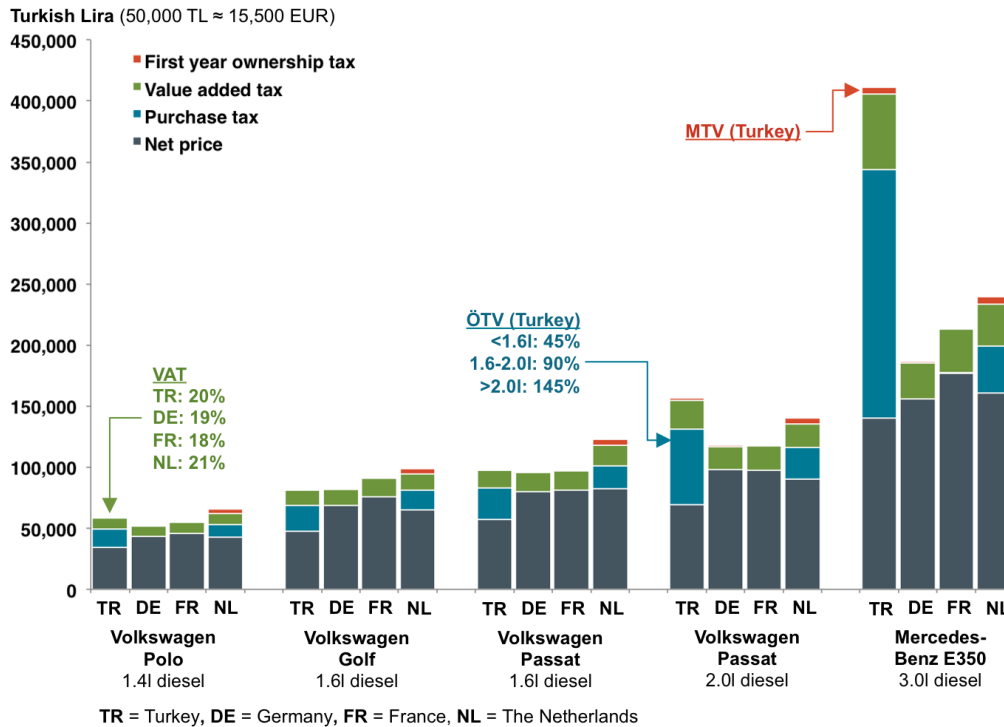


Figure 22. Sales prices and taxation levels for selected vehicle models in Turkey, Germany and France⁷. Data sources: vehicle manufacturers' sales brochures, (ACEA, 2015).

As it was shown, vehicle taxation levels in Turkey are comparably high and, as a result, show a strong effect on consumer purchase behavior. However, currently taxes for passenger cars in Turkey are only linked to the engine displacement and the price of a vehicle. They therefore provide an incentive to choose a vehicle with lower engine displacement and lower net price.

There is a correlation between the engine displacement of a vehicle and its fuel consumption and CO₂ emission level (He and Bandivadekar, 2011). However, this correlation is not particularly strong and it is also not necessarily valid for modern vehicles anymore. For example, a hybrid-electric vehicle generally has a significantly lower fuel consumption and CO₂ emission level than a conventional combustion engine vehicle, despite the fact that its engine displacement might be the same or very similar to that of a conventional petrol or diesel vehicle. Hence, it can be concluded that the current passenger car taxation scheme in Turkey provides a strong steering effect for the vehicle market overall but yet at the same time a weak effect in terms of increasing the demand for new passenger cars with lower fuel consumption and CO₂ emissions.

In recent years, many countries have changed their vehicle taxation schemes to be directly based on the CO₂ emissions or fuel consumption of new vehicles. For example, France introduced a CO₂ based feebate system in 2008 (ACEA, 2015). In a feebate system, vehicles above a certain CO₂ threshold (the so-called pivot point) have to pay a fee (also called malus), while those vehicles with lower CO₂ emissions receive a rebate (also called bonus). In the case of the French feebate system, instead of a straight tax rate line, there are many little steps with specific thresholds that determine the bonus or malus level (Figure 23). As a result, while the French feebate system was found to have a significant steering effect, at the same time it also led to an unintended clustering of new vehicle registrations around the discrete tax thresholds (Mock, 2015b).

⁷ Wherever possible, vehicle prices were adjusted for differences in optional equipment.

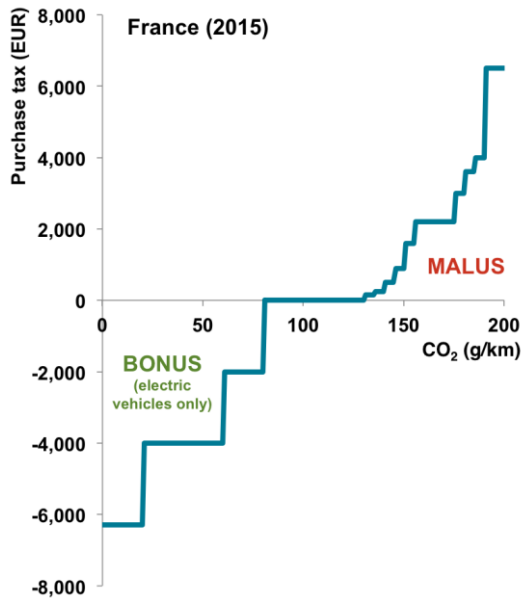


Figure 23. Passenger car sales tax structure in France. *Data source: (ACEA, 2015).*

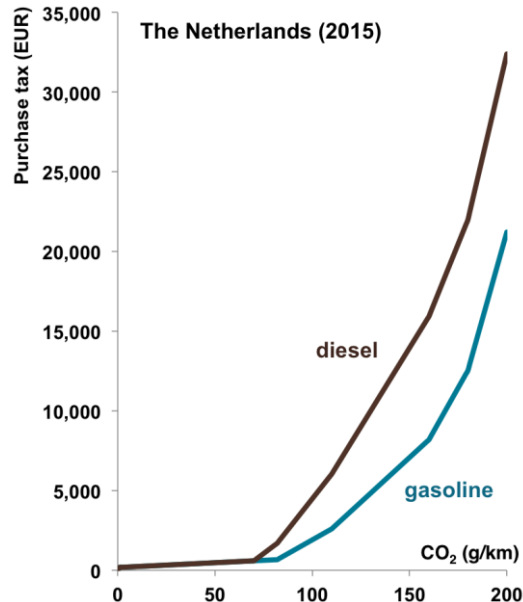


Figure 24. Passenger car sales tax structure in the Netherlands. *Data source: (ACEA, 2015).*

The vehicle taxation scheme in the Netherlands largely avoids clustering of new registrations around discrete tax thresholds by mostly applying a straight tax line, i.e. the tax rate (in EUR per g/km of CO₂) is the same throughout a large CO₂ range. The Dutch system does not offer any bonus payments for vehicles below a certain CO₂ threshold but instead solely imposes a tax on all vehicles, varying drastically depending on the respective CO₂ emissions of a vehicle (Figure 24). The Netherlands switched to a CO₂ based taxation scheme in 2007. Since then, the CO₂ emission level of newly registered passenger cars in the Netherlands fell significantly quicker than in other EU countries (Zacharof et al., 2015).

Figure 25 illustrates schematically the design of a best-practice vehicle taxation scheme that could be implemented for the new vehicle market in Turkey. Taxation basis would be the CO₂ emission level of a vehicle and a linear tax function would be applied, without any discrete tax threshold steps. This means that the tax rate (in TL per g/km of CO₂) is the same for every vehicle, thereby ensuring technology neutrality and avoiding any clustering of vehicles around discrete tax thresholds. Vehicles below a set pivot point would receive a bonus payment while vehicles above the pivot point have to pay a malus. The revenue collected from the malus payments would be used to balance out the bonus payments for low-emission vehicles, thereby ensuring budget neutrality from a government perspective. Additional tax revenue could be collected, if desired by the government, by placing the pivot point in such a way that the sum of revenue collected from malus payments is larger than the sum of bonus payments to low-emission vehicles.

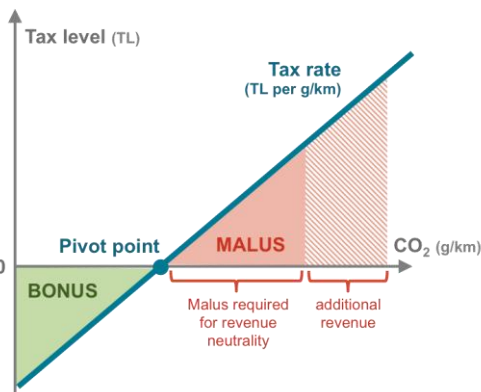


Figure 25. Schematic illustration of best-practice design for a feebate-like vehicle taxation scheme.

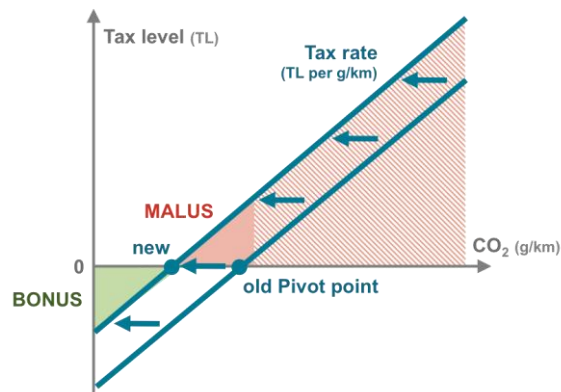


Figure 26. Schematic illustration of adapting a feebate taxation scheme to changes in vehicle market structure.

It should be emphasized that it is important to regularly adapt a feebate-like taxation scheme to ongoing changes in the vehicle market structure. A successful feebate system will have an impact on

customer purchase behavior and will lead to a situation in which the CO₂ emission level of new passenger cars will reduce over time. As a result, the sum of bonus payments will increase and the amount of revenue from malus payments will decrease, thereby threatening government budget neutrality. It is therefore important to regularly adapt either the pivot point and/or the tax rate to ensure that the overall revenue collected remains about the same over time and that the feebate system keeps having an impact on new vehicle purchase behavior. This mechanism for adapting the pivot point of the taxation scheme is illustrated in Figure 26.

Conclusions and outlook

Passenger cars and light commercial vehicles account for three-quarters of the vehicle fleet in Turkey. When taking into account differences in fleet characteristics, such as vehicle weight, size, and engine power, fuel consumption and CO₂ emission levels for new vehicles in Turkey tend to be similar to those on the EU market.

Turkey is one of the few key automotive markets worldwide not yet having introduced mandatory CO₂ standards for cars and light commercial vehicles. If, however, the EU CO₂ targets for new vehicles would simply be transferred to the market situation in Turkey, only a limited steering effect is to be expected. At the same time there are other regions worldwide that have adopted more accelerated emission reduction pathways than the EU. Given Turkey's strong dependence on vehicle exports and with respect to ensuring long-term competitiveness, it should therefore be further assessed whether going beyond the current EU pathway of fuel consumption and CO₂ emission reduction might be more beneficial for the Turkish economy when competing with other global markets.

Taxes on sales and ownership of vehicles (in particular of passenger cars) are relatively high in Turkey. However, these taxes currently are not directly linked to the CO₂ emissions and fuel consumption of a vehicle. Revising the Turkish vehicle taxation scheme to take into account the CO₂ emission level of a vehicle could complement and leverage the effects of CO₂ vehicle standards, thereby further driving technological innovation. Similarly, mandates and incentives specifically for electrified vehicles and alternative fuels should also be assessed in more detail.

Heavy-duty vehicles account for only about one-tenth of the market in Turkey but at the same time are responsible for more than half of fuel consumption and emissions. Currently there are no mandatory fuel consumption and CO₂ emission standards for heavy-duty vehicles, neither in Turkey nor in the EU. However, other regions, such as the United States, Canada, China, and Japan, have recently introduced efficiency standards for new heavy-duty vehicles, and it is likely that the EU will be moving in this direction as well in the near future. Given the particular importance of trucks and buses not only for the local vehicle market in Turkey but also for the export market, the introduction of efficiency standards should be considered and be assessed in more detail.

About half of new cars in Turkey are first registered in the Istanbul area. This highlights the importance of cities, and in particular the city of Istanbul, with respect to the deployment of innovative vehicle technologies. Urban areas are typically most affected by the negative impacts of road transportation, such as high levels of local air pollutants. At the same time, these urban areas can take complementary action, in addition to any policy measures at the national level, to incentivize the deployment of low-emission vehicles. Examples for such measures include an improved infrastructure for alternative fuels and electricity as well as restrictions for high-emission vehicles when entering urban areas. In light of the particular importance of urban areas for the new vehicle market in Turkey, these complementary measures should also be assessed and discussed in more detail.

Acknowledgments

Funding for this work was generously provided through the Mercator-IPC Fellowship Program.

References

ACEA (2015). [ACEA Tax Guide](http://www.acea.be/publications/article/acea-tax-guide). European Automobile Manufacturers Association (ACEA).

<http://www.acea.be/publications/article/acea-tax-guide>

DESTATIS (2015). [Außenhandel - Exporte und Importe \(Spezialhandel\) nach den Güterabteilungen des Güterverzeichnis für Produktionsstatistiken 2014](https://www.destatis.de/DE/ZahlenFakten/GesamtwirtschaftUmwelt/Aussenhandel/Handelswaren/). Statistisches Bundesamt (DESTATIS).

Retrieved from

<https://www.destatis.de/DE/ZahlenFakten/GesamtwirtschaftUmwelt/Aussenhandel/Handelswaren/>

Tabellen/EinfuhrAusfuhrGueterabteilungen.html

EEA (2013). Air pollution fact sheet 2013: Turkey. European Environment Agency (EEA). Retrieved from <http://www.eea.europa.eu/themes/air/air-pollution-country-fact-sheets-2014>

Franco, V., Posada, F., German, J., Mock, P. (2014). Real-world exhaust emissions from modern diesel cars. The International Council on Clean Transportation (ICCT). Publication retrieved from <http://www.theicct.org/real-world-exhaust-emissions-modern-diesel-cars>

He, H., Bandivadekar, A. (2011). Review and Comparative Analysis of Fiscal Policies Associated with New Passenger Vehicle CO₂ Emissions. The International Council on Clean Transportation (ICCT). Publication retrieved from http://www.theicct.org/sites/default/files/publications/ICCT_fiscalpolicies_feb2011.pdf

ICCT (2015a). European Vehicle Market Statistics Pocketbook 2016/16. The International Council on Clean Transportation (ICCT). Publication retrieved from <http://eupocketbook.theicct.org> with additional analyses prepared for this paper based on the underlying vehicle database

ICCT (2015b). Global Transportation Roadmap Model. The International Council on Clean Transportation (ICCT). Retrieved from <http://www.theicct.org/global-transportation-roadmap-model>

ICCT (2016). Global passenger vehicle standards. The International Council on Clean Transportation (ICCT). Retrieved from <http://www.theicct.org/info-tools/global-passenger-vehicle-standards>

IEA (2013). Oil & Gas security - Emergency response of IEA countries: Turkey. International Energy Agency (IEA). Retrieved from https://www.iea.org/publications/freepublications/publication/2013_Turkey_Country_Chapterfinal_with_last_page.pdf

KBA (2015). Statistik Fahrzeuge. Kraftfahrtbundesamt (KBA). Retrieved from <http://www.kba.de/>

Kodjak, D. (2015). Policies to reduce fuel consumption, air pollution, and carbon emissions from vehicles in G20 nations. The International Council on Clean Transportation (ICCT). Retrieved from <http://www.theicct.org/policies-reduce-fuel-consumption-air-pollution-and-carbon-emissions-vehicles-g20-nations>

Mock, P. (2015a). Güven Nasıl Yeniden Sağlanır?. EkoIQ Kasım 2015. Retrieved from <http://ipc.sabanciuniv.edu/wp-content/uploads/2015/10/046-049.pdf>

Mock, P. (2015b). Optimizing to the last digit: How taxes influence vehicle CO₂ emission levels. The International Council on Clean Transportation (ICCT). Retrieved from <http://theicct.org/how-taxes-influence-vehicle-co2-emission-levels>

Mock, P. (2016a). The automotive sector in Turkey – A baseline analysis of vehicle fleet structure, fuel consumption and emissions. The International Council on Clean Transportation (ICCT). Retrieved from <http://theicct.org/automotive-sector-turkey-baseline-analysis>

Mock, P. (2016b). Driving change: a snapshot of the automotive sector in Turkey. IPC-Mercator Policy Brief. Istanbul Policy Center (IPC). Retrieved from http://ipc.sabanciuniv.edu/wp-content/uploads/2016/03/DRIVING-CHANGE-A-SNAPSHOT-OF-THE-AUTOMOTIVE-SECTOR-IN-TURKEY_PeterMock.pdf

OICA (2016). 2005-2015 Sales Statistics. International Organization of Motor Vehicle Manufacturers (OICA). Retrieved from <http://www.oica.net/category/sales-statistics/>

OSD (2014). Aylık Rapor - Automotive Industry Monthly Report, December 2014. Otomotiv Sanayi Derneği (Automotive Manufacturers Association) (OSD). Retrieved from <http://www.osd.org.tr/yeni/wp-content/uploads/2015/01/Rapor2014-12.pdf>

Posada and Façanha (2015). Brazil passenger vehicle market statistics. The International Council on Clean Transportation (ICCT). Publication retrieved from <http://www.theicct.org/brazil-PV-market-statistics>

TUIK (2015). Road Motor Vehicle Statistics 2013. Turkish Statistical Institute (TUIK). Retrieved from <http://www.turkstat.gov.tr/> with updated 2014 data retrieved from

http://www.turkstat.gov.tr/PreTablo.do?alt_id=1051

UNFCCC (2013). Summary of GHG Emissions for Turkey. United Nations Climate Change Secretariat. Retrieved from https://unfccc.int/files/ghg_emissions_data/application/pdf/tur_ghg_profile.pdf

VDA (2015). Annual figures. Verband der Automobilindustrie (Automotive Manufacturers Association) (VDA). Retrieved from <https://www.vda.de/en/services/facts-and-figures/annual-figures.html>

WLPGA (2015). Autogas Incentive Policies - 2015 Update. The World LPG Association (WLPGA). Retrieved from <http://www.wlpga.org/wp-content/uploads/2015/09/autogas-incentive-policies-2015-2.pdf>

Yang, Z. (2015). Improving the conversions between the various passenger vehicle fuel economy/CO₂ emission standards around the world. The International Council on Clean Transportation (ICCT). Publication retrieved <http://www.theicct.org/blogs/staff/improving-conversions-between-passenger-vehicle-efficiency-standards>

Zacharof, N. Tietge, U., Mock, P. (2015). CO₂ emissions from new passenger cars in the EU: Car manufacturers' performance in 2014. The International Council on Clean Transportation (ICCT). Publication retrieved <http://www.theicct.org/co2-new-cars-eu-manufacturer-performance-2014>

Sustainability Enhancement of Urban Traffic Routing via Multi Criteria Optimization

Alberto NAI OLEARI*, Hamady BARRY** & Ali JAAFAR***

*Automotive, Infrastructure & Transportation Division, Altran Technologies, 2 Rue Paul Dautier, 78140 Vélizy-Villacoublay, France.

E-mail: alberto.naioleari@altran.com

**GEP Department, Université Claude Bernard, 43 Boulevard du 11 Novembre 1918, 69100 Villeurbanne, France.

***Altran Research Department, Altran Technologies, 2 Rue Paul Dautier, 78140 Vélizy-Villacoublay, France.

Abstract

In this paper, we propose a novel strategy aimed to improve the environmental footprint of urban traffic. The proposed methodology is based on the representation of a traffic system as an oriented graph, in order to apply the shortest-path algorithms (such as Dijkstra, Bellman-Ford and A). The standard algorithms have been enhanced by multi criteria optimization in order to improve the ecological and economical traffic footprint at the same time. The proposed algorithms have been tested in simulation in order to evaluate the performances of the multi criteria with respect to the mono criterion optimization.*

Key-words: *traffic routing, multi criteria optimization, Link Transmission Model, dynamic traffic flow.*

Dans cet article, nous proposons des techniques d'amélioration de l'empreinte écologique du trafic routier dans les environnements urbains. La méthodologie proposée est basée sur la modélisation d'un réseau routier sous forme d'un graphe orienté afin d'appliquer les algorithmes d'optimisation numérique (algorithme de Dijkstra, Bellman-Ford et A) à la recherche du chemin de moindre coût. L'optimisation multicritère a été utilisée afin d'améliorer collectivement les empreintes écologique et économique du trafic. Les résultats ont été détaillés par algorithme afin de comparer l'optimisation multicritère et monocritère.*

Mots clé: *trafic routier, optimisation multicritère, Link Transmission Model, flux dynamique du trafic.*

Introduction

Traffic control and routing problems have a non-negligible impact on environment, economy and society, where pollution, fuel consumption, travel times and road safety affect the performances of various services, such as delivery, public transportation and other. In these terms, smart management of traffic flows on highways (Nai Oleari, Dominguez Frejo, Fernandez Camacho, & Ferrara, 2015) and urban areas is one of the priorities of the local authorities, in order to improve and ameliorate the environmental and economical footprints in urban areas.

Global Positioning System (GPS) devices are used almost every day to guide drivers along “optimal” routes to their destinations. Such devices are very effective in route calculation, but with the recent development of infrastructures and urbanization they are starting to expose some limitations. Routes are usually only computed from one driver’s point of view, and may not be in the interest of a collective set of drivers. These applications can be seen as “reactive”, being able to respond to real-time traffic state updates and propose corrections. However, these corrections could often be proposed when it’s too late due to the lack of integrating interactions among users. In this case, the risk of congestion displacement is high, since the solution algorithms are often similar as well as the routes they propose.

Moreover, GPS devices can compute their routes according to the type of transportation (by car, by bike, on foot) but not according to the kind of vehicle (electrical, petrol or gas). In other words they do not consider the fact that a route can be optimal for a petrol vehicle and not for an electrical vehicle, since these latter can be equipped with energy recuperation systems (Cassandras, Wang, & Pourazarm, 2014).

As a consequence, such traffic routing does not necessarily provide a good carbon footprint from an urban point of view.

In the Literature, several solutions have been proposed in order to address the optimal routing problem for urban traffic (Du, Han, & Li, 2014) aiming to reduce the negative effects of congestion. In (Cao, Zhang, Kong, Liu, & Wu, 2013), an optimal routing methodology is detailed, based on historical data and on-line data acquisition. In (Fu, Zhang, Feng, & Zheng, 2011) a vehicle-infrastructure integration system with density estimation via fixed sensors is presented. In (Necula, Necula, & Iftene, 2011) the authors developed another method based on client-server architecture for connected vehicles. In (Cassandras, Wang, & Pourazarm, 2014) the authors present a multi-constrained optimization technique applied to a recharging control problem in presence of electrical vehicles with constraints on the energy availability and the recharging times.

In our work, we propose an improvement to the shortest-path routing algorithms, allowing them to compute routes for a given traffic system taking into account the interactions of the different actors, also being able to consider the dynamical evolution of traffic. Before going into the details of the proposed work, it is important to note that we assume that all the vehicles are permanently connected with a traffic control center, in charge of calculating the requested routes. A client-server secured architecture is in charge of managing the data transfer.

The system is considered from a static point of view where the shortest path problem on an oriented graph is formulated (Cao, Zhang, Kong, Liu, & Wu, 2013). Classical algorithms (Dijkstra (Dijkstra, 1959), Bellman-Ford (Bellman, 1958) and A* (Hart, Nilsson, & Raphael, 1968)) are studied and then adapted to a multi criteria (Collette & Siarry, 2002) and multi cost graph. For each graph edge, we consider a vector that can be composed of different costs, such as, for instance, the travelled distance, the travel time (based on speed limit), the energy consumption for electrical and petrol engines, and the pollutant emissions. For electrical vehicles, kinetic energy recovery (Cassandras, Wang, & Pourazarm, 2014) is also taken into account via negative edges costs. In this case, the costs are adapted for the Dijkstra algorithm, by applying a shifting strategy (Eisner, 2011). The objective of the optimization is hence to search for a route on the graph which simultaneously minimizes the different costs. This allows certain flexibility in order to integrate dynamical traffic flow modelling in future works.

The paper is structured as follows. In Section 1 we recall some principles concerning the adopted multi criteria optimization methodology. In Section 2, we describe the modeling approach, while in Section 3 we present the results of the simulated application of the proposed methodology to a case study. Finally, we detail some concluding remarks.

1. Multi criteria optimization principles

Multi criteria optimization techniques are adopted in order to optimize several objective functions (i.e. the criteria) at the same time, which are often in contrast with each other.

In order to adapt the routing algorithms to the multi criteria case, we took inspiration from a strategy based on the weighting of the objective functions presented in (Collette & Siarry, 2002) for linear and nonlinear optimization problems. The mathematical problem is formulated as follows.

$$\begin{cases} \min f_{eq}(\vec{x}) = \sum_{i=1}^k w_i \cdot f_i(\vec{x}) \\ g(\vec{x}) = 0 \\ h(\vec{x}) \geq 0 \end{cases}$$

Where $f_i(\vec{x})$, $i = 1, \dots, k$, $x \in \mathbb{R}^n$ represents the different objective functions (in other words, the optimization criteria), $f_{eq}(\vec{x})$ is the equivalent objective function, w_i are the weighting coefficients subject to $\sum_i w_i = 1$, and $g(\vec{x})$, $h(\vec{x})$ are the associated equality and inequality constraints.

On the basis of this technique, we defined our cost function for a given route as follows.

$$f_{eq}(c) = w_1 \cdot f_1(c) + w_2 \cdot f_2(c) + w_3 \cdot f_3(c)$$

Where in our case $f_1(c)$ is the cost function associated to the travelled distance, $f_2(c)$ is the cost function associated to the estimated energy consumption in the case of electrical vehicles, $f_3(c)$ is the cost function associated to the travel time and $W = [w_1 \ w_2 \ w_3]$ is the weighting vector.

It is important to note that the choice of the weighting coefficients is not given to the end user but is made by the control center itself, according to its environmental and traffic needs. For instance, the control center could choose to assign higher priority to the energy consumption for electrical vehicles.

More criteria can be added to the optimization problem, such as, for instance, the pollutant emissions, the level of congestion, or some others related to road safety.

2. The proposed approach – case study

In route planning problems, a road network can be represented as an oriented graph, against which the standard shortest path algorithms available in the literature can be executed.

To this end, we generated a small scale urban environment with a reduced complexity, which includes some points of interest, as shown in Figure 1. The case study includes also some interesting traffic features, such as critical points for the road network, roads with different speed limits and zones at different levels of altitude.



Figure 1 - The considered case study: a small scale urban environment with points of interest and traffic constraints.

The modelling of an urban environment as an oriented graph is shown in Figure 2 - Figure 3. It is quite intuitive: first of all each intersection is translated into a node (Figure 2), and then each street connecting the intersections is translated into an edge. Street properties such as the length, the speed limit and the slope are used to determine the associated cost vector. We obtained an oriented graph composed of 33 nodes and 88 edges, as the one shown in Figure 3.

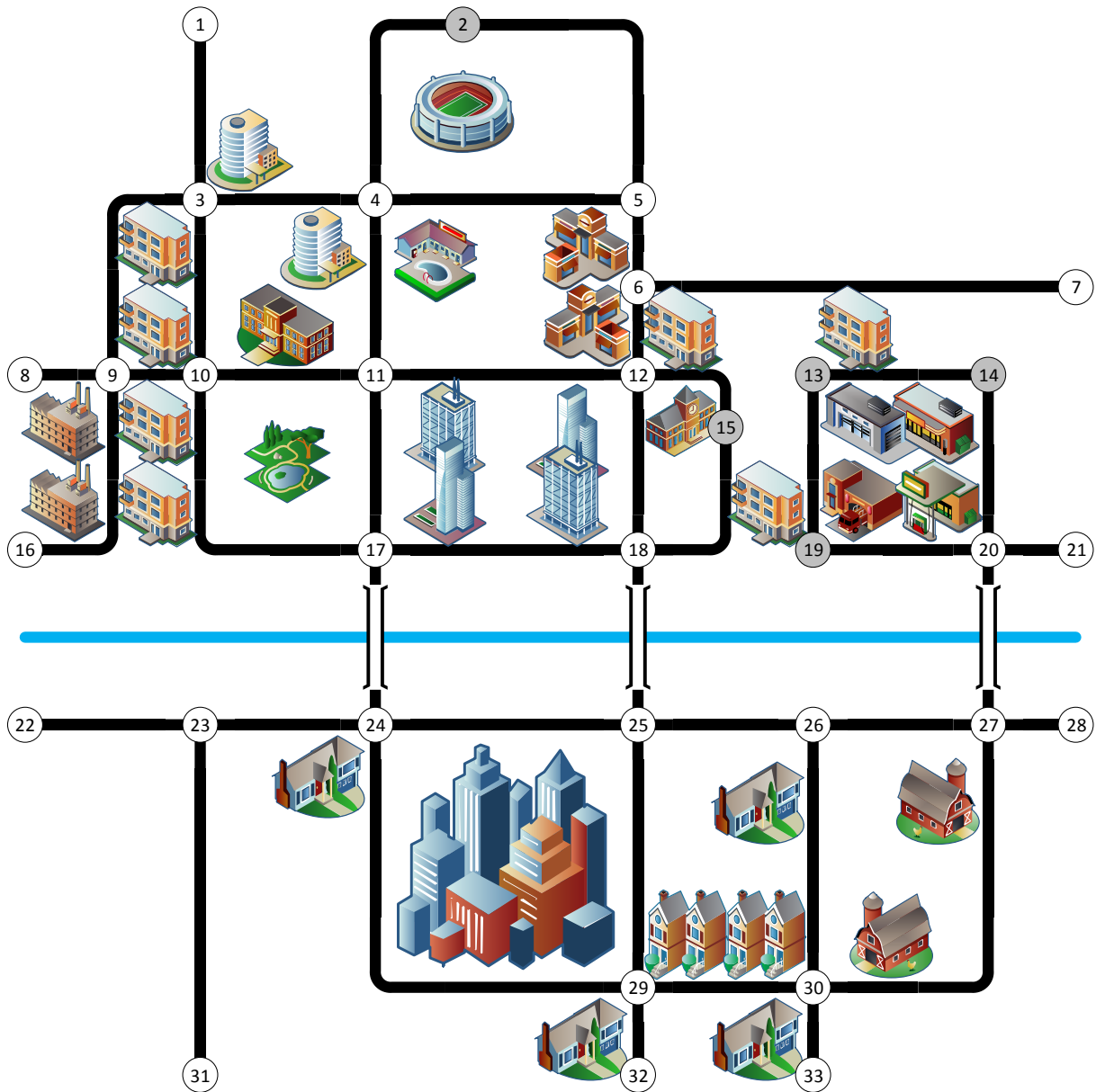


Figure 2 - The considered case study with the nodes put into evidence. The nodes in grey are the ones added in order to eliminate the arcs in double between the nodes.

In this representation, two nodes should not be directly connected by two edges in the same direction. If this case occurs, we must add one or more extra nodes to one of the edges in order to remove the ambiguity. These nodes have been depicted in grey in Figure 2. For instance, node 2 has been added in order to avoid a double direct path from node 4 to node 5 (and vice versa).

In order to have a more realistic test case, we decided to consider the presence of different speed limits on different edges. It is quite common, indeed, that in an urban environment the speed limit of 50 km/h is lowered to 30 km/h in the downtown or near schools and other points of interest. We also decided to consider that some nodes have a different altitude. This is an important factor to take into account when dealing with electric vehicles, since it has a non-negligible impact on energy consumption and recuperation.

In the oriented graph representation, each edge is associated to a cost vector, representing the different costs associated to the passage on the considered edge. It is important to keep in mind that when dealing with multi criteria optimization the choice of the objectives priority is important. This can be done by adjusting the elements of an appropriate weighting vector.

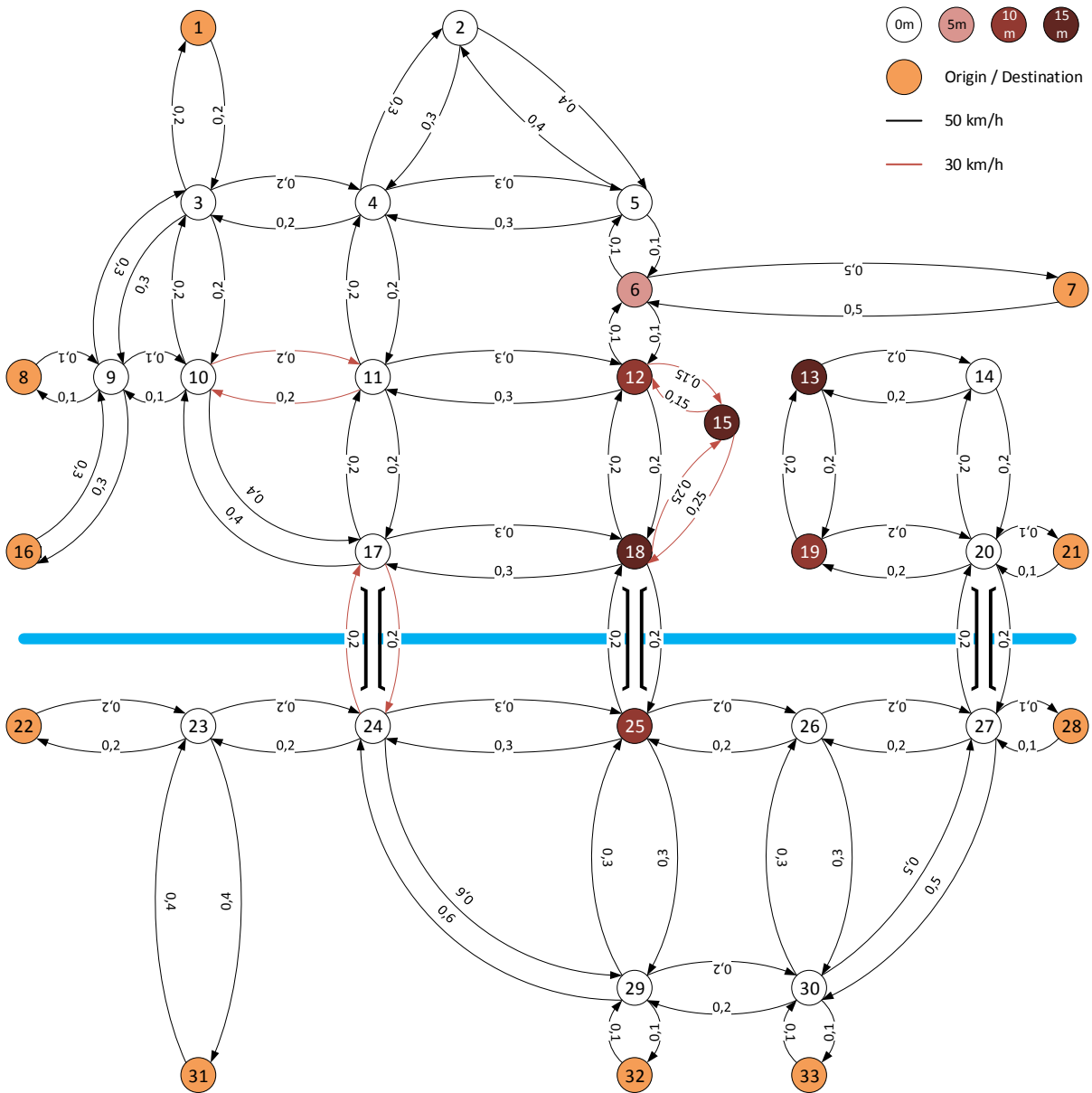


Figure 3 - The oriented graph representing the considered case study. The numbers on the nodes represent their ID and the numbers on the edges represent their length, in kilometers. A color scale represents the different altitudes of the nodes. The edges depicted in black correspond to a speed limit of 50 km/h, while the ones depicted in red correspond to a speed limit of 30 km/h.

3. Simulation Results

The shortest path algorithms have been evaluated on the developed case study and they have been adapted to deal with the multi criteria case. Several simulation tests have been done with different weighting vectors in order to evaluate the performances of the algorithms.

For our simulations we decided to consider the problem from a global point of view and to evaluate all the possible routes in the system, excluding the ones from one node to itself. In our case study, made of 33 nodes and 88 edges, there are 1056 possible routes. For each simulation we measure the effectiveness of the routing algorithm with respect to each of the optimization criteria, which are the total travelled distance, the energy consumption and the total travel time.

In order to analyze the performances of the multi criteria approach, we decided also to consider the results of the mono criteria approach as a reference case. The results have been normalized with respect to the maximum value of each criteria obtained in the mono criterion case.

Figure 4 shows the results of the mono criterion approach, optimizing the travelled distance (Mono 1), the energy consumption (Mono 2) and the travel time (Mono 3) one at a time, with the three algorithms. Such a figure shows that it is well evident how each criterion is being optimized with respect to the others. More detailed results are shown in Table 1.

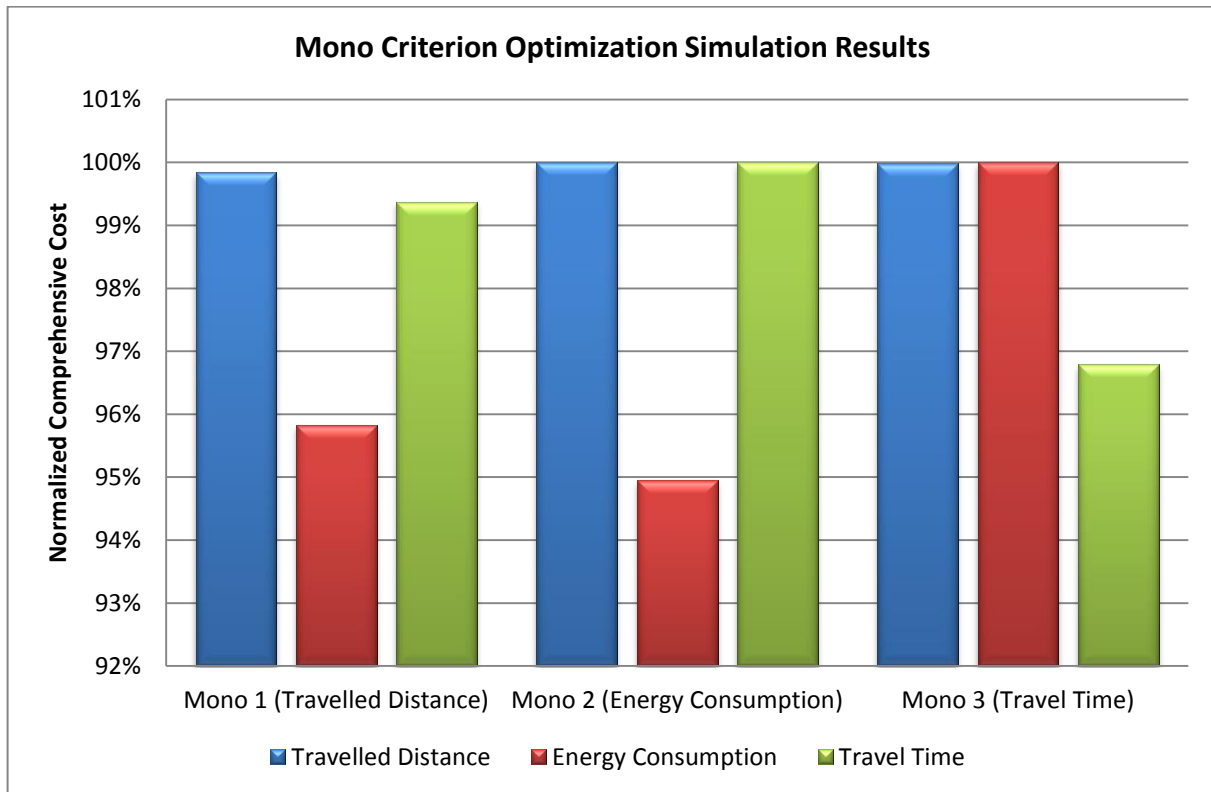


Figure 4 - Mono Criterion Optimization Simulation Results.

Simulation	Travelled Distance	Energy Consumption	Travel Time
Mono 1 (Travelled Distance)	0.9984	0.9582	0.9937
Mono 2 (Energy Consumption)	1.0000	0.9494	1.0000
Mono 3 (Travel Time)	0.9998	1.0000	0.9679

Table 1 – Simulation details and numerical normalized results for the mono criterion case.

The simulation results of the application of the multi criteria approach to the considered test case are shown in Figure 5. Detailed results are shown in Table 2, along with the ponderations that have been chosen. It is well evident how the choice of the weights is important, since it has an impact on the quality of the solution.

In Figure 5 it is possible to observe the benefits of adopting multi criteria optimization with respect to the mono criterion approach. By comparing the case Multi 4 with the case Mono 1 it is well evident how with a very small increase of 0.02% on energy consumption it is possible to achieve a reduction of 1.2 % on the total travel time. Similar considerations can be made for the case Multi 4 and Mono 2: an increase of 1.08 % on the energy consumption allows saving 1.9 % on the travel time. Note that the case Mono 2, even if it achieves the lowest energy consumption, is the one that implies the maximum travelled distance and travel time.

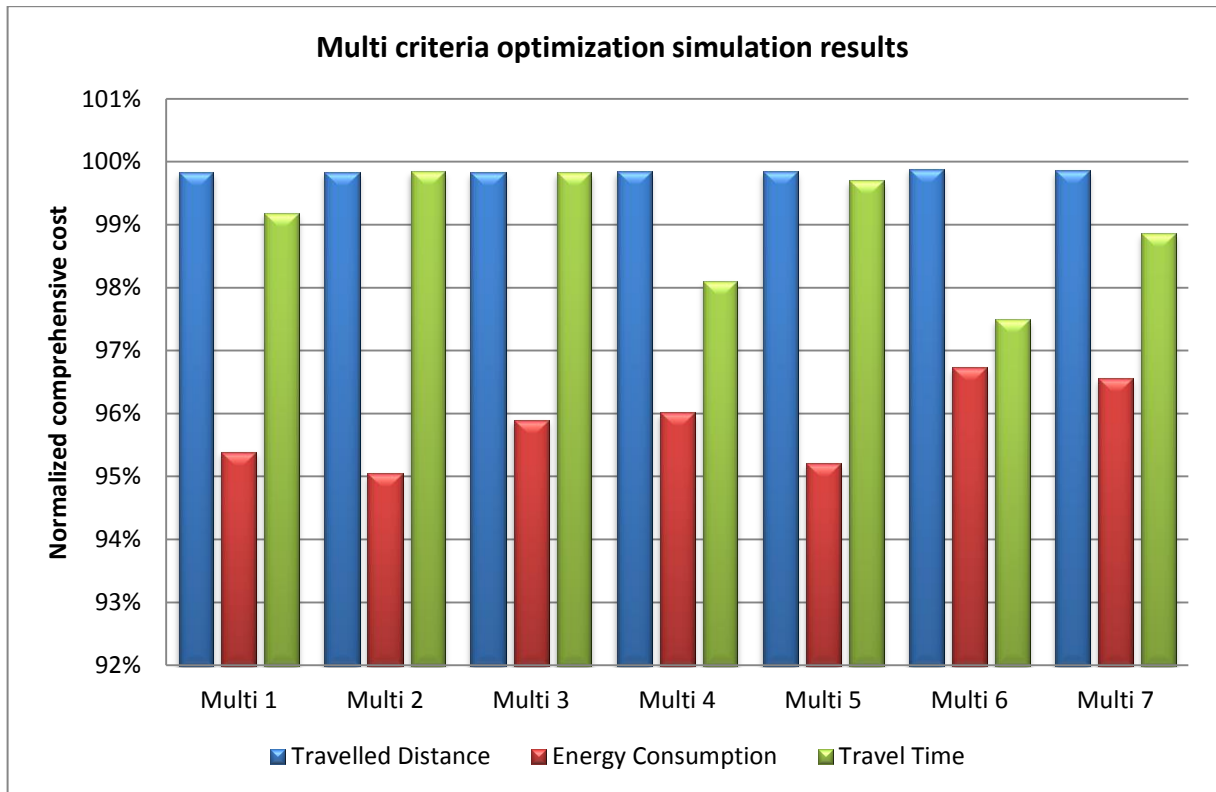


Figure 5 – Normalized simulation results for the multi criteria case.

Simulation	Weights	Travelled Distance	Energy Consumption	Travel Time
Multi 1	[1/3 1/3 1/3]	0.9983	0.9539	0.9919
Multi 2	[0.2 0.6 0.2]	0.9983	0.9505	0.9984
Multi 3	[0.1 0.8 0.1]	0.9983	0.9590	0.9983
Multi 4	[0.25 0.5 0.25]	0.9984	0.9602	0.9810
Multi 5	[0.3 0.4 0.3]	0.9984	0.9521	0.9970
Multi 6	[0.5 0.5 0]	0.9989	0.9674	0.9749
Multi 7	[0.5 0 0.5]	0.9987	0.9656	0.9887

Table 2 – Simulation details and numerical normalized results for the multi criteria case.

Conclusion

In this paper we evaluated the effects of the introduction of multi criteria optimization applied to the standard shortest-path algorithms (Dijkstra, Bellman-Ford and A*). Multi criteria optimization significantly improves the ecological and economical footprint of urban traffic. Unlike the mono-criterion optimization, it allows one to compute routes as good compromises according to a set of criteria at the same time. Simulation results showed that by combining multi criteria optimization techniques with the well-known routing algorithms it is possible to achieve better results with respect to the mono criteria case.

Further work will be devoted to the improvement of the proposed strategies, by adapting the shortest-path algorithms in order to take into account the urban traffic dynamics into the optimization problem. In fact, the introduction of traffic dynamics will allow us to achieve a better traffic management level and to improve the quality of traffic in urban areas. To this end, a traffic dynamical model, known as the Link Transmission Model (Yperman, 2007) has been identified will be adopted in future works.

References

- Bellman, R. (1958). On a Routing Problem. *Quarterly of Applied Mathematics*(16), 87-90.
- Cao, T., Zhang, X., Kong, L., Liu, X.-Y., & Wu, M.-Y. (2013). Traffic Aware Routing in Urban Vehicular Networks. *IEEE Wireless Communications and Networking Conference* (pp. 2004-2009). Shanghai: IEEE.
- Cassandras, C., Wang, T., & Pourazarm, S. (2014). Energy-aware vehicle routing in networks with charging nodes. *IFAC World Congress. 19*, pp. 9611-9616. Cape Town, South Africa: IFAC.
- Collette, Y., & Siarry, P. (2002). *Optimisation Multiobjectif*. Paris: ÉDITIONS EYROLLES.
- Dijkstra, E. (1959). A note on two problems in connection with graphs. *Numeriske Matematik*, 269-271.
- Du, L., Han, L., & Li, X.-Y. (2014, Septembre). Distributed coordinated in-vehicle online routing using mixed-strategy congestion game. *Transportation Research Part B: Methodological*, 67, 1-17.
- Eisner, F. S. (2011). Optimal Route Planning for Electric Vehicles in Large Networks.
- Fu, Q., Zhang, L., Feng, W., & Zheng, Y. (2011). DAWN: A Density Adaptive Routing Algorithm for Vehicular Delay Tolerant Sensor Networks. *49th Allerton Conference on Communication, Control and Computing* (pp. 1250-1257). Monticello, IL: IEEE.
- Hart, P. E., Nilsson, N. J., & Raphael, B. (1968, July). A Formal Basis for the Heuristic Determination of Minimum Cost Paths. *IEEE Transactions on Systems Science and Cybernetics*, SSC-4(2), 100-107.
- Nai Oleari, A., Dominguez Frejo, J. R., Fernandez Camacho, E., & Ferrara, A. (2015). A Model Predictive Control scheme for freeway traffic systems based on the Classification and Regression Trees methodology. *Proceedings of the 2015 European Control Conference* (pp. 3459-3464). Linz, Austria: IEEE.
- Necula, E., Necula, R., & Iftene, A. (2011). A GIS Integrated Solution for Traffic Management. *13th International Symposium on Symbolic and Numeric Algorithms for Scientific Computing (SYNASC)* (pp. 183-190). Timisoara: IEEE.
- Yperman, I. (2007). *The Link Transmission Model for Dynamic Network Loading*. Leuven: Katholieke Universiteit Leuven.

An emissions inventory for non-road mobile machinery (NRMM) in Switzerland

BenediktNOTTER*, Philipp WÜTHRICH* & JürgHELDSTAB**

**INFRA Research and Consulting, Sennweg 2, 3012 Bern, Switzerland*

*** INFRA Research and Consulting, Binzstrasse 23, 8045 Zurich, Switzerland*

Tel+4131 370 19 14–E-mail:benedikt.notter@infras.ch

Abstract

Non-road mobile machinery (NRMM) contributes a significant part of the total energy consumption and air pollutant emissions of mobile sources. The latest update of the Swiss non-road emissions inventory (FOEN 2015) quantifies energy and fuel consumption as well as regulated and four non-regulated pollutants for the period 1980-2050. Emissions are calculated using a bottom-up model in which operating hours segmented by machine type, motor type, size classes with respective nominal power, and age are multiplied with load factors. The resulting energy demand is multiplied with fuel consumption and emission factors.

While energy consumption of NRMM has increased by 5% between 2000 and 2015, the emissions of most air pollutants are decreasing due to the introduction of stricter emission limits. Agricultural and construction machines are the largest sources of NO_x and PM emissions; regarding CO and HC emissions, garden-care appliances are more relevant than construction machinery, however. The share of the non-road sector in total mobile energy consumption has slightly increased to 9% in 2015. The share in air pollutant emissions is even higher due to the time lag in emission standards. The transition from combustion engines towards electric motors is in progress, mainly in the industrial and residential sectors.

Keywords: *Non-road mobile machinery, inventory, modelling, emission control, electric devices.*

Introduction

Non-road mobile machinery (NRMM) is the term used for all mobile machines and devices that are not intended to transport passengers and goods by road. It includes construction machines like excavators, load and dump trucks, mobile industrial, commercial, and municipal appliances like forklifts, snow groomers or street cleaners, agricultural and forestry machines like tractors, harvesters, chain-saws, garden-care appliances like lawn-mowers, boats and ships, rail vehicles, and military machines like tanks. Aircraft are usually not considered part of NRMM. In terms of fuel type, larger mobile machines are mostly diesel-powered, while smaller machines and hand-held devices mostly have spark-ignited two- or four-stroke petrol engines. However, CNG and LPG are also used (mostly for forklifts), and increasingly, electric motors are used to power smaller devices.

NRMM contributes a significant part of the total energy consumption and air pollutant emissions of mobile sources. While its share in total mobile energy consumption in Switzerland remains below 10%, NRMM emits roughly 20% to 40% of the regulated pollutants, depending on the reference year (FOEN 2008, FOEN 2015). The larger share in air pollutant emissions is due to the fact that for many years, the non-road sector was a neglected area of air pollution control. In the EU, the first emission limits for NRMM entered into force in 1999 (TE 2015).

Switzerland compiled its first non-road emissions inventory in 1996 (FOEFL 1996). It has been updated twice since, in 2008 and 2015 (FOEN 2008, FOEN 2015). In this paper, the methodology and key results of the latest update are presented.

1. Objectives

The main objective of the research presented here is the update of the Swiss non-road emissions inventory in order to meet Switzerland's reporting duties towards the international conventions

UNFCCC (UN Framework Convention in Climate Change) and CLRTAP (Convention on Long-Range Transboundary Air Pollution). This includes the update of all activity data, load factors, emission factors, and correction factors, as well as the review of all underlying assumptions. The inventory reports energy and fuel consumption and direct emissions of the following machine categories:

- Construction machinery;
- Industrial machinery (also including commercial/public works machinery);
- Agricultural machinery;
- Forestry machinery;
- Garden-care and hobby appliances;
- Ships and boats;
- Diesel rail vehicles;
- Military machinery.

The current update implements several improvements with respect to previous versions. First, in order to improve the comprehensiveness of the inventory, the list of included machinery is complemented by a few machine types neglected so far:

- Generators in industry, commerce and public administration (so far, only generators in construction and the military had been included);
- Vehicles and mobile machinery of the airside sector of airports;
- Inland barges on the Rhine River.

Second, machines and appliances with electric motors are newly included due to the fact that mainly for small, hand-held devices, electric versions are becoming increasingly popular due to improvements in battery technology. Since the primary aim of this inclusion is the monitoring of the transition from combustion engines to electric motors, only machine types that are traditionally part of NRMM inventories are included; consequently, electric railway transport is excluded, as well as hand-held devices for indoor use that never operated with combustion engines. Since the inventory focuses on direct emissions, only energy consumption but no (indirect) air pollutant emissions from electric devices are reported.

Third, in addition to fuel consumption, CO₂ and the four regulated pollutants carbon monoxide (CO), hydrocarbons (HC), nitrogen oxides (NO_x) and particulate matter (PM) included in the previous inventory, the four non-regulated pollutants methane (CH₄), non-methane hydrocarbons (NMHC), benzene (C₆H₆) and nitrous oxide (N₂O) are included. For PM, only exhaust emissions are considered.

Fourth, since Switzerland has implemented strict particle filter requirements for machinery operated on construction sites through its Ordinance on Air Pollution Control (OAPC), the impacts of this legislation are assessed, as well as the impacts of the current and future emission standards on diesel particle filter (DPF) use.

Fifth, the modelled period (starting in 1980) is extended to 2050 instead of 2020; this implies taking into account longer-term economic forecasts, and most importantly, the Euro-V emission standard.

Sixth and last, the impact of delayed implementation of emission standards due to the sell-off periods and the flexibility scheme provided for in the EU Directive 97/68/EC is assessed.

2. Methodology

General approach

The Swiss non-road emission model implements a bottom-up approach in which operating hours segmented by machine type, motor type, size classes with respective nominal power, and age are multiplied with load factors. The resulting energy demand is multiplied with fuel consumption and emission factors, and corrected with four correction factors:

$$Em = N \cdot H \cdot P \cdot \lambda \cdot \varepsilon \cdot CF_1 \cdot CF_2 \cdot CF_3 \cdot CF_4 \quad (1)$$

Where:

Em = emission per machine type, pollutant, emission standard (in grams or tonnes p.a.)

N = Stock [number of machines/devices]

H = annual hours of operation [h/a]

P = mean nominal capacity [kW]

λ = effective load factor (dimensionless)

ε = emission (or fuel consumption) factor [g/kWh]

CF₁ = correction factor for the deviation of effective load from the standard load in the cycle on which the emission factor is based (dimensionless)

CF₂ = correction factor for dynamic utilisation of the machine (dimensionless)

CF₃ = correction factor for deterioration of the machine (dimensionless)

CF₄ = correction factor for diesel particle filter (DPF) use (dimensionless)

The calculation methodology outlined above refers to fuel consumption and the four regulated pollutants CO, HC, NO_x and PM.

By contrast, CO₂ emissions directly depend on fuel consumption. The fuel-based emission factors in the non-road model (corresponding to the results presented here) are differentiated by fuel type but constant (published in FOEN 2015); for climate reporting from 2015, CO₂ emissions were recalculated using temporally varying CO₂ emission factors (published in FOEN 2016; the deviations to the results presented here are minimal).

Emissions of non-regulated air pollutants are calculated as follows: Components of hydrocarbons (CH₄, NMHC, benzene) are calculated as shares of HC differentiated by type of fuel and engine technology. For benzene, an additional differentiation is made between the periods before and after 2000, since in that year the limit level of 1% for benzene content entered into force. For N₂O, emission factors in g/kWh differentiated by engine technology, are applied (see also FOEN 2015).

Activity data

Inputs on stock, and operating hours were collected from various sources. The approach differs between the periods 1980-2000, 2000-2015, and 2020-2050.

For the period 1980-2000, activity data from the previous non-road emissions inventory (FOEN 2008, stock and operating hours based on EWI 2005) were used in most cases. Stock or operating hours were only retrospectively adjusted if more recent information was available that made a correction necessary.

For the period 2000-2015, official or industry association statistics were used where available. These include the database of the Swiss Federal Motor Vehicle Inspection Office (MOFIS), the inventory data of the Swiss Master Builders Association (SBV 2013), the periodical agricultural census and the federal government's import/export statistics (Swiss-Impex, EZV 2014). Market studies (Off-Highway Research 2005, 2008, 2012) were another important source for the development of construction machinery and tractors. The applications for fuel tax refunds, as well as applications for the use of heating oil, submitted to the Federal Customs Administration, were evaluated. Questionnaires were mailed to manufacturers, importers and operators. To complement the information gathered from these sources, expert workshops were held to discuss the available information and make estimates to fill data gaps. Age distributions were in the majority of cases taken from EWI (2005) and adjusted in a few cases (mostly based on the MOFIS database).

The forecasts up to 2050 are based on various sources. For the construction and the industrial sectors, economic forecasts were available up to 2030 (VÖV 2012), and were extended up to 2050 by taking into account predicted population growth (medium scenario of the Federal Statistical Office, BFS 2014). For agricultural machines, the activity forecast is based on the forward projection of the historical trend in agricultural area. For military and railways, long-term planning information up to 2020-2030 was provided by the Army Logistics Basis (LBA), Swiss Federal Railways (SBB) and the

Bern-Lötschberg-Simplon (BLS) railway; for the subsequent period, the trend was projected forward with gradual levelling-off. For the remaining sectors, the historical trends were projected forward, with a gradual level-off assumed from 2020.

Load factors were basically taken from the previous version of the emissions inventory (FOEN 2008), for which they had been mostly estimated by industry experts. For the 2015 update, they were reviewed during the expert workshops mentioned above, and adapted where necessary. For construction machines and their military equivalents, the load factors were adapted based on the findings of Fridell et al. (2014). For rail vehicles, and partially for large ships, fuel consumption values were available alongside operating hours and nominal power, so that load factors could be calculated from these inputs.

Emission factors

The emission factors for diesel machines not subject to emission regulation (Pre-Euro and small machines <18 kW) are based on EPA (2004) and measurements of black smoke carried out by the Swiss Federal Laboratories for Materials Testing and Research, Agroscope and IVECO (FOEN 2008).

For diesel machines and pollutants subject to the EU emission regulation, the emission factors are based on the respective limit values and the emissions from type approval tests. Where total limit levels from HC + NO_x apply, 90% of these were allocated to NO_x and 10% to HC (in accordance with IFEU 2009). In the case of EU-III A to EU-V for HC, and for EU-III A only for NO_x, 10%-30% were deducted from the limit value to derive the emission factors. For NO_x and PM from EU-III B to EU-V, the limit values are applied as emission factors without any deduction, since it is assumed that manufacturers can hardly keep emissions below these stringent emission limits. For CO, the emission factors amount to between 12% and 37% of the limit values based on type approval emissions.

For petrol-powered devices, the emission factors for the pre-Euro period are based on assumptions deduced from measurements in the framework of an alkylate gasoline study (INFRAS 2008). For the regulated period (Euro stages), the emission factors are derived from the limit values with a deduction of 10%.

The emission factors for ships and boats are largely based on the applicable limit values specified since 1995 in the SAV (Swiss Ordinance on Pollutant Emissions from Ship Motors) and the Euro stages from 2003. Emission limit values up to emission category EU-III A are adopted minus a tolerance of 10%; for the emission stage EU-V, the tolerance of 10% is only applied for HC and CO, and for NO_x and PM the emission limit levels are applied without deduction.

For rail vehicles, the emission factors for older machines correspond to the emission limit recommendations of the UIC and the factors for diesel machines with the same year of manufacture. The emission factors for post-2006 engines correspond to the EU limit values from EU-III A minus a tolerance of 10%. For Euro-V, the manufacturing tolerance of 10% is only applied for HC and CO.

The emission factors of gas-powered machines are based on measurements of engines with different degrees of retrofitting (without after-treatment, with oxidation catalysts, with 50% or 100% of machines with 3-way catalysts).

The emission factors of the non-regulated pollutants CH₄, NMHC, N₂O and C₆H₆ are taken from EEA (2013), IFEU (2009), and Mayer (2005). For CH₄ and NMHC, they are based on complimentary fractions of total HC.

The limit values for the planned EU-V emission standard are based on a draft presented at a 2014 GEME (EU expert group on emissions from Non-Road Mobile Machinery) Meeting (EC 2014); they have not been adapted since.

All emission and fuel consumption factors along with information on their sources can be found in the Annexes of FOEN (2015; see download URL under References).

Fuel and electricity consumption factors

Fuel consumption is calculated in the same way as emissions by applying fuel consumption factors in g/kWh instead of emission factors. The fuel consumption factors in the Swiss non-road emission model are based on the following sources: EPA 2004 (diesel machines), DLG 2008 (petrol devices),

FOEFL 1996 (ships and boats), IFEU 2003 and data from locomotive manufacturers (rail vehicles). For diesel machines, the fuel consumption factors are differentiated by size class but constant in time, whereas for petrol engines, a development parallel to HC emissions is assumed.

For electricity consumption, the reciprocal value of the efficiency level is used instead of a consumption factor in g/kWh. The overall efficiency level is the product of the individual efficiency levels of the motor, the battery and the charger. Different assumptions apply for industrial NRMM and for garden-care/hobby appliances (based on Nipkow 1989, Dieterich 2012, TASPO 2013, Dolder 2014; for details see FOEN 2015). The resulting overall efficiencies are published in FOEN (2015).

Correction factors

The Swiss non-road emission model uses four types of correction factors (see above). All parameter values are published in FOEN (2015).

The *load correction factor* (CF_1 in formula 1 above) adjusts fuel consumption of diesel machines for the deviation of the actual engine load from the average engine load of the test cycle (Non-Road Steady Cycle NRSC, also referred to as ISO 8178-C1) that the fuel consumption factors are based on. It is calculated with the following formula:

$$CF_1 = 2.0095 - 2.1981 \cdot \Delta_{LF} + 1.1886 \cdot \Delta_{LF}^2 \quad (2)$$

Where:

CF_1 = load correction factor

Δ_{LF} = ratio of effective load to standard load

The effect of the load correction factor is that the specific consumption at an effective load of e.g. 20% is around 30% higher than at the NRSC load factor of 48% (see Figure 1).

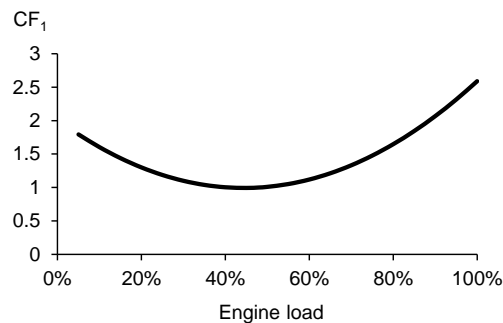


Figure 1. Relationship between engine load and load correction factor CF_1 .

The *correction factor for dynamic use* (CF_2 in formula 1) corrects the emissions of the regulated pollutants due to dynamic machine use (i.e. frequently changing load, as opposed to the stationary load points of the NRSC). The values used for CF_2 up to EU-III A are based on EPA (2004). For EU-III B, CF_2 is set to 1.0 for all machine categories and pollutants. For EU-IV and EU-V, values greater than 1.0 are used for NO_x for all machines between 56 and 560 kW in order to account for the higher specific emissions at low engine loads due to the Selective Catalytic Reduction (SCR) only being activated at higher loads.

The *deterioration correction factor* (CF_3 in formula 1) corrects emissions for deterioration due to wear and tear. It is applied to all machines up to EU-III A after a given period of operation based on the age distribution of the machine park and the annual operating hours. From EU-III B, manufacturers have to prove the stability of emissions over extended operating periods (EC 1997), therefore CF_3 is

set to 1.0 for newer machines.

The *diesel particle filter (DPF) correction factor* (CF_4 in formula 1) applies to all diesel machines equipped with particle filters (ex-works or retrofitted). It corrects PM emissions and fuel consumption for DPF use. Fuel consumption is increased by 3% for machines with DPF; the correction of PM emissions depends on the size class and the emission standard, since also machines without DPF have to meet the applicable limit values, and these differ between EU stages. The limit values of EU-IIIB and EU-IV can be met with either DPF or other after-treatment technologies (Integer 2013), but PM emissions are lower with DPF. For the regulated power range of EU-V engines, it is expected that DPFs will be necessary to meet the emission limits (especially the PN emission limit), therefore the DPF correction factor is set to 1.0.

The share of machines equipped with DPF was estimated separately by machine family and area of operation.

For construction machinery >18 kW operating on construction sites, the Swiss Ordinance on Air Pollution Control (OAPC) prescribes the use of a DPF from 2010, with a grace period for machines >37 up to 2015. For the emission model, it is assumed that this law is implemented (which in fact seems to be the case based on sample inspections).

For diesel machinery operating outside construction sites, the shares of machinery equipped with DPF up to 2010 are based on sales of DPF systems, data cited in the consultation procedure on the revision of the SAV (Swiss Ordinance on Pollutant Emissions from Ship Motors), and information provided by railway operators (SBB 2012, BLS 2012) and the Army Logistics Basis (LBA). For the period 2010-2020, DPF use was estimated based on the emission reduction strategies of machine manufacturers for stages EU-IIIB and EU-IV (Integer 2013; see Table 1), the respective marked shares of these manufacturers in Switzerland (Off-Highway Research 2008, 2012), and the turnover of the machine park depending on the life expectancy by machine category and size class.

Table1.Planned installation of diesel particle filters (DPF) in engines >18 kW in emission stages EU-IIIB and EU-IV, by manufacturer (“partially” indicates that in tendency, higher-powered engines are fitted with DPF).

Manufacturer	Stage EU-IIIB / US Tier 4 Interim	Stage EU-IV / US Tier 4 Final
AGCO	No	No
Caterpillar	Partially	Yes
CNH	No	No
Cummins	Partially	Partially
Deutz	Partially	Yes
IHI	No	No
Isuzu	Partially	No
John Deere	Partially	Yes
Komatsu	Partially	Partially
Kubota	Partially	Yes
Liebherr	Partially	No
Takeuchi	No	No
Volvo CE	Partially	Not yetknown
Volvo Penta	No	No
Weichai	No	No

3. Results and discussion

Activity and emissions in 2015

In 2015, almost three million machines and devices defined as NRMM were active in Switzerland. In total, they were operating for approximately 290 million hours and consumed 17.9 PJ of energy

(Table 2). This amounts to 9% of the total mobile energy consumption (road transport plus NRMM) in Switzerland (Table 4).

Most energy is consumed by large machines in construction (35% of the total), agriculture (28%), and industry (19%). The bulk of the stock (81%) and operating hours (61%), however, is attributed to garden-care appliances, which only account for 3% of the total energy consumption of NRMM. This discrepancy is due to the fact that in garden-care, a large number of small devices with low power (mostly <4 kW) is owned by private households, most of which are operated for short periods only every year. The reason why garden-care appliances account for such a large share of operating hours lies primarily with the lawn robots that operate more or less continuously during the entire vegetation period – however, with minimal energy use (around 25 W).

Diesel is the fuel most used for NRMM with 83%, followed by petrol with about 10%. Electricity already accounts for 5% of non-road mobile energy consumption, while gas and light fuel oil (LFO, used by some passenger ships) account for about 1% each.

Table 2: Stock, operating hours, and energy consumption by machine category in 2015.

Category	No. of machines	Operating hours per machine [h/a]	Total operating hours [million h/a]	Energy consumption [PJ]
Construction machinery	58'900	420	24.8	6.2
Industrial machinery	69'700	680	47.2	3.4
Agricultural machinery	313'600	100	31.5	5.1
Forestry machinery	11'300	190	2.2	0.4
Garden-care/hobby appliances	2'417'200	70	177.1	0.5
Ships and boats	96'400	40	3.4	1.6
Diesel rail vehicles	640	720	0.5	0.4
Military machinery	13'000	70	1.0	0.3
TOTAL	2'981'000	100	287.6	17.9

The absolute emission levels of regulated pollutants and CO₂ in 2015 are presented in Table 3. In total, about 1.25 million tons of CO₂, 7600 t of NO_x and 360 t of PM were emitted in 2015. The share of NRMM in total mobile air pollutant emissions is greater than its share in energy consumption, due to the time lag in emission regulations regarding NRMM compared to road transport: depending on the pollutant, the share of NRMM is between 18% and 33% in 2015. For the greenhouse gas CO₂, the share of NRMM only amounts to 8% - slightly less than its share in energy consumption due to the electric machines that do not emit CO₂ directly (Table 4).

Greenhouse gases are dominated by CO₂, which accounts for 98.6% of total CO₂eq in 2015 (CH₄: 2'900 t CO₂eq or 0.2%, N₂O: 15'200 t CO₂eq or 1.2%). The share of biogenic CO₂ is minimal with 1.1%.

Table 3: Emissions of regulated air pollutants and CO₂ by machine category in 2015.

Category	Carbon monoxide (CO) [t/a]	Total hydrocarbons (HC) [t/a]	Nitrogenoxides (NO _x) [t/a]	Particulate matter (PM) [t/a]	Carbon dioxide (CO ₂) [t/a]
Construction machinery	3'400	299	2'290	40	458'400
Industrial machinery	1'530	115	922	39	192'300
Agricultural machinery	13'500	1'060	2'520	226	374'300
Forestry machinery	1'580	167	129	8	28'700
Garden-care/hobby appliances	10'600	561	72	-	30'300
Ships and boats	4'320	462	1'110	39	114'500
Diesel rail vehicles	210	46	397	4	29'000
Military machinery	452	24	122	3	20'100
TOTAL	35'600	2'730	7'600	359	1'248'000

Depending on the pollutant, different machine categories are the largest sources among NRMM. Regarding CO₂, the ranking is identical to energy consumption (see above), with construction machinery emitting most of the greenhouse gas, followed by agricultural and industrial machinery.

Regarding NO_x, NRMM in agriculture (with 33% of emissions) surpasses construction machinery (30%) in 2015, followed by ships (15%) and industry (11%). With regard to PM emissions, agricultural machinery is by far the largest source accounting for 63% of emissions, leaving behind construction, industry and ships with 11% each. The reason why agriculture surpasses construction in terms of NO_x and PM emissions in spite of lower energy consumption is the longer lifespan of agricultural machines (mostly tractors) that slows down the pervasion of the machine park with new engines with more advanced emission technology. The even more relevant reason regarding PM is the fact that machinery on construction sites is subject to the stringent DPF requirements of the Swiss Ordinance on Air Pollution Control (OAPC), while there are no federal laws going beyond the Euro emission limits affecting agricultural machinery (see also paragraph on DPF use below).

Also in terms of CO and total HC, agricultural machinery is the largest source (accounting for 38% and 39% of emissions, respectively). Here the primary reason is the high petrol use by single-axle mowers which have relatively high nominal power and are operated at high engine load. However, also the large number of small hand-held devices with 2- or 4-stroke petrol engines in agriculture, forestry, and garden-care make an important contribution towards CO and HC emissions, making garden-care the second-most important source of these pollutants (accounting for 30% and 21% of emissions, respectively).

With respect to the non-regulated pollutants, the emission shares per machine category for the hydrocarbon fractions methane, NMHC, and benzene are naturally similar to those of total HC. They vary slightly with fuel type and engine technology distributions among the machine categories, however. For example, garden-care appliances contribute more towards methane emissions than towards NMHC due to the dominance of 2-stroke engines that emit a higher share of methane (about 7% of total HC) than 4-stroke petrol engines (3.4%).

Table 4: Comparison of NRMM and road transport consumption and emissions in 2015.

	Non-road mobile machinery [t/a]	Road transport [t/a] ^{*)}	Share of NRMM in total (road + non-road)
Consumption			
Diesel	352'100	2'057'000	15%
Petrol	40'000	2'425'900	2%
Energy	17.9 PJ	183.8 PJ	9%
Emissions			
Carbon monoxide (CO)	35'600	90'800	28%
Hydrocarbons (HC)	2'730	12'580	18%
Nitrogen oxides (NO _x)	7'600	32'240	19%
Particulate matter (PM)	359	737	33%
Carbon dioxide (CO ₂)	1'248'000	14'132'700	8%

*) Note that road transport refers to fuel used (territorial consumption) and not to fuel sold.

Development of activity and emissions

While in the previous non-road emission inventory (FOEN 2008), a slight decline of total operating hours of NRMM was forecast after a peak around the years 2000-2005, the 2015 update shows that NRMM activity has significantly increased since then. Total energy consumption increased by 5% between 2000 and 2015. The most important driver of this development has been the growing construction sector, while in the other important non-road sectors, i.e. industry and agriculture, energy consumption has stagnated or even decreased. Regarding operating hours, the largest increase is observed with garden-care appliances, again due to the growing popularity of the lawn robots with their long operating hours but low energy consumption (see above).

The emission levels of almost all pollutants modelled for the Swiss non-road emissions inventory increased until the year 1995. Benzene emissions fell sharply with the introduction of the lower limit level for benzene in petrol in 2000. From 2002, i.e. the entry into force of the EU emission standards, emission levels of all pollutants (except the greenhouse gases carbon dioxide and nitrous oxide) began to decrease significantly. The sharpest decline can be observed with PM, the emissions of which have decreased by almost 70% between 2000 and 2015.

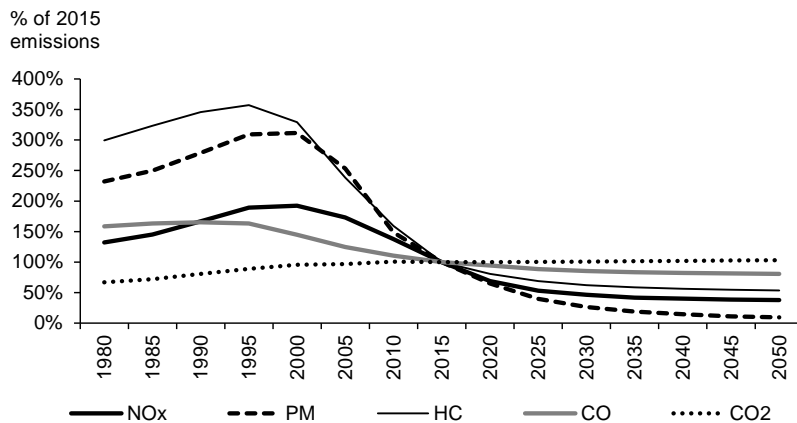


Figure 2. Development of the emissions of regulated air pollutants and CO₂ for the period 1980-2050, expressed in % of emissions in the year 2015.

In the future, a further reduction is expected for the majority of pollutants as a result of the pervasion of the machine park with newer engines with improved technology. The extent of this reduction remains to be verified, however, with emission measurements of EU-III B, -IV and -V

machines (see section on uncertainty below). A further increase of emissions (though at a slower pace) is only anticipated for the greenhouse gases CO₂ and N₂O. The level of PM emissions is expected to fall most sharply: here a reduction to less than 10% of the 2015 level is anticipated by 2050. This reduction is attributable to cleaner engines in general, and to the anticipated use of diesel particle filters (DPF) with the EU-V emission standard in particular.

Currently and in the near future, however, DPF use differs widely between areas of application. As compliance with the EU stage IIIB and IV limits for PM can be achieved without the use of diesel particle filters (DPF), most manufacturers comply with these requirements by the use of SCR (mostly for larger machinery >56 kW) or EGR technologies (mostly for smaller machines <56 kW) (Integer 2013; see also Chapter 2). Only with the particle number (PN) limits of stage V (from 2019/2020), DPF application will be expected to become inevitable for all areas of application. So far, in Switzerland only machinery on construction sites is required to be equipped with DPF. Furthermore, the pervasion of the machine park with DPF depends on the life cycle of machinery, which is longer in agriculture than in the construction or industry sectors. Therefore, estimated DPF use in 2015 varies between 4% in agriculture and 73% in construction machinery (Figure 3). The share of construction machines equipped with DPF does not exceed the latter value due to the fact that on one hand, not all construction machines are actually used on construction sites (other applications like quarrying are not affected by the particle filter legislation), and on the other hand, a sizeable share of construction machines (e.g. mini excavators) is below 18 kW and therefore neither affected by the DPF legislation nor the EU directives. The impact of the Swiss particle filter legislation is still significant, however: In 2015, more than 130 t of PM emissions from construction machinery could be avoided, which is 77% of the amount that would have been emitted without the respective law.

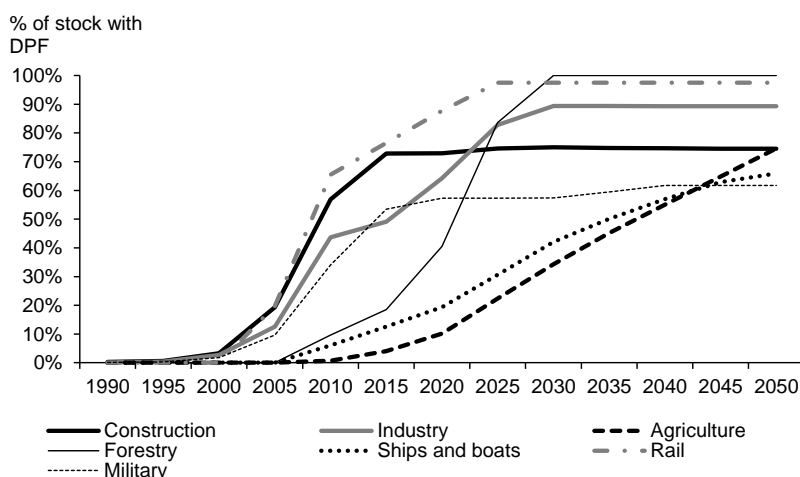


Figure 3. Percentage of machines equipped with diesel particle filters (DPF).

Sources of uncertainty

Emission calculations are always uncertain, and since the total emissions within a geographic region cannot be measured, benchmark figures on which to calibrate the total are lacking. Fuel sales, which are often used to calibrate fuel consumption in road transport emission models, cannot be used for NRMM in Switzerland, as only the total fuel sales for road and non-road are known (except for agriculture, for which there was a time-series on fuel consumption available up to 2004, from which the consumption in the present inventory only deviates by 1-2%). In the following paragraphs, the most relevant sources of uncertainty in the Swiss non-road emissions are discussed.

Regarding *activity data*, sources of uncertainty include the stock of machinery as well as the size class distribution, the respective operating hours and age distributions, the degree of diesel particle filter (DPF) use, and the delayed implementation of emission standards.

For larger machinery in construction and agriculture, stock, operating hours, size class and age distributions are rather well known from official data sources like the Swiss Federal Motor Vehicle registration database (MOFIS) or the agricultural census, or industry association statistics. The same

is valid for large ships, rail vehicles and military machinery, for which there are a few large operators that can provide the necessary information. By contrast, for smaller machinery, especially hand-held devices, information is relatively scant and therefore a large degree of estimation is involved. The uncertainty was reduced as much as possible by validation of the assumptions through industry experts.

The uncertainty of activity data forecasts can be evaluated by comparing the forecasts of the previous emission inventory (FOEN 2008) to the current figures for the year 2015. This corresponds to a forecast period of around 10 years as the previous inventory was based on data from 2000-2005. For 2015, the energy consumption of the current inventory was underestimated by 3% by the previous inventory (not counting electricity, as this was not part of the previous inventory). For some machine categories, the deviations are larger (i.e. the energy consumption of construction machinery was estimated 17% lower in the previous update), but they are partially compensated by deviations in other machine categories.

The *emission technologies used* can be mostly derived from the age distributions and the resulting emission standard that machines implement. There are two additional factors to be considered, however: On one hand, regarding PM, the degree of retrofitting diesel particle filters and the fact that different manufacturers follow different after-treatment strategies (discussed above) leads to uncertainty. Not all manufacturers selling equipment in Switzerland are covered in the Integer (2013) report on emission control technologies for stages EU-IIIB and -IV. Especially for agriculture, the manufacturers covered in the report only account for about half of the market share in Switzerland. Furthermore, the market shares per manufacturer are only known for the historical periods (up to 2012) and they fluctuate over time. Therefore, the percentage of machinery equipped with DPF, especially in agriculture (Figure 3), is uncertain.

On the other hand, the implementation of new Euro emission stages is delayed due to two mechanisms in the EU Directives on non-road emissions that allow placing machinery on the market that conforms to the previous emission stage, i.e. the sell-off period and the flexibility scheme (EC 1997, EC 2014). The extent to which these two mechanisms are used is not known; therefore a sensitivity analysis was carried out. The difference in NO_x emissions between the “best-case” scenario (assuming immediate implementation of emission stages) and the “worst-case” scenario (assuming full exploitation of the two mechanisms) amounts to 14% of total emissions in the period 2015 to 2020. The emissions in the “most likely” scenario, to which the figures presented in this paper correspond (assuming a share 25% of conforming machines in the first year of a new emission stage, 50% in the second year and 100% from the third year, with a somewhat longer delay for stage IIIB), amount to almost exactly the average of the two extreme scenarios.

The *load factors* are generally one of the greatest sources of uncertainty in non-road emission calculations. For many machine categories, the only sources are estimates from industry experts. The changes in emissions due to adapting the load factors of construction machines based on the findings of Fridell et al. (2014; see also Chapter 2) give an impression of the magnitude of uncertainty: For the construction machines alone, energy consumption decreased by about 16% (depending on the reference year) due to the adaptation of the load factors. For the entire non-road inventory, this amounts to a decrease of about 6%.

Emission and energy consumption factors are obviously uncertain as well. This is due to the scarcity of measurements in general, and in particular due to the fact that the existing measurements were mostly carried out using the test cycles NRSC (Non-Road Steady Cycle) and NRTC (Non-Road Transient Cycle). Furthermore, for the emissions inventory presented here, there were virtually no measurements for newer machines (from stage EU-IIIB onwards) available at the time when modelling was carried out. Recent work by the Graz Technical University (Blassnegger 2014) using PEMS (Portable Emission Measurement Systems) measurements and the PHEM model shows that especially for NO_x and newer construction machinery, emission limits are exceeded in real-world applications.

Finally, the *transition towards electric motors* is a large source of uncertainty in the future projections. So far, improvements in battery technology have caused a rise in popularity of electric equipment in areas of application where electric motors have been in use before, albeit less widespread, i.e. for industrial and hand-held devices. In the present Swiss non-road emissions inventory, the future projections for electric motors are limited to these areas of application. This results in a future stagnation of the electric share of non-road energy use, little above the current value

of 5%, since the energy consumption of hand-held devices is low and the relative importance of industrial appliances is decreasing. However, very recent developments indicate that electric motors could become widespread in construction equipment (e.g. Bauwirtschaft Online 2014, Suncar-HK 2016), which could drastically change the outlook on NRMM emissions.

4. Conclusions

The new Swiss non-road emissions inventory delivers up-to-date figures on activity, energy consumption and emissions of NRMM in Switzerland. It documents the increasing activity of NRMM in the past decades and its importance among mobile emission sources. The simultaneous decrease in emissions demonstrates the effectiveness of legislation on emissions – primarily the EU directives on NRMM emissions, but also the Swiss national legislation on particle filter use on construction sites.

However, the modelled sharp decline of air pollutant emissions in the coming years is largely based on limit values and assumptions on the specific values of newer machines. Moreover, load factors remain a large source of uncertainty. The decline in emissions therefore must be verified with more measured data.

In order to do so effectively, increased international exchange of approaches, methods and data, as well as the coordination of measurement programs, are crucial. Currently, an initiative is planned by INFRAS and FOEN to enhance collaboration between non-road emissions experts in Europe.

5. Acknowledgments

The authors wish to thank everyone who has contributed to the research behind this paper. First of all, this is the Transport Section of the Swiss Federal Office for the Environment (FOEN) that has funded the research, contributed expert knowledge, and facilitated contacts with other experts and data providers. Experts from industry, their associations, manufacturers and operators of NRMM have provided valuable data and expertise, namely the Swiss Builders Association (SBV), the Association of Swiss Construction Machinery Manufacturers (VSBM), the Swiss Association for Agricultural Machines (SLV), the Swiss Association of Forestry Enterprises (FUS), the Swiss Forklift Association (swisslifter), Agroscope, the Swiss Federal Institute for Forest, Snow and Landscape Research (WSL), the Swiss Cableway Association (SBS), the Swiss Association of Manufacturers and Dealers of Communal Machinery (SIK), Zurich and Geneva airports, Liebherr, Stihl, Husqvarna, Honda, the Swiss Federal Railways (SBB), the Bern-Lötschberg-Simplon Railway (BLS), the passenger ship companies, the Federal Customs Administration (EZV), the Federal Statistical Office (FSO), the Federal Office for Agriculture (FOAG), and the Army Logistics Base (LBA). Finally we also thank the non-road experts in other countries for their work from which the Swiss emissions inventory has also benefitted.

6. References

- Bauwirtschaft Online (2014): Studenten arbeiten an einem "grünen" Bagger. Bauwirtschaft Online, 18.06.2014. [<http://www.schweizerbauwirtschaft.ch/Artikel-Einzelansicht.20+M5b19422f226.0.html>].
- BFS (2014): Bevölkerungsentwicklung. Ständige Wohnbevölkerung nach den drei Grundscenarien. Bundesamt für Statistik (BFS). [http://www.bfs.admin.ch/bfs/portal/de/index/themen/01/03/blank/key/ent_erw.html].
- Blassnegger, J. (2014): Emission Factor Model for Construction Machinery Based on PEMS Tests. 20th International Transport and Air Pollution (TAP) Conference, Graz, Austria.
- BLS (2012): Geschäftsbericht 2012. BLS AG. [<http://bls.ch/d/unternehmen/investorrelations-geschbericht-2012.pdf>].
- Dieterich, K. (2012): Lösungen für die Energiewende - Energieforschung bei Bosch. In: Zusammenarbeit von Forschung und Wirtschaft für Erneuerbare Energien und Energieeffizienz. FVEE-Jahrestagung 2012, Umweltforum Berlin. ForschungsVerbund Erneuerbare Energien (FVEE). [http://www.fvee.de/fileadmin/publikationen/Themenhefte/th2012-2/th2012_02_02.pdf].

- DLG (2008): DLG-Prüfberichte, Testzentrum Technik & Betriebsmittel. Deutsche Landwirtschaftliche Gesellschaft (DLG). [<http://www.dlg.org/landtechnik.html?&L=51>].
- Dolder (2014): Nennmindesteffizienz und Effizienzklassen von Elektromotoren. Dolder Ingenieure. [http://www.dolder-ing.ch/wissen/Elektro/elektromotor_wirkungsgrad_effizienz.htm].
- EC (1997): Directive 97/68/EC of the European Parliament and of the Council of 16 December 1997 on the approximation of the laws of the Member States relating to measures against the emission of gaseous and particulate pollutants from internal combustion engines to be installed in non-road mobile machinery. European Commission (EC), Brussels.
- EC (2014): Non-Road Mobile Machinery. Revision of Directive 97/68/EC. Presentation held at the GEME (Expert group on emissions from Non-Road Mobile Machinery Engine) Meeting of Feb. 13, 2014. European Commission (EC), not published.
- EEA (2013): EMEP/EEA Air Pollutant Emission Inventory Guidebook 2013. Technical Guidance to Prepare National Emission Inventories. European Environment Agency (EEA). [<http://www.eea.europa.eu/publications/emep-eea-guidebook-2013>].
- EPA (2004): Exhaust and Crankcase Emission Factors for Nonroad Engine Modelling - Compression Ignition. United States Environmental Protection Agency (EPA), Washington, D.C.
- EWI (2005): Neue Offroad-Datenbank 2000. Mengengerüste. Jaakko Pöyry Infra (formerly Elektrowatt Infra, EWI) and Federal Office for Environment, Forestry and Landscape (FOEFL), not published.
- EZV (2014): Swiss-Impex. Eidgenössische Zollverwaltung (EZV). [<https://www.swiss-impex.admin.ch/>].
- FOEFL (1996): Non-road fuel consumption and air pollutant emissions. Federal Office for Environment, Forestry and Landscape (FOEFL), Ittigen.
- FOEN (2008): Non-road fuel consumption and pollutant emissions. Study for the period 1980 to 2020. Environmental studies no. 0828. Federal Office for the Environment (FOEN), Ittigen.
- FOEN (2015): Non-road energy consumption and pollutant emissions. Study for the period 1980 to 2050. Environmental studies no. 1519. Federal Office for the Environment (FOEN), Ittigen. [<http://www.bafu.admin.ch/publikationen/publikation/01828/index.html>].
- FOEN (2016): Switzerland's Greenhouse Gas Inventory 1990-2014. National Inventory Report 2016. Federal Office for the Environment (FOEN), Ittigen. [http://www.bafu.admin.ch/klima/13879/13880/15473/index.html?lang=en&download=NHzLpZeg7t,inp6lONTU042lZ26ln1ad1lZn4Z2qZpnO2Yuq2Z6gpJCHeoB5g2ym162epYbg2c_JjKbNoKSn6A--].
- Fridell, E., Bäckström, S., Jerksjö, M., Lindgren, M. (2014): Emissions from Non-Road Mobile Machinery - Focus on Engine Load. 20th International Transport and Air Pollution (TAP) Conference 2014, Graz, Austria.
- IFEU (2003): Erarbeitung von Basisemissionsdaten des dieselbetriebenen Schienenverkehrs unter Einbeziehung möglicher Schadstoffminderungstechnologien. Institut für Energie- und Umweltforschung (IFEU), Heidelberg.
- IFEU (2009): Aktualisierung des Modells TREMOD - Mobile Machinery (TREMOMM). Endbericht im Auftrag des Umweltbundesamtes. Institut für Energie- und Umweltforschung (IFEU), Heidelberg.
- INFRAS (2008): Einsatzfelder und Nutzung des Alkylatbenzins. Lagebericht für die Schweiz im Auftrag des Bundesamtes für Umwelt und der Schweizerischen Metallunion. Bundesamt für Umwelt (BAFU), Ittigen.
- Integer (2013): Emissions Control in Non-Road Mobile Machinery (NRMM) Markets: 2013 Edition. Integer Research Limited, London.
- Mayer, A. (2005): Elimination of Engine Generated Nanoparticles. expertVerlag, Renningen.
- Nipkow, J. (1989): Elektrizität sparen bei Motoren. Schweizer Ingenieur und Architekt 18(107). [<http://dx.doi.org/10.5169/seals-77095>].

- Off-Highway Research (2005): The Market for Construction Equipment and Agricultural Tractors in Switzerland. September 2005. Off-Highway Research, Wadhurst. [<http://www.offhighway.co.uk/europe.htm#Country>].
- Off-Highway Research (2008): The Market for Construction Equipment and Agricultural Tractors in Switzerland. November 2008. Off-Highway Research, Wadhurst. [<http://www.offhighway.co.uk/europe.htm#Country>].
- Off-Highway Research (2012): The Market for Construction Equipment and Agricultural Tractors in Switzerland. April 2012. Off-Highway Research, Wadhurst. [<http://www.offhighway.co.uk/europe.htm#Country>].
- SBB (2012): Die SBB in Zahlen und Fakten. Schweizerische Bundesbahnen (SBB), Bern. [http://www.sbb.ch/content/sbb/de/desktop/sbb-konzern/medien/publikationen/geschaefts-nachhaltigkeitsbericht/archiv/_jcr_content/contentPar/downloadlist/downloadList/_p_sbb_gb_2012_br_p_.spooler.download.pdf].
- SBV (2013): BIV 2013. Betriebsinterne Verrechnungsansätze und Inventar-Grunddaten. Schweizerischer Baumeisterverband (SBV).
- Suncar-HK (2016): Elektrobagger. Suncar HK AG. [<http://www.suncar-hk.com/de/elektrobagger/technik.php>].
- TASPO (2013): Bosch Gartengeräte-Absatz: "Starke Verkaufsdynamik." TASPO. [<http://taspo.de/aktuell/alle-news/detail/beitrag/56716-bosch-gartengeraeete-absatz-starke-verkaufsdynamik.html>].
- TE (2015): Don't breathe here. Tackling air pollution from vehicles. Transport and Environment (TE). [<https://www.transportenvironment.org/publications/dont-breathe-here-tackling-air-pollution-vehicles>].
- VÖV (2012): Marktanalyse und Marktprognose Schienengüterverkehr 2030. VÖV (Verband öffentlicher Verkehr) in Zusammenarbeit mit INFRAS Forschung und Beratung, BAKBasel und IVT (Institut für Verkehrsplanung und Transportsysteme der ETH Zürich), Bern.

Exhaust emissions from in-service inland waterways vessels

D. Pillot*, B. Guiot**, P. Le Cottier**, P. Perret* and P. Tassel*

* *Laboratoire Transports & Environnement, IFSTTAR, Cité des Mobilités, Bron, 69675, France*
Fax +33 (0)4 72 37 68 37 - email: didier.pillot@ifsttar.fr

** *Centre de Recherche en Machines Thermiques (CRMT), Dardilly, 69570, France*

Abstract

Since the early 1990s, significant reductions of the NO_x (Nitrogen Oxides) and PM (Particulate Matter) emissions from road transport have been observed, especially with Euro VI requirements, whereas current in-service freight vessels are still often equipped with diesel engines free of emission control. However, very few measurements on board freight waterways vessels have been carried out so far, due to both test difficulties and the poor accessibility and availability of commercial vessels. Indeed, only a few hours of emission monitoring could be performed from measurements on-board two freight vessels and a passenger boat, in the frame of a recent project. However, with the steady-state operating conditions observed most of the time, reliable functions could be set up to simply derive pollutant emissions from engine speed, respectively for each pollutant (CO₂, NO_x, PM and CO) and for each boat at various engine cruising speeds. Significant differences are observed between tested vessels, in terms of emissions factors expressed in g/tonne.km, for CO₂, NO_x and PM. Results in g/kWh are analysed as well and confronted with CCNR and European standards. The whole experimental emission factors from current waterways freighters are set against those from heavy-duty trucks. Comparisons are made with Euro II heavy-duty trucks which have similar engine manufacturing years and with the recent Euro V ones.

Keys-words: *exhaust emissions, on-board measurement, inland waterway vessels, freight transport, diesel engine.*

Résumé

Depuis le début des années 1990, des réductions significatives d'émissions de NO_x (Oxydes d'Azote) et de particules (PM en masse) provenant du transport routier ont été observées, particulièrement avec les exigences de la norme Euro VI, alors que les unités fluviales de fret actuellement en service sont encore souvent équipées de moteurs diesel sans traitement des gaz d'échappement. Cependant, très peu de mesures à bord de ce type de navires et sur voies navigables ont été effectuées jusqu'ici, conséquence à la fois des difficultés d'accès à bord et de la faible disponibilité de ces navires commerciaux. De fait, seules quelques heures de suivi d'émissions ont pu être réalisées à bord de deux navires de fret et une vedette passagers, dans le cadre d'un projet récent. Cependant, grâce à des conditions de fonctionnement principalement stationnaires, des relations fiables ont pu être établies pour déduire simplement les émissions de polluants à partir des régimes moteur de chaque bateau, et ceci pour les différents polluants suivis (CO₂, NO_x, PM et CO). Des différences significatives sont observées entre les navires testés, en termes de facteurs d'émissions exprimés en g/tonne.km. Les résultats en g/kWh sont aussi analysés et confrontés avec les limites CCNR et européennes. L'ensemble des facteurs d'émission des unités de transport fluvial relevés sont confrontés à ceux de poids lourds. Les comparaisons sont faites avec des poids lourds Euro II qui avaient des moteurs de technologie semblable et avec les « Euro V » récents.

Mots-clés: *émissions à l'échappement, mesures embarquées, unités fluviales de transport, transport de marchandises, moteur diesel.*

Introduction

As a result of their huge load capacities, inland waterways vessels (IWV) are usually described as an environmentally friendly transport mode, especially when considering CO₂. Indeed, one pusher with 2 fully loaded barges on the river can have the same goods capacity of 150 articulated trucks on the road. Transporting goods in bulk is a significant source of savings, in terms of energy consumption per ton of goods and for many others aspects (manpower, logistical costs...). It is also true that cargo concentration is not adapted to any type of goods or transport, especially when "door-to-door" services or "just in time delivery" is required.

Despite these advantageous specific energy consumption and CO₂ emissions, the introduction of exhaust emission limits for inland and marine vessels came late after the first legislation standards imposed to road transport; in addition, the current certification levels remain lenient for marine engines. Consequently, since the early 1990s, significant reductions of NO_x (Nitrogen Oxides) and PM (Particulate Matter) emissions from heavy-duty road vehicles have been observed, especially with Euro VI requirements, whereas current in-service freight vessels are often equipped with diesel engines free of emission control. Moreover, the long working life of marine engines does not play in favour of a quick renewal towards cleaner engines. It is then suspected that most current IWV have significant emissions of NO_x and particulates, and perhaps higher specific emissions than those from heavy-duty trucks (in g/ton.km). Even if the vessels traffic is small compared to the HGV's one, it seemed relevant to estimate the levels of air pollutants coming from IWV and to compare them with those given for the heaviest truck class.

The interest of a more environmentally friendly transport mode cannot be limited to fuel consumption and CO₂ reductions; it is also necessary to have cleaner ships in terms of particulate matter, nitrogen oxides and unburned hydrocarbons which are typical of diesel engines. The aim is therefore to reduce the impact of the ship traffic on the local air quality, keeping in mind that the traffic of heavy-duty vessels is constantly increasing and that projects of river shuttles within urban areas are flourishing.

In this context, one of the objectives of the research program PROMOVAN launched by "Voies Navigables de France" (VNF or French navigable waterways) was to assess the real exhaust emissions of typical freight vessels during normal operation. One pusher tug with barges and one self-propelled barge could be monitored during usual navigation on the Rhône River. In addition, a passenger boat was tested and emissions from its propulsion engines could be investigated more thoroughly: both port and starboard engines could be measured and data compared and most important, the effect of the navigation direction (upstream and downstream) was investigated. The experimental process is described, with emphasis on sampling and exhaust flow determination.

Very few measurements on board freight waterways vessels have been carried out so far, due to both test difficulties and the poor accessibility and availability of commercial vessels. Indeed, only a few hours of emission monitoring could be obtained and analysed on both freight vessels in the frame of the PROMOVAN project. However, due to the fact that propulsion engines operate mainly in steady-state conditions, reliable functions could be set up to derive simply pollutant emissions from engine speed, respectively for each pollutant (CO₂, NO_x, PM and CO) and for each vessel at various engine cruising speeds.

1. Regulatory context

As we know, emissions limits set by the regulations cannot provide reliable information on emissions during real-world operations as the engines are certified on a test bench along operating cycles that are generally not representative of their average running conditions. Moreover, emissions are expressed in g/kWh, i.e. the rate of emission mass to the energy used, and not to the distance or running time. European guidelines to limit pollutant emissions from IWV were introduced only recently (2007 and 2009 for larger engines), hence after the registration of most of the ships in operation today, including the three river vessels we have monitored.

However, the first environmental regulations for marine engines had previously been set up at a worldwide scale in the frame of the International Maritime Organization (IMO), an agency of the United Nations. In 1958, the first international convention against marine pollution (MARPOL) tackled the oils slicks to prevent environmental disasters on coasts. The "1997 Protocol", which includes Annex VI titled "Regulations for the Prevention of Air Pollution from Ships" set limits on NO_x and induced SO₂ reduction (and indirectly PM reduction) through sulfur abatement imposed in the fuel. Even if it became effective only in 2005 –after being accepted by at least 15 States and with not less than 50% of world merchant shipping tonnage– marine engine manufacturers have been building engines (those greater than 130 kW) compliant with the above NO_x standards since 2000. Accordingly, this regulation has benefited to waterways vessels as they are equipped with the same marine technology engines (same manufacturers). Annex VI amendments adopted in October 2008 introduced new fuel quality requirements and the so-called "Tier II" and "Tier III" NO_x emission standards for new engines, depending on the engine maximum operating speed (n in rpm), as shown in Table 1.

Tier	Date	NOx Limit (g/kWh)		
		n < 130	130 ≤ n < 2000	n ≥ 2000
Tier I	2000	17.0	45.n ^{-0.2}	9.80
Tier II	2011	14.4	44.n ^{-0.23}	7.70
Tier III	2016*	3.4	9.n ^{-0.2}	1.96

* In NOx Emission Control Areas (namely, North American area and the US Caribbean Sea, so far). Tier II standards still apply outside ECAs

Table 1. MARPOL Annex VI, NOx Emission Limits

Tier II standards were met by combustion process optimization (fuel injection timing, pressure and rate, exhaust valve timing, cylinder compression volume, etc...). Tier III standards require dedicated NOx emission control technologies such as various forms of water induction into the combustion process, exhaust gas recirculation and possibly selective catalytic reduction. Experiences of SCR for ships have led to develop well-adapted technologies; for example, one of the main issue, the sulfur content of fuel, is not a poison to marine catalysts (which are most often made of vanadium), unlike SCR catalysts used in the automotive industry.

The MARPOL NOx standards were adopted by the USEPA to make them mandatory from 2003 (Tier 1) for the largest marine engines (category 3, more than 2500 kW) installed on ships sailing in US waters (rivers and seas). A series of US standards was then published, broken down into stage or Tier 2 (2004-2007) and Tier 3 (2009-2014) for the least powered engines (from 37 kW). The limits of CO, HC and particulate matter were then set for the 3 engine categories; particulate limits are not mandatory for bigger engines (category 3) so far. A "Tier 4" was launched for category-1 and -2 engines, applying from 2014 to 2017, respectively for larger engines first to less powerful, the latter being in the range 600-1400 kW, i.e. the ones installed on the tested ships in our project.

At the European scale, the first emission limits for inland waterways were introduced later: they were published in 2004 by the EC to be applied in 2007 or 2009 depending on the engine capacity. However, the countries bordering the Rhine River had defined the so-called "CCNR*" regulations" for application since 2002 and specifically for the Rhine navigation. The 4 major pollutants, CO, HC, NOx and PM are targeted. It is to note that the CCNR-1 limit for NOx was defined identically to the first MARPOL limit (Table 2). Then, the existing CCNR regulation for the Rhine –where a large part of the European inland waterways traffic takes place– can explain why European legislators have postponed to 2007 or 2009 the setting of the first IWV limits, i.e. a long time after the first road vehicles limits.

CCNR Regulations	Power (kW)	CO (g/kWh)	HC (g/kWh)	NOx (g/kWh)	PM10 (g/kWh)
Stage I 2002	37 ≤ PN < 75	6.5	1.3	9.2	0.85
	75 ≤ PN < 130	5.0	1.3	9.2	0.70
	PN ≥ 130	5.0	1.3	n ≥ 2800 rpm : 9.2 500 ≤ n < 2800 rpm : 45.n ^{-0.2}	0.54
Stage II 2007	19 ≤ PN < 37	5.5	1.5	8.0	0.8
	37 ≤ PN < 75	5.0	1.3	7.0	0.4
	75 ≤ PN < 130	5.0	1.0	6.0	0.3
	130 ≤ PN < 560	3.5	1.0	6.0	0.2
	PN ≥ 560	3.5	1.0	n ≥ 3150 rpm : 6.0 343 ≤ n < 3150 : 45.n ^{-0.2} – 3 n < 343 rpm : 11.0	0.2

Table 2. Pollutant emission limits fixed by CCNR for navigation on the Rhine

* CCNR : Central Commission for the Navigation of the Rhine

The limits given for “Stage II” since 2007 are logically close to –if not the same as– the European ones, the latter just apply to a larger scale (Directive 2004/26/EC). With Stage II, it is intended to address emissions from any engine power, even the smallest ones. However, comparisons between CCNR limits (Stage II) and EC ones (Stage III A) are not straightforward because engines are not differentiated by the same features: maximum power (PN) and rated engine speed (n) are used by CCNR whereas EC considers the unit cylinder displacement (D) of the engine, and maximum power (P) in addition for some cases (Table 3). Moreover, EC limits are given for “HC + NOx” but it is easy to derive separately the NOx limits, considering a common limit of 1 g/kWh given to hydrocarbons (HC).

References to next steps of the CCNR regulation can be found in the literature because stage III proposal for 2012 and stage IV for 2016 were long discussed and finally not adopted by the Central Commission (RVBR-CCNR, 2016): the European regulations have been in force since 2007 or 2009 and the proposed future European limits appear to be consistent with the trend drafted by CCNR.

Category	Displacement (D)	Date	CO	HC+NOx	PM
	dm ³ per cylinder		g/kWh		
V1:1	D ≤ 0.9, P > 37 kW	2007	5.0	7.5	0.40
V1:2	0.9 < D ≤ 1.2		5.0	7.2	0.30
V1:3	1.2 < D ≤ 2.5		5.0	7.2	0.20
V1:4	2.5 < D ≤ 5	2009	5.0	7.2	0.20
V2:1	5 < D ≤ 15		5.0	7.8	0.27
V2:2	15 < D ≤ 20, P ≤ 3300 kW		5.0	8.7	0.50
V2:3	15 < D ≤ 20, P > 3300 kW		5.0	9.8	0.50
V2:4	20 < D ≤ 25		5.0	9.8	0.50
V2:5	25 < D ≤ 30	5.0	11.0	0.50	

Table 3. Current European emission standards for Inland Waterway Vessels – Stage III A

Emission limits for inland waterway vessels are significantly tightened under the Stage V proposal. (EC Stage IV was abandoned). The Stage V standards (Table 4), would be applicable to propulsion engines (IWP) above 37 kW and to auxiliary engines (IWA) above 560 kW, including engines of all types of ignition.

Category	Net Power	Date	CO	HC	NOx	PM	PN
	kW		g/kWh				
Propulsion Engines – Category IWP							
IWP-v/c-1	37 ≤ P < 75	2019	5.00	4.70 *	2.10	0.30	-
IWP-v/c-2	75 ≤ P < 130	2019	5.00	5.40 *	2.10	0.14	-
IWP-v/c-3	130 ≤ P < 300	2019	3.50	1.00	2.10	0.11	-
IWP-v/c-4	300 ≤ P < 1000	2020	3.50	0.19	1.20	0.02	1.10 ¹²
IWP-v/c-5	P ≥ 1000	2021	3.50	0.19	0.40	0.01	1.10 ¹²
Auxiliary Engines – Category IWA							
IWA-v/c-1	560 ≤ P < 1000	2020	3.50	0.19	1.20	0.02	1.10 ¹²
IWA-v/c-2	P ≥ 1000	2021	3.50	0.19	0.40	0.01	1.10 ¹²

* HC + NOx

Table 4. Proposal for future emission limits for Inland Waterway Vessels – Stage V

Emission limits of NOx and particulates are significantly tightened in Stage V from 2019: a limit in number of particles (PN) is added for the biggest engines (>300 kW), as it applies already to road vehicles. The limits set in 2021 for vessel engines above 1000 kW are those of the HGV Euro VI values, which are in force since 2013. The very low levels of particle emission, in mass and number expected for 2020 for engines above 300 kW will require a particulate filter. Similarly, the proposed low levels of NOx cannot be achieved without NOx trap or SCR devices. This proposal from the Council of Europe dated 2014 encountered opposition of the shipping industry who asked to adopt

less stringent emission limits in line with the American values (NO_x, 1.8 g/kWh and PM, 0.04 g/kWh), with a phased implementation from 2014 to 2017, from engines above 2000 kW to engines between 600 and 1400 kW (EBU, 2015).

The IWP limits proposed by the EC to apply around 2020 are consistent with the most restrictive values imposed on trucks, in terms of emissions of nitrogen oxides and particulates. However, the fleet renewal delay is much longer for the vessels, so that cleaner diesel engines will make up the majority of the river units not before 2040 / 2050. The graph of Schweighofer (2010a) sums up the comparisons that can be made between both transport modes: first, about the standards of NO_x and particulates that apply for each vehicle type, and secondly for the in-use fleets, with the offsets given for the current situation (2010) and as foreseen in 2020 (Figure 1). As previously mentioned, the limits of stages "CCNR III" and "CCNR IV" are finally not in force, and have to be replaced by European standards "Stage VIII A" and respectively "Stage V" for IWV.

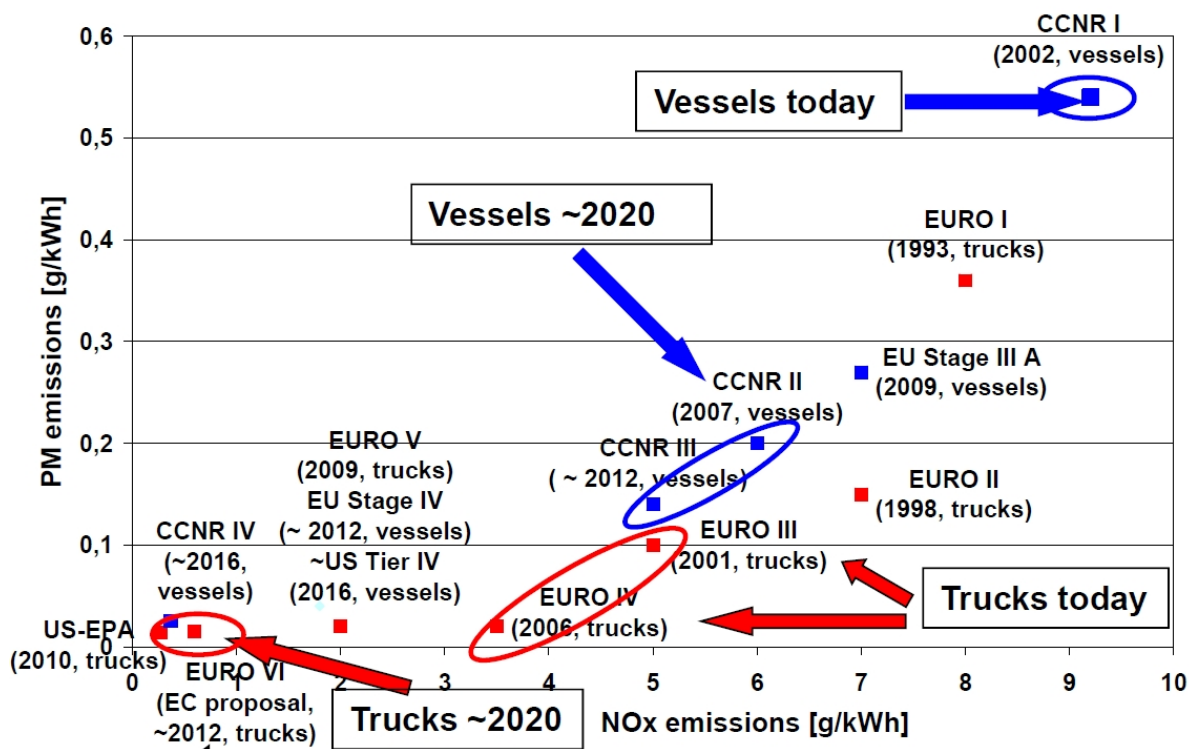


Figure 1. Emission standards and in-use fleets situations – IWV vs trucks (Schweighofer, 2010a)

2. Monitoring Methodology

Two methods of measurement were carried out on board the selected vessels:

- Automated and long-term monitoring (several weeks or months): energy consumption (electricity and fuel) and engine parameters (speed and torque on the propeller axle) were continuously recorded for each vessel. Combined with the GPS parameters, these data were used to thoroughly describe the distances traveled by the ships and to propose patterns of use and consumption of the different machines on board (propulsion engines, generators, pumps, air conditioning and domestic use). It has then been possible to set up a 1000-second operating cycles for each propulsion engine to represent their average energy consumption over the weeks. Moreover, the 1-Hz records of fuel consumption of the engines were needed to derive subsequently the exhaust gas flow rates and by extension, the amount of pollutants emitted by those engines.
- Intermittent monitoring: time-limited and non-automated measurements of pollutant concentrations were performed on exhaust gas by the IFSTTAR team. The sampling and analyzing equipment was heavy and difficult to board and to install at the funnels and it required constant presence of operators during recordings. Several days of measurement were planned to encounter the widest possible variety of engine operations. The emission features of the main pollutants (CO, CO₂, HC, NO_x and

particulates) can be displayed in g/h, g/kWh, g/km or g/t.km according to specific periods, routes or operations. Pollutant emissions are given as well along the average operating cycles which were set up for each vessel from the continuous energy and power recordings (first monitoring results).

The main difficulties to plan and realize on-board measurements were linked to the ship features themselves and to their commercial activity:

- to get on-board personnel and equipment is often difficult on such industrial ships (narrow catwalk, steep staircases and small passageways before reaching the dock close to the funnels). The worst case is "en route" boarding close to a lock.
- loading / unloading barges during daytime at customers' dock is the usual priority of the vessel operators and for one of the selected vessel, it meant that trips were mainly made at night or during weekends, and it could not match with our work schedules,
- business activity and the vagaries of travel (locks) result in very changing and challenging timetables to follow, as far as the 2 cargo vessels are concerned,
- ship crew should not be hindered from doing their job... but they were able to help sometimes !

In addition, meteorological conditions should not be too adverse for the analysers (no cold or rainy weather). As a result, very few days of measurement were carried out and even less records were usable due to some holes in the fuel consumption or engine data that were needed.

Two sets of analysers were used, a PEMS Horiba OBS 2100 (Portable Emission Measurement System) for the gases CO, CO₂, NO_x and HCT, and an AVL "Micro Soot Sensor" (MSS) for the particle mass, both being suitable to give concentrations in exhaust through continuous sampling. No battery packs were necessary to supply the analysers with energy because the on-board electrical network on each of the 3 boats could easily be used and thus there was no power constraint for the measurement campaigns, nor battery to transport.

The gas analysers operate on the same principles as the laboratory analysers; they are more compact and were installed on a narrow carriage (Figure 2). The in-line measurement (1Hz) of the 4 gas concentrations in the exhaust operates according to the following principles:

- CO and CO₂: absorption in the non-dispersive infrared band (NDIR); 0-10% range
- THC (total hydrocarbons): flame ionization detector (FID); works with hydrogen supplied by a hydrogen / helium stable blend (0.15 l/min); 0-1000 ppm range
- NO_x: chemiluminescence detection (CLD); 0-3000 ppm range

The zero point of each analyser was repeated on board before measurement using purified air (bottle of synthetic air). Calibration from reference blends was prior done in laboratory. Following this process, an accuracy of 2% is expected for the PEMS OBS 2100 analysers.



Figure 2. View of the gas analysers on-board a cargo vessel for the exhaust gas sampling (heated line) and concentration measurement



Figure 3. Pitot tube and exhaust gas sampling adapted on one of the propulsion engine funnels (passenger vessel)

To get amounts of emitted pollutants when the analysers measure concentration in a small sampled flow, the PEMS includes a Pitot tube to be placed on the exhaust pipe, to continuously monitor the total flow gas. The Pitot sensor is prior calibrated for a specific pipe diameter. The diameter (120 mm) of the exhaust pipe on the tested passenger vessel and the maximum speed of the propulsion engine are in line with the standard heavy-duty engines. Thus, the calibrated 100 mm probe we had for trucks was used for this ship, by means of adaptation on the funnel (Figure 3). Nevertheless, flow measurement of exhaust gas is often subject to inaccuracy, due to side effects in the exhaust pipe and to the pulsed nature and highly variable velocity of the outlet gas. Accuracy of Pitot tube is usually given about $\pm 5\%$ but can easily exceed it during transient engine operations; however, cargo vessels run mainly on stable cruising speeds between the locks.

The AVL Micro Soot Sensor was managed by the CRMT Company who provided the particulate measurement on behalf of IFSTTAR during this PROMOVAN project. Both devices, PEMS and MSS, were used simultaneously on board and time-synchronised. AVL 483 (MSS) measures the concentration of soot directly in the raw exhaust and without cross-sensitivity to other components. It is based on the photoacoustic measurement method which offers a particularly low detection limit of $5 \mu\text{g}/\text{m}^3$ and a high data rate (10 Hz). Furthermore, this device does not have the drawbacks of the opacimeter (light extinction) with frequent "zero" drift and there is no delicate handling of filters for high precision weighing. A high sensitivity is however not necessary in the case of marine engines with the significant amounts of particulate emissions which were expected.

With the photoacoustic technique, volatile compounds are not detected (same thing with the filter weighing technique) and could lead to underestimation if the proportion of volatile compounds (SOF) is significant. Without estimation of this proportion in the case of marine engines, no correction factor can be applied. However, the loss of particles by thermophoresis (particle deposition on the cold walls) seems significant when sampling is done in the raw exhaust: an AVL document (Schindler, 2012) and a publication from Cao, 2014 describe independent comparative measurements with different particle analysers and both indicate an underestimation with the MSS in the range of 30 – 38% compared to the standard gravimetric filter method (CVS). Therefore, particulates concentrations given by the MSS were constantly multiplied by a factor 1.3 to account for this measurement artefact.

The gas sampling probes for the PEMS and the MSS could not be attached the same way on the 3 types of ship funnel. The sleeve for trucks which was provided initially by Horiba (calibrated with the Pitot tube and bearing temperature probes and sampling line) was used on the passenger vessel (Figure 3). Instead, we had to adapt specific sleeves for the cargo ships with their extra-large funnels (up to 300 mm). Calibration of a pitot tube on such pipe was not possible and moreover, no change in the funnel profile was feasible to avoid any bend upstream the pressure sensors. Indeed, an accurate measurement speed requires that the tube is straight upstream the probe over a length that is at least 10 times the diameter to ensure good homogeneity of the flow speed at any point of the pipe section. Consequently, no gas flow monitoring was possible at the engine outlets of both cargo ships. The PEMS could solely measure the pollutant concentrations in the exhaust gases of these two vessels and subsequent calculation was needed to derive the exhaust gas flow rates from fuel consumption and emission concentrations.

Fuel consumption and mass emissions of carbon compounds are linked as follows:

$$(1) \quad F_{\text{cons}} = (12,011 + 1,008 * r_{\text{HC}} + 16 * r_{\text{OC}}) \times \left[\frac{E_{\text{CO}_2}}{M_{\text{CO}_2}} + \frac{E_{\text{CO}}}{M_{\text{CO}}} + \frac{E_{\text{THC}}}{M_{\text{THC}}} + \frac{E_{\text{EC}}}{M_{\text{EC}}} + \frac{E_{\text{OM}}}{M_{\text{OM}}} \right]$$

with:

- F_{cons} : fuel consumption in g/s (given by flowmeter in the long-term monitoring)
- r_{HC} : atomic ratio H/C of the fuel ($r_{\text{HC}} = 1,855$ for the current fuel used by IWV in France - GNR)
- r_{OC} : atomic ratio O/C ($r_{\text{OC}} = 0,004$)
- E_{CO_2} , E_{CO} , E_{HCT} , E_{EC} et E_{OM} are respectively the emissions of CO₂, CO, Total HC, elementary carbon (soot) and organic mass in g/s. These last 2 terms can be neglected.
- $M_{\text{CO}_2=44,01}$, $M_{\text{CO}=28,01}$, $M_{\text{THC}=13,85}$, $M_{\text{EC}=12,01}$ and $M_{\text{OM}=13,85}$ are the molar masses of the elements in g/mol

Moreover, the mass emission of a given compound ("E" which is unknown) is the product of the exhaust gas flow and the concentration of the compound. The equation for CO₂ is for example:

$$(2) \quad E_{\text{CO}_2} = C_{\text{CO}_2} \times M_{\text{CO}_2} \times Q \times \frac{1}{60} \times \frac{1}{100} \times \frac{1}{22,415} \times \frac{273,15}{293,15}$$

with:

- Q : gas flow in l/min (our unknown)
- E_{CO_2} : emissions of CO₂ in g/s
- M_{CO_2} : molar mass of CO₂ in g/mol
- C_{CO_2} : CO₂ concentration in %

The equations are the same for the other compounds, allowing to identifying Q , the gas flow, as a common factor and ultimately to deduct it every second from consumption and concentrations of major carbon compounds by replacing each E_{XX} in equation (1). Numerical terms of equations (2) can also be put into common factors and it is possible to simplify the equation (1) by applying all numerical values and to give the flow rate Q as :

$$(3) \quad Q = \frac{F_{cons} \times 2,415}{C_{CO_2} + C_{CO} + \frac{C_{THC}}{10^4}}$$

with:

- Q : gas flow in l/min
- F_{cons} : fuel consumption in l/h with a fuel density of 840 g/l
- C_{CO_2} and C_{CO} : concentrations in %
- C_{THC} : concentration of THC in ppm

With the passenger vessel, both methods of determination of the exhaust gas flow were possible: measurement by pitot tube and calculation with equation (3). Comparisons give relative consistent results, except at idle (Figure 4). The average gap is -11.5 % for Q (green line) relatively to measured values by pitot tube (blue line). Considering that our reference is usually the PEMS emissions with its Pitot tubes, in order to minimize a possible underestimation of Q and consequently of the pollutant emissions rates, we adopted a simplified equation (3) by using only the CO₂ concentration. In that case, the discrepancy is reduced to -6 %. Taking in account the fact that pollutants emitted during idling are not significant, the calculation method is acceptable and is adopted to derive exhaust flow, and hence, pollutant emissions from the 2 cargo ships.

The high variability of the calculated flow (green line) is due to the instability of the fuel consumption data given by the flowmeter. Moreover, despite time synchronization between data loggers, an time offset can occur between fuel and gas concentrations data due to line delays. These offsets are difficult to estimate and can distort calculation only during periods of transient running, which are relatively few on heavy-duty vessels.

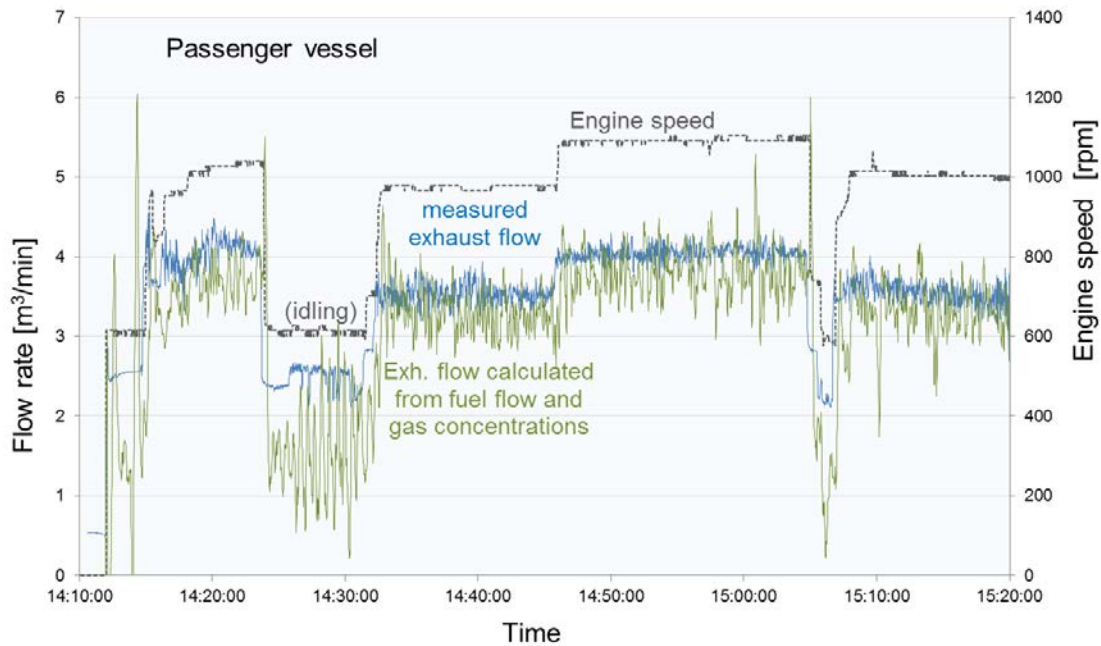


Figure 4. Exhaust flow determination and comparisons of the 2 methods with data from the passenger vessel

3. Results Analysis

Pollutant emissions are analysed for each of the 3 vessels according to various criteria.

The first step was to quantify the pollutant emissions rates relatively to time, distance, energy used –for comparison with the European standard limits and between them– and finally per tonne.km. This unit enables comparisons with the road mode for freight transport. The emission rates or factors are presented both as means of the whole recorded data, and calculated along the representative operation cycle which was set up for each vessel.

Emissions profile along trips

Graphs of ship operating parameters along the route (speed, engine speed, engine torque versus time) enable to clearly distinguish the two navigation directions (upstream / downstream) and provide interesting information (Figure 5):

- Torque and engine speed are directly linked together in steady-state running according to the features of the propeller, with a simple function: $\text{Torque} = a \cdot \text{Speed}^2$ with coefficient “a” being specific to each vessel (Vinot and Derollepot, 2016).
- Torque and engine speed (or propeller speed) are stable most of the time and are kept in the same range for both stream directions, unlike vessel speed; this is especially true in the case of heavy cargo ships. Pilots try to stay on the same cruising engine speeds, the ones which are known to give the best compromise between vessel speed and fuel use.
- The engine steady phases are long and easily identified whereas periods with constant vessel speed are rather brief, showing that resisting forces vary permanently under the influence of currents (depending on the section and longitudinal profile of the canal or river), of the bottoming effect (suction) or canal edge effect (waves), and secondarily, the possible effect of the wind. Heavy units are of course less sensitive to these speed variations due to their inertia.

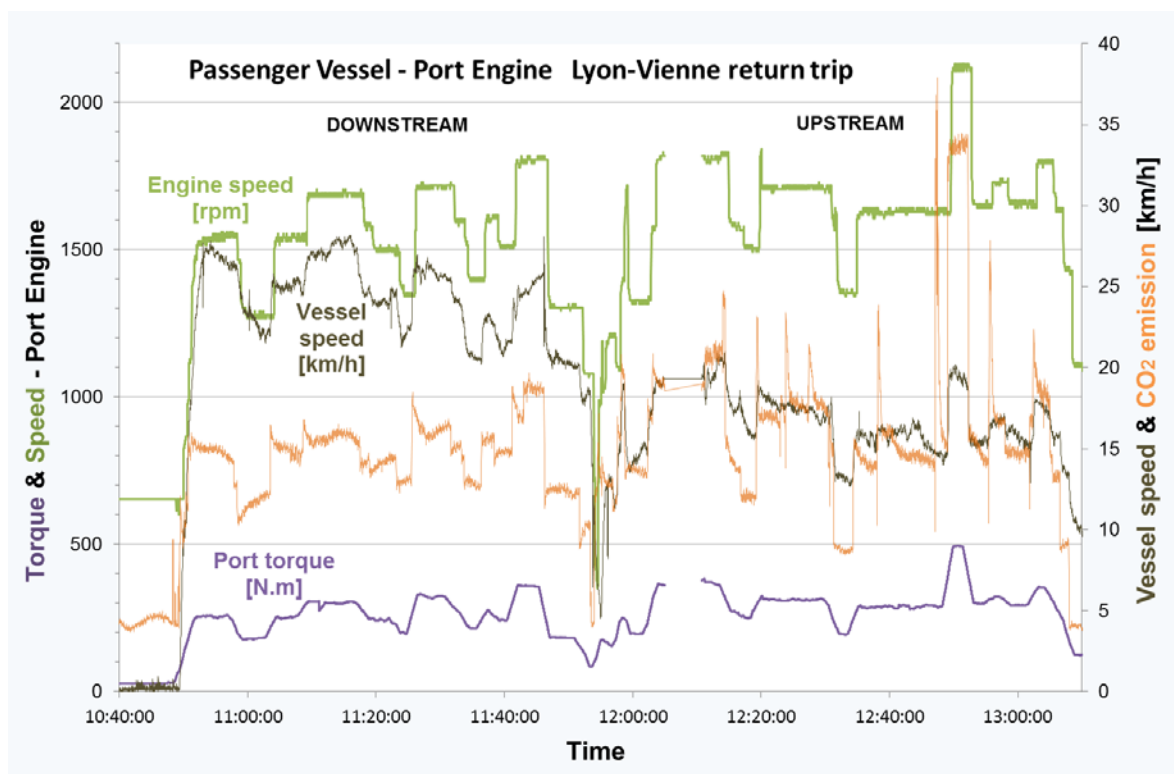


Figure 5. Tracing of engine speed and torque plus vessel speed and CO₂ emission along a return trip on the Rhône River (port side engine)

CO₂ varies simultaneously with engine speed, while being more in line with torque: a sharp CO₂ emission increase occurs (130%) for the high speed phase (2100 rpm) when engine speed increases by about 30% and torque by 70%. CO₂ is also subject to more variability during steady-state phases (especially when going upstream), due also to very high values (maximum of 38 g/s) which remain unexplained as fuel consumption is stable in the same time.

NO_x emissions strictly reproduce the engine speed fluctuations, with the same magnitude.

Particulate emissions are relatively constant around 2 mg/s except at the beginning of the trip; these higher values could be related to a cold engine. However, particulate emissions decrease sharply when engine speed drops below 1500 rpm, and it looks like a threshold effect. Conversely, they become very high when engine speed reaches 2100 rpm, precisely 5 times greater (10 mg/sec) while speed is 30% higher.

CO emissions show a high variability and are therefore difficult to relate to any parameter. Besides, the THC analyser produced sometimes abnormal values during the third trip of the passenger boat (Table 5). Therefore, the THC emission of 4.9 g/km is not reliable and is not included in the global average.

The passenger boat emissions were monitored under various navigation conditions and for each of the two propulsion engines successively. It is easy to see the effect of the navigation direction on emissions (up or down-stream) but no engine comparison can be made at this stage due to non-repeatable conditions of running. However, comparison is made farther from the emission modelling which has been set up specifically for each engine.

Emissions are consistent within each type of travel: pollutant rates are similar when comparing the same trips (even if speeds and distances are not quite the same). We also note the significant increase of emissions with higher cruising speed and more changing running conditions: CO₂ emissions and other gases are multiplied by about 2 while the speed average goes from 11 or 12 km/h to 14 km/h (16.8 km/h without stops) and PM emissions are multiplied by 10 on average between the "urban" trips (smooth cruising) and the "extra-urban" ones (lock and test of various engine speeds)

Passenger Vessel	45 t	Duration	Distance	Average ship speed	CO ₂	NO _x	PM x 1,3	CO	THC
Round trip	Engine	09:56:21	133 km	13.3 km/h	kg/km	g/km	g/km	g/km	g/km
Urban, w/o lock	starboard	01:08:13	12.3	10.84	1.32	31.8	0.04	33.5	10.5
Urban, w/o lock	port	01:32:57	18.5	11.95	1.43	32.2	0.05	23.2	8.3
Extra-urban, 1 lock in each dir.	starboard	03:49:24	54.6	14.28 16.8 w/o stop	2.31	42.4	0.50	78.0	4.9
Extra-urban, 1 lock in each dir.	port	03:25:47	47.3	13.80 16.7 w/o stop	2.99	52.9	0.48	64.2	10.0
Average (1 engine)		(distance-weighted averages)			2.34	43.8	0.39	61.0	9.7
Vessel average (2 engines)					4.68	87.6	0.77	122.0	19.4

Table 5. Average emission of pollutants from the passenger boat (g/m) for both engines and both trip types

PM emissions are measured by the MicroSoot Sensor and data is increased by 30% to compensate for the thermophoresis effect.

Emissions from the pusher tug and the self-propelled barge

Compared to the passenger boat, pollutants are naturally emitted in larger quantities by the freight vessels, due to the higher involved energy and their more powerful engines. Logically, the heaviest vessel produces the highest rates of pollutants. Emissions rate per kWh is a more appropriate indicator to compare the emission characteristics of engines and their impact on air quality.

The pusher tug uses less diesel fuel and emits less CO₂ and NO_x than the self-propelled barge, whereas its larger freight is less favourable. Accordingly the gaps are widening in favour of the pusher when the emission factors are given per tonne of cargo. Conversely CO and THC from the pusher tug are higher than those from the self-propelled barge ; but many problems have occurred in the measuring of these two pollutants and make them unreliable when all the records are taken into account. The selection of steady-state running points with valid measurements offers more valuable comparisons (modelling chapter).

Similar tests on freight IWV were carried out in 2011 on the Seine River, under the initiative of "Port de Paris" and VNF (TL&A and CERTAM, 2011). One difference in the conditions of monitoring is that

pollutants have been recorded only for one cruising speed. Three pusher tugs with similar weight and engine power were part of this previous study and are compared to our cargo vessels. So-called Freycinet vessels in the range 250 - 400 t are part of the database of TL&A and they have engines with power of the same range as our passenger boat, but not the same usage and load. One of them has the same engine and operated empty when monitored and it has nevertheless been added into the comparison (Table 7).

Although in 2011 the pollutants were measured on a unique cruising speed, ultimately, the narrow range of engine speeds encountered with our pusher tug shows that the outlined difference in measurement conditions is not prohibitive to compare vessels emissions from both programmes.

Vessel	Cargo	Power kW	Fuel kg/km	CO ₂ kg/km	NO _x g/km	PM g/km	CO g/km	THC g/km
Passenger boat	-	2x 160	1.4	4.7	88	0.8	122	19.4
Freycinet barge *	0 t	2x 160	-	4.7	79	1.1	12	-
Self-prop. barge	670 t	2x 970	13.6	42.6	873	6.1	205	11.2
Pusher tug	2715 t	2x 920	9.8	30.1	726	7.0	396	56.1
Pusher 1 *	3090 t	2x 660	8.4	32.3	322	3.3	35	-
Pusher 2 *	4000 t	2x 735	11.8	53.8	458	12.5	257	-
Pusher 3 *	2800 t	2x 750	15.1	57.7	427	3.2	77	-

* Vessels of "Port de Paris - VNF" study in 2011. The figures for fuel are the usual consumption given by the pilots and were not measured during tests

Table 6. Average pollutants emissions from the tested vessels of the PROMOVAN programme and in 2011 (g/km) along various trips

Pusher tugs n°2 and 3 of the 2011 study had particularly high CO₂ rates, which are not consistent either with their usual fuel uses, or with engine power and total weight relatively to the other vessels data. Only adverse running conditions (upstream?) can explain these high CO₂ levels, as it was the case for our self-propelled barge during test.

NO_x rates from the three 2011-study pushers are consistent among each other but about 2 times lower than those we measured on the 2 freight vessels. A more recent technology to reduce NO_x in line with the CCNR standards could be part of the explanation for these better results; the other reason could be the lower cylinder capacity of the engines. NO_x emissions from the passenger vessel and the Freycinet barge are very close, and their CO₂ emissions perfectly aligned, which confirms the suitability of this comparison.

Pusher tugs n°1 and 3 have particulate emissions 2 times lower than our freight vessels and no further explanation than those given for NO_x discrepancies can be given. It is indeed difficult to find the reasons for such differences when results from the three 2011-study vessels exhibit such inconsistency for PM emissions.

As far as cargo vessels are concerned, it is interesting to produce the rates of pollutants per ton transported and per km for comparison with the road transport mode. It is clear that the very heavy loads carried by vessels (up to 3700 t deadweight for the pushed barges), play in favour of low emission and fuel rates versus the 25-t payload of the heavy-duty trucks ; on the H-D Vehicles side, NO_x and PM emissions are drastically reduced on the latest Euro VI trucks.

Two categories of trucks were chosen, the Euro II ones certified in the 1996-2000 period because their engine had a technology similar to that of the current in-use vessels, and Euro V models which account for a large share of to-day HGV fleet. The emission values given for trucks (Figure 6) are either obtained from measurements at the UTAC test bench for the Euro II trucks (Pillot et al., 2000), or from realistic models (based on measurements and actual usage) for Euro V trucks (Rexeis et al., 2014).

The pusher tug with its 2700 tons of cargo uses almost 6 times less fuel per tonne transported than the self-propelled barge. It also ranks as the best pusher compared to the 2011 ones in terms of consumption and CO₂ emitted per tonne transported and per km. Euro V HGV use or emit 3 times more fuel or CO₂ respectively with the maximum 25-t load per trip. The self-propelled barge appears

to be poorly efficient in terms of energy consumed per tonne transported compared to the whole pushers, and above all, versus the trucks that are better, and even 2 times better for Euro V trucks.

Thus, inland waterways vessels could be less efficient for goods transport in some cases, unless the cargo is above a 2,000-t threshold as far as the tested self-propelled barge is concerned. This economic threshold would be around 1,000 t of freight for the other tested vessels.

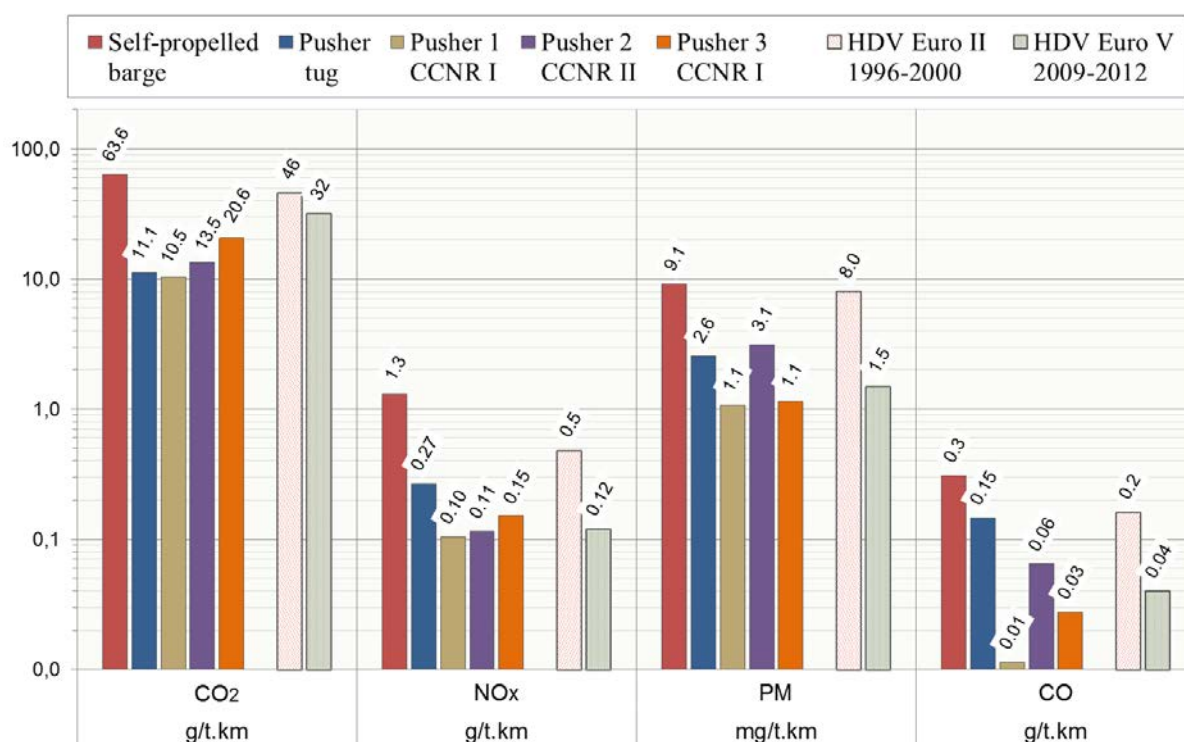


Figure 6. Emissions rates (g/t.km) for the tested vessels and for the Euro II and Euro V heavy-duty trucks along various trips or driving cycles

NO_x emissions from pusher tugs measured in 2011 are in line with the Euro V trucks, but this is not the case of both cargo vessels of this study which are more in the NO_x range of the Euro II trucks, of similar engine technology as regards exhaust pollutants. If Euro V trucks have already benefited from nitrogen oxides treatment devices (SCR or EGR), far lower values are given for Euro VI trucks by Reixis and al. (2013), from models based on NO_x realistic measurements.

Particulate emissions from the best pusher tugs in this domain are the same as the Euro V trucks emissions. However, the other monitored vessels are more polluting than the Euro V trucks as regards PM and much bigger sources of particulates than the most recent trucks which are equipped with particulate filter.

Emission modelling

Beyond the mean vessels emissions recorded along trips and presented so far, emission factors that could be obtained from realistic usage cycles would be better candidates to represent the typical emissions of the 3 vessels. This emission calculation from cycles had been made possible thanks both to the multiple steady-state running phases from which simple functions could be derived and also through the setup of specific operating cycles realised by Vinot and Derollepot (2016). The operating cycles were defined by successive steady engine speeds for a total of 1000 seconds and the breakdown in different engine speeds is representative of the whole monitoring along dozen of running days for each of the 3 vessels. Emission models are also function of the various engine speeds.

Due to the fixed relationships between engine speed and torque, hence linked with the involved energy as well, CO₂ emissions are highly correlated with engine speed (Figure 7). Accordingly, no distinction of the navigation direction can be made on this graph, whereas vessel speed would take two distinct values according to the direction (up and down-stream) if plotted against engine speed or torque.

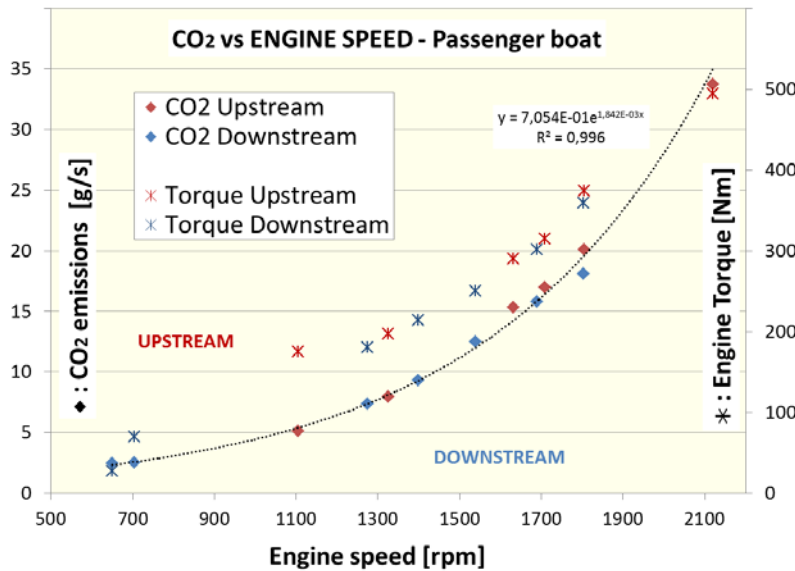


Figure 7.

"CO2 vs engine speed" correlation graph according to the steady-state points identified during one trip of the passenger vessel - Distinction of both navigation directions

A unique function allows then valid calculation of the CO2 emissions from the engine speed. The equation was set up by using the CO2 values for both engines (as regards the passenger vessel) and for all registered trips, after selection of the steady-state phases. This method is used for the other components, NOx, PM and CO the same way.

$$E_{CO_2} = 0,7054 \cdot e^{0,00184 \times Speed} \quad R^2 = 0,996$$

$$E_{NOx} = 1,91 \cdot 10^{-10} \times Speed^3 - 6,98 \cdot 10^{-7} \times Speed^2 + 1,03 \cdot 10^{-3} \times Speed - 0,406 \quad R^2 = 0,983$$

$$E_{PM} = 4,87 \cdot 10^{-9} \times Speed^3 - 1,32 \cdot 10^{-5} \times Speed^2 + 1,17 \cdot 10^{-2} \times Speed - 3,335 \quad R^2 = 0,972$$

$$E_{CO} = 3,63 \cdot 10^{-11} \times Speed^3 + 3,16 \cdot 10^{-8} \times Speed^2 + 1,07 \cdot 10^{-4} \times Speed + 0,1 \quad R^2 = 0,583$$

with: E_{xx} : emission of the pollutant xx in g/s (in mg/s for PM)

$Speed$: Engine speed (rpm)

The function for CO is an attempt of modelling because values are quite scattered, due to measurement problems on the CO analyser. HC emissions are even more dispersed, to the point that no equation can be set up.

A satisfying number of steady-states phases could be identified for one engine of the barge as well. The regression coefficient is excellent and it demonstrates again the strong correlation between propeller speed and engine energy, and by extension, between engine speed and CO2 emissions in stable conditions. Emission values (g/s) for NOx are also well in line with the various steady speeds. Relation for PM with engine speed is less strong but reliable enough to derive mean PM emission from the running cycle (Figure 8) with a larger uncertainty in the lowest and the highest value ranges.

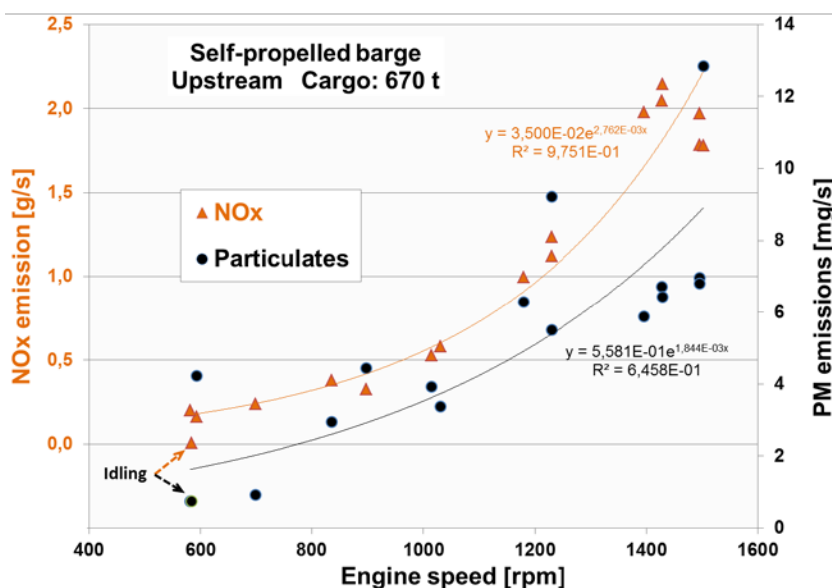


Figure 8.

"NOx & PM vs engine speed" correlation graph according to the steady-state points identified during one trip of the self-propelled barge

With emissions models set up for each vessel, we can assign an emission factor to each class or operating point of the cycle, and in the same way for each measured pollutant. It is done for the engine power as well, and hence it makes it possible to calculate the energy used. We can deduce the average emissions along the representative usage cycle. Comparisons of emissions rates per kWh with the regulatory limits are then possible, even if the conditions of running are not the same. Table 7 gives the 3 vessels emission rates besides recent and future emission standards.

Comparisons between vessels as regards CO₂ / fuel use performances and pollutants bring new information when calculated relatively to the energy used. CO₂ emission rates per kWh are quite the same between barge and pusher, which was not expected with the higher emissions of the self-propelled barge in g/s or g/km, while the cargo was lower (670 against 2715 t). The higher absolute CO₂ levels for the barge do not come from weaker engine efficiency, but from higher power involved during its trips.

Moreover, NO_x emissions rates per kWh are slightly smaller for the barge; it also produces 2 times less particulates for the same dissipated power, which was also the result of comparison with raw data, in g/s (Table 6). The self-propelled barge produces also about 2 times less CO than the pusher, for the same energy supply.

The passenger boat is penalized by its excessive engines power which generates high emissions per kWh, compared to the cargo units. This is about twice as CO₂, NO_x and CO, and nearly 40% higher than the pusher for PM emission rates. The mismatch between the characteristics of its engines and vessel architecture is part of the explanation. Its engines are far too powerful but the vessel was designed originally to reach high speed and lift off from the water.

The IMO limit (MarPol) Tier 1 which addresses only NO_x –for which the self-propelled barge has been certified– is not displayed in table 7 but it is the same regulation as CCNR I: the limit is 10.0 g/kWh for a rated engine speed of 1800 rpm. As already mentioned, the level of NO_x in actual usage has been measured around 14 g/kWh, which is 40% above its maximum value for registration in 2006.

Standard emissions or Vessel id.	Year	Conditions	NO _x g/kWh	PM g/kWh	CO g/kWh	THC g/kWh	CO ₂ kg/kWh
CCNR I	2002	$P^* \geq 130$	9.8	0.54	5.0	1.30	
CCNR II	2007	$130 \leq P^* < 560$	6.0	0.20	3.5	1.00	
EC IWP -3 (proposal)	2019	$130 < P^* \leq 300$	2.1	0.11	3.5	1.00	
Passenger boat 160 kW		cycle	24.1	0.17	19.5	7.30	1.43
CCNR I	2002	$P^* \geq 130$	10.0	0.54	5.0	1.30	
CCNR II	2007	$P^* \geq 560$	7.0	0.20	3.5	1.00	
Self-propelled barge 970 kW		cycle	14.1	0.06	3.9	0.22	0.69
EC V1:4	2009	$2.5 < D^{**} \leq 5$	≈ 7.0	0.20	5.0	HC + NO _x	
EC IWP -4 (proposal)	2020	$300 < P \leq 1000$	1.2	0.02	3.5	0,19	
Pusher tug 920 kW		cycle	17.6	0.12	8.9	1.33	0.71

* P : rated Power (kW) ** D : Displacement per cylinder (dm³)

Table 7. Emissions rates (in g/kWh) for the 3 vessels compared with the CCNR and European standards

The emission rates of NO_x and CO from the pusher tug are far above the CCNR I limits (x 1.8). On the contrary, according to our measurements on both cargo vessels, particulate levels are well below current limits. Actually, the very low levels to be reached for new engines (by 2020) will require the use of particulate filters or to switch to an alternative fuel such as natural gas (compressed or liquefied - GNL) which produces no measurable particles mass. As regards NO_x emissions, EGR and SCR systems that proved to be efficient on truck engines, have to be adapted to marine engines to comply with future limits. Reduction potentials are large and the division by 2 for the NO_x emissions from the 2011 pushers relatively to the pusher tug from 2006 is an illustration.

Experimental programs (e.g. The "Cleanest Ship Project" on the tanker Victoria, Schweighofer, 2010b) have already demonstrated that reductions of 80% in NO_x emissions could be achieved with SCR devices.

Conclusion

In the frame of the PROMOVAN program, pollutant measurements were carried out on board two cargo vessels and one passenger boat and they provide interesting data for this transport mode which is rarely evaluated in actual operation for its impact on air quality. Outlets of the propulsion engines were equipped to collect and analyse mass of the usual regulated pollutants NO_x, PM, CO and THC and CO₂ as well.

Emission profiles observed directly during measurements produce average emission factors in g/s or g/km to identify the most polluting operations and to compare vessels. If the vessel with the largest cargo –the tug had a freight of 2700 t to push– is the highest emitter every second, this rule is not respected when emissions are rated per km, the self-propelled vessel being penalized by greater power requirements. These emission factors in g/s obtained on average trips (averages of several hours of recording), are corrected by the results obtained from the representative running cycles. Emission modelling offer to extrapolate measurements made on some steady-state operating points to those composing the cycle and representative of the mean usages.

Moreover, the emission factors can be expressed per km and tonne transported to compare with road transport typical rates. Euro II trucks (1996-2000) with their 25-t payload emit more pollutant and use more fuel relatively to the cargo vessels, except for CO and HC. The ratio is 5 times less for the pusher tug as regards fuel and CO₂, 3 times less for particulates and almost 2 times less for NO_x. But tighter reductions of emissions obtained on recent heavy goods vehicles (mostly Euro V) have resulted in better rates in g/t.km, and below those of the pusher tug for the main pollutants, but not as regards CO₂ and fuel use. The huge mass capacity of transportation (about 3000 t) by industrial vessels enable them to keep the advantage of reduced fuel consumption per tonne transported, and the gap remains large. In terms of impact on air quality, the pusher tug produces 2 times more NO_x, particulate and CO than trucks for 1 tonne of freight. But these mixed results are going to be corrected with future emission regulations and potential of improvement is large for marine engines as they have not benefitted from aftertreatment devices so far. These devices have been largely tested and improved by the automotive sector. Examples of successful adaptation of such equipment on marine vessels or IVW show that new vessels will become greener quite rapidly. Unfortunately the fleet renewal is a long process.

Acknowledgments

This work was financially supported by the ERDF (European Regional Development Fund) and Rhône-Alpes Region fund.

References

- Pillot D., C. Pruvost, P. Tassel & R. Vidon, 2000, Simplified functions for calculating heavy-duty vehicle emissions, 9th Int. Symposium Transport and Air Pollution, Avignon, Les collections de l'INRETS, Actes, Vol.2, pp.425-430
- Rexeis M., S. Hausberger, J. Kühlwein & R. Luz (2014): Update of Emission Factors for EURO 5 and EURO 6 vehicles for the HBEFA Version 3.2, Final Report, IVT pub., Graz Univ. of Tech.
- RVBR-CCNR, (2016) : Règlement de visite des bateaux du Rhin, Ed. 2016, CCNR pub.
http://www.ccr-zkr.org/files/documents/reglementRV/rv1f_042016.pdf
- Schweighofer J. (2010a): Environmental and technical challenges related to the engine technology of inland waterway vessels, IVR Workshop on Innovations in Inland Waterway Transport, Vienna, May 20, 2010.
- Schweighofer J. (2010b): Recent Developments in Ship Technology and Fleets, Danube Commission – Workshop on Future Fairway Parameters of the Waterway Danube, Budapest
- TL&A & CERTAM (2011) : Étude comparée de rejet de polluants locaux – Transport de marchandises, Rapport de phases 3 & 4, TL&A / CERTAM pub.
- Vinot E. & R. Derollepot (2016): Comparison and sizing of different hybrid powertrain architectures for fluvial boat application, paper submitted to the 13th Vehicle Power and Propulsion Conference, IEEE 2016

Why Own a Hybrid? A Global Total Cost of Ownership Analysis for the Private Car Owner.

Kate PALMER*, James E. TATE**, Zia WADUD*** & John NELLTHORP**

*School of Chemical and Process Engineering, University of Leeds, Leeds, LS9 2JT, UK
Email: pmkhp@leeds.ac.uk

**Institute of Transport Studies, University of Leeds, Leeds, LS9 2JT, UK

Abstract

New powertrain technology such as hybrids can reduce carbon dioxide emissions with the added benefit of reduced fuel cost for the driver. Total Cost of Ownership (TCO) calculations are potentially useful to consumers and policymakers as they combine all the expenses incurred from vehicle ownership such as initial cost, fuel costs and maintenance. No studies to date compare the cost incurred by the owner in different countries, different purchase years, or utilising accurate initial costs, consequently reliable ownership figures are not available.

This research gives a more comprehensive assessment, including a sensitivity analysis between conventional and hybrid vehicle ownership costs in three industrialized countries – the UK, USA (specifically California) and Japan, using the Toyota Prius as a case study. To calculate representative fuel costs real world driving fuel consumption figures are sourced from the Idaho National Laboratory (Idaho Laboratory, 2014) coupled with country specific fuel prices.

Payback periods of the incremental cost incurred by the purchase of the Prius relative to a conventional vehicle have been compared for private car ownership. We conclude that the Prius is most cost effective in Japan due to their vehicle tax breaks for fuel efficient cars despite low annual mileage. In the UK the Prius has been cheaper to own than a conventional vehicle for many years due to historically high fuel prices and increasing fuel economy with each new vehicle generation, whereas in the USA the total cost of ownership of the Prius has reached cost parity despite low fuel prices.

Keywords: Hybrid electric vehicle, Vehicle ownership, Consumer demand, Total Cost of Ownership

Introduction

Globally, there are growing problems in many cities caused by road congestion, air pollution from traffic sources and climate change stemming from transport emissions (among other causes). Low emission vehicles such as hybrids offer a low carbon alternative to conventional petrol or diesel cars. Hybrid vehicles emit lower levels of emissions such as carbon dioxide and NO_x, with associated benefits for climate change and urban air pollution, for this reason the increasing market share of the Prius is of interest.

With a larger battery and features such as regenerative braking, hybrid vehicles historically have a significantly higher initial cost than conventional vehicles. As powertrain technology has matured and hybrid vehicles have moved into mass manufacture this price difference has reduced despite outdated consumer points of view to the contrary. For low emission vehicles the increased initial cost can often be saved through reduced running costs resulting from lower fuel costs, reduced taxes and vehicle subsidies, Total Cost of Ownership (TCO) calculations can be useful to understand the extent of this. For this reason it is important for reliable TCO costs to be available containing all relevant vehicle expenses to assess overall costs compared to conventional alternatives. Such price assessments are useful for the private and fleet market; establishing the cost effectiveness of low emission vehicle can stimulate uptake.

This paper aims to analyse how TCO of hybrids has changed compared to conventional vehicles since hybrid vehicles first entered the mass market in 1997. By comparing different markets where hybrid vehicles have different levels of success, this research aims to analyse the extent of which TCO accounts for consumer choice. This study gives a more comprehensive assessment than most other papers of differences between conventional and hybrid vehicle ownership costs. With over 5.5 million vehicles sold worldwide, the Toyota Prius is currently the most successful hybrid vehicle in the

world (Toyota 2013), for this reason it has been used as a case study in this research. The purpose of this paper is to investigate whether the pricing of the Prius has led to global success; but primarily to shed light on the actual TCO of Hybrid Electric Vehicles (HEVs) compared to standard ICE vehicles in the countries where hybrids have been adopted in large numbers.

To achieve these aims, three countries have been chosen for comparison with different attributes. The Toyota Prius was first introduced in Japan, and with a history of innovation, hybrid vehicles have gained popularity and success, for this reason Japan has been chosen. Another place where hybrid adoption is high despite the need to import these vehicles is California (USA). Like Japan, California has a history of adopting low carbon policies, such as the Zero Emission Vehicle, years ahead of other states in the USA (Greene et al. 2014). Consequently, hybrid vehicles have been more popular in California than anywhere else in America (Muller 2013), for these reasons California has been chosen. In most other markets hybrids have been less successful, despite the high fuel prices in the UK hybrid vehicles still have low market share for this reason the UK is included in the comparison. To analyse the cost evolution of the Prius, all three generations will be considered from the release year in each country.

Literature Review

The current TCO literature has several gaps which need to be addressed for reliable TCO costs. Previous published TCO calculations (see Table 1) have considered different types of hybrid cars (such as mild hybrid versus full hybrid), but do not compare the cost incurred by the private consumer across different countries, which could account for differences in hybrid vehicle market share. Maturing technology leads to decreasing prices, therefore the purchase year is also an important consideration, yet this has not been included in other studies. Other papers do not use the same parameters, leading to incomparable results across the literature, as well as considering only the incremental cost of manufacture as opposed to the actual initial price of a hybrid vehicle from the show room.

Since the introduction of low emission vehicle technology, many TCO calculations for various vehicle types have been published. As early as 2002 Lave & MacLean reported the results of a TCO calculation comparing the Toyota Prius and Toyota Corolla in the USA concluding that at that time the Prius was not cost effective (Lave & MacLean 2002). This is not a surprising result because the comparative inefficiency of the Prius compared to later generations coupled with low gasoline prices in the USA, led to small running cost savings compared to the incremental initial cost of purchasing a Prius over an Internal combustion engine vehicle (ICEV).

Table 1 describes previously published TCO literature by parameters included in each model. Every study considered in Table 1 has very different values of the key parameters in their TCO model. Annual mileage and gasoline price assumptions are used to calculate annual fuel cost which is usually the largest annual cost to the consumer.

The scope of studies reviewed in Table 1 are varied. Many of the studies focus on PHEVs with different battery sizes rather than purely HEVs. They use an incremental cost model where the increased cost of production is estimated, most of this resulting from the larger battery. Due to maturing technology decreases production cost over time, this is not a fair or accurate method of finding the initial cost. Hutchinson et al. is the only study which compares HEV TCO across more than one country. Fuel price, average annual mileage, annual taxes and insurance prices along with driving style and congestion levels are country dependent which mean conclusions from studies from different countries are not transferable. In addition as vehicle technology matures, cost reduces, therefore TCO calculations become outdated very quickly. For this reason, it is difficult to directly contrast and compare the findings of multiple publications.

All the studies considered in this research, except Al-Alawi and Bradley (2013), do not include many of the components necessary to rigorously compare costs of hybrids and conventional vehicles. Most published TCO calculations only include the basic ownership costs, but in this research it is argued that all vehicle ownership costs that differ between hybrid and conventional vehicles should be included for a fair cost comparison. Table 1 details the components of TCO calculations from papers which have been highly cited or use very detailed models. Consumers who purchase new vehicles do not usually keep it throughout the entire vehicle lifetime. In the UK the average vehicle ownership time is three years (Leibling 2008), therefore when a consumer purchases a vehicle they are interested in the resale value. For this reason a depreciation model is important to a TCO

calculation, because many vehicles will change hands several times over their lifetime, a factor that many of the studies in Table 1 neglected. Maintenance costs differ between HEVs and ICEVs, HEVs have lower maintenance costs due to less wear on the brakes and fewer moving parts. The greater the annual mileage, the more significant the difference in maintenance costs, however, few studies consider these differences. Many countries have used tax discounts as incentives for low carbon vehicle purchase. A tax model is therefore necessary to highlight any tax breaks given to low emission vehicles which could significantly cut running costs, again, this factor is not included in many of the TCO publications.

2. Methodology

In this section the systematic methodology used for the TCO calculations in this research will be discussed. The methodology is presented in three sections; study scope, vehicle usage assumptions and modelled components of ownership cost.

Study Scope

This study considers only the mid-sized Toyota Prius (non-plugin) as the hybrid vehicle case study, with the conventional comparison vehicle as the Toyota Avensis for Japan and the UK, and the Toyota Corolla for the USA. The Prius was first released in 1997 exclusively to the Japanese market with a Manufacturer Suggested Retail Price (MSRP) significantly lower than the production cost (Pinkse et al. 2014). Toyota used this first limited release as an opportunity for further on road testing of Priuses. Despite teething problems, the vehicle was released in other markets in 2000 (Sallee 2015). To counteract consumer doubts over reliability of battery technology, Toyota offered a five year mechanical warranty with options to lease rather than purchase the vehicle outright (Toyota GB 2015). By 2008 cumulative global Prius sales passed the one million mark (Toyota Ireland 2008). In the last few years, Toyota have expanded its Hybrid Synergy Drive (HSD) system into other vehicles, such as the Auris, Yaris and Aqua. With a wide choice of Toyota hybrids across different vehicle segments, declining Prius market share may be attributed to vehicle class expansion.

The Toyota Avensis is not available for purchase in the USA (Toyota 2012), but it is used as the comparison vehicle for the Japanese and UK case because it is the most similar Toyota ICEV to the Prius. The diesel model is considered for the UK only because diesel passenger vehicles have reached significant penetrations only in the European market (Bonilla et al. 2014). The release year of purchase for the different Prius generations is generally earlier for Japan than other countries around the world. The TCO is calculated from the model release year as the year of purchase of the vehicles, for example the first generation Prius was first released in 2000 in the UK therefore the purchase for this vehicle model is 2000. The economic countries considered in this study are the UK, USA and Japan. For fair comparison, prices are converted into 2015 pound sterling using historic and projected exchange rates (United States Department of Agriculture Economic Research Service 2015d; United States Department of Agriculture Economic Research Service 2015c). A country dependent Consumer Price Index (CPI) based GDP deflator is used to bring all costs in line with 2015 prices (United States Department of Agriculture Economic Research Service 2015a; United States Department of Agriculture Economic Research Service 2015b; Department for Transport 2016). A CPI based deflator is used because in this study the direct cost to the consumer is the main focus.

Vehicle Usage Assumptions

The annual vehicle miles travelled for the private consumer is assumed to be the national average. It is important to use a representative mileage to compare the different countries. Annual mileage usually declines over vehicle lifetime (Grove 2013). It is clear that using the national average as a constant will be an underestimate for younger vehicles and an overestimate for older vehicles, annual mileage variation will exist between vehicles of the same age. Al-Alawi use a decreasing mileage model, but in the model the initial mileage is still below the national average of the USA. The mileages used in this study are 7900 miles/year, 13 476 miles/year, 6213 miles/year for the UK, USA (CA) and Japan respectively (Federal Highway Administration 2015; Department for Transport 2013; Millard-Ball & Schipper 2011). It is assumed that the average annual mileage in California is in line with the national average for the USA. Average mileage is significantly greater in the USA because of the car culture perhaps as a result of the low fuel price, the extensive road infrastructure and the lack of public transport in many towns and cities.

Table 1. Review of TCO literature

	E PRI (2004)	Simpson (2006)	Lipman & Delucchi (2006)	Lemoine et al. (2007)	AEO (2009)	Al-Alawi & Bradley (2013)	Hutchinson et al. (2014)	This paper.	
Study Scope	Vehicle class	Mid-sized car, Full-sized SUV	Mid-sized sedan	compact or mid-sized large car, pickup, minivan, and SUV	Compact car, Full-sized SUV	Mid-sized sedan	Compact car, Mid-sized car, Mid-sized SUV and Large SUV	Mid –sized car: Toyota Prius (Three generations)	
	Powertrain type	EV, HEV, PHEV20	HEV, PHEV2-60	Five degrees of hybridization	HEV, PHEV20	HEV, PHEV5-60	HEV, PHEV5-60	Conventional, Mild, HSD, Two-Mode, Inline Full, Plug-in HSD, Plug-in Series	HEV
Vehicle Usage Assumptions	Purchase year	2003	2006	2000	2007	2006	2010	2013	Year of release for each generation in each country
	Economic yr country	\$2003 USA (California)	\$2006 USA	\$2000 USA	\$2007 USA (California)	\$2006 USA	\$2010 USA	\$2014 USA and UK	£2015 UK, USA (California), Japan
Vehicle Usage Assumptions	Annual vehicle miles travelled	117 000, 150 000 miles over lifetime	15 000 miles/yr constant	Not specified - decreasing with age	11 000 miles/yr constant	14 000 miles/yr constant	12 000 miles/yr for cars and 15 000 miles/yr for trucks, decreasing with age	130 000 miles over lifetime	10 400 miles/yr, 13 476 miles/yr for UK, USA and Japan.
	Vehicle life	10 years	15 years	15 years	12 years	6 years	5 and 13 years	130 000 miles	3 years
Modellled components of ownership	Fuel economy	EPA adjusted	EPA adjusted	EPA adjusted	EPA adjusted	EPA adjusted	EPA adjusted	Fuel saving tests for urban and highway	The Idaho National Lab and Real world figures.
	Gasoline price model	1.75 (\$/gallon)	5 (\$/gallon)	1.46 (\$/gallon)	2, 3, 4 (\$/gallon)	3, 4,5, 6 (\$/gallon)	Forecasted over vehicle life	3.20, 7.70 for USA, UK (\$/gallon)	Forecasted over vehicle lifetime
Modellled components of ownership	Incremental cost model	EPRI, 2001; ANL	EPRI, 2001	MSRP used	EPRI, 2001 corrected	Includes tax credit	EPRI, 2001; Kalhammer et al., 2007	Brooker et al. 2010; Clearly et al. 2010	None
	Salvage	Battery only	None	None	None	None	Vehicle resale	Vehicle resale	Vehicle resale
Modellled components of ownership	Maintenance cost model	Yes	None	Yes	None	None	Yes	None	Yes
	Insurance cost model	None	None	Yes	None	None	Yes	None	Yes
Modellled components of ownership	Tax model	None	None	Yes	None	None	Yes	None	Yes
	Discount rate	8%	None	none	16%	10%	6%	None	None

Several vehicle ownership lifetimes have been used in this study. The number of ownership years has been calculated for a single owner for 3 years from the year of purchase. Company cars account for approximately half of new vehicle registrations in the UK (SMMT 2013). For this reason a three year TCO is considered as a proxy for lifetime vehicle ownership because this is the average company car vehicle ownership lifetime in the UK (Leibling 2008).

The fuel economy method used in this study is different to that adopted by the other studies in Table 1. TCO calculations need to use realistic real world fuel economy figures otherwise the annual fuel cost in the TCO calculation will be unrepresentative. For the Toyota Prius, the MPG figures used in the TCO calculation in this research are from the The Idaho National Laboratory (U.S. Department of Energy Advanced Vehicle Testing Activity 2015). The testing facility has undertaken comprehensive advanced vehicle testing for the past couple of decades; industry, fleet testing partners and other stakeholders (such as Intertek, Argonne National Labs and Oak Ridge National Labs) help develop the test procedures to accurately model real world driving emissions (Idaho National Laboratory 2014). This is the most comprehensive testing that has been undertaken on all the Prius generations so that the three vehicle MPG figures can be fairly compared. Note that these values are converted from the US gallon to the UK gallon. The hybrid technology of the Prius leads the vehicle to be much more efficient compared to an ICEV under urban rather than motorway conditions (Hutchinson et al. 2014). For this reason, it is important that the MPG figures used have significant shares of motorway and urban driving otherwise the MPG could be unrepresentative. The Idaho National Labs testing has not been extended to the Toyota Avensis or Corolla because these vehicles are conventional and therefore would not merit extensive testing. For this reason, an average across real world MPGs from other sources have been compared to calculate representative MPG values for the ICEVs in this study. The other data sources which have been used are Travelcard (2015), HonestJohn (2015), Spritmoniter (2015), WhatCar (2015) and Edmunds (2015).

The other consideration is the difference in MPG fuel efficiency between different transmission systems. EVs always have an automatic transmission system but most petrol and diesel vehicles are available as either manual or automatic drive cars. In the USA, most cars are automatic, the same is true in Japan; in contrast, manual transmission systems dominate the UK vehicle market. For this reason, where possible, a distinction has been made between the fuel efficiency of manual and automatic vehicles.

Modelled Components of Ownership

After deciding on the study scope the TCO calculation in this section is computed using the following the formula,

$$TCO = I - I * d^t + f * m * e + a + n + x$$

where I = Initial Price (£2015), d = depreciation rate (%), t = time (vehicle age), f = annual fuel price (£2015/litre), m = mileage (miles), e = vehicle efficiency (litre/mile), a = annual maintenance inclusive of vehicle testing (£2015), n = annual insurance (£2015), x = annual tax (£2015).

The initial price of the vehicles is the largest cost to the consumer over the lifetime of the vehicle. Many studies use an incremental cost model that estimates the additional cost of the hybrid powertrain over an ICEV (see Table 1). In this study an incremental cost model is not used because the Prius was initially priced at a loss to stimulate uptake, therefore an incremental cost model is not an appropriate or accurate method of calculating initial price. The MSRP was found for each vehicle and country on car websites such as Edmunds.com for the USA (Edmunds.com 2015), RAC and yourfleet for the UK (RAC 2015; Yourfleet 2015), and goo-net-exchange for Japan (Goo-net-exchange 2015). For third generation Avensis diesel and petrol models, UK MSRPs are available for the vehicles, however, for earlier models the same percentage incremental cost is assumed between petrol and diesel because diesel model costs were not available. Usually a boundary for the MSRP is given without a breakdown, therefore the minimum MSRP price is used.

Initial cost subsidy is often offered as a policy incentive to increase uptake of Low Emission Vehicles (Lemon & Miller 2013). When hybrid vehicles were first introduced to the USA, three manufacturers (Toyota, Honda and GM) introduced their hybrids around the same time (Sallee 2015). The USA government tried to stimulate uptake of HEVs by introducing the clean fuel vehicle deduction for the first 60 000 vehicles sold by each manufacturer with timed phase out (Sallee 2015). The Toyota Prius sold

the fastest and therefore the subsidy was the first to run out. In 2006, this changed to a tax credit system, however, this isn't included in the analysis because the subsidy was not universally available (Sallee 2015). The initial cost subsidy available in Japan was different depending on whether the Ultra-low Emission Vehicle (ULEV) was replacing an existing vehicle or not (Alhulail & Takeuchi 2014). For the purposes of this study, it was assumed that the Prius was replacing an existing vehicle because there are no range constraints like BEVs which are often adopted as the secondary car in the household. In the UK, the plugin places grant only applies to plugin vehicles, no government subsidy is available for the Prius (GOV.UK 2015b). Additionally, in developed countries new vehicle market is primarily a replacement market.

In this model the entire vehicle has a resale value. For a shorter TCO, resale value makes a large difference to the overall TCO calculation result. Part of the reason some people are reluctant to buy ULEVs is because depreciation rate is still uncertain (Hagman et al. 2016). Often even options such as the colour of car are chosen because of vehicle cost retention (fleetcare 2015). Hybrids have historically depreciated at a lower rate due to high demand (Amos 2015). A geometric depreciation rate used for a better approximation, the greatest vehicle cost loss is during the initial vehicle ownership. The depreciation rate of 13.8% is taken from Al-Alawi & Bradley (2013) who calculated this figure from the Toyota Prius generation 1 in the USA. The Toyota Corolla has a similar vehicle cost retention value to the Prius, therefore the same depreciation rate is used (NADA 2014). The same depreciation rate is assumed across Japan, USA and UK. Depreciation is calculated from MSRP, any initial price subsidies are applied to this initial cost after depreciation is calculated.

All the countries considered have significantly different fuel prices because of inherently different tax systems and refinery costs (Dahl 2012). For the UK, the historic and projected petrol and diesel prices were sourced from DECC (Department of Energy and Climate Change) (DECC 2015). For the USA historic petrol prices were sourced for California State from the government website (The California Energy Commission 2015). California has one of the highest fuel prices across the American states, gradually rising above the national average. In 2014, additional state excise tax, state sales tax and local sales tax caused this inconsistency (CA.GOV 2015). Therefore, for future fuel price predictions, the national US average predictions are used with the addition of the 2014 Californian state fuel taxes. Historic Japanese petrol prices were taken from the International Energy Association (IEA) (IEA 2015) but unfortunately future projections were not available. For this reason, future petrol prices were derived from UK price projections using the average difference from 2000-2015.

Maintenance costs are considered to be proportional to length of time the vehicle is owned and miles driven (Electric Power Research Institute 2004). The maintenance model in this study includes an average annual maintenance cost for each vehicle type where costs for diesel maintenance is greater than the other vehicle types. Vehicle repairs are defined as unforeseen costs which do not occur at periodic mileages or years (Al-Alawi & Bradley 2013). For this reason, a repair model is not included as a component of this TCO calculation.

A periodic service fee is payable in all three countries. In the UK, an MOT test is required annually after the vehicle reaches three years of age (GOV.UK 2015a). Historic prices were found since 2000 to accurately model this component. In Japan, the vehicle test is required biennially, with the first test to be within three years of manufacture. This can be expensive and varies significantly from garage to garage as the test price is not regulated (Akita-ken 2015). In California, an annual smog test is required until the vehicle is six years old, after which the test is biennial. Estimated costs are used for this component because the inspection price is not regulated (DMV.ORG 2015). Hybrids and other ULEVs are exempt from the smog test fee (DMV.ORG 2015).

The Prius is classed as an average vehicle for insurance purposes (Carbuyer.co.uk 2015). Therefore, the average comprehensive cover paid should adequately represent the variability in insurance prices, and the difference between the countries in this study. For the UK model, the British Insurance Premium Index is used (The AA 2015). Collating data from approximately 2800 car insurance customers in the UK from a large number of providers, an 'average quoted premium' is calculated. For the Californian model, the comprehensive average premium for California is used for years 2003-2012 (National Association of Insurance Commissioners 2014; Insurance Information Institute 2013; Insurance Information Institute 2009; Insurance Information Institute 2015; Consumer Watch Dog 2007). Because data is not available for 2000-2 and post 2012, prices are assumed to rise in line with inflation (e.g. real price constant after 2012). In California a 10% price reduction on annual

insurance cost is available for low emission vehicles (Hartman 2015). Estimates are used for Japan (Akita-ken 2015). It is assumed that costs change in line with inflation as more detailed information is not available. Mandatory insurance is included in the annual vehicle test costs, but the majority of drivers purchase additional comprehensive cover.

Vehicle tax systems have changed over the time period of the TCO model in this study. In the UK the only vehicle tax is the annual VED (Vehicle Excise Duty) payment. A new CO₂ emissions-based VED system was introduced in 2001, this only affected vehicles purchased in 2001 or later. Under this tax system, hybrids such as the Prius are exempt from annual VED payments (GOV.UK 2015d). A new VED system will be introduced in 2017 but cars registered before this year will still operate under the previous system (GOV.UK 2015c). In the USA a registration and title fee is payable, but this is state dependent (GOV.UK 2015b). The figure used in this study is for California and literature indicates that the amount has not changed over the time period considered. In Japan, three different taxes are payable. When a vehicle is purchased an acquisition fee is due dependent on the MSRP of the vehicle. Additionally, every two years weight tax is owed, and every year an annual tax is due.

In line with other TCO studies, a discount rate of 3.5 %, 4 % and 3.5 % is used for the TCOs representative of the UK, USA and Japan respectively (HM Treasury 2015; Zhuang et al. 2007). The discount rates used in this research are based on social discount rates from the literature, however, these rates are much lower than in other studies (see Table 1). This is partly due to slowing economic growth which lowers the discount rate used. Results are not anticipated to change significantly if the discount rate increases with economic growth.

The TCO model presented in this paper is one of the most complex to be undertaken. However, with such a wide study scope it is difficult to accurately model every cost component, therefore several assumptions have been used. These assumptions do not detract from the results but must be recognised for completeness. Parking and road tolls are not included in this study as they are assumed to be identical for all vehicle types. This is in line with other TCO models such as Delucchi and Lipman (2001). The Prius lifetime is assumed to be less than that of the battery as backed up by empirical evidence (Toyota 2009) and is realistic for a non-plugin hybrid such as the Prius. Detailed tax information has been included in this study. It is assumed that taxes do not change past the base year (2015). In addition, it is assumed that no new policy initiatives will be adopted which significantly change the ownership costs of vehicles already purchased before 2015. With no accurate costs available, it is assumed that scrapping a vehicle in any of the countries considered does not incur a cost. The results of the TCO model only include financial costs and incentives for the vehicles chosen. Non-financial incentives such as designated parking spaces, bus lane or HOV lane access are not included because the financial value could be disputed. In addition, these incentives are worth more to some consumers than others, therefore it is difficult, if not impossible, to allocate a fair price. Finally, social costs of owning a Prius are excluded from this study for the same reasons.

2. Results

The results of the TCO calculation (Fig. 1) demonstrate that the Prius is now cost competitive in the UK and Japan. The largest expense for vehicles in any of the countries considered is depreciation; this cost is significantly more expensive in the UK than the other two countries considered. In Japan, the initial cost has gradually reduced over the first ten years but started to increase since 2010. Annual fuel costs are another significant expense which have been found to be fairly similar between the USA and UK.

The sensitivity analysis on the average annual mileage (Fig. 2) revealed that vehicle TCO in the USA is less sensitive than other countries. The sensitivity analysis on the average fuel price (Fig. 3) leads to the conclusion that if the fuel price in the USA drops significantly below current costs, the Prius will not be cost competitive.

3. Discussion

The results of the TCO calculation (Fig. 1) demonstrate that the Prius is now cost competitive in the UK and Japan. However, the low fuel prices and lack of financial incentives for hybrids in the USA result in higher TCO for the Prius compared to the Corolla. The USA, UK and Japan have very different ownership costs. All the components differ between the countries considered (Fig. 1). Variation in

exchange rate could explain part of the difference in initial and TCO net cost between the UK, USA and Japan over the different years. Annual variation in exchange rate is normal but as all prices are expressed in £2015 this conversion could skew the results for Japan and USA. This may be one reason for the drop in initial cost for the second generation of the Prius. However, without converting all costs into the same currency comparison of total vehicle costs across different countries is not possible.

Depreciation is the largest overall expense associated with vehicle ownership for the first three years of ownership; this cost is significantly more expensive in the UK than the other two countries considered, partly as a result of duty on import vehicles versus home manufacture. The Toyota Prius was initially only manufactured in Japan, with production opening in China in 2005 and Thailand in 2010. In the USA and UK consumers must pay an import cost for these vehicles, it is anticipated that production of the Prius will start in the US before long. The Toyota Corolla has been manufactured on US soil for the time period discussed in this study. The Toyota Avensis has only ever been produced in the UK, and therefore Japanese customers have to pay an import cost for this vehicle, this is one of the reasons for the higher cost of the Avensis compared to the Prius. Historically, there have been difficulties with trade between the US and Japan due to the large US trade deficit caused by sizeable numbers of Japanese vehicles imported into the American market but not vice versa (McAlinden & Chen 2012). In the past the US government has been unhappy with the success of Japanese vehicles

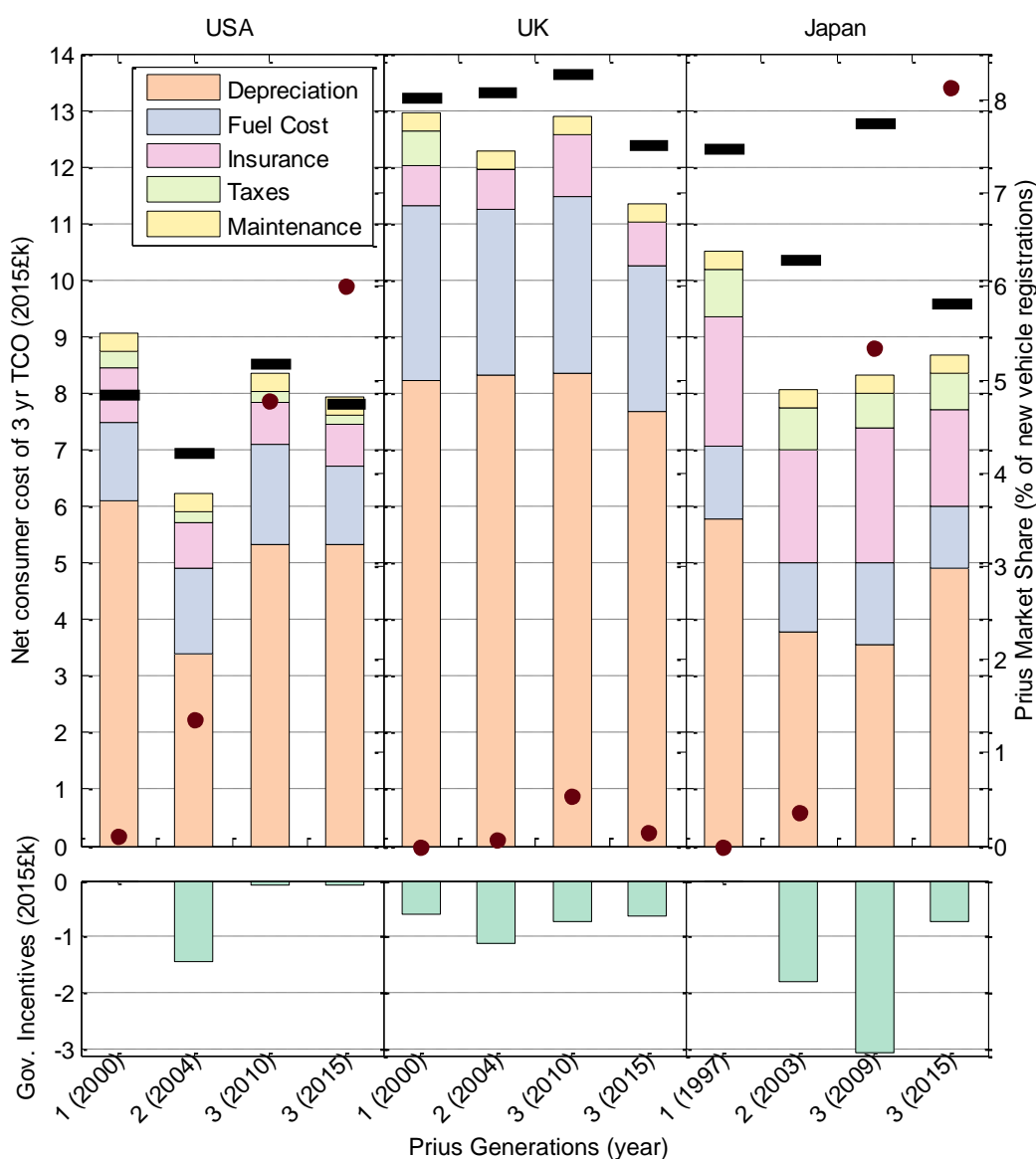


Figure 1. Comparison of TCO for the USA, UK and Japan. Black lines indicate net cost of conventional vehicle, red dots indicate market share.

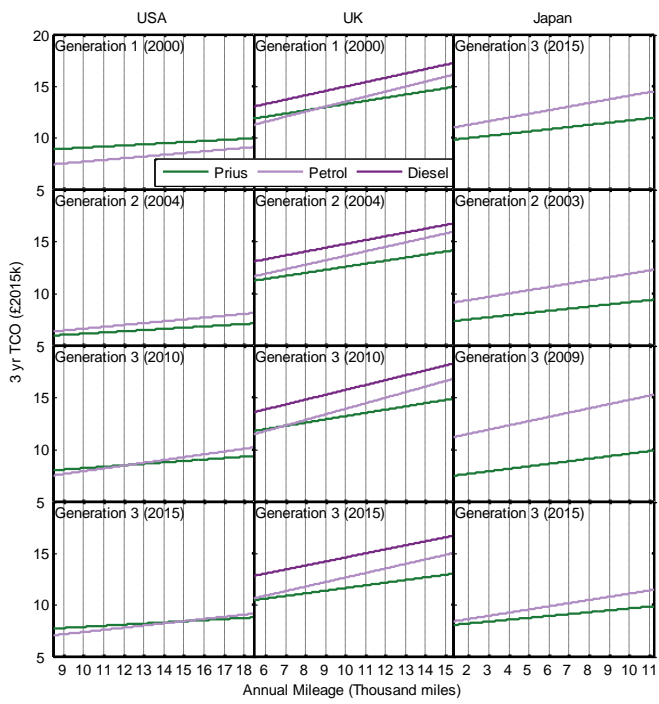


Figure 2. Sensitivity Analysis of annual mileage

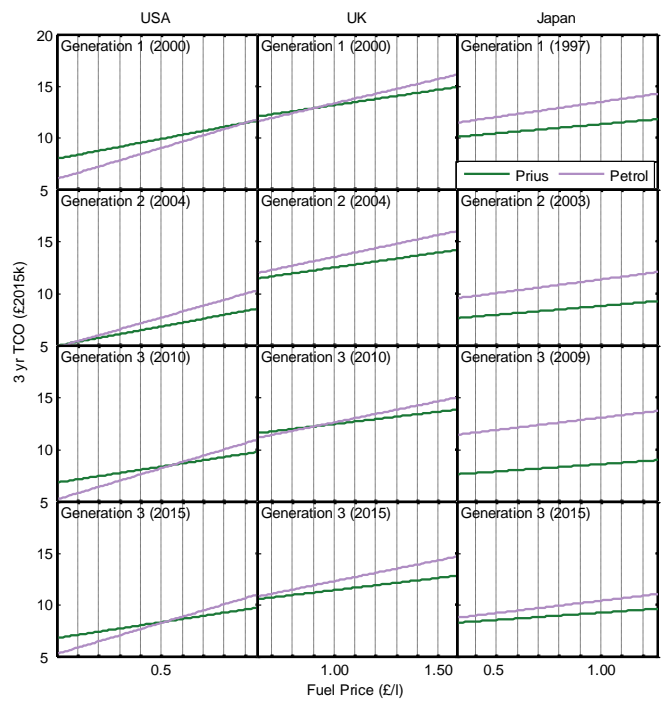


Figure 3. Sensitivity analysis of fuel price

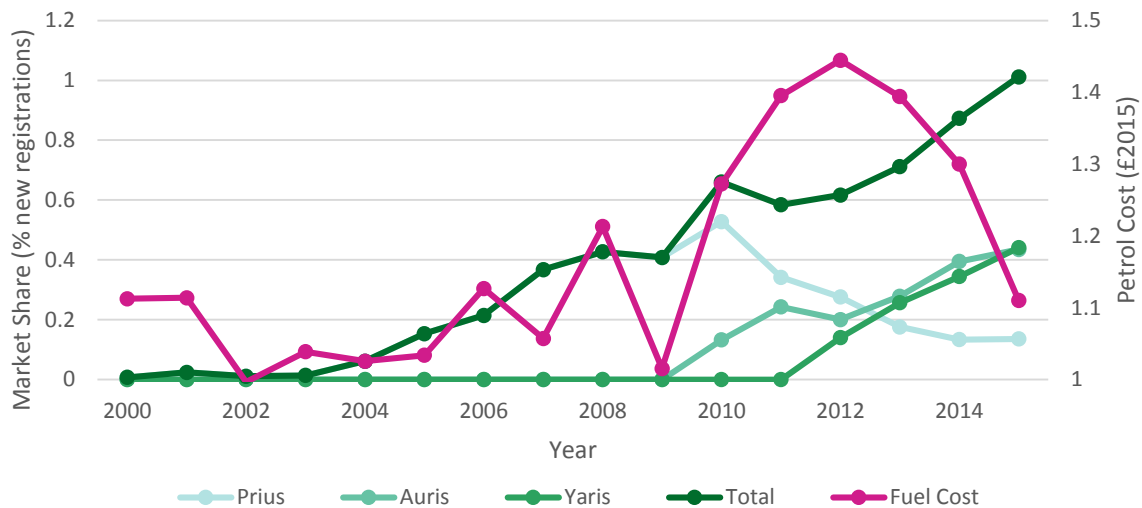


Figure 4. Comparing market share of Toyota hybrids in the UK alongside Petrol fuel price.

displacing American cars on the roads, and the failure of their own manufacturers breaking into the Japanese vehicle market (Banerjee et al. 2007; Ichida 2005). To rectify this, in the past the US government implemented import taxes and voluntary Japanese export quotas limits to discourage US consumers from purchasing Japanese vehicles (Banerjee et al. 2007; McAlinden & Chen 2012; Lee 2011). These quotas were tightened in the early 1990s (Ichida 2005) but Japan countered this by moving production to the USA (Diehl 2001). As a result, Japanese manufacturers reduced vehicle prices in the US auto markets (Banerjee et al. 2007), and combined with the higher efficiency of these vehicles, the US players could not compete with their Japanese counterparts leading to factory closures (Banerjee et al. 2007; Lee 2011). One of the key reasons American vehicles have not broken into the Japanese auto market is that the Japanese vehicle market is dominated by domestic brands with 95% of sales from internal vehicle manufacturers (Lee 2011). In Japanese culture it takes a long time to build trust with a brand. Once this trust is built, loyalty is shown, hence the Japanese tend to only trust their own brands (Lee 2011). The Japanese have not built trust with American brands and along with the large size of US vehicles which do not fit on smaller Japanese roads and the left hand drive setup of US vehicles which are unfavourable on right hand drive Japanese roads, very few US manufactured vehicles have been purchased in Japan (Lee 2011). This brand loyalty does not exist to the same extent in the UK and USA. Many consumers distrust new technology, this is why vehicle manufacturers initially target niche markets for low emission vehicles. For this reason it could be assumed that one reason uptake in the USA and UK may be lagging behind Japan is because potential buyers do not necessarily trust the technology without the trust in the vehicle manufacturer or the loyalty to the brand, therefore the probability of purchasing a new vehicle type is vastly diminished.

In Japan, the initial price has gradually reduced over the first ten years but started to increase since 2010. The reduction in price seen over all three countries may be as a result of reduced production costs associated with mass manufacture. The increased price in Japan and the USA may be from Toyota increasing initial price because of market success. In the UK, market share peaked in 2010 and Toyota may not have increased the initial cost because market share was not sufficient to sustain growth with increased cost. It is possible that the initial cost may have been reduced in the UK since 2010 by Toyota to stimulate sales. It is surprising that market share is significantly higher in California than the UK, when the incremental cost is lower in the UK than California. In the USA, limited Prius supply in earlier years lead to excess demand (Sallee 2015). This may have led to inflated prices, leading to greater incremental cost of the Prius compared to the Corolla. California has a history of innovation and the Prius is seen as an environmental status symbol rather than just a means of mobility (Heffner et al. 2007). New car purchasers consider vehicle depreciation rate of vehicle because they anticipate selling the vehicle before end-of-life. If this is not considered then the payback period for low emission vehicles is longer. Since many vehicles will have more than one owner in their lifetime it is not appropriate to consider payback without incorporating depreciation, but in other studies, comparisons have been made with this technique despite the flaws.

Annual fuel costs are fairly similar between the USA and UK. The price per litre of petrol is much cheaper in the USA than the UK due to lower national and state taxes, however, annual average driving distance is greater. In Japan fuel price per litre is similar to the USA but lower average mileage than either the US or UK leads to lower annual fuel costs. With the falling oil price since 2012 (see Fig 4), net annual fuel cost has reduced. Over the three year TCO this has not made a significant difference to the total cost because of the number of other components calculated in the TCO. Company car mileage is much greater than private car mileage, therefore company cars owners could have an increased saving in purchasing a Prius compared to an ICEV. In the UK, vehicle TCO is more sensitive to changes in annual vehicle mileage than the USA and Japan (Fig. 2). In the UK diesel fuel is more expensive than petrol, consequently, despite better fuel economy, this research has found that diesel vehicles are not cheaper to run than petrol vehicles.

The sensitivity analysis on the average annual mileage (Fig. 2) revealed that vehicle TCO in the USA is less sensitive than other countries due to low fuel price. The improved fuel efficiency of the Prius is indicated by a gentler gradient, indicating that there will be a point where at a certain mileage costs for both vehicle types will be equal. The incentives offered by Japan lead to the conclusion that the Prius is cost effective at any mileage, whereas in the UK mileages of around 5500 lead to the Prius saving the consumer money, finally significantly higher mileages of around 15 000 miles in the USA make the Prius cost competitive. Very high mileage is required in the UK for diesel vehicles to be cost effective compared to UK petrol Prius'. In fact, in the UK, Toyota Prius' are increasingly adopted in the taxi/private hire fleet, it is clear that there is a significant cost saving for high mileage vehicles such as these (Fig. 2).

The sensitivity analysis on the average fuel price (Fig. 3) leads to the conclusion that if the USA drops fuel price significantly, the Prius will not be cost competitive. Fuel cost would have to continue falling in the UK by approximately 20% on today's prices to change the cost effectiveness of the Prius compared to its conventional counterparts. Drops in fuel costs correlate loosely with decline in market share of the Prius in the UK (Fig. 4), however, it is clear that smaller hybrid vehicle types have become more successful since their introduction during the recession.

Taxes and insurance costs are much greater in Japan. The upkeep of vehicles is on the same order of cost to vehicle depreciation. The green car tax incentives in Japan have given low carbon vehicles such as BEVs and HEVs large tax reductions. These incentives were not announced till after the first Prius was introduced in 1997, accounting for the drop in net cost from the first to the second generation of the Prius. These support mechanisms have been gradually phased out in line with increasing AFV market share to show long term commitment to decarbonising the fleet (Fig. 1). In the UK, the financial incentives of owning a hybrid vehicle reduces the running cost rather than the initial cost. Considering the fact that initial cost is the main barrier to purchase for AFVs, incentives that further reduce running costs are not preferable to initial cost subsidies. In the USA, fewer vehicle taxes allow the government fewer opportunities to offer incentives for purchase. The USA is falling behind in the battle against climate change, where several states have imposed additional taxes on low emission vehicles with the reasoning that they cause the same road damage but pay less to the state in fuel tax.

In summary, the pricing strategy of the Toyota Prius has led to the breakthrough from the niche to the mainstream market. The Prius is now successful in more than one vehicle market for different reasons, whether tax breaks (Japan), fuel cost saving (UK) or environmental status symbol (USA). This hybrid is now has a reputation for reliability and dependability (Heffner et al. 2007). The incremental cost between the Prius and the Avensis/Corolla has narrowed as the generations have evolved with greater fuel efficiency and reduced manufacturing costs. Increases in initial cost may have resulted from the Prius moving into the mainstream vehicle market in Japan and California.

Relative TCO between hybrids and ICEVs does explain trend in hybrid market share to a certain extent. In Japan where HEV TCO is much cheaper than for ICEV and there does not exist a barrier for adopting new technologies, high market share can be attributed to significant cost savings. In California, TCO difference between HEV and ICEVs is not as tightly coupled. Perhaps due to the comparative wealth of Californian car purchasers along with their environmental conscience, they do not view cost as a significant barrier. In the UK TCO and Prius market share is not tightly correlated. UK car buyers do not adopt new vehicle technology readily and therefore hybrids have not had the same market success as seen in the other two countries considered.

Conclusion

In the past few years the Toyota Prius has grown in popularity, with the USA (specifically California) and Japan as the countries with the most successful market share. However, the high initial cost of the hybrid powertrain is often quoted to be one of the barriers to uptake. The running costs of the Prius are significantly lower (see Riley et al. (2016)), but without reliable TCO figures it is difficult, if not impossible, to accurately assess whether the Prius is cost effective. This research has contributed to the body of TCO literature by comparing a complex TCO model between different generations of the Toyota Prius to a conventional Toyota vehicle (the Avensis or Corolla) across the USA, UK and Japan.

The results of the TCO calculations show that the Prius has been cost effective for a number of years in the UK, there is evidence that there is hope for cost parity in the USA if fuel prices rise. Significant tax cuts for green vehicles coupled with initial cost similar to an ICEV leads to a cheaper Prius TCO than that of an ICEV in Japan. Now the Prius has entered the mainstream market, trends in initial vehicle cost demonstrate that Toyota may be increasing the price of the Prius for a higher profit margin. Fuel costs are the largest annual running expenses for the consumer after depreciation, therefore a higher mileage, such as that of a company car, increases the costs saving of owning a hybrid. Sensitivity analysis reveals that variation in mileage affects overall TCO for UK more significantly than for the USA or Japan, as a consequence of the greater fuel price in the UK.

The conclusions drawn from this research have the potential to impact stakeholders interested in hybrid vehicles. Policies such as initial price subsidies in the UK and USA could stimulate uptake and increase the cost margin between the Prius and Avensis/Corolla. Unfortunately, potential HEV purchasers are unlikely to read academic papers on this topic. For information on lifetime emissions to be readily accessible to the consumer, this material could be added to the already mandated emissions labels which may increase sales of low emission vehicles. Further research could include extending the TCO comparison to BEVs and PHEVs to investigate how cost has evolved in the same way as the Prius. Researching these vehicle types is more problematic as assumptions must be made over battery charging and usage but useful conclusions could be drawn from this extension.

Acknowledgments

I would like to acknowledge the guidance and support of my PhD supervisors; Dr James Tate of the Institute of Transport Studies, Dr Zia Wadud of the Energy Research Institute and Dr John Nellthorp of the Institute of Transport Studies, all research institutes at the University of Leeds. This project was fully funded by the engineering and Physical research council.

References

- Akita-ken, 2015. Buying a car and car fees. ajet community. Available at: http://akitajet.com/wiki/Buying_a_car_and_car_fees#Shaken [Accessed October 14, 2015].
- Al-Alawi, B.M. & Bradley, T.H., 2013. Total cost of ownership, payback, and consumer preference modeling of plug-in hybrid electric vehicles. *Applied Energy*, 103(2013), pp.488–506. Available at: <http://linkinghub.elsevier.com/retrieve/pii/S0306261912007131> [Accessed November 27, 2014].
- Alhulail, I. & Takeuchi, K., 2014. Effects of Tax Incentives on Sales of Eco-Friendly Vehicles: Evidence from Japan, Available at: <http://www.econ.kobe-u.ac.jp/RePEc/koe/wpaper/2014/1412.pdf> [Accessed May 11, 2015].
- Amos, C.D., 2015. Are Hybrid-Electric Vehicles a Good Buy for Fleet? Government Fleet. Available at: <http://www.government-fleet.com/article/story/2006/09/are-hybrid-electric-vehicles-a-good-buy-for-fleet.aspx> [Accessed October 14, 2015].
- Banerjee, S., Chatterjee, R. & Nag, B., 2007. Changing Features of the Automobile Industry in Asia: Comparison of Production, Trade and Market Structure in Selected Countries. *Asia-Pacific Research and Training Network on Trade Working Paper Series*, 37. Available at: <http://citeseerx.ist.psu.edu/viewdoc/download?doi=10.1.1.551.214&rep=rep1&type=pdf>.
- CA.GOV, 2015. Estimated 2015 Gasoline Price Breakdown & Margins Details. Available at: <http://energyalmanac.ca.gov/gasoline/margins/index.php> [Accessed October 14, 2015].
- Carbuyer.co.uk, 2015. MPG, running costs & CO2. Available at: <http://www.carbuyer.co.uk/reviews/toyota/prius/hatchback/mpg> [Accessed October 14, 2015].
- Consumer Watch Dog, 2007. Proposition 103's Impact on Auto Insurance Premiums in California. Available at: http://www.consumerwatchdog.org/resources/15years_Prop103.pdf [Accessed

- November 11, 2015].
- Dahl, C.A., 2012. Measuring global gasoline and diesel price and income elasticities. *Energy Policy*, 41, pp.2–13. Available at: <http://dx.doi.org/10.1016/j.enpol.2010.11.055>.
- DECC, 2015. DECC fossil fuel price projections. Fossil fuel price projections: 2015. Available at: <https://www.gov.uk/government/publications/fossil-fuel-price-projections-2015>.
- Delucchi, M. a & Lipman, T.E., 2001. An analysis of the retail and lifecycle cost of battery-powered electric vehicles. *Transportation Research Part D: Transport and Environment*, 6(6), pp.371–404. Available at: <http://linkinghub.elsevier.com/retrieve/pii/S1361920900000316>.
- Department for Transport, 2013. National Travel Survey: England 2013, London, UK. Available at: https://www.gov.uk/government/uploads/system/uploads/attachment_data/file/342160/nts2013-01.pdf.
- Department for Transport, 2016. WebTAG: TAG data book, December 2015. Guidance. Available at: <https://www.gov.uk/government/publications/webtag-tag-data-book-december-2015> [Accessed April 29, 2016].
- Diehl, M., 2001. International Trade in Intermediate Inputs: The Case of the Automobile Industry. *Kieler Arbeitspapiere*, 1027. Available at: <http://hdl.handle.net/10419/17738Nutzungsbedingungen>:
- DMV.ORG, 2015. Smog Check in California. Available at: <http://www.dmv.org/ca-california/smog-check.php> [Accessed October 14, 2015].
- Edmunds.com, 2015. Edmunds.com. Available at: <http://www.edmunds.com> [Accessed October 26, 2015].
- Electric Power Research Institute, 2004. Advanced batteries for electric drive vehicles a technology and cost-effectiveness assessment for battery electric vehicles, power assist hybrid electric vehicles and plug-in hybrid electric vehicles., Palo Alto (CA). Available at: <http://www.epri.com/abstracts/pages/productabstract.aspx?ProductId=00000000001009299>.
- Federal Highway Administration, 2015. Average Annual Miles per Driver by Age Group. United States Department of Transportation. Available at: <http://www.fhwa.dot.gov/ohim/onh00/bar8.htm> [Accessed October 13, 2015].
- fleetcare, 2015. Vehicle Colour Choice- Impacts On Depreciation And Visibility. Available at: <http://www.fleetcare.com.au/news-info/fleet-beat-blog/november-2012/vehicle-colour-choice-impacts-on-depreciation-an> [Accessed April 25, 2016].
- Goo-net-exchange, 2015. Toyota Prius car review. Available at: http://www.goo-net-exchange.com/catalog/TOYOTA__PRIUS/ [Accessed October 26, 2015].
- GOV.UK, 2015a. Getting an MOT. Available at: <https://www.gov.uk/getting-an-mot/mot-test-fees> [Accessed October 14, 2015].
- GOV.UK, 2015b. Plug-in car and van grants. Available at: <https://www.gov.uk/plug-in-car-van-grants/overview> [Accessed October 14, 2015].
- GOV.UK, 2015c. Vehicle Excise Duty. Available at: <https://www.gov.uk/government/publications/vehicle-excise-duty> [Accessed October 14, 2015].
- GOV.UK, 2015d. Vehicle tax rate tables. Available at: <https://www.gov.uk/vehicle-tax-rate-tables/overview> [Accessed October 14, 2015].
- Greene, D.L., Park, S. & Liu, C., 2014. Public policy and the transition to electric drive vehicles in the U . S .: The role of the zero emission vehicles mandates. *Energy Strategy Reviews*, 5, pp.66–77. Available at: <http://dx.doi.org/10.1016/j.esr.2014.10.005>.
- Grove, J., 2013. Analysis of vehicle odometer readings recorded at MOT tests, London, UK. Available at: https://www.gov.uk/government/uploads/system/uploads/attachment_data/file/206882/experimental-statistics-mot-data.pdf.
- Hagman, J. et al., 2016. Total cost of ownership and its potential implications for battery electric vehicle diffusion. *Research in Transportation Business & Management*, pp.1–7. Available at: <http://linkinghub.elsevier.com/retrieve/pii/S2210539516000043>.
- Hartman, K., 2015. State Efforts Promote Hybrid and Electric Vehicles. National Conference of State Legislatures. Available at: <http://www.ncsl.org/research/energy/state-electric-vehicle-incentives-state-chart.aspx#ca> [Accessed October 14, 2015].
- Heffner, R.R., Kurani, K.S. & Turrentine, T.S., 2007. Symbolism in California’s early market for hybrid electric vehicles. *Transportation Research Part D: Transport and Environment*, 12(6), pp.396–413. Available at: <http://linkinghub.elsevier.com/retrieve/pii/S136192090700051X> [Accessed July 11, 2014].
- HM Treasury, 2015. The Green Book, Available at: <https://www.gov.uk/government/publications/the-green-book-appraisal-and-evaluation-in-central-government>.

- Honestjohn, 2015. Honestjohn. Available at: <http://www.honestjohn.co.uk> [Accessed October 26, 2015].
- Hutchinson, T., Burgess, S. & Herrmann, G., 2014. Current hybrid-electric powertrain architectures: Applying empirical design data to life cycle assessment and whole-life cost analysis. *Applied Energy*, 119, pp.314–329. Available at: <http://linkinghub.elsevier.com/retrieve/pii/S0306261914000282> [Accessed April 15, 2015].
- Ichida, T., 2005. US-Japan Automobile Trade Negotiation in 1995 - the Analysis on why Japan became assertive toward US negotiators. *早稲田商学*, 404, pp.51–84.
- Idaho National Laboratory, 2014. Advanced Vehicle Testing Activity. Available at: <http://avt.inl.gov/index.shtml> [Accessed October 13, 2015].
- IEA, 2015. Energy Prices and Taxes. Volumes 1999-2015. Available at: <http://www.oecd-ilibrary.org/energy/energy-prices-and-taxes/> [Accessed November 11, 2015].
- Insurance Information Institute, 2015. Average cost for auto insurance, 2005. The Public Policy Institute of New York State Inc. Available at: <http://www.ppiny.org/reports/jtf/autoinsurance.html> [Accessed October 14, 2015].
- Insurance Information Institute, 2013. Average Expenditures for Auto Insurance by State 2008-2012. Available at: <http://www.iii.org/table-archive/21247> [Accessed October 14, 2015].
- Insurance Information Institute, 2009. The Insurance Factbook 2009, New York, USA: Insurance Information Inst., 1984. Available at: https://books.google.co.uk/books?id=PY-aQ_OF0TIC&pg=PA57&lpg=PA57&dq=AVERAGE+EXPENDITURES+FOR+AUTO+INSURANCE+BY+STATE+liability+2006&source=bl&ots=PjvBnxfazV&sig=FPqyTKz-gloJ82qiN1LWk1ffjhE&hl=en&sa=X&ei=Z2GbVei4MYWzUZmeggZAL&redir_esc=y#v=onepage&q&f=false.
- Lave, L.B. & MacLean, H.L., 2002. An environmental-economic evaluation of hybrid electric vehicles: Toyota's Prius vs. its conventional internal combustion engine Corolla. *Transportation Research Part D: Transport and Environment*, 7(2), pp.155–162. Available at: <http://linkinghub.elsevier.com/retrieve/pii/S1361920901000141>.
- Lee, S.M., 2011. A Comparative Study of the Automobile Industry in Japan and Korea. *Asian Survey*, 51(5), pp.876–898.
- Leibling, D., 2008. Car ownership in Great Britain, London, UK. Available at: http://www.racfoundation.org/assets/rac_foundation/content/downloadables/car_ownership_in_great_britain_-_leibling_-_171008_-_report.pdf.
- Lemoine, D., Kammen, D. & Farrell, A., 2007. Effects of Plug-In Hybrid Electric Vehicles in California Energy Markets. In *86th Annual Meeting of the Transportation Research Board*. Washington DC.
- Lemon, S. & Miller, A., 2013. Electric Vehicles in New Zealand: From Passenger to Driver?, Canterbury, New Zealand. Available at: http://www.epecentre.ac.nz/docs/media/Electric_Vehicles_in_New_Zealand_White_Paper-r10.pdf.
- Lipman, T.E. & Delucchi, M. a., 2006. A retail and lifecycle cost analysis of hybrid electric vehicles. *Transportation Research Part D: Transport and Environment*, 11(2), pp.115–132.
- McAlinden, S.P. & Chen, Y., 2012. The Effects a U.S. Free Trade Agreement with Japan would have on the U.S. Automotive Industry, Ann Arbor, USA.
- Millard-Ball, A. & Schipper, L., 2011. Are We Reaching Peak Travel? Trends in Passenger Transport in Eight Industrialized Countries. *Transport Reviews*, 31(3), pp.357–378.
- Muller, J., 2013. Who Buys The Most Hybrid Cars? Northern Californians, Report Says. *Forbes Auto*. Available at: <http://www.forbes.com/sites/joannmuller/2013/01/03/hybrid-landscape-looks-wildly-different-across-the-u-s/>.
- NADA, 2014. NADA Used Car Guide, McLean, VA. Available at: http://www.nada.com/B2B/Portals/0/assets/NADA_Perspective/2014/201406_Hybrid_Car_Market_Review_UPDATED.pdf.
- National Association of Insurance Commissioners, 2014. Auto Insurance Database Report, Washington DC, Kansas City, New York. Available at: http://www.naic.org/documents/prod_serv_statistical_aut_pb.pdf.
- RAC, 2015. Toyota Prius. Available at: <http://www.rac.co.uk/buying-a-car/car-reviews/toyota/prius/301355> [Accessed November 10, 2015].
- Riley, R. et al., 2016. Real-world CO2 emission, and cost benefit, of a switch to hybrid electric vehicles in taxi fleets. In *The 21st International Transport and Air Pollution (TAP) Conference*, Lyon, France, May 24-26.
- Sallee, J.M., 2015. The Surprising Incidence of Tax Credits for the Toyota Prius1. *American Economic Journal: Economic Policy* 3, 3(2), pp.189–219.
- Simpson, A., 2006. Cost-Benefit Analysis of Plug-In Hybrid Electric Vehicle Technology. In *22nd*

- International Battery, Hybrid and Fuel Cell Electric Vehicle Symposium and Exhibition (EVS-22).
Yokohama, Japan.
- SMMT, 2013. The society of motor manufacturers and traders motor industry facts 2013, London, UK.
Available at: <http://www.smmmt.co.uk/wp-content/uploads/sites/2/SMMT-2013-Motor-Industry-Facts-guide.pdf>.
- Spritmonitor, 2015. Spritmonitor.de. Available at: <http://www.spritmonitor.de> [Accessed October 26, 2015].
- The AA, 2015. AA British Insurance Premium Index. Available at:
<http://www.theaa.com/newsroom/insurance/bipi/british-insurance-premium-index.html>.
- The California Energy Commission, 2015. California Average Weekly Retail Gasoline Prices.
CA.GOV. Available at: http://energyalmanac.ca.gov/gasoline/retail_gasoline_prices.html
[Accessed November 11, 2015].
- Toyota, 2009. 2010 Prius: harmony between man, nature, and machine. Toyota Motor Sales U.S.A.,
Inc. Available at: <http://www.toyota.com/byt/pub/buildGeneralEbrochure.do?brochureType=general&modelYear=2010&lang=en&seriesCode=12&zip> [Accessed October 14, 2015].
- Toyota, 2012. Toyota in the world, Available at: http://www.toyota-global.com/company/profile/in_the_world/pdf/2012/databook_en_2012.pdf.
- Toyota, 2013. TOYOTA'S HYBRID SUCCESS STORY. Toyota Media Site. Available at:
<http://media.toyota.co.uk/2013/08/toyotas-hybrid-success-story/> [Accessed April 28, 2016].
- Toyota GB, 2015. History of the Toyota Prius. The Official Blog of Toyota GB. Available at:
<http://blog.toyota.co.uk/history-toyota-prius> [Accessed October 13, 2015].
- Toyota Ireland, 2008. Worldwide Prius Sales Top 1 Million Mark. Available at:
<http://www.toyota.co.jp/en/news/08/0515.html> [Accessed August 26, 2008].
- travelcard, 2015. travelcard: fuel card innovation. travelcard. Available at: <http://www.travelcard.nl/>
[Accessed October 26, 2015].
- U.S. Department of Energy Advanced Vehicle Testing Activity, 2015. 2004 Toyota Prius Electric
Vehicle. HEVAmerica. Available at: <http://avt.inl.gov/pdf/hev/prius2004hevamerica.pdf>,
[Accessed October 26, 2015].
- United States Department of Agriculture Economic Research Service, 2015a. Consumer Price
Indexes (2010 base) Historical. International Macroeconomic Data Set. Available at:
<http://www.ers.usda.gov/data-products/international-macroeconomic-data-set.aspx> [Accessed
November 10, 2015].
- United States Department of Agriculture Economic Research Service, 2015b. Consumer Price
Indexes (2010 base) Projections. International Macroeconomic Data Set. Available at:
<http://www.ers.usda.gov/data-products/international-macroeconomic-data-set.aspx> [Accessed
November 10, 2015].
- United States Department of Agriculture Economic Research Service, 2015c. Real Exchange Rate
Projections. International Macroeconomic Data Set. Available at: <http://www.ers.usda.gov/data-products/international-macroeconomic-data-set.aspx> [Accessed November 11, 2015].
- United States Department of Agriculture Economic Research Service, 2015d. Real Exchange Rates
Historical. International Macroeconomic Data Set. Available at: <http://www.ers.usda.gov/data-products/international-macroeconomic-data-set.aspx> [Accessed November 11, 2015].
- United States Department of Energy (DOE), 2009. Annual energy outlook 2009 with projection to
2030., Washington DC. Available at: [http://www.eia.gov/oiaf/aeo/pdf/0383\(2009\).pdf](http://www.eia.gov/oiaf/aeo/pdf/0383(2009).pdf).
- Whatcar?, 2015. Whatcar? Available at: <http://www.whatcar.com/> [Accessed October 26, 2015].
- Yourfleet, 2015. Toyota Prius Car Review. Available at:
http://www.yourfleet.co.uk/car_reviews/toyota/road_test.php?report_id_1355 [Accessed
November 10, 2015].
- Zhuang, J. et al., 2007. ERD Working Paper Series no. 94, Mandaluyong City, Philippines. Available
at: http://facweb.knowlton.ohio-state.edu/pvinton/courses/crp763/zhuang_et_al.pdf.

Impact assessment of vehicle technology, fuel, and ICT measures on CO₂ emissions from road traffic to 2030

Giannis PAPADIMITRIOU*, Valentini MARKAKI*, Despoina CHATZIKYRIAKOU**, Dorothee LAHAUSSOIS**, and Leonidas NTZIACHRISTOS***

* Emisia S.A., Antoni Tritsi 21, Service Post 2, Thessaloniki, GR-57001, Greece

** Toyota Motor Europe NV/SA, Avenue du Bourget 60, B- 1140 Brussels, Belgium

*** Laboratory of Applied Thermodynamics, Aristotle University of Thessaloniki, GR-54124, Greece

Corresponding authors e-mail: giannis.p@emisia.com, leon@auth.gr

Abstract

This paper presents the outcomes of a study aiming at assessing the CO₂ evolution from road traffic and the impact of vehicle technology, fuel, and ICT/ITS measures to 2030. Feasibility projections of real-world total CO₂ emissions from road transport are presented, taking into account: i) advanced biofuel production pathways, and ii) deployment of ICT/ITS. The context and background of the study is summarized in the 2030 indicative target of -17% reduction (over 2010) in EU28 GHG (CO₂-eq) from all transport modes (2030 Framework for Climate and Energy Policies). This demanding target, together with the fact that ~72% of CO₂ emissions come from road transport, reveals the necessity to undertake actions in all fronts on behalf of the automotive/fuel industry and other stakeholders. The potential impact of alternative fuel pathways on upstream (WtT) and of ICT measures on downstream (TtW) CO₂ emissions is evaluated and the key result is that CO₂ emission evolution in a business-as-usual (baseline) scenario does not reach the 2030 target (-13.1% instead of -17%). Hence, additional technical effort is required. The study shows that by implementing 'higher' effort scenarios, additional reductions of -5.5% in CO₂ can be reached by improved biofuels and enhanced ICT measures. Further -6.6% reductions are possible, based on wider adoption of electrified PCs and improved efficiency in HDVs.

Keys-words: CO₂ emissions reduction, alternative fuel pathways, ICT/ITS measures, fleet projections.

Introduction

Combating global warming and climate change is one of the most important environmental challenges in recent years. As a result of its heavy dependence on fossil fuels, the transport sector is a significant consumer of energy and a major source of GHG emissions. Specifically, it accounted for 31.6% of total final energy consumption in 2013 and was responsible for 24.3% of GHG emissions (including international bunkers) in 2012 in EU28 (European Commission, 2015). Road transport is the dominant mode, emitting 71.9% of all transport-related GHG emissions.

A major concern is that, although total GHG emissions in EU28 decreased from 1990 to 2013, emissions from the transport sector (all modes) increased for the same time period (Figure 1). This is mainly due to the increase of transport activity, both passenger and freight. Nevertheless, by focusing on the time period 2008-2013, reductions in GHG emissions from transport are observed. The latter can mainly be attributed to the economic recession and, secondarily, to specific measures taken at local or global level aiming at reducing fuel consumption. In any case, it is more than obvious that this decrease trend must continue (or even intensify) in order to meet the reduction targets for 2030 and 2050, as shown in Figure 1. Specifically, the 2030 indicative target of -17% reductions (over 2010) is from the 2030 Framework for Climate and Energy Policies¹, while the 2050 target of -69% reductions (over 2010) is from the 2011 White Paper on Transport².

Despite the demanding future targets that have been set on TtW emissions, a key result of the study is that the CO₂ emissions evolution in a business-as-usual (baseline) scenario does not reach the -17% checkpoint in 2030. Specifically, CO₂ reductions in 2030 are projected to reach -13.1% (over 2010) on a fleet level in an integrated approach including WtW CO₂ emissions from total road

¹ http://ec.europa.eu/clima/policies/strategies/2030/index_en.htm

² http://ec.europa.eu/transport/themes/strategies/2011_white_paper_en.htm

transport (PCs, LCVs, HDVs). Another factor that must be taken into consideration is that the EU28 passenger and freight transport activity projection presents a continuous increase from year to year, reaching +23% for passenger transport and +37% for freight transport in 2030 over 2010 (IIASA, Thematic Strategy on Air Pollution)³. This continuous increase in transport activity, together with the fact that ~72% of CO₂ emissions come from road transport, make the future targets even more demanding. Hence, significant additional technical effort is required and actions need to be undertaken in all fronts on behalf of the automotive/fuel industry and other involved stakeholders.

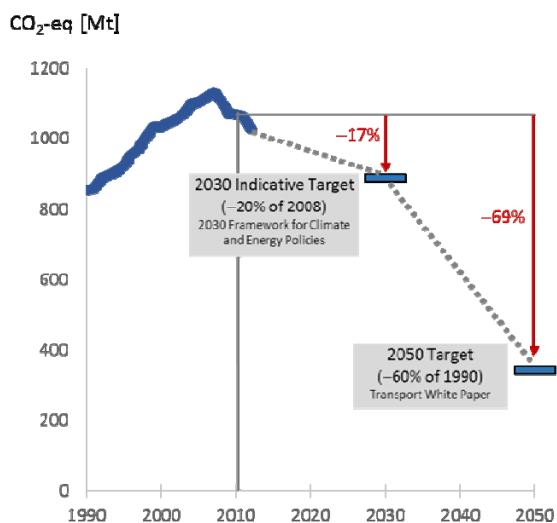


**Figure 1. EU28 all transport GHG (CO₂-equivalent)
(Historical data source: European Environment Agency, 2015)**

The main objective of this paper is to assess the impact of alternative fuel pathways on upstream (WtT) and of ICT measures on downstream (TtW) CO₂ emissions; these measures, combined with advanced vehicle technology, can lead to significant CO₂ reductions. An interesting finding is that the usage of advanced biofuels together with moderate implementation of ICT measures may suffice in order to reach total WtW CO₂ reductions above the -17% indicative target. Further reductions are technically possible by combining advanced biofuels with accelerated deployment of ICT/ITS and advanced vehicle technology measures (fleet renewal with electrified vehicles – battery electric and plug-in hybrid electric – and high efficiency improvements).

In order to assess the evolution of CO₂ emissions from road transport and the impact of vehicle technology, fuel, and ICT measures, feasibility projections of real-world total CO₂ from road transport (calculated on the basis of fuel sales) are presented, taking into account: i) advanced biofuel production pathways, and ii) deployment of ICT/ITS. The projections are based on activity evolution to 2030 agreed in high level EU policy related studies (revision of the Thematic Strategy on Air Pollution). The main methodological components of the study are two fuel and two ICT scenarios applied on two fleet projections. These scenarios explore the possibilities to reduce CO₂ and can be used to inform and guide policy. The numerical results show the CO₂ emission reduction potential.

The software tool that has been used for the fleet projections is SIBYL⁴, a novel vehicle stock projection and scenario evaluation tool with advanced energy consumption and emission modelling capabilities. With SIBYL it is possible to make fleet, activity, energy, and emission estimations and projections up to 2050. Apart from SIBYL, other key research studies used in this paper are:

- _ JEC study (JEC, 2014) and E4tech Auto-Fuel biofuel roadmap (E4tech, 2013) on fuel impacts.
- _ FP7 ICT-Emissions project⁵ on ICT impacts.

The rest of the paper is organized as follows. Section 1 presents the main methodological components. A general overview of the approach is given, followed by a detailed description of the two fuel scenarios, the two ICT scenarios, and the two fleet projections. Section 2 provides the

³ <http://www.iiasa.ac.at/web/home/research/researchPrograms/MitigationofAirPollutionandGreenhousegases/TSAP-reports.html>

⁴ <http://emisias.com/content/sibyl>

⁵ <http://www.ict-emissions.eu/>

numerical results. First, the baseline scenario is described. Next, total CO₂ benefits and relative contribution of the various measures are given. The individual impact of fuels, ICT, and fleet on CO₂ is presented separately. In section 3 there is a short discussion on air pollutants (NO_x), which, although they are not the focus of the study, the impact of the developed scenarios on those should not be ignored in any case. The paper is summarized in the conclusions section.

1. Basic methodological components

The main methodological components are summarized in Figure 2 and shortly outlined below:

- _ 2 *fuel scenarios*: These are based on the JEC study and E4tech Auto-Fuel biofuel roadmap on fuel impacts. The main difference between the two scenarios is that one is built according to policy targets using current feedstock pathways, while the other benefits from increased penetration of advanced biofuels, improved production pathways, and more renewable energy sources.
- _ 2 *ICT scenarios*: These are based on the FP7 ICT-Emissions project on ICT impacts and their main difference is on the penetration to the fleet and their application level.
- _ 2 *fleet projections*: They have been implemented in SIBYL and are based on activity and energy evolution to 2030, as agreed in high level EU policy related studies. Baseline fleet assumes normal fleet renewal and efficiency improvement, while advanced fleet benefits from higher penetration of electrified vehicles and higher efficiency improvements.

The above scenarios can be combined in 8 different ways (2 x 2 x 2 = 8 scenario combinations) for EU28 with time horizon to 2030. Costs and behaviour change limitations have not been considered in the study. All scenarios utilize results of recognized research and policy studies in EU.

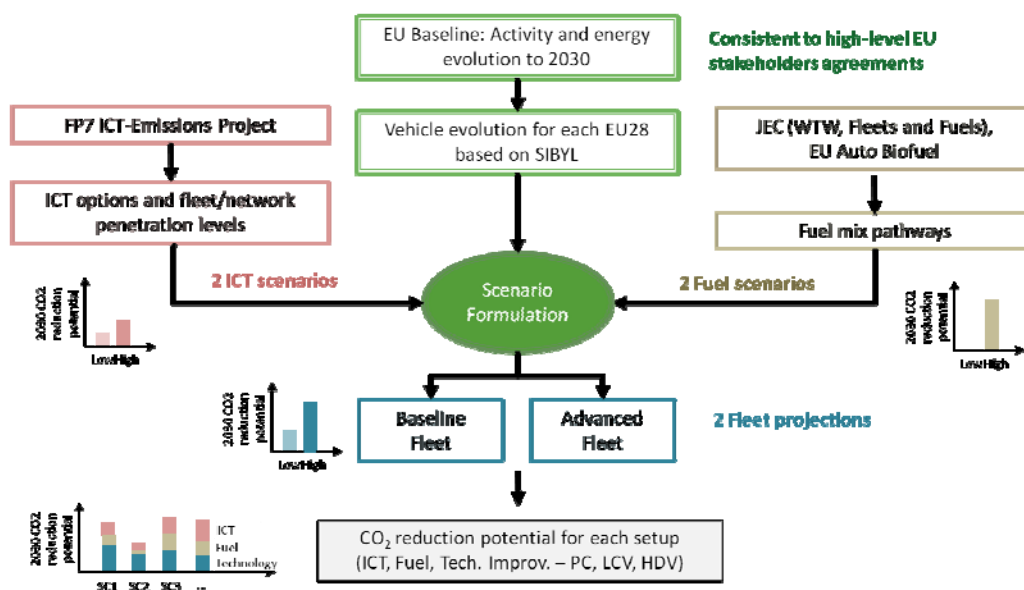


Figure 2. Flowchart of study design

For convenience, fuel and ICT scenarios are distinguished using the terms low/high, which represent how much effort has to be put for implementation. In general, low effort means business-as-usual with no additional policy measures than already agreed; high effort means that significant additional efforts are needed (practically reaching maximum technical feasibility).

Fuel measures and alternative pathways

The methodology followed to create the two fuel scenarios is summarized in Figure 3 and the main components are explained below.

- _ *Main fuels considered*: Fossil diesel and substitutes (biodiesel, HVO, FT), fossil petrol and substitutes (bioethanol, ETBE), electricity, and hydrogen. CNG/LPG are not explicitly mentioned because default SIBYL pathways (with no changes) are used in both scenarios.

- *WtW CO₂ of each pathway*: Impact of each fuel production pathway on CO₂ taken from the JEC study. Of particular importance is the upstream part (WtT) of fuels with renewable production pathways, since these are expected to contribute to the target of total CO₂ reduction.
- *Fuel consumption statistical data (2010-2013)*: Official statistics from Eurostat⁶ and Biofuels Barometer⁷, showing current situation and trends in usage (blending) of biodiesel and bioethanol. Historical data are fully respected in both scenarios.
- *Fuels and pathways for the period 2014-2030*: This is the most important component of the methodology, since it is about deciding the percentage of fossil diesel and petrol to be substituted, and the specific pathways to be used for the production of each fuel substitute (including electricity and hydrogen). The decision is based on the feedstock availability and biofuels supply to 2030 (taken from the EU Auto-Fuel biofuel roadmap) and on the CO₂ impact of each pathway (JEC study). The objective is to select optimum pathways (to reduce total CO₂), while at the same time respecting upper limits of feedstock availability and biofuels supply.

Following the above methodological steps results in the creation of the two fuel scenarios. Each scenario contains exact numerical values of the fuel quantities to be used, sharing of each production pathway and CO₂ impact of each pathway and fuel (weighted average based on pathways sharing).

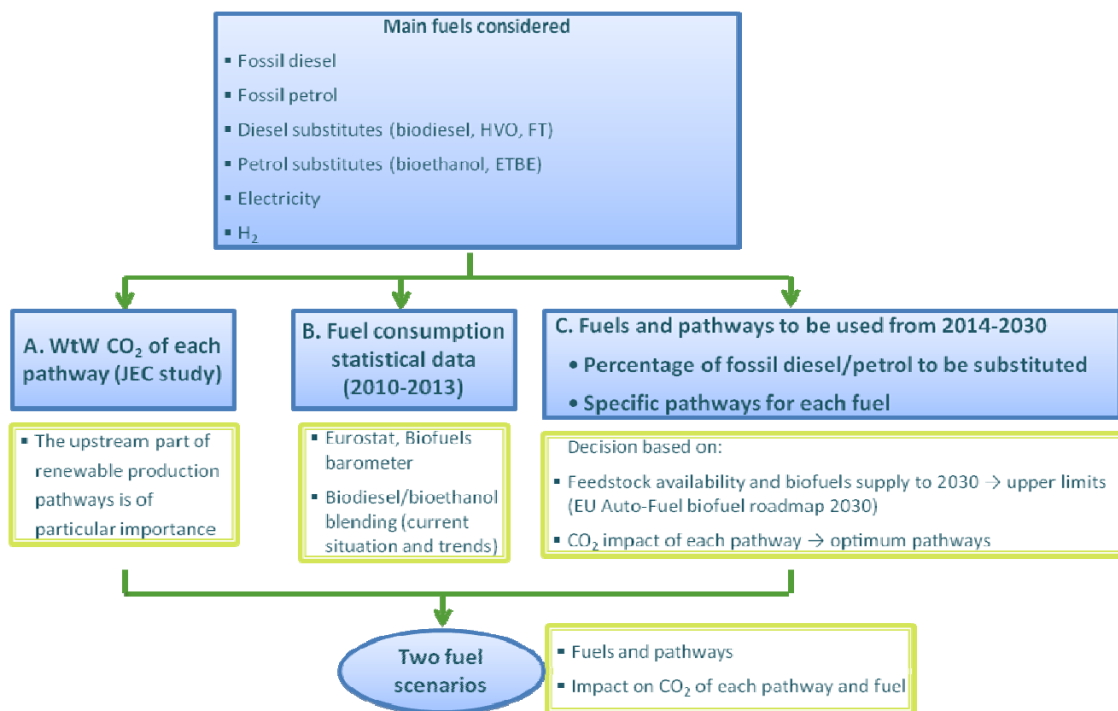


Figure 3. Methodology for the creation of the two fuel scenarios

Both scenarios utilize policy studies in EU and respect policy measures already agreed. This is reflected in Figure 4 which shows the volumetric blending (%) in diesel/petrol mix. Historical statistical data from Eurostat (2010-2013) are fully respected in any case. For diesel, B7 (FAME) is the maximum blend considered in both scenarios; for petrol, the highest blending ratio is E10 (after 2021) with an intermediate step of E7 (from 2016 to 2020). In general, the fuels considered for diesel substitutes are biodiesel (FAME blended) and drop-in fuels (HVO and FT), while the fuels considered for petrol substitutes are bioethanol (EtOH), and bio ETBE. Figure 5 shows indicative examples of volumetric sharing (%) in diesel/petrol mix. In these examples, fossil diesel is 93% while the remaining 7% is split into 5.1% biodiesel (FAME) and 1.9% HVO and FT (drop-in fuels); similarly, fossil petrol is 90% and the remaining 10% is split into 6.4% bioethanol and 3.6% ETBE.

⁶ <http://ec.europa.eu/eurostat/web/energy/data/database>

⁷ <http://www.eurobserv-er.org/biofuels-barometer-2014/>

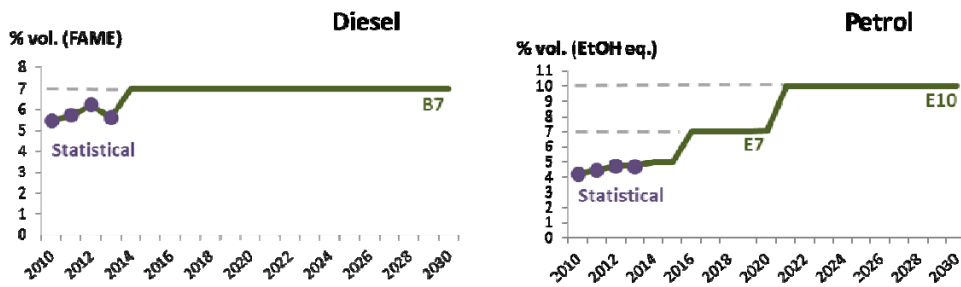


Figure 4: Policy targets respected for diesel (left) and petrol (right)

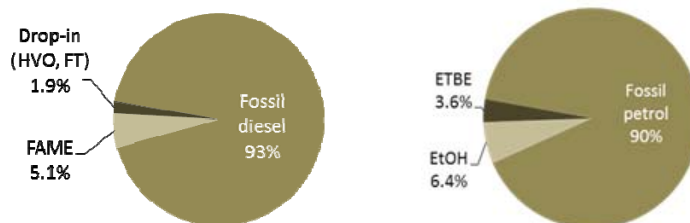


Figure 5: Examples of volumetric sharing (%) in diesel (left) and petrol (right) mix (low effort scenario, year 2021)

Diesel fuel substitute pathways

Figure 6 provides more insight on the differences of the two scenarios concerning the usage of diesel substitutes (indicative years 2010, 2020, 2030). Specifically, the high effort scenario assumes increased penetration of drop-in fuels (HVO and FT); FAME alone remains constant (equal to 7%), while the sum of FAME + HVO + FT continues to increase (9.8% in 2020 and 14.2% in 2030). In the low effort scenario, usage of HVO and FT is moderate (compared to high effort); FAME alone decreases from 2020 to 2030, but the sum of FAME + HVO + FT remains unchanged (equal to 7%). Both scenarios fully respect supply limits from the EU Auto-Fuel biofuel roadmap, which provides HVO and FT production capacity available to the EU to 2030 (low-medium-high case). The main assumption that has been made is that fuel production is considered as fuel consumption in the two scenarios (medium case in the low effort, and high case in the high effort).

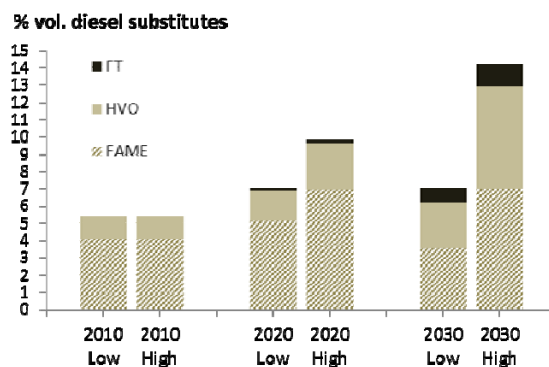


Figure 6: Comparison of low/high effort fuel scenarios in diesel substitutes

Concerning the production pathways of diesel substitutes, low effort scenario assumes FAME, HVO, and FT mostly from food crops (similar to current situation); high-effort scenario assumes some increase of non-food feedstock (e.g. tallow oil, farm/waste wood) to meet ILUC recommendations⁸. The sharing (%) of each pathway (feedstock) in the two scenarios is shown in Table 1. Both scenarios fully respect feedstock availability (supply chains) from the EU Auto-Fuel biofuel roadmap. Changes in high effort scenario (i.e. increase of non-food feedstock) are applied from 2020 to 2030.

⁸ <http://ec.europa.eu/energy/en/topics/renewable-energy/biofuels/land-use-change>

Table 1: Feedstock comparison in the two fuel scenarios for diesel

Biodiesel & HVO	Low Effort	High Effort
Rapeseed	48%	45%
Sunflower	4%	4%
Soy beans	22%	20%
Palm oil	11%	11%
Waste cook oil	15%	15%
Tallow oil	0%	4%
FT	Low Effort	High Effort
Natural Gas	50%	0%
Farm/waste wood	50%	100%

The introduction of tallow oil in biodiesel and HVO in high effort scenario decreases WtW CO₂ (weighted average of pathways used). This WtW improvement is due to the upstream part (less CO₂ for the production of biodiesel and HVO from tallow oil). Significant improvement also exists in WtW CO₂ of FT due to increase of wood. Figure 7 summarizes the positive impact of high effort fuel scenario on CO₂. It is obvious that from 2020 (and until 2030) the CO₂ of diesel substitutes (weighted average of pathways used based on fuel consumption) decreases.

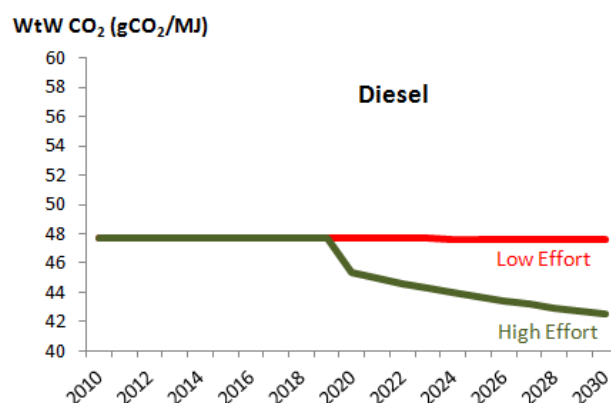


Figure 7: Impact of high effort scenario diesel fuel substitute pathways on CO₂

Petrol fuel substitute pathways

Petrol substitutes today do not offer as significant CO₂ savings as diesel. Noticeable benefits can be achieved only in the high effort scenario (due to improved production pathways). Figure 8 provides more insight on the differences of the two scenarios concerning the usage of petrol substitutes (indicative years 2010, 2020, 2030). In the low effort scenario, bioethanol and ETBE together add up to 7% in 2020 and 10% in 2030. High effort scenario utilizes only bioethanol (7% in 2020 and 10% in 2030).

The assumption made for ETBE is that the 2010 statistical fuel consumption value (1.8Mtoe)⁹ has been used in all years. A parameter that has also been taken into account is that the limit of max oxygen content in petrol 3.7% (mass) has not been exceeded (i.e., E10 vol. is equivalent to ETBE22). The reason for not considering further ETBE in the high effort scenario is that because, according to the JEC study, overall, using ethanol as ETBE would not result in substantial GHG savings (only marginal differences compared to using ethanol as such).

⁹ http://www.iea-amf.org/content/fuel_information/ethanol/ethers

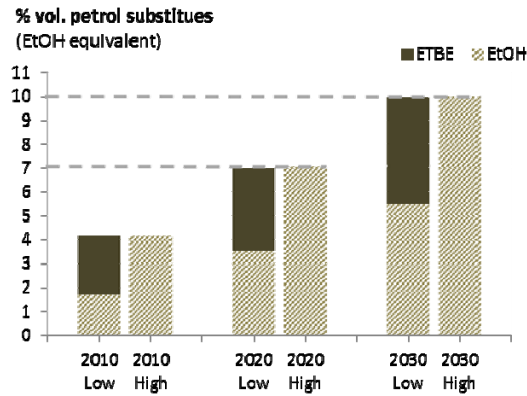


Figure 8: Comparison of low/high effort fuel scenarios in petrol substitutes

Table 2 shows the sharing (%) of each production pathway (feedstock) of petrol substitutes. Specifically, low effort scenario assumes bioethanol from food crops (similar to current situation); high-effort scenario assumes increase in sugar cane imports (a pathway with less CO₂ according to JEC study) and in non-food feedstock (farm/waste wood). Both scenarios fully respect feedstock availability (supply chains) from the EU Auto-Fuel biofuel roadmap.

Table 2: Feedstock comparison in the two fuel scenarios for petrol

Bio-EtOH	Low Effort	High Effort
Sugar beet	30%	30%
Wheat	25%	16%
Barley/rye grain	11%	11%
Corn (maize)	20%	11%
Braz. sugar cane	14%	24%
Farm/waste wood	0%	8%
Bio-ETBE	Low Effort	High Effort
Wheat ethanol and isobutene	100%	-

The increase in sugar cane imports and in non-food feedstock for bioethanol in high effort scenario decreases WtW CO₂ (weighted average of pathways used). This WtW improvement is due to the upstream part (less CO₂ for the production of bioethanol e.g. from wood). Figure 9 summarizes the positive impact of high effort fuel scenario on CO₂. It is obvious that from 2020 (and until 2030) the CO₂ of petrol substitutes (weighted average of pathways used based on fuel consumption) is significantly lower compared to the low effort scenario.

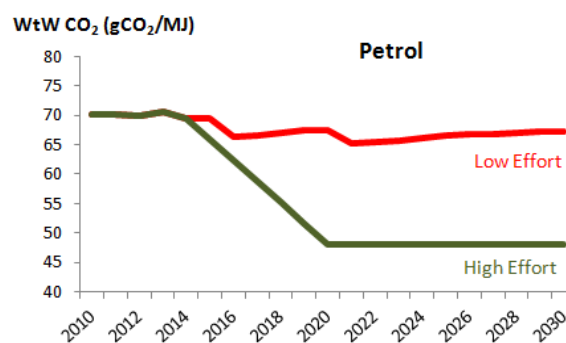


Figure 9: Impact of high effort scenario petrol fuel substitute pathways on CO₂

Electricity and hydrogen carbon intensity

For electricity production, low effort fuel scenario assumes 100% usage of the pathway named as 'EU electricity mix low voltage' in JEC study (current situation). This pathway already utilizes some renewable sources (hydro, wind, waste, other) with 11.7% sharing among all primary energy sources.

The policy targets set for electricity (to be met with the high effort scenario) are the following:

- ~20% share of RES in 2020,
- ~27% share of RES in 2030,
- no change in relative contribution of other pathways.

In order to meet the above targets, the sharing of EU electricity mix pathway has been decreased from 100% to 90% in 2020 and to 82% in 2030, and the remaining percentages have been allocated to other renewable pathways of the JEC study (biogas, wood, wind). Hence, the share of RES in 2020 is $90\% \cdot 11.7\% + 10\% = 20.5\%$, and share of RES in 2030 is $82\% \cdot 11.7\% + 18\% = 27.6\%$, in accordance with the policy targets. The changes applied in the high effort scenario decrease WtW CO₂ (weighted average of production pathways used). This WtW improvement is due to the upstream part (less CO₂ for the production of electricity from biogas, wood, wind) (Figure 10, left).

Regarding hydrogen, it is currently produced mainly from natural gas reforming (thermal process); this pathway is used 100% in the low effort scenario. Renewable pathways are introduced in high effort scenario (via electrolysis and thermal processes) with a sharing percentage 20% (thus, decreasing natural gas reforming to 80%). This change is applied in the high effort scenario gradually from 2015 to 2030 and decreases WtW CO₂ (weighted average of production pathways used). This WtW improvement is due to the upstream part (less CO₂ for the production of hydrogen from wood, electricity-wind) (Figure 10, right).

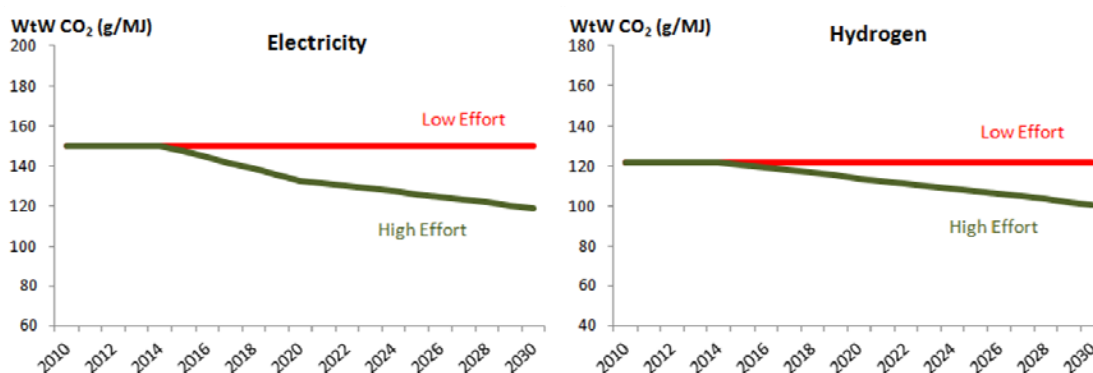


Figure 10: Impact of high effort scenario electricity (left) and hydrogen (right) production pathways on CO₂

RES in view of policy requirements

Both fuel scenarios have been created respecting policy targets for renewable energy sources; this is depicted in Figure 11. The main policy requirements are the following¹⁰:

- ILUC caps first generation biofuels to 7% of transport energy consumption, earliest in 2020.
- ILUC calls for indicative 0.5% advanced biofuels by 2020.
- The renewable directive requires 10% of transport energy in renewables by 2020.

Especially the high effort scenario assumes small, but significant, penetration of non-food crops, beyond moderate expectations at 0.5% in 2020. It is noted that, according to the legislation for 2020, biofuels from waste cooking oil, tallow oil, and wood are double counted (x2), and renewable electricity in electric vehicles counted five times (x5). This multiple counting does not apply in 2030, since there are no targets set yet.

¹⁰ <http://www.biofuelstp.eu/biofuels-legislation.html>

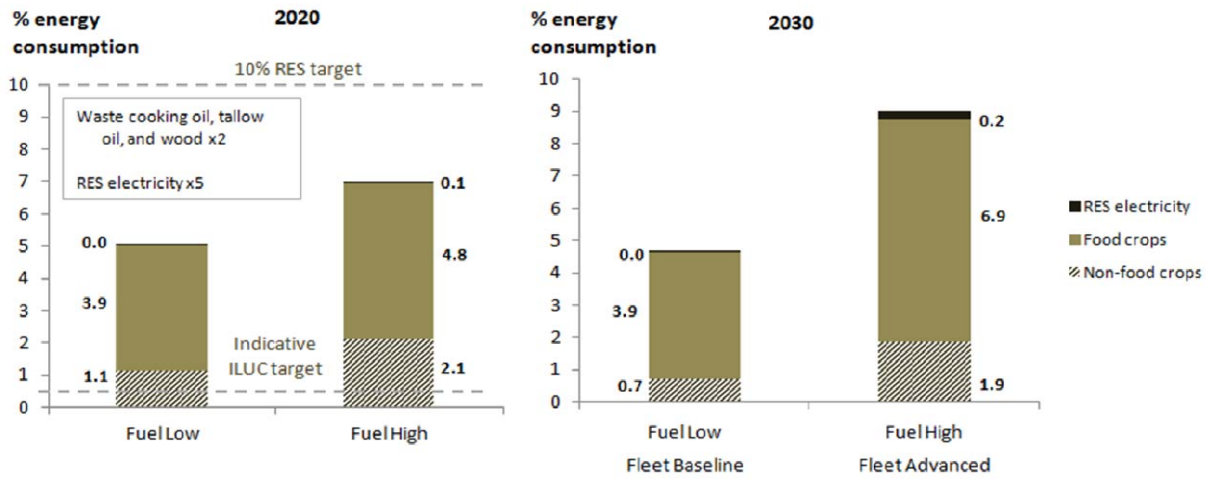


Figure 11: Renewable energy sources used in the two fuel scenarios (2020 and 2030)

ICT/ITS measures

The methodology to assess the impact of ICT/ITS on CO₂ emissions from road transport contains the following measures:

- Green navigation (using historical and real-time traffic information) (GN).
- Adaptive cruise control (ACC).
- Urban traffic control (UTC).
- Variable speed limits (VSL).

For each measure, the optimum CO₂ emissions reduction potential (from the ICT-Emissions project) is adopted and an application level is assigned. The proposed methodology takes into account road type (urban and highway – ICT measures are not applied on rural roads), traffic conditions (peak and off-peak), activity, and different vehicle categories and technologies. The above measures are shortly described below.

Green navigation: A satellite navigation system assigns position to a vehicle on the road and by using the road database it gives directions to other locations along roads in its database. Fuel consumption can be decreased since green navigation avoids extra mileage due to mistakes in the route followed to the destination. Also, the route calculation includes some parameters (shortest distance, fastest road) that can result in fuel savings compared to the route followed without the navigation system. There is a positive impact on traffic distribution, since vehicles with this system on board are guided in less congested routes or better green/eco routes. The combination of historical data (collected from the infrastructure or from the vehicle fleet) with real-time information (e.g. traffic congestion, road works, accidents) can provide optimum results by calculating the best route to reach the destination with the lowest possible fuel consumption. Intelligent parking is an add-on of green navigation and it saves time and fuel by providing available parking slots through the system.

This measure can be applied on both urban and highway road network and should be combined with other measures in order to avoid negative effects in urban areas. Benefits at congested network are substantially larger than at normal and free flow network. However, benefits at a congested road network do not change above a certain penetration level, i.e. maximum benefits (~6% CO₂ reduction) are reached already at 50% penetration level. This is because no further optimization is possible in a congested network above a certain level.

Adaptive cruise control: Systems supporting the driver in the longitudinal control of the vehicle have a positive impact on fuel consumption. The simplest system, cruise control, keeps a constant vehicle speed and reduces CO₂ emissions by avoiding unnecessary speed changes that produce extra fuel consumption. The system can also take into consideration the road geometry and speed limits. Furthermore, if the vehicle is equipped with speed radars, the system can detect the speed of the vehicle in front. In general, an adaptive cruise control system is able to manage the vehicle speed only above a certain threshold. However, more sophisticated systems are capable of managing

situations with very slow or even stopped traffic (ACC + Stop&Go). The parameters affected by an ACC system are the traffic composition, driving dynamics, and average speed. An increased proportion of vehicles equipped with ACC can lead to higher average speed on a transport network. Since the reaction time of an adaptive cruise controller is usually much lower than the reaction time of humans, the safe distances between vehicles can be decreased. A higher average speed is beneficial for the reduction of CO₂ especially in urban road networks.

This measure is applicable on urban and extra-urban networks, as well as on motorways. However, the impact of the measure depends on the share of the on-road vehicles equipped with ACC, since such vehicles affect their surrounding traffic. In general, the ACC can have a major impact on highways where the rate of acceleration largely determines CO₂ emissions (8.9% CO₂ reduction can be achieved in this case). On the other hand, it is less effective on urban road network, since vehicles in the city often have to stop at crossroads and re-accelerate again.

Urban traffic control: This measure includes all infrastructure based systems that are able to measure the level of traffic on a road network, thus, enabling the management or control of traffic in order to optimise the use of the available road capacity. It works by regularizing the movement of vehicles in order to save energy, reduce emissions, and increase safety. For example, traffic light management using traffic sensors can avoid traffic stopped at one way while there is no traffic in the other way. By taking into account speed limits, traffic lights can assist cars in always finding green at the intersections. As a result, the available road capacity is optimized. This measure is applicable on urban road network. The traffic adaptive urban traffic control is the most complex system, but also the most effective one. It can be used in any condition of traffic and it can respond quickly to critical traffic situations. This type of system uses adaptive algorithms to define the best policy of traffic light management, based on the traffic data collected by sensors at intersection, data received by the intersections surroundings, and policies set by the centre. Optimization algorithms are based on traffic patterns; in other words, the knowledge of the network is embedded in the system and it can be used to change the optimization objectives (delay, number of stops, eco-friendly policies).

The fleet structure is important in urban traffic control because the effect of traffic conditions on emissions depends on vehicle technology. Vehicles of the latest technology are more efficient because most of them are equipped with start and stop systems; hence, the impact of stop time on average CO₂ emissions is overall lower. Generally, the UTC can lead to CO₂ reduction of 4.5% up to 8% based on the traffic level. In any case, hybrid and electrified vehicles may show different performance when modifying traffic conditions. This is due to their technology that offers the potential to optimize between different driving modes and take advantage of the possibility to use either the electric motor or the internal combustion engine.

Variable speed limits: Variable (also called dynamic) speed limits use real traffic-flow and weather information to dynamically change the posted speed limit. This measure consists of dynamic message signs deployed along a roadway and connected via a communication system to a traffic management centre. The driver remains responsible for maintaining a safe and proper speed as the system gives only information and warnings, but does not intervene with his behaviour. Variable speed limits can be voluntary or mandatory. The main parameters affected are the average speed, traffic flow, and driving dynamics. Changes in vehicle speeds can have a direct impact on the level of emissions. This measure can be applied on highways and extra-urban networks; significant CO₂ savings are noticed in case of congested traffic (1.6% CO₂ reduction). The impact of this measure on CO₂ emissions is the same regardless of the vehicle technology.

ICT scenarios methodology

The methodology followed to assess the impact of ICT measures on CO₂ emissions results in the creation of two ICT scenarios (low and high effort), combining CO₂ benefits (from the ICT-Emissions project) with real world emission data (from SIBYL). There are four parameters that have been taken into account: the road type (urban/highway), the traffic level (congested and normal flow), the activity (fleet composition and mileage), and the application level (Figure 12). The scenario formation includes combination of ICT measures with minimum and maximum impact on CO₂ emissions (for the low and high effort scenario, respectively). The definitions of the parameters that have been taken into account in the methodology are given next.

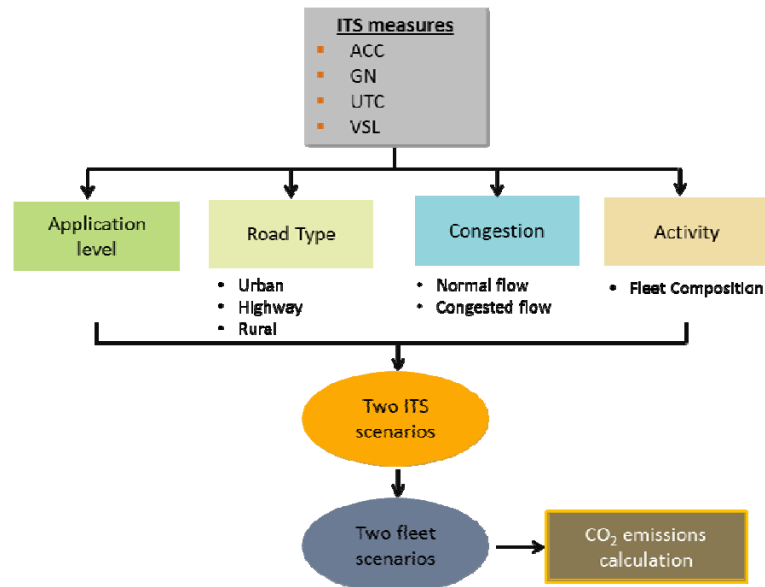


Figure 12: Flowchart of the main methodological components for the ICT scenarios

Road type: The road network is distinguished in three categories:

- Urban,
- Urban-highway,
- Highway.

Urban highways constitute a 20% of the total number of highways (SIBYL data).

Traffic congestion level: The impact of an ICT measure varies according to the traffic level, that is, the number of vehicles running on the roads. Traffic level is distinguished into:

- Peak case (congested traffic),
- Off-peak case (normal flow).

The distinction between peak and off-peak hours was based on the car distribution on all roads by time of the day in Great Britain¹¹ for the period 2006-2013. According to this, 'peak times' are 7-9 am / 4-6 pm on weekdays, and 11-1 am / 4-6 pm on weekends. 'Off-peak times' are all the remaining time slots. It is found that 32% of the vehicle activity occurs during peak times and 68% during off-peak times. This percentage allocation of the vehicle activity remains the same for years 2008-2013.

Activity and fleet composition: Fuel consumption varies according to the type of vehicle, its characteristics, and optionally installed devices. Depending on the ICT measure, the selected type of vehicles can potentially change the results. Hence, it is important to define the fleet composition as:

- Low effort scenario: passenger cars and light commercial vehicles.
- High effort scenario: passenger cars, light commercial vehicles, and buses for the urban network, and passenger cars and light commercial vehicles for the highway network.

The fleet number for the different vehicle categories and the activity of each category (defined according to the road type and traffic level) are obtained from SIBYL.

Combined CO₂ benefit: Initially, the maximum CO₂ benefit at the optimum penetration rate is identified (from the ICT-Emissions project). The optimum penetration rate has high impact with moderate intervention. A combination factor of 70% of the optimum CO₂ benefit is applied when two or more ICT measures are combined to calculate the total combined CO₂ benefit.

Application level: A linearly increasing application level for years 2015-2030 is assigned to both scenarios in order to assess their impact on a yearly basis (Figure 13). A starting level of 10% is assigned to 2015, 30% to 2020, and 70% to 2030. Linear increase is followed for the intermediate

¹¹ <https://www.gov.uk/government/statistical-data-sets/tra03-motor-vehicle-flow#table-tra0308>

years. No specific policy targets are utilized; this linear application level is an estimate of what could be the implementation of the ICT measures to the European traffic activity with time.

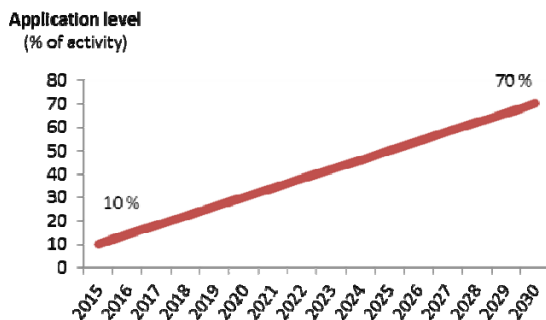


Figure 13: Application level of the ICT scenarios

Table 3 provides an overview of the methodology for the creation of the two scenarios. All four ICT measures are included, as well as the parameters that have been considered. The CO₂ benefit in this table is from the ICT-Emissions project and it is provided as a function of penetration rate.

Table 3: Overview of ICT methodology and CO₂ benefit for different penetration rates

ICT Measures	Road Type & Congestion	Road Type			Split of Highways	Congestion share		Activity	CO ₂ benefit as a function of Penetration rate				
		Urban	Rural	Highway		Peak	Off Peak		10%	25%	50%	75%	90%
Green Nav.	Urban Peak	40%			20%	32%		40% * 32% * vkm	2.0%	4.6%	6.0%	6.1%	5.9%
	Urban Off-Peak					68%		40% * 68% * vkm	1.1%	2.0%	2.4%	2.5%	2.9%
	Urban-Highway Peak		35%	20%	32%		35% * 32% * 20% * vkm	2.0%	4.5%	6.0%	6.1%	5.9%	
	Urban-Highway Off-Peak	68%				35% * 68% * 20% * vkm	1.1%	2.0%	2.4%	2.5%	2.9%		
	Highway Off-Peak			80%		68%		35% * 68% * 80% * vkm	1.1%	2.0%	2.4%	2.5%	2.9%
	Rural		25%					25% * vkm					
ACC	Urban Peak	40%			20%	32%		40% * 32% * vkm	0.8%	0.8%	1.1%	1.4%	1.5%
	Urban Off-Peak					68%		40% * 68% * vkm	0.3%	0.8%	1.4%	1.6%	2.1%
	Urban-Highway Peak		35%	20%	32%		35% * 32% * 20% * vkm	1.5%	2.9%	4.5%	6.3%	7.4%	
	Urban-Highway Off-Peak	68%				35% * 68% * 20% * vkm	1.5%	3.4%	5.3%	6.5%	8.5%		
	Highway Off-Peak			80%		68%		35% * 68% * 80% * vkm	1.5%	3.4%	5.3%	6.5%	8.5%
	Rural		25%					25% * vkm					
UTC	Urban Peak	40%			20%	32%		40% * 32% * vkm	4.5%				
	Urban Off-Peak					68%		40% * 68% * vkm	8.0%				
	Urban-Highway Peak		35%	20%	32%		35% * 32% * 20% * vkm	-					
	Urban-Highway Off-Peak	68%				35% * 68% * 20% * vkm	-						
	Highway Off-Peak			80%		68%		35% * 68% * 80% * vkm	-				
	Rural		25%					25% * vkm	-				
VSL	Urban Peak	40%			20%	32%		40% * 32% * vkm	-				
	Urban Off-Peak					68%		40% * 68% * vkm	-				
	Urban-Highway Peak		35%	20%	32%		35% * 32% * 20% * vkm	1.6%					
	Urban-Highway Off-Peak	68%				35% * 68% * 20% * vkm	1.5%						
	Highway Off-Peak			80%		68%		35% * 68% * 80% * vkm	1.5%				
	Rural		25%					25% * vkm	-				

ICT low effort scenario

The measures considered in this scenario are Green Navigation and Variable Speed Limits. Vehicle fleet involves passenger cars and light commercial vehicles. The combinations of road types and traffic levels are the following:

- Urban peak,
- Urban off-peak,
- Urban-highway peak,
- Urban-highway off-peak,
- Highway off-peak.

Table 4 summarizes the description of the ICT low effort scenario, while Table 5 provides an overview of the methodological process. The first step is the identification of the different cases that this scenario applies to; this involves definition of the road type, the traffic level, and the fleet composition. The maximum CO₂ benefit at the optimum penetration rate is also identified and the combination factor of 70% is applied when the two ICT measures are combined. An application level starting from 10% in 2015 and linearly increasing up to 70% in 2030 is assigned.

Table 4: ICT measures considered per vehicle category and road type in low effort scenario

Type	Condition	GN	ACC	VSL	UTC
Vehicle	PC 	✓	✗	✓	✗
	LCV 	✓	✗	✓	✗
	Urban Bus 		✗		✗
Road	Urban	✓	✗		✗
	Motorway/ Urban Highway	✓	✗	✓	

Table 5: Overview of methodological process for the low effort ICT scenario

				Benefit at optimum penetration rate		Combination factor	Combined CO ₂ benefit	Application level
Road Type & Congestion	Split of Highways	Congestion share	Green Nav	VSL				
A Min Effort	Urban Peak		32%	6.1%	-	-	6.1%	10%-70%
	Urban Off-Peak		68%	2.9%	-	-	2.9%	
	Urban-Highway Peak	20%	32%	6.1%	1.6%	70%	5.4%	
	Urban-Highway Off-Peak		68%	2.9%	1.5%	70%	3.1%	
	Highway Off-Peak	80%		2.9%	1.5%	70%	3.1%	

The CO₂ emissions (obtained from SIBYL) for each vehicle category and for each road type are combined with the above methodological steps in order to calculate the CO₂ benefit as follows:

$$\text{CO}_2 \text{ benefit (ICT measures)} = \text{CO}_2 \text{ emissions (urban/highway Sibil)} \times \text{Split of highways (where applicable)} \times \text{Traffic level (congestion share)} \times \text{Combined CO}_2 \text{ benefit} \times \text{Application level}$$

ICT high effort scenario

The measures considered in this scenario are Green Navigation, Variable Speed Limits, Urban Traffic Control, and Adaptive Cruise Control (combined where applicable). The combinations of road types and traffic levels considered are the same as in the low effort scenario. The vehicle fleet is different for urban and highway road networks. Specifically:

- Urban road types: PCs (conventional, hybrids, electrified), LCVs, buses.
- Highway road types: PCs (conventional, hybrids, electrified), LCVs.

Table 6 summarizes the description of the ICT high effort scenario, while Table 7 provides an overview of the methodological process which, in general, is similar to the low effort scenario. The main difference is that in this high effort scenario there is a classification of passenger cars into conventional, hybrid, and electrified ones (due to their different performance that has a direct impact on the UTC measure and the CO₂ benefit). The UTC CO₂ benefit from hybrid passenger cars is increased by 20% and from electrified by 6% compared to conventional ones. The UTC impact from buses and LCVs is similar to that of conventional cars. The CO₂ benefit is calculated in a similar fashion to that of the low effort scenario.

Table 6: ICT measures considered per vehicle category and road type in high effort scenario

Type	Condition	GN	ACC	VSL	UTC
Vehicle	PC 	✓	✓	✓	✓
	LCV 	✓	✓	✓	✓
	Urban Bus 		✗		✓
Road	Urban	✓	✓		✓
	Motorway/ Urban Highway	✓	✓	✓	

Table 7: Overview of methodological process for the high effort ICT scenario

Road Type & Congestion		Split of Highways	Congestion share	Benefit at optimum penetration rate (%)						Combination factor
				Green Nav	VSL	UTC			ACC	
						Conventional PCs, Buses, LCVs	Hybrid PCs	Electrified PCs		
B Max Effort	Urban Peak		32%	6.1%	-	4.5%	5.4%	4.8%	1.5%	70%
	Urban Off-Peak		68%	2.9%	-	8.0%	9.7%	8.5%	2.1%	70%
	Urban-Highway Peak	20%	32%	6.1%	1.6%	-	-	-	7.4%	70%
	Urban-Highway Off-Peak		68%	2.9%	1.5%	-	-	-	8.9%	70%
	Highway Off-Peak	80%	68%	2.9%	1.5%	-	-	-	8.9%	70%
	Combined CO2 benefit									
					Conventional PCs	Hybrid PCs	Electrified PCs	Buses	LCVs	Application level
					8.5%	9.1%	8.7%	4.5%	8.5%	10%-70%
					9.1%	10.3%	9.4%	8.0%	9.1%	
					10.6%	10.6%	10.6%		10.6%	
					9.3%	9.3%	9.3%		9.3%	
					9.3%	9.3%	9.3%		9.3%	

Vehicle technology measures

The two fuel and the two ICT scenarios described above are applied on two fleet projections which have been implemented in SIBYL and are based on activity and energy evolution to 2030, as agreed in high level EU policy related studies. In general, baseline fleet assumes normal fleet renewal and efficiency improvement, while advanced fleet benefits from higher penetration of electrified vehicles and higher efficiency improvements. The main characteristics of each fleet are summarized below.

- *Baseline fleet:* Business-as-usual fleet, consistent with current legislation (2021 target of 95 g CO₂/km in type approval for passenger cars and 147 g CO₂/km for light commercial vehicles). Normal fleet renewal with moderate sales of electrified vehicles (PHEV, BEV, FCEV).
- *Advanced fleet:* For passenger cars and light commercial vehicles, same as baseline fleet until 2020, but then very high penetration of electrified vehicles (especially PHEV and, secondarily, BEV) and higher efficiency improvements. For heavy duty vehicles, higher efficiency improvements already from the present time based on Ricardo-AEA (2011) study scenarios.

2. Results

Baseline scenario

The baseline scenario is considered a ‘business-as-usual’ case with low technical effort requirements; nevertheless, it does meet policy targets (e.g. for biofuels use, renewable energy sources, type approval CO₂). It consists of the following methodological components:

Baseline scenario = Baseline fleet + Low effort in fuels + No ICT measures

The main technological developments expected from 2010 to 2030 include:

- A gradual increase of the stock of diesel cars and a significant decrease of petrol ones.
- More than doubling the number of alternative fuelled vehicles.
- Limited changes to the number of LCVs and HDVs.

However, despite the expected increase in total fleet, a significant decrease in total energy consumption is projected (Figure 14).

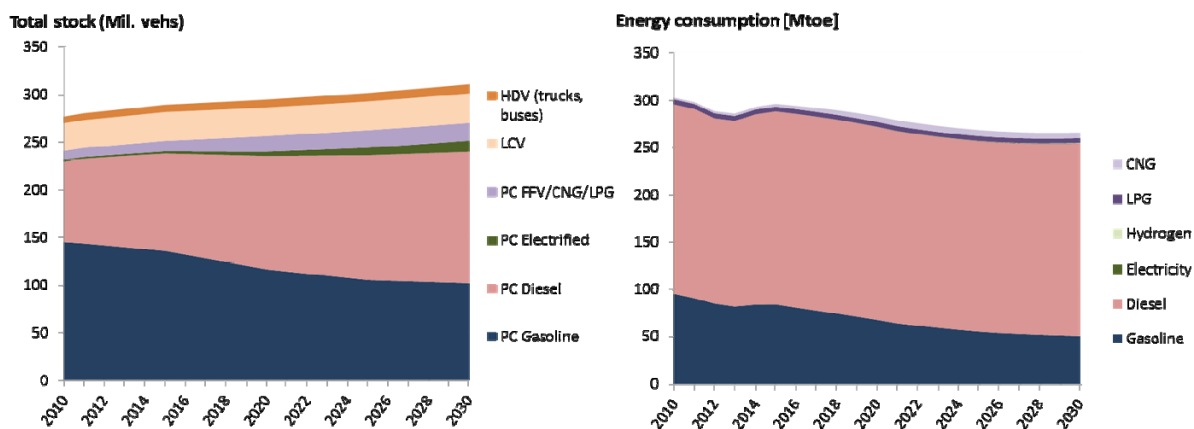


Figure 14. Description of baseline scenario (total vehicle stock and energy consumption)

Total WtW CO₂ reduction and relative contribution of measures

In Figure 15 the total WtW CO₂ reduction that can be achieved with the baseline scenario (-13.1% from 2010 to 2030) is presented. It is obvious from this figure that significant reduction in CO₂ is already achieved in the business-as-usual case, that is, with low effort technological measures (e.g. normal fleet renewal and efficiency improvement) and usage of biofuels according to policy requirements (B7 for diesel and E10 for petrol). However, the -17% indicative target for 2030 (Framework for Climate and Energy Policies) cannot be reached with baseline developments only.

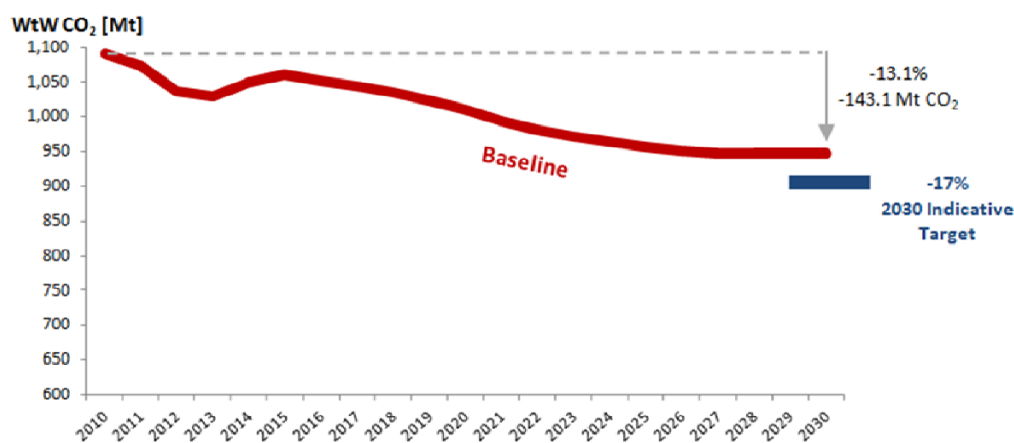


Figure 15. Total WtW CO₂ reduction achieved with baseline scenario

Figure 16 presents total WtW CO₂ reduction potential (%) from 2010 to 2030 for all possible scenario combinations (2 fleet x 2 fuel x 2 ICT = 8 combinations). It is obvious from this figure that the 2030 indicative target can only be met with additional efforts in fuels and ICT measures (Sc. 4: Fleet Baseline, Fuel High, ICT High → -18.6% CO₂ reduction over 2010). Maximum benefit in 2030 can be achieved with the combination of advanced vehicle technology measures and high efforts in fuels and ICT (Sc. 8: Fleet Advanced, Fuel High, ICT High → -25.2% CO₂ reduction over 2010).

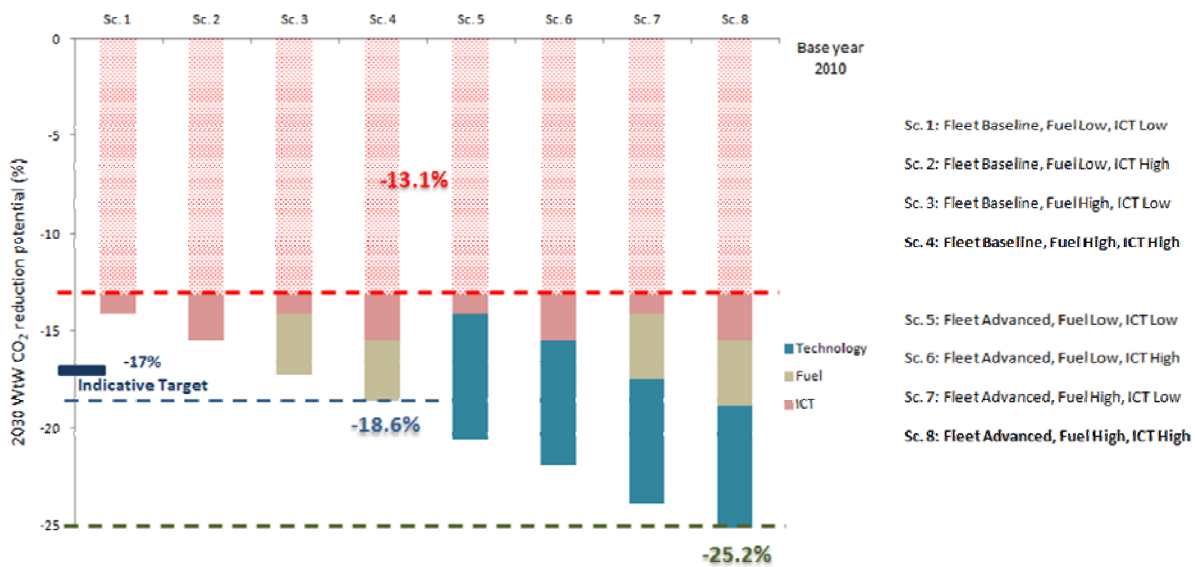


Figure 16. Total CO₂ benefits from all scenario combinations

Figure 17 shows the contribution of different measures in meeting maximum CO₂ reductions in 2030. In general, reductions are split almost equally between vehicle technology (53%) and other (fuel and ICT) measures (47%). Among vehicle technology measures, PC electrification is the single most important contributor with 41%, while the remaining 59% is split to efficiency improvement of PCs, LCVs, and HDVs. Regarding fuel measures, diesel substitutes (biodiesel, HVO, and FT) constitute the most important contributor with 82.3%, followed by electricity (9.4%) and bioethanol (7.6%). The relatively high percentage of electricity is due to the increased number of electrified vehicles in the new car sales of advanced fleet.

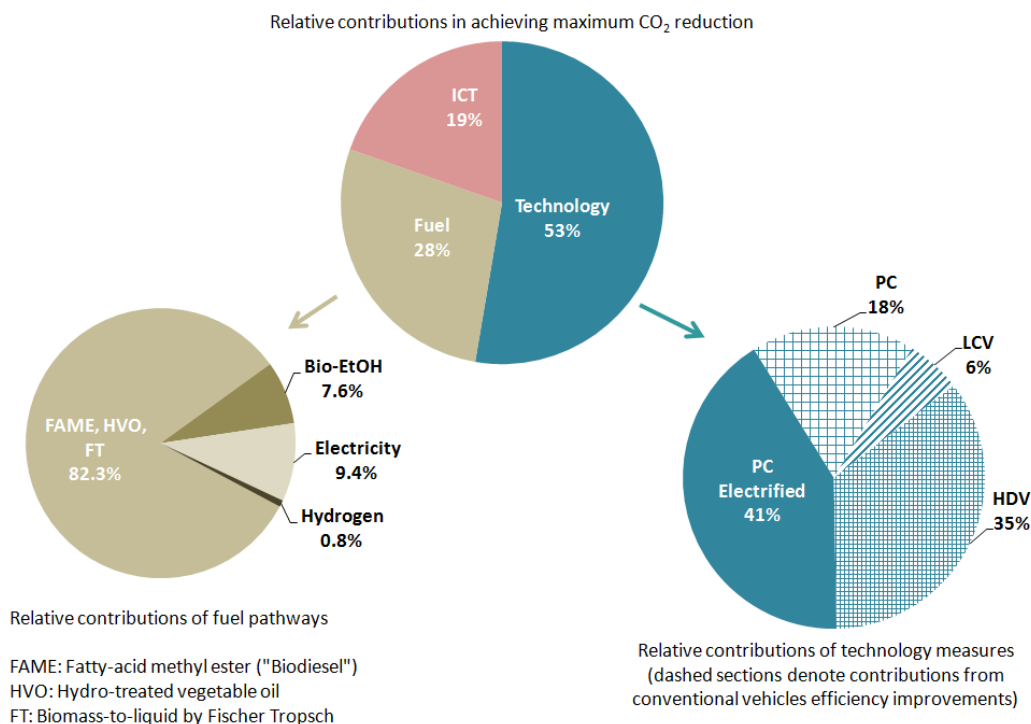


Figure 17. Relative contributions in achieving maximum CO₂ reduction from 2010 to 2030

Impact of fleet on TtW (downstream) CO₂

Figure 18 shows the impact of advanced vehicle technology measures (advanced fleet projection) on TtW (downstream) CO₂ compared to the baseline case (both fleet projections in this figure are

combined with high effort fuel and ICT scenario). It is noted that fuel pathways little contribute to downstream CO₂ differentiation; hence, the TtW part of CO₂ is almost independent of the fuel scenario to be used. The individual impact of ICT on TtW CO₂ is independently discussed later. As observed in this figure, advanced vehicle technology measures (PC electrification and efficiency improvement in all vehicle categories) lead to significant TtW CO₂ benefits.

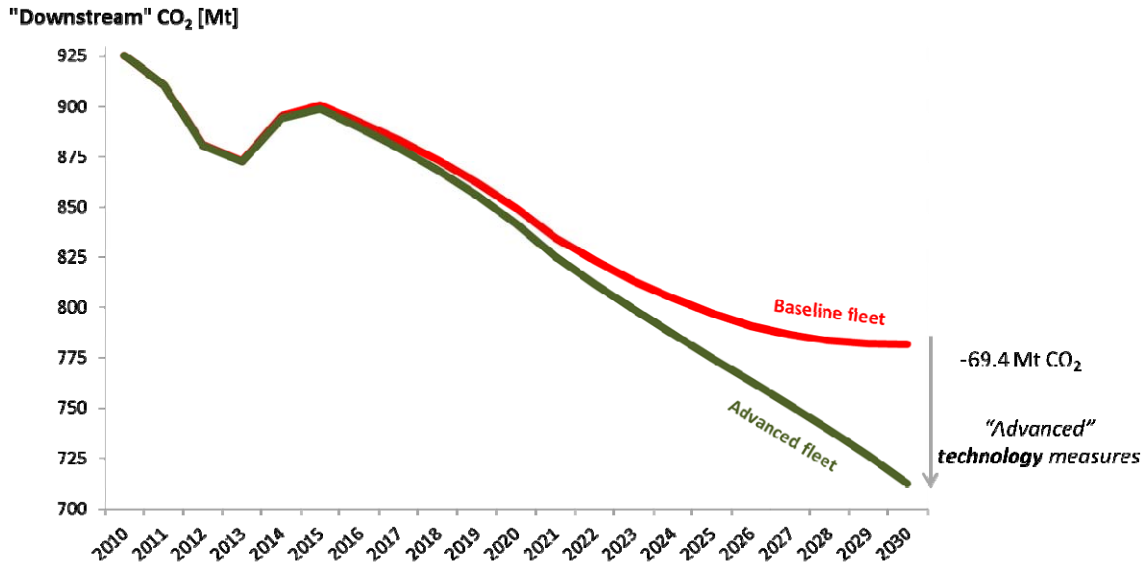


Figure 18. Impact of advanced vehicle technology measures on TtW (downstream) CO₂

Impact of fuels on WtT (upstream) CO₂

Figure 19 shows the impact of advanced fuel measures (high effort scenario) on WtT (upstream) CO₂. In general, WtT CO₂ emissions are approximately 15-20% of TtW ones, depending on scenario (fuel scenarios in Figure 19 are applied on baseline fleet with high ICT). It is observed from this figure that the change in WtT CO₂ over time is insignificant in low effort scenario (mild PC electrification actually leads to increased WtT emissions). High effort scenario on the other hand, with advanced fuels and improved production pathways, leads to substantial reductions (2030 over 2010).

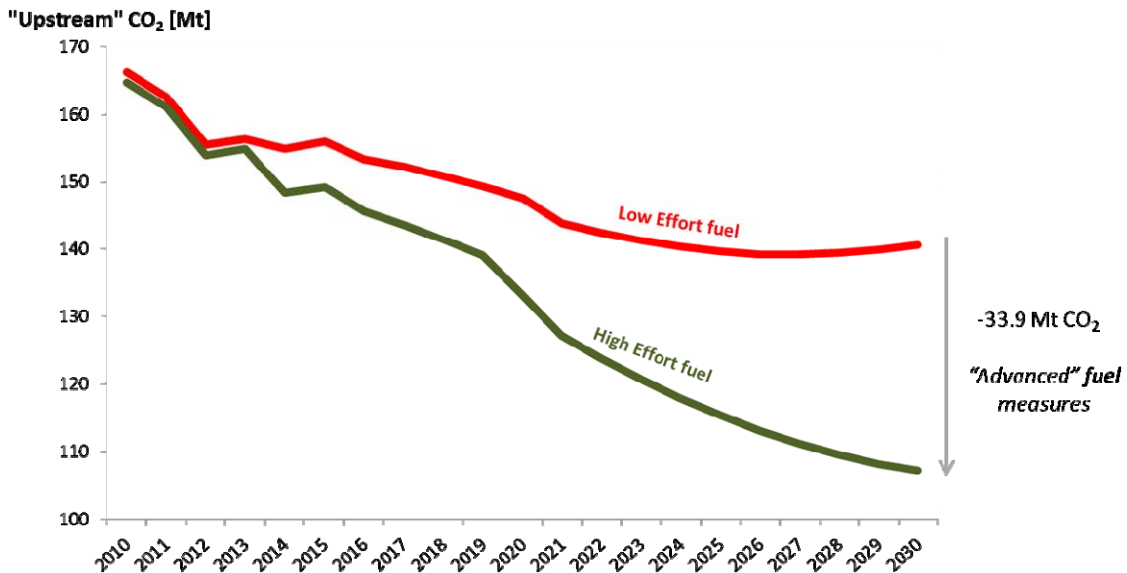


Figure 19. Impact of advanced fuel measures on WtT (upstream) CO₂

Impact of ICT on TtW (downstream) CO₂

Assessment of low effort ICT scenario

Figure 20 (left) shows the impact of ICT measures (low effort scenario) on TtW CO₂ (% savings for years 2015, 2020, 2025, 2030). As observed, there is a continuous increase in the percentage of CO₂ savings, starting from 0.2% in 2015 and reaching 1.2% in 2030. The latter is split to 0.9% savings from passenger cars and 0.3% from light commercial vehicles. A general remark is that even with the low effort scenario, measurable CO₂ savings can be achieved. It is noted that ICT measures present very limited differences for the two fleet configurations (baseline/advanced). The right part of Figure 20 shows the relative contribution of measures in achieving these CO₂ savings in 2030. Most of the benefit is due to green navigation (73%), while the variable speed limits contribute with 27%.

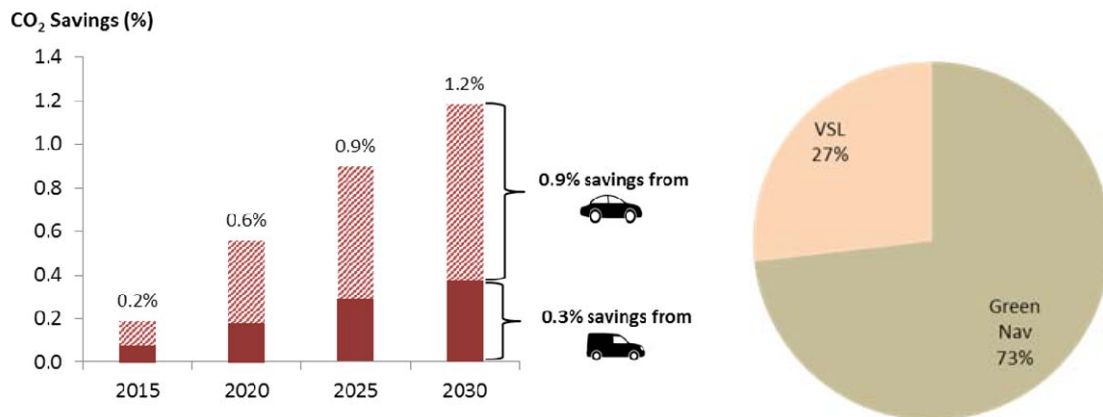


Figure 20: Savings achieved in TtW CO₂ emissions from low effort ICT scenario (left) and relative contribution of measures in achieving these savings in 2030 (right)

Assessment of high effort ICT scenario

Figure 21 (left) shows the impact of ICT measures (high effort scenario) on TtW CO₂ (% savings for indicative years 2015, 2020, 2025, 2030). It is observed that there is again a continuous increase in the percentage of CO₂ savings, starting from 0.5% in 2015 and reaching 2.9% in 2030. These savings are significantly higher than the corresponding ones in the low effort scenario. The 2.9% in 2030 is split to 2.2% savings from passenger cars, 0.6% from light commercial vehicles, and 0.1% from buses. In general, significant CO₂ savings can be achieved from full implementation of ICT measures. The right part of Figure 21 shows the relative contribution of measures in achieving these CO₂ savings in 2030. Most of the benefit is due to urban traffic control (37%), followed by adaptive cruise control (32%), green navigation (23%), and variable speed limits (8%).

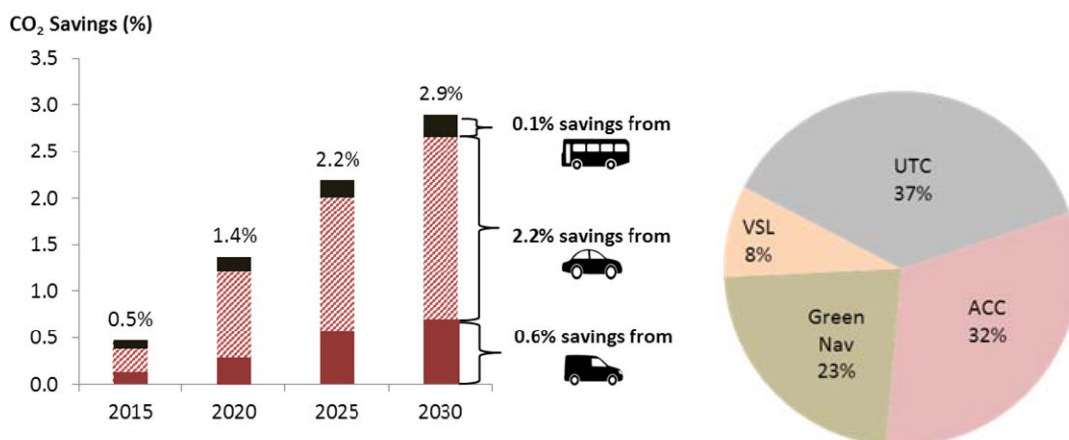


Figure 21: Savings achieved in TtW CO₂ emissions from high effort ICT scenario (left) and relative contribution of measures in achieving these savings in 2030 (right)

3. Discussion on NO_x

Although the focus of the study is on CO₂, the impact of the developed scenarios on air pollutants should not be ignored in any case. As an example of how the current work can be extended, a discussion for NO_x is provided below. Figure 22 presents the evolution of CO₂ and NO_x to 2030 (baseline scenario). An important observation is that the NO_x reduction (as a percentage) is much higher than CO₂ (-75% reduction in NO_x from 2010 to 2030 vs. -13.1% reduction in CO₂). Baseline development of NO_x with SIBYL has been assumed with conformity factor=1.5x for Euro6 RDE.

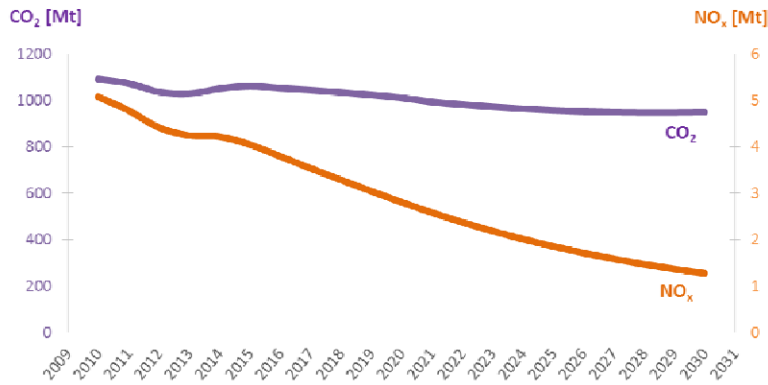


Figure 22. CO₂ and NO_x evolution to 2030 (baseline scenario)

Figure 23 compares the advanced vehicle technology measures with an accelerated replacement scheme (implemented in SIBYL assuming that all conventional vehicles >15 years old are replaced in 2020/21). The figure shows the additional NO_x and CO₂ reductions (as a percentage) that can be achieved in each case compared to the baseline scenario. In addition to CO₂ benefits, which have been analytically discussed earlier, advanced fleet also offers some reductions in NO_x compared to the baseline; this is mostly due to the PHEV introduction which proportionally replace gasoline and diesel vehicles in new car sales. The accelerated replacement scheme on the other hand serves short term rather than long term CO₂ targets; this is reflected by the decrease in corresponding CO₂ percentages from 2020 to 2025 to 2030. Compared to advanced fleet, CO₂ savings achieved in 2030 are significantly lower in the case of accelerated replacement. Regarding NO_x, the positive impact of accelerated replacement is obvious in 2020 and maximized in 2025; compared to advanced fleet, NO_x savings are significantly higher for the whole period 2020-2030, but there is some convergence in 2030 (the difference is not so big for this specific year).

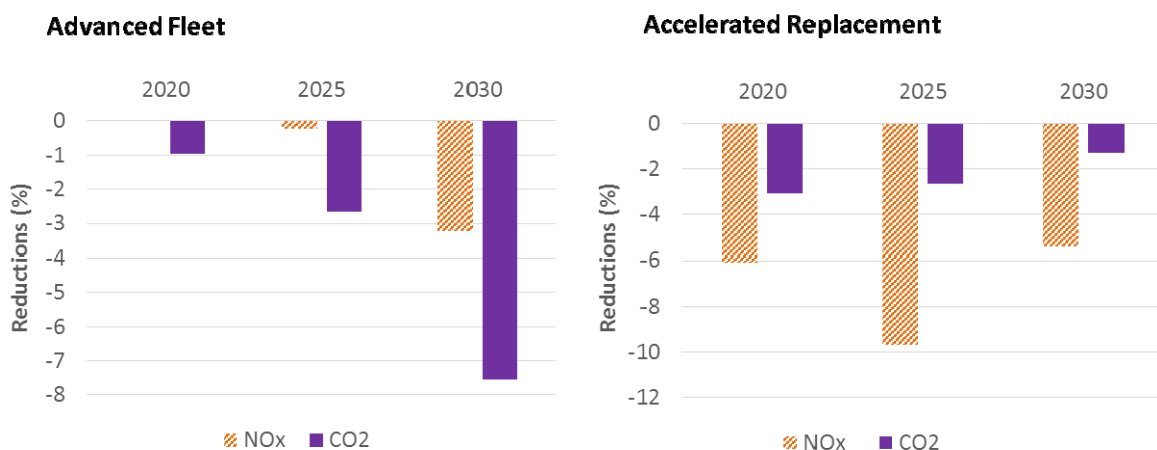


Figure 23. Additional NO_x and CO₂ reductions over the baseline (with advanced fleet and accelerated replacement)

Conclusion

This paper presented an impact assessment study of vehicle technology, fuel, and ICT measures on CO₂ evolution from road traffic to 2030. Feasibility projections of real-world total CO₂ from road transport were provided, considering: i) advanced biofuel production pathways, and ii) deployment of ICT/ITS. The main methodological components were two fuel and two ICT scenarios applied on two fleet projections. Numerical results revealed that CO₂ emissions evolution in a business-as-usual (baseline) scenario does not reach the indicative target for 2030 and, therefore, additional technical effort is required in all fronts on behalf of the automotive/fuel industry and other stakeholders. Specifically, CO₂ reductions to 2030 are projected to reach -13.1% (compared to 2010) on a fleet level in the baseline scenario, which is lower than the -17% target.

As a conclusion, reaching future CO₂ targets does not necessarily mean more advanced vehicle technology; use of more sustainable fuels or moderate ICT implementation may suffice. Additional reductions are technically possible by combinations of concentrated efforts in the introduction of advanced biofuels, accelerated deployment of ICT systems, and fleet renewal with advanced electrified vehicles. Specifically, additional reductions of -5.5% in CO₂ can be achieved by improved biofuels (e.g. drop-in fuels based on waste and tallow) and enhanced ICT measures; the latter show rather small individual potential but are directly applicable on a fleet level. Further reductions in the order of -6.6% are possible, based on technically feasible vehicle technology measures. In the present work, most of the potential of advanced vehicle technology comes from electrified PCs and improved efficiency in HDVs. By adding all the above percentages, the maximum CO₂ reductions can reach -25.2% (with advanced vehicle technology and high efforts in fuels and ICT measures).

List of abbreviations and acronyms

ACC	Adaptive Cruise Control	IIASA	International Institute for Applied Systems Analysis
BEV	Battery Electric Vehicle	ILUC	Indirect Land Use Change
CNG	Compressed Natural Gas	ITS	Intelligent Transport Systems
CO ₂	Carbon Dioxide	JEC	JRC - EUCAR - CONCAWE
ETBE	Ethyl-Tertiary-Butyl Ether	JRC	Joint Research Centre
EtOH	Ethanol	LCV	Light Commercial Vehicle
EU	European Union	LPG	Liquefied Petroleum Gas
EUCAR	European Council for Automotive R&D	NO _x	Nitrogen Oxides
FAME	Fatty Acid Methyl Ester	PC	Passenger Car
FCEV	Fuel Cell Electric Vehicle	PHEV	Plug-in Hybrid Electric Vehicle
FP7	Seventh Framework Programme	RDE	Real Driving Emissions
FT	Fischer-Tropsch	RES	Renewable Energy Sources
GHG	Greenhouse Gas	TSAP	Thematic Strategy on Air Pollution
GN	Green Navigation	TtW	Tank-to-Wheel
H ₂	Hydrogen	UTC	Urban Traffic Control
HDV	Heavy Duty Vehicle	VSL	Variable Speed Limits
HVO	Hydrotreated Vegetable Oil	WtT	Well-to-Tank
ICT	Information & Communication Technologies	WtW	Well-to-Wheel

References

- E4tech (2013): A harmonised Auto-Fuel biofuel roadmap for the EU to 2030. E4tech Final Report, November 2013. Available at <http://www.e4tech.com/reports/report-1/>
- European Commission (2015): EU transport in figures – EU energy in figures. Statistical Pocketbook.
- European Environment Agency (2015): Annual European Union greenhouse gas inventory 1990-2013 and inventory report 2015. EEA Technical Report No 19/2015, 27 November 2015.
- JEC (2014): Well-to-Wheels analysis of future automotive fuels and powertrains in the European context. JRC Technical Report, EUR 26236 EN, 2014. Full set of reports and appendices of JRC-EUCAR-CONCAWE collaboration available at <http://iet.jrc.ec.europa.eu/about-jec/downloads>
- Ricardo-AEA (2011): Reduction and Testing of Greenhouse Gas (GHG) Emissions from Heavy Duty Vehicles – Lot 1: Strategy, Final Report to the EC - DG Climate Action, February 2011.

Influence of pavement management on road traffic emissions and associated costs

Luc PELLECUER***

* Département de génie de la construction, École de technologie supérieure, Montréal, Canada, H3C 1K3

** Institute for Transport Studies, University of Leeds, Leeds, UK, LS2 9JT

Email: luc.pellecuer@etsmtl.ca

Abstract

To achieve sustainable road networks, long-term social and environmental costs and benefits related to traffic emissions should be recognised and incorporated in the decision-making process of pavement management units. A new tool designed to monetize and incorporate social and environmental impacts in decision making processes was used to assess the life cycle social and environmental benefits of pavement management related to traffic emissions. A case study regarding a 1 km long section of an urban collector road located in Montréal, Canada is presented in this paper. The case study shows that pavement surface maintenance provided an estimated social and environmental benefit ranging from \$235 000 to \$5 150 000 over a 40 year analysis period, depending on the maintenance treatment applied and the discount rate used. Despite uncertainties, the results unambiguously show that benefits related to traffic emissions were significant and were the same order of magnitude as the maintenance costs. As such, they deserve to be incorporated in the life cycle assessment of pavement maintenance strategies. Preventive maintenance was also found clearly more effective than corrective maintenance to mitigate exhaust emissions.

Keys-words: road traffic emissions, pavement condition, life cycle cost analysis, environmental impacts, social impacts.

Résumé

Afin de développer de façon durable les réseaux routiers, les unités de gestion des chaussées devraient incorporer dans leur processus de prise de décision les coûts et bénéfices sociaux et environnementaux encourus sur le long terme qui sont liés aux émissions routières. Un nouvel outil, destiné à monétiser les impacts sociaux et environnementaux afin de les incorporer dans les processus de prise de décision, est utilisé dans le but d'estimer, sur le cycle de vie de la chaussée, les bénéfices sociaux et environnementaux liés aux émissions routières des stratégies d'entretien des chaussées. Cet article présente les résultats d'une étude de cas réalisée sur un tronçon d'un kilomètre d'une collectrice en milieu urbain, à Montréal, au Canada. Ces résultats montrent que l'entretien de la surface de roulement induit, sur 40 ans, des bénéfices sociaux et environnementaux d'un montant estimé compris entre 235 000 à 5 150 000 \$ selon le type d'entretien et le taux d'escompte considérés. Malgré les incertitudes liés à ces estimations, les résultats montrent de façon claire que les bénéfices liés aux émissions routières sont significatifs et du même ordre de grandeur que les coûts d'entretien. Ces bénéfices méritent donc d'être incorporés dans l'évaluation sur le cycle de vie des stratégies d'entretien des chaussées. Par ailleurs, l'entretien préventif se révèle bien plus efficace que l'entretien correctif dans la lutte aux émissions routières.

Mots-clés: émissions routières, état de la chaussée, analyse des coûts sur le cycle de vie, impacts environnementaux, impacts sociaux.

Introduction

Road traffic is recognised as a major contributor to the poor air quality in urban areas, but it also affects the environment in suburban and rural areas. The impacts of road traffic emissions on the environment and society include impacts on human welfare (Kunzli et al, 2000), buildings façades (Rabl and Spadaro, 1999), crops (van Essen, 2011), and ecosystems (Signal et al., 2007). From a sustainability perspective, those impacts are now expected to be included in the decision making process of road agencies and pavement management units.

The scope and intensity of those impacts, is significantly influenced by the pavement characteristics. Pavement surface characteristics and condition affect the power required to move

vehicles and, in turn, the associated fuel consumption. Thus, pavement surface characteristics and condition affect exhaust emissions from traffic (Gillespie and McGhee, 2007). Choosing the right pavement maintenance strategy may thus help limit emissions from traffic during the use phase of the pavement life cycle and associated social and environmental impacts. However, those impacts occurring during the use phase are often omitted by road agencies (Santero et al., 2011).

The main objective of this study was to explore and assess the influence of pavement maintenance strategies on social and environmental impacts associated with traffic emissions. This study also aimed to show that, while not including in their decision making process the cost of those impacts along with usual agency costs, pavement management units make decisions that may be unsustainable and non-optimal from society's perspective.

1. Methods

This study relied on the comparison of three different maintenance strategies and their associated social and environmental benefits. The annual social and environmental benefit of a pavement maintenance strategy was calculated as the difference between the costs associated with a “do nothing” base scenario versus the costs associated with the maintenance strategy in question. The next two sections present the tool used to assess the social and environmental costs and the characteristics of the case study, respectively.

1.1. Assessment of impacts

Using the Impact Pathway approach (Bickel et al., 2006), Pellecuer et al. (2016) explore the relationship between pavement surface condition, traffic nuisances (such as exhaust emissions), their impacts on society and the environment, and the associated costs. They developed a model supporting the incorporation of traffic nuisances in the decision making process of pavement management units. Based on that model, the Pavement Environmental Impact Model (PEIM) is the first attempt to adapt the Impact Pathway Approach to assess the emission, dispersion, and impact of traffic emissions, so that social and environmental impacts can be included in the economic models of pavement management units (Pellecuer et al., 2014a).

Figure 1 presents the schematic architecture of PEIM, designed to assign an economic value to impacts associated with noise, air pollutants, and greenhouse gases. The models underlying PEIM require 15 input variables related to the receptors affected by those emissions (population, building and ecosystems) and to the traffic, road, and climate. The study presented in this paper only considered the impacts of air pollutants (excluding greenhouse gases) on health, biodiversity, and buildings.

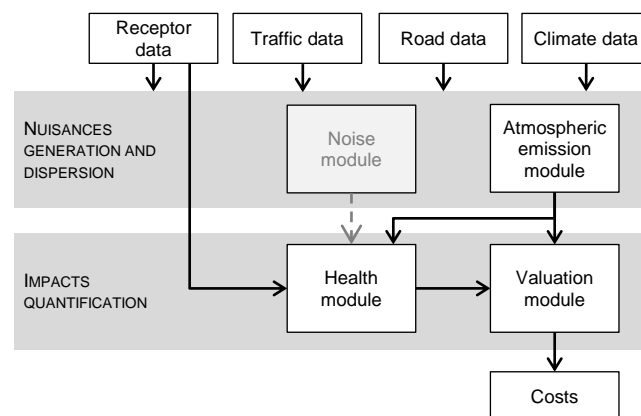


Figure 1. Schematic architecture of PEIM with solid arrows representing the links between inputs, modules and outputs and dashed arrows emphasize the link between modules and intermediate outputs (adapted from Pellecuer et al., 2014b).

The assessment of the social and environmental costs associated with air pollution was performed with PEIM. PEIM computes the fuel consumption and, based on the fuel combustion reaction, estimates the amount of particulate matter (PM10 and PM2.5), sulfur dioxide, and nitrogen oxides released into the atmosphere. Then, to compute the effects on human health, PEIM 1) estimates the concentration of PM10 and PM2.5 at receptors' locations, 2) determines the nature and severity of the impacts with concentration-response functions that provided the number of different health cases, and 3) assigns an appropriate economic value (corresponding to the treatment costs) to each health case. The health outcome considered in this study included mortality, respiratory and cardiac hospital

admission and emergency visit, restricted activity day, asthma symptom day, acute respiratory symptom day, and bronchitis.

On the other hand, to compute the cost of atmospheric emissions on biodiversity and buildings, PEIM directly applies exposure-cost functions to the estimated concentration of chemicals released into the atmosphere. The exposure-cost function for biodiversity is based on the restoration costs of the ecosystem affected by the emissions of SO₂ and NO_x from road traffic. The exposure-cost function for building impacted by particulate matter is inferred from the observed cleaning and renovation expenditures. For more details about the assessment of social and environmental impacts, the reader can refer to Pellecuer et al. (2014a).

1.2. Case study

To explore the effect of pavement management practices on traffic emissions, PEIM was used in a case study about a 1 km long section of a typical urban collector road (50 km/h speed limit) in a densely populated neighbourhood of Montréal, Canada (see Figure 2). The linear population density was 260 people/km. The road section had two traffic lanes each 3.5 m wide and two parking lanes each 2.5 m wide. The house rows were located 2 m away from the road right-of-way. The average daily traffic on this road section was 5 000 vehicle/day, with an annual growth rate of 1.3%, and it included 5% of heavy vehicles.



Figure 2. Typical section of Notre-Dame street, Montréal, Canada (source: Gene Arboit).

We performed an assessment of the life cycle social and environmental benefits of three different maintenance strategies over a base scenario consisting in letting the road surface deteriorate without any maintenance operation. Based on the Ministry of Transport of Québec (MTQ) practices, the analysis covered a period of 40 years, and all costs and benefits were discounted to present at a 6.5% rate.

The traffic supported by the pavement was assumed to be light enough to maintain the deflection of the pavement at its initial value over the analysis period. Consequently, the variation of the surface condition was supposed to be well described by the variation of its roughness only. Therefore, the pavement surface condition was described by a roughness performance index (RPI) based on a 0-100 percentage scale (0 for poorest condition and 100 for new construction).

The three alternative maintenance strategies were as follow:

- two corrective strategies (A and B), with the same maintenance treatment but with different intervention triggers, implying one and two interventions respectively; and
- one preventive strategy, characterised by a less deep maintenance treatment, implying three interventions.

Table 1 details the key characteristics of each maintenance strategy. Figure 3 shows the variations of the pavement surface condition over the analysis period for the base scenario and for the three maintenance strategies. In particular, it shows that the pavement condition deteriorated at a different deterioration rate depending on the maintenance treatment applied, which depended on the maintenance strategy adopted.

Table 1. Characteristics of maintenance strategies (Pellecuer et al., 2014b).

Scenario	Maintenance trigger level	Maintenance treatment	Treatment cost (\$/1000 m ²)	RPI improvement per treatment	RPI deterioration rate (per year)
Base	-	-	-	-	2.23
Corrective A	RPI under 33	Mill and overlay	15,000	100	2.90
Corrective B	RPI under 58	Mill and overlay	15,000	100	2.90
Preventive	Pavement surface age is 10	Seal coat	5,000	20	2.23

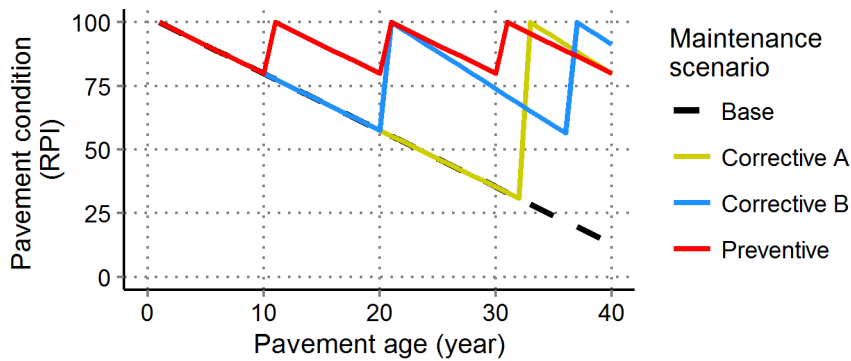


Figure 3. Pavement surface condition of base and alternative scenarios over the analysis period (adapted from Pellecuer et al., 2014b).

2. Results

The valuation of the social and environmental impacts related to traffic emissions is affected by uncertainties that prevented us from estimating the precise absolute value of the costs associated with each maintenance strategy (see Section 3 for a discussion of the uncertainties). The estimation of the relative costs and benefits are however suitable for the comparison of the performance of the maintenance strategies. Thus, the social and environmental benefits over the base scenario were assessed for the three alternative maintenance strategies. Figure 4 shows the variation of the expected annual benefits, in Canadian dollar, provided by each strategy through the analysis period.

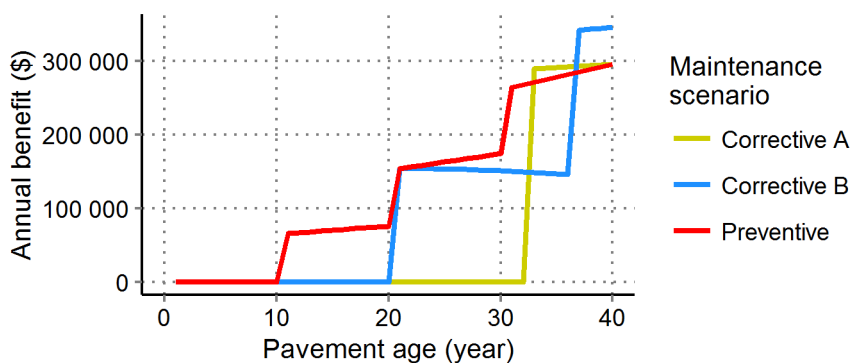


Figure 4. Central estimates of undiscounted annual social and environmental benefits of the alternative maintenance strategies.

In general, the three alternative maintenance strategies provided constantly increasing social and environmental benefits with pavement age. Most of this increase resulted from the change in pavement condition due to each maintenance treatment. This is illustrated in Figure 4 by the visible steps. In addition, the traffic volume growth tended to accentuate the benefits resulting from the maintenance treatments. The social and environmental benefits from pavement maintenance were indeed all the more important as the maintenance impacted more vehicles. The annual increase of benefits associated with the traffic growth is particularly noticeable in Figure 4 for the preventive strategy. An exception arose for corrective strategy B between the years 21 and 36 while the decrease

of the benefits associated with the deteriorating pavement condition was exceeding the increase of the benefits related to the traffic volume growth.

Comparison of pavement maintenance strategies usually relies on the pavement life cycle costs and benefits incurred during the analysis period discounted to present. Figure 5 presents, for the three alternative maintenance strategies, the life cycle social and environmental benefits calculated with two different discount rates: the discount rate usually applied by the MTQ (6.5%), and a zero discount rate used to better apprehend the intrinsic total value of the life cycle benefits. The error bars shown in Figure 5 illustrate the uncertainty pertaining to the quantification and monetization of health effects (Section 3 for a discussion of the uncertainties). These error bars were calculated with the lowest and highest estimates of the parameters involved in the quantification and valuation processes. Therefore, they represent the low and high estimates of the life cycle benefits.

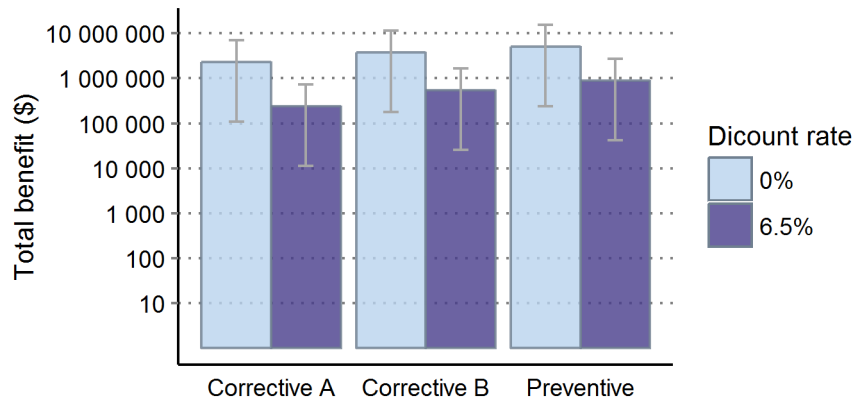


Figure 5. Total social and environmental benefits of the alternative maintenance strategies.

The results reveal that, over the 40 year analysis period, pavement surface maintenance provided central estimate of social and environmental benefits ranging from \$235 000 to \$5 150 000 (from \$11 000 to \$243 000 for low estimates and from \$723 000 to \$15 700 000 for high estimates), depending on the maintenance strategy and the discount rate used. The differences in benefits between the strategies were consistent with their associated pavement condition: the better the pavement condition, the higher the benefit. On the other hand, regardless of the strategy, non-discounted and discounted benefits were found to be significantly different. This was due to the fact that most of the annual benefits occurred at the end of the analysis period.

Based on the MTQ treatment costs (see Table 1), the total costs associated with pavement surface maintenance of each alternative maintenance strategy were computed. Table 2 shows that those costs ranged from \$180 000 for corrective A and preventive strategies to \$360 000 for corrective B strategy, depending on the maintenance strategy and the discount rate. Interestingly, regardless of the strategy, discount rate, and benefits estimate (low, central, or high), life cycle maintenance costs were found to be lower than or similar to the life cycle social and environmental benefits. In particular, central estimates of benefits were consistently higher than maintenance costs.

Table 1. Total pavement surface maintenance costs of the alternative maintenance strategies.

Alternative strategy	Total undiscounted costs (\$)	Total costs discounted at 6.5% (\$)
Corrective A	180 000	22 500
Corrective B	360 000	68 500
Preventive	180 000	58 000

3. Discussion

While analysing the results presented above, it should be kept in mind that assigning an economic value to traffic emission impacts implies unavoidable uncertainties (Bickel et al. 2006, van Essen et al. 2011). As detailed in Pellecuer et al. (2014a), these uncertainties pertain to variable estimation, model parameterisation, and gaps in scientific knowledge. The lack of scientific knowledge affects in particular the health impact quantification (e.g. number of early deaths) and the impact valuation (e.g.

cost of biodiversity loss). However, it is important to stress that these uncertainties are not inherent to the methodology and can be reduced by careful data collection and further research. Moreover, the lack of scientific knowledge prevents from addressing all types of pavement distresses and all types of impacts associated with emissions. This is expected to result in minimizing social and environmental impacts, costs, and benefits (Pellecuer et al. 2014a).

Due to the focus on pavement condition, this study assumed steady free flow traffic conditions. It did not cover the influence of traffic conditions and traffic management devices (e.g. traffic signals) on the impacts and costs associated with traffic emissions. Variable traffic conditions and traffic management devices induce variation in speed and acceleration that causes more traffic emissions. Therefore, it is expected that not assuming steady free flow traffic conditions would have resulted in more intense impacts and higher costs.

Overall, the results presented in this paper are rough estimates of social and environmental benefits associated with traffic emissions. However, they provide a unique opportunity to apprehend the influence of pavement age (and condition) on the social and environmental benefits and to provide an order of magnitude of these benefits, which are essential for comparing the performances of pavement management alternatives. Social and environmental benefits related to traffic emissions were found to be significant and at least the same order of magnitude as the maintenance costs. This suggests that the impacts of traffic emissions were significant and would deserve to be incorporated in the life cycle assessment of pavement maintenance strategies. In particular, it was found that the preventive maintenance strategy was the best to help reduce the impacts associated with traffic emissions, supporting conclusions from Chan et al. (2011).

On the other hand, comparing the discounted and non-discounted benefits reveals that discounting dramatically minimized the total social and environmental benefits of pavement management on the pavement life cycle. This is in accordance with the conclusions of Hellweg et al. (2003) that discounting long-term impacts may influence the total social and environmental benefit of any strategy more than all other factors. This highlights the need to perform a sensitivity analysis of the estimate of the social and environmental benefits to discounting method in order to ensure that the impacts associated with traffic emissions are adequately addressed.

Conclusion

Despite unavoidable uncertainties due to gaps in scientific knowledge, the results unambiguously show that benefits related to traffic emissions were significant and were the same order of magnitude as the maintenance costs. The case study reveals that, over the 40 year analysis period, pavement surface maintenance provided social and environmental benefits ranging from \$235 000 to \$5 150 000 (central estimates), depending on the maintenance strategy and the discount rate. As such, they would deserve to be incorporated in the life cycle assessment of pavement maintenance strategies. Moreover, preventive maintenance was found clearly more effective than corrective maintenance to mitigate social and environmental impacts associated with exhaust emissions. The study also points out the need to take into account the influence of the discounting method for the assessment of the social and environmental benefits.

Acknowledgments

The author would like to thank MTQ for providing data used in this research. This research was supported in part by a fellowship from the FRQNT (Fonds de recherche du Québec – Nature et technologies).

References

- Bickel, P., R. Friedrich, H. Link, L. Stewart and C. Nash (2006): Introducing environmental externalities into transport pricing: Measurement and implications. *Transport Reviews*, vol. 26, n°4, p 389-415.
- Bignal, K. L., M. R. Ashmore, A. D. Headley, K. Stewart & K. Weigert (2007): Ecological impacts of air pollution from road transport on local vegetation. *Applied Geochemistry*, vol. 22, n°6, p 1265-1271.
- Chan, S., B. Lane, T. Kazmierowski and W. Lee (2011). "Pavement preservation: A solution for sustainability." *Transportation Research Record: Journal of the Transportation Research Board*, vol. 2235, p 36-42.

- Gillespie, J. & K. McGhee (2007): Get In, Get Out, Come Back!: What the Relationship Between Pavement Roughness and Fuel Consumption Means for the Length of the Resurfacing Cycle. Transportation Research Record: Journal of the Transportation Research Board, vol. 1990, p 32-39.
- Hellweg, S., T. Hofstetter and K. Hungerbuhler (2003): Discounting and the environment should current impacts be weighted differently than impacts harming future generations? The International Journal of Life Cycle Assessment, vol. 8, n°1, p 8-18.
- Kunzli, N., R. Kaiser, S. Medina, M. Studnicka, O. Chanel, P. Filliger, M. Herry, J. F. Horak, V. Puybonnieux-Textier, P. Quenel, J. Schneider, R. Seethaler, J. C. Vergnaud & H. Sommer (2000): Public-health impact of outdoor and traffic-related air pollution: a European assessment. The Lancet, vol. 356, n°9232, p 795-801.
- Pellecuer, L., G. Assaf & M. St-Jacques (2014a): Influence of Pavement Condition on Environmental Costs. Journal of Transportation Engineering, vol 140, n°10.
- Pellecuer, L., G. Assaf and M. St-Jacques (2014b): Life cycle environmental benefits of pavement surface maintenance. Canadian Journal of Civil Engineering, vol. 41, n°8, p 695-702.
- Pellecuer, L., G. Assaf & M. St-Jacques (2016): Towards the Incorporation of Environmental Impacts into Pavement Management Systems. Transport Reviews, vol 36, n°3, p 361-382.
- Rabl, A. & J. V. Spadaro (1999): Damages and costs of air pollution: An analysis of uncertainties. Environment International, vol. 25, n°1, p 29-46.
- Santero, N. J., E. Masanet & A. Horvath (2011): Life-cycle assessment of pavements. Part I: Critical review. Resources, Conservation and Recycling, vol. 55, n°9–10, p 801-809.
- van Essen, H., et al. (2011): External costs of transport in Europe: Update study for 2008. Technical Report, Publication code: 11.4215.50,CE Delft, Delft, The Netherlands, 161p.

AP-42 approach for PM traffic resuspension estimation over a Milan domain

Nicola PEPE^{***}, Giovanni LONATI^{*}, Guido PIROVANO^{**} & Marco BEDOGNI^{***}

^{*}Politecnico di Milano, 32 Piazza Leonardo da Vinci, 20133 Milano, Italy
email: nicola.pepe@polimi.it

^{**}Ricerca sul Sistema Energetico – RSE S.p.A., 54 Via Raffaele Rubattino, 20134 Milano, Italy

^{***}AMAT s.r.l., 1 Via Tommaso Pini, 20134 Milano, Italy

Abstract

The estimation of temporal and spatial variability of particulate matter and assessment of environmental policies over a urban domain can be conducted using a modelling approach. The modelling chain developed and applied at the regional and urban scale was composed by a meteorological model named WRF, and a chemical and transport models (CTM) named CAMx. Results from 2010 year simulations over Po Valley and Milan urban area showed a steady underestimation of PM₁₀ and PM_{2.5}, especially during winter months. One of the reason would concern a missed emission process for PM overall 2010, associated to a wrong estimation of meteorological input as wind direction, speed wind or planet boundary layer level. Although AP-42 formulation, provided by US EPA, estimates PM emissions due to traffic resuspension was set up for US environment, however this method has been used for a little area of Milan. The first application assessed the contribution of soil resuspension compared to the top-down total emission estimation over the domain.

Keys-words: PMx, soil resuspension, modeling, traffic pollution.

Introduction

In the last few decades governments and policy makers pointed out PM high concentration as a main issue for air quality, particularly over Europe. Milan urban area is located within the Po Valley, region known for high annual mean values of PM concentration together with several peak events leading to the exceedance of the European regulatory threshold for short-term concentrations. Modeling approach is one of the methods to discover how PM disperses over regional or urban domains. However, models predictions are still affected by

In a previous work conducted by Lonati et al. (2010) PM₁₀ e PM_{2.5} concentration levels in the Po valley in 2010 were estimated by a modeling chain set up by Research on Energetic system (RSE) and composed by Weather Research and Forecast model (WRF) by Skamarock (2008), as the meteorological model that provides input meteorological data (wind conditions, ambient temperature, mixing height), and by the chemical and transport model (CTM) named CAMx, (Comprehensive Air Quality model) by ENVIRON (2011). Comparison with monitored data revealed an evident underestimation of both fine and coarse fraction of particulate matter during winter period and a slight underprediction for the summer. Notwithstanding the rather good model performance for PM₁₀ and PM_{2.5}, emission inventories within CAMx could be improved to reduce underestimation by means of the introduction of new emission sources. Actually, in spite of the good quality of national emission inventories used for model simulation, PM traffic resuspension emission was not considered. For this reason the AP-42 approach, formulated by US EPA (2011), was used to estimate PM traffic resuspension emission within a small urban area of Milan city center, even though AP-42 method was based on US guidelines and climate. The results showed that soil contribution could not be considered negligible if compared with residential heating and traffic emissions. Estimation and introduction of soil contribution within the emission inventory for CAMx could improve global performance for both the coarse and the fine fraction of particulate matter.

1. Methods

CAMx was used to simulate dispersion phenomena and chemical processes at regional scale over Northern Italy. In Figure 1 the two innermost domains covering Po Valley and Milan urban area are showed. A 5 km and a 1.7 km grid step resolution were adopted for the wider and smaller domain,

respectively. Simulations run for all 2010 calendar year and the performance was evaluated considering both domains through based on air quality data collected by the regional air quality networks for each region within the domain.

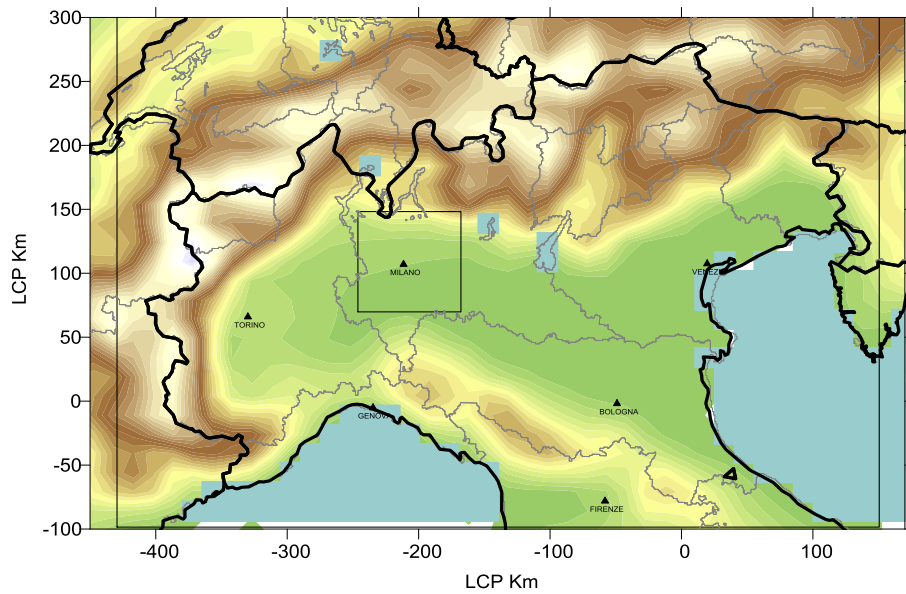


Figure 1. Po Valley and Milan urban area domain

In Figure 2 and Figure 3 CAMx results at different grid step resolution for both pollutants are shown. During the summer period CAMx reproduces quite well the times series of observations while the main problems in terms of reproducibility occur during winter months, when CAMx concentrations underestimate the observations, especially when ambient concentration levels tend to exceed $50 \mu\text{g}/\text{m}^3$.

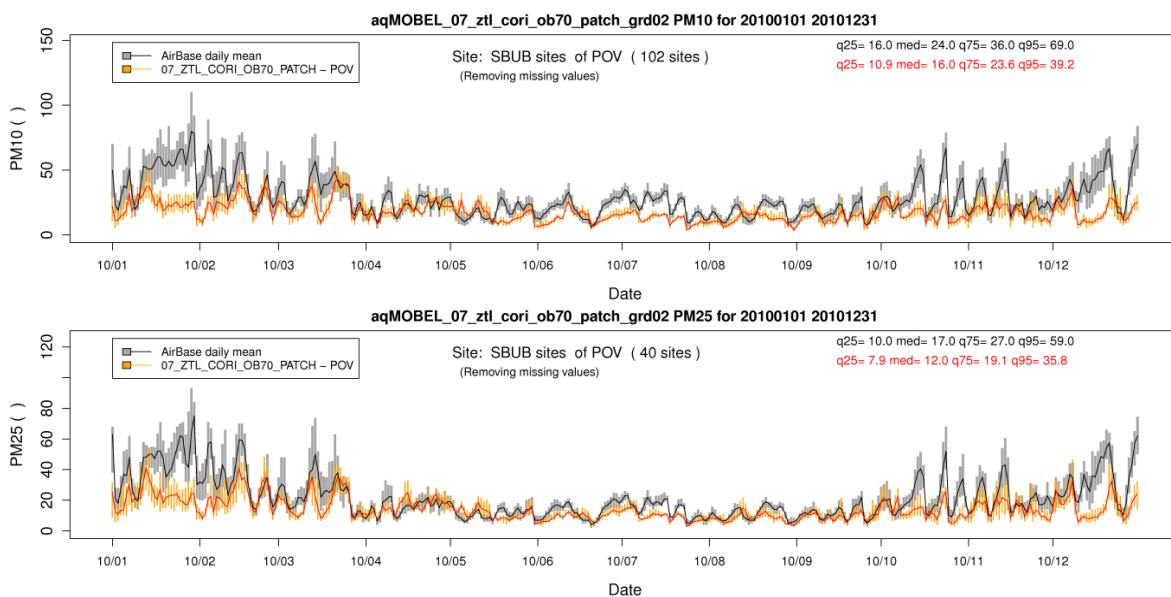


Figure 2. Time series of the box and whiskers plot for the daily distribution of observations (grey/black) and computed values for PM₁₀ (top) and PM_{2.5} (bottom) concentrations expressed as $\mu\text{g}/\text{m}^3$ at Urban and Sub Urban monitoring sites within Po Valley domain for 2010. Bars show the interquartile range, lines the median value. Values for 25th, 50th, 75th and 95th quintile for whole period are reported too.

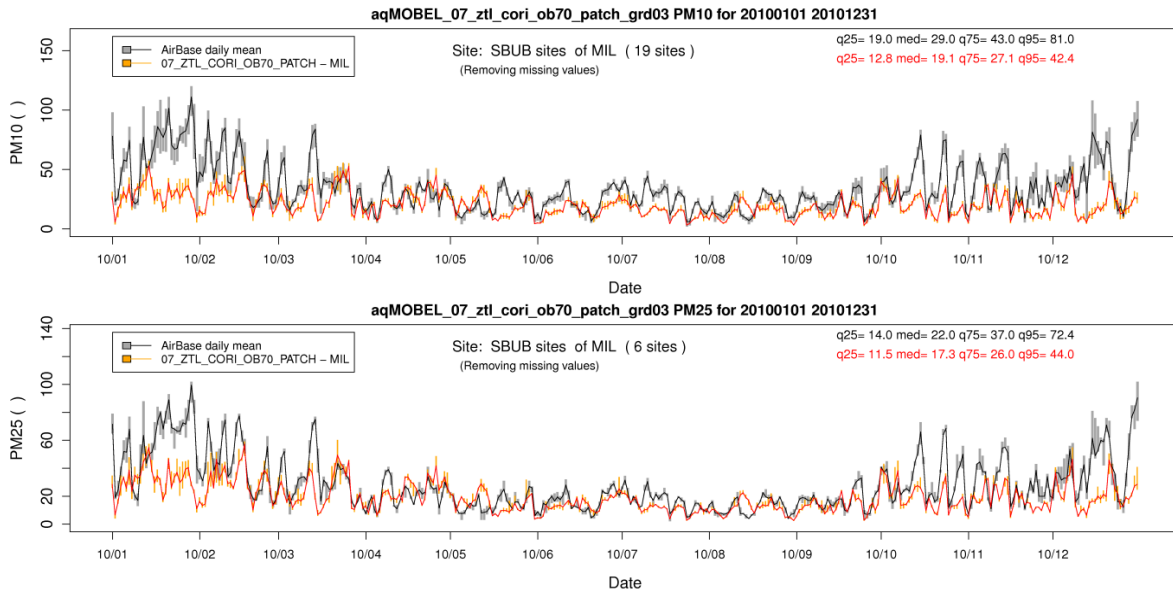


Figure 3. Time series of the box and whiskers plot for the daily distribution of observations (grey/black) and computed values for PM₁₀ (top) and PM_{2.5} (bottom) concentrations expressed as µg/m³ at Urban and Sub Urban monitoring sites within Milan urban domain for 2010. Bars show the interquartile range, lines the median value. Values for 25th, 50th, 75th and 95th quintile for whole period are reported too.

Considering that CAMx provided similar overall performance regardless for the grid step size, the underestimation issue could be explained either by missed emission processes or by meteorological large scale effects not captured by WRF, like low dispersion phenomena or reduced depth of the mixing layer especially during critical winter conditions, as well as inaccurate meteorological input provided by WRF.

In order to reduce the gap between model and observations in the winter period, this work was focused on the introduction of PM traffic resuspension as a new emission source, previously unaccounted because soil resuspension is not considered in national emission inventories. Thus CAMx cannot reproduce its effect on concentration levels. The formulation used to estimate PM traffic resuspension was the AP-42 developed by US Environmental Protection Agency - EPA (2011). This first application covered just a small area of the Milan city center, 1.6x1.6 km² showed in Figure 4, and focused on January 2010 in order to compare soil resuspension with residential heating and traffic emissions. For the study area AMAT (Milan municipality mobility agency) could provide detailed, street-by-street information on traffic intensity and composition.

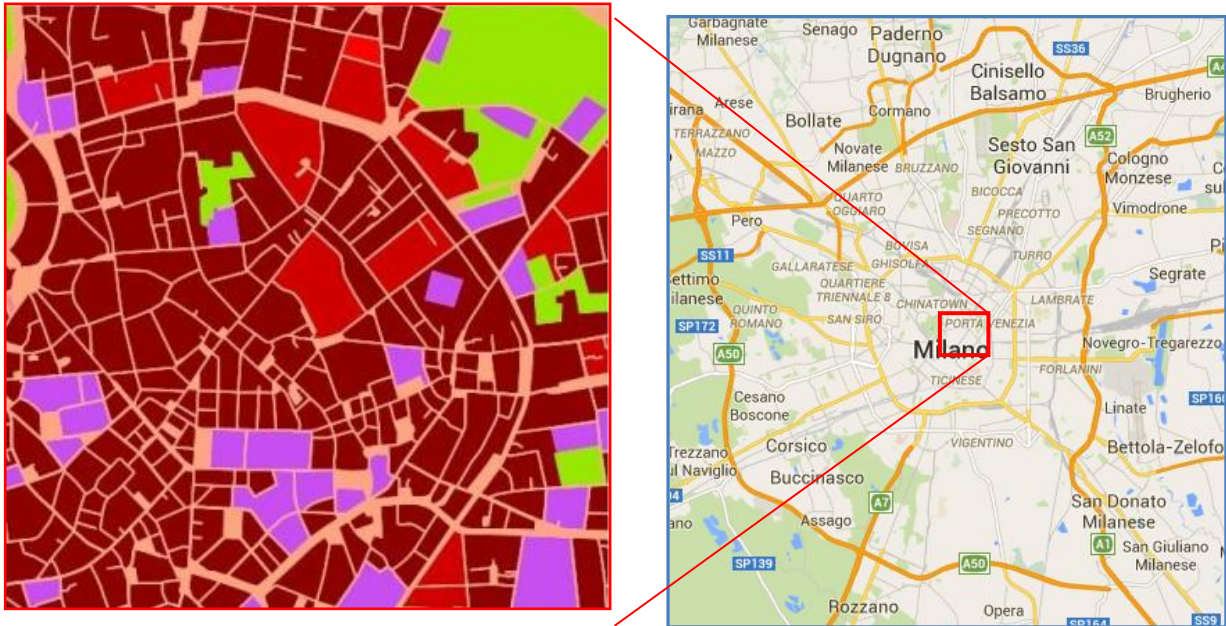


Figure 4. Overview of local domain analyzed for PM traffic resuspension estimation.

AP-42 approach is able to compute the PM emission factor related to a single paved roads for different pollutants. The parameterizations associated to the US formulation allow to consider two different meteorological conditions (baseline and frozen rain), four PM fractions ($PM_{2.5}$, PM_{10} , PM_{15} ; TSP) and the average daily traffic (ADT) through the street, as number of travels. Furthermore, US EPA considered data set variability and provided equations based on daily and hourly data. In this work the following hourly formulation was used:

$$E = (k \cdot sL^{0.91} \cdot W^{1.02}) \cdot \left(1 - 1.2 \cdot \frac{P}{N}\right)$$

where E is the long-term average particulate emission factor computed as g/VKT (VKT is Vehicle Kilometer Traveled); k represents a particle size multiplier having units matching the units of the emission factor (0.15 for $PM_{2.5}$, 0.62 for PM_{10} , 0.77 for PM_{15} and 3.23 for TSP); sL is the road surface silt loading that refers to the mass of silt-size material (equal to or less than 75 micrometers in physical diameters) per unit area of the travel surface parameterized as reported in Table 1; W is the average weight, in tons, of the fleet of all vehicles traveling the road; P is the number of hours with at least 0.254 mm of precipitation during the averaging period; N is the number of hours in the averaging period.

Table 1. Baseline silt loading (sL) default values

ADT	<500	500-5000	5000-10000	>10000
(X) Baseline (g/m^2)	0.6	0.2	0.06	0.03 (0.015 limited access)
Multiplier during months with frozen rain	x 4	x 3	x 2	x 1
Days to return to baseline conditions	7	3	1	0.5

The ADT value was computed based on the number of vehicles traveling during the traffic peak hour provided by AMAT. Silt loading sL and average fleet weight W have been calculated for every single road within the urban domain and AP-42 equation was applied in order to compute first the particulate emission factors and then the monthly emission, according to a bottom-up approach that relies on high quality piece of information on road network and related vehicular traffic.

Conversely, a top-down approach was used to estimate emissions for traffic and residential heating within the urban domain, downscaling regional scale data provided by national/regional inventories (ISPRA, EMEP and INEMAR) to local scale through proxy variables (e.g. land use). The next chapter shows the results from the application of AP-42 equations and the comparison between PM resuspension and the other emissions.

2. Results

Results for fine and coarse fraction of PM are showed in Table 2. The upper part of the table points out the contribution of soil resuspension compared with traffic monthly emissions for January. The process that was not considered within national inventories proves could be not negligible if compared to other urban emissions. PM₁₀ traffic resuspension results in almost 61% of the total traffic emission (exhaust + wear emissions) estimated for the local domain analyzed, while the contribution to PM_{2.5} comes out approximately about 20% with respect to traffic emission.

Table 2. Results for first application of AP-42 equation considering PM₁₀ and PM_{2.5}

Pollutant	Traffic emission [kg]	Soilresuspension [kg]	% [resusp/traff]
PM ₁₀	539,7	329,7	61,1
PM _{2.5}	437,6	79,8	18,2

Pollutant	Heating and traffic emission[kg]	Total emission [kg]	Δ [%]
PM ₁₀	1758,7	2088,4	18,8
PM _{2.5}	1615,4	1695,2	4,9

The overall PM₁₀ and PM_{2.5} emissions for the local domain, computed adding traffic, residential heating, and soil resuspension emissions, are reported in the second column of the lower part of Table 2. The last column in Table 2 summarizes the percentage increment of the total emissions due to resuspension processes. Despite the limited extension of domain, the contribution of soil resuspension appears clearly relevant for PM₁₀ (almost 20%) and less important for PM_{2.5} (5%), coherently with the typical coarse features of resuspended soil dust. As a first rough approximation, assuming that these latter percentage increments of PM emission can directly affect the modeled concentration levels within the urban domain, thus improving the CAMx performance and reducing, partially, the winter underprediction of PM₁₀ and PM_{2.5}.

3. Conclusion

The assessment of urban air quality by means of modeling tools is the alternative approach to air quality monitoring networks that provide hourly concentration levels of atmospheric pollutants. WRF, The meteorological model WRF and the chemical and transport model CAMx were set up in a modeling chain to reconstruct air quality and to assess environmental scenarios (e.g. introduction of electric vehicle, new government regulations). A previous simulation for PM₁₀ and PM_{2.5} for Milan in 2010 showed an underprediction of both pollutants, especially during the winter period, caused by meteorological data or missed emission processes. Focusing on particulate emissions, soil resuspension was not counted within national emission inventories and an approach to estimate this contribution could help reducing CAMx underprediction. AP-42 equation developed by US EPA was used to estimate PM resuspension contribution within an urban domain, covering 1.6x1.6 km² area in Milan. AP-42 application was based on the month of January and soil resuspension emissions were compared to other urban anthropogenic emissions of PM₁₀ and PM_{2.5}, as residential heating and traffic, in order to calculate the absolute and relative contribution of the new process.

Results proved that maybe PM resuspension cannot be considered negligible if compared to the other particulate matter urban sources; monthly PM₁₀ resuspension contribution seemed to be more than 60% of traffic emission while for PM_{2.5} the percentage dropped down to about 20%. Although two different methods to calculate urban emissions were used, top-down approach for residential heating and traffic emission, and bottom-up for soil resuspension, total amounts resulted comparable. Finally, the percentage increment of total emissions when accounting also for soil resuspension were 20% and 5% for PM₁₀ and PM_{2.5} respectively.

PM₁₀ soil resuspension average emission factors (EF) computed in this work, using AP-42 approach and silt loading default values for each street within urban domain, was almost one order of magnitude higher (176.8 mg_{PM10} VKT⁻¹) than in a freeway of Barcelona (22.7 ± 14.7 mg_{PM10} VKT⁻¹), as reported by Amato et al (2012), and higher than other urban values too, such as reported by Ketzler et al. (2007), 17-92 mg_{PM10} VKT⁻¹ at inner-city urban roads in Switzerland, and by Amato et al. (2012), 85 mg_{PM10} VKT⁻¹ in the city center of Barcelona. Gehrig et al. (2004) reported values similar to those estimated in

this work ($198 \text{ mg}_{\text{PM}_{10}} \text{ VKT}^{-1}$), but in Sweden there are different road conditions than in Italy. Thus, a simple AP-42 approach using silt loading default values could overestimate the urban average EFs, maybe because some aspects, such as the periodical road surface cleaning services, were not accounted for in our computations. Indeed, as reported by the AP-42 guidelines too, "the collection and use of site-specific silt loading data for public paved road emission inventories are strongly recommended".

Future works will identify, first of all, the reasons of a possible resuspension EFs overestimation in Milan, and address more in details the time pattern of total PM emissions from soil resuspension as CAMx input in order to improve the overall model performance, in particular the winter underprediction of PM over both the local and regional scale. Additionally, simulations for a larger domain will consider the real urban burden of soil resuspension and improvement on road network data, like real daily number of vehicles traveling will determine a more accurate estimation of emission factors and total emissions.

Acknowledgments

This work has been financed by the Research Fund for the Italian Electrical System under the Contract Agreement between RSE S.p.A. and the Ministry of Economic Development -General Directorate for Nuclear Energy, Renewable Energy and Energy Efficiency in compliance with the Decree of March 8, 2006.

References

- Amato F., A. Karanasiou, T. Moreno, A. Alastuey, J.A.G Orza., J. Lumbreras, R. Borge, E. Boldo, C. Linares & X. Querol (2012): Emission factors from road dust resuspension in a Mediterranean freeway. *Atm.Env.*, vol.61, p580-587.
- ENVIRON (2011): CAMx (Comprehensive Air Quality Model with extensions) User's Guide Version 5.4. ENVIRON International Corporation, Novato, CA.
- Gehrig R., M. Hill, B. Buchmann, D. Imhof, E. Weingarter & U. Baltensprenger (2004): Separate determination of PM10 emission factors of road traffic for tailpipe emissions and emissions from abrasion and resuspension processes. *International Journal for Environment and Pollution*, vol. 22, p 321-332.
- Ketzel M., G. Omstedt, C. Johansson, M. Haakana & R. Berkowicz (2007): Estimation and validation of $\text{PM}_{2.5}/\text{PM}_{10}$ exhaust and non-exhaust emission factors for practical street pollution modeling. *Atm.Env.*, vol 41, p 9730-9385. <http://dx.doi.org/10.1016/j.atmosenv.2007.09.005>
- Lonati G., G. Pirovano, G.A. Sghirlanzoni & A. Zanoni (2010): Speciated fine particulate matter in Northern Italy: A whole year chemical and transport modelling reconstruction. *Atm. Res.*, vol 95, issue 4, p 496-514.
- Skamarock W.C., J.B. Klemp, J. Dudhia, D.O. Gill, D.M. Barker, M.G. Duda, X.Y. Huang, W. Wang & J.G. Powers (2008): A Description of the Advanced Research WRF Version 3, NCAR Technical Note NCAR/TN-475+STR, Boulder, Colorado.
- U.S. Environmental Protection Agency (2011): AP 42, Fifth Edition, Volume I, Chapter 13, Miscellaneous Sources, Chapter Paved roads. <https://www3.epa.gov/ttn/chief/ap42/ch13/final/c13s0201.pdf>

Black Carbon in Lorraine: sources, geographical origins and model evaluation

Jean-Eudes Petit*, Emmanuel Jantzen*, José Nicolas**, Sébastien Conil***, Karine Sellegri** & Alexandre Ockler*

* Air Lorraine, 20 rue Pierre Simon de Laplace, Metz, France
email: je.petit@air-lorraine.org

** Laboratoire de Météorologie Physique CNRS UMR6016, Observatoire de Physique du Globe de Clermont-Ferrand, Université Blaise Pascal, Aubière, France

***Andra, DRD/OS, Observatoire Pérenne de l'Environnement, France

Abstract

Black carbon is mainly emitted by any combustion process: road traffic, wood and coal burning, shipping and various industrial combustions. Given, among others, the health effects of air pollution, and that BC is a good tracer and its sanitary impacts, monitoring of BC at various scales (remote, rural, urban and traffic) has nowadays become widespread. The present study uses long-term BC measurements in Metz (East of France) to determine the contribution of the two main sources, traffic and wood-burning, and their seasonalities. Wood-burning, in 2015, could represent up to 25% of BC during cold months. In parallel, a comparison with measurements at a rural background site located 80 km South-West of Metz during March 2015 helped to assess the role of background concentrations to urban air quality during an intense haze pollution event. Finally, a model evaluation was performed at both sites and showed an air-mass dependence on the performance of the model.

Keys-words: Black Carbon, sources, origin, model

Le carbone suie est majoritairement émis de processus anthropiques, comme entre autre le trafic automobile, la combustion de biomasse ou de charbon ou encore le transport maritime. Et c'est notamment du aux impacts sanitaires de la pollution atmosphérique, que le suivi du BC s'est répandu à plusieurs échelles géographiques (fond atmosphérique, rural, urbain et proximité trafic). L'étude présentée ici utilise des données long-terme de BC en fond urbain à Metz (Est de la France) afin de déterminer la contribution de ses deux principales sources, le trafic et le chauffage au bois, ainsi que leurs saisonnalités. En 2015, le chauffage représentait par exemple jusqu'à 25% du BC pendant les mois les plus froids. Puis, une comparaison avec des mesures en fond rural (effectuées à 80 km au Sud-Ouest de Metz) pendant mars 2015 a permis de quantifier le rôle des niveaux de fonds à la qualité de l'air urbain pendant un intense épisode de pollution. Finalement, une confrontation des mesures au modèle régional de prévision a été effectuée sur les deux sites, et montre une nette dépendance des performances du modèles suivant l'origine des masses d'air.

Mots-clés: Carbone Suie, sources, origines géographiques, comparaison mesures modèle

Introduction

Outdoor air pollution has been, since 2013, considered as carcinogenic for humans (IARC, 2013). The chemical composition of particulate matter (PM) and its granulometry plays a central role in this assessment (Harrison and Yin, 2000). In particular, the physical and chemical structure of Black Carbon (BC) can lead to human health issues. Its small size increases the penetration of soot deep inside our breathing system, and can be associated to (coated with) organic compounds, like Polycyclic Aromatic Hydrocarbons (HAP), potentially intensifying the inflammatory response (Ramgolam et al., 2009). It is for that matter that BC is considered as a good indicator of the impacts of air pollution (Janssen et al., 2011), being closely linked to its sources. BC is emitted from incomplete combustion of fossil fuels and biomass. Thus, in urban areas, where population density enhances the exposure to pollution, BC main sources are traffic and wood-burning. Indeed, Putaud et al. (2004) have highlighted a significant gradient of BC concentrations from rural background to kerbsides. But despite this very local pattern, case studies report examples of long-range advection of

BC, observed in the Himalayas (Ming et al., 2007, 2010), or even in urban environments like Paris (Healy et al., 2012), where up to 21% of BC was determined to have a continental origin. At an European scale, Putaud et al. (2004) also observed geographical heterogeneity.

More specifically, the North-East of France regularly faces pollution episodes during winter and spring usually associated with continental air masses. Paris being located West from this area of France, and oceanic air masses being mainly occurring (Petit et al., 2015), advection from other French regions may be observed. But poor is known about the contribution of the sources of BC and their different geographical scales. This study focuses on Black carbon measurements in Metz, the second largest urban area in Lorraine. Long-term 7-wavelength aethalometer data are presented at urban background during 2015, to investigate the seasonality and the sources of black carbon. A more specific work has been performed during March 2015, associated with an intense pollution episode: a comparison between urban concentrations was performed with a rural background site (OPE), located around 80 km South-West of Metz, to investigate the potential role of rural background on urban BC levels, and inversely.

Moreover, the precise determination of the impacts of mitigation policies in order to improve air quality is closely linked to the capability to model, through mitigation scenarios, BC concentrations. Since few information about this are available in France, a comparison between predicted and observed BC levels at rural and urban environment is presented here during the pollution episode of March 2015.

1. Sites, instrumentation and methods

For the purpose of this study, two measuring sites have been used (Metz and OPE). The first one is located in Metz (49.11°N, 6.22°E), around 5 km South-East of the city center, and is representative of urban background pollution. This station is part of the air quality monitoring network in Lorraine, operated by Air Lorraine. The second site (OPE) is located around 80 km South-West of Metz (49.56°N, 5.51°E), representative of rural background concentrations. Due to this relative proximity, these two sites experience similar meteorology, notably in terms of ambient temperatures and relative humidity. Figure 1 shows the comparison of these 2 parameters at both sites during 2015 (15-min averages).

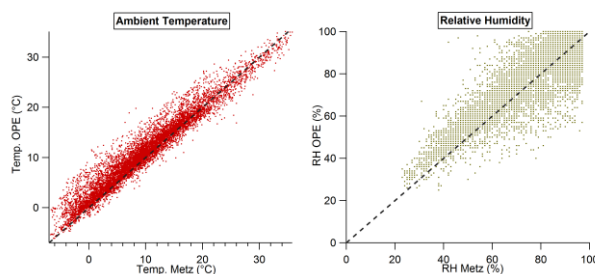


Figure 1. Comparison of ambient temperature and relative humidity between Metz and OPE in 2015 (15-min average)

It is however interesting to note that wind conditions are significantly different (Fig. 2), where OPE seems much more ventilated than Metz, which is mainly associated with calm winds, below 2 m/s. This can be partly associated to the topography of the sites: Metz is located within the valley of the Moselle river and is surrounded by hills, while OPE is on a plateau, cleared from any natural impediment.

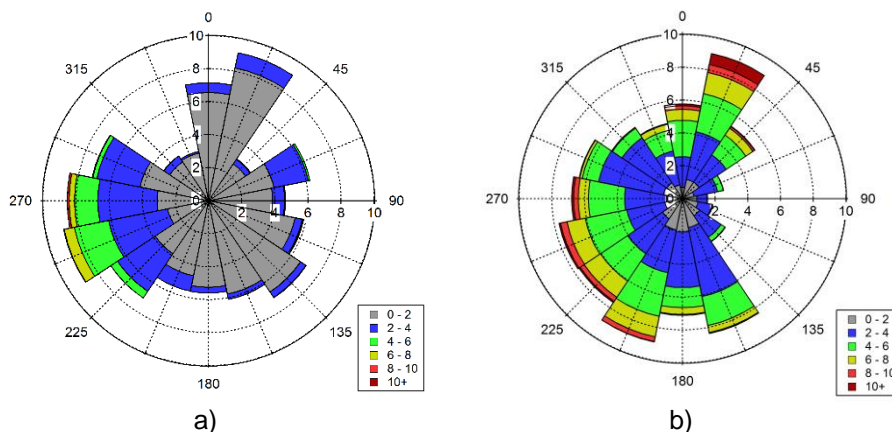


Figure 2. Wind rose in a) Metz and b) OPE, during 2015 (15-min wind data). Radial axis is the frequency (in %), wind speed classes in m/s.

Both sites were equipped with 7-wavelengths aethalometer instruments, AE31 model in OPE, and AE33 model in Metz. Extensive description of these instruments can be found elsewhere (Drinovec et al., 2015 and references therein); they also have been found to be very robust over long term periods (Herich et al., 2011; Petit et al., 2015). In this study, BC concentration at 880 nm were used. Fossil-fuel and wood-burning fractions (BC_{ff} and BC_{wb} , respectively) were calculated in Metz following the algorithm proposed by Sandradewi et al. (2008).

Wind analysis on BC concentrations has been performed at both sites by Non-parametric Wind Regression (NWR, Henry et al., 2009). Calculations were carried out with ZeFir, an Igor© tool for wind and trajectory analyses (Petit et al., submitted). In parallel, backtrajectories arriving hourly at OPE (at 100 m above ground level) were calculated with the PC-based version of Hysplit (Draxler, 1999). Following total spatial variance variations, cluster analysis led to 5 clusters, illustrated in Figure 7.

Black carbon modeled concentrations were determined from the Chemistry-Transport Model (CTM) CHIMERE (Menut et al., 2013), through the regional platform Prev'est. Chemical mechanisms are controlled by MELCHIOR 2 (Lattuati, 1997), thermodynamics by ISORROPIA (Nenes et al., 1998), WRF meteorological fields combined with a regional emission inventory were used. The evaluation of performance of the model was investigated by calculating different statistics: Fraction of predictions within a factor of two (FAC2), Mean bias (MB), Normalised mean bias (NMB), Root mean squared error (RMSE), Pearson correlation coefficient, Coefficient of Efficiency (COE, Legates and McCabe, 2013) and Index of Agreement (IOA, Willmott et al., 2012).

2. Results & Discussion

Figure 3 exposes the monthly averages of BC_{ff} , BC_{wb} and their relative contributions during 2015 at Metz (urban background). BC_{ff} does not exhibit pronounced seasonal variations, despite highest averages being observed in March, October and December, reaching respectively 1.9, 1.8 and 1.6 $\mu\text{g}/\text{m}^3$, while the base level is around 1 $\mu\text{g}/\text{m}^3$, observed during summer. On the contrary, BC_{wb} has a strong seasonal pattern, with highest concentrations during winter, late autumn and early spring. Whatever the season (except for BC_{wb} in summer), both fractions have typical, very pronounced diurnal variations (not shown here): BC_{ff} has a bimodal pattern, with intense peaks in the morning and the evening, corresponding to daily commuting. The station is indeed located near main highways and is thus very reactive to traffic primary emissions. BC_{wb} has only one significant increase during the evening, slightly shifted from the evening traffic peak, and corresponds wood-burning emissions for residential heating. During winter, wood burning represents around 25% of total BC concentrations, underlining the role of this source in urban areas, as this has also been shown in other French cities (e.g. Paris: Bressi et al., 2014; Favez et al., 2009; or Grenoble: Favez et al., 2010) or in Europe (e.g. London: Fuller et al., 2014).

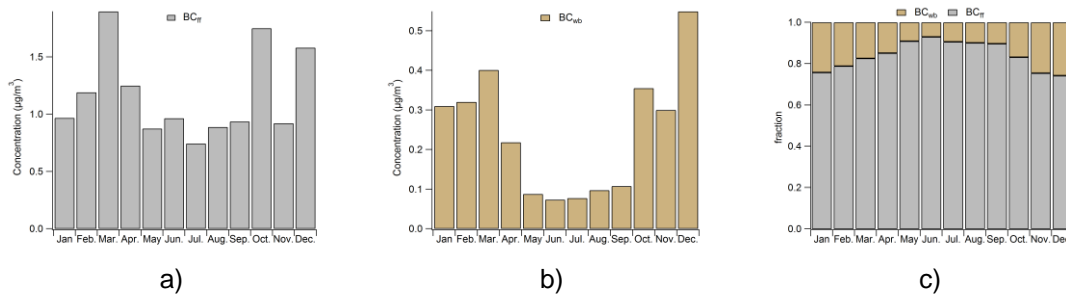


Figure 3. Monthly averages of BC_{ff} (a), BC_{wb} (b), and their relative contributions (c) in 2015

During March 2015, Metz has experienced one of the most intense pollution episode since many years. Briefly, two distinct sub-episodes occurred: the first one, at the beginning of the month (from March 7th to 11th), was characterized by local/regional signals, dominated by primary emissions. The second sub-episode, between March 19th and 22nd exhibited a more advected pattern, with notably a much higher contribution of secondary pollution (especially ammonium nitrate). An in-depth characterization of this episode, spread over most of the French territory, will be available in Petit et al., in prep. However, a specific focus on BC is made here.

A raw comparison of BC levels in Metz and OPE during March reveals a significant contribution of local emissions, rather than rural background (Fig. 4). It represents, in median, around 20% of the concentrations measured at urban background. However, this contribution greatly depends on the concentration, as it decreases with increasing BC masses. It is important to note that this result is representative of this episode only, with all the specificities it may be associated with. A similar work on a longer dataset (e.g. a year), with upwind/downwind discrimination, as performed by Petetin et al. (2014) in Paris, may lead to global/refined conclusions.

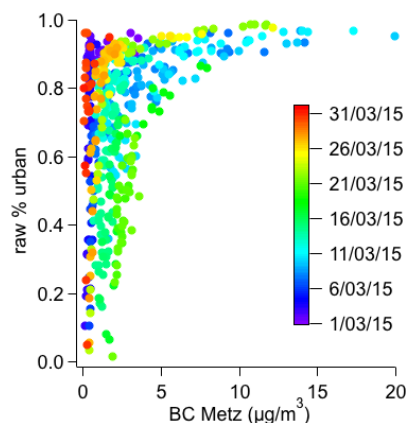


Figure 4. Fraction of urban BC compared to rural background during March 2015.

The wind analyses performed at both sites on BC concentrations during March 2015 show significant discrepancies in terms of geographical origins (Fig. 5). In Metz, highest concentrations are observed at wind speeds close to 0 km/h, confirming the strong influence of local emissions. Also, a clear pathway from the North is observed with intermediate wind speeds (between 5 and 10 km/h). The precise geographical origin of this contribution cannot be precisely determined, mainly because wind speed is not directly proportional to a distance (in km). On the contrary, a completely different pattern is observed at OPE, in relation to dispersion conditions more favourable to advection (Fig. 2). A clear hotspot is observed in the NNE and NE sector, with intermediate wind speeds. Metz and Nancy (the other major city in Lorraine) fall within this sector and could thus significantly influence rural background at OPE. A major motorway connects both urban areas and has dense heavy-duty vehicles, due to the proximity with Belgium and Germany, and could also participate in observed background levels. Finally, long range advection, particularly with NE winds, could occur, since it has

already been shown in Paris (Healy et al., 2012) or Lens (Waked et al., 2014). But the presence major of urban areas like Metz or Nancy upwind of OPE makes this assessment more laborious.

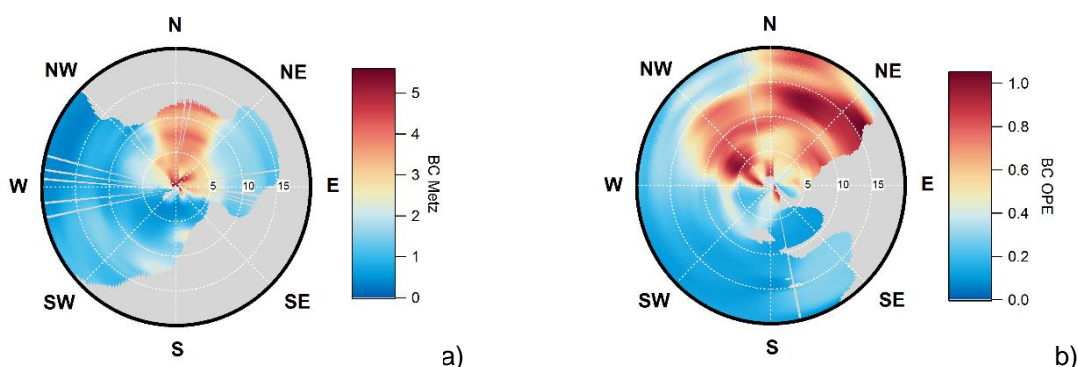


Figure 5. Wind analysis results on BC in a) Metz and b) OPE during March 2015. Radial axis represents wind speed (in km/h), colorscale is relative to the estimated concentrations (in $\mu\text{g}/\text{m}^3$)

Because the evaluation of the effectiveness of mitigation policies on BC comes to a satisfying ability of air quality models to represent its concentrations, it is critical to compare observed and modeled concentrations at different contribution levels (e.g. urban and rural). Such evaluation work is scarce in the literature. Gilardoni et al. (2011) proposed statistical tools to evaluate black carbon modeling using remote and rural sites across the world. Since BC is chemically inert in the atmosphere, the observed discrepancies between measured and modeled BC cannot be attributable to unknown chemical transformation pathways, but more to emission inventory issues and/or meteorological conditions. For example, Gadhavi et al.(2015) have shown seasonal variations in the agreement of the model they used, on a case study at a rural site in India, with highest discrepancies between January and April, associated with Southern air masses which are linked to an underestimation of open biomass burning emissions.

Here, it is very interesting to observe that modeled BC concentrations during the regional pollution episode (07/03 to 11/03) agree very well with the measurements at rural background (OPE), but not at urban background (Metz) (Fig. 6). Overall, Prev'est shows a much better performance at OPE than Metz, with for example a Normalized Mean Bias of -66% in Metz against -34% at OPE. The FAC2, fraction of modeled values within a factor of 2 of the observed values, is also much smaller in Metz (0.39), underlining the fact that the model has been unable to represent the amplitude of concentrations at urban background during this particular episode. On the other hand, modeled BC at rural background (OPE) stayed very low during the second sub-episode (between 19/03 and 22/03), characterized by an advected pattern.

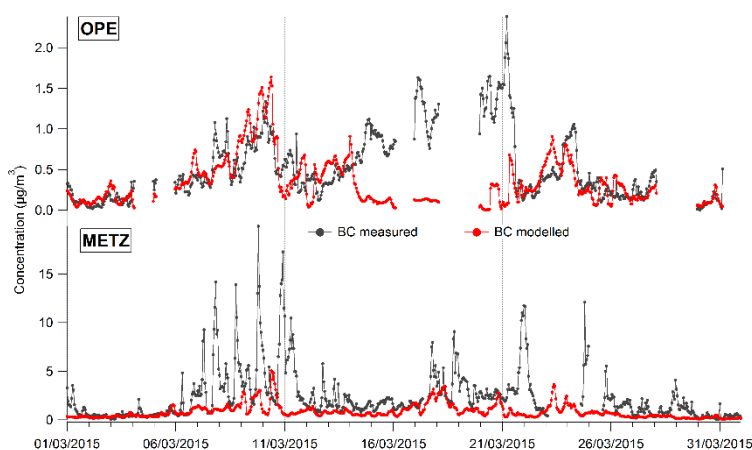


Figure 6. Comparison between BC measured and modeled at OPE and Metz

Table 1. Model evaluation statistics for BC at Metz and OPE during March 2015.

	BC Metz	BC OPE
FAC ₂	0.39	0.625
MB	-1.56 $\mu\text{g}/\text{m}^3$	-0.18 $\mu\text{g}/\text{m}^3$
NMB	-0.66	-0.34
RMSE	2.91	0.51
r	0.34	0.15
COE	0.04	0.03
IOA	0.52	0.52

Figure 7 illustrates the difference between predicted and observed BC concentrations at OPE, colorcoded with the origin of the air masses, defined as clusters, from 1 to 5. Difference values range from +0.6 to -2.3 $\mu\text{g}/\text{m}^3$, highest discrepancies being observe exclusively with cluster 5, corresponding NE air masses. This air mass dependence is particularly highlighted in Fig. 8, illustrating the variations of the model evaluation statistics (described in Table 1) for the 5 clusters. Indeed, each statistic degrades in cluster 5 compared to the other clusters. For example, while RMSE stays below 0.21 for oceanic air masses (cluster 1 to 3), it reaches 0.32 and 0.83 for continental influences (clusters 4 and 5), respectively. This can suggest that the transport of BC from other regions than Lorraine, but also from Metz for example since BC concentrations are badly modeled at urban background, is not well represented. Overall, these results emphasize the critical need of refined emission inventories in urban areas like Metz, but also a better knowledge (and/or consideration) of border emissions.

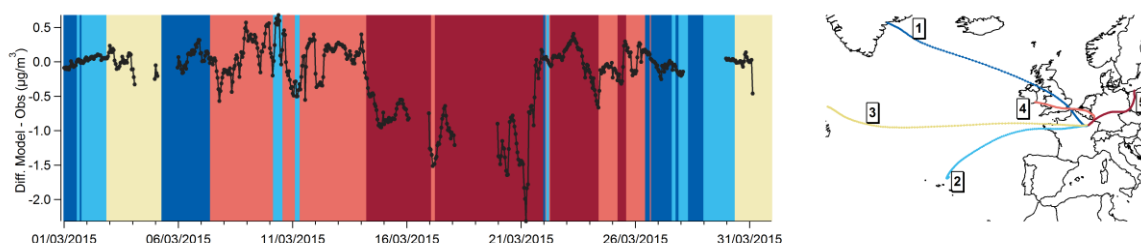


Figure 7. Temporal variation of the difference between BC modeled and observed at OPE. Colors in the background refer to clusters which are described in the right panel.

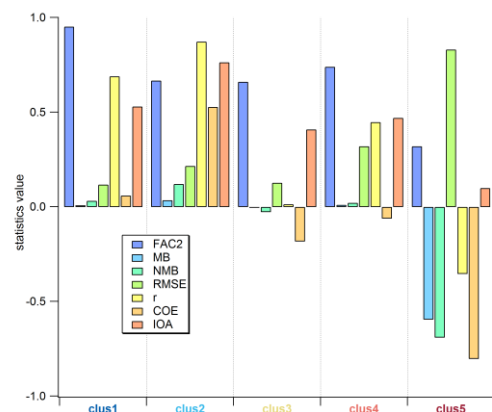


Figure 8. Model evaluation statistics for BC at OPE divided by clusters

Finally, it is important to note that this analysis could suffer from statistical artifact, as the 5 clusters are not temporally equally distributed (e.g. cluster 5 represents 32% of the air masses during this period, against 12% for cluster 2).

Conclusion

This study presents long-term black carbon measurements in a major urban area in the East of France. The fossil fuel fraction, linked to traffic emissions, makes up the majority of BC year long, but wood-burning exhibits a strong seasonality, with highest concentrations during winter and early spring. During March 2015, the comparison between urban and rural levels revealed that most of urban concentrations (80% on median, but up to 98%) are associated with local emissions. Wind analysis performed on BC at the rural site showed that Metz and Nancy, the two major urban areas in Lorraine, influence rural background concentrations during the pollution episode. The role of Paris emissions, yet one the strongest emitter of BC in France, could not be highlighted, mainly because air masses from the West have a low representativeness during the period of study.

Finally, a model evaluation at both sites showed very contrasted results. Overall, the model is more reliable at rural than urban background (relative mean bias of around -34% and -66% respectively). This emphasizes the need of a better knowledge of i) emission factors and ii) emission inventories within urban areas. Also, cluster analysis showed the influence of air mass origin on the performance of the model, which dramatically decreased with continental air masses. Trans-regional modeling work is thus needed for a better prediction of black carbon concentrations.

Acknowledgments

Air Lorraine is greatly acknowledged for financial support. The authors would like to thank Florent Vasbien (ASPA) for providing modeled BC concentrations from Prev'est.

References

- Bressi, M., Sciare, J., Ghersi, V., Mihalopoulos, N., Petit, J.-E., Nicolas, J. B., Moukhtar, S., Rosso, A., Féron, A., Bonnaire, N., Poulakis, E. and Theodosi, C.: Sources and geographical origins of fine aerosols in Paris (France), *Atmospheric Chem. Phys.*, 14(16), 8813–8839, doi:10.5194/acp-14-8813-2014, 2014.
- Draxler, R.: Hysplit4 User's Guide. [online] Available from: <http://www.arl.noaa.gov/documents/reports/arl-230.pdf> (Accessed 14 May 2014), 1999.
- Drinovec, L., Močnik, G., Zotter, P., Prévôt, A. S. H., Ruckstuhl, C., Coz, E., Rupakheti, M., Sciare, J., Müller, T., Wiedensohler, A. and Hansen, A. D. A.: The "dual-spot" Aethalometer: an improved measurement of aerosol black carbon with real-time loading compensation, *Atmospheric Meas. Tech.*, 8(5), 1965–1979,

doi:10.5194/amt-8-1965-2015, 2015.

- Favez, O., Cachier, H., Sciare, J., Sarda-estève, R. and Martinon, L.: Evidence for a significant contribution of wood burning aerosols to PM_{2.5} during the winter season in Paris, France, *Atmos. Environ.*, 43, 3640–3644, 2009.
- Favez, O., El Haddad, I., Piot, C., Boréave, A., Abidi, E., Marchand, N., Jaffrezo, J. L., Besombes, J. L., Personnaz, M. B., Sciare, J., Wortham, H., George, C. and D'anna, B.: Inter-comparison of source apportionment models for the estimation of wood burning aerosols during wintertime in an Alpine city (Grenoble, France), *Atmos Chem Phys*, 10, 5295–5314, doi:10.5194/acp-10-5295-2010, 2010.
- Fuller, G. W., Tremper, A. H., Baker, T. D., Yttri, K. E. and Butterfield, D.: Contribution of wood burning to PM₁₀ in London, *Atmos. Environ.*, 87, 87–94, doi:10.1016/j.atmosenv.2013.12.037, 2014.
- Gadhavi, H. S., Renuka, K., Ravi Kiran, V., Jayaraman, A., Stohl, A., Klimont, Z. and Beig, G.: Evaluation of black carbon emission inventories using a Lagrangian dispersion model – a case study over southern India, *Atmospheric Chem. Phys.*, 15(3), 1447–1461, doi:10.5194/acp-15-1447-2015, 2015.
- Gilardoni, S., Vignati, E. and Wilson, J.: Using measurements for evaluation of black carbon modeling, *Atmospheric Chem. Phys.*, 11(2), 439–455, doi:10.5194/acp-11-439-2011, 2011.
- Harrison, R. M. and Yin, J.: Particulate matter in the atmosphere: which particle properties are important for its effects on health?, *Sci. Total Environ.*, 249(1), 85–101, 2000.
- Healy, R. M., Sciare, J., Poulain, L., Kamili, K., Merkel, M., Mueller, T., Wiedensohler, A., Eckhardt, S., Stohl, A., Sarda-Estève, R., McGillicuddy, E., O'Connor, I. P., Sodeau, J. R. and Wenger, J. C.: Sources and mixing state of size-resolved elemental carbon particles in a European megacity: Paris, *Atmospheric Chem. Phys.*, 12, 1681–1700, doi:10.5194/acp-12-1681-2012, 2012.
- Henry, R., Norris, G. A., Vedantham, R. and Turner, J. R.: Source Region Identification Using Kernel Smoothing, *Environ. Sci. Technol.*, 43(11), 4090–4097, doi:10.1021/es8011723, 2009.
- Herich, H., Hueglin, C. and Buchmann, B.: A 2.5 year's source apportionment study of black carbon from wood burning and fossil fuel combustion at urban and rural sites in Switzerland, *Atmospheric Meas. Tech.*, 4(7), 1409–1420, doi:10.5194/amt-4-1409-2011, 2011.
- IARC: Outdoor air pollution a leading environmental cause of cancer deaths, press release n°221,, 2013.
- Janssen, N. A., Hoek, G., Simic-Lawson, M., Fischer, P., van Bree, L., ten Brink, H., Keuken, M., Atkinson, R. W., Anderson, H. R., Brunekreef, B. and others: Black carbon as an additional indicator of the adverse health effects of airborne particles compared with PM₁₀ and PM_{2.5}, *Env. Health Perspect*, 119(12), 1691–1699, 2011.
- Lattuati M., 1997: Impact des émissions européennes sur le bilan d'ozone troposphérique à l'interface de l'Europe et de l'Atlantique Nord. Rapport de la modélisation lagrangienne et des mesures en altitude. Thèse Université Pierre et Marie Curie Paris, France
- Legates, D. R. and McCabe, G. J.: A refined index of model performance: a rejoinder, *Int. J. Climatol.*, 33(4), 1053–1056, doi:10.1002/joc.3487, 2013.
- Menut, L., Bessagnet, B., Khvorostyanov, D., Beekmann, M., Blond, N., Colette, A., Coll, I., Curci, G., Foret, G., Hodzic, A., Mailler, S., Meleux, F., Monge, J.-L., Pison, I., Siour, G., Turquety, S., Valari, M., Vautard, R. and Vivanco, M. G.: CHIMERE 2013: a model for regional atmospheric composition modelling, *Geosci. Model Dev.*, 6(4), 981–1028, doi:10.5194/gmd-6-981-2013, 2013.
- Ming, J., Zhang, D., Kang, S. and Tian, W.: Aerosol and fresh snow chemistry in the East Rongbuk Glacier on the northern slope of Mt. Qomolangma (Everest), *J. Geophys. Res.*, 112(D15), doi:10.1029/2007JD008618, 2007.
- Ming, J., Xiao, C., Sun, J., Kang, S. and Bonasoni, P.: Carbonaceous particles in the atmosphere and precipitation of the Nam Co region, central Tibet, *J. Environ. Sci.*, 22(11), 1748–1756, doi:10.1016/S1001-0742(09)60315-6, 2010.
- Nenes, A., Pandis, S. N. and Pilinis, C.: ISORROPIA: A new thermodynamic equilibrium model for multiphase multicomponent inorganic aerosols, *Aquat. Geochem.*, 4(1), 123–152, 1998.

- Petetin, H., Beekmann, M., Sciare, J., Bressi, M., Rosso, A., Sanchez, O. and Gherzi, V.: A novel model evaluation approach focusing on local and advected contributions to urban PM_{2.5} levels – application to Paris, France, *Geosci. Model Dev.*, 7(4), 1483–1505, doi:10.5194/gmd-7-1483-2014, 2014.
- Petit, J.-E., Favez, O., Sciare, J., Crenn, V., Sarda-Estève, R., Bonnaire, N., Močnik, G., Dupont, J.-C., Haeffelin, M. and Leoz-Garziandia, E.: Two years of near real-time chemical composition of submicron aerosols in the region of Paris using an Aerosol Chemical Speciation Monitor (ACSM) and a multi-wavelength Aethalometer, *Atmospheric Chem. Phys.*, 15(6), 2985–3005, doi:10.5194/acp-15-2985-2015, 2015.
- Petit, J.-E., Favez, O., Albinet, A., Canonaco, F.: An Igor-based tool for comprehensive evaluation of the geographical origins of atmospheric pollution: wind and trajectory analyses. *Environmental Modelling and Software*, submitted.
- Petit, J.-E., Favez, O., Amodeo, T., Grenier, D., Pellan, Y., Ockler, A., Rocq, B., Meleux, F., Gros, V., Sciare, J.: Characterising an intense PM pollution episode in March 2015 in France : multi-site approach and near real time data, in prep.
- Putaud, J.-P., Raes, F., Van Dingenen, R., Brüggemann, E., Facchini, M.-C., Decesari, S., Fuzzi, S., Gehrig, R., Hüglin, C., Laj, P., Lorbeer, G., Maenhaut, W., Mihalopoulos, N., Müller, K., Querol, X., Rodriguez, S., Schneider, J., Spindler, G., Brink, H. ten, Tørseth, K. and Wiedensohler, A.: A European aerosol phenomenology—2: chemical characteristics of particulate matter at kerbside, urban, rural and background sites in Europe, *Atmos. Environ.*, 38(16), 2579–2595, doi:10.1016/j.atmosenv.2004.01.041, 2004.
- Ramgolam, K., Favez, O., Cachier, H., Gaudichet, A., Marano, F., Martinon, L. and Baeza-Squiban, A.: Size-partitioning of an urban aerosol to identify particle determinants involved in the proinflammatory response induced in airway epithelial cells, *Part. Fibre Toxicol.*, 6(10), doi:10.1186/1743-8977-6-10, 2009.
- Sandradewi, J., Prévôt, A. S. H., Szidat, S., Perron, N., Alfara, M. R., Lanz, V. A., Weingartner, E. and Baltensperger, U.: Using Aerosol Light Absorption Measurements for the Quantitative Determination of Wood Burning and Traffic Emission Contributions to Particulate Matter, *Environ. Sci. Technol.*, 42(9), 3316–3323, doi:10.1021/es702253m, 2008.
- Waked, A., Favez, O., Alleman, L. Y., Piot, C., Petit, J.-E., Delaunay, T., Verlinden, E., Golly, B., Besombes, J.-L., Jaffrezo, J.-L. and Leoz-Garziandia, E.: Source apportionment of PM₁₀ in a north-western Europe regional urban background site (Lens, France) using positive matrix factorization and including primary biogenic emissions, *Atmospheric Chem. Phys.*, 14(7), 3325–3346, doi:10.5194/acp-14-3325-2014, 2014.
- Willmott, C. J., Robeson, S. M. and Matsuura, K.: A refined index of model performance, *Int. J. Climatol.*, 32(13), 2088–2094, doi:10.1002/joc.2419, 2012.

Effects of Alternative Drive Technologies and -Fuels on CO₂-Emissions from Road Traffic in Germany

Conrad PIASECKI*

* Federal Highway Research Institute (BAST), Bergisch Gladbach, 51427, Germany
Phone: +49 (0)2204 43 613, Fax: +49 (0)2204 43 676, email: Piasecki@bast.de

Abstract

Road traffic is in addition to the energy- and industry sector one main source of air pollution and carbon dioxide emissions. Although most countries and manufacturers agreed to environmental regulations to reduce the pollutant emissions, particularly in urban areas with high traffic density, the importance of road traffic emissions on the environment and human health has been growing steadily.

Due to stricter emission standards and the use of emission reducing systems (e. g. catalysts, diesel particulate filter (DPF), selective catalytic reduction (SCR)) emissions from road traffic have been reduced significantly since the last two decades, UBA (2015a). Besides the improvement of conventional vehicle technologies the increasing share of vehicles equipped with alternative drive concepts and -fuels provides an additional option to achieve climate goals and air quality objectives, Küter et al. (2011). These includes an advancing electrification of the powertrain - from micro hybrid systems to battery electric vehicles and fuel cell propulsion systems – as well as the use of alternative fuels as e. g. compressed natural gas (CNG), liquefied petroleum gas (LPG), biomass to liquid (BtL) and biomethan.

In this context, the calculation and forecast of road traffic emissions is an important option to assess the effects of new drive concepts and -fuels on emissions and energy consumption, and to prove compliance of climate goals. For that purpose the Federal Highway Research Institute uses the emission- and calculation tool TREMOD (Transport Emission Model) which provides baseline data and calculated results for pollutants and greenhouse gases in almost every differentiation, Knörr et al., (2012). Moreover, scenarios on future emission trends, fleet composition and traffic development can be carried out.

As a part of a model expansion emission- and fleet datasets of vehicles equipped with alternative drive technologies and -fuels have been implemented into TREMOD. Thus, the effects of these concepts on emissions and fuel/energy-consumption to the total road traffic emissions can be analysed. Within this project trend scenarios are carried out with TREMOD to simulate the fleet composition, the traffic distribution and the CO₂-emissions of passenger cars with different alternative drive and –fuel technologies. As a result preliminary statements about the possible changes in CO₂-emissions due to increasing market penetration of alternative drive concepts by means of modelling can be made.

Keys-words: emission modelling, TREMOD, alternative drive concepts, CO₂-emissions, HBEFA

Introduction

The increase in world population and global economic performance associated with the still increasing demand for energy and mobility, particularly in emerging markets, leads to a series of socio-economic and political changes as well as far-reaching impacts on the environment and climate, Huwart et al., (2014). In addition to the energy and industrial sector, the transport sector contributes significantly to environmental- and climate relevant emissions such as nitrogen oxides (NO_x), hydrocarbons (HC), carbon monoxide (CO), particles (PM) and carbon dioxide (CO₂), UBA (2015b).

In this context, national governments and their associations and authorities developed regulations to mitigate the negative effects of these developments within the framework of national or international agreements. However, the resolution of such agreements requires a full understanding of the processes and polluters, which caused such developments ahead. In this process the calculation and forecast of air pollutants and climate-relevant emissions has a significant role, as it is a scientific basis for the preparation and enforcement of policies and regulations and as it is an option to verify compliance and effectiveness.

The Federal Highway Research Institute (BAST) uses the emission- and calculation tool TREMOD on behalf of the German Federal Ministry of Transport for the calculation and prediction of road traffic emissions, fuel consumption and annual traffic in Germany. The tool was developed in the early 1990's by the Institute for Energy- and Environmental Research Heidelberg GmbH (IFEU) on behalf of the German Federal Environment Agency (UBA) and has been updated steadily in the context of research projects with regard to traffic information and vehicle inventory trends, as well as on current emission data of newly introduced vehicles. TREMOD is used by the governmental institutions as an accepted tool for national and international emission reporting obligations. In addition it allows identifying such road users that contribute disproportionately to road traffic emissions and greenhouse gases and it serves as a scientific basis for the enactment of regulations and laws in Germany.

To ensure the quality of TREMOD calculations in the future, taking into account a changing fleet composition to vehicles with alternative drive systems and fuels, BAST commissioned IFEU to carry out a model extension that reflects these changes and the corresponding effects on emissions adequately. The methodology of TREMOD and its innovations as well as the underlying database Handbook Emission Factors for Road Transport (HBEFA) are described in this report. Finally, trend scenarios are carried out that show the effects of new drive technologies and fuels on passenger car CO₂-emissions in Germany up to the year 2050.

1. Methodology

As a part of the extension of TREMOD all relevant calculation process parameters were examined and adjusted. So, the TREMOD classified vehicle classes were supplemented by alternative drive concepts and fuels, taking into account different fuel mixtures as well. In addition, the vehicle inventory data were expanded to vehicle fleet data sets with alternative drive technologies and fuels based on registration statistics of the German Federal Motor Transport Authority (KBA). The total annual traffic of all relevant vehicle segments was estimated and data sets were implemented into TREMOD. Moreover, assumptions regarding the total amount of consumed alternative fuels and energy consumption were made. Based on results from national and international studies on vehicle emissions, it was possible to estimate emission factors of vehicles with alternative drive concepts and fuels and use them as the basis for the scenario calculation in TREMOD. Besides direct vehicle emissions also the relevant prechain-emissions from the fuel- and energy production and delivery were considered.

The work within this project was carried out in coordination with the parallel development activities on the HBEFA so that the data base of both tools are matching together. Considering the above mentioned steps, finally a trend scenario up to 2050 was defined and calculated with TREMOD. The properties of the selected new fuels and drive concepts and their implementation into the TREMOD model and the results of the scenario calculation were described in detail.

TREMOD

The development of the emission calculation tool TREMOD was initiated in the early 90's on behalf of the German Federal Environment Agency, in order to query detailed information concerning emissions, fuel- and energy consumption for road-, rail-, air-, and waterway transport in Germany, Knörr et al., (2012). Due to the importance of the road traffic sector (the share of CO₂-emissions caused by road traffic to the total CO₂-emissions in Germany was 17.4 % in 2010) this sector is implemented in detail, UBA (2012). TREMOD therefore contains very extensive information on annual traffic, emissions and fuel consumption of all road traffic participants differentiated with regard to the classification in HBEFA.

The input database in TREMOD consists of real emission- and fuel consumption data of all road traffic vehicle categories and their sub- segments in terms of emission factors, which are collected within the HBEFA, as well as on detailed information of annual traffic, also differentiated to vehicle category, road type and local situation, which are collected as a part of driving performance surveys and counting stations carried out on behalf of BAST, Hautzinger et al., (2002), Palm et al., (1994a, 1994b, 1996). Provided that emission factors for one vehicle type in relevant traffic situations are known the total emissions for this class are determined in TREMOD by multiplying the emission factors with the distributed annual traffic of this vehicle class taking into account the vehicle inventory evolution. Information on vehicle inventory and fleet distribution in TREMOD are taken from the Federal Motor Transport Authority and are implemented in TREMOD annually. The prediction of future vehicle stock in TREMOD is done based on estimations of future registrations and on survival curves for actual vehicles. The survival curves describe the percentage decrease within the vehicle stock over

a defined period. Based on the survival curves, the proportion of those vehicles that are eliminated from the market due to age can be determined.

The continuous updating of the input data base in TREMOD by generating emission factors of new vehicle types for HBEFA on the one hand as well as the implementation of actual traffic data and vehicle stock information is necessary to ensure the usability of the calculated results. The results are presented in annual steps retrospectively from the year 1960 up to the current date based on real emission-, annual traffic- and inventory data (basis scenario) and as a trend scenario up to 2050, in which assumptions on future trends in vehicle technology, emission standards and traffic density are made. The actual TREMOD database which is used in this study at hand is the version 5.53.

HBEFA

The Handbook Emission Factors for Road Transports represents a database, which contains information on regulated and non-regulated air pollutants, greenhouse gases and fuel consumption of all relevant vehicle categories in the greatest differentiation. It resulted from a joint cooperation between Germany and Switzerland in the late 1980's, which aimed to bring together the research activities in the field of emission measurements of road vehicles and to increase the quality of the emission data base, Keller et al., (2004). Meanwhile Austria, the Netherlands, Sweden, Norway, France, Greece and the Joint Research Center (JRC) of the European Commission contribute country-specific data sets on emissions and fleet composition in order to improve the development of HBEFA. Thus the number of emission data shown in HBEFA has been extended continuously by nationally funded measurement campaigns. Currently HBEFA Version 3.2 contains emission data sets of the following vehicle categories: Passenger cars, light- and heavy duty vehicles, powered two-wheelers and buses, differentiated into long distance coaches and public buses. These are further divided into segments and sub segments, of which a segment is a group of vehicles with the same engine type (e. g. diesel, gasoline, etc.) and size (displacement / vehicle mass), and this is further differentiated by its sub-segment, which describes the emission level of this vehicle. The emission levels before the introduction of European-wide level Euro 1 in 1992 are summarized within HBEFA as a sub segment "PreEuro". HBEFA includes emission factors for the components shown in table 1.

Table 1. Emission components within HBEFA.

Category	Components
Regulated pollutants	Hydrocarbons (HC), Carbon monoxide (CO), Nitrogen oxides (NO _x), Particulate matter (PM), Non-methane hydrocarbons (NMHC)
Non-regulated components	Nitrogen dioxide (NO ₂), Sulfur dioxide (SO ₂), Ammonia (NH ₃), Benzol (C ₆ H ₆), Particulate number (PN), Fuel consumption (FC)
Greenhouse gases	Carbon dioxide (CO ₂), Methane (CH ₄), Nitrous oxide (N ₂ O)

The emission and fuel consumption of a vehicle depends on numerous parameters such as vehicle speed and load condition as well as on the longitudinal road gradient and dynamic driving parameters. In order to describe the emission behavior of a vehicle, it is therefore necessary to have information on emissions and fuel consumption for their typical driving patterns in real traffic situations. In HBEFA a structure has been created, that classifies the typical real driving situations in the form of driving patterns, and that assigns a corresponding emission- and fuel consumption factor with the unit g/km to each of them. A driving pattern describes the course of velocity over time (driving cycle), which tracks the driving behavior of a vehicle for a particular driving situation, of which are four defined in HBEFA ("Free flow", "Saturated traffic", "Heavy traffic", "Stop + Go"). In addition, a driving pattern is characterized by an average speed. As the driving situations occur on all road types, local situations (rural / agglomeration) and speed limit zones and each of these combinations describes a separate driving pattern (different velocity- and acceleration curves; different average speeds) the classification of "traffic situations" was created in HBEFA. This assigns each combination of local situation, road type (motorway, trunk road, secondary road, district road, local road) and speed limit zone a corresponding driving pattern (e. g. rural/motorway/speed limit 120/saturated). This kind of classification takes into account the effect, that different traffic situations can have a similar average speed, but the underlying driving pattern and the associated emission factor differ. Overall, HBEFA contains 276 individual traffic situations that are linked with emission-, and fuel consumption factors for each vehicle segment and sub-segment. The emission factors are based on exhaust gas measurements in real driving cycles on chassis dynamometers and are derived for the respective driving patterns. Besides operational emissions HBEFA includes also surcharges on cold-start emissions and evaporative emissions that are deposited transaction-based in g HC/transaction for hot-

soak emissions and g HC/day for diurnal losses.

2. Baseline Results

The calculated trend scenario including the new drive technologies represent partly significant changes with regard to the fleet composition, the annual traffic development and the related CO₂-emissions from passenger cars (PC) in Germany within the period 2010 – 2050, as shown in fig. 1.

The total number of passenger cars registered in Germany will remain nearly the same up to 2050, namely about 45 – 48 mio. vehicles. Fig. 1 (a) shows, that there will be a trend within the German fleet composition to vehicles with alternative drives concepts and -fuels from about 2020 onwards, while the number of vehicles powered by conventional drive systems like petrol or diesel will decrease steadily. It turns out, that in a first step vehicles equipped with hybrid or plug-in hybrid systems will replace conventional cars, whereas fully electrified powertrains like battery electric vehicles (BEV) will gain relevant market shares first from 2030 onwards. Up to 2050 nearly 80 % of diesel and petrol vehicles will be replaced by newly introduced drive concepts. The share of BEV in the market is estimated to be about nearly 20 % then.

The development of the annual traffic from passenger cars up to 2050 is similar to that of the fleet composition (see fig. 1 (b)). Currently, about 600 bn. km are driven on German roads by passenger cars. It is expected that there will be a further increase in total annual traffic to a maximum value of about 650 bn. km/a in 2030. Henceforth it is expected that the total annual traffic will decrease due to e. g. demographic effects. Similar to the fleet composition development the share of annual traffic of vehicles powered by conventional drive systems decreases significantly up to 2050; a decline to about 150 bn. km/a is expected within the trend scenario for diesel and petrol cars.

As a consequence the progressive market penetration of vehicles equipped with alternative drive systems and -fuels, particularly from 2020 onwards, effects the amount of CO₂-emissions from passenger cars in Germany. Besides to efficiency improvements of conventional drive systems, a shift to electric vehicles and the drop in annual traffic after 2030 generates a decline in CO₂-emissions of about 60 % up to 2050 in relation to the basis scenario of 2010.

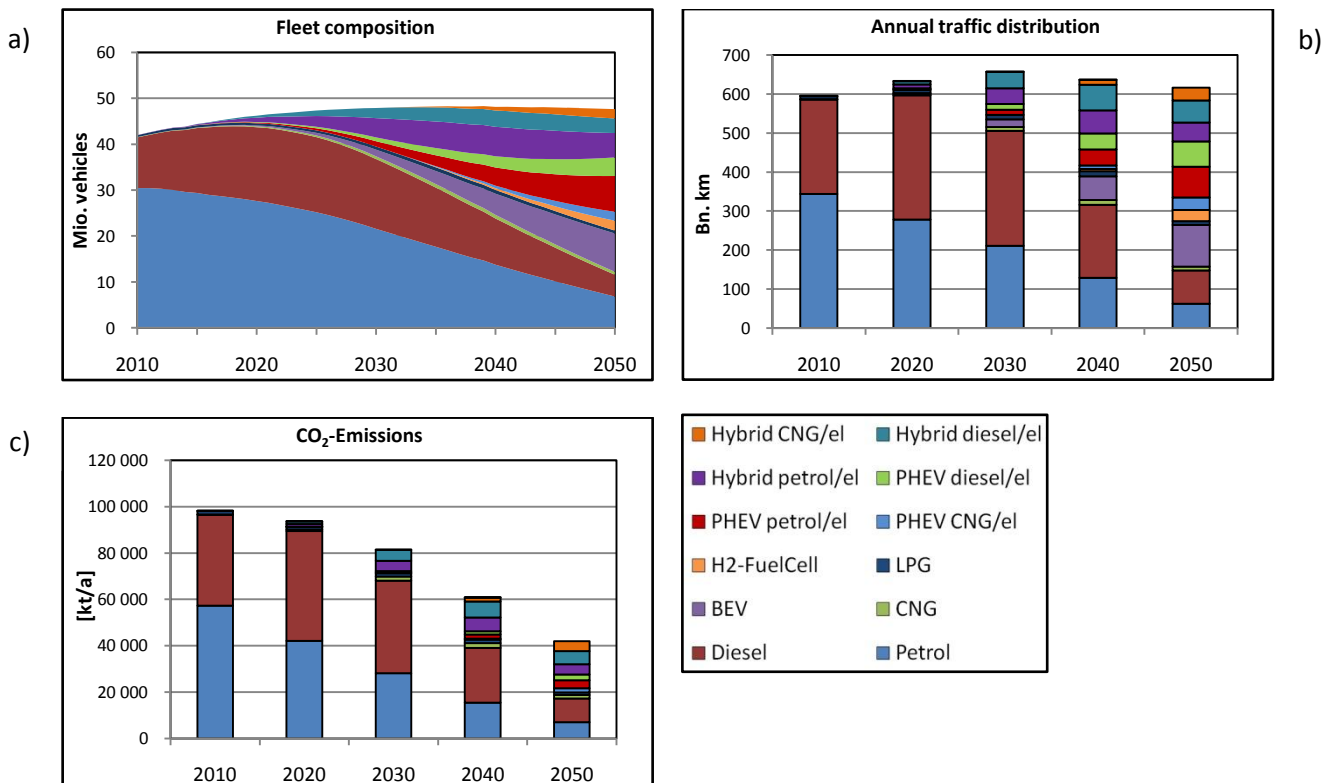


Fig. 1: Trend scenario results differentiated by drive concept, 2010 – 2050
(a) Fleet composition (b) Annual traffic distribution (c) CO₂-Emissions

3. Conclusion

The extension of TREMOD model to alternative drive technologies and fuels allows the calculation of road traffic emissions and fuel- and energy consumption up to 2050 taking into account a changing fleet composition and annual traffic distribution in Germany. In addition to new drive technologies the availability and use of alternative energy sources and their mixtures are included in the calculation. However, the representativeness of the calculations with TREMOD depends largely on the quality of the input data base. So, the continuous updating of the input data base with regard to vehicle inventory, annual traffic and emission factors for all relevant vehicle types to the latest developments and the coordinated work with the HBEFA is required.

References

- Hautzinger, H., Stock, W., Mayer, K., Schmidt, J., Heidemann, D. (2005): Fahrleistungserhebung 2002 Inländerfahrleistung, Bergisch Gladbach, Mai 2005.
- Huwart, J. and L. Verdier (2014): Die Globalisierung der Wirtschaft: Ursprünge und Auswirkungen, OECD Insights, OECD Publishing. <http://dx.doi.org/10.1787/9789264221765-de>.
- Keller, M., de Haan, P., Knörr, W., Hausberger, S., Steven, H.; Handbuch Emissionsfaktoren des Straßenverkehrs 2.1 – Dokumentation. Bern/Heidelberg/Graz/Essen. 18. August 2004.
- Knörr, W., Heidt, C., Schacht, A. (2012): Aktualisierung "Daten- und Rechenmodell: Energieverbrauch und Schadstoffemissionen des Motorisierten Verkehrs in Deutschland 1960 - 2030" (TREMOD, Version 5.3) für die Emissionsberichtserstattung 2013 (Berichtsperiode 1990 - 2011), Heidelberg, 30.09.2012.
- Küter, J., Holdik, H., Pöppel-Decker, M., Ullitzsch, M. (2011): Alternative Antriebstechnologien – Marktdurchdringung und Konsequenzen. Berichtsjahr 2011 – Abschlussbericht. Berichte der Bundesanstalt für Straßenwesen, Reihe Mensch und Sicherheit. Heft M 240. Bergisch Gladbach, 2011, pp. 14 ff..
- Palm, I., Regniet, G., Schmidt, G., Heusch-Boesefeldt (1994a): Nutzfahrzeug-Jahresfahrleistungen 1990 (1986) auf den Straßen in der Bundesrepublik Deutschland; im Auftrag des Bundesministeriums für Verkehr; Aachen 1994.
- Palm, I., Regniet, G., Schmidt, G., Heusch-Boesefeldt (1994b): Ermittlung der Pkw-Jahresfahrleistungen 1990 und 1986 auf allen Straßen in der Bundesrepublik Deutschland; im Auftrag des Bundesministeriums für Verkehr, Aachen 1994.
- Palm, I., Regniet, G., Schmidt, G., Heusch-Boesefeldt (1996): Ermittlung der Pkw und Nfz-Jahresfahrleistungen 1993 auf allen Straßen in der Bundesrepublik Deutschland; im Auftrag des Bundesministeriums für Verkehr, Aachen 1996.
- UBA (2015a): Daten zur Umwelt 2015 – Umwelttrends in Deutschland, Dessau-Roßlau, August 2015, pp. 112 ff..
- UBA (2015b): Nationale Trendtabellen für die deutsche Berichterstattung atmosphärischer Emissionen seit 1990, Emissionsentwicklung 1990 – 2013 (Stand 03/2015).
- UBA (2012): Daten zum Verkehr, Ausgabe 2012. Umweltbundesamt, Dessau, Oktober 2012, p. 44 ff.

Metrological characterization of a remote sensing equipment for on-road emission measurements: Considerations for detecting high-emitter vehicles

Manuel PUJADAS*, Aida DOMÍNGUEZ-SÁEZ*, Josefina De la FUENTE** & Carmen BARRIOS

** CIEMAT, Avda. Complutense, 40, 28040, Madrid, Spain
Tel +34 913466131 - email: manuel.pujadas@ciemat.es

* RemoteSensingLaboratory, Madrid, 28015, Spain.

Abstract

Optical remote sensing techniques were developed in USA for traffic emission measurements more than twenty years ago, giving place to different Remote Sensing Device (RSD) commercial models. These instruments are capable of measuring pollutant emissions produced by individual vehicles in real driving conditions and they have been used widely in the USA for research purposes and for official emission controls. Although these systems have also been used in other countries, outside the USA they are not yet approved instruments. This means that, an eventual future use of RSD instruments in Europe as official control tools will demand a previous metrological evaluation and a subsequent certification of these equipments. Considering this situation, this work has been devoted to assess metrologically the actual performance of the AccuScan RSD4600 model and the results of this study are presented in this paper. This remote sensor has been tested under controlled conditions in on-road and in laboratory essays designed for it. Moreover, as one of the eventual future key applications of these remote sensing techniques should be the detection and identification of "high emitters" vehicles in the European circulating parks, in this paper a short analysis of the conditions that should be fulfilled for this specific purpose is also presented.

Keys-words: Air pollution, traffic emissions, remote sensing, NO_x, high emitters.

Introduction

The definitive solution for anthropogenic air pollution is the drastic reduction of atmospheric emissions produced by pollutant sources. In Europe, E.Commission has tried to brake the negative effect of vehicle emissions by approving the successive Euro Standards for the automotive sector but the effectiveness has not been exactly as expected. Moreover, it is known that all fleets count with a little fraction of circulating vehicles operating very far from their certified characteristics, presenting very high emissions mainly of NO_x and particles. As a consequence, an effective option to improve the air quality in cities is to reduce the presence of these "high emitters" in the circulating fleets. To get it, their detection through no invasive measurements is the key element. Optical remote sensing of on-road exhaust emissions is the most suitable technology to detect efficiently the presence of those high emitter vehicles (Borken-Kleefeld et al, 2012). This kind of technique, developed in USA (Stedman and Bishop, 1993), has been used widely, not only for this purpose but also to improve the accuracy of traffic emission inventories (Chen and Borken-Kleefeld, 2014), to verify inspection and maintenance programs, etc. Nevertheless, as this technology has not yet been certified in Europe, its application has been strictly limited to develop interesting field studies but up its approval it could not be applied by public bodies to official emission controls.

The main goal of this work has been to study (from a metrological point of view) the performance and operation of optical remote sensing techniques applied to on-road emission measurements as well as determine the feasibility of their potential application in the control individualized of exhaust emissions overlooking to the identification of high-emitter (HE) vehicles.

1. Methodology

The equipment tested in this metrological study has been the AccuScanRSD4600 that gives the ratios NO/CO₂, HC/CO₂ and CO/CO₂ present in the exhaust plume of the vehicles. The main goal of this work was to evaluate the quality of those concentration ratios given by this instrument and to achieve this objective, three independent experimental campaigns were carried out:

1.1 On-road measurements of synthetic plumes

Gaseous plumes were synthetically generated from certified gas bottles to determine the measurement uncertainty of the RSD4600 depending on Plume Size (PS) exhaust (% cm CO₂). In real traffic conditions, the PS is influenced by factors like the proper vehicle emissions during the time of measurement, the aerodynamic flows generated by the movement of the vehicle, the position of the exhaust pipe, wind, etc. The objective of these experiments was to document the reproducibility and the uncertainty of the results provided by RSD in a wide range of emission ratios and under different plume sizes.

The procedure used in these essays was based on the production of gaseous plumes of known chemical composition from certified mixtures of CO, NO, HC and CO₂, whose concentrations have been selected to be similar to actual vehicle emissions (synthetic plumes). To do this, certified multicomponent gas bottles were connected to a gas suitable dispenser device, controlled by solenoid valves manually operated, that allowed to emit an actual reference gaseous plume through an open pipe. With this system, different quantities of the distinct gas mixtures used could be released into the atmosphere, producing different types of plumes with known composition. In this way it was necessary to expose the synthetic plumes to the same dispersive conditions (geometry, radio dilution, etc.) produced by a vehicle. To do this, the synthetic plume generation system was installed in a vehicle 100% electric "zero emissions". Under these conditions, the certified gases were emitted from a tube simulating exhaust installed in the electric vehicle. With this system synthetic plumes were generated in both dynamic mode (moving vehicle) and static (stationary vehicle) and from similar heights to an exhaust of a conventional vehicle.

Multiple emissions in different configurations were analyzed by the RSD4600, obtaining a large database of CO/CO₂, NO/CO₂ and HC/CO₂ with varying plume sizes. During these experiments multicomponent bottles supplied by Air Liquide with a nominal uncertainty of 2% for concentrations of all the gases were used. Three different ranges of concentrations were used (see Table 1) in order to simulate three types of emission levels C1, C2 and C3. The range represented by C1 corresponds to a vehicle that can be considered high emitter. For each experiment with a fixed concentration, we use two different certified bottles with nominal concentrations equal but with slightly different in actual concentrations. Concentrations of all bottles used are shown in Table 1.

Table 1. Concentrations and emission ratios of the different bottles used for the experiments

	NO (ppm)	NOx (ppm)	HC (ppm C ₃ H ₈)	CO (%)	CO ₂ (%)	NO/CO ₂ (10 ⁻⁴)	HC/CO ₂ (10 ⁻⁴)	CO/CO ₂
C1_1	6005	6005	1279,1	3,45	12,49	480,78	102,41	0,28
C1_2	6032	6032	1281,6	3,44	12,62	477,97	101,55	0,27
C2_1	409,6	411,4	1120,4	4,91	11,22	36,51	99,86	0,44
C2_2	398,7	401,1	1117,7	4,91	11,2	35,60	99,79	0,44
C3_1	1979,9	1987,1	1205,6	4	12,04	164,44	100,13	0,33
C3_2	1985	1991,4	1207	4	11,99	165,55	100,67	0,33

1.2 Dynamometer engine test bench experiments

Emissions generated by a dynamometer engine test bench (2.0 TDI 140 hp) were measured with the RSD4600 device and simultaneously with an OBS-2200 Horiba. The dynamometer engine test bench is computer controlled. These experiments were aimed to determine the influence on the response of RSD to different values of the VSP parameter (Vehicle Specific Power). VSP is a technical term used in evaluating vehicle emissions defined as the engine power output per vehicle unit mass (kW/t) and is expressed as a function of vehicle speed, road grade and acceleration (Jiménez-Palacios, 1998). In driving conditions the VSP parameter takes into account aerodynamic drag, tire rolling resistance and road grade. To be able to perform suitable on-road remote emission measurements with RSD, it is necessary that the engines of the vehicles circulating in front of the

instrument are at an appropriate point of work, ie, the instant vehicle specific power (VSP) and the instantaneous fuel consumption must be appropriate.

The experiments were conducted in a test bench at CIEMAT premises equipped with a Euro 4 diesel engine (VAG 2.0 TDI 140hp type BKD) and a Schenck W150 dynamometer, both controlled from computer connected to SparKE 2003 Horiba system. From the technical specifications of the vehicle (mass, frontal area, drag coefficient, coefficient of rolling resistance and transmission efficiency), the necessary power for the vehicle is moving at a certain speed and acceleration is obtained. From the known transmission developments and assuming the right gear at each velocity, engine speed and engine torque corresponding to the estimated velocity and acceleration to be reproduced.

During the development of these experiments, six levels of different VSP were reproduced in the bench, covering virtually the entire range of VSP values that are typically recorded during with RSD measurements in real traffic. The following values were selected: 3, 8, 13, 18, 23 and 28 kW/t. In Table 2 the engine operating conditions corresponding to each VSP value are presented. In each essay the concentration ratios provided by RSD4600 were compared with the measurements registered with the OBS-2200.

During the development of these experiments, six levels of different VSP could be reproduced in the bench covering virtually the entire range of VSP values that are typically recorded during with RSD measurements in real traffic. The following values were selected: 3, 8, 13, 18, 23 and 28 kW/t. For each VSP values, the engine operating conditions contained in Table 2 correspond. In each essay the concentration ratios provided by RSD4600 were compared with those obtained from measurements registered with the OBS-2200.

Table2. Engine conditions

VSP	v (km/h)	a ((km/h)/s)	% grade road	Gear	Engine speed (rpm)	Engine torque(N.m)
3	50	0	0	III	2108	24.1
8	85	0	0	IV	2645	50.1
13	106	0	0	V	2719	78
18	106	0	1.6	V	2719	109
23	70	3	0	III	2952	128.7
28	140	0	0.5	VI	2998	150.3

1.3 Field campaigns of on-road measurements in Madrid Region

The database (De la Fuente et al, 2015) was used to evaluate the influence of VSP and PS in concrete cases of circulating vehicles. Three limits on the emission ratios have been suggested ($NO/CO_2 = 88.10^{-4}$, $HC/CO_2 = 80.10^{-4}$ and $CO/CO_2 = 0.18$) for the determination of HE in category M1 through the use of remote techniques (for example with the instrument RSD4600).

2. Results

The results section has been divided into three sections, one for each of the campaigns conducted.

2.1 On-road measurements of synthetic plumes

The large number of tests performed successfully with synthetic plumes (992 experiments), generated a robust set of results for a statistically consistent analysis of quality measurements provided by the RSD4600. Specifically, these experiments allowed to study the uncertainty of the results against the measured concentrations and against the recorded value of the gas plume size (Table 3).

Table3.Main statistical results of experiments with synthetic plumes.

	NO/CO ₂			HC/CO ₂ (10 ⁻⁴)			CO/CO ₂ (10 ⁻⁴)		
Concentration	C1	C2	C3	C1	C2	C3	C1	C2	C3
Number of experiments	321	427	244	321	427	244	321	427	244
Max	628,80	52,15	201,00	140,40	155,60	148,20	3,16E-01	5,31E-01	3,89E-01
Min	397,7	23,22	59,55	77,81	77,83	78,32	0,2567	0,37	0,3129
Mean	500,50	38,16	159,60	105,00	103,00	101,20	2,78E-01	4,36E-01	3,40E-01
Median	499,20	38,19	160,30	103,70	101,00	99,24	2,78E-01	4,38E-01	3,36E-01
Standard deviation	33,29	3,02	12,40	7,87	9,08	9,74	1,08E-02	2,90E-02	1,36E-02
Range	231,10	28,93	142,20	62,59	77,80	69,88	5,91E-02	1,61E-01	7,62E-02
Pattern Ratio	479,38	36,05	165,00	101,98	99,83	100,40	2,74E-01	4,38E-01	3,33E-01
Systematic Error	21,12	2,11	-5,40	3,02	3,17	0,80	4,00E-03	-1,70E-03	6,66E-03
Total uncertainty (%)	6,65	7,92	7,77	7,50	8,81	9,63	3,88	6,64	3,99

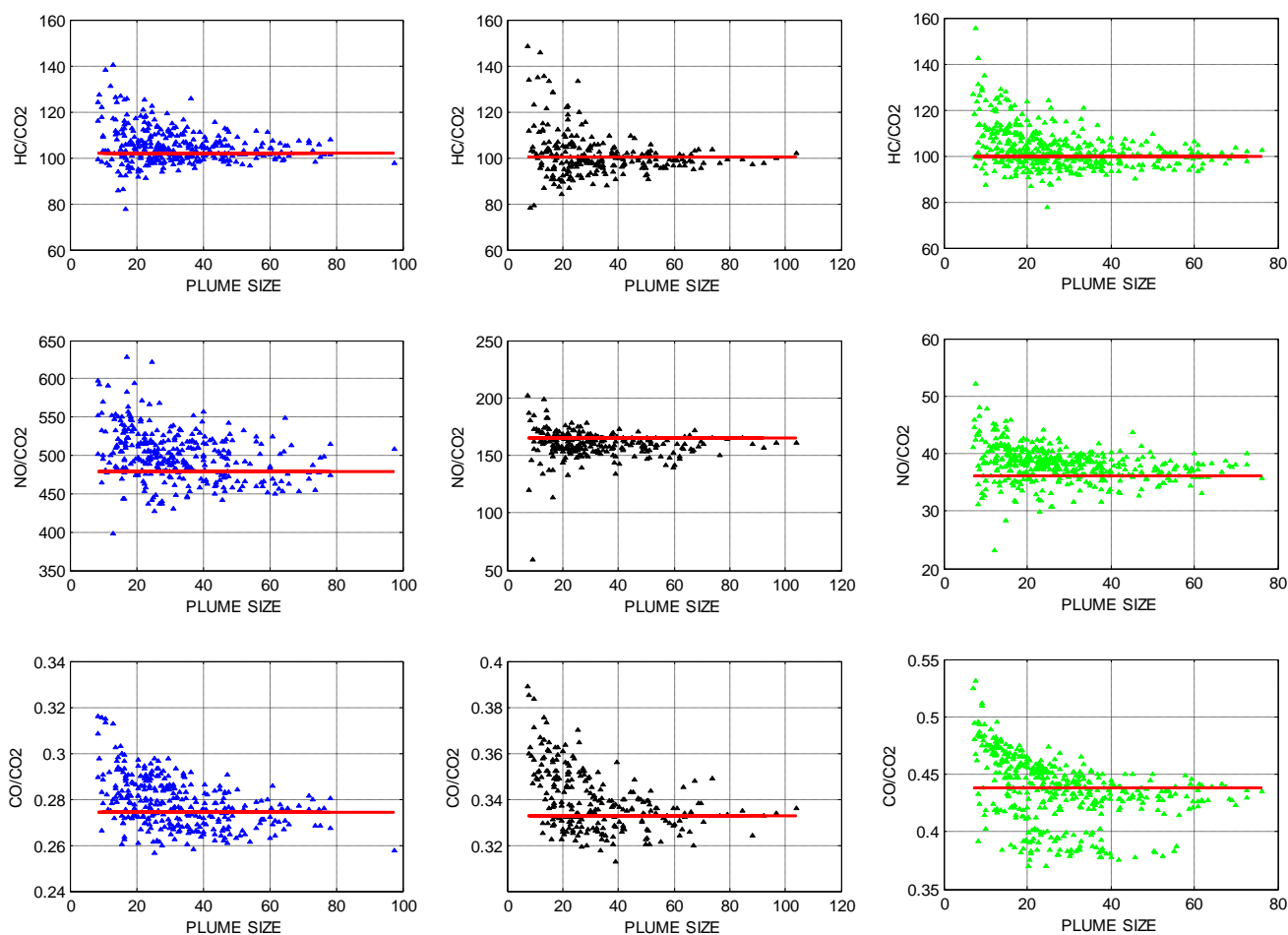


Figure1.Ratios of pollutants measured by RSD with the different synthetic plumes.The values of the reference ratios attending the composition of the certified gas bottles in each case are indicated by the red lines. In blue data corresponding to C1, in black C2 and in green C3.

In figure 1, the measured ratios for each concentration and each pollutant are shown. Greater dispersion of all ratios is observed in the lower ranges of PS. To analyze the dependence of the uncertainty on the value of the PS, it has performed an analysis classifying the results of measurements in three ranges of PS:

$$PS < 20, 20 < PS < 40 \text{ y } PS > 40.$$

Determining that, for values of PS > 20, average uncertainties of the measurements made by the RSD4600 are less than 10% in all cases and for all pollutants. It is important to note the relevance to correctly perform the periodic calibration operations that RSD needs. In the lower right panel of figure 1 a set of measurements affected by a zero drift can be observed. This effect was due to a little error produced during one of the numerous periodic RSD calibration operations that were implemented in these experiments.

2.2 Dynamometer engine test bench experiments

As CO and HC for a modern engine (especially Euro 4) are below the limits of detection of many technologies of emission measurements, in the bench tests only NO/CO₂ measures were performed. Figure 2 shows the ratios of NO/CO₂(RSD4600) or NO_x/CO₂ (OBS 2200) vs the different VSP selected. In table 3 are summarized the main statistical parameters that result of RSD-OBS comparison.

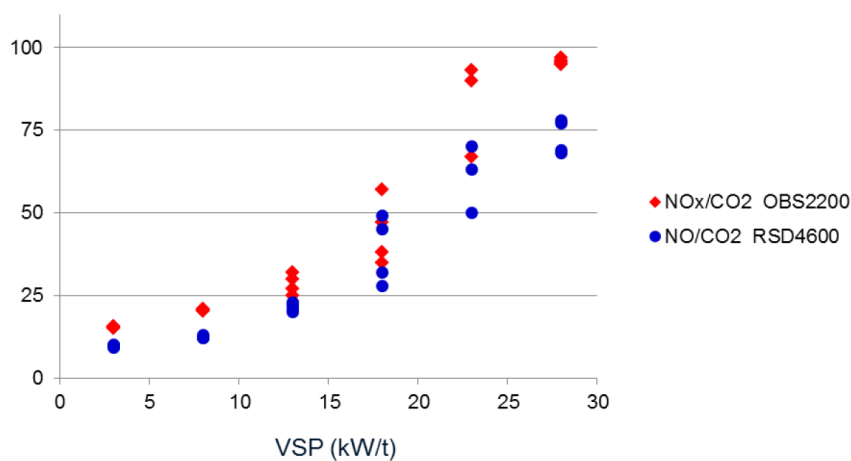


Figure 2. Ratios of NO/CO₂ obtained by RSD4600 (in blue) and NO_x/CO₂ from OBS 2200 measurements (in red) vs VSP values in test bench.

Table 3. Main statistical results of experiments with plumes produced in test bench.

		VSP					
		3	8	13	18	23	28
Number of experiments	RSD	6	6	6	5	5	4
	OBS	6	6	6	5	5	4
NO/CO ₂ (10 ⁻⁴) mean	RSD	7,10	10,33	21,92	37,32	56,66	73,08
	OBS	12,23	21,83	28,50	46,80	78,40	94,00
Standard deviation	RSD	0,87	1,16	1,20	8,69	16,21	5,04
	OBS	0,39	0,41	2,46	12,30	26,70	0,82
Mean PS		47,16	72,02	84,23	103,47	89,65	130,30
Absolute Accuracy Error		5,13	11,50	6,58	9,48	21,74	20,92
Relative Accuracy Error		72,30	111,31	30,04	25,40	38,36	28,63

There is a clear increase of concentration ratio values with VSP and both measuring systems show increasing instability when VSP increases. The table shows that the dispersion of the ratios with both measuring equipment also increases with VSP. This growing trend in emission ratios against the VSP is more representative of diesel engines and must be taken into account in the process of identifying HE vehicles. This point is very important in order to minimize the risk of identifying false positives. As a consequence, it is strongly recommended to establish an appropriate range of VSPs, limiting the maximum value of the VSP to do HE determinations. Otherwise, exceedances of HE limits could occur as a result of excessive instantaneous VSP of vehicles passing in front of the RSD system.

2.3 Field campaigns of on-road measurements in Madrid Region

As the experimental campaign with synthetic plumes emphasized the importance of PS on the measurement uncertainty of the RSD, it has been evaluated the influence of this parameter to detect HE. Overall, the proportion of high emitters for PS values <20 almost double the percentage recorded for PS > 20 (table 4).

Table 4. Percentage of high emitters detected versus plume size measured.

		PS			
		Total	<20	20-40	>40
All vehicles	Total	182804	81377	93994	7433
	HE number	11845	7103	4568	174
	%	6,48	8,73	4,86	2,34
Diesel	Total	141553	62637	73416	5500
	HE number	8720	5058	3558	104
	%	6,16	8,08	4,84	1,89
Gasoline	Total	41251	18740	20578	1933
	HE number	3125	2045	1010	70
	%	7,58	10,91	4,91	3,62

On the other hand, to evaluate the influence of VSP on HE detection, it has performed an analysis of the distribution of the results of measurements of RSD according to the VSP detected and vehicle fuel. In Table 5, figure 3 and figure 4 the results of these distributions are presented. All data were considered, excluding those with PS <20.

Table 5. Distribution of high emitters vehicles in category M1 considering the proposed limits.

		Total	VSP 2-6	VSP 6-10	VSP 10-14	VSP 14-18	VSP 18-22	VSP 22-26	VSP 26-30
All vehicles	Total	101427	13520	24577	25545	18451	10868	5774	2692
	HE	4741	315	767	997	948	763	576	375
	%	4,67	2,33	3,12	3,90	5,14	7,02	9,98	13,93
Diesel	Total	78916	10050	19048	19965	14400	8563	4670	2220
	HE	3662	215	524	704	712	650	518	339
	%	4,64	2,14	2,75	3,53	4,94	7,59	11,09	15,27
Gasoline	Total	22511	3470	5529	5580	4051	2305	1104	472
	HE	1080	101	243	293	236	113	58	36
	%	4,80	2,91	4,40	5,25	5,83	4,90	5,25	7,63

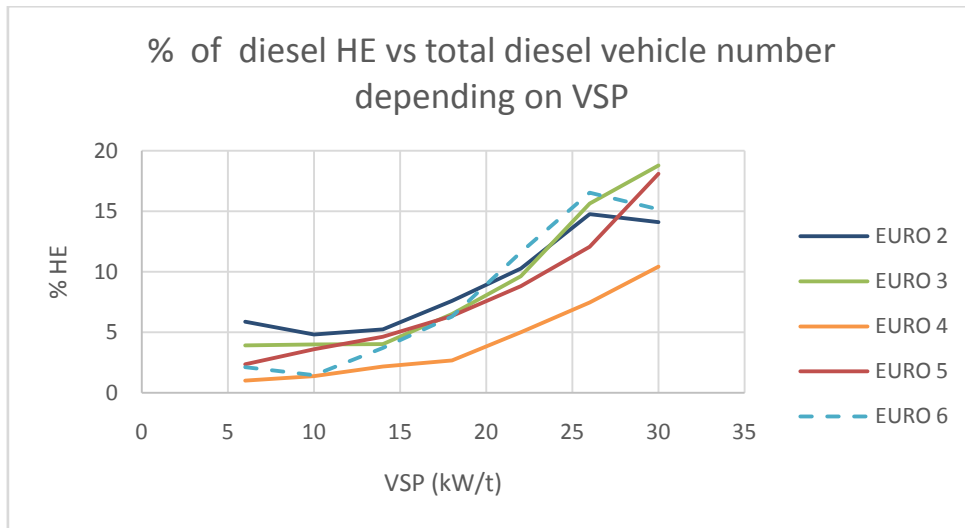


Figure3.High emitter distribution depending on VSP for diesel vehicles.

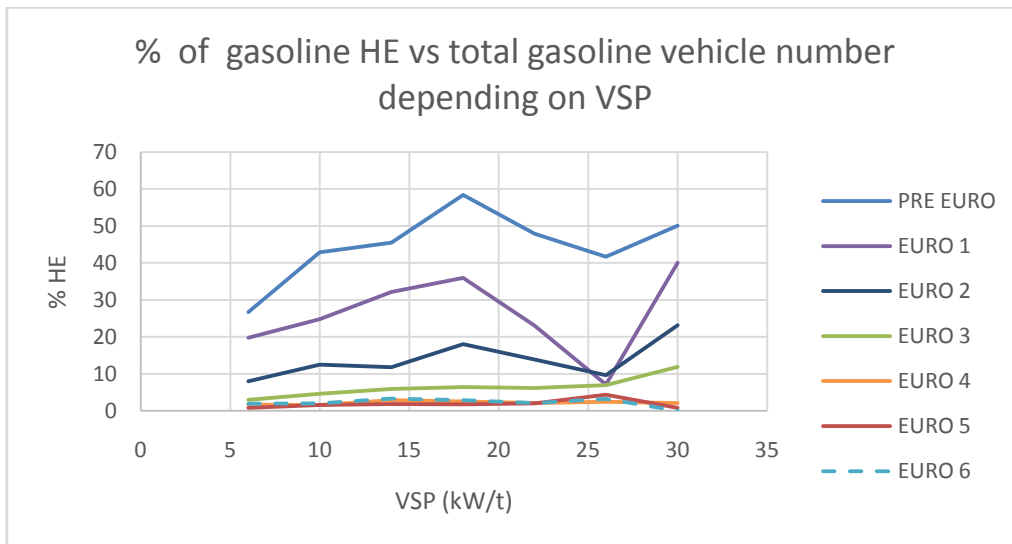


Figure4.High emitter distribution depending on VSP for gasoline vehicles.

Some of the most relevant results of this study are: for PS values > 20 the average uncertainty of the measurements conducted with the RSD-4600 are lower than 10% in all cases; the emission ratio NO/CO₂ depends significantly on the VSP parameter in line with the results obtained by Carslaw et al (2013) and Bishop and Stedman (2008); for VSP values higher than 20, there are possibilities of detecting as high-emitters to vehicles with normal operation. This risk is observed especially for modern diesel (post-Euro 3) vehicles.

Conclusion

The results of controlled experiments implemented to evaluate the metrological performance of an RSD4600 remote sensing equipment have documented the good reliability of the measurements provided by it and has allowed to study the influence on them of different parameters external to the RSD. From the results obtained in these tests, it has been verified that vehicle emission concentration ratios provided by the RSD4600 instrument are governed by quality control applied by the device itself. Specifically, this system only reports the values of the ratios of emission of NO/CO₂, CO/CO₂ and HC/CO₂ that have exceeded the criteria of acceptance/rejection automatically applied by this

instrument. One of those criteria has to do with the value of the parameter called Plume Size (PS) and verified that when this factor is greater than 20 ($PS > 20$) the uncertainty of measured concentration ratios by this equipment is less than 10%.

It has also been shown that, in order to correctly identify truly High Emitters vehicles with RSD measurements, it is also necessary to establish appropriate conditions for their use. If these conditions are not guaranteed, there is a moderate risk of making incorrect identifications of high emitters. This problem would not be due to RSD instrument failure but rather a lack of representation of measured data regarding to the actual emission behavior of the vehicle.

Acknowledgments

The measurement campaigns were developed in the framework of CORETRA project funded by Fundación Biodiversidad (Ministerio de Agricultura, Alimentación y Medio Ambiente of Spain) under Grant CA 2014.

References

- Bishop, G.A., Stedman, D.H., (2008). A decade of on-road emissions measurements. *Environ. Sci. Technol.* 42 (5), 1651-1656.
- Borken-Kleefeld, J., Kupiainen, K., Chen, Y., Hausberger, S., Rexeis, M., Sjodin, A., Jerksjo, M. and Tate, J. (2012). ERMES 2012 Plenary Meeting.
- Carslaw, D.C., Williams, M.L., Tate, J.E. and Beevers, S.D. (2013). New insights from comprehensive on-road measurements of NO_x, NO₂ and NH from vehicle emission remote sensing in London, UK, *Atm. Envi.*, 68, 8–16.
- Chen, Y., Borken-Kleefeld, J. (2014) Real-driving emissions from cars and light commercial vehicles - Results from 13 years remote sensing at Zurich/CH. *Atm. Env.*, 88:157-16
- De la Fuente, J., Domínguez, A. and Pujadas, M. (2016) Study of Traffic Real Driving Emissions in Madrid in 2015 and conclusions., TAP 2016
- Jiménez Palacios, J.L (1999) "Understanding and Quantifying Motor Vehicle Emissions with Vehicle Specific Power and TILDAS Remote Sensing" Thesis, MIT.
- Stedman DH, Bishop GA. (1993) Apparatus for Remote Analysis of Vehicle Emissions, U.S. Patent No. 5, 210, 702, (DU-81 - Multi-Channel FEAT),
http://www.feat.biochem.du.edu/assets/publications/Patent_5210702.pdf

Personal mobility choices and greenhouse gas emissions: which incentives are effective for mitigation?

Charles Raux^{a*}

^a University of Lyon, CNRS, LAET

* corresponding author: email: charles.raux@laet.ish-lyon.cnrs.fr,
address: LAET, ISH, 14 av. Berthelot, 69007 Lyon, France.
Phone: +33472726454, Fax: +33472726448

Abstract

This paper puts in perspective two previous studies analyzing with stated choice experiments the potential of various fiscal instruments combined or not with normative messages (e.g. injunction to reduce GHG emissions). Overall it looks as if fiscal instruments such as carbon tax or carbon trading have limited effects on stated choices on their own. It is only when associated with social norms conveyed by implicit or explicit messaging that they can exhibit their potential. Such results reinforce the case for using psychologically positive framing effects in promoting effective pro-environmental behavior in transport choices. Providing basic CO₂ emissions information on each travel alternative yields effectively intended behavior changes. Normative messages accompanying benchmarking (bonus-malus) or carbon budgeting (quotas) reinforce the incentive especially for larger emitting modes.

Keywords: greenhouse gas emissions; daily mobility; long distance travel; carbon tax; quotas; social norms; stated choices; discrete choice experiments

1 Introduction

There is a majority consensus among climate scientists (and policy makers since the Paris COP 21) on the need for a sharp reduction of anthropogenic greenhouse gas emissions in the next few decades. Transport is one of the main emitter of anthropogenic CO₂ emissions in the world with three-quarters due to road transport and a continuous increase at least since 1990. It is recognized that improvements undertaken in vehicle energy efficiency will not be sufficient in the coming decades and that behavioral changes are also needed, such as shifting from individual to group means of transportation or lower-emission modes per passenger-km or even reducing kilometers travelled.

Regarding behavioral changes, carbon taxes and vehicle taxes are advocated by economists as the most cost-effective instruments. Variants of economic incentives like personal carbon trading have also been proposed. Their roots can be found in the economic literature initially as a combination of economic incentive and quantity control, namely marketable or tradable permits (Baumol and Oates, 1988). Due to the specific nature of tradable permits applied to personal consumption of fuel, potential supplementary outcomes when compared to a carbon tax are expected on psychological grounds rather than economic ones. One effect might come from making carbon visible at the end-user level, with a carbon account delivering frequent feedback on travel behavior (i.e. “carbon budgeting”).

Another effect could come from the social norm associated with a personal allowance fixed within the frame of a public policy. Indeed recent studies in the field of “behavioral economics” have shown that influences devised from social psychology may perform as well and even better than pure economic incentives in generating pro-environmental behavior for instance in the fields of domestic waste management, water or energy consumption.

Given the novelty of the incentives envisaged empirical knowledge regarding their potential effectiveness in changing behavior is limited. This is why the two studies considered thereafter made use of stated choices experiments putting the individuals surveyed in hypothetical but controlled transport choice contexts. In these two studies we have estimated and compared the impacts of economic and psychological incentives in motivating environmentally responsible mobility behavior.

Stated Choice methods are part of the more general Stated Preferences methods which consist of a family of techniques which use individuals’ statements about their preferences when presented with a set of options in a hypothetical context in order to estimate utility functions (Kroes and Sheldon, 1988). In contrast to other stated preferences methods, Stated Choice (SC) methods (Louviere et al., 2000) consist in getting the individuals to make a choice between a set of alternatives on offer.

In a first experiment (Raux et al, 2015a) the potential effectiveness of personal carbon trading (PCT) in changing car travel behavior was compared to the conventional carbon tax (CT) by means of a stated choices survey conducted among French drivers (N~300). The scope of the study was comprehensive annual travel behavior including daily or recurring mobility as well as long distance travel on week-ends or for vacation.

In a second series of experiments (Raux et al, 2015b) we explored the trade-off between (long distance) travel price and travel duration on 900 French participants distributed among seven experiments, while introducing in a controlled setting various effects such as information on CO₂ emissions, injunctive and descriptive social norms, and fiscal incentives such as a carbon tax, a bonus-malus and a personal carbon trading scheme. By “framing” we

mean the ways of presenting a choice based initially on objective economic properties (here the trade-off between travel price and travel time) that do change psychological aspects (information on CO₂ emissions, injunctive and descriptive social norms) and sometimes economic aspects by imposing fiscal incentives (tax, quotas and bonus-malus).

The aim of this paper is to put in perspective these two studies and draw conclusions on the potential of fiscal instruments and psychological incentives based on normative messages to promote pro-environmental behavior in transport choices. The next two sections present successively the two studies with their experimental setting and the recapitulation of their main results. Then these results are discussed before concluding.

2 The first study: comparing carbon tax and personal carbon trading

We first introduce the experimental setting of the first study and then sum up its main results. Details on the methodology and statistical results can be found in Raux et al (2015a).

2.1 Experimental setting

The design of an SC survey includes several steps: sample selection, setting up the context of the experiment and experimental design.

The first stage of the stated choices study consisted in setting up a “fact base”, i.e. the trips carried out by the individual, upon which the hypothetical scenarios (or trade-offs) in the SC survey could be applied. In order to select a sample, interviewers were posted on the street in Lyon city center and at stands in suburban shopping malls (June-July 2009). Those individuals who accepted were given a brief questionnaire about their travel habits for all trip purposes (daily travel, long distance travel, for holidays for instance, but not for business trips) and their car ownership.

Finally the SC survey itself was carried out in January and February 2010. A paper copy of the reported trips along with the set of SC trade-offs had already been sent to the individuals' home in order to facilitate conduct of the survey which was undertaken by phone. Finally after acceptance of the phone survey and questionnaire cleaning the responses of 268 individuals were selected for the statistical analysis.

When compared with the overall profile of the French population this SC sample is younger, more engaged in working activity, more urban, with more presence of minor children in the household, but with roughly the same distribution of income.

In this SC survey, the focus is on respondents' stated behavioral adaptation to various scenarios in which an economic instrument is used (either a CT or PCT), with various levels of taxation (in the case of a CT) or quota prices (in the case of PCT) and various free allowances. An allowance threshold was included in order to make the CT and PCT fully comparable. The individual would be liable to pay the CT above a specific threshold, comparable to the free allowance in the case of PCT. For instance, in the case of the CT, with a threshold of 500 liters of gasoline per year, the individual would have to pay the CT (over and above the current excise tax) on any fuel consumed over 500 liters. Similarly, in the case of PCT, with a free allowance of 500 liters of gasoline per year, the individual would have to buy additional credits for any fuel consumed over 500 liters.

Individuals can reduce their travel emissions in a number of ways: by changing their driving style, by reducing their vehicle-kilometers (for example by increasing the number of passengers in vehicles, reorganizing trips or changing the destinations); by changing their

vehicle or changing transport mode in favor of one which consumes less energy. Some of these actions may be implemented in the short term, while others such as changing one's vehicle or changing one's place of work or residence may take much longer. Since in an SC study respondents must be presented with a closed list of choices, the potential behavioral adaptations have been restricted here to reducing their car mobility (number of trips) in order to reduce or eliminate their need to pay carbon tax or purchase additional carbon credits, or alternatively changing nothing and paying the necessary fiscal amount. The allowance was customized for each individual, depending on their current consumption, in order to maximize the variability of situations in which individuals may find themselves and thus generate statistical information.

Each respondent was presented with four trade-offs (or choice situations), consisting of two with a CT and two with the PCT. For each trade-off, the individuals were presented with three adaptation options, which were personalized according to their travel behavior and the percentage reduction in the number of their trips. The individual had to choose one of these options. The first two combined different levels of car mobility reduction. The third option was in all exercises the "change nothing and pay" option, in which the individual changes nothing in their travel behavior but has to pay a tax (CT) or buy quotas (PCT). Each of the three options included, of course, the payment to be made, i.e. the amount of tax to pay or additional credits to buy, or even the amount earned by selling unused credits.

2.2 *Main results*

The 268 respondents were each presented with 4 choice situations (or trade-offs), which amounted to a potential total of 1072 choice situations, of which 994 received an effective response. 41% of the choices made were option 3 ("change nothing and pay"): this indicates a strong preference for the status quo regarding own mobility behavior even if this involves additional monetary costs. This is confirmed by the estimation of the discrete choice model between the three options where the constant associated with this third option is significant and positive.

One issue is whether this third option was chosen by specific categories of individuals which could reflect constraints (or preferences) regarding their mobility. Among the various socio-demographic attributes such as age, gender, occupation, residential location and presence of children in the household, only the age has a significant influence on behavioral (stated) adaptations. Individuals aged under 25 chose this option less than average while individuals aged between 50 and 65 years chose this option more than average. Again this age effect is confirmed by the discrete choice modeling. This may indicate a generation effect, with middle-aged people being more reluctant to change their mobility behavior.

The second result standing out from the choices stated by the individuals is that the reduction in car trips lessens according to increasing distance categories. The interviewees tend to reduce preferentially their daily trips, i.e. commuting and shopping (corresponding to fairly short distances), while "safeguarding" week-end and holiday trips (corresponding to fairly long distances).

The third result stands out from the comparison (separate modeling) of the CT on the one hand and PCT schemes on the other hand. The CT schemes give coefficient values that are mostly statistically insignificant and erratic. In contrast, in the case of the PCT schemes, the impacts of some variables (such as the income and the distance remaining) are significant.

However the statistical tests show that the absence of a difference in the effectiveness of the two instruments (CT and PCT) cannot be rejected.

3 The second study: comparing various psychological and fiscal incentives

The experimental setting of this second study is introduced, followed by the summary of the main results. The details regarding this study can be found in Raux et al (2015b).

3.1 Experimental setting

Building on the results and perspectives of the previous study, the aim of this second study was to explore in-depth the tradeoff between price and duration of travel in various framing conditions. Contrasting with the previous study which covered the whole car mobility, the field experiment here is long distance leisure travel. Such casual travel choices are distinct from routine daily travel behavior and lead to specific decision at each time. Moreover, the quantity of CO₂ emissions for each such travel decision is sufficiently large to yield significant values of decision parameters and to lead the respondents to play into the assessment of the various alternatives.

Participants were presented with a fictitious scenario in which they had to travel to a destination at about 1,000 km from their home location for a one week of holidays accompanied by a person of their choice. The one week holiday duration aims at making ground transportation a relevant choice given the necessary time to travel this distance. Travelling with somebody else aims at making private car a plausible alternative given its price. Participants had to choose between four different travel modes (air, car, coach, train) or renouncing travel altogether, in a series of choice situations with various combinations of travel price, duration and framing conditions.

The framing conditions refer to various psychological and economic incentives. As in a clinical trials a “baseline control group” was established where only the basic price-time tradeoff between travel modes had to be performed. The survey for this control condition was conducted in June 2013.

For each of the subsequent experimental conditions another group of individuals is selected randomly and assigned to one and only one condition. Because of this random selection, the assumption is made that the responses of any individual assigned to any given experimental condition can be compared to the responses of any other individual assigned to any other experimental condition. Moreover, because each group is assigned to one and only one condition the effect of each condition can be isolated. The differences in responses will allow measurement of the effects only due to differences in experimental conditions.

The next experimental conditions were conducted in December 2013. The aim of the second condition was to see if providing basic information on CO₂ emissions for each trip was encouraging pro-environment behavior compared with control condition. In the screens showing the duration and price tradeoff between alternative transportation modes, the amount of CO₂ emissions associated with each travel mode was added. The same quantity applied for a given mode regardless of travel duration (which is a simplification): 180 Kg of CO₂ for train, 720 kg for air and 124 kg for coach (round trip for two persons for these three transport modes), 408 kg for car (roundtrip for the vehicle).

In the third experimental condition, an “injunctive norm” was added to the CO₂ information in order to assess the impact of such a psychological incentive. This injunctive norm was stated as follows: “The high level of greenhouse gas emissions in the atmosphere (such as CO₂) can cause dangerous climate change for the planet. Climatologists are already seeing many consequences such as melting glaciers or ice field. According to scientists, to limit these effects it is necessary that all humans reduce their emissions by half”.

In the fourth condition, a potential reinforcing effect by a “descriptive norm” is tested. The following sentence is added to the previous injunctive norm: “60% of French people personally contribute through their daily actions to reduce their emissions”.

Finally, the last experimental conditions were conducted in June 2014 and involved fiscal incentives added to the CO₂ information and the injunctive norm. These last two framing effects were kept as necessary to make the introduction of fiscal incentives plausible.

In the fifth experimental condition a carbon tax is applied starting from the first unit of fuel consumed and thus of CO₂ emissions. The aim of this experimental condition is to see if an economic sanction increases or not the use of the least emitter modes of transportation when compared with previous Condition 3 (injunctive norm).

In the sixth condition, a first kind of “social normalization” was tested with a bonus-malus scheme. In this scheme a malus increasing the initial price applies when the CO₂ emissions exceed a given threshold and a bonus decreasing the initial price applies when the emissions are under this threshold.

The last economic instrument, in the seventh condition, is that of quotas (or carbon allowances) allocated to each individual and corresponding to an authorization to emit CO₂. Following her travel choices, the individual account is debited from the allowances in proportion of emissions of the travel mode chosen. If the account balance is in the red the individual must buy allowances as needed, but if it is in credit she may sell her allowances unused. This experimental condition is similar to the bonus-malus one since it combines an economic sanction with a social norm effect. The only difference is in the framing of the policy.

The seven experimental conditions were conducted via an Internet panel on seven different samples, totaling 900 participants in eight French urban areas (Paris, Lyon, Marseille, Toulouse, Lille, Bordeaux, Nice, Nantes). These eight areas were selected as they host an airport connected to the world airline network. Each of the seven samples was representative of the French population according to the quota method (gender x age, job status household, urban area) with individuals aged from 25 to 70.

The experimental design is described in Table 1.

Table 1: Description of the experimental design

Experimental conditions	Description	When	N	N included in analysis
1 (control)	Price and duration combination	June 2013	300	293
2	Price and duration combination + CO ₂ emissions information	December 2013	100	100
3	Price and duration combination + CO ₂ emissions information + injunctive norm	December 2013	100	96
4	Price and duration combination + CO ₂ emissions information + injunctive norm+ descriptive norm	December 2013	100	99
5	Price and duration combination + CO ₂ emissions information + injunctive norm + tax	June 2014	100	99
6	Price and duration combination + CO ₂ emissions information + injunctive norm + bonus/malus	June 2014	100	99
7	Price and duration combination + CO ₂ emissions information + injunctive norm + quotas	June 2014	100	99

3.2 Main results

Firstly, we estimate a model on the control condition (taking into account only the trade-off between travel price and travel time). The four transport modes constants are significant and positive which means that people prefer travelling over renouncing travel. Then we observe that the “renouncing travel” alternative is chosen by very few respondents across all experimental conditions: from 3% to 8% of all responses (choice situations) according to the seven experimental conditions. This is an indication of an overall preference for travelling long distance (in fact for leisure or holidays) despite the various incentives tested.

Then, after eliminating the “renouncing travel” alternative, we pool all the experimental conditions in one sample (N=5010) in order to give an overall estimate of the various framing effects. The travel mode constants are significant and positive meaning that people prefer travelling by air, train or car rather than coach (the reference of comparison). The price and duration coefficients are significant and negative as expected. All the framing effects are significant and negative: they decrease the probability of using air, car and train when compared to coach.

Figure 1 shows the variation of these framing effects according to the travel modes. Overall these effects are stronger on air than on car and then train. Providing CO₂ information on mode emissions is much highly effective in reducing the preference for air and car when compared to train. This effect is reinforced by the injunctive norm (IN) in the case of air and train but not in the case of car. Adding the descriptive norm (DN) decreases the cumulated effect of CO₂ information and injunctive norm. Adding one of the fiscal incentives (tax, bonus-malus or quota) to the combination of CO₂ information and injunctive norm generally decreases this last effect. However, bonus-malus (BM) and then quota schemes appear to have a stronger effect than a tax scheme. Moreover, the effect of the quota scheme is stronger than the effect of the sole injunctive norm in reducing the preferences for the air or train.

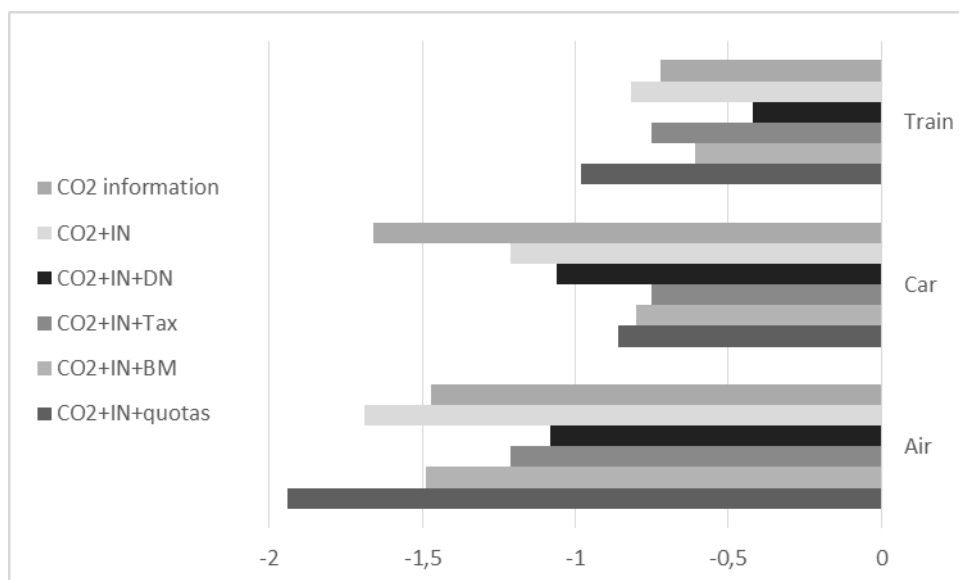


Figure 1: Comparison of framing effects according to travel modes

4 Discussion

First, there is some evidence that an economic instrument like PCT could change travel behavior and hence transport emissions from personal travel. People state they would reduce their car travel in all of the distance categories, but tend to protect their long and very long trips. However, this behavior is not strictly related to distance, since the marginal utility of a kilometer does not differ from one distance category to another, but rather are to trip purpose. It is clear that week-end and holiday trips are the last to be changed.

Second, in the first study people prefer the status quo, as reflected by the significant numbers choosing the “change nothing and pay” option. There is a definite reluctance to reduce car travel, as shown by the negative effects of eliminating trips or the positive marginal utilities of kilometers travelled. Moreover this preference for mobility status quo is stronger for older people than for younger ones.

Third, there is no significant difference in the effectiveness of a CT and PCT when it comes to changing travel behavior. This is in line with economic theory and is indicative of the consistency of the experiment. It also concurs with other findings in the literature (Capstick and Lewis, 2009; Parag et al., 2011; Zanni et al., 2013) despite these studies used different methodologies from ours.

Fourth, however, the CT trade-offs provide erratic and mostly non-significant estimates, while the PCT trade-offs show contrasted and significant effects, which reflects consistency in the respondent’s stated behavior. One possible explanation of this difference could be the novelty of the PCT scheme when compared with CT. Another explanation could lie in a difference in the acceptability of the instruments (the “tax” being straightaway rejected), which could have interfered with the experiment.

The consistency in the responses concerning PCT and its effectiveness in changing (stated) behavior indicates that this instrument has some potential for promoting and

involving people in travel behavior that is more environmentally responsible. The characteristics of PCT, and especially the kind of social norm associated with a personal allowance fixed within a public policy target, could help to activate pro-environmental behavior.

This is why we explored in a second series of experiments the potential of psychological incentives in motivating environmentally responsible behavior in a context of long distance leisure travel with various framing effects: information on CO₂ emissions, injunctive and descriptive norms, in combination or not with a carbon tax, a bonus-malus or a carbon trading (quotas) scheme.

First this experiment confirms the previous one regarding the general preference of individuals in safeguarding long distance travel for leisure or holidays.

Second the various framing conditions all have a significant effect of reducing the intention to choose the most emitting modes. One striking result is that providing CO₂ information on mode emissions is highly effective in reducing the preferences for the most emitting modes (train, air and car). The injunctive norm reinforces this effect in the case of air and train.

Third, another striking result is that adding a descriptive norm or fiscal framing like carbon tax or bonus-malus schemes looks overall counterproductive since the cumulated effect decreases when compared with the only CO₂ information + injunctive norm.

However, bonus-malus and even more quota schemes appear to have a higher effect than the tax scheme. Moreover, for the air and train modes the effect of the quota scheme is higher than the effect of the sole CO₂ information + injunctive norm.

Overall it looks as if fiscal instruments such as carbon tax or carbon trading have limited effects on stated choices on their own. It is only when associated with social norms conveyed by implicit or explicit messaging that they can exhibit their potential.

5 Conclusion

There are some policy implications of such results. First they reinforce the case for using psychologically positive framing effects in promoting effective pro-environmental behavior in transport choices. Providing basic CO₂ emissions information on each travel alternative is likely to yield actual behavior changes. Normative messages accompanying benchmarking (bonus-malus) or carbon budgeting (quotas) may reinforce the incentive especially for larger emitting modes. This indicates that carbon tax or personal carbon trading may have a significant effect only when combined with (social) normative messages.

These two studies add a tangible contribution to the use of behavioral economics in travel behavior analysis, which is still in infancy.

References

- Avineri, E. (2012) On the use and potential of behavioural economics from the perspective of transport and climate change, *Journal of Transport Geography*, 24 (2012) 512–521.
- Baumol, W., Oates, W., 1988. *The theory of environmental policy*. Cambridge University Press, Cambridge, 299p.

- Capstick, S., Lewis, A., 2009. *Personal Carbon Allowances: A Pilot Simulation and Questionnaire*. UKERC, Oxford, 88 p.
- Fawcett, T. and Parag, Y., 2010. An introduction to personal carbon trading. *Climate Policy*, 10(4): 329-338.
- Frey, B., Stutzer, A., 2008. Environmental morale and motivation. In A. Lewis (ed.). *Psychology and economic behavior*. Cambridge: Cambridge University Press (pp. 406-428).
- Hilton, D., Charalambides, L., Demarque, C., Waroquier, L., Raux, C. (2014) A tax can nudge: The impact of an environmentally motivated bonus/malus fiscal system on transport preferences. *Journal of Economic Psychology* 42 (2014) 17–27
- IEA, 2013. *CO₂ Emissions from fuel combustion. IEA Statistics Highlights*. OECD/IEA, 2013.
- IPCC, 2014. Summary for Policymakers, In: *Climate Change 2014, Mitigation of Climate Change. Contribution of Working Group III to the Fifth Assessment Report of the Intergovernmental Panel on Climate Change* [Edenhofer, O., R. Pichs-Madruga, Y. Sokona, E. Farahani, S. Kadner, K. Seyboth, A. Adler, I. Baum, S. Brunner, P. Eickemeier, B. Kriemann, J. Savolainen, S. Schlomer, C. von Stechow, T. Zwickel and J.C. Minx (eds.)]. Cambridge University Press, Cambridge, United Kingdom and New York, NY, USA.
- Kroes, E. P., Sheldon, R. J., 1988. Stated preference methods: an introduction. *Journal of Transport Economics and Policy*, 11-25.
- Louviere, J.J., Hensher, D.A., Swait, J.D., 2000. *Stated Choice Methods: Analysis and Applications*. Cambridge University Press.
- Metcalf, R., Dolan P. (2012) Behavioural economics and its implications for transport, *Journal of Transport Geography*, 24 (2012) 503–511.
- Parag, Y., Capstick, S., Poortinga, W., 2011. Policy Attribute Framing: A Comparison Between Three Policy Instruments for Personal Emissions Reduction. *Journal of Policy Analysis and Management*, Vol. 30, No. 4, 889-905.
- Parry, I.W.H., Walls, M., Harrington, W., 2007. *Automobile Externalities and Policies*. Discussion Paper 06-26. Resources For the Future, Washington, 37 p.
- Raux, C., 2004. The use of transferable permits in transport policy. *Transportation Research Part D*. Vol 9/3, pp 185-197.
- Raux, C., 2010. The Potential for CO₂ emissions trading in transport: the case of personal vehicles and freight, *Energy Efficiency* (2010) 3:133-148.
- Raux, C., 2011. Downstream Emissions Trading for Transport. In Rotthengatter, W., Hayashi, Y., Schade, W. (eds) *Transport Moving to Climate Intelligence: New Chances for Controlling Climate Impacts of Transport after the Economic Crisis*. Springer, pp. 209-226.
- Raux, C., Croissant, Y., Pons, D., 2015a. Would personal carbon trading reduce travel emissions more effectively than a carbon tax? *Transportation Research Part D*, 35 (2015) 72–83
- Raux, C., Marlot, G., 2005. A System of Tradable CO₂ Permits Applied to Fuel Consumption by Motorists. *Transport Policy*, 12 (2005) 255-265.
- Raux, C., Chevalier A., Bougna E., Hilton, D. (2015b) Mobility Choices and Climate Change: Assessing Effects of Social Norms and Economic Incentives Through Discrete Choice Experiments. In *Transportation Research Board 94th Annual*

- Meeting*, Washington DC (USA), January 11-15 2015. <https://halshs.archives-ouvertes.fr/halshs-01158088>
- Stern, N., 2006. *Stern Review on Economics of Climate Change. Executive Summary*. http://www.hm-treasury.gov.uk/media/4/3/Executive_Summary.pdf
- Thaler, R.H., Sunstein, C.R. (2009) *Nudge: Improving Decisions about Health, Wealth, and Happiness*. Penguin, 2009.
- Zanni, A.M., Bristow, A.L., Wardman, M., 2013. The potential behavioural effect of personal carbon trading: results from an experimental survey. *Journal of Environmental Economics and Policy*, vol. 2, No. 2, 222-243.

Real-world CO₂ emission, and cost benefit, of a switch to hybrid electric vehicles in taxi fleets

Richard RILEY*, James TATE**, Hu LI* & Zia WADUD*

*School of Process, Environmental and Materials Engineering, University of Leeds, Leeds, West Yorkshire, LS2 9JT, UK. Email: pm08rjar@leeds.ac.uk

**Institute of Transport Studies, University of Leeds, Leeds, West Yorkshire, LS2 9JT, UK. Email: J.E.Tate@its.leeds.ac.uk

Abstract

This study examines the potential of hybrid electric vehicles to reduce CO₂ emissions from taxi fleets. In the UK hybrid vehicles make up a very small proportion of the fleet, but look set to be an important technology in meeting national CO₂ targets, and air quality standards. This paper focuses on taxis, as they are a good initial focus for policies, encouraging the uptake of hybrid vehicles. This is because taxis predominantly operate in urban stop-start driving conditions, where the efficiency benefits of the hybrid powertrain are the greatest. Taxis also have higher mileage than private vehicles, so emission savings will be greater, and payback times shorter. Legislative test cycles do not represent taxi driving due to their unusual driving pattern, meaning official figures do not accurately inform taxi drivers, or policy makers, about the emissions, or costs of different technologies. To help inform stakeholders, this study recorded vehicle activity, and fuel consumption of a third generation Toyota Prius over a range of representative taxi test routes in Leeds. The vehicle was tested for over 780km (484 miles), using three driving styles. The vehicle activity data, including road gradient, was also simulated by the micro-scale emission model PHEM, which produced fuel consumption data for a comparative petrol, and diesel vehicle. The hybrid outperformed the two conventional vehicles for all driving styles, reducing the fuel consumption by 7.99 L/100km, and 3.49 L/100km, and providing an annual saving of £3,976, and £1,912 compared to the petrol, and diesel respectively.

Keys-words: *Taxi, Hybrid, Emissions, Cost Benefit.*

Introduction

Hybrid electric vehicles are being introduced by motor manufacturers to markets around the world to meet a range of national, and regional vehicle CO₂ emission targets. Despite the technology being available to consumers for around 20 years, and the technology having significantly improved, hybrid vehicle sales are still very low in the UK, making up 0.6% of the fleet, UK Department for Transport (2015a), and 1.6% of new car sales in 2014, UK Department for Transport (2015b). To help meet transport, and wider emission targets, governments should start by encouraging the uptake of low emission vehicles in particularly advantageous markets. At the start of this research, the authors believed taxis could be one of the best early adopter markets for hybrid vehicles in the UK. This assumption was based on several observations.

Firstly, Taxis come under far more government regulation for registration, and use than private vehicles, this provides a greater range of policy levers to encourage hybrid vehicle uptake.

Secondly, while in 2013 there were only around 78,000 taxi vehicles in the UK, making up just 0.27% of the total fleet, UK Department for Transport (2013), their impact is likely to be far larger than their numbers would indicate. Interviews with taxi drivers in Leeds indicate that a taxi will be driven 48,280 km (30,000 miles) a year, while a private hire vehicle with two drivers, completing two shifts per 24 hours, will double this. This mileage is considerably higher than the average UK mileage of 12,713 km (7,900 miles) a year, UK Department for Transport (2014), which means that switching to vehicles with lower emissions will have a greater fuel saving, and emissions benefit for taxis than private cars. As a result taxis benefit from shorter payback times on the high initial cost of low emission vehicles.

Thirdly, hybrid taxis provide far greater exposure of the new technology to the public than private vehicles. While a secondary benefit this could still be important for the uptake of the technology by other users. With around 15 customers a day in Leeds each hybrid taxi could make a real difference to public opinion of hybrid vehicle technologies.

Fourthly, taxis fleets in the UK are dominated by larger engine, diesel vehicles, and their

numbers are focused around urban areas, where they likely do most of their driving. This combination of circumstances suggests there could be great benefits from a switch to hybrid vehicles. Leeds, one of the UK's largest cities, where this research was conducted, has 536 taxis; this fleet is dominated by 2L (41%) and 1.6L (29%) diesel saloons and MPV's (*Leeds City Council, Unpublished Data*). London by far the UK largest city has a taxi fleet of 22,200, making up 28% of all taxis in the UK, UK Department for Transport (2013). London is unusual in having very strict guidelines for taxis, meaning few vehicles are eligible, Transport for London (2007). The London fleet is dominated by vehicles from the London Taxi Company, and the Mercedes Benz Vito, with 2.5L, The London Taxi Company (2015), and 2.1L diesel engines respectively, Mercedes-Benz (2008). London is now realising the damaging effect these polluting vehicles are having on the city air quality, and has specified that all new licenced taxis from 2018 will have to be zero emission capable, which with current technology means plug in hybrids, Transport for London (2015).

Taxis are centred around urban areas, from the source data of the PCO Cenex London Taxi drive cycle, it is estimated that a typical London taxi day has an average speed of 16.33km/h, an average speed excluding stationary data of 25.49 km /h, and spends 29% of the day idling, 28.9% accelerating, 4.7% cruising and 30.5% decelerating (*Millbrook Proving Ground Ltd. Unpublished Data*). These statistics suggests the driving is predominantly stop, start urban driving. The combination of these factors, low speeds, and large diesel engines causes two major problems. Firstly, large engines are very inefficient at low speeds resulting in very high fuel consumption. Secondly, diesel engines, even those having met recent emission limits such as Euro 5, and Euro 6, have been shown to have very high levels of NOx emissions in the real world, Weiss et al (2012).

Hybrid vehicles by comparison, have been shown in several studies to outperform conventional vehicles on fuel consumption, and emissions, especially in urban areas. Costagliola et al. (2015), compared a Euro 4 diesel against a comparable petrol hybrid. Over the Artemis urban cycle, the hybrid had lower emissions for CO, HC, NOx, CO₂, and fuel consumption than the diesel. For CO₂ g/km the diesel was 6, 91, 13, 56% higher than the hybrid over the Urban Drive Cycle (UDC) cold, UDC hot, Extra Urban Drive Cycle (EUDC), and Artemis urban drive cycles respectively. Lenaers(2009), tested a petrol, diesel, and hybrid vehicle in the real world with PEMS equipment. In urban driving the CO₂ emissions from the petrol, and diesel were 70, 39% higher than the hybrid, respectively. Lutsey(2011), looks at the potential of hybrid, and diesel technology to meet future US vehicle emission targets. When comparing hybrid, and diesel CO₂ figures, taken from consumer labels, with comparable petrol vehicles, they found diesel technology could offer a 15% reduction, and hybrids a 30% reduction. The paper also compares the NOx + THC figures from federal test procedure certification data; in this case all diesel vehicles looked at had emissions higher than the fleet average, whereas the average hybrid emissions were 74% lower than the fleet average. It is clear from the literature that hybrids offer great potential benefit both in the reduction of fuel use, and emissions even when compared to modern conventional vehicles technology.

1 Material and Methodology

To test the relative benefits of hybrid vehicle fuel consumption over conventional petrol and diesel vehicles, it was decided to test three comparable vehicles over regular taxi journeys. For ease of use and monetary reasons the vehicles were to be tested using Portable Activity Measurement Equipment (PAMS), rather than Portable Emissions Measurement Equipment (PEMS). This equipment records information from the vehicle Controller Area Network (CAN) bus through the On-Board Diagnostics (OBD II) link. The system records Mass Air Flow (MAF) at the air inlet and lambda which are used to calculate instantaneous fuel consumption. Unfortunately this method only works for petrol engines which operate close to stoichiometric. Due to the difficulty of obtaining and testing three vehicles, it was decided to test a hybrid vehicle, as it is the hardest to model and model the two conventional vehicles. This method also has the benefit that the speed profile is identical for all three vehicles making the fuel consumption output directly comparable on a second by second basis.

Test Vehicle

The vehicle chosen for testing was a 2009, third generation Toyota Prius, at the start of the study the vehicle had 30,000 miles on the clock. This vehicle was chosen because all other hybrid vehicles in the Leeds taxi fleet are second hand 2009-2010 third generation Toyota Prius (*Leeds City Council, Unpublished Data*). The vehicle specifications are summarised in Table 1.

Modelling

The two vehicles modelled were chosen to be closely comparable to the test vehicle and are also summarised in Table 1. The modelling was undertaken using the Technical University of Graz's (TUG)

Passenger car and Heavy duty Emission Model (PHEM). PHEM is a micro-scale emission model; the model inputs are 1Hz vehicle speed and road gradient, from which the model calculates vehicle fuel consumption and emissions (*Luz, R. and S. Hausberger. Unpublished Data*).

Table 1. Specification of test and modelled vehicles.

Registration Year	2009	2010	2010
Vehicle Make and Model	Toyota Prius	Toyota Avensis	Toyota Avensis
Vehicle Classification	1.8 VVT-i T Sprit Hybrid	1.8 V-Matic	2.0D-4D
Fuel Type	Petrol	Petrol	Diesel
Engine Size (cc)	1798	1798	1998
Number Cylinders	4	4	4
Power (ps)	134	147	126
Maximum Torque (Nm)	142	180	310
Kerb Weight (kg)	1370	1375	1500
Vehicle Wheelbase (mm)	2700	2700	2700
CO ₂ Emission Rating (g/km)	92	154	119
Emission Standard	Euro 5	Euro 5	Euro 5

Test Equipment

The vehicle was instrumented using two systems. A Racelogic VBOX Litell connected to a CAN02 and IMU03 modules, and a HEM Data DAWN OBD mini logger. The VBOX Litell has a GPS antenna fixed to the roof of the vehicle and the CAN02 is connected to the CAN using a 'CAN GO Click' which clips onto the CAN wires behind the OBD II port. The Racelogic equipment collected vehicle position, speed, acceleration, pitch, roll and yaw. The HEM Data DAWN OBD mini logger, which plugs directly into the OBD II port, collected 40 variables from the vehicle CAN, including, fuel consumption, power, speed and torque of the major components and battery state of charge. All variables were collected at 2Hz.

Test Routes

The routes driven for the study were chosen after discussion with taxi drivers. From these discussions we learned that a usual taxi drivers shift is 12 hours, consists of 10-15 jobs, 8-9 hours of driving, 3-4 hours of queuing, 50% of jobs travel to around band A, 25% of jobs travel to around band B and the final 25% could be anywhere beyond band B, probably around band C, see Figure 1. Each route starts at a taxi drop off location, heads into the city centre to the train station, queues through the station taxi rank and then head out of the city centre to a different drop off point. Figure 1 shows the routes used, with annotations showing the route start point (S), finish point (F), the location of the train station and the distances for bands A, B and C.

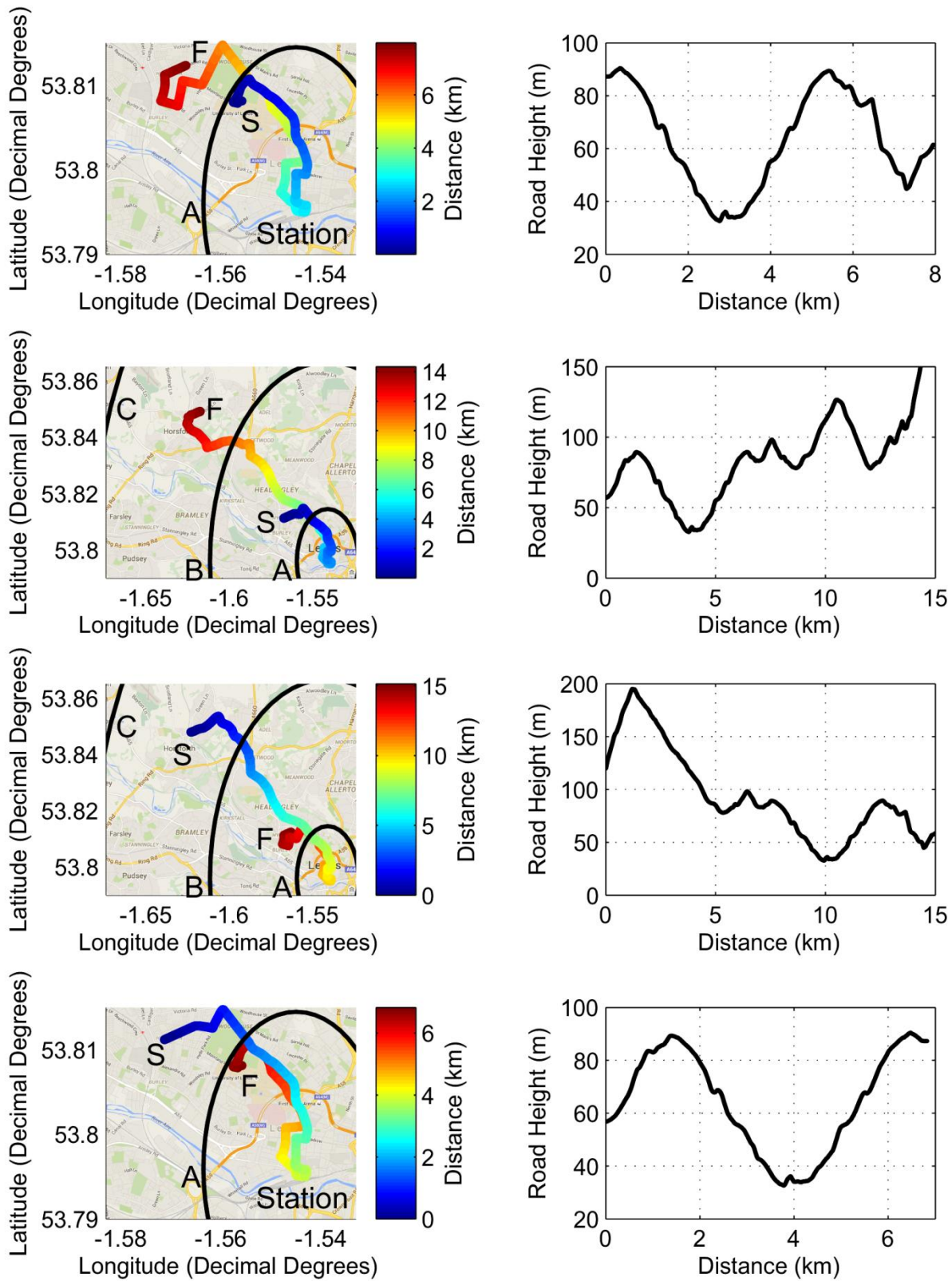


Figure 1. Four test routes with route heights used for Toyota Prius testing.

Testing Procedure

In this study driving tests were conducted between 28th April 2015 and 21st May 2015, this period was chosen as it does not include any school or university holidays that may affect the data. Driving was conducted on Tuesdays, Wednesdays and Thursdays as Mondays and Fridays were expected to be irregular. Each day 8 trips were driven, 4 in the morning starting at 7.15am and ending between 10.00 - 10.30am, and the same 4 trips in the afternoon starting at 2pm and ending between 5.15 – 6.00 pm. The vehicle test routes were chosen to include similar levels of urban and suburban driving as real taxi drivers. The test timings were chosen to include both peak and off peak traffic conditions. Each day of testing is roughly half the number of hours and trips of a real taxi shift. All testing was conducted by one driver, a 25 year old male. As we could not ensure that the test drivers driving style was similar to real taxi drivers, three driving styles were used to cover the full range. Each day the driver tried to drive in a particular driving style; calm, normal or aggressive. Each week contained three days of testing and each day the driver followed one of the three different driving styles. Testing was conducted over three consecutive weeks so each driving style was repeated three times. In total 9 days of driving were conducted, this corresponds to 72 trips, 24 driving calmly, 24 driving normally and 24 driving aggressively. In total over 50 hours corresponding to 780km (484 miles) were driven during testing.

During calm driving, the cars eco mode was selected, which provides the driver with feedback showing the power demanded and suggests an optimum target level to minimise the use of the Internal Combustion Engine (ICE). The driver aims to keep the power demand close to this optimum level while accelerating up to the speed limit. The driver aims to decelerate slowly so that the power from regeneration does not exceed the battery charge rate, this means keeping the bar within the limits of the CHG region in the display. During normal driving the car is left in its default mode (mode the car is in when turned on). In this mode, the driver is given no feedback from the car about their driving style. The driver aims to follow the traffic, matching their driving with the acceleration and speed of the neighbouring cars. During aggressive driving, the cars power mode is selected. In this mode, the driver is given no feedback from the car about their driving style. In these tests the driver aims to pull away from stops quickly and break later coming up to stops. The driver also changes lane more regularly to be in the fastest lane or to move further up the queue at traffic lights, while always obeying road speed limits.

2. Results and Discussion

Taxi Driving Demand

At the beginning of this research we assumed that no legislative CO₂ or fuel consumption data could be used to inform which vehicle would perform best as a taxi in Leeds. This was for two reasons. Firstly, the growing gap between legislative, and real world emission figures is not evenly distributed across, make, segment or technology, making the use of this data for comparison between vehicles very difficult. Secondly, as shown in Figure 2 the driving demand of a taxi is very different to legislative test cycles. Figure 2 a, b, c, d, e, f shows the Toyota Prius test data, with, and without the taxi rank data, the PCO Cenex London taxi driving cycle, the UDDS cycle, the NEDC, and the WLTC respectively. The PCO Cenex cycle was created based on over 500 hours of taxi vehicle tracking data in London, and is therefore a good, representative benchmark of taxi driving in London, and possibly the UK (*Millbrook Proving Ground Ltd. Unpublished Data*).

The test data, and PCO Cenex cycle show very similar speed, and Vehicle Specific Power (VSP) distributions, Jimenez-Palacios (1999), showing that the driving demands of a taxi in Leeds, and London are similar. The closest legislative cycle is the UDDS, which is not surprising considering the central urban data set from which it was created. The UDDS, however, is not the only drive cycle that goes into creating vehicle fuel consumption test figures in USA; the other more aggressive, and highway focused cycles make the test figures more representative of the rest of the fleet, but will make the figures less informative for taxis. The European drive cycles, both the NEDC currently, and the WLTC in the future, lack the low speed power demand, and include too much high speed driving, to provide fuel consumption figures that are useful when comparing technology for taxis.

Another major difference between taxi data, and legislative drive cycles is the idle time. Queuing through the taxi rank adds a significant amount of idling, and engine off phases, to urban driving that already has very high idling percentage. When the test data was collected the test vehicle was kept on for the whole route, but when the speed profile was modelled all stops in the taxi rank longer than one minute where counted as engine off phases for the conventional vehicles. The test data has 10.7% vehicle off, and 27.7% idle data, this is in good agreement with the PCO Cenex source data which has 6.9% vehicle off, and 29% idling (*Millbrook Proving Ground Ltd. Unpublished*

Data). The percentage of idling is very high when compared to test cycles 19.3% UDDS, 27.3% NEDC, and 13% WLTC.

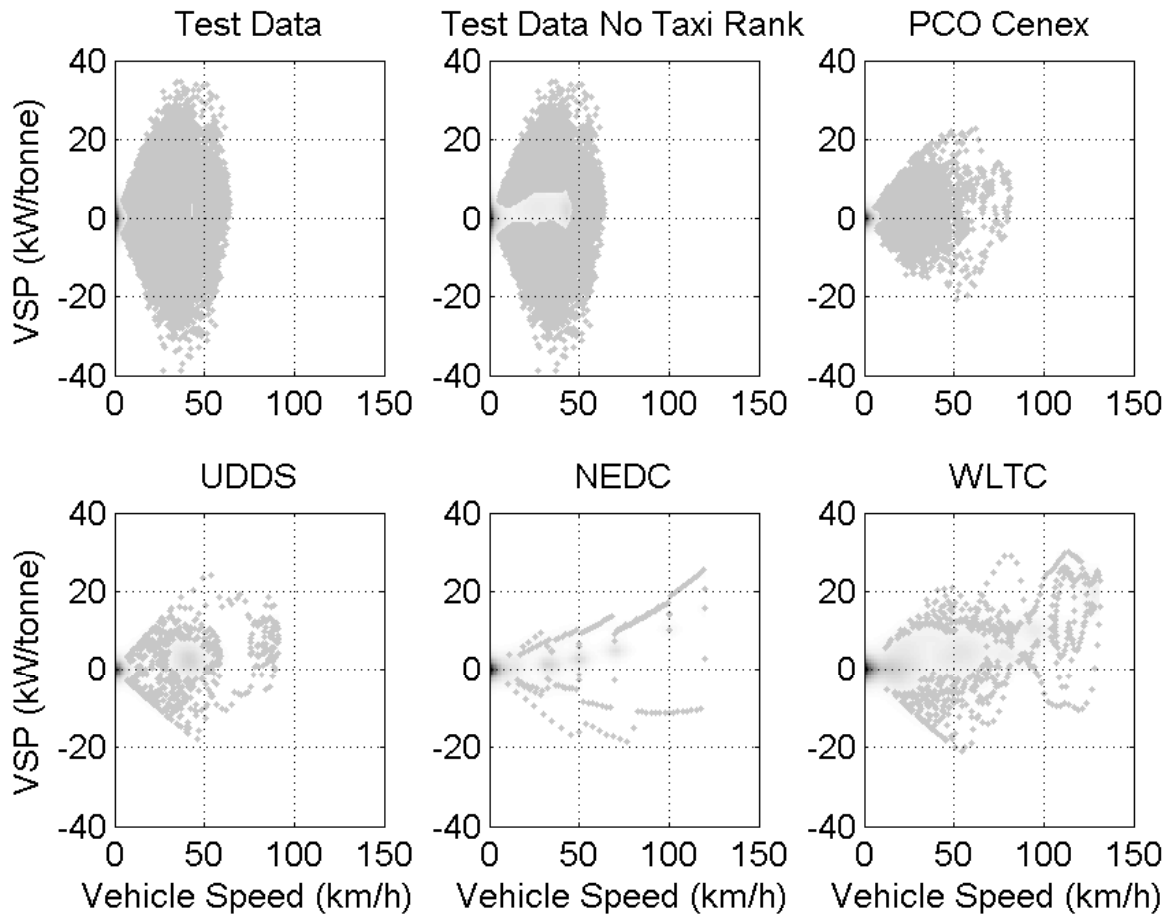


Figure 2. Vehicle Speed against Vehicle Specific Power (VSP) for six data sets. Top-panel (a) Toyota Prius test data, (b) Toyota Prius test data with taxi rank data removed, (c) PCO Cenex London taxi driving cycle. Bottom-panel (d) Urban Dynamometer Driving Schedule (UDDS), (e) New European Drive Cycle (NEDC), (f) Worldwide harmonized Light-duty Test Cycle (WLTC).

Driving Styles

In testing, three different drive styles were used; calm, normal, and aggressive. Figure 3 shows the distribution of speed, and acceleration for the three driving styles, excluding stationary data. These driving styles represent the full range of driving possible in urban conditions. The calm driving accelerated as smoothly as possible, and tried to avoid excessive power, but still had to keep up with the flow of traffic to a large extent. The aggressive driving accelerated as fast as possible, but was limited by the Prius, the traffic flow, and speed limits. The 0.05, 0.25, 0.5, 0.75, 0.95 quantiles, shown in red, clearly show the shift between each driving style. Calm driving has slow acceleration up to the speed limit with a lot of data existing in the acceleration phase. As the driving becomes more aggressive, the low speed acceleration increases, the vehicles moves through the low speeds quickly, and ends up cruising at the speed, or traffic limit. The ranked nonparametric Wilcoxon Mann Whitney test was applied to the test data to check for statistical significant difference between the three driving styles. At 95% confidence level the three driving styles were found to be significantly different from each other for vehicle speed, vehicle acceleration, and fuel consumption.

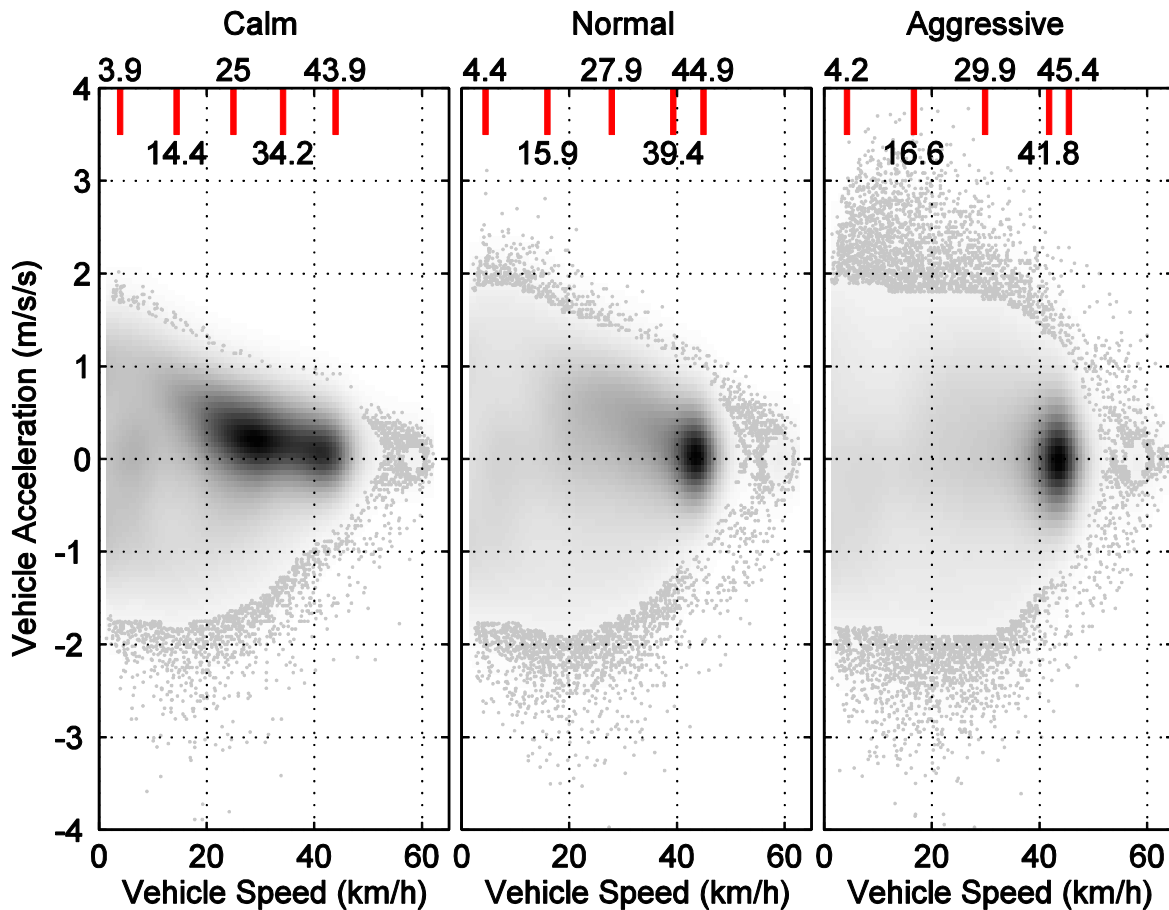


Figure 3. Vehicle speed against vehicle acceleration for three driving styles.

CO₂ Emissions and Fuel Consumption

Table 2 compares the fuel consumption of the three vehicles tested, for the three driving styles. The Prius has the lowest fuel consumption under all three driving conditions, with the lowest fuel consumption in calm driving, and the highest fuel consumption during aggressive driving. The Prius also exhibits the widest range of fuel consumptions, with calm driving saving over 1 l/100km compared to aggressive driving. The Prius switches the engine on for two reasons, because the tractive power demand is too high, or because the battery SOC is too low. During calm driving the vehicle can travel much further before the battery power limit is met, and the engine often turns on due to low battery SOC, whereas during aggressive driving the battery power limit is met soon after the vehicle moves away from a stop, this means that the car cannot utilize the full energy available in the battery. By driving with a calm driving style the percentage time driving in pure electric mode increases by 20%, over aggressive driving. This shift in pure electric mode usage is the main reason why driving style has a greater effect on the Prius than the conventional vehicles. Both of the conventional vehicles are most efficient under normal driving. This is because calm driving forces the engine to operate at low torques, where the engine efficiency is low, and aggressive driving significantly increases the power demand for the cycle.

Table 2. Fuel economy, fuel consumption and CO₂ emissions for three vehicle technologies and three driving styles

	Fuel Economy (MPG _{imperial})	Fuel Consumption (l/100km)	Carbon Dioxide Emissions (g/km)
Hybrid Calm	59.41	4.75	111.11
Hybrid Normal	56.31	5.02	117.24
Hybrid Aggressive	47.94	5.89	137.71
Hybrid All	54.10	5.22	122.02
Petrol Calm	21.10	13.39	312.87
Petrol Normal	21.84	12.93	302.28
Petrol Aggressive	21.21	13.32	311.18
Petrol All	21.38	13.21	308.78
Diesel Calm	32.87	8.59	230.64
Diesel Normal	33.04	8.55	229.49
Diesel Aggressive	31.43	8.99	241.23
Diesel All	32.43	8.71	233.79

Table 3 provides a breakdown of the fuel consumption saving presented in Table 2, by Prius operating mode. With 40% of taxi driving time spent idle, it might appear that a micro hybrid with stop start could achieve much of the benefit of a full hybrid in taxi driving. However, the results show that only around 15% of the fuel consumption benefit of switching to a full hybrid occurs while the vehicle is stationary.

The greatest benefit of the full hybrid architecture, is its ability to drive in pure electric mode. The Prius only has a very small battery, and is therefore only capable of driving at speeds up to 50km/h, and a distance of 2 km, in pure electric mode, Toyota (2015). Never the less, this is enough for the Prius to operate in pure electric mode under low loads when the conventional vehicle is forced to operate its engine at low speeds, and torques, where the engine is particularly inefficient. When the engine is on, it charges the battery through an inefficient electrical power path, if all the battery power came from the engine then the additional engine load would severely limit the benefit of using the vehicle in pure electric mode. The vehicle can also recharge the battery through regenerating power as the vehicles slows down, under taxi driving conditions it was found that around 60% of the power used during pure electric mode comes from regenerated power, and therefore has no associated emissions.

The most surprising find is that the Prius is able to save fuel, compared to the conventional vehicles, when operating in hybrid electric mode, with the engine on. When the Prius engine comes on it must power the vehicle, recharge the battery, and cover efficiency losses through an electrical power path that is far more inefficient than the mechanical power transmission used in conventional vehicles. This means that the Prius engine is operating under higher loads than the conventional vehicles most of the time it is on, and yet it still requires less fuel. This is partially achieved through engine technology, the Prius uses a 1.8L Atkinson cycle engine with cooled EGR at all loads. This technology combination is used to reduce pumping losses at low engine loads, and achieve optimized spark timing, and high compression ratios without engine knock, Kawamoto (2009). The Atkinson cycle is not used in conventional vehicles because it does not deliver the torque requirements, especially at low speeds. The Prius gets around this problem by using the motor to drive the vehicles at low speeds, and by decoupling the engine speed from the vehicle speed, this allows the engine to meet high vehicle torque demands with increased engine speed. The engine efficiency is also achieved through engine control, by decoupling the engine speed from the vehicle speed the engine can be operated along an optimized speed, torque path that avoids engine operation at low, and high torques where the engine efficiency is reduced.

Table 3. Fuel saving achieved by hybrid vehicle in each mode

Mode	Percentage Time (%)	Percentage Fuel Saving Petrol (%)	Percentage Fuel Saving Diesel (%)
Vehicle Stationary	40.6	13.4	16.6
Pure Electric	31.9	54.6	73.1
Hybrid Electric	27.5	32.0	10.3

NOx Emissions

Although this project focuses on CO₂ emissions it is important to mention other emission benefits of switching from a predominantly diesel, to a petrol hybrid taxi fleet. While no emission data was collected during the taxi project, the authors do have data for a Toyota Prius, a petrol Ford Focus, and a diesel Ford Fiesta, tested on a chassis dynamometer, over the nine London drive cycles, Moody et al (2016). The London drive cycles are made up of three urban, three suburban, and three motorway cycles. The urban cycles are a fair representation of taxi driving, with accelerations, and decelerations a little less aggressive than the taxi test data, and much less idling, but overall the vehicle speeds, and accelerations experienced in central London are comparable to taxi driving.

Table 4 presents the NOx saving achieved by switch from a conventional vehicle to a petrol hybrid. The two petrol vehicles have much lower NOx emissions than the diesel vehicles because of their use of three way catalysis. The hybrid has much lower NOx emissions than the petrol vehicle, not because of its use of pure electric mode, as is the case with CO₂, but because the hybrid achieves lower engine out NOx under high engine power events. This is achieved by a combination of engine technologies that are designed to improve fuel consumption, but the large cylinder, reduced compression ratio, and use of cooled EGR at all engine loads, results in lower combustion temperatures which reduces the production of engine thermal NOx.

Table 4. NOx saving achieved by switching from diesel to petrol, or petrol hybrid

Road Type	Percentage reduction in NOx, diesel to petrol (%)	Percentage reduction in NOx, diesel to hybrid (%)	Percentage reduction in NOx, petrol to hybrid (%)
Urban	97.8	99.8	89.1
Suburban	97.6	99.8	93.0
Motorway	95.7	97.8	48.3

Business Case

A second hand conventional vehicle similar to those used as taxi in Leeds costs around £5,000, a second hand Toyota Prius cost £10,700. Table 5 shows the annual fuel saving, and time to repay the higher initial cost, of a switch from a diesel, and a petrol, to a petrol hybrid taxi. These calculations are based on an annual mileage of 48,280 km (30,000 miles) (*Leeds City Council, Taxi Driver Interview. Unpublished Data*), and a fuel price of 104.0 p/L for petrol, and 107.3 p/L diesel (15). Taxis in Leeds must be less than five years old when they enter the fleet, and can be up to ten years old before they must be replaced. Taxi drivers buy vehicles close to five years old as this reduces purchase cost. This is especially true for hybrid vehicles because of the higher initial cost. With a lifetime of five years a hybrid taxi will easily payoff the higher initial cost, and will profit the driver around £3,860, or £14,180 when compared to buying, and running, a diesel, or petrol equivalent respectively.

Table 5. Fuel saving and payback times for purchasing a hybrid taxi

	Switch Diesel to Hybrid		Switch Petrol to Hybrid	
	Annual Fuel Saving (£)	Payback Time (Years)	Annual Fuel Saving (£)	Payback Time (Years)
Calm	2,064	2.8	4,335	1.3
Normal	1,912	3.0	3,976	1.4
Aggressive	1,697	3.4	3,727	1.5

To validate these results, one of the three hybrid taxi drivers in Leeds was interviewed by Leeds City

Council. He calculated that he spent on average £10.50, for every 100 miles travelled in his Toyota Prius, and £17.50 per 100 miles in his previous diesel taxi. Based on the fuel price over the time the two vehicles were owned this converts to 5.52 L/100km for the hybrid, and 8.20 L/100km for the diesel, giving a payback time of 3 years 10 months. Fuel saving is not the only monetary benefit from switching to hybrid vehicles. The taxi driver interviewed, stated higher reliability, lower maintenance costs, and less days of work lost while the vehicle was being repaired, as key factors in his choice to buy a hybrid vehicle. When this is considered as well, the payback times estimated here can be assumed to be conservative estimates (*Leeds City Council, Taxi Driver Interview. Unpublished Data*).

3 Conclusions

There are four key messages for policy makers from this work. Firstly, hybrid vehicles are not a technology for the future that can be introduced when the costs come down. For taxi fleets at least, hybrids are a cost effective solution to transport emissions in cities now. Considering the CO₂, and air quality emission benefits, and the clear business case for hybrid taxis, policies encouraging their uptake should be high on the agenda of all transport policy makers. Secondly, taxi vehicles have a very different driving style to other vehicles on the road, and they are, therefore, poorly represented by legislative test figures. If no taxi specific data is available to make a choice about which technology performs best as a taxi, policy makers are advised to compare vehicles based on UDDS test figures.

Thirdly, one of the two main barriers to the uptake of hybrid vehicles is perception. The growing gap between real, and legislative fuel consumption figures over the last ten years has eroded people's faith in official fuel consumption test figures. The result of this is that people are now unwilling to pay extra for low emission technology that may, or may not, deliver real world fuel cost savings. The key findings of this paper can provide policy makers with real world data, which they can then use in their consultation with the taxi driving community, to inform emission reduction strategies for the taxi fleet.

Fourthly, the second main barrier to the uptake of hybrid vehicles is the initial cost. Even though the payback times are very good, if a taxi driver does not have access to the capital to pay for the higher initial cost of a hybrid vehicle then these vehicles are simply not an option. Central government needs to develop new financing methods that allow taxi drivers to bridge the gap between initial cost, and fuel saving. These financial methods should recognize that this is a very cheap way to encourage technology uptake, especially when compared to the UK preferred policy of grants, and not burden the taxi drivers with high interest loans. Other related areas where policy makers can make a difference is, removing registration fees for hybrid vehicles, and changing policy on taxi colour, as colour restrictions have a big impact on vehicle availability, and price on the second hand market.

If policy makers push for the uptake of hybrid vehicles across all urban taxi fleets, it will have a significant impact on improving city air quality, and meeting national CO₂ targets, through direct emission cuts, and indirectly by proving the technology reliable, and effective to private buyers, and other fleets.

Acknowledgement

I would like to acknowledge the guidance and support of my PhD supervisors; Dr. James Tate of the Institute of Transport Studies, Dr. Hu Li of the Energy Research Institute and Dr. Zia Wadud of the Centre for Integrated Energy Research, all research institutes at the University of Leeds. I would also like to acknowledge the support of Leeds City Council, especially Jon Tubby, and Desmond Broster, who collected data on the Leeds taxi fleet, and for whose support this project would not have been possible. This project was fully funded by the Engineering and Physical Sciences Research Council.

References

Verdi L. & A. Martin (2003): Guidelines to authors. Proc. Int. Symp. "Environment and Transport", Reims, France, 6-10 June, 2003, *Atm. Env.*, vol 169, p415-422.

AA. *Fuel Price Report*. December 2015. <http://www.theaa.com/resources/Documents/pdf/motoring-advice/fuel-reports/december2015.pdf>. Accessed April 28, 2016.

Costagliola, M. A., M. V. Prati, A. Mariani, A. Unich, and B. Morrone (2015). Gaseous and Particulate Exhaust Emissions of Hybrid and Conventional Cars over Legislative and Real Driving Cycles. *Energy and Power Engineering*, Vol. 7, pp. 181–192.

Jimenez-Palacios, J (1999). Understanding and quantifying motor vehicle emissions with vehicle specific power and TILDAS remote sensing. Doctoral Dissertation, Department of Mechanical Engineering, Massachusetts Institute of Technology, Cambridge, MA.

Kawamoto, N., Naiki, K., Kawai, T., Shikida, T. (2009). Development of New 1.8-Liter Engine for Hybrid Vehicles, *SAE Technical Paper* 2009-01-1061, doi:10.4271/2009-01-1061.

Lenaers, G (2009). Real Life CO₂ Emission and Consumption of Four Car Powertrain Technologies Related to Driving Behaviour and Road Type. *SAE Technical Paper*. 2009-24-0127, doi:10.4271/2009-24-0127.

Lutsey, N (2011). Comparison of Emissions, Energy, and Cost Impacts of Diesel and Hybrid Models in the United States in 2010. *Transportation Research Record: Journal of the Transportation Research Board*, No. 2252, pp. 40–48.

Mercedes-Benz. *Vito Taxi*. June 2008. http://www.londonblacktaxis.net/kpmuktaxis_mercedes_vito_taxi.pdf. Accessed July 25, 2015.

Moody, A., Tate, J. In service CO₂ and NO_x emissions of Euro 6/VI cars, light- and heavy-duty goods vehicles in real London driving: Taking the road into the Laboratory. *The 21st International Transport and Air Pollution (TAP) Conference*, Lyon, France, May 24-26, 2016.

The London Taxi Company. *Performance*. <http://london-taxis.co.uk/performance>. Accessed July 25, 2015.

Toyota. *History of the Toyota Prius*. <http://blog.toyota.co.uk/history-toyota-prius>. Accessed April 04, 2015.

Transport for London. *Construction and Licensing of Motor Taxis for use in London. Conditions of Fitness*. 1 January 2007. <https://tfl.gov.uk/cdn/static/cms/documents/taxi-conditions-of-fitness.pdf>. Accessed July 20, 2015.

Transport for London. *New Vision for taxi and private hire services in the Capital*. 1 July 2015. <https://tfl.gov.uk/info-for/media/press-releases/2015/new-vision-for-cleaner-greener-taxi-and-private-hire-services-in-the-capital>. Accessed July 20, 2015.

UK Department for Transport. *Table TAXI0101 Licensed taxis and taxi drivers: England and Wales, from 1965*. August 2013. <https://www.gov.uk/government/statistics/taxi-and-private-hire-vehicle-statistics-england-and-wales-2013>. Accessed July 20, 2015.

UK Department for Transport. *National Travel Survey 2013: Statistical release*. 29 July 2014. https://www.gov.uk/government/uploads/system/uploads/attachment_data/file/342160/nts2013-01.pdf. Accessed July 20, 2015.

UK Department for Transport. *Table VEH0203 Licensing cars by propulsion/ fuel type, Great Britain, annually from 1994*. 9 April 2015. <https://www.gov.uk/government/statistical-data-sets/veh02-licensed-cars>. Accessed July 20, 2015.

UK Department for Transport. *Table VEH0253 Cars registered for the first time by propulsion/ fuel type, Great Britain, annually from 2001*. 9 April 2015. <https://www.gov.uk/government/statistical-data-sets/veh02-licensed-cars>. Accessed July 20, 2015.

Weiss, M., P. Bonnel, J. Kühlwein, A. Provenza, U. Lambrecht, S. Alessandrini, M. Carriero, R. Colombo, F. Forni, G. Lanappe, P. Le Lijour, U. Manfredi, F. Montigny and M. Sculati (2012). Will Euro 6 reduce the NO_x emissions of new diesel cars? – Insights from on-road tests with Portable Emissions Measurement Systems (PEMS). *Atmospheric Environment*, Vol. 62, pp. 657–665.

NO_x Emission Performance Of Vans In Real Urban Driving and The Uptake of Euro 5 Technology Using A Remote Sensing Device

Christopher RUSHTON*, James TATE*, Simon SHEPHERD*

*Institute for Transport Studies, University of Leeds, Leeds, United Kingdom
email: phy4cer@leeds.ac.uk

Abstract (200 / 200 word limit!)

An RSD4600 was deployed in a 10-day survey over 5 sites in Aberdeen in May 2015. LCV's of class N1, type I, II and III were observed and the NO:CO₂ ratio was measured for each vehicle. A NO_x emission factor was calculated for each vehicle pass-through based on the manufacturer's CO₂.

The effectiveness of the LCV technology at reducing emissions in real driving was shown to be poor with 98.8%, 98.3% and 98.1% exceeding the limit values in NI, NII and NIII classes. Emission factors show no improvement between Euro 4 and Euro 5 NO_x emissions. The emission ratios are combined with PHEM CO₂ emission factors and show that 97.9%, 98.6% and 96.8% of NI, NII and NIII emission factors are greater than the limit values across the network.

Registration of Euro 4 and Euro 5 LCV's in the changeover period was monitored. The registration of Euro 5 vehicles as a percentage of total registered LCV's of all types grew from 1.1% in 2009 to 13.5% (2010), to 28.7% (2011) and to 91.0% in 2012. 2015 was the first year where 100% of the vehicles registered were Euro 5. After 2012 1.4% of the vehicles registered each year were Euro 4.

Key-words: NO_x, real driving emissions, light commercial vehicles

Introduction

Light Commercial Vehicles (LCV's) make up 9.1% of the vehicle fleet (Browne *et al* 2010, ICCT 2015) and are responsible for even more journeys (AECOM 2014). They have a lifetime of approximately 5 - 8 years due to their intense usage (<http://www.commercialfleet.org>, <http://uk.reuters.com>). The non-trivial contribution these vehicles make to the total number of journeys made and their hours of operation means that it is important to understand the contribution made by LCV's to the total NO_x in urban street environments. LCV's are subject to different mileage and increased loading compared to passenger cars however they are only occasionally tested in laboratories. LCV tests look at a small number of vehicles under controlled test procedures (Joumard *et al*, 2003). Given their importance in the context of emissions in urban environments it is important to understand their contribution to the emissions inventory.

The type approval date for Euro 5 vehicles is September 2009 however newly registered LCV's did not have to meet Euro 5 standards until January 2011 for LCV-NI class and January 2012 for LCV-NII and LCV-NIII class vehicles. End of line legislation provides an additional mechanism for registering old vehicles. Either 30% of vehicles taken into use in Norway in the previous 12 months or 100, whichever is greater, can be registered in Norway. The result of this legislation is that the new additions to the fleet after the type approval date may not necessarily change as quickly in response to the legislation as would be desirable.

The Remote Sensing Device (RSD) methodology along with the meta-data added through capturing of license plate information can allow monitoring of both the uptake of the new vehicles into the fleet and make a fast and accurate assessment of their total emissions. Vehicle emissions can be calculated both at an instantaneous point on the network and also extrapolate network wide with the combined use of vehicle tracking and PHEM modelling alongside the RSD. This methodology also means that an accurate assessment of the uptake rate of vehicles and their emission can be fed to modellers and policy makers meaning that they can make better informed decisions about policy implementation.

The Euro 6 legislation was introduced in September 2014 and an assessment of the impact is already possible for passenger cars using RSD measurements. It is still too early to assess the change in total fleet characteristics due to introduction of Euro 6 emission limit values as none were measured however it is likely that policy regarding introduction of vehicles from various manufacturers will remain

not differ too much from legislation to legislation. It is now possible to look at the whole lifetime of the Euro 5 legislation using remote sensing data collected in Aberdeen in 2015 and use this information to inform assumptions about the rate of uptake of new technology in the years following the introduction of the Euro 6 legislation.

The aims of this survey are to assess how effective the Euro 5 legislation had been at reducing vehicle emissions, comparing them to the Euro 4 fleet. Furthermore we attempt to describe the uptake rate of new LCV's into the fleet by looking back at the Euro 5 fleet and the overlap time between new type approval of Euro 5 and the date of last registration of Euro 4 vehicles.

Materials and Methodology

A Remote Sensing Device (RSD4600) was deployed at five different locations around Aberdeen in 2015. The RSD4600 uses instrument uses a Non Dispersive Infrared (NDIR) laser system and a Dispersive Ultraviolet laser system. The systems consist of a dual element light source (silicon carbide gas drier igniter and a xenon arc lamp) and a separate detector unit with four non-dispersive infrared detectors that provide an IR reference ($3.9\mu\text{m}$) and measurements of carbon dioxide (CO_2 , $4.3\mu\text{m}$) as well as channels for CO and HC measurements not used in this paper. The frequency window for measuring Nitric Oxide (NO) is centred at the 227nm doublet which allows for elimination of interference by absorption from water molecules at similar frequencies (Bishop *et al*, 1989) (Bishop & Stedman 1990) (Guenther *et al*, 1995) (Popp *et al* 1999). Alongside the RSD a speed and acceleration module (SAM) and a camera are also deployed. The data from these three devices comprises the primary RSD measurement with metadata relating to vehicle type, fuel type, euro class and make and model are sourced from CarWeb (<http://www.carweb.co.uk>).

Five sites in Aberdeen were selected to provide a range of different conditions typical of the road network in the city. Two days of measurements were taken at each site. Power supply issues related to failure of one of the component parts meant that the number of vehicles was reduced slightly however the problems were addressed and the number of missed vehicles was minimised. Data was collected and the LCV subset was extracted from the main fleet using the vehicle category data. The LCV set was further subsetted by type of vehicle. NI, NII and NIII are the legislative type of vehicle and are set based on the vehicle mass. The NI, NII and NIII mass bands are defined as < 2000, 2001 - 2600, 2601 - 3500 kilograms respectively.

The RSD measures the ratio of NO to CO_2 and the vehicle metadata contains the manufacturer carbon dioxide rating ($\text{CO}_{2\text{-base}}$). The base CO_2 value is calculated from the Cold Urban Fuel Consumption entry from the carweb database, initially in litres per 100km. The conversion for litres of diesel per kilometre to grams of CO_2 per kilometre is 26.5. The base CO_2 value is uplifted in line with factors measured by TNO using vehicles fitted with a Smart Emission Measuring System (SEMS) device and driven on-road. The uplift factor used was 1.23 and was calculated using the average of 10 uplift factors measured from different vehicles (TNO, 2015).

A secondary CO_2 emission factor was calculated using the Passenger car and Heavy duty vehicle Emission Model (PHEM) (Hausberger, 2003, Hausberger *et al* 2009) to attempt to estimate the emission factors as they are extrapolated across the whole of the Aberdeen network rather than at a single point on the network. PHEM calculates the mass of emission for a given engine power demand through the use of a lookup table. The CO_2 emission factors for Euro 5 LCVs were calculated as an average over 15 routes driven on the Aberdeen network as part of the same study using the methodology described in Wyatt *et al* (2014). The mean physical parameters of the vehicles were sourced from the carweb database for kerb weight, frontal area and engine power. The payload mass for each class was assigned as NI = 229 kg, NII = 382 kg, NIII = 478 kg (DfT, 2010) and added to the total mass of the vehicle to estimate total mass used as an input for PHEM.

The fractional NO_2 (f- NO_2) was measured using a Remote Sensing Device capable of measuring NO_2 directly in a separate study performed using the prototype FEAT remote sensing device in London. Previous work has cross correlated and validated the measurements performed by the RSD4600 and the fractional NO_2 measurements measured by the prototype FEAT system (Rushton *et al*, 2016). The measured values for f- NO_2 were 0.266 and 0.244 for Euro 4 and Euro 5 LCV's respectively. The f- NO_2 values by vehicle manufacturer are aggregated however the difference between manufacturers is consistent within presented errors (Carslaw & Rhys-Tyler, 2013). Previous work has cross correlated and validated the measurements performed by the RSD4600 and the fractional NO_2 measurements measured by the prototype FEAT system (Rushton *et al*, 2016) The assumption is

therefore made that vehicles from different manufacturers vary little in their f-NO₂ values and the average value is used. The calculation of the total NO_x as an instantaneous emission factor is performed using the following equation and the PHEM emission factor for CO₂ is substituted in unmodified for network wide extrapolation:

$$NO_x = \frac{NO_{RSD}}{(1 - f_{NO_2})} CO_2 \times 1.23$$

The registration information was sourced from the vehicle metadata under the year, month and day of registration elements and this was then converted to a daily value. The number of vehicles registered per day for each Euro class was presented as a frequency density polygon representation of a time series to show a snapshot of the evolution of the fleet after the introduction of Euro 6 technology and in the changeover period from Euro 4 to Euro 5.

Results and Analysis

Vehicle Emissions Analysis

The total number of LCV's measured was 3511 and represented 14.2% of the total measurements. The total number of Euro 5 LCVs was 1895 with 96, 487 and 1312 being of class NI, NII or NIII respectively. Drive cycle tested type approval Carbon Dioxide values were available for 90.64% of Euro 5 LCVs of all classes, or by class 92% for NI, 91% for NII and 86% for NIII. Measurements where no CO₂ values were available were discarded. Of the remaining measurements, 98.8% of NI, 98.3% of NII and 98.2% of NIII measurements for the NO_x emission factor in grams per kilometre were found to be over the limit values required for the Euro 5 type approval. Repeating the analysis using the PHEM CO₂ emission factors for partially loaded LCVs extrapolated over the whole network results in 97.9% of NI, 98.6% of NII and 96.8% of NIII LCVs being over the limit values. These limit values are 0.180, 0.235 and 0.280 grams per kilometre respectively. For the Euro 4 fleet 98.6% of NI, 96.0% of NII and 98.2% of the NIII vehicles' instantaneous emission factor were above the Euro 5 limit and 95.7% of NI, 63.5% of NII and 53.7% of NIII vehicles were above the limit when extrapolated across the network using CO₂ emission factors calculated using PHEM.

The distribution of the measurements varies significantly between manufacturers. Some manufacturers are able to produce many vehicles that whilst over the limit are still relatively closely distributed around it whereas other manufacturers distribution of emissions are spread out to both extremes of the scale. The distributions of NO_x emission factors subset by manufacturer are presented in **Figure 1** for NI, NII and NIII consecutively. Grey histogram bars show the distribution of emission factors as calculated using the uplifted manufacturer rated CO₂ values and red, blue and green histogram bars show the emission factors calculated using the PHEM CO₂ emission factors for NI, NII and NIII respectively. The legislated limit value for Euro 5 vehicles is indicated as a dashed red line in each separate histogram.

It is clear from these results that the emissions produced by these vehicles as of 2015 are contributing a significant amount of pollution to the environment. The results from this analysis show that whilst no manufacturer can claim to be under the limit values some manufacturers are producing vehicles that emit less NO_x than others in the NII class and especially in the NIII class. In the NIII class for example Ford vehicles peak only slightly higher than the limit value whereas Mercedes, Vauxhall and Volkswagen as well as potentially Renault, which have a smaller sample size, have both peaks and spreads that are more in excess of the limit value and covering much more of the range of emission factors than the 'better' manufacturers.

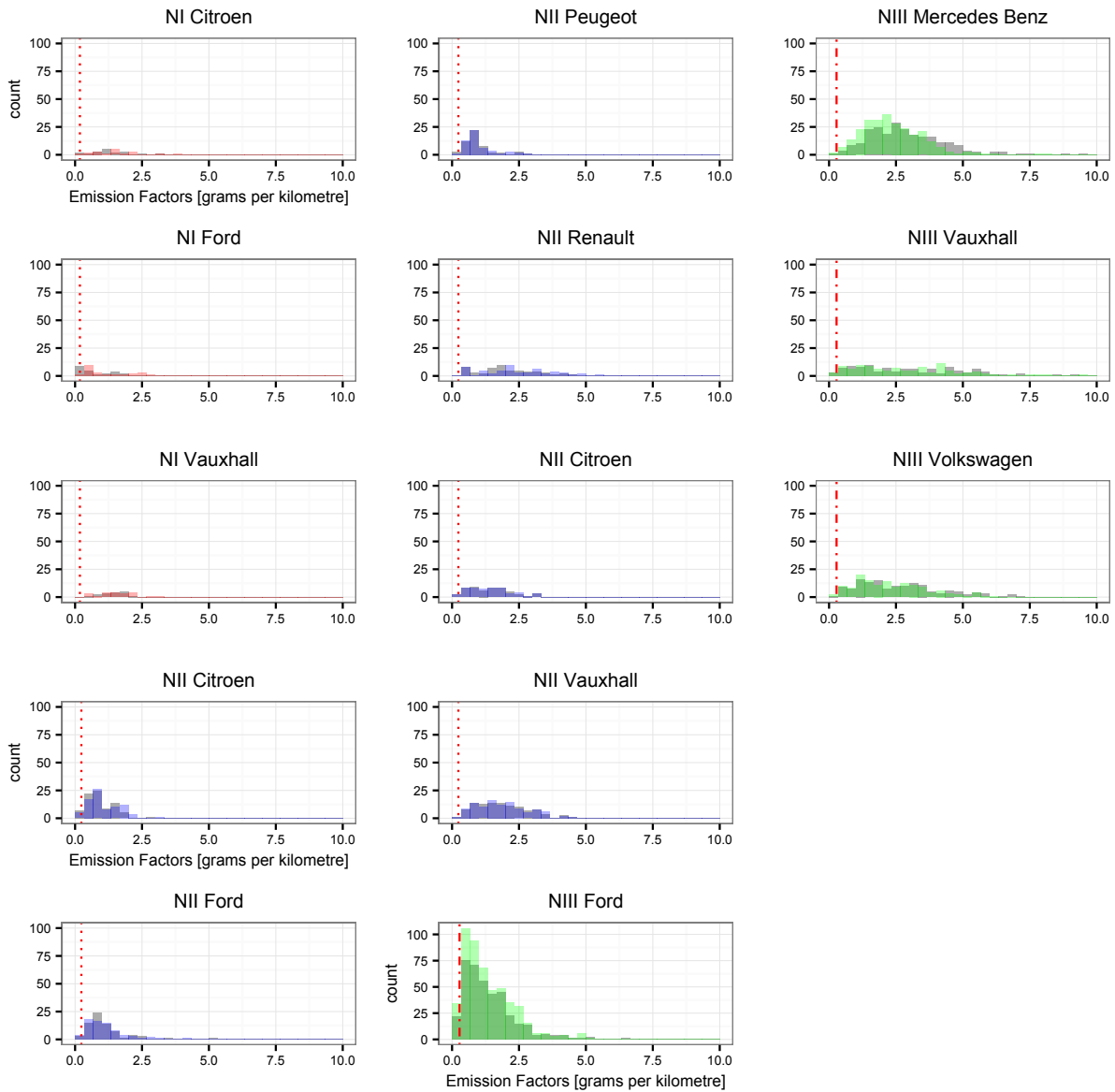


Figure 1: Comparison of emission factors for Euro 5 LCVs measured instantaneously (grey) and extrapolated across the Aberdeen network (coloured) to the legislated limit values (red lines)

Vehicle Introduction Date Analysis

Analysis of the date of first registration for each vehicle was performed to better understand how LCVs were introduced to the vehicle fleet both in the run up to and after the introduction of new legislation. Given the 5-8 year lifetime of a fleet vehicle it is assumed that the majority of vehicles registered since 2007 and almost all registered since 2010 were still present on the road. Given that September 2010 was the introduction date for new type approval the time period of interest should be well represented by the vehicles measured on the road. The measurements were taken after the introduction of Euro 6 vehicles but no vehicles measured were approved to the standard of the new legislation.

The introduction timelines for LCVs fitted with Euro 4 and Euro 5 technology are shown in **Figure 2**. The technology is presented in frequency polygon form with an adjustment resolution of 0.4 years (0.6 for NII Euro 5 for reasons of clarity). Additionally a rug is presented to show individual vehicles' day of registration. Darker grey indicates more vehicles registered on that day. Dashed red lines indicate the type approval date, the last registration date and the end of line cutoff points from left to right respectively with manufacturers indicated by different colours. The rate of introduction of new technology in Aberdeen's LCV fleet is not as clear-cut as might be expected given the apparent nature of the legislation. Based on this analysis the contribution of LCVs to the roadside concentration of pollution should not expect to decrease alongside new type approval legislation. A lag period of one year between the introduction of the Euro 5 type approval and more than just a small number of newly

registered vehicles meeting the Euro 5 emissions limits has been observed. During this time little to no decrease in roadside concentration would be expected due to new LCVs.

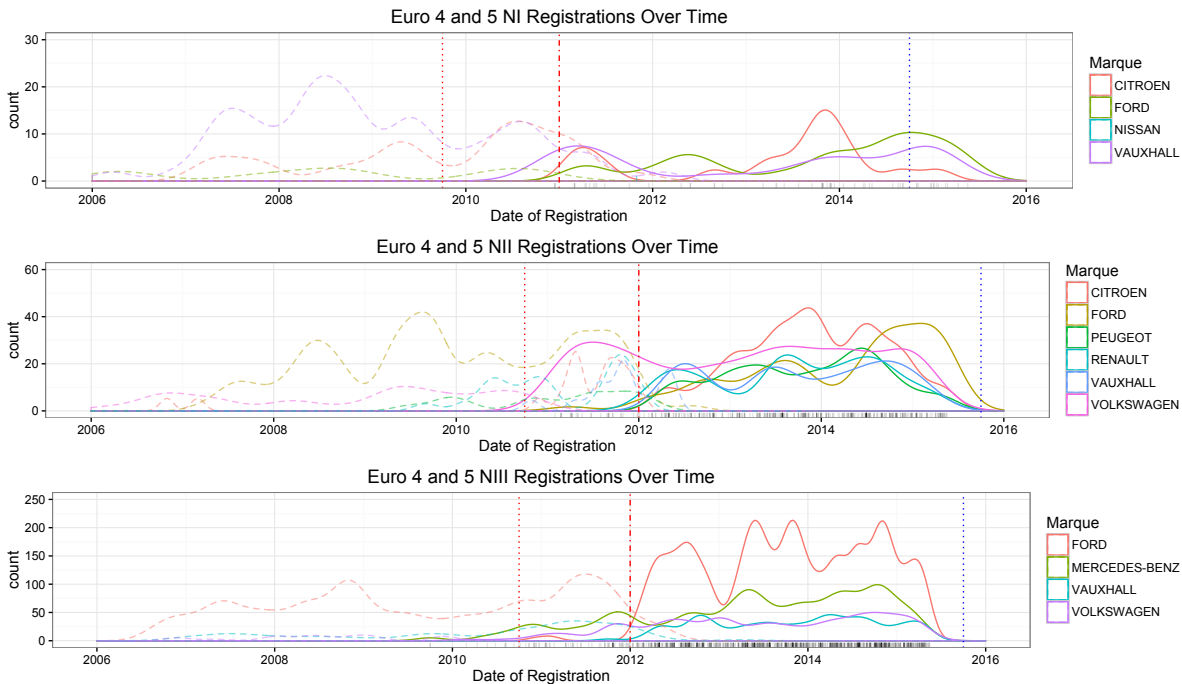


Figure 2: Analysis showing the varying rate of uptake of new technology for the main manufacturers of LCVs compared to the legal last type approval date (dotted red line) and last registration date (dot-dashed line). The Euro 6 type approval date is also shown (dotted blue line). Euro 4 vehicles are shown by dashed lines and Euro 5 vehicles are shown by solid lines.

The analysis undertaken previously is expanded to understand the strategies that different manufacturers use during the period of transition between Euro class legislations. Given the freedom that is afforded these manufacturers by the legislation some variance would be expected.

For class NI the manufacturers appear to have a relatively consistent process of introducing new technology, which is to introduce it as late as possible. For NII and NIII class vehicles manufacturers are diverging noticeably in their strategy. Some manufacturers such as FORD introduce their Euro 5 technology at the latest stage possible whereas other manufacturers such as MERCEDES-BENZ and VOLKSWAGEN introduce their technology as early as possible. Other manufacturers leave the introduction of new technology as long as possible. An overlap of technology has been observed for a small number of cases such as the NII Ford Transit Connect where in January 2011 both Euro 4 and Euro 5 examples were registered albeit with Euro 4 in significantly higher numbers than Euro 5. The incidences of manufacturers registering vehicles fitted with old technology after the limit for vehicle registrations is observed but not shown to be a significant factor.

Conclusions and Discussion

The implications of the results of this research are important from a policy maker's point of view. Firstly it has been shown that Euro 5 vehicles are emitting NO_x at a level considerably higher than the legislated limit values and also that they are performing less well with regards to their emission limit values than Euro 4 vehicles when emissions are extrapolated over the whole network. The limit values cannot be used for any sort of policy-making decisions moving forward as they produce a significant underestimate. The inter-marque effectiveness at reducing NO_x is also striking with some significant differences observed between different manufacturers predominantly in the NIII class. The implications of this result are that there are solutions by certain manufacturers that are more effective than others at removing the NO_x but that not all manufacturers have been as successful at optimizing their use of available technology solutions. This result suggests that better on road monitoring of outcomes is required if regulations on emissions are to be equitable between manufacturers.

The impact of Euro 6 LCVs has not been assessed, as despite the measurements being taken approximately 8 months after the new type approval date there are no examples of Euro 6 LCVs

present in the Aberdeen fleet as measured by the RSD. The lack of vehicles meeting the new limit values further complicates the picture in imposing restrictions on vehicles to limit the total NO_x emissions as limitations based on the first type approval date cannot be trusted to remove all old technology and Euro class would be a better metric however the Euro class of a vehicle is not always obvious to a casual observer and hence more problems may be created. The lack of Euro 6 LCV's is a somewhat surprising result is surprising as Euro 6 cars have been observed in reasonably high numbers since and even prior to the introduction of the new limit values.

It has also been shown that the last change of legislation from Euro 4 to Euro 5 did not produce immediate change in technology that was introduced into the fleet as might be expected. Whilst it remains too early to confirm it appears that this lag between legislation and technology introduction is happening with Euro 6 technology as well. Whilst it would be unrealistic to say that the fleet of Aberdeen can be considered representative of the whole UK fleet without further investigation nor that the sites monitored measured every LCV in Aberdeen the initial stages of the Euro 6 legislation period are similar to the initial stages of the Euro 5 legislation. Any attempt to reduce high NO_x emitting LCV's from a low or ultra-low emission zone should account for this lag.

The RSD and metadata collection methodology has allowed analysis by manufacturer to be performed. This analysis shows that there are noticeable differences between the emissions reductions achieved by different manufacturers. Different manufacturers are likely using different solutions to the NO_x removal problem and some manufacturers are able to reduce the total NO_x they emit significantly more and more consistently than others. It is beyond the scope of the RSD survey to understand what the different solutions and applications of technology are or to suggest ways that manufacturers could improve their real world emissions, only that a difference is clearly visible in the data. This further complicates any attempt to remove high emitters based solely on type approval dates as manufacturers who are able to effectively reduce their NO_x emission may be unfairly penalized or those that are not performing as well may be allowed to emit more NO_x than others.

The rate of introduction of new technology into the vehicles on the forecourt is also shown to vary quite considerably depending on the manufacturer with some being able to get their newest products into the fleet very rapidly whilst other manufacturers are waiting until the last possible moment to introduce theirs. This presents a problem for policy makers because it means that not all LCVs registered in (for example) 2012 are working to equivalent standards. Some may be Euro 4 whilst others may be Euro 5. Any intervention to limit the access of old vehicles or promote access for new vehicles in a low emission zone scenario therefore risks either unfairly punishing a manufacturer who has introduced new technology early or encourages manufacturers who's vehicles are running to an older specification of legislation to not introduce their new technology as soon as possible. In practice the difference between Euro 4 and Euro 5 is limited so the ambiguity caused by different introduction times is largely inconsequential. However if Euro 6 technology can be shown to significantly reduce NO_x in comparison to Euro 5 it is important to understand how to incentivize the uptake of the new technology not just new vehicles that only meet the old standards.

In continuation of this study a measurement of the emissions performance of Euro 6 LCVs is critical as no assessment is currently possible. At the time of writing the vehicle registration deadline has passed for Euro 5 M class vehicles and NI class vehicles however the vehicle registration deadline has not yet passed for Euro 5 NII and NIII class vehicle. The vehicle registration deadline for Euro 5 NII and NIII vehicles is September 2016. As time progresses and the fleet turnover continues the likelihood of measuring these vehicles using the RSD increases. The introduction rate of Euro 6 vehicles should also be monitored. As these deadlines pass the impact of the Euro 6 legislation will be seen in these vehicles and their rate of uptake can be observed in real time by repeated RSD studies between May 2016 and further into the future.

Acknowledgments

This research was completed as part of Aberdeen City Council's Low Emission Zone consultancy and as part of an EPSRC funded PhD project at the University of Leeds Institute for Transport Studies.

References

AECOM: "Van travel trends in Great Britain". *Royal Automobile Club* (2014)

- Browne, Michael, Julian Allen, Toshinori Nemoto, and Johan Visser. "Light goods vehicles in urban areas." *Procedia-Social and Behavioral Sciences* 2, no. 3 (2010): 5911-5919.
- Carslaw, David C., and Glyn Rhys-Tyler. "New insights from comprehensive on-road measurements of NO_x, NO₂ and NH₃ from vehicle emission remote sensing in London, UK." *Atmospheric Environment* 81 (2013): 339-347.
- "Commercial Fleet Case Study: Network Rail". *Commercialfleet.org*. N.p., 2016. Web. 29 Apr. 2016.
- Department for Transport (2010): "Light Goods Vehicle – CO₂ Emissions Study: Final Report"
- Hausberger, S., 2003. Simulation of Real World Vehicle Exhaust Emissions. VKM-THD Mitteilungen, Heft/Vol 82, Verlag der Technischen Universität Graz 2003, ISBN 3-901351-74-4.
- Hausberger, S., Rexeis, M., Zallinger, M., & Luz, R. (2009). Emission Factors from the Model PHEM for the HBEFA Version 3. *Report Nr. I-20/2009 Haus-Em*, 33(08), 679.
- ICCT. "European Vehicle Market Statistics Pocketbook 2015/16" (2015)
- Joumard, Robert, Michel André, Robert Vidon, and Patrick Tassel. "Characterizing real unit emissions for light duty goods vehicles." *Atmospheric Environment* 37, no. 37 (2003): 5217-5225.
- "Research And Markets: Light Commercial Vehicle (LCV) Market In Europe 2015-2019 - Key Vendors Are Daimler Trucks, CNH Industrial, MAN, Renault & Volvo Trucks". *Reuters UK*. N.p., 2016. Web. 29 Apr. 2016.
- Rushton, Christopher, Tate, James, Carslaw, David C., Shepherd, Simon "Inter-Instrument Comparison of Remote Sensing Devices and a New Method For Calculating On Road NO_x Emission and Validation of Vehicle Specific Power." *Awaiting Publication* (2016).
- TNO. "On-road NO_x and CO₂ investigations of Euro 5 Light commercial vehicles" (2015): TNO 2015 R10838
- Wyatt, David W., Hu Li, and James E. Tate. "The impact of road grade on carbon dioxide (CO₂) emission of a passenger vehicle in real-world driving." *Transportation Research Part D: Transport and Environment* 32 (2014): 160-170.

ESPRIT: a new carsharing concept

A socio-economic assessment from Lyon region - France

Shadi SADEGHIAN* & Guy Bourgeois**

* VEDECOM Institute, 77 rue des Chantiers 78000 Versailles, France

Email: shadi.sadeghian@vedecom.fr

** Independent Expert, Lyon, France

Email: guybourgeois69@gmail.com

Abstract

The Easily diStributed Personal Rapld Transit (ESPRIT) is a new one-way carsharing concept based on the use of a purpose-built, light weight electric vehicle that can be stacked together to gain space. Thanks to pioneering coupling systems, up to 8 ESPRIT vehicles can be nested together in a road train, 7 being towed for an efficient redistribution of fleet and a smartly-balanced and cost efficient transport system.

This paper aims to report on the socio-economic impacts of the introduction of this carsharing concept into an existing transport system of a low density area. To this end, a model providing the initial forecasts, based on consolidated costs with simple mode choice, has been developed on a study area situated in Lyon region (France). The model allows both behavioral responses and economic impacts to be assessed. The systemic approach helps to illustrate the permanent interactions between the transport demand and supply at mesoscopic territorial level.

Keys-words: socio-economic assessment, car sharing, electric car, systemic approach, decision making aid

Introduction

People need to travel daily within urban and peri-urban areas to perform their daily and occasional activities. This need for travel has increased due to continuous urban sprawl, and transport systems are put under even greater pressure. Travelers have the choice of using public transport or their own private vehicles. For most of the population in the peri-urban areas, public transport is usually less attractive since unlike the private car it lacks the key ability to provide a rapid 'door to door' service. Thus, private car mode prevails despite its numerous negative footprints (congestion, accident and parking and air pollution issues). For public transport authorities developing conventional public transport networks is economically unsustainable and against current efforts to curb spending and provide revenue generating solutions.

On halfway between private car and transit modes, one-way carsharing systems seem to be a pertinent alternative to car ownership, but the vehicle redistribution in such systems becomes quickly a major hurdle of their development: on one hand, the unbalanced system leaves stations empty and therefore makes the service unreliable and unattractive as users are unable to find a vehicle at the right place and time, especially when most wanted – during peak hours. On the other hand, the regular conventional redistribution's operations are very costly.

The Easily diStributed Personal Rapld Transit (ESPRIT) is a European commission project (H2020)¹ aims to develop a purpose-built, light weight electric vehicle that can be stacked together to gain space. Thanks to pioneering coupling systems, up to 8 ESPRIT vehicles can be nested together in a road train, 7 being towed for an efficient redistribution of fleets and a smartly-balanced and cost efficient transport system.

¹ This project has received funding from the European Union's Horizon 2020 research and innovation program under grant agreement No. 653395.

This paper aims to report on the socio-economic impacts of the introduction of ESPRIT service to an existing transport system of a low density area. To this end, a model providing the initial forecasts, based on consolidated costs with simple mode choice, has been developed on a study area situated in Lyon region (France). The model allows both behavioral responses and economic impacts to be assessed. The systemic approach helps to illustrate the permanent interactions between the transport demand and supply at mesoscopic territorial level.

The study area is a suburban area of about 52 km², located -within the Greater Lyon area (Metropolis of Lyon) - at about 12 km east of the city center of Lyon. The area encompasses three cities of Meyzieu, Decines-Charpieu and Jonage with a total population of approximately 63 000 inhabitants (2012 France Population Census).

We discuss the likely best configuration of the service within the area (ESPRIT stations' localization strategies), the question of complementarity between this new service and the already existing services, the potential impacts on the current transport demand and supply (potential of modal transfer) and we finally measure the effectiveness of the whole panel of transport solutions of the area. The model is developed based on the data provided by the Lyon transport authority (Sytral) and "Metropole de Lyon".

1. An innovative carsharing concept: ESPRIT

One-way carsharing systems have recently been introduced in many city centers across Europe and other parts of the world, and an important number of them are electric. They are used mostly for short trips and seem to be a potential alternative to car ownership, but the vehicle distribution quickly becomes unbalanced leaving stations empty and therefore an unreliable service as users are unable to find a vehicle "at the right location and time", especially when most wanted – during peak hours. To rebalance these existing systems, operators redistribute the vehicles one by one, leading to a very labor intensive, inefficient and expensive system, costly to operate, and a hurdle to further expansion. Furthermore, if the system is electric driven, this requires an important financial investment in electric charging stations (often, more than 2 per vehicle).

The system is composed of the ESPRIT vehicles, charging stations (which also serve as pick-up and drop-off points) supported with business modelling and IT tools to optimize user and logistic requirements. The system will permit single short trips (up to 10 km) to feed public transport networks and park & ride services and to provide "last kilometre" services. Similarly it will balance one-way electric carsharing operations in city centres (ESPRIT project consortium, 2015).

The vehicles' purpose-designed architecture will allow them to be stacked (like shopping trolleys) and driven in articulated road trains of up to 8 vehicles at a time (equivalent to the length of an urban bus [13,3m]), permitting easy and economic redistribution by dedicated operators or, to redistribute two vehicles at a time by the users themselves. This will ensure that the system is continuously balanced and that vehicles are available at all times, which, with the consequent customer loyalty, is expected to double the number of trips per vehicle per day, leading to a significant economy of necessary fleet size and fares. In addition, there will also be significant saving in parking space requirements given the vehicles length and ability to stack (ESPRIT project consortium, 2015).

Compared with existing one-way carsharing vehicles, the ESPRIT vehicle will also be significantly more energy efficient due to its custom-built, light weight architecture and collective, fast-charging battery system and braking energy recovery system (ESPRIT project consortium, 2015).

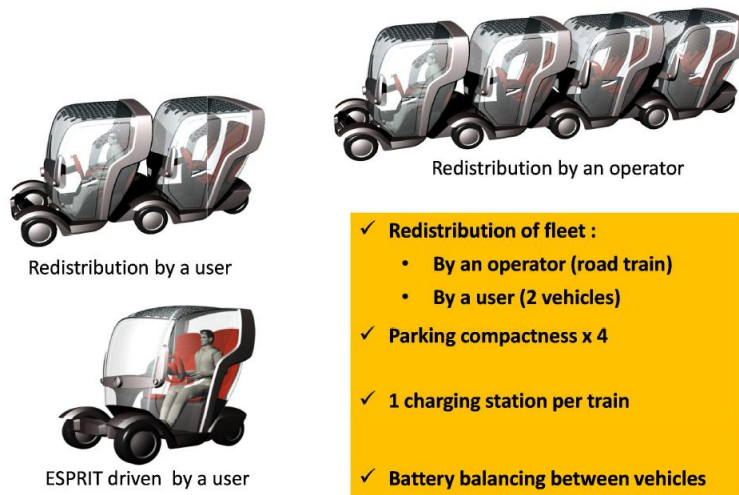


Figure 1. ESPRIT vehicle and key innovations (Communication kit, ESPRIT Project Consortium)

2. Introduction of the study area

The study area “Mezzieu/Decines-Charpieu/Jonage” is a suburban area of 52 km², located -within the Greater Lyon area (Metropolis of Lyon) - at about 12 km east of the city center of Lyon. The area encompasses three municipalities of Mezzieu, Decines-Charpieu and Jonage with a total population of approximately 63 000 inhabitants (2012 France Population Census). The area is slightly smaller, but seven times less dense than the city of Lyon. The figure below shows the position of the study area in Great Lyon urban conglomeration.



Figure 2. Study area: within the bleu boundaries/ City of Lyon: with the black boundaries/ Subway line A shown in red / joint tramway (T3) and Rhône-Express train shown in yellow

As we can observe in the figure above, the study area is connected to the Lyon city center thanks to the structural transit line (Tramway 3) and the Rhône Express train line, sharing the same guideway (shown in yellow) and also thanks to the subway line A (shown in red). The most important employment zones are shown in pink. We can count 3 industrial zones at the extreme east, extreme west and middle of the study area.

Lyon study area identity card	
Area	52 km ²
Population (2012)	63 212
Annual population growth (2007-2012)	1%
Population density (2012)	1213 hab./km ²
Average household size	2.58
Median household net income (2012)	20 294 €

Number of jobs (2012) : A	22 981
Economically active population (2012): B	25 620
Employment concentration rate (A/B)	0.89
Data source: Insee (French National Institute of Statistics and Economic Studies)	

Table 1. Identity card of the study area “Décines-Charpieu/Meyzieu/Jonage”

In general, the area is quite well endowed with rail and road infrastructures and takes advantage of the wide range of transport projects and investments of Lyon Metropolis. Its public transport system consists of several bus lines and a tram line. The area is directly connected to Lyon, the regional airport and the high speed train (TGV) stations. In the last few years, bike lanes have been extended and new Park&Ride facilities have been installed. In addition to these services, the city of Decines-Charpieu provides also a free bus service within the limits of the city, running two mornings per week, dedicated to elderly people. This specific service will not be taken into account in the model. No carsharing service is available in the area.

Despite the quite well- structured public transit system, the modal split is strongly dominated by car. The households’ motorization rate is very important (see figure 3 and table 2 & table 3 below).

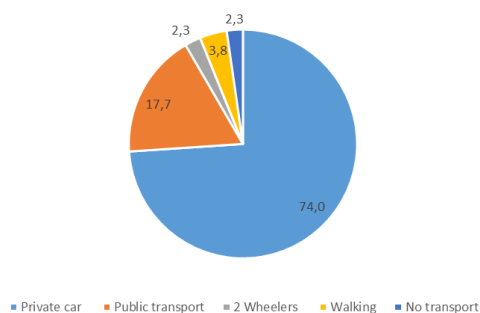


Figure 3. Modal split of the home to work trips in 2012 (Source: Insee)

Cities of the study area	Décines-Charpieu	Meyzieu	Jonage
Private car	70.8 %	75.2%	81.6%
Public transport	20.3%	16.5%	12.3%
2-Wheelers	2.3%	2.4%	1.4%
Walking	4.4%	3.7%	2.1%
No transport	2.3%	2.2%	2.7%

Table 2. Modal Split of the home to work trips in 2012 of 3 cities within the study area (Source: Insee)

As we can observe in the table above, the further, the city is situated from Lyon downtown, the higher is the share of the private car in the home to work trips, but also in the trips realized for the other purposes.

Share of the motorized households (2012)	88%
Share of the multi-motorized households (2012)	51%
Share of the mono-motorized households (2012)	37%

Table 3. Households’ motorization rate in the study area (Source: Insee)

The high-capacity roads are located rather at the border of the area. The internal road network consists of well-connected but low capacity roads, insufficient at peak hours, to ensure the north-south and east-west connection of the area. The Park & Ride sites seem well occupied, and irregular parking practices on the available unbuilt lands around these facilities are commonly observed.

Several future economic and urban developments have been already planned. Particularly, the industrial zone of Meyzieu situated at the eastern part of the area is planned to be extended during the future years, providing new job capacities. As well, the new stadium and sport complex “Grand Stade” is under construction is the east of Décines-Charpieu (in the middle of the study area). This transport generator will be connected to the Tramway T3 and a new activity and commercial zone will be developed around.

The small modal share of public transport and the perspective of future transport demand generated by the multiple development projects of the area emphasize the need of reorganization of

the existing transport system and patterns. The multimodality should be improved in order to encourage amodal shift to alternatives of private cars. The ESPRIT project could be a part of this ambition, as an innovative flexible transport system, at the intermediate of the conventional public transport services and the individual transport.

3. Holistic Model's architecture

A holistic model has been built in order to study the likely potential and impacts of the ESPRIT system's implementation within the study area. The model consists of two sub-models: a transport model and an economic model. The outputs of the transport model are used by the economic model to calculate the operational costs of each transport options for the stakeholders of the transport system: users, transport operators, transport and local authorities and the state.

3.1. Transport model

The figure below (figure. 4) gives an overview of the transport model.

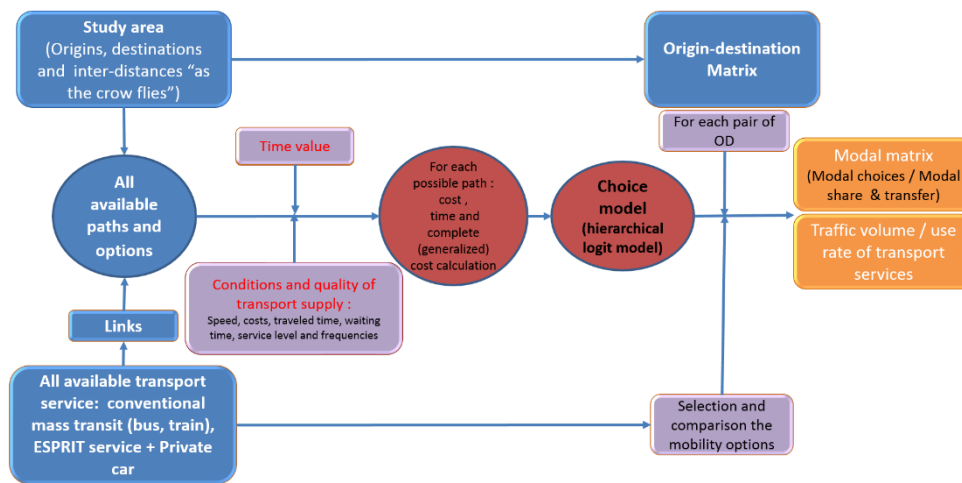


Figure 4. Transport model scheme

At the first step, the transport system of the study area is represented. The process consists of the introduction of transport services and networks available within the area. The combination of the transport services with the existing transport (road and rail) networks of the area constitutes the panel of the transport options for the passengers. The travel costs and time and therefore, the travel generalized cost, given a specific time value, are calculated for all the options and paths linking the different parts of the study area.

Besides, the general OD matrix is introduced into the model, describing the spatial distribution of all the trips (all travel modes and purposes included) within the area (internal flux), but also the trips from or to main daily travel generators of the metropolitan area (different district of Lyon, the main suburbs around Lyon, etc.). The OD matrix are delivered by Lyon local and transport authorities.

At the second step, the model assesses the modal choice of the travelers, based on a comparative analysis of the travel generalized cost (travel quality vs. travel cost) of the available options for each pair of origin-destination. The notion of the quality is defined by the economy of time. We consider a high quality service allowing to have the shortest total travel time which includes access-egress, in-vehicle, and transfer and waiting time. The level of comfort and/or the reliability of the options are not taken into account by the review model. The features of the transport options (speed, fare, frequency, etc.) are the parameters of the model, defined based on local observation and the local travel survey. For each pair of OD, the best option is assigned by the model. Then, the generated traffic by each option is aggregated and the sum of the traffic flux and the modal split is calculated.

The choice model is a hierarchical LOGIT consisted of two levels: a first level of four modes or combinations of modes and a second level with the services attached to the first level modes or their combination.

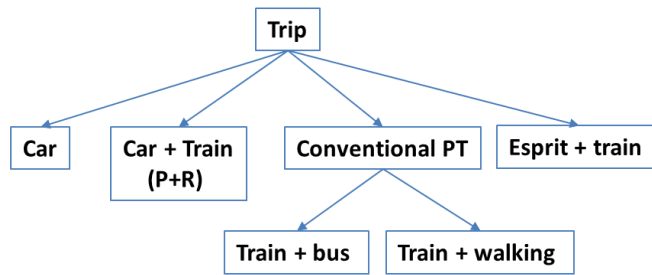


Figure 5. Modal choice in review model

3.2. Economic model

The second sub-model, the economic model calculates the economic balance of the transport operators and measures the interdependencies (e.g. a feeder service can be in deficit, while improving the overall economics of the system). The economic model assesses also the cost (required subsidiaries) and revenues (taxes) generated by the transport services of the area for the public authorities and the state and evaluate the likely impacts of various policies (fare policies) on the public finance. The architecture of the second sub-model is illustrated and detailed in the figure 6:

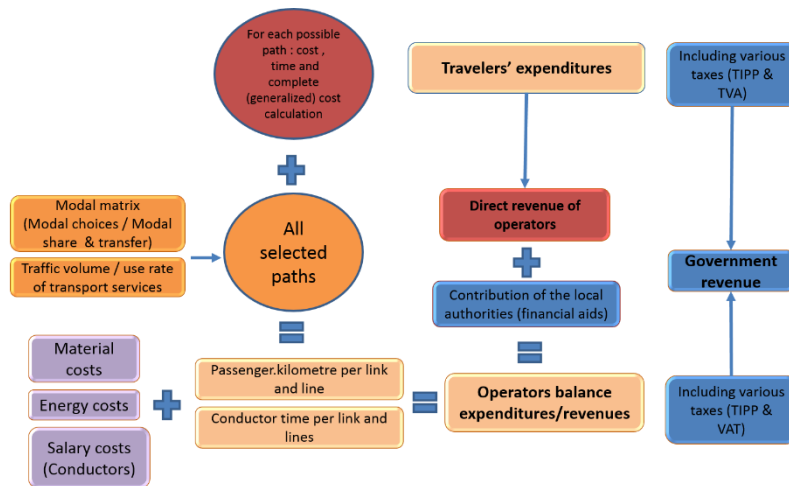


Figure 6. Economic model scheme

The following sections of this paper report on the first sub-model. The economic model is subject to another communication.

4. Zoning design and Implementation strategy of the ESPRIT stations

In the transport model, the zoning design is defined based on how likely a future ESPRIT service could be implemented on the study area. Each zone is defined by an ESPRIT station which constitutes its centroid. The first key assumption is the following: the stations, to be easily accessible, must be situated within a radius of 250m. A first implementation layout was drawn, focusing on the land use interactive maps of the area, available on the local open source databases and thanks to the Google Earth. At the second time, a field visit has been conducted in the aim of confronting the first implementation scheme and the reality of the area. The ESPRIT stations are classed in descending order of importance:

- **ESPRIT stations at transport hubs:** ESPRIT system should serve the 4 stations of the tramway line T3 which crosses the study area (Décines-Centre, Décines Grand-Large, Meyzieu Ville & Meyzieu ZI). These stations insure, in a multimodal approach, the interaction between the rail transport - structural transport system of the area- with the ESPRIT service -which can be considered as a potential feeder system of the area. In Lyon area, the main train station are all equipped with P+R facilities, a part of which can be dedicated to ESPRIT service.

- **ESPRIT stations in the downtown areas:** In the city centers with high urban density, the central points were identified (squares, crossroads, parking places at the foot of the administrative buildings, socio-cultural facilities, shopping centers, etc.), easily accessible, ideally situated to serve nearby clients, while being attractive also for the travelers a little further away. These stations generate inflows and outflows of travelers at any time of the day. We have identified three stations in central Décines- Charpieu, three in the center of Meyzieu and one at the center of Jonage.
- **ESPRIT stations serving the residential area:** ESPRIT service should serve also the residential zones of the area. For the location of the ESPRIT stations, the priority should be given to the multiple-unit dwellings rather than the detached houses, as they represent a more important population density. Décines-Charpieu, as Meyzieu are the cities with a high social mix, and the multiple dwellings are well distributed over the area. These buildings, often surrounded by detached houses, offer good locations for ESPRIT stations. In this category, we have identified five stations in Décines-Charpieu and ten in Meyzieu. Further from the center, at the borders of these two municipalities, as in Jonage, the residential zones are mostly formed by the detached houses, representing a very low density of population. In such these zones, it is difficult to identify “the” most appropriate location for ESPRIT station. The concept of "floating station" or “secondary station” seems corresponding to these areas. The floating/ secondary stations refer to the stations where ESPRIT vehicles can be dropped by users without any charging point, at least at the first stage of the service implementation. Five secondary stations are proposed for Décines-Charpieu, six for Meyzieu and two for Jonage. Finally, it is important to mention that the previous types of ESPRIT stations serve also the residences next to them. Thus, many of ESPRIT station have a mixed use.
- **ESPRIT stations in the industrial and employment areas:** Within the study area, we can count three main industrial zones:
 1. La Soie industrial zone (270 ha), situated at the extreme west of the study area, encompasses more than 600 companies and 9000 employees. This zone is common between Décines-Charpieu and the neighbor city of Vaulx en Velin and accessible from Lyon by the subway line A. An important multimodal hub is situated at its north side. The walking distances are important. It can be considered as an excellent example of a “hostile area” to any alternative of the automobile. Four secondary stations are proposed for La Soie IZ.
 2. The industrial zone of eastern Décines-Charpieu (at the middle of the study zone) is well structured, and two centrality points have been identified to implement ESPRIT stations. A new stadium under construction in this zone, will be surrounded by a new centers of activity in near future. A "secondary station" is proposed on the area.
 3. The industrial zone of Meyzieu (120ha) at the extreme east of the study area, presenting 180 companies and 4600 jobs. This IZ is served directly by the train line. But the train station is located almost at the center of the area. Thus, the walking distances are important. In addition to ESPRIT station of Meyzieu IZ train station, six other stations are proposed, including one "secondary station".

In total, we count 52 ESPRIT stations which we can classify by their level of strategic importance:

ESPRIT network design includes 52 ESPRIT stations corresponding:	
4:	train stations
7:	city down and shopping centers
15:	residential areas (dwelling housing)
7:	industrial zones
+	
19	potential secondary stations:
•	13: residential zones (individual houses)
•	5: less dense industrial zones
•	1: developing area (future activity zone – under development)

Table 4. Initial ESPRIT network design

The figure below represents the zoning design for the three municipalities of the study area.

Whenever possible, the zone is designed so as to align the centroid and the ESPRIT station. This is the case for all the “secondary stations”. If not, the centroid is placed as close as possible to the center of gravity of the area, based on the cartographic assessment.

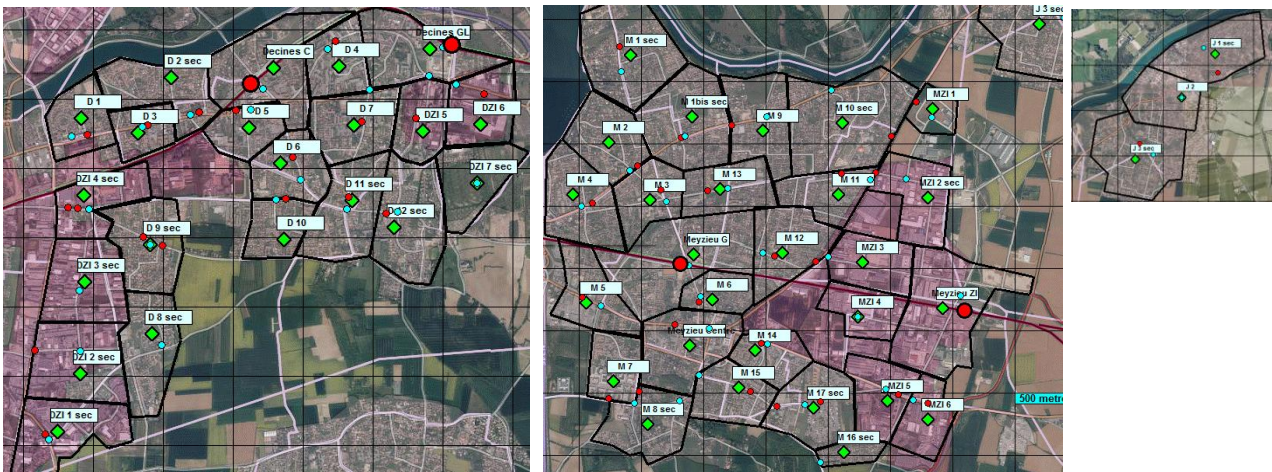


Figure 7. Zoning design of the Study area

4.1. Representation of the rest of the Great Lyon metropolitan area in the model

One of the main objectives of the study is to identify the potential of modal shift, ESPRIT service could generate. It would be necessary to consider all today’s trips that a future ESPRIT user can likely realize using this new mode, whether in case of his internal trips, within the study area or his external trips which have their origin or destination within this area. At this first stage of study, we consider two simplistic choices:

- We eliminate very remote origins and/or destinations, for which surveys show that likely concerned travelers are handful.
- We eliminate also all external trips for which no transit solution is available.

In practical terms, we had at our disposal the OD matrix of the Great Lyon area (148 zones) as it results from the 2006 household travel survey. We eliminate a large number of areas where the sum of the trips (trip generation) to or from the study area is less than 0.5% of total trips of the study area. We also eliminate the rural areas situated at the east and southeast of the study area. We finally eliminate Venissieux and the south east of Lyon, certainly accessible by the transit network, but in very inadequate conditions to challenge the absolute dominance of the private car mode. Following this review, we retain eighteen zones centered on transit stations shown on the following map:

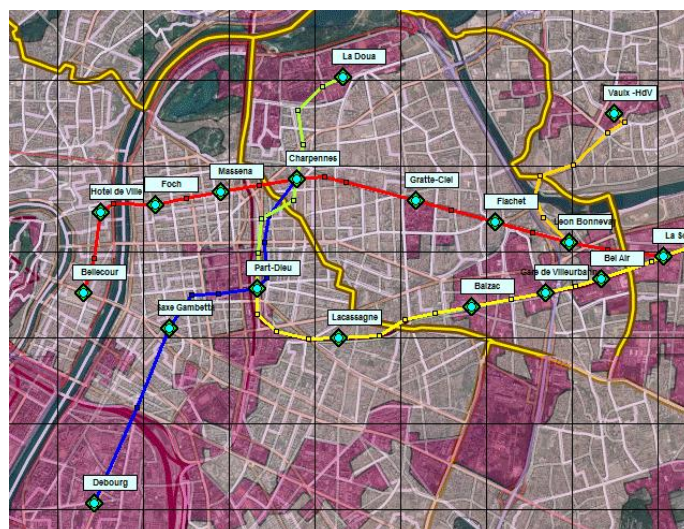


Figure 8. Principal network's nodes (main transport hubs) outside the study area

We add to the panel of external origins and destinations, at east of the study area, Saint- Exupéry airport, an important traffic generator pole connected to the study zone by a particularly fast connection, the Rhone Express train.

Regarding to the 2006 HHs travel survey data and adding these simplifications, we consider in the model, 80% of motorized trips having their origin within the study area, and 73 % of motorized trips having their destination in the study area. The 20 % and 27% “excluded trips” are exclusively on private car mode, for whom, the hope of achieving a modal shift through ESPRIT service is almost zero.

These 19 selected zones can be represented and treated in the model in the same way as the zones within the study area. But it would needlessly complicate the model. We don't place any ESPRIT station in these zones. We consider the transit station as the connecting rail node but also as the centroid of the zone and the average length of 500 meters are applied for the connectors (accessible walking distance). These simplifying hypothesis can be easily modified, if needed.

5. Transport Model's results

The table below represents the potential modal split after the introduction the ESPRIT service into the study area.

Modal split : current transport supply + ESPRIT service					
Modes	PH		Modes	OPH	
PC	6545	57%	PC	4901	75%
PT	667	6%	PT	158	2%
PT STR	529	5%	PT STR	120	2%
ESPRIT	1224	11%	ESPRIT	716	11%
P+R	2595	22%	P+R	623	10%
TOTAL	11561	100	TOTAL	6518	100%

Table 5. Modal split of the study area considering the ESPRIT service

Attention, to correctly interpret these results, it must be remembered that an important part of the travelers (20 % at origin) and (30% at destination) of the study area are characterized as “definitive automobilists” who have no other alternative transport solution to private car and for whom, the ESPRIT service cannot be considered as a modal transfer lever. They have not been taken into consideration in this model.

We see here that, the ESPRIT service, simply added to the existing system, could potentially - considering the availability of service whenever and wherever needed- represent up to 11% of the morning peak hour traffic, and its modal share remains the same during the off peak hours. It is important to We also recognize the efficiency of the free P+R facilities (22% during the morning peak hour, and 10% during off peak hours).

To find out, from which modes and how much, the ESPRIT service would probably take its potential users, we have run the model for the second time, removing the ESPRIT service, all other parameters being strictly identical. The results reveal the 11 % market share of ESPRIT during the morning peak hour, is taken from private car mode (5%), public transport (2%) and the P+R option (4%). During the off peak period, the 11 % market share of ESPRIT comes from for the private mode (8%), public transport (1%), and P+R option (1%).

Modal split : current transport supply					
Modes	PH		Modes	OPH	
PC	7113	62%	PC	5433	83%
PT	880	8%	PT	210	3%
PT STR	568	5%	PT STR	130	2%
ESPRIT	0	0%	ESPRIT	0	0%
P+R	3000	26%	P+R	745	11%
TOTAL	11561	100	TOTAL	6518	100%

Table 6. Modal split of the study area without the ESPRIT service

And to complete, two more tests have been realized.

In the first one, we maintain ESPRIT and exclude the P+R option: the modal share of ESPRIT raises to 23% during the peak period and 16% during the off-peak period.

Modal split : current transport supply - P+R					
Modes	PH		Modes	OPH	
PC	7239	63%	PC	5151	79%
PT	980	8%	PT	206	3%
PT STR	702	6%	PT STR	145	2%
ESPRIT	2640	23%	ESPRIT	1016	16%
P+R	0	0%	P+R	0	0%
TOTAL	11561	100	TOTAL	6518	100%

Table 7. Modal split of the study area considering ESPRIT service and excluding the P+R option

In the second test, we exclude ESPRIT and P+R, the simulation provides an indication of the modal split between private car and public transport, in absence of other possible alternatives.

Modal split : current transport supply - (P+R & ESPRIT)					
Modes	PH		Modes	OPH	
PC	8382	73%	PC	5911	91%
PT	2061	18%	PT	395	6%
PT STR	1118	10%	PT STR	212	3%
ESPRIT	0	0%	ESPRIT	0	0%
P+R	0	0%	P+R	0	0%
TOTAL	11561	100	TOTAL	6518	100%

Table 8. Modal split of the study area without the ESPRIT service and P+R option

Thus, we can conclude in the absence of the free P+R option, ESPRIT could reach a market share of 23% of total trips realized within the area during the morning peak period. These 23% are taken for 10% from PC modal share and 13% from the PT modal share. The availability of free P+R facilities leads to a rather similar result: the solution interests 26 % of travelers, coming respectively for 11% and 15% from PC and PT. By adding ESPRIT service to the free P+R option, PC lost another 5% of its modal share, and PT another 2%.The free P+R may represent a hurdle for the development of a service such ESPRIT.

To verify this observation, we repeat the simulation, modifying the fare hypothesis: charging the P+R for 10 € per day, and proposing the ESPRIT service for free. As result, ESPRIT takes 46% of the market! Excessive? No, the real surprise is elsewhere: we have still 45% of private car modal share, this result means that if we provide the travelers with a combination of i) free and good quality (on demand) local transport service (ESPRIT) and ii) a rapid structural rail transport, largely subsidized, there will be nearly half of travelers who, in all economic rationality, keep using their private cars, allowing a better economy of time.

Modal split : current transport supply & ESPRIT & P+R (10€/day)					
Modes	PH		Modes	OPH	
PC	5157	45%	PC	3889	60%
PT	555	5%	PT	114	2%
PT STR	513	4%	PT STR	95	1%
ESPRIT	5308	46%	ESPRIT	2414	37%
P+R	29	0%	P+R	6	0%
TOTAL	11561	100	TOTAL	6518	100%

Table 9. Modal split of the study area considering a free ESPRIT service and an available P+R option charged 10€ per day

6. Toward the optimization

We have conducted a set of sensitivity analyses in order to study the impacts of different likely service's deployment strategies. For that, we start by deploying the most attractive stations.

In the reference configuration, we had placed a significant number of secondary stations in the areas where we couldn't identify the best station's location. These secondary stations are mostly the "floating stations of the service zones" rather than the fixed station. We will gradually extend the ESPRIT network to these secondary stations, and measure the impacts of these extensions. In the figures below, the priority zones of the study area are presented.

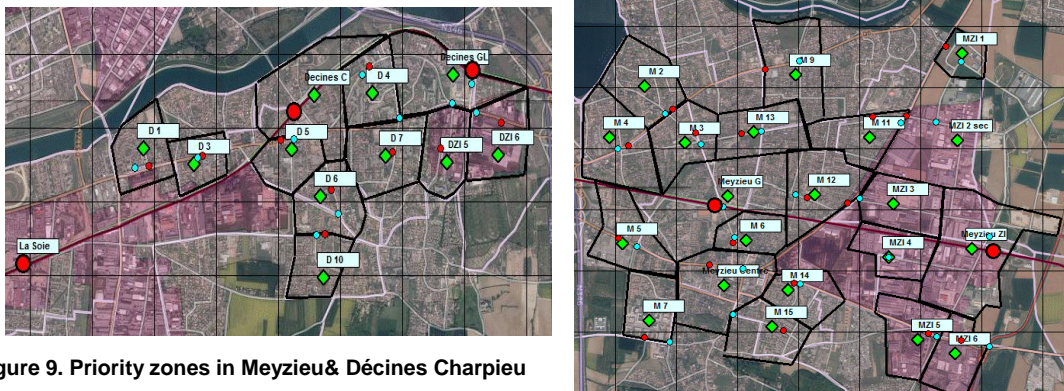


Figure 9. Priority zones in Meyzieu & Décines Charpieu

We run the model with the likely optimal pricing assumptions: P+R at 2€ per half-day and the prices of the ESPRIT service at 3/5th of the Bluey prices. Starting with Meyzieu, we define two subnets, as feeder systems of the nearest tramway T3 stations:

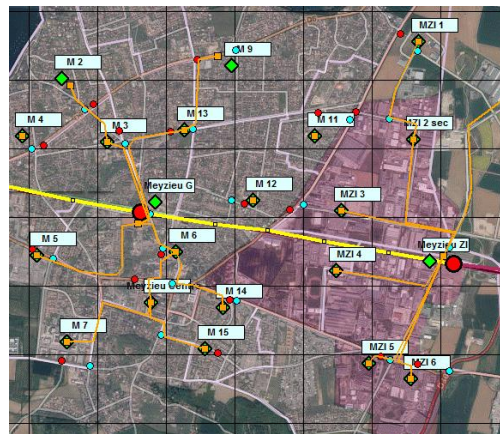


Figure 10. Two Esprit subnets in Meyzieu area (in orange), two tramway stations are shown in red

We have provisionally left out two stations (M11 and M12) that can be connected to both T3 stations of Meyzieu. We also connected Jonage to Meyzieu ZI. Regarding the industrial zone of Meyzieu, private car remains the dominant mode, ESPRIT service is able to take only a very tiny modal share. On the other hand, the ESPRIT station at Jonage has more success. It can potentially take more shares from private car and P+R.

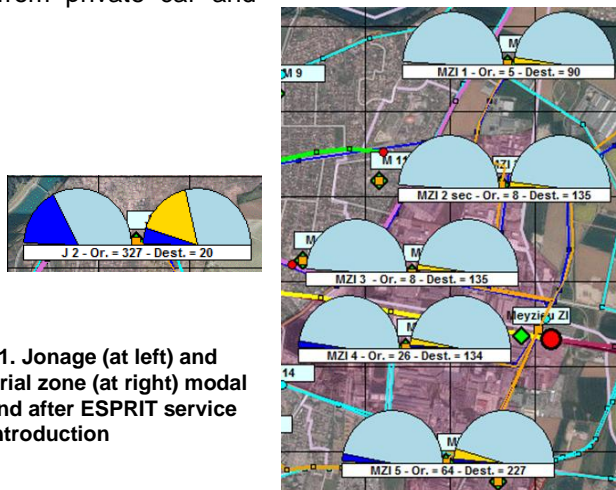


Figure 11. Jonage (at left) and Meyzieu industrial zone (at right) modal split, before and after ESPRIT service introduction

The overview of all the stations of Meyzieu is globally optimistic, while revealing the stations with quite different profiles:

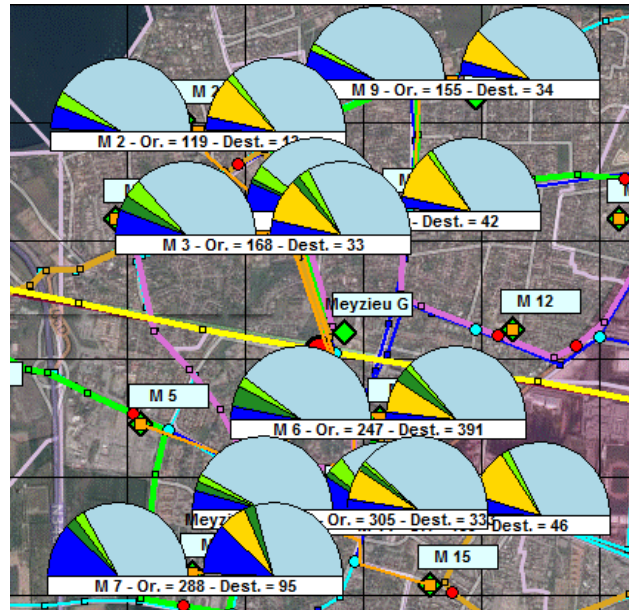


Figure 12. Meyzieu area, modal split before and after introduction of the ESPRIT service

Thus, it would be suitable to start the deployment of ESPRIT service from the downtown and the train station (in case of Meyzieu) and then, progressively, depending on the demand response to the service, extend the network to the further destinations such as Meyzieu industrial zone.

We have built the first two subnets, emphasizing their function as feeder systems of the two train stations. We complete the network, ensuring the full interconnection of all stations to the city, enabling us, to measure and compare the share of internal trips and the share of transfer trips (trips to stations) made by ESPRIT:

- The sub-network of 14 stations arranged radially around the Meyzieu Gare, at which Jonage is also connected, can attract, 619 travelers during PH and 279 during OPH.
- The sub-network of 6 stations arranged radially around the Meyzieu ZI station can absorb 35 travelers at the peak hour and 21 during the off peak hours.
- The interconnection of the two sub-network leads to attract 123 more travelers (+19%) at the peak times and 89 travelers during the off peak hours (+30%).

We do the same exercise on Décines-Charpieu. Going directly to the results, with the ESPRIT network that interconnects all 11 stations in the city (the figure below):

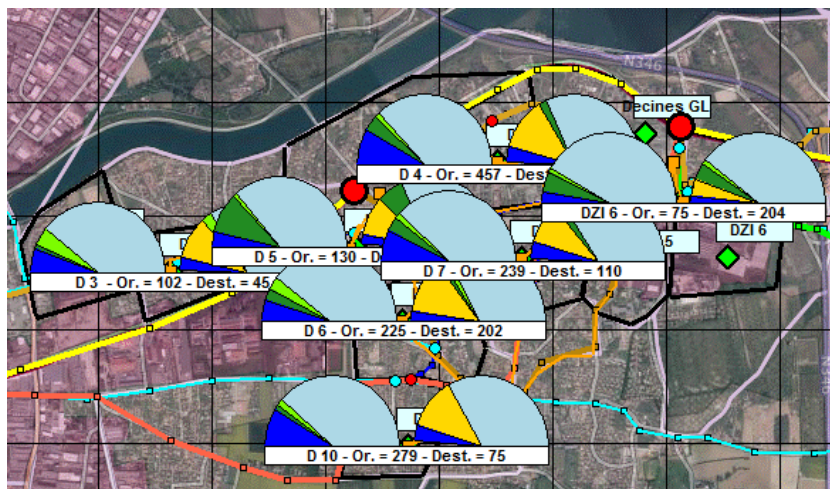


Figure 13. Modal split at Décines Charpieu, before and after introduction the ESPRIT service

The ESPRIT network interests 603 travelers during PH and 213 during OPH: in proportion of the concerned population, it appears as efficient as the ESPRIT network of Meyzieu downtown.

At the final step, we connect the networks of the two cities. This gives us a gain of 159 travelers (12%) during the peak hours and 128 travelers (21%) during the off peak hours. We see again that interconnection brings a more important demand, mostly during the off peak period, which is probably explained by a higher proportion of ESPRIT users for the internal trips during the off peak hours, within the studied area.

We complete this exercise by connecting our entire network to the intermodal train station of La Soie. We earn 118 more travelers (+ 8%) in the peak hour period, and 89 (12%) during the off peak hours.

To conclude this section, we compare the modal split of the reference ESPRIT network and the more compact network we have just described above. We note that with the compact network, the modal share of ESPRIT service shows a decrease of 2.6%: the stations qualified as “secondary” deserve, at the appropriate time, to be added to the network. In some cases, they can outperform the first stations.

Transport modes shares	Reference ESPRIT network	Compact ESPRIT network
Private car	56.5%	60.1%
Public transport	11.5%	11.7%
ESPRIT service	24.2%	21.6%

Table 14. Comparison of the modal splits between reference ESPRIT network and Compact ESPRIT network

Conclusions and perspectives

A pallet of the comprehensive scenarios allowed us to build an initial image of the ESPRIT network in this area and study the different impacts of its deployment of the transport demand and supply of the area.

We notice that the combination of a well-developed and sufficient ESPRIT service and a good pricing strategy can reduce the use of P+R facilities and stop the development of the irregular parking practices around the train stations and thus, liberating the available lands around the transit hubs for housing or economic activities’ development.

The key point is to find the best match between the existing transport services of the area and the future ESPRIT service, in order to boost, in a holistic approach, the whole transit supply (to improve the complementarity between the bus networks and the ESPRIT services) rather than to provoke a competition between the transit services.

The results communicated in this paper are issued from the exploratory simplistic model providing rapid but overall vision of at what an ESPRIT service could look like in a suburban area and to which extent, it could contribute in reorganization of its transport system. The next steps have already launched, consisting in a more detailed representation of the whole transport system of the area, its demand and the ESPRIT service through the more sophisticated activity based demand model and dynamic operational model.

Acknowledgments

We thank Lyon transport authority (Sytral) as well as Lyon local authority (Metropole de Lyon) for providing us with transport data.

References

ESPRIT Project Consortium, Communication kit, 2015

Elucidating the origin of the enrichment in aromatic compounds in Paris megacity atmosphere

Therese SALAMEH*, Agnes BORBON**, Stéphane SAUVAGE***, Nadine LOCOGE***, Stéphane BONNEAU**** & Olivier SANCHEZ****

*Laboratoire Interuniversitaire des Systèmes Atmosphériques (LISA), IPSL, CNRS, UMR 7583, Université de Paris Est Créteil (UPEC) et Paris Diderot (UPD), Créteil, France – email : therese.salameh@lisa.u-pec.fr

**Laboratoire de Météorologie Physique (LaMP), CNRS - UMR 6016, Université de Blaise Pascal, Clermont-Ferrand, France

***Sciences de l'Atmosphère et Génie de l'Environnement (SAGE), Mines Douai, 59508 Douai CEDEX, France

****AIRPARIF, Paris, France

Abstract

Besides their impacts on health, mono-aromatic compounds the so-called BTEX play an important role in the formation of secondary organic aerosols and ozone, which limit values are regularly exceeded in Paris and Ile de France region. A recent study has shown an enrichment in the C7-C9 aromatic fraction in Paris atmosphere by a factor of 3 compared to other northern mid-latitude cities. Here, we combined different approaches to investigate the role of transport-related sources in such enrichment (differences in gasoline composition and in vehicle fleet composition) : a statistical analysis of a large VOC (Volatile Organic Compounds) dataset including multi-year and multi-site speciated measurements (traffic, background, tunnel) by the air quality network AIRPARIF and a coupled experimental and modelling analysis of liquid and headspace composition of representative fuels distributed in Ile de France region (diesel, SP95, SP95 E10, and SP98) regarding C2 to C17 VOCs. First the statistical analysis reveals a high spatial heterogeneity of BTEX composition with lower TEX-to-benzene ratio values at traffic stations, as well as at background sites, in the suburbs and in the outskirts than in Paris intramuros up to a factor of 2. Second, the detailed composition of the fuel liquid phase determined at the laboratory is used to predict the headspace vapour composition that can be compared to the measured one. Modelled and observed compositions are in good agreement with differences up to $\pm 20\%$.

Keys-words: urban air quality, megacity, VOC, BTEX, fuel composition.

Résumé

Les BTEX ont des impacts néfastes sur la santé et jouent un rôle important sur la chimie atmosphérique en tant que précurseurs de composés secondaires comme l'AOS et l'ozone troposphérique. Des travaux précédents ont mis en évidence que la part en composés gazeux aromatiques à l'exception du benzène est deux à trois fois plus riche dans les panaches de pollution parisiens que dans ceux des autres villes de France et de Los Angeles. Les causes de cet enrichissement peuvent être la composition des essences et la composition du parc roulant de véhicules. La méthodologie de travail s'appuie sur une analyse statistique d'une large base de données en COVs, pluriannuelles et multi-sites (trafic, urbain de fond, tunnel) du réseau de qualité de l'air AIRPARIF à Paris et sur une analyse, couplant expérience et modélisation, de la composition de la phase liquide et gazeuse de carburants représentatifs de ceux distribués en Ile-de-France (diesel, SP95, SP95 E10 et SP98) pour les COVs de C2 à C17 afin d'étudier l'impact potentiel de la composition du carburant sur la composition atmosphérique urbaine. Les résultats montrent qu'il existe une hétérogénéité spatiale d'un facteur de 2 des rapports TEX/benzène entre les sites intramuros (trafic et background) et les sites sub-urbains. Les sites «trafic» présentent des rapports plus élevés que les sites «urbains de fond». La comparaison entre la composition de carburants dans la phase gazeuse obtenue par le modèle et celle au laboratoire est satisfaisante à $\pm 20\%$ de différence.

Mots-clés: qualité de l'air, mégapole, COV, BTEX, composition de carburants.

Introduction

As the air quality is increasingly deteriorated in cities world-wide and people are concerned for their health, air quality monitoring has extended beyond the criteria pollutants like carbon monoxide, oxide of nitrogen, ozone, and particulate matter to include measurements of some toxic air pollutants such as

volatile organic compounds (VOCs). Emissions of a large number of anthropogenic volatile organic compounds (VOCs) are prevalent in urbanized areas. VOCs play an important role in the formation of ozone and photochemical oxidants associated with urban smog (Seinfeld and Pandis, 2006). Interest in determining the VOCs in the atmosphere has increased over the last several decades (Lee et al., 2002). Studies have focused on the urban levels of VOCs, especially aromatics, due to the known and suspected carcinogenic nature of these species. Besides their impacts on health, mono-aromatic compounds the so-called BTEX (Benzene, Toluene, Ethylbenzene, and m+p-Xylenes) play an important role in the formation of secondary organic aerosols and ozone.

Paris and its surrounding region named "Ile de France" is one of the most crowded cities in the world, with more than 12 million inhabitants. It was found that the ozone production potential over the urban area of Paris is VOC-sensitive on average over two summers (Deguillaume et al., 2008). Benzene, an important representative of aromatic hydrocarbons has been a prime target for assessment in the urban atmosphere (Brocco et al., 1997) as it is considered to be a genotoxic carcinogen (WHO, 2000; Bolden et al. 2015).

BTEX are generally compounds associated with traffic emissions (exhaust and fuel evaporation) and TEX can be also released with the use of solvents (painting, printing, etc) (Salameh et al. 2014 ; Baudic et al., 2016).

While VOC composition is usually consistent between post-industrialized urban cities, a recent study has shown enrichment in the C7-C9 aromatic fraction in Paris atmosphere by a factor of 3 compared to other European cities (Borbon et al., 2013) including French urban areas (figure 1). The causes of such enrichment would be: (i) differences in gasoline composition (ii) differences in vehicle fleet composition and role of two-wheelers in particular and (iii) differences in solvent use related sources. Note that in Europe, benzene concentration in fuels is restricted to 1% (volume) of the fuels composition since 2000 (Directive 98/70/CE, 1998). The two wheelers are known as large emitters of gaseous aromatics (Saxer et al. 2006, Costagliola et al. 2014, Platt et al. 2014, Li et al. 2015) compared to other VOCs. They contributed to 47% of road transport VOC emissions in 2010 (AIRPARIF, 2013). Adding to that, the vehicle fleet composition in Paris intramuros includes 15% of two wheelers in 2012 compared to 8% in 2002; in outskirts, the two wheelers represented 7% in 2012 compared to 4% in 2002 (AIRPARIF, 2013). Similar trends of two wheelers are seen in other parts of Europe: in Barcelona, 34% in 2012 and 24% in 2002; in London 18% in 2011 compared to 6% in 2000 (Dall'Osto and Querol 2013).

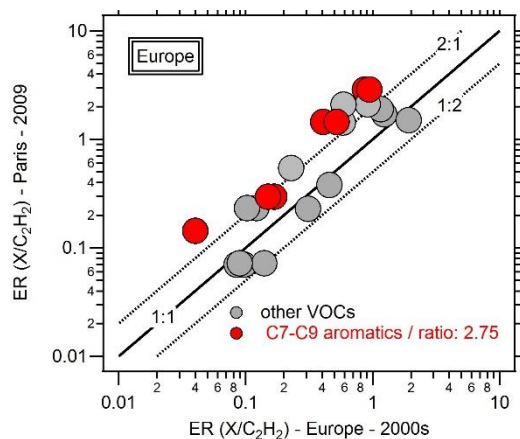


Figure 1: Comparison of NMHC emission ratios relative to acetylene in Paris to previous published studies in Europe (Borbon et al., 2003a, 2003b; Dollard et al., 2007).

Here, we combined different approaches to investigate the two first transport-related hypothesis:

- a statistical analysis of a large VOC (Volatile Organic Compounds) dataset including multi-year and multi-site speciated measurements (traffic, background, tunnel) by the air quality network AIRPARIF in order to investigate their temporal and spatial distribution
- a coupled experimental and modelling analysis of liquid and headspace composition of

representative fuels distributed in Ile de France region (diesel, SP95, SP95 E10, and SP98) regarding C2 to C17 VOCs is used in order to study the potential impact of the fuel composition.

1. Methodology

Ambient observations

In 2001, a long-term monitoring program for VOCs was initiated in France by ADEME (Agence de la Maîtrise de l'Energie et de l'Environnement) and the French Ministry of the Environment. As part of this program, one urban background site in Paris called "Les Halles" was implemented with an on-line TD-GC-FID (thermo-desorption unit Gas Chromatograph coupled to a Flame Ionization detector) for hourly measurements of 31 NMHCs belonging to the European ozone precursor priority list (Badol et al., 2004) and operated by the local Air Quality Monitoring Network (AASQA), AIRPARIF. Since 2011, the sampling site was changed to "Siège Airparif" because of public works at "Les Halles" site. The monitoring station of "Les Halles" is located in the middle of a small park with the closest busy road (>20,000 vehicles per day) located about 100 m distant whereas the "Siège Airparif" site is located at the roof top of the "Airparif" building surrounded by high density of commercial and residential premises as well as vehicular activities. In order to cover all Ile de France region, Airparif has implemented more than 15 monitoring sites (urban background and traffic) for BTEX daily and weekly active sampling with sorbent tubes (figure 2).

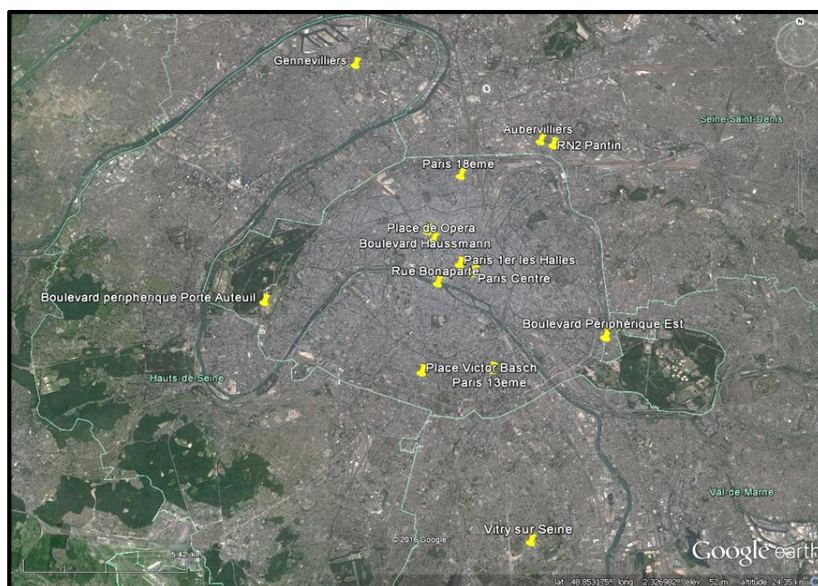


Figure2: Location of the monitoring urban and traffic stations in Paris and Ile de France region.

We have derived the average annual urban enhancement ratios (ER) of TEX relative to benzene concentration from the slope of least-square linear regression fit, from 2003 until 2014 depending on the availability of data at each site. An illustration is provided on figure 3 for toluene vs. benzene at "Auteuil" traffic site and "Les Halles" urban background site in 2010. Significant correlations between toluene and benzene are usually seen at the traffic site than at the urban background site suggesting that these species are emitted by the traffic at Auteuil.

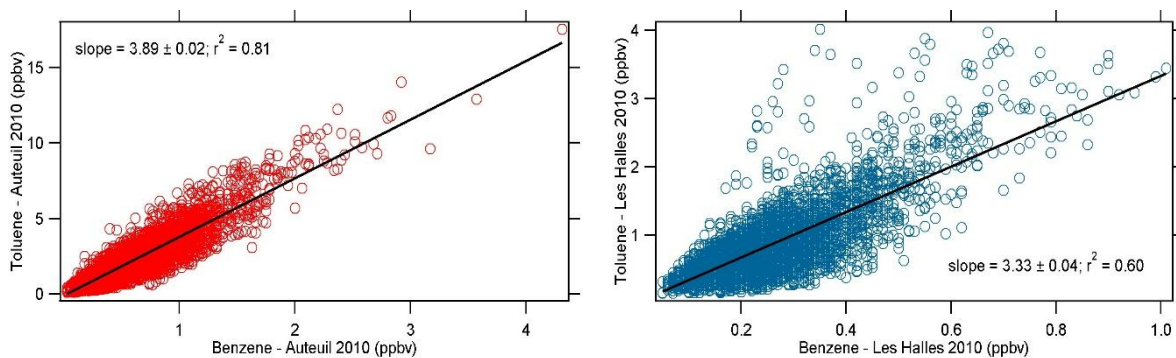


Figure 3: Scatterplots and correlation plots of toluene vs. benzene at the traffic site “Auteuil” and the urban background site “Les Halles” in 2010.

While the effect of photochemical removal cannot be excluded in Paris for the most reactive TEX, Borbon et al. (2013) have shown that there is no evidence of its effect from their diurnal profiles. The impact of photochemistry on TEX concentrations was pointed out in the Paris plume explored by the ATR-42 during the MEGAPOLI campaign at a least/minimum distance of 50 km from the urban center which is not the case of the considered sites in this study.

The BTEX database provided by AIRPARIF gathers different online and offline techniques and the intercomparison of these techniques have been preliminary checked at collocated measurement sites. In particular, we studied the impact of the measurements temporal resolution on the concentrations and on the ER at the urban background site "Les Halles" for which hourly data from 2003 until 2010, daily data from 2003 to 2008, and weekly data in 2009 and 2010 are available. The comparison of hourly data to daily data is satisfactory with a slope at ± 1 and an average coefficient of determination equal to 0.80. The comparison of hourly data to weekly data in 2009 and 2010 shows some differences. They reach a factor of 50% and the r^2 values are lower (0.2 – 0.6). This is partly due to the limited number of points. The comparison of TEX-to-benzene ratios with different temporal resolutions also shows this difference. In the spatial variability study, we will take into account this aspect.

Laboratory observation data

In order to study the potential impact of fuel composition, a coupled experimental and modelling analysis of liquid and headspace composition of representative fuels distributed in Ile de France region (diesel, SP95, SP95 E10, and SP98) regarding C2 to C17 VOCs is applied.

First, we collected three representative types of gasoline (SP95, SP95 E10 and SP98) and diesel distributed in "Ile de France", which were analyzed at the Sciences de l'Atmosphère et Génie de l'Environnement (SAGE) laboratory -Mines Douai in June and July 2015. We examined the composition of fuels at different temperatures and we measured the evaporative emission rates. To do so, we developed a procedure dedicated to analyze the composition of the headspace (figure 4) and of the liquid phase by doping the sorbent tubes, for C2 - C17 VOCs belonging to different chemical families (alkanes, alkenes, alkynes and aromatics).

For the headspace analysis, the system consists on a supply of zero air at a flow rate of hundred milliliters per minute above the capillary connected to the fuel sample. A Tee connector allows another dilution of the sample with zero air before injection into the GC-FID analytical system. We analyzed the same sample at least 4 times to test the repeatability of the results.

For the liquid phase analysis, we diluted 10 times the fuel samples (0.5mL) with pure methanol. Then, we used a syringe of 1 μ L to inject the fuel into the injector and oven at a temperature of 150°C for 3 minutes at a pressure of 8 psi. The liquid injection allows the vaporization of the entire sample in a thermostatic chamber and then it will be introduced directly into the chromatographic column by a carrier gas. We performed the active sampling on Tenax TA tubes allowing the adsorption of C5 to C17 VOCs. The tubes are then analyzed by GC-FID-MS.

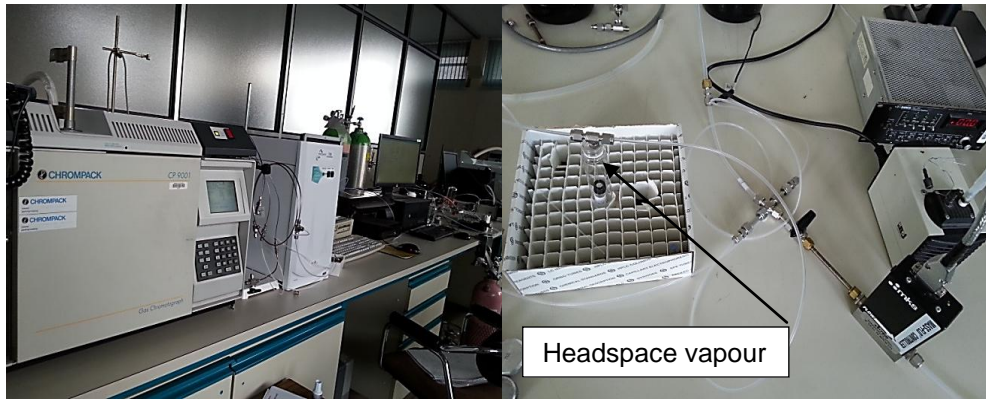


Figure 4: Headspace vapour and liquid phase analysis at the laboratory.

Secondly, we applied a model to predict the headspace composition when changing the liquid phase composition. We designed the model based on the literature (Bennett et al. 1993, Harley and Coulter-Burke, 2000). The model is based on the calculation of the partial pressure of each compound using equation 1 and the Antoine constants at atmospheric pressure and ambient temperature.

Equation 1: Vapor Pressure (P°_i) = $10^{(A - (B / (C + T)))}$ where A, B and C are Antoine constants and T is the temperature in °C.

By applying this model, based on the mole fraction of VOCs in the liquid phase, we will be able to deduce the mole fraction of each compound in the gas phase in equilibrium with the liquid phase.

2. Results and discussion

Spatial variability of the urban enhancement ratios

The results illustrated in figure 5 show that there is a spatial gradient of the ER within Paris and among sites between a 1 to 5 range. The "traffic" sites have higher ratios than "urban background" sites. Moreover, higher ratios are observed in Paris intramuros traffic sites compared to those on the outskirts and suburbs. For the urban-background sites, Paris intramuros also presents higher ratios than those observed in the outskirts and suburbs (Figure 5). Such spatial heterogeneity minimizes the role of solvent use as the main cause of the enrichment of TEX in Paris and point to transport-related sources as the potential main driver. Therefore, we will focus on the two other assumptions (fuel composition and vehicle fleet composition) in the following sections.

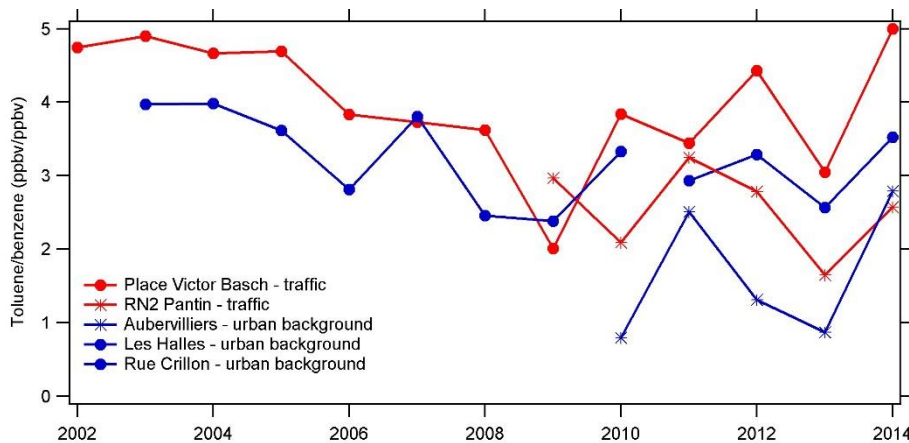


Figure 5: Spatial variability of the urban enhancement ratios at different locations belonging to AIRPARIF network.

Seasonality of the enhancement ratios

In order to study the influence of the TEX-to-benzene ER seasonality on the composition of Paris atmosphere, we computed the ratios from hourly data available for the urban background site "Les Halles" and the traffic site "Auteuil" obtained by the linear regression fit described in previous section (Figure 6) (here for toluene). In winter, the range of ER variability at the two measurement sites are roughly similar; they vary between 2 and 4 at "Les Halles" and between 3 and 4 at the traffic site. During other seasons, especially in summer, the ERs are significantly higher at the background site and reach a value of 5 – 6 compared to 4 - 5 at the traffic site. A less pronounced seasonality is seen at the traffic site "Auteuil" than at "Les Halles". The enrichment could be due to additional gasoline evaporation sources other than traffic in summer and to an increased use of two-wheelers in Paris intramuros in summer. The latter assumption is also consistent with higher ER observed at traffic sites in Paris intramuros over the whole year (figure 5). Therefore, we have first investigated the impact of the fuel composition on the atmospheric composition of aromatic VOCs by coupling experimental and modelling analysis.

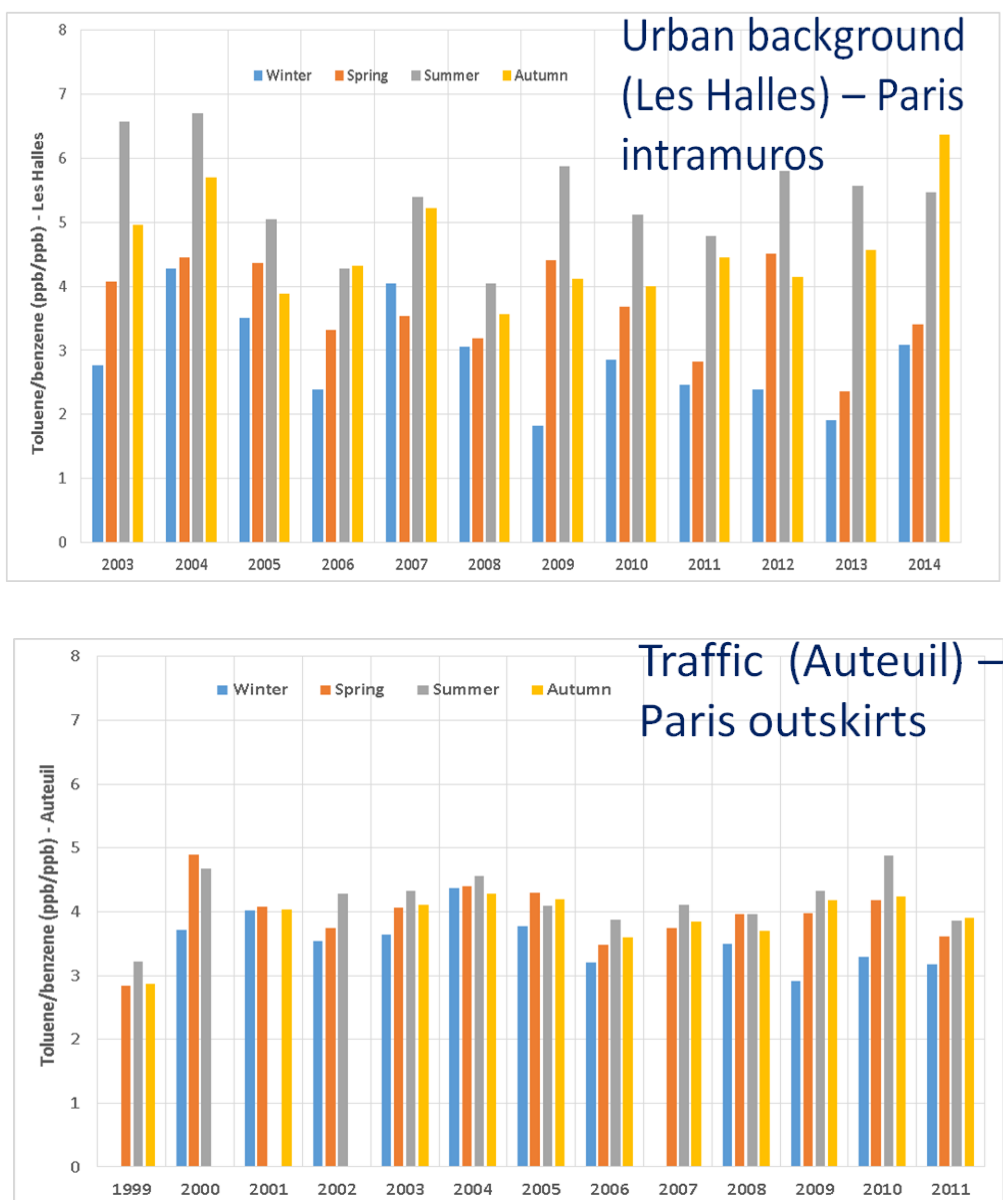


Figure 6: Seasonality of the urban enhancement ratios (toluene/benzene) at an urban background site “Les Halles” and a traffic site “Auteuil”.

Analysis of fuel composition

The comparison of the liquid phase composition of different gasoline distributed in Ile de France region held in figure 7, shows an overall similar fingerprint characterized by aromatics namely (toluene, m,p-xylenes, ethylbenzene, o-xylene) and C5-C8 alkanes (pentane, isopentane, 2-methylpentane, isooctane, hexane). From these data, we can deduce an average profile composition of gasoline in Ile de France region.

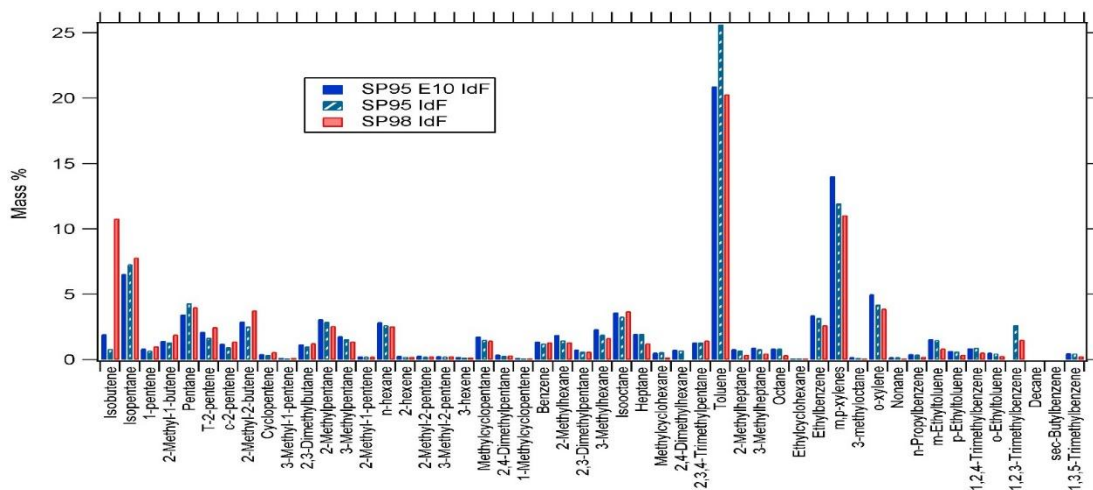


Figure 7: liquid phase composition (mass %) of three types of gasoline (SP95, SP95E10, SP98) distributed in Ile de France region.

Based on the model described above and on the mole fraction of VOCs in the liquid phase of each type of gasoline, we can deduce the mole fraction of each compound in the gas phase in equilibrium with the liquid phase. The comparison between the modelled and measured experimentally, in the laboratory, composition (mass percentages of the different VOCs) of the headspace vapour is very satisfactory for the various species up to $\pm 20\%$ ($r^2 = 0.9$) as illustrated in figure 8.

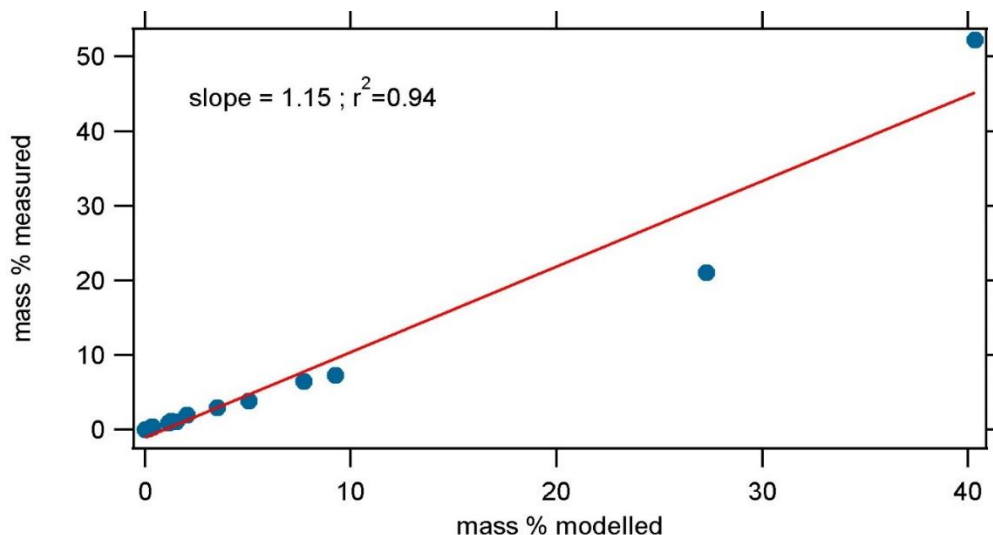


Figure 8: correlation between measured and modelled mass percentages for the SP95.

Once validated the model is a relevant tool to test the sensitivity of BTEX and other VOCs ambient

composition to evaporative emissions of fuels with regards to their composition. It is also possible to simulate a road transport profile by taking into account the fuel evaporation and exhaust emissions. The potential contribution of an additional gasoline evaporation source in summer was estimated at different locations. Preliminary results would suggest that this source, alone, cannot explain the TEX enrichment, pointing out the potential importance of two wheelers emissions. The next step will be to test this last hypothesis.

Conclusion

We conducted a statistical analysis of a large VOC (Volatile Organic Compounds) dataset including multi-year and multi-site speciated measurements (traffic, background, tunnel) by the air quality network AIRPARIF. The objective was to elucidate the causes of TEX enrichment in Paris atmosphere by combining different approaches. First, we assessed the spatial variability and seasonality of urban enhancement ratios in Paris intramuros, outskirts and suburbs. The results show a spatial heterogeneity (up to a factor of two) between the different sites and a significant seasonality at the urban background site especially. We set up a coupled experimental and modelling analysis of liquid and headspace composition of representative fuels distributed in Ile de France region (diesel, SP95, SP95 E10, and SP98) regarding C2 to C17 VOCs. We have developed, optimized and validated a procedure allowing the multi-phase (headspace and liquid phase) analysis of fuel composition. Based on the literature, we have designed a model to test the sensitivity of BTEX and other VOCs ambient composition to evaporative emissions of fuels with regards to their composition and we validated the model with the experimental measurements. This model, predicting the composition of the gas phase from the liquid phase, shows very satisfactory results ($r^2 = 0.9$). The simulation of a road transport profile taking into account the fuel evaporation and exhaust emissions is therefore, possible.

Acknowledgments

This work was supported by the Ile de France region (DIM R2DS – SIPAOS project n°2014-09). We would like to thank Laurence Dépelchin and Thierry Léonardis for technical support and AIRPARIF for providing the data.

References

- AIRPARIF (2013) : Evolution de la qualité de l'air à Paris entre 2002 et 2012. AIRPARIF, Juillet 2013.
- Badol C., A. Borbon, N. Locoge, T. Léonardis & J.C. Galloo (2004) : An automated monitoring system for VOC ozone precursors in ambient air: development, implementation and data analysis. Anal. Bioanal. Chem. Vol. 378, 1815–1827. doi:10.1007/s00216-003-2474-0
- Baudic A., V. Gros, S. Sauvage, N. Locoge, O. Sanchez, R. Sarda-Estève, C. Kalogridis, J.-E. Petit, N. Bonnaire, D. Baisnée, O. Favez, A. Albinet, J. Sciare & B. Bonsang (2016) : Seasonal variability and source apportionment of volatile organic compounds (VOCs) in the Paris megacity (France). Atmos. Chem. Phys. Discuss., doi:10.5194/acp-2016-185.
- Bennett A., S. Lamm, H. Orbey & S.I. Sandler (1993) : Vapor-liquid equilibria of hydrocarbons and fuel oxygenates, J. Chem. Eng. Data, vol. 38, 263-269.
- Bolden A.L., C.F. Kwiatkowski & T. Colborn : New Look at BTEX: Are Ambient Levels a Problem?, Environ. Sci. Technol. vol. 49, 5261–5276. DOI: 10.1021/es505316f, 2015.
- Borbon A., H. Fontaine, N. Locoge, M. Veillerot & J. C. Galloo (2003a) : Developing receptor-oriented methods for non-methane hydrocarbon characterisation in urban air. Part II: Source apportionment, Atmos. Environ., vol. 37(29), 4065–4076.
- Borbon A., H. Fontaine, N. Locoge, M. Veillerot & J. C. Galloo (2003b) : Developing receptor-oriented methods for non-methane hydrocarbon characterisation in urban air: Part I: Source identification, Atmos. Environ., vol. 37(29), 4051–4064.
- Borbon A., J.B. Gilman, W.C. Kuster, N. Grand, S. Chevaillier, A. Colomb, C. Dolgorouky, V. Gros, M. Lopez, R. Sarda-Estève, J. Holloway, J. Stutz, O. Perrussel, H. Petetin, S. McKeen, M. Beekmann, C. Warneke, D.D. Parrish & J.A. de Gouw (2013).: Emission ratios of anthropogenic VOC in northern mid-latitude megacities: observations vs. emission inventories in Los Angeles and Paris, J. Geophys. Res., vol. 118, 2041 - 2057, doi:10.1002/jgrd.50059.

- Brocco D., R. Fratarcangelli, L. Lepore, M. Petricca & I. Ventrone (1997) : Determination of aromatic hydrocarbons in urban air of Rome. Atmos. Environ., vol. 31: 557–566.
- Costagliola M.A., F. Murena & M.V. Prati (2014) : Exhaust emissions of volatile organic compounds of powered two-wheelers: Effect of cold start and vehicle speed. Contribution to greenhouse effect and tropospheric ozone formation. Science of the Total Environment, 468–469, 1043–1049.
- Dall'Osto M. & X. Querol (2013) :New Directions: Four to two – Powered two wheelers changing the European urban motor vehicle census. Atmospheric Environment, 77 (2013) 1083–1084.
- Deguillaume L., M. Beekmann & C. Derognat (2008) : Uncertainty evaluation of ozone production and its sensitivity to emission changes over the Ile-de-France region during summer periods, J. Geophys. Res. Atmos., 113, D02304. Doi: 10.1029/2007JD009081.
- Dollard G. J., P. Dumitrean, S. Telling, J. Dixon & R. G. Derwent (2007) : Observed trends in ambient concentrations of C₂–C₈ hydrocarbons in the United Kingdom over the period from 1993 to 2004, Atmos. Environ., vol. 41, 2559–2569.
- Harley R.A. & S. Coulter-Burke (2000) : Relating liquid fuel and headspace vapor composition for California reformulated gasoline samples containing ethanol, Environ. Sci. Technol. vol. 34, 4088-4094.
- Lee S.C., M.Y. Chiu, K.F. Ho, S.C. Zou & X. Wang (2002) : Volatile organic compounds (VOCs) in urban atmosphere of Hong Kong.Chemosphere,vol. 48, 375–382
- Li L., Y. Ge, M. Wang, Z. Peng, Y. Song, L. Zhang & W. Yuan (2015) :Exhaust and evaporative emissions frommotorcycles fueled with ethanol gasoline blends. Science of the Total Environment vol. 502, 627–631.
- Platt S.M., I. El Haddad, S.M. Pieber, R.-J. Huang, A.A. Zardini, M. Clairotte, R. Suarez-Bertoa, P. Barmet, L. Pfaffenberger, R. Wolf, J. G. Slowik, S.J. Fuller, M. Kalberer, R. Chirico, J. Dommen, C. Astorga, R. Zimmermann, N. Marchand, S. Hellebust, B. Temime-Roussel, U. Baltensperger & A.S.H. Prévôt (2014) : Two-stroke scooters are a dominant source of air pollution in many cities. Nature Communications 5, Article number: 3749 doi:10.1038/ncomms4749.
- Salameh T., C. Afif, S. Sauvage, A. Borbon & N. Locoge (2014) : Speciation of Non- Methane Hydrocarbons (NMHC) from anthropogenic sources in Beirut, Lebanon, Environ. Sci. Pollut. R., vol. 21, 10867–10877, doi: 10.1007/s11356-014-2978-5.
- Saxer C.J., A-M. Forss, C. Rüdý & N.V. Heeb (2006) : Benzene, toluene and C₂-benzene emissions of 4-stroke motorbikes: Benefits and risks of the current TWC technology. Atmospheric Environment vol. 40, 6053–6065.
- Seinfeld J.H.&S.N. Pandis (2006) : Atmospheric chemistry andphysics, from air pollution to climate change,John Wiley & Sons, inc., Hoboken, NJ, USA.
- WHO – World Health Organisation (2000) : Air Quality Guidelines for Europe, 2nd Edn., WHO Regional Publications, No. 91, European Series, Copenhagen.

Investigating the influence of the calibration and validation of cell transmission traffic flow model on average speed-based emission predictions

Arwa SAYEGH*, Richard CONNORS* & James TATE*

**Institute for Transport Studies, University of Leeds, Leeds, UK LS2 9JT*

Tel +44 113 34 35325 - email: ts11ass@leeds.ac.uk

Abstract

Emission and air quality model predictions are used to inform transport policy and investment decisions aimed at reducing road traffic emissions and achieving sustainable mobility. To be effective, such policies must be based on robust models that not only provide predicted policy outcomes, but also inform these with a level of confidence that properly accounts for the propagation of uncertainties through the complex chain of models involved. This paper develops a methodology to calculate the uncertainty in average speed-based emission predictions induced by the uncertainties in its traffic flow data inputs. This paper characterises such uncertainties using an ensemble-based approach for the calibration and validation of a discretised first-order macroscopic traffic flow model, the Cell Transmission Model (CTM), which is often used as input to average speed-based emission models. The propagation of the characterised uncertainties from the CTM is then studied using a Monte-Carlo sampling approach. The paper uses real motorway traffic data for the calibration and validation of CTM and illustrates how the upper and lower bounds of emission predictions can be determined as a result of uncertainty propagation from a calibrated and validated macroscopic traffic flow model, separately.

Key-words: *macroscopic traffic flow modelling, emission modelling, uncertainty propagation, error propagation, real data.*

Introduction

Human exposure to harmful traffic-related air pollutants can, in principle, be assessed using direct measurements of roadside air quality. However, in many current scenarios and particularly for forecasting and policy development, modelling is required. The key inputs to ambient air quality models are source emission estimates or predictions. Road traffic exhaust emissions can either be measured directly or estimated using traffic activity data. However, the limited spatial and temporal resolution of both vehicular emission and traffic activity measurements results in emissions being often predicted using the outputs of traffic flow models as inputs to vehicular emission models.

Various approaches have been developed to integrate traffic flow and emission modelling, depending on the level of detail desired in the emission predictions. The two most straightforward approaches are: whole-link traffic flow models (which are often referred to as static macroscopic traffic flow models) with average speed-based emission models (see for e.g. Namdeo et al, 2002 or Nejadkoorki et al, 2008); and microscopic traffic flow models with instantaneous or power-based emission models (see for e.g. Rakha and Ahn, 2004 or Panis et al, 2006). However, macroscopic traffic flow models, which represent traffic as a continuum and consider only aggregate traffic behaviour, have recently been integrated with different types of emission models in an attempt to improve on the low-fidelity of whole-link traffic flow models while avoiding the high costs in computation, data requirement, and calibration of the microscopic traffic flow models. The Lighthill-Whitham-Richards (LWR)-type models (Lighthill and Whitham, 1955a; 1955b; Richards, 1956) are one of the most commonly used continuum macroscopic traffic flow models in predicting emissions. LWR-type models describe the dynamics of traffic density using one Partial Differential Equation (PDE) and are often referred to as first-order macroscopic traffic flow models (Hoogendoorn and Bovy, 2001).

Cell Transmission Model (CTM) (Daganzo, 1994; 1995), in particular, has been used in a number of studies to predict space-time varying average speed based emissions (e.g. Lin and Ge, 2006; Zhu et al, 2013) or driving-mode based emissions (e.g. Zhang et al, 2013). Similarly, Liu et al (2014) proposed a multi-class form of the CTM and developed a model-based control framework which optimises motorway traffic control systems by minimising both total travel times and total average speed-based emissions predicted using their traffic flow model. Alternatively, Zhou et al (2015) have

integrated Newell's macroscopic traffic flow model (Newell, 1993) with a simple linear car-following model proposed also by Newell (2002) to generate vehicle trajectories and consequently predict power-based emissions. Both CTM and Newell's macroscopic traffic flow models are a finite difference solution schemes for the LWR-type model which are used to predict traffic state variables at short discretised road links and time intervals.

However, a key aspect in using such an integration approach is how well LWR-type models replicate real-world average traffic density and traffic speed which are both used as a basis to predict average speed-based emissions. The main disadvantage of LWR-type models is the use of steady-state speed-density relationship which implies that the average speed adapts instantaneously to traffic density without considering any delay (Hoogendoorn and Bovy, 2001). Despite this limitation, the simplicity of LWR-type models and their ability to replicate time periods of congestion led to their recent widespread integration with average speed-based emission models and to their use both in research and in practice (embedded in commercial software). Nevertheless, calibration and validation studies of LWR-type models against real data are quite limited (mainly Lin and Ahanotu, 1995; Muñoz et al, 2004, 2006; Spilioupilou et al 2014; and Roncoli et al, 2015), especially against real data for the United Kingdom (UK) motorway network (Chow and Li, 2014).

This paper utilises real-world motorway traffic data to study the performance of a first-order traffic flow model, the CTM, for the UK motorway road network using an ensemble-based approach to the calibration and validation. The paper then uses existing methods of incorporating the CTM with average speed-based emissions and uses a Monte-Carlo sampling approach to investigate the influence of both the calibration and validation errors of a commonly used traffic flow model on average speed-based road exhaust emissions. The methodology is applied on the real-world calibration and validation results in order to assess the uncertainty in using first-order macroscopic traffic flow models for predicting road traffic exhaust emissions.

1. Mathematical preliminaries

Lighthill-Whitham-Richard (LWR) model

Mathematically, the LWR model is governed by a system of three independent equations (1-3), two independent variables: location x and time t , and three unknown dependent variables: traffic flow, traffic density, and traffic speed.

$$\partial_t \rho = -\partial_x q \quad (1)$$

$$q(x, t) = \rho(x, t)u(x, t) \quad (2)$$

$$u(x, t) = u^e(\rho(x, t)) \quad (3)$$

Each of the three variables is defined as follows (Hoogendoorn and Bovy, 2001):

- Traffic flow $q(x, t)$ as the number of vehicles flowing past location x during $[t, t+dt]$ per unit time
- Traffic density $\rho(x, t)$ as the number of vehicles on a road segment $[x, x + dx]$ per unit length at time instant t , and
- Traffic speed $u(x, t)$ as the distance travelled by vehicles per unit time.

Equation (1) describes the law of conservation of vehicles. Particularly, it demonstrates that the number of vehicles in segment x changes from time instance t to time instance $t + dt$ according to the balance of traffic inflow at the boundaries x and $x + dx$ of the segment. Equation (2) assumes that the traffic flow at location x and time t is a function of traffic speed and traffic density. The first two equations are considered the basis of any continuum macroscopic traffic flow model. However, in order to solve the system of three unknowns, a third equation is needed; the form of this equation distinguishes between the different types of continuum traffic flow models. For the LWR model, Equation (3) assumes that the equilibrium traffic speed is a function of traffic density; this is the most straightforward approach to solving this system of equations (Hoogendoorn and Bovy, 2001). Accordingly, the resulting non-linear partial differential equation becomes:

$$\partial_t \rho = -\partial_x \{\rho u^e[\rho(x, t)]\} \quad (4)$$

Cell transmission model (CTM)

For the CTM, Equation (4) of the LWR model is approximated by a set of recursive equations

which describe the dynamics of traffic density at each discrete cell and time step. Also, Equation (2) is approximated by a piecewise linear relationship between traffic flow and traffic density, the so-called fundamental diagram. The fundamental diagram proposed initially for the basic CTM in Daganzo (1994) is the isosceles trapezoidal fundamental diagram but then relaxed to the trapezoidal fundamental diagram for the generalised CTM (Daganzo, 1995).

Under the CTM formulation, a motorway section is discretised to a number of cells as shown in Figure 1. The cells are numbered from 0 to N where cell 0 is considered the mainline origin and cell N is considered the mainline destination. Each cell from 1 to $N-1$ can be linked with an external incoming flow for e.g. in the form of an on-ramp and external outgoing flow for e.g. in the form of an off-ramp.

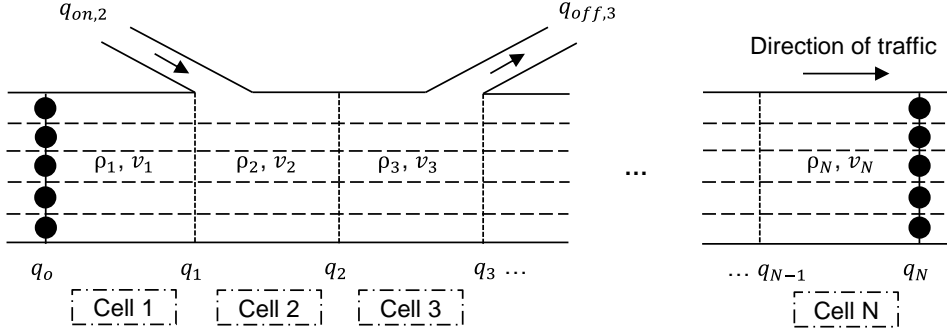


Figure 1: discretisation of a 5-lane motorway section into N cells and the cell's corresponding traffic state variables; q_0 , $q_{on,2}$ and $q_{off,3}$ represent the traffic outflow from origin to cell 1, from on-ramp to cell 2, and from cell 3 to off-ramp.

Accordingly, the evolution of traffic density and traffic flow through space and time is governed by Equations (5-12). A description of the variables and their units are provided in Table 1. In the absence of both off-ramps on a cell and on-ramps on its downstream cell, off-ramp split ratios and on-ramp demand are set to 0 in Equations (8-12). Equations (6-8) illustrate that traffic outflows in the CTM are defined as the minimum of how much an upstream cell can send vehicles to the downstream cell and how much the downstream cell is able to receive. Based on that, CTM can yield three different outflow regimes: (1) free-flow to free-flow when both cells are in free-flow conditions, (2) congested-flow to congested-flow when both cells are in congested conditions, and (3) free-flow to congested-flow when one of the cells is in free-flow conditions and the other is in congested-flow conditions. Also, Equations (10-12) represent a simple queue model at on-ramps used to ensure that the entire on-ramp demand is entering the network (Liu et al, 2014). In calculating the traffic density and traffic flow at each cell and each time step, traffic speed can then be deduced based on the equilibrium relationship as shown in Equation (13).

$$\rho_i(t+1) = \rho_i(t) + \frac{T_s}{l_i \lambda_i} \{ [q_{i-1}(t) + q_{on,i}(t)] - [q_i(t) + q_{off,i}(t)] \} \quad (5)$$

$$S_i(t) = \min\{u_{free,i} \rho_i(t), Q_{m,i}\} \lambda_i \quad (6)$$

$$R_i(t) = \min\{w_i [\rho_{m,i} - \rho_i(t)], Q_{m,i}\} \lambda_i$$

$$s.t \ w_i \leq u_{free,i} \text{ and } Q_{m,i} \leq \frac{\rho_{m,i}}{\frac{1}{u_{free,i}} + \frac{1}{w_i}} \quad (7)$$

$$q_i(t) = \begin{cases} [1 - \beta_i(t)] S_i(t), & [1 - \beta_i(t)] S_i(t) \leq R_{i+1}(t) - d_{on,i+1}(t) \\ \max[0, R_{i+1}(t) - d_{on,i+1}(t)], & \text{otherwise} \end{cases} \quad (8)$$

$$q_{off,i}(t) = \beta_i(t) \frac{q_i(t)}{1 - \beta_i(t)} \quad (9)$$

$$q_{on,i}(t) = \begin{cases} d_{on,i}(t), & [1 - \beta_{i-1}(t)] S_{i-1}(t) \leq R_i(t) - d_{on,i}(t) \\ R_i(t) - q_{i-1}(t), & \text{otherwise} \end{cases} \quad (10)$$

$$d_{on,i}(k) = d_{on,i}(k) + \frac{w_{on,i}(k)}{T_s} \quad (11)$$

$$w_{on,i}(k+1) = w_{on,i}(k) + T_s [d_{on,i}(k) - q_{on,i}(k)] \quad (12)$$

$$u_i(t) = \frac{q_i(t) + q_{off,i}(t)}{\rho_i(t) * \lambda_i} \quad (13)$$

Table 1: description of CTM equation variables

Equation variables	Description	Units
i	cell number with $i = 1, 2, \dots, N-1$ where N is total number of cells	dimensionless
t	time step with $t = 0, 2, \dots, T-1$ where T is total number of time steps	dimensionless
λ_i	number of lanes of cell i	dimensionless
T_s	time step interval	hour
l_i	i^{th} cell length	km
$d_{on,i}(t)$	demand at time step t from the on-ramp located at the start of cell i	veh hr ⁻¹
$\beta_i(t)$	split ratio (fraction) of vehicles exiting to the off-ramp located at the end of cell i at time step t	dimensionless
$\rho_i(t)$	traffic density at cell i and time step t	veh km ⁻¹ lane ⁻¹
$S_i(t)$ and $R_i(t)$	sending and receiving functions of cell i at time step t which are governed by the parameters of the fundamental diagram of each cell	veh hr ⁻¹
$q_{i-1}(t)$ and $q_i(t)$	traffic outflows from cell $i-1$ and cell i , respectively, at time step t	veh hr ⁻¹
$q_{on,i}(t)$ and $q_{off,i}(t)$	outflows at time step t from an on-ramp located at the start of cell i to mainline cell i and outflows from mainline cell i to an off-ramp located at the end of cell i , respectively	veh hr ⁻¹
$w_{on,i}(t)$	queue length at time step t on the on-ramp located at the start of cell i	veh hr ⁻¹
$u_i(t)$	traffic speed at cell i and time step t	km hr ⁻¹
$u_{free,i}$	free-flow traffic speed of cell i	km hr ⁻¹
$Q_{m,i}$	maximum flow rate of cell i	veh hr ⁻¹
w_i	backward wave speed of cell i	km hr ⁻¹
$\rho_{m,i}$	maximum traffic density of cell i	veh km ⁻¹ lane ⁻¹

By substituting Equations (8-10) into (5), CTM can be expressed with the discrete dynamic state Equation (14) where t is the time step, \mathbf{x} is the state vector, \mathbf{d} is the disturbance vector, and \mathbf{z} is the parameter vector.

$$\mathbf{x}(t+1) = \mathbf{f}[\mathbf{x}(t), \mathbf{d}(t), \mathbf{z}]; \mathbf{x}(0) = \mathbf{x}_0 \quad (14)$$

The CTM state vector \mathbf{x} constitutes the cell densities and the disturbance vector \mathbf{d} constitutes the model inputs which are (1) the traffic outflows from the origin to the first cell (q_0), (2) the demand at on-ramps ($d_{on,i}$), (3) the traffic densities at destination (ρ_N), and (4) the split ratios at off-ramps (β_i) at each time step t . The parameter vector \mathbf{z} for the CTM model includes only the four fundamental diagram parameters of each cell. While the parameter vector \mathbf{z} is specified for each cell, Spiliopoulou et al (2014) argued that one fundamental diagram can be considered for all the mainline cells since it is expected that sections with the same infrastructure and driving conditions to have the same fundamental diagram. Also, in order to avoid fake results from the calibration of parameters based on limited data, it is advisable to use a single fundamental diagram for all the cells. In this paper, the same method of a single fundamental diagram has been followed.

Average speed-based emission modelling

Given the traffic density and traffic speed at each cell and at each time interval, the emission $E_i^p(t)$ of pollutant p in grams timestep⁻¹ at time instant t and cell i can be calculated using Equation (15) where $\rho_i(t)$ and $u_i(t)$ are the CTM model outputs as described in Table 1, λ_i and l_i are cell variables as described in Table 1, γ_c is the proportion of vehicles of class c , and $e^{p,c}[u_i(t)]$ is the emission factor for pollutant p and vehicle class c at speed $u_i(t)$. The total emissions E^p in grams over the entire mainline and entire time period can then be calculated as the sum of emissions at each cell i and time step t , as shown in Equation (16).

$$E_i^p(t) = \sum_c \rho_i(t) \lambda_i l_i \gamma_c u_i(t) T_s e^{p,c}[u_i(t)] \quad (15)$$

$$E^p = \sum_i \sum_t E_i^p(t) \quad (16)$$

Emission factors vary depending on the emission model under consideration which is typically developed for different countries dependent on the vehicle classes used and the emission control systems used which can be different from country to country. For the purpose of this study, the COmputer Programme to Calculate Emissions from Road Transport (COPERT) emission factors (Ntziachristos et al, 2000) are used. However, the potential pitfalls of integrating the high-resolution CTM model with average speed-based emission models, in general, and COPERT, in particular, are discussed in the conclusion section. Given Equations (15-16), the uncertainty in the total emissions propagating from the CTM outputs are induced by three terms: $\rho_i(t)$, $u_i(t)$, and $e^{\rho_i \cdot c}(u_i(t))$.

2. Methodology

The Motorway Incident Detection and Automatic Signalling (MIDAS) is a network of traffic sensors providing 1-minute traffic flow and traffic speed data at each lane from more than 8,000 dual loop detectors distributed throughout England's motorway road network. In this study, a 4.79 km motorway section on the anti-clockwise of M25, London has been selected as the case study. The route is equipped with 11 detectors as well as a detector on each of the off-ramp and on-ramp situated along the route. For the calibration and validation of CTM, 6 data sets in year 2014 corresponding to three days during the month of May have been selected. 4 of these data sets (i.e. the AM and PM peak periods of 2 days) are of 3-hour time period and the remaining 2 data sets (i.e. the AM and PM peak periods of 1 day) are of 5-hour time period. Each data set is denoted as ξ^j ($j = 1, 2, \dots, 6$) with $j = 1, 3, 5$ representing the AM peak period data sets and $j = 2, 4, 6$ representing the PM peak period data sets of the 3 days, respectively.

In order to meet the data input requirements of CTM, few raw data transformations have to be made. Mainly, the weighted average traffic speed over all lanes is calculated using the traffic flow and traffic speed data at each lane. Also, traffic density is estimated using the equilibrium speed-density relationship. 1-minute traffic demand at the origin (D^1) and the on-ramp, traffic density at the destination (D^1), and flow rates at the off-ramp are then extracted and a constant interpolation is used in order to input the data at each time step. The time step considered here is $T_s = 3$ seconds and the motorway section is divided into 19 cells (i.e. $N = 19$) with lengths [235, 235, 275, 275, 245, 245, 140, 380, 215, 215, 250, 190, 350, 230, 230, 260, 260, 280, and 280] meters. The minimum cell length is thus 140 meters. It is important to note here that that origin cell 0 is treated as an on-ramp. Accordingly, the measured traffic flow at the origin is considered as traffic demand (Muñoz et al, 2004) and the queue model described in Equations (11-12) is used to ensure that the traffic outflows from the origin does not exceed the receiving capacity of the first cell and that the entire demand has entered the network.

In order to simulate the CTM for data set ξ^j , the optimal parameter vector \mathbf{z} has to be optimised/calibrated and an objective function or Performance Index (PI) to be minimised has to be specified. A number of derivative-free optimisation algorithms has been proposed in different studies such as the Genetic Algorithm (GA) in Poole and Kotsialos (2012), Particle Swarm Alogirthm (PSA) in Poole and Kotsialos (2013), and the 'Nelder-Mead' algorithm (Nelder and Mead, 1965) in Spiliopoulou et al (2014a). Despite the deficiencies of the 'Nelder-Mead' algorithm in terms of its possibility of approximating a local optimum and its dependence on the initial parameter set, Spiliopoulou et al (2015) showed that the algorithm is comparable to other methods such as GA when it is applied several times with different initial parameter sets and at the same time advantageous over other methods in terms of its ease of use and computational time.

Accordingly, the unconstrained 'Nelder-Mead' algorithm has been chosen in this paper. The PI to be minimised by the algorithm is the combined total sum of absolute errors of the measured and predicted traffic speed and traffic density as shown in Equation (17) where D is the total number of loop detectors (including origin and destination ones); M is the total number of 1-minute data; $\tilde{u}(d,m)$ and $\tilde{\rho}(d,m)$ are the measured traffic speed and traffic density at loop detector d and time m ; and $\bar{u}(d,m)$ and $\bar{\rho}(d,m)$ are the time-averaged predicted traffic speed and traffic density at loop detector d and time m . Since the spatiotemporal resolution of measured traffic speed and traffic density are different than that of predicted ones, the 3 second predicted data have been averaged to 1-minute data and only cells where the 9 mainline loop detectors exist are selected for the optimisation problem. The first and the last loop detectors are used as input to the CTM model and thus are not used in the objective function.

$$PI = \frac{1}{D-2} \frac{1}{M} \sum_{d=2}^{D-1} \sum_{m=1}^M [|\bar{u}(d, m) - \tilde{u}(d, m)| + |\bar{\rho}(d, m) - \tilde{\rho}(d, m)|] \quad (17)$$

Since the parameter vector \mathbf{z} has to satisfy the two conditions of Equation (7) and the free-flow traffic speed parameter has to meet the Courant–Friedrichs–Lewy (CFL) condition which states that the minimum cell length should be longer than the free-flow distance i.e. $\min(l_i) \geq u_{free} T_s$ (Daganzo, 1995), three penalty terms are added to ensure that the three conditions are met with the optimisation algorithm. The optimisation algorithm for data set ξ^j is initialised by generating 100 random sample parameter sets X^k ($k = 1, 2, \dots, 100$) within the bounds specified below from a continuous uniform distribution. The bounds have been determined by fitting the fundamental diagram on each weekday of a 3 months traffic data collected for the same motorway section. The range obtained for each parameter is used here.

- $u_{free} \in [99, 107]$ km hr⁻¹
- $Q_m \in [1404, 1712]$ veh hr⁻¹ lane⁻¹
- $w \in [9, 31]$ km hr⁻¹
- $\rho_m \in [77, 160]$ veh km⁻¹ lane⁻¹

The optimisation algorithm is applied 100 times using the corresponding initial parameter set X^k where its output is an optimal parameter vector \mathbf{z} and a minimal PI value. A calibrated CTM model is defined throughout the paper when the CTM is run for data set ξ^j using an optimal parameter vector \mathbf{z} which has been optimised for the same data set ξ^j . A validated CTM model is defined when the CTM is run for data set ξ^j using an optimal parameter vector \mathbf{z} which has been optimised for another data set ξ^n ($n \neq j$). A validated CTM model is used to assess the performance of an optimal parameter vector on data sets which are not used in the optimisation process; these model runs do not necessarily output a minimal PI value. The process of optimisation and simulation of calibrated and validated models is annotated as follows:

- optimise-CTM_k(ξ^j) $\rightarrow \mathbf{z}_k(\xi^j)$; $k = 1, 2, \dots, 100$ & $j = 1, 2, \dots, 6$
- calibrate-CTM_k[$\mathbf{z}_k(\xi^{j,j})$] $\rightarrow PI_k(\xi^j)$
- validate-CTM_k[$\mathbf{z}_k(\xi^{n,j})$] $\rightarrow PI_k(\xi^{n,j})$; $n \neq j$

While $\min[PI_k(\xi^j)]$ over all k and its corresponding parameter $\mathbf{z}_k(\xi^j)$ ($j = 1, 2, \dots, 6$) can be considered as a good local minimum (or even the global minimum) and best parameter vector, respectively, this study follows an ensemble-based approach which identifies all the optimisation runs which converged to a good local minimum and their corresponding parameter vectors using two methods:

- The first method defines the top optimal parameter vectors as those corresponding to the minimum 10% of PI values $PI_k(\xi^j)$ over all k ($j = 1, 2, \dots, 6$). These parameter vectors are referred to as $\mathbf{z}_{M1}(\xi^j)$ ($j = 1, 2, \dots, 6$).
- The second method is a statistical inference method which defines the top optimal parameter vectors as those which lead to capturing both the distribution and variance of measured traffic data. In particular, the CTM is simulated for each optimal parameter vector $\mathbf{z}_k(\xi^j)$ ($k = 1, 2, \dots, 100$ & $j = 1, 2, \dots, 6$) and the time-averaged predicted traffic speed at loop detector locations is obtained. Two non-parametric statistical tests are then applied on the measured traffic speed data and the predicted traffic speed data; these are the Mann-Whitney test which tests whether the measured traffic speed distribution differ from the predicted traffic speed distribution by a location shift or not and the Fligner-Killeen test which tests whether the variance of the measured traffic speed data is different from the predicted traffic speed data or not. A parameter vector is selected if both the distribution and the variance of the measured and predicted traffic speed are not different at a 0.001 significance level. These parameter vectors are referred to as $\mathbf{z}_{M2}(\xi^j)$ ($j = 1, 2, \dots, 6$).

Given the limitations of the 'Nelder-Mead' algorithm, the first method can lead to identifying parameter vectors which do not capture the variability of measured traffic data and/or to disregarding parameter vectors which do capture the variability of measured data. The second method is thus used to ensure that only the parameter vectors which lead to capturing the variability of measured traffic data when simulating the CTM model are selected. However, both methods are used in this paper for

comparison purposes.

To study how uncertainties in predicted traffic speed and traffic density propagate into errors in emission predictions, the normalised error distribution of the bivariate traffic speed and traffic density obtained from the calibrated and validated CTM models using each of the parameter vectors of $\mathbf{z}_{M1}(\xi^j)$ and $\mathbf{z}_{M2}(\xi^j)$ ($j = 1, 2, \dots, 6$) is captured. Based on that, four bivariate error distributions are obtained as follows:

- Two from all the calibrated CTM models using $\mathbf{z}_{M1}(\xi^j)$ and $\mathbf{z}_{M2}(\xi^j)$ ($j = 1, 2, \dots, 6$) parameter vectors, respectively.
- Two from all the validated CTM models using $\mathbf{z}_{M1}(\xi^{n,j})$ and $\mathbf{z}_{M2}(\xi^{n,j})$ ($j = 1, 2, \dots, 6$ & $n \neq j$) parameter vectors, respectively.

In this way an error distribution can be associated with each traffic speed-traffic density input to the COPERT emissions model. Using a Monte-Carlo sampling approach, the impact of the calibration and validation of CTM on NO_x emission predictions is studied across the feasible traffic speed-traffic density region. In particular, for each traffic speed-traffic density point, 10,000 random samples from the bivariate error distribution are drawn and their corresponding emission predictions are obtained. The 2.5th and 97.5th quantile of the final emission predictions are then extracted and considered the lower and upper bounds of emission prediction at the selected $(\xi^{n,j})$ traffic speed-traffic density point at 95% confidence level.

3. Results and discussion

Calibration and validation

As a first step, the optimisation of the CTM for each data set ξ^j ($j = 1, 2, \dots, 6$) has been initialised and the minimised PI value is obtained. Figure 2a shows the convergence of the PI values for each of the 100 optimisation runs applied to each data set. Clearly, the minimum PI value reached is dependent on the data set being calibrated. Figure 2a annotates the PI values obtained from the top optimal parameter vectors obtained using the two methods, $\mathbf{z}_{M1}(\xi^j)$ and $\mathbf{z}_{M2}(\xi^j)$ ($j = 1, 2, \dots, 6$), described in section 2.

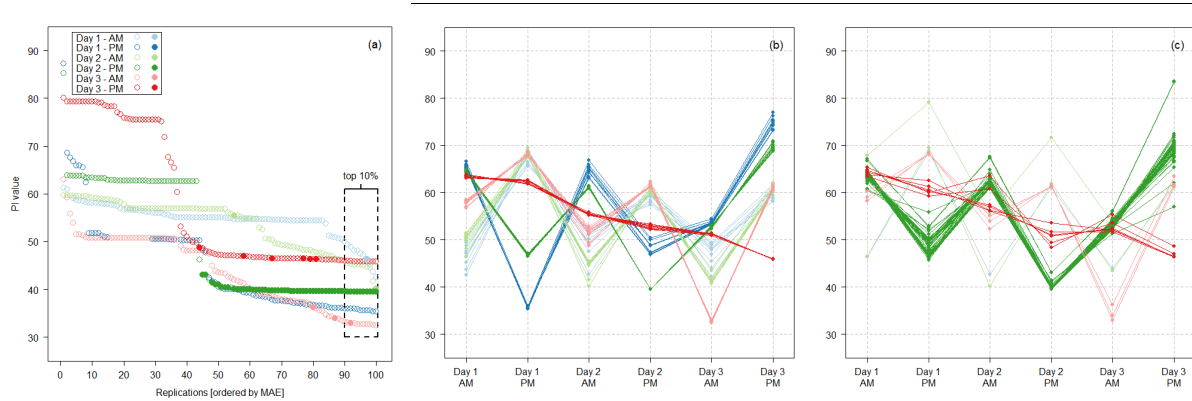


Figure 2: (a) PI values obtained from the optimisation of Cell Transmission Model (CTM) on 6 data sets. PI values of the top calibrated CTM models (total of 60), $\text{PI}_{M1}(\xi^j)$, lie within the dashed rectangle. Filled circles represent top calibrated CTM models (total of 66), $\text{PI}_{M2}(\xi^j)$; (b) PI values obtained from the validated CTM models using $\mathbf{z}_{M1}(\xi^{n,j})$; and (c) PI values obtained from the validated CTM models using $\mathbf{z}_{M2}(\xi^{n,j})$ ($j=1, 2, \dots, 6$ & $n \neq j$).

While the first method identifies 10 top optimal parameter vectors for each data set given its dependence on the 10th quantile of the PI value distribution, the statistical inference method has not identified any parameter vector for the PM period of the first day. The PI values identified by the statistical inference method do not necessarily lie within the lowest 10% of PI values but they are still within [1.1, 1.4] of the minimum PI value obtained for each data set. Figure 2a shows that the PI values have ceased to decrease for the PM period data sets at the 90th replication but have not reached a minimum for the AM period data sets; hence, increasing the number of replications might have led to finding lower PI values for these data sets. Table 2 and Table 3 provide a summary of the top optimal parameter vectors identified by the two methods, respectively. Table 2 shows that the

range of top optimal parameter values is influenced by the peak period under consideration; specifically the w and ρ_m parameters (i.e. backward wave speed and maximum density parameters). However, this is not apparent for the top parameter vectors obtained using the statistical test method as a result of the wider PI value range accepted under this method and the resulting differences in the parameter values which hinder the similarity/dissimilarity of parameters depending on the peak period considered.

Table 2: range [minimum, maximum] of Cell Transmission Model (CTM) top optimal parameter vectors identified by the first method, $z_{M1}(\xi^j)$ ($j = 1, 3, 5$ represent the AM peak periods and $j = 2, 4, 6$ represent the AM peak periods)

Model parameters	$z_{M1}(\xi^1)$ [10 sets]	$z_{M1}(\xi^2)$ [10 sets]	$z_{M1}(\xi^3)$ [10 sets]	$z_{M1}(\xi^4)$ [10 sets]	$z_{M1}(\xi^5)$ [10 sets]	$z_{M1}(\xi^6)$ [10 sets]
u_{free} [km hr ⁻¹]	[96.6,104.3]	[102.9,104.1]	[99.3,101.9]	[102.3,102.8]	[102.9,105.2]	[104.4,105.8]
Q_m [veh hr ⁻¹ lane ⁻¹]	[1736,1910]	[1688,1729]	[1697,1914]	[1710,1758]	[1687,1810]	[1689,1712]
w [km hr ⁻¹]	[27.3,57.4]	[9.4,13.2]	[27.1,65.0]	[13.1,17.1]	[30.1,51.8]	[16.0,17.8]
ρ_m [veh km ⁻¹ lane ⁻¹]	[53,81]	[147,194]	[49,80]	[120,147]	[52,72]	[113,121]

Table 3: range [minimum, maximum] of Cell Transmission Model (CTM) top optimal parameter vectors identified by the second method, $z_{M2}(\xi^j)$ ($j = 1, 3, 5$ represent the AM peak periods and $j = 2, 4, 6$ represent the AM peak periods)

Model parameters	$z_{M1}(\xi^1)$ [1 set]	$z_{M1}(\xi^2)$ [0 sets]	$z_{M1}(\xi^3)$ [2 sets]	$z_{M1}(\xi^4)$ [54 sets]	$z_{M1}(\xi^5)$ [3 sets]	$z_{M1}(\xi^6)$ [6 sets]
u_{free} [km hr ⁻¹]	99.4	-	[100.3,101.2]	[98.3,102.8]	[102.9,103.1]	[103.5,107.5]
Q_m [veh hr ⁻¹ lane ⁻¹]	1830	-	[1454,1914]	[1627,1956]	[1618,1694]	[1696,1809]
w [km hr ⁻¹]	47.8	-	[9.4,65.0]	[6.8,56.7]	[20.4,31.9]	[16.6,30.0]
ρ_m [veh km ⁻¹ lane ⁻¹]	57	-	[49,169]	[58,257]	[70,95]	[80,118]

CTM has been simulated for each data set using its corresponding top optimal parameter vectors, $z_{M1}(\xi^j)$ and $z_{M2}(\xi^j)$. Figure 3 and Figure 4 show the distribution of measured traffic speed and traffic density overlaid by the density distribution of the time-averaged predicted traffic speed and traffic density at loop detector locations obtained from the simulations. Traffic data measurements mostly show a peak representing the free-flow data with traffic speeds between 95 to 105 km hr⁻¹ and traffic density between 65 and 85 veh km⁻¹ lane⁻¹. Congested conditions are distributed along a wider range of traffic speeds and traffic densities. In comparison, CTM simulation results of predicted traffic speed and traffic density show two peaks: one representing the free-flow traffic conditions and matching the peak of measured traffic data; and one representing the congested traffic conditions.

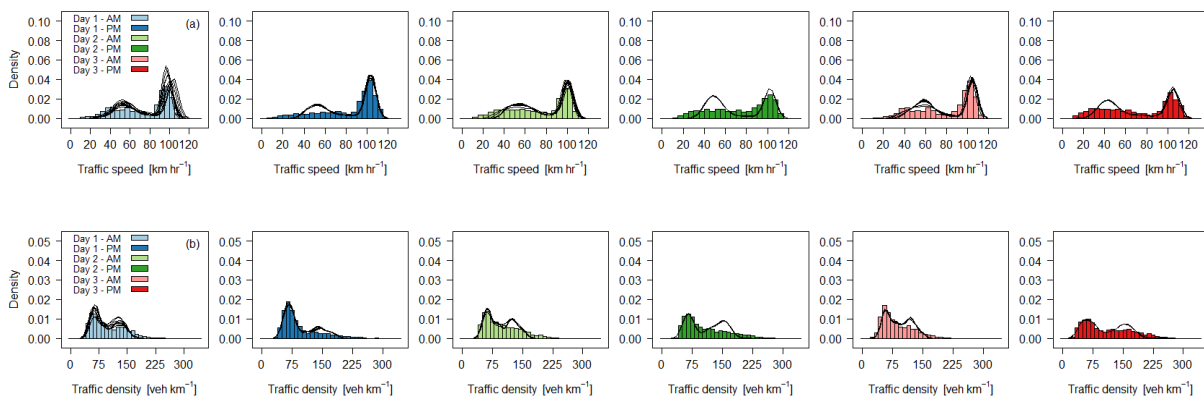


Figure 3: (a) measured traffic speed [km hr⁻¹] distribution and (b) traffic density [veh km⁻¹] as histograms for each of the 6

data sets overlaid by the predicted traffic speed distribution as solid black lines obtained from calibrated CTM models using $z_{M1}(\xi^j)$ ($j = 1, 2, \dots, 6$).

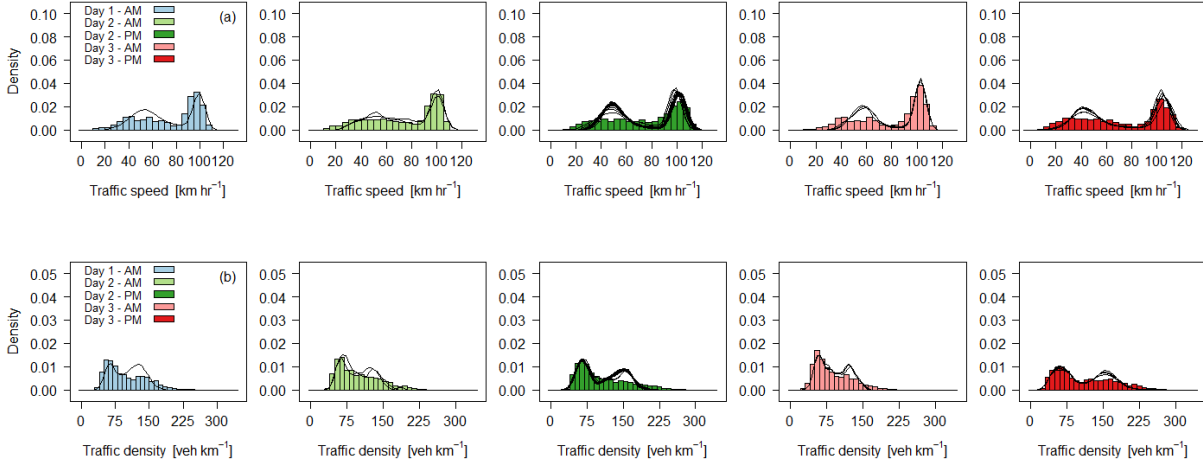


Figure 4: (a) measured traffic speed [km hr^{-1}] distribution and (b) traffic density [veh km^{-1}] as histograms for 5 data sets overlaid by the predicted traffic speed distribution as solid black lines from the calibrated CTM models using $z_{M2}(\xi^j)$ ($j = 1, 3, 4, 5, 6$); Day 2 – PM ($j = 2$) is not included as a result of rejecting all the 100 calibrated models of this data set.

In order to understand this phenomenon more, Figure 5 illustrates an example of the space-time evolution of measured traffic speed and traffic density as well as the predicted traffic speed and traffic density using the best parameter vector solution obtained for data set ξ^4 , i.e. $\min[\text{PI}_{M1}(\xi^4)]$. Figure 5 shows that while the CTM is able to replicate periods of congestion and distinguishes between periods of free-flow and periods of congestion, it does not entirely capture the variability in traffic speed and traffic density conditions; this is primarily a result of CTM's inability to account for fluctuations around the speed-density equilibrium state (Hoogendoorn and Bovy, 2001).

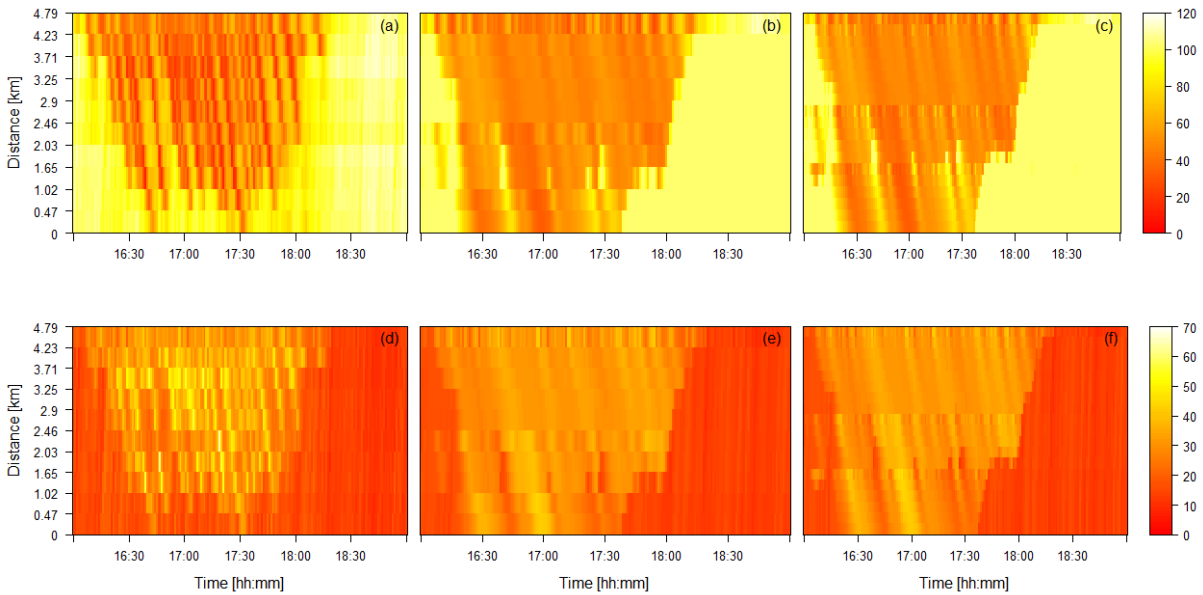


Figure 5: space-time evolution of (a-d) measured traffic speed [km hr^{-1}] and traffic density [$\text{veh km}^{-1} \text{ lane}^{-1}$] for data set ξ^4 , (b-e) time-aggregated predicted traffic speed and traffic density at loop detector locations, and (c-f) predicted traffic speed/traffic density at each segment and each time step (3 seconds) i.e. CTM output without aggregation obtained by simulating CTM using the best parameter vector solution for data set ξ^4 .

In addition to the calibrated CTM model results, the top optimal parameter vectors for each data set have been validated on the remaining data sets as described in section 2 in order to assess the performance of the top optimal parameter vectors when simulated using a data set which has not been included in the optimisation process. Figure 2b and Figure 2c show the PI values obtained from the validation of the top optimal parameter sets $z_{M1}(\xi^j)$ and $z_{M2}(\xi^j)$ ($j = 1, 2, \dots, 6$), respectively. As

discussed earlier, the optimal parameter values lie within the same range depending on the time of the day (i.e. AM/PM), specifically those belonging to $\mathbf{z}_{M1}(\xi^j)$ ($j = 1, 2, \dots, 6$). The validation results also show that the PI values are lower when the model parameters have been optimised for another day with the same time period in comparison with those optimised for different time periods. However, this is not the case when examining the results obtained for the PM period of day 3 (ξ^6) which might be a result of the higher free-flow speed parameter value obtained for this data set in comparison with other data sets as shown in Table 2 and Table 3.

Uncertainty propagation

Using the CTM simulation runs of the top optimal parameter sets obtained above, the bivariate traffic speed and traffic density normalised error distribution is captured from the calibrated and validated CTM models, separately, as described in section 2. Figure 6a and Figure 6c show the bivariate normalised error distribution obtained from the calibration of the top optimal parameter vectors $\mathbf{z}_{M1}(\xi^j)$ and $\mathbf{z}_{M2}(\xi^j)$ (for all j), respectively, while Figure 6b and Figure 6d show the bivariate error distribution obtained from the validation of the top optimal parameter sets. Figure 6 illustrates the lower range of errors obtained from the calibration and validation runs using $\mathbf{z}_{M2}(\xi^j)$ (i.e. statistical inference method) in comparison to using $\mathbf{z}_{M1}(\xi^j)$. Figure 6 also shows that the errors from the validation runs are higher with a range of $[-1, 11]$ for traffic speed and $[-1, 13]$ for traffic density in comparison to those obtained from the calibration runs which range between $[-1, 9]$ for traffic speed and $[-1, 3]$ for traffic density.

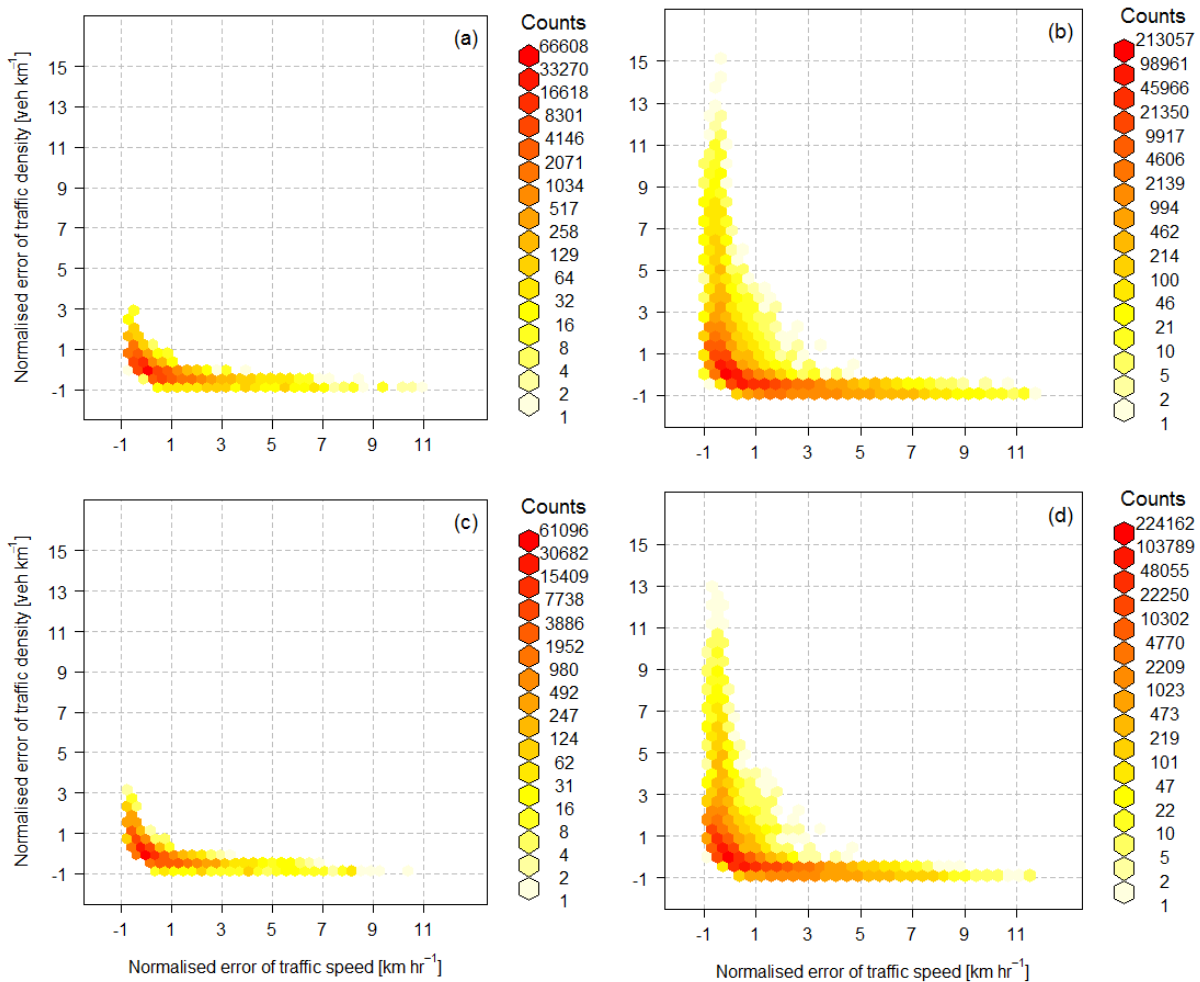


Figure 6: bivariate traffic speed [km hr⁻¹] - traffic density [veh km⁻¹] distribution of the normalized errors (or percent errors) of measured and predicted variables obtained from (a) the calibrated CTM models (total of 60) using $\mathbf{z}_{M1}(\xi^j)$; and (b) the validated CTM models using $\mathbf{z}_{M1}(\xi^{n,j})$; (c) the calibrated CTM models (total of 66) using $\mathbf{z}_{M2}(\xi^j)$; and (d) the

validated CTM models using $z_{M2}(\xi^{n,j})$ (for all j & $n \neq j$).

The feasible traffic speed and traffic density is identified from the real traffic data of the 6 data sets under study which lie between 7 and 120 km hr⁻¹ and 20 and 330 veh km⁻¹. Traffic emissions in grams per minute are calculated according to Equation (15) at each grid point assuming a 1 km link length, a 1-minute time step, and Diesel Euro 6 vehicle class; these predictions correspond to traffic emissions obtained when errors are not accounted for. Errors are then randomly sampled from each bivariate distribution of Figure 6 and added to each traffic speed and traffic density point. The corresponding lower and upper bound of emission estimates at each point are then calculated. This procedure is repeated four times: two using random samples from the calibration results of the top optimal parameters (Figure 6a and Figure 6c) and two using random samples from the validation results (Figure 6b and Figure 6d).

Figure 7a shows the emissions obtained throughout the feasible traffic speed-traffic density region without incorporating the errors. Figure 7b-c and Figure 7f-g show the upper and lower bounds of emissions obtained when incorporating the calibration errors obtained using $z_{M1}(\xi^j)$ and $z_{M2}(\xi^j)$ (for all j), respectively while Figure 7d-e and Figure 7h-i show the upper and lower bounds of emissions obtained when incorporating the validation errors obtained using $z_{M1}(\xi^{n,j})$ and $z_{M2}(\xi^{n,j})$ (for all j & $n \neq j$).

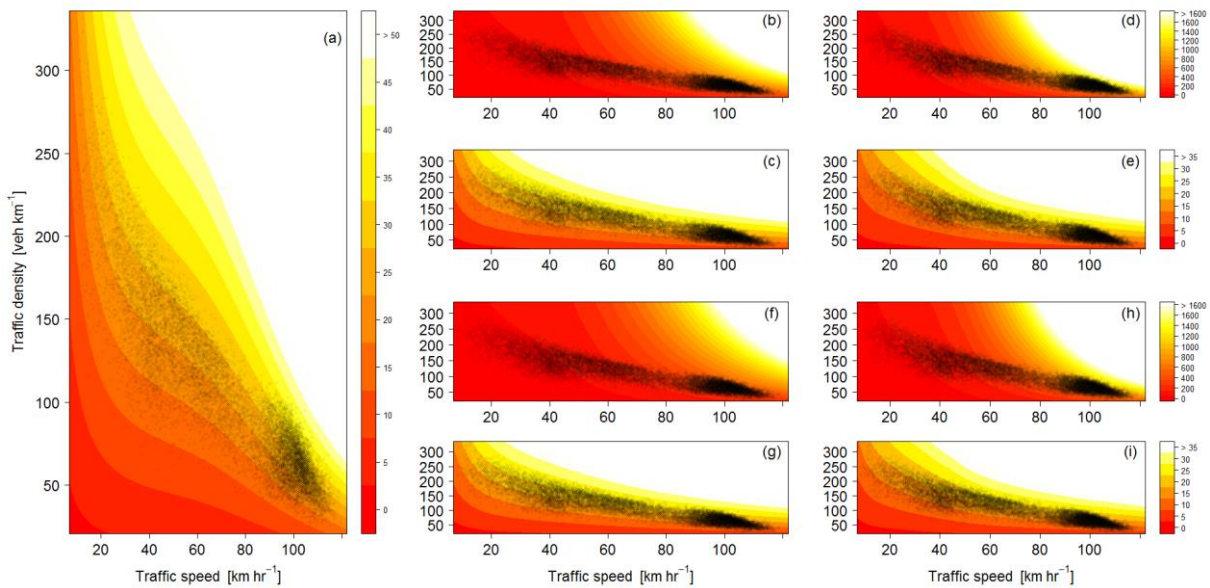


Figure 7: Coloured contours showing NO_x emission estimate map [gram min⁻¹] using COPERT for a Diesel Euro 6 with black dots representing loop detector traffic speed-density data for reference; upper (b) and lower (c) bounds of emission estimates [gram min⁻¹] at 95th confidence level based on the calibrated CTM models obtained using of $z_{M1}(\xi^j)$ (see Figure 6a), upper (d) and lower (e) bounds of emission estimates based on the validated CTM models using $z_{M1}(\xi^{n,j})$ (see Figure 6b), upper (f) and lower (g) bounds of emission estimates based on the calibrated CTM models obtained using of $z_{M2}(\xi^j)$ (see Figure 6c), and upper (h) and lower (i) bounds of emission estimates based on the validated CTM models using $z_{M2}(\xi^{n,j})$ (see Figure 6d).

Conclusion

Cell Transmission Model (CTM) is a discretised first-order macroscopic traffic flow model which describes the dynamics of traffic variables at high spatial and temporal resolution. CTM has recently been used to predict average speed-based emissions on road networks in an attempt to improve on the low-fidelity of whole-link traffic flow models while avoiding the high costs of microscopic traffic flow models. This paper has applied an ensemble-based approach to characterising the uncertainty obtained from the calibration and validation of CTM using real-world measurements of traffic data. While the characterised uncertainties can be related directly to the limited capability of CTM in capturing the dynamics of traffic variables such as traffic speed, uncertainties can also arise due to the use of optimisation algorithms which might not always lead to a global minimum and also to the various assumptions being made when calibrating the CTM using measurements of traffic data, particularly:

- The input data required by the CTM needs to be of the same resolution as the CTM model. In this paper, constant interpolation on the 1-minute traffic data is performed to meet such requirement.
- Traffic density, which is used as a model input to CTM simulations and also for the calibration of CTM parameters, is not directly measured by dual loop detectors. As a result, traffic density has to be estimated using space-mean traffic speed and traffic flow data. However, 1-minute traffic speed data reported by the measurement system is the time-mean traffic speed (i.e. traffic speed of individual vehicles are aggregated arithmetically). Uncertainties can arise due to the use of time-mean traffic speed to estimate the traffic density input and to calibrate the CTM model parameters.

The paper presents the results of the propagation of the characterised uncertainties from the calibration and validation of CTM to uncertainties in average speed-based (COPERT) emission predictions using a Monte-Carlo sampling approach. Nevertheless, uncertainties in average speed-based emission predictions are not only related to the traffic flow model inputs but also to the type of average speed-based emission model used. For instance, emission models such as COPERT are originally developed using trip-based average speeds rather than link-based average speeds. By using link-based average speeds, another type of uncertainty can be propagated to the final emission predictions (see for e.g. Bai et al, 2007). Also, emission models such as COPERT can be limited in terms of their applicability to high-resolution spatial (very short links) and temporal (very short time intervals) traffic data (see for e.g. Samaras et al, 2014). In addition to that, uncertainties also arise from the emission factors themselves depending on their validity in replicating the real-world road traffic exhaust emissions.

In addition to the above, errors are characterised based on space/time-averaged predicted traffic data to meet the spatiotemporal resolution of measured traffic data. The aggregation of traffic data from 3-seconds (time step of the CTM) to 1-minute can also lead to averaging out the variability of measured and/or predicted traffic data and consequently increase and/or reduce the characterised errors arising from the calibration and validation of CTM. Since the average speed-based emissions using CTM are typically made using the high-resolution predicted traffic data (i.e. each cell and each time step), this can consequently lead to an underestimation/overestimation of the uncertainties in the final average speed-based emission predictions.

Macroscopic traffic flow models such as the CTM and those of higher-order (for e.g. the second-order discretised METANET) are integrated not only with average speed-based emission models but also with instantaneous or power-based emission models. Studying such integration approaches using the methodologies developed in this paper is to be considered in future work.

Acknowledgments

Arwa Sayegh would like to thank the Dynamic Systems and Simulation Laboratory (DSSL) Team at the Technical University of Crete for providing feedback on the calibration of macroscopic traffic flow models. The Authors would also like to thank Highways England for providing access to the MIDAS traffic database.

References

- Bai, S., Chiu, Y.C.E. and Niemeier, D.A., 2007. A comparative analysis of using trip-based versus link-based traffic data for regional mobile source emissions estimation. *Atmospheric Environment*, 41(35), pp.7512-7523.
- Chow, A. and Li, Y., 2014. Modeling and optimization of road transport facility operations. *Journal of Facilities Management*, 12(3), pp.268-285.
- Daganzo, C.F., 1994. The cell transmission model: A dynamic representation of highway traffic consistent with the hydrodynamic theory. *Transportation Research Part B: Methodological*, 28(4), pp.269-287.
- Daganzo, C.F., 1995. The cell transmission model, part II: network traffic. *Transportation Research Part B: Methodological*, 29(2), pp.79-93.
- Hoogendoorn, S.P. and Bovy, P.H., 2001. State-of-the-art of vehicular traffic flow modelling. *Proceedings of the Institution of Mechanical Engineers, Part I: Journal of Systems and Control Engineering*, 215(4), pp.283-303.
- Lighthill, M.J. and Whitham, G.B., 1955a. On kinematic waves I: Flood movement in long rivers. In

Proceedings of the Royal Society of London A: Mathematical, Physical and Engineering Sciences, 229(1178), pp. 281-316.

- Lighthill, M.J. and Whitham, G.B., 1955b. On kinematic waves II: A theory of traffic flow on long crowded roads. In *Proceedings of the Royal Society of London A: Mathematical, Physical and Engineering Sciences*, 229(1178), pp. 317-345.
- Lin, J. and Ge, Y.E., 2006. Impacts of traffic heterogeneity on roadside air pollution concentration. *Transportation Research Part D: Transport and Environment*, 11(2), pp.166-170.
- Lin, W.H. and Ahanotu, D., 1995. Validating the basic cell transmission model on a single freeway link. *PATH technical note*; 95-3.
- Liu, S., De Schutter, B. and Hellendoorn, H., 2014, June. Integrated traffic flow and emission control based on FASTLANE and the multi-class VT-macro model. In *Control Conference (ECC), 2014 European*, (pp. 2908-2913). IEEE.
- Muñoz, L., Sun, X., Sun, D., Gomes, G. and Horowitz, R., 2004, June. Methodological calibration of the cell transmission model. In *American Control Conference, 2004. Proceedings of the 2004* (Vol. 1, pp. 798-803). IEEE.
- Muñoz, L., Sun, X., Horowitz, R. and Alvarez, L., 2006. Piecewise-linearized cell transmission model and parameter calibration methodology. *Transportation Research Record: Journal of the Transportation Research Board*, (1965), pp.183-191.
- Namdeo, A., Mitchell, G. and Dixon, R., 2002. TEMMS: an integrated package for modelling and mapping urban traffic emissions and air quality. *Environmental Modelling & Software*, 17(2), pp.177-188.
- Nejadkoorki, F., Nicholson, K., Lake, I. and Davies, T., 2008. An approach for modelling CO₂ emissions from road traffic in urban areas. *Science of the total environment*, 406(1), pp.269-278.
- Nelder, J.A. and Mead, R., 1965. A simplex method for function minimization. *The computer journal*, 7(4), pp.308-313.
- Newell, G.F., 1993. A simplified theory of kinematic waves in highway traffic, part I: General theory. *Transportation Research Part B: Methodological*, 27(4), pp.281-287.
- Newell, G.F., 2002. A simplified car-following theory: a lower order model. *Transportation Research Part B: Methodological*, 36(3), pp.195-205.
- Ntziachristos, L., Samaras, Z., Eggleston, S., Gorissen, N., Hassel, D., Hickman, A.J., Joumard, R., Rijkeboer, R., White, L. and Zierock, L., 2000. *Validation of road vehicle and traffic emission models, a review and meta-analysis: COPERT IV Computer Programme to Calculate Emissions From Road Transport, Methodology and Emissions Factors (Version 2.1)*. Technical Report No. 49. European Environment Agency.
- Panis, L.I., Broekx, S. and Liu, R., 2006. Modelling instantaneous traffic emission and the influence of traffic speed limits. *Science of the total environment*, 371(1), pp.270-285.
- Poole, A.J. and Kotsialos, A., 2012, September. METANET Model validation using a genetic algorithm. In *Control in Transportation Systems* (Vol. 13, No. 1, pp. 7-12).
- Poole, A. and Kotsialos, A., 2013. Deterministic model validation with a new approach to fundamental diagrams of the METANET model. In *Transportation Research Board 92nd Annual Meeting* (No. 13-4046).
- Rakha, H. and Ahn, K., 2004. Integration modeling framework for estimating mobile source emissions. *Journal of transportation engineering*, 130(2), pp.183-193.
- Richards, P.I., 1956. Shock waves on the highway. *Operations research*, 4(1), pp.42-51.
- Roncoli, C., Papageorgiou, M. and Papamichail, I., 2015. Traffic flow optimisation in presence of vehicle automation and communication systems—Part I: A first-order multi-lane model for motorway traffic. *Transportation Research Part C: Emerging Technologies*, 57, pp.241-259.
- Samaras, C., Tsokolis, D., Toffolo, S., Garcia-Castro, A., Vock, C., Ntziachristos, L., and Samaras, Z., 2014. Limits of applicability of COPERT model to short links and congested conditions. In 20th International Transport and Air Pollution Conference 2014.
- Spiliopoulou, A., Kontorinaki, M., Papageorgiou, M. and Kopelias, P., 2014. Macroscopic traffic flow

model validation at congested freeway off-ramp areas. *Transportation Research Part C: Emerging Technologies*, 41, pp.18-29.

Spiliopoulou, A., Papamichail, I., Papageorgiou, M., Tyrinopoulos, I. and Chrysoulakis, J., 2015. Macroscopic traffic flow model calibration using different optimization algorithms. *Transportation Research Procedia*, 6, pp.144-157.

Zhang, L., Yin, Y. and Chen, S., 2013. Robust signal timing optimization with environmental concerns. *Transportation Research Part C: Emerging Technologies*, 29, pp.55-71.

Zhou, X., Tanvir, S., Lei, H., Taylor, J., Liu, B., Roupail, N.M. and Frey, H.C., 2015. Integrating a simplified emission estimation model and mesoscopic dynamic traffic simulator to efficiently evaluate emission impacts of traffic management strategies. *Transportation Research Part D: Transport and Environment*, 37, pp.123-136.

Zhu, F., Lo, H.K. and Lin, H.Z., 2013. Delay and emissions modelling for signalised intersections. *Transportmetrica B: transport dynamics*, 1(2), pp.111-135.

GRETA: Gridding Emission Tool for ArcGIS

Christiane SCHNEIDER*, Michael PELZER*, Nicola TOENGES-SCHULLER*, Michael NACKEN* & Arnold NIEDERAU*

*AVISO GmbH, Am Hasselholz 15, 52074 Aachen, Germany

Abstract

Information on spatial distribution of emissions is of great importance for a number of questions in the field of air quality monitoring, e.g. in the context of compliance to international reporting commitment, provision of input data for dispersion modelling of air pollutants or visualization of spatial distribution structure of the emissions.

Existing inventories at the German Federal Environmental Agency (UBA) either do not contain this spatial information (emission inventory to report emissions, differentiated by NFR sectors) or only show part of total emissions (PRTR) or were prepared for a specific application.

For this reason, an ESRI ArcGIS based software has been developed which allows, independently and on the basis of information generally available, to regularly generate regionalized emission data sets for the complete area of the Federal Republic of Germany.

The software is documented in detail and complies with high standards as to flexibility and extensibility.

Informations sur la distribution spatiale des émissions est d'une grande importance pour un certain nombre de questions dans le domaine de la surveillance de la qualité de l'air, par exemple dans le cadre du respect de l'engagement de rapports internationaux, la fourniture de données d'entrée pour la modélisation de la dispersion des polluants atmosphériques ou la visualisation de la structure des émissions de répartition spatiale.

Inventaires existants à l'Agence allemande pour l'environnement (UBA) soit ne contiennent pas cette information spatiale (inventaire des émissions de déclarer les émissions, différenciés par secteurs NFR) ou seulement montrent une partie des émissions totales (RRTP) ou ont été préparés pour une application spécifique.

Pour cette raison, un logiciel basé ESRI ArcGIS a été développé qui permet, de manière indépendante et sur la base des informations généralement disponibles, pour générer régulièrement des ensembles de données d'émission régionalisées pour la superficie totale de la République fédérale d'Allemagne.

Le logiciel est documenté en détail et est conforme aux normes élevées quant à la flexibilité et l'extensibilité.

Keywords: national emissions, spatial distribution, gridding, distribution parameter, ArcGIS

Keywords French: émissions nationale, répartition spatiale, ArcGIS

Introduction

Information on spatial distribution of emissions is of great importance for a number of questions in the field of air quality monitoring, e.g. in the context of compliance to international reporting commitment, provision of input data for dispersion modelling of air pollutants or visualization of spatial distribution structure of the emissions.

Existing inventories at the German Federal Environmental Agency either do not contain this spatial information (emission inventory to report emissions, differentiated by NFR sectors /UBA 2015/) or only show part of total emissions (PRTR) /PRTR 2013a, PRTR 2013b/ or were prepared for a specific application /PAREST 2010/.

For this reason the aim was to develop an ArcGIS-based software which allows to generate, independently and on the basis of generally available information, highly spatially resolved emission data sets, i.e., a detailed mapping of the only as national total available emission data per source

group carried out over the entire area of the Federal Republic.

The methodology used for spatial distribution of national emissions and the required input data for all relevant source categories (NFR sectors) will be described. Focal point is on development of the software (GRETA – Gridding Emission Tool for ArcGIS). For this purpose, an overview is given and results of sample applications and evaluation are being presented.

1. Methodology used for Spatial Distribution of National Emissions

The methodology for spatial distribution of national emissions is mainly based on the combination of data of the national emission inventory per NFR sector with distribution parameters, which permit a realistic spatial distribution of emissions.

Several reports on spatial distribution of emissions in Europe were considered while deriving the methodology for GRETA /AEA 2006, AEA 2010, AEA 2012, THELOKE 2009, PLEJDRUP 2011, MAAS 2013/.

In GRETA the pollutants NO_x, NH₃, SO₂, CO, NMVOC, PM_{2.5}, PM₁₀ are included. Currently emissions of 127 NFR sectors are reported.

An overview of the necessary steps for spatial distribution, carried out by application of the Gridding Tool, is shown in Figure 1. Key aspects of GRETA are:

- The Gridding Tool includes a full set of required data tables per base year. These include emissions, distribution parameters, geometric data and necessary definition and mapping tables. When developing the Gridding Tool, 2010 was fixed as reference year, for which all necessary data for the Gridding Tool had been prepared, which can be done respectively for any other year.
- Furthermore, boundary conditions have to be set (e.g. consideration of PRTR data for point sources or TREMOD data for the traffic sector). In addition, the relevant distribution parameters per source category / NFR sector for the spatial distribution have to be set, respectively, the default selection has to be modified.
- The PRTR emissions are being checked with respect to the annual national emissions for plausibility and subtracted from these. The remaining national emissions, not covered by way of PRTR point sources per NFR sector, are determined.
- Spatial distribution of these national (remaining) emissions is done by use of distribution parameters, as far as possible to point sources and to line sources. The remaining emissions are spatialized by use of distribution parameters at district level and furthermore under consideration of land-cover data at area source level.
- Finally, gridding for any grid sizes and different coordinate reference systems can be carried out.
- Data export to various nomenclatures (NFR, GNFR, SNAP) and in different formats is possible (NetCDF, ASCII).

Significant factors for spatial distribution of national emissions are so-called distribution parameters. These are characterized in the context of GRETA as follows:

- A distribution parameter represents a function that fully distributes a total sum of emissions (e.g. national emissions Germany) to a specific amount of regional objects.
- The spatial distribution of national emissions is being performed per NFR sector.
- More complex distribution parameters distribute the emissions, for example, to different spatial object classes or by taking into account a further differentiation of the total emissions.
- For each NFR sector emissions are spatially distributed over one or more distribution parameters. For this purpose it has to be determined which part of the emissions is to be distributed over which distribution parameter.

Distribution parameters are used to allocate national emissions, spatially as accurately as possible, to individual point, line or area sources depending on the source group (see Figure 2). The location of a point source is given clearly by coordinates; typical line sources are, for example, streets, which can consist of many sections. Surface sources are defined as areas where many small sources release emissions, for example, small combustion plants in built-up areas.

A substantial database for distribution of national emissions of the 'energy supply' and 'industry' sectors are emissions of individual sites or plants from the PRTR database. In addition, for example, emissions of air traffic are allocated to point sources by location of the airports, whereas in the case of larger airports an additional local distribution is taken into account.

Emissions from road traffic, rail traffic and inland water navigation are spatially assigned to line sources. The respective route networks consist of individual sections. To each of these network segments (line source) a share of the national emissions is assigned.

Figure 1: Overview of the method for spatial distribution of national emissions

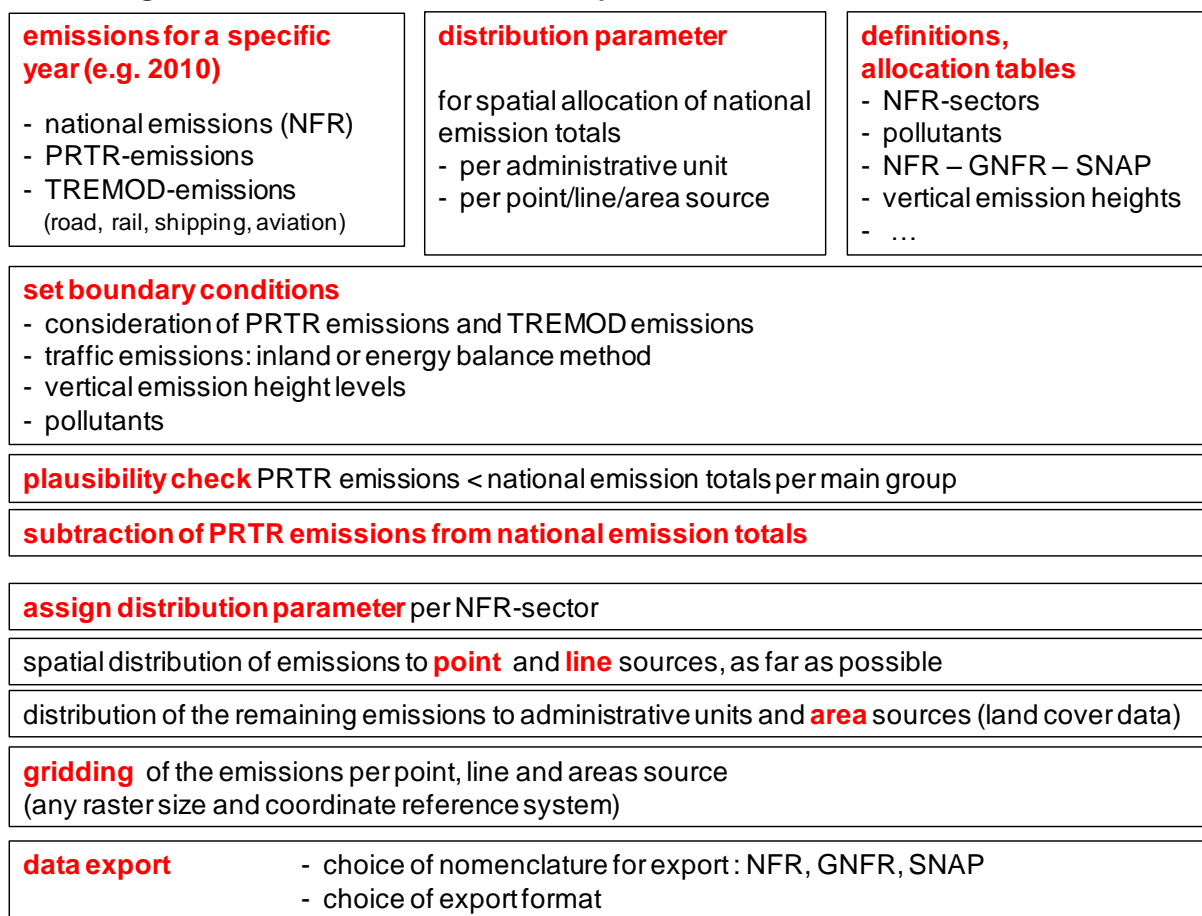
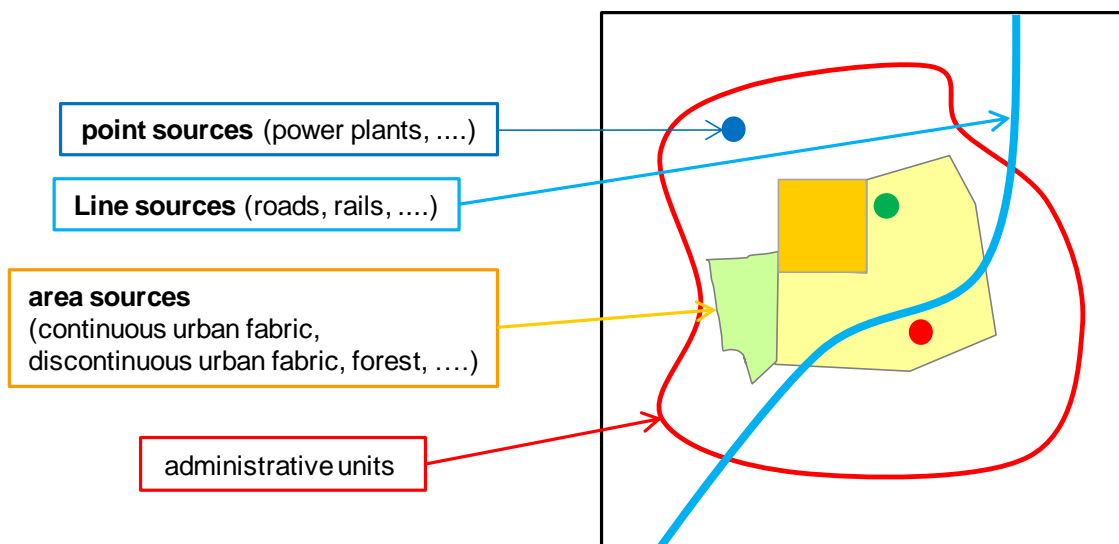


Figure 2: Schematic diagram for the definition of point / line / area sources



The spatial distribution of emissions that are not distributed to point sources or line sources is carried out in two steps on area sources. In the first step, these emissions are distributed by means of suitable distribution parameters to the district level.

In the second step a more accurate spatial allocation of emissions using land cover data is carried out within the districts. Per NFR sector areas of the relevant land use classes are chosen and only to these areas emissions are allocated. Here, emphasis can also be placed on different CLC groups, e.g. land-cover class 'continuous urban fabric' could get a higher rating than land-cover class 'discontinuous urban fabric'. As a result, the national emissions totals previously distributed at district level are now spatially localized to the relevant land-cover areas within the districts.

Aim of the spatial distribution of emissions is the compilation of emissions in a defined grid. For this, the emissions, spatially distributed to individual point, line and area sources, are assigned to the grid cells of the selected grid in a further step. After setting the coordinate reference system and grid size of the raster, the share of each emission source (point / line / area source) per grid cell is determined. The summation of the emissions of all source shares lying within a grid cell leads to the total of emissions of the grid cell.

The spatial distribution of emissions is not only limited to horizontal distribution, but also includes distribution to vertical height levels. Therefore it was necessary to assign to each source category or NFR sector an average characteristic emission height above ground.

2. Determination of Distribution Parameters

The PRTR database of UBA (PRTR = Pollutant Release and Transfer Register; Thru.de) represents an important data source for the spatial distribution of national emissions. The emissions contained in this database are on hand as point source emissions and are taken into account as such for the spatial allocation in the Gridding Tool.

Furthermore, the data of the digital landscape models of the Federal Agency of Cartography and Geodesy (BKG) /DLM 2013/ are used as essential data sources. In detail, these are as follows:

- administrative boundaries (district boundaries, municipal boundaries)
- road network
- streaming water network
- rail network
- location of airports
- land-cover differentiated by classes

As another relevant data source for spatial allocation of emissions that are not assigned by point or line sources, the Corine Land Cover (CLC) data set /CLC 2006/ was used. These data are differentiated in 43 land cover classes. For the usage within the scope of the Gridding Tool these were merged to 6 CLC groups.

Apart from these essential geometric base data sets, further information and data were used for deriving final distribution parameters. These are, for example, data at district level as to the number of inhabitants or employees per business division. The aim was to use those data per NFR sector on the spatial distribution that reflect well the spatial structure of the emission distribution. This also includes typical (effective) vertical heights of sources per NFR sector.

For the main emission source groups below relevant data for spatial distribution used in GRETA are described. More detailed information can be found in /UBA 2016/.

Source Group Energy and Industry

For GRETA a methodology has been developed taking into account PRTR emissions in the spatial distribution of national emissions. Here, the PRTR emissions are subtracted first at national level from the national emission totals. The share of emissions, which is covered by the PRTR emissions, is spatially assigned by the location of PRTR point sources. To avoid negative national residual emissions, this calculation must be done on an aggregated level. For this, the following main groups were defined:

- main group A (energy sector PRTR 1)
- main group B (industrial sectors, PRTR sectors 2,3,4,5,6,8,9)
- main group C (intensive livestock production and aquaculture, PRTR industry 7)

The NFR sectors for which part of the emissions are spatially allocated by means of the PRTR point sources belong to the source groups of energy supply, industry, agriculture and sewage / waste disposal. Thereby affected NFR sectors, national (residual) emissions are distributed in a first step by suitable distribution parameters on district level. The distribution parameters are predominantly based on statistical data on numbers of employees in the various sectors and departments of industry. Within the districts, emissions are distributed via land cover class CLC121 (Industrial and Commercial Units) to the level of area sources.

Source Group Other Non-industrial Combustion Plants

Emissions from non-industrial combustion plants (private households, other small consumers, military, agriculture, etc.) are completely spatially distributed over area sources. For this source group, distribution parameters are mainly based on statistical data at district level. The spatial distribution of emissions from small combustion plants of households was carried out via a more complex distribution function since the national emissions are differentiated into the four sub-categories of oil, gas, wood and other solid fuel combustion plants. Then the emissions per energy source are distributed using different distribution parameters to the district respectively community levels. Within the districts (for wood firing within the communities) emissions are again distributed over the relevant CLC classes to the level of the area sources.

Source group Traffic

For the traffic sector (road, rail, shipping, aviation), at UBA emissions are being determined by TREMOD model /UBA 2013/. These data are available in a more differentiated way than they are shown per NFR sector in national emissions. Therefore, suitable additional information from TREMOD for the spatial distribution is taken into account in GRETA.

For the spatial distribution of national emissions of aviation, in addition to the national totals, additional TREMOD emission data for the 26 largest airports are available. These emissions are spatially allocated directly to their position. For the remaining smaller airports and landing sites in Germany, the national residual emissions from aviation, which are not listed in the TREMOD data separately for each airport, are spatially distributed over the number of flight movements per airport. The location of airports is known as a point source. In addition, for the 15 largest (international) airports in Germany the landing and departure sectors were digitized as funnel-shaped three-dimensional sources. This allows a higher spatial resolution of the distribution of the emissions to local (three-dimensional) sources for these airports.

Emissions of the source group road traffic are composed of exhaust emissions, emissions from abrasions (tires, brakes, roads) and emissions due to fuel evaporation. The exhaust and abrasion emissions from road traffic are fully distributed over line sources, since a digital geometric data basis exists for all roads. The distribution parameter for spatial distribution of emissions were derived from data on mileage per route section. For this purpose, data was processed from different data sources. The evaporative emissions are spatially distributed over area sources to the built-up areas.

For rail traffic, emissions resulting from operation of diesel locomotives are reported. Abrasion-emissions caused by both, electrically and diesel-powered trains are currently not included in the reported emissions and therefore are not taken into account in the sector. The distribution of emissions of rail transport is carried out entirely on line sources. The geometric base is the rail network and significant data base for the derivation of the distribution parameters are the section-related emissions of DB Umwelt AG.

Also the emissions of shipping traffic are completely spatially distributed on line sources. For this purpose, the digital routing network of watercourses as well as the distribution parameters derived from emission data from TREMOD are being applied.

Source group Offroad / Mobile Machinery

This source group includes emissions which are released by the off-road traffic (e.g. in the building and construction industry, forestry and agriculture) and by the use of mobile devices and machines. The emissions from these source categories are allocated completely as area sources. The distribution parameters are mainly based on statistical data at district level.

Source group Solvents and other Product Use

Also emissions that are released by application of solvent-based and other products in the private sector as well as in industrial and other sectors are fully distributed as area sources. The distribution parameters are predominantly based on statistical data at district level, e.g. employees in economic departments of trade and services or inhabitants.

Source group Agriculture

Emissions from agriculture consist of emissions arising from animal husbandry (e.g. cows, pigs etc.), and emissions that occur during agricultural activity on arable land and pastures. An important data source for spatial distribution is the data of the Thünen Institute, which annually determines the emissions from agriculture at district level for Germany. In addition, emissions from stables that underlay reporting obligations are reported in the PRTR database. They only cover a small proportion of national emissions in agriculture. To derive the distribution parameters used in GRETA for the affected NFR sectors, the data of the Thünen Institute and PRTR database were taken into account.

Other NFR Sectors

There are some more NFR sectors, e.g.: 1A4ciii (national fishing), 1B2av (distribution of oil products) and 1A3ei (pipeline compressors), which do not belong to the source groups already described. The distribution parameters for these sectors are based on different data; emissions are predominantly spatially distributed as area sources.

3. Software Gridding Tool (GRETA – Gridding Emission Tool for ArcGIS)

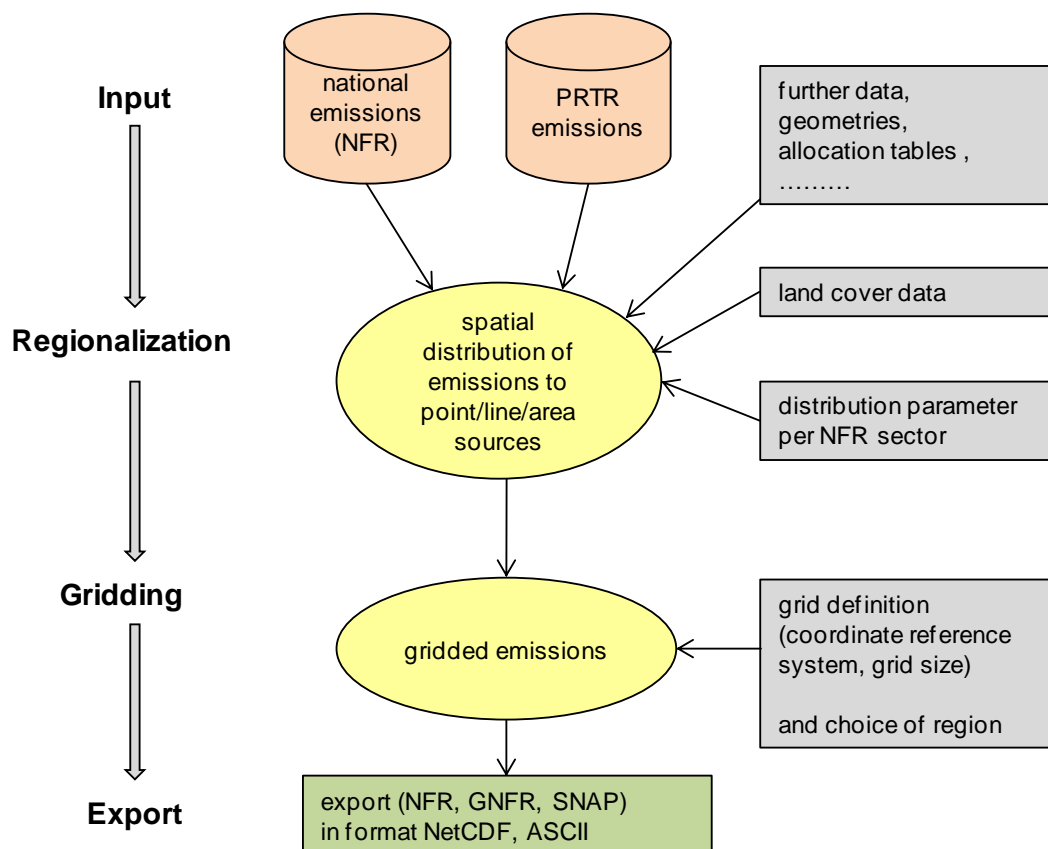
The methodology to spatially distribute national emission totals described above has been implemented when developing the Gridding Tool GRETA. All following descriptions and considerations refer to GRETA version 1.0.3.1. Essential aspects in the development of the software and its programming were the following:

- In the course of the project, GIS Software ESRI ArcGIS10.1 was used initially and changed into the current version ArcGIS 10.3.1.
- The software was implemented as "add-in" (framework in ArcGIS desktop to create and integrate own adjustments and functional extensions) using ArcObjects SDK (software development kit).
- VB.NET is used as programming language.

- Microsoft Visual Studio.NET is used as programming environment.
- Access to the dockable window of Gridding Tool GRETA is carried out on ArcGIS interface via a separate tool button.
- The entire data is stored in a file geodatabase (ArcGIS internal database format to store the geometry and attribute data).
- For the documentation of the software, Wiki System by GitHub was used (web-based service for managing GIT repositories). There, all the programming of the Gridding Tool concerning agreements, definitions and explanations (use cases, data-management and -structures, user management, definition of test cases, programming conventions, runtime environment) are stored.
- All comments in source code documentation were done by using the Microsoft-recommended XML tags. An overview of all functions (internally or with user interaction), which are implemented by the Gridding Tool was created.
- The separation of data, user interface and functional part of the Gridding Tool follows the principle of the MVC concept (Model View Controller).
- In the Gridding Tool all distribution parameters of the same type are encapsulated in their own classes. The concept of "distribution parameter machine" makes it possible to integrate new distribution parameters as separate classes.

An overview of the processes taking place in the Gridding Tool is shown in Figure 3. All relevant input data are provided by the database. The spatial distribution and gridding, as explained above, is carried out in two steps. The distribution parameters needed are available in the tool, a standardized pre-configuration for each NFR sector exists.

Figure 3: Process overview Gridding-Tool



Gridding Tool GRETA is implemented as a class library, which is available within an ArcMap session as a user-defined window acting as an interface between user and tool functions. It works with

objects provided by ArcMap. The tool provides the workflow for emission distributing and gridding, but it is still possible to work “alongside” at any time with the data, e.g. to perform evaluations and presentations of intermediate results.

View and Controller are separated to a large extent, however, parts of the Controller are transcribed by the tool’s window-object respectively by the control elements, and in particular their event treatment routines provided therein. The View functions as a kind of application controller and controls the processes within the tool.

The three components (MVC) are described in the Gridding Tool GRETA as follows:

Model:

Data management and control of data access (to the ArcGIS objects); no strict separation from the View, since in principle within an ArcMap session access to the databases of the Gridding Tool is possible (via standard ArcGIS functions).

View:

ArcMap session with the embedded Gridding Tool GRETA; here both, the review and transfer of user input take place, as well as event handling / forwarding the tool window-related events by accessing the appropriate classes respectively their methods in the controller. There, further processing and application of the program logic are carried out. Event handling by the tool is solely based on the tool window; all other event handlers are within ArcMap internally and will not be intercepted.

Controller:

The functional core of the Gridding Tool GRETA; here the program logic is implemented by responding to events from the View and the Model's data being processed and modified accordingly.

As a result, a very extensive separation of user interface and functional part is achieved. All classes of the tool are organized into namespaces. Here, there was a focus on the defined use cases, i.e. a grouping by function / usage. Each namespace is filed in a separate directory.

The data management of the Gridding Tool GRETA is based on the ArcGIS data format "file geodatabase". A file geodatabase is a collection of geographic and non-geographic datasets and is stored in a folder in the file system.

The filing of all input data used by the tool (tables or layers) is carried out on three levels:

- 1st level: generally valid data (e.g. layer of administrative boundaries)
- 2nd level: data that are valid only for a particular reference year (e.g. emissions)
- 3rd level: data of which contents can be changed by the user (e.g. distribution parameter); multiple user databases/settings are provided

Access to the data is basically carried out also in this staggered way. If a table or a feature layer is needed for displaying / editing, the search is carried out initially in the current user database (level 3). If the data does not exist, search will be executed on level 2 (reference year) and finally on level 1 (global). All produced result data are stored always in the current user database in the results section.

For the development of the Gridding Tool GRETA, 2010 was established as the reference year. There is a filled database for this reference year. This contains all the data (differentiated by NFR sectors) needed for the spatial distribution of national emissions. For each NFR sector, distribution parameters which had been determined in advance from a diverse range of input data set, were preconfigured and their use is recommended as standard assignment. These values can be changed by users of GRETA.

In addition, import tools are available for relevant input data, which may change for different reference years, e.g. for importing national emissions or PRTR emissions.

4. Results

Various sample calculations were performed with GRETA. Amongst others, NO_x emissions of all NFR sectors (with PRTR emissions and under consideration of TREMOD data for the traffic sectors

according to the energy balance principle) were distributed spatially and gridded within a 5 km x 5 km grid (see Figure 4). The spatial emission structure shows clearly the large cities and densely populated areas such as Berlin, Hamburg, North Rhine-Westfalia with the Ruhr area or Stuttgart and Munich. The major highways are also visible. The same data (NO_x emissions of all NFR sectors) gridded within a 1 km x 1 km grid is shown in Figure 5. In GRETA this can be done only by selecting a different grid size definition. Here spatial resolution of the emissions shows significant more details for 5 km x 5 km grid resolution, for example the road network is clearly visible as line sources.

Figure 4: Spatial distribution of NO_x emissions Germany, all NFR sectors, reference year 2010 (with consideration of PRTR emissions and of TREMOD data for the traffic sectors (energy balance principle), 5 km x 5 km grid size

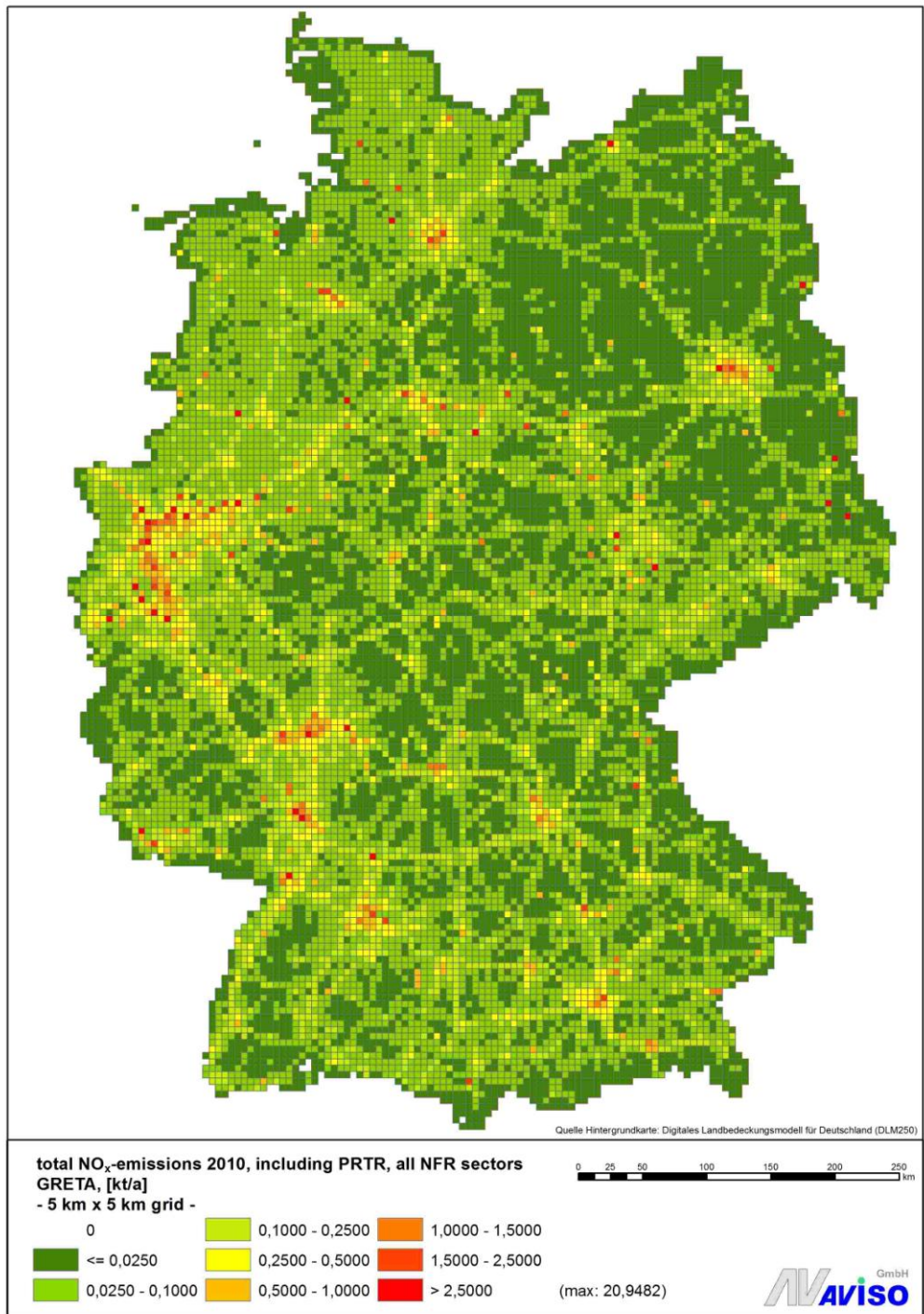
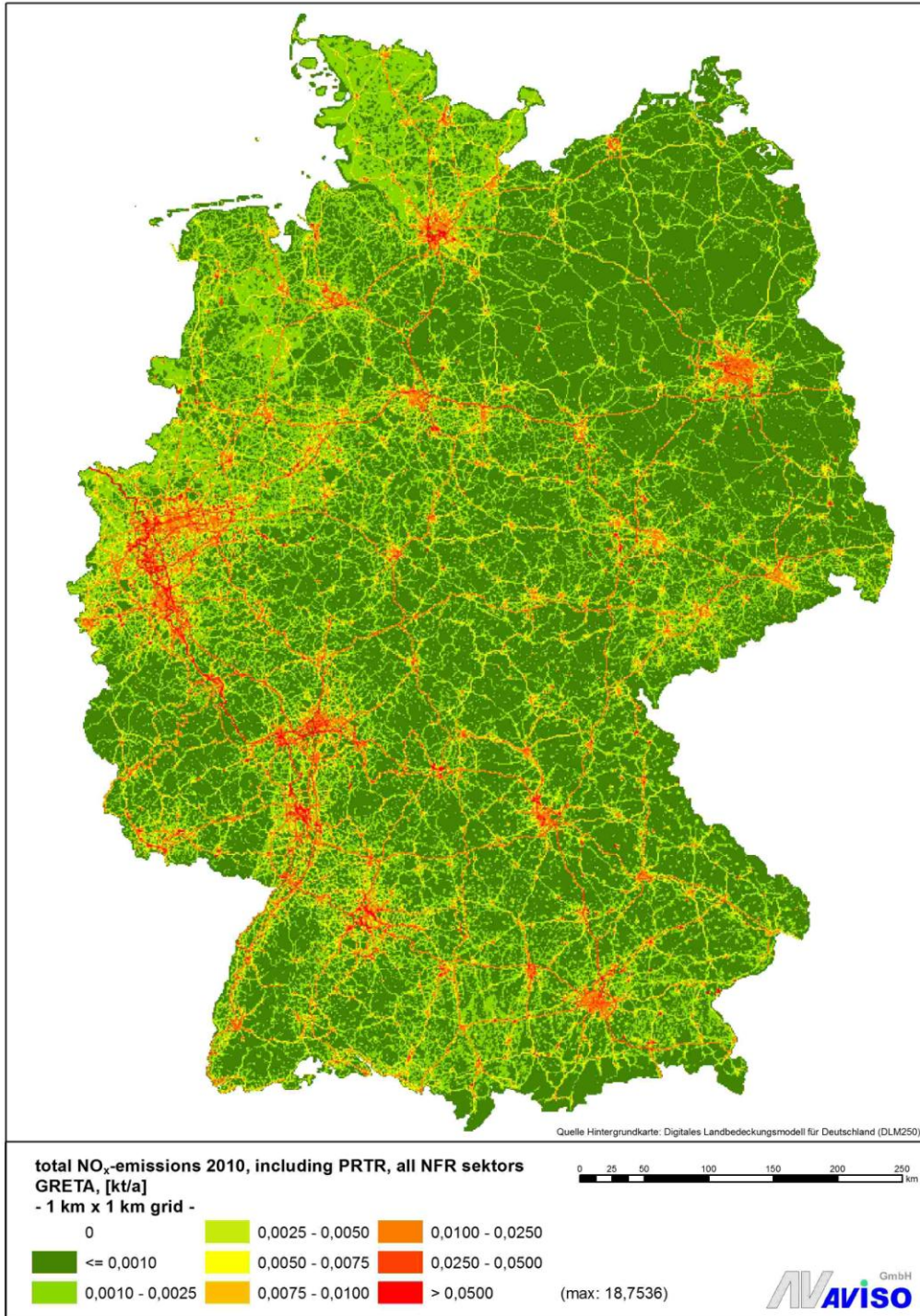


Figure 5: Spatial distribution of NO_x emissions Germany, all NFR sectors, reference year 2010 (with consideration of PRTR emissions and of TREMOD data for the traffic sectors (inland principle), 1 km x 1 km grid size



5. Evaluation

To evaluate Gridding Tool GRETA, emissions calculated with the Gridding Tool have been compared with emissions from other data sources.

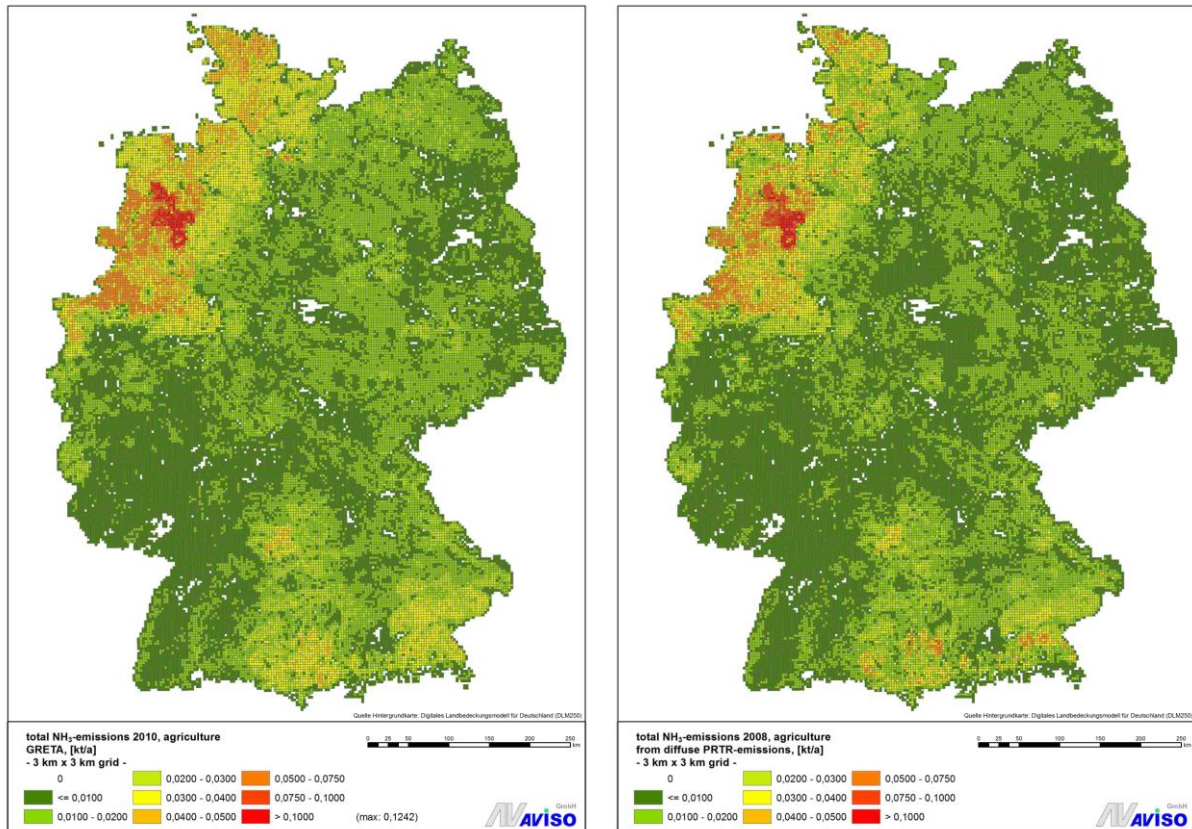
Comparisons of the grid emissions were performed with the following data sets.

- PAREST emissions Germany (1 km x 1km - raster)
- MACC III emissions Germany (1/8 ° x 1 / 16th ° - raster)
- PRTR emissions Germany from diffuse sources (3 km x 3 km - raster)
- emissions from selected small-scaled emission inventories (different raster sizes)

Comparisons were carried out for selected pollutants and source groups and have always been done in the same manner. Grid size of national emissions with the Gridding Tool was set identical to the comparative data sets. Then accumulated emission totals for selected pollutants and areas have been compared to the other data sets. In addition, histograms of the differences in emissions per grid element were created and correlation between the raster data ("pattern matching") determined. Direct comparison of gridded emissions finally took place in form of a differential plot. Possible reasons for striking differences in the spatial distributions were analyzed.

In summary, it was found that emission gridding data sets, produced with the Gridding Tool, basically show a quite similar spatial distribution structure as comparative data sets. When comparing data sets, specified differences originate from the use of different distribution parameters and geometric data sets. An example of the results of the evaluation process is shown below (Figure 6), more examples can be found in /UBA 2016/. The NH₃ emissions of the agriculture sector show in both data sets a quite similar spatial distribution pattern, with highest emissions in the northwest area of Germany, the pattern correlation between the two data sets being 0.96.

Figure 6: Spatial distribution of NH₃ emissions Germany of the agriculture sector, reference year 2010 for the emissions gridded with GRETA (left side) and reference year 2008 for the PRTR emissions of diffuse sources (right side), 3 km x 3km grid size



Acknowledgment

We thank German Environmental Agency (UBA) for supporting (FKZ 3712 63 240 2), the publication of the final report is in preparation.

References

- AEA 2010: I. Tsagatakis et al., UK Emission Mapping Methodology 2008, a Report of the National Atmospheric Emissions Inventory, December 2010, AEAT/ENV/R/3105, Ref: ED48954100 Issue 1
- AEA 2006: K. King, I. Tsagatakis, Mapping Small Industrial Emissions, Local and Regional CO₂ 2005-2006, AEA
- AEA 2012: I. Tsagatakis, Employment based Energy Consumption Mapping in the UK, August 2012, Ref: ED57422 Issue 1
- CLC 2006: CORINE land cover 2006 raster data, <http://www.eea.europa.eu/data-and-maps/data/corine-land-cover-2006-raster-2>
- DLM 2013: www.bkg.bund.de
- EEA 2013: N. Veldeman, W. van der Maas, Emission Inventory Guidebook 2013, 7. Spatial mapping of emissions, www.eea.europa.eu
- MAAS 2013: W. van der Maas, Spatial Allocation of Diffuse Emission Sources, high resolution emission inventory for The Netherlands, National Institute for Public Health and the Environment, Ministry of Health, Welfare and Sport, 17 September 2012
- PAREST 2010a: Thiruchittampalam B., et al., Berechnung von räumlich hochaufgelösten Emissionen für Deutschland, PAREST (Partikel-Reduktions-Strategien), im Auftrag des UBA, UFOPLAN-Nr. 206 43 200/01, 2010
- PLEJDRUP 2011: Plejdrup M.S., Gyldenkoerne S., Spatial Distribution of Emissions to Air – The SPREAD Model, NERI Technical Report Nr. 823, 2011
- PRTR 2013a: Datenabfrage aus www.thru.de zu den Daten für das Berichtsjahr 2010, Stand 2014
- PRTR 2013b: Wursthorn S., Poganietz W., Datenvalidierung/Methodenentwicklung zur verbesserten Erfassung und Darstellung der Emissionssituation im PRTR, FKZ 37 10 91 244, Anhang 5: Thiruchittampalam B., et al., Regionalisierung von nationalen Emissionen im Rahmen von „Diffuse Emissionen im PRTR“, Nov. 2013
- THELOKE 2009: J. Theloke, et al., Methodology Development for a Spatial Distribution of the Diffuse Emissions in Europe, IER Universität Stuttgart, im Auftrag der European Commission, Ref: 070307/2009/548773/SER/C4, 2009
- UBA 2013: TREMOD data for the traffic sector, reference year 2010, per Email from UBA, 11.01.2013, 08.07.2014, 10.07.2014
- UBA 2015: UBA NFR Tabellen 2010, Stand 2015, <http://www.umweltbundesamt.de/themen/luft/emissionen-von-luftschadstoffen>
- UBA 2016. C. Schneider, et al., ArcGIS basierte Lösung zur detaillierten, deutschlandweiten Verteilung (Gridding) nationaler Emissionsjahreswerte auf Basis des Inventars zur Emissionsberichterstattung, im Auftrag des UBA, Forschungskennzahl (FKZ) 3712 63 240 2, 2016, final report, publication in preparation

Intercomparison of three modeling approaches for road dust resuspension using two experimental data sets

Laëtitia Thouron¹, Christian Seigneur¹, Bertrand Carissimo¹, Youngseob Kim¹, Frédéric Mahé², Michel André³, Delphine Lejri³, Daniel Villegas³, Benjamin Bruge², Hervé Chanut⁴, and Yann Pellan⁴

¹CEREA, Joint Laboratory Ecole des Ponts ParisTech / EDF R&D, Université Paris-Est, Champs-sur-Marne, 77455, France

²Airparif, Air quality monitoring network in the Île-de-France region, Paris, 75004, France

³IFSTTAR, Bron, 69675, France

⁴Air Rhône-Alpes, Air quality monitoring network in the Rhône-Alpes region, Saint Martin d'Hères, 38400, France

Keywords. resuspension emissions, exhaust emissions, brake, tire and road wear emissions, air pollutant dispersion

Abstract

Two observational campaigns were conducted, one in the Grenoble area (southeastern France), for the MOCOPo¹ project, near an urban local freeway in 2011 and the other one in a Paris suburb, for the Trafipollu² project, on a major surface street in 2014. PM_{10} concentrations were measured by Air Rhône-Alpes during the last 10 days of September 2011 for MOCOPo and by Airparif during 3 months from April to June 2014 for Trafipollu. It has been shown that abrasion and resuspension processes represent a significant part of the total primary PM_{10} emissions of road traffic. Hereby, resuspended emissions³ originating from the road are estimated with several approaches and compared to PM_{10} measurements. We consider two different models available in the literature: HERMES (Pay et al., 2010) and NORTRIP (Denby et al., 2013), which differ in terms of formulation. We also apply an empirical method developed by Thorpe et al. (2007), based on near-road and background pollutant observations. Those models were combined with atmospheric dispersion models to estimate near-road concentrations. We used a gaussian line-source model for the MOCOPo campaign and a street-canyon model (MUNICH) for the Trafipollu campaign. Our results show satisfactory temporal correlation for PM10 concentrations, especially with HERMES and NORTRIP respectively for MOCOPo and Trafipollu ($r = 0.66$ and $r = 0.5$).

1 Introduction

Resuspension caused by road traffic is defined as the suspension of particles after their deposition on the road surface by air flow. Mollinger et al. (2007) reviewed experiments of the resuspension caused by road traffic. During traffic, the air flow is modified by various factors such as the movement, shape and type of vehicle. Other factors such as the kind of surface and the presence of moisture can also be involved in the amount of resuspension. Beside road dust resuspension, traffic is a major source of air pollutants such as CO , NO_x , SO_2 , PM and metals. We investigate here road dust resuspension in two distinct areas : an urban freeway in the Grenoble area in southeastern France and a major suburban surface street near Paris. Measurements of major traffic air pollutants were conducted at near-road

¹Measuring and Modeling Traffic Congestion and Pollution

²Multi-scale modeling of the pollution emitted from traffic

³Resuspended emissions are defined as pollutants that are resuspended by turbulence and mechanical disturbance (effect of wind and vehicle). As a consequence there is no predefined type of pollutants or particle size range since all pollutants available on the surface area can be potentially resuspended.

monitoring sites for extended periods (ten days in Grenoble and three months in the Paris suburb). We apply here three different methods to estimate road dust resuspension rates: two deterministic models and one empirical method. Near-road PM_{10} concentrations were simulated using atmospheric dispersion models and the effect of taking road dust resuspension by traffic is then assessed by comparison with the near-road measurements.

The Grenoble area is near the border between France and Italy and is subject to local as well as international traffic. As part of the MOCOPo project, several studies have been conducted to assess the level of contamination of air and surface water. For example, Fallah Sorshani et al. (2015) simulated the air pollutant concentrations near-road traffic using a gaussian plume dispersion model augmented with a parametrization for light wind conditions (Venkatram et al., 2013). The same atmospheric dispersion model is used here to calculate near-road concentrations from direct vehicle emissions and road dust resuspension.

The Alsace-Lorraine Boulevard located in an eastern Paris suburb has typical characteristics of a residential/business area impacted mostly by local traffic. Despite reduction in pollutant emissions from tailpipes, the concentrations measured near roadways in the Paris region do not decrease as much as expected and resuspension has been identified as a major indirect source affecting near road air quality.

While the current Nomenclature for Reporting (NFR) air pollutant emissions ignores this process (Amato et al., 2014) further improvements in emission inventory and modelling will necessary need to include resuspension. As a consequence there has been a recent interest in the literature to model resuspension through quantification of emissions. The HERMES emission model, developed in Spain, has been improved with the addition of resuspension (Pay et al., 2010). This model was used to compute resuspension emissions for a domain covering Spain for a whole year of simulation (2004). An evaluation of this model led to a good agreement ($r = 0.41-0.5$), in particular to predict PM_{10} ambient concentrations in dense areas of population in Spain. The ability of this module to simulate resuspension emissions decreases as a function of the distance from the paved road, in particular in background areas where there is little traffic influence. Compared to HERMES, the NORTRIP model (Denby et al., 2013) is more detailed and takes into account traffic speed in addition to traffic flow. It is designed to determine all processes involved in resuspension such as vehicle wear rates, emissions due to traffic, road dust loading and retention of wear particles and suspended emissions based on road surface conditions (dry versus wet). Other estimation methods can be used to estimate resuspension using near-road measurements. For example, Thorpe et al. (2007) calculate the resuspension contribution to PM_{10} concentrations from daily mean PM_{10} , $PM_{2.5}$ and NO_x concentrations. Also, Positive Matrix Factorization (PMF) is one of the principal component methods that has been used to estimate the non-exhaust source based on MOCOPo data measurements (Lucie Polo Rehn, 2013). Over the measurement period, the ratio of the non-exhaust source over the exhaust was estimated to be about 0.76. This PMF result has been used in the work of Fallah Sorshani et al. (2015) to estimate an average resuspension rate. We apply here the three methods mentioned above, HERMES, NORTRIP and that of Thorpe et al. to estimate road-dust resuspension for both the Grenoble freeway and the Paris suburban boulevard.

We first describe the resuspension models and the atmospheric dispersion models used in this study. Next, we present the results for the two sites and compare modeling results to measured PM_{10} concentrations. Finally, we discuss the results and provide conclusions and perspectives for further work.

2 Model descriptions

HERMES

The CALIOPE project was funded by the Spanish Ministry of the Environment and Rural and Marine Affairs. It aims at establishing an air quality forecasting system for Spain (Pay et al., 2010). HERMES is the model used in CALIOPE to compute emissions. To estimate resuspension of PM_{10} the original formula adapted for the whole road network of Spain has been simplified here for a simple road section (Echirrolles near Grenoble), or for a combination of street-segments (Boulevard Alsace-Lorraine) :

$$E_{resuspension} = L_{road} \sum_{v=he,li}^{vehicle} N^v F E_{PM_{10}}^v \quad (1)$$

$E_{resuspension}$ (expressed in $g.h^{-1}$) represents the resuspension emission rate, which depends on the length of the road (L_{road} in km), the traffic flow N^v (in $veh.km^{-1}.h^{-1}$) and the emission factor $FE_{PM_{10}}^v$ specified for each type of vehicle for PM_{10} . The emission factors were measured in Berlin and reported by Düring (2002); the values used are respectively 88 milligrams per vehicle kilometer travelled ($mg.km^{-1}.veh^{-1}$) for light duty and passenger cars and 217 $mg.km^{-1}.veh^{-1}$ for heavy duty vehicles. With traffic evolving during the day and the period of time considered, the resuspension is computed for each situation in the HERMES method. With this model, the resuspension contribution is globally computed depending on vehicle types. It cannot be separated into different source contributions such as resuspension of brake, tire and road wear PM.

NORTRIP

The NORTRIP model is a coupled road dust and surface moisture model implemented by the Norwegian Institute for Air Research to predict road traffic induced particle emissions via resuspension (Denby et al., 2013). The two major differences with the HERMES model are : (1) the use of a PM mass balance on the road surface taking into account deposition and resuspension processes, instead of default resuspension emission rates and (2) the use of vehicle speed, in addition to traffic flow, to calculate the resuspension rate. Initially, a mass balance (M_{road} in $g.km^{-1}.h^{-1}$) is thus computed over time to estimate the mass loading resulting from the consecutive production (via deposition) and sink (via resuspension or drainage) of particles on the road surface. The production term (in $g.km^{-1}.h^{-1}$) corresponds to the retention of wear particles on the road surface ($P_{retention-source}$ in $g.km^{-1}.h^{-1}$). The source of road dust production originates from road, tire and brake wear but it could also originate from background atmospheric deposition and be introduced as an additional term in the formula (background atmospheric deposition was not accounted for in this study). The moisture could also be a retainment factor that leads to increase the amount of particles trapped on the road surface. In this application, we accounted for rain events, but did not apply additional correction associated with moisture as done in Denby et al. (2013). Wear rates W_{source}^v in $g.veh^{-1}.km^{-1}.h^{-1}$ are specified by vehicle category (passenger cars, light-duty and heavy-duty vehicles) and depend on a number of factors as a function of type of wear. The number, speed and types of vehicles and the pavement type are the main input variables to the model. The pavement type is described by hardness(12.5), maximal size grain (10 mm), and amount of grains in the pavement type (95%). Values applied here were obtained from Anne de Bortoli (private communication, LVMT, Mobility, urban planning, and transportation laboratory of Ecole des Ponts ParisTech). They correspond to a semi-coarse asphaltic concrete (BBSG 0/10). The roughness of the pavement could also be a factor that determines retainment of particles on surfaces but it was not taken into account here.

$$\frac{\partial M_{road}^m}{\partial t} = P_{road}^m - S_{road}^m \quad (2)$$

$$P_{retention-source} = \sum_{v=he,li}^{vehicle} N^v W_{source}^v \quad (3)$$

The sink term includes the resuspension process that removes particles from the road surface. The reduction of road dust loading is solved as follows:

$$R_{resuspension}^v = \frac{N^v}{n_{lanes}} h_{0,suspension} \cdot f_{suspension} \cdot (f_{0,suspension} \cdot v_{veh}^v \cdot f_{q,suspension}(g_{road})) \quad (4)$$

It depends on the number of lanes n_{lanes} , the scaling factor to adjust the basic suspension rates for PM_{10} $h_{0,suspension}$, the fraction of resuspension for a given type of vehicle $f_{suspension}^v$ and the retainment fraction of dust on the road surface due to moisture (measured in water mass g_{road}). This last term is neglected here (assumed to be 1).

Finally, the resuspension emission rates are computed via a mass balance on the road dust (M_{road}), which depends on the fraction of the suspended mass in the PM_{10} size fraction. We apply the reference value of 0.18 (an uncertainty of $\pm 30\%$ has been estimated by Denby et al, 2013). The mass of road-dust PM_{10} (Figure 1) is accumulated hours after hours as a function of traffic composition, flow and speeds till the next rainfall (see the fall-off of mass accumulation in the Figure). During the measurement period, 5 rain events were recorded for MOCOPo over the ten-day period. The WRF meteorological

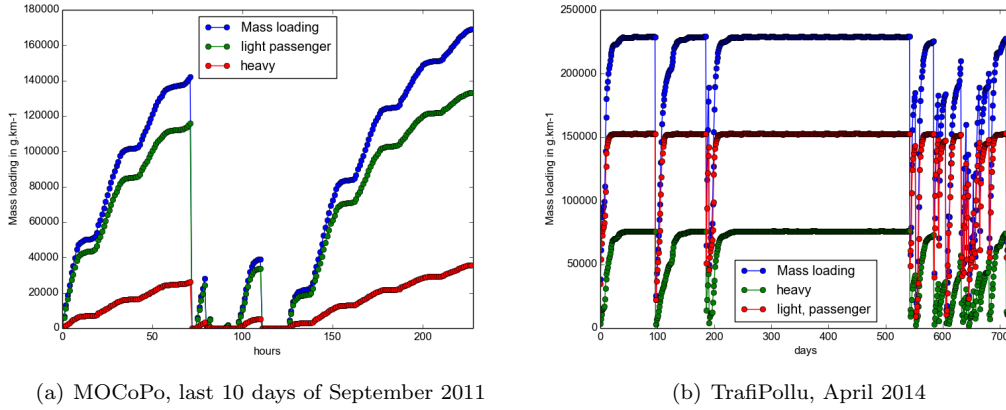


Figure 1: Simulation of PM_{10} mass accumulated on the road surface

model predicts 82 rain events for TrafiPollu, over the three-month period. We assume here that there is no road-dust mass initially. At the next time step, the mass corresponds to the effective deposition of the PM mass produced by tire, brake and road wears, less the amount that enters the ambient atmosphere by resuspension processes. At a given moment t , the PM mass is available for vehicle-induced resuspension as follows:

$$M(t_0 + \Delta t) = P/R + (M(t_0) - P/R)e^{-R \cdot \Delta t} \quad (5)$$

Emissions released to the atmosphere are computed with the loading mass computed with Equation (5) which is affected by the reduction term of the resuspension process.

$$E_{suspension}^x = \sum_{sus-particles} M_{road} \sum_{v=he,li}^{vehicle} R_{resuspension}^v \quad (6)$$

In this model, wear rates are differentiated according to sources and type of vehicle. A driving cycle can be selected among highway, urban, congested, congestion-free, etc. situations and a modified use of brake can be applied to alter the standard brake wear rate. Here, the driving cycle is fixed at 1. Thus, the brake wear rate computed is equal to the standard brake wear rate as given by Boutler et al. (2005). For road and tire wear rate functions are applied depending on the speed of vehicles and on standard wear rates (Table 1) determined respectively by Swedish road wear models (Jacobson and Wagberg, 2007) and by on-road measurements (Snilsberg et al., 2008; Gustafsson et al., 2008). The computed mean wear rates are shown in Table 2. The road abrasion is the mechanism that releases the most particulate matter to the ambient air, Table 2 indicates higher wear rates for road than for tire or brake.

Table 1: Standard wear rates as provided by Denby et al. (2013)

$g.km^{-1}.veh^{-1}$	Light-duty and Passenger	Heavy-duty
Tire	0.01	0.05
Brake	0.01	0.05
Road	0.15	0.75

Table 2: Computed tire and road wear rates as a function of vehicle category

MOCOPO		
Type of wear	Type of vehicle	Mean ($g.km^{-1}.veh^{-1}$)
Tire	heavy	0.4
Tire	light-duty/passenger	0.1
Road	heavy	2.6
Road	light-duty/passenger	0.7
Trafipollu		
Type of wear	Type of vehicle	Mean ($g.km^{-1}.veh^{-1}$)
Tire	heavy-duty	0.02
Tire	light-duty/passenger	0.005
Road	heavy-duty	0.35
Road	light-duty/passenger	0.07

Thorpe method

The method of Thorpe et al. (2007) requires observations to estimate the contribution of resuspension to ambient PM_{10} concentrations. Therefore, unlike HERMES and NORTRIP, which only require traffic-related information, it cannot be applied to sites where near-road measurements are unavailable. Nevertheless, since near-road measurements were available for both the MOCOPO and Trafipollu sites, we applied this empirical method for comparison with the HERMES and NORTRIP deterministic models. The empirical method of Thorpe et al. (2007), relies on direct wear emission factors for brake, tire and road to estimate PM road-dust resuspension. The estimation of particle resuspension was originally applied to a major London road by the Division of Environmental Health and Risk Management of Birmingham University. Emissions of PM_{10} are computed from daily exhaust emissions from the traffic (E_{NO_x}) in $g.h^{-1}$ - which is computed with traffic parameters (flow and speed) and available emission factors - and from the ratio of PM_{10} over NO_x hourly concentrations in $\mu g.m^{-3}$ (excluding the background signal) from the near road observations. Then, the PM_{10} emission term ($E_{PM_{10}}$ in $g.km^{-1}.h^{-1}$) is used to estimate emissions from the fraction of particulate matter comprised between 2.5 and 10 μm according to the same approach. $PM_{2.5}$ are assumed to be exhaust-emitted particles while the coarse fraction of PM_{10} (i.e., $PM_{10} - PM_{2.5}$) represents the non-exhaust source (i.e., that corresponding to PM emissions from tire, brake and road wear). Resuspension emissions (in $g.km^{-1}.h^{-1}$) are deducted from emissions of that fraction comprised between 2.5 and 10 μm from which the direct emissions from brake, tire and road wear are removed. In our MOCOPO and Trafipollu case studies, emissions from brake, tire and road are assumed to be in the fraction between 2.5 and 10 μm coming respectively from CopCETE (MOCOPO) and HEAVEN (Trafipollu) emission simulations.

$$E_{PM_{10}} = E_{NO_x} \left(\frac{\Delta PM_{10,road-background}}{\Delta NO_{x,road-background}} \right) \quad (7)$$

$$E_{PM_{2.5-10}} = E_{PM_{10}} \left(\frac{\Delta PM_{2.5-10,road-background}}{\Delta PM_{10,road-background}} \right) \quad (8)$$

$$E_{resuspension} = E_{PM_{2.5-10}} - (E_{brake} + E_{tire} + E_{road}) \quad (9)$$

Gaussian plume model

The gaussian dispersion model used for the MOCOPO case study has been developed to estimate concentrations near roadways (Briant et al., 2011, 2013), with a modification suitable for light wind conditions (Venkatram et al., 2013). The formulation of the gaussian dispersion is based on an exact gaussian formula for line sources that has been modified for cases when the wind direction is not perpendicular to the road.

$$C_p(x, y, z) = \frac{q(Fz)}{2\sqrt{2\pi}u \cos \theta \sigma_z(d_{eff})} [erf(t_1) - erf(t_2)] \left(\frac{1}{L(x_{wind}) + 1} \right) + E(x_{wind}, y_{wind}, z) \quad (10)$$

The gaussian concentrations emitted from a line source in $g.m^{-3}$ are computed at the distance along the wind direction (x) and at the cross-wind distances from the plume centerline (y, z) decrease with the effective distance d_{eff} from each extremities x_i, y_i , and depend on the vertical standard deviation associated σ_z expressed in meters, the wind velocity (u) in $m.s^{-1}$ and the angle between the wind direction and the normal of the road θ . The rate emission of the line source is q in $g.m^{-1}s^{-1}$. Pollutan dispersion is impacted by the vertical diffusion F_z which depends on vertical dispersion, the height of the emission h_s and the height of the initial plume rise z .

$$t_i = \frac{(y - y_i)\cos\theta - xsin\theta}{\sqrt{2}\sigma_y(d_i)} \quad (11)$$

$$F(z) = \exp\left(-\frac{(h_s - z)^2}{2\sigma_z^2}\right) + \exp\left(-\frac{(h_s + z)^2}{2\sigma_z^2}\right) \quad (12)$$

An error function is introduced (*erf*) when integrating along the line source. Those error functions depend on the distance d_i from each extremity of the line source section in the wind direction.

$$d_{eff} = \frac{x}{\cos\theta} \quad (13)$$

$$d_i = (x - x_i)\cos\theta + (y - y_i)\sin\theta \quad (14)$$

L and E are analytical functions that minimize the error when the wind direction is not perpendicular to the road. Equation (10) is applied for winds direction ranging between 0° and 80° . However, when the wind direction is parallel or nearly parallel ($80^\circ \leq \theta \leq 90^\circ$) to the road, the concentraion C is then calculated as a combination between Equation (10) and a numerical solution ($C_{discretized}$) obtained by discretizing the line source as a set of point sources as follows:

$$C = (1 - \alpha)C_p + \alpha C_{discretized} \quad (15)$$

The coefficient α varies linearly from 0 to 1 when θ varies from 80° to 90° .

A new concentration $C_{light-wind}$ adapted to low wind speed conditions is computed with an ‘‘effective wind speed’’ that advects the plume in a 360° random wind spread:

$$C_{light-wind} = \sqrt{\frac{2}{\pi}} \frac{qF(z)\theta_s}{2\pi u_e \sigma_z} \quad (16)$$

with θ_s the angle subtended by the line source at the receptor,

$$\theta_s = \tanh^{-1}\left(\frac{y_2 - y}{x}\right) + \tanh^{-1}\left(\frac{y - y_1}{x}\right) \quad (17)$$

The effective velocity u_e is specified as follows:

$$u_e = \sqrt{(\sigma_u^2 + \sigma_v^2 + u^2)} \quad (18)$$

The standard deviation of the turbulent velocity fluctuations along the mean flow and in the lateral direction, respectively, are:

$$\sigma_v^2 = u^2 \sinh(\sigma_\theta^2) \quad (19)$$

and

$$\sigma_u^2 = u^2 \cosh(\sigma_\theta^2) - 1 \quad (20)$$

with σ_θ used by default at the 72° value based on the Cirillo and Poli (1992) study.

Concentrations are then corrected as follow:

$$C_{final} = C_{(p)}(1 - f_r) + C_{light-wind}f_r \quad (21)$$

The weighting factor that minimizes the gaussian line source concentrations in presence of calm winds and that gives more importance to recomputation of a local concentration ($C_{light-wind}$) is as follows:

$$f_r = \frac{2\sigma_v^2}{u_e^2} \quad (22)$$

The weighting factor gives here a result close to 95% which means that the gaussian concentrations are weighted with a factor of 5%. For some situations, this factor could be lower and it would be preferable if it was not constant but varying with wind speed in order to adapt for each situation the attenuation of overestimated gaussian concentrations.

MUNICH

The Model of Urban Network of Intersecting Canyons and Highways (MUNICH) is a street-canyon model, which is based on the SIRANE formulation (Soulhac et al., 2011). It was applied to the Trafipollu case study, which is characterized by a suburban morphology. MUNICH computes atmospheric dispersion within a street-canyon according to a simplified description of the urban geometry and parametric relationships for pollutant transfer phenomena within, into, and out of the urban canopy. Two main interconnected components define the model: (1) the street-canyon component and (2) the street-intersection component. The urban background at roof level is also connected to those components via inflow/outflow parameters.

The pollutant concentration in the street-canyon is computed based on mass conservation as described by the following equation :

$$Q_{S,i} + Q_{I,i} = \frac{\sigma_w W L}{\sqrt{2\pi}} (C_{street,i} - C_{background,i}) + HWU_{street} C_{street} + Q_{deposition} \quad (23)$$

where :

$Q_{S,i}$ is the source emission rate (here traffic-related emissions)

$Q_{I,i}$ is the flow rate of air pollutant entering the street from upwin (typically via an intersection)

$Q_{deposition}$ is the pollutant loss rate due to atmospheric deposition (ignored here)

σ_w is the standard deviation of the vertical wind velocity (in $m.s^{-1}$)

The standard deviation of vertical wind velocity depends on atmospheric stability defined by the Monin-Obukhov length (L_{MO})

W , L and H are respectively the street width, street length and building height (in m)

U_{street} is the average wind velocity in the street (in $m.s^{-1}$)

$C_{street,i}$ is the air pollutant concentration in the street (in $\mu g.m^{-3}$)

$C_{background,i}$ is the concentration in the urban background above the street, i.e. at roof level (in $\mu g.m^{-3}$)

The Lemonsu et al. (2004) approach to estimate the vertical profile of the wind speeds, is used here to calculate the mean wind velocity within the street-canyon. The formulation takes into account the street-canyon geometry, which includes a different wind profile.

Thus, in the case of narrow canyons ($H/W > 2/3$) :

$$U_{street,i} = \frac{2}{\pi} U_H \cos(\phi) \exp(\beta(\frac{z}{H} - 1)) \quad (24)$$

and in the intermediate case (i.e, moderate canyons), $H/W < 2/3$:

$$U_{street,i} = [1 + 3(\frac{2}{\pi} - 1)(\frac{H}{W} - \frac{1}{3})] U_H \cos(\phi) \exp(\beta(\frac{z}{H} - 1)) \quad (25)$$

where β is a function of the street aspect ratio such as

$$\beta = \frac{H}{2W} \quad (26)$$

The case where H/W is strictly equal to $2/3$, those formulations give the same result of wind profile. An average wind velocity within the street-canyon is derived from these empirical wind profiles by integrating over the entire street-canyon height.

Turbulent vertical mass transfer at the top of the street-canyon, which is the interface with the background atmosphere, does not depend on the geometry of the canyon. It is only defined by the external flow condition, based on Salizzoni et al. (2009).

$$Q_{H,turb} = \frac{\sigma_w W L}{\sqrt{2\pi}} (C_{street} - C_{background}) \quad (27)$$

where :

C_{street} and $C_{background}$ are the mean concentrations within and above the street (in $\mu g.m^{-3}$)

The street intersection model follows the SIRANE formulation. Air mass flows, P_{street} out of or into a street i are expressed as follows :

$$P_{street,i} = \xi HWU_{street,i} \quad (28)$$

where :

$\xi = 1$ for streets upwind of the intersection (airflow entering the intersection)

$\xi = -1$ for streets downwind of the intersection (airflow leaving the intersection)

In our case study, the Alsace-Lorraine Boulevard is broken down into 15 street-canyon segments. Thus, each segment can be assigned specific street and building characteristics. For each segment, W , L and H are extracted from the BDTOPO database along the Alsace-Lorraine Boulevard; they are presented in Table 3.

Table 3: Street widths, street lengths and building heights along the Boulevard Alsace-Lorraine (in m)

road section	length	width	height
1	30	14.0	7.3
2	65	14.0	7.3
3	34	14.0	7.3
4	45	30.0	8.6
5	34	25.0	8.6
6	36	28.0	8.6
7	344	25.0	8.6
8	57	26.0	8.6
9	178	30.0	8.6
10	59	27.0	8.6
11	43	32.0	8.6
12	44	27.0	8.6
13	124	26.0	8.6
14	38	31.0	8.6
15	182	24.0	8.6

3 Model applications

Input data

Resuspension emissions are computed based on traffic data (speed and flow) that come from SIREDO (MOCOPo), a computerised data collection provided by the French Ministry of Environment, and from AlyceSofreco (TrafiPollu), a French company. In both cases, the traffic was measured in both directions, which were combined for these applications. Road characteristics were obtained as described above (de Bortoli, private communication), and are similar for both cases. Rainfall events were extracted from meteorological observations performed *in situ* for MOCOPo and from WRF, the Weather Research and Forecasting model, for TrafiPollu as no observations were available during the study period.

The gaussian plume model for line sources requires input data, which include an emissions file, a background concentrations file and a meteorological file. The PM_{10} direct vehicle emissions were obtained from the CopCETE model. CopCETE has been implemented by the French Ministry of Environment and is coordinated by the Normandie-Centre Technical Center of Equipment. It is a tool based on the COPERT methodology improved with some emissions factors derived from French research studies. This model computes exhaust and non-exhaust emissions such as wear emissions (brake, tire and road) for a selected road as a function of traffic data. Here, it is applied for the Echirrolles road section in Grenoble and its traffic. The background concentrations file corresponds to observations from the Les Fresnes site, the nearest urban background for the Grenoble area from the local air quality monitoring network (Air

Rhône-Alpes). The meteorological file is the same as that used for rainfall events. The gaussian plume model provides simulated concentrations near the Echirolles freeway. Those simulated concentrations corresponding to direct vehicle emissions are then complemented with concentrations simulated from resuspension emissions models (i.e., HERMES, NORTRIP and Thorpe et al.) and with background concentrations. They are finally compared to PM_{10} near-road concentrations measured by Air Rhône-Alpes.

Similar types of input data are required for MUNICH. Direct emissions have been modeled by Airparif with HEAVEN, the local air quality network, based on traffic data modeled with a microscopic dynamic traffic model, SymuVia, developed and applied here by Ifsttar Lyon. SymuVia was applied to two standard days, a week day and a week-end days, which were then used to construct traffic data for the full 3-month period. Background concentrations were obtained from Airparif rural monitoring stations (Herpin for $PM_{2.5}$ and PM_{10} , and Fontainebleau for NO_2). The meteorological file was extracted from WRF simulations. MUNICH provides simulated concentrations over 15 street sections constituting the Alsace-Lorraine Boulevard. MUNICH concentrations obtained from direct vehicle emissions are added to those obtained from resuspension and to background concentrations in order to obtain the whole pollution measured at the Airparif stations located on the sidewalks of the Boulevard.

Results

Resuspension emission contributions

Mean emissions computed with resuspension models (i.e., HERMES, NORTRIP and Thorpe et al.) are compared to direct PM_{10} vehicle emissions for both case studies (MOCOPO and Trafipollu).

Table 4 indicates the importance of resuspension emissions in both cases. Indeed, resuspension emissions are higher or comparable to direct emissions for most models of resuspension. However, the comparison of the two sites shows a greater contribution from resuspension in the Trafipollu case.

In the MOCOPO case, resuspension from HERMES is commensurate with direct emissions, NORTRIP is almost comparable and represents about 70% of direct emissions. Thorpe et al., is only half that directly emitted by traffic.

Conversely, in the Trafipollu case, HERMES resuspension emissions are much greater (about 5 times) than the direct emissions, while NORTRIP is comparable to the direct emissions. In HERMES, flow is only considered as a key factor to explain resuspension while in NORTRIP speed is taken into account. Vehicle speeds are significantly smaller in this case compared to the MOCOPO freeway case study. Light-duty/passenger and heavy-duty vehicles are driven at an average speed of 32 km.h^{-1} . While traffic speed is low, results show that the resuspension may be high when just taking into account the flow as in HERMES. Nevertheless, NORTRIP gives greater resuspensions than direct emissions, which is due to an important mass loading. Rainfall is regulating the mass of PM deposited on the road over time. Rainfall events are shorter in the Paris suburb than in the Grenoble area. Precipitation data show rain events on the order of 5 hours in the Grenoble area while there are about 2 hours in the Paris suburb. However, the lengths of the precipitation events do not affect our calculations, because it is only the length of the dry period (i.e., between two rain events) that leads to a greater accumulation of particles on the road, as shown in Figure 1. In addition, as traffic is less, there is less PM being resuspended and therefore more accumulation of deposited PM on the road surface, which is then available to be resuspended. Resuspension results from Thorpe et al. model are not shown for Trafipollu study because negative due to the condition imposed (i.e., non-exhaust/exhaust). Indeed, at Trafipollu site, there is a great background contribution.

Considering the temporal evolution of resuspended particles, HERMES follows exactly the direct emissions (Figure 2). Since HERMES resuspension is computed as a function of traffic flow, its profile follows the flow pattern. Direct emissions are a function of vehicle speed, but there little variability of direct emissions with traffic speed in the speed range mostly observed in Grenoble and traffic speed shows limited variation in the Paris suburb boulevard. NORTRIP emissions are impacted by the length of dry periods between rainfall events; consequently they are less correlated to direct emissions (see left side of Figure 2, the right side is only the 1st week of April). As mentioned above, rainfall controls the resuspended mass supply. After each rain event, the PM mass loading present on the road surface is re-set to zero leading to a time-dependent resuspension emission profile over time. The temporal variability of the Thorpe et al. is more heterogenous since those emissions are computed according to observations

ratios, which can be highly fluctuating. For instance, in the MOCOPo case study (see Figure 3), the direct and Thorpe et al. resuspension emissions do not follow the same trend. It suggests that the Thorpe et al. resuspension emissions is not related to direct emissions and that other factors, which may not be accounted for by the models, influence the observed concentrations. Observations could be influenced by another source than traffic emissions.

It is of interest to identify which type of vehicles - heavy-duty or light-duty/passenger vehicles- induces the largest resuspension rate. In Table 8, the relative contributions to resuspension are summarized by types of vehicle. Focusing in HERMES and NORTRIP (since the Thorpe method cannot differentiate emissions by vehicle types), we note that light-duty and passenger vehicles are releasing globally the largest part of the resuspended emissions (more than 80%). Even though emission factors for heavy-duty vehicles are greater than those from light-duty and passenger vehicles (Table 7), the vehicle fleet plays a major role. Light-duty and passenger vehicles account for 96% of traffic in the MOCOPo Grenoble freeway, while heavy-duty vehicles represent only the remaining 4%. A slightly higher proportion (97%) of light-duty and passenger vehicles is also observed in the TrafiPollu suburban street-canyon case study, which leads to a greater contribution of this vehicle type in the amount of resuspended mater modeled in Boulevard Alsace-Lorraine. Among the three types of wears being considered (brake, tire and road), Table 5 shows for both case studies, that road wear is the main mechanical phenomenon at the origin of resuspended particulates and it follows the temporal variability of total NORTRIP emissions. Figure 4 shows resuspension wear emissions and the total resuspension emissions computed with NORTRIP in the TrafiPollu case study. This result is due to higher emission factors applied for road wear compare to tire and brake wear. Road wear is also amplified by flow and speed of vehicles as described by Equation (29), it is also the case for tire wear (Equation (30)) from Denby et al. (2013). Brake wear is a function of the driving cycle as described by Equation (31). It is also possible to compute direct and resuspended emissions for each category of wears with equations and to calculate the proportion of particles that is really resuspended from what is initially emitted (Table 6. Thus, almost all of what is produced by tire and brake is resuspended and more than 70 % for road wear in both case studies.

$$W_{roadwear}^v = W_{0,roadwear}^v * h_{pavement} * (v_{veh}/v_{ref,roadwear})^{a_{wear}} \quad (29)$$

$$W_{tirewear}^v = W_{0,tirewear}^v * (v_{veh}/v_{ref,tirewear})^{a_{wear}} \quad (30)$$

$$W_{brakewear}^v = W_{0,brakewear}^v * h_{drivingcycle} \quad (31)$$

Table 4: Direct and resuspension mean emissions due to traffic

Model	Mean emission MOCOPo ($g.h^{-1}$)	Mean emission TrafiPollu ($g.h^{-1}$)
direct (CopCETE or HEAVEN)	374	45
HERMES	360	199
Thorpe et al.	293	
NORTRIP	262	54

Table 5: Mean emissions computed($g.h^{-1}$)

	MOCOPo		TrafiPollu	
Mean total	309	Contribution	54	Contribution
Mean road	260	84 %	38	70 %
Mean brake	4	1 %	1	2 %
Mean tire	45	15 %	6	10 %

Table 6: Mean direct and resuspended wear emissions computed with NORTRIP ($g.h^{-1}$)

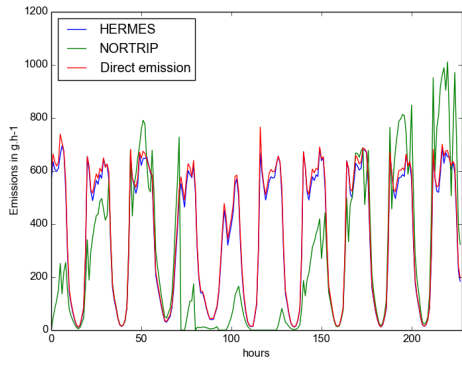
MOCOPo					
Road		Brake		Tire	
Mean direct	Mean resuspended	Mean direct	Mean resuspended	Mean direct	Mean resuspended
845	758	69	69	156	156
Emitted from origin	90 %		100 %		100 %
TrafIPollu					
Road		Brake		Tire	
Mean direct	Mean resuspended	Mean direct	Mean resuspended	Mean direct	Mean resuspended
53	38	1	1	6	6
Emitted from origin	70 %		100 %		100 %

Table 7: Emission factors used for the three models in $g.km^{-1}$

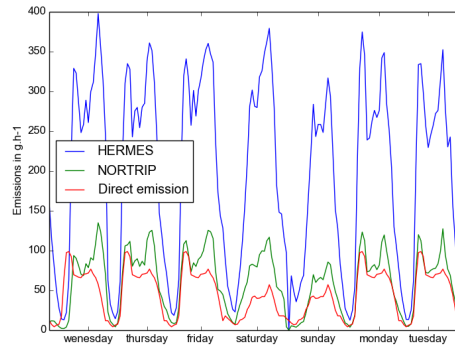
HERMES resuspension			Thorpe et al. direct				NORTRIP direct			
			Brake	Light-duty	0.0177	FAC	Brake	Light-duty	0.01	FAC
			Brake	Heavy-duty	0.0590	3	Brake	Heavy-duty	0.05	5
Light-duty	0.088	FAC	Tire	Light-duty	0.0177	FAC	Tire	Light-duty	0.01	FAC
Heavy-heavy	0.217	2	Tire	Heavy-duty	0.0590	3	Tire	Heavy-duty	0.05	5
			Road	Light-duty	0.0075	FAC	Road	Light-duty	0.15	FAC
			Road	Heavy-duty	0.0380	5	Road	Heavy-duty	0.75	5

Table 8: Resuspension mean emissions due to traffic as a function of vehicle type

Study	Model	Vehicle type	Mean emission ($g.h^{-1}$)
MOCOPo	HERMES	heavy	34
		light-duty/passenger	325
	NORTRIP	heavy-duty	26
		light-duty/passenger	236
TrafIPollu	HERMES	heavy-duty	20
		light-duty/passenger	179
	NORTRIP	heavy-duty	6
		light-duty/passenger	48
		Contribution light-duty/passenger	Contribution heavy-duty
MOCOPo	HERMES	86%	14%
	NORTRIP	94%	6%
TrafIPollu	HERMES	80%	20%
	NORTRIP	65%	35%



(a) MOCOPO, last 10 days of September 2011



(b) Trafipollu, 1st week of April 2014

Figure 2: Traffic emissions : NORTRIP (green), HERMES resuspension (blue) and CopCETE direct emissions (red)

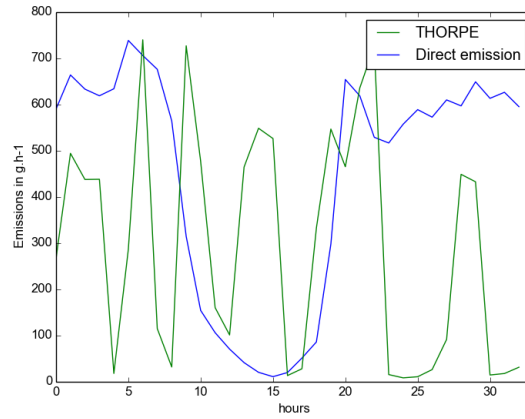


Figure 3: Traffic emissions : THORPE (green) and CopCETE direct emissions (blue)

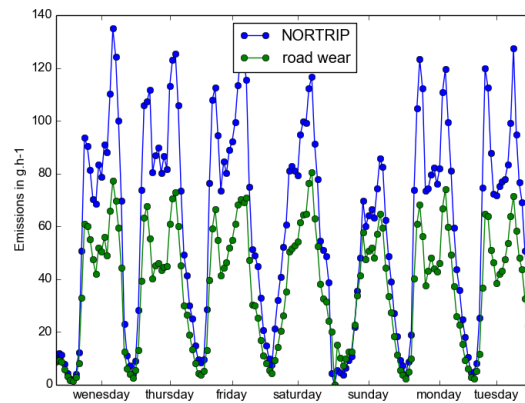


Figure 4: Traffic emissions : total resuspension (blue) and resuspension road wear (green) with NORTRIP at Alsace-Lorraine Boulevard

Simulated concentrations

The simulations were conducted with hourly input and output data, and compared with actual observations. Due to the vicinity of the road to the observations in both case studies, particles may be considered as chemically inert. Concentrations result from the sum of the local concentration being simulated and of the background concentration measured at a site located a couple of kilometers away (see Figure 5). The simulations were performed with the gaussian plume model with light-wind conditions and with resuspension PM_{10} emissions added to the direct ones for the MOCOPO case study. For the other case study (Trafipollu), simulations were performed with MUNICH for Boulevard Alsace-Lorraine taking into account building effects. The main objective of those simulations is to quantify the road traffic contribution to local air pollution taking into account both direct and resuspension emissions. Profiles show observed and simulated concentrations of PM_{10} with and without resuspension added to direct emissions (see Figures ??, 8 and 7). Mean observed concentrations are summarized in Table 9. We obtain the best performance in terms of correlation with modeled PM_{10} concentrations from HERMES (see Table 10 and in Table 11). Indeed, correlation coefficients are 0.5 and 0.66, respectively for Trafipollu and MOCOPO. The correlations obtained with NORTRIP are slightly lower ($r = 0.49$ and 0.36). The correlation coefficients present a slight difference when comparing with and without resuspension, which is consistent with the little improvement (i.e., 2%) reported by Pay et al. (2011) for the whole simulation of Spain. If we compare with Denby et al. (2013), high correlation is obtained when the resuspension module is included in the simulation ($r^2 = 0.77$ - 0.91 ; with a global improvement of 56% due to resuspension). Considering the local meteorology, the use of sanding during winter, the period of simulation (one year against ten days for MOCOPO and 3 months for Trafipollu), and the street configuration (street-canyon type against open roadway for MOCOPO and medium open street-canyon for NORTRIP); it is not surprising to obtain different results. Furthermore, for open street canyon, Denby et al. (2013) found that less than 51% (where resuspension can dominate total emissions) of the variability is explained by the resuspension model, which implies that the resuspension part of the model played a less significant role than in our case studies. The fact that we did not account for the effect of moisture on the road may bias our results and suggests a possible way of improvement.

The final improvement appears to be small compared to the simulation without resuspension because the strong signal of background concentrations tends to dominate those near-road PM_{10} concentrations (see Figure 5). Direct emission correlation to observations ranges from 0.48 to 0.66, while background is already correlated with a range from 0.52 to 0.65. If we check the mean background concentrations in both case studies, they contribute up to 80% of the observations; the rest represents the real traffic signal. In the near-road concentrations, mean concentrations highlight that direct concentrations modeled by the gaussian line plume model contribute to 2% of the mean near-road concentrations. HERMES and NORTRIP accounts for 2% as well. Those results are also influenced by particular meteorological situations occurring in the MOCOPO campaign, such as light winds, and upwind location of the station with respect to the freeway. More details are presented by Fallah Shorshani et al. (2015). Mean concentrations modeled with MUNICH show better performance considering the traffic signal. Direct modeled concentrations contribute to 20% of the near-road concentrations, HERMES resuspension 55% and NORTRIP resuspension 15%.

Simulations are underestimated observations for both cases (see MBE in Table 10 and Table 11).

Another way to calculate the impact of resuspension is to use the conversion factor to convert emissions to concentrations. Equation (32) provides a conversion factor depending on NO_x concentrations (difference between road and background) and emissions. Applied on resuspended emissions, this factor is estimated on average to be 0.02 in MOCOPO, and 0.1 for Trafipollu. As resuspension emissions are 10 times greater at MOCOPO, conversion factors are thus consistent with near-road concentrations. PM_{10} concentrations computed with those factors according to resuspended emission sources (brake, tire, road) and to direct emissions are assumed to represent the total PM_{10} near-road concentrations (see Figure 9). In this Figure, HCAB concentrations from Denby et al. are greater than those of our case studies, especially for concentrations coming from road suspension. This is expected due to the use of road sanding in HCAB case that induce more road particles.

$$f_{con} = [NO_x^{traffic}] - [NO_x^{background}] / NO_x^{emissions} \quad (32)$$

Table 9: Mean observed concentrations ($\mu\text{g}\cdot\text{m}^{-3}$)

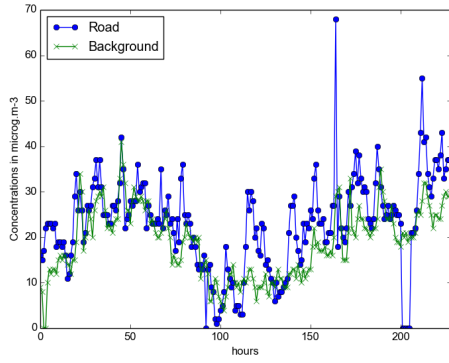
MOCOPo		
Mean NO_x	Mean PM_{10}	Mean $PM_{2.5}$
104	23	15
Mean NO_x background	Mean PM_{10} background	Mean $PM_{2.5}$ background
26	19	14
TrafiPollu		
Mean NO_x	Mean PM_{10}	Mean $PM_{2.5}$
36	19	13
Mean NO_x background	Mean PM_{10} background	Mean $PM_{2.5}$ background
25	18	13

Table 10: Statistical performance for PM_{10} concentrations for the various models including or not resuspension and for MOCOPo study

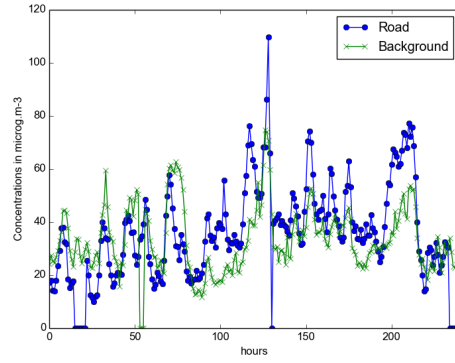
Model	Number of samples	Mean modeled value ($\mu\text{g}\cdot\text{m}^{-3}$)	R	RMSE ($\mu\text{g}\cdot\text{m}^{-3}$)	MBE (%)	FAC 2
PM_{10} (Gaussian plume)	228	18.9	0.66	8.7	-3.9	0.87
PM_{10} (with HERMES)	228	19	0.66	8.7	-3.9	0.87
PM_{10} (with NORTRIP)	228	21.4	0.66	8.7	-3.9	0.85
PM_{10} (with Thorpe et al.)	33	17.7	0.68	23.5	23	0.91
Observations	Number of samples	Mean measured value ($\mu\text{g}\cdot\text{m}^{-3}$)	R			
Road	228	22.9				
Background	228	18.8	0.65			

Table 11: Statistical performance for PM_{10} concentrations for the various models including or not resuspension and for TrafiPollu study

Model	Number of samples	Mean modeled value ($\mu\text{g}\cdot\text{m}^{-3}$)	R	RMSE ($\mu\text{g}\cdot\text{m}^{-3}$)	MBE (%)	FAC 2
PM_{10} (MUNICH)	1968	18.65	0.48	13.62	-2.9	0.64
PM_{10} (with HERMES)	1968	20.6	0.5	13.2	-0.89	0.71
PM_{10} (with NORTRIP)	1968	19.2	0.49	13.5	-2.3	0.66
Observations	Number of samples	Mean measured value ($\mu\text{g}\cdot\text{m}^{-3}$)	R			
Road	1968	21.5				
Background	1968	17.87	0.52			

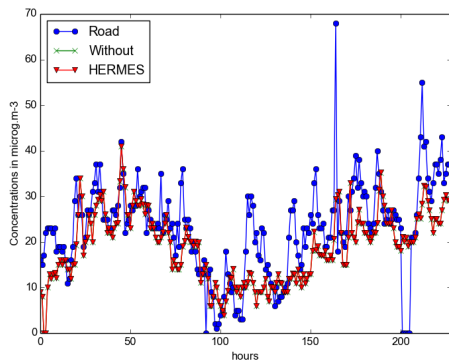


(a) MOCOPo, last 10 days of September 2011

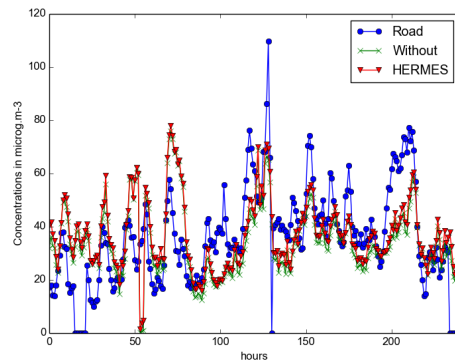


(b) Trafipollu, from April to June 2014

Figure 5: Road (green) and background (blue) concentrations from observations

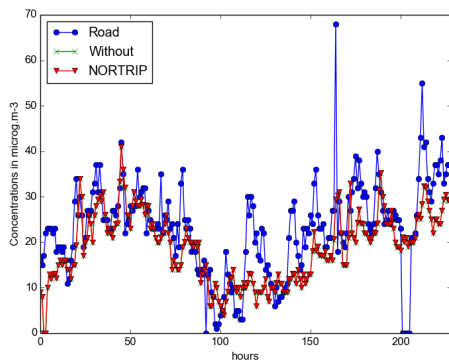


(a) MOCOPo, last 10 days of September 2011

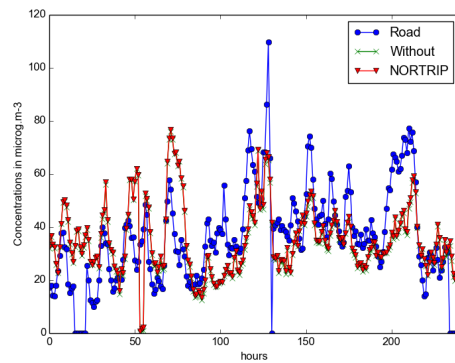


(b) Trafipollu, from April to June 2014

Figure 6: Modeled concentrations using HERMES resuspension and gaussian plume for light wind situations /or MUNICH simulations (red), observed concentrations near road (blue) and without resuspension (green)



(a) MOCOPo, last 10 days of September 2011



(b) Trafipollu, from April to June 2014

Figure 7: Modeled concentrations using NORTRIP resuspension and gaussian plume for light wind situations /or MUNICH simulations (red), observed concentrations near road (blue) and without resuspension (green)

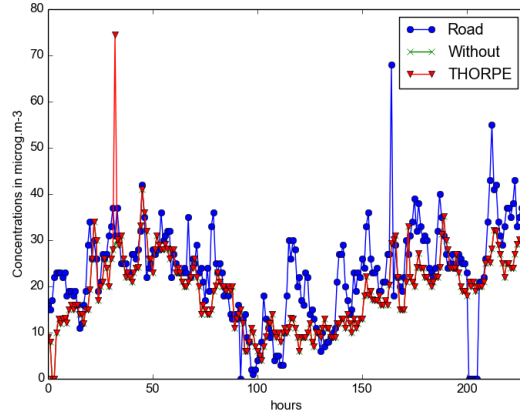


Figure 8: Modeled concentrations using THORPE resuspension and gaussian plume for light wind situations, observed concentrations near road (blue) and without resuspension (green)

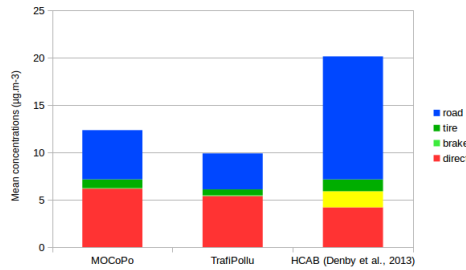


Figure 9: Modeled concentrations using NORTRIP factors at Echirolles freeway 14/09-29/09/2011 (left), Alsace-Lorraine Boulevard 26/03/2014-16/06/2014 (middle) and HCAB 2007-2008 from Denby et al., 2011 (right)

4 Discussion

The total mass of the pollutant emitted during combustion of the fuel mass is defined to be emission factors of traffic pollutants. Basically, emission factors are measured during laboratory tests conducted on dynamometers for exhaust emissions from vehicles. For non-exhaust emissions, empirical emission factors are used. Regarding resuspension, HERMES uses default empirical emission factors, whereas NORTRIP calculates emission factors based on the empirical direct emission factors for brake, tire and road wear, and assumptions on the fraction being resuspended. Therefore, for resuspension, as it is complicated to describe all types of vehicles, fuels, driving behavior, mean representative samples are defined to represent the two vehicles category chosen in this study (light-duty/passenger and heavy-duty vehicles). For this reason, emission factors applied here - beyond uncertainty of measurement - generate another uncertainty due to this impossibility to describe in details all the MOCOPo and Trafipollu fleets. In the literature, many values of emission factors are available. To test our implementation of both resuspension models, values given in the original model articles (Pay et al., 2011; Denby et al., 2013 for abrasion rates) were retained for our numerical modeling (see Table 7). Pay et al., (2011) summarize empirical emission factors from various field campaigns at different locations and road types in central and western Europe. For instance, for light-duty and passenger cars, in the UK emission factors are lower ($14-23 \text{ mg.km}^{-1}.\text{veh}^{-1}$, Thorpe et al., 2007) compared then to those in Germany ($57-67 \text{ mg.km}^{-1}.\text{veh}^{-1}$, Ketzler et al., 2007) or Switzerland ($17-92 \text{ mg.km}^{-1}.\text{veh}^{-1}$, Gehrig et al., 2004). They are higher in Scandinavian countries, probably due to sanding ($121-198 \text{ mg.km}^{-1}.\text{veh}^{-1}$, Ketzler et al., 2007) and in the United States ($63-780$

$mg.km^{-1}.veh^{-1}$, Abul-Allaban et al., 2003). Pay et al. (2011) also mentioned that emission factors applied for Spain are deliberately higher than those for central Europe because there is a higher amount of mineral dust particles in Spain due to climatic conditions (Pataud et al., 2004; Querol et al., 2004). This bias may not be necessarily well adapted to our geographical situation, thus it could be interesting to test other emission factors.

For the Thorpe et al. (2007) method, empirical emission factors were used to obtain the resuspension rate by subtracting brake, tire, and road wear from the estimated coarse PM emission factor deduced from the near-road measurements. Those empirical factors were updated from the last EMEP/CORINAIR emission factors as detailed in EEA (2013). Emission factors from the EMEP/EEA emission inventory guidebook 2013 are calculated based on the Tier 3 method (actually Copert 4), assuming a typical EU-15 fleet and activity data for 1995 in order to be applicable to countries with older vehicle fleets.

In NORTRIP, wear factors based on empirical/simulated standard factors are adjusted with observed speeds (see Equations 29, 30 and 31). Standard wear factors used for the numerical application from Denby et al., (2013) could be compared to wear factors modeled and derived from the EMEP/CORINAIR emission factors as detailed in EEA (2013). Thus, brake and tire wears used in NORTRIP are retrieved from Boulter et al., (2005) and they are about half the EMEP factors for light-duty vehicles, but similar for heavy-duty vehicles. As light-duty vehicles contribute the most to resuspension, this difference could generate an underestimation of tire and brake origin wear using NORTRIP. On the contrary, the road factors from the Swedish road wear model (Jacobson and Wadberg, 2007) used in this model is within a factor of two compared to the EMEP inventory. This leads to a greater contribution of road wear in PM_{10} suspension. The NORTRIP emissions can be converted to traffic fleet-average emission factors by dividing the values by the total number of light-duty, passenger and heavy-duty vehicles. We obtain respectively for light-duty, passenger and heavy-duty vehicles, 80 and $117 mg.km^{-1}.veh^{-1}$ for MOCOPo. This is consistent with the HERMES emissions factors for light-duty vehicles and it is within a factor of two for heavy-duty vehicles.

However, emissions factors alone do not explain why there is such variability in the simulated resuspension emissions,. Indeed, resuspension is also controlled by traffic parameters such as flow and speed. In our case studies, speed and flow are much higher on the MOCOPo Grenoble freeway than on the Trafipollu Paris suburb boulevard. The differences are a factor of two for total mean speed and a factor of five for total mean flow. However, there is some uncertainty in traffic data. First, tools used to estimate the fleet and the speed are based on videos and electromagnetic loops, respectively and such measurements include uncertainties (see discussion by Fallah Shorshani et al, 2015 regarding MOCOPo traffic data). We estimate that traffic data have 30% uncertainty. Second, in Trafipollu, we used only two traffic day types instead of using a real database describing hourly traffic for the full three-month period.

Furthermore, in the case of NORTRIP, the length of the dry period between rain events controls the mass loading on the road and, therefore, the final resuspension emission rate. In the NORTRIP version applied here, we considered that there is no resuspension once it rains. Particles are assumed to be washed away from the pavement by rain or totally retained by moisture on the surface. However, the traffic could be very intense and some resuspension could occur. Another source of uncertainty is the meteorological simulation (conducted only for Trafipollu). Indeed, some difficulty to simulate properly rainfall events precisely have been reported by WRF users.

In the Thorpe et al., method, some constraints are introduced to limit the applicability of the method. First, negative values of the deltas between the near-road and the background are not considered. Second, the ratio of delta PM_{10} between the near-road and the background over delta NO_x between the near-road and the background should not exceed 0.1. Third, the ratio of delta $PM_{2.5}$ between the near-road and the background over delta PM_{10} between the near-road and the background, should be about equal to 0.4 and be fairly constant according to Thorpe et al. (2007) based on values quoted in the literature (Harrison et al., 2001; AQEG, 2005; Charron and Harrison, 2005). In our case study, this ratio is not constant and we applied a threshold value condition to address the first constraint. Furthermore, as done in Thorpe et al. (2007), we also omitted negative values of the estimated resuspension rate. As a result, 85% and 90% of the MOCOPo and Trafipollu values are removed from our analysis.

Conclusion

In 2011, a two-week measurement campaign was conducted near a freeway in Grenoble. Despite a predominantly upwind monitoring site location and mostly calm wind conditions, concentration values were sampled near the roadway than at the background site. According to this set of observations, the results did not allow us to highlight any clear relationship with traffic data - mainly due to a strong dependency on background contributions that tends to hide local effects. In 2014, a three-month measurement campaign was conducted on a boulevard in a Paris suburb. Concentrations simulated with resuspension emissions lead to an improvement in the correlation coefficient, but some overestimation also occurred in our simulation.

A review of current methodologies to model or estimate from available measurements resuspension emissions has allowed us to clarify the relationships between resuspension rates and traffic parameters. Three approaches were applied: two deterministic models, HERMES and NORTRIP, and one empirical method (Thorpe et al.). HERMES depends mainly on traffic flow and emission factors. This method is highly operational and easily workable. NORTRIP is more detailed, as it takes into account many factors such as traffic flow and speed, but also the pavement type. Consequently, it is more complex to apply. For example, rainfall events have to be known with accuracy to apply NORTRIP because they determine the length of the dry periods during which the PM load on the road surface (a major input for the calculation of the resuspension rate) can accumulate. The empirical method of Thorpe et al. is based on PM and NO_x emission factors and on concentration measurements. The fraction between $PM_{2.5}$ and PM_{10} is assumed to be due to resuspension as well as direct emissions from brake, tire and road wear. It can only be applied if such ambient measurements are available; therefore it is mostly a diagnostic tool rather than an operational model.

The traffic fleet characteristics and the associated impact on simulated local concentrations have been assessed by discriminating our calculations according to vehicles types (light-duty/passenger vehicles or heavy-duty vehicles). In both case studies, the traffic fleet was dominated (> 95%) by light-duty/passenger vehicles, which in spite of their lower resuspension of road dust PM than heavy-duty vehicles, lead to more resuspension of particles due to their greater numbers.

Resuspension is a process that mixes a lot of PM origins. The quantification of resuspension is a challenging point because it cannot be validated with observations. Therefore, it is impossible at this point to say which is the best formulation. Thus, an intercomparison and a comparison between simulated concentrations obtained with and without integrating resuspension emissions are currently the best possible way to check which model contributes the most to the concentration simulation performance. NORTRIP, due to its level of details in its formulation should be the preferred model, however, uncertainties in the input data may alter the accuracy of the final results. HERMES has shown encouraging results despite its simpler formulation.

A problem encountered in resuspension investigation is the difficulty to discriminate among different factors affecting it. It is even more difficult if we add the fact that dust collected on the road surface comes from a wide range of sources, not just from vehicles but also from vegetation and nearby sources such as industrial and domestic activities. A review of the literature highlights some studies on the estimation of road pollutants such as brake dust, tire wear and resuspension of non-exhaust traffic particles derived from atmospheric measurements. For instance, Harrison et al. (2012) have shown that the combined use of size distribution information and tracer elements allowed one to separate estimation of the contribution of brake and tire PM and resuspension to particle mass in a the range 0.9-11.5 μm aerodynamic diameter and their mean contributions. This kind of estimation could be complementary to the study of chemical profiles that has been done with PMF (Polo, 2013). It also points out that the definition of resuspension is difficult to characterize as brake and tire particles have both direct and indirect (resuspended) components that are difficult to clearly separate. Furthermore, more work is needed to evaluate the traffic effect on near-road concentrations via processes such as vehicle-induced turbulence. Clearly, the effect of rain and associated moisture needs to be investigated further. Finally, the influence of particles of size larger than 10 μm is of interest for water quality assessment and their resuspension should be investigated.

Acknowledgement

This work was supported by the French National Research Agency (ANR) as part of the Trafipollu project.

References

- Amato F., Cassee F. R., Denier van der Gon H. A. C., Gehrig R., Gustafsson M., Hafner W., Harrison R. M., Jozwicka M., Kelly F. J., Moreno T., Prevot A. S. H., Schaap M., Sunyer J., Querol X. 2014. *Journal of Hazardous Materials* 275. 31-36.
- Boulter P.G. 2013. A Review of Emission Factors and Models for Road Vehicle Non-exhaust Particulate Matter. TRL Limited, Wokingham, UK. (TRL Report PPR065). *Atmospheric Environment*. 77. 283-300.
- Briant R., Korsakissok I. and Seigneur C. 2011. An improved line source model for air pollutant dispersion from roadway traffic. *Atmospheric Environment* 45. 4099-4107.
- Briant, R., Seigneur C., Gadrat M., Bugajny C. 2013. Evaluation of roadway Gaussian plume models with large-scale measurements campaigns. *Geoscientific Model Development* 6. 445-446.
- Cirillo M.C., Poli A. A. 1992. An iter comaprison of semi empirical diffusion models under low wind speed, stable conditions. *Atmospheric Environment* 26A. 765-774.
- Denby B.R., Sundvor I., Johansson C., Pirjola L., Ketzler M., Norman M., Kupiainen K., Gustafsson M., Blomqvist G., Omstedt G. 2013. A coupled road dust and surface moisture model to predict non-exhaust road traffic induced particle emissions (NORTRIP). Part 1: Road dust loading and suspension modelling. *Atmospheric Environment* 77. 283-300.
- Gehrig R., Hill M., Buchmann B., Imhof D., Weingartner E., Baltensperger U. 2004. Separate determination of PM10 emission factors of road traffic for tailpipe emissions and emissions from abrasion and resuspension processes. *International Journal of Environment and Pollution (IJEP)*, Vol. 22, No. 3.
- Gustafsson M., Blomqvist G., Gudmundsson A., Dahl A., Jonsson P., Swietlicki E. 2008. Factors affecting PM10 emissions from road pavement wear. *Atmospheric Environment* 43. 4699-4702.
- Harrison R. M., Jones A. M., Lawrence R. G. 2005. Major component composition of PM10 and PM2.5 from roadside and urban background sites. *Atmospheric Environment* 38. 4531-4538.
- Jacobson T., Wagberg L.G. 2007. The Swedish National Road and Transport Research Institute, Linköping. (VTI notat 7-2007)(in Swedish).
- Ketzela M., Omstedt G., Johansson C., During I., Pohjola M., Oettlg D., Gidhagen L., Wahlina P., Lohmeyere A., Haakanaf M., Berkowicza R. 2007. Estimation and validation of PM2.5/PM10 exhaust and non-exhaust emission factors for practical street pollution modelling. *Atmospheric Environment* 40. 9370-9385.

- Mollinger A. M., Nieuwstadt F. T. M., Scarlett B. 2007. Model Experiments of the Resuspension Caused by Road Traffics. *Aerosol Science and Technology* 9:3. 330-338.
- Pay M., Jimenez-Guerrero P., Baldano J. M. 2011. Implementation of resuspension from paved roads for the improvement of CALIOPE air quality system in Spain. *Atmospheric Environment* 45. 802-807.
- Rehn L. P. 2013. Caractérisation et impacts des émissions de polluants du transport routier : Apports méthodologiques et cas d'études en Rhone Alpes. Doctoral Thesis. Université de Grenoble.
- Salizzoni P., Soulhac L., Mejean P., Perkins R. 2009a. Street canyon ventilation and atmospheric turbulence. *Atmospheric Environment* 43. 5056-5067.
- Shorshani M. F., André M., Bonhomme C., Seigneur C. 2015. Modelling chain for the effect of road traffic on air and water quality: Techniques, current status and future prospects. *Environmental Modelling and Software* 64. 102-123.
- Snilsberg B. 2008. The influence of driving speed and tires in road dust properties. Doctoral Thesis. Norwegian University of Science and Technology, Trondheim.
- Soulhac L., Salizzoni P., Cierco. F-X. Perkins R. 2011. The model SIRANE for atmospheric urban pollutant dispersion; part I, presentation of the model. *Atmospheric Environment* 45. 7379-7395.
- Thorpe A. J., Harrison R.M, Boutler P. G., McCrae I. S. 2007. Estimation of particle resuspension source strength on a major London Road. *Atmospheric Environment*. 41. 8007-8020.
- Venkatram A., Snyder M., Isakov V. Modeling the impact of roadway emissions in light wind, stable and transition conditions. *Transportation Res. D*, 24, 110-119.

Modeling the effect on air quality of Euro 6 emission factor scenarios

Nicola TOENGES-SCHULLER*, Christiane SCHNEIDER*, Arnold NIEDERAU*, Rainer VOGT**, Stefan HAUSBERGER***

* AVISO GmbH, Am Hasselholz 15, 52074 Aachen, Germany
Fax +49 241 470358-9 - email: nicola.toenges-schuller@avisogmbh.de

** Ford Research & Innovation Center, Süsterfeldstrasse 200, 52072 Aachen, Germany

*** Institut für Verbrennungskraftmaschinen und Thermodynamik, TU Graz, Inffeldgasse 19/I, 8010 Graz, Austria

Abstract

To reduce traffic emissions effectively, from September 2017, newly registered cars will have to prove compliance with emission standards on public roads. RDE (real driving emissions) limits will be introduced in two steps. Conformity factors (CF) are introduced to link RDE with laboratory limits. In this study, the effect of several emission factor scenarios on air quality was modeled. Conformity factors were varied between $CF=1.6$ and $CF=3.3$ in step 1 and between 1.2 and 1.8 in step 2. Road traffic emissions and NO_2 concentrations were modeled for three urban main roads in Germany ("Am Neckartor" (Stuttgart, severe limit exceedance of annual mean NO_2 in 2015), "Corneliusstraße" (Düsseldorf, average limit exceedance 2015), "Dachauer Straße" (Munich, compliance with the limit 2015)) for the years 2015, 2020, 2025, and 2030 for each scenario. The results were extrapolated to all German traffic-influenced air quality measurement stations. Depending on scenario, the fraction of traffic-influenced stations exceeding the air quality limit for annual mean NO_2 is expected to be reduced from about 50% in 2015 to 23% up to 28% in 2020, 7% up to 10% in 2025, and 1% up to 4% in 2030.

Abstract French

Pour réduire efficacement les émissions de la circulation les véhicules nouvellement immatriculés devront prouver (à partir de Septembre 2017) la conformité aux normes d'émissions sur les routes publiques. Limites RDE (émissions réelles de conduire) seront introduites en deux étapes. Facteurs de conformité (FC) sont introduits pour relier RDE avec des limites de laboratoire. Dans cette investigation, nous avons modélisé l'effet de plusieurs scénarios de facteurs d'émission sur la qualité de l'air. Les facteurs de conformité ont été variés entre $CF = 1,6$ et $CF = 3,3$ à l'étape 1 et entre 1,2 et 1,8 à l'étape 2. Les émissions de la circulation routière et les concentrations de NO_2 ont été modélisées pour trois routes principales urbaines en Allemagne ("Am Neckartor" (Stuttgart, dépassement gravement la limite de NO_2 en moyenne annuelle en 2015), "Corneliusstraße" (Düsseldorf, dépassement des limites 2015), "Dachauer Straße" (Munich, dans la limite en 2015)) pour les années 2015, 2020, 2025, et 2030 pour chaque scénario. Les résultats ont été extrapolés aux toutes les stations allemandes de mesure de la qualité de l'air influés sur le trafic. Selon le scénario, la fraction des stations dépassant la limite de la qualité de l'air pour le NO_2 annuelle moyenne devrait être réduite d'environ 50% en 2015 à 23% jusqu'à 28% en 2020, 7% à 10% en 2025, et 1% jusqu'à 4% en 2030.

Keywords: NO_x emission factors, Euro 6, real driving emissions, air quality.

Keywords French: Les facteurs d'émission de NO_x , Euro 6, les émissions réelles de conduire, qualité de l'air.

Introduction

The EU air quality limit for the annual mean value of NO_2 was exceeded at many air quality measurement stations all over Europe in recent years. In Germany, about 50% of all traffic-influenced air quality stations did not comply with the limit in 2015. Source apportionment analyses show that road traffic emissions are the main contributor to NO_2 concentrations at these stations; see

e.g. the air quality plan for Stuttgart (2012). In spite of increasingly stringent emission standards for NO_x , road traffic emissions were not reduced accordingly. Until now, compliance with emission limits is tested in laboratories on roller dynamometer test benches. Motor emissions are measured while vehicles perform a given driving cycle under well defined conditions. For passenger cars (PC), the New European Driving Cycle (NEDC), last updated in 1997, is used. Measurements of real world emissions e.g. by Ligterink et al. (2012) showed that, especially for Euro 5 diesel PC, real world NO_x emissions are much higher than emissions on NEDC. As a consequence, according to ERMES (European Research Group on Mobile Emission Sources), NO_x emission factors for Euro 5 diesel PC in the current versions of models such as COPERT (Computer Programme to calculate Emissions from Road Transport), HBEFA (Handbook of Emission Factors), or VERSIT+ (Traffic Situation model), which are used for air quality modeling, are about 4-5 times higher than the emission limit values (ERMES, 2015). Measurements e.g. by Franco et al. (2014) or by Kadijk et al. (2015) showed that real world NO_x emissions are much higher than emissions on NEDC also for Euro 6 diesel PC.

To ensure that emission reductions are achieved in real world, from September 2017 on, newly registered cars will have to prove compliance with emission standards on public roads (RDE, real driving emissions).

RDE limits will be introduced in two steps, step 1 starting from September 2017, and step 2 starting from January 2020. Conformity factors (CF) are introduced to link RDE with laboratory limits. At the meeting of the Technical Committee on Motor Vehicles (TCMV) of the EU on 28/10/2015 in Brussels, the following values were given a positive vote (TCMV, 2015):

- Step 1: $\text{CF}(\text{NO}_x)=2.1$ from September 2017/2019 (new type approvals/all firstly registered vehicles)
- Step 2: $\text{CF}=1.0(\text{NO}_x)$ from January 2020/2021 (new type approvals/all firstly registered vehicles)
- A measurement tolerance for NO_x of 0.5 for step 2 is allowed but subject to an annual review.

In the following paper, the effect of several emissions factor scenarios on air quality was examined; the proceeding for each scenario was the following:

1. Scenario definition: A scenario consists of values for conformity factors, the dates of their coming into effect, and, depending on scenario, the definition of a transfer function.
2. Calculation of emission factors
3. Emission modeling: Calculation of road traffic emissions for three urban main roads ("Am Neckartor" in Stuttgart, "Corneliusstraße" in Düsseldorf, and "Dachauer Straße" in Munich) in Germany for the years 2015, 2020, 2025, and 2030
4. Air quality modeling: Calculation of annual average NO_2 for the three roads and the four years
5. Extrapolation of the results to all traffic-influenced air quality stations in Germany

By this, for each scenario, we determined the number of traffic-influenced air quality stations in Germany which, from today's point of view, are expected to exceed the limit value for annual average NO_2 in the years 2020, 2025, and 2030.

1. Methods

Scenarios

Altogether, ten scenarios were investigated. From these scenarios, six scenarios, as defined in Table 1, are presented in this paper.

In scenario A, the base case, emission factors were taken from HBEFA3.2 (HBEFA, 2014). When HBEFA3.2 was released in 2014, it was known that the type approval procedure for EU 6 PC would be changed in 2017, although details were not fixed yet at the time. So, in HBEFA3.2, there are emission factors for EU 6 (type approval/first registration before 2017/2018) and EU 6c (type approval/first registration after 2017/2018). From today's point of view, emission factors for EU 6 diesel PC are too low in HBEFA3.2 (ERMES, 2015), so in scenario B, these emission factors are increased by 90%.

Table 1: Scenario definition

scenario	base	description	step 1		step 2		transfer function
			CF	date	CF	date	
A	HBEFA3.2	base case					
B	HBEFA3.2	EU 6 diesel PC +90% EU 6c unchanged					
E	B	EU 6 RDE scenario	3.0	Sep 2017	1.5	Sep 2019	no
F	B	EU 6 RDE scenario	3.3	Sep 2017	1.8	Sep 2019	yes
H	B	EU 6 RDE scenario	1.6	Sep 2017	1.2	Sep 2019	no
I	B	EU 6 RDE scenario, TCMV voted	2.1	Sep 2017	1.5	Jan 2020	no

Scenarios E, F, H, and I are RDE scenarios based on scenario B with varying CF. Resulting emission factors for Euro 6 RDE were used instead of HBEFA3.2 emission factors EU 6c. In these scenarios, EU 6 RDE step 1 comes into effect in September 2017 and step 2 in September 2019 (type approval). An exception is scenario I, where step 2 comes into effect in January 2020 (type approval). Thus, scenario I is conform to the values voted for by TCMV (2015).

The resulting phase-in into the fleet is shown in Table 2. The second column shows the phase-in of EU 6c PC according to the current average fleet in Germany according to TREMOD, prepared by ifeu (Institut für Energie- und Umweltforschung Heidelberg GmbH). In line with HBEFA3.2, EU 6c is introduced in one step. The third and fourth column show the phase-in of EU 6 RDE PC, step 1, and step 2, into the fleet as used for scenario E, F, and H. As stated above, in scenario I, step 2 comes into effect four months later.

Table 2: Phase-in of PC: EU 6c according to TREMOD, prepared by ifeu (Institut für Energie- und Umweltforschung Heidelberg GmbH), and two-step introduction as used in scenario E, F, and H

	EU 6c, TREMOD (ifeu)	EU 6 RDE, step 1	EU 6 RDE, step 2
2016	0%	0%	0%
2017	10%	10%	0%
2018	25%	25%	0%
2019	100%	90%	10%
2020	100%	75%	25%
2021	100%	0%	100%
2022	100%	0%	100%

Emission Factors

Emission factors for all chemical compounds needed for air quality modeling (NO_x, NO₂, SO₂, CO, VOC, NH₃, N₂O and CO₂) were taken from HBEFA3.2. Modifications for the emission factors for EU 6 and EU 6 RDE diesel PC were done for scenario B to I.

In all scenarios only the NO_x emission factors were changed compared to scenario A. In reality the exhaust gas recirculation (EGR) for NO_x control is expected to be extended with the RDE demands. This would tend to increase CO and HC emissions. These effects are expected to be quite small on absolute emission levels and were thus not considered to keep the simulation system simple.

While all emission factors for the scenarios A and B have been simulated with the model PHEM for the HBEFA (Rexeis, 2013), the emission factors for urban driving for the vehicles to be type approved under the future RDE legislation were calculated with a different method. Main assumption was that the low real drive emission limit values to be met will need sophisticated control algorithms for engine and after treatment systems. Consequently the controllers were assumed to be tuned to meet the RDE limits (= emission limit x CF) in all driving situations covered by the future legislation with the same safety margin. The safety margin for new vehicles was 0.90 mainly to take aging effects of catalysts into consideration. For the fleet average emission values aged catalysts were assumed, so that the fleet average margin is 0.95.

Without transfer function (TF) the emission factors per vehicle emission class are thus similar for all driving conditions:

Equation 1: $\text{NO}_x \text{ Emission Factor [mg/km]} = \text{CF} * \text{Limit} * 0.95 = \text{CF} * 76 \text{ mg/km}$ for passenger cars

The TF is discussed to be introduced in the RDE legislation to allow somewhat higher emissions under severe driving conditions. The TF shall be overall “environmentally neutral”. This means that higher emissions at severe conditions have to be compensated by lower emissions under mild driving conditions. Since the details of the TF are still under discussion, a worst case scenario for the TF was assumed to show maximum effects under urban driving conditions. The worst case approach assumed that additional emissions are allowed under severe urban driving conditions but the compensation would not be relevant for those driving situations used in the scenarios. Consequently emission factors are in the scenarios F to I for all urban traffic situations 0.95 times the maximum allowed value (Figure 1).

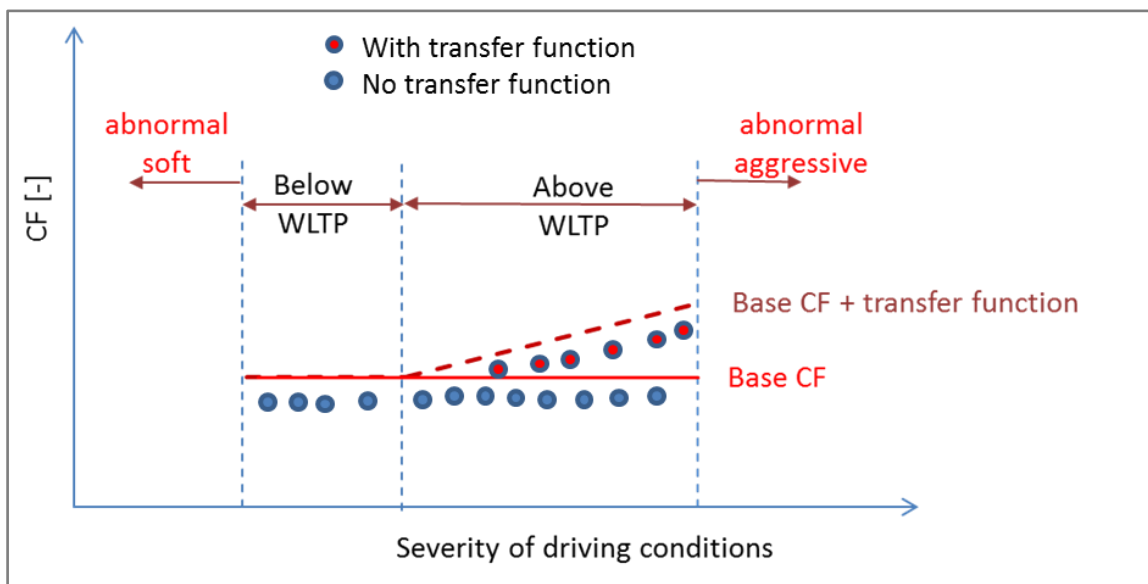


Figure 1: Schematic picture of the emission factor definition with and without transfer function for vehicles type approved under the future RDE legislation

For the scenario with TF the allowance for higher NO_x emissions under increasing dynamic driving behavior (“aggressive driving”) and under increasing cumulative altitude gain was assumed as shown in Figure 2. The allowance for higher NO_x emissions was introduced in the emission factor calculation by adding a ΔCF as function of the dynamic parameter of the driving cycle (95 Percentile of velocity x positive acceleration) and as function of the positive altitude gain. For a combination of very aggressive driving under hilly conditions the maximum CF increase due to the TF was assumed to be limited with +1.0. This gives e.g. in scenario F for stage 2 vehicles CFs between 1.8 (low dynamics, flat road) and 2.8 (aggressive driving, very hilly). For each driving cycle representing urban traffic situations in the HBEFA the corresponding adjustment of the CF by the TF was computed. After adjustment of the CFs for each traffic situation the emission factors were calculated using Equation 1. The emission factors were produced for all passenger car categories from HBEFA depending on vehicle type, motor concept, and traffic situation for all traffic situations. Emission values from HDV were not changed against scenario A.

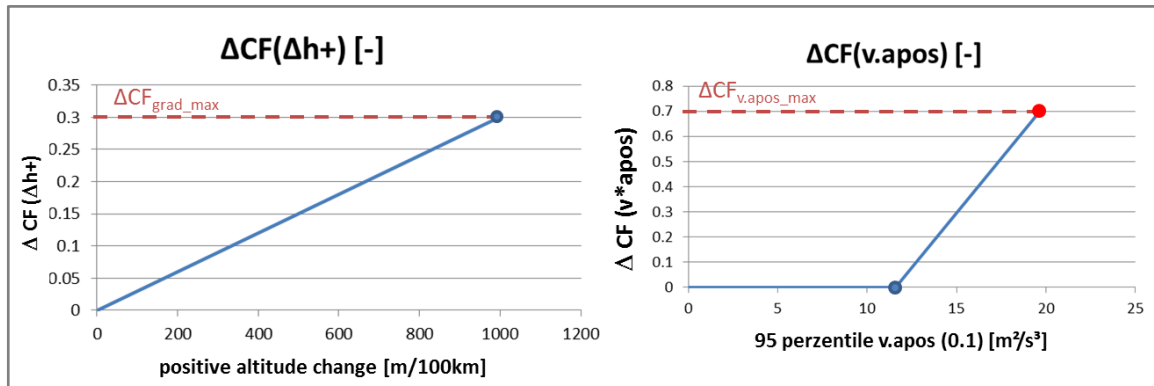


Figure 2: Schematic picture of the transfer functions assumed for positive altitude gains and for driving dynamics for vehicles type approved under the future RDE legislation

Road Traffic Emissions

Specific traffic emissions (pollutant per distance and time unit) for the three urban main roads were calculated as the product of emission factors (pollutant per vehicle and distance, depending on vehicle type, motor concept, and traffic situation) and the traffic volume (vehicles per time unit), weighted by fleet composition. The traffic volume, the fraction of light duty vehicles (LDV, commercial vehicles of permissible maximum weight ≤ 3.5 t), and the fraction of heavy duty vehicles (vehicles of permissible maximum weight > 3.5 t) for the three streets is shown in Table 3. The rest of the vehicles are assumed to be PC.

Table 3: Traffic volume, fraction of light duty vehicles (LDV, commercial vehicles of permissible maximum weight ≤ 3.5 t), and fraction of heavy duty vehicles (vehicles of permissible maximum weight > 3.5 t) at the considered streets

Street	Traffic Volume [veh./24h]	Fraction LDV	Fraction HDV
Corneliusstraße (Düsseldorf)	43.700	3.8 %	1.3 %
Am Neckartor (Stuttgart)	73.500	3.2 %	2.9 %
Dachauerstraße (Munich)	21.600	3.0 %	4.2 %

The traffic situation is derived from street type, speed limit, and hourly values of traffic volume.

The fleet composition, differentiated by energy type and Euronorm concept per vehicle group, is based on the current average fleet in Germany according to TREMOD, prepared by ifeu (Institut für Energie- und Umweltforschung Heidelberg GmbH). For passenger cars, local fleet compositions were considered, taking into account the deviations of local car registration data per Euronorm from German average car registration data. Also, existing low emission zones in Stuttgart and Düsseldorf were taken into account. The resulting PC fleet composition for scenario E, F, and H are shown in Figure 3.

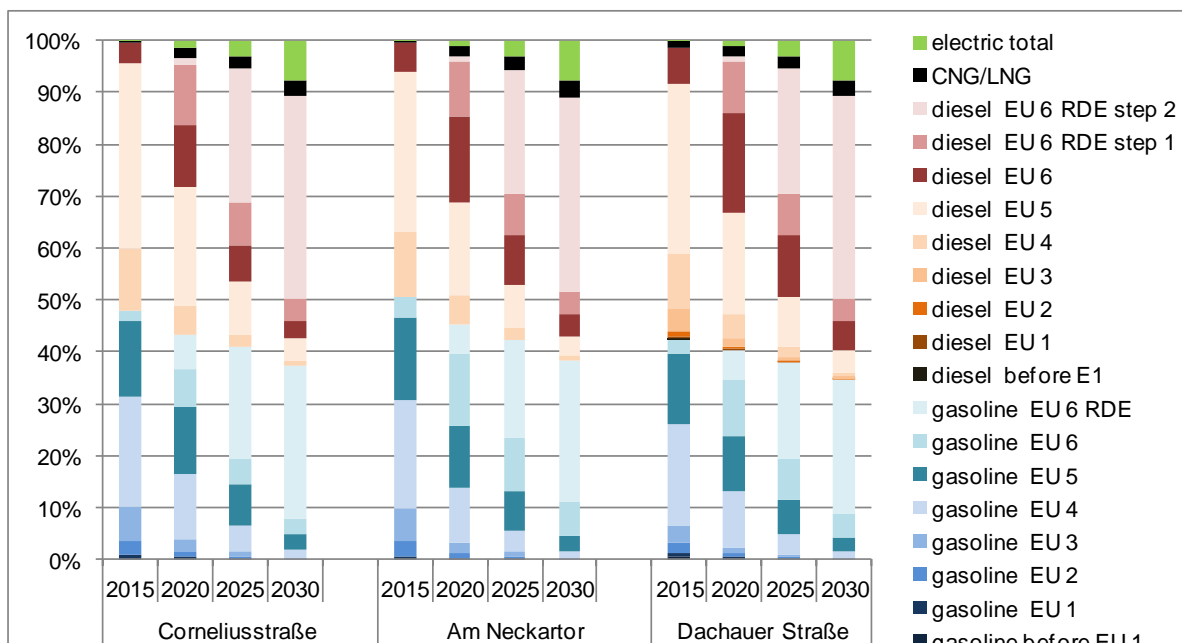


Figure 3: Local composition of the PC fleet in Düsseldorf, Stuttgart, and Munich for scenario E, F, and H

Air quality

Corneliusstraße, “Am Neckartor”, and Dachauer Straße are all street canyons with high building density on both sides of the road. Thus, air quality modeling can be done with a box model: Gas-phase concentrations of pollutants are calculated for the street canyon, which is modeled as a box of infinite length, the width of the street, and the height of roadside buildings, and assumed to be homogeneously mixed. Concentrations in the box correspond to the concentrations typically measured by an air quality station at the kerbside.

The chemistry box model comprises gas-phase chemistry and one-dimensional transport (perpendicular to street). The RADM2 gas-phase chemistry mechanism with 56 species, 140 thermochemical reactions, and 21 photochemical reactions (Stockwell et al., 1990) in combination with the solver of the EURAD-model (Memmesheimer et al., 2007) is used. Not considered are turbulent diffusion, deposition, a variable mixing height, and heterogeneous reactions. As input parameters, urban background concentrations of NO₂, NO and ozone, roadside concentrations of NO and NO₂ (for calibration), wind speed and direction and global radiation, and traffic emissions in the street are needed in an hourly resolution. Background concentrations were taken from air quality measurement stations of the urban background nearby, the trend of the background was taken from UBA (2014).

This box model was already used in the past to simulate NO₂ (Vogt et al., 2010, and Kessler et al., 2010) and particle number (Toenges-Schuller et al., 2013, 2015) in street canyons.

As by Vogt et al. (2010) and Kessler et al. (2010), the box model was calibrated for the year 2006. For this project, it was refitted to the year 2014.

2. Results

Emission Factors

Weighted emission factors for the three considered urban main roads resulting from the scenario definitions in Table 1 are shown in Figure 4. The upper four groups show weighted emission factors according to HBEFA3.2 for EU 5, EU 6 and EU 6c PC (diesel and gasoline). Scenario A is based on these factors. They were derived by weighting the factors for the appropriate traffic situation from HBEFA3.2 with the mileage shares per level of service for the three streets.

According to HBEFA3.2, emission factors for diesel PC cars are reduced by about 2/3 from EU 5 to EU 6, and again by nearly 1/2 from EU 6 to EU 6c. For gasoline PC, according to HBEFA3.2, emission factors for EU 5, EU 6 and EU 6c are the same. They are about a factor of 20 lower than for EU 5 diesel PC.

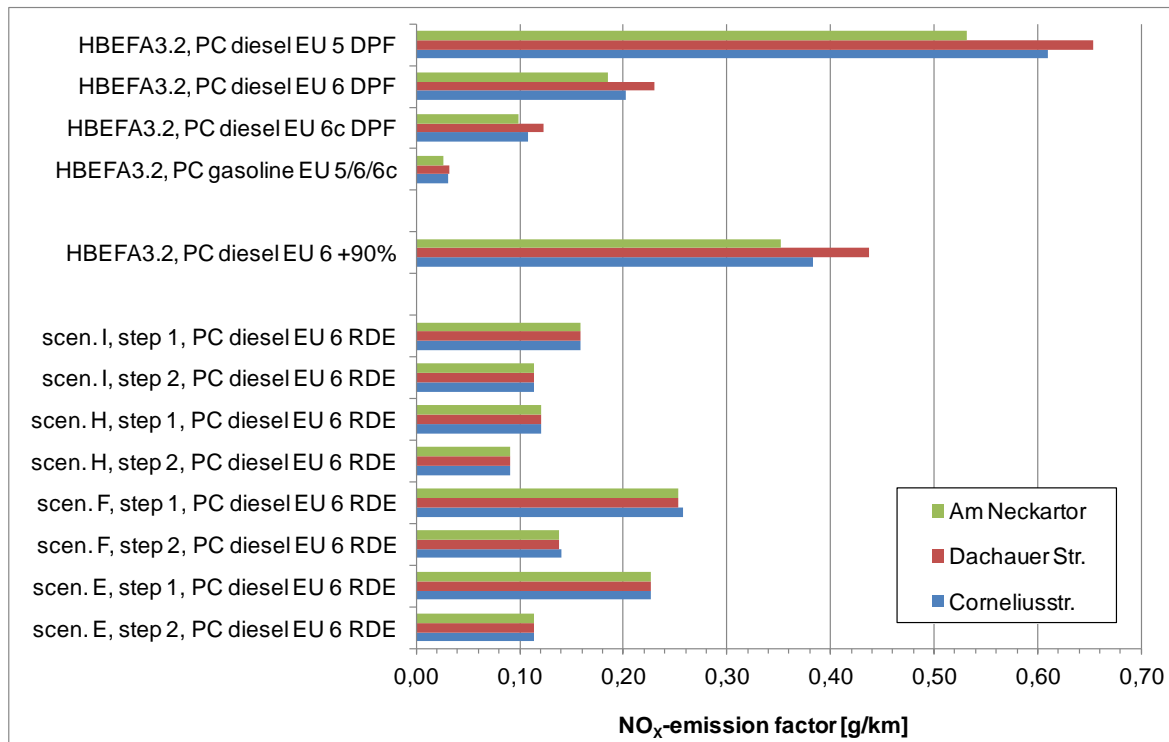


Figure 4: PC emission factors weighted with mileage per level of service for three urban main roads (“Am Neckartor” in Stuttgart, Dachauer Straße in Munich and Corneliusstraße in Düsseldorf)

Below the upper four groups of emission factors based on HBEFA3.2, in Figure 4, one group shows HBEFA3.2 weighted emission factors for EU 6 diesel PC increased by 90% (scenario B). As stated above, from today’s point of view, this is more realistic than scenario A.

The lowest eight groups of weighted emission factors in Figure 4 were derived from the RDE scenarios. Due to the limitations considered, they are the same for the three streets. An exception is scenario F, where a transfer function was applied. However, the differences between the streets are small. As expected (see CF in Table 1), PC diesel EU 6 RDE emission factors are highest in scenario F and lowest in scenario H.

Emissions

For each hour of the year, emissions were calculated as the product of emission factors, depending on traffic situation and fleet composition, and traffic volume. In Figure 5, NO_x-emissions for the three streets are shown for scenario B and the years 2010, 2015, 2020, 2025 and 2030.

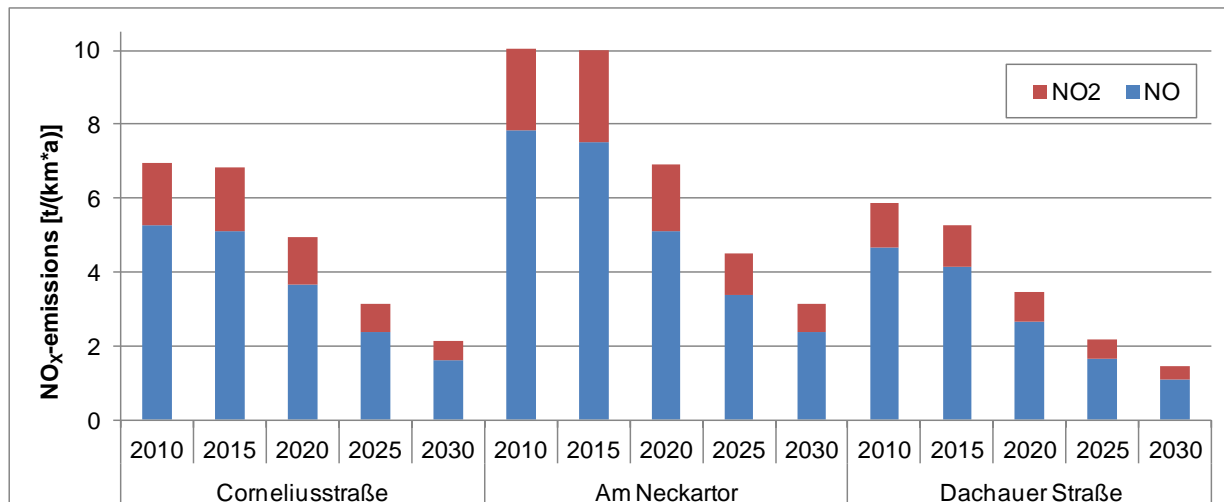


Figure 5: NO_x-emissions (total column, shown as sum of NO (blue column, NO as NO₂) and NO₂ (red column)) for scenario B

At “Am Neckartor”, where traffic volume is highest (see Table 3), also NO_x-emissions are highest, and at Dachauer Straße, NO_x-emissions are lowest. However, due to the higher fraction of heavy duty vehicles, at Dachauer Straße, NO_x-emissions are only slightly lower than at Corneliusstraße. Also, unlike at Corneliusstraße and “Am Neckartor”, there is no low emission zone at Dachauer Straße.

Due to the increasing fraction of vehicles with higher emission standards in the fleet, emissions are expected to reduce considerably until 2030. However, only little emission reduction can be seen between 2010 and 2015, especially for “Am Neckartor” and “Corneliusstraße”. This is a consequence of the fact that, despite lower emission limits, EU 5 diesel NO_x-emissions in real life are not reduced compared to EU 4 NO_x-emissions. The fraction of directly emitted NO₂ (red column) even slightly increases between 2010 and 2015.

In Figure 6, for Corneliusstraße, NO_x-emissions are shown for all scenarios and the years 2010, 2015, 2020, 2025 and 2030. The colors show the contributions of the different vehicle types, for PC, also the contributions of the different motor concepts are shown.

In Figure 7, the same development is shown for NO₂.

In Figure 8, the changes in NO_x-emissions are shown with respect to scenario A (2015) and scenario A (same year, respectively).

In all years, NO_x-emissions are expected to be higher than in scenario A in most scenarios (between 4% and 19%). Due to the stringent conformity factor in scenario H in step 2 (CF=1.2, see Table 1), in 2030, NO_x-emissions in scenario H are expected to be slightly lower than in scenario A.

Compared to 2015, NO_x-emission reductions are expected between 23% and 32% in 2020, between 49% and 56% in 2025, and between 64% and 70% in 2030, depending on scenario.

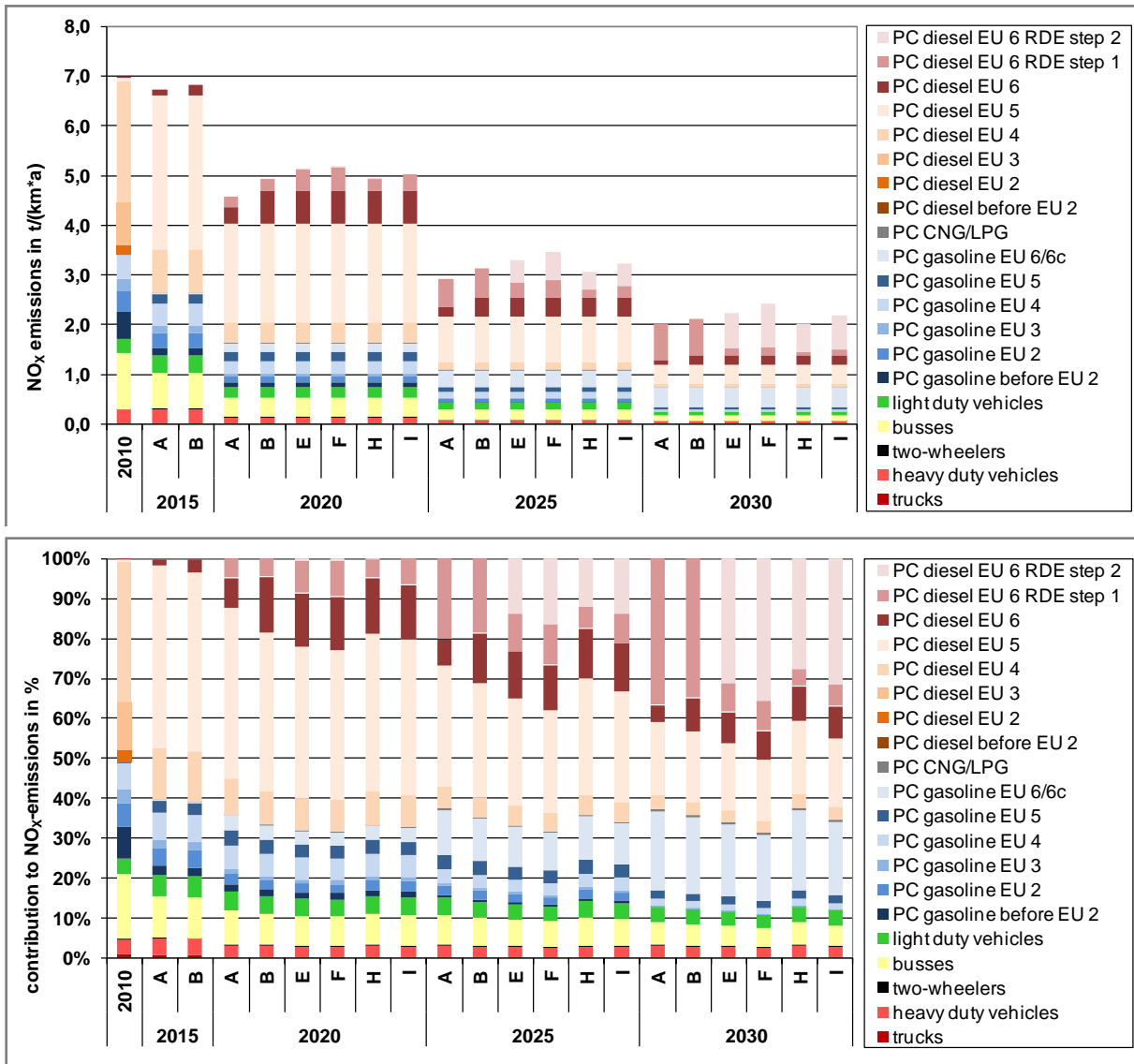


Figure 6: Corneliusstraße: NO_x-emissions for each scenario by vehicle type and motor concept

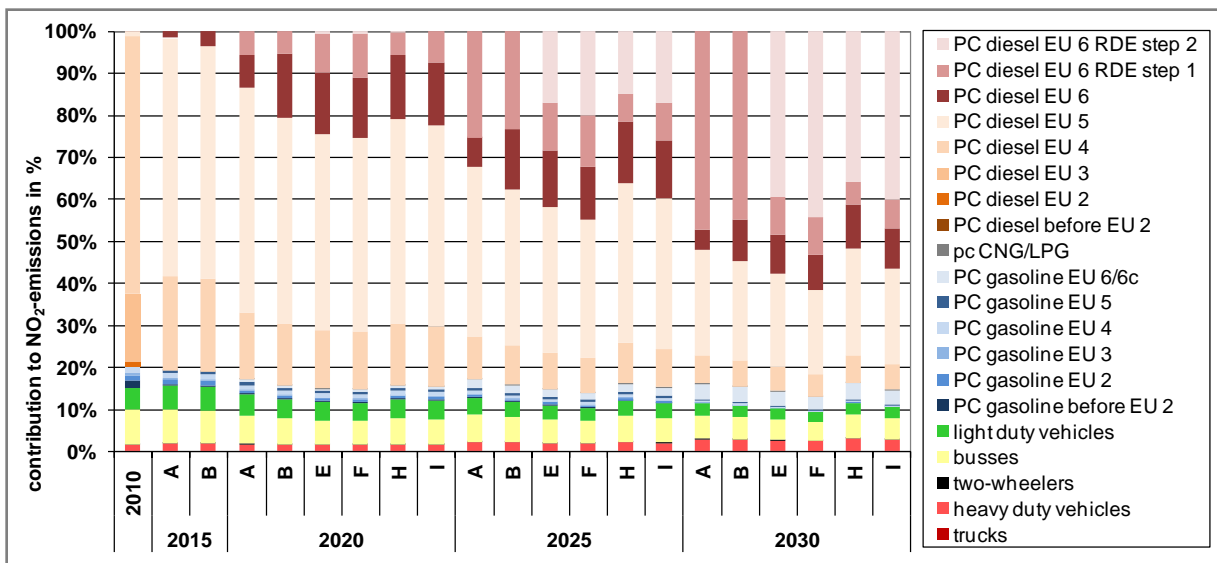
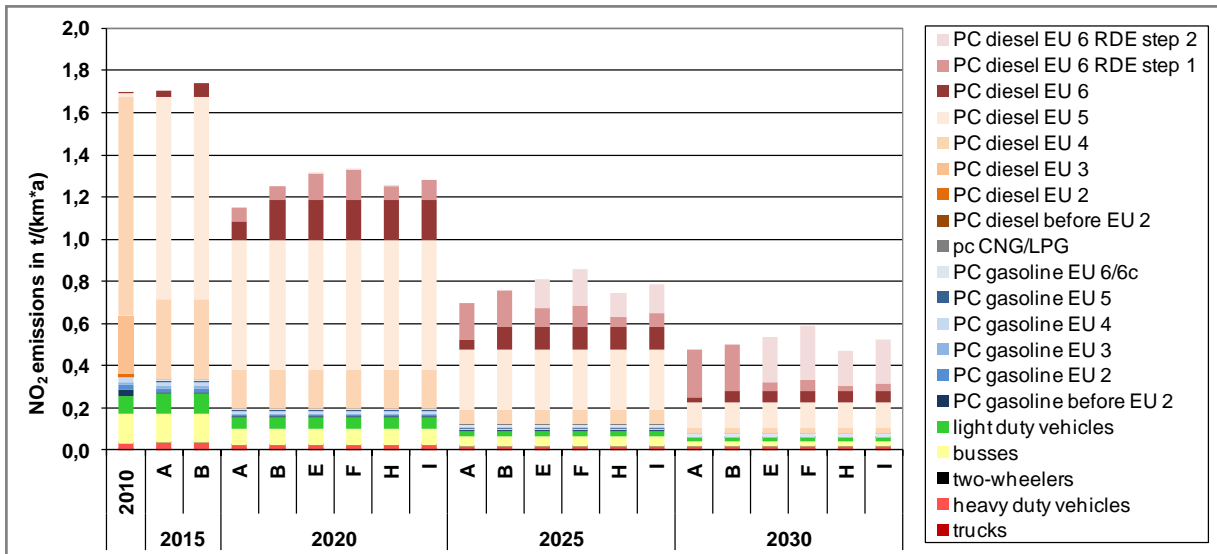


Figure 7: Corneliusstraße: NO₂-emissions for each scenario by vehicle type and motor concept

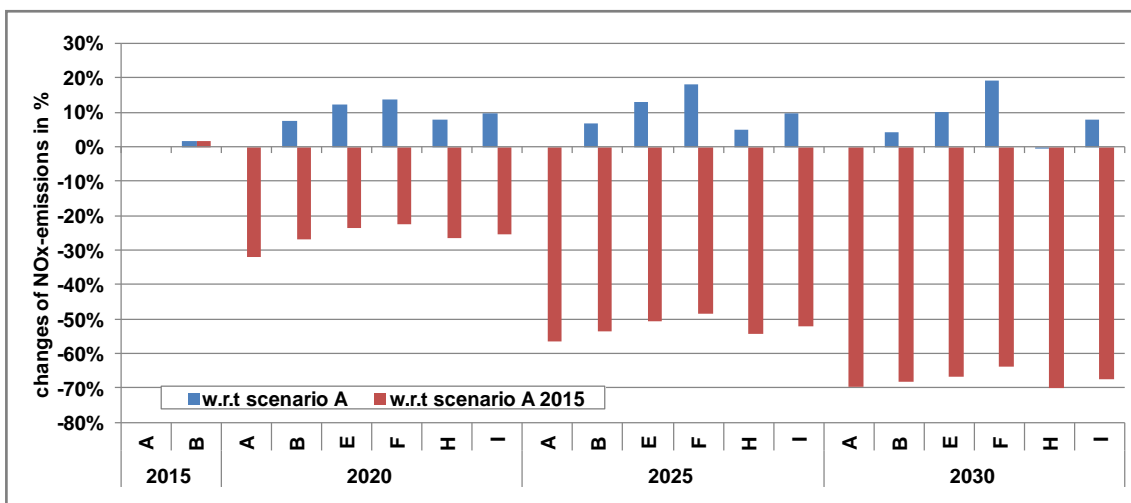


Figure 8: Corneliusstraße: Changes of NO_x-emissions for each scenario w.r.t. scenario A

Air Quality

Based on the emissions calculated above, air quality simulations were done for the three streets for all years and scenarios. The resulting annual mean NO₂ concentrations in the three streets are shown in Table 4.

Table 4: Annual mean NO₂ concentration in µg/m³ for the three considered streets and each scenario

	2015	2020	2025	2030	2015	2020	2025	2030
	scenario A				scenario B			
Am Neckartor	89	66	50	42	90	71	53	43
Corneliusstraße	60	47	36	30	61	49	37	30
Dachauer Straße	31	25	22	20	32	26	22	20
	scenario E				scenario F			
Am Neckartor	90	73	56	45	90	74	57	47
Corneliusstraße	61	50	38	31	61	50	39	32
Dachauer Straße	32	26	22	20	32	26	22	20
	scenario H				scenario I			
Am Neckartor	90	71	53	43	90	72	55	45
Corneliusstraße	61	49	37	30	61	49	38	31
Dachauer Straße	32	26	22	20	32	26	22	20

For all scenarios and all streets, considerable reductions of air pollution are expected until 2030. For “Am Neckartor”, an air quality station at a severely polluted site, the annual mean NO₂ concentration is expected to be reduced from 90 µg/m³ in 2015 to between 42 and 47 µg/m³ in 2030, depending on scenario. However, the air quality limit for the annual mean NO₂ concentration of 40 µg/m³ will still be exceeded in 2030 in all scenarios.

For Corneliusstraße, the annual mean NO₂ concentration is expected to be reduced from 61 µg/m³ in 2015 to between 30 and 32 µg/m³ in 2030, depending on scenario. In all scenarios, compliance with the air quality limit is expected in 2025. For Dachauer Straße, reductions from 32 µg/m³ in 2015 to 20 µg/m³ in 2030 are expected.

In Figure 9, the results are shown graphically. Also shown are calculations with the same model by Kessler et al. (2010) for the years 2006 and 2010 (model calibration 2006) in comparison with measurements. For “Am Neckartor”, the model calculation for 2010 overestimates the measurements. One reason can be that additional actions were taken to reduce emissions at this severely polluted site that were not considered in the model. For Corneliusstraße and Dachauer Straße, model calculations for 2010 agree well with the measurements. For air quality modeling of the scenarios in this study, the model results were refitted to the measurements 2014.

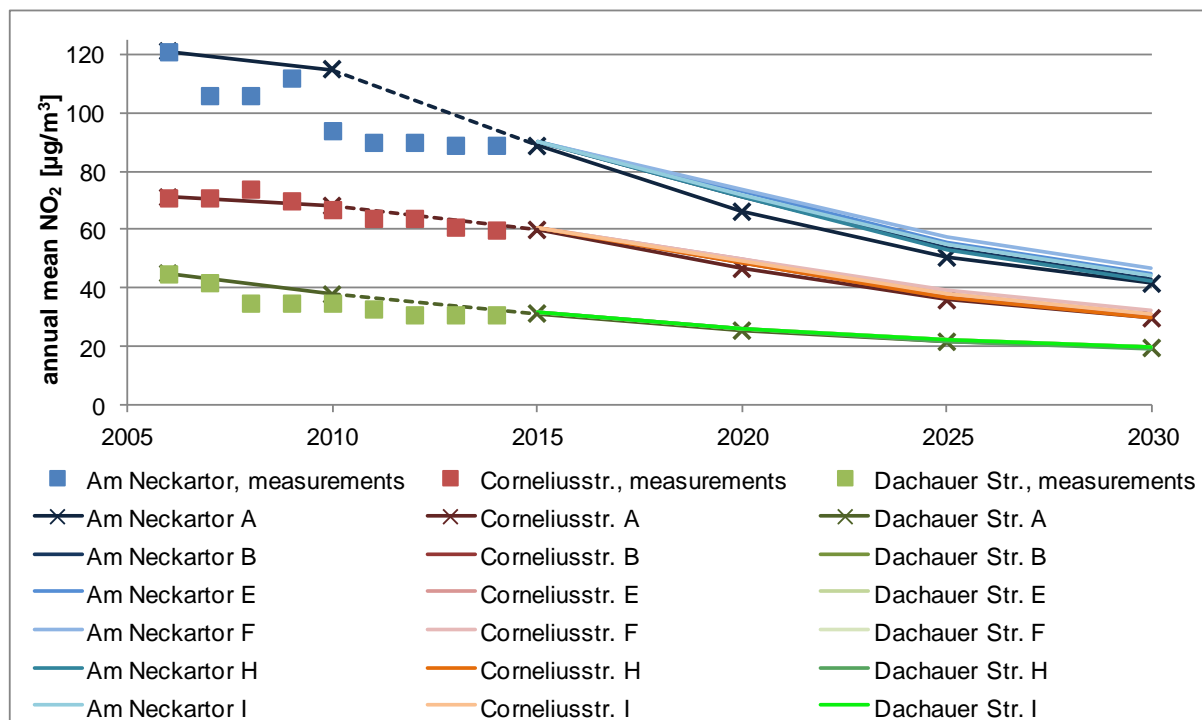


Figure 9: Annual mean NO₂ concentration in µg/m³ for the three considered streets and each scenario; model calculations (2006 and 2010 by Kessler et al. (2010)) and measurements from air quality stations of the federal states of Baden-Württemberg¹, Northrhine-Westphalia² and Bavaria³

Extrapolation to all German Traffic Stations

The results for the three streets were extrapolated to all traffic-influenced air quality measurement stations in Germany as follows. In Figure 10, the annual mean NO₂ values of all German traffic-influenced air quality measurement stations in the EEA (European Environmental Agency) AirBase⁴ 2014 are shown as blue diamonds, sorted by annual mean NO₂. Altogether, there are 144 stations. The model results for the three streets for scenario A 2015 (fitted to the 2014 measurements) are shown as blue circles. To extrapolate the model results, a logarithmic curve was fitted through the three model calculations, shown as blue line. As you can see in Figure 10, this line fairly well captures the behavior of the other measurement stations as well, between station 20 and station 100, the extrapolation slightly underestimates the measurements, between station 1 and station 20, the extrapolation slightly overestimates the measurements. Such a logarithmic extrapolation curve was fitted to the modeled annual mean NO₂ values of all scenarios and years (in Figure 10 shown for scenario A only). Also shown in Figure 10 is the air quality limit for the annual mean NO₂ value (black dotted line). The intersections of the extrapolation curves with the limit line, scaled by a factor to correct for the deviations between measurements and model in 2015, give the number of air quality measurement stations with limit exceedances for all years and scenarios.

¹ <http://www.lubw.baden-wuerttemberg.de/servlet/is/21954/?shop=true>, Reports on annual mean values of the most relevant air pollutants for the air quality stations in Baden-Württemberg between 2005 and 2013

² http://www.lanuv.nrw.de/luft/immissionen/ber_trend/kenn.htm, Annual mean values of the most relevant air pollutants for the air quality stations in Northrhine-Westphalia between 2000 and 2013

³ http://www.muenchen.de/rathaus/Stadtverwaltung/Referat-fuer-Gesundheit-und-Umwelt/Luft_und_Strahlung/Luftreinhalteplan.html, Fifth follow up of the clean air plan for the city of Munich, Bavarian Ministry of Environment and Consumer Protection

⁴ <http://www.eea.europa.eu/data-and-maps/data/airbase-the-european-air-quality-database-8>

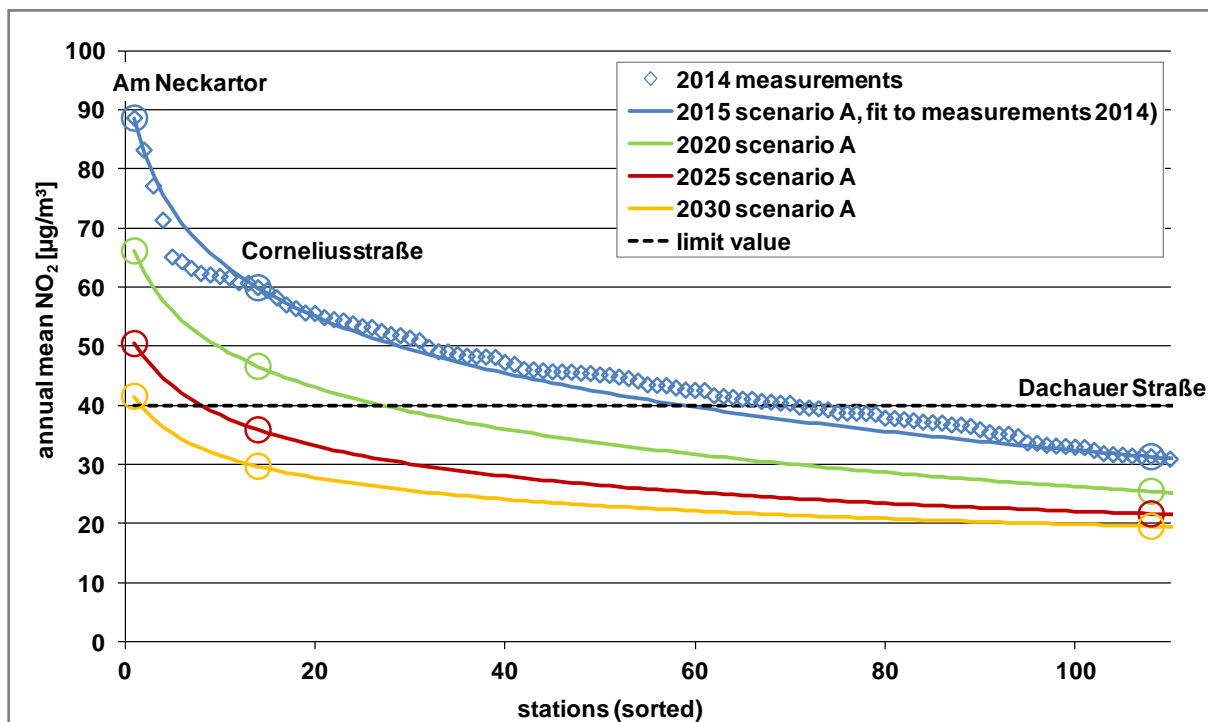


Figure 10: Extrapolation of scenario A to all German Traffic Stations

In Table 5, the number of traffic-influenced air quality stations in Germany expected to exceed the NO₂ air quality limit estimated by this extrapolation is shown for the considered years and scenarios. Also given is the percentage of stations expected to exceed the limit, referring to the total number of 144 traffic-influenced air quality stations in Germany in EEA AirBase. While in 2015 about 50% of all German traffic-influenced air quality stations in EEA AirBase exceeded the limit, this number is expected to be reduced until 2020 to between 23% and 28% (depending on scenario), until 2025 to between 7% and 10% and until 2030 to between 1% and 4% (1% for scenario I, which was TCMV voted).

Table 5: Estimated number and fraction of traffic-influenced air quality stations in Germany which are expected to exceed the NO₂ air quality limit in the considered years and scenarios

		Sc. A	Sc. B	Sc. E	Sc. F	Sc. H	Sc. I
2015	number of stations	70	72	72	72	72	72
	fraction (of 144 stations)	49%	50%	50%	50%	50%	50%
2020	number of stations	33	37	40	41	37	39
	fraction (of 144 stations)	23%	26%	28%	28%	26%	27%
2025	number of stations	10	11	13	14	11	12
	fraction (of 144 stations)	6,9%	7,6%	9,0%	9,7%	7,6%	8,3%
2030	number of stations	1	2	4	5	2	2
	fraction (of 144 stations)	0,7%	1,4%	2,8%	3,5%	1,4%	1,4%

As done by IASA (2012), an uncertainty range was defined by setting an interval of 5 µg/m³ around the NO₂ air quality limit: When the extrapolation of the model results shows an annual mean NO₂ value

- below 35 µg/m³: stations are expected to comply with the limit,
- above 45 µg/m³: stations are expected to exceed the limit,
- between 35 and 45 µg/m³: stations lie within the uncertainty range.

In Figure 11, the estimated number and fraction of traffic-influenced air quality stations in Germany

which are expected to exceed the NO₂ air quality limit in the considered years and scenarios is shown, also shown is the derived uncertainty range.

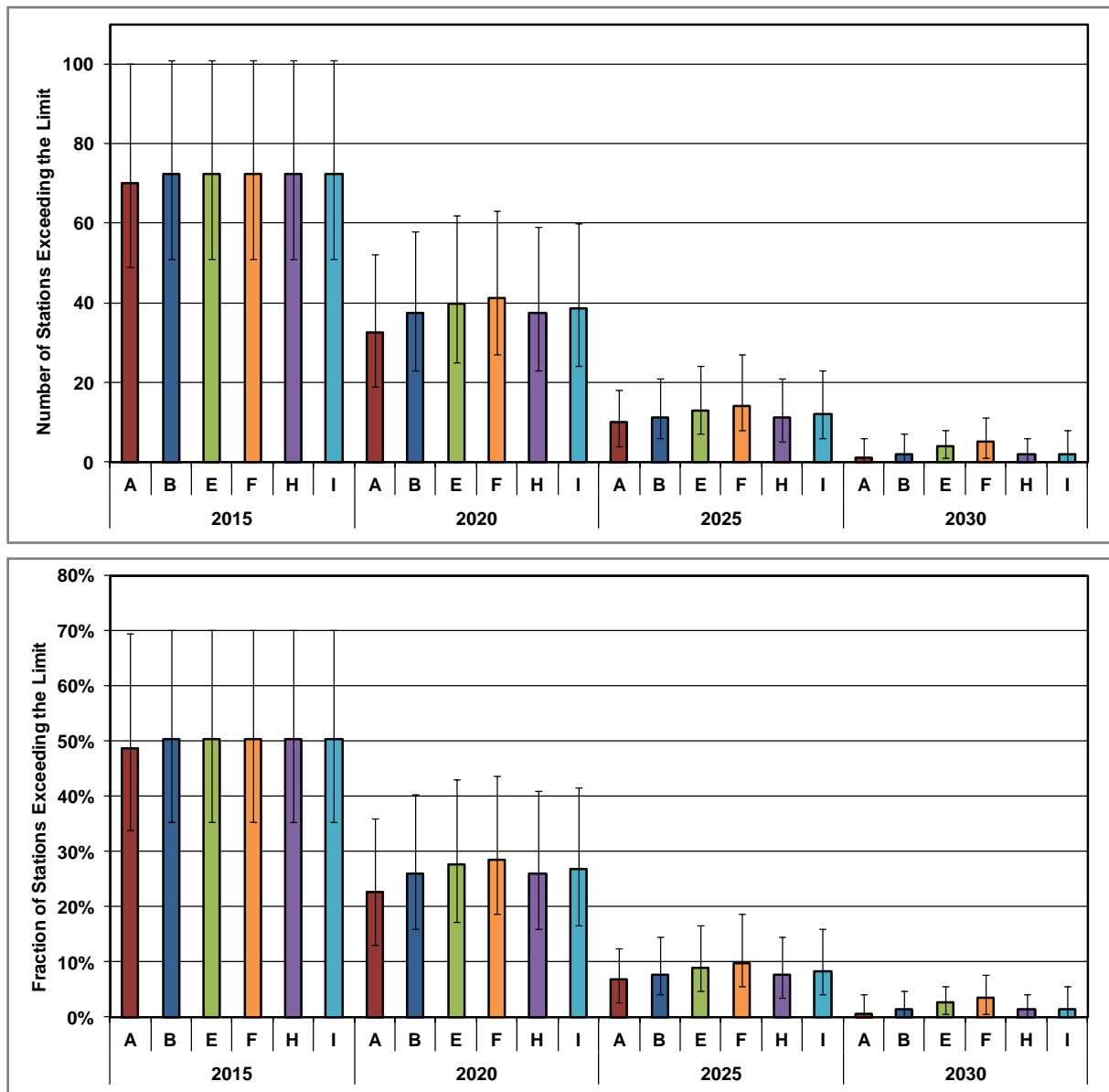


Figure 11: Estimated number of traffic-influenced air quality stations in Germany which are expected to exceed the NO₂ air quality limit in the considered years and scenarios; top: absolute numbers, bottom: fraction of all traffic stations (total: 144)

3. Summary and Conclusions

The effect of several emission factor scenarios on NO₂ air quality was modeled for three urban main roads in Germany, one with severe NO₂ limit exceedances (“Am Neckartor” in Stuttgart), one with average limit exceedances (Corneliusstraße in Düsseldorf) and one compliant with the limit (Dachauer Straße, Munich). Model calculations were done for the years 2015, 2020, 2025, and 2030 for each scenario. The scenarios were defined by conformity factors to limit the emissions of EU 6 diesel PC according to the future RDE regulation. They were varied between CF=1.6 and CF=3.3 in step 1, and between 1.2 and 1.8 in step 2. Step 1 was assumed to be introduced in September 2017, step 2 in September 2019. In scenario I, additionally, the introduction date of step two was changed from September 2019 to January 2020, thus making scenario I conform to what was voted for by TCMV. The results were extrapolated to all German traffic-influenced air quality measurement stations. For all scenarios, PC diesel EU 6 RDE emission factors are expected to be considerably

lower than PC diesel EU 5 emission factors. Due to fleet renewal, this leads to lower road traffic emissions, lower NO₂ concentrations and fewer stations exceeding the NO₂ air quality limit. Depending on scenario, the fraction of traffic-influenced stations exceeding the air quality limit for annual mean NO₂ is expected to be reduced from about 50% (72 stations) in 2015 to 23% up to 28% (33 up to 41 stations) in 2020, 7% up to 10% (10 up to 14 stations) in 2025, and 1% up to 4% (1 up to 5 stations) in 2030. For scenario I (TCMV voted), in 2030, two stations are expected to exceed the NO₂ air quality limit. The differences in modeled NO₂ reduction for the different scenarios and a single year are smaller than the NO₂ reductions modeled for a single scenario between the five-year intervals.

From the model calculations, you can draw the following conclusions:

For all scenarios, air quality is expected to improve considerably until 2030.

In 2020, still 23% to 28% of the traffic-influenced air quality stations are expected to exceed the air quality limit of annual NO₂.

In 2030, most traffic-influenced air quality stations are expected to comply with the NO₂ air quality limit. Only a few stations, where air pollution is especially high, are still expected to show limit exceedances in 2030.

Within the next five to ten years, at many traffic-influenced air quality stations, natural fleet renewal is not fast enough to achieve compliance with the NO₂ air quality limit. Here, additional actions to reduce NO_x-emissions might be considered..

Acknowledgements

We want to say thanks to BMUB (Federal Ministry for the Environment, Nature Conservation, Building and Nuclear Safety, Germany), UBA (Federal Environmental Agency, Germany), ifeu (institute for energy and environmental research, Heidelberg), BASt (Federal Highway Research Institute, Germany), and VDA (German Association of Automotive Industry) for scenario and parameter definition, and to VDA for financial support.

References

- ERMES, 2015: Information Paper: Diesel light duty vehicle NO_x emission factors. http://emisias.com/files/ERMES%20NOX%20EF_V20151009.pdf
- Franco, V., Posada Sanchez, F., German, J., Mock, P., 2014: Real-world exhaust emissions from modern diesel cars. ICCT white paper, Berlin, Germany, 2014
- HBEFA, 2014: <http://www.hbefa.net/e/index.html>
- IIASA, 2012: TSAP-2012 Baseline: Health and Environmental Impacts, TSAP Report #6, Version 1.0, http://ec.europa.eu/environment/air/pdf/tsap_impacts.pdf
- Kadijk, G., van Mensch, P., Spreen, J., 2015: Detailed investigations and real-world emission performance of Euro 6 diesel passenger cars. TNO report 2015 R10702, Delft, the Netherlands, 2015
- Kessler, C., Schneider, C., Vogt, R., 2010. Städtische NO₂-Luftqualität: Quellenanalyse und zukünftige Entwicklung. Immissionsschutz 04.10, pp. 164–170.
- Ligterink, N.E., Kadijk, G., van Mensch, P., 2012: Determination of Dutch NO_x emission factors for Euro-5 diesel passenger cars. TNO report 2012 R11099, Delft, the Netherlands, p.17
- Memmesheimer, M., Wurzler, S., Friese, E., Jakobs, H.J., Feldmann, H., Ebel, A., Kessler, C., Geiger, J., Hartmann, U., Brandt, A., Pfeffer, U., Dorn, H.P., Borrego, C., Eberhard, R., 2007: Chapter 2.8 Long-term simulations of photo-oxidants and particulate matter over Europe with emphasis on North Rhine-Westphalia. Developments in Environmental Science 6, pp. 158–167.
- Rexeis M., Hausberger S., Kühlwein J., Luz R.: Update of Emission Factors for EURO 5 and EURO 6 vehicles for the HBEFA Version 3.2. Final report No. I-31/2013/ Rex EM-I 2011/20/679 from 06.12.2013.

- Stockwell, W.R., Middleton, P., Chang, J.S., Tang, X., 1990: The second generation regional acid deposition model chemical mechanism for regional air quality modelling. J. Geophys. Res. 95, pp. 16343–16367.
- Stuttgart, 2012: Air quality plan Stuttgart: Luftbilanz Stuttgart 2010/2011. Amt für Umweltschutz, https://www.stadtklima-stuttgart.de/stadtklima_filestorage/download/Luftbilanz-Stgt-2010_2011.pdf
- TCMV, 2015: Summary Record of the 51st Meeting of the Technical Committee – Motor Vehicles (TCMV) Meeting, <https://www.eumonitor.eu/>
- Toenges-Schuller et al., 2013: Modellierung der Auswirkungen verkehrsbedingter Partikelanzahl-Emissionen auf die Luftqualität für eine typische Hauptverkehrsstrasse, FAT-Schriftenreihe 262, <https://www.vda.de/de/services/Publikationen/fat-schriftenreihe-262-partikelanzahl-emissionen.html>
- Toenges-Schuller et al., 2015: Modelling particle number concentrations in a typical street canyon in Germany and analysis of future trends. Atmospheric Environment 111 (2015)
- UBA, 2014: Luftqualität 2020/2030: Weiterentwicklung von Prognosen für Luftschadstoffe unter Berücksichtigung von Klimastrategien, TEXTE 35/2014, Umweltforschungsplan des Bundesministeriums für Umwelt, Naturschutz, Bau und Reaktorsicherheit, Forschungskennzahl 3710 43 219, UBA-FB 001945
- Vogt, R., Kessler, C., Schneider, C., 2010. Urban NO₂ Air Quality: Analysis of sources and future projection. VDA Technical Congress, Ludwigsburg, 2010.

Quantification of the effect of WLTP introduction on passenger cars CO₂ emissions

Dimitris TSOKOLIS*, Athanasios DIMARATOS* and Zisis SAMARAS*

Stefanos TSIKMAKIS**, Georgios FONTARAS** and Biagio CIUFFO**

*Laboratory of Applied Thermodynamics, Aristotle University of Thessaloniki, P.O. Box 458, GR 54124, Thessaloniki, Greece, Tel. +30 2310 996066, Fax +30 2310 996016-email: zisis@auth.gr

**Joint Research Centre, Ispra, Via Enrico Fermi 2749, I – 21027, Ispra (VA), Italy

Abstract

In 2014 the United Nations Economic Commission for Europe (UNECE) adopted the global technical regulation No.15 concerning the Worldwide harmonized Light duty Test Procedure (WLTP) while the European Commission is now aiming at introducing the new test procedure in the European type-approval legislation in order to replace the New European Driving Cycle (NEDC) as the certification test. The current paper aims to assess the effect of WLTP introduction on the reported CO₂ emissions from passenger cars presently measured under the NEDC and the corresponding test protocol. The most important differences between the two testing procedures, apart from the kinematic characteristics of the respective driving cycles, is the determination of the vehicle inertia and driving resistance, the gear shifting sequence, the soak and test temperature and the post-test charge balance correction applied to WLTP. In order to quantify and analyze the effect of these differences in the end value of CO₂ emissions, WLTP and NEDC CO₂ emission measurements were performed on 20 vehicles. WLTP CO₂ values range from 125.5 to 217.9 g/km, NEDC values range from 105.4 to 213.2 g/km and the Δ CO₂ between WLTP and NEDC ranges from 4.7 to 29.2 g/km for the given vehicle sample.

French Abstract

En 2014 la Commission Economique des Nations Unies pour l'Europe (UNECE) a adopté le règlement technique mondial No.15 concernant la procédure d'essai Mondiale harmonisée pour les voitures particulières et véhicules utilitaires légers (WLTP), tandis que la Commission Européenne vise désormais à introduire la nouvelle procédure de test afin de remplacer le Nouveau Cycle de Conduite Européen (NEDC) comme le test de certification. Le présent document vise à évaluer l'effet de l'introduction du WLTP sur les émissions de CO₂ rapportées des voitures particulières actuellement mesurées dans le cadre du NEDC et le protocole de test correspondant. Les différences les plus importantes entre les deux procédures d'essai, outre les caractéristiques cinématiques des cycles de conduite respectifs, est la détermination de l'inertie du véhicule et de la résistance à la conduite, la séquence de changement de vitesse, la température de trempage et d'essai et de la correction de la balance de charge après le test appliquée à WLTP. Afin de quantifier et d'analyser l'effet de ces différences dans la valeur finale des émissions de CO₂, mesures des émissions de CO₂ dans WLTP et NEDC ont été effectuées sur 20 véhicules. Les valeurs de CO₂ pour le WLTP vont de 125.5 à 217.9 g/km, les valeurs NEDC vont de 105.4 à 213.2 g/km et la Δ CO₂ entre WLTP et NEDC varie de 4.7 à 29.2 g/km pour l'échantillon des véhicules.

Keys-words: NEDC, WLTP, CO₂, Fuel Consumption, European Regulation.

1. Introduction

Road transport currently accounts for approximately 23% of all carbon dioxide (CO₂) emissions in the European Union (EU), of which about 2/3 come from passenger cars. Emissions from road transport have been increasing until recently (European Environment Agency 2014) undermining reductions made by other sectors and hampering the EU ability to meet its greenhouse gas emission commitments under the Kyoto protocol. Regulation (EC) No 443/2009, setting the target of 95 gCO₂/km for passenger cars to be achieved by 2020, aims at incentivizing investments by the car industry in new technologies and thus

continue improving fuel consumption efficiency and decrease CO₂ emissions.

One of the key challenges for the European legislator is to ensure that reductions in light-duty vehicle emissions at type approval (TA) are representative of those experienced during real world driving and that the fuel consumption values communicated to the customers lay as close as possible to those actually experienced when driving the car. In parallel, the certification procedure has to provide a level playing field for competition of the various OEMs and reflect accurately the competitive advantages of different vehicles in order to support and promote the cars that exhibit better energy efficiency. Several studies have shown that actual on-road emissions and fuel consumption might be substantially higher than values reported during the type approval testing on a chassis dynamometer in testing laboratories (Weiss, Bonnel et al. 2011, Ntziachristos, Mellios et al. 2014, Tietge, Zacharaof et al. 2015, Transport & Environment 2015). One of the reasons for the discrepancy between certified and actual emissions is considered to be the current test cycle, the New European Driving Cycle (NEDC), employed for the TA tests for emissions certification of light-duty vehicles.

The existing TA test in the EU was established in the 70s to measure at the time regulated pollutant emissions but not CO₂ or fuel consumption. The testing of the latter was introduced in the 80s. It is based on the NEDC, which has received a lot of criticism and is currently considered outdated (Mock, German et al. 2013). NEDC does not represent real driving behaviour of a vehicle in actual traffic and thus, does not accurately reflect pollutant emissions and fuel consumption (Joumard, André et al. 2000). NEDC consists of smooth accelerations and decelerations which fail to reflect modern driving patterns (Kågeson 1998, Dings 2013, Marotta, Pavlovic et al. 2015). In addition, the test protocol disregards various real-world conditions like additional weight, number of passengers, use of A/C, realistic gear shifting, cold starts, operation at higher velocities and congestion (Ligterink 2012, Tutuianu, Bonnel et al. 2015), while it examines only a small area of the operating range of the engine (Kågeson 1998).

On top of that, the penetration of modern technologies and alternative drivetrains further aggravate the situation (Millo, Rolando et al. 2014, Rangaraju, De Vroey et al. 2015). The existing test procedure prescribed for plug-in hybrid vehicles mainly considers the CO₂ produced by the engine, while the CO₂ related to the electricity used to charge the battery is only partially taken into account. An experimental investigation on a downsized Euro 5 turbocharged diesel engine managing high/low pressure EGR systems revealed that brake specific fuel consumption decreases around 5-9.5% at low speed/load, 1.7-3.3% at intermediate conditions, both well represented in the NEDC, while no advantages are achieved in higher speed/load conditions (Zamboni, Moggia et al. 2016). Finally, tests in the emissions of petrol and diesel Euro 4, 5 and 6 cars at low temperatures (-7 °C), indicate that current test procedure potentially requires revisions (Dardiotis, Martini et al. 2013).

Apart from the above, specific provisions or interpretations of the current certification procedure, or absence of those, result in the measurement of lower CO₂ emission values. A series of test margins or elasticities have been identified to date like those applied on the speed profile of the test cycle, the test temperature definition, the calculation of vehicle resistances, the vehicle preparation, etc., which make the certified CO₂ value less representative (Kadijk, Verbeek et al. 2012).

The European Commission is currently addressing these open issues by leading the development of a new World-wide harmonized Light duty Test Cycle (WLTC) and a new World-wide harmonized Light-duty Test Procedure (WLTP) and by preparing the ground, including the time-frame, for their introduction in the European TA procedure.

The development of the WLTC has been carried out under a program launched by the World Forum for the Harmonization of Vehicle Regulations (WP.29) of the United Nations Economic Commission for Europe (UNECE) through the working party on pollution and energy transport program (GRPE). The aim of this project was to develop a harmonized light duty test cycle, that represents the average driving characteristics around the world and to have a legislative world-wide-harmonized TA procedure put in place from 2017 onwards.

The first roadmap for the development of the new driving cycle and test procedure was presented in 2009 and it consisted of three phases:

- i. Phase 1 (2009 – 2014): development of the worldwide harmonized light duty driving cycle and associated test procedure for the common measurement of criteria pollutants, CO₂, fuel and energy consumption (Type 1 test of EU type approval procedure).
- ii. Phase 2 (2014 - 2018): low temperature/high altitude test procedure, durability, in-service conformity, technical requirements for on-board diagnostics (OBD), mobile air-conditioning (MAC) system energy efficiency, off-cycle/real driving emissions.
- iii. Phase 3 (2018+): emission limit values and OBD threshold limits, definition of reference fuels, comparison with regional requirements.

After the finalization of WLTP (Tutuianu, Marotta et al. 2013, Tutuianu, Bonnel et al. 2015), the European

Commission decided to propose its introduction in the TA procedure of light duty vehicles already in 2017. This has however an effect on the European Regulations since current CO₂ targets, established for years 2020 and 2021 based on the experience and practices of the old protocol (NEDC), must be adjusted to account for the different severity and boundary conditions of the new test procedure (Ciuffo, Marotta et al. 2015).

In order to tackle this obstacle from 2017 onwards new vehicle registrations will either be measured in both WLTP and NEDC for CO₂ monitoring purposes or it is likely that a back translation of the WLTP measured CO₂ values to their NEDC equivalent will be performed by means of computer simulation, using a dedicated software tool. In order to support this process and provide a first assessment of the impact of the introduction of WLTP in the certification system a series of measurements on real vehicles were performed under both the NEDC and WLTP protocol.

The current paper starts from the results of these measurements and focuses on quantifying the effect of WLTP Regulation, when compared to the NEDC. The results presented here refer to the higher driving resistance configuration of the WLTP (WLTP-High).

2. Methodology

For the scope of this study, and in order to analyze the effect of the introduction of the new test procedure to the European legislation, a series of pollutant and CO₂ emission tests have been performed for a total of 20 passenger cars under the two protocols, NEDC and WLTP-High. The complete test protocol and specifications for some of the tested vehicles can be found in (Tsokolis, Tsiakmakis et al. 2015). In the current paper, a wider vehicle sample is presented, focusing only on CO₂ emissions. The specifications of the vehicles are given in Table 1.

Table 1: Specification of the measured vehicles in NEDC and WLTP-High.

Fuel	Vehicle	Emission Standard	I*/A**/T***	Start/Stop	Displacement [cc]	Max Power [kW]	Max Torque [Nm]	Curb mass [kg]
Gasoline	G01	EURO5	PFI/NA/MT6	YES	1368	125	250	1290
	G02	EURO5	DI/T/MT6	YES	1798	125	318	1450
	G03	EURO6	DI/T/MT6	YES	1600	100	240	1300
	G04	EURO5	DI/T/AT8	YES	1995	180	350	1510
	G05	EURO5	PFI/NA/MT5	YES	875	77	145	930
	G06	EURO5	PFI/NA/MT5	YES	1368	57	115	1025
	G07	EURO5	DI/T/MT6	YES	999	92	170	1179
	G08	EURO5	DI/T/AT7	YES	3498	200	370	1635
	G09	EURO5	PFI/NA/AT5	YES	999	52	92	750
	G10	EURO5	DI/T/AT6	NO	2497	187	360	1456
	G11	EURO5	DI/T/MT5	NO	1197	66	160	1102
	G12	EURO5	DI/T/AT6	YES	1390	110	240	1623
Diesel	D01	EURO5	DI/T/AT8	YES	2967	190	580	1880
	D02	EURO5	DI/T/MT6	YES	1995	120	380	1465
	D03	EURO5	DI/T/MT5	NO	1248	55	190	1090
	D04	EURO5	DI/T/AT7	NO	2030	120	360	2030
	D05	EURO5	DI/T/MT5	YES	1248	70	190	1393
	D06	EURO5	DI/T/AT6	NO	1686	95	300	1309
	D07	EURO6	DI/T/MT6	YES	1598	90	320	1601
	D08	EURO5	DI/T/MT6	YES	1560	82	270	1293

*I = Injection: DI = Direct Injection; PFI = Port Fuel Injection

**A = Aspiration: T = Turbo; NA = Naturally Aspirated

***T = Transmission: ATn = Automatic Transmission with n gears, MTn = Manual Transmission with n gears

The above measurements are complemented with a step-by-step simulation exercise, allowing the better

identification of the sources of differences between the two test protocols, and a further quantification and assessment of the individual effects. The simulation tool used is the AVL's CRUISE, a tool to perform vehicle CO₂ emission simulations and powertrain analysis (AVL 2016). For this activity, two out of thirteen validated vehicle models were used; one small size gasoline (G11) and one medium-large size diesel passenger car (D02), considered to be representative for the current European fleet.

The simulation approach adopted is as follows: both vehicle models are set up to run a WLTP-High. Then, one at a time, a test parameter is modified according to the NEDC protocol, and a new simulation run is performed; i.e. first the test mass is changed, then the RL coefficients, then the driving profile, the gear shifting sequence etc.

3. Results and discussion

The following paragraphs present the main results in terms of the effect on CO₂ emissions between the two protocols as regards the most influential differences between the NEDC and WLTP which are: the driving profile, the vehicle mass (inertia) and road load determination, the chassis preconditioning, the gear-shifting procedure, the temperature, and the REEES (Rechargeable Electric Energy Storage System) Charge Balance (referred to as RCB) correction.

Measurement results

Figure 1 presents the median cold WLTP-High CO₂ bag results vs the median cold NEDC CO₂ bag results for all measurements conducted for the two driving cycles. The pool of tested vehicles included diesel and gasoline fueled engines, with direct or port fuel injection, turbo or naturally aspirated, equipped with manual or automatic transmission, conventional or mild hybrid equipped with Start/Stop (S/S) and regenerative braking. The presented NEDC and WLTP-High results are not corrected for RCB. As explained above, it is expected that the WLTP-High CO₂ values will be higher, if the RCB correction is included, while no RCB correction is foreseen for NEDC.

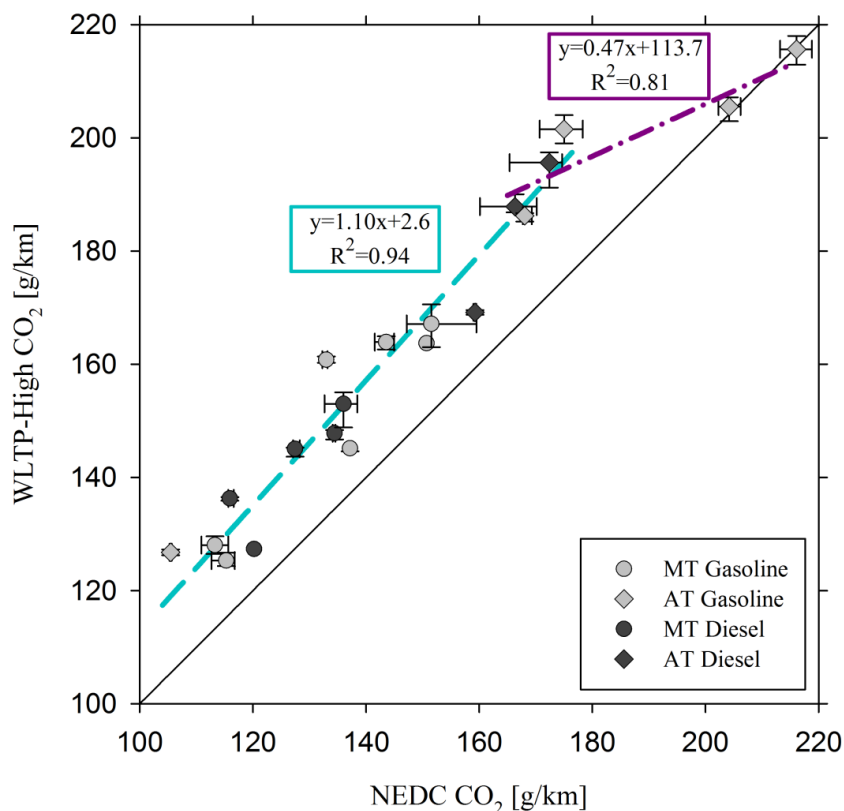


Figure 1: WLTP-High vs NEDC CO₂ measurements for 20 different passenger cars. The points correspond to the median of one to five measurements. The standard deviation of vehicle can also be seen. The dashed trend line corresponds to the increasing trend of WLTP-High vs NEDC CO₂ emissions, while the dotted line corresponds to the decreasing trend.

The WLTP-High vs NEDC CO₂ results can be divided in three main areas according to their NEDC value. The first consists of small, medium and medium-large vehicles with measured CO₂ emissions from 100 to 160 g/km; the second narrow region consists of medium-large and large vehicles with emissions from 160 to 180 g/km and the third consists of executive vehicles with measured NEDC emission values above 180 g/km. In the first area, almost all vehicles were equipped with manual transmission, while the rest were equipped with automatic transmission exclusively.

The WLTP-High results in the range from 100 to 180 g/km demonstrate an increasing trend over the $y=x$ line, especially determined by the vehicles that belong to the second area which can be characterized as “transitional”. Currently, vehicles equipped with automatic transmission are optimized, in terms of gear shifting strategy, to perform best over the NEDC. The measured CO₂ emissions from these vehicles is expected to deliver higher NEDC and lower WLTP values in the future, assuming that the automatic gear shifting strategy will be optimized for the WLTP. Thus, two trends are observed: an increasing trend in the area with WLTP-High CO₂ emission values from 100 to 180 g/km with characteristic $y=1.10x+2.5$, $R^2=0.94$ and a decreasing trend in the area from 180 to 220 g/km with characteristic $y=0.47x+113.7$, $R^2=0.81$.

Driving profile analysis

A significant improvement in the WLTP Regulation is that, in contrast to the NEDC, the driving profile is different for the various vehicles according to their Power to Mass ratio (PMR), which is defined as the ratio of rated power (in Watts) to the curb mass (in kg). Two driving profiles characteristic for low powered vehicles are defined for $PMR \leq 22$ (WLTC class 1) and $22 < PMR \leq 34$ (WLTC class 2). For the rest, vehicles with $PMR > 34$, WLTC class 3 should be used (Tutuianu, Marotta et al. 2013). Most passenger cars fall in the WLTC class 3 category. Since some vehicles close to the borderline PMR values may present drivability problems in high speeds, a downscaling is applied to the speed profile further enhancing the closer-to-reality features of the new approach.

The kinematic characteristics of NEDC and WLTC (Demuyne, Bosteels et al. 2012, Kühlwein, German et al. 2014), as well as their potential effect on pollutant formation (Joumard, Rapone et al. 2006, Sileghem, Bosteels et al. 2014) and CO₂ emissions (Bielaczyc, Woodburn et al. 2014, Mock, Kühlwein et al. 2014) have been sufficiently covered by the scientific community so far. The basic characteristics of NEDC and WLTC class 3, are described in Table 2. Compared to WLTC, NEDC is characterized by shorter duration and distance, longer idling and cruising time and lower speed and acceleration (Figure 1). In addition, a single vehicle operates in lower engine speed and load over the NEDC, which is not representative of real world driving. Although WLTC driving profile is more transient than NEDC, when these two cycles are been tested under the same driving resistance in Euro 5 vehicles, then in most cases WLTC delivers CO₂ results that do not significantly differ from NEDC's (Favre, Bosteels et al. 2013, May, Bosteels et al. 2014, Bielaczyc, Woodburn et al. 2015). The same trend stands for Euro 6 vehicles (Andersson, May et al. 2014, Bielaczyc, Szczotka et al. 2015) and different ethanol fuel blends on gasoline vehicles (Suarez-Bertoa, Zardini et al. 2015).

Table 2: Basic characteristics of NEDC and WLTC class 3.

	NEDC	WLTC class 3
Distance [km]	11.023	23.262
Duration [s]	1180	1800
Idle time [s]	280	235
Phases [#]	2	4
Averagespeed /w idle (w/o idle) [km/h]	33.6 (44.7)	46.5 (53.5)
Max speed [km/h]	120.0	131.3
Max acceleration [m/s²]	~1.0	~1.7

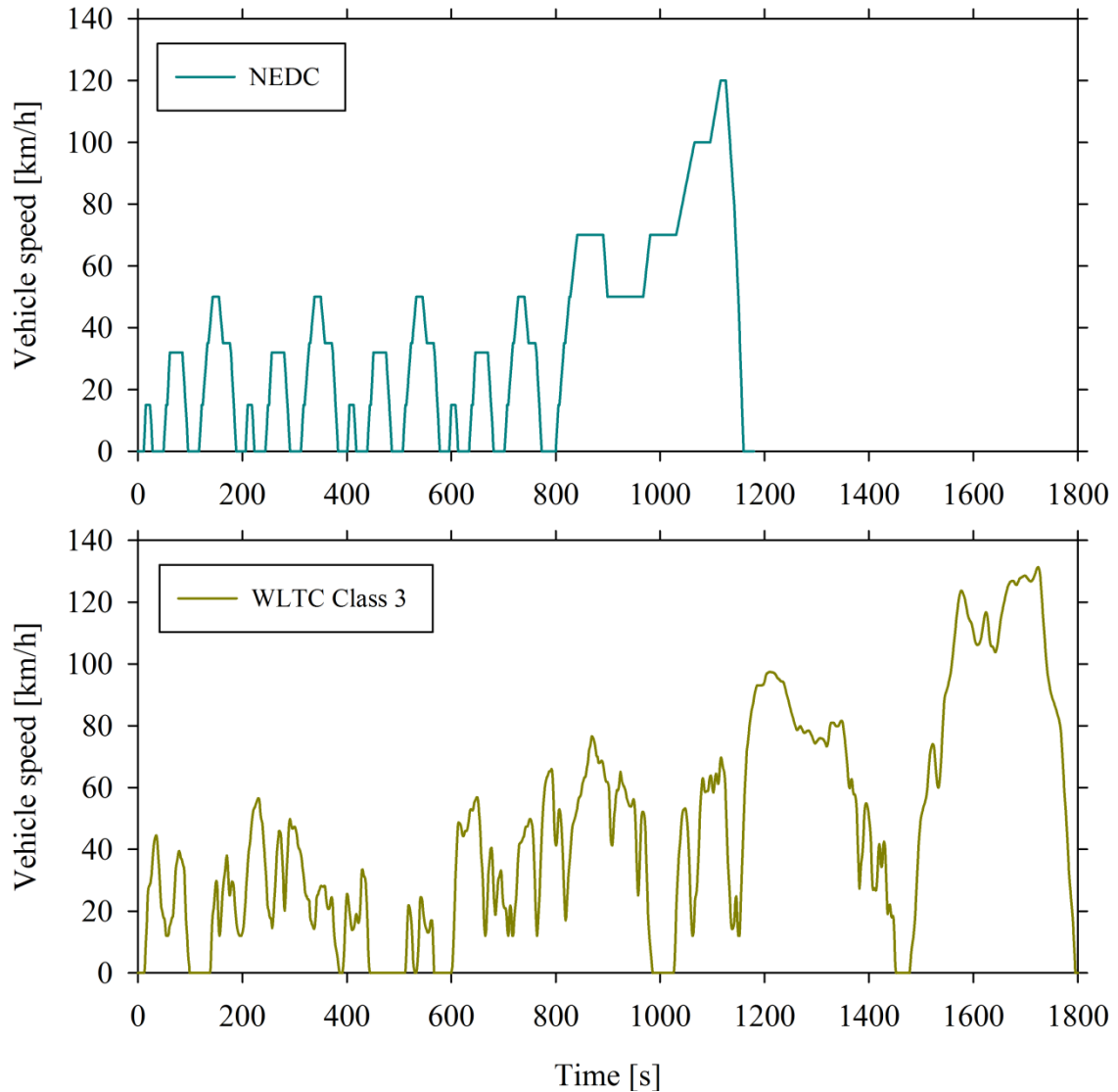


Figure 2: NEDC and WLTC class 3 driving profiles over time.

Test protocol

WLTP substantially differs from the NEDC in the preparation of the vehicle for testing and the post-test management. The latter mainly concerns the corrections applied in the CO₂ values to account for the different contribution of each vehicle's electrical system; a correction which is of crucial importance given the high penetration of micro and mild hybridization systems to modern cars.

A summary of the differences between WLTP and NEDC is given in Table 3. Each of these differences is explained in the following paragraphs.

Table 3: Differences between the NEDC and WLTP measurement protocol.

		NEDC	WLTP
Mass	Test	Reference mass: Unladen + 100 kg	TMH ("worst" case) and TML ("best" case) defined from min/max unladen mass and max laden mass
	Inertia	Inertia classes	Inertia mass = Test mass
	Rotating parts	Not applied	+1.5% for 1-axle chassis dyno
Road load	Origin	Provided by manufacturer – derived by the coast-down	Calculated from NEDC RL taking into account masses, Cd*A,

		method	tyres– derived by the coast-down method in future
	Preconditioning	Vehicle and gear box type dependent (typical values 0 to 20 N)	
Driven wheels	4WD	1-axle dyno allowed	2-axle dyno mandatory
Engine	Preconditioning	1 NEDC + 1 EUDC (gasoline) 3 EUDC (diesel)	WLTP
Gear shifting		Fixed points	Vehicle specific - derived from a function of mass, RL, drivetrain, full load curve
Temperature	Soak	20 to 30 °C	23 °C ± 3 °C
	Oil, coolant	± 2°C to soak temperature	23°C ± 2°C
	Test initiation	25 °C ± 3 °C	23 °C ± 3 °C
RCB Correction		Not applied	Post-test correction

Mass, road load and driven wheels

The procedure which determines the road load (RL) or driving resistance coefficients over the NEDC presents a series of flexibilities which allow lower driving resistances to be applied for the test (Tietge, Zacharaof et al. 2015). These RL coefficients are characteristic for the total driving resistance provided by Equation (1).

$$F = F_0 + F_1 \cdot V + F_2 \cdot V^2 \quad (1)$$

where F represents the total driving resistance in N, F_0 the constant coefficient in N, F_1 the linear coefficient in N/(km/h), F_2 the quadratic coefficient in N/(km/h)² and V the vehicle velocity in km/h.

Achieving lower driving resistance can become feasible by using e.g. low resistance tires or the best aerodynamic and most light weighted version of the same vehicle model during coast down. Additionally, the test mass in NEDC is determined by inertia classes which creates discontinuities in a physical quantity that in reality is continuous and which has significant influence on CO₂ emissions. In WLTP, the RL coefficients for a single vehicle are produced by taking into account its minimum and maximum unladen mass, which is defined as the vehicle's standard weight without driver, fluid or any additional equipment, the maximum permissible weight, the difference in rolling resistance between different tire versions, as well as the difference in aerodynamic resistances expressed as the product of the drag coefficient and the frontal area ($C_d \cdot A$) between the vehicle model with the best and worst aerodynamics. Then, two sets of RL and test mass values are produced; one set characteristic of the best case vehicle (WLTP-Low or WLTP-L), which is the vehicle that is expected to have the lowest energy demand, and one of the worst case vehicle (WLTP-High or WLTP-H), the vehicle of highest energy demand. The equations that were used to calculate the RL coefficients for WLTP can be found in the respective Regulation (Tutuianu, Marotta et al. 2013).

Figure 3 presents different coast down curves for a medium size vehicle. With the NEDC inertia mass and RL coefficients, this vehicle decelerates from 135 km/h to 0 in 215 seconds. Similar coast down time to NEDC is calculated for the WLTP-Low case. In contrast, WLTP-High is associated with lower deceleration time, approximately 180 s. Additionally, individual coast down test performed indicate total deceleration time 20% less than NEDC. The divergence between these individual tests and WLTP-High may be attributed to the experimental difficulties of performing such tests, since they are not fully controlled and identical (wind intensity and direction, road slope, road surface quality, type of tires used etc). Still, a part of the discrepancy between WLTP-High and the real world is expected to remain in the future and possibly rise further (Tietge, Zacharaof et al. 2015).

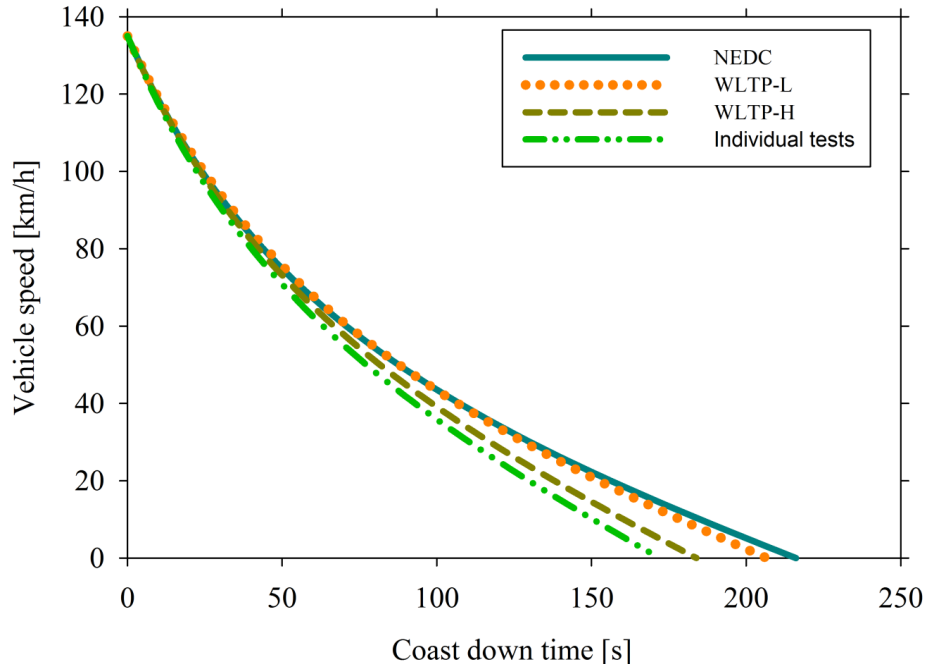


Figure 3: Coast down time for a medium size vehicle.

Chassis preconditioning

Throughout the course of this work, as referred for example in (Tsokolis, Tsiakmakis et al. 2015), it was found that the preconditioning of the chassis dynamometer and the vehicle, during the adjustment of the driving resistance on the dyno, plays a non-negligible role on the CO₂ emissions of the tested cycle. This comes as a direct result of the different resistance that is applied on the vehicle over a driving cycle.

This driving resistance consists of two components: the resistance applied by the electric system (“electric force”, F_{el}) and the friction (“friction force”, F_{fr}). The latter comes from the internal dyno components (such as bearings, the friction of which cannot be zeroed) and the drivetrain of the vehicle (mainly the gearbox, the differential and the tires). Hence, the total force is:

$$F_{tot} = RL = F_{el} + F_{fr} \quad (2)$$

While the former part, F_{el} , depends only on the parameters of the electrical machines, F_{fr} is a function of the thermal state of the test installation. Thus, the hotter the dyno and the vehicle the lower the friction force.

This can be better explained if the two cycles of interest, NEDC and WLTC, are considered. Since WLTC has longer duration and reaches higher speed than NEDC, a single vehicle will be warmer after WLTC than after NEDC (evidently after a start at the same conditions). Since the target is to apply the same F_{tot} in the chassis dyno, different result will be obtained if the chassis setup is performed after a NEDC or a WLTC (or another driving cycle).

Figure 4 shows the effect of different preconditioning on CO₂ emissions. In one case the vehicle was preconditioned by running a NEDC cycle, while in the other case by running for 1180 s at an approximately constant speed in the range 35 - 40 km/h. The results indicate that the average effect in terms of CO₂ emissions is 5 g/km. In the constant speed preconditioning, in fact, the vehicle reached higher temperature, translated in lower F_{fr} , and thus the applied F_{el} by the dyno is higher, so as to achieve the same F_{tot} . This explains the higher CO₂ emissions during the testing of the same driving cycle.

Running as preconditioning a complete WLTC (longer and more dynamic cycle), the results present higher variability for the specific combination of vehicle and tires. An average difference of around 1 gCO₂/km is measured, but for some vehicles this figure goes up to 3-4 gCO₂/km.

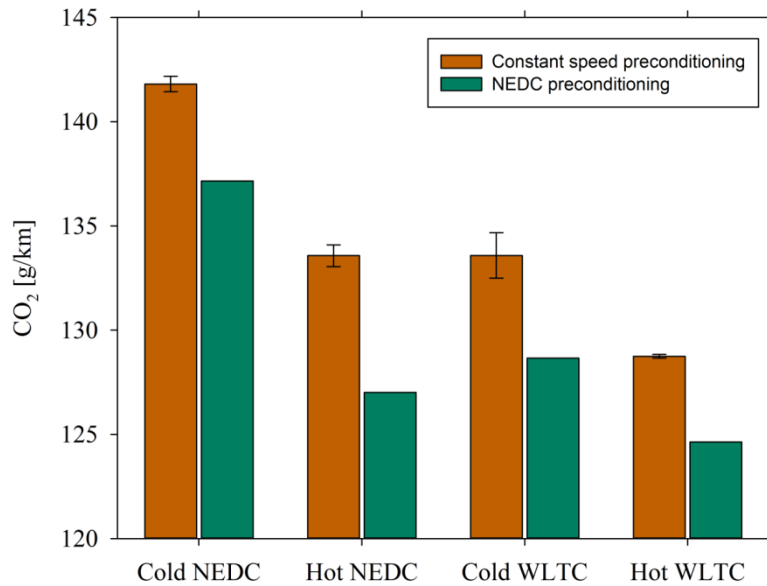


Figure 4: CO2 effect of different chassis preconditioning in NEDC and WLTC for a small 5-gear MT gasoline vehicle.

Gear shifting

This refers to the procedure that defines the gear shifting in WLTP for manual transmission (MT) vehicles; in automatic transmission (AT) vehicles this procedure is not applicable. In NEDC, fixed gear shifting points are defined, without taking into account the different drivetrain configurations. In WLTP first the required (from the driving profile) and available (from the vehicle) power are calculated, then a predefined algorithm decides which gear should be used (Tutuianu, Marotta et al. 2013). This algorithm was designed in a way to emulate the gear shifting experienced in real world driving from normal drivers. As a result, it is highly unlikely for the gear shifting sequence of two randomly selected vehicles to be exactly the same, similar to reality. The generated gear shifting sequence for one diesel and one gasoline vehicle with the characteristics shown in Table 4 is illustrated in Figure 5. Although the driving pattern is the same, the exact shifting points are different due to the differences in the vehicle drivetrain configurations.

Table 4: Vehicle characteristics for the calculation of gear shifting in WLTP-High for two medium size vehicles. For the mass and road load parameters, the delta between these two vehicles is presented if the diesel parameters are used as baseline.

Gear shifting input	Diesel vehicle	Gasoline vehicle
Idle engine speed [RPM]	830	750
Engine speed at maximum power [RPM]	4000	5500
Maximum power [kW]	120	125
Engine to vehiclespeed ratio for 1st gear	98.92	134.85
Engine to vehiclespeed ratio for 2nd gear	54.14	73.23
Engine to vehiclespeed ratio for 3rd gear	33.69	51.31
Engine to vehiclespeed ratio for 4th gear	24.06	38.59
Engine to vehiclespeed ratio for 5th gear	19.25	31.02
Engine to vehiclespeed ratio for 6th gear	15.88	26.52
Delta in curb mass [kg]	-	-200
Delta in WLTP-High mass [kg]	-	-231

Delta in WLTP-High F0 [N]	-	-5.8
Delta in WLTP-High F1 [N/(km/h)]	-	0.0561
Delta in WLTP-High F2 [N/(km/h)²]	-	0.0025

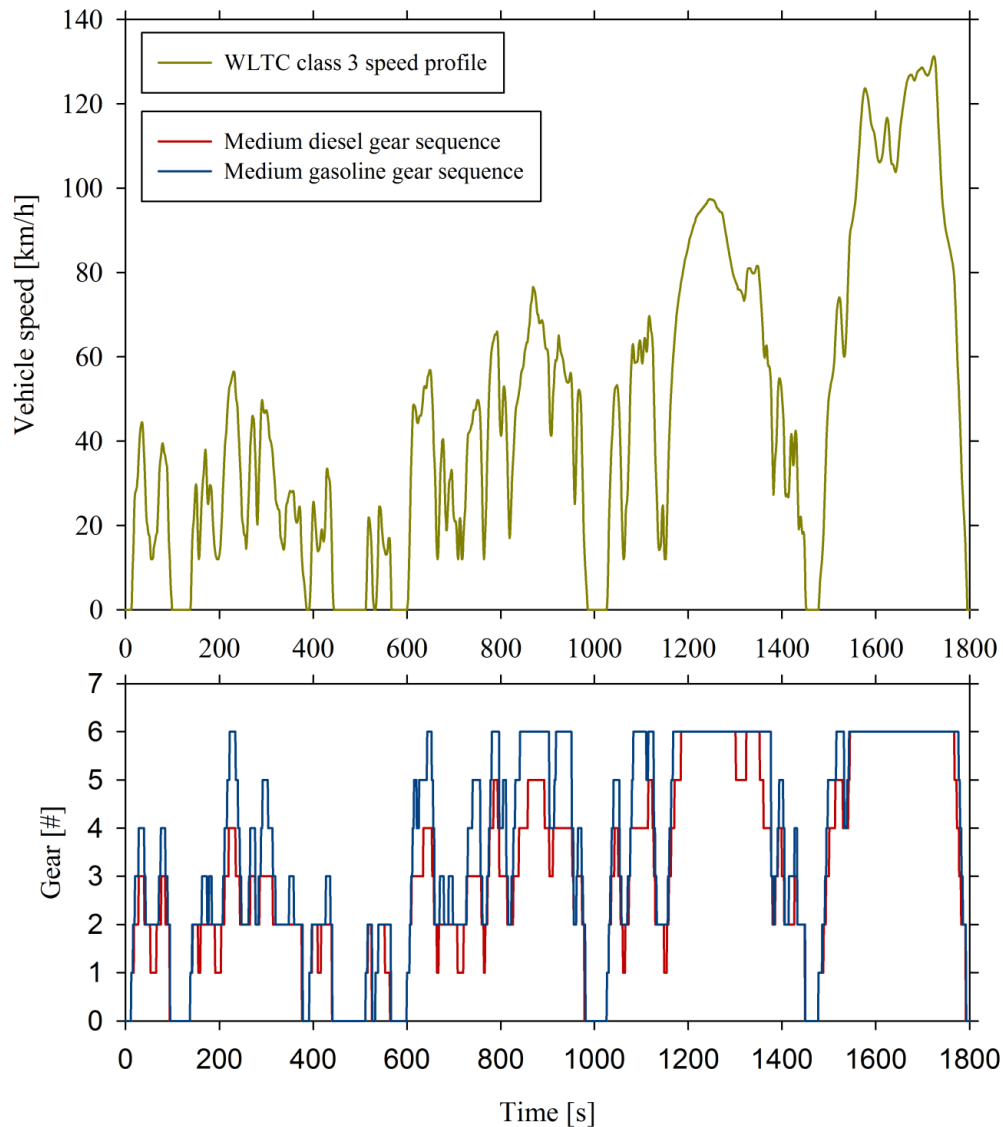


Figure 5: Gear shifting sequence in WLTC for one medium diesel and one medium gasoline vehicle.

One way to investigate the gear shifting effect on WLTP CO₂ emissions is to perform for the two vehicles described in Table 1 (G11, D02), two series of simulations; one with the WLTP-generated gear shifting profile and another with fixed points similar to the NEDC regulation. In both simulations, the total CO₂ emissions were found 1 g/km for the diesel and 6 g/km for the gasoline higher when the NEDC fixed gear shifting points were used. Since the generated gear shifting profile is a function of vehicle specific parameters, it is not odd that the simulated CO₂ effect is not the same for these two case studies.

Temperature

While in NEDC the soak and the test temperature is set between 20 and 30 °C, in WLTP the respective figure is 23±3 °C for both temperatures. These temperatures are not representative of Europe's average annual temperature and even less when compared to Northern Europe's annual average temperature (European Environment Agency 2015). EU is planning to adopt a WLTP test with initial test temperature set at 14 °C, which is closer to the European average.

The temperature difference is expected to have an impact mainly on cold start, which for NEDC is more pronounced given the overall shorter duration of the cycle and the milder driving profile during its first part.

RCB correction

Another parameter that is different between the two procedures is the RCB correction applied to WLTP. So far, the type approval measurement is performed in charge depleting mode because the NEDC regulation does not give any specific prescriptions concerning the state of charge of the battery at the commencement of the test. Therefore, it is common practice to fully charge the battery before the test in order to minimize any extra fuel consumption due to the electrical system. In WLTP, a post-test correction is applied to the measurement, correcting the final CO₂ emissions and fuel consumption value with the total charge balance. The RCB correction is described in Equation (3).

$$RCB\ CO_2\ correction = \frac{\Delta RCB \cdot V_{bat} \cdot Willans\ Factor}{1000 \cdot Alternator\ Efficiency \cdot Distance} \quad (3)$$

where the RCB correction is expressed in g/km, ΔRCB is the RCB difference before and after the measurement in Ah, V_{bat} the nominal voltage of the battery in V, the fuel specific Willans Factor in gCO₂/kWh and the Distance expressed in km. For the Alternator Efficiency typical values are in the order of 0.66-0.67.

Results from four WLTP measurements for a single vehicle and the respective RCB corrections are shown in Figure 6. The tests were performed starting with fully charged battery, discharging during the measurement. When the contribution of the battery is taken into account, the declared value over WLTP is higher than the measured due to the RCB correction. The extra CO₂ produced due to the correction is also shown as charge balance equivalent. The extra consumption due to the battery operation of these tests was on average 9 Ah or 4.6 gCO₂/km. Since this correction was not performed in the NEDC, it is expected that manufacturers will optimize the operation of the electrical system in such a way, as to minimize any additional CO₂ and at the same time maximize the gain from electrical systems such as the Break Energy Recuperation System. The contribution of the electrical system is expected to be different among individual vehicles due to the different requirements and operation strategies.

Simulation results

In order to quantify the differences between the two test procedures, simulation models have been set up, and run sequentially changing one parameter at a time. The delta between WLTP-H and NEDC (ΔCO_2) which is produced from modifying one parameter is shown in Figure 7 for a small gasoline vehicle and in Figure 8 for a medium-large diesel vehicle.

For both vehicles, the largest proportion of the overall ΔCO_2 between WLTP-High and NEDC is due to the change in the RL; 42% for the diesel vehicle and 50% for the gasoline vehicle. If chassis preconditioning is added to RL differentiation, the proportions become 55% and 74% respectively. Significant is also the impact of the different test mass used in WLTP-High, which is calculated to 21% for the diesel and 31% for the gasoline vehicle.

Test parameters such as the driving profile, the gear shifting and the RCB correction may have a negative impact on ΔCO_2 . The sum of the contributions of RL, test mass and chassis preconditioning, exceeds 100% in the case of gasoline vehicles. Although it was expected that with a more aggressive driving profile, compared to NEDC, the divergence between type approval and real world fuel consumption would drop, it was proven otherwise in both EURO 5 (Favre, Bosteels et al. 2013, May, Bosteels et al. 2014, Bielaczyc, Woodburn et al. 2015) and EURO 6 vehicles (Andersson, May et al. 2014, Bielaczyc, Szczotka et al. 2015), as well as when alternative fuels were used (Suarez-Bertoa, Zardini et al. 2015). This may be attributed to the fact that the vehicles are generally driven in a more fuel efficient area for a longer period, which for WLTP is a function of the drivetrain, the engine map, the RL and the generated gear shifting. For the small gasoline vehicle the driving profile had an absolute impact of 0.2 gCO₂/km whereas for the diesel vehicle the impact was 2.1 gCO₂/km. On the other hand, the WLTP gear shifting reduced CO₂ emissions for the gasoline vehicle by 0.9 g/km, while in the diesel vehicle the same figure was less than 0.1 g/km. This was investigated by running WLTC with the NEDC gear shifting strategy.

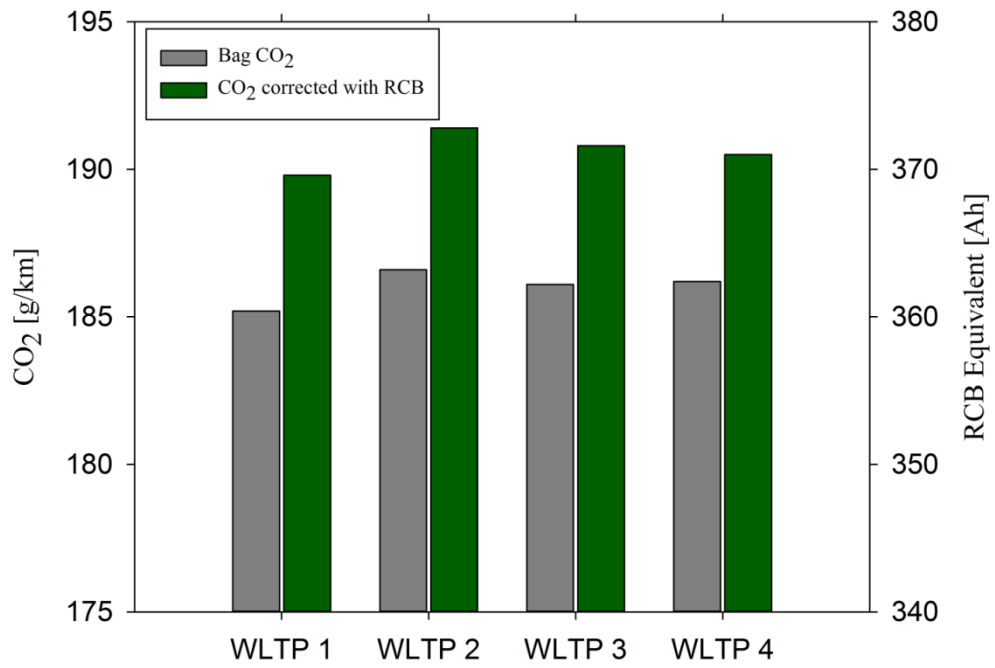


Figure 6: WLTP measurements corrected with RCB for a large gasoline vehicle.

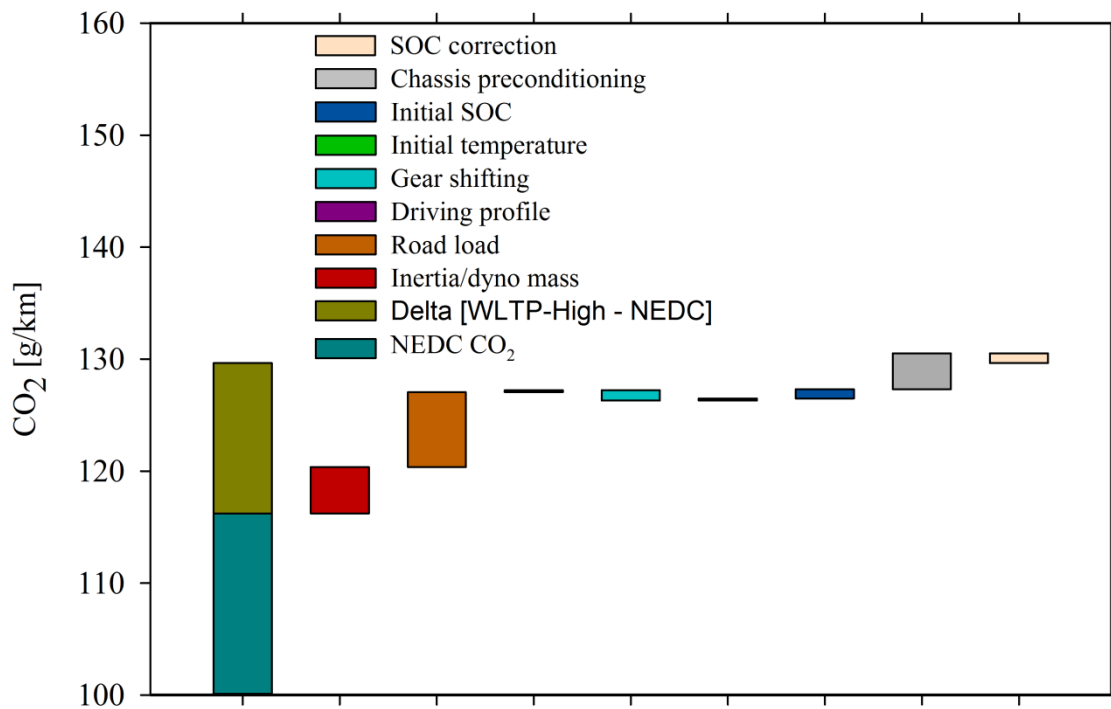


Figure 7: Step-by-step simulated Δ CO₂ between WLTP and NEDC for a small gasoline passenger car.

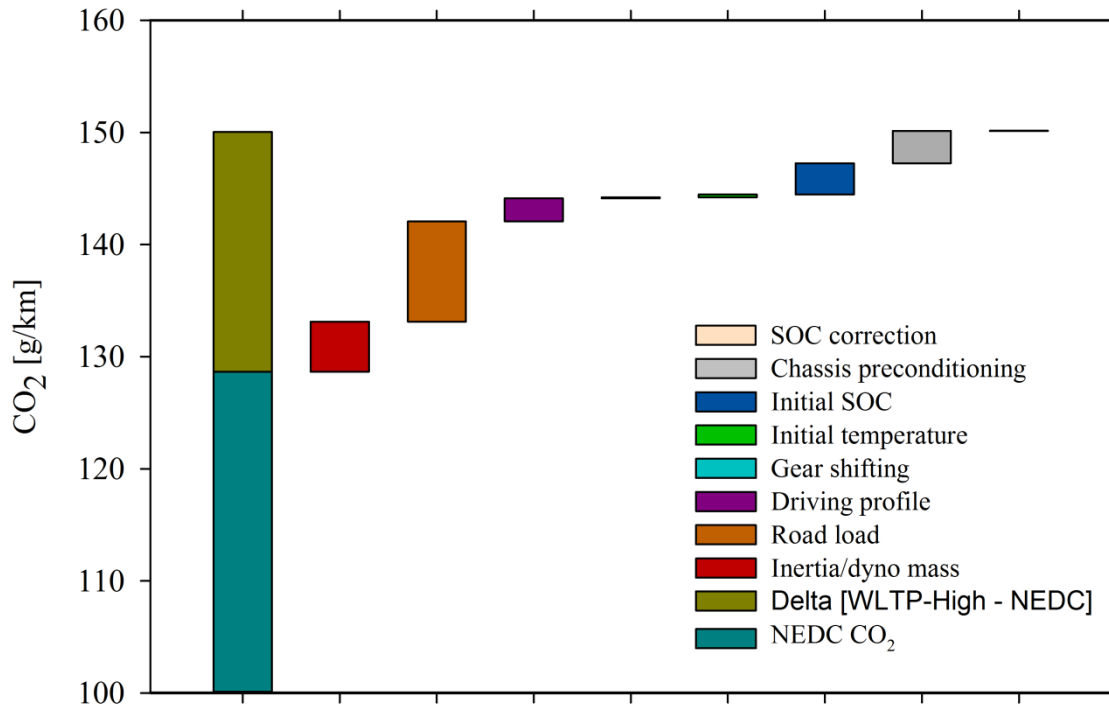


Figure 8: Step-by-step simulated ΔCO_2 between WLTP and NEDC for a medium-large diesel passenger car.

In the specific simulations, the battery SOC effect is investigated by changing its initial value from maximum, which is used in NEDC, to the battery's charge sustain mode operation value, which it is believed that will be used in WLTP. This modification in the simulations has an effect of 13% for the diesel vehicle and 6.1% for the gasoline vehicle in ΔCO_2 . If the final CO_2 values are corrected with RCB from Equation (3), the overall effect for the diesel vehicle remains constant, while surprisingly the effect of the gasoline vehicle is -6.5%, despite the fact that the same electrical system was used for the two vehicles. This highlights the fact that a detailed investigation regarding the optimum initial SOC should be conducted for the gasoline vehicle, in order to minimize the CO_2 correction. Finally, in both vehicles the effect of decreasing the initial test temperature from 25 °C to 23 °C, accounts for less than 1% in the overall ΔCO_2 .

4. Conclusion

CO_2 emission tests for 12 gasoline and 8 diesel passenger cars were performed under the NEDC and WLTP. These tests were used for the calibration and validation of a simulation tool used in the context of the WLTP-NEDC correlation exercise. The current work analyses the differences between the two protocols, and starting from the test results, quantifies the effect of WLTP on CO_2 emissions from passenger cars and comparing it with those of the NEDC.

The two measurement protocols differ in the driving profile and kinematic characteristics, in the determination of the test mass and applied driving resistance, in the gear shifting sequence and RCB correction and in the initial and soak temperature. From the above, the dominant reason for the difference between the WLTP-High and the NEDC was found to be the different test mass and the applied RL coefficients in the chassis dynamometer. These parameters, based on a simulation exercise in a small gasoline and a medium-large diesel car, were found to account for up to 74% in the observed ΔCO_2 between WLTP-High and NEDC.

Comparing cold start WLTP-High against NEDC, two trends were identified as characteristic for the vehicle sample; an increasing trend above the $y=x$ line for emissions from 100 to 180 g/km over NEDC and a decreasing trend from 180 to 220 g/km over the NEDC. In the area of 160-180 g/km belong medium-large automatic transmission vehicles, whose gear-shifting strategy is currently optimized over the NEDC and in the future is expected to be optimized over the WLTP; thus this area is characterized as "transitional". The delta between CO_2 emissions over WLTP-High and NEDC is decreasing as the CO_2 emissions values over NEDC are increasing.

The increase of certified CO₂ emissions when moving from NEDC to WLTP originates from a driving cycle and an overall test procedure, which more closely represents realistic vehicle operation. Introducing WLTP in the type-approval of light duty vehicles therefore represents an important step-forward in the direction of decarbonizing the road transportation sector and of providing customers with more reliable information. Optimizations towards the new procedure by vehicle manufacturers will still be possible, and possibly the overall increase in CO₂ will slightly decrease. But since vehicles will need also to comply with the Euro 6 emission limits on WLTP (for which no adjustment will be carried out) and on the RDE (although with some additional margins), flexibilities will in any case be limited.

Acknowledgments

The authors would like to acknowledge the contribution of the following institutes and their associated personnel in the framework of the NEDC-WLTP correlation exercise: European Commission, TNO, DEKRA, FIAT, Horiba, VELA labs at JRC-Ispra, TU Graz, TUV Nord and UTAC.

References

Andersson, J., J. May, C. Favre, D. Bosteels, S. de Vries, M. Heaney, M. Keenan and J. Mansell (2014). "On-Road and Chassis Dynamometer Evaluations of Emissions from Two Euro 6 Diesel Vehicles." SAE Int. J. Fuels Lubr. 7(3): 919-934.

AVL. (2016). "AVL Cruise - Vehicle System and Driveline Analysis." Retrieved 18 Jan., 2016,, from <https://www.avl.com/cruise>.

Bielaczyc, P., A. Szczotka and J. Woodburn (2015). "Regulated and Unregulated Exhaust Emissions from CNG Fueled Vehicles in Light of Euro 6 Regulations and the New WLTP/GTR 15 Test Procedure." SAE Int. J. Engines 8(3): 1300-1312.

Bielaczyc, P., J. Woodburn and A. Szczotka (2014). The WLTP as a new tool for the evaluation of CO₂ emission. FISITA World Automotive Congress. Maastricht, the Netherlands.

Bielaczyc, P., J. Woodburn and A. Szczotka (2015). A Comparison of Carbon Dioxide Exhaust Emissions and Fuel Consumption for Vehicles Tested over the NEDC, FTP-75 and WLTC Chassis Dynamometer Test Cycles, SAE International.

Ciuffo, B., A. Marotta, M. Tutuianu, K. Anagnostopoulos, G. Fontaras, J. Pavlovic, S. Serra, S. Tsiakmakis and N. Zacharaof (2015). The development of the World-Wide Harmonized Test Procedure for Light Duty Vehicles (WLTP) and the Pathway for its Implementation into the EU Legislation. Transportation Research Board. Washington DC,.

Dardiotis, C., G. Martini, A. Marotta and U. Manfredi (2013). "Low-temperature cold-start gaseous emissions of late technology passenger cars." Applied Energy 111: 468-478.

Demuyneck, J., D. Bosteels, M. De Paepe, C. Favre, J. May and S. Verhelst (2012). "Recommendations for the new WLTP cycle based on an analysis of vehicle emission measurements on NEDC and CADC." Energy Policy 49(0): 234-242.

Dings, J. (2013). "Mind the Gap! Why official car fuel economy figures don't match up to reality." Brussels: Transport and Environment.

European Environment Agency (2014). Tracking progress towards Europe's climate and energy targets for 2020. Trends and projections in Europe 2014. Luxembourg,.

European Environment Agency. (2015, 04/09/2015). "Global and European temperatures." Retrieved 12/01/2016, 2016, from <http://www.eea.europa.eu/data-and-maps/indicators/global-and-european-temperature/global-and-european-temperature-assessment-3>.

Favre, C., D. Bosteels and J. May (2013). "Exhaust Emissions from European Market-Available Passenger Cars Evaluated on Various Drive Cycles." SAE Int. J. Engines.

Joumard, R., M. André, R. Vidon, P. Tassel and C. Pruvost (2000). "Influence of driving cycles on unit emissions from passenger cars." Atmospheric Environment 34(27): 4621-4628.

Joumard, R., M. Rapone and M. Andre (2006). Analysis of the cars pollutant emissions as regards driving cycles and kinematic parameters: 132p.

Kadijk, G., M. Verbeek, R. Smokers, J. Spreen, A. Patuleia, M. van Ras, J. Norris, A. Johnson, S. O'Brien, S. Wrigley, J. Pagnac, M. Seban and D. Buttigieg (2012). Supporting Analysis on Test Cycle and Technology Deployment for Reviews of Light Duty Vehicle CO₂ Regulations Final Report,.

Kågeson, P. (1998). "Cycle-Beating and the EU Test Cycle for Cars. European Federation for Transport

and Environment, Brussels."

Kühlwein, J., J. German and A. Bandivadekar (2014). Development of test cycle conversion factors among worldwide light-duty vehicle CO₂ emissions. White Paper, The International Council on Clean Transport (ICCT).

Ligterink, N. E. (2012). Real world CO₂ emissions: causes and effects. lowCVP conference. London, TNO.

Marotta, A., J. Pavlovic, B. Ciuffo, S. Serra and G. Fontaras (2015). "Gaseous Emissions from Light-Duty Vehicles: Moving from NEDC to the New WLTP Test Procedure." Environmental Science & Technology.

May, J., D. Bosteels and C. Favre (2014). "An Assessment of Emissions from Light-Duty Vehicles using PEMS and Chassis Dynamometer Testing." SAE Int. J. Engines 7(3): 1326-1335.

Millo, F., L. Rolando, R. Fuso and F. Mallamo (2014). "Real CO₂ emissions benefits and end user's operating costs of a plug-in Hybrid Electric Vehicle." Applied Energy 114: 563-571.

Mock, P., J. German, A. Bandivadekar, I. Riemersma, N. Ligterink and U. Lambrecht (2013). From laboratory to road: A comparison of official and 'real-world' fuel consumption and CO₂ values for cars in Europe and the United States, International Council on Clean Transportation.

Mock, P., J. Kühlwein, U. Tietge, V. Franco, A. Bandivadekar and J. German (2014). The WLTP: How a new test procedure for cars will affect fuel consumption values in the EU. Working Paper The International Council on Clean Transport (ICCT).

Ntziachristos, L., G. Mellios, D. Tsokolis, M. Keller, S. Hausberger, N. E. Ligterink and P. Dilara (2014). "In-use vs. type-approval fuel consumption of current passenger cars in Europe." Energy Policy 67(0): 403-411.

Rangaraju, S., L. De Vroey, M. Messagie, J. Mertens and J. Van Mierlo (2015). "Impacts of electricity mix, charging profile, and driving behavior on the emissions performance of battery electric vehicles: A Belgian case study." Applied Energy 148: 496-505.

Sileghem, L., D. Bosteels, J. May, C. Favre and S. Verhelst (2014). "Analysis of vehicle emission measurements on the new WLTC, the NEDC and the CADC." Transportation Research Part D: Transport and Environment 32(0): 70-85.

Suarez-Bertoa, R., A. A. Zardini, H. Keuken and C. Astorga (2015). "Impact of ethanol containing gasoline blends on emissions from a flex-fuel vehicle tested over the Worldwide Harmonized Light duty Test Cycle (WLTC)." Fuel 143(0): 173-182.

Tietge, U., N. Zacharaof, P. Mock, V. Franco, J. German, A. Bandivadekar, N. Ligterink and U. Lambrecht (2015). A 2015 update of official and "real-world" fuel consumption and CO₂ values for passenger cars in Europe. White Paper, The International Council on Clean Transportation.

Transport & Environment (2015) "Mind the Gap."

Tsokolis, D., S. Tsiakmakis, G. Triantafyllopoulos, A. Kontses, Z. Toumasatos, G. Fontaras, A. Dimaratos, B. Ciuffo, J. Pavlovic, A. Marotta and Z. Samaras (2015). "Development of a Template Model and Simulation Approach for Quantifying the Effect of WLTP Introduction on Light-Duty Vehicle CO₂ Emissions and Fuel Consumption " SAE Int. J. Engines.

Tutuianu, M., P. Bonnel, B. Ciuffo, T. Haniu, N. Ichikawa, A. Marotta, J. Pavlovic and H. Steven (2015). "Development of the World-wide harmonized Light duty Test Cycle (WLTC) and a possible pathway for its introduction in the European legislation." Transportation Research Part D: Transport and Environment 40: 61-75.

Tutuianu, M., A. Marotta, H. Steven, E. Ericsson, T. Haniu, N. Ichikawa and H. Ishii (2013). Development of a World-wide Worldwide harmonized Light duty driving Test Cycle (WLTC). Transmitted by the WLTP DHC Chair.

Weiss, M., P. Bonnel, R. Hummel, A. Provenza and U. Manfredi (2011). "On-Road Emissions of Light-Duty Vehicles in Europe." Environmental Science & Technology 45(19): 8575-8581.

Zamboni, G., S. Moggia and M. Capobianco (2016). "Hybrid EGR and turbocharging systems control for low NO_x and fuel consumption in an automotive diesel engine." Applied Energy 165: 839-848.

Real world performance of ventilation systems for reducing nitrogen oxides or particulate matter levels in road tunnels

Bruno VIDAL*, Jean François. BURKHART*, David PRETERRE**, Frantz GOURIOU** & Jean François PETIT***

*Centre D'Étude des Tunnels [Centre for Tunnel Studies] (CETU), 25 Avenue François Mitterrand, Bron, France

Fax +33 04 72 14 33 70 - email: bruno.vidal@developpement-durable.gouv.fr

** CERTAM, 1 Rue Joseph Fourier, Saint Etienne du Rouvray. France

*** CEREMA DTer Ile de France, 12 Rue Teisserenc de Bort, Trappes. France

Abstract

In a context where the findings of scientific studies converge on a proven health risk and where the opportunities for reducing emissions are limited, the question of motorists' exposure to road pollutants is becoming more and more a sensitive subject. Despite the short exposure time, travel through road tunnels must be subject to careful examination due to the confined nature of these structures. The prevailing pollutants could see their concentrations reach exaggerated levels during traffic congestion if they are not diluted with fresh air via sanitary ventilation systems.

A series of four on-site measurement campaigns has demonstrated the positive impact of this regulatory measure. Despite methodological limitations, the results have revealed a significant reduction in the levels of gaseous pollutants thanks to their dilution with fresh air. This strategy has been adequate to achieve concentrations that meet regulatory criteria with regards to air quality in road tunnels. A slower decrease in particulate pollution has also been observed. However, the fight against this pollutant also involves the regular washing of roads tunnels. Finally, the positive effects of sanitary ventilation have been more easily characterised for longitudinal systems (jet fans hanging from the ceiling) than for transverse systems (injection of fresh air distributed along the tube) which seem to have greater inertia.

Key words: Road tunnel ventilation, efficiency tests, on road measurements, NO₂, particulate matter.

Résumé

Dans un contexte où les conclusions des études scientifiques convergent vers un niveau de risque sanitaire avéré et où les possibilités de réduction des émissions deviennent limitées, la question de l'exposition des automobilistes aux polluants routiers est de plus en plus sensible. Malgré une durée d'exposition courte, le passage dans les tunnels routiers doit faire preuve d'un examen attentif en raison du caractère confiné de ces ouvrages. Les polluants qui y règnent pourraient voir leurs concentrations atteindre des valeurs exagérées lors des congestions de trafic si on ne les diluait pas par apport d'air frais grâce aux dispositifs de ventilation sanitaire.

Une série de quatre campagnes de mesure in situ a pu montrer l'impact positif de cette mesure régulatrice. Malgré des limitations d'ordre méthodologique, les résultats ont montré une réduction significative des niveaux des polluants gazeux grâce à leur dilution par l'air frais. Cette stratégie a permis d'atteindre des concentrations respectant les critères réglementaires sur la qualité de l'air en tunnel routier. Une diminution de la pollution particulaire, moins rapide, a également pu être observée. Mais la lutte contre ce polluant passe aussi par un lavage régulier des tunnels. Enfin, les effets positifs de la ventilation sanitaire ont plus facilement été caractérisés sur les systèmes de type longitudinal (accélérateurs en voûte) que sur ceux de type transversal (injection d'air frais répartie le long du tube) qui semblent présenter plus d'inertie.

Mots clés: Ventilation, tunnel routiers, tests d'efficacité, mesures embarquées, NO₂, particules.

INTRODUCTION

In 2013, outdoor air pollution was classified by the WHO as carcinogenic for humans, WHO (2013). Many air-borne pollutants originate from road traffic which constitutes one of the main producers of particles and nitrogen oxide. In 2012, the WHO classified diesel engine exhaust effluents as definite carcinogenic to humans, WHO (2012). Over the course of scientific studies, the causal relationship

between outdoor air pollution and respiratory and cardiovascular pathologies, as well as effects on foetal or neurological development, or on reproduction has been strengthened, WHO (2016). In addition, data concerning the acute and chronic effects of NO₂ resulting from studies of humans highlights respiratory symptoms, a change in bronchial responsiveness, an inflammation of airways, as well as decreased immunity defences originating from an increased susceptibility to respiratory infections, ANSES (2013). Finally, in 2011, the conclusions of the APHEKOM project stressed the importance of developing urban policies to reduce the exposure of populations living within close proximity to streets and roads with high traffic density, APHEKOM (2011).

Road users, who are exposed to pollutants at the site of their emission, are particularly affected by road emissions. In 2015, the CYCLO-POL study considered the concentration of NO₂ in a vehicle's cabin to be 2 to 3 times greater than the level observed within close proximity of traffic, which was itself twice as high as background pollution levels, ADEME (2015). Just as an individual's total exposure to pollution is the sum of multiple exposures that occur throughout the day (work, leisure, sporting activities, rest ... and transport), the total exposure of a road user to road emissions is the result of exposures encountered during their journey, which vary depending on the volume of traffic encountered, traffic conditions (free flow, slow speed or severe congestion), weather conditions or even the surrounding environment (countryside, peri-urban, city centre).

Travel through road tunnels, because of the confined nature of such structures, constitutes a situation where the risk of encountering significant pollution levels is high. However, users' exposure is generally limited, as they only remain within these structures for short periods of time (from several tens of seconds to several minutes, depending on the length of the structure and the fluidity of the traffic). Thus, the amount of pollutant received when travelling through a tunnel is not, most of the time, significant in relation to the total dose received over an entire journey. Travelling through a tunnel may even be beneficial if it means avoiding a route, which, even though outside, results in a higher exposure. This may be the case for a longer and congested alternative route with high pollution levels.

In a review published in June 2014, the ADEME stated that the successive application of EURO standards has drastically reduced exhaust emissions from new vehicles with the exception of NO_x emissions from diesel vehicles. It then emphasised that subsequent reductions will be increasingly difficult to achieve for cars beyond the EURO 6 standard, ADEME (2014). Furthermore, every new exhaust pollution control device is likely to generate other types of primary or secondary pollutant emissions.

On 31 March 2016, the European Union published EC Regulation no. 2016/427 (modification to EC regulation no. 692/2008) in the Official Journal of the European Union concerning emissions from private and light commercial vehicles (Euro 6). This regulatory evolution came in response to discrepancies between pollutant emissions observed during approval procedures and those measured in normal use conditions on roads, especially for nitrogen oxides. This text provides for a derogation in relation to emissions in actual driving conditions (ADC). For NO_x, this tolerance would be set initially to 110% in relation to the upper limit of the Euro 6 standard – which is 168 mg/km compared to 80 mg/km now – and, from January 2020, this rate would be reduced to 50%, which is 120 mg/km.

Thus, in constant traffic, there is little hope of significant improvements to the volume of motor vehicle emissions. NO₂ remains and could continue to remain for a long time the most worrying gaseous pollutant in road tunnels, knowing that the share of NO₂ has increased significantly to the detriment of NO – significant increase in the ratio [NO₂]/[NO_x] over the last 20 years, Bernagaud et al (2014). On the other hand, and despite the widespread use of particle filters which has significantly reduced primary particle exhaust emissions, the problem of fine particles however has not been resolved with the persistence of secondary particles (formed from gas precursors) and primary particles formed through

abrasion (floor, tyres, breaks, etc.) which can easily accumulate in confined spaces like tunnels and then being resuspended by whirlwinds created by the traffic.

The regulation concerning air quality applicable to road tunnel users in normal conditions of use is presented in the circular of the Direction Générale de la Santé [French General Health Directorate] 99-329 of 08 June 1999, Ministère de la Santé [French Ministry of Health] (1999), based on the recommendation of 14 December 1998 issued by the Conseil Supérieur d'Hygiène Publique de France [French Higher Public Health Council], Conseil supérieur d'hygiène publique de France (1998). In addition, the CETU recommends that opacity does not exceed 5 km^{-1} at any point in the tunnel at any time, CETU (2003).

Table 1: Summary of French legislation

Pollutant	Time	Limit value	Location
Carbon monoxide (CO)	15 minutes	90 ppm	On average over the entire length of the structure
	30 minutes	50 ppm	
Nitrogen dioxide (NO ₂)	15 minutes	0.4 ppm	

In order to reduce the impact of exposure for road tunnel users, air quality must be controlled in accordance with the regulatory criteria applicable for these structures [Table 1]. The results of the AIRTURIF project, Guilloteau et al (2010), which focussed on several measurement campaigns in road tunnels in the Île de France, showed that in the absence of sanitary ventilation:

- CO levels requirements were still respected;
- NO₂ levels requirements were sometimes exceeded in some tunnels and under certain conditions;
- The tunnels with the greatest sensitivity to pollution peaks were tunnels with one or more of the following characteristics: Congested, two-way, long or featuring a declivity, Vidal et al (2014).

To significantly reduce tunnel users' exposure to road pollutants, road network operators have two key means at their disposal. The first, which must be given priority, is ensuring the fluidity of traffic, even if this leads to congestion outside the tunnel. This measure is also an essential means of minimising the consequences of a fire inside the tunnel, by limiting the number of people present and facilitating the intervention of the emergency services. The second means of reducing pollution levels is the dilution of pollutants by providing outside fresh air. This is known as "sanitary ventilation" as opposed to "smoke control ventilation" which is used in the case of a fire. A draught moving at 3 to 5 m/s inside a structure is generally sufficient to comply with air quality requirements within road tunnels, Vidal et al (2014). This draught is usually generated by the traffic itself, due to a sustained piston effect maintained on air masses. In the event of traffic congestion, sanitary ventilation can mechanically generate draught and thus reduce the concentration of pollutants.

Tunnel engineering terminology distinguishes between two types of ventilation systems, CETU, (2003):

- The longitudinal system, where fans (generally called accelerators or jet fans – hanging from the ceiling) push the air mass around the tunnel, providing fresh air or removing exhausted air only through the portals;
- The transverse system, fitted with a blowing circuit which injects air into the tunnel at regular intervals on the one hand and an extraction circuit which extracts air from the tunnel at regular intervals on the other. Except for very particular configurations, this type of system requires ventilation shafts that run the full length of the tunnel. We talk about a "semi-transverse system"

when the system is not fitted with an extraction circuit or “use in semi-transverse mode” when the system is able to exhaust out of the tunnel the polluted air but this functionality isn’t used.

For economic reasons, a single ventilation system is installed to meet both smoke extraction and sanitary needs. Constraints which determine the choice of ventilation system are therefore not only fire safety requirements (often the most demanding constraints) but also fresh air needs for diluting in-tunnel pollutants (particularly for structures with high traffic volumes and regularly saturated traffic). In some cases, the environmental impact of air discharged outside the tunnel and the maximum acceptable speed of the draught can influence the choice. Simpler longitudinal systems are generally well suited to one-way tunnels without recurring congestion. Transverse ventilation is generally reserved for two-way tunnels or one-way tunnels with recurring congestion.

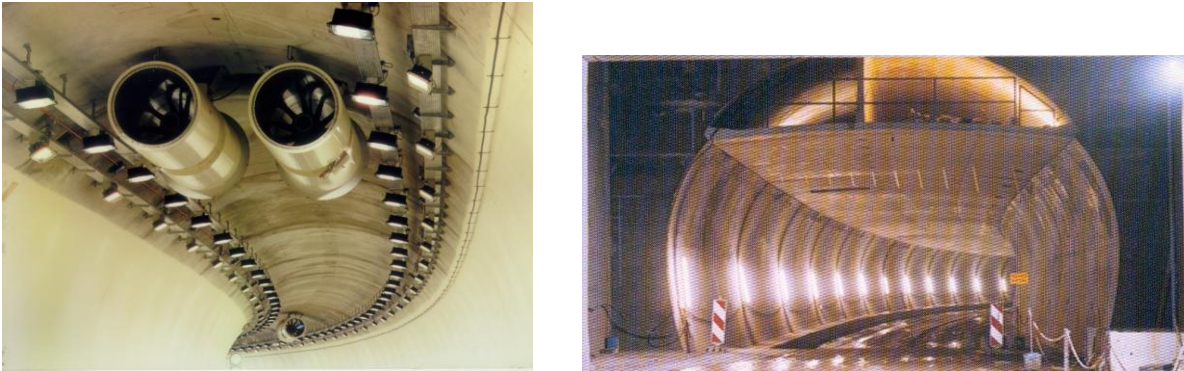


Figure 1: Jet fans in a longitudinal system (left) ventilation ceiling ducts and vertical blowing ducts in a transverse system (right)

Sanitary ventilation systems are designed to supply the necessary amount of fresh air to dilute vehicle emissions. In a specific approach to the issue of road tunnels, the AIPCR’s tunnel committees have listed the exhaust emission factors of various pollutants (CO, NO_x and particles) as well as the emission factors of particulate matter that are non-exhausted particles sources, PIARC (2012). The minimum quantities of fresh air needed to ensure compliance with in-tunnel air quality values are calculated from these emission factors, taking into account the specific vehicle fleet on the concerned route, CETU (2012). The distribution of pollutants along the tunnel – and its potential access roads – when in steady state, can also be modelled, CETU (2011), in order to complete the specifications of the ventilation system. In design studies, the consideration of the dispersion of the discharge from the structure’s portals may also be indispensable.

In normal operating conditions, sanitary ventilation is generally managed automatically according to algorithms that determine fresh air needs via sensors (CO, NO₂, opacity) distributed throughout the tunnel. The operator can also operate it manually. Finally, as the use of fans requires significant electric power, the tunnel operator must optimise the duration of their use so as to effectively manage operating costs. Ventilating at just the right level is key from an economic and sanitary perspective as well as within a more global approach which includes sustainable development.

Based on on-site experiments, this article provides an assessment of the effective capacity of sanitary ventilation systems to curb situations of excessive concentrations of in-tunnel pollutants. After outlining measurement performance conditions, this article shall discuss the benefits and constraints of each ventilation system based on tests conducted in various type of structures:

- One-way tunnel with longitudinal ventilation; Guy Môquet tunnel;
- Two-way tunnel with a transverse ventilation system; Siaix tunnel;
- One-way tunnel with transverse ventilation; Landy and Bobigny tunnels.

1. Methodology

The aim of these tests is to demonstrate the impact of sanitary ventilation on air quality. The difficulty in defining a test method lies in the fact that these tests are carried out in real operating conditions and many parameters are therefore not controlled - like, for example, the type and volume of emissions in the structure and the atmospheric conditions as well as the evolution of these parameters during the test. Ideally, to compare situations with or without the operation of ventilation, the experimental conditions need to be identical. However, each situation within a structure is unique and therefore cannot be perfectly reproduced. The methodology consists of finding conditions that can be considered adequately similar.

In addition to pollutant concentration measurements, other parameters that should ideally be monitored ideally during ventilation tests are the flow and speed of vehicles inside the structure, as well as the draught speed inside the tunnel.

- For a tunnel with longitudinal ventilation, fresh air is sucked in via the structure's entrance and the polluted air is discharged through the exit portal; a single draught speed measurement point is sufficient.
- For semi-transverse ventilation, fresh air is injected along the structure and exhausted air is expelled via the two portals with distribution depending on traffic conditions, outdoor wind conditions, a potential chimney effect in the tunnel (if there is a gradient) or even a pressure difference between the two portals. For this type of ventilation, in order to assess the draught leaving the tunnel, an anemometer should be placed at each of the structure's portals.

Finally, note that anemometers can only be installed on the outside of the circulated space, meaning very close to the walls. Thus, to ascertain the exact draught at a measurement point, we need to carry out a calibration correction per anemometric grid to estimate the average speed in the ventilated section. Practically speaking, implementing such calibration during ventilation tests in an operational tunnel is very complex. Therefore, anemometric measurements are given here for information purposes only; they do not provide exact average draught speed values for the measurement sections (by dividing the values provided in this paper by a coefficient of around 0.9 we can get close to this, but this coefficient is variable and depends on the shape of the tube and the positioning of the sensor, among other things). However, the draught measurements presented make it possible to differentiate between various situations: High, moderate, low and almost zero draught and thus observing the main effects of the activation of sanitary ventilation systems (off, operating at 50% or 100%).

Tests were deliberately carried out when the pollutant concentrations were at their highest because on the one hand sanitary ventilation is designed to manage this type of event and because on the other it's in these type of situations that we see more easily how pollutants are diluted through injection of fresh air. For one-way tubes, test runs focussed on congestion situations as draught speed in the structure is lower and the effect of sanitary ventilation can be more easily detected (first of all with anemometric measurement). Rainy days were eliminated as even inside the tunnel (excluding long structures) the floor and walls become wet due to runoff and water projection from vehicles. On these days, particles were not resuspended nearly as much.

As such, the tests consisted of comparing high pollution situations during congestion periods, which are theoretically repeatable, whilst activating or deactivating the sanitary ventilation:

- For the Guy Môquet tunnel, the recurring congestion period – between around 7.30 a.m. and 9.30 a.m. – was chosen, with the ventilation in operation (full speed or half speed depending on the tests) for 45 minutes between 8.00 a.m. and 8.45 a.m. Provided that the traffic congestion is present and stable for the duration of the test, this method permits the observation of the actual contribution of the ventilation – when it's activated – and the impact of its absence – when it's turned off – and also makes it possible to observe the response time in both cases.

- For the Siaix tunnel (access route to the Tarentaise valley in the Alps), the tests were carried out on Saturdays when vehicles were travelling to or returning from winter sports activities, when this structure experienced congestion in both directions. This two-way tunnel is fitted with transverse ventilation. As the pollution started to build up from 7.00 a.m., we chose to operate the ventilation permanently between 9.00 a.m. and 9.00 p.m., alternating between full and half-speed at 1.5 hour intervals. Only two tests could be validated as on the other Saturdays when measurements were taken it rained.
- For the Landy tunnel, there was congestion throughout the morning, often from 6.30 a.m. and sometimes until 1.00 p.m., with easily repeatable traffic and pollution profile conditions. During an 8 week measurement campaign in June/July 2002, two Friday mornings were dedicated to ventilation tests (28 June between 8.25 a.m. and 11.25 a.m. and 5 July between 7.00 a.m. and 9.00 a.m. with the ventilation operating at full speed) whilst during the 4 previous Friday mornings the ventilation was not activated to provide reference values.
- For the Bobigny tunnel, as with the Guy Môquet tunnel, the decision was made to carry out the tests in the middle of congestion periods, either from 10.30 a.m. until 12.00 p.m. or from 4.00 p.m. until 6.30 p.m., and to then observe the concentration gradients recorded at the fixed station when the ventilation was in operation or turned off. These tests were performed by activating the ventilation at one of the three operating speeds, depending on the day. This measurement campaign was also subject to on-board vehicle measurements to enable the comparison of longitudinal concentration profiles over the length of the structure depending on the ventilation speed applied during each journey, for similar traffic situations. This part of the study was carried out with the technical support of CERTAM (Centre d'Études et de Recherche Technologique en Aérothermique et Moteurs [Centre of Aerothermal and Engine Studies and Technological Research]) within the scope of the AIRTURIF project, Vidal et al (2014).

The specific methodological features of each test are presented in the results section.

2. Results

One-way tunnel with longitudinal ventilation - Guy Môquet tunnel

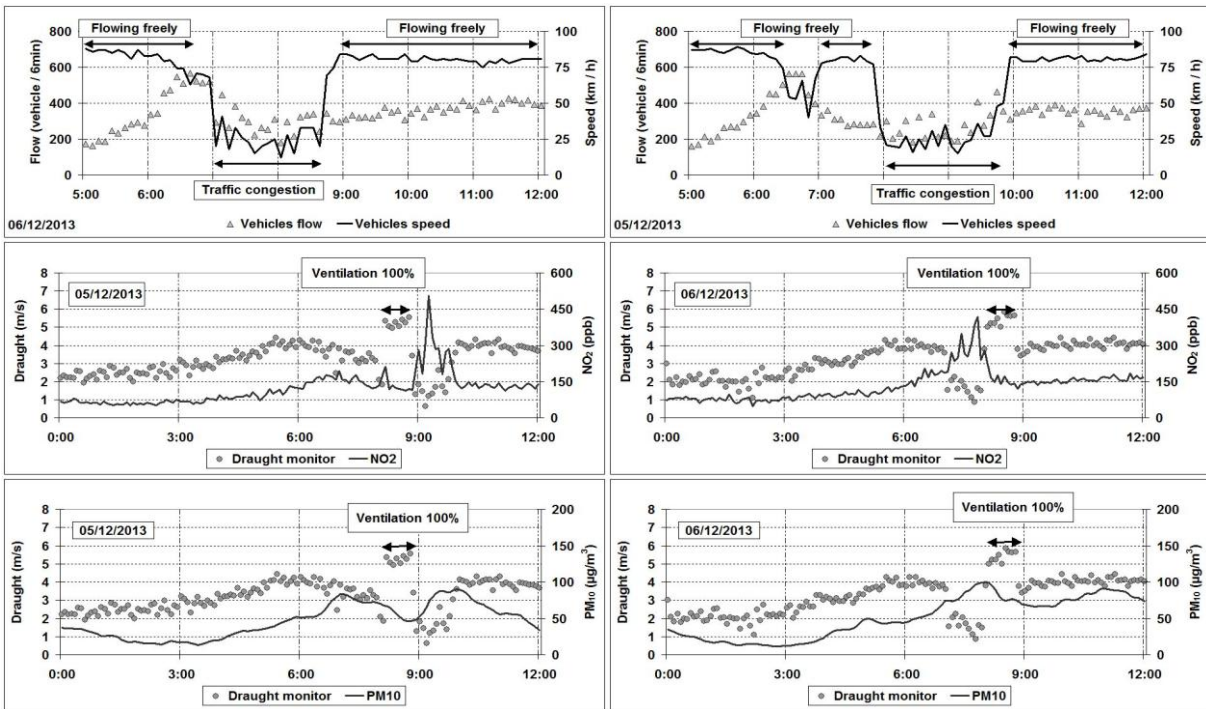
The Guy Môquet tunnel is a 560 m long structure located on the A86 motorway on the outskirts of Paris. It is ventilated longitudinally by 12 booster fans with a respective unitary thrust of 1,100 N, arranged in two banks of 6. The ventilation can be operated at full speed (ventilation at 100%) or at moderate speed (ventilation at 50%). The tunnel was equipped, 125 metres from the exit portal of the north tube, with:

- An APNA (Horiba) chemiluminescence analyser for nitrogen oxide concentrations;
- A TEOM (Thermo Scientific) for particle concentrations with a diameter of less than 10 μm (PM_{10});
- A Tunnel rotating vane anemometer (Thies) installed on the side wall to monitor variations in the draught speed.

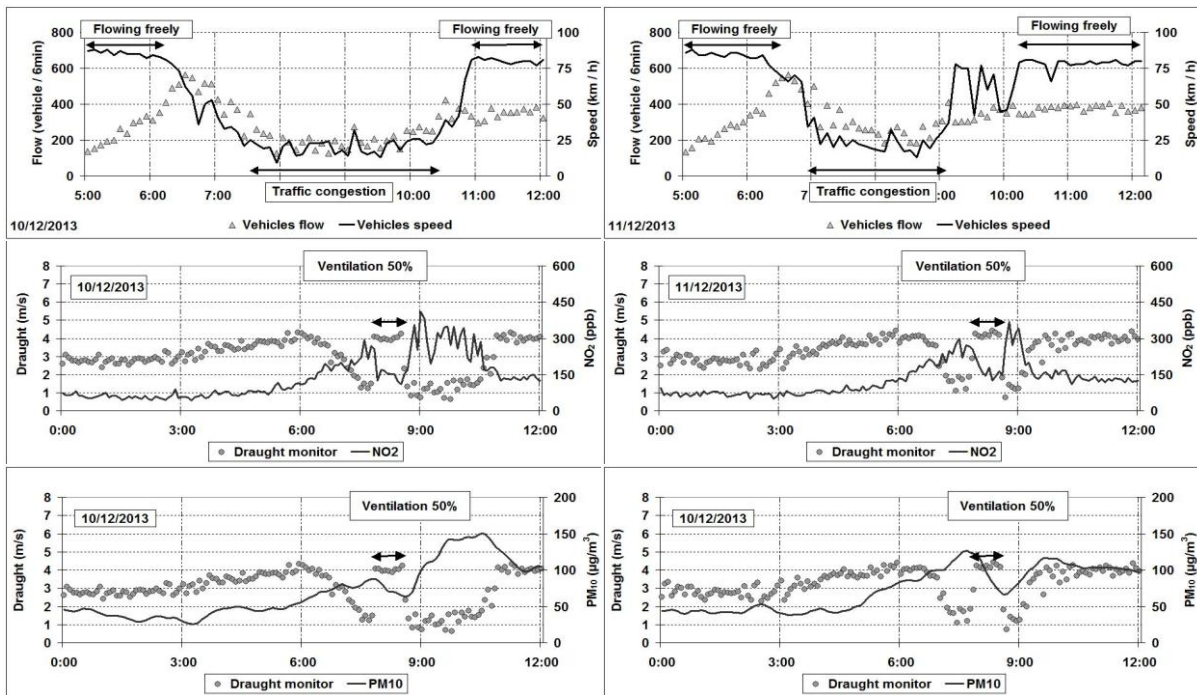
The measurement campaign lasted for around 3 weeks (from 27 November to 7 December 2013) including 9 days of ventilation tests. The average NO_2 concentrations (throughout the tunnel and for 15 minutes) were always lower than the regulatory level, however, they did reach this value on 3 December between 4.10 p.m. and 4.40 p.m. In a congestion situation, vehicle speeds drops to between 10 and 30 km/h, the draught in the tunnel becomes low and pollutant concentrations are high. As soon as the ventilation is activated, the draught increases, thus leading to an injection of fresh air. There is a fairly rapid drop in NO_2 concentrations. There is a slower response time for PM_{10} .

During the two tests carried out on 5 and 6 December 2013 [Figures 2 to 7], the ventilation operated at 100%, resulting in draught speed of around 5.5 m/s in the tube. On 5 December, congestion began to

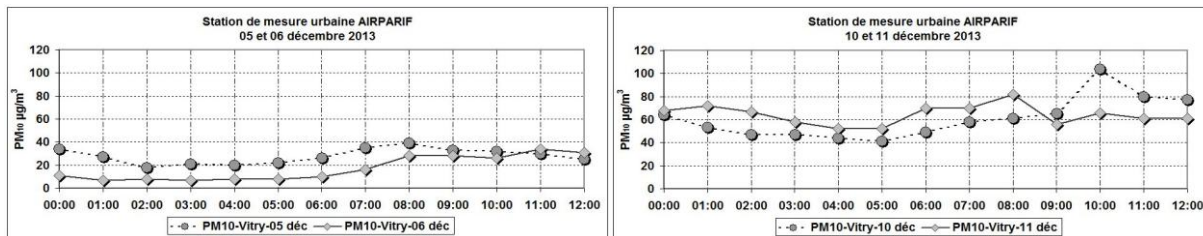
build up from 8.00 a.m. and continued 9.45 a.m. When the sanitary ventilation was turned off, the airflow speed decreased dropping to 1 m/s, creating a situation conducive to the formation of a peak in pollution which remained until the traffic was flowing again. On 6 December, congestion started to build up from 7.00 a.m. and continued until 8.45 a.m. The peak in pollution preceded the activation of the sanitary ventilation. When this was turned off, the traffic was moving again, resulting in an draught speed of 4 m/s, and the NO₂ and PM₁₀ concentrations remained stable



Figures 2 to 7: Traffic flow and speed, NO₂, PM₁₀ concentrations and draught speed during the mornings of 5 and 6 December 2013 in the Guy Môquet tunnel



Figures 8 to 13: Traffic flow and speed, NO₂ and PM₁₀ concentrations and draught speed during the mornings of 10 and 11 December 2013 in the Guy Môquet tunnel



Figures 14 and 15: Background concentrations of PM₁₀ on the mornings of 5, 6, 10 and 11 December 2013 at the Vitry sur Seine air quality monitoring station (Airparif data)

The 8 to 13 figures show the tests carried out on 10 and 11 December with the sanitary ventilation operating at 50% of its maximum power resulting in an draught speed of around 4.0 m/s in the tube, which is sufficient to result in a fast and significant reduction in NO₂ concentrations. The impact on PM₁₀ is less immediate and inconsistent in terms of amplitude depending on the day.

In conclusion:

- At night, a low draught of 2.5 to 3 m/s dilutes the moderate emissions visible at this time;
- During the day, when traffic is moving, a more pronounced draught (4 m/s) maintains NO₂ concentrations at reasonable levels;
- In congestion situations, the flow is extremely low and no longer allows pollutants to be diluted, which are emitted in greater volumes during these periods;
- In congestion situations, when sanitary ventilation is activated, NO₂ concentrations are maintained at the levels observed when traffic is moving. Ventilation operating at 50 % provides enough draught to maintain NO₂ concentrations at reasonable levels;

The dilution of particles is less rapid and seems more problematic. The effects of ventilation on days (10 and 11 Dec) when outdoor PM₁₀ concentrations were higher (see Figures 14 and 15), are less visible. In contrast, draught tends to resuspend particles and, at the start of a ventilation session, causes the inverse effect to that sought. Sanitary ventilation only had a moderate effect on eliminating particles during tests in the Guy Môquet tunnel and it would have been wise to ventilate for longer to better observe the beneficial effects. This also highlights how important it is to regularly clean tunnels as this removes a large portion of the matter that may be resuspended.

Table 2 : Summary of the ventilation in the Guy Môquet tunnel

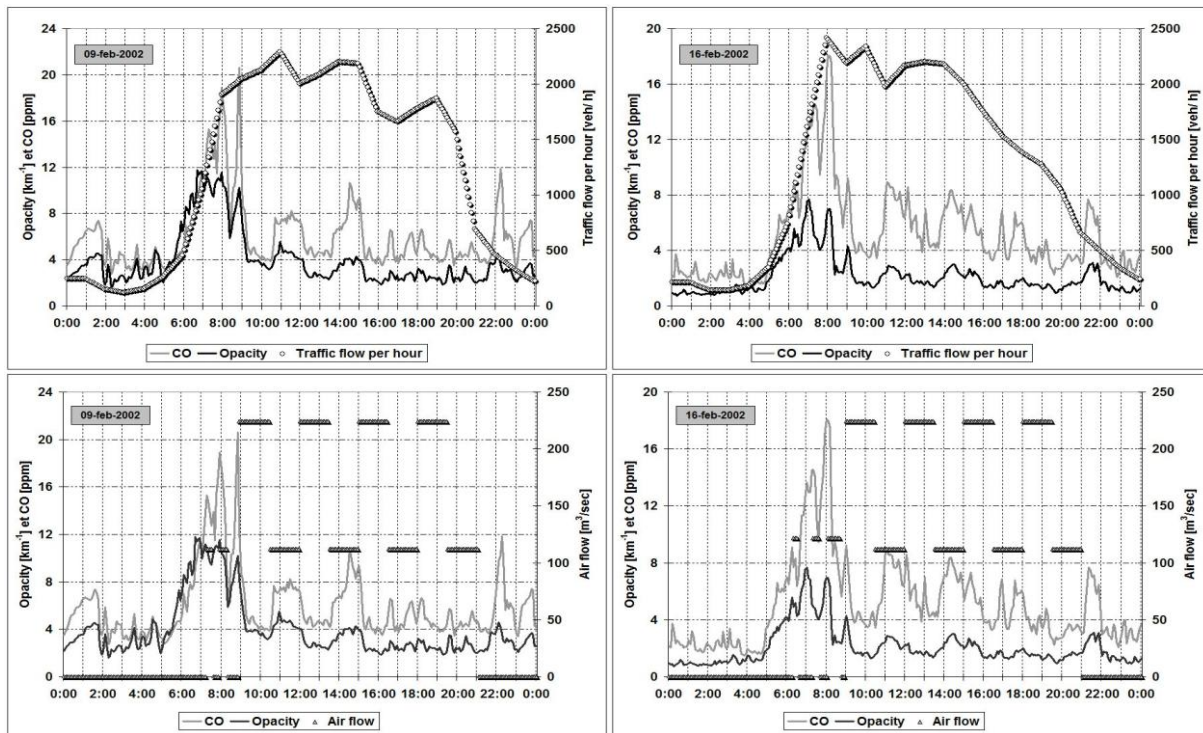
Parameters	Date	Night	During the peak in pollution	With sanitary ventilation	Fluid traffic situation
Draught speed y (m/s)	05 Dec	2.5	1.5	5.5	4.0
	06 Dec	2.5	1.5	5.5	4.0
	10 Dec	2.8	1.0	4.0	4.0
	11 Dec	3.0	1.5	4.0	4.0
NO ₂ (ppb)	05 Dec	70	500 ⁽¹⁾	130	130
	06 Dec	80	400 ⁽²⁾	150	150
	10 Dec	60	380 ⁽³⁾	140	140
	11 Dec	75	320 ⁽⁴⁾	150	140
PM ₁₀ (µg/m ³)	05 Dec	15	90	50	50
	06 Dec	15	100	75	80
	10 Dec	35	150	65	100
	11 Dec	40	125	65	100

Average estimate of NO₂ concentrations throughout the tunnel: ⁽¹⁾ 350ppb, ⁽²⁾ 280ppb, ⁽³⁾ 270ppb, ⁽⁴⁾ 230 ppb.

Two-way tunnel with semi-transverse ventilation – Siaix tunnel

The Siaix tunnel is a 1590 metre long two-way tunnel located on the RN90 National Road in the Alps. During the tests, the ventilation was operated in semi-transverse mode, which supplies fresh air at a rate of 112 m³/s via each of its two ventilation stations (one station at each of the structure's portals). The tunnel was fitted with a SICK VICOTEC 404 opacimeter 950 metres from the south portal (Moutiers side) which made it possible to measure the opacity and carbon monoxide through infra-red absorption.

The recording period lasted for around 6 months (first half of 2002). The opacity rate, which was generally low during this period (average = 1.4 km⁻¹ and 50th percentile = 0.6 km⁻¹) did however present rather high episodes, sometimes with some very prominent peaks, greater than the value of 5 km⁻¹ recommended for opacity. During the winter period, observed pollution levels (averages or peaks) were considerably higher than those recorded during the spring, which were higher than those in summer. Dry dust, much of which wasn't generated by internal combustion engines, was suspended in the air, creating a significant opacity rate. This structure was only occasionally congested, only during departures for winter sport activities. As traffic travelled in both directions, draught was generally low (average of 0.6 m/s, with a standard deviation of ± 1.2 m/s, during the six months of measurements) thus resulting in the stagnation of pollutants due to insufficient air renewal.



Figures 16 to 19: Flow and traffic, CO concentrations and opacity on Saturday 9 and 16 February 2002 in the Siaix tunnel

Two days of ventilation tests could be validated: Saturday 9 and 16 February 2002. Congestion appeared between 7.00 a.m. and 8.00 a.m. and remained until 6.00 p.m. From 9.00 a.m., the ventilation was operated manually for 1.5 hour periods, alternating between half and full power. We observed the beneficial effects of fresh air intake on the CO as well as on the opacity:

- At 9.00 a.m., there was a sudden drop in concentrations when the ventilation was activated at 100%;
- Each time the speed was switched from 100% to 50% (at 12.00 p.m., 3.p.m. or 6.00 p.m.), we noted a decrease in concentrations;

- In contrast, when the speed was switched from 50% to 100%, the levels of pollutants increased once again, however the opacity did not reach the recommended value of 5 km⁻¹;
- Finally, when it was turned off at 9.00 p.m., as the traffic hadn't yet reduced sufficiently, we noted a final increase in pollutant concentrations:

In conclusion, these two tests show the intended effect of the ventilation. The reduction in opacity levels was significant, but lower levels could have been reached if the structure had been cleaned regularly to remove any dust which levels were particularly significant on this route. The 50% speed was found to be sufficient to produce a significant decrease in the two pollutants observed. Additional equipment would have been needed to assess compliance with regulatory criteria over the entire length of the structure.

Two-way tunnel with semi-transverse ventilation – Landy tunnel

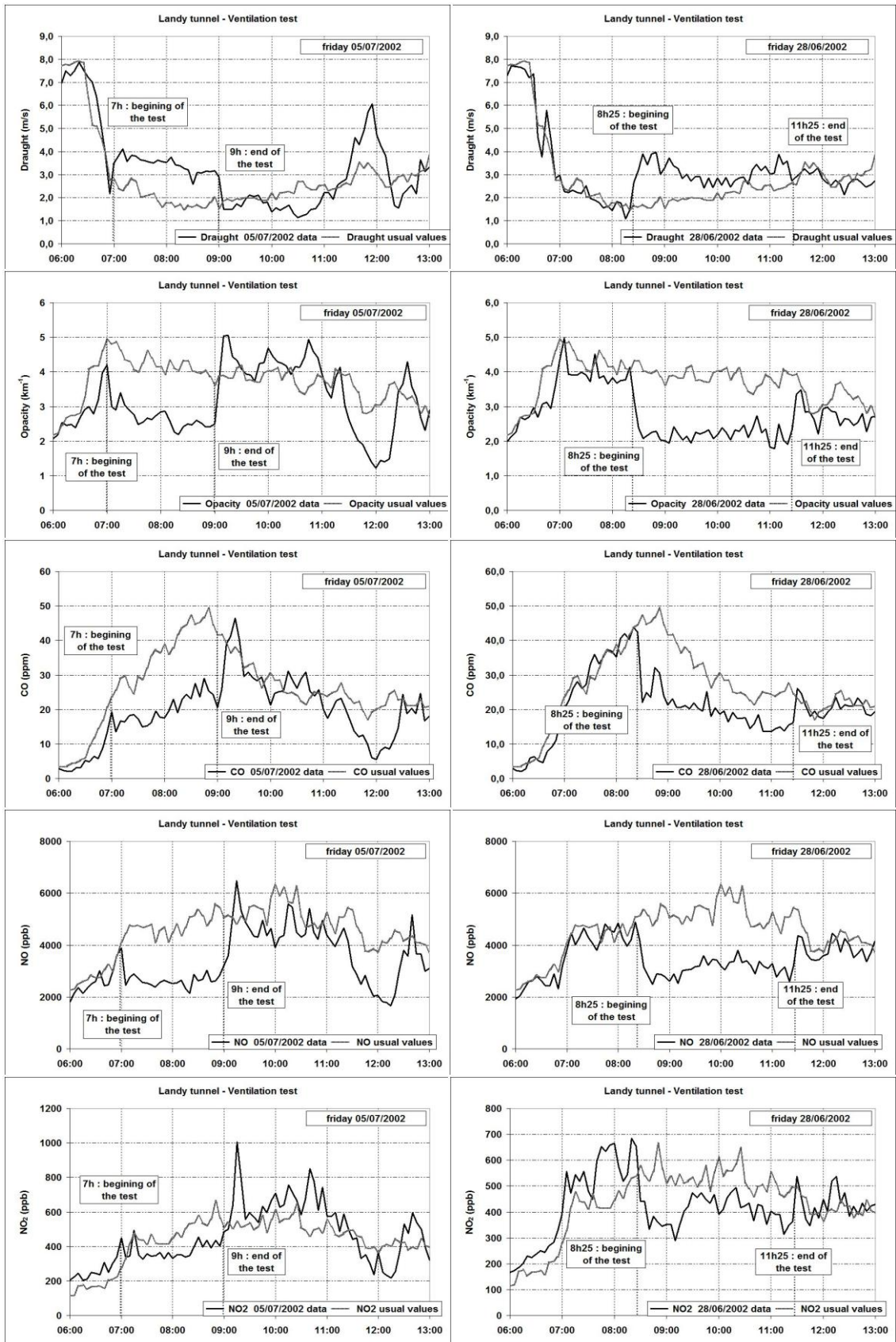
The Landy tunnel is a 1360-metre-long covered section located on the A1 motorway at the north entrance to Paris. At the time of the tests, in 2002, the ventilation device comprised four ventilation sections. Three of them were managed by a ventilation station, the fourth was ventilated equally by 62 ventilation sections (each housing a small capacity reversible motorised fan unit). The tests were carried out by operating the ventilation at full speed (blowing fresh air only), namely at 447 m³ /s. Note that since 2012, the Landy tunnel has been fitted with roof-mounted jet fans which make it possible to control draught in the event of a fire and potentially to manage pollution peaks more effectively.

As part of a study evaluating discharge at the tunnel's south portal, Brousse et al (2005), the west tube (Province → Paris direction) was equipped, 16 metres from the exit portal of the south tube, with:

- A SERES chemiluminescence analyser for nitrogen oxide concentrations;
- An infra-red UNOR MAIHAK analyser for carbon monoxide concentrations;
- A SICK VICOTEC 401 opacimeter for measuring opacity;
- A Tunnel rotating vane anemometer (Thies) installed on the side wall to monitor variations in the draught speed.

With a 98th percentile of 1300 mg/m³, Brousse et al (2005), the NO₂ levels observed in 2002 at the exit of the structure without sanitary ventilation, suggests that the regulatory value for this pollutant (average along the tunnel and over 15 minutes) was respected the vast majority of the time. To further refine this judgement, it would however be necessary to have precise longitudinal profiles of NO₂ concentrations in traffic congestion situations. A relatively high repeatability of the build-up of congestion was observed in this tunnel during the 8 weeks of testing. Two ventilation tests were carried out (see the methodology) in the middle of the peak in morning traffic. Note that we only have access to anemometric data at the tunnel's exit and when activating a semi-transverse ventilation system some of the polluted air is evacuated through the structure's entrance.

The graphs [Figures 20 and 21] show that the draught speeds were high when the traffic was moving (8 m/s before 6.30 a.m.) but quickly decreased when congestion began to build up (1 to 2 m/s). The activation and then the deactivation of the ventilation is clearly visible, but the measurements taken at the structure's south portal do not make it possible to assess the total flow of polluted air, seeing as some of the discharge occurred at the north portal. The instability of air speeds at the south portal during both tests suggests that that the distribution of flows between each portal may have varied during the tests. The impact of the ventilation during the congestion situation is clearly visible in the CO, NO and opacity recordings [Figures 22 to 27], with steep gradients when the ventilation was activated and deactivated.



Figures 20 to 29: Draught speed, level of opacity and CO, NO and NO₂ concentrations on the mornings of 28 June and 5 July 2002 in the Landy tunnel

Whilst there is no reason why the NO₂ wasn't diluted by the fresh air, the impact on NO₂ concentrations was however less visible in the recordings [Figures 28 and 29]. We can offer several explanations that could be cumulative:

- The flaws in the comparison method for measurements of traffic and environmental situations which were sometimes too different. NO₂ concentrations outside of the ventilation phase on test days seems slightly higher than the average on the reference days (also see the comment below on ozone contributions);
- The measurement technique is based on a differential measurement of NO then NO_x which is likely to lead to an accumulation of errors, combined with low levels of NO₂ compared to NO – ratio levels [NO₂/NO_x] between 6 and 10 %.
- The injection of fresh air into the tunnel which eventually leads to an injection of ozone in the structure [O₃ outside levels depending on the season and weather conditions], ozone which combines rapidly with the NO to form NO₂, leading to a further decrease in NO concentrations, but slightly opposing the decrease in NO₂.

One-way tunnel with semi-transverse ventilation - Bobigny tunnel

The Bobigny tunnel is a 2220 metre long covered section located on the A86 motorway to the north of Paris. It's comprised of two rectangular cross-section tubes for one-way traffic. At the time of the tests, in 2010, the south tunnel, in which the fixed measurement station was installed, was fitted with 132 fans with a maximum blowing capacity of 396 m³/sec (note that this structure has since been renovated and now boasts roof-mounted jet fans which make it possible to control draught in the event of fire and potentially to manage pollution peaks more effectively via longitudinal ventilation). Each of the tunnel's tubes comprises one entry ramp in the first third and an exit ramp in the second third. The operation of the structure's ventilation is therefore very complex, the injected air, which has several exit options, may cause poor ventilation homogeneity.

As part of the AIRTURIF project, the south tube (clockwise direction) was fitted, at around 400 m from the tunnel's exit, with:

- A HAPNA HORIBA chemiluminescence analyser for nitrogen oxide concentrations;
- Two GRIMM particle detectors (model 1.108) for the detection of particles in terms of number and mass;
- A SIGRIST VISGUARD opacimeter for measuring the opacity;
- A Tunnel rotating vane anemometer (Thies) installed on the side wall to monitor variations in the draught speed. (Note that for ventilation tests, it would have been appropriate to install devices at both portals and the tube's two exit ramps to properly assess the distribution of the air expelled from the tunnel).

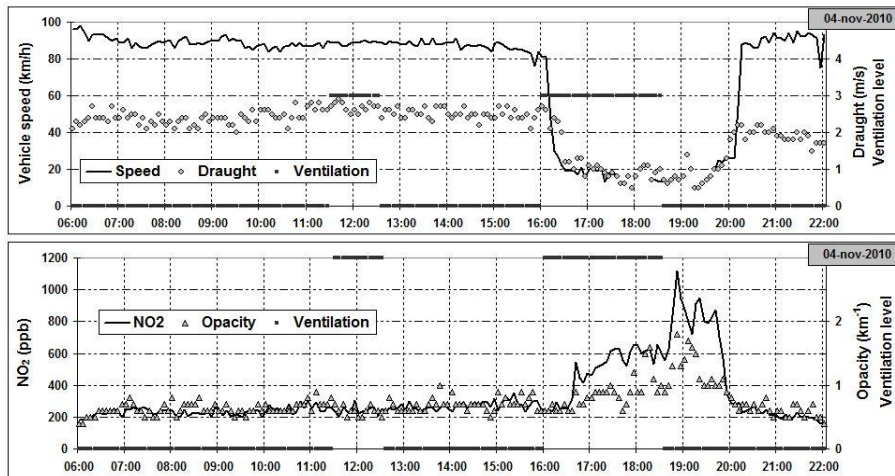
The on-board measurements, also completed as part of the AIRTURIF project, consisted of the continuous recording of pollution levels by the CERTAM laboratory vehicle which travelled through the Bobigny tunnel one hundred times. This vehicle is a van with two seats specially equipped to accommodate:

- A Topaze 32M (Environnement SA) double-chamber chemiluminescence analyser for the measurement of nitrogen oxides [frequency: 1 Hz; measurement scale: 0-10 ppm]
- An Environnement SA CO12M model infra-red correlation carbon monoxide analyser, set to a frequency of 3 seconds;
- An ELPI (Dekati) low-pressure electrostatic impactor for the measurement of particles.

This measurement campaign, which took place from Monday 18 October to Tuesday 9 November 2010 was characterised by low traffic volumes and low congestion rates (fuel shortage linked to a labour dispute during the first week and then school holidays during the second week). This context was not favourable for carrying out ventilation tests, due to the non-repeatability of the congestion situations. With

these tests it was possible to test three different sanitary ventilation modes: Low speed (LS, 132 m³/s of fresh air supply), Moderate Speed (MS, 264 m³/s) and High Speed (HS, 396 m³/s).

In the test conditions, the NO₂ levels observed suggested that the regulatory value for this pollutant (average throughout the tunnel and over a 15 minute period) was exceeded around 4% of the time, during certain congestion situations, depending on the operating speed of the sanitary ventilation.



Figures 30 and 31: Ventilation test in the Bobigny tunnel – Measurements taken at the fixed station on 04 November 2010

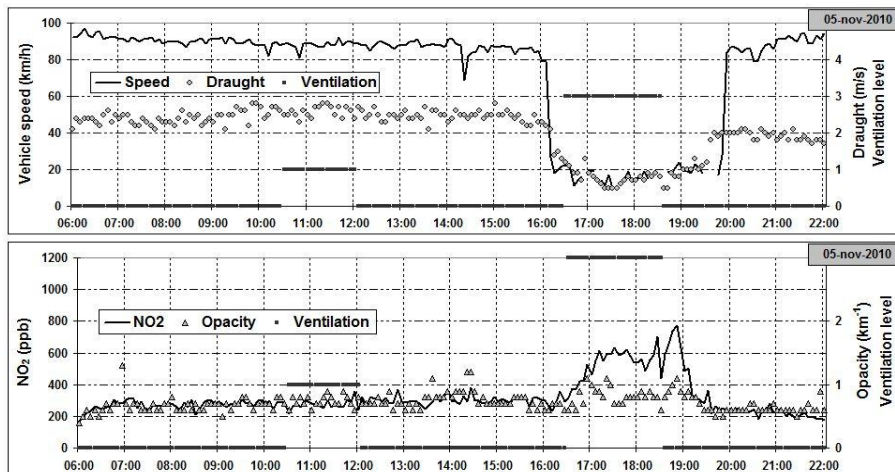


Figure 32 and 33: Ventilation test in the Bobigny tunnel – Measurements taken at the fixed station on 05 November 2010

Throughout the campaign, the draught speeds at the fixed stations remained low; they varied between 1 and 3 m/s whilst following the same evolutions as the speed of the vehicles travelling through the structure. On 4 and 5 November, the draught speed reached 2 to 3 m/s at the measurement point when the traffic was moving and was limited to between 0.5 and 1 m/s during congestion. On both days, the operation of the ventilation had no impact on the draught speed at the measurement point, both at Low Speed and High Speed, as well as in congestion and moving traffic situations. The addition of ventilation did not have a noticeable effect on NO₂ concentrations or opacity at the fixed measurement point when the traffic was moving. During congestion situations, NO₂ concentrations at the fixed measurement point – and to a lesser extent the opacity – increased despite the sanitary ventilation operating at High Speed, but the beneficial effect of the sanitary ventilation was shown, as its deactivation resulted in a slight increase in pollutant levels.

With regards to the on-board measurements, NO was used as a tracer of the gaseous pollution in the structure. The NO₂ measurements were in effect subject to too many uncertainties such as the CO levels being too low to be significant, Vidal et al (2014), the particles being too influenced by resuspension and the time which had elapsed since the structure was last cleaned.

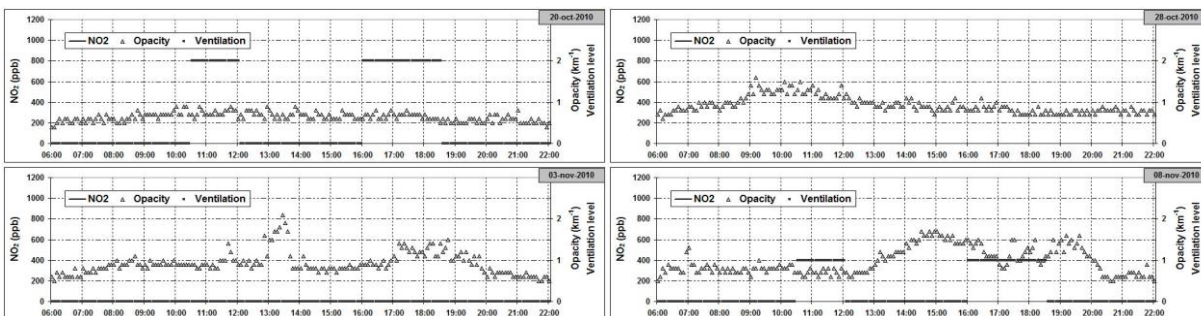
The results include a statistical analysis showing average trends. It should be noted that this analysis lacks robustness due to the insufficient number of journeys through Bobigny's south tube in traffic congestion situations (see table no.3).

Table 3: Statistics relating to on-board measurements

Ventilation speed	No ventilation	Ventilation at 33% (LS)	Ventilation at 66% (MS)	Ventilation at 100% (HS)	
Journey number	2	3	2	12	
Speed of the CERTAM vehicle (km/h)	Minimum speed	14.0	8.6	17.8	8.9
	Average speed	19.7	10.3	20.1	17.0
	Maximum speed	33.2	16.2	23.0	31.0
Duration of the journey through the south tube	Minimum duration	4:01	8:12	06:17	04:18
	Average duration	06:45	12:57	06:53	07:49
	Maximum duration	09:29	15:29	07:29	15:03
Dates	28 Oct - PM 03 Nov – 12:00	08 Nov - PM	20 Oct - PM	2 on 22 Oct - PM 6 on 04 Nov - PM 4 on 05 Nov - PM	
NO (ppm) – journey average	1.942	2.035	1.276	1.435	
NO ₂ (ppb) (*) – average	486 (*)	509 (*)	319 (*)	359 (*)	

(*) Estimation of average NO₂ concentrations based on a ratio $[NO_2/NO_x] = 0.25$ throughout the structure. Value most likely exaggerated and punitive (Vidal et al, 2014). Note for the record: average ratio $[NO_2/NO_x] = 0.19$ measured at the fixed station from 19 October to 8 November over the period from 6.00 a.m. until 10.00 p.m.

The [34 to 37] graphs showing the evolution of the opacity for the days between 20 and 28 October as well as the 3 and 8 November reveal few highlights: A peak in the opacity on 3 November at around 12.00 p.m. and fluctuations in the opacity during the period of Low Speed ventilation on 8 November, which are difficult to interpret.

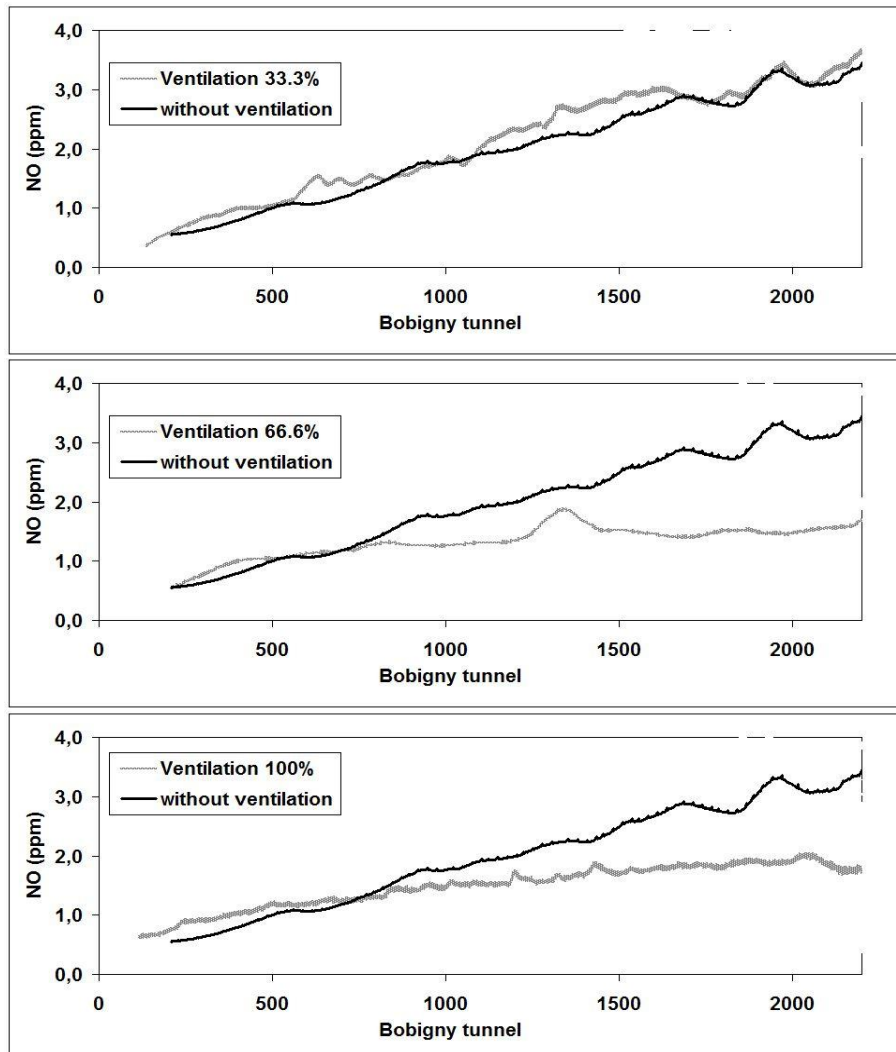


Figures 34 to 37: Opacity levels at the fixed measuring station during the ventilation tests on 20 and 28 October and 3 and 8 November.

The [38 to 40] graphs shows average NO concentrations for the different ventilation modes. These graphs, as well as the statistical table, indicate more significant concentrations of pollutants in no ventilation or Low Speed ventilation situations. In both situations, the regulatory value of NO₂ was

probably exceeded. In contrast, when the ventilation is operating in Medium Speed or High Speed mode, the average NO concentrations are reduced. This reduction is especially visible at the structure's exit. At the entrance, the concentrations are however slightly more pronounced in this situation, as some of the pollutants exit via the entrance portal.

In conclusion, when we only consider recordings taken from a fixed measurement point, the effect of ventilation is clearly less visible in this complex structure fitted with semi-transverse ventilation than in structures fitted with longitudinal ventilation. The concentration profiles over the length of the structure obtained from on-board measurements allow us to better assess the global contribution of sanitary ventilation: the collected results, even if they are limited in number, suggest that sanitary ventilation has significant effects when operated at Moderate and High Speeds, making it possible to reduce NO₂ concentrations efficiently so as to meet regulatory criteria.



Figures 38 to 40: Ventilation test in the Bobigny tunnel with the CERTAM laboratory vehicle – Average longitudinal profiles of NO concentrations according to the different ventilation modes (this is the average of all the laboratory vehicle's journeys)

3. Discussion

The aim of these tests was to highlight the decrease in the concentration of pollutants as a result of the activation of sanitary ventilation and, if applicable, to assess if this process enabled compliance with

regulatory air quality values inside road tunnels. These tests have provided positive answers, but many questions remain.

Indeed, these studies have faced several methodological limitations:

- The fact that the situations could not be fully repeated, even if the pollution phenomena in each structure are recurrent;
- The difficulty of not being able to install enough devices in the tunnels at the risk of only a partial interpretation of the results. For simple tunnels with semi-transverse ventilation, such as the Siaix or Landy, 3 measurement points (one close to each portal and one, a third of the way through the tube) for nitrogen oxides and the anemometry would therefore have been valuable beneficial;
- The difficulty in interpreting the results increased for complex tunnels such as Bobigny which has access ramps and which makes the structure's ventilation behaviour less predictable and may mitigate air renewal in certain areas;
- The difficulty in collecting a significant number of records to establish robust statistics, mainly in the case of on-board measurements, as this measurement method is a very time-consuming procedure, especially for experiencing traffic congestion situations. However, these measurements should be favoured as they provide concentration profiles over the entire length of the structure;
- Finally, in certain cases, interference caused by variations in weather conditions which can greatly influence draught in the structure. Depending on the prevailing winds or the difference in pressure between each portal, the effect of longitudinal ventilation can be significantly diminished or, in the case of semi-transverse ventilation, the distribution of discharges at each portal can be radically reversed, especially for tubes with two-way traffic. These atmospheric events, which can have a significant effect on the longitudinal profiles of pollutants over the length of the structure, have not been taken into account in this study.

The quality of the dilution of pollutants in the structure depends on the ventilation device's capacity to inject enough fresh air at any given point to obtain sufficient dilution throughout the structure so as to comply with the various air quality criteria, whether it's an average over the length of the tube (CO, NO₂) or single point values (opacity). Yet the fixed points – which were unique in four of the tested tubes – and the on-board measurements – which were only performed in the Bobigny tunnel – could only give a very fragmented view of compliance with these criteria.

Moreover, beyond the regulated pollutants, we should not forget other the road pollutants that are a danger to public health, ANSES (2012). However, we can assume, for gaseous pollutants, that if sanitary ventilation allows for a significant reduction in the “tracer” pollutant used during the measurements, then the reduction of other pollutants will generally follow a similar process (note however that ozone inputs may combine with NO to create NO₂ at fresh air injection points).

Despite these limitations, the tests presented in this report show that for gaseous pollutants, the desired effect (dilution) is obtained clearly enough for longitudinal ventilation, and less obviously – due to a lack of data – for other types of ventilation.

However, for particulate pollutants, whose mobility and lifespan in the tunnel are directly influenced by their size, mass and nature (mineral or carbon chain), these tests have not provided us with much experimental data. Nevertheless, this data, which was limited to measurements of PM₁₀ in the Guy Môquet tunnel, has shown the positive impact of longitudinal sanitary ventilation, despite a longer response time.

However, ventilation is not the only solution for reducing particulate pollution in tunnels. Regular washing of the structure is recommended for removing a large portion of it. Sanitary ventilation tests with

particle measurements taken before and after a cleaning session would be appropriate for assessing its impact. This cleaning would be more required the longer the tunnel is (and therefore likely to accumulate larger quantities of particulate matter) and for those where there is not usually a steady and sustained draught (for example 3 to 5 m/s).

With regards to compliance with regulatory criteria, the tests have only given a partial answer in support of more or less solid assumptions:

- For NO₂ (or NO) and CO, for which we would need to calculate more reliable averages over the length of the tunnel, it would be advisable to have several measurement points or to accumulate a large number of longitudinal profiles using a laboratory vehicle. For a simple structure (without a by-pass road), in a longitudinal ventilation situation – that is to say with either natural ventilation (draught of at least 2 m/s) or the activation of longitudinal sanitary ventilation – the concentration profile is linear and increases in the direction of the draught, CETU (2003). Two measurement points are sufficient (at a push, only one by making assumptions about C₀ concentration at the structure's entrance) to estimate an average longitudinal concentration. In semi-transverse ventilation situations, where the natural draught is low (between ± 2 m / s), the concentration profiles in the structure are harder to evaluate and we can only really visualise them by having either a sufficient number of measurement points distributed along the tube or concentration profiles established by the laboratory vehicle (see the illustration of the concentration profiles in figures 41 and 42).
- With regards to opacity, for which we should check that no recommended value has been exceeded, we would need to have a large number of sensors distributed over the entire length of the tunnel.

However, it's advisable to look at the issue in the context of each pollutant : CO emissions are now very low, leading to in-tunnel concentrations which are much lower than regulatory values, even at peak hours. As for opacity peaks, they are exceptional in nature and are generally linked to technical incidents (damaged turbo or cylinder head gasket for example). Only NO₂ levels may be problematic. Various measurement campaigns, Vidal et al (2014), have shown that only situations with low draught and/or traffic congestion in the structure presented a risk of exceeding the regulatory NO₂ value – often exacerbated by a lengthened exposure period for the user due to low traffic speeds (up to 15 min 29 sec to travel through the Bobigny tunnel during the tests presented above).

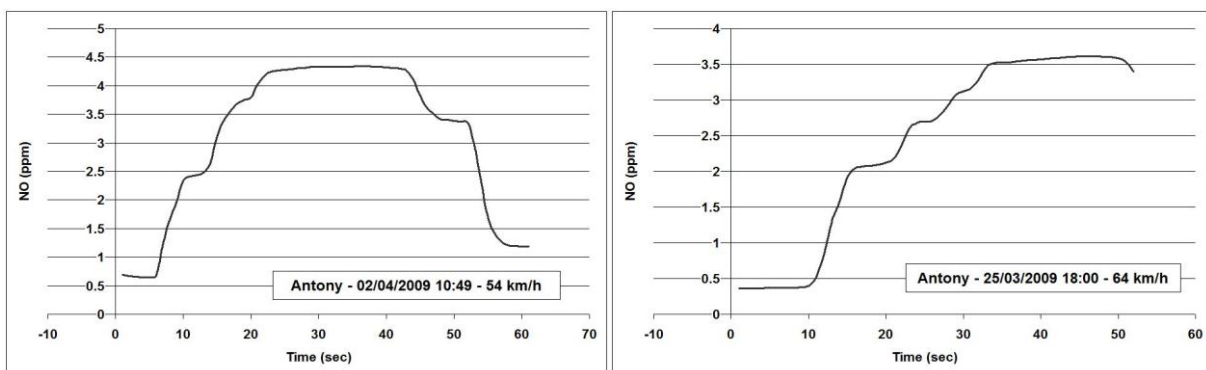


Figure 41 and 42: NO concentration profiles in the Antony tunnel (two-way traffic – sanitary ventilation not activated) recorded by the CERTAM laboratory vehicle – On the right, draught is established in the direction of movement of the laboratory vehicle and pushes pollutants towards to the exit portal.

The estimation of the average NO₂ concentrations in the structure was based on various methods for the four tests presented:

- Guy Môquet tunnel: It's a relatively short tunnel where the NO₂ concentrations at the measurement point (close to the exit portal) rarely reach the regulatory value, without activating

the sanitary ventilation. As the ventilation in the structure is longitudinal, the pollutant concentration profiles are linear and the average NO₂ concentration values are therefore lower than the threshold of 0.4 ppm. It was observed that activating the sanitary ventilation improved the situation.

- Siaix tunnel: As it was initially an opacity study and the opportunities to install NO_x analysers were, at the time, very limited, we have no information on NO₂ levels in this structure at this time.
- Landy tunnel: The single measurement point, located several metres from the west tube's exit portal, gives an idea of the average concentrations present as long as the ventilation is longitudinal and there is sufficient airflow (higher than 2 m/s). The regulatory criteria for NO₂ was therefore respected. When the draught is low, the pollutants stagnate and we are no longer able to estimate the longitudinal NO₂ concentrations but everything seems to indicate that (NO₂ concentrations reaching 600 to 800 ppb at the exit portal) the risk of exceeding regulatory criteria is high and that there are probably violations. When the sanitary ventilation is activated, we no longer know the longitudinal average of NO₂ concentrations but as concentrations at the exit portal are more moderate (around 400 ppb), it is reasonable to presume that this average is significantly less than the regulatory threshold of 400 ppb.
- For the Bobigny tunnel, the issue is the same as with the Landy tunnel. But we also have several metres of on-board measurements which indicate an almost linear concentration profile over the length of the structure whether the ventilation is activated or not. When the sanitary ventilation operates at High or Moderate Speeds, there was no violation of the regulatory criteria for NO₂. The frequency of violations of this criteria without sanitary ventilation depends on the assumptions used to extrapolate the NO₂ value from NO measurements. By using a "large" value for an average ratio [NO₂/NO_x] of 0.25 over the length of the tube, we notice that there are situations when the regulatory value is exceeded when the ventilation is not activated. But by choosing the average value of 0.19 during the measurement campaign (period from 6 a.m. until 10 p.m.) reported by the fixed measurement station [NO₂/NO_x], we no longer observe violations of the regulatory criteria.

In conclusion, these tests have shown that outside of congestion periods, the regulatory criteria were well respected. But it also shows that to properly understand congestion situations with low draught, or even to properly understand the effects of semi-transverse ventilation, we would need to deploy more metrological resources.

Conclusions

The aim of the sanitary ventilation tests in this paper was to evaluate the capacity of ventilation to reduce pollution levels according to the typology of the tunnel and, if possible, according to various operating configurations. The measurements carried out have therefore shown that controlling in-tunnel pollution depends on several fundamental parameters:

- The type of traffic flow with:
 - In the case of one-way tunnels, a generally significant draught in the structure (except in the case of traffic congestion) which favours air renewal;
 - In the case of a two-way structure, a direction and force of draught that depends on the traffic ratio in each direction and atmospheric conditions on each side of structure. This generally leads to low draught and poor air renewal;
- The traffic density which, when it's too high, causes congestion situations in which vehicle emissions are higher (individually and globally) and air renewal through the piston effect of air masses is low or even non-existent;
- The nature of the ventilation device, with:
 - Longitudinal devices (fan hanging from the ceiling) whose effects are easy to observe and which have shown pretty fast response times and good efficiency;

- Semi-transverse devices (fresh air supply over the length of the tube) whose effects have been more difficult to assess (complex profiles of pollutant concentrations along the structure) and which have proved to be less reactive as they can at least partially oppose the favourable effects of the piston effect of traffic.

The tests presented in this paper focused on traffic congestion situations as they present higher concentrations of pollutants and may result in violations of regulatory criteria. The four experiments (one with longitudinal ventilation and the other three with transverse ventilation, including one case of two-way traffic) have shown the positive impact of the use of sanitary ventilation on the “tracer” pollutants observed. In congestion situations, the introduction of sanitary ventilation enables compliance with regulatory criteria on NO₂ (regulatory pollutant threshold may pose problems), which isn't always the case if we don't activate it.

However, these tests would merit further development as it's difficult to develop a very rigorous methodology. More equipment would allow us to better understand aerodynamic phenomena in structures with semi-transverse ventilation. The use of a laboratory vehicle producing longitudinal profiles of concentrations is very useful but requires many journeys through the tunnel under the test conditions sought to be able to establish sufficiently robust statistics.

Finally, the problem of particulate pollution could not be sufficiently addressed. The dilution of particles seems less rapid than that of gaseous pollutants. Explanations may be found in the different origins of this pollution, in its ability to accumulate in the structure and then become resuspended because of the effects of draught (traffic or sanitary ventilation). A specific experiment would need to be conducted to assess the impact of regular cleaning which should be recommended in addition to ventilation.

REFERENCES

- ADEME (2014): Emissions de Particules et de NO_x par les véhicules routiers [Particle and NO_x emissions by road vehicles] www.ademe.fr.
- ADEME (2015): CYCLO-POL Etude comparative sur l'exposition des cyclistes / automobilistes et risques sanitaires associés pendant les pics de pollution atmosphérique [CYCLO-POL comparative study of cyclist's/motorist's exposure and the associated health risks during peaks in atmospheric pollution]. www.ademe.fr.
- ANSES (2012): Avis relatif à la sélection des polluants à prendre en compte dans les évaluations des risques sanitaires réalisées dans le cadre des études d'impact des infrastructures routières [Review relating to the selection of pollutants to take into account in the assessment of health risks completed within the scope of road infrastructure impact studies]; www.anses.fr
- ANSES (2013): Proposition de valeurs guides de qualité d'air intérieur – Le dioxyde d'azote [Proposal of indoor air quality reference values – Nitrogen oxide]. Avis de l'Anses [Anses opinion], Rapport d'expertise collective [Collective expert appraisal], Édition scientifique [Scientific edition]. www.anses.fr
- APHEKOM (2011): Summary report of the Aphekom project 2008-2011. www.aphekom.org.
- Bernagaud C., J.F. Burkhart, B. Vidal, T. Lepriol, J.F. Petit, T. Brunel, F. Gouriou & D. Préterre (2014): Observations of the [NO₂]/[NO_x] ratio in road tunnels. Pollution Atmosphérique n° 221.
- Brousse B., B. Vidal, X. Ponticq, G. Goupil, R. Alary (2005): Pollution dispersion at an urban motorway tunnel portal: Comparison of the small-scale predictive study with the actual conditions measured on the site. Atmospheric Environment 39 (2005) 2459–2473
- CETU (2003): Les dossiers pilotes du CETU – Ventilation. [CETU pilot records - Ventilation] www.cetu.developpement-durable.gouv.fr

- CETU (2011): Logiciel de calcul monodimensionnel anisotherme transitoire en tunnel CAMATT 2.20 [CAMATT 2.20 one-dimensional transitional anisothermal in-tunnel calculation software] www.cetu.developpement-durable.gouv.fr.
- CETU (2012): Calcul des émissions de polluants des véhicules automobiles en tunnel [Calculation of motor vehicle exhaust emissions in tunnels]. www.cetu.developpement-durable.gouv.fr.
- Conseil Supérieur d'Hygiène Publique de France [Supreme Council for Public Hygiene in France] (1998): Qualité de l'air dans les ouvrages souterrains ou couverts [Air quality in underground and covered structures].
- Guilloteau A., B. Vidal, L. Paillat, G. Thiaut, D. Preterre and V. Dunez (2010): Air Quality in the Ile de France road tunnels (AIRTURIF project): presentation, methodology and preliminary results, Transport and Air Pollution 2010.
- Ministère de la Santé [French Ministry of Health] (1999): Circular no. 99.329.
- PIARC (2012): Road tunnels – vehicle emissions and air demand for ventilation. www.piarc.org
- Vidal B., C. Bernagaud, J.F. Burkhart, J.P. Grand, D. Preterre, F. Gouriou, J.F. Petit, T. Le Priol, A. Guilloteau, P. Barbe & M. Bouquet (2014): Nitrogen oxides and particles matter levels in the tunnels of the Ile-de-France motorways network. Transport and Air Pollution 2014.
- WHO (2012) IARC – Diesel engine exhaust carcinogenic. Press release n°213.
- WHO (2013) IARC – Outdoor air pollution a leading environmental cause of cancer deaths. Press release n°221.
- WHO (2016) Expert Consultation – Available evidence for the future update of the WHO Global Air Quality Guidelines (AQGs). Meeting report, Bonn, Germany, 29 September-1 October 2015

A comprehensive evaluation method for instantaneous emission measurements

Konstantin WELLER*, Martin REXEIS*, Stefan HAUSBERGER* & Bernhard ZACH**

**Institute for Internal Combustion Engines and Thermodynamics, Graz University of Technology
Inffeldgasse 19, 8010 Graz, Austria*

Fax: +43 31687330262 - email: weller@ivt.tugraz.at

*** JustBits.at Software Design and Development, Mühlenweg 36, 8036 Graz/Stattegg, Austria*

Abstract

The effects of variable gas transport times are well known to be a challenge for generating high quality test results from emission measurements. This is especially valid for correct allocation of modal emission mass signals to the operating points of internal combustion engine and exhaust aftertreatment system. These time shift effects occur both at test benches and at portable emission measurement systems.

At the ICE (Institute for Internal Combustion Engines and Thermodynamics) of the TU Graz (University of Technology Graz) an algorithm was developed, which allows for consideration of variable gas transport times based on measured exhaust mass flow and volumes and temperatures in the measurement system. This algorithm was implemented into the software "ERMES tool" which is capable to perform evaluations of measurement data from any kind of emission test systems (diluted from CVS, undiluted from engine dyno or PEMS measurement). The tool now provides methods to correct emission test results for effects of analyser response behaviour and transport times in diluted and undiluted parts of the measurement equipment.

Keywords: *Instantaneous emission measurement, transport time, emission modelling.*

Introduction

High quality data from emission testing is a key factor for development and simulation of complex internal combustion engines and exhaust aftertreatment systems. A crucial point in the evaluation of data from any kind of emission test system is to provide a correct temporal allocation of modal emission mass signal to the correlated engine operating point. Especially the consideration of variable transport times of the exhaust gas in the exhaust pipe and the emission measurement system is a well known challenge, for which so far no common scientific method has been established. Provisions as defined in the different emission legislations (e.g. UNECE R49.06) do only foresee a constant time shift for modal measured emissions which considers the average transport time over an emission test. This is acceptable as only the averaged results per cycle (or per phase of the cycle) are the relevant results from legislative emission testing. However, for research and development purposes a much higher demand on the quality of the data from emission data is given. In the last two decades several methods on the post-processing on modal emission data have been published. The method as developed by (Franco V., (2014)) for example uses CO₂ as tracer gas which allows for "reconstruction" of emission behaviour at the engine via correlation of CO₂ as measured on the test bed with the fuel consumption signal as measured at the engine. Other papers e.g. (Ajtay D. et al, (2004)) use methods from signal theory to correct for transport dynamics in the emission measurement system.

At the ICE (Institute for Internal Combustion Engines and Thermodynamics) of the TU Graz (University of Technology Graz) a novel algorithm was developed, which allows for compensation of variable gas transport times based on a physical model. Main input data for the correction algorithm are the measured exhaust mass flow and volumes and temperatures in the measurement system. This method was implemented into the software "ERMES tool" which is capable to perform evaluations of measurement data from any kind of emission test systems (diluted from CVS, undiluted from engine dyno or PEMS measurement). The tool now provides methods to correct emission test results for effects of analyser response behaviour and transport times in diluted and undiluted parts of the measurement equipment. This paper shall give an overview on the developed methods by providing:

- An introduction into the main effects which distort instantaneous data from emission testing (chapter 2)
- A description on the correction algorithms as implemented in the “ERMES tool” (chapter 3) and
- Examples for application of the method (chapter 4).

1. Main effects which distort instantaneous data from emission testing

This chapter gives an introduction into the main effects which cause a distortion and a time shift of instantaneous emissions as measured on a test bed compared to the emissions at engine outlet. The explanations are given on the example of a diluted measuring system where the sampling of modal emissions is performed at the end of the dilution tunnel of a CVS system. A scheme of such a system is given in Figure 1. The exhaust system of the car ranges from the engine (position E) to the beginning of the undiluted part of the CVS system at position D. From that point the exhaust gas flows through the CVS undiluted pipe till reaching the mixing point (position C) and entering the diluted part of the system. At position B a sample of the diluted exhaust is extracted and flows towards the analysers (position A).

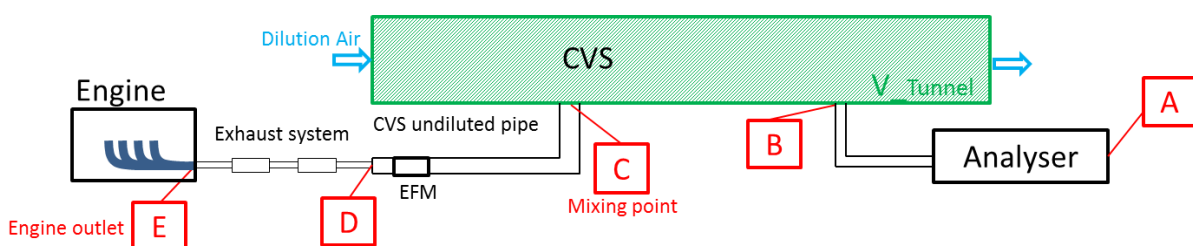


Figure 1: CVS system of the dynamometer of the ICT Graz

In the following a synthetic “test case” is used to demonstrate the course of emissions for a rectangular signal (“low” – “high” – “low” step both for emission concentrations and exhaust mass flow) originating at the engine and flowing downwards the emission measurement system. This test case correlates to a sudden change in engine operation point, where total exhaust volume flow (“ExVF”), the concentration of a certain emission component (“EC”) and – as a consequence – the mass flow of the emission component (“EMF”) are varied. Figure 2 shows the three quantities of this test case at engine outlet position E.

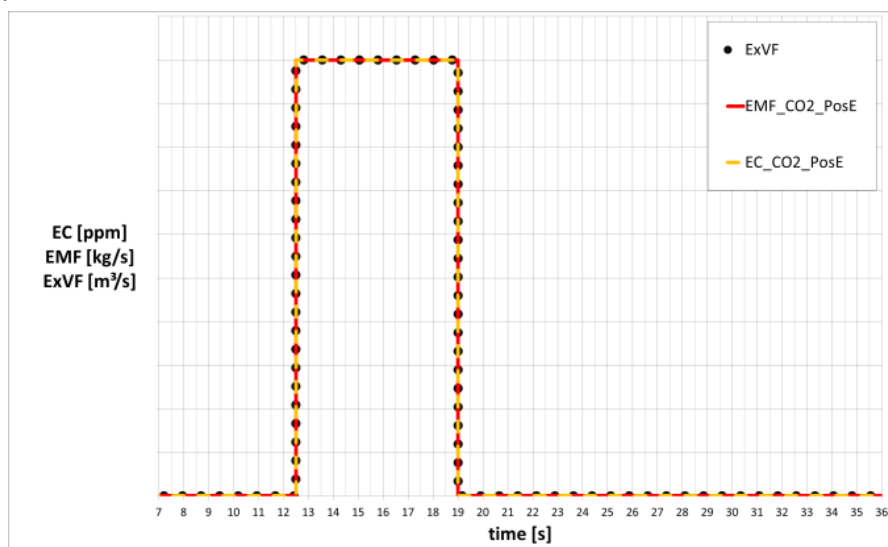


Figure 2: Test case, emission mass flow at position E (engine outlet)

From position E the exhaust gas flows downwards the vehicles exhaust system (passing position D) and the CVS undiluted part to the “mixing point” with the dilution air at position C. Position C can also be interpreted as sampling point of an undiluted measurement system. This signal behaviour is shown in Figure 3. At the mixing point C the changes of volume flow and emission concentration arrive

at different time steps: The change of the volume flow spreads with velocity of sound, in contrast the step of emission concentration flows with exhaust flow velocity in the undiluted system. Consequently the emission mass flow of the exhaust component under consideration rises in two steps: First with rising volume flow (1: concentration remains low, but exhaust flow steps up) and second with the rising emission concentration (2: high volume flow and high emission concentration). When the exhaust flow steps back to “low” level again the undiluted pipe is still filled with high emission concentration. Because of the low volume flow this remaining high concentration needs a long time to leave the exhaust pipe (3).

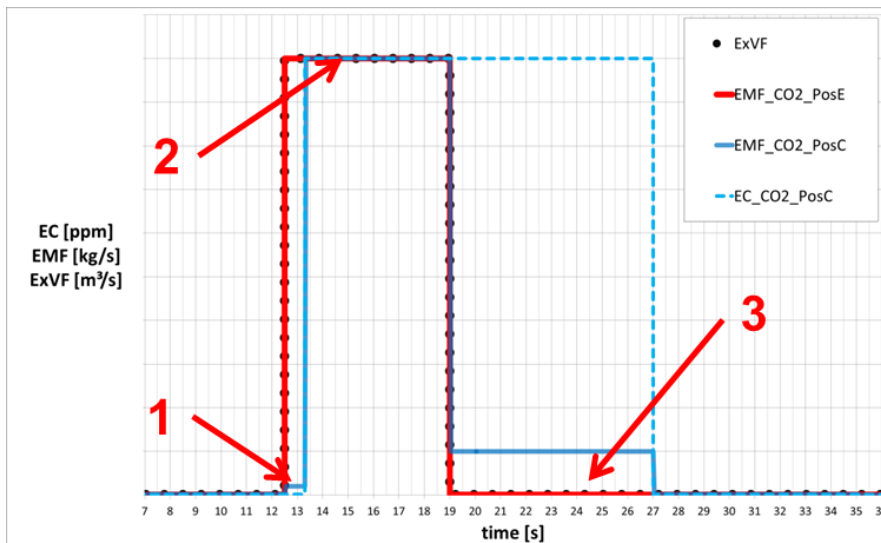


Figure 3: Test case, emission mass flow at position C (mixing point with dilution air)

When entering the CVS tunnel the exhaust gas gets diluted by background air achieving a nearly constant volume flow. The dilution does not change the emission mass flow of the pollutant under consideration, but lowers the associated emission concentration in the CVS tunnel. This emission concentration gets time shifted about a nearly constant transport time through the CVS tunnel towards position B (sampling point), see Figure 4.

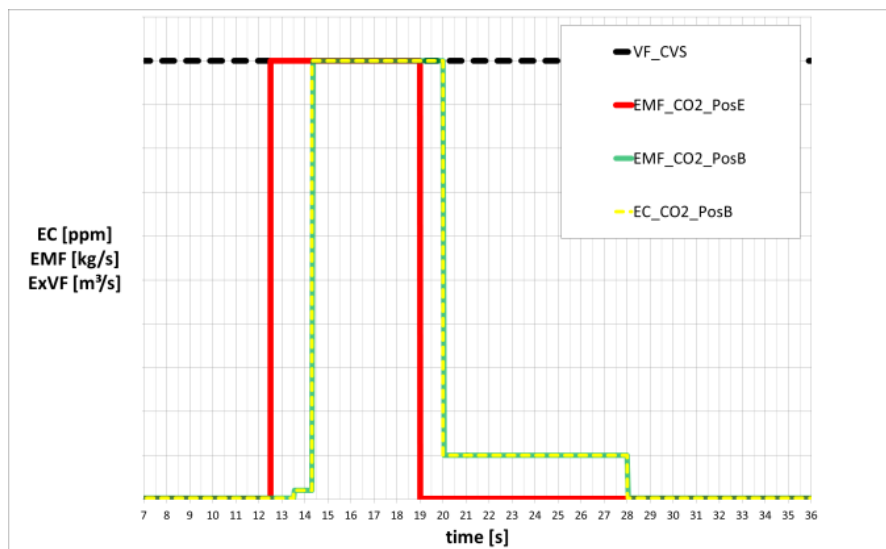


Figure 4: Test case, emission mass flow at position B (sampling point in CVS tunnel)

At sampling point B a constant probe of the CVS volume flow is taken and sucked with constant volume flow towards the analysers. Because of the transport time through the sampling line and the limitations in the response behaviour of the analysers (position A), the signal for emission concentrations is again time shifted and distorted resulting in the purple signal as shown in Figure 5. If the mass flow of the emission component under consideration would be calculated without applying any corrections just from the analyser signal and the constant CVS volume flow, the resulting course of emission mass flow would have a similar shape than the purple line in Figure 5. This signal is not only time shifted to the original signal in point E but also shows a remarkably different shape.

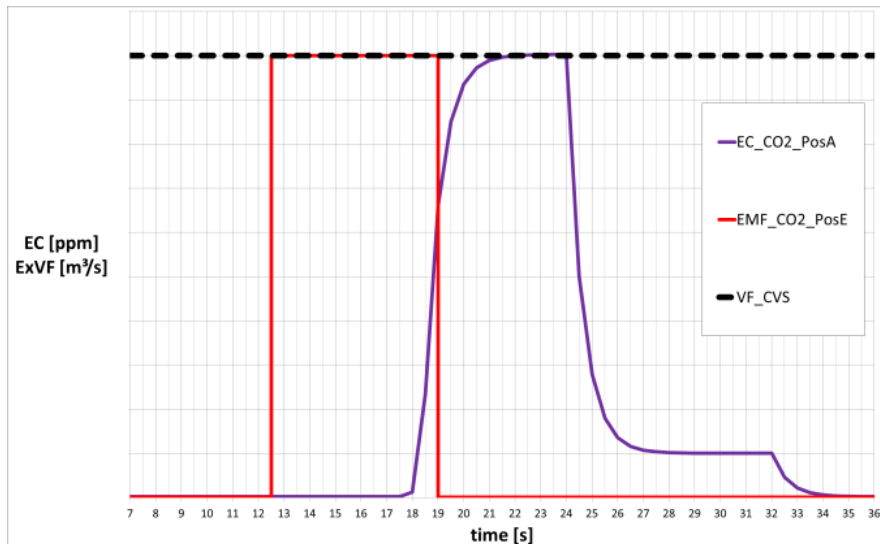


Figure 5: Test case, emission concentration as measured by an analyser at position A

The correction algorithms as presented in the next chapter aim to reconstruct the original signal at position E. The list of distorting effects as presented in this chapter does only cover the main relevant mechanisms as identified for the test beds at the ICE. Other mechanisms are e.g. the smoothening of emission concentrations by turbulent mixing effects. However, according to ICE internal analysis, these effects are less important compared to the mechanisms which are corrected by the ERMES tool.

2. Algorithms for emission mass calculation from the analysers to the engine

In this section the different correction algorithms to calculate the signal for emission mass flow at the engine from the signal for emission concentration measured by the analyser are explained.

Analyse response and dead time correction

Starting point is the correction of the response characteristics of the analysers, which is approximated by an inverse PT1 (first order low-pass) element. The resulting emission concentration signal is then subject to a constant time shift, which comprises the constant transport time of the sample gas from position B to position A as well as an analyser specific dead time in the response characteristics. The applied parameters for PT1 time constant as well as analyser specific dead times have been determined by test measurements, where a distinctive rectangular signal for emission concentrations has been injected at point B and the related valve position as well as the analyser signal have been recorded.

Based on the emission concentration signal at position B and the actual volume flow in the CVS system in a next step the emission mass flow for the component under consideration at point B is calculated. From this point on, any further algorithms are based on the emission mass flow but not on concentrations.

Correction of transport time in the diluted measurement system

For each time step the transport time in the diluted part of the measurement systems is calculated by division of the known volume of the CVS tunnel between point B and C with the actual value for CVS volume flow. This transport time is then applied as a time shift to calculate the emission mass signal at C. As the volume flow as well as the temperatures in the CVS tunnel are nearly constant, a simplified algorithm is applied for transport time correction compared to the method as used for correction in the undiluted pipe system (see "Correction of variable transport time in the undiluted measurement system").

Correction of variable transport time in the undiluted measurement system

The next and final step in the calculation procedure is the variable time shifting through the undiluted part of the measurement system till the emission mass reaches the engine at position E. For this purpose the emission mass as calculated at position C for each time step gets shifted through the

undiluted part which is split into different volume sections with varying temperatures and pressures.

Main calculation principle

The calculation is performed reverse to the flow direction and is done for each “packet”. A packet denotes the properties:

- volume,
- the mass of the emission component, as well as
- the total exhaust mass

which correlates to a single data point in the emission mass flow calculated first at position C which is then in the correction algorithm virtually shifted “upstream” towards position E. The emission mass as well as the total exhaust mass of each packet are constant independent of the position. The volume of each packet at a certain position is depending on the temperature and the pressure at the certain time and position. Every time step, the current calculated packet at position C is virtually shifted into the undiluted system and “pushes” the packets which are located inside the system towards position E until they reach the end. From this calculation the individual transport time of each packet can be calculated. This principle is illustrated in Figure 6 **Erreur ! Source du renvoi introuvable.**, where every horizontal line represents a single time step and every coloured cell represents a packet. In this simplified example the transport time of packet 13 is calculated to be 2 seconds by shifting packets 12, 11 and 10 backwards into the undiluted system.

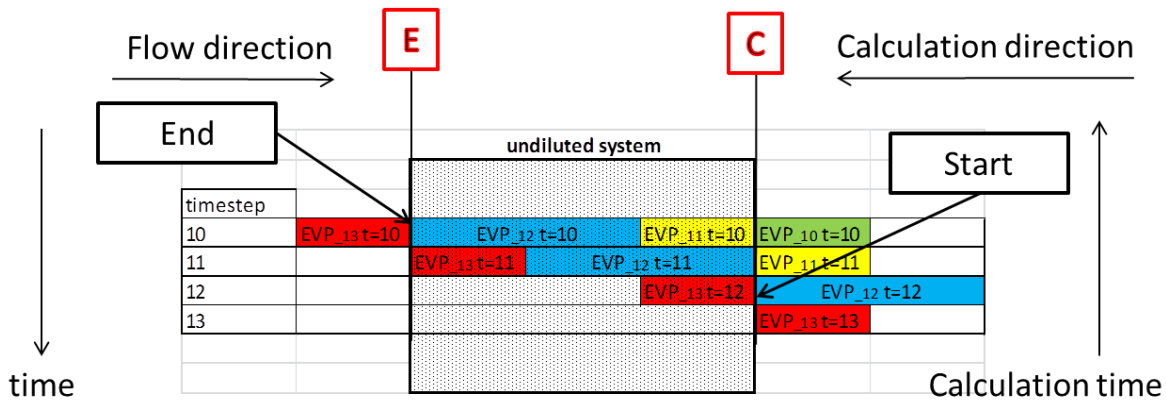


Figure 6: Principle of pushing packets through the undiluted section

Calculation of the packet position

The calculation of the position of a packet inside the undiluted system is based on the cumulative mass of exhaust gas inside the system with position C as zero-point. As already defined above each packet has its specific values for mass of exhaust gas and for mass of emission component. The exhaust mass represents the whole mass of the packet which is measured by an exhaust mass flow meter (EFM). Regarding gas properties the exhaust gas of every packet is considered as ambient air.

The whole undiluted volume is divided into different volume sections. Each of them has its own size (equal in this example) and separate temperature and pressure at the beginning and the end. Within these volume sections temperature and pressure are assumed to be linear. These volume sections are divided into smaller partial volume sections (equal sized). Within a partial volume section pressure, temperature and consequently density are assumed to be constant and represent average values. The explained division is illustrated in Figure 7.

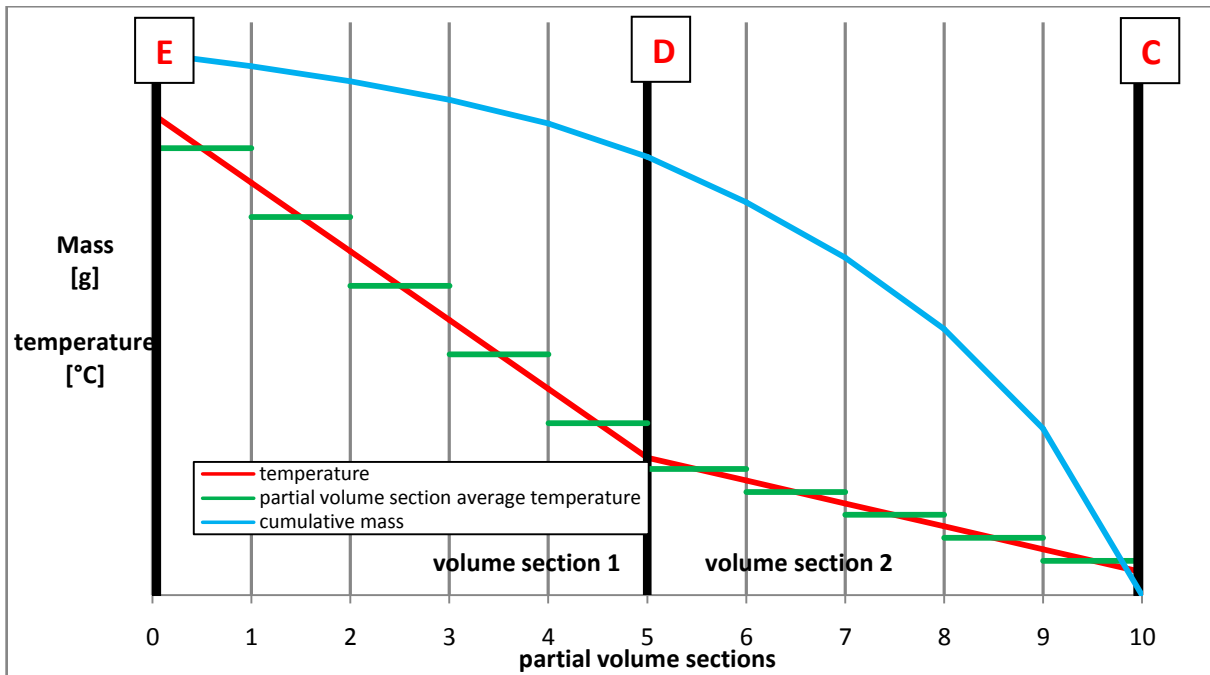


Figure 7: Division in partial volume sections

As a function of volume, temperature and pressure, each partial volume section can be filled linear with a separate exhaust mass. The ideal gas equation is used for this calculation. By adding up the separate masses starting at position C the course of the cumulative mass (blue line in Figure 7) in the undiluted part of the system can be calculated. With varying pressure and temperature in the undiluted system over time, this cumulative curve has to be calculated once for every time step. With this function the position and the size of a packet (starting at position C) can be calculated using the exhaust mass as describing parameter. This approach is exemplarily shown in Figure 8.

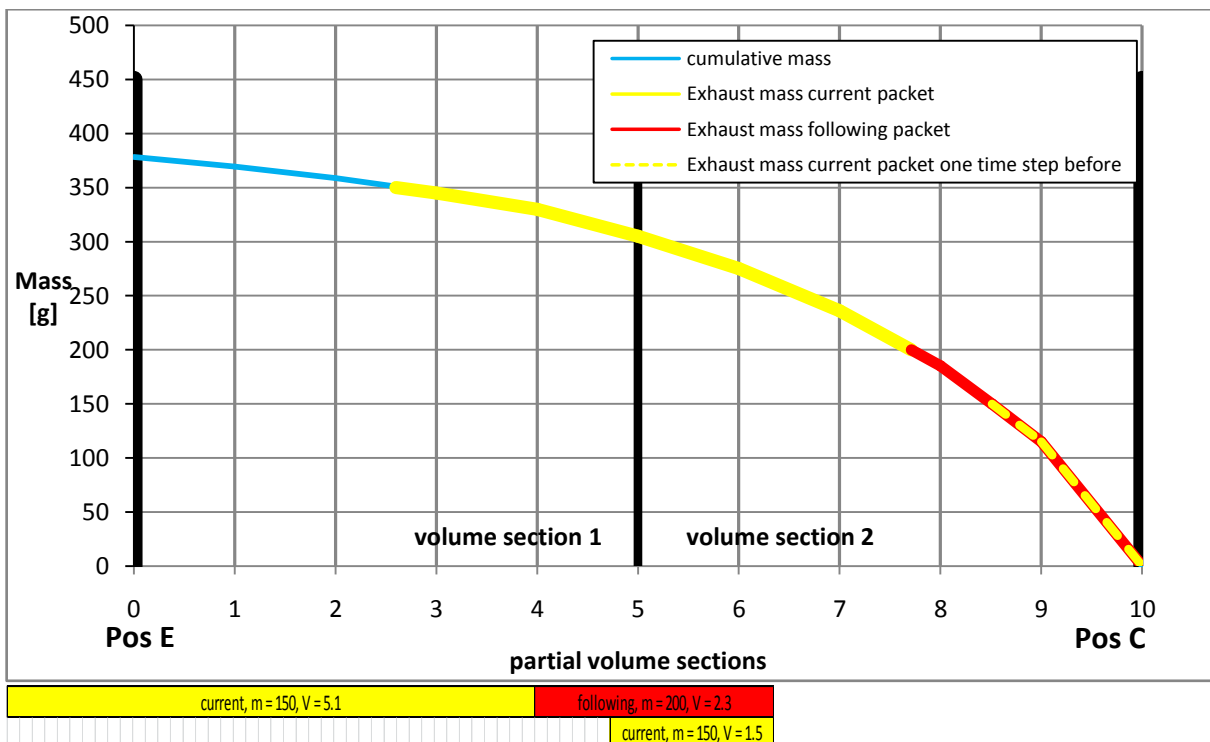


Figure 8: Mass curve, illustration of various packet volumes in the undiluted system

The curve (blue, in the background of the entire graph) represents the cumulative mass of the partial volume sections. Due to the measured exhaust mass of the packets their position can be calculated out of this cumulative mass function.

For every time step the position calculation starts with the packet, which just entered the undiluted system at C (partial volume section 10 in this example). With its mass the covered volume from the system border is computed. At the time of entering the system, the volume of the yellow packet (mass = 150 g) is 1.5 partial volume sections. For the calculation of the packet volume and position at the next time step (one line higher), the mass of the next packet entering the undiluted system at the considered time step (red one) is added to the mass of the first packet and the covered volume for the whole mass is calculated. One time step before the red packet (mass = 200 g) was measured. With the reverse calculation direction this packet is the next to enter the undiluted system with the volume 2.3 partial volume sections. The cumulative mass of these two packets is 350 g and consequently the volume for both packets 7.4 partial volume sections. The new packet volume of the yellow one is calculated by subtracting the volume of the red one from the cumulative volume of both packets. Therefore the volume of the yellow packet grows from 1.5 to 5.1 partial volume sections. At every time step this procedure is repeated until the packets have left the tunnel completely.

The number of partial volume sections per volume section can be decided manually regarding calculation time and accuracy. With an increasing number of partial volume sections the accuracy of the calculation increases, but the calculation time is increasing as well.

Final temporal allocation of the packets to engine operation point

When a packet leaves the undiluted system, the emission mass gets assigned to this time step at position E, shown in Figure 6. However in most cases at the end of one time step a volume packet will overlap the system border as shown in Figure 9. This has to be considered by splitting and assigning the mass at different time steps.

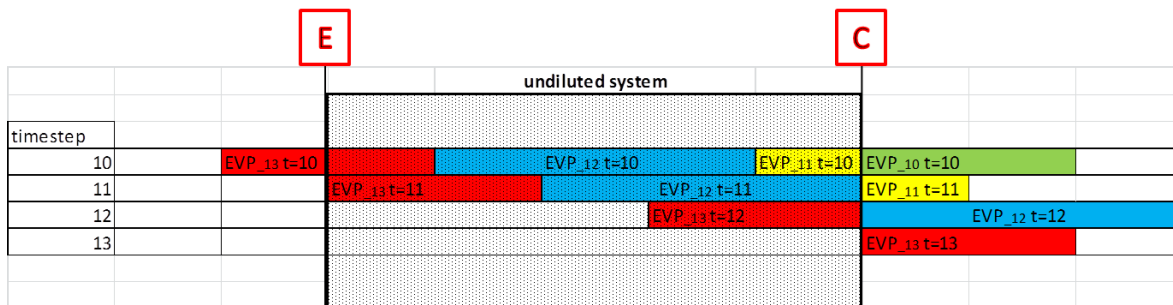


Figure 9: Overlapping of packets while dynamic time shift

Caused by the shift of packet 11 (yellow, allocated to point C at time step 11) into the undiluted system in time step 10 packet 13 (red) overlaps the border. As a consequence the emission mass of this packet has to be allocated to two different time steps (10 and 9 in this example). Figure 10 and equations 1 to 4 describe the applied method. Every time step the emission mass denoted with EM_{out} gets assigned to that engine operating point. EM_{in} represents the not assigned emission mass of the packet and will be assigned in the next time step(s). Depending on the variation of exhaust flow during the emission test it is also possible that multiple packets are allocated to single time steps at engine out. The presented method is also able to depict this case correctly.

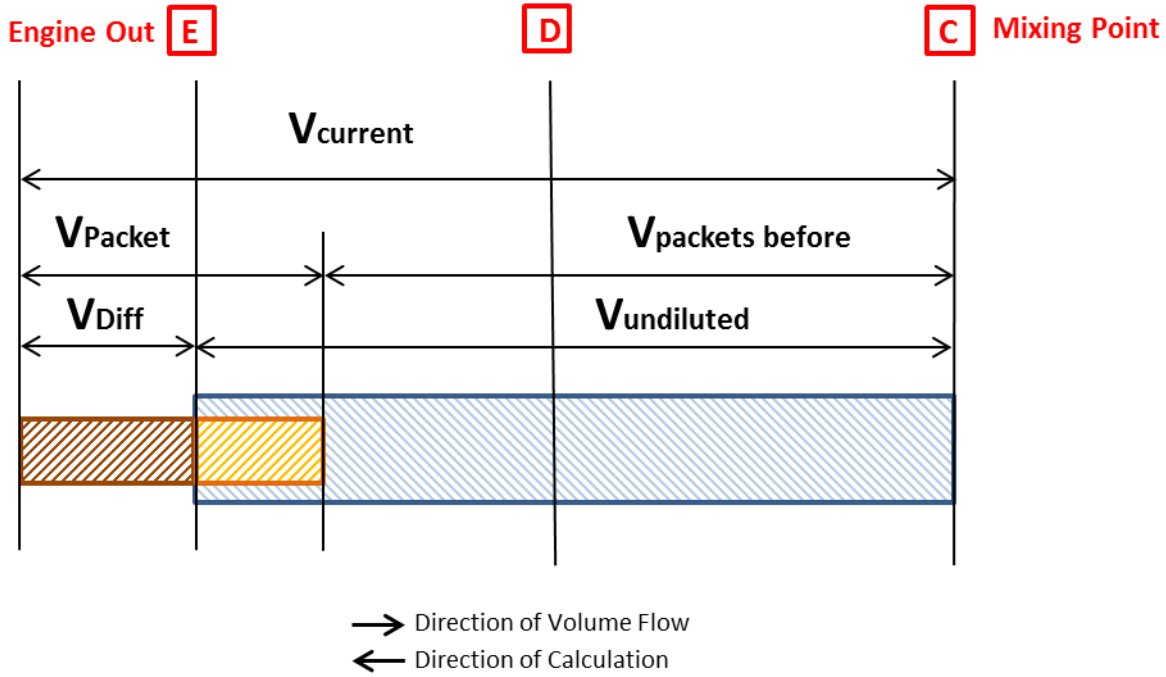


Figure 10: Time shift of overlapping volume packets

Notation:

$V_{undiluted}$... Volume of undiluted pipe system

V_{Packet} ... Volume of the considered emission volume packet

$V_{packets\ before}$... Aggregated Volume of all the emission volume packets measured before and filled into the tunnel

V_{Diff} ... Part of considered volume packet which already left the tunnel

$V_{current}$... Volume of considered volume packet and previous volume packets

EM_{Packet} ... Emission mass of the considered volume packet

EM_{out} ... Part of the emission mass of the considered packet which already left the tunnel

EM_{in} ... Part of the emission mass of the considered packet which is still located in the tunnel

$$V_{current} = V_{packet} + V_{packets\ before} \quad (\text{Eq. 1})$$

$$V_{Diff} = V_{current} - V_{undiluted} \quad (\text{Eq. 2})$$

$$EM_{out} = EM_{Packet} * \frac{V_{diff}}{V_{Packet}} \quad (\text{Eq. 3})$$

$$EM_{in} = EM_{Packet} - EM_{out} \quad (\text{Eq. 4})$$

Application example

This section demonstrates the effect of the variable time shift method for the undiluted exhaust system for the synthetic test case as discussed in chapter 1 of this paper. Figure 11 shows the temporal assignment of emission masses from position C (upper graph) to position E (lower graph). In the top diagram the coloured boxes filling the area below the blue line represent the emission mass as allocated to time at position C. All these coloured boxes are shifted to different time steps at position E depending on their individual transport time. The emissions in the blue area (time step 19 to 27 at C) are shifted back to time step 18 to 19 at E because of the increasing transport time caused by the low exhaust mass flow during the last phase of the test. All emissions as represented in the yellow box are shifted from C to E by about the same transport time because of the constant mass flow during this phase of the test. The first box on the left side (around time step 13 at position C dark green) is shifted to the first "low" phase of the test at position E (higher emission mass is distributed to more time

steps). Consequently the hole between the long-time shifted normal idling emissions and the short shifted high phase (running time 8 seconds before throttling and 0.8 seconds while throttling) is filled up. As a consequence in this test case the emission mass flow signal at E is calculated by the method correctly.

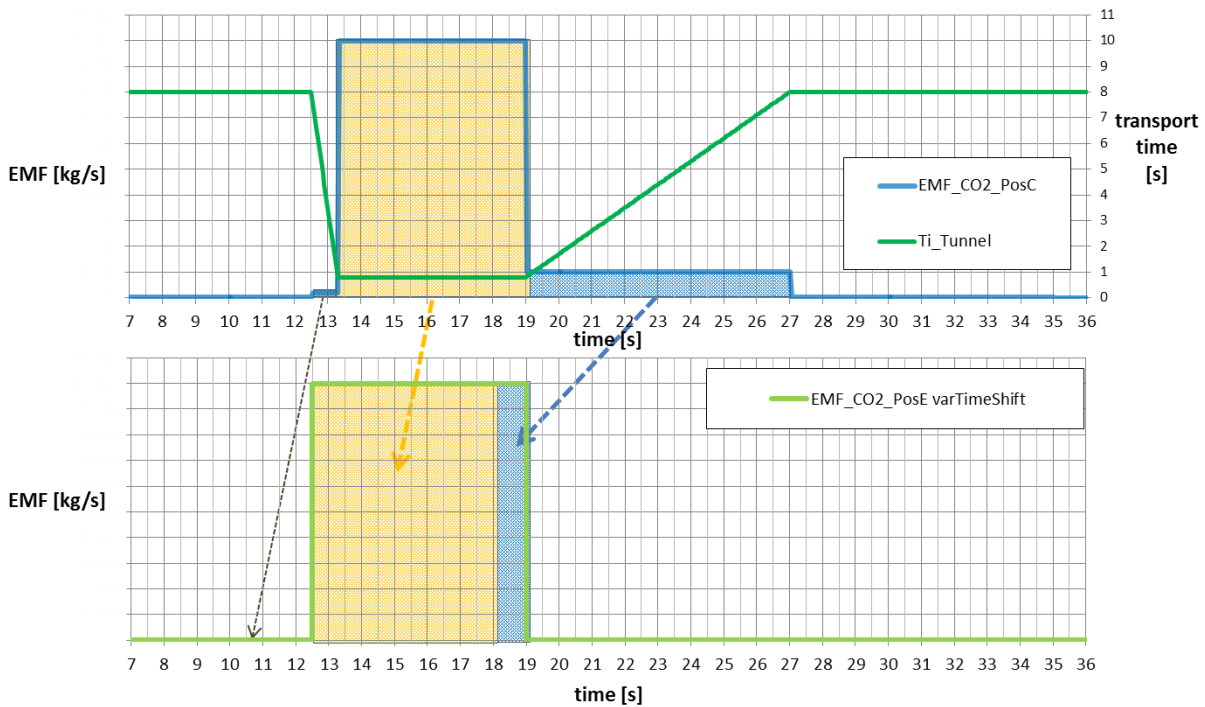


Figure 11: Assignment of emission masses with variable time shift

Important to note is that the method of correction of variable transport times as introduced in this paper only changes the allocation of emission mass flow over time but does not change the cumulative emission mass over an entire emission test.

4. Practical applications

In this chapter practical applications of the variable time shift method are demonstrated. These results show the benefit by using the method. Therefore these results are compared with the constant time shift method which is currently used. First the result of a test measurement is shown followed by results for vehicle emission tests. Furthermore some special cases important for the parametrisation of the evaluation methods are discussed.

Application to test measurements with known reference signal

Figure 12 shows a test measurement representing a step response test performed at the CVS system at the ICE in Graz. The object of the test is to check the entire signal correction methods as implemented in the ERMES tool by a test measurement with known reference result. The exhaust mass flow is generated by a fan and CO₂ gas from a calibration gas bottle is injected into measurement system at tailpipe position. The exhaust mass flow and the CO₂ concentration is changed at the same time from "low" to "high" and back to "low" again similar to the synthetic test case as discussed in the previous chapters. Figure 12 illustrates the results of the whole process of the ERMES tool with the measured CO₂ concentration at the analysers "EC_CO2" and the exhaust mass flow "ExMF" as input signals and the corrected emission mass flow at the engine "EMF_CO2_Var" as result. Compared to the emission mass flow calculated by the simple constant time shift method "EMF_CO2_Const" a much better temporal correlation of the emission mass flow with the reference result can be achieved.

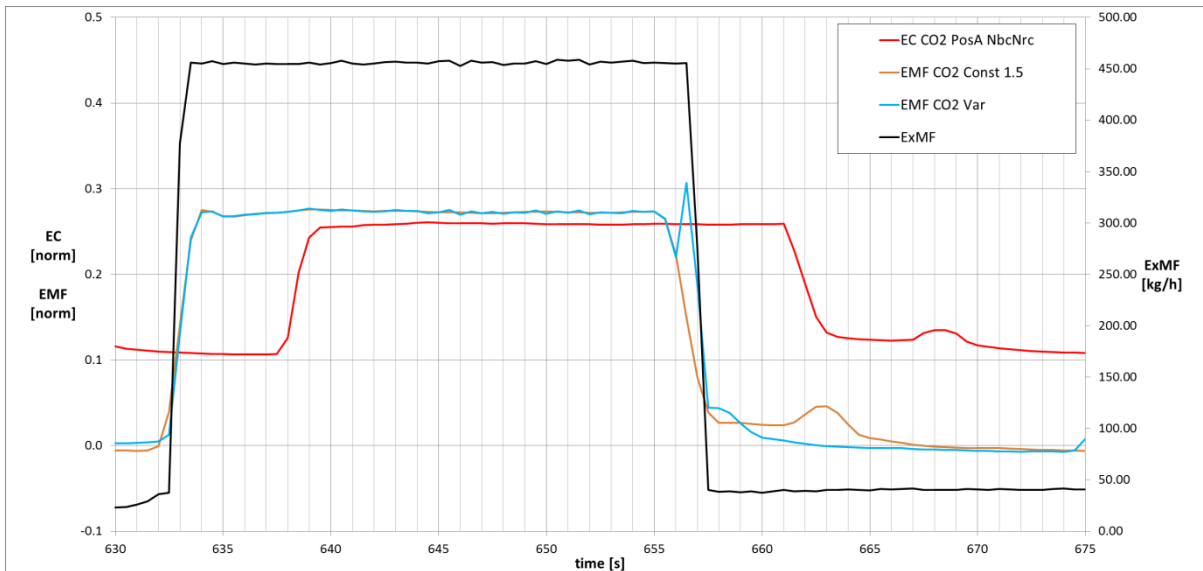


Figure 12: Evaluation of a test measurement representing a step response test

Application to full vehicle tests

Measurements with modal sampling in the diluted exhaust (CVS system)

In this section the evaluation methods as implemented in the ERMES tool are demonstrated using data from a full vehicle measurement at a chassis dynamometer with modal sampling in the diluted exhaust. The results for mass flow of CO₂ emissions are compared to the results based on the constant time shift method. As reference signal the engine power as calculated from vehicle dynamics and drivetrain efficiencies is used. An excerpt of the data is shown in Figure 13. A high quality signal for CO₂ mass flow is expected to qualitatively follow the engine power signal (blue). Both CO₂ emission peaks and phases of low emissions correlate very well with the power signal using the ERMES tool method (green). This is obviously much less the case for the CO₂ signal obtained from the constant time shift method (red).

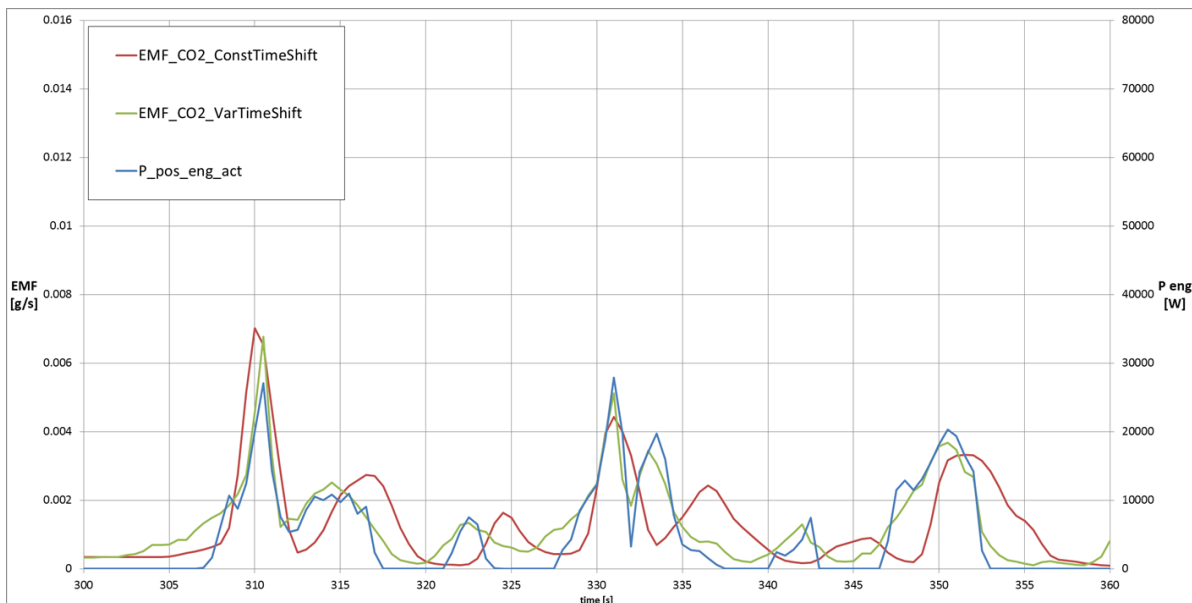


Figure 13: Comparison of CO₂ emission mass flow with engine power for an emission test at a chassis dyno with emission sampling in diluted exhaust (CVS system)

The advantage of transient emission data with a higher signal quality can be demonstrated by using the data in instantaneous emission models. Such models, e.g. PHEM (Luz and Hausberger (2013)), use the information recorded in emission testing to setup engine emission maps, where the emission mass flow or other engine relevant parameters are modelled over engine speed and engine power. The common method for setup of PHEM emission maps is to use emission data from transient real world cycles (e.g. the CADC and/or the ERMES cycle). For creation of emission maps based on

constant time shift data, the input signals for engine speed, power and emission mass flow have been averaged over 3s to reduce the well known temporal assignment problem. Using the ERMES tool data such an averaging procedure is not necessary anymore. To demonstrate the benefit of the ERMES tool method, emission maps have been created with both approaches. The quality of the resulting emission maps can be checked looking at the emission mass flow on the engine drag curve, which should be close to zero. Such a comparison of engine map data for CO₂ on the drag curve is shown in in Figure 14. The emission map compiled based on the constant time shift method has much higher emissions on the drag curve than the map created based on the ERMES tool data. However, also the variable time shift method cannot fully correct for all existing “distorting mechanisms” in the emission measurement setup perfectly. As a consequence the emissions are not zero at the drag curve but obviously smaller.

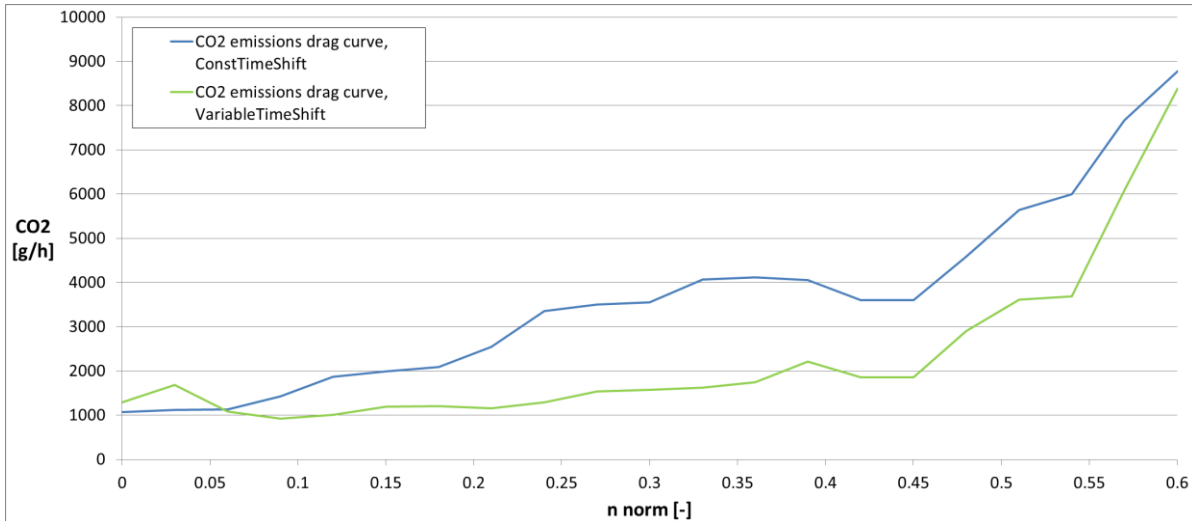


Figure 14: Comparison of NOx emissions on the drag curve

Measurements with modal sampling in undiluted exhaust

The ERMES tool correction methods can also be applied to test data from modal emissionsampling in undiluted exhaust, e.g. from PEMS measurements. In most cases due to the much smaller volume of the undiluted parts of the measurement system compared to CVS sampling the variability of the gas transport time decreases. As a consequence also the influence of the variable time shift method on the calculated mass flows from the constant time shift method is much less pronounced as for a CVS system (Figure 15).

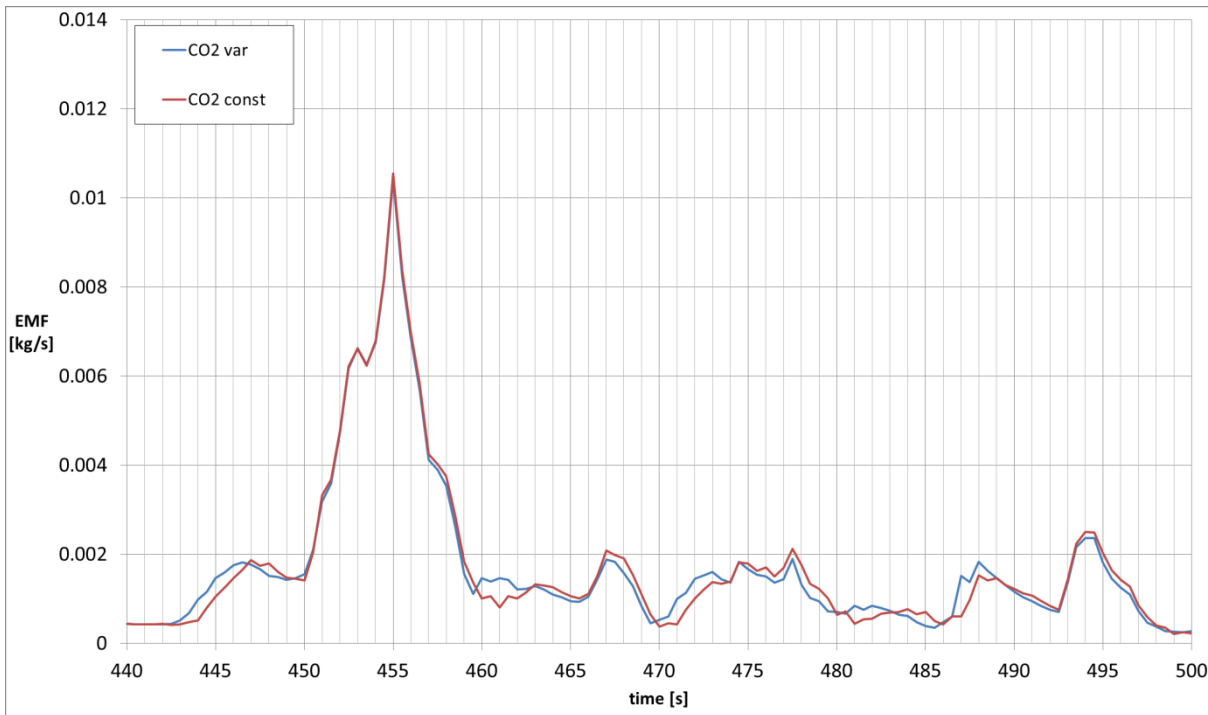


Figure 15: Comparison of variable and constant time shift method for a PEMS measurement

“Short test” for calibration of volume of vehicles’ exhaust system

The parameterisation of the volumes in the exhaust system has a significant effect on the assignment of the emission masses to their right operating point. Consequently exact information about the different volume sections is necessary. The volumes of test bench specific pipes (all pipes except the exhaust system of the car) can be measured once and can then be defined as default values in the evaluation process. However, the volume of the vehicles exhaust system has to be determined for each tested vehicle. To avoid these efforts at the ICE a “short test” was developed which fulfils two purposes:

1. The implicit determination of the exhaust system volume (engine out to tailpipe)
2. A verification that the ERMES tool correction algorithms provide reasonable results for the tested vehicle

This short test consist of the variation of engine speed from idling followed by a short phase of engine rated speed (target: approximately 10 seconds) and followed again by engine idling. The driver has the instruction to perform the engine speed changes as quickly as possible. Due to this simple test setup such a short test can be performed both on the chassis dyno as well as in real world PEMS testing. In the test evaluation the volume of the vehicles exhaust systems is varied within a reasonable range and the results for CO₂ mass flow are compared with the recorded engine speed signal. Figure 16 gives an example for the evaluation of a short test.

Accompanied by the beginning of throttling the CO₂ emission mass and the engine speed are raising at the same time. After the acceleration phase the engine speed is hold close to the rated speed with a somewhat smaller CO₂ emission mass compared to the peak in the acceleration phase. While removing throttle, no fuel is injected until reaching the idling speed. With decreasing engine speed the exhaust volume flow is going down and as a consequence the zero CO₂ emissions from fuel cut-off are delayed in the measurement system due the small gas transport speed. This low CO₂ level should be at idling level again once the engine speed reaches idling speed, the point where the fuel injection starts again. According to the various volumes, which are shown in the legend of the diagram, both the assignment of the slope at the beginning of throttling and the “filling up” of the zero CO₂ emission phase are solved differently. In this case exhaust and undiluted volume of 68 litres (red line) provides the most reasonable result. The blue line representing a volume of 88 litres shifts the emission packets too far and the smaller ones cannot correct the zero emission phase completely. Especially the “filling” of the zero emission phase until the engine speed reaches the idling speed is the most valuable indication and shows the sensitivity of the correction methods to different volumes of the exhaust system.

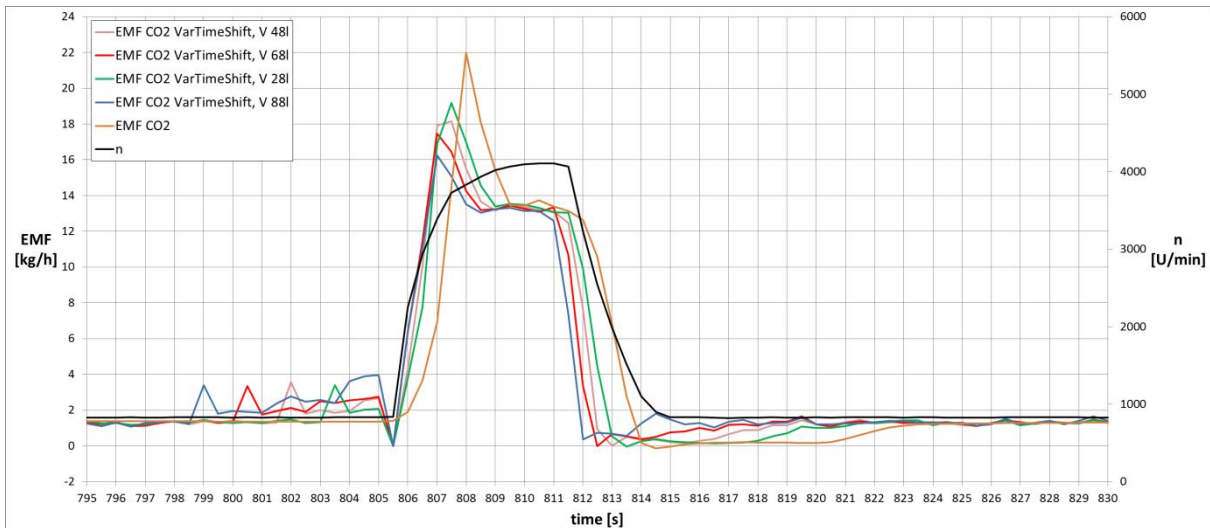


Figure 16: Volume determination (exhaust system + CVS connection pipe) based on the results of the short test

By the evaluation of the test in the ERMES tool the volume of the exhaust system of the car can be determined with very low efforts.

Influence of differences in the response characteristics of exhaust mass flow and concentration measurement on the results of the variable time shift method

The variable time shift method corrects the signal optimally when the response characteristics (delay and duration) of the measurement of exhaust mass flow and emission concentration match. To demonstrate this influence in Figure 17 the emission mass flow at position C (sampling point at the end of the undiluted system) are shown.

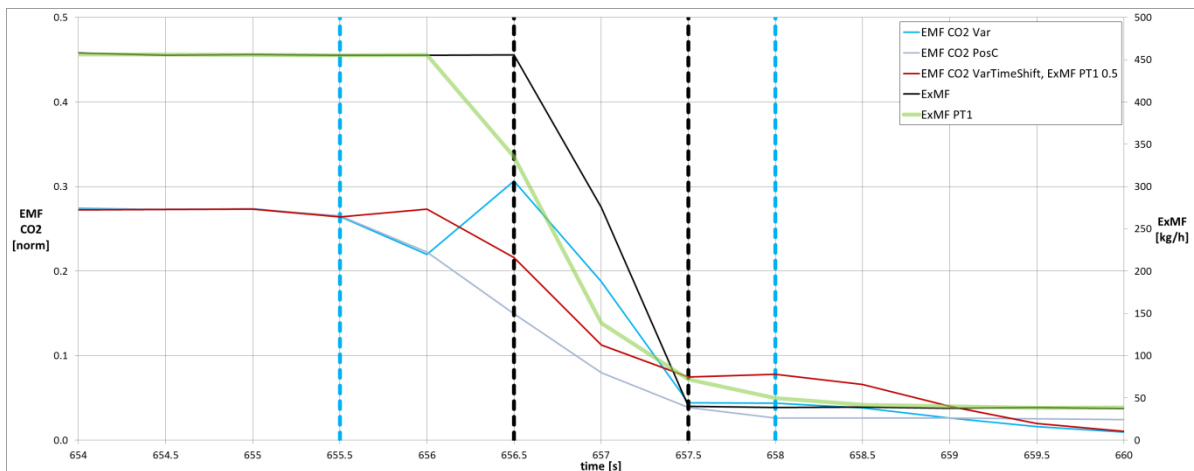


Figure 17: Coherence of response characteristic

This example represents the decrease from a high constant emission and mass flow level to a lower one. The dotted lines in the respective colours show the beginning and the end of the different signal changes. It is obvious that the change of the response corrected (described in Figure 17 and the corresponding explanation) emission concentration (represented by the emission mass at position C, purple) takes a longer time than the turn of the mass flow (black). For that reason the different concentrations are inverse PT1 corrected, but the effect is limited and cannot compensate the difference of the response characteristics completely. Consequently the variable time shift method does not work perfectly. The valley at second 656 is formed because of the falling concentration with the constant volume flow before the first black dotted line. The missing emission mass is shifted to second 656.5 and the result is a peak at that position. One possibility for the equalization of the different response characteristics additional to the inverse PT1 correction of the concentrations could be a PT1 correction of the ExMF. With this flattened signal (green) the response delay would be extended and consequently the signals would better match regarding the peak at second 656.5 (dark

red signal). But the long delay implies high idling emissions and the signal is just corrected to the “new” flattened exhaust mass flow. Despite the improvement of the response characteristic by the inverse PT1 correction of the measured concentration, this method downgrades the fast measured exhaust mass flow. Moreover the different concentration measuring sensors have different response characteristics. Thus the adaptation of the PT1 correction of the exhaust mass flow has to be done for an average signal.

The coherence of the response characteristic has to be checked for every test bed because of different sensors and mass flow measurement equipment. A decision concerning the separate signal correction possibilities has to be made after regarding the test results.

Conclusions

At the Institute for Internal Combustion Engines and Thermodynamics an algorithm was developed, which allows for correction of variable gas transport times in the analysis of instantaneous emission measurements. The corrections are performed using a physical model based on measured exhaust mass flow and volumes and temperatures in the measurement system. This algorithm was implemented into the software “ERMES tool” which is capable to perform evaluations of measurement data from any kind of emission test systems (diluted from CVS, undiluted from engine dyno or PEMS measurement). The tool now provides methods to correct emission test results for effects of analyser response behaviour and transport times in diluted and undiluted parts of the measurement equipment.

For the determination of the vehicle specific volume of the exhaust system – which is a crucial parameter in the correction algorithm – a short test was developed which has to be performed only once for each measured vehicle and only takes few minutes. Main benefits of the application of the ERMES tool methods are a significantly improved quality of the emission mass signals regarding temporal allocation to the operation point of engine and exhaust aftertreatment.

Acknowledgements

The work presented in this paper as well as the ERMES tool is internal research at the ICE. The authors want to thank all colleagues in the ERMES group and especially Martin Weilenmann for the inspiring discussions on how to understand and to improve instantaneous emission test results.

References

- Franco Garcia V. (2014): Evaluation and improvement of road vehicle pollutant emission factors based on instantaneous emissions data processing. Dissertation Universität Jaume
- Ajtay D., Weilenmann M. (2014): Compensation of the Exhaust Gas Transport Dynamics for Accurate Instantaneous Emission Measurements. *Environ. Sci. Technol.* 2004, 38, 5141-5148
- Luz R., Hausberger S. (2013): User Guide for the Model PHEM, Version 11.2; Institute for Internal Combustion Engines and Thermodynamics TU Graz, Graz, 2013

Greenhouse gas emissions from heavy duty vehicles using upgraded biogas as a fuel

Morten WINTHER* & Steen Solvang JENSEN**

Aarhus University, Department of Environmental Science, Frederiksborgvej 399, 4000 Roskilde, Denmark

*mwi@envs.au.dk,

**ssj@envs.au.dk

Abstract

This paper examines the CH₄ loss and the total greenhouse gas emission (GHG emissions) savings associated with the use of upgraded biogas as a fuel for heavy duty vehicles in Denmark. The study focuses on the emissions related to the operation of the vehicles and the emissions from fuel tanking. Emission calculations are made in two scenarios for 2035 using low and high loss CH₄ input factors derived from the literature. Results suggest that engine loss/tank boil off is the largest source of CH₄ followed by CH₄ leaks at the fuel station and the CH₄ emissions from exhaust. The low[high] loss emission percentage shares are 57 %[62 %] for engine loss/tank boil off, 43 %[23 %] for fuel station and 0.4 %[15 %] for exhaust. The calculated low and high loss GHG emission reductions are 91 % and 86 % from "tank-to-wheel" (engine loss/tank boil off and exhaust) and 88 % and 84 % from "pump-to-wheel" (engine loss/tank boil off, exhaust and fuel station), in relation to the diesel reference scenario.

Key-words: CNG, LNG, CH₄, CO₂, biogas, heavy duty vehicles

Introduction

Today the transport sector almost entirely uses fossil fuels except for a few percent biofuels added, and electric vehicles generally penetrates the car market very slowly. In order to meet the global challenges in terms of climate protection, Denmark has adopted a climate law establishing the strategic frame for the transformation into a low carbon society by the year 2050. For road transport alone, a few technological solutions exist to achieve this political goal.

In the light vehicle segment of the road transport fleet, the technological development within battery electric vehicles and plug-in hybrids should allow passenger cars and vans to become mainly electric in the future. Also fuel cell cars powered by hydrogen is likely to penetrate the market in the future as they will provide driving range similar to nowadays cars.

Trucks instead, will most likely not be electric in the future - except in small niches of the fleet and for limited applications - as they are too heavy and cannot be frequently charged during normal operational use. Urban buses on short distance routes and opportunities for fast charging as part of the timetable have a potential to become battery electric or battery/hybrid in the future. As a second likely alternative, trucks and buses can be using solely biodiesel, but in this case the provision of second-generation biofuels from Danish sources may be limited by the availability of bio-resources and might not be provided in the quantities needed.

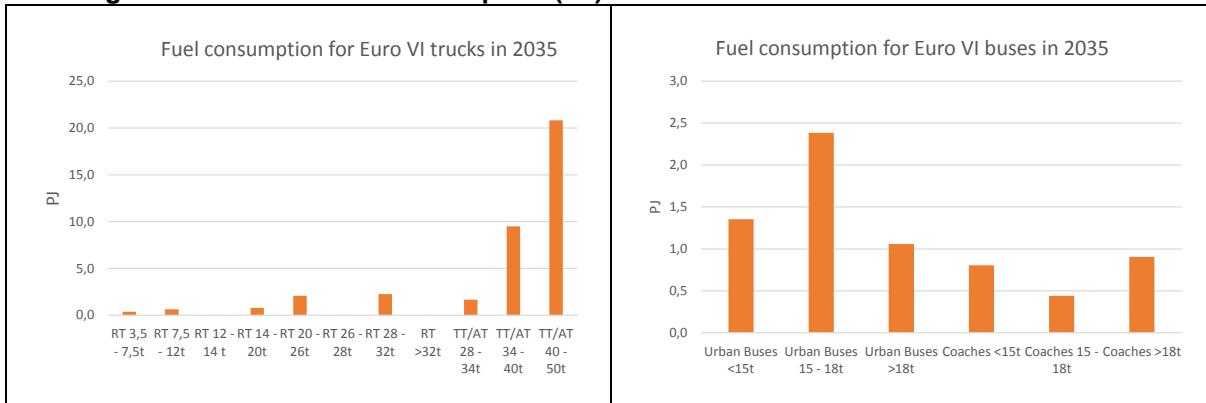
Instead, natural gas (methane or CH₄) seems like the most promising fuel alternative for heavy duty vehicles in Denmark. Denmark has a large potential for biogas production from different organic sources, e.g. manure, straw and household waste, and after upgrading biogas can be distributed in the existing natural gas grid. Due to these advantages, there is a strong political, administrative and commercial interest for the deployment and use of biogas in Denmark.

Since the Danish Government's plan for Green Growth in 2009 there is a political objective to use up to 50% of the livestock manure in Denmark for energy production (probably primarily biogas) towards 2020. This goal was further pursued in the National Energy Agreement from 2012, supporting biogas development, and a task force was formed for realising the targets. In addition a resource strategy of the Danish Government from 2013 stresses that more organic waste from households, restaurants and grocery shops should be collected and used to produce biogas (Ministry of

Euro VI vehicles are relevant for natural gas substitution and therefore the fuel consumption picture is analyzed in more details for 2035. This is shown in Figure 2 (note the axis scaling).

The estimated total fuel consumption for Danish heavy duty vehicles becomes 45 PJ in 2035. The calculated fuel consumption (percentage shares in brackets) for TT/AT trucks, rigid trucks, urban buses and tourist buses are 32 PJ (71 %), 6.1 PJ (14 %), 4.8 PJ (11 %) and 2.2 PJ (5 %), respectively. A break down of fuel consumption by vehicle size categories for trucks shows the vehicle category 40-50t uses 21 PJ (46 %) and the vehicle category 34-40t 9.5 PJ (21 %). The fuel result figures are also shown in Table 2.

Figure 2. Forecast of fuel consumption (PJ) for Danish Euro VI trucks and buses in 2035.



1.2 CNG and LNG vehicles in the biogas scenario

CNG (Compressed Natural Gas) vehicles are available on the market today up to 320 hp (see e.g. www.gasbiler.info). The CNG vehicles have CNG fuel stored on board in pressurized tanks (200-260 bar) and are equipped with SI (spark ignition) engine that operates similarly to a gasoline engine. Today's vehicles are certified as Euro VI and are equipped with a three-way catalyst to ensure compliance with the EU emission standards.

One disadvantage of CNG vehicles is the smaller km range between fuel stops compared to their conventional diesel counterparts. Another drawback for CNG is the relatively low fuel economy vs diesel. Only limited fuel economy data is currently available for Euro VI CNG engines to compare with diesel. Fuel economy data for Euro VI CNG vs. Euro VI diesel examined by Danish Technological Institute for the Danish Energy Agency (2014) showed large variations depending on vehicle model and emission test cycles. An average of 19 % more MJ/km for CNG compared to diesel could be derived from the data material¹. However, it is believed that a future introduction of throttle-less gas engines will bring considerable fuel efficiency improvements maybe in the order of 15 % compared to today's CNG vehicles (e.g. Danish Energy Agency, 2014).

LNG (Liquefied Natural Gas) vehicles have fuel stored onboard in vacuum insulated storage tanks (3-10 bar, -160 °C). The LNG vehicles are equipped with dual fuel engines that operate similarly to a diesel engine and use 5 % diesel to pilot the ignition of fuel in the cylinder during each combustion stroke. Due to the higher energy density of the LNG fuel stored the km range between fuel stops for LNG vehicles is considerably longer than for CNG.

In Europe LNG sales have only recently started, and in Denmark only one LNG truck is available at the moment. LNG trucks are, however, more widespread in use in other parts of the world. This is e.g. the case in the United States, where a national network of public LNG fueling centres has been established with new LNG filling stations continuously being added to the network. The commercially available LNG dual fuel engines in the US today cover the entire engine size range for freight vehicles up to 600 hp. Although only certified for the US market the engines are equipped with SCR catalysts, DOC catalysts and DPF's in order to meet the most stringent US emission standards for heavy duty vehicles. In terms of fuel economy, LNG suffers from the same drawback as for CNG. The International

¹ The same study found no significant NO_x and PM (Particulate Matter) emission differences between Euro VI CNG and diesel based on the limited measurement data available

Council on Clean Transportation (ICCT, 2015) estimate a 10 % lower fuel economy for LNG vehicles compared to their modern diesel counterparts.

By all means, LNG trucks will also become commercially available in Europe. The introduction of LNG for transport in Europe is not least supported by the adoption of the EU directive 2014/94 that places on member countries to establish a LNG tank facility infrastructure along the main arterial roads (TEN T: Trans European road network) in the EU by 2025.

In the present project CNG vehicles replace rigid trucks and buses and for TT/AT trucks the vehicle replacement is made with LNG trucks. For both CNG and LNG vehicles, a 10 % lower fuel economy compared to diesel is assumed in the biogas scenario calculations.

1.3 Emission factors and CH₄ loss factors

A fuel related CO₂ factor of 66.6 g/MJ is used in the diesel reference scenario. The factor relies on the country specific CO₂ emission factor of 74 g/MJ for neat diesel and the 10 % blend percentage of (CO₂ neutral) biodiesel in the diesel fuel assumed by the Danish Energy Agency for 2035. N₂O and CH₄ emission factors in the reference case come from COPERT IV.

The source of CH₄ emission factors for CNG vehicles is measurements made by Danish Technological Institute (DTI), see also DTI(2015). The latter study reports measurements of among others CH₄ for two CNG buses and one Euro CNG truck - all certified as Euro VI- obtained during chassis dynamometer tests using different test driving cycles. The measurements obtained during the World Harmonized Vehicle Cycle (WHVC) were selected as realistic values for the present study, and the measured emissions were believed to represent LNG vehicles also. High/low emission percentages of 0.196/0.003% CH₄ per unit of fuel consumed were derived from the measurements. An assessment of the measurement results for other emission components (CO, NMVOC) gave DTI reason to believe that the high emission factor was measured during rich fuel engine running conditions. Transformed into g/kWh the high factor equals 0.47 that is just below the Euro VI emission limit value of 0.5 g/kWh valid for natural gas engines.

In addition to direct CH₄ emitted from the tail pipe, other CH₄ emissions occur from CNG and LNG vehicles directly related to the vehicles. These sources of CH₄ have been summarized in the assessment study for heavy duty vehicle natural gas emissions made by ICCT (2015) and low/high emission factors are proposed based on the literature. The ICCT emission factors are adopted for the present study.

For CNG vehicles, CH₄ is emitted from the crankcase as so-called "blow by emissions" occurring from CH₄ leaking between piston rings and cylinder walls, being vented to the atmosphere. LNG vehicles use diesel-like HPDI (high pressure direct injection) engines, and in this case, CH₄ occasionally needs to be vented due to pressure control in the fuel injection system. In addition CH₄ from LNG vehicles is vented from the vehicle fuel tank during "boil off" pressure release, which is made for safety reasons. In the following crankcase/dynamic venting/tank boil off emissions are referred to as engine loss/tank boil off emissions.

ICCT (2015) also propose factors for CH₄ leaks and escapes from natural gas fueling stations. CH₄ leaks occur from valves, pipes and fittings at the tanking facilities and small escapes of CH₄ occur during nozzle connection and disconnection during the tanking of the vehicles. In addition for CNG compressor loss occurs at the station, whereas for LNG, methane is boiled off in storage tanks and is manually vented from vehicle fuel tanks prior to refueling.

Table 1. CH₄ loss (% of fuel delivered).

Source of CH ₄ loss	Low estimate	High estimate
Tail pipe exhaust	0.003	0.2
Engine loss/tank boil off	0.4	0.8
Fueling station	0.3	0.3

1.4 Calculation of CH₄ loss

The source specific emissions of CH₄ in the biogas scenario are calculated as follows:

$$E_{CH_4} = \frac{FC_{GJ} \times 1.1}{LHV_{CH_4}} \times LF_{CH_4}/100$$

Where:

E_{CH_4} = Mass based emissions of CH₄ (tonnes)

FCPJ = Fuel consumption (GJ) for diesel vehicles in the reference scenario (Section 1.1, table 2)

1.1: Fuel economy adjustment factor for CNG/LNG vehicles replacing diesel vehicles (Section 1.2).

LHV_{CH₄} = Lower heating value for CNG/LNG fuel (47.96 GJ/tonnes; Danish Energy Agency, 2014)

LF_{CH₄} = Source specific loss factor of CH₄ (% of fuel delivered, Table 1)

2. Results

The emission results for the reference scenario and the biogas scenario are shown in Table 2.

Table2.Emission results for the reference scenario and the biogas scenario.

	Reference scenario				Biogas scenario									
	FC	CO ₂	CH ₄	N ₂ O	Fuel consumption				CO ₂	CH ₄ exhaust		CH ₄ engine loss/tank boil off		CH ₄ Fuel station
					CH ₄	Diesel	CH ₄	Diesel		low	high	low	high	
	PJ	kTonnes	Tonnes	Tonnes	Tonnes	Tonnes	PJ	PJ	kTonnes	Tonnes		Tonnes		Tonnes
Total Trucks	38.1	2540	5.1	189	837	41	40.1	1.8	117	25.1	1621	3347	6694	2518
RT	6.1	409	1.0	27	140	0	6.7	0.0	0	4.2	272	561	1121	422
TT/AT	32.0	2131	4.1	162	697	41	33.4	1.8	117	20.9	1350	2787	5573	2096
Total Buses	6.9	466	0.8	28	159	0	7.6	0.0	0	4.8	309	638	1275	480
Urban buses	4.8	320	0.5	20	110	0	5.3	0.0	0	3.3	213	440	880	331
Coaches	2.2	146	0.3	7	49	0	2.4	0.0	0	1.5	96	197	395	149
Grand total	45.0	3006	5.9	217	996	41	47.8	1.8	117	29.9	1930	3985	7970	2998

In Table 3 the emission results for the reference scenario and the biogas scenario are shown transformed into CO₂ equivalents by using the global warming potential factor of 25 for CH₄ and 298 for N₂O (IPCC, 2007).

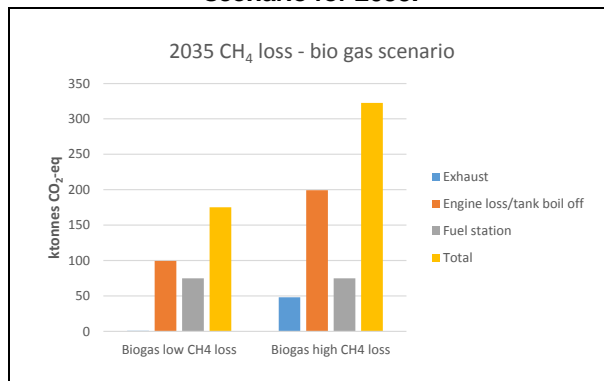
Table3.Emission results for the reference scenario and the biogas scenario counted in CO₂ eq.

	Reference scenario			Biogas scenario								
	CO ₂	CH ₄	N ₂ O	CO ₂	CH ₄ exhaust		CH ₄ engine loss/tank boil off		CH ₄ Fuel station	CH ₄ Total		
					low	high	low	high		low	high	
	kTonnes CO ₂ -eq.			kTonnes	kTonnes CO ₂ -eq.		kTonnes CO ₂ -eq.		kTonnes CO ₂ -eq.	kTonnes CO ₂ -eq.		
Total Trucks	2540	0.13	56	117	0.63	40.5	83.7	167.4	62.9	147	271	
RT	409	0.02	8	0	0.11	6.8	14.0	28.0	10.5	25	45	
TT/AT	2131	0.10	48	117	0.52	33.7	69.7	139.3	52.4	123	225	
Total Buses	466	0.02	8	0	0.12	7.7	15.9	31.9	12.0	28	52	
Urban buses	320	0.01	6	0	0.08	5.3	11.0	22.0	8.3	19	36	
Coaches	146	0.01	2	0	0.04	2.4	4.9	9.9	3.7	9	16	
Grand total	3006	0.15	65	117	0.75	48.3	99.6	199.2	74.9	175	322	

Measured in CO₂ equivalents the low and high estimates of CH₄ loss for the biogas scenario become 175 ktonnes and 322 ktonnes, respectively (Table 3 and Figure 3). The CH₄ losses from each

source are proportional to their fuel related emission factors (Table 1), and needless to say, for each source category the internal emission shares correspond with the fuel consumption share per vehicle category. In both cases the engine loss/tank boil off is the largest source of CH₄ followed by CH₄ leaks at the fuel station and the CH₄ emissions from exhaust. Derived from the numbers in Table 3, the engine loss/tank boil off [fuel station, exhaust] emission shares are 57 % [43 %, 0.4 %] and 62 % [23 %, 15 %] in the low and high case, respectively.

Figure3. Total CH₄ loss (ktonnes CO₂ eq.) from Danish heavy duty vehicles calculated in the biogas scenario for 2035.

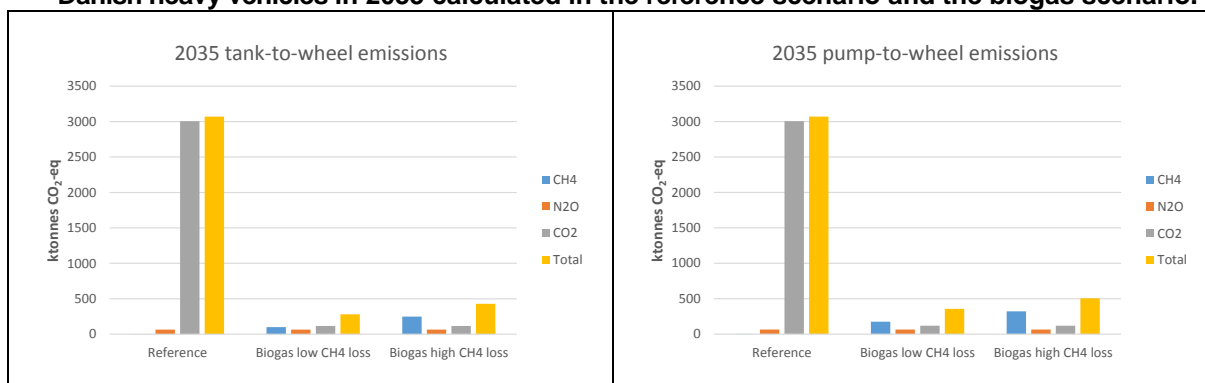


The total GHG emissions calculated in the low/high biogas scenarios are shown in Figure 4 for the “tank-to-wheel” (engine loss/tank boil off and exhaust) and “pump-to-wheel” (engine loss/tank boil off, exhaust and fuel station) chain of emissions. The CO₂ emissions calculated in the biogas scenario originates from the 5 % diesel pilot fuel (explained in Section 1.2). Due to lack of emission information, the diesel heavy duty N₂O emission factors are used for the gas vehicles as well.

The calculated low and high loss GHG emission reductions are 91 % and 86 % from tank-to-wheel and 88 % and 84 % from pump-to-wheel, in relation to the diesel reference scenario.

For tank-to-wheel the calculated low [high] GHG percentage contributions for CO₂, CH₄ and N₂O become 42 % [27 %], 36 % [58 %] and 23 % [15 %], respectively. In the pump-to-wheel case, the low [high] CO₂, CH₄ and N₂O GHG contributions become 33 % [23 %], 49 % [64 %] and 18 % [13 %].

Figure4. Total tank-to-wheel and pump-to-wheel greenhouse gas emissions (ktonnes CO₂-eq.) for Danish heavy vehicles in 2035 calculated in the reference scenario and the biogas scenario.



3. Conclusion

This paper examines the CH₄ loss and the total GHG emissions savings associated with the use of upgraded biogas as a fuel for heavy duty vehicles in Denmark. The study focuses on the emissions related to the operation of the vehicles and the emissions from fuel tanking. Emission calculations are made in two scenarios for 2035 using low and high loss CH₄ input factors derived from the literature.

Results suggest that engine loss/tank boil off is the largest source of CH₄ followed by CH₄ leaks at the fuel station and the CH₄ emissions from exhaust. The low [high] loss emission percentage shares

are 57 % [62 %] for engine loss/tank boil off, 43 % [23 %] for fuel station and 0.4 % [15 %] for exhaust.

The calculated low and high loss GHG emission reductions are 91 % and 86 % from “tank-to-wheel” (engine loss/tank boil off and exhaust) and 88 % and 84 % from “pump-to-wheel” (engine loss/tank boil off, exhaust and fuel station), in relation to the diesel reference scenario.

The input data for CH₄ loss are regarded as relatively uncertain (ICCT, 2015) and the resulting emissions might change if new CH₄ loss factors become available.

The GHG emissions calculated from tank-to-wheel are small in comparison with the emissions from the diesel reference scenario, and the GHG emissions are still quite low even if we include the CH₄ loss from the fueling stations (pump-to-wheel emissions). As a side remark, the calculated GHG emissions will be additionally 4 percent point lower by assuming that the LNG pilot fuel consist of neat biodiesel rather than diesel with a 10 % content of biodiesel, based on the energy forecast from the Danish Energy Agency.

To gain a complete overview of the total GHG emission consequences of a 100 % fuel switch from diesel to natural gas for heavy duty vehicles, we need to estimate the emission loss during the production of the natural gas from biogas, distribution of gas to fueling stations and the changed emissions in the society due to the use of bio resources for biogas production instead of alternative usage.

Jørgensen & Kvist (2015) examined the CH₄ loss during the production of biogas. Measurements made at nine biogas plants showed a significant average loss of 4.2 % of the produced biogas quantity. A subsequent work made to seal the leaks discovered brought down the CH₄ percentage loss to 0.8 % (Agrotech, 2015). By using 0.8 % and 4.2 % as low and high CH₄ loss factors, respectively, for biogas production, the “production-to-wheel” (excluding gas distribution) GHG emission reductions are roughly estimated to 82 % and 50 % compared with the diesel reference scenario.

On the other hand, the upstream Danish emission savings from alternative usage of the bio resources will be very large. A large amount of the bio resource is foreseen to consist of manure from animal production that consequently will not emit methane from the various manure management steps, including in stables and storage tanks.

The upstream emission loss during natural gas production and plant to fueling station distribution, and the emission savings from alternative bio resource usage will be investigated in an ongoing project carried out at Danish Centre for Environment and Energy (DCE), Aarhus University that the present study is also part of.

Acknowledgments

The work presented in this paper is a part of the multidisciplinary research project “Biogas for transport - resources, environment and welfare economics” carried out from 2014-2016 and funded by the Danish Centre for Environment and Energy (DCE), Aarhus University.

References

- Agrotech (2015). Methane emission from Danish biogas plants. Climate effects of methane leakages from biogas plants, 11 pp., May 2015.
- Danish Technological Institute (2015): Measurement program for heavy CNG vehicles, 60 pp, Oct. 2015.
- Danish Energy Agency: Framework conditions for using natural gas in heavy duty road transport, 150 pp., December 2014 (in Danish).
- Danish EPA (2014): Denmark without waste. Resource plan for waste treatment 2013-2018. Guidelines from the Danish EPA no. 4, 2014.
- EMEP/EEA (2013): Air Pollutant Emission Inventory Guidebook, prepared by the UNECE/EMEP Task Force on Emissions Inventories and Projections (TFEIP). Available at: <http://www.eea.europa.eu/publications/emep-eea-guidebook-2013> (12-01-2016).
- IPCC (2007): Climate Change 2007: The Physical Science Basis. Contribution of Working Group I to the Fourth Assessment Report of the Intergovernmental Panel on Climate Change [Solomon, S.,

D. Qin, M. Manning, Z. Chen, M. Marquis, K.B. Averyt, M. Tignor and H.L. Miller (eds.]. Cambridge University Press, Cambridge, United Kingdom and New York, NY, USA, 996 pp.

Jørgensen, L. & Kvist, T. (2015): Methane emission from Danish biogas plants - Quantification of methane losses, Project report, 44 pp., ISBN: 978-87-7795-385-9, Danish Gas Technology Centre, June 2015. Ministry of Environment (2013): Denmark without waste. More recycling – less combustion. October 2013 (in Danish).

Nielsen, O-K., Plejdrup, M. S., Winther, M., Hjelgaard, K., Nielsen, M., Fauser, P., Thomsen, M. (2015): Projection of greenhouse gases 2013-2035. Aarhus University, DCE – Danish Centre for Environment and Energy. (Scientific Report from DCE - Danish Centre for Environment and Energy; Nr. 129).

The International Council on Clean Transportation (ICCT) (2015): Assessment of heavy-duty natural gas vehicle emissions: Implications and policy recommendations, White Paper, 34 pp., July 2015.

Analysis of Diurnal Trends in Vehicle Fleet Composition and their Emission Contribution on an Urban Arterial Road in Leeds, UK.

David WYATT*, Hu LI** & James TATE***

* Doctoral Training Centre in Low Carbon Technologies, University of Leeds, Leeds, LS2 9JT, UK
Email: pmdww@leeds.ac.uk

** Energy Research Institute, University of Leeds, Leeds, LS2 9JT, UK

*** Institute for Transport Studies, University of Leeds, Leeds, LS2 9JT, UK

Abstract

This research investigates diurnal variation in vehicle fleet hot exhaust Carbon Dioxide (CO₂) emissions through development of a coupled traffic simulation and vehicle emission model. An AIMSUN traffic micro-simulation was developed for a road network around a 3.8km portion of one of the main arterial corridors into and out of Leeds, the third largest city in the UK. The model was separately calibrated and validated for five time periods, AM Peak (AM), Inter-Peak (IP), PM Peak (PM), Evening (EV) and Night (NI). For each time period in AIMSUN, the second-by-second vehicle trajectories for all vehicles in the simulation were extracted using an Application Programming Interface (API) tool. The Technical University of Graz's (TUG) Passenger car and Heavy duty Emission Model (PHEM) was used to calculate CO₂ emissions estimates from the 1Hz trajectory data. Parameters within the coupled model, such as the vehicle fleet and vehicle dynamics, were customised for the specific study area and time period. This work represents the development of a coupled micro-simulation and instantaneous emission model which could provide a very cost effective way of conducting high-resolution emission estimation, thereby providing accurate estimation of real-world vehicle fleet emission factors whilst also characterising the relative emission contribution from every vehicle category within the fleet.

Keywords: CO₂, Micro-simulation, PHEM, AIMSUN, Fleet Emissions.

1. Introduction

Over the last decade an increase in computing power and improved data capture for model validation and calibration, have enabled the development of sophisticated microscopic traffic simulation tools such as AIMSUN (TSS 2013), VISSIM (PTV 2004) and PARAMICS (Quadstone 2005). These models can be used to simulate the movement and interactions of all vehicles, over a defined time period, in a well specified road network (i.e. a simulated network where the real-world traffic signal control timings, speed limits and road geometry are accurately described). If the model is well calibrated, the modelled second-by-second speed profiles of the simulated vehicles should be representative of the on-road speed profiles for such vehicles in real-world driving (Kraschl-Hirschmann, Zallinger et al. 2011).

In order to ascertain how emission from the vehicle fleet in the network varies over a typical working day, five individually calibrated and validated AIMSUN Headingley network simulations were developed. These five time periods represent different traffic flow conditions observed during diurnal analysis of the vehicle fleet data captured by Automatic Number Plate Recognition (ANPR) survey. The time periods modelled were the AM-Peak traffic (07:30 – 09:30); an Inter-Peak (IP) period (13:00 – 15:00); the PM-Peak (16:00 – 18:00); the Evening (EV) period (20:00 – 22:00) and Night (NI) period (01:00 – 03:00), with a half hour warm-up period before each, to ensure that the starting traffic conditions for the recorded simulation were suitably defined. To account for the stochastic nature of the AIMSUN micro-simulation process, ten simulation runs were conducted for each of the 2 hour time periods (AM, PM, IP, EV and NI) and the simulated drive cycle data from each were processed in PHEM to generate second-by-second emission estimates for each simulated vehicle. In total the coupled AIMSUN-PHEM model produced emission estimates for 377,062 simulated vehicles over the 50 simulations runs, generating a total of 119.2 million seconds of vehicle emission data.

A number of recent studies have demonstrated methods utilising second-by-second vehicle trajectory data from microscopic traffic simulation as input to an emission model to estimate real-world emission. Kraschl-Hirschmann, Zallinger et al. (2011) linked the traffic simulation model VISSIM and the emission model PHEM to compare PHEM estimates of emission from Portable Emission Measurement System (PEMS) recorded vehicle speed with PHEM estimates using VISSIM simulated speed profiles. Zallinger, Tate et al. (2009) used AIMSUN to generate 50 virtual drive cycles through a simulated

network and recorded 50 on-road drive cycles through the network using an instrumented vehicle. Emission estimates from both sets of drive cycles were generated using PHEM and a roller test-bed for comparison. Swidan (2011) employed AIMSUN and a PEMS based Vehicle Specific Power (VSP) modal method for emission estimation, evaluating the difference between PEMS vehicle field data to simulated AIMSUN vehicle trajectories. Similarly (Anya, Roupail et al. 2014) used AIMSUN and MOVES to compare simulated vehicle emission and activity to on-road PEMS data. Song, Yu et al. (2012), employed VISSIM for traffic simulation and compared real-world PEMS data to VISSIM simulated data using a VSP bin MOVES methodology to estimate emission from both datasets. Ahn, Kronprasert et al. (2009) used microscopic traffic simulation models INTEGRATION and VISSIM to replicate driver behaviour at a roundabout, at a signalised intersection and at a stop sign. They then used the emission model VT-Micro and the comprehensive emission model (CEM) to estimate fuel consumption and the emission level for each traffic control form.

The difference between previous studies and the work in this paper is predominantly one of scale and definition. Previous research using coupled traffic simulation and emission models has either primarily investigated small geographical areas, such as a single junction, to demonstrate the impact of varying traffic control measures, or has focused on comparison of a small number of simulated vehicles and evaluated the estimated emission against real-world measurements. This research instead encompasses a relatively large and detailed network and generates emission estimates using the second-by-second movement of all simulated vehicles in the network over two-hour simulation periods. The measurement of the real-world fleet vehicle fleet through an ANPR survey ensured that the simulated fleet is representative of the on-road traffic in the network and quantified the diurnal changes in vehicle fleet composition. Studies that rely on average vehicle fleet data or model default settings are unlikely to reflect the real-world emission within the specific simulation area.

A factor that is almost universally absent in previous similar studies is road grade. A majority of the traffic simulations developed during such research conclude that the modelled test area was flat enough to set the road grade to 0. In this research, a road grade for each of the 374 road links described in the Headingley AIMSUN model was included in the simulation, derived from Digital Terrain Model (DTM) data to account for the potential influence of the topography of the network.

The development of a properly calibrated traffic simulation model facilitates the generation of second-by-second data which describe the movement of all vehicles passing through a road network in a set time period. This is particularly important as collecting a similar volume of real world data, for a large number of drivers under a full range of traffic conditions, is both impractical and prohibitively expensive (Jackson and Aultman-Hall 2010). The development of a coupled micro-simulation and instantaneous emission model could provide a very cost effective way of conducting high-resolution emission estimation, enabling the estimation of real-world vehicle fleet emission factors whilst also identifying the relative emissions contribution from each vehicle category within the fleet.

2. Vehicle Fleet Analysis – 24hr ANPR Survey

A typical vehicle fleet is a combination of different types of vehicle, of varying ages, covering a wide range of engine sizes and technologies. There are substantial differences in the emission of vehicles both between different vehicle categories (primarily due to average engine size and vehicle weight) and within vehicle categories (due to technology evolution over time). Vehicle fleet distributions vary both by location and time and these variations in the on-road fleet composition can cause significant differences in overall fleet emissions (Granell, Guensler et al. 2002; Malcolm, Younglove et al. 2003; Liu, Tok et al. 2011). Research conducted by Palmgren, Berkowicz et al. (1999) showed how fleet composition varies over a 24hr period, highlighting that the ratios between vehicle types are not constant.

The AIMSUN model developed for the Headingley network incorporates nine discreet vehicle types comprising Passenger Car; Taxi; Rigid Heavy Goods Vehicle (HGV), Light Commercial Vehicle (LCV), Tractor Trailer (Articulated HGV), Articulated Bus, Double-decker Bus, Single-decker Bus and Extra Bus, which correspond to defined vehicle categories within PHEM. In order to simulate the vehicle fleet emissions specific to the research network, it was necessary to quantify the composition of the traffic in the test area by these vehicle categories and then to further differentiate within the categories at the individual vehicle level by EURO standard, fuel type and vehicle weight. It is important that the vehicle fleet is correctly described within the simulation, not only because it defines the proportion of vehicles assigned to each specific PHEM vehicle type and sub-category power-emission map and thus the rate of emission, but also because the dynamic characteristics of each vehicle type vary and therefore the composition of the fleet may influence the overall behaviour of the traffic flows within the AIMSUN model.

General fleet composition data for urban areas (outside London) are available from The Department

for Environment Food and Rural Affairs (DEFRA) National Atmospheric Emissions Inventory (NAEI) (DEFRA 2014). However as this “Base 2013 Fleet Composition Data” provides only an aggregated national fleet average based on vehicle kilometres travelled (VKM), it was considered unlikely to provide an accurate measure of the vehicle fleet in the Headingley test area. Aggregate figures are designed for regional analysis, however, micro-scale simulation requires a greater spatial resolution (Liu, Tok et al. 2011). In addition, the NAEI figures lack sufficient detail to inform the diurnal analysis of fleet composition, so to develop network simulations that represent the traffic conditions in the five, two-hour segments it is necessary to have a detailed fleet distribution specific to those time periods.

To determine the operational vehicle fleet proportions throughout the Headingley network an ANPR survey was undertaken on Monday 9th February 2015, by Nationwide Data Collection on behalf of Leeds City Council and the ITS. The survey was conducted using ANPR cameras positioned on the A660 (at 53.816552N, 1.567555W) capturing the northbound and southbound traffic flows over a continuous 24 hour period from midnight to midnight. The ANPR cameras recorded the number plate (Vehicle Registration Mark, VRM) on each occasion a vehicle passed through the survey point. These cameras were positioned facing the oncoming traffic and used infra-red to capture the VRM data both during daylight hours and when dark. The 24hr survey logged a total of 16,930 vehicles with a VRM capture rate of 94.86% indicating that the survey recorded a large majority of the vehicle fleet.

To obtain detailed metadata for each vehicle passing through the survey area, the VRM database of 16,060 records (10,999 distinct number plates, due to multiple captures of the same vehicle) was cross-referenced by CarwebUK Ltd (www.carweb.co.uk) with the UK Motor Vehicle Registration Information database, which matches each number plate to specific information about that vehicle. The Motor Vehicle Registration Information database comprises 94 information fields, including vehicle make / model, vehicle specifications, EURO emission standard and pollutant emission performance. The VRM database was also cross-referenced against the Leeds taxi licence register for March 2015. This facilitated identification of the taxi fleet component of the observed Headingley vehicle fleet.

The comprehensive vehicle registration information enables a detailed evaluation of the vehicle fleet that uses the A660. Table 1 presents a comparison of the observed Headingley 24 hour fleet from the ANPR survey with the NAEI’s Base 2013 Fleet Composition Data (DEFRA 2014). The Headingley fleet composition is shown alongside the NAEI fleet projections for urban traffic conditions in England (outside London) for the years 2014, 2015 and 2016. The NAEI data are based on the DfT’s traffic forecast projection from actual 2011 road traffic statistics (DfT 2013). Cars form the major fraction of the recorded fleet, with 79.99% of the valid fleet data, followed by Light Commercial Vehicles (12.04%), Buses (4.97%) and Heavy Goods Vehicles (3.00%).

Table 1. Comparison of the Headingley ANPR Survey 24 Hour Vehicle Fleet with the NAEI Base 2013 England (outside London) Urban Fleet Composition for 2014, 2015 and 2016.

	Headingley 24hr ANPR Survey		NAEI Base 2013 Fleet Composition - England (outside London); Urban					
			NAEI 2014 Fleet		NAEI 2015 Fleet		NAEI 2016 Fleet	
	Vehicle Count	Proportion by Count	Proportion by VKM	Difference to ANPR	Proportion by VKM	Difference to ANPR	Proportion by VKM	Difference to ANPR
Electric car	4	0.03%	0.05%	-0.02%	0.07%	-0.04%	0.10%	-0.07%
Petrol car	6692	42.23%	46.70%	-4.46%	44.82%	-2.58%	43.09%	-0.85%
Diesel car	5979	37.73%	36.43%	1.31%	38.26%	-0.53%	39.85%	-2.12%
Electric LCV	4	0.03%	0.05%	-0.02%	0.08%	-0.06%	0.13%	-0.10%
Petrol LCV	19	0.12%	0.35%	-0.23%	0.31%	-0.19%	0.29%	-0.17%
Diesel LCV	1884	11.89%	12.88%	-0.99%	12.87%	-0.98%	13.01%	-1.12%
Rigid (HGV)	406	2.56%	1.71%	0.85%	1.75%	0.81%	1.73%	0.83%
Artic (HGV)	69	0.44%	0.41%	0.03%	0.41%	0.03%	0.40%	0.03%
Bus	788	4.97%	1.43%	3.54%	1.42%	3.55%	1.40%	3.57%
TOTAL	15845	100.00%	100.00%	MAE = 1.27%	100.00%	MAE = 0.98%	100.00%	MAE = 0.99%

The Mean Absolute Error (MAE) calculations comparing the Headingley Fleet proportions with the NAEI basic fleet projections reveal their compositions to be very similar. Whilst the Bus and Rigid HGV fractions are consistently greater in the Headingley fleet than accounted for by the NAEI fleets, the proportions of Electric, Petrol and Diesel cars and LCVs are a good match. The high fraction of Buses is likely due to the A660 being atypical of the average urban road, as it is the busiest and most crowded

bus corridor into and out of Leeds, with many bus stops and a large number of high-frequency bus services, >5 buses per hour (TfL 2015). Likewise, the Rigid HGV fraction is likely greater than a typical urban road as the A660 arterial corridor provides a direct route to and from the city to the northern section of the Leeds outer ring road (A6120).

The metadata for the observed Headingley fleet enabled a detailed description of the composition of the fleet for each vehicle type, by fuel type and EURO emission standard to be made. For example Figure 1 shows the observed Petrol and Diesel car fleets (including taxis) from the ANPR survey, separated by EURO emission standard in comparison to the NAEI's vehicle fleet projections (DEFRA, 2014).

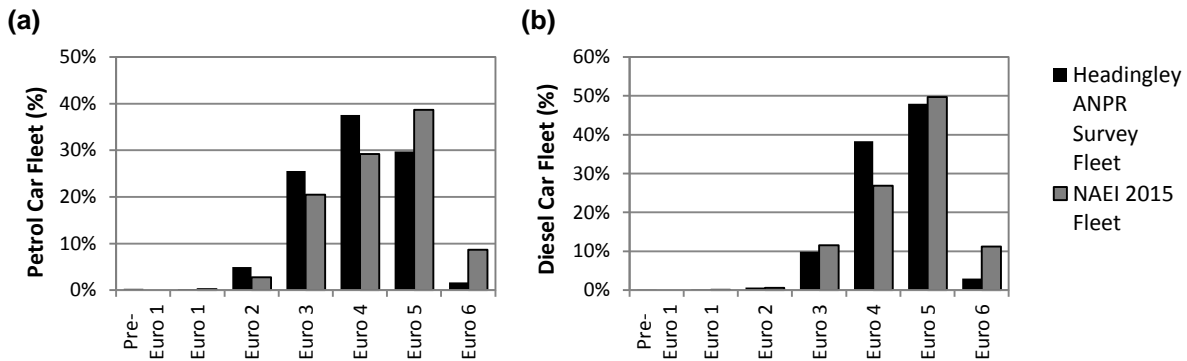


Figure 1. Car fleet composition by EURO Emission Standard in the Headingley ANPR Survey and NAEI 2015 Vehicle Fleets: (a) Petrol and (b) Diesel

Understanding the composition of the Headingley fleet by vehicle age (for which EURO emission standard is a proxy indicator) is very important as the EU legislation on CO₂ emissions in tandem with other pollutants, has seen technological developments to the vehicles that have influenced the rate of pollutant emission. In consequence, the overall fleet average pollutant emission can be related to the age composition of the vehicle fleet being studied. The observed data suggest that the car fleet travelling on A660 is slightly older than the national average, as it contained a greater percentage of EURO 4 cars and fewer EURO 6 cars than predicted by the NAEI 2015 car fleet distributions. This trend was common to each of the vehicle types, which showed a greater percentage of older vehicles in the Headingley fleet than the national average. The ANPR observed Bus fleet, for example, was found to contain 95.3% EURO 3 emission standard or earlier vehicles, which is a considerably greater proportion than that of the NAEI 2015 projection, which estimated that 58.5% of the fleet should be of EURO 5 or EURO 6.

Using the timestamp on each VRM record in the ANPR survey, it was possible to analyse changes in traffic flow and fleet composition during the 24-hour survey. The diurnal variation in traffic flow, for the combined northbound and southbound directions on the A660 is illustrated in Figure 2. For each of the 24 surveyed hours the number of vehicles captured by the ANPR cameras is shown and this total flow is presented with the fraction from each vehicle type.

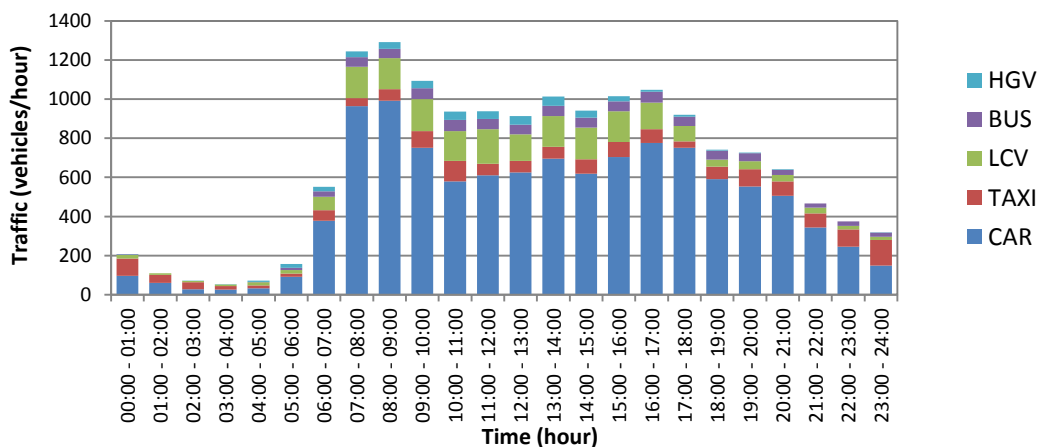


Figure 2. Diurnal Variation in Traffic Flow on the A660 by Vehicle Type.

The weekday variation in traffic flow reveals a clear morning peak flow on the A660 between 7am and 9am, as morning rush-hour traffic enters Leeds, and a less distinct afternoon peak between 3pm and 6pm. The observed traffic flow in the afternoon peak is lower than the morning peak as the capacity of the northbound A660 is lower than the southbound A660 at the location of the ANPR survey. In the afternoon peak, as traffic leaves the centre of Leeds at the end of the working day, the traffic flow on the northbound A660 is often greater than the roads capacity, resulting in substantial delays to the northbound traffic. These delays limit the traffic flow possible on the northbound A660.

In order to accurately describe the real-world Headingley vehicle fleet composition in the AIMSUN-PHEM model simulations, the ANPR data were analysed for each of the two and a half hour time periods, which represent the AM, IP, PM, EV and NI traffic conditions. Figure 3 presents both the number of vehicles recorded during each time period and the vehicle fleet composition. Whilst the total flow varies throughout the day, so too does the composition of the vehicle fleet. During daylight hours Passenger Cars form the bulk of the vehicle fleet, whilst the proportion of Taxis increases substantially during the evening and night hours. The figure shows a significant fraction of HGV vehicles during the morning peak and inter-peak hours; however that fraction decreases before the afternoon peak as the commercial drivers presumably try to avoid the delay associated with the very congested evening rush hour.

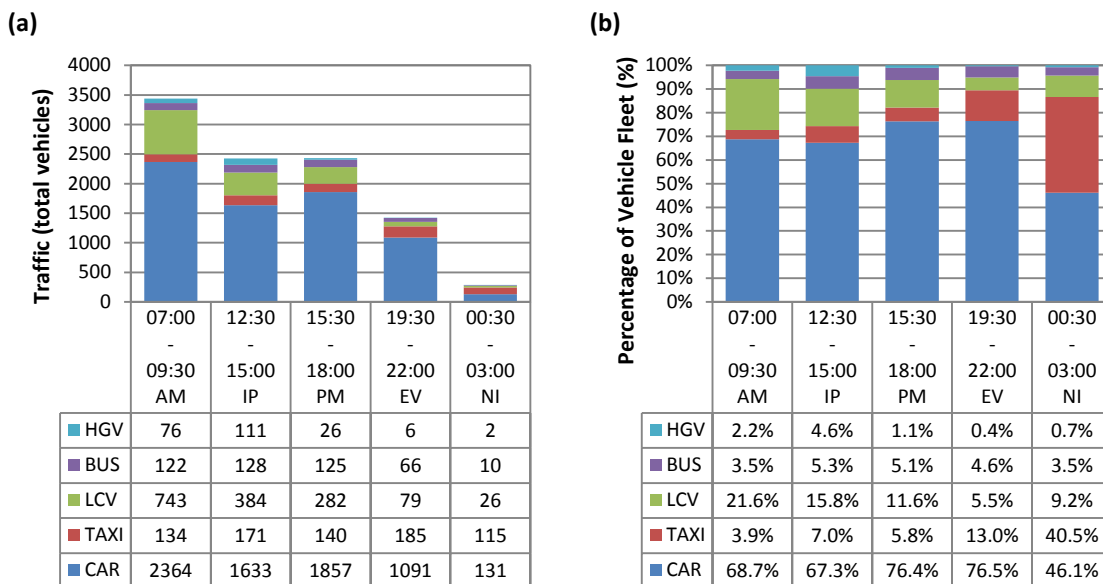


Figure 3: Variation in Traffic Count (a) and Vehicle Type Fleet Composition (b) for the Five AIMSUN-PHEM Test Periods (AM, IP, PM, EV and NI)

For the AIMSUN simulations the HGV vehicle type was further sub-divided into the percentages of HGV Rigid and HGV Articulated, and the Bus vehicle type was also sub-divided into four categories, Articulated Bus, Double-Decker Bus and Single-Decker Bus (for the scheduled bus fleet) and Bus Extra (which provides the percentage of buses and coaches that are not part of the scheduled fleet). For the fleet composition detail in PHEM, all vehicle types were further classified by the percentage in each EURO emission standard; Cars, Taxis and LCV vehicles were also sub-divided by fuel type and LCV and HGV Rigid were further segregated into weight categories.

Confidence in the representativeness of the recorded weekday fleet composition would be strengthened with further ANPR data, as this analysis was reliant on only one recorded 24 hour period. The difficulty with obtaining such data is that commissioning such surveys entails substantial cost as does obtaining the vehicle specific data for many thousands of vehicles from the Motor Vehicle Registration Information database. However, accepting the limited sample size, the level of detail provided by the ANPR survey in this research facilitated vital characterisation of the changes in fleet composition throughout the day in the test network. This is in contrast to many traffic modelling and emission modelling projects which assess only AM and PM peak periods. The high capture rate of the ANPR survey method, with access to the Motor Vehicle Registration Information database, gives great confidence that the observed vehicle fleet captured the composition of the real-world fleet and has provided a wealth of vehicle metadata.

3. Method: AIMSUN-PHEM Model

Figure 4 describes the modelling approach for the coupled traffic simulation and instantaneous emission model used to generate network emissions estimates in this research. The modelling framework was originally developed and evaluated at the University of Leeds Institute for Transport Studies (ITS), in collaboration with the Institute of Internal Combustion Engines and Thermodynamics at the Technical University of Graz (TUG), Austria (Zallinger, J. et al. 2008). This study used the microscopic traffic simulation model AIMSUN to simulate the road network around a 3.8km section of an arterial corridor passing through Headingley, a suburb in the city of Leeds, UK.

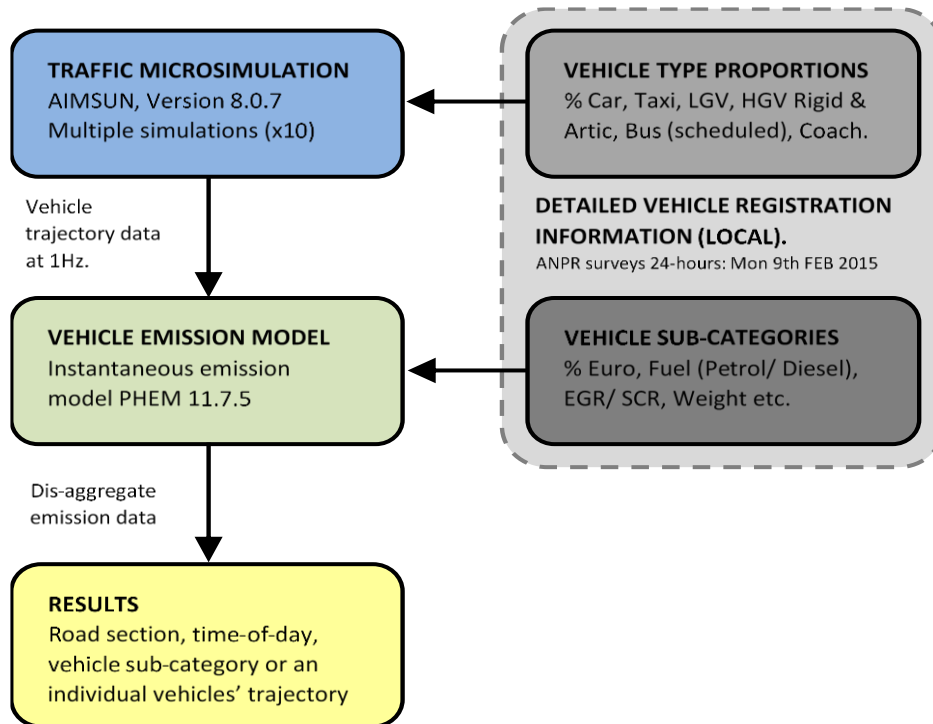


Figure 4. AIMSUN-PHEM Coupled Traffic-Emission Modelling Framework (Tate 2015)

AIMSUN was employed in this research to generate the required second-by-second output for emission modelling in PHEM. AIMSUN continuously models each vehicle in a network throughout a simulation time period. The movement of vehicles within the network is controlled by behavioural models that dictate each vehicle's longitudinal (e.g. acceleration; deceleration) and lateral response (e.g. overtaking; lane-changing) to stimuli within the system. These reactions are driven by operational algorithms which describe behaviours such as car-following, lane-changing and gap-acceptance (Dia, Gondwe et al. 2006; TSS 2013; Anya, Roupail et al. 2014).

The operational algorithms and hence the speed profiles of vehicles within the model are influenced by controllable parameters within the simulation package at three scales. Vehicle attributes, including maximum desired speed, maximum acceleration, normal deceleration, maximum deceleration, which are specific to each vehicle category in the model (e.g. Car, Bus, LCV, HGV); local parameters (e.g. road section speed limit); and global parameters, which are universal across the network (e.g. simulation step and reaction time).

The parameters within the Headingley AIMSUN model were defined to accurately reflect the real-world conditions of the modelled area. The simulation process required the specification of a large number of factors including network layout, traffic demand data, traffic control plans and public transport plans. The high-resolution nature of the coupled traffic micro-simulation and vehicle emission model necessitates a substantial amount of detailed input data. Throughout the modelling process, every effort was made to identify, obtain and utilise the highest quality and most appropriate, data sources available.

The AIMSUN simulated Headingley network developed for this research built on previous work by the University of Leeds ITS, which had developed a smaller scale AIMSUN 'beta' model for the A660 through Headingley (Tate 2011). Traffic control signal data, junction turning movements and local and global model parameters used in the calibration of the beta model were used to inform the new AIMSUN

simulation. For this study, the Headingley network layout was redrawn and extended using geo-referenced aerial photography downloaded from the Landmap Kaia (Millin-Chalabi, Schumm et al. 2011), and the network topography was described using data from a 5m resolution DTM (Bluesky 2013). The extent of the Headingley A660 AIMSUN model is shown in Figure 5 and comprises 374 road sections and 145 junctions. The speed limit on a majority of the roads in the network is 30 mph, however, a number of the smaller residential side roads have speed limits of 20 mph.

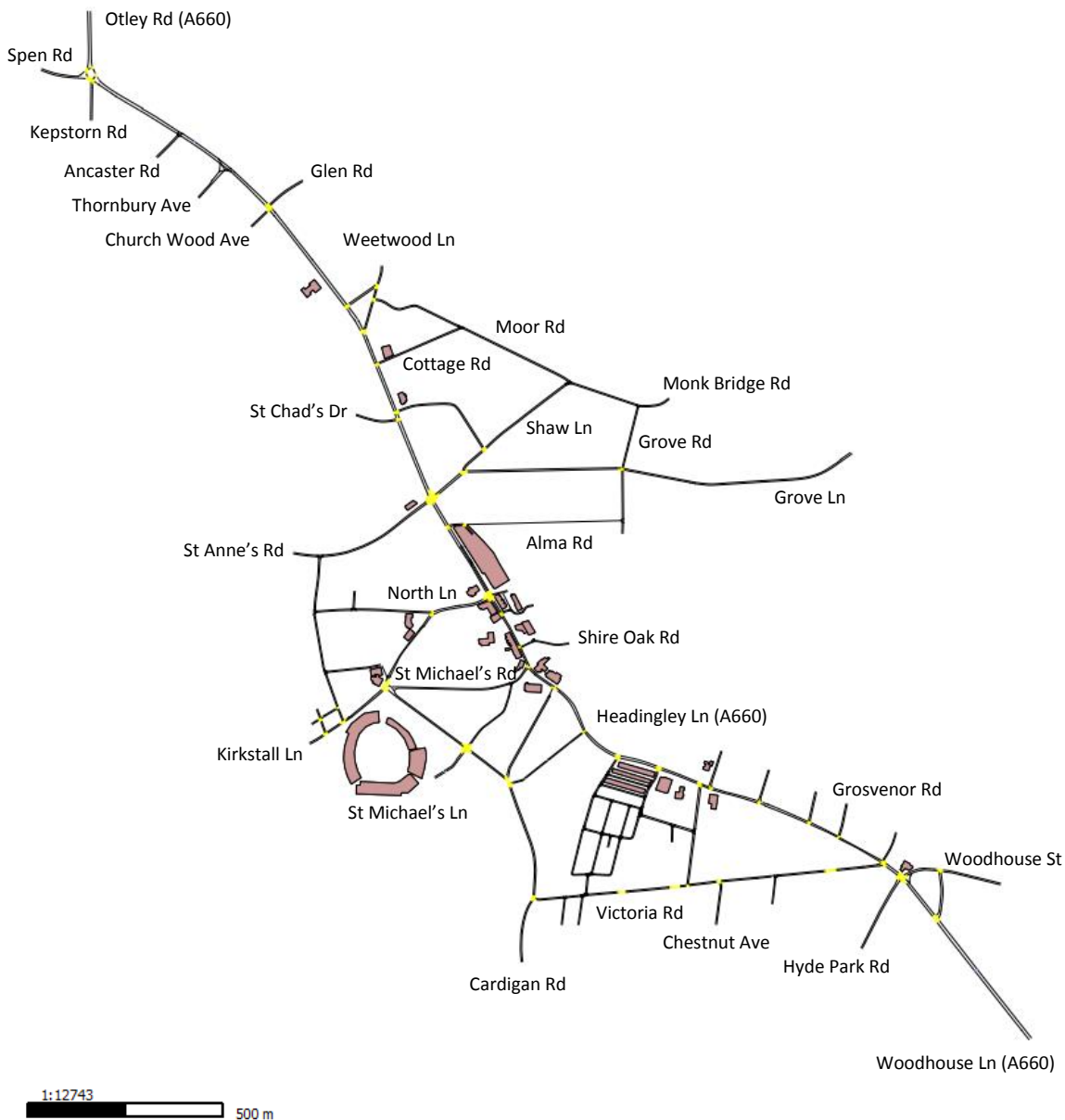


Figure 5. Extent of the Headingley A660 AIMSUN Model

The network contains six traffic signal controlled junctions, which have been coded to accurately reflect the on-street situation at each time period. The Leeds City Council Urban Traffic Management and Control team made available traffic control signal timing data for junctions that had not previously been described in the beta model. The stages, green times and intergreen times have been ratified by direct field observation. There are twelve pedestrian crossings within the network area. Detailed information could not be found regarding the frequency of use of the crossings or duration of crossing times, so these have been estimated from limited field observations at each location. A more rigorous survey would improve the quality of this element of the AIMSUN simulation.

Traffic flow input data were provided by way of Automatic Traffic Count (ATC) and Manual Classified Count (MCC) data supplied by the Highways and Transportation department of Leeds City Council. In total, there were 42 ATC surveys and 20 MTC surveys for calibration of the traffic networks, collected between March 2006 and July 2014, with the majority of surveys recorded post-2008. Wherever

possible the most recent data were used and data recorded between September and November were given priority in an effort to minimise any seasonal disparities. The vehicle fleet composition (by vehicle type, fuel type, EURO emission standard and vehicle size) was derived by means of the Automatic Number Plate Recognition (ANPR) survey and cross-referencing against a Motor Vehicle Registration Information database, as described previously. The AIMSUN input flow data for each simulated time period were defined in 30-minute 'traffic states' which designate the vehicles per hour entering the model from each of the 36 input road links. Each time period (e.g. AM, IP, PM, EV and NI) was described by five traffic states for each vehicle type; one, a half hour warm up period and four for the duration of the two-hour recorded simulation. The traffic states were vehicle type specific describing the input flow of each vehicle type separately. The ATC data used to create the traffic states, were records only of total vehicle flow. In order to calculate the input flow for each of the traffic state vehicle types, the total flow was multiplied by the fleet composition percentages for each of these vehicle types as recorded by the ANPR survey. The fleet compositions were specific to the simulated time period (AM, IP, PM, NI and EV).

The values influencing vehicle dynamics within the simulation package, such as maximum acceleration and deceleration, were estimated for Cars, Taxis and LCVs from PEMS data recorded in the network and for the Bus and HGV vehicle categories were drawn from relevant literature.

In-line with 'best practice' (Dowling, Skabardonis et al. 2004) calibration was conducted using comparison of real-world observed and model simulated flows as the 'measure of performance'. A total of 26 virtual detectors were included within the AIMSUN model for sites, independent of the input flows, at which real-world traffic count data were available. The simulated model flows were compared to the real-world flows (defined by the traffic count data) at each of the 26 detector sites using a goodness of fit GEH statistic (Dowling, Skabardonis et al. 2004; DfT 2014). The DfT Transport Analysis Guidelines (TAG) for link flow validation was followed and the initial calibration phase of model development was considered complete when all individual flows for the simulation had a GEH of < 3 for each 30 minute traffic state and for the overall two hour simulation, and the flow count criteria were met in all cases.

To determine whether the model was an accurate representation of the observed network, ten simulations of the AIMSUN Headingley model were run for each time period (AM, IP, PM, EV and NI), each with a unique random seed to ensure different vehicle entry times and paths for each simulation. The vehicle flows in the ten simulations, for each of the five time periods, were then validated according to the DfT TAG guidelines and were completed with a minimum of 25 of the 26 (96%) of the detectors flows having a GEH statistic of < 5 for each 30 minute traffic state, and 100% of calculated GEH values < 5 for each of the two-hour simulations. The simulation flows in the Headingley AIMSUN model therefore met and exceeded the DfT TAG guidelines which set validation criteria acceptability at greater than 85% of individual flows having a GEH statistic < 5 .

In order to conform to the WebTag guidelines for model validation, analysis should be conducted to assess the difference between simulated and real-world journey time through the network. However at the time of validation, journey time data were not available for the network so the validation was performed using only modelled and observed traffic flows. An important element of future work with the simulation will be to improve the robustness of the validation by performing this journey time analysis.

An Application Programming Interface (API) written by the ITS, was used to export simulated vehicle trajectory data from the AIMSUN Headingley network for input into the University of Graz's (TUG) Passenger car and Heavy duty Emission Model (PHEM) to generate emissions estimates. During a simulation run of the AIMSUN network, the API made records every 0.5 seconds for each vehicle in the network of the individual vehicle ID, the road link / junction number on which the vehicle was currently travelling, the vehicle type, the vehicle speed, the geographical position and road link gradient. The open source software 'R' (R 2006) was then employed to process the AIMSUN output data into a 1Hz drive cycle format for use in PHEM.

The PHEM emission modelling process takes the simulated second-by-second speed and road grade for each simulated vehicle during its transit through the network and uses this drive cycle data to calculate the instantaneous engine power output and engine speed of the vehicle at each second in the network (Luz and Hausberger 2015). From the calculated engine power output and engine speed, the fuel consumption and vehicle emissions for each second of trajectory data are then interpolated from measured engine maps specific to the simulated vehicle (defined by vehicle type, fuel type and EURO standard). PHEM contains a background vehicle specification data file for each sub-category (by EURO emission standard, fuel type and weight) of each modelled vehicle type. The file for each vehicle type sub-category contains average parameters for that vehicle, including vehicle mass; cross-sectional area; rated engine power; rated engine speed and engine idling speed that influence the instantaneous power output estimate. Utilising the vehicle metadata garnered from the ANPR survey, the PHEM vehicle specifications files were adjusted to reflect the average values (vehicle weight, engine power,

etc.) for each vehicle category from the observed Headingley fleet. Where insufficient data were available from the ANPR survey data, default PHEM values were used. By adjusting the background files, the vehicle specifications within the model better reflect the Headingley fleet, which should provide better emissions estimates than those simply calculated from the generic European fleet vehicle specification data which are the default values in PHEM.

The nature of the PHEM output enables this emissions data to be analysed at a variety of scales, ranging from analysis of one individually selected vehicle trip to calculation of the entire aggregate fleet emission. As each second of data is also labelled with details of the specific vehicle responsible for the emission and its location within the network, the emissions contributions from each vehicle type, fuel type and EURO standard can be assessed, along with emissions analysis of specific road links.

4. Results

Although a robust validation of journey times within the model was not possible due to a lack of real-world journey time data within the network, a comparison was undertaken between the AIMSUN-PHEM simulated car journey times and CO₂ emission factors with a PEMS data set recorded in the network. A PEMS was utilised to record the second-by-second absolute position, vehicle speed and CO₂ emission of a EURO 4 passenger car over the northbound and southbound transit of a 1.5km section of the A660 within the simulated Headingley network. The instrumented vehicle completed these sections 16 times in the AM-Peak, 14 times in the Inter-Peak, 11 times in the PM-Peak and 6 times in the Evening period. There were no test runs during the Night time period. The links in the AIMSUN simulation which make up the northbound and southbound sections were identified and the drive cycle data for all simulated Cars and Taxis completing the 1.5km sections were extracted. In order to assess the accuracy of the simulated drive cycle CO₂ emission estimates from PHEM, the northbound and southbound simulated Car and Taxi drive cycles (including the link road grades from the AIMSUN model) were processed in PHEM using vehicle specifications set up to represent the instrumented EURO 4 vehicle. By this means of the simulated Car and Taxi drive cycles generated a CO₂ emission estimate which can be evaluated against the real-world CO₂ PEMS recorded emissions.

Figure 6 shows data generated by three different methods for estimating the EURO 4 test vehicle gCO₂/km emission rate over the AM model southbound section against the time taken to complete the journey. The red points indicate the 15 real-world gCO₂/km values from the PEMS recorded journeys between 07:00 and 09:30 on the southbound section in the Headingley network. The green points describe 15 PEMS-PHEM generated estimates of the gCO₂/km emission from the PEMS recorded vehicle speed data and a LiDAR-GIS calculated road grade for each second of data (Wyatt, Li et al. 2014). The blue points present the gCO₂/km emission estimates from the AIMSUN-PHEM AM model simulated drive cycles for all Cars and Taxis completing the southbound section. From the 10 replications of the AM model 4722 Cars and Taxis completed the southbound section and the API extracted drive cycles from these vehicles were then processed in PHEM using the EURO 4 vehicle specifications.

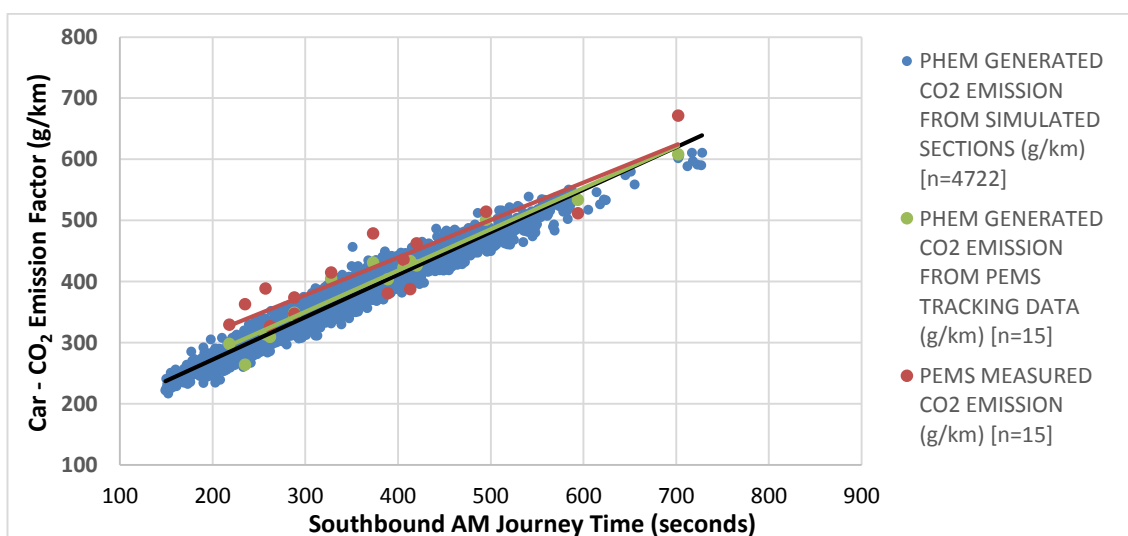


Figure 6. Southbound AM: PEMS, PEMS-PHEM and AIMSUN-PHEM Model CO₂ Emission Factors by Journey Time for a EURO 4 Passenger Car.

Although ideally the AIMSUN-PHEM simulated data should replicate the PEMS real-world recorded CO₂ emission value, it is, in fact, more relevant to assess the ability of the AIMSUN-PHEM model output to reproduce the PEMS-PHEM emission factors. The closer the AIMSUN-PHEM CO₂ emission estimates are to the PEMS-PHEM values, the more likely it is the simulated second-by-second drive cycle data are a good approximation of the PEMS recorded real-world vehicle speed data.

The simulated southbound journey times generated by the AIMSUN AM model cover the entire observed range of PEMS recorded journey times, which indicates that the model captures the range of real-world congestion for this section of the network. The average journey time from the 15 PEMS recorded runs was 378s, with a range from 218s to 702s. The average journey time of the 4722 simulated journeys is slightly faster than the real-world data at 333s and has a slightly greater range from 149s to 728s. A further dataset from Trafficmaster (www.teletrac.co.uk) was made available by Leeds City Council with average times to complete set road links on the A660 for the AM-Peak and PM-Peak Traffic. Analysis of this dataset of approximately 1500 observations suggests an average AM journey time on the southbound section of 303s.

In order to assess the accuracy of the AIMSUN-PHEM model CO₂/km estimates at each journey time, lines of best fit were calculated through the journey time and emission plots for each of the three methods of CO₂ emission estimation. The average difference between these lines of best fit was then calculated within the range of PEMS observed journey times. The average difference (in the range 149s to 728s) between the AIMSUN-PHEM model CO₂ emission estimate and PEMS measured CO₂ emission was found to be -4.9% and the average difference between the AIMSUN-PHEM model and the PEMS-PHEM CO₂ estimates, -1.2%. This suggests that the AIMSUN simulated vehicle trajectory data produces emission estimates from PHEM which are on average within 1.2% of the PHEM estimates made with the on-road GPS tracking data, which would indicate that the AIMSUN model is well calibrated for the southbound section in the AM model.

Figure 7 presents the PEMS, PEMS-PHEM and AIMSUN-PHEM AM model CO₂ emission estimates by journey time to complete the northbound section. The 10 AM model replications generated 3582 simulated Car and Taxi drive cycles over the northbound section. The simulated northbound journey times (133 to 540s) do not completely cover the range of PEMS measured journey times with the instrumented vehicle (171s to 680s), with a number of the PEMS journeys being considerably longer than the simulated times. The Trafficmaster data average journey time of 272s is however closer to the simulated average of 244s than the PEMS observed average journey time of 374s. It is possible that the congestion during the PEMS testing week on the northbound section was greater than the average network congestion at this time.

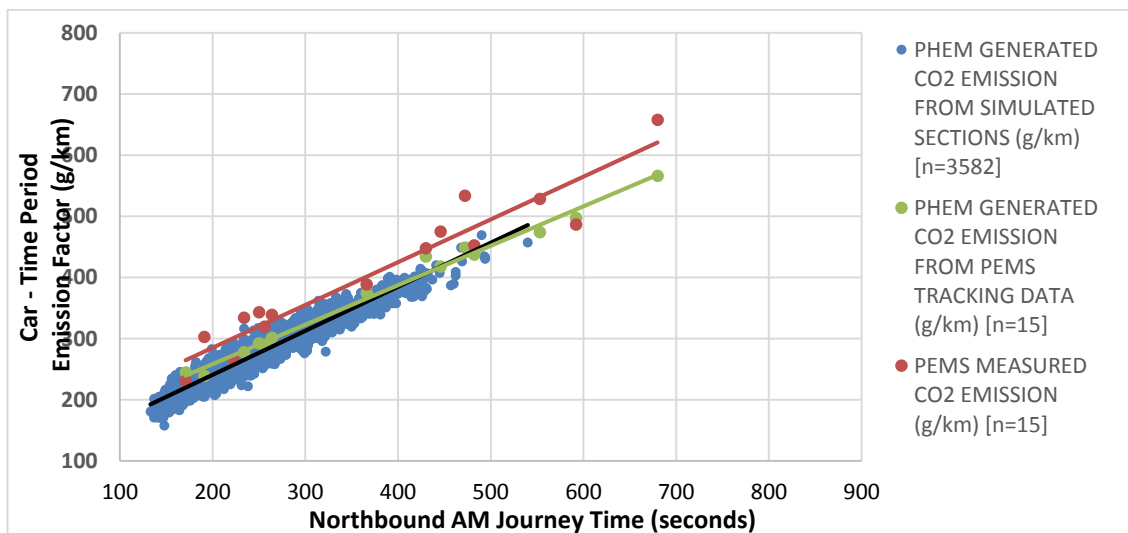


Figure 7. Northbound AM: PEMS, PEMS-PHEM and AIMSUN-PHEM Model CO₂ Emission Factors by Journey Time for a EURO 4 Passenger Car.

Evaluating the accuracy of the AM model northbound CO₂ emission estimates over the range 171s to 680s, the AIMSUN-PHEM model CO₂ emission estimate line of best fit is 9.0% lower than the PEMS measured CO₂ emission but the difference between the AIMSUN-PHEM model and the PEMS-PHEM CO₂ estimates is calculated at an average of -0.2%. This again suggests that a simulated journey from

the AM model would generate a similar rate of CO₂ emission in PHEM as a PEMS recorded vehicle speed profile of the same journey time.

The same analysis was conducted for the IP, PM and EV periods. Aside from the IP period in which the simulated journey times were significantly quicker than the PEMS recorded journey times, the other simulated time periods in general captured the correct range of journey times and have approximately the same average. The IP discrepancy is possibly the result of the inability of the AIMSUN simulation to account for factors such as interaction with pedestrians and cyclists and may be related to increased use of pedestrian crossings on the route, for which there were no detailed survey data. The A660 road section used in the analysis also features two large bus bays outside a busy shopping centre and, with the bus service at peak frequency during the IP hours it is conceivable that there is some interaction between the bus bays and the traffic network which is not accounted for in the simulation.

The line of best fit for the simulated CO₂ emissions and journey time data are consistently very close to that of the PEMS-PHEM generated emission estimates, suggesting that the simulated second-by-second data is a close match for the real-world tracking data. The AIMSUN-PHEM model CO₂ emissions estimate line of best fit was found to be, for the southbound and northbound transits respectively, on average 6.7% and 3.5% lower than the PEMS-PHEM CO₂ estimate line of best fit for the IP period, 5.8% lower and 0.7% greater for the PM period and 6.1% and 8.2% lower for the EV period. Given the limited sample size of the PEMS survey, further data will be required to assess whether the PEMS surveyed journey times provide a fair reflection of the real-world journey times, if so the IP AIMSUN-PHEM model may require some improvement to better reflect the network conditions.

To confirm that the simulated second-by-second trajectory data are representative of the real-world data, it is also necessary to confirm that the power output profile of the simulated journey data is comparable to the power output profile of the PEMS recorded journey data. Without checking the comparability of the power distributions, it would be possible that the simulated vehicle journeys result in different power distributions to vehicles driven in the real-world but arrive at similar CO₂ emission estimate because the average positive Vehicle Specific Power (VSP) over the journey time is similar. Whilst this would generate reasonable CO₂ emission estimates because of the linear relationship between CO₂ emission and engine power output, for other pollutants the relationship is not linear and differences in engine power output distribution may cause large emission estimation errors.

To assess the simulated and real-world engine power distributions, time segments of approximately 20s were chosen from the simulated journey time data over the 1.5km road section (either northbound or southbound), corresponding to points at which a number of PEMS journey time values were grouped. The duration of the time segments was set at values such that there were approximately 200 simulated journeys to compare to at least three PEMS journeys. The power output for each second of the simulated and real-world journeys was calculated using the equation for VSP derived by Jimenez-Palacios (1999) which is shown in Equation 1, with the rolling resistance term coefficient of 0.128 and aerodynamic drag term coefficient of 0.000318 calculated to correspond to the specific EURO 4 passenger car employed in the PEMS study.

Equation 1

$$VSP_{EURO4} = v \times ((1.1a) + (9.81 \times \sin(\text{atan}(\text{grade}))) + 0.128) + (0.000318v^3)$$

Where: VSP is vehicle specific power (kW/tonne); v is vehicle speed (m/s); a is vehicle acceleration (m/s²); and grade is road grade (dimensionless).

Figure 8 compares the VSP distribution of 208 simulated southbound section journeys between 237s and 257s in length, with the VSP distribution of five PEMS recorded southbound section journey times of 241s, 247s, 247s, 247s and 251s. The simulated data are presented as boxplots of the maximum, minimum, interquartile range and median percentage for the percentage of each simulated journey in that VSP bin. For example, over the 208 journeys, the average journey VSP distribution would have 52.2% of the journey at a VSP <0, however one of those 208 journeys had a high percentage (59.9%) of the journey at VSP values <0 and one had a low percentage (34.7%) of the journey at VSP <0. The coloured points mark the actual VSP distribution of the PEMS recorded journeys. For example, the 241s real-world journey had a VSP distribution with 57.9% of VSP values <0, 3.2% were in the VSP 0-1 bin, 4.9% were in the VSP 2-3 bin, etc.

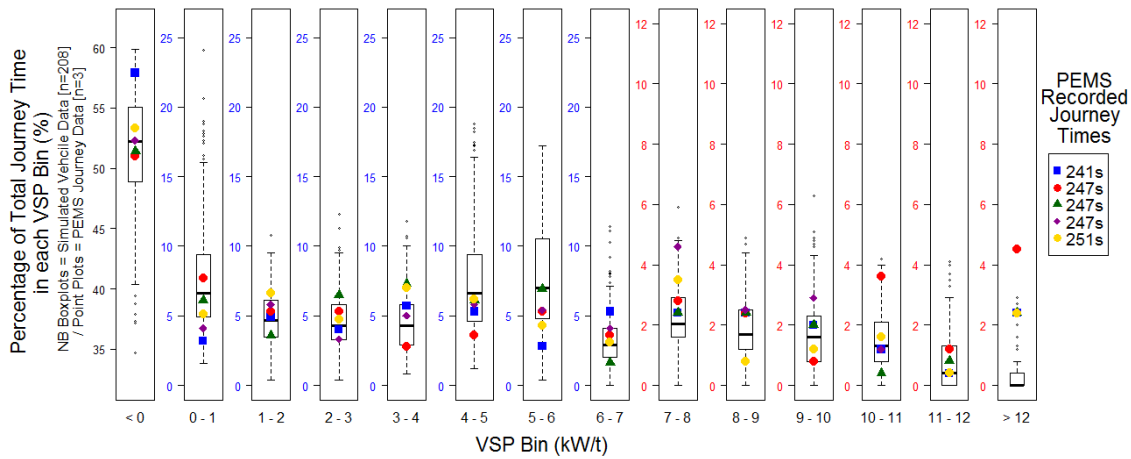


Figure 8. Comparison of Simulated and PEMS 1Hz VSP Distributions: Southbound 237-257s

The simulated distributions, in this case, look to be a good fit with the real-world data, with a large number of the VSP bins having IQ ranges (the middle 50% of the data) which overlap with the real world values.

However, the simulated and real-world VSP distributions were not a good fit in all instances. Figure 9 is a comparison of the VSP distributions of 344 simulated northbound journeys between 208 and 217s in length with three PEMS recorded journeys of 208s, 216s and 217s in length. There appears to be a slight anomaly with the VSP 1-2 bin where the simulated journeys contain a much greater percentage of power values than is reflected in the PEMS distributions. The simulation also seems to underestimate the percentage of VSP values in VSP 6-7 and VSP 7-8, when compared to the real world distributions.

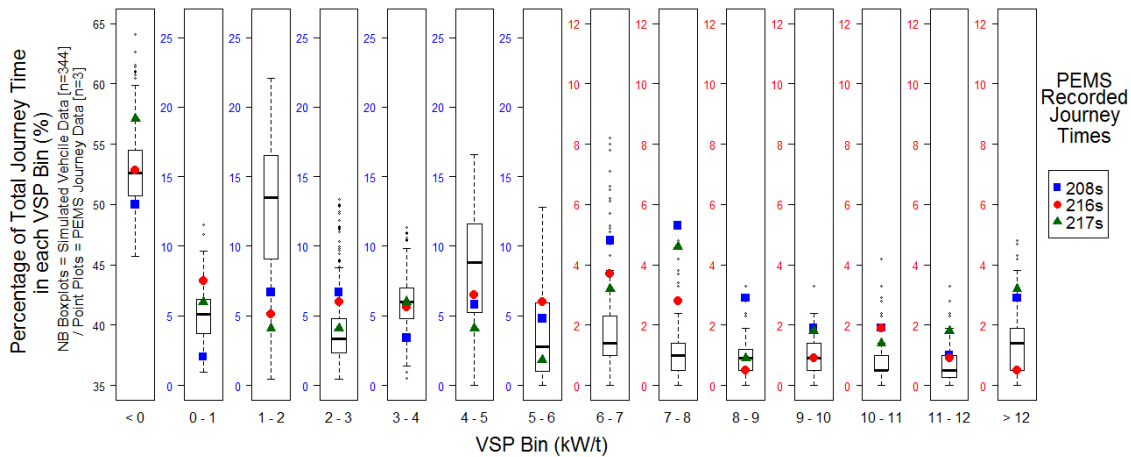


Figure 9. Comparison of Simulated and PEMS 1Hz VSP Distributions: Northbound 208-217s

The analysis of simulated and PEMS distributions, for vehicles completing similar length journeys, suggests that the calibrated AIMSUN simulations produce second-by-second transient vehicle data that are representative of real-world driving. However, anomalies such as found in Figure 9 indicate further calibration work may be required since differences in the distributions may cause more significant errors for other emission species. Sensitivity testing of the AIMSUN simulation vehicle dynamics may reveal ways to improve the match between the VSP distributions.

Diurnal Variation in Network CO₂ Emission

Aggregating the CO₂ emission from all AIMSUN-PHEM simulated vehicles in the network reveals that the greatest rate of CO₂ emission is generated by the vehicle fleet during the PM-peak with an average emission over the 10 simulation runs of 5770 kgCO₂ in the two-hour simulation period. The PM-peak had the greatest average flow of vehicles through the network, with 5604 veh/h and the greatest average vehicle kilometres travelled with 10137 km per hour covered by traffic in the network. The average total network vehicle fleet CO₂ emission over the other two hour time periods was 5168 kg,

4451 kg, 2507 kg and 428 kg, for the AM, IP, EV and NI respectively.

Dividing the average total network CO₂ emission by the average vehicle kilometres travelled in the network in each simulated time period gives average network emission factors for the AM, IP, PM, EV and NI periods of 272.8 gCO₂/km, 284.4 gCO₂/km, 284.6 gCO₂/km, 212.0 gCO₂/km and 181.9 gCO₂/km respectively; with the perhaps surprisingly high IP emission the result of a greater proportion of HGV vehicles during the IP, as can be seen in Figure 3.

The high-resolution nature of the coupled traffic simulation and instantaneous emission model allows results like those presented above to be disaggregated into much smaller constituent elements. In fact, the ability to present analysis at this sub-category level is one of the major advantages of the coupled model methodology. Figure 10 presents the same data, but sub-divided into the contribution from each vehicle type, revealing petrol passenger cars as the leading source of CO₂ emission, for all periods except at night, when the primarily diesel taxi fleet becomes a significant fraction of the traffic. The average on-road emission factors of the combined passenger car and taxi fleet (including both petrol and diesel vehicles) are calculated by the AIMSUN-PHEM model at 228 gCO₂/km, 212 gCO₂/km, 243 gCO₂/km, 191 gCO₂/km and 166 gCO₂/km for the AM, IP, PM, EV and NI simulations respectively. These factors are considerably greater than the SMMT calculated 2014 average rated emission of a car in the UK fleet of 156.6 gCO₂/km (SMMT 2015) and larger than the DEFRA calculated emission factors for 2015 that suggest average emission for a petrol car of 190.7 gCO₂/km and 180.6 gCO₂/km for a diesel (DEFRA 2015). Only in the free flowing NI conditions, are the network emission factors for passenger cars as low as the suggested emission for the average car from these two sources.

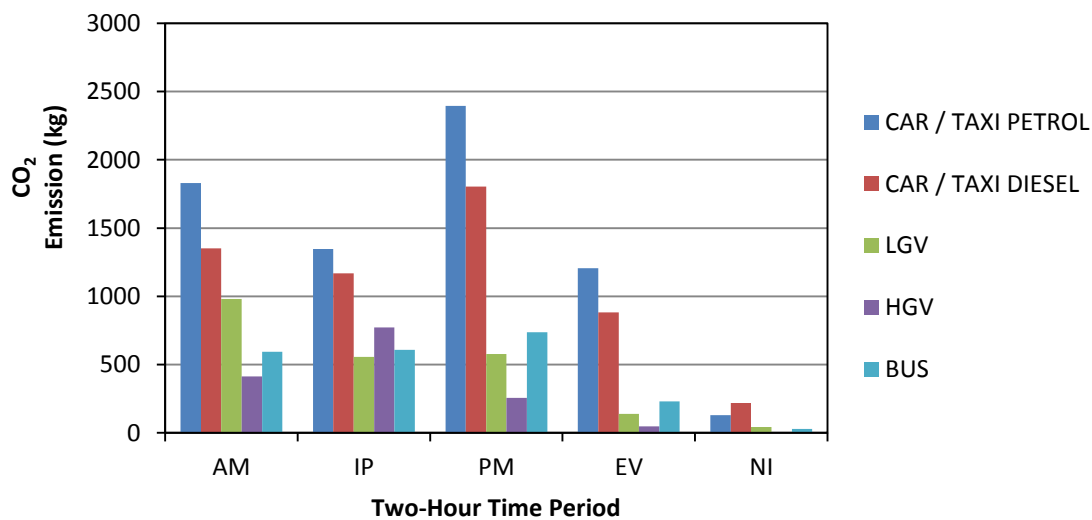


Figure 10. Total Network CO₂ Emission in each two-hour Time Period by Vehicle Type

Figure 11 presents the CO₂ g/km emission factors for passenger cars separated by fuel type and emission standard. The illustrated increase in CO₂ emission from EURO 2 to EURO 4 for both petrol and diesel is perhaps counter-intuitive, as the trend might be expected to show an improvement in efficiency and therefore in fuel consumption and CO₂ emission. The rise in emission is, however, a reflection of the increase in average rated engine power observed in the Headingley fleet by the ANPR survey. The drop in EURO 5 emission may be the result of the introduction of the EU's New Car CO₂ Regulation in 2009 which forced manufacturers to reduce the CO₂ emission from their vehicle fleets (EC 2009). The rise in the EURO 6 emission factor is derived from a limited sample size of new vehicles (≈300) and the average engine size of the EURO 6 vehicle observed by the ANPR survey was considerably larger than for previous emission standards. The figures reveal a clear trend in increased average CO₂ emission with congestion. In the NI free-flowing conditions the average CO₂ emission rate per km is 32% lower for petrol passenger cars and 27.2% lower for diesel passenger cars than the emission rate during congested PM conditions.

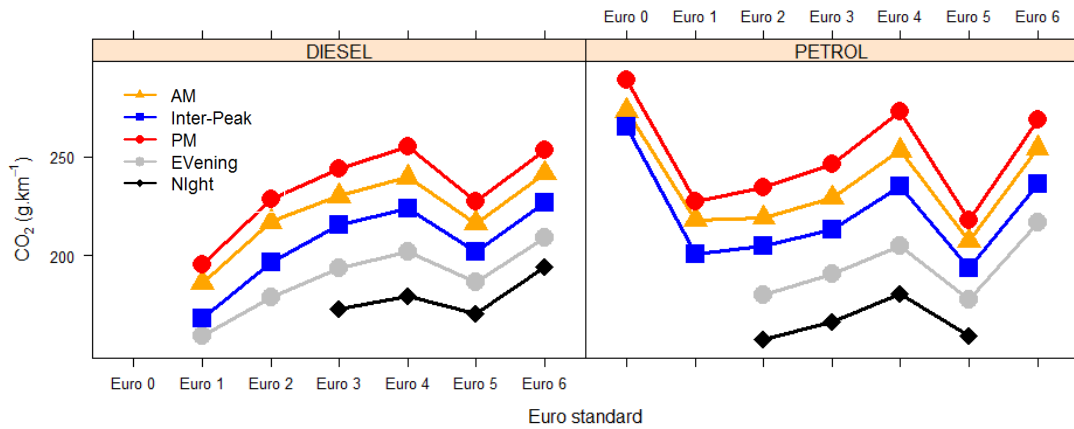


Figure 11: Diesel and Petrol Passenger Car CO₂ Emission Factors by EURO Emission Standard

The same emission pattern by time period is evident in the simulated taxi fleet, Figure 12, with congested stop-start conditions and lower average network speeds during the PM peak resulting in the highest CO₂ emission factors. The diesel taxi CO₂ emission factors are lower than the diesel passenger car fleet. This is unsurprising given that vehicle fuel economy will have an important bearing on profit for the industry. The metadata from the ANPR survey reveals a decrease in engine size in taxis from EURO 3 to EURO 5 which is contrary to the trend in passenger cars and is probably the result of efforts to reduce costs in the face of increasing fuel prices. The generated average emission factors for diesel taxis were 188.8 gCO₂/km for the AM model, 185.1 gCO₂/km in the IP, 210.3 gCO₂/km in the PM, 174.8 gCO₂/km in the EV and 155.9 gCO₂/km in the NI model. The petrol taxis fleet's CO₂ emission values are noticeably greater than those of the diesel taxis. As diesel engines offer better like-for-like fuel consumption than similar sized petrol engines this difference is not unexpected. The gap is widened further by the fact that the average engine size of the petrol taxis in the Headingley fleet is larger than the diesel taxis. It should be noted that the EURO 5 petrol taxi CO₂ emission rates are likely an overestimation of the actual real-world emission rate. Of the 72 EURO 5 petrol taxis observed in the Headingley fleet on the A660, 48 were hybrid vehicles. As there is currently no provision in PHEM for hybrid vehicles these vehicles had to be coded as standard petrol vehicles.

The magnitude of the difference in Taxi CO₂ emission rates between the PM-Peak and the NI period is similar to that observed with the passenger car values, with the average gCO₂/km figure from the NI model 25.8% and 32.1% lower than the PM figure for diesel and petrol taxis respectively.

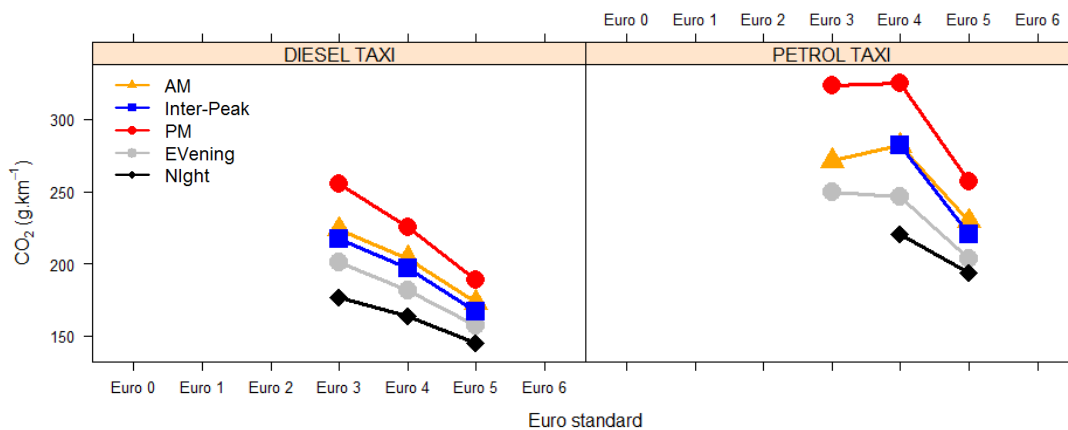


Figure 12: Diesel and Petrol Taxi CO₂ Emission Factors by EURO Emission Standard

Figure 13 presents the average network CO₂ emission factors by EURO emission standard for four sizes of LCV including the added N₂ category between 3.5 – 5 t (identified in the graph as DIESEL IV). Although this category is technically classified as HGV all observed ANPR vehicles had the same engines as the lighter N₁ Class III LCVs. Relatively few LCVs were observed by the ANPR survey on the A660 in the EV and NI periods resulting in gaps in the graphs at a number of EURO emission standards where there are no data to report. The trend of increased CO₂ emission with increased

congestion is once again clear, with the NI periods reporting the lowest values and the PM the greatest. For the Class III diesel (1.76 to 3.5 t) which covered 66.2% of the VKM in the simulations, the range in average CO₂ emission rate from the five models is from 198.4 gCO₂/km in the NI simulations to 268.2 gCO₂/km in the PM simulations, a difference of 26%.

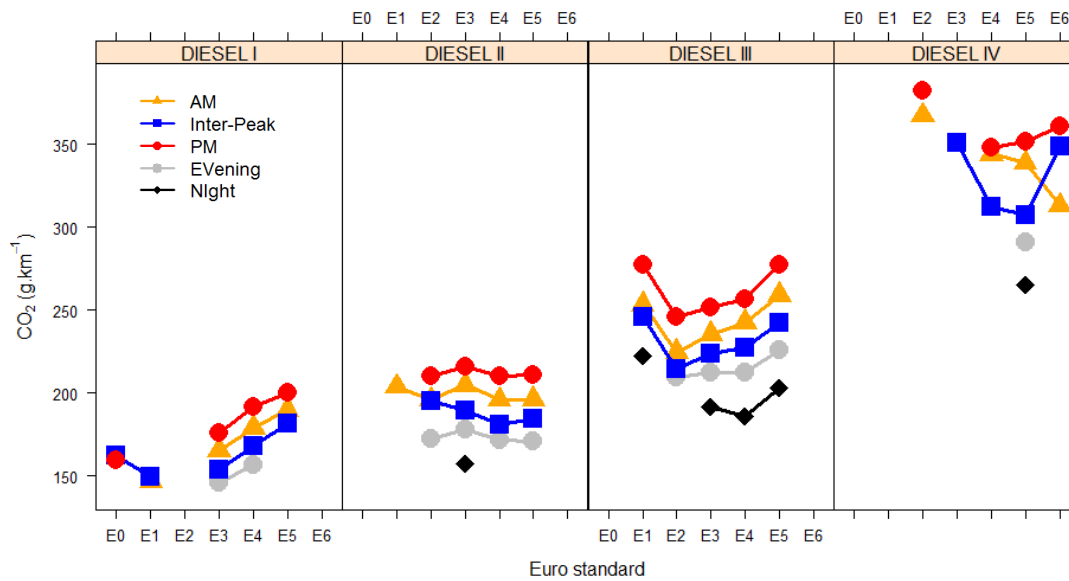


Figure 13. LCV CO₂ Emission Factors for Different Weight Classes

For each LCV vehicle category, the emissions at each EURO standard tend to follow the trend in observed average engine size calculated from ANPR A660 survey metadata. For example, the newer Class II LCVs were found to have only a slight increase in average rated engine power and any resultant CO₂ emission increase from this is offset by a trend in reduced vehicle mass, leaving the modelled CO₂ emission factors from this category relatively stable. However, for the observed Headingley LCV Classes I and III, the data reveal increasing average engine size and mass in service from EURO 2 to EURO 5, resulting in the observed increase in average modelled CO₂ emission. The data set for the N₂ Class IV vehicles was small with fewer than 5 observed vehicles in all but the EURO 5 emission standard categories, making it difficult to draw any conclusions.

The modelled CO₂ emission factors presented in Figure 14 show the emission of CO₂ per km travelled for 12t Rigid (2-Axle) HGVs, 26t Rigid (3-Axle) HGVs and Articulated HGVs. As would be expected, the greater weight and engine sizes of these vehicle types lead to significantly greater average emission rates than those of the LCV categories. The increase of emission factor with network congestion is once again clear but, due to the scarcity of HGV vehicles in the EV and NI model it is not possible to properly assess the rate of emission in free-flowing traffic conditions. For the 12t Rigid HGV category, where a number of vehicles in this category were recorded during free-flowing conditions the average emission rate in the EV was 23.9% lower than in the PM model, decreasing from 735.5 gCO₂/km to 559.4 gCO₂/km.

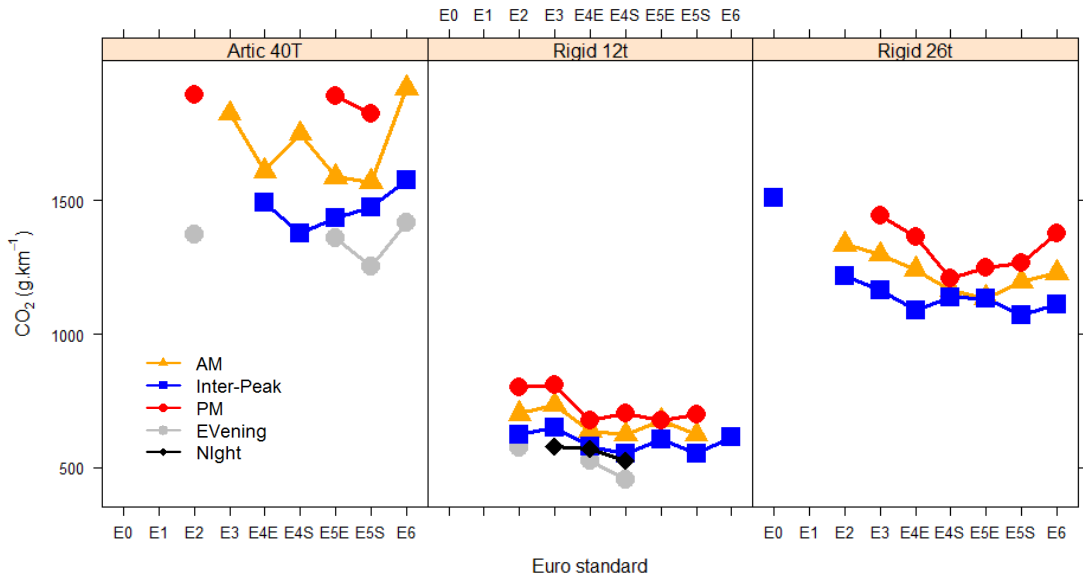


Figure 14. HGV CO₂ Emission Factors for Articulated and Rigid HGVs

Figure 15 displays the simulated Headingley bus fleet CO₂ emission per km at each EURO standard. The observed Headingley bus fleet was found to be composed of almost exclusively of EURO 2 and EURO 3 emission standard vehicles, with 87% of the fleet being double-decker buses. As the night time bus service on the A660 is run with single-deck buses there is no double-decker CO₂ emission factor at this time for comparison. The average evening CO₂ emission rate calculated from the simulation data for double-decker buses is 27.8% lower during the EV simulation than during the PM-Peak, at 1306.6 gCO₂/km and 1810.4 gCO₂/km, respectively. In reality, the difference may be greater than this as a constant rate of loading (number of passengers) was applied in the model throughout all time periods. It is likely that the loading would be significantly greater in the peak travel periods which could be accounted for within the AIMSUN-PHEM model were a detailed bus occupancy survey carried out in the network.

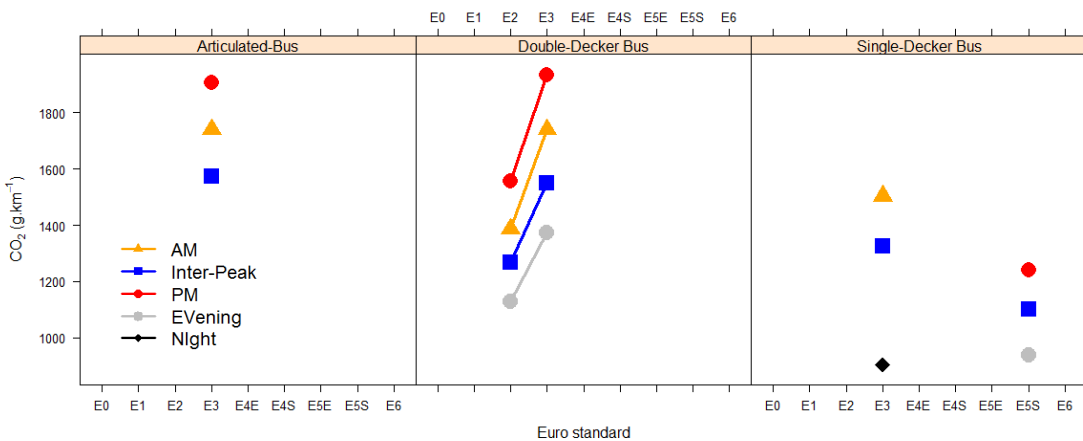


Figure 15: Bus CO₂ Emission Factors for Articulated, Double and Single-Decker

In summary, the figures presented in this section clearly reveal a range of average emission rates at different time periods in the day, resulting from diurnal variations in traffic demand that cause fluctuation between congested and free flowing traffic in the network. The AIMSUN-PHEM simulations suggest that average network CO₂ emission per km rates under free-flowing conditions are approximately 32% lower for petrol vehicles and 25% lower for diesel vehicles than in the most congested traffic conditions.

5. Summary and Conclusions

This paper has presented the development and application of an AIMSUN-PHEM coupled traffic micro-simulation and instantaneous emission model for an urban road network around a 3.8 km section of one of the main arterial corridors into and out of Leeds, UK. Five separately calibrated and validated versions of the model were created to represent five time periods; AM-Peak, Inter-Peak, PM-Peak, Evening and Night to investigate the diurnal variation in vehicle fleet CO₂ emissions which result from changes in traffic demand and fleet composition over a typical 24-hour weekday.

A 24-hour ANPR survey was undertaken to provide an accurate composition of the Headingley vehicle fleet, both for modelling the fleet in AIMSUN and describing the correct proportion of vehicles by vehicle type, EURO emission standard and fuel type in PHEM. This survey method was demonstrated to deliver a high capture rate (94.86%) giving confidence that the ANPR observed fleet is representative of the real-world fleet. The ANPR survey also provided a large quantity of metadata for each recorded VRM, which was used to update the background vehicle specification files in PHEM, making the average vehicle data representative of the Headingley fleet rather than relying on the PHEM default settings.

As with any model, the AIMSUN-PHEM Headingley simulations could be improved with better input data, such as a comprehensive traffic count conducted simultaneously across the network to mitigate the effect of seasonal influences on traffic flow, a longer ANPR survey to ensure the observed fleet represents the real-world fleet, and a greater quantity of instrumented vehicle PEMS data to assess the accuracy of the simulated CO₂ emission estimates and inform the vehicle dynamics parameters within AIMSUN. In reality, such detailed data collection exercises are outside of the scope and budget of a study such as this. However, every effort was made to identify, obtain and utilise the highest quality and most appropriate, data sources available. Including a road grade estimate for each road link and utilising PEMS data recorded within the network to inform the AIMSUN vehicle dynamics parameters likely improved the ability of the AIMSUN-PHEM model to generate trajectory data comparable to on-road vehicle movements in the real-world.

Comparing the AIMSUN-PHEM simulated CO₂ emission rates to the PHEM CO₂ emission estimates calculated from the PEMS trajectory data, by journey time (Figure 6), suggests that in general, the 1Hz simulated vehicle data from AIMSUN generated very similar results to the PEMS 1Hz data, indicating that simulated data can be used to generate real-world CO₂ emission estimates. In a further check of the AIMSUN-PHEM method, analysis was conducted to compare the distribution of second-by-second VSP calculated from AIMSUN simulated journey data with the VSP distribution from PEMS real-world trajectories, for cars completing a 1.5 km road section in similar journey times. This showed the simulated data to have a similar VSP distributions to the PEMS real-world data. However, a number of anomalies suggest that further calibration work may be required to improve the simulated values, as differences in distribution may have a more significance for other emission species.

The coupled model facilitated evaluation of CO₂ emission in the network at a variety of scales, from total network emission factors to individual vehicle type emission factors by fuel type and emission standard, demonstrating the ability of this method to provide both aggregated and highly disaggregated emission factors. The Headingley AIMSUN-PHEM model displayed significant diurnal variation in emission factor, with the average network CO₂/km emission rate under free-flowing conditions approximately 32% lower for petrol vehicles and 25% lower for diesel vehicles than in the most congested traffic conditions observed in the network.

Whilst the calculated CO₂ emission factors in this study are specific to the Headingley test area, this research advances the development, calibration and validation of the AIMSUN-PHEM coupled traffic micro-simulation and instantaneous emission model method. The study demonstrated the relative ease with which AIMSUN can be coupled to PHEM, and although the modelling process requires a large amount of detailed input data, this type of data is increasingly available. As more AIMSUN networks are developed to model traffic flows for traffic management purposes, as long as the parameters within AIMSUN are representative of the real-world network and the model is well calibrated, then a coupled AIMSUN-PHEM model can be utilised to provide improved assessment of the environmental impact of traffic networks. The coupled model offers the possibility to generate current emission factors with networks as well as assess the potential emission impact of different junction designs, speed limit reductions, the addition of bus lanes and different fleet mixes. As PHEM is able to generate emission estimates for a number of emission species, the tool also offers the possibility to assess the emission of pollutants which have a greater influence on local air quality such as Nitrogen Oxides (NO_x).

Acknowledgments

David Wyatt is supported by the Doctoral Training Centre in Low Carbon Technologies at the University of Leeds funded through the UK EPSRC.

References

- Ahn, K., N. Kronprasert, et al. (2009). "Energy and environmental assessment of high-speed roundabouts." Transportation Research Record: Journal of the Transportation Research Board(2123): 54-65.
- Anya, A., N. Roupail, et al. (2014). "Application of AIMSUN Microsimulation Model to Estimate Emissions on Signalized Arterial Corridors." Transportation Research Record: Journal of the Transportation Research Board(2428): 75-86.
- Bluesky. (2013). "LiDAR Height Data." Retrieved 05/11/2013, 2013, from <http://www.bluesky-world.com/products/lidar/>.
- DEFRA. (2014). "National Atmospheric Emissions Inventory: Vehicle fleet composition projections (Base 2013) " Retrieved 05/11, 2015, from <http://naei.defra.gov.uk/data/ef-transport>.
- DEFRA. (2015). "Greenhouse Gas Conversion Factor Repository." from <http://www.ukconversionfactorscarbonsmart.co.uk/>.
- DfT. (2013). "Road transport forecasts 2013." Roads reform: management of the strategic road network and Road network and traffic, from <https://www.gov.uk/government/publications/road-transport-forecasts-2013>.
- DfT. (2014). "Transport Analysis Guidance (TAG) Unit M3.1 Highway Assignment Modelling ", 2015, from https://www.gov.uk/government/uploads/system/uploads/attachment_data/file/427124/webtag-tag-unit-m3-1-highway-assignment-modelling.pdf.
- Dia, H., W. Gondwe, et al. (2006). A traffic simulation approach to evaluating the benefits of incident management programs. AUSTRALASIAN TRANSPORT RESEARCH FORUM (ATRF), 29TH, 2006, GOLD COAST, QUEENSLAND, AUSTRALIA, VOL 29.
- Dowling, R., A. Skabardonis, et al. (2004). "Guidelines for calibration of microsimulation models: framework and applications." Transportation Research Record: Journal of the Transportation Research Board(1876): 1-9.
- EC (2009). Regulation (EC) No. 443/2009 of the European Parliament and of the Council of 23 April 2009 Setting Emission Performance Standards for New Passenger Cars as Part of the Community's Integrated Approach to Reduce CO₂ Emissions from Light-duty Vehicles, Official Journal of the European Union, L140/1. 443/2009/EC, European Commission.
- Granell, J., R. Guensler, et al. (2002). Using Locality-Specific Fleet Distribution in Emissions Inventories: Current Practice, Problems and Alternatives. In Proceedings of the 81st Annual Meeting of the Transportation Research Board, Washington, D.C. .
- Jackson, E. and L. Aultman-Hall (2010). "Analysis of Real-World Lead Vehicle Operation for Modal Emissions and Traffic Simulation Models." Transportation Research Record(2158): 44-53.
- Jimenez-Palacios, J. (1999). Understanding and quantifying motor vehicle emissions with vehicle specific power and TILDAS remote sensing. . Doctoral Dissertation, Department of Mechanical Engineering, Massachusetts Institute of Technology, Cambridge, MA.
- Kraschl-Hirschmann, K., M. Zallinger, et al. (2011). A method for emission estimation for microscopic traffic flow simulation. Integrated and Sustainable Transportation System (FISTS), 2011 IEEE Forum on, IEEE.
- Liu, H., Y. C. A. Tok, et al. (2011). "Development of A Real-Time On-Road Emissions Estimation and Monitoring System." 2011 14th International IEEE Conference on Intelligent Transportation Systems (Itsc): 1821-1826.
- Luz, R. and S. Hausberger (2015). PHEM User Guide for Version 11, Technische Universitat Graz.
- Malcolm, C., T. Younglove, et al. (2003). "Mobile-source emissions - Analysis of spatial variability in vehicle activity patterns and vehicle fleet distributions." Energy, Air Quality, and Fuels 2003(1842): 91-98.
- Millin-Chalabi, G., J. Schumm, et al. (2011). "The Landmap Service: Reaching New Horizons in Data Management and E-Learning." RSPSoc Annual Conference 2011, Bournemouth University, UK.
- Palmgren, F., R. Berkowicz, et al. (1999). "Actual car fleet emissions estimated from urban air quality measurements and street pollution models." Science of the Total Environment 235(1-3): 101-109.
- PTV (2004). VISSIM User Manual Version 3.70, PTV Group - [www.http://vision-traffic.ptvgroup.com/](http://www.vision-traffic.ptvgroup.com/).
- Quadstone (2005). Quadstone Paramics V5.0: Modeller Reference Manual, Quadstone - <http://www.paramics-online.com/>.
- R. (2006). "A language and environment for statistical computing. R Foundation for Statistical Computing, Vienna, Austria. ISBN 3-900051-07-0." from <http://www.R-project.org>.
- SMMT. (2015). "New Car CO₂ Report 2015: The 14th Report." Retrieved 17/11, 2015, from [http://www.smmt.co.uk/wp-content/uploads/sites/2/101924_SMMT-CO₂-Report-FINAL-270415.pdf](http://www.smmt.co.uk/wp-content/uploads/sites/2/101924_SMMT-CO2-Report-FINAL-270415.pdf).

- Song, G., L. Yu, et al. (2012). "Applicability of traffic microsimulation models in vehicle emissions estimates: case study of VISSIM." Transportation Research Record: Journal of the Transportation Research Board(2270): 132-141.
- Swidan, H. (2011). "Integrating AIMSUN Micro Simulation Model with Portable Emissions Measurement System (PEMS): Calibration and Validation Case Study."
- Tate, J. E. (2011). Improved assessment of Environmental Traffic Management Policies - Headingley - Leeds City Council, Institute For Transport Studies, University of Leeds.
- Tate, J. E. (2015). Wakefield Modelling of Action Plan Measures - Vehicle Emission Modelling, Institute For Transport Studies, University of Leeds.
- TfL. (2015). "Bus routes & borough reports." Retrieved 10/11, 2015, from <https://tfl.gov.uk/forms/14144.aspx>.
- TSS (2013). Aimsun Version 8 User's Manual July 2013 © 2005-2013 TSS-Transport Simulation Systems, Transport Simulation Systems, Barcelona, Spain, www.aimsun.com.
- Wyatt, D. W., H. Li, et al. (2014). "The impact of road grade on carbon dioxide (CO₂) emission of a passenger vehicle in real-world driving." Transportation Research Part D-Transport and Environment **32**: 160-170.
- Zallinger, M., T. J., et al. (2008). An Instantaneous Emission Model For The Passenger Car Fleet. 6th International Transport and Air Pollution Congress, Graz, Austria
- Zallinger, M., J. Tate, et al. (2009). Evaluation of a Coupled Micro-scopic Traffic Simulator and Instantaneous Emission Model. Air Quality Conference. Istanbul.

Study on reducing commuters' in-vehicle exposure to ultrafine particles

Bin Xu* and Yu Gong*

*College of Environmental Science and Engineering, Tongji University, NO.1239 Siping Road, Shanghai, China 200092

Fax +86-21-65981831 - email: binxu@tongji.edu.cn

Abstract

Vehicular-emitted ultrafine particles (UFPs) exposure in-cabin is of concern, since the high concentrations and reported toxicity. To determine ways to reduce commuters' UFP exposure, the study measured factors that govern the in-cabin to on-roadway (I/O) UFP concentration ratios quantitatively using a previously developed in-cabin UFP dynamic model (Xu and Zhu, 2009). Such factors included ventilation condition, mechanical airflow rate, driving speed, cabin air filter quality, and cabin air filter usage. The results showed that 20% I/O ratio reduced when the fan was set to Recirculation (RC)-on versus when the fan was set to RC-off due to less UFP exchange between inside the cabin and outside. Also, when the fan was set to RC-off, 40% I/O ratio reduced by at lower mechanical airflow rates. In addition, I/O ratio was decreased 30% compared to the thinnest filter resulted from the thickest cabin air filter. Thus, the lowest UFP I/O ratio is occurred when the vehicle is operating with a high efficiency cabin filter, the ventilation set to Fan-on and RC-on, and at a high ventilation airflow rate. Furthermore, a promising approach to significantly reduce in-cabin UFP exposure was detected, HEPA filter.

Keys-words: Ultrafine particle, I/O ratio, vehicular emissions, in-cabin exposure, driving condition.

Introduction

Increasing evidence has shown that the currently-regulated larger particles are less toxic per unit mass than ultrafine particles (UFPs, diameter < 100 nm) (Ferin et al., 1990, Peters et al., 1997, Alessandrini et al., 2006). Because of their small size and large surface area, cell membranes can be crossed and they can reside in the mitochondria (Li et al., 2003). Redox-active chemicals that can lead to systemic inflammation are abundant in vehicular-emitted UFPs (Sioutas et al., 2005, Elder et al., 2007). Many studies reported that high UFP concentrations were happened on and near interstate freeways and urban roadways (Zhu et al., 2002a, b, Westerdahl et al., 2005, Morawska et al., 2008), which highlights the importance of UFP exposures in in-cabin microenvironments. Although a small amount of their daily time (~1.5 hours) people spend on commuting (Klepeis et al., 2001), the proportion of a person's total daily UFP exposure is substantial when traveling inside vehicles on roadways (Zhu et al., 2007, Fruin et al., 2008).

There are two essential factors that determine in-cabin exposure to vehicle-emitted UFPs, on-roadway concentrations and in-cabin to on-roadway (I/O) concentration ratios. In general, on-roadway UFP concentrations are determined by emissions from all the surrounding vehicles and thus, are beyond the control of an individual commuter. However, in-cabin UFP exposure can be effectively controlled by commuters; various techniques can be employed to reduce the I/O ratios. Recently, Xu and Zhu formulated and validated a mathematical model that incorporates the major physical processes of UFP transport and transformation from on-roadway to in-cabin (Xu and Zhu, 2009). In subsequent studies, researchers began to identify and study some important physical processes, such as penetration across vehicle cracks, filtration through the cabin filters, and deposition inside the vehicles (Gong et al., 2009, Xu et al., 2010a, b). Therefore, the foundation for the current paper was built by these previous studies.

In this study, vehicle driving conditions were studied in relation to UFP I/O ratios, including vehicle ventilation conditions (Fan-off, Recirculation (RC)-off; Fan-on, RC-off; Fan-on, RC-on), mechanical ventilation flow rate, driving speed, and cabin filter usage. In addition, it is also discussed that techniques to reduce UFP exposure that are not currently widely employed but can be easily implemented, such as a high efficiency particulate air (HEPA) cabin filter.

1. In-Cabin UFP Dynamics

Driving conditions can affect the I/O UFP ratio directly. To investigate the effect of driving conditions on the I/O ratio, this study employed a previously developed model that studied the fundamentals of in-cabin UFP dynamics (Xu and Zhu, 2009). Experimental on-road measurements for different vehicles at different ventilation settings verified the model (Zhu et al., 2007). Briefly, a material-balance can describe the UFP transport and transformation of exposure from on-roadway to in-cabin on, as shown in Eq. 1 (Xu and Zhu, 2009).

$$\frac{d(C_i V)}{dt} = C_0 [Q_S (1 - \eta_S) + Q_L P] - C_i [Q_F \eta_F + \beta V + (Q_S + Q_L)] \quad (1)$$

There are two pathways that outdoor UFPs can enter the in-cabin microenvironment: through the mechanical air supply at a flow rate of Q_S ($\text{m}^3 \text{h}^{-1}$) and leakage at a flow rate of Q_L ($\text{m}^3 \text{h}^{-1}$). For a particular particle size, d , the in-cabin particle concentration is C_i (particles cm^{-3}), the on-roadway concentration is C_0 (particles cm^{-3}), and V (m^3) is the volume of the vehicle's interior. The variables, P , η_S , η_F , and β , are the penetration factor (-), filtration efficiency (-), removal fraction by respiratory (-), and deposition coefficient (h^{-1}), respectively. Among the in-cabin UFP dynamics, Q_S , V , P , η_S , and β have been determined experimentally in our previous studies (Gong et al., 2009, Xu et al., 2010a, b), and Q_L can be calculated theoretically (Baker et al., 1987).

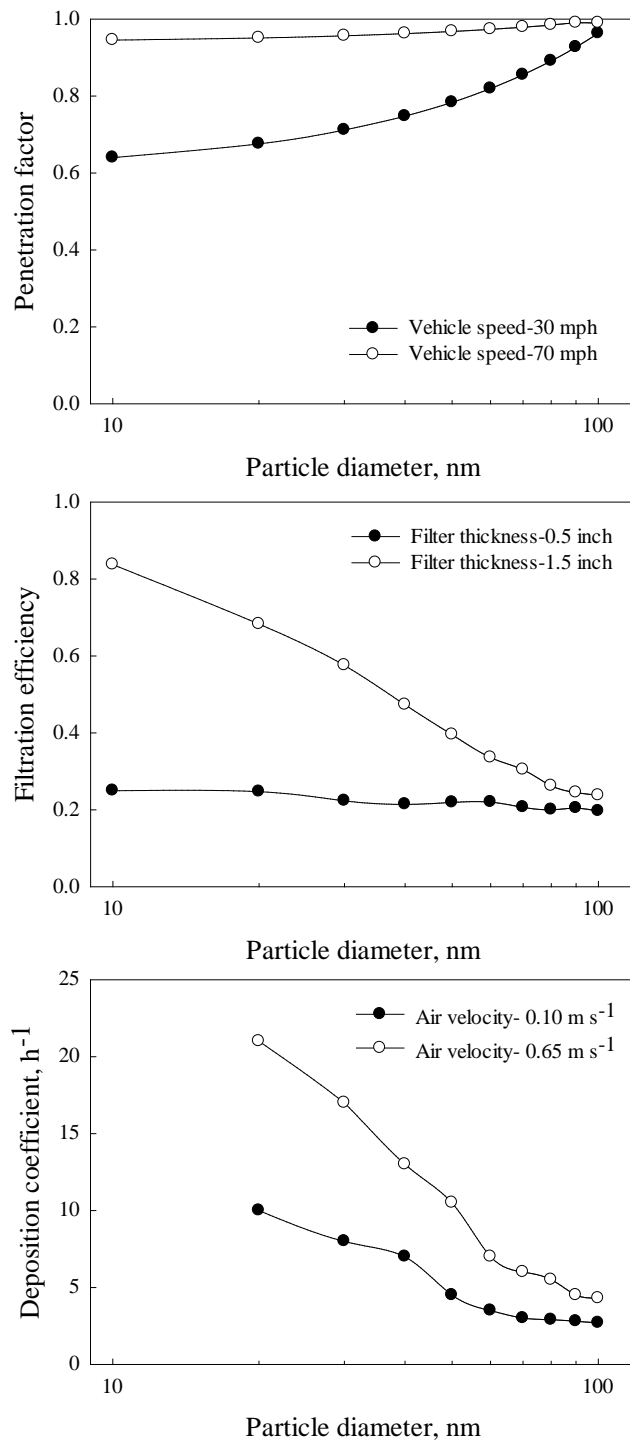


Figure 1. Size-segregated parameters governing in-cabin UFP transport and transformation dynamics: (a) penetration factor (Xu et al., 2010a), (b) filtration efficiency (Xu et al., 2010b), and (c) deposition coefficient (Gong et al., 2009).

The range of size-segregated parameters that affect UFP transport and transformation is illustrated in Figure 1. Penetration factor, P define as the fraction of particles from on-roadway to in-cabin through leakage airflow, which was measured at different crack sizes on the vehicle envelope under different pressure drops across the cracks. The smallest P was found at the lowest pressure drop (30 Pa), whereas the largest P across the cracks was found at the highest pressure drop (200 Pa). For the detailed experimental setup and protocol, see Xu et al., 2010a. The filtration efficiency (η_s) was different with three commercially-available cabin filters with different thicknesses (1.5 inches, 1 inch, and 0.5 inch) over a range of filter face velocities (0.1-0.5 $m s^{-1}$). Figure 1b shows that the filtration

efficiency varied significantly with respect to different filter thicknesses. The detailed experimental setup and protocol can be found in Xu et al., 2010b. The deposition coefficient (β) was determined in three vehicles at three different ventilation settings (Fan-off, RC-off; Fan-on, RC-off; Fan-on, RC-on). Figure 1c shows that the highest deposition coefficient occurred at the highest in-cabin air velocity. The detailed experimental setup and protocol can be found in Gong et al., 2009.

Under different ventilation conditions, i.e., (i) Fan-off, RC-off; (ii) Fan-on, RC-off; and (iii) Fan-on, RC-on, Eq.1 can be simplified with respect to different UFP entry pathways from the on-roadway atmosphere to the in-cabin environment. For example, under condition (i), there is no mechanical air

supply ($Q_S=0$), and Eq. 1 is reduced to: $\frac{C_i}{C_0} = \frac{Q_L P}{Q_F \eta_F + \beta V + Q_L}$. It is shown that commuters can

lower the UFP I/O ratio by minimizing the penetration factor (P) and leakage flow rate (Q_L). Similarly, under condition (ii), decreasing the mechanical air supply (Q_S) and increasing the filtration efficiency (η_S) reduce the UFP I/O ratio; under condition (iii), decreasing the penetration factor (P) and leakage air flow rate (Q_L) reduce the UFP I/O ratio.

All mentioned parameters above that govern the in-cabin UFP dynamics, are related to vehicles' driving condition, of which the commuters can control, the ventilation conditions, ventilation airflow rate, driving speed, and cabin filter usage. The following sections present how the in-cabin UFP I/O ratios were affected by these adjustable vehicle driving conditions.

2.Ventilation Conditions

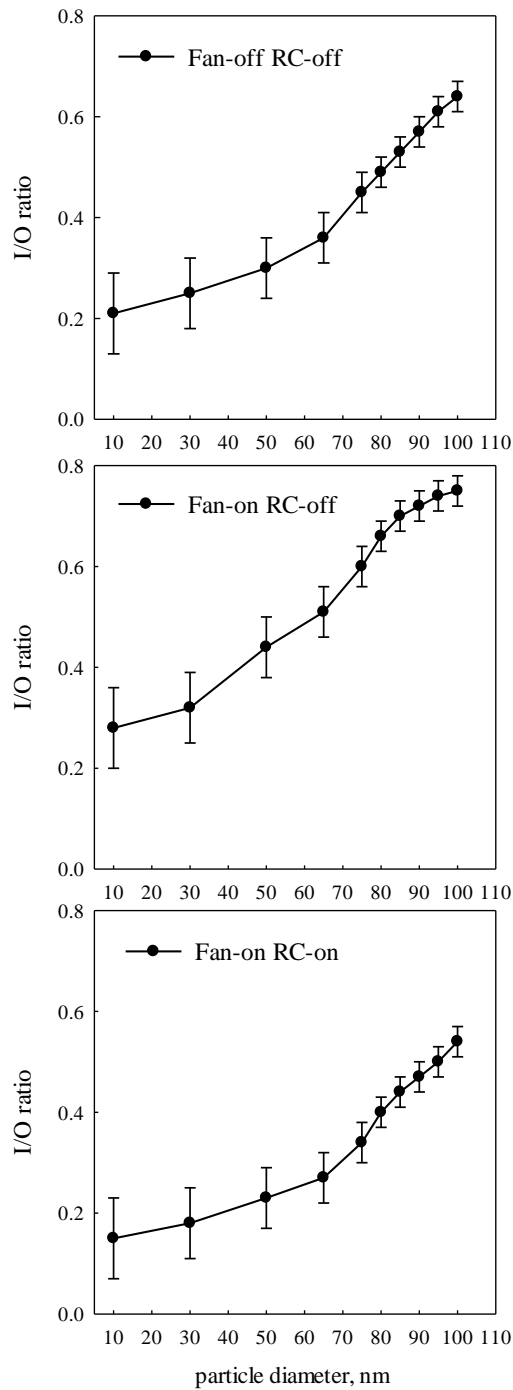


Figure 2. The range of the modeled I/O ratios under different ventilation settings: Fan-off, RC-off, Fan-on, RC off, and Fan-on, RC-on. Volume of the vehicle was 6 m³.

The modeled UFP I/O ratios as a function of particle size under different ventilation conditions: (i) Fan-off, RC-off, (ii) Fan-on, RC-off, and (iii) Fan-on, RC-on, is shown in Figure 2. To calculate the I/O ratios, the measured UFP transport and transformation parameters (penetration factor, filtration efficiency and deposition coefficient, shown in Figure 1) were implemented into the model. Under all ventilation conditions, when the largest penetration factor, lowest filtration efficiency, and lowest deposition coefficient were combined, the largest I/O ratios were found. The largest penetration factor occurred with the largest driving speed, largest crack height, and shortest crack length (Xu et al., 2010a). At the lowest filter face velocity, the lowest filtration efficiency was found with the thinnest

filter (Xu et al., 2010b). With the smallest interior surface to volume ratio and at the lowest in-cabin air velocity, the lowest deposition coefficient occurred (Gong et al., 2009). In general, driving an old, leaky, large vehicle with a poor quality in-cabin filter at a high speed is reflected under this condition.

As shown in Figure 2b, the smaller particle sizes under condition (ii), the greatest variability in the I/O ratio, ~40%, occurred due to the large difference in filtration efficiencies with respect to different filter thicknesses. A large variability of median I/O ratios (up to 20%) was observed among different ventilation conditions. Under conditions (ii) and (iii), the average highest (55%) and lowest (35%) I/O ratios were observed, respectively. In addition, the I/O trends were similar for all three ventilation conditions at first sight, but the underlying mechanisms resulting in each trend are significantly different. The I/O ratios increased with increasing particle size under condition (i) is attributed to the larger penetration factor for larger particles. Differently, for condition (ii), this trend is due to the lower filtration efficiency for larger particles. For condition (iii), the trend is because of the larger penetration factor and the smaller deposition coefficient for larger particles.

Under condition (i), the predominant pathway for air and UFP exchange between the in-cabin and the outside is the leakage airflow. It was found that the most important parameters that affect the UFP I/O ratios are the penetration factors and the leakage rate under this ventilation setting. Under condition (ii), the mechanical airflow which exceeds the leakage airflow is the dominant air exchange process for the in-cabin microenvironment. The air exchange rate was lower under conditions (i) and (iii) than condition (ii) because the leakage flow has a lesser effect than the mechanical airflow (Xu and Zhu, 2009), which leads to the lowest median I/O UFP ratio, as shown in Figure 2. Under condition (iii), the predominant pathway for air and UFP exchange is the leakage airflow. When the ventilation setting was switched from condition (i) to condition (iii), the UFP deposition on the vehicle interior surfaces was enhanced with increasing the in-cabin air velocity and resulted in a lower median I/O UFP ratio. As shown in Figure 2, under condition (iii), the median UFP I/O ratio is the lowest, which is consistent with the previous measurement during freeway and tunnel travel (Zhu et al., 2007; Knibbs et al., 2010). Therefore, in order to minimize the in-cabin UFP levels, it is recommended that commuters set ventilation conditions to Fan-on, RC-on. It should be noted that under this ventilation condition, however, there is a minimal air exchange between the in-cabin and the outside, which results in a quick build-up of in-cabin CO₂ levels. Thus, the ventilation condition should be used with caution during a long commute.

3. Mechanical Ventilation Airflow Rate

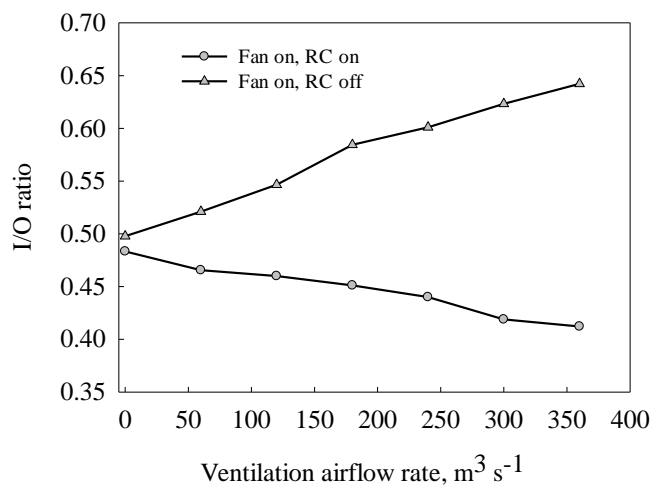


Figure 3. The range of the modeled I/O ratios at different mechanical air flow rates under two ventilation settings (ii) Fan-on, RC-off and (iii) Fan-on, RC-on. All the other UFP transport dynamics were set to average values. The volume of vehicle was 6 m³, and the speed of vehicle was 50 mph.

Besides the ventilation conditions, the UFP I/O ratio was also significantly affected by the mechanical ventilation airflow rate. As shown in Figure 3, the I/O ratio significantly increased (20-30%) under condition (ii). This is because the mechanical air supply was the predominant airflow and

determined the in-cabin air exchange rate which influences the filtration efficiency well. Thus, I/O ratio increased with the larger air exchange rate and the lower filtration efficiency. In contrast, 10-15% I/O ratio reduced under condition (iii). This is attributed to more UFPs deposited on the vehicle interior surface with the in-cabin air velocity increased (Gong et al., 2009). Therefore, under condition (ii), commuters should choose a lower ventilation airflow rate to achieve a lower in-cabin UFP exposure. A higher ventilation airflow rate, however, should be chosen to achieve a lower in-cabin UFP exposure under condition (iii).

4. Driving Speed

In addition to the ventilation settings and the airflow rate, the UFP I/O ratio was also significantly affected by vehicle driving speed. In an earlier study, it was found that the larger leakage airflow (Ott et al., 2007) and greater particle penetration (Xu et al., 2010a) was produced by a larger pressure differential between the in-cabin and the outside created by a larger driving speed. As the differential pressure, the leakage airflow could bring UFPs into the vehicle through cracks in the vehicle envelope. Previously, it was found that the pressure differential increased from 30 ± 5 Pa to 150 ± 40 Pa with the vehicle driving speed increased from 30 mph to 70 mph under different ventilation settings (Xu and Zhu, 2009).

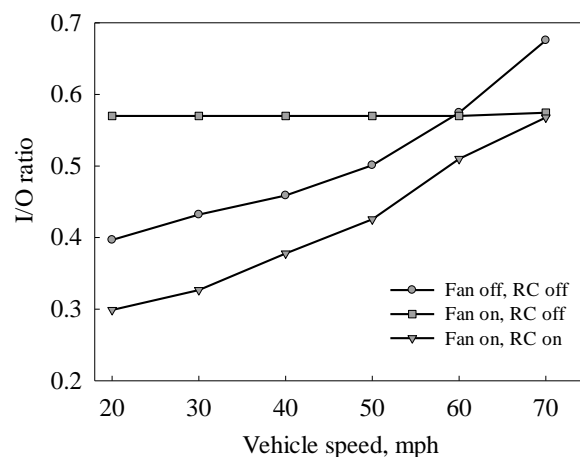


Figure 4. The range of the modeled I/O ratios at different vehicle speeds under three ventilation settings: (a) Fan-off, RC-off, (b) Fan-on, RC-off and (c) Fan-on, RC-on. The volume of the vehicle was 6 m^3 , and the ventilation airflow rate was $180 \text{ m}^3 \text{ h}^{-1}$.

Based on the model calculation, the relationship between the UFP I/O ratios and the vehicle driving speeds for different UFP sizes (10-100 nm) were illustrated in Figure 4. The I/O ratios were largest for the 100-nm particles under three ventilation conditions. While at the same vehicle speed, the same differential pressure between the outside and the in-cabin, and the same amount of leakage airflow, the more particles being leaked into the vehicle was caused by a larger penetration factor of the larger particles.

A larger driving speed results in higher I/O ratios. However, the relative importance of the vehicle speed is related to different ventilation settings. Compared with conditions (i) and (iii), the vehicle speed is less significant under condition (ii). The differential pressure between the in-cabin and the outside, which determines the leakage airflow rate, is directly affected by the vehicle driving speed. When there is no mechanical ventilation air supply from the on-roadway atmosphere into the in-cabin (conditions (i) and (iii)), the UFPs penetration is predominantly through leakage and thus, a greater increase (up to 30%) of the I/O ratio. In contrast, when mechanical airflow from outside enter into the cabin under condition (ii), the I/O ratio isn't significantly affected by the vehicle speed (<10%).

Besides on-roadway UFP level and I/O ratio, commuters' exposure to UFP inside vehicles is determined by another important parameter, commuting time. M (particle cm^{-3} hour) denotes the total UFP exposure during commuting, can be calculated as $M = C \times y \times t$. Where C is the on-roadway total UFP concentration, y (-) is total UFP I/O ratio, and t (hour) is commuting time. For a given distance, assuming constant on-roadway total UFP concentration, the product of y and t that both are related to vehicle speed determine the exposure. To achieve an explicit relationship between M and

vehicle speed, the quantitative relationship between total UFP I/O ratio and vehicle speed was shown in Figure 5. It was obvious that linear relationships under all three ventilation conditions. Similar to Figure 4, the effect of vehicle speed on UFP I/O ratio under condition (i) and (iii) is greater significant than those under condition (ii) due to the mechanical air supply through the ventilation system under condition (ii). A quantitative relationship between total UFP exposure, M and vehicle speed, x (m s^{-1}) can then be derived from applying the linear regression equations in Figure 5. For example, under condition (i), $M = C \times (0.005x + 0.34) \times \frac{L}{x} = 0.005CL + \frac{0.34CL}{x}$ where L (mile) is the distance vehicle traveled. The other two conditions have the similar equations. Quantitatively, to commute 14 miles, it takes 0.7 and 0.2 hours at 20 mph and 70 mph, respectively. If on-roadway UFP concentration is a constant, $10^5 \# \text{cm}^{-3}$, the accumulative in-cabin exposure levels are 3.08×10^4 particle cm^{-3} hour and 1.38×10^4 particle cm^{-3} hour at 20 mph and 70 mph, respectively.

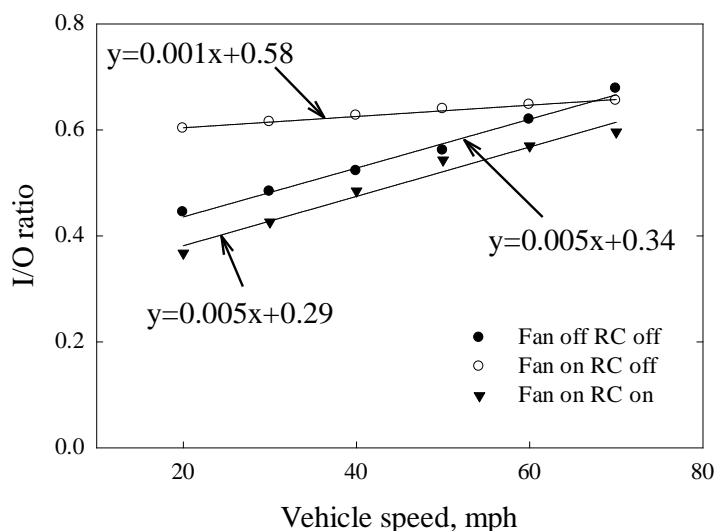


Figure 5. Relationship between modeled total UFP I/O ratios and vehicle speeds under three ventilation settings: (a) fan off RC off, (b) fan on RC off and (c) fan on RC on. Volume of the vehicle is 6 m^3 . Ventilation airflow rate is $180 \text{ m}^3 \text{ h}^{-1}$.

5. Cabin Filter Quality and Usage

Cabin air filters that may reduce in-cabin UFP concentrations commonly equipped in modern vehicles (Pui et al., 2008). In a previous study, it is reported that a large range of filtration efficiencies (up to 60%, Figure 1b) for different commercial cabin air filters and the greatest filtration efficiency occurred for the thickest commercially available cabin filter (Xu et al., 2010b). Due to the variability in the filtration efficiency, the quality of the cabin filter can greatly affect the UFP I/O ratios. The modeled UFP I/O ratio with different cabin filters under condition (ii) is shown in Figure 6 (Xu and Zhu, 2009). The average UFP I/O ratio for the different size ranges was $\sim 50\%$ with the thickest filter, while the average UFP I/O ratio increased to $\sim 75\%$ with the thinnest and worst quality filter. Instead of an existing commercial cabin air filter, in-cabin UFP exposure can significantly lower equipping a High Efficiency Particulate Air (HEPA) filter. The filtration efficiency of a HEPA filter is greater than 99.97% in the UFP size range (Schroth, 1996). It means that the amount of UFPs entering the in-cabin can be effectively reduced through the ventilation system. As shown in Figure 6, the mean UFP I/O ratio decreased by $\sim 50\%$, and especially for the larger UFPs.

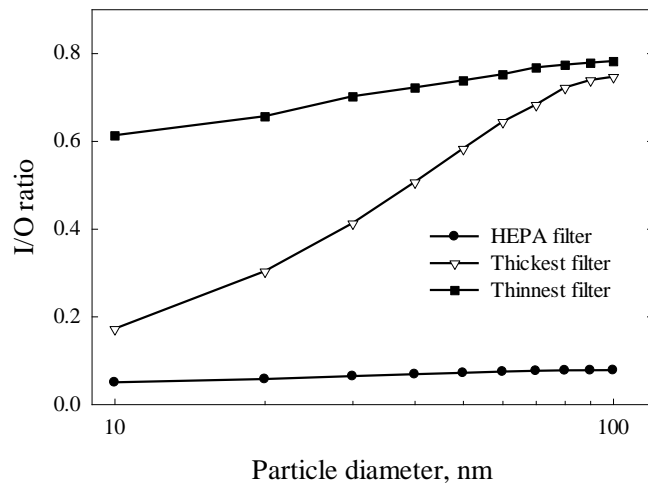


Figure 6. The range of the modeled I/O ratios with different filter qualities under the ventilation setting of Fan-on, RC-off. The thickness of thickest filter and thinnest filter were 1.5 inches and 0.5 inch, respectively. The ventilation airflow rate was $180 \text{ m}^3 \text{ h}^{-1}$.

The UFP I/O ratios can be affected by another important parameter, the filter usage, which can be also controlled by commuters. Filter usage can be increased by the filtration efficiency or the pressure drop across the filter. The UFP I/O ratios can be reduced by increased filtration efficiency under Fan-on, RC-off (Xu and Zhu, 2009). However, due to the pressure drop not only decreases the mechanical flow rate but also affect the pressure differential, it is more complicated that the pressure drop affects the UFP I/O ratios (Xu and Zhu, 2009, Xu et al., 2010a). For instance, an increased differential pressure can push more UFPs into the in-cabin through leakage, which results in a higher I/O ratio (Xu et al., 2010b).

Traffic conditions also determined the effect of the filter usage on the I/O ratio. For the same filter usage, the results showed that the particle loading on the filter was accelerated under heavy traffic (PM_{10} : $100\sim 135 \mu\text{g m}^{-3}$), which caused a larger pressure drop across the filter and a greater UFP I/O ratio compared with when under light traffic (PM_{10} : $20\sim 45 \mu\text{g m}^{-3}$) (Xu et al. 2010b). The modeled UFP I/O ratios as a function of filter usage at a condition of moderate traffic (PM_{10} : $45\sim 75 \mu\text{g m}^{-3}$) with the Fan-on and RC-off is shown in Figure 7. The I/O ratio was observed to increase nearly 20% with the filter usage over 30 months. Therefore, to avoid a large I/O ratio increase, it is recommended to change the cabin filter after a certain period. Guidelines and discussion on this are provided elsewhere (Xu et al. 2010b).

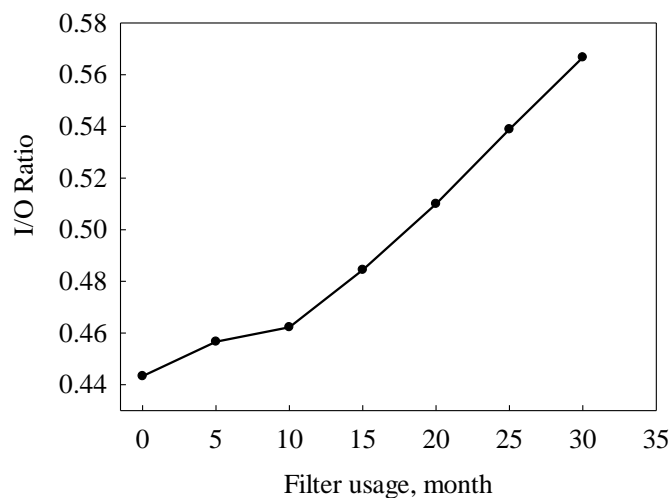


Figure 7. Modeled total UFP I/O ratios as a function of filter usage. The best quality filter was used in the model calculation. The volume of the vehicle was 6 m^3 , and the ventilation airflow rate was $180 \text{ m}^3 \text{ h}^{-1}$.

In addition to ventilation condition, a few techniques such as vehicle driving speed, and filter usage, exist that have not yet been practically employed in the current vehicle fleet. These techniques that may be implemented in the future have the potential to reduce in-cabin UFP exposure. One of those techniques is discussed as follows, re-circulation of air through a cabin air filter.

6. Recirculation Air Passing Through Cabin Air Filter

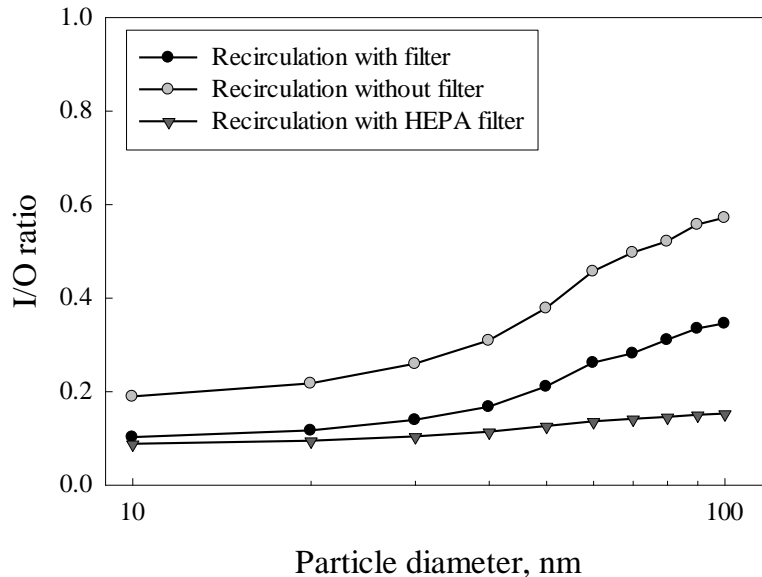


Figure 8. The range of the modeled I/O ratios under the ventilation setting of Fan-on, RC-on for: (a) Recirculation with filter and (b) Recirculation without filter. The ventilation airflow rate was $180 \text{ m}^3 \text{ h}^{-1}$.

In the previous sections, the model calculated the UFP I/O ratio under condition (iii) is the common practice of the current vehicle fleet. Passing recirculating air through the cabin air filter, however, may result in a substantial in-cabin UFP reduction. In addition to breathing and deposition, if considering the cabin air filter at a rate of $Q_S \eta_S$, then Eq. 1 can be modified to Eq. 2.

$$\frac{d(C_i V)}{dt} = C_0 Q_L P - C_i (Q_F \eta_F + \beta V + Q_S \eta_S + Q_L) \quad (2)$$

At steady-state, the UFP I/O ratio can be calculated as $\frac{C_i}{C_0} = \frac{Q_L P}{Q_F \eta_F + \beta V + Q_S \eta_S + Q_L}$. As

shown in Figure 8, the modeled UFP I/O ratios as a function of particle size under condition (iii) with and without recirculation air passing through the cabin air filter. The UFP I/O ratio decreased 10%-30% when the recirculating air passed through the cabin air filter compared with the recirculating air does not pass through in the ventilation system (~30%). It was observed that the lowest I/O ratio occur when the recirculating air passed through a HEPA filter (~10.1%).

Conclusion

The research studied the relationship between vehicle driving conditions and the UFP in-cabin to on-roadway concentration (I/O) ratios. It was found that the I/O ratios varied significantly with the driving conditions. From an environmental health perspective, driving at the speed limit using the largest ventilation airflow rate with condition (iii) (Fan-on; RC-on) and using a high-efficiency filter to reduce exposure to in-cabin UFPs are recommended to commuters. In addition, the study also found

a promising technique to greatly reduce in-cabin UFP exposures, recirculating in-cabin air through a HEPA filter.

References

- Alessandrini, F., Schulz, H., Takenaka, S., Lentner, B., Karg, E., Behrendt, H., and Jakob, T. (2006) 'Effects of ultrafine carbon particle inhalation on allergic inflammation of the lung' Journal of Allergy and Clinical Immunology, 117, 824-830.
- Baker, P., Sharples, S., and Ward, I. (1987) 'Air-flow through cracks' Building and Environment, 22, 293-304.
- Elder, A., Couderc, J., Gelein, R., Eberly, S., Cox, C., Xia, X., Zareba, W., Hopke, P., Watts, W., Kittelson, D., Frampton, M., Utell, M., Oberdorster, G. (2007) 'Effects of on-road highway aerosol exposures on autonomic responses in aged, spontaneously hypertensive rats' Inhalation Toxicology, 19, 1-12.
- Ferin, J., Oberdorster, G., Penney, D., Soderholm, S., Gelein, R., and Piper, H. (1990) 'Increased pulmonary toxicity of ultrafine particles? I. Particle clearance, translocation, morphology' Journal of Aerosol Science, 21, 381-384.
- Fruin, S., Westerdahl, D., Sax, T., Sioutas, C., and Fine, P. M. (2008) 'Measurements and Predictors of On-road Ultrafine Particle Concentrations and Associated Pollutants in Los Angeles' Atmospheric Environment, 42, 207-219.
- Gong, L., Xu, B., and Zhu, Y. (2009) 'Ultrafine particles deposition inside passenger vehicles' Aerosol Science and Technology, 43, 544-553.
- Klepeis, N., Nelson, W., Ott, W., Robinson, J., Tsang, A., Switzer, P., Behar, J., Hern, S., and Engelmann, W. (2001) 'The National Human Activity Pattern Survey (NHAPS): a resource for assessing exposure to environmental pollutants' Journal of Exposure Analysis and Environmental Epidemiology, 11, 231-252.
- Knibbs, L., De Dear, R., and Morawska, L. (2010) 'Effect of cabin ventilation rate on ultrafine particle exposure inside automobiles' Environmental Science and Technology, 44, 3546-3551.
- Li, N., Sioutas, C., Cho, A., Schmitz, D., Misra, C., Sempf, J., Wang, M., Oberley, T., Froines, J., and Nel, A. (2003) 'Ultrafine particulate pollutants induce oxidative stress and mitochondrial damage' Environ Health Perspect, 111, 455-460.
- Morawska, L., Ristovski, Z., Jayaratne, E. R., Keogh, D. U., and Ling, X. (2008) 'Ambient nano and ultrafine particles from motor vehicle emissions: Characteristics, ambient processing and implications on human exposure' Atmospheric Environment, 42, 8113-8138.
- Ott, W., Klepeis, N., and Switzer, P. (2007) 'Air change rates of motor vehicles and in-vehicle pollutant concentrations from secondhand smoke' Journal of Exposure Science and Environmental Epidemiology, 17, 1-14.
- Peters, A., Wichmann, H., Tuch, T., Heinrich, J., and Heyder, J. (1997) 'Comparison of the number of ultra-fine particles and the mass of fine particles with respiratory symptoms in asthmatics' The Annals of Occupational Hygiene, 41, 19-23.
- Pui, D., Qi, C., Stanley, N., Oberdorster, G., and Maynard, A. (2008) 'Recirculating air filtration significantly reduces exposure to airborne nanoparticles' Environmental Health Perspect, 116, 863-866.
- Schroth, T. (1996) 'New HEPA/ULPA filters for clean-room technology' Filtration & Separation, 33, 245-250.
- Sioutas, C., Delfino, R., and Singh, M. (2005) 'Exposure Assessment for Atmospheric Ultrafine Particles (UFPs) and Implications in Epidemiologic Research' Environ Health Perspect, 113, 947-955.
- Westerdahl, D., Fruin, S., Sax, T., Fine, P.M., and Sioutas, C. (2005) 'Mobile platform measurements of ultrafine particles and associated pollutant concentrations on freeways and residential streets in Los Angeles', Atmos. Environ., 39, 3597-3610.
- Xu, B., Liu, S., and Zhu, Y. (2010a) 'Ultrafine particle penetration through idealized vehicle cracks' Journal of Aerosol Science, 41, 859-868.
- Xu, B., Liu, S., Liu, J., and Zhu, Y. (2010b) 'Effects of cabin filter on in-cabin to on-roadway ultrafine

particle ratios' Aerosol Science and Technology, in press.

- Xu, B. and Zhu, Y. (2009) 'Quantitative analysis of the parameters affecting in-cabin to on-roadway (I/O) ultrafine particle concentration ratios' Aerosol Science and Technology, 43, 400-410.
- Zhu, Y., Hinds, W., Kim, S., Shen, S., and Sioutas, C. (2002a) 'Study of ultrafine particles near a major highway with heavy-duty diesel traffic' Atmospheric Environment, 36, 4324-4435.
- Zhu, Y., Hinds, W., Kim, S., and Sioutas, C. (2002b) 'Concentration and size distribution of ultrafine particles near a major highway' Journal of Air and Waste Management Association, 52, 1032-1042.
- Zhu, Y., Eiguren-Fernandez, A., Hinds, W., and Miguel, A. (2007) 'In-cabin commuter exposure to ultrafine particles on Los Angeles freeways' Environmental Science and Technology, 41, 2138-2145.

Exposure of Volatile Organic Compounds inside Vehicle Cabins in China

Bin Xu^{1,2,*}, Yu Gong¹, Ya Wu¹

1. Department of Environmental Engineering, Tongji University, Shanghai 200092, China
Fax +86-21-65981831 -email: binxu@tongji.edu.cn
2. Shanghai Key Laboratory of Atmospheric Particle Pollution and Prevention (LAP3)
Shanghai, China 200433

Abstract

This study measured the concentrations of nine volatile organic compounds (VOCs) inside vehicle cabins under three different driving conditions ((i) fan off and recirculation (RC) off, (ii) fan on and RC off, and (iii) fan on and RC on) in China. The mean concentrations of benzene, toluene, xylene, ethylbenzene, styrene, formaldehyde, acetaldehyde, acetone, and acrolein, were 16.73 mg/m³, 66.02 mg/m³, 14.20 mg/m³, 6.78 mg/m³, 28.09 mg/m³, 16.43 mg/m³, 12.47 mg/m³, and 20.65 mg/m³, respectively. Compared with ventilation condition (ii), the VOCs concentrations were larger (up to 31.15%) than the concentration under ventilation condition (i) and (iii). The results indicated that VOCs exposure inside vehicle cabins with higher fraction of leather is larger than vehicles with fabric interiors. Compared with old vehicles, the concentrations of benzene, toluene, xylene, methylbenzene, formaldehyde, acetaldehyde, acetone and acrolein inside new vehicles were found 12.89%, 103.54%, 123.14%, 104.20%, 6.26%, 6.31%, and 10.67% larger, respectively. The concentrations of toluene, styrene, methylbenzene, and xylene increased 513.6%, 544.8%, 767.0%, and 597.7% as the ambient temperature increased from 11 °C to 25 °C, respectively.

Key words: Volatile Organic Compounds, ventilation condition, vehicle age, temperature

Introduction

Exposure to volatile organic compounds (VOCs) in vehicle cabins has increasingly become an important public concern. Several studies have found that mucosal irritation, non-specific symptoms, and even numerous long-term health problems are caused by VOCs (Wolkoff et al., 2005; Araki et al., 2010; Abraham et al., 2016). Previous study reported the fact that the time spent inside vehicle cabins was considerable (~8% of the daily time) (Wallace, 1996). Many studies indicated that the mean concentration of VOCs inside vehicle cabins significantly exceeds the ordinary indoor or outdoor level (Chien, 2007; Geiss et al., 2009; Leung and Harrison, 1999). Taking all these into consideration, it is essential to investigate the in-cabin VOC exposure levels and the key factors on them.

Various air pollutants inside vehicle cabins have been investigated in many studies. However, assessing the in-cabin VOCs under various driving conditions have been few studied and systematical analysis focused on the parameters which affect in-cabin VOCs transport or concentrations was also scarce. Besides, there is even no analytical or quantitative model that can be used to simulate in-cabin VOCs transport or facilitate the suggestions to lower in-cabin VOCs concentration.

This study measured the concentration of nine VOCs (benzene, toluene, xylene, methylbenzene, styrene, formaldehyde, acetaldehyde, acetone and acrolein), which were limited according to a national standard of China (MEPC, 2012), and investigated the major factors that affect in-cabin VOCs concentrations. The factors included ventilation conditions (fan off and recirculation (RC) off, fan on and RC off, fan on and RC on), vehicle age (old, new), interior temperature and interior trims (leather, fabric). In order to systematically analyze the changes of VOCs concentrations inside vehicle cabins, the concentrations of TVOC, CO₂, CO, H₂S were also monitored.

1. Methodology

1.1 Test vehicles and conditions

This study was performed between July and November, 2015 in four biggest cities in China: Beijing, Shanghai, Chengdu, and Shenzhen. The location of the cities, which had the largest ownership of automobiles in China, was shown in Figure 1. Based on different background temperature of them, the VOCs emission from the trims inside vehicle cabins would be significantly affected. All the vehicles under investigation were rented from private owner or car rental agency. As listed in Table 1, Volkswagen Passat and Chevrolet Cruze were the selected vehicle models. Two typical materials: leather (Passat) and fabric (Cruze) decorated their interiors. According to the usage years, old (more than 5 years) and new vehicles (less than one year) in the test were defined. To minimize the potential variability to the result, the same new cabin air filters (Serial NO. PQ35 SVW, Mann+Hummel Inc., Germany) equipped in all vehicles and all of the excess things inside the cabins were removed. Meteorological conditions were similar during all test days (sunny days, relative humidity was 40.0±5.0%).

Three ventilation settings were investigated in the study: (i) circulation fan off and RC off; (ii) fan on and RC off; and (iii) fan on and RC on. Compared with condition (ii), the supply air to the in-cabin environment under condition (iii) was not from outside but from inside. Fan speed of the outlets was kept at ~5.0 m/s.



Figure 1. The tested four cities: Beijing, Shanghai, Chengdu, and Shenzhen.

Table 1. Summary of test vehicle characteristics and test conditions

No.	City	Vehicle Models	Vehicle condition	Ventilation conditions*	Background Temperature (°C)
1	Beijing	Passat	Old	i, ii, iii	11.8±2.2
2	Beijing	Passat	New	i, ii, iii	11.8±2.2
3	Beijing	Cruze	Old	i, ii, iii	11.8±2.2
4	Beijing	Cruze	New	i, ii, iii	11.8±2.2
5	Shanghai	Passat	Old	i, ii, iii	25.1±0.9
6	Shanghai	Passat	New	i, ii, iii	25.1±0.9
7	Shanghai	Cruze	Old	i, ii, iii	25.1±0.9
8	Shanghai	Cruze	New	i, ii, iii	25.1±0.9
9	Chengdu	Passat	Old	i, ii, iii	17.4±2.4
10	Chengdu	Passat	New	i, ii, iii	17.4±2.4
11	Chengdu	Cruze	Old	i, ii, iii	17.4±2.4
12	Chengdu	Cruze	New	i, ii, iii	17.4±2.4
13	Shenzhen	Passat	Old	i, ii, iii	15.8±1.9
14	Shenzhen	Passat	New	i, ii, iii	15.8±1.9
15	Shenzhen	Cruze	New	i, ii, iii	15.8±1.9

*Ventilation condition (i) = Fan off RC off, Ventilation condition (ii) = Fan on RC off, Ventilation condition (iii)= Fan on RC on.

1.2 Field Measurements and Sampling

This study measured the concentrations of various in-cabin air pollutants, e.g. TVOC, CO₂, CO, H₂S, benzene, toluene, xylene, methylbenzene, styrene, formaldehyde, acetaldehyde, acetone, and acrolein. The TVOC concentration was measured by a portable TVOC monitor (ppbRAE 3000, RAE Systems, Inc., USA) with a photoionization detector. The CO₂ and CO concentrations, air velocity, temperature, relative humidity, and air pressure were measured by a Q-trak (model 7575, TSI Inc., US) with two different probes (model 962 and 982, TSI Inc., US). The H₂S concentrations were measured with a portable hydrogen sulfide analyzer (Jerome 631-X, Arizona Instrument LLC, US).

Measurements of nine VOCs (benzene, toluene, xylene, methylbenzene, styrene, formaldehyde, acetaldehyde, acetone, and acrolein) were divided into a sampling step and an analytical step. Two different methods were adopted to sample and analyze gaseous aromatic hydrocarbons and carbonyl compounds, respectively. Sampling pumps (TWA-300XB, XBX Inc. China) were portable and set at a constant air flow rate during the tests. They were correctly calibrated by gas flow meter (model 4045, TSI Inc., USA) with high accuracy. For the aromatic hydrocarbons (benzene, toluene, xylene, methylbenzene, styrene), the sample air was extracted through a stainless steel tube (PerkinElmer Inc., US) for 20 min at a fixed air flow rate of 200 mL/min. Tenax TA filled in the tube can adsorb aromatic hydrocarbons in the air. Before sampling, all the Tenax TA tubes were conditioned in helium for 2 h at 225 °C. For the carbonyl compounds (formaldehyde, acetaldehyde, acetone, and acrolein), the sample air was extracted through a silica cartridge (Anpel Inc., China) coated 2, 4-dinitrophenylhydrazine (DNPH) for 20 min at a fixed air flow rate of 400 mL/min. The DNPH would react with the carbonyl compounds in the sampling air. An ozone scrubber (Anpel Inc., China) was linked before the DNPH-silica cartridge to prevent the reaction of ambient ozone and DNPH.

The tests were usually conducted between 5 pm and 7 pm when the traffic was busy. During the field measurements, the test vehicles were driven at a constant speed as 30±5 km/h on the selected routes. Each test vehicle was driven at least 1.5 h on the roads. Testing and sampling procedures were detailed as follows: (1) Keeping all the windows opened, Online instruments would monitor outside pollutant concentrations and atmospheric parameters for 20 min and record every 2 min. The air samples were collected out of the window for 0.2 m, in high of driver's breath position. (2) Then close the windows and run the tests under three ventilation modes in turn. The air samples were collected in height of driver's breath position in the middle of the cabin. Online instruments would monitor in-cabin pollutant concentrations and atmospheric parameters.

1.3 Analysis

The ATD-GC/MS method was employed for identification and quantification of in-cabin concentrations of benzene, toluene, xylene, methylbenzene, and styrene in the study. The aromatic hydrocarbons adsorbed by Tenax TA were thermally desorbed by thermal desorber (TurboMatrix 350 ATD, Perkin-Elmer Inc., US). Quantification analyses were performed by gas chromatography-mass spectrometry (GC/MS, DSQ-II, Thermo Fisher, US).

The gas chromatograph (GC) capillary column model was DB-5MS (30m×0.25mm, Agilent Inc., US). The oven of the GC was programmed from 40 °C (holding time 3 min) to 60 °C at 2 °C/min and to 250 °C at 20 °C/min (holding time 3 min) . Data were acquired in electron impact mode (70 eV) by full scanning between 35 and 350 mass units.

High-performance liquid chromatography (HPLC) was employed to quantify in-cabin concentrations of formaldehyde, acetaldehyde, acetone, and acrolein. The sampled cartridges were eluted by 5.0mL acetonitrile (HPLC gradient grade, Sinoreagent Inc., China) and analyzed by HPLC (1200-DAD, Agilent Inc., US). The analytical conditions were as follows: Athena C18-WP column (3µm, 250×4.6 mm, CNW); gradient mobile phase: 0~20 min from 60% acetonitrile and 40% Milli-Q water; mobile-phase flow rate: 1.0mL/min; injection volume: 25 µL; detector: UV at 360nm.

Standard solutions are used to determine the concentrations of the VOCs. For the aromatic hydrocarbons, the original liquid standard (Catalog NO.: 120212-1, o2si smart solutions Inc., USA) was diluted by methanol (HPLC gradient grade, Sinoreagent Inc., China) to five grades. Same volume of the diluted standards would be injected directly into adsorbent bed in the Tenax TA tubes. These standard tubes would be analyzed as the same ATD-GC/MS method to the samples. To carbonyl compounds, the original liquid standard (Catalog NO.: 132520-03, o2si smart solutions Inc., USA) was diluted to five grades. The diluted standards would be injected directly into DNPH-silica bed in the cartridges. These standard cartridges would be eluted by 5.0mL acetonitrile (HPLC gradient grade, Sinoreagent Inc., China) and analyzed by HPLC method used for the field samples. The Standard solutions forced to pass through the origin were calculated from the test results with one replicate at each concentration.

Table 2. The equations and correlation coefficients (R^2) of standard curves for VOCs

Compounds	Standard Curve Equations	Correlation Coefficients(R^2)
Benzene	$y=48742x$	0.9974
Toluene	$y=107522x$	0.9994
Ethylbenzene	$y=140473x$	0.9999
P-xylene and M-xylene	$y=269184x$	0.99995
Styrene	$y=100715x$	0.99996
O-xylene	$y=150612x$	0.9998
Formaldehyde	$y=28.193x$	0.9977
Acetaldehyde	$y=20.937x$	0.9987
Acetone and Acrolein	$y=38.168x$	0.9980

2. Result and discussion

Table 3 presented the average concentrations of TVOC, VOCs, CO, CO₂, H₂S in all the tested vehicle cabins. It was obvious that toluene was the primary pollutants among the measured 9 VOCs inside vehicle cabins. As shown in the table, a broad range was found between the measured pollutants concentrations, which indicated that there was high variance under different conditions. The conditions included ventilation conditions, vehicle age, interior temperature and interior trims in the study.

Table 3.Summary of in-vehicle gaseous pollutant concentrations

Compounds		Min	Max	Ave	SD
	TVOC	257.85	961.89	612.25	188.92
	Benzene	7.76	48.58	16.73	7.45
	Toluene	6.64	250.23	66.02	62.00
Organic pollutants ($\mu\text{g}/\text{m}^3$)	Ethylbenzene	1.06	56.21	14.20	12.14
	Styrene	0.90	26.73	6.78	5.55
	Xylene	2.49	122.04	28.09	28.72
	Formaldehyde	8.42	29.82	16.43	4.95
	Acetaldehyde	5.83	22.89	12.47	4.49
	Acrolein,acetone	3.70	46.04	20.65	11.44
	CO (ppm)	0.10	2.10	1.20	0.53
	CO ₂ (ppm)	481.0	3659.0	1553.7	798.09
	H ₂ S (ppb)	1.00	25.00	5.04	2.58

2.1 Concentrations of TVOC, CO, CO₂, H₂S

In the test, the concentrations of TVOC, CO, CO₂, and H₂S were measured by online instruments logged every two minutes. As shown in Figure 2, highly variability of the concentrations of TVOC, H₂S, and CO₂ were presented during the 80min under different ventilation conditions (outside, fan off RC off, fan on RC off, and fan on RC on, respectively). The concentrations of CO measured in this study were constant, which was comparable with the previous study (Zhu et al., 2007). Change of TVOC concentrations was consistent with CO₂ and opposite with H₂S. During the roadway period, the concentrations of the TVOC and CO₂ were generally lowest level and remain stable. When the ventilation fan was off, little external air was brought into the in-cabin environment. Thus, the concentrations of TVOC and CO₂, rapidly increased to 614.54 $\mu\text{g}/\text{m}^3$ and 2756.7 ppm. Under ventilation condition (ii), the concentrations of TVOC and CO₂ decreased to 513.58 $\mu\text{g}/\text{m}^3$ and 650 ppm due to the air exchange with outside. Under condition (iii), the average concentrations of TVOC and CO₂ increased by 38.5% and 64.1%, respectively. On the contrary, the in-cabin H₂S concentration was maintained at a high level under roadway period and ventilation condition (ii). In-cabin CO₂ is generally considered by the body's metabolism emission. The origin of H₂S is emitted from the tailpipe. All the results indicated that the main sources of VOCs were from the inside vehicles, as well as CO₂, which was consistent with previous research that vehicle interiors, such as plastic moldings, upholstery, carpeting, adhesives, and lubricants, can emit VOCs (Chien, 2007).

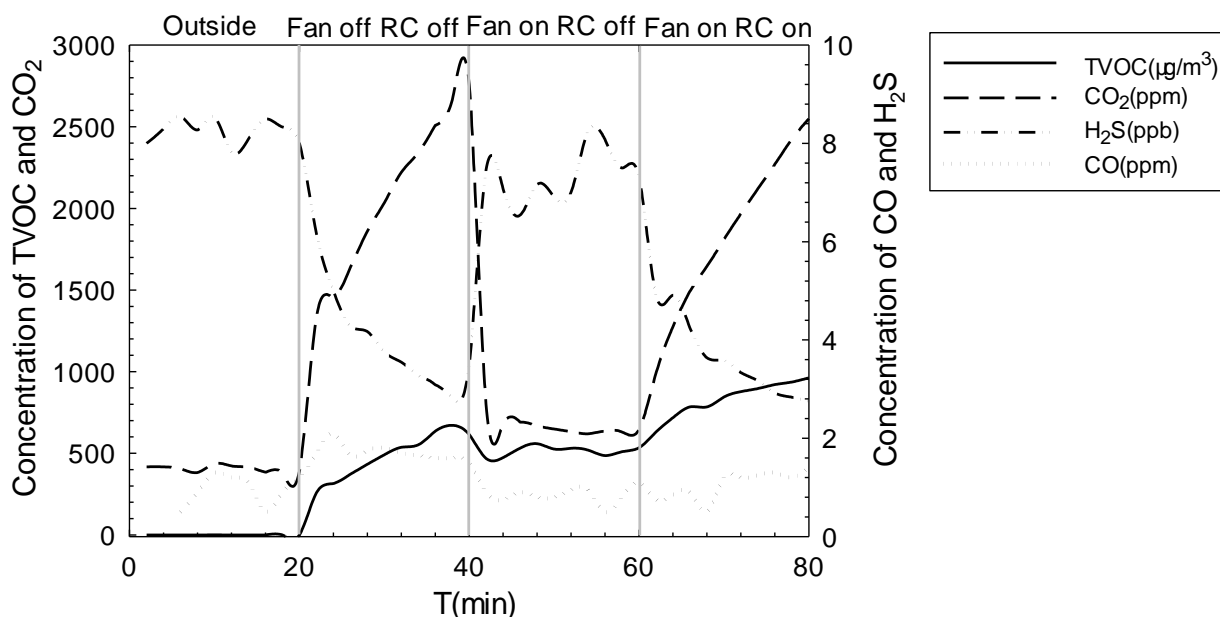


Figure 2. In-cabin concentrations of TVOC, H₂S, CO₂, and CO under different ventilation conditions.

2.2 Factors that affects the VOCs concentrations

Significant change of the VOCs concentrations under different ventilation conditions was found in this study. The mean concentrations of in-cabin benzene, toluene, xylene, methylbenzene, styrene, formaldehyde, acetaldehyde, acetone and acrolein were $16.73\mu\text{g}/\text{m}^3$, $66.02\mu\text{g}/\text{m}^3$, $14.20\mu\text{g}/\text{m}^3$, $6.78\mu\text{g}/\text{m}^3$, $28.09\mu\text{g}/\text{m}^3$, $16.43\mu\text{g}/\text{m}^3$, $12.47\mu\text{g}/\text{m}^3$, and $20.65\mu\text{g}/\text{m}^3$, respectively. Toluene was abundant among the measured VOCs, which was up to $85.32\mu\text{g}/\text{m}^3$. Compared with ventilation condition (ii), the VOCs concentrations were larger (up to 31.15%) than the concentration under ventilation condition (i) and (iii). In addition, the study also found that in-cabin VOC concentrations were twice larger than the ambient levels. All of them indicated that introducing outside air into vehicle cabin under condition (ii) lowered the in-cabin VOCs concentrations.

The study measured two vehicle models (Volkswagen Passat and Chevrolet Cruze). The materials decorated interiors in different vehicle models were different: leather and fabric. The result indicated that VOCs exposure inside vehicle cabins with higher fraction of leather is larger than vehicles with fabric interiors. The mean concentration of toluene measured inside new Passat vehicles (leather interiors) was $102.77\mu\text{g}/\text{m}^3$, which is 39.09% larger than the level in the new Cruze (fabric interiors).

Another factor that affected the in-cabin VOCs exposure was vehicle age. The concentrations of benzene, toluene, xylene, methylbenzene, formaldehyde, acetaldehyde, acetone and acrolein inside new vehicles were found 12.89%, 103.54%, 123.14%, 104.20%, 6.26%, 6.31%, and 10.67% larger than the concentrations inside old vehicles, respectively. Compared with old vehicles, the air tightness of vehicle envelop is sound and the air exchange

rate between in-cabin and outside is generally little in new vehicles. Besides, after a period of usage time, the VOCs emission rate continuously decreased due to the decreasing VOCs residual in the interior trims. As a result, the in-cabin VOCs levels were found lower for the old vehicles.

The study compared in-cabin VOC concentrations between four cities: Beijing, Shanghai, Chengdu, and Shenzhen under different ambient temperatures. Table 1 listed the geographical information of the four cities during the testing period. For most VOCs, the concentrations increased as a function of the increasing temperatures in the four cities. This was due to the fact that higher temperature led to more VOCs emissions from interior trims. Toluene, styrene, methylbenzene, and xylene were found as the most sensitive VOCs to the ambient temperature for all measurements. The concentrations of toluene, styrene, methylbenzene, and xylene increased 513.6%, 544.8%, 767.0%, and 597.7% as the ambient temperature increased from 11 °C to 25 °C, respectively. In addition, the ambient VOCs concentrations were measured and found much lower than the in-cabin concentrations, which means the ambient VOCs hardly affect the in-cabin VOC concentrations in different cities.

Conclusion

This study found that VOCs exposure inside vehicle cabins with higher fraction of leather is larger than vehicles with fabric interiors. The concentrations of measured VOCs inside new vehicles were found larger than the old vehicles. In addition, the concentrations of toluene, styrene, methylbenzene, and xylene increased 513.6%, 544.8%, 767.0%, and 597.7% as the ambient temperature increased from 11 °C to 25 °C, respectively. Therefore, in order to reduce in-cabin VOCs exposure, choosing a car with fabric interiors, decreasing ambient temperature and driving under ventilation condition (i) (fan off; RC off) or ventilation condition (iii) (fan on; RC on) is advisable.

Acknowledgments

This material is based on the work partially supported by the Fundamental Research Funds for the Central Universities (Grant NO. 2013KJ020) and Opening Project of Shanghai Key Laboratory of Atmospheric Particle Pollution and Prevention (LAP3) (Grant NO. FDLAP13001).

Reference

- Atsuko Araki, Toshio Kawai, Yoko Eitaki, Ayako Kanazawa, Kanehisa Morimoto, Kunio Nakayama, et al. (2010): Relationship between selected indoor volatile organic compounds, so-called microbial VOCs, and the prevalence of mucous membrane symptoms in single family homes. Science of the Total Environment, 408, 2208–2215.
- Chien Y.C (2007): Variations in amounts and potential sources of volatile organic chemicals in new cars. The Science of the total environment, 382, 228-239.
- Chien Y.C (2007): Variations in amounts and potential sources of volatile organic chemicals in new cars. Science of the Total Environment, 382; 228-239.
- Ministry of Environment Protection of the People's Republic of China(MEPC) (2012): Guideline for air quality assessment of passenger car. <http://www.zhb.gov.cn/>.
- Michael H. Abraham, Joelle M.R. Gola, J. Enrique Cometto-Muñiz (2016): An assessment of air quality reflecting the chemosensory irritation impact of mixtures of volatile organic compounds. Environment International, 86, 84-91.
- Otmar Geiss, Salvatore Tirendi, Josefa Barrero-Moreno, Dimitrios Kotzias (2009): Investigation of volatile organic compounds and phthalates present in the cabin air of used private cars. Environment International, 35; 1188-1195.
- Pei-Ling Leung, Roy M. Harrison (1999): Roadside and in-vehicle concentrations of monoaromatic hydrocarbons. Atmospheric Environment, 33; 191-204.
- P. Wolkoff, C. K. Wilkins, P. A. Clausen, G. D. Nielsen (2006): Organic compounds in office environments—sensory irritation, odor, measurements and the role of reactive chemistry. Indoor Air, 16: 7-19.
- Wallace L. (1996): Indoor particles: A review. Journal of the Air & Waste Management Association, 46, 98-126.
- Zhu Y, Eiguren-Fernandez A., Hinds W.C., Miguel A.H (2007): In-cabin commuter exposure to ultrafine particles on Los Angeles freeways. Environmental science & technology, 41, 2138-2145.

TOWARDS AN INTEGRATED TOOL OF A LIFE CYCLE ASSESSMENT FOR CONSTRUCTION OF ASPHALT PAVEMENTS IN EGYPT

Mohamed YOUNES¹, Yue HUANG², and Ibrahim HASHIM¹

¹Department of Civil Engineering, Menoufia University, Shebin El Kom, Menoufia, Egypt
Email: m.a.younes@ljamu.ac.uk, hashim1612@hotmail.com

²Department of Civil Engineering, Liverpool John Moores University, Liverpool, England, UK
Email: y.huang@ljamu.ac.uk

Abstract

The complexity of climate change and research on its causes and impacts has resulted in new developments and approaches to decrease the life-cycle greenhouse gas (GHG) emissions connected with construction and maintenance of roads. Tools and databases have developed by national agencies to facilitate the measurement using life-cycle approaches that account for acquisition and production of raw material, construction, use, maintenance, and end-of-life of roads. There are several tools established or commercialized for the performance of life cycle assessment (LCA) like SimaPro, GaBi, PaLATE, ROAD-RES, UK model, CHANGER, asPECT, Athena Impact Estimator for Highways, PAS 2050, and Umberto each of them special country specific. From abovementioned, Egypt do not have LCA tool to estimate emissions from construction of asphalt pavements, thus the paper highlights on UK model to take advantage from it, moreover to be a guide in creating LCA Tool. Therefore, the fundamental objective of this paper is to build up a tool to evaluate the life cycle inventory for construction of asphalt pavements in Egypt. The paper presents the methodology that will be followed for the development of an Egyptian LCA tool for construction of road pavements.

Key-words: road construction, life-cycle assessment, air pollutants, pavement, Egypt.

1. INTRODUCTION

The roads construction is continually seeking resolutions to increase construction efficiency, enhance pavement performance, protect resources and advance environmental protection. Because of the continuous increase in the population, economic and social development worldwide, it has become an urgent need for development and increase of road networks. Roads construction could cause negative environmental impacts and pollution effects of air, water and soil (Ghazy et al., 2016).

Egypt is one of the most populous countries in Africa and the Middle East. Because of the continuous increasing in population and Urban Development, there is a marked expansion in the construction of road networks. The road network in Egypt has a total length of 121.4 thousand km consists of 108.8 thousand km paved roads with percentage 90% and 12.6 thousand km unpaved roads with percentage 10% (ESCWA, 2015). All type of roads existed in the road network.

The construction of roads causes emissions and pollution to surrounding environment. The emissions occur during the raw materials extraction, manufacture and transportation, manufacturing and transportation of asphalt mix, as well as construction and maintenance processes. Therefore, towards an integrated tool to estimate the life cycle inventory for construction of asphalt pavements in Egypt is the main goal of this paper.

Life Cycle Assessment (LCA) is a tool for assessing the ecological impact of a product through every step of its life (cradle to grave) from the extraction of natural resources to the final disposal. For instance, five phases often considered in a pavement system (Santero, 2009). These include the acquisition and production of raw material, construction, use, maintenance, and end-of-life phases. In its 14040 series, publications the International Standards Organization (ISO, 2006) outlines four phases for execution an LCA encompass: 1) *goal and scope definition*; defining study goal, system boundaries, functional unit, and determine data collection method. 2) *Inventory analysis*; include all of the environmental inputs and outputs data associated with a product. 3) *Impact assessment*; is to convert and dividing the life cycle inventory (LCI) results into impact categories (e.g., global warming potential, acidification, and human toxicity) to understand their environmental significance. 4) *Interpretation* is the final phase to analyse results, reach conclusions, provide recommendations, identify analysis improvements, as well as aid in the decision-making operation. These four steps

illustrated in Figure 1. Based on the different system scopes and theory, LCA can be classified as *process LCA*, *input-output LCA* and *hybrid LCA* (Lenzena et al., 2003).

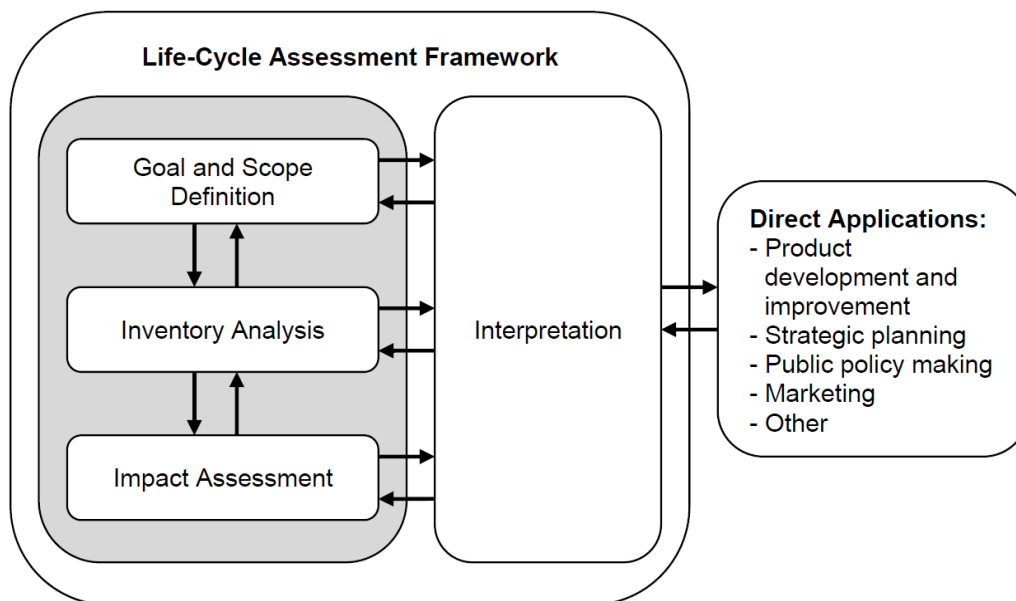


Figure 1. Basic LCA framework (ISO, 2006)

2. PAVEMENT LCA LITERATURE

Roads are responsible for more than 80% of the final energy used in Europe caused by transportation (European Commission, 2010). Moreover, energy use and emissions of GHG are in increasing trend within the transport sector while most of economy sectors have a decreasing trend (European Commission, 2010). Thus, measures need to take to decrease the environmental impact and energy demand in the transport sector. In addition, a considerable amount of energy used in construction and rehabilitation of the highway infrastructure can be saved by selecting road surface characteristics and road alignment that can reduce fuel consumption of vehicles (ECRPD 2010).

The area of pavement engineering had a number of LCA studies, with various LCA models proposed. In general, each model is partitioned into different modules, which carry disparate functionalities to contribute to the final results. A module, also named as part, component, phase, or stage in various LCA studies, is the unique term to represent the functional block of LCA model in this research. The specific modules in the LCA study vary greatly and have not reached consensus among the pavement community (Yu, 2013). Different practitioners disaggregate LCA models into different modules. For instance, Roudebush (1999) evaluated the environmental impacts of asphalt and concrete highway pavement systems by dividing the LCA model into ten modules, including: natural resource formation, exploration and extraction, material production, design, component production, construction, use, demolition, natural resource recycling, and disposal. Santero (2009) split the LCA model into five individual modules, including material, construction, use, maintenance, and end-of-life (EOL). Zhang et al. (2010) preferred to view the LCA model as six-fold, including material, construction, distribution, congestion, usage, and EOL modules.

Yu (2013) stated that a complete LCA model should consist of material, construction, maintenance, congestion, usage, and EOL modules. However, most LCA models are incomplete, with focus mainly on material and construction modules while ignoring others, especially the usage module. According to the findings from research that did incorporate usage module, it would dominate analysis results or at least is a counterpart to the material module (Häkkinen and Mäkelä 1996; Zhang et al. 2010; Santero 2009). Thus ignoring the usage module would also ignore a great portion of environmental burdens in LCA model (Yu, 2013).

As have been pointed out by Santero (2009), many of the so-called pavement LCAs are, strictly speaking, LCIs, meaning lack of impact assessment. Even without a further impact assessment step, LCIs follow the same process as performed by the LCA models, provide valuable data for further research, and will not be differentiated from LCA models in this review.

There are several previously LCA studies to evaluate the environmental impact of different road materials or road construction types for whole or specific life-cycle phases (Häkkinen and Mäkelä 1996; Horvath and Hendrickson 1998; Roudebush 1999; Berthiaume and Bourchard 1999; Mroueh et al., 2000; Striple 2001; Chappat and Bilal 2003; Treloar et al. 2004; Kendall 2004; Zapata and Gambatese 2005; Hoang et al. 2005; Athena 2006; Chan 2007; Weiland 2008; Huang et al. 2009; Weiland and Muench 2010; Zhang et al. 2010; ECRPD 2010; Gschosser et al. 2012; Yang 2014).

3. LCA TOOLS AND DATABASES

The European Commission site for the Joint Research Centre (JRC) contains a homepage with a list of a several LCA databases and tools, few of them are free to download. *SPINE@CPM* database is open source LCA database developed by the Swedish Life Cycle Centre, where data is transparent and quality reviewed (www.cpm.chalmers.se). These databases and tools is proper for LCA-studies of pavements and roads but no evaluation made on it (Carlson, 2011).

Some tools developed specifically intended at roads and pavements through recent years. In light of the consequence of their research, Mroueh et al. (2001) established an Excel program for road construction. It overlays all phases from raw material production to maintenance of road.

A model, called Road Model constructed by Striple (2001), was developed using Excel and focused largely on compiling a comprehensive inventory. Data collected for both material and construction processes, specific to the Swedish context. The entire life cycle analysed without impact assessment, and the use phase marginally considered traffic, as the inventory collection was the focus of the report.

Two of pavement LCA tools have been released in 2004 and 2005. The *Pavement Life cycle Assessment Tool for Environmental and Economic Effects* (PaLATE) is an open-source spreadsheet tool that covers the entire life cycle except for the use phase (Horvath, 2003). First released in 2004 by California University, Berkeley, the tool followed a hybrid LCA approach by supplementing primary and literature data with economic IO-LCA. In 2005, Birgisdóttir (2005) described an LCA software model based on Paradox database and C++ called ROAD-RES. Which can assess leaching impacts of waste residues in road construction. The LCI included data from Danish contractors and producers as well as European literature sources.

Hoang et al. (2005) developed LCA model called ERM/GRM (*Elementary Road Modulus/Global Road Modulus*) model. The extraction of raw material and EOL phases excluded from the model. The system boundaries include manufacturing and transportation of raw material to construction site. In addition, construction and maintenance tools.

LCA tool developed by Huang et al. (2009) based on spreadsheet in Excel excluding the use and EOL phases. A case study also investigated, that involved using recycled waste glass and Recycled Asphalt Pavement (RAP). It comprises of five spreadsheets for estimating and presenting results of the inventory. There are calculation formulas linked these spreadsheets. The tool designed to analyse pavements in the UK.

Zhang et al. (2010) detailed an LCA tool for pavement overlay systems that covered the entire life cycle, with special care to traffic delay, roughness, and the use of Engineered Cementitious Composites (ECC) in Portland Cement Concrete (PCC). Each of the three pavement types considered (asphalt, PCC, and PCC with ECC) given different distress indexes over time based on their maintenance schedules and predicted deterioration.

PAS 2050 tool was developed for calculating the GHG emissions of goods and services (BSI, 2011). It contains a methodology that can also be used in other areas, and it is used in wide rang in Europe and the UK (Sinden, 2009).

The asphalt Pavement Embodied Carbon Tool (asPECT) was first released in 2010 to calculate the carbon footprint of asphalt pavements (TRL, 2010). The asPECT tool calculates GHG emissions for all phases of the life cycle, specially dealing with asphaltic material processes and thus omitting the use phase.

CHANGER (*Calculator for Harmonised Assessment and Normalisation of Greenhouse gas Emissions for Roads*) first released in November 2009. It was developed by International Road Federation (IRF) in Geneva. It enables calculation of emissions of roads construction activities. Its database covers a comprehensive range of construction processes and materials, including impacts from (pre-construction, on-site, materials, and machinery) (Huang et al., 2013).

Athena released the Athena Impact Estimator for Highways software in 2013, which is currently the most developed and accessible pavement LCA tool (Athena, 2013). The entire life cycle accounted for, including impacts from fuel consumption in the use phase due to stiffness and roughness of the pavement surface layer. The inventory is proprietary and includes collected data relevant to the North American region.

Gabi (GaBi, 2013) and SimaPro (SimaPro, 2013) are the most prominent LCA software packages. These programs evaluate the environmental impact of certain products or processes from cradle to grave.

4. DEVELOPMENT OF EGYPTIAN LCA TOOL (EGY-LCA TOOL)

From abovementioned, Egypt do not have LCA tool to estimate emissions from roads construction, EGY-LCA Tool must include roads life cycle, and be devised to permit input and output of Egyptian LCI database for the relevant phases of this life cycle. Moreover, allow comparison between alternatives is necessary, and to display the results of analyses. The research will study UK model (Huang's model) to take advantage from it, furthermore to be a guide in creating EGY-LCA Tool. EGY-LCA Tool should have these inputs to developed; fuel efficiency and transport distance, energy consumption of each processes, materials recipe, pavement dimension, and the materials tonnage in the project.

Huang's LCA model based on spreadsheet in Excel consists of five worksheets as shown in Figure 2. These worksheets are used for calculation and graphical presentation of inventory results in this model and linked by calculation formulas. 'Process parameters' and 'Pavement parameters' worksheets contain specific project data. 'Unit inventory' worksheet is made of calculating formulas and the LCI for each unit process. 'Project inventory' worksheet presented the LCI results for the overall pavement project. 'Characterisation results' worksheet presented the inventory results after classification and characterisation for impact assessment. The framework of the LCA model followed the ISO14040 standards.

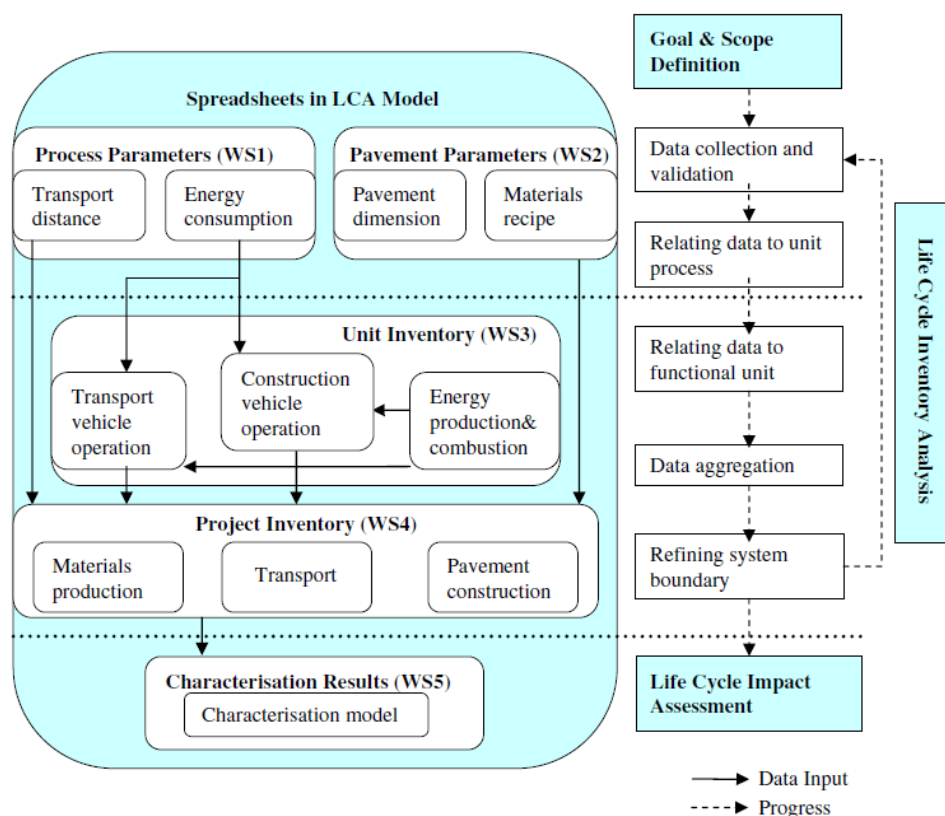


Figure 2. Overview of the Huang's model (Huang et al., 2009).

In order to achieve the research objectives, a research methodology is set consisting of the following phases:

Phase One: Developing of EGY-LCA Tool: LCA model cannot be implemented directly from one country to another because of different construction systems, pavement materials, and the validity and applicability of data. Therefore, a new EGY-LCA Tool will be generated, based on Huang's model (Huang, 2007). This model was established in accordance with the ISO14044. Firstly, this model will be applied and tested on a real pavement in the UK, as a case study. The primary sources of process data comes from the UK plants and contractors, as well as other LCA literature. Secondly, the results will be compared with other software's results to validate the model. Finally, this model will be implemented in Egypt after developing a national LCI database.

Phase Two: Developing of Egyptian National LCI Database: includes the collection of quantitative data on the inputs and outputs of materials, energy and transportation associated with a product over its entire life cycle so that its whole-life environmental impacts can be determined.

This stage will be done by doing field surveys in Egyptian agencies of Energy and Environmental studies and performing questionnaires with pavement engineers General Authority for Roads, Bridges & Land Transport (GARBLT), and factories that manufacture the mainly pavement construction materials in Egypt.

Phase Three: Applying the Data in EGY-LCA Tool: The collected data from the second phase will be the input data of the new Egyptian tool as a web-based tool. Figure 3 shows the suggested framework of EGY-LCA Tool to calculate emissions from roads construction in Egypt.

Phase Four: Verification and Validation of the Egyptian Tool: This phase concern with applying the tool after finishing the modelling in roads construction in Egypt, as a case study.

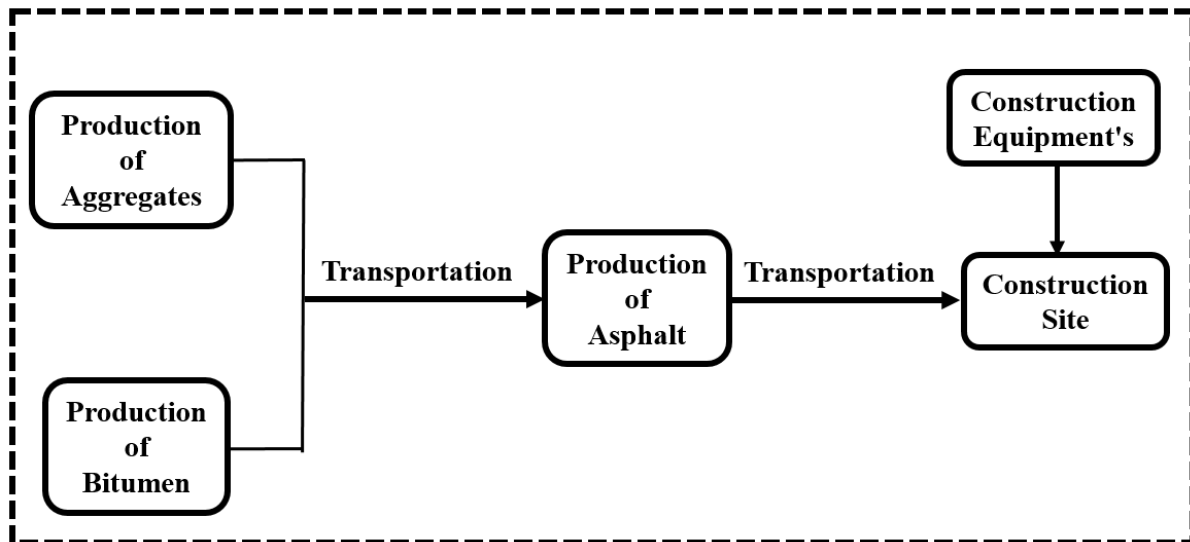


Figure 3. Suggested framework of EGY-LCA Tool: Construction phase

5. CONCLUSION

LCA tools became significant for assessing the environmental impact of materials and products. The ISO 14040 series outlines how to execute an official LCA in which the materials production, construction, use, maintenance, and EOL of road construction, beside illustration of resources consumption and released emissions. These results are useful to road designers, site engineers, contractors, and government interested in expecting environmental impacts during pavement's life.

The findings of this research will help to bind air pollution measurements from traffic to life cycle modelling of construction in order to undertake transport-related air pollution assessment.

The review can summarize that calculation of emissions and energy consumption from pavement construction in Egypt from LCA view is more difficult because Egypt does not have any LCA tool/program to estimate emissions from road construction. EGY-LCA Tool must include a road's life cycle, and be devised to permit input and output of Egyptian LCI database for the relevant stages of this life cycle. The findings from this review study can be used to standardize the study of life cycle assessment concept in Egypt because it has a lack of LCA studies and to put the base of Egyptian tool framework EGY-LCA Tool to build more cleanly environment from air emissions.

FURTHER WORK

Simulation software will be used to measure the environmental impacts of road maintenance works and the disrupted traffic on it. The simulation results will be fed into a traffic emissions model. The emissions from road works and the distributed traffic will be compared.

ACKNOWLEDGEMENTS

The first author want to express gratitude toward Ministry of Higher Education in Egypt (MoHE) for affording the financial support (PhD scholarship) for this research in addition to the Liverpool John Moores University for presenting the required tools and facilities to execute this work.

REFERENCES

- Athena Institute, (2006). *A Life Cycle Perspective on Concrete and Asphalt Roadways: Embodied Primary Energy and Global Warming Potential*. Prepared for the Cement Association of Canada.
- Athena Institute, (2013). *Athena Impact Estimator for Highways [Software]*. Ottawa, Canada.
- Berthiaume, R., and Bouchard, C. (1999). *Exergy Analysis of the Environmental Impact of Paving Material Manufacture*. Transactions of the Canadian Society for Mechanical Engineering. Vol. 23, No. 1B, pp. 187-196.
- Birgisdottir, H. (2005). *Life cycle assessment model for road construction and use of residues from waste incineration*. PhD thesis, Institute of environment & Resources, Technical University of Denmark, Kgs Lyngby, Denmark.
- BSI, (2010) PD 6691: *guidance on the use of BS EN 13108 bituminous mixtures material specifications*. British Standards Institution, London.
- Carlson, A. (2011). *Life cycle assessment of roads and pavements – Studies made in Europe*. MIRIAM project, VTI rapport 736A, The Swedish Transport Administration.
- Chan, A.W.C. (2007). *Economic and Environmental Evaluations of Life Cycle Cost Analysis Practice: A Case Study of Michigan DOT Pavement Projects*. Master of Science Thesis in Natural Resource and Environment, University of Michigan.
- Chappat, M., and Bilal, J. (2003). *The Environmental Road of the Future, Life Cycle Analysis*. Report from COLAS Group, 40p.
- ECRPD (2010). Energy conservation in road pavement design, maintenance and utilisation, Intelligent Energy Europe, www.roadtechnology.se/ecrpd.eu/.
- ESCWA (2015). *Promoting Energy Efficiency Investments for Climate Change Mitigation and Sustainable Development case study EGYPT*. United Nations.
- European Commission (2010). EU energy and transport in figures, Statistical pocketbook 2010.
- GaBi (2013). *GaBi v6. PE International*. Retrieved August 10, 2013. <http://www.gabi-software.com/solutions/life-cycleassessment/>.
- Ghazy, M.R., Abdallah A.M., Basiouny, M.A., & Saad, M.A.S. (2016). *Life Cycle Assessment of Flexible Pavement Construction*. British Journal of Applied Science & Technology. 12(1): 1-17, Article no.BJAST.20620. ISSN: 2231-0843, NLM ID: 101664541.
- Gschösser, F., Wallbaum, H., & Boesch, M.E, (2012). *Life cycle assessment of the production of Swiss road materials*. Journal of Materials in Civil Engineering, ASCE, 24(2), 168–176.
- Häkkinen, T., and Mäkelä, K. (1996). *Environmental adaption of concrete environmental impact of concrete and asphalt pavements*. Technical research center of Finland. Research Notes 1752.
- Hoang, T., Jullien, A. & Ventura, A. (2005). *A global methodology for sustainable road – Application to the environmental assessment of French highway*. 10DBMC International Conference on Durability of Building Materials and Components, Lyon.
- Horvath, A. (2003). *Pavement Life-cycle Assessment Tool for Environmental and Economic Effects (PaLATE) [Software]*. Consortium on Green Design and Manufacturing, University of California, Berkeley.
- Horvath, A., and Hendrickson, C. (1998). *Comparison of Environmental Implications of Asphalt and Steel-Reinforced Concrete Pavements*. Transportation Research Record. Vol. 1626, pp. 105-113.

- Huang, Y. (2007). *Life Cycle Assessment of Use of Recycled Materials in Asphalt Pavements*. PhD Thesis, School of Civil Engineering and Geosciences. Newcastle upon Tyne, Newcastle University.
- Huang, Y., Bird, R., & Heidrich, O. (2009). *Development of a life cycle assessment tool for construction and maintenance of asphalt pavements*. Journal of Cleaner Production, Volume 17, Issue 2, pp. 283-296.
- Huang, Y., Hakim, B., & Zammataro S. (2013). *Measuring the carbon footprint of road construction using CHANGER*. International Journal of Pavement Engineering, Vol. 14, No. 6, 590–600, <http://dx.doi.org/10.1080/10298436.2012.693180>.
- International Organization for Standardization (2006). *Environmental Management - Life Cycle Assessment - Principles and Framework*. ISO 14040:2006(E). International Organization for Standardization: Geneva, Switzerland.
- Kendall, A. (2004). *A dynamic Life Cycle Assessment Tool for Comparing Bridge Deck Designs*. Master thesis, University of Michigan.
- Lenzena, M.S.A., Murray, S.A., Kortec, B., & Deya, C.J. (2003). *Environmental impact assessment including indirect effects – A case study using input– output analysis*. Environ. Impact Assess. Rev., vol. 23, no. 3, pp. 263–282.
- Mroueh, U.M., Eskola, P., & Laine-Ylijoki, J. (2001). *Life-cycle impacts of the use of industrial by-products in road and earth construction*. Waste Management 21 (2001) 271–277.
- Mroueh, U.M., Eskola, P., Laine-Ylijoki, J., Wellman, K., Mäkelä, E., Juvankoski, M., & Ruotoistenmäki, A. (2000). *Life cycle assessment of road construction*. Finnish National Road Administration. Finnra Reports 17/2000.
- Roudebush, W.H. (1999). *Environmental Value Engineering (EVE) Assessment of Concrete and Asphalt Pavement*. Portland Cement Association. PCA R&D Serial No. 2088a.
- Santero, N.J. (2009). *Pavements and the Environment: A life Cycle Assessment Approach*. PhD dissertation, University of California, Berkeley.
- SimaPro (2013). *SimaPro 7.3 LCA tool. PRe-sustainability*. Retrieved August 10, 2013. <http://www.pre-sustainability.com/SimaPro-lca-software>.
- Sinden, G. (2009). *The contribution of PAS 2050 to the evolution of international greenhouse gas emission standards*. Int J Life Cycle Assess 14:195–203.
- Stripple, H. (2001). *Life Cycle Assessment of Road: A Pilot Study for Inventory Analysis (Second Revised Edition)*. Swedish National Road Administration. IVL B 1210 E.
- Transport Research Laboratory (TRL) (2010). *asphalt Pavement Embodied Carbon Tool (asPECT) [Software]*. Version 3.0.04. United Kingdom.
- Treloar, G.J., Love, P.E.D., & Crawford, R.H. (2004). *Hybrid Life-Cycle Inventory for Road Construction and Use*. Journal of Construction Engineering and Management. Vol. 130, No. 1, pp. 43-49.
- Weiland, C., and Muench, S.T. (2010). *Life-cycle assessment of reconstruction options for interstate highway pavement in Seattle*. Washington, Transportation Research Record, pp. 18–27.
- Weiland, Craig D. (2008). *Life cycle assessment of Portland cement concrete interstate highway rehabilitation and replacement*. Master thesis, Civil Engineering, University of Washington.
- Yang, R. (2014). *Development of a Pavement Life Cycle Assessment Tool Utilizing 16 Regional Data and Introducing an Asphalt Binder Model*. M.S. thesis. University of Illinois at Urbana-Champaign, Champaign, IL.
- Yu, Bin. (2013). *Environmental Implications of Pavements: A Life Cycle View*. University of South Florida. Graduate Theses and Dissertations. <http://scholarcommons.usf.edu/etd/4619>.
- Zapata, P., and Gambatese, J.A. (2005). *Energy Consumption of Asphalt and Reinforced Concrete Pavement Materials and Construction*. Journal of Infrastructure Systems. Vol. 11, No. 1, pp. 9-20.
- Zhang, H., Lepech, M.D., Keoleian, G.A., Qian, S., & Li, V.C. (2010). *Dynamic life-cycle modelling of pavement overlay systems: capturing the impacts of users, construction, and roadway deterioration*. Journal of Infrastructure Systems, 16(December), 299–309.

Evaluation of emissions and fuel consumption of Heavy-Duty Vehicles in urban areas

Giorgio ZAMBONI* & Michel ANDRÉ**

*Internal Combustion Engines Group (ICEG) – Department of Mechanical, Energy, Management and Transportation Engineering (DIME) - University of Genoa, via Montallegro 1, 16145, Genoa, Italy
email:giorgio.zamboni@unige.it

**French Institute of Science and Technology for Transport, Spatial Planning, Development and Networks (IFSTTAR) – Laboratory Transports and Environment (LTE), Cité des Mobilités, Case 24, 69675, Bron Cedex, France

Abstract

An investigation referred to the city of Genoa was made jointly by ICEG - University of Genoa and the Transports and Environmental Laboratory - IFSTTAR, aiming at the definition of specific information on heavy-duty vehicle (HDV) activities in urban and port zones. Circulating fleet, mileage and speed patterns were assessed, in order to evaluate pollutant emissions and energy consumption of different vehicle classes.

Several issues were considered within the study. Firstly, HDV flows entering and leaving the urban area at the different highway exits and the relevant share involved in port operations were evaluated. Then, typical trips connecting the highway exits to the port gates and the relevant HDV mission profile within selected port terminals were identified, followed by an experimental campaign focused on the acquisition of instantaneous speed related to these trips and the selection of the most representative speed patterns. Finally, an instantaneous model (Passenger car and Heavy duty Emission Model, PHEM) was applied to the experimental speed profiles to estimate fuel consumption and emission factors for selected HDV classes. It was therefore possible to deepen the influence of urban trips and port activities on the environmental impact of HDV traffic flows, outlining peculiar aspects.

As a further step of the study, taking into account the outcomes of previous analysis, a comparison between pollution from different fleets of heavy-duty vehicles circulating in Genoa (HDV involved in commercial and shipping activities, public transport buses, waste collection vehicles, etc.) was developed. This allowed identifying the most interesting ones for dedicated measures aiming at emissions reduction through suitable transport actions.

Keys-words: Heavy-Duty Vehicles, Urban driving mode, Port activities, Exhaust emissions, Fuel consumption

Résumé

Une expérimentation a été menée conjointement par ICEG - Université de Gênes, Italie et le laboratoire Transports et Environnement de l'IFSTTAR, France, en vue de caractériser la circulation et la pollution des véhicules lourds en zones urbaines et de desserte portuaire de la ville de Gênes en Italie.

Le parc automobile, les kilométrages et vitesses de circulation ont été caractérisés. On a ainsi considéré les flux de camions accédant à l'agglomération via les différentes entrées et sorties du réseau autoroutier, et la part de ce trafic à destination de la zone portuaire. Des trajets représentatifs ont été identifiés ainsi que des profils de manœuvre et activités dans les terminaux du port. L'instrumentation de véhicules a permis l'enregistrement et la sélection de profils de vitesses représentatifs, utilisés ensuite pour la détermination des consommations et émissions de polluants de véhicules types grâce au modèle d'émission instantané PHEM (Passenger car and Heavy duty Emission Model, PHEM). Les trafics urbains et activités portuaires des véhicules lourds peuvent ainsi être analysés en détail.

L'analyse est ensuite étendue aux autres catégories de véhicules lourds circulant dans la ville de Gênes : camions de livraison, autobus urbains, collecte des déchets, etc., permettant d'anticiper les mesures de réduction des émissions les plus pertinentes.

Mots-clefs: Camions, véhicules lourds, circulation urbaine, activités portuaires, émissions de polluants atmosphériques, consommation, carburant

Introduction

Most large urban agglomerations record today important air pollution levels, and the road traffic is one of the main contributors to this pollution. According to different simulations conducted in Nantes and Paris big areas, the heavy duty vehicles (HDVs) traffic (buses and trucks, etc.) could account for 40-50% of the road traffic NO_x emission and about 20-40% of the PM (André et al. 2015, Carteret et al. 2014), while they would represent only 7-8% of the total road traffic.

In cities with a significant industrial activity and an important traffic of heavy vehicles, it can be expected that their influence on the environment would be really significant. Cities with a maritime port - such as Genoa, Italy - record also important air pollution, due to the shipping activity but also to the road (and rail) traffic connected to the port.

However, the traffic of heavy-duty vehicles in urban areas and its influence on the air pollution is weakly known and rarely investigated, while the characterization of the vehicles, their activities and driving conditions, would be necessary to have an accurate idea of their environmental impact. Furthermore, operations and working conditions in port areas, with several loading and unloading maneuvers and very low driving speeds are not at all investigated, while they are badly approached by the current tools for emissions estimation, although they could result in significant local emissions.

The objective of this work was an in-depth investigation of the heavy-duty vehicles traffic in a maritime city (Genoa), for characterizing the vehicles fleets, their operations and driving speeds, while focusing on both urban- and port-related activities.

1. Methodologies

Three main categories of trucks and buses were analyzed in different investigations referred to the city of Genoa. Waste collection trucks (Capobianco et al. 2005), buses for public transport (Zamboni et al. 2009) and heavy-duty vehicles having port terminals as Origin-Destination area (Zamboni et al. 2013 and 2015). Being the most recent and extended study and due to the relevance of the developed methodology, more details will be given on the activities of HDVs in port area and the relevant environmental impact and energy consumption.

The methodology consists in the following main steps: 0- characterization of the heavy-vehicles fleet; 1- identification of the main itineraries from the highway network to the city and to the port areas, 2- selection of representative trips, 3- instrumentation of vehicles and monitoring of the driving conditions, 4- development of speed patterns representing the urban driving and HDVs operation in the port areas, 5- calculation of fuel consumption and emissions associated to the representative speed profiles, 6- evaluation of the pollutant emissions from other heavy vehicles categories and comparison between the different truck classes.

Highway network in Genoa

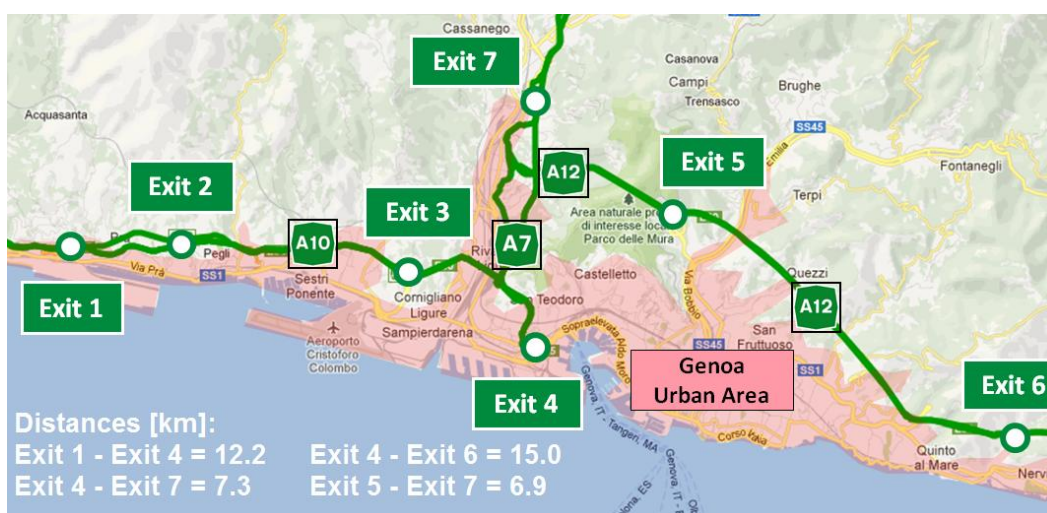


Figure1.Highway exits in Genoa urban area.

The city of Genoa is located in the north-western part of Italy. Densely populated residential areas and industrial/commercial zones can be identified, being mainly distributed on a 30 km long and

narrow coastal plain and along two valleys, characterized by a perpendicular direction referring to the coastline. Genoa represents an important node of the northern Italy highway network. Four different motorways (A7, A10, A12 and A26) start to link France, northern and central regions. Seven exits are distributed in the whole urban area, reflecting the city structure, as shown in Fig.1.

The evaluation of vehicle flows entering and leaving the urban area from the seven exits can be made considering average daily flows calculated on a yearly basis by the Highways Society. Flows are classified according to the five different categories implementing the toll collection system. Vehicles with two axles belong to A and B classes, being differentiated according to the heights on the front axle. The number of axles identifies classes 3, 4 and 5, including trucks and specific vehicles (cars with trailers, coaches, etc.), whose number is generally negligible. Through a survey within the Truckers' Association, it was possible to estimate the distribution of heavy-duty vehicles involved in port activities between the three classes (3, 4 and 5-axles), as discussed in the dedicated section.

Selection of port accesses

The development of the urban layout and road network is deeply related to port and shipping activities. This is proved by the number of accesses to the port and its terminals located in Genoa urban area (more than twenty), involving an extension of about fifteen kilometers of the city coastal zone. Data from the Genoa Port Authority on vehicle flows allowed to identify five main gates. The first one (Goods Terminal 1, GT1) is located in the western part of the city and is interested by HDVs traffic. Its link to the highway network is Exit 1 (Fig.2), which is mainly dedicated to truck activities.



Figure2.GT1 link to Exit 1.



Figure3.GT3 link to Exit 4.

Four main port gates are located near the city center, leading to major interactions between vehicles entering/exiting the port area, other highway flows and urban mobility and to a significant contribution to air pollution. Exit 4 is their connection to the highway network (Fig.3). Two gates (Goods Terminal 2 and 3) are involved in HDV flows. The third access (GT4) is an intermodal gate (road/railway). The last one is a Ferry Terminal (FT) access, where traffic flows of different vehicle categories are observed, with high peak of cars in the summer period.

Taking into account the relevant daily number of vehicles, investigations were focused on terminals GT1 and GT3, also aiming at a sound evaluation of HDV activities.

HDV working cycle in port terminals and experimental assessment of the relevant driving speed patterns

The typical activity performed in selected terminals GT1 and GT3 is identified as Lift-on/Lift-off (LoLo). After its access to the terminal, a reach stacker or a port/ship crane unloaded the container from the truck and loaded it with another one. These operations can be made in the same or in different locations, while the number of containers can vary according to their lengths.

The different operations performed inside urban and port areas are identified following the scheme presented in Fig.4, including all the phases from the highway exit to the port terminal, inside it and back to the highway entrance. A short description is provided for each operation, together with the driving mode or the association to a different “macro-activity” within the terminals. Four macro-activities were identified, in order to evaluate the most polluting and fuel consuming phases in each terminal: entrance (Get in and P1), terminal internal movement (P2, T1 and P3), unload/load (LM1 and LM2) and exit (P4 and Get out). Processing of the measured speed patterns allowed to define the number of unload/load phases and of the transition movements, taking into account the most frequent set of these specific operations.

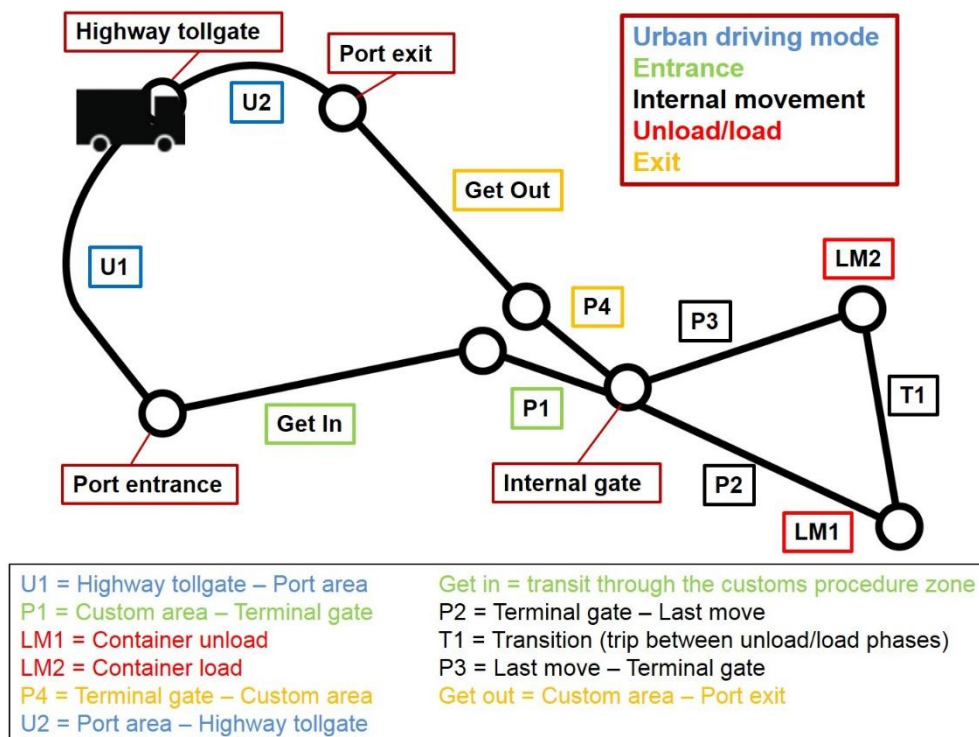


Figure4.HDV activities (highway exit – port terminal – highway entrance).

In a first step, characteristics and duration of each working phase were defined according to a survey among transport and logistics companies involved in port activities, presented in Zamboni et al. (2013). An experimental validation of the average drivers perception was then performed, measuring instantaneous speed inside Goods Terminal 1 and 3, including the different phases within the port area and their urban connections to highway exits (1 and 4, respectively). Different HDVs were therefore equipped with a Global Positioning System (GPS) and a data logger. Data processing was divided in three steps:

1. Validation of each acquisition. Check of the number of tuned GPS satellites and verification of the

correct position of speed trace on a map of the port area.

2. Detection of working cycle phases. On the base of the geographical position (latitude and longitude) of the internal gate and other significant locations of the port terminal, each activity was identified in the speed pattern.
3. Definition of the representative speed profiles for each terminal and phase considered.

In the second step, several kinematic parameters were computed (average speed and acceleration, travelled distance, etc.). Stop duration also represented a key parameter for phase detection, in particular for unload and load operations. In the third step, a statistical procedure was applied to the whole set of data for a given phase, identifying the most representative curves in terms of speed and acceleration distribution. These speed patterns were given in input to the PHEM model (Passenger car and Heavy duty Emission Model) to calculate the associated exhaust emissions and fuel consumption for a wide range of HDV classes.

Calculation of HDV fuel consumption and exhaust emissions in urban and port areas

Different approaches can be followed to evaluate road vehicle fuel consumption and exhaust emissions, taking into account average speed, as in Copert, or traffic situations, as in HBEFA. Functions applied in these models cover an extended range of traffic conditions, but don't include very low speed levels (typically below 6 or 10 km/h), which were measured in specific phases of the HDVs working cycle in port terminals depicted in Fig.4. Therefore, the Passenger car and Heavy duty Emission Model (PHEM) was selected for the calculation of fuel consumption and pollutant emissions on the base of speed traces resulting from the experimental campaign and the relevant processing procedure previously described. More details on PHEM structure and HDVs database, including data for 118 trucks belonging to classes from EURO 0 to EURO 5, are given in Hausberger et al. (2010).

Calculations were made considering vehicles with different weights (16, 26, 30 and 44 t), selected taking into account the most frequent truck classes involved in port activities (Fig.6) and different Euro standards. For Euro 5 vehicles, two further classes are available in PHEM, according to the fitted NO_x control systems (EGR/SCR catalyst). Instantaneous profiles for fuel consumption (FC) and different pollutants (NO_x, NO₂, HC, CO, PM and PN) were obtained, allowing to derive FC and emission factors or the overall values associated to the macro-activities defined in Fig.4.

Public transport buses

Different investigations were developed in the past aiming at the evaluation of exhaust pollutants emitted by road vehicles circulating in the urban area of Genoa, presented in Capobianco and Zamboni (2003) and Zamboni et al. (2009). Eight vehicle categories were defined (spark ignition and Diesel passenger cars and light duty vehicles, heavy duty commercial vehicles, buses, motorcycles and mopeds), further split in classes with reference to various parameters (i.e., legislation class, engine displacement, combustion system, vehicle reference weight, year of production, 2 or 4 stroke engine, etc.). As regards buses, data supplied by the local transport company were considered for both fleet composition and mileage. As buses proved to travel distances about ten times the average level of other vehicle categories, on a yearly base, their contribution to the total mileage in Genoa urban area was not negligible. Moreover, taking into account their NO_x and PM emission factors, the corresponding share of total emissions were significant, as presented in Tab.2.

Data on fleet composition and mileage were recently updated in order to check overall trends, mainly referring to official statistics of the local transport company, usually defined on a yearly base. In recent years, a decreasing number of circulating vehicles and total travelled distances were apparent (Fig.13), while the fleet renewal was strongly limited, due to the economic crisis and to specific financial problems supported by the company.

Waste collection vehicles

Within the overall category including Heavy-Duty vehicles, trucks for waste collection and other related services represent a particular case, since their use is quite different from the typical road vehicles mission. The evaluation of fuel consumption and pollutants emission during the working time with engine running at part load conditions, while the vehicle is stationary, is a difficult task. As they may represent a significant share of the total emission and the pollution effect is concentrated, it may be worth to be assessed or considered (Fontaras et al. 2012, Karavalakis et al. 2013).

A first study referring to the city of Genoa was presented in Capobianco et al. (2005), focusing on the definition of exhaust emission factors for the waste collection vehicles fleet managed by the local company, taking into account the specific mission profiles to perform the requested services (waste collection, transportation and disposal, container cleaning, streets cleaning and auxiliary). Different classification criteria were firstly applied based on the fleet characteristics, aiming at the identification of suitable vehicle classes according to their mass, UN-ECE category, emission standard, fuel and service. Then, the calculation of the exhaust emissions for each vehicle was based on a two terms equation, the first related to the daily vehicle travel, the second to the daily equipment use. The first contribution was evaluated with a conventional approach, considering different sources for the relevant emission factors and deriving information on the travelled distances from the company database. The second term was estimated taking into account the average daily use of the specific working equipment (always derived from the company information service) and a mean vehicle speed representing the equipment use in terms of engine operating conditions. Suitable emission factors were applied for this phase, estimated from the results of an experimental study on buses and waste collection trucks (Callera et al., 2003), whose real stationary working time was simulated through periods at constant vehicle speed.

A computational code was then set up for the evaluation of the daily pollutants emission for the whole fleet and each required service. Available results were processed to define the distribution of total emissions between the different vehicles categories and classes, to calculate the waste fleet contribution to the overall pollution due to road transport in Genoa urban area and to estimate the effects of the fleet renewal.

Following that investigation, an update of the overall contribution of the waste collection fleet working in Genoa should be performed, taking also into account the statistics on urban waste production (Fig.13).

2. Results

The different steps of the activities allowed defining quantitative information on several aspects of HDV activities in urban and port contexts. Traffic flows and classification of commercial vehicles according to type, mass and legislation phase were firstly assessed. Representative speed patterns of commercial vehicles involved in port operations were derived through an experimental campaign. Their input in PHEM allowed the estimation of fuel consumption and exhaust emissions of selected truck classes. Finally, a comparison between pollution from different fleets of heavy-duty vehicles circulating in Genoa (HDVs involved in commercial and shipping activities, public transport buses, waste collection vehicles) was developed. This allowed identifying the most interesting ones for dedicated measures aiming at emissions reduction through suitable transport actions. The most important results of the different investigation steps are presented and discussed in the following subsections.

HDV flows in Genoa (highway exits, urban road network and port area)

Data collected from the different sources previously described were processed in order to assess HDV flows from highway exits and their relevant share involved in port activities. Referring to average daily traffic flows and to HDVs belonging to highway classes 3, 4 and 5, Fig.5 presents the overall number of trucks passing through the seven highway exits located in Genoa urban area, exits 1 and 4 and port accesses for selected years between 2002 and 2015. The relevant share of vehicles having the port as Origin – Destination area are also shown.

An increasing trend is apparent for highway flows between 2002 and 2010. A slight rise can also be observed in port flows between 2002 and 2008, while figure for 2010 is very close to the previous level. Consequently, ratios between port and exits flows show decreasing tendencies, especially for the comparison with exits 1 and 4. In recent years, a significant growth in port activities is outlined by Port Authorities' statistics, with the number of vehicles going over the 3000 threshold. On the other hand, a slight reduction of highway flows is shown in Fig.5. Therefore, the relevance of port terminals as Origin – Destination area for trucks is grown. Most of HDVs passing through exits 1 and 4 in 2014 and 2015 were involved in port activities, while their share against the total flows was around 58%.

As a reference, it should be taken into account that registered vehicles in Genoa at the end of 2014 were 4091, considering trucks and trailers of the same highway classes.

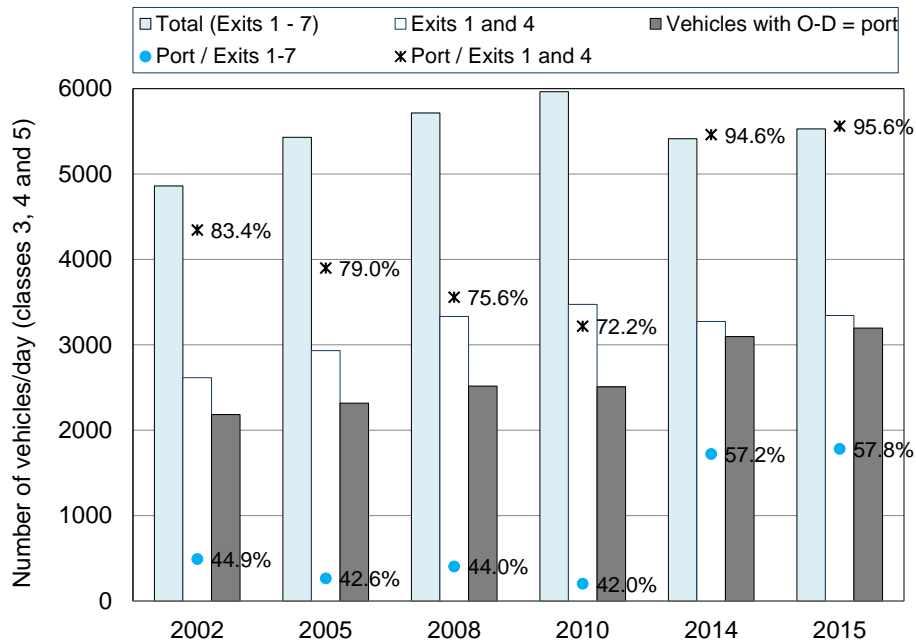


Figure 5. Comparison between average daily flows of HDV through highway exits and port accesses in different years.

A further result of this step is related to the classification of vehicles circulating within the port area. To this aim, a survey within the Truckers' Association allowed to estimate the share of HDV groups referring to vehicle type (rigid trucks, RT, or truck trailers, TT, and articulated trucks, AT), mass range and number of axles. As shown in Fig. 6, fleet involved in port activities mainly belongs to 4 and 5-axle classes, with a full load mass over 28 t. The overall figure for these classes is 70%, with a higher contribution from trailers and articulated trucks (56%) and a lower figure (14%) of rigid trucks. Trailers and articulated trucks in 14 ÷ 28 t classes cover most (24%) of the remaining share. As contribution from shorter and lighter classes is lower, neglecting class B values when processing highway flows appears to be a correct assumption.

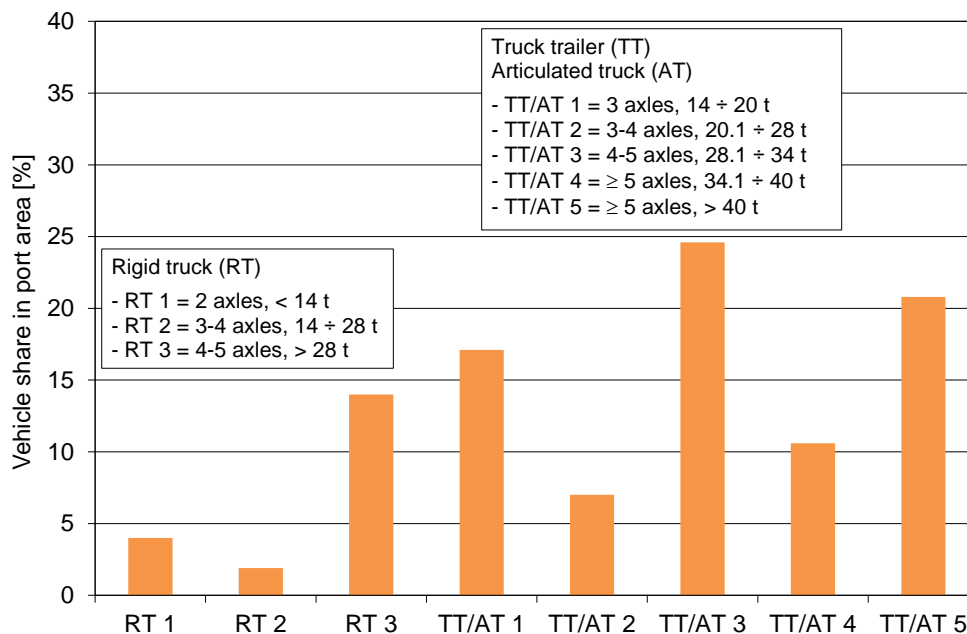


Figure 6. Main HDV classes circulating in Genoa port area.

Taking into account the classification shown in Fig. 6 and considering the distribution of registered trucks and road tractors in Italy (data from the National Register Office available in ACI (2016), referred to 31/12/2014) according to the legislation phases on exhaust emissions, the corresponding

allocation of HDVs involved in port activities was estimated. The resulting distribution is shown in Fig.7. Even under the strong assumption that the circulating fleet is represented by the registrations, it is interesting to outline that most of the trucks belongs to Euro 3 and Euro 5 classes, while older vehicles represent a significant share (around one third). The negligible number of Euro 6 trucks is probably due to the limited period available for the fleet renewal. One should add that the general economic situation did not support a quick promotion of the less polluting vehicles.

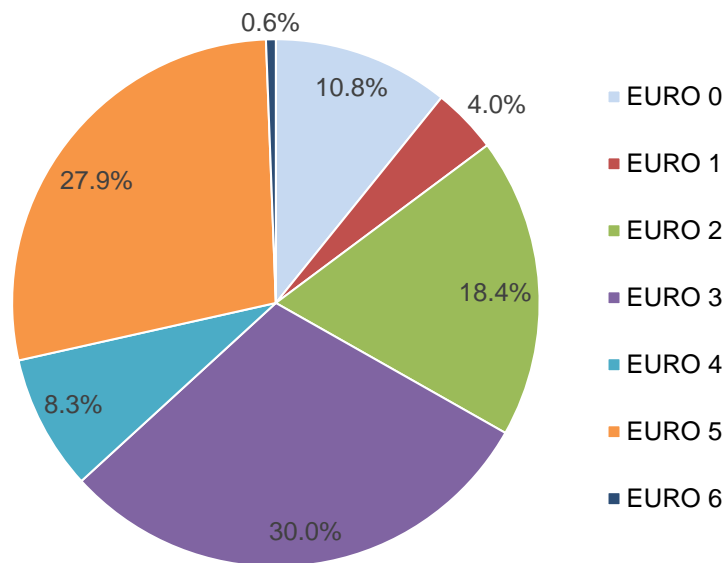


Figure7. Distribution of HDVs circulating in Genoa port area according to legislation phases on exhaust emissions (Reference: total registered trucks and road tractors in Italy, December 2014).

Kinematic characteristics of HDV in port and urban areas

Speed profiles obtained by the application of the statistical procedure previously described (presented in Fig.8) allowed to estimate a number of significant kinematic parameters, whose values are presented in Table 1, referring to each macro-activity and to the complete driving pattern. Levels referred to urban trips U1 and U2 are also shown.

Terminal or Driving mode	Macro-activities	Duration	Distance	Average speed	Running speed	Stop duration
		[s]	[km]	[km/h]	[km/h]	[%]
Goods Terminal 1	Entrance	2002	0.74	1.3	12.6	89.5
	Internal movement	1271	5.42	15.3	19.0	19.1
	Exit	762	0.37	1.8	15.4	88.6
	Unload/load	1270	0.02	0.1	-	-
	Overall	5305	6.55	4.4	17.4	74.5
Goods Terminal 3	Entrance	1736	1.80	3.7	16.8	77.8
	Internal movement	520	1.16	8.1	9.1	11.9
	Exit	283	0.77	9.7	13.2	26.5
	Unload/load	1445	0.09	0.2	-	-
	Overall	3984	3.82	3.5	10.8	68.1
U1		232	1.6	22.6	24.7	8.4
U2		150	1.4	33.2	34.8	4.7

Table 1 – Main characteristics of representative speed patterns for selected terminals and urban trips.

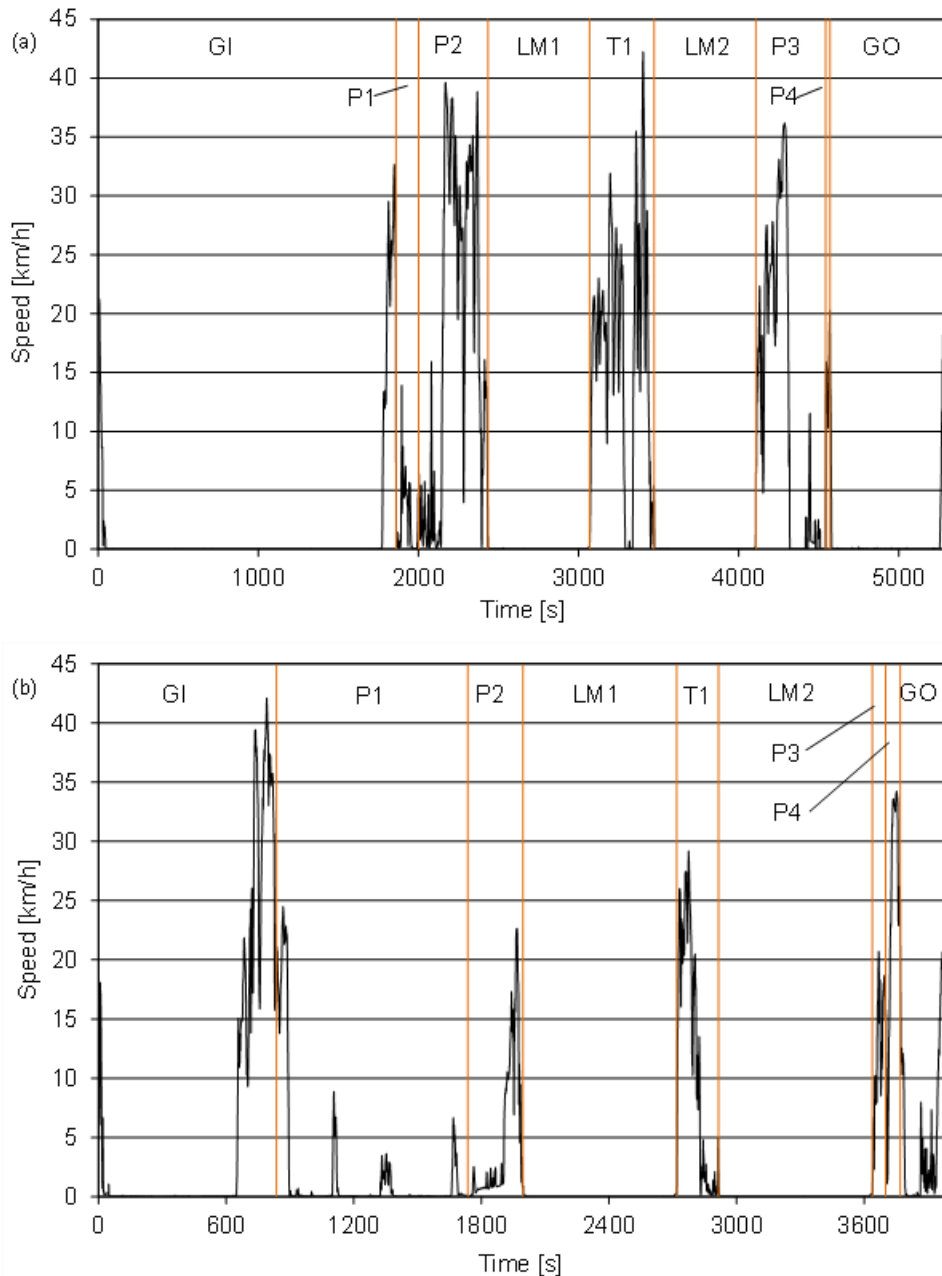


Figure 8. Representative speed traces for Terminal 1 (a) and 3 (b) (Zamboni et al. 2015).

Comparing terminals 1 and 3, durations and travelled distances are different, mainly due to the wider extension of the last move area in GT1, outlined by the corresponding distance for the internal movement phase. In both cases, overall average speed values are very low, due to the peculiar mission profile and driving behavior within the port area. Different aspects influenced this result: the number of circulating vehicles, speed limits in the working areas and the engine operation in idling mode during the customs procedure and the unload/load phases. Consequently, stop duration represents a major share of each pattern.

In order to quantify driving dynamics for each terminal, other parameters can be considered, i.e., relative positive acceleration (RPA), as defined in Sileghem et al. (2014) and number of stops for kilometers. As discussed in Zamboni et al. (2015), GT3 presents a higher dynamics, as its representative speed profile is associated to higher values of RPA and stops number. On the other hand, urban speed profiles show lower RPA levels and dynamics.

Referring to macro-activities, similar behavior between the terminals can be identified for entrance (i.e., transit through the zone for customs procedure) and unload/load phases.

Finally, the comparison of kinematic characteristics between port speed profiles and urban driving

mode trips shows strong differences, which will be confirmed by the relevant fuel consumption and emission factors.

Macro-activities contribution to fuel consumption and emissions

As presented in methodologies section, phases of working cycles were grouped in four macro-activities, namely entrance, internal movements, unload/load and exit (Table 1). Fuel consumption and exhaust emissions, calculated by PHEM with a time base of one second, were summed-up according to the macro-activities, in order to estimate their share. FC, NO_x and PM emissions in terminals 1 and 3 are shown in Figs.9 and 10, referring to a Euro 3 TT/AT with a mass over 40 t and to a Euro 5 TT/AT with a mass within 28.1 and 34 t, respectively.

As far as Gross Terminal 1 is concerned, highest contributions are due to internal movements, mainly due to the distance travelled within the involved phases (P2, T1 and P3, around 83% of the total trip length in GT1). On the other hand, entrance provides around 25% in fuel consumption and emissions, due to the long extension in time.

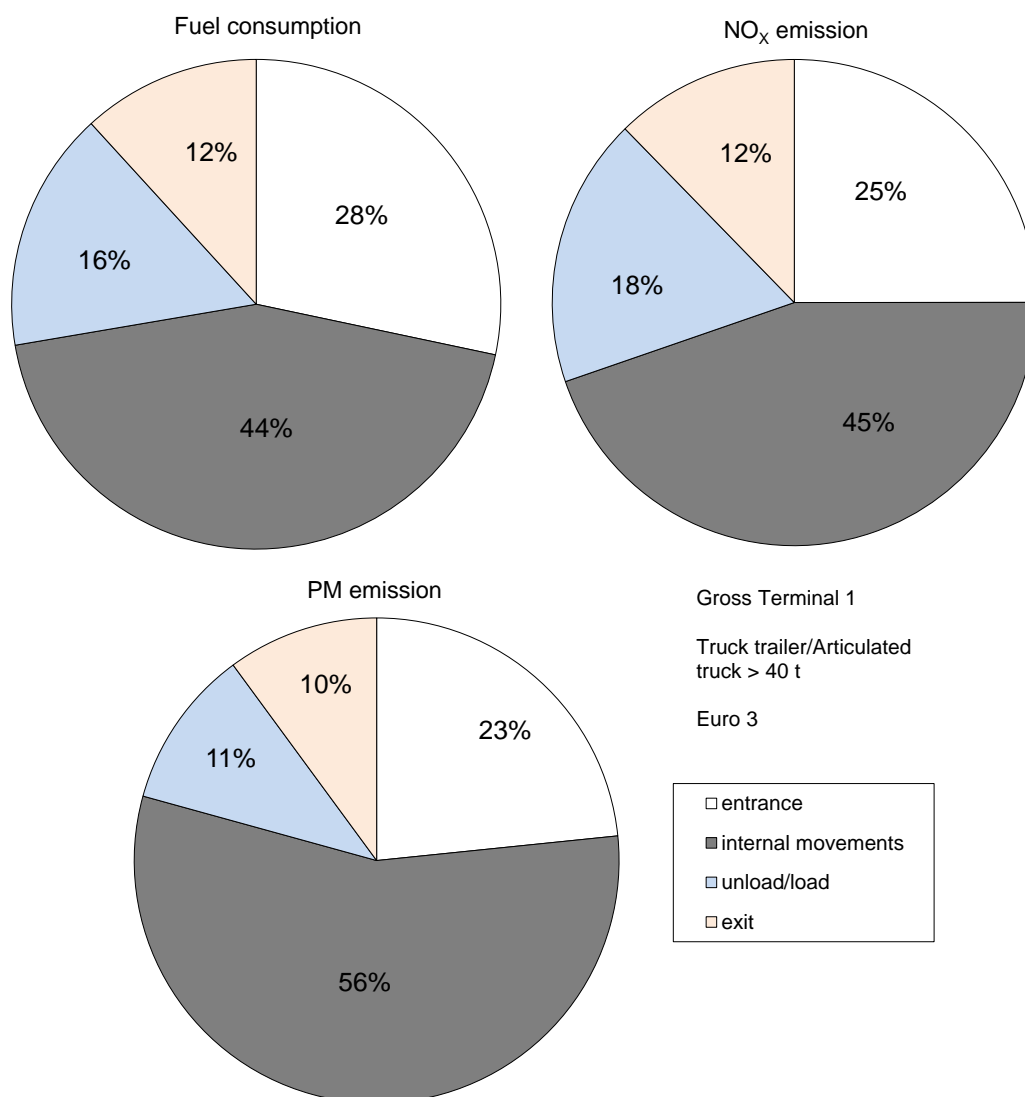


Figure9. Contribution of macro-activities to fuel consumption and emissions in Terminal 1.

For a similar reason, the entrance is the most fuel consuming and polluting activity for Gross Terminal 3. In this case, share of FC, NO_x and PM emissions are very close, with the travelled distances in phases GI and P1 accounting for a similar figure, about 47% of the total length (Tab.1). On the other hand, internal movements cover around 30% of the total distance, but their contribution to fuel consumption and emissions is lower, probably due to a limited dynamics of speed profile, as this

phase shows a low stop duration and close levels of average and running speed.

The contributions of unload/load phases, with engine in idling mode, are around 15% for GT1 and 20% for GT3, with a higher percentage for NO_x and a lower one for PM. These quantities correspond to what may be avoided if the engine would be switched off within these operations.

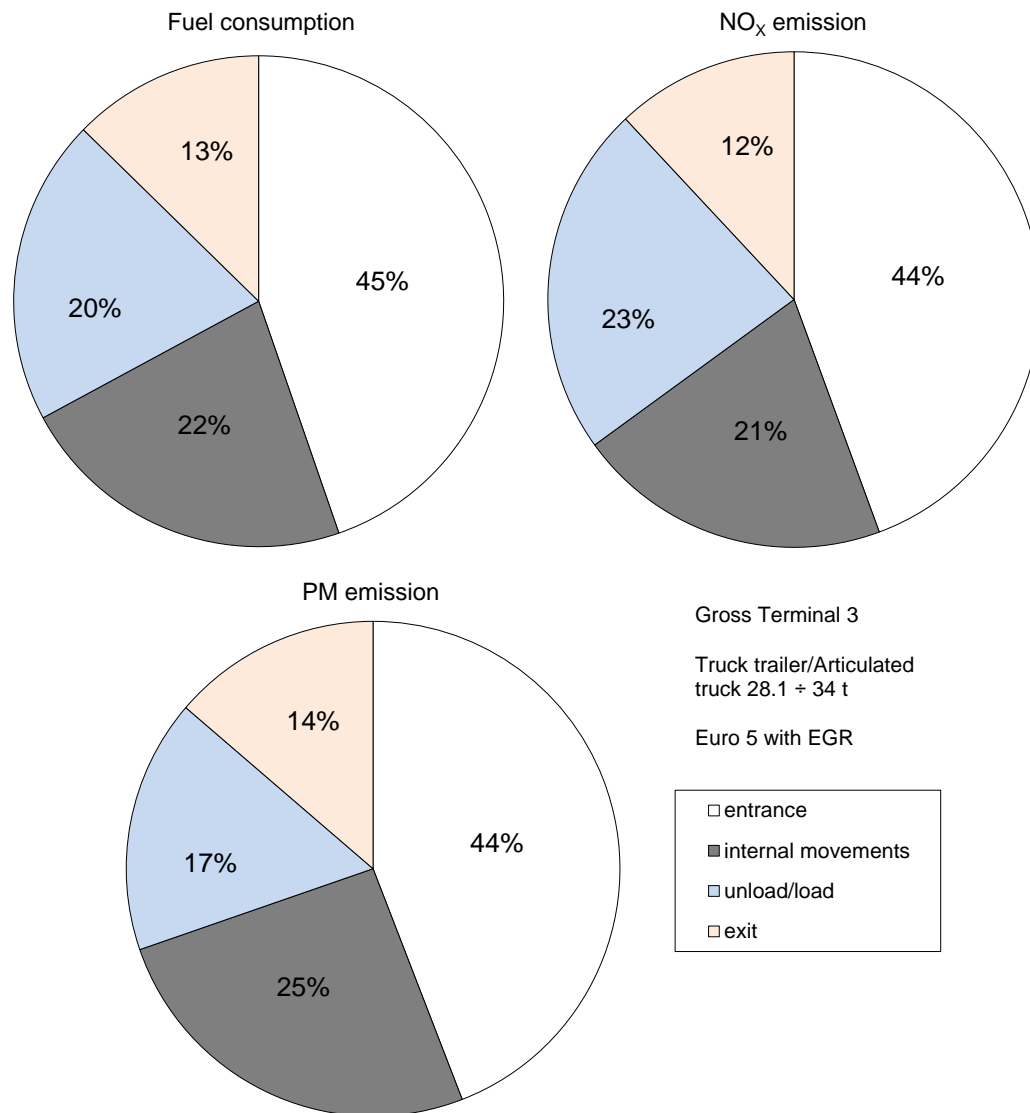


Figure 10. Contribution of macro-activities to fuel consumption and emissions in Terminal 3.

Evaluation of HDV fuel consumption and exhaust emissions in port terminals and urban areas

Outputs from PHEM allowed to calculate factors for fuel consumption and exhaust emissions referring to driving profiles in port terminals and in urban mode.

Figures 11÷13 present FC, NO_x and PM emission factors for Euro 3 and Euro 5 vehicles belonging to three mass classes (i.e., 14 ÷ 20, 28.1 ÷ 34, > 40 t). As previously outlined, Euro 5 trucks are further divided on the base of the NO_x control device (SCR system or EGR circuit). In each figure, a reference value is also shown, in order to compare calculated levels with data related to the assessment of emission inventories. To this aim, average fuel consumption and factors for NO_x and PM emitted quantities were obtained from the National Agency for the Environment Protection website (ISPRA, 2016), referring to the urban driving mode for the Italian HDV fleet in 2013.

As far as fuel consumption is concerned (Fig. 11), levels decrease for reduced vehicle weight when considering data for a given terminal, while lower figures are generally observed for Euro 5 trucks. Higher fuel consumption were calculated for each vehicle class circulating in terminal 3. This result can be related to the stronger dynamics of the relevant speed pattern.

When comparing FC levels in port areas and in urban driving mode, strong differences are apparent, with factors ranging between 1.9 and 4.3 (GT1/urban) or 2.8 and 5.8 (GT3/urban). Higher variations are commonly found for Euro 3 vehicles in both cases, followed by Euro 5 trucks with SCR. These results are related to the significant differences in corresponding vehicle speed and dynamics between urban and terminal driving conditions (Tab.1). On the other hand, reference value is comparable with calculated levels for urban conditions, being therefore much lower than factors for port activities.

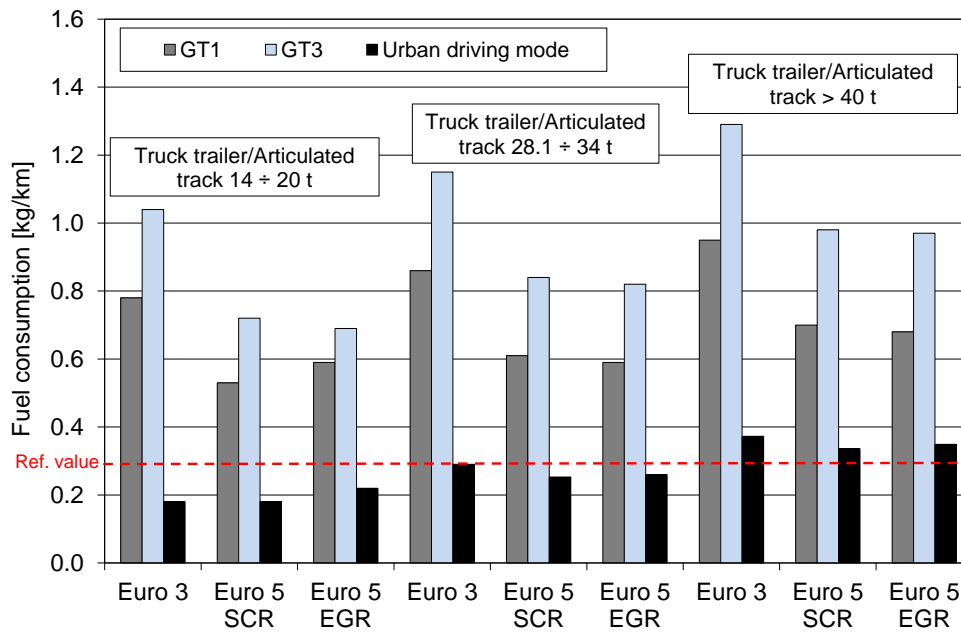


Figure11. Fuel consumption in urban and port areas for different HDV classes.

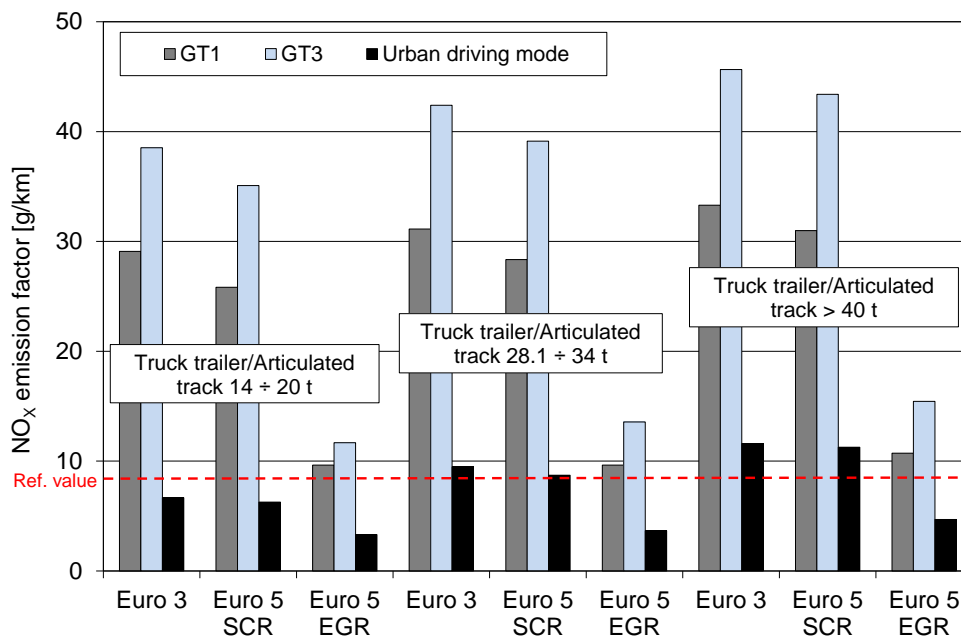


Figure12.NO_x emission factors in urban and port areas for different HDV classes.

The influence of vehicle mass and terminal on NO_x emission factors (Fig.12) is similar to that outlined for FC. On the other hand, comparing emission levels for Euro 5 trucks fitted with SCR systems or EGR circuits, a negative situation is apparent for the first type, probably related to low levels of exhaust temperature at reduced speeds, leading to inadequate values of SCR conversion efficiency, as shown in Guan et al. (2014). As a result, NO_xemission factors are only slightly below Euro 3 HDV emissions.

Port and urban driving conditions lead again to strong differences, with a ratio between 2.3 and 4.4 (GT1/urban) or 3.3 and 5.8 (GT3/urban). In this case, Euro 3 vehicles and Euro 5 trucks with SCR show higher and similar ratios. Reference value is in line with calculated levels for urban conditions for Euro 3 and Euro 5 trucks with SCR, but also for Euro 5 vehicles with EGR in port terminals, therefore showing a significant difference in urban mode for this class. Consequently, high levels of NO_x for Euro 5 vehicles fitted with SCR systems were also assessed in urban mode.

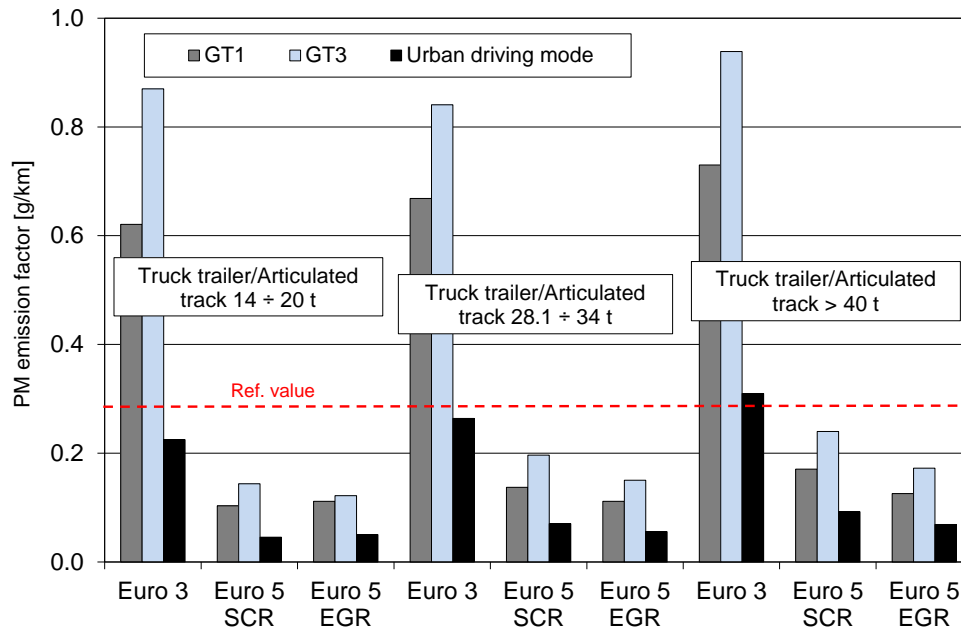


Figure 13. PM emission factors in urban and port areas for different HDV classes.

Considering PM emission factors (Fig.13) similar trends can be generally observed referring to vehicle mass and terminal. A strong reduction is apparent between Euro 3 and Euro 5 vehicles, with only slight differences between the two Euro 5 technological options.

For this pollutant, ratios between port and urban driving conditions factors are included in a range between 1.8 and 2.8 (GT1/urban) or 2.4 and 3.9 (GT3/urban). Euro 3 vehicles show the highest increase, while similar ratios were computed for Euro 5 trucks fitted with either of the NO_x control systems. Finally, reference value is generally above the calculated PM emission factors, except for Euro 3 trucks working in port terminals.

Comparison of exhaust emissions from HDVs and overall circulating fleets

In order to make a first assessment of the importance of heavy-duty vehicles involved in different activities, calculated values from previous investigations (Capobianco et al., 2005; Zamboni et al., 2009) referred to the Genoa urban area were processed, while historical trends of indicators for significant transport activities were defined, for the same geographical zone.

Year	Type of vehicles	Share of the total travelled distance/emissions [%]		
		Mileage	NO _x	PM
2000	HDVs	4.1	30.7	26.3
	Buses	1.9	25.2	11.1
2004	Waste collection trucks	0.4	3.5	1.7
2010	HDVs	4.5	40.0	33.2
	Buses	1.9	25.1	9.8

Table 2 – Contribution of the considered vehicles to the overall values in Genoa urban area (data from Capobianco et al., 2005; Zamboni et al., 2009).

Table 2 presents the first group of data with reference to different years, i.e., 2000 and 2010 for HDVs and buses, 2004 for waste collection trucks. It is apparent that contribution of HDVs and buses to NO_x and PM emissions was always significant in past years, notwithstanding the limited share for mileage. Moreover, an increasing trend is apparent if comparing 2000 and 2010 levels. This result is due to the relevant average emission factors, higher than those of other vehicle categories, as shown in Zamboni et al.(2009).

On the other hand, contribution from trucks for waste collection is limited, mainly due to the very low mileage, even if it is confirmed that the contribution to emissions is larger in percentage. In this case, the equipment use in the different working phase was also accounted, according to the procedure described in Capobianco et al. (2005), giving a further contribution to emitted pollutants.

Referring to transport indicators, six parameters were selected in order to outline their historical trends, always referred to the city of Genoa. These are the total number of registered vehicles, the statistics on gasoline and diesel fuel sales, the average number of container entering and exiting the port area, the total mass of waste collected (ISPRA, 2010 and ISPRA, 2014), truck flows in highway exits 1 and 4 and the urban mileage of buses of local transport company (AMT, 2016). Numbers of registered vehicles include passenger cars, light and heavy-duty vehicles, buses and motorcycles and were obtained from the National Register Office (ACI 2016). Fuel sales are referred to the use in road transport sector and are available from the energy statistics of the Italian Ministry of Economic Development (2016).

Data were normalized considering 2005 values as reference. Calculated levels are presented in Fig.14. Even if some values are missing, three different behaviors can be identified in recent years: while buses mileage and fuel market decreased (even if with a turnaround in 2014 for fuel), vehicle fleet and waste collection show a value close to 1, highlighting a nearly constant trend. Finally, HDV flows at selected highway exits and, in particular, port traffic are characterized by a significant increase, above 10 and 30%, respectively.

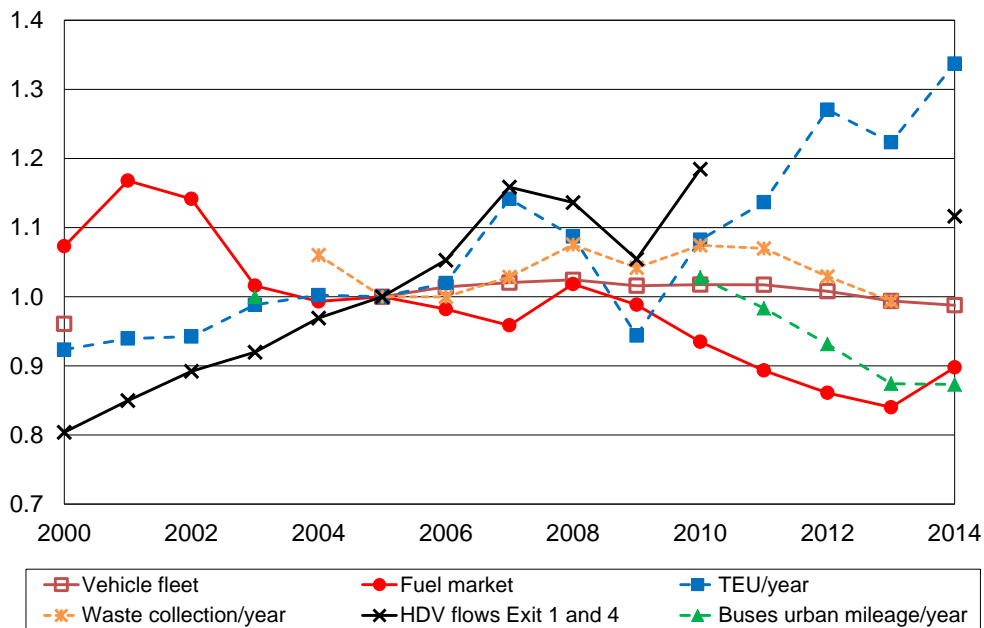


Figure 14. Trends of different transport activities indexes in Genoa.

Taking into account the contribution of HDVs to emissions (Tab.2) and calculated values of transport indexes (Fig.14), it can be concluded that measures to reduce pollution should be mainly focused on trucks involved in port activities, as their number and share are increasing (Fig.5). A better evaluation of their contribution have to be made, considering a more realistic classification of vehicles according to the legislation on emissions and applying fuel consumption and emission factors (such as those presented in Figs.11÷13) derived from the investigation on port terminals for the whole set of vehicle classes. On the other hand, updated values of overall circulating fleet, referring to private and public mobility and specific vehicles, should be estimated, in order to allow a more reliable evaluation of energy consumption and emissions due to road transport and the distribution between the different

vehicle categories.

Conclusion

European cities involved in industrial, commercial and/or shipping activities are interested by significant flows of heavy-duty vehicles, whose energy consumption and environmental impact have to be carefully evaluate in order to apply effective actions for air pollution reduction in the short, medium and long term. To this aim, a range of suitable measures are available, such as the deployment of alternative fuels, the adoption of ITS solutions, the application of multimodal transport schemes and the development of new infrastructures. Due to their different costs and complexity, a reliable assessment of the initial situation and the benefits deriving from each action are mandatory for a careful selection of the measures with the highest potential for air quality enhancement and energy consumption reduction.

Therefore, investigations on trucks operation in urban and port areas looks important, in order not only to characterize vehicle fleet, their activities and driving conditions, but also to define proper methodologies for data collection and validation. Furthermore, the comparison of contribution to exhaust emissions from HDVs involved in different tasks can help in identifying the best target of the above-mentioned actions.

The first result of the investigation developed jointly by the Internal Combustion Engines Group (ICEG) of the University of Genoa and the Transports and Environmental Laboratory (LTE) of IFSTTAR is the methodological approach to define HDV port and urban activities, designed and focused in co-operation with national and local entities (Italian Highways Society, Genoa Port Authority and Truckers' Association). The assessment of the total traffic flows through the highways network and the relevant share entering and exiting the port terminals, the classification of vehicles according to their type, mass and legislation class, the definition of working cycle within the port terminals are the preliminary phases requested for a general evaluation of the issue importance while giving it a correct framing. The experimental definition of the driving conditions in urban areas connecting highway exits and port accesses and in terminals, the development of a suitable statistical procedure for their processing aiming at the selection of representative speed profiles and their application in PHEM to calculate fuel consumption and exhaust emissions of different truck classes are the most innovative steps, taking into account the peculiar mission profile, characterized by specific maneuvers and very low driving speeds.

This approach allowed defining a wide database on trucks circulating in Genoa urban areas and involved in port activities, referring to their flows, classes, driving characteristics, fuel consumption and emissions factors. Results demonstrate that fuel consumption and emissions in the port areas constitutes a very significant share (ranging between 80–90% of total calculated values considering representative speed profiles, depending on vehicle class and technology), while their contribution in the urban area remain more limited (10–20%). Therefore, this share cannot be neglected for a reliable assessment of energy and emission inventories, while its evaluation has to be carefully developed due to the peculiar kinematic behavior, showing low speed levels and extended periods in idling mode.

Other studies on public transport buses and waste collection trucks allowed to assess the relevant emissions and to compare the different contribution of HDV fleets. Taking into account an analysis of transport indicators, historical trends prove that trucks involved in port activities are one of the main source of pollution, requiring suitable solutions for the reduction of their impact.

Finally, the presented statistics demonstrate that heavy duty vehicles contribute to a large extent to the local pollution due to road traffic (around 65% of the NO_x emissions and 43% of PM in 2010), despite their limited share in the total travelled distance (slight below 7%) of the overall vehicle fleet circulating in Genoa urban area.

Acknowledgments

Authors would like to thank Italian Highways Society for the availability of updated information on traffic flows at the toll gates in Genoa urban area.

References

André M. & E. Brutti-Mairesse (2015): Évaluation de l'impact d'un PDU : problématique de l'émission de polluants atmosphériques. *Rech. Transp. Secur.*, 2015, pp 121-133,

doi:10.4074/S0761898015002058.

- Callera G., F. Alberici&S. Florio (2003): Determinazione Sperimentale delle Emissioni allo Scarico di Motori Diesel di Mezzi Adibiti al Trasporto Pubblico ed al Servizio di Raccolta RSU ed Estensione Relativa all'Uso di Biodiesel, Rapporto Finale Studio Regione Emilia Romagna, (in Italian).
- Capobianco M. & G. Zamboni (2003): PROGRESS: a Computer Programme for Road Vehicles Emissions Evaluation. Proc. 6th International Conference on "Engines for Automobile" (ICE2003), paper SAE-NA 2003-01-61, Capri, Italy, 14-19 September 2003, doi: 10.13140/2.1.2544.4648.
- Capobianco M., M. Cerulli, P. Cinquetti& G. Zamboni (2005): Exhaust Emissions from a Waste Collection Vehicles Fleet: a Case Study. Proc. 7th International Conference on "Engines for Automobile" (ICE2005), SAE Paper 2005-24-023, Capri, Italy, 11-16 September 2005.
- Carteret M., M. André& A. Pasquier (2014): Observation des parcs automobiles en circulation et évaluation de l'impact de mesures de restriction d'accès sur les émissions de polluants. ProjetPrimequalZaParC. (in French) Rapport IFSTTAR LTE, Bron (France). 150p.
- Fontaras G., G. Martini, U. Manfredi, A. Marotta, A. Krasenbrink, F. Maffioletti, R. Terenghi& M. Colombo (2012): Assessment of on-road emissions of four Euro V diesel and CNG waste collection trucks for supporting air-quality improvement initiatives in the city of Milan. Sci. Total Environ., vol426, p 65–72, doi:10.1016/j.scitotenv.2012.03.038.
- Guan B., R.Zhan, H.Lin, Z.Huang, (2014): Review of state of the art technologies of selective catalytic reduction of NO_x from diesel engine exhaust. Appl. Therm. Engineering 66, 395–414,doi:10.1016/j.applthermaleng.2014.02.021.
- Hausberger S., M. Rexeis, M. Zallinger&R. Luz (2010): PHEM User guide for version 10. TUG/FVT Report, Graz, Austria, 57 p.
- <http://dgsaie.mise.gov.it/dgerm/>, Energy statistics, Italian Ministry of Economic Development website, in Italian, 2016.
- <http://www.aci.it/studiericerche/datiestatistiche/>, Statistical data 2014, Automobile Club d'Italia (ACI) website, in Italian, 2016.
- http://www.amt.genova.it/amministrazione_trasparente/bilanci.asp, Statistics, AMT website, in Italian, 2016.
- <http://www.sinanet.isprambiente.it/it/sia-ispra/fetransp>, Higher Institute for Environment Protection and Research (ISPRA) website, in Italian, 2016.
- ISPRA (2010): Rapporto Rifiuti Urbani Edizione 2009, Rapporto 108/2010 (in Italian).
- ISPRA (2014): Rapporto Rifiuti Urbani Edizione 2014, Rapporto 202/2014 (in Italian).
- Karavalakis G., M.Hajbabaie, T. D. Durbin, K. C. Johnson, Z. Zheng& W. J. Miller (2013): The effect of natural gas composition on the regulated emissions, gaseous toxic pollutants, and ultrafine particle number emissions from a refuse hauler vehicle. Energy, vol 50, p 280-291, doi:10.1016/j.energy.2012.10.044.
- Sileghem L., D. Bosteels, J. May, C. Favre, S. Verhelst, (2014): Analysis of vehicle emission measurements on the new WLTC, the NEDC and the CADC. Transportation Res. Part D 32, 70–85, doi:10.1016/j.trd.2014.07.008.
- Zamboni G., M. Capobianco&E.Daminelli (2009): Estimation of road vehicle exhaust emissions from 1992 to 2010 and comparison with air quality measurements in Genoa, Italy. Atm. Env., vol 43, n°5, p 1086 - 1092, doi:10.1016/j.atmosenv.2008.11.014.
- Zamboni G., S. Malfettani, M. André, C. Carraro, S. Marelli& M. Capobianco (2013): Assessment of heavy-duty vehicle activities, fuel consumption and exhaust emissions in port areas. Appl. Energy, vol 111, p 921-929, doi:10.1016/j.apenergy.2013.06.037.
- Zamboni G., M. André, A. Roveda& M. Capobianco (2015): Experimental evaluation of Heavy Duty Vehicle speed patterns in urban and port areas and estimation of their fuel consumption and exhaust emissions. Transport. Res. Part D, vol 35, p 1-10, doi:10.1016/j.trd.2014.11.024.

Study of Traffic Real Driving Emissions in Madrid in 2015 and conclusions

Josefina de la FUENTE*, Aida DOMÍNGUEZ-SÁEZ** & Manuel PUJADAS**

*RemoteSensingLaboratory, Madrid, 28015, Spain.

Tel +34 658 579 766 / +34 91 559 28 68 - email: josefina.fuente@rslab.es

**CIEMAT, Avda. Complutense, 40, 28040, Madrid, Spain

Abstract

Concerns about high levels of air pollutants, together with the observed differences between the vehicle emission running under normal operating conditions and the limits specified in the homologation tests, has encouraged to conduct in Spain a study to meet the actual emissions of the circulating vehicle fleet. For this purpose Madrid metropolitan area was selected to carry on this study, considering that the characteristics of its circulating park can be extrapolated to the rest of the country fleet. The measuring technology used was optical remote sensing that allows to measure the emissions in terms of ratios of each emitted pollutant versus CO₂ in the exhaust plume. Some of the most relevant results are the high levels of NO/CO₂ registered for euro 5 and euro 6 diesel vehicles, and the big differences among the emissions when they are evaluated comparing the results of brands of the Spanish fleet.

Keys-words: RSD, Remote Sensing-Laboratory, traffic emissions.

Introduction

The use of remote emission measurements for characterizing emissions vehicles running in real traffic conditions has grown in the last two decades. The main applications of these remote sensing techniques are: fleet monitoring emissions, inspection and maintenance programs (I/M), and detection of high emitters. Due to the most demanding application of emission standards and technological developments especially focused on after-treatment systems, it is necessary to conduct periodic reviews of the characterizations of fleet emissions. The use of remote sensing devices has been and is a quick and economical tool for the characterization of fleets operating in real traffic conditions and also allows a characterization in-situ and in a non-intrusively mode. Remote sensing equipment of emissions can be used to analyze how an expected emission reductions (conditional on the introduction of a stricter emission regulations) result in a change in the trend of emissions on the road. Its use is particularly widespread in the US as inventors and precursors of this methodology are installed there. Some of the most significant recent work has shown the collection of data acquired during a decade (Bishop and Stedman, 2008) showing among its main conclusions a significant reduction in global emissions and a high reliance on these emissions with the VSP ("Vehicle Specific Power"). Other remarkable campaigns were conducted by Kuhns et al, 2004 or Fujita et al, 2012. The results of those campaigns cannot be extrapolated to Europe because the weight of diesel vehicles in the European passenger car fleets is very higher. In Europe, remote sensing measurements of emissions have also been used for the characterization of fleets, highlighting Switzerland, Sweden and England. During 2000-2013, in a unique location in Zurich in the same season of year, emissions data they were taken using remote sensing devices (Chen and Borcken-Kleefeld, 2014). In total more than 100,000 vehicles were registered, dominated by diesel vehicles, making the classification by type of emission regulations and fuel type. The main conclusion of this study emphasizes that, as other authors (Weiss et al, 2011) had indicated, new NO_x emission controls are not effective in actual driving. They also indicated that it is necessary to determine the amount of primary NO₂ and identify systematic differences among emissions of the different dominant brands in European fleets. Along the same lines highlight the work done by the King's College London (Carslaw et al, 2011; Carslaw et al, 2013a, Carslaw et al, 2013b). The campaign was conducted from 2007 to 2010 (7 campaigns at different points) with a total of more than 80,000 valid records, the high values of the emission of NO_x/CO₂ for modern vehicles (Euro 4/5) were also detected contrary to expected emissions due to stricter emissions standards. All studies emphasize that recent technologies do not adequately reduce this type of emission. These studies also found that for the post-2000 vehicles (Euro 3, Euro 4 and Euro 5) diesel vehicles show a high dependence on the VSP in NO_x emissions, which was not observed in previous models or other contaminants. Other campaigns have been conducted in Europe

have been Sjödín and Jerksjö, 2008 in Sweden (15,000 vehicles).

This work presents a part of the results of CORETRA project (Control Remoto de Emisiones de Tráfico) devoted to assess the performance of Remote Sensing Devices and also to apply this kind of technology to study the Spanish circulating fleet. This paper is specifically focused on presenting and discussing the results of the current park that mostly is formed by diesel vehicles (in a much higher proportion than those presented in the rest of the works). The measurements were developed in Madrid region and the sample is very representative of the national fleet. The work also includes a comparison of results considering the different brands.

1. Methodology

This on-road emission study has been based on remote measurements implemented with an AccuScan™ RSD4600 instrument. This remote sensing device allows performing emissions measurements of vehicles in real road traffic conditions by non-intrusive optical technology. The system uses two light beams, one in the ultraviolet (UV) and other one in the infrared range (IR), so that these beams crossing the street or highway on a path perpendicular to the axis of the road on which the measurements are made emissions and more or less in a path parallel to the surface. The beams are reflected in a Corner Cube Mirror (CCM) and return where a similar way to the measurement equipment where they are detected and analyzed. Emission specific concentrations of Hydrocarbon (HC), carbon oxide (CO), carbon dioxide (CO₂) and nitrogen oxide (NO) in the vehicle exhaust are calculated based on the absorption of characteristic frequencies of IR/UV light. During the measurement process the system also collects information on the speed and acceleration of each vehicle registered and takes pictures of it (OCR or optical character recognition). The emissions and other related data are merged into an individual vehicle record stored in a computer housed in a roadside van. This entire process is accomplished in less than a single second. Trained operators customarily monitor and periodically audit mobile roadside units to ensure data integrity. Through the study of number plates it is possible to obtain the technical characteristics of all registered vehicles.

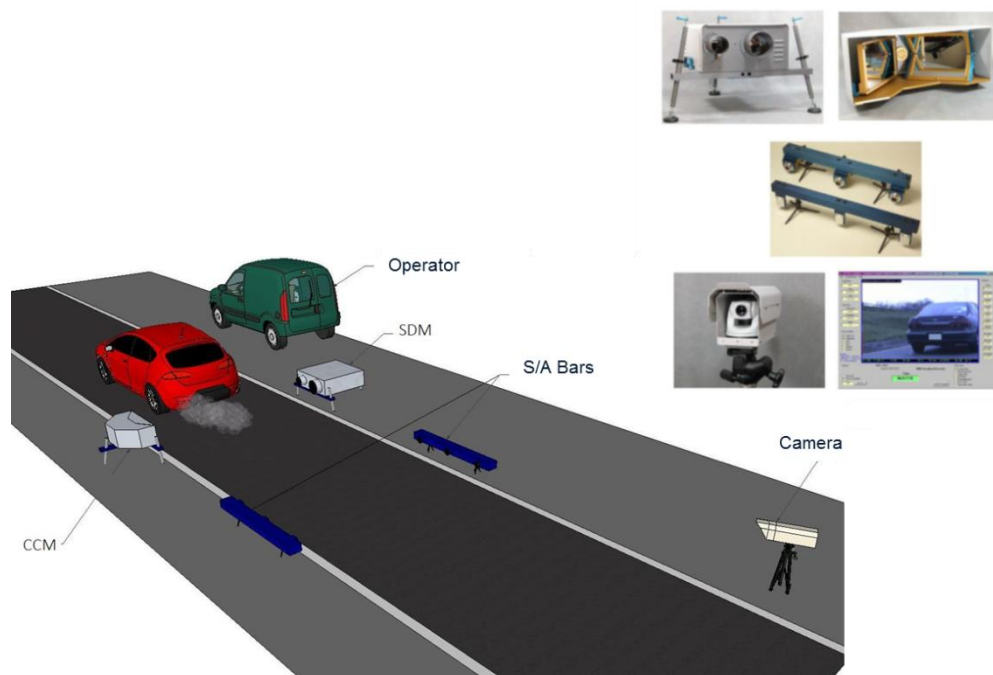


Figure 1. RSD configuration in the road. CCM: Corner Cube Mirror. SDM: Enclosed Source/Detector Module. S/A: Speed Acceleration

The RSD 4600 equipment provides as output ratios of the concentrations of CO/CO₂, NO/CO₂ and HC/CO₂ present in each measured plume and the manufacturer's technical information (table 1) provides the uncertainty of these data to two possible situations:

Table 1. Static background conditions and mean value CO₂ plume (>20 and <20)

CO ₂ plume > 20%-cm	
CO% / CO ₂ %	+/- 0.007 or 10% of reading, whichever is greater
HC ppm /CO ₂ %	+/- 6.6 or 10% of reading, whichever is greater
NO ppm /CO ₂ %	+/- 10 or 10% of reading, whichever is greater
CO ₂ plume < 20%-cm	
CO% / CO ₂ %	+/- 0.015 or 15% of reading, whichever is greater
HC ppm /CO ₂ %	+/- 10 or 15% of reading, whichever is greater
NO ppm /CO ₂ %	+/- 10 or 15% of reading, whichever is greater

The Quality Assurance and Quality Control protocols applied during the campaigns were based on the use of on-site calibration procedure with audited “puff” release of reference blended gas (13.6% CO₂, NO 1000 ppm, 2% CO, propane 1000ppm). The response of the instrument was periodically verified in situ every 4 hours, following the specific procedure designed by the manufacturer. The device used was the RSD 4600 and the fieldwork according to ISO 17025 methodologies was performed by RSLAB.

The field work was conducted in 25 different locations around Madrid City during two experimental campaigns (2014 and 2015). The 25 locations are shown in figure 2. A total number of 191,632 vehicles were registered of which 139,450 were unique (no repetitions) and the rest were representing 73% of the total measurements. The vehicle number distributions of these vehicles in the different points are shown in figure 3.

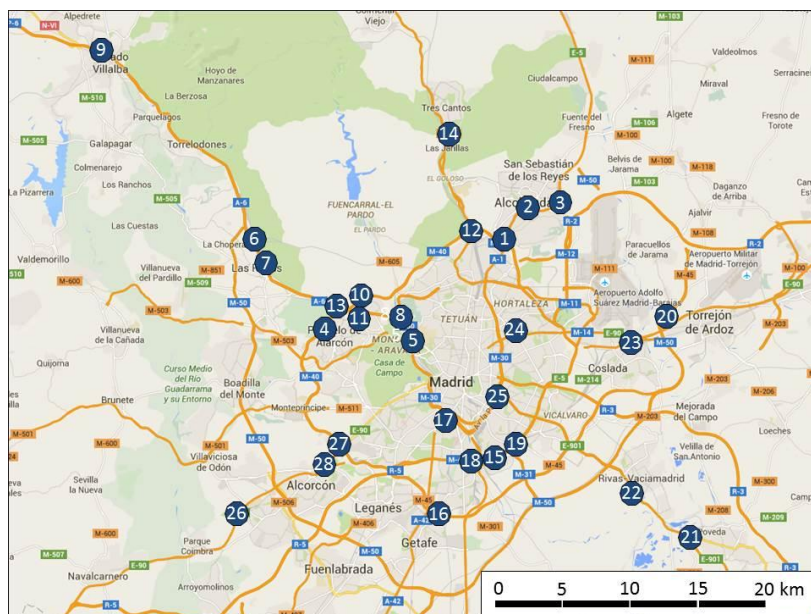


Figure 2. Geographical locations of the 25 measurement points in Madrid region.



Figure3.Vehicle numberdistributions in each of the 25 locations.

Diesel vehicles are a large part of the fleet (78%), while 22% represent the gasoline vehicles. It is noteworthy that the vast majority of measured vehicles (92%) were passenger cars (M1), having a small percentage (7% and 1%) of light commercial vehicles (N1-I \leq 1305 kg, N1-II between 1305 and 1760 kg, N1-III between 1760 and 3500 kg) and heavy commercial vehicles (M2, M3, N2, N3 \geq 3500 kg) respectively. 67% of registered vehicles during the campaigns were Euro 4 or Euro 5 and most of the registered vehicles circulated with speeds in the range 16-70 km/h.

Table 2.Number of vehicles depending on European emission standard, type of fuel and vehicle category.

	PRE EURO		EURO 1		EURO 2		EURO 3		EURO 4		EURO 5		EURO 6		Total Nº Veh	Total % Veh
	Nº Veh	% Veh	Nº Veh	% Veh	Nº Veh	% Veh	Nº Veh	% Veh	Nº Veh	% Veh	Nº Veh	% Veh	Nº Veh	% Veh		
DIÉSEL	219	0.13%	521	0.33%	4576	3.03%	24541	17.06%	40959	29.11%	38258	27.51%	2691	1.81%	111765	78.97%
M1	96	0.06%	334	0.22%	4096	2.74%	21920	15.40%	37238	26.72%	34788	25.11%	2443	1.62%	100915	71.86%
N1-I	30	0.02%	52	0.03%	59	0.04%	447	0.27%	1032	0.66%	906	0.60%	116	0.07%	2642	1.69%
N1-II	48	0.03%	64	0.04%	138	0.08%	793	0.51%	1010	0.64%	1023	0.69%	0	0.00%	3076	2.00%
N1-III	22	0.01%	48	0.03%	197	0.12%	1038	0.65%	1311	0.81%	1158	0.77%	0	0.00%	3774	2.39%
M2,M3,N2,N3	23	0.01%	23	0.01%	86	0.06%	343	0.23%	368	0.28%	383	0.33%	132	0.12%	1358	1.04%
GAS	679	0.39%	879	0.59%	3024	1.96%	8632	5.84%	9004	6.28%	8143	5.59%	559	0.37%	30920	21.03%
M1	653	0.38%	870	0.59%	3020	1.96%	8601	5.82%	8950	6.25%	8126	5.58%	558	0.37%	30778	20.94%
N1-I	24	0.01%	7	0.00%	2	0.00%	28	0.02%	42	0.03%	9	0.01%	1	0.00%	113	0.07%
N1-II	0	0.00%	2	0.00%	2	0.00%	3	0.00%	4	0.00%	2	0.00%	0	0.00%	13	0.01%
N1-III	2	0.00%	0	0.00%	0	0.00%	0	0.00%	8	0.01%	6	0.00%	0	0.00%	16	0.01%
Total	898	0.52%	1400	0.92%	7600	4.99%	33173	22.90%	49963	35.40%	46401	33.09%	3250	2.18%	142685	100.00%

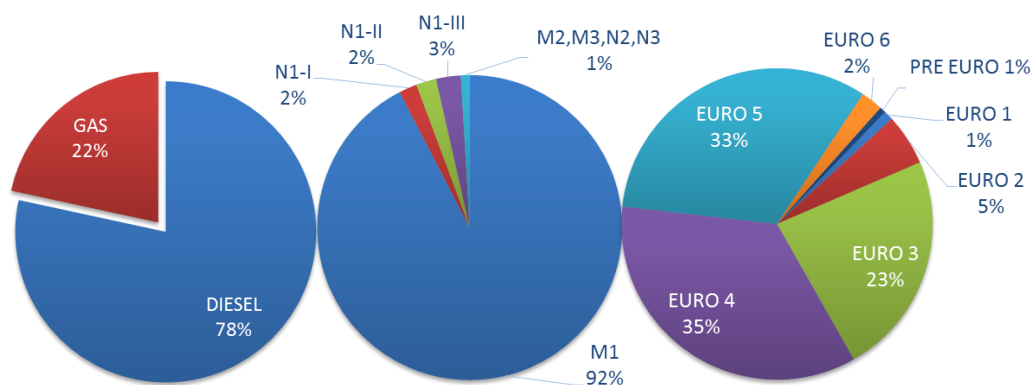


Figure 4.Vehicle distribution depending on fuel, vehicle category, and European emission standard.

2. Results

The average values of the emission ratios of all registered vehicles are shown in table 3. In Figure 5 are shown the mean ratio emission for M1 category versus the European emission standard. The general trend is that average vehicle emissions have been reduced with the application of each newer European emission standards, although some exceptions have been observed. In the case of CO, Heavy commercial vehicles (M2, M3, N2 and N3) exceed the limit established from Euro 3. In the case of HC, the average emissions are above a certain level, however, for vehicles belonging to the Euro 5 and 6 Standards, the emission ratios are below.

NO is a separate case. In general, since before the existence of any Euro standard to the current standard the NO_x has been consecutively reduced, but it should be stressed that the actual emission levels are well above those thresholds, except for some gasoline vehicle group.

In the case of M1 diesel vehicles, the behavior of NO/CO₂ average ratios for modern cars is very similar to pre-Euro models.

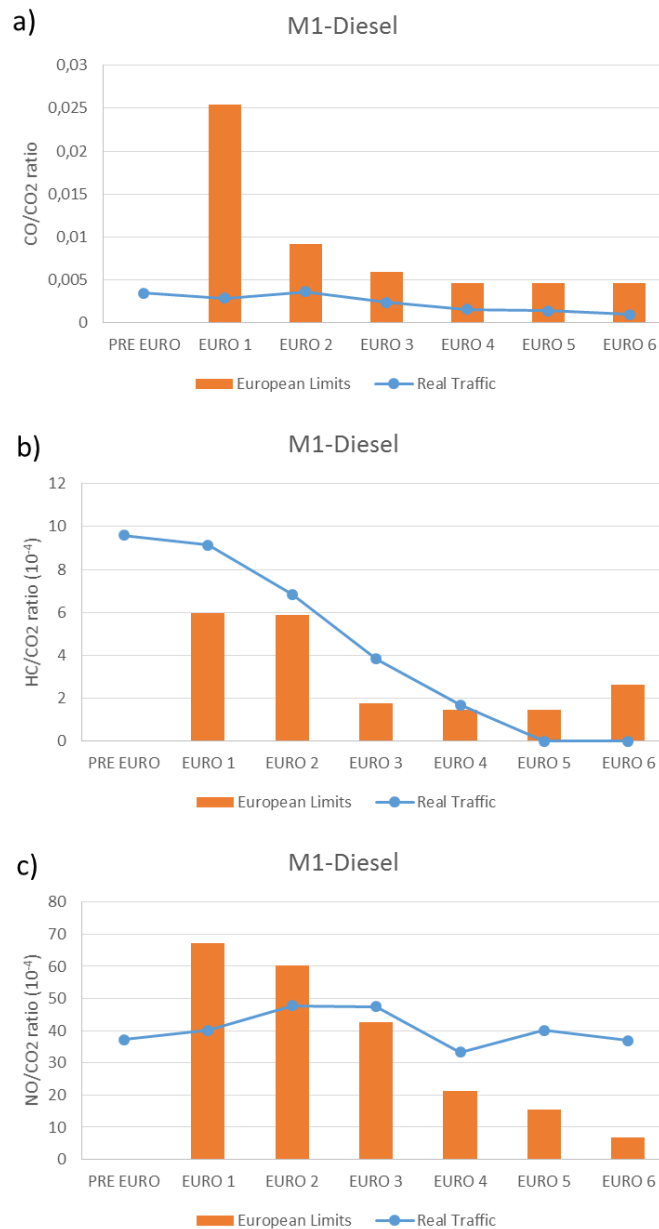


Figure 5. European limit vs mean ratio of CO/CO₂, HC/CO₂ and NO/CO₂ obtained in real traffic conditions. For calculating the European emission limit ratio, the limit value of this legislation for each pollutant, by the average CO₂ emitted in the NEDC cycle for this legislation has been used. Converting all values to volume concentrations.

Table 3. Values of average emissions from vehicles by fuel type, category and standard Euro (shaded in blue). Limit set by the Euro standard (shaded in orange).

DIESEL	M1			N1-I			N1-II			N1-III			M2,M3,N2,N3		
	CO/CO ₂	HC/CO ₂	NO/CO ₂	CO/CO ₂	HC/CO ₂	NO/CO ₂	CO/CO ₂	HC/CO ₂	NO/CO ₂	CO/CO ₂	HC/CO ₂	NO/CO ₂	CO/CO ₂	HC/CO ₂	NO/CO ₂
PRE EURO	0,0034	9,60	37,21	0,0037	7,94	37,52	0,0082	12,48	60,05	0,01	16,49	87,22	0,01	14,69	134,80
EURO 1	0,0028	9,14	40,09	0,0051	4,93	41,37	0,0104	9,64	41,49	0,01	9,29	85,06	0,01	10,28	116,93
Limit	0,0254	5,95	67,23	*	*	*	*	*	*	*	*	*	0,01	6,82	145,44
EURO 2	0,0036	6,85	47,77	0,0011	4,72	38,26	0,0047	7,91	44,76	0,00	8,01	78,47	0,01	6,77	99,05
Limit	0,0092	5,86	60,15	*	*	*	*	*	*	*	*	*	0,01	6,81	127,13
EURO 3	0,0024	3,82	47,48	0,0014	3,88	42,91	0,0023	5,06	43,07	0,01	7,02	63,92	0,01	4,36	80,57
Limit	0,0059	1,75	42,72	0,0040	1,20	29,30	0,0050	1,40	38,14	0,01	1,60	45,82	0,00	4,06	90,33
EURO 4	0,0016	1,67	33,36	0,0013	2,67	34,88	0,0020	3,46	31,98	0,00	3,67	40,80	0,01	3,75	73,67
Limit	0,0046	1,45	21,33	0,0031	1,00	14,64	0,0040	1,20	19,34	0,00	1,40	22,87	0,00	2,83	63,11
EURO 5	0,0014	<<	40,19	0,0013	0,14	47,08	0,0022	0,38	41,96	0,00	1,48	51,41	0,01	2,41	52,67
Limit	0,0046	1,45	15,36	0,0031	1,00	10,54	0,0040	1,20	13,77	0,00	1,40	16,42	0,00	2,83	36,06
EURO 6	0,0009	<<	37,00	0,0014	<<	47,71	**	**	**	**	**	**	0,00	1,69	33,97
Limit	0,0046	2,62	6,83	0,0031	1,80	4,69	0,0040	1,80	6,16	0,00	1,80	7,33	0,00	0,80	7,20
GAS	M1			N1-I			N1-II			N1-III					
	CO/CO ₂	HC/CO ₂	NO/CO ₂	CO/CO ₂	HC/CO ₂	NO/CO ₂	CO/CO ₂	HC/CO ₂	NO/CO ₂	CO/CO ₂	HC/CO ₂	NO/CO ₂	CO/CO ₂	HC/CO ₂	NO/CO ₂
PRE EURO	0,1562	70,11	95,43	0,2933	88,44	83,11	***	***	***	0,01	10,97	107,88	<<: The value of average emission tends to zero. *: There is no limit to the three types of pollutant separately for Euro 1 and Euro 2 standards, the values of hydrocarbons and nitrogen oxides (HC + NOx) were added. **: There are no vehicles for the category and standard Euro, as it enters into force in September 2015. ***: No registered vehicles for the category and Euro standard		
EURO 1	0,0714	35,18	55,56	0,1682	111,47	38,79	0,0072	0,60	49,66	***	***	***			
Limit	0,0250	5,31	65,97	*	*	*	*	*	*	*	*	*			
EURO 2	0,0314	13,57	34,20	0,0025	-0,33	29,59	0,0004	2,26	36,91	***	***	***			
Limit	*	*	*	*	*	*	*	*	*	*	*	*			
EURO 3	0,0133	4,76	16,42	0,0392	34,41	25,93	0,0027	1,73	42,99	***	***	***			
Limit	0,0210	5,29	12,80	0,0117	2,93	7,09	0,0213	3,70	8,60	0,03	4,32	10,09			
EURO 4	0,0067	0,54	6,61	0,0365	16,11	8,37	0,0007	1,30	19,34	0,00	4,24	38,83			
Limit	0,0090	2,61	6,74	0,0050	1,45	3,76	0,0091	1,90	4,71	0,01	2,34	5,20			
EURO 5	0,0041	0,16	3,76	0,0007	<<	16,73	<<	<<	10,09	0,00	<<	40,63			
Limit	0,0090	2,61	5,05	0,0050	1,45	2,82	0,0091	1,90	3,54	0,01	2,34	3,88			
EURO 6	0,0020	2,06	3,87	0,0000	<<	48,60	**	**	**	**	**	**			
Limit	0,0090	2,61	5,05	0,0050	1,45	2,82	0,0091	1,90	3,54	0,01	2,34	3,88			

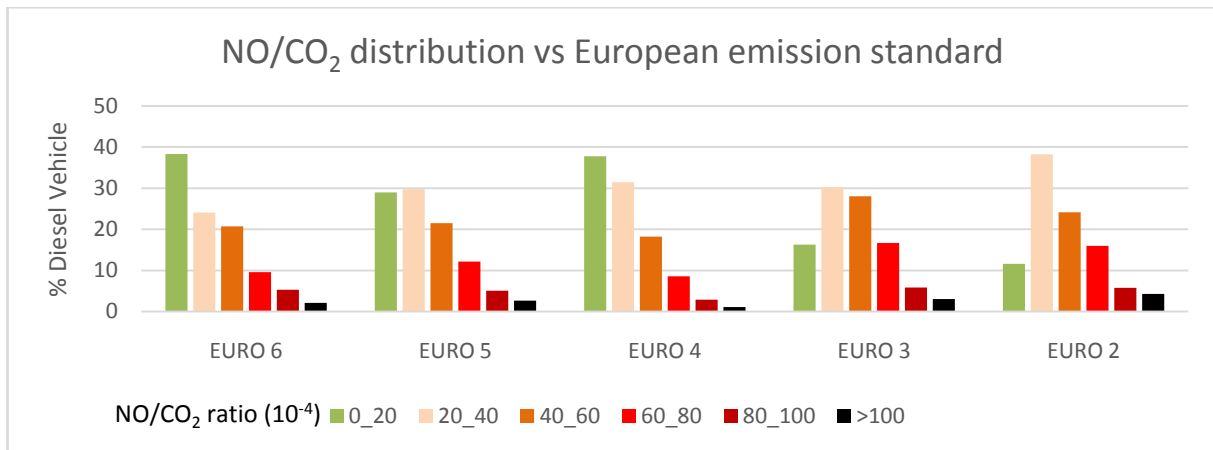


Figure 6. NO/CO₂ distribution depending on European emission standard and emission range of the ratio NO/CO₂ for diesel vehicles

Furthermore, as shown in Figure 6, there is a great dispersion in the NO/CO₂ ratio values that is very significant. The graph shows the distribution of ratios only from Euro 2, since for the Euro 1 and PREEURO there is a no significant number of vehicles. Euro 5 has more than 40% of their vehicles with ratios that exceed the value of 40. 10⁻⁴, while the Euro 4 standard only 30% of the registered vehicles showed this behavior. From a technological point, there are differences among the abatement pollutant solutions adopted for the last three Euro standards. Oxidation catalyst and DPF was used in Euro 4, in the Euro 5, EGR, DPF and complex electronic control were the most common technologies, and finally DPF, LNT or SCR and EGR for Euro 6. Kadijk et al (2016) report that no NO_x reduction in modern engines, especially Euro 5, might be the result of failing emission control at high power demand. This high dispersion in the emission ratios could point to failures in some control technologies due to cost reduction and technology differences between vehicle manufacturers. To test this hypothesis, the values of NO/CO₂ ratios of diesel vehicles corresponding to the most numerous brands in the circulating fleet registered in the campaigns are shown in the following figures.

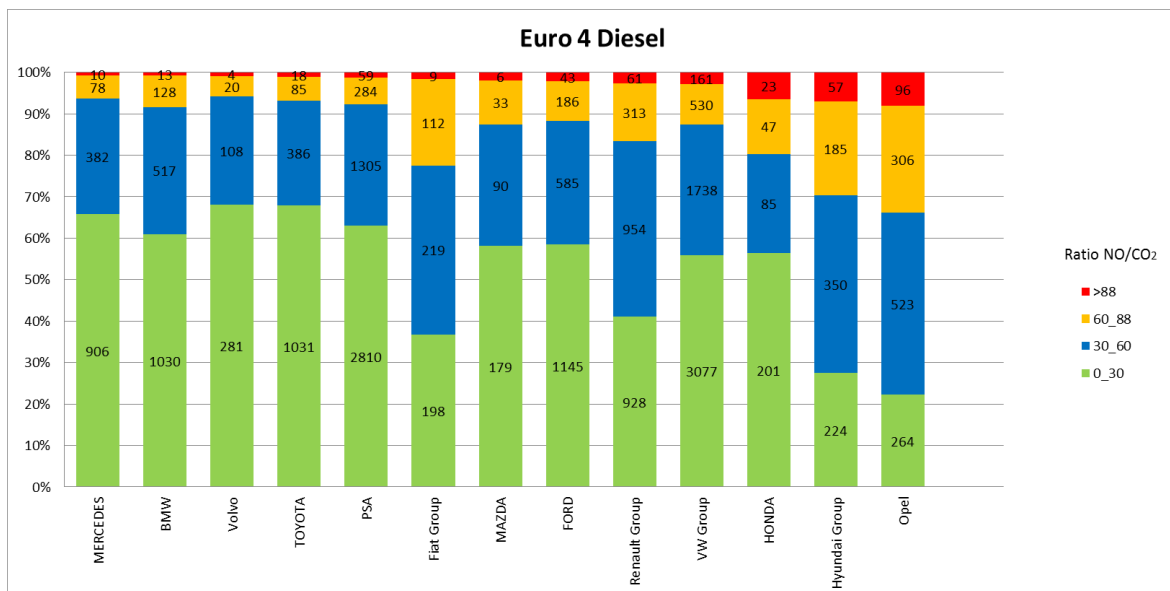


Figure 7. NO/CO₂ ratio distribution of diesel Euro 4 vehicle by brand. In the bars is shown the vehicle number registered of each brand and each ratio group.

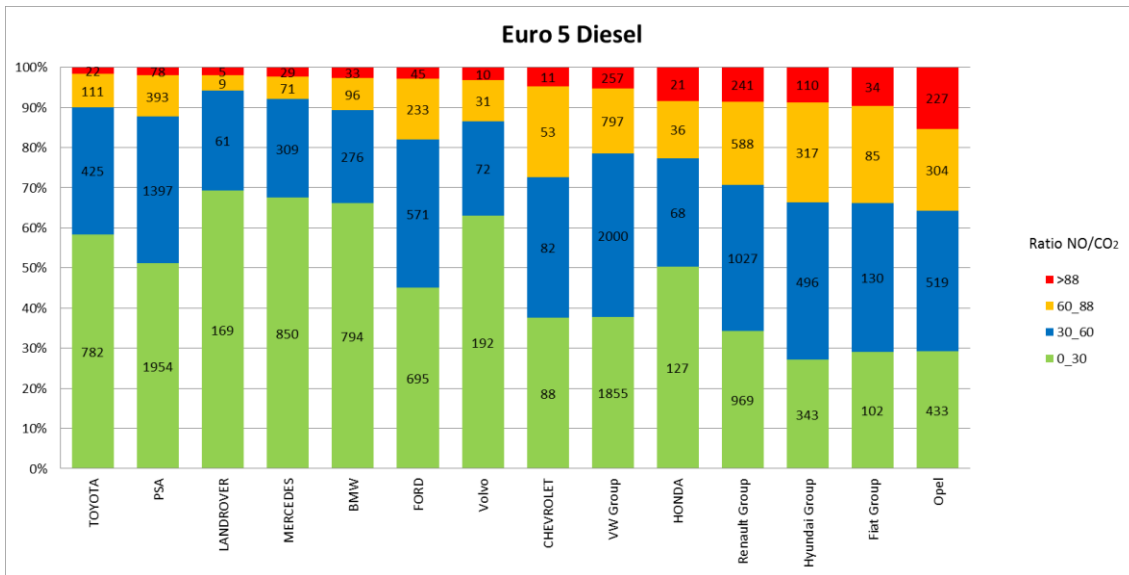


Figure 8. NO/CO₂ ratio distribution of diesel Euro 5 vehicle by brand. In the bars is shown the vehicle number registered of each brand and each ratio group.

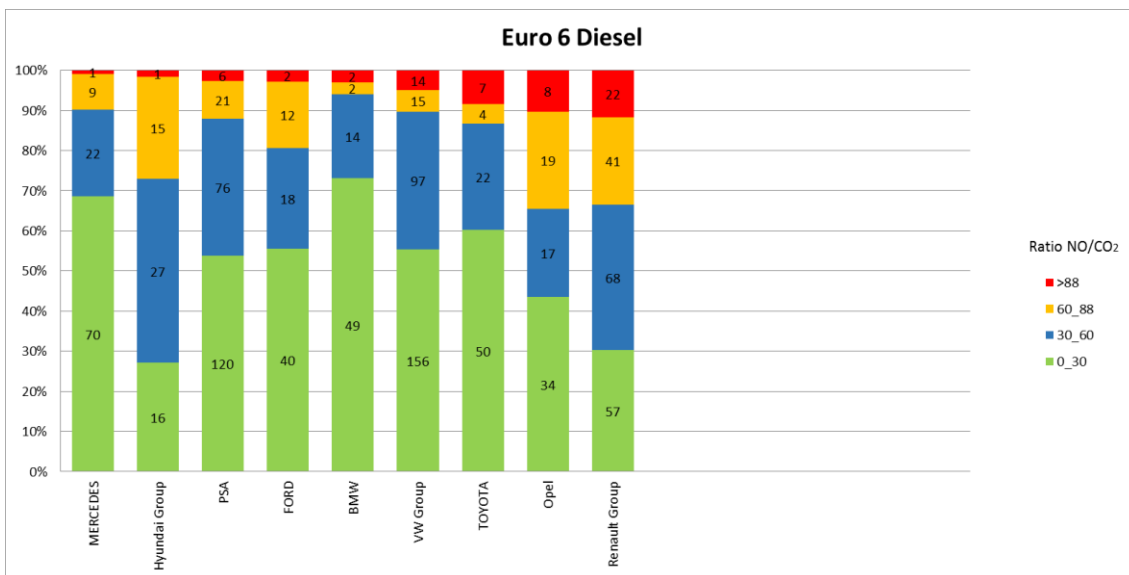


Figure 9. NO/CO₂ ratio distribution of diesel Euro 6 vehicle by brand. In the bars is shown the vehicle number registered of each brand and each ratio group.

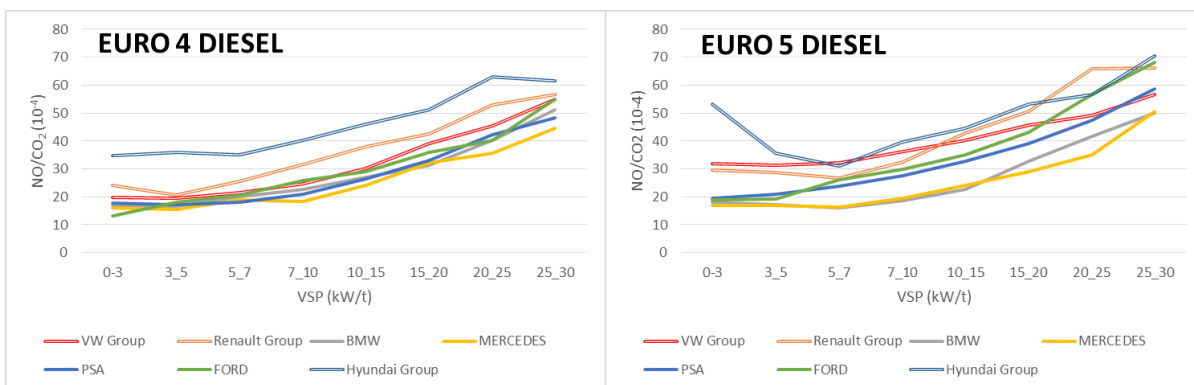


Figure 10. Average NO/CO₂ ratio vs VSP and brand. Only a few representative brands have been represented.

Some general remarks can be concluded from these results: Opel diesel vehicles have high emissions in all regulations (figures); GroupHyundai engines were the most pollutants with Euro 4 standard, and while remaining the most pollutants in the Euro 5 and Euro 6 standards they came closer to other manufacturers, especially with high VSP. Renault group's vehicles have high emissions, especially in the Euro 6. Mercedes, BMW and Volvo pollute the least, but with the entry of the EURO 5 standard, the difference became more evident. Ford and PSA group have average emissions in both EURO 4 and EURO 5. Volkswagen group in Euro 4 standard presents a mean NO/CO₂ ratio noneespecially high but after the approval of Euro 5 standard its engines present a clear increase in the general pollutant level of the brand even under low VSP conditions as shown in figure 10.

Conclusions

Remote sensing has been demonstrated as an effective technology to update vehicle emission inventories, to study trends and to detect abnormalities of the circulating fleet. The emitting behavior of a representative sample of the Spanish circulating fleet has been studied with a RSD 4600 instrument in Madrid region during 2014 and 2015. One of the most relevant results of this study is related to the trends of the NO_x emissions produced by diesel cars that present clear anomalies because the average NO/CO₂ ratios do not correlate with the Euro standards and have certain dependency from the vehicle brands. In Euro 5 and Euro 6 diesel vehicles, these ratios are too high regarding the expected NO_x emission levels determined by the correspondent standards.

Given that emissions of nitrogen oxides are very high in European cities and considering that diesel vehicles are predominant in the Spanish fleet, it is necessary to deepen the study of these emissions and determine why vehicles in real traffic conditions emit more than expected.

Acknowledgments

The measurement campaigns were developed in the framework of CORETRA project funded by FundaciónBiodiversidad (Ministerio de Agricultura, Alimentación y Medio Ambiente of Spain) under Grant CA 2014.

References

- Bishop, G.A., Stedman, D.H., 2008. A decade of on-road emissions measurements. *Environ. Sci. Technol.* 42 (5), 1651-1656.
- Carslaw, D.C., et al., 2011. Recent evidence concerning higher NO_x emissions from passenger cars and light duty vehicles. *Atmos. Environ.* 45 (39), 7053-7063.
- Carslaw, D.C., et al., 2013a. The importance of high vehicle power for passenger car emissions. *Atmos. Environ.* 68, 8-16.
- Carslaw, D.C., Rhys-Tyler, G., 2013b. New insights from comprehensive on-road measurements of NO_x, NO₂ and NH₃ from vehicle emission remote sensing in London, UK. *Atmos. Environ.* 81, 339-347.
- Chen, Y., Borken-Kleefeld, J. (2014) Real-driving emissions from cars and light commercial vehicles - Results from 13 years remote sensing at Zurich/CH. *Atmospheric Environment*, 88:157-16
- Fujita, E. M., Campbell, D. E., Zielinska, B., Chow, J. C., Lindhjem, C. E., DenBleyker, A., Bishop, G. A., Schuchmann, B. G., Stedman, D., Lawson, D. R. (2012) Comparison of the MOVES2010a, MOBILE6.2, and EMFAC2007 mobile source emission models with on-road traffic tunnel and remote sensing measurements, *Journal of the Air & Waste Management Association*, 62:10, 1134-1149, DOI: 0.1080/10962247.2012.699016
- Kadijk, G., Ligterink, N., Mensch P., Smokers, R. (2016). TNO 2016 R10083 NO_x emissions of Euro 5 and Euro 6 diesel passenger cars – test results in the lab and on the road. TNO report | TNO 2016 R10083 | 9 March 2016.
- Kuhns, H.D., Mazzoleni, C., Moosmüller, H., Nikolic, D., Keislar, R.E., Barber, P.W., Li, Z., Etyemezian, V., Watson, J.G., 2004. Remote sensing of PM, NO, CO, and HC emission factors for on-road

gasoline and diesel engine vehicles in Las Vegas, NV. *Science of the Total Environment* 322, 123–137.

McClintock, P, 2011. "Enhanced Remote Sensing Performance Based Pilot Program". Tiburon, CA/USA: Environmental Systems Products Inc.

Sjodin, VA., and M. Jerksjö. 2008. "Evaluation of European Road Transport Emission Models Against On-road Emission Data as Measured by Optical Remote Sensing." In 17th International Transport and Air Pollution Conference.

Weiss, M., et al., 2011. On-road emissions of light-duty vehicles in europe. *Environ. Sci. Technol.* 45 (19), 8575e8581.

Prediction of Airport Noise with CadnaA Model and GIS (Case Study: IKIA Airport)

Maryam kiani Sadr¹, Amir Arefian²

1. Assistant Professor, Islamic Azad University of Hamedan, Iran
2. Faculty of Civil Engineering, Islamic Azad University of Shahriar, Iran

Abstract

The issue of airport noise pollution has paramount importance to the community in vicinity of airports. This study investigated the broad issue of prediction of airport noise by employing Remote Sensing, Geographic Information System (GIS) in conjunction with an optimization algorithm, integrated with CadnaA software, to establish the various potential effects and consequences of aircraft noise in study area. The case of the Imam Khomeini International Airport in Iran, (considered as a “large airport”), is presented. CadnaA is a computer model used to develop Noise Exposure Maps, to determine noise impacted areas. The results indicate the compatibility of existing landuses around the IKIA airport with airport noise levels and alert for the development of residential areas in the near future.

Key words: Airport Noise Pollution, Geographic Information System, CadnaA

1. Introduction

The aim of this study is to investigate the broad issue of land-use planning around airports by employing aircraft noise prediction model, namely CadnaA and using Arc GIS software and remote sensing to establish the various potential effects and consequences of aircraft noise, in study area.

Also, another objective of this study is to establish that communities experience annoyance from aircraft noise and Devise an inclusive airport noise and land-use planning framework to be used around new or existing airports. Aviation has grown tremendously since the 1970s. Yet, due to the introduction of new aircraft technologies noise exposure patterns surrounding airports in the world have greatly shrunk. In the future, however, less is expected from new technology, which is why the number of exposed people is expected to grow. As a result, aircraft noise is regarded as a prominent issue facing capacity expansion efforts. Indeed, noise considerations have played a significant role in recent decisions not to expand airports and in supporting costly relocations (Girvin, 2010). Exposure to aircraft noise can negatively impact health. These effects range from subjective and behavioral effects, like annoyance or sleep disturbance (Miedema, 2007), to physical effects, such as high blood pressure (Babisch, 2006). (Miedema, 2007), to physical effects, such as high blood pressure (Babisch, 2006). While the attributable burden of cardiovascular disease due to community noise exposure (including aircraft noise) has been estimated at 0.1% of the total national disease burden (in the Netherlands), a burden expressed in ‘severe annoyance’ adjusted life-years may amount to 2% of the total disease burden (DeHollander, 2004). To reduce the negative effects of aircraft noise exposure, the Federal Aviation Administration has primarily focused on the source with successively stringent certification standards for new aircrafts. Later, policies also addressed other means to reduce exposure to aircraft noise. Illustrative is ICAO’s balanced approach, which (in addition to source reductions) focuses on land-use planning, noise abatement operational procedures and aircraft operating restrictions (ICAO, 2004). Noise mapping is an important tool for supplying the necessary relevant information for both global and local action plans (Klæboe et al., 2006; WG-AEN, 2006). Imam Khomeini International Airport is located in Ahmadabad, Iran. The airport is located about 30 kilometres (19 mi) southwest of the city near the localities of Robat-Karim and Eslamshahr. It was designed to replace Mehrabad International Airport, which is in the west of the city, now inside the city boundaries. The airport originally designated as Ahmadabad but was later renamed to Imam

Khomeini International Airport in honor of Ruhollah Khomeini. (IKIA, 2012). The total airport site is about 13 500 Ha and it is divided in two parts, a northern one and a southern one, separated by an important spine road connected to Tehran. Today, only the northern site of the airport is developed but it represents already about 1400 Ha. The large wide areas surrounding the airport offer an important development potential in order to turn IKIA into the main prestigious gateway to Iran (IKIA, 2012). Imam Khomeini Airport is accessible from Tehran by Car, taxi and bus via the Tehran-Qom Freeway. An airport access road connects the freeway to the airport terminal, continuing to serve Robat-Karim via an interchange with Saidi Highway. An extension to the southern part of Line 1 of Tehran Metro for IKIA airport is currently under construction. There is also plan to have Line 3 of the Tehran Metro to reach its southern terminus at IKIA in future. One runway is already built and the closest taxiway to the runway was built to be used as an emergency runway, but it is not authorized to operate yet.

2. Material and Method

The Noise Exposure Maps (NEM) are designed to clearly identify an airport's present and future noise patterns as well as land uses which are not compatible with those noise patterns. Airport's NEM serves as a standard reference to the airport's existing and future noise impacts for anyone proposing sensitive development in the vicinity of the airport. The scope of work consisted of the production of noise exposure contours by using the United States Federal Aviation Administration's Integrated Noise Model version 7.0c. The noise exposure contour sets were developed for three time frames detailed in the table 1. Fig. 1 shows the study area. Based on the three time frames defined previously, three scenarios (in years of 2011, 2020, 2030) were developed to evaluate the airport noise impact on the surrounding communities and the future airport city. The different runway layouts used in each scenario.

Table (1) Scenarios Characteristics in noise airport modeling

Scenario 1 (In 2011)			Scenario 2 (In 2020)			Scenario 3 (In 2030)		
Runway	Annual Passenger Traffic	Average Daily Aircraft Movements	Runway	Annual Passenger Traffic	Average Daily Aircraft Movements	Runway	Annual Passenger Traffic	Average Daily Aircraft Movements
11 / 29	12 Mpax	290 movements	11L / 29R	27 Mpax	580 movements	11L / 29R	92 Mpax	1705 movements
			11R / 29L			11R / 29L		
						12L / 30R		
						12R / 30L		

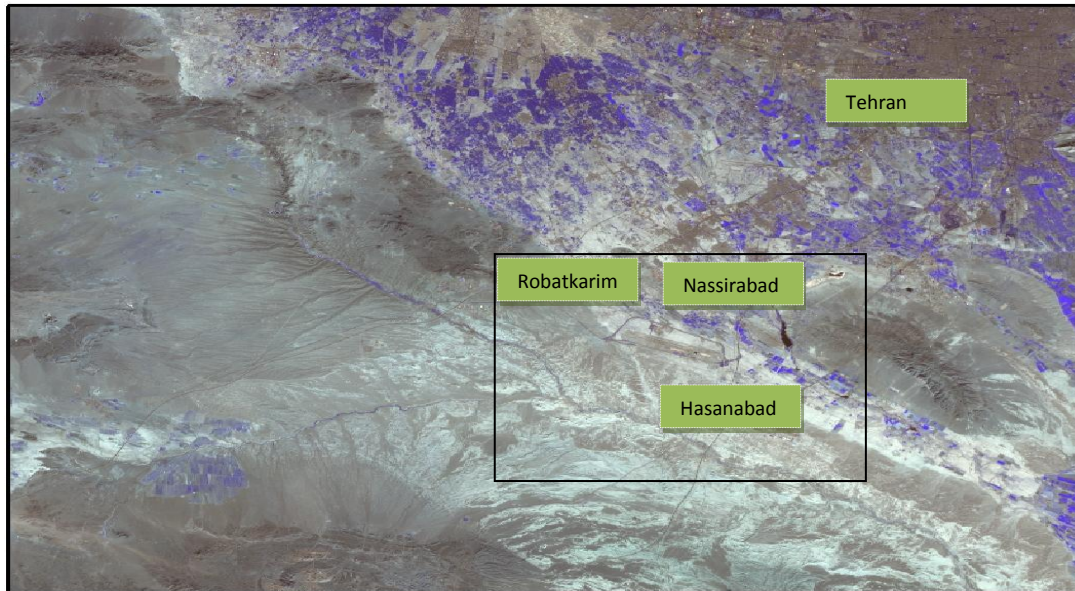


Figure 1 : Study area- IRS- image (2012/03/02)

Aircraft operations are expected to be accommodated on a single runway oriented east/west in scenario 1. An additional staggered parallel runway is planned to be constructed in scenario 2. The ultimate phase presents long-term development at the airport which would comprise two pairs of close spaced parallel runways with a mid-field terminal.

The following tasks were completed for all the above 3 scenarios:

- (a) Analytic aircraft traffic assessment per day/runway/flight path
- (b) Distribution of aircraft types in categories, per day hour/runway/ flight paths in the three partial period's day–evening–night
- (c) Airport Operations: Percentage of aircraft operations per period of the day is presented in the table 2.

Table (2) Percentage of Aircraft Operations PER Period of the Day

Time Period	Existing	Mid-Term	Long-Term
Day	70%	71%	72.5%
Evening	14%	15%	15%
Night	17%	14%	12.5%

The aircraft fleet mix per ICAO Code is presented in the table (3).

Table (3) Percentage of Operations per ICAO Code

ICAO Code	Scenario 1	Scenario 2	Scenario 3
A	0 %	0 %	0 %
B	0%	0%	0%
C	59%	68%	69%
D	36%	18%	0%
E	5%	14%	29%
F	0%	0%	2%

- (d) Runway Utilization : At IKIA, 60 percent of the landing and take-off procedures will be operated to the west on runway 29L/R and 30L/R.

(e) Aircraft Fleet Mix: Based on the forecast of the future air traffic demand, a typical aircraft fleet mix was assumed for the existing, mid-term and long-term conditions

(f) Flight Tracks: The exit radials were used to CadnaA model the flight tracks by the various aircraft that will be accommodated at IKIA airport.

Then used of the “Report on Standard Method of Computing Noise Contours around Civil Airports”, (ECAC.CEAC, Doc 29, 2–3 July, 1997). For the needs of the present study “CadnaA” software was used which completely ensures the demands of the above report “ECAC.CEACDoc29”. CadnaA is the leading software for calculation, presentation, assessment and prediction of environmental noise. With more than 30 implemented standards and guidelines, powerful calculation algorithms, extensive tools for object handling, outstanding 3D visualization and the very user-friendly interface. CadnaA is the perfect software to handle national and international noise calculation and noise mapping projects of any size. The following national and international standards and guidelines are implemented in CadnaA: Aircraft Noise: (ECAC Doc. 29, 2nd edition 1997 (International, EC-Interim) , DIN 45684 (Germany) , AzB (Germany) , AzB-MIL (Germany) , LAI-Landeplatzleitlinie (Germany) , AzB 2007, draft (Germany). The results of the aircraft noise modelling with software CadnaA for all scenarios are given in the following Strategic Noise Maps — SNM (figs. 2-5)

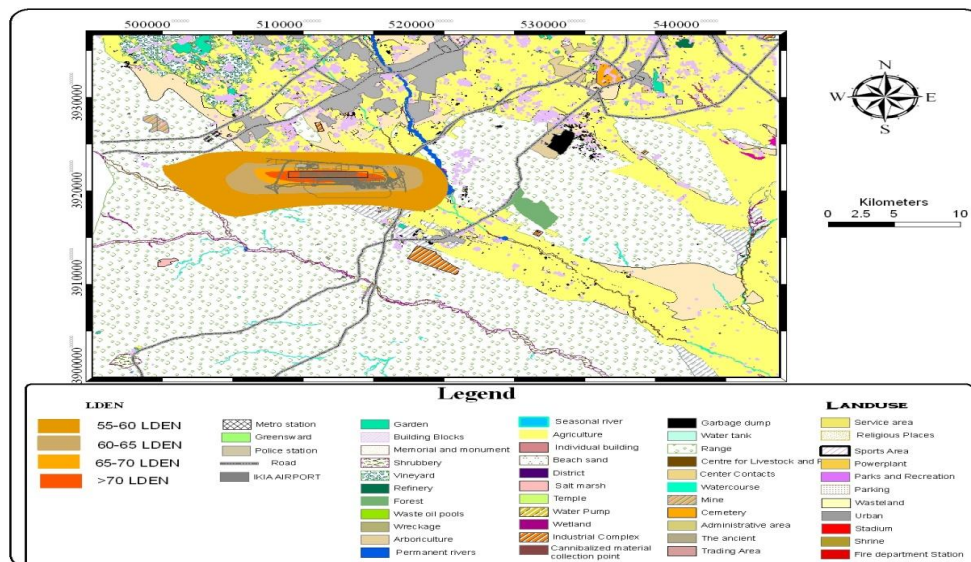


Figure 2 : IKIA Airport SNM 2011, noise index L_{den} (Modelling by CadnaA)

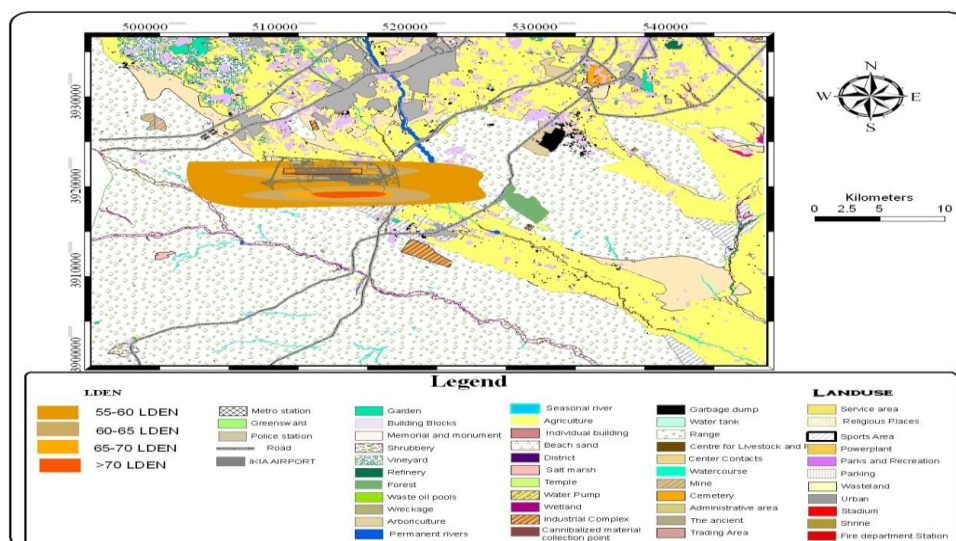


Figure 3 : IKIA Airport SNM 2020, noise index L_{den} (Modelling by CadnaA)

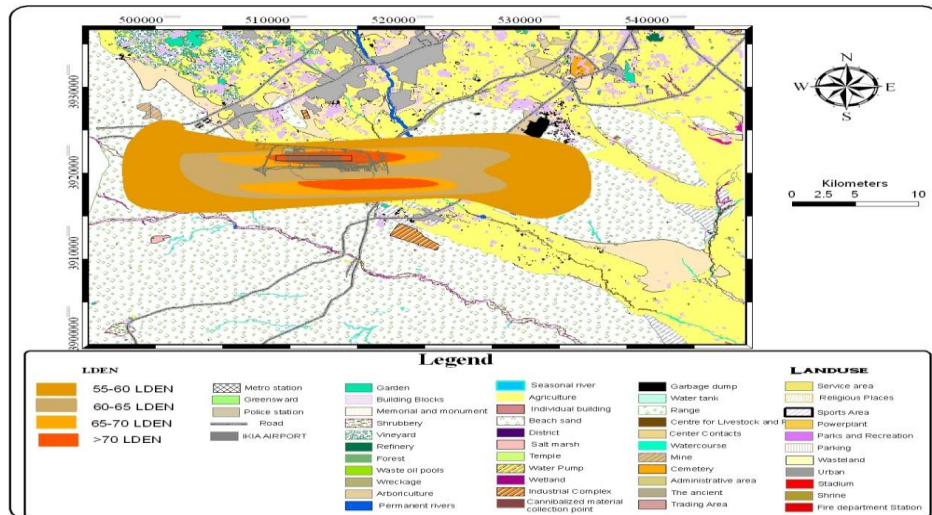


Figure 4 : IKIA Airport SNM 2030, noise index L_{den} (Modelling by CadnaA)

The author set up and used this model and Arc GIS software to further the aims of the study. ArcGIS Desktop is a state-of-the-art GIS software package developed by ESRI. The software can be used in a wide area of general as well as specific GIS applications and can be extended easily via its Application Interface (API). The API gives fine grain access to data stored as well in general data base formats as topologically indexed vector data in the industry standard "shape" format as well as different GRID and geo-referenced raster formats (Farçaş a, 2010). In this study a georeferenced GIS database was built in IDRISI (a GIS software) comprising elevation data, land use, results of CadnaA model and project data. The results obtained overlay map of landuse and CadnaA output.

The materials and data for this part of the project were from two main sources and they are:

- IRS images (IRS 2012), (fig. 1)

- Coordinates of runway extension which was observed directly on the site

In order to use the IRS image for the required analysis, they were processed. The processing of the image was done in ERDAS Imagine (a remote sensing software). The first operation was stacking the images. Stacking involves joining the different IRS image bands to produce one image containing the seven bands. To do this in ERDAS Imagine, the Layer Stack function was used. After the stacking, it is obvious that the area covered by the IRS Image covers a very large area that is far beyond the area of study. Therefore, there was a need to subset the image which involved the cutting out of a particular part of an image that is the area of interest. This was also done in ERDAS Imagine through the Subset Image function. The next process after the subset was derived was to classify the image. Classification was carried out on the IRS image to determine the land use of the various parts of the area around the runway. This was done in ERDAS Imagine by using the Classifier function. The unsupervised method of classification was used to classify the land use (Uche et al., 2011). Unsupervised classification was made using 47 classes in order to establish a good representation of the various land use classes. To ascertain the accuracy of the classified map, a classification accuracy assessment was carried out on the recoded map. To achieve a mean accuracy, 100 reference points were used for the accuracy assessment. In continued overlay of NEM and land use map .

Noise metric:

Noise Exposure Contour are computed by using the L_{DEN} noise metric which considers noise events that occurs between 7 a.m. and 6:59 p.m. without penalty and adds additional decibels to aircraft noise events occurring in the evening from 7 p.m. to 10:59 p.m., and at night from 11 p.m. to 6:59 a.m. These penalties include 5 dB (A) for the evening hours and 10 dB (A) for the night-time hours. The L_{DEN} was commonly adopted in Europe in 2002 in the European Noise Directive 2002/49/EC. The FAA has developed guidelines for noise and land use compatibility evaluation on the basis of yearly

DNL (FAA, 1998). the Day-Night Average Sound Level (DNL) used in the United States which does not add decibels to aircraft noise occurring during the evening, the L_{DEN} takes into account the annoyance perceived by the airport surrounding communities between 7 p.m. and 10:59 p.m. This noise metric was selected for the computation of the noise exposure maps as it is more restrictive when considering land use planning in the vicinity of an airport.

The definition of the L_{den} level (day-evening-night) is defined by the following formula:

$$L_{den} = 10 \log \frac{1}{24} (12 * 10^{\frac{L_{day}}{10}} + * 10^{\frac{L_{evening} + 5}{10}} + 8 * 10^{\frac{L_{night} + 10}{10}})$$

Where: (a) L_{day} is the A-weighted long-term average sound level as defined in ISO 1996-2: 1987, determined over all the day periods of a year,

(b) $L_{evening}$ is the A-weighted long-term average sound level as defined in ISO 1996-2: 1987, determined over all the evening periods of a year,

(c) L_{night} is the A-weighted long-term average sound level as defined in ISO 1996-2: 1987, determined over all the night periods of a year. (Vogiatzis, 2012)

The study area includes the areas affected by IKIA airport noise. For indicate the suitable position for sampling, at first some samples were taken randomly as pilot sampling. Based on the results of pilot sampling 30 stations were indicated as suitable sample numbers using formula. Then gridding method was used to obtain the samples, the surface of the study area was divided into some stations, where the grid intersect diameter as the sample was determined. In assessing human responses to the aircraft noise, the authors employed a field survey that consists of physical measurements and social surveys using a questionnaire. This study assesses the effects of aircraft noise on residential satisfaction, an important indicator of subjective well-being, and it was administered to residents living within study area. A questionnaire set by the community Response to Noise Team of ICEN is a commonly used tool to evaluate the subjective annoyance due to noise (ISO, 2003). Questionnaires were comprised of questions relating to the assessments of aircraft noise, as well as some general questions of residents, even if they do not relate to noise. Questions were arranged in three basic sections. The first section sought to obtain demographic data, the second asked questions about nuisance perception from aircraft noise, and the third dealt with health-related symptom questions. Therefore, the questionnaire contained demographic questions, degree of noise annoyance, interferences with daily activities, psychological and physiological health-related symptoms, and reaction to aircraft noise. In order to assess the annoyance responses to aircraft noise, specifically, people were asked questions like “how much were you bothered or annoyed by the aircraft noise, while staying at home, in the last 12 months (Lim and Lee, 2003). The respondents then used an 11 category response ranging from 0 (not annoyed at all) to 10 (extremely annoyed). The 11-point numerical scale was chosen over the shorter 7 or 9-point numeric scales with the assumption that respondents are more cognitively familiar with the 0 to 10 scaling (ISO, 2003). The sampling frame is best described as a modified probability sample after Hazard (1971). An experimental population had to be located in the vicinity of the airport’s flight paths where there was likelihood that they would be exposed to noise from aircraft operations. The control population were required to be located a similar distance from the airport but not directly under the flight paths. An experiment group (subdivided into two groups) and a control group were selected. The requirements for the control group were (a) to consist of houses of similar construction, type and materials to the experiment group, and (b) to be located at similar distances from the airport, but the control group not lying directly under flight paths. Two separate data flows had to be collected. Firstly the survey was administered with questionnaires, and this data collected. Secondly, measurement of airport noise for the same time of the survey was collected, and noise contours for these flight operations produced. The CadnaA was used to generate L_{DEN} contour. Then the relationship between the measured noise levels and the public discontent was investigated. The chi-square test was used to test whether there is a difference between two samples of data expressed in frequency form. The control group and the suburb group were treated as a random cross-section of the population at large and also as two random samples for the purpose of the chi-square test. A large value of chi-square indicates that there is a large amount of difference between the observed and the expected frequencies (Ebdon, 1977). Each questionnaire took about 15 min to complete and the social surveys were carried out within a given period of the noise measurement at each site. 75% of the randomly selected respondents participated in this survey, resulting in a total of 890 respondents for the analysis of exposure-effect relationships between aircraft noise levels and annoyance responses.

3. Results

The results of the special aircraft noise computation software CadnaA for all scenarios are given in the Strategic Noise Maps — SNM. The noise exposure map for the existing condition is slightly bigger than in the mid-term conditions due to the shift of the fleet mix toward quieter aircraft. No aircraft operations of Airbus A300 and A310 are expected to be accommodated in the mid-term and long-term scenario. The Noise exposure map for the long-term condition will serve as a basis to define compatible land uses within the area covered by the noise exposure map. Land use management in the vicinity of IKIA airport is essential to avoid conflicts with existing and future surrounding communities as well as providing sufficient flexibility for the development of the airport. The United States Federal Aviation Administration has established restrictive guidelines relating types of land use to airport sound level. This table presents these guidelines and detailed the compatibility parameters for residential, public (schools, places of worship, nursing homes, hospitals, libraries), commercial, manufacturing and production, and recreational land uses. All land uses within the areas below 65 dB are considered to be compatible with airport operations. Residential land uses are generally incompatible with noise levels above 65 dB. In some areas, residential land use may be permitted in the 65-70 dB with appropriate sound insulation measures implemented. Schools and other public facilities located between 65 and 70 dB are generally incompatible without sound insulation. Above 75 dB, schools, hospitals, nursing homes and places of worship are considered as incompatible land uses.

Respondents reporting high levels of annoyance to aircraft noise during the time of 10 to 2 March 2011 between 19:00 and 07:00 are shown in Fig. 5 where it is clear that the experimental group reported a much greater level of annoyance (66.2%) to aircraft noise than the control group (33.8%). This result creates an initial impression that evening and night-time aircraft noise is a problem. As shown in fig. 5, the annoyance responses of experiment group are much higher than those of control group.

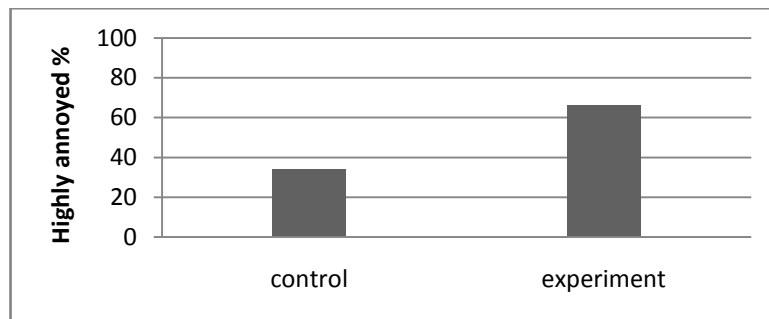


Figure 5: HA % Control group and experiment group

A t test is used to analysis whether the means of two groups (control and experimental groups) are statistically significant or not. The statistical software to compare the means of two groups was SAS ver. 9.2. As shown in this analysis, the variances of the two groups are significantly different. Therefore, the significance level of the t value is less than 0.0001 (t value = -7.96) where the variances of the two groups are statistically different ($P < 0.05$).

The results of the statistical analysis show that there is significant difference in the annoyance responses of aircraft noise between control group and experimental group. 51 percent of the respondents were male and 49% were female. The ages of the respondents exhibit a wide range: younger than 20 years (8%), 20–40 (34%), and 40–60 (42%) and older than 60 years (16%). In addition to the analysis of annoyance, which is a general state of mind, four activities which take place at home were identified for analysis to see whether aircraft noise interferes with them. They were sleep, television viewing, telephone conversations, and work or study this section reports on the interference of aircraft noise on these activities as reported by the survey respondents. About 8% of the control group reported that aircraft noise interferes with sleep (Fig. 6) whereas no control group

respondents reported that there was interference with their television watching, telephone conversations or work/study activities very often.

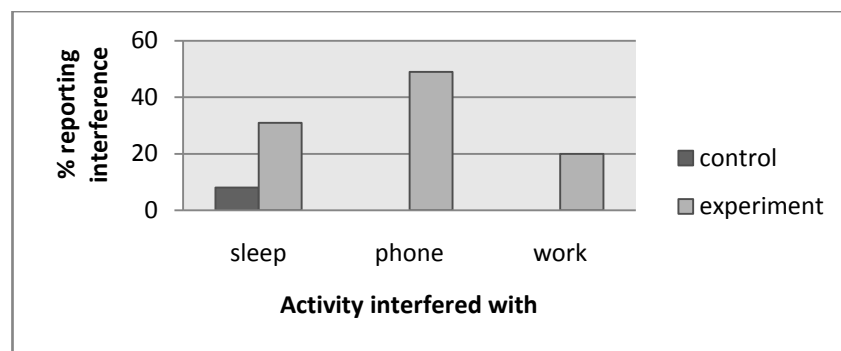


Figure 6: Percentage of responses about home activities in interference with aircraft noise

Experimental group reported the highest percentages of interference with sleep, television watching, telephone conversations and work/study. In this section, the survey results are interpreted according to L_{DEN} noise contours. This section considers the degree of reported annoyance to aircraft noise as it varies according to L_{DEN} zone. Borrowing a concept from GIS, this section may be seen as an attempt to ‘ground-truth’ the survey results at a local level (Brown, 1999), by checking them against international experience. Of the respondents living outside the $55L_{DEN}$ zone, 60% reported being highly annoyed while 40% reported not being annoyed. Aircraft noise is a problem for neighborhoods around the airport. Result of this research show that as the average noise levels increase within the noise zones, there is a general trend in increasing annoyance.

4. DISCUSSION:

Airport capacity continues to be one of the air transport issues that create the most concern regarding the degradation of the acoustic environment (Suau-Sanchez et al., 2011)

In this article, based on the results of an extended and comprehensive Strategic Noise Mapping research, introducing and evaluating the impacts of the IKIA International Airport future development. According to the survey results, areas adjacent to the airport that received L_{DEN} level of 60 to 65 dB (A), has land use of agricultural and poor pasture lands and often are arid lands that it is in accordance with FAA standards.

Areas with L_{DEN} of 65 to 70 dB (A) and 70 dB (A), which affected residents and workers IKIA airport, in the field of management measures for these individuals should considered.

In addition to, it should be noted that the above results (annoyed of residents from noise level Airport) is the current situation airport. While the results of CadnaA modeling of intermediate and future phases in IKIA airport indicate that noise levels in the future with the development of the airport, more residents are exposed to higher levels of L_{DEN} . Obviously annoyed levels of noise pollution levels will increase. Results of social study show that experimental group received the highest percentages of interference with sleep, television watching, telephone conversations and work/study. Wagner (2000) reports that two thirds of the individual variance in the reaction to noise is dependent on individual traits and the surrounding environment. He gives an example of how in visually attractive streets residents feel less annoyed than in visually unpleasant streets with the same level of noise. Wallenius (2004) reports that physiological effects and health complaints are more closely related to subjective reactions to noise than to the noise itself. The degree of human response to aircraft noise is not only a function of acoustic variables but also of certain non-acoustic variables. Insight in these variables is important in order to predict noise annoyance reactions better (Fidell, 1999) and also to deal with the problem of aircraft noise more effectively (Findell and Stallen, 1999). Although demographic characteristics significantly affect human reaction to noise (Miedema and Vos, 2005), research has shown that the most influential variables are social-psychological in nature, compromising attitudes towards the source, future expectations and feelings of control (Guski, 1999;

Kroesen et al., 2008). These findings confirm that the level of annoyance according to noise only is difficult to explain. Note that when residents are at home, they feel aircraft noise so they reaction to $L_{Aeq} (night)$ should be investigated. Therefore in this study, the analysis examined people's reactions to the parameter $L_{Aeq} (night)$. These parameters were obtained from field measurements and prediction by CadnaA model. The residents' responses according to the 12-hour night L_{Aeq} contour were statistically extracted according to the noise zone they were located in. The degree of annoyance increases directly with increasing noise level zone. IN $L_{Aeq} > 60$ dB (A) the combined moderately to highly annoyed responses indicate that all the respondents in this zone were annoyed by aircraft noise at night. Comparison of the two parameters (L_{DEN} and L_{Aeq}) has shown that people respond sever than L_{Aeq} parameter, the parameter is L_{DEN} . Distribution of residences per L_{den} and L_{night} for the three scenarios detailed in the following figures. (figs. 7-9).

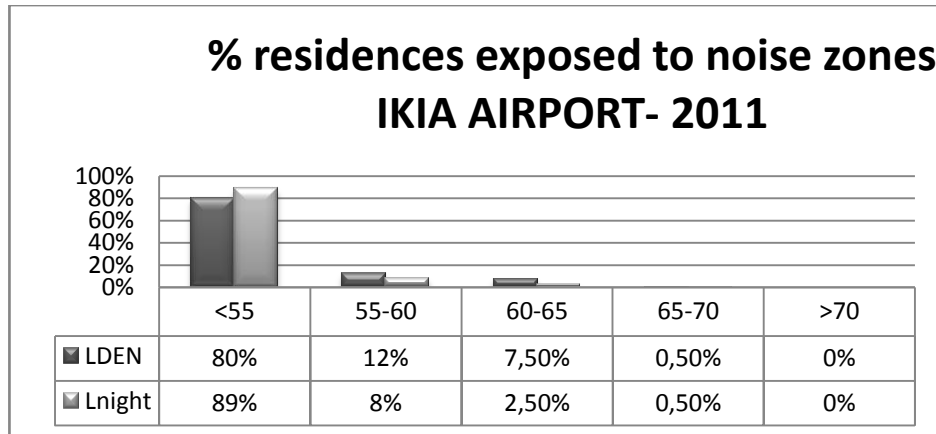


Figure 7: Distribution of residences per L_{den} and L_{night} for the scenario-2012

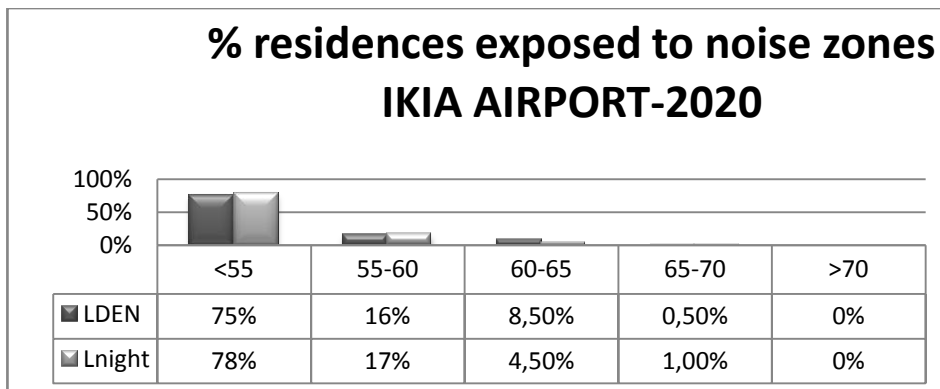


Figure 8: Distribution of residences per L_{den} and L_{night} for the scenario -2020

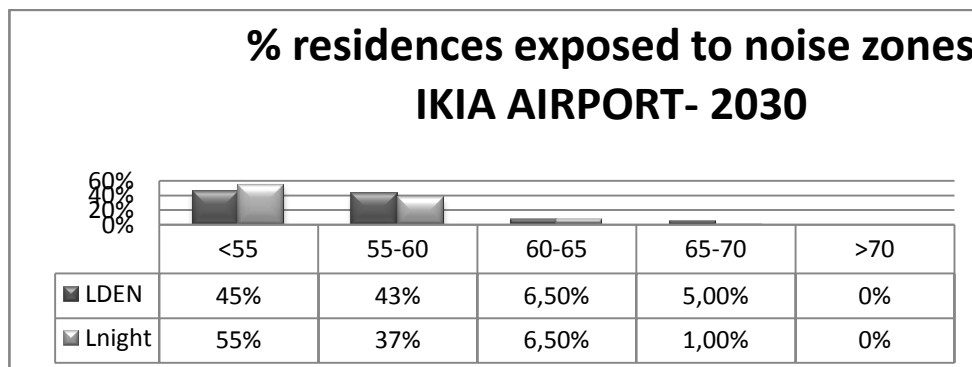


Figure 9: Distribution of residences per L_{den} and L_{night} for the scenario -2030

Given these findings, management and control of noise pollution from the IKIA airport is essential. ICAO has established the program, so called “Balanced Approach” for managing noise around airports, which includes four elements: reducing noise at source, planning and land use management, operational procedures to reduce noise and operational restrictions. This approach recommends that noise reduction measures should not seek a single solution, but a combination of different ones (Netjasov, 2012). The airport may choose to reduce noise levels by modifying operations with the use of a preferential runway system, special flight tracks, noise abatement flight procedures, and airport use restrictions. For large airports with multiple runways, a noise-preferential runway system can be used to change noise exposure patterns. With this procedure, a runway is utilized based on the noise impact it generates, along with other environmental factors such as wind direction. Using the same principles, some airports will modify flight paths based on noise exposure. With these tools, aircraft can be routed around noise sensitive areas (Horonjeff, 2010. Girvin, 2009).

While all of these mitigation strategies help reduce the negative impacts of excessive airport noise, only the coordination of development between airports and surrounding communities addresses the underlying land use conflict. Some municipalities have acknowledged the limitations of existing noise mitigation strategies and moved to implementing land use regulation to manage the problem. Early capacity and expansion planning can inform environmental planning officials in advance of potential noise impacts. Municipal governments, working with airport authorities, can plan for land use that complements airport economic activity while restricting incompatible uses (McDowall, 2012).

5. Conclusion:

Overall, the results indicate the compatibility of existing landuses around the IKIA airport with airport noise levels and alert for the development of residential areas in the near future.

In recent years, due to wrong policies, the land around the IKIA airport has been speculation and trading by land speculation and speculators have been common, So that perhaps the next decade around the airport is crowded. Current distance from residential areas surrounding the Airport include: Distance from Rabat Karim: 1400 meters, 2. Distance from Eslamshahr: 6 Km, 3. Distance from Hassan Abad: 4 Km. According to the growth in the residential areas of the IKIA airport, surely "the next decade with the problem of noise pollution in the area of IKIA airport will be met. CadnaA software results also indicate that developing airports with residential development will increase the airport's noise. Given the above, the need for proper management control and reduce noise from the airport is essential. Land use management measures used include both preventive and corrective techniques. Preventive land use management techniques seek to prevent the introduction of additional noise sensitive land uses within existing and future airport noise contours. Corrective land use management techniques seek to remedy existing and projected future unavoidable noise impacts in existing areas of incompatible land use. The responsibility for determining the acceptable and permissible land uses and the relationship between specific properties and specific noise contours rests with the local authorities. Also, the results showed that already moderate aircraft noise levels lead to intensive annoyance due to aircraft noise. Annoyance from aircraft noise depends on both acoustical and non-acoustical factors. The latter include fear of aircraft crashing, potential benefits, housing availability, possibilities for compensation, sensitivity to noise and so on. (Zaporozhets et al., 2011.)

6. References:

1. AzB. (1999). Neue zivile Flugzeugklassen für die Anleitung zur Berechnung von Lärmschutzbereichen (Entwurf). Berlin: Umweltbundesamt.
2. Babisch, W. (2006). Transportation noise and cardiovascular risk: Updated review and synthesis of epidemiological studies indicate that the evidence has increased. *Noise and Health*, 8, pp. 1-29.
3. Brown, V.A. (1999). Ground-truthing ecologically sustainable development. In Buckingham-Hatfield S & Percy S (eds) *Constructing local environmental agendas. People, places and participation*, pp. 140-155. London: Rutledge.
4. De Hollander, A. E. M. (2004). *Assessing and evaluating the health impact of environmental exposures*. Utrecht: Universities Utrecht.
5. Ebdon, D. (1977). *Statistics in geography. a practical approach*. Oxford: Basin Blackwell.
6. ECAC. (1997). CEAC, Doc 29. Report on standard method of computing noise contours around civil airport. adopted by the Twenty-First Plenary Session of ECAC; 2–3.

7. Farçaş a, F., Sivertun, Å. (2010). Road Traffic Noise: Gis Tools for Noise Mapping And A Case Study For Skåne Region. *The International Archives of the Photogrammetric, Remote Sensing and Spatial Information Sciences*, 34, pp. 1-10.
8. Federal Aviation Administration. (1998). *Airport Noise Compatibility Planning*, pt. 150, Federal Aviation Regulation, Washington, D.C.
9. Fidell, S. (1999) Assessment of the effectiveness of aircraft noise regulation. *Noise and Health*, 1, pp. 17-25.
10. Fleming, G., Malwitz, A., Balasubramanian, S., Roof, C., Grandi, F., Kim, B., Usdrowski, S., Elliff, T., Eyers, C., Horton, G., Lee, D. and Owen, B. (2008). Trends in global noise and emissions from commercial aviation for 2000 through 2025. 26th International Congress of the Aeronautical Sciences. Anchorage, Alaska.
11. Flindell, I. H. and Stallen, P. J. M. (1999). Non-acoustical factors in environmental noise. *Noise and Health*, 1, pp. 11-16.
12. Girvin, R. (2010). Aircraft noise regulation, airline service quality and social welfare: The monopoly case. *Journal of Transport Economics and Policy*, 44, pp. 17-35.
13. Girvin, Raquel. (2009). Aircraft noise-abatement and mitigation strategies. *Journal of Airport Transport Management*, 15, pp. 14-22.
14. Guski, R. (1999). Personal and social variables as co-determinants of noise-annoyance. *Noise and Health*, 3, pp. 45-56.
15. Hazard, WR. (1971). Predictions of noise disturbance near large airports. *Journal of Sound and Vibration* 15 (4), pp. 425-445.
16. Horonjeff, Robert M. and Francis, X. (2010). *Planning and Design of Airports*. New York: McGraw Hill Professional.
17. ICAO. (2004). A35-5: Consolidated statement of continuing ICAO policies and practices related to environmental protection. Published by authority of the Secretary General.
18. International Standard Organization (ISO). (2003). "Acoustics—Assessment of noise annoyance by means of social and socio-acoustic surveys," ISO/TS 15666.
19. Klæboe, R., Engeli, E., Steinnes, M. (2006). Context sensitive noise impact mapping. *Appl Acoust*;67:620–42.
20. Ko, J.H., Chang, S.I. & Lee B.C. (2011). Noise impact assessment by utilizing noise map and GIS: A case study in the city of Chungju, Republic of Korea, *Applied Acoustics*, Vol. 72, Issue 8, pp. 544-550. (doi:10.1016/j.apacoust.2010.09.002).
21. Kreshover, J., Larson, Ph., Lough, S., Merkt, E. (2000). *Integrated Noise Model Route Optimization for aircraft*, Systems Engineering Capstone Conference.
22. Kroesen, M., Molin, E. J. E. and Van Wee, G. P. (2008). Testing a theory of aircraft noise annoyance: A structural equation analysis. *Journal of the Acoustical Society of America*, 123, pp. 4250-4260.
23. Lim, C. and Lee, S. (2003). "Questionnaire on environmental noise: The core set," Center for Environmental Noise and Vibration Research. pp. 766-771.
24. McDowall, D. (2012). *planning on noise: the implementation of noise compatibility zoning in the northeast united states* , Submitted in partial fulfillment of the requirement for the degree Master of Science in Urban Planning, Columbia University, pp.1-40.
25. Miedema, H. M. E. (2007). Annoyance caused by environmental noise: Elements for evidence-based noise policies. *Journal of Social Issues*, 63, pp. 41-57.
26. Miedema, H. M. E., Fields, J. M. and Vos, H. (2005). Effect of season and meteorological conditions on community noise annoyance. *Journal of the Acoustical Society of America*, 117, pp. 2853-2865.
27. Netjasov, F. (2012). Contemporary measures for noise reduction in airport surroundings , *Applied Acoustics*, 73, pp. 1076-1085.
28. Suau-Sanchez, P., Pallares-Barbera, M., Paül, V. (2011). Incorporating annoyance in airport environmental policy: noise, society response and community participation. *J Transp Geogr* March 2011;19 (2):275–84.
29. che, O. Onyebuchi, U. (2011). *Using GIS for Analysis of the Runway Extension of Margaret Ekpo International Airport, Calabar, Nigeria*. Thesis for Master Degree in Geomatics, pp. 1-52.
30. Vogiatzis, K. (2012). Airport environmental noise mapping and land use management as an environmental protection action policy tool. The case of the Larnaka International Airport (Cyprus). *Journal of Science of the Total Environment*, 424, pp. 162-173
31. Wagner, D. (2000). German planning principles preventing and reducing environmental spillovers in urban areas. In Miller D & de Roo G (eds) *Resolving urban environmental and spatial conflicts*, pp. 39-62. Groningen: GeoPress.
32. Wallenius, MA. (2004). the interaction of noise stress and personal project stress on subjective health. *Journal of environmental psychology*, 24, pp. 167-177.
33. www.ikia.ir
34. Zaporozhets, O., Tokarev, V. and Attenborough, K. (2011). *Aircraft Noise Assessment, prediction and control*, published by Spon Press, ISBN 13: 978-0-415-24066-6 (hbk), pp. 1- 433.

Economies of scale and density in the public road transport: Empirical evidence for Tunisia

Mohamed Amine MEZGHANI and Younes BOUJELBENE

Department of Management, University of Management and Economic Sciences of Sfax, Street of Airport km 4.5, LP 1088, 3018, Sfax, Tunisia 1 E-mail: amine-mezghani@hotmail.com

Abstract

This study seeks to broaden the knowledge in the impact of the economies of scale and density drawn in and by the road transport sector in Tunisia so as to not only grasp the possibility of a substitutability of the production factors used but also highlight the importance of the global productivity achieved in the operation of means of transport for the users and the community. The study of the twelve urban, suburban and interurban regional public road transport companies of passengers and goods in Tunisia reveals the existence of a homogeneity in the total production of these companies which vary with the size of the networks, the number of stops, the number of employees, although it exists a strong heterogeneity concerning.

Keywords : *Economics of scale; Density; Transport sector; Translogarithmic function*

1. Introduction

Transportation is lifeline of economic development, and also an important component of the support, services and security system in sustainable and healthy development of national economy, Wang and Lu (2014). Since the seminal work by AMarshall (2006), when a company reduces costs and increases production volume, the internal economies of scale have been achieved. External economies of scale (EES) occur outside of the firm, within an industry. In fact, when an industry's scope of operations expands (due to the creation of a better transportation network that resulting in a subsequent decrease in cost for a company working within that industry), the EES are said to have been achieved.

During the last decades, many scientific analytical and empirical works have attempted to study the findings of the economies of scale and density in the public road transport sector. In the seventies of last century these works were interested in the concept of the substitutability, their total productivity and the relative concept to price elasticity and costing as well as economies of scale and density.

The previous main empirical works were based on cost estimates and production technology that can influence the charging structure in the transport sector. More precisely, these inputs were based on linear cost functions, Cobb-Douglas functions, Keller functions and Diwert second order translog arbitrary cost.

The rest of this paper is organized as follows. Section 2 focuses in the most relevant research finding in the literature. Section 3 deals with methodology and proposed approach. Section 4 describes the data. Section 5 presents results and empirical findings. Section 6 gives some recommendations and concludes this study.

2. Previous research finding

Many researches were undertaken on road transport building on a sequence of function of translogarithmic cost (Ayadi A and Hammami S 2012). According to Viton (1981), on a sample of 54 urban and suburban American agglomerations for the year 1975, who estimated his function by Sure-Zeller method (1962). The last drew that the American group bus network produces short-term and long-term rising economies of scale and density. Viton (1981) also noticed the existence of

substitutability between the two factors of production, that's to say the two inputs: work and energy (AES, $\hat{\nu}_{LF} = 0,22$) while stating that labor demand for urban small transport firms is inelastic to the price ($\mu_{LW} = -0,03$); which is not the case for the large firms ($\mu_{LW} = -0,19$). Besides, he concluded by maintaining that the energy demand is elastic to the price according to the various classification of the different firms with $(-0,19 \leq \mu_{FC} \leq 0,57)$.

For their part, Karlaftis and Mc Carthy (2002) estimated function of the variable translogarithmic cost from a sample of 256 urban and suburban group haulers in the period of time between 1986 and 1994 in the United State. Through their model, on the basis of Sure-Zeller method, they used the cluster analysis which allowed them to identify the gathering of individuals who shared the same attributes. Moreover, resorting to the variable (vehicles/miles) measuring the output in the road transport sector, they reached the following results: the existence of a common and increasing economy of scale and density with (ES = 1, 28) and (ED = 1, 33) where the two inputs work and energy are complementary ($\dot{\nu}_{LF} = -0, 55$). The demand of work and that of faintly elastic compared with their prices with ($\mu_{LW} = -0,17$) and ($\mu_{FC} = -0,45$). These results concern a common sample. On the other hand, when the sample was divided into six groups, the authors concerned affirmed the existence of an economy of scale and density between a constant value evolving towards another one sharply increasing ES is for (0,99 to 11) ; ED is for (0,99 to 20).

As a result, the two inputs work and energy are at the same time substitutable and complementary according to each group of haulers ($0,63 \leq \dot{\nu}_{LF} \leq -0,53$); while the demand of work and that of energy are faintly elastic comparing to their price ($-0.16 \leq \eta_{LW} \leq 0,24$) ; ($-0.45 \leq \mu_{FC} \leq -0.17$).

Keho.Y (2005) analyzed the contribution of the public investments to the private capital formation in Ivory Coast, using a co-integration test and an estimation of error correlation during the period 1965-2001. His analysis was concerned with the impact of the global public investment on the private investment which gave rise to a positive, significant relation between the two variables that means the first investment exerted a ratchet effect on the second one. This public capital was divided on six main components (education transport and communication, services, health, agriculture, mines and industries) and had a positive compact on the accumulation of the private capital with long term elasticity varying between (0.54) and (0.80) and this is thanks to the contribution, especially, of the transport, communication and education sector, since the compact exerted by the other sectors is not significant. Keho (2005) concluded by stating that the politic of public investment in the economic infrastructure is in the transport and communication sector or in the formation of human capital is an efficient instrument to stimulate growth and development of the private investment forming a fundamental factor for the attractiveness of the direct foreign investments.

Piacenza (2006) estimated a function of a variable translogarithmic cost by the maximum likelihood method using a cross-sectional database with a trend where its sample containing 45 transport company giving urban and suburban vehicles haulers during a period of six year from 1993 to 1999 in Italy. He used as variables the « place-vehicle/kilometers » and average speed as output. The chosen sample is heterogeneous; which encouraged him to work on a common sample and a classified one composed of various group. He could draw the existence of an economy of short and long term growing density.

These authors chose, as inputs, two variables representing the work factor which corresponds to the number of half time and full time employees; the capital factor contains the number of used buses. Furthermore, they have also chosen 2 outputs: « Place/km and Vehicle/ Kilometers ». They noticed in their studies that the economy of scale is increasing for small and medium-size enterprises and that there's a small increase of the technical efficiency during the average of the period. There is also a low increase of the average efficiency due to additional constraints.

Starting from these analytic and empirical results which are coherent and pertinent as for the study of the existence of an economy of scale and density in the urban, suburban and interurban road transport operation for certain developed and developing countries; starting from that we are going to wonder if such situations exist or not in the Tunisian public road transport? In other words does transport operation generate an economy of scale and density or not? In both cases how to grasp these situations? The answers for these questions prompt us to undertake an empirical analysis.

3. Methodology and proposed approach

We approximate the variable size of network by the total length of lines reserved for the twelve regional transport companies in Tunisia. We also estimate the variable number of stops by the stop indicating the place where vehicles stop to pick up or drop the passengers which concern the collection centre for captive transport. Furthermore, we determine the variable. Vehicle Park building on the acquired vehicles on the occasion of the creation or extension of the urban and interurban public transport service or the renewal of the used park for these services: buses, coaches, articulated buses, comfort coaches and minibus, etc. This allows us to calculate the number of employees by the total number of the company employees which is composed of: The administrative staff, the working and technical staff. Finally we estimate the production of the public transport service in the regional companies as a homogenous variable marked (Y). The variable production is calculated from the vehicle/kilometers travelled. This production gives a better representation not only of the average efficient capacity used to guarantee the service, but also of the distance traveled by the vehicles simultaneously.

To study the economies of scale and density in the public road transport for the twelve regional Tunisian companies from 1995 to 2014 on annual frequency, we refer to an artificial econometric model. Historically, the economies of scale and density are expressed by the production of the public transport service of these regional companies. This production (Y) corresponds to the endogenous variable for our data base. On the other hand, the explanatory variables are: the size of network (SN), the number of stops (NS), the Fleet (F), the number of employees (NE) and the production (Y). Indeed, empirically speaking, the link between the economies of scale and density in the public road transport sector in Tunisia concerns, the total length of lines reserved for the twelve regional transport companies (TR) the number of vehicle stops to pick up or drop the passengers (NS) the vehicle acquired on the occasion of the urban and interurban public transport service or the renewal of the fleet (F) and the number of employees (NE) to establish this link between these different variables, we refer to the main works of Viton (1981), De borger (1984), d'Obeng (1985), Thiry and Lawarée (1987) et d'Abbes and Bulteau (2003), to draw a base model which is presented in the form of the following Cobb-Douglass function:

$$Y_{it} = A_i (SN)_{it}^{\alpha_i} (NS)_{it}^{\beta_i} (F)_{it}^{\theta_i} (NE)_{it}^{\lambda_i} e^{\varepsilon_{it}} \quad \forall t = 1995 \rightarrow 2014 \text{ et } i = 1, \dots, 12$$

To test the homogeneity of all the coefficients and constants of our below reference model and to give an exact specification to this model, we use the logarithmic linear operation on the right and on the left. After its transformation our modal takes the following from:

$$\text{Log}(Y_{it}) = \text{Log}(A_i) + \alpha_i \text{Log}(SN)_{it} + \beta_i \text{Log}(NS)_{it} + \theta_i \text{Log}(F)_{it} + \lambda_i \text{Log}(NE)_{it} + \varepsilon_{it}$$

To give an exact specification of the temporal-individual double dimension we use Fisher homogeneity and heterogeneity tests. For this purpose, we adopt the two statistics of fisher (F1 et F3) to identify the common and different feature of all the parameters of our base model relating to the twelve regional public transport companies (SRT) in Tunisia for the period 1995-2014.

4. The descriptive statistics

The data base was extracted from the directorate general research and planning of the ministry of transport and from regional public road transport company balance sheets (land transport directorate). This base has a double dimension individual or spatial and temporal. The first corresponds to the twelve regional transport companies which are: Beja, Bizerte, Gabes, Gafsa, Jendouba, Kairouan, Kasserine, Kef, Medenine, Nabeul, Sfax and Sousse. The second represents the period from 1995 to 2014¹ on annual basis.

The analysis of the economy of scale and density in the public transport sector requires the implementation of a road infrastructure and the use of production factors. The optimal allocation of these factors, that's to say the labor and the rolling stock, is the fundamental determinant of the total factor productivity.

The combination of these two productions factors requires a dose of technology to achieve a certain level of output. The last represents the public transport service in our article. Our base for the

¹ Noticing that the information concerning 2014 are approximate; they estimated from anterior data.

temporary individual data concerns the explanatory and endogenous variables including: the Size of Network (SN), the Number of Stops (NS), the Fleet (F), the Number of Employees (NE) and the Production (Y).

In this statistical study we are going to choose the indicators of positions, dispersions and forms in order to study the normality, the adjustment and the estimation quality of each component of our base model. For this goal, Tables (1, 2 and 3) correspond to a descriptive analysis of the explanatory variables and the endogenous variable during a period of study from 1995 to 2014 on annual frequency concerning the twelve regional transport companies

Table 1 : The indicators of positions

Indicators Variables	Average	Médian	Maximum	Minimum	Observation
Log(Y)	9.97798	10.00462	11.51692	4.884089	240
Log(SN)	8.704679	8.772821	11.48018	3.763987	240
Log(NS)	9.0342	8.954139	11.54245	4.145513	240
Log(F)	5.132474	5.02703	10.23917	4.110874	240
Log(NE)	6.13845	6.001403	10.23917	5.293305	240

According to Table 1, we can conclude that on one hand, that the average for the five explanatory variables and the production of the companies transport services are a little high since the values of these variables are quite strong the median which shares the cumulated increasing frequency of each variable of our theoretical model which is grouped also into two is also strong for the explanatory variables and the endogenous variable of the base model. On the other hand, we must study the quality of estimation and the adjustment each component of this model by the indicators of absolute and relative dispersions. In order to achieve this, Table 2 corresponds to the dispersion criteria of these variables.

Table 2 : The indicators of dispersions

Indicator Variables	The Variance	Standard deviation	Coefficient of variation
Log(Y)	0.725634	0.8518415	0.0853721
Log(SN)	0.6426829	0.801675	0.092097
Log(NS)	0.4907143	0.70051	0.0775398
Log(F)	0.589895	0.7680462	0.1496444
Log(NE)	0.5253896	0.7248376	0.1180815

From the result of Table 2, we observe that the quality of estimation of these variables is very good since the variance of each variable below is too low. The linear adjustment of each previously mentioned variable is efficient because the standard deviations are low as well. Therefore we can conclude that is exists a good linear adjustment for the explanatory variables and the endogenous variables of our base model. Furthermore, it's necessary to study the normality of each variable of our reference model by the bias of the indicators of forms and Jarque and Berra statistics presented in the Table 3.

Table 3 : The indicators of forms

Indicators Variables	Kurtosis	Skewness	Jarque & Berra	Significance of JB
Log(Y)	7.385253	-0.8213214	0.0853721	0.9741264
Log(SN)	8.172581	-0.9443931	0.092097	0.961352
Log(NS)	12.84983	-1.121977	0.0775398	0.951423
Log(F)	25.42775	3.741124	0.1496444	0.901423
Log(NE)	13.6683	2.448337	0.1180815	0.914212

Table 3 shows that these variables follow a normal law because the statistics of Jarque and Berra are two degrees of freedom lower than the critical value of Khi-two. Likewise, these variables are asymmetric since the statics of Kurtosis are greater than three. Thus, we conclude that all these variables have parabolic branches with asymptotic direction towards the abscissa axis but these statics of Skewness tend this to zero. We could conclude that the production, the size of network and the number of stops are shifted to the left. However, the other variables are shifted to the right.

5. Results and discussions

5.1. Causal and correlational relationships

The study of dependencies relationships between the explanatory variables and the production of public transport services for the twelve regional companies during a period of study from 1995 to 2014 on annual frequencies is given the total matrix correlation describing the interrelations between the variables of our model.

Variables	Log(Y)	Log(TR)	Log(NS)	Log(F)	Log(NE)
Log(Y)	1.0000				
Log(SN)	0.8743	1.0000			
Log(NS)	0.8620	0.9382	1.0000		
Log(F)	0.5659	0.7160	0.6627	1.0000	
Log(NE)	0.6897	0.7278	0.6893	0.9288	1.0000

From this matrix we can say that it exists positive dependencies relationship between the endogenous variable and all the explanatory variables. Thus, there is a positive dependence between the production of public transport services for the regional companies, the size of the network, the number of stops, the vehicle fleet and the number of employees. So it exists, by the end of the day, a positive correlation between the number of employees and the other explanatory variables. The vehicle fleet exerts positive influences on the production, the size of the network and the number of employees. That's to say the transport services provided by these companies are according to the vehicle park, the more we increase the number of vehicles in use the more the available seats increase. We notice that the dependencies between the explicatory variables and the endogenous variable are very high. So, there's a strong correlation between the explanatory variables. As a result, there will be a multi-collinearity problem between these explanatory variables.

5.2. Specification tests

The static estimate of the linear function, relating the logarithm of the productions of the public transport services according to explanatory variables in log for the twelve regional companies during a study period from 1995 to 2014 on annual frequencies, requires as in a first step, the homogenous or heterogeneous verification and specification of the generative process of individual-temporal data. On the econometric front, this comes down to test the equality of coefficients our theoretical model studied in its individual dimension. On the economic front, the specifications tests amount to determining if we have the right to suppose that this production is perfectly identical for the twelve Tunisian regional companies of public road transport; or it's quite the reverse; there are specificities which are peculiar to each company. Our theoretical model could be written in the following from:

$$\text{Log}(Y_{it}) = \text{Log}(A_i) + \alpha_i \text{Log}(SN)_{it} + \beta_i \text{Log}(NS)_{it} + \theta_i \text{Log}(F)_{it} + \lambda_i \text{Log}(NE)_{it} + \varepsilon_{it}$$

The innovations ε_{it} are supposed to be «iid» with mean zero and variance of $\sigma_{\varepsilon}^2, i \in [1, N]$. Thus, we suppose that the constants $Log(A_i)$ of our model can vary in the individual² dimension..., but they are invariant in time. This model has many possible configurations (see Christophe Hurlin 2006)

Table 5 represents the tests of homogeneity heterogeneity of the model parameters.

Table 5 : The tests of homogeneities-heterogeneities		
	Homogeneity of constantes	Homogeneity of coefficients
$Log(Y_{it})$	55.06 (0.000)	0.63 (0.9124)

From Table 5, we conclude that all the production coefficients of the public road transport services are identical for the twelve regional companies even though the invariant effects are heterogeneous among these companies. Accordingly, our reference model is specified in the form of a panel with individual effects taking these following specifications:

$$Log(Y_{it}) = Log(A_i) + \alpha Log(SN)_{it} + \beta Log(NS)_{it} + \theta Log(F)_{it} + \lambda Log(NE)_{it} + \varepsilon_{it}$$

5.3. Static estimate of the production of the public road transport services in Tunisia

The specification tests show that our theoretical model can be formalized as a Panel with individual effects. In order to estimate the production of the public transport services of the twelve Tunisia regional companies of road transport during the period from 1995 to 2014 on annual frequencies we use Within and du GLS techniques. Table 6 recapitulates these two estimation procedures. In fact, in the observation of the static relation which links the production of the public transport services according to explanatory fundamental and behavioral variables?

Table 6 : Static estimation				
	Estimation Within		Estimation GLS	
Variables	Coefficients	Significativities	Coefficients	Significativities
Log(SN)	0.7710577	0.000	0.7770208	0.000
Log(NS)	0.1827413	0.000	0.1844504	0.000
Log(F)	0.5667019	0.000	0.5901751	0.000
Log(NE)	0.5098013	0.000	0.5415531	0.000

From table 6 we could say that the estimation, using these two techniques, gives positive and significant results for all the explanatory variables of our reference model. The production of public transport services is elastic with respect to the size of network that means the growth of road networks has a big influence on the rise of this public production even on the presentation of the provided services. This result matches Hirshhausen and Cullmann work (2010) for collective public and private transport system in Germany. However, the production of public transport services is less sensitive but positive to the number of stops. This interpretation is in agreement with Hirshhausen and Cullman's conclusion (2010) where the number of stops in Germany exerts a positive effect on the increase of production's volumes of the public services. The vehicle park, also, and the number employees have a positive impact on these volumes of transport production in Tunisia for both estimation procedures Within and GLS.

² With the exception of innovation variance which we suppose identical for all individuals.

Nevertheless, to arbitrate between the two estimation techniques, we must turn to Hausman's test (1979); Table 7 corresponds well to Hausman's test (1978) for the logarithm of the production of public road transport services.

Table 7 : Hausman test (1978)	
Log(Y) _{it}	
Stat-Hausman	$\chi^2(4) = 2.98 (0.5604)$

Table 7 shows that the production of public transport services for the twelve regional companies is specified by a Panel with random individual effects since Hausman's statistics is lower than Khi-two is 4 degrees of freedom below. This drives us to stick with the estimation results of this production using GLS techniques. The elasticities of the public transport production with respect to the explicatory variables are positive and significant, that means it exists or strong sensitivity between this production, the size of the network, the number of stops, the vehicle park and the number of employees.

These results are expected because the accumulation of the production of the public transport services requires an innovation of lines. Such an innovation can have a positive effect for the existence of an economy of density in the management of Tunisian public road transport concerned companies. The improvements of stops or stations for the used vehicles as well as a well-planned, efficient staff increase of the regional transport companies can have a positive impact on the management of these data. Table 8 corresponds to the constant estimation or the Random individual effects for the twelve companies using the GLS technique.

Table 8 : Estimation of Random individual effects		
Indicators	Estimation GLS	
Variables	Coefficients	Significant
Log(SN)	0.7770208	0.000
Log(NS)	0.1844504	0.000
Log(F)	0.5901751	0.000
Log(NE)	0.5415531	0.000
Estimation of Random individual effects		
Beja constant	1.470082	0.000
Bizerte constant	1.352885	0.001
Gabes constant	1.345887	0.001
Gafsa constant	1.076482	0.008
Jendouba constant	1.323406	0.000
Kairouan constant	1.64515	0.000
Kasserine constant	1.126698	0.002
Kef constant	0.9230292	0.013
Médenine constant	1.749658	0.000
Nabeul constant	1.126266	0.007
Sfax constant	1.626183	0.000
Sousse constant	1.967576	0.000

Finally, we can indicate that the estimation of individual effects by the generalized least-square method GLS gives expected and significant results. The estimated values of the constants are also very low; these ones mean that the average effects of the omitted variables are very low. Hence, it's a question of a good specification of the production of the public transport service with respect to the explanatory services since the unforeseen uncertainties are so low. We represent these random individual effects in the figure 1.

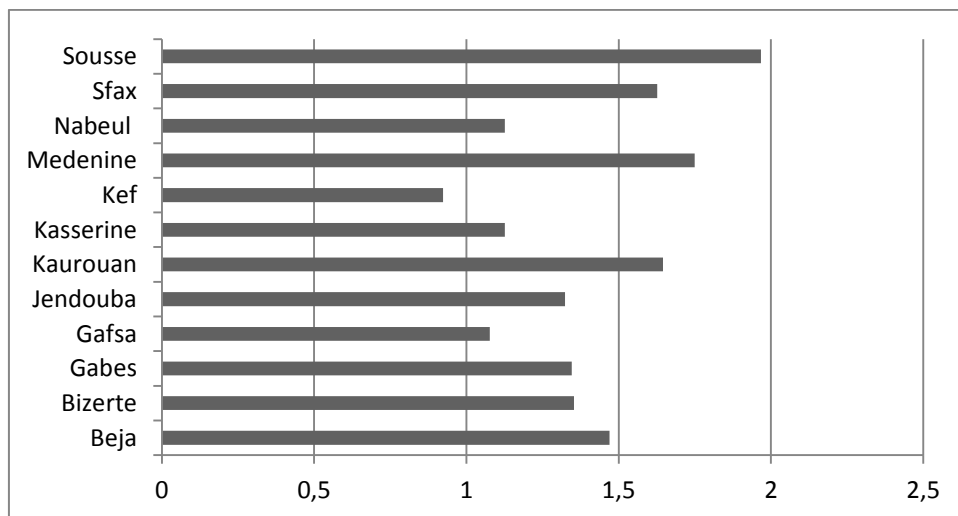


Figure 1, random individual effect.

6. Conclusion and recommendations

This paper provides some important evidence on the impact of the economies of scale and density drawn in and by the road transport sector in Tunisia, and the understanding of officials' perceptions of the role of transport in facilitating city growth. The trans-logarithmic production function has been used in order to detect the relationship between the used variables. We have concentrated on the twelve regional transport companies which are: Beja, Bizerte, Gabes, Gafsa, Jendouba, Kairouan, Kasserine, Kef, Medenine, Nabeul, Sfax and Sousse during the period 1995-2014 with annual data. Results show a big interdependence between the production of public transport services for the regional companies, the size of the network, the number of stops, the vehicle fleet and the number of employees. In fact, the principal findings of our study reveals the existence of a homogeneity in the total production of these companies which vary with the size of the networks, the number of stops, the number of employees, although it exists a strong heterogeneity concerning. Thus, despite of the shortage in staff and in rolling stock which are necessary for a proper operation of the public road transport run by the twelve regional companies, the focus of our study, we could affirm, considering our study on the urban suburban and interurban transport network, that the situation requires a strengthening not only in the field of infrastructure but also in the operation of the public road transport lines in Tunisia.

References

Abbes S and Bulteau J (2003) Analysis of the productive efficiency of the urban transport networks in France. University of Calgary,

De Borger L (1984) Cost and Productivity in Regional Bus Transportation: The Belgian Case. The Journal of Industrial Economics, Vol. 33, No. 1. pp. 37-54.

Diewert W E (1974) Functional Forms for Revenue and Factor Requirement Functions. International Economic Review, Vol 15 (1), pp 119-130.

Hausman J (1979) The Econometrics of Labour Supply and Convex Budget Sets », Economics Letters, 3, pp. 171-174.

Hausman J (1978) Specification Test in Economics. Econometrical, Vol.46, n°6, pp.1251-1271.

Hirschhausen C V and Cullmann A A (2010): «A Nonparametric Efficiency Analysis of German Public Transport Companies», *Transportation Research Part E*, Vol 46(3): pp 436-445.

Hurlin Christophe (2006) Network Effects of the Productivity of infrastructure in Developing Countries. Policy Research Working Paper No. 3808, WorldBank.

Karlaftis M G and Mccarthy P (2002) Cost structures of public transit systems: a panel data analysis. *Transportation Research Part E*, Vol 38, pp.1-18.

Keeler T E (1974) Railroad Costs, Returns to Scale and Excess Capacity. *Review of Economics and Statistics*, Vol 56, pp.201-8.

KEHO Yaya (2005) Efficacité macroéconomique du crédit bancaire en Côte d'Ivoire, Document de travail n°118, CAPEC, Côte d'Ivoire.

Obeng K (1985) Bus transit cost, productivity and factor substitution. *Journal of transport economics and policy* may, pp.183-203.

Piacenza M (2006) Regulatory Contracts and Cost Efficiency: Stochastic Frontier Evidence from the Italian Local Public Transport. *Journal of Productivity Analysis*, Vol 25(3), pp. 257-277. <http://www.hermesricerche.it/elements/wp02-2.pdf>.

Thiry B and Lawaree J (1987) Productivité, coût et caractéristiques technologiques des sociétés belges de transport urbain. *Annales de l'économie publique, sociale et coopérative*, Vol 4, pp 369-96.

Viton P (1981) A Translog Cost Function for Urban Bus Transit. *The Journal of Industrial Economics*, Vol. XXIX, 3 (March), pp. 287-304.

Zellner A (1962) An Efficient Method of Estimating Seemingly Unrelated Regressions (SUR) and Tests for Aggregation Bias. *Journal of the American Statistical Association*, Vol 57, pp. 348-368.

Wang, Z., & Lu, M. (2014). An empirical study of direct rebound effect for road freight transport in China. *Applied Energy*, 133, 274-281.

Marshall, Alfred. (2006). Industry and trade. Vol. 2. Cosimo, Inc.,.

Air quality in an urban public transportation network: local-scale determinants

Bogdan MURESAN* & Denis FRANÇOIS*

*LUNAM Université, Ifsttar, AME, EASE, F-44344 Bouguenais, France (EU)
Fax +33 (0)2 40 84 59 92 - email: bogdan.muresan-paslaru@ifsttar.fr

Abstract

Air quality, in terms of particles and particulate polycyclic aromatic hydrocarbons (PAHp), is probed in vehicles, stations and the ambient environment of a public transportation network located in a major French agglomeration. The network under examination comprises conventional and specific site public transports (SSPT). The objective of this study is to find determinants for air quality in urban public transport systems. Mobile measurements show that the air quality proposed to public transport users is driven by transport-system independent (external) and dependent (internal) variables or a combination of both. External variables consist of outdoor processes that partake into the build-up or clearance of ambient particulate pollution. Internal variables instead include the particulate generation and transfer processes relating to the configuration, structure and use of public transports and related equipment. Hence, air quality in transports and served stations is highly volatile and hardly explicable by means of large-scale (i.e. regional and/or urban background) pollutions. It exhibits sharp temporal and spatial variations (i.e. at the scales of seconds or meters), which in some cases, superimpose on durable (i.e. up to tens of minutes or over kilometers) evolutions. The array of variables further results in a variety of particulate pollutions including, but not limited to: authigenic particles in certain SSPT, coarse particles from transports' passageways or PAHp-loaded fines from road traffic.

Key-words: *urban area, specific site public transport, particulate pollution, mobile measurements.*

1. Introduction

For several decades, air quality is a public health concern. A poor air quality may be responsible of various pathologies. This is especially true in urban areas where the transportation sector is one of the most important causes of air quality deterioration [Joumard et al. (1996), Vlahov and Galea (2002)]. Among other things, this regards the airborne particulate matter and polycyclic aromatic hydrocarbons (PAH), and their respective increased risks of cardiovascular and respiratory diseases or cancer [Vuković et al. (2014), Chart-asa and Gibson (2015)].

Airborne particles and PAH levels are two parameters widely considered for the evaluation of urban air quality [Gros et al. (2007), Silva and Mendes (2012)]. Despite wide variations among sites, around 25% of particulate matter (PM) in the atmosphere is thought to originate from road transport, and particularly, from diesel engines (combustion of gasoil) [Barbusse and Plassat (2005)]. Exhaust PM is initially made of carbon nucleus (few nanometers in diameter) on which various organic species can adsorb (unburned hydrocarbons, oxygen derivatives and PAH). Hence, PAH-loaded fine particles are often considered as indicators of high temperature combustion sources typical of environments affected by road transport emissions. Several PAH are known for their carcinogen, mutagen and teratogen risks for human being [Azevedo et al. (2013)]. Benzo[a]pyren is often used to set exposure threshold values [e.g. 1 pg/L for particulate with a 50 % efficiency cut-off at 10 μm aerodynamic diameter (PM_{10}), yearly average value; EU (2005)]. Through collisions, the fine exhaust particles agglomerate (nucleation phenomenon) and can reach up to several tens of microns. Exhaust particles in the atmosphere further sums with micrometric dust particles that partly originate from local or distant sources (including industries and agriculture) as well as from the wear of urban materials (e.g. re-suspended road-particles or abrasion of metallic or concrete surfaces). The accumulation of PM in the atmosphere, even at relatively low concentrations (50 ng/L), may result in respiratory effects in short time scale. In longer time scales, ambient particles can result in mutagen and carcinogen risks.

Many initiatives have been taken in several urban areas around the world to promote the shift from private car to public transport. These are intended to reduce the transportation sector total emissions: i.e. through decreased amounts of vehicles in transit; less congestion [Almasri et al. (2011), Batty et al. (2015), Schindler and Caruso (2014)]. In certain places, Park and Ride (P+R) facilities are implemented

as elements of urban sustainability strategies in order to help incoming drivers to leave their car at the periphery and to ease the use of public transport toward the city center [Dijk et al. (2013)]. To reach a maximal benefit such P+R facilities are often associated with urban public transports having specific right-of-way, also called specific site public transports (SSPT). Indeed, compared to conventional public transport, SSPT have the advantage of facilitating the movement of vehicles in urban traffic, improving the efficiency of service to users (speed, punctuality) and allowing to reduce vehicle fuel consumption through improved regularity of engine pace (vehicles escaping congestion, reducing traffic stop-and-start episodes). SSPT can further be equipped with less emissive engines (e.g. electric or natural gas-powered), thus reducing the local concentrations of pollutants inherent to the diesel or gasoline fuels (especially PM or NO_x) [Gonçalves et al. (2009)].

The relationship between air quality inside and outside of vehicles can vary according to various parameters [Chan and Chung (2003), Tartakovsky et al. (2013)]. More specifically, the objective of this research is to find clear determinants for air quality in urban public transport systems. To reach this goal, mobile measurements are carried out inside public transport vehicles (PTV), at different stations where they stop and in the surrounding air. The aim is to identify the greatest possible range of causes of variation in the quality of the air inhaled by public transport users in the different phases of their travels. Herein, air quality is assessed through its particulate content, and PAH associated to particles (PAHp). The measurements are conducted in a given urban background submitted to usual urban pollution sources, among which road-traffic [Zamboni et al. (2009)].

Engaged in a transport policy intended to favor the shift toward public transports, in addition to P+R facilities, the city of Nantes (west of France; 47°12'17" N, 1°32'46" W) presents a large variety of SSPT modes. This provides the additional opportunity to assess the in-vehicle and the immediate outdoor air quality offered to users for different SSPT modes. Hence, a secondary objective is to assess the possible significant differences in air quality between different SSPT modes.

The methodology and the material used in order to examine pollutants concentrations in the air, the characteristics of the study site and the organization of measurements are presented first. Then, results are given and discussed for the various urban areas located in the scope of the study. The latter results give elements of interpretation for air quality signals recorded at (as well as in the vicinity of) the stations and PTV of each SSPT line. Ultimately, interrelations are sought between outdoor particulate pollution levels and the air quality at stations and in PTV. This is done for different categories of particles with respect to the configuration of the transport lines, the typology of transports, the local urban contexts, the road-traffic density, etc.

2. Materials en methods

Study site characteristics

The study focuses on an urban renewal area of the Nantes center, located between two arms of the Loire River (namely Ile-de-Nantes). The extent of this island is 4.9 km from East to West, and 1 km at the maximum in width. This area is a major path between the center and the south parts of Nantes' urban area (circa 600,000 inhabitants). In its central part, the island is crossed by a tramway (hereafter referred as TW) line. Parallel, in the east of the island, is a busway (RBW) line. More recently (in 2013) a chronobus (PBW) line has been implemented from the west end of the island to its east part. This cuts perpendicularly the tramway and busway lines, and finally joins the Nantes railway station. Both the TW and the two kinds of buses (bus rapid transits - BRT) offer to users a high level of service. The RBW, similarly to the tramway, benefits from a reserved part of the street, not accessible to other vehicles and is priority at crossroads. The PBW benefits from a specific lane in the street delineated with ground marks but, in some areas, equally displays mixed traffic sections. PBW vehicles have also priority at crossroads. Both the RBW and PBW are powered by natural gas (NG), while the tramway is electric. To allow comparison with conventional public transports, an ordinary bus line (OB, consisting of NG-powered vehicles) is further considered in this study. The location of the latter is chosen on the possible route of a SSPT project.

The study area gathers the three types of SSPT + OB line in a single urban domain of 3.4 km². The proximity among transports helps to keep meteorological conditions and the road-traffic relatively homogeneous in the course of each campaign. From this point of view, this would allow more reliable comparisons between SSPT modes than from distinct sites [Choi et al. (2013), Font et al. (2014)]. Moreover, this choice highlights the contrasts due to different urbanization strategies at the scale of districts.

Data collection periods and protocol

The study is carried out from 4 measurement campaigns with a duration of 4-5 hours each, on the 5th and 13th of June 2014, and on the 10th and 11th of July 2014. The measures are all carried out in the morning in order to fit with a single time slot, corresponding furthermore to the daily gradual traffic increase. The weather conditions are cloudy or overcast. The air temperature is 15-21 °C. A light wind mainly blows northeasterly or southeasterly though it once veers southwesterly.

The investigation method is to adopt the posture of a public transport user by browsing the different public transport lines of the study site with a portable device of data acquisition. The protocol is based on measurements into in-use vehicles and in a number of stop stations (1 to 11): 4, 5 and 4 stations for PBW, RBW and TW, respectively. The numbering of stations follows the data collection path (Table 1). An extra station (n° 0) serves as a terminal site for measurement conducted in OB vehicles (i.e. 11-0 section). Two stations are interconnections between SSPT lines; namely, Station 2 (PBW/TW) and Station 3 (PBW/RBW). As elements of comparison and interpretation of results on the monitored public transport lines, air quality measurements are also carried out on some journeys made on foot: sections 4-5, 8-9 and 0-1. On the same days, three additional areas, located in the center of Nantes (namely Sites S_A, S_B and S_C), are monitored to supplement the existing data with respect to the influence of urban environment and traffic conditions on ambient pollution levels.

Transport	Index	Land-use typology	Urban framework	Road traffic (veh./d)
PBW	Station 1	Recreational	Spaced	11,900
PBW	Section 1-2	Recreational/Residential	Spaced	6200-13,100
PBW/TW	Station 2	Residential	Spaced	16,400
PBW	Section 2-3	Residential	Mixed	10,200
PBW	Station 3	Residential	Confined	23,100
PBW	Section 3-4	Residential	Mixed	6900-20,600
PBW	Station 4	Industrial (transport sector)	Spaced	10,800
On foot	Section 4-5	Residential/Industrial	Spaced	11,700
RBW	Station 5	Residential/Recreational	Spaced	21,100
RBW	Section 5-6	Residential	Confined	20,400
RBW	Station 6	Residential	Confined	19,700
RBW	Section 6-3	Residential	Confined	21,400
RBW/PBW	Station 3	Residential	Confined	23,100
RBW	Section 3-7	Residential	Confined	23,400
RBW	Station 7	Residential	Confined	23,700
RBW	Section 7-8	Residential	Mixed	25,100
RBW	Station 8	Residential	Spaced	22,400
On foot	Section 8-9	Residential	Spaced	18,600
TW	Station 9	Residential	Spaced	21,600
TW	Section 9-10	Residential	Spaced	34,600
TW	Station 10	Residential	Mixed	14,600
TW	Section 10-2	Residential	Mixed	14,300
TW/PBW	Station 2	Residential	Spaced	16,400
TW	Section 2-11	Residential	Spaced	16,700
On foot	S _A	Residential	Confined	5600-28,900
On foot	S _B	Residential	Spaced	4000-15,000
On foot	S _C	Recreational	Spaced	6400
TW/OB	Station 11	Residential	Confined	23,300
OB	Section 11-0	Residential	Spaced	12,800-21,500
OB	Station 0	Industrial (food sector)	Spaced	21,300
On foot	Section 0-1	Recreational	Spaced	10,800-20,500

Table 1. Indexes, land-use, urban framework and local road traffic for the monitored stations and sections. Travels are from top to bottom indexes. The daily mean road traffic values are for 2012 [Auran (2014)].

Stop stations are all equipped with shelters for users on hold. When the configuration of shelters is favorable, measurements of air quality are carried out not only on the front side of the shelter (location where users are typically waiting for PTV), but also behind the glass of the shelter, in the aim to assess any screen effect toward the pollution from the traffic or the surrounding. Table 1 shows all the sections and stations of measurement of the study.

Air quality measurement

Measurements of air quality are carried out in real time by using an autonomous particle counter (Grimm EDM 1.108) connected in series with a particle-bound PAH (referred as PAHp) detector (Grimm 130). Data is stored on-site on a mobile computer. Particle concentrations are measured every 6 seconds via re-diffusion of a laser beam. PAHp measures are obtained every minute (photo-ionization of aromatic cycles exposed to UV rays). This measurement doesn't differentiate PAH congeners.

The particle counter is able to measure from 1 particle/L to $2 \cdot 10^6$ particles/L. Here, liter (L) is used instead of cubic meter (m^3) since it is consistent with the lung volumes and capacities of public transport users. After gravimetric measurement of internal filters (GF/F grade glass microfiber and/or PTFE disks), the accessible mass concentrations are from 0.1 ng/L to 100 $\mu g/L$. The size of detected particles ranges from 0.35 μm to 23 μm . After appropriate calibration by measuring (through GC/MS analysis) PAH in the filter sample extracts, the PAHp detector is able to measure from 0.001 ng to 5 ng of PAHp per liter. The accuracy of measurement is above 85%, for a variability below 5% regarding the particle counter, and below 10 % regarding the PAH detector.

The analytical system (particle counter + PAHp detector + computer) is implemented in a 2-wheel shopping trolley, allowing easy moving into PTV and along the streets (total weight less than 15 kg). The outlet of the air intake pipe (antistatic) is set circa 1 m above the ground. This is an intermediary height between airborne particles from the regional / urban background and particles from immediate sources (exhausts, dust (re-)suspension, wheel and asphalt abrasion, etc.). This also corresponds to the mean height for children and individuals seated at stations as well as in PTV.

3. Results and discussion

Air quality in various urban areas

Air quality in PTV likely depends on the ambient pollution levels. On foot measurements show that some industrial areas (Station 4, which account for Nantes' central railway station; see thereafter) and zones displaying dense road-traffic (i.e. over 20,000 veh./day like Station 11 and S_A) are depicted by elevated number concentrations (PN) (Fig. 1). The latter zones concentrate both individual vehicles and PTV, which might locally account for increased PAHp concentrations (punctually up to 83 ± 3 pg/L). Since $94 \pm 2\%$ of PN consist of $< 1 \mu m$ in diameter particles, it is probable that measured PAHp-loaded particles originate from vehicular exhausts and/or a

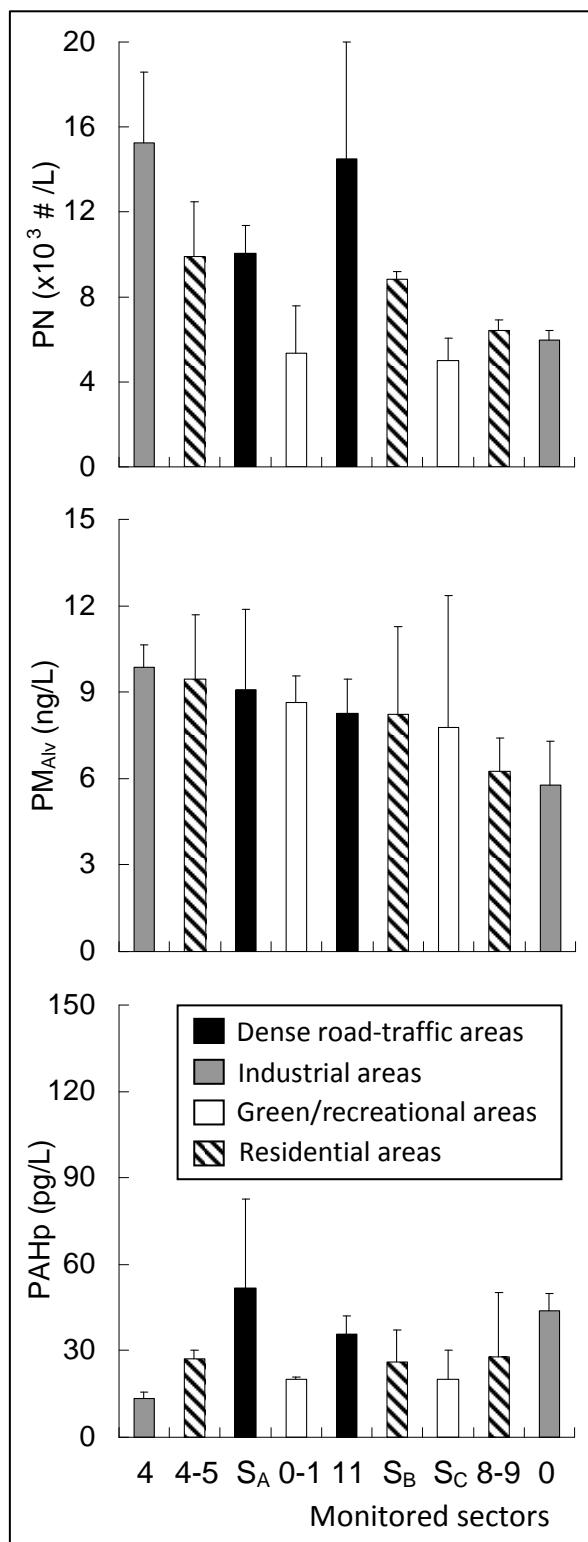


Figure 1. Air quality as a function of urban sectors. Areas S_A , S_B and S_C account for additional surveys carried out at the same date in central Nantes. These were intended at probing the role of urban texture on particulate pollution levels.

(re-)suspension of fines from road surface. The significant preponderance of $<1 \mu\text{m}$ particles may also contribute to keep alveolar mass concentration (PM_{Alv}) low: i.e. comparable to this in recreational areas. Accordingly, by exclusively basing onto mass concentrations, one may fail to capture the actual degree of particulate pollution in densely trafficked zones. This is apparent when considering the absence of significant difference in PM_{Alv} concentrations between industrial/trafficked zones and green/recreational areas.

The industrial activity in Nantes mainly involves light and intermediate industries in order to produce consumer-/business-oriented goods or services. This often takes place in small or medium size facilities such as commercial platforms or warehouses. Measurements indicated that distinct industrial activities partake in different pollutions. Indeed, industrial area related to Nantes' central train station shows increased PN and PM_{Alv} concentrations but low PAHp levels. Comparatively, the truck-trafficked zone near Station 0, which corresponds to an area dedicated to food industry, exhibits low PN and PM concentrations but significant PAHp levels (Fig. 1). Hereafter, PM refers to PM_{Alv} , PM_{Tho} and PM_{Inh} group. Put differently, the PAHp content of dust almost doubles. This accompanies a step-up in the contribution of coarser particles (i.e. $>1 \mu\text{m}$): from $6\pm 2\%$ to $11\pm 1\%$ of PN. Possible reasons would be the (re-)suspension of polluted soils, tire wear and/or tear of asphalt fragments by passing trucks.

The texture (i.e. the arrangement, dimensions and shapes of constructions) of urban areas and local road traffic density partly control the quality of immediate air. This, in turn, may condition pollution levels in PTV. For instance, open urban areas, i.e. depicted by spaced environments (Area S_B) surrounded by low-rise buildings, and areas that adjoin large water bodies (Section 8-9 or 0-1), display moderate PM and/or PAHp levels, in spite of notable road-traffic. Conversely, confined urban environments result in degraded air quality *via* local accumulation of industrial, residential and road traffic emissions. This is the case for Area S_A , and, to a lower extent, Station 11 and Section 4-5. The latter partly undergoes particulate emissions from the nearby industrial area around Station 4.

Air quality in public transport vehicles and at stations

The mean PN and PM concentrations at PBW stations (in this part of the manuscript, we focus on the front side of shelter where users are usually waiting for PTV) rapidly increase between Station 1 and 2 then stabilize at intermediate levels: $(9.3\pm 0.4) 10^3 \text{ \#}/\text{L}$ and 10.6 ± 0.8 (PM_{Alv}), 23.9 ± 0.8 (thoracic, PM_{Tho}) and 32 ± 1 (Inhalable, PM_{Inh}) ng/L, respectively (Fig. 2). Furthermore, Stations 2 and 3 show more pronounced PAHp concentrations (50 ± 20 and 47 ± 2 pg/L, respectively). As could be expected, and unlike for Station 1 (relating to a recreational area) or 4 (associated to an industrial area), these locate in more heavily trafficked zones (Table 1). This confirms the previous results on the central role of road-traffic on outdoor pollution levels and, presumably, on air quality at stations. The in-vehicle PN and PM concentrations, however, exceed by a 2.8-3.4 factor these at stations. This demonstrates a lowering in in-vehicle air quality that is not commensurate with the outdoor pollution levels. The highest degradation is measured at Section 1-2. There, mean PM_{Alv} , PM_{Tho} and PM_{Inh} concentrations reach up to 35 ± 10 , 90 ± 10 and 120 ± 20 ng/L, respectively. As the PBW vehicles run towards Station 4, PM levels tend to progressively decrease whereas PN exhibits a clear maximum at Station 3. On the one hand, this pattern suggests the existence of in-vehicle sources of coarse particles. These coarse particles, which amount to 15-20% of PN, are emitted before PBW vehicles leave the terminal stations. On the other hand, it indicates a localized (i.e. near Station 3) contamination of the in-vehicle air with outdoor PAHp-loaded fines. Actually, it is possible that the nominal size of PAHp-loaded fines, which is not accessible using our measurement system, rapidly increases as these come in contact with coarse particles previously generated into PBW vehicles.

The mean PN and PM concentrations at RBW stations are comparable to these at PBW stations: mean differences range from 3 to 19%. Largest PN concentrations are from Station 5 and Station 3. The latter also presents the highest PM levels (Fig. 2). As previously indicated, Station 5 in part undergoes PN emissions from the nearby industrial area around Station 4. Station 3, accounts for the central part of a confined urban environment (a transportation corridor surrounded medium-size and tall (>10 -storey) buildings that runs from Station 6 to Station 7). Furthermore, the corridor concentrates road traffic (from 19,700 to 25,100 veh./d). This urban context likely contributes to the pronounced PAHp levels at stations as well as in PTV that run through the area (Fig. 2). As a matter of fact, between Station 5 and Station 7, PAHp concentrations increase by a factor 3 and +50% at stations and RBW vehicles, respectively. It is also worth noticing the strong PM concentration in RBW vehicles (especially of coarse PM fractions) at Section 5-6. The latter section immediately follows a terminal/departure station. The larger coarse particle contributions (10-15% of PN) and significant

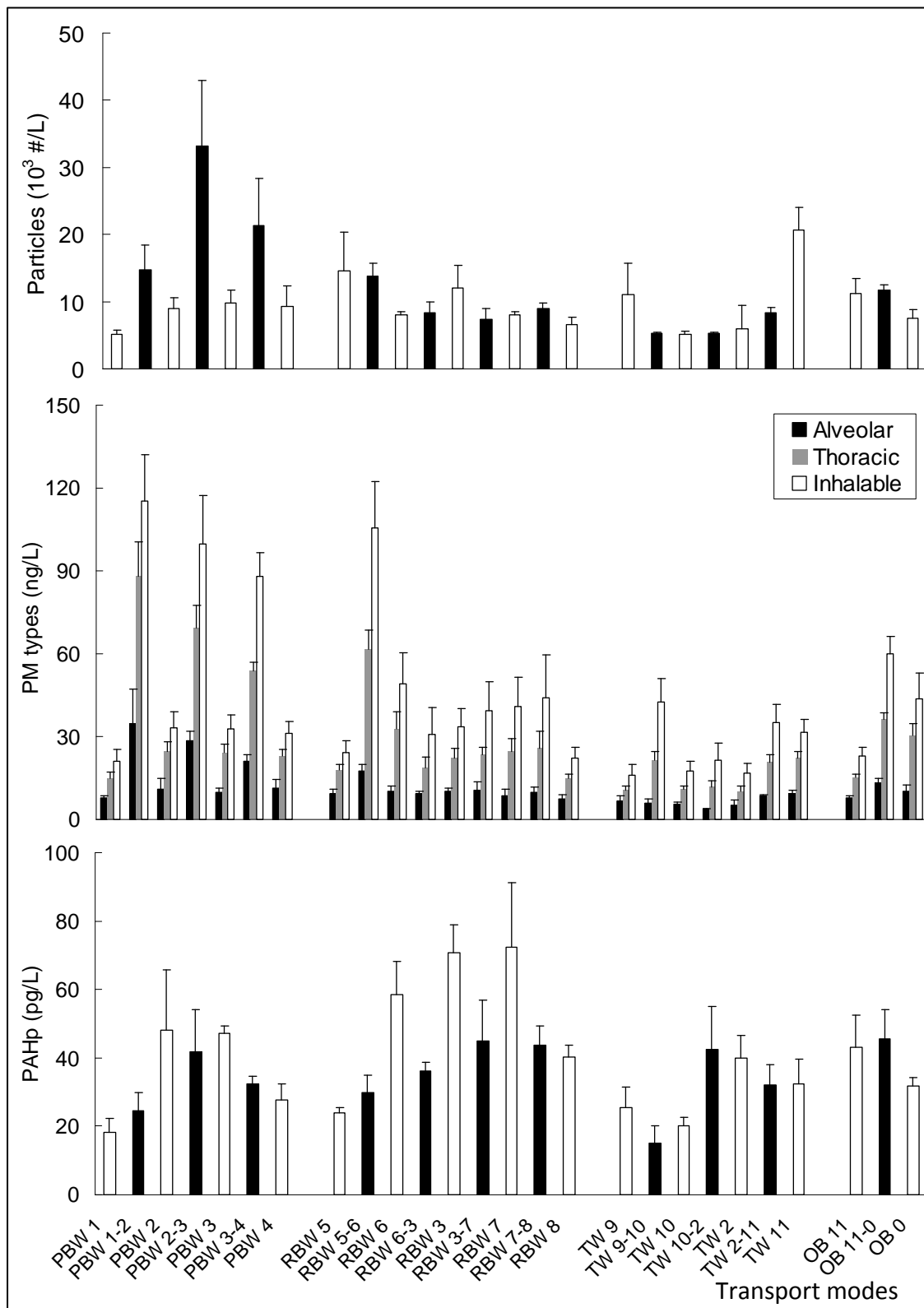


Figure 2. Mean (\pm standard error) particulate and PAHp concentrations at stations (front side of the shelter) and in PTV. Distinction is made in the middle panel between alveolar, thoracic and inhalable particulate matters.

decreases in in-vehicle pollution levels as RBW vehicles stop at Station 6, indicates an initial contamination of in-vehicle air. This is consistent with measurements carried out in PBW vehicles. Alternatively, gained results suggest that certain RBW users and the driver would be exposed, at least, to the internally generated coarse particles and the PAHp-loaded fines from the outdoor immediate pollution.

Comparatively to PBW and RBW, TW measurements indicate an overall improved air quality: mean PN, PM and PAHp concentrations at TW stations and in transports stand for 0.4-0.9 and 0.2-0.9 of these for PBW or RBW lines, respectively. This probably comes from the apparent absence of major particulate sources around TW line. The densely trafficked section 9-10 (Table 1) accounts for a bridge crossing the Loire River, which, as previously mentioned, may act as an immediate sink for vehicular emissions of fines and related PAHp. Elsewhere, the surrounding urban texture is usually characterized by family houses and medium-size buildings, which also tends to limit particulate accumulation in the immediate atmosphere. Besides, since TW vehicles are electricity-powered, their direct emissions of combustion-type particles are practically zero. In-vehicle particulate generation processes, however, cannot be fully refuted (see below). It is worth noticing that, at Station 2 and in TW vehicles that run through Section 10-2, larger PAHp concentrations (close to 40 pg/L, Fig. 2) are observed. Since the associated PN and PM levels are low, it is possible that PAHp-loaded (up to 4 ± 1 ng/g) (ultra) fines, which, unlike PAHp, cannot not be detected by using our analytical system, locally accumulate. TW Station 2 is circa 50 m away from PBW Station 2: both stations are therefore located in a relatively trafficked zone. The distance between TW and PBW stations, along with the time difference between measurements (about 3 h), may be responsible for the discrepancy in PM concentrations. The previous data for TW line air quality does not take into account the high concentrations measured at Station 11: there, PN and PM concentrations exceed by a factor 1.9-2.8 these in the rest of the TW stations. It has been previously mentioned that Station 11 is depicted by a dense road-traffic (including individual vehicles and PTV) within a confined urban environment. Yet, since this is in the central square of Nantes, and due to the low/medium size of buildings, the confinement is less marked than for other highly trafficked zones. Hence, the mean PAHp levels are comparable to these observed at Station 2 (32 ± 7 vs. 40 ± 7 pg/L) but significantly (50-60%) lower than these observed at RBW stations. Gained values must nevertheless be proportioned to the local road traffic estimated to 23,300 veh./d.

On the one hand, OB stations display PN and PM concentrations similar to, or lower than, RBW stations (from 0.6 to 1.2 of multiplicative factor) (Fig. 2.). On the other hand, except for Section 5-6 data (which account for in-vehicle generated PM), PN and PM concentrations in OB vehicle are significantly higher than in RBW vehicles (multiplicative factors ranging from 1.4 to 1.6). This means that in the absence of in-vehicle particulate generation, and despite increased outdoor/at-station pollution levels, SSPT vehicles may offer an enhanced air quality with respect to the PN and PM of ordinary buses. Yet, this is not true for all SSPT modes, day-period, types of pollutants or travelled areas. To exemplify, PAHp concentration in a particular PTV is in part driven by PAHp levels at served stations or crossed sections (see above). Providing accumulation (resp. removal) dynamics in SSPT (resp. OB) vehicles is fast enough, PAHp concentrations in SSPT vehicles would eventually exceed these in OB vehicles. This is the case for RBW vehicles running in Section 3-7 and 7-8: mean concentrations of 43-45 pg/L (vs. 43 pg/L in OB vehicles). Besides, the SSPT vehicles that undergo in-vehicle particulate generation processes exhibit, at least temporarily, larger PM and PN concentrations than OB ones. These results underline the importance of the equilibrium between in-vehicle particulate build-up and removal along lines.

Particulate pollution levels around stations

Significant changes in air quality are observed around stations for all but the public transport lines (Table 2). In most cases, the highest mass concentration values are measured at the front side of stations (where the users typically wait for PTV). The contrast between the front side and the rear of stations is especially pronounced for coarser particles (including $PM_{T_{ho}}$ and $PM_{I_{nh}}$) whereas lower or insignificant spatial variations are seen for finer (PN or $PM_{A_{lv}}$) fractions. Furthermore, as the d/D ratio values indicate, over the 0.35-23 μm range, the number contribution of $>1 \mu m$ in diameter particles is also increased at the front side of stations. This suggests that the recorded spatial variability in mass concentrations around stations would not only come from the direct proximity to PTV exhaust emissions but also from induced (re-)suspension of coarse particles and their subsequent dispersal/deposition dynamics. All these observations support the fact that both the tested BRT and, to a higher degree, the OB transport mode contribute to accentuate the particulate pollution with coarse particles in the vicinity of public transport passageways. This is less the case for the TW line. Despite a slight trend of higher concentrations at the front site of stations, no significant (at a 95% level) values could be observed. Beside, as previously discussed, TW line offers to its users an overall improved air quality with respect to bus-type public transport lines. This presumably signifies that, from the individuals waiting at station point of view, the monitored TW vehicles do not behave as an immediate major source of particulate pollution.

Ratio _{Front/Rear}	n	PN	PM _{AIV}	PM _{Tho}	PM _{Inh}	PAHp	d/D
PBW	12	1.4±0.2	1.3±0.2	1.6±0.3	1.5±0.5	0.7±0.2	0.89±0.05
RBW	15	1.0±0.1 (0.8±0.1)	1.3±0.1 (1.2±0.2)	1.4±0.3 (1.3±0.3)	1.9±0.5 (1.9±0.5)	1.1±0.2 (0.4±0.2)	0.7±0.2 (0.72±0.05)
TW	8	1.1±0.4	1.1±0.1	1.1±0.3	1.3±0.3	1.0±0.1	1.1±0.1
OB	8	1.7±0.4	1.8±0.3	2.7±0.5	3.1±0.8	1.1±0.3	0.83±0.06

Table 2. Ratios of mean particulate concentrations at stations (in front side of the shelter to concentrations measured behind the shelter). n is the total number of data monitoring series. Values in parentheses account for the confined and heavily trafficked RBW Section 3-7. Values in bold differ significantly ($p < 0.05$) from unit. d/D is the ratio of (PN) fraction below 1 μm in diameter to this over 1 μm .

A more detailed look at data allows discriminating between different urban situations. As regards RBW line, when considering the values for Station 3 and 7 together (both located in the central part of a confined and densely trafficked zone, Table 1), PAHp concentrations behind the shelter are more than twice that measured at the front side of stations (i.e. near RBW passageway) (Table 2). This is despite relatively high local mean PAHp concentrations, i.e. 45 ± 11 pg/L. Indeed, as previously evoked, 2-3 m behind these stations passes a highly trafficked road. When positioned behind the station shelters, and providing several cars wait at a nearby traffic light, a smelling of exhaust gases is perceptible. When the cars start and/or the traffic intensifies, mean PAHp concentrations exceed 150 pg/L (up to 180 pg/L) whereas the mean PN and d/D values rise by 65-80% and 25-50%, respectively. This highlights the local occurrence of episodes of atmospheric loading with PAH-loaded fines. In the same situations, yet, parameters remain relatively steady in the front side of stations: 15-25%, 2-9% and 3-11% of relative variations, respectively. This either supports the role of barrier played by the shelter or the rapid agglomeration then deposition of PAH-loaded fines. Overall, the contamination with coarse particles from buses' passageway and the accumulation of PAHp-loaded fines from the adjacent road make particulate matter levels around RBW stations highly variable. Along with the confinement of the area and additional contributions from surrounding urban materials, these momentarily, yet, repeatedly, take part in the degradation of the quality of air proposed to individuals waiting at stations.

Particulate transfers between vehicles and the immediate atmosphere

The figure 3 evidences a wide panel of distributions for particulate concentrations and d/D values. Plotted against the values at surrounding stations, in-vehicle PAHp concentrations and d/D values overall exhibit close to linear relationships. However PM_{Inh}, PM_{Tho} and, to a lower degree, PM_{AIV} and PN concentrations demonstrate less predictable evolutions. This means that, the coarse particle exchanges between the in-vehicle air and the immediate outdoor atmosphere play a limited role with respect to in-vehicle or outdoor particle generation/removal mechanisms. Another possible explanation would be that the coarse particulate concentrations at stations hardly account for these estimates between stations: inter-station values are calculated as the mean of values measured at surrounding stations. Although possible, series of measurements conducted between stations (i.e. along the public transport lanes) show that, in a given urban context and in the absence of localized sources, the overall PM variations are low to moderate. As mentioned earlier, larger variations in coarse particles levels are observed with the distance from the lanes used by PTV or the nearby trafficked roads. Inter-station variability in air quality thus hardly accounts for the observed deviations from $y=x$ line. Most of the upward deviations actually reflect the in-vehicle coarse particulate generation processes (cases of PN, PM_{Inh}, PM_{Tho} and PM_{AIV} in PBW vehicles) whereas the downward ones are associated with areas where road-traffic particulate emissions accumulate in the atmosphere at the neighborhood scale (cases of PM_{Inh}, PM_{Tho} and PM_{AIV} concentrations between Station 6 and Station 7 and PN near the TW Station 11).

As regards PBW data, significant ($p > 0.05$) correlations are only found for PAHp and d/D. For both parameters, the slope of best-fitting line (using Pearson's r^2) linking the measurements conducted in PBW vehicles and corresponding inter-station data demonstrate 0.6-0.7 values. This means that, when travelling into contaminated areas, only a fraction of the outdoor PAHp pollution reaches the in-vehicle air. It further points out that, compared to the variations in the immediate atmosphere, changes in the proportion of particles < 1 μm in diameter are less marked into PBW vehicles than between stations. In other words, air quality in PBW vehicles exhibits a relative inertia in relation to the contamination with fines and PAHp-loaded particles. Alternatively, this inertia in air quality results in sluggish decreases in the proportion of fines and PAH-loaded particle concentrations when vehicles leave any particularly

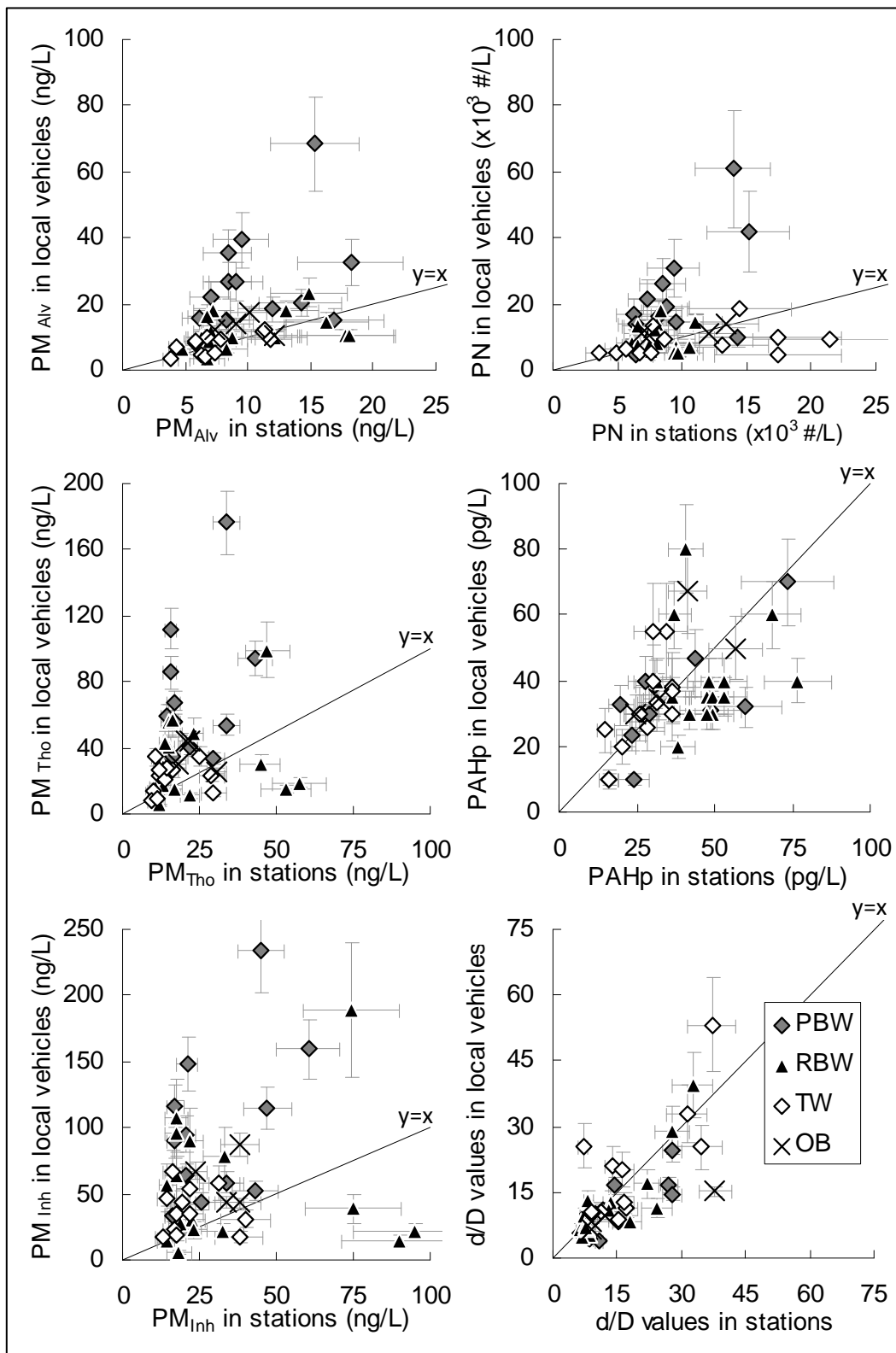


Figure 3. Mean particulate concentrations (resp. d/D values) in PTV plotted against the average of mean concentrations (resp. d/D values) in surrounding stations. Distinction is made between tested public transport modes.

polluted area. Based on the recorded variations in PAH_p and d/D PBW profiles, and depending on the duration of travels in polluted areas as well as on the related mean air contamination, it would take from <1 to 2 stations for the in-vehicle PAH_p and d/D levels to equilibrate with external air values. The calculated equilibration distance is rather short, which would limit the exposure of passengers beyond the polluted areas. This is less the case for the initial contaminations with PM_{Inh}, PM_{Tho} or PM_{AV}. These are thought to be internally generated before PBW vehicles leave terminal stations. After the vehicles'

departure, PM_{Inh} , PM_{Tho} or PM_{Alv} concentrations progressively decrease yet remain significant until the end of the line is reached. Accordingly, providing any extra contributions of other internal or external PM sources can be neglected, the equilibrium with the outdoor atmosphere would be attained after 20-35 stations. This is longer than the PBW line itself, which has a total of 13 stations.

Two categories of particles can be clearly identified for the RBW line. These differ in the inter-station coarse particulate (mostly PM_{Tho} and PM_{Inh}) concentrations (Fig. 3). The category with the highest inter-station PM_{Tho} (i.e. >40 ng/L) and PM_{Inh} (i.e. >70 ng/L) concentrations is also apparent for TW and PBW modes. The corresponding measurements have been carried out during a sunny weather period that followed several days of heavy rains. These also corresponds to morning rush. Comparisons between consistent urban areas (in terms of urban texture and land-use) demonstrate significantly lower PM_{Tho} and PM_{Inh} concentrations (i.e. 17 ± 4 ng/L and 21 ± 8 ng/L, respectively) in low traffic zones. Hence, it is highly probable that the large inter-station PM_{Tho} and PM_{Inh} levels originate from localized remobilization processes: i.e. through the wear or asphalt concrete, of automotive parts and/or the (re-)suspension of remnant particles as well as newly deposited dust. Besides, because of the relatively low d/D values (i.e. 15 ± 3) and PAHp concentrations (30 ± 10 pg/L), the (re-)suspension of coarse dust, as well as the wear of asphalt uppermost aggregate and/or of metallic automotive parts, appear the more likely. When excluding RBW data associated to in-vehicle coarse particle generation, the in-vehicle moderate PM_{Tho} (20 ± 8 ng/L) and PM_{Inh} (30 ± 20 ng/L) concentrations show that the supposedly wear/(re-)suspension particles are barely transferred into PTV. Knowing the exact origin and fate of this particulate category would require further investigation. As for the second particulate category, of lower inter-station PM_{Tho} (i.e. <30 ng/L) and PM_{Inh} (i.e. <45 ng/L) concentrations, most of in-vehicle PN and PM data lies above the $y=x$ equation line. This thereby indicates the preponderance of in-vehicle particulate pollution over outdoor pollution along RBW line. The few RBW data ($n=3$) below $y=x$ equation line exclusively comes from measurements performed within the highly trafficked corridor between Station 6 and Station 7. Finally, it is worth noticing that unlike for PN and PM, most of PAHp and d/D data is below the $y=x$ equation line. This supports that PAHp and fines from the adjacent highly trafficked road contribute in a limited proportion to the pollution increase into RBW vehicles (as it is also apparent in Fig. 2). The ratio of cumulated PAHp increase in vehicles to this at stations ranges from $1/6$ to $1/4$. It would take >4 stations for the in-vehicle PAHp levels to equilibrate with external air values. Accordingly, PAHp concentrations in RBW vehicles exhibit a more pronounced inertia than in PBW ones. The limited PAHp increase into vehicles is further testified by the previous data about reduced propagation and/or rapid deposition of PAH-loaded fines around stations.

Except for PM_{Tho} , PM_{Inh} as well as data for Station 11 and the supposedly wear/(re-)suspension coarse particle category (see above), TW mean PN, PM_{Alv} , PAHp and D/d values homogeneously distribute around the $y=x$ equation line (Fig. 3). The values of slopes of simple linear regressions and the related Pearson's r^2 coefficients ($n >8$) are 0.7-1.3 and 0.45-0.75, respectively. This demonstrates that, in the absence of notable road traffic near TW line or particulate sources in the crossed confined urban areas, the mean concentrations of fines and PAHp in vehicles smoothly follow these estimated between stations. A careful observation of the recorded signal further shows that mean contamination then is the net result of a quick succession of air contamination (i.e. traveling periods) and pollution removal (during stops at the served stations) events. As for PM_{Tho} and PM_{Inh} , the mean concentrations in vehicles broadly exceed these inter-stations: i.e. the mean multiplicative factors are 1.7 ± 0.2 and 2.2 ± 0.3 , respectively. The values for multiplicative factors nevertheless are lower than in RBW (2.0 ± 0.3 and 2.6 ± 0.6) or PBW (3.5 ± 0.7 and 3.7 ± 0.8) vehicles. This demonstrates an actual but relatively limited build-up of coarse particles into TW vehicles (as it is apparent at the densely trafficked Section 9-10). Since the mean PM_{Tho} and PM_{Inh} concentrations in TW vehicles do not depend on the traveled distance (Fig. 2) and to a limited extent on inter-station pollution levels (Fig. 3), these may substantially differ from PM_{Tho} and PM_{Inh} particles in PBW or RBW vehicles. The associated extremely low PAHp levels indicate that these may primarily not consist of combustion-type particles. However, at this time, the nature and the origin of these particles remain unclear (e.g. sand used to increase wheel/rail adhesion performance, outdoor dust and/or authigenic particles from passengers or on-board equipment). This calls for further research in order to examine the specific contribution of all the potential sources.

Only a limited amount of OB data is available ($n=4$). Most of the concentration data lies above $y=x$ line whereas d/D values are below (Fig. 3). This means that, in the monitored urban area, air quality in OB vehicles is seemingly lower than between stations. Below $y=x$ line, d/D values also indicate that the air in vehicles contains a relatively higher proportion of coarse particles (>1 μm particles account for 6-13% of PN). This further displays substantial mean PAHp concentrations: from 30 ± 3 to 70 ± 10 pg/L. A

more detailed analysis of the recorded concentration signals demonstrates that in-vehicle PN, PM and PAHp concentrations are the highest at Station 11, then progressively decrease with travel time. Since the monitored OB vehicles locally travel from a highly trafficked and confined residential area toward a less trafficked and spaced urban/industrial domain, the recorded evolutions may reflect the progressive removal, presumably through dilution and/or deposition processes, of pollutants accumulated from past sections, including Station 11. The outdoor base levels (considered at Station 0) are attained for travels exceeding 4 stations. This distance, unlike the variability of the concentration signal (coarser particles exhibit more pronounced variations), does not markedly vary among PM_{Inh} , PM_{Tho} or PM_{Alv} . Finally, due to the high in-vehicle PAHp concentrations, extra inputs from road traffic emissions (comprising OB exhausts) or contamination with internally generated particles cannot be excluded.

Conclusion

It is now widely accepted that the in-vehicle air quality may be lower than in the travelled urban area. However, the extent and modalities of this degradation are only partially characterized in PTV and, especially, in SSPT. This scarcity of information is problematical since today many urban areas are developing fast (in emerging countries and mature economies) and local authorities face the pressing request of millions of commuters for the implementation of rapid mass transit systems. Our research shows that air quality in PTV and served stations cannot be durably neglected without eventual sanitary effects. Indeed, it is not unusual to measure PM concentrations that enduringly and significantly exceed the short-term standards established in the EU and US (e.g. case of the coarse particulate pollution in PBW vehicles). Besides, in the absence of data on the nature, physical characteristics and potential transformations of particles and particle-bound pollutants, any regular PM levels do not guarantee an acceptable air quality (i.e. case of air contamination with PAHp-loaded (ultra)finest around Station 2 and Station 3, as well as in SSPT vehicles passing through these stations). All these results underline the dynamic character of the air quality offered to public transport users. This depends on many external variables, among which: meteorological conditions, the specific emissions from distant and immediate sources, the presence of sinks (such as large water-bodies) and the urban texture. This equally is a complex function of transport equipment-dependent variables comprising: the location and structure of stations, the positioning of individuals at stations and, presumably, the proximity to in-vehicle particle generation spots as well as vehicles' capacity to concentrate or dilute pollutants. This panel of variables affects, to greater and lesser extents, all the tested transport modes thereby demonstrating that, compared to conventional bus lines, SSPT lines do not systematically partake in the enhancement of the air quality proposed to users. There is an actual need for more detailed investigations on air quality determinants in PTV and related stations. Until further information is available, common sense actions could be introduced in order to limit users' exposure. These may involve: positioning stations away from intersections and traffic lights, increasing the distance between densely trafficked roads and the public transport lanes, closing temporarily the external air vents in polluted areas, shutting down the engine when PTV stop for a longer period (eg. during regulation at terminals), making sufficient clean/filtered air to come in so as to ensure the dilution or removal of contaminated air.

Acknowledgments

The authors thank Sébastien Rabuel, Head of Investments at the General Directorate of Urban Transports of Nantes Métropole, for his help in allowing the monitorings. We also acknowledge the transport network operator (Semitan) and drivers for providing access to stations and in-use PTV. This research was financially supported by the French Ministry of Ecology, Sustainable Development and Energy (MEDDE) as part of axis "Assessment of state zero for implementation of SSPT" of the Orevadd project. For this, we are grateful to Odile Heddebaut (Ifsttar) and Bernard Halphen (Cerema).

References

- Almasri R., T. Muneer & K. Cullinane (2011): The effect of transport on air quality in urban areas of Syria. *Environ. Policy*, vol. 39, n°6, p 3605-3611.
- Auran (2014): Road traffic in the Loire-Atlantique Department: 2012 counts. Nantes Region urban planning agency / Loire-Atlantique Department / Nantes Métropole, n°118.14, Nantes, France, 1 p.
- Azevedo J.A.H., R.S. Araùjo & G.M.M. Silva (2013): Polycyclic aromatic hydrocarbons atmospheric from automotive sources: a brief review. *Holos*, vol. 29, n°1, p 102-114.

- Barbusse S. & G. Plassat (2005): Les particules de combustion automobile et leurs dispositifs d'élimination. Reference data. 2nd Ed. ADEME report, n° 5728, Paris, France, 132 p.
- Batty P., R. Palacin & A. González-Gil (2015): Challenges and opportunities in developing urban modal shift. Travel Behav. Soc., vol. 2, n°2, p 109-123.
- Chan A.T. & M.W. Chung (2003): Indoor–outdoor air quality relationships in vehicle: effect of driving environment and ventilation modes. Atm. Env., vol. 37, n°27, p 3795-3808.
- Chart-asa C. & J.M. Gibson (2015): Health impact assessment of traffic-related air pollution at the urban project scale: Influence of variability and uncertainty, STOTEN, vol. 506-507, p 409-421.
- Choi W., S. Hu, M. He, K. Kozawa, S. Mara, A.M. Winer & S.E. Paulson (2013): Neighborhood-scale air quality impacts of emissions from motor vehicles and aircraft. Atm. Env., vol. 80, p 310-321.
- Dijk M., J. de Haes & C. Montalvo (2013): Park-and-Ride motivations and air quality norms in Europe. J. Transport Geogr., vol. 30, p 149-160.
- European Union (EU) (2005): Directive 2004/107/EC of the European Parliament and of the Council of 15 December 2004 relating to arsenic, cadmium, mercury, nickel and polycyclic aromatic hydrocarbons in ambient air. J. Europe, vol. 23, p 3-16.
- Font A., T. Baker, I.S. Mudway, E. Purdie, C. Dunster & G.W. Fuller (2014): Degradation in urban air quality from construction activity and increased traffic arising from a road widening scheme. STOTEN, vol. 497-498, p 123-132.
- Gonçalves M., P. Jiménez-Guerrero & J.M. Baldasano (2009): High resolution modeling of the effects of alternative fuels use on urban air quality: Introduction of natural gas vehicles in Barcelona and Madrid Greater Areas (Spain). STOTEN, vol. 407, n°2, p 776-790.
- Gros V., J. Sciare & T. Yu (2007): Air-quality measurements in megacities: Focus on gaseous organic and particulate pollutants and comparison between two contrasted cities, Paris and Beijing, C.R. Geosci., vol. 339, n°11-12, p 764-774.
- Joumard R., C. Lamure, J. Lambert & F. Tripiana (1996): Air quality and urban space management. STOTEN, vol. 189-190, p 57-67.
- Schindler M. & G. Caruso (2014): Urban compactness and the trade-off between air pollution emission and exposure: Lessons from a spatially explicit theoretical model. Comput., Environ. Urban, vol. 45, p 13-23.
- Silva L.T. & Mendes J.F.G., (2012): City Noise-Air: An environmental quality index for cities. Sustain. Cities Soc., vol. 4, p 1-11
- Tartakovsky L., V. Baibikov, J. Czerwinski, M. Gutman, M. Kasper , D. Popescu, M. Veinblat & Y. Zvirin (2013): In-vehicle particle air pollution and its mitigation. Atmospheric Environment, vol. 64, p 320-328.
- Vlahov D & S. Galea (2002): Urbanization, Urbanicity and Health. J. Urban Health, vol. 79, n°1, p 1-12.
- Vuković G., A. Urošević, M., Razumenić, M. Kuzmanoski, M. Pergal, S. Škrivanj & A. Popović (2014): Air quality in urban parking garages (PM₁₀, major and trace elements, PAHs): Instrumental measurements vs. active moss biomonitoring. Atm. Env., vol. 85, p 31-40.
- Zamboni G., M. Capobianco & E. Daminelli (2009): Estimation of road vehicle exhaust emissions from 1992 to 2010 and comparison with air quality measurements in Genoa, Italy. Atm. Env., vol. 43, n°5, p 1086-1092.

Using a simplified Willans line approach as a means to evaluate the savings potential of CO₂ reduction measures in heavy-duty transport

Stephan (P.S.) VAN ZYL*, Veerle (V.A.M.) HEIJNE*, Norbert (N.E.) LIGTERINK*

*Sustainable Transport and Logistics, TNO, Delft, 2628 XE, The Netherlands

Tel: +31 (0)88 866 27 05, Email: stephan.vanzyl@tno.nl

Abstract

In this study a simplified Willans line approach is used to model the CO₂ emissions of a long-haul tractor-semitrailer combination. The results are validated with PEMS measurements and show that high accuracy levels can be achieved, if the vehicle and cycle specific parameters are known. It is shown that the same approach can be used to calculate and predict the savings potential of a reduction measure and that the effectiveness strongly depends on the vehicle weight and the velocity profile. Based on the measured effects of vehicle and system measures from recent studies, the generic approach is used to determine the cumulative effect of a given package of fuel efficiency measures, including: energy carriers, vehicle technologies and operational improvements. The cumulative savings potential is determined for two use cases: a city distribution rigid truck and a long-haul tractor-semitrailer. The results show that large CO₂ savings can be achieved when using an integrated approach of vehicle and system measures together. For the city distribution rigid truck, large CO₂ reductions are achieved with electric drivetrains in combination with a clean well-to-tank electricity production whereas improved engine efficiency, reduced road load and logistic options are more promising solutions for the long-haul tractor-semitrailer.

Keys-words: Heavy-Duty, CO₂-modelling, Willans line, integrated approach, fuel efficiency.

Introduction

The reduction of greenhouse gas emissions is one of the large societal challenges faced by mankind. At the annual Conference of Parties in Paris (CoP21), 190 countries have agreed on the significance of global warming and the need to globally reduce greenhouse gas emissions by 50% in 2050 with reference to 1990. According to EC (2011a), the EU is committed to reducing greenhouse gas emissions even further to 80-95% in the context of necessary reductions by developed countries as a group. In EC (2011b), the above mentioned goals are translated to a CO₂ reduction of at least 60% for the transport sector alone.

While CO₂ emissions for new cars and vans are already regulated under EU legislation, no specific targets have yet been defined for the heavy-duty sector including trucks, buses and coaches. A first step to curbing heavy-duty emissions has been made by introducing certification and monitoring of heavy-duty emissions. For this purpose the computer simulation tool VECTO has been developed to measure CO₂ emissions from new vehicles. With the support of this tool the Commission intends to propose a new legislation. One of the considered options is setting mandatory limits on average CO₂ emissions for newly-registered heavy-duty vehicles – comparable to the current light-duty legislation - and the stimulation of fuel efficiency measures. When comparing efficiency measures at the level of individual vehicles and engines, with specific calibration and optimization, the side-by-side comparison may fail. In detailed models much information is needed to be able to run a simulation. Such information is often not available. Moreover, detailed modelling requires detailed validation. The latter is often absent and the effects can be attributed to the wrong aspect in detailed modelling. A generic approach is needed to recover generic effects and their interaction in normal vehicle usage.

In this paper a more generic approach is presented by using Willans lines in combination with user-specific mission profiles. This approach groups effects in such a way that they can be validated with vehicle testing data and vehicle monitoring data, like PEMS data. Determining the overall savings potential of a group of reduction measures is difficult to determine from first principles and often requires highly detailed vehicle models, the relative saving potential however can be determined more easily. In the presented approach, the actual vehicles and the vehicle usage observed in monitoring programs will be used as the baseline to determine the saving effects. It is shown that the presented approach can be used to determine the cumulative savings potential of a range of reduction measures. The

forthcoming results indicate that large CO₂ savings can be achieved when taking into account vehicle as well as system measures that cover the entire spectrum of the supply chain in the use of a vehicle. Specifically, these are: alternative energy carriers, powertrain and vehicle technologies, behavioral effects as well as optimized logistic operations and intelligent traffic systems.

1. The Willans line approach to modelling CO₂ emissions

The CO₂ emission of a vehicle is closely related to the vehicle's power demand. This relation can be derived for any specific vehicle from PEMS measurements and is visualized in Figure 1 for a heavy-duty tractor-semitrailer combination. The relationship between power demand and CO₂ is referred to as the Willans line, see TNO (2008). The relationship can be expressed by a linear function

$$\text{CO}_2 \text{ [g/s]} = \alpha \text{ [(g/s) / kW]} \times P_{\text{load}} \text{ [kW]} + \beta \text{ [g/s]},$$

where α is a measure for the efficiency of the powertrain [η_{PT}] as well as the carbon content of the fuel [γ], P the power demand and β a measure of the internal losses in the powertrain.

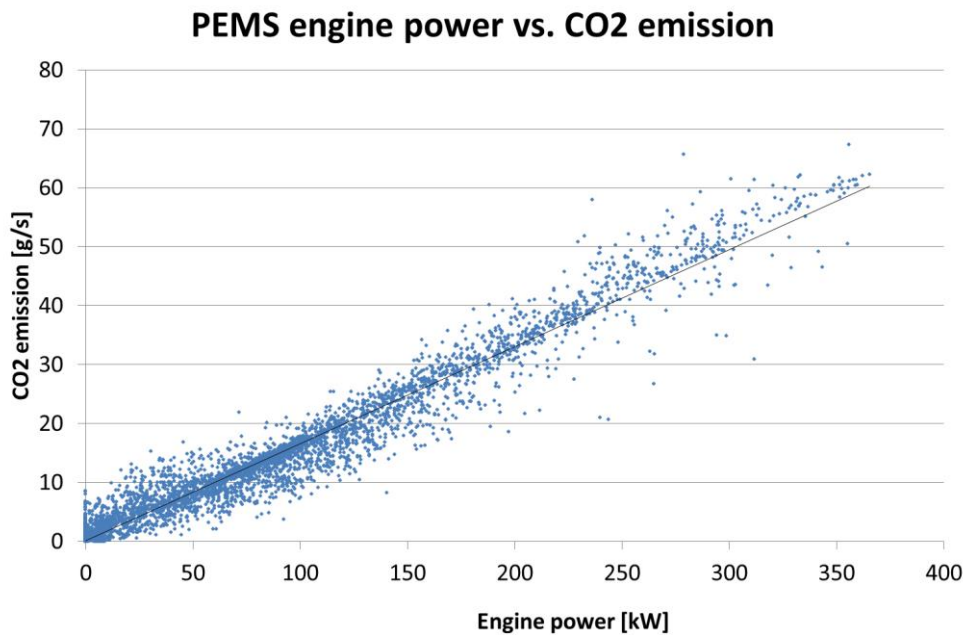


Figure 1. The Willans line for a tractor-semitrailer combination derived from PEMS measurement

With the knowledge of the Willans line coefficients α and β , modelling CO₂ for a specific vehicle is simply a matter of calculating the road load equation

$$\begin{aligned} P_{\text{load}} &= P_{\text{rrc}} & + P_{\text{air}} & + P_{\text{inertia}} & + P_{\text{regen}} & + P_{\text{gradient}} \\ P_{\text{load}} &= MC_{\text{rr}}\cos(\theta)v & + \frac{1}{2}\rho C_d A v^3 & + M_0 a^+ v & + \eta_{\text{regen}} M a^- v & + M g \sin(\theta) v \end{aligned}$$

and the following vehicle and cycle specific parameters:

- C_{rr} – coefficient of rolling resistance
- C_d – drag coefficient
- g – earth's acceleration
- ρ – air density
- A – frontal area of the vehicle
- η_{regen} – regenerative braking efficiency [only applicable for regenerative brakes]
- M – vehicle mass [empty weight + payload]
- θ – road gradient
- v – instantaneous velocity
- a^+ – vehicle acceleration
- a^- – vehicle deceleration

The linear approach uses fixed values for all parameters, except for the road gradient, the velocity and the acceleration which are transient. This also reflects the limitations of the approach. The relation between power and CO₂ emission is only linear by approximation. Some variation is to be expected,

even though many aspects are already covered from the fit of emission data, including variations with engine speed. The lower the power, the larger the residual variation around the straight line approximation. This does not invalidate the approximation, as on average the fit provides the correct relation, and the typical variations are for a great part related to transients not covered by the Willans line. For example, the engine rotating inertia stores kinetic energy visible in the CO₂ emission, but not in the power output. As a result, in acceleration from a stop to high velocity, with numerous gear shifts in between, the fuel rate, engine speed and engine power output vary rapidly, but not synchronously. At gear shift the power output and the fuel consumption are zero, and the engine is motoring. Gear shift therefore shows up as a large variation in the relation between CO₂ rate and power output at low powers. Short periods of high fuel consumption are also used, apart for acceleration, to overcome engine losses at intermediate times when the clutch is engaged. Little energy is lost in this process as it is released at motoring. At longer time scales the buffering of energy in for example rotational inertia, cancels out and the linear relation is even more prominent than on a second-by-second basis.

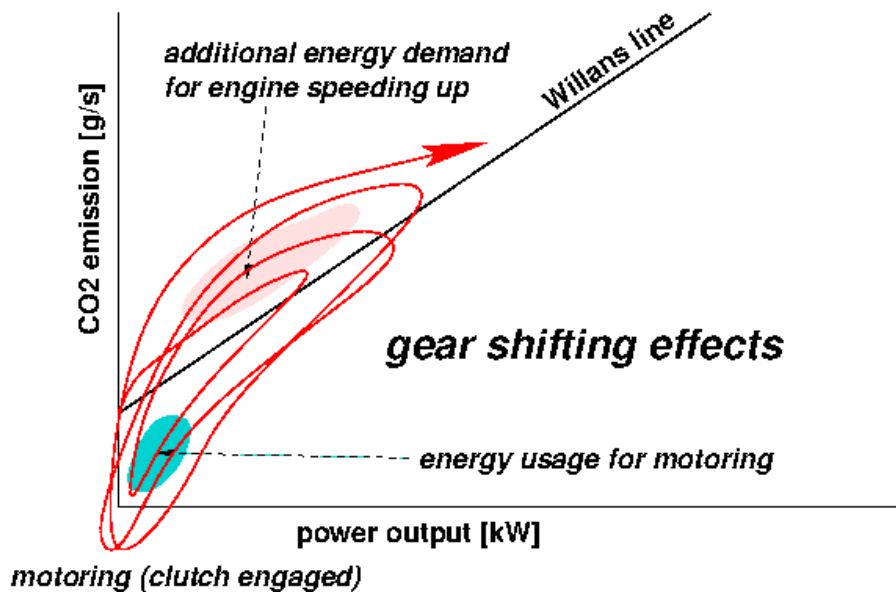


Figure 2. The spread of the data around the Willans line due to gear shifting. The additional energy to speed up the engine is released at intermediate motoring. The net effect is the Willans line, as no energy is lost.

With the given model, the savings potential of various CO₂ reduction measures can be determined. Each reduction measure interacts differently with the vehicle and therefore changes either the vehicle, the cycle specific parameters, or both. A schematic overview of how parameters are influencing the vehicle and cycle specific parameters is shown in Figure 3. The following reduction measures can be differentiated:

- Energy carriers like gas (LPG, CNG, LNG), electricity and hydrogen have an effect on the carbon content of the energy carrier, mostly in combination with a change in engine efficiency η_{PT} .
- Engine and driveline efficiencies, for example a hybrid transmission, control strategies, improved fittings and higher combustion pressures, have an effect on the powertrain efficiency η_{PT} and β , the internal losses.
- Vehicle measures effect the rolling resistance, the air drag and the vehicle weight (C_{rr} , C_d and M).
- High-over system measures, that influence the vehicles behavior, the traffic systems and the logistic supply chain have their main effect on the vehicle's velocity and its payload.

In the following sections, it is shown that the Willans line provides a relatively accurate modelling approach, given the knowledge of the vehicle and cycle specific parameters described above. For this purpose, the modelling accuracy of a Willans line is evaluated using PEMS measurement data of a tractor-semitrailer combination. Furthermore, it is shown that the Willans line is suited to model the savings potential of a CO₂ reduction measure without detailed knowledge of the engine map or the underlying control strategy. This is particularly useful, since in practice the control strategy of a specific make is often unknown. At last, the Willans line approach is used to evaluate the overall potential of two heavy-duty cases in order to demonstrate that the roadmap towards low emissions differ strongly per case.

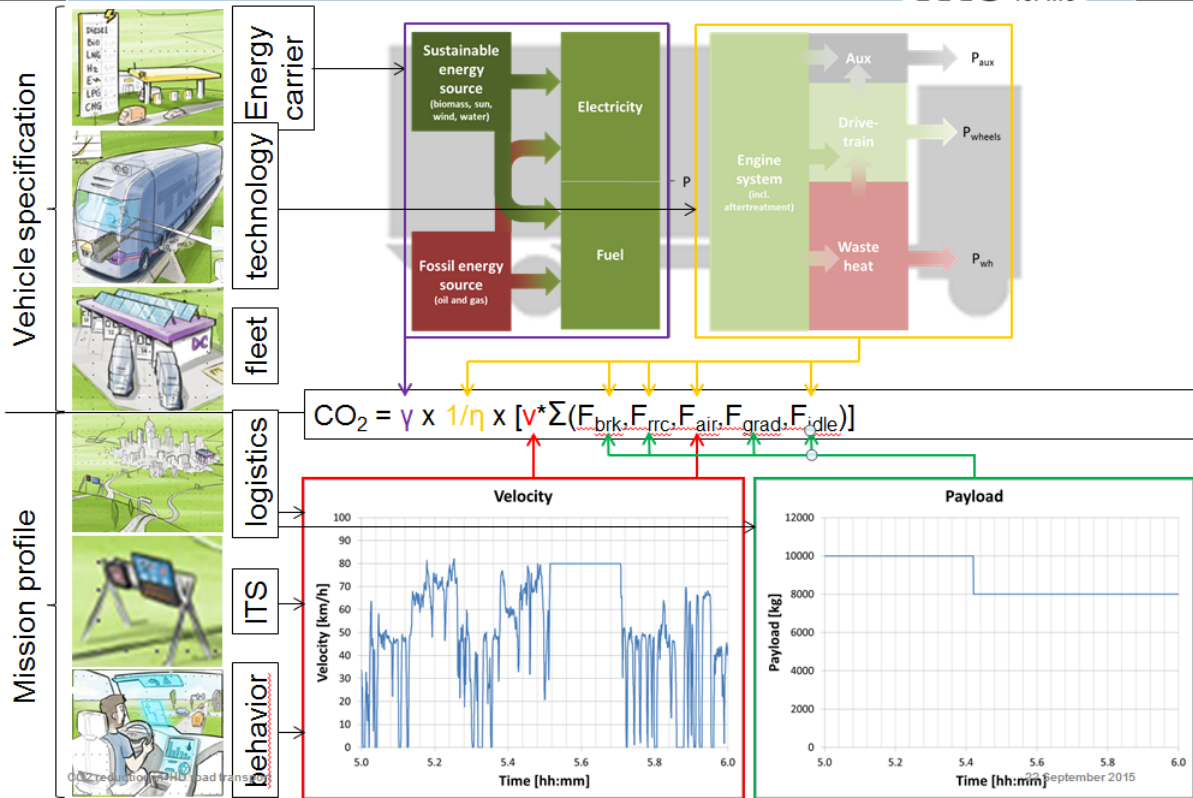


Figure 3. Schematic overview of the effects of reduction measures on the vehicle and cycle specific parameters and the CO₂ emissions in general

2. Validation of the Willans line approach with PEMS measurements

PEMS measurement data was used to validate the Willans line approach. For this purpose, three similar trips were logged with a tractor-semitrailer combination. For each trip, the payload was varied between 10% (3370 kg), 55% (17220 kg) and 100% (31120 kg) of the maximum load. The tailpipe CO₂ emission was measured and compared with the results from the model. The model specifications shown in Table 1 were determined from the vehicle subparts where possible. If this information was not available, an estimate was made based on values from literature such as UBA (2015), ICCT (2014) and ICCT (2015). Since internal losses depend on the engine load, with higher losses occurring at high loads, the internal losses have been assumed to be in the order of 2-4% of the rated power which corresponds to observed values from TNO in-house PEMS measurement results.

Table 1. Vehicle specific modelling parameters used for the PEMS validation

	Parameters	Tractor-semitrailer
Energy carrier	γ [gCO ₂ -WTW/MJ]	89.7 (Diesel)
Powertrain	Prated [W]	340000
	η_{PT} [%]	40.0
	β [W]	6800 – 13600
Auxiliaries	Paux [W]	1360
Air drag	CdA [m ²]	6
Rolling resistance	Crr [N/kN]	6
Vehicle weight	Empty weight [kg]	15380

A comparison of the real-world PEMS measurements and the model is shown in Figure 4. The left figures provide a direct comparison of the CO₂ emissions between model (red) and measurements (black). The figures on the right show that the share of certain physical forces in the overall energy consumption of the trip.

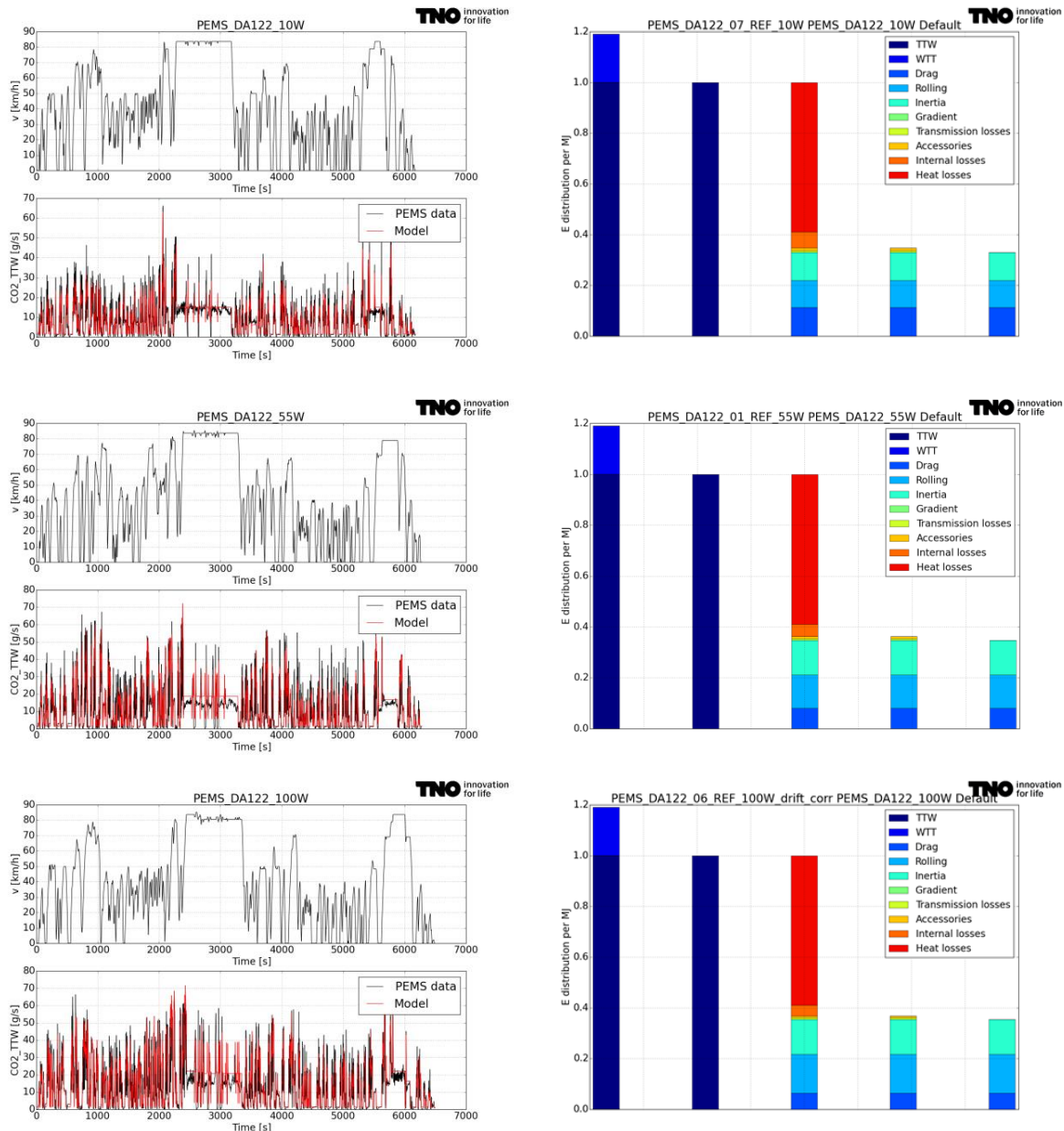


Figure 4. Validation results PEMS vs. model for three different load cycles (top to below: 10%, 55% and 100% loaded vehicle, left to right: CO₂ emissions and normalized share of energy consumption per trip

A number of observations are made:

- The modelled data clearly follows the same trend as the measurement data. The overall performance of each trip, both model and measurement, is shown in Table 2. From the results it can be concluded that the overall estimation accuracy is in the range of +/- 5%.
- Heat losses account for about half of the overall energy use. This is expected and is directly related to the thermal efficiency of the engine and the driveline efficiency. Although in practise exhaust and cooling losses of the engine system will differ depending on the load, in the model these losses remain constant over all three trips. This is due to the assumption that the powertrain efficiency η_{PT} is constant.
- The share of internal losses accounts for about 3% of the energy consumption and is higher at low loads (= low payload). This is to be expected, since the internal losses are assumed to be load-variant. The losses mimic the real-life performance of pumping and friction losses in the engine.

- As a result of the increased payload, the inertial forces and rolling resistance increase as well. This leads to overall higher CO₂ emissions of the vehicle, an increased share of inertia and rolling resistance and a decreased share of air drag in the overall energy consumption.
- The trips were all performed in the Netherlands and hardly had any road gradients. In the Alps for example, the road gradient might have a significant share of the overall energy consumption.
- Transmission losses are small (1-2%) and are accounted for in the efficiency of the powertrain η_{PT} .

Table 2. CO₂ emissions model vs. PEMS

Payload	Model	PEMS	Ratio model/PEMS
Trip 1 – 10% payload	771 [g/km]	809 [g/km]	95.3 [%]
Trip 2 – 55% payload	1092 [g/km]	1057 [g/km]	103.3 [%]
Trip 3 – 100% payload	1322 [g/km]	1280 [g/km]	103.3 [%]

The results show that the Willans line approach is suitable way to determine the CO₂ emission of a vehicle with an accuracy of +/- 5%. It also illustrates that the savings potential of a reduction measure will vary strongly depending on the cycle, as the share on the different forces are amongst other influenced by the payload and the velocity profile. The large range of the effectiveness of reduction measures can best be demonstrated with two examples, low rolling resistance tyres and aerodynamic side skirts. According to the following sources: TNO (2014) and WABCO (2014),

- low rolling resistance tyres account for a reduction in rolling resistance of roughly 10%.
- aerodynamic side skirts can reduce the aerodynamic drag Cd of a Tractor-semitrailer by about 15%.

A 10% reduction in Crr is expected to reduce the CO₂ emissions by about 3-4% (10% reduction of Crr and 30-40% share of rolling resistance in the total road load). A drag reduction of 15% is expected to reduce CO₂ emissions by 3% (15% reduction of Cd and 30% share of air drag in the overall energy consumption). The exact savings potential depends on the payload and the velocity profile of the vehicle and is calculated using the Willans line approach. The results are summarized in the table below (Table 3) for two different vehicle payloads and two different mission profiles. The range of both savings potential are compared with the measurement results from the Future-Truck program in the Netherlands, TNO (2013a).

Table 3. CO₂ savings potential of low rolling resistance tyres and aerodynamic side skirts

	Vehicle type	Mission profile	Low rolling resistance tyres	Aerodynamic side skirts
Modelled	Tractor-semitrailer (light)	city distribution	1.9%	3.1%
	Tractor-semitrailer (heavy)	city distribution	2.3%	1.7%
	Tractor-semitrailer (light)	long-haul	2.9%	6.7%
	Tractor-semitrailer (heavy)	long-haul	4.1%	4.2%
Measured	Tractor-semitrailer (mix)	mix	2 - 4%	2.7 - 6%

The results show that the effectiveness of a reduction measure is not just a fixed number but a range that depends on the vehicle type and its use. The range of the savings potential for both, low rolling resistance tyres and aerodynamic side skirts, is large. While rolling resistance measures are most effective for heavy vehicles at high velocities, air drag measures are most effective for light vehicles at high velocities. It can be seen that the model results are well in-line with the measurement results. Small differences can be explained by the fact that the future truck program monitored a range of vehicles with marginally different payloads and velocity profiles than modelled.

3. Outlook 2020-2030

In the past years, large monitoring programs like the U.S. Super-Truck program or the Dutch Future-Truck program have shown that there are large CO₂ saving potentials to be harvested for heavy-duty transport, TNO (2013a) and ICCT (2014). However, these programs mainly focus on the technological feasibility of vehicle technologies, hereby excluding important aspects from system technologies like logistics, behaviour and intelligent traffic systems. The provided saving potentials therefore only represent a subset of the overall picture. This study aims at presenting a truly integrated approach which takes into account the overall savings potential of energy carriers, vehicle and system technologies.

This paper uses the Willans line approach to estimate the overall savings potential of fuel reduction measures in the 2020-2030 timeframe. In the approach, references from the knowledge domains of powertrains, logistics and smart mobility are used to form an overall picture. By using Willans lines, the

physical relationships between the one domain and the other are taken into account, instead of oversimplifying the calculation by cumulating effects. To demonstrate the range of possibilities, two use cases were studied: a rigid truck with a city distribution cycle and a Tractor-semitrailer combination driving long-haul distances. EURO VI truck technology was taken as the baseline.

Baseline scenario – current state of the art

Vehicle and cycle specific modelling parameters as shown in Table 4 were derived from in-house PEMS measurements (see above) and compared with recent studies UBA (2015) and ICCT (2015). Average cycle payloads were taken from TNO (2013b) and assumed to be constant over time. When dealing with daily logistic operations this is obviously not the case as the payload typically changes between empty and full. The cycle and weight of loading and unloading however is very operations specific and does not provide a general insight, as provided in TNO (2013b) for Dutch average payloads.

Table 4. Baseline scenario - vehicle and cycle specific modelling parameters

		Parameters	Rigid truck	Tractor-semitrailer
Vehicle specific parameters	Energy carrier	γ [gCO ₂ WTW/MJ]	89.7 (Diesel)	89.7 (Diesel)
	Powertrain	Prated [W]	185000	310000
		η_{PT} [%]	40	41
		β [W]	3700 – 7400	6800 - 13600
		Auxiliaries	Paux [W]	750
	Air drag	CdA [m ²]	4.4	5.85
	Rolling resistance	Crr [N/kN]	7	6
	Vehicle weight	Empty weight [kg]	8820	15380
Cycle specific parameters	Payload [kg]		2376	17220
	Velocity profile		see below	

The velocity profiles of a city distribution and long-haul cycle were taken from subsections of in-house PEMS measurements and are shown in Figure 5 and Figure 6, respectively. In both figures are shown from top to below the velocity profile, the histogram of velocities and acceleration as well as the relative shares of CO₂ emission at specified velocity bins.

In order to make cycles more representative for daily operation, several cycles were repeated to attain a realistic distance. From the histogram of velocities it can be seen that the long-haul cycle is dominated by motorway driving at 80 km/h, whereas in city distribution the velocity profile is more balanced between urban (<50 km/h) and motorway (70-80 km/h) driving. The acceleration profile for both cases is relatively similar, however for the long-haul case it is observed that on average the tractor-trailer combination decelerated harder than the rigid truck in city distribution. This is possibly due to the heavier tractor-trailer combination, but could also be effected by driving behavior. The relative shares in CO₂ emissions are split apart for heat losses, auxiliaries, internal and transmission losses as well as the road load. For combustion engines, heat losses account for the largest share of the energy consumption. It can be seen that internal losses have a high share in overall emissions at low velocities. At velocities between 10 and 50 km/h, inertia losses have the highest share in the emissions contributed to road load. At velocities above 50 km/h, rolling resistance and air drag contribute most, while air drag dominates the emissions at velocities higher than 70 km/h.

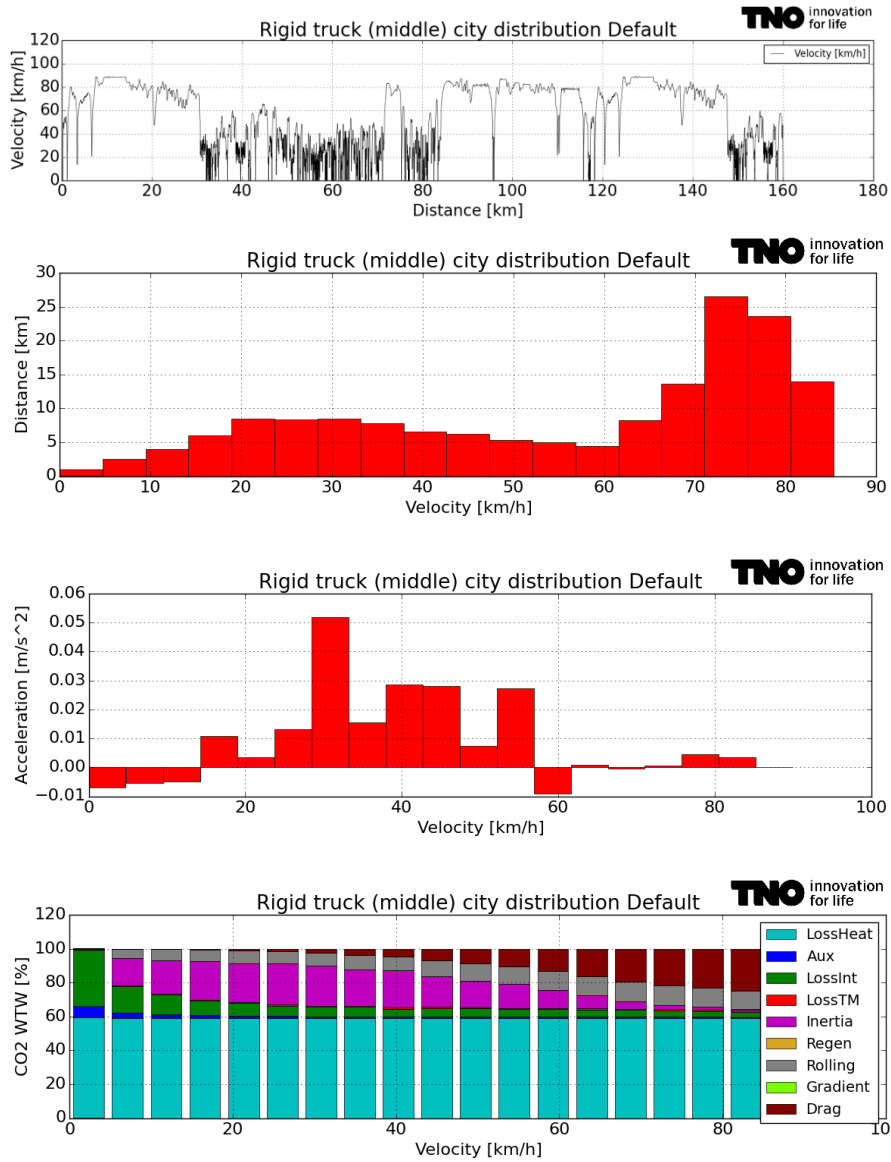


Figure 5. City distribution rigid truck – from top to bottom: velocity profile, histogram of velocities, histogram of acceleration and relative CO₂ emission at different velocity bins

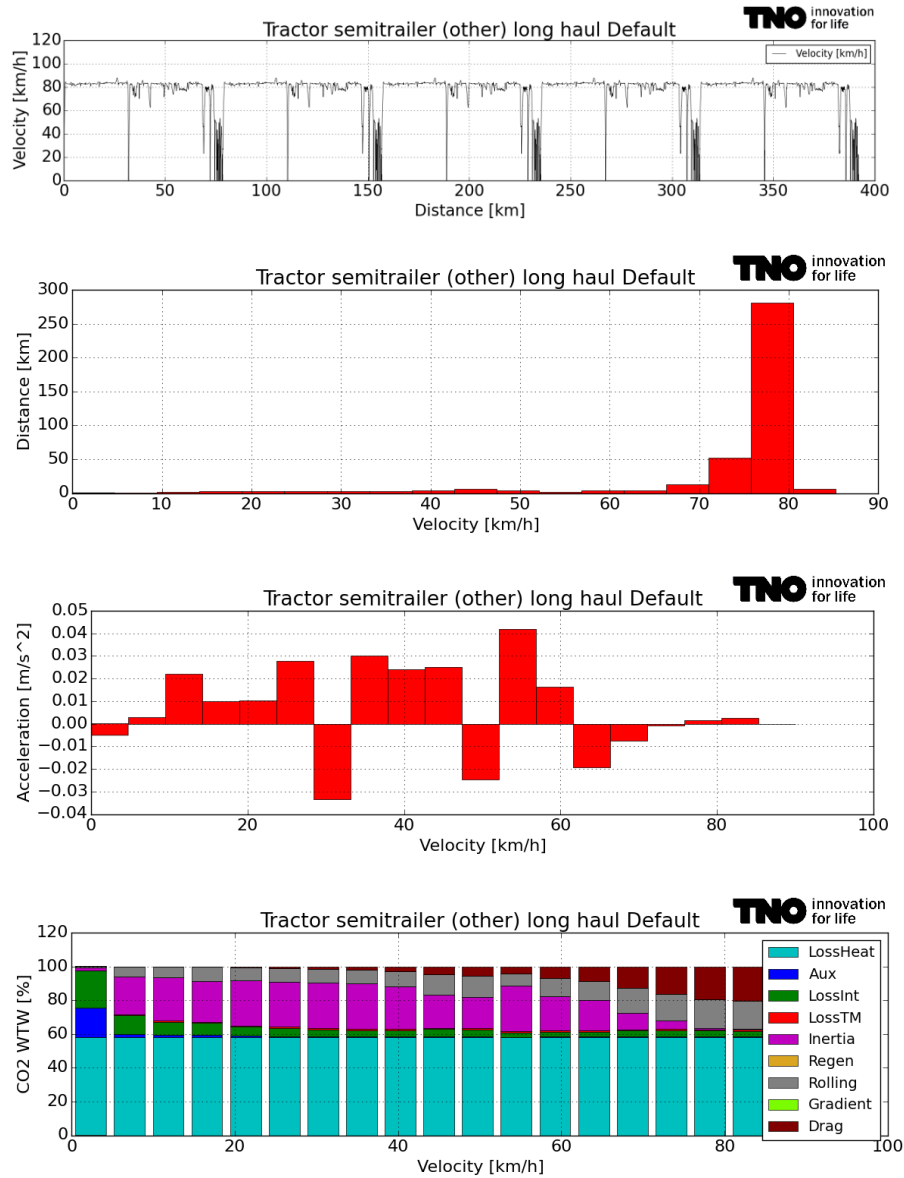


Figure 6. Long-haul tractor-trailer – from top to bottom: velocity profile, histogram of velocities, histogram of acceleration and relative CO₂ emission at different velocity bins

Fuel efficient scenario – fuel efficiency technologies in 2020-2030

The effectiveness of fuel efficiency technologies have been studied in previous publications, separately for vehicle technologies in ICCT (2015), logistics in TNO (2013c) and smart mobility solutions in RAEA (2015b). The following analysis aims at determining the overall effectiveness when combining the underlying assumptions of these three domains. For this purpose the baseline scenario is used as starting point to successively incorporate ready-to-market technologies in the timeline of 2020-2030 into the Willans line model. The results of all three domains are shown apart in Figure 7 and Figure 8, respectively for the city distribution rigid truck and the long-haul tractor-trailer combination. The underlying assumptions that lead to these results are detailed underneath.

The assumptions for the vehicle technology packages are shown in Table 5 and are based on ICCT (2015), RAEA (2011), RAEA (2015b) and TIAX (2011).

Table 5. Vehicle measures and their effect on the vehicle specific modelling parameters

	Parameters	Rigid truck	Tractor-semitrailer
Energy carrier	γ [gCO ₂ WTW/MJ]	125 (Electricity NL _{mix2015})	89.7 (Diesel)
Advanced powertrain solutions	Prated [W]	E-motor [150kW, 160kWh]	Advanced diesel engine [280 kW]
	η_{PT} [%]	80%	50% (+20%)
	η_{regen} [%]	50%	50%
	β [W]	n.a.	-10% downsized engine -20% downspeeding
Auxiliaries	Paux [W]	375 (-50%)	620 (-50%)
Reduced air drag	CdA [m²]	3.06 (-30% CdA)	4.1 (-30% CdA)
Low rolling resistance	Crr [N/kN]	4.2 (-30% Crr)	4.2 (-30% Crr)
Lightweighting	Empty weight [kg]	7500 (-14% mass) + 1600 (mass E-motor) = 9100	13370 (-14% mass)

In ICCT (2015), a vision was formulated for the development path of diesel-powered heavy-duty vehicles up to the year 2030. This vision is largely based on the outcome of the U.S. Super-Truck program in which the commercial parties and RTOs Cummins, Daimler, Navistar and Volvo have demonstrated how to increase freight efficiency with 50% by applying cutting-edge vehicle technologies which are not yet ready-to-market but expected penetrate the market in the future. Based on these findings, different technology packages were defined, starting from moderate (2017), phase 1 (2020+), advanced (2020+ WHR) up to long term (2030+). In this study, the assumptions for 2020-2030 are largely based on the availability of the following technology packages.

- Energy carrier: According to EMOSS (2015), a 12 ton rigid truck with 80% payload, comparable to the rigid truck in the use case, achieves an energy consumption of about 0.8 kWh/km. With the Willans line approach, an energy consumption of 0.85 kWh/km is determined when taking into account the improved motor efficiency of 80% (vs. 40% of the Diesel engine), 50% regenerative braking efficiency and when accounting for the additional weight of the battery pack of roughly 1600 tons (10 kg/kWh times 160 kWh). In comparison to EMOSS, the estimated energy consumption is probably even a conservative estimate. Since the diesel powertrain is completely replaced with an electric one, no further powertrain improvements are expected for the rigid truck. Carbon content levels of the current electricity mix in the Netherlands is assumed. This is a conservative estimate, since the renewable share of the electricity mix in Europe is planned to be 20% in 2020 and even higher beyond.
- Improved engine efficiency of 52% BTE_{peak}. This is achieved by reducing the friction losses in the engine, using on-demand accessories, optimized combustion control and waste heat recovery: In the Willans line approach, this translates to a increased powertrain efficiency of 50% including transmission losses and a reduction of the energy demand of all accessories (e.g. the steering pump, AC, compressor, etc.). Based on RAEA (2011), a maximum reduction of accessory energy demand of up to 50% is assumed. Hybrid powertrains could reduce energy consumption further by making use of regenerative brakes. A regenerative braking efficiency of 50% is assumed based on TNO (2012).

- 20% engine downspeeding is achieved by use of a dual clutch transmission. Furthermore, a 10% engine downsizing is assumed feasible. Both measures are reflected in the internal losses of the Willans line approach.
- The road load is expected to be reduced by 30% less air drag, 30% less rolling resistance and 14% less weight. Although not explicitly stated in ICCT (2015), it is assumed that the rigid truck can achieve the same road load reductions. According to FAT (2013), large air drag reductions can be achieved with side skirts and boat tails, both for rigid and tractor-trailer combinations. It is also clear that low rolling resistance tyres, TNO (2014), and TPMS technology, TNO (2013c), can improve rolling resistance. However, it must be stated that a reduction of 30% in air drag and rolling resistance are very ambitious targets. Weight reductions in the range of roughly 2000 kg (14%) can only be achieved when taking into account innovations like an aluminium chassis [DAF (2015)], cabin size reduction and further material innovations mentioned in RAEA (2015).

The assumptions for the system technology packages are shown in Table 5. System measures typically influence the cycle specific modelling parameters like the velocity and acceleration profile as well as the vehicle payload. According to RAEA (2011) driver training can result in fuel economy reductions of 5 to 10%. Truck platooning technologies are also expected to result in fuel savings of up to 10%, see TNO (2015a). Driver education can be expressed in a reduced amount of inertial forces, while all other road load forces remain the same. Ideally the driver learns to coast for longer distances, instead of braking abruptly, and also reduces speeding. In the Willans line approach, this translates to a reduction in acceleration and deceleration levels. Truck platooning reduces the aerodynamic drag of both the leading and the following vehicle and thus yield a reduced fuel consumption. In the following analysis it is assumed that driver training will be most effective in dynamic driving conditions like city distribution, whereas truck platooning is effective on the motorway at long-haul cycles. For both use cases a fuel consumption reduction of 10% is assumed due to these technologies.

Longer Heavier Vehicles (LHVs) have a large CO₂ savings potential which is directly related to the increased freight efficiency. According to Daimler (2015), two LHVs can replace three standard tractor-semitrailers, hereby reducing the fuel consumption by 15-20%. It will be assumed that this is only applicable for the tractor-semitrailer. When dimensioning an electric rigid truck, the weight of the battery packages will be trade with payload in daily operation. Therefore, it is assumed that no further logistic optimization can be realized for the rigid truck.

Table 5. System measures and their effect on the cycle specific modelling parameters

	Parameters	Rigid truck	Tractor-semitrailer
Behaviour and ITS	Acceleration [m/s²]	-10% fuel consumption	-10% fuel consumption
Logistic solutions	Payload [kg]	n.a.	+8t (additional trailer) +30% payload
	Distance [km]	n.a.	-30%

The results in Figure 7 show that even with the current electricity mix in the Netherlands, electric rigid trucks can achieve a great WTW CO₂ reduction of more than 30%. Obviously, when this mix is 100% renewable, WTW emissions will even reduce to zero. Apart from this, large savings of nearly 20% can still be achieved with road load reductions and behavioral measures. Even if the above described measures only achieve 80% of their target value and when excluding further renewable energy sources in the electricity mix, the cumulative savings potential for a rigid truck with a city distribution cycle is still 40%.

According to ICCT (2015), the development potential of a diesel engine is not yet saturated. This is reflected in the results below (see Figure 8). Without alternative powertrains and energy carriers, a long-haul tractor-trailer combination also achieves savings of at least 40% CO₂ WTW. The savings potential associated to the powertrain is roughly half as large as in the electric case above, however larger savings can be achieved with a reduction of road loads, ITS solutions like truck platooning and LHVs. Using HVO from waste cooking oil instead of Diesel can reduce CO₂ savings even up to 90% (carbon content of 8.1 MJ/l instead of 89.9 MJ/l), but just as with other biofuels the availability of sufficient resources remains uncertain. HVO from waste cooking oil is only mentioned in this analysis to illustrate the maximum range of the savings potential. With biofuels the origin of the energy source as well as the chemical composition of the fuel is always crucial, see TNO (2015b). A counter example is given with FAME from rape seed where in the best case no saving is achieved and even if using FAME from a different energy source, it is only intended as drop-in fuel up to 30% which reduces its savings potential drastically.

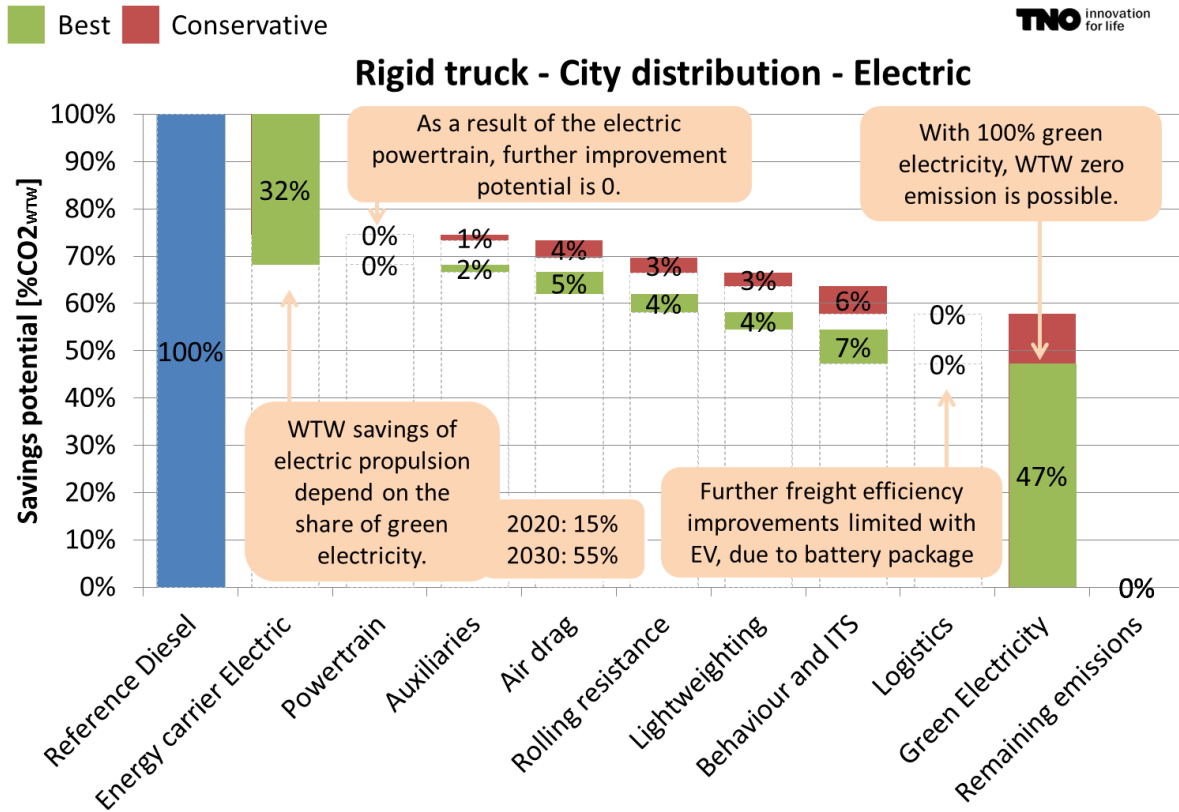


Figure 7. Savings potential for a city distribution rigid truck– route EV

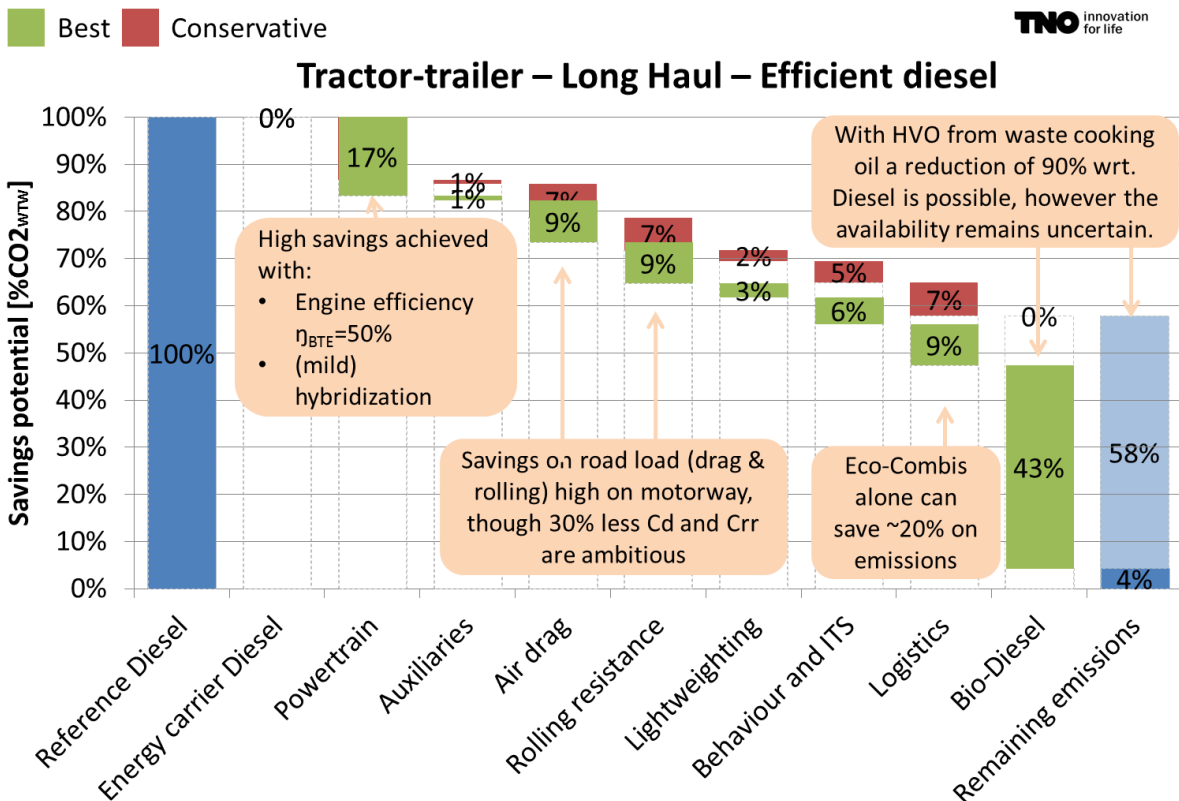


Figure 8. Savings potential for a long-haul tractor-semitrailer – route efficient diesel

4. Discussion and Conclusion

In this paper, a simplified Willans line approach was presented as an alternative tool to calculate the savings potential of heavy-duty reduction measures. For this purpose, PEMS measurements were used to derive vehicle specific modelling parameters and validate the modelling approach. By tuning the parameters according to suggested values from recent studies, the cumulative savings potential of two use cases was determined.

The results show that the heavy-duty transport sector can yet achieve large CO₂ reductions when considering vehicle as well as system measures. Depending on the vehicle and its daily operational cycle, the route towards low emission levels will differ and thus needs to be determined for different use cases and logistic sectors apart. The two cases illustrate that the choice of an energy carrier also lays out the path for further reductions. Obviously, choosing for an electric energy carrier eliminates the options of diesel engine measures which are applicable and optimized for diesel engines only. The same applies for logistic options which aim at higher truck loads, since in many cases the use of an electric truck is a trade-off between payload, designated battery package and the required loading infrastructure. The room for further logistic optimization in electric trucks remains something to be further explored for different logistic operations. Disregarding the choice of the energy carrier, road load reductions by means of reduced air drag, rolling resistance and weight provide large cumulative potentials. However, it is highlighted that the here assumed reductions mentioned in the 'advanced package' of ICCT (2015) are very ambitious and will require much research and development efforts. The road load can be even further reduced by behavioral and ITS measures which influence the inertial forces of the vehicle. The range of saving potentials for renewable energy carriers is large and always depends on the energy source and its chemical composition.

A good strategy to reach low emission targets could be to first improve the freight efficiency further, before relying on the availability of sustainable energy carriers.

References

- DAF (2015): DAF Future Truck Chassis Concept (FTCC) – press release, [DAF \(www.daf.com\)](http://www.daf.com), 2015.
- Daimler (2015): Presentation of results from field test “Efficiency Run 2015”: Long-haulage trucks: integrated approach reduces CO₂ emissions by up to 14 percent, [Daimler \(www.daimler.com\)](http://www.daimler.com), 2015
- EC (2011a): Communication from the Commission to the European Parliament, the Council, the European Economic and Social Committee and the Committee of the Regions - Energy Roadmap 2050, [European Commission \(www.ec.europa.eu\)](http://www.ec.europa.eu), 2011.
- EC (2011b): White paper for transport – Roadmap to a single European Transport Area, towards a competitive and resource-efficient transport system, [European Commission \(www.ec.europa.eu\)](http://www.ec.europa.eu), 2011.
- EMOSS (2015): e-Truck full electric, [EMOSS \(www.emoss.biz/electric-truck\)](http://www.emoss.biz/electric-truck), 2015.
- FAT (2013): Numerische Untersuchungen zur Aerodynamik von Nutzfahrzeugkombinationen bei realitätsnahen Fahrbedingungen unter Seitenwindeinfluss, [Verband der Automobilindustrie \(www.vda.de\)](http://www.vda.de), 2013
- FREVUE (2013): State of the art of the electric freight vehicles implementation in city logistics, [FREVUE \(www.frevue.eu\)](http://www.frevue.eu), 2013.
- ICCT (2014): The U.S. Super-Truck Program – Expediting the development of advanced heavy-duty vehicle efficiency technology, [ICCT \(www.theicct.org\)](http://www.theicct.org), 2014.
- ICCT (2015): Advanced tractor-trailer efficiency technology potential in the 2020-2030 timeframe, [ICCT \(www.theicct.org\)](http://www.theicct.org), 2015.
- TNO (2013c): Kennisborging Lean and Green, [TNO \(www.tno.nl\)](http://www.tno.nl), 2013
- RAEA (2011): Reduction and Testing of Greenhouse Gas (GHG) Emissions from Heavy Duty Vehicles – Lot 1: Strategy, [European Commission \(www.ec.europa.eu\)](http://www.ec.europa.eu), 2011.
- RAEA (2015): Light-weighting as a means of improving Heavy Duty Vehicles’ energy efficiency and overall CO₂ emissions, [European Commission \(www.ec.europa.eu\)](http://www.ec.europa.eu), 2015.
- RAEA (2015b): Study on the Deployment of C-ITS in Europe: Summary Report, [European Commission \(www.ec.europa.eu\)](http://www.ec.europa.eu), 2015. NOT YET PUBLISHED.
- TIAX (2011): European Union Greenhouse Gas Reduction Potential for Heavy-Duty Vehicles, [European Commission \(www.ec.europa.eu\)](http://www.ec.europa.eu), 2011.
- TNO (2008): Correlation Factors between European and World Harmonised Test Cycles for heavy-duty engines, [European Commission \(www.ec.europa.eu\)](http://www.ec.europa.eu), 2008.
- TNO (2012): Report Concerning Standard Component Dimensioning Classes, [HCV \(www.hcv-project.eu\)](http://www.hcv-project.eu), 2012, p 18-19.
- TNO (2013a): De Truck van de Toekomst – Brandstof- en CO₂-besparing anno 2013, [TNO \(www.tno.nl\)](http://www.tno.nl), 2013.
- TNO (2013b): Voertuigcategorieën en gewichten van voertuigcombinaties op de Nederlandse snelweg op basis van assen-combinaties en as-lasten, [TNO \(www.tno.nl\)](http://www.tno.nl), 2013.
- TNO (2013c): Study on Tyre Pressure Monitoring Systems (TPMS) as a means to reduce Light-Commercial and Heavy-Duty Vehicles fuel consumption and CO₂ emissions, [TNO \(www.tno.nl\)](http://www.tno.nl), 2013
- TNO (2014): Potential benefits of Triple-A tyres in the Netherlands, [TNO \(www.tno.nl\)](http://www.tno.nl), 2014.
- TNO (2015a): Truck platooning – driving the future of transportation, [TNO \(www.tno.nl\)](http://www.tno.nl), 2015
- TNO (2015b): LNG for trucks and ships: fact analysis Review of pollutant and GHG emissions Final, [TNO \(www.tno.nl\)](http://www.tno.nl), 2015
- WABCO (2015): Opti-Flow SideWings – sales brochure, [WABCO \(www.wabco-optiflow.com\)](http://www.wabco-optiflow.com), 2015.

Comparative study of three digestion methods for airborne PM10-bound metallic elements in an urban site

Amina Kemmouche*, [Hocine Ali-Khodja*](#), Xavier Querol**, Fayrouz Bencharif-Madani*

*Laboratoire Pollution et Traitement des Eaux (LPTE), Département de Chimie, Faculté des Sciences Exactes, Université des Frères Mentouri, Constantine, Algérie.

** Institut de l'Évaluation Environnementale et de la Recherche sur l'Eau (IDAEA), Conseil Supérieur de la Recherche Scientifique (CSIC), Barcelone, Espagne.

Author email: hocine_ak@yahoo.fr

Abstract

A comparative study of three different aerosol extraction processing techniques was carried out on ten quartz fiber PM10 sampling filters and a standard material (P1633b Fly Ash). Simultaneous sampling of PM10 was conducted at an urban background site in the town of Constantine. Three different mixtures of reagents were chosen in order to achieve the extraction procedure: mix 1 (HF / HClO₄ / HNO₃), mix 2 (HCl / HNO₃), mix 3 (HCl / H₂O₂ / HNO₃). A standard material (P1633b) was used to quantify and compare the extraction efficiencies of the three techniques. The solutions obtained after dust mineralization were analyzed by two analytical techniques. Pb, Cu, Co and Ni were analyzed by ICP-MS, while Zn and Mn were determined by ICP-AES. The first digestion technique proved to be the most efficient for all samples. The differences in extraction efficiencies between the three techniques varied from one sample to another according to the element analyzed.

Keywords: PM10, partial extraction, metallic elements, digestion methods

Introduction

Particulates are compounds with a health issue and their study is important because they are small enough to penetrate the respiratory system (Al Masri *et al.*, 2005). These pollutants can be primary when they are directly emitted to the atmosphere or secondary when they result from the transformation of gaseous pollutants. The emission sources of aerosols are diverse. They may be natural such as soil erosion, the bursting of waves bubbles allowing the formation of sea spray, volcanic activity, etc. (Azimi, 2004). Anthropogenic sources are also responsible for particulate pollution; farming activities using fertilizers and pesticides, industry with the various pollutants it rejects, petroleum refining, combustion and finally road transport (Lamaison 2006; Tombette, 2007; Han *et al.*, 2006). According to the IUPAC definition, MTE (metallic trace elements) is: "Anything with an average concentration below 100 ppm." The term "ultra-trace" is a name that has no strict definition, but which is frequently used in the literature (Brown & Milto, 2005). MTE are part of air pollutants and their determination in the fine particles is an important parameter in the assessment of the health risk induced by these particles (Perez *et al.*, 2004). Recent studies have developed methods for the determination of harmful MTE such as: Cd, Co, Cr, Cu, Ni and Pb present in aerosols (Castillo *et al.*, 2008; Moreno *et al.*, 2006). Analysis of MTE present in dust samples taken from the ambient air at very low concentrations is a challenge. The low weights of the samples increase the risk of loss and contamination. Research has mainly focused on the development of new methods to increase the sensitivity and selectivity of the analysis of trace elements. Direct methods include X-ray fluorescence (XRF), X-ray emission induced by proton (PIXE) analysis and instrumental neutron activation (INAA). However, matrix effects can cause major interferences while using these techniques. The most common methods used today for the determination of metallic elements in environmental samples involve highly sensitive spectroscopic techniques, such as atomic absorption spectroscopy (FAAS, ETAAS), inductively coupled plasma mass spectrometry and inductively coupled plasma atomic emission spectrometry (ICP-MS and ICP-AES). The use of these techniques requires dissolving the samples before the determination of the metal contents. In recent years, analysts have

recognized increasingly that most systematic errors could be introduced during the sampling and sample preparation steps. Currently, the influence of the sample preparation step on the quality of the analysis results is recognized worldwide (Ehi-Eromosele et al., 2012). Different digestion methods for trace metals present in aerosols can be used. The extraction efficiency depends on several factors: the sample nature and its matrix, the time available for analysis and the optimal time of acid digestion (Ehi-Eromosele et al., 2012).

In the scientific literature, several extraction protocols of trace elements in aerosols are reported without specifying whether the type of extraction is exhaustive allowing the total dissolution of metals or selective for a specific metallic fraction. Several techniques are used for the extraction of metal elements contained in solid environmental matrices (aerosols, sediments, soil, marine and dust samples). Some studies are based on the extraction in a single step and use different mixtures of reagents such as: $\text{HNO}_3 + \text{HCl}$ (aqua regia), HNO_3 alone, $\text{HNO}_3 + \text{H}_2\text{O}_2$, $\text{HNO}_3 + \text{HF} + \text{H}_2\text{O}_2 + \text{H}_3\text{PO}_4$, $\text{HNO}_3 + \text{HCl} + \text{HF}$, $\text{HNO}_3 + \text{HF}$, etc. (Pérez et al., 2004; Petterson & Olsson, 1998; Ragosta et al., 2008; Bettinelli et al., 2000). Other studies implement the sequential extraction based on the principle of the attack of the sample by gradually stronger mineralizing solutions (Grotti et al., 2002; Ryan et al., 2008; Jimoh, 2012). A total digestion method must include the use of hydrofluoric acid HF which, despite its harmful health effects, remains the only reagent capable of releasing the silicates bound metal fraction. However, in many studies, other techniques such as aqua regia proved equally effective for some metals (Sastre et al., 2002).

The purpose of this study is to conduct a comparative study between a total digestion technique ($\text{HF} / \text{HNO}_3 / \text{HClO}_4$) and two partial extraction techniques ($\text{HNO}_3 / \text{HCl}$) and ($\text{HNO}_3 / \text{HCl} / \text{H}_2\text{O}_2$) to measure the efficiency of such techniques towards the metallic elements: Cd, Co, Cr, Cu, Ni and Pb.

1. Material and methods

1.1. Samples

A standard material (UPM 1648 Fly Ash) and ten PM10 quartz fiber filters were used for sampling PM10 in the period between 15/01/2015 and 13/03/2015 at the Slimane Zouaghi campus of the university of Constantine using a high volume sampler, model Tisch-TE-6001 (Fig. 1).

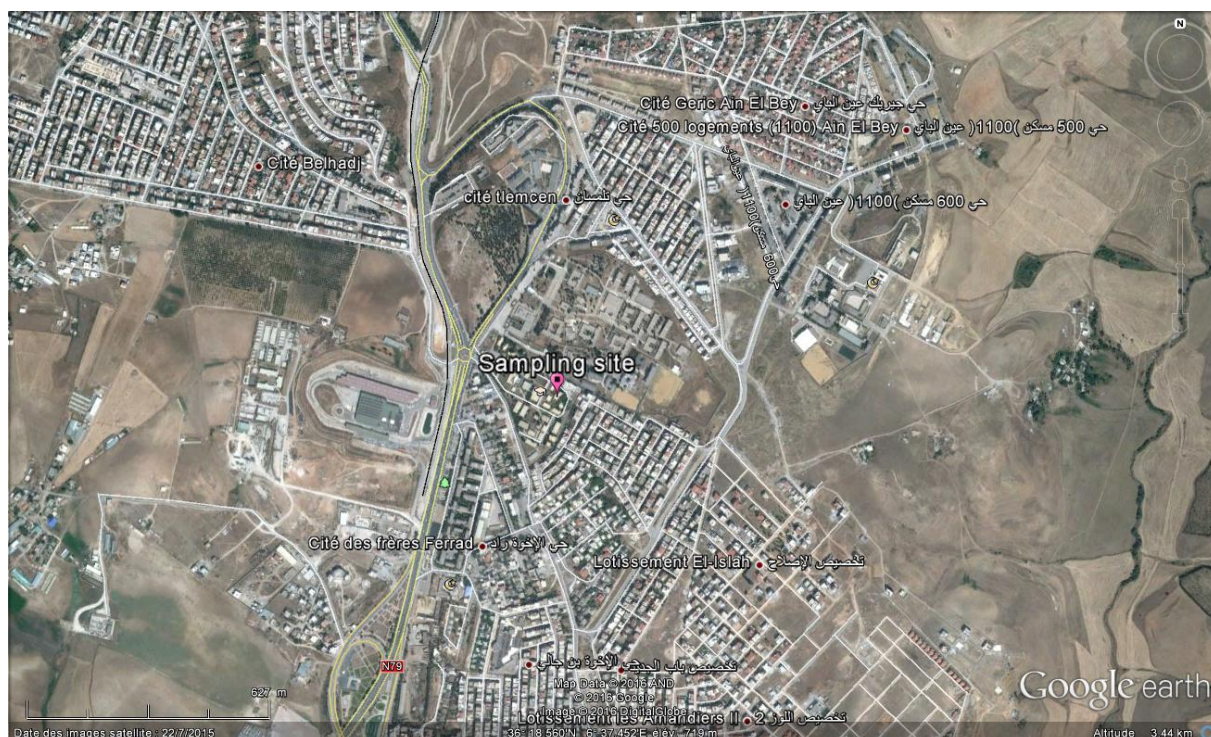


Figure 1. Map of PM10 sampling site

1.2. Dust mineralization

Experimental protocols used for PM₁₀ sample dissolution are shown below. To complete each extraction protocol, circular 30 mm diameter discs were cut from the ten PM₁₀ filters.

1.2.1. First Protocol (P1)

Samples were digested in a solution containing 1 ml HNO₃ and 2 ml HF in a closed PFA bottle at 90 °C for at least 8 hours. After cooling, the containers were opened and 1 ml of HClO₄ was added. The acids were then completely evaporated by placing the PFA containers on a hot plate at 240 °C. The remaining dry residue was dissolved with 2.5 ml of HNO₃ before being diluted with distilled water (MilliQ) to 25 ml, to obtain solutions of 10% HNO₃ that were centrifuged for 20 minutes at 3000 rpm (Querol et al., 2001).

1.2.2. Second Protocol (P2)

The samples were introduced into PFA vials. A 10 ml solution of a (3:1) mixture (12M HCl and 17M HNO₃) was left at room temperature for 24 h. Then the solution was digested on a hot plate at 130 °C for 15 min. After cooling at room temperature, the suspension was filtered and diluted to 25 ml with 0.17 M HNO₃ (Pena-Icart et al., 2011).

1.2.3. Third Protocol (P3)

The extraction of the filters was carried out using the following reagents: HCl (37%), H₂O₂ (35%) and HNO₃ (65%). Samples were put in a PFA flask and a solution containing 30 ml HCl and 5 ml H₂O₂ was added. After heating for 1 hour on a hot plate at 120 °C, the solution was filtered and 20 ml HCl (1+1) were added to the residue for 15 min to complete the extraction. The PFA flask content was filtered again and the filtrate was added to the filtrate of the previous step. The solution was concentrated on a hot plate until a small volume was left in the flask. The latter was then transferred to a volumetric flask of 25 ml. This volume was filled up with a HNO₃ solution (2+98) (Awan et al., 2011).

1.2.4. Analytical techniques

The resulting solutions were then analyzed by ICP-AES (IRIS Solutions Advantage Thermo TJA) for elements, Zn and Mn and by ICP-MS (X Series II Thermo) for elements Cu, Pb, Co and Ni.

2. Results and discussion

2.1. Evolution of PM₁₀ concentrations

Ten PM₁₀ samples were collected during from 15/01/2015 to 13/03/2015. The daily concentrations of PM₁₀ are shown in Fig. 2.

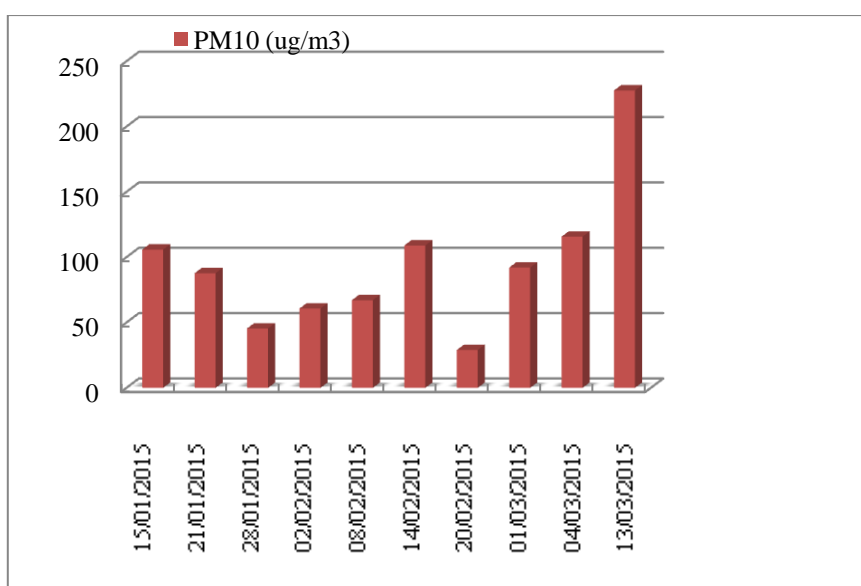


Figure 2. Daily atmospheric levels of PM₁₀

Table 1 summarizes the results for PM10.

Table 1. PM10 concentrations measured at the study area

Number of samples	10
Sampling period	15/01/2015 - 13/03/2015
Unit	$\mu\text{g}/\text{m}^3$
Average daily concentration	94
Maximum daily concentration	227
Minimum daily concentration	28

PM10 concentrations range from 28 $\mu\text{g}/\text{m}^3$ to 227 $\mu\text{g}/\text{m}^3$ with an average value of 94 $\mu\text{g}/\text{m}^3$. The results obtained show that daily levels of PM10 vary widely. This variation is linked both to fluctuations in the intensity of emission sources (road traffic, various industrial activities) and to natural influences (desertic sand, biomass fires, dust resuspension) and weather parameters (wind direction and intensity, humidity, precipitation, temperature) (Kerbach et al., 2009).

2.2. Concentrations of the standard material (P1633b) bound metal elements extracted according to the three extraction protocols

The most common approach for measuring the efficiency of digestion procedures is the estimation of the percentage recovery of metals contained in standard materials having a composition and a structure similar to those of the samples (Celo et al., 2010). Table 2 shows the certified values and reference values of the six studied metallic elements contained in the standard material (P1633b) and the measured concentrations obtained after analysis of the same material using the three extraction protocols.

Using the data from Table 2, we calculated the percentage recovery of each metal element and for each extraction protocol. The results are shown in Table 3.

Table 2. Certified values and reference values and measured concentrations for Cu, Pb, Zn, Co, Mn and Ni contained in the standard material (P1633b)

Element	Certified and reference values	Measured concentrations		
		P1	P2	P3
Cu (mg/kg)	113	102	47	68
Pb (mg/kg)	68	58	31	37
Zn (mg/kg)	210	266	123	173
Co (mg/kg)	50	40	17	24
Mn (mg/kg)	131,8	137	65	81
Ni (mg/kg)	120	130	44	59

Table 3. Percentage recovery of metal elements contained in the standard material (P1633b)

R%	P1	P2	P3
Cu	90%	42%	60%
Pb	85%	46%	54%
Zn	127%	59%	83%
Co	80%	34%	48%
Mn	104%	49%	61%
Ni	108%	37%	49%

In order to interpret the observed differences between the three extraction techniques, it is essential to define the metallic fraction targeted by each extraction method. The mixture HF / HClO₄ / HNO₃ (P1) allows the determination of the total contents of the analyzed elements (Bettineli et al., 2000). The aqua regia extraction method (P2) is a technique that is frequently used for the extraction of metals in different environmental matrices. This technique solubilizes most of the residual minerals (Bettineli et al., 2000). The addition of oxygenated water in the third solution (P3) makes it possible to solubilize the oxidizable phase metals such as sulphides and organic matter (Grotti et al., 2002).

The extraction efficiency is relatively better for method P3 compared to method P2 for all studied elements with percentage recoveries ranging from 48% to 83% for P3 and from 34% to 59% for P2. The addition of H₂O₂ in method P3 improved the percentage recoveries by 18% for Cu, 8% for Pb, 24% for Zn, 14% for Co, 12% for Mn and Ni.

The addition of HF in the first extraction protocol P1 improved significantly the extraction efficiency for all elements with percentage recoveries ranging from 85% to 127%. This method improved the percentage recoveries achieved by protocol P3 by 50% for Cu, 31% for Pb, 32% for Co, 39% for Mn and 51% for Ni, considering that percentage recoveries cannot exceed 100%. The overestimated observed Zn concentration was due to possible contamination.

2.3. Concentrations of the metal elements contained in aerosols and obtained according to the three extraction protocols

Figure 3 allows a comparison between the mean concentrations of six metallic elements present in the solutions obtained by the three extraction protocols for ten PM10 samples represented by: S1, S2, S3, S4, S5, S6, S7, S8 S9 and S10.

P1 allows the highest extraction efficiency of the three digestion methods for the elements determined, in most individual samples. Exceptions concern Pb contained in samples S3 and S8, Ni contained in samples S1, S3, S8 and S10 and Zn contained in samples S3 and S10. This may be due to possible contamination of the samples while performing protocols P2 and P3.

P2 and P3 protocols are two partial extraction techniques. The absence of HF in the P2 and P3 reagent mixtures does not allow the release of the metal bound silicate fraction (Hong et al., 2005). This fraction varies from one sample to another depending on the element considered and this explains the significant difference in extraction efficiency between the total extraction protocol P1 and the two partial extraction protocols P2 and P3. Both protocols present a more or less similar efficiency for elements Mn, Ni and Co. Protocol P2 is on average more efficient than P3 protocol for the extraction of Cu and Zn.

The behavior of Pb is exceptional with concentrations very close to each other for protocols P1, P2 and P3 for almost all samples. This element has a high affinity for organic matter (Mathews et al, 2012). The organic fraction may well be completely dissolved by the various mixtures used in the three digestion methods.

For sample S7 which shows the minimum PM10 concentration, significant differences were not found in the amounts of metal elements extracted by the three digestion methods in each studied sample.

2.4. Comparison of the results obtained for the standard material (P1633b) and PM10 samples

The efficiency of an extraction technique can only be quantified by using standard samples having certified values and reference values for the elements of interest because these materials are easier to analyze than real environmental samples (Gerboles et al., 2011). Therefore, such standard samples can not confirm the digestion efficiency of real samples because of different inherent matrices and element concentration ranges (Celo et al., 2010). Figure 4 compares the concentrations of metal elements extracted by the three extraction methods on standard material and the average concentrations of the same elements contained in the ten studied PM10 samples.

For Pb, Zn, Co, and Mn and despite the different concentrations ranges between samples and between samples and the standard material, the same findings apply for the three extraction protocols for the standard material (P1633b) and for the studied PM10 samples. The extraction efficiency increases in the order P2, P3, P1.

The total digestion method P1 is most efficient for the six elements analyzed in both the standard material and the studied PM10 samples.

The addition of H₂O₂ in the third method has improved the percentage of recovery of all elements contained in the standard material (P1633b) in comparison to the second extraction method. However, the average concentrations of Cu, Zn and Ni contained in the PM10 samples are higher when they are extracted by method P2 in comparison to method P3. This could be explained by the difference in composition of the samples studied in both cases.

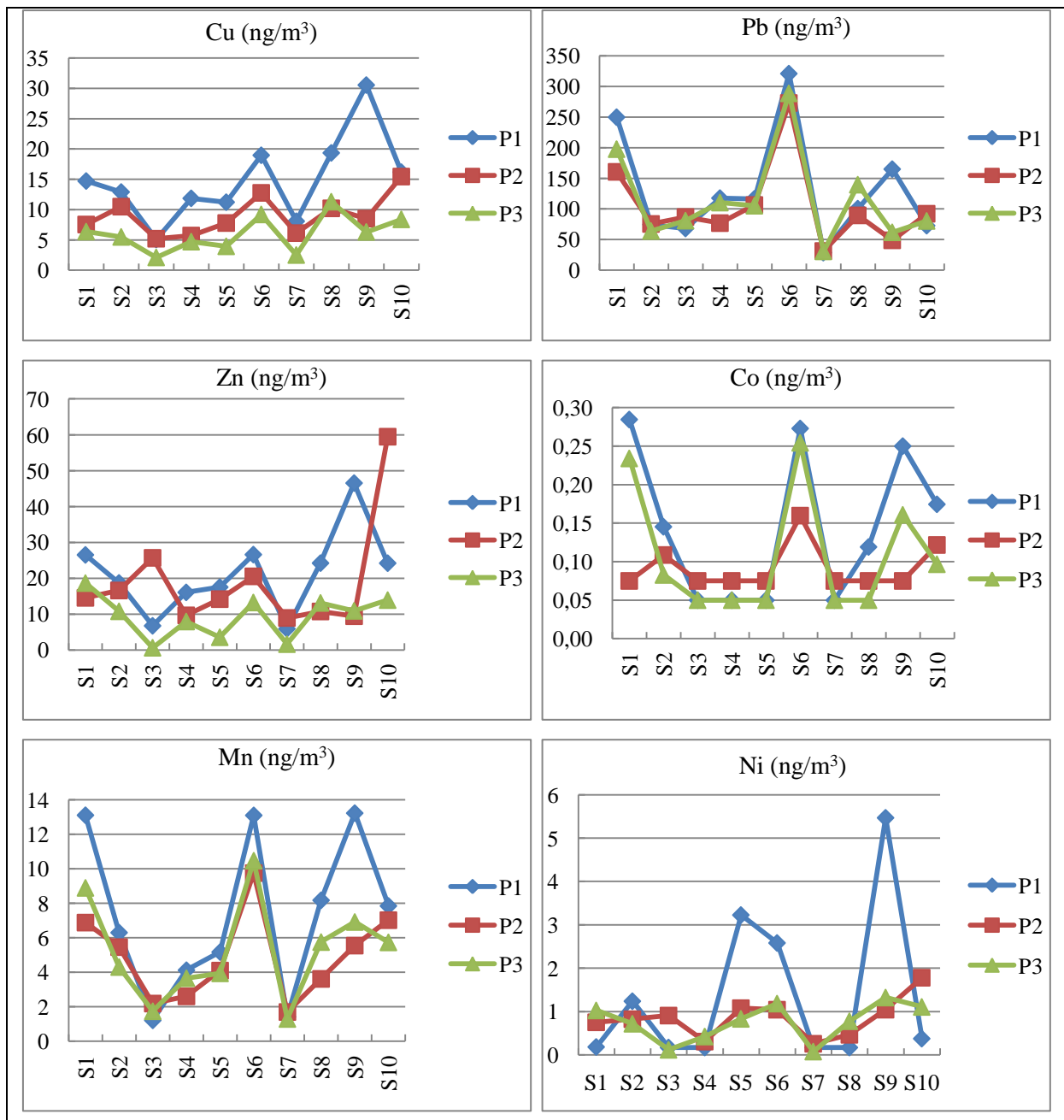
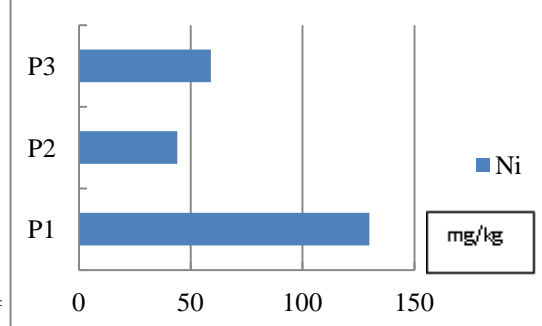
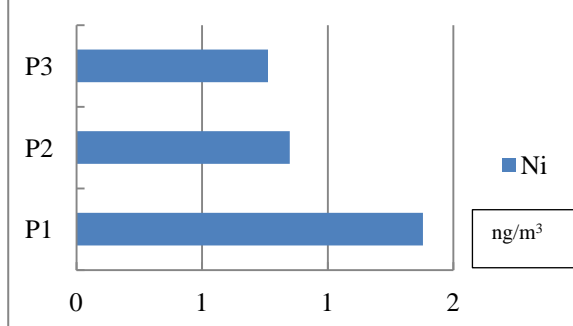
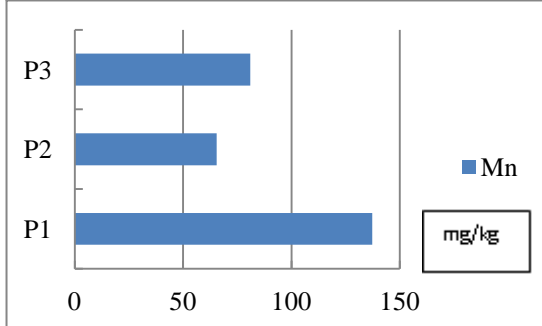
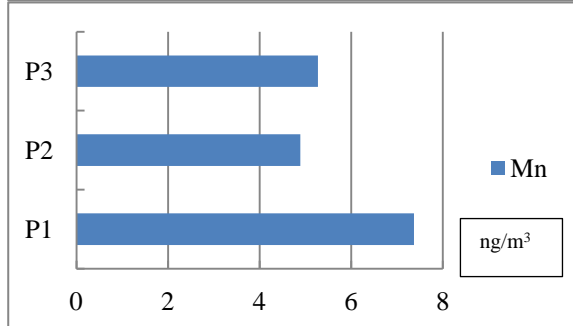
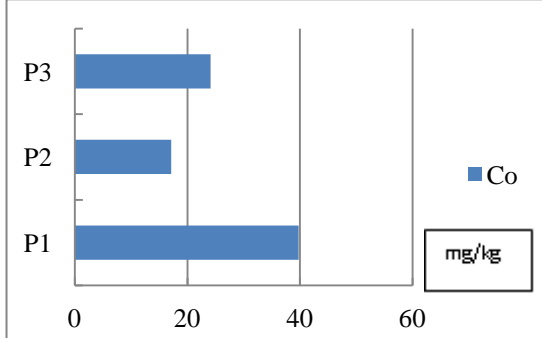
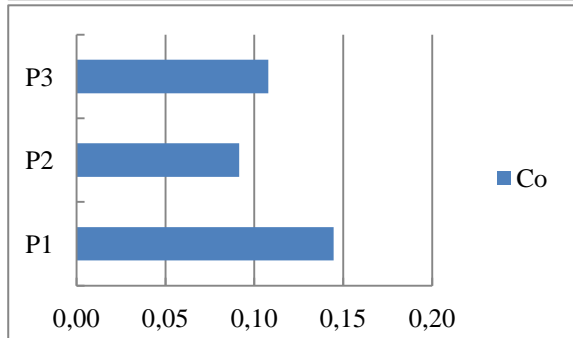
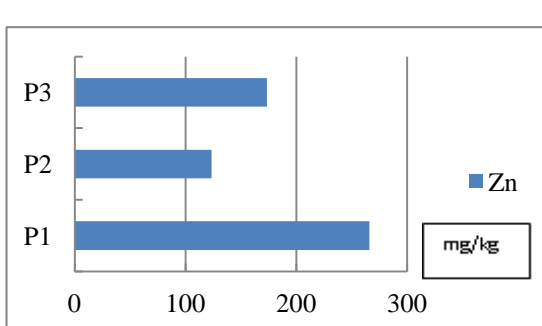
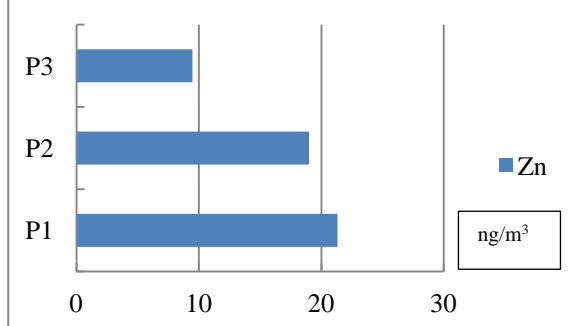
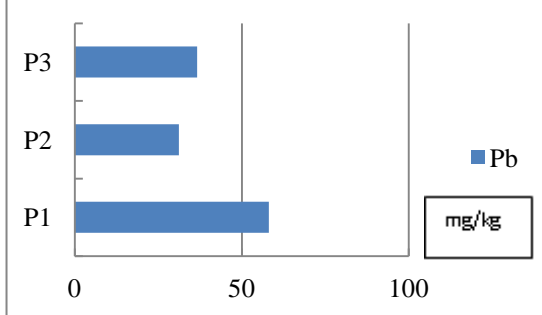
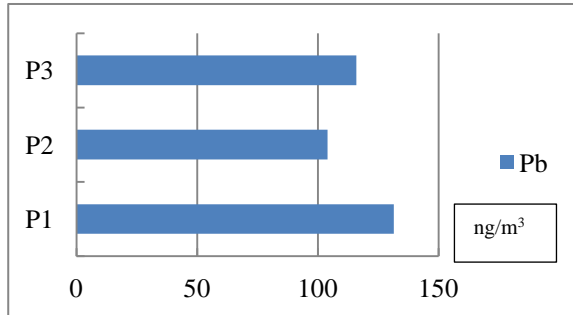
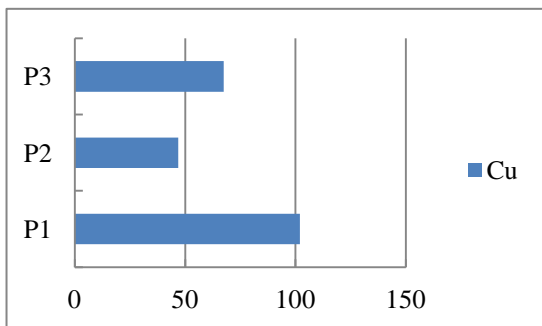
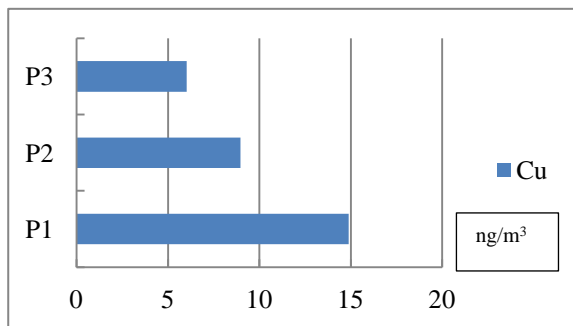


Figure 3. Comparison of the concentrations of Cu, Pb, Zn, Co, Mn, and Ni extracted from PM10 by the three digestion methods

Figure 4. Comparison of the concentrations of metal elements extracted from the PM10 samples (left) and the certified material P1633b (right) by the three digestion methods



Conclusion

This study highlights the different metal extraction capacities of three digestion methods. Extraction efficiencies were shown to vary greatly between these methods. This emphasizes the need for normalization of digestion methods in order to be able to harmonize results for comparison purposes.

The addition of H₂O₂ to aqua regia has improved the percentage of recovery of all elements contained in the standard material (P1633b). Such an improvement concerned only Co and Mn and to a lesser extent Pb. Extraction of Cu, Zn and Ni in PM10 samples was better with aqua regia. The silicate phase could be poorly attacked by the solvents used with respect to some elements. Mn oxides and hydroxides which are not completely dissolved by aqua regia could explain the small amount of extracted Mn.

The total digestion method proved to be the most efficient for extracting Cu, Pb, Zn, Co, Mn and Ni in a standard material and in ten PM10 samples. No reagent mixture can replace the presence of HF which, despite its harmful effects, is the only reagent capable of releasing the metal fraction associated with silicates. Significant differences between extraction protocols vary with samples, matrices and elements. The efficiency of an extraction technique depends on several factors: the extraction solution, the nature of the sample matrix, the analysis time available as well as the optimal time of digestion acids (Ehi-Eromosele et al., 2012).

References

- Al Masri, M.S, K. Al-Kharfan, & K. Al-Shamali (2005). Speciation of Pb, Cd and Zn determined by sequential extraction for identification of air pollution sources in Syria. *Atm. Environ.*, 40 (2006) p 753–761.
- Awan, M.A., S.H. Ahmed, M.R. Aslam & I.A. Qazi (2011). Determination of total suspended particulate matter and heavy metals in ambient air of four cities of Pakistan. *Iran. J. Energ. & Environ.* 2 (2): 128-132.
- Azimi, S. (2004). Sources, flux et bilan des retombées atmosphériques de métaux en Ile-de France. Thèse présentée pour l'obtention du diplôme de docteur de l'Ecole nationale des ponts et chaussées, spécialité : sciences et techniques de l'environnement. 30-36.
- Bettinelli, M., G.M. Beone, S. Spezia, & C. Baffi (2000). Determination of heavy metals in soils and sediments by microwave-assisted digestion and inductively coupled plasma optical emission spectrometry analysis. *Anal. Chim. Act.* 424, p 289-296.
- Brown, R & M. Milto (2005). Analytical techniques for trace element analysis : an overview. *Trends Anal. Chem.*, vol. 24, n°3, p 266-274.
- Castillo, S., T. Moreno, X. Querol, A. Alastuey, E. Cuevas, L. Herrmann, M. Mounkaila, M & W. Gibbons (2008). Trace element variation on size-fractionated African Desert dusts. *J. of Arid Environ.* vol. 72, p 1034-104.
- Celis, V., E.D. Zlotorzynska, D., Mathieu, & I. Okonskaia (2010). Validation of a simple microwave-assisted acid digestion method using microvessels for analysis of trace elements in atmospheric PM2.5 in monitoring and Fingerprinting studies. *Open Chem. Biomed. Method. J.* 3, p 143-152.
- Ehi-Eromosele, C.O., A.A. Adaramodu, W.U., Anake, C.O., Ajanaku & A., Edobor-Osoh (2012). Comparison of three methods of digestion for trace metal analysis in surface dust collected from an e-waste recycling site. *Nat. Sci.* vol. 10, n° 10, p 1-6.
- Gerboles, M et al. (2011). Interlaboratory comparison exercise for the determination of As, Cd, Ni and Pb in PM10 in Europe. *Atm. Environ.* vol. 45, n° 20, p 3488-3499.
- Grotti, M. C., Ianni, & R. Frache (2002). Inductively coupled plasma optical emission spectrometric determination of trace elements in sediments after sequential selective extraction: effects of reagents and major elements on the analytical signal. *Talanta*, vol. 57, n° 6, p 1053–1066.
- Han, X. & Luke P. Naeher (2006). A review of traffic-related air pollution exposure assessment studies in the developing world. *Environ. Int.* p 106-120.
- Nguyen, H.L., M. Braun & M. Leermakers (2005). Comparison of two digestion procedures used for trace metals extraction from reference sediments. *Environ. Tech.* ES04.
- Jimoh, W. (2012). A sequential extraction method for the chemical speciation of metals in Harmattan dust collected from Kano and Zaria cities in Northern Nigeria. *Int. J. Res. Chem. Environ.*, vol. 2, n° 2, p 76-82.

- Kerbachi, R., N. Oucher, A. Bitouche, N. Berkouki, B. Demri, M. Boughedaoui, & R. Jourmard (2009). Pollution par les particules fines dans l'agglomération d'Alger. Colloque international Environnement et Transports dans des Contextes Différents, Ghardaïa, Algérie, 16-18 février 2009.
- Lamaison, L. (2006). Caractérisation des particules atmosphérique et identification de leurs sources dans une atmosphère urbaine sous l'influence industrielle. Thèse de doctorat en Structure et dynamique des systèmes réactifs, Lille, France.
- Mathews, A., C. Omono, C. & S. Kakulu (2012). Comparison of digestion methods for the determination of metal levels in soils in Itakpe, Kogi State, Nigeria. *Int. J. Pure Appl. Sci. Technol.*, 13(2) p 42-48.
- Moreno, T., X. Querol, A. Alastuey, M. Viana, P. Salvador, A. Sanchez, A. Begona, S. Dela Rosa, & W. Gibbons (2006). Variation in atmospheric PM trace metal content in Spanish towns: Illustrating the chemical complexity of the inorganic urban aerosol cocktail. *Atm. Environ.* 40, p 6791-6803.
- Pena-Icart, M. (2011). Comparative study of digestions methods EPA 3050B (HNO₃, H₂O₂, HCl) and ISO 11466.3 (aqua regia) of Cu, Ni and Pb contamination assessment in marine sediments. *Marine Environmental Research* 72, p 60-66.
- Querol, X., A. Alastuey, S. Rodriguez, F. Plana, E. Mantilla, & C.R. Ruiz (2001). Monitoring of PM10 and PM2.5 ambient air levels around primary anthropogenic emissions. *Atm. Environ.* vol. 35, n° 5, p 848–858.
- Pérez, C., J. Pinerio, P. Mahia, S. Lorenzo, E. Fernandez, & D. Rodriguez (2004). Hydride generation atomic fluorescence spectrometric determination of As, Bi, Sb, Se(IV) and Te(IV) in aqua regia extracts from atmospheric particulate matter using multivariate optimization. *Anal. Chim. Act.*, vol. 526, p 185-192.
- Petterson, R.P. & M. Olsson (1998). A nitric acid–hydrogen peroxide digestion method for trace element analysis of milligram amounts of plankton and periphyton by total-reflection X-ray fluorescence spectrometry. *J. Anal. At. Spectrom.*, vol. 13, p 609–613.
- Ragosta, M., R. Caggiano, M. Macchiato, S. Sabia, & S. Tripetta (2008). Trace elements in daily collected aerosol : Level characterization and source identification in a four-year study. *Atm. Res.*, vol. 89 p 206-217.
- Ryan, P.C., S. Hillier, & A.J. Wall (2008). Stepwise effects of the BCR sequential chemical extraction procedure on dissolution and metal release from common ferromagnesian clay minerals: A combined solution chemistry and X-ray powder diffraction study. *Sci Total Environ.*, vol. 407,
- Sastre, J., A. Sahuquillo, M. Vidal, & G. Rauret. (2002). Determination of Cd, Cu, Pb and Zn in environmental samples: microwave-assisted total digestion versus aqua regia and nitric acid extraction. *Anal. Chim. Act.*, vol. 462, n° 1, p 59-72.
- Tombette, M. (2007). Modélisation des aérosols et de leurs propriétés optiques sur l'Europe et l'Ile de France : validation, sensibilité et assimilation de données. Thèse présentée pour l'obtention du diplôme de docteur de l'Ecole nationale des ponts et chaussées, spécialité : sciences et techniques de l'environnement, p 30-36.

Identification of anthropogenic and natural sources of atmospheric particulate matter and trace metals in Constantine, Algeria

Hocine ALI-KHODJA**, Mahfoud KADJA**, Ahmed TERROUCHE* & Kanza LOKORAI*

* *Laboratoire Pollution et Traitement des Eaux, Université des Frères Mentouri, Constantine, Algérie*
Fax +213 31 81 13 08 - email: hocine_ak@yahoo.fr

** *Laboratoire d'Energétique Appliquée et de Pollution, Université des Frères Mentouri, Constantine, Algérie*

Abstract

The purpose of this study was to identify the different Sources of PM₁₀ and some metallic elements (Pb, Cu, Zn, Fe, K, Ca, Na, Mg) at a traffic site at Zouaghi, in the south of Constantine, using factor analysis (FA) to categorise the different trace elements according to their origin and the enrichment factor (EF) to identify terrigenous elements and those having a marine origin. We also used back-trajectories clustering to identify potential distant sources that contribute to particulate pollution and metallic elements in our site. Sources of coarse particles are the most important due to the significant contribution of resuspended coarse particles and Saharan dust intrusions. Anthropogenic, soil resuspension, sea salt and traffic were identified as the main PM₁₀ sources. Enrichment factors in relation to soil and seawater average concentrations indicate that Mg is of marine origin and K originates mainly from the soil while Pb, Cu and Zn are derived from anthropogenic sources. Results point at the Sahara desert as a major source of PM₁₀ and Fe.

Keywords: *Traffic site, factor analysis, back-trajectories, enrichment factors.*

Introduction

Motor vehicles strongly affect air quality within urban areas (Pastuszka et al. 2010). Several studies have provided evidence that the exposure to high concentrations of aerosols is associated with adverse health effects (Pateraki et al. 2012). Multi-city extensive studies conducted in the United States and in Europe reported positive associations between PM₁₀ and death. In a multicentre study involving four European cities, consistent positive associations were found between coarse particles central sites concentrations and prevalence of respiratory symptoms. Another particulate matter health study in China revealed a 10- $\mu\text{g}/\text{m}^3$ increase in 2-day moving-average PM₁₀ was associated with a 0.35% increase of total mortality, 0.44% increase of cardiovascular mortality and 0.56% increase of respiratory mortality (Chen et al, 2012). In a study that examines the relation of lung cancer incidence with long-term residential exposures to ambient particulate matter, it was established that a 10- $\mu\text{g}/\text{m}^3$ increase in 72-month average PM₁₀ was positively associated with lung cancer. Moreover, adverse health effects may be caused by mineral dusts originating from the Sahara.

Lim et al. (2012), in the framework of the WHO driven evaluation of the Global Burden of Disease (GBD), evidenced that particulate atmospheric pollution is the 4th cause of worldwide mortality in developing countries and the 11th one in central Europe. REVHIHAAP (Review of evidence on health aspects of air pollution) (WHO 2013) evidenced that mean life expectancy of European citizens is reduced by 9 months due to increase on premature mortality due to cardiovascular, respiratory and cerebro-vascular causes. These reports also indicate that atmospheric particulate matter (PM) is the main pollutant causing these health outcomes.

Studies on traffic-related airborne particulate matter, are scarce or even not available in many cities in the developing world and particularly in Africa. This is in spite of the high levels of atmospheric particulate pollution observed in African cities.

In the developing countries, the particulate matter forms the major contributor to air pollution and hence the pressure to understand its sources better. Emissions from combustion of fossil fuels are expected to increase significantly in African cities in the near future. Atmospheric particulate pollution is more severe in developing countries than in developed countries because of rapid urbanization and a sudden expansion in the number of vehicles. It was reported that annual PM levels in Northern Africa exceeded annual and 24-h WHO guidelines, with annual PM₁₀ levels exceeding 150 $\mu\text{g}/\text{m}^3$ in

different sites of Cairo while mean PM10 levels across a network of four monitoring stations that was established in Algiers ranged from approximately 38 to 129 $\mu\text{g}/\text{m}^3$ between 2002 and 2003.

The Mediterranean area is also affected by natural mineral dust transport from the Sahara (Rodriguez et al. 2007).

The main objectives of this study were: 1) to assess the temporal variations of atmospheric particulates and associated metallic elements; 2) to identify distant sources of PM10 by calculating 3-day back trajectories; 3) to identify potential pollution sources of PM10 and metallic elements based on factor analysis and cluster analysis (CA).

1. Methods

The paper must include in order: the title, author(s), address, an English abstract, keywords in English, if possible a French abstract and keywords in French, the introduction, a limited number of sections (e.g: 1. the method; 2. the results; 3. discussion), and then the conclusion, acknowledgements and references. Main sections will be numbered 1, 2, 3. The titles of sub-sections will not be referenced.

Site description

The sampling site was located at the entrance to the campus of the Faculty of Earth Sciences located at Zouaghi, Constantine, nearby National Road 79, which is one of the busiest traffic highways in the city of Constantine, (36°22'N, 6°40'E, 640 m.a.s.l), Algeria. The sampling device was placed about 5 m above the ground, and about 6 m from the road. The position of the sampling site was such that it could be considered a traffic station because it is directly influenced by vehicular emissions. Sampling was scheduled at midnight.

Measurement of fine particulate matter

A portable low volume air sampler Model Minivol TAS with a rate of 5 liters/minute was used. Ambient air particulates were trapped by a quartz filter (47 mm in diameter with a porosity of 0.2 microns). After each sampling interval, the collection media were returned to the weighing laboratory and allowed to equilibrate for 24 h in a dessicator before weighing to a precision less than ± 0.01 mg using a Shimadzu balance (model AUW120D). The initial weights were determined after a similar period of desiccation.

Analysis of trace elements

Each filter was digested according to the method of Kuvarega and Taru (2008). A Shimadzu-7000 AAS supporting an acetylene flame was used to analyse metallic elements Fe, Na, Mg, Ca, Zn and K, while Pb and Cu were analysed using polarography (VA Computrace797). To minimize the effects of matrices, the standard addition technique was used for the determination of all metals. The results of the analysis of ten blank samples were used to estimate the element concentration produced by the filter and sample preparation.

Factor analysis attempts to identify underlying variables, or factors, that explain the pattern of correlations within a set of observed variables. The primary interest of this type of analysis is to replace the original variables, generally correlated with more easily treated uncorrelated variables (Dagnelie, 1975). This technique tries to explain a set of data in a number smaller than the number of starting dimensions. The technique is to summarize the data-matrix with minimal and controlled loss of initial information by a reduced number of factors as differentiated as possible. This is a linear transformation whose general pattern is written in the form:

$$X_i = A_{i1}F_1 + A_{i2}F_2 + \dots + A_{ik}F_k + U_i$$

with X: variable.

F: the common factor.

U: single factor.

A: coefficient used to combine k factors.

The data were processed using IBM SPSS Statistics 20.0 software. The main sources of PM10 were identified by performing a varimax rotation which has reduced the initial number of variables to a

lesser number of independent variables (factors), and which estimated values of the factors (factor score) for each sample.

2. Results

Contribution of local Traffic to PM10 Levels

Figure 1 shows the evolution of the difference in concentration of PM10 between the traffic and background sites. Daily concentrations of roadside PM10 are almost always higher than those of background site (positive days), but for 9 days (of 116 days), background pollution exceeds the pollution along road (negative days) and for 22 days, the levels of PM10 in the background and roadside sites are identical.

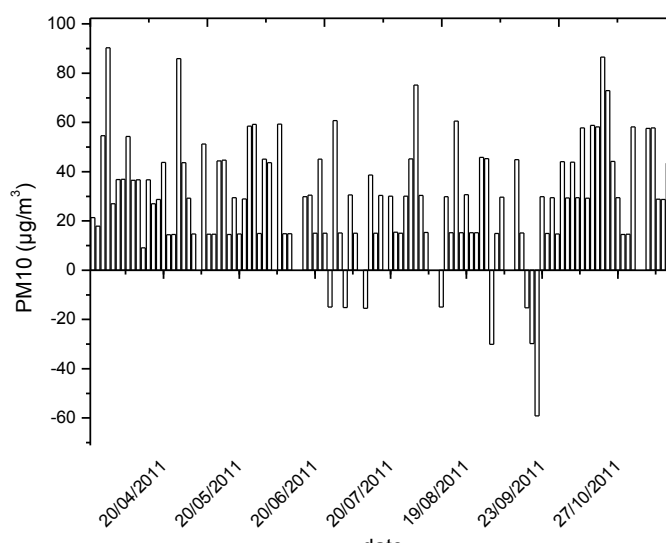


Figure 1. Time variation of the difference in PM10 concentrations between traffic and background sites

Several studies (Charron & Harrison, 2003) reported the influence of weather conditions on levels of particulate emitted by vehicles. To well understand this phenomenon we analyzed the meteorological data during the positive and negative days (Table 1, Figure 2).

In the positive days, the temperature and humidity are different from those observed during the negative days (Table 1). These two parameters have a significant influence on the number and size of particles. A rise in temperature favors the formation of finer and thus more mobile particles. In addition, a high temperature and a high air humidity effectively reduce the density of air causing a reduction in the oxygen content in the air and thus influence the air-fuel ratio of the burnt mixture resulting in elevated levels of particle emissions (Jamriska et al., 2008).

We also observe that the average wind speed is higher during the negative days than during the positive days (1.4 and 1.2 m/s respectively). The wind speed is greater than 3.6 m/s in 12% of the time during the negative days (Fig. 2) and only in 5% of the time during the positive days (Fig. 2B). High wind speeds promote the dispersion of the particles and eliminate the difference between traffic and background sites. The predominance of light winds at measurement sites promotes the accumulation of dust from transportation on the roadside leading to higher pollution than in the background site.

We also note that for the positive days, prevailing winds are westerly and tend to bring dust from arid lands situated to the west of National Road 79.

Table 1. Average values of some meteorological parameters

	Negative days	Positive days
Wind speed	1.4	1.2
Rainfall	0.7	2.2
Temperature	22.6	19.4
Humidity	31.8	41.4
Pressure	948	968.2

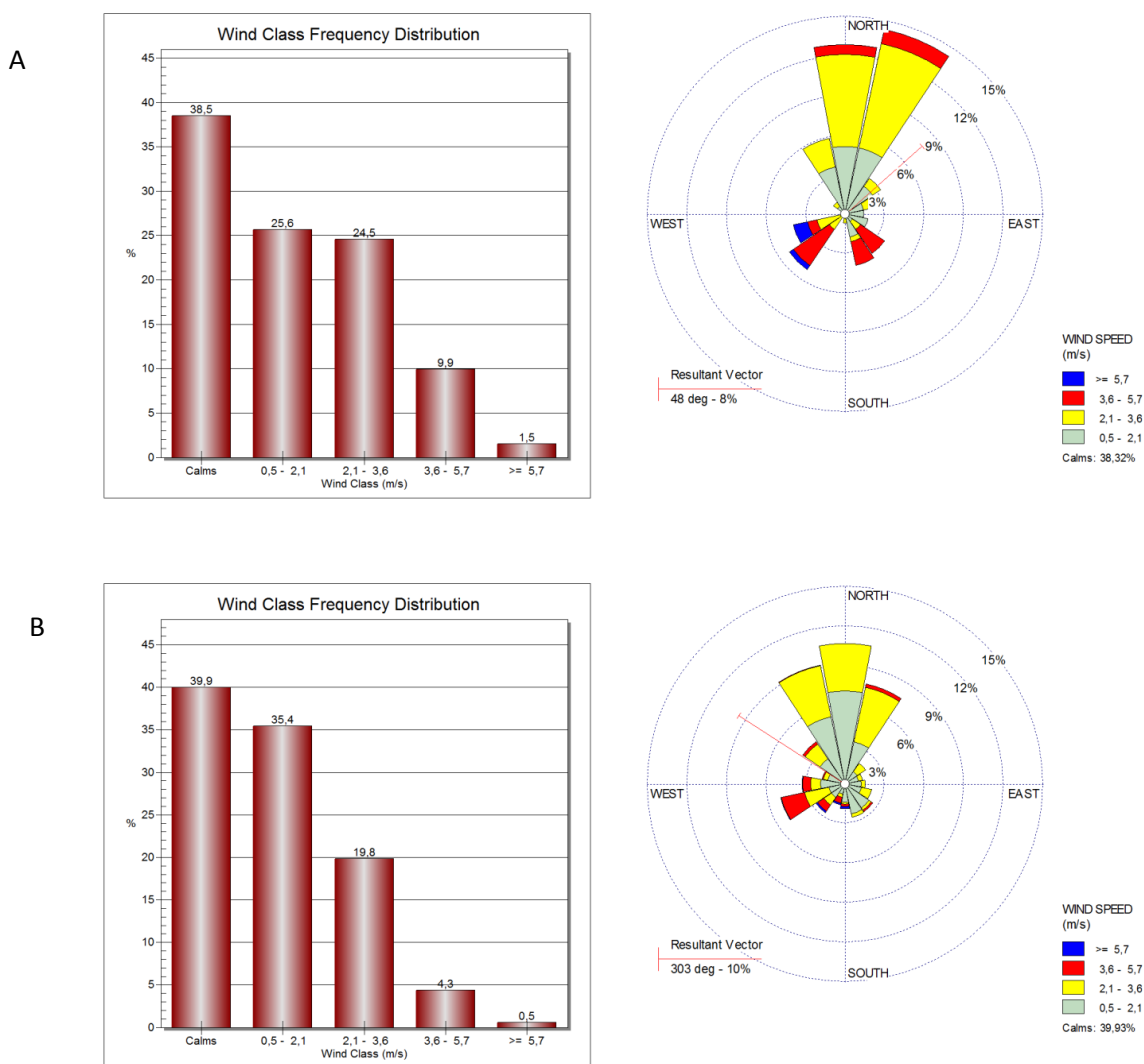


Figure 2. Wind roses in Zouaghi, Constantine (A) Negative days (B) Positive days

Table 2 shows the contribution of road traffic to PM₁₀ and some metal elements. Traffic contributes 39.8% to PM₁₀, either by direct emissions such as Pb (62.4%), Zn (50.3%), Cu (55.6%), and/or the resuspension of soil dust originating from earth such as Fe (57.9%), Ca (65.1%), K (56.8%) and from marine elements like Na (29.5%) and Mg (49.6%). It is assumed that traffic emits Pb, Zn and Cu by a single channel (direct emission) and the other elements are resuspended by vehicle movement. The direct emission and resuspension contribute up to 55.49% and 49.55% respectively to PM₁₀ levels.

Table 2. Difference in pollution between traffic and the background sites

	<i>Traffic site</i>	<i>Background site</i>	<i>Increment*</i>	<i>Contribution due to traffic**</i>
	$\mu\text{g}/\text{m}^3$		$\mu\text{g}/\text{m}^3$	%
PM ₁₀	81,71	49,23	32,48	39.75
Pb	1,09	0,41	0,68	62.39
Cu	0,63	0,28	0,35	55.56
Zn	1,47	0,73	0,74	50.34
Direct emission	3.19	1.42	1.77	55.49
Fe	4,11	1,73	2,38	57.90
Ca	3,93	1,37	2,56	65.14
K	5,93	2,56	3,37	56.83
Mg	2,34	1,18	1,16	49.57
Na	6,92	4,88	2,04	29.48
Resuspension	23.23	11.72	11.51	49.55

*Increment = concentration in traffic site - concentration in background site

**Contribution = [(concentration in traffic site – concentration in background site) / concentration in traffic site]* 100

Conclusion

PM₁₀ concentrations were measured at a sampling traffic site situated at Zouaghi, Constantine between 23 March 2011 and 22 November 2011. The results presented in this work allow us to conclude that PM₁₀ concentrations are excessive in light of the WHO and the EU standards. The latter seem hardly feasible in view of the contribution of natural aerosols to ambient PM levels. The average daily concentration of PM₁₀ (80,42 $\mu\text{g}/\text{m}^3$) was observed for the period extending from 23 March 2011 to 22 November 2011. During the study period implying the sampling of PM₁₀, the average concentration of PM₁₀ was 105.2 $\mu\text{g}/\text{m}^3$. Sources of PM₁₀ particles are related to the significant contribution of resuspended coarse particles and Saharan dust intrusions.

In this work some statistical techniques have been successfully used to identify and characterize PM₁₀ sources. The application of Varimax rotated factor analysis, a multivariate technique, has allowed us to qualitatively identify anthropogenic, soil resuspension, sea salt and traffic as the main PM₁₀ sources, at a traffic site in Constantine (Algeria).

Enrichment factors in relation to soil and seawater average concentrations indicate that Mg is of marine origin and K originates mainly from the soil while Pb, Cu, Zn are derived from anthropogenic sources.

To identify external sources and their geographical origin, air mass back-trajectories have been calculated with the HYSPLIT 4 model. Results point at the Sahara desert as a major source of PM₁₀ and Fe. The contribution to Na results from long-range transport of air masses originating from the North (Mediterranean sea) or from the South (salt marshes).

On the other hand, salt marshes located south of the study station are identified as the path followed by dust plumes originated in the desert region. They have been derived for Na.

The mediterranean sea has been identified as the major source of Na, Mg, K and Ca. Iron is of crustal origin, either from nearby sources such as the soil surrounding the site or distant sources such as the Sahara to the south. Calcium and potassium have also an anthropogenic origin. Anthropogenic sources are related to the construction works of the tram on the other side of the road along the measurement site. Zn, Cu and Pb are derived from anthropogenic sources: traffic and industry. Traffic is the major source of the high Pb levels observed since gasoline still contains lead additives in Algeria.

Traffic contributes 39.8% to PM₁₀, either by direct emissions or by the resuspension of soil dust originating from earth and from marine elements.

References

- Charron A and R M Harrison (2003): Primary particle formation from vehicle emissions during exhaust dilution in the roadside atmosphere, *Atmospheric Environment*, Vol. 37, p 4109–4119
- Rodriguez S, Querol X, Alastueya A and J de la Rosa (2007): Atmospheric particulate matter and air quality in the Mediterranean: a review. *Environ Chem Lett* 5, p 1–7. doi: 10.1007/s10311-006-0071-0
- Jamriska, M., L. Morawska and K. Mergersen,(2008): The effect of temperature and humidity on size segregated traffic exhaust particle emissions. *Atmos. Environment*, 42, p 2369-2382.
- Pastuszka JS, Rogula-Kozłowska W and E Zajusz-Zubek (2010): Characterization of PM10 and PM2.5 and associated heavy metals at the crossroads and urban background site in Zabrze, Upper Silesia, Poland, during the smog episodes. *Environ Monit Assessment* 168: 613-627. doi: 10.1007/s10661-009-1138-8
- Chen R, Kan H, Chen B, Huang W, Bai Z ,Song G and G Pan (2012): Association of particulate air pollution with daily mortality: the China Air Pollution and Health Effects Study. *Am J Epidemiol* G Vol. 175, n°11, p 1173-1181. doi: 10.1093/aje/kwr425
- Lim SS, Vos TD, Flaxman AD, Danaei G, and K Shibuya K (2012): A comparative risk assessment of burden of disease and injury attributable to 67 risk factors and risk factor clusters in 21 regions, 1990-2010: a systematic analysis for the Global Burden of Disease Study 2010. *Lancet*, 380, p 2224-2260. doi: 10.1016/S0140-6736(12)61766-8.
- Pateraki St, Asimakopoulos DN, Flocas HA, Maggos Th and Ch Vasilakos (2012): The role of meteorology on different sized aerosol fractions (PM10, PM2.5, PM2.5–10). *Sci Total Envir* 419, p 124-135. doi: 10.1016/j.scitotenv.2011.12.064
- WHO (2013): Review of evidence on health aspects of air pollution- REVHIHAAP. WHO Regional Office for Europe.

A real-world test and demonstration project for assessing consumption and emission of Natural Gas Heavy Good Vehicles: Equilibre Project

F. BAUCHE^{1,*}, R. TRIGUI¹, B. SCHNETZLER¹, N.-E. EL FAOUZI¹ and P. MÉGEVAND²

¹ French Institute of Science and Technology for Transport, Spatial Planning, Development and Networks (IFSTTAR), Lyon, 69500, France

² Mégevand Logistics, Association Equilibre, 01600 Sainte Euphemie, France

Keywords: Natural gas vehicle, heavy Good Vehicles, pollutant emission, fuel consumption.

Abstract

Interest in Natural Gas Vehicles (NGV) has received increasing interest in recent years. The potential environmental benefits and the savings in fleet operational costs drive this evolution. To anticipate the NGV expansion, a large-scale demonstration project, called Equilibre was launched with support of the French Environment and the Energy a gas distribution company GrDF, 100% subsidiary of ENGIE with the active involvement of a six Freight Logistic Operators (Equilibre Association). This association aims at promoting and assessing the GNV freight logistics from economical standpoint.

To achieve this goal, a sample of 16 heavy Good Vehicles (HGV) are instrumented including diesel and NGV (Compressed natural gas – CNG, and Liquefied natural gas –LNG) powered engines. The HGV fleet is monitored in real-world conditions and context data is collected (e.g. road topology such as altitude, road type,...), weather and traffic data.

The collected data will be then used ultimately to build a decision support system (DSS) that predict gas consumption according to the trip characteristics, type of HGV and loads.

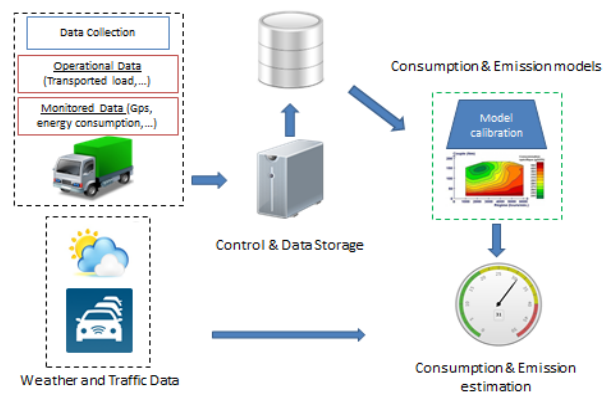


Figure 1. GENERAL METHODOLOGY

Table 1. EQUILIBRE HGV FLEET

Number of Trucks	Engine
5	Gazole
6	CNG
5	LNG

In this paper, we focus on the experimental phase and report the effort of data collection from the monitoring of the Equilibre HGV Fleet in real-world conditions.

* Corresponding Author

Potential of In-Motion Charging Buses for the Electrification of Urban Bus Lines

Fabian BERGK*, Kirsten BIEMANN*, Udo LAMBRECHT*, Prof. Dr. Ralph PÜTZ** & Hubert LANDINGER***

* ifeu – Institut für Energie- und Umweltforschung Heidelberg GmbH, Heidelberg, D-69120, Germany
phone: +49 (0) 6221 / 47 67 -38, e-mail: fabian.bergk@ifeu.de

** Department of mechanical engineering, HAW Landshut, Landshut, D-84036, Germany

*** Ludwig-Bölkow-Systemtechnik GmbH (LBST), Munich, D-85521, Germany

Abstract

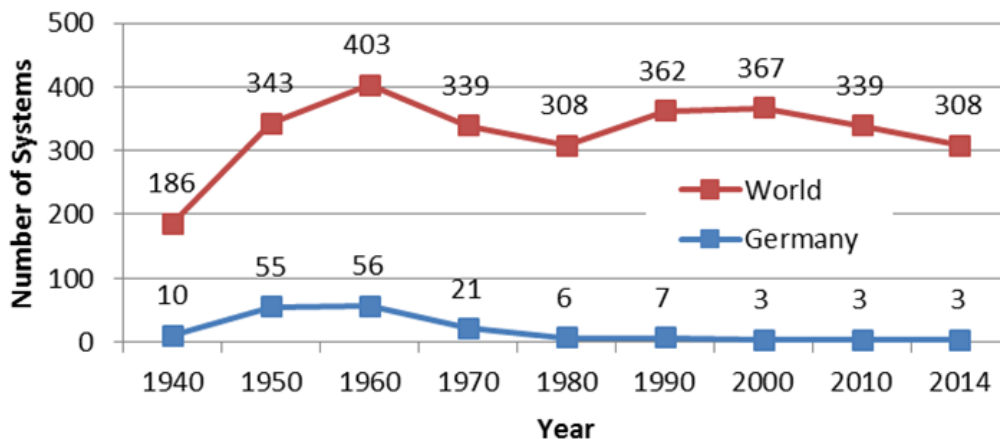
Electric buses can help to reduce energy consumption, greenhouse gas emissions, pollutants and noise. One possible electric bus concept is the in-motion charger. As a combination of a trolleybus and a battery electric bus, the in-motion charger is able to operate relevant stretches in battery mode and therefore the amount of installed catenary wires can be significantly reduced. As a part of the German 'Mobility and Fuels Strategy' (BMVI, 2013), the aim of the article's underlying work was to identify possible applications for the in-motion charger. This included a comparison of the environmental and economic performance of the different traction systems of urban buses (in-motion charger, opportunity charger, overnight charger, fuel cell hybrid and diesel buses). The analysis focused on an urban bus line, running with articulated buses and is covering the whole lifespan of vehicles and infrastructure. The analysis showed that in a lifetime perspective all electric systems can significantly reduce greenhouse gas emissions compared to buses fuelled with fossil diesel. But even until 2025 the diesel bus will be the most economic bus technology under the assumed framework conditions. In comparison with other electric buses, the in-motion charger is the most cost-effective bus system for high capacity lines.

Keywords: electric mobility, buses, environmental impact, economic analysis.

Introduction

Public transport buses play an important role in urban mobility. Already today buses are reducing transport greenhouse gas emissions due to the shift from private cars. But for the long term goal of a climate neutral economy also public transport has to abandon fossil fuels and switch to renewables. The direct usage of electricity is the most energy efficient way of using renewable power. Today this technology is used in rail-bound public transport and in three trolley systems in Germany (see figure 1) with a cumulated number of less than one percent of the German urban bus fleet (see Association of German Transport Companies' 2014 statistics: <https://www.vdv.de/english.aspx>).

Figure 1. Number of trolleybus systems in Germany and the world from 1940 until 2014; (Spousta et al. 2013), <http://www.solingen-internet.de/>



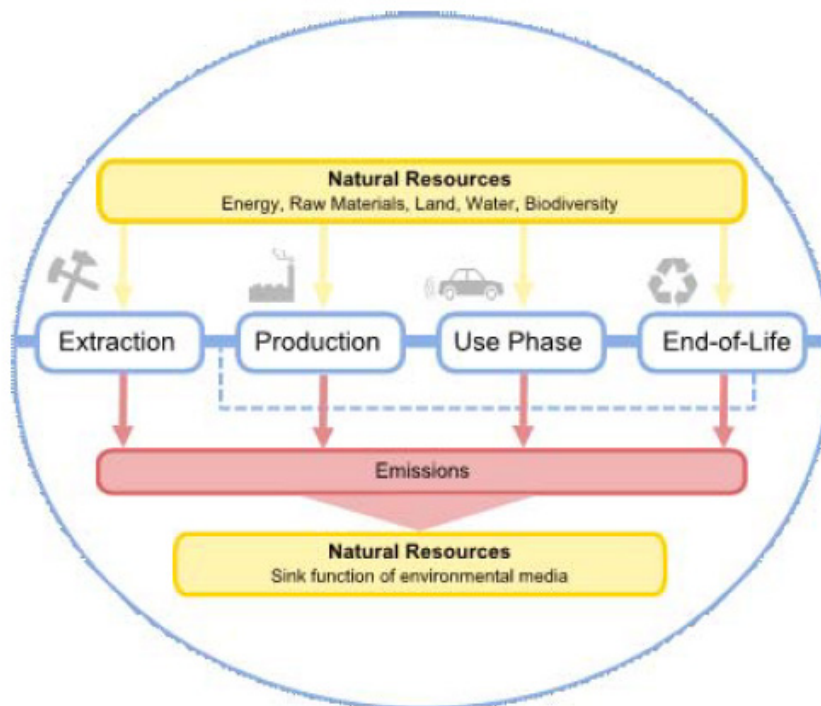
Nowadays electric buses are again on the agenda of decision makers (e.g. reflected in Hamburg's goal to stop the purchase of conventional buses in 2020): They can help reduce energy consumption, greenhouse gas emissions, pollutants and noise. Furthermore, they can support the introduction and integration of renewable energy sources and thus promote a diversification of energy sources. One possible electrification option is the In-Motion Charger (IMC). In contrast to a conventional trolleybus with electric auxiliary unit the battery of an IMC has a considerably higher capacity. This allows the IMC to operate relevant stretches in battery mode. Therefore the amount of installed catenary wires can significantly be reduced.

Goal of the study as part of the German 'Mobility and Fuels Strategy' (BMVI, 2013) was to identify possible applications of the IMC and the resulting IMC's environmental benefit. The main steps were an in-depth analysis of the environmental and economic performance of the different electric bus systems (IMC, opportunity charger, overnight charger, fuel cell battery hybrid and diesel buses) followed by two workshops with stakeholders to identify usage and acceptance constraints.

1. Method

The comparison of the environmental performance is based on a detailed Life Cycle Assessment (LCA) (see figure 2). The functional unit is a bus kilometre or a passenger kilometre. The analysis focused on the production and the use phase of the bus.

Figure 2. Schematic of LCA approach (Jöhrens, Helms, 2014)



The global warming potential ($\text{CO}_2\text{-eq}$) is calculated including the emissions of carbon dioxide, methane and nitrous oxide. The assessment of pollutants is focusing on nitrogen oxide (NO_x) and particle mass (PM) emissions, which are currently most debated in respect to the compliance with European air quality standards.

Use case

The drivetrain concepts are compared for an articulated bus (length ~18 m) on an urban line with an annual mileage of 60,000 km. These buses are widely used in Germany, particularly on lines with high passenger demand. The characteristics of the use case are chosen to represent an average German urban line with a length of 15 km in easy urban traffic (Standardised On-Road Test cycle (SORT) 2). Bus intervals from 15 to 4 minutes are examined which leads to a line capacity from 560 to 2,100 passengers per hour and direction (pphd).

The technical details of the buses are shown in table 1:

Table 1. Technical parameters of compared electric bus concepts (articulated buses)

Power train parameter		IMC	OC	ONC	FC
Battery capacity	kWh	70	150	400	30
Power (engine, power electronics)	kW	250	250	250	250
Average charging power	kW		250	80	
Fuel cell power	kW				160
Hydrogen storage	kg				35
IMC = In-Motion Charger, OC = Opportunity Charger, ONC = Overnight Charger, FC = Fuel Cell Hybrid					

Electric bus systems need proper infrastructure, but economic (lean) infrastructure and operational performance are often a trade-off. For this study, the infrastructure has been dimensioned after intense discussions with technology suppliers and public transport consultants.

Table 2. Energy supply infrastructure for different electric bus systems, example for 7.5 minute interval (15 buses/ line)

	Infrastructure	Scale	Number
IMC	Catenary (two-sided)		7.5 km (50 % of the line)
	Substation	750 kW	4
OC	Fast charging point (including substation)	300 kW	4
	Charging point depot	25 kW	15
	Substation depot	400 kW	1
ONC	Charging point depot	100 kW	15
	Substation depot	1.5 MW	1
FC	Hydrogen refuelling station	Middle sized station	25 % degree of capacity utilization
IMC = In-Motion Charger, OC = Opportunity Charger, ONC = Overnight Charger, FC = Fuel Cell Hybrid			

Energy consumption

The total consumption of the different power train concepts reflects the following losses and consumers:

- The energy of the engines to provide traction energy,
- the energy for the operation of auxiliary equipment (e.g. heating),
- the losses in the provision of energy (e.g. in charging infrastructure) and
- the losses in the vehicle (e.g. charging and discharging of batteries, losses in power electronics).

The energy consumption without heating/ air-conditioning was determined by Belicon GmbH at HAW Landshut using extensive measurements on different buses (see <http://belicon-forschung.jimdo.com/>). The consumption of heating or air-conditioning of electric buses could not be determined from measurements as this would have required year-long testing in different climatic conditions. Moreover, the majority of the vehicles measured were equipped with chemical auxiliary heaters, which are not part of the case study. Therefore, the consumption for heating/ air-conditioning had to be modelled. Major data input for modelling were:

- The Test Reference Years (TRY) of 'Deutscher Wetterdienst' (see <http://www.dwd.de/DE/leistungen/testreferenzjahre/testreferenzjahre.html?nn=507312>),
- the heating/ air-conditioning energy need of a bus as a function of the temperature difference

between outside and inside (www.spheros.de/Media/Documents/3680/HVAC%20in%20E-Bussen.pdf) and

- the efficiency of a heating/ air-conditioning system consisting of a combination of a heat pump and a heating resistor dependent on outside temperature and heating/ cooling demand.

Emission factors (exhaust and upstream emissions of energy carriers)

Tailpipe emissions of conventional buses are calculated using the 'Handbook Emission Factors for Road Transport (HBEFA, version 3.2)' database. The use phase emissions of electric buses are determined by the electricity production. The electricity production mix is based on work of the AG Energiebilanzen (Working Group on Energy Balances, <http://www.ag-energiebilanzen.de/4-1-Home.html>), Bundesverband Erneuerbare Energien (German Renewable Energy Federation, <http://www.bee-ev.de/english/>) and Fraunhofer Institut für Solare Energiesysteme (Fraunhofer Institute for Solar Energy Systems, https://www.ise.fraunhofer.de/en?set_language=en). Future electricity mixes are based on the Leitstudie 2011's 'Scenario A' (BMU 2012). The calculated emission factors for electricity production include the emissions of power plants and the supply of the primary energy carriers.

Table 3. Upstream emissions for different energy carriers

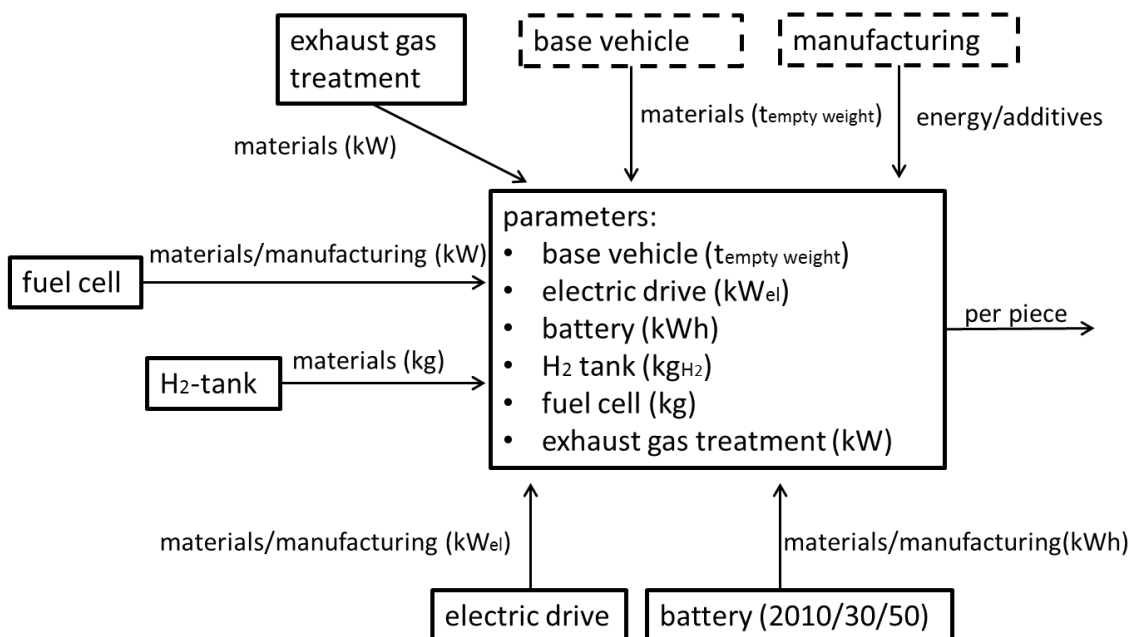
Year	CO ₂ -eq [g/kWh]			NO ₂ [g/kWh]			PM ₁₀ [g/kWh]		
	Diesel	Electricity	H ₂	Diesel	Electricity	H ₂	Diesel	Electricity	H ₂
2015	58	584	381	0.14	0.62	0.33	0.01	0.16	0.03
2025	62	355	175	0.14	0.44	0.14	0.01	0.08	0.01

Production emissions

To determine the environmental impact of bus production an LCA model for buses with different power train concepts has been developed by ifeu. For the comparison of the different technologies the buses have been broken down into their essential components, as shown in figure 3.

The component approach allows for individual accounting of vehicles with different drive concepts. The LCA model contains detailed information for each component in respect to material input, production energy and transportation effort. The background data to for the material upstream-emissions is taken from the ecoinvent database (version 3.1).

Figure 3. Schematic representation of the LCA model for bus production



In this work the emissions of the infrastructure could only be estimated roughly, as there is a lack of primary data on this topic. However, the available data show that the emissions for the construction of electric bus infrastructure should not exceed 80 g CO_{2-eq}/Bus-km (Ebrahimi, 2014).

Cost analysis

The Life Cycle Costs (LCC) of an urban bus line comprises vehicles, infrastructure, replacement, drivers, energy as well as service and maintenance costs. All costs are calculated with the annuity method and an interest rate of 5 %.

In the standard case, a 12 year service life and a 5 % residual value are considered. The assumed vehicle costs are calculated from the component's cost. Therefore, the derived costs are independent of the current market situation. The projection of future component costs is derived from learning curves, see table 4 for batteries and fuel cells.

Table 4. Battery and fuel cell costs (nominal in €, 2015)

		Source	2015	2020	2025	2030
Battery	€/kWh	2015: expert guess Prof. R. Pütz Development 2015 – 2030: Wietschel et al. (2013)	1,000	784	684	622
Fuel cell	€/kW	FCH JU, 2012: 'Production-at-Scale'- Scenario	1,161	609	542	432

The infrastructure is depreciated of the whole lifespan and then has a residual value of zero. Maintenance costs are assumed to be 2 % of the investment costs.

Table 5: Infrastructure costs (nominal in €)

Infrastructure	Unit	Costs [€]
Catenary (two-sided)	per km	350,000
Substation	per unit, 0.4 - 1.5 MW	430,000 - 1,720,000
Fast charging point (including substation)	per unit, 300 kW	250,000
Charging point depot	per unit, 25 kW	15,900

2. Energy Consumption and Emissions

This chapter contains the results of the LCA divided in the sections energy use, greenhouse gas emissions and pollutants.

Energy consumption

The 2015 energy consumption of the buses is derived from measured and modelled data (see chapter 1). The assumptions on the development of energy efficiency until 2025 are made based on interviews with manufactures.

Table 6. Average yearly energy consumption of articulated buses

Drive train concept		Unit	2015	2025
IMC	Electricity	kWh/km	2.1	1.9
OC	Electricity	kWh/km	2.1	1.9
ONC	Electricity	kWh/km	2.4	2.2
FC	Hydrogen	kWh/km	4.8	4.5
	Hydrogen	kg/ 100 km	14.4	13.5
Diesel	Diesel	kWh/km	5.2	5.0
	Diesel	l/ 100 km	52	50

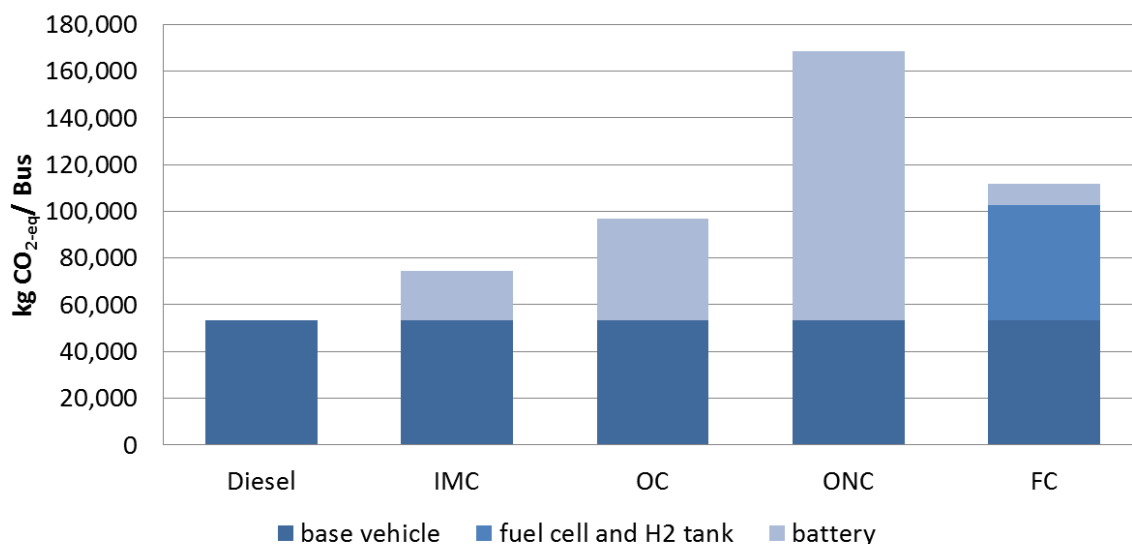
IMC = In-Motion Charger, OC = Opportunity Charger, ONC = Overnight Charger, FC = Fuel Cell Hybrid

The average yearly energy demand for heating is 0.31 kWh/km and therefore less than 15 % of the overall energy demand. In winter it can be up to 50 % (4.7 MWh in January) in the coldest region of Germany and become an important factor for the dimensioning of batteries and charging infrastructure.

Greenhouse gas emissions

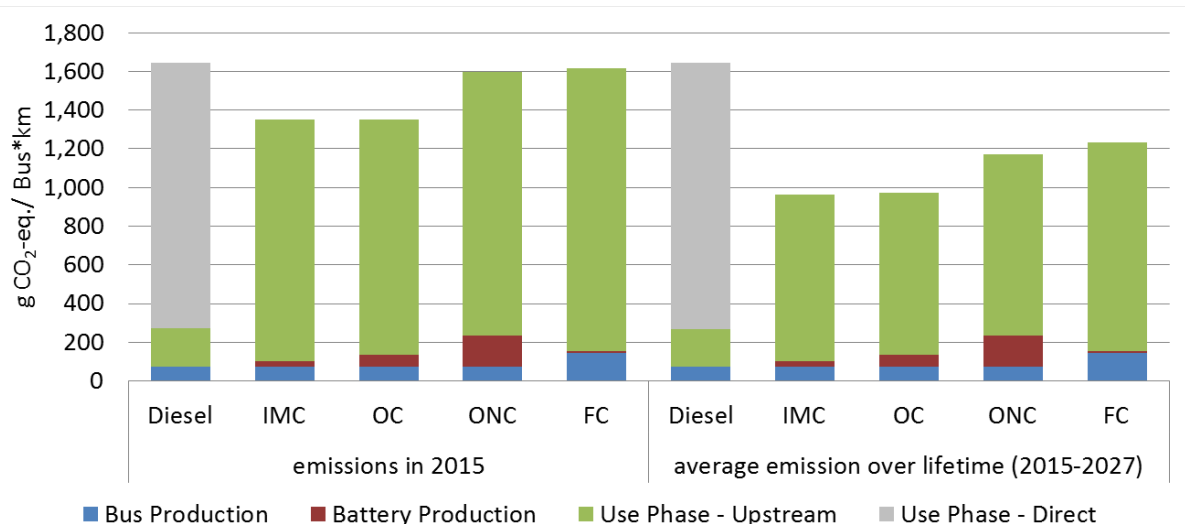
The greenhouse gas emissions of the bus production are shown in figure 4. All alternative concepts have increased emissions in the production phase compared to the diesel bus. They are highly influenced by the size of the batteries in the respective electric bus concept. But also fuel cell hybrid buses have significant higher emissions due to vehicle production. The higher emissions of the fuel cell bus are mainly due to the Carbon-Fibre-Reinforced Polymer (CFRP) used in the hydrogen tank and platinum used in the fuel cell. More efficient production processes for CFRP, the use of electricity with a higher share of renewable energy and a higher share of recycled platinum could reduce these environmental impacts in the future.

Figure 4. Greenhouse gas emissions per produced bus in 2015; IMC = In-Motion Charger, OC = Opportunity Charger, ONC = Overnight Charger, FC = Fuel Cell Hybrid



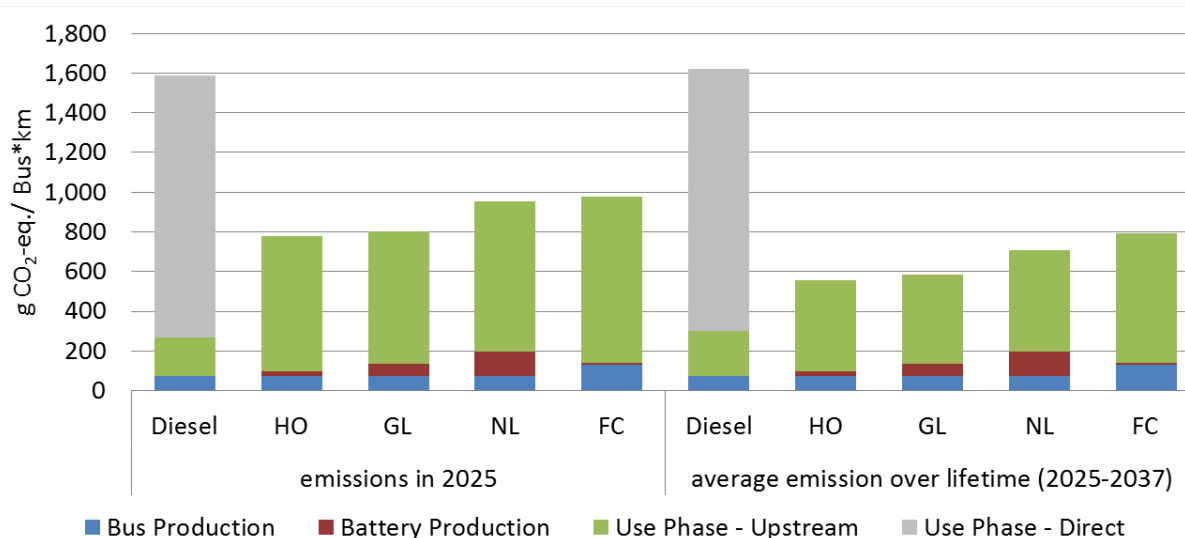
For the sum of production and use phase all electrified concepts have lower greenhouse gas emissions than the diesel bus (see figure 5). With an increasing share of renewable energy in the electricity mix, the use phase emissions' benefit will increase to almost 40 % for the IMC and the opportunity charger. Overnight charger and fuel cell hybrid buses have significantly higher emissions due to higher production emissions and lower efficiency. Infrastructure construction emissions are negligible.

Figure 5. Production and in-use greenhouse gas emissions of different bus concepts in 2015; IMC = In-Motion Charger, OC = Opportunity Charger, ONC = Overnight Charger, FC = Fuel Cell Hybrid



Comparing the situation with newly registered buses in 2015, all 2025 buses can increase their greenhouse gas advantage against the fossil fuelled diesel bus. This is partly due to improved components (batteries and fuel cells), but mainly due to the raising share of renewables in the energy mix. In contrast, the diesel bus has a slight increase in emissions due to a raising share of unconventional oil.

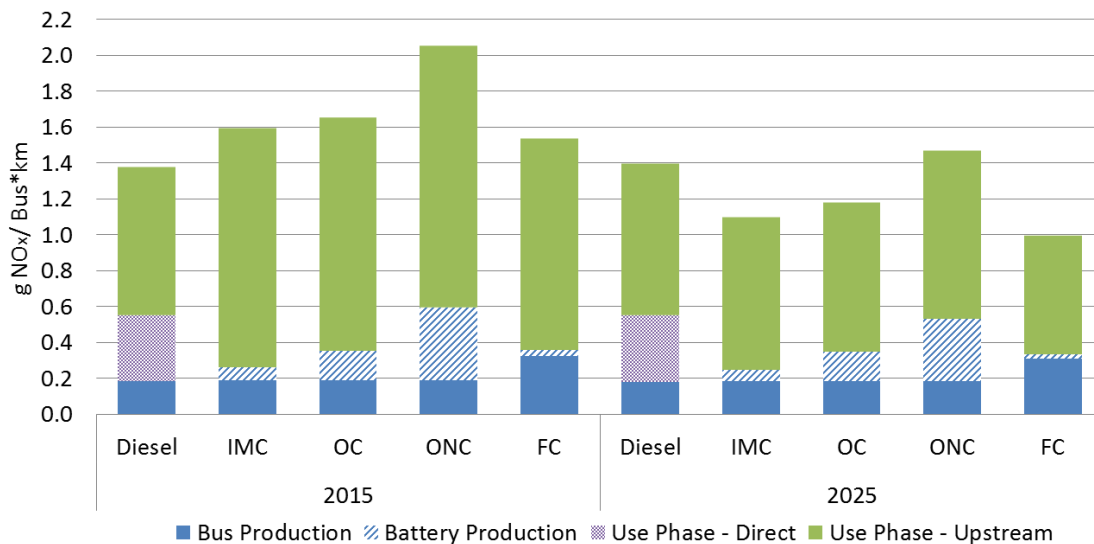
Figure 6. Production and in-use greenhouse gas emissions of different bus concepts in 2025; IMC = In-Motion Charger, OC = Opportunity Charger, ONC = Overnight Charger, FC = Fuel Cell Hybrid



Nitrogen oxide and particle mass emissions

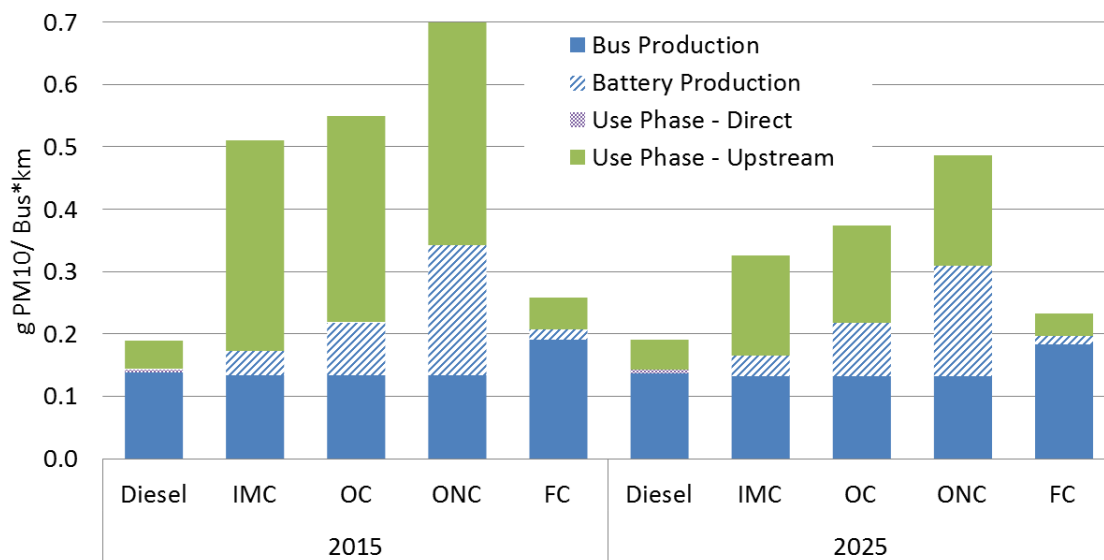
It is expected that NO_x and PM emissions of diesel buses will decrease with the introduction of the Euro-6 standard, but electric buses are already local zero emission vehicles. This is in particular relevant, as the EU air quality directive (Directive 2008/50 / EC ‘Clean Air for Europe’) is violated in many cities in Germany.

Figure 7. Nitrogen oxide emissions for different drivetrain concepts in urban buses; IMC = In-Motion Charger, OC = Opportunity Charger, ONC = Overnight Charger, FC = Fuel Cell Hybrid



But zero local emissions in total are overcompensated by higher upstream emissions, which, however, mainly arise outside the urban areas. The electricity production (particularly for the electric buses in the use phase) could still lead to higher background pollution. Until 2025 the electricity mix is becoming cleaner and the environmental impact of battery production is decreasing (see figure 8).

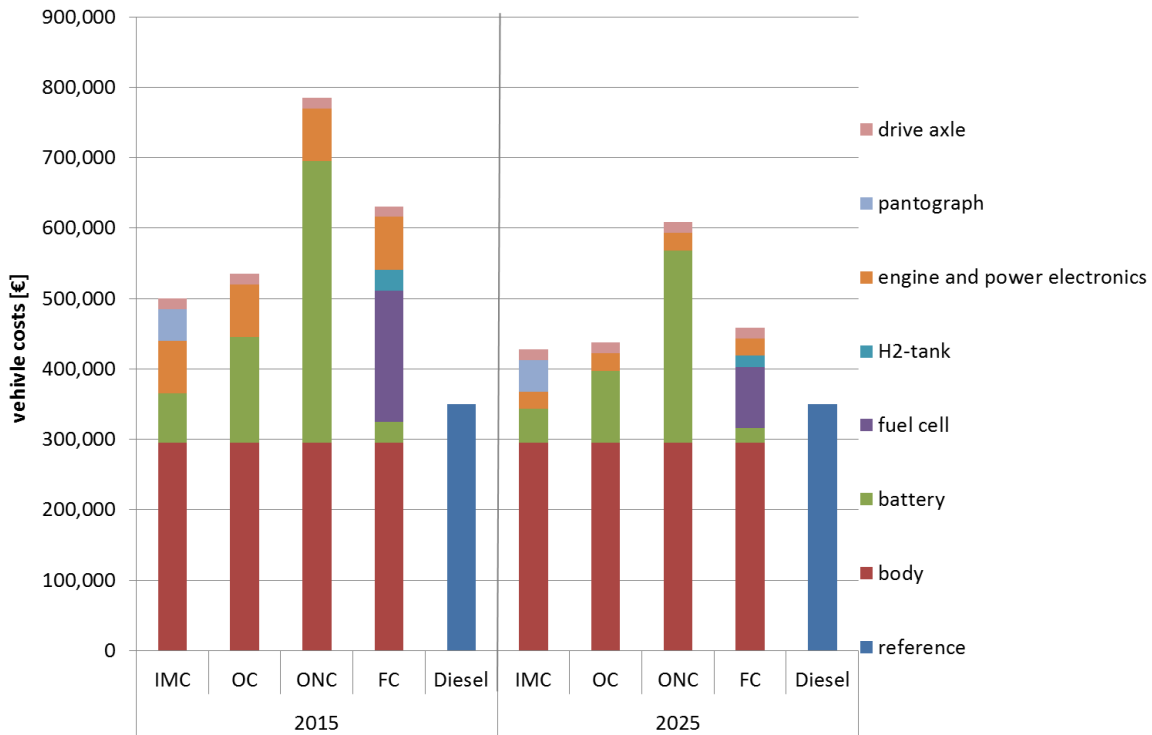
Figure 8. Particle emissions for different drivetrain concepts in urban buses; IMC = In-Motion Charger, OC = Opportunity Charger, ONC = Overnight Charger, FC = Fuel Cell Hybrid



3. Life cycle costs

The results of the vehicle's cost analysis are illustrated in figure 9. The vehicle costs are calculated based on the costs of the individual components in order to improve the comparability and on a projection of the future development of costs. It shows that in large-scale production bus prices could significantly lowered against today's market prices (actual market prices in 2015 are approximately 100,000 € higher than calculated costs).

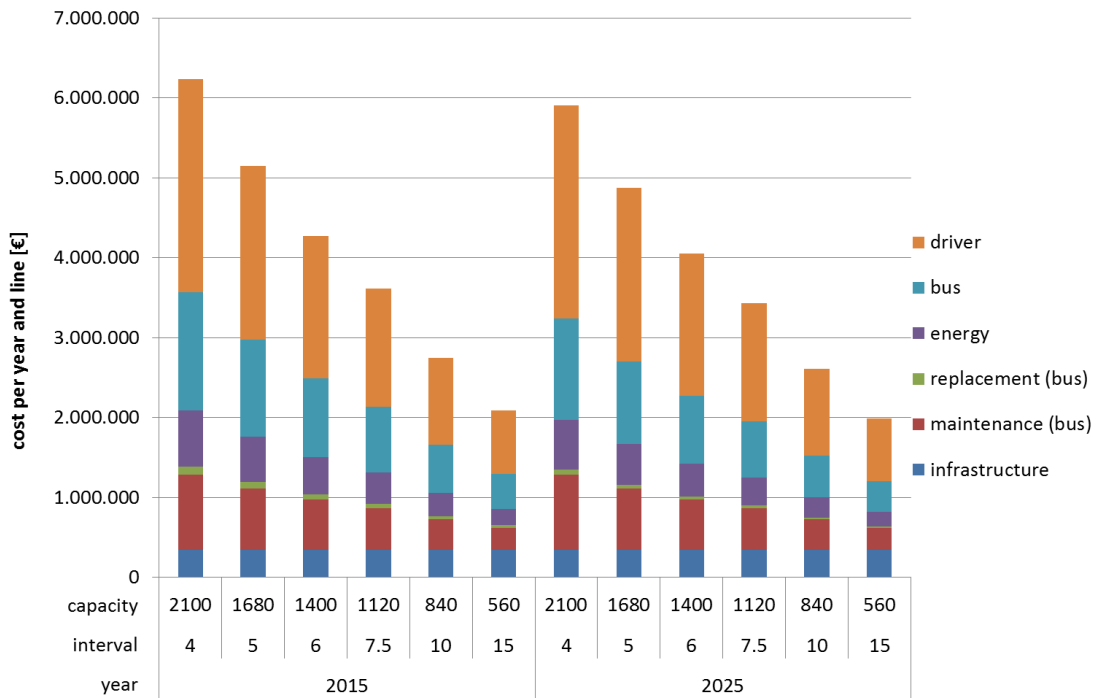
Figure 9. Vehicle costs of different power train technologies in 2015, 2025; IMC = In-Motion Charger, OC = Opportunity Charger, ONC = Overnight Charger, FC = Fuel Cell Hybrid



The IMC's infrastructure costs are significantly higher than for the other bus concepts and therefore have to be considered in the economic analysis. The main parameters influencing the share of infrastructure costs at the IMC's LCC are the interval and the catenary system costs:

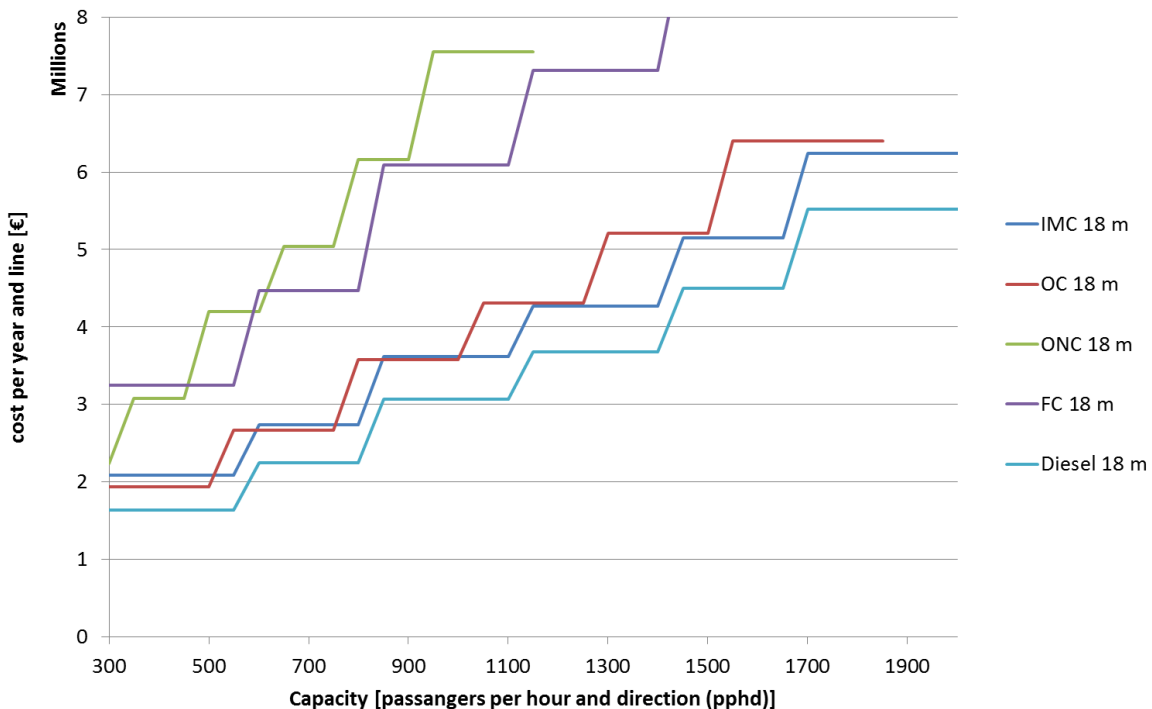
- While the infrastructure costs are independent from the interval, energy, driver and vehicle costs are increasing nearly linear (see figure 10). Therefore, the cost share of infrastructure is largely dependent on the interval, from 7 % in a 5 minute to 13 % for a 10 minute interval.
- The costs for the catenary system depend on its length and the specific costs. For an economic configuration of the catenary system it is favourable to choose sections with slow speeds (allowing longer charging time with shorter catenary length). Also, the specific costs per length can be lowered choosing sections with a low demand for superstructure (e.g. long straight roads).

Figure 10. Costs per IMC bus line in 2015, 2025 for different intervals



Today the IMC has additional costs compared to a diesel bus of about 495,000 € per line and year for a ten minute interval (22 % cost difference per capacity). Compared to other electric buses, it is the most economical bus for below ten minute intervals (more than 1,100 pphd) (see figure 11).

Figure 11. Costs per capacity in 2015; IMC = In-Motion Charger, OC = Opportunity Charger, ONC = Overnight Charger, FC = Fuel Cell Hybrid



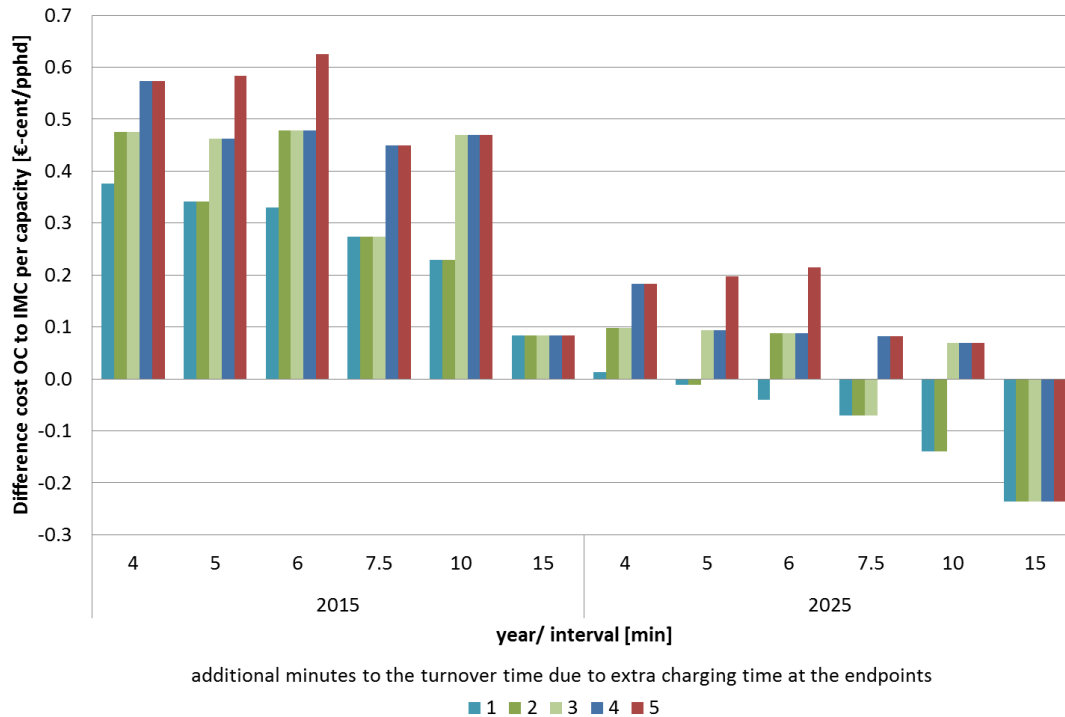
IMC's higher infrastructure costs can be compensated through lower vehicle demand and lower vehicle costs compared to overnight and opportunity chargers. Higher vehicle demand in case of overnight and opportunity chargers derives from following aspects:

- The overnight charger's higher battery mass is reducing the payload leading to a lower capacity per bus. Therefore more vehicles and drivers are needed. As the driver is the largest cost position in operating a line with at least 39 % share of total costs, higher driver demand can significantly lower economic performance. In 2015 the capacity costs for the overnight

charger are twice as high as for the IMC (10 minute interval/ 92,000 pphd).

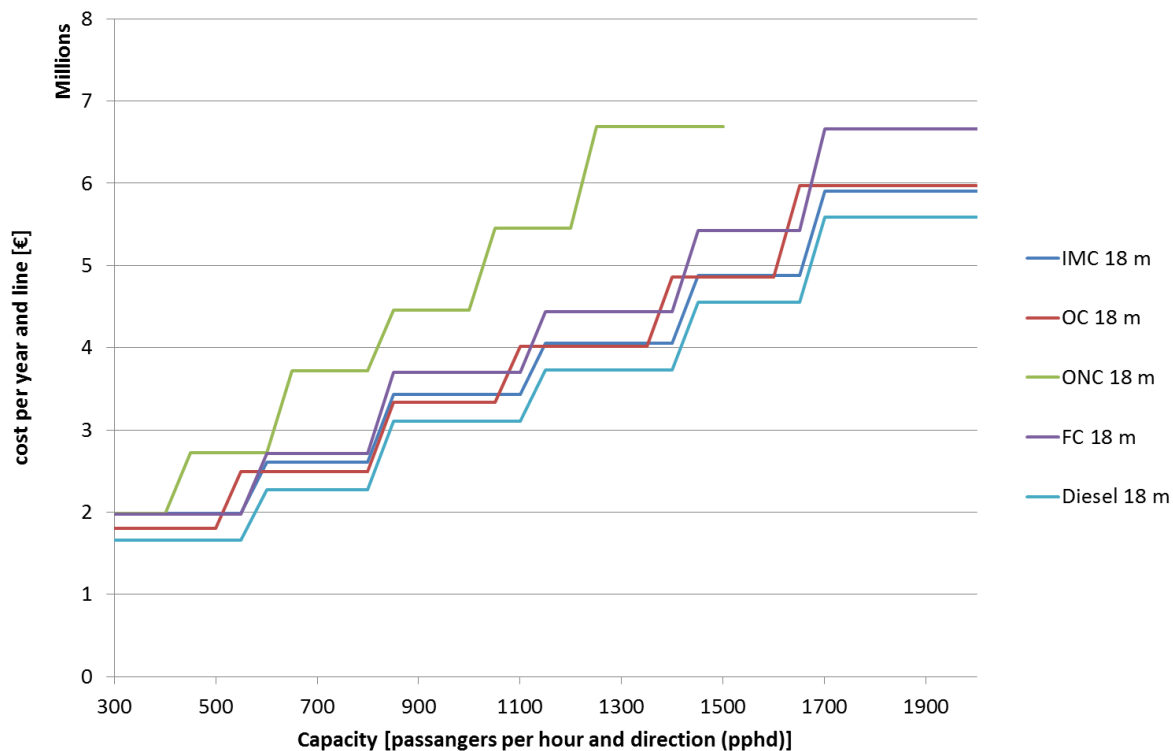
- The opportunity charger requires sufficient turnaround time to ensure minimum charging even under heavy traffic conditions. Rogge et al. (2015) shows that in the example of the City of Münster for about 40 % of the lines this leads to an increase in the scheduled turnaround time. This can lead to a higher number of vehicles and drivers needed for a line (see figure 12). In addition to the results shown in figure 12, three additional minutes turnaround time could lead to additional costs compared to the IMC of 92,000 € per year in a ten minute interval in 2015.

Figure 12. Additional costs of the opportunity charger (OC) compared to the IMC dependent on extra turnaround time for the OC in 2015 and 2025



With advances in battery technology (costs, energy density) until 2025 the LCC per capacity for the different electric concepts is converging (see figure 13). Technologies without trackside infrastructure (fuel cell hybrid, overnight charger) are remaining more expensive than those concepts with trackside infrastructure (IMC, opportunity charger). For a wide range of possible use cases, the costs of IMC and opportunity charger are becoming almost equal. Urban design aspects and operational performance are becoming more important. The IMC will stay the most economical electric bus concept for high capacity until 2025.

Figure 13. Costs per capacity in 2025; IMC = In-Motion Charger, OC = Opportunity Charger, ONC = Overnight Charger, FC = Fuel Cell Hybrid



4. Potential of In-Motion Charger Buses

In this chapter the results of the analysis are mirrored to the situation of public transport in Germany. The chapter will give a short overview about mitigation obstacles for the IMC and current trends in the public transport sector.

Economic situation

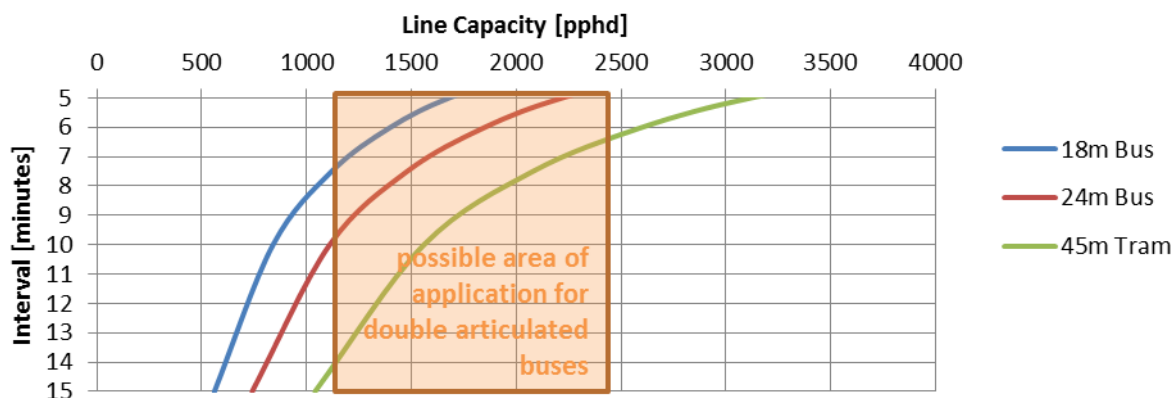
Funding for public transport is severely limited in Germany; especially the municipalities are not in a position to transact larger investments. Therefore, local public transport remains on the status quo, as long as investments are not funded in large parts by the federal states and/ or the federal government. In almost all counties there are already incentive programs for electric buses. For the economic viability of the IMC the inclusion of the infrastructure in these programs is crucial.

The economics of IMC are much more attractive, if compared to a tram instead of a diesel bus. This has to be seen in the light of the ongoing establishment of double-articulated buses in various European cities. Due to the low number and the legal restrictions of double-articulated buses in Germany, they were not in the focus of this investigation. However, with the results of this study they seem to be an ideal field of application for IMC and being significantly more economic than trams for a wide range of applications.

Figure 14. Hess LighTram3 in Zürich, by Micha L. Rieser (own work) [CC BY-SA 3.0] <https://commons.wikimedia.org/wiki/File%3ALighTram3-Linie-31-Z%C3%BCrich-Bild-2.jpg>



Figure 15. Capacity of public transport systems dependent on type of vehicles and service interval (18 m articulated bus - 140 places, 24 m double articulated bus - 185 places, 45 m tram - 260 places)



Implementation efforts

Particularly for the public transport operator, the change to IMC's is accompanied by some efforts. The most relevant are:

- Complex operations due to the presence of several different drive train systems (at least in the transition phase).
- Changing job profiles to the employees. Therefore, extensive training is needed for a generally older workforce. Also the recruitment of highly skilled mechatronics is challenging because of competition with the automotive industry. This effort can be smaller if the public transport operator is already using electric means of transport like tram or light rail.
- Termination of established manufacturer relations if the usual supplier does not offer IMCs. Today, the only company with a relevant market share offering IMCs in Germany is Solaris. Currently, there is no German manufacturer offering IMCs.

Acceptance

Higher environmental awareness and regulatory requirements are leading to an increasing loss of acceptance of the diesel bus. The IMC's image with the key stakeholders (local policy makers, administration, public transport operators and citizens) is hampered by the perception as an outdated vehicle technology with extensive overhead line structures. This image is largely influenced by the conditions of the German trolley systems in their last years of existence (excluding the small systems which continued operation also after the 1970's). Therefore, the disruption in trolley development and trolley culture (in contrary to Italy or Switzerland) is seen as a severe drawback for the implementation of IMC today. The creation of a best practice example for integrating IMC in an urban environment seems to be one of the most relevant measures to overcome this image.

Conclusion

Our analysis shows that a diesel bus running with conventional diesel remains the most economic technology until 2025 as long as the regulatory framework remains unchanged. But it contributes very little to the central goals of the German 'Mobility and Fuels Strategy' (MFS), like the reduction of energy consumption and greenhouse gas emissions or the introduction of new technologies. In contrary, electric buses could significantly contribute to these goals. With progress in the energy transition ('Energiewende') and the further development of battery technology electric buses will become more beneficial, particularly from the environmental point of view. For electric buses, the IMC is seen as the most economical technology for high capacity lines (frequent service, high capacity vehicles) or lines with a high energy demand. Therefore, the IMC is seen as an essential part of an electrification strategy for public transport.

Acknowledgments

This work was funded by the German Federal Ministry for Transport and Digital Infrastructure (BMVI).

References

- BMU (2012): Leitstudie 2011 - Langfristszenarien Und Strategien Für Den Ausbau Der Erneuerbaren Energien in Deutschland Bei Berücksichtigung Der Entwicklung in Europa Und Global. National aeronautics and space research centre (DLR), Fraunhofer Institute for Wind Energy and Energy System Technology (IWES), Ingenieurbüro für neue Energien (IFNE) [http://www.fvee.de/publikationen/publikation/?sb_damorder\[juid\]=4636&cHash=06b2c3f1ab6b2757a44b77db72802b87](http://www.fvee.de/publikationen/publikation/?sb_damorder[juid]=4636&cHash=06b2c3f1ab6b2757a44b77db72802b87), Berlin, 345 p.
- BMVI (2013): The Mobility and Fuels Strategy of the German Government (MFS). <http://www.bmvi.de/SharedDocs/EN/Artikel/G/G-MKS/mfs-mobility-and-fuels-strategy.html>, Berlin, Germany, 92 p.
- Ebrahimi, B. E. (2014): Life Cycle Assessment of High Speed Rail Electrification Systems and Effects on Corridor Planning. <http://www.diva-portal.org/smash/get/diva2:752204/FULLTEXT01.pdf> NTNU Trondheim, 202 p.
- FCH JU, 2012: Urban buses: alternative power trains for Europe. Fuel Cells and Hydrogen Joint Undertaking, McKinsey, <http://www.fch.europa.eu/studies>
- Rogge, M., Wollny, S., Sauer, D. (2015): Fast Charging Battery Buses for the Electrification of Urban Public Transport - A Feasibility Study Focusing on Charging Infrastructure and Energy Storage Requirements. In: *Energies*. Vol. 8, No.5, pp. 4587–4606.
- Wietschel et al. (2013): Market evolution scenarios for electric vehicles. Fraunhofer Institute for systems and innovation research (ISE), http://www.isi.fraunhofer.de/isi-en/e/projekte/316741_Markthochlaufszzenarien-E-Fahrzeuge_Wi2014.php, Karlsruhe, Germany
- Spousta, J., Németh, Z. Á., Wolek, M., Weiß, A., Chick, D. G. (2013): Trolleybus Intermodal Compendium. <http://www.trolley-project.eu/index.php?id=44>, ISBN 978-80-86502-50-2, Brno, Czech Republic, 68 p.
- Jöhrens, J., Helms, H. (2014): How to Green Electric Vehicles Analysis of Key Factors for Reducing Climate Impacts of Electric Vehicles. Proceedings of IEEE International Electric Vehicle Conference, ISBN 9781479960750, Florence.

Photocatalytic Oxidation of Volatile Organic Compounds for Cleaning Vehicle Cabin Air

Marième BOUHATMI*, Frédéric DAPPOZZE*, Chantal GUILLARD* & Philippe VERNOUX*

*Université de Lyon, Institut de Recherches sur la Catalyse et l'Environnement de LYON, UMR 5256, CNRS, Université Claude Bernard Lyon 1, 2 avenue Albert Einstein, 69626 Villeurbanne, France

Tel +334 72 44 54 03 - email: marieme.bouhatmi@ircelyon.univ-lyon1.fr // bouhatmimarieme@live.fr

Abstract

The photocatalytic degradation of *n*-pentane in gas phase has been investigated under different conditions on a TiO₂ DEGUSSA P25 at room temperature, in dry air, in a flow through reactor. Several parameters have been studied such as the concentration of *n*-pentane [25-500]ppmv for a total flow of 120mL/min, the molar flow rate (0.10-2.5mmol/min), and the modulation of the irradiance at 365nm. The degradation and the mineralization into CO₂ were followed through a gas analysis with a GC/FID/Catalytic Methanizer. Preliminary results showed that a complete mineralization of *n*-pentane into CO₂ seems to be always achieved whatever the operating conditions. Moreover, the degradation rate of *n*-pentane reached about 0.05mmol/min. This work shows also that the a conversion rate of 44% is reached for a molar flow rate of 0.10mmol/min.

L'étude de la dégradation photocatalytique du *n*-pentane en phase gazeuse a été menée sous différentes conditions expérimentales sur un TiO₂ DEGUSSA P25 à température ambiante, à 0% d'humidité relative dans un réacteur en flux traversant. L'impact de plusieurs paramètres a été étudié tels que : la concentration en *n*-pentane pour une gamme de 25-500ppm pour un débit total de 120mL/min, le débit molaire de 0.10-2.5mmol/min, et la puissance lumineuse à 365nm. Il a ainsi été observé qu'une minéralisation totale du *n*-pentane en CO₂ semble toujours être obtenue quelques soient les conditions expérimentales. Par ailleurs, la vitesse de dégradation du *n*-pentane atteint environ 0.05mmol/min. Ces travaux montrent également qu'un taux de conversion de 44% a été atteint pour un flux molaire en pentane de 0.10mmol/min

Keys-words: VOC, *n*-pentane, photocatalysis, indoor air, vehicle.

COV, *n*-pentane, photocatalyse, air intérieur, automobile

Introduction

The Volatile Organic Compounds (VOCs) represent a major health issue because of their important presence in the vehicle cabin air, a closed space in which people spent the most party of their time (Müller (2011)), causing allergies, respiratory and skin problems....

The most of the depollution systems are based on filtration or adsorption over active charcoal, cheap systems, which store the pollutants at the surface, requiring the regular change of them. In addition, Destailats *et al.* (2011) showed that the VOCs adsorbed over those systems can produce secondary VOCs by reacting with atmospheric ozone, and so represent a supplementary risk for the human health.

On the other hand, some systems can degrade the VOCs such as ozonation systems, but represent a real danger for human health because ozone can react with lung tissues, and produce during the degradation other VOCs (EPA, 2005).

As a matter of fact, the photocatalysis, appears as a good alternative to those systems, because it's a well known sustainable way to degrade the major part of pollutants (Zhao, 2002).

The photocatalysis is based on the activation of a semi-conducting material upon irradiation providing an energy equal or superior to its band gap, which creates an electron and a hole in the bulk. After migration to the surface they react with the adsorbed molecules creating activated species such as O_2° and HO° . Those radicals will finally react with the adsorbed pollutants at the surface and so degrade them (Linsebigler (1995), Herrmann (2005)).

It's quite difficult to give the exact composition of VOCs present in the vehicle cabin air, because of the impact of several parameters on their nature, such as the brand/ the model of the car, the interior of this one, the temperature, the relative humidity (r.h), the age of the vehicle (Muller (2011)).

However, 3 majors groups of VOCs are distinguishable: the cycloalkanes ($533.5\mu\text{g}/\text{m}^3$ either 19.8%), the aromatics ($521.2\mu\text{g}/\text{m}^3$ either 19.8%) and the alkanes ($1363.5\mu\text{g}/\text{m}^3$ either 50.6%) (Faber (2013), Brodzik (2014), Yoshida (2006)). From these studies, it appears that alkanes are mainly represented in the vehicle cabin air. Among them, the n-pentane derivatives are fully represented (Debono (2013)). To the best of our knowledge the degradation of the n-pentane by photocatalysis is not widely studied. That's why this preliminary work is focused on the photocatalytic degradation of the n-pentane under several conditions described below.

1. Objectives

The main objective of these preliminary works is to study the degradation of n-pentane in presence of TiO_2 under UV irradiation. Several parameters will be under study to understand how the n-pentane could be degraded by photocatalysis over a TiO_2 . First, the impact of the concentration will be studied for a given total flow. From this result, the influence of the molar flow of n-pentane will be studied to allow us to work closer to the real conditions of a vehicle cabin air. Finally, the impact of the irradiance which plays an important role in photocatalysis will be considered.

2. Material and Methods:

Photocatalytic Reaction: The degradation of n-pentane was done at room temperature ($\sim 24^\circ\text{C}$) in dry air, in a flow through reactor equipped of an optical window of 4cm diameter which cut the wavelengths inferior at 340nm. The photocatalyst (30 mg of EVONIK® P25 powder, 86wt.% Anatase, 14wt.% Rutile) is deposited and scattered on a filter provided by Durapore® (Millipore, diameter: 5cm, porosity: $0.4\mu\text{m}$) placed into the reactor.

The irradiation is performed by a Philips Mercury Lamp PL-L 18 W, with a major irradiation in UV-A (315-400nm), placed directly on the reactor's window. The irradiance is measured by a radiometer at the outlet of the lamp.

VOC generation: In order to generate the n-pentane at different concentrations, a n-pentane cylinder provided by Air Liquide®, at 1000ppmv in air (with 959 ± 29 mol-ppm of n-pentane and 19.94 ± 0.40 mol-% of O_2) is used. The dilutions are performed with a dry air flow composed by 300ppbv of CO_2 (obtained by an air compressor equipped by particles/ CO_2 /relative humidity filters) via a Brooks Instrument® mass flow controller.

Photocatalytic degradation measurements: All the gases were analysed by a GC-Flame Ionization Detector GC CP-3800 Varian equipped with a catalytic methanizer for the CO_2 detection. The separation is performed by two capillary columns in series: a CPSIL-5 and a PLOTQ provided by Agilent®.

A first analysis is done by by-passing the reactor to have the blank of the mixture sent into the reactor. Then, a second analysis is done to observe the adsorption of n-pentane on TiO_2 in dark (without

irradiation). Finally, a last analysis is done upon irradiation in the reactor. For all the analysis the stationary state is reached.

Tested conditions: The impact of the n-pentane concentration has been tested for a total flow of 120mL/min, and irradiation power of 5mW/cm² for the following range: [25-500]ppmv. The experiments are performed at room temperature, in dry air.

Then, different molar flows, from 0.10 to 2.50mmol/min, were tested in order to be closer to the real conditions in vehicle cabin air. Indeed, if we consider that in a vehicle cabin, the averaged concentration of a specific pollutant is around 100ppb (Faber (2013)), and that the usual air flow used by the usual ventilation system is superior or equal to 20m³/h, which corresponds to a molar flow of the pollutant superior or equal to 1.37mmol/min. At the same time, the irradiance has been modulated from 5mW/cm² to 0.5mW/cm².

The conversion rate of n-pentane and the mineralization into CO₂ of the degraded n-pentane are calculated by the followed equations:

$$\tau_{C_5H_{12}} = \left(\frac{n_{(C_5H_{12})i} - n_{(C_5H_{12})f}}{n_{(C_5H_{12})i}} \right) \times 100 \qquad v_{CO_2} = \left(\frac{n_{(CO_2)f}}{5n_{(C_5H_{12})i}} \right) \times 100$$

with:

$\tau_{C_5H_{12}}$: the conversion rate of n-pentane during the photooxidation

v_{CO_2} : the conversion into CO₂ of the degraded n-pentane during the photooxidation

$n_{(C_5H_{12})i}$: the initial number of moles of n-pentane

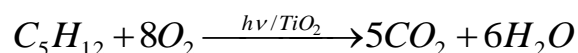
$n_{(C_5H_{12})f}$: the final number of moles of n-pentane

$n_{(CO_2)f}$: the final number of mole of CO₂

Impact of the concentration: The degradation rate of n-pentane and the production rate of CO₂ under different concentrations are presented in Figure 1.

It appears that for low concentrations the degradation rate increases, and reaches a plateau at a value of about 0.05mmol/min. The photocatalysis following a Langmuir-Hinshelwood model (Herrmann (2005)), the reaction rate is directly dependent of the surface coverage Θ of the catalyst by the molecules of pollutant (if we neglect the adsorption of O₂ and of reaction products). At low concentrations of reactant, the coverage rate is less than 1, and the degradation rate is directly related to the pollutant concentration (apparent order reaction 1). At higher concentrations, the coverage rate is nearly 1, the surface is saturated, and the degradation rate is no more dependent of the reactant adsorption (apparent order reaction 0).

Moreover, a complete mineralization seems to be always achieved whatever the initial concentration. Indeed, the production rate of CO₂ is equal to around 5 times to the degradation rate of n-pentane confirming the equation of n-pentane oxidation:



From these results it also appears that for an initial concentration of n-pentane of 25ppmv, a conversion of 23% is reached. As expected, the conversion rate is decreasing when the concentration increases.

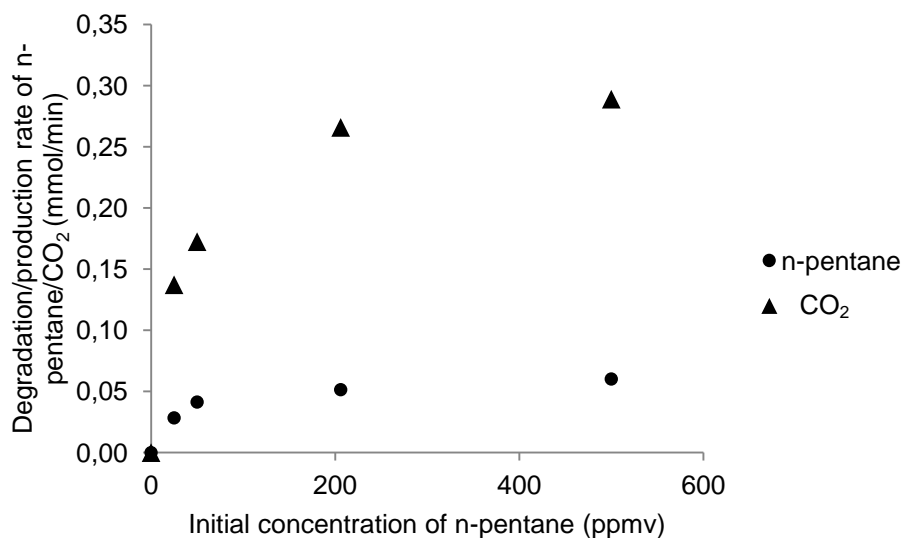


Figure 1: Degradation rate of n-pentane (dots) and production rate of CO₂ (triangles) as a function of the initial concentration of n-pentane.

Total flow: 120mL/min. Irradiance: 5mW/cm².

Impact of molar flow: In the same way, different molar flows have been tested; the results are represented in the Figure 2. When the molar flow increases, the conversion rate is decreasing. Indeed, the contact time decreases. A conversion rate of 44% is reached for a molar flow of 0.10mmol/min corresponding to a degradation rate of 0.05mmol/min, maximal degradation rate of n-pentane obtained in presence of 30 mg of TiO₂ P25 and under 5mW/cm² of irradiance.

This study highlights an important result: for a molar flow close to the real conditions 1.03mmol/min or more, the degradation rate is about 0.05mmol/min. It means that in a recirculation system of indoor air, to degrade a molar flow of pollutant (n-pentane) of 1.03mmol/min, it requires in these conditions about 20 minutes.

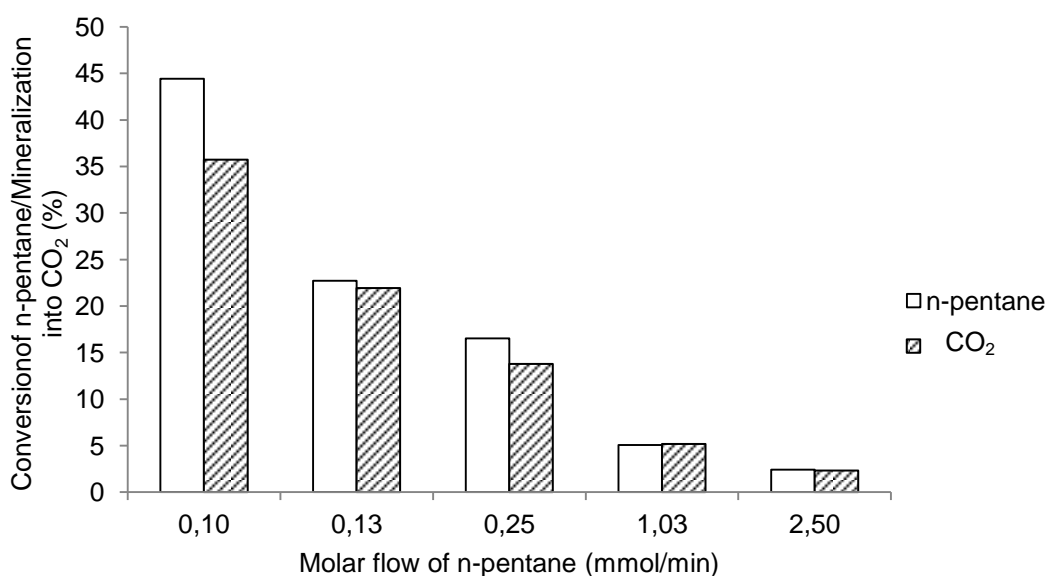


Figure 2: Conversion of n-pentane (unshaded) and percentage of mineralization into CO₂ (shaded) as a function of the molar flow of n-pentane. Irradiance: 5mW/cm².

Impact of the irradiance on the mineralization rate: The impact of the irradiance power has been tested for a same molar flow of 0.10mmol/min. We clearly observed after a diminution of 90% of the irradiance power, a diminution of more or less 90% of the conversion rate (44% to 4%), and a complete oxidation of n-pentane seems to be still observed. In photocatalysis, the conversion rate is directly depending on the irradiance power of the irradiation source, because it's related to the number of electron/hole pairs formed. The more the irradiance power is, the more the number of electron/hole pairs increases and the photocatalytic activity increases

Irradiance Power (mW/cm ²)	Molar flow (mmol/min)	Conversion (%)	Mineralization into CO ₂ (%)	Rate (mmol/min)
5	0.10	44	80	0.05
0.5	0.10	4	100	0.01

Table 1. Impact of the irradiance on the conversion rate of the n-pentane by photocatalysis.

Conclusions

The photocatalytic oxidation of n-pentane on TiO₂ P25 was investigated under different conditions in dry air, at room temperature in a flow through reactor. A complete mineralization seems to be always achieved whatever the investigated operating conditions. No reaction intermediates were detected.

The impact of the concentration and molar flow of n-pentane have been demonstrated. Due to surface saturation, the degradation rate of n-pentane (production rate of CO₂) remains constant for high hydrocarbon concentrations, or high molar flows, and reaches a degradation rate of 0.05 mmol/min. Moreover, a maximum conversion of 44% is achieved for a molar flow of 0.10 mmol/min of n-pentane. Increasing the contact time could probably enhance the hydrocarbon conversion. This study also highlighted that even if the irradiance is decreased by 90% leading to similar drop of the conversion, a total mineralization was still achieved.

According to these results, the required time to clean a cabin air vehicle exposed to 100 ppb of n-pentane can be estimated at around 20 and 200 minutes under an irradiation of 5mW/cm² and 0.5mW/cm², respectively. This estimation takes into account a photocatalytic device equipped with a ventilation system delivering a flow of 20m³/h, and 30mg of TiO₂ P25. This preliminary work seems to show that the n-pentane can be degraded and mineralized in conditions close to the real operations.

Acknowledgments

The authors would like to thank the French Ministry of National Education Higher Education and Research for the PhD grant of Marième BOUHATMI.

References

- Brodzik K., J. Faber, D. Lomankiewicz & A. Golda-Kopek (2014): In vehicle VOCs composition of unconditioned newly produced cars. *J. Environ. Sci.*, vol. 26, p 1052-1061
- Debono O., F. Thévenet, P. Gravejat, V. Héquet, C. Raillard, L. Le Coq & N. Locoge (2013): Gas phase photocatalytic oxidation of decane at ppb levels: removal kinetics, reaction intermediates and carbon mass balance, *J. Photoch. Photobio. A*, vol. 258, p 17–29
- Destailats H., W. Chen M. G. Apte, N. Li , M. Spears , J. Almosni, G. Brunner, J.J. Zhang & W. J.

- Fisk (2011): Secondary pollutants from ozone reactions with ventilation filters and degradation of filter media additives. Atmos. Environ., vol. 45, p 3561-3568
- Faber J., K. Brodzik, A. Golda-Kopek & D. Lomankiewicz, (2013): Air pollution in new vehicle as a result of VOC emissions from interior materials. Pol. J. Environ. Stud., vol. 22, n°6, p 1701-1709
- Herrmann J-M., (2005): Heterogeneous photocatalysis: state of the art and present applications. Topics in Catalysis, vol. 34, n°1-4, p 49-65
- Linsebigler A.L., G. Lu & J.T. Yates, Jr, (1995): Photocatalysis on TiO₂ surfaces: principles, mechanisms, and selected results. Chem. Rev., vol. 95, p 735-758
- Müller D., D. Klingelhöfer, S. Uibel & D. A. Groneberg, (2011): Car indoor air pollution-analysis of potential sources. J Occup Med Toxicol, vol. 6, p 1701-1709
- United States Environmental Protection Agency (EPA), Residential Air Cleaners. Indoor Air Quality, EPA report, Second Ed., 402-F-09-002, 2009
- Yoshida T. & I. Matsunaga, (2006) : A case study on identification of airborne organic compounds and of their concentrations in the cabin of a new car for private use. Environ. Int., vol. 32, p 58-79
- Zhao J. & X. Yang, (2003): Photocatalytic oxidation for indoor air purification: a literature review . Build. Environ., vol. 38, p 645-654

A sensitivity study of road transportation emissions at metropolitan scale

Ruiwei CHEN*, Vincent AGUILÉRA**, Vivien MALLET***, Florian COHN****, David POULET**** & Fabien BROCHETON****

* CEREAs, Joint Laboratory École des Ponts ParisTech/EDF R&D, Université Paris-Est, 6 – 8 Avenue Blaise Pascal, 77455 Marne-la-Vallée, France
- email: ruiwei.chen@enpc.fr

** CEREMA, 110 rue de Paris - BP 214 - 77487 Provins Cedex

*** INRIA, 2 rue Simone Iff, 75012 Paris

**** NUMTECH, 6, allée Alan Turing - CS 60242 - Parc Technologique de la Pardieu63178 Aubière, France

Abstract

Road traffic transportation emissions depend on both the traffic flow and the vehicles emission factors. They are very sensitive to the input data of both traffic assignment models and emissions calculation methods. In this study, we investigate the influences of the input data on a simulation chain from traffic flow assignment to emissions calculations, based on a case study in the agglomeration of Clermont-Ferrand in France. In order to better represent the congestion phenomenon and the temporal and spatial evolution of traffic flow, we use a dynamic traffic assignment model, LADTA, to compute the traffic flow at street resolution. The model is evaluated by comparison between model predictions and traffic flow observations captured by inductive loop traffic detectors. The traffic flow outputs of LADTA are then coupled with COPERT model to calculate emissions of air pollutants (nitrogen oxides NO_x for example). A sensitivity study is then carried out by varying the input parameters in the traffic emission modeling chain: the total traffic volume injected into the network, the average speed, the vehicle fleet composition, etc. The study shows that the emissions are very sensitive to these factors, especially during the transition from a free traffic network to a congested one.

Key-words: road traffic emissions, dynamic traffic assignment, COPERT, sensitivity study, congestion

Introduction

The emissions of road traffic are one of the main sources of air pollutants in urban area. In Île-de-France for instance, the road traffic is responsible for more than 55% of nitrogen oxides (NO_x) and more than 30% of particulate matter (Airparif (2014)). To analyze how traffic influences the air pollutant emissions at an agglomeration scale, traffic assignment models are needed for predicting the traffic volume at street resolution. There exist both static and dynamic traffic assignment models to reach this goal. The resulting traffic information is then used in emission calculation methods to estimate the air pollutants emitted by road traffic.

Our study focuses on the sensitivity of the emissions calculation outputs to the inputs of a dynamic traffic assignment model. The latter lets us better understand the effects of congestions resulting from the temporal evolution and time-dependent interactions of traffic flows. This paper is divided into 4 sections. The first section recalls the fundamentals of traffic assignment models, and presents briefly the dynamic traffic assignment (DTA) model, LADTA (for Lumped Analytical DTA), that we use in this study. Section 2 presents an analysis of the real-time traffic measurement data in Clermont-Ferrand, in order to study the road network users' behaviors and prepare the input data for LADTA simulation. Section 3 presents the main results from the simulation of traffic assignment and emission calculation, in the agglomeration of Clermont-Ferrand. Finally, the sensitivity analyses are presented in Section 4.

1. Description of traffic assignment model and emissions model

Traffic assignment aims at determining the network traffic flows according to network users' route choices when they travel from their origins to their destinations. It can also be considered as an economical equilibrium between the demand and the supply. The Origin-Destination matrix (O-D matrix) describes the total flux from original zones to destination zones. The road network shows limited capacities to absorb all the demand. One of the main hypotheses for traffic assignment problems is that every network user makes their route choice by minimizing their own travel cost, such as travel time, toll,

etc. The cost is often converted to one general criterion, such as time, which is called generalized cost of route choice. At equilibrium when every traveler succeeds in finding an optimal route, all used routes associated with the same O–D pair should have the same minimum generalized cost, so that there is no possibility for users to shift to another route. This is the user equilibrium condition (Wardrop (1952)), and it was proved to be adequate for both static and dynamic traffic assignment models, with a certain number of assumptions (Leurent (2003b), Aguiléra and Leurent (2009), Wagner (2012)).

In both static and dynamic traffic assignment models, the travelers are assumed to have complete information about each link in a network (the supply): physical capacity, length, speed limit and toll price (if any), in order to estimate the generalized travel cost of each available route. In a static model, the effect of road capacity on travel time is modeled by a volume-delay function (VDF): the travel cost (or time) is a strictly increasing function of the traffic volume. For example, the Bureau of Public Roads (1964) in the USA proposed a commonly used function as Equation (1),

$$t = t_0[1 + \alpha(V/C)^\beta] \quad (1)$$

where t is the link travel time to determine, t_0 is the link free flow travel time, V is the volume on the link, C is the capacity, α and β are coefficients to be adjusted. Figure 1 illustrates this type of VDFs with $\alpha = 1$ and a varying β . It is observed that VDFs are very sensitive to β . To represent the fact that the link travel time increases with the volume loaded on a link in congested cases, the volume may increase indefinitely and exceed the link capacity. This is not possible in reality, and it is also unrealistic to assume that the travel cost depends only on the flow of the link. In other words, in congested condition, the travel time calculated by VDF in static models does not depend on physical features of congestion (such as travel speed, density, or queue) (Ortuzar and Willumsen (2011)). This is a motivation to seek for dynamic traffic assignment models (DTA) in order to better represent the congestion phenomenon.

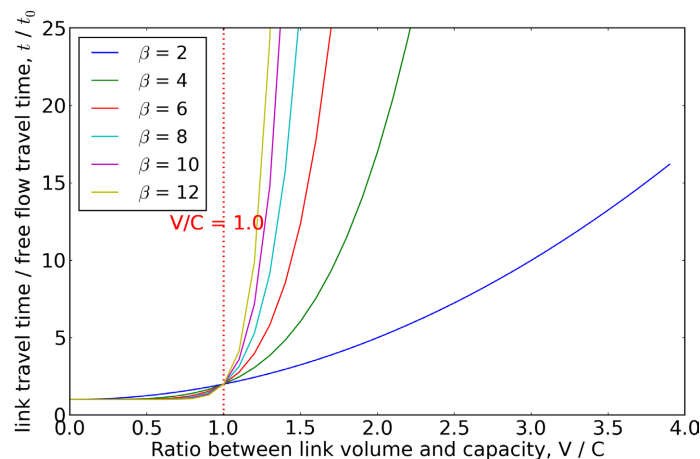


Figure 1. An example of volume delay functions in static traffic assignment models. When volume loaded on a link exceeds the capacity, the link travel time (t) can be calculated with $\alpha = 1$ and different β .

In dynamic assignment, the speed decreases when the link density increases, and the link travel time will therefore increase. The link travel time also depends on the vehicles' entrance time on the network. In fact, the traffic already existing on the link can decrease the link capacity. This may result in an increase of link travel time if the actual inflow volume exceeds the actual capacity of the link. There are different methods to calculate the link travel time in DTA, such as the fundamental diagram of traffic flow to represent the density – speed relationship (Lighthill and Whitman (1955), Rechards (1956), Geroliminis and Daganzo, (2008a)). Another method is bottleneck modeling where queue appears in upstream junction when the volume assigned to the link exceeds the capacity (Vickrey (1969)). In this model, the time spent in queue is taken into consideration to compute the link travel time.

Since the traffic emissions depend on both the traffic volume and the average speed of the vehicles and these two factors are correlated when congestion appears, a DTA model is used in our study to better represent and analyze the sensitivity of traffic emissions.

1.1 Introduction of LADTA

The LADTA model is one of the link-time-based DTA models which can be applied to a large-scale real network. Together with its software, LADTA ToolKit (LTK), it can handle the DTA problem of a metropolitan network frame within a reasonable time (Aguiléra and Leurent (2009)). It needs a dynamic O-D matrix as input data, as well as full information of the network. Then it computes the dynamical user equilibrium between the supply and the demand. Its outputs are the traffic flow and travel time for every link. The calculation of link travel time is based on bottleneck model.

1.2 COPERT IV method for calculations of emission factors

To calculate the traffic emissions, the tier 3 method of EMEP/EEA (2013) is used. The total exhaust emissions from road transport are calculated as the sum of hot emissions and cold-start emissions. In this study, only exhaust hot emissions from passenger cars are considered.

For each link in the network, the hot emissions can be estimated by the following equation:

$$E_{\text{hot},i,j}(g) = e_{\text{hot},i,j}(g \cdot \text{km}^{-1}) \times N_j(\text{veh}) \times M_j(\text{km} \cdot \text{veh}^{-1}) \quad (2)$$

where E_{hot} is the link's hot emission of a certain type of pollutant, and a certain vehicle type j , e_{hot} is the hot emission factor for the corresponding pollutant and vehicle type j , N is the vehicle number of vehicle type j on this link, and M is the distance traveled by this corresponding category of vehicles.

The vehicle number of each link can be obtained by traffic assignment models, and the distance traveled by vehicles is link length. The hot emission factors for each pollutant and each category of vehicles are calculated according to the COPERT IV method in EMEP/EEA (2013). Briefly speaking, the hot emission factors mainly depend on vehicle's average speed and the vehicle fleet.

1.3 The simulation scenario from traffic flow assignment to emission calculations

With the help of a static O-D matrix during evening peak period, a dynamic O-D matrix is built by applying a daily temporal evolution profile of the traffic flow in Clermont-Ferrand, as observed by the inductive loop traffic detectors in the network. A LADTA simulation can be launched for a complete day, and the traffic flow of each interval of simulation (15 minutes) can be obtained as well as the link travel time. The link travel time resulting from LADTA model is used in calculating the average travel speed on each link. Using the vehicle fleet composition data and the flow data of LADTA model, the air pollutant emissions can be calculated for each 15 minutes during a full day.

2. Analyses on real-time traffic flow observational data of Clermont-Ferrand

2.1 Description of stationary inductive detectors in road network of Clermont-Ferrand

Clermont-Ferrand has 535 inductive loop traffic detectors in the road network, which are generally located in main city boulevards and/or crossroads, as presented in Figure 2. They collect the traffic density and flow information every minute. These precious and rich traffic data help us analyze the network users' behavior and set up the LADTA simulation. The City of Clermont-Ferrand has provided two years of observational data of every detector with a resolution of 15 minutes, from September 2013 to September 2015. The data for the first year have been analyzed in detail in order to set up and calibrate LADTA model, and the data for the second year are then used to evaluate the traffic flow results predicted by LADTA.

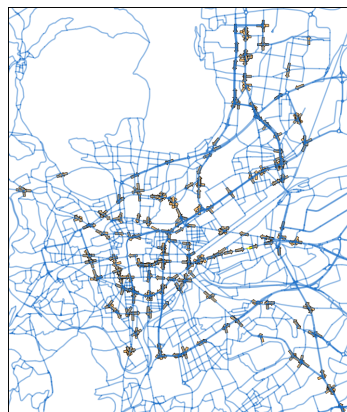


Figure 2. Detector locations in Clermont-Ferrand. The blue lines represent the roads of Clermont-Ferrand. The yellow arrows represent the position and direction of traffic detectors.

2.2 The analysis of observational data

The observational data of the real road traffic help us better understand the behaviors of road network users. It is observed that the network users in Clermont-Ferrand almost always behave the same for the same day type. Figure 3 shows temporal evolution profiles of flow for each Tuesday during 2013.9 – 2014.9.

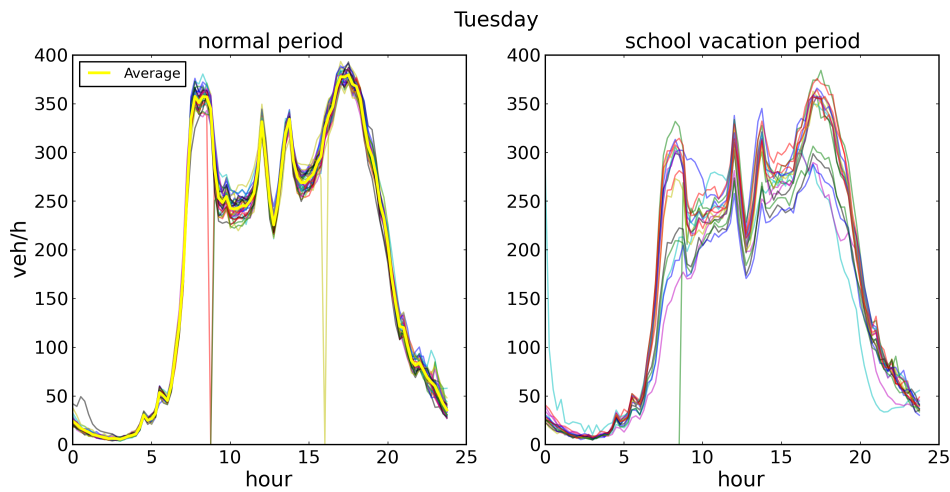


Figure 3. Temporal profiles of traffic flow averaged over all detectors of all Tuesdays. Each thin line represents a temporal profile of traffic on each Tuesday during normal periods (left) and scholar vacation periods (right), during 2013.9 – 2014.9, and the yellow line on the left profile is the average temporal profile of traffic flow over all Tuesdays in normal periods. Several points reach zero when no data was collected. This rarely happens (less than 5%), and the data in these cases have not been taken into account for calculating of average temporal profile.

The left profile in Figure 3 presents the temporal profile of traffic during a normal period. The right profile is the traffic during vacation period. It is clear that for every working day, the morning peak appears almost at the same moment of the day around 08:00, so is the evening peak, around 17:00. The differences among traffic flows during peak hours of different days are not significant. Moreover, the total volume of traffic during a day remains almost unchanged from one Tuesday to another. The same feature is observed for other weekdays, and the temporal profile of the same weekday during a year can be easily represented by an average temporal profile (yellow line). Furthermore, it is also shown in the Figure 4 that the total daily volume of the traffic slightly changes from Monday to Friday, but remains quite stable from month to month during non-vacation periods. This allows us to simplify the construction of dynamic O-D matrix for LADTA. However, as shown in the right profile in Figure 3 and daily volume in Figure 4, during the vacation period, the total daily volume and the temporal profile of the traffic are harder to predict, and the traffic flow during peak hours are not the same. It would not be reasonable to represent these days by only one temporal profile, and individual profiles should be used when simulating the traffic flow of these days.

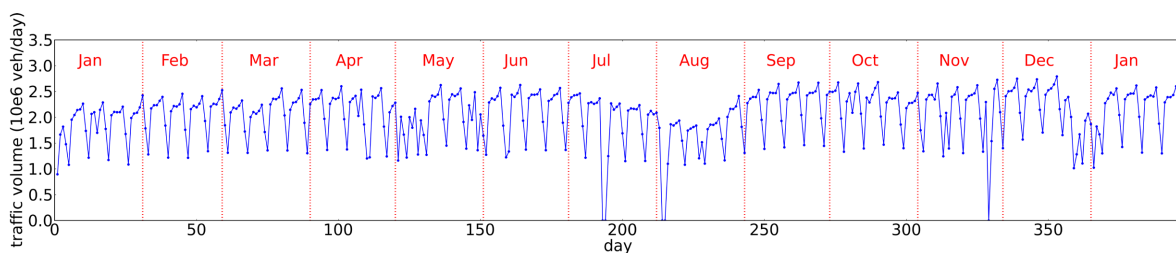


Figure 4. Daily traffic volume measured during the year 2014 (in 10^6 veh/day). The value of each point shows the sum of observational data of all detectors during each day. The value reaches zero when no data was collected.

In the following sections, the case study is for a working Tuesday during non-vacation period for the agglomeration of Clermont-Ferrand.

3. Traffic assignment and emission calculations for agglomeration of Clermont-Ferrand

3.1 Input data

The traffic demand and the physical road network supply in the traffic assignment problem need to be mathematically modeled respectively by an oriented graph with nodes and links, and an O-D matrix of traffic demand flux between each O-D pair. Figure 5 presents the modeled domain of the agglomeration of Clermont-Ferrand for LADTA. The simulation results will be presented only on red rectangle domain.



Figure 5. Modeled network for LADTA simulation. The road network of Clermont-Ferrand is modeled by links and nodes. Bold lines represent links with a capacity higher than 1600 veh/h, e.g. highways, national roads, departmental roads, etc.

(1) Zoning and dynamic OD matrix

The whole simulation domain is divided in 124 zones, and the O-D matrix of traffic demand during the evening rush hour is already given by the Syndicat Mixte des Transport en Commun de l'agglomération Clermontoise (SMTC – Clermont-Ferrand). Then, we use the temporal evolution of a typical day, a Tuesday during working week (as in Figure 3) to generate our dynamic O-D matrix for LADTA simulation. This temporal profile is calculated by the observational data during the period from September 2013 to June 2014. The starting hour of simulation is from 03:15. to minimize errors, since this is the time when the total traffic volume in the network is minimum, and LADTA model has to assign the network from zero vehicle.

(2) Oriented graph to model the road network

For the agglomeration of Clermont-Ferrand, the modeled network in the simulation domain has 19628 links and 8844 nodes. There is detailed information for each link, including its head node, tail node, length, capacity, speed limit and number of lanes. The free flow travel time is calculated from the link's length and speed limit.

With these two main input data, a LADTA assignment simulation is then launched for a complete day. The results and the corresponding statistical analysis are presented in the next sub-section.

3.2 Traffic assignment results simulated by LADTA model

(1) Temporal evolution and vehicle travel time during 24h

Figure 6 shows the average temporal evolution of the traffic during 24h. The flow results are averaged over of all inductive loop detectors. The LADTA simulation results have been compared with observational data during the period from September 2014 to June 2015. This shows that LADTA can very well simulate the temporal profile.

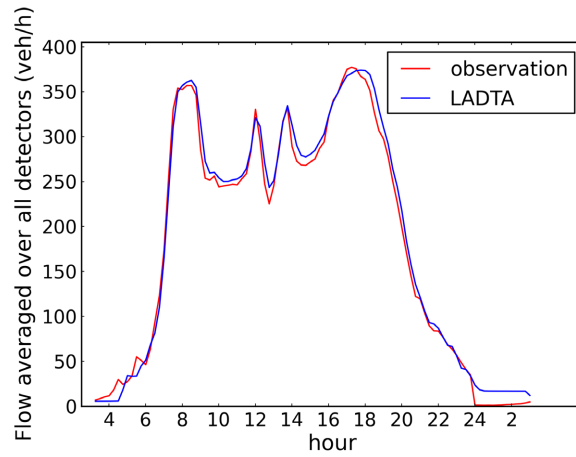


Figure 6. Temporal profile of spatial average flow on a normal Tuesday during non vacation periods from 2014/09/01 to 2015/06/30.

(2) Spatial distribution of the traffic in the network

Figure 7 and Figure 8 show the traffic assignment and the congestion distribution of Clermont-Ferrand from 07:00 to 08:30, for each 15 minutes. In this section, a link is considered to be congested when the associated average travel time (t) is 50% more than its free flow travel time (t_0). The results show the links with higher capacities have been assigned more traffic volume, and the congestions appear firstly and more frequently on crossroads. These fit well to the reality of urban traffic situation. The spatial distributions at different time periods show that the transition to the morning peak is almost immediate, and some links become congested within a quarter of an hour. Moreover, from 07:45 to 08:30, no significant difference can be seen in Figure 7 for traffic flows, as they have already reached the maximum, i.e. the link capacity. However, Figure 8 shows that during the same period, the link travel time continues increasing and there are more and more congested links. This congestion phenomenon may affect the emissions, since the latter depend on both the vehicle number and the average travel time. The dynamic traffic assignment model can then give more detailed information of traffic temporal evolutions than the static assignment model.

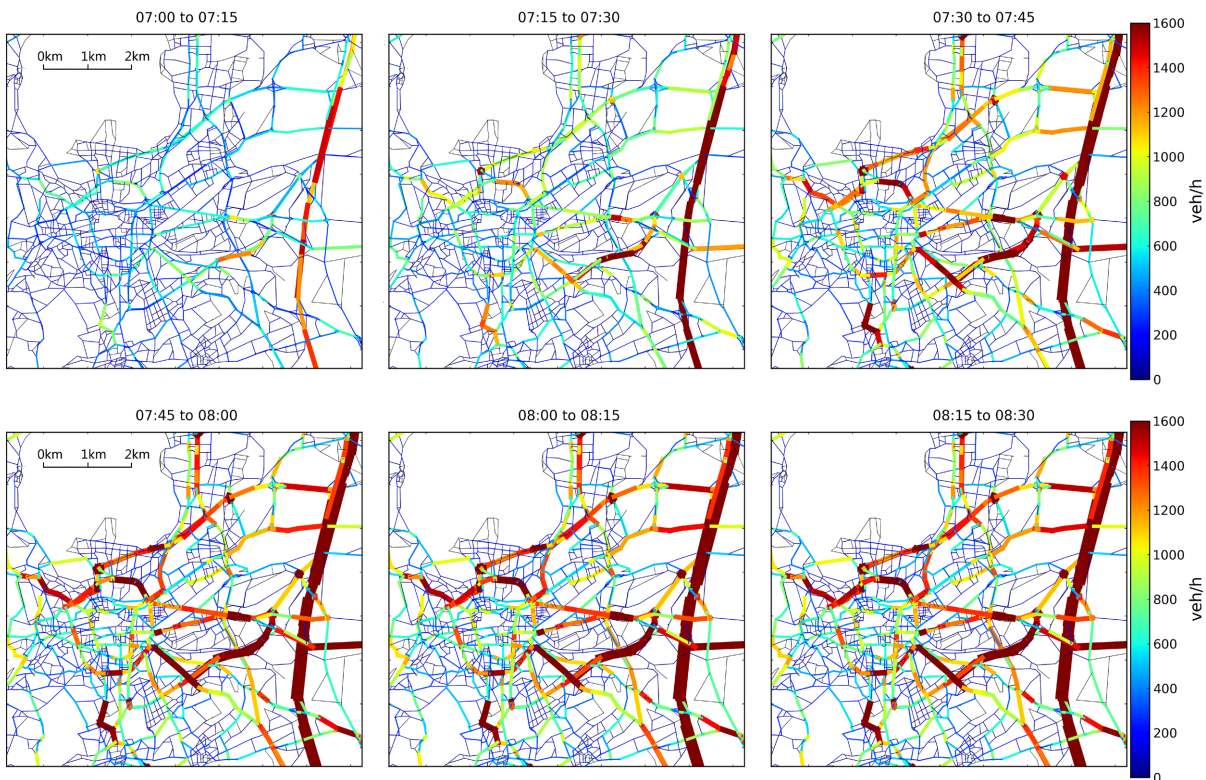


Figure 7. The traffic assignment results of LADTA from 07:00 to 08:30. Black lines represent unused links. The line width is proportional to the traffic flow on the link.

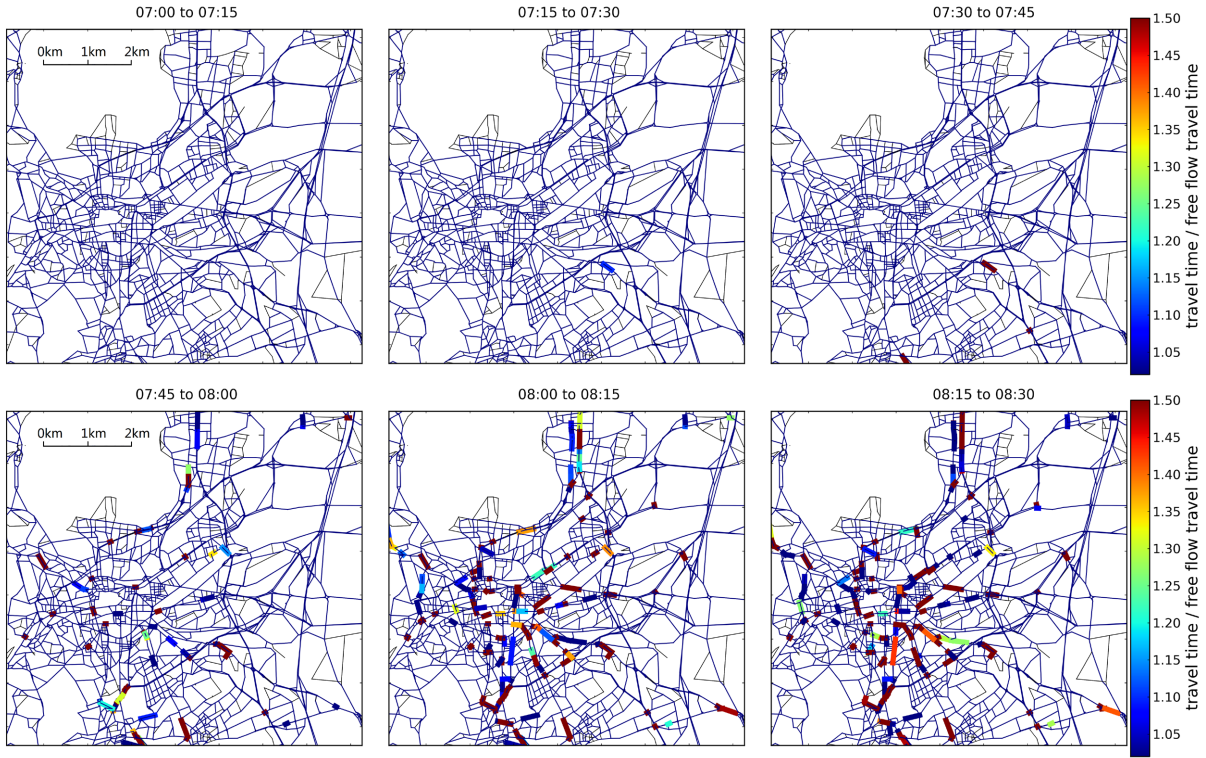


Figure 8. The spatial distribution of congestion from 07:00 to 08:30. Black lines represent unused links. Thin blue lines represent links whose travel time equals to its free flow travel time. Bold lines with various colors represent links with travel time larger than its free flow travel time.

(3) Comparison of simulation results and observational data

With the coordinate information, we can determine the corresponding link in the modeled network for each detector. One detector can only collect data of one lane and there may be several detectors on the same link. If we divide the simulated traffic flow of each link by its lane number, we can obtain the simulated traffic flow for each detector, for each 15 minutes during the day. For observational data, we have M detectors, N Tuesdays and T time steps during the day. The total size of observational data is $M \times N \times T$. We assume that for each detector, the simulation results are the same at the same time for each Tuesday. Then we can build the simulation data sequence of the same size as observational data, i.e. $M \times N \times T$. Table 1 shows the statistical values and scores for evaluating the model, where $o_{m,n,t}$ is the observed sequence and $s_{m,n,t}$ is the corresponding simulated sequence.

Table 1. Statistical values and scores for evaluation of LADTA.

Statistical values	Formula
Global mean value	$\bar{o}_{\text{global}} = \frac{1}{M \times N \times T} \left(\sum_{m=1}^M \sum_{n=1}^N \sum_{t=1}^T o_{m,n,t} \right)$ $\bar{s}_{\text{global}} = \frac{1}{M \times N \times T} \left(\sum_{m=1}^M \sum_{n=1}^N \sum_{t=1}^T s_{m,n,t} \right)$
Spatial average flow sequence	$\bar{o}_{\text{spatial}}^{(t)} = \frac{1}{M \times N} \left(\sum_{m=1}^M \sum_{n=1}^N o_{m,n,t} \right), \quad \bar{s}_{\text{spatial}}^{(t)} = \frac{1}{M \times N} \left(\sum_{m=1}^M \sum_{n=1}^N s_{m,n,t} \right)$
Temporal average flow sequence	$\bar{o}_{\text{temporal}}^{(m)} = \frac{1}{N \times T} \left(\sum_{n=1}^N \sum_{t=1}^T o_{m,n,t} \right), \quad \bar{s}_{\text{temporal}}^{(m)} = \frac{1}{N \times T} \left(\sum_{n=1}^N \sum_{t=1}^T s_{m,n,t} \right)$
Mean bias error	$e_{\text{global}} = \frac{1}{M \times N \times T} \sum_{m=1}^M \sum_{n=1}^N \sum_{t=1}^T (s_{m,n,t} - o_{m,n,t})$ $e_{\text{temporal}} = \frac{1}{T} \sum_{t=1}^T (\bar{s}_{\text{spatial}}^{(t)} - \bar{o}_{\text{spatial}}^{(t)})$

$$e_{\text{spatial}} = \frac{1}{M} \sum_{m=1}^M (\bar{s}_{\text{temporal}}^{(m)} - \bar{o}_{\text{temporal}}^{(m)})$$

$$\text{RMSE}_{\text{global}} = \sqrt{\frac{1}{M \times N \times T} \sum_{m=1}^M \sum_{n=1}^N \sum_{t=1}^T (s_{m,n,t} - o_{m,n,t})^2}$$

Root mean square error (RMSE)

$$\text{RMSE}_{\text{temporal}} = \sqrt{\frac{1}{T} \sum_{t=1}^T (\bar{s}_{\text{spatial}}^{(t)} - \bar{o}_{\text{spatial}}^{(t)})^2}$$

$$\text{RMSE}_{\text{spatial}} = \sqrt{\frac{1}{M} \sum_{m=1}^M (\bar{s}_{\text{temporal}}^{(m)} - \bar{o}_{\text{temporal}}^{(m)})^2}$$

Normalized mean square error (NRMSE)

$$\frac{\text{RMSE}}{\bar{o}}$$

Correlation

$$R_{\text{global}} = \frac{\sum_{m=1}^M \sum_{n=1}^N \sum_{t=1}^T [(s_{m,n,t} - \bar{s}_{\text{global}})(o_{m,n,t} - \bar{o}_{\text{global}})]}{\sqrt{\sum_{m=1}^M \sum_{n=1}^N \sum_{t=1}^T (s_{m,n,t} - \bar{s}_{\text{global}})^2} \sqrt{\sum_{m=1}^M \sum_{n=1}^N \sum_{t=1}^T (o_{m,n,t} - \bar{o}_{\text{global}})^2}}$$

$$R_{\text{temporal}} = \frac{\sum_{t=1}^T [(\bar{s}_{\text{spatial}}^{(t)} - \bar{s}_{\text{spatial}})(\bar{o}_{\text{spatial}}^{(t)} - \bar{o}_{\text{spatial}})]}{\sqrt{\sum_{t=1}^T (\bar{s}_{\text{spatial}}^{(t)} - \bar{s}_{\text{spatial}})^2} \sqrt{\sum_{t=1}^T (\bar{o}_{\text{spatial}}^{(t)} - \bar{o}_{\text{spatial}})^2}}$$

$$R_{\text{spatial}} = \frac{\sum_{m=1}^M [(\bar{s}_{\text{temporal}}^{(m)} - \bar{s}_{\text{temporal}})(\bar{o}_{\text{temporal}}^{(m)} - \bar{o}_{\text{temporal}})]}{\sqrt{\sum_{m=1}^M (\bar{s}_{\text{temporal}}^{(m)} - \bar{s}_{\text{temporal}})^2} \sqrt{\sum_{m=1}^M (\bar{o}_{\text{temporal}}^{(m)} - \bar{o}_{\text{temporal}})^2}}$$

LADTA is evaluated with the observational data sequence of all Tuesdays during non-vacation period from September 2014 to June 2015. The statistical scores of LADTA model are presented in Table 2. It is shown that LADTA model can well predict the temporal evolution of the daily traffic. The model performed perfectly with high correlation and low bias or RMSE. However, the model has limitations to predict the spatial distribution of the traffic in the network. This may be due to at least three reasons: (i) the method to estimate the simulated results for each detector by dividing link volume with lane number, ignoring that left side lanes and right side lanes might have different traffic flows, (ii) the hypotheses that all the travelers choose their route by minimizing their generalized travel cost, while different users may use several different criteria for routing in reality, (iii) the nature of origin – destination pairs according to the nature of zones. Indeed, the temporal evolution profile of LADTA inputs might be different for an O-D pair from an industrial zone to a residence zone, and for a pair from a residence zone to an industrial zone.

Table 2. Comparison of traffic flow results between LADTA and measurements.

	Global	Temporal	Spatial
RMSE (veh / h)	149	12	112
Mean bias error (veh / h)	6	6	5
Mean value of observations (veh / h)	183	183	183
NRMSE (%)	81.4	6.6	61.2
Correlation	0.73	0.99	0.57

The results of LADTA are then used in calculations of the emissions for air pollutant at street resolution in agglomeration of Clermont-Ferrand, combining with links' information and vehicle fleet data.

3.3 Calculation of air pollutant emissions for agglomeration of Clermont-Ferrand

The national vehicle fleet composition data of 2013 have been used in the calculation of emissions, as shown in Table 3 and Table 4. Using the average travel time on each link, the traffic flow results from LADTA, and the link length, the hot emissions of nitrogen oxides (NO_x) emitted by passenger cars are calculated, during each 15 minutes for a normal working day. The results are presented in Figure 9.

Table 3. Distribution of engine type and capacity (André et al. (2013)).

Engine type		Engine capacity	Percentage within each category (in %)
Gasoline	70.6	< 1.4 L	66.9
		1.4 – 2 L	30.2
		> 2L	2.9
Diesel	29.2	< 1.4 L	9.3
		1.4 – 2 L	78.3
		> 2L	12.4

Table 4. Composition of the vehicle fleet for passenger cars according European emission standards, i.e. the Euro standard. (sum of veh.km in %, André et al. (2013)).

Euro standard	percentage
Pre Euro	3.6
Euro 1	6.6
Euro 2	14.0
Euro 3	33.5
Euro 4	39.9
Euro 5	2.4

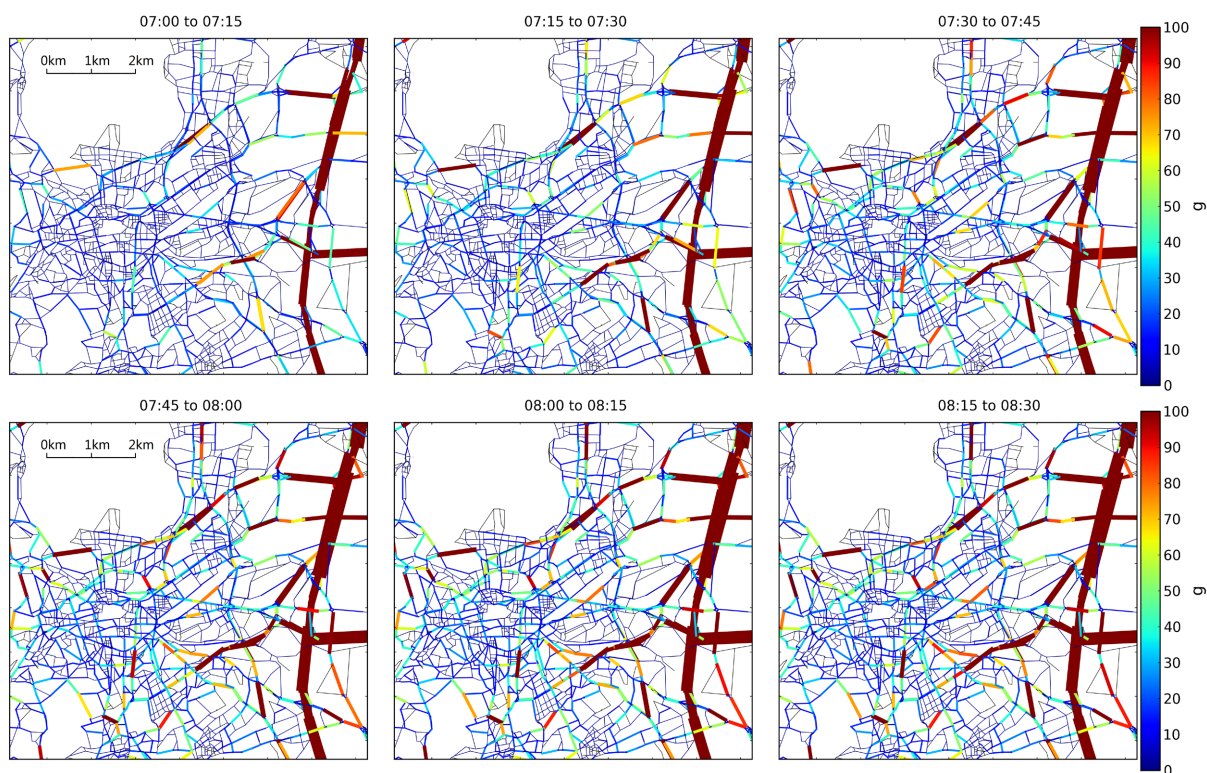


Figure 9. Emission map of NO_x in Clermont-Ferrand from 07:00 to 08:30. Black lines represent links with zero emission. The line width is proportional to the traffic flow on the link.

In Figure 9, we can see that the highways are the most polluted links in the network since there is more traffic and the speed is higher. During the transition from normal period to rush hours, the emissions of NO_x change with the evolution of time, and the spatial distribution of emissions has also changed. It is also observed that the emissions are very sensitive to the traffic flow affected in the network, and the sensitivity studies are presented in the next section.

4. Sensitivity analyses

In this section, we are interested in three main factors for calculating emissions: the total traffic demand in the network, the vehicle average speed and the vehicle fleet composition. The results in Section 3 are considered as references. We take three outputs as indicators: the total vehicle travel time, the proportion of congested links and the total NO_x emissions in the whole network. For the

second indicator, a link is considered as congested with the same criterion as in Section 3: travel time 50% higher than the free flow travel time. The congestion proportion is then calculated as the ratio between the total length of congested roads in the network, and the total length of the whole network.

4.1 The total demand of traffic volume in the network

We vary the total demand volume from -50% to $+100\%$, with the same temporal profile as for dynamic O-D matrix as Section 3. The data for links' information and vehicle fleet composition remain unchanged. Then the vehicle travel time, the proportion of congested roads in the whole network, and the emissions are calculated for each link during each 15 minutes.

The Figure 10 shows the spatial distribution of these three indicators during the period from 07:45 to 08:00, with a total traffic demand volume of -50% , 0% and $+50\%$ comparing with the referenced simulation case in Section 3. It can be observed that the traffic volume and the link travel time are more influenced by the evolution of the total demand volume entered to the LADTA model than the link emissions. In order to analyze the sensitivity in detail, the total values of these indicators of the whole network during 24 h are calculated for each case with different total demand volume. The sensitivity analyses of these three global indicators are presented from Figure 11 to Figure 13.

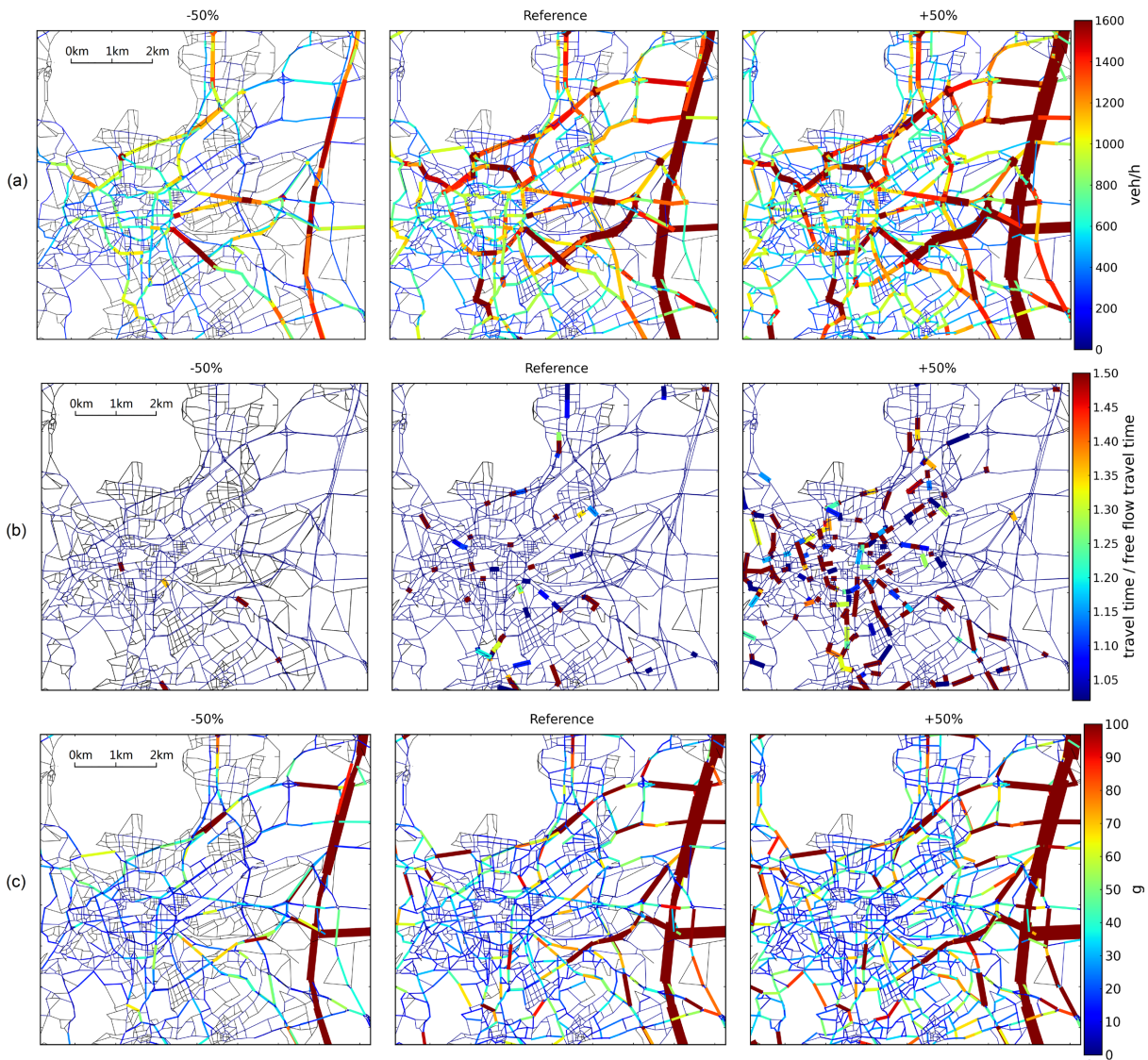


Figure 10. The spatial distribution of (a) traffic flow, (b) congestion and (c) emission of NO_x during 07:45 to 08:00, with change of total demand volume of -50% , reference case, and $+50\%$. Black lines represent unused links in LADTA model. The line width is proportional to link's vehicle travel time in (a) and to link's emission in (c). In (b), thin blue lines represent links where the travel time equals to the free flow travel time.

Figure 11 to Figure 13 show the influence of the total traffic demand volume on the three outputs. We see that the total vehicle travel time and the congestion rate of the network are very sensitive to

the total demand volume, especially when congestion phenomenon appears. Figure 11 and Figure 12 show that the total vehicle travel time and the network's congestion proportion become about 10 times higher than the reference case, when the total demand is doubled. In Figure 11 (b) and Figure 12 (b), below the reference total demand volume, the increase of vehicle travel time and the congestion rate is almost linear with the increase of the demand. After that, the network becomes more and more congested and the growth of travel time of vehicles becomes increasingly fast.

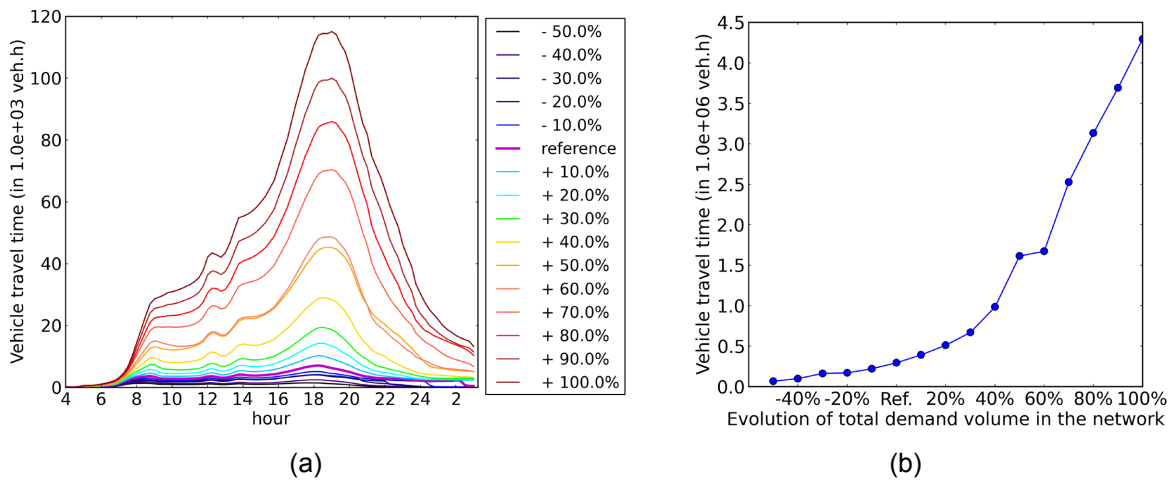


Figure 11. Sensitivity of vehicle travel time to the total demand volume. (a) Evolution during the day (in 10^3 veh.h), (b) evolution of the total vehicle travel time in the whole network (in 10^6 veh.h).

Furthermore, it is interesting to notice that the road traffic during the evening peak period is more congested than during the morning peak, and travelers suffer a longer travel time during evening peak with congestions. The network before evening peak hour is no longer empty and the traffic appearing before evening peak can affect the dynamic assignment traffic results. This is the phenomenon that we can only observe in DTA models. In fact, the existing traffic before evening peak hours might decrease the link capacity, and the capacity varies with the increase of traffic demand when peak hour arriving. This phenomenon cannot be simulated by static traffic assignment models even with separate time periods since the static models do not take into account the existing traffic on the network, and there is no interaction between traffic flow assigned and the link capacity.

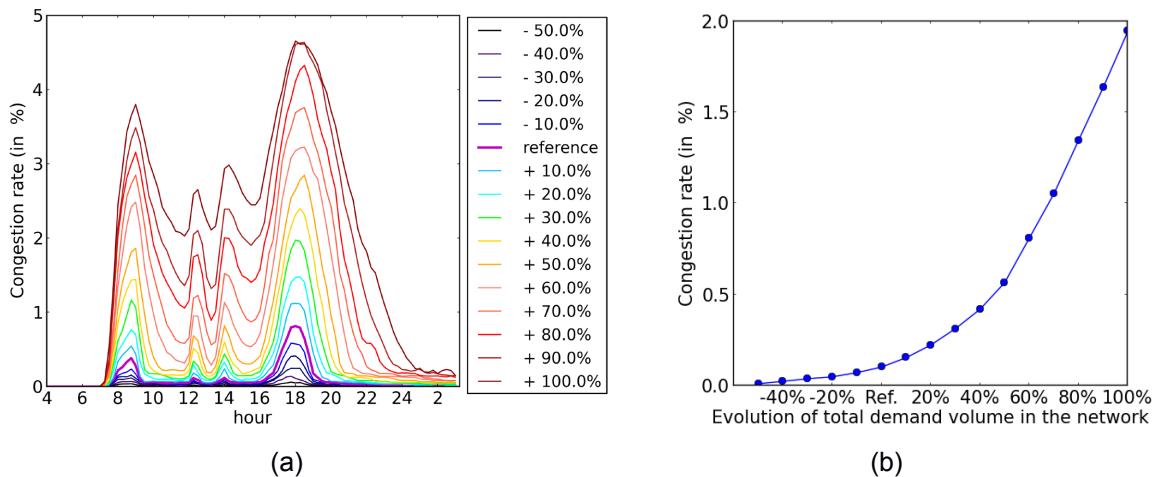


Figure 12. Sensitivity of the congestion rate to the total demand volume (in %). (a) evolution during the day, (b) evolution of the proportion of congested links in the whole network.

Concerning the total emission, as shown in the Figure 13, the influence of the total volume is not linear either, but the non-linearity of the total emissions is not as obvious as in the vehicle travel time. The total emissions tripled when we double the total demand volume comparing with the reference case. In fact, the emission factor of NO_x changes with the average travel speed as shown in Figure 14. With the increase of traffic volume, roads are becoming congested and the travel time increases. This leads to the decrease of vehicle speed, and decrease of emission factors for most of the links.

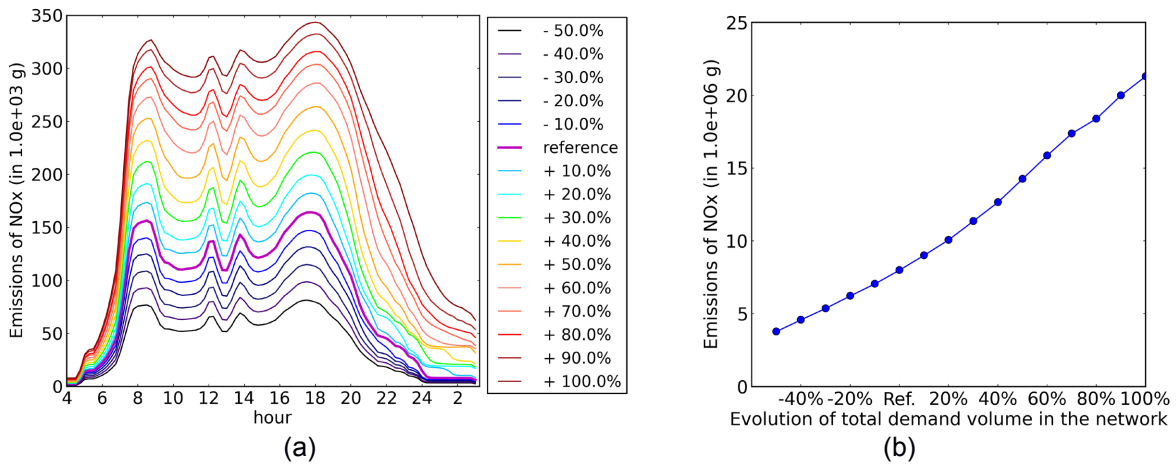


Figure 13. Sensitivity of the total emissions of the network to the total demand volume. (a) evolution for the whole day (in 10^3 g), (b) evolution of the total vehicle travel time in the whole network (in 10^6 g).

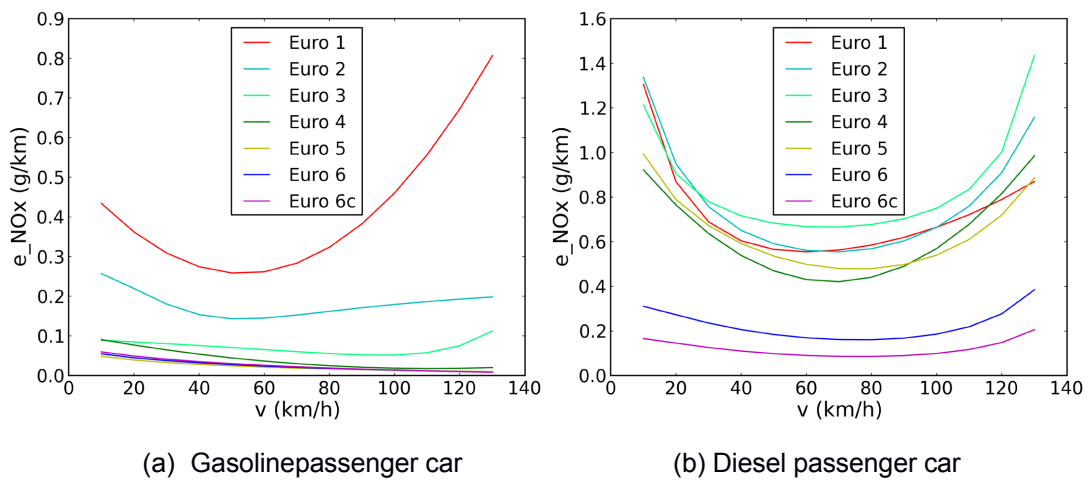


Figure 14. Sensitivity of hot emission factor of passenger cars for NO_x to the average speed.

4.2 Links' speed limit

This sub-section analyzes the sensitivity of traffic emission to the road's average speed in a more direct way. The maximum authorized speed of each road has been decreased by 5%, 10%, 15%, 20%, 25%, 30%, 35%, 40%, 45%, and 50%. It is found that the total vehicle travel time and the network total emissions are less sensitive to the speed limitation than to the total demand, as shown in Figure 15 and Figure 16. Figure 16 (b) shows that the variation of the total emissions is not monotonic with the speed limitation. A minimum is reached for a decrease of 25%. For higher limitation of the speed, more emissions are released. We observe that limiting the link's speed does not strongly change the traffic flow in the network. The emissions follow the same non-monotonic trend as in Figure 14, and the variation of the amplitude depends on the vehicle fleet.

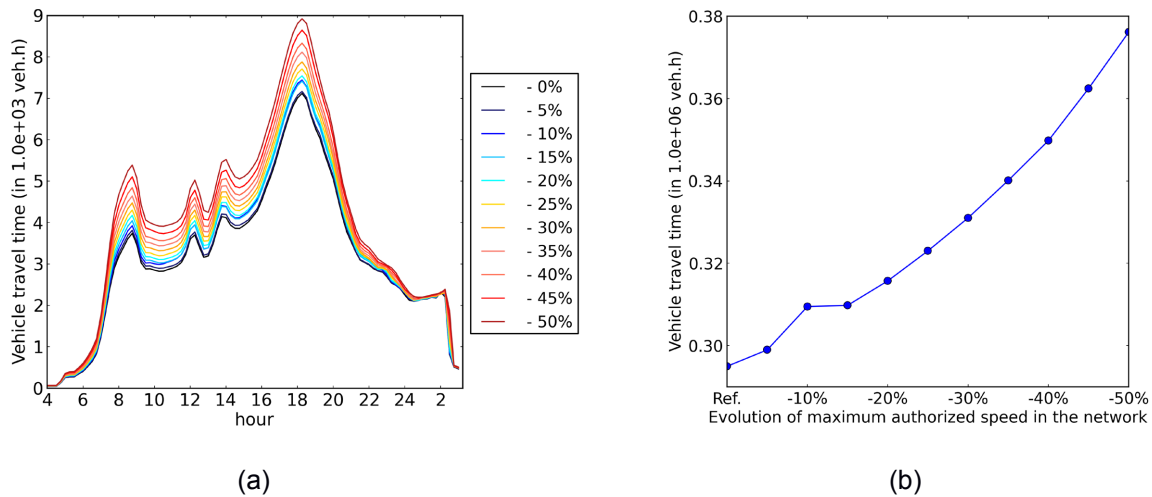


Figure 15. Sensitivity of total vehicle travel time to the links' speed limit. (a) temporal profile for the day (in 10^3 veh.h), (b) daily total value (in 10^6 veh.h).

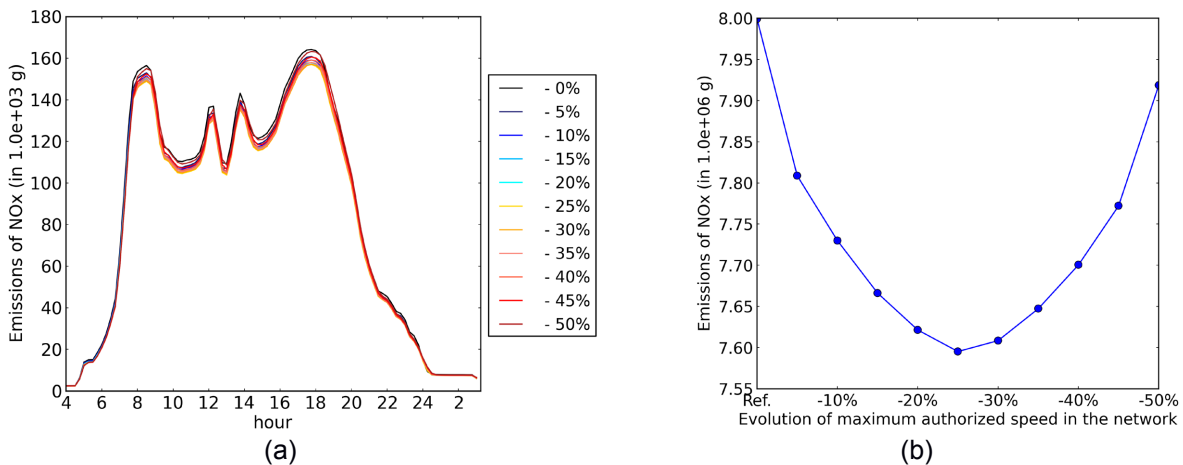


Figure 16. Sensitivity of the networks' total emissions to the links' speed limit. (a) temporal profile for the day (in 10^3 g), (b) daily total value (in 10^6 g).

4.3 Vehicle fleet composition

(1) Effects of vehicle emission Euro standards

In this subsection, we divide passenger cars into two big categories: (i) the “Euro 4 +” vehicles with Euro standards of Euro 4 and higher, (ii) the “Euro 3 –” vehicles with Euro standards from pre-Euro to Euro 3. In the reference simulation, the percentage of “Euro 4 +” vehicles is about 42.3% for passenger cars. For the sensitivity study, we increase the percentage of “Euro 4 +” cars from 42.3% to 80%. Within each category, we keep the same distribution of car standards. Figure 17 (a) shows that the NO_x emissions decrease when the proportion of “Euro 4 +” category increases.

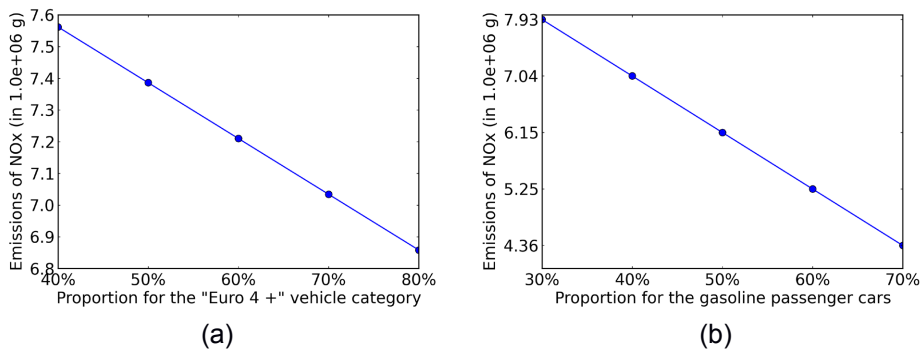


Figure 17. Sensitivity of total emissions of NO_x to (a) Euro Standard and (b) vehicle fleet type.

(2) Effects of the proportion for gasoline passenger cars and diesel passenger cars

In the reference case, the percentage of diesel passenger cars is 70.6% and that of gasoline passenger cars is 29.2%. We increase the proportion of gasoline passenger cars from 30% to 70% with steps by 10%. The results in Figure 17 (b) show that we can decrease the total NO_x emission of 45% by doubling the percentage of gasoline passenger cars.

Conclusions

In this study, we have presented a simulation chain for emission calculations combined with a dynamic traffic assignment model called LADTA, and the COPERT IV method. The case study is carried out for a typical working day during non-vacation period for the agglomeration of Clermont-Ferrand. We have firstly analyzed users' travelling behavior in the network during the year and then used this information to calibrate and evaluate LADTA. The emission calculations are based on traffic flow results of LADTA for each link during every 15 minutes for the day. At last, we studied the sensitivity of the emissions to LADTA model and COPERT inputs.

Both the vehicle travel time and the total emissions increase with the total demand volume onto the network. The total vehicle time grows increasingly fast when total demand increases linearly, which leads to congestions. However, the non-linearity of emissions evolution is less significant since the decreased average speed may lead to the decrease of emission factors of NO_x.

The variation of the link speed has less influence on the network total vehicle travel time and total emissions. As we decrease the links' speed limits, the total emissions firstly decrease and then increase. The minimum value is reached when the speed decreases by about 25%. This is mainly due to the influence of vehicle travel speed on the hot emission factors of NO_x.

It is also found that the total emissions of NO_x are sensitive to the vehicle fuel type as well as the Euro emission standards: emissions decrease strongly when we increase the percentage of gasoline passenger cars or vehicles with European emission standard of Euro 4 and higher.

This study shows the importance to take into account the congestion phenomenon by using a dynamic traffic assignment model. The emissions are very sensitive to the traffic flow, which can be increased immediately within a quarter of an hour. The static assignment model during peak hours or with separate hours may not be sufficient. Furthermore, the sensitivity analysis shows that when the total traffic demands change, emissions can change non-linearly. The actual variation of the total demand from one day to another might be significant enough to trigger large emission variations. In further studies, we will take into account the distribution of vehicle speed for emission calculations during heavy traffic periods, in order to better handle vehicles' unstable stopping and starting on congested links. Meanwhile, we will improve LADTA model to reduce its spatial errors. For example, we can apply different temporal profiles to different kind of O-D pairs for generating the input dynamic O-D matrix.

Acknowledgements

This work is funded by the French National Research Agency (Agence Nationale de la Recherche, i.e. ANR), project ESTIMAIR. The City of Clermont-Ferrand provided the traffic flow observational data. SMTC provided the modeled network, the static O-D matrix and a static traffic assignment for Clermont-Ferrand.

References

- Aguiléra V. & F. Leurent (2009): Large Problems of Dynamic Network Assignment and Traffic Equilibrium: Computation Principles and Application to Paris Road Network. Transportation Research Record, 2132, p 122 – 132.
- Airparif (2014): Inventaire regional des émissions en Île-de-France. Airparif report, p 5.
- André M., A.L. Roche & K. F. Moore (2013): Statistiques de parcs et trafic pour le calcul des émissions transports routiers en France. Rapport IFSTTAR-LTE, mars 2013, p 87 – 88.
- Bureau of Public Roads (1964). Traffic Assignment Manual. U.S. Dept. of Commerce, Urban Planning Division, Washington D.C.
- EMEP/EEA (2013): air pollutant emission inventory guidebook, 1.A.3.b. Road transport, p 40 – 66.

- Geroliminis N. & C.F. Daganzo (2008a): Existence of urban-scale macroscopic fundamental diagrams: some experimental findings. Transportation Research Part B. 42(9), p 759 – 770
- Leurent F. (2003b): On network assignment and supply demand equilibrium: an analysis framework and a simple dynamic model. European Transport Conference (CD Rom edition).
- Lighthill M. & J. Whitman (1955): On kinematic waves, ii: A theory of traffic flow on long crowded roads. Proceeding of Royal Society, A229, p 281 – 345.
- Ortuzar J.D. & L. G. Willumsen (2011): Modeling Transportation 4th edition, p353.
- Richards P.I. (1956): Shock waves on the highway. Operations Research 4, p 42 – 51.
- Vickrey W. (1969): Congestion theory and transport investment. American Economic Review, vol. 59, p 251 – 261.
- Wagner N. (2012): Dynamic equilibrium on a transportation network: mathematical properties and economic application. Ph.D Thesis.
- Wardrop J.G. (1952): Some theoretical aspects of road traffic research. Proceedings of the Institution of Civil Engineers, Part II 1, p 325 – 350.

Reducing the Negative Impacts of Transport Fuel Subsidies in Mexico

Ernesto Sanchez Triana
World Bank, Washington DC (USA)

Abstract:

Between 2005 and 2009, Mexico's electricity, diesel, gasoline, and liquefied petroleum gas subsidies represented 1.8 percent of the country's GDP (on average Mex\$200.4 bn. per year). Transport fuel subsidies account for about 0.8 percent of GDP.

Subsidies on gasoline alone are equivalent to 25 percent of revenues collected from the value-added tax (VAT). Subsidies on fuel have varied tremendously, ranging from levels of light taxation in the years 2000-2004, to net subsidies thereafter. Fuel subsidies climbed steadily from being close to zero in 2005, to a peak of 350 billion in 2008. In 2009 and 2010 they decreased to around 160 billion pesos, but in 2011 they increased again to 276 billion pesos. These variations signal to the complex political economy nature behind these fuel subsidies.

Fuel subsidies are inefficient because they encourage consumers to use more fuels than they would if they were priced at market prices. About a third of total energy subsidies corresponded to gasoline and diesel. Deadweight loss, or the inefficiency loss amounts to 2.1 percent for Magna gasoline and 1.6 percent for Premium gasoline. This means that for every Mex\$100 of subsidy on Magna and Premium gasoline, society loses Mex\$2.1 and Mex\$1.6, respectively. In the case of diesel consumption, we estimate that the deadweight loss is of 2.7 percent.

Fuel subsidies are regressive: the richest 20 percent of Mexico's citizens – the ones who own most of the cars – receive 55 percent of the subsidy, while the poorest 20 percent get only the 3.4 percent. In Mexico, it is estimated that removing government energy subsidies alone would increase GDP by about 1.5 percent by 2030 even if the subsidy money were not reallocated to more-productive use. Finally, the net effect of fuel subsidies is to increase fossil fuel consumption thus exacerbating both emissions of local pollutants (such as particulates, NOx, SOx, and VOC) and CO₂.

Eliminating subsidies to fuels leads to lower use of fossil fuels and thus to a reduction in global emissions (e.g., CO₂). Approximately 41.7 million tons of CO₂ would be abated every year through a decrease in fossil fuel usage due to elimination of fuel subsidies. It is estimated that cutting fuel subsidies would result in abating 80 percent of the carbon dioxide emissions that Mexico tried to achieve under its first Special Program on Climate Change (2009-2012).

Additionally, the decrease in fossil fuel consumption would improve urban population health. This will have a particularly significant impact in Mexico's cities, where illnesses related to air pollution amount to 1.5 percent of annual GDP.

In conclusion, a number of lessons from transport fuel subsidy reforms undertaken by countries around the globe are relevant for Mexico, including: (i) reductions should be part of a comprehensive, long-term strategy for the energy sector, developed in consultations with stakeholders; (ii) a clear and extensive communication strategy should be carried out, emphasizing the negative effects of the subsidies and explaining how those resources will be used in the future; (iii) subsidy removals should be complemented with targeted measures to protect the poor; and (iv) the reduction of subsidies should be based on automatic and transparent pricing mechanisms, with the aim of depoliticizing the issue.

Performance of in-use buses retrofitted with diesel particle filters

Rafael FLEISCHMAN*, Ran AMIEL*, Jan CZERWINSKI**, Andreas MAYER*** & Leonid TARTAKOVSKY*

*Faculty of Mechanical Engineering, Technion – Israel Institute of Technology, Haifa, 3200003, Israel

Phone +972-4-8291654 – email: rafael.fleischman@gmail.com

**Labs for IC-Engines & Exhaust Emission Control, University of Applied Sciences, Biel, 2501, Switzerland

*** TTM – Technik Thermische Maschinen, Niederrohrdorf, 5443, Switzerland

Abstract

Inhalation of combustion generated nanoparticles leads to major adverse health effects. Public road transportation heavily depends on diesel fueled vehicles, which greatly contribute to air pollution in urban centers. Retrofitting polluting older buses with diesel particulate filter (DPF) is a cost-effective measure to quickly reduce particulate emissions. This study experimentally analyses the impact of DPF retrofitting on particulate emissions and engine performance aspects of in-use diesel buses. DPFs from three different major manufacturers were installed in 18 urban and intercity Euro III buses of a major Israeli bus company. Particulate number (PN) concentration and size distribution were measured both before and after DPF at different engine operating regimes. The average increase in fuel consumption due to DPF retrofitting was measured to be less than 2.5%, and backpressure increase is about one third of the acceptable limit. No deterioration of buses engine, as well as vehicle drivability were detected. The average reduction in total PN emissions was found to be higher than 97%, with no substantial difference between the different DPF manufacturers.

Introduction

The link between inhalation of particulate matter and adverse health effects has been extensively studied and is well documented (Dockery et al. (1993), Pope III and Dockery, (2006), Lelieveld et al. (2015) and Ware and Thibodeau (1981)). Boffetta and Silverman (2001) and Vermeulen et al. (2014) have related the exposure to diesel engine exhaust with cancer incidence. Nonetheless, only relatively recent studies have established the connection with particulate size, suggesting that the smaller the particles, the greater the toxicity, as indicated by Dellinger et al. (2008).

Road transport represent a great challenge in attempts to achieve better air quality levels. It is the main source of air pollution in Israel's cities and population centers, while public transportation in the country, both urban and intercity, is based almost entirely on diesel engines.

Exhaust emission regulations have progressively become more constrict in the last years, especially since the advent of the European emission standards. However, heavy-duty diesel engine vehicles may be kept in service for periods as long as 15 years or more. For example, approximately a half of Israeli buses fleet is composed of Euro III or older technology vehicles. As a result, their emission control technologies become obsolete and they turn into a major source of particulate emissions. Retrofitting older in-use buses with recently developed technologies, such as DPF, is a cost-effective measure to reduce particulate matter emissions, Mayer (2008), Tartakovsky et al. (2004).

The main goals of this study were to evaluate the reduction in nanoparticle emissions of in-use diesel buses retrofitted with DPF and to assess the impact of retrofitting on the buses performance in real-world usage conditions.

1. Methodology

Vehicles used

For the purpose of the study, a pilot group composed of 18 in-use buses from a major Israeli bus company were selected for DPF retrofitting. 9 of them were urban buses and 9 intercity coaches. Popular models from leading European bus manufacturers were chosen for retrofitting. All the vehicles were produced under the Euro III emission standards, and had travelled a distance compatible with its age. Every vehicle had an original engine and had been submitted to appropriate maintenance. The main engine parameters of the tested buses are shown in Table 1.

A control group composed of 18 identical vehicles was also defined. Data on fuel consumption, engine performance, maintenance and bus drivability aspects of both groups were compared. By means of that, it was possible to isolate the effect of the DPF retrofitting from the natural aging of the vehicles. All the considered buses, both the pilot and the control group were appropriately checked before the test and found to be in a well-tuned condition.

The content of maintenance operations, as well as their frequency, were monitored, for vehicles in both the pilot and the control group. The obtained results were compared, and abnormalities in maintenance activities were searched.

After driving the DPF-retrofitted buses, experienced bus drivers were asked to fill a simple questionnaire about their impressions on the bus performance and engine behavior.

Table 1: Main parameters of bus engines

Parameter	Intercity Coach	Urban Bus
Bus Model	Mercedes-Benz OC500	Man NL313F
Engine Model	OM457	D2866 (LUH 28)
Combustion System	Four-stroke diesel direct injection	Four-stroke diesel direct injection
Number of cylinders	6	6
Bore × Stroke, Displacement	128 × 155 mm, 11967 cm ³	128 × 155 mm, 11967 cm ³
Compression ratio	18.5:1	18:1
Rated power [kW]	260	228

In-use buses from three regions were chosen: Tel Aviv area, Jerusalem area and North area. These regions have different topographies, and might be characterized as flat, hilly and mixed, respectively. The vehicles were evenly divided in each area (three urban buses and three intercity coaches in each of them). After DPF installation, the vehicles were returned to service at their usual routes, at their original sites.

Ultra-low-sulfur diesel fuel, with sulfur content not exceeding 10 ppm, was used in the buses, in accordance to the EU practice. High quality low-ash lubricant oil, recommended for heavy-duty diesel vehicles with DPF was used in the bus engines.

There is a large variety of DPF types and technologies, with different characteristics, which could be more or less appropriate for installation on the selected buses. In order to choose DPF type suitable for retrofitting in the tested buses, temperature profiles of exhaust gas before the bus silencer have been measured. For this purpose, thermocouples were installed in the exhaust manifold of the selected buses, and the temperature profile was monitored for a couple of months. As an example, Figure 1 shows the obtained temperature profile for bus I3 in the period from January to March 2015

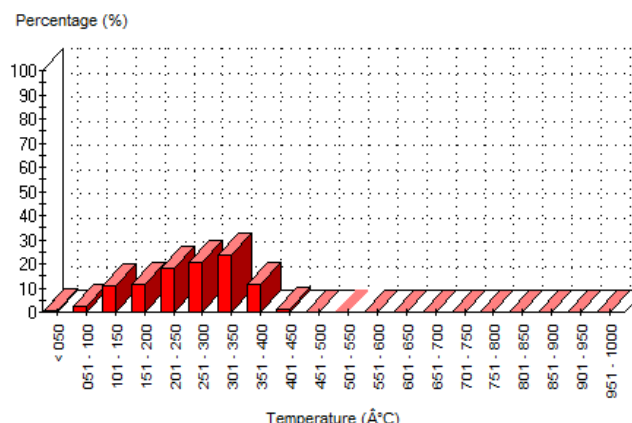


Figure 1: Exhaust gas temperature profile of bus I3

As can be seen from Figure 1, the temperature of the exhaust gas is higher than 100°C, 200°C, 300°C and 400°C during 97%, 75%, 36% and 1% of total usage time, respectively. Moreover, the mean temperature during engine operation was found to be 258°C.

DPFs selected for retrofit

Only VERT-certified DPFs, as published in the VERT-Filter List, were selected for the experiment. Filters from three leading manufacturers were selected. The different filters were evenly divided by area and bus type, as can be seen in Table 2.

The regeneration mechanism used by all of the chosen filters is based on the passive regeneration of Continuous Regeneration Trap (CRT) technology, developed by Johnson Matthey, Cooper et al. (1990) and Allansson et al. (2002). With this method, the accumulated soot is continuously oxidized using NO₂-oxidation mechanism.

Table 2: Selected Buses

Bus Code	Area	Bus Type	Bus Manufacturer	DPF Manufacturer	Distance travelled at DPF installation date [km]
I1	North	Intercity	Mercedes OC500	"A"	1,521,700
I2	South	Intercity	Mercedes OC500	"A"	1,161,895
I3	Jerusalem	Intercity	Mercedes OC500	"A"	1,319,521
I4	North	Intercity	Mercedes OC500	"B"	1,451,936
I5	South	Intercity	Mercedes OC500	"B"	1,441,011
I6	Jerusalem	Intercity	Mercedes OC500	"B"	1,406,971
I7	North	Intercity	Mercedes OC500	"C"	1,297,858
I8	South	Intercity	Mercedes OC500	"C"	1,404,728
I9	Jerusalem	Intercity	Mercedes OC500	"C"	1,581,330
U1	North	Urban	Man NL313F	"A"	463,398
U2	South	Urban	Man NL313F	"A"	451,465
U3	Jerusalem	Urban	Man NL313F	"A"	560,386

U4	North	Urban	Man NL313F	"B"	539,626
U5	South	Urban	Man NL313F	"B"	474,150
U6	Jerusalem	Urban	Man NL313F	"B"	534,047
U7	North	Urban	Man NL313F	"C"	568,681
U8	South	Urban	Man NL313F	"C"	462,893
U9	Jerusalem	Urban	Man NL313F	"C"	577,739

Measurement procedure

To assess how the influence of DPF retrofitting varies with time, three measuring rounds were planned. The first one shortly after DPF installation, and the second and the third about 4 and 9 months later, respectively. The data presented on this paper does not include the third measuring round.

Different operating regimes were selected for particle emissions measurements. According to Tartakovsky et al. (2015), these regimes reflect in some way real conditions of buses usage. Three steady-state regimes (low idle, high idle and 85% of rated speed at engine's full load) and one transient (free acceleration) operating mode were selected for measurements carrying out. Idling regimes were chosen because of their great contribution to particle emissions, especially in the events of passengers' collection. Table 3 presents the bus operating modes applied in the tests.

For the load-regime measurements, experienced dyno-operators and bus drivers operated the vehicles over a chassis dynamometer, used to impose load on the wheels. Due to the difficulty to sustain steady-state operation, fluctuations on the engine speed, load imposed on the wheels and on bus velocity were perceived, even after the goal load was reached. Fluctuations, however, were usually small, as can be seen in Table 3.

Table 3: Operating regimes of the buses tested

Bus Number	Low Idle	High Idle	Free Acceleration	Load		
	Engine speed [rpm]	Engine speed [rpm]	Engine speed [rpm]	Engine speed [rpm]	Power on wheels [kW]	Minimum Bus velocity [km/h]
I1	550	1700	550-1700	1600-1200	155-149	79-77
I2	550	1700	550-1700	1950-1900	186-185	70-71
I3	580	1700	580-1700	1950-1900	157-145	70-71
I4	550	1700	550-1700	1400-1250	179-141	80-78
I5	550	1700	550-1700	1920-1900	179-180	70-71
I6	550	1700	550-1700	1970-1950	179-172	70-71
I7	680	1800	680-1800	1400-1300	154-151	83-80
I8	550	1700	550-1700	1900-1600	157-149	70-71
I9	560	1700	560-1700	1920-1900	169-168	70-71
U1	650	2400	650-2400	1650-1600	130-129	68-65
U2	650	2450	650-2450	1700-1680	150-149	68-69

U3	680	2680	680-2680	1950-1920	123-122	68-69
U4	720	2600	720-2600	1900-1700	140-134	70-69
U5	700	2450	700-2450	1700-1720	153-154	69-68
U6	700	2700	700-2700	1820-1800	122-121	68-69
U7	650	2450	650-2450	1800-1650	129-127	74-68
U8	700	2700	700-2700	2020-2000	145-140	68-69
U9	700	2650	700-2650	1920-1900	124-123	69-70

For every bus at each operating regime, PN concentrations and size distributions in the bus exhaust gases were measured both upstream and downstream the DPF.

The PN weighted concentration per channel, n_i was used to estimate particle mass (PM) weighted concentration per channel, m_i and is described by the equation:

$$m_i = \rho \frac{\pi d_i^3}{6} n_i$$

Here the subscript i indicates the measuring channel, ρ is the particle density (assumed to be 1 g/cc) and d_i is the particle mobility size. Due to the fact that this study devotes more concern to PN, the simplification assumption that all particles are spheres was made. A more sophisticated method for calculating particle mass was developed by Maricq and Xu (2004) and takes into account effective density and fractal dimension.

Total PN and PM concentrations were calculated, respectively, by:

$$TPN = \sum_{i=1}^u n_i$$

$$TPM = \sum_{i=1}^u m_i$$

DPFs filtering efficiencies in terms of number and mass, PNFE and PMFE, respectively, were calculated by the following equations, where the subscripts "B" and "A" stand for before and after the DPF, respectively:

$$PNFE = \frac{(TPN_B - TPN_A)}{TPN_B} \cdot 100$$

$$PMFE = \frac{(TPM_B - TPM_A)}{TPM_B} \cdot 100$$

Particle emissions measurement

All the measurements were performed at the bus company garages. The garages were equipped with a chassis dynamometer. Figure 2 shows the experimental setup.

TSI-made Engine Exhaust Particle Sizer (EEPS) Spectrometer 3090 model was used for particles size distribution measurements. Particles pass through an electrical diffusion charger where they get a

predictable charge level based on their size. An electric field drags the particles in the sizing region where 22 sensing electrometers are installed. Particles, which land on the sensing electrodes transfer their charge. The equipment measures particles from 5.6 to 560 nm with particle size resolution of 16 channels per decade (32 total) and time resolution of 10 readings per second.

TSI-made Rotating Disk Thermodiluter Thermal conditioning device 379020A-30 was used for diluting the sample. The equipment is composed of two separate parts, the Thermodiluter Head and Thermal Conditioner Air Supply. It is suited for sampling, diluting, and conditioning exhaust particles prior their measurement in dedicated equipment. A small quantity of the raw exhaust is captured by a cavity of the rotating disk and transported to the measurement channel where it is mixed with HEPA-filtered, particle-free dilution air. It performs a two-stage dilution and can heat the sample up to 400°C.



Figure 2: Experimental setup: 1: DPF; 2: 379020A-30 Thermodiluter Head; 3: 379020A-30 Thermal Conditioner Air Supply; 4: EEPS 3090

A warm-up period was allowed prior each measurement. A two-stage dilution and heating to 300°C were performed to prevent condensation of the volatile particles, in accordance with the ECE-PMP-Protocol as described in UN ECE (2010, 2013a, 2013b).

The average value of the PN measurements was assumed to adequately characterize the given regime under steady-state measurements. 60 seconds measuring duration was used for idling regimes and about 45 seconds for measurement under load. Since the EEPS collects values at a frequency of 10 Hz, averages of 600 and about 450 readings were taken into account, respectively.

For the transient free-acceleration regime, six consecutive accelerations were performed, with intervals that allowed engine's speed returning to low idling values (typically about 5 to 10 seconds). The average of the higher PN concentration of each peak were considered in filter efficiency assessment.

Total PN concentration, as well as PN size distribution, were measured. Data collected from the measuring equipment includes particles with diameters from 5.6 nm up to 560 nm. Nonetheless, current Particle Measurement Program procedure prescribes PN measurement for particles with diameter greater than 23 nm. Thus, all data regarding smaller particles was not considered in the provided analysis results.

Fuel Consumption

The travelled distance and amount of diesel fuel refueled were used to calculate the vehicles monthly fuel consumption (in kilometers per liter). This analysis includes a period from 19 months prior DPF installation to 7 months after it. Monthly fuel consumption of the retrofitted buses was compared with that of the control group. Herewith, it's possible to know how DPF retrofitting affects fuel consumption.

The average value of fuel consumption of the period from January to July 2014 was compared to that of the same months of the year 2015 for vehicles in both the pilot and the control group. It was chosen to consider the average of all the 36 vehicles to increase sample size and minimize the effects caused by the fact that the buses don't always ride on the same routes and are not always conducted by the same driver. In both periods all the buses worked without DPF retrofitting. By means of that, the average natural deterioration of fuel efficiency of the buses due to vehicle aging was evaluated for urban and intercity vehicles.

Then, the fuel consumption of the vehicles in the pilot group for the period of 9/2014-3/2015 was compared to that for the period 9/2015-3/2016, i.e. exactly one year later. In the first period, buses worked without DPF retrofitting, and in the second period they had already had it. The difference in the results of fuel consumption is the gross fuel efficiency deterioration. By subtracting the fuel efficiency deterioration due to natural aging, the net fuel efficiency deterioration due to DPF retrofit was obtained.

Backpressure

Pressure sensors were installed in the exhaust manifold of the retrofitted buses, upstream the DPFs. The frequency of reading of the pressure sensors is 0.1 Hz. Pressure sensors worked only when the engine was operating.

Analysis of the obtained data allows evaluation of the increase in backpressure due to the DPF retrofitting and assessment of the backpressure built-up during the buses real-world operating.

2. Results and Discussion

Nanoparticle emissions

Figure 3 and Figure 4 show examples of typical obtained particle size distributions for intercity and urban buses, respectively. Results for the 4 analyzed operating regimes are presented, for both measurements performed upstream and downstream the DPF.

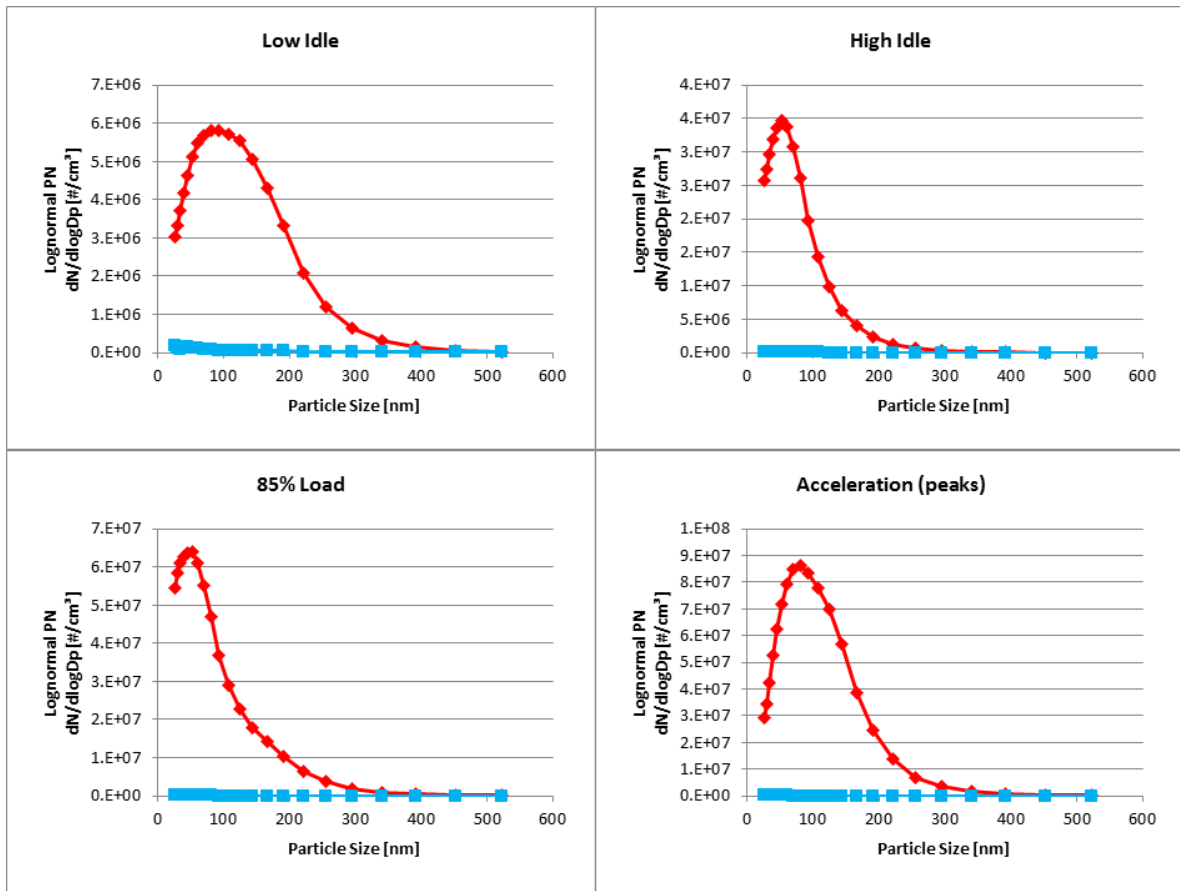


Figure 3: Particle Size Distribution of Bus I3. Red: Before DPF; Blue: After DPF

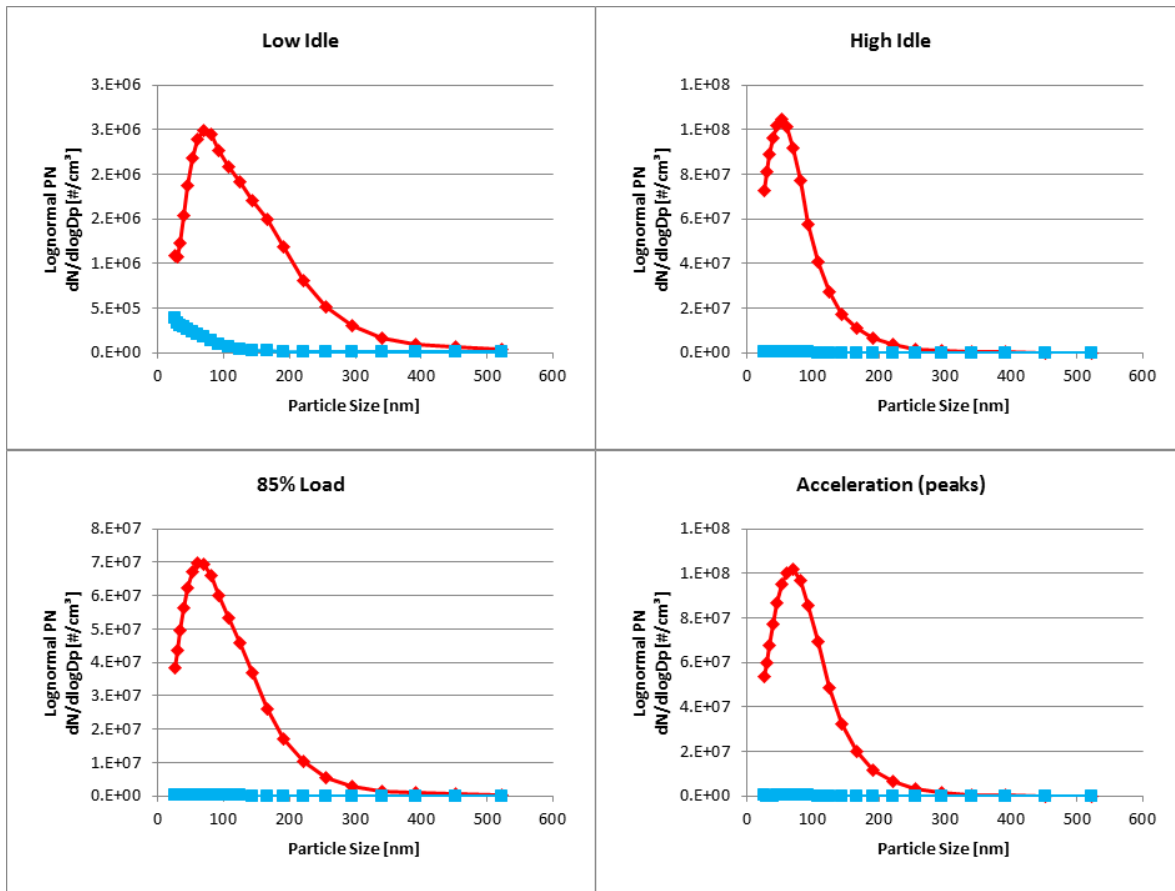


Figure 4: Particle Size Distribution of Bus U3. Red: Before DPF; Blue: After DPF

Table 4 and Table 5 summarize the Total PN concentration, Total PM concentration, PNFE and PMFE for the graphs presented in Figure 3 and Figure 4. DPF efficiency, for both PN and PM was found to be very high. The average PNFE for all the DPFs installed in the 18 analyzed vehicles was found to be higher than 97%.

It can be noticed that PNFE values were always higher than PMFE. This is due to the relatively higher PN concentration of smaller sized particles, whose contribution to total PM is small. Nonetheless, at low idle regime, filtration efficiencies were found to be the smallest. At this regime, the residence time of the gases inside the cylinder and in the exhaust manifold is higher, thus allowing a greater agglomeration of the particles, resulting into less and larger particles.

It was found that the three DPFs from different manufacturers behave similarly and present the same PN distribution patterns. It was also found that PNFE tend to be slightly higher for interurban buses, most probably because of smaller contribution of low-load operating modes. Figure 5 presents a comparison of average PNFE values of intercity and urban buses for all the 18 vehicles in the pilot group.

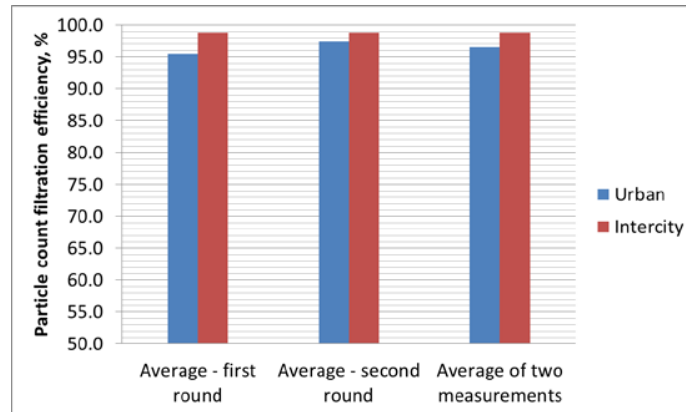


Figure 5: Comparison of PNFE values for intercity and urban buses

Table 4: PN and PM emissions, and Filtration Efficiencies of Bus I3

		Total PN Concentration [#/cm ³]	Total PM [μg/m ³]	PNFE [%]	PMFE [%]
Low Idle	Before Filter	4.70E+06	5.81E+03	98.14	96.27
	After Filter	8.76E+04	2.17E+02		
High Idle	Before Filter	2.08E+07	6.12E+03	99.73	98.96
	After Filter	5.71E+04	6.38E+01		
Full load, 85% rated speed	Before Filter	4.20E+07	2.22E+04	99.83	99.67
	After Filter	7.28E+04	7.25E+01		
Free acceleration (peaks)	Before Filter	5.76E+07	4.75E+04	99.83	99.80
	After Filter	9.74E+04	9.62E+01		

Table 5: PN and PM emissions, and Filtration Efficiencies of Bus U3

		Total PN Concentration [#/cm ³]	Total PM [μg/m ³]	PNFE [%]	PMFE [%]
Low Idle	Before Filter	1.81E+06	2.60E+03	90.9	95.11
	After Filter	1.65E+05	1.27E+02		
High Idle	Before Filter	6.13E+07	1.71E+04	99.82	99.16
	After Filter	1.12E+05	1.44E+02		
Full load, 85% rated speed	Before Filter	4.90E+07	3.65E+04	99.79	99.42
	After Filter	1.05E+05	2.11E+02		
Free acceleration (peaks)	Before Filter	6.36E+07	2.80E+04	99.88	99.61
	After Filter	7.39E+04	1.10E+02		

Fuel Consumption

As expected, it was found that compared to urban buses, intercity coaches achieve a better fuel efficiency. Figure 6 presents the averaged fuel consumption of all 9 urban buses and 9 intercity coaches of the pilot group.

Moreover, the seasonal variation in fuel consumption is made very clear. Due to the use of air conditioning during the hot Israeli summer, fuel consumption increases significantly, for both urban and intercity coaches. Average of the 36 vehicles of both the pilot and the control group indicate that fuel consumption increases by about 4 and 8 percent for intercity and urban buses, respectively, during summer, as can be seen in Figure 7. This is a result of higher relative influence of power demand for air conditioning at urban driving, due to lower engine loads at the latter operating mode.

Natural deterioration of the fuel efficiency due to vehicle aging was evaluated in this study. The result was used to isolate the effect of DPF on fuel consumption, which is shown in Figure 8. It was found that the average increase of fuel consumption due to DPF retrofitting is 2.5% and 2.1% for intercity and urban buses, respectively. The usage of DPFs had a higher impact on fuel consumption of intercity buses most probably due to the greater percentage of time they operate under higher load regimes with respectively higher values of backpressure due to bigger flow rate of exhaust gases.

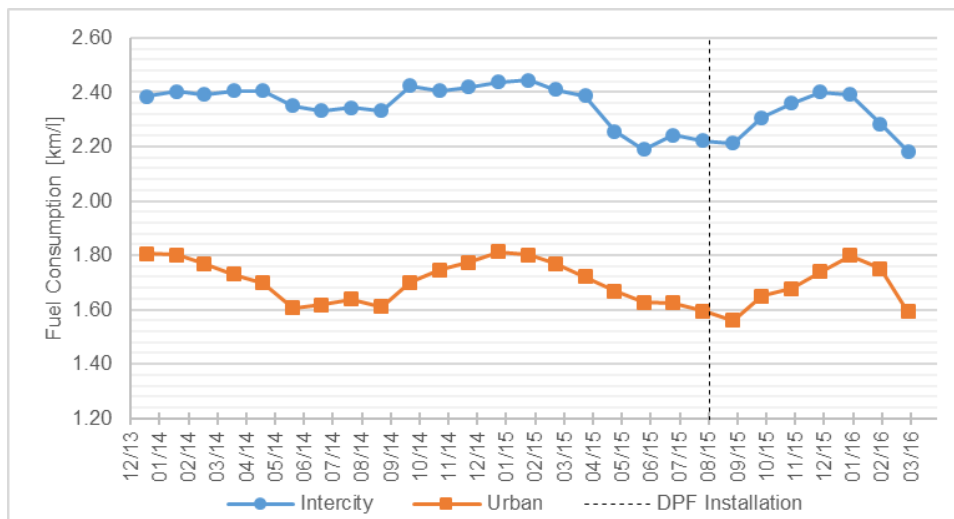


Figure 6: Fuel consumption of intercity and urban buses of the pilot group

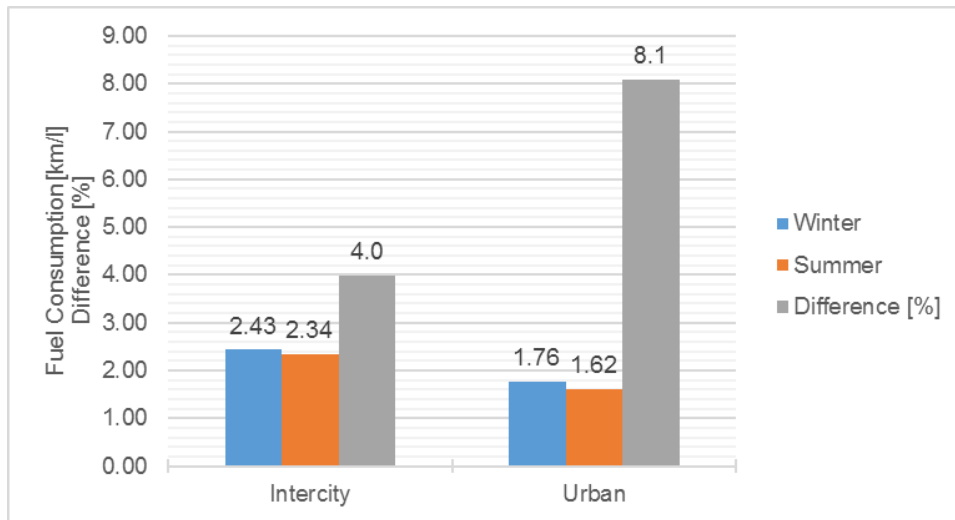


Figure 7: Seasonal variation in fuel consumption of buses of the pilot and control groups

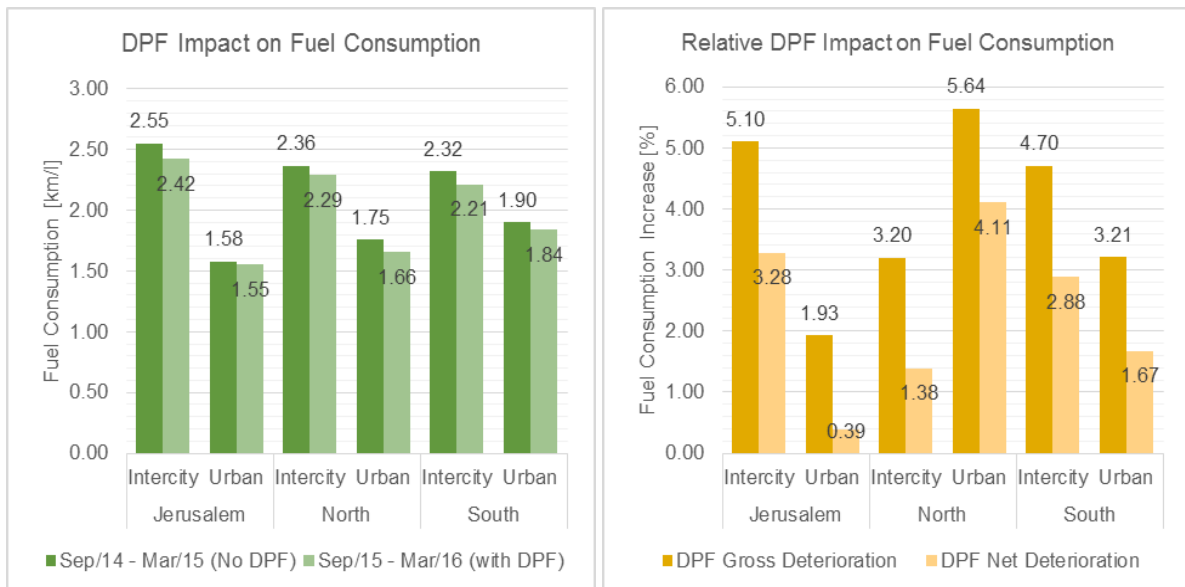


Figure 8: DPF effect on fuel consumption

Backpressure

Data from the pressure sensors installed in the exhaust manifold at the entrance to the DPF was logged and analyzed. The average daily backpressure increase due to the DPF was calculated and is presented in Figure 9. It can be seen that after half a year of real-world usage, DPF doesn't cause backpressure increase greater than 60 mbar, and is far from the maximal recommended value of 150 mbar.

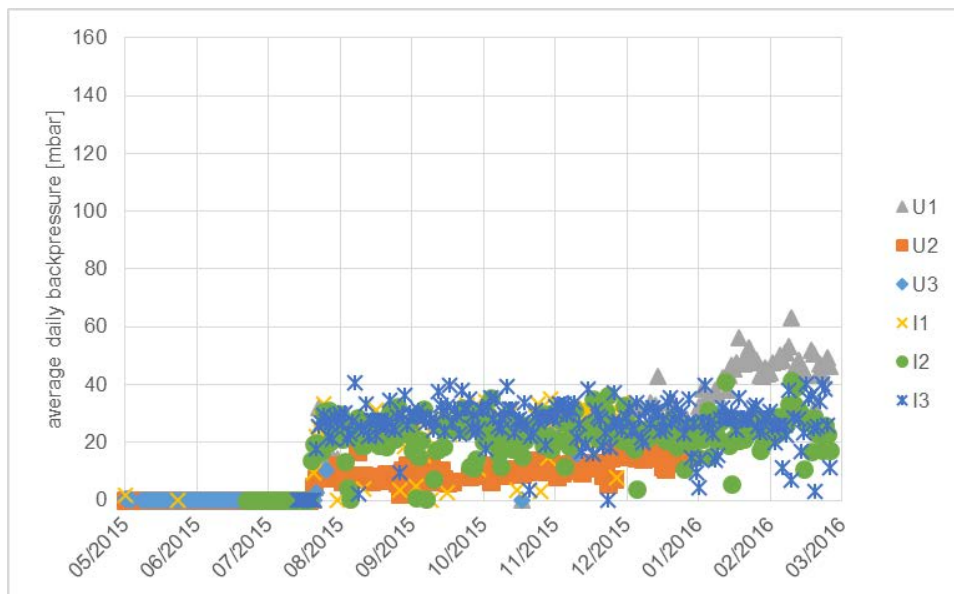


Figure 9: Backpressure increase due to DPF: buses U1, U2, U3, I1, I2 and I3

Moreover, it should be noticed that DPF was installed replacing the bus silencer, which also imposed some resistance to exhaust gases flow. In this manner, the actual backpressure increase due to DPF retrofitting is somewhat lower.

Maintenance and drivability

The maintenance actions of the vehicles of the pilot group were compared with that of the control group. No influence of DPF retrofitting on the maintenance operations, as well as their frequency was detected till now. Moreover, drivers didn't report on any deterioration in buses drivability.

Conclusions

Comparison of the measured engine-out and tailpipe nanoparticle number concentrations clearly demonstrates the potential of nanoparticle emissions mitigation by DPF retrofitting. The average values of PNFE were found to be higher than 97% for all the measured bus operating regimes. Low idle regime presents slightly lower efficiencies, possibly because of the higher agglomeration values at this regime. It was also noticed that DPF's PNFE values are somewhat higher for intercity coaches.

The increase of fuel consumption due to DPF retrofitting was found to be 2.5% and 2.1% for intercity and urban buses, respectively.

The backpressure values measured upstream a DPF after retrofitting lay below 60 mbar after half a year of buses operation with retrofitted DPFs and don't approach the limit value of 150 mbar. No deterioration in vehicle drivability was reported, as well as unusual repairs or changes in maintenance volumes.

Acknowledgments

The authors are grateful to the Egged Transportation Company for the financial support that made this work possible and readiness to contribute to the efforts toward air quality improvement. Special thanks to VERT Association for the fruitful cooperation and assistance in the experiments carrying-out.

References

- Allansson, R., Blakeman, P. G., Cooper, B. J., Phillips, P. R., Thoss, J. E., & Walker, A. P. (2002). The use of the continuously regenerating trap (CRTTM) to control particulate emissions: minimising the impact of sulfur poisoning. SAE paper, 01-1271.
- Boffetta, P., & Silverman, D. T. (2001). A meta-analysis of bladder cancer and diesel exhaust exposure. *Epidemiology (Cambridge, Mass.)*, 12(1), 125–30.
- BJ Cooper, HJ Jung and JE Thoss, US Patent 4,902,487 (1990) Cooper, B. J., Jung, H. J., & Thoss, J. E. (1990). US Patent 4,902,487.
- Dellinger, B., D'Alessio, A., D'Anna, A., Ciajolo, A., Gullett, B., Henry, H., ... Zimmermann, R. (2008). Report: Combustion Byproducts and Their Health Effects: Summary of the 10th International Congress. *Environmental Engineering Science*, 25(8), 1107–1114.
- Dockery, D. W., Pope, C. A., Xu, X., Spengler, J. D., Ware, J. H., Fay, M. E., ... Speizer, F. E. (1993). An association between air pollution and mortality in six US cities. *New England Journal of Medicine*, 329(24), 1753–1759.
- Lelieveld, J., Evans, J. S., Fnais, M., Giannadaki, D., & Pozzer, A. (2015). The contribution of outdoor air pollution sources to premature mortality on a global scale. *Nature*, 525(7569), 367-371.
- Maricq, M. M., & Xu, N. (2004). The effective density and fractal dimension of soot particles from premixed flames and motor vehicle exhaust. *Journal of Aerosol Science*, 35(10), 1251-1274.
- Mayer, A. (2008). *Particle filter retrofit for all diesel engines*. (Vol. 97). Expert Verlag. Germany
- Pope III, C., & Dockery, D. (2006). Health effects of fine particulate air pollution: lines that connect. *Journal of the Air & Waste Management Association* 56.6 (2006): 709-742.
- Tartakovsky, L., Czerwinski, J., Aleinikov, Y., Aronov, B., Baibikov, V., Gutman, M., Veinblat M. and Zvirin Y. (2004). Retrofitting of urban buses in Israel with particulate traps – first results. Proc. of the 13th World Clean Air and Environmental Protection Congress (IUAPPA), Transport, Environment and the Sustainable City, Paper No. 1, 6p, London (UK), August 22-27, 2004.
- Tartakovsky, L., Baibikov, V., Comte, P., Czerwinski, J., Mayer, a., Veinblat, M., & Zimmerli, Y. (2015). Ultrafine particle emissions by in-use diesel buses of various generations at low-load regimes. *Atmospheric Environment*, 107, 273–280.
- UNECE (United Nations Economic Commission for Europe). (2010). Addendum 82: Regulation No. 83 Revision 4 - Uniform provisions concerning the approval of vehicles with regard to the emission of pollutants according to engine fuel requirements, (March 1958).
- UNECE (United Nations Economic Commission for Europe). (2013a). Addendum 48: Regulation No. 49 Revision 5 – Amendment 1 - Uniform provisions concerning the measures to be taken against the emission of gaseous and particulate pollutants from compression- ignition engines for use in vehicles, and the emission of gaseous pollutants from positive-ignition engines fuelled with natural gas or liquefied petroleum gas for use in vehicles.
- UNECE (United Nations Economic Commission for Europe). (2013b). Addendum 48: Regulation No. 49 Revision 5 - Uniform provisions concerning the measures to be taken against the emission of gaseous and particulate pollutants from compression- ignition engines for use in vehicles, and the emission of gaseous pollutants from positive-ignition engines fuelled with natural gas or liquefied

petroleum gas for use in vehicles.

Vermeulen, R., Silverman, D. T., Garshick, E., Vlaanderen, J., Portengen, L., & Steenland, K. (2014). Exposure-response estimates for diesel engine exhaust and lung cancer mortality based on data from three occupational cohorts. *Environmental Health Perspectives (Online)*, 122(2), 172.

VERT Filter List (2015), www.vert-certification.eu

Ware, J. H., Thibodeau, L. A., Speizer, F. E., Colóme, S., & Ferris Jr, B. G. (1981). Assessment of the health effects of atmospheric sulfur oxides and particulate matter: evidence from observational studies. *Environmental Health Perspectives*, 41, 255.

PM10 emission effects of new studded tyre regulations

Mats GUSTAFSSON*, Olle ERIKSSON*, Karl Idar GJERSTAD**, Martin JUNEHOLM***, Brynhild. SNILSBERG** and Bruce DENBY****

* Swedish National Road and Transport Research Institute, Linköping, SE-58195, Sweden, Fax +46 13 14 14 36 – email : mats.gustafsson@vti.se

** Norwegian Public Roads Administration, Oslo, NO-0033, Norway

***Swedish Transport Administration, Borlänge, SE-781 89, Sweden

**** The Norwegian Meteorological Institute, Oslo, NO-0313, Norway

Abstract

Emissions from road wear is an important contributor to PM10 concentrations in the Nordic countries. Due to new regulations and an alternative test method for approval, studded tyres on the market presently have stud numbers ranging from 96 to 190 studs per tyre (at 205/55R16). In the present study, the particle generation from studded tyres was tested in the VTI road simulator. The results show that the tyre with the most studs (190) generates significantly higher PM10 levels than all other tyres, whilst the tyre that generates the least mass of inhalable particles has 96 studs and follows the stud number regulations. Increased number of studs and increased stud force significantly increases the concentration of PM10. Temperatures in the tyre, pavement and air as well as relative humidity also have an effect on the particle levels. A calculation example using the NORTRIP emission model demonstrated that the effect of variations in the studded tyre wear on both PM10 - levels and the number of limit value exceedances for the current data set used was significant.

Keys-words: *studded tyres, regulation, wear, PM10, NORTRIP.*

Introduction

New restrictions on the number of studs on studded tyres were introduced in Sweden and Finland in 2013. Regulations now allows 50 studs per meter rolling circumference. Alternatively, the tires can be tested in a special wear test, the so-called over-run test, to be approved. This has resulted in that studded tyres following the regulations, but also tyres that pass the over-run test, even though they have considerably more spikes, are present on the market. The over-run test shall ensure that the tested tire will not cause more road wear than a tire with a maximum of 50 studs per meter rolling circumference. Since studded tires are a major source of inhalable particles (PM10) in road and street environments, it is of interest to investigate the difference between the various studded tyre types also from particle emission point of view.

1. Methods

In the present study, the particle generation from seven studded tyres was tested in the VTI road simulator (Figure 1). The road simulator (Figure 1) consists of four wheels that run along a circular track with a diameter of 5.3 m. A separate motor is driving each wheel and the speed can be varied up to 70 km h⁻¹. An excentric movement of the vertical axis is used to slowly side shift the tyres over the full width of the track. Any type of pavement can be applied to the simulator track and any type of tyre can be mounted on the axles. An internal air cooling system is used to temperate the simulator hall to below 0°C. From wear studies it is well known that the wear in the simulator is accelerated but with a good correlation to test surfaces of the same pavements on real road (Jacobson och Wågberg, 2007).

A pavement ring, including 14 different asphalt pavements with different rocks, and constructions, tested for wear in a previous research project was used for the tests. The pavements were mainly stone mastic asphalts (SMA), some with rubber modified bitumen.



Figure 1. The VTI road simulator. Photo: Mats Gustafsson, VTI.

The studded tyres used in the tests were of four types:

1. Studded tyres complying with current regulations in Norway today and regulations in Sweden and Finland before 1/7 2013. 130 studs
 - a. Nokian Hakkapeliitta 5
2. Studded tyres complying with regulations in Sweden and Finland after 1/7 2013, but has passed the over-run test. 130 studs
 - a. Pirelli Ice Zero
 - b. Goodyear Ultragrip Ice Arctic
 - c. Continental Ice Contact
3. Studded tyres complying with new regulations in Sweden and Finland after 1/7 2013. 96 studs
 - a. Michelin X-Ice North
 - b. Gislaved Nord Frost 100
4. Studded tyres that have passed the over-run test despite more studs than both old and new regulations. The only tyre not approved in Norway but with an exemption. 190 studs.
 - a. Nokian Hakkapeliitta 8

Tyre 4.a. is used as a reference tyre in the tests.

All tyres were tested at 50 km/h in a statistically optimal sequence for comparing tyres (Table 1) during four test days where various order of tyres used each day of testing. For details on choice of experiment design, see Gustafsson & Eriksson (2015). PM10 were measured during the experiments,

as well as environmental parameters (temperature and humidity). In the statistical analysis of particle data was partly analysed as constants and partly as depending on ambient and tyre-specific parameters.

Table 1. Chosen design for analyses. Bold numbers refer to a certain set of tyres.

Day	Order during day				
	1	2	3	4	5
1	4	1	0	5	4
2	2	0	6	1	2
3	0	3	5	6	0
4	3	1	4	2	3

Test time series data for PM10 for all four test days are shown in figures in Appendix C. The results of the regression analysis are shown in Table 6.

Table 2. Results of the regression analysis of PM10 -data.

	Estimate	Std. Error	t value	P-value
<i>Intercept day1</i>	12.78	0.56	22.93	0.000
<i>Slope day1</i>	-0.43	0.15	-2.90	0.027
<i>Intercept day2</i>	11.92	0.51	23.48	0.000
<i>Slope day2</i>	-0.36	0.15	-2.47	0.048
<i>Intercept day3</i>	10.96	0.52	20.94	0.000
<i>Slope day3</i>	-0.24	0.15	-1.61	0.158
<i>Intercept day4</i>	9.62	0.58	16.59	0.000
<i>Slope day4</i>	0.14	0.15	0.94	0.385
<i>Pirelli compared to ref</i>	-2.55	0.40	-6.41	0.001
<i>Goodyear compared to ref</i>	-4.03	0.40	-10.04	0.000
<i>Continental compared to ref</i>	-2.75	0.40	-6.89	0.000
<i>Michelin compared to ref</i>	-3.82	0.40	-9.62	0.000
<i>Gislaved compared to ref</i>	-6.51	0.41	-15.92	0.000
<i>Nokian Hakka 5 compared to ref</i>	-1.77	0.41	-4.32	0.005

2. Results

2.1 Statistical analyses of PM10 data

The PM10 data are shown in Figure 2. The bullets show the observations and the circles show the fitted values. The vertical distances between circles and bullets are estimates of the random variation. The reference lines represent the general behavior during the days, which is also the fitted emission for the reference tyre if it would have been tested on any day as any number within day.

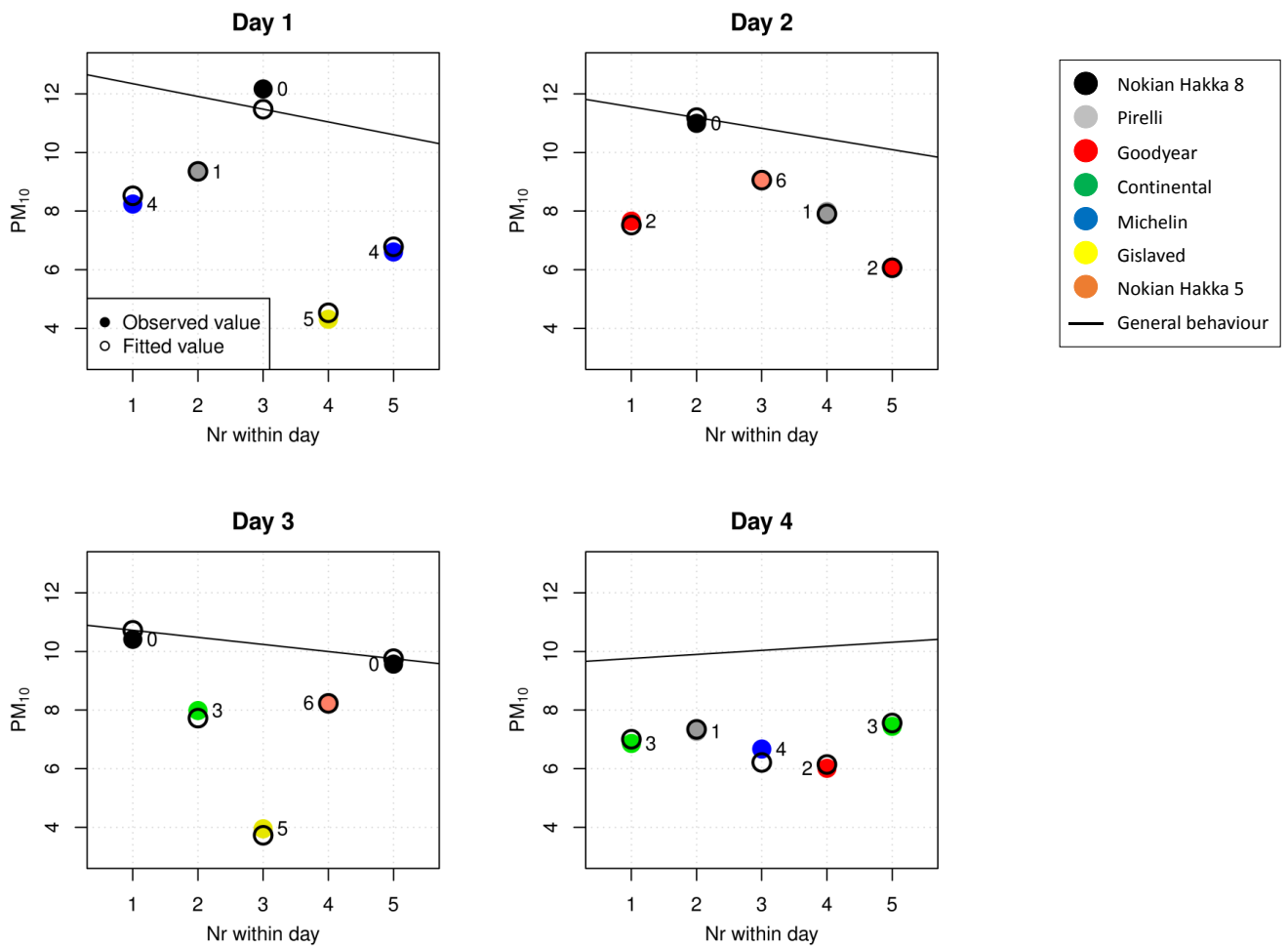


Figure 2. Observed and fitted PM₁₀ values with tyre labels for all days.

Looking at the results in order from highest to lowest emission, we observe that the tyres can be divided into 4 groups (Table 3 and Figure 3), where the tyres within groups do not differ significantly on 5 % level while the P-values between closest neighbors in groups are written in the list. P-values are not corrected for multiple comparisons.

Table 3. Significantly separated tyre groups for PM₁₀ results.

Group	Tyre	Type
1	Nokian Hakka 8	4
<i>0.005</i>		
2	Nokian Hakka 5	1
2	Pirelli	2
2	Continental	2
<i>0.043</i>		
3	Michelin	3
3	Goodyear	2
<i>0.003</i>		
4	Gislaved	3

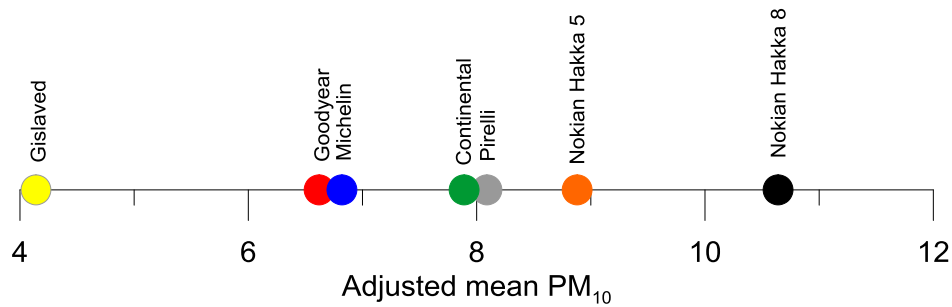


Figure 3. Order of adjusted mean PM10.

2.2 Results for tyre properties and experimental environment

The data supports that a model that does not use stud weight or any interactions is a good choice for PM10. This model is also supported by current knowledge about which variables causes PM10 emissions.

Table 4. Results of statistical analysis of parameters influencing PM10.

	Estimate	Std.Error	P(> t)
(Intercept)	-23.294	26.319	0.397
Road temp ($mg\ m^{-3}C^{\circ-1}$)	-2.323	1.289	0.102
Air temp ($mg\ m^{-3}C^{\circ-1}$)	3.132	1.185	0.025
Humidity ($mg\ m^{-3}\%^{-1}$)	0.135	0.052	0.026
Tyre temp ($mg\ m^{-3}C^{\circ-1}$)	-0.709	0.247	0.017
Speed ($mg\ m^{-3}km/h^{-1}$)	0.298	0.460	0.532
Mean protrusion during test ($mg\ m^{-3}mm^{-1}$)	2.273	1.423	0.141
Number of studs ($mg\ m^{-3}stud^{-1}$)	0.047	0.010	0.001
Stud force ($mg\ m^{-3}N^{-1}$)	0.037	0.009	0.002
Rubber hardness ($mg\ m^{-3}shore^{-1}$)	-0.133	0.075	0.107

R^2 for this analysis is 0.952. The first set of variables describes the environment. Three significant result can be seen, that PM10 emission increase with higher air temperature and humidity and decrease with higher tyre temperature. The second set of variables describes the tyres. Emissions increase with higher number of studs and higher stud force, and decrease with higher rubber hardness (not significantly, though). Possibly, the studs wearing of the surface should be expressed as the number of studs times the stud force, but adding this interaction to the model did not improve the explanation significantly.

Two types of analyses have been done here. The first type only models tyre effects as constants, the second tries to describe the tyre effects as a function of stud weight etc. Both have high R^2 , indicating that both models fit good to the data. Also, in Figure 2, the similarity in level and pattern between circles and bullets indicate that the model fits well and has the same structure as the data.

2.3 Estimation of implications for air quality

Laboratory results in a road simulator are, naturally, not directly applicable for estimating effects on air quality in cities by changing type of studded tyre. Using the NORTRIP emission model, where road wear is included together with meteorological, road operation and traffic related parameters and processes can be used for a rough estimate of effects on PM10 emission for a certain street for changes in road wear (Denby et al., 2013a; Denby et al., 2013b). In Figure 4, a dataset for Hornsgatan in Stockholm, for the winter season 2012-2013, has been used as an example. Hornsgatan is one of the most polluted streets in Stockholm and a studded tyre ban has been in use for some years. Despite the ban, the studded tyre use is about 30 % during the winter season. In the rest of Stockholm the figure is about 50 %.

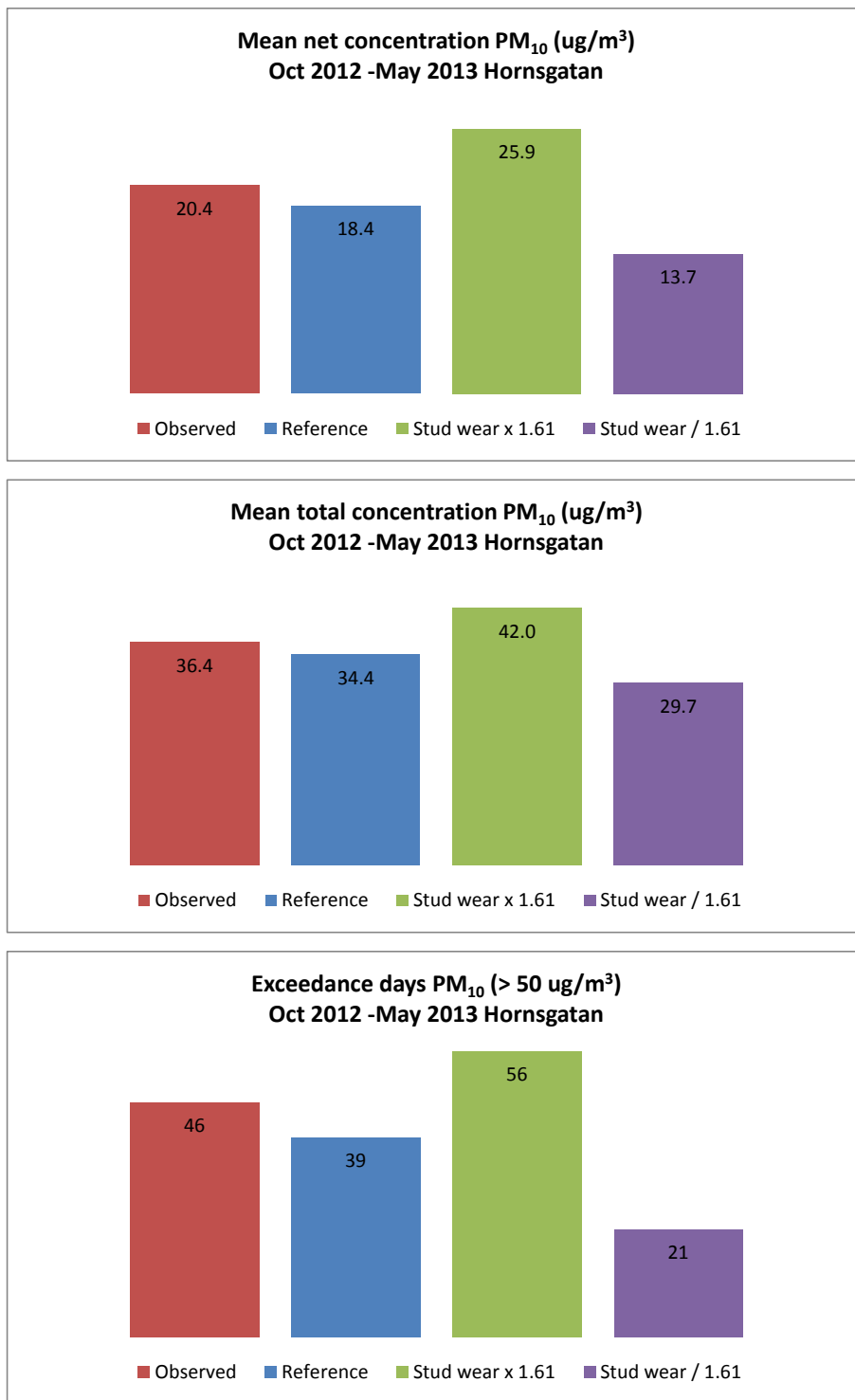


Figure 4. Effects on mean net and total PM₁₀ as well as on limit value exceedance days on Hornsgatan, Stockholm of 1.6 times span of the reference wear (see text for explanation).

The modelled PM₁₀ concentrations in a situation where everyone using studded tyres used the lowest and the highest emitting tyres in this study is shown in comparison to the observed and the modelled reference concentrations. The modelled reference is the wear and resulting PM₁₀ emission that the model produces when using standards settings for studded tyre use and wear. The highest emitting tyre has about 2.6 times higher PM₁₀ emission than the lowest emitting tyre. The modelled reference is the wear used in the model. If the reference road wear is assumed to be on a level right between the results of the tyres used in this test, the highest emitting tyre is 1.6 times higher than the reference and the lowest emitting tyre 1.6 times lower. Figure 4 shows the results of this calculation on the mean total PM₁₀ concentration and the number of exceedances of the PM₁₀ directive during

October – May. The increase in net (only the local contribution of PM10 from the street environment) and mean total (including background PM10) PM10 concentration is 41 and 22 % respectively compared to the reference case and the limit value is exceeded 17 more days. The corresponding decrease is 25 and 14% and 18 exceedance days less.

3. Discussion

All studded tyres tested emit PM10 when wearing the pavement ring, but there are significant differences related to tyre and tyre properties.

The road simulator is a laboratory equipment and as such not directly comparable to reality. The main draw-back of the simulator is the small diameter inducing a rather sharp curve of the track. This, in turn generates a turn-slip motion in the contact between the tyres and the pavement, which is not equivalent to normal driving. As mentioned in the methods chapter, studies at VTI despite this have shown very good correlation between the studded tire wear on the road and in the machine. Jacobson & Wågberg (2007) reported a coefficient of determination (R^2) from 0.93 to over 0.95.

Two types of statistical analyses have been used. The first type only models tyre effects as constants, the second tries to describe the tyre effects as a function of stud weight etc. Both have high R^2 , indicating that both models fit good to the data. The particle emissions have about the same level each day and not a steep slope. The experiment behaves similar from day to day without any major drift during any day. Also the drift during the days does not have the same direction each day meaning that there is no sign of a problem of an ongoing drift in the experiment or the environment itself that reoccurs on each day.

Regarding the tyre properties significantly affecting PM10, higher stud weight and stud number increased both while harder rubber decreased the concentrations. A combination of both stud weight and number of studs into “stud mass per tyre”, did not improve the model results. The higher stud weight and number of studs are expected to increase the emissions of wear particles. Rubber hardness, and especially its relation to temperatures are harder to interpret. While higher temperature in tyres and/or pavement should make materials softer and more yielding, which should result in lower wear, harder rubber should also result in higher wear, which is not the case. An interaction is suspected but has not been further analysed. An alternative speculation is that the turn-slip movement of the studs in the simulator is reduced by higher rubber hardness and therefore results in lower wear particle emissions.

The Nokian Hakkapeliitta 8 is producing more PM10 than the rest of the tyres. Even though the stud weight is lower, the number of studs are more than double than the tyres with the lowest number of studs. It also has the softest rubber, which might affect both the movement of the studs in the turn-slip contact and the ability to suspend dust on the tests track surface. The Gislaved tyre is at the other end of the PM10 emission scale and has 96 studs per tyre together with the Michelin tyre. The significantly lower production of PM10 indicate an additional property affecting the emission, which is not covered by the statistical analyses. The shape of the stud pin (trident star) might be an explanation, but a quantitative estimate of the importance of the shape has not been feasible in this study.

The Goodyear tyre has 130 studs and a higher stud protrusion than the rest of the tyres, but still ranks as the second lowest emitting tyres. Compared to the two other tyres of type 2, it has a harder rubber. The Pirelli, Continental and Nokian Hakka 5 tyres have similar emission of PM10. Generally, the type 3 tyres with fewer studs per tyre emit less particles than the rest, except for the Goodyear tyre.

The NORTRIP modelling example shows that the effects on local air quality would be large if all studded tyres were swapped to new low or high PM10- emitting tyres, but the result should be seen as merely an indication since there are many uncertainties to this estimate. E.g. it is not known if the assumption that today's studded tyre fleet is actually emitting PM10 in between the two extremes in this specific test.

Conclusion

The combined approval procedure of both regulations and an approval test have resulted in high variation of number of studs in studded tyres. The statistical analysis showed that PM10 levels produced by the tyres could be sorted in four significantly different groups, where the tyre with most studs

(approved through the test method) emitted most PM10 while one of the tyres with least number of studs had the lowest emissions. Emissions increase with higher number of studs and higher stud force. Environmental factors also affect the PM10 emissions, which increase with higher air temperature and humidity and decrease with higher tyre temperature. A model simulation for a single street using the NORTRIP model shows a relatively large effect of the span in PM10 emission within this specific range of tyres.

Acknowledgments

This work was financed by The Swedish Transport Administration and The Norwegian Road Authority. The authors would like to thank Tomas Halldin for running and maintaining the road simulator.

References

- Denby BR, Sundvor I, Johansson C, Pirjola L, Ketzel M, Norman M, Kupiainen K, Gustafsson M, Blomqvist G, Kauhaniemi M, Omstedt G. (2103a): A coupled road dust and surface moisture model to predict non-exhaust road traffic induced particle emissions (NORTRIP). Part 2: Surface moisture and salt impact modelling. *Atm. Env.*, vol. 81, p 485-503.
- Denby BR, Sundvor I, Johansson C, Pirjola L, Ketzel M, Norman M, Kupiainen K, Gustafsson M, Blomqvist G, Omstedt G. (2013b): A coupled road dust and surface moisture model to predict non-exhaust road traffic induced particle emissions (NORTRIP). Part 1: Road dust loading and suspension modelling. *Atm. Env.*, vol. 77, p 283-300.
- Jacobson T, Wågberg L. Utveckling och uppgradering av prognosmodell för beläggningsslitage från dubbade däck samt en kunskapsöversikt över inverkan faktorer. *VTI-notat 7*. Swedish National Road and Transport Research Institute, Linköping, Sweden, 2007.

Particle mass size distribution relation to train traffic and type in a railway tunnel

Mats GUSTAFSSON*, Göran BLOMQVIST*, Anders GUDMUNDSSON**, Sara JANHÄLL*, Christer JOHANSSON*** & ****, Michael NORMAN***, Ulf OLOFSSON*****

* Swedish National Road and Transport Research Institute, Linköping, SE-58195, Sweden, Fax +46 13 14 14 36 – email : mats.gustafsson@vti.se

** Department of Ergonomics and Aerosol Technology, Lund University, Lund, SE-22100, Sweden

*** SLB-analys, Box 8136, Stockholm, SE-10420, Sweden

**** Department of Environmental Science and Analytical Chemistry (ACES), Stockholm University, Stockholm, SE-10691, Sweden

***** Department of Machine Design, Royal Institute of Technology (KTH), Stockholm, SE-10044, Sweden

Abstract

Concentrations of inhalable particles (PM₁₀) have been shown to be exceptionally high in railroad and subway tunnel environments. The elemental composition usually indicates that particles originate in wear from rails, wheels, brake systems and pantographs. To be able to study and abate the contribution to PM₁₀ from different train types, or even individual train sets, detailed traffic data is needed. Most studies are from subways where train types are rather uniform. This study was made in a rail road tunnel, where five different train types traffic the platform. A measurement system for train passages was set up and the data combined with traffic data from the Swedish Transport Administration to pinpoint if certain train types or individual train sets are more important than others for high PM₁₀ concentrations. The results show that an older type of train, with mechanically braking wagons seem to produce most peaks of high PM₁₀ concentrations.

Key-words: railroad, PM₁₀, size distribution, train type.

Introduction

Even though not trafficked by combustion vehicles, high levels of particulate air pollution have been recognized in several railroad environment, especially in subway stations, e g Stockholm, London, New York city, Tokyo, Helsinki, Mexico City, Taipei, Prag, Budapest, Seoul and Rome (Aarnio et al., 2005; Birenzvice et al., 2003; Johansson and Johansson, 2003; Ripanucci et al., 2006; Seaton et al., 2005, Nieuwenhuijsen et al 2007, Kim et al, 2008, Raut et al., 2009; more references are given in Abbasi et al. (2013) and Järholm et al., 2013). Typically, super-micron particles generated during mechanical wear dominate the particle mass concentration. Wheels, rails and brake systems are dominating sources and particles consist to a large part of different oxidized forms of iron. In a Stockholm subway station around 60% of the PM₁₀ was found to be iron or iron oxides, both magnetite (Fe₃O₂) and hematite (Fe₂O₃) (Johansson, 2005). Many other trace metals and metalloids have been found in elevated concentrations in subway environments, e g chromium, nickel, arsenic, calcium, barium, copper, antimony and aluminium (e g Querol et al., 2012). Also organic material has been identified.

While rails and wheels mainly consist of iron, brake wear systems have diverse techniques and compositions with potential to emit both different amounts of wear particles and with different compositions. The variation in contribution to PM₁₀ from different trains and even from individual train sets might be high depending on brake system and brake materials used as well as on the maintenance state of the systems.

The aim of this study was to investigate the relation between particle emission and properties and train types trafficking a railroad tunnel.

1. Methods

The subterranean station Arlanda Central (C) is situated north of Stockholm below Arlanda airport. The platform is 400 m long with one track on both sides with traffic in opposite directions. The tunnel is approximately 5 km long and the station is trafficked by mixed long distance, regional and commuter trains passing the airport. The tunnels are self-ventilated. The only active ventilation is smoke evacuation fans only activated if fire occurs.

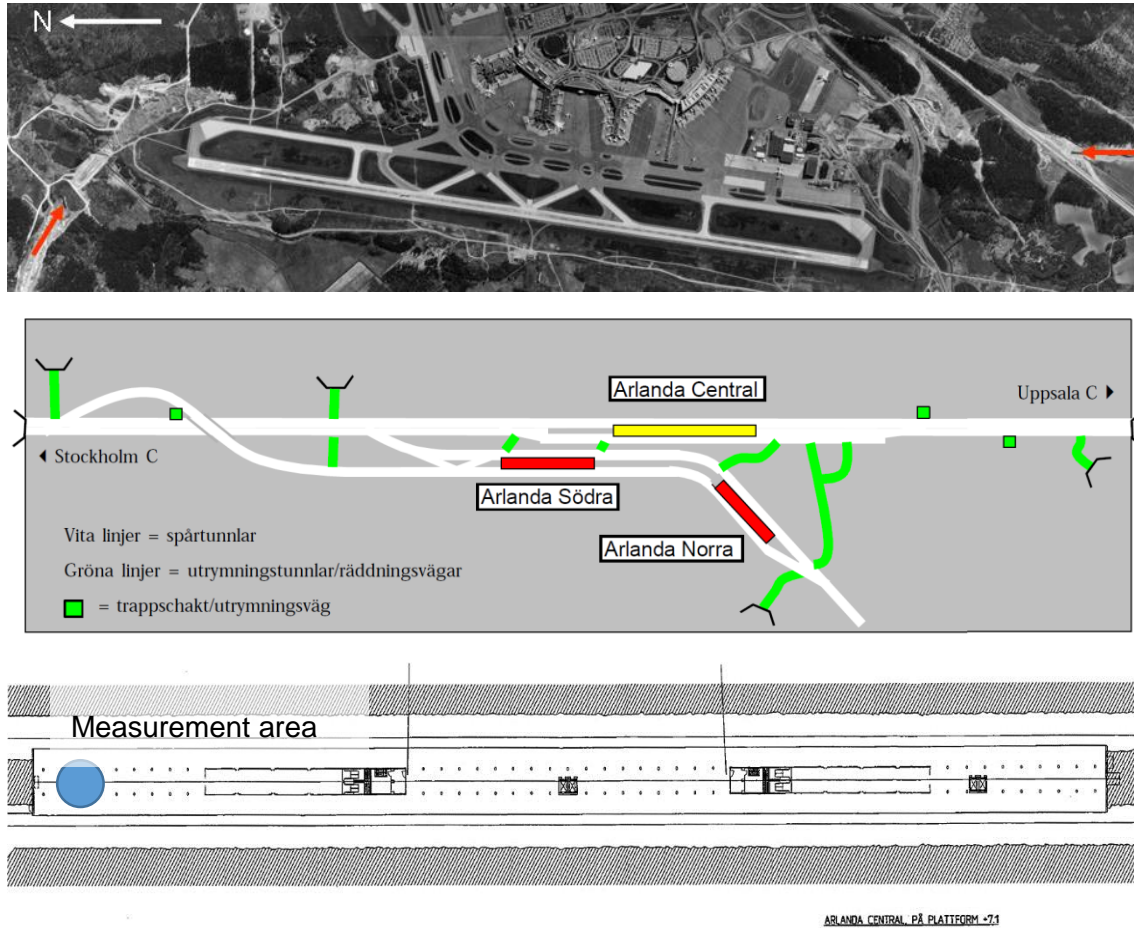


Figure 1. Arlanda tunnel and its entrances (upper) and Arlanda C platform with placement of the measurements.

The traffic in the tunnel is a mix of electrical trains, from long distance to commuter trains of different age and construction (Figure 2).



Figure 2. Train types trafficking Arlanda C. All photos from järnväg.net.

Apart from these electric trains, different types of maintenance vehicles traffic the tunnel, mainly in night time, when there is no regular train operations ongoing. These vehicles can be either electrically or diesel driven.

The train traffic at Arlanda C was detected by a photocell equipment designed at VTI registering each train arrival approximately 10 meters before the Arlanda C train station platform at each track (track 1= northbound, track 2 = southbound). The two rays were placed perpendicular to the rail, two meters apart, why the speed could be calculated. Since both the train front speed (by disrupting the rays) and train aft speed (by resuming the rays) could be calculated, the train length and speed retardation could be calculated. The photocells (brand: IR transmitter IFM Efector 200 OA5101, IR receiver IFM Efector 200 OA5102) were fixed two meter apart on aluminum rods held by two tripods at approximately 130 cm above the rails (Figure 3). The timing of ray disruption and resuming was logged by a TA89-logging equipment (VTI notat T147). During the measurement period 2013-01-28–2013-02-11, a total of 885 northbound and 959 southbound train arrivals were registered. Train definitions are: Length 20–400 m, acceleration/retardation between 2 and -2 m s^{-2} , front speed above 2 m s^{-1} . Using the traffic system LUPP (access provided by the Swedish Transport Administration), it was possible to identify each train registered by the traffic measurements system.



Figure 1. Train traffic counting equipment in the tunnel. Measurement rays across the rail is indicated by red lines in the photo.

Monitoring of PM₁₀ was performed using tapered element oscillating microbalance (TEOM) instruments (Thermo Fischer Inc., USA, model 1400a). The inlet at Arlanda were placed 2 m above the platform. Particle size distributions over the range 0.523-14.6 μm were measured using TSI Aerodynamic Particle Sizer (TSI APS 3321) and are presented as mass distribution. The time resolution for APS was 20 s. In the conversion from number to mass, a particle density of 5.0 kg m^{-3} is used for particles > 0.5 μm (density of iron oxide). For APS the Stokes correction was used which corrects for APS's overestimate of the particle size when the particle density is much higher than 1.0 kg m^{-3} .

2. Results

Traffic density shows obvious traffic peaks in the morning and afternoon (Figure 4), with a main minimum during late night and a secondary during mid-day. PM₁₀ concentration correlates reasonably well with traffic density ($R^2=0.58$ for hourly mean values).



Figure 4. Mean traffic density and mean hourly PM₁₀ concentration at Arlanda C.

The average mass size distribution of PM10 at Arlanda C is unimodal and peaks at slightly above 2 μm (Figure 5). From data on time series of particle size distributions, trains related to peaks in mass size distributions of PM10 have been identified on individual level using the LUPP-system and traffic data collected during the measurements. In Figure 6, a size distribution time series from the APS instrument during one day (February 3rd, 2013) is shown. On this scale, pinpointing the arrival of RC-trains (older trains with locomotive and coaches) seem to initiate mass peaks of the coarse fraction detected by the APS. It can also be seen that the arrival of the specific train set RC6 1419 three times during the day in Figure 6 results in similar particle mass peaks with a maximum around 3-4 μm , while other RC trains are connected to finer mass peaks.

In opposite to the irregular arrival pattern of the regional trains (RC, X40 and X55), the X60 commuter trains arrive almost simultaneously from both directions every 30 minutes between 8 AM to 11 PM. The lack of periodically recurring mass concentration peaks that coincide with the periodical commuter traffic indicates that these train sets are not major particle sources. Also the X50/X55 and the X40 train sets seldom coincide with particle peaks, but are harder to discern from the RC arrivals.

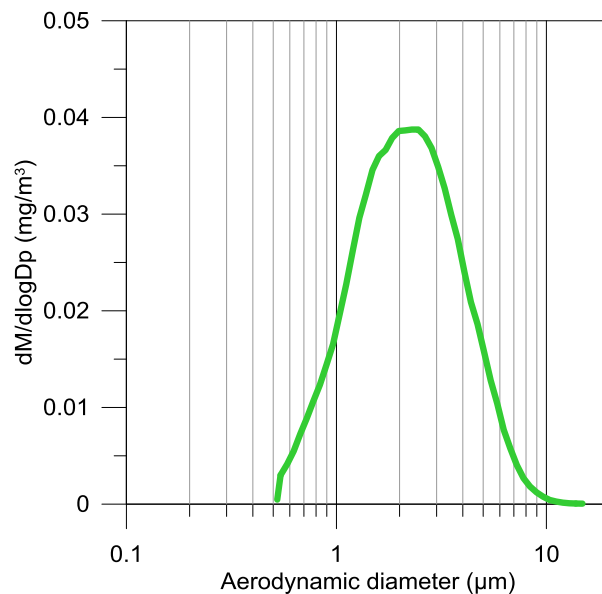


Figure 5. Mean mass size distribution for PM10 at Arlanda C.

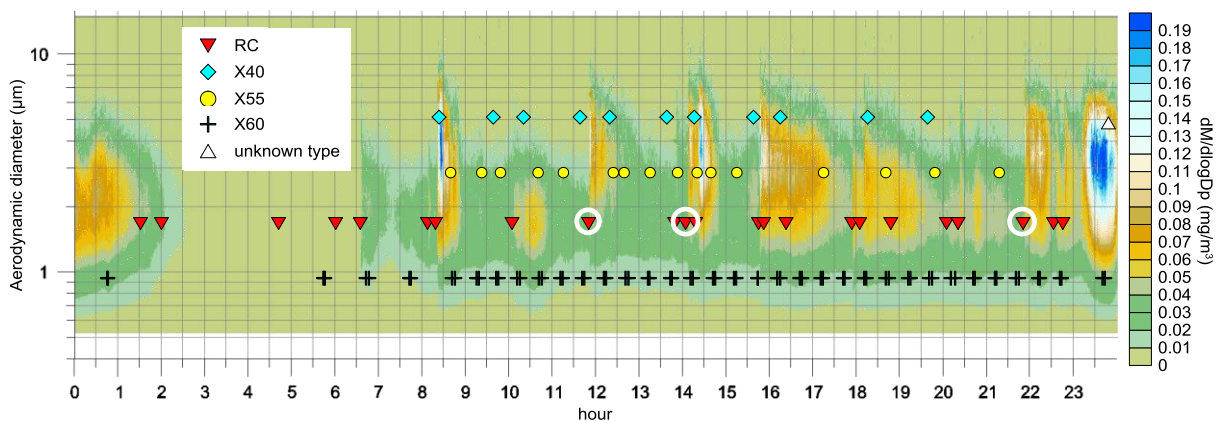


Figure 6. Mass size distributions and train type passages at Arlanda C during February 3rd, 2013. White rings indicate passages of the train RC6 1419.

3. Discussion

This study shows that electric train sets emit PM10 when trafficking an underground station and different train types and individuals are connected to different concentration peaks. The older type of trains (RC) are more often connected to high particle concentrations than other, more modern train sets.

A possible explanation for the connection between particle peaks and RC trains, is that the RC trains have longer braking time and also more individual behaviour since braking time depends on the number of wagons that are mechanically braked. Also in terms of electrical braking the RC locomotives are different since the locomotive itself is electric braked and the wagons are mechanically braked. The longer braking time may also make the particle emissions from the RC trains longer and therefore also easier to detect depending on the sampling time of the instruments.

It is likewise obvious though, that not all RC trains are connected to high PM10 concentrations and that some other train types occasionally are connected to particle concentration peaks, indicating that there are differences in the systems emitting the particles and/or how systems are used during the deceleration before finally stopping at the station. Differences could be associated to materials, state of system maintenance or differences in driving pattern.

Even though not studied in this work, it is probable that emissions made in other parts of the tunnel might result in contaminated air pulses that are moved to the platform due to piston effects (Coke et al., 2000) and natural ventilation, which makes the interpretation of the data more complex.

From an air quality abatement perspective, it would be beneficial to reduce stops of RC trains in the tunnel, through exchanging them for more modern trains with electrical brakes or to modernize the wagon brake systems.

Conclusion

Electrical trains cause high concentrations of PM10 in tunnel platform environment. PM10 has a unimodal, mean mass distribution peaking at 2-3 μm . Data support that the older type of trains (RC), with mechanically braked wagons and longer braking time are responsible for most PM10 emission peaks. Since not all RC trains cause high PM10 concentrations, data could be used to identify the individual high- emitters to investigate the origin of particle sources. PM10 concentrations in the tunnel could be improved by reducing RC train stops or by identifying and abate high-emitting train sets.

Acknowledgments

This project was financed by BVFF, an industry program for research, development and innovations in road and railway construction and maintenance. The authors would like to thank Anna Kryhl at the Swedish Transport Administration for data out-take from LUPP and A-train for admittance to the platform, help and information during the work.

References

- Aarnio P, Yli-Tuomi T, Kousa A, Makela T, Hirsikko A, Hameri K, Raisanen M, Hillamo R, Koskentalo T, Jantunen M. (2005): The concentrations and composition of and exposure to fine particles (PM2.5) in the Helsinki subway system. *Atm. Env.*, vol. 39, p 5059-5066.
- Bigert C, Alderling M, Svartengren M, Plato N, de Faire U, Gustavsson P. (2008): Blood markers of inflammation and coagulation and exposure to airborne particles in employees in the Stockholm underground. *Occupational and Environmental Medicine*, vol. 65, p 655-658.
- Abbasi S, Sellgren U, Olofsson U. (2013): Technical note: Experiences of studying airborne wear particles from road and rail transport. *Aerosol and Air Quality Research*, vol. 13, p 1161-1169.
- Coke LR, Sanchez JG, Policastro AJ. (2000): A model for the dispersion of contaminants in the subway environment. *10th International Conference, Aerodynamics and Ventilation of Vehicle Tunnels*. Argonne National Lab., IL (US), Boston, MA (US).
- Johansson C. (2005): Källor till partiklar i Stockholms tunnelbana. SLB analys, Rapport 6-2005, Miljöförvaltningen i Stockholm, Stockholm (in Swedish).
- Johansson C, Johansson P-A. (2003): Particulate matter in the underground of Stockholm. *Atm. Env.*, vol. 37, p 3-9.

- Kim KY, Kim YS, Roh YM, Lee CM, Kim CN. (2008): Spatial distribution of particulate matter (PM10 and PM2.5) in Seoul Metropolitan Subway stations. Journal of Hazardous Materials, vol. 154, p 440-443.
- Nieuwenhuijsen MJ, Gomez-Perales JE, Colvile RN. (2007): Levels of particulate air pollution, its elemental composition, determinants and health effects in metro systems. Atm. Env., vol. 41, p 7995-8006.
- Querol X, Moreno T, Karanasiou A, Reche C, Alastuey A, Viana M, Font O, Gil J, De Miguel E, Capdevila M. (2012): Variability of levels and composition of PM 10 and PM 2.5 in the Barcelona metro system. Atmospheric Chemistry and Physics, vol. 12, p 5055-5076.
- Raut JC, Chazette P, Fortain A. (2009): Link between aerosol optical, microphysical and chemical measurements in an underground railway station in Paris. Atm. Env., vol. 43, p 860-868.
- Ripanucci G, Grana M, Vicentini L, Magrini A, Bergamaschi A. (2006): Dust in the underground railway tunnels of an Italian town. Journal of Occupational and Environmental Hygiene, vol. 3: p 16-25.
- Seaton A, Cherrie J, Dennekamp M, Donaldson K, Hurley JF, Tran CL. (2005): The London Underground: dust and hazards to health. Occupational and Environmental Medicine, vol. 62, p. 355-362.

REMI model: Bottom-up emissions inventories for cities with lack of data

Sergio Ibarra-Espinosa*, Rita Ynoue*

*Departamento de Ciências Atmosféricas, Instituto de Astronomia, Geofísica e Ciências Atmosféricas, Universidade de São Paulo, Rua do Matão, 1226 - Cidade Universitária São Paulo-SP - Brasil - 05508-090
email: sergio.ibarra@iag.usp.br

Abstract

*Emissions inventorying is a complex task with regulatory and/or scientific environmental purposes. In South American cities, when the task is performed, the common denominator is lack of data and documentation, and vehicles are usually the main source of pollutant of emerging and consolidated megacities. Therefore, emissions inventories is becoming more important, especially for mobile sources. In this manuscript we present the model REMI (**R-EM**issions-Inventory) for developing bottom-up emissions inventory for vehicles in cities with lack of data (Ibarra & Ynoue, 2016).*

The program was written in R (R CORE TEAM 2016) using several libraries. The program consists in several R scripts organized in folders with Inputs& Outputs. For traffic inputs uses counts or simulations, and also, it can be as a top-down method with statistical traffic information. REMI classifies vehicle data by fuel, size of motor, use and gross weight annually up to 50 years, according to EEA/EMEP guidelines and Copert (Ntziachristos, 2014). REMI has several options for emission factors, 1) Emission factors from Ntziachristos (2014), 2) local emission factors or 3) mixed emission factors. In the future REMI will include HBEFA emission factors. REMI also incorporates deterioration factors. Currently REMI estimate hot-engine emissions of 27 pollutants.

Keys-words: REMI, vehicular, emissions inventory, R, bottom-up.

Abstrait

*Emissions inventoriage est une tâche complexe avec des fins réglementaires et / ou scientifiques environnementales. Dans les villes d'Amérique du Sud, lorsque la tâche est effectuée, le dénominateur commun est le manque de données et la documentation, et les véhicules sont généralement la principale source de polluants des mégapoles émergentes et consolidées. Par conséquent, les inventaires d'émissions est de plus en plus important, en particulier pour les sources mobiles. Dans ce manuscrit, nous présentons le modèle REMI (**R-EM**issions-Inventaire) pour développer bottom-up inventaire des émissions pour les véhicules dans les villes avec le manque de données (Ibarra & You, 2016).*

Le programme a été écrit en R (R CORE ÉQUIPE 2016) en utilisant plusieurs bibliothèques. Le programme se compose de plusieurs scripts R organisés dans des dossiers avec entrées et sorties. Pour les entrées de trafic utilise les chiffres ou les simulations, et aussi, il peut être aussi une méthode descendante avec les statistiques de circulation. REMI classe les données VEHICULE par le carburant, la taille du moteur, l'utilisation et le poids brut annuellement jusqu'à 50 ans, selon l'EEE / lignes directrices de l'EMEP et Copert (Ntziachristos, 2014). REMI dispose de plusieurs options pour les facteurs d'émission, les facteurs 1) d'émission de Ntziachristos (2014), 2) les facteurs d'émission locaux ou 3) des facteurs d'émission mélangés. Dans l'avenir REMI comprendra des facteurs d'émission HBEFA. REMI intègre également des facteurs de détérioration. Actuellement REMI estimer les émissions à chaud moteur de 27 polluants.

Clés mots: REMI, véhicules, inventaire des émissions, R, bottom-up.

1. Introduction

“Emission Inventories always seem to be available at a very late point in time ... and are easily seen as the scapegoat if a mismatch is found between modeled and observed concentrations of air pollutants” Tim Pulles (2010). So, the task of emissions inventories compilation ideally should be faster enough in order that It can be updated before deadline. Emissions inventories, scientific or regulatory, must to be comprehensive, with quality and documented but all these requirements faces the common difficulty of lack of data. The uncertainty of estimation depends on the type of sources considered, because there are sources with required information more accesible than other. Per example, usually there are legal obligation that indubstries must report their emissions, like the Pollutant Release and Transfer Registry (PRTR) emissions inventory (<http://prtr.ec.europa.eu/>). But in other cases, sources like mobiles are hard estimate because vehicles are in movement in space. Vehicle emissions inventory can have a top-down approach with activity data as registered fleet, or can be bottom-up based on traffic simulations. Either case, there are inherent uncertainties and the agreement between top-down and bottom-up is hard to accomplish. In order to solve this problem, we developed the REMI model, for elaborating emissions inventories of vehicles, which can be adapted to the information that compiler has, and also is fast.

2. Objectives

To develop a model to estimate vehicular emissions based on road network

3. Method

Structure

REMI works with a working directory placed in any part of the computer and inside it there are folders “functions” and “data” and these folder divide in several sub-folders as showed in figure 1, where black words are folders and blue ones are files.

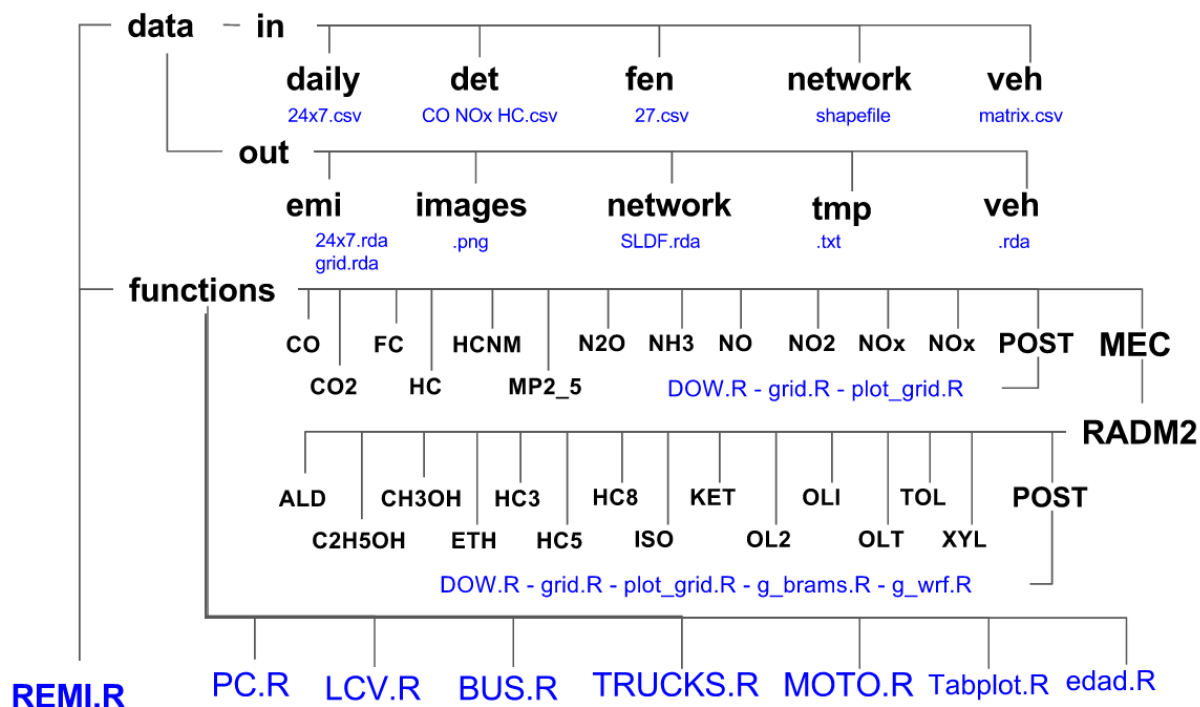


Figure 1. Structure of REMI.

This work consists in present the model REMI for developing bottom-up emissions inventory for vehicles in cities with lack of data (Ibarra & Ynoue, 2016). The program was written in R (R CORE TEAM 2016) using libraries sp (Bivand et al, 2013), rgeos (Bivand & Rundel, 2015), maptools (Bivand & Lewin-Koh, 2015), ggplot2 (Wickham, 2009) and ggmap (Kahle & Wickham, 2013). Activity: Reads traffic simulations, traffic counts and interpolates, or road network and assigns interpolation. Splits categories by fuel, size of motor, use and gross weight annually up to 50 years. Data classification is according to EEA/EMEP guidelines and Copert (Ntziachristos, 2014). The pollutants covered Are CO,

NO_x, NO₂, NO, HC, HCNM, PM_{2.5}, N₂O, NH₃, SO₂, CO₂, Fuel Consumption; and speciate HCNM according experimental analysis of tunnel emissions factors in São Paulo for Aldehyde (ALD), C₂H₅OH, CH₃OH, ETH, HC₃, HC₅, HC₈, HCHO, ISO, ketone (KET), OL₂, OLI, OLT, TOL and xylenos (XYL).

The file REMI.R works like a namelist where all scripts are called and include options to type of estimation, grid resolution for output, title of imags, etc. REMI.R has an order, first it calls NETWORK.R which produce “data/out/network/red.rda”, then the activity functions PC.R, LCV.R and so on. Each of these functions produce graphics with ggplot saved in “data/out/images/*.png”, tables saved in “data/out/tmp/*.txt ” and the most important, the activity saved in “data/out/veh/na_*.rda”. An advantage of working with .rda files instead of .csv or shapefiles is that it's possible save different objects with the same extension, and it's light and faster to load in R.

data

Input data

The input data are locate in “data/in” and the folders are daily, fen, det, network and veh.

daily: it contains files with a normalized profile at 08:00-09:00 of the traffic counts 24 hours from monday to sunday. There profiles for Passenger Cars (PC), Light Commercial Vehicles (LCV), Trucks and Buses. It depends on the available data, Ibarra & Ynoue (2016) used traffic counts of a near downtown toll station.

veh: it's a comma-delimited .csv file of 25 vehicles in circulation, that is, vehicles sales after applying survival functions for 50 years. It's a dataframe (R object to store data tables) with header indicating the type of vehicle.

fen: it's a .csv file, a dataframe very similar to veh.csv, but it counts emission factors to the 25 type of vehicles over 50 years of use. There is one file per pollutant.

det: it's a .csv file for the 25 vehicles over 50 years indicating deterioration ate year of use. There deterioration factors for CO, HC and NO_x.

network: it contains the road network in a spatial format. It can read virtually any spatial format with rgdal library being shapefile one of the most popular, but as it's called on REMI.R, it can be modified as the user prefers. The road network has mandatory fields depending if it's from openstreetmap or a traffic simulation. As traffic simulation varies greatly, here is presented the mandatory fields when performing an emissions inventory with traffic counts and openstreetmap:

- ⑩ “highway”: field with type of streets: “motorway”, “motorway_link”, etc.
- ⑩ “xlong1”: first longitude coordinate in EPSG:4326.
- ⑩ “xlong2”: last longitude coordinates in EPSG:4326
- ⑩ “ylat1”: first latitude coordinate in EPSG:4326.
- ⑩ “ylat2”: last latitude coordinate in EPSG:4326.
- ⑩ “longkm”: Length ot the link in km.

Output data

The input data are locate in “data/out” and the folders are emi, images, tmp, network and veh.

emi: it contains all the resulting emissions with 4 types:

1) emissions inventory tables according 5, 20 and 142 types of vehicles, df.rda, ta_cetesb.rda and E_df.rda, respectively. Also the same for RADM2 speciation: df_hcx.rda, ta_cetesb_hcx.rda and E_df_hcx.rda.

2) Hourly emissions by each link from Monday to Sunday to each pollutant,

3) Gridded emissions with resolution selected by compiler, hourly of a Monday (ex; g_NO₂.rda),

4) Two text files .txt of the gridded hourly emissions of a Monday. Each file has all the pollutants considering a RADM2 estimation. These files are used one generate WRF-Chem (DF_wrf.txt) (Grell *et al*, 2005) input data, an the other to BRAMS (DF_brams.txt) input data. These files require that the user indicate the time zone of the area where the emissions were estimated because it stores the emissions in GMT.

images: Here are stored all the images generated by different scripts. There are images of fleet distribution, emissions plot in bars, gridded emissions maps and network maps.

tmp: In this folder there are all the .txt tables generated indicating fleet, accumulated fleet, fleet by fuel standard, and also an emissions table ta_cetesb.csv.

network: It contains the file red.rda of the network which is a SpatialLineDataFrame (SLDF) format, in other words, an sp object. The following fields were added: "ID","V" the rush hour speed, "Vlibre" free flow speed, "Vmedia" the average speed between "V" and "Vlibre", "dcentro" which is the distance between the mid point of each link and the chosen center of the city, and "dcentroC" which is the same as "dcentro" with a limit in the distance calculation to avoid overestimation of trucks in streets far outside the city.

veh: it includes 5 files of activity level: na_bus.rda, na_lcv.rda, na_m.rda, na_pc.rda and na_trucks.rda. Each file contains the amount of vehicle in each link at 08:00-09:00 of a Monday to each type year of use, from 0 to 50 and by technological composition: na_pc.rda has 348, na_lcv.rda 171, na_trucks.rda 255, na_bus.rda 102 and na_m.rda 171.

functions

Here there are the vehicles function PC.R, LCV.R, TRUCKS.R, BUS.R and MOTO.R. These functions assign vehicles to the road network applying a survival function over 50 years of use and classifies by fuel, size, weight and emissions standard. These functions returns dataframes called na_pc.rda, na_lcv.rda, na_trucks.rdam na_bus.rda and na_m.rda as showed in last section. These functions also create fleet plots and dataframes saved as text files.

Other functions are Tabplot.R and edad.R. edad.R stores a wide range of survival functions resulting in different average years for each type of vehicle (PC, LCV, TRUCKS, BUS and MOTO). The user must choose the respective average age of the fleet. Tabplot.R is to plot emissions bar later after the estimation process ended, it reads df.rda.

There are also pollutant functions, that are the core functions of REMI. Each pollutant has a folder with scripts for the emission factors of each type of vehicle and also the estimations procedure, described in following section.

This folder also contains subfolders POST and MEC. POST include functions to produce SpatialLineDataFrames with 24 emissions for each day of the week, to generate grid with spatial resolution chosen by the user, and functions to plot grids with ggmap library. MEC the chemical mechanism, so far it has RAMD2 functions which speciate the Non-Methane HydroCarbons (NMHC) in fifteen pollutants Aldehyde (ALD), C2H5OH, CH3OH, ETH, HC3, HC5, HC8, HCHO, ISO, ketone (KET), OL2, OLI, OLT, TOL and xylenos (XYL), according experimental observations performed at Departament of Atmospheric Sciences of IAG/USP (<http://www.iag.usp.br/>). This folder includes a subfolder also called POST with same functions to the respective pollutants, but also includes two special functions to generate text files used to generate WRFR-Chem and BRAMS emissions inputs.

Finally, each folder has a delete.R function used to exclude temporary files.

Emissions estimation process

One all the activity .rda files were generated starts the emissions estimation process. In oder to clarify we present a small part of REMI.R

First, define the working directory and call the libraries.

Then it reads the road network with the respective spatial reference. It's important to note that the original road network could be in any spatial reference, but in order to run in REMI, it must be in EPSG:4326, which is WRG84 LAT LON.

Then are defined the considered latitude and longitude for center in order to calculate its euclidean distance with midpoint of each link (in future it will calculate the geographical (geodesic) distance) .when used the method of interpolation of traffic counts.

```
R> setwd("/your/path")
R> library(maptools); library(rgeos); library(ggmap);
R> red <- readShapeLines("data/in/network/sp.shp", proj4string=CRS("+init=epsg:4326"))
R> xlongCENTRO <- -46.633949
R> ylatCENTRO <- -23.550391
R> system.time(source("functions/NETWORK.R"))
R> rm(list = ls())
```

The activity functions are called following. They assign the vehicles to the road network if it is an interpolation, or read from traffic simulation, and then split it by type of fuel, size of motor and gross weight in a 50 years distribution reading the file data/in/veh/veh.csv. As a result, we have the amount of vehicles at each link with vehicles age distribution and type of fuel, so it's possible to assign respective emissions standard, resulting in a dataframe names data/out/veh/na*.rda. It also produces different fleet plots and tables. The procedure, for Passenger Cars, is just:

```
R > system.time(source("functions/PC.R")) # na_pc.rda
```

The emissions estimations starts loading the emission factors. REMI uses local emissions factors from measurements made by the manufacturers in Brazil with FTP-75 driving cycle (CETESB, 2013), and uses (Ntziachristos, 2014). to incorporate the speed variation at other speeds than 34.12 km/h, the mean speed at this driving cycle. As the emission factors are available to each year of use, it incorporates deterioration factor identifying 50 years. The following lines show the procedure in R:

```
R> det <- read.csv("data/in/det/detco.csv", h=T)
R> fen <- read.csv("data/in/fen/fenco.csv", h=T)
R> F_CO_A_2012_G_L5_1000 <- function(V) {
R>   ((1.36E-01 + -8.91E-04*V + 0*V^2)/(1 + -1.41E-02*V + 4.99E-05*V^2))
R> }
R> FFE_1 <- fen[1,1]/F_CO_A_2012_G_L5_1000(34.12)
R> F_CO_A_2012_G_L5_1000 <- function(V) {
R>   ((1.36E-01 + -8.91E-04*V + 0*V^2)/(1 + -1.41E-02*V + 4.99E-05*V^2))*FFE_1*det[1,1]
R> }
```

Then the emissions are then calculated loading the activity na*.rda file and red.rda. REMI considers three mean speeds for rush hour (V), free flow (Vlibre) and an averaged speed (Vmedia) distributed over 24 hours. The emissions are calculated for 50 years of use calculating first to each hour, as follows:

```
R> E_CO_OU_2012_D_P7_seg_8 <- OU_0_D_P7 * F_CO_OU_2012_D_P7 (red$V)*red$longkm
...
R> E_CO_OU_2012_D_P7_seg_8_vl <- OU_0_D_P7 * F_CO_OU_2012_D_P7 (red$Vlibre)*red$longkm
...
R> E_CO_OU_2012_D_P7_seg_8_vm <- OU_0_D_P7 * F_CO_OU_2012_D_P7 (red$Vmedia)*red$longkm
...
```

In this case the base-year is 2012, so the emissions are calculated till year 1962 and summed by the emission standard classification of type of vehicle. Then comes the part of extrapolate the emissions to the hours and days of the week. The emissions s are calculated with traffic flow of morning peak hour of 08:00-09:00 and with three average speeds, rush hour, free flow and averaged, and the extrapolation process uses a profile of 24 hours and each day of the week normalized to 08:00-09:00. So, three type of emissions (by each mean speed) were allocated to 24 hours and then multiplied with this profile at 24 hours and each day of the week. The allocation assumes the following speed distribution:

- ⑩ 00:00-06:00 Free Flow mean speed (Vlibre).
- ⑩ 06:00-07:00 Averaged mean speed (Vmedia).
- ⑩ 07:00-10:00 Rush Morning hour (V).
- ⑩ 10:00-17:00 Averaged mean speed (Vmedia).
- ⑩ 17:00-20:00 Rush Evening hour (V).
- ⑩ 20:00-21:00 Averaged mean speed (Vmedia).
- ⑩ 21:00-00:00 Free Flow mean speed (Vlibre).

So, the emission are multiplied with the normalized profile at each respective hour. Per example, the 00:00 hour emissions are the emissions calculated with free flow speed and multiplied with the profile of 00:00 hour. The following lines show the process:

```
#Monday
R> E_CO_OU_D_P7_seg_0 <- E_CO_OU_D_P7_seg_8_vl *profile[1,1]
...
R> E_CO_OU_D_P7_seg_6 <- E_CO_OU_D_P7_seg_8_vm *profile[7,1]
...
```

```
R> E_CO_OU_D_P7_seg_7 <- E_CO_OU_D_P7_seg_8 *profile[8,1]
...
# Tuesday
R> E_CO_OU_D_P7_ter_0 <- E_CO_OU_D_P7_seg_8_v1 *profile[1,2]
...
```

Once the emissions are calculated to all the hours of the week, are summed to tons/year and stored as dataframe E_df.rda. Then, the emissions are summed to each hour and day of the week ate each link and also stored as dataframe.

```
R> E_CO_BUS_seg_0<-E_CO_OU_D_P7_seg_0 + E_CO_OU_D_P5_seg_0 + ...
```

Benchmark

REMI runs in a machine with GNU/Linux operational system Debian 8.2 Jessie, kernel x_86_64 Linux 3.15.0-4-amd64, CPU of Intel Core i7-4770 3.9GHz and 16 Gb RAM. When calculating the emissions, including gridding and all the plots takes:

Table 1. Performance of REMI

REMI for Metropolitan Area of São Paulo	Time
<p>Count interpolation 105468 links 27 pollutants 24 hours, 7 days of the week</p>	4 hours
<p>Traffic Simulation 34733 links 27 pollutants 24 hours, 7 days of the week</p>	1 hour

4. Discussion

In order to run this model properly it's needed with traffic interpolation it's needed traffic counts, local emissions factors and fleet statistics over 50 years. But this information is not always available when performing an inventory. In REMI model with traffic count interpolation, the amount of vehicles basically depends on road network of open street map (<http://www.openstreetmap.org/>). So, a bigger city will have a bigger road network and a smaller city a smaller network. Keeping that in mind, it's possible to assign the interpolation of one city into another, while those cities shares relatively the same level of congestion per street. As a result, a bigger city will have more vehicles circulating and a smaller one less. It's always important take into account the peculiarities of each city, per example, a city near an important economic activity that requires circulation of heavy duty vehicles, like ports of mining industry. Also, the fleet distribution by type of vehicle, per example, cities with larger amount of motorcycles, like asian cities. Another important aspect is the average age of the fleet of the city, because, despite that the city could have high emissions standards, if the average age of th fleet is old, that city will have more older vehicles circulating, resulting in higher emissions.

With those considerations it was applied REMI model (called REMI in that time) to estimate the vehicular emissions of 58 urban centers of South America (Ibarra *et al*, 2015a). The pollutants covered were CO, PM2.5, HC and NOx. The figure 2 and 3 shows the results by country for CO and by city for PM2.5. In this study were corrected the different type of fuels used in each city, and it was considered the average age of fleet in each country with a statistically significant association with GDPpp for 2012.

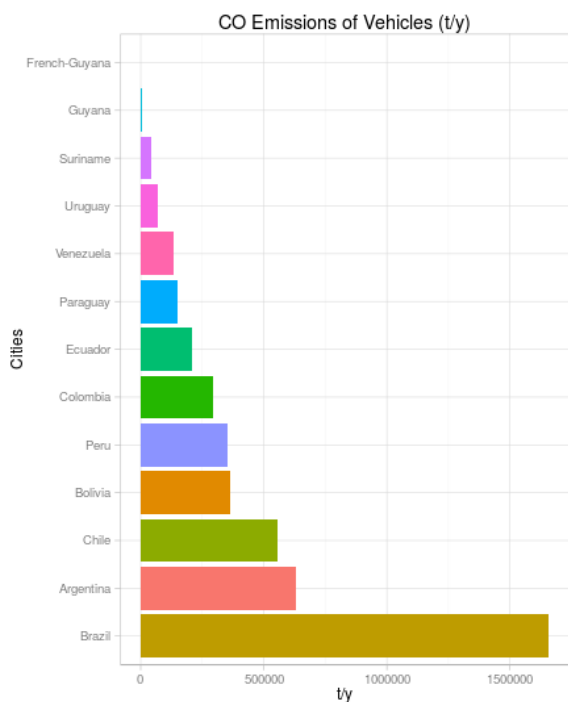


Figure 2. Vehicle emissions of CO by country in 2012 (Ibarra et al., 2015a).

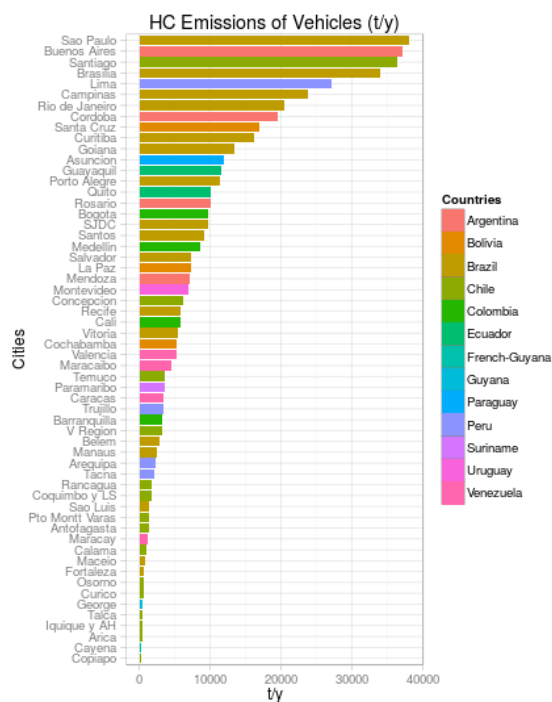


Figure 3. Vehicle emissions of HC by city in 2012 (Ibarra et al., 2015a).

This model was also used to estimate emissions and simulate air pollutant concentrations for the city of Porto Alegre, Brazil (Ibarra et al, 2015b). The air pollutant concentrations could not be compared with observations due to lack of data, but the results were meteorological and chemically consistent. Figure 4 and 5 show results of CO emissions and concentrations.

The model is still in development and a new version it's planned to produce an R package which must be very versatile. This characteristic is for adequate to the reality of different cities. Also, as it's this packages will have different emission factors, allowing projections and estimation of past scenaries. REMI will also include a more type of vehicles, emission factors and it would be applicable to region in the world.

Conclusion

REMI model is a program to estimate bottom-up vehicular emissions inventory which, unders certain assumptions, can be adapted to availability of data to any city. Right now it represents Brazilian conditions, but it can be adapted to other realities, including emission factors. SO far, it does not include evaporative and cold start emissions, but it's planned to include them near in future. This work is part of the PhD in meteorology program of the University of São Paulo, Brazil.

Acknowledgments

We would like to thank María de Fátima Andrade of Laboratório de Processos Atmosféricos (LAPAT) for all the support, as scholarships progams CAPES of Ministry of Education, Brazil, and Becas Chile, from Conicyt, Chile.

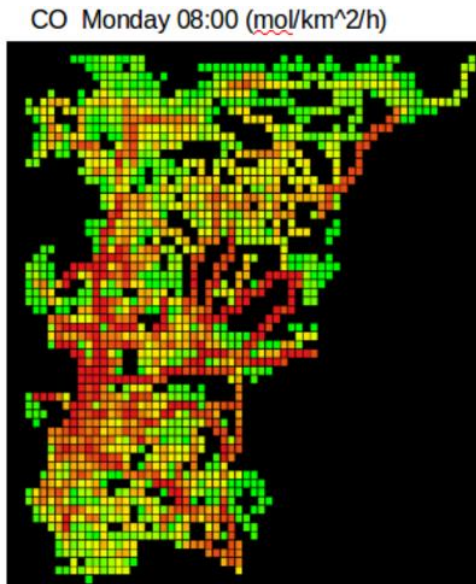


Figure 4. Vehicle emissions of CO Porto Alegre 2012 (Ibarra et al., 2015b).

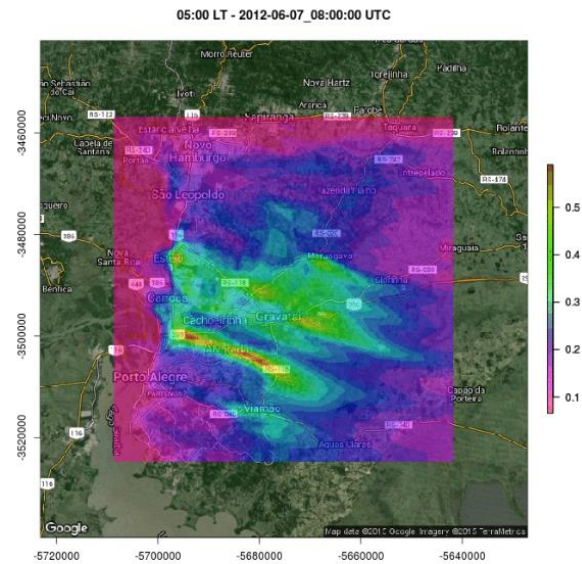


Figure 5. CO concentration (ppm) Porto Alegre 2012 (Ibarra et al., 2015b).

References

- CETESB, 2012. Emissões veiculares no estado de são paulo. <http://veicular.cetesb.sp.gov.br/relatorios-e-publicacoes/>.
- D. Kahle and H. Wickham. ggmap: Spatial Visualization with ggplot2. *The R Journal*, 5(1), 144-161. URL <http://journal.r-project.org/archive/2013-1/kahle-wickham.pdf>
- Grell, G. A., Peckham, S. E., Schmitz, R., McKeen, S. A., Frost, G., Skamarock, W. C., & Eder, B. (2005). Fully coupled "online" chemistry within the WRF model. *Atmospheric Environment*, 39(37), 6957-6975.
- H. Wickham. ggplot2: Elegant Graphics for Data Analysis. Springer-Verlag New York, 2009.
- Ibarra S. and Ynoue R. (2016) High resolution vehicular emissions inventory for the megacity of São Paulo. Manuscript to be sent to *Atmospheric Environment*.
- a) Ibarra S., Ynoue R., Vela A., Vehicular Bottom-up Emissions Inventory And Atmospheric Simulation For 58 Urban Centers Of South America. 11TH International Conference On Southern Hemisphere Meteorology And Oceanography. October 5TH TO 9TH 2015, Santiago, Chile.
- b) Ibarra S., Vela A., Rehbein A., Ynoue R., High Resolution Air Pollutant Simulation For The Metropolitan Region Of Porto Alegre. IX Workshop Brasileiro De Micrometeorologia. 11-13 Novembro 2015, Santa Maria, RS, Brasil.
- Ntziachristos, L., and Z. Samaras. "EMEP/EEA emission inventory guidebook." *European Environment Agency, Copenhagen* (2009).
- R Core Team (2016). R: A language and environment for statistical computing. R Foundation for Statistical Computing, Vienna, Austria. URL <https://www.R-project.org/>.
- Roger S. Bivand, Edzer Pebesma, Virgilio Gomez-Rubio, 2013. Applied spatial data analysis with R, Second edition. Springer, NY. <http://www.asdar-book.org/>
- Roger Bivand and Colin Rundel (2015). rgeos: Interface to Geometry Engine - Open Source (GEOS). R package version 0.3-15. <https://CRAN.R-project.org/package=rgeos>
- Roger Bivand and Nicholas Lewin-Koh (2015). mapproj: Tools for Reading and Handling Spatial Objects. R package version 0.8-37. <https://CRAN.R-project.org/package=mapproj>
- Tim Pulles and Dick Heslinga. "The art of emission inventoring." TNO, Utrecht (2010).

Active diesel particulate filters and nitrogen dioxide emission limits

Osama IBRAHIM^{1,2}, Sorour ALOTAIBI¹, and Hans WENGHOEFER²

¹Department of Mechanical Engineering, College of Engineering & Petroleum, Kuwait University
email: osama.ibrahim@ku.edu.kw

²RYPOS Inc., Franklin, MA 02038, USA

Abstract

Diesel engines are major source of nitrogen oxides (NO_x). NO_x, primarily nitric oxide (NO) and nitrogen dioxide (NO₂), are formed at high temperatures during diesel fuel combustion. While neither NO nor NO₂ are desirable, NO₂ is the more reactive gas associated with health problems. Both US Environmental Protection Agency (US-EPA) and California Air Resources Board (CARB) initiated rulings for diesel emissions retrofit technologies to limit NO₂ emissions increase "slip" to 20% over the engine baseline emissions. In this paper, an active diesel particulate filter that reduces NO₂ emissions is presented. The active diesel particulate filter utilizes a porous sintered metal filter medium, which is divided into pleated filter strips. These filter strips are regenerated (cleaned) by applying direct electric heating to burn off accumulated soot. Exhaust emissions measurements show that a degreened active diesel particulate filter reduces NO₂ by 42% from the diesel engine exhaust. The data also show that the efficiency of NO₂ emissions reduction improves with aging. Following a break-in or "aging" period, the active diesel particulate filter achieved 96% NO₂ reductions. This far exceeds latest US-EPA and CARB verification standards on NO₂.

Key-words : diesel emissions, nitrogen dioxide, retrofit technologies, diesel particulate filter

Les filtres actifs à particules diesel et les limites d'émissions du dioxyde d'azote

Résumé

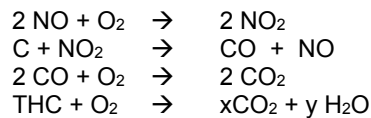
Les moteurs diesel sont une source majeure d'oxyde d'azote (NO_x). Les NO_x, principalement l'oxyde nitrique (NO) et le dioxyde d'azote (NO₂), se forment à des températures élevées pendant la combustion du carburant diesel. Bien que ni le (NO) ni le (NO₂) sont souhaitables, le NO₂ est le plus réactif gaz associé aux problèmes de santé. Le US Environmental Protection Agency (US-EPA) et le California Air Resources Board (CARB) ont lancé des décisions pour régulariser les émissions des moteurs diesel et les techniques de réajustement pour limiter l'accroissement des émissions de NO₂ à 20% au-dessus de la ligne de référence des émissions du moteur. Ce document est une présentation du filtre actif à particules pour le moteur diesel qui réduit les émissions de NO₂. Le filtre actif à particules pour le moteur diesel utilise un filtre fait de métal fritté poreux, qui est divisé en bandes de filtre plissé. Ces bandes de filtre sont régénérées par l'application directe d'échauffement électrique pour brûler la suie accumulée. Les mesures des émissions d'échappement montrent qu'un filtre actif à particules pour le moteur diesel nouvellement utilisé réduit NO₂ par 42% de la sortie d'échappement du moteur diesel. Les données montrent également que l'efficacité de la réduction des émissions s'améliore avec l'âge. À la suite de la période de vieillissement, Le filtre actif à particules pour le moteur diesel atteint une réduction de 96% en NO₂. Cela dépasse de loin les plus récentes normes de vérification du NO₂ par l'US-EPA et du CARB.

Mots-clés : émissions de diesel, dioxyde d'azote, technologies de rénovation, filtre à particules diesel

Introduction

Diesel emissions consist of different exhaust components that include particulate matter (PM), carbon monoxide (CO), total hydrocarbons (THC), and nitrogen oxides (NO_x). PM is a complex mixture of extremely small particles (soot) and liquid droplets, primarily incompletely burnt fuel. The small particles adsorb other toxins from the engine and engine exhaust, which can cause adverse health effects including cancer and other pulmonary and cardiovascular diseases. In enclosed spaces, CO resulting from incomplete fuel combustion, is known to cause headaches, dizziness and lethargy, and in extreme cases, death. THC, a contributor to smog, will cause lung irritation in similar environments. NO_x, primarily nitric oxide (NO) as well as some nitrogen dioxide (NO₂), are formed at high temperatures during diesel fuel combustion. While neither NO nor NO₂ is desirable, NO₂ is the more reactive gas associated with significant health problems. Scientific evidence links NO₂ exposures, with adverse respiratory effects, Schindler (1998) and Ponsonby (2001). Several studies were also done to investigate the health effect of children exposure to diesel exhaust in school buses, Shima and Adachi (2000), Ponsonby et al. (2001), and Wargo (2002). Their conclusions show that diesel emissions have been associated with health problems, being potentially harmful to children near school buses.

Passive Regeneration: Regeneration of Passive Diesel Particulate Filters (PDPF) relies on NO₂ as an oxidizer of carbon to clean the filter and maintain low engine backpressure. This technique requires that NO₂ be generated by the oxidation catalyst of the remediation device. During passive regeneration, NO, C, THC, and CO in the exhaust stream are oxidized in the following manner:



In most PDPFs, an excess of NO₂ is produced and only partially used in the carbon oxidation process, thus causing NO₂ slip to the atmosphere. NO₂ slip from exhaust remediation devices is highly undesirable and is the main reason why US-EPA and CARB have limited NO₂ increase to 20% of engine baseline for diesel retrofits US-EPA (2007), US-EPA (2010), and CARB (2011). The National Institute for Occupational Safety and Health (NIOSH) studies have also shown a significant increase in NO₂ concentrations in mine air, resulting from the use of catalyzed filters, Mischler and Cauda (2009). Because NO₂ is a lung irritant, a ceiling value of 5 ppm has been set to lower miners' exposure.

Active Regeneration: Active regeneration of diesel particulate filters is done through different ways and strategies. In this paper, the focus on an Active Diesel Particulate Filter (ADPF), shown in Figures 1 and 2, uses direct electrical heating to burn the accumulated PM and regenerate or “clean” the filter. The ADPF utilizes a filter media made of porous sintered metal fibers, shown Figure 3, made of Fecralloy, which contains iron, chromium, aluminum and yttrium. The added aluminum improves resistance to corrosion at high temperature, while yttrium, a rare earth metal, serves to anchor the protective aluminum oxide layer to the surface of the base metal. The filter media consists of multilayers with different fiber size. The graded filter medium is designed for maximum dirt holding capacity and high filter efficiency.

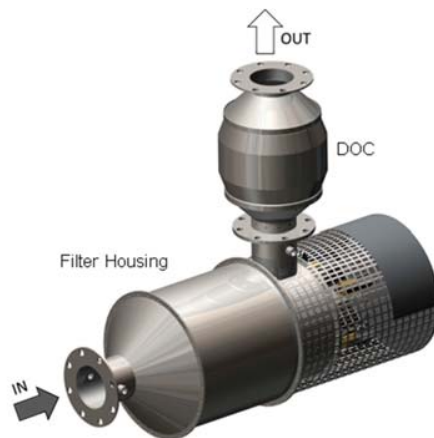


Figure 1. Active Diesel Particulate Filter (ADPF) with Diesel Oxidation Catalysts (DOC) downstream.

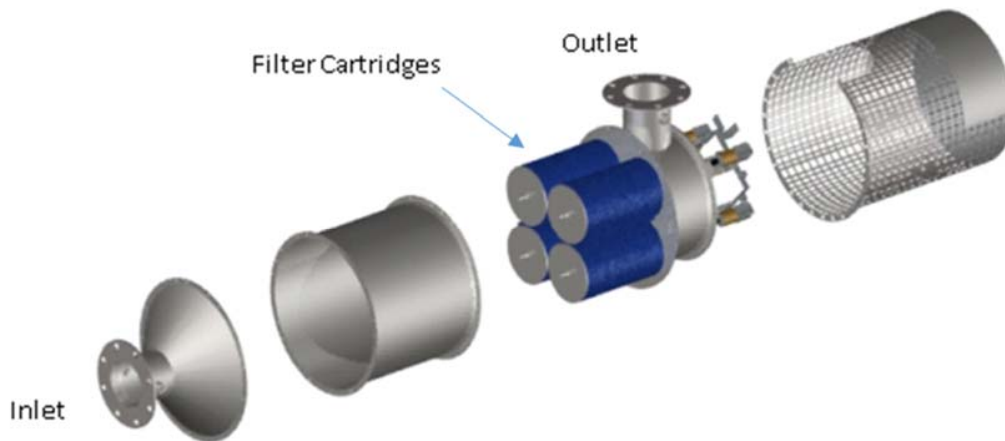


Figure 2. Exploded view of an Active Diesel Particulate Filter (ADPF).

The total area of the filter is divided into pleated filter strips, which are packaged as active filter cartridges shown in Figure 4. Dividing the filter area into strips allows for partial regeneration of the total filter area, which reduces the maximum electric power requirements for regeneration. To manage regeneration cycles for the whole filter system, a microprocessor controller is used to monitor and keep the filter cartridges functioning at low backpressure during normal operation.

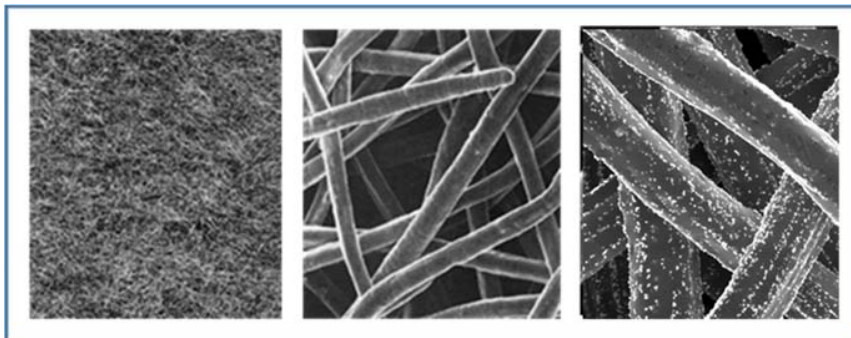


Figure 3. Sintered metal fibers.

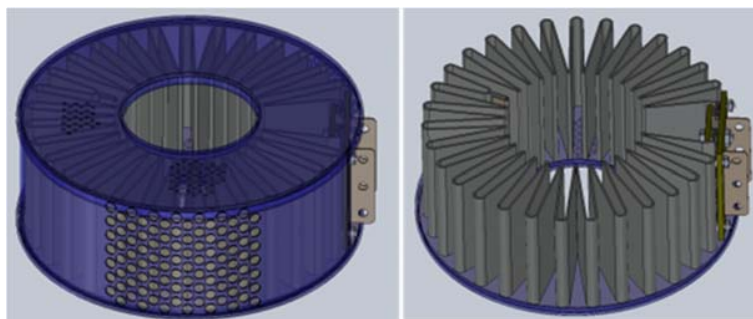


Figure 4. Active filter cartridge, flow from outside to inside.

Active regeneration does not rely on NO₂ as an oxidizing agent of carbon (soot), keeping NO₂ at or below engine baseline levels. Specially designed oxidation catalysts, attached to the outlet, reduce CO and THC without converting NO to NO₂. ADPF provides a method of reducing NO₂ from the diesel engine exhaust stream directly by reacting with carbon, C. To increase the probability of NO₂ reacting with carbon, particulates are collected on the filter in fluffy layers resulting in high surface area.

During normal operation or active regeneration, C, THC, and CO in the exhaust stream is oxidized in the following manner:

- a) During normal operation
 $\text{NO}_2 + \text{C} \rightarrow \text{CO} + \text{NO}$
 Using special oxidation catalysts downstream
 $2\text{CO} + \text{O}_2 \rightarrow 2 \text{CO}_2$
 $\text{THC} + \text{O}_2 \rightarrow x \text{CO}_2 + y \text{H}_2\text{O}$
- b) During Active Regeneration Cycle-Thermal Oxidation
 $\text{NO}_2 + \text{C} \rightarrow \text{CO} + \text{NO}$
 $2 \text{C} + \text{O}_2 \rightarrow 2 \text{CO}$
 $\text{C} + \text{O}_2 \rightarrow \text{CO}_2$
 Using special oxidation catalysts downstream
 $2 \text{CO} + \text{O}_2 \rightarrow 2 \text{CO}_2$
 $\text{THC} + \text{O}_2 \rightarrow x \text{CO}_2 + y \text{H}_2\text{O}$

Test Bed

The test bed was a diesel generator set (genset). Details on the genset are provided in Table 1.

Table 1. Genset specification.

Type	225 kW Generator
Manufacturer	Caterpillar
Engine Model	3306B
Year	1994
Displacement	10.45 L
Rated Power	281 kW (377hp)@ 1800rpm
Engine Configuration	InLine 6, Turbo, AA cooling
Power	300 hp
Engine SN	9NR00796
Hours on Engine	1890

Test Cycle

Two active diesel particulate filters (ADPFs) were tested: the first ADPF had been aged in a durability test of 525 hours; the second ADPF had been degreened for 25 hours. Testing took place over the five modes described in ISO 8178-4 Cycle D2, shown in Table 2. The fuel used was Eastern Region Ultra Low Sulphur Diesel fuel (< 15 ppm sulfur).

Table 2. ISO 8178-4 D2 five mode test cycle.

Torque, %	100	75	50	25	10
Speed	Rated Speed (1800 rpm)				
Weighting Factors	0.05	0.25	0.3	0.3	0.1

Test Results and Comments

The test was performed by Emission Research and Measurement Division (ERMD) of Environment Canada. The emissions were sampled and analyzed using the ERMD Dynamic Dilution On/Off-road Emissions Sampling System. Emission rates were determined for CO, NO_x, NO₂, THC and TPM. The

average weighted emission rates in grams per kilowatt-hour can be found in Table 3. Each test configuration had a minimum of three valid tests.

Table 3. Summary the average weighted emissions in g/kWh.

Test Configuration	CO	NOx	NO2	THC	TPM
OEM (base line)	1.92	9.1	0.47	0.95	0.168
AfterTreatment: Degreened ADPF	0.31	8.4	0.27	0.23	0.022
AfterTreatment: Aged ADPF	0.11	8.5	0.02	0.22	0.011

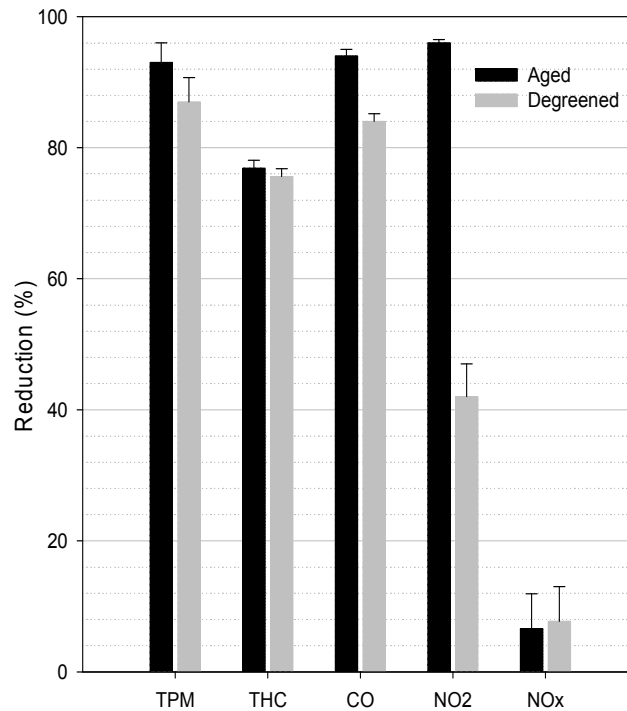


Figure 5. Emission reductions.

As shown in Figure 5, PM was reduced by 87% for the degreened unit, and 93% for the aged unit. Both units show reductions of 84 and 94% in CO, and reductions greater than 75% in THC. The results show a significant reduction in NO₂ for aged system, over 90% compared to 42% for the degreened units. In Figure 6, the NO₂ emissions of the Original Engine Manufacturer (OEM) baseline, the degreened and aged units are plotted as function of exhaust temperature. The results show that the aged unit has a significant reduction in NO₂ in the entire temperature range. The degreened unit, however, shows much less reduction in NO₂ emissions especially at high temperature. The uncertainty in NO₂ measurements were low for the aged unit compared to the OEM baseline and the degreened unit.

Both the degreened and aged units show small reductions in NO_x, about 7%. Plotted in Figure 7, is NO_x emissions as a function of temperature for the OEM baseline, the degreened unit, and the aged unit. It clear from the plots, there is slight reduction in NO_x emissions and that both the degreened and aged units have the same NO_x emissions output.

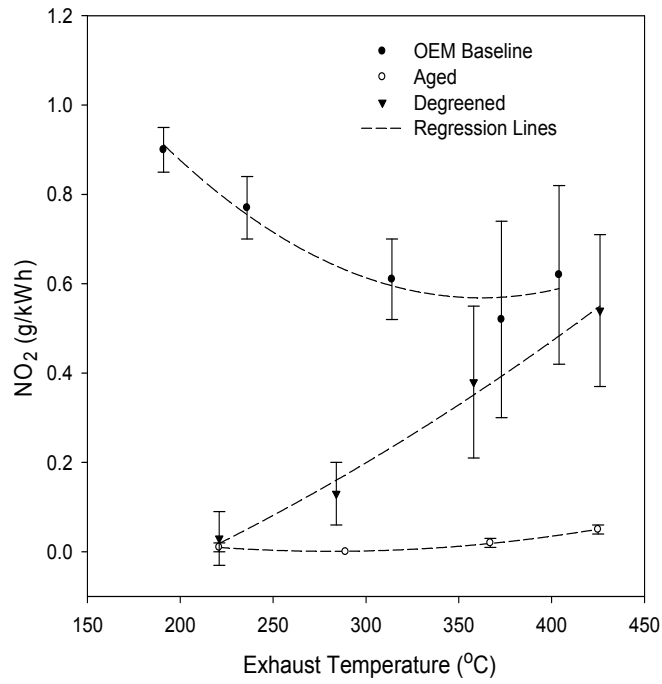


Figure 6. Nitrogen dioxide emissions vs. exhaust temperature.

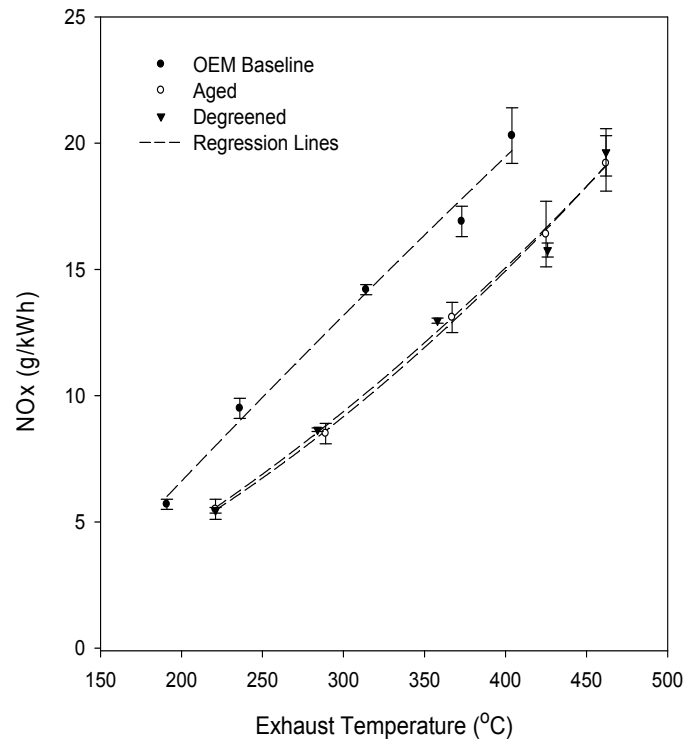


Figure 7. Nitrogen oxides emissions vs. exhaust temperature.

Conclusions

Regeneration of passive diesel particulate filters mostly relies on NO₂ as an oxidizer to regenerate (clean) the filter. This technique requires that NO be oxidized into NO₂ by platinum based diesel catalysts. In most passive diesel particulate filters, an excess of NO₂ is produced, and only partially used in the carbon oxidation process, thus causing NO₂ slip into the atmosphere. NO₂ is considered potentially one of the most harmful emission gases in diesel exhaust. On a world-wide basis, recommendations are being made to limit the conditions under which NO₂ are produced. These include diesel engine management and exhaust after-treatment. US-EPA and CARB have proposed and initiated rulings to limit NO₂, especially for emission control systems that increase these levels >20% over engine baseline levels. Active regeneration, using direct electrical heating, does not rely on NO₂ as an oxidizing agent of carbon. It has demonstrated a novel process to significantly reduce NO₂. NO₂ reduction was accomplished by using soot as a reducing agent. Special oxidation catalysts, which are designed to minimize the oxidation of NO into NO₂, were used downstream of the filter systems. The result is over 90% reduction in NO₂ for an “aged” system.

References

- US Environmental Protection Agency (December 20, 2007): Nitrogen Dioxide Limits for Retrofit Technologies. Letter EPA420-B-08005.
- California Air Resources Board (2011), California Code of Regulations, Title 13, Division 3, Chapter 14, Section 2706.
- Ibrahim, O. and H. Wenghoefer (2009) : Optimization and Verification of Hybrid Diesel Particulate Filter with NO_x Reduction”, Final Report, submitted to Houston Advanced Research Center, Project number N-13.
- Hendren, J. (2006): The Evaluation of the Effects of the RYPOS INC. HDPF/C on the Exhaust Emissions of a 1994 Model Year Caterpillar 3306B Genset. ERMD Report # 06-17-2, Environment Canada, Ottawa, Ontario.
- Strand, V. et al (1998): Repeated Exposure to an Ambient Level of NO₂ enhances Asthmatic Response to a nonsymptomatic Allergen Dose. *European Respiratory Journal*, 12: 6–12.
- Schindler, C. et al (1998): Associations between Lung Function and estimated average Exposure to NO₂ in eight Areas of Switzerland. *Epidemiology*, 9: 405–411.
- Ponsonby, A. L. et al (2001): The Relationship between low Level Nitrogen Dioxide Exposure and Child Lung Function after cold Air Challenge. *Clinical and Experimental Allergy: Journal of the British Society for Allergy and Clinical Immunology*, 31: 1205–1212.
- US Environmental Protection Agency (2010): Primary National Ambient Air Quality Standards for Nitrogen Dioxide Final Rule, 40 CFR Parts 50 and 58. Federal Register / Vol. 75, No 26.
- Mischler, S., and E. Cauda (2009): NO₂ Emission Increases Associated with the Use of Certain Diesel Particulate Filters in Underground Mines, CDC. <http://blogs.cdc.gov/niosh-science-blog/2009/02/03/no2/>
- Wargo, J. (2002): Children’s Exposure to Diesel Exhaust on School Buses. North Haven, Connecticut: Environment & Human Health, Inc., 7 February 2002. 29. <http://www.ehhi.org/reports/diesel/diesel.pdf>
- Shima, M. and M. Adachi (2000). Effect of Outdoor and Indoor Nitrogen Dioxide on Respiratory Symptoms in School Children. *International Journal of Epidemiology*, 29: 862–870.

Acknowledgements

We gratefully acknowledge the support of Kuwait Foundation for the Advancement of Sciences, Kuwait University, and Rypos Inc., USA.

Development of Road Transport Emissions: Case Study of Singapore for 2004-2014

Arimbi JINCA, Maximilian STORP, Tobias MASSIER, Andreas RAU
TUM CREATE Pte. Ltd., 1 CREATE Way, CREATE Building, 138602 Singapore
arimbi.jinca@tum-create.edu.sg; maximilian.storp@googlemail.com; tobias.massier@tum-
create.edu.sg; andreas.rau@vt.bv.tum.de

Abstract

Singapore as an island city-state in South East Asia is well known for its magnificent implementation of land transport management measures such as vehicle ownership control and alternative vehicular technologies. These measures and their combinations are consequently effect on travel behaviour which end up reducing directly and indirectly the impact of air pollutants and greenhouse gases (GHG) emissions. However, an information on road transport related emissions sources is still missing. Therefore, Singapore has to establish an inventory of (GHGs) and air pollutants from anthropogenic activities such as road transport activities to understand the magnitude of their activities.

The main objective of this paper is to develop road transport emissions inventory in Singapore from 2004 to 2014. The estimation covers major emission sources (CO, VOC, NO_x, PM_{2.5}, and CO₂). Both bottom-up (COPERT IV) and top-down (fuel sales) approaches were implemented to compile the inventory from various sources where possible. One of the results indicates that there is a small discrepancy of CO₂ emissions estimation with an average value of 9.27% between the top-down and the bottom-up approaches. Moreover, a clear trend of emissions reduction was identified for CO, VOC, NO_x and PM_{2.5}.

Keywords: Road transport, COPERT, Fuel consumption, Emissions, Singapore

1. Introduction

The transportation sector has been developing fast along with the rapid development of motorization and urbanization in the world. Consequently, the problems of traffic congestion, energy consumption and traffic accidents are progressively noticeable (Xing & Hu 2013). Furthermore, the growing number of motor vehicles and their activities are the primary source of pollutants and air toxics. Incomplete fuel combustion produces unburned hydrocarbons (UHCs) and other volatile organic compounds (VOCs), carbon monoxide (CO), and particulate matter (PM). Sulphur dioxide (SO₂) is a product of mostly diesel fuel combustion. These pollutants cause direct impact on human health, whereas carbon dioxide (CO₂) is produced by complete combustion of fuel molecules and it is a greenhouse gas contributing to climate change.

The transportation sector is responsible for about 23% of overall CO₂ emissions and 19% of global energy use in the world (International Energy Agency 2009)(Organisation for Economic Co-operation and Development (OECD) 2010). Its emissions have increased by 45% from 1990 to 2007 (Johnson & Adams 2011). Without any strategic intervention, the global CO₂ emissions are predicted to continue to grow by roughly 40% from 2007 to 2030 (OECD & International Transport Forum 2010) In Asia, although China and India constitute the largest share of total emissions, Malaysia and Singapore have the highest per capita CO₂ emissions (Clean Air Asia 2012). Nevertheless, the road transport per capita CO₂ emissions from these countries are much lower compared to OECD (Organization for Economic Co-operation and Development) countries' per capita emissions.

Singapore is a city-state island in South East Asia with a land area of approximately 718 km² and a population of about 5.4 million people in 2014 (Singapore Department of Statistic 2015). It is a tropical country located close to the equator line with uniform temperature and high humidity along the year. The average daily temperatures range from 23°C - 34°C while average humidity is at 84%. Singapore is a highly urbanized country, with an urbanization rate of 100%. Currently, 12% and 14% of total area of Singapore are taken by roads and housing (Land Transport Authority of Singapore 2013). Around 800.000 vehicles are registered in Singapore which make it as one of the lowest vehicles per population

share among developed countries. Therefore, Singapore meets a challenge issue to manage the mobility without expending more roads but in a sustainable way.

Singapore is actively involved in the international climate change negotiation. It is noticed that in 2009, Singapore pledged to undertake mitigation measures leading to a reduction of greenhouse gas emissions (GHGs) by 16% below 2020 Business as Usual (BAU) level, contingent on a legally binding global agreement, in which all countries implement their commitments in good faith (National Climate Change Secretariat 2012). Therefore, Singapore has to establish a national inventory of greenhouse emissions (GHGs) and associated air pollutants from anthropogenic activities such as transport to understand the magnitude of its transport activities. On the other hand, a range of policies in the transport sector have been taken by the Singapore government to improve the public transport system, to control vehicle ownership and vehicle usage and to introduce environmental friendly vehicles.

One of the measures that has been implemented to control vehicle ownership and influence the use of vehicle is the fiscal measures. These fiscal measures can be divided into a single measure such as open market value (OMV), additional registration fee (ARF), vehicle quota system (VQS), area licencing scheme (ALS) which is replaced by electronic road pricing (ERP). These measures and their combinations are consequently effect on travel behaviour which end up reducing directly and indirectly the impact of air pollutants and GHG emissions. A related topic about Singapore's innovative transportation policies as part of environmental instruments has been studied by several researchers in the last two decades, as evidenced by literature on the subject (e.g. (Olszewski 2007)(Chin 2000)). Unfortunately, those statements remained to be verified since less relevant quantitative studies have so far been conducted.

Limited studies attempted to estimate the air pollution and GHG emissions from road transport in Singapore. One of the studies held in 2005, the Land Transport Authority (LTA) of Singapore quantified emissions of road transport (LTA Academy 2013). It turned out that the contribution of different vehicle types to the overall emissions differed significantly. For instance, taxis account for only 3% of the overall vehicle population in Singapore, but it is estimated for about 17% of CO₂ emissions due to their higher travel mileage. Similar results were obtained for buses and commercial vehicles. Motorcycles and private cars contributed to approximately 36% of CO₂ emissions, despite accounting for 78% of the total vehicle population.

The main objective of this paper is to develop road transport emission inventory in Singapore from 2004 to 2014. The estimation is based on two approaches:

(1) Bottom-up approach which is based on road traffic activities. This approach covers the impact of transport activities on selected air pollutants and emissions, viz. CO, NO_x, VOC, PM_{2.5} and CO₂ from fuel combustion sources. Moreover, the outcome of this approach highlights some significant emissions estimation result and identifies the relation to the Singapore's fleet and traffic activities.

(2) Top-down approach or fuel based method is based on fuel consumption in road transport sector. In this case, only CO₂ is estimated. A comparison of CO₂ emissions based on bottom-up and top-down approach is performed to check the consistency of the results.

Furthermore, this paper figures out few shortcomings and recommends suggestions for the development of better emissions quantification to support environmentally friendly mobility in Singapore.

2. Methodology

Since Singapore is an island state, it makes the territorial boundary clear for the emission estimation. In this situation, the influence of national transport policies reflected directly on the transport activities of inhabitants which determine the emission in the territory. However, transport activities of inhabitants covered not only territory area but also small part of transboundary road traffics from and to Malaysia. Additional traffic activities from overseas vehicles were not included in this study.

For our estimation of emissions sources, we implemented both bottom-up (CO, NO_x, PM_{2.5}, VOC and CO₂) and top-down (only CO₂) approaches to compile the inventory from various sources where possible. Moreover, the results of both approaches for CO₂ emissions is compared to identify the consistency of different emissions estimation approaches.

For the bottom-up approach, selecting a proper emission model for a particular area is always a challenging issue since there is no emission models can provide details and comprehensive calculation that can be applied to all situations. It is likely more compromising matters of some criteria; modelling objective, modelling scale, modelling approach, data availability, and local condition (Jinca et al. 2014). In this case, the modelling objective is clearly defined for emission inventory for a city-state scale of Singapore. For the modelling scale, in terms of time and spatial scale which is fit to the associated emissions and air pollutants, it is recommended to use several approaches such as aggregated emissions factor, average speed, and traffic situations. However, not all approaches can be applied considering the availability and accessibility of the data. Inaccuracy of data pose a risk using a full bottom-up methodology. Furthermore, local condition of Singapore need to be considered into account such as meteorological concerns (such as higher temperature and humidity), typical fleet composition, and practicability (such as resources of human, budget, effort). An assessment has been done to identify a proper emission model for Singapore based on those defined criteria. Therefore an average speed model is selected for a city-state island.

Average speed models (e.g. COmputer Programme to calculate Emissions from Road Transport, COPERT) are based on a principal that the emission factor for certain pollutants and vehicle types varies over a trip according to the average speed. Since vehicle emissions depend on the engine operation (i.e. driving situation), exhaust emissions are calculated as a function of average speed, for three driving conditions: urban, rural and highway.

COPERT is the most commonly used methodology in Europe for official national inventories of emissions from road transport. For this case, bottom up approach based on transport activity using COPERT (version 11.0) has been chosen as an appropriate model for Singapore considering that the model is regularly updated, uses the same emission standard as Singapore, the model is accessible and affordable and it is widely used in the last two decades for emission quantification in most European countries and some other parts of the world. This model is famous for medium and large scale applications (Ajtay 2005). In the last decade, this model was used for different application scales such as done by Agyemang-Bonsu et.al (K.W et al. 2010) on city scale, Fameli et.al (Fameli & Assimakopoulos 2015) for a bigger scale agglomeration area, and Soylu (Soylu 2007) for nation-wide analysis. Furthermore, the COPERT model has been localize into COPERT Australia which precisely reflects the local emission factors and fleet characteristic (Smit & Ntziachristos 2012)(Ntziachristos et al. 2013)(Smit & Ntziachristos 2013).

The top-down approach using fuel-based is typically used for city or regional area sources. The approach describes total polluting activity in a geographical area of interest, such as total energy sales or fuel consumption. CO₂ emissions can be determined impartially accurately based on total amount of fuel combusted and the carbon content of the fuels. Only CO₂ emissions are estimated in this case because other air pollutants depend on the combustion technology and operating conditions which vary significantly. Due to these factors, using energy sales data or fuel consumption for air pollutants for enormous variability in technological and over the time will induce reasonably uncertainties. CO₂ emissions obtained from the total amount of fuel consumed by road transport multiply by emission factor. A uniform average CO₂ emission factor according to Intergovernmental Panel on Climate Change (IPCC) will be used for all motor vehicles according to the fuel type (gasoline and diesel) (Waldron et al. 2006).

A detailed methodology for bottom-up and top-down is presented below in Figure 1. In principle, the road transport emissions estimations using bottom-up and top-down approaches are carried out independently. In each case, the most reliable information from various data sources were formed as the basis of estimation. Uncertain parameters are then considered to relevant knowledge and realistic assumptions. For the bottom-up approach, an average speed model (COPERT IV methodology) was used with Singapore traffic activities and local characteristics. Input parameters for emission calculations are specific vehicle stocks, emission concepts, traffic activities, emission factors and related local contents (see bottom-up input 01 to 05 in Figure1). While for top-down approach, the estimation relies on statistical fuel consumption data of road transport Singapore and default emission factor given by the IPCC guideline (see top-down input 01 to 02 in Figure1)(Waldron et al. 2006). The calculated CO₂ emissions and fuel consumptions of both approaches are compared to identify the consistency of the results.

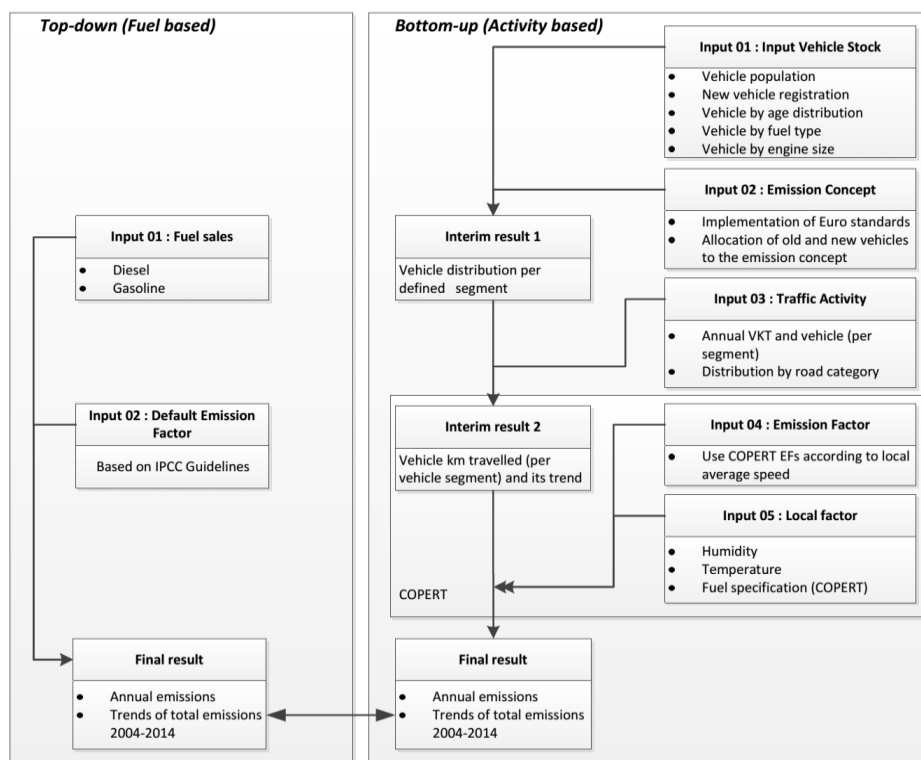


Figure 1. Model structure

3. Data Analysis

Several lines of evidence were used to simulate the emissions accurately according to the selected methodology. The Land Transport Authority (LTA) of Singapore annually publishes prevailing facts on land transport statistics including the Singapore land transport statistics, transport infrastructure, traffic matters, public transport, and motor vehicles facts. However, these data are available only to varying extent. Therefore, some secondary data such as previous related studies and some technical data from different research projects were also used to default an assumption.

3.1. Bottom-up

3.1.1. Vehicle Characteristics and its distribution

In Singapore, vehicle population and fleet characteristics are strongly affected by a string of transportation management policies such as vehicle ownership control. Vehicle ownership control include fiscal measures to moderate the growth of the motor vehicle population such as VQS (see Annex 1 for the summary of fiscal measures). With introduction of the VQS in 1990, the government set an annual vehicle growth rate started from 3% in 1990 to 0.5% from 2013 onwards to control the growth of vehicle population due to the limited land supply. Furthermore, starting from February 2015, the rate growth is more stringent which is set at 0.25% per annum (Land Transport Authority of Singapore 2013). In fact, the annual vehicle growth rate increased sharply over the limit from 2005 and reached a peak growth rate of 6% in 2007. Then from 2007 onwards, the vehicle growth rate decreased continuously up to -0.25% in 2014. In 2014, vehicle population decrease affected by the stringent vehicle growth rate policy. The vehicle population slowly increased over the last decade (2002-2013) and decreased in 2014. An illustration of the vehicle population according to the general vehicle distribution and the growth rate is described in the following figure (see Annex 2 for more details).

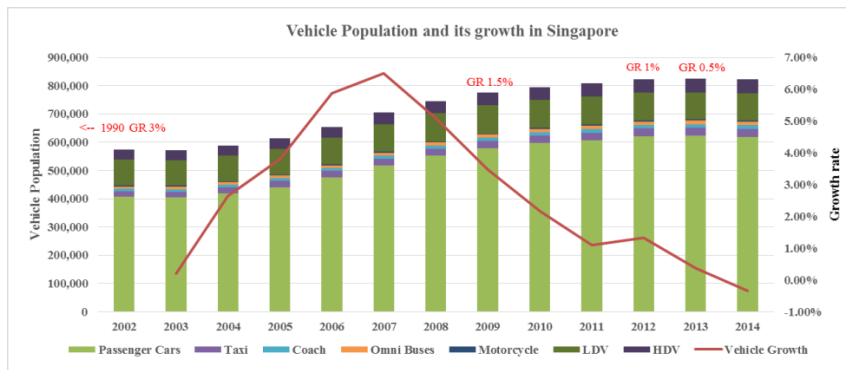


Figure 2. Vehicle population and its annual growth

According to the Singapore condition, the fleet is divided into seven main categories: passenger cars (PC), taxis (T), coaches (C), omnibuses (B) (hereinafter called public bus), motor cycles (MC), light duty vehicles (LDV) and heavy duty vehicle (HDV). These vehicle categories can be subdivided further according to the certificate of entitlement (COE), new registration under vehicle quota system (VQS), age distribution, fuel used, cc rating (hereinafter called engine size), and make (hereinafter called car manufacturer) (Land Transport Authority of Singapore 2015b). The total vehicle population based on those categories is available from 2004. However, this subdivision fleet information did not always provide synergy information among subdivision categories.

The engine size of PC has been evolving over the years. A clear trend of owning bigger engine size PC (>1.6 l) is observed. More distribution of gasoline (98%-99%) is the trend of the last ten years (Land Transport Authority of Singapore 2015b). However, in the last few years, more alternative energy sources for PC, like petrol, electric, petrol-CNG, and diesel electric with an amount of 1% arose. In contrast to PC, taxis mainly use diesel. In 2004, 99% of all taxis in Singapore ran on diesel (See Annex 4 for fuel share trend of vehicles). Until 2014, the share of diesel taxis decreased to 85% (Land Transport Authority of Singapore 2015b).

Table 1. Engine size of passenger cars in 2004 and 2014

Year	Engine Size				
	< 1.0 l	>1.0 – 1.6 l	>1.6 – 2.0 l	>2.0 – 3.0 l	> 3.0 l
2004	4%	58 %	23 %	11 %	1 %
2014	1%	54 %	27 %	15 %	3 %

Similar to European countries, Singapore follows the Euro standard band to tighten vehicle emission standards for a better air quality. Vehicle classification data based on emission control technology is unfortunately not yet reported in the yearly statistic. The authors were initiated to default an assumption of emission standard classification based on assortment information of new registration vehicles, vehicles age, phasing out rate, announced date and implementation of emission standard which are pledged by the National Environmental Agency of Singapore on behalf of the government.

Classification of the local fleet was adopted to the fleet structure of the COPERT methodology (Dimitrios Gkatzoflias et al. 2012). These subdivision categories (e.g. COE, VQS, age distribution) were converted to COPERT vehicle categorization (per investigated year) for which emission factors are directly linked to the combination of vehicle type, fuel used, engine size and vehicle technology parameters (D Gkatzoflias et al. 2012). In summary, the following assumptions were taken into account for converting the Singapore fleet distribution into COPERT's fleet distribution:

- PCs comprise private cars, company cars, tuition cars, rental cars and off peak cars, whereas taxis are generally categorized as passenger cars but simulated independently since taxis have a higher mileage and most of them use diesel as fuel.
- It was assumed that coaches were intended for mini buses, school buses, private buses, private hire buses and excursion buses while omnibuses were addressed to the entire type of public transport buses which are operated by two registered public transport companies in Singapore.

- Due to the different categorization of engine sizes for PC, an adjustment has been done for the entire fleet PC from Singapore to COPERT methodology. For example, PCs for <1,000 cc & below and 1,001 – 1,600 cc in Singapore situation are assumed as PC for <1.4 l in COPERT methodology. See Table 2 for details.

Table 2. Engine size categorization of PC

Singapore	COPERT
<1,000 cc	< 1.4 l
1,001 – 1,600 cc	
1,600 – 2,000 cc	1.4 - 2.0 l
2,001 – 3,000 cc	> 2,0 l
> 3,001 cc	

A similar adjustment has been performed for MC. In Singapore, MC are categorized into < 100 cc, 101-200 cc, 301 – 400 cc, 401-500 cc, 501-1000 cc and > 1001 cc. An adjustment into COPERT engine size distribution is described in the following table.

Table 3. Engine size categorization of MC

Singapore	COPERT
(1) <100 cc	Mopeds 2S <50 cc = 25% x (1) Mopeds 4S <50 cc = 25% x (1) Mopeds 4S >50 cc = 50% x (1)
(2) 101 - 200 cc	MC 4S < 250 cc = (2) + (50% x (3))
(3) 201 - 300 cc	
(4) 301 - 400 cc	MC 4S 251 cc - 750 cc = (50% x (3)) + (4) + (5) + (50% x (6))
(5) 401 - 500 cc	
(6) 501 – 1000 cc	MC > 750 cc = (50% x (6)) + (7)
(7) 1001 cc & above	

Table 4. Engine size categorization of LDV and HDV

Singapore	COPERT		
	LDV	HDV Rigid	HDV Articulated
(1) <3500 kg	<3500 t	-	-
(2) 35000 – 7000 kg	-	<7.5 t	-
(3) 7001 – 11000 kg	-	7.5 – 12 t	-
(4) 11001 – 16000 kg	-	12 – 14 t	-
(5) 16001 – 20000 kg	-	14 – 20 t	14 – 20 t
(6) 20001 – 26000 kg	-	20 – 26 t	20 – 28 t
(7) 26001 – 32000 kg	-	28 – 32 t	28 – 34 t
(8) 32001 – 40000 kg	-	>32 t	34 – 40 t
(9) 40001 – 50000 kg	-	-	40 – 50 t
(10) > 55000 kg	-	-	50 – 60 t

- For new alternative energy sources such as petrol electric or diesel electric vehicles, COPERT simulated them as hybrids category whereas petrol CNG was simulated as CNG category.

3.1.2. Traffic Activity

3.1.2.1. Vehicle kilometre travelled (VKT)

Data on VKT is annually provided by the LTA at Land Transport Statistics in Brief (Land Transport Authority of Singapore 2014a). Due to insufficient data of vehicle segregation, average annual VKT in each year was applied generally based on vehicle type in the COPERT model. It is observed that the average annual VKT for PC decreased during 2004-2014 from 20,298 km to 16,600 km primarily due to the expansion and improvement of the public transportation system, non-motorized transport facilities and further control measures such as the ERP. Other surveys from mandatory inspection and maintenance during 2012-2013 showed slightly different values of the mean annual VKT of about 18,000 km (Chu 2015). These numbers are comparable to the VKT of PC in Chicago city (LTA Academy 2010), but Singapore's land area is very limited being about 23 km long and 42 km wide. Moreover, the VKT is much higher than Hong Kong and Tokyo as compared to Asian cities with similar efficient and

highly developed public transport systems (Chu 2015). Higher number of VKT for PC is strongly affected by the higher cost of owning a vehicle in Singapore which is mostly bundled to the fixed costs (i.e. road tax, additional registration fee, COE, extra duty) rather than the variable costs (i.e. fuel, oil, inspection and maintenance) (De Jong 1990). Still, this statement is not entirely precise due to some facts on the effect on car restraint policies and mileage in Singapore. It is identified that PC drivers tend to make an extra detour and value less time to avoid some ERP gantries through the city centre (Chu 2015).

In Singapore, taxis are considered as public transport which serve the most efficient means of travel. Consequently, their VKT values are very high. The fleet-average annual mileage decreased from an estimated 145,031 km to 136,658 km over the last decade. With introduction of the Taxi Availability Standards (TA Standards) in 2013, the proportion of two-shift taxis increased from 53% to 66% in 2014. Furthermore, the share of taxis driving at least 250 km a day increased from 82% to 87% (Land Transport Authority of Singapore 2014b).

For the public bus fleet, the annual VKT decreased from 95,249 km in 2004 to 81,228 km in 2014 because of small re-routing in some bus lines and more population of buses to support the overall public transport improvement program. In contrary to that, the fleet-average VKT for coaches increased from 45,789 km to 57,450 km over the last decade. HDVs showed increasing VKT between 2004 and 2011. However, because of efficiency improvement, the annual mileage of HDVs rapidly decreased from 44,100 km to 30,000 km in the last three years (2011-2014). The fleet-average annual VKT values for LDV and motorcycles remained stable over the last decade (See Annex 3 for detailed VKT in 2004-2014).

Table 5. VKT of Singapore's vehicles in 2004 and 2014

Year	Vehicle type						
	PC	Taxi	Coach	Bus	MC	LDV	HDV
2004	20,298	145,031	45,789	95,249	13,744	29,374	39,158
2014	16,600	136,658	57,450	81,228	13,100	29,300	30,000

3.1.2.2. Average Vehicle Speed

Average vehicle speed influences vehicular emissions. Average speed of vehicle is estimated based on peak hour speed values provided from the LTA as well as the value resulting from the Singapore driving cycle for PC (Ho et al. 2014). COPERT allows the distribution between the three different road type; highway (hereafter expresway), rural, and urban. Since Singapore is a city state, the estimation considered only the driving share into expresway and urban.

Expressways play a major role as a backbone of the road network system in Singapore. It is observed that the share of distance travelled increased from 1990 to 2005 due to the increase share of expressways from the total road network. In 2005, 44.63% share of the total distance travelled by passenger car is served by expressways while expressways only representing around 4.61% of total road network (Fwa & Chua 2007). The distance travelled share is expecting progress in 2014 following the previous pattern since they recently opened more expressways such as Kallang Paya Lebar Expressway (KPE) and Marina Coastal Expressway (MCE).

In central business district (CBD), the ERP has helped to increase the average travel speed during peak hours from 25.8 km/h in 2004 to 28.9 km/h in 2014 (Land Transport Authority of Singapore 2015a). Average journey speeds at CBD in earlier 1990 were estimated about 20.1 km/h to 25.5 km/h. (Olszewski et al. 1995). Whereas in expressways the average speed during peak hours increased from 62.9 km/h in 2004 to 64.1 km/h in 2014.

Average speed values for other vehicle types are estimated based on the total average speed of PCs, V_{Total} :

$$V_{Total} = \alpha \cdot V_{Expressway} + (1 - \alpha) \cdot V_{Urban} \quad (1)$$

$$V_{Expressway} = \beta \cdot \gamma \cdot V_{Expressway} \quad (2)$$

$$V_{Urban} = \beta \cdot \delta \cdot V_{CBD/Urban} \quad (3)$$

whereas V_{Total} is the average speed of PCs in the total area of Singapore and α is the share of vehicle activity on expresway. $V_{Expressway}$ is the measured average speed during peak hours on expressways and $V_{CBD/Urban}$ is the measured average speed during peak hour in the arterial roads and in the CBD

area. β is the conversion factor between peak hour speed and total average speed and assumed 1.05. Since the two published values $V_{Expressway}$ and $V_{CBD/Urban}$ are snapshots at specific streets, acceleration and deceleration as well as idling because of traffic condition is not considered. In order to estimate the actual average vehicle speed we used the two correction factors γ and δ for highways, respectively arterial roads. γ is estimated 0.85, δ is assumed 0.5.

By reason of the vehicle restriction strategies and policies, fleet-average vehicle speed of PCs slightly increased from 32.44 km/h in 2004 to 34.93 km/h in 2014. Average speed for LDVs, HDVs, MCs, and coaches is based on these values with the following correlation

$$V_{Total,i} = \theta_i \cdot V_{Total} \quad (4)$$

whereas θ_i is the adjustment factor for MCs (1), LDVs (0.93), HDVs and coaches (both 0.9) based on secondary data given by LTA. Public buses are measured at 18.44 km/h in average (Zhou & Mischalski 2015), taxis were found to travel at 31.59 km/h (Moeker 2014).

3.1.3. Emission Factors

The emission factors that have been used in this calculation are obtained from COPERT 4 methodology (Version 11.0). Practically, it means the specific emission factor is used according to detailed vehicle category (vehicle type, fuel type, engine size, emission standard) and its activity (VKT, area, speed, etc.) in a case study of Singapore.

Local information such as fuel quality and meteorological conditions are needed as input parameters for COPERT model. Even though the emission factors follow COPERT 4 methodology which are based on vehicles test on laboratory measurement test and typical European driving cycle, still these local information (such as temperature and humidity) play a role in defining proper emission factor by using a correction factor according to the typical local condition input parameter. The data on fuel specification was not available at certain detailed because in the reality the specifications vary from grade to grade and brand to brand because of different crude oil quality or refinery technology. However, National Environmental Agency (NEA) has announced the minimum fuel specification regulation (National Environment Agency 2013). Based on this regulation, it is observed that the fuel quality in Singapore is still within a range with a typical fuel quality given in COPERT model which is confirmed with Euro standards.

3.2. Top-down

Road transport energy use and CO₂ emissions can be analysed based on fuel consumption. Diesel and gasoline fuel consumption from the road transport sector were regularly measured from 1990 to 2009 according to the World Bank (Trading Economics n.d.). The consumption of gasoline and diesel increased considerably in the last two decades from 1990 to 2009. However, a sharp increase of diesel consumption can be seen from 2007-2009. It could be due to the increase of diesel vehicles and the use of diesel vehicles on the road.

In terms of time line in this study framework, only year 2004 to 2009 is successfully recorded (Figure 4 and Table 3). A significant increase of diesel consumption is observed within period of 2004-2009, from 1,930 kt in 2004 to 2,600 kt in 2009. At years 2004-2007, the share of diesel remained the same at 65% but increased to 67% since 2008 until 2009.

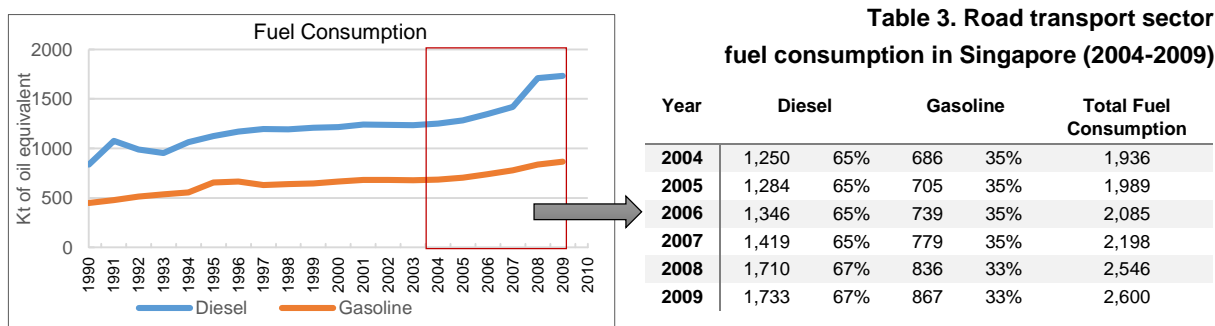


Figure 4. Road transport sector fuel consumption in Singapore (1990-2009)

4. Results and discussion

4.1. Bottom-up results

For bottom-up results, the following illustrations (Figure 5.) show the estimation results for selected emissions simulated using COPERT methodology. The illustrations describe the emission trends 2004-2014 time series by vehicle category. General emissions trend of CO, VOC, NO_x and PM_{2.5} shows the emissions level declined gradually even though the vehicle population increased at the same period of time 2004-2014. These trends were happened due to the implementation of strategic policies and improvement of vehicle technologies from time to time in Singapore.

CO emissions declined considerably by about -10% from 75.7 kt in 2004 to 26kt ton in 2014. The reduction was about one-third in the last decade. The significant reduction of CO is clearly visible and mainly caused by the passenger cars as the greatest main sources. These reductions are supported by the transition of gasoline Euro standards for passenger vehicles from Euro II to Euro IV during that period and due to the higher passenger cars turnover rate.

Similar to CO emissions, significantly declined trend was observed for emissions of VOC from 2004 to 2014. VOC emissions decreased approximately by -10% from 8.7 kt in 2004 to 3.5 kt in 2014. As seen in figure 5 (part VOC), passenger cars with high turnover rate were one of the main causes of VOC reductions in Singapore. In the first year of the timeline (2004), passenger cars were contributed the most (45%) for VOC emissions among all vehicle categories followed by motorcycles (33%), HDVs (8%), LDVs (5%), coaches (4%), public buses (4%) and taxi (1%). However, since emissions standards policy have been tightened and combination of other policies have been implemented within the time, passenger cars (23%) were not contributed dominantly to the VOC emissions but motorcycles with a contribution of 51% in 2014.

NO_x emissions trend, compare to other pollutants showed a slightly different declining trend with a slowly reduction curve during the period of time. About -1% of average annual decline was identified in NO_x emissions (28.4 kt ton in 2004 to 22.7 kt in 2014). HDVs, coaches and public buses which are mostly powered by diesel were the main contributors of NO_x emissions. Increasing number of vehicle population and vehicle share using diesel as a fuel consumption during that period might be responsible for the slightly NO_x emissions reductions.

As illustrated in Figure 5 (part PM_{2.5}), PM_{2.5} emissions decreased moderately from 1.3 kt in 2004 to 0.8 kt in 2014. The emissions of PM_{2.5} had a similar trend to NO_x emissions since both of air pollutants are closely related to the diesel vehicles. Highest reduction (-14%) was found in 2013 to 2014 compare to the annual reduction was about -4% from 2004 to 2014. HDVs were dominated source of PM_{2.5} in 2014 (24%), followed by LDVs (20%), taxis (16%), PCs (14%), coaches (13%), public bus (9%), and motorcycles (4%).

The CO₂ emissions increased gradually with an annual growth of 4% from about 5.6 Mt in 2004 and reached the peak with 7.2 Mt in 2011. The emissions were increased due to the growth of VKT and number of fuel consumptions in that period of time. Since 2011, the CO₂ emissions decreased leisurely to 6.6 Mt in 2014. A significant CO₂ emissions reduction (-5%) was identified for year 2013 to 2014 due to the implementation of carbon emissions-based vehicle scheme (CEVS) that started from 1 January 2013. The CEVS was intended to encourage vehicle buyers to buy a new low-emission cars and charge or provide rebate according to average carbon emissions per km (CO₂/km).

Passenger cars contributed the most CO₂ emissions during the period of time. In 2014, passenger cars had a share of 44% of total CO₂ emissions, followed by HDVs with 14%, LDVs with 11%, coaches with 11%, public buses with 8%, taxis for 10% and motorcycles by 2%. Another highlight can be found in taxis. With a share of 3% of total vehicles population in 2014, taxis contributed 10% of total CO₂ emissions due to the highest VKT. Furthermore, coaches and buses with a share of 1% and 0.5% of total vehicle population contributed around 11% and 8% of total CO₂ emissions. However, if we considered the efficiency of vehicle in terms of CO₂ emissions per passenger kilometre travelled, still the CO₂ emissions of coaches and buses will be the lowest compared to other passenger vehicles.

Regarding CO₂ emission factor, the efficiency gain for passenger cars nowadays. The efficiency of vehicles also takes effect in Singapore even though in certain stage the citizens tend to buy larger PCs in the last decade (see Annex 5 for changes in the composition of car fleet by engine size, 2004-2014). Furthermore, due to the vehicle restriction policies in a form of various fiscal measures (Annex 1), the turnover of PCs in Singapore is substantial higher comparing to other countries. As shown in Annex 6, the 80% of total cars in 2014 are below eight years old.

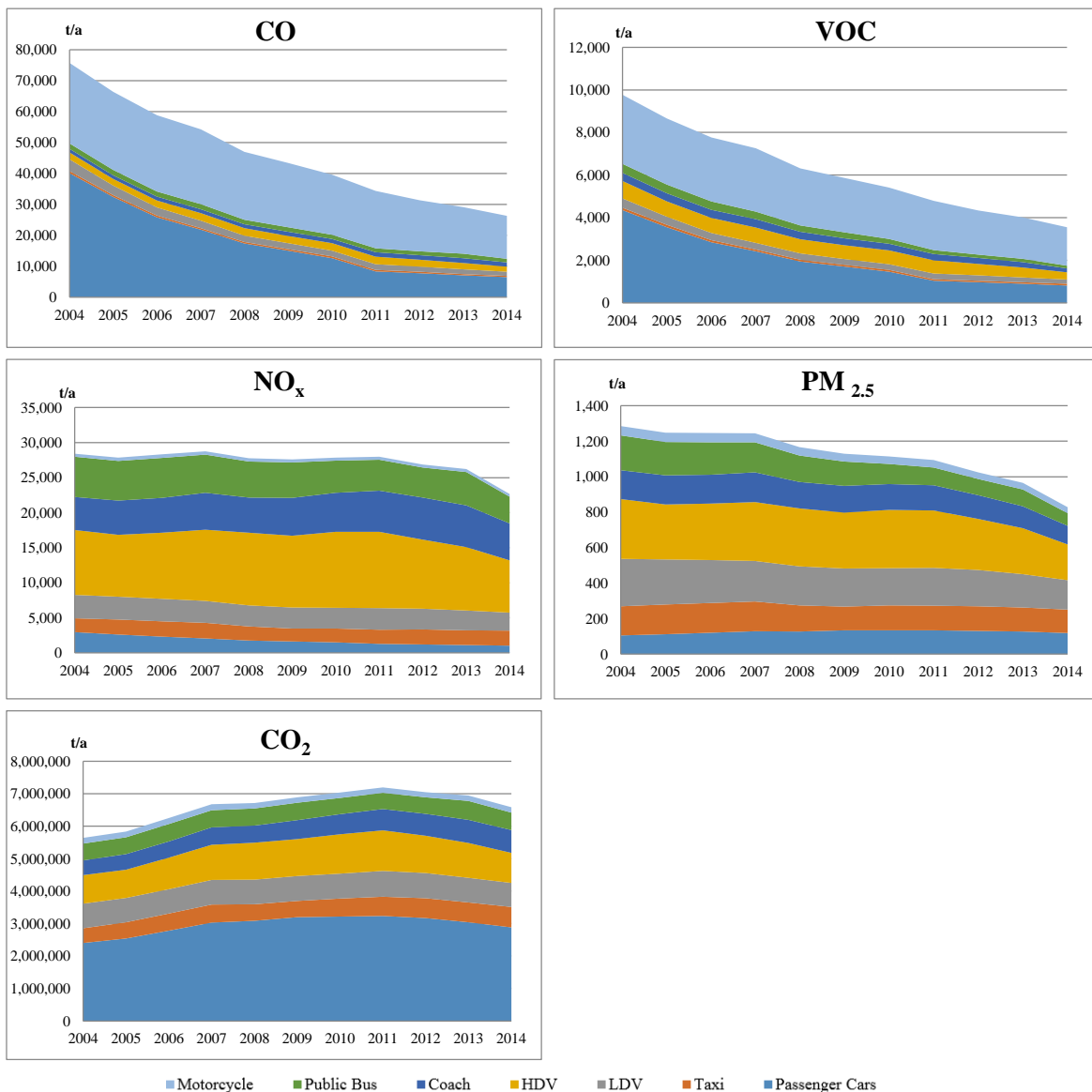


Figure 5. Singapore's emission trends by vehicle category

4.2. Top-down results

For the top-down approach, CO₂ emissions have been estimated under fuel sales principle using fuel sales data from road transport for the period of 2004-2009 (see Figure 3). This approach is inline with the CO₂ Act, for greenhouse gas inventory in accordance with the Kyoto Protocol and IPCC Guideline (Waldron et al. 2006). In this case, default emission factors were used according to the guideline for certain fuel type consumed. It shows that the consumption of gasoline and diesel increased considerably from 6,106 kt in 2004 to 8,198 kt in 2009 with an average annual growth rate of 6%. The share of diesel remained the same from 2004 to 2007 at 65% but increased to 67% since 2008 until 2009. The development of diesel consumption was supported by a series of evidence from the entire fleet data. For instance, taxis, buses and HDVs with high VKT are mostly consume diesel, while other vehicles use gasoline with less VKT.

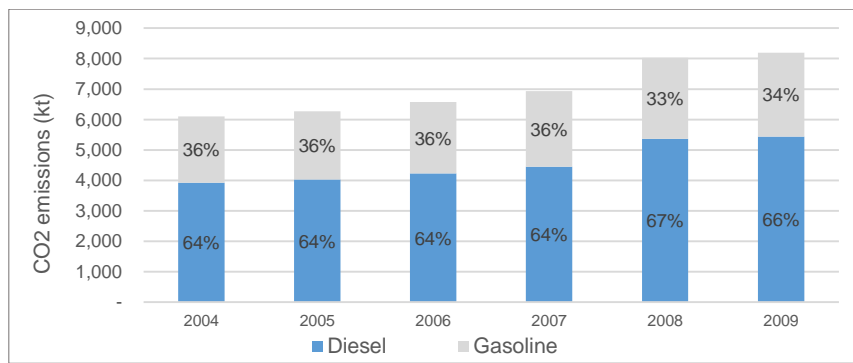


Figure 6. Singapore's road transport CO₂ emissions based on top-down approach (2004-2009)

4.3. Comparison of bottom-up and top-down results

A comparison of CO₂ emission using top-down and bottom-up estimation was performed in Table 6 and figure 7. The quantitative analysis has shown considerable differences over the period from 2004 to 2009, as each approach is subject to different data sources and quality. It is seen that CO₂ emission calculated based on fuel sales principle are higher than the estimated by traffic activity inhabitants. Moreover, the average absolute difference value was 9.27% correspond to the calculated CO₂ emission from national fuel consumption given by the World Bank (Trading Economics n.d.). Still, the national fuel consumption data is missing for the period from 2010 to 2014. Nevertheless, the result shows that the calculation meets a certain level of agreement regarding consistency of the calculation using both approaches.

Table 6. Top-down vs. Bottom-up CO₂ emissions estimation

	Top-down (kt)	Bottom-up (kt)	Absolute difference (%)
2004	6,106.48	5,642.24	7.60%
2005	6,273.66	5,831.85	7.04%
2006	6,576.46	6,248.38	4.99%
2007	6,932.88	6,674.30	3.73%
2008	8,027.88	6,716.98	16.33%
2009	8,198.68	6,890.47	15.96%
average	-	-	9.27%

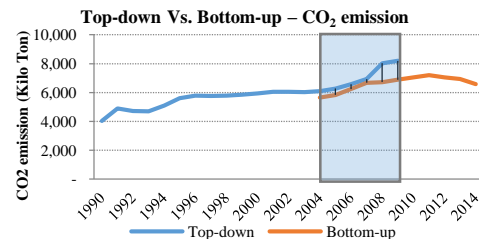


Figure 7. Top-down vs. Bottom-up results

5. Limitation and further scope of the study

There were certain constraints related to the standard data and methodology adopted in this study. For instance, the bottom-up calculation did not cover tax exempted¹ vehicles for goods and other vehicles, including for the off road use. However, the small number of vehicles in this category consumed also fuel which was not included yet in the calculation. Limitations and uncertainties of the bottom-up approach related to the boundary have also been found for fleet categorization, specific fleet activity and its distribution. Due to the data limitation, the fuel quality was assumed the same for overall years simulated. Therefore, this study has further scope to be revised as and when a detailed fleet model, vehicle activities, driving cycle and emissions factors are available and accessible based on local Singapore condition. A better methodology such as applying a traffic situation approach can be done further once the detailed data requirement is accessible. For the top down approach, apart from the statistical data uncertainties given by the source, the difference is largely contributable during to the practice of transport activity to neighbourhood country of Malaysia especially for logistic purpose. Also, petrol and diesel have always been cheaper and the quality of fuel is continually lower in Malaysia comparing to Singapore. Furthermore, it is also essential to validate especially the air pollutants trend with ambient air quality data monitored along roadside locations.

¹ Tax exempted vehicles include vehicles registered with exemption of road tax payment, vehicles for off-the-road use and engineering plants, etc.

6. Conclusion

The modelled fleet and activity data have been simulated using COPERT methodology to estimate the road transport emissions in Singapore for every year from 2004 to 2014. It is observed that the emissions loads for all the pollutants showed decreasing trend for year 2004 to 2014. A clear reduction trend for pollutants CO and VOC were found especially caused by the PCs as the ultimate main factors. This indication is a clear impact of steps taken by the government through the implementation of tighten emission standard, VQS and some fiscal measures. NO_x and PM_{2.5} emissions trends were decreased slowly due to the increasing number of vehicle population using diesel as a fuel consumption. Despite of some reduction trends of pollutants, the vehicle and fleet characteristics were highly affected by series of transportation policies that is being executed by the government such as vehicle control policies and combination of other fiscal measures.

The CO₂ emissions estimation from bottom-up approach is compared with the CO₂ emissions estimation from fuel sales data (top-down) for evaluation purposes. The result showed a significant agreement with an absolute difference of 9.27% even though there were still some limitations and uncertainties within the calculation. Moreover, it is also necessary to validate the emission trends with ambient air quality data monitored along the roadside locations. Nevertheless, this emissions estimation is a good foundation for setting a baseline of emissions estimation and to develop better emissions quantification to support environmentally friendly mobility. The estimation will stimulate the related stakeholders to continue implementing with sustainable transport policies and mitigation actions (such as ERP, VQS). Further estimation of emissions reduction from certain or combination of mitigation actions will influence the effectiveness of any mitigation scheme in the transport sector which is being planned and implemented by the government Singapore.

Acknowledgement

This work was financially supported by the Singapore National Research Foundation under its Campus for Research Excellence And Technological Enterprise (CREATE) programme.

References

- Ajtay, D. Iisabeta, 2005. *Modal Pollutant Emissions Model of Diesel and Gasoline Engines*. Swiss Federal Institute of Technology Zurich.
- Chin, A.T.H., 2000. Sustainable urban transportation: abatement and control of traffic congestion and vehicular emissions from land transportation in Singapore. *Environmental Economics and Policy Studies*, 3(4), pp.355–380.
- Chu, S., 2015. Car restraint policies and mileage in Singapore. *Transportation Research Part A*, 77, pp.404–412. Available at: <http://dx.doi.org/10.1016/j.tra.2015.04.028>.
- Clean Air Asia, 2012. *Assessing ASIA : Air Pollution and Greenhouse Gas Emissions Indicators for Road Transport and Electricity*.
- Fameli, K.M. & Assimakopoulos, V.D., 2015. Development of a road transport emission inventory for Greece and the Greater Athens Area: Effects of important parameters. *Science of the Total Environment*, 505(July 2015), pp.770–786.
- Fwa, T.F. & Chua, G.K., 2007. Passenger Car Travel Characteristics in Singapore – Analysis of Changes from 1990 to 2005 –. *International Association of Traffic and Safety Sciences*, 31(2), pp.48–55. Available at: [http://dx.doi.org/10.1016/S0386-1112\(14\)60222-3](http://dx.doi.org/10.1016/S0386-1112(14)60222-3).
- Gkatzoflias, D. et al., 2012. COPERT 4 Computer programme to calculate emissions from road transport. , (February).
- Gkatzoflias, D. et al., 2012. *COPERT 4. Computer Program to calculate emissions from road transport. User Manual (Version 9.0)*.
- Ho, S., Wong, Y. & Chang, V.W., 2014. Developing Singapore Driving Cycle for passenger cars to estimate fuel consumption and vehicular emissions. *Atmospheric Environment*, 97, pp.353–362. Available at: <http://dx.doi.org/10.1016/j.atmosenv.2014.08.042>.
- International Energy Agency, 2009. *Transport, Energy and CO2 Moving Toward Sustainability*.
- Jinca, A. et al., 2014. *Selecting a Suitable Traffic Emission Model for a Particular Application*, Available at: http://baq2014.org/wp-content/uploads/Full-Souvenir-Program_20Jan2015.pdf.
- Johnson, L. & Adams, S., 2011. *Transport Outlook 2010*, Available at: www.nmc.org.
- De Jong, G.C., 1990. An indirect utility model of car ownership and private car use. *European Economic Review*, 34(5), pp.971–985.

- K.W, A.-B. et al., 2010. Traffic-data driven modelling of vehicular emissions using COPERT III in Ghana : A case study of Kumasi. , 134350, pp.32–40.
- Kouridis, C. & Ntziachristos, L., 2012. Copert 4.
- Land Transport Authority of Singapore, 2015a. Facts and Figures - Traffic Flow. Available at: <https://www.lta.gov.sg/content/dam/ltaweb/corp/PublicationsResearch/files/FactsandFigures/TrafficFlow.pdf> [Accessed November 1, 2015].
- Land Transport Authority of Singapore, 2015b. Land Transport Publications and Research. Available at: <http://www.lta.gov.sg/content/ltaweb/en/publications-and-research.html> [Accessed February 8, 2016].
- Land Transport Authority of Singapore, 2014a. *Land Transport Statistics in Brief 2014*,
- Land Transport Authority of Singapore, 2014b. Taxi Availability Improves for Second Consecutive Year. Available at: <http://www.lta.gov.sg/apps/news/page.aspx?c=2&id=b7c17d30-f5d3-4d15-9ccc-e017d4fb43bb> [Accessed November 1, 2015].
- Land Transport Authority of Singapore, 2013. *The Singapore Land Transport Master Plan 2013*, LTA Academy, 2013. *Asia regional exchange on NAMAs in the transport sector*, Singapore.
- LTA Academy, 2010. Journeys - Sharing Urban Transport Solutions. *Journeys - Sharing Urban Transport Solutions*, (4).
- Moeker, S., 2014. *Driving Profile and Energy Demand Analysis for Electrical Vehicles based on GPS Trajectories*. Technische Universitaet Muenchen.
- National Climate Change Secretariat, 2012. *Singapore's National Climate Change Strategy*,
- National Environment Agency, 2013. Factsheet on Singapore Air Quality Abatement Measures. Available at: <http://www.nea.gov.sg/docs/default-source/corporate/COS-2014/singapore-air-quality-abatement-measures.pdf> [Accessed April 7, 2016].
- Ntziachristos, L. et al., 2013. Air Pollutant and Greenhouse Gas Road Transport Inventory using COPERT Australia. , (2), pp.1–6.
- OECD & International Transport Forum, 2010. *Reducing transport greenhouse gas emissions. Trends & Data 2010*,
- Olszewski, P., Fan, H.S.L. & Tan, Y., 1995. Area-wide traffic speed flow model for the Singapore CBD. *Transportation Research Part A*, 29(4), pp.273–281.
- Olszewski, P.S., 2007. Singapore motorisation restraint and its implications on travel behaviour and urban sustainability. *Transportation*, 34(3), pp.319–335.
- Organisation for Economic Co-operation and Development (OECD), 2010. *Reducing Transport Greenhouse Gas Emissions Trends and Data 2010*,
- Singapore Department of Statistic, 2015. Singapore in Figures: 2015.
- Smit, R. & Ntziachristos, L., 2013. COPERT Australia : a new software to estimate vehicle emissions in Australia. , (October), pp.1–11.
- Smit, R. & Ntziachristos, L., 2012. *COPERT Australia : Developing Improved Average Speed Vehicle Emission Algorithms for the Australian Fleet*.
- Soylu, S., 2007. Estimation of Turkish road transport emissions. *Energy Policy*, 35(8), pp.4088–4094. Available at: <http://linkinghub.elsevier.com/retrieve/pii/S0301421507000560> [Accessed September 26, 2014].
- Trading Economics, Road sector fuel consumption in Singapore. Available at: <http://www.tradingeconomics.com/singapore/road-sector-diesel-fuel-consumption-kt-of-oil-equivalent-wb-data.html> [Accessed October 10, 2015].
- Waldron, C.D. et al., 2006. *IPCC Guidelines for National Green House Gas Inventories Volume 2 : Energy*,
- Xing, P. & Hu, T., 2013. Urban Low Carbon Transport System. In F. Chen, Y. Liu, & G. Hua, eds. Berlin, Heidelberg: Springer Berlin Heidelberg. Available at: <http://link.springer.com/10.1007/978-3-642-34651-4> [Accessed August 13, 2013].
- Zhou, Y. & Mischalski, M.G., 2015. *Public Transport Modelling of Singapore*, Singapore.

Annexes

Annex 1

Table 7. A summary of the fiscal measures in Singapore has implemented to manage the car population growth

Measure	Description
Registration Fee	A Registration Fee of S\$140 covers the costs of registering a vehicle in Singapore. It is collected upon registration of the vehicle.
Additional Registration Fee (ARF)	The Additional Registration Fee (ARF) is a tax imposed upon registration of a vehicle. It is calculated based on a percentage of the Open Market Value (OMV) of the vehicle.
Preferable Additional Registration Fee (PARF)	The Preferential Additional Registration Fee (PARF) benefit is granted to a vehicle owner who de-registers his car by scrap or export before the car reaches ten years old. This fee ensures a relatively young and roadworthy fleet for smooth flowing traffic.
Excessive Duty	Excise Duty is a tax imposed and collected by Singapore Customs. Like the ARF, the Excise Duty is also calculated based on a percentage of the OMV of the vehicle, 20% of OMV.
Road Taxes	Levied progressively based on engine capacity as follows Additional road tax surcharge for vehicles over ten years
Vehicle Quota System	Implemented on 1 May 1990 the scheme requires buyers of all new vehicles other than public buses and school buses to take part in a public tender to get a license to buy a fixed number of vehicles.
Special Tax	A Special Tax is levied on diesel cars and is payable in addition to the Road Tax of the vehicle. The quantum of the Special Tax for diesel cars takes into account the particulate matter (PM) emissions. A petrol duty is imposed to encourage fuel conservation and discourage excessive use of vehicles that may contribute to congestion and pollution. However, there is currently no equivalent duty imposed on diesel.

Annex 2

Table 8. Singapore road transport vehicle population by year. Source: LTA Statistic (2004-2014)

Year	Vehicle type								
	AGR ^a	Total	PC	Taxi	Coach	Bus	MC	LDV	HDV
Share 2004		100%	58.54%	2.85%	1.29%	0.50%	19.12%	12.64%	5.04%
2004	2.65%	716,507	419,470	20,407	9,274	3,618	137,029	90,579	36,130
2005	3.81%	743,813	440,583	22,383	9,621	3,599	139,434	91,588	36,605
2006	5.87%	787,459	474,717	23,334	10,046	3,785	142,736	93,244	39,597
2007	6.50%	881,208	517,041	24,446	10,431	3,761	144,340	97,019	41,585
2008	5.08%	911,749	552,846	24,300	11,122	3,854	146,120	98,986	43,980
2009	3.47%	911,749	579,371	24,702	11,614	4,045	147,215	99,956	44,846
2010	2.17%	931,528	597,746	26,073	11,955	3,981	148,160	98,569	45,044
2011	1.09%	941,700	606,280	27,051	12,540	4,112	146,559	99,112	46,046
2012	1.32%	954,145	620,011	28,210	12,556	4,212	144,110	98,058	46,988
2013	0.36%	957,584	623,688	27,695	12,513	4,552	144,934	95,483	48,719
2014	-0.31%	954,583	619,023	28,736	12,535	4,756	145,026	95,599	48,908
∅	2.91%								
Share 2014		100%	64.85%	3.01%	1.31%	0.50%	15.9%	10.01%	5.12%

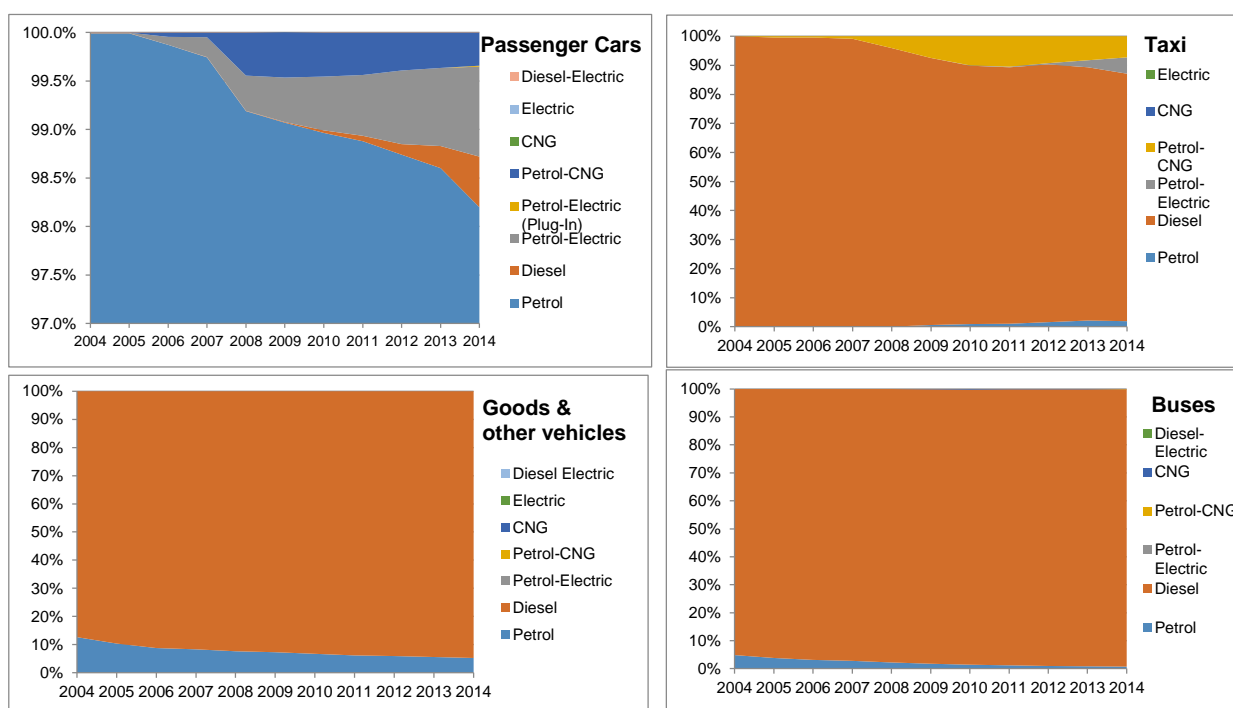
^aAGR is annual growth rate

Annex 3

Table 9. VKT of Singapore's vehicles in 2004 and 2014. Source: LTA Statistic (2004-2014)

Year	Vehicle type						
	PC	Taxi	Coach	Bus	MC	LDV	HDV
2004	20,298	145,031	45,789	95,249	13,744	29,374	39,158
2005	20,603	145,031	46,905	95,849	13,711	29,248	38,768
2006	21,100	144,205	47,300	95,103	13,700	29,300	40,400
2007	20,800	141,933	48,500	94,665	13,800	28,100	42,400
2008	19,700	131,472	46,350	92,345	13,300	27,900	42,000
2009	19,600	124,742	48,400	91,374	13,200	28,000	41,200
2010	19,100	130,756	49,800	88,199	13,000	28,500	44,100
2011	19,000	131,935	51,450	85,771	13,400	29,900	44,100
2012	18,200	131,161	53,450	84,866	13,300	29,700	39,400
2013	17,400	134,603	55,450	92,443	13,200	29,500	34,700
2014	16,600	136,658	57,450	81,228	13,100	29,300	30,000

Annex 4



Note: All motorcycles use petrol.

Figure 8. Fuel share trend per vehicle type. Source: LTA Statistic (2004-2014)

Annex 5

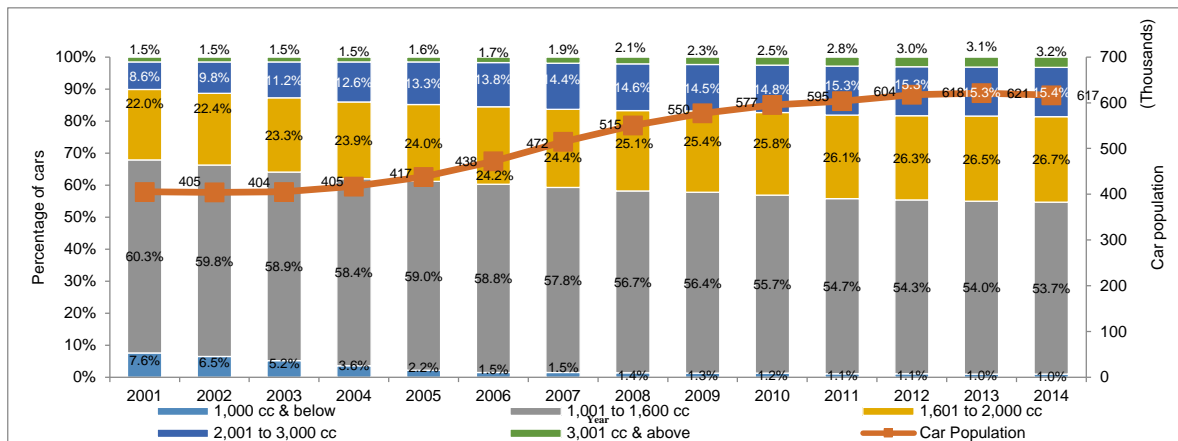


Figure 9. Changes in the composition of car fleet by engine size, 2004-2014.
Source: LTA Statistic (2004-2014)

Annex 6

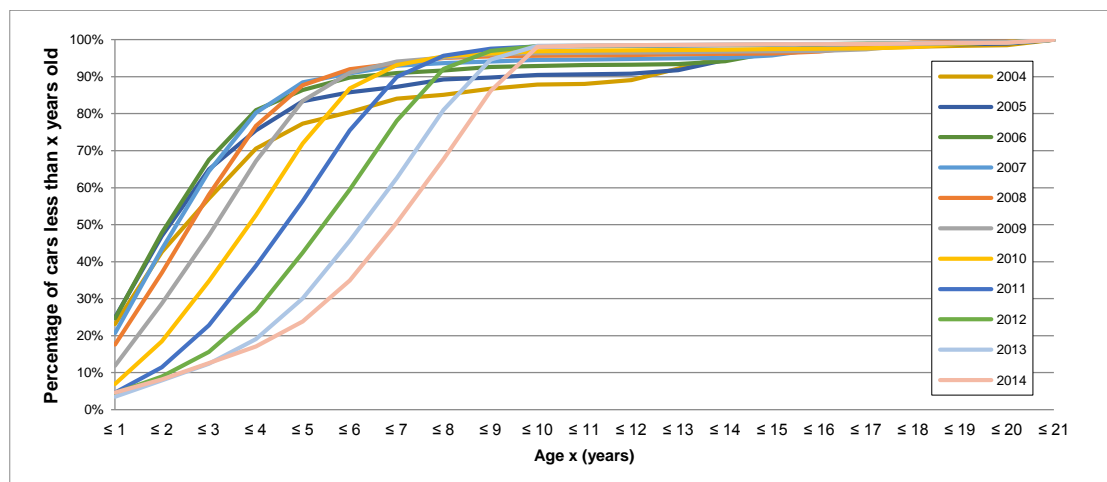


Figure 10. Changes in cumulative age distribution of cars in Singapore.
Source: LTA Statistic (2004-2014)

Variations of real world NO_x emissions of diesel Euro 5 and 6 light-duty vehicles

Gerrit KADIJK, Pim van MENSCH & Norbert E. LIGTERINK

TNO, Van Mourik Broekmanweg 6, 2628 XE Delft, The Netherlands.

Fax +31 88 866 3010 - email: gerrit.kadijk@tno.nl

** Lab. Environment, TNO Automotive, Automotive Campus 30, 5708 JZ Helmond, The Netherlands

Abstract

In order to gain insight into trends in real-world emissions of light-duty diesel vehicles under conditions relevant for the Dutch and European situations, eighteen Euro 6 passenger cars and ten Euro 5 light commercial vehicles (LCV's) were extensively tested in the laboratory and on the road. These measurements also form a basis for the annual update of Dutch emission factors. The majority of the vehicles comply in type approval emission tests but on the road real-world NO_x emissions are on average 5 to 6 times higher than the type approval limit value. Euro 6 passenger cars emit in the range of 50-2000 mg/km. The average NO_x emissions of the N1 class III Euro 5 commercial vehicles range from 1421 to 1670 mg/km. In general the difference between real-world emissions and type approval emissions has been growing over the years. Improvement of real world NO_x emissions of future diesel vehicles is possible with Real Driving Emission legislation. Currently the relative expensive PEMS is foreseen as the type approval standard for on-road testing. TNO applies also a NO_x-O₂ sensor based system with data logger (SEMS) as a NO_x screening tool. In the RDE legislation it is prescribed to normalize the measured data of RDE test trips. The current normalization tools (EMROAD and CLEAR) show a variation in the results.

Keys-words: Real-world NO_x emissions, light-duty vehicles, RDE, PEMS, SEMS.

Introduction

Commissioned by the Dutch Ministry of Infrastructure and the Environment, TNO regularly performs test programmes to determine real-world emission performance of vehicles in the Netherlands (Kadijk 2015 a,b,c & 2016a). The main goal of the programs is to gain insight into trends in real-world emissions of light-duty vehicles under conditions relevant for the Dutch and European situations. Between 2013 and 2015 in total eighteen Euro 6 passenger cars and ten Euro 5 light commercial vehicles (LCV's) were extensively tested. These measurements also form a basis for determining the annual update of the Dutch emission factors, used in national emission inventories and air-quality models

Based on the performed emission measurements, TNO develops and annually updates vehicle emission factors that represent real-world emission data for various vehicle types and different driving conditions. Vehicle emission factors are used for emission inventory and air quality monitoring. TNO is one of the few institutes in Europe who perform independent emission tests for real-world conditions. Dutch emission factors are based on these tests. The emission factors are one of the few independent sources of information on the growing difference between legislative emission limits and real-world emission performance of cars.

To minimize air pollutant emissions of light-duty vehicles, in 1992 the European Commission introduced the Euro emission standards. In the course of time, these standards have become more stringent. Since September 2014 all new type approved light-duty vehicles must comply with Euro 6 regulations and from September 2015 onwards all registered vehicles needs to comply with the Euro 6 limits, therefore the tested vehicles are relatively early models. The focus of the test program were compression ignition (diesel) vehicles. The standards apply to vehicles with spark ignition engines and to vehicles with compression ignition engines and cover the following gaseous and particulate emissions: CO (carbon monoxide), THC (total hydrocarbons), NO_x (nitrogen oxides), PM (particulate mass) and PN (particulate number).

As a result of the Euro emission standards, the pollutant emissions of light-duty vehicles as observed

in type approval tests have been reduced significantly over the past decade. However, under real driving conditions some emissions substantially deviate from their type approval equivalents. The real driving nitrogen oxides, or NO_x, emissions of diesel vehicles are currently the largest issue with regard to pollutant emissions. As NO_x represents the sum of NO and NO₂ emitted, reducing NO_x emissions of vehicles are an important measure in bringing down the ambient NO₂ concentration. In the Netherlands, the ambient NO₂ concentration still exceeds European limits at numerous road-side locations.

TNO regularly performs emission measurements within the “in-use compliance program for light-duty vehicles”. Whereas in the early years, i.e. in 1987 to 2000, many standard type approval tests were executed, in recent years the emphasis has shifted towards the gathering of real-world emission data. Real-world emission data is collected by means of:

1. Performing emission measurements on a chassis dynamometer using various non-standard driving cycles, for example driving cycles that better reflect real-world driving conditions, and;
2. Equipping vehicle with an on-board emission measurement system and subsequently measuring the emissions of the vehicles while driving on the public road.

1. Objective

The objective of this research is to assess the real-world emission performance of Euro 6 passenger cars and Euro 5 light commercial vehicles (mainly N1 class III) and to assess the NO_x reduction performance of Euro 5 and 6 diesel technologies.

2. Methods

Emission tests were performed on the chassis dynamometer and on the road.

Chassis dynamometer tests: The Type Approval (TA) value for NO_x emissions of light-duty vehicles is based on a chassis dynamometer test in a laboratory. TNO tested most of the Euro 6 passenger cars in chassis dynamometer tests with a total number of approximately 130 tests. All vehicles were tested according to the official test procedure (UNECE Reg 83) and they nearly all comply with the NO_x limit value of 80 mg/km. Also different driving cycles were conducted, such as the CADC and WLTC.

On-road testing: TNO performs real-world tests on the road with a Portable Emission Measurement System (PEMS) and/or a Smart Emission Measurement System (SEMS). PEMS equipment measures CO, CO₂, HC, NO and NO₂ emissions. SEMS is an emission screening tool which contains a data logger and a NO_x – O₂ sensor. Moreover, with SEMS NH₃ emissions are monitored.

PEMS testing: Emission tests with different vehicles were performed on the road under real-world conditions. During the PEMS tests, the vehicle was loaded with a test driver, a test engineer and the test equipment (including a battery and a generator), amounting to a total test weight of approximately 200 kg.

SEMS testing: In recent years, TNO has developed the so-called Smart Emission Measurement System or SEMS (Vermeulen et al. 2012 & 2014). Most vehicles in this testing program were also tested using SEMS. SEMS is an emission screening tool which contains a data logger, a NO_x – O₂ sensor (Continental, UniNOx) and a thermocouple, the latter two of which are installed in the tailpipe of the vehicle. It measures the exhaust gas temperature and the O₂ and NO_x volume concentrations in vol% or ppm. SEMS also measures geographical data and logs the CAN data of the vehicle with a measuring frequency of 1 Hz. On the basis of the measured O₂ readings and the carbon and hydrogen content of the fuel, the CO₂ concentrations are calculated. In former projects, the accuracy and the reliability of the SEMS equipment and method has been proved (2012), (2014b). However, the absolute emission results are calculated with data from the CAN bus of the vehicle and these can deviate which may lead to deviations in the end results. In this project, the air mass rate of the vehicle CAN bus has been applied for calculations of the NO_x and CO₂ mass flow rates [mg/km]. The quality of the air mass rate signal has a large influence on the accuracy of the NO_x and CO₂ mass emissions.

Moreover, the NO_x – O₂ sensor is sensitive for temperature and pressure which may have an effect on the accuracy.

The test and data processing procedure contains the following steps:

1. The CO₂ volume concentration is determined from the measured O₂ volume concentration and the fuel C:H ratio.
2. The exhaust mass flow rate is determined from the vehicle Mass Air Flow signal, augmented with combustion products CO₂ and H₂O using the fuel C:H ratio and the normal air density
3. The CO₂ and NO_x mass flow rates are determined from the measured volume concentrations and the exhaust mass flow rate.

This analysis requires three input parameters:

- the C:H ratio of the fuel, which is assumed to be 1.95 for modern market-fuel diesel, and;
- the ambient oxygen content of air at 20.8% for on-road conditions;
- Normal air density of 1.29 kg/m³ at standard conditions to calculate the exhaust gas density

Test routes:

PEMS and SEMS register real-world conditions and real-world emissions. In order to be able to compare the individual real-world vehicle emissions, the TNO-designed 'reference trip' is always part of the investigation. The reference trip consists of urban, rural and highway driving. Additionally, some other trips are driven: a constant speed trip, a trip mainly containing urban driving and a trip consisting mainly of highway driving. Table 1 shows the main characteristics of the test trips. All trips are started in Helmond, the Netherlands. For the LCV's tests are carried out with different payloads.

Table 1: Specifications of PEMS and SEMS test trips.

	TNO City route Helmond	TNO Reference route	Constant speed route (Germany)
Type	City	City, rural and highway	Highway
Cold/Hot start	Hot start	Cold and hot start	Hot start
Distance [km]	25.6 km	73.5 km	189 km
Duration [min]	57 min	89 min	119 min*
Av. speed [km/h]	32 km/h (excluding idle time)	55 km/h (excluding idle time)	93 km/h (total route)*
Load [-]	Driver** + test equipment	Driver** + test equipment	Driver** + test equipment

*Constant speed measurements are part of this route; constant speed tests have duration of approximately 300 to 600 seconds.

**For PEMS trips a driver and a test engineer run the test.

Driving styles in on-road measurements:

The test driver is given instructions for the required driving style. This can be 'regular', 'economic' or 'dynamic'. Some vehicles are tested with all driving styles. After every trip the fuel tank of the vehicle is filled off at the same pump of the same filling station.

Test vehicles:

Table 2,

Table 3 and **Table 4** show the sixteen tested Euro 6 vehicles per phase in the measurement programme. The three phases in the measurement programme are defined as follows:

- Phase 1: Euro 6 prototype vehicles, tested in 2010;
- Phase 2: First Euro 6 production models, tested in 2012 and 2013
- Phase 3: Selection of Euro 6 vehicles with an SCR system, tested in 2014 and 2015.

In Table 5 the types of test per passenger vehicle are specified.

In Table 6 the tested diesel light commercial Euro 5 vehicles are specified.

Table 2: Phase 1: Tested Euro 6 prototype vehicles in 2010.

Vehicle ID	-	veh: H2	veh: H3	veh: A2	veh:E4*
Engine Power class	[kW]	>150	>150	>150	100 - 125
Engine capacity class	[cm3]	>2000	>2000	>2000	1750 - 2000
Odometer	[km]	2.354	16.634	9.466	9.400
Fuel	-	Diesel	Diesel	Diesel	Diesel
Inertia	[kg]	1700	1930	2040	1590
Emission class	-	Euro 6	Euro 6	Euro 6	Euro 6
Type	-	Sedan	Sedan	Sedan	Sedan
Applied system for NO _x reduction	-	LNT	LNT	SCR	SCR

*Three vehicles

Table 3: Phase 2: First Euro 6 production models, tested in 2012 and 2013.

Vehicle ID	-	veh: H4	veh: H6	veh: H7	Veh: E6	Veh: J1	Veh: J2
Engine Power class	[kW]	125 - 150	100 - 125	100 - 125	100 - 125	100 - 125	100 - 125
Engine capacity class	[cm3]	1750 - 2000	1750 - 2000	1750 - 2000	1750 - 2000	1750 - 2000	1750 - 2000
Odometer	[km]	10.965	28.376	3.000	26.200	20.100	11.616
Fuel	-	Diesel	Diesel	Diesel	Diesel	Diesel	Diesel
Inertia	[kg]	1590	1470	1810	1590	1590	1590
Emission class	-	Euro 6	Euro 6	Euro 6	Euro 6	Euro 6	Euro 6
Type	-	Wagon	Sedan	Sedan	Sedan	MPV	MPV
Applied system for NO _x reduction	-	LNT	LNT	LNT	SCR	EGR	EGR

Table 4: Phase 3: Selection of Euro 6 vehicles with SCR system, tested in 2014 and 2015.

Vehicle ID	-	Veh. K1	Veh. K2	Veh. L1	Veh. M1	Veh. N1	Veh. O1
Engine Power class	[kW]	100 - 125	100 - 125	75 - 100	100 - 125	>150	>150
Engine capacity class	[cm3]	1500 - 1750	1500 - 1750	1500 - 1750	>2000	>2000	>2000
Odometer	[km]	3.500	15.000	10.125	20.000	19.500	11.400
Fuel	-	Diesel	Diesel	Diesel	Diesel	Diesel	Diesel
Inertia	[kg]	1700	1700	1250	1590	2270	1930
Emission class	-	Euro 6	Euro 6	Euro 6	Euro 6	Euro 6	Euro 6
Type	-	MPV	MPV	Wagon	Sedan	MPV	Sedan
Applied system for NO _x reduction		SCR	SCR	SCR	SCR	SCR	LNT+SCR

Table 5: Types of tests per vehicle.

Phase of measurement programme	Type of vehicle	Vehicle ID	Chassis dynamometer tests	PEMS tests	SEMS tests
[-]	[-]	[-]	[#]	[#]	[#]
Phase 1	Prototype models	Veh: H2	6	-	-
		Veh: H3	3	-	-
		Veh: A2	3	-	-
		Veh: E4	6	-	-
Phase 2	First Euro 6 production models	Veh: H4	7	-	-
		Veh: H6	9	-	-
		Veh: H7	0	14	-
		Veh: E6	8	15	-
		Veh: J1	8	-	-
		Veh: J2	10	-	-
Phase 3	Selection of Euro 6 SCR models	Veh. K1	19	-	-
		Veh. K2	7	16	-
		Veh. L1	12	11	16
		Veh. M1	7	14	37
		Veh. N1	7	-	55
		Veh. O1	7	-	20
Total			119	70	128

Table 6: Tested diesel commercial Euro 5 vehicles

Vehicle ID	[-]	1	2	3	4	5	6	7	8	9	10
Engine Power class	[kW]	65-70	50-55	60-65	60-65	95-100	70-75	90-95	65-70	75-80	95-100
Engine capacity class	[dm ³]	1.6	1.6	2.2	2.0	2.1	2.1	2.0	2.0	2.3	2.2
Odometer	[km]	18.500	42.000	41.700	23.400	91.000	52.200	12.800	99.000	99.000	10.000
Empty vehicle mass	[kg]	1.700	1.400	1.850	1.750	2.300	1.900	2.100	2.000	2.200	1875
Emission class	[-]	Euro 5	Euro 5	Euro 5	Euro 5	unknown	Euro 5	Euro 5	Euro 5	Euro 5	Euro 5
Type	[-]	Van	Van	Van	Van	Van	Van	Van	Van	Van	Van
Category	[-]	N1 cl III	N1 cl II	N1 cl III	N1 cl III	N1 cl III	N1 cl III	N1 cl III	N1 cl III	N1 cl III	N1 cl III
Date of production	[-]	11-2012	03-2013	01-2013	02-2014	05-2011	02-2013	08-2014	02-2012	01-2012	04-2014
CO ₂ Type approval	[g/km]	177	136	183	176	223	195	211	Not declared	Not declared	199

3. Results

Most vehicles were tested on a chassis dynamometer. Between 2013 and 2015 five Euro 6 vehicles were tested using PEMS with a total of approximately 70 tests. Fifteen vehicles were tested with SEMS (four Euro 6 passenger cars and eleven Euro 5 LCV's), approximately 220 SEMS tests were performed.

Chassis dynamometer test results Euro 6 vehicles:

CO emissions: In chassis dynamometer tests the CO emissions of most vehicles are well below the type approval limit value of 500 mg/km.

THC emissions: The combined type approval limit value of THC+NO_x is 170 mg/km. As already shown, the NO_x emissions exceed their limit value of 80 mg/km. In most tests the THC emission is well below 90 mg/km.

PM emissions: The PM emissions of most vehicles are well below the type approval limit value of 4.5 mg/km. This is caused by the diesel particulate filters which have high filter conversion rates.

NO_x emissions: In Figure 1 the NO_x emissions of sixteen Euro 6 vehicles in various test cycles are shown. The range of NO_x emission results in chassis dynamometer tests is very broad; 40 – 800 mg/km. In the type approval test (NEDC) nearly all vehicles comply with the NO_x limit value of 80 mg/km, depicted as a red line in the figure.

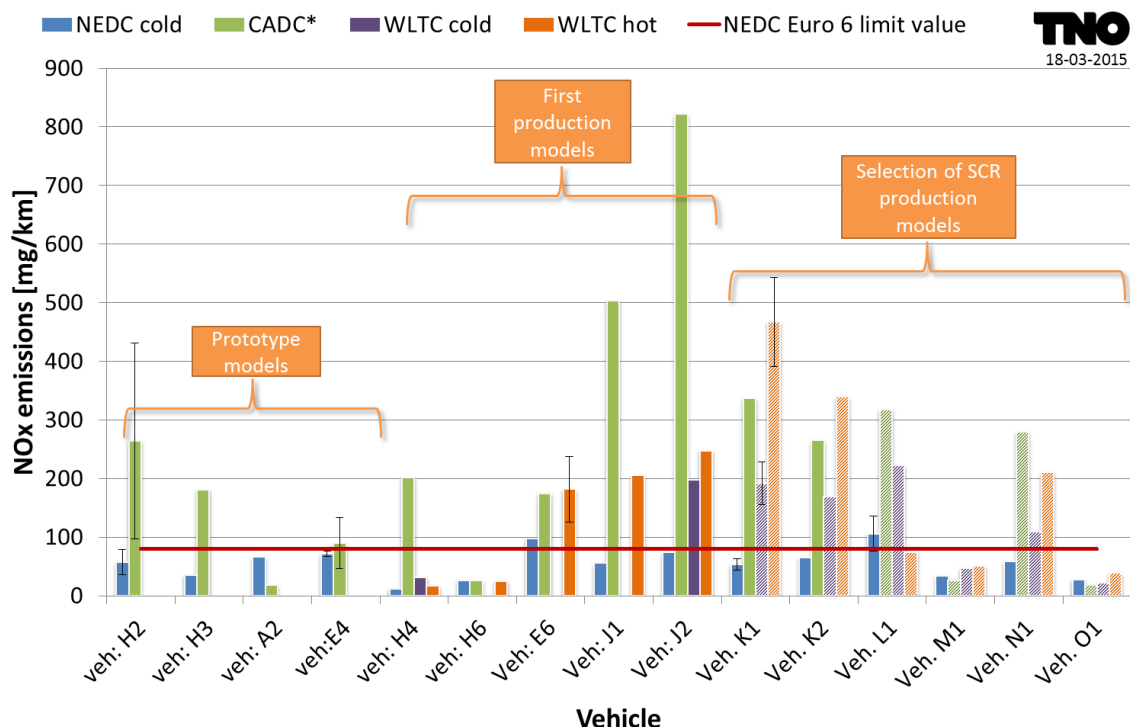


Figure 1: NO_x emissions on the chassis dynamometer per driving cycle of Euro 6 diesel vehicles

- In CADC tests the NO_x emissions of the vehicles are 4 - 10 times higher (200-800 mg/km) than in NEDC tests. Especially vehicle J1 and J2 have extreme high NO_x emissions in the CADC test (up to 1150 mg/km). These vehicles are not equipped with a NO_x aftertreatment device but NO_x emissions are controlled with an engine with a lowered compression ratio and an EGR system.
- The NO_x emissions on WLTC tests are also often higher than the NEDC test results. Moreover the vehicles K1, K2 and N1 show significant higher NO_x emissions in the WLTC with hot start compared to the WLTC with cold start. These results indicate that emission optimization is related to the applicable type approval test cycle.
- The vehicles A2, E4, M1 and O1 perform very well in all chassis dynamometer tests (< 80 mg/km). These vehicles are equipped with a SCR system, most likely in combination with EGR. But other SCR vehicles (K1, K2 and N1) have elevated emissions in test cycles that better represent real-world conditions (100-500 mg/km, or up to 6 times the type approval limit value).
- Vehicles H2, H3, H4, H6 are equipped with an LNT for NO_x reduction, most likely in combination with

EGR. The vehicles H4 and H6 perform well below 80 mg/km but H2 and H3 emit 180-280 mg/km.

In the CADC tests of Figure 2 the urban phase with cold and hot start of most vehicles gain equal NO_x emissions. However vehicles M1, N1 and O1 clearly show higher emissions after cold start; probably the SCR-catalyst operates after the cold start below the light off temperature. Most vehicles have high NO_x emissions in the motorway phase (200–1200 mg/km). Vehicles J1 and J2 which are not equipped with LNT or SCR show high emissions, while vehicle J2 even exceeds the value of 1000 mg/km. On the contrary the vehicles A2, E4, H6, M1 and O1 show relatively low emissions in all CADC-phases. These vehicles are all equipped with LNT or SCR technology. The residual SCR-equipped vehicles have relatively high emissions on the highway phase (200-400 mg/km)

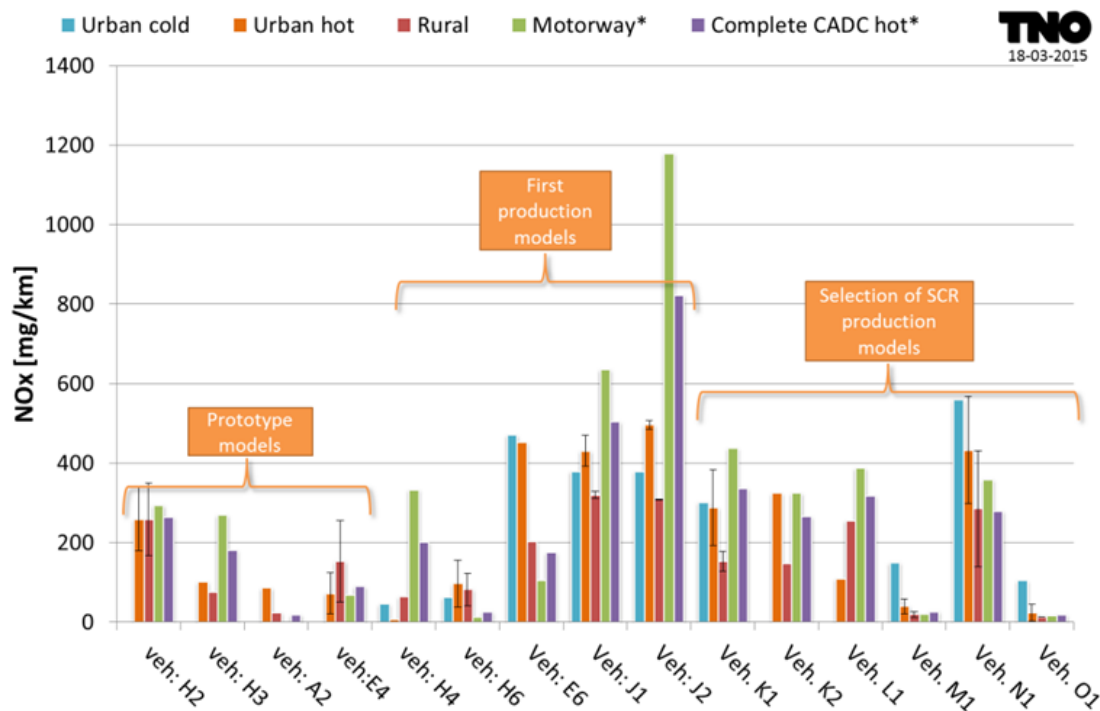


Figure 2: NO_x emissions per phase in CADC tests

NO_x emissions in on-road urban, reference and highway trips:

Figure 3 shows the on-road NO_x emissions of urban, reference and highway trips. The urban and reference trips are in some way comparable because they were started with a hot engine and driven with a regular driving style. The highway trips are not comparable because the average vehicle speed already differs significantly per trip. The error bars at the highway trips show the variation of the trip speed (horizontal) and the variation of NO_x emissions (vertical).

In urban and reference trips the NO_x emissions are between approximately 80 to 700 mg/km. In highway trips NO_x emissions range from 80 to around 1100 mg/km. Overall, on-road NO_x emissions of the measured vehicles show a very scattered pattern, with values ranging from 80 to 1100 mg/km, the latter value being 14 times higher than the Euro 6 NEDC limit value. In highway trips the NO_x emission performance is not stable because the average vehicle speed per trip differs. Only one vehicle has relatively low NO_x emissions in all trips, ranging from 50 to 200 mg/km. Remarkably, both the best-performing vehicle and the worst-performing vehicle are equipped with SCR technology. However the best performing vehicle also has a LNT.

The real-world NO_x emission of Euro 6 diesel passenger cars is in the range of 50 to >2000 mg/km. On average real-world NO_x emissions are 5 to 6 times higher than the type approval limit value of 80 mg/km. This seems to indicate that emission control technologies perform differently on the road than they do on the chassis dynamometer. Moreover, the real world NO_x emission per road type of the different vehicles differ widely. Also driving behavior and gear shift patterns can strongly influence the NO_x emission results. Proper RDE-legislation, possibly in combination with independent testing can improve these real driving emissions.

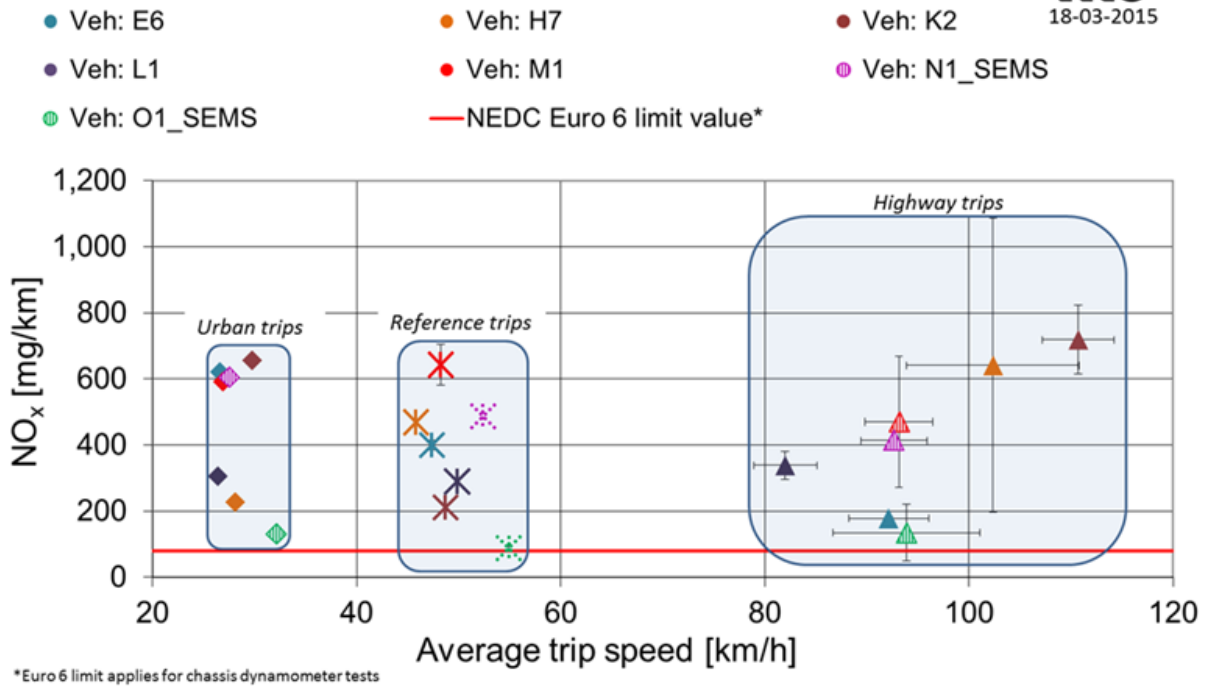


Figure 3: On road NO_x emission test results Euro 6 passenger vehicles

Performance of SEMS test equipment on a chassis dynamometer:

The sensors of the SEMS equipment are calibrated, however the quality of the OBD mass air flow signal is not known. Therefore, independent verification with fuelling data was used to determine the quality of the air flow signal of the different vehicles. The total CO₂ between fuelling, as determined from the fuel and from the air flow signal was equal for all vehicles, within a 5% range. No systematic deviation from this 5% variation was found. It is noted that at very low concentrations of NO_x, the SEMS sensor is less accurate for transient signals. However, in the range of concentrations of the current measurements the correlation and calibration tests carried out in the last four years provide a good evidence for the accuracy of the measurements.

In order to validate the SEMS test results, validation tests were performed on a chassis dynamometer while testing vehicle N1. The CO₂ and NO_x test results are shown in Figure 4 and Figure 5. The SEMS test results are well in line with the chassis dynamometer test results. SEMS test results are partly based on Mass Air Flow data of the CAN-bus of the vehicle, the accuracy of which is unknown. In all emission tests the CO₂ deviation is 8% and the NO_x deviation is -14% to +12%. Both standard deviations for CO₂ are approximately 1%; for NO_x these equal 8 and 12%. The results show that SEMS is a screening tool which yields repetitive indicative results. One should keep in mind that the accuracy of these test results is directly related to the accuracy of the mass air flow signal of this vehicle type. Other vehicle types may gain different accuracies.

Although SEMS is less accurate than PEMS, the system is well suited for a quick screening of NO_x emissions of a vehicle. Its error margins are sufficiently low to identify emissions that are well beyond emission limits.

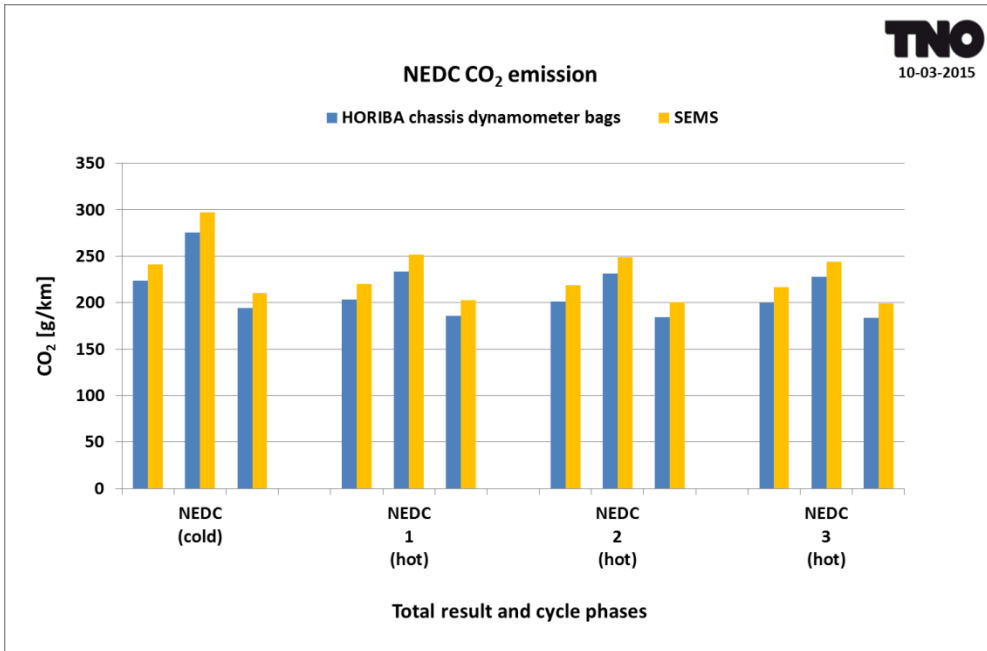


Figure 4: Validation CO₂ test results SEMS-chassis dynamometer on one vehicle (per test the total result and urban and extra urban results are shown) .

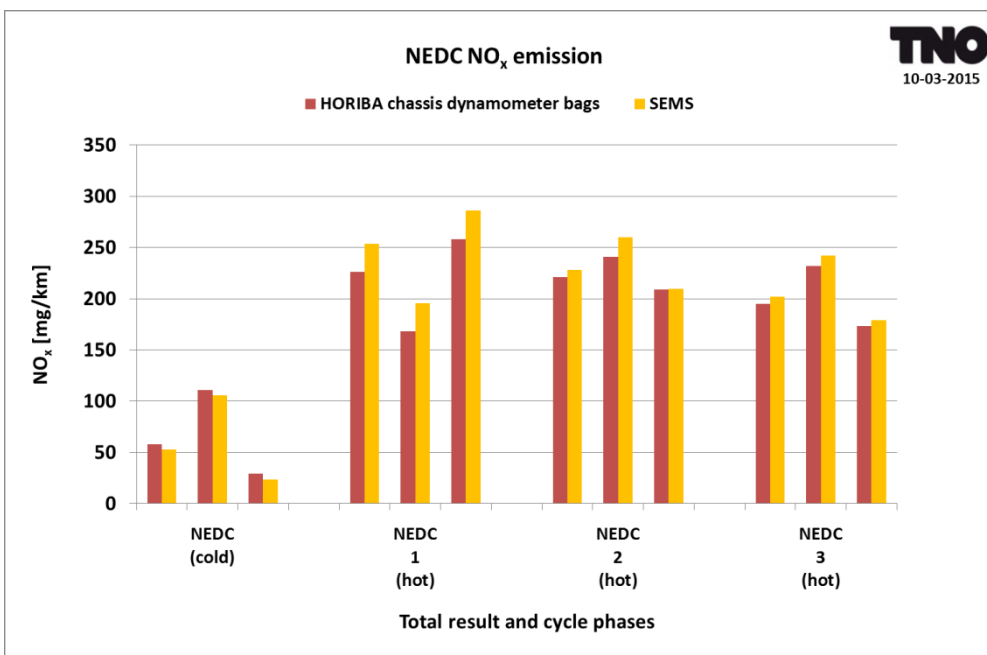


Figure 5: Validation NO_x test results SEMS-chassis dynamometer of one vehicle (per test the total result and urban and extra urban results are shown).

Evaluation of Real Driving Emissions

Table 7 shows the NO_x emissions of seven vehicles which are tested on the chassis dynamometer as well as on the road. The TNO reference trips have been normalised and weighted (1/3 for each road area) according to EMROAD (version 5.80) and CLEAR (version 1.8.6). The EMROAD and CLEAR results are reported in the final two columns of Table 7 and plotted in Figure 6.

In general the EMROAD tool applies small correction, ranging from -11% to +3%. The CLEAR tool applies larger corrections in both directions: the corrections vary from -26% to +23%. The executed TNO reference trips, with a normal driving style are comparable with the RDE reference hence it is notable that the result is in some cases lowered and in some cases increased. Moreover, in some

cases CLEAR lowers the result where EMROAD increases the result. Obviously the tools choose a different method for normalisation. In order to obtain a more balanced view on the performances of EMROAD and CLEAR more results of on-road test trips need to be evaluated.

Table 7: NOx emissions on the chassis dynamometer and on the road with hot start.

NO _x emissions in mg/km	NEDC	NEDC	CADC	TNO reference trip**		
	cold	Hot	hot	hot		
Vehicle	Average			Average	EMROAD Result and CF	CLEAR result and CF
E6	98	210	201	409	419 / 5.2	389 / 4.9
H7	27	16	79	451	402 / 5.0	422 / 5.3
K2	65	58	253	181	182 / 2.3	134 / 1.7
L1	106	11	126	293	-	360 / 4.5
M1	34	27	27	603	618 / 7.7	526 / 6.6
N1*	58	214	370	466	-	451 / 5.6
O1*	28	28	16	79	-	72 / 0.9

*SEMS data

** Not corrected for drift

The EMROAD correction values range from -11% to +3% and CLEAR applies corrections between -26 and + 23%, see Figure 6.

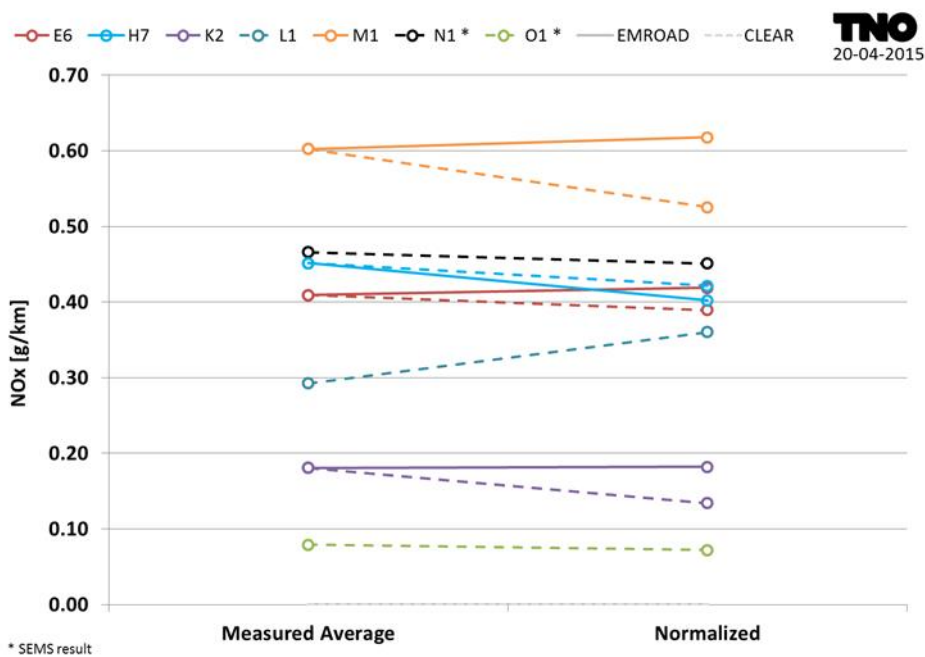


Figure 6: Measured and normalised NOx emissions of 7 vehicles in a reference trip with a hot start.

Driving style and driving at higher speeds

The TNO reference trip was executed with two driving styles (regular and sportive). Table 8 shows the differences in trip characteristics, mainly the higher average acceleration and RPA (Relative Positive

Acceleration) indicate the sportive driving style. Additionally trips at higher speeds were performed and analysed with the normalisation tools.

Figure 7 shows the measured and normalised NO_x emissions of vehicle K2 in a reference trip with regular and sportive driving style. With EMROAD no overall normalised results were calculated, the trip was too sportive. The results as shown in **Error! Reference source not found.** were calculated based on the results per road area.

CLEAR yields an overall result, with a reduction of 40% after normalisation the result is lowered substantially.

Additionally a TNO reference trip with highway speeds of 150 km/h was processed with EMROAD. It seems that EMROAD does not take these higher speeds in to account at all for the overall result.

From these results it seems that the normalisation tools do not report sportive driving and driving at high speeds or the result is lowered substantially, however, in real world operation this kind of driving does occur.

Table 8: Trip characteristics

Reference trip	Trip distance	Average speed	Average acceleration	Average Relative Positive Acceleration
Vehicle	[km]	[km/h]	[m/s ²]	[m/s ²]
K2_regular	76.5	49.8	0.43	4.85
K2_sport	76.3	49.4	0.55	6.98

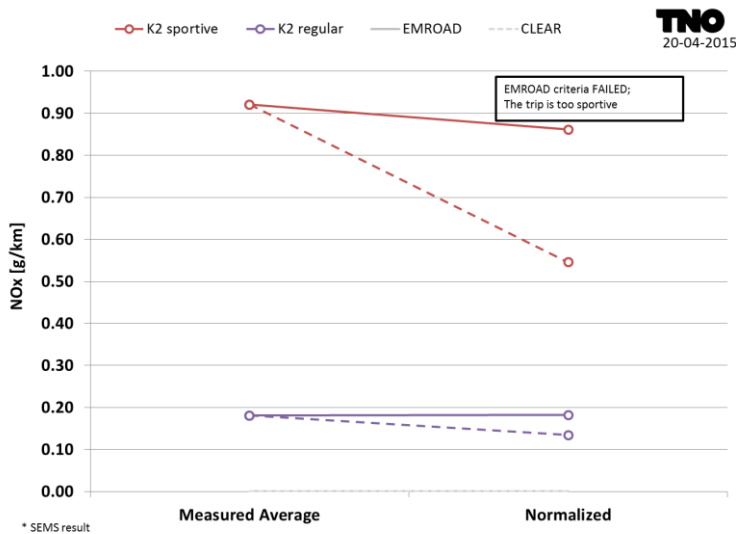


Figure 7: Measured and normalised NO_x emissions of vehicle K2 in a reference trip with regular driving style versus a reference trip with sportive driving style.

Investigations of NO_x reductions and SCR conversion rates of tested vehicles:

In Figure 8 the relationship of the converted NO_x in the SCR catalyst and the pre-SCR NO_x emissions (also measured with a Continental UniNO_x sensor) of the different vehicles are reported. From this figure the following observations can be made:

- the maximum amount of converted NO_x of these SCR catalysts is 400 to 600 mg/km.
- with low engine-out emissions, i.e. less than 400 mg/km, the SCR catalysts are able to reduce a large amount of NO_x. High SCR conversion rates are possible.
- with higher engine out emissions, i.e. over 500 mg/km, the SCR catalyst does not seem able to reduce all residual NO_x. Operating temperatures and adverse exhaust gas flow conditions are

likely to restrict the performance of SCR catalysts in some cases. In other cases, where the operating conditions are in fact favourable, a lack of injected AdBlue is the cause for elevated vehicle emissions.

For vehicles L1, M1 and N1 to achieve post-SCR emissions like vehicle O1, their engine-out NO_x emissions would need to be lowered *and* the SCR system would to reduce a larger share of NO_x.

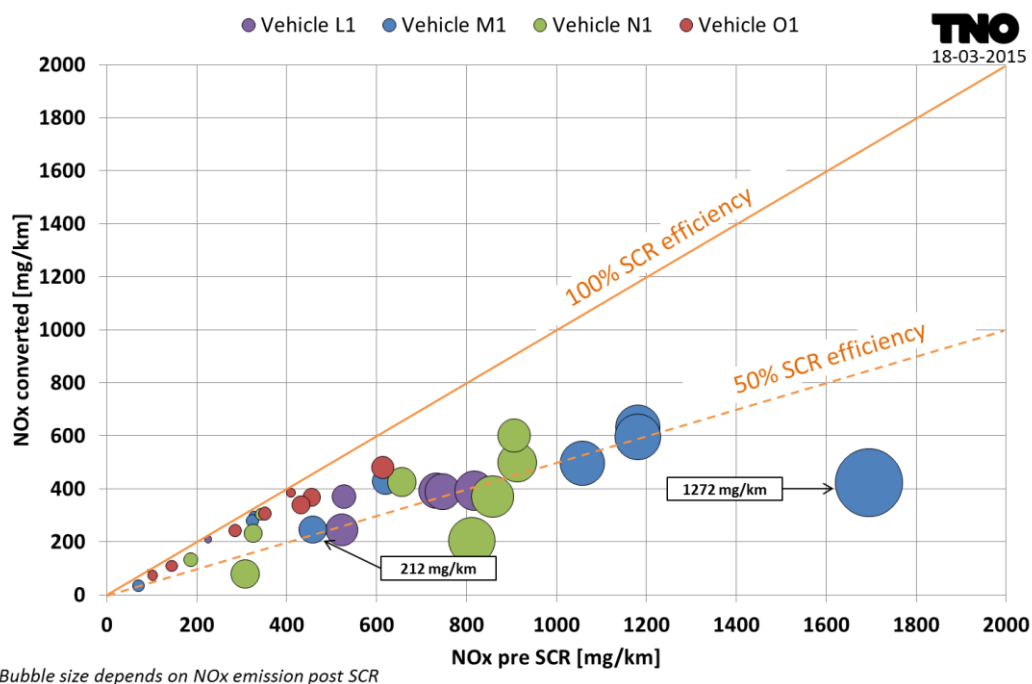


Figure 8: Converted NOx related to engine out NOx emissions in chassis dynamometer and on-road tests.

On-road test results of Euro Light Commercial Vehicles:

Figure 9 shows the (SEMS) NO_x emission test results of the on-road test trips of 10 Euro 5 commercial vehicles. In the three trips with two different payloads the average NO_x emissions range from 1421 – 1670 mg/km. These emission levels are 5-6 times higher than the type approval emission limit value of 280 mg/km. These measurement results confirm findings in another study of another European research institute, IIASA from Austria, which found comparable real-world NOx emissions of 1300 mg/km in a Remote Emission Sensing experiment in Zurich (Borken-Kleefeld 2014a). Vehicle 2 has relatively low NO_x emissions, which is mainly due to the fact that it is a N1 class II vehicle with a lower weight and more stringent emission limit than the nine N1 class III vehicles. An increase of the payload from 28 to 100% in city and reference trips results in an average increase of NO_x emissions of 11-15%.

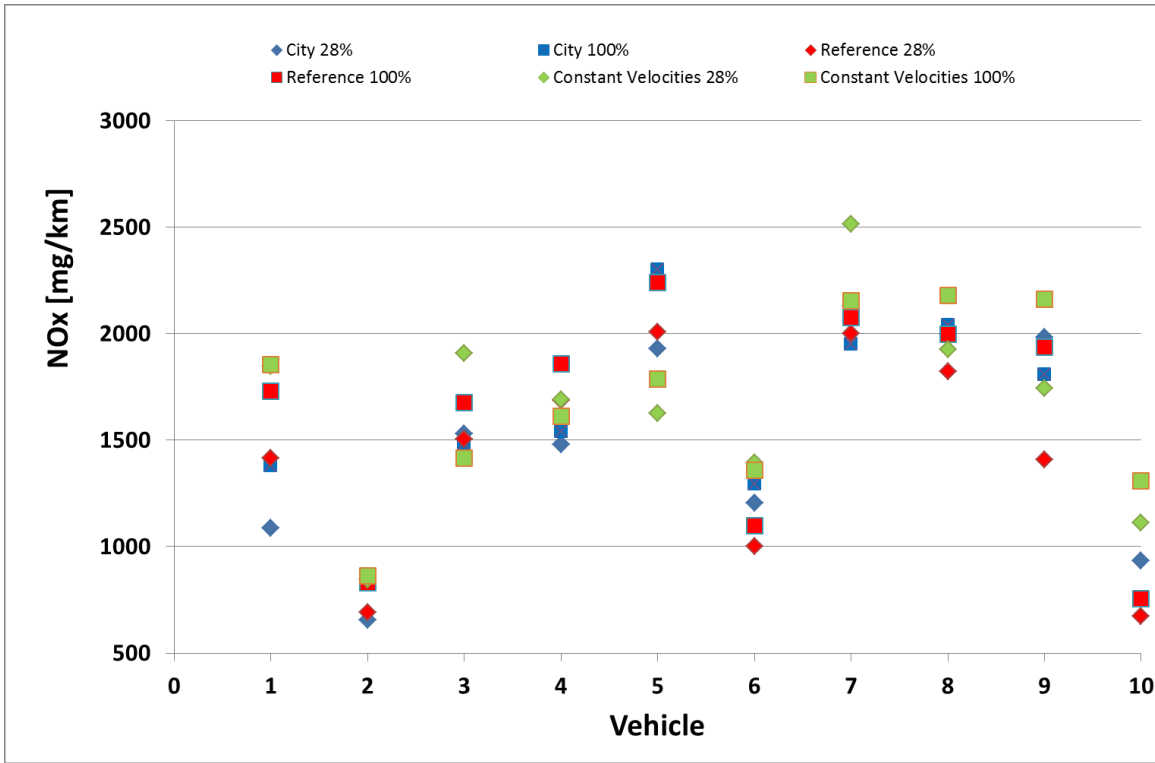


Figure 9: NOx emission SEMS test results of 10 Euro 5 commercial vehicles.

The CO₂ emission (SEMS) test results of the on-road test trips are shown in Figure 10. In real-world tests the CO₂ emissions per kilometre are 7% to 52% higher than the declared CO₂ emissions in the type approval tests. Some LCV's (i.e. number five) are built up with a square box which results in a relative large frontal area without an aerodynamic spoiler; this results in relative high CO₂ emissions at higher vehicle velocities.

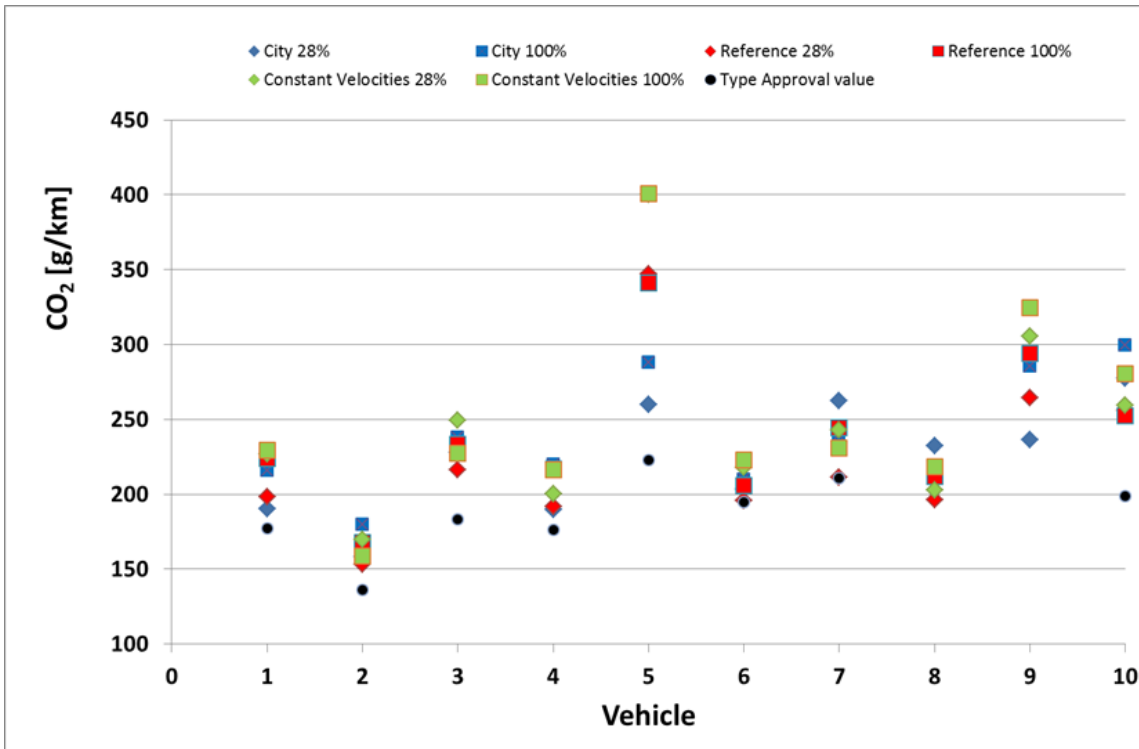


Figure 10: CO₂ emission SEMS test results per trip of 10 Euro 5 commercial vehicles

These new emission data are input for an upgrade of current emission factors.

In Table 9 the old and newly proposed NO_x emission factors of Euro 4 and 5 N1 class III commercial vehicles are reported. The Euro 4 are expected to perform similar to the Euro 5 vehicles. Except from the emission factor of the motorway (congested), the NO_x emission factors increase with 33 to 85%.

Table 9: Old and newly proposed NO_x emission factors of Euro 4 and 5 N1 class III commercial vehicles.

[g/km]	Emission estimate	NO _x Old	NO _x New	Increase
Urban	Congested	1.66	2.45	48%
	Normal	0.98	1.44	47%
	Free-flow	0.90	1.40	56%
Rural	Normal	0.54	0.86	59%
Motorway	Congested	1.57	1.53	-3%
	80 km/h strict	0.65	0.92	42%
	80 km/h	0.73	0.99	36%
	100 km/h strict	0.80	1.06	33%
	100 km/h	0.82	1.16	41%
	120 km/h	0.90	1.53	70%
	130 km/h	0.95	1.76	85%

Discussion

Euro 6 passenger vehicles:

What are the main emission characteristics of the tested Euro 6 diesel passenger vehicles?

The test results of the sixteen tested vehicles show good CO, THC and PM10 real-world emissions because the applied technologies for controlling these emissions are intricately robust. In almost all conditions the emissions are low. However the real-world NO_x emission of all vehicles varies from 0 to 2000 mg/km. Although the type approval emissions of all vehicles are below 80 mg/km, the average real-world NO_x emission of all tested Euro 6 vehicles varies between 150 and 650 mg/km.

What are the characteristics of the vehicle with the lowest real-world NO_x emissions and the vehicle with the highest real-world NO_x emissions?

The real-world NO_x emission of vehicle O1 is 150 mg/km and the corresponding Conformity Factor (CF) is less than 2. Measuring data show clearly that the pre-SCR NO_x emissions of this vehicle are relatively low, ranging from 350 to 750 mg/km, indicating an effective EGR system and LNT catalyst which avoid the emission of NO_x. In addition the residual NO_x is mainly reduced in the SCR catalysts which results in an average tailpipe emission of 150 mg/km. In most trips up to 500 mg/km is reduced by the SCR catalyst at an operational temperature up to 380 °C. These data provide clear evidence for the fact that low real-world NO_x emissions can be achieved by means of adequate appliance of an EGR, which, in turn, facilitates the maximum SCR performance as SCR operating temperatures in that case are higher allowing for higher SCR conversion rates. At low engine load the LNT seems effective in the conversion of NO_x to harmless components.

On the contrary vehicle M1 has a real-world pre-SCR NO_x emission up to 1250 mg/km. This value deviates strongly from pre-SCR emissions in chassis dynamometer tests, which amount to 50 to 150 mg/km. In real-world tests 0 to 750 mg/km NO_x is reduced by the SCR catalyst at an operational temperature up to 250 °C. This results in an average tailpipe emission ranging from 0 to 2000 mg/km, with an average value of about 650 mg/km.

These large differences between NO_x emissions in a chassis dynamometer tests and NO_x emissions in real-world operation are most likely caused by the control strategy dependence on ambient temperatures, the differences in EGR system settings and adjustments. Contrary to the EGR performance, the performances of the different SCR systems are relatively at a constant level: for all tested vehicles the maximum SCR NO_x reduction performance ranges from 350 to 750 mg/km.

Would injecting more AdBlue result in a larger NO_x reduction by the SCR?

Theoretically, more AdBlue could result in a larger NO_x reduction. However, the size of the SCR catalyst, operating conditions of the engine and the operating temperature of the SCR catalyst together determine its maximum NO_x reduction performance. Moreover, ammonia slip is undesirable. The test results of some vehicles show a maximum quantity of reduced NO_x of around 600 to 750 mg/km. It is likely that the maximum performance of these SCR catalysts is already reached and injecting more AdBlue would yield an ammonia slip, which would cause penetrant odours which are not desirable.

Test results do however indicate that for some of the tested vehicles, such as vehicle M1, which has low SCR conversion rates and relatively cold exhaust gas, injecting more AdBlue may result in improved NO_x reduction.

Are the test results representative for all Euro 6 diesel vehicles?

The sixteen tested vehicles can be classified as medium and large vehicles. Most of these vehicles are equipped with LNT or SCR technology and are not representative for the whole Euro 6 diesel fleet. It is expected that the bulk of the small and medium size diesel vehicles, that will become available in September 2015, will be equipped with cheaper technology. Especially their NO_x emissions on the highway are expected to be relatively high. Possibly, the overall real-world NO_x emission performance of Euro 6 vehicles will turn out to be equal to Euro 4 and Euro 5 diesel vehicles.

How can real-world NO_x emissions of Euro 6 vehicles be improved?

In order to improve real-world emissions Real Driving Emission legislation (RDE) is needed. This legislation describes the test procedure and data evaluation methods for determination of real-world emission levels or Conformity Factors. Currently negotiations between the European Commission and the automotive industry are ongoing and it is expected that RDE-legislation for light duty vehicles will be implemented in 2017 or 2020.

How can SCR-technology be assessed?

In order to assess SCR-technology it is benchmarked with two other technologies. From 1988 onwards the three-way catalyst technology on petrol engines has been applied. Currently the engine control systems and the catalyst technologies are well developed and the real world CO, THC and NO_x emissions have been reduced with 90-99%. Since 2002 the closed diesel particulate filters have entered the market and their PM-filter efficiencies of more than 99% are remarkable. Furthermore, this technology is robust against varying circumstances because all exhaust gas is filtered. Fortunately Euro VI heavy duty vehicles show significant reductions of their real world NO_x emissions. The only cause for this huge NO_x reduction can be found in the emission legislation. On the contrary the real world NO_x emission of Euro 5 and 6 light duty vehicles still strongly exceed the type approval limit values (3 – 10 times) because no RDE legislation is in to force. Some current Euro 6 vehicles have been equipped with DPF, EGR and SCR technologies and they have the potential to yield low real world emissions but the EGR and SCR technologies are only partly activated.

Summarizing the current status and real world emission of Euro 6 diesel vehicles and the available engine and aftertreatment technologies and the current status of heavy duty vehicles it is clear that the next step must be a proper RDE legislation for Euro 6 vehicles. This RDE legislation will be the main actor to ensure low real world emissions of light duty vehicles and will determine the real world effectiveness of NO_x aftertreatment technologies.

Euro 5 light commercial vehicles:

The selected and tested vehicles are mainstream light commercial vehicles and cover a large part of the Dutch fleet of commercial vehicles. Due to a lack of accurate fleet data of the numbers of commercial vehicles it is not possible to determine the quantitative rate of representativeness of specific vehicle models.

In this project the NO_x and CO₂ emission mass rates are based on measured volume concentrations, fuel parameters, calculations and the measured air mass rates. Although the air mass rate signals of the vehicles might deviate (i.e. +/- 10%) it is clear that the on-road vehicle NO_x emissions are far higher than the type approval emissions. Independent comparison of the CO₂ emissions with the recorded fuel consumption, based on the same signals, yields typical deviations of less than 5% for the accumulated CO₂ over a few trips.

Despite of the continuous tightening of the NO_x type approval limit values from Euro 1 to Euro 5 real-world NO_x emission factors have stabilized at around 1430 mg/km in the last decade, as **Figure 11** clearly shows. In other words: the difference between type approval NO_x emissions and real-world NO_x has grown significantly over the year. Compared to the current type approval limit value of 280 mg/km, the difference between type approval emissions and real-world is substantial.

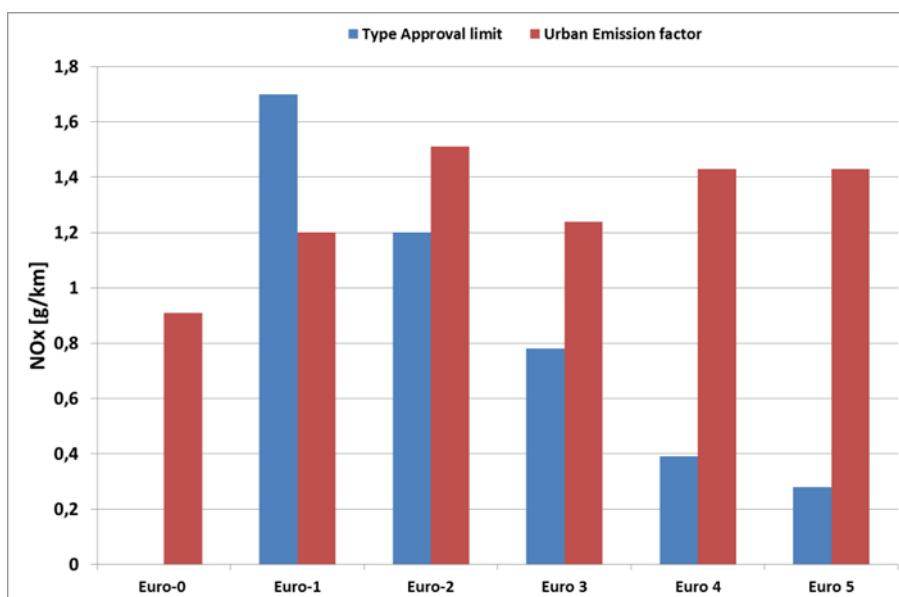


Figure 11: NO_x emission factors in the city and type approval limit values of diesel commercial vehicles.

The test results of this study proved a limited effect of driving behaviour, engine load and external circumstances, causing typically less than 15% variation per vehicle between the extreme cases. To determine the actual cause of the difference between real-world emissions and type approval emissions, however, a different type of investigation is required. Euro-4 and older vehicles, the typical velocities and engine loads comparable with the type-approval test still led to comparable emissions with the type-approval values. With Euro-5 it is no longer the case: for the same velocities and engine loads as on the type-approval the real-world NO_x emissions are also factors higher than the type-approval value. Moreover, test execution and vehicle state may explain a few percent difference between one test and another, but not such magnitude. Concluding, emission tests were executed on the conservative side, not to produce high emissions due to special test circumstances, however, still they were high. Moreover, variations found among vehicles and among test circumstances were much smaller than the factor 5 to 6 difference between type-approval value and real-world emissions.

Conclusions

In several emission test programs TNO has tested sixteen Euro 6 diesel passenger cars and 10 Euro 5 Light Commercial Vehicles. The tests were carried out on a chassis dynamometer and on the road with mobile test equipment. From the measurements, TNO draws the following conclusions:

1. all sixteen Euro 6 diesel passenger cars comply with or perform very near the type approval CO, THC, NO_x, PM and PN limit values. Especially the prototypes in the test program of 2010 performed well on the chassis dynamometer. These vehicles were however not tested on the road.
2. for all tested vehicles the effect of a hot start on NO_x emission differs widely; for some vehicles the NO_x emission decrease but for other vehicles it increases a factor 3.
3. the range of NO_x emissions of Euro 6 diesel passenger cars in real-world tests is very large with values from 50 to more than 2000 mg/km. On average real-world emissions are 5 to 6 times higher than the type approval limit value of 80 mg/km. This seems to indicate that emission control technologies perform differently on the road than they do on the chassis dynamometer. Moreover the real world NO_x emission per road type of the different vehicles differ widely. Only proper RDE-legislation can improve these real driving emissions.
4. current Euro 6 diesel vehicles with low real-world NO_x emissions run with active and well-functioning EGR and SCR systems. Vehicles with higher real-world emissions seem to operate with EGR systems that are inactive or partly inactive. In that case, the SCR system is not able to reduce the high engine-out NO_x emissions.
5. it is expected that for Euro 6 compact cars the simplest and cheapest emission control technology will be applied, i.e. it is likely that these vehicles will be equipped with limited emission control technology. This signifies a risk of high NO_x emissions similar to Euro 5, in particular on the motorway.
7. TNO's Smart Emission Measurement System yields repetitive emission test results which are in line with chassis dynamometer test results. Therefore SEMS is classified as a road vehicle emission screening tool.
8. normalisation of real-world NO_x emissions of a couple of TNO reference trips with two normalisation tools, EMROAD and CLEAR, yield different results. EMROAD correction values range from -11% to +3% and CLEAR applies corrections between -26 and + 23%. However these results only represent a regular driving style. In order to judge the quality of these two normalisation tools more data and more research with different driving styles is needed.
9. the average NO_x emissions of the N1 class III Euro 5 commercial vehicles tested in this project range from 1421 to 1670 mg/km and are 5 to 6 times higher than the type approval emission limit value of 280 mg/km. The measurements confirm findings in another study, which found comparable real-world NO_x emissions of around 1300 mg/km in a Remote Emission Sensing experiment. The only vehicle showing relatively low NO_x emissions was an N1 class II vehicle, with a relatively low weight. The effect of payload on NO_x emissions is moderate. In city trips and reference trips an increase of the payload from 28% to 100% results in an average increase of NO_x emissions of 11-15%. The average CO₂ emissions per kilometre during the road tests are 7% to 52% higher than the CO₂ emissions in the type approval certificates.
10. The large and increasing difference between the NO_x emission limit and the real world emissions of modern diesel vehicles is remarkable result. This, and previous studies, have shown that vehicles that perform well during a type approval test, generally and almost with no exception have far higher NO_x emissions under real-world conditions. Moreover, the difference between real-world emissions and type approval emissions has been growing over the years.
11. The new emission data have been used to update the current Dutch emission factors for light commercial vehicles. Except for the emission factor for congested motorway operation, NO_x emission

factors increase with 33% to 85%.

Acknowledgments

This work is part of the in-use compliance programme of light-duty vehicles, which is financed since 1987 by the Dutch Ministry of Infrastructure and The Environment (I&M).

References

- Borken-Kleefeld, J. (2014a) Real World Emissions from Road Vehicles: Results from Remote Sensing, Emission Measurements and Models, International Institute for Applied Systems Analysis (IIASA), Laxenburg/Austria (TAP conference 2014, Graz, Austria)
- Kadijk, G. Ligterink, N.E. Spreen, J.S. (2015a) On-road NO_x and CO₂ investigations of Euro 5 Light Commercial Vehicles. TNO report TNO 2015 R10192 (30 p).
- Kadijk, G. van Mensch, P. Spreen, J.S. (2015b) Detailed investigations and real-world emission performance of Euro 6 diesel passenger cars. TNO report TNO 2015 R10702 (75 p).
- Kadijk, G. Ligterink, N.E. van Mensch, P. Spreen, J.S. Vermeulen, R.J., Vonk, W.A. (2015c) Emissions of nitrogen oxides and particulates of diesel vehicles. TNO report TNO 2015 R10838 (16 p).
- Kadijk, G. Ligterink, N.E. van Mensch, P. Smokers, R.T.M. (2016a) NO_x emissions of Euro 5 and Euro 6 diesel passenger cars – test results in the lab and on the road. TNO report TNO 2016 R10083 (33 p).
- Vermeulen et al. (2012) A smart and robust NO_x emission evaluation tool for the environmental screening of heavy-duty vehicles, TNO and Ministry of Infrastructure and the Environment, the Netherlands. Paper TAP conference 2012, Thessaloniki, Greece
- Vermeulen et al. (2014b), SEMS operating as a proven system for screening real-world NO_x and NH₃ emissions, TNO and Ministry of Infrastructure and the Environment, the Netherlands. Paper TAP conference 2014, Graz Austria

Real-world driving, energy demand and emissions of electrified vehicles

U. KUGLER, S. EHRENBERGER, M. BROST, H. DITTUS, E. D. ÖZDEMİR, M. KONRAD & F. PHILIPPS

Institute of Vehicle Concepts, German Aerospace Center, Stuttgart, 70569, Germany, email: ulrike.kugler@dlr.de

Abstract

Knowledge on real-world driving, charging patterns, energy consumption and well-to-tank/tank-to-wheel emissions of electrified vehicles (EV) still has to be enhanced. For this, first results of two measurement campaigns on battery electric vehicles (BEV) and plug-in hybrid electric vehicles (PHEV) are presented.

In order to evaluate on-road energy consumption and user behavior, a number of BEV has been equipped with data loggers. The data includes hours of operation, state of charge (SOC), mileages driven, speed statistics and GPS information to determine energy used from the traction battery and energy regeneration. Results for one analyzed BEV show that the specific traction battery energy demand varies with a 60% higher demand in winter months and is 17 kWh/100 km on average in 2015. Electric meter readings of charging stations show that the total energy demand can be up to 30% higher than the energy demand at traction battery. Using that information, well-to-tank air pollutant emissions during charging are calculated in combination with hourly data of the German electricity mix. Attitudes and experiences with EV are surveyed via user questionnaires. First results indicate that EV technical benefits such as their pronounced acceleration are not commonly known. Although their image concerning environmental benefits is positive, only a minority is convinced that EVs are suitable for daily use.

In a further measurement campaign, different EURO6 passenger cars are tested on a dynamometer and various exhaust gases are quantified. In this paper, we present the results for a mid-size PHEV combining a gasoline ICE with an E-motor in a parallel hybrid drivetrain in detail. PHEV direct emissions strongly vary depending on the operating strategy and ambient temperature.

Keys-words: real word energy demand, electric vehicles, emission measurement

1. Introduction

Electrified vehicles (EV) are seen as one instrument towards a mitigation of local air pollution and climate change (European Commission, 2011). However, it is yet not fully clear whether these mitigation effects will happen as was hoped for under real-world driving and charging conditions (these being part of a number of studies, e.g. Fetene et al., 2015; Plötz et al., 2015; Ligterink et al., 2013). In Germany as of yet, user experiences with EV are still relatively rare and acceptance could pose a potential threshold towards a further EV penetration. Thus, knowledge on driving and charging patterns, user acceptance, energy consumption and well-to-tank/tank-to-wheel emissions of EV still has to be enhanced. Furthermore, the real life direct emissions of PHEV which depend on driver behavior, driving patterns and ambient conditions are still an open question.

In this paper, first results of two EV measurement campaigns will be presented, focusing on battery electric vehicles (BEV) and plug-in hybrid electric vehicles (PHEV). Measurement devices and measured parameters differ, using OBD data loggers and user questionnaires for the BEV campaign and chassis dynamometer emission tests for the PHEV campaign.

2. BEV campaign: energy consumption and indirect emissions

The BEV measurement campaign is part of the project 'InitiativE-BW' (2014-2016) that aims for electrification of commercial fleets in southern Germany. Over 40 BEV, mostly used for social services or as shared cars, have been equipped with OBD data loggers. Data includes hours of operation, state of charge (SoC), mileages driven, speed statistics and GPS information. On top of that data, users are asked for completing the questionnaires for their experiences with BEV to gain insights on user acceptance and potential barriers. For some users, further data is available, e.g. on the vehicle specific energy demand at their respective charging station, helping to assess the energy demand of BEV at the electric grid.

Traction battery energy demand

From the OBD loggers, information on SoC and mileages driven was combined to get the amount of energy used at the traction battery and the amount of energy regenerated by decelerating or downhill driving.

First results for one BEV (B segment) located in the southern black forest region show, as expected, that ambient temperatures have a significant influence on its energy consumption. The car had an annual average energy traction battery demand of 17 kWh/100 km in 2015, varying from 14 kWh/100 km in July to 23 kWh/100 km in January (Figure 1). During this period, the traction battery was fully charged in over 90% of the time (SoC = 100%), starting at a SoC of $\geq 50\%$ in 70% of the time. The car is used on a daily basis except on week-ends. 80% of the trips in 2015 had a length up to 80 km, 80 km being the range given at the beginning of a winter trip. Annual mileage in 2015 was about 13,000 km.

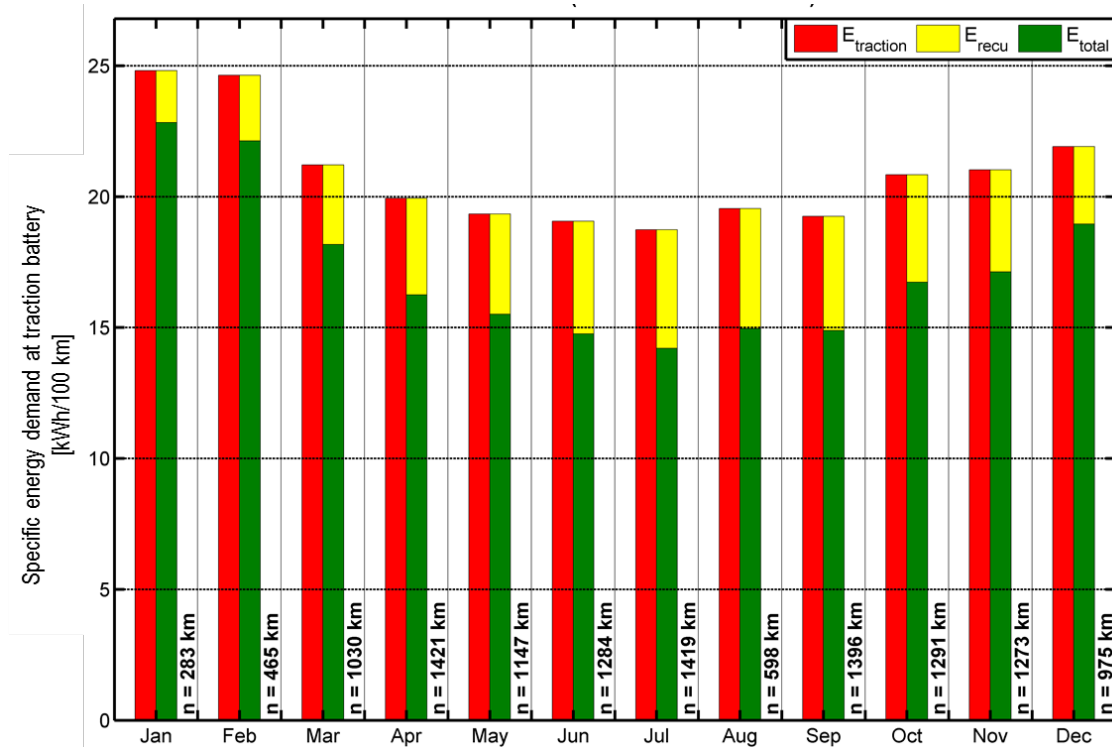


Figure 1. Measured traction battery energy demand (B-Segment car, southern black forest region).

Total energy demand

In addition to the logged traction battery energy demand, total energy demand of a number of vehicles was assessed by manually tracking electric meter readings of their charging stations over a 3 days period in September 2015 and January 2016 (Figure 2). All charging stations are provided by the same manufacturer with a type 2 connector and 22 kW charging power. The analysis shows that the overall energy efficiency (from charging station to traction battery) varies between 72% and 96% meaning that up to 30% of the energy charged at the station is used elsewhere (e.g. for auxiliaries such as heating or infotainment) or lost due to technical inefficiencies. These findings are in line with Peht and Höpfner (2007) who give charging losses of 10-30%.

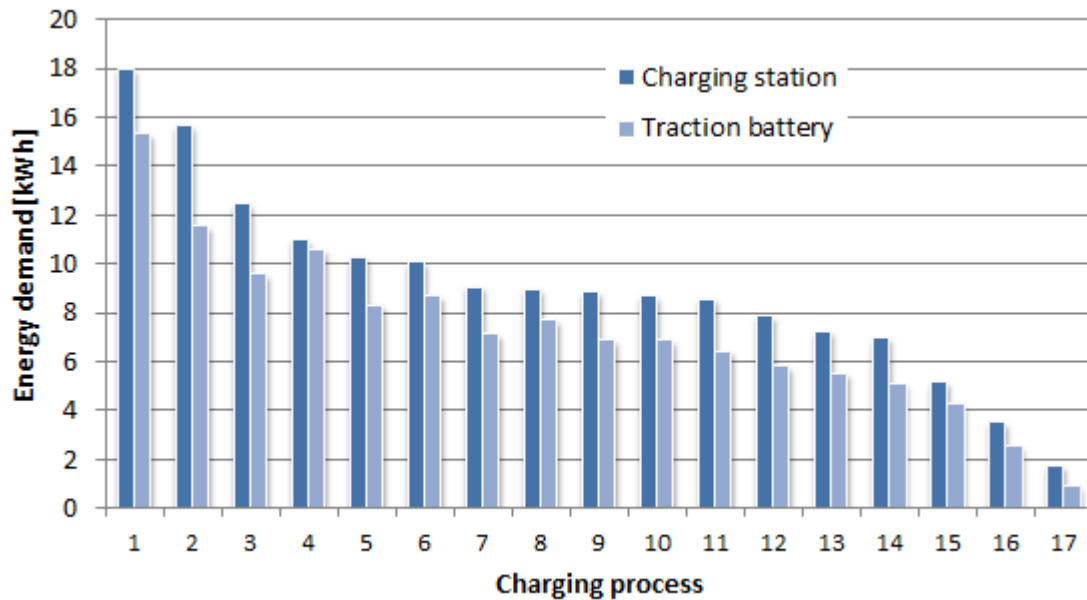


Figure 2. Energy demand: charging station vs. traction battery (each pair of bars represents one charging process per individual vehicle)

Taking into account the measured energy demand of the vehicles' traction battery (17 kWh/100 km, see above) plus the monitored overall charging losses, the average total energy demand of that BEV will be around 20 kWh/100 km.

Well-to-tank emissions of air pollutants

Several studies assessed air quality and climate effects of electric vehicles in combination with an electricity mix (JRC, 2014; Jungmeier et al, 2014). However, most of these studies are based on yearly average values. In combination with hourly data of the German electricity mix, well-to-tank emissions during charging can be computed much more accurately. Figure 3 shows monitored data on the hourly electricity mix in Germany during the winter months November and December in 2014 (Agora 2015). Fossil sources, especially lignite and hard coal, were dominating the electricity production with negative effects on air quality and greenhouse gas emissions.

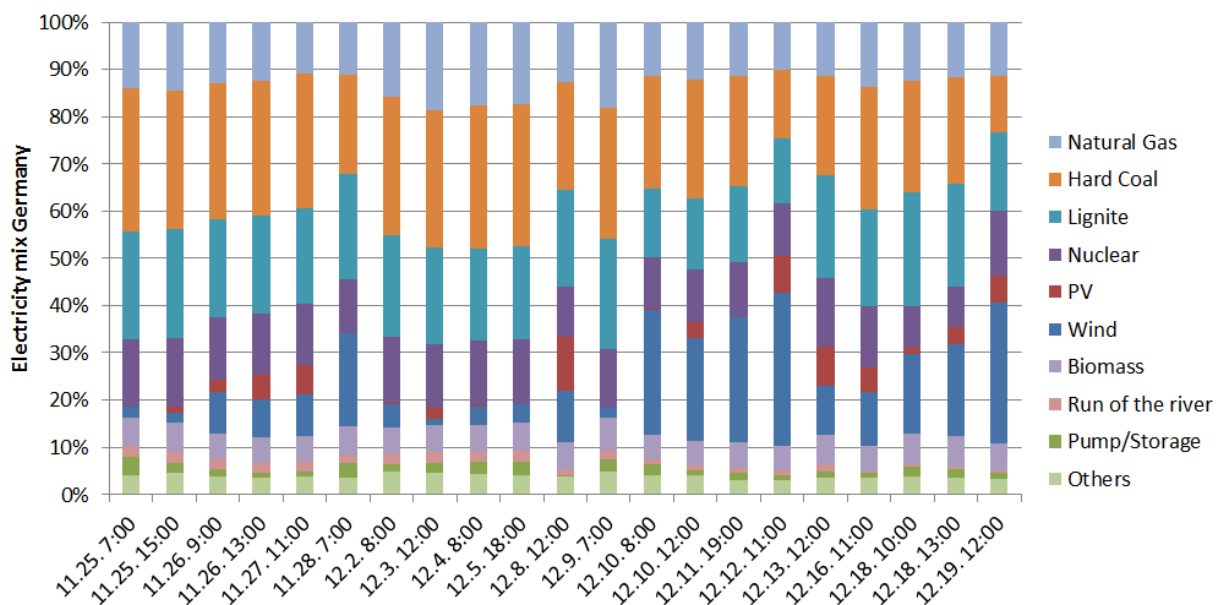


Figure 3. Hourly electricity mix in Germany, November – December 2014 (Agora 2015)

In combination with BEV charging processes and taking into account overall charging losses of 20%, the respective NO_x and PM_{2.5} well-to-tank (WTT) emissions on basis of the above mentioned electricity mix are computed using emission factors from the database ecoinvent 3.2 (Ecoinvent 2016, Figure 4).

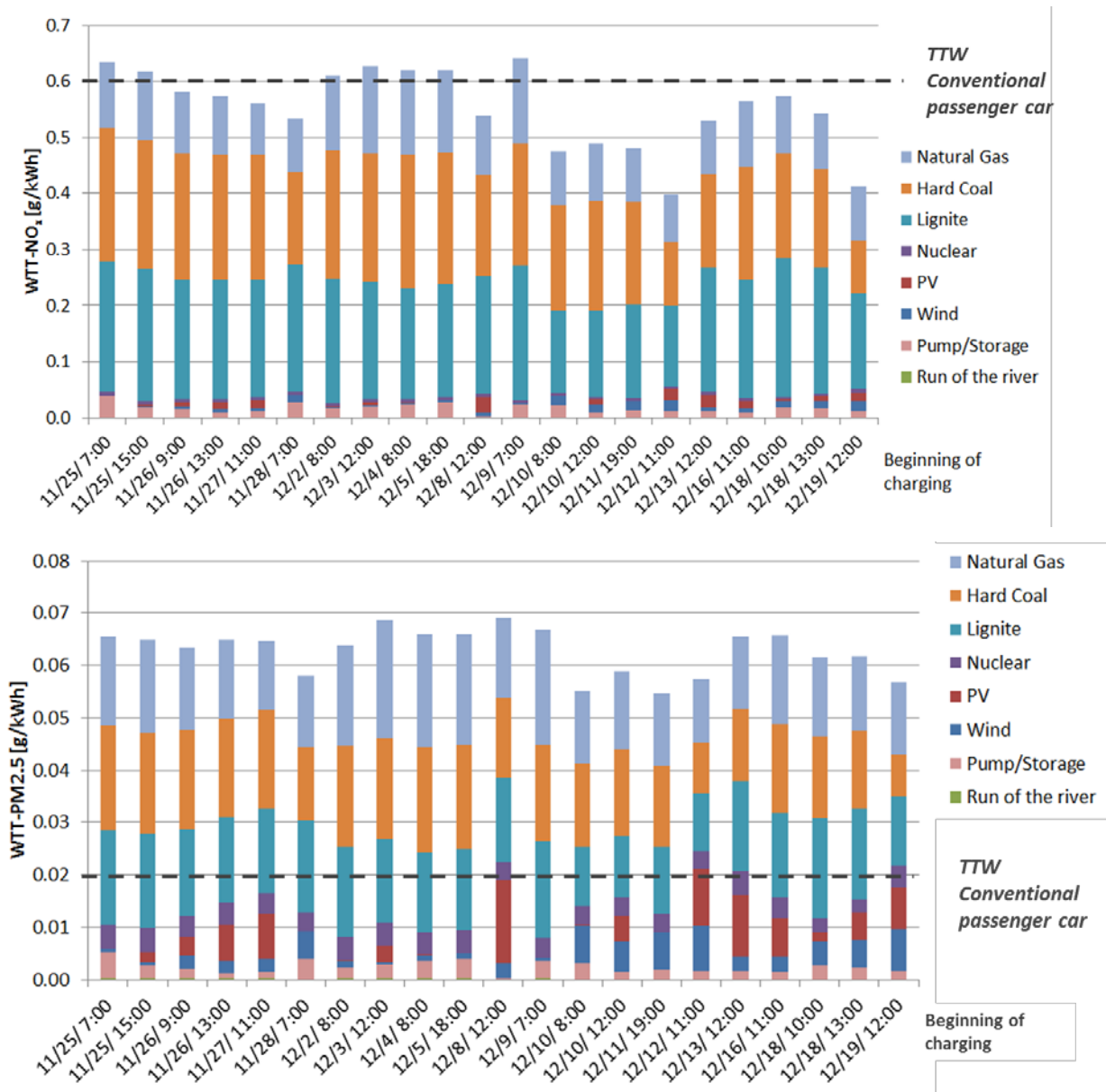


Figure 4. Well-to-wheel NO_x emissions (top) and PM_{2.5} emissions (bottom) due to charging events of one BEV (B segment); German conventional electricity mix, November – December 2014

Depending on the time of charging, 0.4 – 0.6 grams of NO_x and 60 – 70 mg of PM_{2.5} are emitted per kWh when the average German electricity mix of that respective period is taken as a basis. Compared to conventional passenger cars (directly emitted tank-to-wheel (TTW) air pollutants due to fuel combustion, neglecting WTT emissions due to fuel production and transport), this is about the same amount for NO_x emissions and 2-3 times higher for PM_{2.5} emissions. TTW emission factors of 0.37 g NO_x/km and 0.02 g PM_{2.5}/km were taken from HBEFA (2014).

User attitudes and acceptance

Among all participants of InitiativE-BW, attitudes and experiences with leased EVs (90% BEV, 10% plug-in hybrid electric vehicles (PHEV) and range-extended electric vehicles) as well as information on user costs, electricity tariffs, expected mileages and predicted needs for electric ranges are surveyed via two-stage (first one before EV lease and the second one after ca. 1 year) questionnaires up to the end of 2016.

So far, survey results indicate that EV technical benefits such as their pronounced acceleration are not commonly known before the usage of the vehicle (Figure 5). 49% stated that acceleration would be the same or inferior to conventional vehicles, and around 10% did not have any knowledge on any of the asked EV features.

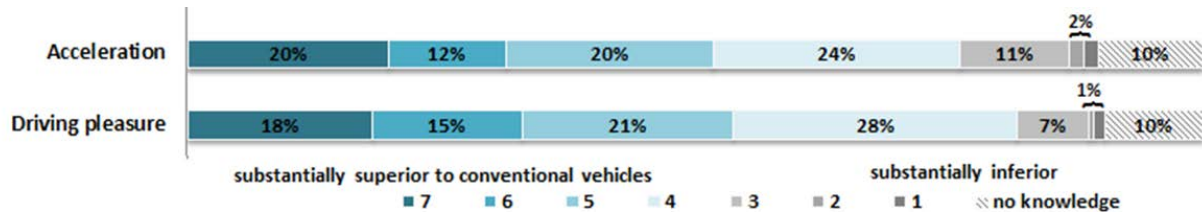


Figure 5. Survey results on technical aspects and handling: attitudes towards EV in comparison to conventional vehicles (198 users)

On the other hand, the image of EV concerning environmental benefits is positive (Figure 6). Around 70% of the users think that EV will be superior to conventional vehicles concerning the improvement of local air quality and the mitigation of noise as well as climate change. However, only 28% are convinced that an EV is suitable for their daily use.

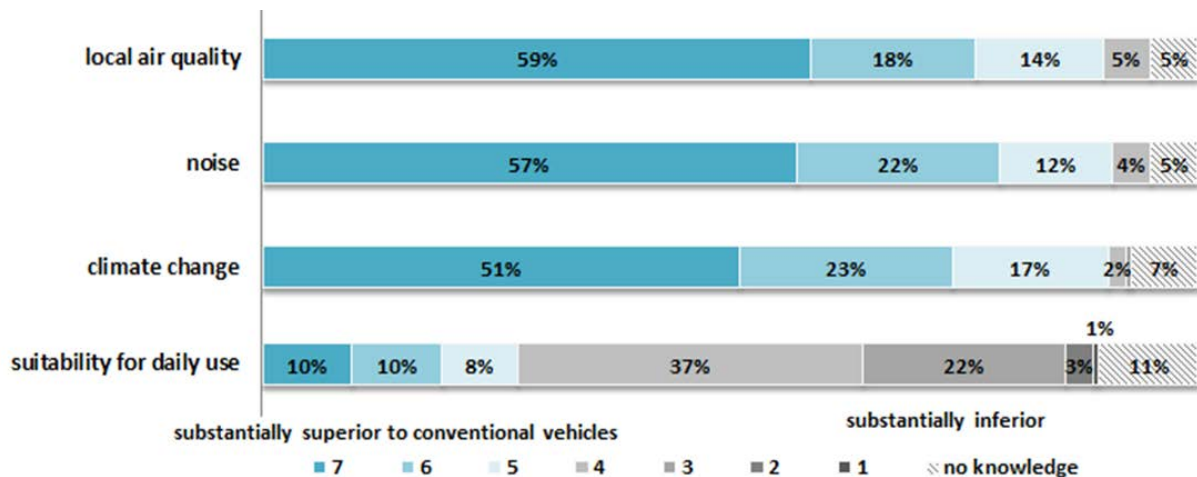


Figure 6. Survey results on perception and environmental effects: attitudes towards EV in comparison to conventional vehicles (198 users)

3. PHEV campaign: energy consumption and direct emissions

Background

Alternative vehicle drivetrain technologies as used in PHEVs are expected to play a major role in future passenger car markets. Yet, there is still a lack of knowledge about the emission and energy efficiency of such vehicles. As current vehicles are still certificated based on the NEDC cycle and procedure, a gap to real world emissions and efficiency is expected. In order to assess the emissions of a PHEV drivetrain, a measurement campaign with three different PHEV models has been started, focusing on the analysis of exhaust emissions from mid-size vehicles under different ambient conditions. Additionally to the PHEV technology, conventional vehicles fulfilling EURO 6 have been tested. Here, results for a mid-size PHEV combining a gasoline internal combustion engine (ICE) with an E-motor in a parallel hybrid drivetrain are presented in detail. We show the influence of different ambient temperatures at 0°C and 23°C in terms of emissions of air pollutants and energy efficiency. Additionally, we compare the emissions during cold and hot start tests.

Test set-up

The measurements have been taken on a four-engine all-wheel roller dynamometer with climate control. Several driving cycles have been analyzed to detect the influence of traffic situations (urban, suburban and motorway) on vehicle emissions. The influence of temperature is studied by performing the measurements at 23 °C and 0 °C and by comparing the emissions of both hot and cold starts. 22 different gases have been detected online during the measurement on a secondly basis using a FTIR analyzer. NO_x emissions have been detected separately with a CLD measuring instrument. In order to derive the absolute amount of emissions, the volume flow rate is needed. Therefore, the flow rate has been detected separately using a real-time ultrasonic exhaust gas flow meter. Apart from exhaust emissions, the data of the On Board Diagnostics (OBD) has been logged in order to monitor various vehicle parameters like revolutions per minute, catalyst temperature, etc.

We present results of WLTC tests, as this cycle contains a representative share of urban, extra urban and highway driving situations and will be mandatory in the EU from 2017 on. The tests have been conducted in different modes and at different ambient temperatures (Table 1). The tests at 0°C have the same vehicle conditions as at 23°C. In order to evaluate the energy efficiency and the emissions as close to real life as possible, the tests have been performed with air condition running and without any changes in tire pressure. Cold starts are assumed to take place after vehicle charging in the morning and are driven with a charge depleting driving mode (CD mode). In addition to the CD mode tests, the results for the tests with charge sustaining (CS) mode are presented. These tests are supposed to represent the situation where the electric range of the vehicle is exceeded and the driver uses the car as a common gasoline vehicle. Although the vehicle recuperates the braking energy also in this mode, the electric driving share in this case is negligible.

Table 1: Overview of test conditions of the presented WLTC tests

Test	Temperature	Driving Mode	Starting condition
WLTC-1-0°	0 °C	CD	cold
WLTC-2-0°	0 °C	CS	hot
WLTC-1a-23°	23 °C	CD	cold
WLTC-1b-23	23 °C	hybrid ¹	cold
WLTC-2-23°	23 °C	CD / CS	hot
WLTC-3-23°	23 °C	CS	hot

¹ In the hybrid mode, the vehicle operates both in the electric and ICE mode according to an internal operation strategy.

Results

The WLTC driving cycle has different dynamic speed intervals which represent the driving situation in urban and non-urban environments and on highways. The measured speed and acceleration curves for this driving cycle are equal within a defined tolerance range (Figure 7). The urban part of the cycle is characterized by low speeds and idle periods. The highway section with speeds higher than 100 km/h is less dynamic, but due to the high speed the ICE motor is used also in the all-electric driving modes (Figure 9).

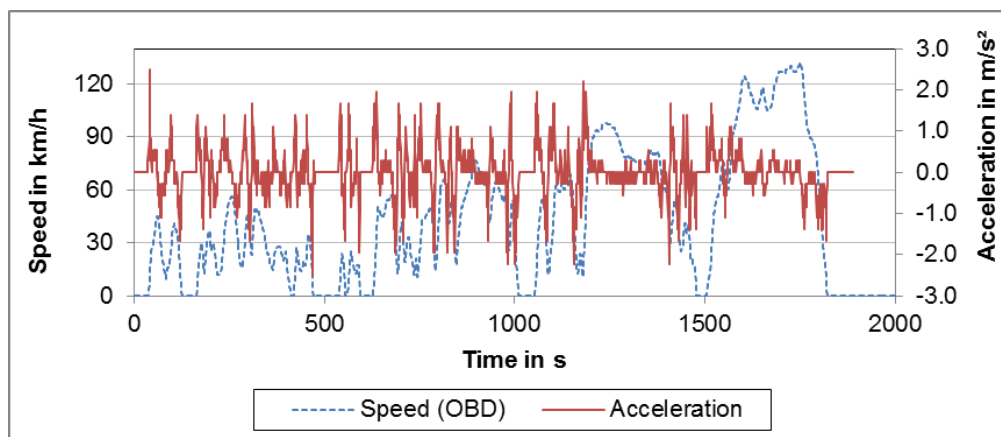


Figure 7: Measured acceleration and speed for the WLTC test

The energy consumption of the tested PHEV in the CD mode changes notable with lower temperatures (Figure 8, upper part). The settings of the air condition are identical for both ambient temperatures with a passenger compartment temperature of 23°C and the blower controls set on automatic mode. In the 23°C test, WLTC test in the CD mode has to be performed twice as the battery has not been discharged after the first WLTC test.

In contrast to this, the 0°C test revealed that the battery is discharged faster and reaches the status of constantly low SOC at the end of the first WLTC. Furthermore, the battery lost about 2.4 percentage points SOC during a standstill time of 220 s before the cold start WLTC and 4 percentage points SOC during the 20 minutes break between the two WLTC test drives at 0°C (see Figure 8). A similar, but much lower discharging is observed between the tests at 23°C ambient temperature. Assuming a linear decrease of SOC in this range, the energy loss per second during the break time between the tests at 0°C was lower than the loss before the test at the same ambient temperature. This relatively lower loss between the tests can be explained by the fact that after the first cycle, the vehicle interior was already warmed by the air conditioning for 30 minutes. We assume that the energy lost before the test and during the break was mainly used for air conditioning (heating). If the same amount of power would be used for heating during the driving as in stand still, the loss for one WLTC cycle would be between 8 to 19 percentage points. If about 19 percentage points SOC are subtracted for heating, this would still leave a difference of 17 to 7 percentage points to the SOC delta of the cold start WLTC at 23°C. This indicates an increased power loss of the battery at lower temperatures.

The recuperation of braking energy is visible in an increase of SOC and is particularly high when decelerating at the end of the highway part at the end of each WLTC.

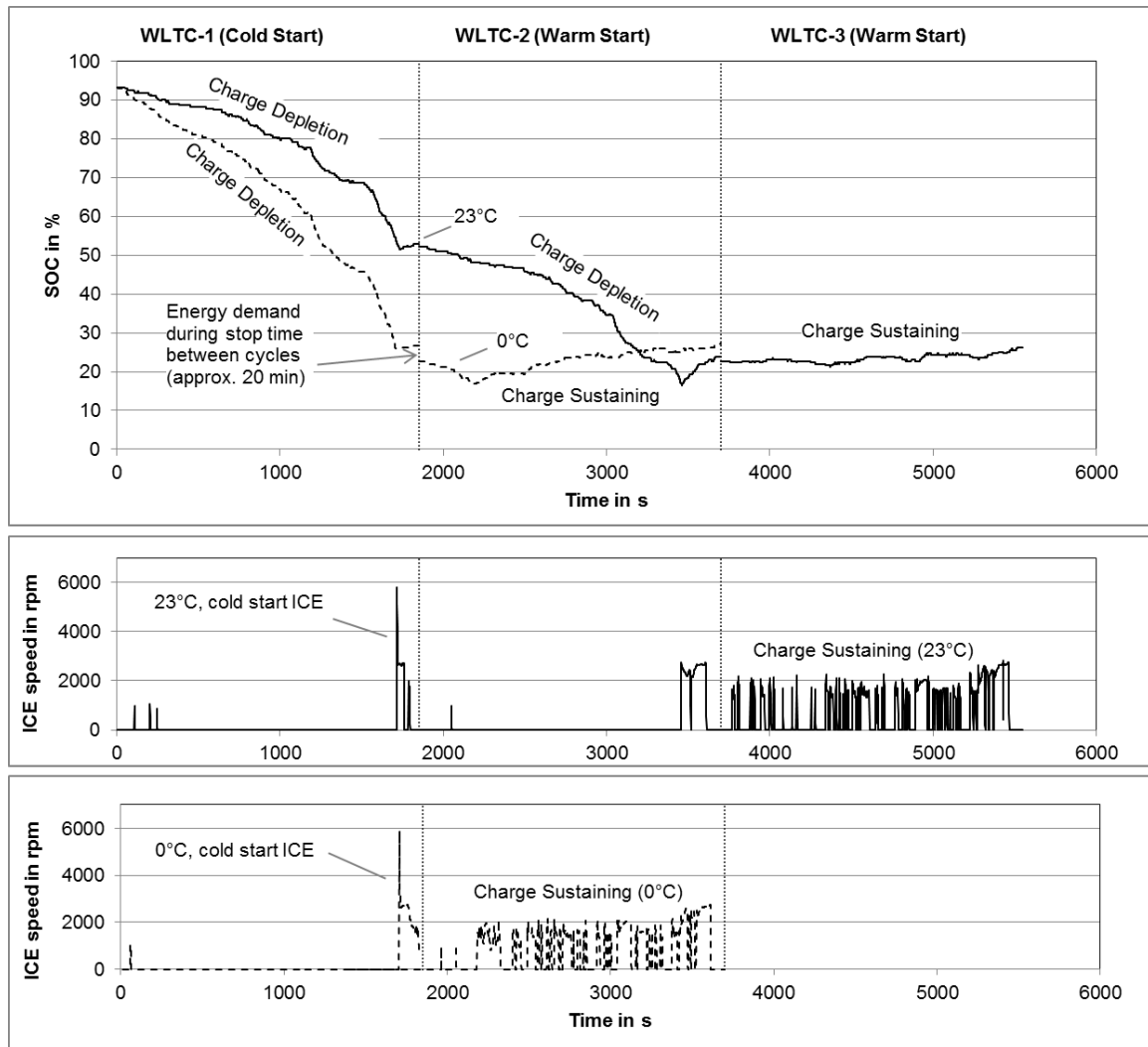


Figure 8: Development of the SOC during the WLTC at different temperatures (top) ICE speed vs. time (bottom)

Although the cold start tests have been driven in the CD mode, none of the WLTC could be driven purely electric, as the ICE started automatically during the highway section at a speed higher than 125 km/h due to the implemented operation strategy of the tested PHEV. This behavior could be observed for an ambient temperature of 23°C as well as for 0°C and is shown by the curve of the ICE speed vs. time in Figure 8 (bottom). The start of the ICE leads to direct emissions from the fuel combustion and shows peaks for CO and NO_x emissions, as the catalyst has not reached its optimal operating temperature yet (Figure 9). For both tests, higher emissions could be observed at 0°C.

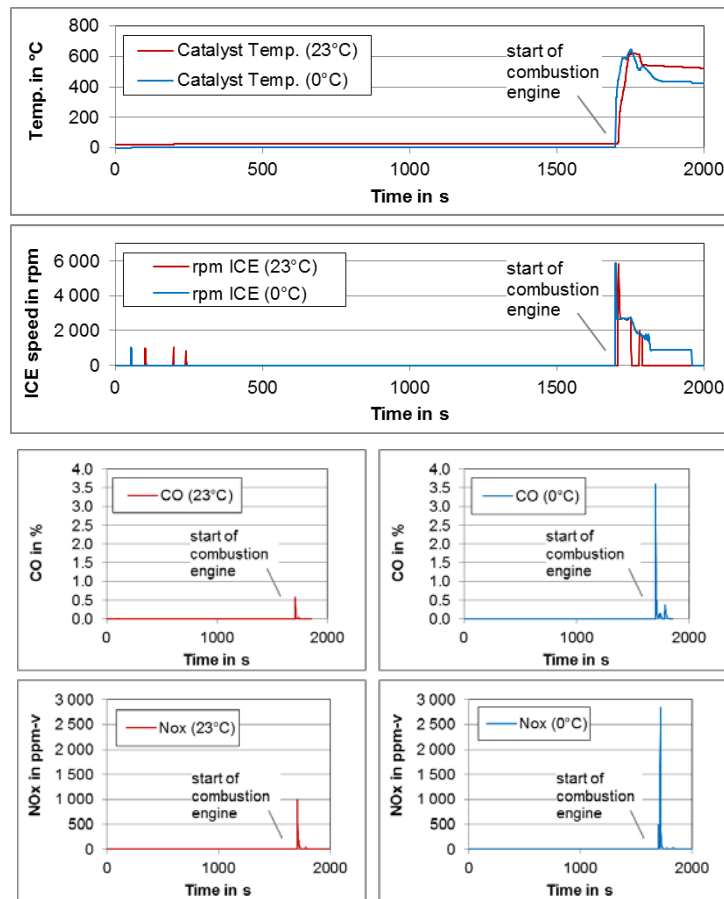


Figure 9: Cold start WLTC test at 0°C and 23°C in charge depletion mode (WLTC-1-0° and WLTC-1a-23°)

In order to compare the cold start in different modes, an additional cold start test at 23°C has been carried out in the hybrid mode. In this driving mode, the vehicle software alternates between the electric and ICE drive or combines both of them following an internal operation strategy. As the ICE is only used in specific situations during the test, the catalyst temperature reaches its optimum only in late stage of the cycle (Figure 10). This leads to several CO emission peaks during the test every time the ICE is started. These peaks completely disappear when the catalyst runs in optimal conditions. As the catalyst is not preheated during electric drive time (see Figure 9, top) the disadvantageous effect of an insufficient catalyst temperature can be assumed to be more important for the hybrid mode in lower ambient temperatures.

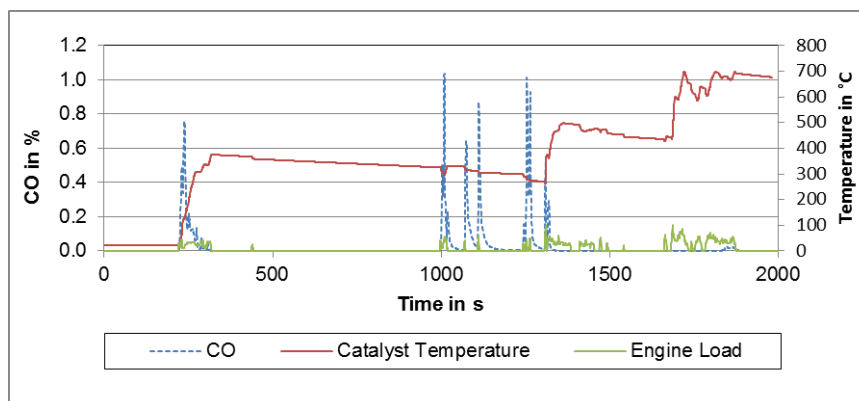


Figure 10: Cold start WLTC test at 23°C in hybrid mode

For the evaluation of absolute exhaust emissions, the volume flow rate is correlated to the relative concentration of exhaust gases. In order to assess the potential emissions of the PHEV in cases where the battery is discharged and the vehicle operates as gasoline vehicle, hot start WLTC tests have been

performed as both 0°C and 23°C after the PHEV reached the maximum electric mileage and the battery showed a constant low SOC. In this case, the vehicle operation strategy switches to the CS mode, but the remaining and recuperated battery energy is still used at low speeds in the urban part of the WLTC. The HC and CO emissions show higher concentrations in the comparatively dynamic urban part of the WLTC (Figure 11). The CO₂ emissions are higher at high motor loads during the highway part as expected. The NO₂ and especially the NO emissions are highest when the acceleration of the driving cycle is most intensive. What is most notable is that the emissions of all exhaust gas emissions are significantly higher at 0°C than at 23°C. Two main possible reasons can be identified: the higher energy consumption for heating and the less effective exhaust gas treatment. In both cases, the catalyst has reached its optimal temperature in the prior tests. In the 0°C test, the catalyst cools down significantly during the 20 minutes break between the two WLTC tests (WLTC-1-0° and WLTC-2-0°).

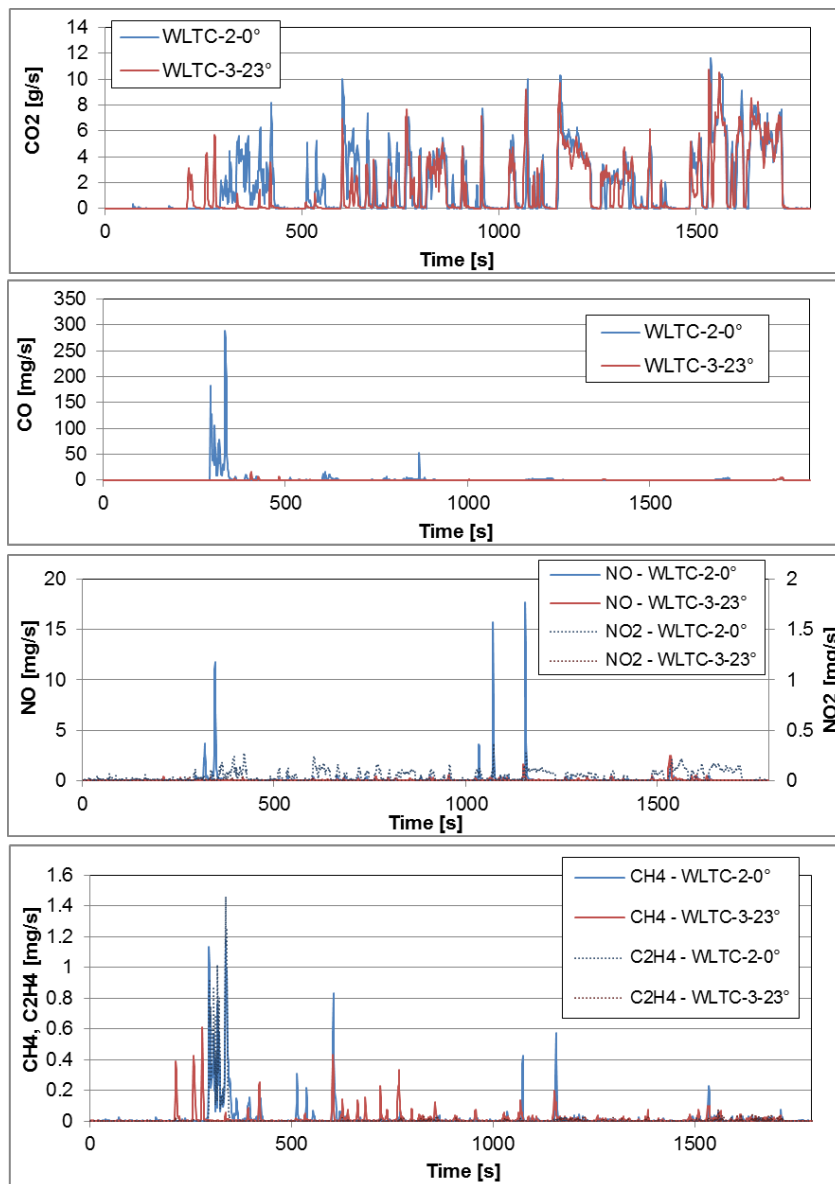


Figure 11: Absolute emissions of the WLTC-2-0° and the WLTC-3-23° tests in g/s for different exhaust gases

The evaluation of the average emissions shows, that for all pollutants and for CO₂ a temperature dependency is observed (Table 2). This is a direct result of higher emissions per time as shown in Figure 11. Additionally, the ICE-in-use share is higher when the temperature is low which again increases the absolute emissions during the WLTC. The emissions refer to the length of the entire WLTC test and therefore include phases without local emissions. This results from the recuperation of the battery and to the use of this energy for certain driving situations. The CO₂ emissions of the test in the CS mode at 23°C are below the limit of 130 g/km which is currently the target for the average passenger car vehicle in the EU, while the emissions at

0°C are above this limit. Although 130 g CO₂/km is the target for the fleet average, the emissions of mid-size vehicles are a good indicator for the potentials of reaching this goal with certain technologies. In contrast to the CO₂ limits, the emission standards for other pollutants are valid for every single vehicle. In our WLTC tests, the gasoline PHEV meets the EU standards with the analyzed exhaust gases, but the benefits from the PHEV technology are significantly lower in periods with low ambient temperatures.

Table 2: Average emissions of the presented WLTC tests in g/km for different emitted gases

Test	CO ₂ [g/km]	CO [mg/km]	NO [mg/km]	NO ₂ [mg/km]	SO ₂ [mg/km]
WLTC-1-0°	23	333	27	1	0.4
WLTC-2-0°	133	186	10	3	5
WLTC-1a-23°	14	25	6	1	0.4
WLTC-1b-23	74	209	9	0.4	3
WLTC-3-23°	104	10	3	0.1	5

The strong influence of a low ambient temperature has been observed in other tests of this measurement project as well. Especially in the case of a tested diesel PHEV, the temperature influenced the share of ICE driving considerably. Furthermore, the temperature and cold start effects are visible not only for NO_x and CO, but also for HC and VOC emissions. Such effects need to be considered when the emissions from passenger cars are quantified and the effects of such emissions on air pollution and climate changed are modelled.

4. Conclusions

EV have the potential to reduce local air pollution and greenhouse gas emissions. User acceptance is positive concerning environmental benefits, although technical benefits are not commonly known. As expected, real-world driving and real-world charging will lead to a higher energy demand. Monitoring a BEV on-road during 2015, it could be shown that its average traction battery energy demand is 17 kWh/100 km. When taking overall charging losses due to inefficiencies or auxiliaries into account, the total energy demand of that BEV model is 20 kWh/100 km on average. The electricity mix as of today in Germany with a 50% share of hard coal and lignite is resulting in well-to-tank NO_x and PM2.5 emissions per kWh that are comparable to directly emitted tank-to-wheel emissions of conventional passenger cars. Still, air pollutants from electricity production are emitted at higher heights and usually in less densely populated areas such that urban air quality will benefit from the use of BEV.

The shift of emissions to the power plant locations also takes place in the case of electric driven PHEV. Basically, these vehicles have the potential to reduce local emissions, but our dynamometer measurements indicate that the actual saving potential strongly depends on ambient conditions. The tests show that the ambient temperature influences the range, the share of ICE use and the catalyst temperature notably, which is directly reflected by the exhaust emissions. Though cold start effects are avoided by electric driving in the beginning, such effects are shifted to later stages when either a higher speed or acceleration or a low SOC is reached. Additionally, PHEV emissions strongly depend on the user behavior, but due to the low number of registered vehicles little is known about a representative or typical PHEV user behavior. Data from a Dutch study indicate that the actual electric driving share is lower than expected due to the individual charging habits (Ligterink, Smokers, and Bolech, M. 2013).

The presented studies feed into our scenario work on future vehicle energy consumption and emissions and will provide improved input data for air quality and climate change models.

Acknowledgments

This work is supported by the Federal Ministry for the Environment, Nature Conservation, Building and Nuclear Safety (BMUB) in the frame of the project InitiativeE-BW (www.initiative-bw.de) and by the DLR Centre of Excellence project 'Environment and Transport (EnvITrans)'. The results of the studies presented in this paper will be used for the DLR project "Transport and the Environment" (www.dlr.de/VEU).

References

- Agora Energiewende (2015): Agorameter. Available at <https://www.agora-energiewende.de/de/themen/-agothem-/Produkt/produkt/76/Agorameter/>
- ecoinvent Center (2014): *Ecoinvent Version 3.1*. www.ecoinvent.org. European Commission
- European Commission (2011): White Paper - Roadmap to a Single European Transport Area, COM(2011) 144 final, European Commission.
- Fetene, G. M., Prato, C. G., Kaplan, S., Mabit, S. L., Jensen, A. F. (2015): Harnessing Big-Data for Estimating the Energy Consumption and Driving Range of Electric Vehicles. Final manuscript for presentation at the 95th Annual Meeting of the Transportation Research Board, January 10-14, 2016, Washington D.C.
- HBEFA (2014): Handbook emission factors for road transport. <http://www.hbefa.net/e/index.html>
- JRC (2014): Well-To-Wheels Report Version 4.A, JEC Well-To-Wheels Analysis, JRC Technical Reports
- Jungmeier, G., Dunn, J., Elgowainy, A., Gaines, L., Ehrenberger, S., Özdemir, E. D., Althaus, H.-J., Widmer, R. (2014): Life cycle assessment of electric vehicles – Key issues of Task 19 of the International Energy Agency (IEA) on Hybrid and Electric Vehicles (HEV). Transport Research Arena 2014, 14.-17. April 2014, Paris, France
- Ligterink, N.E., R.T.M. Smokers, and Bolech, M. (2013): Fuel-Electricity Mix and Efficiency in Dutch Plug-in and Range-Extender Vehicles on the Road. EVS 27, Barcelona, Spain.
- Pehnt, M. and U. Höpfner (2007): Elektromobilität und erneuerbare Energien (Electric mobility and renewable energy). Working paper No. 5. Heidelberg, Wuppertal, November 2007
- Plötz, P., Funke, S. and P. Jochem (2015): Real-world fuel economy and CO2 emissions of plug-in hybrid electric vehicles. Working Paper Sustainability and Innovation No S1/2015, Fraunhofer ISI, Karlsruhe, Germany

Emissions of NO, NO₂, and PM from inland water transportation

Ralf KURTENBACH, Kai VAUPEL, Jörg KLEFFMANN, Ulrich KLENK, Eberhardt SCHMIDT & Peter WIESEN

Bergische Universität Wuppertal (BUW), Institute for Atmospheric and Environmental Research, 42097 Wuppertal

Fax +49 202 439 2757 - email: kurtenba@uni-wuppertal.de

Abstract

Particulate matter (PM) and nitrogen oxides NO_x (NO_x = NO₂ + NO) are key species for urban air quality in Europe and are emitted by mobile sources. According to European recommendations, a significant fraction of road freight should be shifted to waterborne transport in the future. In order to better consider this changed emission pattern in future emission inventories, in the present study, inland water transport emissions of NO_x (NO_x = NO₂ + NO), CO₂ and PM were investigated under real world conditions at the river Rhine, Germany in 2013. An average NO₂/NO_x emission ratio of 0.08 ± 0.02 was obtained, which is indicative of ship diesel engines without after-treatment systems. For all measured motor ship types and operation conditions overall weighted average emission indices of EI_{NO_x} = 54 ± 4 g/kg and a lower limit EI_{PM₁} = ≥ 2.0 ± 0.3 g/kg were obtained. EIs for NO_x and PM₁ were found to be in the range of 20–161 g kg⁻¹ and ≥ 0.2–8.1 g kg⁻¹, respectively. A comparison with threshold values of national German guidelines shows that the NO_x emissions of all investigated motor ship types are above the threshold values, while the obtained lower limit PM₁ emissions just within. To reduce NO_x emissions to acceptable values, implementation of after-treatment systems is recommended.

Key-words: *Air pollution, city air quality, emission factors, guidelines, inland water transport.*

Introduction

Particulate matter (PM) and nitrogen dioxide (NO₂) are key species for urban air quality in Europe. Whereas the exceedence of PM limiting values has attracted considerable public attention during the last decade, NO₂ is a topical problem, which became mature through the introduction of new European limiting values in January 2010.

The reduction of nitrogen oxide (NO_x = NO + NO₂) emissions has been historically one of the key objectives for improving air quality in Europe. NO_x emissions have started to decrease considerably since the mid eighties of the last century in many European areas. However, emissions from mobile sources are still important contributors to air pollution, in particular for NO_x. Together with NO_x, non-methane volatile organic compounds (NMVOCs) undergo photochemical reactions producing secondary pollutants such as ozone (O₃), peroxyacetyl nitrate (PAN) and others (Chameides et al. 1997, Atkinson 2000).

According to the European Commission's White Paper (2011), 30% of road freight transported over more than 300 km distance should shift to other transport modes such as waterborne or rail transport by 2030, and more than 50% by 2050 (European Commission 2011). Accordingly, such a shift will result in an increase of emissions from inland water transportation in the next years.

Today in Germany the contribution of inland navigation to the total freight traffic is about 12% (BDA 2015a). In the Rhine corridor the contribution is 16-18%, respectively (BDA 2015b). With respect to the goods categories "coal, crude oil and petroleum gas", "ores, industrial rocks and minerals, other mining products" and "coking plant and petroleum products" inland water navigation is the most important transportation mode. In comparison to road transport, inland navigation has a contribution of 72% for these goods categories and 52% for container transport. Inland water navigation is a competitive alternative to road and rail transport, because the energy consumption per km and ton of transported goods is only approximately 17% of road and 50% of rail transport (ECT 2015). As a consequence of the lower energy consumption, inland water transportation emits significantly less CO₂ and, therefore, has a direct impact on climate change.

In the EU-15 the emission of NO_x, VOC, PM and CO from road and rail transport decreased from 1990 to 2000, whereas emissions from inland navigation remained more or less constant and emissions from sea transport slightly increased (Trends 2003). However, in the Netherlands a slight reduction in inland shipping emissions were observed in the same time period when modern engines were introduced in the fleet (Adviesdienst Vereer en Vervoer 2003).

It has been also conclusively demonstrated that the fuel has an important impact on the emissions. Using liquid natural gas (LNG) as fuel for inland water vessels leads to substantial emission reductions, i.e. 75% for NO_x, 97% for PM and 10% for CO₂ (Van der Werf 2013).

The emissions from inland water transportation have been regulated by several national and international guidelines. In 2005 the German national guideline "Binnenschiffabgasverordnung, BinSchAbgasV" was implemented for national water ways, defining engine dependent emission indices, i.e. emitted mass of pollutant per kg burnt fuel, for NO_x and PM of EI_{NO_x}: 30 - 42 g/kg and EI_{PM}: 1.2 - 2.4 g/kg, respectively (BinSchAbgasV9 2005). In 2011 an international guideline for the Rhine river "RhineSchUO" was implemented with engine dependent EI_{NO_x}: 28 - 36 g/kg and an EI_{PM}: 0.9 - 3.1 g/kg (RheinSchUO 2011). In addition, for river-sea-ships the MARPOL guideline (International Convention for the Prevention of Pollution from Ships) (IMO 2012) has to be applied. For example, for marine diesel engine with a medium-speed of 720 min⁻¹ NO_x-emission indices of 58 g/kg since 2000 (Tier I), 56 g/kg since 2011 (Tier II) and 11 g/kg since 2016 (Tier III) have been introduced.

The correct determination of emission indices (EI) is prerequisite for establishing and developing emission inventories (VBD 2001, Klimont et al. 2002, Browning and Bailey 2006, Rohacs and Simongati 2007, TNO 2008, CBS 2009, UBA 2013). Up to now, several studies have been published in which NO, NO₂, SO₂ and PM emissions from sea ships (Sinha et al. 2003, Chen et al. 2005, Eyring et al. 2005, Petzold et al. 2008, Moldanova et al. 2009, Murphy et al. 2009, Schrooten et al. 2009, Williams et al. 2009, Eyring et al. 2010, Beecken et al. 2014, Jonsson et al. 2011, Lack et al. 2011, Alföldy et al. 2013) and, in particular, from sea ferries (Cooper et al. 1996, 1999, Copper 2001, 2003, Copper and Ekström 2005, Tzannatos 2010, Pirjola et al. 2014) were investigated. Motor test bed studies can also be used for the determination of EIs from single ship's engines (Petzold et al. 2008). However, up to now only three studies have reported on inland water transportation emissions (Trozzi and Vaccaro 1998, Kesgin and Vardar 2001, Schweighofer, and Blaauw 2009, Van der Gon and Hulskotte 2010)

In the present study, inland water transport emissions were investigated under real world conditions at the riverside of the river Rhine in Germany during a field campaign from February 20, to February 22, 2013.

1. Description of the Experimental Procedures

Measurement site

The measurement campaign was carried out at the river Rhine in Germany close to the "Wunderland Kalkar" at Rhine kilometre 843. Figure 1 shows a map of the measurement site. During the campaign emissions from both, upstream and downstream driving inland ships were studied. The sampling point was located 50 m downwind from the river bank.

It is reasonable to assume that the engines of the ships passing the sampling site, were under warm operation conditions.

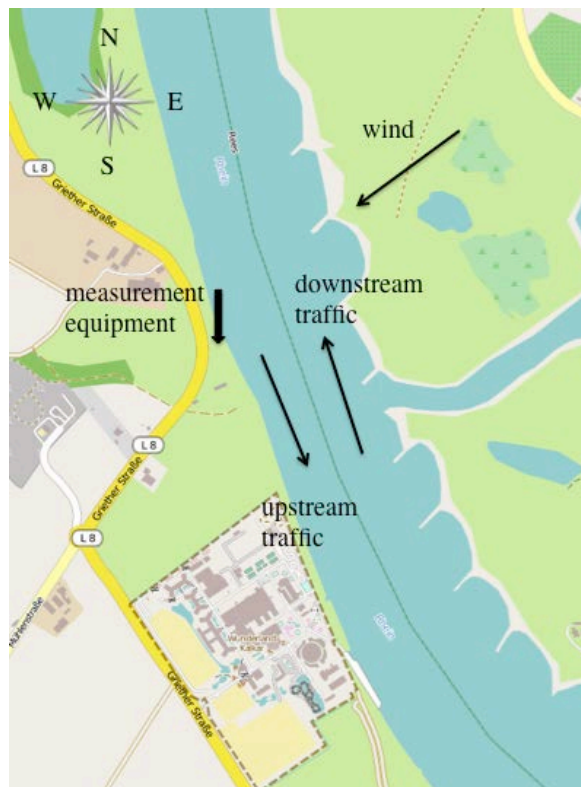


Figure 1: Location of the measurement site at Rhine kilometre 843.

(This map is made available under the Open Database License: <http://opendatacommons.org/licenses/odbl/1.0/>. Any rights in individual contents of the database are licensed under the Database Contents License: <http://opendatacommons.org/licenses/dbcl/1.0/> - See more at: <http://opendatacommons.org/licenses/odbl/#sthash.hMw4LqYT.dpuf>).

Analytical Equipment

The analytical equipment used was installed in a mobile van with an external power supply. NO and NO₂ were measured on-line with a commercial NO_x chemiluminescence analyzer (Environnemental, AC 31M with molybdenum converter). The time resolution was 10 s and the detection limit, which was calculated from the variation of the zero signal was 2 ppbV for NO and 3 ppbV for NO₂. The NO channel of instrument was directly calibrated by diluted standard NO calibration mixtures (Messer, stated accuracy 5 %). The NO₂ channel was calibrated by using a NO titration unit (Environnemental, GPT). NO₂ was produced by the reaction of NO with O₃ in a flow reactor leading to the quantitative conversion of the calibrated NO ($\Delta\text{NO} = \Delta\text{NO}_2$).

Ozone (O₃) was measured on-line with a commercial O₃ monitor (Environnemental, O3 41M with UV absorption). The time resolution was 10 s and the detection limit, which was calculated from the variation of zero measurements, was 1 ppbv. O₃ was calibrated by using an O₃ calibration unit (Environnemental, K-O₃, accuracy 10 %). O₃ was produced by the photolysis of synthetic air in a flow reactor leading to the quantitative formation of O₃.

Carbon dioxide (CO₂) was measured on-line with a commercial CO₂ monitor (LICOR 7100 with IR absorption). The time resolution was 1 s and the detection limit, which was calculated from the variation of background concentrations, was 0.5 ppmv. CO₂ was directly calibrated by diluted standard CO₂ calibration mixtures (Messer, stated accuracy 2 %).

PM was measured by an optical particle counter (OPC) (Grimm Aerosol Technik GmbH, DustMonitor EDM 107). The OPC counts particles in a size range from 0.25 and 32 μm in 31 size-channels. The time resolution was 6 s and the detection limit 0.1 μg/m³. However, the instrument only provided the concentrations of the fractions PM₁, PM_{2.5} and PM₁₀.

Meteorological parameters, such as temperature, pressure, relative humidity and wind speed were also measured. In addition to the measurement of compounds in the ambient air, the number and types of ships passing the measurement site were counted.

2. Results and discussion

Inland water transportation emissions

NO, NO₂, O₃, CO₂, PM₁ and PM₁₀ concentrations, wind speed and wind direction at the measurement site as well as movements of the ships were measured. During the campaign more than 170 emission peaks from motor ships were observed. From these peaks almost 140 could be attributed to single ships and were analyzed accordingly. Figure 2 shows as an example the temporal variation of NO, NO₂, O₃ and CO₂ mixing ratios at the measurement site on February 20, 2013 from 11:30 to 14:00. The perfect correlation between NO and NO₂ with CO₂ confirms that these compounds were emitted from the same source, i.e. the engine exhaust. The anti-correlation between NO₂ and O₃ provides information about NO_x chemistry in the ship exhaust plumes, i.e. the formation of NO₂ by the titration reaction of NO with O₃.

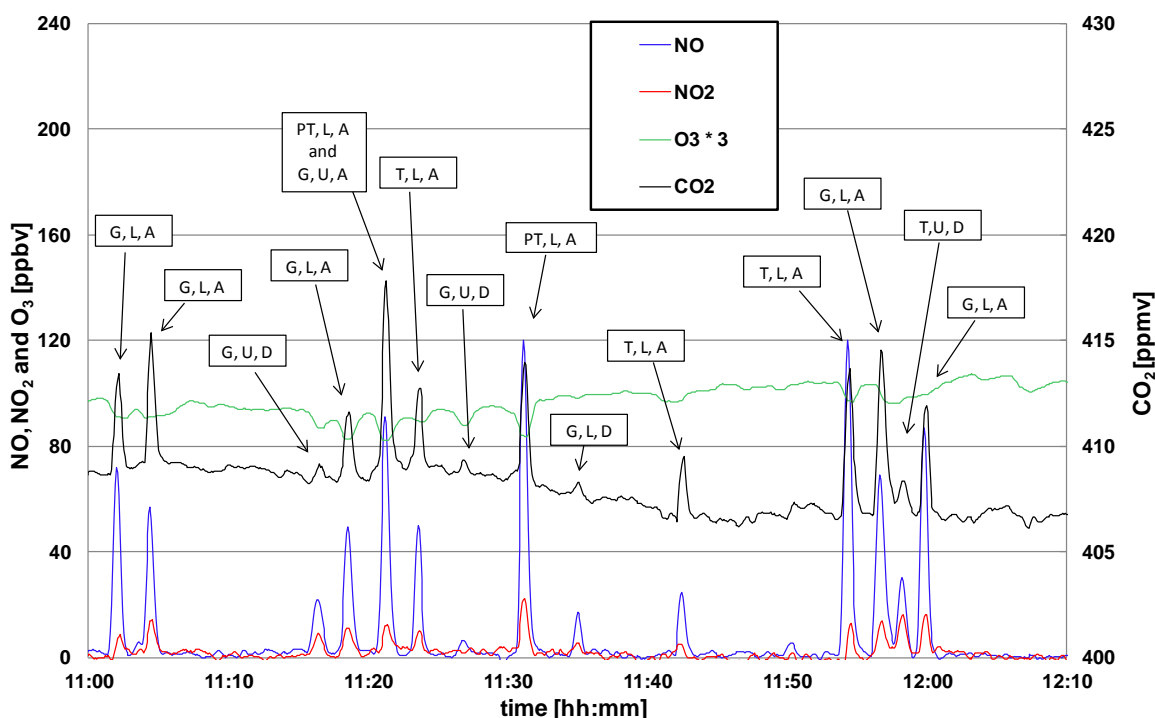


Figure 2. Temporal variation of the NO, NO₂, O₃ and CO₂ concentration at the measurement site on February 20, 2013 from 11:30 to 14:00 from different ship types (G=goods ship, T=petroleum tanker, PT=push tow) and at different operation parameters (L=loaded, U=unloaded, A=upstream and D=downstream).

NO₂/NO_x emission ratio

In order to obtain information about the ships engine types and to estimate the impact of ship emissions on the ozone formation the NO₂/NO_x ratio in the exhaust plume is an important parameter. It is well known that diesel engines without after-treatment systems show NO₂/NO_x ratios of 0.10 – 0.12 for road traffic (Kurtenbach et al. 2001, Kousoulidou et al. 2008, Carslaw and Rhys-Tyler 2013) and (0.14 ± 0.04) for navigation (Cooper 2001, Grice et al. 2009). In contrast, the NO₂/NO_x ratio from road traffic diesel engines with after-treatment systems such as oxidation catalyst or PM filter systems are in the range of 0.25 – 0.30. The NO₂/NO_x emission ratio from navigation diesel engines with selective catalytic NO_x reduction systems (SCR) is (0.009 ± 0.003) (Cooper 2001).

In order to obtain the correct NO₂/NO_x emission ratio from the measurements it is important to distinguish between primarily emitted NO₂ and NO₂, which is being formed by the reaction of NO with ozone in the exhaust plume. The correct NO₂/NO_x ratio is obtained by plotting O_x, which is the sum of NO₂ and O₃ versus the measured NO_x concentration as shown in Figure 3 (Clapp and Jenkin 2001). The NO₂/NO_x emission ratio and the local O₃ background mixing ratio are obtained from the slope and

intercept of the regression line, respectively. From the data shown in Fig. 3 a NO_2/NO_x emission ratio of (0.08 ± 0.02) and a local ozone background volume mixing ratio of (23 ± 2) ppbv were obtained. The obtained NO_2/NO_x ratio indicate that the ships passing the measurement site were equipped with conventional diesel engines without exhaust after-treatment.

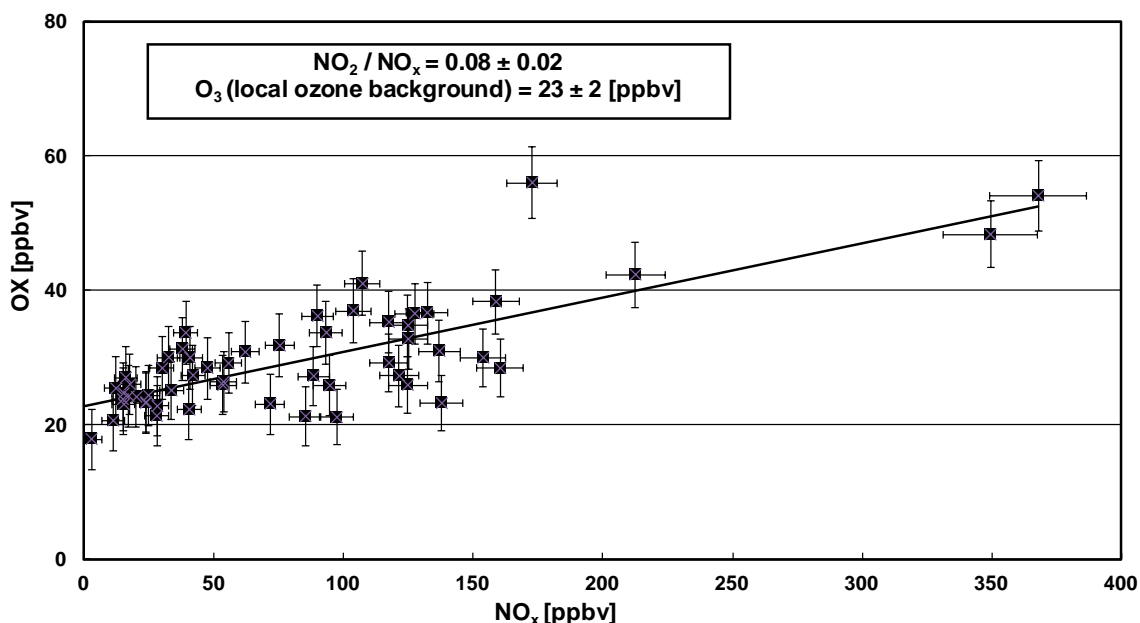


Figure 3. Plot of O_x vs. NO_x

PM₁ and PM₁₀ emissions

Figure 4 shows the temporal variation of CO_2 , PM_{10} and PM_1 concentrations at the measurement site on February 20, 2013 from 11:50 to 12:10. Some PM_1 peaks are well correlated with those of CO_2 mixing ratios, therefore, with ship plumes. In contrast, some PM_{10} peaks showed no correlation with ship emissions. This indicates that the main PM emissions from ships diesel engines are in the PM_1 range. This result is in good agreement with other studies e.g. from the US-EPA (1996), Petzold et al. (2008), Beecken et al. (2014), Pirjola et al. (2014) and Westerlund et al. (2015). Therefore, in the present study particle ship emissions are defined as PM_1 . According to Westerlund et al. (2015) the maximum in the particle number size distribution was observed at about 10 nm and the maximum particle mass distribution at 250 nm. Therefore the used optical particle counter (OPC) detect only a lower limit of the emitted particle mass.

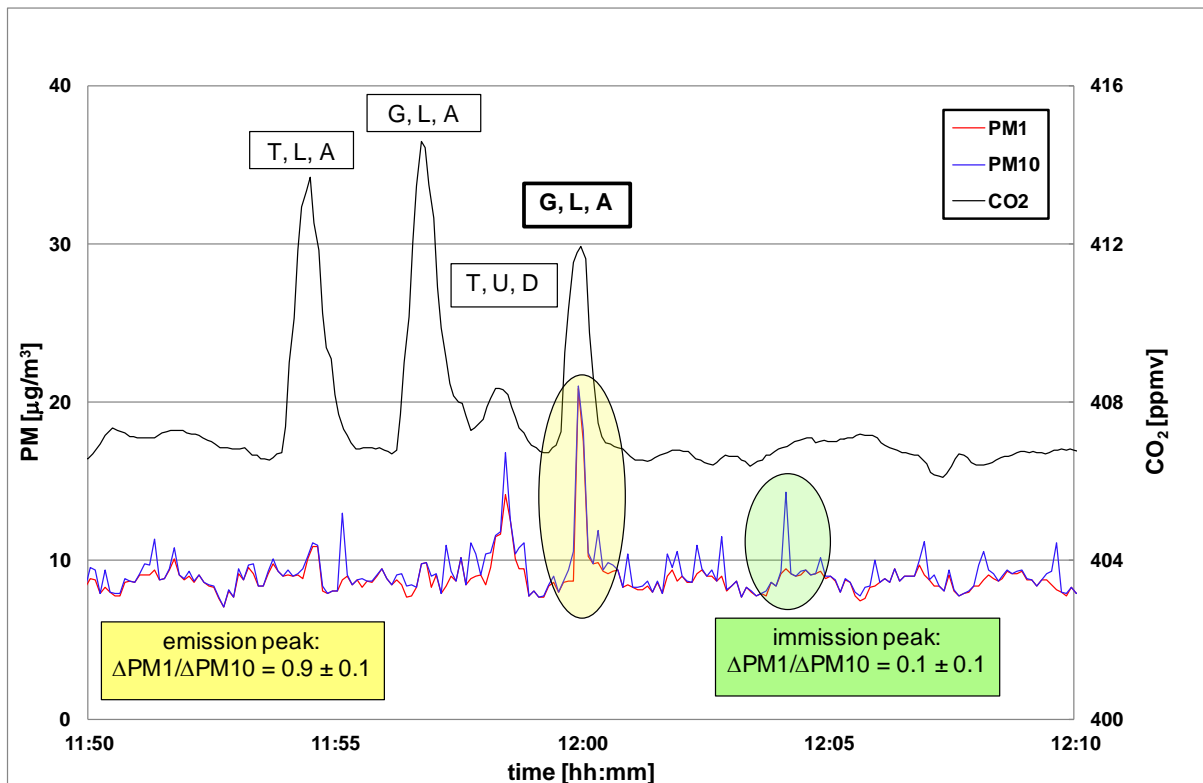


Figure 4. Temporal variation of CO₂, PM₁₀ and PM₁ at the measurement site on February 20, 2013 from 11:50 to 12:10 for different ship types (G=goods ship, T=petroleum tanker) and different operation parameters (L=loaded, U=unloaded, A=upstream and D=downstream).

Emission indices

From the measurement data, emission indices (EIs) for NO_x (NO calculated as NO₂) and PM₁ (unit: mass per kg burnt fuel) were calculated. In Figure 5 the integrated emission peak (peak area) for NO, NO₂, CO₂ and PM₁ as ΔNO , ΔNO_2 , ΔCO_2 and ΔPM_1 are shown as an example for a single motor ship. If one assumes that the increase of NO, NO₂, PM₁ and CO₂ in the plume is proportional to the emission strength of the ship engine, an emission ratio to CO₂, e.g. $\Delta\text{NO}_x/\Delta\text{CO}_2$, can be easily calculated (Petzold et al. 2008). In addition the ΔNO , ΔNO_2 , ΔCO_2 and ΔPM_1 were also calculated by the difference between background and plume mixing ratios (Schlager et al. 2008) and considering the precision errors of the background data of typically ± 1.7 ppbv, ± 3.6 ppbv, ± 1.4 ppbv, ± 0.7 ppmv and ± 2 $\mu\text{g}/\text{m}^3$ for NO, NO₂, O₃, CO₂ and PM₁, respectively.

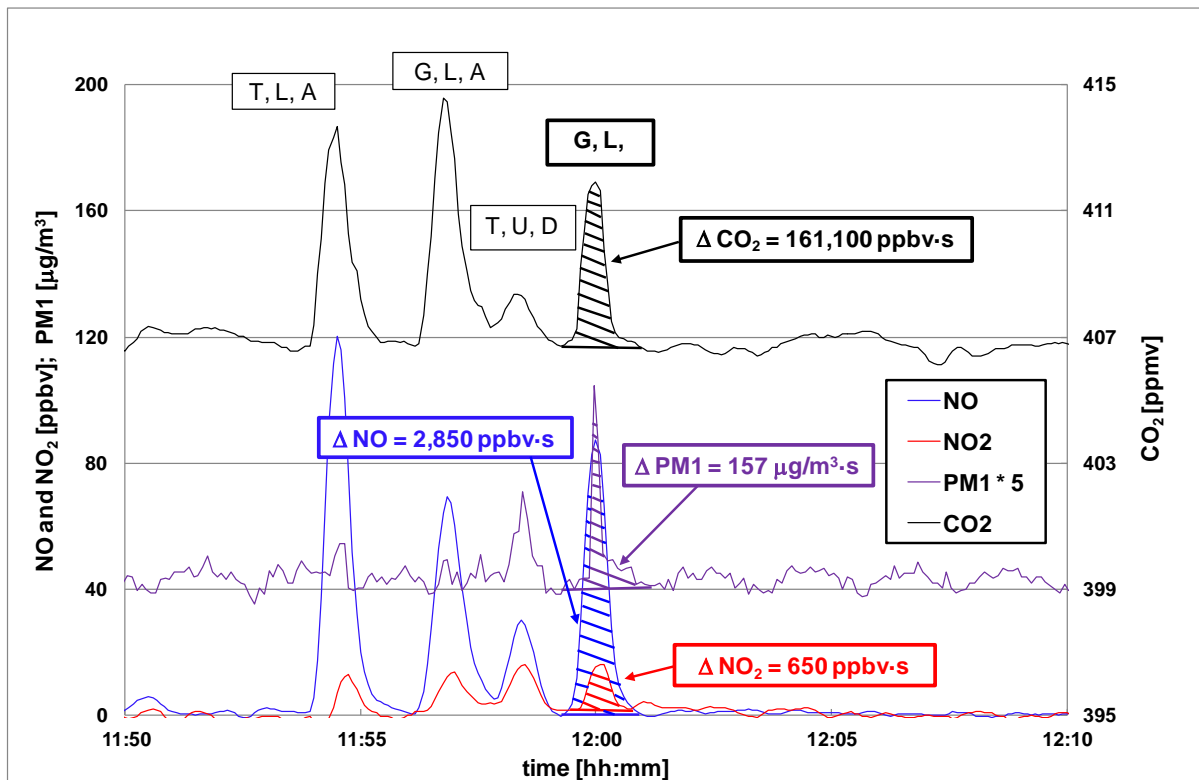


Figure 5. Temporal variation of the NO, NO₂, CO₂ and PM₁ concentration and the integrated emission peaks as ΔNO, ΔNO₂, ΔCO₂ and ΔPM₁ peak area at the measurement site on February 20, 2013 from 11:50 to 12:10 for a goods ship (G) under loaded (L) and upstream (A) conditions.

Both approaches were used to calculate the emission indices and were in good agreement, in general better than ± 6 %. Caused by the slightly different time responses of the instruments, finally the integrated peaks results were specified. Elementary analysis of a typical ship diesel fuel yielded: 86 wt% carbon and 14 wt% hydrogen (Cooper 2001). From the wt% carbon and under the assumption that all fuel is burnt to the final end product CO₂ an emission index EI (CO₂) of 3,150 g CO₂ per kg burnt fuel was calculated and further used to calculate the corresponding emission index (EI) for the ship engines. The emission index (EI) is calculated by the following equation (Petzold et al. 2008):

$$EI(X) = EI(CO_2) \times \frac{M(X)}{M(CO_2)} \times \frac{\Delta(X)}{\Delta(CO_2)}$$

where *M* denotes the molecular weight and Δ the peak area, mixing ratios, column densities, etc. of the species. *M* (CO₂) with 44g/mol and *M* (NO_x) with 46 g/mol, NO_x as NO₂ were used for the subsequent calculations.

Figure 6 shows as an example the emission index for NO_x (as NO₂) (EI_{NO_x}) of single motor ships [goods] and the weighted average EI_{NO_x} for different operation parameters, i.e. L=loaded, U=unloaded, A=upstream and D=downstream.

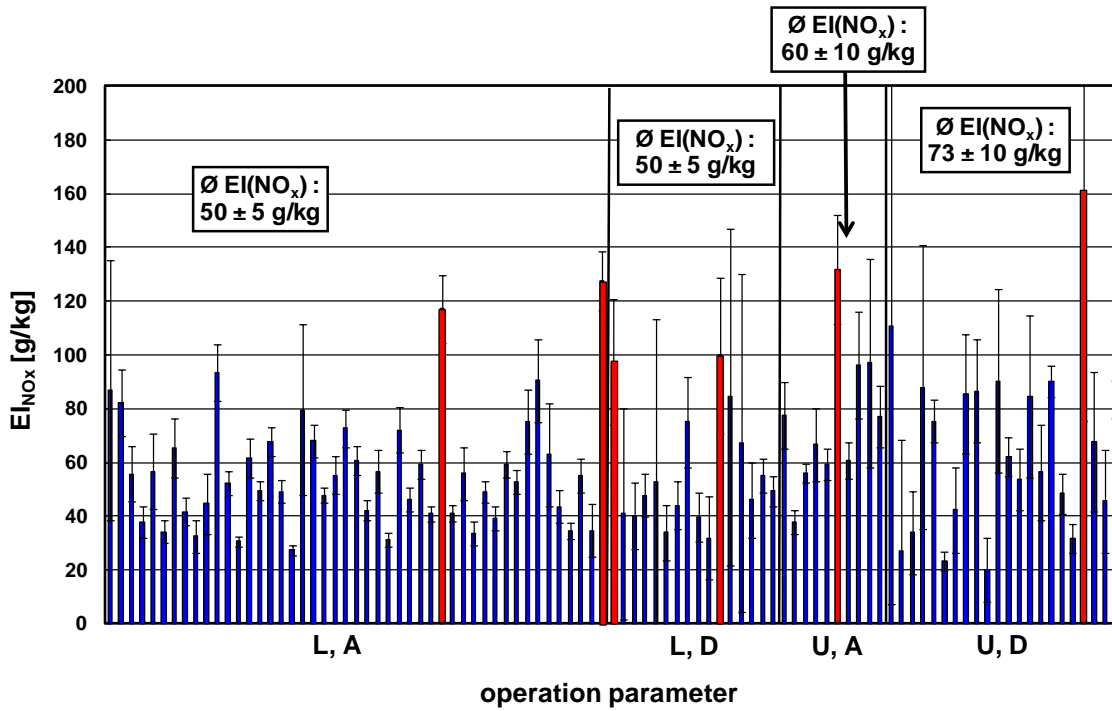


Figure 6. EI_{NO_x} (as NO_2) of single motor ships [goods] and the weighted average value of EI_{NO_x} for different operation parameters, L=loaded, U=unloaded, A=upstream and D=downstream. Red bars show outliers (4σ limit) and were not taken into account in the calculation of the weighted average value.

Figure 7 shows as an example the obtained lower limit PM_1 emission index (EI_{PM_1}) for single motor ships [goods] and the weighted average EI_{PM_1} for different operation parameters, i.e. L=loaded, U=unloaded, A=upstream and D=downstream. Red bars show outliers (4σ limit) and were not taken into account in the calculation of the weighted average value. Values are lower limits because of the detection range of the OPC system.

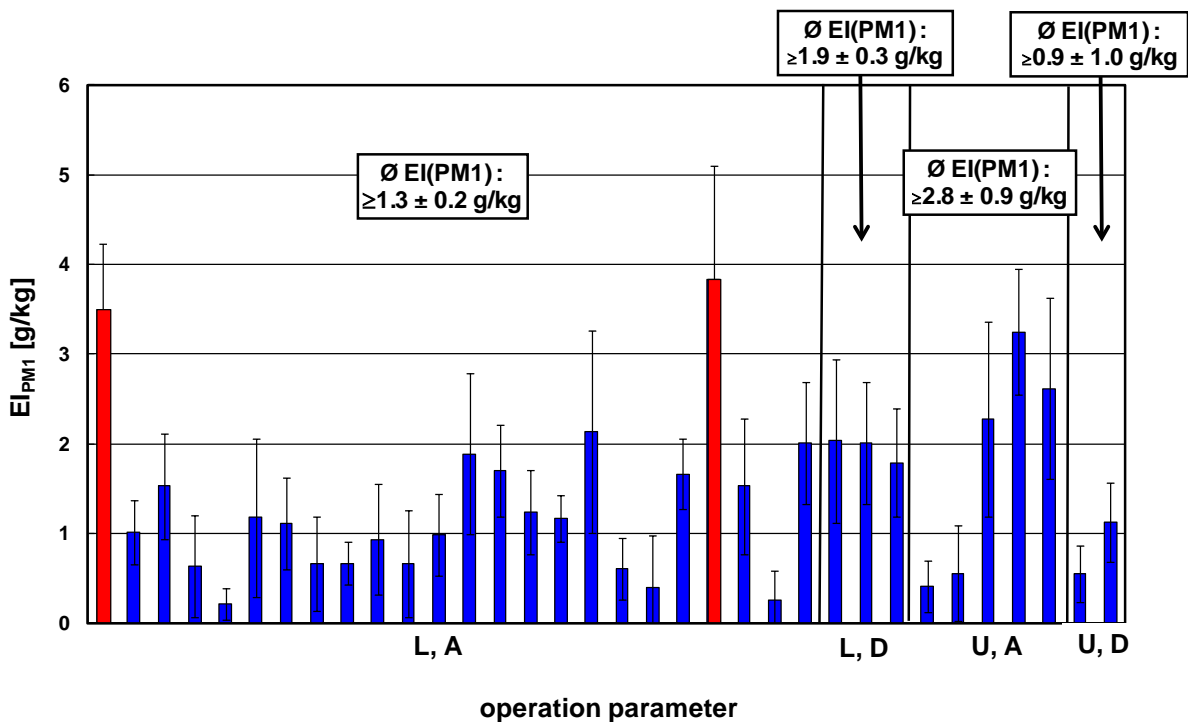


Figure 7. Lower limit EI_{PM_1} of single motor ships [goods] and the weighted average EI_{PM_1} for different operation parameters, L=loaded, U=unloaded, A=upstream and D=downstream.

Although Fig. 6 and 7 show a large variation of the EIs for NO_x and PM_1 , the average data exhibit that the EI_{NO_x} are almost independent of engine operation parameters within the given error limits. The same was found for tankers and push tows, see weighted average emission index figures 8 and 9.

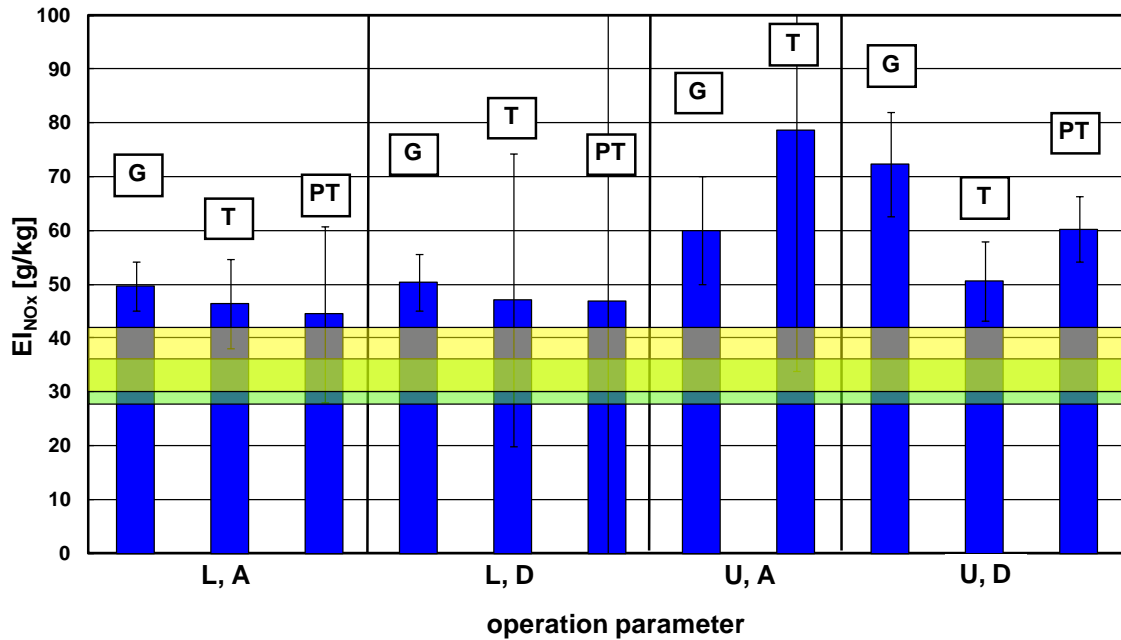


Figure 8. Weighted average emission index for NO_x (EI_{NO_x}) for different motor ship types (G=goods, T=tanker and PT=push tow) at different operation parameters, (L=loaded, U=unloaded, A=upstream and D=downstream) in comparison with German guide lines (BinSchAbgasV 2005 [yellow] and RheinSchUO 2011 [green])

Figure 8 exhibits that the NO_x emission indices of all motor ship types investigated are above the engine rotation speed dependent limit values of the German guide lines, which are 29 – 37 g/kg for the RheinSchUO and 36 – 46 g/kg for the BinSchAbgasV guide lines.

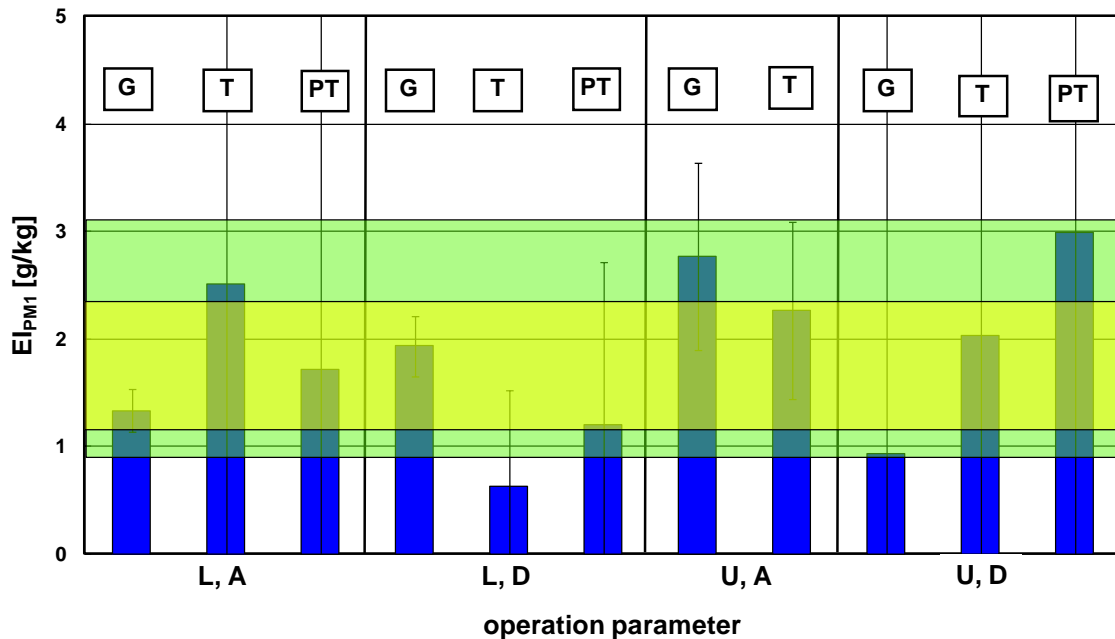


Figure 9. Weighted average lower limit emission index for PM₁ (El_{PM₁}) for different motor ship types (G=goods, T=tanker and PT=push tow) at different operation parameters, (L=loaded, U=unloaded, A=upstream and D=downstream) in comparison with German guide lines (BinSchAbgasV 2005 [yellow] and RheinSchUO 2011 [green]).

Figure 9 exhibits that the obtained lower limit PM₁ emissions values for almost all motor ship types are just within the limit values of the German guide lines, which are 0.9 – 3.1 g/kg for the RheinSchUO and 1.2 – 2.4 g/kg for the BinSchAbgasV guide lines depending on the engine rotation speed.

For comparison with literature data, uncertainty(2σ)-weighted averaged El_{NO_x} and El_{PM₁} were calculated for all motor ship types and operation condition investigated. An El_{NO_x} of 52 ± 3 g/kg and a lower limit El_{PM₁} of ≥ 1.9 ± 0.3 g/kg were obtained. Minimum and maximum EIs for NO_x and PM₁ were found to be in the range of 20 – 161 g/kg and ≥ 0.2 – 8.1 g/kg, respectively. Table 1 show the emission indices NO_x and PM₁ in g/kg fuel calculated from the measured values in comparison with different literature data. Errors were calculated using error propagation for the different measured compounds.

Between 1998 and 2013 only a few studies reported El_{NO_x} and El_{PM₁} from inland water navigation (Trozzi and Vaccaro 1998, Kesgin and Vardar 2001, Schweighofer, and Blaauw 2009, Van der Gon and Hulskotte 2010) in the range 39 – 57 g/kg and 0.7 – 1.9 g/kg, respectively, see table 1. The uncertainty(2σ)-weighted averaged El_{NO_x} and El_{PM₁} were 48 ± 4 g/kg and El_{PM₁} 1.3 ± 0.2 g/kg, which are in good agreement with the present study.

Emission indices for NO_x and PM₁ from inland water navigation have been used in emission inventories by Klimont et al. (2002), Rohacs and Simongati (2007), TNO (2008), CBS (2009) and UBA (2013). The authors reported El_{NO_x} and El_{PM₁} in the range 46 – 51 g/kg and 1.5 – 4.0 g/kg, respectively (see table 1). From these data uncertainty(2σ)-weighted average values for El_{NO_x} of 48 ± 2 g/kg and El_{PM₁} 2.7 ± 1.2 g/kg were derived, which are in a good agreement with the present study.

In order to comply with the limit values of the current RheinSchUO guide line for inland water navigation for NO_x with 29 – 37 g/kg a further significant reduction of the NO_x emission is necessary. This can be achieved e.g. by using exhaust after-treatment systems, whose functional capability have been demonstrated in recent studies (Cooper 2001, Schweighofer and Blaauw 2009, BMVBS 2012, Future Carrier 2012, Hallquist et al. 2013, Pirjola et al. 2014). For example, the European project “The cleanest ship” (Schweighofer and Blaauw 2009) shows that NO_x and PM emission of a ship diesel engine equipped with an SCR (selective catalytic reduction) system and particle filter can be reduced to 4 g/kg and 0.02 g/kg, respectively.

Table 1. Emission indices NO_x and PM_1 in g/kg fuel calculated from the measured values in comparison with different literature data.

Reference	Location	Sampling period	EI_{NO_x} [g/kg]	EI_{PM_1} [g/kg]	Ship types
A) field measurements (inland, engine without after-treatment system)					
This study	Germany, Rhine (inland)	2013	54 ± 4	$\geq 2.0 \pm 0.3$	different
Kesgin and Vardar (2001)	Turkey; Bosporus (inland)	1998	57	1.2	domestic passenger ships (a)
Trozzi and Vaccaro (1998)	Italy, Tyrrhenian Sea (inland)	1998	51	1.2	domestic passenger ships (a)
Van der Gon and Hulskotte (2010)	Netherlands (inland)	2010	45	1.9	different
Schweighofer and Blaauw (2009)	inland	2009	39	0.73	research vessel (b)
B) field measurements (inland, engine with after-treatment system)					
BMVBS (2012)	inland	2011	n.d.	0.08 – 0.48	research vessel
Futura Carrier (2010)	inland	2009	n.d.	0.29 ± 0.01	research vessel
Schweighofer and Blaauw (2009)	inland	2009	11 - 39	0.02	research vessel (c)
C) inventories					
Rohacs and Simongati (2007)	Average EU (inland)	2007	47	3.2	inventory
TNO (2008), CBS (2009)	Netherlands (inland)	2008-2009	46	1.9	inventory
Klimont et al. (2002)	RAINS, EU (inland)	2002	51	4.0	inventory
UBA (2013)	TREMODO, Germany (Inland)	2013	49 ± 6	1.5 ± 0.2	inventory

Remarks: n. d. no data, a) domestic passenger ships with diesel engine (medium-speed), b) without after-treatment system, c) with after-treatment system

3. Summary and Conclusion

The present study has shown that the measurement site at the Rhine river provided representative real world emission data from inland navigation. Emissions of NO , NO_2 , CO_2 , and particulate matter from a large number of individual ships were monitored and analyzed.

Particulate emissions measured in the ship plumes were dominated by PM_1 . An average NO_2/NO_x emission ratio of 0.08 ± 0.02 was obtained, which is typical for ship diesel engines without after-treatment systems such as oxidation catalysts or PM filter systems.

The emission indices for NO_x (EI_{NO_x}) and PM_1 (EI_{PM_1}) determined for different motor ship types (cargo, petroleum tanker and push tow) and for different operation parameters (L=loaded, U=unloaded, A=upstream and D=downstream) exhibited a large variation and were almost independent of the ship types and operation parameters. For the motor ship types and operation conditions investigated a weighted average EI_{NO_x} of 54 ± 4 g/kg and lower limit EI_{PM_1} of $\geq 2.0 \pm 0.3$ g/kg was obtained with minimum and maximum values ranging from 20 – 161 g/kg for NO_x and ≥ 0.2 – 8.1 g/kg for PM_1 , respectively. The EI_{NO_x} and EI_{PM_1} from the present study are in a good agreement with literature data.

The comparison of emission indices for NO_x and PM_1 with limit values of the German Guidelines (BinSchAbgasV 2005, RheinSchUO 2011) showed that NO_x emissions of all motor ship types investigated were above the limit values whereas the obtained lower limit PM_1 emissions for almost all motor ship types were just within the limit values.

In order to meet the limit values for NO_x and PM, in particular the NO_x emissions have to be

reduced significantly, e.g. by the introduction of specific exhaust after-treatment systems, some of which have been proven to be very effective.

References

- Adviesdienst Vereer en Vervoer (Dutch Transport Research Centre), 2003. Inland Shipping Emissions Protocol, [EMS-protocol](#) - emissies door de binnenvaart: verbrandingsmotoren versie 3, Rotterdam 22 Nov 2003.
- Alfödy, B., Lööv, J. B., Lager, F., Mellqvist, J., Berg, N., Beecken, J., Weststrate, H., Duyzer, J., Bencs, L., Horemans, B., Cavalli, F., Putaud, J.-P., Janssens-Maenhout, G., Csordas, A. P., Van Grieken, R., Borowiak, A., Hjorth, J., 2013. Measurements of air pollution emission factors for marine transportation in SECA. *Atmospheric Measurement Techniques*, 6, 1777-1791.
- Atkinson, R., 2000. Atmospheric chemistry of VOCs and NO_x, *Atmospheric Environment*, 34, 2063-2101.
- Binnenschifffahrt Abgasverordnung (BinSchAbgasV9, 2005), Richtlinie EU2004/26/EG. <http://eur-lex.europa.eu/LexUriServ/LexUriServ.do?uri=OJ:L:2004:225:0003:0107:DE:PDF>.
- BMVBS, 2012. Bundesministerium für Verkehr, Bau und Stadtentwicklung: Erprobung von Partikelfilter für den Einsatz in der Binnenschifffahrt, *Projektbericht*. <http://www.bmvbs.de>.
- Bundesverband der Deutschen Binnenschifffahrt e.V. (BDA), 2015a. Daten und Fakten 2014/2015 <http://binnenschiff.de/content/wp-content/uploads/2015/08/150827-Daten-Fakten-2014-2015.pdf>.
- Bundesverband der Deutschen Binnenschifffahrt e.V. (BDA), 2015b. *Pressemitteilung* http://bdbev.de/aktuell/2015/150205_Binnenschifffahrt_boomt_im_Rheinkorridor.pdf.
- Beecken, J., Mellqvist, J., Salo, K., Ekhol, J., Jalkanen, J.-P., 2014. Airborne emission measurements of SO₂, NO_x and particles from individual ships using a sniffer technique. *Atmospheric Measurement Techniques*, 7, 1957-1968.
- Browning, L., and Bailey, K., 2006. Current Methodologies and Best Practices for Preparing Port Emission Inventories. *ICF Consulting and EPA*, Fairfax, Virginia, USA, Final Report for US.
- CBS, StatLine., 2009. Luchtverontreiniging, emission naar luct. *CBS*, Den Haag/Heerlen.
- Carlaw, D. C. and Rhys-Tyler, G., 2013. New insights from comprehensive on-road measurements of NO_x, NO₂ and NH₃ from vehicle emissions remote sensing in London, UK. *Atmospheric Environment*, 81, 339-347.
- Chameides, W. L., Fehsenfeld, M. O., Rodgers, C., Cardelino, J., Martinez, D., Parrish, W., Lonneman, D. R., Lawson, R. A., Rasmussen, P., Zimmerman, J., Greenberg, P., Middleton and T. Wang, 1992. Ozone Precursor Relationships in the Ambient Atmosphere. *Journal Geophysical Research*, 1992, 97, 6037-6055.
- Chen, G., Huey, L. G., Trainer, M., Nicks, D., Corbett, J., Ryerson, T., Parrish, D., Neuman, J. A., Nowak, J., Tanner, D., Holway, J., Brock, C., Crawford, J., Olson, J. R., Sullivan, A., Weber, R., Schauffler, S., Donnelly, S., Atlas, E., Roberts, J., Flocke, F., Hübler, G., Fehsenfeld, F., 2005. An investigation of the chemistry of ship emission plumes during ITCT 2002. *Journal of Geophysical Research*, Vol. 110, D10S90.
- Clapp, L. J. and Jenkin, M. E., 2001, Analysis of the relationship between ambient levels of O₃, NO₂ and NO as a function of NO_x in UK. *Atmospheric Environment*, 35, 6391-6405.
- Cooper, D. A., Peterson, K., Simpson, D., 1996. Hydrocarbon, PAH and PCB emissions from ferries: a case study in the Skagerak-Kattegatt-Oresund region. *Atmospheric Environment*, 30 (14), 2463-2473.
- Cooper, D. A. and Andreasson, K., 1999. Predictive NO_x emission monitoring on board a passenger ferry. *Atmospheric Environment*, 33, 4637-4650.
- Cooper, D. A., 2001. Exhaust emissions from high speed passenger ferries. *Atmospheric Environment*, 35, 4189-4200.
- Cooper, A. D., 2003. Exhaust emissions from ships at berth. *Atmospheric Environment*, 37, 3817-3830.

- Cooper, D. A. and Ekström, M., 2005. Applicability of the PEMS technique for simplified NO_x monitoring on board ships. Atmospheric Environment, 39, 127-137
- European Commission, White paper (2011); 52011DC0144: Roadmap to a Single European Transport Area – Towards a competitive and resource efficient transport system, SEC(2011)391 final, <http://eur-lex.europa.eu/legal-content/EN/TXT/?qid=1433420196688&uri=CELEX:52011DC0144>.
- European Commission Transport, 2015. Inland waterways. What do we want to achieve? http://ec.europa.eu/transport/modes/inlad/index_en.htm.
- Eyring, V., Köhler, H. W., van Aardenne, J., Lauer, A., 2005. Emissions from international shipping: 1. The last 50 years. Journal of Geophysical Research, Vol. 110, D17305. doi:10.1029/2004JD005619.
- Eyring, V., Isaksen, I. S. A., Berntsen, T., Collins, W. J., Corbett, J. J., Endresen, O., Grainger, R. G., Moldanova, J., Schlager, H. and Stevenson, D. S., 2010. Transport impact on atmosphere and climate: Shipping. Atmospheric Environment, 44, 4735-4771.
- FUTURE Carrier, New Logistics® GmbH, 2012. <http://www.new-logistics.de/new-logistics/pdf/uebersichtsbroschuere.pdf>.
- Grice, S., Stedman, J., Kent, A., Hobson, M., Norris, J., Abbott, J., Cooke, S., 2009. Recent trends and projections of primary NO₂ emissions in Europe. Atmospheric Environment, 43, 2154-2167.
- Hallquist, A. M., Fridell, E., Westerlund, J., Hallquist, M., 2013. Onboard Measurements of Nanoparticles from a SCR-Equipped Marine Diesel Engine. Environmental Science & Technology, 47, 773-780
- International Maritime Organisation (IMO), 2012. Nitrogen Oxides – Regulation 13. [http://www.imo.org/ourwork/environment/pollutionprevention/airpollution/pages/nitrogen-oxides-\(nox\)-regulation-13.aspx](http://www.imo.org/ourwork/environment/pollutionprevention/airpollution/pages/nitrogen-oxides-(nox)-regulation-13.aspx).
- Jonsson A. M., Westerlund, J., Hallquist, M., 2011. Size-resolved particle emission factors for individual ships. Geophysical Research Letters, 33, L13809.
- Kesgin, U. and Vardar, N., 2001. A study on exhaust gas emissions from ships in Turkish Straits. Atmospheric Environment, 35, 1863–1870.
- Klimont Z., Cofala, J., Bertok, I., Aman, M., Heyes, C., Gytas, F., 2002. Modelling Particulate Emissions in Europe. A Framework to Estimate Reduction Potential and Control Costs. Interim Report IR-02-076, IIASA, Laxenburg.
- Kousoulidou, M., Ntziachristos, L., Mellios, G., Samaras, Z., 2008. Road-transport emission projections to 2020 in European urban environments. Atmospheric Environment, 42, 7465-7475.
- Kurtenbach, R., Becker, K. H., Gomes, J. A. G., Kleffmann, J., Lörzer, J. C., Spittler, M, Wiesen, P., Ackermann, R., Geyer, A., Platt, U., 2001, Investigations of Emissions and Heterogeneous Formation of HONO in a Road Traffic Tunnel. Atmospheric Environment, 35, 3385-3394.
- Lack, D. A., Cappa, Ch. D., Langridge, J., Bahreini, R., Buffaloe, G., Brock, Ch., Cerully, K., Coffman, D., Hyden, K., Holloway, J., Lerner, B., Massoli, P., Li, Sh.-M., Middlebrook, A. N., Moore, R., Nenes, A., Nuaaman, I., Onasch, Th. B., Peischl, J., Perring, A., Quinn, P. K., Ryerson, T., Schwartz, J. P., Spackman, R., W. St. C., Worsnop, D., Xiang, B., Williams, E., 2011. Impact of Fuel Quality Regulation and Speed Reductions on Shipping Emission: Implications for Climate and Air Quality. Environmental Science & Technology, 45, 9052-9060.
- Moldanova, J., Fridell, E., Popovicheva, O., Demirdjian, B., Tishkova, V., Faccineto, A., Focsa, C., 2009. Characterisation of particulate matter and gaseous from a large ship diesel engine. Atmospheric Environment, 43, 2632-2641.
- Murphy, S. H., Agrawal, H., Sorooshian, A., Padro, L. t., Gates, H., Hersey, S., Welch, W. A., Jung, H., Miller, J. W., Cocher III, D. R., Nenes, A., Jonsson, H., Flagan, R. C., Seinfeld, J. H., 2009. Comprehensive Simultaneous Shipboard and Airborne Characterization of Exhaust from a Modern Container Ship at Sea. Environmental Science & Technology, 43, 4626-4640.
- Petzold, A., Hasselbach, J., Lauer, P., Baumann, R., Franke, K., Gurk, C., Schlager, H., Weingartner, E., 2008. Experimental studies on particle emissions from cruising ships, their characteristic properties, transformation and atmospheric lifetime in the marine boundary layer. Atmospheric Chemistry and Physics, 8, 2387-2403.

- Pirjola, L., Pajunoja, A., Walden, J., Jalkanen, J.-P., Rönkkö, T., Kousa, A., Koskentalo, T., 2014. Mobile measurements of ship emissions in two harbour areas in Finland. Atmospheric Measurement Techniques, 7, 149-161.
- RheinSchUO, Zentralkommission für die Rheinschifffahrt, 2011. http://www.ccr-zkr.org/files/documents/reglementRV/rv1a_122011.pdf.
- Rohacs, J., and Simongati, G., 2007. The role of inland water navigation in a sustainable transport system, TRANSPORT – 2007, Vol XXII, No 3, 148-153.
- Schlager, H., Baumann, R., Lichtenstern, M. Petzold, A., Arnold, F., Speidel, M., Gurk, C., Fischer, H., 2008. Aircraft-based trace gas measurements in a primary European corridor. In: Proceedings of the International Conference on Transport, Atmosphere and Climate (TAC), Oxford, UK, pp.83-88.
- Schrooten, L., De Vlieger, I., Panis, L. I., Chiffi, C. and Pastori, E. Emission of maritime transport: A European reference system. Science of the Total Environment, 2009, 408, 318-323.
- Schweighofer, J. and Blaauw, H., 2009. The Cleanest Ship, Final Report. http://www.via-donau.org/uploads/project_downloads/The_Cleanest_Ship_report.pdf.
- Sinha, P., Hobbs, P. V., Yokelson, R. J., Christian, T. J., Kirchstetter, T. W., Bruintjes, R., 2003. Emissions of trace gases and particles from two ships in southern Atlantic Ocean. Atmospheric Environment, 37, 2139-2148
- TNO, 2008. Trans-Tool data. <http://www.inro.tno.nl/transtool>
- Trends, 2003. Calculation of indicators of environmental pressure caused by transport: main report, European Commission, Office for Official Publications of European Communities, Luxembourg, 2003.
- Trozzi, C., and Vaccaro, R., 1998. Methodologies for estimating air pollutant emissions from ships. Technical Report MEET. (Methodologies for Estimating Air Pollutant Emissions from Transport) RF98.
- Tzannatos, E., 2010. Ship emissions and their externalities for the port of Piraeus – Greece. Atmospheric Environment, 44, 400-407.
- UBA, 2013. Aktualisierung der Emissionsberechnung für die Binnenschifffahrt und Übertragung der Daten in TREMOD. Endbericht, 371145105.
- US Environmental Protection Agency, 1996. Compilation of air pollutant emission factors-AP42, Vo. I, 5th Edition (Chapter 3.4 Large Stationary Diesel Engines) Office of the Federal Register National Archives and Records Administration. US Government Printing Office, Washington, D.C., USA.
- Van der Gon, H. D. and Hulskotte, J., 2010. Methodologies for estimating shipping emissions in the Netherlands. A documentation of currently used emission factors and related activity data. BOP report. www.pbl.nl.
- Van der Werf, H., 2013. LNG as Fuel in Inland Navigation. Secretary General. Central Commission for the Navigation of the Rhine (CCNR), http://www.mariko-leer.de/cms_uploads/files/hans-van-der-werf-zkr.pdf.
- Versuchsanstalt für Binnenschifffahrt e. V. (VBD): Emissionen luftverunreinigender Stoffe durch den Schiffverkehr in Nordrhein-Westfalen – Ein Modell zur Berechnung der Schadstoffverteilung auf Wasserstraßen, in Schleusen und Häfen, 2001, http://www.lanuv.nrw.de/veroeffentlichungen/materialien/mat56_web.pdf.
- Westerlund, J., Hallquist M., Hallquist A. S., 2015. Characterization of fleet emissions from ships through multiindividual determination of size-resolved particle emissions in a coastal area. Atmospheric Environment, 112, 159-166.
- Williams, E. J., Lerner, B. M., Murphy, P. C., Herdon, S. C., Zahniser, M. S., 2009. Emission of NO_x, SO₂, CO, and HCHO from commercial marine shipping during Texas Air Quality Study (TexAQS) 2006. Journal of Geophysical Research, Vol. 114, D21306.

Effects of bike lane features on cyclists' exposure to black carbon and ultrafine particles

Giovanni LONATI*, Senem OZGEN*, Giovanna RIPAMONTI* & Stefano SIGNORINI**

* Department of Civil and Environmental Engineering, Politecnico di Milano, Milano, Italy
Fax +39 02 23 99 64 99 - email: giovanni.lonati@polimi.it

** Energy and Environment Laboratory Piacenza, Piacenza, 29121, Italy

Abstract

Cyclists might experience increased exposure to air pollution due to their active travel mode and to the proximity to traffic. Several local factors, like meteorology, road and traffic features, and bike lanes features, affect cyclists' exposure. This paper investigates the effect of the features of the bike lanes on cyclists' exposure to airborne fine and ultrafine particulate matter and black carbon in the mid-sized city of Piacenza, located in the middle of the Po Valley, Northern Italy. Monitoring campaigns were performed by means of portable instruments along a 40-min urban bike route with bike lanes, characterized by different distances from the traffic source (on-road cycle lane, separated cycle lane, green cycle path), during morning and evening workday rush hours. The proximity to traffic significantly affected cyclists' exposure to UFP and BC: exposure concentrations measured for the separated lane and for the green path were 1-2 times and 2-4 times lower for the on-road lane. Conversely, exposure concentrations to PM₁₀, PM_{2.5} and PM₁ particle mass were not influenced by traffic proximity, without any significant variation between on-road cycle lane, separated lane or green cycle path.

Keys-words: cyclists' exposure, black carbon, ultrafine particles, urban air quality, mobile monitoring.

Introduction

The shift from motor vehicle use to an active transport mode like bicycling for short trips in urban areas has been considered helpful to reduce traffic volume and related air pollution emission but also to improve public health thanks to the increased physical activity (Jarjour et al., 2013; de Nazelle et al., 2010). However, due to their proximity to the traffic source cyclists might be exposed to higher concentrations of traffic-related atmospheric pollutants (MacNaughton et al., 2014). Some studies that directly compared the exposure concentrations, i.e.: the concentrations to which a person is exposed, among different urban transport modes (Suárez et al. 2014; Quiros et al., 2013; Ragetti et al., 2013) reported contrasting results and highlighted the dependency of the exposure levels on a large number of variables, such as road characteristics and meteorological conditions (de Nazelle et al. 2012; Int Panis et al., 2010). However, most of the available evidence for urban cycling suggests that: i) the higher the volume of motorized traffic the greater the cyclists' exposure to traffic-related pollutants, and in particular to ultrafine particles (UFPs, diameter smaller than 0.1 μm) and black carbon; ii) bicycle paths that offer lateral separation between the cyclists and the motorized traffic reduce the concentration they are exposed to, as increased exposure concentrations are associated with increased proximity to traffic (Schepers et al., 2015). Additionally, exposure to both high-average levels and to short-duration concentration peaks of UFPs and black carbon particles is more likely to occur because of the proximity to the emission sources (Spinazzè et al. 2015; Kendrick et al., 2013). Furthermore, bike riding can result in higher particle deposition in the alveolar region since an active travelling mode (e.g., cycling) results in higher minute ventilation, because of increasing breathing frequency and larger tidal volume due to physical effort (Hofmann, 2011), and in higher lung deposition rate of inhaled particles which increases with exercise (Daigle et al., 2003; Chalupa et al., 2004).

Conversely, reductions in cyclists' exposure have been observed when they take alternative routes along lower trafficked roads (Good et al., 2015; Strak et al., 2010; Zuurbier et al., 2010). Thus, a

proper selection of the travelling route through an urban area, as well as travelling outside rush hours, can reduce the exposure of cyclists to both primary traffic-related pollutants and to secondary pollutants (Hertel et al., 2008). However, as far as cycling networks and infrastructures are concerned, there is still a lack of knowledge and little research on how they can affect cyclists' exposure to traffic related atmospheric pollutants (Farrel et al., 2015).

This work provides some additional piece of information by investigating the effect of cycle lane and road features on cyclists' exposure concentration to airborne particulate matter, namely focusing on ultrafine particles and black carbon, based on field measurements performed while travelling different routes in a mid-sized city in Northern Italy. Comparisons between the UFP and BC exposure levels measured along the selected routes are presented, accounting for the season and for the time of the day. The impact of route choice on cyclists' exposure during commuting trips is also estimated through a Monte Carlo approach, based on the measured data.

1. Methods

Monitoring routes

Monitoring campaigns were performed in the urban area of Piacenza, Italy, a mid-sized city with about 100,000 inhabitants located right in the middle of the Po Valley at about 60 m a.s.l.. Despite its location in a context mostly rural and less urbanized compared with the largest metropolitan areas of the region, PM levels in Piacenza hardly comply with the air quality limits, especially as far as the PM10 daily limit is concerned.

Monitoring campaigns were performed during two weeks in July and September 2011 with two daily sessions, on morning (9.00-10.00) and evening workdays' rush hours (17.30-18.30); an additional 1-week monitoring campaign, still with morning and evening sessions, was performed in December 2012. In order to investigate the role of cycle lane and road features on cyclists' exposure concentration, four route sectors were travelled during each monitoring session:

- Sector 1 - on-road cycle lane: in this city-centre road the cycle lane is marked on the right side of road and cyclist and vehicles travel adjacent without a real separation. The road is bordered on both sides by 3-4-storey buildings creating a street canyon.
- Sector 2 - green cycle path: in this sector the cycle path passes through a green area where motorized vehicle are banned. The cycle path is paved with asphalt. The green area is about 50 meters large and it is bordered by the Sector 1 and Sector 2 roads.
- Sector 3 - separated cycle path: in this sector the cycle lane is separated from the motorized vehicles lane by a row of parallel parking lots. A minimum distance of about 2.5 m exists between cyclists and traffic flow. The road is bordered by buildings on one side and by a green area on the other side, where the cycle path runs. Sector 3 is part of the ring road that runs around the historical city centre.
- Sector 4 - no cycle lane: in this road sector cyclists and vehicles share the same lanes, without any kind of separation. The road is bordered on both sides by 3-4-storey buildings as for Sector 1, still creating a street canyon but with cross section wider than in Sector 1. Sector 4 is part of the outer ring road of the city centre.

Crossing the city in the East-West direction, the four sectors were selected because they may be taken by cyclists travelling from the South-Western residential areas to the train station (North-East of the city centre) for daily commuting. Route sectors, each about 1.5 km long, were travelled consecutively (i.e. not in parallel) following the same order (S1, S2, S3, and S4) in each session. Due to their rather small length, during each session the sectors were travelled three times, collecting about 15-20 concentration data.

Instruments

During the monitoring campaigns two portable instruments for particle number and black carbon measurement were held in a backpack keeping the instrument inlets near the breathing zone

Real-time particle number concentration (PNC) was measured by means of a portable condensation particle counter (P-Trak, TSI Model 8525, USA). P-Trak is able to measure the PNC in the 20-1000 nm size range (PNC_{0.020-1}) at 1-min time resolution, detecting particle concentration up to

$5 \cdot 10^5 \text{ cm}^{-3}$. Ambient air drawn into the instrument is first saturated with isopropyl alcohol vapour that then condenses onto the particles, causing them to grow into a larger droplet detectable by means of a photo-detector when flashed by a focused laser beam. Despite its measurement range extending beyond 100 nm, P-Trak data are commonly regarded as UFP concentration data since in urban areas particles with diameter below 100 account for the majority of the total particle number (Morawska et al. 2008); therefore, in this work $\text{PNC}_{0.020-1}$ data are presented as UFP data.

Concurrently with PNC measurements, equivalent black carbon concentration (EBC) was measured by means of a portable micro-aethalometer AE51 with 1-min time resolution. Ambient air is drawn by a pump inside the instrument through a Teflon-coated borosilicate glass fiber filter where particles are collected. The rate of change in the attenuation of transmitted light (880 nm wave length) due to continuous collection of aerosol deposit on the filter is measured. Then, black carbon concentration is derived based on the assumption that the change in aerosol light attenuation is proportional to black carbon concentration through a constant called mass absorption cross section. Following literature recommendations (Petzold et al. 2013), hereafter the term equivalent black carbon (EBC) is used instead of black carbon (BC) because the absorption properties have been measured by an optical technique.

2. Results

The distributions of 1-minute concentration data for EBC and UFP measured along the selected sectors during the morning and evening sessions are summarized in the box-plots presented in Figure 1-2 and in Figure 3-4 for the cold and warm season, respectively. Peak concentration data, identified as outliers according to Tukey's method (Tukey, 1977) are also plotted. Though regarded as outliers from the statistical standpoint, these data actually correspond to infrequent situations of high exposure concentrations occurring at busy crossroads or as a consequence of "big emitters" exhaust plumes.

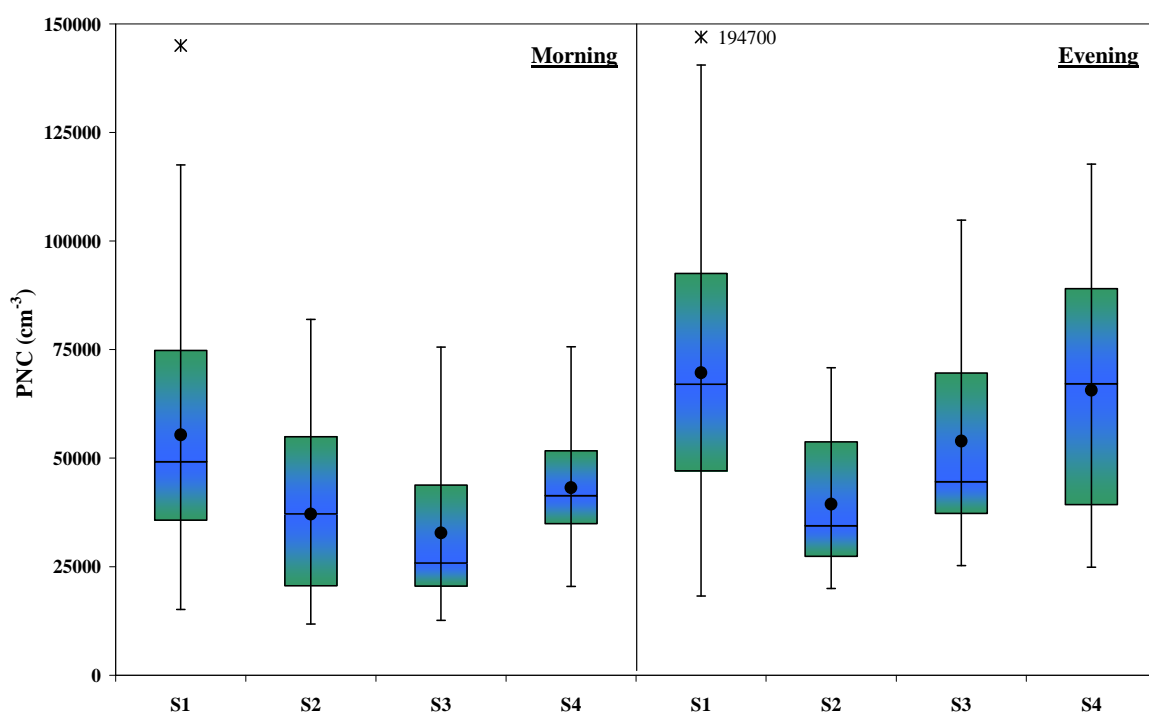


Figure 1. Box-plots of 1-min concentration data for UFP in the cold season.

As usually observed, cold season concentrations are always higher than the corresponding warm season values, as a consequence of both less favorable meteorological conditions (lower wind speed, shallower boundary layer) and of stronger emissions (traffic and space heating, including biomass burning for domestic heating). However, it can be noticed that the cold/warm season ratio is larger for UFPs than for EBC (3.7 vs. 2.1), because of the additional contribution of secondary particle formation, particularly favored by low-temperature conditions.

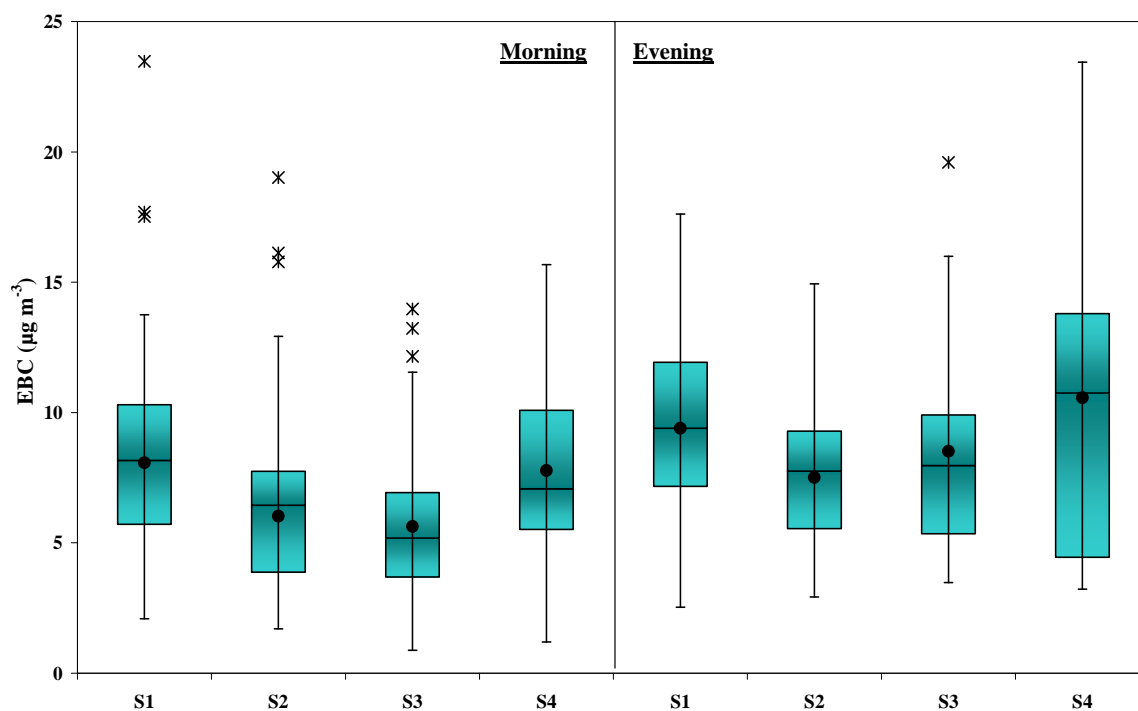


Figure 2. Box-plots of 1-min concentration data for EBC in the cold season.

In the cold season the sector-averaged concentrations for the morning session are in the $3.3 \cdot 10^4$ - $5.5 \cdot 10^4 \text{ cm}^{-3}$ range for UFPs and in the 5.6 - $8.1 \text{ } \mu\text{g m}^{-3}$ range for EBC; concentration ranges for the evening session are $3.9 \cdot 10^4$ - $7.0 \cdot 10^4 \text{ cm}^{-3}$ and 7.5 - $10.6 \text{ } \mu\text{g m}^{-3}$, respectively. Corresponding figures for the warm season are $1.1 \cdot 10^4$ - $2.1 \cdot 10^4 \text{ cm}^{-3}$ and 2.5 - $8.0 \text{ } \mu\text{g m}^{-3}$ for the morning session and $0.8 \cdot 10^4$ - $1.7 \cdot 10^4 \text{ cm}^{-3}$ and 1.5 - $6.6 \text{ } \mu\text{g m}^{-3}$ for the evening session. Maximum concentration values in the cold season are in the $7.1 \cdot 10^4$ - $1.4 \cdot 10^5 \text{ cm}^{-3}$ range for UFPs and in the 12 - $23 \text{ } \mu\text{g m}^{-3}$ range for EBC, but mostly around $15 \text{ } \mu\text{g m}^{-3}$; warm season maxima are much lower, ranging between $2 \cdot 10^4$ - $4 \cdot 10^4 \text{ cm}^{-3}$ for UFPs and between 4 - $15 \text{ } \mu\text{g m}^{-3}$ for EBC. As the warm season distributions are shifted towards lower concentrations values, outliers are mainly observed in this season both for UFPs and EBC and more frequently for the sectors where the proximity to vehicle exhaust is higher (i.e.: S1 and S4). However the highest UFPs outliers are around $5 \cdot 10^4 \text{ cm}^{-3}$, that is in the same orders of the average values for the cold season; conversely, EBC outliers at the most trafficked sectors are up to about $20 \text{ } \mu\text{g m}^{-3}$, that is even greater than the cold season maximum levels. The comparison between morning and evening data shows an opposite seasonal behavior: in the cold season concentrations are basically higher in the evening than in the morning whereas in the warm season evening data are similar or slightly lower than the morning data. This behavior is related to the diurnal development of the planetary boundary layer (PBL), significantly different in the two seasons: indeed, the evening session took place after sunset in the cold season with a reduced PBL depth as solar radiation was no longer active; conversely, in the cold season the PBL was still high in the morning, thus providing a similar volume for the dispersion of the pollutants. Regardless for the season, sector-averaged UFPs and EBC concentrations are strongly correlated (cold season: $R^2 = 0.85$; warm season: $R^2 = 0.67$; overall: $R^2 = 0.72$), thus confirming the relevant role of primary emission from traffic on roadside levels for both the pollutants. Such a correlation suggests that cyclists can be concurrently exposed to high UFPs and EBC levels while riding the bike route.

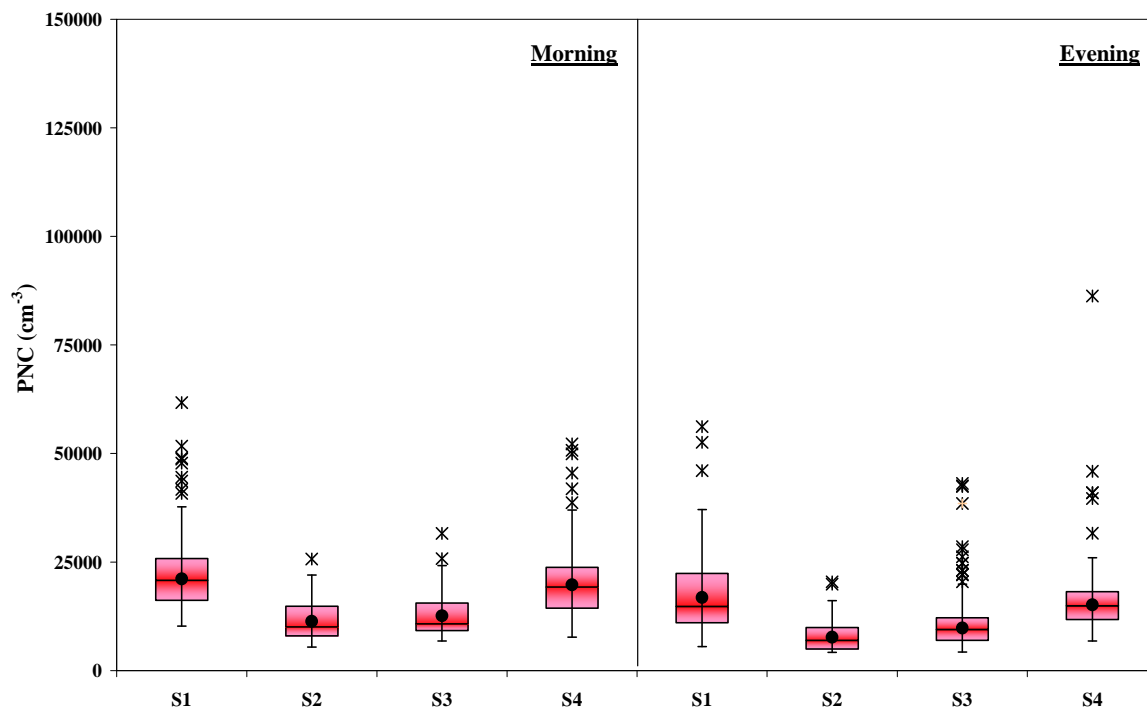


Figure 3. Box-plots of 1-min concentration data for UFP in the warm season.

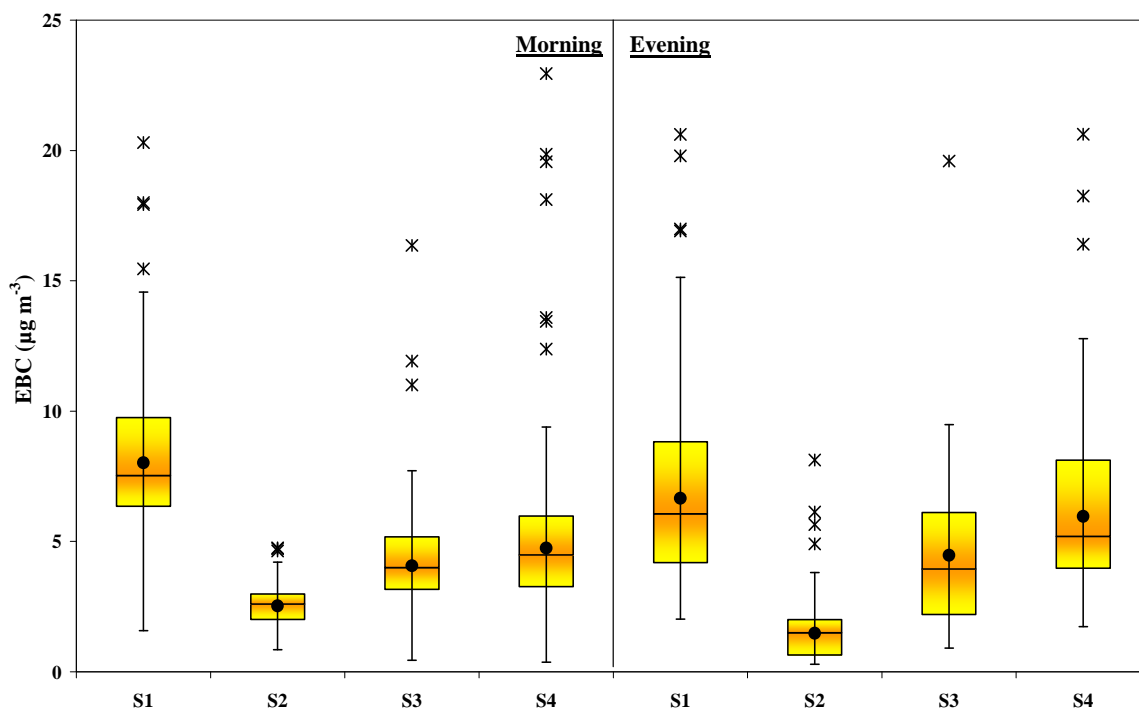


Figure 4. Box-plots of 1-min concentration data for EBC in the warm season.

3. Discussion

UFPs exposure concentration levels reported in this work are in substantial agreement with literature data, reporting cyclists' exposure levels in the $1.6 \cdot 10^4$ - $2.8 \cdot 10^4$ cm^{-3} range in Italy, Switzerland, Belgium and The Netherlands (Spinazzè et al. 2015; Ragetti et al., 2013; Int Panis et al., 2010; Strak et al., 2010; Berghmans et al., 2009) but up to $4.5 \cdot 10^4$ - $8.4 \cdot 10^4$ cm^{-3} in other Dutch studies and in Spain (de

Nazelle et al., 2012; Zuurbier et al., 2010; Kaur et al., 2006); reported summertime exposure concentration levels for cyclists in a trafficked road in Milan are about $3 \cdot 10^4 \text{ cm}^{-3}$ (Ozgen et al., 2016).

Relative differences between average road sectors exposure concentrations observed in our work are summarized in Table 1. With respect to sector S1, in Sectors S2 and S3, where proximity to traffic is reduced, the average exposure concentrations show reductions in the 22%-54% range for UFPs and in the 9%-78% range for EBC depending on season and time of the day. Less relevant reductions are observed for Sector S4, where proximity to traffic doesn't change significantly but the wider cross road section reduces the urban canyon effect present in the narrower sector S1.

Table 1. Relative differences between the average exposure concentrations for road sectors S2, S3 and S4 with respect to Sector S1.

	Season	Morning session			Evening session		
		S2	S3	S4	S2	S3	S4
UFPs	Cold season	32.9%	40.8%	22.0%	43.4%	22.5%	5.7%
	Warm season	46.3%	40.2%	6.5%	54.2%	41.9%	9.9%
EBC	Cold season	25.3%	30.3%	3.6%	20.1%	9.4%	-12.5%
	Warm season	68.4%	49.3%	40.9%	77.8%	32.9%	10.4%

Similar relative reductions for cycling infrastructures are reported in literature. Comparing cyclists' exposure concentrations between roadside cycle lane and separated cycle track (through parallel parking lots) in Portland, Kendrick et al. (2011) reported significantly lower average levels for UFPs, with differences ranging between 8%-38% depending on traffic volume, and fewer exposure concentration peaks on the cycle track. Cole-Hunter et al. (2013) reported a 35% decrease in particle number exposure concentration on alternative route of lower proximity to traffic in Brisbane. Farrel et al. (2015) reported a 41% decrease in UFP levels between bike trails and major roadways and almost no change between separated bike tracks and major roadways in Montreal; conversely, they report a decrease in black carbon levels for both separated bike tracks (19%) and bike trails (40%). Influence of vehicular volume is also reported as concentration decrease is less relevant for local roads than for major roads. MacNaughton et al. (2014) reported 20% and 50% increased average exposure concentration levels to black carbon on designated bike lanes and bike lanes compared with bicycle paths in Boston.

Despite some overlap in the distributions of concentration data, most of the sector-averaged values are statistically different, especially in the warm season, according to paired t-test results at 5% significance level. In particular, S2 mean concentrations (i.e.: green path data) are always statistically lower than those of all the other sectors in the warm season, with the only exception for UFPs on mornings when compared to sector S3. Conversely, the average concentrations for sectors S1 and S4 (i.e.: the most trafficked sectors with roadside bike lanes) never show statistically significant differences except for EBC on mornings, when the S1 mean is almost twice as high as S4 mean ($8.0 \mu\text{g m}^{-3}$ vs. $4.7 \mu\text{g m}^{-3}$).

In the cold season, most of the differences still remain significant, namely those between sector S2 and sectors S1 and S4, or non-significant, as those for sectors S1 and S4 (this time with the only exception for UFPs instead of EBC on mornings). Conversely, t-tests for the evening session data involving sector S3 show non-significant differences with sectors S1 and S4 for EBC, with average concentration levels still lower ($8.5 \mu\text{g m}^{-3}$ vs. 9.4 and $10.6 \mu\text{g m}^{-3}$) but no longer significantly different as in the warm season; additionally, a non-significant difference in UFPs levels with respect to sector S4 for the evening session is also observed, contrary to morning data.

Overall, in spite of the rather limited extension of the dataset, these results confirm that proximity to the traffic source is one of the main drivers affecting exposure concentration for cyclists. Indeed, sector S2, passing through a non-traffic area, and sector S3, thanks to the parking lots separating the bike

lane, experience lower concentration levels than sectors S1 and S4, where the bike lane is simply on the rightmost part of the road. The impact of bike lane design is particularly strong for sector S3 where peak-hour traffic flow is higher than in Sectors S1 and S4 (about 2300 vehicles hour⁻¹ vs. about 1400-1500 vehicles hour⁻¹): indeed, the lower distance from traffic and the canyon-like configuration of these latter sectors overbalance the lower primary emissions. Canyon-like road features are particularly relevant for the narrow sector S1 where, regardless for season and time of the day, the highest concentrations are usually observed for both UFPs and EBC. However, sector-averaged concentration levels are also influenced by seasonality: actually, in the cold season concentrations levels tend to be more uniform as a consequence of the high background that reduces the effect of local scale emissions; additionally, the poor atmospheric dispersion favors the build up of airborne pollutants at the urban scale smoothing the contrasts between the sectors.

As these results suggest that a proper choice of the travel route across the city may affect the overall exposure to UFPs and EBC, the impact of route choice on cyclists' exposure during commuting urban trips has been assessed considering four alternative routes travelling from the South-Western residential areas to the train station for daily commuting. All routes are about 3.5 km long and are supposed to be ridden in 12 minutes. For each route, composite concentration subsets have been randomly generated drawing concentration data distributions from the sector-related distribution through iterative Monte Carlo technique. Such a probabilistic approach allows accounting for data variability within each sector, thus providing a more reliable assessment than simply relying of sector-averaged concentration values. Subsets for a reference route were formed based on sector S4 data (12 concentration data); the subsets for the three alternative routes were formed considering 6 data from the data distribution of sector S4 and 6 from those of sectors S1, S2, and S3. Cumulative exposure travelling to (in the morning) and from (in the evening) the train station have been then estimated in terms of total number of inhaled UFPs and total mass of inhaled EBC. As all routes are flat, no variation in exercise is considered and the same ventilation rate was used. The resulting frequency distributions of the computed cumulative exposures have been then compared in order to assess their variability in relation to the route choice. As shown in Figure 5, a worst-route choice can result in an increased cumulative exposure to UFPs up to about 50% with respect to the best option route, without any relevant difference between cold and warm season. Conversely, for EBC seasonality strongly affects the difference in cumulative exposure between worst- and best-route choice: indeed, a worst-route choice leads to an increased exposure around 20% in the cold season, but up to 90% in the warm season.

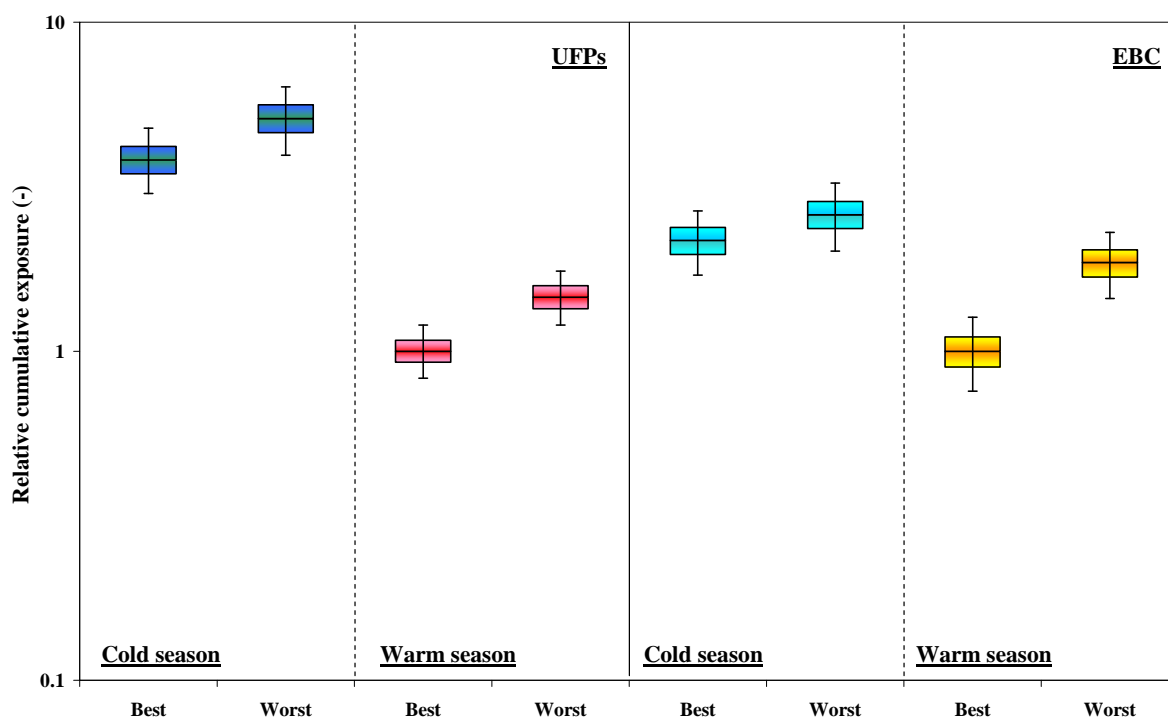


Figure 5. Box-plots of computed cumulative exposure to UFPs and EBC for best- and worst-case route choice for a commuter's ride in the urban area.

In the warm season, the best- and the worst-route choice are the same for UFPs and EBC: best choice is to pass through sector S2 on both trips, while the worst one is to pass through sector S1. In the cold season, as concentration levels tend to be more uniform, route choices also consider passing through sector S3 (morning trip) and Sector S2 (evening trip) as best option for both UFPs and EBC; for UFPs the worst-route choice is still the one passing through Sector S1 on both trips, whilst for EBC Sector S4 route on the evening trip leads to the higher exposure. Even though quite obvious, given the different concentration levels for the selected road sectors, these results provide a comparative and quantitative assessment of the extent of the different cyclists' exposure according to the travel route they choose. In particular, the route choice has a huge effect on EBC exposure in the warm season as the distance from the traffic source takes greater value when the concentrations of primary pollutants, as black carbon, are at their lowest levels and spatial concentration gradients within the urban area are stronger.

4. Conclusion

Ultrafine particles number and black carbon concentration have been measured in a mid-sized city in Northern Italy while travelling by bike urban routes in order to assess cyclists' exposure concentration levels and to investigate the effect of cycle lane and road features on their exposure.

Despite some limitations, mainly related to the limited dataset and to the non-concurrent route monitoring, the results confirm that reducing cyclists' proximity to traffic results in significantly lower exposure concentration levels. Indeed, where proximity to traffic is reduced, the average exposure concentrations show reductions in the 22%-54% range for UFPs and in the 9%-78% range for EBC depending on season and time of the day. Exposure concentrations are also affected by road features as the wider cross road section reduces the urban canyon effect, thus favoring the dispersion of traffic related pollutants. Seasonality is another relevant factor affecting exposure: the high concentration background in the cold season reduces the effect of local scale traffic emissions, thus smoothing the contrasts between the bike routes.

The impact of route choice in cyclists' exposure during commuting trips has been also estimated through a Monte Carlo approach, based on the measured data. These results show that, even for a short commuting trip in the urban area, a worst-route choice can result in an increased cumulative exposure to UFPs up to about 50% with respect to the best option route, without any relevant difference between cold and warm season. Conversely, for EBC seasonality strongly affects the difference in cumulative exposure between worst- and best-route choice: indeed, a worst-route choice leads to an increased exposure around 20% in the cold season, but up to 90% in the warm season.

Acknowledgments

The financial support by Fondazione di Piacenza e Vigevano for funding the UPUPA project (Ultrafine Particles in Urban Piacenza Area) is acknowledged.

References

- Berghmans P., N. Bleux, L. Int Panis et al. (2009) Exposure assessment of a cyclist to PM10 and ultrafine particles. Sci. Total Environ., vol. 407, p 1286-1298.
- Chalupa D.C., P.E. Morrow, G. Oberdörster et al. (2004). Ultrafine particle deposition in subjects with asthma. Environ. Health Perspect., vol. 112, p 879-882.
- Cole-Hunter T., R. Jayaratne, I. Stewart et al. (2013). Utility of an alternative bicycle commute route of lower proximity to motorised traffic in decreasing exposure to ultra-fine particles, respiratory symptoms and airway inflammation – a structured exposure experiment. Environmental Health, vol. 12, 29
- Daigle C.C., D.C. Chalupa, F.R. Gibb et al. (2003) Ultrafine Particle Deposition in Humans During Rest and Exercise. Inhal. Toxicol., vol. 15, p 539-552.
- de Nazelle A., B.J. Morton, M. Jerrett, D. Crawford-Brown (2010). Short trips: an opportunity for reducing mobile-source emissions? Transport Res. Part D-Transport Environ., vol. 15 p 451-457.
- de Nazelle A., S. Fruin, D. Westerdahl, et al. (2012) A travel mode comparison of commuters' exposures to air pollutants in Barcelona. Atm. Env., vol. 59, p 151-159.

- Farrel W.J., S. Weichenthal, M. Goldberg, M. Hatzopoulou (2015) Evaluating air pollution exposures across cycling infrastructure types: Implications for facility design. J. of Transport and Land Use, vol. 8 p 131-149
- Good N., A. Mölter, C. Ackerson et al. (2015) The Fort Collins Commuter Study: Impact of route type and transport mode on personal exposure to multiple air pollutants. J. Expo. Sci. Environ. Epidemiol., doi: 10.1038/jes.2015.68
- Hertel O., M. Hvidberg, M. Ketzel et al. (2008). A proper choice of route significantly reduces air pollution exposure - A study on bicycle and bus trips in urban streets. Sci. Total Environ., vol. 389, p 58-70
- Hofmann W. (2011). Modelling inhaled particle deposition in the human lung: a review. J. Aerosol. Sci., vol. 42, p 693-724.
- Int Panis L., B. de Geus, G. Vandenbulcke et al. (2010) Exposure to particulate matter in traffic: a comparison of cyclists and car passengers. Atm. Env., vol. 44, p 2263-2270.
- Jarjour S., M. Jerrett, D. Westerdahl et al. (2013). Cyclist route choice, traffic-related air pollution, and lung function: a scripted exposure study. Environ. Health, vol. 12, p 14
- Kaur S., R. Clark, P. Walsh et al. (2006) Exposure visualization of ultrafine particle counts in a transport microenvironment. Atm. Env., vol. 40 p 386-398.
- Kendrick C.M., A. Moore, A. Haire et al. (2011). Impact of bicycle lane characteristics on exposure of bicyclists to traffic-related particulate matter. J. of the Transportation Research Board, vol. 2247, p 24-32.
- MacNaughton P., S. Melly, J. Vallarino et al. (2014). Impact of bicycle route type on exposure to traffic-related air pollution. Sci. Total Environ., vol. 490, p 37–43
- Morawska L., Z. Ristovski, E.R. Jayaratne et al. (2008) Ambient nano and ultrafine particles from motor vehicle emissions: characteristics, ambient processing and implications on human exposure. Atm. Env., vol. 42, p 8113-8138.
- Ozgen S., G. Ripamonti, A. Malandrini et al. (2016). Particle number and mass exposure concentrations by commuter transport modes in Milan, Italy. AIMS Environ. Sci., vol. 3, p 168-184.
- Petzold A. et al. (2013) Recommendations for reporting “black carbon” measurements. Atmos. Chem. Phys., vol. 13, p 8365-8379.
- Quiros D.C., E.S. Lee, R. Wang et al. (2013) Ultrafine particle exposures while walking, cycling, and driving along an urban residential roadway. Atm. Env. vol. 73, 185-194.
- Ragetti M., E. Corradi, C. Braun-Fahrländer et al. (2013) Commuter exposure to ultrafine particles in different urban locations, transportation modes and routes. Atm. Env., vol. 77, p 376-384.
- Schepers P., E. Fishman, R. Beelen et al. (2015) The mortality impact of bicycle paths and lanes related to physical activity, air pollution exposure and road safety. J. of Transport & Health, vol. 2, p 460-47
- Spinazzè A., A. Cattaneo, D.R. Scocca et al. (2015): Multi-metric measurement of personal exposure to ultrafine particles in selected urban microenvironments. Atm. Env., vol. 110, p 8-17
- Strak M., H. Boogaard, K. Meliefste et al. (2010) Respiratory health effects of ultrafine and fine particle exposure in cyclists. Occup. Environ. Med., vol. 67, p 118-124
- Suárez L., S. Mesías, V. Iglesias et al. (2014) Personal exposure to particulate matter in commuters using different transport modes (bus, bicycle, car and subway) in an assigned route in downtown Santiago, Chile. Environ. Sci. Processes Impacts, vol. 16, p 1309-1317.
- Tukey J. (1977): Exploratory Data Analysis. Addison-Wesley Pub. Co., Reading, Massachusetts, 688 p.
- Zurbier M., G. Hoek, M. Oldenwening et al. (2010) Commuters' exposure to particulate matter air pollution is affected by mode of transport, fuel type, and route. Environ. Health Persp., vol. 118, p 783-789.

The interactions of the Exhaust Ultrafine Particle with the vehicle near-wake flow

Amine MEHEL*, Frederic MURZYN** & Romain RODRIGUEZ**

* Department of Composite Materials Mechanics and Environment, ESTACA, 78180, Montigny-Le-Bretonneux, France Fax +33 01 76 52 11 43 - email: amine.mehel@estaca.fr

** Department of Composite Materials Mechanics and Environment, ESTACA, 53061, Laval, France

Abstract

Reduction of pollution emission coming from automotive engines has become a key strategy leading to some significant improvements in the last two decades in Europe with the implementation of new and tighter regulations. To date, the most important remaining problem concerns the increased emission of ultrafine particles (nanoparticles) especially with the reduction of larger and solid carbonaceous particles. Recent studies have shown that these ultrafine particles (most important in number rather than in mass) are the worst and most harmful particles in terms of health effects. Indeed, they are able to reach the respiratory system in its deepest part, the alveolar region where they can readily penetrate the blood stream leading to major cardiovascular diseases or cancer. Furthermore, it is well-known that these ultrafine particles can infiltrate the vehicle in-cabin and accumulate inside. This enhances the risk exposure of the passengers. In this study, we are not only interested in investigating their dispersion downstream of a reduced-scale square-back car model, but also in studying their interaction with the dynamic of the model near-wake flow turbulence in a wind tunnel. The results show that a high correlation is found between the ultrafine particles dispersion/accumulation zones and the turbulent vortices that are generated in the vehicle near-wake.

Keys-words: Aerosol dispersion, Ultrafine Particles, Particle concentration, Turbulence, Wind tunnel, LDV

Introduction

For many decades the particles emissions were not regulated or only limited to the mass concentration. This explains why road traffic has become one of the major sources of fine and ultrafine particles number concentrations (PNC). Emission measurements campaigns suggest that motor vehicles are the primary direct emission sources of fine and ultrafine particles to the atmosphere in urban areas (Shi et al., 1999; Hitchins et al., 2000; Biswas et al., 2008). They roughly count for 90% or more of the total particle number in areas influenced by on-road vehicles emissions (Morawska et al., 2008). They are in the size range 20–130 nm for diesel engines (Morawska et al., 1998) and 20–60 nm for gasoline engines (Ristovski et al., 1998). The exposure to such ultrafine particles result in causing several adverse health effects. Recent toxicological studies have showed that these ultrafine particles are more toxic than larger particles with the same chemical composition and at the same mass concentration (Brown et al., 2000; Oberdorster, 2001). Indeed, they are able to reach the respiratory system in its deepest part, the alveolar region where they can readily penetrate the blood stream leading to major cardiovascular diseases or cancer (Valberg, 2004; Silverman et al., 2012, Ostro et al., 2015). Thus, the need of particle number concentration (PNC), together with the size distribution (PSD) of ultrafine particles, has led to several studies where measurements have been conducted to better assess ambient air quality and its potential health effects. Among them, Zhu et al. (2002), Janssen et al. (2001), Kozawa et al. (2012) assessed PNC and PSD near major highways and roads. These ultrafine particles are then transported from these regions with very high concentrations to all over the surrounding local environments where they can infiltrate vehicles in-cabin, building, schools and indoor environments. Consequently they can cumulate resulting in the exposure of the passengers, pedestrians, bikers...The exposure to such pollutants has been assessed through local/individual measurements. Particularly, they recent studies have evaluated the individual exposure when commuting in the transportation microenvironment (Adams et al., 2001; Zuurbier et al., 2010), buses or bicycle (Gee & Raper; 1999), vehicles in-cabin (Joodatnia et al.,

2013; Zhu et al., 2007). Other investigations have been conducted to compare exposure depending on transport mode (Panis et al., 2010; Knibbs et al., 2011) or during day-time activities including, outdoor commuting in traffic environments (Gu et al. 2015). All these studies have underlined the importance of two major parameters (among others) in assessing the exposure, i.e. the concentration and particle size. This has led some authors to characterize them during different stages of the transportation process. During the infiltration process, it has been shown that parameters such as vehicle mileage, age and ventilation fan speed have strong influence on the indoor to outdoor concentration ratio (Hudda et al., 2012). The pollutants dispersion is also influenced by the local topology as mentioned in Goel & Kumar (2015) or Takano and Moonen (2013). They showed the influence of signalized traffic intersections or of the street canyon roof shape on PNC respectively on pollutants concentration levels.

This brief overview demonstrates the importance of treating particle dynamics at different urban scales as concluded by Kumar et al. (2011). This is the reason why we focus on the dispersion of the UFP in the vehicle wake flow where the PNC levels are very high and the risk due to exposure elevated. The dispersion process of the UFP at this stage is mostly influenced by the flow and particularly by the turbulent structures. Studying their correlations with PNC would be helpful to identify some key-parameters that may affect particle dispersion. To achieve this goal, we undertake wind tunnel investigations. Across the literature, we notice that only very few experimental studies dealt with that topic (Kanda et al., 2006; Carpentieri et al., 2012). Then, we present new wind tunnel experiments to assess the dynamic of carbonaceous UFP downstream of a reduced-scale truck model. While Carpentieri et al. (2012) used a passive tracer gas, we resort to solid particles. Furthermore, in our experimental conditions, the tailpipe flow and wind tunnel flow mixing are supposed to be representative of an urban vehicle moving at 30km/h (kinematic scale). PNC and velocity field measurements are achieved to bring new understanding regarding UFP interaction with the vehicle near wake flow and its consequence on their dispersion. Results are mostly compared and discussed with Carpentieri et al. (2012). Further perspectives and future works are presented.

1. Experimental method

The present experiments are conducted in two different wind tunnels. The Particle Number Concentrations (PNC) measurements are undertaken in the experimental facility located at ESTACA Paris. The corresponding wind tunnel has a test section of 800mm in length, a width of 600mm and a height of 600mm. The velocity measurements are recorded at ESTACA Laval in the second wind tunnel which is 1m in length, 0.3m in width and 0.3m in height. The same upstream air velocity is ensured and set at $U_{\text{mean}}=14.4\text{m/s}$ so as to get the same flow conditions in both wind tunnels. This velocity is recorded either with a Pitot tube (Paris) or with a 2D LDV system (Laval). Walls are made of transparent altuglass allowing flow visualization and use of optical devices. The studied car model is shown in Fig. 1 (left). It has a common rear part of a truck with a reduced size. Here, the scale factor is 1/20 compared to a real prototype. The length of the model is $L=122\text{mm}$, its width is $W=49\text{mm}$ and its height is $H=65\text{mm}$. For all conditions, the blockage ratio was less than 4%. No raised false floor is installed contrary to Carpentieri et al. (2012) where one was used for some experimental conditions. Nevertheless, a calibration of the wind tunnel is carried out prior to the present experiments to ensure a well-defined knowledge of the undisturbed flow developing in the measurement section. For both wind tunnels, the turbulence intensity of the incoming flow is less than 1%.



Figure 1. Car model used during the experiments (Left) and the Cartesian coordinate system with incoming flow from top left to bottom right (Right)

The experimental conditions are supposed to correspond to a real truck prototype speed $U_p=8.33\text{m/s}$ (30km/h) according to an imposed kinematic scale of 1.73 (U_{mean}/U_p). This scale is imposed by some experimental constraints related to the flow rate of the exhausted particles. Hence, the dynamic similarity of the tailpipe jet and wind tunnel air flows is ensured. The associated Reynolds number based on the truck height and kinematic viscosity of air is 6.10^5 ($Re=U_{\text{mean}}*H/\nu=6.10^5$). This is significantly larger than critical value of 10^4 from which the boundary layer at the rear of the car becomes turbulent. According to Hucho (1998), above this limit, little sensitivity to the Reynolds number is expected. During the experiments, the kinematic scale between prototype and model is kept constant for exhausted gas/particle velocity considering a given engine speed of 2500 rpm. It is worthwhile to note that this condition is a novelty in comparison to the previous studies on pollutant dispersion in wind tunnels. The nanoparticles are generated by a PALAS DNP 2000 spark discharge aerosol generator using graphite electrodes and Nitrogen. The aerosol is injected in the model tailpipe at a given flow rate of $Q_{cp}=0.133\text{L/s}$. The size distribution of ultrafine carbon particles ranges from 20 to 100nm. An Electrical Low Pressure Impactor (ELPI) is used for Particle Number Concentration (PNC) measurements. Altogether these experimental conditions are supposed to be typical of urban areas. Additional details dealing with experimental conditions are given by Mehel and Murzyn (2015).

The Particle Number Concentrations are measured at 66 different locations downstream of the car corresponding to distinct positions in the longitudinal (x), vertical (y) and transversal (z) directions. Altogether they cover a domain given by $0.25 < X=x/H < 5$, $0.25 < Y=y/H < 1$ and $-0.5 < Z=z/H < 0.5$ where H is the height of the truck. This finite volume is imposed by the size of the wind tunnel section. Therefore, according to the dimensions of the experimental facilities, we are mostly focused on the near-wake region ($x/H < 5$). For completeness, the origin of the axis system (Fig. 1, right) is taken on the centerline of the wind tunnel ($z=0$), on the ground ($y=0$) and on the rear face of the car model ($x=0$). In the dimensionless coordinate system, the injection point representing the tailpipe is located at $X=x/H=0$, $Y=y/H=0.25$ and $Z=z/H=-0.25$.

For PNC measurements, data acquisition lasts 120 seconds and the data rate is kept constant and equal to 1 Hertz. The acquisition duration is long enough compared to the time scale of the flow. So the convergence of the concentration data is ensured.

The velocity fields are measured using a 2D LDV system (DANTEC) mounted on a 2D displacement table. Both streamwise (U) and vertical (V) components of the velocity are recorded at 560 different locations downstream of the truck. The corresponding investigated area spreads such as $0.25 < X < 5$, $0.25 < Y < 1$ and $-0.55 < Z < 0$. The measurement grid consists of $20 \times 7 \times 4$ points. On the x-axis, the step between 2 points is 16.25mm while it is 8.25mm on the y-axis and 12mm on the z-axis. Data acquisition lasts 60 seconds or ends as soon as 5000 samples are acquired. To avoid any erroneous measurements, velocity data are filtered based on the rms value of U and V. That is, if $U-U_{\text{mean}}$ (or $V-V_{\text{mean}}$) is larger than $3u'$ ($3v'$ respectively) where u' and v' are the rms values of U and V, then the pair (U, V) is replaced by $(U_{\text{mean}}, V_{\text{mean}})$. This filtering technique only concerns few points (less than 1%) and does not significantly affect U_{mean} , V_{mean} , u' and v' (Murzyn and Belorgey, 2005). Furthermore, measured points where data rate is below 5Hz are systematically removed as they may not represent the real flow dynamic where rapid fluctuations occur. Nevertheless, this only represents a very low number of points (less than 2%) and may be explained by possible invisible scratches on the wind tunnel walls for instance.

For all measurements, we acknowledge a constant air speed (steady conditions) and no heat flux from engine is considered. Lastly, it should be noticed that even if the aerosol is not heated, the particles are less sensitive to the buoyancy effect than if a gaseous passive tracer was used. Indeed, their density is approximately 2000kg/m^3 (carbon particle). This point is a main difference compared to the experimental investigations of Kanda et al. (2006) and Carpentieri et al. (2012) where a gas tracer was used.

2. Results and Discussion

For the following figures, black marks indicate the measurement positions. An absence of symbol means unavailable data due to data rate below 5Hz and/or possible scratch on the side of the wind tunnel.

Mean velocity fields

Figure 2 presents a 2D vertical map (xy) of the dimensionless mean streamwise velocity (U/U_{mean}) measured at the centreline of the channel ($z/H=0$). Our results indicate that a negative streamwise velocity component is found close to the rear of the vehicle ($x/H < 1$) over a height which approximately corresponds to $0.80H$. The minimum streamwise velocity ($U \sim -0.23\text{m/s}$) is found at $x/H=0.5$ and $y/H \sim 0.38$. Overall, this finding is in accordance with results from Carpentieri et al. (2012). Out of this very near-wake region, positive streamwise velocities are measured with increasing values when the distance to the vehicle increases. This characterizes a recirculating flow that appears in the near-wake of the vehicle Ahmed et al (1984). From the present measurements, the length of this region is estimated at approximately $1H$ when Carpentieri et al. (2012) suggested $2H$. This is not in contradiction as they did not strictly use the same shape for the vehicle model. Far downstream (top right of figure 2), the flow recovers the same mean streamwise velocity as upstream ($U/U_{\text{mean}} \sim 1$) for $x/H > 4$ and $y/H > 0.90$. The transition between the recirculation and the “far wake” regions is gradual. This is also in agreement with Carpentieri et al. (2012).

Figure 3 presents the same 2D vertical map for the dimensionless mean vertical velocity (V/U_{mean}) measured at the centreline of the channel ($z/H=0$). For $0 < x/H < 0.75$ and y/H up to 0.90 , positive values are found depicting an upward mean flow motion. Similarly, at $x/H=0.50$, an upward motion occurs up to $y/H \sim 0.50$. Everywhere else, negative values are encountered. For $x/H > 0.75$, dimensionless values are between -0.20 and -0.05 (-2.90m/s and -0.7m/s). Far downstream ($x/H=5$), the dimensionless vertical component of the velocity is roughly homogeneous with an average value of -0.05 . The flow is back to a quasi 1D structure similar to the upstream conditions. Combining with the above results, this clearly denotes the apparition of recirculation vortex in the vicinity of the car model. From the mean velocity field, we put in evidence its development close to the car model. This is in accordance with past results (Carpentieri et al., 2012). The structure and the dynamic of the flow in this near-wake region are of importance and have significant impact on the PNC measurements as it will be seen in the next section.

For completeness, Figs 4 and 5 present the same characteristics relative to the mean flow but for a different 2D cross section. Here, the (yz) map is considered at $x/H=0.50$ (near-wake). It only represents half of the symmetrical near-wake flow. Taking into account the width of the car model, it is worthwhile to note that the lateral sides of the car are situated at $z/H \sim \pm 0.38$. From these figures, some relevant information can be deduced. From the lower vertical position $y/H=0.25$ to $y/H \sim 0.75$, negative horizontal streamwise velocities are encountered when $z/H < 0.20$. In the same time, vertical component of the velocity vector is mostly positive when $y/H < 0.50$ whatever z/H is. It is believed that the recirculation area may be symmetrical but does not spread over the whole width of the vehicle. Out of this very near-wake region (for $x/H > 2$), our results show that horizontal streamwise velocity is always positive. This is also true at $x/H=1$ except for the position $y/H=0.25$ and $z/H=0$ where a negative horizontal streamwise velocity is recorded. This reveals that the recirculation region is limited to the closest vicinity of the car model.

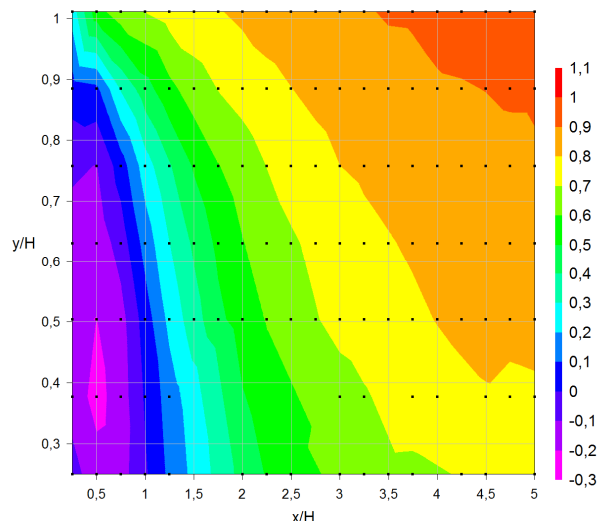


Figure 2. 2D map (xy) of dimensionless mean streamwise velocity ($z/H=0$)

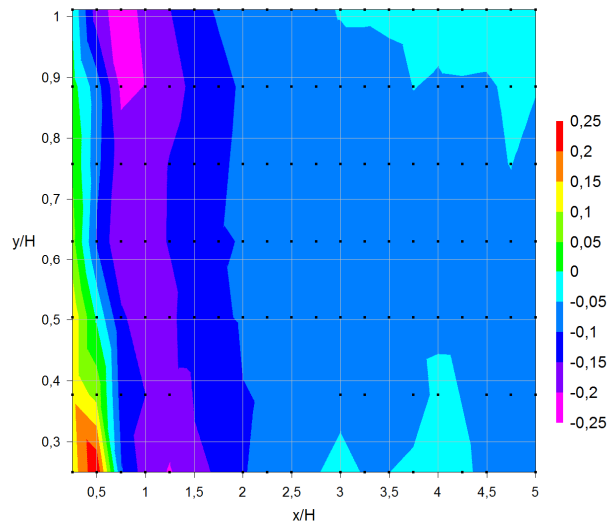


Figure 3. 2D map (xy) of dimensionless mean vertical velocity ($z/H=0$)

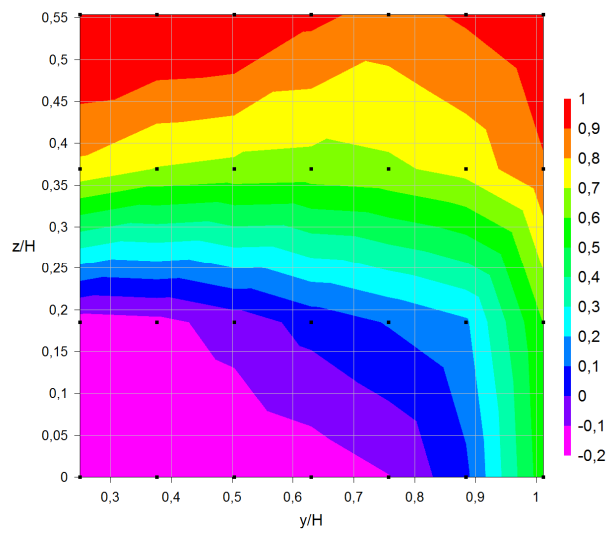


Figure 4. 2D map (yz) of dimensionless mean streamwise velocity ($x/H=0.50$)

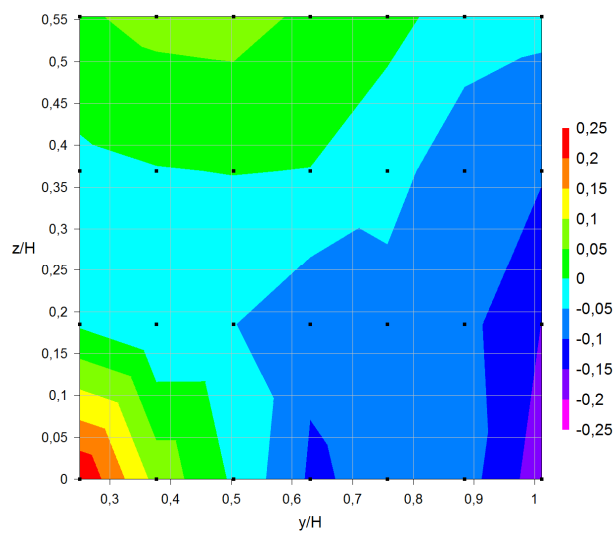


Figure 5. 2D map (yz) of dimensionless mean vertical velocity ($x/H=0.50$)

Turbulent velocity fields

Figures 6 and 7 present the turbulence intensity in both longitudinal (I_x) and vertical (I_y) directions respectively. I_x and I_y are expressed as the ratio between rms of the corresponding velocity component and U_{mean} . The displayed data correspond to the centreline of the wind tunnel ($z/H=0$). Note that the scale is kept identical to make the comparison easier.

For the given transverse position $z/H=0$, our results for the turbulence intensity levels (Figs 6 and 7) exhibit that the turbulence level is overall more intense close to the vehicle and decreases with the dimensionless distance x/H . Except for one position ($x/H=0.50$ and $y/H=0.25$ where I_x reaches 25.5%) the turbulence intensity does not exceed 17%. Peaks are mainly measured at heights corresponding to upper ($0.80 < y/H < 1$) and lower ($y/H < 0.40$) surfaces of the car model. This behaviour was previously observed by Carpentieri et al. (2012) within a comparable range. Furthermore, a similar behaviour is highlighted. Indeed, at the roof height ($y/H \sim 1$), we found the highest turbulence level at $x/H=0.75$ ($I_x=16.8\%$). Close to the ground, the maximum is measured at $x/H=0.50$ ($I_x=25.5\%$). This longitudinal gap between both peaks has been reported by Carpentieri et al. (2012) as well. Regarding I_y (Fig. 7), the highest level is estimated slightly below 20% but average results are pretty much the same as I_x (Fig. 6).

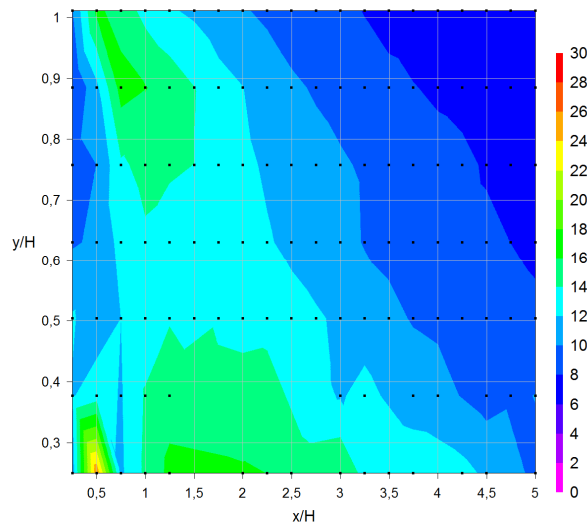


Figure 6. 2D map (xy) of turbulence intensity I_x ($z/H=0$)

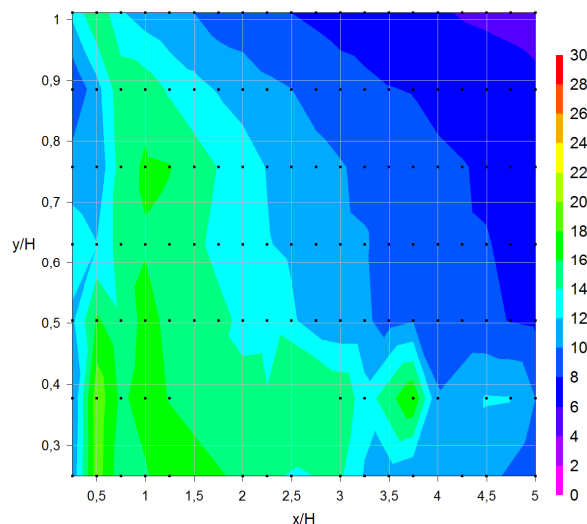


Figure 7. 2D map (xy) of turbulence intensity I_y ($z/H=0$)

Far downstream, both average levels of turbulence (I_x and I_y) fall below 10%. The wake is still disturbed compared to the upstream flow conditions and a larger distance is required to get back to the upstream flow conditions.

Particle Number Concentration (PNC)

Two different 2D maps of Particle Number Concentrations are presented on Figs 8 and 9.

Figure 8 corresponds to a vertical section at the centreline of the channel ($z/H=0$). It shows that the most important PNC ($\text{PNC} > 2 \cdot 10^6$) is observed in the vicinity of the car ($x/H < 1$). This is not surprising since it corresponds to the emission point region. The maximum PNC reaches $3.38 \cdot 10^6$ for $x/H=0.50$ and $y/H=0.25$ (height of the tailpipe). In the spanwise direction (vehicle width), the PNC evolves according to a particular behaviour: close to the vehicle ($x/H < 1$), nanoparticles are entrapped by the recirculation cell leading to highest concentrations in the centreline at $z/H=0$. By looking at these PNC contours for $z/H=-0.30$ (approximated position of the tailpipe), the maximum of PNC is found between $x/H=0.50$ and 1 for $y/H=0.25$. The corresponding levels are $1.21 \cdot 10^6$ ($x/H=0.50$ and $y/H=0.25$) and $1.29 \cdot 10^6$ ($x/H=1$ and $y/H=0.25$). For $z/H=-0.50$ and 0.50 (outer of the vehicle width), peaks are mostly found from $x/H=5$ rather than in the very near wake region ($x/H < 1$).

This is strongly related to the near wake flow structure pointed out from the velocity measurements. At $z/H=0$, nanoparticles are sucked by this large recirculating structure and accumulate in this part of the flow. It has an approximated size of 0.50 to $1H$ in length and 0.50 to $0.80H$ in height. Once the nanoparticles are trapped by the large recirculating vortex, the mechanism of turbulence diffusion takes place driving them to the area where I_x and I_y are lower which corresponds to $x/H < 0.75$ and $y/H > 0.5$ as noticed above (Figs 6 and 7). As a result, the plume is enhanced in the vertical direction. The highest PNC correspond to highest levels of I_y . Interaction between turbulence and particles is then obvious. This behaviour was previously mentioned by Mehel and Murzyn (2015) and illustrates the strong influence of the vehicle wake on the development of the plume.

In the cross-section at $x/H=1$ (Fig. 9), the cloud of dispersed nanoparticles enlarges and spreads in the spanwise direction. At $x/H=1$, the shape of the plume is roughly Gaussian but not centred around $z/H=0$. Far downstream ($x/H=2$ to 5), we show that a clear dissymmetry appears and the most important PNC are found between $z/H=-0.50$ and -0.30 (Fig. 10). This clearly denotes that the dynamic of the nanoparticles is strongly influenced by the pair of lateral longitudinal outer vortices that develop and propagate from both edges of the car. The highest number of particles is also found in the lower part of the flow ($y/H < 0.50$) which corresponds to the position of the tailpipe. For $x/H=0.50, 1, 2$ and 5 , the highest PNC values are $3.38 \cdot 10^6$ ($y/H=0.25$ and $z/H=0$), $1.29 \cdot 10^6$ ($y/H=0.25$ and $z/H=-0.30$), $0.548 \cdot 10^6$ ($y/H=0.25$ and $z/H=-0.30$), $0.293 \cdot 10^5$ ($y/H=0.25$ and $z/H=-0.30$). Therefore, the decay rate is inversely proportional to the dimensionless distance to the car model and is related to the dilution process.

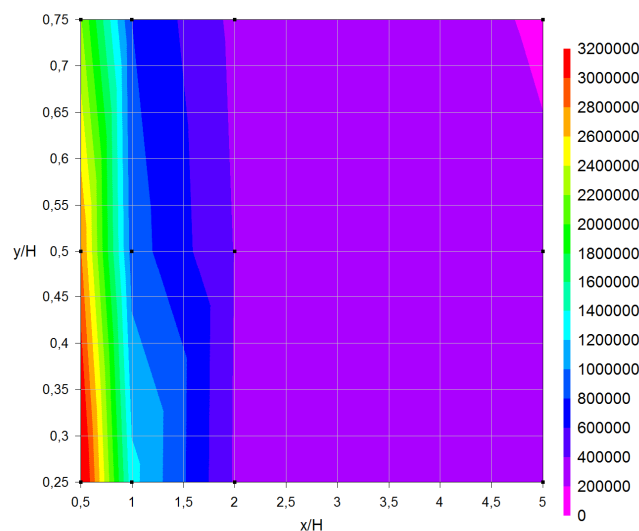


Figure 8. 2D map (xy) of PNC ($z/H=0$)

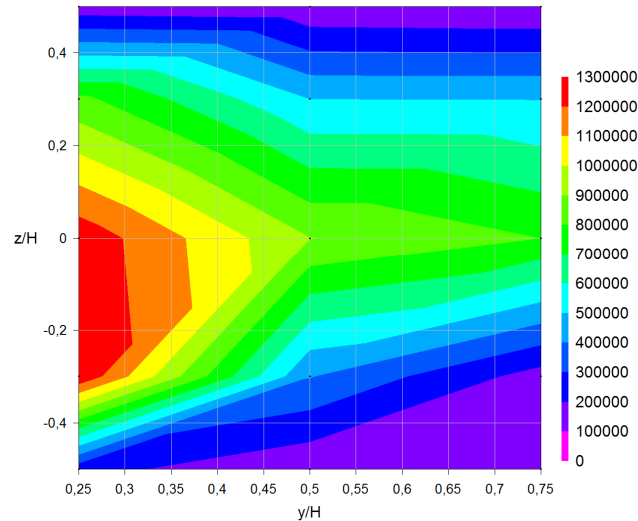


Figure 9. 2D map (yz) of PNC (x/H=1)

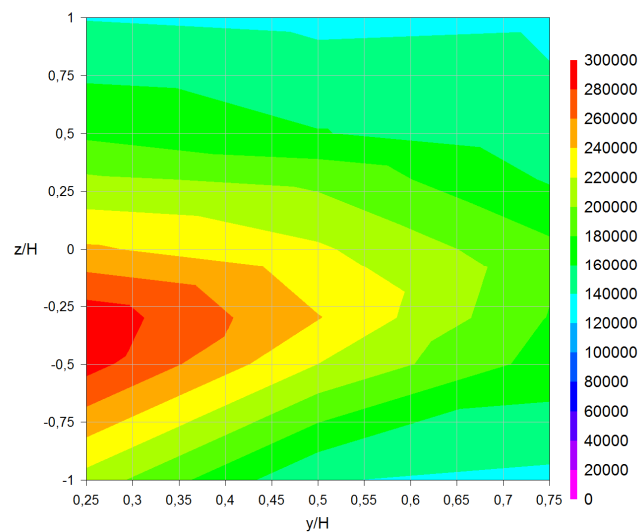


Figure 10. 2D map (yz) of PNC (x/H=5)

At the same time, at $x/H=0.50$, the maximum PNC is found at $z/H=0$ while it is shifted to $z/H=-0.30$ for $x/H=1, 2$ and 5 . It is worthwhile to note that $z/H=-0.30$ roughly corresponds to the position of the lateral side of the car model and the tailpipe position. For $x/H=1$, a second peak close to the first one ($PNC=1.27 \cdot 10^6$) is measured showing that lateral dispersion really starts downstream of $x/H=1$. According to the literature, this is also related to lateral vortices that develop in this region from the edge of the car (Hucho, 1998). Our results confirm that the vortices appearing in the near wake flow strongly influence the dispersion of the emitted particles. Accordingly, the turbulence plays an important role in the dispersion of nanoparticles emitted from the tailpipe of a car and the development of the corresponding plume.

Conclusion

In the present paper, we present experimental results of wind tunnel investigations regarding the correlation between flow dynamic and Particle Number Concentration in the wake of a vehicle model. Prior to this contribution, only few studies have been undertaken to assess this link. Here, we measure the mean and turbulent properties of the near-wake flow developing downstream of a passenger car and the Particle Number Concentration (PNC). The experimental flow conditions are defined so as to be representative of a real car at 30km/h (urban cycle) according to a kinematic scale. The flow developing downstream of the car is characterized using a 2D LDV system and a grid of 560 points is defined for velocity measurements while PNC are recorded at 66 locations. Although we acknowledge that some

improvements may be brought by reducing the step between 2 measurement points, by exploring the 3D flow or by considering more accurately the boundary layer effect, it is also expected that these preliminary results will be helpful for the community. From the measurements, our main conclusions highlight that:

- A recirculating flow develops in the close vicinity of the car model which size is estimated and compared with the previous work of Carpentieri et al. (2012) showing interesting consistency;
- The longitudinal and vertical turbulence intensities are investigated showing peaks around 25% and 20% for I_x and I_y respectively;
- Two main regions of intense turbulence activity are revealed either at the roof level or close to the ground with a longitudinal gap;
- PNC measurements in the near-wake depict a strong influence of the recirculation region which is able to suck particles leading to highest concentrations at the centreline of the channel for lowest values x/H . Then they are diffused in the vertical direction towards low level of turbulence intensities I_x and I_y ;
- When increasing the distance to the vehicle, our results indicate that lateral vortices developing from the edge of the car are capable of trapping particles. This is put in evidence by looking at the off-centre distribution of PNC. Far downstream, the peak of PNC is found to be in-line with the tailpipe. This point is important for numerical modelling as the position of the tailpipe must be taken into account with accuracy.

Altogether, these results are an added value to the existing literature and supplement interestingly some preliminary PNC measurements published earlier (2015). They particularly show the narrow relation existing between flow turbulence dynamics and particle dispersion. Nevertheless, the remaining questions are still numerous. As a consequence, some further experimental measurements and in-situ campaigns will be scheduled in the context of two new PhD research project startings focusing on correlation between wake flow and PNC.

References

- Adams, H. S., Nieuwenhuijsen, M. J., Colvile, R. N., McMullen, M. A. S., & Khandelwal, P. (2001). Fine particle (PM 2.5) personal exposure levels in transport microenvironments, London, UK. *Science of the Total Environment*, 279(1), 29-44.
- Ahmed, S. R., Ramm, G., & Faitin, G. (1984). Some salient features of the time-averaged ground vehicle wake (No. SAE-TP-840300). Society of Automotive Engineers, Inc., Warrendale, PA.
- Brown, D. M., Stone, V., Findlay, P., MacNee, W., & Donaldson, K. (2000). Increased inflammation and intracellular calcium caused by ultrafine carbon black is independent of transition metals or other soluble components. *Occupational and Environmental Medicine*, 57(10), 685-691.
- Carpentieri, M., Kumar, P., & Robins, A. (2012). Wind tunnel measurements for dispersion modelling of vehicle wakes. *Atmospheric environment*, 62, 9-25.
- Janssen, N. A., van Vliet, P. H., Aarts, F., Harssema, H., & Brunekreef, B. (2001). Assessment of exposure to traffic related air pollution of children attending schools near motorways. *Atmospheric environment*, 35(22), 3875-3884.
- Joodatnia, P., Kumar, P., & Robins, A. (2013). The behaviour of traffic produced nanoparticles in a car cabin and resulting exposure rates. *Atmospheric environment*, 65, 40-51.
- Gee, I. L., & Raper, D. W. (1999). Commuter exposure to respirable particles inside buses and by bicycle. *Science of the Total Environment*, 235(1), 403-405.
- Goel, A., & Kumar, P. (2015). Zone of influence for particle number concentrations at signalised traffic intersections. *Atmospheric Environment*, 123, 25-38.
- Gu, J., Kraus, U., Schneider, A., Hampel, R., Pitz, M., Breitner, S., ... & Cyrus, J. (2015). Personal day-time exposure to ultrafine particles in different microenvironments. *International journal of hygiene and environmental health*, 218(2), 188-195.
- Hitchins, J., Morawska, L., Wolff, R., Gilbert, D., (2000). Concentrations of submicrometer particles from vehicle emissions near a major road. *Atmospheric Environment* 34, 51–59.
- Hucho W.H. (1998), *Aerodynamics of road vehicles: From fluid mechanics to vehicle engineering*, Society of Automotive Engineering.
- Kanda, I., Uehara, K., Yamao, Y., Yoshikawa, Y., & Morikawa, T. (2006). A wind-tunnel study on exhaust gas dispersion from road vehicles—Part I: Velocity and concentration fields behind single vehicles. *Journal of wind engineering and industrial aerodynamics*, 94(9), 639-658.

- Knibbs, L. D., Cole-Hunter, T., & Morawska, L. (2011). A review of commuter exposure to ultrafine particles and its health effects. *Atmospheric Environment*, 45(16), 2611-2622.
- Kozawa, K. H., Winer, A. M., & Fruin, S. A. (2012). Ultrafine particle size distributions near freeways: Effects of differing wind directions on exposure. *Atmospheric Environment (Oxford, England)*: 1994), 63, 250–260.
- Kumar, P., Ketzel, M., Vardoulakis, S., Pirjola, L., & Britter, R. (2011). Dynamics and dispersion modelling of nanoparticles from road traffic in the urban atmospheric environment—a review. *Journal of Aerosol Science*, 42(9), 580-603.
- Mehel, A., & Murzyn, F. (2015). Effect of air velocity on nanoparticles dispersion in the wake of a vehicle model: Wind tunnel experiments. *Atmospheric Pollution Research*, 6(4), 612-617.
- Morawska, L., Ristovski, Z., Jayaratne, E.R., Keogh, D.U., Ling, X. (2008). Ambient nano and ultrafine particles from motor vehicle emissions: characteristics, ambient processing and implications on human exposure. *Atmospheric Environment* 42, 8113-8138.
- Morawska, L., Bofinger, N.D., Kocis, L., Nwankwoala, A., (1998). Submicrometer and super micrometer particles from diesel vehicle emissions. *Environmental Science and Technology* 32, 2033–2042.
- Murzyn, F. and Belorgey, M. (2005). Experimental investigations of the grid-generated turbulence features in a free-surface flow, *Experimental Thermal and Fluid Science*, 29, pp925-935.
- Oberdorster, G., (2001). Pulmonary effects of inhaled ultrafine particles. *International Archives of Occupational and Environmental Health* 74 (1), 1–8.
- Ostro B, Hu J, Goldberg D, Reynolds P, Hertz A, Bernstein L, Kleeman MJ. 2015. Associations of mortality with long-term exposures to fine and ultrafine particles, species and sources: results from the California Teachers Study cohort. *Environ Health Perspect* 123:549–556
- Panis, L. I., De Geus, B., Vandenbulcke, G., Willems, H., Degraeuwe, B., Bleux, N., ... & Meeusen, R. (2010). Exposure to particulate matter in traffic: a comparison of cyclists and car passengers. *Atmospheric Environment*, 44(19), 2263-2270.
- Ristovski, Z.D., Morawska, L., Bofinger, N.D., Hitchins, J., (1998). Submicrometer and supermicrometer particles from spark ignition vehicles. *Environmental Science and Technology* 32, 3845–3852.
- Shi, J.P., Khan, A.A., Harrison, R.M., (1999). Measurements of ultrafine particle concentration and size distribution in the urban atmosphere. *Science of the Total Environment* 235, 51–64.
- Takano, Y., & Moonen, P. (2013). On the influence of roof shape on flow and dispersion in an urban street canyon. *Journal of Wind Engineering and Industrial Aerodynamics*, 123, 107-120.
- Zhu, Y.; Hinds, W.C., Kim, S., Shen, S. & Sioutas, C., (2002). Study of ultrafine particles near a major highway with heavy-duty diesel traffic, *Atmospheric Environment*, Volume 36, Issue 27, Pages 4323-4335
- Zhu, Y., Eiguren-Fernandez, A., Hinds, W. C., & Miguel, A. H. (2007). In-cabin commuter exposure to ultrafine particles on Los Angeles freeways. *Environmental science & technology*, 41(7), 2138-2145.
- Zuurbier, M., Hoek, G., Oldenwening, M., Lenters, V., Meliefste, K., van den Hazel, P., & Brunekreef, B. (2010). Commuters' exposure to particulate matter air pollution is affected by mode of transport, fuel type, and route. *Environmental health perspectives*, 118(6), 783.

Impact of train braking systems on particle levels in the Paris subway

Romain Molle¹ & Sophie Mazoué¹

¹ RATP, Paris Public Transport, 54 Quai de la Râpée. Paris, France

email: romain.molle@ratp.fr

Abstract

Several factors can explain the high levels of particle concentrations in underground transportation systems. One of the main particle sources is train's mechanical braking system. The mechanical braking is decreasing with the renewal of rolling stock, new trains have other brake kind : the electrodynamic braking. This technology decreases the mechanical braking use and this one is more and more efficient on new trains.

Two stages have been planned to study the brake technology (with electrodynamic braking //without electrodynamic braking) on particulate air pollution. PM2.5 mass concentration and PM10 mass concentration were simultaneously measured at Colonel Fabien subway platform. The chemical composition of the fine particle fraction (PM2.5) and the coarse fraction (PM10-2.5) is measured using PIXE analysis.

In this campaign, the brake technology has an impact on the air quality. The electrodynamic braking use lowers the PM10 mass concentration by a factor of 4.3. Moreover, the train's mechanical braking system is responsible for a higher iron mass percentage in the coarse particle fraction.

Keys-words: subway, air quality, train, indoor

Introduction

Paris Public Transport (RATP) services include sixteen subway lines and parts of the Paris regional express railway network. High levels of particle concentrations have been observed by Delaunay et al. (2010) in subway stations. Several particle sources explain these levels in subway systems : wear of rail tracks, wheels and braking pads. The station characteristics (area, volume), the air change rate and train traffic are decisive parameters on particulate matter levels in subway system.

1. Objectives

In railway environments, one of the main particle sources is train's mechanical braking system. The mechanical braking is decreasing with the renewal of rolling stock, new trains have other brake kind : the electrodynamic braking. This technology decreases the mechanical braking use and this one is more and more efficient on new trains. When the electrodynamic braking is performed, the motors operate as generators and convert the kinetic mechanical energy into electrical energy. This study has been planned to study the brake technology on particulate air pollution (two stages, step I : with electrodynamic braking ; step II : without electrodynamic braking).

Both braking modes were studied on a part of the subway line 2 between October 3 and December 19, 2013 at the Colonel Fabien subway platform. Monitoring of PM10 and PM2.5 were performed using tapered element oscillating microbalance instruments (TEOM). The chemical composition of the fine particle fraction (PM2.5) and the coarse fraction (PM10-2.5) is measured by PIXE analysis (Particle Induced X-ray Emission). Metals analyzed by this method are : Cr, Mn, Fe, Ni, Cu, Zn, As, Sr, Cd, Zr, Mo, Sn, Sb, Ba and Pb.

2. Results

PM10 and PM2.5 mass concentration means during the campaign are summarized in Table 1.

Table 1. PM10 and PM2.5 mass concentration means for each stage.

Stage	PM10 ($\mu\text{g}/\text{m}^3$)	PM2.5 ($\mu\text{g}/\text{m}^3$)
I	220	110
II	960	380

PM10 mean concentrations were higher without the electrodynamic braking (II) compared to the stage I by a factor 4.3. PM2.5 mean concentrations were also higher without electrodynamic braking (II) by a factor 3.4. Therefore the electrodynamic braking has a greater impact on the reduction of PM10 mass concentration. The chemical composition of the fine particle fraction (PM2.5) and the coarse fraction (PM10-2.5) for each stage highlights the large presence of iron in the mass percentage. This large presence of iron can be explained by a previous study. According to Fischer (2003), wear of braking pads reveals the preponderant presence of iron (between 50 and 80% of the dust mass). Copper, barium, manganese, silicon, calcium and sulfur are also present in the studied braking pads. The mass percentage of iron in each stage is presented in the Table 2.

Table 2. Mass percentage of iron in the coarse fraction and the fine particle fraction

Stage	PM2,5-10 (%)	PM2.5 (%)
I	38	38
II	33	28

Conclusion

Without electrodynamic braking, the results reveal a higher iron mass percentage in the coarse particle fraction compared to the fine fraction. Therefore train's mechanical braking system increases iron mass percentage in the coarse particle fraction. Furthermore the brake technology has an impact on the particle levels. In this campaign, electrodynamic braking lowers the PM10 mass concentration by a factor of 4.3. The renewal of rolling stock with an electrodynamic braking optimized on the new trains is carried out on several subway lines.

Acknowledgments

The authors acknowledge the valuable assistance from the Rail Rolling Stock team (RATP).

References

- Delaunay, C., Mazoué, S., Morawski, F., Goupil, G., Ravelomanantsoa, H., Person, A. (2010). *City dwellers exposure to atmospheric pollutants when commuting in Paris urban area*. Primequal/Predit (RATP, LCPP, LHVP).
- Fischer, N. (2003). PhD, compréhension des mécanismes d'aérocontamination croisés (gaz et aérosols) dans les espaces d'une station du métro parisien. Université Paris-Est Créteil Val de Marne.

In service CO₂ and NO_x emissions of Euro 6/VI cars, light- and heavy-duty goods vehicles in real London driving: Taking the road into the Laboratory.

Adam MOODY* and James TATE**

*Transport for London (TfL), UK

**Institute for Transport Studies, Faculty of Earth and Environment, University of Leeds, UK.

Email: j.e.tate@its.leeds.ac.uk

Abstract

Driving on-the-road has more frequent and prompt acceleration/decelerations than in the type-approval light-duty test conditions (NEDC), with Real Driving Emissions (RDE) of CO₂ and NO_x known to be considerably higher. Despite permissible limits of NO_x emissions at type approval reducing significantly, in-service emissions from diesel vehicles have, in reality, not reduced at all through the Euro 1–5 / I–V emission standards. TfL commissioned a programme of laboratory testing to better understand the in-service emission performance of Euro 6/VI vehicles over the TfL London Drive Cycle (LDC). This cycle was constructed from instrumented car data making repeated circuits of a set route at different times of day. Twelve Euro 6 passenger cars were tested over the entire 140 kms of the LDC from a warm-start. Three HGVs were tested over the suburban sub-cycle (40kms) in laden and un-laden condition.

NO_x emissions from the petrol cars were at a low level and below, or at, their type approval limit of 0.06 g.km⁻¹. Only one SCR equipped diesel car achieved NO_x emissions close to their 0.08 g.km⁻¹ type approval limit. NO_x emissions from diesel cars with only LNT NO_x controls were between 3 and 13 times higher than their type approval limit (conformity factors). A diesel supermini was emitting NO_x at the same level as the fully laden 40T artic HGV tested.

Keys-words: real driving emissions (RDE), CO₂, NO_x, Euro 6/VI, laboratory testing.

Résumé

La conduite sur route est caractérisée par des accélérations et décélérations plus fréquentes et soudaines que lors des essais d'homologation des véhicules légers (NEDC), résultant ainsi en des émissions de CO₂ et NO_x en condition réelle (RDE) considérablement plus importantes. Malgré l'abaissement significatif des limites tolérées des émissions de NO_x lors des essais d'homologation, les émissions des véhicules à moteur diesel, observées en condition réelle, n'ont pas du tout été réduite lors des adoptions successives des normes Euro 1-5 / I-V. Transport for London (TfL) a engagé un programme d'essai en laboratoire basé sur leur propre cycle de conduite (London Drive Cycle – LDC). Son but est de mieux comprendre la performance en condition réelle qu'offrent les véhicules Euro 6/VI en matière d'émission. Ce cycle a été construit à partir des mesures enregistrées sur des véhicules effectuant plusieurs passages le long d'un même itinéraire à différentes périodes de la journée. Douze voitures ont été testées sur les 140 km du LDC avec démarrage à chaud. Trois camions ont été testés sur des cycles suburbain de 40 km, en pleine charge et à vide. Les émissions de NO_x des voitures à moteur essence étaient relativement basses et demeuraient en-dessous ou au niveau de la valeur limite d'homologation, soit 0.06 g.km⁻¹. Une seule des voitures à moteur diesel équipées d'un système RCS produisait des émissions de NO_x proche de la valeur limite d'homologation, soit 0.08 g.km⁻¹. Les émissions de NO_x des voitures à moteur diesel simplement équipées de pièges à NO_x étaient entre 3 et 13 fois supérieures à la valeur limite d'homologation. Un véhicule supermini à moteur diesel émettait autant de NO_x que le semi-remorque de 40 tonnes qui était testé chargé.

Introduction

In Europe, all new vehicles must go through a process of type-approval to ensure that they conform to common standards. Part of this process includes standards for the control of emissions from the vehicle. The latest Euro 6 standards for diesel and petrol passenger cars came into force in September 2014, with NO_x not to exceed 0.08 and 0.06 g.km⁻¹ respectively over the NEDC test.

The Euro 6 standard for emissions from light duty cars and vans was defined in UN ECE Regulation 715/2007. The main change is a reduction in the limit for NO_x from diesel engines of 55 percent, whilst the other legislated emissions remain unchanged from Euro 5b. Euro 5b has been mandatory for new cars since January 2013 and introduced a particle number limit for diesel engines, the first time that a count of particles, rather than a total mass, has been regulated. Euro 6 petrol engine emissions limits are unchanged from Euro 5, except for the introduction of a particle number limit, in line with that of diesel engines.

European Regulation UN ECE 595/2009 introduces the Euro VI standard for heavy duty diesel engines. It reduces the limit for NO_x emissions by 77 percent, whilst continuing to set demanding limits for control of particulates and other gases. In addition, the test protocol has been changed to broaden the range of speed/load conditions over which the engine must meet the emissions limits. This is followed up by a requirement to verify the emissions performance over a period of on-highway driving with portable emissions equipment (PEMS). Additionally, for Heavy Duty diesel engines, an ammonia (NH₃) concentration limit of 10 ppm applies to diesel (WHSC + WHTC) and gas (WHTC) engines. This has been introduced to control ammonia slip from Selective Catalytic Reduction (SCR) systems used to control NO_x emissions. A further proposed measure to limit the NO₂ component of NO_x emissions (known as primary NO₂) may be defined at a later stage. Some Euro VI provisions, including an extended on-board diagnosis (OBD) and certain testing requirements are to be phased-in by 2016 for new types and 2017 for all new vehicles.

It is crucial that Euro 6/VI vehicles emit less NO_x and other pollutants than their predecessors if London and Europe's air quality is to improve. It is especially important for central London that Euro 6/VI diesel vehicles are cleaner as it plans to operate the 'world's first' Ultra-Low Emission Zone (ULEZ), which will come into force on 7th September 2020. The plans follow a consultation on the proposed scheme in 2015 and 2016. The emission standard that diesel vehicles (cars, LGVs, HGVs and Bus/ Coach) must attain to drive without a charge in the zone is Euro 6/VI. Euro 4 (and newer) petrol cars and vans may drive without a charge in the zone as their NO_x emission standard is at the same level or less than comparable Euro 6 diesel limits. The charge if a vehicle is not compliant with the ULEZ standard is expected to be £12.50 for light-duty and £100 for heavy-duty vehicles.

1. Objective

TfL commissioned a Programme of laboratory testing, carried out at Millbrook Proving Ground Ltd, to better understand the in-service emission performance of Euro 6/VI vehicles. A key objective for this work was to strengthen the evidence on the effectiveness of Euro 6/VI regulations in lowering vehicles NO_x emissions in real London driving conditions.

2. Method

A laboratory testing approach was adopted so direct comparisons between vehicles could be carried out, and the results benchmarked against earlier testing of Euro 4/IV and 5/V (TfL, 2016). The test-cycle speed profile was created from real (observed) driving in London.

THE TfL LONDON DRIVE CYCLE

A 'London Drive Cycle' for light-duty vehicles has been developed by TfL as part of an on-going Vehicle Emission Study (TfL, 2016). The drive cycle was developed in association with www.millbrook.co.uk, who tracked a car (VBox GPS and CAN Bus link) being driven by an experienced driver, driving normally, making repeated circuits of a set route in the North-East of London (see Figure 1) at different times of day (AM peak, Inter-peak and in Free-flow conditions). The route contained sections of (urban) motorway, suburban and urban (central London) roads. The speed profiles for the (urban) motorway, suburban and urban sub-cycles are presented in Figure 2. The LDC doesn't consider fluctuations in road gradient i.e. it assumes that London is flat.

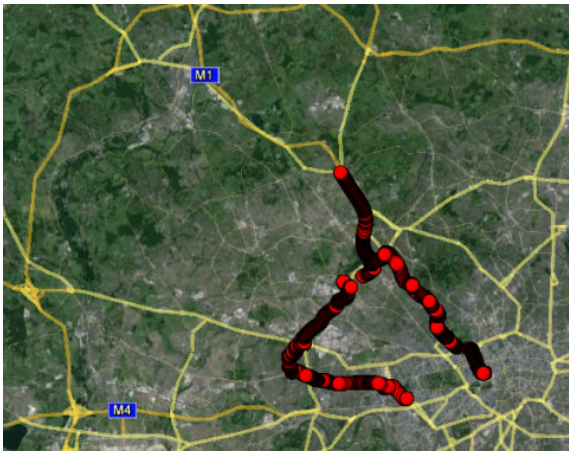


Figure 1. The TfL London Drive Cycle route
{Background © Copyright GoogleTM 2015}

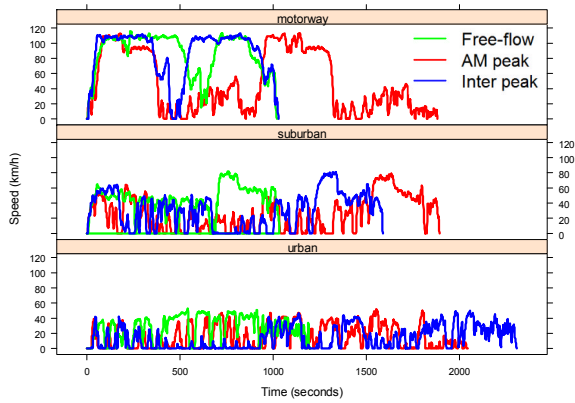


Figure 2. The London Drive Cycle Speed Profile
(a) motorway; (b) suburban; (c) urban.

The distribution of the LDC's speed, acceleration and VSP (Vehicle Specific Power - Jimenez-Palacios, 1999) are compared against the NEDC and WLTP cycles in Figures 3 and 4 respectively. In Figure 5 the VSP distribution for the AM peak, Inter-peak and Free-flow LDC sub-cycles are disaggregated. VSP sums the loads on an engine resulting from acceleration, aerodynamic drag, rolling resistance and hill climbing, which is divided by the mass of the vehicle. VSP therefore expresses in a single term an estimate of the work an engine is doing, per vehicle tonne mass, at any instance in a journey. Positive VSP have been found (Wyatt et al, 2014) to correlate well with fuel consumption and is now commonly applied in vehicle emission studies, particularly in the US (Liu et al, 2015). For clarity, idling periods (defined as vehicle speed < 0.5 ms⁻² and acceleration in the range ± 0.1 ms⁻²) are removed from the distributions. The proportion of time spent idling during the LDC, NEDC and WLTP cycles is 16.4, 13.1 and 27.2 % respectively. Summary statistics for the drive cycles are documented in Table 1.

Table 1. Drive-cycle summary.

Drive Cycle	Road Type	Time Period	Duration (seconds)	Distance (km)	Average Speed (km.h ⁻¹)	Maximum Acceleration (m.s ⁻²)
TfL London Drive Cycle (LDC)	Urban	Free-flow	1202	8.92	26.73	2.67
		AM peak	2048	8.93	15.69	1.97
		Inter-Peak	2311	8.93	13.91	2.48
	Suburban	Free-flow	1036	13.33	46.31	2.4
		AM peak	1894	13.33	25.33	2.67
		Inter-Peak	1591	13.33	30.16	2.31
	Motorway	Free-flow	1023	24.61	86.60	1.62
		AM peak	1884	24.61	47.03	1.69
		Inter-Peak	1030	24.61	86.02	2.46
NEDC	-	-	1220	11.01	32.47	1.06
WLTP	-	-	1800	23.14	46.26	1.80

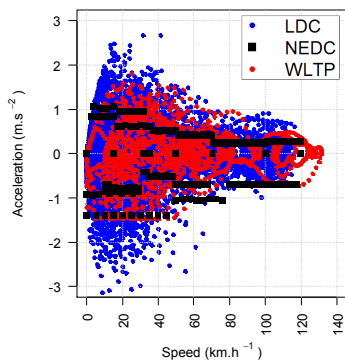


Figure 3. Distribution of Speed and Accelerations over the LDC, NEDC and WLTP cycles

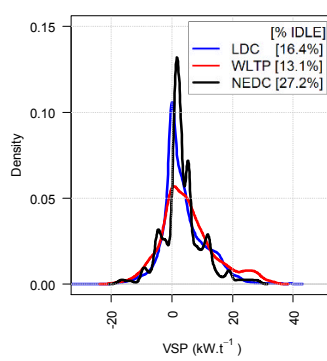


Figure 4. VSP density distributions for the LDC, NEDC and WLTP cycles (idling periods excluded)

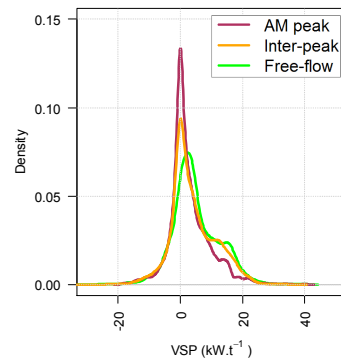


Figure 5. VSP density distributions for the LDC in Free-flow, AM- and Inter-peak periods (idling periods excluded)

The LDC covers a broad range of low and high speed driving conditions, with maximum accelerations in all but the motorway sub-cycles greater than those in the WLTP (and therefore NEDC). The LDC VSP range (positive and negative) is also greater than the WLTP. This indicates the London test driver is driving slightly more aggressively than driving represented in the WLTP when road space is available to do so. However in London AM peak and even Inter-peak periods there is little opportunity to drive freely, instead being limited to the behavior of the processions of vehicles circulating the UK's capital City. This explains why the proportion of time spent with the engine under moderately high power demands (VSP in the range 20 – 30 kW.t⁻¹) in the LDC is lower than on the WLTP. Pellecuer et al's (2016) analysis of high resolution vehicle telematics data also found that in high demand, slow moving traffic conditions drivers' behaviour was constrained, with lower VSP than the norm. The LDC is considered to be a long (140kms) real-driving cycle, representative of vehicle speed profiles on heavily trafficked UK and perhaps European city streets.

LABORATORY TESTING

The Euro 6 passenger cars were tested over the entire 140 kms of the LDC from a warm-start in the Millbrook Vehicle Emission testing laboratories that meet the requirements of Directive 2007/46 EC Article 41, Section 3 and have been designated as a Category A Technical Service for Individual Vehicle Approvals (IVA). The sample of 12 passenger cars included a range of:

- Powertrains | petrol (2), diesel (9) and petrol-HEV (1);
- Exhaust after-treatments | 3 way Cat, LNT and SCR;
- Market segments | Compact, Supermini, Small family, Family/MPV, SUV/4x4, Prestige/sports and Hybrid; and
- Marques | BMW, Fiat, Lexus, Mercedes, Peugeot, Volvo and Volkswagen.

Three Heavy-Goods Vehicles (HGVs) were tested over the suburban sub-cycle (only) in both laden and un-laden conditions. The vehicles included: Rigid HGV N2 7500kg, Rigid HGV N3 18000kg and Artic HGV N3 40000kg.

3. Results

PASSENGER CARS

The passenger car average NO_x and CO₂ emission performance in relation to their type-approval figure are illustrated in Figure 6. The data is also documented in Table 2. NO_x emissions from the petrol cars were at a low level and below or at their type approval limit of 0.06 g.km⁻¹. The petrol-HEV was an order of magnitude cleaner than the petrol-ICE's. Only one SCR (selective catalytic reduction) equipped diesel car achieved NO_x emissions close to their 0.08 g.km⁻¹ type approval limit. There was significant variation in the NO_x performance of the diesel cars equipped with only LNT (Lean NO_x Trap) NO_x controls (conformity factors 2.9 - 13.2). The average Euro 6 diesel car NO_x emission factor over the 'real' LDC speed profiles was 0.36 g.km⁻¹. This is less than its predecessors but 4.5 times greater than their type approval limit (Laboratory, NEDC).

The average NO_x and CO₂ results are presented for each road type (motorway, suburban, urban) and time period (AM peak, Inter-peak and Free-flow) in Figure 7. The impact of driving conditions (time of day) on the discrepancy between the measured and type-approval CO₂ figures is greatest in the urban setting. In the AM and Inter-peak periods speeds fall from the Free-Flow average of 26.8 km.h⁻¹ to 15.7 and 13.9 km.h⁻¹ respectively. The increased frequency of stop-start motions (see Figure 2) in the AM and Inter-peak periods come with a fuel and therefore CO₂ penalty. The petrol-HEV has the lowest discrepancy between the type-approval CO₂ figure and measured values for the slower LDC urban AM and Inter-peak sub-cycles. This is expected as the hybrid powertrain captures and re-uses energy that would have otherwise been lost under braking. The benefit of the HEV powertrain is greatest in more intensive stop-start driving conditions.

The single high NO_x emitting Euro 6 diesel super-mini performs worst in the urban (central London) driving conditions tested. It is concerning that the diesel super-mini with poor NO_x exhaust controls emitted so much of a critical air pollutant in normal urban driving conditions. In urban areas population density and therefore exposure to associated air pollution is considerably higher, such as in central London. This is exacerbated by high buildings restricting the dispersion of vehicle emissions from streets.

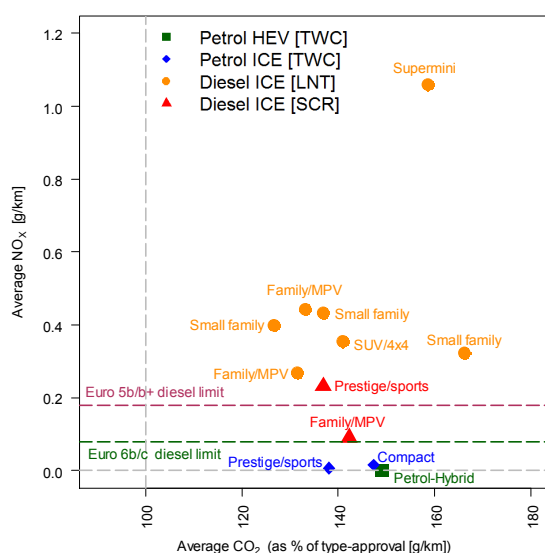


Figure 6. The Euro 6 passenger car average NO_x and CO₂ emissions in relation to their type-approval over the TfL London Drive Cycle

Table 2. Euro 6 passenger cars tested and summary results recorded over the urban and suburban sections of the LDC

Market segment	Fuel	Transmission	Emission Controls	type-approval CO ₂ (g.km ⁻¹)	Average CO ₂ (g.km ⁻¹) over LDC	CO ₂ as % type-approval	Average NO _x (g.km ⁻¹) over LDC	f-NO ₂ over LDC
Compact Exec	Petrol-HEV	CVT	3 way Cat	82	122	149	0.0004	N/a
Compact	Petrol	Manual	3 way Cat	99	146	147	0.0151	N/a
Prestige/sport	Petrol	Auto	3 way Cat	195	269	138	0.0066	N/a
Small family (*)	Diesel	Auto	LNT	111	141	127	0.399	0.347
Small family	Diesel	Manual	LNT	98	134	137	0.433	0.336
Family/MPV	Diesel	Manual	LNT	107	141	132	0.268	0.218
Family/MPV	Diesel	Manual	LNT	109	145	133	0.443	N/a
Small family	Diesel	Manual	LNT	97	161	166	0.321	N/a
SUV/4x4	Diesel	Auto	LNT	124	175	141	0.353	N/a
Supermini	Diesel	Manual	LNT	88	140	159	1.059	N/a
Prestige/sport	Diesel	Auto	SCR	110	151	137	0.232	0.609
Family/MPV	Diesel	Auto	SCR	103	147	142	0.090	0.308

There was a high variability in the primary NO₂ emissions from diesel cars and between driving conditions as illustrated in Figure 8, with averages documented in Table 2. Primary NO₂ emissions from petrol cars were at a low-level, around the lower-detectable limit of the test bench so are not reported. The NO₂ fraction of total NO_x was only speciated for 5 of the 9 diesel passenger cars tested. The fraction of NO_x emissions emitted as NO₂ (termed f-NO₂) from one SCR equipped diesel car exceeded 0.8 in free-flow motorway driving, falling to 0.4 in congested urban conditions. The average diesel car f-NO₂ was 0.363. There was no discernable relationship between f-NO₂ and speed/ acceleration or VSP.

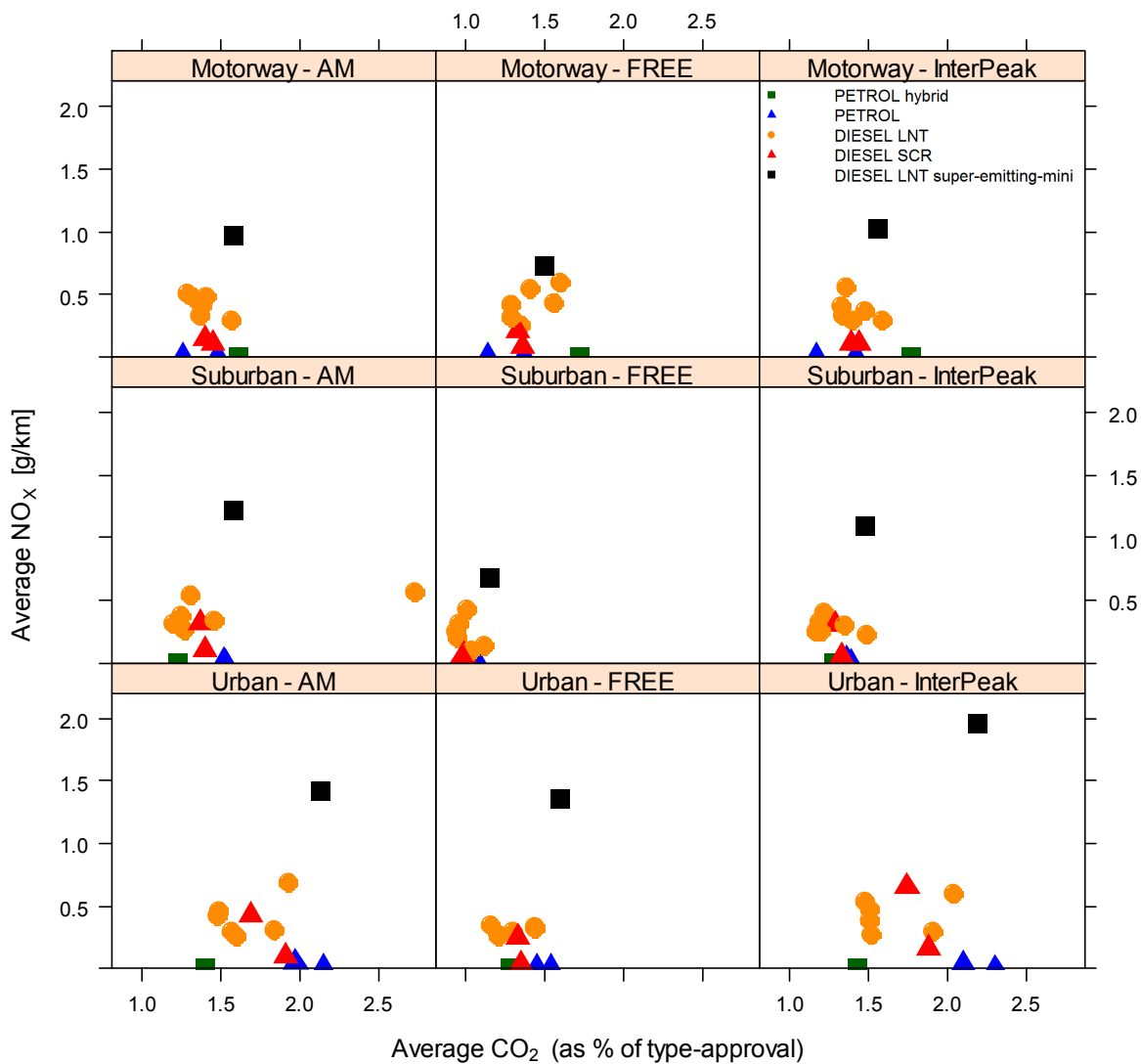


Figure 7. The Euro 6 passenger car average NO_x and CO₂ emissions in relation to their type-approval over the TfL London Drive sub-Cycles
 (top-row) motorway; (middle-row) suburban; (bottom-row) urban
 (left-column) AM peak; (middle-column) Free-Flow; (right-column) Inter-peak

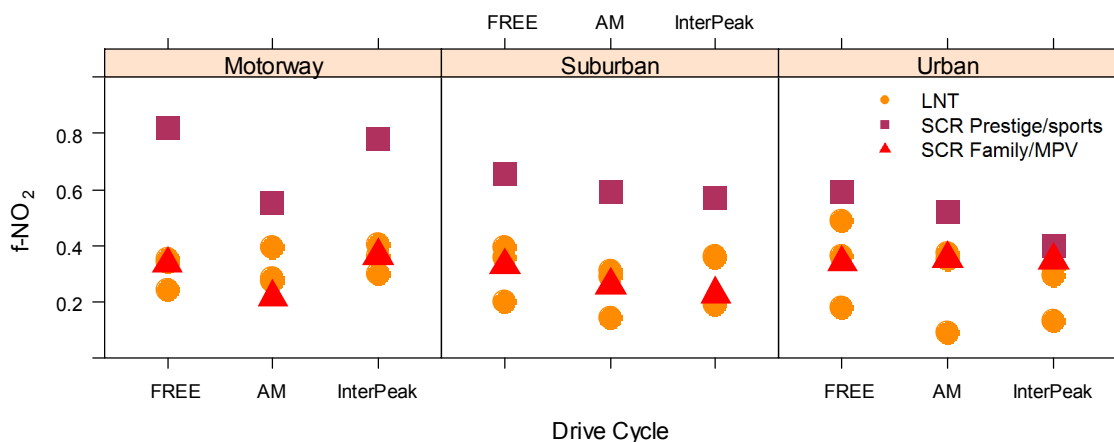


Figure 8. The fraction of NO_x emissions emitted as NO₂ (f-NO₂) for Euro 6 diesel passenger cars
 (a) motorway; (b) suburban; (c) urban

The sensitivity of CO₂ and NO_x emission rates (grams.sec⁻¹) relative to the load on the engine for one illustrative diesel passenger car (annotated * in Table 2) are explored in Figures 9 and 10 respectively. This analysis is conducted to illustrate the influence a more aggressive driving style (drive cycle) would have on emissions. In Figure 9 the second-by-second emission rates are plotted against the calculated VSP for that instant (second). The measurements are also grouped by driving mode (idle, acceleration, cruise and deceleration). The driving mode definitions proposed by Frey et al (2003) are used:

- Idle | Vehicle speed < 0.5 ms⁻² and Acceleration in the range ± 0.1 ms⁻²;
- Cruise | Vehicle speed > 0.5 ms⁻² and Acceleration in the range ± 0.1 ms⁻²;
- Acceleration | > 0.1 ms⁻²; and
- Deceleration | < - 0.1 ms⁻².

As reported by Frey et al (2003) and Wyatt et al (2014), positive VSP correlates well with instantaneous fuel consumption and CO₂ emissions. As expected, higher power demands and therefore emission rates of CO₂ are seen when the vehicle is accelerating. For the vehicle speeds, rates of acceleration and VSP range of the LDC, the correlation of positive VSP with CO₂ is linear. The NO_x emission rate increases exponentially with positive VSP. This analysis and data illustrates that NO_x emissions are much more sensitive to driving style than fuel consumption / CO₂ emissions.

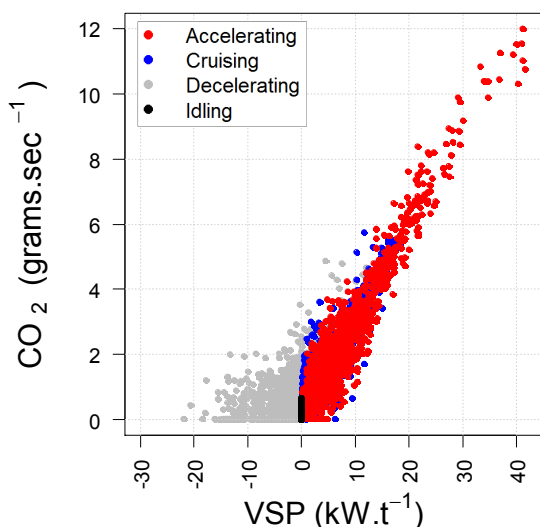


Figure 9. The influence of VSP on CO₂ emission rates for an illustrative (*) Euro 6 diesel small family car (by driving mode)

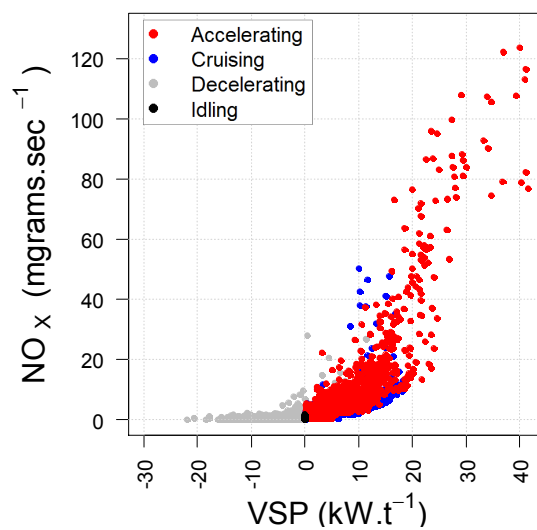


Figure 10. The influence of VSP on NO_x emission rates for an illustrative (*) Euro 6 diesel small family car (by driving mode)

HEAVY GOODS VEHICLE

Three HGVs were tested over the suburban cycle (only) in both laden (fully) and un-laden condition. As the Millbrook VTEC laboratory is only capable of 20,000kgs inertia simulation the larger 40T class N3 HGV was tested using a PEMS (Portable Emission Measurement System) with the vehicle following the drive cycle whilst driving on the large, flat circular track at the Millbrook testing ground. The summary results are presented in Table 3. A total PM measure was only available for the combined AM peak and Free-flow suburban sub-cycles. No NO_x recording was available for the for the N3 rigid 18000kg un-laden Free-flow suburban sub-cycle.

The levels of PM emissions remained consistent regardless of payload, controlled by the diesel particulate filter (DPF). It is interesting to note that the NO_x emissions are considerably lower in the fully loaded condition for each vehicle type. This may be attributed to the increased engine exhaust temperatures on the laden vehicle allowing for more effective dosing of the SCR catalyst. In a number of cases, these cycle average emission levels are almost as low as those of diesel passenger cars, indicating the effectiveness of Euro VI (heavy-duty) at controlling NO_x from heavy-duty engines, under the right conditions.

NO_x emissions from the three HGVs tested were highest when un-laden vehicles were driven in AM peak driving conditions with frequent stops-and-starts and extended idling periods. The change in NO_x emissions from laden to un-laden, and between AM peak and Free-flow conditions, was greatest for the 40T N3 artic. In fully laden (GVW 40 tonnes) NO_x emissions were at a moderate level of moderate level in the AM peak, roughly halving when completing the same route in Free-flow traffic conditions as less fuel intensive stops-and-starts are undertaken. When running empty (un-laden) NO_x emissions are at a low-level, around the Euro 6 emission standard for a category N₁-III Light-Commercial Vehicle (1750 – 3500kg GVW). When the same vehicle follows the same route in congested AM peak driving conditions, NO_x emissions increase 18 times. This analysis indicates Euro VI emission controls are now able to control NO_x emissions in all but extreme low average engine load situations, when the SCR is not able to maintain an operational/ effective temperature.

Table 3. Euro VI HGV tests and summary results over the suburban AM peak and Free-flow sub-cycles of the LDC

HGV class	GVW (kg)	Fuel	Loading	LDC suburban phase	Average Speed (km.h ⁻¹)	NO _x (grams.km ⁻¹)	CO ₂ (grams.km ⁻¹)	PM (grams.km ⁻¹)	
N2 rigid	7500	Diesel	0 %	AM	25.3	1.082	356.5	0.003	
				FreeFlow	46.2	0.271	289.6		
			TOTAL			32.7	0.676		323.1
			100 %	AM	24.6	0.472	546.7		
				FreeFlow	45.3	0.177	419.7		
			TOTAL			31.9	0.325		483.2
N3 rigid	18000	Diesel	0 %	AM	25.0	0.776	774.1	0.006	
				FreeFlow	46.0	N/a	569.7		
			TOTAL			32.4	N/a		671.9
			100 %	AM	24.6	0.798	1024.5		
				FreeFlow	45.2	0.128	758.7		
			TOTAL			31.9	0.463		891.6
N3 artic	40000	Diesel	0 %	AM	25.1	2.473	995.8	0.007	
				FreeFlow	45.8	0.137	731.5		
			TOTAL			32.4	1.305		863.7
			100 %	AM	24.4	1.559	2075.0		
				FreeFlow	45.2	0.818	1519.9		
			TOTAL			31.8	1.188		1797.4

4. Summary and Conclusions

It can be seen from this analysis of test results that, in urban driving, Euro 6 petrol cars emit very low levels of NO_x. Diesel cars at Euro 6 show a significant improvement over those at Euro 5. Some models of light-duty diesel vehicles may require re-calibration to satisfy the RDE protocol for emission verification, which is expected to be introduced from 2017 onwards, and for all new cars from 2019 following the introduction of a new World Light Duty Test Protocol (WLTP) in 2017. It is understood that conformity factors for the RDE testing have been agreed with the European Commission, to be phased in in two stages (initially 2.1 moving to 1.5 later), but that some important details such as 'dynamic boundary conditions' for the testing are still to be finalized. This process will be similar to that already in place for heavy duty engines where substantial reductions in real-world NO_x emissions have been observed.

TfL has also tested examples of heavy-duty buses (MLTB cycle) and heavy-duty goods vehicles (TfL Suburban Cycle) at Euro VI. In each case, the results have been impressive, with emissions of NO_x significantly reduced from vehicles at Euro V. This is especially true at lower road speeds, which is clearly advantageous for urban and suburban areas. Heavy-duty Euro VI emission controls on the sample of tested vehicles were found to be able to control NO_x emissions in all but the most extreme low average engine load situations i.e. empty running (un-laden) in congested driving conditions. As the SCR is not able to maintain an operational/ effective temperature NO_x emissions were found to increase by an order of magnitude. Sustainable road freight management and logistics should therefore avoid running HGVs empty in peak periods, preventing un-necessarily high emissions of NO_x.

One area of concern, and for possible further research, is that of primary NO₂ emissions. This is the fraction of total NO_x which is constituted of NO₂ at the point that it leaves the vehicle tailpipe. There are suggestions that this may be more important when considering human exposure in urban streets than the emissions of NO (which later oxidise in the atmosphere to form secondary NO₂). Some diesel exhaust after-treatment systems increase the fraction of total NO_x which is NO₂, despite reducing the total mass emission of NO_x. There are discussions at the European Commission about a potential primary NO₂ limit, which may even constitute a future Euro standard (Euro VII ?).

Acknowledgments

The data used in this report was compiled as part of a study by Transport for London into 'real-world' emissions performance of road vehicles under urban driving conditions. Test cycle development and laboratory emissions testing and pollutant analysis was carried out by Millbrook Proving Ground Ltd on behalf of Transport for London.

References

- Frey, H.C., Unal, A., Rophail, N.M., Colyar, J.D., 2003. On-road measurement of vehicle tailpipe emissions using a portable instrument. *J. Air Waste Manag. Assoc.* 53 (8), 992–1002.
- Jimenez-Palacios, J., 1999. Understanding and quantifying motor vehicle emissions with vehicle specific power and TILDAS remote sensing. , Doctoral Dissertation, Department of Mechanical Engineering, Massachusetts Institute of Technology, Cambridge, MA.
- Liu, B., Frey, C. 2015. Variability in Light-Duty Gasoline Vehicle Emission Factors from Trip-Based Real-World Measurements. *Environ. Sci. Technol.*, 2015, 49 (20), pp 12525–12534, DOI: 10.1021/acs.est.5b00553
- Pellecuer, L., Tate, J. and Chapman, S. 2016. How do traffic flow and emissions it produced vary through the day, week, season and year: evidence from big telematics data. The 21st International Transport and Air Pollution (TAP) Conference, Lyon, France, May 24-26, 2016.
- TfL. 2016. London Exhaust Emissions Study: Developing a test programme, and analysis of emissions data from passenger cars in London. [Accessed 12/04/2016 <http://content.tfl.gov.uk/london-exhaust-emissions-study-developing-a-test-programme.pdf>]
- Wyatt, D., Li, H., Tate, J. 2014. The impact of road grade on carbon dioxide (CO₂) emission of a passenger vehicle in real-world driving. *Transportation Research Part D: Transport and Environment*, 32, pp 160-170, October 2014, DOI: 10.1016/j.trd.2014.07.015

On the potential for lightweight electric vehicles to facilitate one-way trips in and around cities

Richard MOUNCE & John NELSON

Centre for Transport Research, University of Aberdeen, Kings College, Aberdeen, UK
Email: r.mounce@abdn.ac.uk

Abstract

One reason for the growing momentum behind electric vehicles is the emergence of mobility operators such as car-sharing companies. There is currently rapid growth in one-way car-sharing, although vehicle redistribution can be a problem in such systems. The Easily diStributed Personal Rapld Transit (ESPRIT) vehicle is a lightweight electric vehicle designed primarily to facilitate short one-way trips in and around cities. A key feature of the ESPRIT system is the capability for ESPRIT vehicles to be stacked together and driven in road trains; this makes the redistribution between locations much easier. A second key feature is the possibility of an entire train of vehicles being charged off a single charging facility. The paper details the ESPRIT system as well as its potential benefits, which include a) providing a convenient way to access public transport modes for people with and without cars; b) improving the air quality in city centres (since the vehicles are non-polluting) and c) reducing pressure on parking due to both their parking compactness (as they require around only a quarter of the space that conventional cars require) and the elimination of the need to park at popular locations such as train stations.

Keywords: Car-sharing, electric vehicle, charging, intermodality, redistribution.

Introduction

Cities (and to a lesser extent towns) are extremely significant to transport and travel patterns. First, they have large populations which mean that many trips originate and terminate in cities. Secondly, they have numerous attractions (e.g. employment locations, shopping and recreational facilities etc.) which mean that many trips by those living outside the city have their destination within the city. Many of these trips are facilitated by motorised transport and this means that there is generally a lot of traffic concentrated within cities.

There are downsides to having large volumes of traffic in cities. These high volumes of traffic often lead to congestion, which amounts to a huge waste of time, energy and money. Emissions from traffic are a major contributor to greenhouse gases. High levels of traffic have a major impact on urban air quality (Fenger, 1999). The adverse health effects of particulate matter are well documented and there are growing concerns regarding nitrogen dioxide (World Health Organisation, 2013). Other downsides include increased accident rates and noise pollution. In general, the extent of these problems is particularly striking in some of the larger cities in developing countries, but this is perhaps largely because cities in developed countries have had longer to refine their strategies for dealing with these traffic-related problems. Such strategies include:

- 1) *Car-free zones.* Car-free living is most easily satisfied in cities due to them affording better access to services and better public transport.
 - a) *Car-free cities.* The most extreme form of this is when cities are completely car-free. There are actually a reasonable number of such towns and cities across Europe, e.g. Venice which utilises water transport and Mdina in Malta which does not allow motor traffic inside the city walls.
 - b) *Pedestrianisation.* Most cities do allow cars into their centres, but many cities do have pedestrianised zones, which are streets or areas for use solely by pedestrians (and perhaps cyclists in some cases). The first purpose-built pedestrian street in Europe was the Lijnbaan in Rotterdam, opened in 1953. A large number of European towns and cities have made part of their centres car-free since the early 1960s. The impacts of pedestrianisation are assessed in Hass-Klau (1993).
 - c) *Car-free neighbourhoods.* Underlying car-free neighbourhoods is the exclusion of traffic and non-ownership of vehicles. There is evidence that car-free neighbourhoods are friendlier and more socially cohesive (Ornetzeder et al., 2008).

- d) *Car-free periods*. Many cities have had car-free days as a means of demonstrating the benefits to their citizens.
- 2) *Congestion charging*. Congestion charging is a form of road pricing. With road pricing, drivers must pay monetary fees in order to traverse some of the roads on the network. Economists have long advocated road pricing, but there is a debate about its economic efficiency (Raux et al., 2012). Road pricing ideally charges users the marginal congestion cost, which is the additional cost that users place on existing users (Button, 2004). Congestion charging attempts to deter road users from entering congested city centre areas by charging them a monetary fee, which can be fixed or variable (e.g. it might increase as the congestion increases). Congestion charging can result in time savings for travellers (Raux et al., 2012) as well as lowering rates of car ownership in the long term. However, the successful implementation of congestion charging relies not only on its design and implementation, but also on its public acceptability (Jaensirisak et al., 2005). Probably the most high profile scheme is the London Congestion Charge, which was introduced in 2003 and remains one of the largest congestion charge zones in the world. The charge's primary aim is to reduce high traffic flow in the central area, but has also raised investment funds for London's transport system (Zheng and Hensher, 2012).
 - 3) *Low emission zones*. A low emission zone (LEZ) is an area from which vehicles emitting pollutants over a given threshold are restricted access to, e.g. hybrid vehicles may be allowed, but internal combustion vehicles would not be. There are also ultra-low emission zones (ULEZs), which have extremely low emissions thresholds; and zero emission zones (ZEVs), which do not permit any vehicle emissions at all (so only fully electric vehicles would be allowed and not hybrids, along with pedestrians, cyclists and fully electric public transport). The aim of LEZs, ULEZs and ZEVs is to improve air quality in the area. The first LEZs in Europe were established in Stockholm in 1996. More than 200 cities and towns in 10 countries around Europe already have in place, or are preparing to launch LEZs. The EU air quality directive (2008/50/EC) required the limit values for particulate matter and nitrous dioxide to be achieved by 2005 and 2010- but these limits are exceeded by many European cities. Many cities have introduced LEZs to help meet these targets. Holman et al. (2015) investigated the effectiveness of LEZs in improving air quality.
 - 4) *Improvements to public transport and walking/cycling infrastructure*. The number of motorists in city centres can be reduced by making public transport more attractive since this will induce a modal shift away from the car. In terms of public transport, service reliability is a key factor for passengers. Intermodal connections are also important, since in replacing trips that might otherwise only be possible by car, it may be necessary to undertake these using multiple modes. An example of this is Park and Ride, in which drivers park outside of the city and take buses into the city centre. Provision of sufficient walking and cycling infrastructure is also important in encouraging use of these slow modes instead of the car. The availability of new technology (especially apps accessed via smartphones) is also being used to promote public transport and active travel.

There are trends emerging that are extremely relevant to the problem of city centre traffic as well as the measures listed above used to tackle them. These include:

- 1) *The decline in car ownership in the developed nations*. Car ownership rates have generally levelled off in developed countries (Goodwin, 2012) and has particularly dropped off amongst young men (Noble, 2005). Historically, the car-ownership saturation level was thought of in terms of everyone who wants a car having, whereas the reality is that congestion is reducing the private car's appeal in many areas. Hence, there has been a shift from car ownership towards car access.
- 2) *The emergence in the motor car market of electric vehicles*. This is also hugely important, in particular with reference to air quality and emissions. Section 1 will give more detail about the electric vehicle industry and how this relates to the above issues.
- 3) *The development of autonomous vehicles*. This has great potential to be a disruptive technology, since it has the potential to radically alter the way we approach transport.
- 4) *The potential shift towards 'mobility as a service'*. The essential idea of which is to see transport or mobility not as a physical asset to purchase (e.g. a car) but as a single customised service available on demand and potentially incorporating all transport services from cars to buses to rail. This would lessen the need to own a vehicle (or multiple vehicles as is often the case for families in the

developed world).

- 5) *The rapid emergence of car-sharing.* This is also hugely important to the issues above, since it has the potential to drastically reduce car ownership as well as reduce pressure on parking space. More detail will be given on car-sharing in Section 2. The ESPRIT one-way car-sharing system will be detailed in Section 3.
- 6) *The emergence of lift-sharing.* Lift-sharing, also known as ride-sharing and car-pooling, is when one or more distinct groups of travellers make use of a single vehicle at the same time. It has been growing rapidly and has the potential to make a sizeable reduction in the number of cars on the road. It has been promoted in the US by the introduction of dedicated car-pooling lanes on highways.

1. The electric vehicle industry

The internal combustion engine was not always the favoured engine used to power the motor vehicle. In fact, at the turn of the twentieth century there were more battery-operated electric motor cars in use in the USA than either steam or gasoline-powered (Hoffman, 1967). The severe range and speed limitations of storage batteries meant that it was not long before they went out of fashion. There was renewed interest in the USA in the 1960s and 1970s due, mainly due to the negative effects of air pollution and rising oil prices (Hoffman, 1967). However, they could not compete on price or performance with their petrol-fuelled counterparts and interest waned again. A renewed surge of interest in electric vehicles began in the early 1990s, but was somewhat dampened by the subsequent rather limited progress in battery technology, meaning that consumers were not satisfied with range, function and price. On the other hand, hybrid vehicles, which combine the internal combustion engine with the electric motor, flourished during the same period when electric vehicle take-up was faltering, with a noticeable example being the Toyota Prius. As well as electric vehicles, there has also been significant interest recently in hydrogen vehicles.

Recently there has been new momentum for battery electric vehicles resulting from both technological advances as well as developments in the social context of car mobility (Dijk et al., 2013). One of the key factors has been climate protection policies and targets, motivated by political concerns about climate change. A landmark event in the development of such policies was the Kyoto Protocol, ratified in 2002 and in effect from 2005, which established targets for emissions of greenhouse gases for nations signing up to it. As a consequence of Kyoto, green and fuel-efficient vehicles were subsidised in the developed countries; these subsidies not only encouraged production, but also provided much-needed investment in research and development. This investment was most needed in the battery sector. Car manufacturers recognised that battery technology was the key to improving electric vehicle performance and so started collaborating with battery manufacturers. Not only were electric vehicles beginning to become more affordable, their range was increasing to the point where it was becoming less of an issue. There has also been substantial investment in the charging infrastructure, which is vital to the practical operation and hence success of electric vehicles. The emergence of mobility operators, in particular car-sharing operators, has also been a major factor in boosting the electric vehicle industry. In car-sharing, a car is rented on a per-ride basis from the operator, who both owns and is responsible for the maintenance of the vehicle. Car-sharing will be covered in greater detail in Section 2.

Dijk et al. (2013) identify a number of factors that are crucial to the success of electric car mobility, including:

1. *The degree of investment in the necessary infrastructure.* There needs to be sufficient charging points, in terms of coverage (so that consumers are reassured about not running out of fuel) and capacity (to support a larger number of electric vehicles on the road, particularly in and around cities where traffic is much higher).
2. *Developments in mobility.* These include the trends mentioned above, i.e. the shift towards mobility as a service and also the rise of car-sharing. The success of car-sharing will boost the electric vehicle industry since it overcomes one of the main barriers in the high purchase price of electric vehicles. In addition, better systems of intermodality will also benefit the electric vehicle industry, because an electric vehicle may be used for part of a trip in conjunction with other modes; this is particularly relevant when viewed in the context of car-sharing which eliminates the need for parking once a user finishes with the vehicle. This leads directly to and expands potential for car-sharing, particularly as technological

advances can help address the demands of all age groups more effectively than in the past.

3. *Developments in the global car manufacturing industry.* There has been significant growth in automobile sales in developing countries (Zhou, 2011). Of particular importance is China, which has focussed more on electric vehicle production. Electric vehicles require fewer parts than cars using the internal combustion engine (e.g. an engine or exhaust), meaning that the modular nature of car production poses less of a barrier to their production by emerging enterprises than for cars using the internal combustion engine. The ever-increasing efficiency of cars using the internal combustion engine, combined with their generally lower price, should not be forgotten, in terms of their competition with electric vehicles.
4. *Energy sector and climate policies.* Peak oil is the point in time when the maximum rate of extraction of petroleum is reached, after which it is expected to enter terminal decline (Hirsch et al., 2005). There have been many predictions of when peak oil might occur, many of which have now been shown to be incorrect given that oil production has continued to grow, albeit slowly, mainly due to innovations in oil field technology. If production does start to slow, it will put upward pressure on oil prices. Electricity prices will rise too, but to a lesser extent. Climate policies are stimulating renewable energy generation and contributing to electric mobility, since transport emissions are a key source of greenhouse gases. In turn, the fact that renewable energy generation is characterised by intermittent supply suggests the opportunity for BEVs to be used to store such electricity, via smart-grid systems.

There are a number of positive feedback mechanisms working in favour of electric vehicles (Dijk et al., 2013). Shepherd et al. (2012) provide a systems dynamics model of the UK take-up of electric vehicles over the next forty years.

2. Car-sharing

Car-sharing is a model of car rental in which customers rent cars for short periods of time, e.g. by the hour, from a car-sharing operator, who owns all of the vehicles and is responsible for their maintenance. The prime driver behind car-sharing is the fact that cars are massively underutilised, given that most cars are used to transport a single person and are used for less than an hour a day. In fact, consumers often purchase vehicles that exceed their needs. They also have different needs for different types of trips. Car-sharing enables people to have access to a car without the need to own one; this is attractive to customers who make only occasional use of a car, since everything is on a pay-as-you-use basis. A car-sharing operator typically has a fleet of vehicles incorporating different types (e.g. sports car, passenger carrier, four-wheel drive etc.) and hence can cater to customers who want to make use of different vehicle types for different types of trip. Car-sharing membership eliminates the purchase price of cars and reduces the costs associated with car ownership such as insurance, maintenance and depreciation. Electric vehicles have been burdened by their high purchase price, but car-sharing operators can utilise electric vehicles and yet be competitive. Car-sharing also fits in with the new paradigm of 'mobility as a service'. Car-sharing can play a key role in reducing the number of cars on the road, since replacement rates can be as high as 15:1, i.e. 15 prior car owners can be accommodated by 1 vehicle on average. In addition, car clubs often have incentives for people to trade in their car when joining the scheme. People who have driven electric vehicles have increased willingness to forgo a private car purchase (Finkorn and Muller, 2015). Car-sharing is able to perform different roles depending on the user. Travellers with a tendency towards car use may use car-sharing as a substitute for public transport, whereas those with a tendency towards public transport user will use car-sharing in conjunction with public transport rather than making the same journey by car. Overall, car-sharing is considered to be complementary to public transport use, since it makes possible journeys that would otherwise only be possible using a car for the whole journey.

The first known car-sharing program was the Selbstfahrergenossenschaft car-share program in a housing cooperative that got underway in Zürich in 1948 (Shaheen et al., 1998), but there was no known formal development of the concept in the next few years. A much more ambitious project called the Witkar was launched in Amsterdam by the founders of the 1968 white bicycles project, and it endured into the mid-1980s before finally being abandoned. There was slow growth in the 1980s and the early 1990s, mainly of smaller non-profit systems. Zipcar, Flexcar (which was bought by Zipcar in 2007) and City Car Club were all formed in 2000. Several car rental companies launched their own car sharing services beginning in 2008, including Hertz, Enterprise and Avis. By 2010, when various peer-to-peer

car-sharing systems were introduced, Zipcar accounted for 80% of the U.S car sharing market and half of all car-sharers worldwide, with 730,000 members sharing 11,000 vehicles by September 2012. Car-sharing has also spread to the developing world because population density is often a critical determinant of success for car-sharing and developing nations often have highly dense urban populations. At time of writing there are hundreds of car-sharing operators in operation throughout the world. Car-sharing is thriving in Germany, where there were 1.26 million car-sharing customers registered at the start of 2016.

In one-way car-sharing, the user picks up the vehicle from a station or some other location and drops it off at their destination. This often means that vehicles become unbalanced over time, i.e. end up in locations where they are not needed. This then poses a problem of the operator having to redistribute the vehicles, which can be costly. The Autolib' car-sharing service, begun in Paris in 2011, offers its users an incentive (e.g. a free trip) to help redistribute its vehicles.

In free-floating car-sharing systems, cars can be picked up and dropped off at any location. Generally users utilise a smartphone app to locate available vehicles. The first free-floating car-sharing system was car2go, launched by the car manufacturer Daimler in 2009 in the city of Ulm, Germany, and offering a mixed fleet of electric and gasoline vehicles. A new trend is for combined car-sharing services that provide both free-floating and station-based cars within one tariff; these now operate in four German cities and in the Rhein-Main region. Europe has more than two thirds of all free-floating car-sharing operators.

The rise of car-sharing and particularly one-way car-sharing has been rapid. However, there are a number of barriers that need to be overcome for car-sharing to become more widespread; these include regulatory issues, the need for the necessary charging infrastructure (for electric vehicle fleets) and changes in users' mobility and car ownership patterns. At the same time there are many factors working in favour of car-sharing. Many building developers are now incorporating share-cars into their developments as an added value to tenants, and this is being promoted by municipal government bodies (Melia, 2014). There is also clearly synergy with the emergence of electric as well as autonomous vehicles. Fully autonomous vehicles have the potential to completely transform urban mobility: when vehicles complete their trips they would simply be able to drive themselves back to the depot, which would make free-floating car-sharing much easier. The success of car-sharing systems depend on a number of preconditions for success: urban populations of significant scale and diversity (including not just predominantly commuters); having adequate infrastructure including both charging and parking facilities; and having the local authorities on board with the scheme.

3. The ESPRIT one-way car-sharing system

ESPRIT is an EU-funded Horizon 2020 project which is aiming to develop a purpose-built, lightweight L-category electric vehicle with novel elements including the capacity for forming road trains of up to eight vehicles and the capability to charge the entire road train from a single charging point. A preliminary test and demonstration of three prototype vehicles will take place in 2018 at three different geographical pilot sites: Glasgow (UK), Lyon (France) and L'Hospitalet de Llobregat (Spain).

Two main use-case scenarios are foreseen for the ESPRIT vehicle (see Figure 1):

1. *A one-way redistributed car-sharing system within city centres.* These trips will generally be short and will be for a variety of trip purposes, e.g. commuting, shopping, tourism, etc.
2. *A first and last kilometre personal mobility system to and from existing public transport interchanges in suburban areas.* For these trips ESPRIT will be used for part of a trip in conjunction with other modes. These first and last kilometre journey legs will mainly be between travellers' homes and suburban transport interchanges. ESPRIT will also facilitate such trips on business parks and campuses.

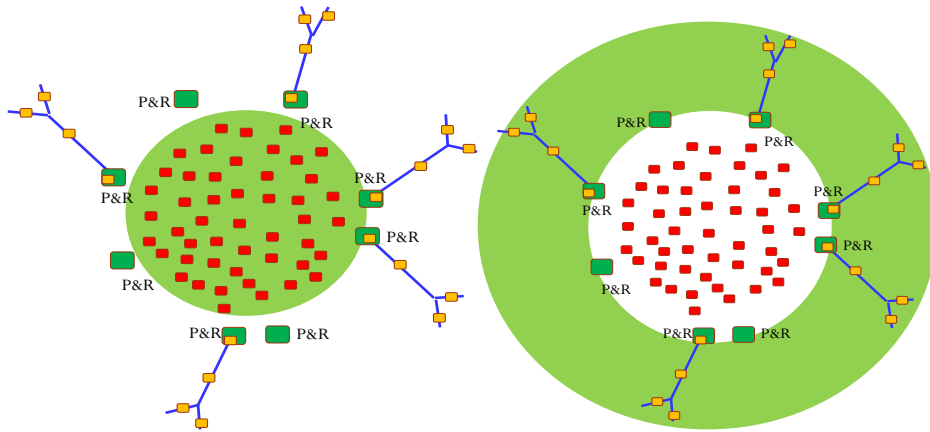


Figure 1. ESPRIT use case scenarios

The capability of ESPRIT vehicles to be driven in road trains is a key feature of the vehicle. Pioneering coupling systems mean that up to 8 ESPRIT vehicles can be nested together in a road train, which consists of the lead vehicle towing the other seven. The ESPRIT vehicle includes the following systems related to the vehicle's operation in a road train:

1. *A Guiding and Coupling System.* This allows the vehicles to be linked together electromechanically and performs the coupling action in a semi-automatic way. This is particularly critical in terms of security and operating safety of the system).
2. *A Powertrain and Steering Control System.* This is linked to the steering, propulsion and braking equipment and enables the road train to work safely in forward and reverse gear. In particular, it will prevent lateral oscillations (sway) and toppling, jack-knifing and trajectory drift of the road train.

The capability for ESPRIT vehicles to be driven in road trains enables the efficient redistribution of vehicle fleets and contributes to a smartly-balanced and cost-efficient transport system.



Figure 2. The ESPRIT road train

A train of ESPRIT vehicles can be charged using a single charging station. Battery loads are dynamically balanced in order to prioritise charging towards the front of the road train, ensuring that the lead vehicle is ready for the user to drive away when required. The capability for charging in road trains means that fewer charging facilities are needed compared to conventional charging.

It was noted in section 2 that the biggest challenge in one-way car-sharing is vehicle redistribution: vehicles accumulate in places where they are not required and there are no vehicles available where demand is high. The ESPRIT transport system is well placed to tackle this challenge through its ability to redistribute up to eight vehicles at a time in a road train, which will vastly reduce redistribution costs. Boldrini et al. (2016) study the spatial and temporal patterns of station utilisation in a one-way car-sharing system. The ESPRIT project is targeting, and seeking to demonstrate through simulation, that the ESPRIT system can achieve a 90% availability rate across all stations; this compares favourably with many of the current one-way car-sharing systems which have 50% of stations empty several times per day.

In order to bring the ESPRIT vehicles to the market, they have to comply with various legal and technical requirements in different countries. The ESPRIT single vehicle could be classified as vehicle

type L7e-CP (heavy quadri-mobile for passenger transport). However, there is no applicable legal framework for the homologation of the ESPRIT road train as such. The ESPRIT consortium are working towards producing recommendations for development of regulations and standards to enable ESPRIT vehicles to be driven in road trains by an operator, as well as to enable the general public to drive an ESPRIT vehicle in a road train of two vehicles.

The introduction of ESPRIT will have impacts which will result in a number of benefits, including:

1. *Modal shift away from conventional private car.* It is anticipated that the introduction and success of ESPRIT will encourage citizens to use conventional public transport and car-sharing solutions, which will contribute towards lowering both congestion and pollution.
2. *Better integration with public transport.* Since ESPRIT is designed to be complementary to public transport by linking in with it, it will contribute to a move towards seamless intermodal transport. Reduced pressure on parking. Increases capacity as ESPRIT vehicle is smaller and more utilised.
3. *Reduced pressure on parking.* The intermodal and one-way nature of ESPRIT should eliminate the need for parking once a user finishes with the vehicle. In addition, the compactness of the ESPRIT vehicle results in significant space saving when they are parked since they require around only a quarter of the space that conventional cars require.

The ESPRIT project will utilise a number of modelling and simulation tools to predict the effects of deploying ESPRIT vehicles. The ESPRIT business model estimation tool will be able to accurately predict the economic viability of deploying the ESPRIT transport system in a variety of different urban/suburban configurations as well as the public transport modal share induced by the system. The model includes a number of sub-models, including:

1. *Demand and Revenue Model.* This will predict the demand for ESPRIT from analysing citizens' lifestyle criteria and their specific requirements for last kilometre and one-way car-sharing services.
2. *Operations Model.* This model determines how the car-sharing system operates in terms of where the charging stations are located and how vehicles are optimally redistributed.
3. *Business Case Model.* This model predicts the operating profits and cash flows using the operating costs and predicted demand and revenue.
4. *Review Model.* This model will provide initial forecasts as well as the facility to permit the testing of the influence of key variables such as cost, time, speed, fares, value of time, etc. on the modal choice, operating costs and revenues.

The ESPRIT project consortium will manufacture three fully-functional demonstrator vehicles as well as three additional appropriately weighted 'shell' vehicles (with the latter only being used as vehicles to be towed in the road train, of a maximum length of six vehicles in the demonstration as opposed to a maximum of eight as in the design). This will enable a complete functional validation of all sub-systems (including road testing) to be performed. It will also enable ESPRIT to be physically presented to end users, e.g. citizens, operators, decision makers and government authorities. Exposing these groups to ESPRIT will not only contribute to disseminating the ESPRIT concept, but will also provide feedback to the process of industrialisation, exploitation, further progressive deployment and overcoming regulatory barriers to implementation. The initial demonstration will function as a stepping stone towards further deployment of ESPRIT vehicles.

Conclusion

High volumes of traffic in cities can cause problems such as congestion and pollution. The use of electric vehicles can contribute towards better air quality in urban areas. The emergence of car-sharing operators is giving momentum to electric vehicles. One-way car-sharing is growing rapidly, but vehicle redistribution can be a problem. The ESPRIT vehicle is a lightweight electric vehicle designed for one-way car-sharing. The ESPRIT vehicles can be stacked together and driven in road trains; these features facilitate easy redistribution between locations. Another novel feature of the ESPRIT vehicle is that an entire train of vehicles can be charged off just a single charging facility. ESPRIT has the potential to deliver a number of benefits including improving urban air quality; reducing pressure on parking; and

promoting intermodal transport solutions.

Acknowledgments

This research was funded under grant agreement no. 653395 of the European Union's Horizon 2020 research and innovation programme.

References

- Boldrini, C., Bruno, R. and Conti, M. (2016) Characterising demand and usage patterns in a large station-based car sharing system. *IEEE Smart City 2016*.
- Button, K. (2004) The rationale for road pricing: standard theory and latest advances. *Research in Transport Economics* 9, 3-25.
- Dijk, M., Orsato, R.J. and Kemp, R. (2013) The emergence of an electric mobility trajectory. *Energy Policy* 52, 135-145.
- Fenger, J. (1999) Urban air quality. *Atmospheric Environment* 33 (29), 4877–4900
- Firnkorn, J. and Müller, M. (2015) Free-floating electric car-sharing-fleets in smart cities: The dawning of a post-private car era in urban environments? *Environmental Science and Policy* 45, 30–40.
- Goodwin, P. (2012) Peak Travel, Peak Car and the Future of Mobility: Evidence, Unresolved Issues, Policy Implications, and a Research Agenda. Discussion Paper No. 2012-13 Prepared for the Roundtable on Long-Run Trends in Travel Demand. DOI:10.1787/5k4c1s3l876d-en.
- Hass-Klau, C. (1993) Impact of pedestrianization and traffic calming on retailing: A review of the evidence from Germany and the UK. *Transport Policy* 1(1), 21–31.
- Hoffman, George A. (1967) Systems design of electric automobiles. *Transportation Research* 1, 3–19.
- Holman, C., Harrison, R. and Querol, X. (2015) Review of the efficacy of low emission zones to improve urban air quality in European cities. *Atmospheric Environment* 111, 161–169.
- Hirsch, R. L., Bezdek, R. and Wendling, R. (2005) Peaking of world oil production: Impacts, mitigation and risk management. http://www.netl.doe.gov/publications/others/pdf/Oil_Peaking_NETL.pdf, US Department of Energy.
- Jaensirisak, S., Wardman, M. and May, A.D. (2005) Explaining variations in public acceptability of road pricing schemes. *Journal of Transport Economics and Policy* 39(2), 127–153.
- Melia, S. (2014) Carfree and low-car development. *Parking Issues and Policies (Transport and Sustainability, Volume 5)*. Emerald Group Publishing Limited, 5, 213-233.
- Noble, B. (2005) Why are some young people choosing not to drive. Department for Transport, London.
- Ornetzeder, M., Hertwich, E. G., Hubacek, K., Korytarova, K. and Haas, W. (2008) The environmental effect of car-free housing: A case in Vienna. *Ecological Economics* 65(3), 516-530.
- Raux, C., Souche, S. and Pons, D. (2012) The efficiency of congestion charging: Some lessons from cost-benefit analyses. *Research in Transportation Economics* Emerald 36, 85-92.
- Shaheen, S., Sperling, D. and Wagner, C. (1998) Car-sharing in Europe and North America: Past, Present and Future. *Transportation Quarterly* 52 (3), 35–52.
- Shepherd, S., Bonsall, P. and Harrison, G. (1998) Factors affecting future demand for electric vehicles. *Transport Policy* 20, 62–74.
- World Health Organisation (2013) Review of the evidence on health aspects of air pollution- REVIHAAP Project Technical Report, Copenhagen.
- Zhou, L. (2011) The Strategies for Entering the Next Generation Automotive Market in China: Frontiers of Local Innovations. Nikkei BP, Tokyo.

Portable Emissions Measurement System (PEMS) data for Euro 6 diesel cars and comparison with emissions modelling

R.S. O'Driscoll¹, H.M. ApSimon², T. Oxley³, N. Molden⁴

^{1,2,3} Centre for Environmental Policy, Imperial College London, London, SW7 1NA, United Kingdom

⁴ Emissions Analytics, Kimball Smith Limited, Kings Worthy House, Court Road, Kings Worthy, Winchester, SO23 7QA, United Kingdom

Abstract

This paper reviews the emissions performance of 39 Euro 6 diesel passenger cars using a Portable Emissions Measurement System (PEMS). Comparisons are made with current emissions regulations (in particular the Euro 6 standard for nitrogen oxides ($\text{NO}_x = \text{NO} + \text{NO}_2$) of 0.80 g km^{-1}) and predictions by the speed dependent emission factors of COPERT.

The mean NO_x emission was $0.36 \pm 0.36 \text{ g km}^{-1}$, the mean nitrogen dioxide (NO_2) emission was $0.17 \pm 0.19 \text{ g km}^{-1}$. The average fraction NO_x emitted as NO_2 (known as primary NO_2 or fNO_2) was 44%. Each vehicle was analysed over a test route composed of urban and motorway driving. On average NO_x emissions were 5.3 times the Euro 6 limit for urban driving and 3.8 times the limit for motorway. A wide range of deviation ratios (ratio between real world measurements and type approval limit) were found, the highest being 27.3 for an urban section. The average PEMS measured NO_x emission was 1.6 times COPERT's average estimate. Similarly with primary NO_2 (44% compared to 30% assumed by COPERT).

Scenario analysis was then performed to assess the sensitivity of the mean annual roadside concentrations of NO_2 to the discrepancies between type approval limits, COPERT estimates and on road emissions measured by PEMS.

Key-words: Euro Standards, Primary NO_2 , Nitrogen oxides (NO_x), COPERT, On-road emissions, Diesel passenger cars, Portable Emissions Measurement System (PEMS), Euro 6

Introduction

Successive Euro Standards have failed to effectively reduce urban concentrations of nitrogen dioxide (NO_2) (Beevers et al. 2012; Carslaw et al. 2011; Franco et al. 2013). In this paper we will investigate the real world nitrogen oxides ($\text{NO}_x = \text{NO} + \text{NO}_2$) emissions of the latest Euro 6 standard diesel vehicles, compare these to estimates from emissions modelling and evaluate what this could mean for future urban air quality.

A key focus of this paper is primary NO_2 ($f\text{NO}_2$, the amount of NO_x emitted directly as NO_2). When NO_x is released into the atmosphere as a mixture of NO and NO_2 chemical reactions take place with ozone (O_3), which reacts with the NO component to produce nitrogen dioxide. This is balanced by the photo-dissociation of NO_2 to NO . Given well mixed air and sufficient time this results in an equilibrium ratio of NO_2 to NO_x (depending on the total oxidant as the sum of ozone and NO_2 (Clapp & Jenkin 2001)). However at road-side locations there is insufficient time for such reactions during dispersion and mixing of fresh emissions, and often ozone is already depleted in busy streets limiting reaction with NO . In these circumstances the proportion of NO_x emitted directly as primary NO_2 becomes very important. Hence primary NO_2 is particularly important for road-side concentrations of NO_2 near busy roads. Introduction of successive Euro standards has marked an increase in the percentage $f\text{NO}_2$, mainly attributed to the addition of oxidative after-treatment systems known as diesel oxidation catalysts (DOCs) (Grice et al. 2009; Alvarez et al. 2008; Carslaw et al. 2011).

To evaluate the real world performance of Euro 6 diesel vehicles a Portable Emissions Measurement System (PEMS) has been used. PEMS devices can be fitted to the tailpipe of nearly all vehicles without any modification, they then record real time emissions as the vehicles drive on open roads. PEMS were approved for EU engine certification of heavy duty engines in 2009, becoming mandatory for heavy duty type approval in 2011 (EC, 2011, 2009). Their introduction into test procedure is expected to reduce the problem of NO_2 exceedances in urban areas (Degraeuwe et al., 2015; Weiss et al., 2012). As of September 2017 new models being registered for sale in the EU will be subject to a real driving emissions (RDE) test procedure using PEMS (EC, 2015a). The on road NO_x emission limit will be higher than the Euro 6 standard of 0.08 g km^{-1} . The RDE emission limit will take the form of a not-to-exceed (NTE) value dependant on a conformity factor, the agreed conformity factor for NO_x of 2.1 (NTE limit of 0.168 g km^{-1}) will be legally binding from September 2017 (Europarl, 2016).

The emissions model used for comparison in this study is COPERT (Computer Program to Calculate Emissions from Road Transport). COPERT is developed by the European Environment Agency and is the tool recommended by the European Monitoring and Evaluation Program (EMEP). It is currently used in 22 out of the 28 EU member states for road transport emissions and projections (Kioutsioukis et al. 2010). To evaluate the possible implications of discrepancies between PEMS measurements and COPERT 4v11 estimates modelling was performed for different road flows and backgrounds for the year 2030.

Method

39 Euro 6 diesel passenger cars were monitored by Emissions Analytics over a set route in the Greater London area. All vehicles were tested on the same route (with minor variation due to unavoidable circumstances such as road works). The route

chosen was composed of motorway and urban driving (here urban is taken to mean a road in an urban/ residential area with a speed limit of 30mph). To analyse the difference in emissions between urban and motorway driving each trip was also broken down (by purpose built software which identified locations by GPS) into its composite urban and motorway parts. These shall be referred to as urban/ motorway sections whereas the whole journey shall be referred to as the trip.

As driving style (i.e. aggressive acceleration) can have large effect on the emissions of a vehicle the tests were evaluated to ensure the driving style was representative of normal driving and uniform throughout the study. The driving style for each trip was evaluated using the Relative Positive Acceleration (RPA) (Weiss et al. 2011; Thompson et al. 2014) metric and found to be within the World Harmonised Light-Duty Test bounds for normal European driving (average 0.1 m s^{-2} and 0.2 m s^{-2} for motorway and urban respectively (Tutuianu et al. 2013)).

Test Vehicles

The vehicles ranged in engine size from 1.4ℓ- 3ℓ and deployed the three main NO_x after treatment technologies Lean NO_x Traps (LNT), Selective Catalytic Reduction (SCR) and Exhaust Gas Recirculation (EGR) (vehicles in the study fitted with LNT and SCR were also fitted EGR in combination, vehicles referred to as EGR are fitted with EGR alone). Vehicles were tested from 13 different manufactures. The distribution of engine sizes (average 2 ℓ), abatement technologies (7 EGR, 19 LNT and 13 SCR) and manufactures are comparable to the EU average to ensure the study is representative; the 13 manufactures sampled provided 70% of the new car fleet in 2016 (Eurostat 2013; ICCT 2015; SMMT 2016). Table 1 lists the vehicles in the study and their characteristics.

Data Analysis

Cold starts (classified as the first 300 seconds of the journey (Weiss et al. 2011)) have been removed, this was to ensure continuity as all vehicles were not able to soak overnight.

Emissions are reported as the trip or section average in grams per kilometre (g km^{-1}) which is calculated by summing the total emissions in a section/ trip and dividing by total distance travelled. The Deviation Ratio (DR, sometimes called conformity factor) is also used to evaluate results. The DR is a measure of by how many times a vehicles emissions exceed the relevant Euro Standard. In this study-

$$\text{Deviation Ratio} = \frac{\text{average section emission in } \text{g km}^{-1}}{\text{Euro 6 standard } (0.08 \text{ g km}^{-1})}$$

Results are presented as the mean and standard deviation.

Table 1. Specification of test vehicles

Vehicle ID	Year of manufacture	Engine displacement [l]	Mileage at start [km]	NO _x after treatment
E1.5	2015	1.5	1675	EGR
E1.6	2014	1.6	2363	EGR
E2.2a	2012	2.2	6013	EGR
E2.2b	2012	2.2	225	EGR
E2.2c	2013	2.2	1164	EGR
E2.2d	2015	2.2	590	EGR
E2.2e	2015	2.2	531	EGR
L1.4a	2014	1.4	2245	LNT
L1.4b	2014	1.4	1463	LNT
L1.5	2015	1.5	1263	LNT
L2.0a	2015	2.0	1059	LNT
L2.0b	2014	2.0	2568	LNT
L2.0c	2014	2.0	745	LNT
L2.0d	2015	2.0	451	LNT
L2.0e	2015	2.0	1312	LNT
L2.0f	2013	2.0	2019	LNT
L2.0g	2014	2.0	640	LNT
L2.0h	2014	2.0	2563	LNT
L2.0i	2015	2.0	2910	LNT
L2.0j	2014	2.0	1000	LNT
L2.0k	2014	2.0	1492	LNT
L2.0l	-	2.0	742	LNT
L2.0m	2014	2.0	4356	LNT
L2.0n	2015	2.0	4276	LNT
L2.0o	2014	2.0	1696	LNT
L2.0p	2014	2.0	4192	LNT
S1.6a	2014	1.6	2406	SCR
S1.6b	2014	1.6	544	SCR
S1.6c	2013	1.6	2178	SCR
S1.6d	2014	1.6	2028	SCR
S2.0a	2015	2.0	2502	SCR
S2.0b	2015	2.0	2093	SCR
S2.0c	2014	2.0	2567	SCR
S2.0d	2014	2.0	5270	SCR
S2.0e	2013	2.0	4061	SCR
S2.0f	2014	2.0	3842	SCR
S2.0g	2015	2.0	1184	SCR
S3.0h	-	3.0	1861	SCR
S3.0i	-	3.0	1393	SCR

- data not available

PEMS testing

The on- road tail pipe emissions were measured by Emissions Analytics using a SEMTECH-DS, developed by Sensors Inc (Sensors Inc 2010). SEMTECH-DS PEMS measurements fulfil official emissions testing requirements of the EU and US and have been found to be accurate within the range of lab based testing methods (EPA 2008b; EPA 2008a; EC 2011; Weiss et al. 2012).

The SEMTECH unit includes multiple gas analysers, a GPS receiver (recording vehicle speed, latitude, longitude and altitude), exhaust flow meter and an interface for connection to the vehicles on- board engine diagnostics (OBD) port. Non-Dispersive Ultraviolet (NDUV) is used to measure nitric oxide (NO, reported as NO₂) and NO₂ simultaneously and separately with NO_x calculated as the sum of both (Sensors Inc 2014). For further detail on PEMS installation and SEMTECH-DS see (Hu et al. 2012; Weiss et al. 2012; Kousoulidou et al. 2013). Leak tests along with zero and span calibration tests were performed before and after each trip in line with recommendation.

PEMS are powered by external batteries meaning engine operation is not effected apart from by additional weight. The PEMS weigh 95kg (equivalent to an additional passenger) the drivers then bring the additional weight to 220kg. This weight is uniform for each test. Additional weight may bias results by affecting the power to mass vehicle ratio (Weiss et al. 2012) and potentially increasing CO₂ emission by up to 3%; it is reasonable to assume a similar margin for NO_x (Fontaras & Samaras 2010; Weiss et al. 2012).

COPERT

The latest COPERT (4v11) speed dependant emission factors were used to generate an average COPERT emission estimate for each trip. This is done using the road links method previously used by the INCERT model (Kousoulidou et al. 2013) whereby the PEMS speed profile is split into equal one km lengths, the average speed of each link calculated and the relevant speed dependent emission factor applied to each length. In turn this generated a COPERT emissions profile from which an average can be taken. This process was performed by specialised software created by the authors and the iMove model (Valiantis et al. 2007).

Results and Discussion of PEMS data

Figure 1 shows the trip average NO and NO₂ emissions of each vehicle, there was huge variability within the results. 2 vehicles (S2.0e, L2.0b) met the Euro 6 limit of 0.08 g km⁻¹, a further 2 vehicles (L2.0a, S2.0b) were within 10% of the Euro 6 limit. This shows that with current technology both LNT and SCR (when used in conjunction with EGR) are capable of meeting the Euro 6 emission limit during real world driving. The mean trip average emissions (0.36 ± 0.36 g NO_x km⁻¹) correspond

to a DR of 4.5, the highest deviation ratio was 22 by vehicle S3.0h. 11 vehicles met the not-to-exceed limit (DR < 2.1).

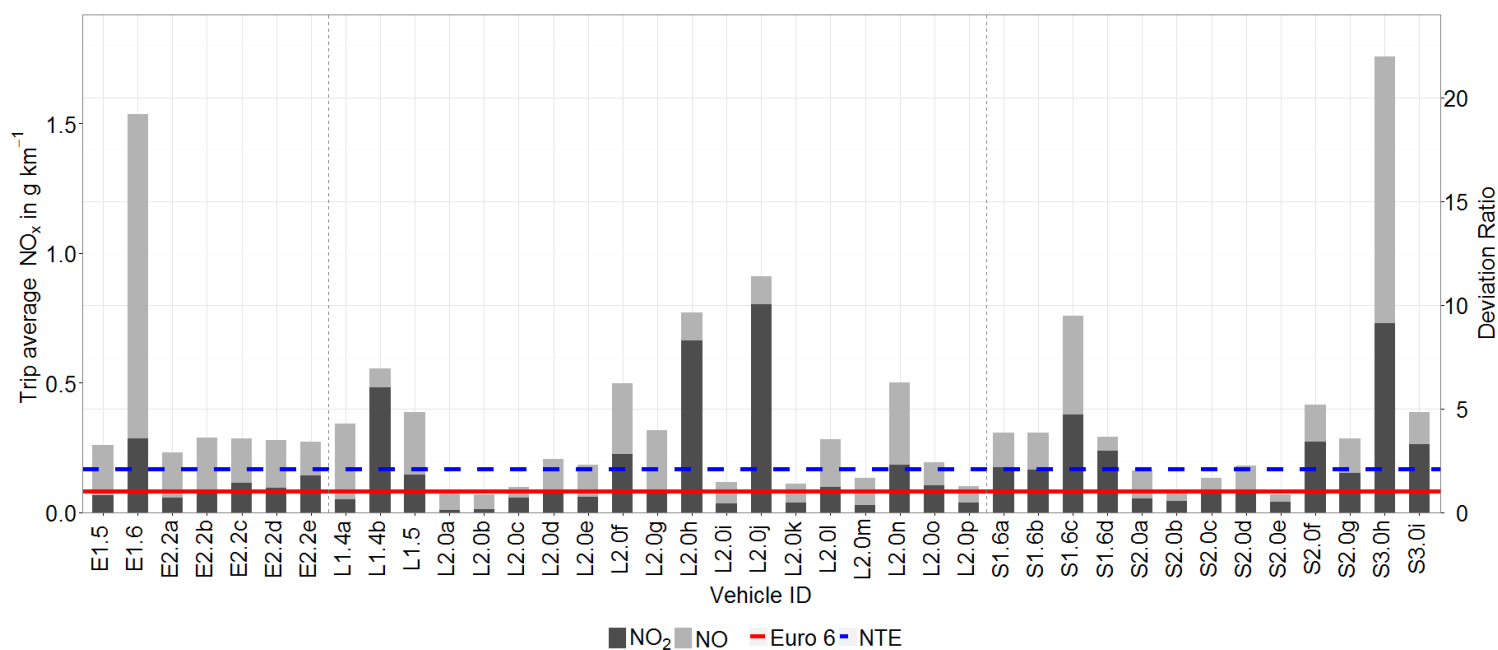


Figure 1. PEMS measurements showing trip average NO_x and NO₂ for 39 Euro 6 diesel vehicles

Of the 39 vehicles, 22 exceeded the Euro 6 NO_x standard with NO₂ (dark grey) emissions alone (i.e. trip average over 0.08 g NO₂ km⁻¹). The PEMS average NO₂ emission was 0.17 ± 0.19 g NO₂ km⁻¹, over double the Euro 6 limit for total NO_x. Our results show high values of absolute NO₂ emissions with the highest being 0.801 g km⁻¹, ten times the Euro 6 limit for total NO_x. The average fNO₂ of the trip was 44 ± 20%. Of the 11 vehicles that met the NTE limit one (S2.0c) exceeded the Euro 6 limit with NO₂ alone, this highlights the problem with regulating NO_x levels whilst having no legal limit for NO₂.

Comparison with COPERT

In Figure 2 we compare the PEMS measurements (red) for NO_x and NO₂ to the COPERT estimates (green). As expected (due to all trips having very similar speed and distance characteristics) COPERT's estimates display very little variation, this is because COPERT aims to provide an average for the fleet. The PEMS averages were higher in some instances and lower in others but overall were higher. The PEMS average NO_x was 1.6 times the COPERT average of 0.23 ± 0.01 g NO_x km⁻¹ (DR=2.9), the average NO₂ estimate, 0.07 ± 0.003 g NO₂ km⁻¹, was 2.5 times lower than the PEMS measured average. The PEMS average fNO₂ (44 ± 20%) was higher than the 30% assumed by COPERT.

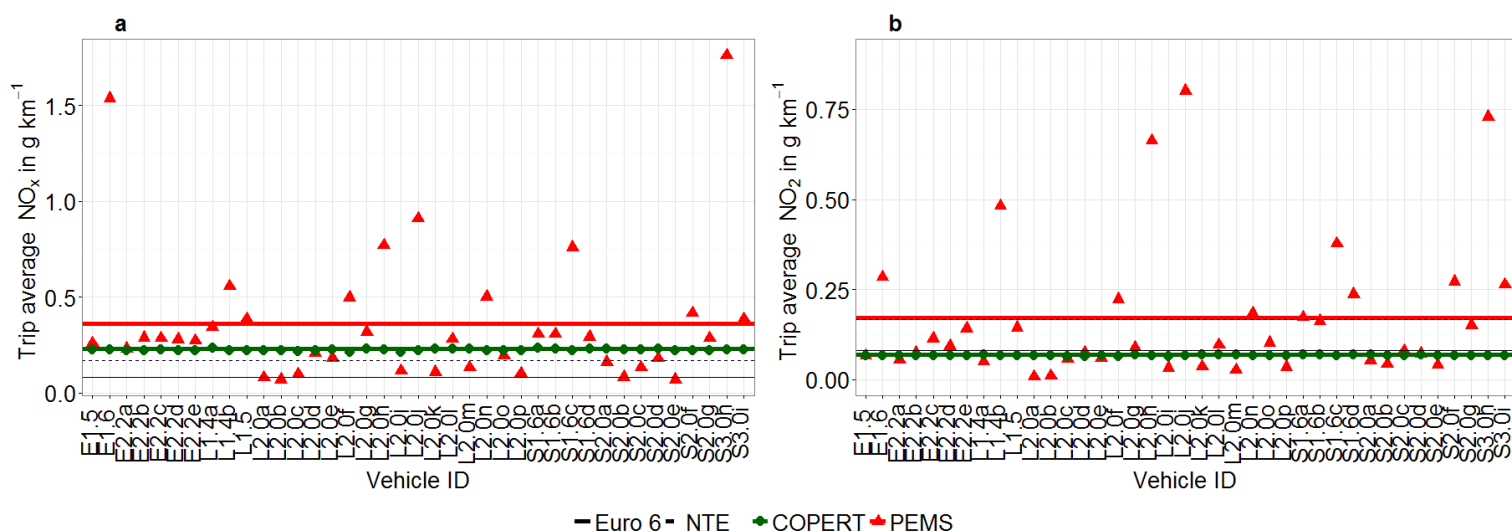


Figure 2. Comparison of COPERT 4v11 projections to PEMS measurements for NO_x (a) and NO₂ (b). Green line is COPERT average, red line is PEMS average

Within the results 5 vehicles particularly stand out as the worst; L2.0h, S3.0h, E1.6, S1.6c and L2.0j. These vehicles all have on road emissions higher than 0.63 g NO_x km⁻¹ (the average COPERT 4v11 emission factor for Euro 5). We find that when these 5 are removed the PEMS average becomes much more aligned to the COPERT average estimate and the standard deviation is greatly reduced. This indicates that to effectively reduce NO₂ concentrations in hotspot urban areas policy makers should consider discriminating on the basis of actual on road emissions as opposed to Euro class.

Table 2. Effect of removing 5 worst vehicles

	PEMS average before	PEMS average worst 5 removed	COPERT average
NO_x	0.36 ± 0.36 g NO _x km ⁻¹ DR=4.5	0.25 ± 0.13 g NO _x km ⁻¹ DR=3.1	0.23 ± 0.01 g NO _x km ⁻¹ DR=2.9
NO₂	0.17 ± 0.19 g NO ₂ km ⁻¹	0.11 ± 0.10 g NO ₂ km ⁻¹	0.07 ± 0.003 g NO ₂ km ⁻¹

Urban and Motorway sections

The sections of the trip identified by GPS as urban and motorway driving are now analysed. When compared to their motorway counterparts urban NO_x emissions were 1.7 ± 1.0 times higher, though there was large variability and in some cases urban emissions were lower. Urban sections average NO_x emissions were 0.43 ± 0.42 g km⁻¹, DR = 5.4, motorway section emissions were 0.31 ± 0.37 g NO_x km⁻¹, DR = 3.9. The highest urban deviation ratio was 27.3 for vehicle S3.0h. fNO₂ was not significantly different (45 ± 21%) to the trip average.

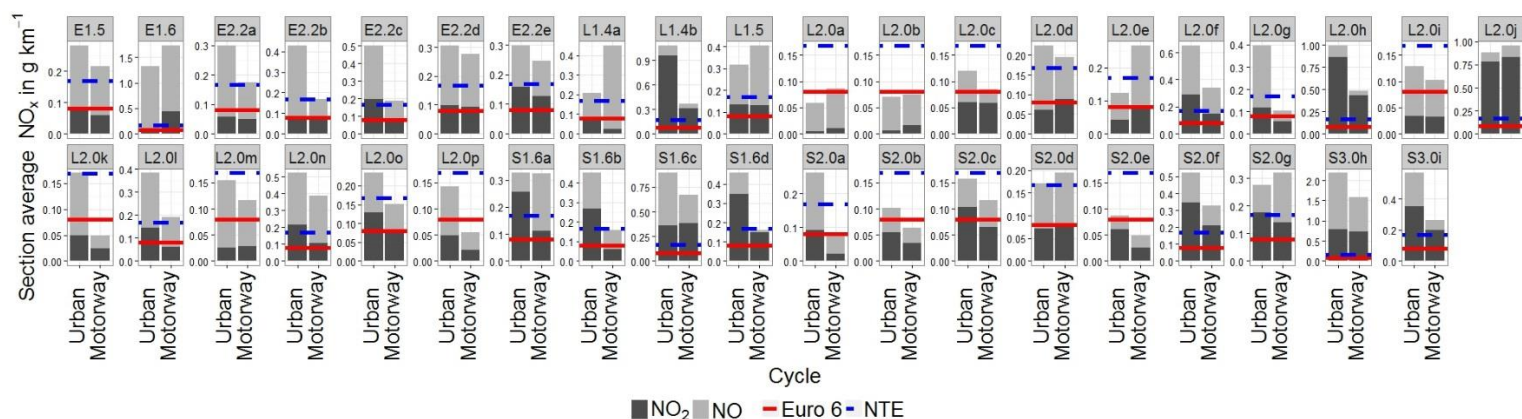


Figure 3. Comparison of urban and motorway trip average NO_x emissions (caution y-axis scale varies)

Modelling of implications for roadside concentrations

COPERT speed dependant emission factors, emissions regulation and the findings from the PEMS measurements have been used to inform six Euro 6 diesel NO_x emission factors and fraction primary NO₂ scenarios. These six scenarios have been modelled for the year 2030 by the UK Integrated Assessment model UKIAM (Oxley et al. 2013; Oxley. More specifically the Background, Road and Urban Transport modelling of Air quality (BRUTAL (Oxley et al. 2009)), which is the road transport high resolution (1km) module of the UKIAM designed to model roadside concentrations of air quality pollutants in urban environments. BRUTAL takes aggregated vehicle and technology dependant emissions factors for PM₁₀ and NO_x from iMove and applies them spatially (using a bottom up approach). The scenarios have been chosen to represent the different deviation ratios of the Euro 6 diesel cars and also variation in the percentage primary NO₂.

Table 3. Description, average NO_x emissions factors and NO₂ fraction of scenarios

Average Euro 6 emissions...	Scenario name	NO _x [g/km]	Average DR	f-NO ₂	
				a – 0.3	b – 0.44
S1 ... meet the Euro 6 standard	S1	0.08	1.0	a – 0.3	b – 0.44
S2 ... meet the Euro 6c standard (as modelled by COPERT 4v11)	S2	0.10	1.3	a – 0.3	b – 0.44
S3 ... meet the 2017 not-to-exceed real world limit	S3	0.17	2.1	a – 0.3	b – 0.44
S4 ... as modelled by COPERT 4v11 speed dependant emission factors	S4	0.19	2.4	a – 0.3	b – 0.44
S5 ... are those found by the O’Driscoll et al. PEMS study	S5	0.34	4.5	a – 0.3	b – 0.44
S6 ... are those found by the O’Driscoll et al. PEMS study differentiating between motorway and urban driving	S6 Motorway	0.31	3.9	a – 0.3	b – 0.44
	A, B,C	0.43	5.4		

Results of modelling (2030)

Figure 4 shows the results of the scenario analysis; a, b, and c represent different background levels of NO₂ categorised as low (8-11µg m⁻³), medium (13-16 µg m⁻³) and high (18-22 µg m⁻³). At each background level 5 different roads with different flows (in vehicles per day) were modelled, these are labelled with the corresponding flow in the legend (e.g F = 25000). All locations represent urban driving (i.e. A, B or C roads in built up urban or residential areas) and have the same traffic mix of diesel cars (44% diesel with 91% Euro 6). Each scenario has its own tile for each background level and the line joins Sa (fNO₂ = 0.3) to Sb (fNO₂ = 0.44). The steeper the positive gradient the greater the increase in annual mean roadside concentration between Sa and Sb.

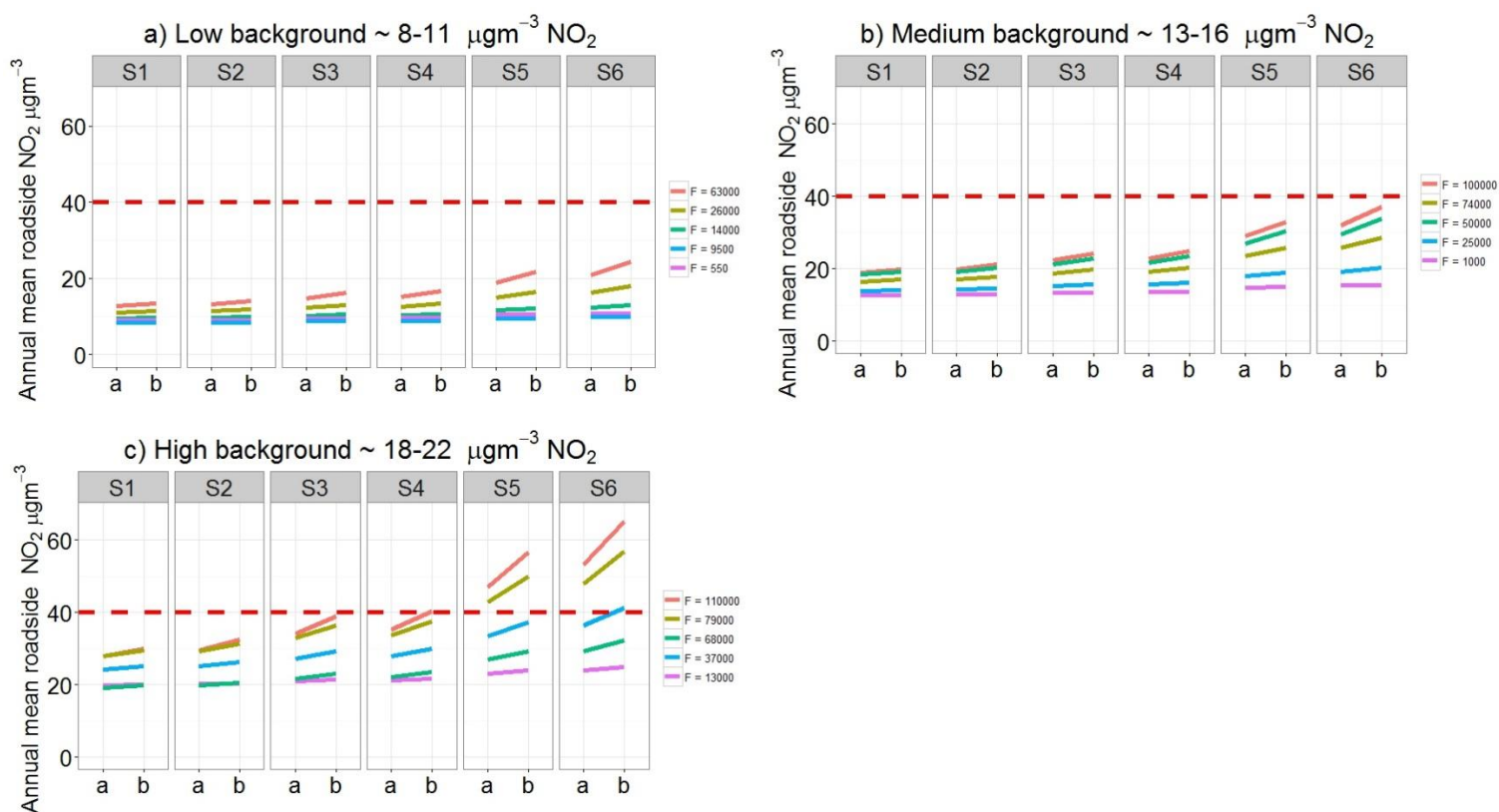


Figure 4. Roadside concentrations for roads with varying flows and a) low, b) medium and c) high backgrounds

Figure 4 shows an increase in roadside concentrations as the deviation ratio of the scenarios increases (from S1 – S6). As expected increase is most prevalent in locations with highest vehicles flows at higher background concentrations. This indicates the importance of lowering on road emissions of Euro 6 diesel cars by 2030.

At locations with low background and low flows there was little difference in roadside concentrations between the a) $fNO_2 = 0.3$ and b) $fNO_2 = 0.44$ scenarios. However in areas with higher background (Figure 4c) roadside concentrations significantly increased. The biggest increase was for the high background road with an 110,000 vehicle flow, annual mean roadside concentration between S6a and S6b increased by $8.4 \mu g m^{-3}$.

Conclusion

Our study found that NO_x and primary NO_2 emissions from Euro 6 diesel passenger cars varied widely, the average NO_2 emission ($0.17 \pm 0.19 g km^{-1}$) was over double the Euro 6 limit for total NO_x . The average fNO_2 was $44 \pm 20\%$. Two vehicles (one deploying Lean NO_x Traps the other Selective Catalytic Reduction) were able to meet the Euro 6 emissions standard for NO_x ($0.08 g km^{-1}$) during real world driving.

The average NO_x emission of $0.36 \pm 0.36 \text{ g km}^{-1}$ equates to a deviation ratio of 4.5 which rose to 5.4 for urban driving. Urban section NO_x emissions were 1.7 ± 1.0 times those of motorway sections and had an average deviation ratio of 5.4. To effectively reduce NO₂ concentrations in areas with danger of limit value exceedance policy makers should consider discriminating on the basis of actual on road emissions as opposed to Euro standards of vehicles, as removal of the five worst polluting vehicles was required to reduce the average emissions to a level comparable with COPERT.

Trip average measured emissions were higher than COPERT estimates in the majority of cases. Real world emissions NO₂ emissions were on average 2.5 times COPERT estimates. The study average fNO₂ of 44% was higher than the COPERT assumption of 30%. Scenario analysis showed that this 14% variation in fNO₂ or Euro 6 diesels could lead to a $8.4 \mu\text{g m}^{-3}$ increase in annual mean roadside concentrations in 2030 for busy urban roads.

Acknowledgements

All PEMS data was provided by Emissions Analytic. This research was funded as part of a DEFRA studentship.

References

- Alvarez, R., Weilenmann, M. & Favez, J.-Y., 2008. Evidence of increased mass fraction of NO₂ within real-world NO_x emissions of modern light vehicles — derived from a reliable online measuring method. *Atmospheric Environment*, 42(19), pp.4699–4707. Available at: <http://www.sciencedirect.com/science/article/pii/S1352231008000964> [Accessed February 3, 2016].
- Beevers, S.D. et al., 2012. Trends in NO_x and NO₂ emissions from road traffic in Great Britain. *Atmospheric Environment*, 54, pp.107–116. Available at: <http://www.sciencedirect.com/science/article/pii/S1352231012001434> [Accessed January 19, 2016].
- Bush, T. et al., 2008. *NAEI UK Emission Mapping Methodology 2005*, Available at: https://uk-air.defra.gov.uk/assets/documents/reports/cat07/0803111358_NAEIMappingMethodReport2005-v3_issue1.pdf [Accessed April 22, 2016].
- Carslaw, D. et al., 2011. Recent evidence concerning higher NO_x emissions from passenger cars and light duty vehicles. *Atmospheric Environment*, 45(39), pp.7053–7063. Available at: <http://www.sciencedirect.com/science/article/pii/S1352231011010260> [Accessed March 6, 2015].
- Clapp, L.J. & Jenkin, M.E., 2001. Analysis of the relationship between ambient levels of O₃, NO₂ and NO as a function of NO_x in the UK. *Atmospheric Environment*, 35(36), pp.6391–6405. Available at: <http://www.sciencedirect.com/science/article/pii/S1352231001003788>.
- EC, 2011. *COMMISSION REGULATION (EU) No 582/2011 of 25 May 2011 implementing and amending Regulation (EC) No 595/2009 of the European*

- Parliament and of the Council with respect to emissions from heavy duty vehicles (Euro VI) and amending Annexes I and III to Directive 2005/69/EC, Official Journal of the European Union L 167/1. Available at: <http://eur-lex.europa.eu/LexUriServ/LexUriServ.do?uri=OJ:L:2011:167:0001:0168:en:PDF> [Accessed November 10, 2015].
- EPA, 2008a. *40 CFR Part 1065, Subpart J - Field Testing and Portable Emission Measurement Systems | US Law | LII / Legal Information Institute*, EPA - United States Environmental Protection Agency. Available at: <https://www.law.cornell.edu/cfr/text/40/part-1065/subpart-J> [Accessed February 9, 2016].
- EPA, 2008b. *Determination of PEMS Measurement Allowances for Gaseous Emissions Regulated under the Heavy-duty Diesel Engine In-use Testing Program. Revised Final Report*, EPA - United States Environmental Protection Agency. Available at: <http://nepis.epa.gov/Exe/ZyNET.exe/P10024XU.txt?ZyActionD=ZyDocument&Client=EPA&Index=2006> Through 2010&Docs=&Query=&Time=&EndTime=&SearchMethod=1&TocRestrict=n&Toc=&TocEntry=&QField=&QFieldYear=&QFieldMonth=&QFieldDay=&UseQField=&IntQFieldOp=0&ExtQFieldOp=0 [Accessed January 21, 2016].
- Eurostat, 2013. *Passenger cars in the EU - Statistics Explained*. Available at: http://ec.europa.eu/eurostat/statistics-explained/index.php/Passenger_cars_in_the_EU#Further_Eurostat_information [Accessed February 4, 2016].
- Fontaras, G. & Samaras, Z., 2010. On the way to 130gCO₂/km—Estimating the future characteristics of the average European passenger car. *Energy Policy*, 38(4), pp.1826–1833. Available at: <http://www.sciencedirect.com/science/article/pii/S0301421509009094> [Accessed May 26, 2015].
- Franco, V. et al., 2013. Road vehicle emission factors development: A review. *Atmospheric Environment*, 70, pp.84–97. Available at: <http://www.sciencedirect.com/science/article/pii/S1352231013000137> [Accessed March 31, 2015].
- Grice, S. et al., 2009. Recent trends and projections of primary NO₂ emissions in Europe. *Atmospheric Environment*, 43(13), pp.2154–2167. Available at: <http://www.sciencedirect.com/science/article/pii/S1352231009000508> [Accessed May 25, 2015].
- Hu, J. et al., 2012. Real-world fuel efficiency and exhaust emissions of light-duty diesel vehicles and their correlation with road conditions. *Journal of Environmental Sciences*, 24(5), pp.865–874. Available at: <http://www.sciencedirect.com/science/article/pii/S1001074211608784> [Accessed March 18, 2015].
- ICCT, 2015. *European Vehicle Market Statistics, Pocketbook 2015/16*. Available at: http://theicct.org/sites/default/files/publications/ICCT_EU-pocketbook_2015.pdf [Accessed March 1, 2016].
- Kioutsioukis, I. et al., 2010. Uncertainty and Sensitivity Analysis of National Road Transport Inventories Compiled with COPERT 4. *Procedia - Social and Behavioral Sciences*, 2(6), pp.7690–7691. Available at: <http://www.sciencedirect.com/science/article/pii/S1877042810013224> [Accessed November 4, 2015].
- Kousoulidou, M. et al., 2013. Use of portable emissions measurement system

- (PEMS) for the development and validation of passenger car emission factors. *Atmospheric Environment*, 64, pp.329–338. Available at: <http://www.sciencedirect.com/science/article/pii/S1352231012009363> [Accessed March 11, 2015].
- Oxley, T. et al., 2009. Background, Road and Urban Transport modelling of Air quality Limit values (The BRUTAL model). *Environmental Modelling & Software*, 24(9), pp.1036–1050. Available at: <http://www.sciencedirect.com/science/article/pii/S1364815209000437> [Accessed April 21, 2016].
- Oxley, T. et al., 2013. Modelling future impacts of air pollution using the multi-scale UK Integrated Assessment Model (UKIAM). *Environment International*, 61(0), pp.17–35. Available at: <http://www.sciencedirect.com/science/article/pii/S0160412013002031>.
- Oxley, T. et al., 2003. The UK Integrated Assessment Model, UKIAM: A National Scale Approach to the Analysis of Strategies for Abatement of Atmospheric Pollutants Under the Convention on Long-Range Transboundary Air Pollution. *Integrated Assessment*, Vol. 4(No. 4), pp.236–249. Available at: http://journals.sfu.ca/int_assess/index.php/iaj/article/viewFile/143/98 [Accessed February 19, 2015].
- Sensors Inc, 2014. NO/NO Gas Analyzer - A SEMTECH ECOSTAR Product. Available at: <http://www.sensors-inc.com/brochures/SEMTECH-NOx.pdf> [Accessed May 25, 2015].
- Sensors Inc, 2010. SEMTECH-DS On Board Vehicle Emissions Analyzer User Manual. , (2.01).
- SMMT, 2016. SMMT new car registrations- December 2015. Available at: <http://www.smmt.co.uk/smmt-membership/member-services/market-intelligence/vehicle-data/monthly-automotive-data/> [Accessed February 29, 2016].
- Thompson, G.J. et al., 2014. *In-use emission testing of light duty vehicles in the united states*, Available at: http://www.theicct.org/sites/default/files/publications/WVU_LDDV_in-use_ICCT_Report_Final_may2014.pdf [Accessed January 4, 2016].
- Tutuianu, M. et al., 2013. *Development of a World-wide Worldwide harmonized Light duty driving Test Cycle (WLTC)*, Available at: <https://www.unece.org/fileadmin/DAM/trans/doc/2014/wp29grpe/GRPE-68-03e.pdf> [Accessed March 7, 2016].
- Valiantis, M., Oxley, T. & ApSimon, H., 2007. Assessing alternative transport scenarios in relation to the UK air quality strategy. In *6th International Conference on Urban Air Quality, Cyprus*. pp. 27–29.
- Weiss, M. et al., 2011. On-Road Emissions of Light-Duty Vehicles in Europe. *Environmental Science & Technology*, 45(19), pp.8575–8581. Available at: <http://dx.doi.org/10.1021/es2008424>.
- Weiss, M. et al., 2012. Will Euro 6 reduce the NOx emissions of new diesel cars? – Insights from on-road tests with Portable Emissions Measurement Systems (PEMS). *Atmospheric Environment*, 62, pp.657–665. Available at: <http://www.sciencedirect.com/science/article/pii/S1352231012008412> [Accessed March 30, 2015].

Air-noise observatory: regional and local scale exposure to air and noise pollution in Rhône-Alpes

Philippe OLIVIER*, Didier CHAPUIS*, Bruno VINCENT**, Sebastien CARRA**, Xavier OLYNY***, Bernard MIEGE***

*Air-Rhône-Alpes, Air Quality Monitoring Network, Bron, Rhône-Alpes, 69500, FRANCE

**Acoucité, Environmental Noise Observatory of Greater Lyon, Lyon, Rhône-Alpes, 69003, FRANCE

***CEREMA, L'Isle d'Abeau, Rhône-Alpes, 38080, France

Abstract

Air Rhône-Alpes, Acoucité and the Technical French State Services (CEREMA) have developed an environmental platform combining air quality and noise pollution on the Rhône-Alpes region. This platform, named ORHANE (Observatoire RHônalpin des Nuisances Environnementales - Rhône-Alpes region's Observatory of Environmental Nuisances) has been developed to identify and prioritize areas of overexposure to air and noise pollution. The information is delivered to the public as well as the decision makers who need reliable diagnoses in order to implement action plans.

Transport activity is the major source of nuisance for both air and noise pollution. Therefore, a very precise work was conducted on atmospheric and acoustic emissions of transport and on their dispersion modeling. Thus the result is a regional map of air quality and noise pollution. Thanks to the combination of models at different scales, this map is consistent and precise for both regional and local scale.

Currently, work is in progress to extend this platform to the larger territory of the new region Auvergne Rhône-Alpes and to update the current database. Moreover, this platform will be opened to the public in 2016 and its current results will be promoted to the local authorities in order to identify the overexposed areas and gradually lower them.

Keywords: *air pollution, noise pollution, numerical modeling, observatory, environmental nuisances*

Mots-clés: *pollution atmosphérique, pollution sonore, modélisation numérique, observatoire, nuisances environnementales*

Introduction

The approach of environmental diagnosis at European level is nowadays strongly oriented and encouraged by the European policy, through scientific and technical-oriented directive. Member States are often faced with a three-part issue consisting in:

- Harmonizing the European regulatory requirements with the pre-existing national regulatory procedures,
- Consolidating the link between the different environmental crossed diagnoses, both in terms of territory and in terms of kind of sources (air, noise...),
- Ensuring the consistency of approaches mostly delegated to the local authorities as regions or urban community.

This article offers to describe from an experimentation conducted on a 44 000 km² territory and 6 million inhabitants, Rhône-Alpes, with an approach among the different stakeholders for a crossed diagnosis with themes such as noise and air quality. This approach steps forward a future information portal oriented towards the general public and decision makers. Furthermore, it intends to offer a methodology mainly aiming at minimizing the uncertainty related to the input data quality of the calculation methods.

The European directives in matters of noise and air impose a detailed knowledge of the impact of human activity on territories. The National Environmental Health Plans (PNSE) 2 and 3, declined in regional plans as PRSE, have placed the resorption of environmental black spots as a national priority. Simultaneously, the European regulation is being reinforced and calls for the implementation of perspectives and action plans evaluations.

For nearly 10 years, ACOUCITE and AIR Rhône-Alpes have been cross-cooperating and cross-intervening on the main tools acting at the local and regional levels in matters of transport policies and environmental impacts: Urban Transports Plan (PDU), Territorial COherence Strategy (SCOT), Plan for the Prevention of Noise in the Environment (PPBE), Atmosphere Protection Plan (PPA), Climate Air Energy Regional Strategy (SRCAE), etc. Both are more and more commonly solicited on the impact of road projects (Rocade Est, Aménagement Mermoz in Lyon ...).

Rhône-Alpes is a pioneer region with effective expertise poles on noise (ACOUCITE) and air quality (AIR Rhône-Alpes). Through partnership with CEREMA (the Technical French State Services), these three structures have engaged into innovative works, which aim at providing local decision-makers with cartography on Air and Noise fragile points, by developing an index integrating data on air (PM₁₀ particles and nitrogen dioxide) and noise condition, revealing a co-exposure to both of these environmental nuisances. A web platform, named ORHANE (<http://orhane.fr>), will make these results public. The Rhône-Alpes DREAL and the Auvergne Rhône-Alpes Region financially support these works.

1. The method

The determination of fine scale cartography on the co-exposure to air and noise nuisances is based on a four-step methodology:

- Development of a regional basis of common sources of noise and atmospheric pollution;
- Development of an annual map of atmospheric pollution and of noise levels, in high spatial resolution (10m);
- Cross-referencing both maps in order to establish a unique map with an air and noise co-nuisance index;
- Cross-referencing the air-noise map with the population to establish a spatial diagnosis on exposition.

1.1. Regional basis of common sources of air-noise nuisances

The regional common database gathers all of the useful data to estimate the impacts of air quality and noise pollution associated to road, rail and air transport.

The work on road transport is greater, in terms of impact on cartographies and of the complexity of implementation. It consists in collecting all characteristics data on traffic travelling on major public roads of the study area (average flow of vehicles, ratio of heavy good vehicles, circulation speed of each type of vehicle...). This data is essentially generated from the results of traffic count and traffic modelling in agglomerations. Concerning noise pollution calculations, additional information on the topography of traffic lanes and noise protection devices should be gathered.

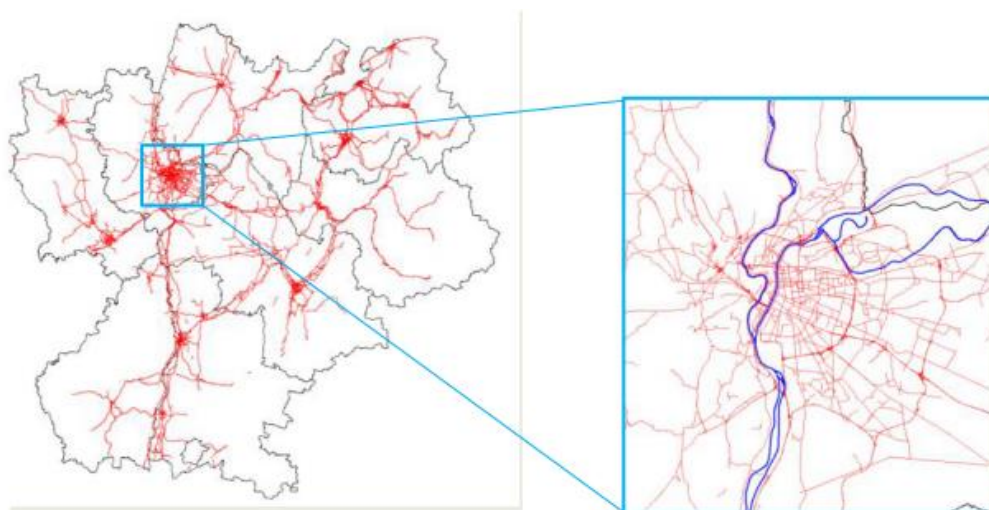


Figure 1. Harmonised regional traffic overview with a zoom on Lyon

In the same manner, a regional rail network was built, and each section of this network was documented in terms of traffic volumes, distinction of its activities (freight, major lines/TGV and TER), and proportion of diesel and electric locomotives by section. The tunnels were also identified, so that entry and exits could be treated as punctual sources for concentrations calculations, and hence ignored for the noise.

The work on air transport takes into consideration a dozen of airports, for which data on activities (number of commercial and non-commercial flights, type of airplanes) is gathered. A particular focus was brought on the location of airstrips and take-off and landing tracks.

1.2. Elaboration of annual maps of atmospheric pollution and noise levels

1.2.1. Air emissions calculations

The elaboration of an annual fine-scale map of atmospheric pollution first requires measuring emissions. The pollutants taken into consideration for this project are nitrogen oxide and PM₁₀ particles.

The calculation of road transport pollutant emissions is based on a tool developed by Air Rhône-Alpes, which relies on the COPERT European methodology (Computer Programme to Estimate Emissions from Road Transport).

The calculation of rail transport emissions takes into account its diverse origins: combustion for diesel locomotives, which are mainly circulating on non-electrified railways, the wear of wheels, rails and breaks, and of catenaries for electrified railways at the origin of particles emission.

The emissions of air transport also have various origins (taxiing and take-off, climbing or approaching phases, abrasion...), which match diverse spatial representations.

In the context of this project, work has also been led to represent on a fine-scale the contribution of the most important industrial emitters. Thus, the 100 emitting sites of nitrogen oxides and PM₁₀ particles have been specifically treated.

Finally, all of the other emitting activities, especially in residential, service and agriculture sectors are quantified in order to be taken into consideration on a surface-based approach.

1.2.2. Elaboration of cartographies on atmospheric pollutants concentrations

The cartographies of atmospheric pollutants produced by Air Rhône-Alpes are generated from a modelling chain commonly used for the production of annual cartographies on air quality, thus benefiting from validation and feedback for over ten years. The main principle of this chain resides in the combination of two concentration cartographies, each related to a specific treatment scale, regional and proximity.

The first cartography is generated from a calculation of regional models, the WRF meteorological model and the CHIMERE chemical-transport model (Menut and al. 2013). A statistical treatment enables the application of a correction on the modelled concentration fields, by exploiting the data on the network of Air Rhône-Alpes measuring stations.

The second cartography is generated from the SIRANE model (Soulhac and al. 2011), developed by the École Centrale de Lyon, which allows for the calculation of pollutants concentrations from a network of streets, taking into consideration the existing constructions, and the modelling of spatial distribution of pollutants concentrations, on a scale of almost ten meters.

This combination of models allows the conjoint phenomena representation of dispersion and chemical transformation of pollutants on a regional scale, and very precisely on a fine-scale neighbouring the principal emitting sources, for the production of high-resolution cartographies of pollution levels of nitrogen dioxide and PM₁₀ particles.

1.2.3. Elaboration of noise levels cartographies

The elaboration of a noise map at the regional scale required beforehand a modelling for each of these three sources: road, rail and air traffic. This procedure involves the work of three partners: Acoucity, the CEREMA and the Safety Civil Aviation Centre-East Directorate (DSAC-CE):

- Acoucity, using the Mithra SIG software, and the NMPB2008 calculation standard for the calculation of acoustic emission and propagation, calculated the road noise cartography.
- The rail noise cartography was the result of the calculation undertaken by the CEREMA, using the Mithra SIG software and the NMPB-Fer-2008 calculation standard.
- The DSAC-CE provided the air noise maps for airports and aerodromes near the

agglomerations. These maps were calculated with INM and use data based on short or average term traffic hypothesis (Noise Exposition Plan or Noise Annoyance Plan).

For each of these three sources, a 10x10 metres matrix is produced with the global noise index L_{DEN} . A noise index is then calculated, on each geographical point, combining the 3 indexes (multi-exposure), according to the principle of accumulation of the “annoyance equivalent road noise reference”, admitted by the European Union.

1.3. Elaboration of a unique cartography of an air and noise co-nuisance index

The cross-referencing of both fine-scale cartographies, respectively atmospheric and noise pollution, required the creation of a unique composite index. To this end, two specific indexes were developed, one for the air, the other for the noise, on a 6 classes scale, of which the boundaries were conditioned to the existing regulation:

- The NO_2 class refers to the average annual concentration of NO_2 projected on the 6 classes scale;
- The PM_{10} class refers to the daily threshold exceedence (daily average of $50 \mu g/m^3$) projected on the 6 classes scale;
- The Air sub-index refers to the maximum value of sub-index NO_2 and PM_{10} , rounded to a whole number;
- The level of global noise annoyance is also converted into a “noise multi-exposure” index that can vary from 1 to 6.

Lastly, the final co-nuisance index is calculated with the average of the air index and the noise index.

		index value - area	1 - Very low exposure area	2 - Low exposure area	3 - Impaired area	4 - Degraded area	5 - Priority area	6 - High- priority area
Air quality	NO_2	Air Concentrations ($\mu g/m^3$)	≤ 11	11 - 29	29 - 35	35 - 40	40 - 60	> 60
	PM_{10}	Number of days of exceedence	≤ 10	10 - 25	25 - 31	31 - 35	35 - 53	> 53
Noise	L_{DEN} ref. road	Noise multi- exposure index	≤ 55	55 - 60	60 - 65	65 - 70	70 - 75	> 75

Figure 2. Determination matrix of the air and noise co-nuisance index

1.4. Population exposure

From the exposure and co-exposure indexes, and an affectation of population in residential buildings, a statistical estimation of the number of persons affected by the noise, the air pollution or both is realised. This information is compatible to those asked by Europe in matters of reporting.

The cross-referencing of “pollution x population” is aggregated to the municipality, while retaining the distribution data by index class. This index provides a weighted vision of the issues on the territory, highlighting the coincidental situations between pollution and human presence.

2. The results

The estimation results of the index of co-exposure to the air and noise environmental nuisances, and exposure of the population, are made available to the public on a dedicated website, which is expected to be operating in 2016.

This website offers a cartographic interface allowing the visualisation of the Air-Noise index at different scales, throughout the Rhône-Alpes region, up to a 10 meter resolution through successive zooms. The cartographies proposed here provide a very detailed geographical delimitation of the areas exposed to the different classes of the index. An example of the visualisation is presented on the following figure:

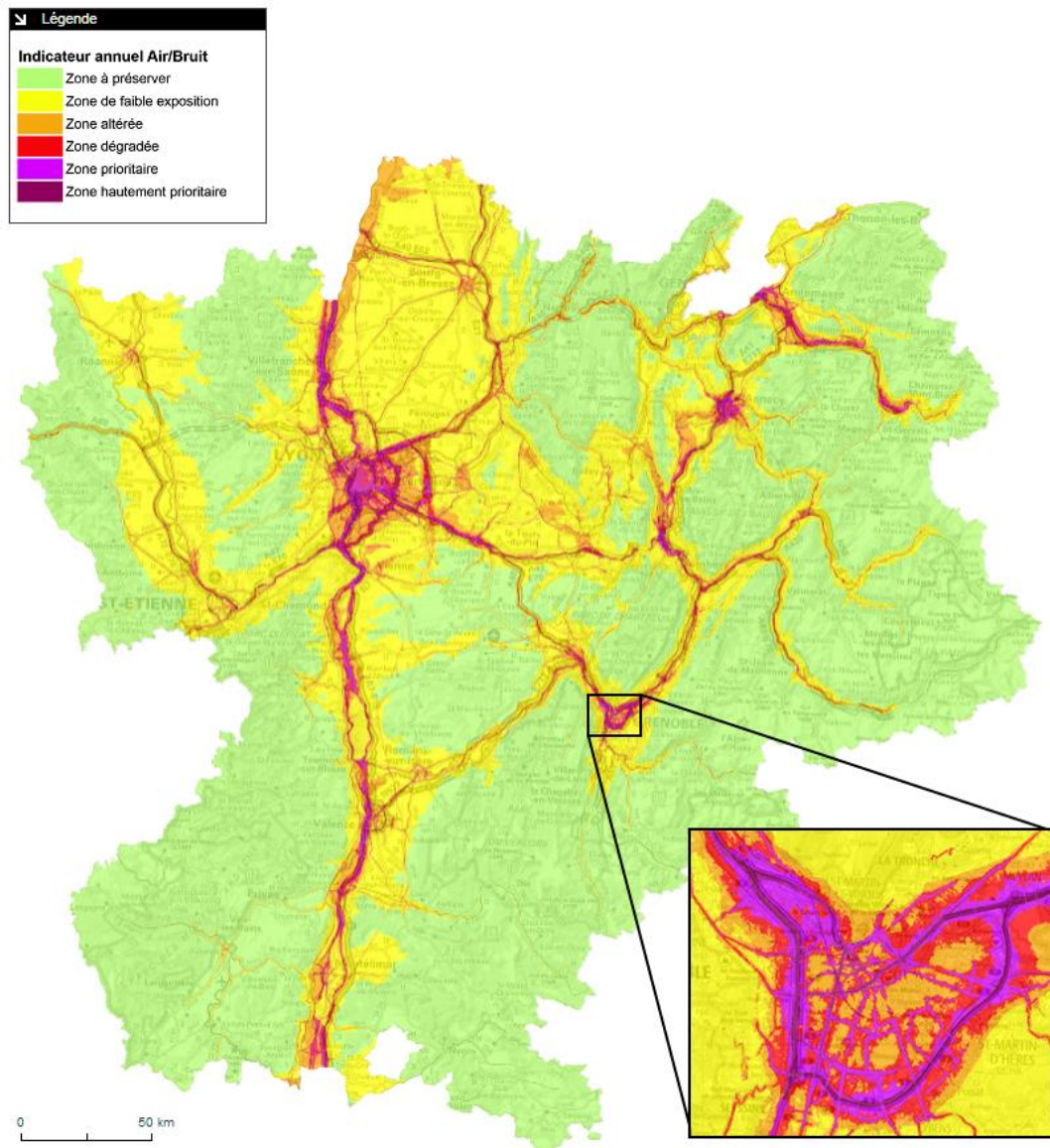


Figure 3. Example of the Air-Noise index cartographies: Rhône-Alpes region and zoom on the Grenoble agglomeration

The maps of the population co-exposure to the air and noise nuisances are presented on the website on a municipality scale, in the form of histograms of population distribution according to the 6 classes of the Air-Noise index (portion of the municipality population exposed to each class of the index). An example of the visualisation is presented in the following figure:



Figure 4. Example of cartographies of co-exposure of population to the air and noise nuisances

3. Perspectives

This first work fuels a thematic to which the interest, in terms of environmental health and territorial socio-environmental inequalities, is growing.

A first challenge is located at a technical level:

- The law n° 2015-991 of August 7th, 2015, based on a new territorial organisation of the Republic, effectively merges the Auvergne and Rhône-Alpes regions. In this context, the works and the platform will be extended to the Auvergne territory, as of 2017, following the same methodology, involving an update of data on road traffic (traffic counting), pollutants emissions, population data, etc.
- The tool created may allow the integration of other parameters describing environmental nuisances. It is a perspective that will be carefully studied, for example in the context of the National Environmental Health Plan 3 (PRSE3).

A second challenge lies on a rather political and strategic level. It aims at promoting this diagnosis tool towards the territorial communities, city and urban planners, in order to reduce the exposition of populations to nuisances in areas identified as overexposed or to not degrade this exposition in preserved areas.

Acknowledgments

The stakeholders of this project thank the Auvergne Rhône-Alpes region and the DREAL Rhône-Alpes for their financial support, as part of the PRSE2.

References

- Ben Salem N., Garbero V., Salizzoni P., Lamaison G., Soulhac L. (2015): Modelling Pollutant Dispersion in a Street Network, *Bound.-Layer Meteorol.* vol 155, p 157–187
- Miedema (2002), Position paper on dose response relationships between transportation noise and annoyance
- Soulhac L., Salizzoni P., Cierco F.-X., Perkins R. J., (2011). The model SIRANE for atmospheric urban pollutant dispersion: PART I: Presentation of the model. *Atmospheric Environment.* vol 45, p 7379-7395
- Menut L., Bessagnet B., Khvorostyanov D., Beekmann M., Blond N., Colette A., Coll I., Curci G., Foret G., Hodzic A., Mailler S., Meleux F., Monge J.-L., Pison I., Siour G., Turquety S., Valari M., Vautard R., and Vivanco M. G. (2013): CHIMERE 2013: a model for regional atmospheric composition modelling, *Geosci. Model Dev.*, vol 6, p 981-1028

How do traffic flow and the emissions they produce vary through the day, week, season and year: evidence from big telematics data

Luc PELLECUER**, James Tate** and Sam Chapman***

* *Département de génie de la construction, École de technologie supérieure, Montréal, Canada, H3C 1K3. Email: luc.pellecuier@etsmtl.ca*

** *Institute for Transport Studies, University of Leeds, Leeds, UK, LS2 9JT*

*** *The FLOOW Ltd., Sheffield, UK, S3 8GW*

Abstract

To better estimate and forecast the air quality variation over time, and to improve the efficiency of air quality plans, the temporal variability of traffic emissions warrants further study. This paper presents the analysis of a telematics dataset providing information, sampled at 1 Hz, about 35 000 journeys of a fleet of private vehicles located in the Sheffield area. Variation of vehicle specific power (VSP), which is a good predictor of exhaust emissions, were examined through the day, the week and the year, across different types of day, and against weather and visibility conditions. Whatever the time scale, traffic conditions and the type of the day (regular, weekend, or holiday) were found to affect the value of VSP by up to 30.1% and 56.7%, respectively. Bad weather conditions were found to induce 26.7% lower VSP values whereas daylight was found to induce 8.7% lower VSP values. Consequently, the results suggest that in order to accurately estimate and forecast emissions exhausted from motor vehicle traffic and air quality, ad hoc models should at least take into account the type of day and include diurnal variation. Moreover, the results demonstrate that the influence of traffic on vehicle emissions can be captured qualitatively even in the absence of traffic data.

Keys-words: *exhaust emissions, motor vehicle traffic, diurnal variation, type of day, telematics data.*

Résumé

Afin de mieux estimer et prévoir les variations de la qualité de l'air dans le temps ainsi que d'améliorer l'efficacité des plan de lutte contre la pollution atmosphérique, il est nécessaires d'étudier en détails la variabilité temporelle des émissions routières. Cet article présente l'analyse de données prélevées à une fréquence de 1 Hz sur une flotte de presque 35 000 véhicules particuliers circulant dans la région de Sheffield. Les variations de la puissance spécifique des véhicules (VSP), qui est un bon indicateur des émissions routières, ont été analysées sur la journée, la semaine, et l'année, en fonction du type de journée ainsi qu'en fonction des conditions météorologiques et de visibilité. Quelle que soit l'échelle de temps considérée, il apparaît que le niveau de trafic et le type de journée (normale, weekend, ou vacances) influent sur la valeur de la VSP jusqu'à 30,1% et 56,7% respectivement. Il apparaît que de mauvaises conditions météorologiques induisent une VSP jusqu'à 26,7% plus faible tandis que la lumière du jour induit une VSP 8,7% plus faible. Par conséquent, les résultats suggèrent qu'afin d'estimer et prévoir de façon précise les émissions routières ainsi que la qualité de l'air, les modèles ad hoc devraient au moins tenir compte du type de journée et inclure des variations quotidiennes. De plus, les résultats démontrent que l'influence du niveau de trafic sur les émissions routières peut être évaluée qualitativement sans même avoir de données de comptage à disposition.

Mots-clés: *émissions routières, trafic routier motorisé, variation quotidienne, type de journée, données télématiques.*

Introduction

Emissions from motor vehicle traffic are a major contributor to urban air pollution. To help study and design efficient air quality plans, models include traffic emissions based on emission factors aggregated over time (Franco et al., 2013). However, those traffic-related emissions, and exhaust emissions in particular, vary over time with traffic conditions and density, weather conditions, and drivers' behaviour. Moreover, emission regulations rely not only on yearly or daily targets but also on hourly ones. For example, the European legislation for air quality establishes the maximum hourly concentration in nitrogen dioxide (Henshel et al., 2015).

Therefore, to better estimate and forecast the air quality variation, and to improve the efficiency of air quality plans, the temporal variability of traffic emissions needs to be explored in details. The objective of the study presented in this paper was to examine the variation of traffic emissions through different time scales, and with weather and visibility conditions. The paper also aims to demonstrate that telematics data provides an interesting opportunity to study traffic emissions at high time-resolution.

1 Methods

In order to examine the temporal variability of traffic emission, this study relied on the analysis of vehicle tracking data. Based on this data, the vehicle specific power (VSP – used as a proxy for emissions) was computed. Then, the variation of VSP was examined on different time scales (day, week, and year), across different categories of day (business, weekend, and bank holiday day, during or out of school and university terms), and against weather conditions (temperature and rainfall) and visibility conditions (daylight).

1.1 Data

The telematics dataset used in this study provided information on the journeys of a fleet of private vehicles equipped with GPS tracking system for insurance purposes. The dataset consisted of GPS vehicle tracking records of 34 425 journeys, sampled at 1 Hz rate. Data provided was anonymised to protect the privacy of drivers following a privacy impact assessment. This included removing any journeys starting or ending in the target region, which were <0.5% of the available vehicle trips. In total, this represents 2 440 580 records and a little more than 15 000 travelled km (i.e. around 440 m per journey). The journeys were collected during one year between 01/05/2014 and 30/04/2015 in the Sheffield city centre over an area of 1.8 km². (see Figure 1). An important traffic generator, the University of Sheffield, is found in this area. Because records were available only in the area presented in Figure 1, most of the journeys in the dataset were not complete, i.e. from beginning to end. They were rather the portions of the actual journeys that fall in this area.

For each record, the dataset provided information on the journey from the GPS tracking system (location, time, bearing, and speed) and on the car by post-treatment and coupling with the information from the insurance company (make, model and year). For the purpose of the study, the speed provided by the GPS, which only took a few discrete values, was not accurate enough to capture small variations of speed. Therefore another speed was derived from the successive vehicle positions, calculated as the distance between two consecutive points divided by 1 s. Then, to avoid unrealistic speed values due to GPS errors, the speed was smoothed with the Kalman filter smoothing function available in the “dlm” R package (with a 3rd degree polynomial model).

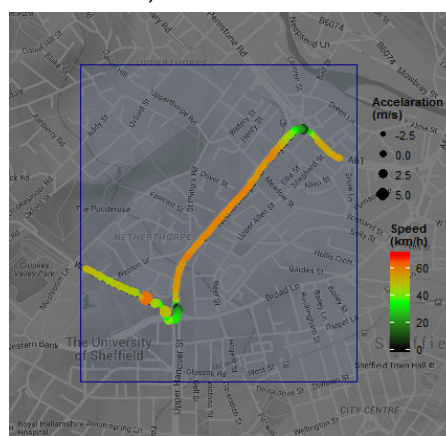


Figure 1. Study area (blue rectangle) and example of an anonymous recorded journey. Produced with ggmap (Kahle and Wickham, 2013).

1.2 Vehicle specific power

To explore the variation of traffic emissions through different time scale, we first computed the vehicle specific power (VSP) at each second of every journey. VSP is a convenient and good predictor of instantaneous CO₂ vehicle emissions. As such, computing VSP allows one to estimate vehicle emissions without having to run emission models. VSP is used in many studies about instantaneous exhaust emissions (see Moody and Tate, 2016, and Ligterink et al., 2016) and is the primary metric of the motor vehicle emissions simulator (MOVES) of the United States Environmental Protection Agency

Supposing that all journeys were made with the same average car, VSP was computed with Equation (1), adapted from Jiménez-Palacios (1999), and expressed in kW/tonne:

$$VSP = v \cdot (a \cdot (1 + \varepsilon) + g \cdot \sin(\text{grade}) + g \cdot C_R) + \frac{1}{2} \cdot \rho_a \cdot \frac{C_D \cdot A}{m} \cdot (v + v_w)^2 \cdot v \quad (1)$$

where v is the speed of the vehicle (m/s), a the acceleration of the vehicle (m/s²), ε the mass factor (0.1, dimensionless), g the acceleration of gravity (9.8 m/s²), grade the road grade (degree), C_R the coefficient of rolling resistance (0.013, dimensionless), ρ_a the ambient air density (1.207 kg/m³), C_D the drag coefficient (0.328, dimensionless), A the frontal area of the vehicle (2.13 m²), m the mass of the vehicle (1500 kg), v_w the velocity of the headwind into the vehicle (neglected – 0 m/s).

The speed of the vehicle is the speed computed as described above. The acceleration of the vehicle was derived from the speed and computed as the difference in speed between two consecutive points divided by 1 s.

The road grade was derived from elevations retrieved from the 50 cm horizontal resolution digital terrain model (DTM) produced by the UK environment agency. The road grade was computed as the arctangent of the ratio rise/run, where the rise was the difference of elevation between two consecutive points divided by the distance between those two points. When the speed of the vehicle is low and the position of the vehicle moves from one DTM tiles to another, the value of the run may be significantly smaller than the value of the rise, resulting in an overestimation of the grade. To avoid such overestimation, the road grade was computed following the method developed by Wyatt et al. (2014) when the speed of the vehicle falls under 1 m/s. In that case, the road grade at the vehicle position was calculated between the last point where the vehicle was farther than 0.5 travelled meters from the vehicle position considered and the first point where the vehicle was farther than 0.5 travelled meters from the vehicle position considered. Thus, the minimum travelled distance over which the road grade is calculated is 1 m.

2 Results and discussion

VSP values can be either positive when the vehicle needs power to move or negative when it does not. Vehicle emissions levels are low and relative constant for negative values of VSP, e.g. when a vehicle is breaking. Consequently, records with negative values of VSP were discarded from the study, and the results presented below are based on positive values of VSP only.

Whatever the time scale, the results suggest that VSP variation may be explained by traffic conditions (Section 2.1) and by whether it is a typical day or a holiday (Section 2.2). VSP variation may also be observed according to change in the driver's environment such as change in weather conditions (Section 2.3) or daylight (Section 2.4).

2.1 Variation of VSP over time

VSP was found to vary significantly through the year, week, and day. Figure 2 shows the variation of the mean VSP through the year, the transparency level of each bar reflecting the number observations, and the error bars representing the 5th and 95th percentile of VSP. Overall, VSP appeared to vary by up to 24.5% on average depending on the month. VSP was higher from March to September (5.77 kW/tonne vs 5.19 kW/tonne), with a maximum value in August (6.30 kW/tonne) when many people are on holidays. This may suggest that the driving conditions during this period allowed people to adopt their "natural" driving behaviour, i.e. without being constrained by the bad weather conditions of winter or by heavy traffic conditions.

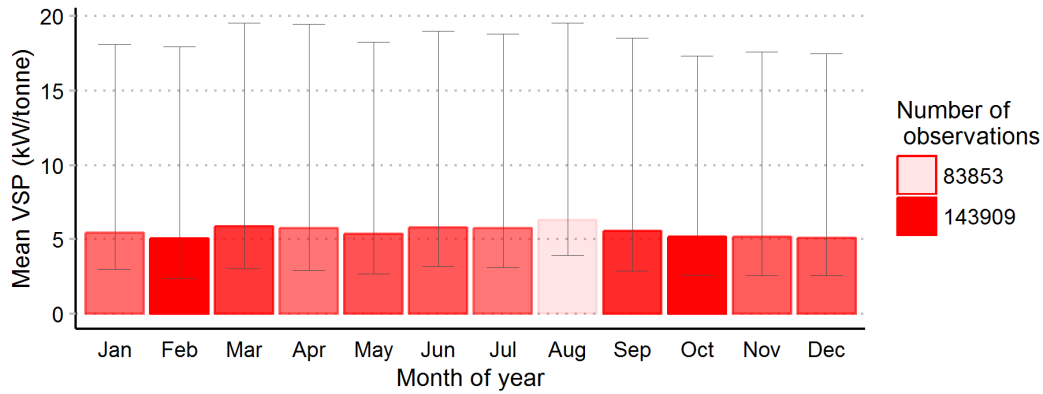


Figure 2. Variation of VSP with the month of the year.

VSP also varied through the week, with higher VSP values during the weekend (6.57 kW/tonne) and lower VSP values on week days (5.29 kW/tonne). Overall, VSP varies by up to 24.1% on average depending of the day of the week. As illustrated in Figure 3, this remained true for every month of the year, supporting the idea that higher VSP values occur in light traffic conditions.

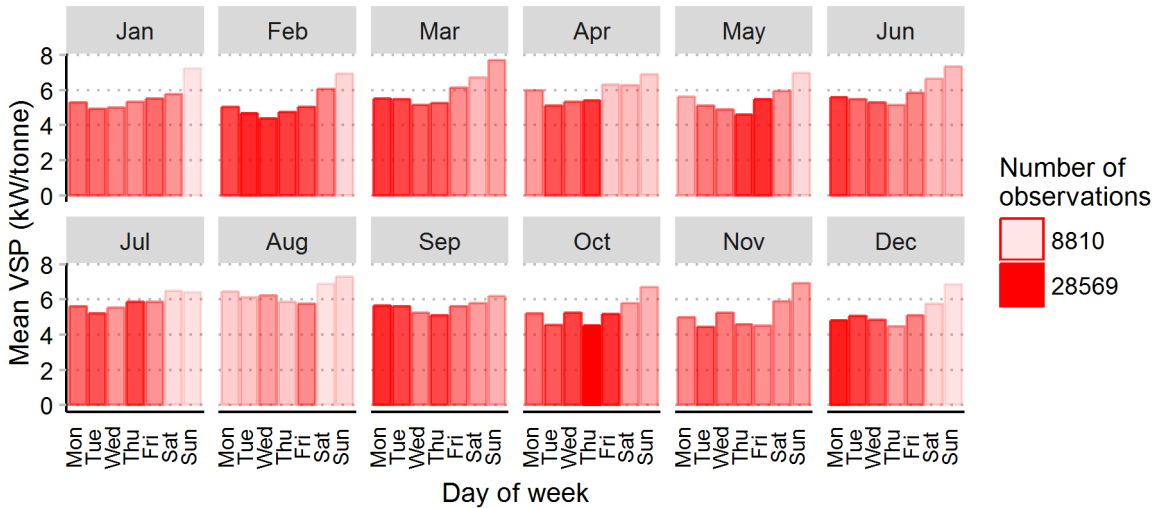


Figure 3. Variation of VSP with the day of the week

VSP also varied through the day. The variation of VSP with the hour of the day is presented in Figure 4. The same pattern was followed across week days. A later, reduced onset of more constrained behaviour occurred on weekend days. On week days, the mean value of VSP was constantly significantly lower (30.1% lower on average) during morning and evening traffic peak periods, i.e. between 7:00 and 9:59, and between 16:00 and 18:59. On weekend days, the variation of the mean value of VSP is not as obvious, explained by the absence of a noticeable traffic peak period.

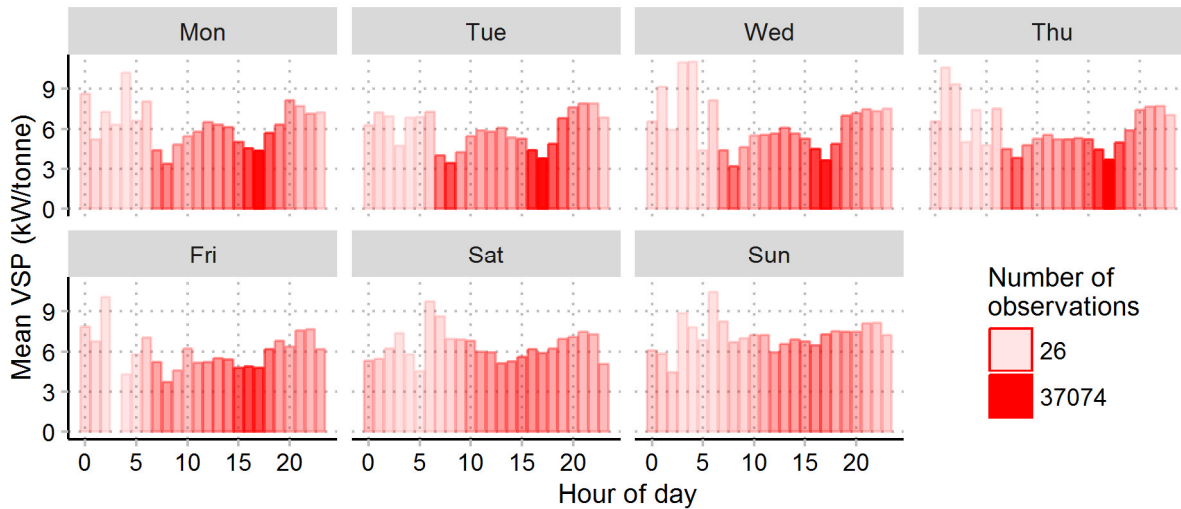


Figure 4. Variation of VSP with the hour of the day.

2.2 Influence of the type of day on VSP

To examine the influence of traffic conditions on VSP, we compared the mean values of VSP for different types of day for which different level of traffic are expected. Bank holidays dates were retrieved from the UK government website (<https://www.gov.uk/bank-holidays>). Dates of school and university holidays were retrieved from the holiday calendar of the Sheffield City Council (<https://www.sheffield.gov.uk/education/schools/holidays.html>) and the University of Sheffield (<https://www.sheffield.ac.uk/about/dates>) respectively.

Figure 5 illustrates the mean values of VSP for different type of days including regular week and weekend days, bank holidays, and school and university holidays. VSP was found to be higher on days for which light traffic conditions were expected (e.g. during periods with school and university holidays). The highest value of VSP was observed on days which are bank, school and university holidays at the same time (7.82 kW/tonne on average). The lowest VSP value was observed on regular week days (4.99 kW/tonne), when the traffic conditions are expected to be the heaviest. On regular week-end days and bank holidays, VSP values are intermediate at 6.45 kW/tonne and 5.88 kW/tonne respectively. Overall, VSP varied by up to 56.7% depending on the type of day

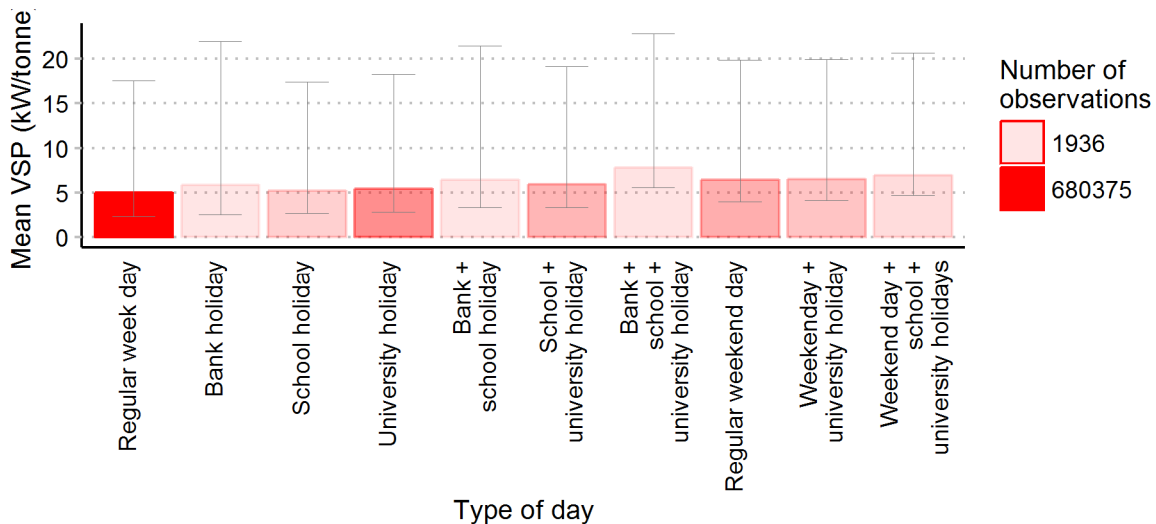


Figure 5. Influence of the type of day on VSP. Error bars represent the 5th and 95th percentiles.

Coupling the vehicle tracking data with traffic data, when available, would be relevant and could support these findings. However, the results show that, even in the absence of traffic data, the influence of traffic on VSP can be captured qualitatively.

2.3 Influence of the weather conditions on VSP

Bad weather conditions are expected to constrain the drivers' behaviour. In particular, poor visibility due to rain or fog and slippery road due to freezing temperature could induce the driver to be more cautious than usual, resulting in less intense accelerations and decelerations. The driver adapting to weather conditions would thus imply lower VSP, and ultimately lower associated vehicle emissions.

Historical hourly weather data were obtained from the UK Met Office datasets (MIDAS) through the Centre for Environmental Data Analysis (CEDA – <http://browse.ceda.ac.uk/browse/badc/ukmo-midas/data>). Because no visibility data was available in this database for the study area, descriptors of weather conditions were limited to rainfall and temperature. The data used in this study included hourly temperature and rainfall measured at a station located within the study area. The resolutions of the data were 0.1°C and 0.2 mm respectively.

To illustrate the influence of the rain on VSP, rainfall intensity was used to form four categories. No, low, medium, and high rainfalls corresponded to 0 mm, less than 1mm, between 1 and 2 mm and more than 2 mm rainfalls per hour respectively. Moreover, in order to capture the influence of the rain on VSP while minimising influence of other parameters, only records collected during the off-peak period of regular week days (between 10:00 and 14:59) were used. Figure 6 shows that the mean value of VSP remained roughly the same across the first three categories (5.4 kW/tonne) but was 20% lower for rainfall of more than 2 mm per hour (4.5 kW/tonne). This suggests that drivers might adopt less aggressive driving behaviour when the road visibility was reduced by the rain and when the road was wet and slippery.

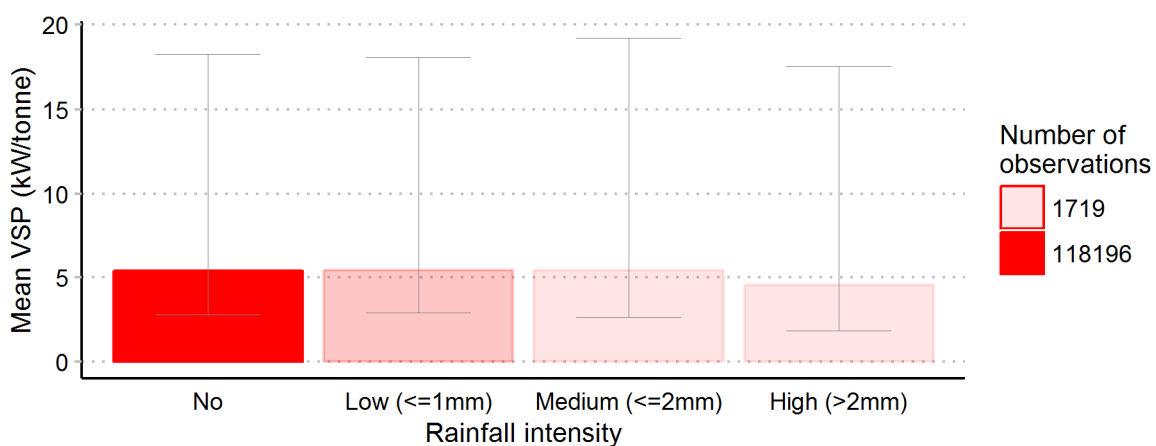


Figure 6. Influence of the rain on VSP.
Error bars represent the 5th and 95th percentiles.

To illustrate the influence of the temperature on VSP, the temperature was categorised into five classes. Negative, very low, low, medium, and high temperatures corresponded to temperatures below 0°C, between 0 and 2°C, between 2 and 7°C, between 7 and 12°C, and above 12°C respectively. Moreover, in order to capture the influence of the temperature on VSP while minimising influence of other parameters, only records collected during the regular week days were used. Because negative to low temperatures are likely to occur during the morning peak period, only records collected during this period (7:00 to 8:59) were used. Figure 7 demonstrates that the mean value of VSP remained relatively constant for temperature above 2°C (between 3.7 and 4.0 kW/tonne) but was clearly lower for low and negative temperature (between 2.9 and 3.1 kW/tonne). This 26.7% difference can be explained by drivers adopting a more cautious driving behaviour, either because of their own perception of the slipperiness of the road or because of the driving assistant warnings.

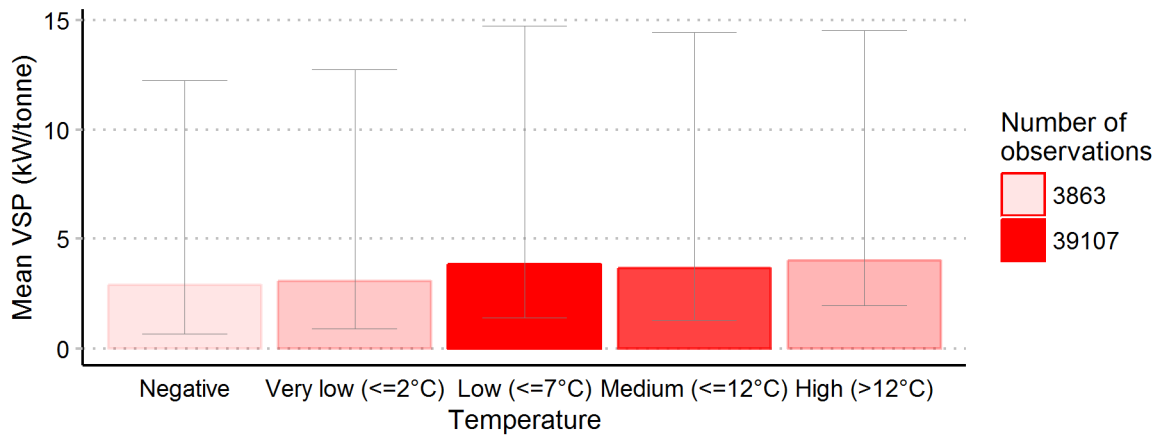


Figure 7. Influence of the type of day on VSP.
Error bars represent the 5th and 95th percentiles.

2.4 Influence of the daylight on VSP

Road visibility is not affected by weather conditions only. Daylight is likely to affect road visibility and consequently influence the drivers' behaviour in the same way weather conditions do.

The sunrise and sunset functions of the "mapprools" R package enabled us to determine whether each record was collected during daytime or night time, depending on the day of the year and the time of the day. In the study area, the earliest and latest times at which the sun rises were 04:53 and 08:21 respectively, while the earliest and latest times at which the sun sets were 15:47 and 21:37 respectively. To capture the influence of daylight on VSP while minimising influence of other parameters, only records collected during those two periods of the day were used.

Figure 8 shows the mean values of VSP during daytime (over 296 513 observations) and night time (over 444 303 observations). The 0.4kW/tonne (8.7%) difference in mean VSP was statistically significant (p -value < 0.001) and proved that daylight had an impact on VSP. This impact could appear counterintuitive as VSP was lower during daytime than during night time, implying that drivers' behaviour was more aggressive during night time despite the reduced visibility. An explanation of this finding could lie in the hypothetical drivers' preference to drive in daylight. This preference would induce relatively heavier traffic conditions in daytime, constraining the drivers' behaviour and, in turn, lowering the mean value of VSP.

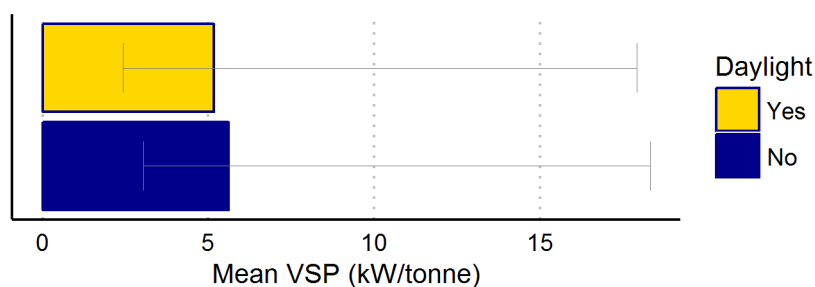


Figure 8. Influence of the daylight on VSP.
Error bars represent the 5th and 95th percentiles.

Conclusion

Exploring big telematics data from Sheffield city centre, it was found that the average vehicle specific power (VSP) varies significantly through the year, week and day. Also, differences in VSP were observed depending on the type of day, whether normal, holiday or weekend. The results suggest that heavy traffic conditions constrained drivers' behaviour so that associated VSP values remained low. Similarly, it was found that bad weather conditions induced low VSP values. VSP being a good predictor of vehicle exhaust emissions, it would be expected that the same results would have been found with emissions.

Therefore, the results suggest that to accurately estimate and forecast air quality and emissions, ad

hoc models should take into account the type of day and should include diurnal variation. Most advanced models should include the influence of the weather and daylight as well. Moreover, those results demonstrate that the influence of traffic on VSP, and consequently on vehicle emissions, can be captured qualitatively even in the absence of traffic data. Further work is underway to directly capture the variation of emissions (instead of the variation of VSP). To this end, PHEM will be used to model vehicle emissions from the telematics data.

Acknowledgments

The authors would like to thank the UK Met Office for their support in retrieving the weather data.

The authors acknowledge the financial support provided by the École de Technologie Supérieure, Montréal.

References

Franco, V., M. Kousoulidou, M. Muntean, L. Ntziachristos, S. Hausberger and P. Dilara (2013): Road vehicle emission factors development: A review. Atmospheric Environment, vol. 70, p 84-97.

Henschel, S., A. Le Tertre, R. W. Atkinson, X. Querol, M. Pandolfi, A. Zeka, D. Haluza, A. Analitis, K. Katsouyanni, C. Bouland, M. Pascal, S. Medina and P. G. Goodman (2015): Trends of nitrogen oxides in ambient air in nine European cities between 1999 and 2010. Atmospheric Environment, vol. 117, p 234-241.

Jiménez-Palacios, J. L. (1999): Understanding and quantifying motor vehicle emissions with vehicle specific power and tunable infrared laser differential absorption spectrometer remote sensing. Ph.D. thesis, Massachusetts Institute of Technology.

Kahle, D. and H. Wickham (2013): ggmap: Spatial Visualization with ggplot2. The R Journal, vol. 5, n°1, p 144-161.

Koupal, J., M.Cumberworth, H. Michaels, M. Beardsley, D. Brzezinski (2002): Draft Design and Implementation Plan for EPA's Multi-Scale Motor Vehicle and Equipment Emission System (MOVES). United States Environmental Protection Agency Report, n°420-P-02-006

Ligterink, N.E., J.E. Tate and V.A.M. Heijne (2016): Vehicle emission model for traffic simulations. In 21st International Transport and Air Pollution Conference, Lyon, France, 24th-26th May 2016.

Moody, A. and J.E. Tate (2016): In service CO₂ and NO_x emissions of Euro 6/VI cars, light- and heavy-duty goods vehicles in real London driving: Taking the road into the Laboratory. In 21st International Transport and Air Pollution Conference, Lyon, France, 24th-26th May 2016.

Wyatt, D. W., H. Li and J. E. Tate (2014): The impact of road grade on carbon dioxide (CO₂) emission of a passenger vehicle in real-world driving. Transportation Research Part D: Transport and Environment, vol. 32, p 160-170.

Reducing Freight Transport Pollution by using electric vehicles

Christophe RIZET* & Antoine MONTENON**

*IFSTTAR-AME-DEST, 14-20 bd. Newton. Marne-la-Vallée, France
Email: christophe.rizet@ifsttar.fr

** IFSTTAR-AME-SPLOTT, 14-20 bd. Newton. Marne-la-Vallée, France

Abstract

To mitigate the pollution of road transport, several cities in Europe have implemented 'Low Emission Zones' (LEZ). In order to plan the future of such questions for the Paris area, and to assess their impacts on traffic and air pollution, LEZ scenarios have been defined for freight vehicles: a 'Business as Usual (BAU) scenario, a LEZ scenario, in which only the most recent vehicles are authorized, and two 'electric scenarios, in which only electric vehicles can enter the zone limited by the motorway A86, an area of 385 km² for about 4.8 million inhabitants. The difference between the two electric scenarios is related to the hypothesis on the evolution of the technologies: In the first scenario, Diesel trucks can be replaced by equivalent electric powered trucks of the same payload. In the second scenario, only the vehicles with a payload below 5 tons could be replaced by the electric equivalent. So, every vehicle with a load over 5 tons has to be replaced by several smaller vehicles in the LEZ area.

This communication follows the RETMIF project (Reduction of Emissions from Freight Transport in the Greater Paris Region). Its main objective is to understand the potential impacts of a LEZ in the Paris metropolitan area, in particular for goods vehicles. In conjunction with this development of LEZ, there has been a huge evolution in the motor technologies for commercial diesel vehicles. The industrial companies have also began to develop new hybrid and electric technologies, in anticipation of the scarcity of fossil oil and the future potential regulations only enabling non-polluting vehicles.

Keys-words: (5 words) LEZ, freight, electric, pollution, companies

Introduction

Air quality is a very important topic for cities. Proportion of population exposed to air quality problems is high: in 2012, 36% of European urban population is concerned by a day limit on air concentration of PM₁₀ (EEA, 2013). The city of Paris follows this assessment. In 2013, more than 9 on 10 inhabitants of the city were concerned by an overexposure to NO₂ and PM₁₀ in the air. Peaks of pollution levels in 2014 and 2015 reopened the debate on that topic into media and politics.

Above the punctual regulations, the city of Paris actually wants to lower the pollutant emissions, and become a model to follow in Europe. Some initiatives have been taken: reduction of parking places, peak-hour restrictions, working groups on "100% non-Diesel deliveries", prefiguration of a Low Emission Zone, etc.

Low Emission Zones (LEZ) is one of the solutions proposed by European Commission to lower the air pollution. Some have already been implemented in Europe, but their effect on the city economy, on workers, and on the environment is poorly known. The objective of the RETMIF project, funded by ADEME (French Agency on Energy and Environment) is to better know the effects of this regulation on companies and environment. Phase 1 of the project aimed to specify the different characteristics of Low Emission Zones in Europe, interviews with professionals throughout Europe, especially in London, Berlin, Göteborg and Paris, have been lead during the phase 2.

This paper follows the phase 3 of RETMIF. The objective is to know what effect a Low Emission Zone would have on goods transport in the Paris Region. It is structured as follows. Section 1 explains the impacts of European, national and local environmental programs, especially Low Emission Zones, with a focus on the reactions of companies concerning environment, as well as the difficulties that could be created by these regulations. Section 2 introduces the methodology of the quantitative part of

the study, by defining 4 scenarios of transport regulations for Paris region from now to 2025: 1 “Business as Usual scenario”, 1 Low Emission Zone scenario, and 2 scenarios 100% electric: one with goods vehicles replaced by electric vehicles with the same capacity, one with a maximum payload of 5 tones for goods vehicles (gross weight of 12 tones).

Politics for Environment and Transport

In 2002, European Commission implemented the sixth Environmental Action Program which set out to achieve a high level protection of human health. Different environmental goals have been defined to be achieved in 2020 or 2050. This program has been reinforced by the seventh Environmental Action Program which aims to define new higher standards for air quality. Current European goals in terms of pollution follow the Directive 2008/50/EC. This directive is based on Euro standards for vehicles. These standards, defined by a number (roman for HGV, Arabic for other vehicles), correspond to a limit of pollution mass per energy unit developed depending on the type of vehicle, the type of engine, the year of commercialization, and the type of pollutant. This limit is calculated through a driving-cycle standard (NEDC).

Member countries of the European Union and the European Environment Agency have to apply these programs by implementing national action programs in order to satisfy the pollution criteria. In France, two roadmaps for Environment have been set out during the past ten years : “the Grenelle Environnement (1 et 2)” and the “Loi pour la transition énergétique”. These two roadmaps consider the Environment as a global initiative, which has to be interpreted in the different faces of the national economy : energy, housing, transport, etc.

The goals of the Directive 2008/50/EC are not being reached in Europe, especially in urban areas. The European Commission launched in 2014 legal proceedings against countries in order to enhance the respect of the Directive.

Road transport is one of the main sources of pollutants, especially Nitrogen Oxides (NO_x) and Particulate Matters (PM). In 2011, road transport produced 47% of all NO_x and 14% of all PM10 (EEA, 2013). Diesel engines particularly are concerned by these pollutions, by being 4 to 100 times more polluting for NO_x than gasoline engines – equivalent power and weight. Urban goods transport is a great contributor of pollution and greenhouse gases. In London, in 2010, freight transport was responsible for 24% of the CO₂ emitted by road transport, 38% for the NO_x and 37% for the PM10 according to Allen et al. (2012) and In French cities, this type of transport represent 35% of the NO_x, and about 50% of the PM10 emitted by road transport, according to Gonzales-Feliu (2010).

In parallel, the most recent white paper on transport for European Union stresses the need to develop new sustainable transport systems, which consumes less energy, especially in urban areas. In France, the “Loi pour la Transition Énergétique” has the ambition to reach a relative energetic independence in the country. That means to use less petrol and more biogas and electrical power (France has the capacity of producing more electricity than needed). It therefore enhances the use of electrical power within all the faces of economy, especially transport. At present, two types of electrical engines are promoted by the Ministry of Sustainable Development: direct electric engines using batteries and fuel cell engines powered by hydrogen, which creates the needs of new production and value chains in the energy economy, but which is much less restricting for vehicles by reducing the size and the weight of batteries.

One of the reasons of the growth of pollution in urban areas is the growth of mobility, and the use of older vehicles for doing short routes. This assessment has been verified for big cities like Paris through interviews during the RETMIF project.

A tool which is enhanced by the European Commission is Low Emission Zones (LEZ). These are “geographically limited zones that cover more than a very local area where there are problems from the point of view of atmospheric pollution, noise, the quality of urban life, traffic congestion and/or safety and in which specific restrictions are applied with regard to the volume and/or the nature of traffic in the zone” (UE, 2005).

The types of vehicles and associated Euro standards concerned by the LEZ are defined by the national, regional and local authorities. In 2015, there are about 210 LEZ in Europe, in 11 countries. Half of them are combined with a toll. The areas covered by these zones vary between 0.6 km² in Lisbon and 5700 km² in Styria (Austria). 99% of them concern HGVs, and about 75% concern personal cars and LCVs.

The method of enforcement widely influences the efficiency of the LEZ. In Europe, the two main methods of enforcement are the automatic enforcement by cameras reading the license plate on the vehicles, and the manual enforcement by municipal or national agents. In Amsterdam, the compliance rate rose from 66% in 2008 to 97% in 2010, while cameras have been implemented in 2009 (Broaddus et al., 2012).

Low Emission Zones are environmental policies, which has to be implemented and applied by the transport departments in the municipalities. That creates some troubles around the measure.

In fact, goods transport is often “forgotten” by the authorities (Dabanc, 2013), and is seen as the biggest pollution (air and noise) problem. But, reducing pollution by banishing different types of HGVs and LCVs creates number of evolutions in this economic sector, especially when speaking about investments for alternative fuel engines.

Low Emission Zones and Road Freight Transport.

This part is directly following two previous publications (Cruz et al., 2015, Dabanc et al. 2015) and the qualitative part of the RETMIF project.

The part 2 of the RETMIF project aims at interviewing goods transport professionals (companies, federations, associations, researchers, public authorities) in four cities : Paris, which hadn't any LEZ at this time, London, Berlin and Göteborg (+ Stockholm), which have implemented their LEZ few years before. These interviews were separated in several parts: presentation of the company/institution, what they know and think about the environmental policies in their city/country, how they implement the notion of sustainable development in their institution, how they welcome the LEZ, what has changed several years after.

Most of goods transport companies and companies which use own-account transport can be divided in three types, which we won't define precisely because of the fuzziness of the limits between them:

- Larger companies. They have enough funds for renewing their fleet quickly, by modifying their business models or not. In these companies, HGVs are renewed every 5 or 6 years, LCVs between every 6 months and every 3 years. Very few LEZ concern vehicles which are less than 6 years. Therefore, the measure doesn't concern them at all, except for special vehicles, like waste collection vehicles. These companies have to ask an exemption pass, or redefine the routes of the vehicles for the time just after the implementation of the LEZ. The older vehicles drive outside the LEZ and the newer ones inside the LEZ.
- SMEs which depend on larger ones. Most of the time, the larger companies ask their subcontractor to have new vehicles in order to get a greener image. So, the LEZ doesn't have any influence on them. We have the same thing for SMEs for which environment is a great part of their business model and competitiveness. But, LEZ can be a little loss of their competitiveness in comparison of other SMEs.
- The smaller companies have big troubles for complying with the LEZ. Some decide to merge with others or to use vehicle location for long time, but a lot have to shut up because the investment can be too high, or the subsidies provided by public authorities are too low. This case is very common in bigger cities because the vehicles cover less kilometers and therefore can be used longer.

Speaking about the link between environment and transport, especially goods transport, can have a different meaning depending on the location and the policies. When German, Swedish or Italian transport companies speak about environment, they speak more about ISO 14001 or gas and hybrid vehicles. In France and in London, most of the companies say: “we actually try to be aware of the new electric technologies for vehicles, but actually we don't have a right business model for using it”. From a first point of view, big cities like Paris or London are particularly adapted for using electric vehicles: smaller trucks, less need of range, lots of stops in a small area, low speed, etc.

Environment concerns everybody, adapting it in a business way can be hard. Therefore, almost everybody feel reticent for using electric vehicles for a lot of reasons:

- A lack of supply for vehicles. Vehicle manufacturers have the financial capacity for conceiving

and market electrical trucks, but because of the price and of the small market, public authorities have to be very clear about what the future program on transport for cities and the regulations that will be defined. The regulations would help and constraint users for using electric vehicles. The business model for manufacturers is already too tight for evolving that way, in comparison to hybrid or gas vehicles.

- The supply of energy and fuel. There are quite few gas and electricity supply stations in France. And, refueling trucks during the night would be complicated; today, a lot of drivers take their trucks at home, in order to avoid the travel time between their home and the warehouse in the morning before doing their deliveries.
- The very low payload, compared to the GVW. The battery needed for bigger urban trucks is much too heavy, so there are no such trucks in the market. There are no such hybrid vehicles for the same reason. A change of regulations would force companies to use a number of smaller vehicles to replace one bigger. The price of the vehicles would not be a problem (with public funds, the price could be cheaper), but every vehicle would need a driver, which costs much more than the vehicles.
- But, thanks to the new developments works on electric vehicles, especially new fuel cells systems which are tanked by hydrogen composites, the battery and size problems about electric vehicles would be partially cleared.

Methodology

The scenarios

- The Business As Usual (BAU) scenario
- The Low Emission Zone (LEZ) scenario
- The 2 'electric' scenarios

These two scenarios "100% electric" scenarios aim at quantifying what could be the evolution of emissions in a hypothetical situation where all freight vehicles would be electric. These two scenarios are the following:

In the first electrical scenario, we assume that any freight vehicle - regardless of its total maximum weight - is replaced by an electric vehicle of the same capacity. In this scenario, we assume that in 2025, the commercial vehicle manufacturers will manufacture electric vehicles with a payload up to 25 tons. Thus, the utility park used is identical to that found in the BAU scenario for capacity, but all vehicles run on electricity.

In the second electrical scenario, the maximum payload of an electric vehicle is assumed to be 5 tons, with a maximum gross weight of 12 tones. All vehicles with a payload higher than 5 tones are replaced by smaller electric vehicles, while maintaining constant total payload to keep a constant volume of potentially cargo. For simplicity, we consider two types of electric trucks: GVW vehicles included in 7.5 and 12 tones (maximum payload of 5 tons) and vehicle gross weight less than 7.5 tons (maximum payload of 2 tones). Eg a 11 tons of payload diesel truck, will be replaced in the second scenario by two electric L 5 tons of payload trucks and a two tones of payload truck. In contrast, a truck 14 tons of payload will be replaced in the second electric scenario by three trucks with a payload of 5 tons to minimize the increase in traffic : More electric commercial vehicles than today will be needed to transport the same load. We will estimate the increase in traffic

In each scenario, we will focus on CO₂ and PM emissions, the only pollutants generated by electric vehicles. We study the same road sections and therefore the same traffic in each scenario.

In order to calculate road transport pollutant emissions in Paris region, and their evolution according to the different scenarios, the software CopCETE v4 has been used. CopCETE v4 has been developed by the CEREMA, and uses a Copert v4 basis with French data and adapted for a use with a Microsoft Excel interface.

CopCETE, as Copert, uses the following characteristics of vehicles:

- Personal cars, Light Commercial Vehicles, Rigid Trucks, Articulated Trucks and Buses

- Different types of fuel: gasoline, Diesel, electric, hybrid, LPG
- Different sizes of engines
- Euro standards from Euro 0 to Euro 6.

30 types of emissions can be calculated in CopCETE but we will calculate only 3 of them:

- Nitrogen oxides (NOx). In 2011, about 61% of the NOx emissions in France come from road transport (CITEPA, 2014)
- Particulate matter (PM10). In 2011, about 15% of the PM10 emissions in France come from road transport
- Carbone dioxide (CO2). In 2011, 33% of the CO2 emissions in France come from road transport.

CopCETE also distinguish hot engine and cold engine tail pipe emissions, and non-tail pipe emissions (PM, HAP, some metals) for brake and tires use.

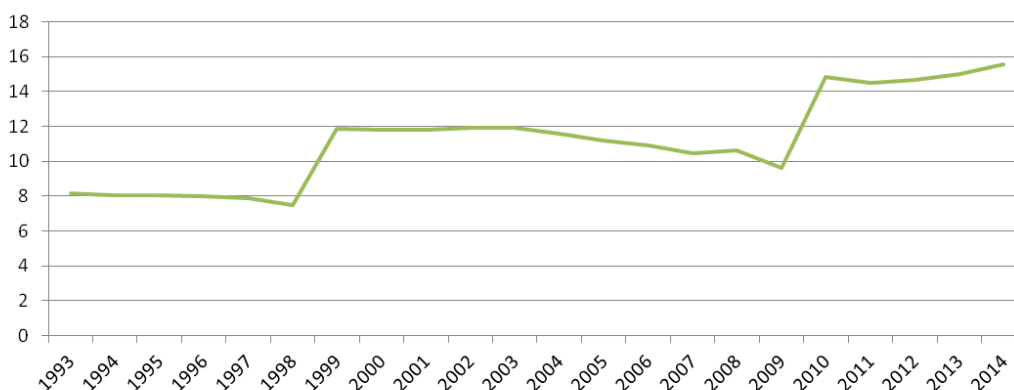
Fleet evolution

To simulate the fleet evolution, we computed from statistical data on fleet, for each type of vehicles and for each year, the rate of vehicles still working for a given generation. On the other hand, we estimated the number of new vehicles entering the fleet per vehicle type, from what has been observed in other LEZ and from our scenarios. From the computed rate of survival, we estimate a theoretical law, in order to smooth the irregularities and to simulate the future evolution of the fleet, using the parameters of the statistical law. As suggested by Koli (2012), we used a Weibull statistical law, in which the rate of survival is : $S(t) = e^{-\left[\frac{t}{\beta}\right]^\alpha}$

α determines how ‘incurved’ the function is and β is a parameter of temporal scale, which influences the vehicle median duration of life. Given the available statistics, we assumed α to be independent of the type of vehicle and we used the α estimated by Bourdeau (1997), which means that the speed of wear per type of vehicle does not varies along the years. The matching between the data observed and the Weibull law is then done by optimizing the parameter β for two types of vehicles: ‘road tractors’ and ‘trucks and vans’.

We are therefore interested in the categories of commercial vehicles, for which data of registrations are available far enough in the past. We then compare the results of optimal beta in the case of tractors and the trucks and vans, and then trace the evolution of optimal beta coefficient obtained between 1993 and 2014.

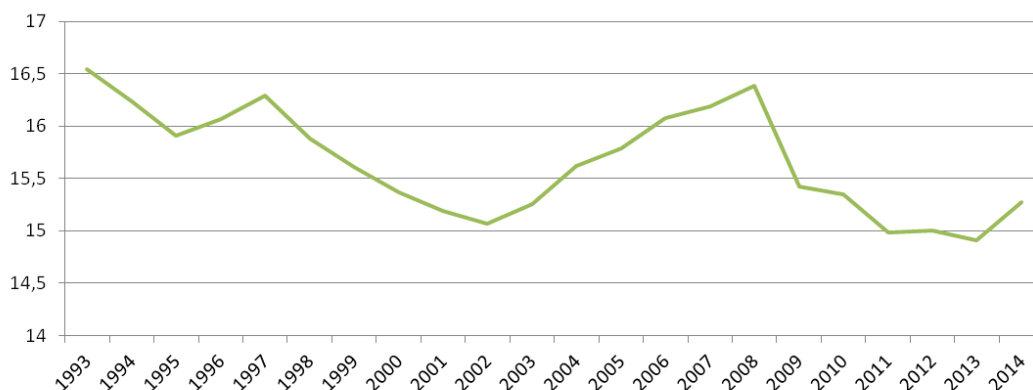
Figure 1: Determination of beta for vans (<3.5 t.)



In the case of vans (Figure 1), beta varies in steps: around 8 between 1993 and 1998 and between 10 and 12 until 2010 when it stabilizes at 14.9. These different levels can have various explanations, including buyer behavior can be encouraged by policy measures favoring renewal. But the landing between 2009 and 2010 was most likely a change in the way of counting vehicles: before 2009 were accounted for all vehicles less than twenty years after that date then only vehicles less

than fifteen years old are counted.

Figure 2 : Determination of beta for trucks



The variations of beta are much more pronounced in the case of heavy goods vehicles (Figure 2). Beta increases or decreases over long periods. As in the previous chart, we see the peak in 2009 probably due to the change in the way of counting. The beta value is between 15 and 17. Finally, to define the forecast changes, we retain the alpha values of Bourdeau, and we hold the average value of beta from 2009 as shown in the table below.

Table 1 : The coefficients alpha and beta we used

	Vans	Rigide trucks	Tractors & trailers
Alpha	2,1	3,3	3,9
Beta	14,9	15,17	15

Implementation for fleets of the studied areas:

We evaluated the fleets circulating in four distinct areas: inner Paris, the first ring road (boulevard périphérique), the intra- A86 area and the A86 (second ring road). For each area, the categories of vehicles have been adapted to the structure of CopCETE software. Not having enough accurate data to estimate the parameters for each vehicle types, we assume that all types of vehicles of the same category (i.e. personal cars, vans, rigid trucks or trailer) follow the same law and, within the class, the types of vehicles are only differentiated by the data of the initial year.

In addition, as observed in the cases of Berlin and London during the RETMIF project, we assumed that the total traffic remains constant per vehicle subcategory, that is to say that any abandoned vehicle is replaced by a newer model of the same vehicle. This assumption allows analyzing the impact of fleet renewal, regardless of the trends between different subcategories.

Moreover, given that the share of electric vehicles is extremely low, and no regulatory or strong political will exists today on their development, we keep constant the percentage in both scenarios "over water" and "Reduced Emissions Zone." » The "electric" scenario will assess the possible impact of a change of clean vehicles.

The fleets in the 'Business as Usual' scenario

Our approach is therefore to estimate the fleet in each of the different area, implementing our statistical laws of survival defined above. Specifically, for a given vehicle type (eg diesel PL standard Euro 4), we assume that it is as likely to have been made in each year the standard was the latest in the market (Tables 2 and 3), and then we apply the survival coefficient corresponding to the years ahead.

For example, PL for Euro 4 diesel in 2014, about a third was registered in 2006 and the same for 2007 and 2008. For Euro 6, the number of vehicles also split in the different years, according to the

previous assumption of replacement of discarded vehicles.

Table 2: Years of registration of each Euro standard for HDV

Conventionnel	1988	1989	1990	1991	1992
Euro 1	1993	1994	1995		
Euro 2	1996	1997	1998	1999	2000
Euro 3	2001	2002	2003	2004	2005
Euro 4	2006	2007	2008		
Euro 5	2009	2010	2011	2012	2013
Euro 6	2014	2015	...		

Table 3 : Years of registration of each Euro standard for vans

Conventionnel	1990	1991	1992	1993	1994
Euro 1	1995	1996	1997	1998	
Euro 2	1999	2000	2001		
Euro 3	2002	2003	2004	2005	2006
Euro 4	2007	2008	2009	2010	
Euro 5	2011	2012	2013	2014	
Euro 6	2015	...			

This enabled to estimate the fleets in the "Business As Usual" scenario on each area for the years following the counting. These BAU fleets, compared to the "LEZ" scenario fleets, show the impact of a LEZ on the fleet. To determine the LEZ fleets scenario, we rely on rates of compliance of the LEZ observed in Berlin and London, taking into account the specificities of each of the capitals (eg Parisian fleet is initially oldest) and the type of control implemented. This gives the following table of compliance:

Table 4 : compliance rate of the LEZ per area and per year

	2018 (manual control)	2021 (RFID control)
Inside Paris	Limitation : E5 VUL 70%, PL 65%	Limitation : E6 VUL 96%, PL 93%
Ring road (Périphérique)	Limitation : - E5: VUL 65%, PL 60%	Limitation : E5 E6 : VUL 90%, PL 85% E5 : VUL 95%, PL 90%
Intra A86	Limitation : - E5: VUL 65%, PL 60%	Limitation : E5 E6 : VUL 90%, PL 82% E5 : VUL 95%, PL 90%
A 86	Limitation : - E5: VUL 65%, PL 60%	Limitation : - E6 : VUL 85%, PL 80% E5 : VUL 90%, PL 85%

These rates have been obtained by modifying the beta coefficient of the Weibull distribution from the year of announcement of the new regulation, which corresponds to the acceleration of the fleet renewal observed in all low emission zones. Beta determines the median age of survival and its decrease leads to a lower lifetime for old vehicles. Figure 3 shows an example of a van registered in 2008).

Figure 3: changes in the law of survival: for a van registered in 2008

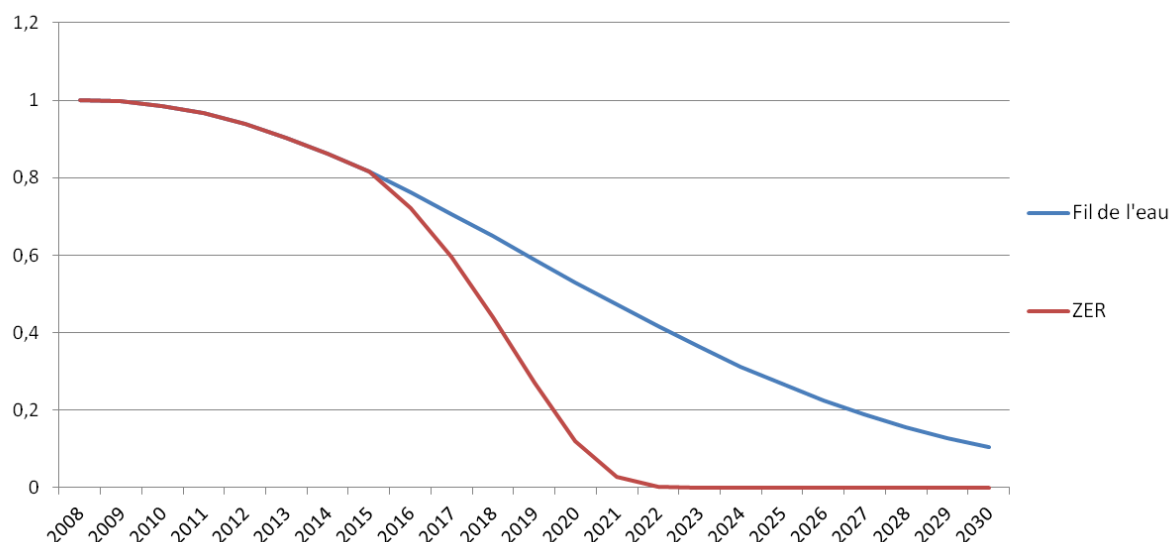


Table 5: The beta values used for the previous graph

2008	2009	2010	2011	2012	2013	2014	2015	2016	2017
14,9	14,9	14,9	14,9	14,9	14,9	14,9	14,9	13,6	12,3
2018	2019	2020	2021	2022	2023	2024	2025	2026	2027
11	9,7	8,4	7,1	7,1	7,1	7,1	7,1	7,1	7,1
2028	2029	2030							
7,1	7,1	7,1							

So we get ultimately estimates of the structure of the fleet (percentage of each traffic) for each year, for each zone and for scenarios BAU and LEZ.

Without a LEZ, 'natural' renewal of the old fleet with new vehicles in the latest Euro standard is gradual; the announcement and the implementation of a LEZ accelerates this renewal. Table 6 take the example of the evolution of trucks in Paris and allows us to further analyze the impact of the LEZ.

Table 6 : Evolution of the split of trucks in Paris according to their Euro norm

Euro standard	BAU				LEZ			
	2014	2018	2021	2025	2014	2018	2021	2025
Conventional	1,5%	0,2%	0,04%	0,02%	1,5%	0,03%	0,00%	0,00%
Euro I	1,2%	0,4%	0,1%	0,05%	1,2%	0,1%	0,00%	0,00%
Euro II	11, 6%	5,5%	2,3%	1,1%	11,6%	3,0%	0,00%	0,00%
Euro III	23,5%	16,6%	10,6%	5,1%	23,5%	13,2%	0,00%	0,00%
Euro IV	23,4%	20,3%	16,1%	10,1%	23,4%	18,7%	0,2%	0,1%
Euro V	29,5%	28,3%	25,7%	21,7%	29,5%	27,7%	6,8%	3,3%
Euro VI or more	9,4%	28,7%	45,2%	61,9%	9,4%	37,3%	93,0%	96,6%

La part des poids lourds les plus anciens (<= Euro II) est faible en 2021 dans le scénario au fil de l'eau et devient nulle ou négligeable dans notre scénario ZER ; l'impact de la mise en place d'une ZER sur ce parc ancien est donc faible (2,5%). En revanche, ces vieux véhicules ayant des

émissions très importantes par kilomètre, l'impact sur les émissions est beaucoup plus important.

Pour les poids lourds plus récents (Euro III à V) qui représente 76 % du parc en 2014, l'impact de la ZER est beaucoup plus sensible sur l'évolution du parc : dans Paris la part de ces PL passe de 76% en 2014 à 7% dans le scénario ZER 2021 (-69%) contre 52% en 2021 dans le scénario fil de l'eau (-24%). La tendance est la même pour les VUL dans Paris.

Pour les zones géographiques hors Paris, le fait que les véhicules Euro 5 sont en service depuis 2009 pour les PL et 2011 pour les VUL implique que le scénario ZER 2021 n'aura que peu d'influence sur le renouvellement effectif du parc. Le taux de renouvellement naturel (au fil de l'eau) des PL et VUL est suffisamment rapide pour que la ZER ne provoque pas de bouleversement important. Dans Paris, l'impact est plus fort car la ZER implique de l'Euro 6 donc des véhicules 4 à 5 ans plus récents (**Erreur ! Source du renvoi introuvable.** et **Erreur ! Source du renvoi introuvable.**).

La ZER va augmenter la proportion (et donc le nombre) de véhicules utilitaires 'propres' de façon significative. Cette modernisation accélérée du parc a été déjà observée dans les autres pays (Londres et Berlin).

The share of the oldest trucks (<= Euro II) is low in 2021 in the BAU scenario and becomes nil or negligible in our LEZ scenario; the impact of the implementation of the LEZ on this old stock is low (2.5%). However, for these older vehicles with very high emissions per kilometer, the impact on emissions is much more important than the impact on fleet.

For newer trucks (Euro III to V) representing 76% of the park in 2014, the impact of the LEZ is much more sensitive on the evolution of the park: in Paris the share of these trucks from 76% in 2014, decreases to 7% in the 2021 LEZ scenario (minus 69%) against 52% in 2021 in the BAU scenario (-24%). The trend is similar for vans in Paris.

For locations outside Paris, the fact that the Euro 5 trucks are in operation since 2009 (2011 for vans) means that the LEZ 2021 scenario will have little effect on the actual fleet renewal. The natural turnover (BAU) for trucks is fast enough for the LEZ does not cause major upheaval. In Paris, the impact is stronger because the LEZ involves Euro 6 vehicles, therefore 4-5 years more recent.

LEZ will increase significantly the proportion and therefore the number of clean freight vehicles. This accelerated modernization of the park following the implementation of a LEZ has already been observed in London and Berlin.

Computing emissions for electric vehicles

Electric vehicles do not emit CO₂ directly during a journey, but we take into account the CO₂ emissions upstream from the production of electricity used to operate the vehicle. For passenger cars (PC), the estimated average consumption (ADEME, 2014) per 100 km is 20 kWh. We will assume that all cars have the same consumption. Knowing that the French electricity emission factor is 53 gCO₂ / kWh (MEDDE, 2012), a private car therefore emits around 10.6 gCO₂ / km. For goods vehicles, emissions are calculated according to the power consumption, estimated by the following formula (Rizet et al, 2014b):

$$\text{Electricity consumption per km (kWh / km)} = 0.43 + 0.033 \times \text{GVW (tones)}$$

This formula was found from consumption data of different types of electric trucks literature on the assumption that the relationship between power consumption and the GVW is linear. For light commercial vehicles (vans), the average gross weight is taken equal to 3 tons. In the same way as cars, we will use the emission factor of 53 g CO₂ / kWh for the CO₂ emissions for each type of commercial vehicles (Heavy Commercial Vehicles).

From the number of trucks and vans and composition of fleet in the four zones in 2025, we were finally able to calculate, for each zone, the CO₂ emissions per linear kilometer of road. In the different scenarios

- Calculation method of PM emissions

Electric vehicles do not emit directly particulate matters out of their tailpipe like other ICE vehicles,

but they produce emissions of particles, by resuspension as well as abrasion (tires, brakes and road surface).

Table 7 : Non tail pipe PM emissions per vehicle type, in g/km.

Vehicle type	Trucks	Vans	Cars
Non tail pipe PM emission (g/km)	0,5732	0,05	0,0444

The values shown in Table 7 are the unit emissions per vehicle class data CopCETE. By summing the products of unit emissions by the number of vehicles, we finally get the PM emissions generated by the traffic of electric vehicles.

Results: vehicles and emissions

Local pollution of freight vehicles: the situation in 2011

Within the RETMIF project, the city of Paris sent us the data of the survey 'number plates' realized in 2011 to know various vehicle types circulating to Paris. These data were used with the software COPCETE V4 which calculates emissions by vehicle type, using the equations of COPERT 4. We present here the results of this analysis, focusing on the share of freight vehicles in the traffic and in its emissions.

In this plates survey, vehicle registration numbers are raised at various points, allowing, with the file of French vehicles registrations, to know their type, their energy, their year of first registration and pollution standard (Euro norm). The survey was conducted in week, 22 to 23 and June 28, 2011 from 8am to 10am and from 14h to 16h. The recorded sample of registrations recovered with a comprehensive traffic count.

We used these data for three types of roads: Motorways arriving in Paris, the ring road around central Paris (périphérique) and inside Paris. In this latter category, the survey points are mostly located on relatively large boulevards. The result of a road type is obtained by the weighted average traffic results of each point of inquiry of this type of road. For example Table 8 for motorway is the average of results from 3 survey points, one on the motorway A1, one on the motorway A4 and the third on the motorway A13, on their arrival in the capital. Emissions and traffic tables below are for 1 km of road, for 4 hours x 3 days of the week. Unfortunately we had not sufficient information to make an estimate of the overall emissions over the city for a year or even over a year at a given point, or even over 24 hours in a given point.

Importance of freight vehicles in the road traffic emissions in 2011: results by type of road:

In Table 1, freight vehicles account in 2011 for 23% of the number of registered vehicles (vans 17% HGV 6%), 53% of CO₂ emissions (23 and 30%), 68% of NO_x (21 and 47%) and 54% of PM (15 and 39%).

Table 8 : Motorways arriving in Paris - % of freight vehicles in the traffic and in the emissions

Motorways	Vehicles km (x1000)	tones CO ₂	Kg NO _x	Kg PM
Vans	5,08	0,95	3,85	0,42
%	17%	23%	21%	15%
Trucks	1,72	1,24	8,77	1,13
%	6%	30%	47%	39%
∑ freight vehicles	6,80	2,19	12,6	1,55
%	23%	53%	68%	54%
All vehicles	30,1	4,16	18,6	2,88

On the ring road (Table 2), freight vehicles account for 28% of traffic (19 and 8% respectively for vans and trucks), 63% of CO₂ emissions (25 and 38), 77% NO_x (19 and 58) and 64% PM (15 and 49). Compared to motorways, the volume of traffic is close, the share of commercial vehicles is somewhat higher (28% against 23%) and the share of emissions from these freight vehicles is more

important: 63% against 53% for CO₂, 77% against 68% for NO_x and 64% against 54% for PM.

Table 9 : Ring road (périphérique) - % of freight vehicles in the traffic and in the emissions

Ring road	Vehicles km (x1000)	tones CO ₂	Kg NO _x	kg PM
Vans	6,09	1,43	5,65	0,55
%	19%	25%	19%	15%
Trucks	2,61	2,19	17,4	1,81
%	8%	38%	58%	49%
Σ freight vehicles	8,70	3,62	23,0	2,35
%	28%	63%	77%	64%
All vehicles	31,3	5,78	29,9	3,68

Inside Paris (Table 3), the traffic is on average much lower than on motorways or on the ring road (about 6 times less) and freight vehicles account for 24% of traffic but with less truck (2%). The share of emissions from freight vehicles is also lower: 48% for CO₂ (11% for PL), 61% of NO_x (25%) and 46% PM (18%).

Table 10 : Inside Paris - % of freight vehicles in the traffic and in the emissions

In Paris	Vehicles km (x1000)	tones CO ₂	kg NO _x	kg PM
Vans	1,12	0,33	1,28	0,12
%	22%	36%	36%	28%
Trucks	0,10	0,10	0,88	0,076
%	2%	11%	25%	18%
Σ freight vehicles	1,22	0,44	2,15	0,19
%	24%	48%	61%	46%
All vehicles	5,12	0,92	3,51	0,43

For the 3 types of roads where traffic is known, freight vehicles (vans and trucks) are much more important for their emissions than for their traffic. They represent overall around a quarter of road traffic (23, 28 and 24% of vehicles km), half (53, 63 and 48%) of CO₂ emissions, two thirds of NO_x (68, 77 and 61%), and half of the particles (54, 64 and 46%). This share of freight vehicles in the total road emissions is higher than previous estimate for NO_x (35%, according to Gonzales-Feliu 2010) and close for PM. So specific regulations on emissions of commercial vehicles could have a significant impact on the total emissions in the capital. We also noted that commercial vehicles have a greater share in traffic on motorways and ring road than within Paris.

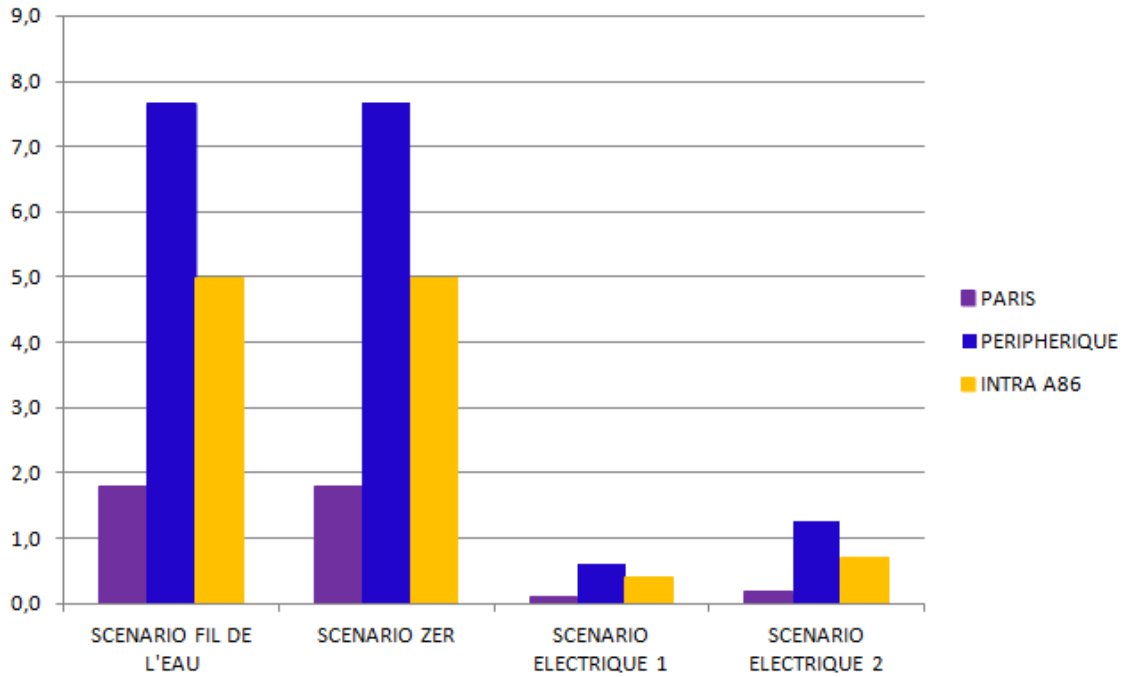
Freight vehicles emissions in the 2025 scenarios

Calculating emissions

Within Paris, an average emission value, weighted by the amount of traffic, is calculated from emissions on the different sections considered in the plate survey of the City of Paris in 2011. It is the same for the value of the emissions on the ring road (périphérique), where three sites are considered.

For non-electric scenarios, BAU and LEZ, we used the CopCETE tool for computing CO₂ emissions and PM. So we can make a comparison of emissions based on different scenarios. Figures 4 (for CO₂) and Figure 5 (for PM) here under show the evolution of computed emissions for different scenarios in 2025 for the three areas: Paris, ring-road (périphérique) and intra A86 motorway.

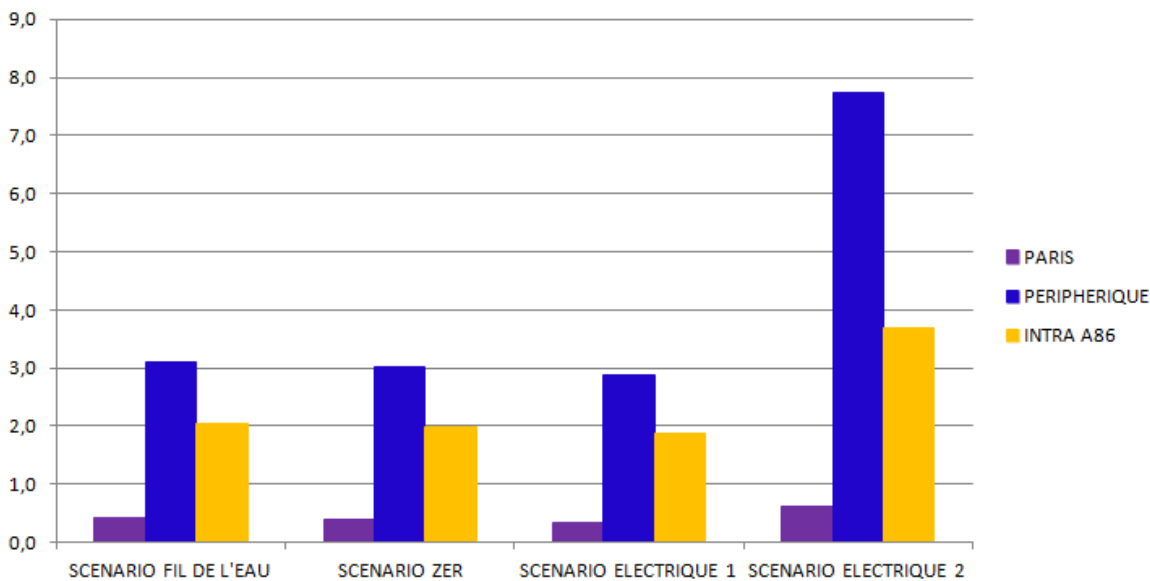
Figure 4 : CO₂ emissions (tones / km of road) by scenario and zone in 2025



For CO₂ emissions there is not much difference between BAU and LEZ scenarios: The LEZ has very little influence on CO₂ emissions since CO₂ is not included in the emission Euro norms.

In electrical scenarios 1 and 2, the CO₂ emissions have been considerably reduced in 2025 regardless of the geographical area. The reduction is less for electric scenario 2 because the number of vehicles increases. Indeed, the maximum threshold of 5 tones payload causes an increase in the number of vehicles and thus traffic. Compared with the BAU scenario, in the city of Paris CO₂ emissions declines of 95% for the electric scenario 1 and 90% for the electricity scenario 2. These decreases are very important because the French electricity emission factor is low (53 g CO₂ / kWh, ADEME, 2014), thanks to the high proportion of nuclear generation. These scenarios "100% electric" are extremely effective in terms of reducing CO₂ emissions, for the three areas concerned, from the current French context. The energy situation may however change in the coming years.

Figure 5: Estimation of PM emissions (kg/km of road) by zone in 2025 for the different scenarios



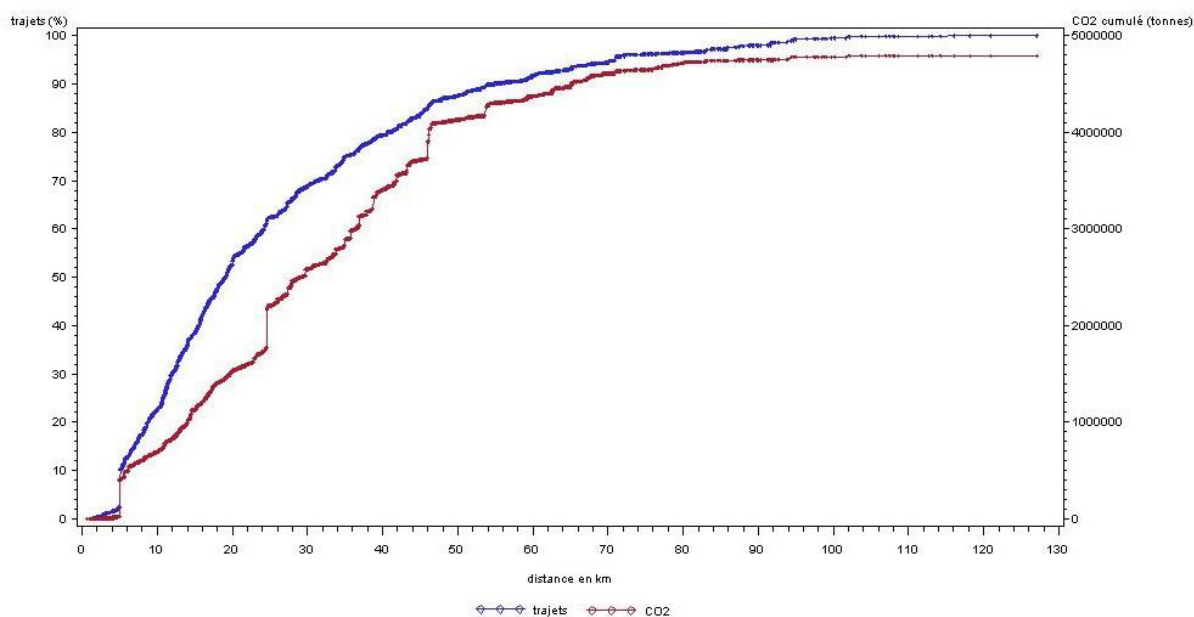
On PM emissions (Figure 5), the results are surprising at first. Indeed, we observe a very small decrease in emissions for the electricity scenario 1 compared to BAU and a real increase in emissions for electric Scenario 2. These phenomena are explained by the PM emission processes. The emissions in electric scenario 1, compared with the BAU scenario, decreased by 14.2%, respectively, 7.6% and 7.0% for Paris, the ring road and intra A86. These decreases are low because non tailpipe emissions (abrasion and re suspension) predominate for PM. For example, for a Euro 5 truck of less than 7.5 tones gross weight, non tailpipe PM emissions represent 96.6% of total PM. The phenomena of abrasion and resuspension also explain the significant increase in PM emissions for the electric scenario 2. Indeed, the traffic of trucks and vans increased by 293% 363% and 278% respectively, 2% for Paris, the ring-road and the intra A86. Thus the increase in emissions of the most important PM, 148.9% was observed for the ring-road, which is experiencing the greatest increase in traffic.

These results allow us to step back on the benefits of an electric scenario. But we must remember that the PM and indirect (upstream) emissions of CO2 are almost the only emissions of electric vehicles. For example, electric trucks don't emit NOx nor PAH.

Urban trip distances and electric vehicles range

The electric trucks range is an important constraint for the electrification of urban freight¹: we analyzed the distribution of freight traffic according to the distance of the legs in the electrical scenarios. The graph below (Fig. 6) shows the distribution of the number of urban legs according to their distance and thus the proportion of these legs which could be electrified in the electric scenario, according to the maximal distance considered for electric trucks. Nearly 90% of the legs are less than 50 km long. The figure below also shows the distribution of the urban CO2 emissions according to this distance.

Figure 6: Trip legs number and CO2 distribution according to the trip leg distance.



(Computed from Echo Survey, Cf. Rizet et al. 2015)

The percentage of trip legs can be read on the left axis and the corresponding CO2 emission level on the right axis: 87.6% of trip legs are less than 50 km and they emit 86% of the whole CO2 of the urban freight in the data base. At the opposite, legs beyond 100 km only represent 0.45% of the legs. The range currently announced for electric vans (around 100 km) would thus allow covering approximately 90% of the return electric routes of a French urban scenario. For the remaining 10%, it would be advisable either to improve electric trucks range (up to approximately 140 km), or to find a way to recharge battery before ending the round trip, or still to optimize the location of platforms by

¹ Cf. Rizet et al. 2015 (City Logistics)

agreeing to reduce the zones of limitation of the Diesel traffic of freight below urban areas.

Electric vehicle capacity and the congestion in electric scenario 2

In electric scenario 2, a diesel truck with a payload of 11 tones will for example be replaced by two trucks of 5 tons payload and one 2 tones payload. In contrast, a 14 tons payload truck will be replaced in this second electric scenario by three 5 tons payload trucks, to minimize the increase in traffic.

More electric freight vehicles will be needed to transport the same quantity of goods than today with large diesel trucks. The increase in traffic in electric scenario 2 compared with BAU, expressed in truck miles, is presented by region in Table 11

Tableau 11: Induced traffic in the electric Scenario 2 (% increase of freight vehicles) by Zone

Area	Paris	Ring-road (Périphérique)	Intra A86
Increase in the number of freight vehicle	293 %	363 %	278 %

Conclusion

The implementation of a LEZ will force road transport professionals to adapt their behavior to the new regulations. Impacts will depend on the size of actors: bigger ones will not be much concerned by the measure, thanks to rental services and adaptation of their business models, smaller ones will have more trouble, they have less long-term visions and their evolution will depend on the time of preparation and the helps (services or funding) provided by authorities.

But, in Paris, despite the great funding provided by the city of Paris and the national funding for buying an electric vehicle, the cost of such vehicles seems to be too high for a punctual use. Another difficulty will be that most of these companies have no time for doing complicated administrative tasks. The companies which count more than 10 employees won't have any funding from the municipality, so time for the evolution of the restriction has to be long enough for enabling these companies to comply.

Quantitatively speaking, the Low Emission Zone speeds up the modernization of the fleet. The impact the use of oldest vehicles will be low, but the resulting emissions will decrease much, due to the high emission factors. For newer vehicles, the LEZ would not have a great influence on their renewal, because the natural renewal of these utility vehicles is fast enough.

The impact on the fleet is higher in Paris than around the city, and reducing the flow of the utility vehicles is a priority because of the resultant polluting emissions. The highest impact would be for the NOx. The most realistic electric scenario shows an increase of the congestion and of the non-exhaust emissions.

With these results, the industrialization of new fuel cell engines tanked by alternative fuels like hydrogen seems to be a good complement of the regulations, by reducing the cost of the vehicles (mostly due to the price of the battery). Therefore, such "electric policies" have to go with most globalized industrialization plans, developing technological and logistics solutions.

References

Allen, J., Browne, M. and Woodburn, A. London Freight Data report 2012 update. 2012
 Boogaard, H., Janssen, N., Fischer P., Kos G., Weijers E., Cassée F., Van der Zee S., Hartog J., Meliefste K., Wang M., Brunekreef B., and Hoek G.. Impact of Low Emission Zones and Local Traffic

Policies on Ambient Air Pollution Concentrations. *Science of the Total Environment*, Vol. 435–436, 2012, pp. 132–140.

Bourdeau, B. 1997. Evolution du parc automobile français entre 1970 et 2020. PHD Thesis, Université de Savoie – Chambéry

Carteret M., André M., Pasquier A. 2014. Méthode d'estimation des parcs automobiles et de l'impact de mesures de restriction d'accès sur les émissions de polluants. Projet ZAPARC. Réalisé pour le compte de l'ADEME. 184 p.

Cruz, C., Montonen, A. Implementation and Impacts of Low Emission Zones on Freight Activities in Europe: Local Schemes Versus National Schemes. *Transportation Research Procedia*. Vol. 12, 2016, pp. 544–556.

Dablanc, L. Une grande oubliée, la logistique. In SEURA (Eds) , Les rendez-vous de la mégapole, AIGP2 saison 2. Atelier international du Grand Paris, 2013, pp 13-32.

Dablanc, L., Montonen, A., Impacts of Environmental Access Restrictions on Freight Delivery Activities - Example of Low Emissions Zones in Europe. *Transportation Research Record: Journal of the Transportation Research Board* Vol. 2478, 2015, pp. 12–18.

EEA, 2013 : Air Quality in Europe—2013 Report. European Environment Agency, Copenhagen, Denmark, 2013.

Gonzales-Feliu, J., Toilier, F. and Routhier, J.-L. End consumer goods movement generation in french medium urban areas. *Procedia Social and Behavioral Sciences*, Vol.2, 2010, pp. 6189-6204.

Hugrel, C., Joumard, R. 2004. Transport routier – Parc, usage et émissions des véhicules en France de 1970 à 2025. Document de l'INRETS

Kolli, Z. 2012. Dynamique de renouvellement du parc automobile. Projection et impact environnemental. PHD Thesis in economics, Université Paris 1

Rizet, C., Cruz, C., Vromant, M. The Constraints of Vehicle Range and Congestion for the Use of Electric Vehicles for Urban Freight in France, 9th Conference on City Logistics, Tenerife June 2015, Elsevier *Procedia*, pp 500-507

UE, 2005 : Report from the Working Group on Environmental Zones—Exploring the Issue of Environmentally-Related Road Traffic Restrictions. Joint Expert Group on Transport and Environment, Brussels, Belgium, 2005.

1 **DPF regeneration of Euro5 Diesel vehicles as source of fine and ultrafine** 2 **particles in the atmosphere**

3 B. R'Mili¹, A. Boréave¹, A. Meme¹, Charbonnel N., ¹ P. Vernoux¹, M. Leblanc², L. Noël², S.
4 Raux², B. D'Anna^{1*}

5 ¹*Université de Lyon, Institut de Recherches sur la Catalyse et l'Environnement de Lyon, UMR 5256,*
6 *CNRS, Université Claude Bernard Lyon 1, 2 avenue A. Einstein, 69626 Villeurbanne, France*

7 ²*IFP Energies nouvelles - Direction Systèmes Moteurs et Véhicules, Etablissement de Lyon, Rond-*
8 *point de l'échangeur de Solaize - BP 3, 69360 Solaize – France*

9

10 *Corresponding Autor : barbara.danna@ircelyon.univ-lyon1.fr

11

12 **Abstract**

13 Exhaust after treatment systems are commonly employed in passenger cars to comply with
14 current pollutant emission standards. This paper evaluated the characteristics of particles
15 emissions (particulate number (PN), size distribution, morphology and chemical composition)
16 released during the active regeneration of Diesel Particulate Filters (DPF) of two Euro 5
17 vehicles. The first vehicle was equipped with an oxidation catalyst (DOC) and a catalyzed-
18 Diesel Particle Filter (cDPF), while the after treatment of the second one was ensured by a
19 close-coupled DOC and non-catalyzed DPF combined with fuel borne catalyst. Exhaust
20 particulate emissions were monitored using several instruments including SMPS+E, MAAP,
21 AMS and MPS to determine PN size distribution, black carbon weight concentration,
22 chemical composition of the volatile fraction adsorbed on the particles and by off line TEM
23 analysis to study particles morphology and elemental composition. Emission profiles varied
24 during the regeneration process depending on the evaluated technologies. The emitted
25 particles mainly consist of small droplets formed by nucleation process and soot aggregates in
26 the accumulation mode. The first are mainly formed by ammonium sulfate and sulfuric acid,
27 predominantly found in lubricants, stored in the DPF during normal driving conditions. The
28 second consists of carbonaceous material (aggregate soot) coated by semi-volatile materials
29 including organics, ammonium sulfate and sulfuric acid. Emissions in the accumulation mode
30 are due to a gradual decrease in the filtration efficiency (due to the soot cake oxidation)
31 throughout the regeneration process.

32

33 Keywords : DPF active regeneration, Euro5, Diesel exhaust, black carbon, ultrafine and fine particles,
34 chemical composition, TEM-EDX, AMS

35

37 1. Introduction

38

39 | Aerosol particles have important effects on air quality, human health, and climate.[*IPCC. and*
40 *Stocker, 2013; WHO, 2012*] In particular, transports and specifically Diesel engines are
41 important source of ultrafine particles in urban environments. Diesel engine's particles mainly
42 consist of carbonaceous species, including soot particles and organic matter (OM). The latter
43 resulting from low volatility organic compounds originated by incomplete fuel combustion
44 and/or lubricant.[*Chow et al., 2011; Matti Maricq, 2007*] The OM is primarily composed of
45 aliphatic hydrocarbons and may contain various amount of polycyclic aromatic hydrocarbons
46 (PAHs) known to be toxic and carcinogenic.[*Humans, 1983; Nielsen et al., 1996; Soontjens et*
47 *al., 1997*] Ashes such as metals traces (S, Fe, Ni, Mg, Zn, Cr, Na, K, Mn, Cu...), originating
48 from combustion (fuel or lubricant) or from engine wear, are also found in exhaust
49 emissions.[*Cheung et al., 2010; Sharma et al., 2005; Wang et al., 2003*] Diesel exhaust PM
50 composition highly depends on the engine operation and mileage, fuel composition, lubricant
51 and exhaust after treatment technology.[*Chow et al., 2011*] In Europe, all Diesel cars are
52 equipped with a combination of Diesel Oxidation Catalyst (DOC) and Diesel Particulate Filter
53 (DPF) to meet, from 2011 Euro 5b regulation (limited PN = 6.0×10^{11} #/km ($D_p > 23$ nm)
54 and PM = 4.5 mg/km), or from 2014 Euro 6b (regulation (EC) [692/2008, 2008]).

55 The DOC promotes chemical oxidation of CO and soluble organic fraction (SOF) of diesel
56 PM. It also oxidizes exhaust nitric oxide (NO) to form nitrogen dioxide (NO₂), which assists
57 particulate matter oxidation in the DPF.[*Shrivastava et al., 2010*] However, at high exhaust
58 gas temperature, DOC can release and oxidize SO₂ to SO₃. In the presence of sufficient water
59 vapor, this yields sulfuric acid, which can promote nucleation alone or upon neutralization
60 with NH₃, it can also rapidly condense on soot. [*Giechaskiel et al., 2014; Matti Maricq, 2007*]
61 DPF drastically reduces PM emissions (between 90-98%) through filtration or physical
62 deposition mechanisms, i.e. inertial impaction, interception, Brownian diffusion and
63 thermophoresis. [*Adler, 2005; Herner et al., 2011; Mayer, 2008*] Continuous particle
64 deposition on the DPF's walls forms a so-called deep bed or soot-cake, which significantly
65 improves filtration efficiency. [*Choi et al., 2014*] To avoid excessive back pressure on the
66 engine, regeneration of the accumulated soot is periodically required. The commonly used
67 process consists in oxidizing the soot by an exothermic reaction. The so-called active
68 regeneration is activated by means of post-injections in the engine's cylinders during the late
69 expansion stroke or directly in the exhaust line in order to generate exothermic energy across

70 the DOC.[*Fino and Specchia, 2008; Van Setten et al., 2001*] During active regeneration
71 process, the filter temperature sharply increases (over 600 °C) while the pressure gradually
72 drops, due to the soot-cake combustion. High emission of PM (both in number and mass) are
73 observed during active DPF regeneration.[*Beatrice et al., 2012; Bikas and Zervas, 2007;*
74 *Campbell et al., 2006; Dwyer et al., 2010*] Particle bimodal distribution is generally observed:
75 the nucleation mode is attributed to the stored semi-volatile compounds inside the DPF
76 originating from unburned fuel or engine lubricating oil and in certain studies to the
77 fragmentation of soot particle aggregates; the accumulation mode mainly consists in
78 carbonaceous soot particles coated with small fraction of ash and organic
79 compounds.[*Beatrice et al., 2012; Cauda et al., 2007; Cauda et al., 2006*]
80 In order to gain a better understanding of Euro 5 Diesel passenger cars emissions and their
81 impact on the environment, a detailed investigation of particle chemical composition,
82 morphology, size and PN was undertaken. This study presents a complete view of PM
83 emissions measured on a dynamometer test bench, combining multiple analytical techniques
84 that allow, an accurate assessment of ultrafine particles in the range 2-37 nm and size resolved
85 information on the chemical composition and morphology of the emitted particles.

86

87 **2. Experimental set-up and methodology**

88 **2.1. Vehicles and fuels specifications**

89 Two vehicles with different Diesel engine types and after treatment technologies were
90 evaluated during the testing phases; both were equipped with a common-rail direct injection
91 and meet Euro 5 emission standard.

- 92 1. Vehicle 1: fitted with two DOCs and a catalyzed DPF (cDPF).
- 93 2. Vehicle 2: fitted with a close coupled DOC and non-catalyzed DPF combined with a
94 Fuel Borne Catalyst (FBC-DPF).

95 The main vehicles characteristics are summarized in Table 1. The after treatment
96 configurations evaluated in this study correspond to the most widespread technologies and
97 Diesel exhaust control configurations for passenger cars in Europe. The fuel used during the
98 testing meets the EN590 standard representative of current commercial fuels with low sulfur
99 content (< 2 ppmv), mass spectra are shown in Figure S3 and S4. The lubricants used in the
100 two engines were analyzed (their elemental compositions are presented in table S1, while
101 Figure S1 and S2 show their mass spectra).

102

103 Table 1: Vehicle specifications

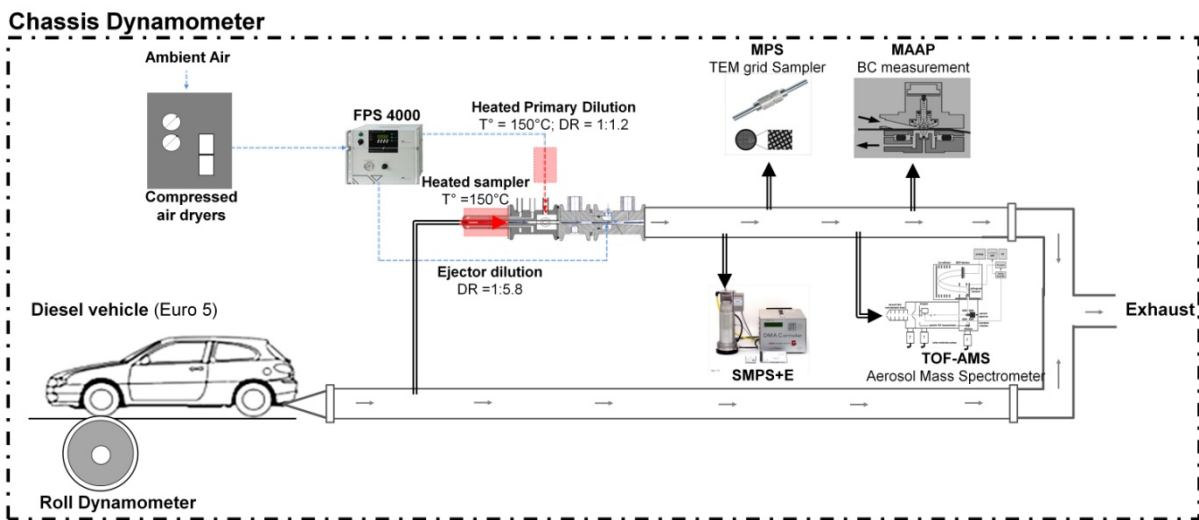
	Vehicle 1	Vehicle 2
Weight (kg)	1200	1300
Mileage (km)	13000	27000
Emissions standard	Euro 5	Euro 5
Engine displacement (cc)	1461	1560
Number of cylinders	4	4
Rated power (kW)	66	84
Peak torque (Nm)	200	270
Fuel Delivery	Common Rail	Common Rail
After-treatment	Underfloor DOCs+CDPF	Close-coupled DOC+FBC-DPF

104

105 **2.2. Measurement protocol**

106 The tests were conducted at IFPEN facilities. A dedicated instrumentation was deployed
107 inside the dynamometer test bench to follow a wide range of vehicles and exhaust emissions
108 parameters (among which : vehicle speed, exhaust composition, temperature and pressure,
109 pressure drop across the DPF,...), in order to characterize the active regeneration process of
110 the two DPFs.

111 The experimental set-up is shown in **Figure 1**



112

113 **Figure 1.** Concept diagram of the experimental set-up.

114

115 | **∇**Exhaust gases were sampled using a two-stage dilution and sampling system with perforated
116 tube and ejector diluter, FPS-4000 Dekati®. This device provides a primary hot or cold
117 dilution through a perforated tube, limiting therefore condensation and coagulation
118 phenomena. A second dilution is realized using an ejector (please insert dilution ranges).
119 Temperatures and pressures are measured in different parts of the diluter enabling real time

120 calculation of the dilution factor and the sampling rate. The FPS-4000 was used with a
121 dilution rate of about 6.1:1, calculated from the CO₂ concentrations continuously measured in
122 the exhaust line and downstream of the FPS-4000 corresponding to sampling rate of about 21
123 l/min.

124 Particulate emissions were monitored by several instruments. A Scanning Mobility Particle
125 Sizer with Faraday Cup Electrometer (SMPS+E GRIMM) equipped with a small Differential
126 Mobility Analyzer (DMA) was chosen for particle number concentration and size distribution
127 measurements. The SMPS+E was operated with a sheath air flow of 20 l/min and an aerosol
128 flow of 1 l/min. Aerosols size distribution measurements between 2 and 35 nm were achieved
129 every 37 seconds. On-line time resolved measurements of particle composition were
130 performed using a compact time-of-flight (c-TOF ToFwerk) aerosol mass spectrometer (AMS,
131 Aerodyne Inc. USA). The AMS operating principles, calibration procedures and analysis
132 protocols are described in details elsewhere (e.g.[*Drewnick et al.*, 2009; *Drewnick et al.*,
133 2005]). The instrument provides quantitative size-resolved mass spectra of the non-refractory
134 components empirically defined as vaporizable species over a 1s time interval at 700°C and
135 | 10⁻⁷ torr. These typically include OM, ammonium nitrate and sulfate (NH₄⁺, NO₃⁻ and SO₄²⁻),
136 chloride and water. This instrument combines the mass spectrometer system with
137 aerodynamic particle sizing and thus provides information on the aerodynamic size
138 distribution of particles. Particles were sampled through a critical orifice of 100 μm at
139 approximately 85 mL/min. A Thermo Scientific Model 5012 MAAP (Multi-Angle
140 Absorption Photometer) was used for Black Carbon (BC) mass concentration measurements
141 of vehicle 2 (FBC-DPF) at a single nominal wavelength 670 nm. The instrument measures
142 both light attenuation and scattering at specific angles 0°, 130° and 165° reducing
143 significantly the influence of scattering, even if material other than BC is also sampled in the
144 filter.[*Petzold and Schonlinner*, 2004] The technique is mainly applied for ambient air
145 measurements but has recently been successfully applied to combustion particles.[*Petzold and*
146 *Schonlinner*, 2004] Correction for measurements artifact at high BC mass concentration levels
147 were taken into account as suggested by Hyvarinen et al. [*Hyvarinen et al.*, 2013] A MPS
148 (mini-particle sampler) was used to collect exhaust particles. This technique, based on
149 filtration through TEM-porous grids, enables sampling of particles directly on a specific
150 support minimizing additional sample preparation procedure and sampling artifact.[*R'mili et*
151 *al.*, 2013] A solenoid valve system was used to perform sampling at specific times of the
152 regeneration events with a flow rate of 0.3 l/min. The deposited particles were then

153 investigated by TEM, coupled with energy-dispersive X-ray (EDX) with respect to their size,
154 morphology and elemental composition (JEOL 2010F microscope operated at 200 kV).

155 **2.3. Test methodology**

156 To allow the DPFs to be regenerated, it was first necessary to load them. Due to the use of in
157 service vehicles during this study, two different loading ways were encountered in order to
158 help to improve regeneration conditions. First, a regeneration was launched at the vehicle
159 arrival to take advantage of its real driving loading and thereafter, to start the DPF loading
160 procedure defined for the study with a nearly empty DPF in each case. After that, the DPFs
161 were loaded on the dynamometer test bench during approximately 800 kms, on random
162 successive cycles (10 NEDC, 6 WLTC, 4 CADC and 12 urban CADC), steady speed haulages
163 arised from the NEDC and with different conditions of engine starts (from cold to hot). The
164 random order was chosen not to favor one of the after treatment technologies in terms of
165 potential continuous regenerating conditions and to avoid systematic bias.

166 Finally, DPF regenerations were triggered at constant vehicle speed of 90 km/h. The engine
167 load remained constant during the whole regeneration process, but was primarily set to
168 achieve an upstream DPF temperature of about 390 °C, in order to characterize the
169 regeneration process with similar and stable initial conditions for both DPFs [R'mili et al.,
170 2013]. Then, a decoy was applied to the DPF back pressure sensor to simulate an increase in
171 the DPF loading and the need of a DPF cleaning. This decoy forced the engine control unit
172 (ECU) to initiate the active regeneration process and to switch to the dedicated cartography.

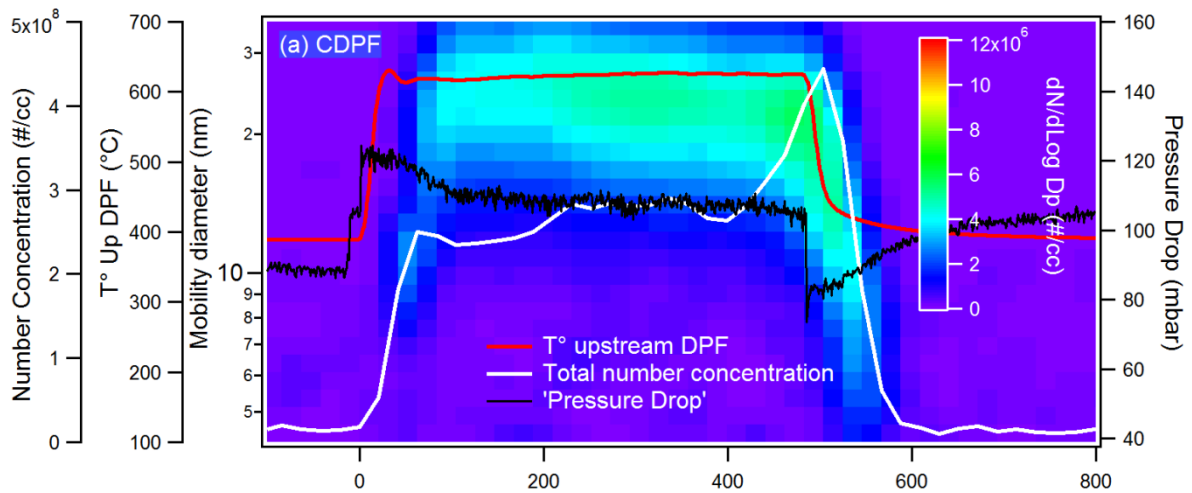
173

174 **3. Results and Discussion**

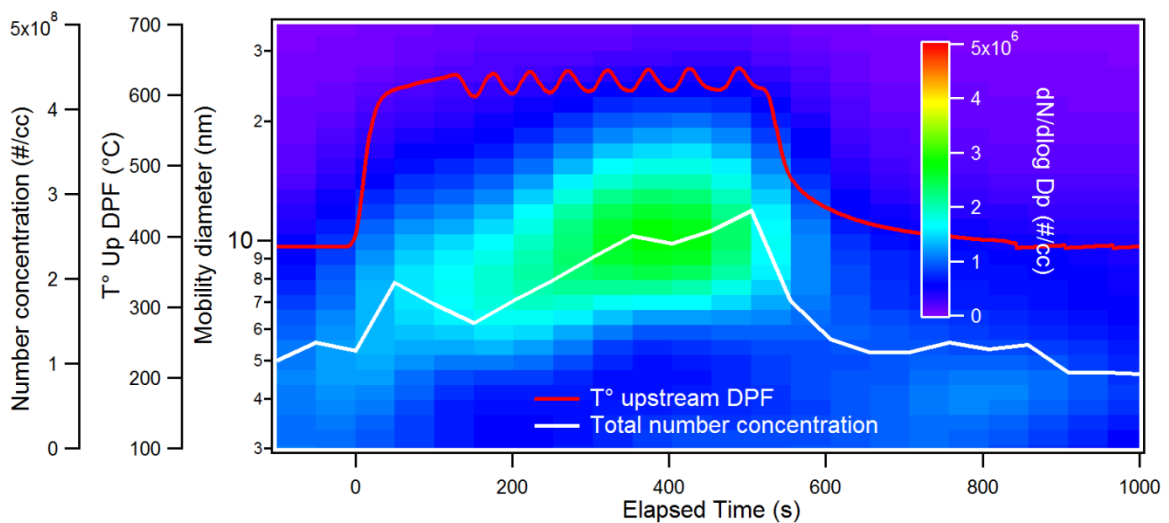
175 Three regenerations were analyzed for each vehicle. They are similar in terms of trend,
176 duration and targeted temperature (even between vehicles) but particulate emissions were
177 quite different whether it is between the vehicles or between the different regenerations with
178 the same vehicle. . For brevity, only the results from one regeneration for each vehicle will be
179 presented and discussed in details. The choice...

180 Figure 2 reports the time evolution of the ultrafine particles (size distribution and
181 concentrations between 2-35 nm) measured at the outlet of the DPFs by the SMPS+E during
182 the regeneration of the vehicle 1 (CDPF) and 2 (FBC-DPF) respectively, as well as the DPF
183 upstream temperature. The temperature profiles for vehicle 1 (Figure 2a) and vehicle 2 (Figure
184 2b) are slightly different even if the average upstream DPF temperature is approximately
185 610°C for both vehicles. For vehicle 1, the temperature sharply increases up to the target

186 temperature of about 620 °C involving a temperature overshoot at the beginning of the
 187 regeneration process before to be stabilized at approximately 610 °C. For vehicle 2, the
 188 temperature first quickly increases up to 600 °C, then gradually reaches 630 °C and then starts
 189 to oscillate between 600 °C and 630 °C. The post-injected fuel seems to be managed along the
 190 process in order to guarantee the required regeneration temperature and to avoid the filter
 191 breakup.



192



193

194 **Figure 2.** SMPS+E measurements – temporal evolution of ultrafine particles (Dp below 35 nm)
 195 concentration and size distribution during regeneration events: (a) the CDPF and (b) FBC-DPF
 196 vehicles.

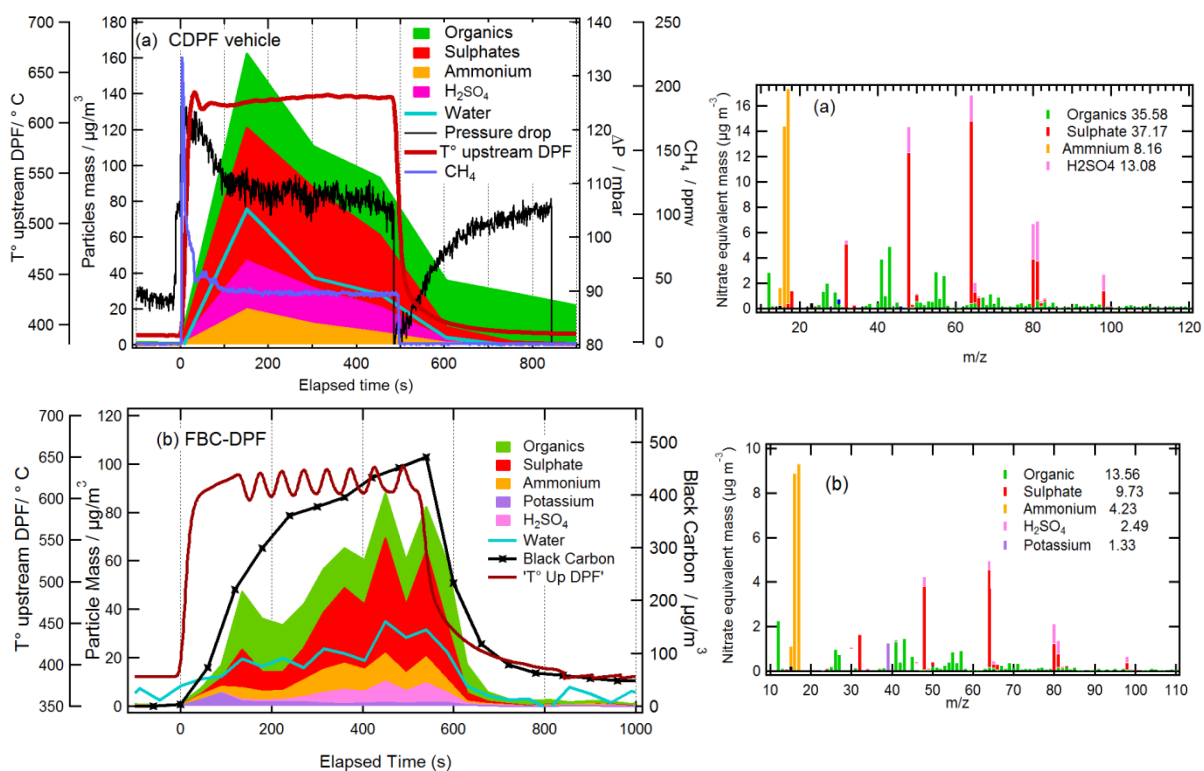
197

198 As the post-injection starts, a rapid increase in ultrafine PN is observed for vehicle 1 (Figure
 199 2a) whereas for vehicle 2 (Figure 2b) , a progressive and smaller PN -increase is observed. In
 200 both cases, the ultrafine particulate emissions last as long as the active regeneration process
 201 take place, that is to say during less than 600 seconds. This duration is likely related to the

202 post-injection strategy (fuel quantity and duration), which relies on the estimated DPF soot
203 load, traffic conditions met by the vehicle, but also on fuel savings and minimum sootload
204 preservation in the DPF allowing an optimal filtration efficiency.[Konstandopoulos and
205 Papaioannou, 2008] The observed size distribution indicates that nucleation events occur
206 during DPF regeneration, as already reported by several groups. [Beatrice et al., 2012; Bikas
207 and Zervas, 2007; Cauda et al., 2007; Dwyer et al., 2010] Even if it is difficult to directly
208 relate the present work to previous studies since the DPF, the test procedures and the
209 instrumentations are different, some similarities emerge. Previous works link ultrafine particle
210 emission during DPF regeneration to the purge of stored volatile material originating from
211 unburned fuel and lubricant [Giechaskiel et al., 2007] or to sulfur oxides that may lead in
212 presence of water to the formation of sulfuric acid droplets and ammonium sulphate.[Bikas
213 and Zervas, 2007; Campbell et al., 2006] Other authors [Beatrice et al., 2012; Cauda et al.,
214 2007; Harris and Maricq, 2002; Kostoglou and Konstandopoulos, 2003] suggest possible
215 fragmentation of the soot cake in the DPF during regeneration due to the fast combustion
216 process, resulting in emission of such soot fragments. Chemical composition and morphology
217 analysis of the emitted particles during the regeneration process have been investigated in this
218 study and will be presented in the next paragraphs in order to achieve a better characterization
219 and understanding of their evolution.

220 Real time chemical composition of condensable species was monitored using an Aerosol
221 Mass Spectrometer (Aerodyne C-ToF). The temporal evolution of the main measured
222 chemical families are shown in Figure 3a for vehicle 1 and in Figure 3b for vehicle 2,
223 respectively. Spectral analysis show the presence of ammonium sulfate, sulfuric acid, organic
224 compounds and water (average mass spectra are shown on the right side of Figure 3). Water
225 mainly from the gas phase is also observed, therefore it is not accounted as particle mass. For
226 vehicle 1 (Figure 3a), the regeneration start is characterized by a rapid increase in emissions
227 of sulfur species (ammonium sulfate and sulfuric acid) and water followed by organic species.
228 A similar behavior in the chemical composition is observed in the second regeneration (SI
229 Figure S1). Sulfuric acid may additionally be formed inside the ionization chamber of the
230 AMS by reaction of SO_3 with the high water content present in the exhaust plume (SI,
231 equations I-III). Sulfate and sulfuric acid dominate the particulate phase composition at the
232 beginning of the regeneration event of the CDPF vehicle. These emissions lasted for about
233 450 to 600 seconds, while the organic fraction continued to be emitted beyond 500-600
234 seconds most likely associated with soot emissions, this can be explained by a reduced

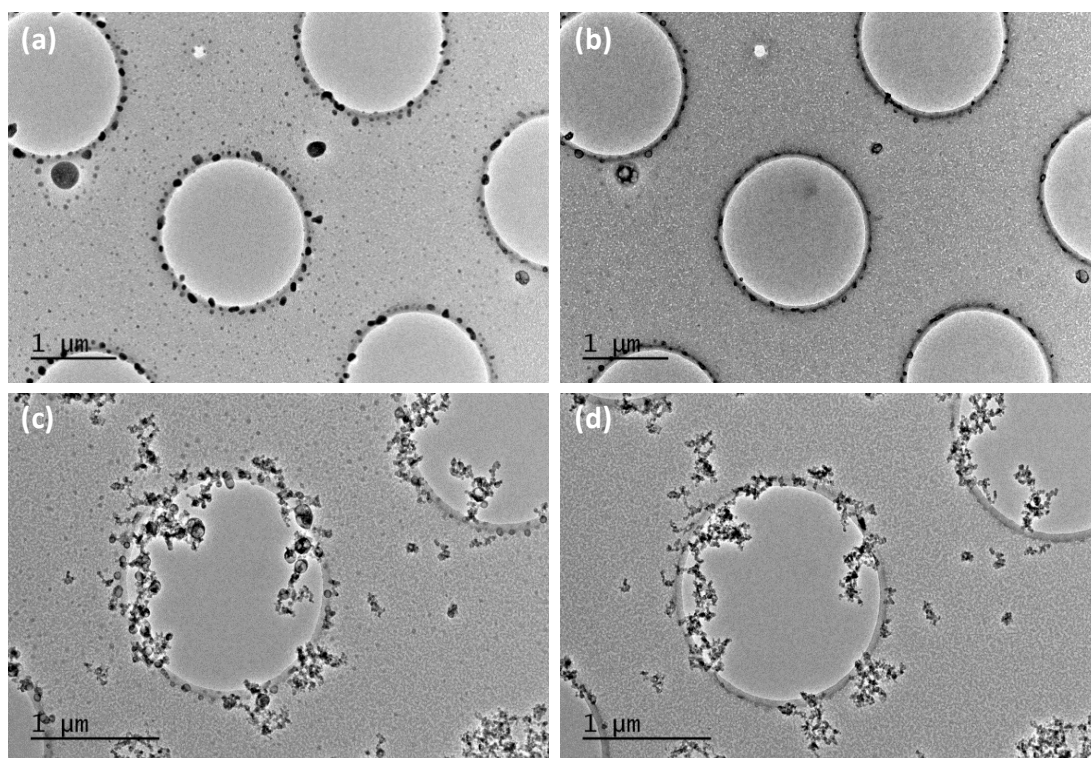
235 filtration efficiency just after the regeneration due to the removal of the soot layer on the DPF.
 236 For vehicle 2 (Figure 3b) the regeneration event induced progressive emission of ammonium
 237 sulfate and sulfuric acid, water and BC while the organic fraction in the exhaust reaches a
 238 relatively constant value two minutes after the post-injection beginning. The regenerations
 239 observed for the FBC-DPF vehicle presented good repeatability in term of time evolution (SI
 240 Figure 2S). BC emissions (measurements performed only for vehicle 2) increased
 241 progressively as the regeneration event started and lasted about 540 seconds reaching about
 242 $450 \mu\text{g}/\text{m}^3$ in the last phase of regeneration, then dropped to about $60 \mu\text{g}/\text{m}^3$ at the
 243 regeneration end due to reduced DPF filtration efficiency. A similar behavior was observed
 244 by Cauda et al. and Beatrice et al. [Beatrice et al., 2012; Cauda et al., 2007] who suggested
 245 that the time profile of emitted soot (dependent also on the post-injection) followed the
 246 reduction of DPF filtration efficiency due to the soot layer oxidation throughout the
 247 regeneration process.



248
 249 **Figure 3.** AMS and MAAP measurements - temporal evolution of the major identified chemical
 250 species and average mass spectra for (a) the CDPF and (b) the FBC-DPF vehicles.

251 TEM images of the particles sampled during the regeneration event of vehicle 1 (CDPF) are
 252 shown in Figure 4a, 4b, 4c and 4d. The first two images were obtained with a sample of 80
 253 seconds from the beginning of the regeneration. Many small droplets with average projected
 254 diameter of about 19 nm (using ImageJ® software) were observed; they easily evaporated

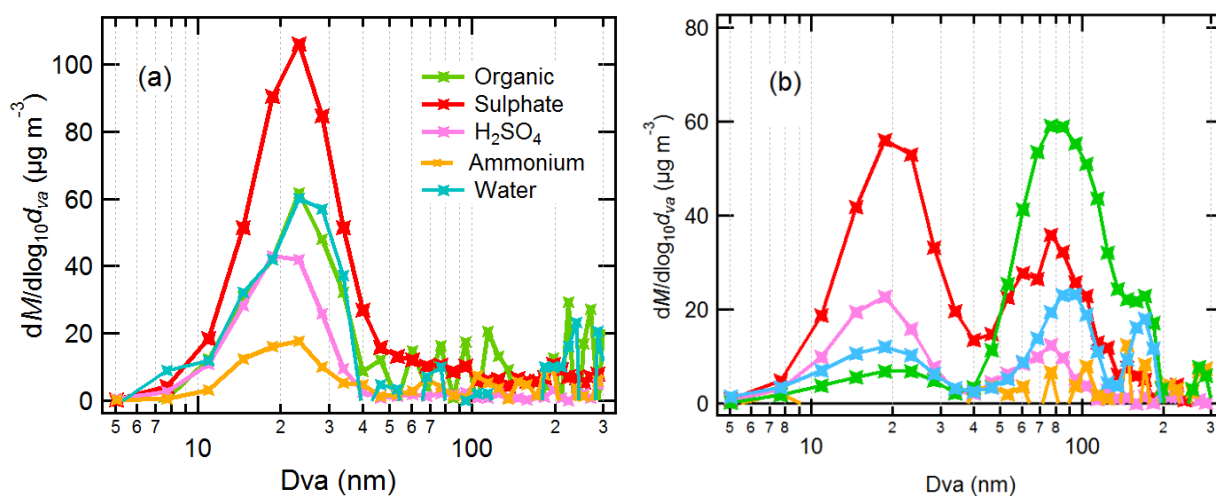
255 within seconds of exposure under the TEM electron beam as can be seen by comparing the
256 two images (Figure 4a and 4b) taken at the same location. EDX analysis of small particles is
257 somehow challenging even though elemental sulfur was detected as main component. Figures
258 4b and 4c show a second TEM image for the same regeneration event; the sampling was
259 operated 120 seconds after the first one. Again, evaporation of the small droplets under the
260 electron beam is noticeable by comparing Figure 4c and Figure 4d. Fractal soot was observed
261 here and a fraction of containing sulfur particles was observed (EDX analysis) and seemed to
262 be adsorbed on soot aggregates.



263
264 **Figure 4.** TEM analysis results – samples taken during the regeneration event of the CDPF: (a) sample
265 of 80 seconds from the regeneration start; (b) same image after few seconds under the electron beam;
266 (c) sample of 120 seconds from the end of the first sample; (d) same image after few seconds under the
267 electron beam.

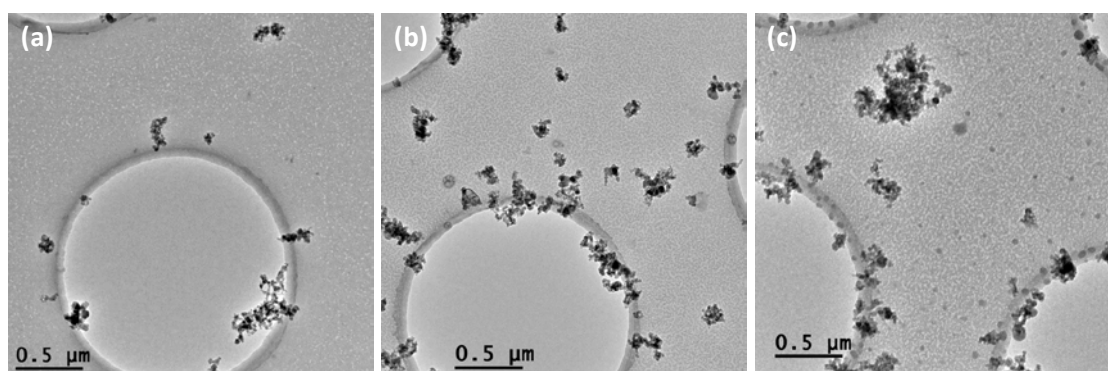
268 TEM-EDX observations are further confirmed by the chemically resolved mass normalized
269 particle Time-of-Flight size distributions shown at two stages of the regeneration events of the
270 vehicle 1 (figure 5a and 5b). Even if the AMS should not be able to measure particles below
271 60 nm, due to their losses in the aerodynamic lens, the amount of ultrafine particles emitted
272 during the first regeneration of the CDPF vehicle was so high that their presence was
273 monitored by the instrument. As can be seen in figure 5a, the nucleation mode dominates the
274 first minutes of the regeneration, with particle's average diameter of 23 nm (aerodynamic
275 vacuum diameter, D_{va}), their composition was dominated by ammonium sulfate and sulfuric

276 acid, water and to a minor extent organic matter. After a couple of minutes, a bimodal
 277 distribution appeared (figure 5b) showing a lower second mode composed by organic material
 278 and to a minor extent sulfates, both probably adsorbed onto soot aggregates at 80-90 nm.



279 **Figure 5.** Chemically resolved mass normalized pToF size distributions (aerodynamic vacuum
 280 diameter) for vehicle 1 (CDPF) : (a) during the first 180 seconds from the start of the regeneration and
 281 (b) 380-400 seconds after the regeneration start. Color codes in Figure 5a indicated the size resolved
 282 chemical composition.

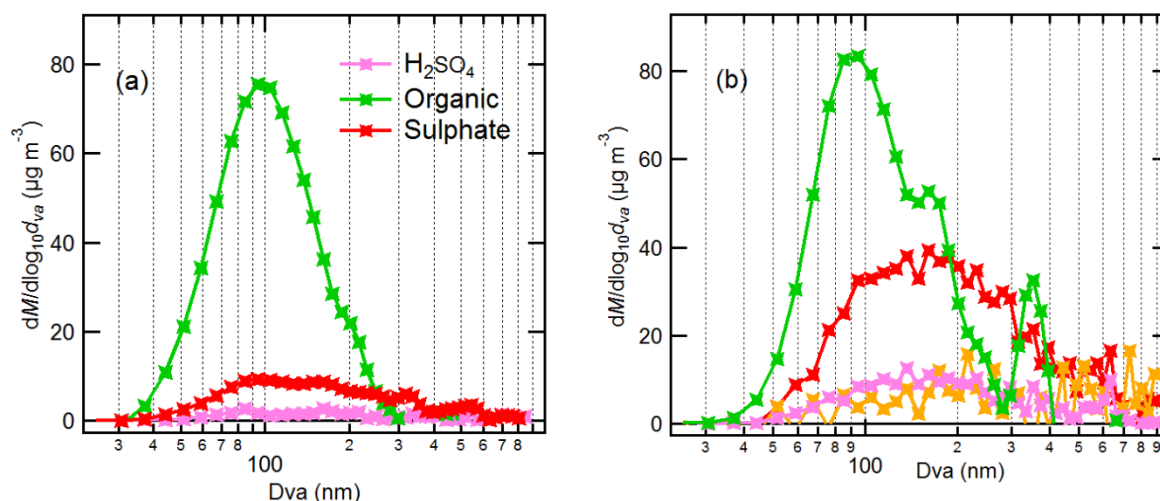
283 For vehicle 2, the particles were sampled on TEM grids at three successive times; the results
 284 are shown in Figure 6a, 6b and 6c. A first sample was collected over a period of 120 seconds
 285 followed by two samples collected over 120 and 240 seconds respectively. Small amounts of
 286 carbon soot are observed at the beginning of the regeneration; as this evolves small droplets
 287 with median projected diameter of about 15 nm appear in addition to the soot particles,
 288 emission of both type of particles increases at the end of the regeneration.



289 **Figure 6.** TEM analysis results of samples collected during the regeneration of vehicle 2 : (a) sample
 290 of 120 seconds from the regeneration start. (b) 120 seconds from the end of the first sample and (c)
 292 240 seconds from the end of the second sample.

293 AMS chemically resolved mass normalized pToF size distributions for vehicle 2 are shown in
 294 Figure 7a and 7b. From the beginning of the regeneration an accumulation mode around 100

295 nm is observed, mainly composed by organic material most likely adsorbed onto soot
 296 particles. A second broader mode with median diameter of about 180 nm is observed,
 297 composed by sulfates and to a lesser extent by sulfuric acid ; this latter mode increased at the
 298 end of the regeneration process (Figure 7b). The nucleation mode is not observed here by the
 299 AMS, because of a poor lens transmission efficiency and a relatively lower concentration of
 300 ultrafine particles emitted during the regeneration of the FBC-DPF, as can be observed by
 301 SMPS+E analysis (Figure 2b).



302 **Figure 7:** Chemically resolved mass normalized pToF size distributions (aerodynamic vacuum
 303 diameter) for vehicle 2: (a) after 120 seconds and (b) after 400-460 seconds from the post-injection
 304 start. Color codes in 7a indicated the size resolved chemical composition.

305 Discussion

306 According to the SMPS+E, AMS and TEM analysis, the trigger of the post-injection during
 307 these two regenerations is accompanied by emission of both fine and ultrafine particles.
 308 Particles emission is rapid for vehicle 1 (CDPF) and progressive for vehicle 2 (FBC-DPF) due
 309 to the different after treatments design and regeneration strategies. Granulometry (SMPS+E),
 310 morphology (TEM) and chemical analysis (AMS and TEM-EDX) suggest that the ultrafine
 311 particles (below 30 nm) are small droplets composed by sulfuric acid and ammonium sulfate
 312 and to a minor extent by organic material most likely coming from lubricant and unburned
 313 fuel (see SI Figure 4S).

314 Ultrafine particles are mainly linked to desulfation of the catalyst. The adsorbed sulfur is
 315 desorbed from the catalyst (DOC and /or DPF?) as the temperature rises, it is then oxidized to
 316 SO_3 which can further react with water vapor leading to sulfuric acid formation and, after
 317 neutralization by ammonia, to ammonium sulfate. Soot particles or its fragments were not

318 clearly observed in the nucleation mode. The accumulation mode observed for both vehicles
319 (even if at slightly different diameters) is characterized by an organic fraction adsorbed onto
320 soot aggregates and sulfates, this later can or not be adsorbed onto the soot aggregates, as
321 shown in Figure 5b and 7b. Particles in the accumulation mode are mainly emitted during
322 regeneration process when the soot cake oxidation gradually reduces the DPF filtration
323 efficiency allowing to a fraction of soot to pass through the DPF walls.

324 The two vehicles clearly showed different emissions in terms of time evolution, particle
325 number, size and morphology. The rapid emission of ultrafine particles or droplets observed
326 for vehicle 1 (CDPF) could be explained by the direct contact between the catalyst layer
327 incorporated into the DPF walls and the stored semi-volatile material originating mainly from
328 lubricant oil (which contains relatively 0.12 wt of sulfur, see SI table 1S). In fact, SOF
329 (Soluble Organic Fraction) viscosity rapidly decreases with increasing temperature inside the
330 DPF, it could therefore slip through the soot layer and become in contact with the catalyst
331 layer. As the regeneration starts and the temperature rises t , the decomposition of sulfates
332 previously stored may initiate leading to emission of SO_3 that could bring to nucleation
333 events.

334 For vehicle 2 the FBC is added to the fuel inside the engine cylinder, therefore it will be
335 deposited in the DPF in close contact with soot particles [*Song et al.*, 2006] and distributed
336 throughout the soot layer. As the regeneration process starts and the temperature rises, the
337 previously deposited metals can catalyze soot oxidation. After their oxidation, the FBC may
338 come progressively in contact with organic material and the sulfur compounds and gradually
339 increase the release into the gas phase of the nucleation precursors. This dynamic might
340 explain the gradual increase in the number concentration and size distribution of particles
341 observed during regeneration events. The unburned post-injected fuel can also play a role in
342 the nucleation process and droplets formations when the soot layer is oxidized and the
343 filtration efficiency reduced. These aspects of DPF regeneration deserve to be depth to better
344 understand the mechanisms that lead to the nucleation process and droplets formation
345 according to the after treatment technology.

346 The present work introduces a new analytical approach based on the coupling of different
347 measurement techniques to assess particles emissions during regeneration event of Euro 5
348 light-duty vehicles equipped with the most commonly used after treatment systems. The
349 results provide new informations regarding to particulate emissions morphology and

350 composition during this particular process . The regeneration events may cause strong particle
351 emissions both in terms of total number and mass concentration if the duration of post-
352 injection is not properly controlled. Emission of ultrafine particles can be important whatever
353 the vehicle and the after-treatment technology used and is mainly associated to sulfates and
354 sulfuric acid (volatile materials). These particles contain a complex chemical mixture
355 (ammonium sulfate, sulfuric acid, organics and traces of potassium). Therefore, attention
356 should be given to this particular phase of the operation of modern vehicles and further
357 research is needed to characterize the actual environmental and health impact of the emitted
358 particles. However, it can be already concluded that in order to minimize such emissions,
359 regeneration strategies should avoid full removal of the soot cake.

360

361 **Acknowledgements**

362 The authors would like to thank ADEME agency for financing the project CAPPNOR
363 (CORTEA program).

364

365

366

367 **References**

- 368 692/2008, C. R. E. N. (2008), Implementing and amending regulation (EC) N. 715/2007 of the
 369 European parliament and of the council on type-approval of motor vehicles with respect to
 370 emissions from light passenger and commercial vehicles (Euro 5 and Euro 6) and on access to
 371 vehicle repair and maintenance information, *Official Journal of the European Union*.
- 372 Adler, J. (2005), Ceramic Diesel Particulate Filters, *International Journal Applied Ceramic Technology*, 2
 373 (6), 429-439.
- 374 Beatrice, C., S. D. Iorio, C. Guido, and P. Napolitano (2012), Detailed characterization of particulate
 375 emissions of an automotive catalyzed DPF using actual regeneration strategies, *Experimental
 376 Thermal and Fluid Science*, 39(0), 45-53.
- 377 Bikas, G., and E. Zervas (2007), Regulated and Non-Regulated Pollutants Emitted during the
 378 Regeneration of a Diesel Particulate Filter, *Energy & Fuels*, 21(3), 1543-1547.
- 379 Campbell, B., M. Peckham, J. Symonds, J. Parkinson, and A. Finch (2006), Transient gaseous and
 380 particulate emissions measurements on a diesel passenger car including a DPF regeneration
 381 event, SAE Technical Paper.
- 382 Cauda, E., D. Fino, G. Saracco, and V. Specchia (2007), Secondary nanoparticle emissions during diesel
 383 particulate trap regeneration, *Topics in Catalysis*, 42-43(1-4), 253-257.
- 384 Cauda, E., S. Hernandez, D. Fino, G. Saracco, and V. Specchia (2006), PM0.1 Emissions during Diesel
 385 Trap Regeneration, *Environmental Science & Technology*, 40(17), 5532-5537.
- 386 Cheung, K., L. Ntziachristos, T. Tzamkiozis, J. Schauer, Z. Samaras, K. Moore, and C. Sioutas (2010),
 387 Emissions of particulate trace elements, metals and organic species from gasoline, diesel, and
 388 biodiesel passenger vehicles and their relation to oxidative potential, *Aerosol Science and
 389 Technology*, 44(7), 500-513.
- 390 Choi, S., K.-C. Oh, and C.-B. Lee (2014), The effects of filter porosity and flow conditions on soot
 391 deposition/oxidation and pressure drop in particulate filters, *Energy*, 77, 327-337.
- 392 Chow, J. C., J. G. Watson, D. H. Lowenthal, L. W. A. Chen, and N. Motallebi (2011), PM2.5 source
 393 profiles for black and organic carbon emission inventories, *Atmospheric Environment*, 45(31),
 394 5407-5414.
- 395 Drewnick, F., S. S. Hings, M. R. Alfarra, A. S. H. Prevot, and S. Borrmann (2009), Aerosol quantification
 396 with the Aerodyne Aerosol Mass Spectrometer: detection limits and ionizer background
 397 effects, *Atmospheric Measurement Techniques*, 2(1), 33-46.
- 398 Drewnick, F., S. S. Hings, P. Decarlo, J. T. Jayne, M. Gonin, K. Fuhrer, S. Weimer, J. L. Jimenez, K. L.
 399 Demerjian, S. Borrmann, and D. R. Worsnop (2005), A new time-of-flight aerosol mass
 400 spectrometer (TOF-AMS) - Instrument description and first field deployment, *Aerosol Science
 401 and Technology*, 39(7), 637-658.
- 402 Dwyer, H., A. Ayala, S. Zhang, J. Collins, T. Huai, J. Herner, and W. Chau (2010), Emissions from a
 403 diesel car during regeneration of an active diesel particulate filter, *Journal of Aerosol Science*,
 404 41(6), 541-552.
- 405 Fino, D., and V. Specchia (2008), Open issues in oxidative catalysis for diesel particulate abatement,
 406 *Powder technology*, 180(1), 64-73.
- 407 Giechaskiel, B., R. Munoz-Bueno, L. Rubino, U. Manfredi, P. Dilara, G. De Santi, and J. Andersson
 408 (2007), Particle Measurement Programme (PMP): Particle Size and Number Emissions Before,
 409 During and After Regeneration Events of a Euro 4 DPF Equipped Light-Duty Diesel Vehicle, SAE
 410 Technical Paper.
- 411 Giechaskiel, B., M. Maricq, L. Ntziachristos, C. Dardiotis, X. Wang, H. Axmann, A. Bergmann, and W.
 412 Schindler (2014), Review of motor vehicle particulate emissions sampling and measurement:
 413 From smoke and filter mass to particle number, *Journal of Aerosol Science*, 67(0), 48-86.
- 414 Harris, S. J., and M. M. Maricq (2002), The role of fragmentation in defining the signature size
 415 distribution of diesel soot, *Journal of Aerosol Science*, 33(6), 935-942.

416 Herner, J. D., S. Hu, W. H. Robertson, T. Huai, M.-C. O. Chang, P. Rieger, and A. Ayala (2011), Effect of
417 advanced aftertreatment for PM and NO_x reduction on heavy-duty diesel engine ultrafine
418 particle emissions, *Environmental Science & Technology*, 45(6), 2413-2419.

419 Humans, C. I. D. R. S. L. C. W. G. O. T. E. O. T. C. R. O. C. T. (1983), *Polynuclear Aromatic Compounds,*
420 *Part 1: Chemical Environmental and Experimental Data*, International Agency for Research on
421 Cancer.

422 Hyvarinen, A. P., V. Vakkari, L. Laakso, R. K. Hooda, V. P. Sharma, T. S. Panwar, J. P. Beukes, P. G. Van
423 Zyl, M. Josipovic, R. M. Garland, M. O. Andreae, U. Poeschl, and A. Petzold (2013), Correction
424 for a measurement artifact of the Multi-Angle Absorption Photometer (MAAP) at high black
425 carbon mass concentration levels, *Atmospheric Measurement Techniques*, 6(1), 81-90.

426 IPCC., and T. F. Stocker, D. Qin, G.-K. Plattner, M. Tignor, S.K. Allen, J. Boschung, A. Nauels, Y. Xia, V.
427 Bex and P.M. Midgley (Eds.) (2013), *Climate Change 2013: The Physical Science Basis.*
428 Contribution of Working Group I to the Fifth Assessment Report of the Intergovernmental,
429 *Cambridge University Press, Cambridge, United Kingdom and New York, NY, USA, , 1535 pp,*
430 *doi:10.1017/CBO9781107415324.*

431 Konstandopoulos, A. G., and E. Papaioannou (2008), Update on the science and technology of diesel
432 particulate filters, *KONA Powder and Particle Journal*, 26, 36-65.

433 Kostoglou, M., and A. G. Konstandopoulos (2003), Oxidative fragmentation and coagulation of diesel
434 soot aggregates, *Journal of Aerosol Science*, 34, S1061-S1062.

435 Matti Maricq, M. (2007), Chemical characterization of particulate emissions from diesel engines: A
436 review, *Journal of Aerosol Science*, 38(11), 1079-1118.

437 Mayer, A. (2008), *Particle filter retrofit for all diesel engines*, expert verlag.

438 Nielsen, T., H. E. Jørgensen, J. C. Larsen, and M. Poulsen (1996), City air pollution of polycyclic
439 aromatic hydrocarbons and other mutagens: occurrence, sources and health effects, *Science of*
440 *the Total Environment*, 189, 41-49.

441 Petzold, A., and M. Schonlinner (2004), Multi-angle absorption photometry - a new method for the
442 measurement of aerosol light absorption and atmospheric black carbon, *J. Aerosol Sci.*, 35(4),
443 421-441.

444 R'mili, B., O. L. C. Le Bihan, C. Dutouquet, O. Aguerre-Charriol, and E. Frejafon (2013), Particle
445 Sampling by TEM Grid Filtration, *Aerosol Science and Technology*, 47(7), 767-775.

446 Sharma, M., A. K. Agarwal, and K. Bharathi (2005), Characterization of exhaust particulates from
447 diesel engine, *Atmospheric Environment*, 39(17), 3023-3028.

448 Shrivastava, M., A. Nguyen, Z. Zheng, H.-W. Wu, and H. S. Jung (2010), Kinetics of Soot Oxidation by
449 NO₂, *Environmental Science & Technology*, 44(12), 4796-4801.

450 Song, J., J. Wang, and A. L. Boehman (2006), The role of fuel-borne catalyst in diesel particulate
451 oxidation behavior, *Combustion and Flame*, 146(1-2), 73-84.

452 Soontjens, C. D., K. Holmberg, R. N. Westerholm, and J. J. Rafter (1997), Characterization of polycyclic
453 aromatic compounds in diesel exhaust particulate extract responsible for aryl hydrocarbon
454 receptor activity, *Atmospheric Environment*, 31(2), 219-225.

455 Van Setten, B. A., M. Makkee, and J. A. Moulijn (2001), Science and technology of catalytic diesel
456 particulate filters, *Catalysis Reviews*, 43(4), 489-564.

457 Wang, Y.-F., K.-L. Huang, C.-T. Li, H.-H. Mi, J.-H. Luo, and P.-J. Tsai (2003), Emissions of fuel metals
458 content from a diesel vehicle engine, *Atmospheric Environment*, 37(33), 4637-4643.

459 WHO (2012), IARC: DIESEL ENGINE EXHAUST CARCINOGENIC, *PRESS RELEASE N° 213.*

460

461

How selection techniques on traffic data sets can help in estimating network vehicle emissions

Nicole SCHIPER*, Delphine LEJRI* & Ludovic LECLERCQ*

*Laboratoire Ingénierie Circulation Transport (LICIT), ENTPE/IFSTTAR, Lyon, 69518, France - email : nicole.schipper@ifsttar.fr

Abstract

Road traffic is a major source of air pollution in urban areas. Policy makers are pushing for different solutions including new traffic management strategies that can directly lower pollutants emissions. To assess the performances of such strategies, the calculation of pollution emission should take into account traffic dynamics.

The use of traditional on-road sensors (e.g. inductive loops) for collecting real-time data is necessary but not sufficient because of their expensive cost of implementation. It is also a disadvantage that such technologies, for practical reasons, only provide local information. Some methods should then be applied to expand this local information to large spatial extent. These methods currently suffer from the following limitations: (i) the relationship between missing data mechanisms/patterns and the estimation accuracy, both cannot be easily determined and (ii) the calculations on large area is computationally expensive. Given a dynamic traffic simulation, we take a novel approach to this problem by applying selection techniques that can identify the most relevant locations to estimate the network vehicle emissions. This paper explores the use of a statistical method, i.e. the Lasso regularized generalized linear models, as powerful tool for selecting the most relevant traffic information on a network to determine the total pollution emission.

Keys-words: vehicle emissions, traffic data selection, inductive loops, lasso, spatial-temporal correlation.

Résumé

Le trafic routier reste une source importante de pollution de l'air dans les zones urbaines. Face à ce constat, l'enjeu est de proposer des stratégies de réductions des émissions de polluants, y notamment des stratégies de gestion du trafic permettant réduire les congestions. Pour évaluer les performances de ces stratégies, le calcul des émissions des polluantes devrait prendre en compte la dynamique du trafic.

L'utilisation de capteurs traditionnels sur la route (par exemple des boucles inductives) pour la collecte de données en temps réel est nécessaire mais pas suffisante en raison de leur coût élevé de mise en œuvre. D'autre part, l'inconvénient de telles mesures de trafic, est de fournir des informations localisées. Certaines méthodes permettent d'étendre cette information locale afin de représenter les états de trafic sur l'ensemble du réseau. Ces méthodes souffrent actuellement des limitations suivantes : (i) la détermination des données manquantes n'est pas aisée à déterminer et (ii) les calculs à grande échelle impliquent des traitements des données coûteuses en temps. A partir d'une simulation dynamique et microscopique de trafic, nous proposons une nouvelle approche à ce problème en appliquant des techniques de sélection qui peuvent aider à identifier les endroits les plus pertinents pour estimer les émissions des véhicules du réseau. Cet article explore l'utilisation d'une méthode statistique, à savoir le Lasso, puissant outil de sélection des données de trafic sur un réseau pour déterminer les émissions totales de polluants.

Mots-clés : émissions de véhicules, sélection des données de trafic, boucle de comptage, lasso, corrélation spatiale et temporelle.

Introduction

Over the years the transportation industry has been directly associated with different environmental problems. Among these problems are the air pollutant emissions. The vehicle emissions are generated by various chemical reactions occurring inside the internal combustion engine. These compounds are primarily responsible for degradation of atmospheric air, which results in a loss of quality of life of all inhabitants (breathing problems, degradation of structures), especially in large urban centers (Smit et al, 2010). The emissions generated by vehicles are also responsible for greater magnitude of problems related to climate change (Franco et al, 2013).

According to the European Union (European Commission, 2015), road traffic accounted for 65% of Carbon Monoxide (CO), 41% of hydrocarbons (HC), 48% of Nitrogen Oxides (NO_x) and 30% carbon dioxide (CO₂) released into the atmosphere. Measures such as technological innovation for vehicles and the use of cleaner fuels have contributed to a significant reduction in vehicle emissions per kilometer traveled. However, the growth of the vehicle fleet and the increase in distances traveled has contributed to an increase in generated vehicle emissions (Andre et al, 2009), offsetting the benefits already achieved. The policymakers wish to reduce emissions without reducing mobility. The challenge, therefore, is to provide an improved air quality without compromising the mobility of the population.

Reducing emissions can be achieved also with the implementation of measures to modify the pattern of car use, either by reducing car use, either by reducing the events that produce high emissions rates (i.e. congested periods). The impact of transport control measures on emissions is typically measured in terms of reduction of vehicle emissions brought about by these strategies. In this context, the environmental impact of road transport is becoming increasingly a concern for planners and transportation managers. Currently, many of the transport models incorporate technologies to measure pollutants from road traffic, in order to assist in the evaluation of transport strategies taking into account their respective environmental impacts.

Most of these proposals is associated with new technologies for vehicles and fuels. This type of measurement, however, presents results only in a long term. To ensure a future decrease in transport-related CO₂ emissions, it is essential that most of users exploit cleaner vehicles, use low-Sulphur and unleaded fuels, and increase the turn-over rate of their ageing vehicle fleet. This type of strategies need years to be implemented and to get the first results of pollutants reduction. However, measures related to planning traffic influence on vehicle operating characteristics have a good result in a short-term (Franceschetti et al, 2013). The extent of the results of the implementation of planning measures traffic and cost/benefit, however, can not be evaluated without the use of quantitative models for pollutants estimate from road traffic, or simply, emission models (De Vlieger, 2000).

In general, the emission models perform quantification of contaminants in two stages. The first consists in determining a set of emission factors that specify the rate at which the emissions are generated. The second step involves estimating the activities of vehicles. The emission inventory is calculated by multiplying the results of these two steps. The emission models need, therefore, data on the activity and behavior of the traffic. It is commonly used for this purpose, driving cycles developed to represent the operation of a vehicle in a manner similar to the real world (Ahn and Rakha, 2008). However, sometimes these cycles can represent traffic behavior of a refined form (Al Barakeh, 2012). Currently we observe the great use of emission models that aggregates the traffic models. The direct use of traffic models for the calculation of vehicle emissions becomes interesting as it provides a refined description of traffic conditions both in space and time. Furthermore, there are able to predict the impacts of new traffic management strategies or new road layouts.

Good understanding of traffic dynamics is fundamental to assist in choosing the most effective study strategy to be adopted for each type of problem being treated. In this context, simulations can reproduce the effect that any changes will have on traffic, predicting their behavior, can be instrumental in defining appropriate strategies to be adopted to improve the traffic in question. This work allows taking into account more precisely, the effects of traffic dynamics on network and for that precision, a significantly increase of volume processed data and time calculation to get some results. This complexity is necessary when it comes to describe a fine resolution of space and time the evolution of emissions. It may seem excessive, but when it is fair to compare different projects in relation to their global impacts.

The aim of the paper is to work on the sampling of data traffic to reduce significantly the volume of data to be processed while keeping an accurate estimate of the overall results in terms of air pollution. It is thus to define the minimum sample in time and in space as a function of the emission model. For example, rather than making calculations on each part of the network, a set of links and reference time periods will be identified to perform the calculations. Compared to this objective, the main challenges are related to the integration of spatial and temporal correlations between the traffic information and, more generally, to the inclusion of the time dimension. The spatial-temporal correlations are linked to waves of congestion and changes in demand that propagate through the network. Thus it is important to define a methodology able to take into account the correlations for the segmentation of the population to define a representative sample. Moreover, the dynamic traffic and the traffic conditions changes on different time horizons (from the second to the day). It is important to correctly estimate the emissions but also their temporal estimation to consider the time factor. This may lead to a particular sampling differentiated according to the periods of the day. For this, a good understanding of the coupling between

traffic models and emission models will be profitable.

1. Objectives and methodology

Traffic data sampling is the research topic that is presented. It comes to identify effective methods of sampling in order to determine with a sufficient degree of accuracy the characteristics of pollutant emissions in the total population (average, total...). We explore the use of a statistical method, i.e. the Lasso regularized generalized linear models (Friedman et al, 2010), as powerful tool for selecting the most relevant traffic information on a network to determine the total pollution emissions. A neighborhood of Paris, part of the 6th district, was used as the basis for our study. The network was built as part of the project ISpace & Time (2013) funded by the ANR (the french national research agency). The network is composed of 234 links, 93 crossroads, 19 entries, 21 exits including 4 parking's inside and 27 traffic lights. All links have directions, bus lane, traffic lights times and allowed turning movements inside crossroads. This network was implemented in the microscopic traffic simulator called Symuvia developed by the laboratory LICIT (*Laboratoire Ingénierie Circulation Transport*). This traffic simulator is used to define the traffic settings which represents, in the most realistic way, the traffic conditions on the neighborhood. There are three main settings that should be taken into account: temporal evolution of demand, origin-destination matrix and assignment matrix. In order to avoid long calculation time to simulate 24 hours of traffic, the 6 most relevant hours for typical daily traffic are considered. The temporal evolution of the demand is represented by two peak hour's traffic: morning and evening. The first one corresponds to the intense demand distributed in short period of time while the evening peak have a moderate demand distributed in a longer time.

In order to simulate the traffic in the proposed network, only passenger cars were modeled. On each link are placed the two types of sensors. The 6 hours of simulation will be divided in 24 periods of 15 minutes, and for each one the traffic information will be recovered in every link of the network.

Two types of virtual sensors are used during the simulation. MFD loops provide a complete information of the local traffic as: total travel time, travelled distances by cars and their mean speeds. Inductive loops just give the number of vehicles and the mean speed observed in the middle of each link. This loop type is an example of traffic data used by policymakers to evaluate their strategies to regulate the networks. It is important to note that the spatial traffic information at link level only come from MFD sensors. This can only be derived by simulation. A sensibility analysis between both to quantify emissions will be discussed in the next section.

In order to be statistically representative, a great number of observations (i.e. simulations) and various traffic states in space and time are needed. To this end, the number of simulations has been set at 400, so the traffic simulator will be launched 400 times to represent more of a year of traffic data. The difference between them will be the demand randomly for each entry and period of time.

In order to assess traffic emissions, the main purpose of emission models consists in estimating emission data on different spatial and temporal scale. The current state-of-art in vehicle emission models comprise a set of methodologies. They range from calculations at a microscopic scale (i.e. for a single vehicle or for a street) to a macroscopic calculation (i.e. regional, national and global levels) through the inventory of an urban transport network. Furthermore, the models differ by the way they take into account the following parameters: pollutants "covered"; type of emissions; fleet composition (vehicles categories and age); driving patterns (average speed only or instantaneous speed and acceleration). For our study will be used COPERT IV emission model to estimate the pollutants from the variables described above.

This paper is organized as follow: First will be presented how different source of traffic information can affect emissions; The second part presents the sampling method used to select the most relevant traffic and the datasets used; Finally, the results will be discussed.

2. Influence of variable definition on emissions

Once all simulations have been launched on Symuvia, the traffic data for each loop was recovered using the software Matlab. From the MFD loops were recovered 4 important traffic information from each time period in every link: total travel time, total travelled distance and mean speed. Total travel time and total travelled distance (i.e. travel production) means the total time spent by vehicles respectively the

total travelled distance in each link during the time period settled. The spatial mean speeds are calculated as the ratio of the total travelled distance and the total time spent by vehicles for every link and time period.

Inductive loops give only vehicle flows and mean speeds at the location of the sensors (i.e. in the middle of each lane in every link of the network). In order to calculate emissions using COPERT IV, two traffic information are required: travelled distance and mean speed. Using the inductive loops as traffic information source, travelled distances need to be calculated from the vehicle flows. To this end, two link length definitions will be used. The two definition for link lengths are static and dynamic one: The first called static length, considers the geometric link length, so the length between its begin and end including the distance between the exit of link and barycenter from the upstream crossroad, if it exists. The second length called dynamic, takes into account the extra distances of allowed movements inside of the crossroads. The latter allows to know the real distance travelled by vehicles on the link and inside of the crossroad, according to flow, instead of estimated them using geometric measures. It is interesting to understand that the geometric link length is a static magnitude and does not depend to traffic flow. Unlike that, the dynamic link length depends completely of the traffic flow on each link and crossroad, hence the name dynamic.

As described above, the traffic data will be used as input in emission models to calculate pollutant emissions. Two pollutants will be considered, the CO₂ (carbon dioxide) that have most impact in greenhouse effect and the NO_x (nitrogen oxides) which impact the public health. The emission assessment is done according to the choice of parameter settings such as fleet composition, type of emissions and speed-dependent emissions. The 2015 french fleet composition was chosen and the study will concentrate on hot emissions. To calculate the amount of each pollutant, the speed-dependent curves will be used. The latter provide emission factors for each average speed bigger than 10 km/h. Considering that, for average speeds less than 10 km/h, the emissions will be calculated using the emission factor equal to 10 km/h. The equation that will be used to quantify emissions with the speed curve is shown below:

$$E(t) = P(t) \cdot \mathbf{EF}(S)$$

Where:

$E(t)$ → Total Emission for each period

$P(t)$ → Total travelled distance for given period

$\mathbf{EF}(S)$ → Emission factor based on the mean speed for given period

As said before, the MFD travel production is used as reference to evaluate the calculation methods of the total traveled distance using traffic data from inductive loops. To remember, this last one recover, for each time period, only mean speed and vehicle flows for each point settled in the middle of each lane. To obtain the total traveled distance to use as input on the emission model, two hypotheses are explored: calculate it as function of the full link length including the barycenter length of the upstream crossroad if exists multiplied by the flow in each period of time (namely geometric); and calculate it as function of traveled distance by cars on the link plus the allowed movements travelled inside of the upstream crossroad (namely dynamic). Figure 1 shows the comparison of these two hypothesis with the reference.

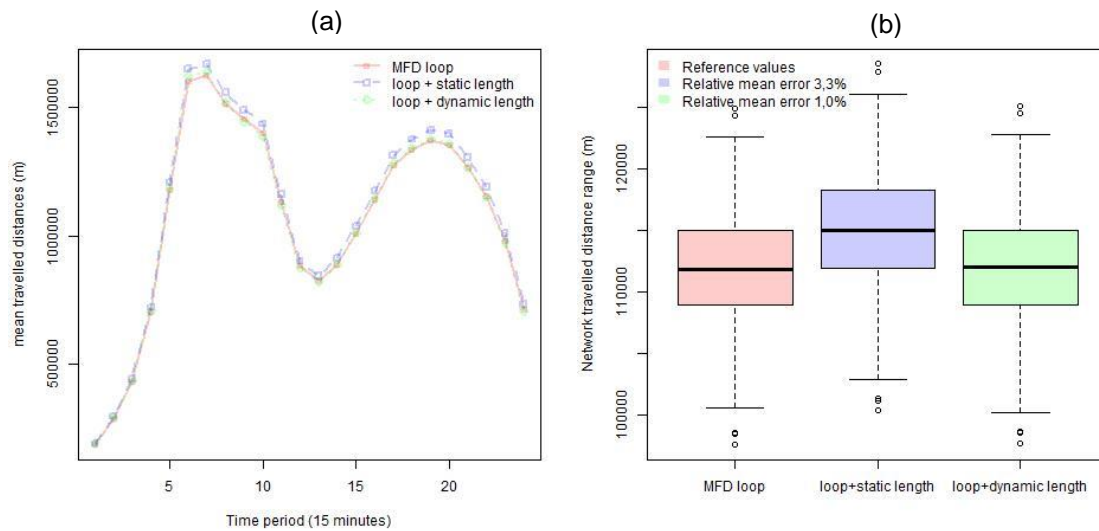


Figure 1. Network travelled distance comparison.

Both figures make comparison of network travel productions. Network travelled distances is defined by the total travelled distance considering the entire network (all links gathered). “MFD loop” is the reference values, “Loop + static length” corresponds to total travelled distances considering the geometric link length and finally the “Loop + dynamic length” are the values considering the dynamic length. The last one is the method that better corresponds with the reference values with only 1% of average error (over 400 simulated values). It is interesting to observe that the travelled distances calculated using geometric length have almost the same distribution than the travelled distances calculated using the dynamic link length. In fact, this last is not surprising because the total travelled distances are the product between the number of vehicles that pass at the sensor in a given link and the mean travelled distance of the same link. Considering that, we assume that all vehicles passed through the sensor did the same travelled distance. Consequently, this travelled distance will be a bit overestimated, at about 3% as shown in Figure 1(b), because it considers that all vehicles passed in front of sensor run through the totality of geometric link length and sometimes it is not the case. The differences between them are small considering they were calculated at network level (i.e. time and space gathered). This difference also can be seen in figure 1(b) that shows distribution values of each one and the relative mean error of each method in comparison to the reference values. Within a perspective of policymakers and considering the low errors of travelled distances (under 3,5% in average over 400 simulations) the method using geometric length allows, in an easy way, to determine the travelled distance of a link or network directly using the data collected by a sensor and geo-referenced maps without having to use simulations to this purpose.

The second traffic variable that need to be analyzed to estimate emissions is the mean speed. The network under study represents an urban area which has low mean speed over 15 minutes and its variation is between 1 km/h and 50 km/h locally. Speeds are the ratio between distances and times and, considering the low difference between static travelled distance (i.e. using geometric link length) and dynamic one (i.e. using dynamic link length), both give almost the same results. The mean speeds from inductive loops are both overestimated and reached great relative mean errors, at about 115% in average error, as shown in figure 2. The range of mean speeds at network scale are very different when MFD and inductive loops are compared. The range of mean speeds values vary between 5 and less than 35 km/h. These low speeds are totally normal when an urban area is represented. Furthermore, these low speeds have an importance when the emissions are calculated, because they have higher emission factors. The great differences between the mean speed from MFD and Inductive loops are more evident in the periods of free-flow (traffic lights influence), and can reach 14km/h of difference between both, than the periods which the network is considered congested, so this difference vary according to the traffic state. This fact is explained in how the mean speed is considered at link level. For inductive loops, the mean speed considered to all link length is measured from a point in the middle of each lane. As most of links have small length, so the vehicles run through the sensor are still accelerating. Unlike the inductive loops, the MFD sensors calculate the mean speed considering the full-length of each link (spatial approach) and not a point and it is possible only through simulations. These considerations explain the differences between mean speeds from the sensors. The spatial mean speed needs the

simulation environment to determine it precisely.

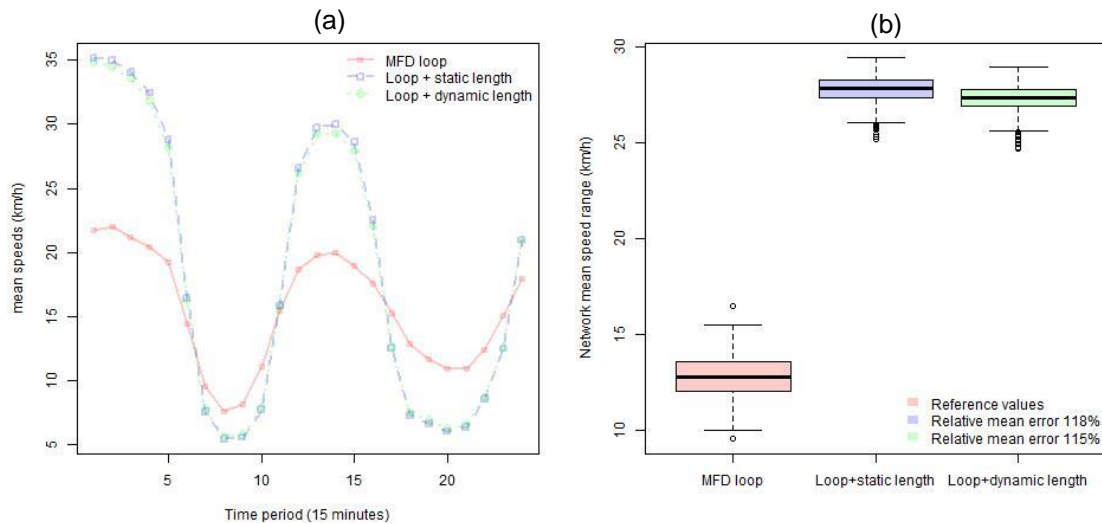
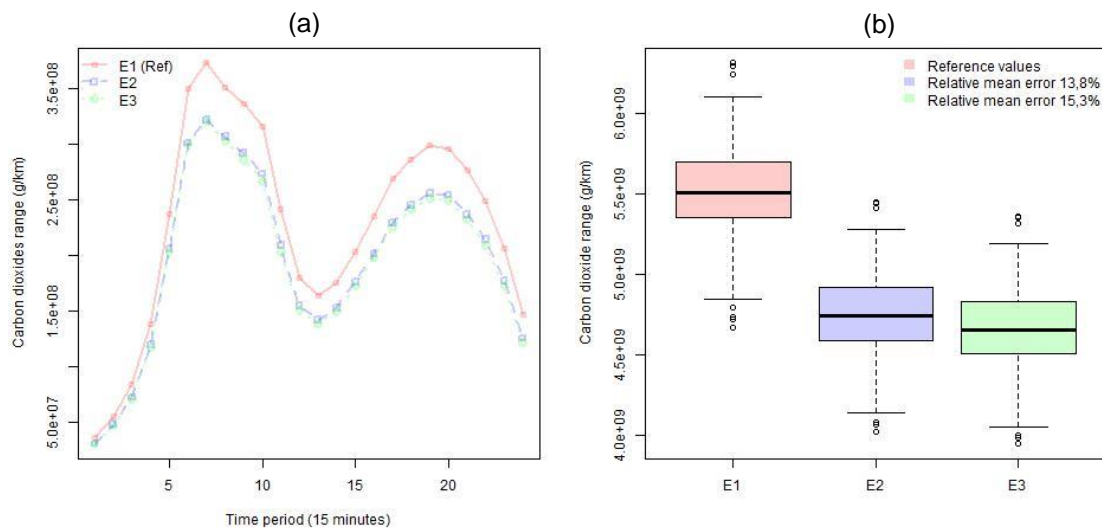


Figure 2. Network mean speeds comparison.

The definition of emissions is the pollutant's sum on each link and time period. The network pollutants were calculated using the total travelled distance and mean speed recovered by sensors for each 15 minutes' time range. Then, it was made the sum of emissions for all links and period of time per daily traffic (i.e. simulations).

This method was used to get the emissions from MFD and inductive loops, knowing that the last one have two options of travel productions, accordingly two possibilities of emission values. For all studies about emissions, the MFD results from local calculation were our reference values, because they used a finest description of traffic and represent the exact values on each simulation.

The figure 3 compares the pollutant emissions from both sensors: (a) and (b) correspond to carbon dioxide network emissions; and (c) and (d) for NO_x network emissions. As can be seen, the pollutant emissions calculated using local traffic data from inductive loops show lower values than from MFD sensors. These lower amounts of emissions are due to the fact that inductive loops consider much higher speeds than MFD sensor and consequently lower emission factors; these differences are most evident in congested state.



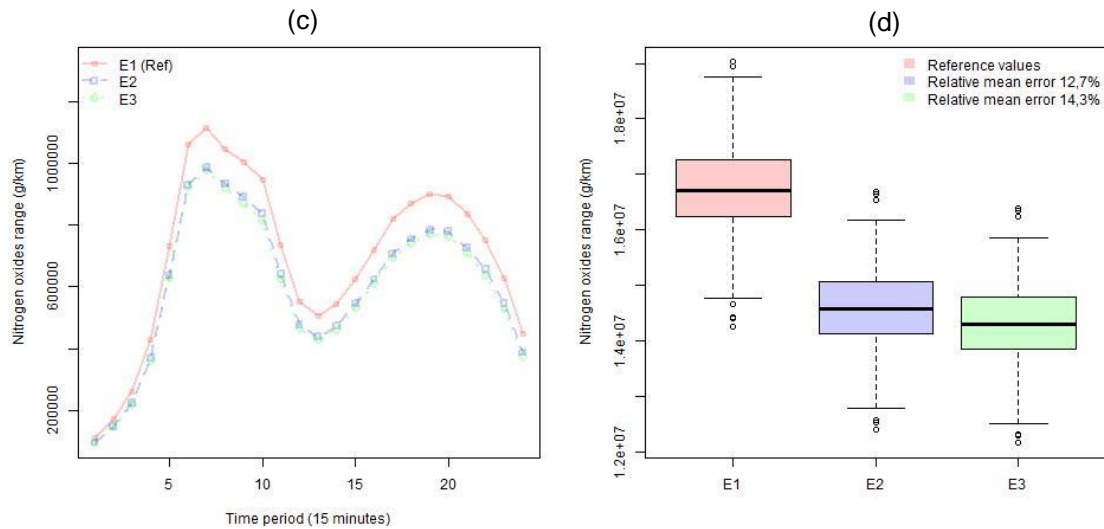


Figure 3. Network pollutant emission comparison: (a) and (b) corresponds to CO₂ network emissions; and (c) and (d) corresponds to NO_x network emissions.

As shown in figure 2 the network mean speeds from inductive loops are between 5km/h and 35km/h instead of 7km/h and 25km/h from MFD loops, consequently high speed values tend to have lower coefficient of emissions.

The pollutant emission is the product of traveled distance and the corresponding emission factor for given pollutant determined by mean speed. The difference between the three travelled distances are very small (figure 1) but the mean speed comparison shows different speeds from both sensors and that ending to underestimate around 14% the network emissions using the traffic data from this loop ((b) and (d) in figure 3).

Two sources of information were analyzed: MFD and inductive loops. Both provide the necessary traffic data to estimate emissions. Traffic data from inductive loops tends to be overestimated in comparison to MFD values. Travelled distance has a little average increase of 2% in average while mean speed can reach over 100% of disparity. These gaps lead to an underestimation of emissions around 14% at network level. For free-flow periods this disparity is at about 1% compared to congested periods that can reach 14% of difference. To assess the emissions accurately and to obtain a selection using the accurate values, after having compared all variables and how they affect the emissions, the traffic data from MFD loops will be used to apply the selection methods

3. The sampling method

The LASSO is a regression method that involves penalizing the absolute size of the regression coefficients. By penalizing (or equivalently constraining the sum of the absolute values of the estimates) you end up in a situation where some of the parameter estimates may be exactly zero. The larger the penalty applied, the further estimates are shrunk towards zero.

The least absolute shrinkage and selection operator (LASSO) is a modern statistical method that has gained much attention over the last decade as researchers in many fields are able to measure far more variables than ever before. Linear regression suffers in two important ways as the number of predictors becomes large: First, over fitting may occur, meaning that the fitted model does not reliably generalize beyond the particular data observed; second, it becomes difficult to interpret the fitted models. The Lasso addresses both of these issues by identifying a small number of predictors on which a reliable model can be built.

We have a set of explanatory variables (X_i) for $1 < n < p$ to explain a variable Y linearly and nothing ensure of all variables involved are explanatory. So we have a set of potentially explanatory variables or candidates. Our goal is to identify the explanatory ones. Therefore, it is necessary to choose a model among 2^p possibilities. How to choose the right model? Study all possibilities it not possible when p is large, more importantly, knows whether a model is better than the others. The LASSO method offers, in some cases, a solution to this problem. This is convenient when dealing with highly correlated predictors, where standard

regression will usually have regression coefficients that are 'too large'(Tibshirani,1996).

We are looking to explain a variable Y linearly by p variables potentially explanatory of X_i . To this end, we simulate n observations. The variable model Y is described below:

$$Y^n = X^n \beta^n + \varepsilon^n$$

where, $\varepsilon^n = (\varepsilon_1, \dots, \varepsilon_n)^T$ is a vector of n random variables with average value equal zero and variance σ^2 which corresponds to the noise in observations (which may contain all the explanatory variables not taken into account in the model); $Y^n \in \mathbb{R}^n$ corresponds to n observation of Y variable and X^n matrix. The $X^n = (X_1^n, \dots, X_p^n) = ((X_1^n)^T, \dots, (X_p^n)^T)^T$ is a $n \times p$, where X_j^n is the column j^{th} that corresponds to the predictor j^{th} of X_j . The X_i^n is the line i^{th} that corresponds to the observation i^{th} . The $\beta^n \in \mathbb{R}^p$ is the parameter that need to be estimated and is indexed by n to allow its coefficients and its size vary as n increases (p may depend on n).

If X_i variables are not all relevant, the goal is to eliminate the unnecessary variables and only those ones. The idea of LASSO is not to make a classical linear regression but a regularized regression that makes equal zero some of β coefficients. This involves estimate for $\lambda \in \overline{\mathbb{R}_+}$:

$$\widehat{\beta}^n(\lambda) = \underset{\beta \in \mathbb{R}^p}{\operatorname{argmin}} \left(\frac{1}{2} \| Y^n - X^n \beta \|_2^2 + \lambda \| \beta \|_1 \right)$$

where $\| x \|_2^2 = \sum_{i=1}^n x_i^2$ and $\| x \|_1 = \sum_{i=1}^p |x_i|$.

The parameter $\lambda \geq 0$ that controls the power of regularization. If $\lambda = 0$, the Lasso method corresponds to classical linear regression (if $p \geq n$). Contrariwise, if $\lambda = \infty$, all $\widehat{\beta}^n(\infty)$ are equal zero. Increasing λ induces decrease of some $\widehat{\beta}^n(\lambda)$ coefficients to zero until exactly zero. The last model is equivalent to the following:

$$\widetilde{\beta}^n(t) = \underset{\beta, \| \beta \|_1 \leq t}{\operatorname{argmin}} (\| Y^n - X^n \beta \|_2^2)$$

considering for all $\lambda \in \overline{\mathbb{R}_+}$, it exists $t \geq 0$ such that: $\widetilde{\beta}^n(t) = \widehat{\beta}^n(\lambda)$. Indeed, just take $t = \| \widehat{\beta}^n(\lambda) \|_1$ then for all β such that $\| \beta \|_1 \leq t$, $\lambda \| \beta \|_1 \leq \lambda \| \widehat{\beta}^n(\lambda) \|_1$ therefore, by definition of $\widehat{\beta}^n(\lambda)$, $\| Y^n - X^n \beta \|_2^2 \geq \| Y^n - X^n \widehat{\beta}^n(\lambda) \|_2^2$.

The algorithm that was applied to solve LASSO uses cyclical coordinate descent computed along the regularization path (Friedman et al, 2010). It consists in determining $\widehat{\beta}^n(\lambda)$ for all $\lambda \geq 0$. The next step is to determine the right λ that can keep only true explanatory variables and eliminate others. One general approach is to use prediction error to guide this choice. One of this method is called tenfold cross-validation.

Cross-validation works by dividing the training data randomly into ten equal parts. The learning method is fitted—for a range of values of the λ (namely complexity parameter) — to nine-tenths of the data, and the prediction error is computed on the remaining one-tenth. This is done in turn for each one-tenth of the data, and the ten prediction error estimates are averaged. From this we obtain an estimated prediction error curve as a function of the complexity parameter. It is always necessary divide the data into training set and test set. Cross-validation is applied to the training set, since selecting the shrinkage parameter is part of the training process. The test set is there to judge the performance of the selected model.

The chosen algorithm computes an entire path of solution in λ for any particular model, leaving the user to select a particular solution from the ensemble. It is possible to evaluate the prediction performance at each value of λ , and pick the model with the best performance. To evaluate the models, the mean-square prediction error was used as measure of risk. From the mean cross-validated error curve, two models are highlighted, one line that corresponds to the minimum error and gives a model with p number of predictors and, another line that gives the largest value of lambda such that the error is within one standard-error of the minimum error - the so called "one standard-error rule". The two highlighted models have best performance, but the difference between them are the number of selected predictors on each model. The one-standard error rule gives a model with less predictors than the model defined by minimum error. When we compare the relatives' errors values from the predicted values on both models, they have a similar error. For our purpose, the model using the "one standard-error" rule is the best choice because has a minimal number of selected regressors and from that, all analyses will be made. The comparison between both models to confirm the choice made are detailed in Friedman et al (2010).

4. The datasets

Two types of datasets were built to help characterizing the dynamic behavior of network. They were built for each variable as total travelled distance, mean speed, CO₂ and NO_x emissions. The datasets structures are explained below.

The first dataset called static considers only the daily traffic values for each link on the network. The purpose is to estimate variables values at network level considering daily traffic values for travel production, mean speed and emissions. All links have their periods of time gathered, giving the total or mean values for each one.

For example, considering the travel production variable, each link has the total traveled distance for daily traffic, which means the values for each link are the sum of travelled distances of all time periods. Each value (X_i^n) that corresponds to the links (X_j^n) on the network was provided by a simulation. To illustrate, the regressors are the links and their observations are the total traveled distance with all period gathered for each simulation. In the same way this dataset was built for CO₂ and NO_x emissions, they are represented as sum of total emissions in periods of time. In contrast to, the average speed on links are calculate in function of their means speeds and travel times. The values represent the average mean speeds over periods of time and are calculate for each link separately.

Mathematically speaking, the variables as travelled distance, mean speed and pollutants emissions were represented as $X_{i \times j}$ matrix. The column j^{th} corresponds to the predictor j^{th} of $X_{i \times j}$. For all variables in the static dataset, the j^{th} corresponds to the links of the network and each column j^{th} are represented by singular link. The line i^{th} of each j^{th} corresponds to the observations. The observations can be represented by: the total travelled distance, or the spatial mean speed or the total pollutants emissions. Each i^{th} corresponds to daily values (all time periods gathered) of the j^{th} links. Each i^{th} corresponds a variable values of i^{th} simulation. The method of selection was applied in these matrices based in the vector Y with i^{th} lines. The vector Y represent the daily network variable values (all links and periods gathered). Each i^{th} line can be represented according to the variable: total travelled distance in the network; mean speed of the network; total pollutants emissions values of the network. The matrices and vectors in this datasets have 400 observations.

The second dataset that will be studied is called dynamic and considers the traffic data for each 15 minute' periods on each link. But its structure was built to have as regressors: links and their periods of time. The selection methods will be applied both on link and time period. The idea is to identify for each link which time periods are really relevant. The observations are their respective values for each simulation. This dataset allows to estimate the network daily values using 15 minute' period traffic data.

This dataset is structured to allow possible have links and their most relevant periods of time selected. The X_j are represented by links and periods of time. Each j^{th} corresponds to one link and singular period of time. The X_i are the observations that correspond to the variables values of $X_{i \times j}$ from the i^{th} simulation. The matrices have 5520 possibilities of predictors (one predictor represents a link and period of time) with 400 observations each one. The selection method was applied on these matrices based on the Y vectors that represents the daily network variable values as the same vectors in static dataset.

Both datasets provide as results network values, that means the variables values considering the entire network for a daily traffic. The results from the selection method and a comparison between them will be study in the next section.

5. Results

Both datasets have 4 different variables: travel production, mean speed, CO₂ and NO_x emissions. These variables are structured as $n \times p$ matrix, which p are the links represented in the network while n are the observations values for each link. Each link has 400 observations and they were split up randomly in two parts: the first represents 2/3 of the matrix and was used as training set where LASSO was applied and settled a model; and the second part, 1/3 of original matrix, represents the validation set where the LASSO settled model defined in training set will be validated and the errors associated will be quantified.

Static datasets

As explained before, the model proposed by λ with one standard-error from the minimum square error was the model retained for all variables. The results are presented only for this model. In figure 5 are shown the λ cross-validated for each variable in static dataset. The figure 5 represents the estimated prediction error curves and their standard errors for the variables in static datasets: (a) is the model settled for travelled distance, (b) for mean speed, (c) for CO₂ and (d) for NO_x emissions. Each curve is plotted as a function of the corresponding complexity parameter λ . The horizontal axis has been chosen so that the model complexity increases as we move from right to left. The estimates of prediction error and their standard errors were obtained by tenfold cross-validation. The least complex model within one standard error of the best is chosen, indicated by the vertical lines. The left vertical line is the model with minimum error and the right one is the model settled using the one standard error rule (the model that will be studied). The top of each plot is annotated with the size of models.

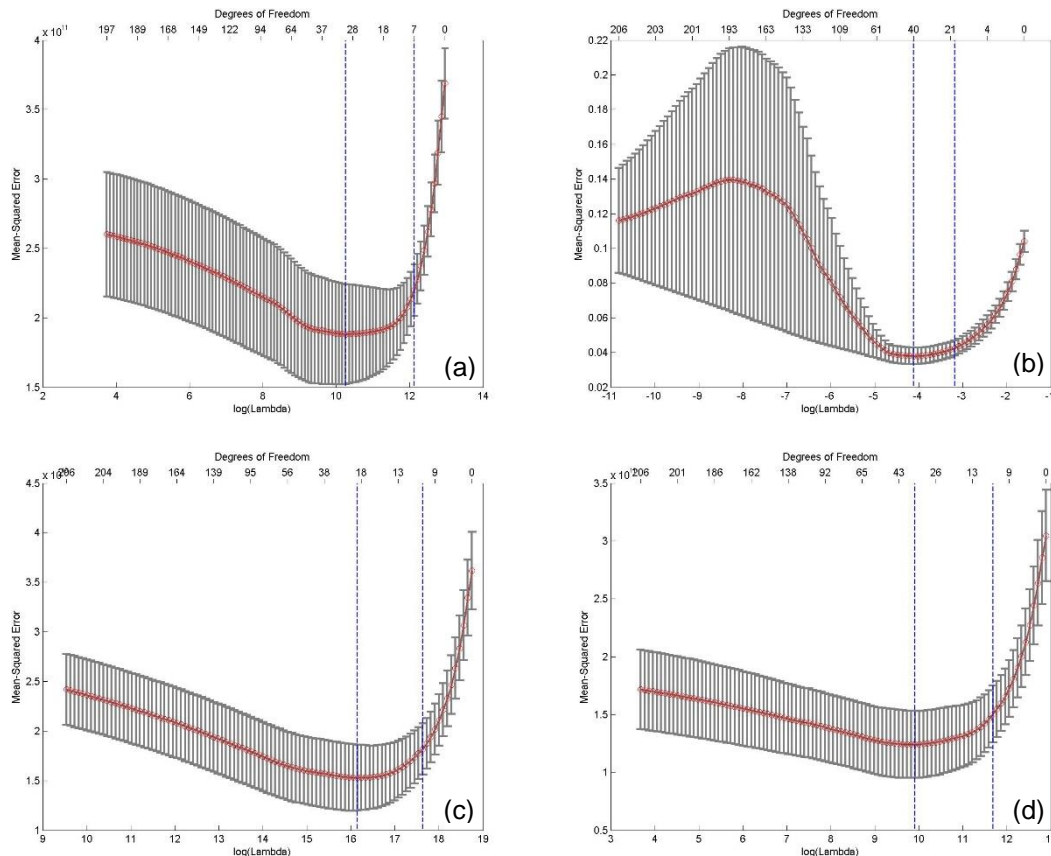


Figure 5. The λ cross-validated for each variable in static dataset: (a) represents travel production, (b) is the mean speed, (c) is the CO₂ and (d) is the NO_x emissions. The model retained for each variable corresponds to the rightest vertical line.

The LASSO made a selection over 230 links of the network and gives us models with: 7 links for travelled distance which the model that can explain the data in 43% considering the confidence interval of 95%; selected 19 links for mean speed with 64% of data explained by the model; and 11 links for both pollutants emissions with model that explain 54% of data in CO₂ emissions and 55% of data explanation in NO_x emissions. The relatives' errors were calculated comparing the results (values predicted by the model established) with the reference values (Y). The figure 6 shows the distribution of associated errors in each variable for the static dataset.

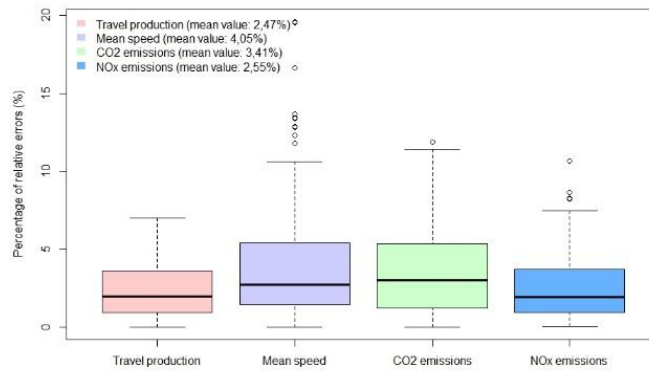


Figure 6. Percentage of error between the resulting variable values of the model with selected links and the original values of variables (Y).

All variables have small average error considering models that have less than 10% of the links of the network selected. More than 50% of the data has errors less than 5% considering average errors between 2,50% and 4%. A cross-analysis was made to observe if one of the 4 models could be used to determine other variables values with the goal to have a set of selected links that can be used to quantify network values for all variables. The table below shows the average percentage of error of the selected links model established by the variables in the columns applied on the variables disposed in the lines.

<i>Models settled by Lasso with variable Applied on variable</i>	Travelled distance model	Spatial mean speed model	CO₂ emissions model	NO_x emissions model
<i>Travel Production</i>	2,5%	2,0%	1,6%	1,7%
<i>Mean speed</i>	5,9%	4,0%	5,9%	5,3%
<i>CO₂ emissions</i>	2,7%	2,7%	3,4%	2,8%
<i>NO_x emissions</i>	1,9%	2,2%	1,9%	2,5%
<i>Model size</i>	7	19	11	11
<i>Sampling rate</i>	3,0%	8,3%	4,8%	4,8%

Table 1. The average error of the model established with one variable applied to another.

The table 1 shows the average error on validation set of the selected links from one variable applied to another one and the average error for the Lasso applied on the variables. The aim here is to investigate the possibility of using a set of selected links to determine all other variables. To this end, in the same training set, a linear regression was performed on the links selected by Lasso. The objective is to find the beta values of each selected link adapted to the variable under study. In general, for all cases, the average errors values remain in the same range as the Lasso method. The links selected in common for the 4 variables were also compared and the ratio is presented in the table 2 to complete the analysis.

	Travelled distance model	Spatial mean speed model	CO₂ emissions model	NO_x emissions model
<i>Travel Production model</i>	100%	0%	36,4%	27,3%
<i>Mean speed model</i>	0%	100%	0%	0%
<i>CO₂ emissions model</i>	57,1%	0%	100%	72,7%

<i>NO_x emissions model</i>	42,8%	0%	72,7%	100%
---------------------------------------	-------	----	-------	------

Table 2. Ratio of common selected links between variables.

It is possible to observe in table 2 that travelled distance and spatial mean speed variables have no common selected links. That can be explained by their opposite behavior: the travelled distance is a linear variable over the links whereas the spatial mean speed is not. In the light of these considerations, two conclusions can be observed: (i) the strong correlation between travelled distance and spatial mean speed allows to determine each emissions from their sampling, because they are dependent from these both traffic variables; and (ii) the fact that both can be used to determine other variable values using a simple linear regression, leads us to conclude that it does not exist just only one acceptable sampling (set of links). Thus there is ample evidence of the selection flexibility. The model with less selected links will be the best choice, especially in practical point of view, for transportation managers when they decide to outfit links on the network.

All models defined by Lasso or by linear regression were validated on a validation set completely different from the training set used to apply them. Yet, to be able to compare the results, the training data and the validation data were the same throughout this study. The average errors remain in the same range with the four links sets: 2% for NO_x emissions and travelled distance and 3% for CO₂ emissions. So, various sampled links could provide an estimation of traffic and emission variables over the network with reasonable error.

Considering the low sampling rate in each variable, and also their low average errors and taking into account that they have some common selected links, it also was considered to study the possibility to make the union or/and the intersection between the traffic variables and between the emissions pollutants. For example, the selected links identified by the shrinkage method for the traffic data, total travelled distance and spatial mean speed, will be put together (union of selected links between two variables) to apply a linear regression and obtain a new model with adjusted beta values for each predictor (links). In the same way, the union between CO₂ and NO_x was considered. Taking into account that some variables have common links, it was considered the intersection between them. The advantage of the intersection between them is the possibility to have a model with less predictors than the model established by the union of them. The associated errors were quantified for each resulting variable values. The average error of each linear regression is shown in table 3 and was calculated for each variable considering each situation (union or intersection).

<i>Link selection method/ Variables to which was applied</i>	Total travelled distance selection union spatial mean speed selection	Total travelled distance selection intersection spatial mean speed selection	CO₂ emissions selection union NO_x emissions selection	CO₂ emissions selection intersection NO_x emissions selection
<i>Total travelled distance</i>	1,8%	-	1,6%	1,7%
<i>Spatial Mean speed</i>	3,5%	-	5,3%	6,6%
<i>Total CO₂ emissions</i>	2,5%	-	2,8%	3,0%
<i>Total NO_x emissions</i>	2,2%	-	2,1%	2,1%
<i>Model size</i>	26	-	14	8
<i>Sampling rate</i>	11,3%	-	6,10%	3,48%

Table 3. The average percentage of error from the linear regression model settled on the union or intersection between variables of the same nature.

The selected links in total travelled and spatial mean speed are completely different, so they have no common links. The union of traffic variables allows estimating all variables values with the same accuracy as the Lasso selection applied in each one separately. The distribution of error values varies from 0,1% to less than 7% considering 95% of confidence interval in general for all variables. When selection in travelled distance showed in table 1 is compared with the union between the traffic variables and also with the union of the pollutants emissions, it is possible to observe that the distribution of errors

is less dispersed with the union of selected links. In contrast to, the union models have more links than the model established by travelled distance in table 1, which explains the fact that the errors are less dispersed.

When the same comparison is made with the intersection between the selected links of the pollutants, they have almost the same amount of selected links and average error values. If we compare the models of the pollutants in table 1 with the intersection between them, it is interesting to observe that even if it reduces the selection's size (in this case the selection passes from 11 to 8), the results remain the same.

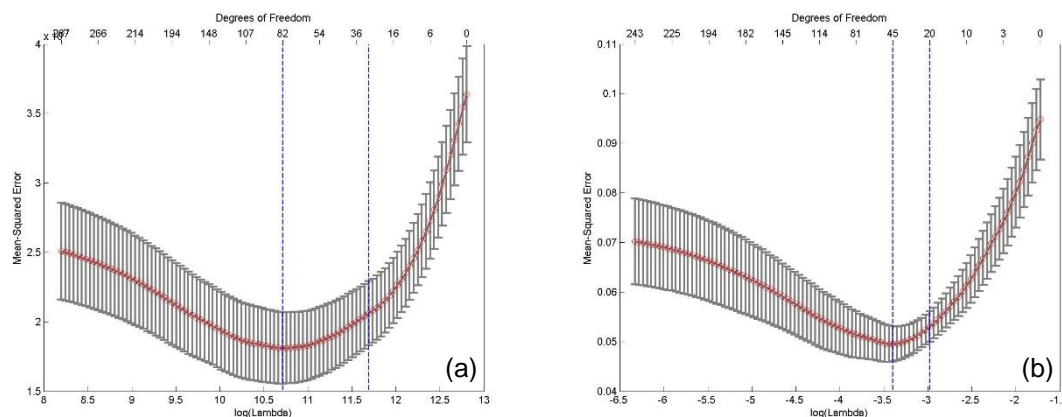
So, the union of selected links identified by the shrinkage method for the two variables that characterize daily values of the traffic and the linear regression model established with these ones, can estimate the network daily values with a low average error and using just 11% of the network links. When it comes to the emissions, the best choice is the intersection between them. Considering only 8 links (3,5% of the network), all the variables can be estimate with acceptable error, around 2% for travelled distance, 3% for pollutants emissions and less than 7% for spatial mean speed.

The shrinkage method called Lasso was used as linear regression selection method to perform a selection of the most relevant links on the network for traffic and emissions variables. For each one, a model was established with a set of links and the weights of each one. Using total/mean daily information as input is enough to estimate with accurateness the variables. The analysis concludes that the links selected on the travelled distance presents better results in terms of minimum number of links necessary to estimate with accuracy traffic and emissions daily values. To sum up, we can deduce that a finest traffic data is not necessary to quantify and determined daily traffic and emissions at network level, the daily values are enough information to obtained it.

Dynamic datasets

This dataset has 4 different variables: travelled distance, mean speed, CO₂ and NO_x emissions. These variables are structured as $n \times p$ matrix, where p are the links represented for each period of time (230 links and 24 time periods: 5520 predictors) and n are the simulations values. Each predictor has 400 observations and they were split up randomly in two parts: the first represents 2/3 of the matrix and was used as training set where LASSO was applied; the second part, 1/3 of original matrix, represents the validation set where the LASSO selection will be validated and the errors associated will be quantified.

As explained before the model proposed by λ with one standard-error from the minimum square error was the model retained for all variables. The results are presented only for this model. In figure 7 are shown the λ cross-validated for each variable.



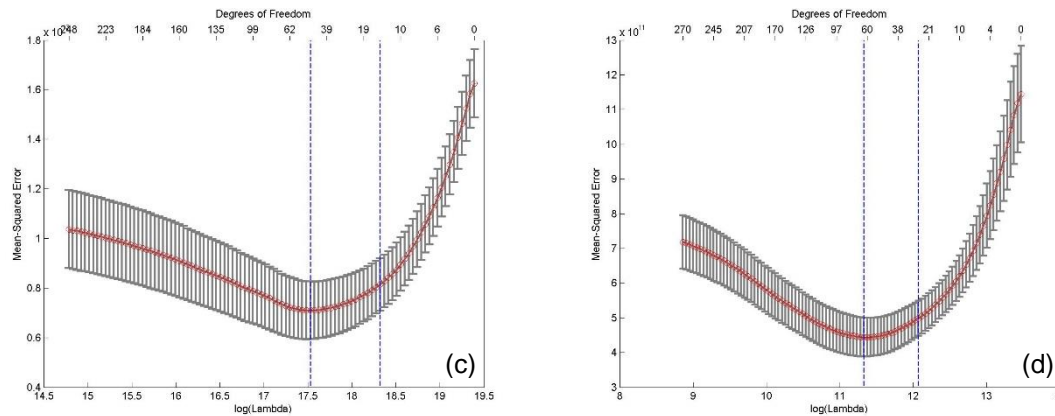


Figure 7. Estimated prediction error curves and their standard errors for the variables in dynamic/dynamic datasets. Each curve is plotted as a function of the corresponding complexity parameter λ . The horizontal axis has been chosen so that the model complexity increases as we move from right to left. The estimates of prediction error and their standard errors were obtained by tenfold cross-validation. The least complex model within one standard error of the best is chosen, indicated by the rightmost vertical line. The top of each plot is annotated with the size of models. Each plot represents: (a) travelled distances, (b) spatial mean speed, (c) CO₂ and (d) NO_x emissions.

In travelled distance, the 30 predictors selected represents 25 links on the network. 14 predictors correspond to morning traffic against 16 in the evening (the morning traffic are represented by periods of time from 1 to 12 and the evening from 13 to 24). It is interesting to observe that the selected periods of time represent the free-flow periods. These datasets provide as result the daily values of the network as static datasets. The models established for travelled distance can explain the data at 52% (which refers to 95% of confidence interval) and give us the results with a mean error equal to 3,6%. If we compare the travelled distance selection between static and dynamic datasets, we have 6 common links, which means that 6/7 selected links on travelled distance with static dataset are included in the model established with the dynamic dataset.

The spatial mean speed had 20 periods of time selected, which represents 18 links. In the 20 predictors, 12 are from morning peak and 8 are from the evening. The model can explain 56% of the data with average error of 5,11%. All periods selected represents a free-flow state in the network. This dataset gives us as result the average daily speed in the network. If we compare with the selection made in static dataset (which have 19 links on its model), they have in common only 6 ones.

The figure 7(c) represents the selection made in CO₂ emissions: 12 predictors are selected. They represent 11 links on the network. 5 among the selected time periods are in the morning assignment, respectively 7 in the evening assignment. 8 predictors among 12 are the same (link and period of time) between CO₂ and travelled distance. Any predictors selected in mean speed were selected in CO₂. The periods selected represent also a free-flow state on the network. The model built by LASSO can explain 56% of the data with average error at about 3,6% as show in figure 8.

The figure 7(d) represents the selection made in the NO_x emissions. This variable has 29 predictors selected and they are represented by 23 links with 6 predictors that represent morning assignment and 23 predictors for evening assignment. This variable selected more evening time periods than the other variables in this dataset. The model built by Lasso using the selected links and time periods can explain 64% of data with average error of 2,8%.

Analyzing the results of all variables, in most of them, the free-flow time periods are selected, which means states that the network is charged by vehicles but traffic flows normally. The number of selected time periods are equilibrated between morning and evening assignment with exception the NO_x that have more selected periods in the evening. The emissions models provide selected links and time periods completely different in comparison to the selection obtained with mean speed.

The daily values of each variable were calculated using the validation set and their relative errors were calculated. The average errors are almost the same as the other dataset. 75% of the data have an error lower than 7%. In figure 8, the percentage of error in the validation set are shown, when network variables were calculated using the model with selected predictors.

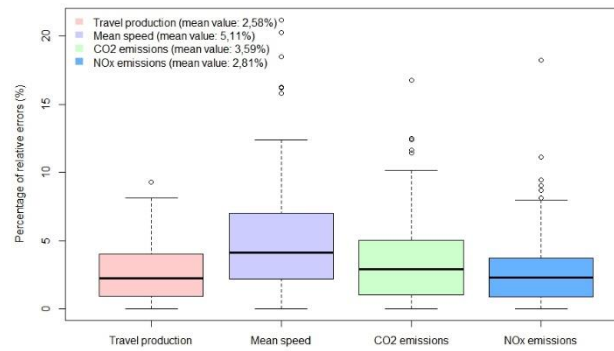


Figure 8. Percentage of error between the resulting variable values of the model with selected links and time periods and the original values of variables (Y).

As in static dataset, a cross-analysis was conducted to observe if one of the 4 models could be used to determine other variables' values. The table below shows the average percentage of error on the validation set of the model established by selection on the variables in the columns and applied on the variables disposed in the lines.

<i>Models settled by Lasso/ Variables to which was applied</i>	Travelled distance model	Spatial mean speed model	CO₂ emissions model	NO_x emissions model
<i>Travel Production</i>	2,6%	2,7%	2,2%	2,7%
<i>Mean speed</i>	5,9%	5,1%	6,3%	4,2%
<i>CO₂ emissions</i>	3,0%	3,4%	3,6%	3,4%
<i>NO_x emissions</i>	2,5%	3,0%	2,5%	2,8%
<i>Model size</i>	30	20	12	29
<i>Nb of links</i>	25	18	11	23
<i>Sampling rate</i>	11%	7,8%	4,8%	10%

Table 4. The average error of the model established with Lasso selection on one variable applied on another.

As noted in the table 4, the same considerations made for static dataset are applied here. It is possible to use selected links of one variable to determine the other ones with the same accuracy as Lasso did. The predictors selected for all variables were analyzed. Unlike the spatial mean speed, the other three variables have predictors (link and time period) in common and they are shown in table 5. The most important conclusion is that the model defined in CO₂ emissions has 75% of same selected links and time periods, which means a strong dependence of the CO₂ with travelled distance for time period.

	Travelled distance model	Spatial mean speed model	CO₂ emissions model	NO_x emissions model
<i>Travel Production model</i>	100%	0%	75%	27,6%
<i>Mean speed model</i>	0%	100%	0%	0%
<i>CO₂ emissions model</i>	30%	0%	100%	13,8%

<i>NO_x emissions model</i>	26,7%	0%	33,3%	100%
---------------------------------------	-------	----	-------	------

Table 5. The common selected links and time periods between variables.

A second study was conducted to observe if a linear regression model including a set of selected predictors could be used to determine all variables values. We considered the union between traffic variables, the union between emissions and the intersection on the last one. In the table 6 are presented the average percentage of error between the linear regression model and their respective reference values (Y) of the validation set.

<i>Method/ Variables to which was applied</i>	Total travelled distance selection union spatial mean speed selection	Total travelled distance selection intersection spatial mean speed selection	CO₂ emissions selection union NO_x emissions selection	CO₂ emissions selection intersection NO_x emissions selection
<i>Total travelled distance</i>	2,6%	-	2,1%	2,5%
<i>Spatial Mean speed</i>	4,4%	-	5,4%	-
<i>Total CO₂ emissions</i>	2,9%	-	2,7%	3,3%
<i>Total NO_x emissions</i>	2,4%	-	2,6%	2,8%
<i>Model size</i>	50	-	37	4
<i>Nb of links</i>	43	-	30	3
<i>Sampling rate</i>	19%	-	13%	1%

Table 6. The average percentage of error from the linear regression model settled on the union or intersection between variables of the same nature.

The model size of the linear regression corresponds to the selected predictors of the two variables with the same nature, traffic or emissions. Each predictor corresponds to a singular link and time period. All linear regression models applied on all variables have low average percentage of errors in the validation set. The union between the traffic variables has a model size equal to 50 predictors that corresponds to 43 links of the network with all of periods with free-flow state. The union between the two pollutants emissions is composed of 37 selected predictors over the 5520 of the original matrix. Its model corresponds to 30 selected links with also most of periods in free-flow state. The last linear regression model, the intersection between CO₂ and NO_x, has only 4 predictors that represent 3 links of the network with all periods in free-flow. The last model can accurately assess, with 15 minutes' traffic data on only 3 links identified by Lasso, the daily values of the network for travelled distance and pollutants emissions considering that the data are explained in, at about 60%, considering the confidence interval of 95%. The linear regression on the selected links intersection does not have statistical representativeness for the network spatial mean speed. In practice, this type of results needs a finest traffic data over a year and a pre-processing data to obtain local emission and finally a model that can estimate 3 of 4 variables with reasonable error.

Conclusion and discussion

In this paper we aimed to use traffic data from MFD loops and inductive loops in order to assess traffic variables required to estimate the related emissions: mean speed and total travelled distance at a quarter scale (6th district of Paris) and for each 15min periods. A sensibility analysis between both loops was made to understand how they could affect the quantification of pollutants emissions. Inductive loops tend to underestimate emissions in comparison to MFD loops. The sampling method, called Lasso, was applied on MFD data. The aim is to construct a model that can estimate emissions from a small group of predictors (links or links with their periods of time) based on observations values. Four variables were studied: travelled distance, mean speed, CO₂ and NO_x emissions.

The static dataset and dynamic dataset give the same type of results: the daily traffic and emissions values. The difference between both are: (i) the static one has as predictors the links of the network and

as observations the daily values of each link according to the variables under study; (ii) the dynamic dataset has as predictors the periods of time of each link and as observations the 15 minutes' variable values that respectively correspond to the link and period of time. Both matrices are compared with a vector that represents the network daily values (all links and period of time gathered) for each simulation. The idea of the first dataset is to identify the most relevant links in the network using daily values. With the second dataset, the aim is to identify in each link which time periods are really relevant. This method can help to identify where it is possible to place, in reality, on-road sensors to estimate network variables. This first analysis leads us to conclude that using the selection on daily travelled distance is the best model that can estimate the spatial mean speed and both pollutants emissions. The last selected only 3% of the network' links with an average error less than 6%.

In order to qualify the effectiveness of Lasso method for environmental assessment, these results have to be confirmed with other data sets and compared to other selection methods. However, the daily emission value is often not sufficient if we are interested in population exposure to pollutants. Thus, further analysis will first be conducted in order to find the best link selection to assess 15 min 's emissions.

The applications of such techniques are numerous. In addition to significant improvement in computing time, the development of appropriate sampling methods could also help to identify key areas of a network or travel types and thus, help to improve the assessments a posteriori (optimal positioning stations measurement, definition references tours for vehicles with embedded measurement means, ...). The technique covered by this work could also be useful in real-time assessments of quantify emissions. Indeed, sensor networks for air pollution are generally sparse and does not discriminate specifically the contribution of road traffic.

References

- Ahn, KyoungHo, and Hesham Rakha (2008): The Effects of Route Choice Decisions on Vehicle Energy Consumption and Emissions. Transportation Research Part D : Transport and Environment 13 (3) : 151–67. doi:10.1016/j.trd.2008.01.005.
- Al Barakeh, Zaher (2012) : Suivi de Pollution Atmosphérique Par Système Multi-Capteurs–méthode Mixte de Classification et de Détermination D'un Indice de Pollution. Saint-Etienne, EMSE. <http://www.theses.fr/2012EMSE0677>.
- André, Michel, and Mario Rapone (2009a). Analysis and Modelling of the Pollutant Emissions from European Cars Regarding the Driving Characteristics and Test Cycles. Atmospheric Environment 43 (5): 986–95. doi:10.1016/j.atmosenv.2008.03.013.
- da Rocha, Thamara Vieira (2013): Quantification Des Erreurs Associées à L'usage de Trajectoires Simplifiées, Issues de Modèles de Trafic, Pour Le Calcul de La Consommation En Carburant. École Nationale des Travaux Publics de l'État. <https://tel.archives-ouvertes.fr/tel-00932609/>.
- De Vlioger, I., D. De Keukeleere, and J. G. Kretzschmar (2000a): Environmental Effects of Driving Behaviour and Congestion Related to Passenger Cars. Atmospheric Environment 34 (27): 4649–55.
- European Commission (2015). European Union energy and transport in figures: statistical pocketbook. Luxembourg: Office for Official Publications of the European Communities.
- Europäische Kommission, and Europäische Gemeinschaften, eds (1999): Meet: Methodology for Calculating Transport Emissions and Energy Consumption. Transport Research Strategic Research 99. Luxembourg: Office for Official Publ. of the Europ. Communities.
- Fallahshorshani, Masoud, Michel André, Céline Bonhomme, and Christian Seigneur (2012): Coupling Traffic, Pollutant Emission, Air and Water Quality Models: Technical Review and Perspectives. Procedia - Social and Behavioral Sciences 48: 1794–1804. doi:10.1016/j.sbspro.2012.06.1154.
- Franceschetti, Anna, Dorothee Honhon, Tom Van Woensel, Tolga Bektaş, and Gilbert Laporte (2013) The Time-Dependent Pollution-Routing Problem. Transportation Research Part B: Methodological 56 (October): 265–93. doi:10.1016/j.trb.2013.08.008.
- Franco, Vicente, Marina Kousoulidou, Marilena Muntean, Leonidas Ntziachristos, Stefan Hausberger, and Panagiota Dilara (2013): Road Vehicle Emission Factors Development: A Review. Atmospheric

Environment 70 (May): 84–97. doi:10.1016/j.atmosenv.2013.01.006.

Friedman, J., Hastie, H. and Tibshirani, R. (2010) Regularization Paths for Generalized Linear Models via Coordinate Descent, *Journal of Statistical Software*, Vol. 33, Issue 1.

Gkatzoflias, D., Chariton, K., Ntziachristos, L. and Samaras, Z. (2012) COPERT 4: Computer programme to calculate emissions from road transport, *European Environmental Agency*.

ISpace & Time (2013): Constitution d'un environnement de simulation à grande échelle et production de données synthétiques pour le trafic routier et étude des données mobiles pour l'analyse des déplacements piétons. *IFSTTAR Livrable D4.4*.

Smit, Robin, Leonidas Ntziachristos, and Paul Boulter (2010): Validation of Road Vehicle and Traffic Emission Models – A Review and Meta-Analysis. *Atmospheric Environment* 44 (25): 2943–53. doi:10.1016/j.atmosenv.2010.05.022.

Tibshirani, R. (1996) Regression Shrinkage and Selection via the Lasso. *Journal of Royal Statistical Society, Series B*, Vol. 58, Issue 1, 267-268.

Parametric study on trajectory optimization

S.Javanmardi^{1,2,3}, E.Bideaux¹, R.Trigui², E.Nicouleau Bourles³, S.Dehoux³, Hervé Mathieu³

¹ AMPERE UMR CNRS 5005, 25, Av. Jean Capelle, Bat. Saint Exupery, F-69622 Villeurbanne Cedex, France

² IFSTTAR, LTE, 25, Av. Francois Mitterand, F-69675 Bron, France

³RENAULT, 1, Allée Cornuel 91510 Lardy, France

Keywords: Trajectory optimization, Eco driving, Dynamic Programming, Fuel consumption.

Author email: setareh.javanmardi@insa-lyon.fr

Energy consumption and pollutant emissions reduction has become one of the most important research subjects in automotive sector. Regarding the worldwide growing demand for transportation, there is not a single development that can solve the problems of fuel consumption and greenhouse gas emissions alone. Therefore, developments in different technological and usage fields should continue in parallel to resolve these issues. One of the recently popular methods to reduce fuel consumption by the driver's action is ecodriving. Ecodriving could be defined as using the existing vehicles and motorization in the most efficient way.

Many studies on economic and ecological effects of ecodriving behavior can be found in the literature. Results of Mensing's research in her thesis show that driving with high accelerations and higher gears is favorable for eco driving. The constraints on pollutants emissions should be considered in order to respect emission regulations. This way the driving would be both economical and ecological.

In this research we have performed a parametric study on the impact of several road and trip constraints on optimal trajectory. For this purpose, the trajectory optimization algorithm developed by Mensing in her thesis was used. The algorithm is based on dynamic programming method for finding the optimal velocity and gear choice for a conventional passenger vehicle. By applying the numerical trajectory optimization method on an inverse vehicle model, the best vehicle operation for a given trip is determined.

We have applied the trajectory optimization algorithm on two different vehicle missions. The first one is a short trajectory of 500 meters long. We studied the impact of time constraint, road grade and discretization size on optimization results. We have observed that time constraint has an important role on acceleration

rates, thus affects considerably the fuel consumption and the optimal velocity profile. Figure 1 shows the comparison of optimization results for trajectories with and without time constraint. Results demonstrate that when a time constraint is applied, higher acceleration rates and velocities are used, thus increasing fuel consumption. Meanwhile, if the time is set free, smoother accelerations have been observed.

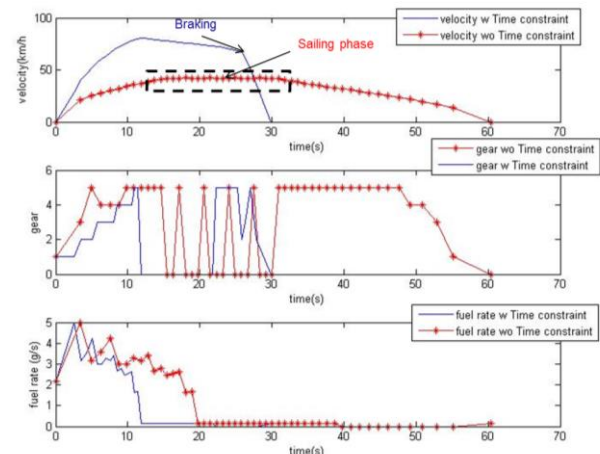


Figure 1 : optimal velocity, gear choice & fuel consumption w/wo time constraint

The second vehicle mission studied is a complete real driving cycle on a sloped road. We have compared the results of with and without considering road slope in the optimization process. Results show that optimal vehicle operation depends widely on the road slope. We have observed that in downhill phases driving with injection cut-off is preferable. While on flat roads, driving at engine dead point (sailing mode) could be interesting for fuel optimization. This can be observed on *Figure 1*.

This work is a collaboration PhD study between IFSTTAR research institute, Renault Company and Ampère laboratory in INSA de Lyon.

- Ericsson, E. (2000) *Variability in urban driving patterns. Transportation Research Part D 5 (2000) 337-354.*
- Mensing, F. et al. (2011) *Vehicle trajectory optimization for application in ECO-driving. VPPC, pages 1_6. IEEE, September 2011. ISBN 978-1-61284-248-6.*
- Mensing, F. (2013) *Optimal energy utilization in conventional, electric and hybrid vehicles and its application to Eco-Driving. Doctoral thesis in Energy and Systems, University of Lyon.*

REMI model: Bottom-up emissions inventories for cities with lack of data

Sergio Ibarra-Espinosa*, Rita Ynoue*

*Departamento de Ciências Atmosféricas, Instituto de Astronomia, Geofísica e Ciências Atmosféricas, Universidade de São Paulo, Rua do Matão, 1226 - Cidade Universitária São Paulo-SP - Brasil - 05508-090
email: sergio.ibarra@iag.usp.br

Abstract

Emissions inventorying is a complex task with regulatory and/or scientific environmental purposes. In South American cities, when the task is performed, the common denominator is lack of data and documentation, and vehicles are usually the main source of pollutant of emerging and consolidated megacities. Therefore, emissions inventories is becoming more important, especially for mobile sources. In this manuscript we present the model REMI (**R-EM**issions-Inventory) for developing bottom-up emissions inventory for vehicles in cities with lack of data (Ibarra & Ynoue, 2016).

The program was written in R (R CORE TEAM 2016) using several libraries. The program consists in several R scripts organized in folders with Inputs & Outputs. For traffic inputs uses counts or simulations, and also, it can be as a top-down method with statistical traffic information. REMI classifies vehicle data by fuel, size of motor, use and gross weight annually up to 50 years, according to EEA/EMEP guidelines and Copert (Ntziachristos, 2014). REMI has several options for emission factors, 1) Emission factors from Ntziachristos (2014), 2) local emission factors or 3) mixed emission factors. In the future REMI will include HBEFA emission factors. REMI also incorporates deterioration factors. Currently REMI estimate hot-engine emissions of 27 pollutants.

Keys-words: REMI, vehicular, emissions inventory, R, bottom-up.

Abstrait

Emissions inventoriage est une tâche complexe avec des fins réglementaires et / ou scientifiques environnementales. Dans les villes d'Amérique du Sud, lorsque la tâche est effectuée, le dénominateur commun est le manque de données et la documentation, et les véhicules sont généralement la principale source de polluants des mégapoles émergentes et consolidées. Par conséquent, les inventaires d'émissions est de plus en plus important, en particulier pour les sources mobiles. Dans ce manuscrit, nous présentons le modèle REMI (**R-EM**issions-Inventaire) pour développer bottom-up inventaire des émissions pour les véhicules dans les villes avec le manque de données (Ibarra & You, 2016).

Le programme a été écrit en R (R CORE ÉQUIPE 2016) en utilisant plusieurs bibliothèques. Le programme se compose de plusieurs scripts R organisés dans des dossiers avec entrées et sorties. Pour les entrées de trafic utilise les chiffres ou les simulations, et aussi, il peut être aussi une méthode descendante avec les statistiques de circulation. REMI classe les données VEHICULE par le carburant, la taille du moteur, l'utilisation et le poids brut annuellement jusqu'à 50 ans, selon l'EEE / lignes directrices de l'EMEP et Copert (Ntziachristos, 2014). REMI dispose de plusieurs options pour les facteurs d'émission, les facteurs 1) d'émission de Ntziachristos (2014), 2) les facteurs d'émission locaux ou 3) des facteurs d'émission mélangés. Dans l'avenir REMI comprendra des facteurs d'émission HBEFA. REMI intègre également des facteurs de détérioration. Actuellement REMI estimer les émissions à chaud moteur de 27 polluants.

Clés mots: REMI, véhicules, inventaire des émissions, R, bottom-up.

1. Introduction

“Emission Inventories always seem to be available at a very late point in time ... and are easily seen as the scapegoat if a mismatch is found between modeled and observed concentrations of air pollutants” Tim Pulles (2010). So, the task of emissions inventories compilation ideally should be faster enough in order that It can be updated before deadline. Emissions inventories, scientific or regulatory, must to be comprehensive, with quality and documented but all these requirements faces the common difficulty of lack of data. The uncertainty of estimation depends on the type of sources considered, because there are sources with required information more accesible than other. Per example, usually there are legal obligation that indubstries must report their emissions, like the Pollutant Release and Transfer Registry (PRTR) emissions inventory (<http://prtr.ec.europa.eu/>). But in other cases, sources like mobiles are hard estimate because vehicles are in movement in space. Vehicle emissions inventory can have a top-down approach with activity data as registered fleet, or can be bottom-up based on traffic simulations. Either case, there are inherent uncertainties and the agreement between top-down and bottom-up is hard to accomplish. In order to solve this problem, we developed the REMI model, for elaborating emissions inventories of vehicles, which can be adapted to the information that compiler has, and also is fast.

2. Objectives

To develop a model to estimate vehicular emissions based on road network

3. Method

Structure

REMI works with a working directory placed in any part of the computer and inside it there are folders “functions” and “data” and these folder divide in several sub-folders as showed in figure 1, where black words are folders and blue ones are files.

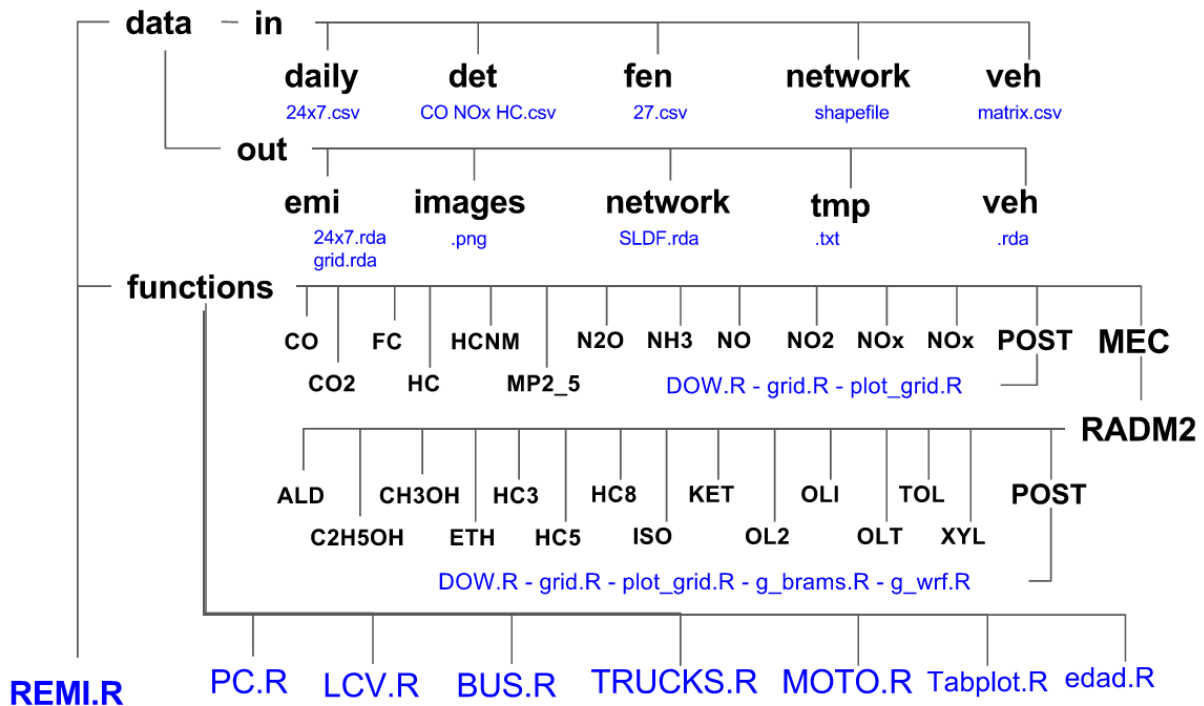


Figure 1. Structure of REMI.

This work consists in present the model REMI for developing bottom-up emissions inventory for vehicles in cities with lack of data (Ibarra & Ynoue, 2016). The program was written in R (R CORE TEAM 2016) using libraries sp (Bivand et al, 2013), rgeos (Bivand & Rundel, 2015), maptools (Bivand & Lewin-Koh, 2015), ggplot2 (Wickham, 2009) and ggmap (Kahle & Wickham, 2013). Activity: Reads traffic simulations, traffic counts and interpolates, or road network and assigns interpolation. Splits

categories by fuel, size of motor, use and gross weight annually up to 50 years. Data classification is according to EEA/EMEP guidelines and Copert (Ntziachristos, 2014). The pollutants covered are CO, NO_x, NO₂, NO, HC, HCNM, PM_{2.5}, N₂O, NH₃, SO₂, CO₂, Fuel Consumption; and speciate HCNM according to experimental analysis of tunnel emissions factors in São Paulo for Aldehyde (ALD), C₂H₅OH, CH₃OH, ETH, HC₃, HC₅, HC₈, HCHO, ISO, ketone (KET), OL₂, OL₁, OL_T, TOL and xylenes (XYL).

The file REMI.R works like a namelist where all scripts are called and include options to type of estimation, grid resolution for output, title of images, etc. REMI.R has an order, first it calls NETWORK.R which produces "data/out/network/red.rda", then the activity functions PC.R, LCV.R and so on. Each of these functions produces graphics with ggplot saved in "data/out/images/*.png", tables saved in "data/out/tmp/*.txt" and the most important, the activity saved in "data/out/veh/na_*.rda". An advantage of working with .rda files instead of .csv or shapefiles is that it's possible to save different objects with the same extension, and it's light and faster to load in R.

data

Input data

The input data are located in "data/in" and the folders are daily, fen, det, network and veh.

daily: it contains files with a normalized profile at 08:00-09:00 of the traffic counts 24 hours from Monday to Sunday. These profiles are for Passenger Cars (PC), Light Commercial Vehicles (LCV), Trucks and Buses. It depends on the available data, Ibarra & Ynoue (2016) used traffic counts of a near downtown toll station.

veh: it's a comma-delimited .csv file of 25 vehicles in circulation, that is, vehicles sales after applying survival functions for 50 years. It's a dataframe (R object to store data tables) with header indicating the type of vehicle.

fen: it's a .csv file, a dataframe very similar to veh.csv, but it counts emission factors for the 25 types of vehicles over 50 years of use. There is one file per pollutant.

det: it's a .csv file for the 25 vehicles over 50 years indicating deterioration at year of use. There are deterioration factors for CO, HC and NO_x.

network: it contains the road network in a spatial format. It can read virtually any spatial format with the rgdal library being shapefile one of the most popular, but as it's called on REMI.R, it can be modified as the user prefers. The road network has mandatory fields depending if it's from openstreetmap or a traffic simulation. As traffic simulation varies greatly, here is presented the mandatory fields when performing an emissions inventory with traffic counts and openstreetmap:

- "highway": field with type of streets: "motorway", "motorway_link", etc.
- "xlong1": first longitude coordinate in EPSG:4326.
- "xlong2": last longitude coordinates in EPSG:4326
- "ylat1": first latitude coordinate in EPSG:4326.
- "ylat2": last latitude coordinate in EPSG:4326.
- "longkm": Length of the link in km.

Output data

The output data are located in "data/out" and the folders are emi, images, tmp, network and veh.

emi: it contains all the resulting emissions with 4 types:

1) emissions inventory tables according to 5, 20 and 142 types of vehicles, df.rda, ta_cetesb.rda and E_df.rda, respectively. Also the same for RADM2 speciation: df_hcx.rda, ta_cetesb_hcx.rda and E_df_hcx.rda.

2) Hourly emissions by each link from Monday to Sunday to each pollutant,

3) Gridded emissions with resolution selected by compiler, hourly of a Monday (ex: g_NO₂.rda),

4) Two text files .txt of the gridded hourly emissions of a Monday. Each file has all the pollutants considering a RADM2 estimation. These files are used to generate WRF-Chem (DF_wrf.txt) (Grell *et al*, 2005) input data, and the other to BRAMS (DF_brams.txt) input data. These files require that the

user indicate the time zone of the area where the emissions were estimated because it stores the emissions in GMT.

images: Here are stored all the images generated by different scripts. There are images of fleet distribution, emissions plot in bars, gridded emissions maps and network maps.

tmp: In this folder there are all the .txt tables generated indicating fleet, accumulated fleet, fleet by fuel standard, and also an emissions table ta_cetesb.csv.

network: It contains the file red.rda of the network which is a SpatialLineDataFrame (SLDF) format, in other words, an sp object. The following fields were added: "ID","V" the rush hour speed, "Vlibre" free flow speed, "Vmedia" the average speed between "V" and "Vlibre", "dcentro" which is the distance between the mid point of each link and the chosen center of the city, and "dcentroC" which is the same as "dcentro" with a limit in the distance calculation to avoid overestimation of trucks in streets far outside the city.

veh: it includes 5 files of activity level: na_bus.rda, na_lcv.rda, na_m.rda, na_pc.rda and na_trucks.rda. Each file contains the amount of vehicle in each link at 08:00-09:00 of a Monday to each type year of use, from 0 to 50 and by technological composition: na_pc.rda has 348, na_lcv.rda 171, na_trucks.rda 255, na_bus.rda 102 and na_m.rda 171.

functions

Here there are the vehicles function PC.R, LCV.R, TRUCKS.R, BUS.R and MOTO.R. These functions assign vehicles to the road network applying a survival function over 50 years of use and classifies by fuel, size, weight and emissions standard. These functions returns dataframes called na_pc.rda, na_lcv.rda, na_trucks.rdam na_bus.rda and na_m.rda as showed in last section. These functions also create fleet plots and dataframes saved as text files.

Other functions are Tabplot.R and edad.R. edad.R stores a wide range of survival functions resulting in different average years for each type of vehicle (PC, LCV, TRUCKS, BUS and MOTO). The user must choose the respective average age of the fleet. Tabplot.R is to plot emissions bar later after the estimation process ended, it reads df.rda.

There are also pollutant functions, that are the core functions of REMI. Each pollutant has a folder with scripts for the emission factors of each type of vehicle and also the estimations procedure, described in following section.

This folder also contains subfolders POST and MEC. POST include functions to produce SpatialLineDataFrames with 24 emissions for each day of the week, to generate grid with spatial resolution chosen by the user, and functions to plot grids with ggmap library. MEC the chemical mechanism, so far it has RAMD2 functions which speciate the Non-Methane HydroCarbons (NMHC) in fifteen pollutants Aldehyde (ALD), C2H5OH, CH3OH, ETH, HC3, HC5, HC8, HCHO, ISO, ketone (KET), OL2, OLI, OLT, TOL and xylenos (XYL), according experimental observations performed at Department of Atmospheric Sciences of IAG/USP (<http://www.iag.usp.br/>). This folder includes a subfolder also called POST with same functions to the respective pollutants, but also includes two special functions to generate text files used to generate WRFR-Chem and BRAMS emissions inputs.

Finally, each folder has a delete.R function used to exclude temporary files.

Emissions estimation process

One all the activity .rda files were generated starts the emissions estimation process. In oder to clarify we present a small part of REMI.R

First, define the working directory and call the libraries.

Then it reads the road network with the respective spatial reference. It's important to note that the original road network could be in any spatial reference, but in order to run in REMI, it must be in EPSG:4326, which is WRG84 LAT LON.

Then are defined the considered latitude and longitude for center in order to calculate its euclidean distance with midpoint of each link (in future it will calculate the geographical (geodesic) distance) .when used the method of interpolation of traffic counts.

```
R> setwd("/your/path")
```

```
R> library(maptools); library(rgeos); library(ggmap);
R> red <- readShapeLines("data/in/network/sp.shp", proj4string=CRS("+init=epsg:4326"))
R> xlongCENTRO <- -46.633949
R> ylatCENTRO <- -23.550391
R> system.time(source("functions/NETWORK.R"))
R> rm(list = ls())
```

The activity functions are called following. They assign the vehicles to the road network if it is an interpolation, or read from traffic simulation, and then split it by type of fuel, size of motor and gross weight in a 50 years distribution reading the file data/in/veh/veh.csv. As a result, we have the amount of vehicles at each link with vehicles age distribution and type of fuel, so it's possible to assign respective emissions standard, resulting in a dataframe names data/out/veh/na*.rda. It also produces different fleet plots and tables. The procedure, for Passenger Cars, is just:

```
R >system.time(source("functions/PC.R")) # na_pc.rda
```

The emissions estimations starts loading the emission factors. REMI uses local emissions factors from measurements made by the manufacturers in Brazil with FTP-75 driving cycle (CETESB, 2013), and uses (Ntziachristos, 2014). to incorporate the speed variation at other speeds than 34.12 km/h, the mean speed at this driving cycle. As the emission factors are available to each year of use, it incorporates deterioration factor identifying 50 years. The following lines show the procedure in R:

```
R> det <- read.csv("data/in/det/detco.csv", h=T)
R> fen <- read.csv("data/in/fen/fenco.csv", h=T)
R> F_CO_A_2012_G_L5_1000 <- function(V) {
R>   ((1.36E-01 + -8.91E-04*V + 0*V^2)/(1 + -1.41E-02*V + 4.99E-05*V^2))
R> }
R> FFE_1 <- fen[1,1]/F_CO_A_2012_G_L5_1000(34.12)
R> F_CO_A_2012_G_L5_1000 <- function(V) {
R>   ((1.36E-01 + -8.91E-04*V + 0*V^2)/(1 + -1.41E-02*V + 4.99E-05*V^2))*FFE_1*det[1,1]
R> }
```

Then the emissions are then calculated loading the activity na*.rda file and red.rda. REMI considers three mean speeds for rush hour (V), free flow (Vlibre) and an averaged speed (Vmedia) distributed over 24 hours. The emissions are calculated for 50 years of use calculating first to each hour, as follows:

```
R> E_CO_OU_2012_D_P7_seg_8 <- OU_0_D_P7 * F_CO_OU_2012_D_P7 (red$V)*red$longkm
...
R> E_CO_OU_2012_D_P7_seg_8_vl <- OU_0_D_P7 * F_CO_OU_2012_D_P7 (red$Vlibre)*red$longkm
...
R> E_CO_OU_2012_D_P7_seg_8_vm <- OU_0_D_P7 * F_CO_OU_2012_D_P7 (red$Vmedia)*red$longkm
...
```

In this case the base-year is 2012, so the emissions are calculated till year 1962 and summed by the emission standard classification of type of vehicle. Then comes the part of extrapolate the emissions to the hours and days of the week. The emissions s are calculated with traffic flow of morning peak hour of 08:00-09:00 and with three average speeds, rush hour, free flow and averaged, and the extrapolation process uses a profile of 24 hours and each day of the week normalized to 08:00-09:00. So, three type of emissions (by each mean speed) were allocated to 24 hours and then multiplied with this profile at 24 hours and each day of the week. The allocation assumes the following speed distribution:

- 00:00-06:00 Free Flow mean speed (Vlibre).
- 06:00-07:00 Averaged mean speed (Vmedia).
- 07:00-10:00 Rush Morning hour (V).
- 10:00-17:00 Averaged mean speed (Vmedia).
- 17:00-20:00 Rush Evening hour (V).
- 20:00-21:00 Averaged mean speed (Vmedia).

- 21:00-00:00 Free Flow mean speed (Vlibre).

So, the emission are multiplied with the normalized profile at each respective hour. Per example, the 00:00 hour emissions are the emissions calculated with free flow speed and multiplied with the profile of 00:00 hour. The following lines show the process:

```
#Monday
R> E_CO_OU_D_P7_seg_0 <- E_CO_OU_D_P7_seg_8_vl *profile[1,1]
...
R> E_CO_OU_D_P7_seg_6 <- E_CO_OU_D_P7_seg_8_vm *profile[7,1]
...
R> E_CO_OU_D_P7_seg_7 <- E_CO_OU_D_P7_seg_8 *profile[8,1]
...
# Tuesday
R> E_CO_OU_D_P7_ter_0 <- E_CO_OU_D_P7_seg_8_vl *profile[1,2]
...
```

Once the emissions are calculated to all the hours of the week, are summed to tons/year and stored as dataframe E_df.rda. Then, the emission are summed to each hour and day of the week ate each link and also stored as dataframe.

```
R> E_CO_BUS_seg_0<-E_CO_OU_D_P7_seg_0 + E_CO_OU_D_P5_seg_0 + ...
```

Benchmark

REMI runs in a machine with GNU/Linux operational system Debian 8.2 Jessie, kernel x_86_64 Linux 3.15.0-4-amd64, CPU of Intel Core i7-4770 3.9GHz and 16 Gb RAM. When calculating the emissions, including gridding and all the plots takes:

Table 1. Performance of REMI

REMI for Metropolitan Area of São Paulo	Time
<p>Count interpolation 105468 links 27 pollutants 24 hours, 7 days of the week</p>	4 hours
<p>Traffic Simulation 34733 links 27 pollutants 24 hours, 7 days of the week</p>	1 hour

4. Discussion

In order to run this model properly it's needed with traffic interpolation it's needed traffic counts, local emissions factors and fleet statistics over 50 years. But this information is not always available when performing an inventory. In REMI model with traffic count interpolation, the amount of vehicles basically depends on road network of open street map (<http://www.openstreetmap.org/>). So, a bigger city will have a bigger road network and a smaller city a smaller network. Keeping that in mind, it's possible to assign the interpolation of one city into another, while those cities shares relatively the same level of congestion per street. As a result, a bigger city will have more vehicles circulating and a smaller one less. It's always important take into account the peculiarities of each city, per example, a city near an important economic activity that requires circulation of heavy duty vehicles, like ports of mining industry. Also, the fleet distribution by type of vehicle, per example, cities with larger amount of motorcycles, like asian cities. Another important aspect is the average age of the fleet of the city, because, despite that the city could have high emissions standards, if the average age of th fleet is old, that city will have more older vehicles circulating, resulting in higher emissions.

With those considerations it was applied REMI model (called REMI in that time) to estimate the vehicular emissions of 58 urban centers of South America (Ibarra *et al*, 2015a). The pollutants

covered were CO, PM2.5, HC and NOx. The figure 2 and 3 shows the results by country for CO and by city for PM2.5. In this study were corrected the different type of fuels used in each city, and it was considered the average age of fleet in each country with a statistically significant association with GDPpp for 2012.

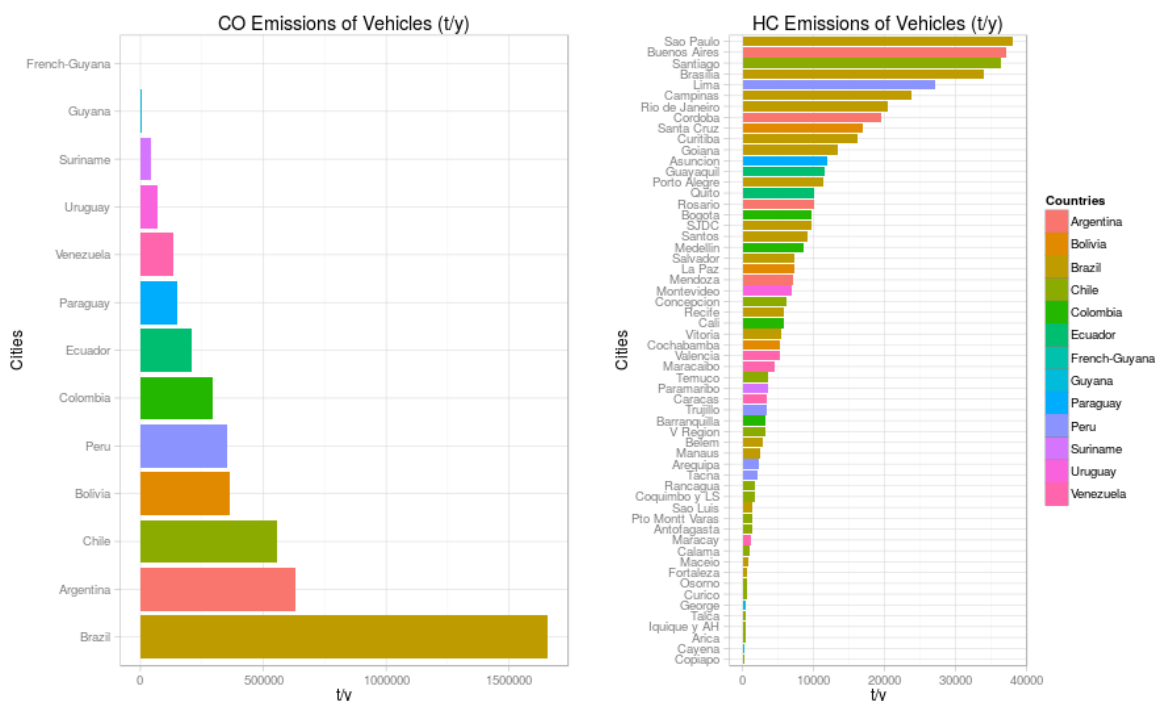


Figure 2. Vehicle emissions of CO by country in 2012 (Ibarra et al., 2015a). **Figure 3. Vehicle emissions of HC by city in 2012 (Ibarra et al., 2015a).**

This model was also used to estimate emissions and simulate air pollutant concentrations for the city of Porto Alegre, Brazil (Ibarra et al, 2015b). The air pollutant concentrations could not be compared with observations due to lack of data, but the results were meteorological and chemically consistent. Figure 4 and 5 show results of CO emissions and concentrations.

The model is still in development and a new version it's planned to produce an R package which must be very versatile. This characteristic is for adequate to the reality of different cities. Also, as it's this packages will have different emission factors, allowing projections and estimation of past scenaries. REMI will also include a more type of vehicles, emission factors and it would be applicable to region in the world.

Conclusion

REMI model is a program to estimate bottom-up vehicular emissions inventory which, unders certain assumptions, can be adapted to availability of data to any city. Right now it represents Brazilian conditions, but it can be adapted to other realities, including emission factors. SO far, it does not include evaporative and cold start emissions, but it's planned to include them near in future. This work is part of the PhD in meteorology program of the University of São Paulo, Brazil.

Acknowledgments

We would like to thank María de Fátima Andrade of Laboratório de Processos Atmosféricos (LAPAT) for all the support, as scholarships progams CAPES of Ministry of Education, Brazil, and Becas Chile, from Conicyt, Chile.

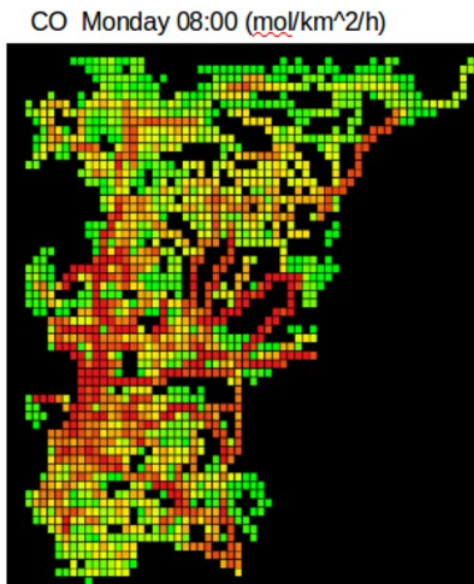


Figure 4. Vehicle emissions of CO Porto Alegre 2012 (Ibarra et al., 2015b).

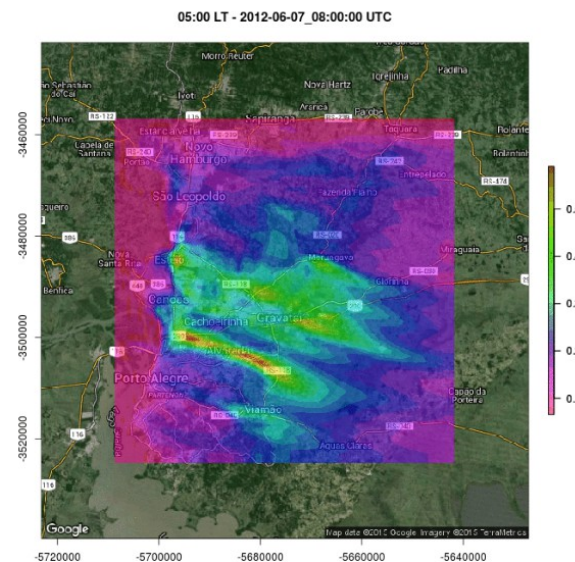


Figure 5. CO concentration (ppm) Porto Alegre 2012 (Ibarra et al., 2015b).

References

- CETESB, 2012. Emissões veiculares no estado de são paulo. <http://veicular.cetesb.sp.gov.br/relatorios-e-publicacoes/>.
- D. Kahle and H. Wickham. ggmap: Spatial Visualization with ggplot2. The R Journal, 5(1), 144-161. URL <http://journal.r-project.org/archive/2013-1/kahle-wickham.pdf>
- Grell, G. A., Peckham, S. E., Schmitz, R., McKeen, S. A., Frost, G., Skamarock, W. C., & Eder, B. (2005). Fully coupled "online" chemistry within the WRF model. *Atmospheric Environment*, 39(37), 6957-6975.
- H. Wickham. ggplot2: Elegant Graphics for Data Analysis. Springer-Verlag New York, 2009.
- Ibarra S. and Ynoue R. (2016) High resolution vehicular emissions inventory for the megacity of São Paulo. Manuscript to be sent to Atmospheric Environment.
- a) Ibarra S., Ynoue R., Vela A., Vehicular Bottom-up Emissions Inventory And Atmospheric Simulation Fof 58 Urban Centers Of South America. 11TH International Conference On Southern Hemisphere Meteorology And Oceanography. October 5TH TO 9TH 2015, Santiago, Chile.
- b) Ibarra S., Vela A., Rehbein A., Ynoue R., High Resolution Air Pollutant Simulation For The Metropolitan Region Of Porto Alegre. IX Workshop Brasileiro De Micrometeorologia. 11-13 Novembro 2015, Santa Maria, RS, Brasil.
- Ntziachristos, L., and Z. Samaras. "EMEP/EEA emission inventory guidebook." *European Environment Agency, Copenhagen* (2009).
- R Core Team (2016). R: A language and environment for statistical computing. R Foundation for Statistical Computing, Vienna, Austria. URL <https://www.R-project.org/>.
- Roger S. Bivand, Edzer Pebesma, Virgilio Gomez-Rubio, 2013. Applied spatial data analysis with R, Second edition. Springer, NY. <http://www.asdar-book.org/>
- Roger Bivand and Colin Rundel (2015). rgeos: Interface to Geometry Engine - Open Source (GEOS). R package version 0.3-15. <https://CRAN.R-project.org/package=rgeos>
- Roger Bivand and Nicholas Lewin-Koh (2015). maptools: Tools for Reading and Handling Spatial Objects. R package version 0.8-37. <https://CRAN.R-project.org/package=maptools>
- Tim Pulles and Dick Heslinga. "The art of emission inventorying." TNO, Utrecht (2010).

Evaluation of E-mobility benefits in Klagenfurt

Ulrich UHRNER*, Rafael REIFELTSHAMMER*, Gerhard BACHLER*, Martin Dippold*, Wolfgang HAFNER**, & Peter J. STURM*

*Traffic & Environment, IVT, Graz University of Technology, 8010 Graz, Austria
Fax +43 316 873 30202 - email: ulrich.uhrner@ivt.tugraz.at

** Department of Environmental Protection, City of Klagenfurt, 9020 Klagenfurt, Austria

Abstract

Promoting E-mobility in Klagenfurt and realizing environmental co-benefits are major objectives of CEMOBIL. In Klagenfurt, there is a high share of light diesel vehicles (> 60 % VKT) and NO₂ levels at air quality stations have remained high near major roads within the last couple of years. Due to Klagenfurt's location in a sheltered alpine basin, there is a strong sensitivity of air quality towards emissions released close to the ground. The impact of increased E-mobility (20 % electric light vehicles, 25 % electric buses) in the Klagenfurt area was assessed for 2025 and compared with a BAU 2025 reference scenario. Additional electricity related emissions were estimated.

Emission reductions were computed for CO₂ (-14 %), NO_x (-8.8 %) and PM₁₀ (-0.6 %). An area-wide reduction potential of -0.8 µg/m³ AM NO₂ was computed for the city center and up to -1.5 µg/m³ at major road kerbside locations compared to the BAU scenario 2025. For PM_{2.5} and PM₁₀ the computed improvements are up to -0.1 µg/m³ at busy roads. The comparison BAU 2025 versus Base 2014 revealed that the reduction potential of improved exhaust aftertreatment technologies along with fleet renewal is larger than the E-mobility reduction potential for NO₂ and PM.

Keys-words: E-mobility, benefits, air pollution, NO_x, CO₂

1. Introduction and Background

Depending on its market penetration as well as electricity mix, E-mobility technologies have a great potential in reducing greenhouse gases (GHG) and air pollutant emissions such as nitrogen oxides (NO_x) or particulate matter (PM). In addition, urban noise levels can be reduced. Demonstrating and facilitating E-mobility in order to realize future environmental co-benefits in Klagenfurt are major objectives of the EU-Life+ project CEMOBIL (CO₂ neutral Electro-MOBILity for the reduction of air pollutants and noise in European cities, for example Klagenfurt; <http://www.cemobil.eu/>).

In the sheltered Klagenfurt basin (population ~100 000) located south of the Alpine bow, air quality problems (PM₁₀, NO₂) have been encountered frequently over the last years (see Figure 1). There, frequently low wind speeds and inversions are encountered. Eastward of Klagenfurt, 67 % of the recorded winds were below 1.5 m/s in 2010 (Uhrner et al., 2014). In Klagenfurt there is not much industry and the city is not located close to area-wide extensive sources of high pollution. Therefore, a strong sensitivity of air quality particularly towards emissions released close to the ground results. Traffic is the main NO_x source and a major PM source in Klagenfurt (Sturm et al., 2012, Uhrner et al., 2014). A specific aspect of E-mobility is that almost no harmful air pollutants are emitted close to the ground. Their most promising application is urban transport and commuting. Due to the high share of diesel light vehicles in Austria, which is over 60 % on vehicle kilometers travelled (VKT), the reduction potential of electric vehicles on NO_x and PM exhaust emissions is high. Within the framework of CEMOBIL future E-mobility scenarios and a business as usual scenario (BAU) have been developed to evaluate the potential impact of electric vehicles on air quality in Klagenfurt in the near future.

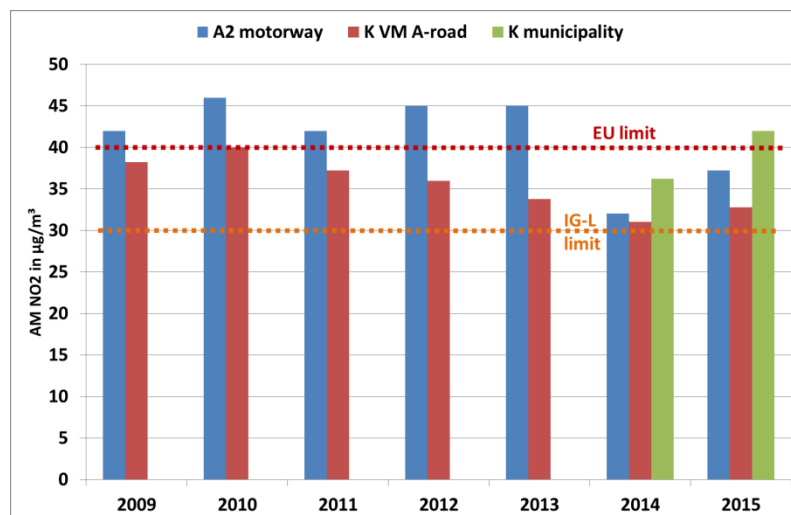


Figure 1: Measured annual mean (AM) NO₂ at monitoring station located near busy roads. The red dotted line indicates the EU limit of 40 µg/m³, the orange one the Austrian limit (IG-L).

2. Objectives

Within this work the emission reduction potential of one E-mobility scenario as well as improved engine and exhaust aftertreatment technologies along with fleet renewal will be evaluated and discussed. The additional electricity demand for electric light vehicles and busses is computed and resulting power generation related emissions were estimated for CO₂, NO_x and PM₁₀. Annual mean (AM) NO_x, NO₂, PM_{2.5} and PM₁₀ concentrations were computed to assess the impact on air quality of these three cases. Another objective was to evaluate the E-mobility reduction potential on air quality in case the emission reductions related to improved engine exhaust technologies are delayed or their effect significantly lessened in extent.

3. Methodology

Traffic data and emissions: Traffic model results using the VISUM traffic model containing traffic densities for light vehicles (LV) (mostly cars and vans), heavy duty vehicles (HDV) and buses on the Klagenfurt road network, as well as average speeds were provided by Klagenfurt municipality for 2014 and form the basis of this work. These traffic count data, together with vehicle speed data, were used as an input to compute traffic related air pollutant emissions for the road network. For this purpose the vehicle emission prediction model (NEMO 3.7, Dippold et al., 2012), which contains the Austrian vehicle registration data along with future fleet projections, was used. The computed emissions were allocated in space to approx. 34 000 road sections. Tunnel emissions were integrated over the tunnel length and calculated as portal area sources.

Scenarios: Based on the experiences in Klagenfurt and latest traffic numbers, no further increase in traffic volume for 2025 was assumed in the BAU 2025 scenario and E-mobility scenario. The aim of the Klagenfurt BAU scenario was twofold: 1) to assess the impact of technological progress in exhaust after-treatment, driven by more stringent emission standards until 2025 in combination with the ongoing fleet renewal; 2) to provide a basis to evaluate the E-Mobility Scenario of a 20 % share of electrically driven LV (cars, vans) in Klagenfurt, 10 % share of electrically driven LV at the motorways around Klagenfurt and 25 % share of electrically driven city buses in 2025. Emissions from both scenarios were computed using NEMO and allocated in space to road sections.

Dispersion: In order to compute dispersion of NO_x, PM_{2.5} and PM₁₀ the GRAMM (Graz Mesoscale Model, Almbauer et al. 2000) and GRAL (Graz Lagrangian Model, Öttl 2015) models were used. For the flow field computations, digital elevation model data and land use data (Bossard et al., 2000) were processed on 250 m x 250 m grids. Meteorological data from a meteorological station located eastward of Klagenfurt were classified into different prevailing flow conditions (wind speed classes, 10° wind sectors and 7 stability classes, Uhrner et al. 2014). Finally, CPU intensive dispersion

computations were carried out for the selected area around Klagenfurt, 16.5 km by 16 km in size, using a counting grid resolution of (10 m x 10 m) to compute dispersion. AM NO_x, PM_{2.5}, PM₁₀ concentrations were modelled. NO_x to NO₂ conversion was computed using a Romberg type empirical conversion formula (Bächlin et al., 2006, Romberg et al., 1996). Residential heating, in particular wood burning is a major PM source within the area of interest. Within the PMinter project (Uhrner et al., 2014) emissions from residential heating have been assessed bottom-up and validated. In order to represent the strong contributions and concentration gradients resulting from residential heating the PMinter data have been used. Homogeneous constant background values for NO_x, PM_{2.5} and PM₁₀ were used to compensate for neglected sources and regional transport towards the model domain. Air quality monitoring data from 5 to 6 stations were used to adjust NO_x, PM_{2.5} and PM₁₀ background values and for validation of the modelling approach.

4. Results and Discussion

Emissions

Internal combustion engine related traffic emissions were computed for all road sections of the modelling domain using the model NEMO. NO_x, PM_{2.5}, PM₁₀ exhaust and non-exhaust emissions were allocated to respective road sections for light vehicles, buses and heavy duty vehicles for all three cases respectively. **Figure 2** shows the dispersion modelling domain and results from traffic emission modelling for NO_x using NEMO for the Klagenfurt road network. Maximum emissions are found near the motorway, the main arterial roads and within the city centre.

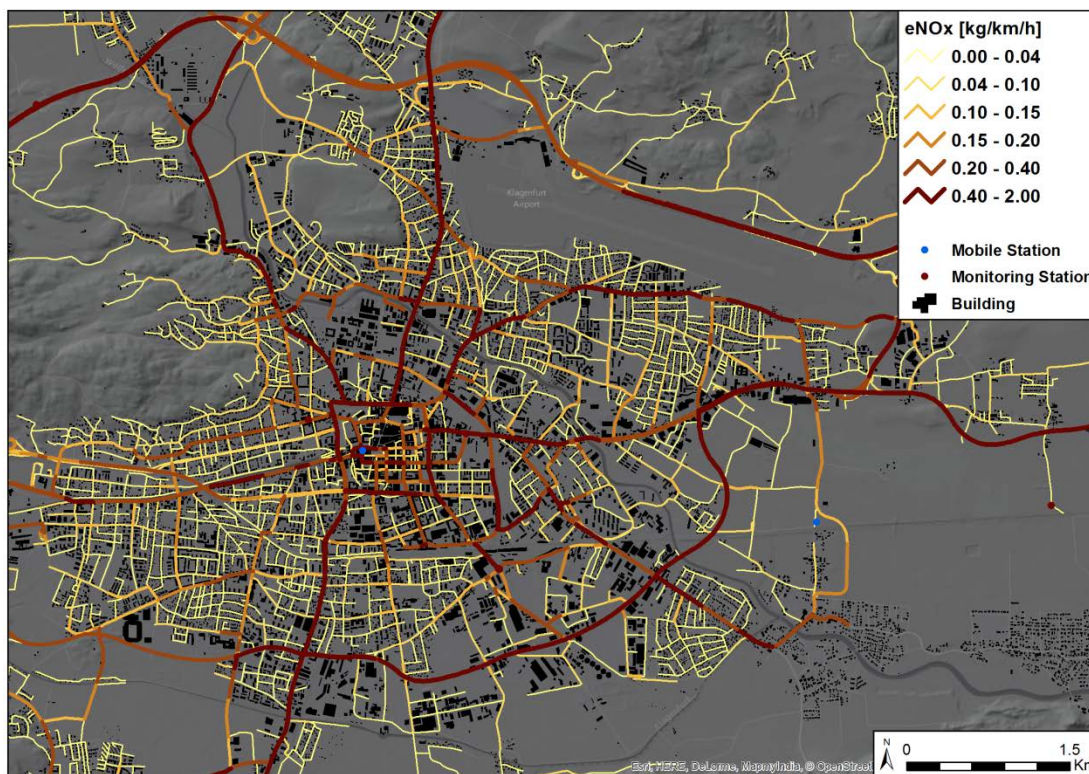


Figure 2: Dispersion modelling domain and location of air quality monitoring comprising Klagenfurt municipality and modelled line source emissions for NO_x, base case 2014.

For the E-mobility 2025 scenario (20 % E-LV in the municipality, 10 % E-LV on motorways and 25 % E-buses in the municipality) the required electricity consumption was computed using NEMO. Table 1 summarizes for all vehicles the total annual power consumption, CO₂, NO_x, PM_{2.5} and PM₁₀ exhaust as well as non-exhaust emissions. In total 1003 million vehicle kilometres travelled per annum were computed. For the base case 2014 and the BAU 2025 scenario the actual CEMOBIL fleet was

taken into account. In addition, the E-mobility power production related NO_x, PM₁₀ and CO₂ emissions were computed based on the Austrian 2013 power mix (Stromkennzeichnungsbericht 2014) and the continental Europe ENTSO-E (European Network of Transmission Systems Operators) power mix. The Austrian power mix comprises electricity from 68.1 % hydro power, 10.5 % other renewables, 18.7 % fossil fuels and 2.6 % nuclear power. In contrast, the ENTSO-E 2014 power mix contains less hydro power but large shares of fossil fuel and nuclear power produced electricity (18.5 % hydro power, 10.5 % other renewables, 40.5 % fossil fuels and 26.4 % nuclear power). Electrical power consumption related emission factors (in g/kWh el) from ÖKO (2010), GEMIS 4.6 and PROBAS data bases were used to estimate the power production related emissions for both power mixes (Table 1).

Table 1: Total electricity consumption (Cons el) and traffic emissions per annum for the Klagenfurt area. The * indicates power production related emissions according to the Austrian power mix and additionally ENTSO-E, ex denotes exhaust, and Nex non-exhaust PM emissions.

	Cons el [GWh/a]	CO ₂ [t/a]	CO ₂ * [t/a]	NO _x [t/a]	NO _x * [t/a]	PM ₁₀ ex [t/a]	PM ₁₀ Nex [t/a]	PM ₁₀ * [t/a]	PM _{2.5} Ex [t/a]	PM _{2.5} Nex [t/a]
Base 2014	0.20	205024	27.1	743.6	0.05	19.9	44.7	0.00	19.9	24.3
BAU 2025	0.20	176283	27.1	251.4	0.05	5.02	44.8	0.00	5.02	24.3
Emob 2025	49.3	144624	6631	216.5	12.9	4.1	44.8	0.62	4.12	24.3
ENTSO-E			13528		31.1			0.89		

BAU 2025 CO₂ emissions from internal combustion engines (ICE) driven vehicles are reduced by -28741 t/a (-14 %) compared to the base case 2014. E-mobility 2025 CO₂ ICE emissions are reduced by -31659 t/a (-18 %) compared to the BAU 2025 scenario. 49.3 GWh/a electricity are required for the electric vehicles (from the plug-in, without production and line losses). If the required electricity is produced according to the Austrian 2013 power mix, 6631 t/a power production related CO₂ emissions would result (Table 1), assuming 5 % line losses. With the ENTSO-E 2014 power mix (40.5 % fossil fuels) the positive impact of E-mobility on CO₂ declines, but is still positive (Figure 3, Table 1).

BAU 2025 ICE NO_x emissions are reduced by -492 t/a (-66 %) compared to the base case 2014. E-mobility 2025 NO_x ICE emissions are further reduced by -34.9 t/a (-14 %) compared to the BAU 2025 scenario. The substantial NO_x reductions of both 2025 scenarios compared to the base case 2014 are mainly attributable to improved exhaust aftertreatment technologies driven by emission legislation (Euro 6) and fleet renewal. It should be noted that the computed substantial NO_x exhaust emission reductions (BAU 2025 – Base 2014) include as well NO_x reductions of HDV. With the Austrian power mix, 12.9 t/a electricity production related NO_x emissions would result (Table 1). With the ENTSO-E 2014 power mix the positive impact of E-mobility on NO_x emissions is almost counter balanced, see Figure 3.

BAU 2025 PM_{2.5} and PM₁₀ exhaust emissions (ICE) are reduced by -14.9 t/a (-75 %) compared to the base case 2014. E-mobility 2025 PM_{2.5} ICE emissions are reduced by -0.9 t/a (-17 %) compared to the BAU 2025 scenario. PM_{2.5}/10 exhaust emissions comprise 45 %/31 % of the total PM_{2.5}/10 emissions and in BAU 2025 the share of PM_{2.5}/PM₁₀ exhaust emission is reduced to 17 %/10 %. The related reductions are limited to exhaust PM, consequently the total reduced PM mass is low, see Figure 3.

The computed substantial NO_x exhaust emission reductions (BAU 2025 – Base 2014) are only realistic if future real world emissions will not deviate significantly from the upcoming “Real Driving Emission” RDE legislation (September 2017 Step 1, September 2019 Step 2). In principal, the impact of realistic dynamic driving situation on NO_x emissions is implemented within the NEMO model. However deactivation of exhaust aftertreatment components at low temperatures or malfunctioning of complex exhaust aftertreatment components cannot be represented. For future PM exhaust emission computations leaking of old regenerating particle may pose as well a major uncertainty of emission computations.

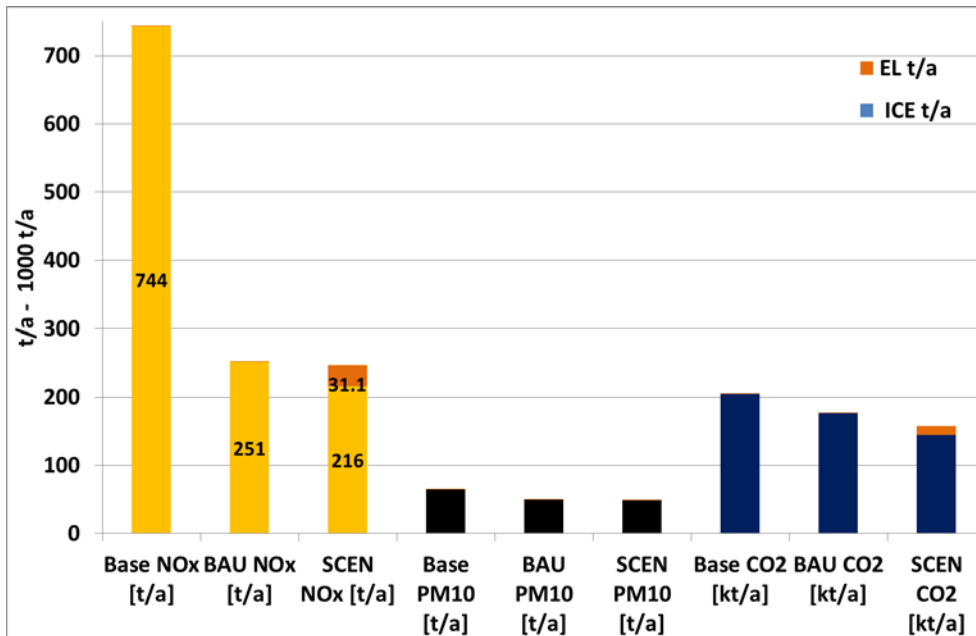


Figure 3: Total traffic NOx, PM10 (t/a) and CO2 (in 1000t/a) emissions from internal combustion engines (ICE) and power production related emissions according to ENTSO-E mix.

Air Quality

Base case 2014: Figure 4 shows the result for the AM NO₂ for the base case 2014 for the entire domain. The locations of the monitoring sites are indicated. Results of the comparison monitoring results versus simulations are shown in Figure 5. For NO₂ the agreement is good, for PM_{2.5} and PM₁₀ (not shown, R² = 0.74) the agreement is fair. The measurements have been used for the evaluation of background values which were also used in both scenarios:

- 7 µg/m³ for NO_x (as NO₂ mass equivalent)
- 8 µg/m³ for PM_{2.5}
- 10 µg/m³ for PM₁₀

Generally, within the inner city of Klagenfurt elevated NO₂ levels of up to 30 µg/m³ are computed. At some locations near the ring road and inner city the Austrian (IG-L) air quality standard is exceeded; close to busy roads even the EU air quality standard. Generally, the AM NO₂ is low around the city centre, i.e. less than 20 µg/m³. However, near main arterial roads, near the motorway and the tunnel portals, very high elevated AM NO₂ concentration levels above the air quality standards (IG-L/EU) of 30/40 µg/m³ were computed. Generally AM PM_{2.5} and AM PM₁₀ levels are low in Klagenfurt, near major roads AM PM_{2.5} / PM₁₀ levels up to 19 µg/m³ / 25 µg/m³ are computed (not shown). However, particularly during winter time high PM_{2.5} and PM₁₀ levels are monitored exceeding frequently the daily mean of 50 µg/m³, dominated by PM attributable to secondary inorganics, solid fuels used in residential heating and traffic non-exhaust (Uhrner et al., 2014).

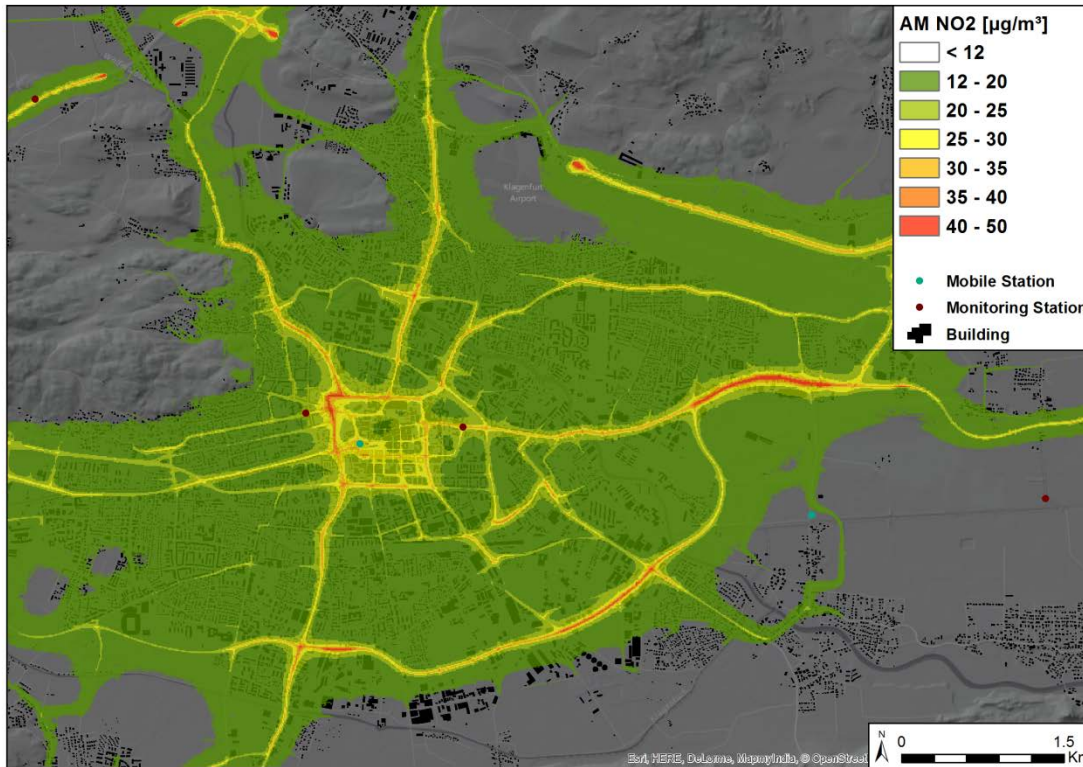


Figure 4: Simulated AM NO₂ concentration for Klagenfurt base case 2014, and location of air quality monitoring.

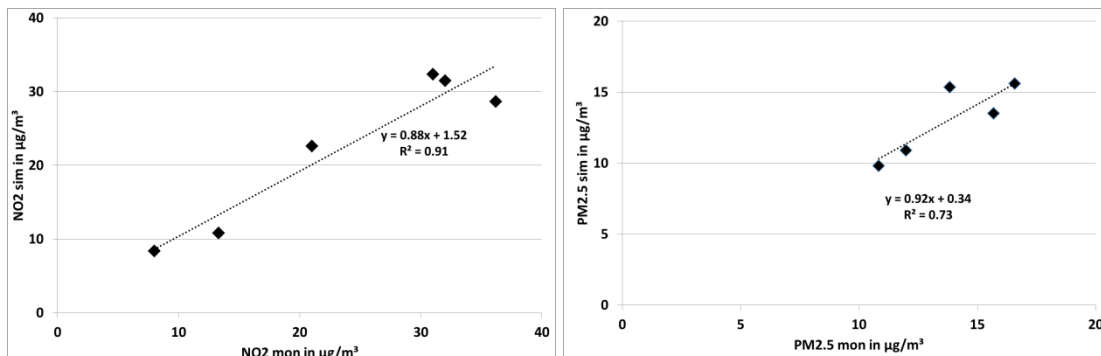


Figure 5: Comparison of monitored versus simulated base case AM NO₂ and AM PM_{2.5}, 2014.

BAU 2025 Scenario: After verification of the model approach on the basis of the 2014 simulations, the impact of technological progress in exhaust aftertreatment in combination with ongoing fleet renewal until 2025 was analysed. AM NO₂ concentration levels are significantly decreased, values above the IG-L limit of 30 µg/m³ result only near major roads and the tunnel portals (Figure 6, left). Levels above 40 µg/m³ were only computed at the tunnel portal locations. The reduction of BAU 2025 NO_x emissions results in substantial area-wide NO₂ concentration reductions. AM NO₂ is reduced area-wide by up to -11 µg/m³ in the city centre and in the vicinity of busy roads. Maximum reductions amount up to -14 µg/m³ close to busy roads (Figure 7, left). Figure 6 shows the simulated AM PM_{2.5} which is dominated by PM_{2.5} from solid fuels used in residential heating; concentration gradients are even at major roads low. According to the definition of the scenario, PM Reductions are limited to exhaust emissions. The share of exhaust particle emissions has been significantly reduced since the introduction of the Diesel particle filters (in most cases together with the introduction of the Euro 4 emission standard in 2005). In 2014, 53 % of the diesel LV were equipped with regenerating particle traps. Consequently, the future impact on PM exhaust emissions can be expected to be small as long as pre-Euro 4 diesel vehicles are not replaced in large quantities. BAU 2025 simulations for PM_{2.5} yield area-wide reductions of about -0.7 µg m⁻³

and up to $-1.5 \mu\text{g m}^{-3}$ in the vicinity of busy roads (Figure 7).

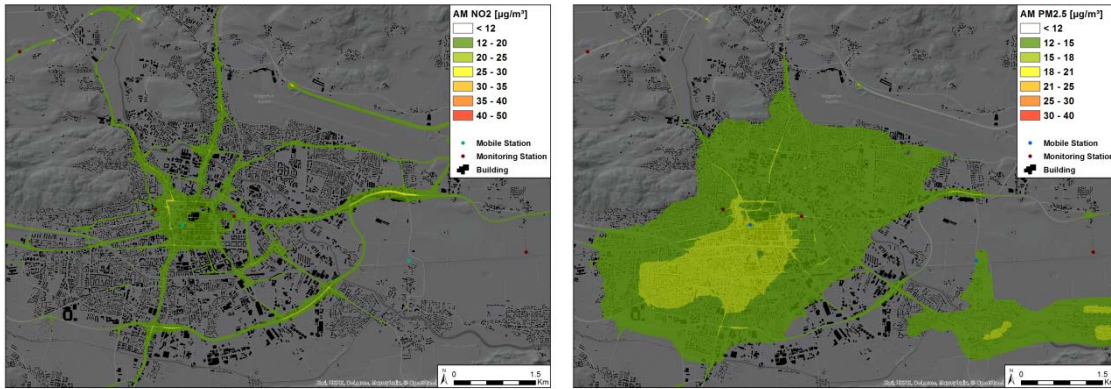


Figure 6: Simulated AM NO2 concentration (left) and simulated AM PM2.5 concentration for Klagenfurt BAU 2025.

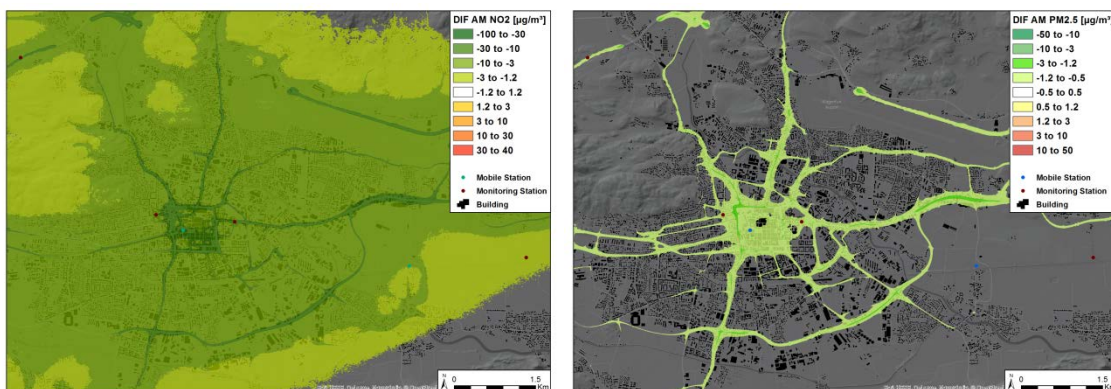


Figure 7: Difference AM NO2 (left) and difference AM PM2.5 (right) BAU 2025 vs. Base 2014.

E-Mobility 2025 Scenario: Compared to the BAU 2025 scenario AM NO2 concentration levels are significantly decreased (Figure 8). Within the city centre and the main roads air quality may improve by -0.5 to $-1.5 \mu\text{g}/\text{m}^3$ at major road kerbside locations. Compared to the BAU 2025 scenario, computed PM2.5 reductions are very small, up to $-0.1 \mu\text{g}/\text{m}^3$ at busy roads (Figure 8). These improvements (Emob 2025 - BAU 2025) are small compared with BAU 2025 – Base 2014. However, the reductions compared to the base case are large, i.e. in principal the superposition of the differences in NO2 and PM2.5 of Figure 7 (BAU 2025 - Base 2014) and Figure 8 (Emob 2025 – BAU 2025). The reduction potential of improved exhaust aftertreatment along with fleet renewal is larger than the E-mobility reduction potential. However, in case the expected impact of technological progress is delayed or considerably lessened, the E-mobility reduction potential is increased. Figure 9 shows the results for the E-mobility reduction potential for the extreme scenario of stagnating conditions in NOx and PM exhaust emissions related to the base case 2014. The E-mobility reduction potential is improved to $2.5 \mu\text{g}/\text{m}^3$ for AM NO2 and up to $0.5 \mu\text{g}/\text{m}^3$ for AM PM2.5 at city centre kerbside locations. It should be noted that the air pollution reduction potential of E-Mobility can be maximized, if ICE vehicles with extremely high NOx and/or PM exhaust emissions are replaced. Finally, considering the event of reduced or delayed future exhaust aftertreatment the reduction potential of electric vehicles may range between the two cases illustrated in Figure 8 and Figure 9, given a high share of electric light vehicles and electric buses in 2025.

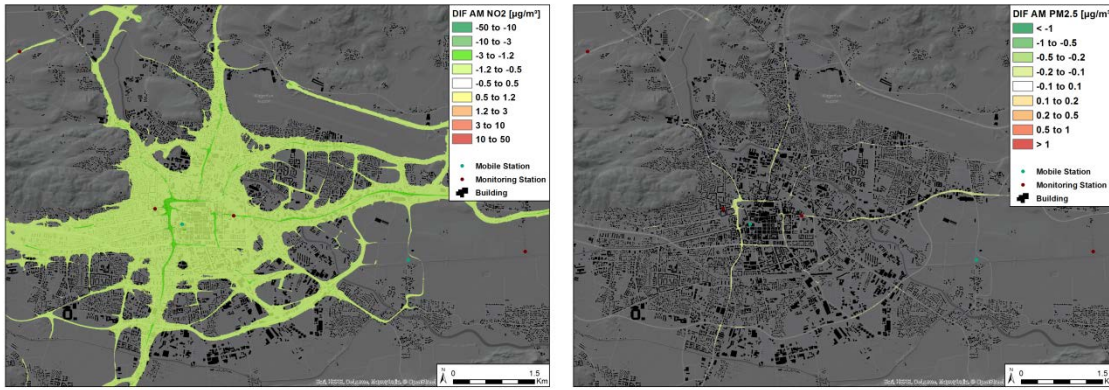


Figure 8: Difference AM NO2 E-mobility Scen 2025 vs. BAU 2025 (left), Difference AM PM2.5 E-mobility Scen 2025 vs. BAU 2025 (right).

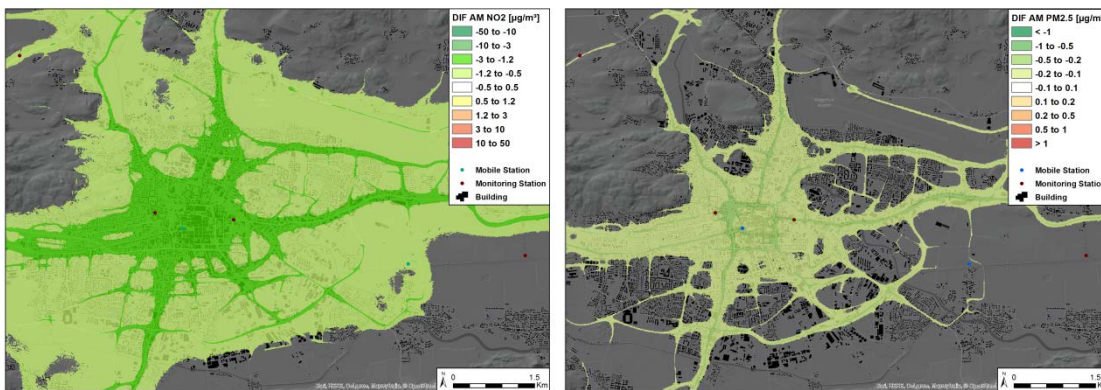


Figure 9: Reduction potential of E-mobility on AM NO2 (left) and AM PM2.5 for the extreme case of absent advances in future exhaust aftertreatment related to the base case 2014.

5. Conclusions

The impact of increased E-mobility on CO₂, NO_x and PM_{2.5} emissions and air quality (NO₂, PM_{2.5} and PM₁₀ exposure) was studied for the Klagenfurt municipality (~100 000 pop.) for 2025. The E-mobility scenario comprised a replacement of light vehicle ICE traffic by 20 % VKT in Klagenfurt municipality and 10 % replacement at the surrounding motorways, city buses were replaced by 25 % electric busses until 2025. A business as usual (BAU) scenario for 2025 was used as a reference case, to account for technological advances in exhaust after-treatment driven by more stringent emission standards and ongoing fleet renewal until 2025.

Substantial ICE emission reductions were computed for CO₂ by -28741 t/a (-18 %) as well as NO_x -34.9 t/a (-14 %) compared to the BAU 2025 scenario. PM exhaust emissions were reduced by -0.90 t/a (-3.1 % of total PM_{2.5} and -1.8 % of total PM₁₀ vehicle emissions) indicating that the future reduction potential for PM is exhausted due to the prognosed high share of vehicles with efficient state of the art or future exhaust aftertreatment technologies, e.g. regenerating particle traps. A power demand of 49.3 GWh/a was computed to run the electric vehicles. Additional power generation related emissions were estimated using the Austrian power mix which is characterized by a high share of hydro power (68 %). CO₂ emissions increase by 6631 t/a (+3.8 %), NO_x by 12.9 t/a (+5.1 %) and PM₁₀ by 0.62 t/a (+1.2 %). A comparison with the continental European ENTSO-E power mix (41 % fossil fuels) revealed power generation related CO₂ emissions of 13528 t/a (+7.7 %) and NO_x emissions of +31.1 t/a (+12.3%). Here NO_x emission reductions due to replacement of ICE vehicles are almost counter balanced by high NO_x emissions emitted by power plants using fossil fuels for power and heat generation.

However, a specific aspect of E-mobility is that almost no harmful air pollutants are emitted close to the ground and that effect was studied by running flow field and dispersion simulations to compute

annual means (AM) for NO₂, PM_{2.5} and PM₁₀. An area-wide reduction potential of -0.8 µg/m³ AM NO₂ was computed for the city center and up to -1.5 µg/m³ at major road kerbside locations, compared to the BAU scenario 2025. For PM_{2.5} and PM₁₀ the computed improvements are very small, only up to -0.1 µg/m³ at busy roads. The comparison BAU 2025 versus Base 2014 revealed that the reduction potential of improved exhaust aftertreatment technologies along with fleet renewal is larger than the E-mobility reduction potential. In case, the expected impact of technological progress is delayed or considerably lessened, the E-mobility reduction potential would be increased. It should be noted that the air pollution reduction potential of E-Mobility can be maximized, if ICE vehicles with extremely high NO_x and/or PM exhaust emissions are replaced.

Acknowledgments

This work was supported by the EU-Life+ programme.

References

- Almbauer R.A., D. Oetl, M. Bacher & P.J. Sturm (2000): „Simulation of the air quality during a field study for the city of Graz”, Atm. Env. 34, p 4581-4594
- Bächlin W., R. Böisinger, A. Brandt & T. Schulz (2006): Überprüfung des NO-NO₂-Umwandlungsmodells für die Anwendung bei Immissionsprognosen für bodennahe Stickoxid-freisetzung, Gefahrstoffe - Reinhaltung der Luft, 66, p 154-157
- Bossard M, J. Feranec & J. Otahel (2000) "CORINE Land Cover Technical Guide - Ad-dendum 2000". Technical report No 40, Copenhagen (EEA)
- Dippold M., M. Rexeis & S. Hausberger (2012): NEMO – A Universal and Flexible Model for Assessment of Emissions on Road Networks. 19th International Conference „Transport and Air Pollution“, 26. – 27.11.2012, Thessaloniki
- GEMIS-Österreich Modell Version 4.5
- ÖKO 2010: (Öko-Institut – Institut für angewandte Ökologie e.V.) Globales Emissions-Modell Integrierter Systeme (GEMIS) Version 4.6; internet-release auf www.gemis.de
- Öttl, D. (2015): Evaluation of the revised Lagrangian particle model GRAL against wind-tunnel and field experiments in the presence of obstacles. Boundary-Layer Meteorol, 155, 271-287
- Probas: Prozessorientierte Basisdaten für Umweltmanagementsysteme
<http://www.probas.umweltbundesamt.de/php/index.php>
- Romberg E., R. Böisinger, A. Lohmeyer, R. Ruhnke & E. Röth (1996): NO-NO₂-Umwandlung für die Anwendung bei Immissionsprognosen für Kfz-Abgase. Gefahrstoffe-Reinhaltung der Luft, 56, p 215-218.
- Stromkennzeichnungsbericht (2014): E-Control, 9. September 2014.
- Sturm J.P., C. Kurz & G. Bachler (2012): „Dispersion Modelling“ in Advances of Atmospheric Aerosol Research in Austria, Verlag der Österreichischen Akademie der Wissenschaften, ÖAW, ISBN 978-3-7001-7364-9.
- Uhrner U., B.C. Lackner, R. Reifeltshammer, M. Steiner, R. Forkel & P.J. Sturm (2014): Inter-Regional Air Quality Assessment, - Bridging the Gap between Regional and Kerbside PM Pollution, Results of the PMinter Project, VKM-THD Mitteilungen, Volume 98, Verlag der Technischen Universität Graz, ISBN: 978-3-85125-364-1
- VISUM Version 14.00-16, PTV AG

PM10 non-exhaust emission factors from tunnel measurements using a novel approach accounting for deposition and resuspension

Ulrich UHRNER*, Thomas NÖST* & Peter J. STURM*

*Traffic & Environment, IVT, Graz University of Technology, 8010 Graz, Inffeldgasse 21a, Austria
Fax +43 41 15 12 46 25 - email: uhrner@ivt.tugraz.at

Abstract

An improved understanding of PM non-exhaust sources from abrasion and resuspension processes is important for ambient air quality management and tunnel air management. Traffic tunnels are often used for real world air pollutant emission measurements. In contrast to ambient air quality measurements, flow and dilution conditions are well defined, driven speeds are typically constant. Data from two monitoring campaigns in a 10 km long tunnel with different distances between the air quality monitoring stations (3380 m/7180 m) have been re-analysed. The objective was to study the role of traffic volume on emission factors and to examine if PM10 deposition as opposed to resuspension needs consideration in road tunnel emission measurements. Without accounting for potential prevailing deposition processes non-exhaust emission factors evaluated from concentration gradient measurements in long road tunnels approach 0 or are even negative. Non-exhaust emission factors were significantly increased by using an effective deposition velocity as a sink term accounting for the interplay of wall deposition losses and resuspension of PM10. Average light vehicle (LV) PM10 non-exhaust EF ranged between 0.015 g/km/LV (35000 LV/day) to 0.060 g/km/LV (6500 LV/day). Average heavy duty vehicle (HV) PM10 non-exhaust EF ranged between 0.080 g/km/HV (6000 HV/day) to 0.300 g/km/HV (1500 HV/day).

Keys-words: PM10 non-exhaust emission factor, tunnel measurements, deposition, resuspension.

1. Introduction and Background

Road traffic non-exhaust emissions are a major particulate matter (PM) source in Europe. In contrast to PM exhaust emissions, non-exhaust emission factors (EF) are difficult to characterize and have large uncertainties. An improved understanding of PM non-exhaust sources is important for ambient air quality management but also tunnel air and waste management.

In contrast to exhaust pipe particles, mechanically produced particles from road traffic abrasion and resuspension processes are still poorly characterised, detailed quantitative information is missing. These non-exhaust or often termed diffuse road traffic emissions consist of brake, tire and road wear generated particles, as well as vehicle induced resuspension of deposited road dust. Wet road surface conditions may retain particles, under dry conditions particles get resuspended (Denby et al., 2013). Measurements to characterize non-exhaust PM emissions in ambient air are influenced by complex atmospheric processes such as flow, turbulence, rain, snowfall acting upon road conditions. Non-exhaust emissions may also be influenced by different speed, acceleration or deceleration. Uni-directional traffic tunnels have been used for real world emission measurements as flow and dilution conditions are mainly controlled by traffic and the tunnel geometry. Emission factors for gaseous species and PM2.5/PM10 have been assessed by Kristensson et al. (2004), Meier et al., (2015) and Hinterhofer et al., (2015), using approaches described by Equation 1. Average fleet emission factors (EF_{fl-avg}) were determined by monitoring the concentration difference $\Delta C (= C_{down} - C_{up})$ at the traffic related upstream (C_{up}) and downstream (C_{down}) locations with distance ΔL apart and monitoring the number of vehicles (N_{veh}) passing by in a certain time interval and by assessing the airflow in the tunnel by the longitudinal velocity (V_L) multiplied by the tunnel cross section (A).

$$\text{Equation 1: } EF_{fl-avg} = \frac{\Delta C \cdot V_L \cdot A}{\Delta L} \cdot \frac{\Delta t}{N_{veh}}$$

Multiple linear regression is typically used to split fleet average (fl-avg) total PM emissions between light vehicles (LV, i.e. cars and vans) and heavy duty vehicles (HV, i.e. coaches, trucks, tractor-trailer), see Equation 2. There, $Emis_{tot}$ denotes the total amount of emissions, N_{LV} and N_{HV} the number of light

and heavy duty vehicles, respectively. Generally, considerable uncertainty may be introduced by splitting the fleet emission factors into vehicle type specific emission factors (Buckowiecki et al., 2010). These total PM10 emission factors for light vehicles and heavy duty vehicles are further split into exhaust and non-exhaust emission. The exhaust part is frequently specified by using emission models or emission data bases, e.g. HBEFA.

$$\text{Equation 2: } Emis_{tot} = EF_{LV} \cdot N_{LV} + EF_{HV} \cdot N_{HV}$$

Table 1 presents a compilation of non-exhaust emission factors from three tunnel monitoring studies and four studies based on ambient air monitoring. The vehicle speed conditions of the cited studies are similar to the present study. The non-exhaust PM10 EF analysed in long tunnels appear to be significantly lower than non-exhaust EF from ambient air monitoring. In the almost 5 km long Islisberg tunnel in Switzerland air pollutants were measured at a distance $\Delta L = 4756 m$ apart. Interestingly, the PM10 non-exhaust EF for LV analysed was negative -0.0025 g/km and 0.003 mg/km for HV (Meier et al., 2015). Hinterhofer et al., (2015) analyses as well very low EF for the 10 km long Plabutsch tunnel near Graz. Using the Network Emission model NEMO (Dippold et al., 2012) to compute PM10 exhaust emissions resulted in low non-exhaust emissions. Using HBEFA, slightly higher non-exhaust emissions resulted (Table 1) due to lower exhaust emissions computed with HBEFA compared to NEMO. The differences between the NEMO and HBEFA exhaust emission results are related to the assignment of the traffic situation and emission factor. In contrast to HBEFA, NEMO assigned for the given speed a mean of similar traffic situations.

On the one hand, traffic flow in road tunnels is constant which may minimize brake, tyre and road wear. On the other hand, deposition velocities for coarse PM (2.5 to 10 μm) are high compared to gaseous species such as NO_x. In tunnels the wall surface area is large and at close distance related to the PM emission sources which leads to high PM impingement at all surfaces.

Table 1: Compilation of PM10 non-exhaust emission factors (EF) for motorway, speed ~100 km/h conditions, LV are cars, vans and HV are buses, trucks, tractor-trailer.

Study	Location/Conditions	Methodology	EF LV g/km/LV	EF HV g/km/HV
Meier et al. (2015)	Islisberg-Tunnel (CH), 2014, $\Delta L = 4756$, 100 km/h	Monitoring, exhaust HBEFA3.1	-0.003	0.003
Hinterhofer et al. (2015)	Plabutsch-Tunnel (A) 2012, $\Delta L = 3380$ m, 100 km/h	Monitoring, exhaust NEMO	0.007	0.044
		exhaust HBEFA 3.1	0.015	0.063
	Plabutsch-Tunnel (A) 2013, $\Delta L = 7180$ m, 100 km/h	Monitoring, exhaust NEMO	0.002	0.019
		exhaust HBEFA 3.1	0.010	0.050
Kristensson et al. (2014)	Söderledstunnel Stockholm (S) $\Delta L = 595$ m , 75-90 km/h, 5% HV	Monitoring PM10 - PM0.9	fleet-avg 0.268	
Bukowiecki et al. (2010)	Reiden (CH), motorway, ambient, 120 km/h	monitoring down/upwind, HBEFA 2.1 AB_120	0.030 ± 0.014	0.169 ± 0.082
Gehrig et al. (2004)	Humlikon (CH), motorway, ambient	monitoring down/upwind PM10-PM1	0.022	0.144
Düring et al. (2003)	Analysis monitoring stations in Saxony (D), motorway, ambient	Monitoring & NOx tracer method/modelling, HBEFA, motorway	0.030	0.200
Düring et al. (2011)	Analysis monitoring stations in Saxony (D), motorway, ambient	Monitoring & NOx tracer method/modelling, HBEFA, motorway	0.022	0.130

2. Objectives

The aim of this work is to analyse non-exhaust emissions as a function of mean traffic volumes and to what extent PM₁₀ deposition as opposed to resuspension may play a role in the evaluation of emission factors.

3. Methodology and Results

In this work, we re-analyse two data sets from the Plabutsch tunnel near Graz in Austria (Hinterhofer et al., 2014, Hinterhofer et al., 2015) from two different campaigns. The monitoring set-ups from two tunnel campaigns 2012 and 2013 are shown in Figure 1. In 2012 the air quality monitoring equipment was placed at two break-down bays located 3380 m apart, and in 2013 the equipment of the upstream location was moved further up, a distance of 7180 m resulted. In both campaigns the monitoring locations near the end of the tunnel were identical. The 2012 campaign took place from 24.08.12 to 07.09.12 and the 2013 campaign from 30.08.13 to 16.09.13. The Plabutsch tunnel is part of the A9 motorway, which bypasses Graz at its western periphery underneath the Plabutsch hill range. Both tunnel tubes are about 10 km long with unidirectional traffic. The monitoring took place in the eastern bore (direction towards Linz) using break-down bays to place the monitoring equipment. Approximately 20 000 to 30 000 vehicles pass through each tunnel bore per day. The tunnel has a gentle roof profile with slopes of 1 %. For the analysis, data were only used when the complex ventilation system was not operated, meaning that the vehicles pushed the air forward within the tunnel tube. The resulting vehicle induced longitudinal velocity (V_L) was monitored. Traffic volumes are operationally monitored outside the tunnel, 332 m after the north portal. All monitored data were recorded with one minute time resolution.

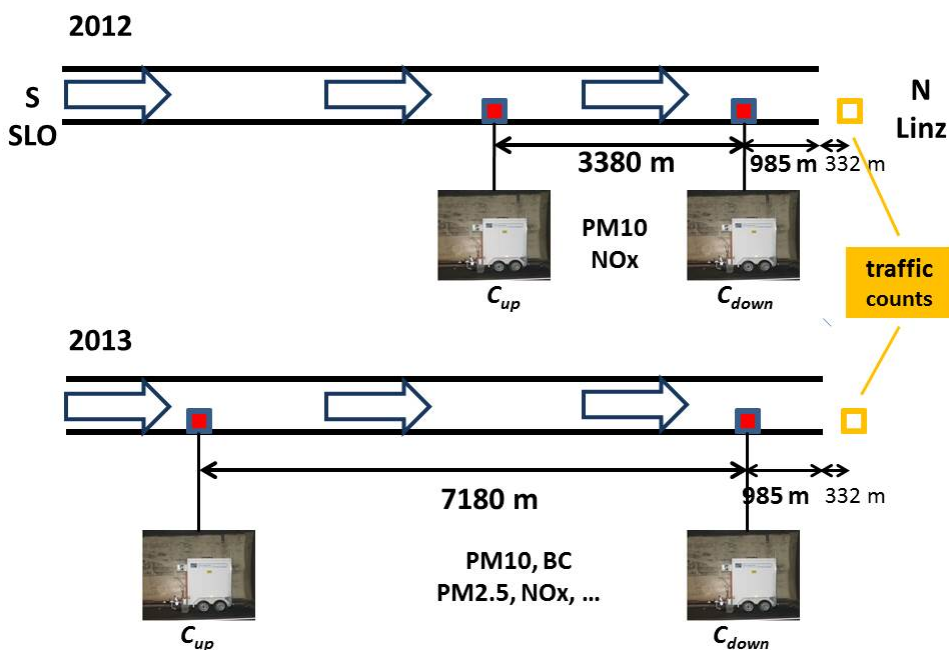


Figure 1: Schematic illustration of the monitoring set-ups used 2012 (top) and 2013 (bottom).

The approach of this work is to bring together both data sets by grouping both of them into different traffic volume levels to complement the aforementioned approach (Equation 1) with an additional term accounting for coexisting PM wall deposition losses and resuspension at road surface, tunnel side walls and ceiling. Therefore, Equation 1 may be modified by a simplified approach to account for PM wall deposition and resuspension using an exponential term which described the interplay between deposition and resuspension by using an “effective” wall deposition velocity V_{Def} (Equation 3). If V_{Def} is 0, all deposited PM₁₀ is immediately resuspended. If V_{Def} is > 0 depositional losses predominate and consequently the emission factor derived from the monitored difference between two monitoring

locations would increase due to wall losses. W is the tunnel width and H the tunnel height.

$$\text{Equation 3: } EF_{fl-avg} = \left(\frac{C_{down}}{\exp(-2V_{Deff}(1/W + 1/H) \cdot \Delta L/V_L)} - C_{up} \right) \cdot \frac{V_L \cdot W \cdot H \cdot \Delta t}{\Delta L \cdot N_{veh}}$$

According to Equation 3, the higher the effective deposition velocity or the higher emissions and concentration levels within the tunnel and the longer the distance between monitoring stations the stronger is the deposition effect.

4. Results and Discussion

In order to use the monitoring results of the two tunnel data sets, traffic counts were classified into 9 different daily traffic volume (DTV) ranges using 5000 vehicles per day as step size (Table 2). For the chosen DTV ranges, mean DTV, mean measured concentrations and mean V_L were used for further emission analysis. In order to obtain reliable results only those data were taken into account, which fulfilled the following conditions: $\Delta NO_x > 100 \mu\text{g}/\text{m}^3$, $\Delta PM_{10} > 5 \mu\text{g}/\text{m}^3$, number of light vehicles passing the traffic counter > 1 vehicles per minute, and $V_L > 1.5 \text{ m/s}$.

Table 2: Daily traffic (DTV) volume based classification, number of valid data and related mean parameters from Plabutsch campaigns $\Delta L = 3380 \text{ m}$ (2012) and $\Delta L = 7180 \text{ m}$ (2013), NO_x was calculated as NO₂.

DTV range veh/day	N data [1]	DTV veh/day	%- HV	ΔNO_x $\mu\text{g}/\text{m}^3$	ΔPM_{10} $\mu\text{g}/\text{m}^3$	V_L [m/s]
0-5000	515	3574	26%	2309	62.0	3.6
5000-10000	1015	7726	17%	2859	94.8	4.3
10000-15000	1138	12291	14%	3225	116.1	4.7
15000-20000	673	17565	15%	3908	147.0	5.5
20000-25000	1015	22771	17%	4518	149.8	6.4
25000-30000	1755	27595	17%	5025	164.5	6.8
30000-35000	1831	32615	15%	5123	175.8	6.9
35000-40000	1457	37157	14%	5292	185.6	7.0
> 40000	712	42929	14%	5558	198.5	7.2

DTV range veh/day	N data [1]	DTV veh/day	%- HV	ΔNO_x $\mu\text{g}/\text{m}^3$	ΔPM_{10} $\mu\text{g}/\text{m}^3$	V_L [m/s]
0-5000	988	3151	29%	1318	10.5	3.9
5000-10000	1632	7532	15%	1510	32.8	4.5
10000-15000	1005	12187	13%	1585	33.2	5.1
15000-20000	540	17525	14%	1901	47.0	6.1
20000-25000	462	22833	17%	2179	55.7	7.1
25000-30000	712	27694	16%	2431	57.5	7.3
30000-35000	787	32288	14%	2432	62.6	7.3
35000-40000	323	36925	14%	2516	67.3	7.6
> 40000	114	42841	14%	2622	69.3	7.8

Figure 2 shows the distribution of light and heavy duty vehicles of the two data sets and Figure 3 the relative differences. Generally, the difference between the two data sets in DTV for all vehicles as well as DTV light vehicles is small (within $\pm 2.5 \%$) except for the smallest class (< 5000 vehicles/day). The 2013 data set (7189 m) shows generally higher numbers of heavy duty vehicles compared to the 2012 data (3380 m). The relative difference is up to 15 % in the 5000 to 10000 DTV range. To summarize,

significant differences (> 5%) in DTV and fleet composition are at the DTV ranges < 10 000 and 25000 to 30000 vehicles. Due to the lower number of total vehicles, differences in DTV light vehicles and DTV heavy vehicles have a greater weight in the determination of emission factors. Particularly the results below 10000 vehicles per day must be interpreted with caution.

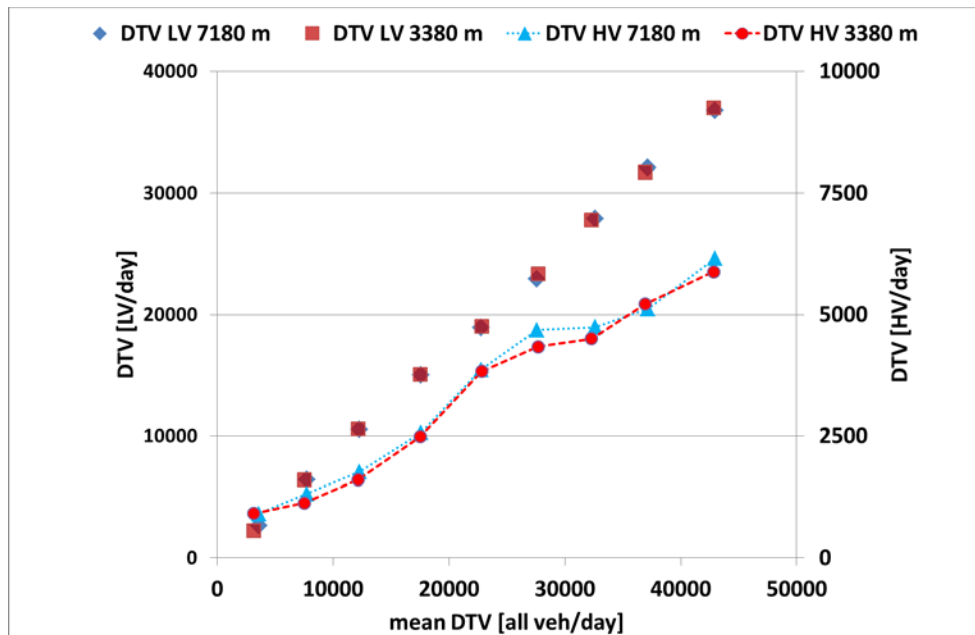


Figure 2: Distribution of daily traffic volumes (DTV) from the two data sets for light vehicles (LV, left y-axis) and heavy duty vehicles (HV, right y-axis) versus DTV all vehicles.

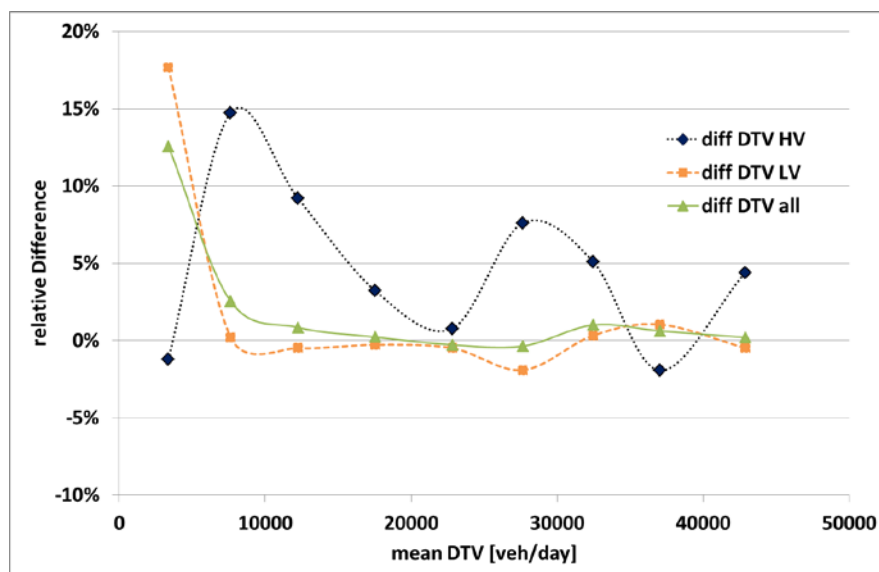


Figure 3: Relative differences (7180 m vs. 3380 m) LV, HV and all vehicles.

Mean NO_x and PM₁₀ longitudinal concentration gradients were computed for the different traffic volume ranges of both campaigns and are shown in Figure 4. Averaged monitored NO_x concentrations gradients increase almost linearly with increasing traffic volume for both data sets. The computed NO_x gradients from both data sets compare well. Deviations and the large intercept below 10000 DTV can be attributed to differences in traffic volumes, fleet composition and higher dynamic driving behaviour (less constant) at low traffic densities. Averaged monitored PM₁₀ concentrations gradients increase as well with increasing traffic volume for both data. In contrast to NO_x, in tunnel PM₁₀ concentration gradients for the two data sets deviate significantly. Figure 5 shows fleet average NO_x and PM₁₀ emission factors for both campaigns using the approach of Equation 1. EF from both

campaigns decrease with increasing traffic volume (DTV). The total PM10 fleet average EF shown in Figure 5 are low compared to cited emission factors from Bukowiecki et al. (2010), Kristensson et al., (2004), and Gehrig et al., (2004). Emission factors determined for $\Delta L = 3380\text{ m}$ are lower than those for $\Delta L = 7180\text{ m}$ using Equation 1. A possible explanation may be a net loss of PM10 due to prevailing wall deposition losses as opposed to resuspension of PM10. Moreover, over three days black carbon was monitored in the 2013 campaign. Black carbon can be regarded as an indicator for exhaust emissions. Only 18 % of the total PM sampled consisted of black carbon. In Figure 6, total PM10 (exhaust & non-exhaust) emission factors for light vehicles (left) and heavy duty vehicles (right) are shown. The approach of Equation 1 was used. Also the modelled exhaust emission factors assigned by NEMO are shown. As a consequence non-exhaust emission factors are very low and 18 % black carbon content appears not in line with the results presented. Several data points are below the modelled ones which would imply negative non-exhaust emission factors.

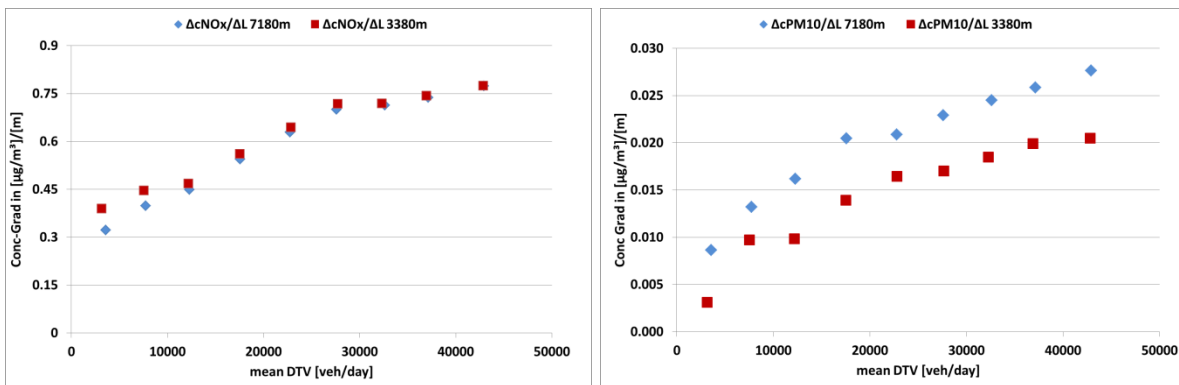


Figure 4: Mean longitudinal concentration gradients for NOx (left) and PM10 (right) between the monitoring stations 7180 m and 3340 m apart.

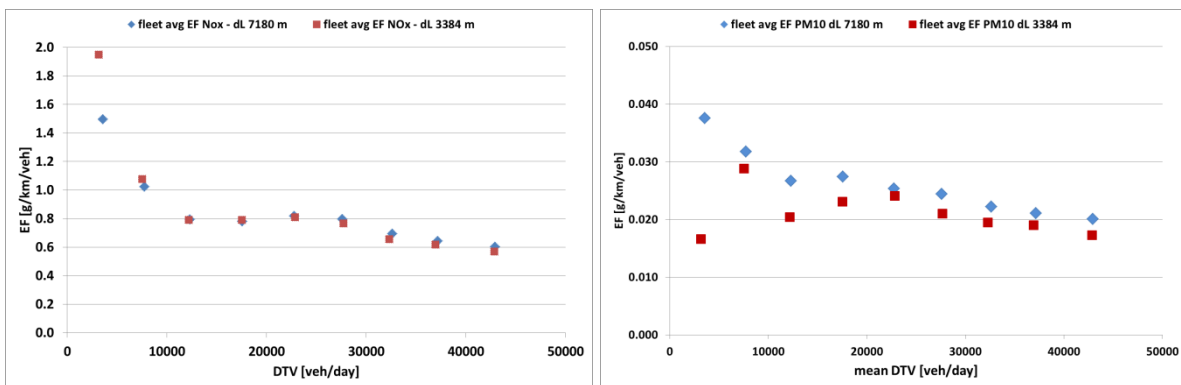


Figure 5: Fleet average total (exhaust & non-exhaust) PM10 EF using Equation 1.

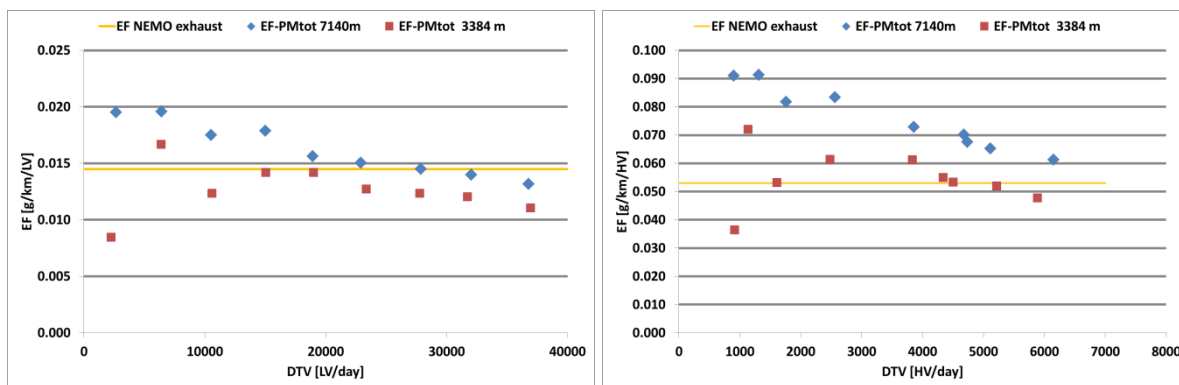


Figure 6: PM10 total EF for light vehicles (LV, left) and heavy duty vehicles (HV, right) versus LV/HV traffic volume using Equation 1. The NEMO exhaust EF is also shown.

Accounting for deposition and resuspension

Equation 3 was employed by adjusting the effective deposition velocity V_{Def} to match the fleet average emission factors of both data sets. By utilizing an effective V_{Def} of 0.001 m/s affecting the PM10 fleet average emission factors of both data sets ($\Delta L = 7180$ m in 2013, $\Delta L = 3380$ m in 2012) significantly increased total PM10 fleet average emission factors are obtained and shown in Figure 6. The emissions factors from both data sets agree well. The derived emission factors decrease with increasing traffic volume. At low traffic densities (< 5000 DTV) very high emission factors are obtained. However, these results must be carefully evaluated. Firstly, the shares of heavy duty vehicles is significantly higher than within the other traffic volume ranges (Table 2) and secondly both data sets show some significant difference in DTV light vehicles, and thirdly due to the low traffic volume comparably low mean longitudinal velocities with high variation result. Hence, the uncertainties can be expected as larger. The adjusted effective deposition velocity is small. For particles, deposition velocities vary with particle diameter (Sehmel, 1980), for PM10 typically a value of 0.01 m/s is frequently applied. Compared to the deposition velocity of NO 0.00016 m/s (Seinfeld & Pandis, 1997) the adjusted effective deposition velocity of 0.001 m/s is considerably higher. Neglecting resuspension processes and setting V_{Def} to 0.01 m/s would result in extremely large i.e., unrealistic emission factors. Moreover, the indicated functional relationship between the two data sets in Figure 6 would disappear.

The emission factors presented relate to dry conditions. Due to the length of the Plabutsch Tunnel, only near the entry portal wet conditions within the tunnel may be encountered with heavy rainfall. The tunnel section where the monitoring took place remained practically always dry.

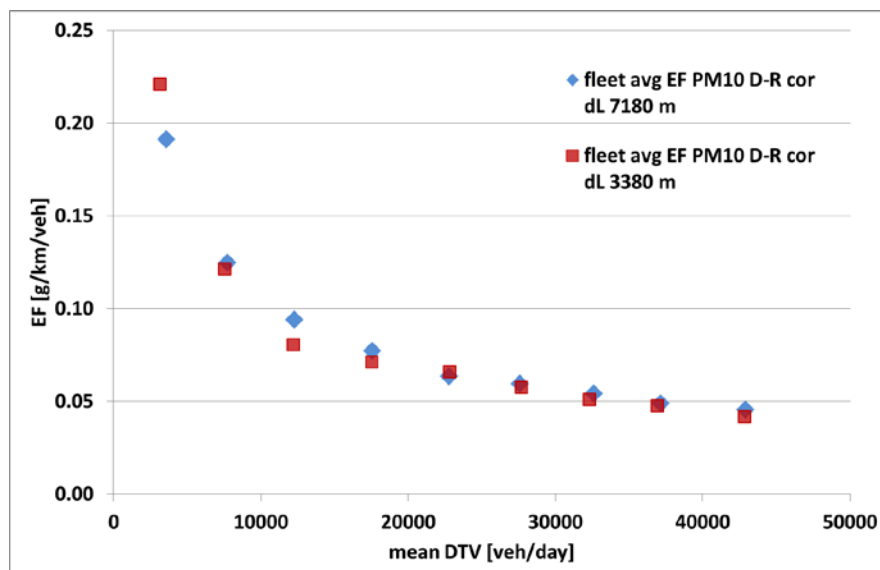


Figure 7: Deposition and resuspension corrected total PM10 fleet average vehicle EF versus traffic volume. % heavy duty vehicles for both campaigns.

The total PM10 fleet average vehicle emissions (Figure 6) can be further specified by using multiple linear regression to split between light vehicles (LV, i.e. cars and vans) and heavy duty vehicles (HV, i.e. coaches, trucks, tractor-trailer). Here, the factors from the analysis by Hinterhofer et al., (2014) were used. These factors relate to the analysis of the entire data set (no classification into different DTV levels). Therefore, the data for DTV < 5000 vehicles/day must be scrutinized because the percentage of heavy duty vehicles deviates significantly from the average (Table 2). The Network Emission Model NEMO (Dippold et al., 2012) was used to compute PM10 exhaust emission factors. By subtracting them from total PM10 LV and HV emission factors, finally non-exhaust emission factors for LV and HV were obtained and are shown in Figure 7.

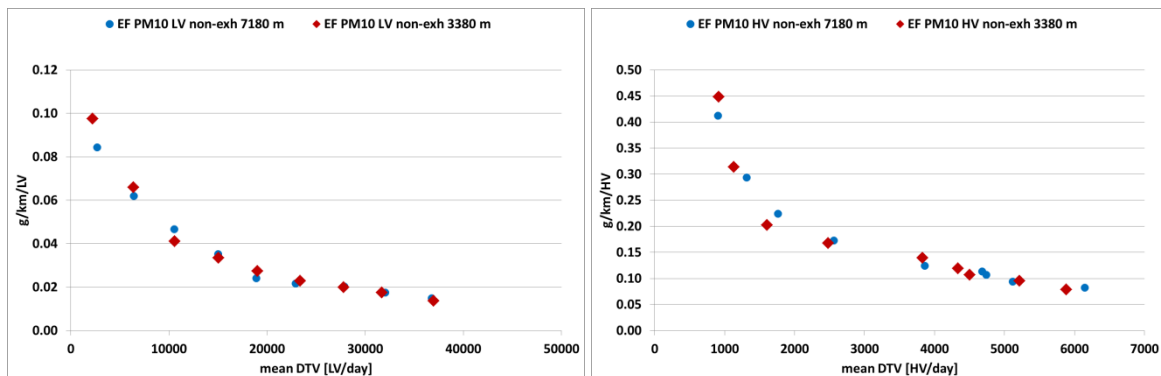


Figure 8: PM10 non-exhaust EF for light vehicles (LV) and heavy duty vehicles (HV) versus traffic volume.

PM10 non-exhaust EF-LV range from 0.015 g/km/LV (at ~35000 LV/day or 42000 vehicles/day) to 0.060 g/km/vehicle (at ~6500 LV/day or 7500 vehicles/day). Average PM10 non-exhaust EF for heavy duty vehicles range from 0.080 g/km/HV (at ~6000 HV/day or ~42000 vehicles/day) to 0.300 g/km/HV (at ~1500 HV/day or ~7500 vehicles/day). The determined PM10 non-exhaust EF for LV and HV increase with decreasing traffic volume. The non-exhaust EF are for light vehicles and traffic volumes larger than 10000 LV/day are comparable in magnitude compared to the studies cited in Table 1 based on ambient measurements. Non-exhaust EF for heavy duty vehicles and HV traffic volumes larger than 1500 HV/day are in the same size range compared to the studies cited in Table 1 based on ambient measurements.

Non-exhaust emission factors for light vehicles below 10000 LV/day are comparable to levels found near Birrhard at a Swiss motorway (0.047 g/km/LV, Gehrig et al., 2004) or a very busy road intersection in Zürich (0.045 g/km/LV, Hüglin, 2000). Results for heavy duty vehicles are on the same level as analysed for a street canyon in Zürich (0.498 g/km/HV) by Buckowiecki et al., (2010). At lower traffic volumes e.g. during night time, there is more time for PM fractions larger than 10 µm for gravitational settling. Hence, the dust loading at the road surface would be increased compared to conditions with high traffic volumes (> 20000 DTV). Moreover, there is more time for PM10 deposition. Therefore, the higher emission factors found at lower traffic volumes may be explained by increased abrasion and resuspension per passing vehicle.

5. Conclusion

Two data sets from two air pollutant tunnel measurement campaigns have been analysed in a 10 km long tunnel to study the potential role of traffic volume and PM10 deposition interacting with resuspension on non-exhaust emission factors.

Neglecting sink processes in the determination of non-exhaust emission factors resulted in very low PM10 non-exhaust emission factors. The comparison of black carbon PM measurements with PM10 tunnel measurements indicated 18 % black carbon content. Exhaust particle measurements showed that black carbon is the main PM exhaust fraction. In-tunnel PM10 concentration gradients from two different campaigns in the same tunnel indicate stronger PM10 gradients at the front section compared to the rear section at comparable traffic volumes. Therefore, the impact of a correction for mass losses due to wall deposition was hypothesised using an effective deposition velocity. A small effective deposition velocity of 0.001 m/s, i.e. approximately one-tenth of the PM10 deposition velocity found in literature would significantly increase the non-exhaust emission factors derived from two monitoring stations in tunnels with long distances apart. This correction would imply different concentration gradients for PM10 and a larger share of non-exhaust PM10.

PM10 non-exhaust emission factors for light vehicles range from 0.015 g/km/LV (at ~35000 LV/day) to 0.060 g/km/LV (at ~6500 LV/day). Average PM10 non-exhaust emission factors for heavy duty vehicles range from 0.080 g/km/HV (~6000 HV/day) to 0.300 g/km/HV (at ~1500 HV/day). The determined PM10 non-exhaust EF for LV and HV increase with decreasing traffic volume. At low traffic volumes e.g. during night time, there is more time for PM fractions larger than 10 µm for gravitational settling and PM10 deposition. Hence, the dust loading at the road surface would be increased compared to conditions with high traffic volumes (> 20000 DV). Therefore, emissions due to increased abrasion and resuspension per vehicle may result.

A correction term for long tunnel studies is proposed. Ideally, in order to measure in tunnels non-exhaust emission factors and to account for simultaneous PM deposition and resuspension effects, at least three monitoring locations equipped with identical monitoring devices should be operated at the same time in a tunnel.

Acknowledgments

This work was supported by the Austrian Ministry of Traffic Innovation and Technology and ASFINAG BMG.

References

- Bukowiecki, N., P. Lienemann, M. Hill, M. Furger, A. Richard, F. Amato, A.S.H. Prévôt, U. Baltensperger, B. Buchmann & R. Gehrig, (2010): PM10 emission factors for non-exhaust particles generated by road traffic in an urban street canyon and along a freeway in Switzerland, Atmos. Environ., 44, pp. 2330–2340
- Denby, B.R., I. Sundvor, C. Johansson, L. Pirjola, M. Ketzel, M. Norman, K. Kupiainen, M. Gustafsson, M., G. Blomqvist, & G. Omstedt (2013): A coupled road dust and surface moisture model to predict non-exhaust road traffic induced particle emissions (NORTRIP). Part 1: road dust loading and suspension modelling. Atmos. Environ. 77, 283-300.
- Dippold M., M. Rexeis & S. Hausberger (2012): NEMO – A Universal and Flexible Model for Assessment of Emissions on Road Networks. 19th International Conference „Transport and Air Pollution“, 26. – 27.11.2012, Thessaloniki
- Düring I., A. Lohmeyer., A. Moldenhauer, E. Nitzsche, M. Stockhausen (2004): Projektbericht zum Forschungsvorhaben "Berechnung der Kfz-bedingten Feinstaubemissionen infolge Aufwirbelung und Abrieb für das Emissionskataster Sachsen", November 2004.
- Handbook Emission Factors for Road Transport (HBEFA) Version 3.1 (2010): <http://www.hbefa.net/>
- Handbook Emission Factors for Road Transport (HBEFA) Version 2.1 (2004): <http://www.hbefa.net/>
- Hinterhofer, M., P.J. Sturm, T. Nöst (2015): in Rauch (ed): Proceedings of the 12th Urban Environment Symposium, Oslo, Norway.
- Hinterhofer, M., T. Nöst, P.J. Sturm, Plabutschunnel, zwei Messungen, Ermittlung von aktuellen Emissionsfaktoren für limitierte und nicht limitierte Schadstoffkomponenten von KFZ-Flotten, Bericht Nr. FVT-117/14 V&U 12/45/6200.
- Hüglin, C. (2000). Anteil des Strassenverkehrs an den PM10- und PM2.5 Immissionen; Chemische Zusammensetzung des Feinstaubes und Quellzuordnung mit einem Rezeptormodell, Nationales Forschungsprogramm NPF41 Verkehr und Umwelt, Bericht C4, Bern.
- Meier, M., R. Eugster, V. Delb, P. Federer, & P. Maly (2015), Schadstoffmessungen im Islisbergtunnel, Ostluft Schlussbericht US + FZ.
- Gehrig, R., M. Hill, B. Buchmann, B., D. Imhof, E. Weingartner & U. Baltensperger (2004): Separate determination of PM10 emission factors of road traffic for tailpipe emissions and emissions from abrasion and resuspension processes, Int. J. Environment and Pollution, Vol. 22, No. 3, 14 p.
- Schmidt, W., I. Düring, A. Lohmeyer: Einbindung des HBEFA 3.1 in das FIS Umwelt und Verkehr sowie Neufassung der Emissionsfaktoren für Aufwirbelung und Abrieb des Straßenverkehrs (2011)
- Seinfeld, J.H. & S.N. Pandis (1997): Atmospheric Chemistry and Physics: From Air Pollution to Climate Change, John Wiley & Sons, New York.
- Sehmel, G.A. (1980); Particle and gas deposition, a review, Atmos. Environ., 14, 983-1011.

Light-Duty Vehicles Emissions and Urban Air Quality: Past, Present, and Future Perspectives

T.J. Wallington

Research & Advanced Engineering, Ford Motor Company, Dearborn, Michigan 48121, USA

Keywords: light duty vehicles, NO_x, VOCs, PM, smog.

Author email: twalling@ford.com

The co-evolution of automotive fuels and light-duty vehicle technology over the past 50 years and their likely future trajectory will be discussed with respect to vehicle emissions and their impact on urban air quality. In conjunction with engine advancements, automotive fuel composition has been fine tuned to balance efficiency and power demands while minimizing emissions. Pollutant emissions from internal combustion engines (ICE) result from complex processes involving interactions between the fuel and engine parameters. Engine hardware and operating conditions, after-treatment catalysts, and fuel composition all affect the amount and composition of emissions leaving the vehicle tailpipe. While engine and after-treatment effects are generally larger than fuel effects, engine and after-treatment hardware can require specific fuel properties. The best prospects for achieving the highest efficiency and lowest emissions lie with optimizing the entire fuel-engine-after-treatment system.

Vehicle emissions of volatile organic compounds (VOCs), CO, nitrogen oxides (NO_x), and particulate matter (PM) contribute to photochemical smog in urban atmospheres. As illustrated in Figure 1, there have been large reductions in the emissions of NO_x, volatile organic compounds (VOC), and particulate matter (PM) emissions from new vehicles over the past 50 years. Emissions from the on-road fleet are expected to continue to decline mainly reflecting fleet turn-over with new vehicles with modern emission control systems replacing older vehicles.

The reduction of emissions from traffic has been an important factor in the observed improvements in air quality in U.S. and European cities. As an example, Figure 2 shows the 84% reduction in the national average level of CO in air in U.S. cities from 1980 to 2013 (USEPA, 2015). The global trend of reduced emissions from road traffic and reduced contribution of vehicle emissions to air quality issues will be presented and discussed.

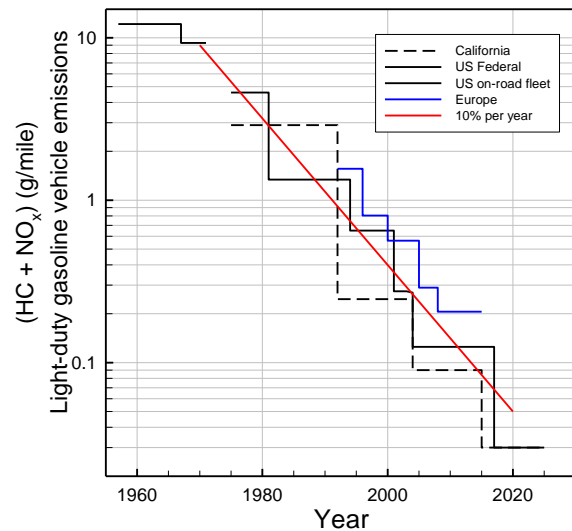


Figure 1. International emission standards for gasoline light-duty vehicles. Data taken from Fegraus et al (1973) and TransportPolicy.net website (<http://transportpolicy.net>)

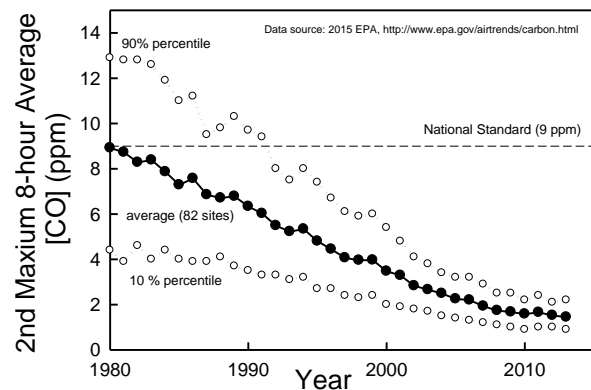


Figure 2. Trend for CO concentrations in U.S. cities. Data taken from USEPA (2015)

Fegraus, C.E. Domke C.J. and Marzen, J. (1973) *Contribution of the vehicle population to atmospheric pollution*, Society of Automotive Engineers Technical Paper 730530.

USEPA (2015) *Air trends*, <http://www3.epa.gov/airtrends>

Author Index

- łutczyk Grzegorz, 255–262
- Akter Shamema, 2–20
Ali-Khodja Hocine, 21–26, 291–299
Anagnostopoulos Konstantinos, 160–171
André Michel, 726–741
Archer Greg, 66–79
Arcidiacono Vincenzo, 160–171
Arefian Amir, 752–762
- Badin Anne-Laure, 27–37
Barrios Carmen, 500–507
Barry Hamady, 401–408
Bayram Abdurrahman, 136–145
Bechkit Walid, 50–65
Bedogni Marco, 480–485
Bencharif-Madani Fayrouz, 291–299
Benhassine Sana, 38–49
Bonneau Stéphane, 550–558
Bonnell Pierre, 354–362
Borbon Agnès, 125–135, 550–558
Boreave Antoinette, 319–337
Bouaoun Liacine, 146–151
Boubrima Ahmed, 50–65
Bourgeois Guy, 537–549
Breuil Philippe, 188–199
Brochier Cedric, 314–318
Bugajny Christine, 112–124
Burkhart Jean-François, 636–655
- Camilleri Pierre, 80–97
Champelovier Patricia, 146–151
Chatzikyriakou Despoina, 453–472
Ciuffo Biagio, 160–171, 621–635
Clavel Aurore, 27–37
Conil Sébastien, 486–494
Connors Richard, 559–572
Consuegra Sara, 98–103
Cuenot Francois, 66–79
Czerwinski Jan, 104–111
- D'anna Barbara, 319–337
Dablanc Laetitia, 80–97
De La Fuente Josefina, 500–507, 742–751
Dimaratos Athanasios, 160–171, 621–635
- Doğan Güray, 136–145
Domínguez-Sáez Aida, 500–507
Dominguez Aida, 742–751
Dominutti Pamela, 125–135
Dumanoglu Yetkin, 136–145
Dunez Philippe, 112–124
Dunez Virginie, 112–124
- Elbir Tolga, 136–145
Evrard Anne-Sophie, 146–151
- Fameli Kyriaki-Maria, 152–159
Fontaras Georgios, 160–171, 621–635
Fornaro Adalgiza, 125–135
François Denis, 772–783
Francois Cyrille, 172–187
- Galineau Julien, 200–207
Geilenkirchen Gerben, 208–224, 346–353
Gondran Natacha, 172–187
Gong Yu, 698–718
Gouriou Frantz, 636–655
Grondin Didier, 188–199
Guillard Chantal, 314–318
Guiot Bernard, 423–437
- Hashim Ibrahim, 719–725
Hausberger Stefan, 225–238, 605–620, 656–669
Heijne Veerle, 784–797
Heldstab Jürg, 409–422
Helms Hinrich, 263–272
Huang Yue, 719–725
- Ibarra Sergio, 239
- Jaafar Ali, 401–408
Jantzem Emmanuel, 486–494
Jensen Steen, 670–678
Jerksjö Martin, 240–254
Joehrens Julius, 263–272
Johansson Håkan, 255–262
- Kadja Mahfoud, 21–26
Kaemper Claudia, 263–272
Katsis Petros, 273–290
Kemmouche Amina, 291–299

- Kiani Sadr Maryam, 752–762
 Kontses Anastasios, 160–171
 Kooli Elyes, 38–49
 Kotrikla Anna, 152–159
 Kouridis Chariton, 300–313

 Lahaussais Dorothee, 453–472
 Lamaa Lina, 314–318
 Lambert Jacques, 146–151
 Laumon Bernard, 146–151
 Le Cottier Patrick, 423–437
 Leblanc Mickael, 319–337
 Leclerq Ludovic, 27–37
 Lefevre Marie, 146–151
 Lejri Delphine, 27–37, 338–345
 Li Hu, 519–529, 679–697
 Ligterink Norbert, 208–224, 346–353, 784–797
 Lipp Silke, 225–238
 Lo Ting-Shek, 273–290
 Locoge Nadine, 550–558
 Lodi Chiara, 354–362
 Lokorai Kanza, 21–26
 Lonati Giovanni, 480–485

 Müezzinoğlu Aysen, 136–145
 Malfettani Stefano, 354–362
 Markaki Valentini, 453–472
 Matzer Claus, 225–238
 Mehel Amine, 363–372
 Mellios Giorgos, 373–381
 Mezghani Amine, 763–771
 Mock Peter, 382–400
 Mraih Rafaa, 38–49
 Muresan Bogdan, 772–783
 Murzyn Frederic, 363–372

 Nacken Michael, 573–584
 Nai Oleari Alberto, 401–408
 Nellthorp John, 438–452
 Nicolas Jean-Pierre, 172–187
 Niederau Arnold, 573–584, 605–620
 Noel Ludovic, 319–337
 Nogueira Thiago, 125–135
 Notter Benedikt, 409–422
 Ntziachristos Leonidas, 273–290, 300–313, 453–472

 Oğuz Kuntasal öznur, 136–145
 Ockler Alexandre, 486–494
 Odabaşı Mustafa, 136–145
 Olny Xavier, 27–37

 Palmer Kate, 438–452

 Papadimitriou Giannis, 453–472
 Papageorgiou Thomas, 300–313
 Pekey Beyhan, 136–145
 Pekey Hakan, 136–145
 Pellecuer Luc, 473–479
 Pelzer Michael, 573–584
 Pepe Nicola, 480–485
 Perret Pascal, 423–437
 Peruchon Laure, 314–318
 Petit Jean-Eudes, 486–494
 Petit Jean-François, 636–655
 Piasecki Conrad, 495–499
 Pillot Didier, 423–437
 Pirovano Guido, 480–485
 Poliscanova Julia, 66–79
 Preterre David, 636–655
 Pujadas Manuel, 500–507, 742–751

 Querol Xavier, 291–299

 R'mili Badr, 319–337
 Raux Charles, 508–518
 Raux Stéphane, 319–337
 Rexeis Martin, 225–238, 656–669
 Riley Richard, 519–529
 Rivano Hervé, 50–65
 Rodriguez Romain, 363–372
 Ruas Anne, 50–65
 Rushton Christopher, 530–536

 Sadeghian Shadi, 537–549
 Salameh Thérèse, 550–558
 Samaras Zisis, 160–171
 Samaras Zissis, 621–635
 Sanchez Olivier, 550–558
 Sandvik Kjell Ottar, 255–262
 Sauvage Stéphane, 550–558
 Sayegh Arwa, 559–572
 Schneider Christiane, 573–584, 605–620
 Sellegri Karine, 486–494
 Seyfioğlu Remzi, 136–145
 Shepherd Simon, 530–536
 Smit Robin, 273–290
 Sofuoğlu Sait, 136–145
 Sorand Caroline, 27–37

 Tassel Patrick, 423–437
 Tate James, 438–452, 519–536, 559–572, 679–697
 Terrouche Ahmed, 21–26
 Thouron Laëtitia, 585–604
 Toenges-Schuller Nicola, 573–584, 605–620
 Tsiakmakis Stefanos, 160–171, 621–635

Tsokolis Dimitrios, 160–171
Tsokolis Dimitris, 621–635
Tuncel Gürdal, 136–145

Valverde - Morales Victor, 160–171
Van Zyl Stephan, 784–797
Vernoux Philippe, 188–199
Vidal Bruno, 636–655
Viricelle Jean-Paul, 188–199
Vittoz Therese, 27–37
Vogt Rainer, 605–620

Wüthrich Philipp, 409–422
Wadud Zia, 438–452, 519–529
Weller Konstantin, 656–669
Westermann Alexandre, 188–199
Winther Morten, 670–678
Wong Carol, 273–290
Wu Ya, 710–718
Wyatt David, 679–697

Xu Bin, 698–718

Yılmaz Civan Mihriban, 136–145
Ynoue Rita, 239
Younes Mohamed, 719–725

Zach Bernhard, 656–669
Zamboni Giorgio, 726–741
Zsidákovits József, 255–262

List of participants

- Adhikari Ghanshyam
- Ake Sjodin
- Akter Shamema
- Alam Md Saniul
- Ali-Khodja Hocine
- André Michel
- Andre Jean-Marc
- Anfosso Ledee Fabienne
- Anguita Paola
- Arimbi Jinca
- Azaiez Mohamed
- Badin Anne-Laure
- Baouche Fouad
- Batra Mukul
- Benjamin Rocher
- Bergk Fabian
- Bhatta Sitaram
- Boreave Antoinette
- Bouhatmi Marième
- Bourquin Frédéric
- Bugajny Christine
- Bütler Thomas
- Camilleri Pierre
- Caravaggio Gianni
- Chao Wang

- Chaudhary Omkar
- Chen Ruiwei
- Chopin Caroline
- Consuegra Sara
- Coudon Thomas
- Coyle Finn
- Cuenot Francois
- Czerwinski Jan
- D Anna Barbara
- De La Fuente Josefina
- Degraeuwe Bart
- Derrough Samir
- Doğan Güray
- Dominutti Pamela
- Dubois-Brugger Isabelle
- Dunez Virginie
- Dunez Philippe
- Ehrler Verena
- Evrard Anne-Sophie
- Fays Sebastien
- Fleischman Rafael
- Fleischman Rafael
- Fleischman Rafael
- Françon Gérard
- Galassi Maria Cristina
- Galigneau Julien
- Garcia Vargas Jesus Manuel
- George Christian
- Ghimire Radhika Khanal
- Gil Villarino Sonia
- Giroir-Fendler Anne
- Gopaul Ramesh

- Grondin Didier
- Gross Robert
- Gruber Karin
- Guensler Randall
- Guillard Chantal
- Guitard Nathalie
- Gustafsson Mats
- Gustafsson Mats
- Hammond Janelle Katharine
- Hardej Monika
- Harizi Bisma
- Hategekimana Jean Damascene
- Hausberger Stefan
- Hazan Gilad
- Heidegger Fabian
- Hemon Pierre
- Hernando Anta Pablo
- Hitchcock Kristen
- Ibarra Sergio
- Ibrahim Osama
- Ismerie Cécile
- Jacyna Marianna
- Janhäll Sara
- Javanmardi Setareh
- Jeanneret Bruno
- Jenk Harald
- Jerksjö Martin
- Johansson Håkan
- Jones Charlotte
- Juneholm Martin
- Kadijk Gerrit
- Kaemper Claudia

- Katsis Petros
- Khardi Salah
- Kim Youngseob
- Koehl Arnaud
- Kokkulunk Gorkem
- Kotrikla Anna Maria
- Kouridis Chariton
- Kugler Ulrike
- Kurtenbach Ralf
- Lacroix Lucson
- Lamaa Lina
- Leblanc Mickaël
- Lejeune Marc
- Lejri Delphine
- Leprovost Julien
- Lesage Thierry
- Ligterink Norbert
- Liu Yao
- Liu Huan
- Lonati Giovanni
- Long Marlène
- Louis Cédric
- Lulić Zoran
- Mahe Frédéric
- Malfettani Stefano
- Man Hanyang
- Martinet Simon
- Matzer Claus
- Mehel Amine
- Mellios Giorgos
- Mendy Albert
- Merkisz Jerzy

- Merkisz-Guranowska Agnieszka
- Meyer Martine
- Mezghani Amine
- Mock Peter
- Molina Gonzalez Sonia
- Montenon Antoine
- Mounce Richard
- Muresan Bogdan
- Murzyn Frédéric
- Nai Oleari Alberto
- Newton Maxuel
- Niederau Arnold
- Noaen Mohammad
- Notter Benedikt
- O'driscoll Rosalind
- Olivier Philippe
- Palmer Kate
- Pandey Varun
- Pasquier Anaïs
- Pellecuer Luc
- Pepe Nicola
- Peruchon Laure
- Perugu Harikishan
- Petit Jean-Eudes
- Piasecki Conrad
- Pierrefeu Charlotte
- Pillot Didier
- Queron Jessica
- R'mili Badr
- Raballand Wilfried
- Raux Charles
- Resetar Marko

- Rexeis Martin
- Richard Alexandra
- Riley Richard
- Rivano Hervé
- Rolstad Denby Bruce
- Romain Souweine
- Rouleau Mathieu
- Rushton Christopher
- Sadeghian Shadi
- Salameh Thérèse
- Samaras Zisis
- Sanchez Celia
- Sanchez Célia
- Sánchez Alfredo
- Sayegh Arwa
- Schäfer Klaus
- Schiper Nicole
- Schiper Nicole
- Schodl Barbara
- Sciencesconf.org Administrateur
- Sihaib Zakaria
- Stierlin Philippe
- Stranner Gudrun
- Sturm Peter
- Tamang Ratna Man
- Tate James
- Tate James
- Teichmann Ulrich
- Thouron Laëtitia
- Tilagone Richard
- Toenges-Schuller Nicola
- Tritscher Torsten

- Tsokolis Dimitris
- Turan Eda
- Uhrner Ulrich
- Vanhulsel Marlies
- Vernoux Philippe
- Vidal Bruno
- Vieira Da Rocha Thamara
- Viricelle Jean-Paul
- Wakeling Daniel
- Wallington Timothy
- Weller Konstantin
- Winther Morten
- Wojtowicz Jacek
- Wuethrich Philipp
- Wyatt David
- Xu Bin
- Yaghzar Marouane
- Yahya Mohammad-Reza
- Yang Daoyuan
- Younes Mohamed
- Zamboni Giorgio
- Zimmermann Eric
- łutczyk Grzegorz